ILLUSTRATED SOURCEBOOK
of
MECHANICAL COMPONENTS

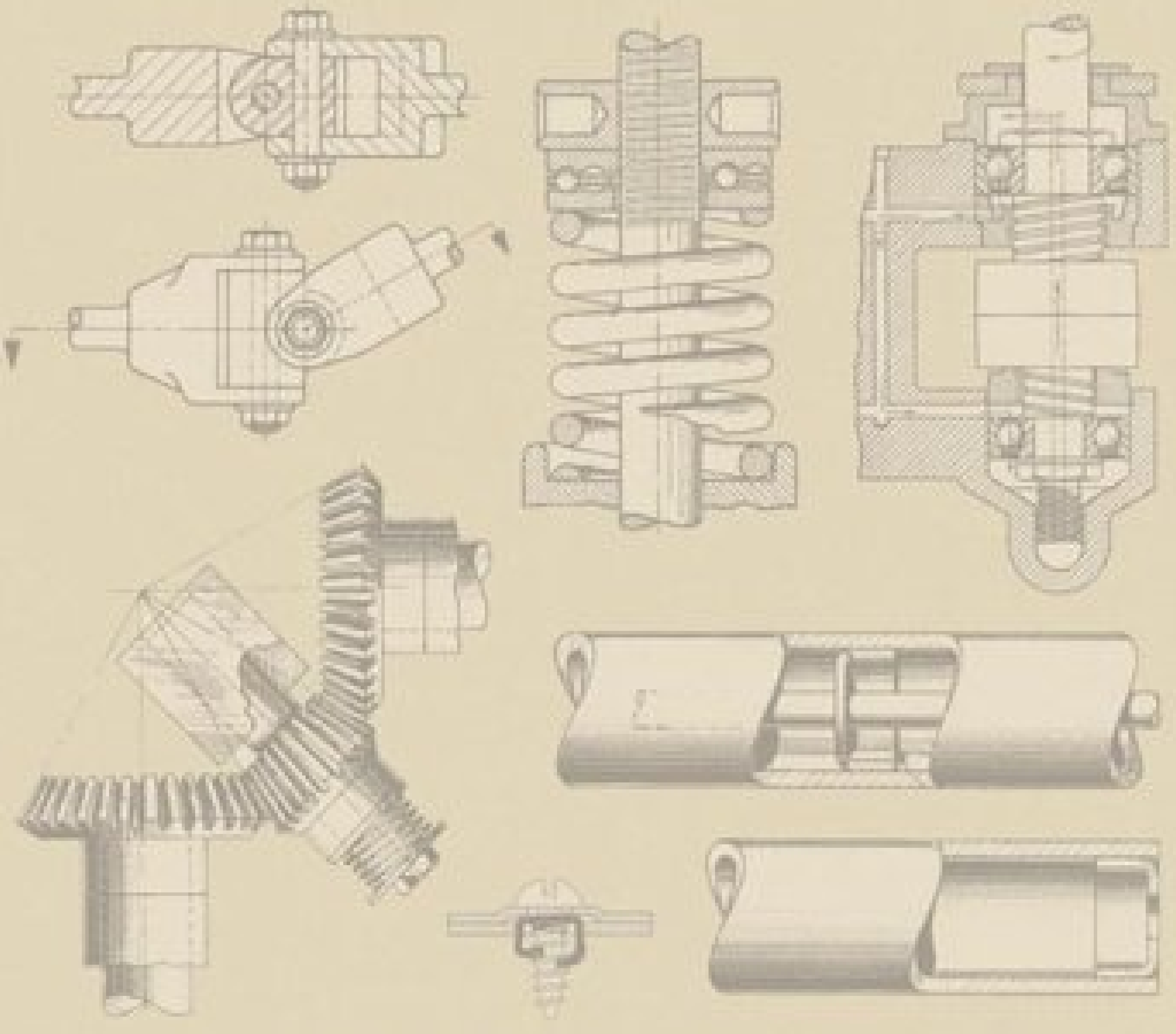

ROBERT O. PARMLEY, P.E.

ILLUSTRATED SOURCEBOOK
of
MECHANICAL COMPONENTS

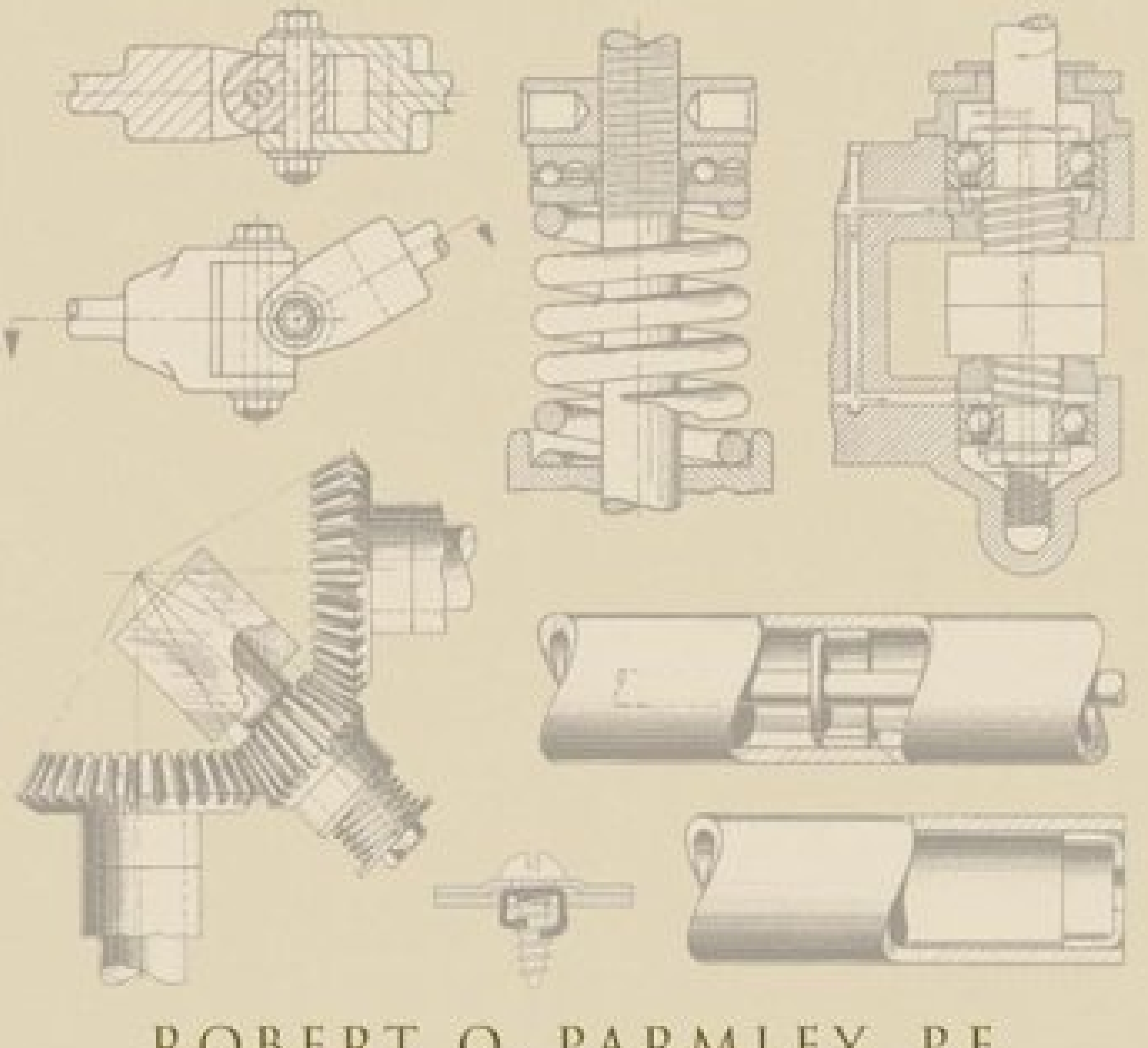

ROBERT O. PARMLEY, P.E.

ILLUSTRATED SOURCEBOOK *of* MECHANICAL COMPONENTS

ROBERT O. PARMLEY, P.E.
EDITOR-*in*-CHIEF

McGraw-Hill
New York San Francisco Washington, D.C. Auckland Bogotá
Caracas Lisbon London Madrid Mexico City Milan Montreal
New Delhi San Juan Singapore Sydney Tokyo Toronto

McGraw-Hill

A Division of The ***McGraw-Hill*** *Companies*

1 2 3 4 5 6 7 8 9 0 KGP/KGP 0 6 5 4 3 2 1 0

ISBN 0-07-048617-4

The sponsoring editor for this book was Linda Ludewig and the production supervisor was Pamela A. Pelton.

It was set in Goudy and designed by Wayne C. Parmley.

Printed and bound by Quebecor/Kingsport.

This book is printed on recycled, acid-free paper containing a minimum of 50% recycled, de-inked fiber.

Dedicated to the memory of Geo. H. Morgan, P.E., co-founder of Morgan & Parmley, Ltd., civil engineer, mentor, partner, trusted friend and a true professional.

ABOUT *the* EDITOR-*in*-CHIEF

Robert O. Parmley, P.E., CMfgE, CSI, is co-founder, President and Principal Consulting Engineer of Morgan & Parmley, Ltd., Professional Consulting Engineers, Ladysmith, Wisconsin. He is also a member of the National Society of Professional Engineers, the American Society of Mechanical Engineers, the Construction Specifications Institute, the American Design Drafting Association, the American Society of Heating, Refrigerating, and Air-Conditioning Engineers, and the Society of Manufacturing Engineers, and is listed in the AAES *Who's Who in Engineering*. Mr. Parmley holds a BSME and a MSCE from Columbia Pacific University and is a registered professional engineer in Wisconsin, California, and Canada. He is also a certified manufacturing engineer under SME's national certification program and a certified wastewater plant operator in the State of Wisconsin. In a career covering four decades, Mr. Parmley has worked on the design and construction supervision of a wide variety of structures, systems, and machines - from dams and bridges to municipal sewage treatment facilities and municipal water projects. The author of over 40 technical articles published in leading professional journals, he is also the Editor-in-Chief of the, *Field Engineer's Manual*, Second Edition, the *HVAC Field Manual*, the *Hydraulics Field Manual*, the *HVAC Design Data Sourcebook*, the *Mechanical Components Handbook*, and the *Standard Handbook of Fastening & Joining*, Third Edition, all published by McGraw-Hill.

PREFACE

The major mission of this sourcebook is to intensify and highlight the importance of typical mechanical components by illustrating their versatility, innovative applications, history and artistry. Hopefully, this presentation will stimulate new ideas by giving the reader a graphic kaleidoscopic view of mechanical components, as well as an appreciation for their geometric grace and adaptability into complex mechanisms.

The contents of this presentation have many sources. We searched legions of past journals and publications for articles about creative uses of mechanical components and selected only the best for inclusion in this book. Many of these classic ideas were originally printed in *Product Engineering*, a great magazine which ceased publication in the mid-1970s.

Product Engineering was a truly unique magazine. Many issues featured a two or three page illustrated article that highlighted an innovate mechanical design. I was a contributor to that series for many years and have repeatedly received requests for reprints. Unfortunately, they are extremely difficult to obtain. Except for Douglas Greenwood's books, published in the late 1950s and early 1960s and Chironis' *Mechanisms & Mechanical Devices Sourcebook*, most of those great presentations have faded from the technical literature. I believe they should be preserved in a hardbound reference. The innovation captured in these illustrated articles is monumental and should be a source of inspiration for decades to come. Innovation and invention generally does not spring forth easily. It takes prior thought, hard work, and tenacity to generate novel concepts; which are followed by the struggle of their development.

In addition, other technical magazines, like *American Machinist*, *Machine Design*, *Power and Assembly*, have generously supplied valuable articles and material from their past issues. Some appropriate data from classic handbooks has been included, with permission, to round out their respective topic.

Several leading manufacturing companies and technical institutes have kindly furnished layouts and designs depicting creative applications of many mechanical components. The design files of Morgan & Parmley, Ltd., (Professional Consulting Engineers) were combed and several of their layouts incorporated into various sections to flesh out the manuscript.

We have, also, included some design material that is not typically available in general handbooks. This data has been placed in the sourcebook to help designers through those unusual or non-typical phases often present during a project.

As previously noted, a major portion of the material displayed throughout the following pages has been selected from five decades of technical publications. Therefore, the reader will undoubtedly notice the wide variety of graphic styles and printing techniques. Since these differences do not affect the technical data, we have let these variations remain and believe they add a historical quality and flavor to the overall presentation.

This sourcebook attempts to help pave the way for designers by having thousands of good, solid ideas at their fingertips from which to consult. Any mechanical engineer, designer or inventor, must have not only technical competence but access to a broad scope of things mechanical. This sourcebook attempts to provide that data in abundance.

Many key mechanical components in use today have been in existence since time immemorial. We must not forget those ingenious individuals of old who solved mechanical problems with truly original solutions. In many cases, their ideas have blended into our technological fabric and are today taken for granted by the public and go unheralded; even by many professionals. We must never lose sight of the fact that knowledge comes slowly and often only through a difficult struggle. Therefore, it is mandatory that successful details and ideas be preserved in order to continue the advancement of technology. It was the discovery of ancient manuscripts, depicting the inventive genius of past civilizations, that helped ignite the European Renaissance. Without that discovery, it is this writer's opinion, the modern technological era would have been significantly delayed and certainly much more difficult to achieve. Good technical ideas are priceless and must be respected by properly recording them for future reference.

Most of this data and information can not be found in conventional handbooks, which tend to present merely condensed basic engineering information. The material selected for this sourcebook represents the product of shirtsleeve engineering which often goes beyond academic training. Here is the distilled experience and valuable knowledge of engineers in the everyday trenches of design; the "Yankee ingenuity" that built America and lead the world into the modern age. Competitive design creates many innovative solutions to complex problems and this sourcebook's goal is to aid in the continuation of that noble process.

Frank Yeaple, former editor of *Product Engineering*, generously supplied hundreds of tear sheets from his collection of past *Product Engineering* publications. It is safe to say that this sourcebook would be severely limited in its content were it not for his valuable assistance. In addition, I want to note Frank's encouragement and support for this project. His wise council is much appreciated.

It is next to impossible to fully list all of the individuals, organizations, societies, institutes and publishers who have assisted in the development of this sourcebook. Their spirit of cooperation and support for this effort has encouraged me numerous times and I salute all of them. Where appropriate, credit has been listed. We have made a special attempt to list the names of original authors of each article. However, any oversight of acknowledgment is purely unintentional.

I must make special note of Harold Crawford's contribution to this effort. Hal was the sponsoring editor for the first book I had published and for the past twenty-five years has been a good friend and advisor. Just before his well earned retirement from McGraw-Hill in 1998, he helped me develop the format for this sourcebook. I trust that our effort meets with his approval.

This project also provided a rare opportunity for me to work "elbow-to-elbow" with my son over an extended period of time. Wayne's contribution greatly influenced the final appearance and general style of this sourcebook. His patience with an aging engineer, who struggles against the operation of computers, is a mark of a true professional. However, our collaboration seemed to ironically bridge the gap between conventional or classic methods and the emerging electronic process. In the final analysis, we both feel this presentation has preserved a large segment of valuable information and innovative designs that would have otherwise remained obscure and perhaps lost forever. The ingenious concepts and artistry of many of these designs should launch future innovative devices and systems to propel technology ever forward; we trust, for the good of society. Hopefully, this sourcebook will have a permanent place in the history of mechanical technology.

A special thanks to Lana and Ethne for transcribing my notes and not complaining when I buried them with last minute revisions. At last, this sourcebook is now complete and ready for public viewing. We have made a special effort to organize its contents into a usable format and trust that it will be of value for decades. If you enjoy this sourcebook as much as we have preparing it, then I know the project was worthwhile.

ROBERT O. PARMLEY, P.E.
Editor-in-Chief
Ladysmith, Wisconsin

INTRODUCTION

Before the reader or user embarks upon a tour of this sourcebook or even randomly leafs through its pages, it should be noted that both the detailed Table of Contents (at the beginning of each Section) and the cross-referenced Index will serve to find specific topics. The format has been structured to insure user-friendliness.

Great effort was taken to arrange each Section and its contents to present a logical continuity, as well as a speedy locate for specific material.

THE COMPONENT:

The building blocks of mechanical mechanisms consist of many typical individual components; just as electrons, protons and neutrons are basic parts of an atom. In each case, these pieces must be properly selected and precisely arranged in a predetermined pattern to result in a functioning unit. As each assembly is fit into a larger and more complex device, the individual component becomes less and less noticeable, until a malfunction occurs. Remember the Challenger's o-ring which triggered a chain of events that resulted in a terrible accident. Think of the literally hundreds of thousands of separate components that performed properly in the space shuttle, the support equipment and control facilities. Yet, apparently, one individual component failed and the world focused its attention on that specific part for months. Similar catastrophic events have been recorded, reminding one of the story that ends with the phrase, "For the lack of a nail the kingdom was lost." Therefore, the weakest link in a chain is the one that fails first and thereby instantly becomes the most important component. Whether it's an automobile that won't start or a lock that will not open, it usually is caused by a single mechanical component gone awry. We must never underestimate the importance of each specific component in any mechanical design and how it fits into the total mechanism.

THE ORIGIN:

The origin of many classic mechanical components, illustrated in this sourcebook, date back to the Greek and Roman civilizations. Others have their roots in the Renaissance, while scores were developed during the modern era of industrial development. As tools and machinery became more refined, designs of mechanical components were also improved. Standards were organized so each typical component had fixed tolerances for manufacture; thereby insuring common usage and interchangeability.

THE DEBT:

Before continuing our discussion, it seems prudent to pause for a moment and reflect upon how much we are indebted to those who preceded us. Modern innovators generally owe a debt of gratitude to those earlier and most often anonymous inventive geniuses. Most of the building blocks on which modern technology rests are the work of unheralded engineers, craftsmen, inventors, millwrights and artisans who left models, descriptions and drawings as their only legacy. Hopefully, this sourcebook will instill in the reader a respect for their invaluable contributions.

Modern wonders of design such as the jet engine, antilock brake system, computer hard-drive, industrial robot and the multi-use laser, utilize basic mechanical components. Upon inspection of these units, one sees springs, pins, fasteners, rings, washers, gears, cams, and many other standard components. These individual components have an unlimited variety of applications in larger and more complex mechanisms.

Over four centuries ago the Renaissance genius, Leonardo da Vinci, drafted hundreds of engineering drawings and notebook sketches of his mechanical designs and technological dreams. Fortunately for us, many have been preserved in his personal manuscripts and have been reproduced. The emerging mechanical technology of that era certainly was a major milestone upon which the industrial revolution sprang. It is assumed that da Vinci's ingenious ideas could not have been universally disseminated had it not been for the printed page. Therefore, in the spirit that motivated Leonardo and others like him, this sourcebook is dedicated to continue that tradition by preserving basic, practical and innovative design information for dissemination.

THE DESIGN:

Good designs rarely come easy. They are generally developed over an extended period; often through experiments, trial & error or structured research and development. When experience is insufficient, a prudent designer consults his technical library and reference files. Therefore, the professional designer who has a broad resource will have a distinct advantage in arriving at a solution. Often designs that were originally developed for one purpose can be slightly modified or easily retrofitted to serve an entirely different solution. In the proper setting and with well illustrated reference material, the designer can review past designs and concepts which should inspire and trigger new arrangements of mechanical components to serve innovative uses.

THE ART:

The art of good mechanical design is a topic seldom discussed. Perhaps it is because the main purpose is to solve a specific problem by producing a machine or mechanism. The grace of geometry and the flow of its contour somehow is not paramount and is lost in its higher calling. Nevertheless, it is this writer's opinion that good mechanical design has an elegance or grace that reveals an artistic expression. Everyone acknowledges the beauty of a well designed automobile or a piece of quality furniture. In the same token, we should see the beauty in the precision of a gear train or a mechanical watch mechanism. The splendor with which each part interacts with its companion to blend, unassumingly, into the whole. That mathematical and mechanical beauty which is displayed is above and beyond its function and should be classified as a work of art.

The ability to visualize a mechanical device, containing various individual components arranged in position to perform a task, and then accurately record that idea on paper in graphic form, is apparently not a common skill. One must be naturally able to think in pictures and either through training or inherited talent sufficiently skilled to draft the device on to paper.

Up until the development of modern drafting principles and the refinement of perspective drawing, man was severely limited in his graphic representations. A combination of art, mathematics, visual proportions, geometry, cross-sectioning, drafting aids and standardization orthographic projection are all needed, in addition to the individual, to produce a truly accurate presentation on paper. This vehicle carries the three dimensional concept from one person's mind to another's. Truly, "a picture is worth a thousand words." This form of communication is not only a technical transmitter, but on another level can be considered an art form.

W. N. WOODRUFF.

SHAFT KEY.

No. 368,744. Patented Aug. 23, 1887.

Fig. 1.

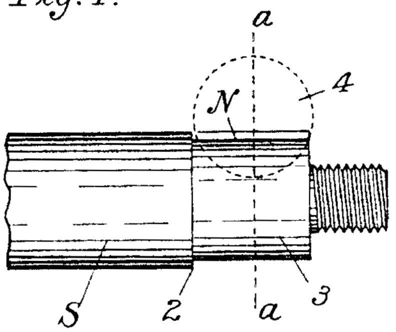

Fig. 2.

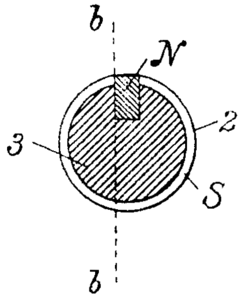

Fig. 3.

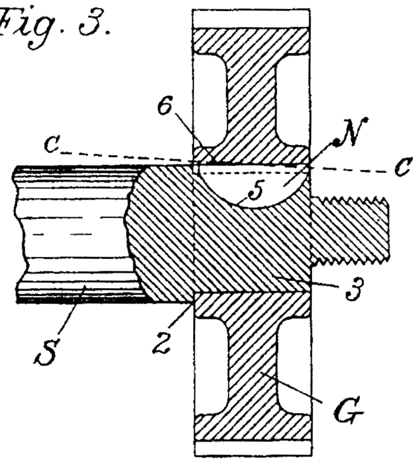

Fig. 4.

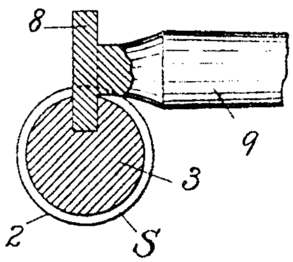

Fig. 5.

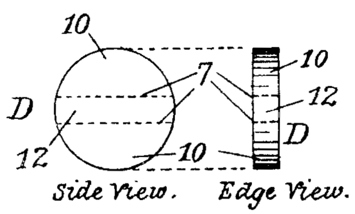

Fig. 6.

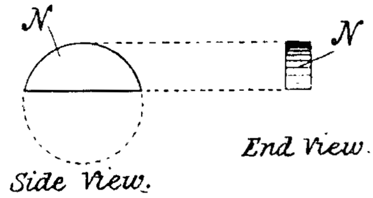

Witnesses:
Geo. W. Drake
W. M. Stone.

Inventor:
Wm. N. Woodruff,
By his Attorney, F. H. Richards.

A good painting has mathematical balance, eye appeal, harmony, conveys a message and pleases the viewer. A well conceived mechanical design has all of these segments. I have viewed thousands of technical drawings during my life that have literally been a vision of beauty. Many have inspired new concepts and mechanical innovations. The very spark that ignited a fresh idea as if one has, for a brief moment, stepped into another mind and shared the idea. Often, just browsing through various technical drawings, something is set in motion in one's own mind that triggers a chain of events that is reminiscent of touring a museum of technology; i.e. the gateway to innovation.

THE KEY:

I had the pleasure to work briefly with a fine gentlemen by the name of William Edgerton in the early 1980s. Bill developed a section on chains & sprockets for me which was included in the *Mechanical Components Handbook* that I edited. At that time, he had served 37 years as chief engineer at Whitney Chain Company.

Upon his retirement in 1985, he wrote me praising the recent publication of MCH. In that letter, Bill noted that Clarence Whitney purchased William Woodruff's patent and his small factory in 1896 and was the sole producer of Woodruff keys until the patent expired. He said that the original patent document, complete with ribbon, was given to him as a souvenir of his decades of service to Whitney Chain. Bill was kind enough to send me a copy of Woodruff's patent and the figure illustrations are reproduced here. Note the masterful simplicity and basic geometry of this universal component which has stood the test of time. This is an excellent example of a single component that revolutionized mechanical technology and continues, to this day, as an element in countless assemblies. This is a true testimony to its inventor; whose ame will always be tied to its identification.

THE RAIL:

In the fall of 1830, a brilliant engineer, named Robert Livingston Stevens was on a ship crossing the Atlantic Ocean headed for England. His mission was to purchase a locomotive and rail tracks for his family's infant Camden & Amboy Railroad which recently received a New Jersey charter and was destined to be one of the first railways in the United States.

Robert was the second generation of a three generation lineage, known as America's "First Family of Inventors". For three generations, the Stevenses of New Jersey displayed their inventive genius in naval warfare equipment, steamboats, agriculture, railroads and a variety of other technical pursuits.

During his passage to England, Robert became concerned with the faulty design of the rail tracks currently being produced. Most of the tracks were iron straps connected to wood rails. The straps tended to loosen and often pierced the carriage underside. This instability was dangerous to freight as well as passengers. Stevens knew that something much stronger would be required if their proposed railway service were to grow and prosper at the rate that he envisioned. The so-called Birkenshaw rail, an English design, had a splendid T profile, but was supported by crude base clamps. Since metalworkers in America, at that time, were scarce, he had to develop something far better.

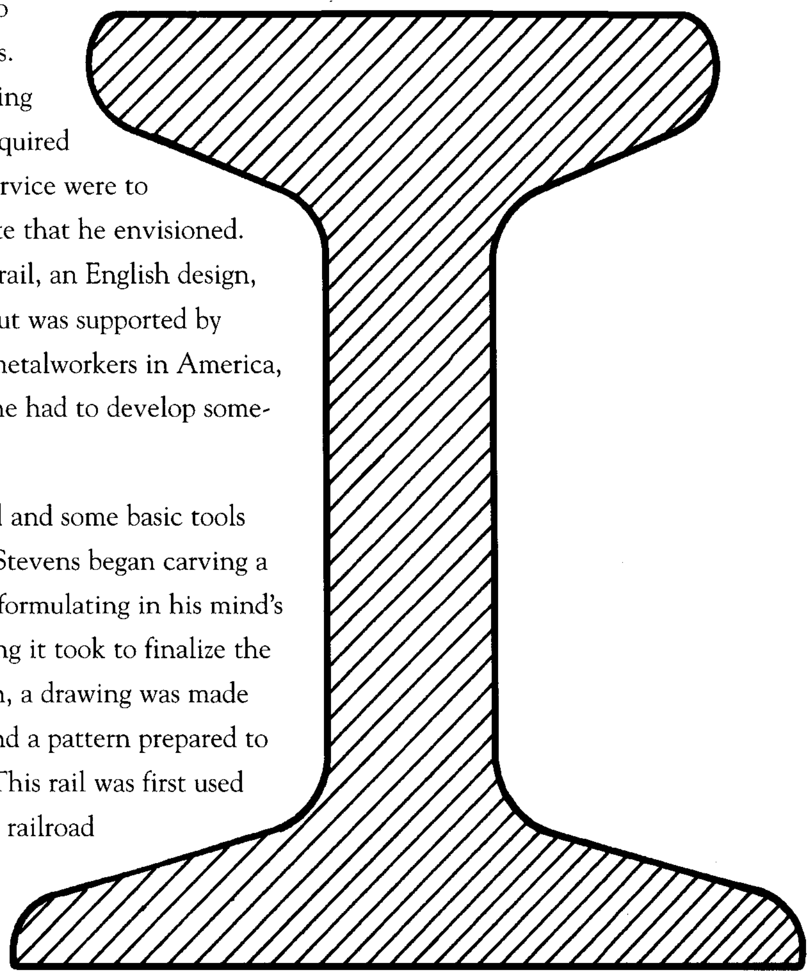

Borrowing a block of wood and some basic tools from the ship's carpenter, Stevens began carving a model of the rail that was formulating in his mind's eye. It is unknown how long it took to finalize the profile, but upon his return, a drawing was made from the wooden model and a pattern prepared to produce the Stevens rail. This rail was first used on the Camden & Amboy railroad carrying the epoch-making John Bull. Stevens' rail design was gradually accepted world-wide and became the industry standard. Even to this day, Stevens' basic rail design is still in use. Thus proving that a good design is universal and will stand the test of time.

As a footnote, Stevens later designed the spike that fastens the rail to the tie and the fish plate that connects the rail ends to each other. He also simplified railway construction by introducing crushed rock as the embedment for wooden ties.

THE ASSEMBLY:

The end product is the final assembly of mechanical components into a device, machine, system or mechanism. With this in mind, several sections at the later portion of this sourcebook illustrate many innovative and complex assemblies. As you study these assemblies, be continually aware of the individual components and their linkage to one another.

THE SUMMARY:

We must never forget the inheritance that was left to us by our predecessors who struggled with technical problems and developed innovative solutions to complex situations. This sourcebook attempts, in a small way, to honor those inventive and resourceful individuals; many of which remain unknown. Their creative skills and adaptability have fueled the advancement of technology for untold centuries. While most of the names remain unsung because records are lacking, this sourcebook has made every effort to faithfully list the original contributor of each presentation reproduced herein, if reliability available. The engineers, designers, technicians, inventors and artisans who generously shared their ideas and took the time to prepare the original material reveals the spirit of the true professional. They certainly represent the heart or spark plug of technology.

ROBERT O. PARMLEY, P.E.
Editor-in-Chief

CONTENTS

SECTION 1

GEARS & GEARING

Design of Bevel Gears

Yesterday's rule of thumb isn't good enough today. With this systematic approach you can quickly predict gear life for a given load capacity.

Wells Coleman

TIME was when the gear designer could rely on rule of thumb, conservative factors of safety, backglances at previous designs. Today he must often design for specific load capacity and life.

Fortunately, though design goals are higher, the approach can be simpler. With the charts given here you can go directly to the proper range of gear sizes; with the rating formulas you can pinpoint the best gear rapidly. The data are based on two key factors, surface durability (pitting resistance) and strength (resistance to tooth breakage). Included are recommendations for diametral pitches, number of teeth, face widths, spiral angles, tooth proportions, mounting design, and gear lubrication—and a completely worked-out design problem. A previous article (see Editor's Note, p 80) compares in detail the various types of bevel gears.

Loads and conditions

You will need to know something about anticipated loads and operating conditions:

Normal operation: What is the normal load and speed, desired number of hours of life? Is operating temperature range to be above the normal 160 to 180 F? If so, you must allow for this in your design.

Peak operation: What will be the maximum torque, the expected duration of maximum torque during gear life, the temperature at peak load?

Starting loads: What is the peak starting torque, frequency of occurrence, and duration of starting loads at each start?

Shock loads: Suggested overload factors are shown in Table I. Shock loads, however, cannot be predicted accurately. Energy absorption methods of load measurement are unreliable because the time duration is so short. Strain-gage measurements must be made with extreme care if results are to be reliable. Repetitive shock is, of course, more damaging than occasional shock loads, but these should not be ignored.

Duration of loads: This information may be known from past experience. More often it is a matter of making an estimate based on a rational premise. Prepare time-torque curves if possible.

Gear lubrication: The rating formulas given in this article assume that the gears will be properly lubricated. Some lubrication hints, however, are also given.

Once the loads and operating conditions are known, the next step is to determine approximate gear size, num-

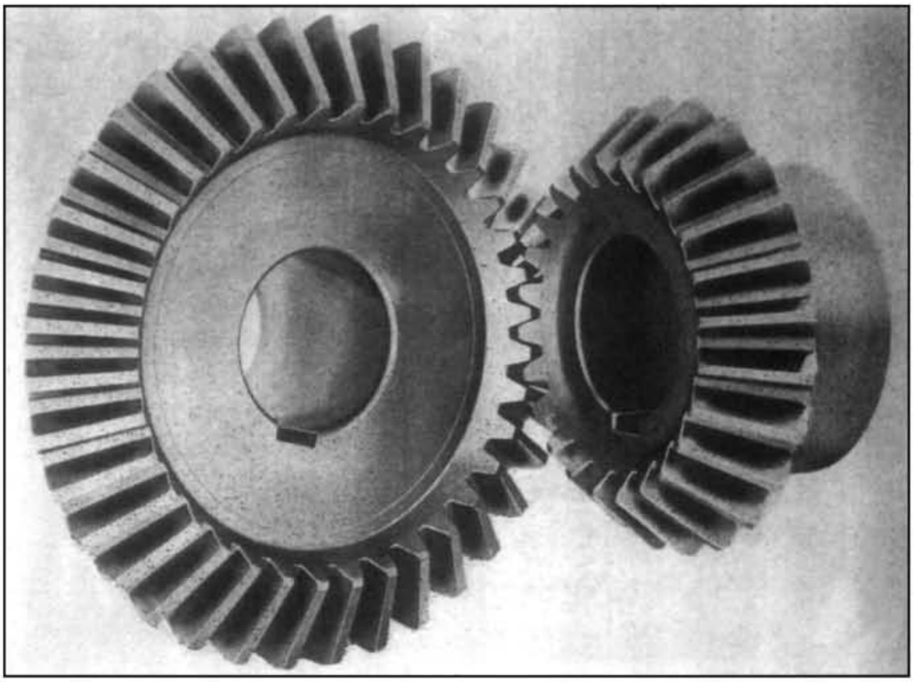

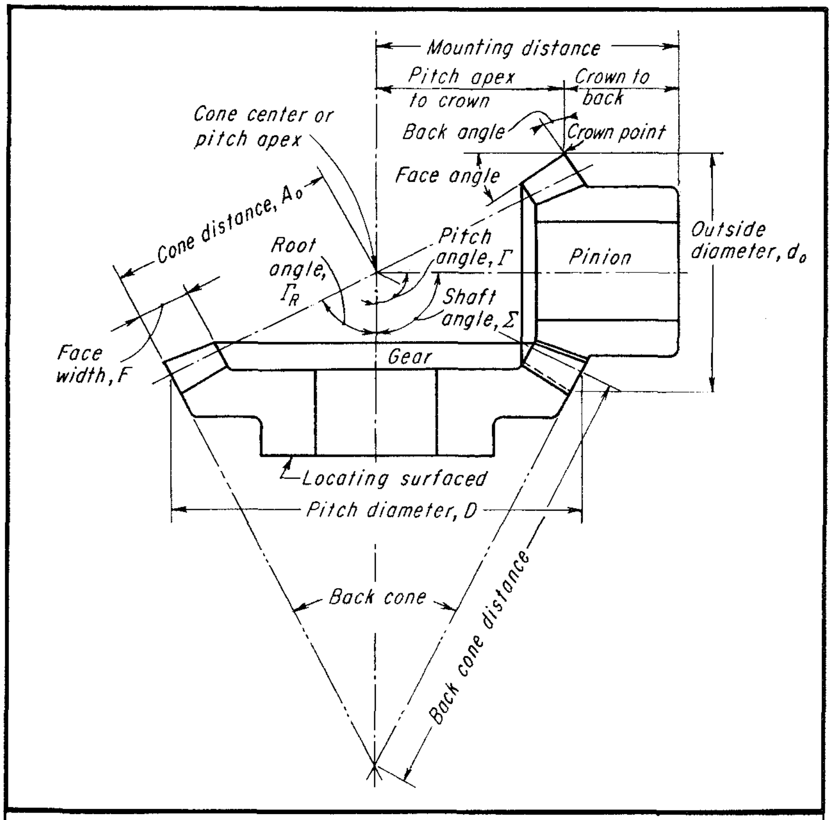

Symbols

a_o = addendum, in.
A_o = outer cone distance, in.
b_o = dedendum, in.
c = clearance, in.
C_M = material factor
d = pinion pitch dia, in.
d_o = outside dia, in.
D = gear pitch dia, in.
F = face width, in.
h_k = working depth, in.
h_t = whole depth, in.
K = circular thickness factor
I = durability geometry factor
J = strength geometry factor
m = speed ratio
m_F = face contact ratio
n = pinion speed, rpm
N_C = number of teeth in crown gear
N_G = number of gear teeth
N_P = number of pinion teeth
P = maximum operating horsepower, hp
P_d = diametral pitch
t = circular tooth thickness, pinion, in.
T = design pinion torque, lb-in.; also circular tooth thickness, pinion, in.
T' = maximum operating torque, or one-half peak pinion torque, or full peak pinion torque, lb-in.
V = pitch line velocity, ft/min
X_o = pitch apex to crown, in.
δ = dedendum angle
γ = pinion pitch angle, deg
Γ = gear pitch angle, deg
γ_o = pinion face angle
Γ_o = gear face angle
γ_R = pinion root angle
Γ_R = gear root angle
ϕ = pressure angle, deg
Ψ = spiral angle, deg
Σ = shaft angle, deg

bers of teeth, diametral pitch, and face width.

GEAR SIZE

Peak loads

First determine what fraction of the peak load to employ for estimating the gear size. This has been our experience:

If the total duration of the peak load exceeds ten million cycles during the total expected life of the gears, use the peak load for estimating the gear size.

If, however, the total duration of the peak load is less than ten million cycles, use one half the peak load, or the value of the highest sustained load, whichever is greater.

The pinion torque requirement (torque rating) can now be obtained as follows:

$$T = T' \tag{1}$$

or

$$T = \frac{63{,}000P}{n} \tag{2}$$

where T = design pinion torque, lb-in.
T' = maximum operating pinion torque, or one half peak pinion torque, or full peak pinion torque, as outlined above.
P = maximum operating horsepower
n = pinion speed, rpm

For general industrial gearing the preliminary gear size is based on surface durability (long gear life in preference to minimum weight). The design chart, Fig 1, is from durability tests conducted with right-angle spiral-bevel gears of case-hardened steel. Given pinion torque and the desired gear ratio, the chart gives pinion pitch diameter.

For other materials, multiply the pinion diameter given in Fig 1 by the material factor given in Table II.

Straight bevels and Zerol bevels will be somewhat larger. Multiply the values of pinion pitch diameter from Fig 1 by 1.3 for Zerol bevels and by 1.2 for Coniflex straight bevels. (Zerol and Coniflex are registered trademarks of the Gleason Works.)

For high-capacity spiral bevels (case-hardened, with ground teeth), the preliminary gear size is based on both surface capacity and bending strength. Based on surface capacity, the pinion diameter from Fig 1 should be multiplied by 0.80. Based on bending strength, the pinion diameter is given by Fig 2. Choose the larger pinion diameter of these two.

Statically loaded gears should be

designed for bending strength rather than surface durability. For statically loaded gears which are subject to vibration, multiply the pinion diameter from Fig 2 by 0.70. For statically loaded gears not subject to vibration, multiply the pinion diameter from Fig 2 by 0.60.

Tooth numbers

Although tooth numbers are frequently selected in an arbitrary manner, it has been our experience that for most applications the tooth numbers for the pinion from the charts, Fig 3 and 4, will give good results. Fig 3 is for spiral bevels and Fig 4 for straight and Zerol bevels. The number of teeth in the mating gear is of course governed by the gear ratio.

For lapped gears: Avoid a common factor in the numbers of teeth in the gear and mating pinion. This permits better and more uniform wear in the lapping process on hardened gears.

For precision gears: Accuracy of motion is of prime importance; hence the teeth of both pinion and gear should be hardened and ground. Also, use even ratios. Gears made for even ratios are easier to test, inspect, and assemble accurately.

Automotive gears: These are generally designed with fewer pinion

1. . PITCH DIAMETERS BASED ON SURFACE DURABILITY

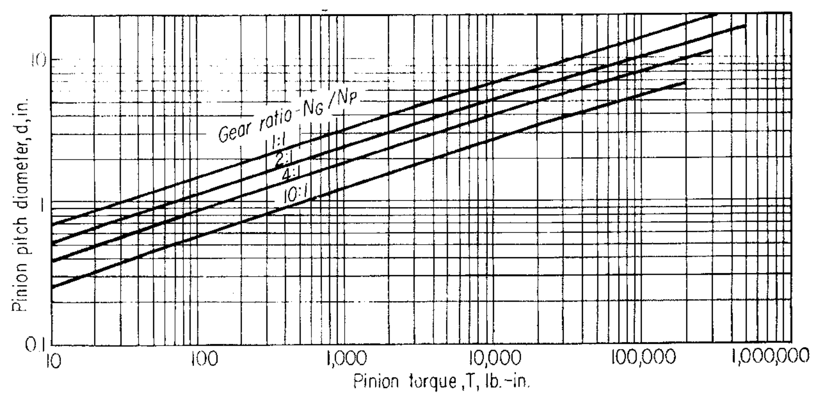

2. . PITCH DIAMETERS BASED ON TOOTH BENDING STRENGTH

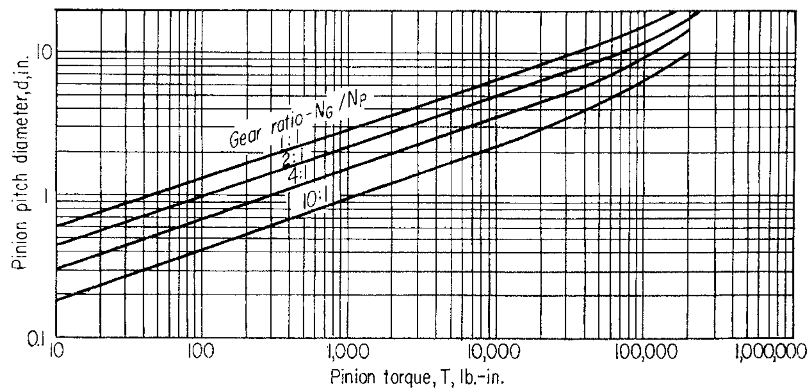

Table I . . Overload factors

Values in this table are for speed decreasing drives; for speed increasing drives add $0.01(N_G/N_P)^2$ to these factors.

POWER SOURCE	CHARACTER OF LOAD ON DRIVEN MACHINE		
	Uniform	**Medium shock**	**Heavy shock**
Uniform	1.00	1.25	1.75
Light shock	1.25	1.50	2.00
Medium shock	1.50	1.75	2.25

Table II . . Material factors for gear mesh

GEAR		PINION		Material Factor
	Minimum hardness		Minimum hardness	C_M
Case-hardened steel	58 R_C	Case-hardened steel	60 R_C	0.85
Case-hardened steel	55 R_C	Case-hardened steel	55 R_C	1.00
Flame-hardened steel	50 R_C	Case-hardened steel	55 R_C	1.05
Flame-hardened steel	50 R_C	Flame-hardened steel	50 R_C	1.05
Oil-hardened steel	375-425 Brinell	Oil-hardened steel	375-425 Brinell	1.20
Heat-treated steel	250-300 Brinell	Case-hardened steel	55 R_C	1.45
Heat-treated steel	210-245 Brinell	Heat-treated steel	245-280 Brinell	1.65
Cast iron	....	Case-hardened steel	55 R_C	1.95
Cast iron	....	Flame-hardened steel	50 R_C	2.00
Cast iron	....	Annealed steel	160-200 Brinell	2.10
Cast iron	....	Cast iron	....	3.10

3 . . NUMBER OF TEETH FOR SPIRAL BEVEL GEARS

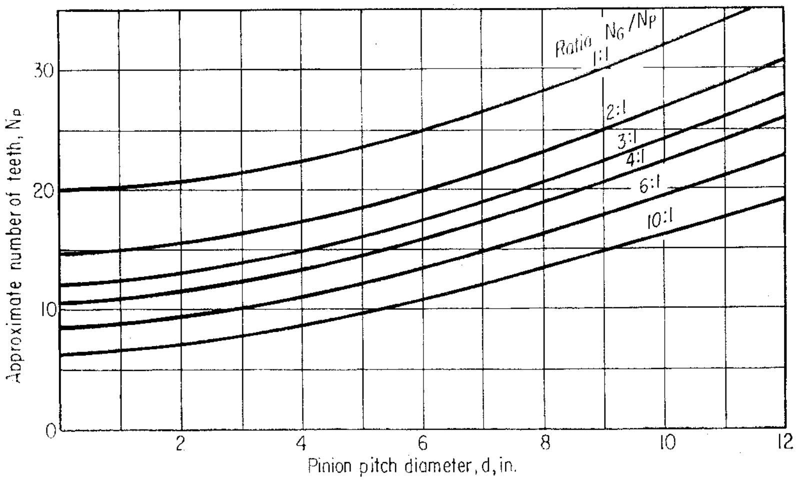

4 . . NUMBER OF TEETH FOR STRAIGHT AND ZEROL BEVELS

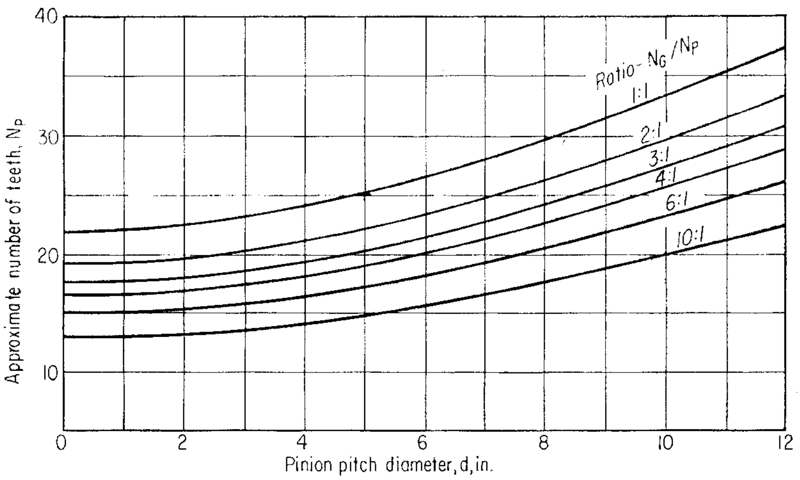

Table III..Pinion teeth for automotive applications

Approximate ratio, N_G/N_P	Preferred number of pinion teeth, N_P	Allowable range, N_P
2.0	17	15-19
2.5	15	12-16
3.0	11	10-14
3.5	10	9-12
4.0	9	8-10
4.5	8	7-9
5.0	7	6-9
6.0	6	5-8
7.0	6	5-7
8.0	5	5-6

teeth. Table III gives suggested tooth numbers for automotive spiral bevel drives. The numbers of teeth in the gear and mating pinion should not contain a common factor.

Face widths

The face width should not exceed 30% of the cone distance for straight-bevel and spiral-bevel gears and should not exceed 25% of the cone distance for Zerol bevel gears. In addition, it is recommended that the face width, F, be limited to

$$F \leqq 10/P_d$$

where P_d is the diametral pitch. Practical values of diametral pitches range from 1 to 64.

The design chart in Fig 5 will give the approximate face width for straight-bevel and spiral-bevel gears. For Zerol bevels the face width given by this chart should be multiplied by 0.83. The chart is based on face width equal to 30% of cone distance.

Diametral pitch

The diametral pitch can now be determined by dividing the number of teeth in the pinion by the pinion pitch diameter. Thus

$$P_d = N_P/d$$

Because tooling for bevel gears is not standardized according to pitch, it is not necessary that the diametral pitch be an integer.

Spiral angle

The spiral angle of spiral-bevel gears should be so selected as to give a face-contact ratio, m_F, of at least 1.25. We have found that for smoothness and quietness, a face-contact ratio of 2.00 or higher will give best results.

The design chart, Fig 6, gives the spiral angle for various face-contact ratios. It is assumed that you have already determined the diametral pitch and face width to obtain the product, P_dF. The curves are based on the equation

$$m_F = P_dF[K_1 \tan \psi - K_2 \tan^3 \psi]$$

where
Ψ = spiral angle
$K_1 = 0.2865$
$K_2 = 0.0171.$

The values for K_1 and K_2 are dependent upon the ratio of face width to outer cone distance of $F/A_0 = 0.3$.

Whenever possible, select the hand of spiral to give an axial thrust that tends to move both the gear and pinion out of mesh. As a second choice, select the hand of spiral to give an axial thrust that tends to move the pinion out of mesh.

Standard bevel systems

There are three standardized AGMA systems of tooth proportions for bevel gears: 20-deg straight bevel, spiral bevel, and Zerol bevel. There are also several special bevel-gear tooth forms which result in minor modifications to the above proportions. These special forms are used for manufacturing economy or to accommodate special mounting considerations. Because they are very closely tied to the method used in producing the gears, the means of achieving them and the effects they have on standard tooth proportions are beyond the scope of this article.

20-deg straight bevels

General proportions for this system are given in Table IV. The tooth form is based on a symmetrical rack, except where the ratio of tooth top lands on pinion and gear would exceed a 1.5 to 1 ratio. A different value of addendum is employed for each ratio to avoid undercut and to achieve approximately equal strength. If these gears are cut on modern bevel-gear generators they will have a localized tooth bearing. Coniflex gears have this tooth form. To provide uniform clearance, the face cone elements of the gear and pinion blanks are made parallel to the root cone elements of the mating member. This permits the use of larger edge radii on the generating tools, with consequent greater fatigue strength.

Note that the data in Table IV apply only to straight bevel gears that meet the following requirements:

1) The standard pressure angle is 20 deg. See Table V for ratios which may be cut with 14½, 22½, and 25-deg pressure angles.

2) The teeth are full depth. Stub teeth are avoided because of resulting reduction in contact ratio, which can increase both wear and noise.

3) Teeth with long and short addenda are used throughout the system (except on 1:1 ratios) to avoid undercut, increase strength, and reduce wear.

4) The face width is limited to one third the cone distance. The use of a greater face width results in an excessively small tooth size at the inner end of the teeth and, therefore, impractical cutting tools.

The American Gear Manufacturers Assn standard for this system is AGMA 208.02.

Spiral bevels

Tooth thicknesses (see Table IV) are proportioned so that the stresses in the gear and pinion will be approximately equal with a left-hand pinion driving clockwise or a right-hand pinion driving counterclockwise. These proportions will apply to all gears operating below their fatigue endurance limit. For gears operating above the endurance limit, special thickness proportions will be required. The standard for this system is AGMA 209.02.

The tooth proportions shown are based on the 35-deg spiral angle. A smaller spiral angle may result in undercut and a reduction in contact ratio. The data in this system do not apply to the following:

1) Automotive rear-axle drive gears, which normally are designed with

5 . . FACE WIDTHS FOR SPIRAL BEVELS AT 90° SHAFT ANGLE. FOR ZEROL, MULTIPLY BY 0.83.

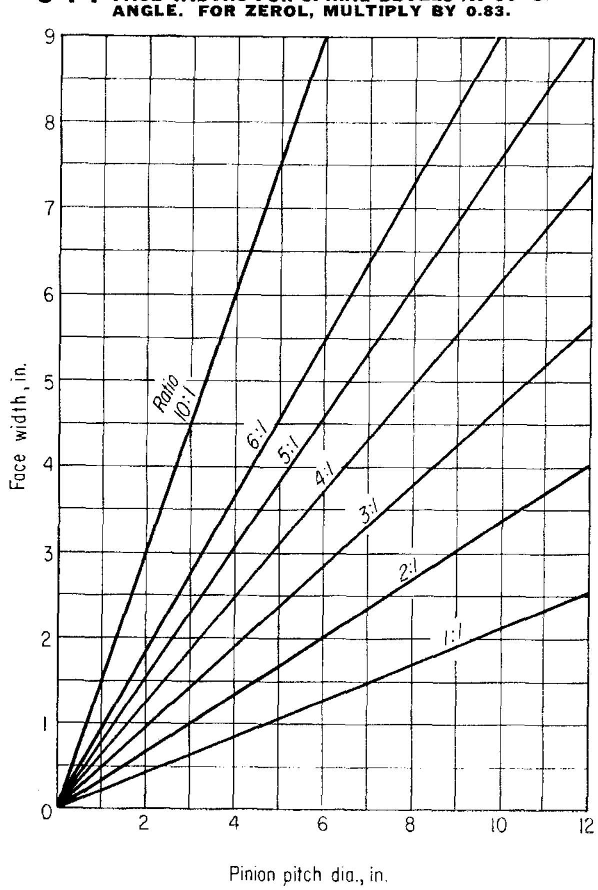

6 . . FACE-CONTACT RATIO FOR SPIRAL BEVELS

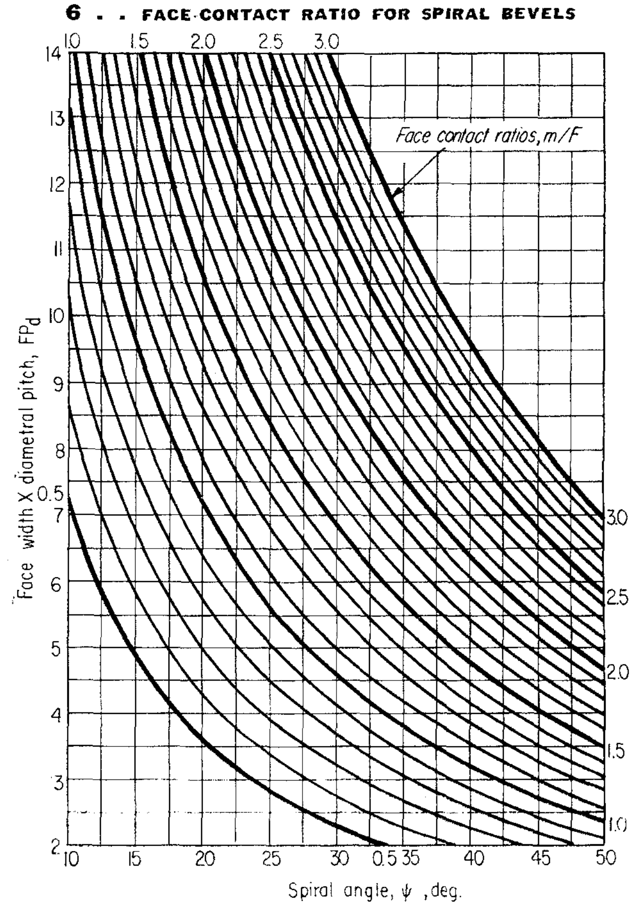

Table IV..Tooth Proportions for Standard Bevel Gears

Item	STANDARD BEVELS (*see Table V for other cases*)		
	Straight	**Spiral**	**Zerol**
Pressure angle, ϕ, deg	20	20	20, 22½, 25
Working depth, h_k, in.	$2.000/P_d$	$1.700/P_d$	$2.000/P_d$
Whole depth, h_t, in.	$(2.188/P_d)+0.002$	$1.888/P_d$	$(2.188/P_d)+0.002$
Clearance, c, in.	$(0.188/P_d)+0.002$	$0.188/P_d$	$(0.188/P_d)+0.002$
Gear addendum, a_G, in.	$\frac{0.540}{P_d}+\frac{0.460}{P_d(N_G/N_P)^2}$	$\frac{0.460}{P_d}+\frac{0.390}{P_d(N_G/N_P)^2}$	$\frac{0.540}{P_d}+\frac{0.460}{P_d(N_G/N_P)^2}$
Face Width, F, in. (Use the smaller value from the two formulas)	$F \leqq \frac{A_o}{3}$ or $F \leqq \frac{10}{P_d}$	$F \leqq \frac{3A_o}{10}$ or $F \leqq \frac{10}{P_d}$	$F \leqq \frac{A_o}{4}$ or $F \leqq \frac{10}{P_d}$
Spiral angle, ψ, deg	None	25 to 35 (See note 1)	0
Minimum number of teeth (Note 2)	13	12	13
Diametral pitch range	no restriction	12 & coarser	3 & finer
AGMA reference number	208.02	209.02	202.02

Notes

1. 35 deg is the standard spiral angle. If smaller spiral angles are used, undercut may occur and the contact ratio may be less.
2. This is the minimum number of teeth in the basic system. See Table V for equivalent number of teeth in the gear member.

fewer pinion teeth than listed in this system.

2) Helixform and Formate (registered Gleason trademarks) pairs, which are cut with a nongenerated tooth form on the gear.

3) Gears and pinions of 12 diametral pitch and finer. Such gears are usually cut with one of the duplex cutting methods and therefore require special proportions.

4) Ratios with fewer teeth than those listed in Table V.

5) Gears and pinion with less than 25-deg spiral angle.

Zerol bevels

Considerations of tooth proportions to avoid undercut and loss of contact ratio as well as to achieve optimum balance of strength are similar to those for the straight-bevel gear system.

The Zerol system is based on tooth proportions (Table IV) in which the root cone elements do not pass through the pitch cone apex. The face cone element of the mating member is made parallel to the root cone element to produce uniform clearance.

The basic pressure angle is 20 deg. Where needed to avoid undercut, 22½-deg or 25-deg pressure angles are also used (see Table V). The face

Table V.. Minimum number of teeth

Pressure angle, deg	STRAIGHT Pinion	STRAIGHT Gear	SPIRAL Pinion	SPIRAL Gear	ZEROL Pinion	ZEROL Gear
20 (standard)	16	16	17	17	17	17
	15	17	16	18	16	20
	14	20	15	19	15	25
	13	30	14	20		
			13	22		
			12	26		
14½	29	29	28	28	Not Used	
	28	29	27	29		
	27	31	26	30		
	26	35	25	32		
	25	40	24	33		
	24	57	23	36		
			22	40		
			21	42		
			20	50		
			19	70		
16	Not Used		24	24	Not Used	
			23	25		
			22	26		
			21	27		
			20	29		
			19	31		
			18	36		
			17	45		
			16	59		
22½	13	13	14	14	14	14
					13	15
25	12	12	12	12	13	13

width is limited to one quarter of the cone distance because, owing to the duplex taper, the small-end tooth depth decreases rapidly as the face width increases.

The standard for this system is AGMA 202.02.

Gear-dimension formulas

Table VI gives the formulas for bevel-gear blank dimensions. Tooth proportions are based on data from Table IV. A sample design problem later in the article illustrates the use of these formulas.

Rating formulas

Once the initial gear size has been determined from the above charts, the gears are checked for surface durability and strength, using the following two equations. Surface durability is the resistance to pitting and involves the stress at the point of contact, using Hertzian theory. Strength is the resistance to tooth breakage and refers to the calculation of bending stress in the root of the tooth.

Surface durability:

$$T = \frac{FIK_v}{2K_m}\left(\frac{S_c d}{C_p}\right)^2 \qquad (3)$$

Strength:

$$T = \frac{FJK_v}{2K_s K_m}\left(\frac{S_t d}{P_d}\right) \qquad (4)$$

where

T = maximum allowable torque, lb-in. Use the smaller of the two values.
S_c = allowable contact stress. For recommended values see Table VIII.
S_t = allowable bending stress (also from Table VIII)
d = pinion pitch diameter at larger end of tooth, in.
P_d = diametral pitch at large end of tooth
F = face width, in.
C_p = elastic coefficient (see Table IX)
I = geometry factor (durability) from the design curves in Fig 9 and 10. Fig 9 is for spiral bevel gears with 20-deg pressure angle and 35-deg spiral angle, Fig 10 for straight-bevel and Zerol-bevel gears with 20-deg pressure angle.
J = geometry factor (strength) from the design curves in Fig 11 and 12. Fig 11 is for spiral-bevel gears with 20-deg pressure angle and 35-deg spiral angle. Fig 12 is for straight-bevel and Zerol-bevel gears with 20-deg pressure angle.
K_m = load distribution factor. Use 1.0 when both gear and pinion are straddle-mounted; use 1.1 when only one member is straddle-mounted. Somewhat higher values may be required if the mountings deflect excessively.
K_v = dynamic factor from the design curves in Fig. 13. Use curve 1 for high-precision ground-tooth gears, curve 2 for industrial spiral bevels, curve 3 for industrial straight-bevel and Zerol-bevel gears.
K_s = size factor from Fig 14.

If the computed value of T from either of the above torque equations is less than the design pinion torque,

7 . . CIRCULAR THICKNESS FACTORS, STRAIGHT AND ZEROL BEVELS

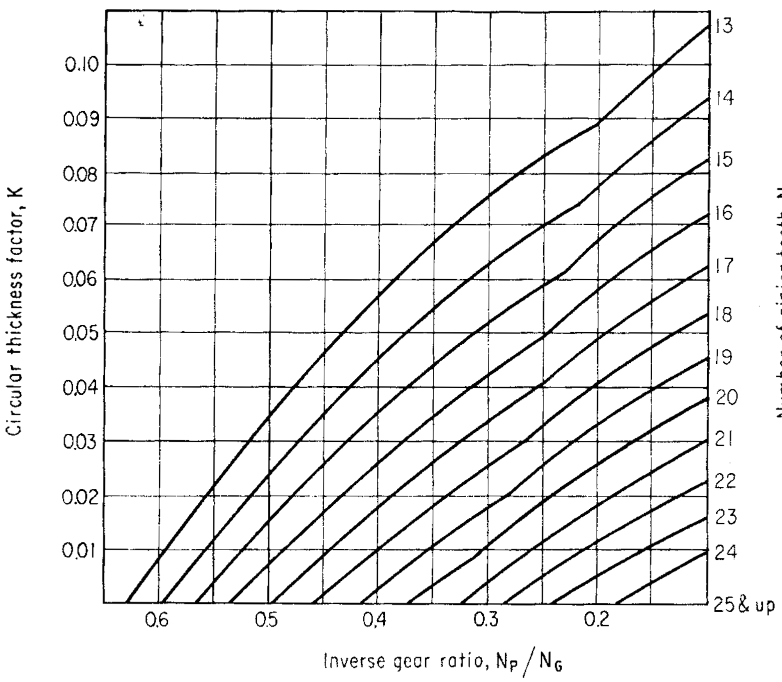

8 . . CIRCULAR THICKNESS FACTORS FOR SPIRAL BEVELS

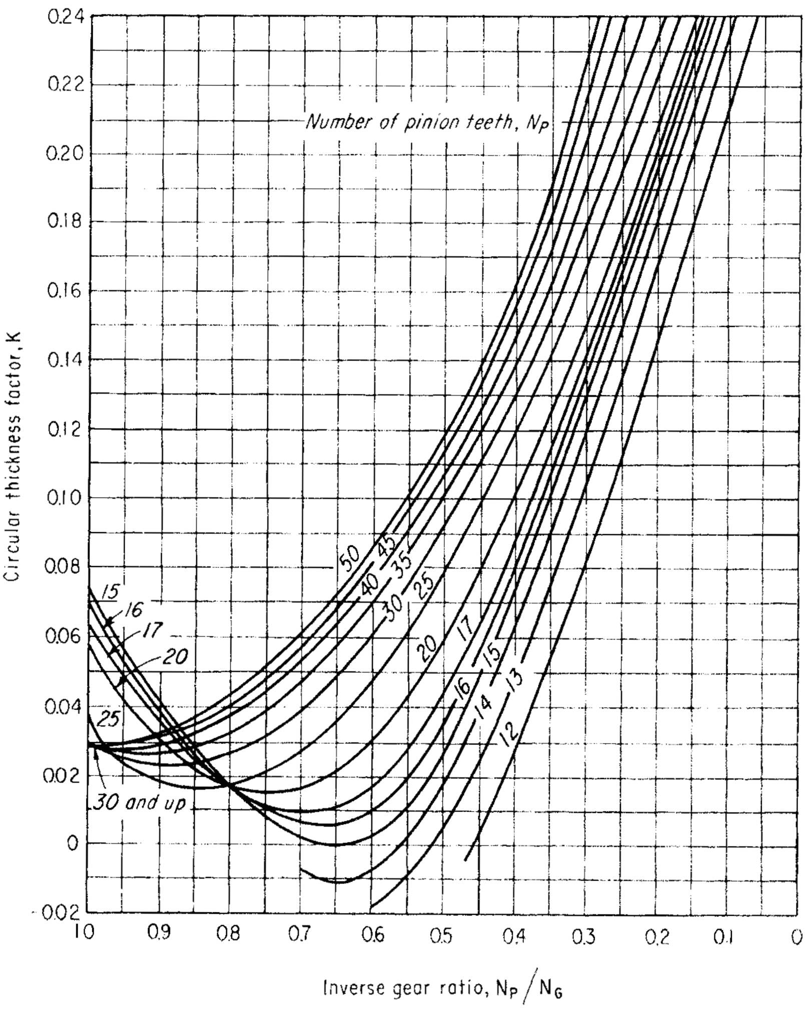

the gear sizes should be increased and another check should be made.

Design example

Select a bevel gear set to connect a small steam turbine to a centrifugal pump with the following specifications: The turbine is to deliver 29 hp at 1800 rpm to a centrifugal pump. The pump is to operate at 575 rpm.

Gear ratio:

$$m = 1800/575 = 3.13$$

Normal operating torque:

$$T' = 63{,}000(29)/1800$$
$$= 1015 \text{ lb-in.}$$

For a centrifugal pump driven by a steam turbine, only light shock with uniform load is anticipated. Therefore an overload factor of 1.25 is selected from Table I.

Design torque:

$$T = 1.25(1{,}015) = 1270 \text{ lb-in.}$$

Because the speed is above 1000 rpm, spiral-bevel gears are used.

Pinion pitch diameter: From Fig 1, for $T = 1{,}270$ lb.-in. and $N_G/N_P = 3.13$, $d = 2.2$ in. Because this is an industrial design, Fig 2 need not be consulted.

Number of teeth: From Fig 3, the pinion will have $N_P = 13$ teeth. Thus, for the gear, $N_G = 13(3.13) = 41$ teeth.

Face width: From Fig 5, the face width of both gears will be approximately $F = 1.1$ in.

Pitch line velocity:

$$V = \frac{3.14(2.2)(1800)}{12}$$

$$= 1030 \text{ ft/min}$$

The approximate size of the gear set has quickly been determined. Now check it for durability and strength using these factors:

$S_c = 200{,}000$ psi, from Table VIII, assuming that both pinion and gear are to be made from case-hardened steel
$C_p = 2800$, from Table IX
$I = 0.116$, from Fig 9
$K_m = 1.1$ for overhung pinion mounting
$K_v = 0.84$ from curve 2, Fig 13

Durability evaluation:

$$T = \frac{(1.1)(0.116)(0.84)(200{,}000)^2(2.2)^2}{(2)(1.1)(2800)^2}$$

$T = 1210$ lb-in.

Since the gears must be designed to carry 1270 lb-in. torque, the gear size should be increased slightly. To approximate the new size, multiply the

Table VI..Bevel-gear dimensions

Dimension *All dimensions in in. and deg*	Formulas, chart or table	
1. Number of pinion teeth, N_P	Figs 3, 4; Tables III, V	
2. Number of gear teeth, N_G	$N_G = m\ N_p$	
3. Diametral pitch, P_d	Practical range, 1 to 64 P_d	
4. Face width, F	Fig 5; Table IV	
5. Working depth, h_k	Table IV	
6. Whole depth, h_t	Table IV	
7. Pressure angle, ϕ	Table IV	
8. Shaft angle, Σ	Practical range, 10 to 180 deg	
	Pinion	**Gear**
9. Pitch diameter; d, D	$d = \frac{N_P}{P_d}$ (Figs 1, 2)	$D = \frac{N_G}{P_d}$
10. Pitch angle; γ, Γ	$\gamma = \tan^{-1}\frac{\sin\Sigma}{\frac{N_G}{N_P}+\cos\Sigma}$	$\Gamma = \Sigma - \gamma$
11. Outer cone distance, A_o	$A_o = \frac{D}{2\sin\Gamma}$	
12. Circular pitch, p	$p = \frac{3.1416}{P_d}$	
13. Addendum, a_{oP}	$a_{oP} = h_k - a_{oG}$	$a_{oG} =$ (Table IV)
14. Dedendum, b_{oP}	$b_{oP} = h_t - a_{oP}$	$b_{oG} = h_t - a_{oG}$
15. Clearance, c	$c =$ (Table IV)	
16. Dedendum angle, δ (See Note 1)	$\delta_P = \tan^{-1}\frac{b_{oP}}{A_o} + \Delta\delta$	$\delta_G = \tan^{-1}\frac{b_{oG}}{A_o} + \Delta\delta$
17. Face angle of blank; γ_o, Γ_o	$\gamma_o = \gamma + \delta_G$	$\Gamma_o = \Gamma + \delta_P$
18. Root angle; γ_R, Γ_R	$\gamma_R = \gamma - \delta_P$	$\Gamma_R = \Gamma - \delta_G$
19. Outside diameter; d_o, D_o	$d_o = d + 2\,a_{oP}\cos\gamma$	$D_o = D + 2\,a_{oG}\cos\Gamma$
20. Pitch apex to crown; x_o, X_o	$x_o = A_o\cos\gamma - a_{oP}\sin\gamma$	$X_o = A_o\cos\Gamma - a_{oG}\sin\Gamma$
21. Circular thickness; t, T (See Note 2)	$t = p - T$	$T = \frac{p}{2} - (a_{oP} - a_{oG})\frac{\tan\phi}{\cos\Psi} - \frac{K}{P_d}$

Notes:

1. The change in dedendum angle, $\Delta\delta$, is zero for straight bevel and spiral bevel gears; $\Delta\delta$ is given by Table VII for Zerol bevel gears.
2. Factor K is given by Fig 7 for straight bevel and Zerol bevel gears with 20 deg pressure angle, and by Fig 8 for spiral bevel gears with 20 deg pressure angle and 35 deg spiral angle. For other cases K can be determined by the method outlined in "Strength of Bevel and Hypoid Gears" published by the Gleason Works.

Table VII..Formulas for $\Delta\delta$ — Zerol bevel gears

Pressure Angle, deg	Change in Dedendum Angle, $\Delta\delta$, min
20	$\Delta\delta = \frac{6668}{N_C} - \frac{300}{F}\sqrt{\frac{1}{N_C\,P_d\,(\tan\gamma+\tan\Gamma)}} - \frac{14\,P_d}{N_C}$
22½	$\Delta\delta = \frac{4868}{N_C} - \frac{300}{F}\sqrt{\frac{1}{N_C\,P_d\,(\tan\gamma+\tan\Gamma)}} - \frac{14\,P_d}{N_C}$
25	$\Delta\delta = \frac{3412}{N_C} - \frac{300}{F}\sqrt{\frac{1}{N_C\,P_d\,(\tan\gamma+\tan\Gamma)}} - \frac{14\,P_d}{N_C}$

Note:
$N_C = 2\,P_d\,A_o =$ number of teeth in crown gear.

Table VIII..Allowable stresses

Material	Heat treatment	Minimum surface hardness	Contact Stress S_C, psi	Bending Stress S_t, psi
Steel	Carburized (*Case Hardened*)	55 R_C	200,000	30,000
Steel	Flame or Induction hardened (*Unhardened root fillet*)	50 R_C	190,000	13,500
Steel	Hardened and Tempered	300 Brinell	135,000	19,000
Steel	Hardened and Tempered	180 Brinell	95,000	13,500
Steel	Normalized	140 Brinell	65,000	11,000
Cast Iron	As Cast	200 Brinell	65,000	7,000
Cast Iron	As Cast	175 Brinell	50,000	4,600
Cast Iron	As Cast	....	30,000	2,700

Table IX...Elastic coefficients, C_P

	GEAR MATERIAL				
Pinion	Steel	Cast iron	Aluminum	Aluminum bronze	Tin bronze
Steel, $E = 30 \times 10^6$	2800	2450	2000	2400	2350
Cast iron, $E = 19 \times 10^6$	2450	2250	1900	2200	2150
Aluminum, $E = 10.5 \times 10^6$	2000	1900	1650	1850	1800
Aluminum bronze, $E = 17.5 \times 10^6$	2400	2200	1850	2150	2100
Tin bronze, $E = 16.0 \times 10^6$	2350	2150	1800	2100	2050

trial pinion pitch diameter by the square root of the design torque divided by the allowable torque from the first trial.

New pinion pitch diameter:

$$d = 2.2\sqrt{\frac{1270}{1210}} = 2.25 \text{ in.}$$

New face width, from Fig 5:

$$F = 1.125$$

All other values in Eq 3 remain the same. Use Eq 3 to again check the allowable torque:

$$T = \frac{(1.125)(0.116)(0.84)(200{,}000)^2}{(2)(1.1)(2800)^2} \times (2.25)^2$$

$$T = 1290 \text{ lb-in.}$$

This exceeds the required 1270 lb-in.

Strength evaluation

Now make a check of tooth strength, using these factors in Eq 4:

$J = 0.228$, from Fig 11

$K_s = 0.645$, from Fig 14

$S_t = 30{,}000$ psi, from Table VIII

$$P_d = \frac{N_P}{d} = \frac{13}{2.25} = 5.78$$

All other factors remain the same as for the durability evaluation, hence

$$T = \frac{(1.125)(0.228)(0.84)(30{,}000)}{(2)(0.645)(1.1)(5.78)} \times (2.25)$$

$T = 1770$ lb-in. (allowable for strength)

Safety factors:

$$\frac{1290}{1270} = 1.01 \text{ for surface durability}$$

$$\frac{1770}{1270} = 1.39 \text{ for strength}$$

The selected gears, therefore, are correct for surface durability but are conservative for strength. In, say, aerospace applications, strength would dominate over durability and a smaller (and lighter) pinion and gear set would be selected. However, on heavily loaded gears where special surface treatment is given to increase the surface resistance to wear, actual test experience has shown that fatigue breakage in the root fillet rather than a breakdown of the tooth surface does occur. Thus, in applications such as aircraft and automotive, adequate fatigue strength must be assured.

The detail gear dimensions are now obtained.

Gear diameter:

$$D = \frac{N_G}{P_d} = \frac{41}{5.78} = 7.093 \text{ in.}$$

Spiral angle:

$$FP_d = (1.125)(5.78) = 6.5$$

The spiral angle is now selected with reference to Fig 6. From the curves the face contact ratio, m_F, will be 1.72 with a 35-deg spiral angle or 2.03 with a 40-deg spiral angle. If maximum smoothness and quietness is required, the 40-deg spiral angle is recommended. However, in this case the 35-deg spiral angle should give adequate smoothness. The lower spiral angle reduces the bearing loads and thereby reduces the cost of the unit.

Working depth, Table IV:

$$h_k = \frac{1.700}{5.78} = 0.294$$

Whole depth, Table IV:

$$h_t = \frac{1.888}{5.78} = 0.327$$

MOUNTING DESIGN

With regard to the mountings, the designer should keep three points in mind:

1) Designing the gear blanks, the shafts, bearings, and gear housings to provide the good rigidity as well as accuracy.

2) Designing the entire unit for ease of assembly.

3) Designing the blanks in a simple geometrical form for ease of manufacture.

The entire success of the bevel-gear drive depends not only on the design but also on care in manufacturing the unit. The gears must be assembled accurately.

Recommended methods for mounting bevel gears are shown in Fig 15 and 16, and poor vs good design points

9 . . DURABILITY FACTORS FOR SPIRAL BEVELS

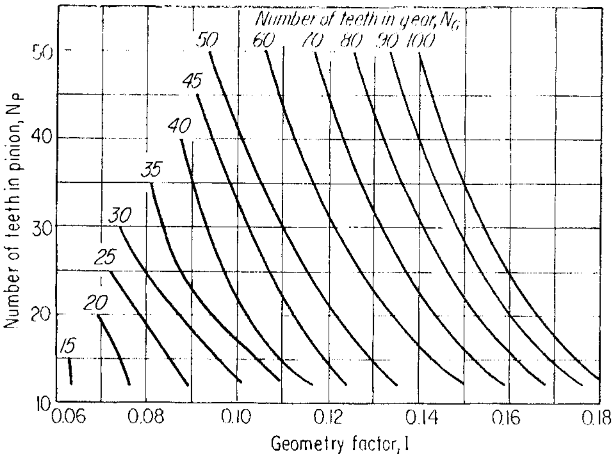

10 . . DURABILITY FACTORS, STRAIGHT AND ZEROL BEVELS

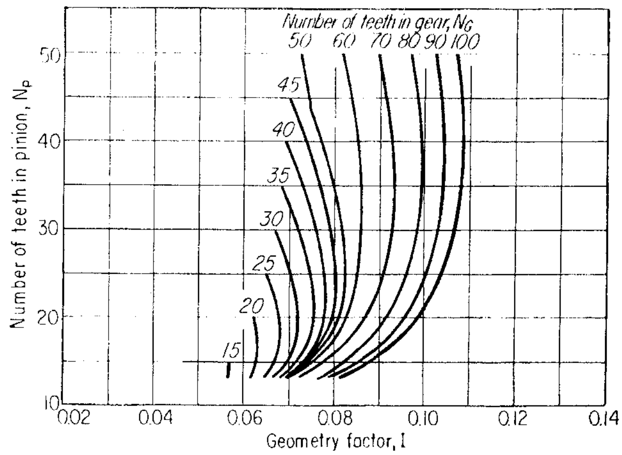

11 . . STRENGTH FACTORS FOR SPIRAL BEVELS

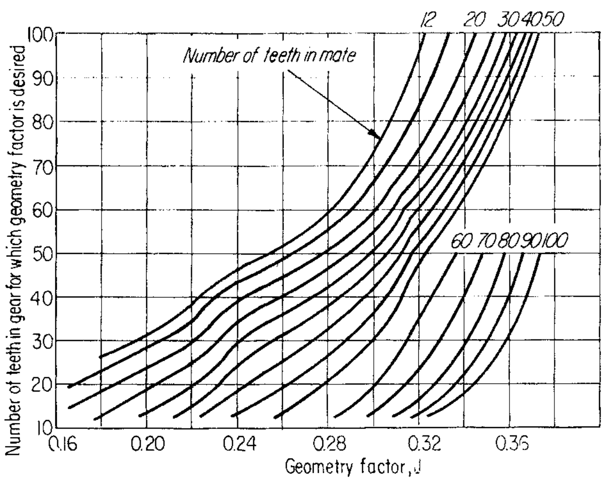

12 . . STRENGTH FACTORS, STRAIGHT AND ZEROL BEVELS

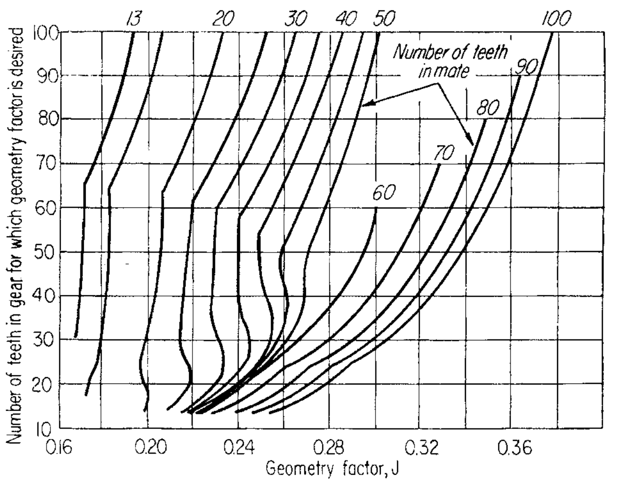

13 . . DYNAMIC FACTORS FOR ALL BEVELS

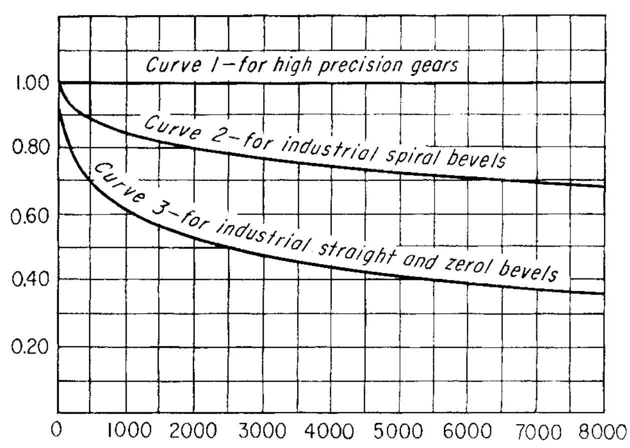

14 . . SIZE FACTORS FOR ALL BEVELS

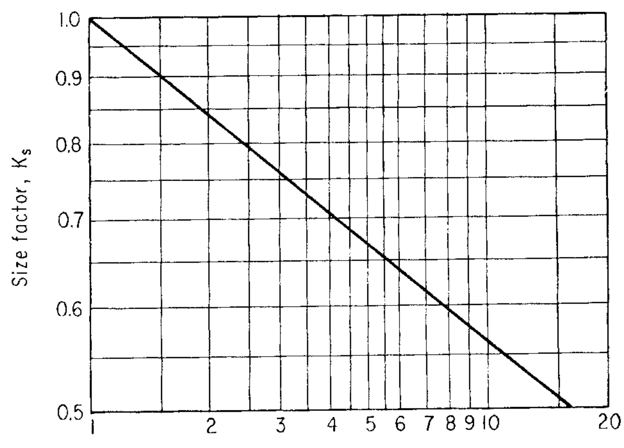

below. As a general rule rolling-friction bearings are superior to plain bearings for bevel gear mountings. This is especially true for spiral-bevel and hypoid gears because these types must be held within recommended limits of deflection and locked against thrust in both directions.

Gear lubrication

There are two methods recommended for lubricating bevel gears—the splash method and the pressure or jet method. The splash method, in which the gear dips in an oil sump in the bottom of the gear box, is satisfactory for gears operating at peripheral speeds up to 2000 fpm. At higher speeds churning of the oil is likely to cause overheating. For speeds above 2000 fpm a jet of oil should be directed on the leaving side of the mesh point to cover the full length of the teeth on both members. If the drive is reversible, jets should be directed at both the entering and leaving mesh.

Some present-day gear lubricants will operate continuously at temperatures of 200 F and above. However, 160 F is the recommended maximum for normal gear applications. Special oils are not normally required for bevel gears; the lubricants for spur and helical gears are also used for straight, Zerol and spiral bevels.

Typical mounting details

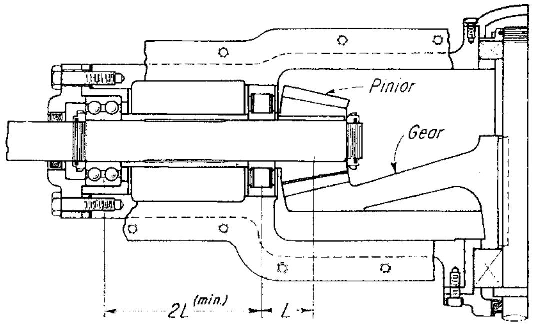

15. OVERHUNG MOUNTING: THE DISTANCE BETWEEN BEARING CENTERS SHOULD BE GREATER THAN TWICE THE OVERHUNG DISTANCE, L.

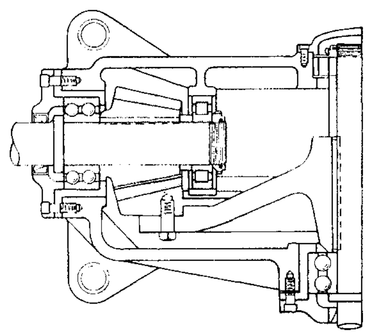

16. STRADDLE-MOUNTING FOR BOTH MEMBERS OF A SPIRAL BEVEL PAIR. FOR HIGH-RIGIDITY APPLICATIONS.

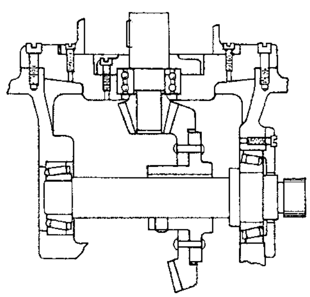

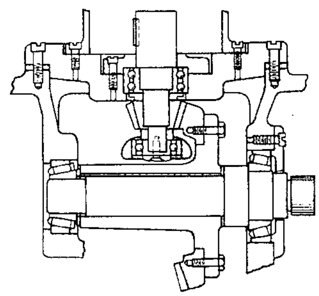

POOR DESIGN

- ☐ Face width too great, more than one third of cone distance.
- ☐ Metal at small end of pinion between teeth and bore too thin.
- ☐ Webbed steel ring gear adds to cost of material and machining.
- ☐ Use of rivets to hold gear to hub introduces danger of runout.
- ☐ A setscrew is inadequate to hold gear in correct axial position and tends to "cock" the gear.
- ☐ Pinion held on shaft only by fit.
- ☐ An overhung pinion cannot be held in line by one double-row bearing.
- ☐ No means of adjustment for gears.

GOOD DESIGN

- ☐ Face width reasonable, less than one third of cone distance.
- ☐ Sufficient metal at small end of pinion to provide strength.
- ☐ Section of ring gear simpler and more direct in design.
- ☐ Screws hold gear to hub.
- ☐ Gear positively held in position.
- ☐ Pinion locked in position by washer and screw.
- ☐ Pinion rigidly supported by addition of inboard bearing.
- ☐ Adjusting washers provided, to be ground to thickness required to correctly position gears.
- ☐ Pinion and bearings can be assembled as a complete unit.

Worksheet Streamlines Bevel-Gear Calculations

B. J. Mumken

The following worksheet neatly gathers together the many mathematical problems that need solving when designing straight bevel-gears. And they are numbered in the correct sequence—no need to hunt "all over the place" as when using formulas in the usual bevel-gear tables. In fact, there are no formulas as such—and, therefore, no need for working with the many Greek symbols found in them.

Instead, the language here is in terms of the actual working operations. For example, space (9) tells you to obtain pitch diameter of the pinion—simply divide the value in space (1) by the value in space (3). And to get root angle for the gear, you are told to subtract the value in space (24) from the value in space (14). Each bracketed number refers you to a value previously filled in.

Just fill in the known values for pinion and gear in the first eight spaces, then work through the sheet, which is based on the Gleason system for 90° straight bevel-gears. Final result (next page) is gear-blank dimensions.

Colored numbers show values obtained in a sample problem worked out by this method.

1	No. of teeth, pinion	40	5	Working depth = $\frac{2.000}{(3)}$	0.200
2	No. of teeth, gear	80	6	Whole depth ("D+F") = $\frac{2.188}{(3)}$ + 0.002	0.2208
3	Diametral pitch	10	7	Pressure angle	20°
4	Face width	0.750	8	Total backlash	0.003

	PINION			GEAR	
	(Thick underlining indicates working dimensions)				
9	Pitch dia. $\frac{(1)}{(3)}$	4.000	10	Pitch dia. $\frac{(2)}{(3)}$	8.000
11	Tan $\frac{(1)}{(2)}$	0.5000	12	Tan $\frac{(2)}{(1)}$	2.0000
13	Pitch angle (11), in deg.	26° 34′	14	Pitch angle (12)	63° 26′
15	2 X cos (13)	1.7888	16	Cone distance $\frac{(10)}{(15)}$	4.4722
18	Addendum (5) − (17)	0.135	17	Addendum = $\frac{\text{(see table)}}{(3)}$	0.065

Gear Addendum for 1 D.P.
Ratio = (No. of gear teeth)/(No. of pinion teeth)

Ratios From	Ratios To	Addendum, in.	Ratios From	Ratios To	Addendum, in.	Ratios From	Ratios To	Addendum, in.	Ratios From	Ratios To	Addendum, in.
1.00	1.00	0.850	1.15	1.17	0.750	1.41	1.44	0.650	1.99	2.10	0.550
1.00	1.02	0.840	1.17	1.19	0.740	1.44	1.48	0.640	2.10	2.23	0.540
1.02	1.03	0.830	1.19	1.21	0.730	1.48	1.52	0.630	2.23	2.38	0.530
1.03	1.05	0.820	1.21	1.23	0.720	1.52	1.57	0.620	2.38	2.58	0.520
1.05	1.06	0.810	1.23	1.26	0.710	1.57	1.63	0.610	2.58	2.82	0.510
1.06	1.08	0.800	1.26	1.28	0.700	1.63	1.68	0.600	2.82	3.17	0.500
1.08	1.09	0.790	1.28	1.31	0.690	1.68	1.75	0.590	3.17	3.67	0.490
1.09	1.11	0.780	1.31	1.34	0.680	1.75	1.82	0.580	3.67	4.56	0.480
1.11	1.13	0.770	1.34	1.37	0.670	1.82	1.90	0.570	4.56	7.00	0.470
1.13	1.15	0.760	1.37	1.41	0.660	1.90	1.99	0.560	7.00	α	0.460

19	Dedendum = $\frac{2.188}{(3)}$ − (18)	0.0838	20	Dedendum = $\frac{2.188}{(3)}$ − (17)	0.1538
21	Tan $\frac{(19)}{(16)}$	0.0187	22	Tan $\frac{(20)}{(16)}$	0.0343
23	Ded angle (21)	1° 4′	24	Ded angle (22)	1° 58′
25	Face angle (13) + (24)	28° 32′	26	Face angle (14) + (23)	64° 30′
27	Root angle (13) − (23)	25° 30′	28	Root angle (14) − (24)	61° 28′

29	cos (13)	0.8944	30	cos (14)	0.4472
31	[2 x (18)] x (29)	0.2414	32	[2 x (17)] x (30)	0.0581
33	OD = (9) + (31)	4.2415	34	OD = (10) + (32)	8.0581
35	(18) x (30)	0.0603	36	(17) x (29)	0.0581
37	Pitch-apex to crown = [0.5 x (10)] − (35)	3.9396	38	Pitch-apex to crown = [0.5 x (9)] − (36)	1.9419
39	Circular pitch = $\frac{3.1416}{(3)}$	0.3141	41	(18) − (17)	0.0700
40	0.5 x (39)	0.1570	42	(41) x tan (7)	0.0254
44	Circular tooth thickness = (39) − (43)	0.1825	43	Circular tooth thickness = (40) − (42)	0.1316
45	$(44)^3$	0.0060	46	$(44)^3$	0.0022
47	$(9)^2$	16.0000	48	$(10)^2$	64.0000
49	6 x (47)	96.0000	50	6 x (48)	384.000
51	$\frac{(45)}{(49)}$	0.00006	52	$\frac{(46)}{(50)}$	0.0000
53	Chordal tooth thickness = (44) − (51) − [0.5 x (8)]	0.181	54	Chordal tooth thickness = (43) − (52) − [0.5 x (8)]	0.1301
55	$(44)^2$ x (29)	0.0298	56	$(43)^2$ x (30)	0.0077
57	4 x (9)	16.0000	58	4 x (10)	32.0000
59	$\frac{(55)}{(57)}$	0.0019	60	$\frac{(56)}{(58)}$	0.0002
61	Chordal addendum (18) + (59)	0.1369	62	Chordal addendum (17) + (60)	0.0652
63	sin (28)	0.8785	64	sin (27)	0.4771
65	cos (28)	0.4776	66	cos (27)	0.8788

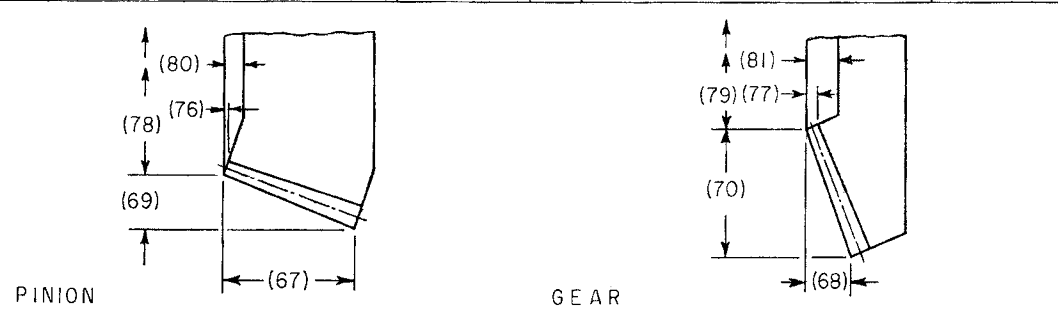

67	(4) x (63)	0.6589	68	(4) x (64)	0.3579
69	(4) x (65)	0.3583	70	(4) x (66)	0.6591
71	$\frac{(16) - (4)}{(16)}$	0.8323			
72	(18) x (71)	0.1124	73	(17) x (71)	0.0541
74	(19) x (71)	0.0697	75	(20) x (71)	0.1280
76	[(72) + (74)] x (30)	0.0815	77	[(73) + (75)] x (29)	0.1629
78	(33) − [2 x (69)]	3.5249	79	(34) − [2 x (70)]	6.7399
80	(76) + mfg. std.	0.125	81	(77) + mfg. std.	0.250

Special Angle Table Simplifies Helical Gear Design

A Helix angle whose cosine is a simple fraction permits rapid calculation of center distances and pitch diameters.

W. U. Matson

HELICAL gears are used when both high speed and high horsepower are required. Although the 45-deg helix angle is most popular for stock gears, as the gear can be used for either parallel or crossed shafts, the large helix angles—30 to 45 deg—impose high thrust loads on bearings when single helicals are used and unless precisely cut and installed increase gear backlash. These helix angles also increase gear weight without proportionally increasing either the strength of the gear or the power and load the helical gear can transmit.

As Table I indicates, based on the use of disks, weights would increase as the square of the diameter. Hence a disk for a 45-deg helix angle of the same normal diametral pitch would be $(1.4142)^2$, or twice as heavy for the same face width as a spur gear (0-deg helix angle). The table also points out the percentage of rise in thrust and bearing loads imposed by the higher-angle gears.

Smaller helix angles—below 30 deg—may increase gear wear slightly but improve backlash tolerance and give lower bearing loads. One helix angle—20° 21′ 50.887″—adds a majoi advantage, ease of design.

Why a small helix angle

Thrust on the bearings caused by helix angles above 20 deg can be mitigated by double-helical or herringbone teeth. However, face width increases and manufacturing is complicated. Most ball or tapered roller bearings capable of being preloaded can be used with gears of about 20-deg helix angle, as the thrust is less than 50% of the tangential load.

Backlash in the plane of rotation

TABLE I - **Effect of helix angle on various parameters**

HELIX ANGLE ψ DEG	INCREASE IN PITCH DIA OVER STANDARD SPUR GEAR %	AXIAL PRESSURE ANGLE AT PITCHLINE, ϕ	TANGENTIAL PITCHLINE LOAD THRUST %	BEARING %
*0	0	20	0	106.4
10	1.54	20°17′	17.6	106.6
20° 21′ 50.877″	6.66	21°13′	37.1	107.3
30	15.47	22°48′	57.7	108.4
40	30.54	25°25′	83.9	110.7
45	41.42	27°14′	100.0	112.5
	$\%_{Inc} = 100(1/\cos\psi - 1/\cos 0°)$	$\tan\phi = \frac{\tan\phi_n}{\cos\psi}$	$\%_T = 100\tan\psi$	$\%_B = 100\frac{1}{\cos\phi}$

**Spur gear*

TABLE II -Values for one normal diametral

Helix angle, Ψ, = 20° 21′ 50.887″ Pressure angle = 20° For Other Normal Diametral Pitches, Except for

NUMBER OF TEETH IN GEAR, N	PITCH DIAMETER FOR $P_N = 1$ D_1	OUTSIDE DIAMETER FOR $P_N = 1$ D_{o1}	MEASUREMENT OVER $1.728/P_N$ WIRES FOR $P_N = 1$ M_1*
17*	18.1333	20.1333	20.5249
18	19.2000	21.2000	21.5948
19	20.2666	22.2666	22.6641
20	21.3333	23.3333	23.7334
21	22.4000	24.4000	24.8026
22	23.4666	25.4666	25.8714
23	24.5333	26.5333	26.9402
24	25.6000	27.6000	28.0089
25	26.6666	28.6666	29.0773
26	27.7333	29.7333	30.1457
27	28.8000	30.8000	31.2139
28	29.8666	31.8666	32.2821
29	30.9333	32.9333	33.3502
30	32.0000	34.0000	34.4182
31	33.0666	35.0666	35.4860
32	34.1333	36.1333	36.5539
33	35.2000	37.2000	37.6217
34	36.2666	38.2666	38.6894
35	37.3333	39.3333	39.7571
36	38.4000	40.4000	40.8247
37	39.4666	41.4666	41.8923
38	40.5333	42.5333	42.9599
39	41.6000	43.6000	44.0274
40	42.6666	44.6666	45.0949
41	43.7333	45.7333	46.1623
42	44.8000	46.8000	47.2297
43	45.8666	47.8666	48.2971
44	46.9333	48.9333	49.3645
45	48.0000	50.0000	50.4318
46	49.0666	51.0666	51.4990
47	50.1333	52.1333	52.5663
48	51.2000	53.2000	53.6336
49	52.2666	54.2666	54.7008
50	53.3333	55.3333	55.7680
51	54.4000	56.4000	56.8352
52	55.4666	57.4666	57.9022
53	56.5333	58.5333	58.9695
54	57.6000	59.6000	60.0367
55	58.6666	60.6666	61.1037
56	59.7333	61.7333	62.1709
57	60.8000	62.8000	63.2380
58	61.8666	63.8666	64.3050
59	62.9333	64.9333	65.3722
60	64.0000	66.0000	66.4392
61	65.0666	67.0666	67.5062
62	66.1333	68.1333	68.5733
63	67.2000	69.2000	69.6404
64	68.2666	70.2666	70.7073

NUMBER OF TEETH IN GEAR, N	PITCH DIAMETER FOR $P_N = 1$ D_1	OUTSIDE DIAMETER FOR $P_N = 1$ D_{o1}	MEASUREMENT OVER $1.728/P_N$ WIRES FOR $P_N = 1$ M_1*
65	69.3333	71.3333	71.7743
66	70.4000	72.4000	72.8413
67	71.4666	73.4666	73.9081
68	72.5333	74.5333	74.9752
69	73.6000	75.6000	76.0422
70	74.6666	76.6666	77.1091
71	75.7333	77.7333	78.1761
72	76.8000	78.8000	79.2432
73	77.8666	79.8666	80.3100
74	78.9333	80.9333	81.3770
75	80.0000	82.0000	82.4439
76	81.0666	83.0666	83.5107
77	82.1333	84.1333	84.5777
78	83.2000	85.2000	85.6446
79	84.2666	86.2666	86.7115
80	85.3333	87.3333	87.7784
81	86.4000	88.4000	88.8454
82	87.4666	89.4666	89.9121
83	88.5333	90.5333	90.9790
84	89.6000	91.6000	92.0460
85	90.6666	92.6666	93.1128
86	91.7333	93.7333	94.1797
87	92.8000	94.8000	95.2465
88	93.8666	95.8666	96.3133
89	94.9333	96.9333	97.3802
90	96.0000	98.0000	98.4471
91	97.0666	99.0666	99.5139
92	98.1333	100.1333	100.5807
93	99.2000	101.2000	101.6476
94	100.2666	102.2666	102.7144
95	101.3333	103.3333	103.7813
96	102.4000	104.4000	104.8482
97	103.4666	105.4666	105.9150
98	104.5333	106.5333	106.9818
99	105.6000	107.6000	108.0486
100	106.6666	108.6666	109.1154
101	107.7333	109.7333	110.1823
102	108.8000	110.8000	111.2491
103	109.8666	111.8666	112.3158
104	110.9333	112.9333	113.3826
105	112.0000	114.0000	114.4495
106	113.0666	115.0666	115.5163
107	114.1333	116.1333	116.5831
108	115.2000	117.2000	117.6499
109	116.2666	118.2666	118.7166
110	117.3333	119.3333	119.7834
111	118.4000	120.4000	120.8503
112	119.4666	121.4666	121.9170
113	120.5333	122.5333	122.9838
114	121.6000	123.6000	124.0506

***For odd tooth gears—divide measurement over wires by 2 and make radial measurement.**

increases with helix angle. For larger helix angles, greater precision of gear cutting is required where the backlash desired is small in the direction of rotation.

Manufacture by hobbing of gears with high helix angles is sometimes limited by the extent to which the hobs can be rotated or swiveled. Gears of high helix angle sometimes require special setups and equipment.

Face width is usually planned to give complete pitch-line contact overlap. For very small helix angles the face required to do this is large, as sin ψ becomes small in the denominator of the equation. The small faces afforded by large helix angles can not be used because of forces during cutting. But, face widths for gears of about 20-deg helix angle are of reasonable size for the various normal diametral pitches.

Ease of design can not be ignored.

pitch for full depth helical gears

Number of Teeth, Divide Values by Normal Diametral Pitch (Hob Cutter Pitch).

NUMBER OF TEETH IN GEAR, N	PITCH DIAMETER FOR $P_N=1$ D_1	OUTSIDE DIAMETER FOR $P_N=1$ D_{o1}	MEASUREMENT OVER $1.728/P_N$ WIRES FOR $P_N=1$ M_1*
115	122.6666	124.6666	125.1174
116	123.7333	125.7333	126.1842
117	124.8000	126.8000	127.2510
118	125.8666	127.8666	128.3177
119	126.9333	128.9333	129.3845
120	128.0000	130.0000	130.4513
121	129.0666	131.0666	131.5180
122	130.1333	132.1333	132.5848
123	131.2000	133.2000	133.6516
124	132.2666	134.2666	134.7182
125	133.3333	135.3333	135.7850
126	134.4000	136.4000	136.8519
127	135.4666	137.4666	137.9186
128	136.5333	138.5333	138.9854
129	137.6000	139.6000	140.0522
130	138.6666	140.6666	141.1188
131	139.7333	141.7333	142.1856
132	140.8000	142.8000	143.2524
133	141.8666	143.8666	144.3191
134	142.9333	144.9333	145.3859
135	144.0000	146.0000	146.4527
136	145.0666	147.0666	147.5193
137	146.1333	148.1333	148.5861
138	147.2000	149.2000	149.6529
139	148.2666	150.2666	150.7196
140	149.3333	151.3333	151.7864
141	150.4000	152.4000	152.8532
142	151.4666	153.4666	153.9198
143	152.5333	154.5333	154.9866
144	153.6000	155.6000	156.0534
145	154.6666	156.6666	157.1201
146	155.7333	157.7333	158.1869
147	156.8000	158.8000	159.2536
148	157.8666	159.8666	160.3203
149	158.9333	160.9333	161.3870
150	160.0000	162.0000	162.4538
151	161.0666	163.0666	163.5205
152	162.1333	164.1333	164.5872
153	163.2000	165.2000	165.6540
154	164.2666	166.2666	166.7206
155	165.3333	167.3333	167.7874
156	166.4000	168.4000	168.8542
157	167.4666	169.4666	169.9208
158	168.5333	170.5333	170.9876
159	169.6000	171.6000	172.0543
160	170.6666	172.6666	173.1210
161	171.7333	173.7333	174.1878

NUMBER OF TEETH IN GEAR, N	PITCH DIAMETER FOR $P_N=1$ D_1	OUTSIDE DIAMETER FOR $P_N=1$ D_{o1}	MEASUREMENT OVER $1.728/P_N$ WIRES FOR $P_N=1$ M_1*
162	172.8000	174.8000	175.2546
163	173.8666	175.8666	176.3213
164	174.9333	176.9333	177.3881
165	176.0000	178.0000	178.4548
166	177.0666	179.0666	179.5214
167	178.1333	180.1333	180.5882
168	179.2000	181.2000	181.6549
169	180.2666	182.2666	182.7216
170	181.3333	183.3333	183.7883
171	182.4000	184.4000	184.8550
172	183.4666	185.4666	185.9217
173	184.5333	186.5333	186.9884
174	185.6000	187.6000	188.0551
175	186.6666	188.6666	189.1218
176	187.7333	189.7333	190.1885
177	188.8000	190.8000	191.2553
178	189.8666	191.8666	192.3219
179	190.9333	192.9333	193.3887
180	192.0000	194.0000	194.4554
181	193.0666	195.0666	195.5220
182	194.1333	196.1333	196.5887
183	195.2000	197.2000	197.6555
184	196.2666	198.2666	198.7221
185	197.3333	199.3333	199.7889
186	198.4000	200.4000	200.8556
187	199.4666	201.4666	201.9222
188	200.5333	202.5333	202.9890
189	201.6000	203.6000	204.0557
190	202.6666	204.6666	205.1223
191	203.7333	205.7333	206.1891
192	204.8000	206.8000	207.2558
193	205.8666	207.8666	208.3225
194	206.9333	208.9333	209.3892
195	208.0000	210.0000	210.4560
196	209.0666	211.0666	211.5226
197	210.1333	212.1333	212.5894
198	211.2000	213.2000	213.6561
199	212.2666	214.2666	214.7227
200	213.3333	215.3333	215.7894
300	320.0000	322.0000	322.4590
400	426.6666	428.6666	429.1270
500	533.3333	535.3333	535.7946
600	640.0000	642.0000	642.4618
700	746.6666	748.6666	749.1288
800	853.3333	855.3333	855.7958
900	960.0000	962.0000	962.4627
1000	1066.6666	1068.6666	1069.1295

And the cosine of 20° 21′ 50.887″ is equal to 0.9375 = 15/16, a simple fraction. Thus, many design calculations can be done in longhand or with slide rule, eliminating some tedious calculations. For example, if a 20-deg angle is used the cosine value equals 0.93969262, much harder to manipulate than 15/16, although the difference in helix angle is slight.

There are many other angles whose cosines are simple fractions such as 4/5, 6/7, 7/8, etc. These range from helix angles of 36° 52′ 11″ to 16° 15′ 36″ and many have simple sine values. Many of these might be good choices.

Why standardize on an angle

Manufacturing and engineering can be simplied, as stocks of helical gears could be made and cataloged for the trade as is done with spur gears. In addition, expensive cam guides for gear shapers could be purchased with certainty of full use by gear manu-

EXAMPLE—DESIGN OF HELICAL GEARS — $\psi = 20° \ 21' \ 50.887''$

$P_N = 48, \quad PA = 20°, \quad N_P = 38, \quad N_G = 64$

STEP	FORMULA	PINION	GEAR
1	$P = (P_N)(15/16)$	45	45
2	PA = pressure angle (given)	20°	20°
3	P_N = normal diametral pitch (given)	48	48
4	N = number of teeth (given)	38	64
5	ψ = helix angle (given)	20° 21′ 50.887″	20° 21′ 50.887″
6	$D = D_1(\text{table})/P_N$	0.8444	1.4222
7	$a = 1/P_N$	0.02083	0.02083
8	Hand	Right	Left
9	Whole depth	Not required	Not required
10	$D_o = D_{01}(\text{table})/P_N$	0.8861	1.4638
11	$G = 1.728/P_N$	0.036	0.036
12	$M = M_1(\text{table})/P_N$	0.8949	1.4730
13	$F = 9.03/P_N = 0.188$	Use 0.250	Use 0.218
14	$C = (D_G + D_o)/2$	1.1333	1.1333

facturers. And, it is now possible to achieve enough precision to manufacture fully interchangeable helical gears rather than furnish them in pairs of special design. Mathematical tables such as those that follow can be used to simplify design and manufacturing calculations.

Tables reduce mathematics

Helical gears can be manufactured by hobbing with standard spur gear cutters as easily as spur gears, once the essential calculations have been made. For this reason, the following set of helical gears with a helix angle of 20° 21′ 50.887″ is suggested for use where smoothness, lack of vibration and quietness of drive are desired.

Tables have been prepared in terms of one normal pitch, with the effects on the dimensions caused by the helix angle already incorporated. To obtain the values to be tabulated for a gear, the one-normal-pitch dimensions are divided by the normal (or cutter) diametral pitch. Steps in using the table are:

1) Complete pitch diameters by either of these two methods:

a) By formula:

$$D = N/P = N/P_N \cos\psi = N/P_N(15/16) = 16N/15P_N$$

b) By table:

Choose value D_1 and divide by the cutter or normal diametral pitch, P_N.

2) Compute outside diameter of gears by either of these two methods:

a) By formula

Add $2/P_N$ to pitch diameter

b) By table:

Choose value D_{01} and divide by normal diametral pitch, for full-depth involute gears only.

3) Compute minimum face width, F. Very wide faces should be avoided.

$$F = \pi/P_N \sin\psi = 9.03/P_N$$

4) Compute measurement over wires. This has been done for one normal diametral pitch; hence divide table M_1 values by normal diametral pitch, P_N. Use radial measurements for odd-toothed gears.

5) Compute thrust. Any ball or tapered roller bearing of the same shaft bore that has provisions for axial preloading or thrust will usually be adequate to handle thrust of these helical gears. Where doubt exists, thrust load W_T equals $W \tan\psi$, which is 0.371 W. W is tangential pitch-line load. Bearings should be free of end play and kept close to gears for rigid support.

How to use tables

A design example is shown above. A summary of the formulas used for the example in order of gear tabulation for drawings would be:

1) Diametral pitch in plane of rotation, P

$$P = P_N \cos\psi$$

2) Normal pressure angle, ϕ_N

3) Normal diametral pitch, P_N

4) Number of teeth, N

5) Helix angle, ψ

6) Pitch diameter, D

$$D = D_1(\text{table})/P_N$$

7) Addendum, a

$$a = 1/P_N$$

8) Hand, one gear must be left, the other right

9) Whole depth, not required

10) Outside diameter, D_o

$$D_o = D_{01}(\text{table})/P_N$$

11) Wire diameter, G

$$G = 1.728/P_N$$

12) Measurement over wires

$$M = M_1(\text{table})/P_N$$

13) Minimum face width, F

$$F = 9.03/P_N$$

14) Center distance, C

$$C = (D_G + D_P)/2$$

All other values such as index gears, feed gears, machine constant, feed, material, etc, must be determined on the basis of gear application and machine type and cutter type to be used. This information must come from the gear consultant and is based on manufacturing equipment available for generating the gear teeth.

Form Cutters for Helical Gears

Oliver Saari

Most handbooks and other sources still give the formula for the selection of the proper spur tooth cutter for milling involute helical gear teeth as being

$$N_c = \frac{N}{\cos^3 \psi} \qquad (1)$$

where

N = actual number of teeth in gear to be cut
ψ = helix angle of gear to be cut
N_c = number of spur gear teeth for which cutter has been made.

No spur-tooth form cutter can give an exact involute shape when used to mill helical teeth—in fact, even for spur gears the form is correct for only one number of teeth in the range specified for a given cutter. But Formula (1) gives a needlessly poor approximation, particularly with small numbers of teeth and helix angles above 20°. Its continued presentation to the gear-cutting public is strange in view of the fact that thirty years ago Ernest Wildhaber published a much more exact and almost as simple formula for finding the cutter number (*AM*—Dec. 20, 1923). This formula is

$$N_c = \frac{N}{\cos^3 \psi} + (P_n D_c) \tan^2 \psi \qquad (2)$$

where the symbols are the same as before, and in addition

P_n = normal diametral pitch of gear and cutter
D_c = pitch diameter of cutter = OD of cutter − 2 × dedendum of gear

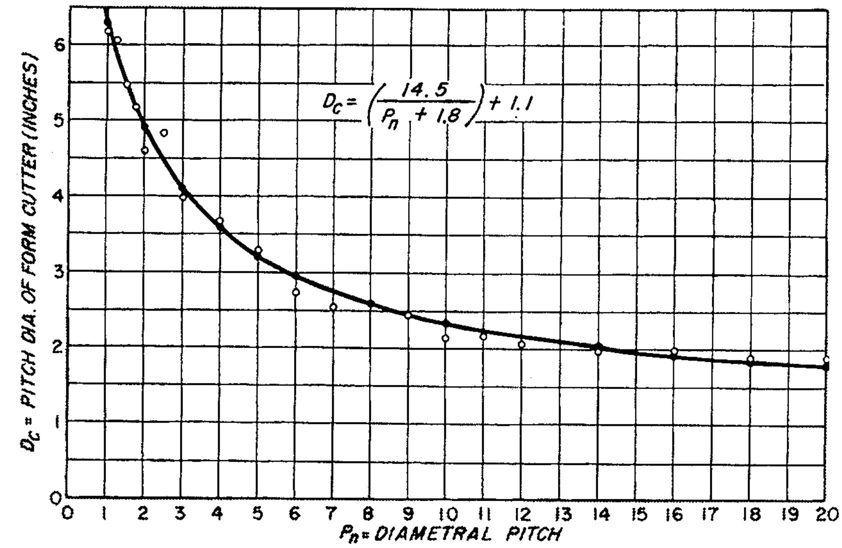

FIG. 1 . . . Empirical relationship of gear-cutter pitch diameter to diametral pitch (Standard ITW cutters)

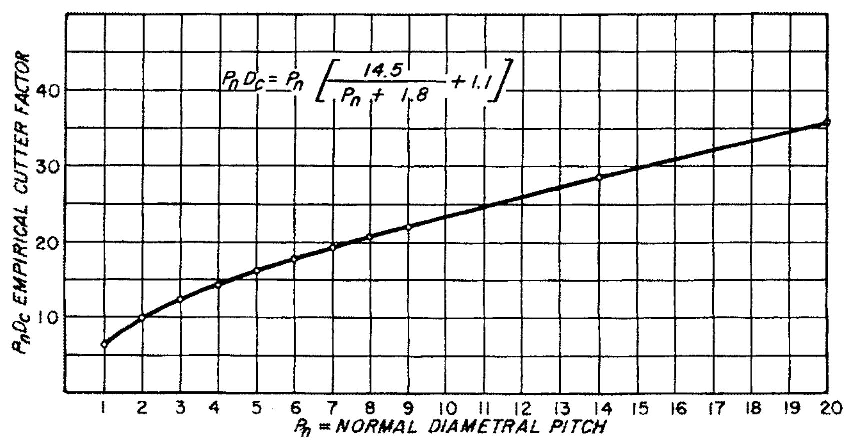

Fig. 2 . . . Empirical relationship of $P_n D_c$ to diametral pitch for standard ITW cutters

This formula gives values which are theoretically exact in both tooth-thickness and pressure angle at one point of the tooth profile, and the spur cutter itself provides a crowning or relieving effect above and below this point.

Possibly one reason that this simple formula has not been included in the readily available gear literature is the fact that it involves the cutter pitch diameter. This varies with the diametral pitch and with the various manufacturers. It is not generally known to the tool designer or anyone except the man in the shop who actually gets the cutter from the tool crib. Then it is too late to do anything but "cut and try."

This difficulty can be eliminated by establishing an empirical relationship between the cutter diameter and diametral pitch. Spur cutter sizes can be directly related to diametral pitches, even though such a relation may not be intentional on the part of the manufacturer, because the proportions of the tooth form and the size of hole required almost automatically dictate the "natural" size of the cutters. A curve of this relationship, together with an empirical formula, is shown in Fig. 1. Even though the individual cutters may deviate slightly from this curve, the errors caused by the deviation are far smaller than those resulting if the effects of cutter diameter are ignored altogether.

The combined relationship of the product P_nD_c, which appears in the exact equation (2), to the diametral pitch is shown in the curve and empirical formula of Fig 2. This curve and Equation (2) are sufficient for all calculations in the range of pitches from one to 20. A combined formula which may be used alternatively if Curve (2) is not available is

$$N_c = \frac{N}{\cos^3 \psi} + P_n\left(\frac{14.5}{P_n + 1.8} + 1.1\right)\tan^2 \psi \quad (3)$$

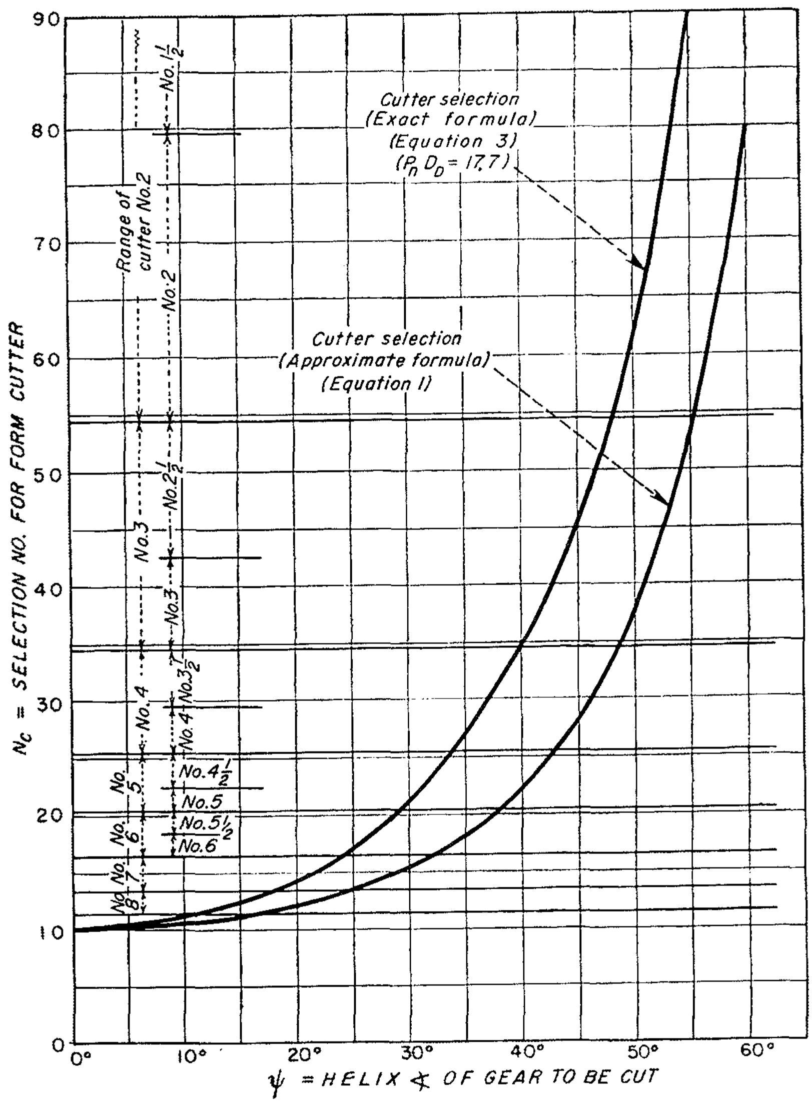

FIG. 3 ... Curves for 6-DP gear, 10 teeth, showing the variation in form-cutter number determined by the exact and approximate selection formulas

A comparison of the values obtained by the use of Equations (1) and (3) for one particular case—10-tooth, 6-pitch gears of various helix angles — is shown by the curves of Fig 3. These curves show that the exact formula gives a better choice of cutter number for all helix angles above 17°.

Planetary Gear Systems

Efficiency and Speed-Ratio Formulas

Here are complete torque, speed, and power analysis, a new method for finding efficiencies and final formulas ready for use.

John H. Glover

THE remarkably high speed reductions that are produced in relatively small spaces by planetary gear systems fascinate gear designers. New gear arrangements are periodically developed—you might say invented—and it is surprising to note how similar many of them look when compared to each other. Yet, slight differences can cause one arrangement to have a much higher or lower speed-reduction ratio than another.

But speed reduction is not the only design criterion. Just as important is the overall efficiency of the gear system. This determines the amount of power that the gear system consumes (mostly in the form of heat), and hence the horsepower requirements of the motor that drives the planetary.

Most designers would find it difficult to calculate the overall efficiency of a complex planetary. And when they derive the efficiency formula they cannot be sure that the formula is correct. In fact, the types with multiple carriers and split power, such as Ex 8, p 76, seldom have been analyzed in the literature.

This article, then, not only provides new easy-to-use "cook-book" formulas for overall efficiency and speed ratio, but also presents torque and angular speed values for the member-gears of the planetaries which are needed for the design of the gears themselves.

Planetary assembly...

and its schematic, torque-flow, fixed carrier and power-flow diagrams. The 20 systems that follow use the same notation system, and include speed-ratio formulas, R, and overall-efficiency formulas, E.

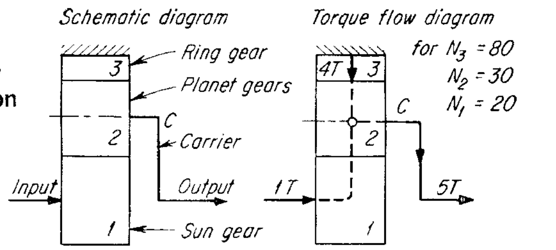

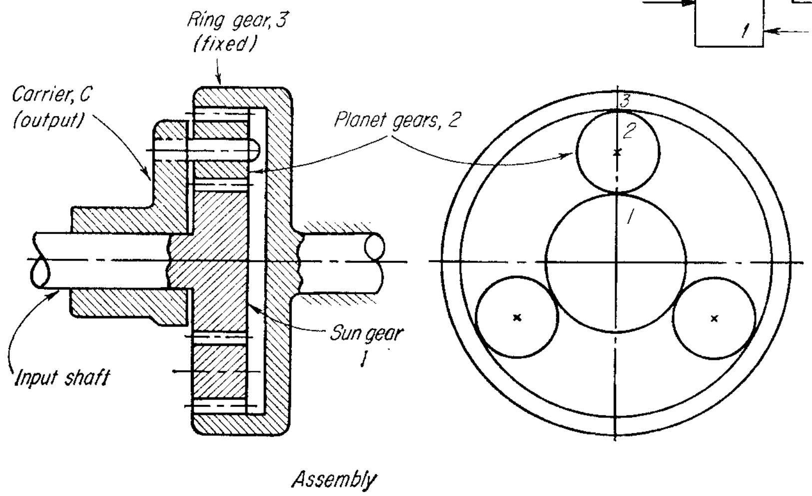

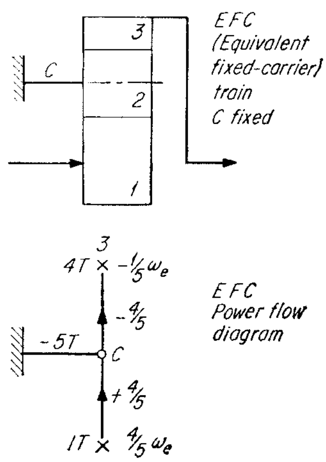

Such torque and speed values are also needed for the design of clutches or fastenings to lock the reaction gears from turning (the gears that do not rotate in the assembly).

How to use the boxed examples

The basis for deriving speed-ratio, efficiency, and torque values is given on p 1-28. It will help you develop formulas for your own planetary arrangements should you need them. But chances are good that the planetary system you want is in the group of planetary systems that begin with Ex 1 below (there are 20 systems to select from). **Thus you can go directly to the boxed systems to obtain:**

Schematic diagrams displaying the skeletal structure of the various gears and planet carrier hook ups (see the illustrations below, left, for an explanation of the diagrams). The schematics also show the torque flow and power flow through all the members of the gear assembly.

Formulas for the overall speed ratio, R. This is a function of the number of teeth of the gears (N_1, N_2, etc). Typical values for the number of teeth have been selected in the examples to illustrate how torque and power splits or combines while flowing through the gears.

Formulas for overall efficiency, E. These formulas require knowing only the number of teeth and the efficiency between meshing teeth. For example, $\epsilon_{1,4}$ is the mesh efficiency between gears 1 and 4. You can assume a mesh efficiency of $\epsilon = 0.98$ (98%) for each external mesh and $\epsilon = 0.99$ for each internal mesh, in keeping with common practice. Because power losses are always *positive* in sign, the terms in the efficiency equations which constitute losses are frequently enclosed in bars to indicate that an absolute (positive) value is always to be used.

Table of torque and speed values for the various members of the system. Each member is listed in the first column. The letter C stands for carrier (see list of symbols on p 1-28); the numbers represent gears.

The second column in the table shows the role that each member plays in the gear set. It may be the input or output member; it may be a reaction member, as is the case with the ring gear (3) in Example 1; or it may be an idler gear with no influence on the gear ratio.

The third column gives the torque acting on each member in relative terms. The torque on the input is set at 1, idlers have zero torque, and the torque on the other members is usually in terms of the speed ratio, R. Hence in Example 1, the torque on the output member is equal to $-R$, or for the number of teeth shown, $R = 1/5$, and the output torque will be 1/5 the input torque. The reaction member takes up 4/5 of the input torque. Input speed is assigned 1.

The fourth column gives the absolute angular speed, ω, of the member around its own axis (which includes the speed imparted to the member by a moving carrier.

The fifth column gives the angular speed of tooth engagement, ω_ϵ, which is its absolute speed minus the speed of the carrier.

By multiplying the T and ω values you obtain the power transmitted through a member. Also, by multiplying the T and ω_ϵ values you obtain the power circulating in its tooth engagement (if it is a gear).

The boxed systems also display an "equivalent fixed carrier" power-flow diagram. By assuming that the carrier is fixed you quickly see a nondimensional, relative-value flow of torque, speed, and power, starting with assigned values of unity for input torque and input angular speed.

How to derive new formulas

The method which produced all the formulas and relationships in the boxed examples is based on the use of ratio factors, called R-factors,

Boxed formulas continue on next page
Derivation continues on page 1-28

1. Simple planetary system -- input to carrier

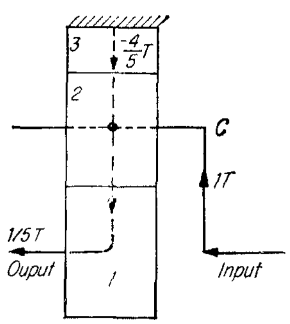

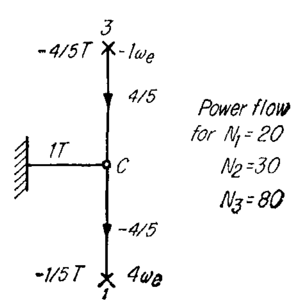

Speed-ratio formula

$$R = \frac{1}{1 + \frac{N_3}{N_1}}$$

Efficiency formula

$$E = \frac{1}{1 + \left[\frac{N_3}{N_1 + N_3}\left(\frac{1}{\epsilon_{32}\epsilon_{21}} - 1\right)\right]}$$

Member	Role	T	ω	ω_e
C	Input	1	1	–
1	Output	$-R$	1/5	$\omega - \omega_C$
		$-1/5$	5	4
3	Reaction	$R-1$	0	$\omega - \omega_C$
		$-4/5$		-1
2	Idler	0	–	$m_{21}\omega_{e1}$
				$-8/3$

2. Simple planetary system -- input to sun

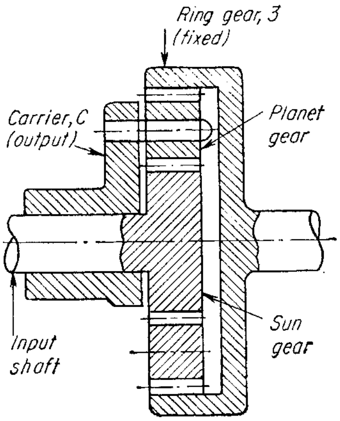

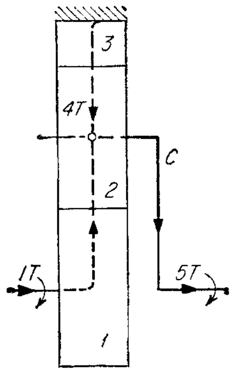

Power & torque flow for $N_1 = 20$, $N_2 = 30$, $N_3 = 80$

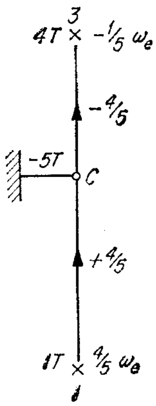

$$R = 1 + \frac{N_3}{N_1}$$

$$E = 1 - \left[\frac{N_3}{N_1 + N_3}(1 - \epsilon_{12}\,\epsilon_{23})\right]$$

Member	Role	T	ω	ω_e
1	Input	1	1	$\omega - \omega_c$
C	Output	−R	1/R	—
3	Reaction	R−1	0	$\omega - \omega_c$
2	Idler	0	—	$m_{21} - \omega_{e1}$

3. Simple planetary system -- with carrier fixed

Torque flow

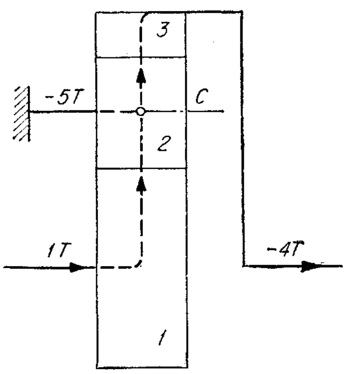

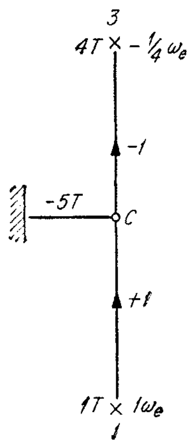

Diagrams for
$N_1 = 20$
$N_2 = 30$
$N_3 = 80$

$$R = -\frac{N_3}{N_1}$$

$$E = \epsilon_{12}\,\epsilon_{23}$$

Member	Role	T	ω	ω_e
1	Input	1	1	$\omega - \omega_c$
3	Output	−R	1/R	$\omega - \omega_c$
C	Reaction	R−1	0	—
2	Idler	0	—	$m_{21} - \omega_{e1}$

4. Compound planetary -- input to carrier

Torque flow

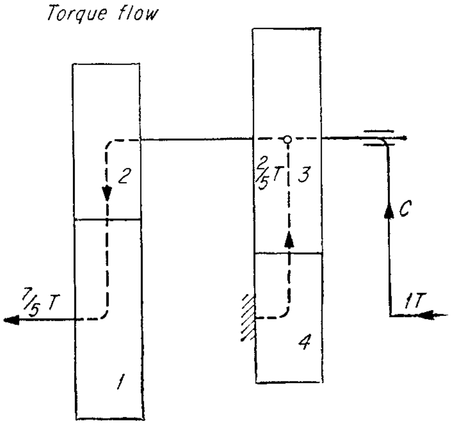

Power flow

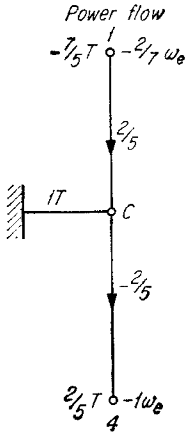

Diagrams for
$N_1 = 30$
$N_2 = 20$
$N_3 = 35$
$N_4 = 15$

$$R = \frac{1}{1 - \frac{N_2 N_4}{N_1 N_3}}$$

when $N_1 N_3 < N_2 N_4$

$$E = \frac{1}{1 + \left[\frac{-N_2 N_4}{N_1 N_3 - N_3 N_4}\right]\left[\left(\frac{1}{\epsilon_{43}\,\epsilon_{21}} - 1\right)\right]}$$

when $N_1 N_3 > N_2 N_4$

$$E = \frac{1}{1 + \left[\frac{-N_2 N_4}{N_1 N_3 + N_3 N_4}\right]\left[(1 - \epsilon_{12}\,\epsilon_{34})\right]}$$

Member	Role	T	ω	ω_e
C	Input	1	1	—
1	Output	−R	1/R	$\omega - \omega_c$
4	Reaction	R−1	0	$\omega - \omega_c$
2 − 3	Compound Idler	—	—	$m_{21} - \omega_{e1}$

5. Compound planetary -- input to sun

$$R = 1 - \frac{N_2 N_4}{N_1 N_3}$$

When $N_1 N_3 < N_2 N_4$

$$E = 1 - \left/ \frac{-N_2 N_4}{N_1 N_3 - N_2 N_4} \right/ (1 - \epsilon_{12}\, \epsilon_{34})$$

When $N_1 N_3 > N_2 N_4$

$$E = 1 - \left/ \frac{-N_2 N_4}{N_1 N_3 - N_2 N_4} \right/ \left(\frac{1}{\epsilon_{43}\, \epsilon_{21}} - 1 \right)$$

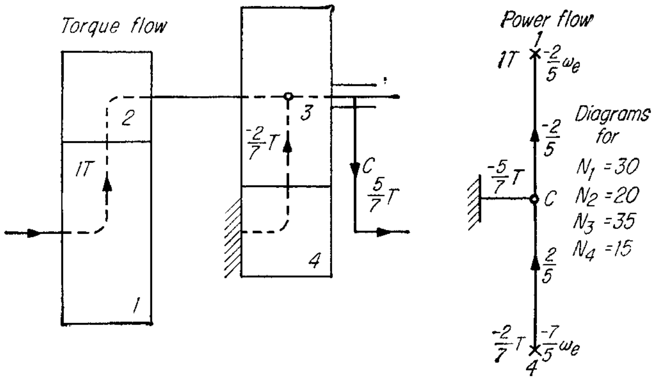

Member	Role	T	ω	ω_e
1	Input	1	1	$\omega - \omega_c$
C	Output	- R	1/R	–
4	Reaction	R - 1	0	$\omega - \omega_c$
2 – 3	Compound Idler	0	–	$m_{21}\, \omega_{e1}$

6. Double-eccentric planetary

$$R = \frac{1}{1 - \frac{N_5\, N_3\, N_1}{N_6\, N_4\, N_2}},$$

$$E = \frac{1}{1 + \left/ \frac{-N_5\, N_3\, N_1}{N_6 N_4 N_2 - N_5 N_3 N_1} \right/ \begin{cases} \left(\frac{1}{\epsilon_{12}\, \epsilon_{34} \epsilon_{56}} - 1 \right) & \text{if } N_6\, N_4\, N_2 < N_5\, N_3\, N_1 \\ (1 - \epsilon_{65} \epsilon_{43} \epsilon_{21}) & \text{if } N_6\, N_4\, N_2 > N_5\, N_3\, N_1 \end{cases}}$$

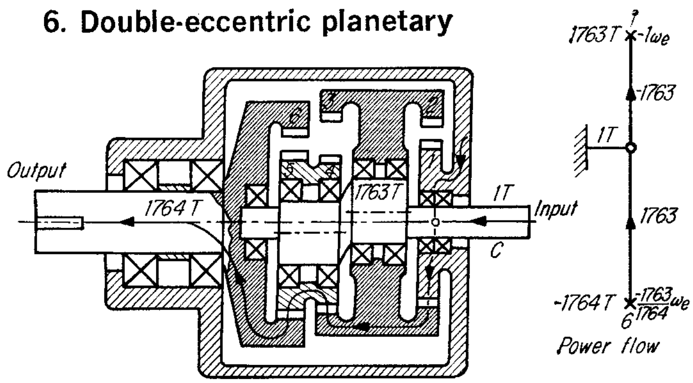

For $N_1 = 82$ $N_2 = 84$ $N_3 = 86$
$N_4 = 82$ $N_5 = 82$ $N_6 = 84$
$R = 1764$

Member	Role	T	ω	ω_e
C	Input	1	1	–
6	Output	-R	1/R	$\omega - \omega_c$
1	Reaction	R-1	0	$\omega - \omega_c$
2,3	Compound Idler	0	–	$m_{21}\, \omega_{e1}$
4,5	Compound Idler	0	–	$m_{56}\, \omega_{e6}$

7. Triple-planet planetary

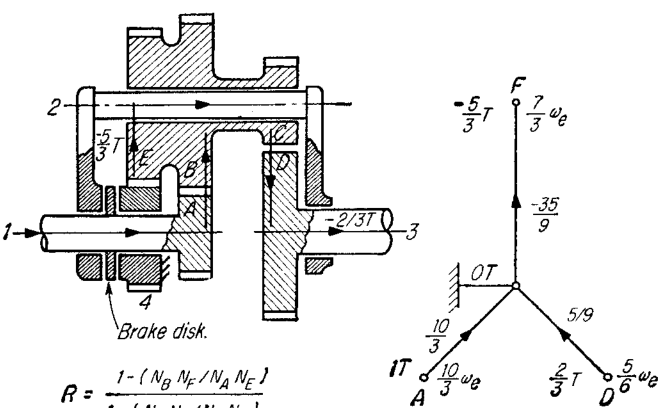

$$R = \frac{1 - (N_B\, N_F / N_A\, N_E)}{1 - (N_C\, N_F / N_D\, N_E)}$$

Member	Role	T	ω	ω_e
A	Input	1	1	$\omega - \omega_c$
D	Output	-R	1/R	$\omega - \omega_c$
F	Reaction	R-1	0	$\omega - \omega_c$
2 (Carrier)	Neutral	0	$\frac{N_A N_E}{N_A N_E - N_B N_F}$	–
E-B-C	Compound Idler	–		$m_{EF}\, \omega_{ef}$

$N_A = 20 = N_C$ $N_E = 35$
$N_B = 40 = N_D$ $N_F = 25$

$$E = \frac{1 - \left/ \frac{-N_B\, N_F}{N_A\, N_E - N_B\, N_F} \right/ \begin{cases} (1 - \epsilon_{AB} \epsilon_{EF}) & \text{if } N_A N_E < N_B N_F \\ \left(\frac{1}{\epsilon_{FE} \epsilon_{BA}} - 1 \right) & \text{if } N_A N_E > N_B N_F \end{cases}}{1 + \left/ \frac{-N_C\, N_F}{N_D\, N_E - N_C\, N_F} \right/ \begin{cases} \left(\frac{1}{\epsilon_{FE} \epsilon_{CD}} - 1 \right) & \text{if } N_D N_E < N_C N_F \\ (1 - \epsilon_{DC}\, \epsilon_{EF}) & \text{if } N_D N_E > N_C N_F \end{cases}}$$

8. Triple ring-gear drive

$$R=\left(1+\frac{N_3}{N_1}\right)\left[\left(1+\frac{N_6}{N_4}\right)\left(-\frac{N_9}{N_7}\right)-\frac{N_6}{N_4}\right]-\frac{N_3}{N_1}$$

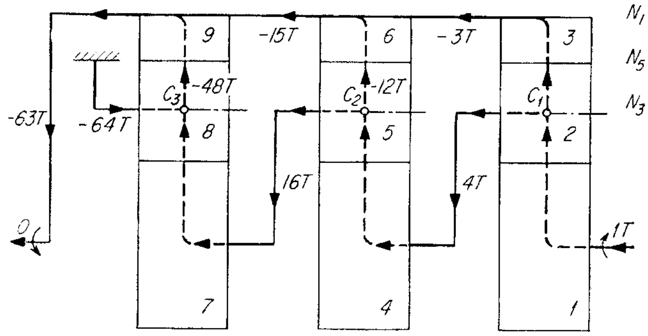

Torque flow numbers for

$N_1=N_2=N_4=20$

$N_5=N_7=N_8=20$

$N_3=N_6=N_9=60$

$$E=1-\frac{16}{21}(1-\epsilon_{12}\,\epsilon_{23})-\frac{16}{21}(1-\epsilon_{45}\,\epsilon_{56})-\frac{16}{21}(1-\epsilon_{78}\,\epsilon_{89})$$

Member	Role	T	ω
1	Input	1	1
10	Output	$-R$	$1/R$
C_3	Reaction	$R-1$	0
3	Split output from 1	$-m_{13}$	ω_0
C_1		$-(1-m_{13})$	ω_4
4	Input to 2	$-T_{c1}$	$\omega_e+\omega_{e2}$

Member	Role	T	ω
6	Split output from 2	$-(1-m_{13})m_{46}$	ω_0
C_2		$T_{c1}(1-m_{46})$	ω_7
7	Input to (3)	$-T_{c2}$	ω_e
9	Output from (3)	$-T_7\ m_{73}$	ω_0
2	Idler	0	$m_{21}\,\omega_{e1}$
5	Idler	0	$m_{54}\,\omega_{e4}$
8	Idler	0	$m_{87}\,\omega_{e7}$

9. Minuteman-cover drive

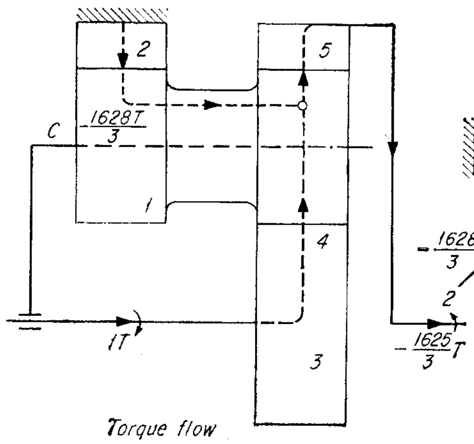

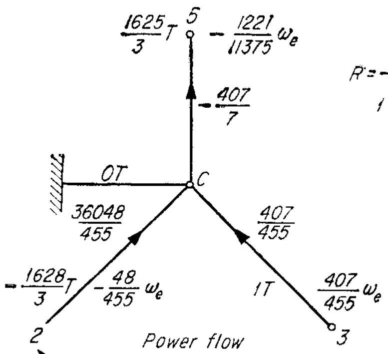

$$R=\frac{1+\dfrac{N_4\,N_2}{N_3\,N_1}}{1-\dfrac{N_4\,N_2}{N_5\,N_1}}=-541\tfrac{2}{3}\ \text{for}\ N_1=32,\ N_2=74,\ N_3=9,\ N_4=33,\ N_5=75$$

Member	Role	T	ω	ω_e
3	Input	1	1	$\omega-\omega_c$
5	Output	$-R$	$1/R$	$\omega-\omega_c$
2	Reaction	$R-1$	0	$\omega-\omega_c$
C	Neutral	0	$-\omega_c=\frac{N_3N_1}{N_4N_2+N_3N_1}$	
1 – 4	Idler	0	—	$m_{43}\,\omega_{e3}$

$$E=\frac{1-\left|\left[N_4N_2/(N_3N_1+N_4N_2)\right](1-\epsilon_{34})\right|}{1+\left|\left[\dfrac{-N_4\,N_2}{N_5N_1-N_4N_2}-\dfrac{N_4N_2}{N_3N_1+N_4N_2}\right]\left(\dfrac{1}{\epsilon_{21}\,\epsilon_{45}}-1\right)\right|+\left|\dfrac{N_4\,N_2}{N_3N_1+N_4N_2}\left(\dfrac{1}{\epsilon_{45}}-1\right)\right|}$$

Coupled planetary drives

10.

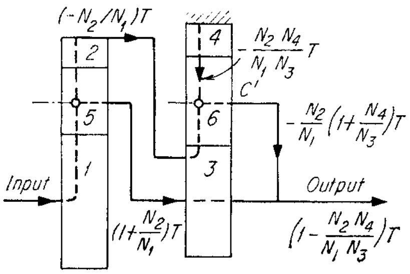

$$R=1-\frac{N_2\,N_4}{N_1\,N_3}$$

$$E=1-\left|\frac{-N_2\,N_4}{N_1\,N_3-N_2\,N_4}(1-\epsilon_{15}\epsilon_{52}\epsilon_{36}\epsilon_{64})\right|$$

11.

$N_2=N_4=60$

$N_1=N_3=20$

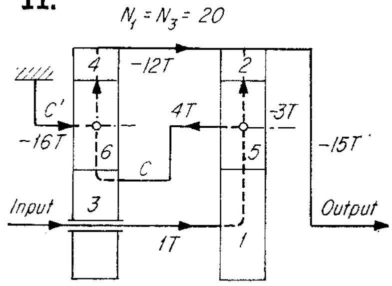

$$R=\left(1+\frac{N_2}{N_1}\right)\left(-\frac{N_4}{N_3}\right)-\frac{N_2}{N_1}$$

$$E=1-\left|\tfrac{4}{5}(1-\epsilon_{15}\epsilon_{52})\right|-\left|\tfrac{4}{5}(1-\epsilon_{36}\epsilon_{64})\right|$$

12.

$N_2=N_4=60$

$N_1=N_3=20$

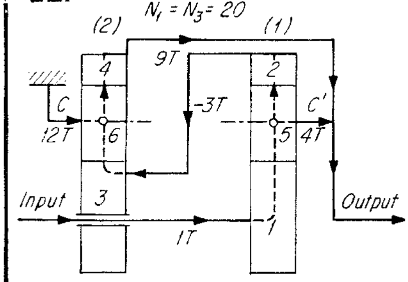

$$R=1+\frac{N_2}{N_1}\left(1+\frac{N_4}{N_3}\right)$$

$$E=1-\left|\tfrac{12}{13}(1-\epsilon_{15}\,\epsilon_{52})\right|-\left|\tfrac{9}{13}(1-\epsilon_{36}\,\epsilon_{64})\right|$$

13. Coupled planetary drives (continued)

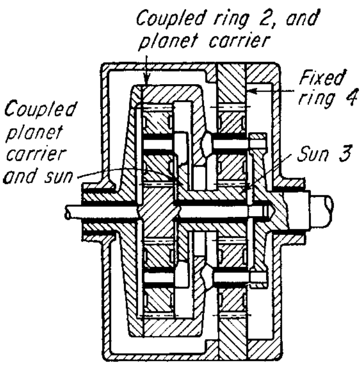

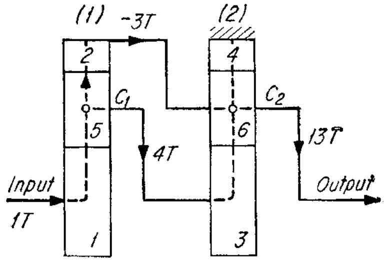

Power flow for $N_2 = N_4 = 60$, $N_1 = N_3 = 20$

$$R = 1 + \frac{N_4}{N_3}\left(1 + \frac{N_2}{N_1}\right)$$

$$E = 1 - \left|\frac{3}{4}(1 - \epsilon_{15}\epsilon_{52})\right| - \left|\frac{12}{13}(1 - \epsilon_{36}\epsilon_{64})\right|$$

14. Differential drive

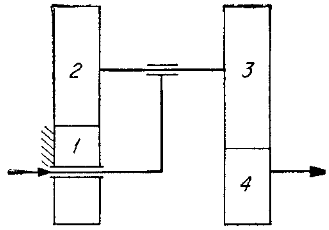

$$R = \frac{1}{1 - \frac{N_3 N_1}{N_4 N_2}}$$

$$E = 1 \Big/ \left[1 + \left|\frac{-N_3 N_1}{N_4 N_2 - N_3 N_1}(1 - \epsilon_{43}\epsilon_{21})\right|\right]$$

Fixed differential drives

15.

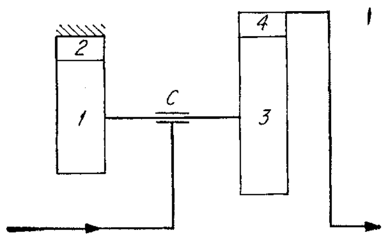

$$R = \frac{1}{1 - \frac{N_3 N_2}{N_4 N_1}}$$

$$E = \frac{1}{1 + \left|\frac{-N_3 N_1}{N_4 N_2 - N_3 N_1}\right| \left|\begin{matrix}\left(\frac{1}{\epsilon_{21}\epsilon_{43}} - 1\right) \text{ if } N_3 N_2 > N_4 N_1 \\ (1 - \epsilon_{43}\epsilon_{21}) \text{ if } N_3 N_2 < N_4 N_1\end{matrix}\right|}$$

16.

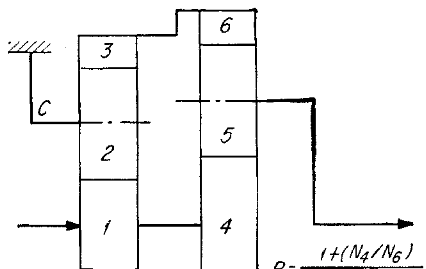

$$R = \frac{1 + (N_4/N_6)}{(N_4/N_6) - (N_1/N_3)}$$

$$E = \frac{1 - \left|\frac{N_6}{N_4 + N_6}(1 - \epsilon_{45}\epsilon_{56})\right|}{1 + \left|\frac{-N_6 N_1}{N_4 N_3 - N_6 N_1}\right| \left|\begin{matrix}\left(\frac{1}{\epsilon_{12}\epsilon_{23}\epsilon_{15}\epsilon_{54}} - 1\right) \text{ if } N_6 N_4 > N_4 N_3 \\ (1 - \epsilon_{45}\epsilon_{56}\epsilon_{32}\epsilon_{21}) \text{ if } N_6 N_4 < N_4 N_3\end{matrix}\right|}$$

17.

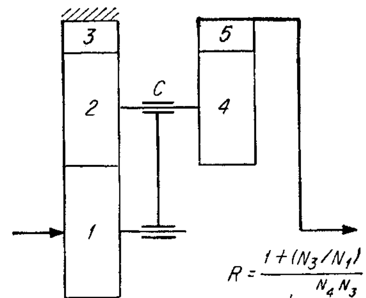

$$R = \frac{1 + (N_3/N_1)}{1 - \frac{N_4 N_3}{N_5 N_2}}$$

$$E = \frac{1 - \left|\frac{N_3}{N_1 - N_3}\left(\frac{1}{\epsilon_{32}\epsilon_{21}} - 1\right)\right|}{1 + \left|\frac{-N_4 N_3}{N_5 N_2 - N_4 N_3}\right| \left|\begin{matrix}\left(\frac{1}{\epsilon_{32}\epsilon_{45}} - 1\right) \text{ if } N_4 N_3 > N_5 N_2 \\ (1 - \epsilon_{54}\epsilon_{23}) \text{ if } N_4 N_3 < N_5 N_2\end{matrix}\right|}$$

18. Fordomatic transmission planetary

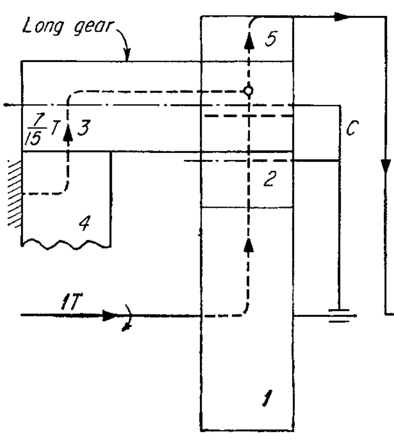

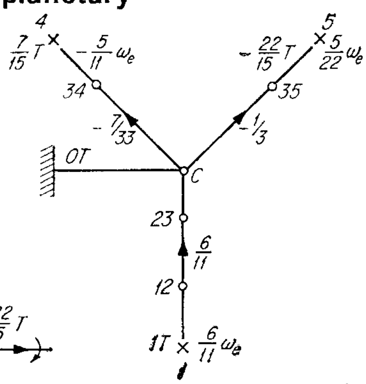

Power flow for:
$N_1 = 30$, $N_2 = N_3 = 18$, $N_4 = 36$, $N_5 = 72$

Member	Role	T	ω	ω_e
1	Input	1	1	$\omega -$ e
5	Output	−R	$1/R$	$\omega -$ c
4	Reaction	R − 1	0	$\omega - \omega_c$
C	Neutral	0	$\frac{1}{1+(N_4/N_1)}$	—
2	Idler	0		$m_{21}\omega_{e1}$
3	Idler	0		$m_{35}\omega_{e5}$

$$R = \frac{1 + (N_4/N_1)}{1 + (N_4/N_5)}$$

$$E = \frac{1 - \left|\left(\frac{N_4}{N_1 + N_4} - \frac{N_4}{N_5 + N_4}\right)(1 - \epsilon_{12}\epsilon_{23}\epsilon_{34})\right| - \left|\frac{N_4}{N_5 + N_4}(1 - \epsilon_{12}\epsilon_{23})\right|}{1 + \left|\frac{N_4}{N_5 + N_4}\left(\frac{1}{\epsilon_{35}} - 1\right)\right|}$$

19. GM Hydramatic planetary

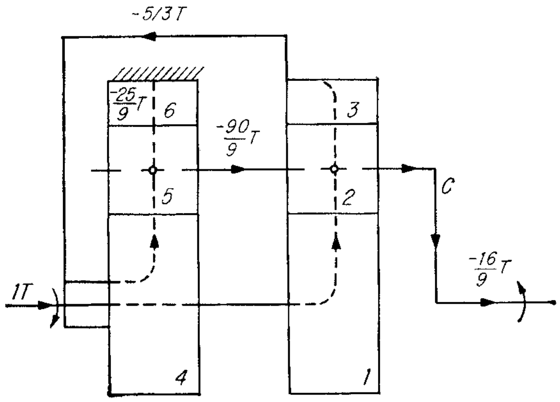

$N_1 = 45 = N_4$

$N_2 = 15 = N_5$

$N_3 = 75 = N_6$

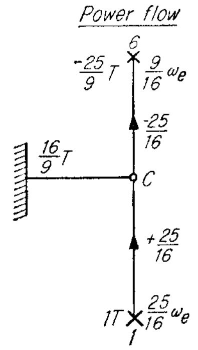

$$R = -\frac{N_3}{N_1}\left(1 + \frac{N_6}{N_4}\right) + \left(1 + \frac{N_3}{N_1}\right)$$

$$E = 1 - \left/ \frac{-N_3 N_6}{N_1 N_4 - N_3 N_6}(1 - \epsilon_{12}\,\epsilon_{23}\,\epsilon_{45}\,\epsilon_{56}) \right/$$

SYMBOLS

C = carrier (also called "spider")—a non-gear member of a gear train whose rotation affects gear ratio
m = fixed gear ratio (for a train with no rotating carriers)
N = number of teeth
R = overall speed reduction ratio = ω_i/ω_o
f = follower (in a gear train)
d = driver (in a gear train)
t = gear train
ω = angular speed
T = torque
ϵ = efficiency between meshing teeth
E = overall planetary gear mesh efficiency

Subscripts
o = output
i = input
r = reaction
c = carrier
e = equivalent
1, 2, 3, etc.— gears in a train

Use of double subscripts
m_{13} = gear ratio for the train starting at gear *1* as input and proceeding to gear *3* as output
ϵ_{13} = mesh efficiency between gears *1* and *3*

which give the ratio between individual members of the assembly in terms of m, the gear ratio for the assembly if the carriers are assumed fixed.

When carrier is input

$$R_i = \frac{1}{1 - m_{or}}$$

When carrier is output

$$R_o = 1 - m_{ir}$$

When carrier is a reaction member (locked to frame)

$$R_r = m_{io}$$

Subscript *or* refers to the ratio between output (o) and reaction (r) members, etc. See list of symbols for definition of other symbols and subscripts.

Speed ratio formulas

The R-factors lead directly to the speed ratio formulas. For example, for a complicated planetary with five gears, the Minuteman cover drive, Example 9, in which one ring gear is fixed and the second is the output, the overall ratio is

$$R = R_o R_i = \frac{1 - m_{ir}}{1 - m_{or}}$$

1) Write out the m-train sequence, as shown after Step 6 below.

2) Place a plus sign over the number of the first driver.

3) Mentally turn the first driver and note the direction of rotation of the next gear in mesh with it.

4) Place the appropriate sign over the number of this next gear.

5) Continue in this manner to the end of the train.

6) Signs of m are the same as that of the last follower.

$$t_{ir} = \begin{matrix} (+) & & (-) & & (-) & & (-) \\ 3 & - & 4 & - & 1 & - & 2 \\ (d) & & (f) & & (d) & & (f) \end{matrix}$$

$$t_{or} = \begin{matrix} (+) & & (+) & & (+) & & (+) \\ 5 & - & 4 & - & 1 & - & 2 \\ (d) & & (f) & & (d) & & (f) \end{matrix}$$

7) Magnitude of m = product of N_f's/product of N_d's.

$$m_{ir} = m_{32} = N_4 N_2 / N_3 N_1$$
$$m_{or} = m_{52} = N_4 N_2 / N_5 N_1$$

$$R = \frac{1 - \left(-\dfrac{N_4 N_2}{N_3 N_1}\right)}{1 - \dfrac{N_4 N_2}{N_5 N_1}} = \frac{1 + \dfrac{N_4 N_2}{N_3 N_1}}{1 - \dfrac{N_4 N_2}{N_5 N_1}}$$

Thus for the number of teeth selected (see Example 9) you obtain a 541⅔ speed reduction. The final formulas derived by this method are given in the boxed examples.

Efficiency formulas

The overall gear-mesh efficiency formula for planetary gear systems is

$$E = \frac{1 - \text{Total } R_o \text{ and } R_r \text{ losses}}{1 + \text{Total } R_i \text{ losses}}$$

20. Tractor transmission planetary

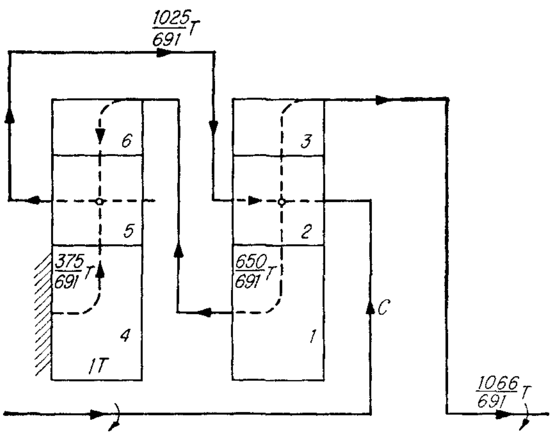

$N_1 = 50$

$N_2 = 17 = N_5$

$N_3 = 82$

$N_4 = 45$

$N_6 = 78$

$$R = \frac{1}{1 - \dfrac{N_1 N_4}{N_3 N_6}}$$

$$E = \frac{1}{1 + \left/ \dfrac{-N_6 N_1}{N_3 N_4 - N_6 N_1} (1 - \epsilon_{32}\epsilon_{21}\epsilon_{65}\epsilon_{54}) \right/}$$

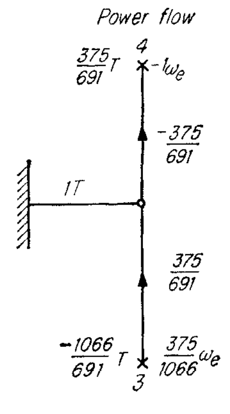

with their mates. These losses can be determined by first computing "ρ factors" from the following equations:

$$\rho_i = \frac{m_{or} - m_{or}}{1 - m_{or}}$$

$$\rho_o = \frac{-m_{ir}}{1 - m_{ir}}$$

Then, in computing R_i loss, when ρ_i comes out positive, use the equation

$$R_i \text{ loss} = \rho_i \left[\frac{1}{\epsilon_{ro}} - 1\right]$$

When ρ_i is a negative value, use

$$R_i \text{ loss} = |\rho_i| (1 - \epsilon_{or})$$

Note that you employ the absolute value of ρ_i in the second equation (you assume that it is a positive value).

In the same manner, when ρ_o is positive

$$R_o \text{ loss} = \rho_o (1 - \epsilon_{ir})$$

When ρ_o is negative

$$R_o \text{ loss} = |\rho_o| \left[\frac{1}{\epsilon_{ri}}\right] - 1$$

Also, in all cases

$$R_r \text{ loss} = 1 - \epsilon_{io}$$

The ρ-factor is a "signed" quantity. Its sign indicates the direction of power flow in the equivalent fixed carrier (EFC) train (power flow diagram), and its size indicates the magnitude of the equivalent power. In the power flow diagram the law of direct-current flow for electrical circuits applies. The flow to a junction point in the power flow diagram must be equal to the flow from the junction point.

As can be noted in Fig 1, input is to gear 1 and output is from carrier C with gear 3 fixed (reaction member). Equivalent power, P_e, flows from 1 to 2 through gear meshes 12 and 23, and input power carries a plus sign and output power a minus sign. The power losses sustained in driving these gears through mesh with their mates in the EFC train is the same as (equivalent to) the power losses circulating in the same tooth engagements in the train.

The external torque, T, acting on each member remains the same in the EFC train, but the speed, ω, of each member is reduced algebraically by the speed of the carrier, ω_c (since the carrier is artificially stopped). Therefore $\omega - \omega_c = \omega_e$ or *equivalent speed.*

Turn now to Example 1, where a specific planetary gear set with numbers of teeth given is shown. Here gear 3 is fixed, the EFC train schematic is omitted, and the EFC power flow is shown, this time with actual torque and equivalent speed values shown on the EFC power flow diagram corresponding to T and ω_e values in the table.

The ρ_i factor for Example 1 is

$$\rho_i = \frac{-m_{13}}{1 - m_{13}} = \frac{N_3}{N_1 + N_3}$$

If $N_1 = 20$, $N_2 = 30$ and $N_3 = 80$, then $\rho_i = +4/5$. The plus sign means that the equivalent power flow is "like" the flow in the planetary system, and 4/5 means that the equivalent power is 4/5 of the planetary transmitted power. The term "like" is carefully chosen, because the flow is not identical. In the planetary train the transmitted power flows from i to o or C to 1. In the EFC train equivalent power flows from r to o or 3 to 1. The flow is "like" because in both cases the flow is *to o*. (Had the sign of ρ_i been minus then the flow would have been *from o* to r and therefore "unlike".)

Returning to the equation for efficiency, it can be rewritten as

$$E = \frac{1}{1 + |\rho_i| \left(\dfrac{1}{\epsilon_{ro}} - 1\right)}$$

This equation is then put into the form you see in Ex 1, with the number of teeth replacing ρ. This is done for every example for ease of use.

To better understand the flow of power in a planetary, it is helpful to know that the equivalent speed of a member is equal to its speed of tooth engagement. Equivalent power and power circulating in tooth engagement likewise are identical, since power is proportional to the product of torque and speed. This means that frictional power losses due to gear tooth action in planetary trains and power losses in EFC trains are the same and are equal to the difference between equivalent input and output power.

Checklist for Planetary-Gear Sets

These five tests quickly tell whether the gears will mesh, and whether there is room for them to fit together.

Hugh P. Hubbard

SYMBOLS

CP = Circular pitch, in.
L = Distance from center of sun gear to center of planet gear, in.
M = Major or outside diameter of gear, in.
DP = Diametral pitch, teeth/in.
m = Minor, or working depth diameter of gear, in.
N = Number of teeth per gear
PD = Pitch diameter, in.
x = The whole number in dividend when N_s is divided by number of planets
y = The whole number in dividend when N_r is divided by number of planets
z = Increment for locating planet gear
α = Angular location of planet gear

You have decided to design a planetary-gear system with a certain gear ratio, and have chosen the number of teeth for each gear to get that ratio. Will it work? Will the gears fit together to make a workable system?

If they can pass the following five tests, they will.

1—Do all gears have the same circular pitch?

If they do not, the gears will not mesh.

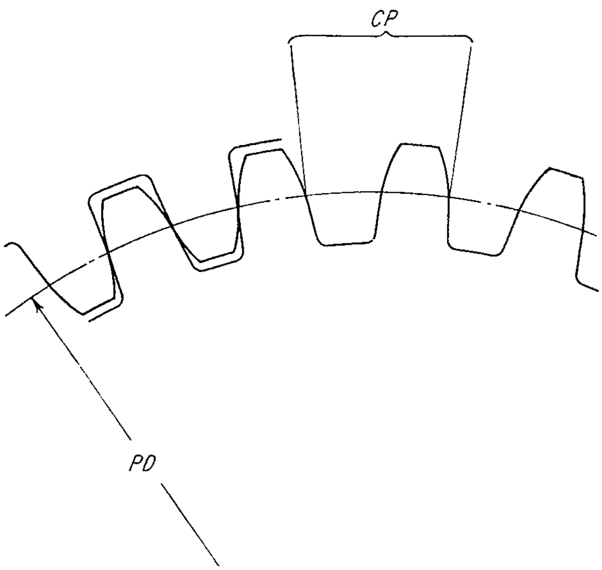

Circular pitch $CP = \pi/DP = PD/N$

Circular pitch and number of teeth determine pitch diameter, which leads to the next test:

2—Will the gears mate at the pitch diameters?

This equation shows whether the planet gear will fill the space between the sun gear and the ring gear:

$$N_p = \frac{N_r - N_s}{2}$$

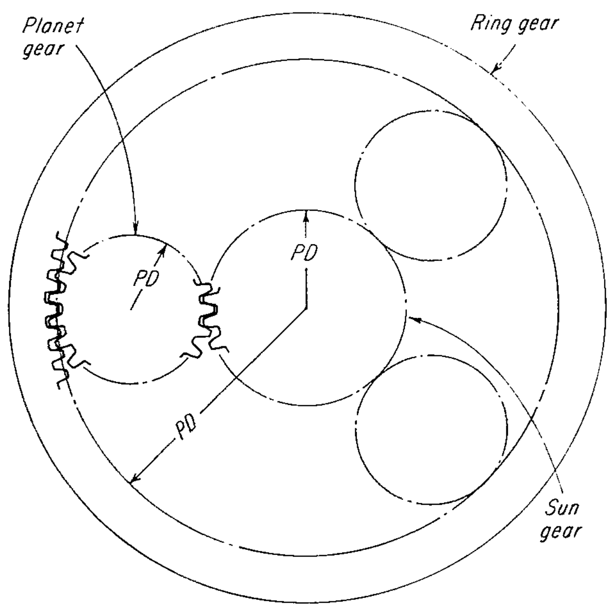

3—Will the teeth mesh?

Gears that pass the first two tests will not necessarily pass this one. If the gears have the wrong number of teeth, the planet gear will not mesh with the sun gear and the ring gear at the same time. Gears with numbers of teeth divisible by three will mesh. There are two other possible cases.

Case I—The number of teeth on the sun gear divides evenly into the number of teeth on the ring gear. This set will mesh, if allowance is made by spacing the planet gears unevenly around the sun gear.

EXAMPLE: In a set of planetary gears the ring gear has 70 teeth, the sun gear 14 teeth and each of the three planet gears 28 teeth. Even spacing would place the planet gears every 120°, but in this case they must be placed slightly to one side of the 120° point to mesh. Since N_s divides evenly into N_r there is a tooth on the ring gear opposite every tooth on the sun gear. Therefore, it is possible to fit a planet gear opposite any tooth on the sun gear. Tooth 6, five circular pitches from tooth 1, is the choice because it is closest to being one-third of the way around. It is opposite tooth 26 on the ring gear, because Nr/Ns = 70/14 = 25/5.

Case II—The number of teeth on the sun gear does not divide evenly into the number of teeth on the ring gear. This set may or may not mesh; the following example shows how to tell.

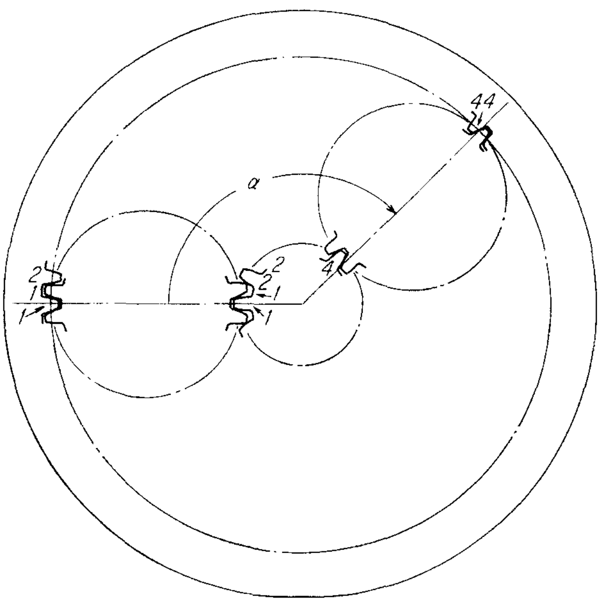

EXAMPLE: In a set of planetary gears with three planets, the ring gear has 134 teeth, the sun gear 14 and the planet gears 60 each. $N_s/3$ = 14/3 = 4.67, so the whole number x = 4. $N_r/3$ = 134/3 = 44.67, so the whole number y = 44.

Plug these numbers into the locating equation

$$(x+z)\,N_r/N_s = y+(1-z) = (4+z)\,134/14 = 44+(1-z)$$
$$10.57\,z = 6.72$$
$$z = 0.636$$

Location of the planet gear as a fractional part of the circular distance around the set is $(x + z)/N_s$ = 4.636/14 = 0.3311, and $y + (1 - z)/N_r$ = 44.364/134 = 0.3311. The answers agree to four places, so the gears will mesh. If the answers don't agree to four places, there will be interference.

Angle α = 0.3311 x 360 = 119.2°

4—Can three planets fit around the sun gear?

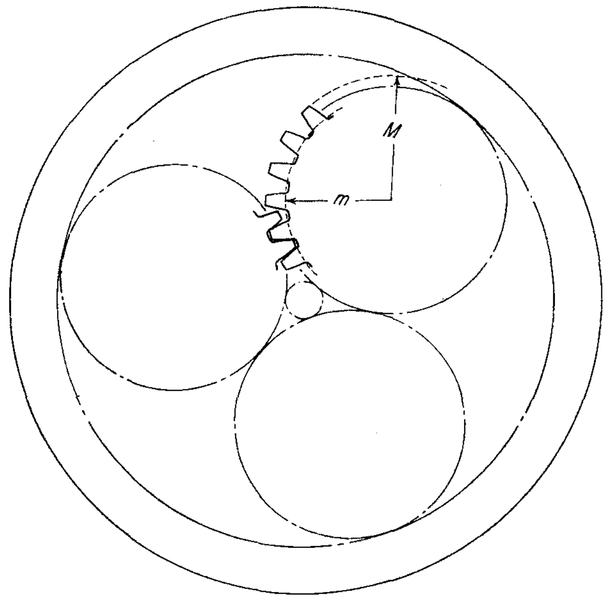

They will if the major diameters adhere to the limitation $M_p + m_s/2 < m_r$ by a safety clearance of $\frac{1}{32}$ in. more than maximum tolerances.

5—Will irregularly spaced planets hit each other?

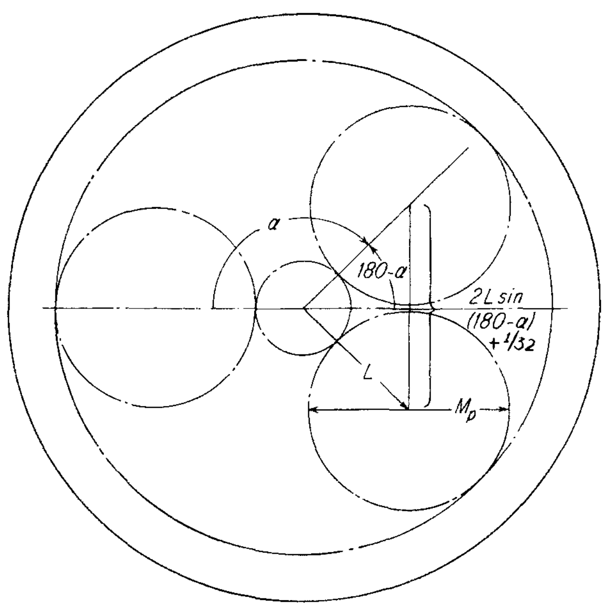

Two adjacent planets will not hit each other if $2L \sin(180 - \alpha) > M_p + \frac{1}{32}$ in. safety clearance. Sun-to-planet center-to-center distance $L = (PD_s + PD_p)/2$. ■

Cardan-Gear Mechanisms

These gearing arrangements convert rotation into straight-line motion, without need for slideways.

Sigmund Rappaport

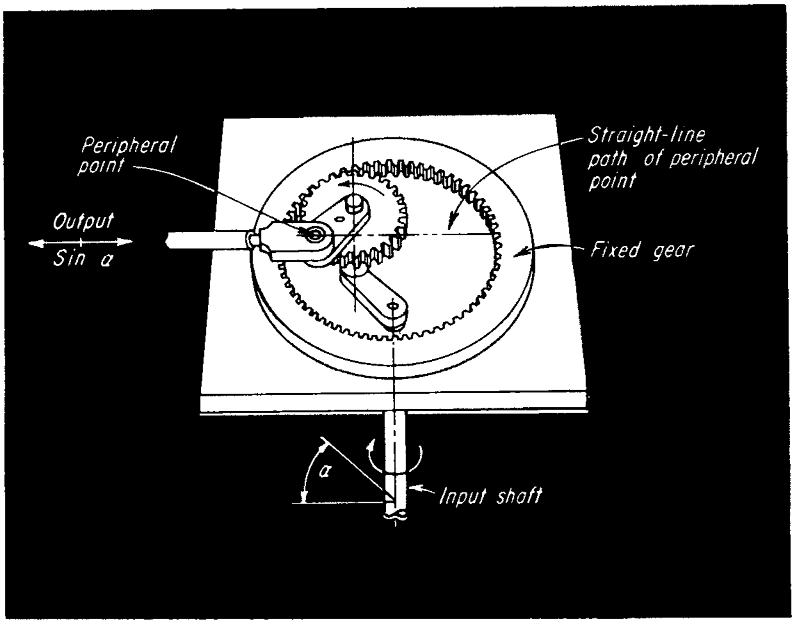

1

Cardan gearing . . . works on the principle that any point on the periphery of a circle rolling on the inside of another circle describes, in general, a hypocycloid. This curve degenerates into a true straight line (diameter of the larger circle) if diameters of both circles are in the ratio of 1:2. Rotation of input shaft causes small gear to roll around the inside of the fixed gear. A pin located on pitch circle of the small gear describes a straight line. Its linear displacement is proportional to the theoretically true sine or cosine of the angle through which the input shaft is rotated. Among other applications, Cardan gearing is used in computers, as a component solver (angle resolver).

2

Cardan gearing and Scotch yoke . . . in combination provide an adjustable stroke. Angular position of outer gear is adjustable. Adjusted stroke equals the projection of the large dia, along which the drive pin travels, upon the Scotch-yoke centerline. Yoke motion is simple harmonic.

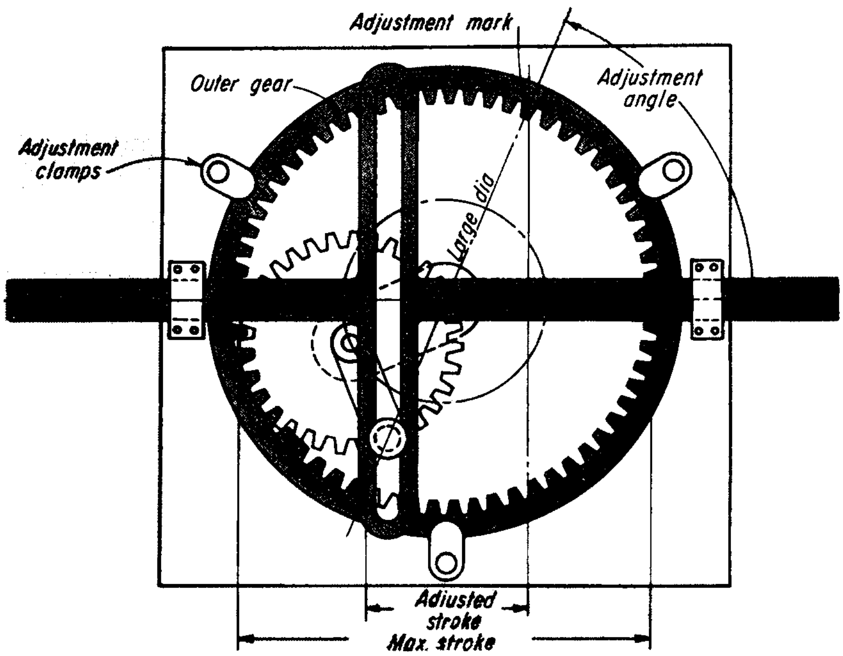

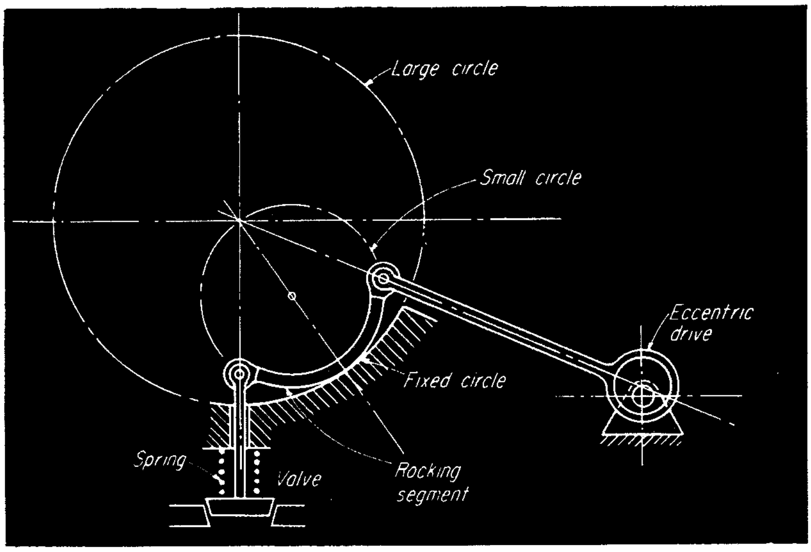

3

Valve drive . . .
exemplifies how Cardan principle may be applied. A segment of the smaller circle rocks to and fro on a circular segment whose radius is twice as large. Input and output rods are each attached to points on the small circle. Both these points describe straight lines. Guide of the valve rod prevents the rocking member from slipping.

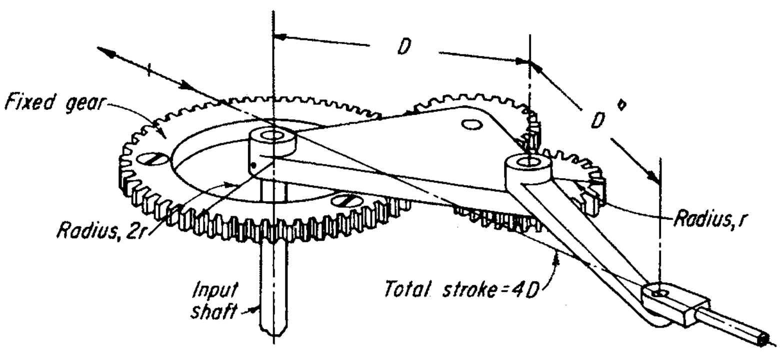

4

Simplified Cardan principle . . .
does away with need for the relatively expensive internal gear. Here, only spur gears may be used and the basic requirements should be met, i.e. the 1:2 ratio and the proper direction of rotation. Latter requirement is easily achieved by introducing an idler gear, whose size is immaterial. In addition to cheapness, this drive delivers a far larger stroke for the comparative size of its gears.

5

Rearrangement of gearing . . .
in (4) results in another useful motion. If the fixed sun-gear and planet pinion are in the ratio of 1:1, then an arm fixed to the planet shaft will stay parallel to itself during rotation, while any point on it describes a circle of radius *R*. An example of application: in conjugate pairs for punching holes on moving webs of paper.

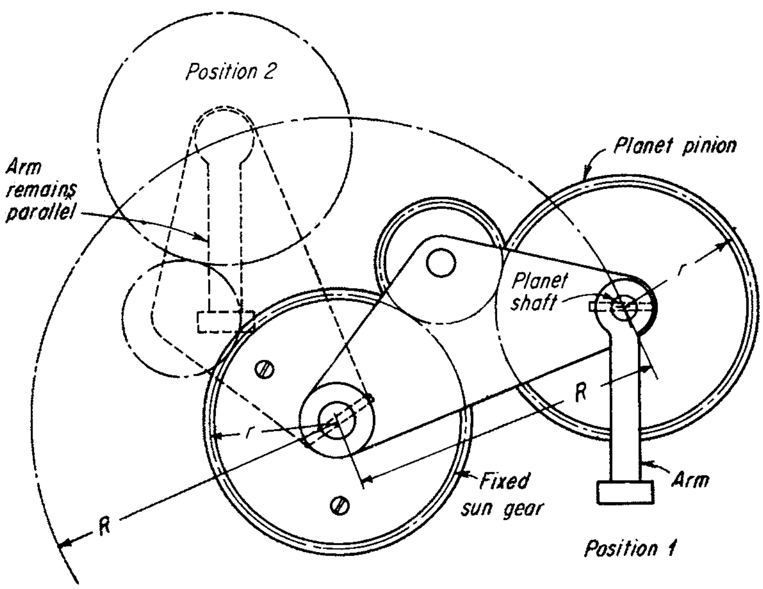

Geneva Wheel Design

These diagrams and formulas will help.

Douglas C. Greenwood

The Geneva wheel was originally used as a stop for preventing overwind in watch springs—leave one of the slot positions unslotted and the number of turns the drive can make is limited. Now, the Geneva wheel is one of the most useful mechanisms for providing high-speed, intermittent, rotary motion.

In the position shown in the first diagram the roller is on the point of entering the slot and about to begin driving the star wheel. Drive ceases when the roller has moved through angle a. The star is locked during its rest periods because the concentric shoulder of the driving member has engaged the corresponding edge of the star. To permit the drive wheel to continue turning it must have a recess for star clearance.

When a Geneva mechanism is used in a machine, the machine speed depends upon the speed at which the star can be driven. Although, on balance, no advantage is gained, some modifications have been investigated that reduce the maximum acceleration and the resulting force. If, for example, the slots are not exactly tangential to the crank circle at their entrance, acceleration forces are reduced. Drive speed can, therefore, be increased. Such design changes, while decreasing acceleration, increase deceleration. Also, hammering will occur at the concentric surface, with a resultant noisy operation.

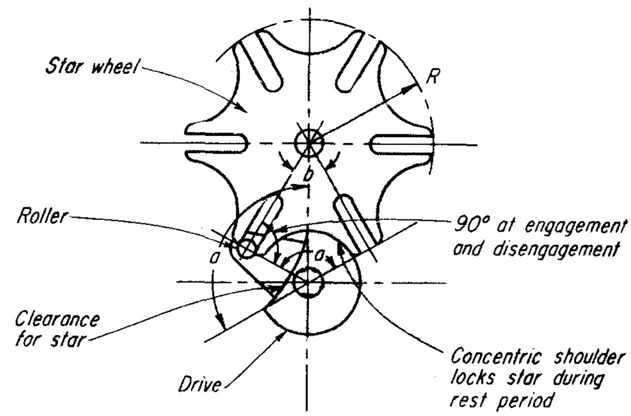

Complete Geneva Mechanism

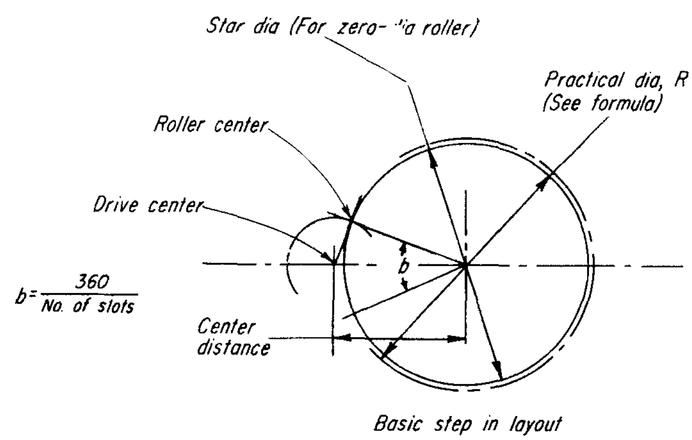

Basic step in layout

Geneva mechanism . . .

can theoretically have from 3 to any number of slots. In practice from 4 to 12 is enough to cover most requirements. Once the number of slots and crank dia are known, the layout can be started by constructing a right-angled triangle on the center distance. A tangent to the star dia where it is cut by a leg of the angle b is the crank radius. The clearance angle on the drive is 180 minus b. Layout is completed by drawing the rest of the mechanism outline. Roller and slot dimensions will depend on forces to which the mechanism will be subjected.

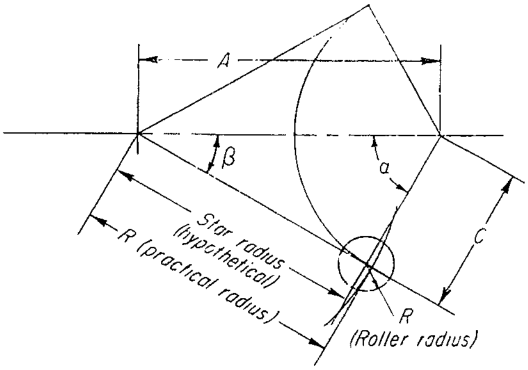

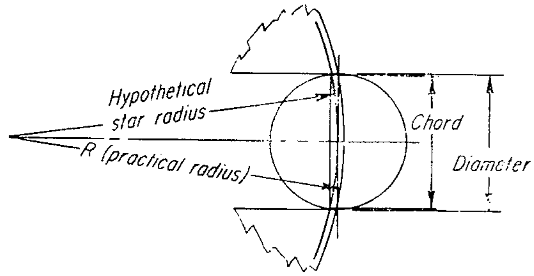

DESIGN FORMULAS

Values such as angular position at any instant, velocity, acceleration and practical star-wheel dia can be calculated from the formulas that follow. Illustrated in the sketch above are symbols that appear in the formulas.

Hypothetical star radius . . .

would be practical only for a roller of zero dia. Otherwise R will always be the greater radius. This ensures that correct roller and slot clearance is maintained at entrance and exit. Difference between chord and dia would be the excess clearance that would result (at time of entry and exit) from using incorrect radius.

Center distance A

$$= CM \text{ where } M = \frac{1}{\text{Sin} \frac{180}{\text{no. of slots}}}$$

Angular displacement:

$$\text{Tan } \beta = \frac{\text{Sin } \alpha}{M - \cos \alpha}$$

Angular velocity

$$= \frac{d\beta}{dt}$$

$$= \omega \left(\frac{M \cos \alpha - 1}{1 + M^2 - 2M \cos \alpha} \right)$$

where Ω = radians/sec

Angular acceleration, radians/sec²

$$= \frac{d^2\beta}{d t^2}$$

$$= \omega^2 \left(\frac{M \sin \alpha \, (1 - M^2)}{(1 + M^2 - 2M \cos\alpha)^2} \right)$$

Max acceleration occurs when

$$\cos\alpha = \pm \sqrt{\left[\left(\frac{1 + M^2}{4\,M} \right)^2 + 2 \right]} - \left(\frac{1 + M^2}{4\,M} \right)$$

Max acceleration and therefore max wear occurs at about $\frac{1}{3}$ to $\frac{1}{4}$ distance down the slot length from the wheel edge.

Practical star-wheel dia

$$2R = \sqrt{A^2 - C^2 + \mu^2}$$

ANGULAR DISPLACEMENT OF DRIVE
during periods of star-wheel rest and motion

Slot angle	No. of drive rollers	Drive crank: Degrees of driving stroke (motion period)	Drive crank: Degrees of free turning (dwell period)
90° 4 slot	1	90	270
	2	180	180
	3	270	90
	4	360	0
72° 5 slot	1	108	252
	2	216	144
	3	324	36
60° 6 slot	1	120	240
	2	240	120
45° 8 slot	1	135	225
	2	270	90
36° 10 slot	1	144	216
	2	288	72
30° 12 slot	1	150	210
	2	300	60

Modified Geneva Drives and Special Mechanisms

These sketches were selected as practical examples of uncommon, but often useful mechanisms. Most of them serve to add a varying velocity component to the conventional Geneva motion.

Sigmund rappaport

Fig. 1—(Below) In the conventional external Geneva drive, a constant-velocity input produces an output consisting of a varying velocity period plus a dwell. In this modified Geneva, the motion period has a constant-velocity interval which can be varied within limits. When spring-loaded driving roller *a* enters the fixed cam *b*, the output-shaft velocity is zero. As the roller travels along the cam path, the output velocity rises to some constant value, which is less than the maximum output of an unmodified Geneva with the same number of slots; the duration of constant-velocity output is arbitrary within limits. When the roller leaves the cam, the output velocity is zero; then the output shaft dwells until the roller re-enters the cam. The spring produces a variable radial distance of the driving roller from the input shaft which accounts for the described motions. The locus of the roller's path during the constant-velocity output is based on the velocity-ratio desired.

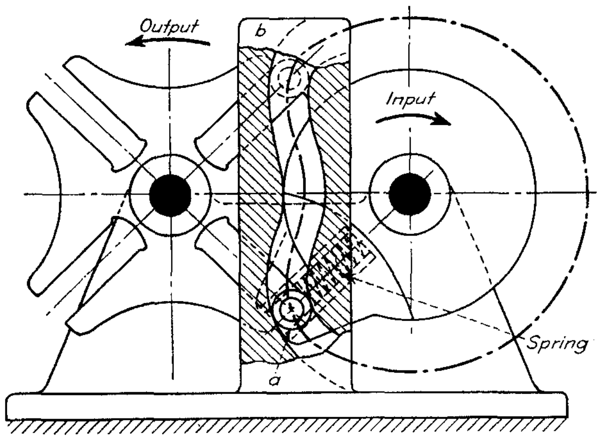

Saxonian Carton Machine Co., Dresden, Germany

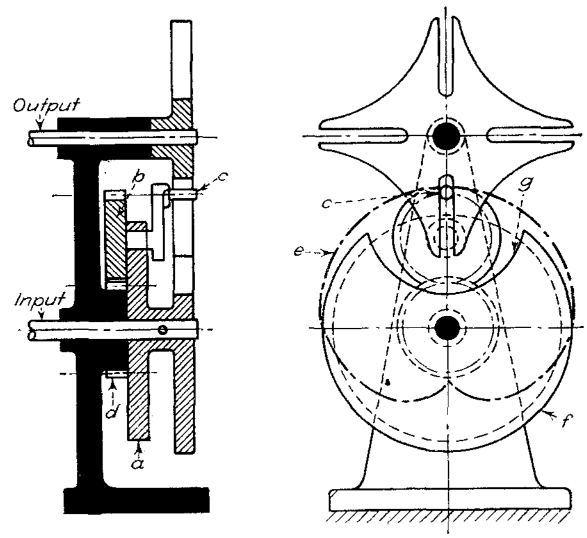

Fig. 2—(Above) This design incorporates a planet gear in the drive mechanism. The motion period of the output shaft is decreased and the maximum angular velocity is increased over that of an unmodified Geneva with the same number of slots. Crank wheel *a* drives the unit composed of plant gear *b* and driving roller *c*. The axis of the driving roller coincides with a point on the pitch circle of the planet gear; since the planet gear rolls around the fixed sun gear *d*, the axis of roller *c* describes a cardioid *e*. To prevent the roller from interfering with the locking disk *f*, the clearance arc *g* must be larger than required for unmodified Genevas.

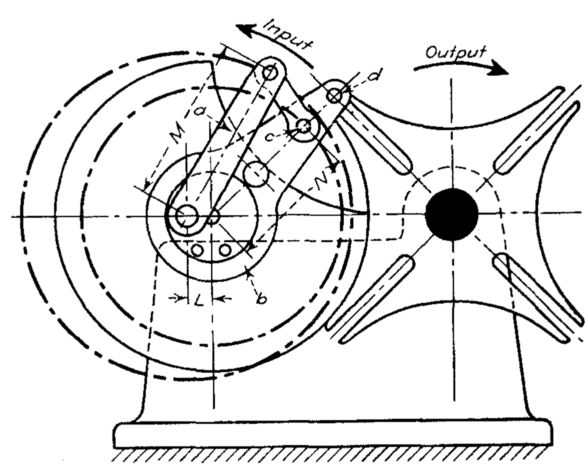

Fig. 3—A motion curve similar to that of Fig. 2 can be derived by driving a Geneva wheel by means of a two-crank linkage. Input crank *a* drives crank *b* through link *c*. The variable angular velocity of driving roller *d*, mounted on *b*, depends on the center distance *L*, and on the radii *M* and *N* of the crank arms. This velocity is about equivalent to what would be produced if the input shaft were driven by elliptical gears.

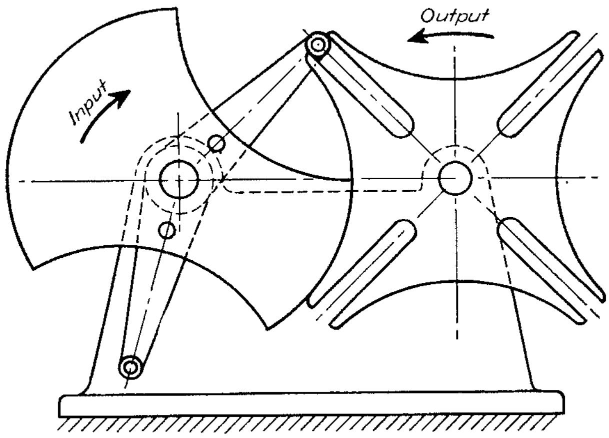

Fig. 4—(Left) The duration of the dwell periods is changed by arranging the driving rollers unsymmetrically around the input shaft. This does not affect the duration of the motion periods. If unequal motion periods are desired as well as unequal dwell periods, then the roller crank-arms must be unequal in length and the star must be suitably modified; such a mechanism is called an "irregular Geneva drive."

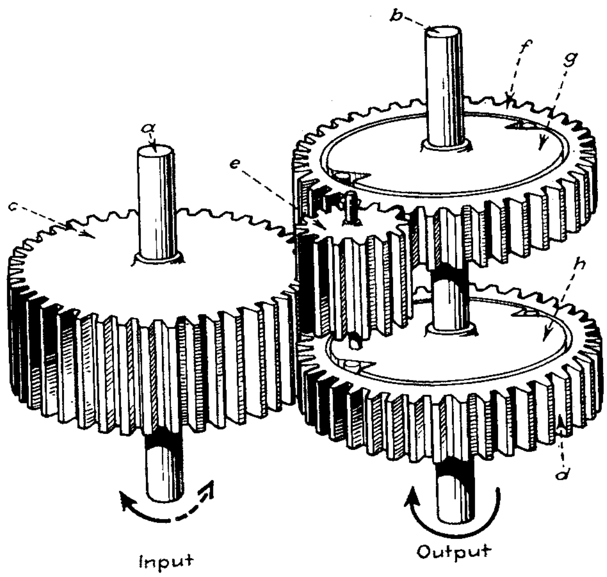

Fig. 5—(Below) In this intermittent drive, the two rollers drive the output shaft as well as lock it during dwell periods. For each revolution of the input shaft the output shaft has two motion periods. The output displacement ϕ is determined by the number of teeth; the driving angle, ψ, may be chosen within limits. Gear *a* is driven intermittently by two driving rollers mounted on input wheel *b*, which is bearing-mounted on frame *c*. During the dwell period the rollers circle around the top of a tooth. During the motion period, a roller's path *d* relative to the driven gear is a straight line inclined towards the output shaft. The tooth profile is a curve parallel to path *d*. The top land of a tooth becomes the arc of a circle of radius *R*, the arc approximating part of the path of a roller.

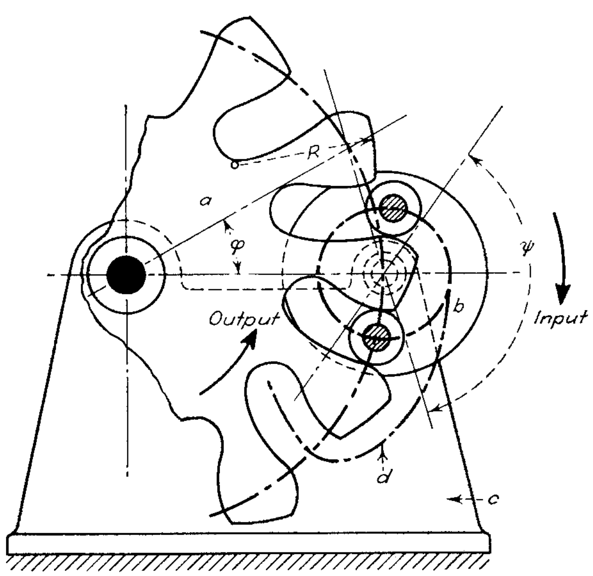

Fig. 6—This uni-directional drive was developed by the author and to his knowledge is novel. The output shaft rotates in the same direction at all times, without regard to the direction of the rotation of the input shaft; angular velocity of the output shaft is directly proportional to the angular velocity of the input shaft. Input shaft *a* carries spur gear *c*, which has approximately twice the face width of spur gears *f* and *d* mounted on output shaft *b*. Spur gear *c* meshes with idler *e* and with spur gear *d*. Idler *e* meshes with spur gears *c* and *f*. The output shaft *b* carries two free-wheel disks *g* and *h*, which are oriented uni-directionally.

When the input shaft rotates clockwise (bold arrow), spur gear *d* rotates counter-clockwise and idles around free-wheel disk *h*. At the same time idler *e*, which is also rotating counter-clockwise, causes spur gear *f* to turn clockwise and engage the rollers on free-wheel disk *g*; thus, shaft *b* is made to rotate clockwise. On the other hand, if the input shaft turns counter-clockwise (dotted arrow), then spur gear *f* will idle while spur gear *d* engages free-wheel disk *h*, again causing shaft *b* to rotate clockwise.

Epicyclic Gear Trains

M. F. Spotts

EPICYCLIC GEAR TRAIN shown in Fig. 1 has Arm A integral with the right hand shaft. Gears C and D are keyed to a short length of shaft which is mounted in a bearing in Arm A. Gear C meshes with the fixed internal gear B. Gear D meshes with internal gear E which is keyed to the left hand shaft.

To find the ratio of the speed of shaft E to the speed of shaft A proceed as follows. Let N_b be the number of teeth in gear B, N_c the number in gear C, and so on. Let arm A, which was originally in a vertical position, be given an angular displacement θ. In so doing gear C will traverse through arc ab on gear B. Arc bc of gear C must be equal to arc ab of gear B. Since angles are inversely proportional to radii, or to the number of teeth, gears C and D will have turned through angle $\theta N_b/N_c$.

While the foregoing was taking place gears D and E were rotating on each other through the equal arcs ed and ef. Gear E will have been turned in the reverse direction through angle

$$\theta N_b/N_c \times N_d/N_e$$

The net effect of these two operations is to move the point of gear E, which was originally vertical at g, over to location f. Gear E has thus been rotated through angle

$$(1 - N_bN_d/N_cN_e)\,\theta$$

This latter value when divided by θ, the angular movement of shaft A, gives the ratio of the rotations of shafts E and A respectively.

This method of analysis gives a graphical representation of the movement of all the parts. It may be easily applied to all types of epicyclic systems including those containing bevel gears. Additional examples are shown in Figs. 2 to 6 inclusive. Either of shafts A or E may be used as the driver.

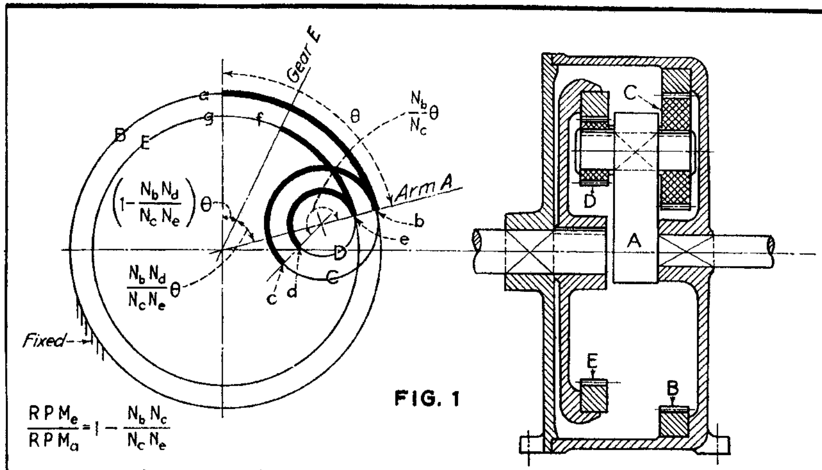

$$\frac{RPM_e}{RPM_a} = 1 - \frac{N_bN_c}{N_cN_e}$$

FIG. 1

Drive and driven shafts rotate in **same** direction

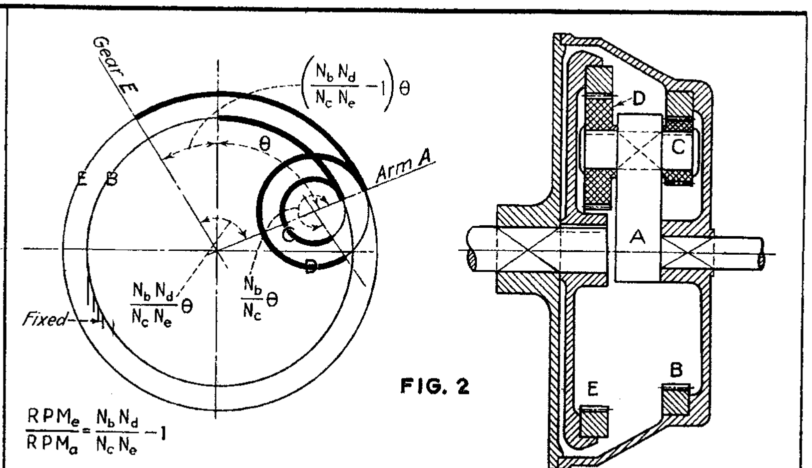

$$\frac{RPM_e}{RPM_a} = \frac{N_bN_d}{N_cN_e} - 1$$

FIG. 2

Drive and driven shafts rotate in **opposite** directions

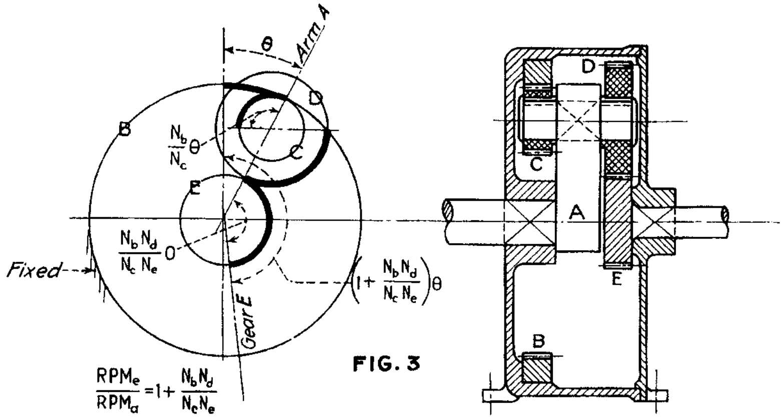

FIG. 3

$$\frac{RPM_e}{RPM_a} = 1 + \frac{N_b N_d}{N_c N_e}$$

Drive and driven shafts rotate in **same** direction
Equation is valid for $N_c = N_d$, and for $N_c > N_d$

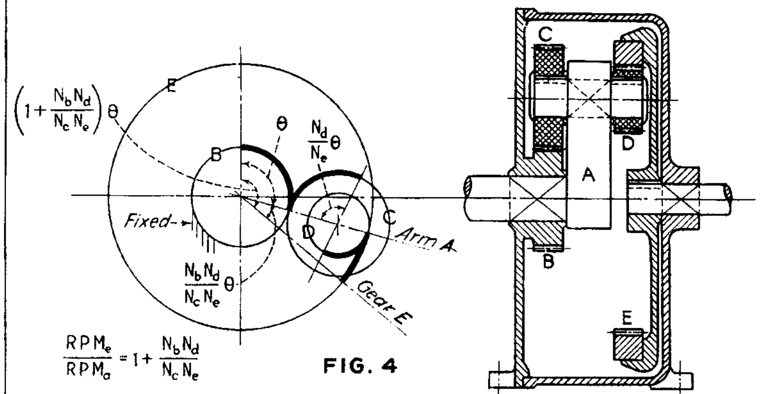

FIG. 4

$$\frac{RPM_e}{RPM_a} = 1 + \frac{N_b N_d}{N_c N_e}$$

Drive and driven shafts rotate in **same** direction
Equation is valid for $N_c = N_d$, and for $N_c > N_d$

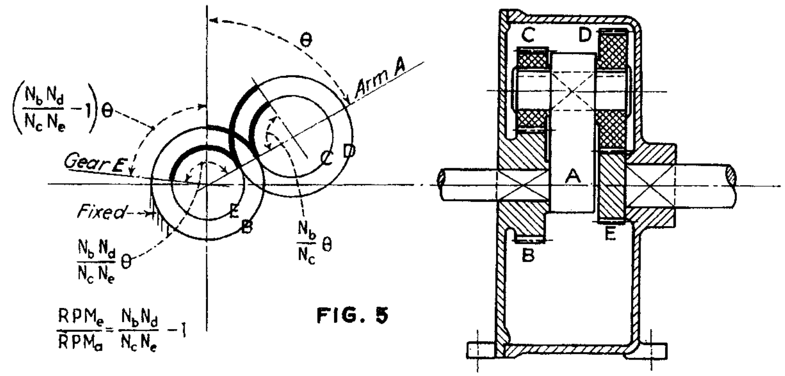

FIG. 5

$$\frac{RPM_e}{RPM_a} = \frac{N_b N_d}{N_c N_e} - 1$$

Drive and driven shafts rotate in **opposite** directions

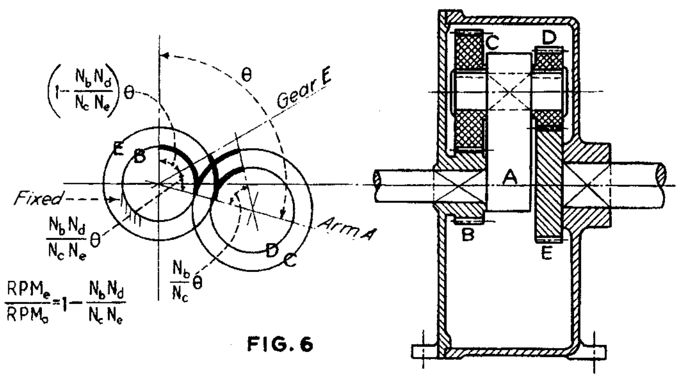

$$\frac{RPM_e}{RPM_a} = 1 - \frac{N_b N_d}{N_c N_e}$$

FIG. 6

Drive and driven shafts rotate in **same** direction

Cycloid Gear Mechanisms

Cycloidal motion is becoming popular for mechanisms in feeders and automatic machines. Here are arrangements, formulas, and layout methods.

Preben W. Jensen

THE appeal of cycloidal mechanisms is that they can easily be tailored to provide one of these three common motion requirements:

- **Intermittent motion**—with either short or long dwells
- **Rotary motion with progressive oscillation**—where the output undergoes a cycloidal motion during which the forward motion is greater than the return motion
- **Rotary-to-linear motion with a dwell period**

All the cycloidal mechanisms covered in this article are geared; this results in compact positive devices capable of operating at relatively high speeds with little backlash or "slop." The mechanisms can also be classified into three groups:

Hypocycloid—where the points tracing the cycloidal curves are located on an external gear rolling inside an internal ring gear. This ring gear is usually stationary and fixed to the frame.

Epicycloid—where the tracing points are on an external gear which rolls in another external (stationary) gear

Pericycloid—where the tracing points are located on an internal gear which rolls on a stationary external gear.

HYPOCYCLOID MECHANISMS

1. Basic hypocycloid curves

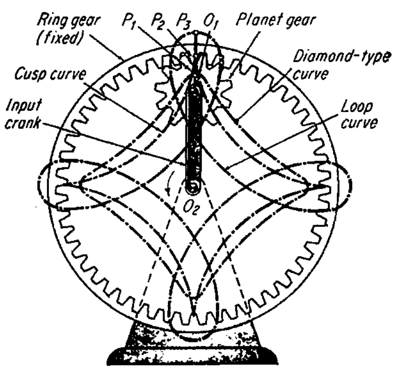

Input drives a planet in mesh with a stationary ring gear. Point P_1 on the planet gear describes a diamond-shape curve, point P_2 on the pitch line of the planet describes the familiar cusp curve, and point P_3, which is on an extension rod fixed to the planet gear, describes a loop-type curve. In one application, an end miller located at P_1 was employed in production for machining a diamond-shape profile.

2. Double-dwell mechanism

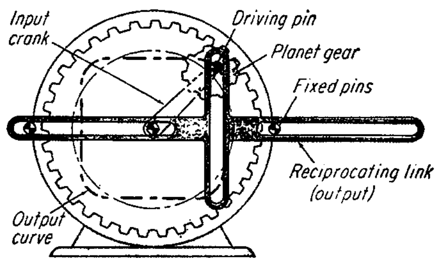

Coupling the output pin to a slotted member produces a prolonged dwell in each of the extreme positions. This is another application of the diamond-type hypocycloidal curve.

3. Long-dwell geneva drive

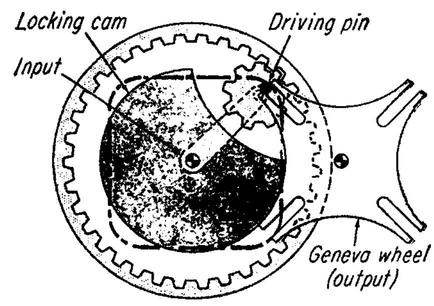

As with standard four-station genevas, each rotation of the input indexes the slotted geneva 90 deg. By employing a pin fastened to the planet gear to obtain a rectangular-shape cycloidal curve, a smoother indexing motion is obtained because the driving pin moves on a noncircular path.

4. Internal-geneva drive

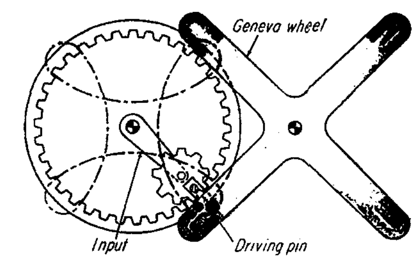

Loop-type curve permits driving pin to enter slot in a direction that is radially outward from the center, and then loop over to rapidly index the cross member. As with the previous geneva, the output rotates 90 deg, then goes into a long dwell period during each 270-deg rotation of the input.

5. Cycloidal parallelogram

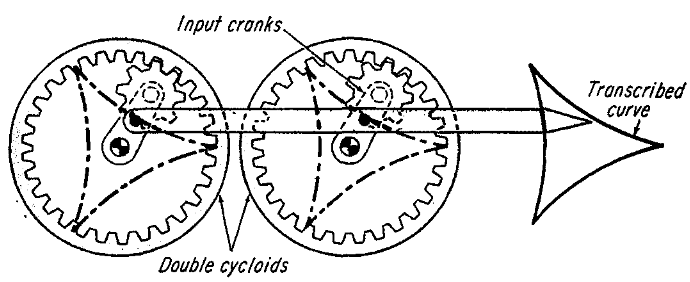

Two identical hypocycloid mechanisms guide the point of the bar along the triangularly shaped path. They are useful also in cases where there is limited space in the area where the curve must be described. Such double-cycloid mechanisms can be designed to produce other types of curves.

6. Short-dwell rotary

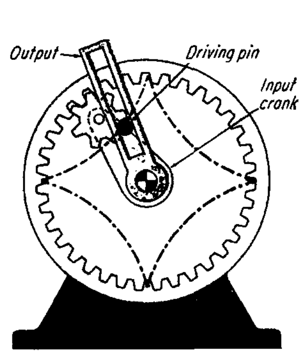

Here the pitch circle of the planet gear is exactly one-quarter that of the ring gear. A pin on the planet will cause the slotted output member to have four instantaneous dwells for each revolution of the input shaft.

7. Cycloidal rocker

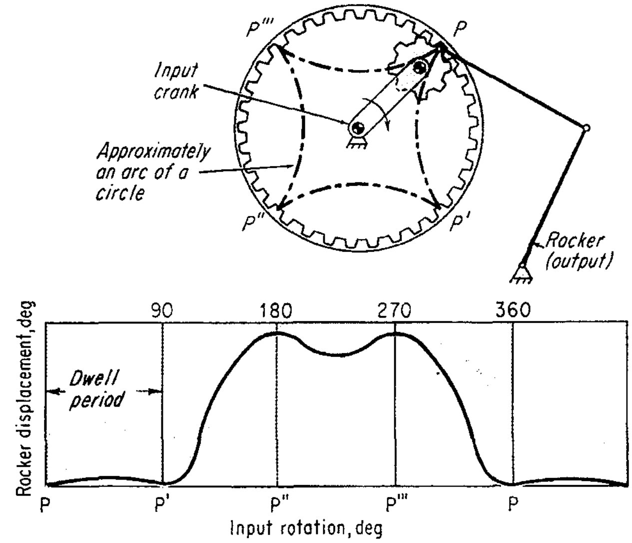

The curvature of the cusp is approximately that of an arc of a circle. Hence the rocker comes to a long dwell at the right extreme position while point P moves to P'. There is then a quick return from P' to P'', with a momentary dwell at the end of this phase. The rocker then undergoes a slight oscillation from point P'' to P''', as shown in the displacement diagram.

8. Cycloidal reciprocator

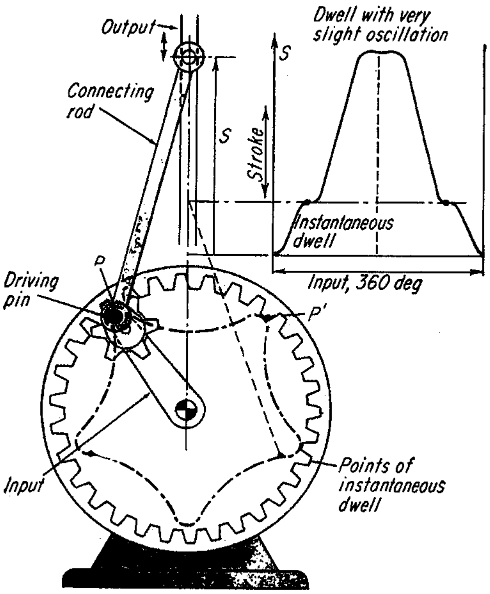

Portion of curve, *P-P'*, produces the long dwell (as in previous mechanism), but the five-lobe cycloidal curve avoids a marked oscillation at the end of the stroke. There are also two points of instantaneous dwell where the curve is perpendicular to the connecting rod.

9. Adjustable harmonic drive

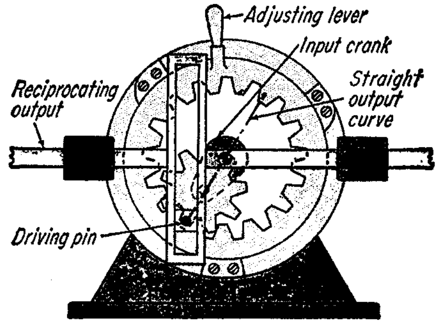

By making the planet-gear half that of the internal gear, a straight-line output curve is produced by the driving pin which is fastened to the planet gear. The pin engages the slotted member to cause the output to reciprocate back and forth with harmonic (sinusoidal) motion. The position of the fixed ring gear can be changed by adjusting the lever, which in turn rotates the straight-line output-curve. When the curve is horizontal, the stroke is at a maximum; when the curve is vertical, the stroke is zero.

10. Elliptical-motion drive

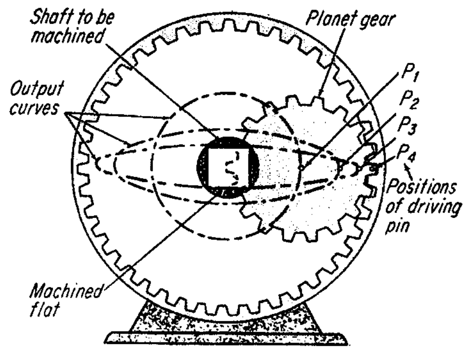

By making the pitch diameter of the planet equal to half that of the ring gear, every point on the planet gear (such as points P_2 and P_3) will describe elliptical curves which get flatter as the points are selected closer to the pitch circle. Point P_1, at the center of the planet, describes a circle; point P_4 at the pitch circle describes a straight line. When a cutting tool is placed at P_3, it will cut almost-flat sections from round stock, as when machining a bolt. The other two sides of the bolt can be cut by rotating the bolt, or the cutting device, 90 deg. (Reference: H. Zeile, *Unrund- und Mehrkantdrehen,* VDI-Berichte, Nr. 77,1965.)

EPICYCLOID MECHANISMS

11. Epicycloid reciprocator

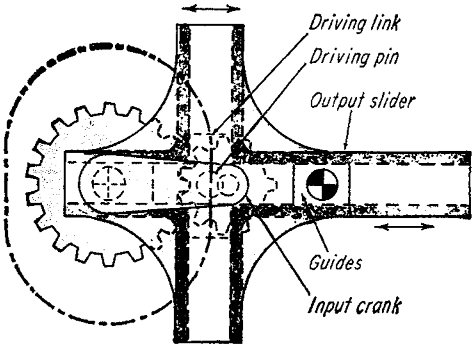

Here the sun gear is fixed and the planet gear driven around it by means of the input link. There is no internal ring gear as with the hypocycloid mechanisms. Driving pin *P* on the planet describes the curve shown which contains two almost-flat portions. By having the pin ride in the slotted yoke, a short dwell is produced at both the extreme positions of the output member. The horizontal slots in the yoke ride the end-guides, as shown.

12. Progressive oscillating drive

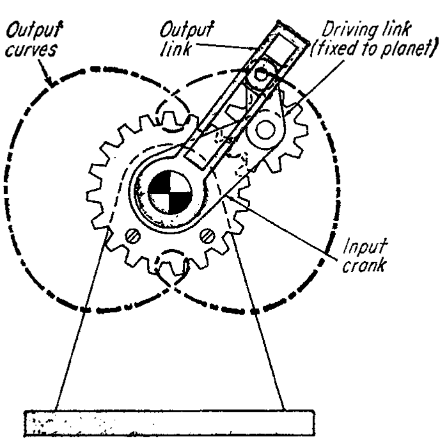

By fixing a crank to the planet gear, a point *P* can be made to describe the double loop curve illustrated. The slotted output crank oscillates briefly at the vertical portions.

13. Parallel-guidance mechanisms

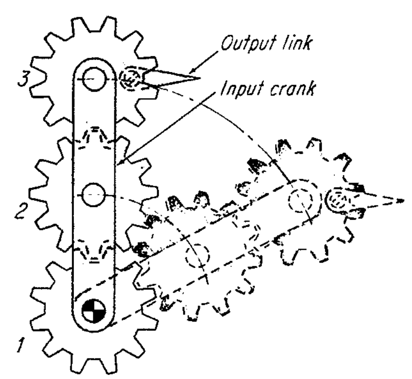

The input crank contains two planet gears. The center sun-gear is fixed as in the previous epicycloid mechanisms. By making the three gears equal in diameter and having gear *2* serve as an idler, any member fixed to gear *3* will remain parallel to its previous positions throughout the rotation of the input ring crank.

MOTION EQUATIONS

14. Equations for epicycloid drives

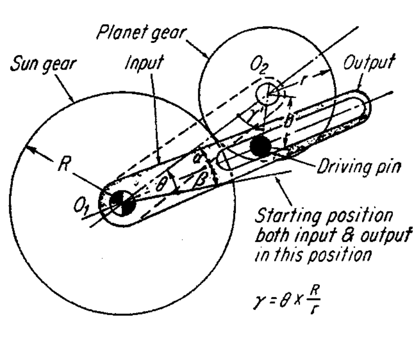

The equations for angular displacement, velocity and acceleration for basic epicyclic drive are given below. (Reference: Schmidt, E. H., "Cycloidal Cranks," *Transactions of the 5th Conference on Mechanisms,* 1958, pp 164-180):

Angular displacement

$$\tan\beta = \frac{(R+r)\sin\theta - b\sin(\theta+\gamma)}{(R+r)\cos\theta - b\cos(\theta+\gamma)} \qquad (1)$$

Angular velocity

$$V = \omega\,\frac{1 + \dfrac{b^2}{r(R+r)} - \left(\dfrac{2r+R}{r}\right)\left(\dfrac{b}{R+r}\right)\left(\cos\dfrac{R}{r}\theta\right)}{1 + \left(\dfrac{b}{R+r}\right)^2 - \left(\dfrac{2b}{R+r}\right)\left(\cos\dfrac{R}{r}\theta\right)} \qquad (2)$$

Angular acceleration

$$A = \omega^2\,\frac{\left(1 - \dfrac{b^2}{(R+r)^2}\right)\left(\dfrac{R^2}{r^2}\right)\left(\dfrac{b}{R+r}\right)\left(\sin\dfrac{R}{r}\theta\right)}{\left[1 + \dfrac{b^2}{(R+r)^2} - \left(\dfrac{2b}{R+r}\right)\left(\cos\dfrac{R}{r}\theta\right)\right]^2} \qquad (3)$$

Symbols

- A = angular acceleration of output, deg/sec^2
- b = radius of driving pin from center of planet gear
- r = pitch radius of planet gear
- R = pitch radius of fixed sun gear
- V = angular velocity of output, deg/sec
- β = angular displacement of output, deg
- γ = $\theta R/r$
- θ = input displacement, deg
- ω = angular velocity of input, deg/sec

15. Equations for hypocycloid drives

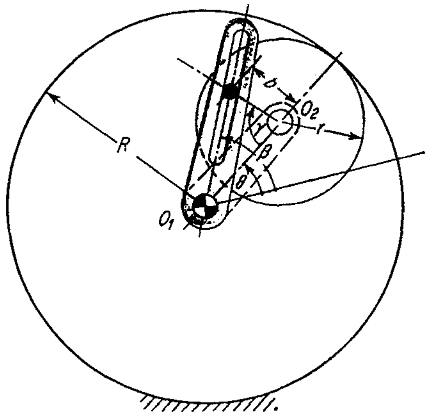

$$\tan \beta = \frac{\sin \theta - \left(\frac{b}{R-r}\right)\left(\sin \frac{R-r}{r}\theta\right)}{\cos \theta + \left(\frac{b}{R-r}\right)\left(\cos \frac{R-r}{r}\theta\right)} \tag{4}$$

$$V = \omega \frac{1 - \left(\frac{R-r}{r}\right)\left(\frac{b^2}{(R+r)^2}\right) + \left(\frac{2r-R}{r}\right)\left(\cos \frac{R}{r}\theta\right)}{1 + \frac{b^2}{(R+r)^2} + \left(\frac{2b}{R+r}\right)\left(\cos \frac{R}{r}\theta\right)} \tag{5}$$

$$A = \omega^2 \frac{\left(1 - \frac{b^2}{(R+r)^2}\right)\left(\frac{b}{R+r}\right)\left(\frac{R^2}{r^2}\right)\left(\sin \frac{R}{r}\theta\right)}{\left[1 + \frac{b^2}{(R+r)^2} + \left(\frac{2b}{R+r}\right)\left(\cos \frac{R}{r}\theta\right)\right]^2} \tag{6}$$

DESCRIBING APPROXIMATE STRAIGHT LINES

16. Gear rolling on a gear—flatten curves

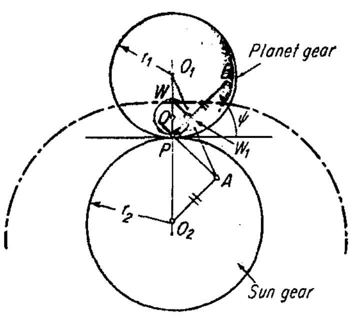

It is frequently desirable to find points on the planet gear that will describe approximately straight lines for portions of the output curve. Such points will yield dwell mechanisms, as shown in Fig 2 and 11. Construction is as follows (shown at left):

1. Draw an arbitrary line *PB*.
2. Draw its parallel O_2A.
3. Draw its perpendicular *PA* at *P*. Locate point *A*.
4. Draw O_1A. Locate W_1.
5. Draw perpendicular to PW_1 at W_1 to locate *W*.
6. Draw a circle with *PW* as the diameter.

All points on this circle describe curves with portions that are approximately straight. This circle is also called the inflection circle because all points describe curves which have a point of inflection at the position illustrated. (Shown is the curve passing through point *W*.)

17. Gear rolling on a rack—vee curves

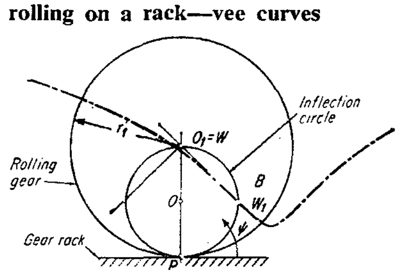

This is a special case. Draw a circle with a diameter half that of the gear (diameter O_1P). This is the inflection circle. Any point, such as point W_1, will describe a curve that is almost straight in the vicinity selected. Tangents to the curves will always pass through the center of the gear, O_1 (as shown).

18. Gear rolling inside a gear—zig-zag

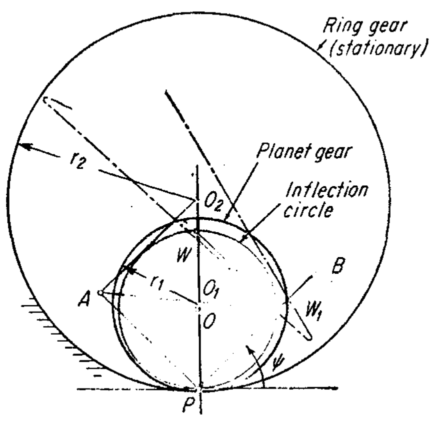

To find the inflection circle for a gear rolling inside a gear:

1. Draw arbitrary line *PB* from the contact point *P*.
2. Draw its parallel O_2A, and its perpendicular, *PA*. Locate *A*.
3. Draw line AO_1 through the center of the rolling gear. Locate W_1.
4. Draw a perpendicular through W_1. Obtain *W*. Line *WP* is the diameter of the inflection circle. Point W_1, which is an arbitrary point on the circle, will trace a curve of repeated almost-straight lines, as shown.

19. Center of curvature—gear rolling on gear

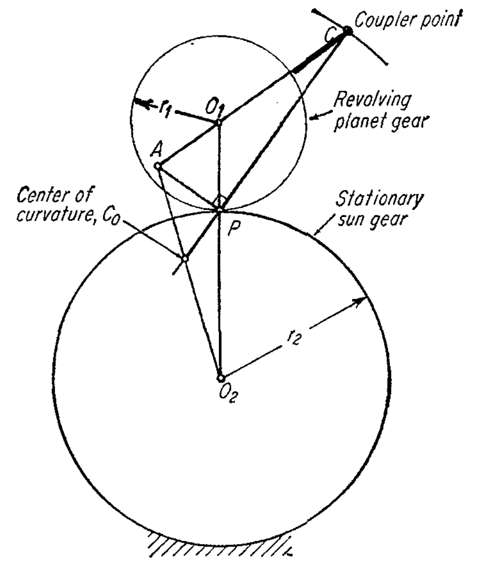

By locating the centers of curvature at various points, one can then determine the proper length of the rocking or reciprocating arm to provide long dwells (as required for the mechanisms in Fig 7 and 8), or proper entry conditions (as for the drive pin in the mechanism in Fig 3).

In the case of a gear with an extended point, point C, rolling on another gear, the graphical method for locating the center of curvature is given by these steps:

1. Draw a line through points C and P.
2. Draw a line through points C and O_1.
3. Draw a perpendicular to CP at P. This locates point A.
4. Draw line AO_2, to locate C_o, the center of curvature.

20. Center of curvature—gear rolling on a rack

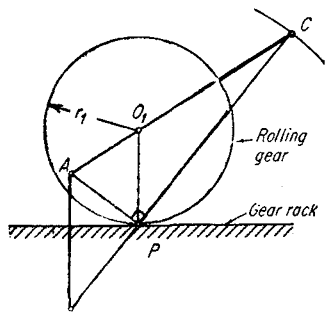

Construction is similar to that of the previous case.

1. Draw an extension of line CP.
2. Draw a perpendicular at P to locate A.
3. Draw a perpendicular from A to the straight suface to locate C_o.

21. Center of curvature—gear rolling inside a gear

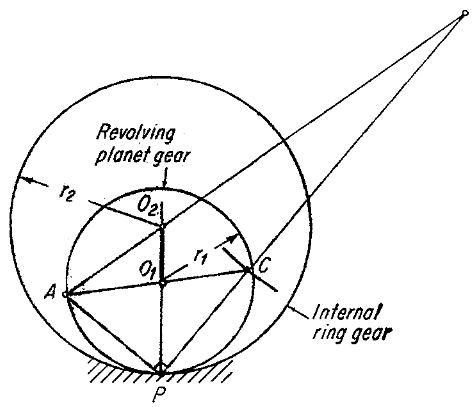

1. Draw extensions of CP and CO_1.
2. Draw a perpendicular of PC at P to locate A.
3. Draw AO_2 to locate C_o.

22. Analytical solutions

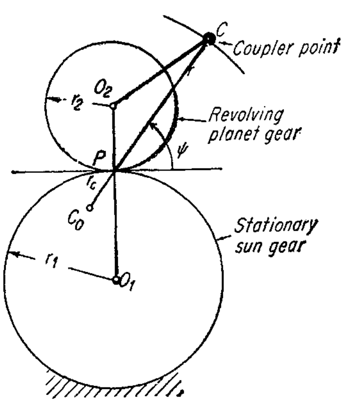

The centure of curvature of a gear rolling on a external gear can be computed directly from the Euler-Savary equation:

$$\left(\frac{1}{r} - \frac{1}{r_c}\right)\sin\psi = \text{constant} \quad (7)$$

where angle ψ and r locate the position of C.

By applying this equation twice, specifically to point O_1 and O_2 which have their own centers of rotation, the following equation is obtained:

$$\left(\frac{1}{r_2} + \frac{1}{r_1}\right)\sin 90^\circ = \left(\frac{1}{r} + \frac{1}{r_c}\right)\sin\psi$$

or

$$\frac{1}{r_2} + \frac{1}{r_1} = \left(\frac{1}{r} + \frac{1}{r_c}\right)\sin\psi$$

This is the final design equation. All factors except r_c are known: hence solving for r_c leads to the location of C_o.

For a gear rolling inside an internal gear, the Euler-Savary equation is

$$\left(\frac{1}{r} + \frac{1}{r_c}\right)\sin\psi = \text{constant}$$

which leads to

$$\frac{1}{r_2} - \frac{1}{r_1} = \left(\frac{1}{r} - \frac{1}{r_c}\right)\sin\psi$$

23. Hypocycloid substitute

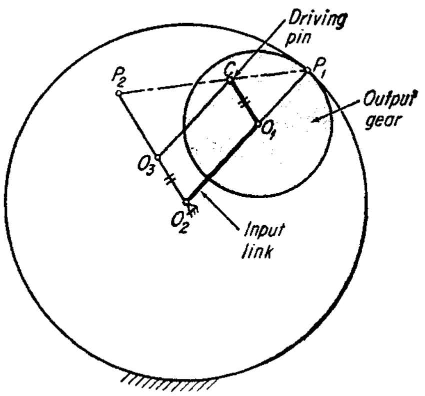

Original mechanism

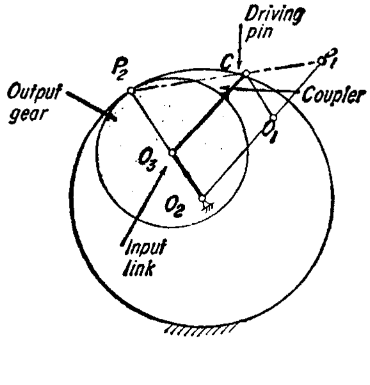

Substitute

It is not always realized that cycloid mechanisms can frequently be replaced by other cycloids that produce the same motion and yet are more compact.

The mechanism (right) is a typical hypocycloid. Gear *1* rolls inside gear *2* while point *C* describes a hypocycloid curve. To find the substitute mechanism, draw parallels O_3O_2 and O_3C to locate point P_2. Then select O_2P_2 as the new radius of the large (internal) gear. Line P_2O_3 becomes the radius of the small gear. Point *C* has the same relative position and can be obtained by completing the triangles. The new mechanism is about two-thirds the size of the original.

24. Epicycloid substitute

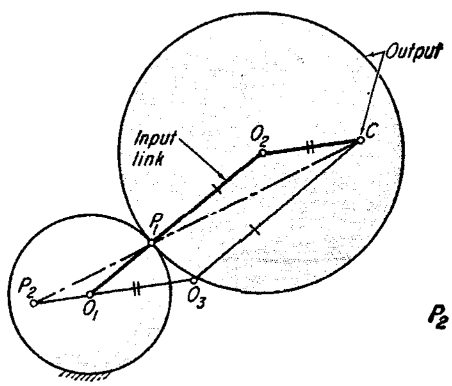

Original mechanism

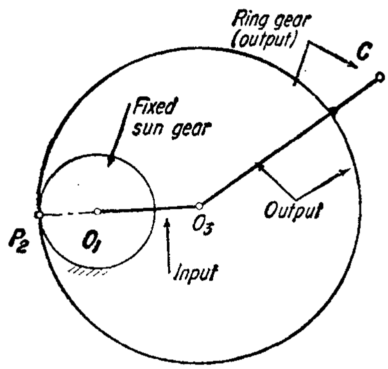

Substitute

The equivalent mechanisms of epicycloids are pericycloids in which the planetary gear is stationary and the output is taken from the ring gear. Such arrangements usually lead to a more-compact design.

In the above mechanism, point *C* traces an epicycloidal curve. Draw the proper parallels to find P_2, then use P_2O_3 to construct the compact substitute mechanism shown at right of original.

25. Multigear substitute

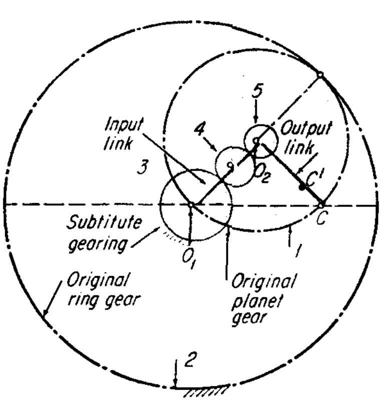

This is another way of producing a compact substitute for a hypocycloid mechanism. The original mechanism is shown in dashed lines—gear *1* rolls inside gear *2* and point *C* describes the curve. The three external gears (gears *3*, *4*, and *5*) replace gears *1* and *2* with a remarkable savings in space. The only criterion is that gear *5* must be one-half the size of gear *3*: gear *4* is only an idler. The new mechanism thus has been reduced to approximately one-half that of the original in size.

Limit-Switch Backlash

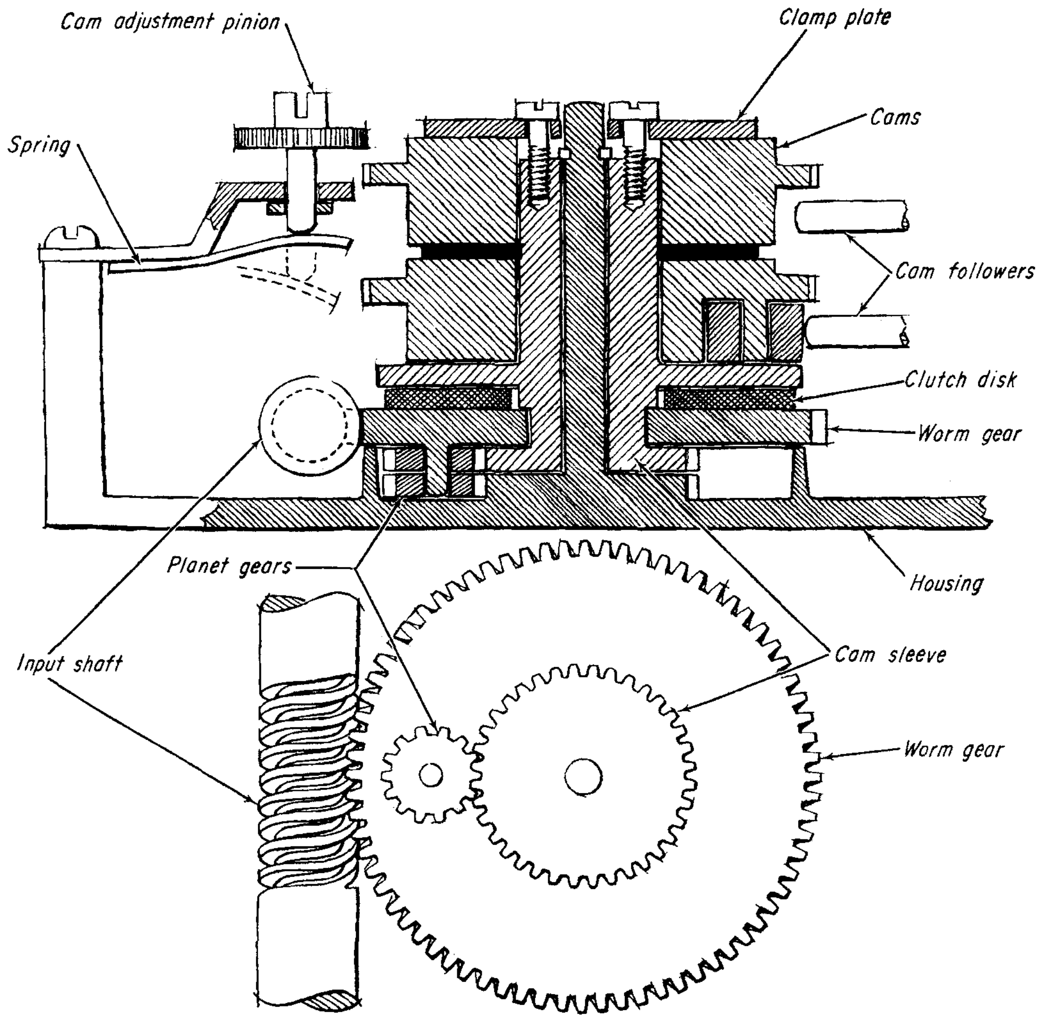

SWITCH-ACTUATING CAMS are driven by double-reduction gearing. The first pass is the input worm and its worm gear. The second reduction consists of a planetary system with two keyed planets pivoted on the worm gear. The two planets do not have the same number of teeth. When the worm gear is rotated the planet gears move around a sun gear cast into the base of the housing. The upper planet meshes with gear teeth on the sleeve. The cams clamped to the sleeve actuate the switches. The ratio of the planetary reduction can be altered by changing the planets.

A friction clutch between the sleeve flange and the worm gear makes the switch exceedingly sensitive to reversals at the input worm. When a switch is actuated to reverse input direction, the cams are driven directly by the input worm and gear through the friction clutch until the backlash has been taken up. At this point the clutch begins to slip. The immediate reversal of the cams resets switches in ⅓ to 1 revolution depending on the worm-gear ratio.

In some of the reduction ratios available a deliberate mismatch is employed in planetary gear sizes. This intentional mismatch creates no problems at the pitch velocities produced, since the 3500 rpm maximum at the input shaft is reduced by the step-down of the worm and worm gear. The low torque requirements of the switch-operating cams eliminate any overstressing due to mismatch. The increased backlash obtained by the mismatch is desirable in the higher reduction ratios to allow the friction clutch to reset the switches before the backlash is taken up. This permits switch reset in less than 1 rpm despite the higher input gear reductions of as much as 1280:1.

4 Ways to Eliminate Backlash

Wedges take up freedom in threads and gears, hold shaft snug against bearing.

L. Kasper

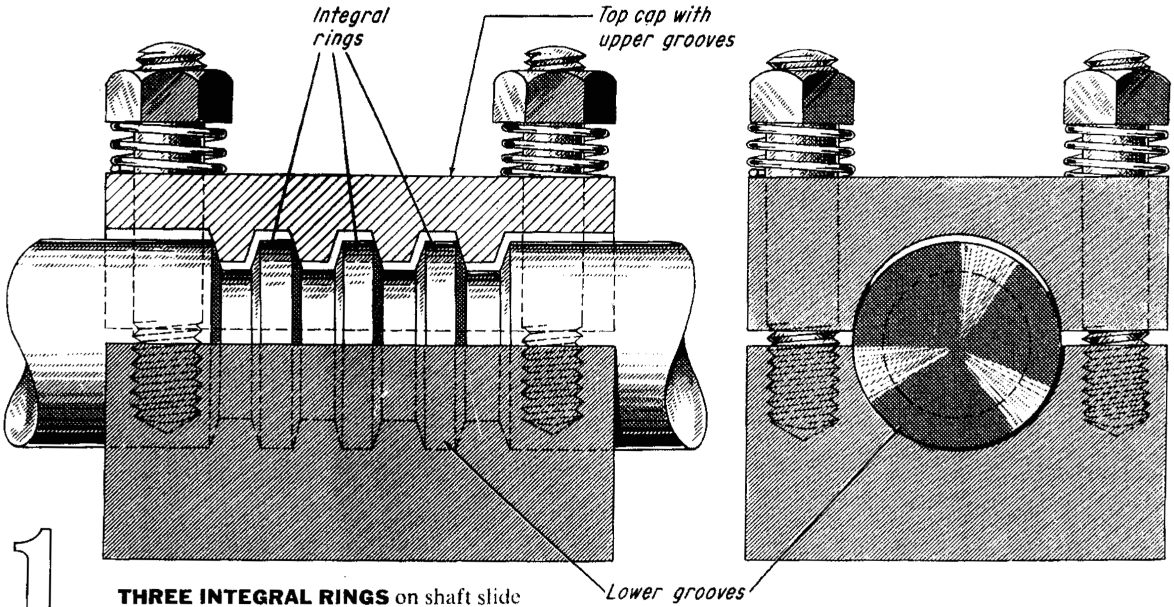

1 **THREE INTEGRAL RINGS** on shaft slide in grooves to prevent axial movement of shaft. Grooves in cap are offset axially.

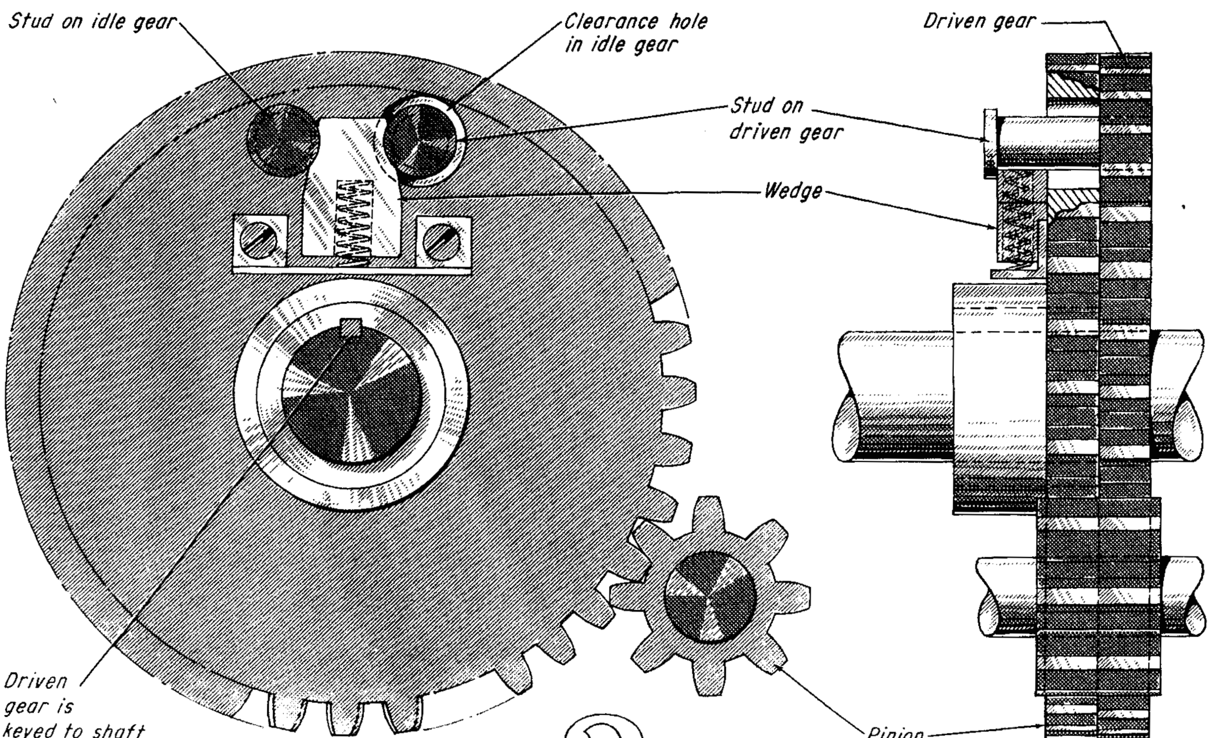

3 **SPRING-LOADED WEDGE** forces driven and idle gears to move relative to one another to take up backlash between gears and pinion.

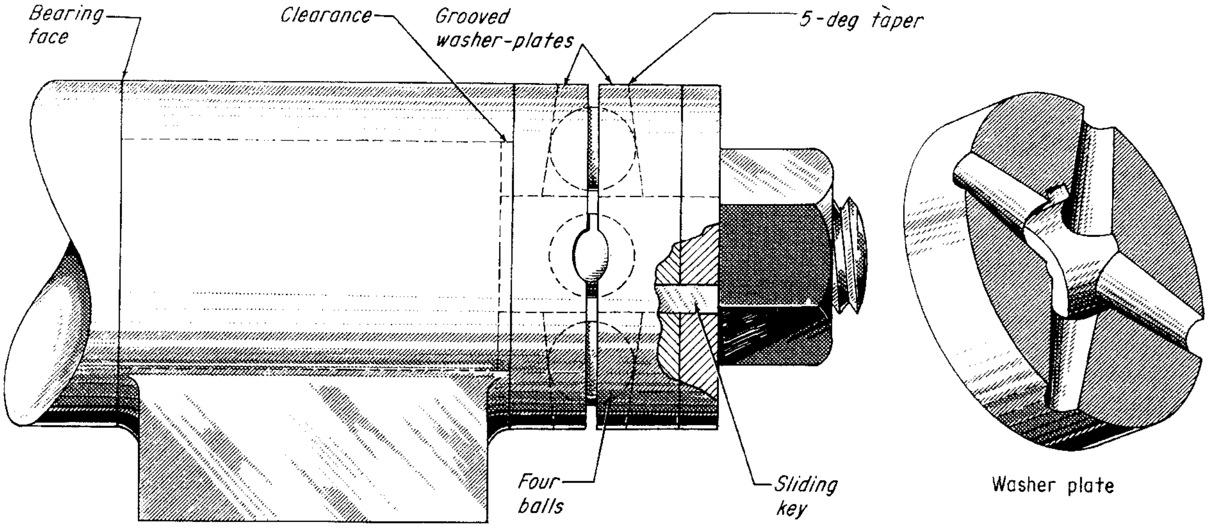

2

CENTRIFUGAL FORCE causes balls to exert force on grooved washer-plates when shaft rotates, pulling it against bearing face.

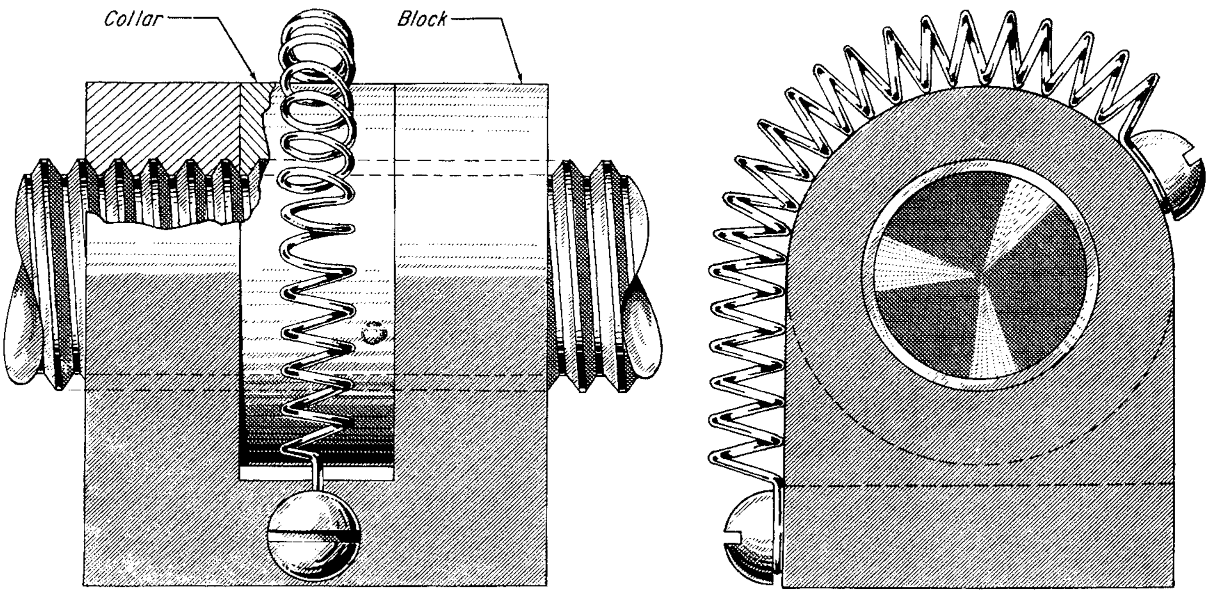

4

COLLAR AND BLOCK have continuous V-thread. When wear takes place in lead screw, the collar always maintains pressure on threads.

4 More Ways to Prevent Backlash

Springs combine with wedging action to ensure that threads, gears and toggles respond smoothly.

L. Kasper

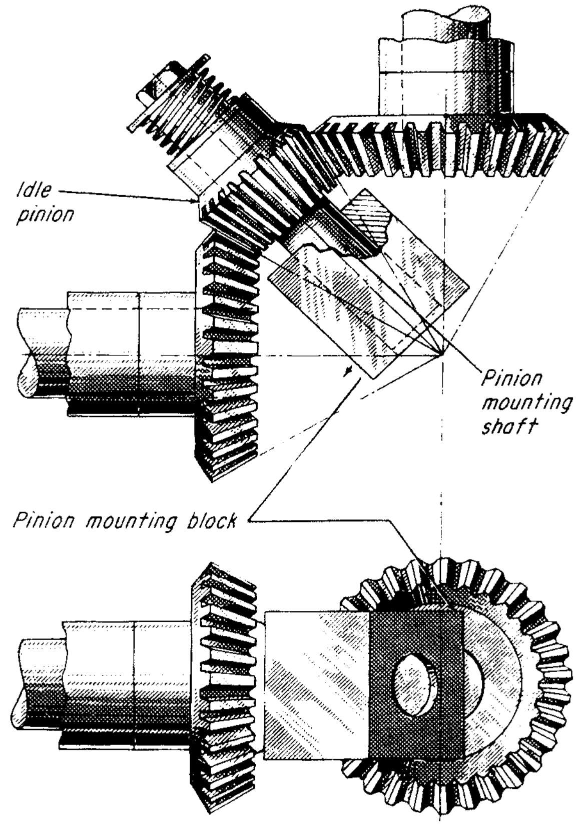

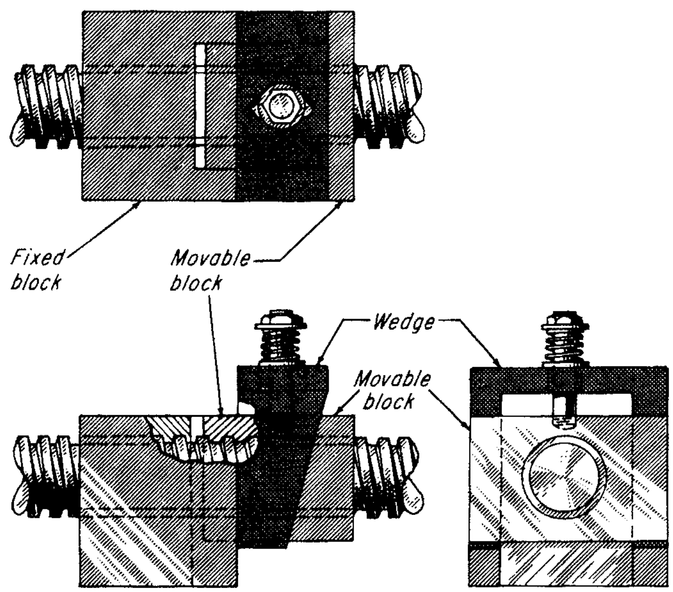

2 SPRING-LOADED PINION is mounted on a shaft located so that the spring forces pinion teeth into gear teeth to take up lost motion or backlash.

1 MOVABLE BLOCK is forced away from fixed block by spring-loaded wedge. Pressure is applied to both sides of lead screw, thus ensuring snug fit.

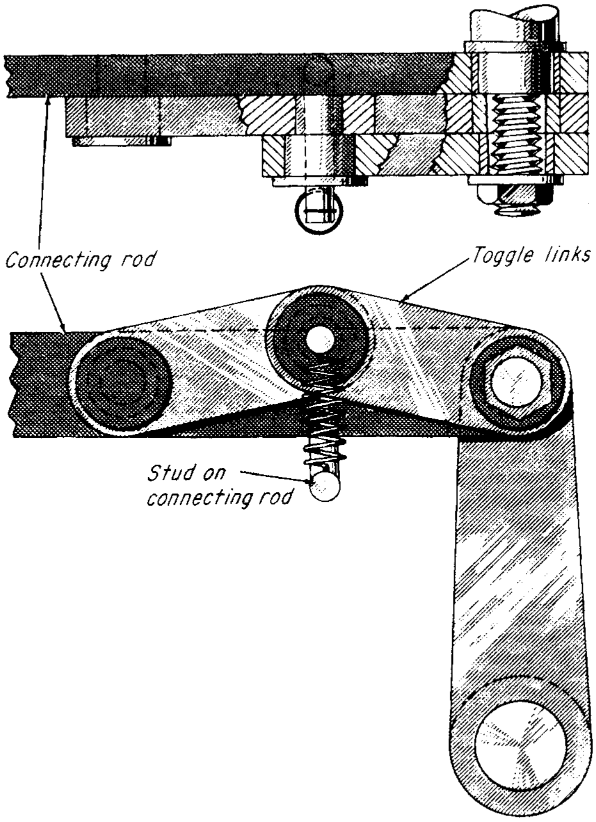

3 **TOGGLE LINKS** are spring-loaded and approach alignment to take up lost motion as wear in the joint takes place. Smooth response is thus gained.

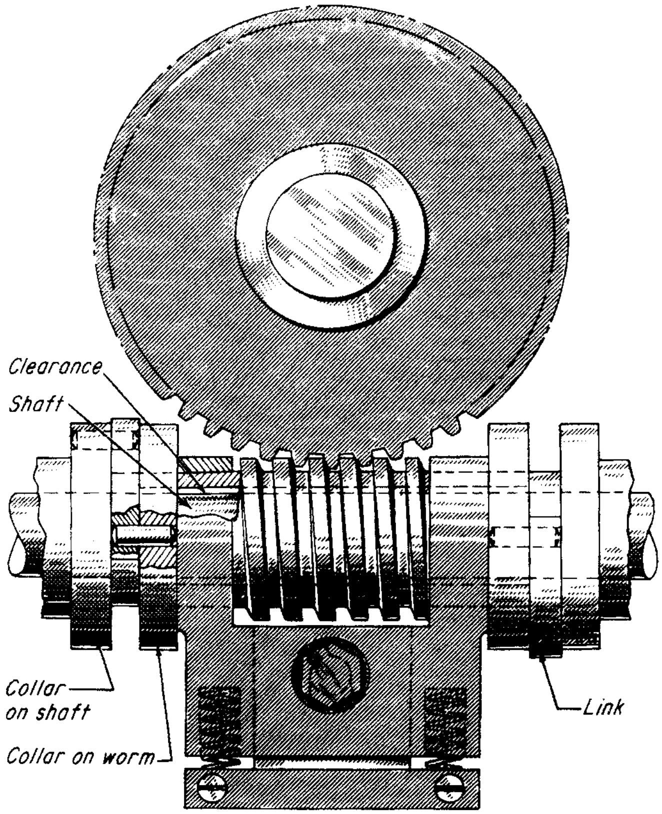

4 **HOLLOW WORM** has clearance for shaft, which drives worm through pinned collars and links. As wear occurs, springs move worm into teeth.

1-Way Output from Speed Reducers

When input reverses, these 5 slow-down mechanisms continue supplying a non-reversing rotation.

Louis Slegel

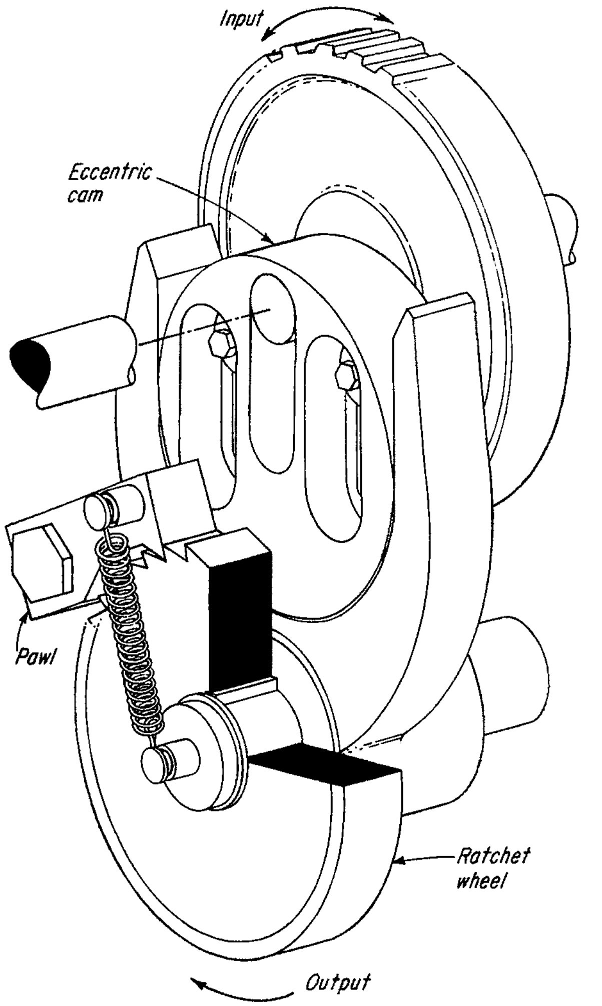

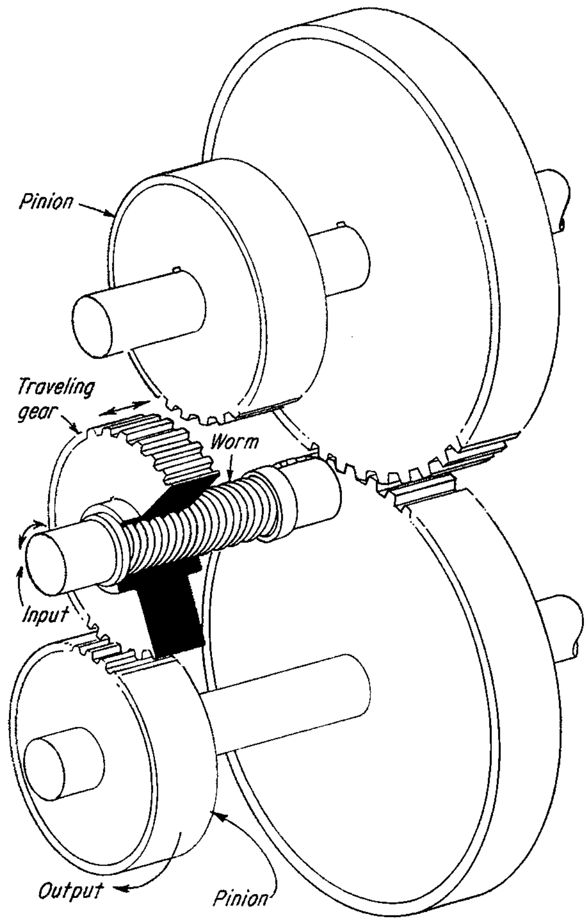

1 ECCENTRIC CAM adjusts over a range of high-reduction ratios, but unbalance limits it to low speeds. When direction of input changes, there is no lag in output rotation. Output shaft moves in steps because of ratchet drive through pawl which is attached to U-follower.

2 TRAVELING GEAR moves along worm and transfers drive to other pinion when input rotation changes direction. To ease engagement, gear teeth are tapered at ends. Output rotation is smooth, but there is a lag after direction changes as gear shifts. Gear cannot be wider than axial offset between pinions, or there will be interference.

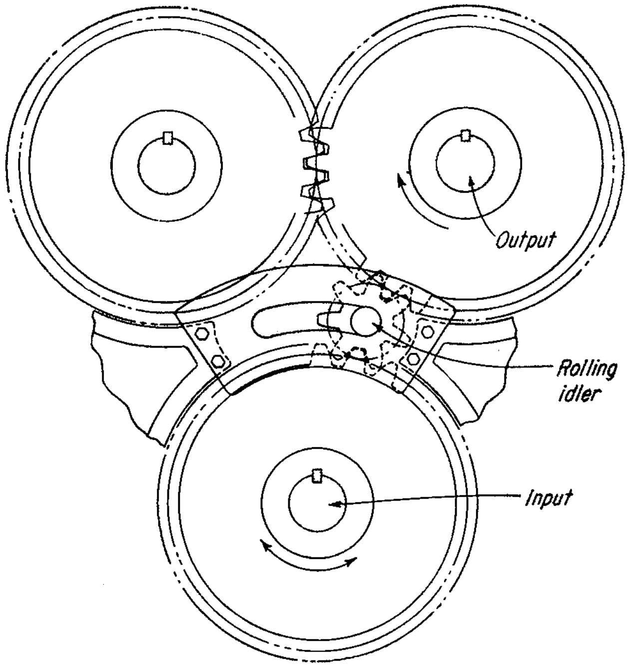

3 ROLLING IDLER also gives smooth output and slight lag after input direction changes. Small drag on idler is necessary, so that it will transfer into engagement with other gear and not sit spinning in between.

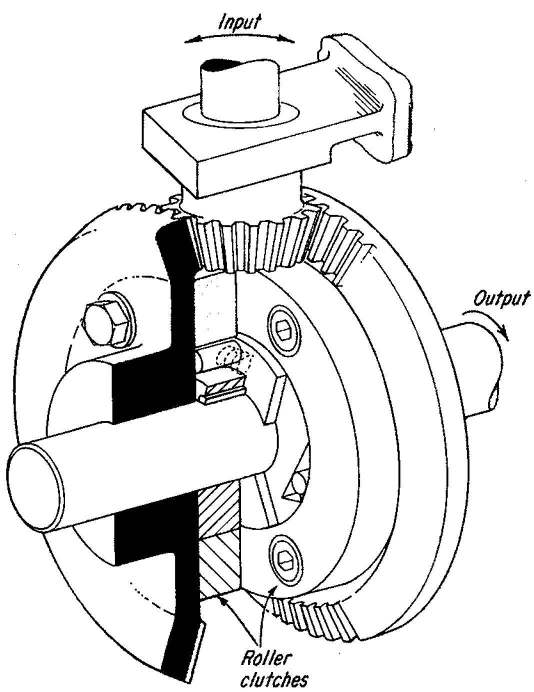

4 TWO BEVEL GEARS drive through roller clutches. One clutch catches in one direction; the other catches in the opposite direction. There is negligible interruption of smooth output rotation when input direction changes.

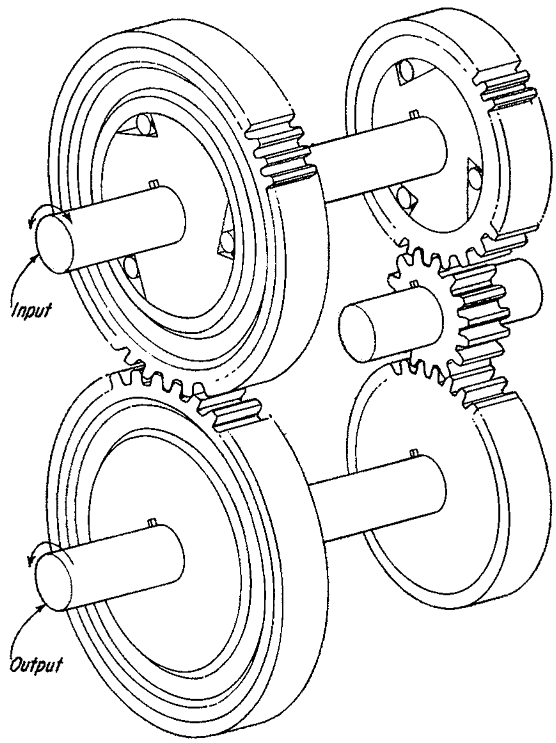

5 ROLLER CLUTCHES are on input gears in this drive, again giving smooth output speed and little output lag as input direction changes.

6 Ways to Prevent Overloading

These "safety valves" give way if machinery jams, thus preventing serious damage.

Peter C. Noy

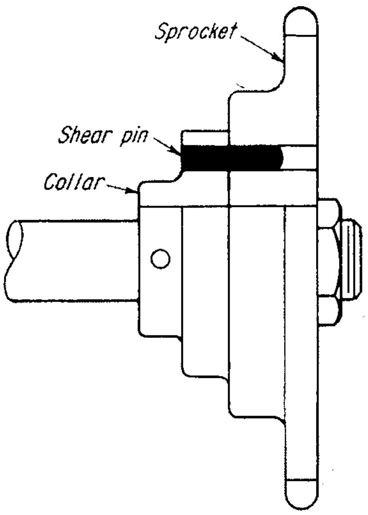

1
SHEAR PIN is simple to design and reliable in service. However, after an overload, replacing the pin takes a relatively long time; and new pins aren't always available.

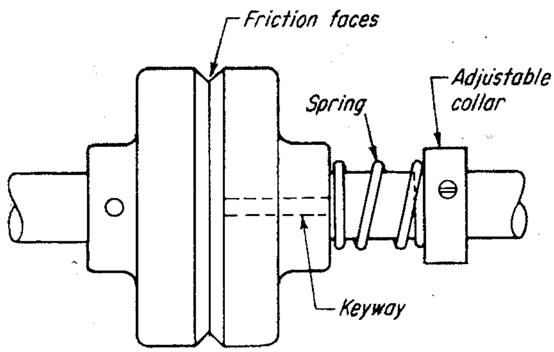

2
FRICTION CLUTCH. Adjustable spring tension that holds the two friction surfaces together sets overload limit. As soon as overload is removed the clutch reengages. One drawback is that a slipping clutch can destroy itself if unnoticed.

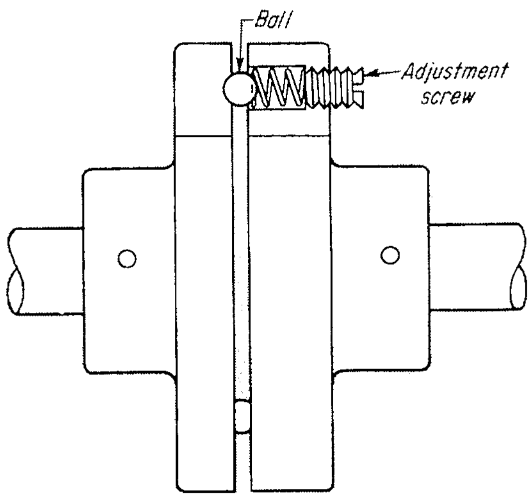

3
MECHANICAL KEYS. Spring holds ball in dimple in opposite face until overload forces the ball out. Once slip begins, wear is rapid, so device is poor when overload is common.

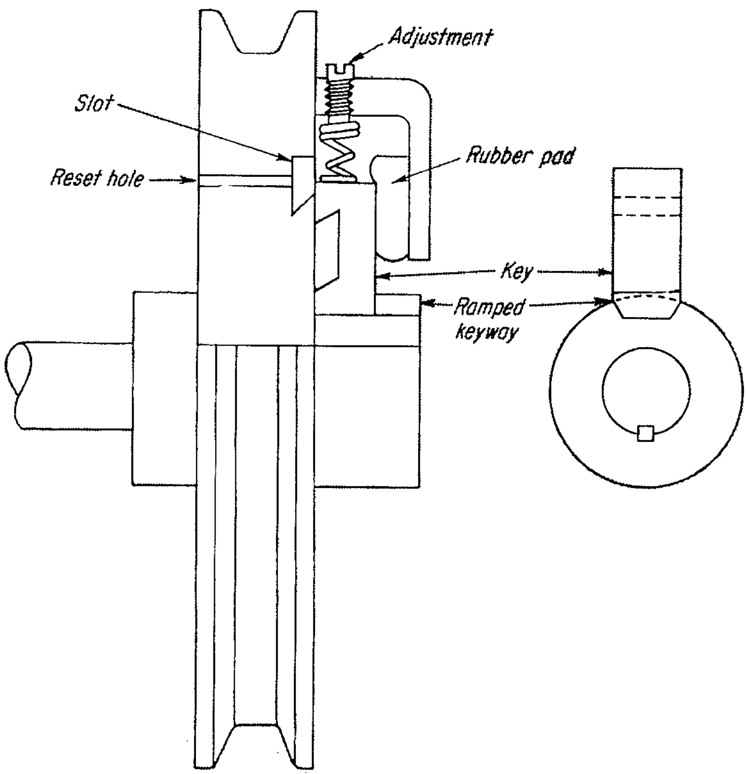

4
RETRACTING KEY. Ramped sides of keyway force key outward against adjustabe spring. As key moves outward, a rubber pad—or another spring—forces the key into a slot in the sheave. This holds the key out of engagement and prevents wear. To reset, push key out of slot by using hole in sheave.

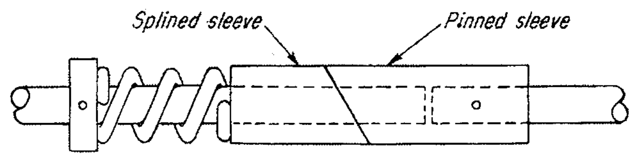

5
ANGLE-CUT CYLINDER. With just one tooth, this is a simplified version of the jaw clutch. Spring tension sets load limit.

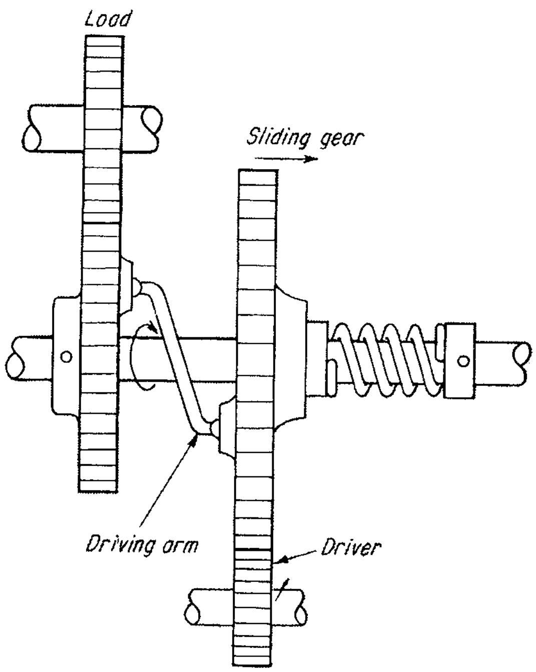

6
DISENGAGING GEARS. Axial forces of spring and driving arm balance. Overload overcomes spring force to slide gears out of engagement. Gears can strip once overloading is removed, unless a stop holds gears out of engagement.

Torque-Limiters Protect Light-Duty Drives

In such drives the light parts break easily when overloaded. These eight devices disconnect them from dangerous torque surges.

L. Kasper

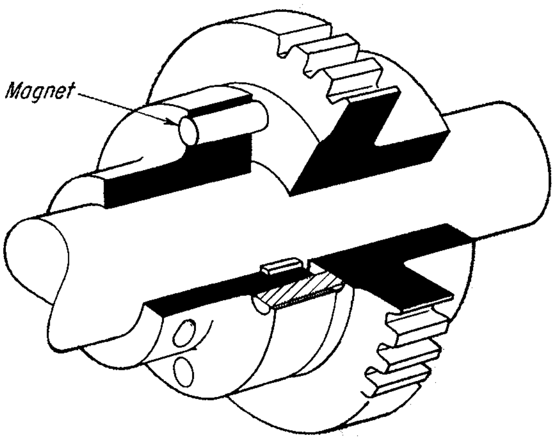

1
MAGNETS transmit torque according to their number and size. In-place control is limited to lowering torque capacity by removing magnets.

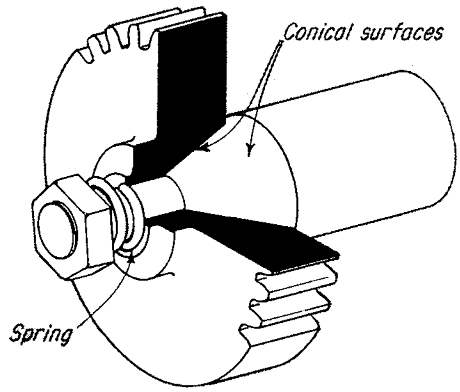

2
CONE CLUTCH is formed by mating taper on shaft to beveled hole through gear. Tightening down on nut increases torque capacity.

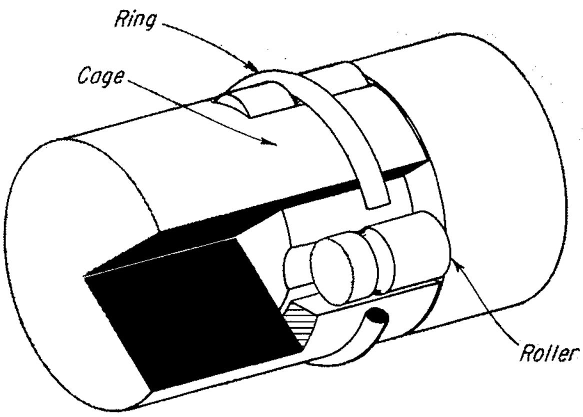

3
RING fights natural tendency of rollers to jump out of grooves cut in reduced end of one shaft. Slotted end of hollow shaft is like a cage.

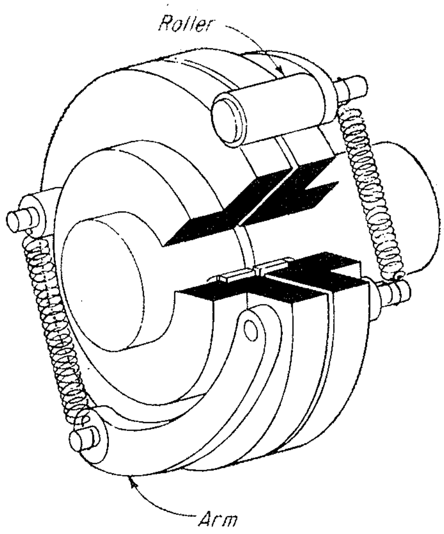

4
ARMS hold rollers in slots which are cut across disks mounted on ends of butting shafts. Springs keep rollers in slots; over-torque forces them out.

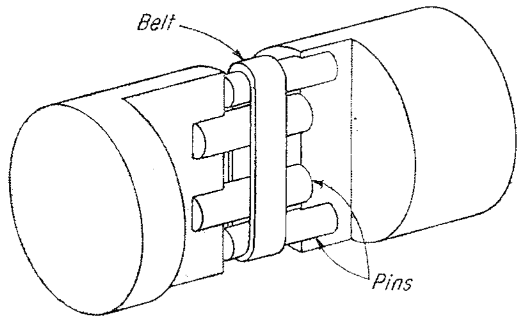

5
FLEXIBLE BELT wrapped around four pins transmits only lightest loads. Outer pins are smaller than inner pins to ensure contact.

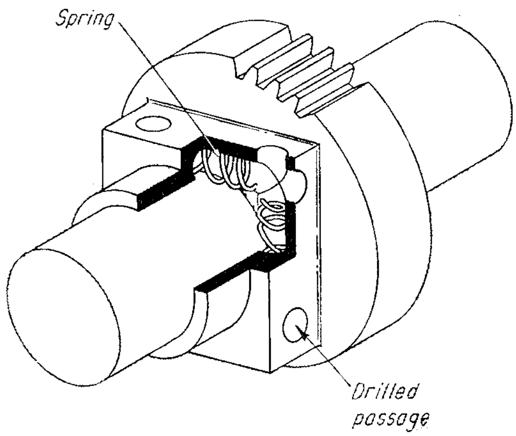

6
SPRINGS inside drilled block grip the shaft because they distort during mounting of gear.

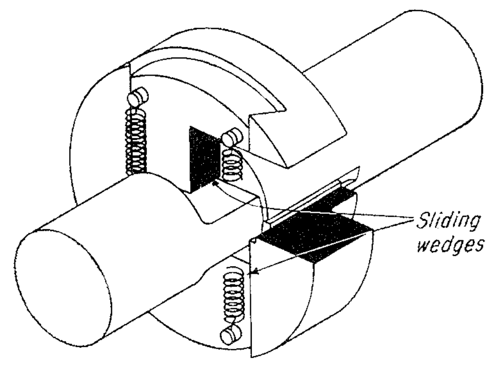

7
SLIDING WEDGES clamp down on flattened end of shaft; spread apart when torque gets too high. Strength of springs which hold wedges together sets torque limit.

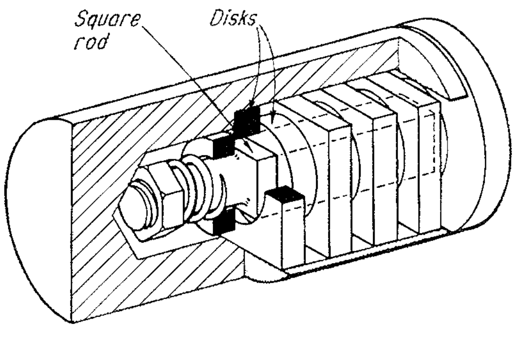

8
FRICTION DISKS are compressed by adjustable spring. Square disks lock into square hole in left shaft; round ones lock onto square rod on right shaft.

SECTION 2

CHAINS, SPROCKETS & RATCHETS

History of Chains

William R. Edgerton

The fundamental concept of creating a strong, yet flexible, chain structure by joining together a consecutive series of individual links is an idea that dates back to the earliest human utilization of metals. The use of iron for this purpose probably dates to the eighth century B.C.

The second step in the development process was the fashioning of wheels adapted to interact with the flexible chains, by the provision of teeth and pockets on the circumference of the wheels. These specially adapted wheels, known as "sprocket wheels," but usually referred to simply as "sprockets," were first developed by the military engineers of Greece some 22 centuries ago. From the writings of Philo of Byzantium, c. 200 B.C., we learn of chain and sprocket drives being used to transmit power from early water wheels, of a pair of chains fitted with buckets to lift water to higher elevations, and of a pair of reciprocating chain drives which acted as a tension linkage to feed and cock a repeating catapult.

The first two of these instances of chain and sprocket interaction probably used simple round-link chain, but the third involved a flat-link chain concept designed by Dionysius of Alexandria while working at the Arsenal at Rhodes. The design conceived by Dionysius employed what is now known as the inverted-tooth chain-sprocket engagement principle, a major advance over the cruder round-link design.

Despite its very early origins, rather little practical use was made of chain and sprocket interaction for the transmission of power or the conveyance of materials until the advent of the Industrial Revolution, which took place largely during the nineteenth century. The development of machinery to mechanize textile manufacture, agricultural harvesting, and metalworking manufacturing brought with it a need for the positive transmission of power and accurate timing of motions that only a chain-and-sprocket drive could provide.

The earliest sprocket chains manufactured in the United States employed cast components, usually of malleable iron, and many configurations of detachable link chain and pintle chain were produced in large quantities. As the need for higher strength and improved wear resistance became evident, chains employing heat-treated steel components were introduced. The use of rolled or drawn steel as a raw material required manufacturing machinery which provided greater dimensional accuracy than was possible in foundry practice, with the result that certain of the new types of sprocket chains came to be known as "precision chain." This developed somewhat earlier in Great Britain than in the United States, starting with the Slater chain, patented in England in 1864. The Slater design was further refined by Hans Renold with the development of precision roller chain, patented in England in 1880.

Chain manufacture in the United States continued to be principally concerned with cast and detachable link designs until the American introduction of the "Safety Bicycle" in 1888. Drop-forged steel versions of the cast detachable chains were first used, then precision steel block chain for bicycle driving, and progressively larger sizes were manufactured in the U.S. as the horseless carriage craze swept the country in the 1890s.

Precision inverted-tooth chain, popularly known as "silent chain," was introduced in the late 1890s, with many proprietary styles being developed during the early part of the twentieth century.

The first efforts toward standardization of roller chain were begun in the 1920s, resulting in the publication of the first chain standard, American Standard B29a, on July 22, 1930. Since that time, eighteen B29 standards have been developed, covering inverted-tooth chain; detachable chain; pintle and offset-sidebar chains; cast, forged, and combination chains; mill and drag chains; and many other styles.

There are eighteen American National Standards which relate to the various types of sprocket chains in general use. This family of standards is the result of over 50 years of standardization activity, which had its beginning in the work that led to the publication of *American Standard B29a—Roller Chain, Sprockets, and Cutters* in 1930. The chain types covered by the current standards are as follows:

ANSI B29.1	Precision roller chain
ANSI B29.2	Inverted-tooth (or silent) chain
ANSI B29.3	Double-pitch roller chain for power transmission
ANSI B29.4	Double-pitch roller chain for conveyor usage
ANSI B29.6	Steel detachable chain
ANSI B29.7	Malleable iron detachable chain
ANSI B29.8	Leaf chain
ANSI B29.10	Heavy-duty offset-sidebar roller chain
ANSI B29.11	Combination chain
ANSI B29.12	Steel-bushed rollerless chain
ANSI B29.14	Mill chain (H type)
ANSI B29.15	Heavy-duty roller-type conveyor chain
ANSI B29.16	Mill chain (welded type)
ANSI B29.17	Hinge-type flat-top conveyor chain
ANSI B29.18	Drag chain (welded type)
ANSI B29.19	Agricultural roller chain (A and CA types)
ANSI B29.21	Chains for water and sewage treatment plants
ANSI B29.22	Drop-forged rivetless chain

The basic size dimension for all types of chain is pitch—the center-to-center distance between two consecutive joints. This dimension ranges from 3/16 in (in the smallest inverted-tooth chain) to 30 in (the largest heavy-duty roller-type conveyor chain).

Chains and sprockets interact with each other to convert linear motion to rotary motion or vice versa, since the chain moves in an essentially straight line between sprockets and moves in a circular path while engaged with each sprocket. A number of tooth-form designs have evolved over the years, but the prerequisite of any tooth form is that it must provide:

1. Smooth engagement and disengagement with the moving chain
2. Distribution of the transmitted load over more than one tooth of the sprocket
3. Accommodation of changes in chain length as the chain elongates as a result of wear during its service life

The sprocket layout is based on the pitch circle, the diameter of which is such that the circle would pass through the center of each of the chain's joints when that joint is engaged with the sprocket. Since each chain link is rigid, the engaged chain forms a polygon whose sides are equal in length to the chain's pitch. The pitch circle of a sprocket, then, is a circle that passes through each corner, or vertex, of the pitch polygon. The calculation of the pitch diameter of a sprocket follows the basic rules of geometry as they apply to pitch and number of teeth. This relationship is simply

$$\text{Pitch diameter} = \frac{\text{pitch}}{\sin\,(180°/\text{number of teeth})}$$

The action of the moving chain as it engages with the rotating sprocket is one of consecutive engagement. Each link must articulate, or swing, through a specific angle to accommodate itself to the pitch polygon, and each link must be completely engaged, or seated, before the next in succession can begin its articulation.

Source: Mechanical Components Handbook by Robert O. Parmley ©1985

Ingenious Jobs for Roller Chain

How this low-cost industrial workhorse can be harnessed in a variety of ways to perform tasks other than simply transmitting power.

Peter C. Noy

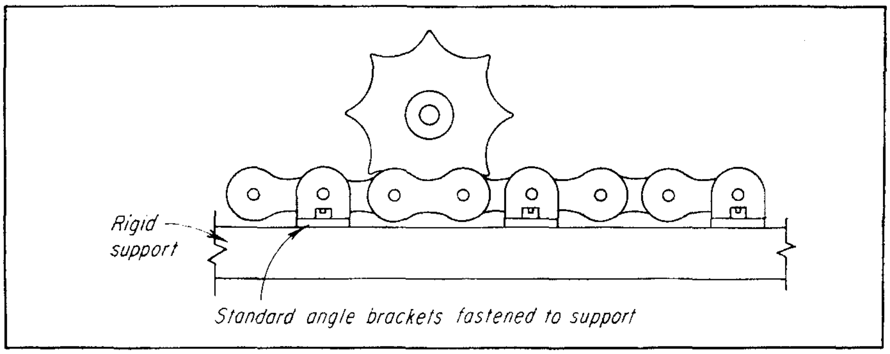

1 LOW-COST RACK-AND-PINION device is easily assembled from standard parts.

2 AN EXTENSION OF RACK-AND-PINION PRINCIPLE— soldering fixture for noncircular shells. Positive-action cams can be similarly designed. Standard angle brackets attach chain to cam or fixture plate.

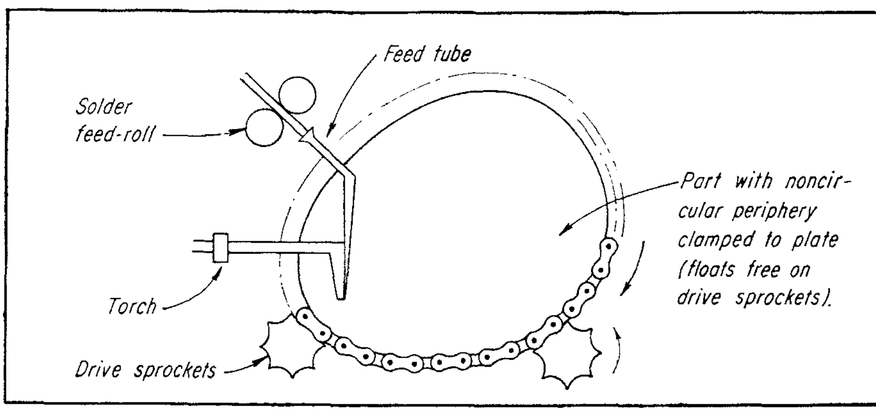

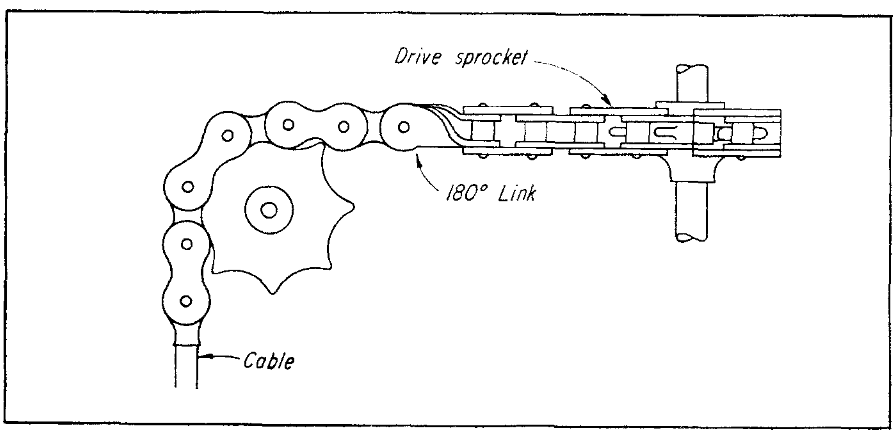

3 CONTROL-CABLE DIRECTION-CHANGER extensively used in aircraft.

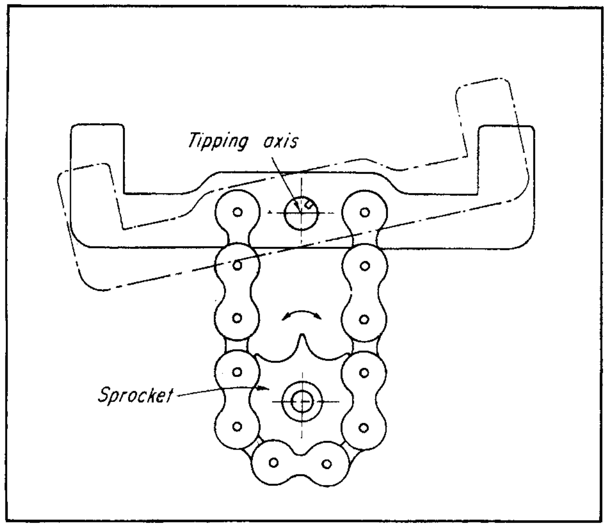

4 TRANSMISSION OF TIPPING OR ROCKING MOTION. Can be combined with previous example (3) to transmit this type of motion to a remote location and around obstructions. Tipping angle should not exceed 40° approx.

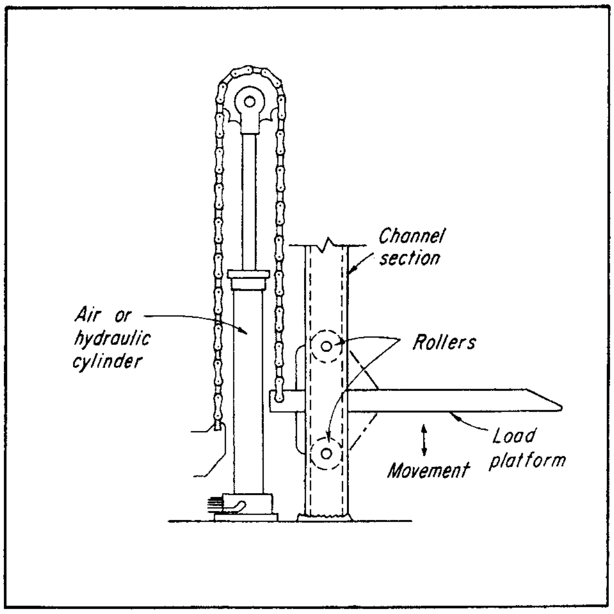

5 LIFTING DEVICE is simplified by roller chain.

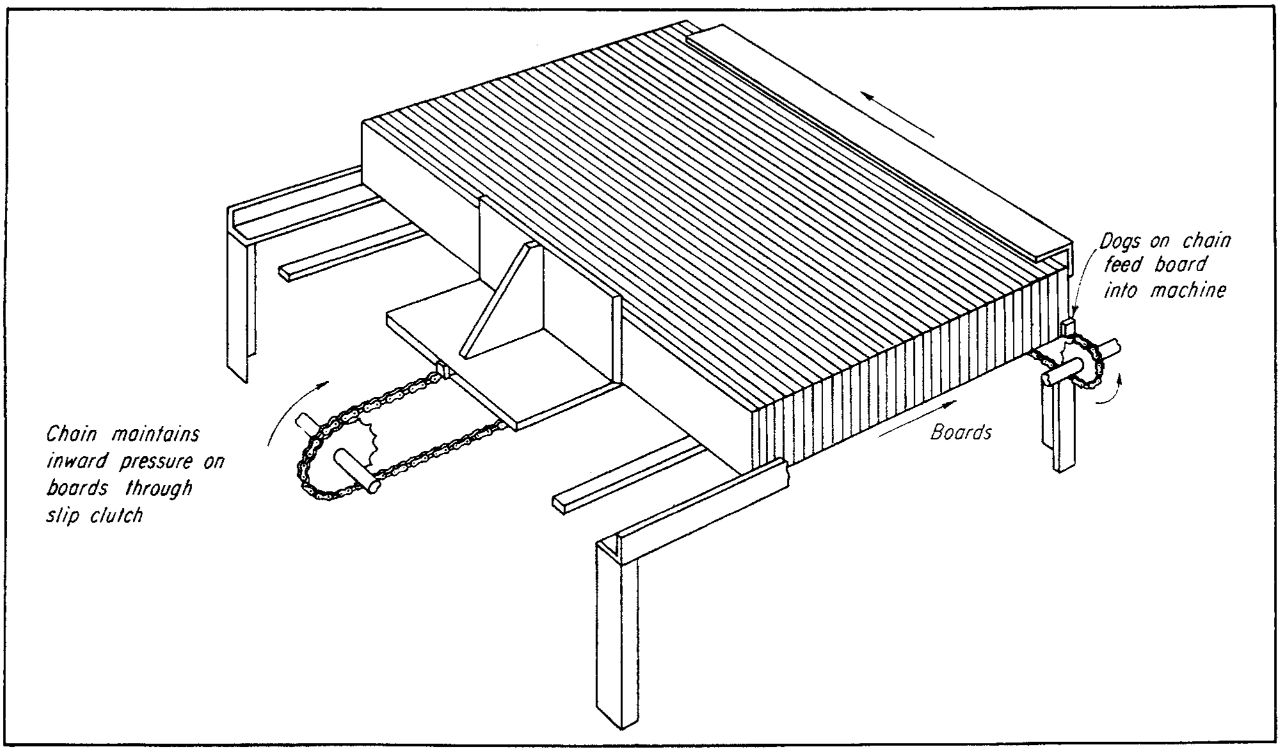

6 TWO EXAMPLES OF INDEXING AND FEEDING uses of roller chain are shown here in a setup that feeds plywood strips into a brush-making machine. Advantages of roller chain as used here are flexibility and long feed.

Examples of how this low-cost but precision-made product can be arranged to do tasks other that transmit power.

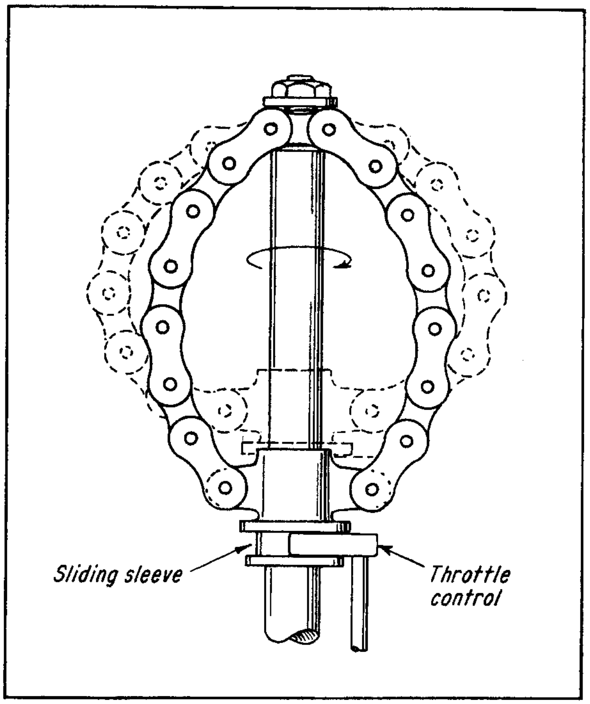

7 **SIMPLE GOVERNOR**—weights can be attached by means of standard brackets to increase response force when rotation speed is slow.

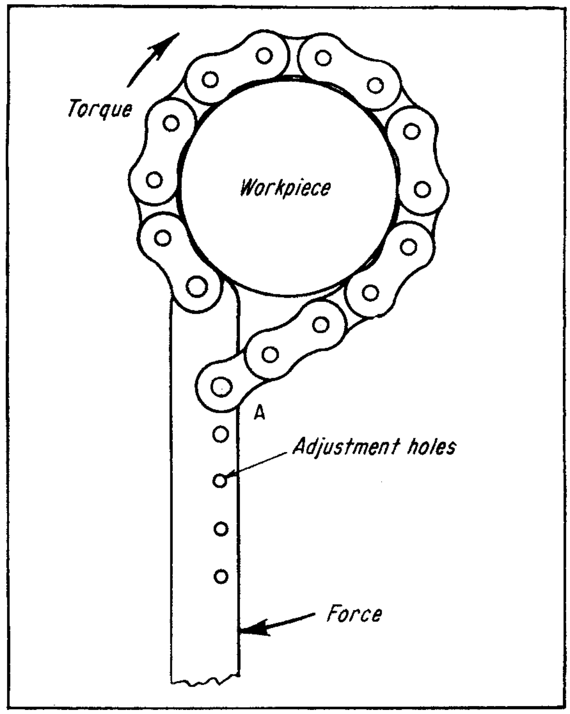

8 **WRENCH**—pivot A can be adjusted to grip a variety of regularly or irregularly shaped objects.

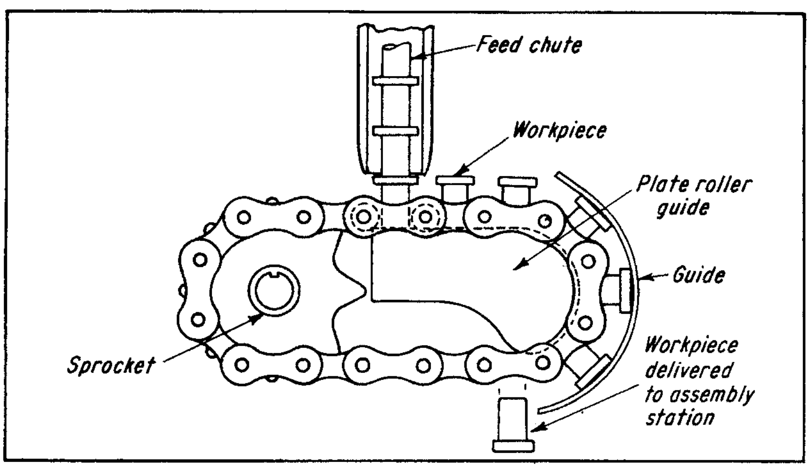

9 **SMALL PARTS CAN BE CONVEYED**, fed, or oriented between spaces of roller chain.

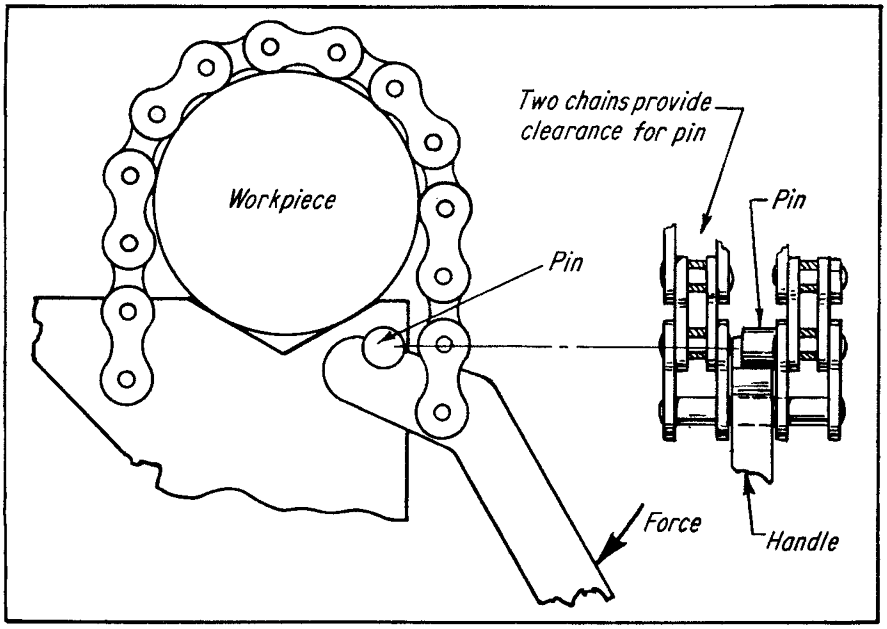

10 CLAMP—toggle action is supplied by two chains, thus clearing pin at fulcrum.

11 LIGHT-DUTY TROLLEY CONVEYORS can be made by combining standard roller-chain components with standard curtain-track components. Small gearmotors are used to drive the conveyor.

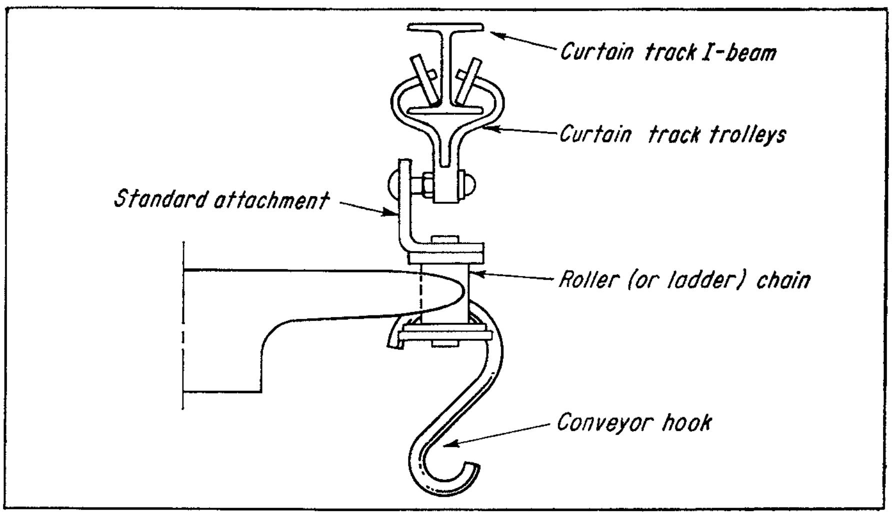

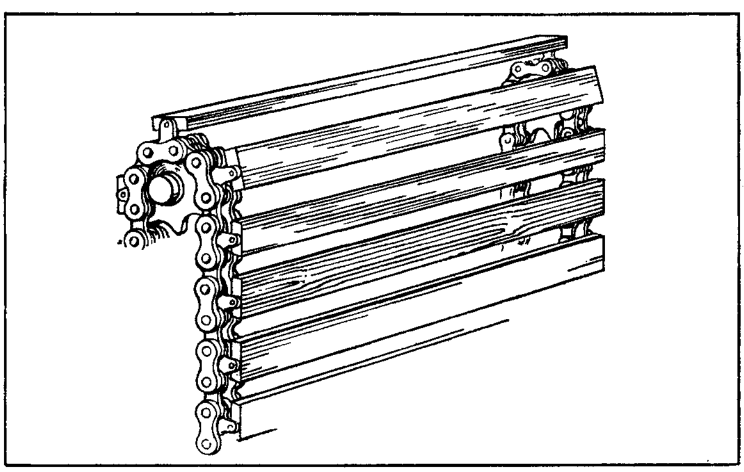

12 SLATTED BELT, made by attaching wood, plastic or metal slats, can serve as adjustable safety guard, conveyor belt, fast-acting security-wicket window.

Bead Chains for Light Service

Bernard Wasko

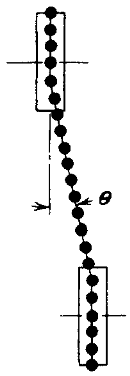

Fig. 1—Misaligned sprockets. Nonparallel planes usually occur when alignment is too expensive to maintain. Bead chain can operate at angles up to θ=20 degrees.

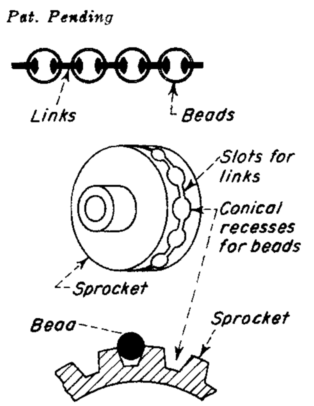

Fig. 2—Details of bead chain and sprocket. Beads of chain seat themselves firmly in conical recesses in the face of sprocket. Links ride freely in slots between recesses in sprocket.

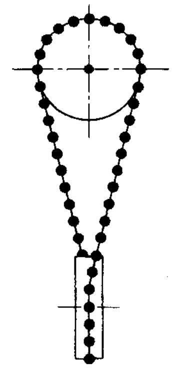

Fig. 3—Skewed shafts normally acquire two sets of spiral gears to bridge space between shafts. Angle misalignment does not interfere with qualified bead chain operation on sprockets.

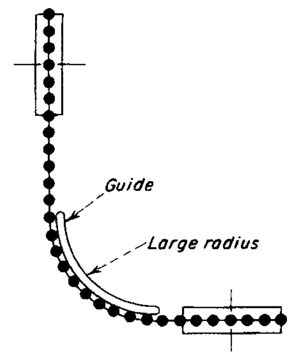

Fig. 4—Right angle drive does not require idler sprockets to go around corner. Suitable only for very low torque application because of friction drag of bead chain against guide.

Table I-Load capacity of bead chains. Capacity varies with bead diameter, chain speed and lubrication

Bead dia (in.)	Beads per ft	Max working tension(lb)
3/32	102 - 103	20
1/8	72 - 73	35
3/16	50 - 51	70
1/4	36 - 37	150

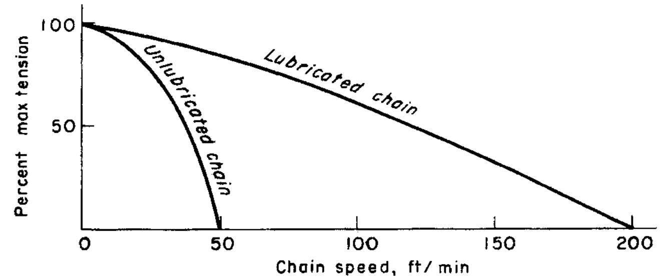

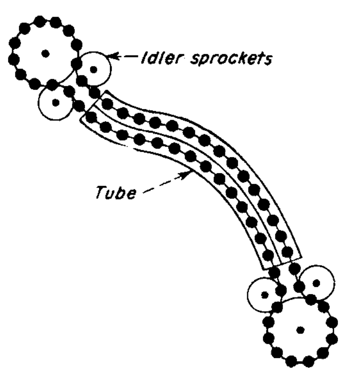

Fig. 5—Remote control through rigid or flexible tube has almost no backlash and can keep input and output shafts synchronized.

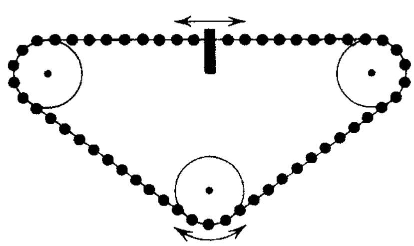

Fig. 6—Linear output from rotary input. Beads prevent slippage and maintain accurate ratio between the input and output displacemonts.

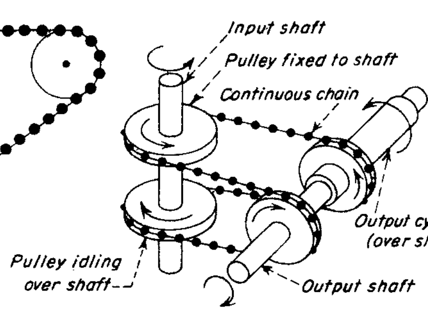

Fig. 7—Counter-rotating shafts. Input shaft drives two counter-rotating outputs (shaft and cylinder) through a continuous chain.

Where torque requirements and operating speeds are low, qualified bead chains offer a quick and economical way to: Couple misaligned shafts; convert from one type of motion to another; counter-rotate shafts; obtain high ratio drives and overload protection; control switches and serve as mechanical counters.

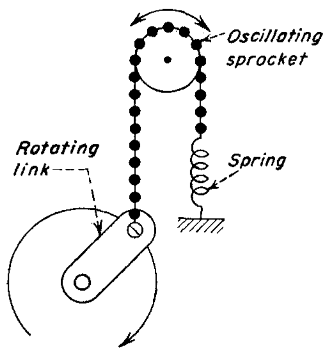

Fig. 8—Angular oscillations from rotary input. Link makes complete revolutions causing sprocket to oscillate. Spring maintains chain tension.

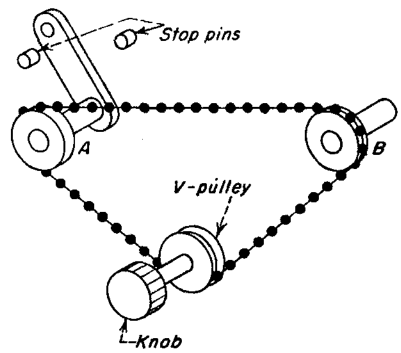

Fig. 9—Restricted angular motion. Pulley, rotated by knob, slips when limit stop is reached; shafts A and B remain stationary and synchronous.

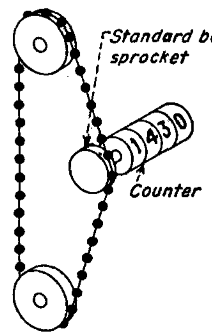

Fig. 10—Remote control of counter. For applications where counter cannot be coupled directly to shaft, bead chain and sprockets can be used.

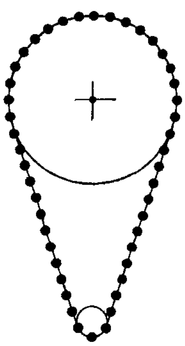

Fig. 11—High-ratio drive less expensive than gear trains. Qualified bead chains and sprockets will transmit power without slippage.

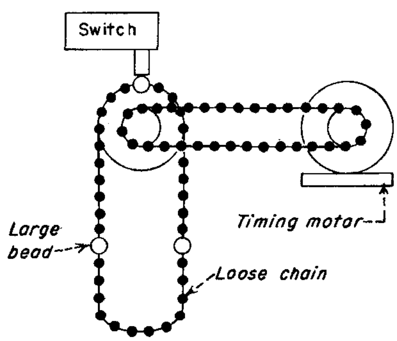

Fig. 12—Timing chain containing large beads at desired intervals operates micro-switch. Chain can be lengthened to contain thousands of intervals for complex timing.

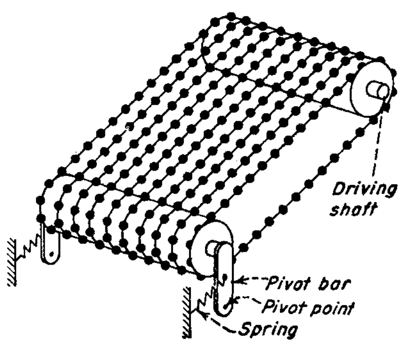

Fig. 13—Conveyor belt composed of multiple chains and sprockets. Tension maintained by pivot bar and spring. Width of belt easily changed.

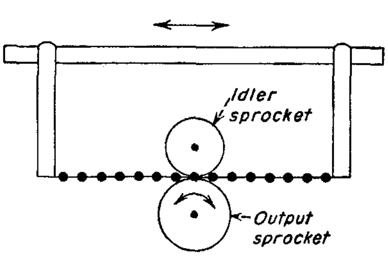

Fig. 14—Gear and rack duplicated by chain and two sprockets. Converts linear motion into rotary motion.

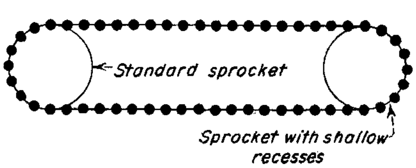

Fig. 15 — Overload protection. Shallow sprocket gives positive drive for low loads; slips one bead at a time when overloaded.

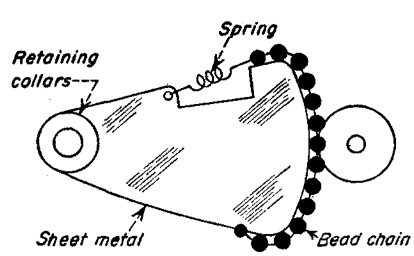

Fig. 16—Gear segment inexpensively made with bead chain and spring wrapped around edge of sheet metal. Retaining collars keep sheet metal sector from twisting on the shaft.

Types of Trolley Conveyor Chain Links and Joints

Sidney Reibel

JOINTS used in conveyor chain systems are designed for specific applications. The type of joint specified for a certain installation depends entirely on the layout of the supporting track. Joints can be designed for use with bends in the vertical or horizontal planes, and for combination service.

VARIOUS TYPES OF JOINTS

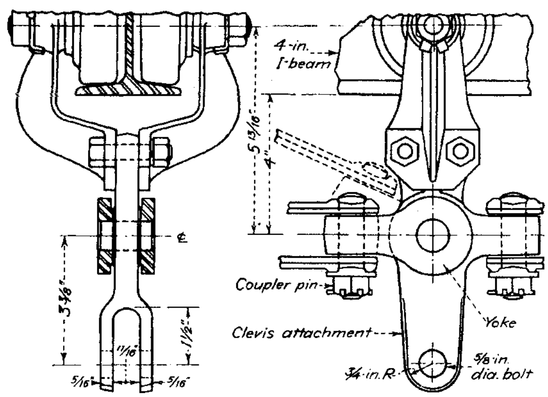

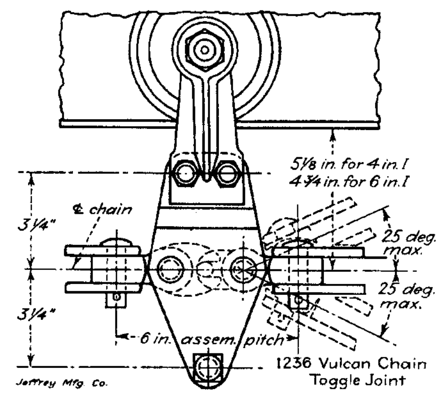

1236 Vulcan Chain Toggle Joint

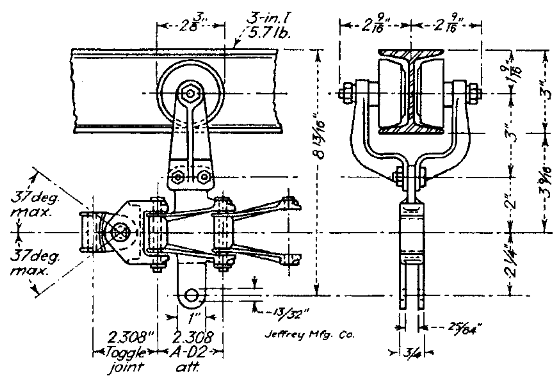

60 Reliance (H-60) Chain-Toggle Joint

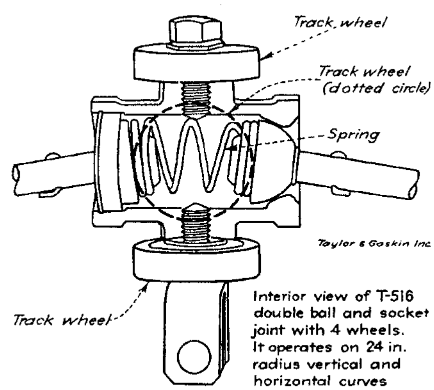

Interior view of T-516 double ball and socket joint with 4 wheels. It operates on 24 in. radius vertical and horizontal curves

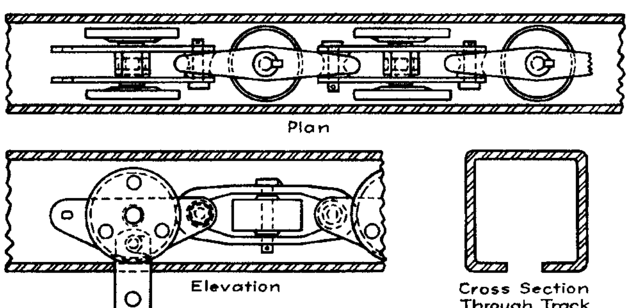

Universal Joint Operates on 24-in. Radius Vertical and Horizontal Curves

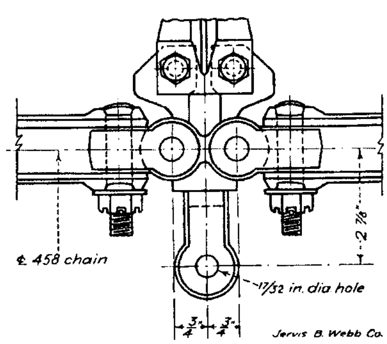

458 Chain-Universal Link Assembly

THE SUCCESS of the overhead trolley conveyor is largely the result of the development and use of drop-forged, rivetless, Keystone chain. The dimensions of several sizes of Keystone chain links are shown below with two examples of pin-jointed chain. Standard Keystone chain parts are shown in three views.

DETAILS FOR PARTS OF STANDARD KEYSTONE CHAIN

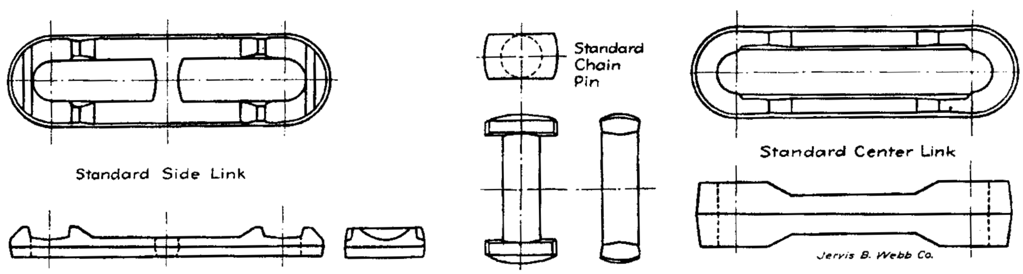

PIN-JOINTED LINKS

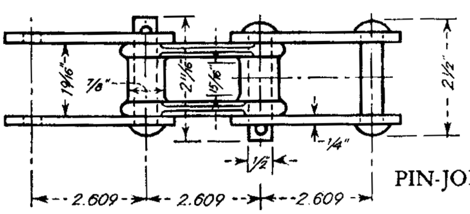

C-188 Chain

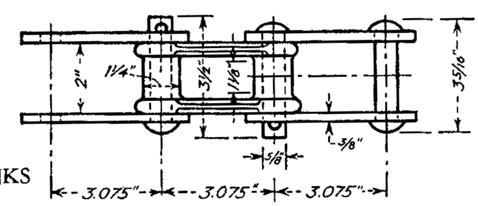

C-131 Chain

DIMENSIONS OF KEYSTONE LINKS

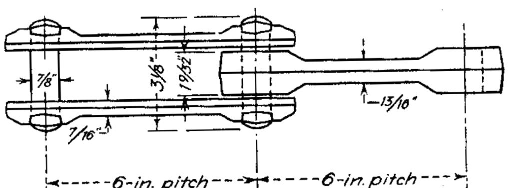

678 Chain

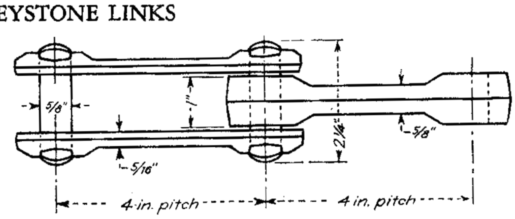

458 Chain-Standard Center Link

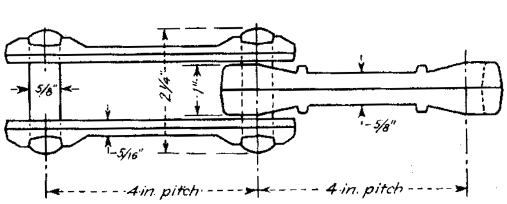

458 Chain-Modified Center Link

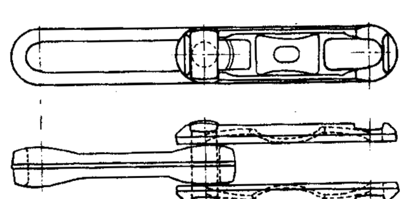

X-458 Chain– An Improved Type, Interchangeable with 458 Chain

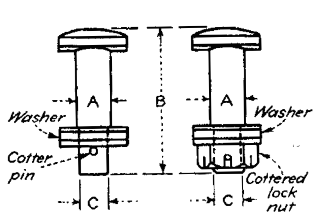

Coupler Pins for Keystone Chain

Chain size	A	B	C
348	½"	2⅜"	⅜"
458	⅝"	3¼"	½"
468	¾"	4"	⅝"
678	⅞"	4¼"	⅝"

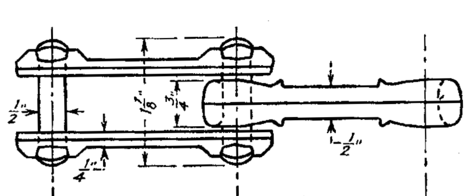

348 Chain Modified Center Link

Methods for Reducing Pulsations in Chain Drives

Pulsations in chain motion created by the chordal action of chain and sprockets can be minimized or avoided by introducing a compensating cyclic motion in driving sprockets. Mechanisms for reducing fluctuating dynamic loads in chain and the pulsations resulting therefrom include non-circular gears, eccentric gears, and cam activated intermediate shafts.

Eugene I. Radzimovsky

Fig. 1—The large cast-tooth non-circular gear, mounted on the chain sprocket shaft, has wavy outline in which number of waves equals number of teeth on sprocket. Pinion has a corresponding noncircular shape. Although requiring special-shaped gears, drive completely equalizes chain pulsations.

Fig. 2—This drive has two eccentrically mounted spur pinions (1 and 2). Input power is through belt pulley keyed to same shaft as pinion 1. Pinion 3 (not shown), keyed to shaft of pinion 2, drives large gear and sprocket. However, mechanism does not completely equalize chain velocity unless the pitch lines of pinions 1 and 2 are noncircular instead of eccentric.

Fig. 3—Additional sprocket 2 drives noncircular sprocket 3 through fine-pitch chain 1. This imparts pulsating velocity to shaft 6 and to long-pitch conveyor sprocket 5 through pinion 7 and gear 4. Ratio of the gear pair is made same as number of teeth of spocket 5. Spring-

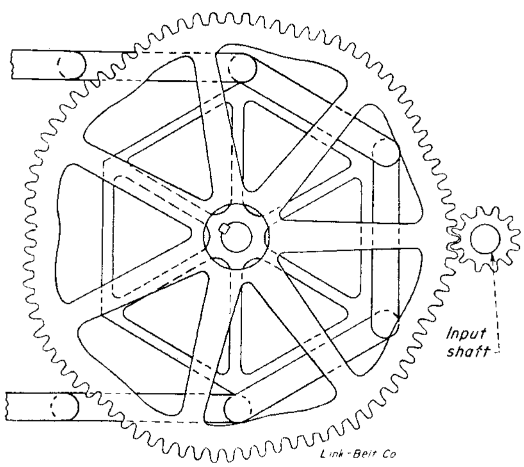

Fig. 1

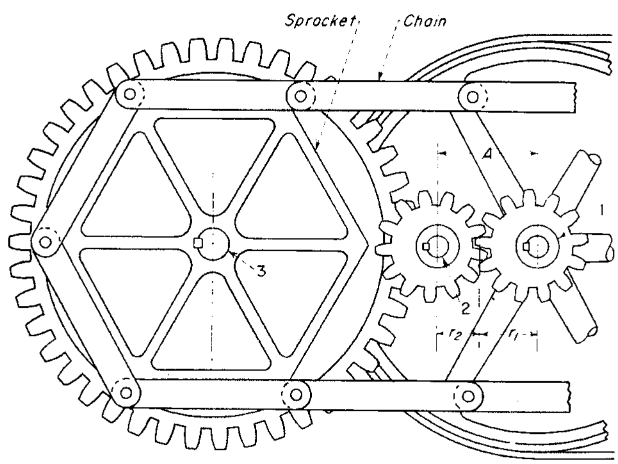

Fig. 2

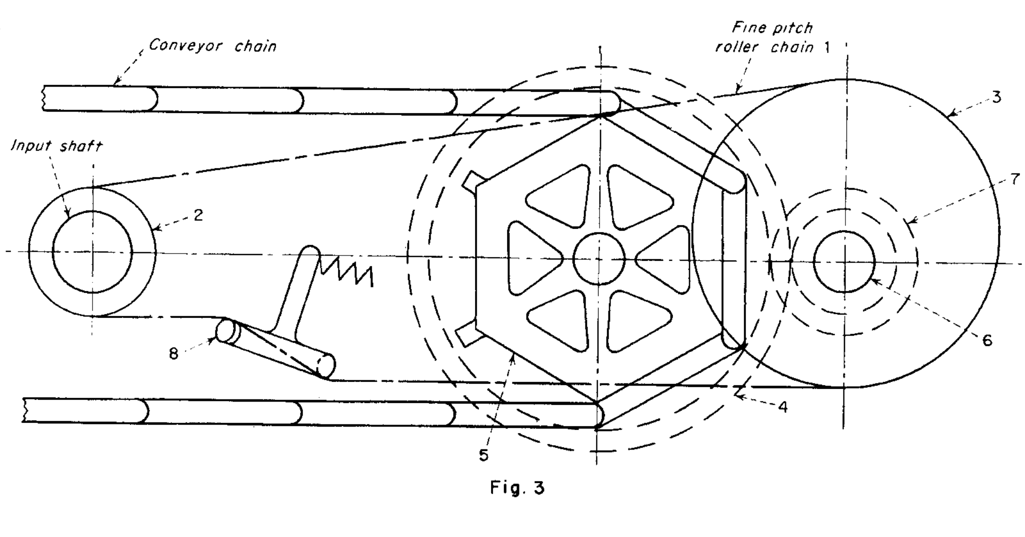

Fig. 3

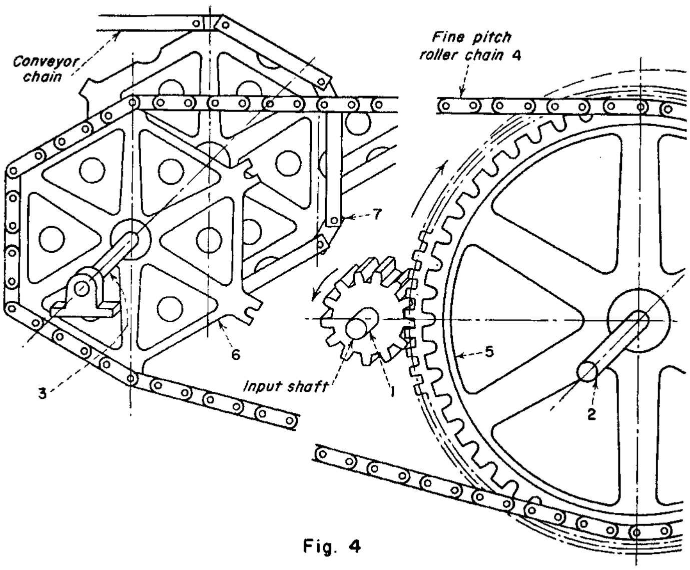

Fig. 4

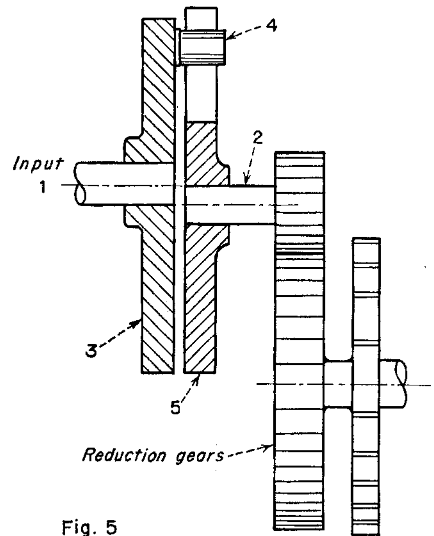

Fig. 5

actuated lever and rollers 8 take up slack. Conveyor motion is equalized but mechanism has limited power capacity because pitch of chain 1 must be kept small. Capacity can be increased by using multiple strands of fine-pitch chain.

Fig. 4—Power is transmitted from shaft 2 to sprocket 6 through chain 4, thus imparting a variable velocity to shaft 3, and through it, to the conveyor sprocket 7. Since chain 4 has small pitch and sprocket 5 is relatively large, velocity of 4 is almost constant which induces an almost constant conveyor velocity. Mechanism requires rollers to tighten slack side of chain and has limited power capacity.

Fig. 5—Variable motion to sprocket is produced by disk 3 which supports pin and roller 4, and disk 5 which has a radial slot and is eccentrically mounted on shaft 2. Ratio of rpm of shaft 2 to sprocket equals number of teeth in sprocket. Chain velocity is not completely equalized.

Fig. 6—Integrated "planetary gear" system (gears 4, 5, 6 and 7) is activated by cam 10 and transmits through shaft 2 a variable velocity to sprocket synchronized with chain pulsations thus completely equalizing chain velocity. The cam 10 rides on a circular idler roller 11; because of the equilibrium of the forces the cam maintains positive contact with the roller. Unit uses standard gears, acts simultaneously as a speed reducer, and can transmit high horsepower.

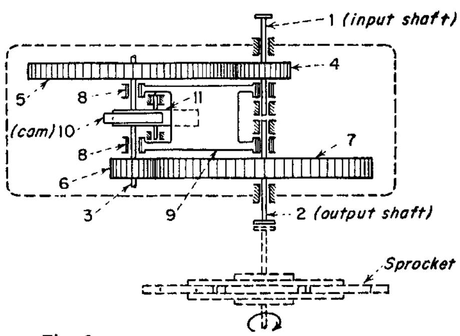

Fig. 6

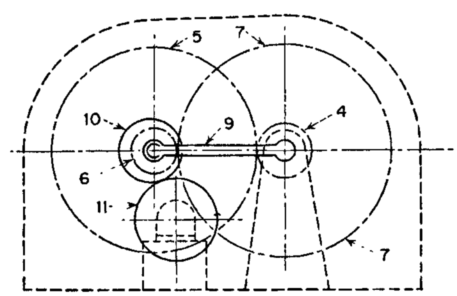

Patent applied for # 425,076

Pave the Way for Better Chain Drives

Roller-chain horsepower ratings are catching up with the realities of improved chain design, better materials, and more precise machining methods. New proposed ratings from the U.S.A. Standards Institute replace ratings that were too conservative about power capacity at high speeds.

By relying on the new USASI ratings, the designer can avoid overspecifying chain for a given drive. Manufacturers hope the effect will be to make chains more competitive with belt drives and gear drives.

The new tables take into account the important factor of lubrication. USASI recommends four types of lubrication for power capacities and speeds from lowest to highest: manual, drip, oil-bath, and oil-stream. Chief engineer John J. Scales of Rex Chainbelt, Springfield, Mass., notes that lubrication becomes critical at the increased speed limits in capacity ratings. Under such conditions, he says, a force-feed method should be used.

Importance of lubrication. Horsepower ratings in the new tables are based on 15,000 hr. of full-load service and are valid only when the USASI-recommended method of lubrication is used. With less effective lubrication, life expectancy may be shortened unless the horsepower is reduced accordingly.

USASI bases its ratings on dynamic testing and on the fatigue properties of chain rather than ultimate tensile strength or wear properties. According to Scales, the wear life-expectancy for chains at the listed horsepower values can range from less than 1 hr. to more than 15,000 hr. depending on the amount of lubrication they receive. If lubrication is inadequate, a more expensive drive must be used for greater wear capacity.

Scales also points out that if a chain drive is properly installed, is well lubricated, and has some means of take-up, it shouldn't wear out even in 15,000 hr.

Service life. Not all chain drives have to last 15,000 hr. If a designer needs less than that life expectancy in a drive, he should use experience factors in conjunction with the ratings in making his selection or to increase the horsepower load. Cross-hatched area in the middle chart shows how horsepower capacity can be increased as service life demand is reduced from 15,000 to 1000 hr.

The same chart shows the changing ratio between capacity and life expectancy as speed is varied. At speed A, the ratio is substantial, but at speed B, the ratio is down to unity. From speed B to speed C, the capacity rating remains the same for 1000-hr. and 15,000-hr. life. Beyond speed C, it changes again.

Thus, the USASI 15,000-hr. rating cannot be converted to another life expectancy by applying a simple ratio factor. The rating is a function of speed, sprocket size, center distances, and components that limit the life of the drive at a given speed. If a designer wants a chain to operate for 15,000 hr. but for only, say, 1000 hr. of full load, he would be well advised to check with the chain manufacturer for the performance data he needs.

Intermittent peaks. In using the new ratings, the designer must also take into account the degree of intermittency of the speed in high-speed applications. In some applications, bursts of speed for a few seconds can exceed the rated speed without damage to the drive, as the bottom chart shows.

However, for continuous high-speed operation of a drive, the USASI limit must be kept in mind if the drive is to operate satisfactorily.

For intermittent high-speed operation, it has been found to be difficult to determine a maximum practical speed limit in all applications. Possible chain combinations and operating variants are too numerous for generalization. For instance, well lubricated chains in hoists can tolerate at least twice the rated speeds in the USASI charts if the bursts of speed last less than a minute and the rest time between bursts of speed amount to more than a minute. ☐

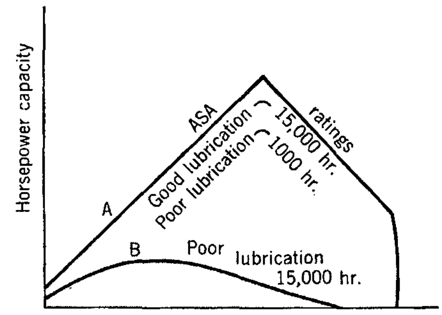

With good lubrication, a chain can transmit more horsepower at higher speeds and for a longer time. Graph shows a typical lifecurve.

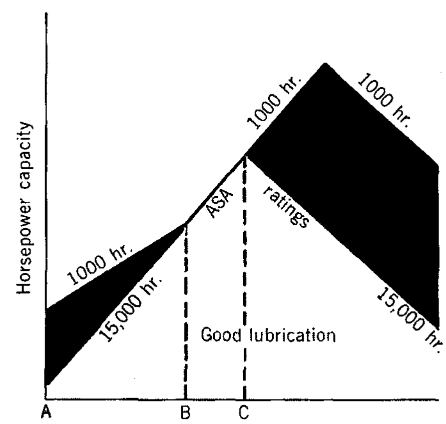

If full loads are infrequent, a 1000-hr.-rating chain will often meet need for a 15,000-hr. service life. Hatched area shows how hp is increased thereby.

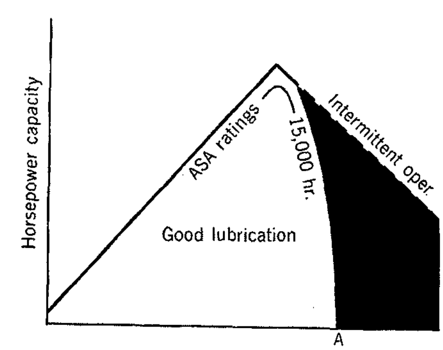

If speed is intermittent in a given application, more speed can be obtained than basic USASI ratings show. At times, the speed may be doubled.

Lubrication of Roller Chains

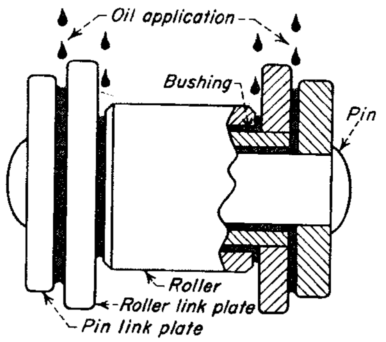

Fig. 1

Fig. 1—APPLY OIL DROPS between roller and pin links on lower strand of chain just before chain engages sprocket so that centrifugal force carries oil into clearances. Oil applied at center of roller face seldom reaches the area between bushing and roller.

Fig. 2—MANUAL APPLICATION OF LUBRICANT by (A) flared-lip oil can, or (B) hand brush, is simplest method for low-speed applications not enclosed in casings. New chains should be lubricated daily until sufficiently "broken-in," after which weekly lubrication programs should suffice.

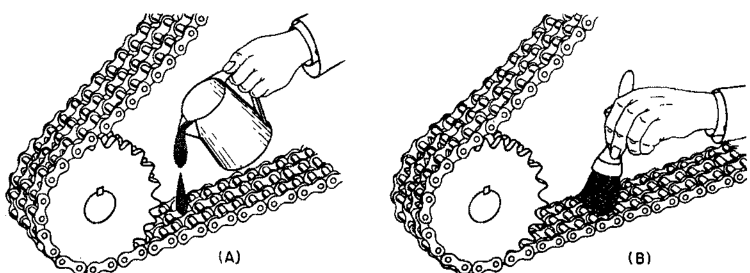

Fig. 2

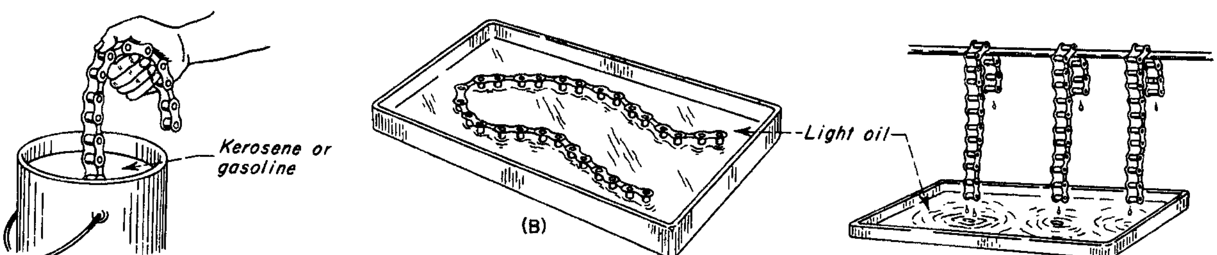

Fig. 3

Fig. 3—CHAINS WITHOUT CASING should be: (A) removed periodically and washed in kerosene, (B) soaked in light oil after cleaning, and (C) draped to permit excess oil to drain.

Fig. 4—DRIP LUBRICATION can be adjusted to feed oil to edges of link plates at rate of 4 to 20 drops per minute depending on chain speed. Pipe contains oil-soaked wick to feed multiple-width chains.

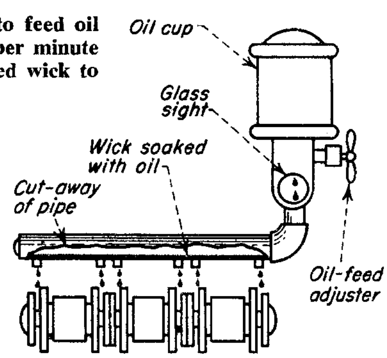

Fig. 4

Fig. 5—CONTINUOUS LUBRICATION systems for open chains: (A) Wick lubrication is lowest in cost to install; (B) Friction wheel lubrication uses wheel covered with soft absorbent material and pressured by flat spring.

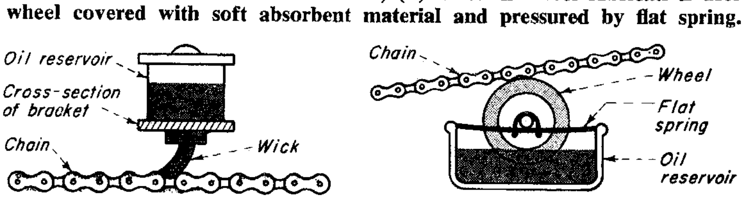

Fig. 5

Unsatisfactory chain life is usually the result of poor or ineffective lubrication. More damage is caused by faulty lubrication than by years of normal service. Illustrated below are 9 methods for lubricating roller chains. Selection should be made on basis of chain speed as shown in Table I. Recommended lubricants are listed in Table II.

Table I—Recommended Methods

Chain Speed, ft/min	Method
0–600	Manual: brush, oil can Slow Drip: 4–10 drops, min Continuous: wick, wheel
600–1500	Rapid Drip—20 drops, min Shallow Bath, Disk
over 1500	Force Feed Systems

Table II—Recommended Lubricants

Pitch of chain, in.	Viscosity at 100 F, SUS	SAE No.
¼–⅝	240–420	20
¾–1¼	420–620	30
1½–up	620–1300	40

Note: For ambient temperatures between 100 to 500 F use SAE 50.

Fig. 6—SHALLOW BATH LUBRICATION uses casing as reservoir for oil. Lower part of chain just skims through oil pool. Levels of oil must be kept tangent to chain sprocket to avoid excessive churning. Should not be used at high speeds because of tendency to generate excessive heat.

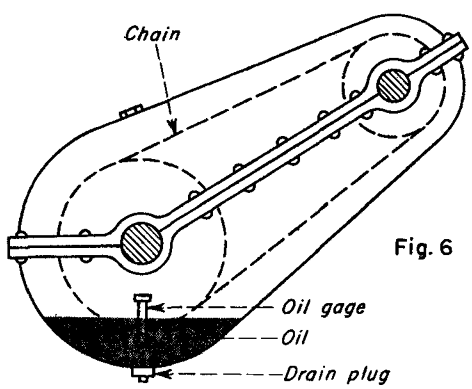

Fig. 6

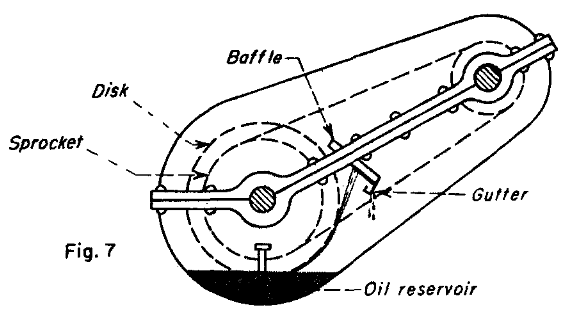

Fig. 7

Fig. 7—DISK OR SLINGER can be attached to lower sprocket to give continuous supply of oil. Disk scoops up oil from reservoir and throws it against baffle. Gutter catches oil dripping down from baffle and directs it on to chain.

Fig. 8—FORCE-FEED LUBRICATION for chains running at extremely high speeds. Pump driven by motor delivers oil under pressure to nozzles that direct spray on to chain. Excess oil collects in reservoir which has wide area to cool oil.

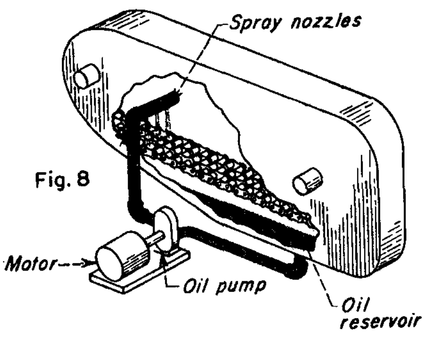

Fig. 8

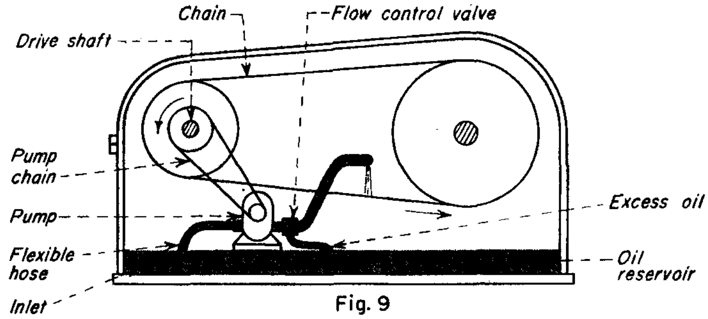

Fig. 9

Fig. 9—CHAIN-DRIVEN FORCE-FEED system has pump driven by main drive shaft. Flow control valve, regulated from outside of casing, by-passes excess oil back to reservoir. Inlet hose contains filter. Oil should be changed periodically—especially when hue is brown instead of black.

One-Way Drive Chain Solves Problem of Sprocket Skip

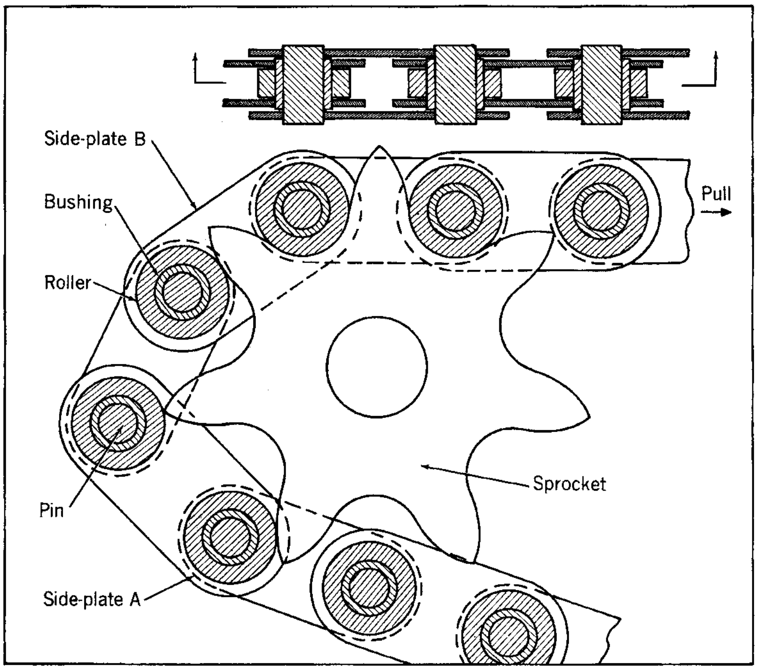

Link can skip a tooth in conventional chain (above), because tension on chain squeezes bushing, which forces next link to rotate and rise. But if all links are offset (below) and chain is properly applied, it will drape freely around sprockets.

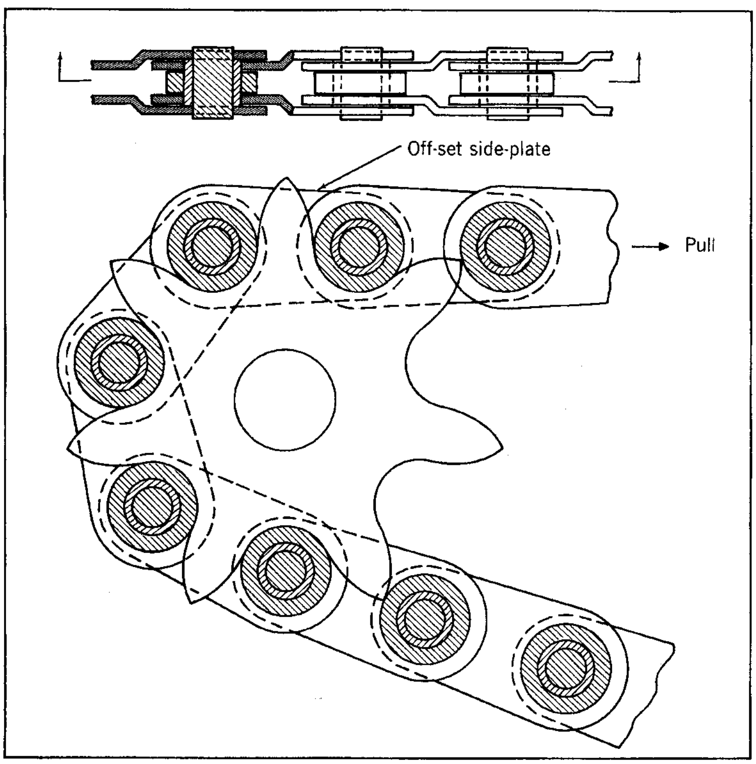

Double or nothing—that's the principle Milton Morse, president of APM Hexseal Corp., Englewood, N. J., followed when he developed his grease-free, skip-free, Kleen-chain drive-chain for bicycles. And depending upon the way it is used, it can be either the best chain drive or the worst. Morse uses it the best way and plans to make it available soon.

Alternate pairs of side plates "B" (drawing left) are attached to bushings and are carried within side-plates "A." These outer side-plates are secured in pairs to pins that are carried, but still free to move in the bushings. The bushings also carry rollers that contact, and tend to rotate with, the sprocket teeth. But it is this tendency for the bushings to rotate, plus the friction between the roller and the bushing when the chain is under tension, that causes the chain to rise and skip over sprocket teeth in conventional design.

This condition occurs only on alternate teeth where pin-supported side-plates are applying tension to the chain. The adjacent bushing-supported side plate is forced to roll on the tooth and rise as the bushing is squeezed between roller and pin.

No-skip link. On the next tooth, bushing-supported side-plates are transferring the tension to the chain and only the roller is squeezed—this time between the tooth and the bushing. The pins supporting the link following are not under pressure and are free to let the approaching links drape in the ideal manner around the sprocket. Regardless of how small the sprocket is, the chain will not attempt to skip.

Morse's chain doesn't skip, because he made it out of only one type of link, by using offset links (drawing left). One end of the side-plates is connected to bushings, and the other is connected to pins. If the chain is applied so the tension is transferred to the tooth only by bushings, the adjacent link will always be pin-supported, and the chain will drape freely around the smallest sprocket. By using smaller sprockets, it is possible to make larger reductions with fewer stages.

Chain Hoist for Dam's Radial Arm Gate

From partial plan to retrofit control dam structure

Robert O. Parmley

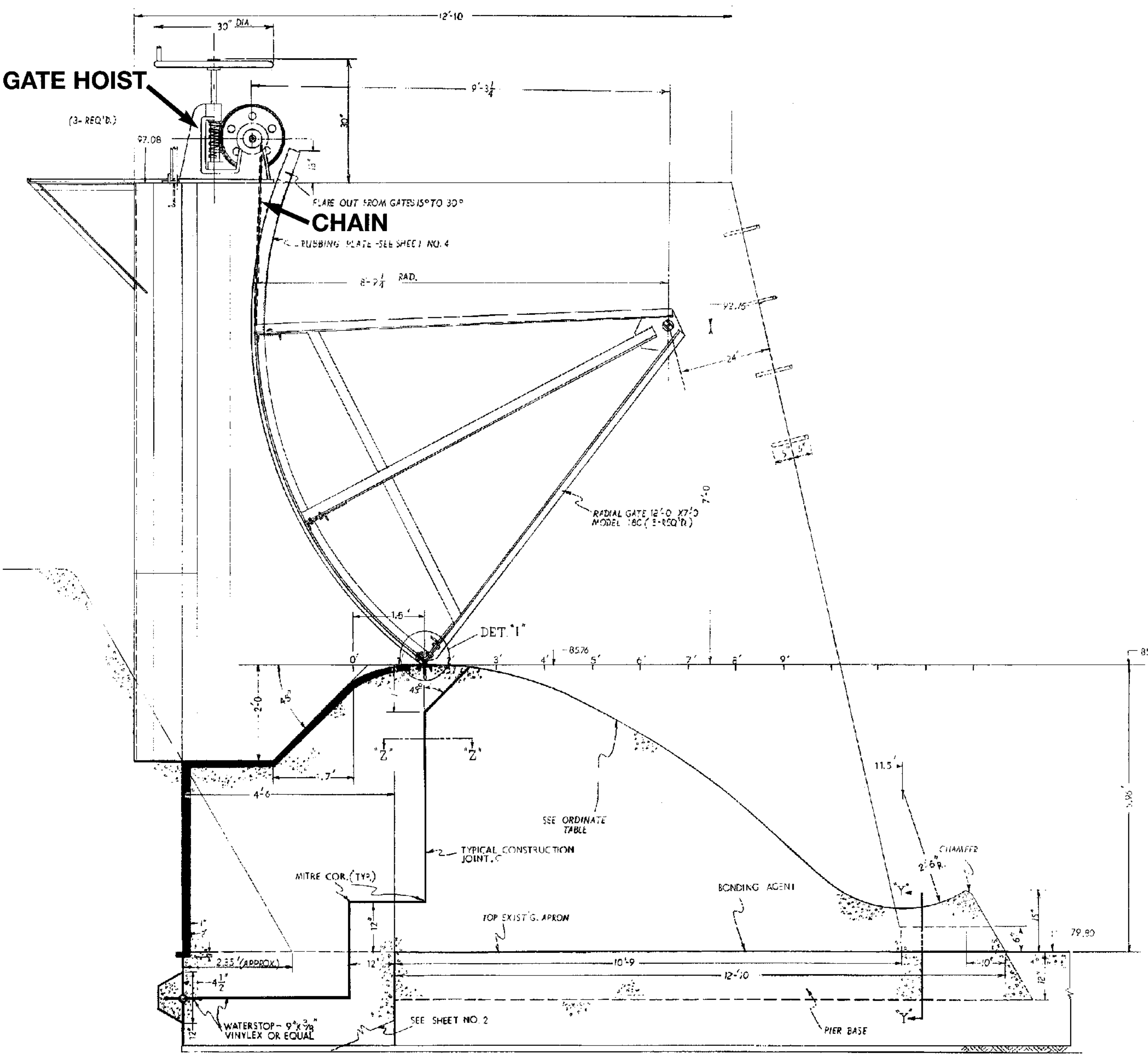

Courtesy: Morgan & Parmley, LTD.

Portable Chain Hoist for Motors

Robert O. Parmley

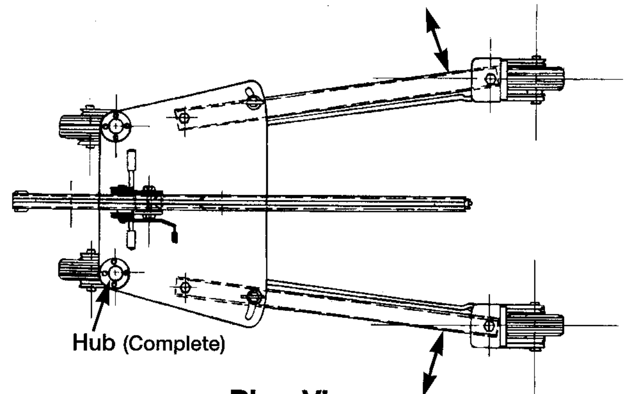

Plan View

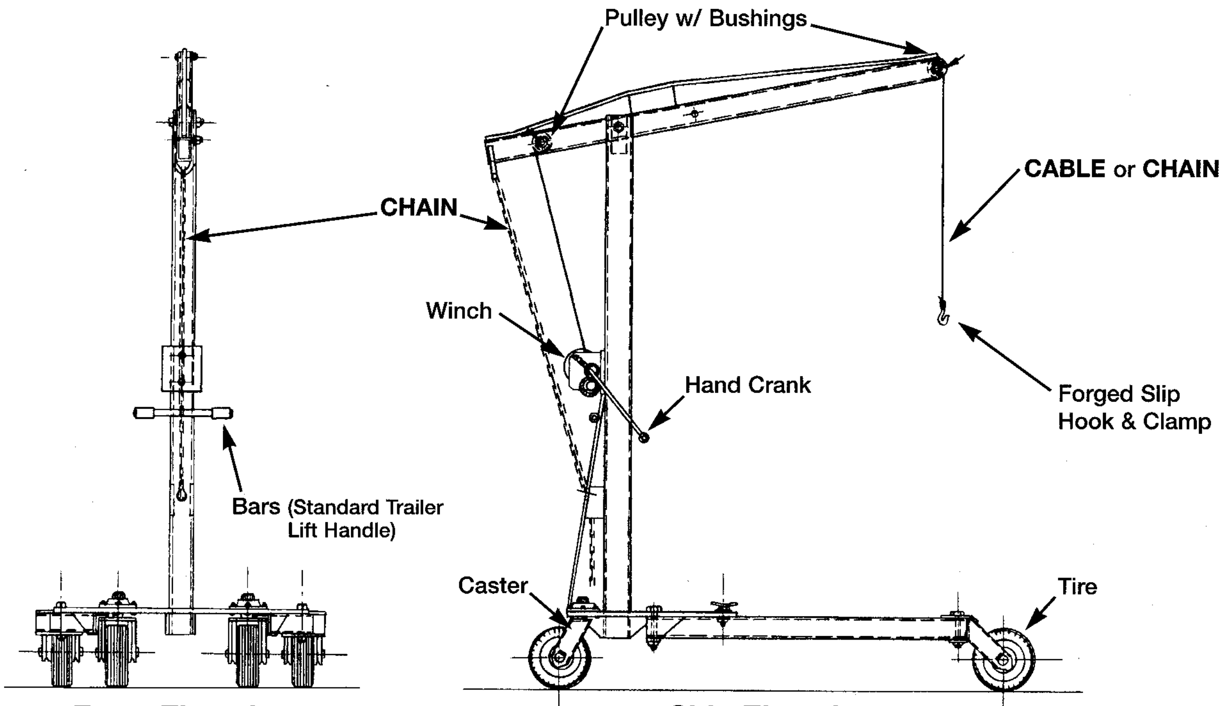

Front Elevation

Side Elevation

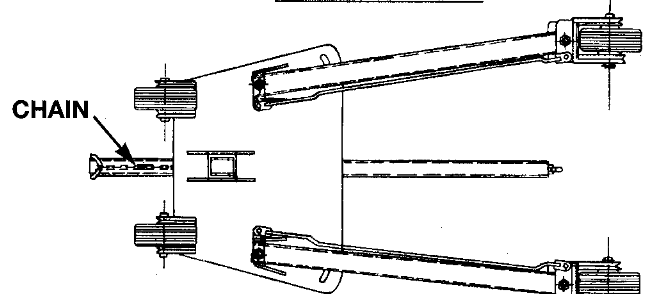

Bottom View

Design of Precision Sprockets

Arthur Hill

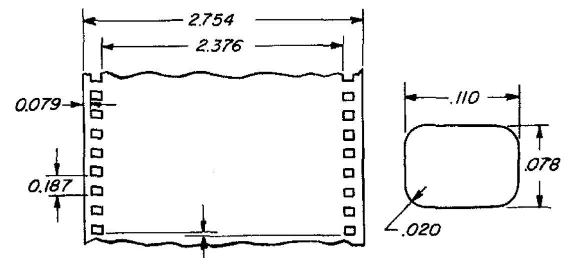

FIG. 1

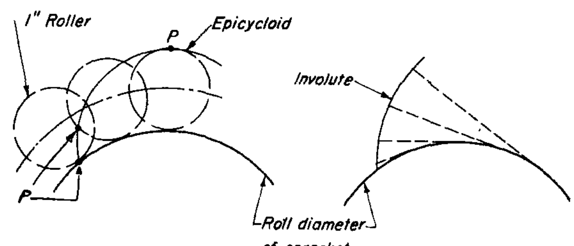

FIG. 2 (a) (b)

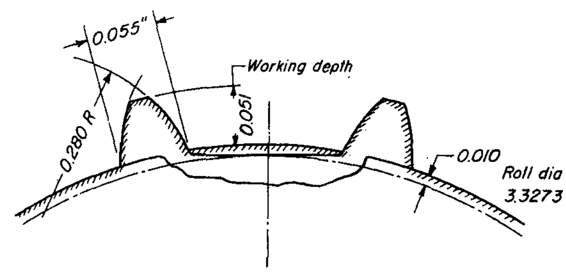

FIG. 3

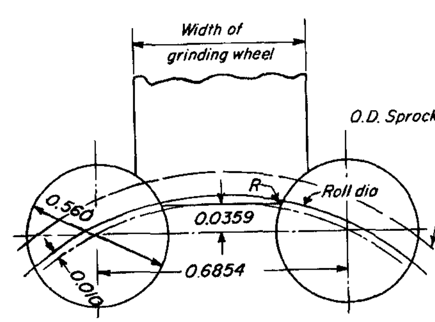

FIG. 4

Camera-type sprockets are being adapted to computers. Here are gear-tooth calculations and data for dimensioning and generating a precision sprocket, as normally used in a tracking camera or a computer for the accurate transmission of tape or film.

The sprocket will accommodate standard 70 mm perforated film, manufactured in accordance with Military Standard MS33525 (see Fig. 1). The sprocket has 56 teeth, a roll diameter of 3.3273 in. that will provide a mean diameter to the film (0.006 in. thick) of 3.3333 in.

In the design of this particular sprocket, the teeth are shaped to meet two different conditions: the film can leave the sprocket on a 1-in. dia roller, or the film can be pulled off in a tangential path. These two extremes call respectively for a tooth contour not exceeding an epicycloid or an involute using the roll diameter of the sprocket as a base circle, see Figs. 2*a* and 2*b*.

A tooth radius is chosen coincident with both curves at their base and lying just inside at the tip of the tooth. A radius of 0.280 in. with its center 0.010 in. below the roll diameter is found to be satisfactory. It is now necessary to compute data to design and make a templet that can be used on the Panto-Crush grinder. The templet is used for dressing a wheel to grind the space between the sprocket teeth as shown in Figs. 3 and 4. Note: the computations and process described here are not restricted to any specific kind of gear grinder. In fact, this information can also be used for any kind of a gear hobbing machine by simply making a hob to the same proportion and with the same profile as the grinding wheel shown in Fig. 7. It will be noticed that the tooth fillet radius *R* must originate below the roll diameter, and that the circumference of the wheel may be straight in section, i.e., parallel to the axis of the wheel.

One method of fabricating the sprocket is to make it from a 3-piece sandwich construction utilizing ground aluminum side plates of a diameter equal to the roll diameter. The center plate is made of steel equal in thickness to the sprocket tooth thickness, and hardened and ground from the crushed wheel, Fig. 4. The work piece is indexed 56 times to grind the gear tooth spaces; however this method is extremely time consuming for a production setup.

A better production method was devised as a result of a study conducted to determine if it is practical to grind the sprocket teeth on the Reishauer gear grinder. This method requires dressing the grinding wheel to fabricate a tooth form that would satisfy the conditions as stated above. The tooth now has an involute form instead of only a radius.

The first step in this preferred production method is to establish the correct pressure angle for the involute tooth form. As indicated above, the tooth profile must be generated in such a manner that there will not be any interference with the epicycloid or involute take-off.

If the involute has a base circle below the roll diameter of the sprocket the tooth form will clear the perforations in the film while the film is being loaded or unloaded tangent to the roll diameter.

To help determine the correct pressure angle, it is necessary to establish how many degrees of rotation on the sprocket are needed to satisfy an epicycloid profile tooth. This information can be established as follows (See Fig. 5) and these computations:

R_o—Outside radii of sprocket teeth, 1.7146 in.

r —Mean radii of the film rolled on 1-in. dia roller, 0.503 in.

C —Center distance between the sprocket and roller with film in between, 2.1697 in.

R —Mean radii of film rolled on roll diameter of sprocket, 1.6667 in.

$$\cos\theta = \frac{r^2 + C^2 - R_o^2}{2\ r\ C}$$

$$\theta = \frac{0.503^2 + 2.1697^2 - 1.7146^2}{2 \times 0.503 \times 2.1697}$$

$$= 0.92567$$

$$\theta = 22.2302^\circ$$

$$\cos\Psi = \frac{1.7146^2 + 2.1697^2 - 0.503^2}{2 \times 2.1697 \times 1.7146}$$

$$= 0.99382$$

$$\Psi = 6.37202^\circ, \text{ or } 0.1112 \text{ radians}$$

Because the roller r rolls on the radius R and does not slip, they both roll off an equal amount of their circumference. Therefore, their arcs AB and BD are equal. Employing the theorem—radius multiplied by the included angle expressed in radians equals the length of arc in the included angle; then because the two arcs are equal to each other, their equations are also equal to each other.

$$\frac{\theta\ \pi}{180} \times r = \frac{\delta\ \pi}{180} R$$

$$\therefore\ \delta = \frac{\theta\ \pi\ r}{180} \times \frac{180}{R\ \pi} = \frac{\theta\ r}{R}$$

$$\delta = \frac{22.2301 \times 0.503}{1.667}$$

$$= 6.709^\circ, \text{ or } 0.1171 \text{ radians}$$

$$\phi_E = \delta - \Psi = 0.0059 \text{ radians}$$

It is important to make certain that the pressure angle of the teeth at the outside diameter of the sprocket when generated is an involute greater than 14°47′, which would be the pressure angle of an involute tooth whose involute function is equal to ϕ_E. Because the pitch diameter of the gear in the follow-

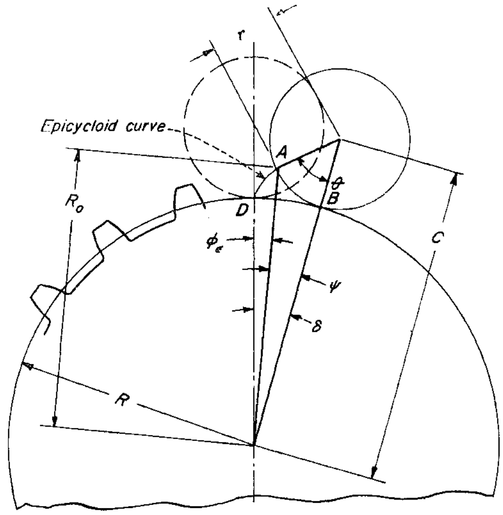

FIG. 5

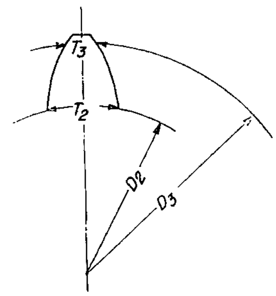

FIG. 6

ing computations is just about equal to the outside diameter of the sprocket, a pressure angle of 15° 3½′ is selected because the base circle for this gear would then fall approximately 0.011 in. below the roll diameter. Furthermore, by providing a minimum radius of 0.004 in. on the wheel, the sprocket tooth will not be undercut.

This data is now converted into information similar to gear calculations in order to setup the Reishauer gear grinder, or any other gear-generating machine tool. From the Reishauer manual PZA 75 a gear train can be setup as follows:

$$\frac{12}{DP} = \frac{G_1}{G_2} \times \frac{G_3}{G_4}$$

From the selection of change gears a 16 1/3 DP is easily obtained.

$$\frac{12}{DP} = \frac{40}{70} \times \frac{54}{42}$$

$$\therefore\ DP = 16\ 1/3$$

Computing the imaginary gear

No. of teeth	N	$= 56$
Diametral Pitch	P	$= 16\ 1/3$
Pressure angle	ϕ_2	$= 15°\ 3\frac{1}{2}'$
Pitch diameter	D_3	$= 3.4286$
Circular pitch	C	$= \frac{\pi}{P} = 0.1923$
Outside diameter	OD	$= \frac{N+2}{P} = 3.5510$
Whole depth	D	$= \frac{2.156}{P} = 0.132$
Root diameter	R D	$= 3.2870$

$$D_3 = \frac{N}{P} = 3.4286$$

Base dia. $= 0.9915 \times 3.3333 = 3.3048$

Referring to Fig. 3, the sprocket tooth shows a height of 0.051 in. and an undercut of 0.10 in. below roll diameter. Therefore, the wheel will penetrate 0.061 in. below the outside diameter of the sprocket. Also note that the tooth has a chordal thickness of 0.055 in. at the roll diameter. The arc tooth thickness is 0.055 in. at the point of contact with the mean thickness of the film. However, for the purpose of dimensioning the grinding wheel the arc tooth thickness must be determined at the pitch diameter of the imaginary gear.

T_2 = Arc tooth thickness of tooth at $D_2 = 0.055$
T_3 = Arc tooth thickness of tooth at D_3
ϕ_1 = Pressure angle at point where the mean diameter of the film makes contact with the tooth
D_2 = mean dia of film = 3.3333
D_3 = pitch dia = 3.4286

$$\text{Cos } \phi_2 = 15°\,3\tfrac{1}{2}' = 0.9639$$

$$\text{Cos } \phi_1 = \frac{D_3 \text{ Cos } \phi_2}{D_2} = \frac{3.4286 \times 0.9639}{3.3333} = 0.99145$$

$$\phi_1 = 7°\,30'$$

$$\text{Inv } \phi_1 = 0.00075 \quad \text{Inv } \phi_2 = 0.00622$$

$$T_3 = D_3\left[\frac{T_2}{D_2} \times \text{Inv } \phi_1 - \text{Inv } \phi_2\right]$$

$$T_3 = 3.4286\left[\frac{0.055}{3.3333} + 0.00075 - 0.00622\right] = 0.0343$$

The root diameter of the sprocket is equal to the roll diameter minus 0.020 in. as indicated in Fig. 3, or 3.3073 in. This figure is 0.1213 in. less than the pitch dia of the imaginary gear. Therefore, to determine the dimension for the width of the groove in the grinding wheel at the point of deepest penetration, Fig. 7, multiply 0.1213 in. by the tangent of ϕ_2 and add this value to T_3.
ie: $0.26904 \times 0.1213 + 0.0343 = 0.067$ in.

From *this* information the grinding wheel can now be dimensioned.

It should be noted that the dimensions given in Fig. 7 are normal to the tooth and not parallel to axis of wheel.

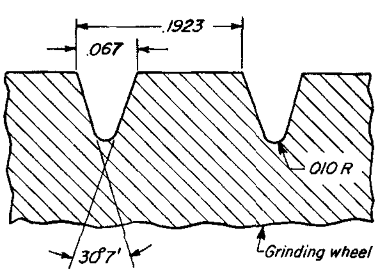

FIG. 7

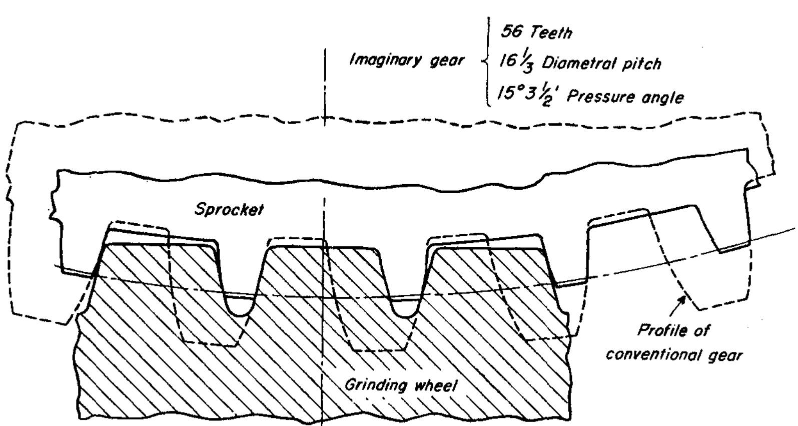

FIG. 8

Sheet Metal Gears, Sprockets, Worms & Ratchets

Haim Murro

When a specified motion must be transmitted at intervals rather than continuously, and the loads are light, these mechanisms are ideal because of their low cost and adaptability to mass production. Although not generally considered precision parts, ratchets and gears can be stamped to tolerances of ± 0.007 in. and if necessary, shaved to closer dimensions. Sketches indicate some variations used on toys, household appliances and automobile components.

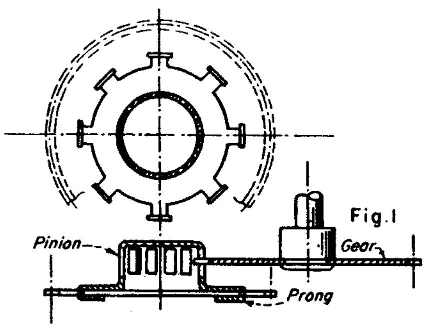

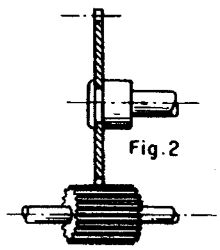

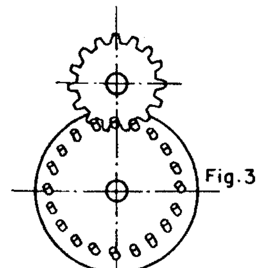

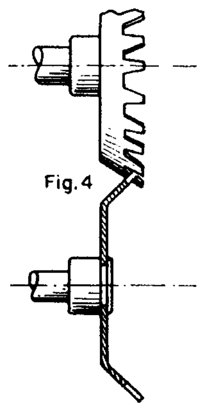

Fig. 1—Pinion is a sheet metal cup, with rectangular holes serving as teeth. Meshing gear is sheet metal, blanked with specially formed teeth. Pinion can be attached to another sheet metal wheel by prongs, as shown, to form a gear train.

Fig. 2—Sheet metal wheel gear meshes with a wide face pinion, which is either extruded or machined. Wheel is blanked with teeth of conventional form.

Fig. 3—Pinion mates with round pins in circular disk made of metal, plastic or wood. Pins can be attached by staking or with threaded fasteners.

Fig. 4—Two blanked gears, conically formed after blanking, make bevel gears meshing on parallel axis. Both have specially formed teeth.

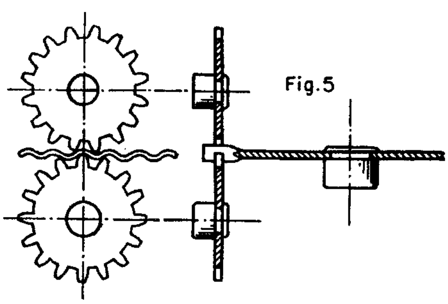

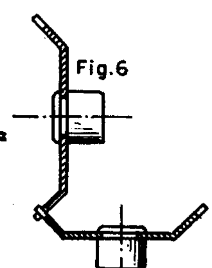

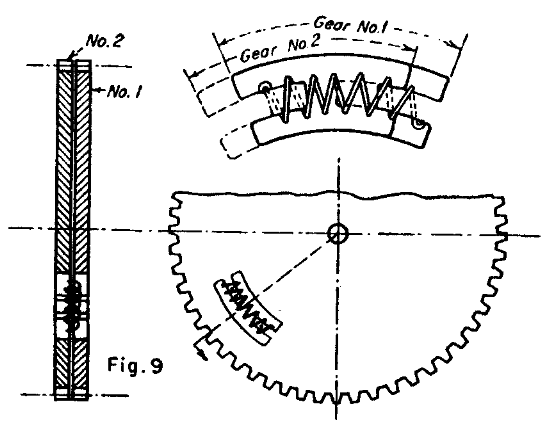

Fig. 5—Wheel with waves on its outer rim to replace teeth, meshes with either one or two (shown) sheet metal pinions, having specially formed teeth, and mounted on intersecting axes.

Fig. 6—Two bevel type gears, with specially formed teeth, mounted for 90 deg intersecting axes. Can be attached economically by staking to hubs.

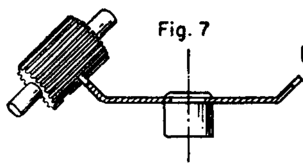

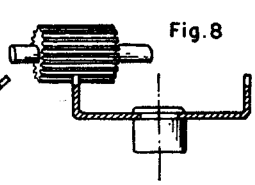

Fig. 7—Blanked and formed bevel type gear meshes with solid machined or extruded pinion. Conventional form of teeth can be used on both gear and pinion.

Fig. 8—Blanked, cup-shaped wheel meshes with solid pinion for 90 deg intersecting axes.

Fig. 9—Backlash can be eliminated from stamped gears by stacking two identical gears and displacing them by one tooth. Spring then bears one projection on each gear taking up lost motion.

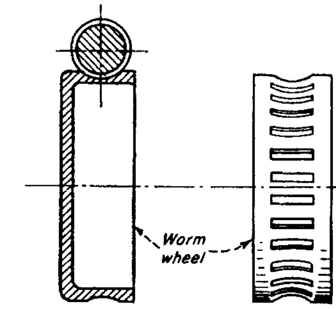

Fig.10

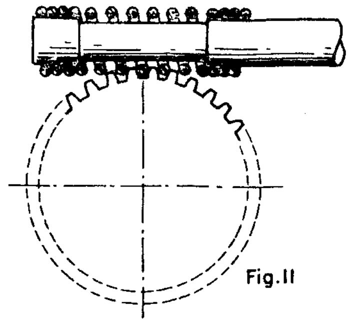
Fig.11

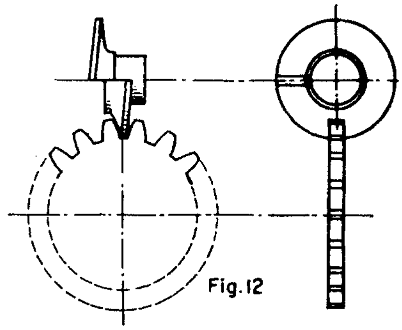
Fig.12

Fig. 10—Sheet metal cup which has indentations that take place of worm wheel teeth, meshes with a standard coarse thread screw.

Fig. 11—Blanked wheel, with specially formed teeth, meshes with a helical spring mounted on a shaft, which serves as the worm.

Fig. 12—Worm wheel is sheet metal blanked, with specially formed teeth. Worm is made of sheet metal disk, split and helically formed.

Fig. 13—Blanked ratchets with one sided teeth stacked to fit a wide, sheet metal finger when single thickness is not adequate. Ratchet gears can be spot welded.

Fig. 14—To avoid stacking, single ratchet is used with a U-shaped finger also made of sheet metal.

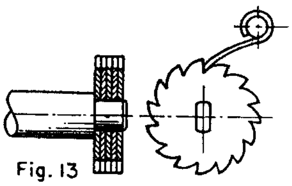
Fig. 13

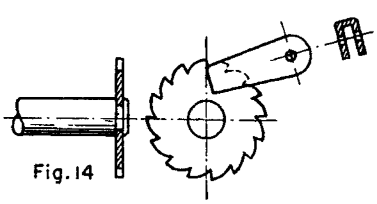
Fig. 14

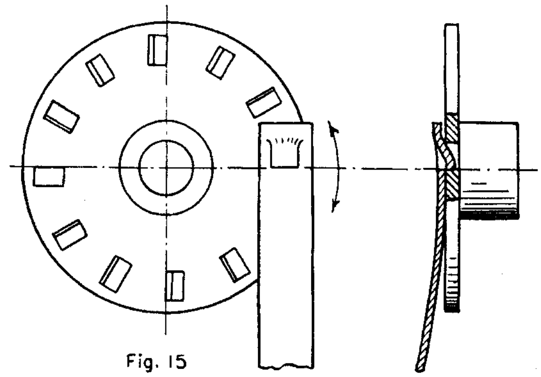
Fig. 15

Fig. 15—Wheel is a punched disk with square punched holes to selve as teeth. Pawl is spring steel.

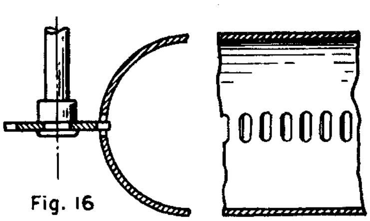
Fig. 16

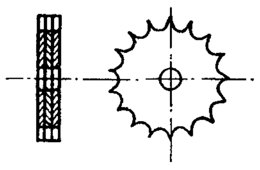
Fig. 17

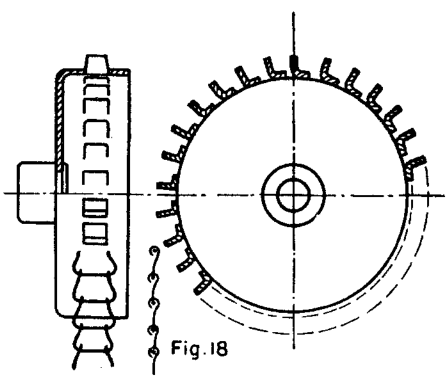
Fig. 18

Fig. 16—Sheet metal blanked pinion, with specially formed teeth, meshes with windows blanked in a sheet metal cylinder, to form a pinion and rack assembly.

Fig. 17—Sprocket, like Fig. 13, can be fabricated from separate stampings.
Fig. 18—For a wire chain as shown, sprocket is made by bending out punched teeth on a drawn cup.

Ratchet Layout Analyzed

Here, in a brief but comprehensive rundown, are generally unavailable formulas and data for precise ratchet layout.

Emery E. Rossner

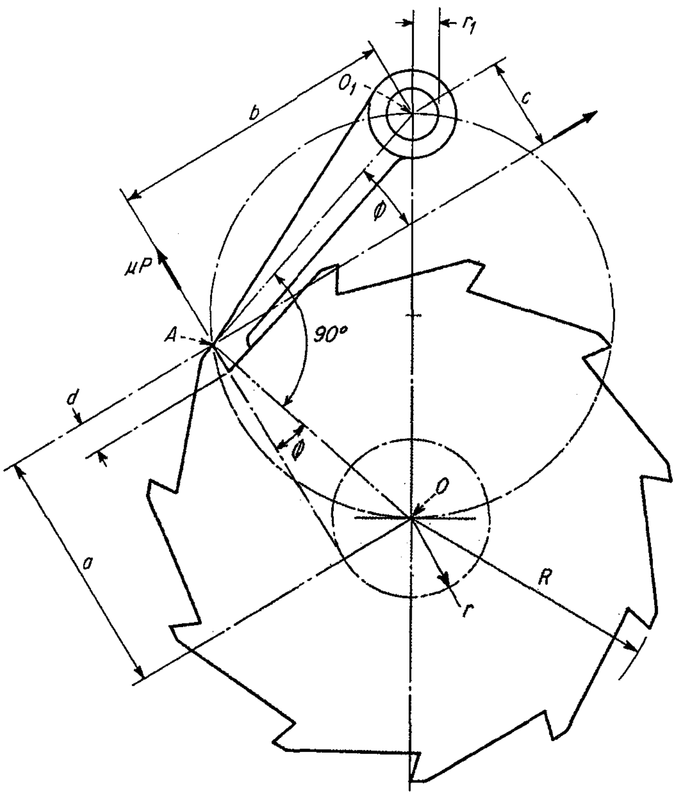

Pawl in compression . . .
has tooth pressure *P* and weight of pawl producing a moment that tends to engage pawl. Friction-force μP and pivot friction tend to oppose pawl engagement.

Symbols

a	= moment arm of wheel torque
M	= moment about O_1 caused by weight of pawl
0, 0_1	= ratchet and pawl pivot centers respectively
P	= tooth pressure = wheel torque/a
$P\sqrt{(1+\mu^2)}$	= load on pivot pin
μ, μ_1	= friction coefficients

Other symbols as defined in diagrams

The ratchet wheel is widely used in machinery, mainly to transmit intermittent motion or to allow shaft rotation in one direction only. Ratchet-wheel teeth can be either on the perimeter of a disc or on the inner edge of a ring.

The pawl, which engages the ratchet teeth, is a beam pivoted at one end; the other end is shaped to fit the ratchet-tooth flank. Usually a spring or counterweight maintains constant contact between wheel and pawl.

It is desirable in most designs to keep the spring force low. It should be just enough to overcome the separation forces—inertia, weight and pivot friction. Excess spring force should not be relied on to bring about and maintain pawl engagement against the load.

To insure that the pawl is automatically pulled in and kept in engagement independently of the spring, a properly layed out tooth flank is necessary.

The requirement for self-engagement is

$$Pc + M > \mu Pb + P\sqrt{(1+\mu^2)}\,\mu_1 r_1$$

Neglecting weight and pivot friction

$$Pc > \mu Pb$$

or

$$c/b > \mu$$

but $c/b = r/a = \tan\phi$, and since $\tan\phi$ is approximately equal to $\sin\phi$

$$c/b = r/R$$

Substituting in term (1)

$$rR > \mu$$

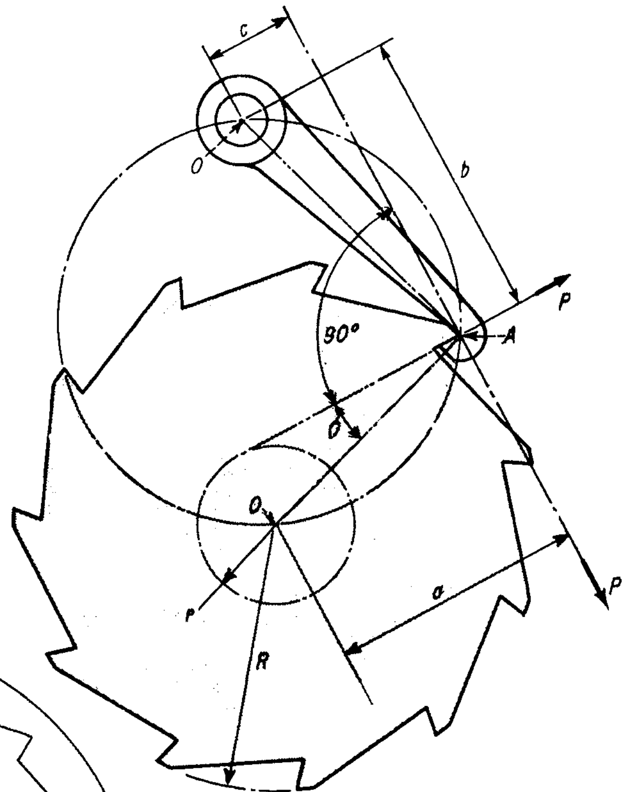

Pawl in tension . . .
has same forces acting on unit as other arrangements. Same layout principles apply also.

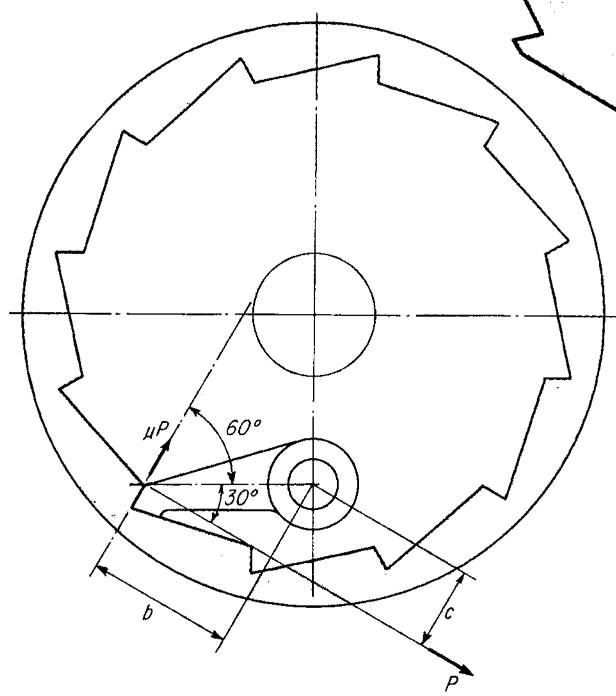

Inner teeth . . .
allow compact assembly of pawl and ratchet.

For steel on steel, dry, $\mu = 0.15$. Therefore, using

$$r/R = 0.20 \text{ to } 0.25$$

the margin of safety is large; the pawl will slide into engagement easily. For internal teeth with ϕ of 30°, c/b is tan 30° or 0.577 which is larger than μ, and the teeth are therefore self engaging.

When laying out the ratchet wheel and pawl, locate *points* O, A and O_1 on the same circle. AO and AO_1 will then be perpendicular to one another; this will insure that the smallest forces are acting on the system.

Ratchet and pawl dimensions are governed by design sizes and stress. If the tooth, and thus pitch, must be larger than required in order to be strong enough, a multiple pawl arrangement can be used. The pawls can be arranged so that one of them will engage the ratchet after a rotation of less than the pitch.

A fine feed can be obtained by placing a number of pawls side by side, with the corresponding ratchet wheels uniformly displaced and interconnected.

No Teeth Ratchets

With springs, rollers and other devices they keep going one way.

L. Kasper

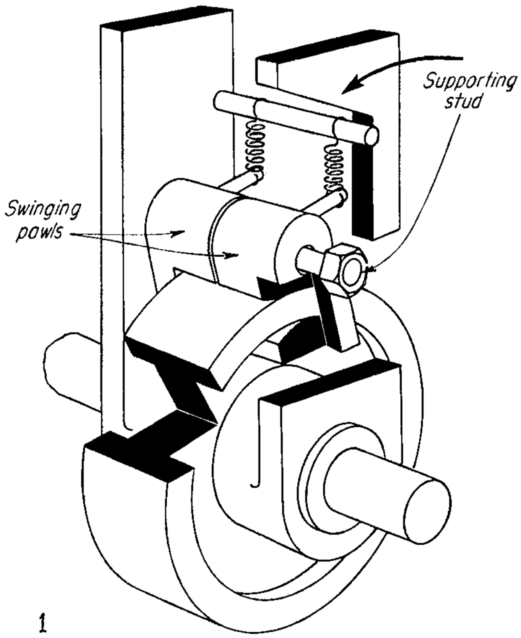

1

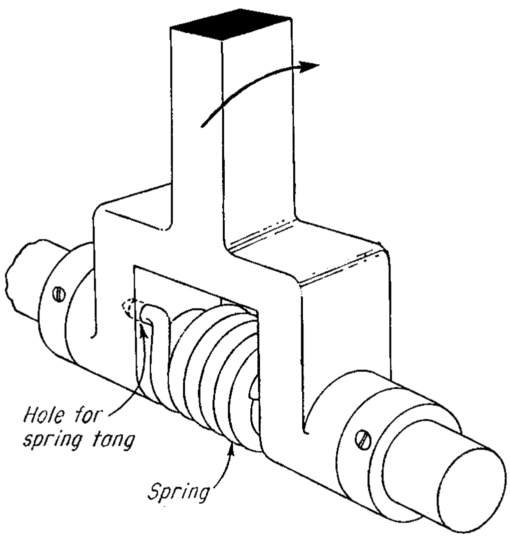

2

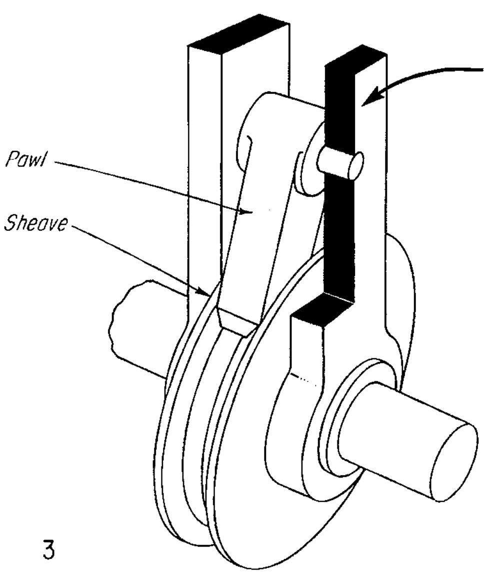

3

1 **SWINGING PAWLS** lock on rim when lever swings forward, and release on return stroke. Oversize holes for supporting stud make sure both top and bottom surfaces of pawls make contact.

2 **HELICAL SPRING** grips shaft because its inner diameter is smaller than the outer diameter of shaft. During forward stroke, spring winds tighter; during return stroke, it expands.

3 **V-BELT SHEAVE** is pushed around when pawl wedges in groove. For a snug fit, bottom of pawl is tapered like a V-belt.

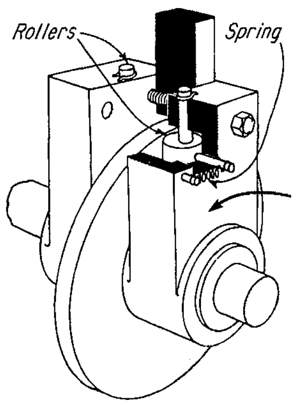

4

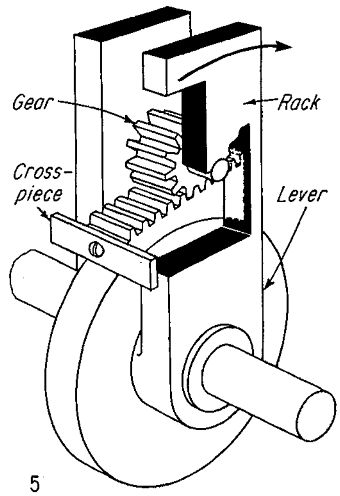

5

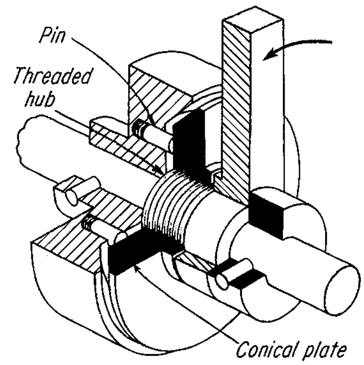

6

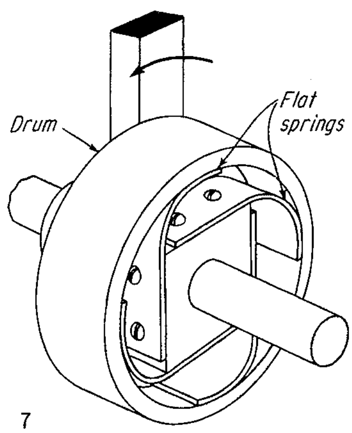

7

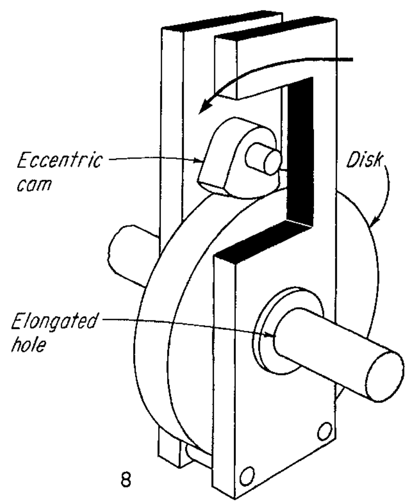

8

4 ECCENTRIC ROLLERS squeeze disk on forward stroke. On return stroke, rollers rotate backwards and release their grip. Springs keep rollers in contact with disk.

5 RACK is wedge-shape so that it jams between the rolling gear and the disk, pushing the shaft forward. When the driving lever makes its return stroke, it carries along the unattached rack by the cross-piece.

6 CONICAL PLATE moves as a nut back and forth along the threaded center hub of the lever. Light friction of spring-loaded pins keeps the plate from rotating with the hub.

7 FLAT SPRINGS expand against inside of drum when lever moves one way, but drag loosely when lever turns drum in opposite direction.

8 ECCENTRIC CAM jams against disk during motion half of cycle. Elongated holes in the levers allow cam to wedge itself more tightly in place.

SECTION 3

BELTS & BELTING

Unique Belt Applications

Brent Oman

Belt power transmission systems have been in operation in industry for over 200 years, going back to early flat belt drives. These early flat belts were typically composed of leather and cotton or hemp rope, used to transmit power from steam engines or water wheels to early industrial production machinery. Belt technology has increased dramatically, with modern engineered belt systems handling loads and applications with a design flexibility that other power transmission systems cannot match. Modern belt drives can handle a wide variety of loads and speeds that would not have been possible in the past.

An example of an extremely harshly loaded belt application is the supercharger belt drive system used on the supercharged, nitromethane consuming Top Fuel and Funny Car classes in professional drag racing. The belt drive is used to drive the supercharger, transmitting power from the engine crank-shaft. Vehicles in these drag racing classes commonly traverse the 1/4 mile track in under 5 seconds. Belt tensioning is provided by the addition of an idler. The superchargers used to develop such high vehicle speeds can require in excess of 1000 HP to operate, at speeds in excess of 10,000 RPM. Engine acceleration at the start of a race can be nearly 5,000 RPM in 0.2 seconds. Such extreme operating conditions requires a belt with equally extreme capabilities. A polyurethane synchronous belt with high strength aramid tensile cords and a modified curvilinear tooth form is the only belt which can handle such a demanding load requirement. Supercharger drive belts are commonly 14mm pitch (distance from the center of one belt tooth to the center of an adjacent belt tooth) and approximately 3 inches wide.

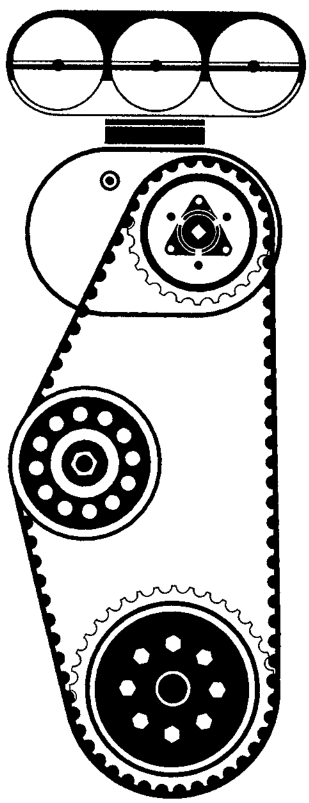

An example of a Top Fuel or Funny Car supercharger driven from engine crankshaft

While the supercharger drive, racing application is highly visible and glamorous, the same polyurethane belt is used in industry to replace roller chain on a wide variety of applications. Roller chain requires lubrication and regular maintenance in order to perform at its peak level. Roller chain can stretch up to 3% of its length over the life of the chain. The high capacity, polyurethane synchronous belt provides superior horsepower capacity, with virtually no stretch.

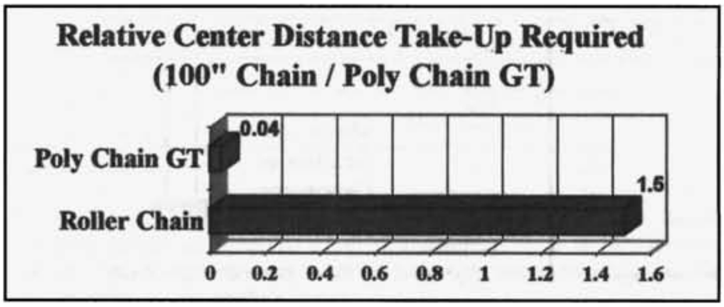

Stretch comparison of high performance polyurethane synchronous belt vs. roller chain.

Over time, stretch of flexible power transmission products may require re-tensioning for optimum performance. Note that the high performance polyurethane belt system is virtually free of stretch over the life of the belt drive.

Additionally, no lubrication is necessary with the synchronous belt. The lack of lubrication allows the polyurethane synchronous belt to replace roller chain on applications where cleanliness is necessary to prevent contamination of product. As an example, conveying and paper converting applications are typically very sensitive to grease and contaminants contacting the product being manufactured.

Live roller conveyors are used for controlled movement of a great variety of regular or irregular shaped commodities, from light and fragile to heavy and rugged unit loads. The term "live roll" indicates that the conveyor rolls are connected and driven by a power source. Where roller chain previously had to be used due to its capacity at low speeds, the latest generation of polyurethane, modified curvilinear tooth, aramid tensile cord synchronous belt drives have horsepower capacities in excess of similarly sized roller chain drives.

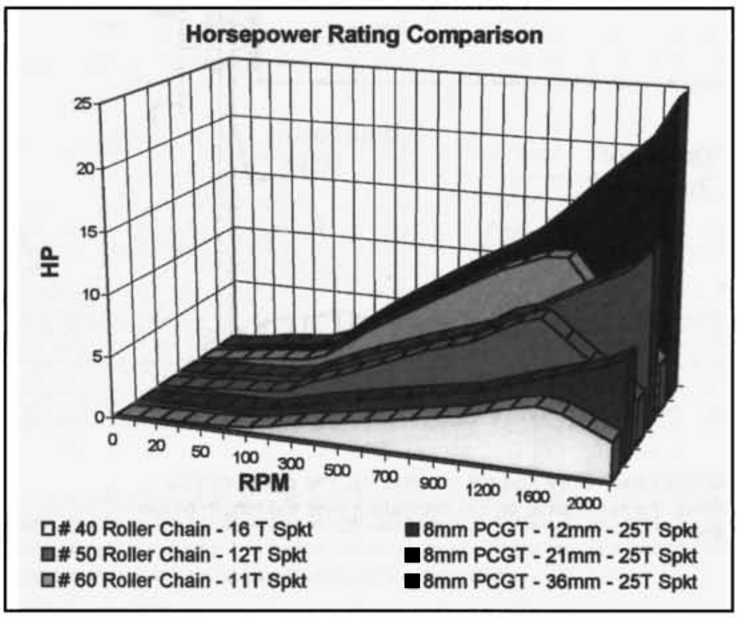

Comparison of Horsepower Ratings for roller chain and high performance polyurethane synchronous belts. Note that it is quite possible to replace roller chain with comparably sized belt drives which will eliminate lubrication and maintenance concerns.

The high capacity synchronous belt allows for driving live roll conveyors by an arrangement of "roll to roll" belt drives, connecting adjacent rolls. At times, idler rolls are inserted between driven rolls.

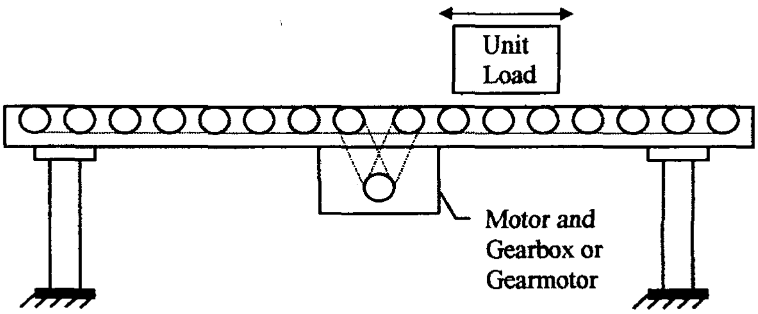

Typical conveyor arrangement showing general roll to roll drive configuration

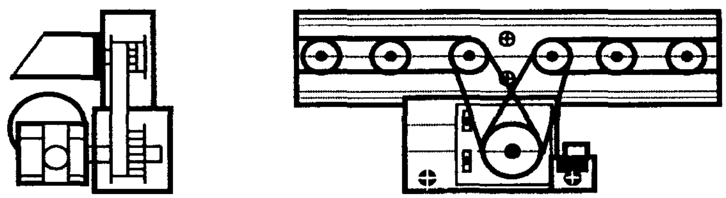

Detail showing motor and gearbox driving sets of live rolls.
Note the belt drives connecting pairs of live rolls.

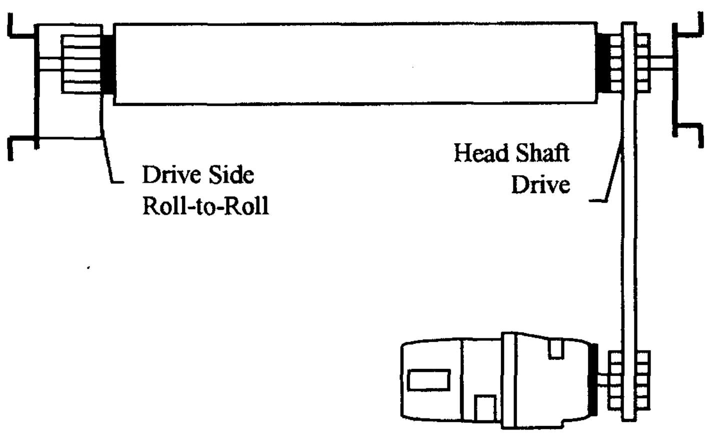

Detail showing head shaft drive and roll to roll drive. The drives can be on opposite sides, the same side, or a combination over the length of the conveyor system.

The major advantages of the polyurethane synchronous belt compared to roller chain are their high load capacity, wide range of operating speeds, lack of lubricant contamination, and virtual elimination of maintenance. The polyurethane synchronous belts can be used to replace roller chain with performance advantages in a wide variety of industries, including lumber, pulp, and paper; packaging; food processing; and sand/gravel/concrete processing. An additional conveying application for synchronous belts is transporting product on the belt's back.

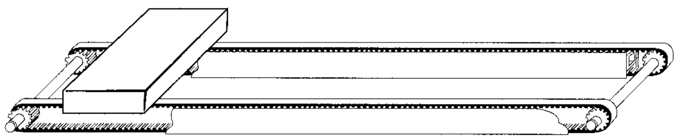

This pallet conveyor transports product on the back of a synchronous belt. Typically, the belt span will be supported on a low friction surface. Special high durability backings are available which will reduce wear on the back belt contact surface. Special backings are also available in non-marking constructions.

Another unique product which demonstrates the design flexibility available belts provide is long length synchronous belting. This is a synchronous belt which is available in a continuous length of up to 100 feet, in a variety of pitches and constructions. Rubber trapezoidal tooth profile belts with pitches from .080″ to .500″ are available; as well as rubber curvilinear tooth profile belts with pitches from 2mm to 8mm. Urethane long length belting with aramid or steel tensile cords is also available in both trapezoidal and modified curvilinear tooth profiles.

Long length belting is a cost effective, efficient and low maintenance alternative to chain. It is particularly suited for linear movement applications (automatic doors, automated warehouse or production conveying systems) and positioning applications (machine tools, x-y coordinate machines, printers, office equipment). Synchronous long length belting offers high positioning accuracy, length stability, low maintenance, and simple mechanical attachment using belt clamping fixtures. The clamping fixtures are easily machined, providing an effective method of attaching the ends of the belting to the device or product being positioned.

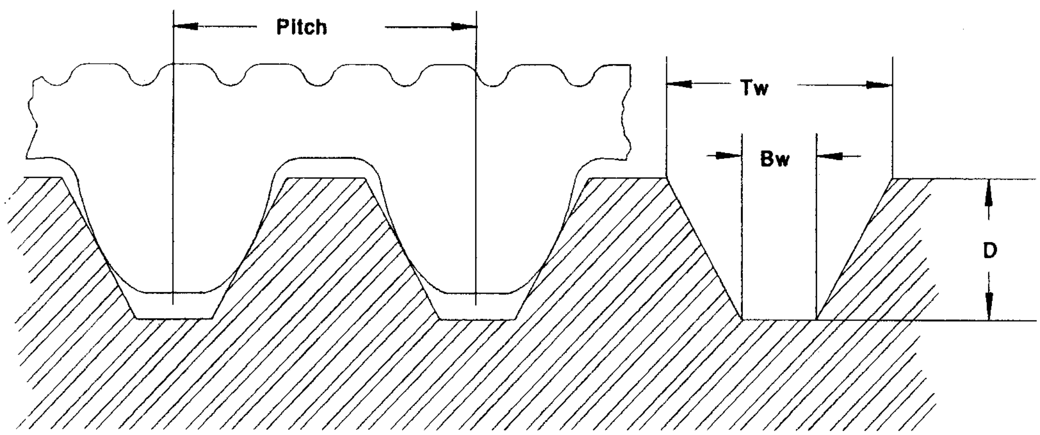

An example of a clamp groove profile which is used for attaching modified curvilinear tooth profile polyurethane long length belting to a fixture. A top plate is typically used to mechanically clamp the belt into the grooves. The fixture is mechanically attached to the component being positioned by the belt drive.

It is not uncommon for a pair of long length belts to be used in an industrial manufacturing environment to move a production mechanical device linearly. The belt is typically clamped to the device being positioned. Examples of applications include cutters, knives, print heads, and component movement equipment.

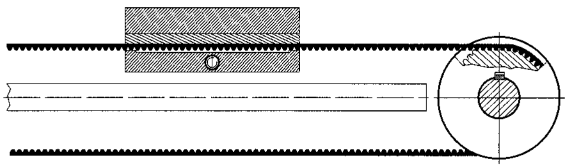

Belt clamp fixture attached to belt. The fixture would be attached to the machine element being positioned by the belt drive.

One of the advantages of synchronous belts is their very high efficiency. Efficiency of any power transmission system is a measure of the power loss associated with the motor, the bearings and the belt drive. Any loss of power is a loss of money. By minimizing the losses in the system, the cost of operating the drive is minimized. Since the passage of the U.S. Energy Policy Act (1992), higher efficiency motors are more often being used by Original Equipment Manufacturers (OEM) to reduce power loss. The U.S. Energy Policy Act is aimed at increasing the efficiency standards for all types of appliances and equipment (including electric motors). However, even a high efficiency motor's advantages can be under-utilized if the most efficient belt drive alternative is not chosen. Synchronous belts are more energy efficient than V-belts, providing a cost effective method of improving the overall system efficiency.

Efficiency can be defined by the following formula:

Efficiency = HPout/HPin = (TORQUEout x RPMout)/(TORQUEin x RPMin)

As this equation shows, energy losses in belt drives can be separated into two categories, torque and speed loss. Torque loss results from the energy required to bend the belt around the sprocket or sheave. Energy lost as heat (due to friction) also causes torque loss.

Speed losses are the result of belt slip and creep. Belt slip is self-explanatory. Creep happens as the belt elongates or stretches as it moves from the slack side to the tightside as tension increases. This causes a slightly longer belt to leave the sheave than what entered.

Since V-belts generally have a much thicker cross section than synchronous belts, they use more energy bending around the sheave. Also, V-belts operate through a wedging action with the sheave, thus creating friction. There is generally more heat lost through this wedging action than from the minimal friction generated as a synchronous belt tooth enters and exits the sprocket grooves.

V-belt drives, especially if poorly maintained, will slip. But synchronous belts are a positive drive system and do not slip. The V-belt drive will show a decrease in driveN speed (rpm) over time and the synchronous drive will not. Also, due to its low stretch properties, a synchronous belt does not experience creep.

Even though properly maintained V-belts drives can run as high as 95-98% efficient at the time of installation, this often deteriorates over time by as much as 5% during operation. Poorly maintained V-belt drives may be up to 10% less efficient. Synchronous belts remain at an energy efficiency of around 98% over the life of the belt.

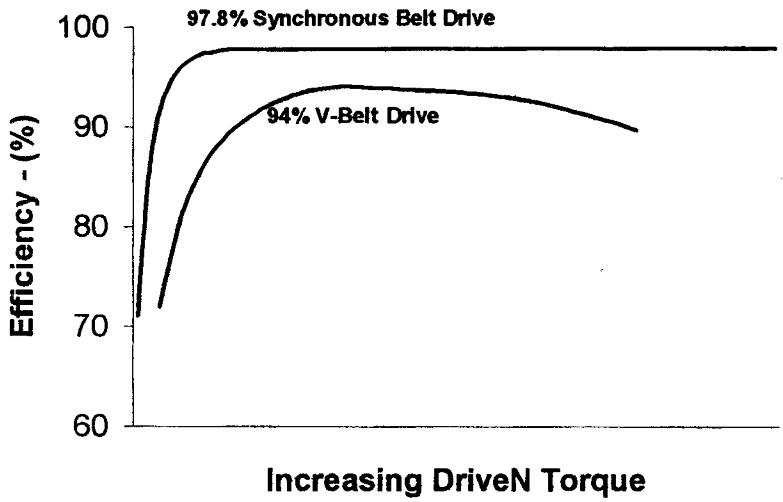

Synchronous belts are often used where precise positioning of components is required. Sophisticated machine tool applications, pick and place applications, and printing applications are just a few examples of potential synchronous belt drive applications.

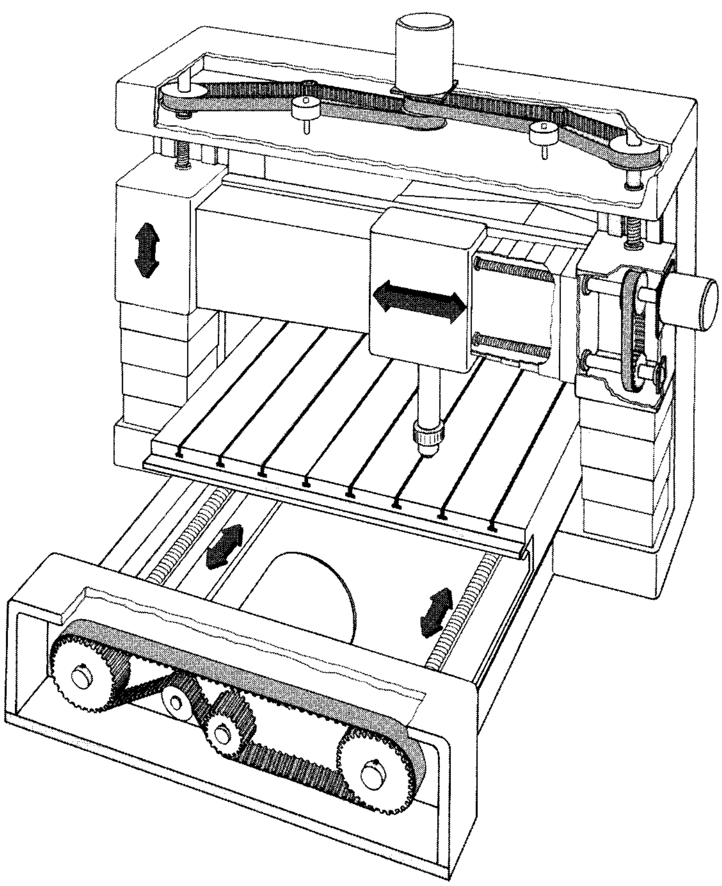

This machining station uses synchronous belts to drive lead screws which position a machining spindle.

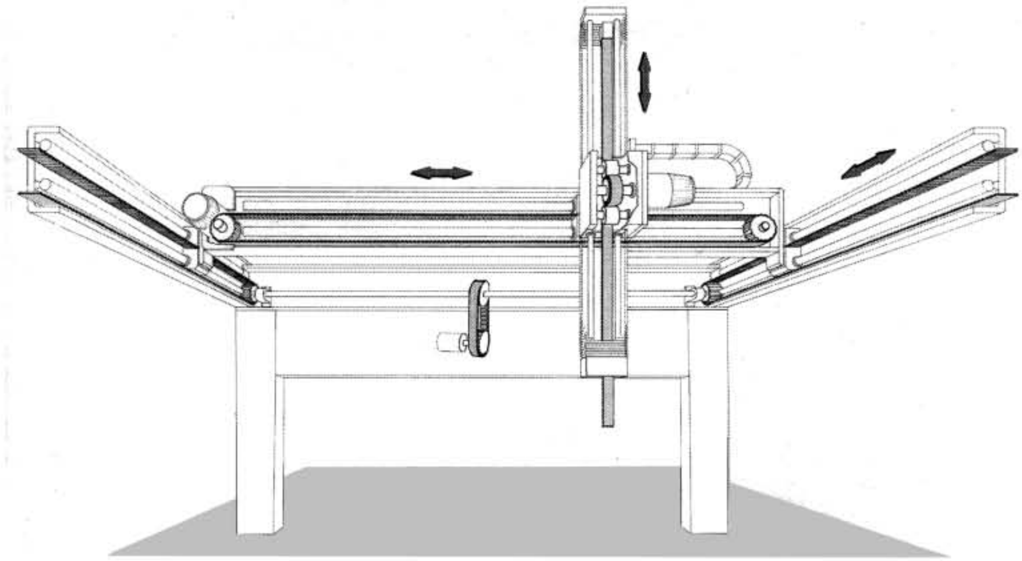

Synchronous belts are used to drive and position components in this pick and place application.

V-belt drives offer robust power transmission systems which can be designed for many unique applications. One example is the use of spring loaded idlers to minimize maintenance by means of automatic tensioning. An additional benefit is that a spring loaded idler provides lower overall drive tensions for drives subjected to large peak loads as compared to the drive's average load. This increases the life of the V-belt and drive components.

Fixed, manually adjusted, idlers function by forcing the idler into the belt until proper belt tension is achieved and the idler is locked into place. Belt tension in fixed idler drives is not constant, but decreases with time due to sheave wear, belt wear, and belt elongation. When retensioning is required, the idler must be manually adjusted to provide proper tension. With a fixed idler, static tension is imposed on the drive to transmit the peak load. With varying loads, this can result in higher belt tensions, reducing belt life.

The spring loaded idler system automatically compensates for sheave and belt wear as well as belt elongation. Spring loading is often designed to provide constant tension over the life of the V-belt drive. Additionally, on applications subject to extremely wide variations in horsepower requirements, properly designed spring loaded idlers produce a constant slack side tension. Since the slack side tension remains constant, the tight side tension increases with increasing loads but drops as the loads decrease. This results in lower overall tensions and longer belt life.

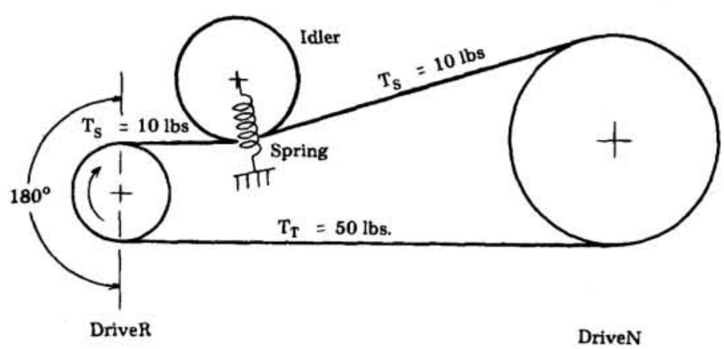

V-belt drive with spring loaded idler

Specific design procedures must be followed to properly calculate the required spring forces. However, the long term application benefits greatly outweigh the initial design time required. Examples of V-belt applications which commonly use spring loaded idlers are lawn mower deck drives and agricultural machinery.

The driveR and driveN sheaves of a typical V-belt drive are usually in the same plane, but there are occasions which require that the two sheaves be in different planes. Two of the most common two-plane V-belt drives are quarter turn drives, which have the sheaves 90° apart, and eight-turn drives, which have the sheaves at 45°. Quarter turn drives are more widely used, example applications include irrigation pumps driven by a PTO, agricultural equipment, lawn and garden equipment, and lineshafts.

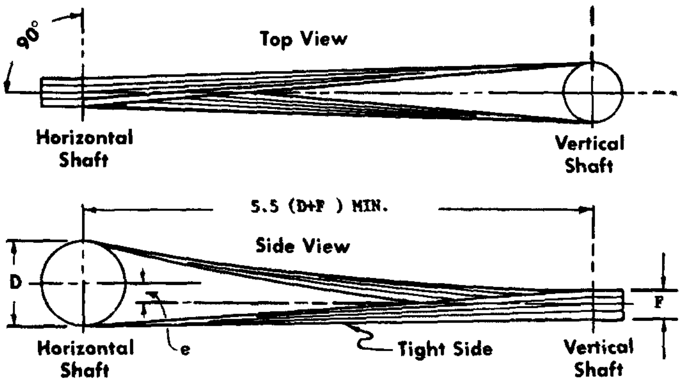

Quarter drive configuration showing dimensional design considerations.

Specific design considerations must be followed when designing drives operating in more than one plane. Minimum drive center distances, alignment positioning of the two shafts, rotational direction, and belt tensioning are all factors which must be examined in order to obtain optimum belt performance. It is suggested that belt manufacturers be consulted for specific application recommendations when designing a two plane drive.

Serpentine drives are commonly defined as those having three or more sheaves or sprockets, in which the belts can drive from either inside or backside surfaces. There are many types of applications for serpentine drives, but several of the more common types include automotive front end accessory drives, roll drives in printing or paper equipment, machine tools, and conveyors. Many belt types can be used, including Micro-V, Double-V, conventional V-belts, and double sided synchronous belts. Double sided synchronous belts not only allow for power transmission from both sides of the belt, but also synchronize shaft speeds. This is typically critical in roll drives used in the paper or printing industry. Double sided synchronous belts are a clean, low maintenance alternative to roller chain for these types of applications.

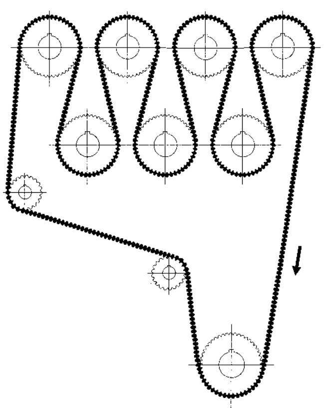

Double sided synchronous belts provide design flexibility for systems requiring shaft counter-rotation and positive positioning.

In addition to providing a cost effective means of power transmission, belts can also be supplied in a variety of special constructions which might be required for unique applications. Alternate tensile member types, high or low temperature constructions, non-marking constructions, and special backings are just a few of the special constructions that are available to solve equipment designer's problems.

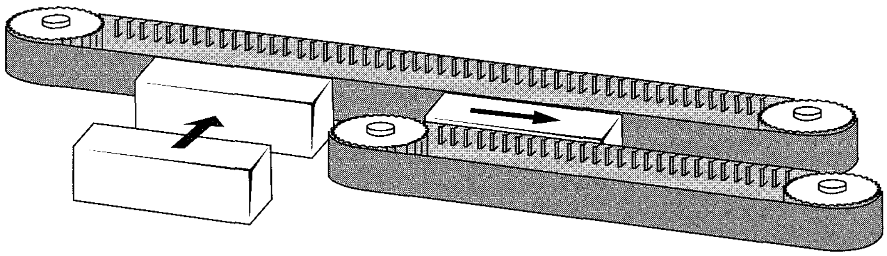

Synchronous belts can be supplied with special backings for unique applications. Product is captured between the backs of two belts and moved in an assembly or conveying process. Similarly, belts with special backings can be used for wire drawing applications or bottling applications.

Information provided: Courtesy of The Gates Rubber Company

Author: Brent Oman, Project Application Engineer
The Gates Rubber Company

Leather Belts–Hp Loss and Speeds

From 0-10,000 ft/min and 435-3450 rpm, for pulley diameters up to 30 in.

Douglas C. Greenwood

Horsepower ratings and correction factors for various leather belt sizes, tensions, and operating conditions are given by most engineering handbooks or manufacturers' catalogs. Such data, however, are usually not corrected for centrifugal force. This chart may be entered at any axis or pulley-speed curve. As shown, secants parallel to the axes connect any four values in correct relationship. In the sample construction, a 12 in. dia pulley at 1150 rpm gives a belt velocity of about 3620 fps at which speed there is a 12% hp reduction. Consult belt manufacturer regarding suitability, efficiency and other factors in high-speed applications.

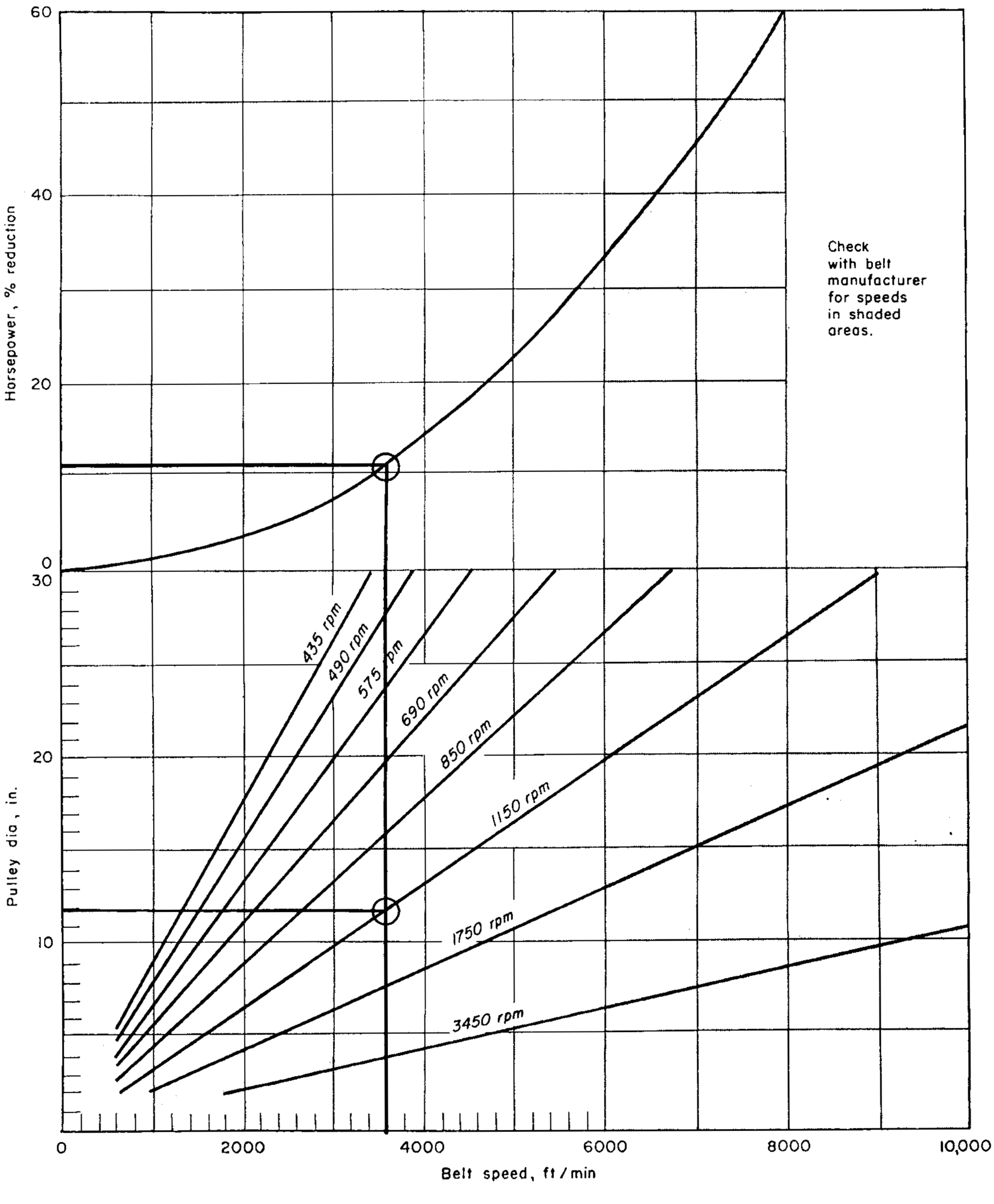

Find the Length of Open and Closed Belts

The following formulas give the answers (see the illustrations for notation):
Open length, $L = \pi D + (\tan\theta - \theta)\ (D - d)$
Closed length, $L = (D + d)\ [\pi + (\tan\theta - \theta)]$
You can find θ from (for open belts): $\cos\theta = (D - d)/2C$; (for closed belts) $\cos\theta = (D + d)/2C$.

When you want to find the **center distance of belt drives,** however, it is much quicker if you have a table that gives you $y = \cos\theta$ in terms of $x = (\tan\theta) - \theta$. **Sidney Kravitz,** of Picatinny Arsenal, has compiled such a table. Now, all you need do to find C is first calculate $x = [L/(D + d)] - \pi$ for open drives.

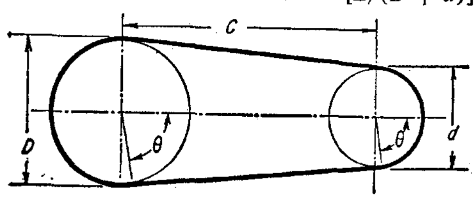

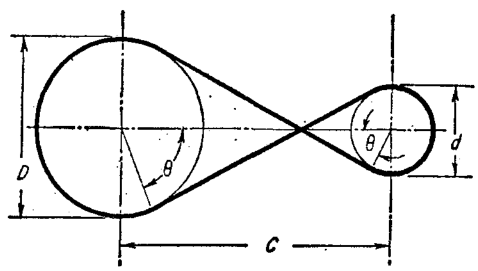

y values[1]

x	0.00	0.01	0.02	0.03	0.04	0.05	0.06	0.07	0.08	0.09
0.0	1.00000	0.95332	0.92731	0.90626	0.88804	0.87175	0.85690	0.84318	0.83039	0.81839
0.1	.80705	.79630	.78606	.77629	.76693	.75795	.74931	.74098	.73295	.72518
0.2	.71767	.71038	.70332	.69646	.68980	.68332	.67701	.67086	.66487	.65902
0.3	.65331	.64774	.64230	.63698	.63177	.62668	.62169	.61681	.61202	.60733
0.4	.60274	.59822	.59380	.58946	.58520	.58101	.57690	.57286	.56889	.56499
0.5	0.56116	0.55738	0.55367	0.55002	0.54643	0.54289	0.53941	0.53598	0.53260	0.52927
0.6	.52600	.52277	.51958	.51645	.51336	.51031	.50730	.50433	.50141	.49852
0.7	.49567	.49286	.49009	.48735	.48465	.48198	.47935	.47675	.47417	.47164
0.8	.46913	.46665	.46420	.46179	.45940	.45703	.45470	.45239	.45011	.44785
0.9	.44562	.44342	.44123	.43908	.43694	.43483	.43274	.43068	.42863	.42661
	.0	.1	.2	.3	.4	.5	.6	.7	.8	.9
1	0.42461	0.40568	0.38850	0.37284	0.35848	0.34526	0.33304	0.32170	0.31115	0.30130
2	.29208	.28344	.27531	.26766	.26043	.25359	.24712	.24098	.23515	.22960
3	.22431	.21926	.21445	.20984	.20544	.20121	.19717	.19328	.18955	.18596
4	.18251	.17918	.17598	.17289	.16991	.16703	.16424	.16156	.15895	.15644
5	0.15400	0.15163	0.14935	0.14712	0.14497	0.14287	0.14084	0.13886	0.13694	0.13508
6	.13326	.13149	.12977	.12810	.12646	.12487	.12332	.12181	.12033	.11889
7	.11748	.11611	.11477	.11346	.11217	.11092	.10970	.10850	.10733	.10618
8	.10506	.10396	.10289	.10183	.10080	.09979	.09880	.09783	.09688	.09594
9	.09503	.09413	.09325	.09238	.09153	.09070	.08988	.08908	.08829	.08751
	0	1	2	3	4	5	6	7	8	9
10	0.08675	0.07980	0.07389	0.06879	0.06436	0.06046	0.05701	0.05393	0.05116	0.04867
20	.04641	.04435	.04246	.04073	.03914	.03766	.03629	.03502	.03384	.03273
30	.03169	.03072	.02980	.02894	.02812	.02735	.02663	.02594	.02528	.02466
40	.02406	.02350	.02296	.02244	.02195	.02148	.02103	.02059	.02018	.01978
50	0.01939	0.01903	0.01867	0.01833	0.01800	0.01768	0.01737	0.01708	0.01679	0.01651
60	.01624	.01598	.01573	.01549	.01525	.01502	.01480	.01459	.01438	.01417
70	.01397	.01378	.01359	.01341	.01323	.01310	.01289	.01273	.01257	.01241
80	.01226	.01211	.01197	.01183	.01169	.01155	.01142	.01129	.01117	.01104
90	.01092	.01080	.01069	.01057	.01046	.01036	.01025	.01015	.01004	.00994
100	0.00985 (see note below for x > 100)									

[1]If $x = (\tan\psi) - \psi$; then $y = \cos\psi$.

If $x > 100$, calculate C from $C = \frac{L}{2} - \frac{\pi}{4}(D + d)$ for both open and closed belts.

$$x = \frac{L}{D + d} \quad \text{for closed drives}$$

Then

$$C = \frac{D - d}{2y} \quad \text{for open drives}$$

$$C = \frac{D + d}{2y} \quad \text{for closed drives}$$

Example: $L = 60.0$, $D = 15.0$, $d = 10.0$, $x = (L - \pi D)/(D - d) = 2.575$, $y = 0.24874$ by linear interpolation in the table. $C = (D - d)/2y = 10.051$.

• • • •

Morton P. Matthew's letter on fractional derivatives (*PE*—July 22 '63, p 105) drew several interesting comments from readers. Here's what Professor Komkov of the University of Utah had to say on the subject. He pointed out that the question raised by Mr Matthew is well known in mathematics, but very little publicized.

"The definition of fractional derivatives goes back to Abel, who developed around 1840 this fascinating little formula:

$$D^s(f) = \frac{d^s f(x)}{dx^s} = \frac{1}{\Gamma(-s)} \int_0^x (\xi - t)^{(-s-1)} f(t)\, dt$$

($\Gamma(n)$ is the Euler's Gamma Function).

An elementary proof of this formula is given for example in Courant's *Differential and Integral Calculus,* Part II, page 340. Abel claimed that the formula works for all real values of S, although there is no guarantee that the range of values obtained can be bounded. For a negative S Abel's operator D^s becomes an integral operator:

$$\iota^s(f(x)) = D^{-s}(f(x)) = \frac{1}{\Gamma(s)} \int_0^x (\xi - t)^{s-1} f(t)\, dt.$$

All results quoted by Mr Matthew may be easily obtained by application of Abel's Formula.

"There exists a generalization to partial differential equations of the fractional derivative. This is the so-called Riesz Operator. In one dimensional case it becomes Abel's derivative of fractional order.

"Details of the Riesz technique are explained, for example, in Chapter 10 of *Partial Differential Equations* by Duff. Unfortunately I know of no textbook which devotes more than a few pages to the subject of fractional derivatives. However, there exists a large number of papers on the subject in mathematical journals. I remember reading one by Professor John Barrett in the Pacific Journal of Mathematics (I think it was 1947) which discussed the equation:

$$\frac{d^s y}{dx^s} + \iota y = 0 \quad \text{where } 1 \leqq s \leqq 2$$

"There are some interesting applications in engineering and science for this theory. I was interested some years ago in formulation of elasticity equations for some plastics. I have never completed that investigation but I have established that in some cases, the behavior of plastics may be better simulated by assuming stress-strain relationship to be of the type:

$$\iota_{ij} = C_{ijkl} \frac{d^s \epsilon^{kl}}{dt^s}$$

where s is some number between 0 and 1, than by the usual assumption of linear superposition of Hooke's law and Newtonian Fluid properties. In case of some rubbers s worked to be close to 0.7."

Ten Types of Belt Drives

Although countless types of belt drives are possible, these ten will solve most industrial applications. These pertain to power transmission only; the tooth type of timing belt is not included. For each drive are given: design pitfalls; speed and capacity ranges; and suggestions for application.

George R. Lederer

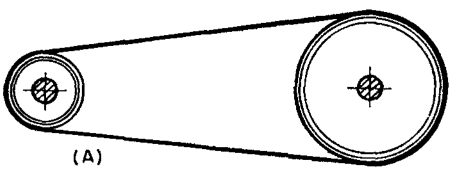

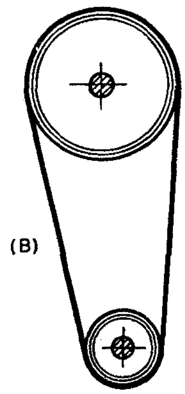

Fig.1 OPEN DRIVE
(V, Flat or Poly V Belts)

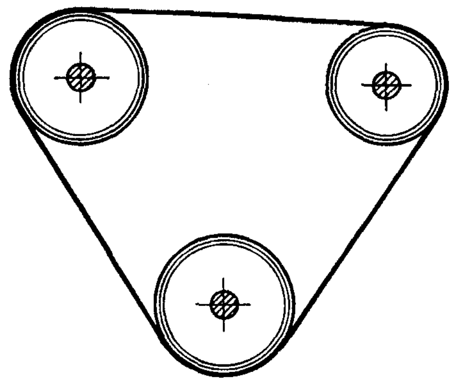

Fig. 2 THREE PULLEY DRIVE
(V, Flat or Poly V Belts)

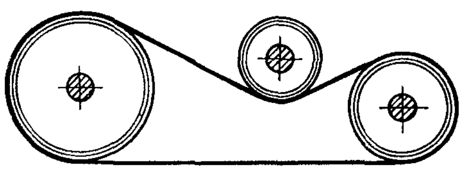

Fig.4 REVERSE BEND IDLER
(Poly V, V, or Flat Belts)

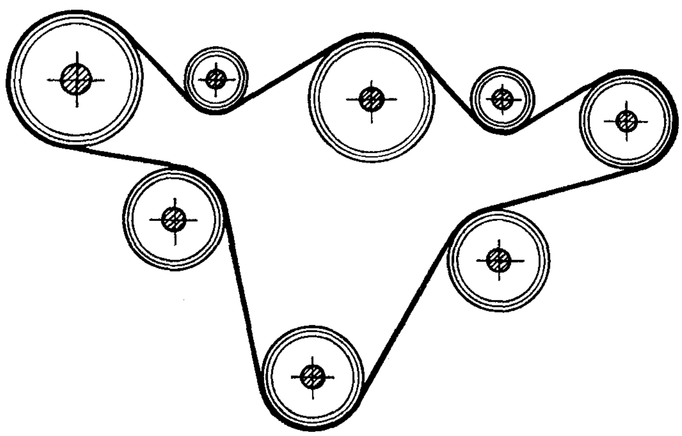

Fig.3 SERPENTINE DRIVE
(Poly V, V, or Flat Belts)

FIG. 1—Can be either horizontal (A), or vertical (B). Used on equipment ranging from washing machines to oil well pumps. Ideal for high capacity drives; allows wider range of speed ratios than any other type. Provisions must be made for take-up. No minimum or maximum center distance limits other than available belt lengths.

FIG. 2—Limited in capacity to 8-10 hp because of small high-speed pulleys and limited provisions for take-up. Usually used with one unit hinge-mounted, as in automotive fan belt drives. Large belts would stretch beyond capacity of hinged unit to take up slack.

FIG. 3—Useful where several units are driven from a central shaft. The Vv belt that resembles two v-belts joined back-to-back was developed especially for this drive. For Vv operation all pulleys must be grooved. For regular V-, Poly-V or flat-belt operation, only those driven by the belt face are grooved, others are flat and are driven by the back of the belt. Driving capacity range from 15-25 hp. Sheaves are small, speed is slow and belt flex is extremely high, which affects belt life.

FIG. 4—Used where driver and driven sheaves are fixed and there is no provision for take-up. Idler is placed on the slack side of the belt near the point where the belt leaves the driver sheave. Idler also gives increased wrap and increased arc of contact. Applications range from agricultural jackshaft drives to machine tools and large oil field drives. Idler can be spring loaded to keep belt tight if drive is subject to shock. For maximum belt life, the larger the idler, the better.

FIG. 5—Driver and driven sheaves are at right angles; belt must travel around horizontal sheave, turn, go over vertical sheave and return. Bend must be gradual to prevent belt from leaving sheave. Minimum center distance for V-belts is 5.5 in. × (pitch dia of largest sheave + width of sheave).

For Poly-V, minimum center distance = 13 × pitch dia of small sheave or 5.5 × (pitch dia + belt width). For flat belts it is 8 ×

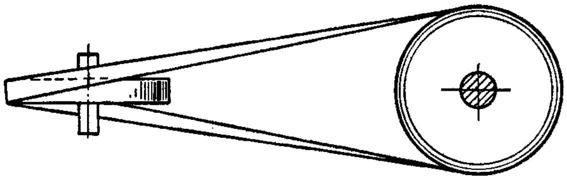

Fig. 5 QUARTER-TURN DRIVE (OPEN)
(Poly V, V, or Flat Belts)

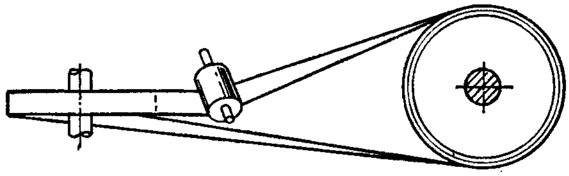

Fig. 6 QUARTER-TURN DRIVE (REVERSE BEND IDLER)
(Poly V, V, or Flat Belts)

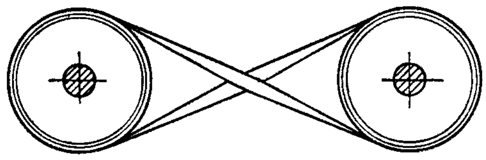

Fig. 7 CROSSED BELT DRIVE
(Flat Only)

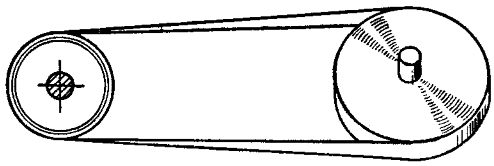

Fig. 8 ANGLE DRIVE (EIGHTH TURN)
(Poly V, V, or Flat Belts)

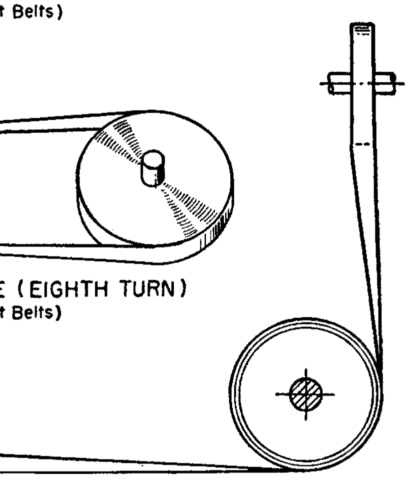

Fig. 9 MULE DRIVE
(Poly V, V, or Flat Belts)

(pitch dia + width). V-belt sheaves must be deep grooved and close matching is essential. Speed usually ranges from 3,000-5,000 rpm; hp from 75-150.

FIG. 6—Similar to Open Quarter-Turn but has higher capacity with shorter centers and increased wrap. Tracking is a problem with flat belts. With Poly-V drive, speed ratio is unlimited. Angle of entry (angle between belt and a line perpendicular to face of the sheave) is limited to 3 deg or less.

FIG. 7—Limited to flat belts because either V-belt or Poly-V would rub against itself and burn or wear rapidly. Desirable only where the direction of rotation must be reversed such as on planers, woodworking tools in general and line shaft drives.

FIG. 8—Used where driver and driven sheave cannot be on the same plane. Has same center distance and angle of belt entry limitations as Quarter-Turn. Drive can be open if take-up can be accomplished at either end or it can be fitted with a reverse bend idler, but not an inside idler. Angle between shaft can be from zero to 90 deg.

FIG. 9—Especially developed for drill presses and special applications where driver and driven sheaves are at right angles to each other and yet on the same plane. Can operate around a corner or from one floor to another. The center sheave is 90 deg from the driver and driven sheave and acts as an idler. Twists affect belt life.

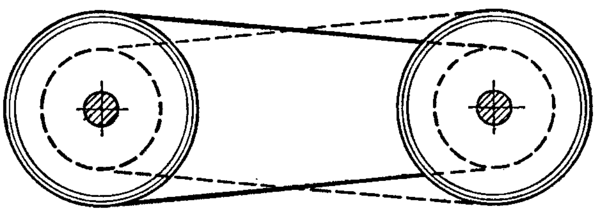

Fig. 10 VARIABLE SPEED DRIVE
(V Belts Only)

FIG. 10—Sheaves must be grooved to change the pitch diameter for variable or adjustable pitch operation. With two sheaves and one belt, it is possible to have a range of four different speeds. Widely used on propulsion drives and cylinder drives on agricultural combines and machine tools. Drive has same high capacity and advantage as standard open drive, with wider speed range. They are mostly single belt drives 1¼ to 2 in. wide. Small pulleys are not advisable. Most applications require special vari-speed cylinder or traction belt.

Mechanisms for Adjusting Tension of Belt Drives

Sketches show devices for both manual and automatic take-up as required by wear or stretch. Some are for installations having fixed center distances; others are of the expanding center take-up types. Many units provide for adjustment of speed as well as tension.

Joseph H. Gepfect

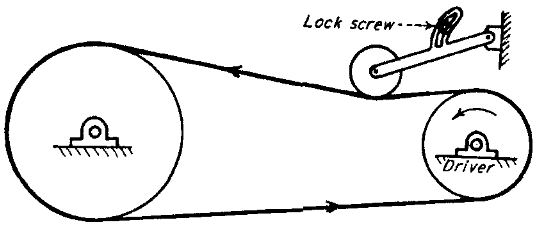

Fig. 1—Manually adjusted idler run on slack side of chain or flat belt. Useful where speed is constant, load is uniform and the tension adjustment is not critical. Can be adjusted while drive is running. Horsepower capacity depends upon belt tension.

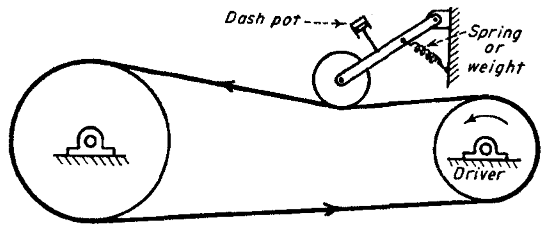

Fig. 2—Spring or weight loaded idler run on slack side of flat belt or chain provides automatic adjustment. For constant speed but either uniform or pulsating loads. Adjustments should be made while drive is running. Capacity limited by spring or weight value.

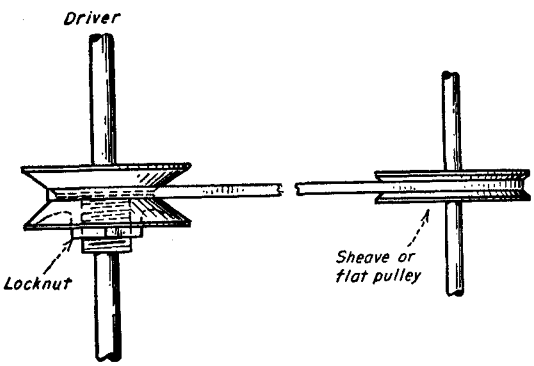

Fig. 5—Screw type split sheave for V-belts when tension adjustment is not critical. Best suited for installations with uniform loads. Running speed increases with take up. Drive must be stopped to make adjustments. Capacity depends directly upon value of belt tension.

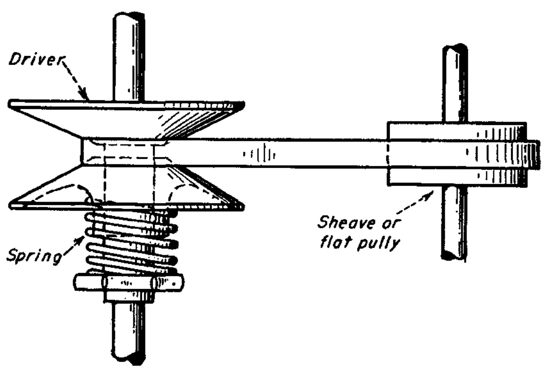

Fig. 6—Split sheave unit for automatic adjustment of V-belts. Tension on belt remains constant; speed increases with belt take up. Spring establishes maximum torque capacity of the drive. Hence, this can be used as a torque limiting or overload device.

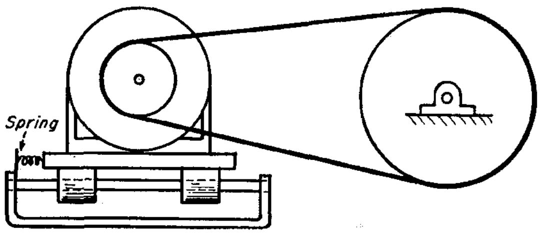

Fig. 9—Spring actuated base for automatic adjustment of uniformly loaded chain drive. With belts, it provides slipping for starting and suddenly applied torque. Can also be used to establish a safety limit for the horsepower capacity of belts.

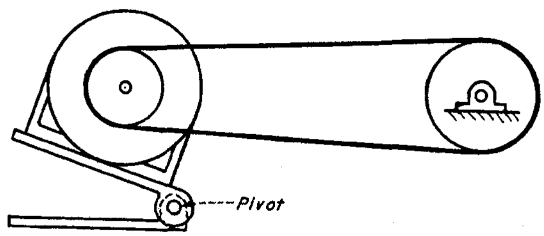

Fig. 10—Gravity actuated pivoting motor base for uniformly loaded belts or chains, only. Same safety and slipping characteristics as that of Fig. 9. Position of motor from pivot controls the proportion of motor weight effective in producing belt tension.

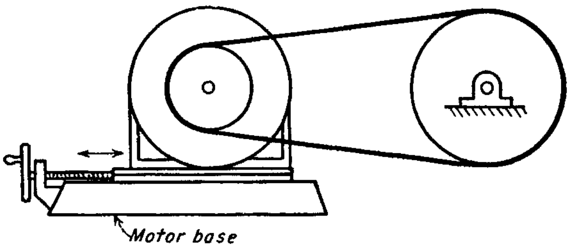

Fig. 3—Screw-base type unit provides normal tension control of belt or chain drive for motors. Wide range of adjustments can be made either while unit is running or stopped. With split sheaves, this device can be used to control speed as well as tension.

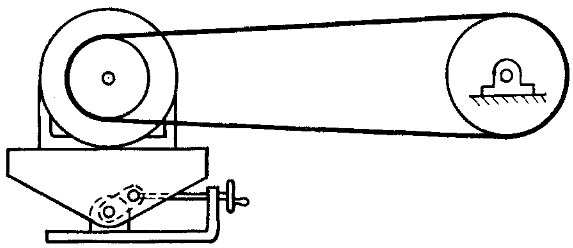

Fig. 4—Pivoting screw base for normal adjustment of motor drive tension. Like that of Fig. 3, this design can be adjusted either while running or stopped and will provide speed adjustment when used with split sheaves. Easier to adjust than previous design.

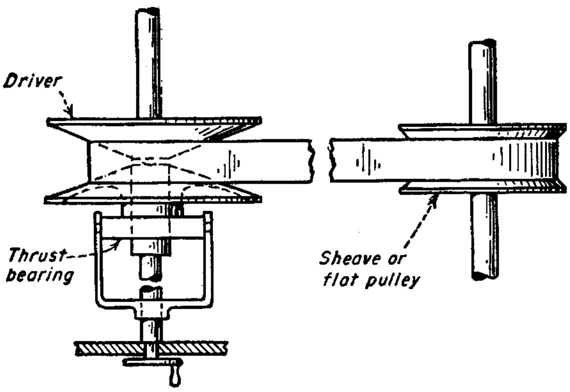

Fig. 7—Another manually adjusted screw type split sheave for V-belts. However, this unit can be adjusted while the drive is running. Other characteristics similar to those of Fig. 6. Like Fig. 6, sheave spacing can be changed to maintain speed or to vary speed.

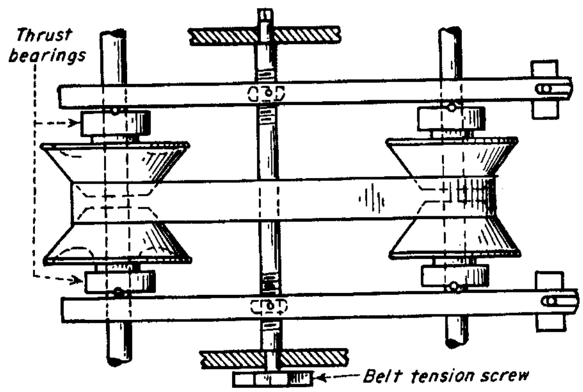

Fig. 8—Special split sheaves for accurate tension and speed control of V-belts or chains. Applicable to parallel shafts on short center distances. Manually adjusted with belt tension screw. No change in speed with changes in tension.

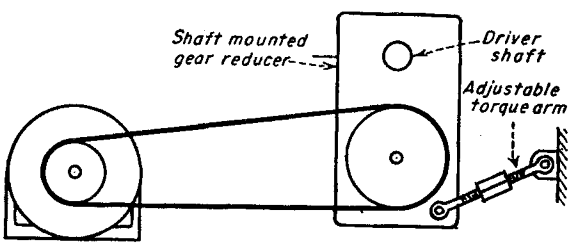

Fig. 11—Torque arm adjustment for use with shaft mounted speed reducer. Can be used as belt or chain take up for normal wear and stretch within the swing radius of reducer; or for changing speed while running when spring type split sheave is used on motor.

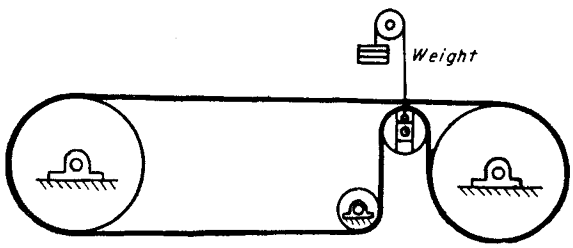

Fig. 12—Wrapping type automatic take-up for flat and wire belts of any width. Used for maximum driving capacity. Size of weight determines tension put on belt. Maximum value should be established to protect the belt from being overloaded.

Equations for Computing Creep in Belt Drives

Don't confuse slippage caused by overloading with creep found in all belt drives. These equations give the creep rate and power loss in various pulley systems

Peter L. Garrett

When a belt is transmitting power there exists a tension T_1 on the tight side that is greater than the tension T_2 on the slack side. This is due to friction between belt and pulley. By the rules of equilibrium, the maximum possible tension ratio, T_1/T_2, that can be transmitted without slip is given by the following equation (refer to figure below):

$$\left(\frac{T_1}{T_2}\right)_{max} = e^{\mu\theta} \qquad (1)$$

where

T_1 = tension at tight side, lb
T_2 = tension at slack side, lb
e = natural logarithm base = 2.718
μ = coefficient of friction
θ = angle of wrap, radians

For velocities substantially below the speed of sound this equation has been confirmed by tests. For those sufficiently curious to note the effect of extremely high speeds, Eq 1 can be modified to include the Mach number, M.

$$\left(\frac{T_1}{T_2}\right)_{max} = e^{\left(\frac{\mu\theta}{1-M^2}\right)} \qquad (1A)$$

Any load greater than $e^{\mu\theta}$ in Eq 1 will cause belt slippage, loss of synchronism and serious wear. Coefficients of friction for belts and ropes are listed in the table of belt and rope properties on page 89.

The relationship between the driving torque, τ, and the belt tension is

$$\tau = (T_1 - T_2)R_B \qquad (2)$$

where R_B = radius of pulley B plus one half the belt thickness.

Therefore, the initial belt tension and ratio T_1/T_2 can be increased to prevent slip without affecting the torque equation (or, more specifically, the difference in tensions, $T_1 - T_2$). The limiting factors in this case are the belt stress and bearing loads.

Yet even when there is no slip the belt inexorably creeps backward over the pulleys, an effect that is particu-

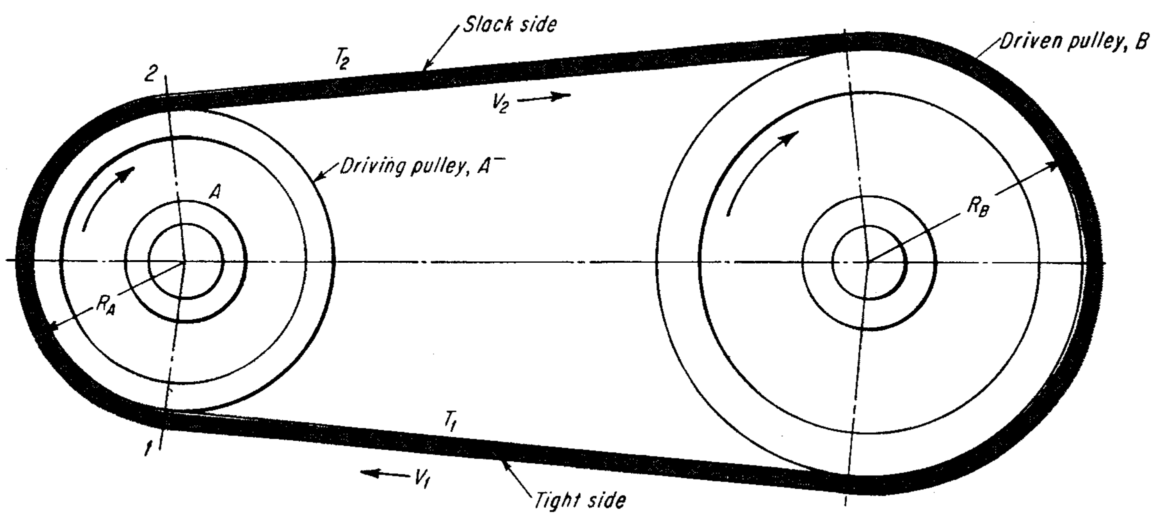

DUAL-PULLEY DRIVE

larly obvious if the drive never reverses. For zero slip, one revolution of pulley A will pull $2\pi R_A$ inches of belt at tension T_1. However, as the belt approaches point 1, the tension drops to a lower value, T_2, and the belt contracts by an amount d equal to

$$d = (T_1 - T_2)\frac{2\pi R_A}{K} \qquad (3)$$

where K = spring constant of belt. Typical K values are included in the table of properties on page 89.

This change in length causes localized slippage between belt and pulley with consequent power dissipation. Thus, pulley A unwinds only $(2\pi R_A - d)$ inches of belt per revolution, and the belt creeps backward an amount equal to d inches each revolution.

The K factors

Factor K in Eq 3 is the spring constant of the belt in units of force per unit strain. Thus

$$K = \frac{\text{lb}}{\text{in./in.}}$$

These units for K simplify calculations with belts of different length. The K factor is constant for all belts of a particular material and cross section. It can be calculated easily for belts of uniform material and measurable section. For example, for a steel band with a ¼ x 0.020-in. cross section

$$K = \frac{F}{FL/AE}$$

where
A = area of belt cross section, in.²
L = segment of belt length, in.
E = modulus of elasticity, psi
F = tensile loading

If L = 1 in., then

$$K = AE$$

or

$$K = (\tfrac{1}{4})(0.020)(30 \times 10^6)$$
$$= 150{,}000 \text{ lb/in./in.}$$

For laminated belts, the calculations are more complex. Belt manufacturers usually can give you the K factor for a belt, but it is a simple matter to obtain the value by test if they do not.

For example, 30 in. of belting elongates ⅛ in. under a 20-lb load. What is the K factor?

$$\text{Strain} = \frac{\text{deflection}}{\text{length}}$$

$$= \frac{1/8}{30} = \frac{1}{240} \text{ in./in.}$$

$$K = \frac{20}{1/240}$$

$$= 4800 \text{ lb/in./in.}$$

Velocity relationships

Returning to Eq 3, this relationship can be put into terms of velocity. During a specific time, Δt, pulley A will have rotated through an angular displacement of θ_A. Hence the velocity of the tight side is

$$V_1 = \frac{R_A\theta_A}{\Delta t} \qquad (4)$$

and of the slack side

$$V_2 = \frac{R_A\theta_A - R_A\theta_A(T_1 - T_2)\left(\frac{1}{K}\right)}{\Delta t} \qquad (5)$$

Hence

$$\frac{V_1}{V_2} = \frac{R_A\theta_A/\Delta t}{R_A\theta_A\left[1 - (T_1 - T_2)\left(\frac{1}{K}\right)\right]\Big/\Delta t}$$

$$\frac{V_1}{V_2} = \frac{1}{1 - \frac{T_1 - T_2}{K}} \qquad (6)$$

Velocity V_1 can be considered as the nominal belt velocity, and V_2 as being equal to V_1 minus the creep rate, or

$$V_2 = V_1 - V_1C$$

$$\frac{V_2}{V_1} = 1 - C \qquad (7)$$

where creep factor, C, is the fractional loss in speed due to elastic effects. Combining Eq 6 and 7 gives

$$1 - \frac{T_1 + T_2}{K} = 1 - C$$

$$C_A = \frac{T_1 - T_2}{K} \qquad (8)$$

Since the torque load is equal to $\tau = (T_1 - T_2)R_B$, then

$$C_A = \frac{\tau}{R_AK} \qquad (9)$$

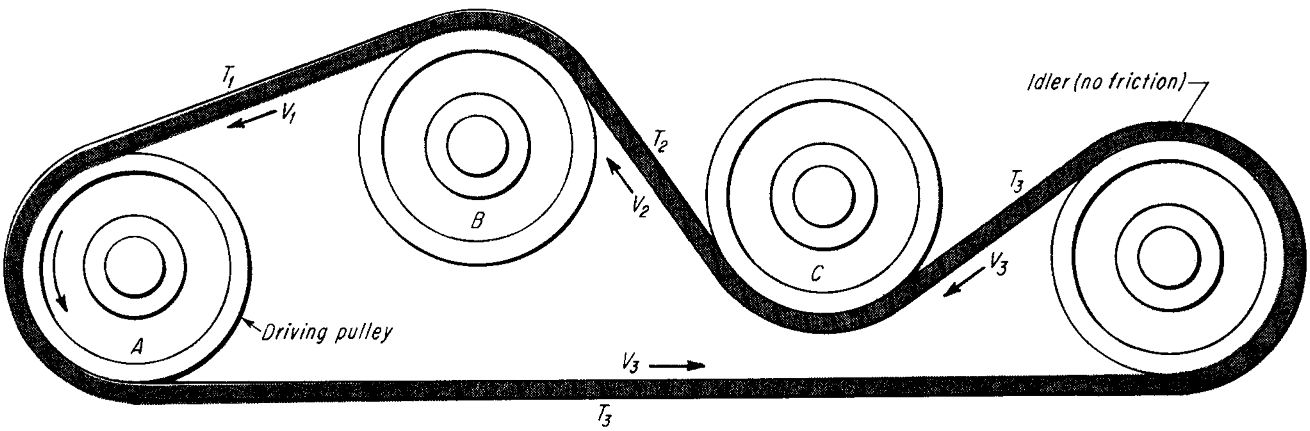

MULTIPLE-PULLEY DRIVE

SYMBOLS

C = CREEP FACTOR, DIMENSIONLESS	t = TIME, SEC
d = CHANGE IN BELT LENGTH, IN.	T = TENSION, LB
K = SPRING CONSTANT OF BELT, LB/(IN./IN.)	V = LINEAR VELOCITY OF BELT, IN./SEC
L = SEGMENT OF BELT LENGTH, IN.	VC = CREEP RATE, IN./SEC
M = MACH NUMBER—THE RATIO OF THE VELOCITY OF A MOVING BODY TO THAT OF SOUND	θ = ANGLE OF WRAP, RADIANS
P = POWER, LB-IN./SEC.	θ' = FINITE ANGULAR DISPLACEMENT, RADIANS
R = PULLEY RADIUS + ½ BELT THICKNESS, IN.	τ = TORQUE OF LOAD, LB-IN.
	μ = FRICTION COEFFICIENT

SUBSCRIPTS A, B, AND C REFER TO PULLEYS A, B, AND C, RESPECTIVELY.

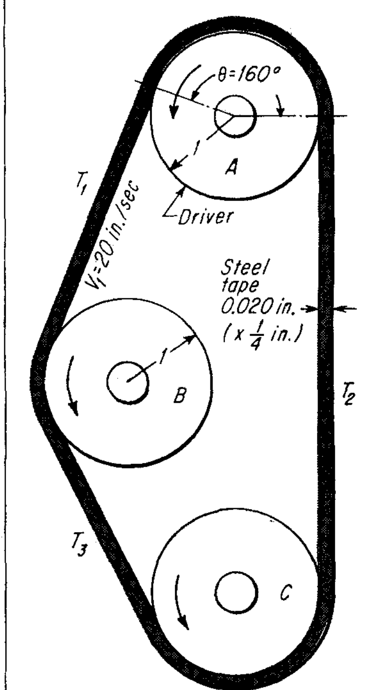

STEEL-TAPE DRIVE

Factor $1/K$ is frequently referred to as the "compliance" of the belt, in units of strain per pound. Thus from Eq 9 it can be noted that *creep is directly proportional to the product of load and compliance.*

Power losses

Ignoring windage and hysteresis losses (the energy converted into heat by the belt during the stretch and relaxation cycles), the power relationships are

Driven pulley

$$P_{in} = T_1V_1 - T_2V_2 \quad (10)$$

$$P_{out} = V_2(T_1 - T_2) \quad (11)$$

The power loss is

$$P_{loss} = P_{in} - P_{out}$$

Thus

$$P_{loss} = T_1(V_1 - V_2) \quad (12)$$

Driving pulley

$$P_{out} = T_1V_1 - T_2V_2 \quad (13)$$

An ideal driving pulley will recover the power T_2V_1 and its power output will be

$$P_{out} = T_1V_1 - T_2V_1 \quad (14)$$

Hence, subtracting Eq 14 from Eq 13, the power loss is equal to

$$P_{loss} = T_2(V_1 - V_2) \quad (15)$$

Because T_1 is greater than T_2, comparing Eq 15 with Eq 12 shows that the *power loss at the driven pulley is slightly greater than the loss at the driver.*

Belt creep—multiple pulleys

Employing the same analytical approach to arrangements with three or more pulleys results in the following equations (refer also to the illustration of the multiple-pulley drive on previous page):

$$\frac{V_1}{V_2} = \frac{1}{1 - C_B} \quad (16)$$

$$\frac{V_2}{V_3} = \frac{1}{1 - C_C} \quad (17)$$

where

$$C_B = \frac{T_1 - T_2}{K} \quad (18)$$

$$C_C = \frac{T_2 - T_3}{K} \quad (19)$$

Hence

$$V_3 = V_2(1 - C_C) \quad (20)$$

$$V_2 = V_1(1 - C_B) \quad (21)$$

Therefore

$$V_3 = V_1(1 - C_B)(1 - C_C) \quad (22)$$

and

$$V_n = V_1(1 - C_1)(1 - C_2)\cdots(1 - C_{n-1}) \quad (23)$$

From this it can be concluded that the creep with respect to the driving pulley speed will increase as we go from pulley to pulley through the driven series of belts. Therefore it is not possible to have a reversible drive with a constant ratio between any two pulleys if there are more than two pulleys in the chain (not counting idlers).

Power loss—multiple pulleys

The power loss is due to friction in the areas, where the belt must slip to transmit the difference in tension. For all drivers and loads, this area of slippage begins at the unreeling line of tangency and ends *short* of the other line of tangency.

Pulley A (driver)

Similar to Eq 12:

$$P_{loss} = T_1(V_1 - V_3)$$

Pulley B (1st driven)

$$P_{in} = T_1V_1 - T_2V_2$$
$$P_{out} = V_2(T_1 - T_2)$$
$$P_{loss} = T_1(V_1 - V_2)$$

Pulley C (2nd driven)

$$P_{in} = T_2V_2 - T_3V_3$$
$$P_{out} = V_3(T_2 - T_3)$$
$$P_{loss} = T_2(V_2 - V_3)$$

To add the power losses of the two driven pulleys, note that $T_1 > T_2 > T_3$, and $V_1 > V_2 > V_3$; hence

$$T_1(V_1 - V_2) + T_2(V_2 - V_3) < T_1(V_1 - V_2) + T_1(V_2 - V_3)$$

or

$$T_1(V_1 - V_2) + T_2(V_2 - V_3) < T_1(V_1 - V_3)$$

Thus, the power losses of all the driven pulleys together is slightly greater than the loss at the driver.

Example—steel-tape drive

To show the use of the design equa-

BELT AND ROPE PROPERTIES					
TYPE	MATERIAL	COEFFICIENT OF FRICTION, μ (ON CAST IRON PULLEYS)	DENSITY LB/IN.[3]	MODULUS OF ELASTICITY, PSI	WORKING STRENGTH (MAXIMUM TENSION), PSI
FLAT BELT	LEATHER	0.25 TO 0.35	0.035	20,000	300 TO 500
	WOVEN COTTON	0.2 TO 0.3	0.035	40,000	300 TO 400
	WOVEN HAIR	0.2 TO 0.3	0.035	30,000	300 TO 400
	BALATA	0.3 TO 0.4	0.04	50,000	400 TO 500
	RUBBER	0.2 TO 0.3	0.045	30,000	400 TO 500
	STEEL	0.15 TO 0.25	0.28	30×10^6	10,000
V-BELT	FABRIC SET IN RUBBER	0.25 TO 0.35	0.04	35,000	400
COTTON ROPES	STRANDED COTTON	0.2 TO 0.3	$0.28D^2$ LB/FT D IN.=DIA	VARIABLE	200
WIRE ROPES	STRANDED STEEL WIRE	0.15 TO 0.25	$1.5D^2$ LB/FT D IN.=DIAMETER	VARIABLE	4000

From G. H. Ryder

tions, assume that the three-pulley drive, at left, employs a 0.020 x ¼-in. steel tape. To avoid overstressing the tape, the drive uses 2-in.-dia pulleys.

Pulley A drives the belt system.

Pulley B is coupled to an indicator with a 0.5-in.-lb load.

Pulley C is coupled to a mechanism with a 5-in.-lb load.

Other design specifications are:

Coefficient of friction for steel tape (see table), $\mu = 0.2$.

Angle θ for pulley A = 160 deg.

Belt speed, $V_1 = 20$ in./sec.

Tension, T_1, by preloading the belt = 10 lb. Thus

$$T_1 = \frac{10}{(0.020)\,(0.25)} = 2000 \text{ psi}$$

This amount is sufficient for proper belt seating, yet within the 10,000-psi limit (from the table) for the steel belt.

Calculations for the tape tensions are as follows:

$$T_2 = T_1 e^{\mu\theta_A}$$

$$T_2 = 10\, e^{(0.2)\,(2.79)} = 17.5 \text{ lb}$$

This value is the maximum permissible tension at the high-tension side of the drive—the belt will slip with higher tensions. (The actual T_2 value will depend on the driven loads and should be less than 17.5 lb.) Thus the tension drop available for work is

$$(T_2 - T_1)_{max} = 17.5 - 10 = 7.5 \text{ lb}$$

Because $R = 1$ in., the maximum torque that can be transmitted is (1) (7.5) = 7.5 in.-lb, which is greater than the 5.5 in. lb total load requirement.

It has been shown that the design is adequate at the driver pulley. The two driven pulleys will now be examined.

Pulley C—major load

To determine the minimum angle of wrap at pulley C, it is convenient and conservative to ignore the tension drop across the ½-in.-lb load. In other words, assume that

$$T_3 = T_1 = 10 \text{ lb}$$

To support this contention, note that for the equation

$$\frac{T_3}{T_1} = e^{\mu\theta_B}$$

when $\theta_B = 0$, $T_3/T_1 = 1$. But at any positive value of θ, $T_3/T_1 > 1$, or $T_3 > T_1$.

Returning to the analysis of pulley C, the maximum possible torque is 5 in.-lb, or 5 lb at the 1-in. radius. Hence the actual T_2 tension will be

$$T_2 = T_3 + 5 \text{ lb} = 10 + 5 = 15 \text{ lb}$$

$$e^{\mu\theta_C} = \frac{T_2}{T_3} = \frac{15}{10} = 1.5$$

$$\mu\theta_C = \ln 1.5 = 0.405$$

$$\theta_C = 0.405/0.2 = 2.02 \text{ rad} = 115 \text{ deg}$$

A wrap angle of less than 115 deg may cause slippage at pulley C.

Pulley B—minor load

In a similar manner

$$e^{\mu\theta_B} = \frac{0.5 + 10}{10}$$

$$\theta_B = 0.25 = 15 \text{ deg}$$

The power loss at the driver is

$$C_A = \frac{\tau}{R_A K}$$

$$= \frac{5.5 \text{ in.-lb}}{(1 \text{ in.} \times 150{,}000 \text{ lb/in./in.})}$$

$$C_A = 3.7 \times 10^{-5}$$

where the value for K was previously computer on page 87.

$$\frac{V_2}{V_1} = \frac{1}{1 - 3.7 \times 10^{-5}}$$

$$\approx 1.000{,}037$$

$$\begin{aligned} P_{loss} &= T_1(V_2 - V_1) \\ &= (15.5)(20)(1.000{,}037 \quad - 1) \\ &= 310(0.37)(10^{-4}) \\ &= 0.011 \text{ in.-lb/sec} \end{aligned}$$

It is safe to assume that the power losses for both driven pulleys are very nearly equal to the loss at the driver. Hence, the total power loss is approximately 0.022 in.-lb/sec.

Input power = 20 in./sec x 5.5 lb = 110 in.-lb/sec; therefore the efficiency of the tape drive is

$$\frac{110 - 0.022}{110} \approx 1 - 0.00022 \text{ or } 99.98\%$$

This example shows why X-Y curve plotters and other instruments often use steel tapes for drives. The low creep rate resulting from the high modulus of steel permits use of a band that is not indexed to any pulley in the drive and can still indicate position repeatably.

Typical Feeders, Take-ups, Drives and Idlers for Belt Conveyors

FEEDERS

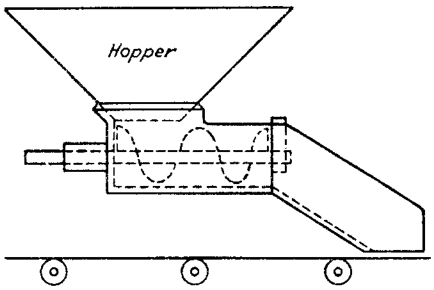

Spiral Feeder

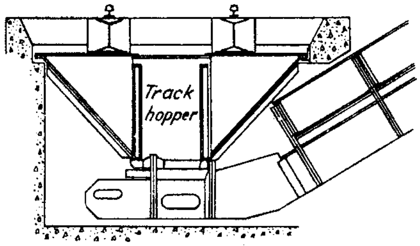

Horizontal and Inclined Apron Feeder

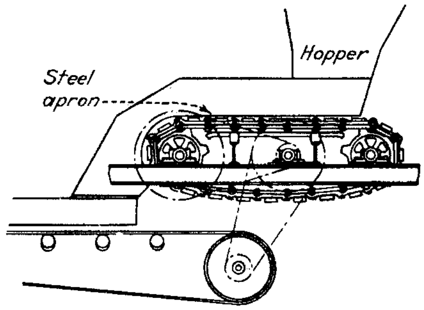

Self-Contained Apron Feeder

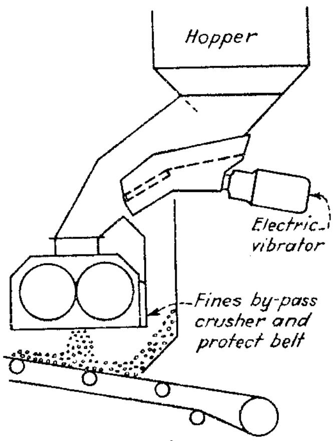

Crusher Feeder

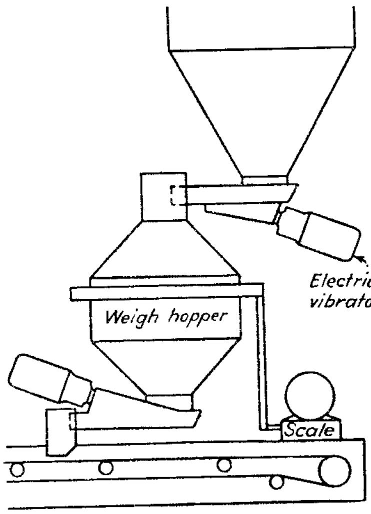

Batch Feeder

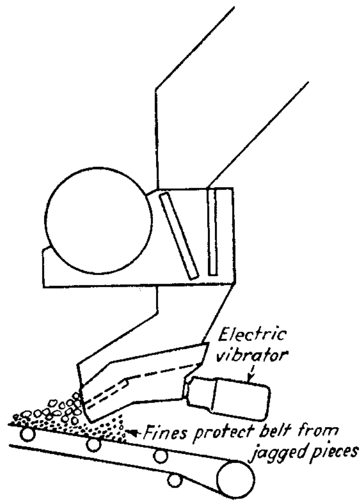

Crusher Products Feeder

TAKE-UPS

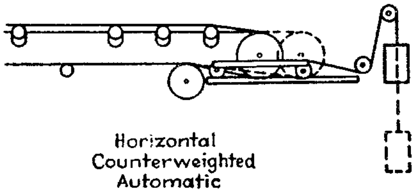

Horizontal Counterweighted Automatic

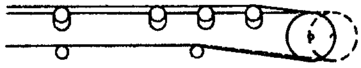

Screw Take-Up

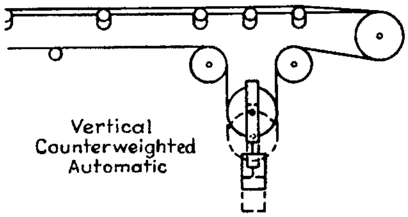

Vertical Counterweighted Automatic

DRIVES

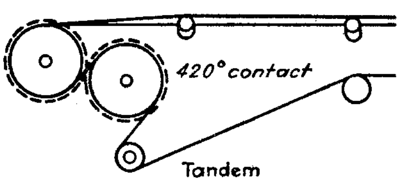

Tandem

Snub

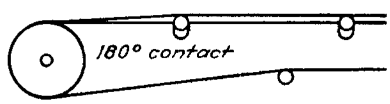

Plain

IDLERS

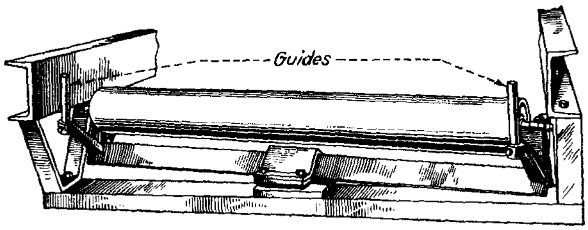

Self-Aligning Return Idler
(Positive Type)

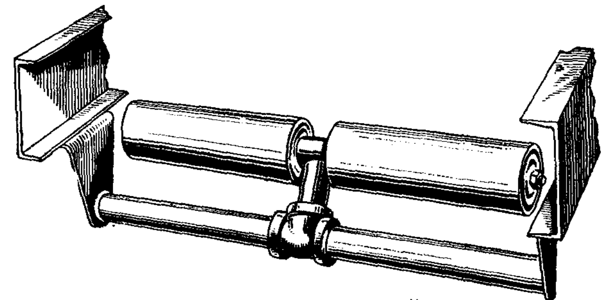

Self-Aligning Return Idler
(Inclined Pivot Type)

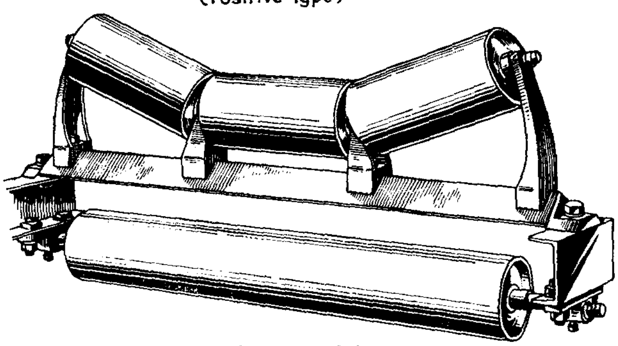

Troughing and Return Idler

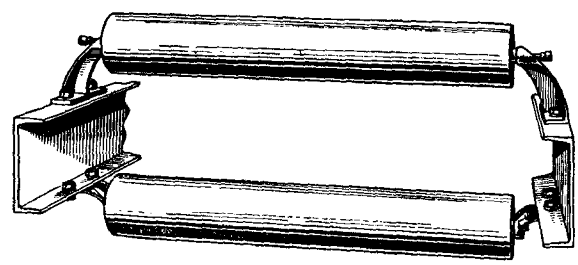

Flat Belt and Return Idler

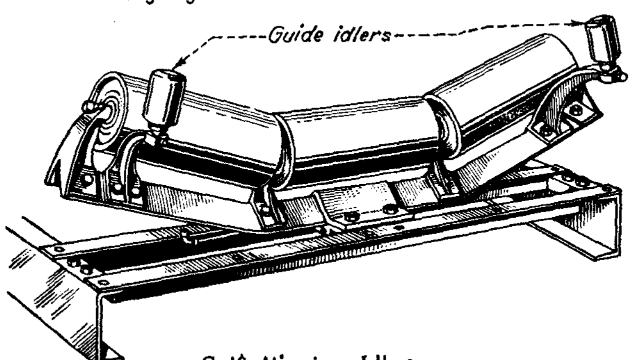

Self-Aligning Idler
(Positive Type)

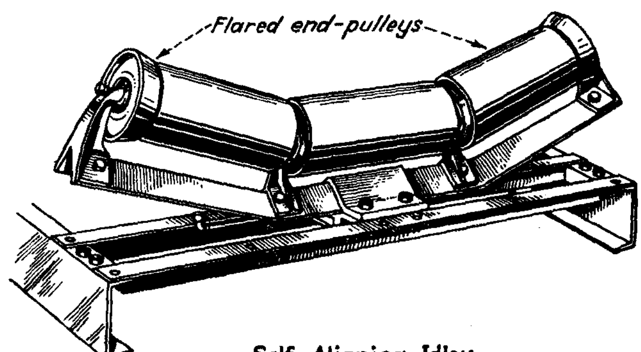

Self-Aligning Idler
(Friction Type)

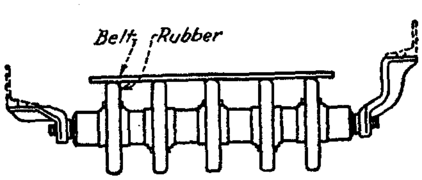

Spool Return Idler

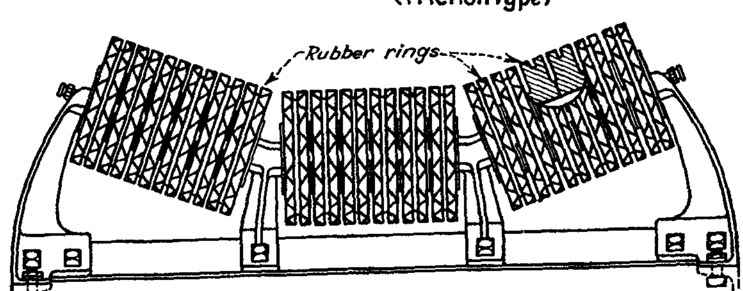

Impact Absorption Idler

SECTION 4

SHAFTS & COUPLINGS

Overview of Shafts & Couplings

Robert O. Parmley (from Mechanical Components Handbook)

SHAFTS

A rotating bar, usually cylindrical in shape, which transmits power is called a shaft. Power is delivered to the shaft through the action of an outside tangential force, resulting in a torsional action set up in the shaft. The resultant torque allows the power to be distributed to other machines or to various components connected to the shaft.

4-1 Usage and Classification

Shafts and shafting may be classified according to their general usage. The following categories are presented here for discussion only and are basic in nature.

Engine Shafts An engine shaft may be described as a shaft directly connected to the power delivery of a motor.

Generator Shafts Generator shafts, along with engine shafts and turbine shafts, are called prime movers. There is a wide range of shaft diameters, depending on power transmission required.

Turbine Shafts Also prime movers, turbine shafts have a tremendous range of diameter size.

Machine Shafts General category of shafts. Variation in sizes of stock diameters ranges from ½ to 2½ in (increments of 1/16 in), 2½ to 4 in (increments of ⅛ in), 4 to 6 in (increments of ¼ in).

Line Shafts Line shafting is a term employed to describe long and continuous "lines of shafting," generally seen in factories, paper or steel mills, and shops where power distribution over an extended distance is required. Stock lengths of line shafting generally are 12 ft, 20 ft, and 24 ft.

Jackshafts Jackshafts are used where a shaft is connected directly to a source of power from which other shafts are driven.

Countershafts Countershafts are placed between a line shaft and a machine. The countershaft receives power from a line shaft and transmits it to the drive shaft.

4-2 Torsional Stress

A shaft is said to be under torsional stress when one end is securely held and a twisting force acts at the opposite end. Figure 4-1 illustrates this action. Note that the only deformation in the shaft is the rotation of the cross sections with respect to each other, as shown by angle ϕ.

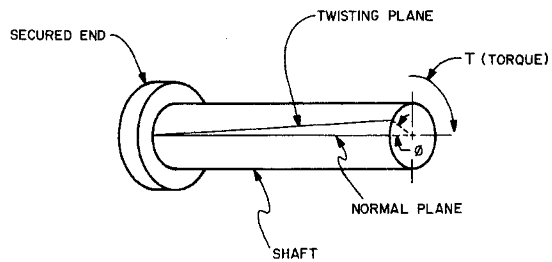

FIG. 4-1 Shaft subjected to torsional stress.

Shafts which are subjected to torsional force only, or those with a minimal bending moment that can be disregarded, may use the following formula to obtain torque in inch-pounds, where horsepower P and rotational speed N in revolutions per minute are known.

$$T = \frac{12 \times 33{,}000\,P}{2\pi N} \tag{4-1}$$

4-3 Twisting Moment

Twisting moment T is equal to the product of the resultant P_r of the twisting forces multiplied by its distance from the axis R. See Fig. 4-2.

$$T = P_r \times R \tag{4-2}$$

4-4 Resisting Moment

Resisting moment T_r equals the sum of the moments of the unit shearing stresses acting along the cross section of the shaft. This moment is the force which "resists" the twisting force exerted to rotate the shaft.

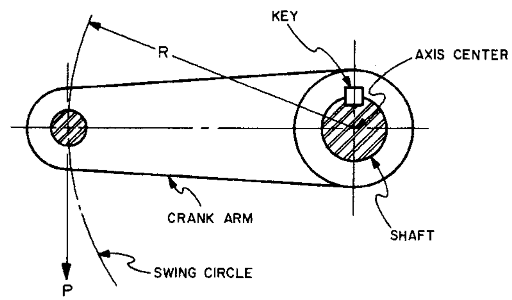

FIG. 4-2 Typical crank arm forces.

4-5 Torsion Formula for Round Shafts

Torsion formulas apply to solid or hollow circular shafts, and only when the applied force is perpendicular to the shaft's axis, if the shearing proportional limit (of the material) is not exceeded.

Conditions of equilibrium, therefore, require the "twisting" moment to be opposed by an equal "resisting" moment. The following formulas may be used to solve the allowable unit shearing stress τ if twisting moment T, diameter of solid shaft D, outside diameter of hollow shaft d, and inside diameter of hollow shaft d_1 are known.

Solid round shafts:

$$\tau = \frac{16T}{\pi D^3} \tag{4-3}$$

Hollow round shafts:

$$\tau = \frac{16Td}{\pi(d^4 - d_1^4)} \tag{4-4}$$

4-6 Shear Stress

In terms of horsepower, for shafts used in the transmission of power, shearing stress may be calculated as follows, where P = horsepower to be transmitted, N = rotational speed in revolutions per minute, and the shaft diameters are those described previously. Maximum unit shearing stress τ is in pounds per square inch.

Solid round shafts:

$$\tau = \frac{321{,}000P}{ND^3} \tag{4-5}$$

Hollow round shafts:

$$\tau = \frac{321{,}000Pd}{N(d^4 - d_1^4)} \tag{4-6}$$

The foregoing formulas do not consider any loads other than torsion. Weight of shaft and pulleys or belt tensions are not included.

4-7 Critical Speeds of Shafts

Shafts in rotation become very unstable at certain speeds, and damaging vibrations are likely to occur. The revolution at which this mechanical phenomenon takes place is called the "critical speed."

Vibration problems may occur at a "fundamental" critical speed. The following formula is used for finding this speed for a shaft on two supports, where W_1, W_2, etc. = weights of rotating components; y_1, y_2, etc. = respective static deflection of the weights; g = gravitational constant, 386 in/s^2.

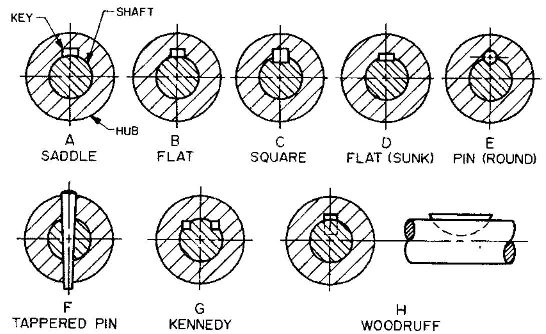

FIG. 4-3 Types of keys.

$$f = \frac{1}{2\pi}\sqrt{\frac{g(W_1y_1 + W_2y_2 + \cdots}{W_1y_1^2 + W_2y_2^2 + \cdots}} \quad \text{cycles/s} \tag{4-7}$$

A thorough discussion of this phenomenon is beyond the scope of this book. Readers should consult the many volumes devoted to vibration theory for an in-depth technical presentation.

4-8 Fasteners for Torque Transmission

Keys Basically keys are wedge-like steel fasteners that are positioned in a gear, sprocket, pulley, or coupling and then secured to a shaft for the transmission of power. The key is the most effective and therefore the most common fastener used for this purpose.

Figure 4-3 illustrates several standard key designs, including round and tapered pins. The saddle key (*a*) is hollowed to fit the shaft, without a keyway cut into the shaft. The flat key (*b*) is positioned on a planed surface of the shaft to give more frictional resistance. Both of these keys can transmit light loads. Square (*c*) and flat-sunk (*d*) keys fit in mating keyways, half in the shaft and half into the hub. This positive holding power provides maximum torque transfer. Round (*e*) and tapered (*f*) pins are also an excellent method of keying hubs to shafts. Kennedy (*g*) and Woodruff (*h*) keys are widely used. Figure 4-4 pictures feather keys, which are used to prevent hubs from rotating on a shaft, but will permit the component part to move along the shaft's axis. Figure 4-4*a* shows a key which is relatively long for axial movement and is secured in position on the shaft with two flat fillister-head matching screws. Figure 4-4*b* is held to the hub and moves freely with the hub along the shaft's keyseat.

A more in-depth presentation of keys will be found in Sec. 12, "Locking Components."

Set Screws Set screws may be used for light applications. A headless screw with a hexagon socket head and a conical tip should be used. Figure 4-5 illustrates both a "good" design and a "bad" design. The set screw must be threaded into the hub and tightened on the shaft to provide a positive anchor.

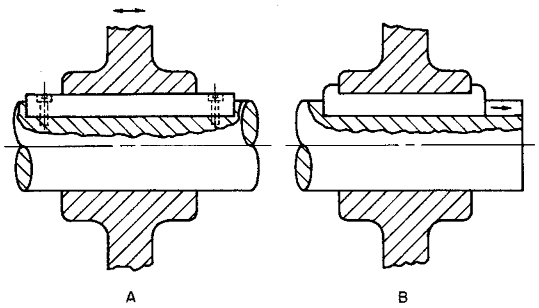

FIG. 4-4 Feather keys.

Pins Round and taper pins were briefly discussed previously, but mention should be made of the groove, spring, spiral, and shear pins. The groove pin has one or more longitudinal grooves, known as flutes, over a portion of its length. The farther you insert this pin, the tighter it becomes. The spring or slotted tubular pin is a hollow tube with a full-length slot and tapered ends. This slot allows the pin's diameter to be reduced somewhat when the pin is inserted, thus providing easy adaptation to irregular holes. Spirally coiled pins are very similar in application to spring pins. They are fabricated from a sheet of metal wrapped twice around itself, forming a spiral effect. Shear pins, of course, are used as a weak link. They are designed to fail when a predetermined force is encountered.

4-9 Splines

Spline shafts are often used instead of keys to transmit power from hub to shaft or from shaft to hub. Splines may be either square or involute.

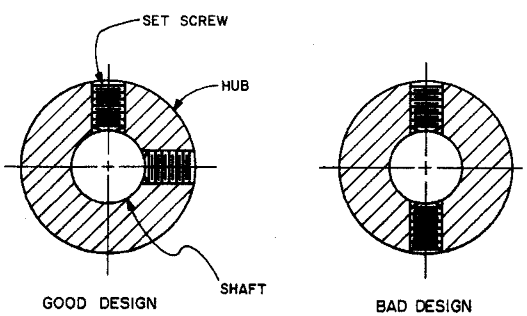

FIG. 4-5 Use of set screws.

One may think of splines as a series of teeth, cut longitudinally into the external circumference of a shaft, that match or mate with a similar series of keyways cut into the hub of a mounted component. Splines are extremely effective when a "sliding" connection is necessary, such as for a PTO (power take-off) on agricultural equipment.

Square or parallel-side splines are employed as multispline shaft fittings in series of 4, 6, 10, or 16.

Splines are especially successful when heavy torque loads and/or reversing loads are transmitted. Torque capacity (in inch-pounds) of spline fittings may be calculated by the following formula:

$$T = 1000NrhL \qquad \text{in}\cdot\text{lb} \tag{4-8}$$

where N = number of splines
r = mean radial distance from center of shaft/hub to center of spline
h = depth of spline
L = length of spline bearing surface

This gives torque based on spline side pressure of 1000 lb/in^2. Involute splines are similar in design to gear teeth, but modified from the standard profile. This involute contour provides greater strength and is easier to fabricate. Figure 4-6 shows five typical involute spline shapes.

SHAFT COUPLINGS

In machine design, it often becomes necessary to fasten or join the ends of two shafts axially so that they will act as a single unit to transmit power. When this parameter is required, shaft couplings are called into use. Shaft couplings

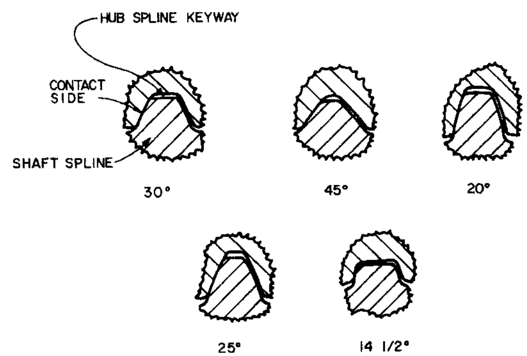

FIG. 4-6 Involute spline shapes.

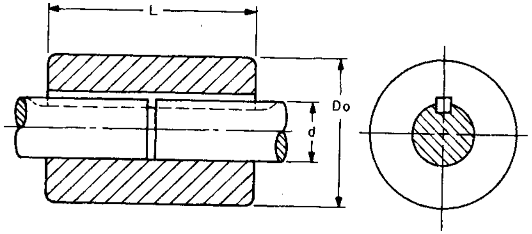

FIG. 4-7 Sleeve coupling.

are grouped into two general classifications: rigid (or solid) and flexible. A rigid coupling will not provide for shaft misalignment or reduce vibration or shock from one shaft to the other. However, flexible shaft couplings provide connection of misaligned shafts and can reduce shock and/or vibration to a degree.

4-10 Sleeve Coupling

Sleeve coupling, as illustrated in Fig. 4-7, consists of a simple hollow cylinder which is slipped over the ends of two shafts fastened into place with a key positioned into mating keyways. This is the simplest rigid coupling in use today. Note that there are no projecting parts, so that it is very safe. Additionally, this coupling is inexpensive to fabricate.

Figure 4-8 pictures two styles of sleeve couplings using standard set screws to anchor the coupling to each shaft end. One design is used for shafts of equal diameters. The other design connects two shafts of unequal diameters.

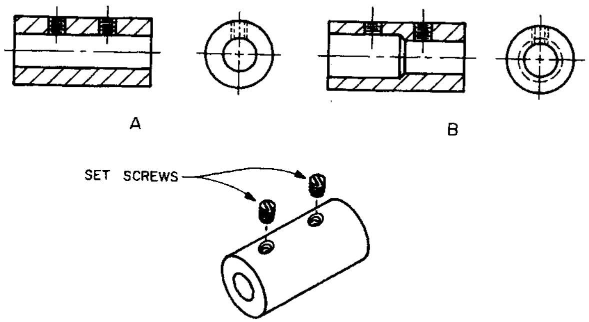

FIG. 4-8 Sleeve shaft coupling.

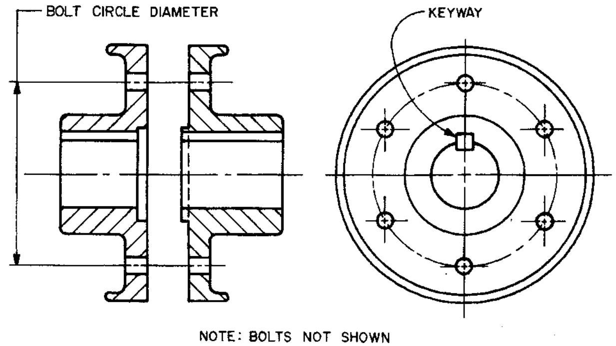

FIG. 4-9 Solid coupling.

4-11 Solid Coupling

The solid coupling shown in Fig. 4-9 is a tough, inexpensive, and positive shaft connector. When heavy torque transmission is required, a rigid coupling of this design is an excellent selection.

4-12 Clamp or Compression Coupling

The rigid coupling shown in Fig. 4-10 has evolved from the basic sleeve coupling. This clamp or compression coupling simply splits into halves, which have recesses for through bolts that secure or clamp the mating parts together, producing a compression effect on the two connecting shafts. This coupling may be used for transmission of large torques because of its positive grip from frictional contact.

4-13 Flange Coupling

Flange couplings are rigid shaft connectors, also known as solid couplings. Figure 4-11 illustrates a typical design. This rigid coupling consists of two components, which are connected to the two shafts with keys. The hub halves

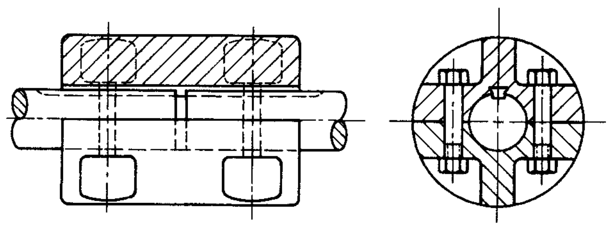

FIG. 4-10 Clamp or compression coupling.

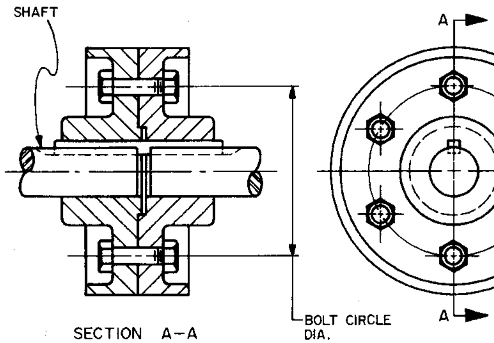

FIG. 4-11 Flange coupling.

are fastened together with a series of bolts arranged in an even pattern concentrically about the center of the shaft. A flange on the outside circumference of the hub provides a safety guard for the bolt heads and nuts, while adding strength to the total assembly.

4-14 Flexible Coupling

Flexible couplings connect two shafts which have some nonalignment between them. The couplings also absorb some shock and vibration which may be transmitted from one shaft to the other.

There are a wide variety of flexible-coupling designs. Figure 4-12 pictures a two-part cast-iron coupling which is fastened onto the shafts by keys and set

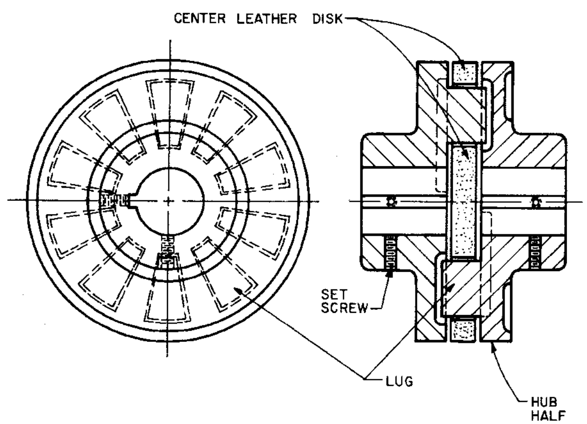

FIG. 4-12 Flexible coupling.

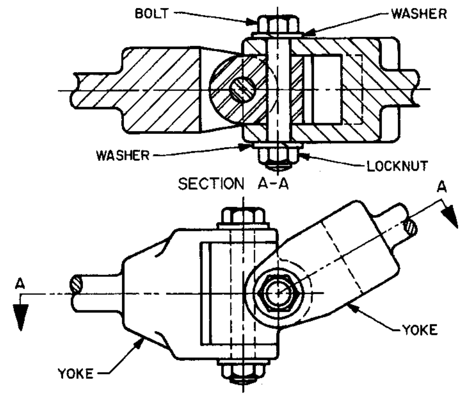

FIG. 4-13 Universal coupling.

screws. The halves have lugs, which are cast an an integral part of each hub half. The lugs fit into entry pockets in a disk made of leather plies which are stitched and cemented together. The center leather laminated disk provides flexibility in all directions. Rotation speed, either slow or fast, will not affect the efficiency of the coupling.

4-15 Universal Coupling

If two shafts are not lined up but have intersecting centerlines or axes, a positive connection can be made with a universal coupling. Figure 4-13 details a typical universal coupling.

Note that the bolts are at right angles to each other. This makes possible the peculiar action of the universal coupling. Either yoke can be rotated about the axis of each bolt so that adjustment to the angle between connected shafts can be made. A good rule of thumb is not to exceed 15° of adjustment per coupling.

4-16 Multijawed Coupling

This rigid-type shaft coupling is a special design. The coupling consists of two halves, each of which has a series of mating teeth which lock together, forming a positive jawlike connection. Set screws secure the hubs onto the respective shafts. This style of coupling is strong and yet easily dismantled. See Fig. 4-14.

4-17 Spider-Type Coupling

The spider-type or Oldham coupling is a form of flexible coupling that was designed for connection of two shafts which are parallel but not in line. The two end hubs, which are connected to the two respective shafts, have grooved

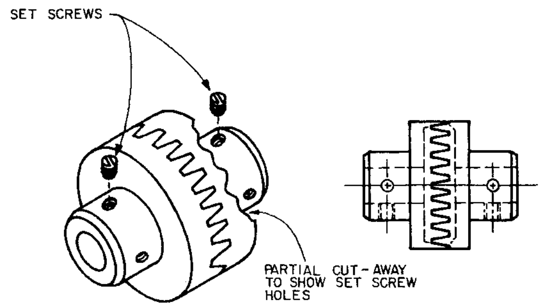

FIG. 4-14 Multijawed coupling.

faces which mate with the two tongues of the center disk. This configuration and slot adjustment allow for misalignment of shafts. Figure 4-15 shows an assembled spider-type coupling.

4-18 Bellows Coupling

Two styles of bellows couplings are illustrated in Fig. 4-16. These couplings are used in applications involving large amounts of shaft misalignment, usually combined with low radial loads. Maximum permissible angular misalignment varies between 5° and 10°, depending on manufacturer's recommendation. Follow manufacturer's guidelines for maximum allowable torque. Generally, these couplings are used in small, light-duty equipment.

4-19 Helical Coupling

These couplings, also, are employed to minimize the forces acting on shafts and bearings as a result of angular and/or parallel misalignment.

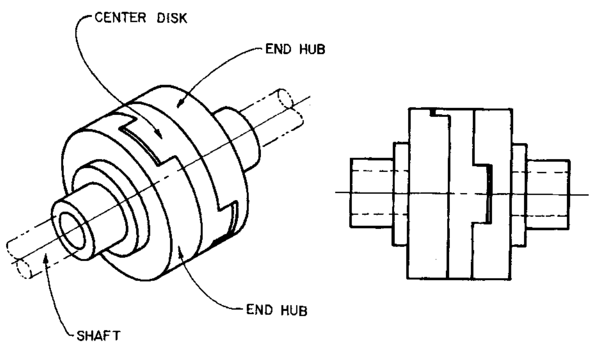

FIG. 4-15 Spider-type coupling.

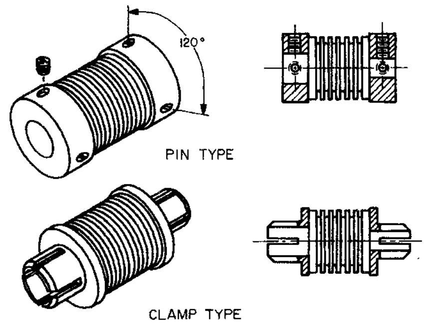

FIG. 4-16 Bellows couplings.

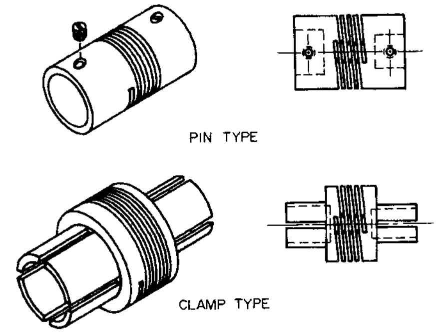

FIG. 4-17 Helical couplings.

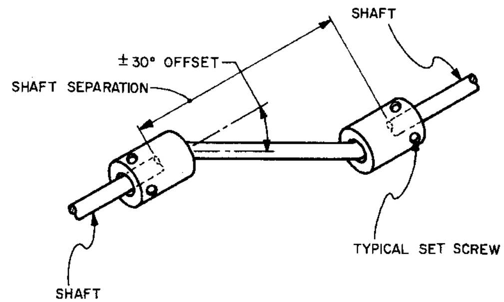

FIG. 4-18 Offset extension shaft coupling.

These couplings are used when motion must be transmitted from shaft to shaft with constant velocity and zero backlash.

The helical coupling achieves these parameters by virtue of its patented design, which consists of a one-piece construction with a machined helical groove circling its exterior diameter. Removal of this coil or helical strip results in a flexible unit with considerable torsional strength. See Fig. 4-17, which pictures both the pin- and clamp-type designs.

4-20 Offset Extension Coupling

Figure 4-18 depicts an offset extension shaft coupling. This coupling is used to connect or join parallel drive shafts that are offset ±30° in any direction, with separations generally greater than 3 in. Shafts are secured to the coupling with set screws.

REFERENCES

Master Catalog 82, Sterling Instrument Division of Designatronics, Inc., New Hyde Park, N.Y.
Levinson, Irving J.: *Machine Design*, Reston Publishing Co., Reston, Va., 1978.
Parmley, R. O.: *Standard Handbook of Fastening and Joining*, McGraw-Hill, New York, 1977.
Spotts, M. F.: *Design of Machine Elements*, 5th ed., Prentice-Hall, Englewood Cliffs, N.J., 1978.
Winston, Stanton E.: *Machine Design*, American Technical Society, Chicago, 1956.
Carmichael, Colin, ed.: *Kent's Mechanical Engineer's Handbook*, 12th ed., Wiley, New York, 1958.

Beams & Stepped Shafts

Equations simplify analysis. Two general equations can now handle any type of loading and number of stepped contours. The method is exact and avoids integration.

William Griffel

IN practice, it is quite common for beams or shafts to be subjected to a combination of concentrated loads, distributed loads, and moments. Also, the beams may have cross-sections that vary by distinct steps.

To find the deflection and slope at any point on a beam with, say, only three loads, as shown in Fig 1, pages of calculations are needed, and you will certainly turn for help from a computer, if one is available. Thus, the value of the simplified method given here becomes apparent. It can handle any number and combination of loads, and any number of steps in the contour. The method is similar to the one developed by W. H. Macaulay of Great Britain (see "Note on the Deflection of Beams," *Messenger Math,* Vol 48, Cambridge, England), but its application to stepped beams is new.

The method makes use of two design equations, one for deflection and the other for slope. There is no integration—simple algebraic calculations are all that's needed. There is no approximation involved: The method is exact. But it has its limitations in that it is applicable only to cases where the reactions are known—statically indeterminate beams are beyond the scope of the methods. Most beams and cantilever problems, however, *are* statically determinate.

The derivation of these two general equations (Eq 7 and 8) which follows gives a clearer picture of the concepts underlining the method. But if you wish, you may skip directly to the sample problems starting on p 84 to see how easily the equations can produce beam formulas (starting with simple loadings), and to the stepped-shaft problem, p 86.

Symbols

a, b, c = distance along a beam locating points of application of moment M, concentrated load P, and the point where the uniform load w begins

C, D = constants of integration

E = modulus of elasticity, psi

I = moment of inertia, in.[4]

x = point on the beam where the deflection is calculated, in.

x_1, x_2, etc = specific values of x for segments of the beam, in.

y_1, y_2, etc = deflections at points x_1, x_2, etc., in.

y_0 = deflection at the origin of the coordinate system, in.

w = uniform distributed load, lb/in.

θ = slope of the beam at point of interest, r, radians

θ_0 = slope at the origin of the coordinate system, radians

Upward deflections and clockwise moments to the left of a section are considered positive. See illustration on facing page.

DESIGN EQUATIONS FOR UNIFORM BEAMS

Although integration is employed in deriving the method, it is not required in the actual solution of problems.

The usual method of determining the curved line of a beam under load is to start with the functional equation:

$$EI \frac{d^2y}{dx^2} = M \tag{1}$$

and integrate it twice, whereby the equation is obtained of the deflection curve $y = f(x)$. (Most of the current methods, such as the *moment-area method* and the *conjugate-beam method,* are based on carrying out in some way this double integration.) The constants of integration, C and D, are easily determined from the boundary conditions. As a rule:

$$C = EI\theta_0$$
$$D = EIy_0$$

where y_0 and θ_0 are the deflection and angle of rotation at the origin of coordinate system (see list of symbols).

For example, for a cantilever beam with a uniformly distributed load w, if the origin of the coordinates is placed at the free end, then Eq 1 can be written as:

$$EI\frac{d^2y}{dx^2} = -w\frac{x^2}{2} \quad (2)$$

Integrating twice

$$EI\frac{dy}{dx} = -w\frac{x^3}{6} + C \quad (3)$$

$$EIy = -w\frac{x^4}{24} + Cx + D \quad (4)$$

For $x = 0$, Eq 3 and 4 become

$$EIy_0 = D \quad (5)$$
$$EI\theta_0 = C \quad (6)$$

where upward deflection and clockwise movement to the left of a section are considered positive.

Note that the relationships in Eq 5 and 6 are valid on the condition that the same origin be used for the x coordinate no matter what portion of the beam is considered.

For the cantilever beam with all three types of loading, Fig 1, we denote the four segments of the beam as *A-B, A-C, A-D, A-E,* as defined by their coordinates, x_1, x_2, x_3, x_4. Each of these segments has its own differential equation describing the elastic line, and each equation if solved separately, introduces two constants of integration. Thus, *eight constants of integration* must be determined from appropriate boundary conditions. This requires an involved procedure, but the number of integration constants can be reduced to two, *regardless of the number of segments,* by following these steps:

1. Obtain the equation for the bending moment at a desired section by considering the external forces lying between that section and the origin.
2. Integrate the moment equation without opening the brackets.
3. Introduce a beam factor $(x - a)^0$, for convenience. Because this factor is raised to the zero power and hence must be equal to unity, it will not affect the equations, as will be seen.

For segment A-B (where coordinates of a point are x_1,y_1):

$$EI\frac{d^2y_1}{dx_1^2} = 0$$

Double integration gives

$$EI\frac{dy_1}{dx_1} = C_1$$

$$EIy_1 = C_1x_1 + D_1$$

For segment A-C (coordinates x_2, y_2)

$$EI\frac{d^2y_2}{dx_2^2} = M$$

Multiplying by the beam factor

$$EI\frac{d^2y_2}{dx_2^2} = M(x_2 - a)^0$$

Integrating twice gives

$$EI\frac{dy_2}{dx_2} = M(x_2 - a) + C_2$$

$$EIy_2 = M\frac{(x_2 - a)^2}{2} + C_2x_2 + D_2$$

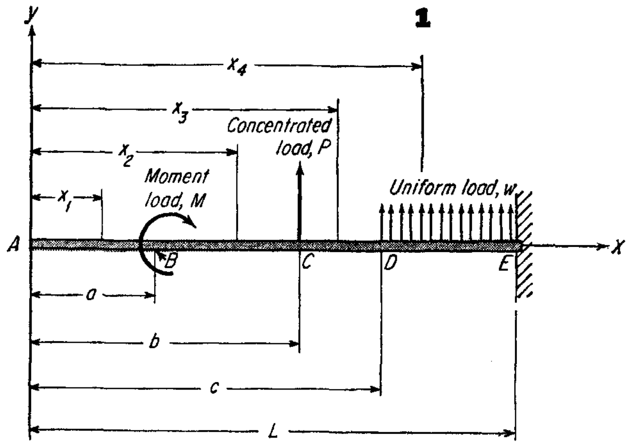

Note—Moments and loads are positive in the directions indicated

For segment A-D; (x_3, y_3)

$$EI\frac{d^2y_3}{dx_3^2} = M(x_3 - a)^0 + P(x_3 - b)$$

$$EI\frac{dy_3}{dx_3} = M(x_3 - a) + P\frac{(x_3 - b)^2}{2} + C_3$$

$$EIy_3 = M\frac{(x_3 - a)^2}{2} + P\frac{(x_3 - b)^3}{6} + C_3x_3 + D_3$$

For segment A-E; (x_4, y_4)

$$EI\frac{d^2y_4}{dx_4^2} = M(x_4 - a)^0 + P(x_4 - b) + w\frac{(x_4 - c)^2}{2}$$

$$EI\frac{dy_4}{dx_4} = M\frac{(x_4 - a)}{1} + P\frac{(x_4 - b)^2}{2} + w\frac{(x_4 - c)^3}{6} + C_4$$

$$EIy_4 = M\frac{(x_4 - a)^2}{2} + P\frac{(x_4 - b)^3}{6} + w\frac{(x_4 - c)^4}{24} + C_4x_4 + D_4$$

The eight constants of integration are now determined from the boundary conditions of the segments. For example, when $x_1 = x_2$, then both are equal to a, and the deflections y_1 and y_2 will be equal to each other. Following this type of reasoning we get

When	$x_1 = x_2 = a$	then	$y_1 = y_2$	and $\theta_1 = \theta_2$
	$x_2 = x_3 = b$		$y_2 = y_3$	$\theta_2 = \theta_3$
	$x_3 = x_4 = c$		$y_3 = y_4$	$\theta_3 = \theta_4$
	$x_4 = L$		$y_4 = 0$	$\theta_4 = 0$

These values for y and θ are substituted into the previous equations for each sector to yield:

$$C_1 = C_2 = C_3 = C_4 = C$$
$$D_1 = D_2 = D_3 = D_4 = D$$

Thus, the substitution of $(x - a)^0$ caused all constants to be equal to each other, except two, C and D. These two can be determined from the fourth condition which was already calculated (Eq 5 and 6):

$$C = EI\theta_0, \qquad D = EIy_0$$

Now, considering a case where there may be a multiplicity of forces and moments, we turn to segment *A-E*, and from its equation obtain a general formula good for any arrangement of forces *M, P, w*:

Design equation for deflection

$$EIy = EIy_0 + EI\theta_0 x + \sum \frac{M(x-a)^2}{2} + \sum \frac{P(x-b)^3}{6} + \sum \frac{w(x-c)^4}{24} \quad (7)$$

Design equation for slope (by differentiating Eq 7)

$$EI\theta = EI\theta_0 + \sum M(x-a) + \sum \frac{P(x-b)^2}{2} + \sum \frac{w(x-c)^3}{6} \quad (8)$$

Because the reactions of the supports are included in the external forces and moments, Eq 7 and 8 are applicable to beams with any type of support.

The term that contains the distributed load w is valid only if the distributed load continues at least to the section where y and θ are to be determined. If the load breaks off before the section of interest, it should be continued to the section and an equivalent load of opposite direction should be added (example 6 illustrates this).

Thus, one equation is all that is needed to calculate the deflection of a beam with any supports, any type of loading and number of applied loads.

Example 1—Fixed-end with concentrated load

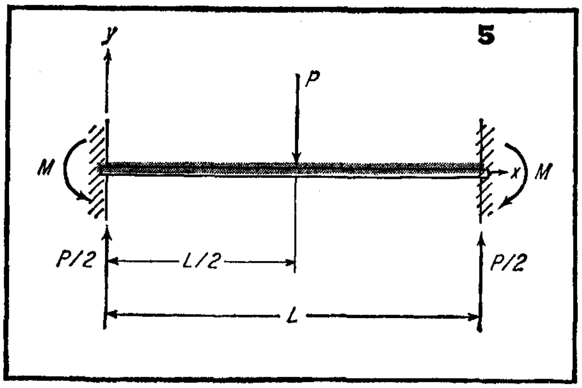

Determine the maximum deflection for a beam with both ends fixed subjected to a center load.

Solution

You can place the origin of the coordinates at either the left or right end of the beam. In both cases, $x_0 = 0$ and $y_0 = 0$. Thus, in the equation for deflection, Eq 7, the first two terms drop out. Also, because of symmetry, it is best to calculate y_{max} at $x = ½$. Include in Eq 7 all forces and moments lying between the origin and the section under consideration (which is at $x = L/2$). This means that the reactive force $R = P/2$ and reactive moment $M = ½ \times L/2 \times P/2 = PL/8$ at the built-in end should be used too. Because the direction of the reactive moment is counter-clockwise, it will enter in the general equation with a minus sign. Also $a = b = c = 0$.

Thus y_{max}, for $x = L/2$, is

$$EIy_{x=L/2} = -\frac{PL}{8}\,\frac{(L/2-0)^2}{2} + \frac{P}{2}\,\frac{(L/2-0)^3}{6}$$

$$= -\frac{PL^3}{192} \quad \text{or} \quad y_{max} = -\frac{PL^3}{192EI}$$

From the sign convention, the minus sign designates a downward deflection.

Example 2—Fixed-end with distributed load

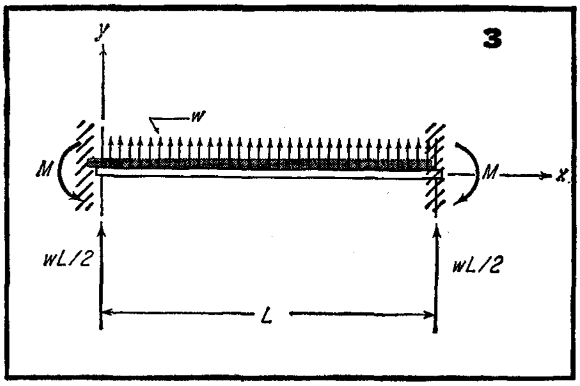

Here, too, the location of the origin is arbitrary. Maximum deflection y_{max} is at $x = L\ 2$ and $a = b = c = 0$. Thus from Eq 7:

$$EIy_{x=L/2} = -\frac{wL^2}{12}\,\frac{(L/2-0)^2}{2} + \frac{wL}{2}\,\frac{(L/2-0)^3}{6} - \frac{w(L/2-0)^4}{24}$$

$$= -\frac{wL^4}{384} \quad \text{or} \quad y_{max} = -\frac{wL^4}{384EI}$$

Note that the downward load w was entered with a minus sign.

Example 3—Cantilever with distributed load

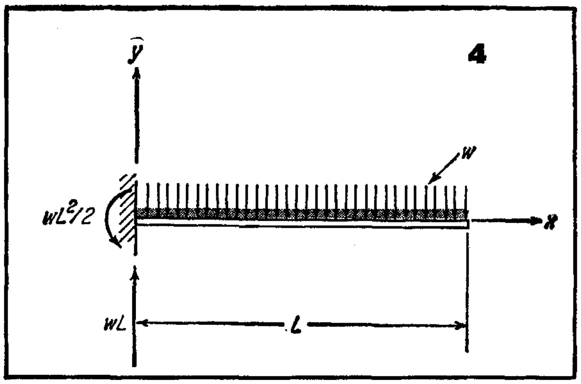

In this case find the maximum deflection and slope (Fig 4).

Solution

It is best to place the origin at the built-in end. Then $y_0 = 0$ and $\theta_0 = 0$, and maximum deflection and slope, y_{max} and θ_{max} are at $x = L$. With $a = 0$, $b = 0$, $c = 0$, obtain from Eq 7:

$$EIy_{x=L} = -\frac{wL^2}{2}\frac{(L-0)^2}{2} + \frac{wL(L-0)^3}{6} - \frac{w(L-0)^4}{24}$$

$$= -\frac{wL^4}{8}$$

From Eq 8:

$$EI\theta_{x=L} = -\frac{wL^2}{2}(L-0) + \frac{wL(L-0)^2}{2} - \frac{w(L-0)^3}{6}$$

$$= -\frac{wL^3}{6}$$

Example 4—Simple beam with fixed ends

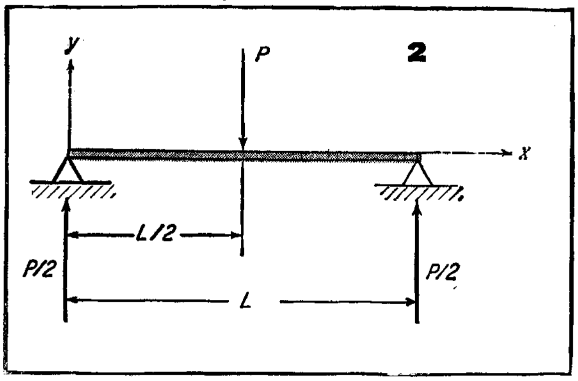

Find y_{max}, θ_{max} for the beam in Fig 5.

Solution

Because Eq 7 contains both y_0 and θ_0, choose the location of the origin such that either of the two terms (or both) are equal to zero. By placing the origin at the left end, you can determine θ_0 by making use of the condition that at $x = L$ the deflection is zero. Hence

$$EIy_{x=L} = EI\theta_0 L + \frac{P}{2}\frac{(L-0)^3}{6} - \frac{P(L-L/2)^3}{6} = 0$$

and

$$\theta_0 = -\frac{PL^2}{16EI} = \theta_A = \theta_{max}$$

$$\theta_B = -\theta_A = \frac{PL^2}{16EI}$$

The maximum deflection is at $x = L/2$:

$$EIy_{x=\frac{L}{2}} = -\frac{PL^2}{16}\left(\frac{L}{2}\right) + \frac{P}{2}\frac{(L/2)^3}{6} = -\frac{PL^3}{48}$$

Note that the distance from the origin to the reactive force $P/2$ is zero, but to the applied load P it is $L/2$.

Example 5—Beam with complex loading

Find the deflection at point D, and the slope at point A, of the beam loaded as shown in Fig 6.

Solution

Place the origin at the left support where $y_0 = 0$. The

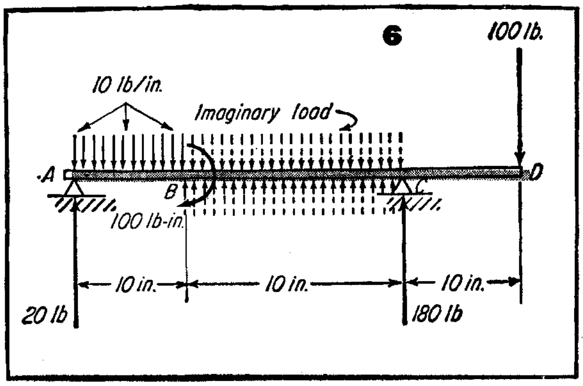

angle of rotation θ_0 then will be determined from the condition that $y = 0$ at $x = 20$ in.

$$EIy_{x=20} = EI\theta_0 20 + \frac{100(20-10)^2}{2} + \frac{20(20-10)^3}{6} - \frac{10(20-0)^4}{24} + \frac{10(20-10)^4}{24} = 0$$

or $\quad \theta_0 = -\dfrac{225}{EI}$

As was pointed out before, the design equations recognize only a distributed load that does not break off before the section where y or θ are to be determined. Because the uniform load in Fig 6 breaks off at point B, you must extend the load to point C. To compensate for this addition, add a uniform load of opposite direction (upward) in the portion BC of the beam. The last member in the equation below reflects this change.

Deflection at point D ($x = 30$ in.):

$$EIy_D = -225(30) + \frac{100(30-10)^2}{2} + \frac{20(30-0)^3}{6} + \frac{180(30-20)^3}{6} - \frac{10(30-0)^4}{24} + \frac{10(30-10)^4}{24} = -137{,}583$$

In the previous cases of beams with moment of inertia constant all along the length of the beam, only M was integrated as a function of x. But when the moment of inertia I also varies with x, Eq 1 can be written as:

$$\frac{d^2y}{dx^2} = \frac{M}{I_0/I}\left(\frac{1}{EI}\right) \qquad (9)$$

where I is arbitrarily chosen as a basis to which we refer the varying I_0. Integrating the $M/(I_0/I)$ function gives the deflection line.

Because I_0/I is dimensionless, $M/(I_0/I)$ has the dimension of bending moment and represents as a function of x, a corrected bending-moment for the beam with uniform moment of inertia I. Hence, it follows that the M moment diagram on the beam of constant inertia will result in the same deflection curve as the $M/(I_0/I)$ moment diagram on the beam of varying moment of inertia. In other words, a certain $P/(I_0/I)$ loading system, which originates the $M/(I_0/I)$ diagram, will produce exactly the same deflection curve on the beam of constant cross

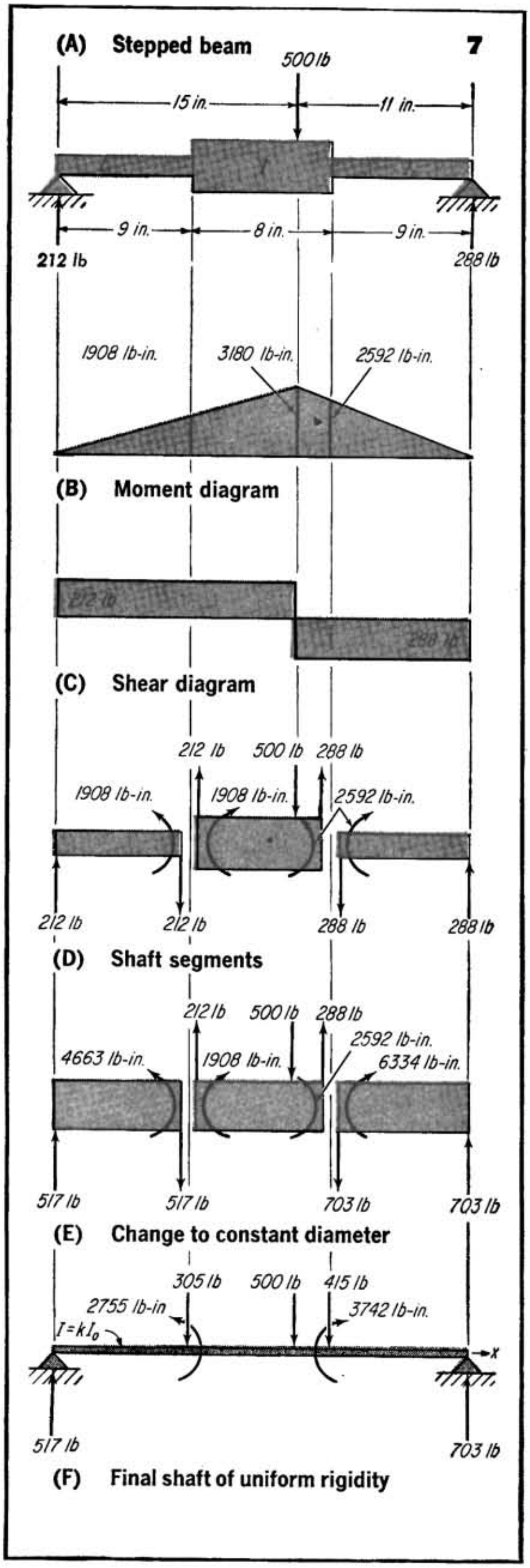

section as the original P loading (which gave the M diagram) would do on the beam of variable moment of inertia.

Thus, if you replace a beam or a portion of a beam with a moment of inertia I_0, by a beam with a moment of inertia $I = KI_0$, and at the same time change all the loads and reactions acting upon the beam by a factor of $K = I/I_0$, the elastic curve of the two beams will be the same. Therefore, to apply the general formulas, Eq 7 and 8, to a beam whose cross section varies by steps, you must replace the beam of variable rigidity by a beam of constant rigidity in the manner described above. This is illustrated in the following numerical example:

Example 6—Stepped shaft

Determine the end slope θ_0, and the deflection under the 500-lb load of a steel stepped shaft, Fig 7A. The shaft has a 1 in. dia with $I_0 = 0.049$ in.^{4} and 1¼ in. dia with $I = 0.120$ in.^{4}. $E = 30 \times 10^6$ psi.

Solution

Construct a bending moment diagram, Fig 7B, where $M = 212 \times 15 = 3180$ lb-in., followed by a shear diagram, Fig 7C. Fig 7D shows the shaft with moments and shears at the discontinuities.

In Fig 7E the stepped shaft is replaced by a shaft with a constant diameter of 1¼ in. Now transform the loads by a factor of $I/I_0 = 2.444$. The loads acting upon the middle portion of the shaft remain unchanged, because we have not changed the moment of inertia of this portion. Finally, in Fig 7F, the shaft of uniform rigidity is schematically shown *for which the general equations, Eq 7 and 8, apply*. Thus, the effect of the change in the cross section has been established as identical to that of a certain force system, and it is possible to find the deflection in a beam with any number of steps and discontinuities by a simple expedient of using one equation.

Continuing the numerical computations, assume the origin of coordinates at the left support. Thus, at $x = 26$ in. $y_0 = 0$, and Eq 7 yields:

$$EIy_{x=26} = EI\theta_0 26 - \frac{2755(26-9)^2}{2} + \frac{3742(26-17)^2}{2} + \frac{517(26-0)^3}{6} - \frac{305(26-9)^3}{6} - \frac{500(26-15)^3}{6} - \frac{415(26-17)^3}{6} = 0$$

Hence

$$\theta_0 = -\frac{32{,}948}{EI} = -0.0092 \text{ radians}$$

Now again, from Eq 7, but at a new position ($x = 15$), and with inclusion of the θ_0 value:

$$EIy_{x=15} = -32{,}948(15) - \frac{2755(15-9)^2}{2} - \frac{305(15-9)^3}{6} + \frac{517(15-0)^3}{6}$$

$$= -264{,}518$$

or

$$y_{x=15} = -\frac{264{,}518}{(30 \times 10^6)(0.12)} = 0.073 \text{ in.}$$

Shafts:
5 Steps Find Strength & Defection

Charles Tiplitz

Bending or torsional stresses, or a combination, may be limiting requirements in shaft design. Shaft stress diagrams usually deal with combined stress only. Three supplementary graphs presented here, together with a step-by-step example, bring quick aid to difficult shaft design problems.

EXAMPLE

Design a shaft that will transmit at 1200 rpm, 0.1 hp through a 4-in.-dia, 20° gear, centrally mounted between self-aligning bearings 2 in. apart. Limiting combined shear stress to be 10,000 psi, deflections must not exceed 0.05° or 0.0002 in.

Step 1.

Find:

$$\text{Torque} = \frac{\text{hp} \times 63{,}025}{\text{rpm}} = \frac{0.1 \times 63{,}025}{1{,}200} = 5.25 \text{ in. lb}$$

Tangential force at the gear pitch-radius (2 in.) is, th**Step 1** $5.25/2 = 2.63$ lb. From chart 1, a 2-in. radius interpolated for 2.6 lb gives $D = 0.14$ in. for 10,000 psi shear.

(CONTINUED)

1. Force vs radius and shaft dia to produce 10,000 psi shear stress

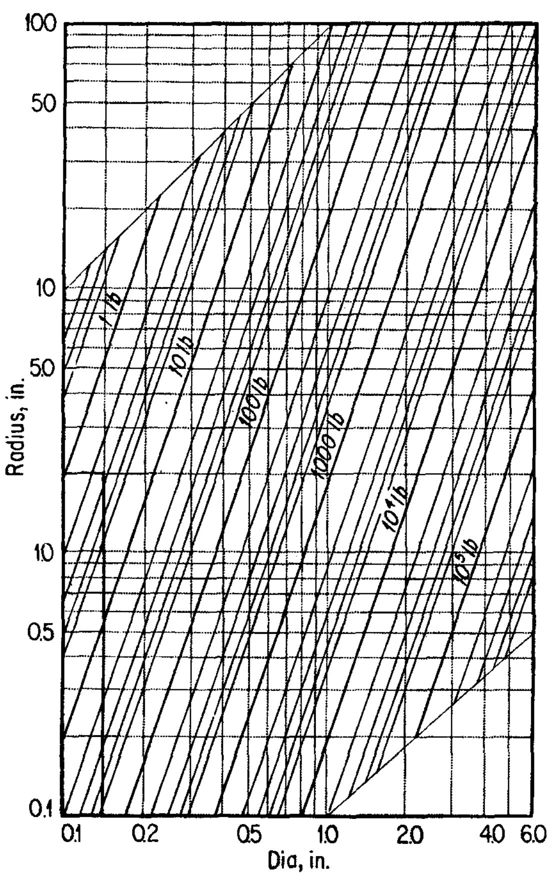

2. Deflection and load of uniformly loaded steel shaft.
(For 10,000 psi stress, and $E = 30 \times 10^6$ psi)

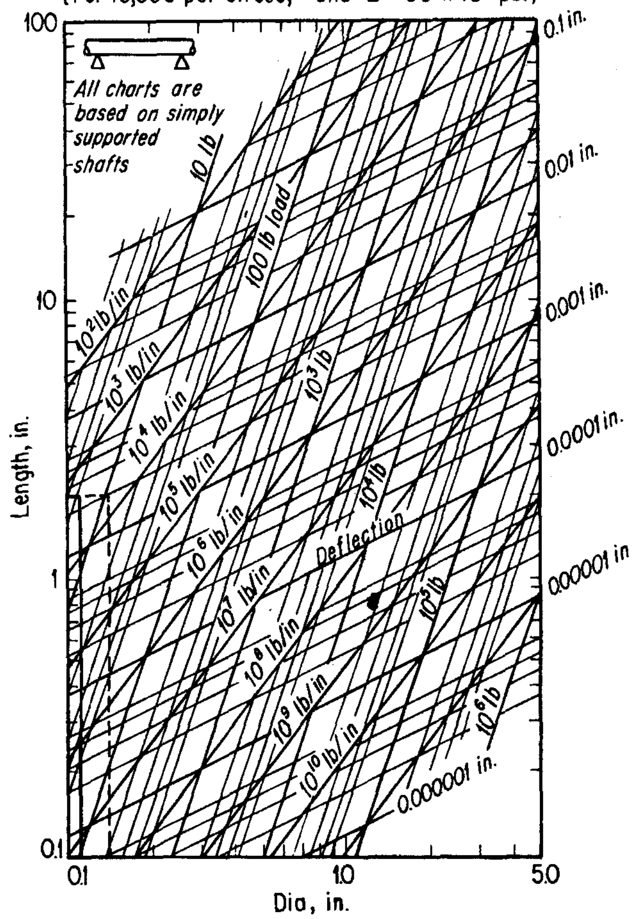

Step 2

Since the bearings are self aligning and there is a central load, correction factor is 0.5 (see table, simple supports). Since a 20° gear-tooth is transmitting the power, the bending force on the shaft will be greater than the tangential force.

Resolving: $2.63 \times \text{secant } 20° = 2.8$ lb. Therefore, uncorrected force to stress the shaft to 10,000 psi will be $2.8/0.5 = 5.6$ lb. Therefore, enter chart 2 at 5.6 lb, at which point $D = 0.11''$ (solid line).

Step 3

Check combined stress on the 0.14 shaft dia found in step 1. Bending capacity on chart 2 for this dia is approximately 11 lb (dotted line). The load correction factor is 0.5 so actual (corrected) load to produce 10,000 psi is 5.5 lb. Load is proportional to stress, hence a 2.8 lb load will cause a bending stress of 5,100 psi. Combined stress

$$S = \sqrt{\left(\frac{\text{actual stress}}{2}\right)^2 + (\text{max stress})^2}$$

3. Angular deflection and torsional elasticity—steel shaft.

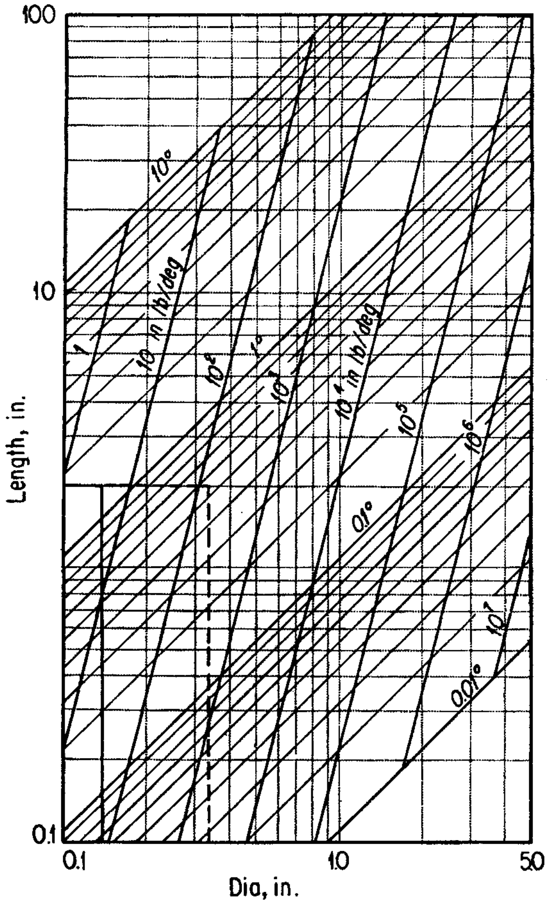

$$S = \sqrt{\left(\frac{5{,}100}{2}\right)^2 + 10{,}000^2} = 10{,}600 \text{ psi}$$

Read deflection of 0.0026 in. at junction of 2 in. length and 0.11 in. dia. Deflection factor from table is 0.8, therefore correct value is $(0.8)(0.0026) = 0.0022$ in.

Step 4

Target deflection is 0.0002 in.; check for deflection and torsion instead of adjusting for combined stress requirement. Desired deflection is $0.0002/0.0022 = 1/9$ of the deflection of the 0.11 in.-dia shaft. Interpolate between lines for 1000 lb/in. and 10,000 lb/in. for an elasticity of about 2000 lb/in. Elasticity factor is 0.625 so actual elasticity is 1250 lb/in. Value on diagram should be 9×2000 lb/in or 18,000 lb/in. to reduce deflection correctly. Interpolate between 10^4 lb/in. and 10^5 lb/in.: shaft dia is 0.20 in.

Step 5

Obtain torsional deflection from chart 3. Angular deflection is based on a stress of 10,000 psi; chart 1 showed that a shaft 0.14 in. dia would be stressed this much by the design torque. A 2 in. length will be twisted approximately 1.3° according to interpolation of chart 3 (solid line). Desired deflection is 0.05°. Estimate torsional elasticity of 5.5 in. lb/deg by interpolating between 1 in.lb/deg on chart 3. Elasticity must be greater by the factor $1.3/0.05 = 26$. Calculate: $26 \times 5.5. = 143$. Interpolate between 10^2 and 10^3 in.lb/deg. (dotted line) to find a dia of 0.034 in. This is the correct shaft dia to use.

CORRECTION FACTORS

Condition	Load	Deflection	Elasticity lb/in.
Simple supports, uniformly loaded (the charts are based on this condition)	1.0	1.0	1.0
Simple supports, one concentrated load at center	0.5	0.8	0.625
Fixed ends, uniformly distributed load	1.5	0.3	5.0
Fixed ends, one concentrated load at center	1.0	0.4	2.5
Cantilever, one end fixed, other unsupported, one concentrated load at unsupported end	0.125	3.2	0.0391
Square shafts, length of side same as shaft dia.	1.698	0 589	2.882

Shaft Torque:
Charts Find Equivalent Sections

An easy way to convert solid circular shafts to equivalent-strength shafts of hollow circular, elliptical, square, and rectangular sections.

Dr. Biswa Nath Ghosh

1—ROUND and ELLIPTICAL SHAFTS

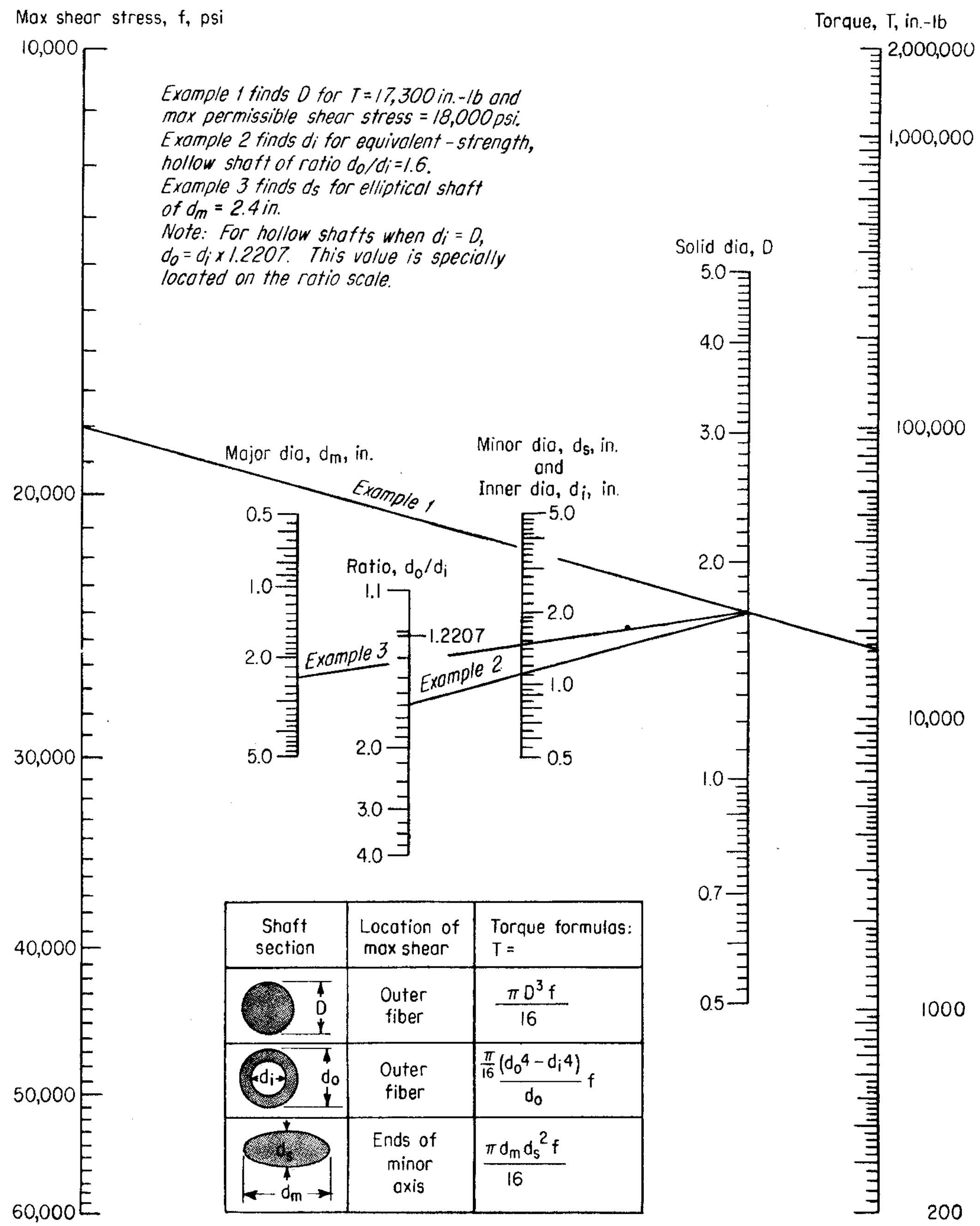

Shaft section	Location of max shear	Torque formulas: T =
D	Outer fiber	$\frac{\pi D^3 f}{16}$
d_i, d_o	Outer fiber	$\frac{\frac{\pi}{16}(d_o{}^4 - d_i{}^4)}{d_o} f$
d_s, d_m	Ends of minor axis	$\frac{\pi d_m d_s{}^2 f}{16}$

CONTINUED

2—SQUARE and RECTANGULAR SHAFTS

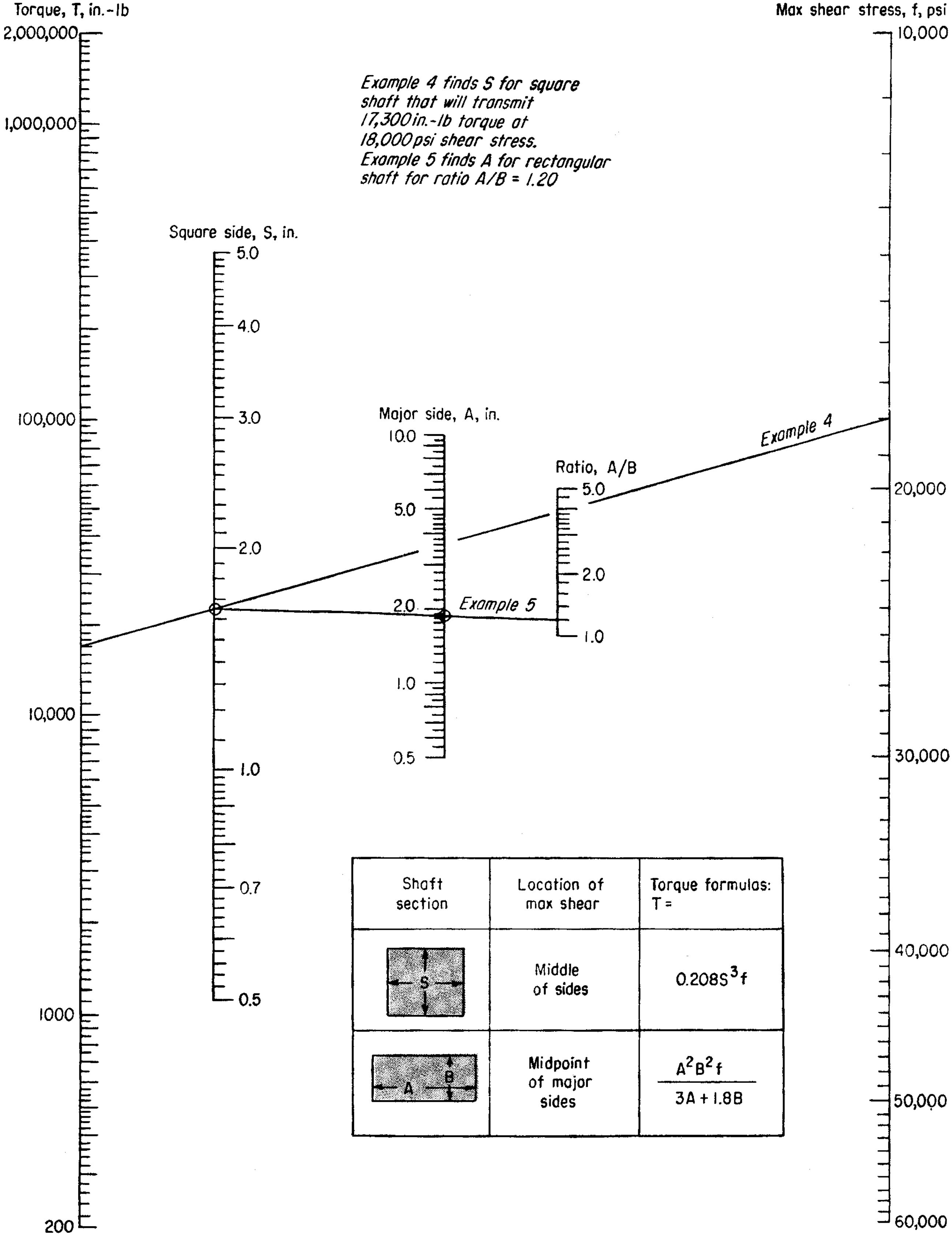

Shaft section	Location of max shear	Torque formulas: T =
S	Middle of sides	$0.208S^3f$
A, B	Midpoint of major sides	$\dfrac{A^2B^2f}{3A+1.8B}$

Critical Speeds of End Supported Bare Shafts

L. Morgan Porter

THIS NOMOGRAM solves the equation for the critical speed of a bare steel shaft that is hinged at the bearings. For one bearing fixed and the other hinged multiply the critical speed by 1.56. For both bearings fixed, multiply the critical speed by 2.27. The scales for critical speed and length of shaft are folded; the right hand sides, or the left hand sides, of each are used together. The chart is valid for both hollow and solid shafts. For solid shafts, $D_2 = 0$.

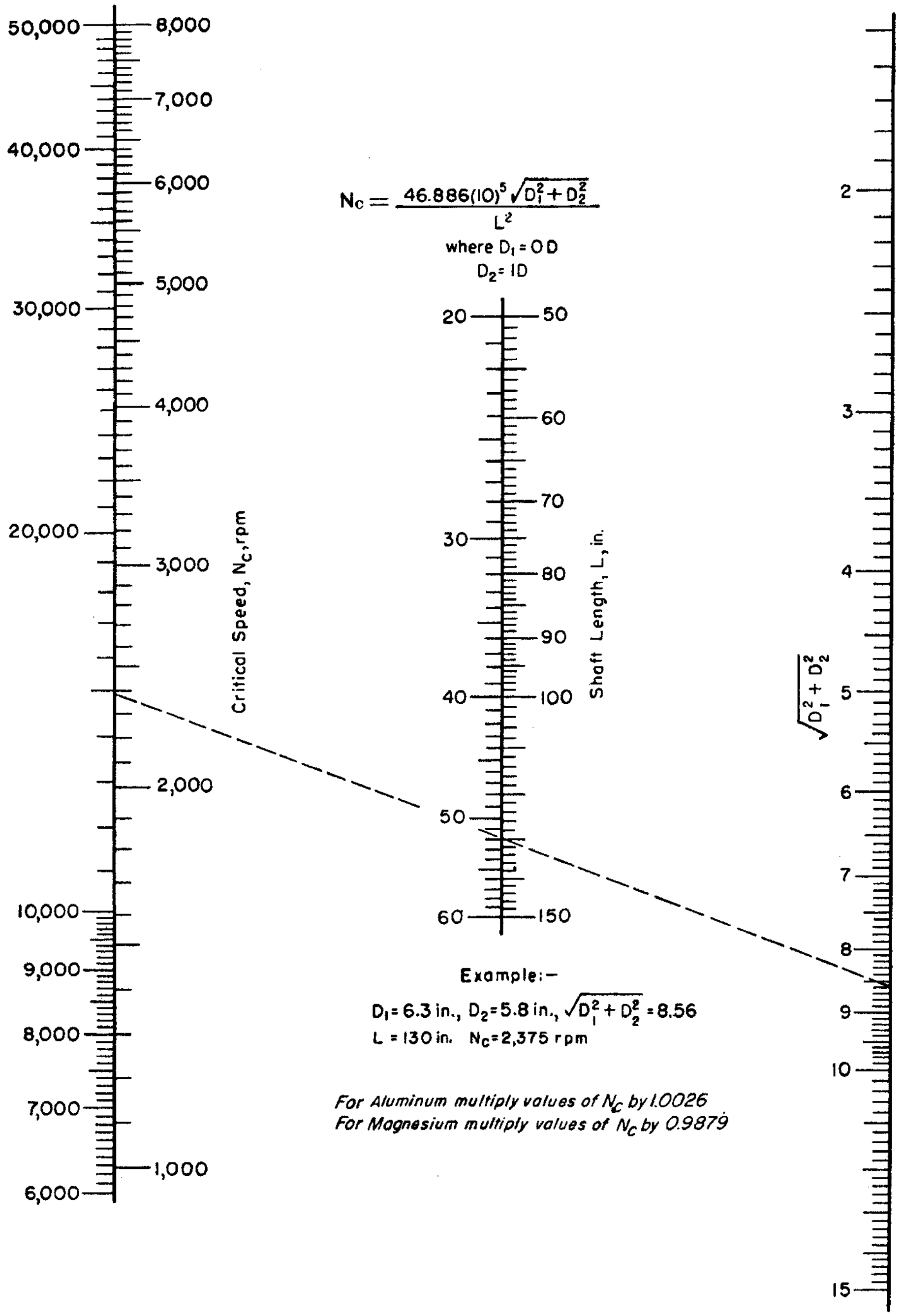

Torsional Strength of Shafts

Formulas and charts for horsepower capacity of shafts from 1/2 to 2 1/2 inch diameter and 100 to 1000 rpm.

Douglas C. Greenwood

For a maximum torsional deflection of 0.08° per foot, shaft length, diameter and horsepower capacity are related in

$$d = 4.6\sqrt[4]{\frac{hp}{R}}$$

where d = shaft diameter, in.; hp = horsepower; R = shaft speed, rpm. This deflection is recommended by many authorities as being a safe general maximum. The two charts are plotted from this formula, providing a rapid means of checking transmission-shaft strength for usual industrial speeds up to 20 hp. Although shafts under 1-in. dia are not transmission shafts, strictly speaking, lower sizes have been included.

When shaft design is based on strength alone, the diameter can be smaller than values plotted here. In such cases use the formula

$$d = \sqrt[3]{\frac{k\,hp}{R}}$$

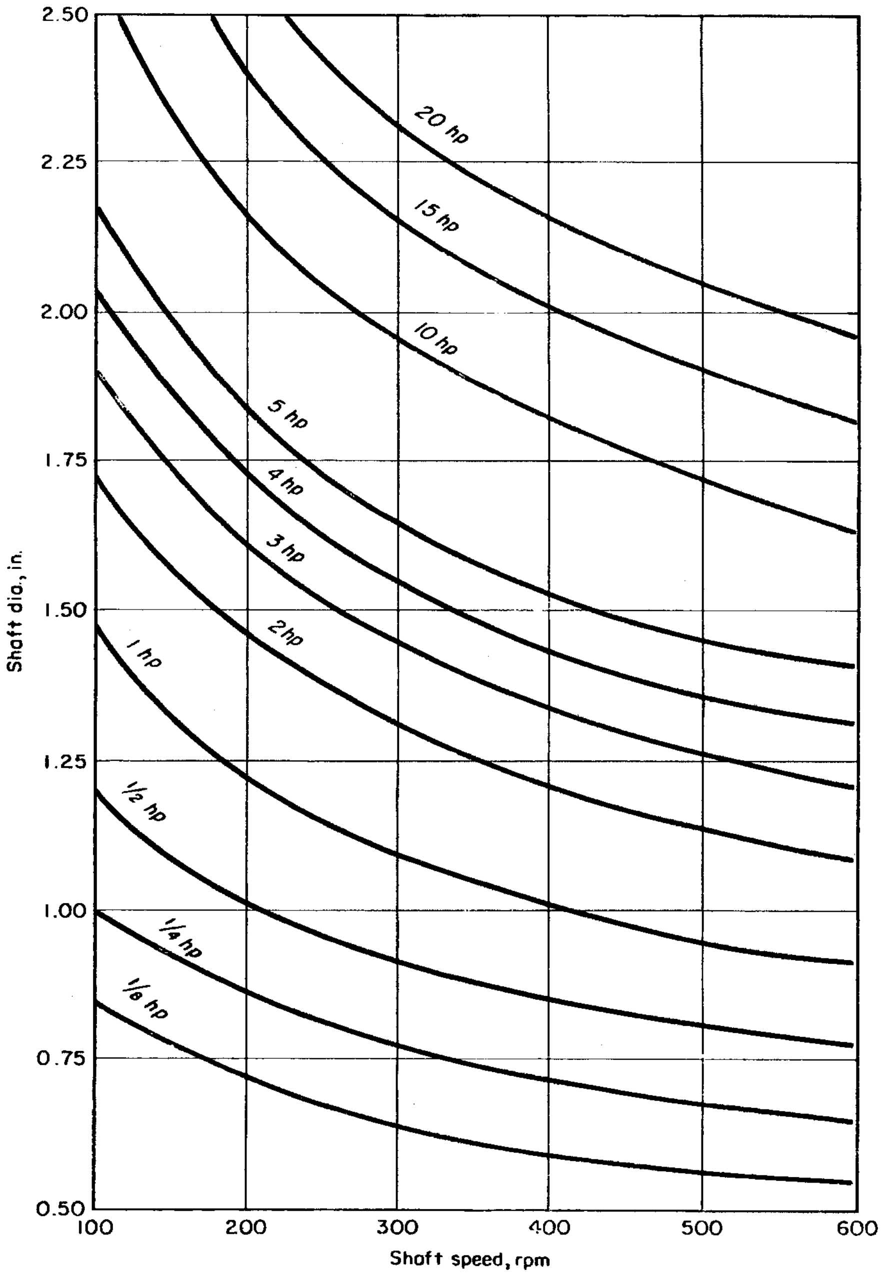

k	LOADING CONDITION
125 (2600 psi)	Head shafts subject to heavy strains. (Intermittent loads and slow speeds, clutches or gearing carried)
100 (3200 psi)	Lineshafts 75–100 ft long, heavily loaded. Bearings 8 ft apart.
90 (3550 psi)	Lineshafts 50–75 ft long, medium load, bearings 8 ft apart.
75 (4300 psi)	Lineshafts 20–50 ft long, lightly loaded, bearings 6 ft apart.

The value of k varies from 125 to 38 according to allowable stress used. The figure accounts for members that introduce bending loads, such as gears, clutches and pulleys. But bending loads are not as readily determined as torsional stress. Therefore, to allow for combined bending and torsional stresses, it is usual to assume simple torsion and use a lower design stress for the shaft depending upon how it is loaded. For example, 125 represents a stress of approximately 2600 psi, which is very low and should thus insure a strong-enough shaft. Other values of k for different loading conditions are shown in the table.

When bending stress is not considered, lower k values can be used, but a value of 38 should be regarded as the minimum.

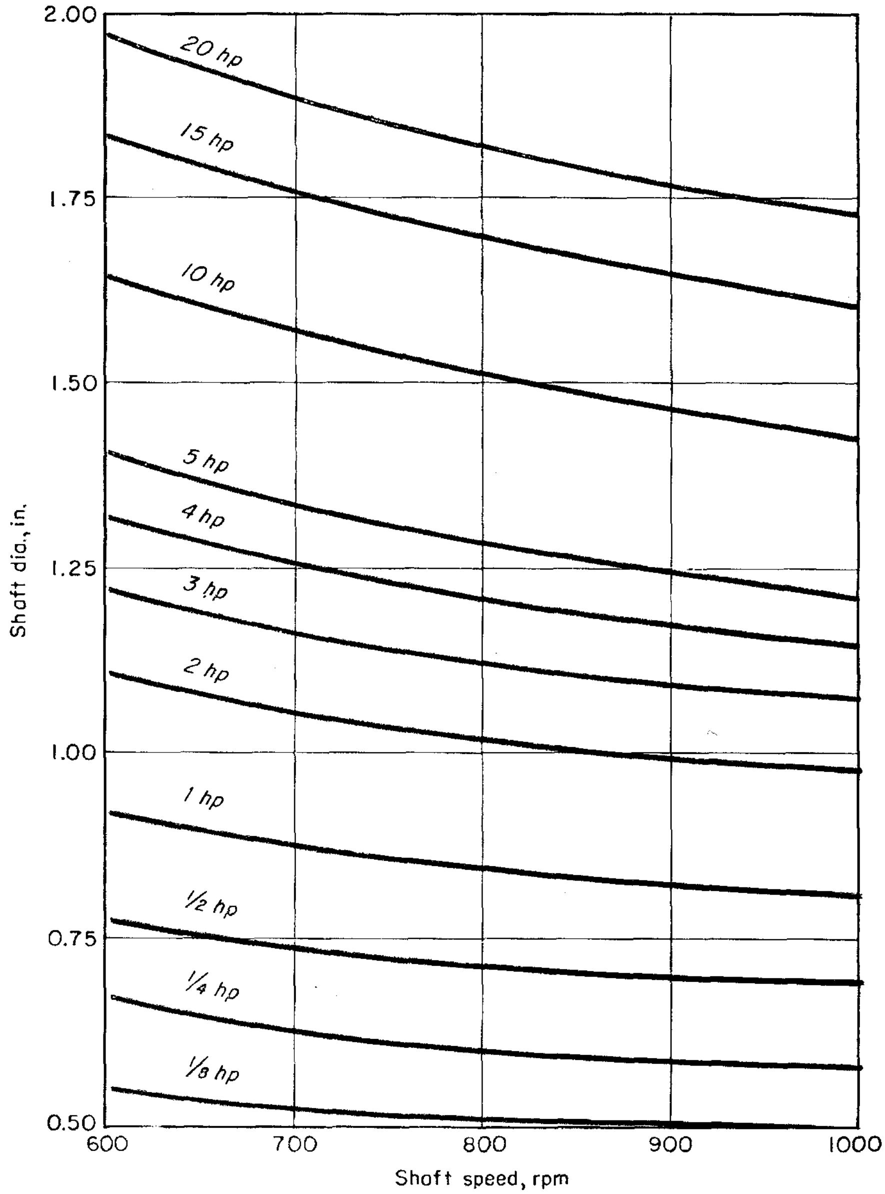

Bearing Loads on Geared Shafts

Simple, fast and accurate graphical method of calculating both direction and magnitude of bearing loads.

Zbigniew Jania

To calculate the bearing loads resulting from gear action, both the magnitude and direction of the tooth reaction must be known. This reaction is the force at the pitch circle exerted by the tooth in the direction perpendicular to, and away from the tooth surface. Thus, the tooth reaction of a gear is always in the same general direction as its motion.

Most techniques for evaluating bearing loads separate the total force acting on the gear into tangential and separating components. This tends to complicate the solution. The method described herein uses the total force directly.

If T is the torque transmitted by a gear, the tangential tooth force is

$$F_T = 2T/D,$$

Also, from Fig. 1,

$$F = F_T \sec \phi \quad \text{(spur gears)},$$
$$F = F_T \sec \phi_t \quad \text{(helical gears)}.$$

Since a force can be replaced by an equal force acting at a different point, plus a couple, the total gear force can be considered as acting at the intersection of the shaft centerline and a line passing through the mid-face of the gear, if the appropriate couple is included. For example, in Fig. 2 the total force on gear B is equivalent to a force F_B applied at point X plus the couple $b \times F_B$. In establishing the couples for the other gears, a sign convention must be adopted to distinguish between clockwise and counterclockwise moments.

If a vector diagram is now drawn for all couples acting on the shaft, the closing line will be equal (to scale) to the couple resulting from the reaction at bearing II. Knowing the distance between the two bearings, the load on bearing II can be found, the direction being the same as that of the couple caused by it.

The load on bearing I is found in the same manner by drawing a force vector diagram for all the forces acting at X including the load on bearing II found from the couple diagram.

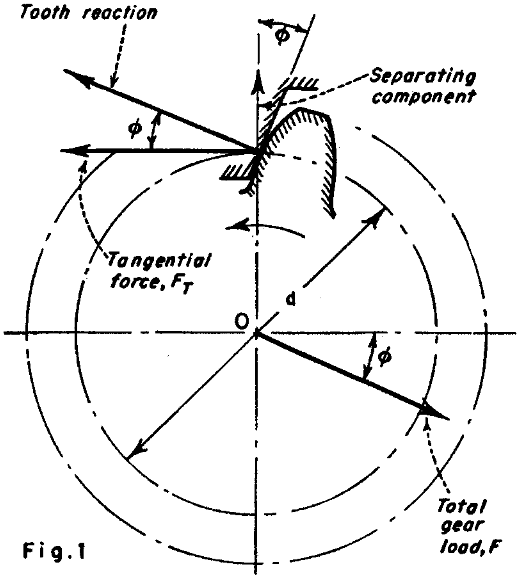

Fig.1

The construction of both diagrams is illustrated on page 213. Referring to Fig. 2 the given data are

Pitch Dia. of Gears, in.		Moment Arm, in.	
A	2.00	a	1.50
B	1.50	b	3.50
C	4.00	c	5.00
Driver	1.75	d	7.00

Angle, deg			
		Torque on driver	100 lb-in.
α	55	Torque delivered by A	40 per cent of torque on center shaft
β	48	Torque delivered by B	60 per cent of torque on center shaft
γ	45	Pressure angle of all gears, ϕ	20 deg

Then,

$$\text{Tangential force of driver} = 200/1.75 = 114 \text{ lb}$$
$$\text{Torque on center shaft} = 2 \times 114 = 228 \text{ lb-in.}$$

Gear loads are

$$F_A = \frac{0.4 \times 2 \times 228}{2.00} \sec 20 \text{ deg} = 97 \text{ lb}$$

$$F_B = \frac{0.6 \times 2 \times 228}{1.5} \sec 20 \text{ deg} = 195 \text{ lb}$$

$$F_C = 114 \sec 20 \text{ deg} = 121.5 \text{ lb}$$

Before drawing the diagrams, it is convenient to collect all the data as in Table I.

Then, the couple diagram, Fig. 3, is drawn. It is important to note that:

(a) Vectors representing negative couples are drawn in the same direction but in opposite sense to the forces causing them;

(b) The direction of the closing line of the diagram should be such as to make the sum of all couples equal to zero. Thus, the direction of 7 P_{II} is the direction of bearing reaction. The bearing load has the same direction but is of opposite sense.

Fig. 2

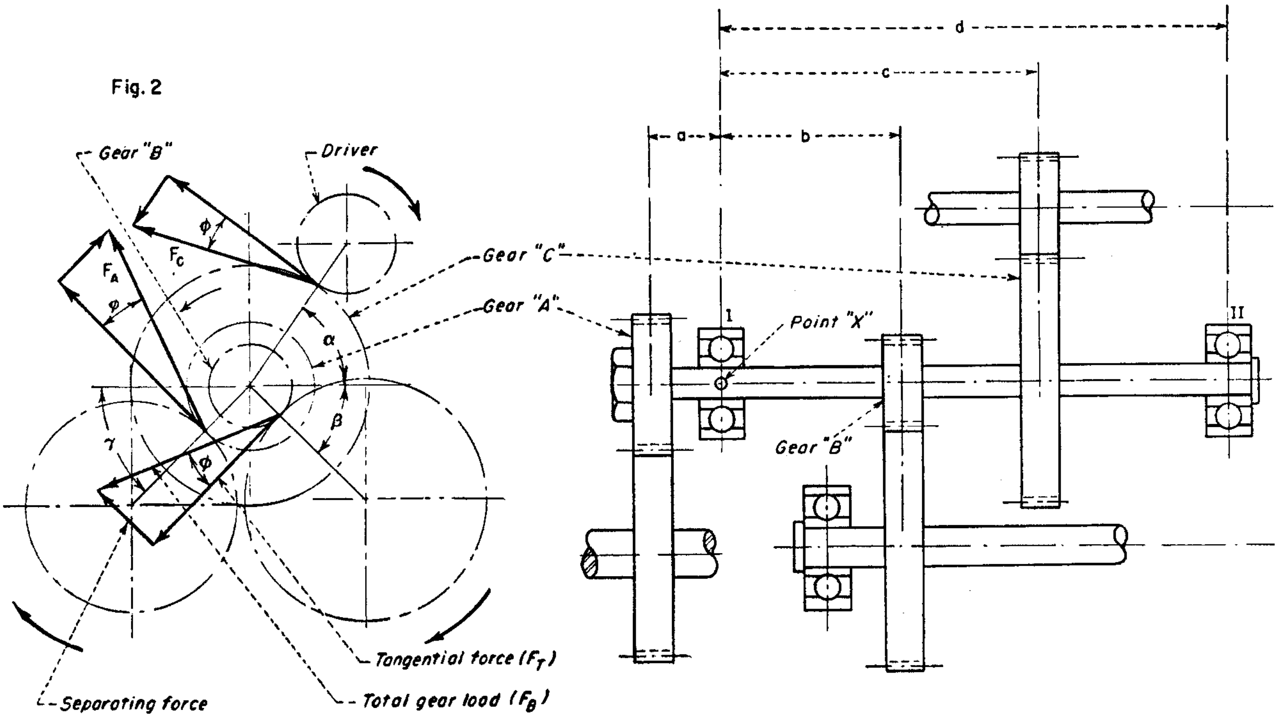

7 Ways to Limit Shaft Rotation

Traveling nuts, clutch plates, gear fingers, and pinning members are the bases of these ingenious mechanisms.

I. M. Abeles

Mechanical stops are often required in automatic machinery and servomechanisms to limit shaft rotation to a given number of turns. Two problems to guard against, however, are: Excessive forces caused by abrupt stops; large torque requirements when rotation is reversed after being stopped.

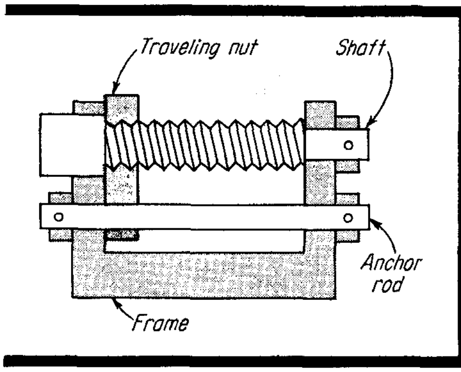

1

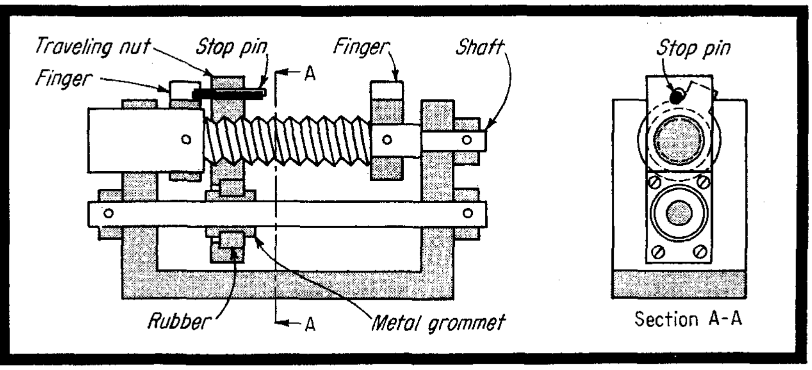

2

TRAVELING NUT moves (1) along threaded shaft until frame prevents further rotation. A simple device, but nut jams so tight that a large torque is required to move the shaft from its stopped position. This fault is overcome at the expense of increased length by providing a stop pin in the traveling nut (2). Engagement between pin and rotating finger must be shorter than the thread pitch so pin can clear finger on the first reverse-turn. The rubber ring and grommet lessen impact, provide a sliding surface. The grommet can be oil-impregnated metal.

3

CLUTCH PLATES tighten and stop rotation as the rotating shaft moves the nut against the washer. When rotation is reversed, the clutch plates can turn with the shaft from A to B. During this movement comparatively low torque is required to free the nut from the clutch plates. Thereafter, subsequent movement is free of clutch friction until the action is repeated at other end of the shaft. Device is recommended for large torques because clutch plates absorb energy well.

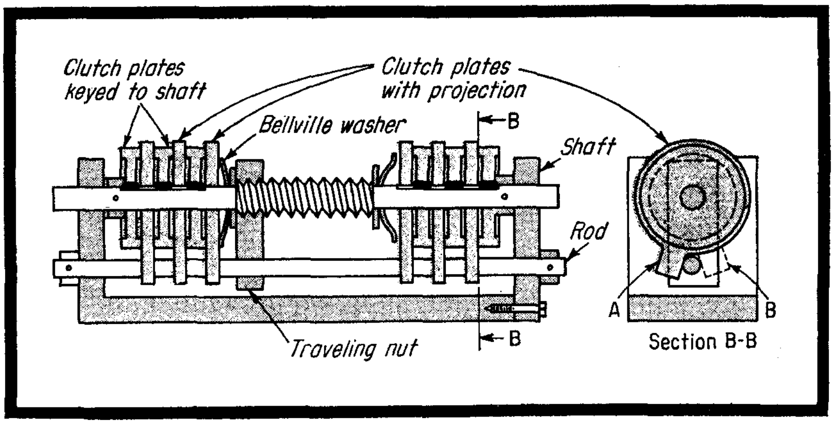

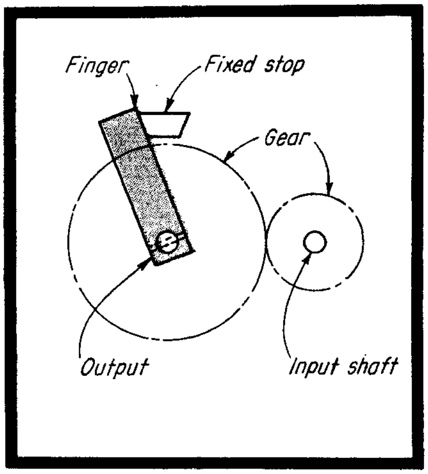

4

SHAFT FINGER on output shaft hits resilient stop after making less than one revolution. Force on stop depends upon gear ratio. Device is, therefore, limited to low ratios and few turns unless a worm-gear setup is used.

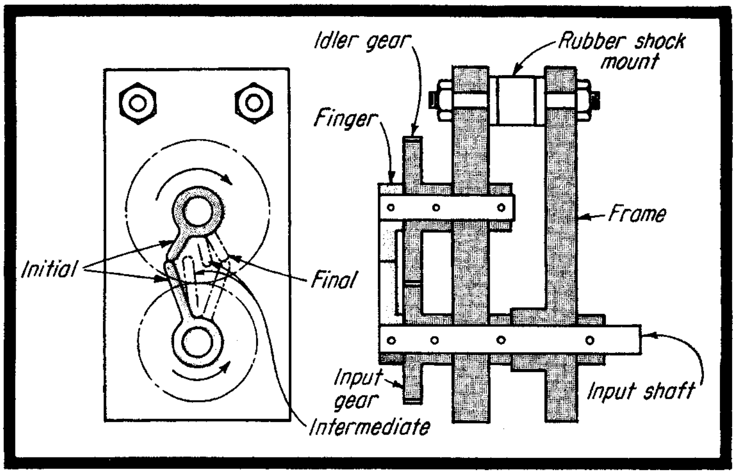

5

TWO FINGERS butt together at initial and final positions, prevent rotation beyond these limits. Rubber shock-mount absorbs impact load. Gear ratio of almost 1:1 ensures that fingers will be out of phase with one another until they meet on the final turn. Example: Gears with 30 to 32 teeth limit shaft rotation to 25 turns. Space is saved here but gears are costly.

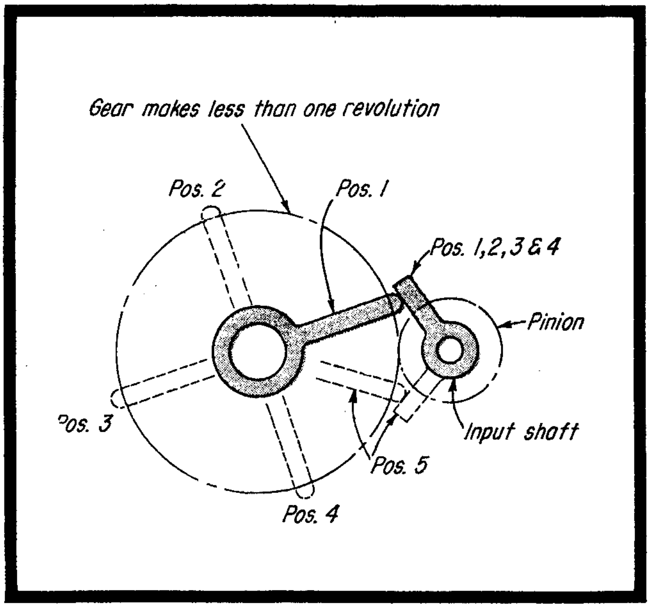

6

LARGE GEAR RATIO limits idler gear to less than one turn. Sometimes stop fingers can be added to already existing gears in a train, making this design simplest of all. Input gear, however, is limited to a maximum of about 5 turns.

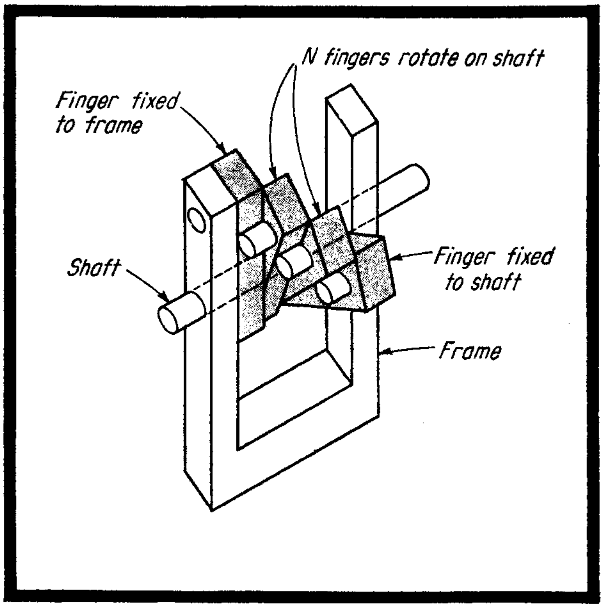

7

PINNED FINGERS limit shaft turns to approximately N + 1 revolutions in either direction. Resilient pin-bushings would help reduce impact force.

Friction for Damping

When shaft vibrations are serious, try this simple technique of adding a sleeve to the shaft can keep vibrations to a minimum. Here's how to design one and predict its effect.

Burt Zimmerman

WHEN BOOSTING THE OPERATING SPEED of any machine, the most formidable obstacle to successful operation that the designer faces is structural vibration. There is always some vibration in a system, and as the speeds are increased the vibration amplitudes become large (relatively speaking, for they may still be too small to be seen).

These amplitudes drastically reduce life by causing fatigue failures and also damage the bearings, gears, and other components of the machine. It is not over-simplifying the case to say that the easiest way to prevent vibration damage is to damp the vibration amplitudes.

An interesting but little-known technique for vibration damping is to apply a small amount of dry friction (coulomb friction) at key places of the structure. This produces a greater amount of damping than one would normally expect, and the technique is used with success by some product designers and structural engineers but, it seems, *only after the machine or structure has been built.* There seems to have been little attempt to apply this concept to initial design or to develop the equations necessary for the proper location of the friction points.

We will apply this concept here to the solution of torsional vibrations of shafts, as this is a serious problem in both industrial machinery and in military systems such as submarines, missiles, and planes. The necessary design formulas are developed and put to work to solve a typical shaft problem from industry.

How the technique works

Vibration amplitudes in a shaft become a problem when the shaft length to the thickness ratio, L_1/D_1, becomes large. One can of course make the shaft thicker. But this would greatly add to its weight.

Symbols

$a = L_1/L_2$
$C = D_2/D_1$
D_1 = Diameter of shaft
D_2 = Diameter of sleeve
G = Shear modulus of elasticity
H = Thickness of the sleeve wall
J = Polar moment of inertia (for the shaft: $\pi D_1^4/32$)
$J_{EG} \approx \pi D_1^3 H/4$
L_1 = Length of shaft
L_2 = Length of sleeve
$m = D_1/8HC^3$ = ratio of torsional stiffness of the shaft to that of the sleeve
$r = 1 + m$
R = Damping ratio
T = Applied torque on the shaft
T_s = Resisting frictional torque applied by the sleeve
U = Residual internal energy of shaft and sleeve
U_1 = Internal energy of the shaft
U_2 = Internal energy of the sleeve
W = Energy dissipated in a half oscillation
$\lambda = T_s/T$
θ = Angular displacement of the shaft
θ_s = Angular displacement of the sleeve

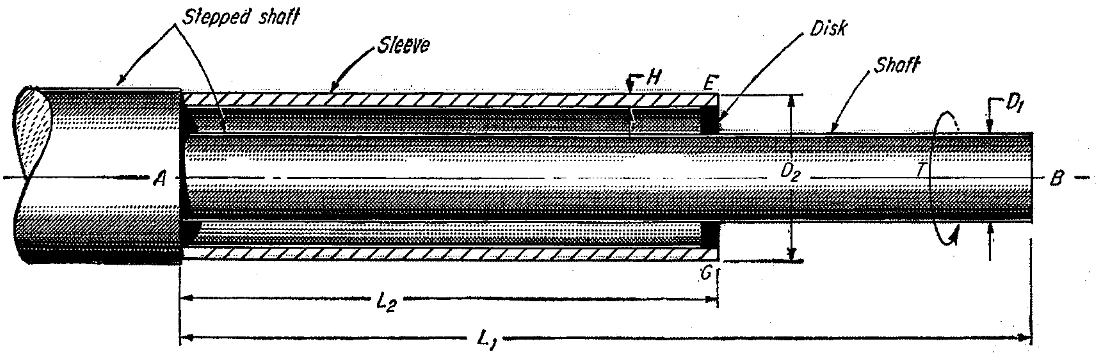

1. Thin sleeve added to rotating shaft greatly reduces torsional vibrations. The disk is rigidly attached to the shaft and has a snug fit with the sleeve. Extending the sleeve over the entire length provides the most effective damping condition.

To apply the friction-damping technique to a shaft, Fig 1, a sleeve is added which is attached to the shaft at one end (A). The sleeve is extended along the shaft length and makes contact with some point on the shaft. In this particular design, a disk is rigidly attached to the shaft (by welding it or tightly pressing it on), and there is a snug fit between the disk and the sleeve.

The exact amount of fit is not too important, but it must be neither too loose nor too tight: If the fit is too tight, the shaft and sleeve will tend to move together as a unit and there will be no damping (just an increase in the moment of inertia); if too loose, with a clearance between disk and sleeve, again there will be no damping.

The frictional forces in question occur at the contact between the inside surface of the sleeve and the edge of the disk, and their magnitude depends on the coefficient of friction and on the pressure between the surfaces.

The most effective damping condition is when the sleeve extends the entire length of the shaft, but there may be cases, depending on the product design and application, where this is impossible. Therefore, the general case where the sleeve length is variable is considered here.

To avoid corrosion or fretting at the interface, try a layer of viscoelastic stripping (elastomer) at the edge of the disk.

Analysis of concept

When a shaft is rotating, a resisting torque is developed in the shaft which varies along the length of the shaft. Because the angular displacement is a function of this resisting torque, the surface fibers of the shaft will undergo different angular displacements which depend on the distance of the specific fiber from the point of

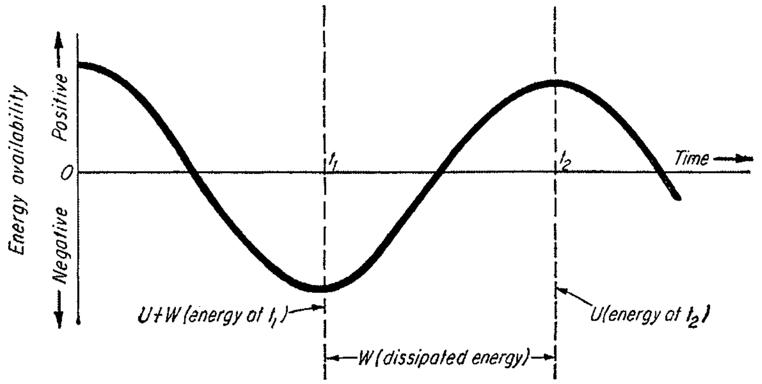

2. Energy present in a rotating shaft through one complete cycle of vibration with damping taking place for one half of the cycle. At t_1, the energy in the shaft is equal to its residual internal energy, **U**, plus the energy dissipated during half the cycle, **W**. At t_2, the energy is equal to **U**, which indicates that the energy dissipated through dry friction damping is **W**.

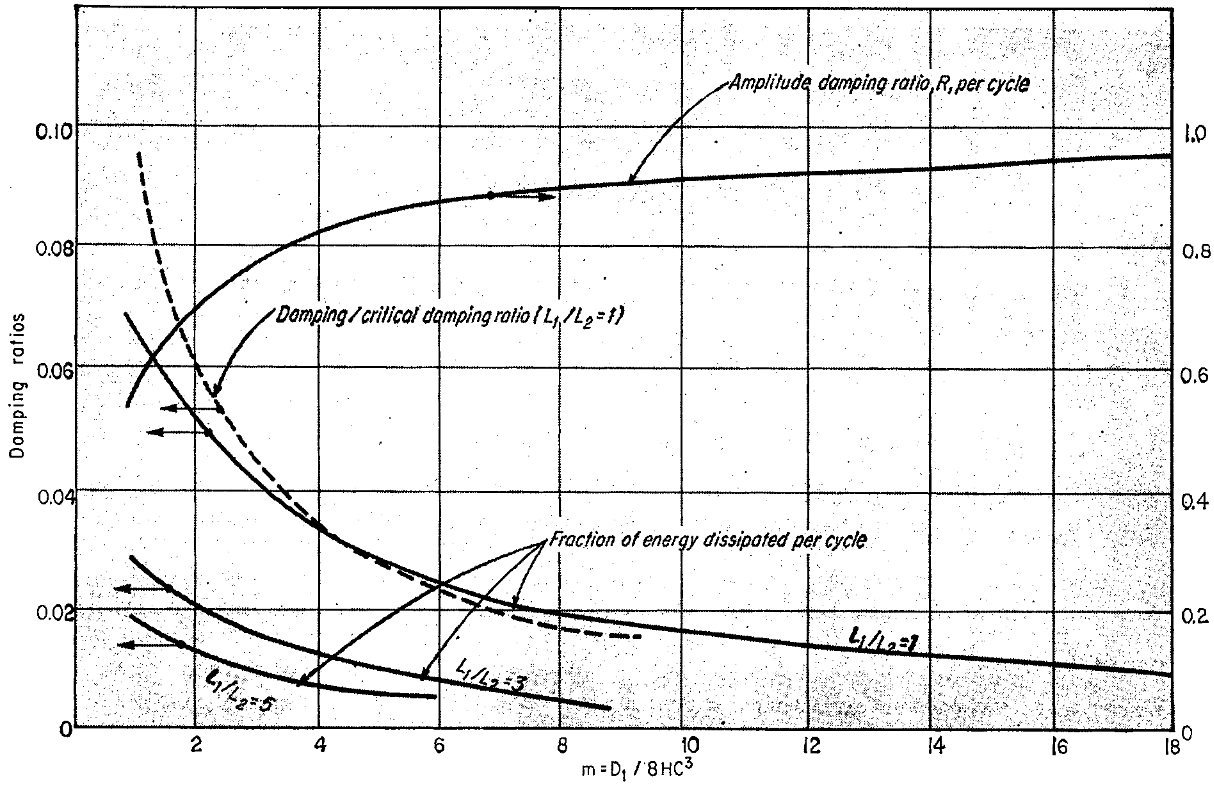

3. Design chart for different values of the dimensional constant, m. The frictional amount of energy dissipated per cycle is a function of the sleeve-shaft length ratio. Critical damping is the amount of damping above which the sleeve-disk interface will stick. The curve for the amplitude-damping ratio (which is read at the right scale) can be used for most design problems, as illustrated in the numerical example.

the applied torque. The magnitude of the torsional vibration is measured by the difference of displacements along the shaft length.

The torque difference on the shaft (applied torque, T, minus the torque at the disk, T_{eg}) is greater than the corresponding torque difference along the length of the sleeve. Therefore, there will be an angular difference between the sleeve and the disk. Because the inside edge of the sleeve and the outside surface of the disk have a pressure contact (however slight) this tends to resist relative motion, hence, torsional vibration damping. One can see that as the sleeve diameter approaches infinity and as the length of the sleeve approaches the length of the shaft, the damping becomes more and more efficient. (The point to remember here is that it is not the contact pressure which causes damping but rather the frictional torque, T_s, which opposes the direction of the applied torque on the shaft.)

Because a shaft is usually driving a load at its end, it is safe to assume (to simplify the equations without much error) that the system consists of two rotating masses connected by a shaft whose inertia is negligible as compared to the end masses. So we can say that the applied torque is a constant along the shaft length.

If the angular displacement is assumed to be zero at the end (A) of the shaft, the displacement at the disk (at EG) is in the form (see list of symbols):

$$\theta = \frac{TL}{JG} \tag{1}$$

or

$$\theta_{EG} = \frac{(T - T_s)(L_2)}{\pi D_1^4 G/32} \tag{2}$$

And that the displacement at the end B in the form

$$\theta_B = \theta_{EG} + \frac{T(L_1 - L_2)}{\pi D_1^4 G/32} \tag{3}$$

The angular displacement of the sleeve at EG (with zero displacement at the fixed end A) is

$$(\theta_S)_{EG} = \frac{4\lambda T L_2}{\pi D_1^3 C^3 HG} \tag{4}$$

The strain energy of the shaft caused by vibration is

$$U = U_1 + U_2 \tag{5}$$

The maximum strain energy of the shaft can be derived as

$$U_1 = \tfrac{1}{2}[T(1 - \lambda)\theta_{EG} + T(\theta_B - \theta_{EG})] \tag{6}$$

The corresponding energy in the sleeve is

$$U_2 = \tfrac{1}{2}\lambda T(\theta_S)_{EG} \tag{7}$$

The difference between the energies in the shaft and th sleeve must be the energy dissipated by friction:

$$W = 2\lambda T[\theta_{EG} - (\theta_S)_{EG}] \tag{8}$$

Chenea and Hansen (Ref 1) proved that the reduction in amplitude (and hence dissipated energy) is 50% of the maximum strain for a half cycle. Therefore, for

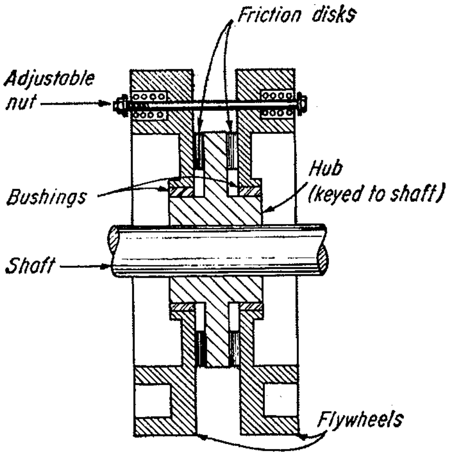

4. Application of the friction-damping technique to dampen torsional vibrations in an engine flywheel system. Both flywheels are free to rotate on bushings and are driven by a crankshaft through friction disks. The flywheels are pressed against the disks by means of loading springs and adjustable nuts. When, due to resonance, large deflections (vibrations) of the shaft and hub occur, the inertia of the flywheel prevents them from duplicating the vibrations; there is relative motion between the hub and the flywheels. As a result, friction energy (of vibration) is dissipated. The change of total system energy from a torsional deflection results in a decrease in the amplitudes of vibrations.

each full cycle of damping, the amplitude is reduced by a factor of 4 or, in other words, the energy dissipated is raised by a factor of 4. This accounts for the factor 2 in Eq 8.

Note at this point that when the relative displacement ϕ_{EG}-$(\phi_x)_{EG}$ is zero there is no relative motion, and hence no damping action.

Determination of damping

The amount of damping in any system can be expressed in terms of a ratio (and is shown in Fig 3):

$$R = \frac{\text{Magnitude of energy after damping}}{\text{Magnitude of energy before damping}}$$

$$= \frac{U}{U + W}$$

where $U = U_1 + U_2$

If the damping action is to be a maximum, the ratio of R must be so chosen as to make $U/(U + W)$ a minimum or $W/(U + W)$, which is the percentage of energy dissipated, a maximum.

$$\frac{W}{U + W} = \frac{1}{\dfrac{U}{W} + 1}$$

The ratio U/W must be a minimum, hence W/U must be a maximum. Using the previous equations (Eq 1 to 8)

$$\frac{W}{U} = \frac{4(T_S/T - (T_S/T)^2 - T_S^2 D_2^3/8T^2 H D_1^2)}{(1 - T_S/T)^2 + T_S^2 D_2^3/8T^2 H D_1^2 + \dfrac{L_1 - L_2}{L_2}} \quad (9)$$

Differentiating with respect to T_s/T, and equating the result to zero, results in a value for T_s/T which is the optimum value.

$$\frac{T_S}{T} = \lambda^2 - 2a\lambda + \frac{a}{r} = 0 \quad (10)$$

where $\lambda = T_S/T$.

Solving the quadratic for λ, results in:

$$\lambda = a[1 - \sqrt{1 - (1/ar)}] \quad (11)$$

where $r = 1 + D_1/8HC^3 = 1 + m$
$c = D_2/D_1$
$a = L_1/L_2$

The ratio m, which is equal to $D_1/8HC^3$, is the ratio of the torsional stiffness of the shaft to that of the sleeve.

The corresponding fractional value of the energy dissipated per oscillation at optimum λ is equal to 1-R.

The key to the design chart, Fig 3, is the fact that the fractional energy curve is not in direct proportion to the ratio L_2/L_1 of the sleeve length to the shaft length. This allows the designer a choice between a full-length sleeve and a stiffer sleeve placed over part of the shaft length.

The chart shows that for the same damping capacity, a sleeve 1/3 or 1/5 the length of the shaft must be many times stiffer than one covering the entire length of the shaft.

Damping vs forced vibration

Suppose a cyclic forcing function is imposed upon the shaft, causing a vibration at its fundamental natural frequency. The resulting increment per half oscillation of torsional displacement in the absence of damping, is equal to $\Delta\theta$. As a result of introducing dry friction damping, this displacement will become zero when the losses due to the energy dissipated are equal to the gain from the forcing function. It is desirable to have the energy dissipated at the smallest possible torsional displacement; in other words when

$$\theta/\Delta\theta = \text{minimum} \quad (12)$$

This can only be true when λ is equal to 1-R. Therefore, the inverse of Eq 12, $\Delta\theta/\theta$, is a ratio of energy dissipated, and

$$\Delta\theta/\theta = 1 - R \quad (13)$$

or

$$\theta = \frac{\Delta\theta}{1 - R} \quad (14)$$

Thus, if we know the increment of amplitude $\Delta\theta$ produced by the forcing function (assuming the forcing frequency equals the natural frequency and that damping is zero), we can calculate the torsional displacement to which the system can be limited for any value of the damping ratio, R.

Application to an engine

Actually, this procedure could be used for any application of rotating parts where space and weight considerations are critical. The general effect of torsional vibrations is to decrease the allowable stresses on a transmission shaft.

One of the earliest applications of coulomb friction to reduce torsional vibrations is found in gasoline and diesel engines and is called the "Lanchester Damper."

It is shown in Fig 4 (see "Vibration Problems in Engineering," 3rd Edition, Van Nostrand Co, pp 265-268).

Other design considerations

If weight is a primary objective, make the damping sleeve diameter as large as possible to gain the largest weight saving.

If weight is not important, it is probably best to go to a sleeve diameter only slightly larger than the shaft itself.

You have a choice for the length of sleeve, ranging from a full-length sleeve to one of one-tenth the total length. In the latter case, make sure that you design into the sleeve sufficient rigidity and stiffness.

Reduce the wall thickness at the end of the sleeve in contact with the disk so that the contact pressure will not induce large stresses in the sleeve. Make sure that this contact pressure is uniform around the periphery of the friction end of the sleeve.

Frictional torque depends on the coefficient of friction and the normal pressure exerted by the sleeve. It is not easy to measure the coefficient of friction under dynamic conditions, but there are values tabulated by many authors. You can vary the pressure by using a variable-diameter disk. In this way, the optimum value of damping can be empirically determined.

Don't worry too much about fretting corrosion at the friction surfaces because: 1) the friction torque is low (relative to shaft torque); 2) the normal force is distributed over a large area so as to limit the pressure to low values; 3) even if fretting occurs to some slight degree, it will not affect the torque-carrying shaft; 4) the friction surfaces need not be metallic (an elastomer or any viscoelastic material works well)

Numerical problem

A sleeve is to be designed for a shaft transmitting power to an air compressor for a supersonic wind tunnel, Fig 5. The shaft has a diameter of $D_1 = 7.5$ in. and a length of $L_1 = 8$ ft $= 96$ in. Thus L_1 and D_1 are fixed and L_2, H and D_2 are values which must be determined. As will be seen in this problem, L_2 and D_2 are selected on a trial and error basis, and H, which is the thickness of the sleeve wall and thus the important parameter which influences the total weight of the shaft, is determined from the chart in Fig 3 and its abscissa equation.

Solution

It is generally accepted that with most dry-friction damping there will be approximately 3% of damping taking place per cycle. If the forcing torque were removed for one cycle, the strain energy would drop to 97% of its maximum value and the angular displacement would likewise drop to 0.97 θ. Therefore, the forcing torque must be such as to increase the angular displacement by an amount, or (in the absence of damping):

$$\Delta\theta = 0.03\theta \text{ per cycle} = 0.015\theta \text{ for half cycle}$$

We would like to limit the $\Delta\theta$ value of torsional vibration to 10% of the steady displacement which is a result of the mean torque in the shaft.

Substituting in Eq 14 and solving for R,

$$R = 1 - \frac{0.015\theta}{0.1\theta} = 1 - 0.15 = 0.85$$

From Fig 3, this value of R (damping ratio) requires an m-value equal to 5.2 and a damping/critical damping value of 2.6%. Thus

$$m = D_1/8HC^3 = 5.2$$

Since $D_1 = 7.5$ in.

$$HC^3 = 0.1802$$

We can now choose how the produce HC^3 is to be made up. If we pick D_1 to be twice D_2, then $C = D_1/D_2 = 2$, and $H = 0.1802/8 = 0.0225$.

This provides a sleeve thickness of about 24 gage, which has only 2.7 per cent of the weight of the shaft. Thus we obtained a 10:1 reduction in the amplitude or vibration at the cost of very little extra weight. To compute the resisting friction torque, from Eq 11 we obtain

$$\lambda = \frac{T_s}{T} = 1\left[1 - \sqrt{1 - \frac{1}{(1)(6.2)}}\right] = 0.09$$

From the engine characteristics, it is known that $T = 800{,}000$ lb-in. Therefore, the frictional torque is

$$T_s = 800{,}000(0.09) = 72{,}000 \text{ lb-in.}$$

With a diameter of 15 in. on the sleeve, the friction force is equal to 1528 lb/in. If we further assume a material will be used with a coefficient of friction equal to 0.6, the normal force per inch of periphery is 2,547 lb. This amount of pressure is small compared with the kind of pressure usually associated with fretting fatigue.

References

1. P. F. Chenea and H. M. Hansen, *Mechanics of Vibration,* John Wiley and Sons Inc, 1952, pp 319-324.
2. D. Williams, *Damping of Torsional Vibrations by Dry Friction,* Royal Aircraft Establishment, 1960 (Fig 3).

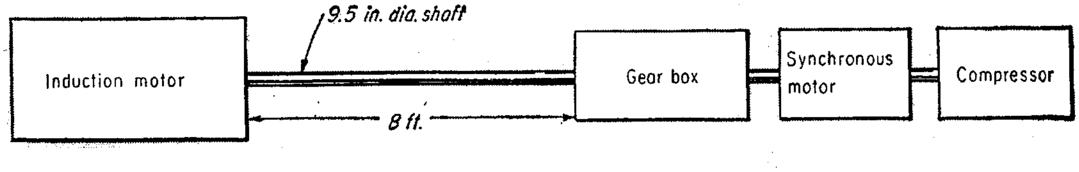

5. Transmission system designed for friction-damping. Numerical example below shows how the addition of a very thin sleeve with a wall thickness of 0.023 in. reduces the amplitude of vibration by 10 to 1.

15 Ways to Fasten Gears to Shafts

So you've designed or selected a good set of gears for your unit–now how do you fasten them to their shafts? Here's a roundup of methods–some old, some new–with a comparison table to help make the choice.

L. M. Rich

1 PINNING

Pinning of gears to shafts is still considered one of the most positive methods. Various types can be used: dowel, taper, grooved, roll pin or spiral pin. These pins cross through shaft (A) or are parallel (B). Latter method requires shoulder and retaining ring to prevent end play, but allows quick removal. Pin can be designed to shear when gear is overloaded.

Main drawbacks to pinning are: Pinning reduces the shaft cross-section; difficulty in reorienting the gear once it is pinned; problem of drilling the pin holes if gears are hardened.

Recommended practices are:

- For good concentricity keep a maximum clearance of 0.0002 to 0.0003 in. between bore and shaft.
- Use steel pins regardless of gear material. Hold gear in place on shaft by a setscrew during machining.
- Pin dia should never be larger than ⅓ the shaft–recommended size is 0.20 D to 0.25 D.
- Simplified formula for torque capacity T of a pinned gear is:

$$T = 0.787\, Sd^2D$$

where S is safe shear stress and d is pin mean diameter.

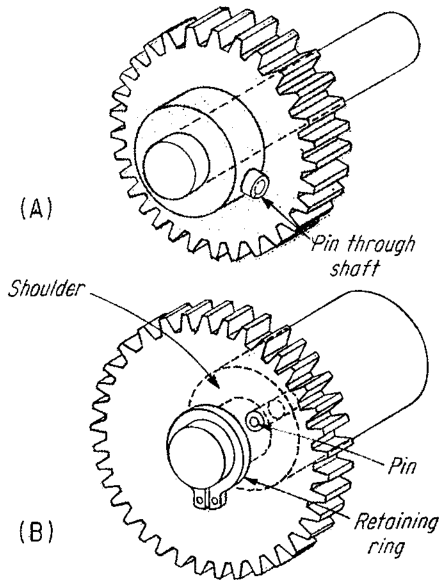

2 CLAMPS AND COLLETS

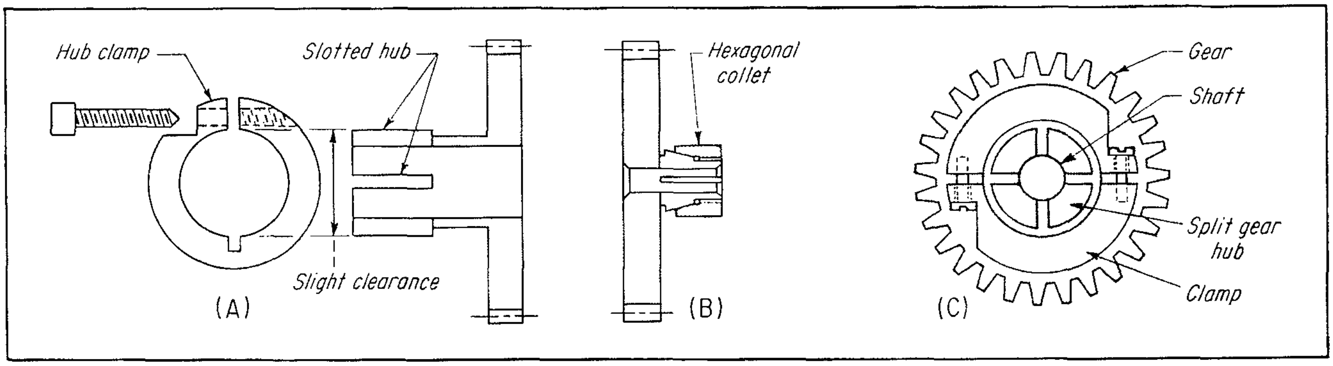

Clamping is popular with instrument-gear users because these gears can be purchased or manufactured with clamp-type hubs that are: machined integrally as part of the gear (A), or pressed into the gear bore. Gears are also available with a collet-hub assembly (B). Clamps can be obtained as a separate item.

Clamps of one-piece construction can break under excessive clamping pressure; hence the preference for the two-piece clamp (C). This places the stress onto the screw threads which hold the clamp together, avoiding possible fracture of the clamp itself. Hub of the gear should be slotted into three or four equal segments, with a thin wall section to reduce the size of the clamp. Hardened gears can be suitably fastened with clamps, but hub of the gear should be slotted prior to hardening.

Other recommendations are: Make gear hub approximately same length as for a pinned gear; slot through to the gear face at approximately 90° spacing. While clamps can fasten a gear on a splined shaft, results are best if both shaft and bore are smooth. If both splined, clamp then keeps gear from moving laterally.

Material of clamp should be same as for the gear, especially in military equipment because of specifications on dissimilarity of metals. However, if weight is a factor, aluminum-alloy clamps are effective. Cost of the clamp and slitting the gear hub are relatively low.

3 PRESS FITS

Press-fit gears to shafts when shafts are too small for keyways and where torque transmission is relatively low. Method is inexpensive but impractical where adjustments or disassemblies are expected.

Torque capacity is:

$$T = 0.785\, f D_1 L e E \left[1 - \left(\frac{D_1}{D_2}\right)^2\right]$$

Resulting tensile stress in the gear bore is:

$$S = eE/D_1$$

where f = coefficient of friction (generally varies between 0.1 and 0.2 for small metal assemblies), D_1 is shaft dia, D_2 is OD of gear, L is gear width, e is press fit (difference in dimension between bore and shaft), and E is modulus of elasticity.

Similar metals (usually stainless steel when used in instruments) are recommended to avoid difficulties arising from changes in temperature. Press-fit pressures between steel hub and shaft are shown in chart at right (from Marks' Handbook). Curves are also applicable to hollow shafts, providing d is not over 0.25 D.

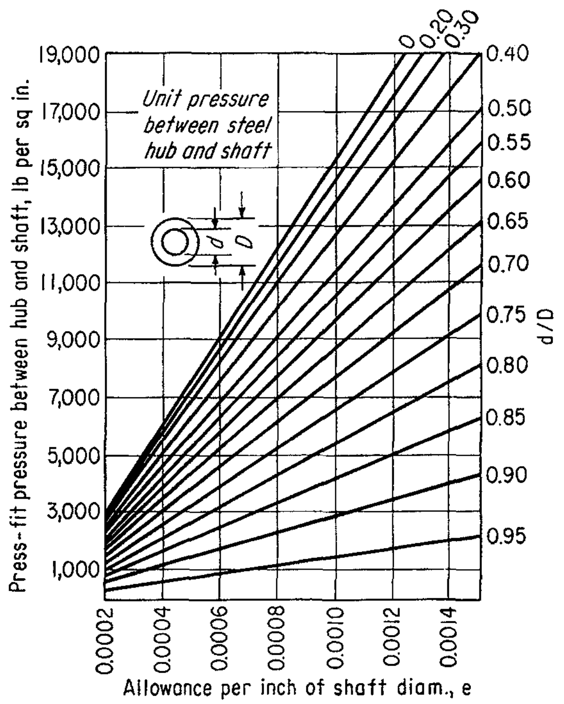

Comparison of Gear-Fastening Methods

Method	Torque Capacity	Ease of Replacing Gear	Reliability Under Operation	Versatility in Applications	Ability to Meet Environment Specs	Machining Requirements	Ability to Use Prehardened Parts	Relative Cost
—Pinning	Excellent	Poor	Excellent	Excellent	Excellent	High	Poor	High
—Clamping	Good	Excellent	Fair	Fair	Good	Moderate	Excellent	Medium
—Press fits	Fair	Fair	Good	Fair	Good	Moderate	Excellent	Medium
—Loctite	Good	Good	Good	Excellent	Excellent	Little	Excellent	Low
—Setscrews	Fair	Excellent	Poor	Good	Fair	Moderate	Good	Low
—Splining	Excellent	Excellent	Excellent	Fair	Excellent	High	Excellent	High
—Integral shaft	Excellent	Poor	Excellent	Good	Excellent	High	Excellent	High
—Knurling	Good	Poor	Good	Poor	Good	Moderate	Poor	Medium
—Keying	Excellent	Excellent	Excellent	Poor	Excellent	High	Excellent	High
—Staking	Poor	Fair	Poor	Poor	Good	Moderate	Poor	Low
—Spring washer	Poor	Excellent	Good	Fair	Good	Moderate	Excellent	Medium
—Tapered shaft	Excellent	Excellent	Excellent	Good	Excellent	High	Excellent	High
—Tapered rings	Good	Excellent	Good	Excellent	Good	Moderate	Excellent	Medium
—Tapered bushing	Excellent	Excellent	Excellent	Good	Good	Moderate	Excellent	High
—Die-cast assembly	Good	Poor	Good	Excellent	Good	Little	Fair	Low

4 RETAINING COMPOUNDS

Several different compounds can fasten the gear onto the shaft—one in particular is "Loctite," manufactured by American Sealants Co. This material remains liquid as long as it is exposed to air, but hardens when confined between closely fitting metal parts, such as with close fits of bolts threaded into nuts. (Military spec MIL-S-40083 approves the use of retaining compounds).

Loctite sealant is supplied in several grades of shear strength. The grade, coupled with the contact area, determines the torque that can be transmitted. For example: with a gear $\frac{3}{8}$ in. long on a $\frac{3}{16}$-in.-dia shaft, the bonded area is 0.22 in.^{2} Using Loctite A with a shear strength of 1000 psi, the retaining force is 20 in.-lb.

Loctite will wick into a space 0.0001 in. or less and fill a clearance up to 0.010 in. It requires about 6 hr to harden, 10 min. with activator or 2 min. if heat is applied. Sometimes a setscrew in the hub is needed to position the gear accurately and permanently until the sealant has been completely cured.

Gears can be easily removed from a shaft or adjusted on the shaft by forcibly breaking the bond and then reapplying the sealant after the new position is determined. It will hold any metal to any other metal. Cost is low in comparison to other methods because extra machining and tolerances can be eased.

5 Setscrews

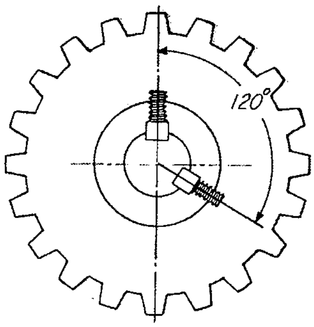

Two setscrews at 90° or 120° to each other are usually sufficient to hold a gear firmly to a shaft. More security results with a flat on the shaft, which prevents the shaft from being marred. Flats give added torque capacity and are helpful for frequent disassembly. Sealants applied on setscrews prevent loosening during vibration.

6 GEARS INTEGRAL WITH SHAFT

Fabricating a gear and shaft from the same material is sometimes economical with small gears where cost of machining shaft from OD of gear is not prohibitive. Method is also used when die-cast blanks are feasible or when space limitations are severe and there is no room for gear hubs. No limit to the amount of torque which can be resisted—usually gear teeth will shear before any other damage takes place.

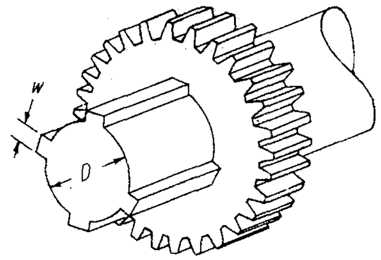

	4-spline	6-spline
D	W	W
1/2	0.120	0.125
3/4	0.181	0.188
7/8	0.211	0.219
1	0.241	0.250
1-1/4	0.301	0.313

7 SPLINED SHAFTS

Ideal where gear must slide in lateral direction during rotation. Square splines often used, but involute splines are self-centering and stronger. Nonsliding gears are pinned or held by threaded nut or retaining ring.

Torque strength is high and dependent on number of splines employed. Use these recommended dimensions for width of square tooth for 4-spline and 6-spline systems; although other spline systems are some times used. Stainless steel shafts and gears are recommended. Avoid dissimilar metals or aluminum. Relative cost is high.

8 KNURLING

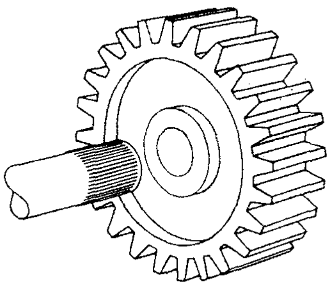

A knurled shaft can be pressed into the gear bore, to do its own broaching, thus keying itself into a close-fitting hole. This avoids need for supplementary locking device such as lock rings and threaded nuts.

The method is applied to shafts $\frac{1}{4}$ in. or under and does not weaken or distort parts by the machining of groove or holes. It is inexpensive and requires no extra parts.

Knurling increases shaft dia by 0.002 to 0.005 in. It is recommended that a chip groove be cut at the trailing edge of the knurl. Tight tolerances on shaft and bore dia are not needed unless good concentricity is a requirement The unit can be designed to slip under a specific load—hence acting as a safety device.

9 KEYING

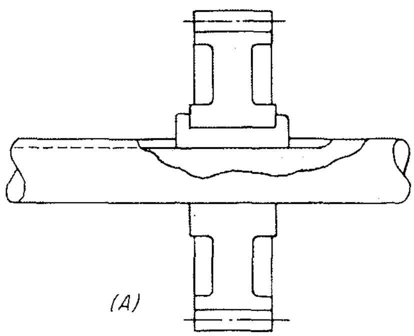

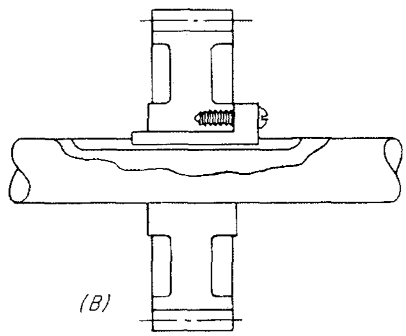

Generally employed with large gears, but occasionally considered for small gears in instruments. Feather key (A) allows axial movement but keying must be milled to end of shaft. For blind keyway (B), use setscrew against the key, but method permits locating the gear anywhere along length of shaft.

Keyed gears can withstand high torque, much more than the pinned or knurled shaft and, at times, more than the splined shafts because the key extends well into both the shaft and gear bore. Torque capacity is comparable with that of the integral gear and shaft. Maintenance is easy because the key can be removed while the gear remains in the system.

Materials for gear, shaft and key should be similar preferably steel. Larger gears can be either cast or forged and the key either hot- or cold-rolled steel. However, in instrument gears, stainless steel is required for most applications. Avoid aluminum gears and keys.

10 STAKING

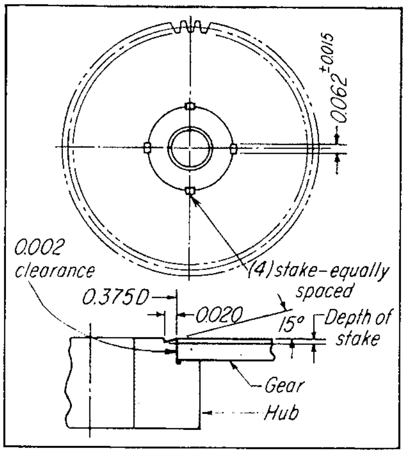

No. of stakes	Depth	Clearance	Torque in.-lb.
4	0.015	0.0020	27
4	0.015	0.0025	20
4	0.020	0.0020	28
4	0.020	0.0020	30
8	0.020	0	52

It is difficult to predict the strength of a staked joint—but it is a quick and economical method when the gear is positioned at the end of the shaft.

Results from five tests we made on gears staked on 0.375-in. hubs are shown here with typical notations for specifying staking on an assembly drawing. Staking was done with a 0.062-in. punch having a 15° bevel. Variables in the test were: depth of stake, number of stakes, and clearance between hub and gear. Breakaway torque ranged from 20 to 52 in.-lb.

Replacing a gear is not simple with this method because the shaft is mutirated by the staking. But production costs are low.

11 SPRING WASHER

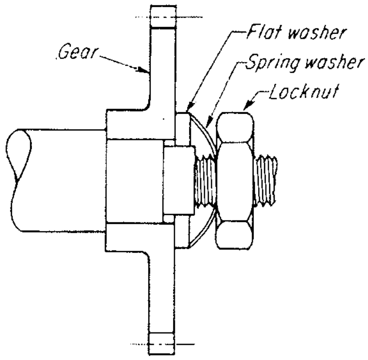

Assembly consists of locknut, spring washer, flat washer and gear. The locknut is adjusted to apply a predetermined retaining force to the gear. This permits the gear to slip when overloaded—hence avoiding gear breakage or protecting the drive motor from overheating.

Construction is simple and costs less than if a slip clutch is employed. Popular in breadboard models.

12 TAPERED SHAFT

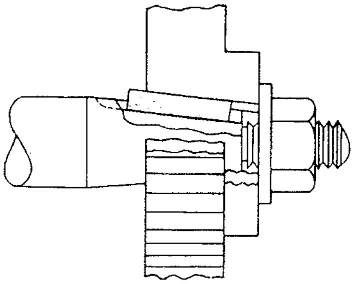

Tapered shaft and matching taper in gear bore need key to provide high torque resistance, and threaded nut to tighten gear onto taper. Expensive but suitable for larger gear applications where rigidity, concentricity and easy disassembly are important. A larger dia shaft is needed than with other methods. Space can be problem because of protruding threaded end. Keep nut tight.

13 TAPERED RINGS

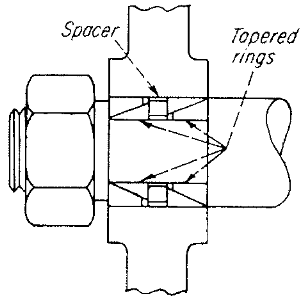

These interlock and expand when tightened to lock gear on shaft. A purchased item, the rings are quick and easy to use, and do not need close tolerance on bore or shaft. No special machining is required and torque capacity is fairly high. If lock washer is employed, the gear can be adjusted to slip at predetermined torque.

14 TAPERED BUSHINGS

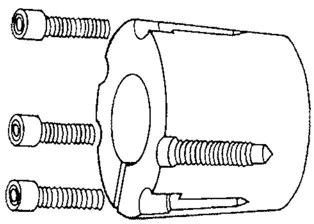

This, too, is a purchased item—but generally restricted to shaft diameters ½ in. and over. Adapters available for untapered bores of gears. Unthreaded half-holes in bushing align with threaded half-holes in gear bore. Screw pulls bushing into bore, also prevents rotational slippage of gear under load.

15 DIE-CAST HUB

Die-casting machines are available, which automatically assemble and position gear on shaft, then die-cast a metal hub on both sides of gear for retention. Method can replace staked assembly. Gears are fed by hopper, shafts by magazine. Method maintains good tolerances on gear wobble, concentricity and location. For high-production applications. Costs are low once dies are made.

14 Ways to Fasten Hubs to Shafts

M. Levine

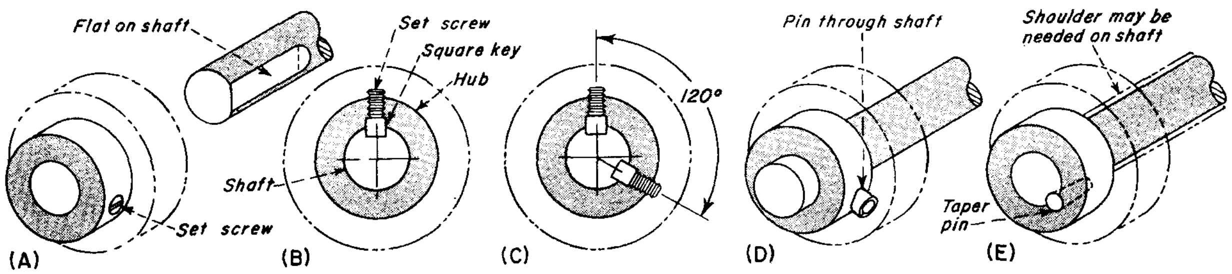

1 Cup-point setscrew . . .

in hub (A) bears against flat on shaft. Fastening suitable for fractional horsepower drives with low shock loads. Unsuitable when frequent removal and assembly necessary. Key with setscrew (B) prevents shaft marring from frequent removal and assembly. Not suitable where high concentricity is required.

Can withstand high shock loads. Two keys 120° apart (C) transmit extra heavy loads. Straight or tapered pin (D) prevents end play. For experimental setups expanding pin is positive yet easy to remove. Gear-pinning machines are available. Taper pin (E) parallel to shaft may require shoulder on shaft. Can be used when gear or pulley has no hub.

4 Splined shafts . . .

are frequently used when gear must slide. Square splines can be ground to close minor diameter fits but involute splines are self-centering and stronger. Non-sliding gears may be pinned to shaft if provided with hub.

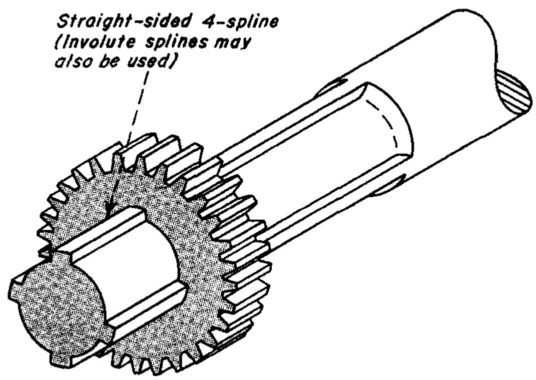

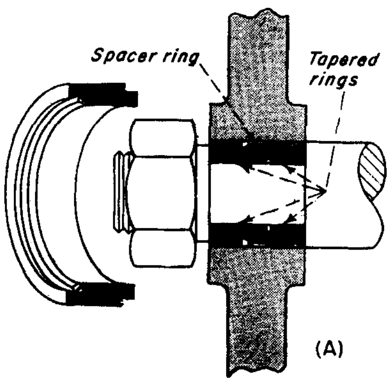

7 Interlocking . . .

tapered rings hold hub tightly to shaft when nut is tightened. Coarse tolerance machining of hub and shaft does not effect concentricity as in pinned and keyed assemblies. Shoulder is required (A) for end-of-shaft mounting; end plates and four bolts (B) allow hub to be mounted anywhere on shaft.

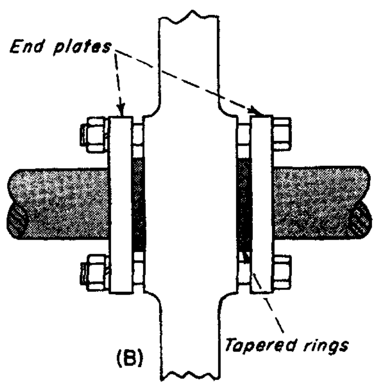

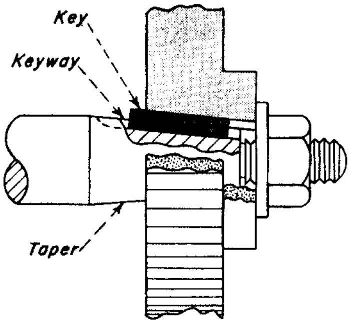

2 Tapered shaft . . .

with key and threaded end provides rigid, concentric assembly. Suitable for heavy-duty applications, yet can be easily dissasembled.

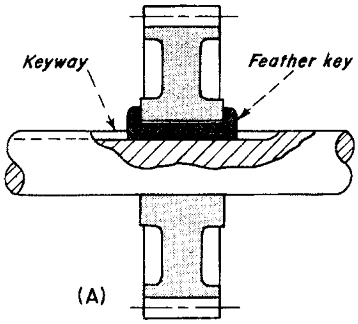

3 Feather key . . .

(A) allows axial movement. Keyway must be milled to end of shaft. For blind keyway (B) hub and key must be drilled and tapped, but design allows gear to be mounted anywhere on shaft with only a short keyway.

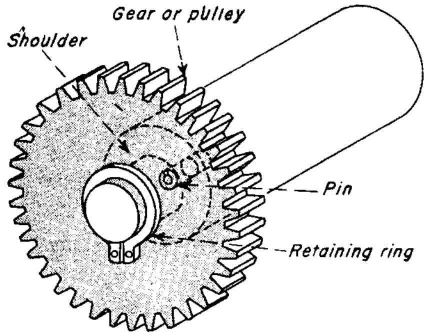

5 Retaining ring . . .

allows quick removal in light load applications. Shoulder on shaft necessary. Pin securing gear to shaft can be shear-pin if protection against excessive load required.

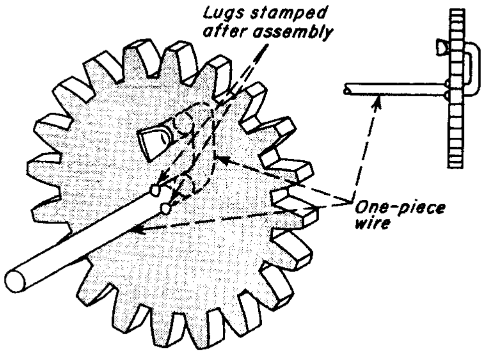

6 Stamped gear . . .

and formed wire shaft used mostly in toys. Lugs stamped on both legs of wire to prevent disassembly. Bend radii of shaft should be small enough to allow gear to seat.

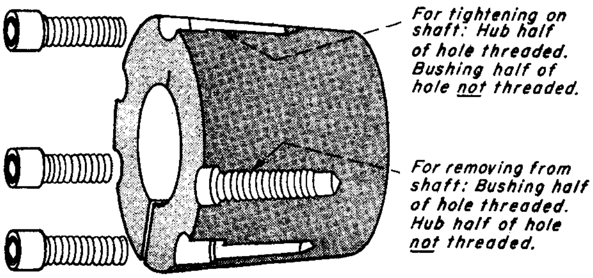

8 Split bushing . . .

has tapered outer diameter. Split holes in bushing align with split holes in hub. For tightening, hub half of hole is tapped, bushing half is un-tapped. Screw therefore pulls bushing into hub as screw is screwed into hub. Bushing is jacked from hub by a reverse procedure. Sizes of bushings avaliable for ½- to 10-in. dia shafts. Adapters are available for untapered hubs.

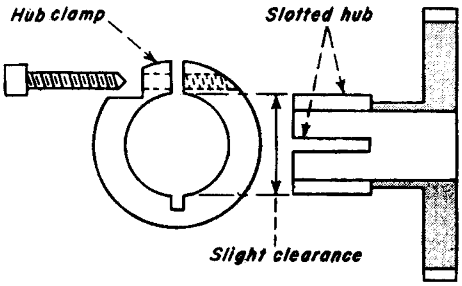

9 Split hub . . .

of stock precision gear is clamped onto shaft with separate hub clamp. Manufacturers list correctly dimensioned hubs and clamps so that efficient fastening can be made based on precision ground shaft. Ideal for experimental set-ups.

Attaching Hubless Gears to Shafts

Thin gears and cams save space–but how to fasten them to their shafts? These illustrated methods give simple, effective answers.

L. Kasper

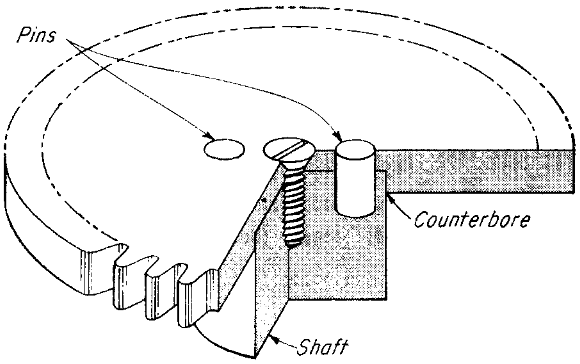

1 COUNTERBORE with close fit on shaft ensures concentric mounting. Torque is transmitted by pins; positive fastening is provided by flathead screw.

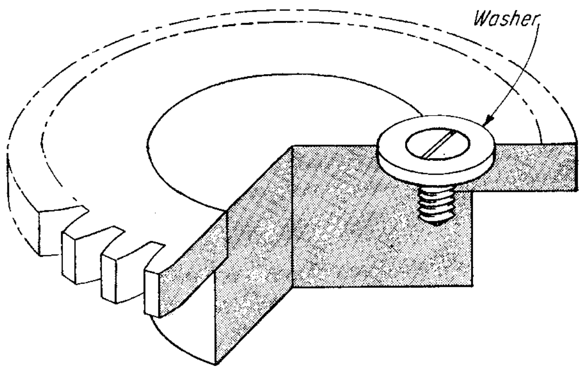

2 TIGHT-FITTING washer in counterbored hole carries the radial load; its shear area is large enough to ensure ample strength.

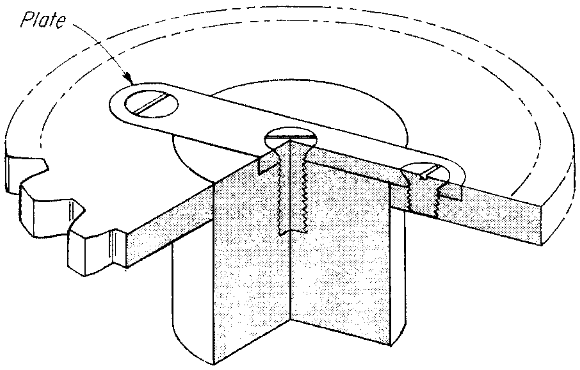

3 PLATE gives greater resistance to shear when radial loads are likely to be heavy. When the gear is mounted, the plate becomes the driver; the center screw merely acts as a retainer.

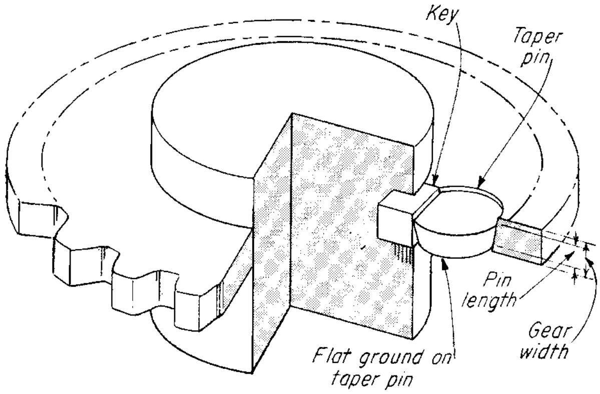

4 KEY AND FLATTED TAPER-PIN should not protrude above surface of gear; pin length should be slightly shorter than gear width. Note that this attachment is not positive—gear retention is by friction only.

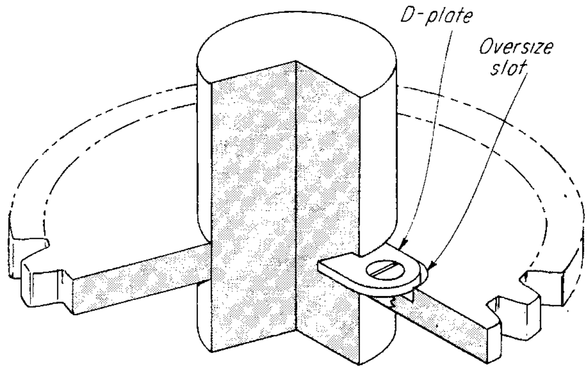

5 D-PLATE keys gear to shaft; optimum slot depth in shaft will depend upon torque forces and stop-and-start requirements—low, constant torque requires only minimum depth and groove length; heavy-duty operation requires enough depth to provide longer bearing surface.

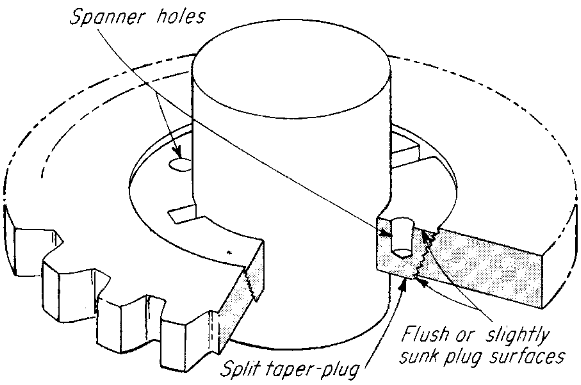

6 TAPERED PLUG is another friction holding device. This type mounting should be used so that the radial load will tend to tighten rather than loosen the thread. For added security, thread can be lefthand to reduce tampering risk.

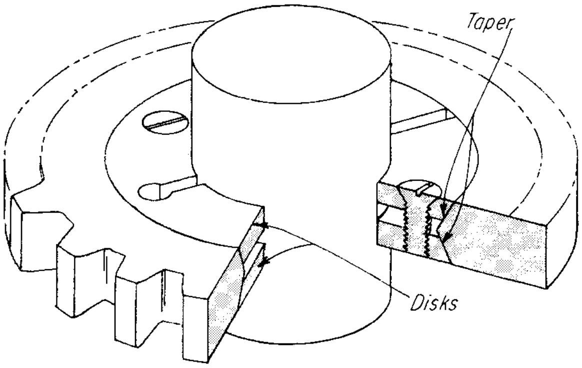

7 TWO FRICTION DISKS, tapered to about 5° included angle on their rims, are bored to fit the shaft. Flathead screws provide clamping force, which can be quickly eased to allow axial or radial adjustment of gear.

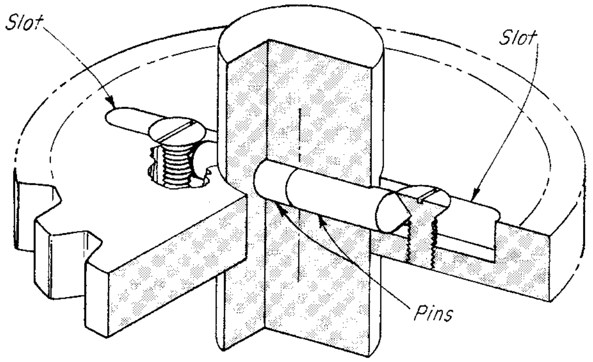

8 TWO PINS in radial hole of shaft provide positive drive that can be easily disassembled. Pins with conical end are forced tightly together by flathead screws. Slot length should be sufficient to allow pins to be withdrawn while gear is in place if backside of gear is "tight" against housing.

10 Different Types of Splined Connections

W. W. Heath

CYLINDRICAL TYPES

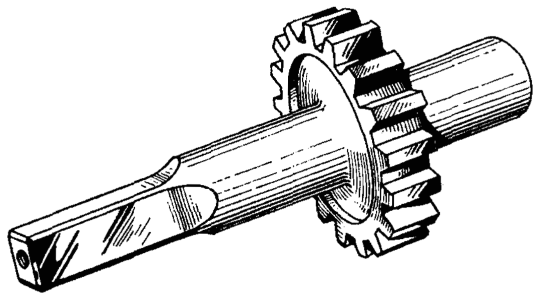

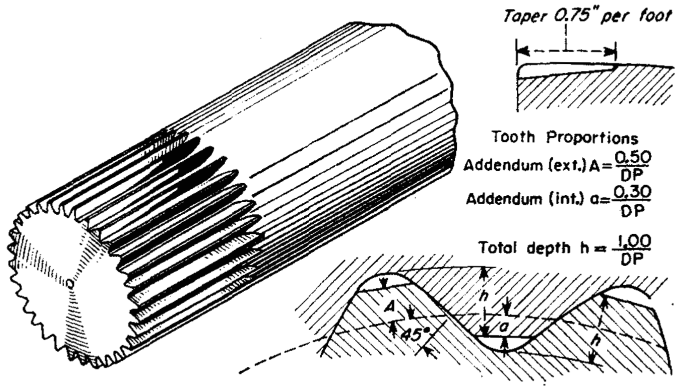

1 SQUARE SPLINES make a simple connection and are used mainly for applications of light loads, where accurate positioning is not important. This type is commonly used on machine tools; a cap screw is necessary to hold the enveloping member.

2 SERRATIONS of small size are used mostly for applications of light loads. Forcing this shaft into a hole of softer material makes an inexpensive connection. Originally straight-sided and limited to small pitches, 45 deg serrations have been standardized (SAE) with large pitches up to 10 in. dia. For tight fits, serrations are tapered.

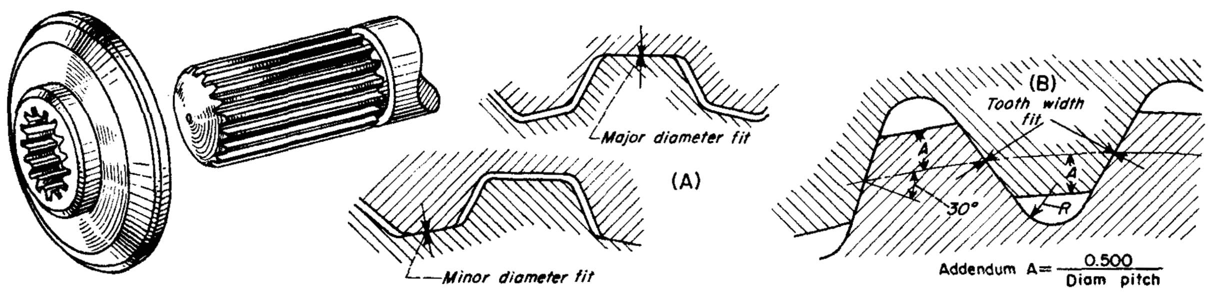

5 INVOLUTE-FORM splines are used where high loads are to be transmitted. Tooth proportions are based on a 30 deg stub tooth form. (A) Splined members may be positioned either by close fitting major or minor diameters. (B) Use of the tooth width or side positioning has the advantage of a full fillet radius at the roots. Splines may be parallel or helical. Contact stresses of 4,000 psi are used for accurate, hardened splines. Diametral pitch above is the ratio of teeth to the pitch diameter.

FACE TYPES

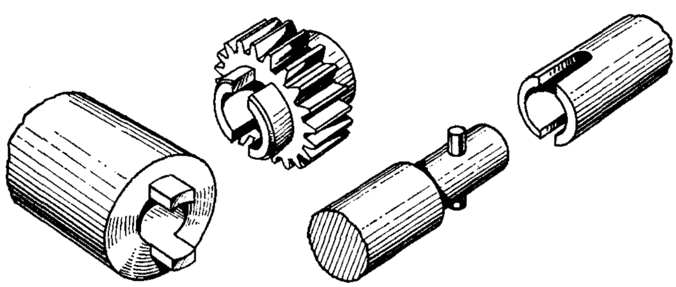

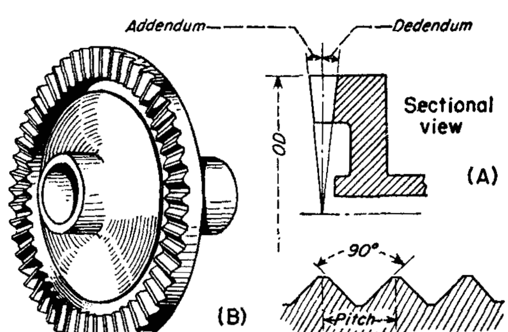

FELLOWS GEAR SHAPER CO

8 MILLED SLOTS in hubs or shafts make an inexpensive connection. This type is limited to moderate loads and requires a locking device to maintain positive engagement. Pin and sleeve method is used for light torques and where accurate positioning is not required.

9 RADIAL SERRATIONS by milling or shaping the teeth make a simple connection. (A) Tooth proportions decrease radially. (B) Teeth may be straight-sided (castellated) or inclined; a 90 deg angle is common.

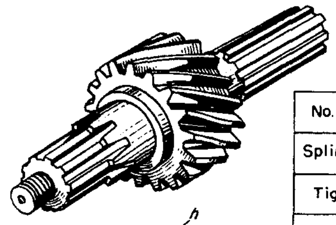

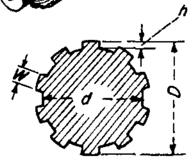

SAE STANDARD SPLINE PROPORTIONS

No. of splines			4	6	10 or 16
Spline width		W	0.241 D	0.250D	0.156D*
Tight fit		h	0.075D	0.050D	0.045D
Sliding fit	Unloaded	h	0.125D	0.075D	0.070D
	loaded	h	—	0.100D	0.095D
* Width of 16-tooth spline is 0.098D					
Root dia, d=D−2h					

3 STRAIGHT-SIDED splines have been widely used in the automotive field. Such splines are often used for sliding members. The sharp corner at the root limits the torque capacity to pressures of approximately 1,000 psi on the spline projected area. For different applications, tooth height is altered as shown in the table above.

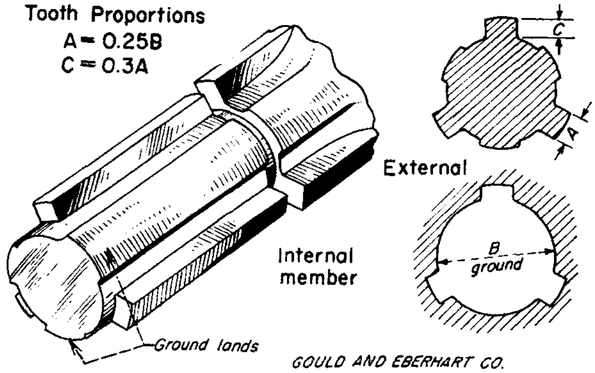

4 MACHINE-TOOL spline has a wide gap between splines to permit accurate cylindrical grinding of the lands—for precise positioning. Internal parts can be ground readily so that they will fit closely with the lands of the external member.

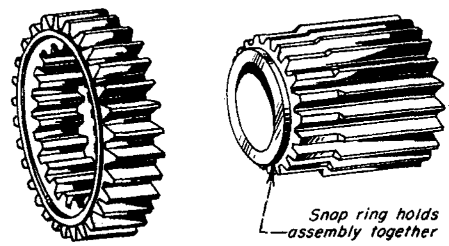

6 SPECIAL INVOLUTE splines are made by using gear tooth proportions. With full depth teeth, greater contact area is possible. A compound pinion is shown made by cropping the smaller pinion teeth and internally splining the larger pinion.

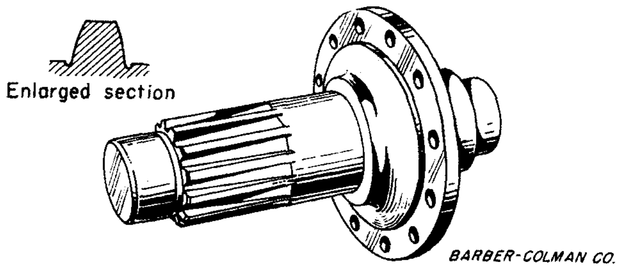

7 TAPER-ROOT splines are for drives which require positive positioning. This method holds mating parts securely. With a 30 deg involute stub tooth, this type is stronger than parallel root splines and can be hobbed with a range of tapers.

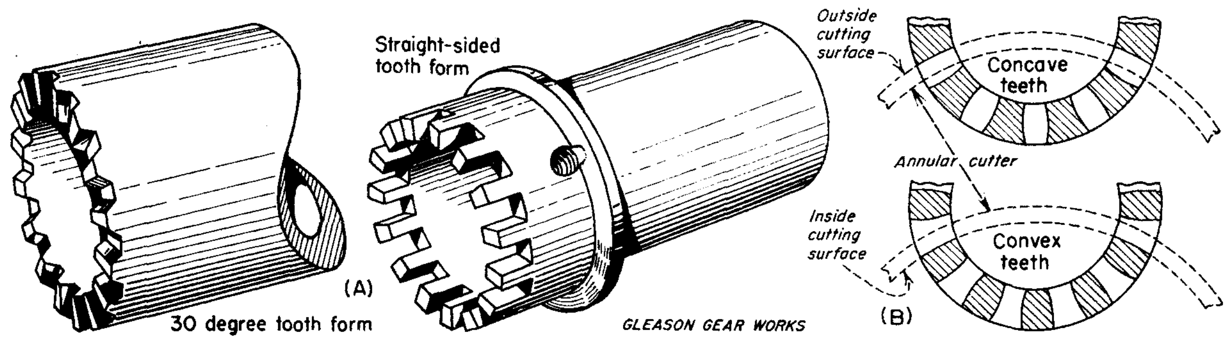

10 CURVIC COUPLING teeth are machined by a face-mill type of cutter. When hardened parts are used which require accurate positioning, the teeth can be ground. (A) This process produces teeth with uniform depth and can be cut at any pressure angle, although 30 deg is most common. (B) Due to the cutting action, the shape of the teeth will be concave (hour-glass) on one member and convex on the other—the member with which it will be assembled.

Typical Methods of Coupling Rotating Shafts I

Methods of coupling rotating shafts vary from simple bolted flange constructions to complex spring and synthetic rubber mechanisms. Some types incorporating chain, belts, splines, bands, and rollers are described and illustrated below.

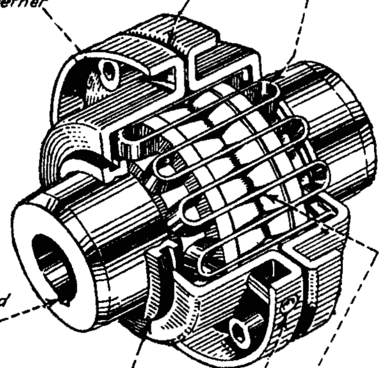

FIG. 1

The Falk Corp.

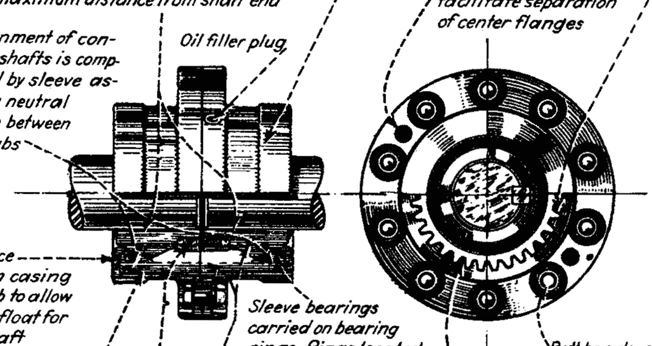

FIG. 2

Bartlett - Hayward Div., Koppers Co., Inc.

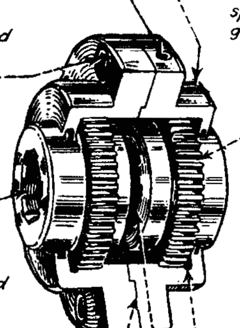

FIG. 3

Barcus Engineering Co., Inc.

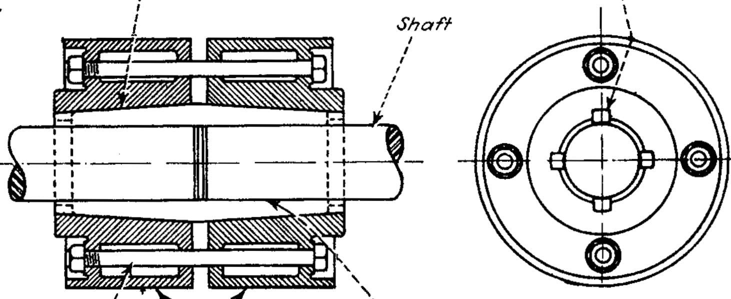

FIG. 4

W. H. Nicholson and Co

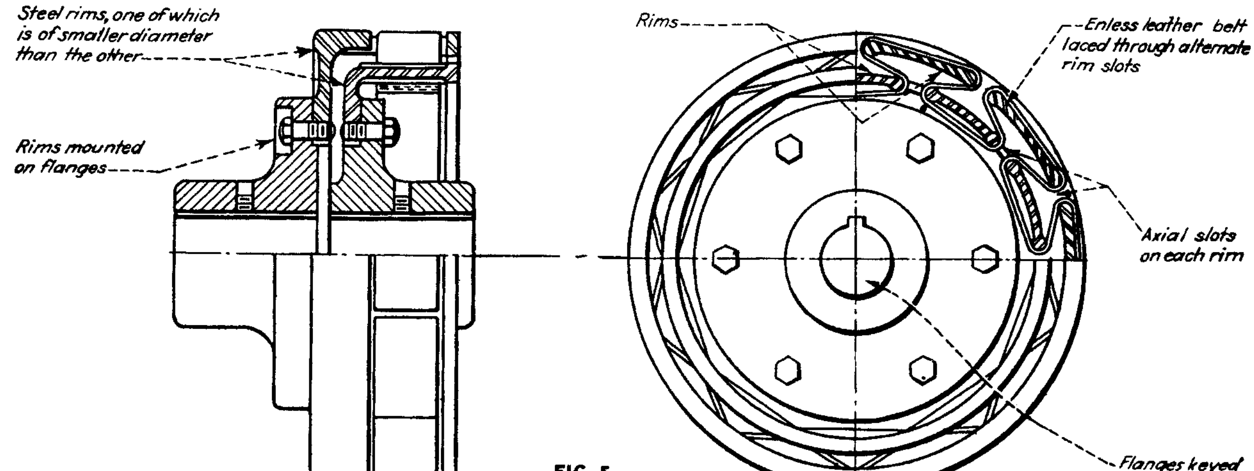

FIG. 5

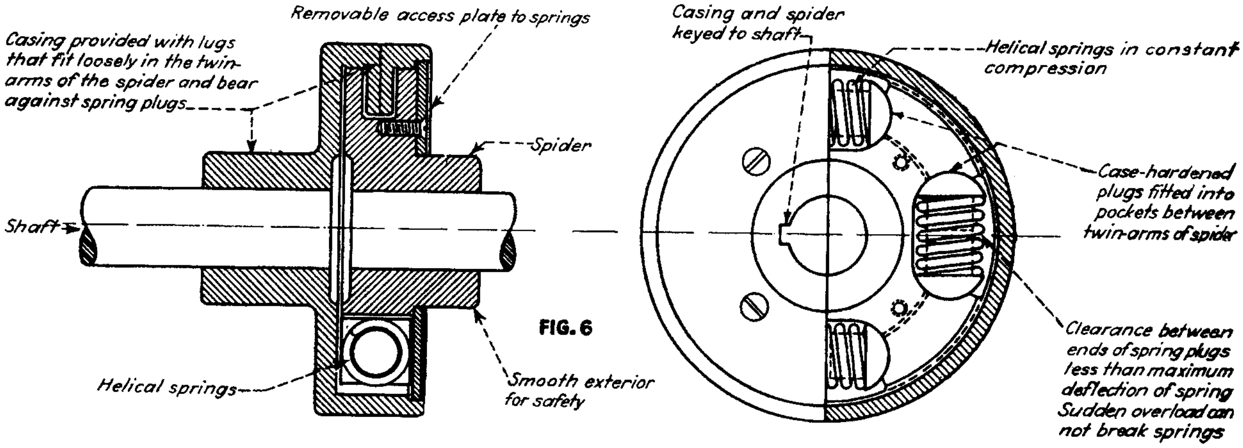

FIG. 6

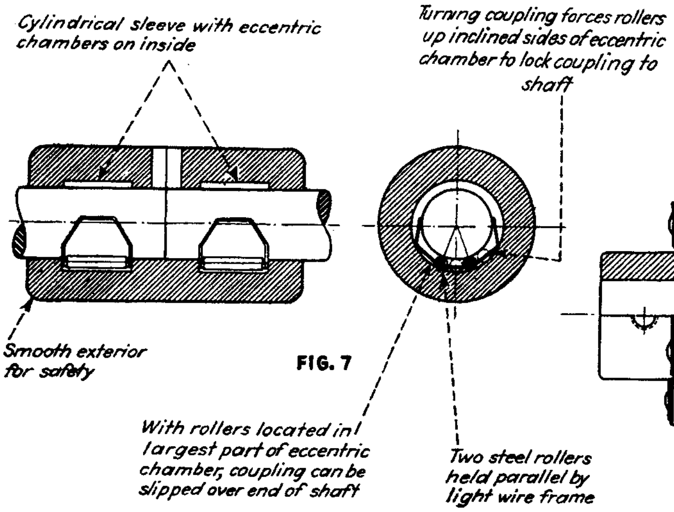

FIG. 7

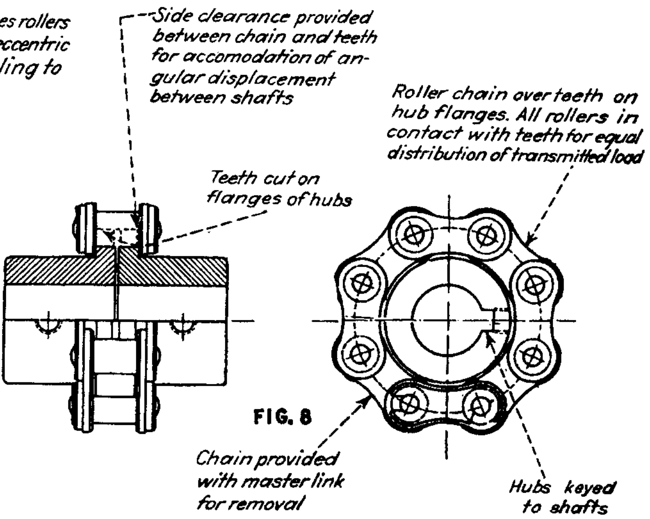

FIG. 8

Typical Methods of Coupling Rotating Shafts II

Shafts couplings that utilize internal and external gears, balls, pins and non-metallic parts to transmit torque are shown herewith.

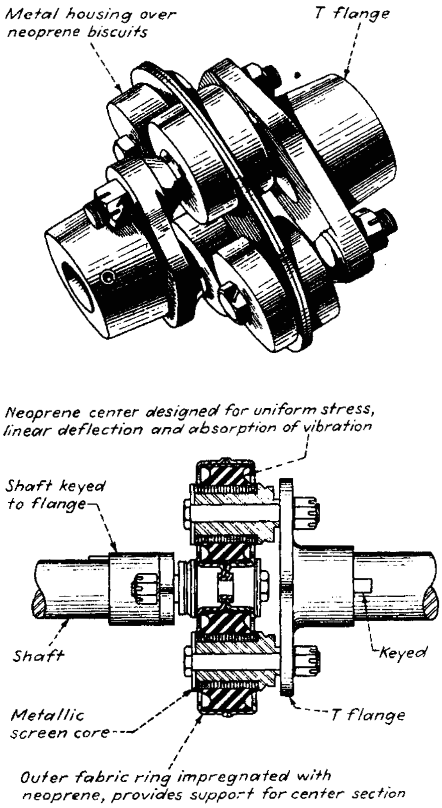

FIG.1 Morse Chain Co

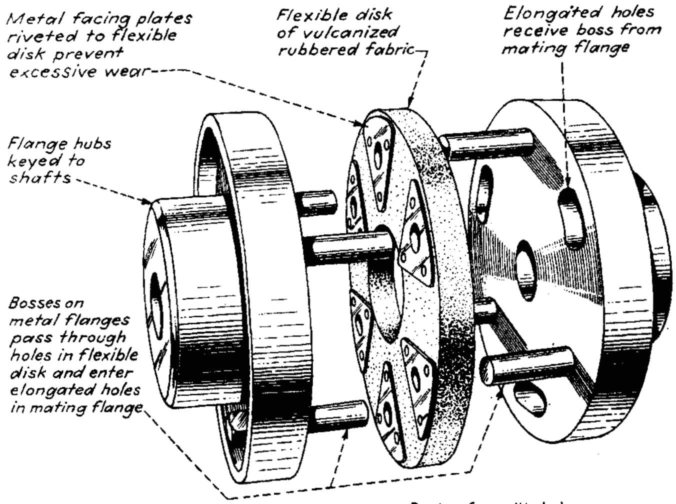

FIG.2 Boston Gear Work, Inc.

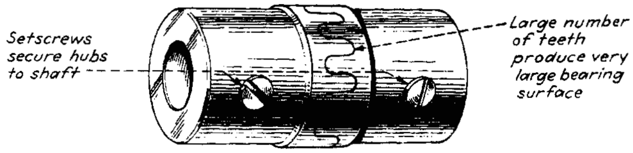

FIG.3 Boston Gear Works, Inc.

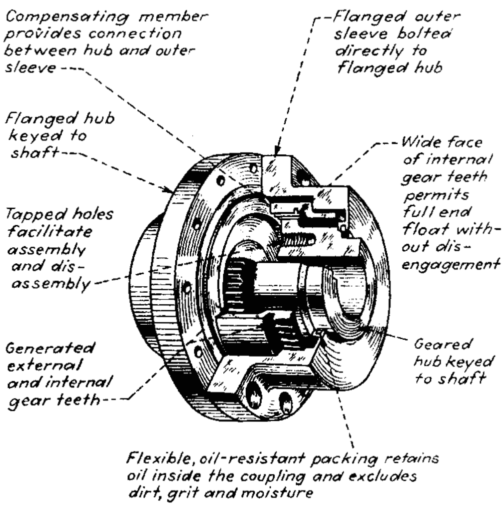

FIG.4 Farrel-Birmingham Co., Inc.

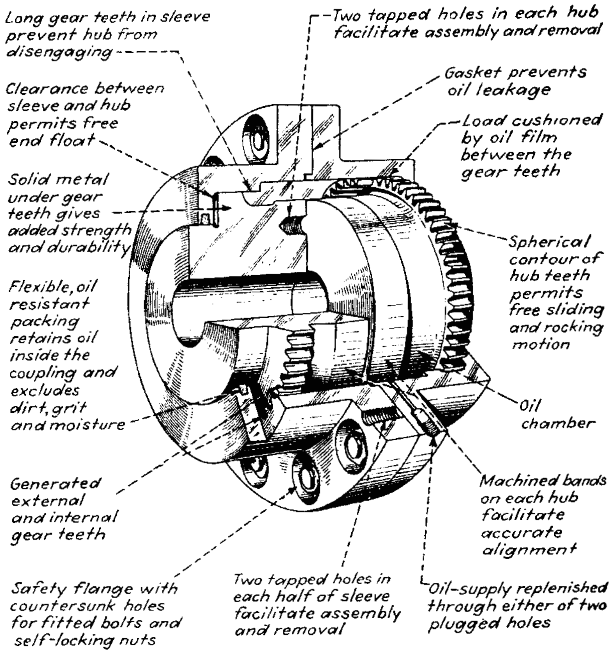

FIG.5 Farrel Birmingham Co., Inc.

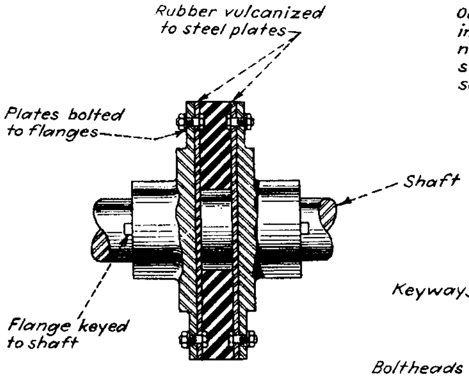

FIG. 6

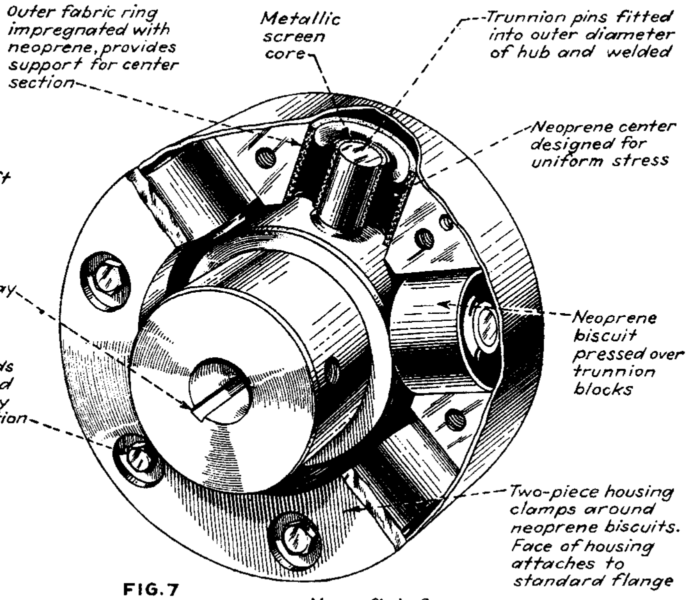

FIG. 7 Morse Chain Co.

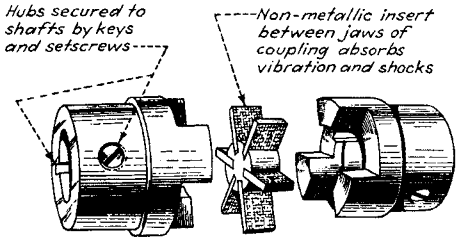

FIG. 8 Boston Gear Works, Inc.

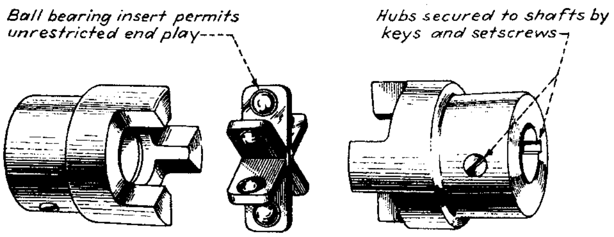

FIG. 9 Boston Gear Works, Inc.

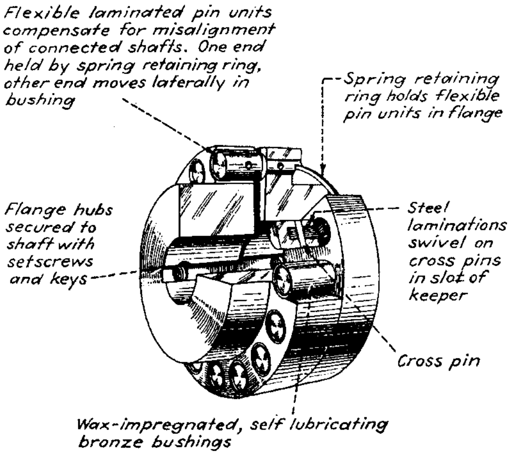

FIG. 10 John Waldron Corp.

No lubrication is required on this coupling

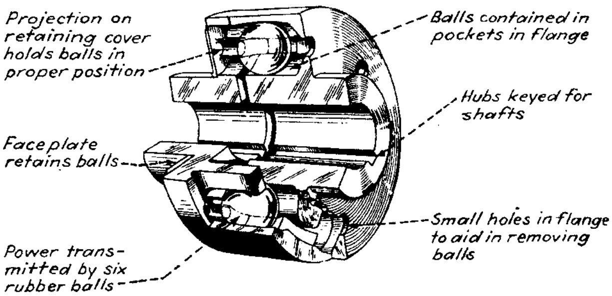

FIG. 11 Crocker-Wheeler Div., Joshua Hendy Iron Works

Typical Designs of Flexible Couplings I

Cyril Donaldson

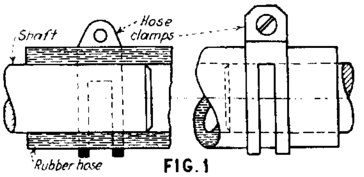

FIG. 1

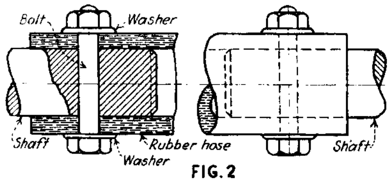

FIG. 2

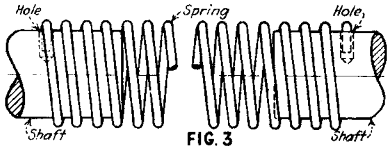

FIG. 3

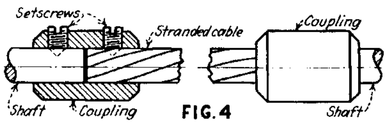

FIG. 4

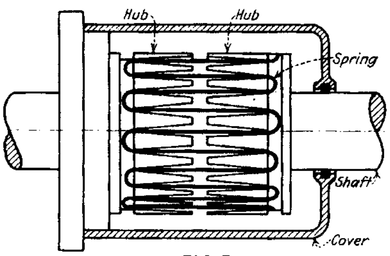

FIG. 5

Fig. 1—A rubber hose clamped to two shafts. For applications where the torque is low and slippage unimportant. It is easily assembled and disconnected without disturbing either machine element. Adaptable to changes in longitudinal distance between machines. This coupling absorbs shocks, is not damaged by overloads, does not set up end thrusts, requires no lubrication and compensates for both angular and offset misalignment.

Fig. 2—Similar to Fig. 1, but positive drive is assured by bolting hose to shafts. Has same advantages as type in Fig. 1, except there is no overload protection other than the rupture of the hose.

Fig. 3—The use of a coiled spring fastened to shafts gives the same action as a hose. Has excellent shock absorbing qualities, but torsional vibrations are possible. Will allow end play in shafts, but sets up end thrust in so doing. Other advantages are same as in types shown in Figs. 1 and 2. Compensates for misalignment in any direction.

Fig. 4—A simple and effective coupling for low torques and unidirectional rotation. Stranded cable provides a positive drive with desirable elasticity. Inertia of rotating parts is low. Easily assembled and disconnected without disturbing either shaft. Cable can be encased and length extended to allow for right angle bends such as used on dental drills and speedometer drives. Ends of cable are soldered or bound with wire to prevent unraveling.

Fig. 5—A type of Falk coupling that operates on the same principle as design shown in Fig. 6, but has a single flat spring in place of a series of coiled springs. High degree of flexibility obtained by use of tapered slots in hubs. Smooth operation is maintained by inclosing the working parts and packing with grease.

Fig. 6—Two flanges and a series of coiled springs give a high degree of flexibility. Used only where the shafts have no free end play. Needs no lubrication, absorbs shocks and provides protec-

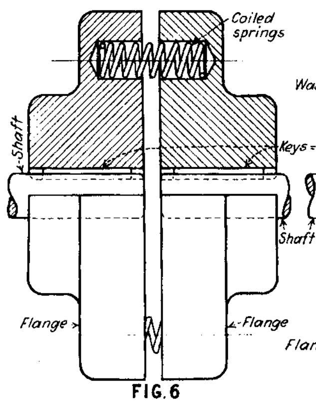

FIG. 6

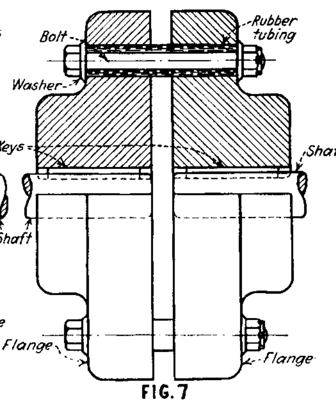

FIG. 7

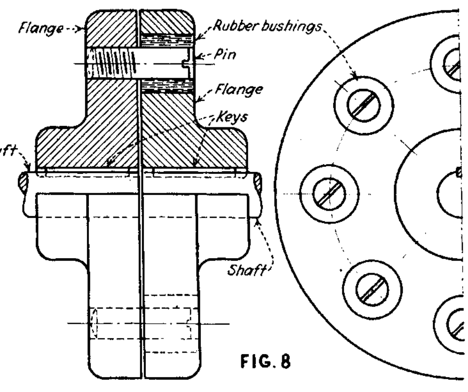

FIG. 8

tion against overloads, but will set up torsional vibrations. Springs can be of round or square wire with varying sizes and pitches to allow for any degree of flexibility.

Fig. 7—Is similar to Fig. 6, except that rubber tubing, reinforced by bolts, is used instead of coiled springs. Is of sturdier construction but more limited in flexibility. Has no overload protection other than shearing of the bolts. Good anti-vibration properties if thick rubber tubing is used. Can absorb minor shocks. Connection can be quickly disassembled.

Fig. 8—A series of pins engage rubber bushings cemented into flange. Coupling is easy to install. Flanges being accurately machined and of identical size makes accurate lining-up with spirit level possible. Will allow minor end play in shafts, and provides a positive drive with good flexibility in all direction.

Fig. 9—A Foote Gear Works flexible coupling which has shear pins in a separate set of bushings to provide overload protection. Construction of studs, rubber bushings and self-lubricating bronze bearings is in principle similar to that shown in Fig. 10. Replaceable shear pins are made of softer material than the shear pin bushings.

Fig. 10—A design made by the Ajax Flexible Coupling Company. Studs are firmly anchored with nuts and lock washers and bear in self-lubricating bronze bushings spaced alternately in both flanges. Thick rubber bushings cemented in flanges are forced over the bronze bushings. Life of coupling said to be considerably increased because of self-lubricated bushings.

Fig. 11—Another Foote Gear Works coupling. Flexibility is obtained by solid conically-shaped pins of metal or fiber. This type of pin is said to provide a positive drive of sturdy construction with flexibility in all directions.

Fig. 12—In this Smith & Serrell coupling a high degree of flexibility is obtained by laminated pins built-up of tempered spring steel leaves. Spring leaves secured to holder by keeper pin. Phosphor bronze bearing strips are welded to outer spring leaves and bear in rectangular holes of hardened steel bushings fastened in flange. Pins are free to slide endwise in one flange, but are locked in the other flange by a spring retaining ring. This type is used for severe duty in both marine and land service.

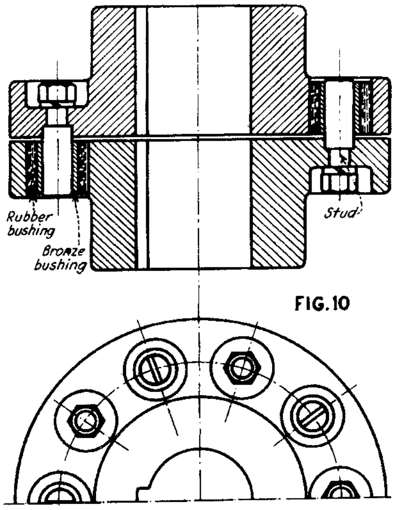

FIG. 10

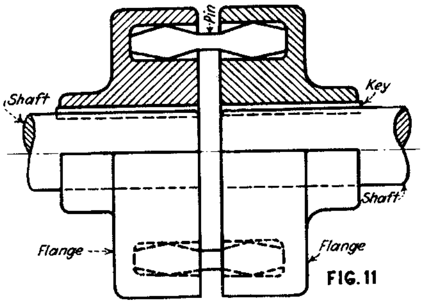

FIG. 11

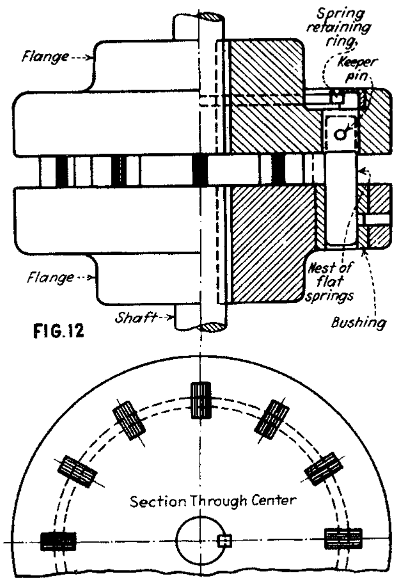

FIG. 12

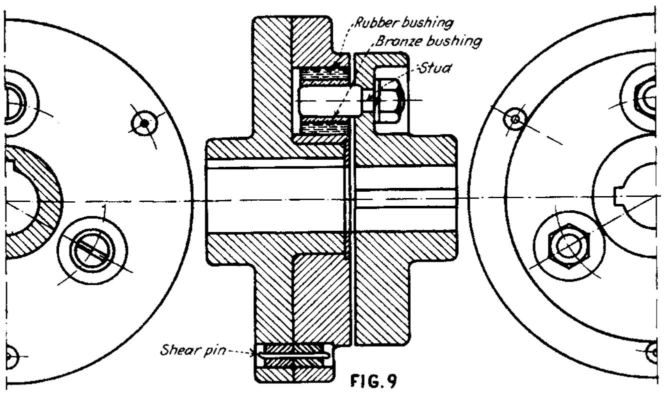

FIG. 9

Typical Designs of Flexible Couplings II

Cyril Donaldson

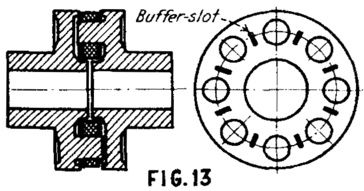

FIG. 13

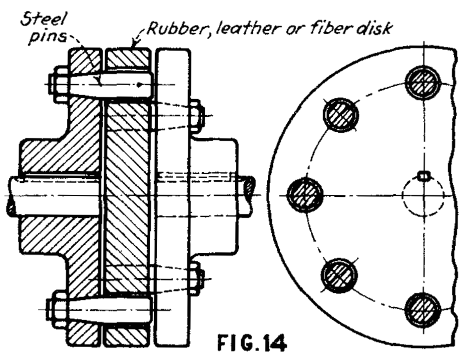

FIG. 14

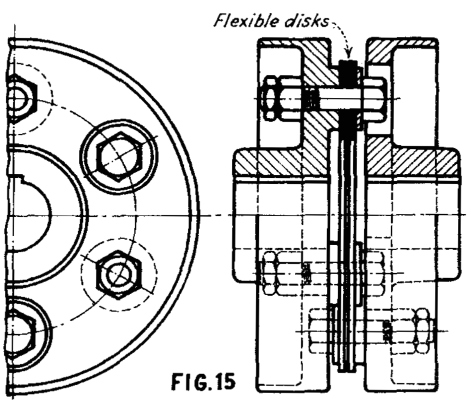

FIG. 15

Fig. 13—In this Brown Engineering Company coupling flexibility is increased by addition of buffer-slots in the laminated leather. These slots also aid in the absorption of shock loads and torsional vibration. Under parallel misalignment or shock loads, buffer slots will close over their entire width, but under angular misalignment buffer slots will close only on one side.

Fig. 14—Flexibility is provided by resilience of a rubber, leather, or fiber disk in this W. A. Jones Foundry & Machine Company coupling. Degree of flexibility is limited to clearance between pins and holes in the disk plus the resilience of the disk. Has good shock absorbing properties, allows for end play and needs no lubrication.

Fig. 15—A coupling made by Aldrich Pump Company, similar to Fig. 14, except bolts are used instead of pins. This coupling permits only slight endwise movement of the shaft and allows machines to be temporarily disconnected without disturbing the flanges. Driving and driven members are flanged for protection against projecting bolts.

Fig. 16—Laminated metal disks are used in this coupling made by Thomas Flexible Coupling Company. The disks are bolted to each flange and connected to each other by means of pins supported by a steel center disk. The spring action of the center ring allows torsional flexibility and the two side rings compensate for angular and offset misalignment. This type of coupling provides a positive drive in either direction without setting up backlash. No lubrication is required.

Fig. 17—A design made by Palmer-Bee Company for heavy torques. Each flange carries two studs upon which are mounted square metal blocks. The blocks slide in the slots of the center metal disk.

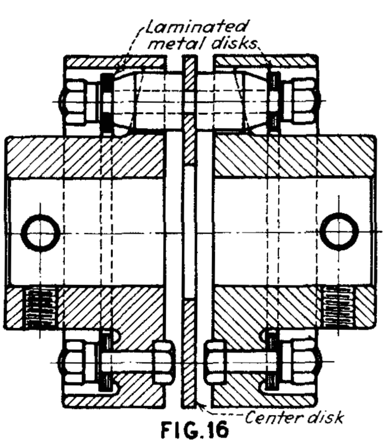

FIG. 16

FIG. 17

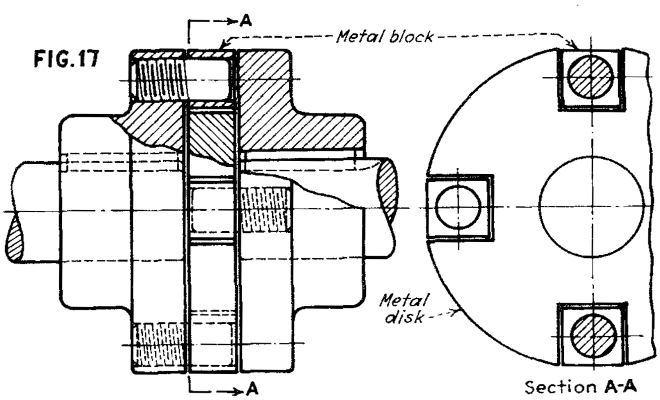

Section A-A

Fig. 18—In this Charles Bond Company coupling a leather disk floats between two identical flanges. Drive is through four laminated leather lugs cemented and riveted to the leather disk. Compensates for misalignment in all directions and sets up no end thrusts. The flanges are made of cast iron and the driving lug slots are cored.

Fig. 19—The principle of the T. B. Wood & Sons Company coupling is the same as Fig. 18, but the driving lugs are cast integrally with the metal flanges. The laminated leather disk is punched out to accommodate the metal driving lugs of each flange. This coupling has flexibility in all directions and does not require lubrication.

Fig. 20—Another design made by Charles Bond Company. The flanges have square recesses into which a built-up leather cube fits. Endwise movement is prevented by through bolts set at right angles. The coupling operates quietly and is used where low torque loads are to be transmitted. Die-castings can be used for the flanges.

Fig. 21—Similar to Fig. 20, being quiet in operation and used for low torques. This is also a design of Charles Bond Company. The floating member is made of laminated leather and is shaped like a cross. The ends of the intermediate member engage the two cored slots of each flange. The coupling will withstand a limited amount of end play.

Fig. 22—Pins mounted in flanges are connected by leather, canvas, or rubber bands. Coupling is used for temporary connections where large torques are transmitted, such as the driving of dynamometers by test engines. Allows for a large amount of flexibility in all directions, absorbs shocks but requires frequent inspection. Machines can be quickly disconnected, especially when belt fasteners are used on the bands. Driven member lags behind driver when under load.

Fig. 23—This Bruce-Macbeth Engine Company coupling is similar to that of Fig. 22, except that six endless wire cable links are used, made of plow-steel wire rope. The links engage small metal spools mounted on eccentric bushings. By turning these bushings the links are adjusted to the proper tension. The load is transmitted from one flange to the other by direct pull on the cable links. This type of coupling is used for severe service.

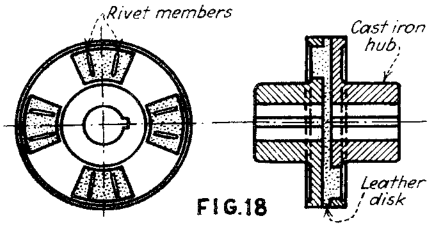

FIG.18

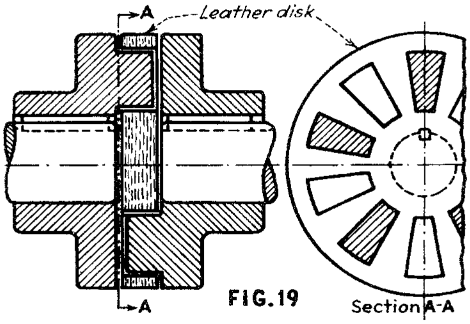

FIG.19

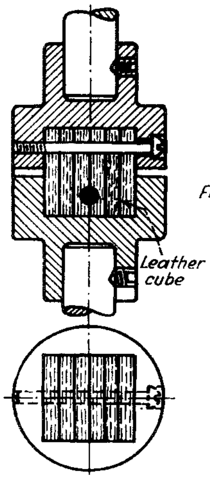

FIG.20

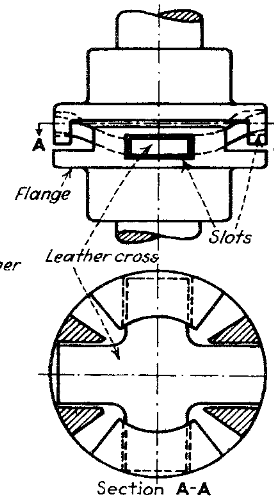

FIG.21

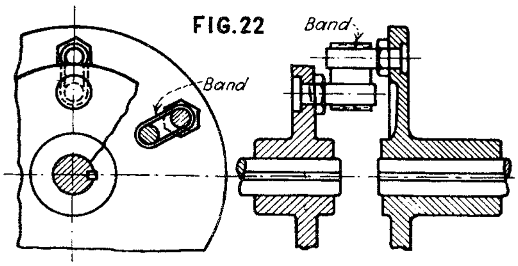

FIG.22

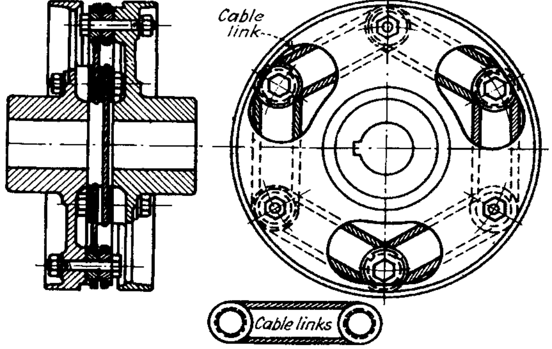

FIG.23

Typical Designs of Flexible Couplings III

Cyril Donaldson

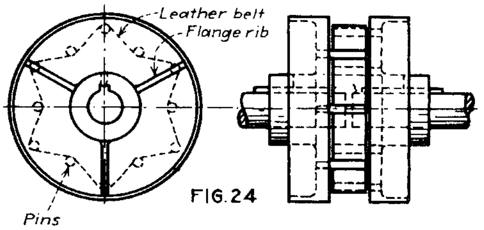

FIG. 24

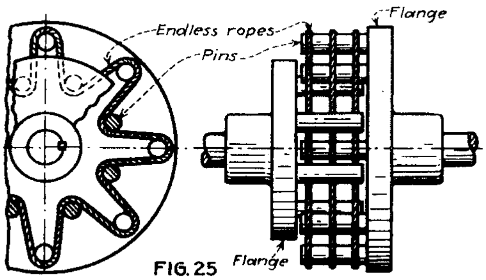

FIG. 25

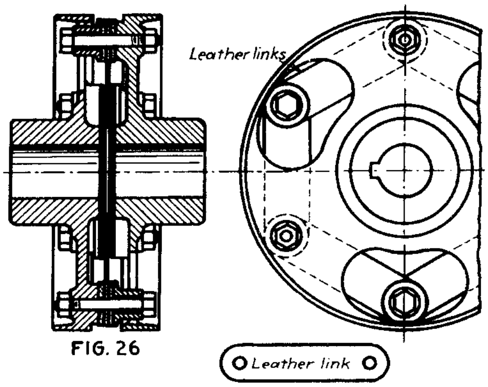

FIG. 26

Fig. 24—This Webster Manufacturing Company coupling uses a single endless leather belt instead of a series of bands, as in Fig. 22. The belt is looped over alternate pins in both flanges. Has good shock resisting properties because of belt stretch and the tendency of the pins to settle back into the loops of the belt.

Fig. 25—This coupling made by the Weller Manufacturing Company is similar to the design in Fig. 24, but instead of a leather belt uses hemp rope, made endless by splicing. The action under load is the same as in the endless belt type.

Fig. 26—This Bruce-Macbeth design uses leather links instead of endless wire cables, as shown in Fig. 23. The load is transmitted from one flange to the other by direct pull of the links, which at the same time allows for the proper flexibility. Intended for permanent installations requiring a minimum of supervision.

Fig. 27—The Oldham form of coupling made by W. A. Jones Foundry and Machine Company is of the two-jaw type with a metal disk. Is used for transmitting heavy loads at low speed.

Fig. 28—The Charles Bond Company star coupling is similar to the cross type shown in Fig. 21. The star-shaped floating member is made of laminated leather. Has three jaws in each flange. Torque capacity is thus increased over the two-jaw or cross type. Coupling takes care of limited end play.

Fig. 29—Combination rubber and canvas disk is bolted to two metal spiders. Extensively used for low torques where compensation for only slight angular misalignment is required. Is quiet in operation and needs no lubrication or other attention. Offset misalignment shortens disk life.

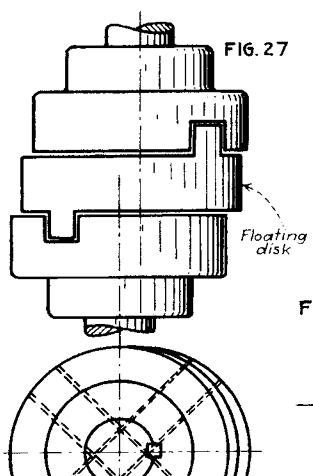

FIG. 27

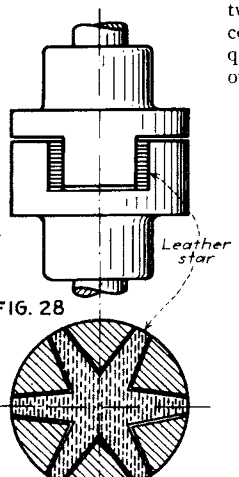

FIG. 28

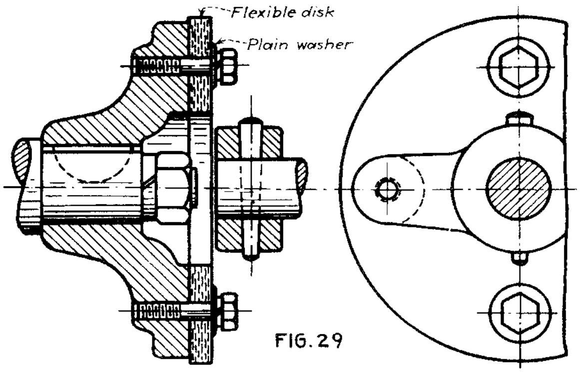

FIG. 29

Fig. 30—A metal block as a floating center is used in this American Flexible Coupling Company design. Quiet operation is secured by facing the block with removable fiber strips and packing the center with grease. The coupling sets up no end thrusts, is easy to assemble and does not depend on flexible material for the driving action. Can be built in small sizes by using hardwood block without facings, for the floating member.

Fig. 31—This Westinghouse Nuttall Company coupling is an all-metal type having excellent torsional flexibility. The eight compression springs compensate for angular and offset misalignment. Allows for some free endwise float of the shafts. Will transmit high torques in either direction. No lubrication is needed.

Fig. 32—Similar to Fig. 29, but will withstand offset misalignment by addition of the extra disk. In this instance the center spider is free to float. By use of two rubber-canvas disks, as shown, coupling will withstand a considerable angular misalignment.

Fig. 33—In this Smith & Serrell coupling a flexible cross made of laminated steel strips floats between two spiders. The laminated spokes, retained by four segmental shoes, engage lugs integral with the flanges. Coupling is intended for the transmission of light loads only.

Fig. 34—This coupling made by Brown Engineering Company is useful for improvising connections between apparatus in laboratories and similar temporary installations. Compensates for misalignment in all directions. Will absorb varying degrees of torsional shocks by changing the size of the springs. Springs are retained by threaded pins engaging the coils. Overload protection is possible by the slippage or breakage of replacable springs.

Fig. 35—In another design by Brown Engineering Company, a series of laminated spokes transmit power between the two flanges without setting up end thrusts. This type allows free end play. Among other advantages are absorption of torsional shocks, has no exposed moving parts, and is well balanced at all speeds. Wearing parts are replacable and working parts are protected from dust.

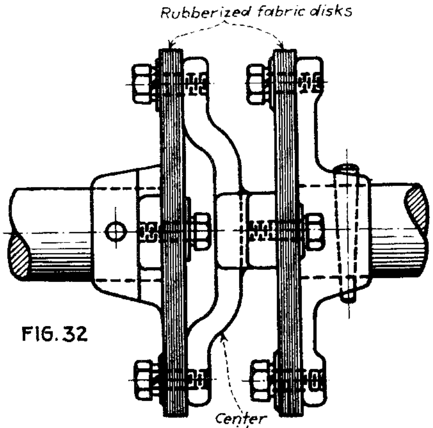

FIG. 32

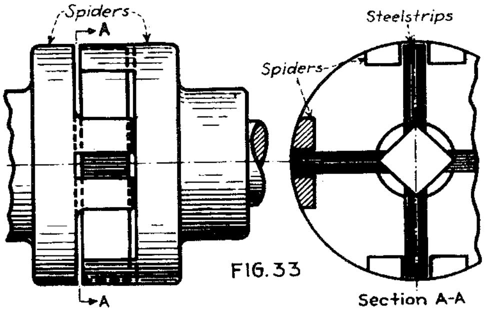

FIG. 33

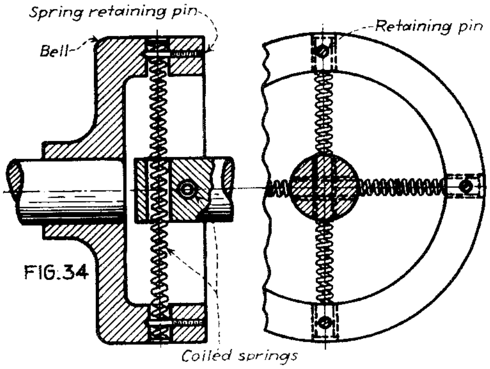

FIG. 34

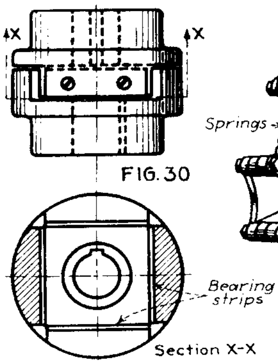

FIG. 30

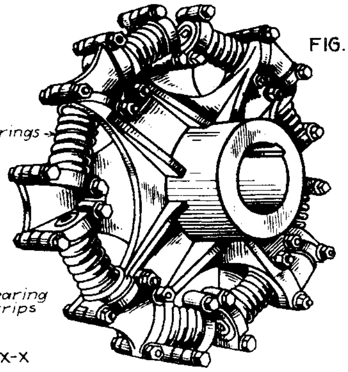

FIG. 31

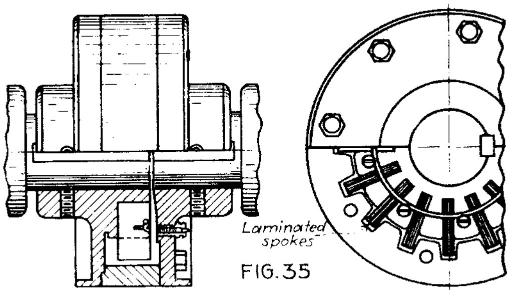

FIG. 35

Low Cost Methods of Coupling Small Diameter Shafts

Sixteen types of low cost couplings, including flexible and non-flexible types. Most are for small diameter, lightly loaded shafts, but a few of them can also be adapted to heavy duty shafts. Some of them are currently available as standard commercial parts.

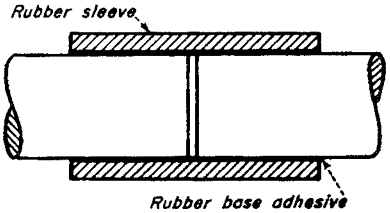

Fig 1—Rubber sleeve has inside diameter smaller than shaft diameters. Using rubber-base adhesive will increase the torque capacity.

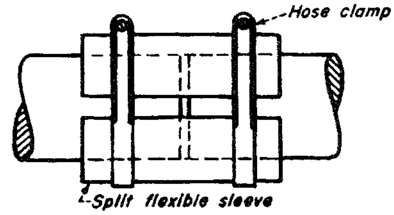

Fig 2—Slit sleeve of rubber or other flexible material is held by hose clamps. Easy to install and remove. Absorbs vibration and shock loads.

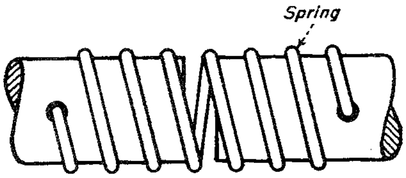

Fig 3—Ends of spring extend through holes in shafts to form coupling. Dia of spring determined by shaft dia, wire dia determined by loads.

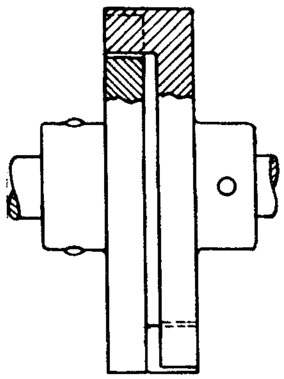

Fig 7—Jaw-type coupling is secured to shafts with straight pins. Commercially available; some have flexible insulators between jaws.

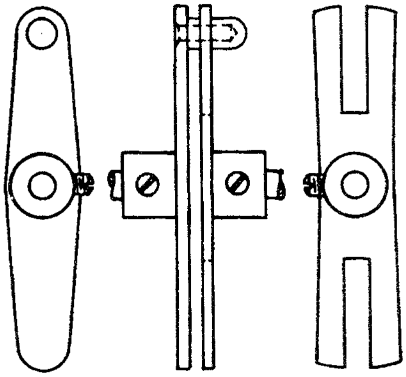

Fig 8—Removable type coupling with insulated coupling pin. A set screw in the collar of each stamped member is used to fasten it to the shaft.

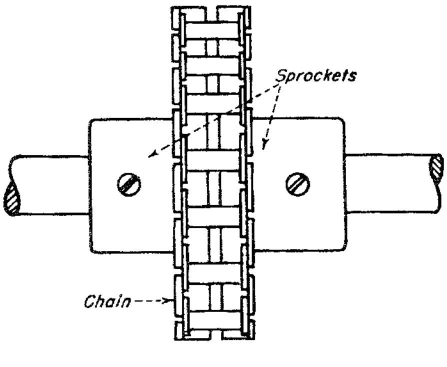

Fig 9—Sprockets mounted on each shaft are linked together with roller chain. Wide range of torque capacity. Commercially available.

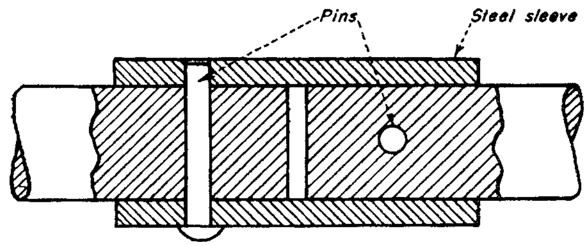

Fig 13—Steel sleeve coupling fastened to shafts with two straight pins. Pins are staggered at 90 degree intervals to reduce the stress concentration.

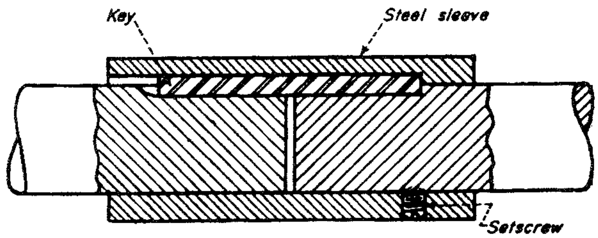

Fig 14—Single key engages both shafts and metal sleeve which is attached to one shaft with setscrew. Shoulder on sleeve can be omitted to reduce costs.

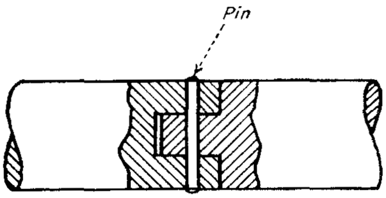

Fig 4—Tongue-and-groove coupling made from shaft ends is used to transmit torque. Pin or set screw keeps shafts in proper alignment.

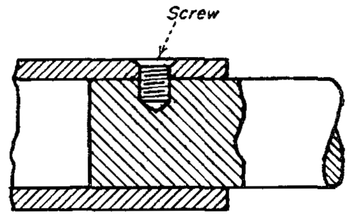

Fig 5—Screw fastens hollow shaft to inner shaft. Set screw can be used for small shafts and low torque by milling a flat on the inner shaft.

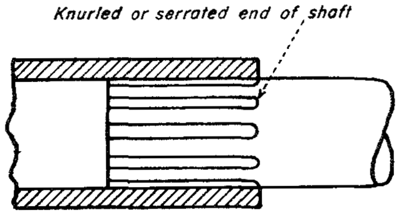

Fig 6—Knurled or serrated shaft is pressed into hollow shaft. Effects of misalignment must be checked to prevent overloading the bearings.

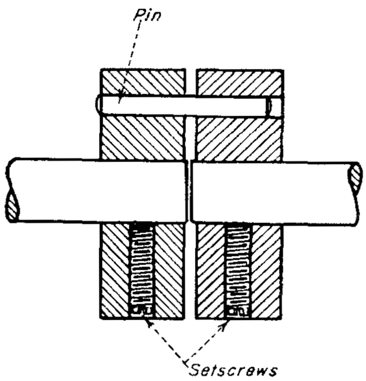

Fig 10—Coupling made of two collars fastened to shafts with set screws. Pin in one collar engages hole in other. Soft spacer can be used as cushion.

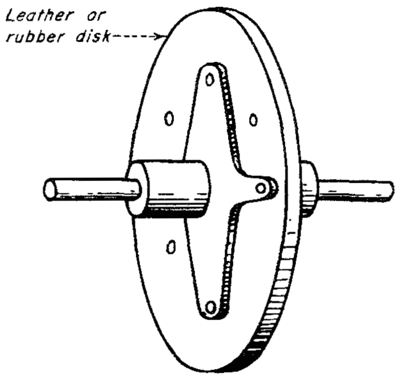

Fig 11—Coupling is made from two flanges rivited to leather or rubber center disk. Flanges are fastened to the shafts by means of setscrews.

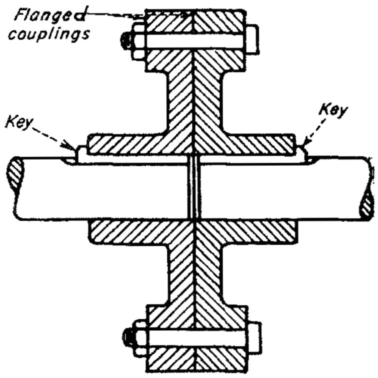

Fig 12—Bolted flange couplings are used on shafts from one to twelve inches in diameter. Flanges are joined by four bolts and are keyed to shafts.

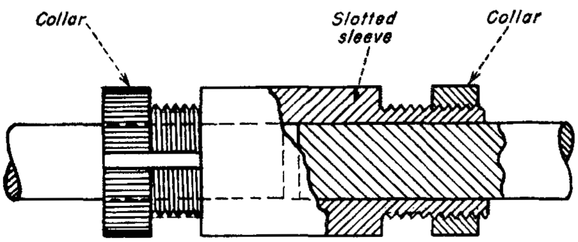

Fig 15—Screwing split collars on tapered threads of slotted sleeve tightens coupling. For light loads and small shafts, sleeve can be made of plastic material.

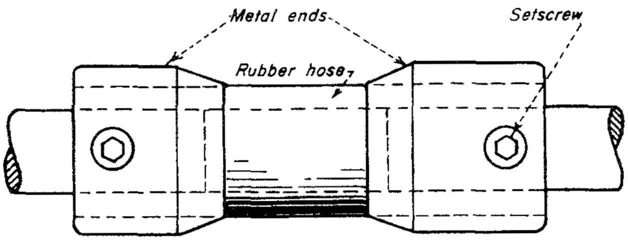

Fig 16—One-piece flexible coupling has rubber hose with metallic ends that are fastened to shafts with set screws. Commercially available in several sizes and lengths.

Coupling of Parallel Shafts

H. G. Conway

FIG. 1—A common method of coupling shafts is with two gears; for gears may be substituted chains, pulleys, friction drives and others. Major limitation is need for adequate center distance; however, an idler can be used for close centers as shown. This can be a plain pinion or an internal gear. Transmission is at constant velocity and axial freedom is present.

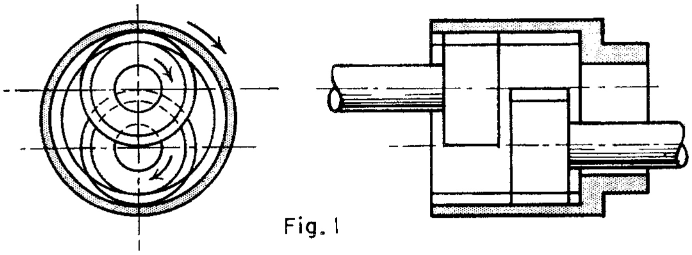

Fig. 1

FIG. 2—Two universal joints and a short shaft can be used. Velocity transmission is constant between input and output shafts if the shafts remain parallel and if the end yokes are disposed symmetrically. Velocity of the central shaft fluctuates during rotation and at high speed and angles may cause vibration. The shaft offset may be varied but axial freedom requires a splined mounting of one shaft.

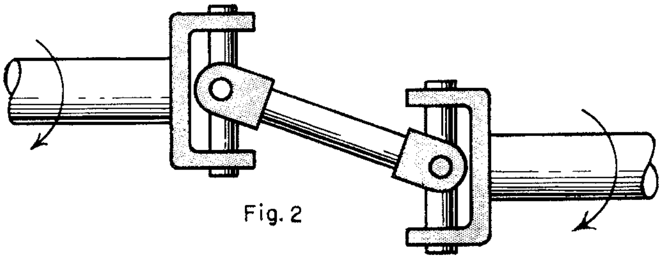

Fig. 2

FIG. 3—Crossed axis yoke coupling is a variation of the mechanism in Fig. 2. Each shaft has a yoke connected so that it can slide along the arms of a rigid cross member. Transmission is at a constant velocity but the shafts must remain parallel, although the offset may vary. There is no axial freedom. The central cross member describes a circle and is thus subjected to centrifugal loads.

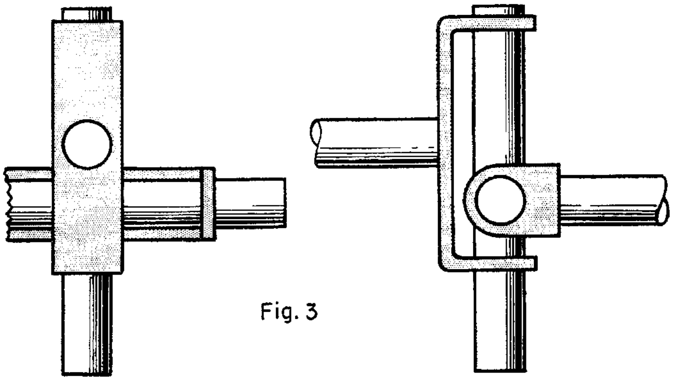

Fig. 3

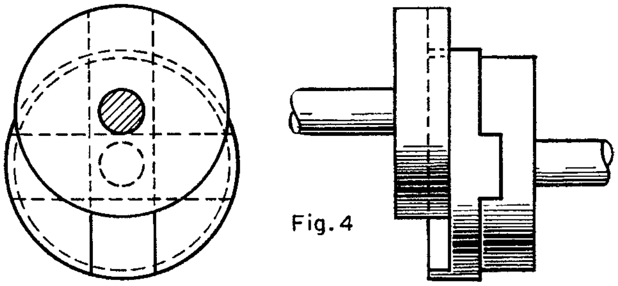

Fig. 4

FIG. 4—Another often used method is the Oldham coupling. The motion is at constant velocity, the central member describing a circle. The shaft offset may vary but the shafts must remain parallel. A small amount of axial freedom is possible. A tilting action of the central member can occur caused by the offset of the slots. This can be eliminated by enlarging the diameter and milling the slots in the same transverse plane.

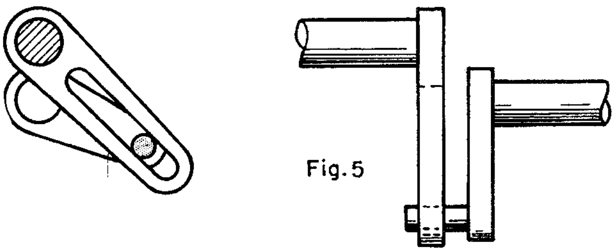

Fig. 5

FIG. 5—If the velocity does not have to be constant a pin and slot coupling can be used. Velocity transmission is irregular as the effective radius of operation is continually changing, the shafts must

The coupling of parallel shafts so that they rotate together is a common machine design problem. Illustrated are several methods where a constant 1:1 velocity ratio is possible and others where the velocity ratio may fluctuate during rotation. Some of the couplings have particular value for joining two shafts that may deflect or move relative to each other.

remain parallel unless a ball joint is used between the slot and pin. Axial freedom is possible but any change in the shaft offset will further affect the fluctuation of velocity transmission.

FIG. 6—The parallel-crank mechanism is sometimes used to drive the overhead camshaft on engines. Each shaft has at least two cranks connected by links and with full symmetry for constant velocity action and to avoid dead points. By using ball joints at the ends of the links, displacement between the crank assemblies is possible.

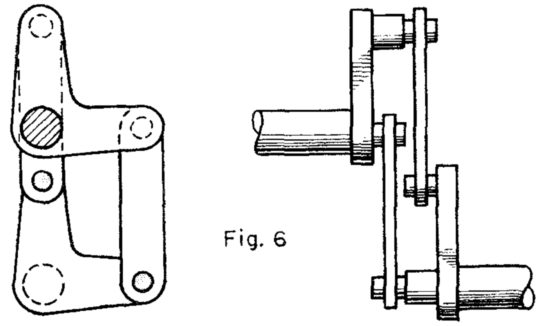

Fig. 6

FIG. 7—A mechanism kinematically equivalent to Fig. 6, can be made by substituting two circular and contacting pins for each link. Each shaft has a disk carrying three or more projecting pins, the sum of the radii of the pins being equal to the eccentricity of offset of the shafts. The lines of center between each pair of pins remain parallel as the coupling rotates. Pins do not need to be of equal diameter. Transmission is at constant velocity and axial freedom is possible.

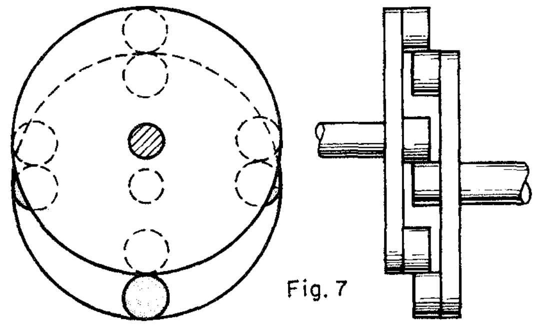

Fig. 7

FIG. 8—Similar to the mechanism in Fig. 7, but with one set of pins being holes. The difference of radii is equal to the eccentricity or offset. Velocity transmission is constant; axial freedom is possible, but as in Fig. 7, the shaft axes must remain fixed. This type of mechanism is sometimes used in epicyclic reduction gear boxes.

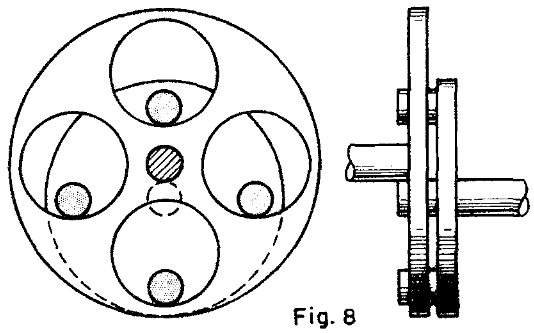

Fig. 8

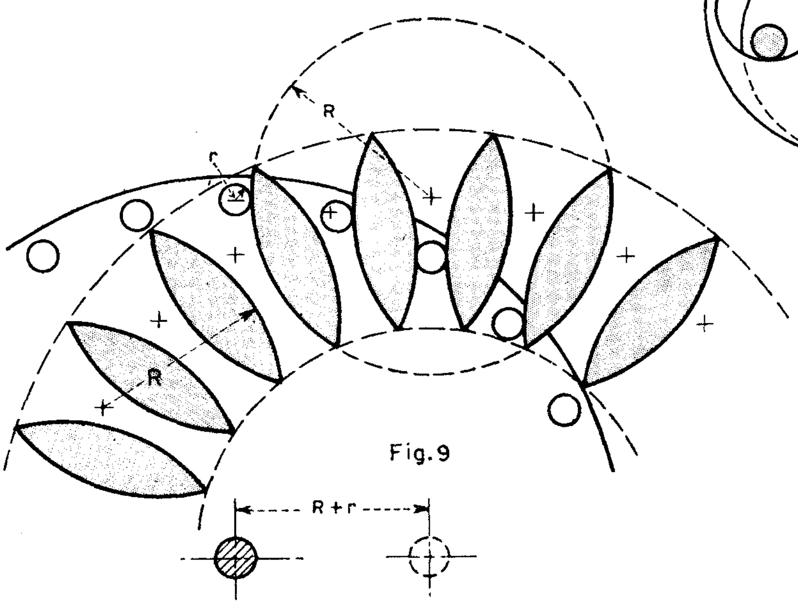

Fig. 9

FIG. 9—An unusual development of the pin coupling is shown left. A large number of pins engage lenticular or shield shaped sections formed from segments of theoretical large pins. The axes forming the lenticular sections are struck from the pitch points of the coupling and the distance $R + r$ is equal to the eccentricity between shaft centers. Velocity transmission is constant; axial freedom is possible but the shafts must remain parallel.

Novel Linkage for Coupling Offset Shafts

...simplifies the design of a variety of products.

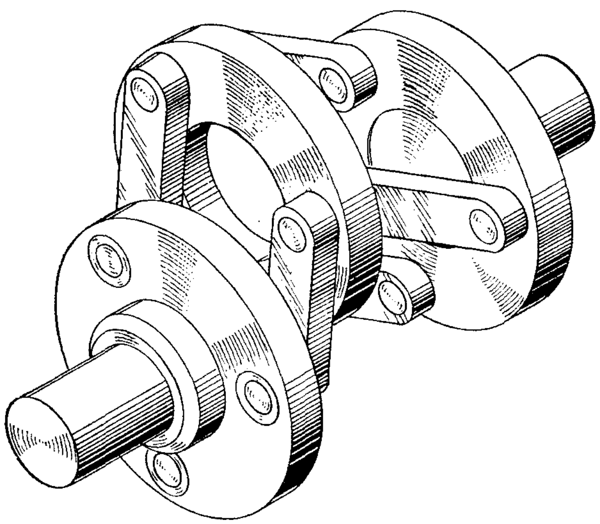

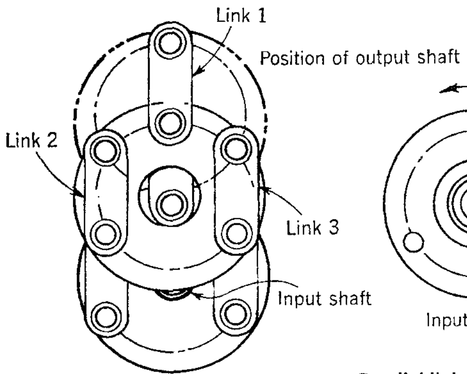

Maximum displacement (rear view)

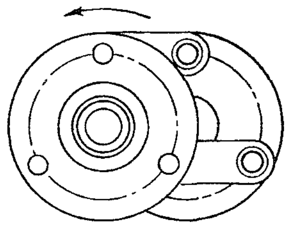

Input and output shafts in line
Zero displacement

Parallel-link connections between disks (sketch at upper left) exactly duplicate motion between input and output shafts—the basis of a new principle in coupling. Lower diagrams show three positions of links as one shaft is shifted with respect to the other shaft in the system.

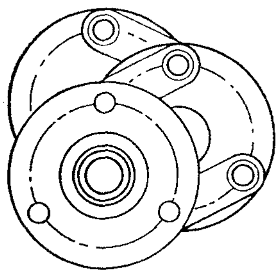

Midway position

An unorthodox yet remarkably simple arrangement of links and disks forms the basis of a versatile type of parallel-shaft coupling. This type of coupling—essentially three disks rotating in unison and interconnected in series by six links (drawing, left)—can adapt to wide variations in axial displacement while running under load.

Changes in radial displacement do not affect the constant-velocity relationship between input and output shafts, nor do they initial radial reaction forces that might cause imbalance in the system. These features open up unusual applications in automotive, marine, machine-tool, and rolling-mill machinery (drawings, facing page).

How it works. The inventor of the coupling, Richard Schmidt of Schmidt Couplings, Inc., Madison, Ala., notes that a similar link arrangement has been known to some German engineers for years. But these engineers were discouraged from applying the theory because they erroneously assumed that the center disk had to be retained by its own bearing. Actually, Schmidt found, the center disk is free to assume its own center of rotation. In operation, all three disks rotate with equal velocity.

The bearing-mounted connections of links to disks are equally spaced at 120 deg. on pitch circles of the same diameter. The distance between shafts can be varied steplessly between zero (when the shafts are in line) and a maximum that is twice the length of the links (drawings, left). There is no phase shift between shafts while the coupling is undulating. □

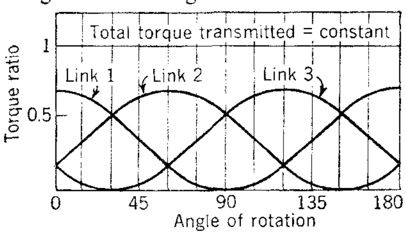

Torque transmitted by three links in group adds up to a constant value regardless of the angle of rotation.

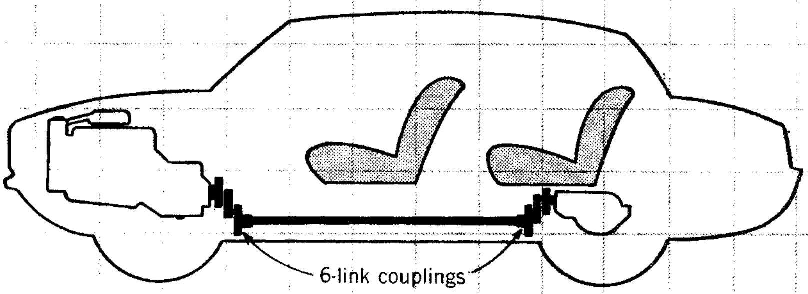

Drive shaft can be lowered to avoid causing hump in floor of car. Same arrangement can be applied to other applications to bypass an object.

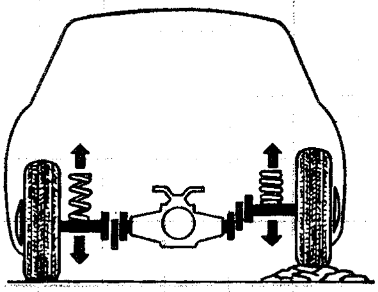

Car differential can be mounted directly to frame, while coupling transmits driving torque and permits wheels to bounce up and down. Arrangement also keeps wheels vertical during shock motion.

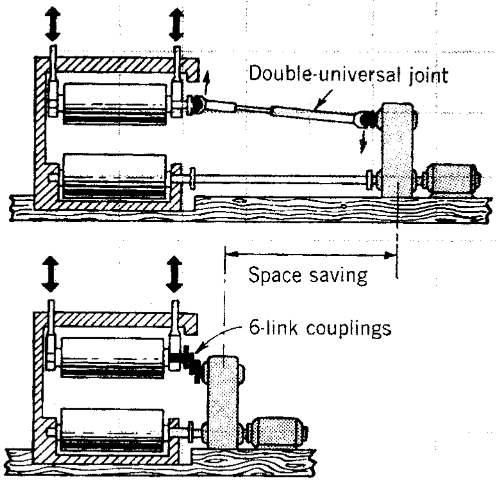

Rolling mill needs a way to permit top roller to be adjusted vertically. Double universal joint, normally used, causes radial forces at the joints and requires more lateral space than the 6-link coupling.

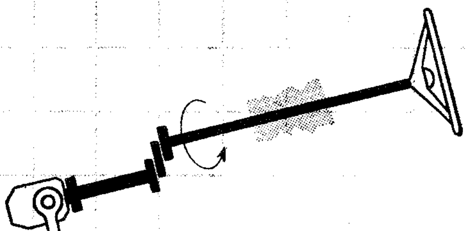

Steering column can be rotated around main axis for better comfort or driving position.

Machine for pounding road beds uses unbalanced shaft to induce large-amplitude vibration. Coupling prevents vibrations from passing on to transmission and frame.

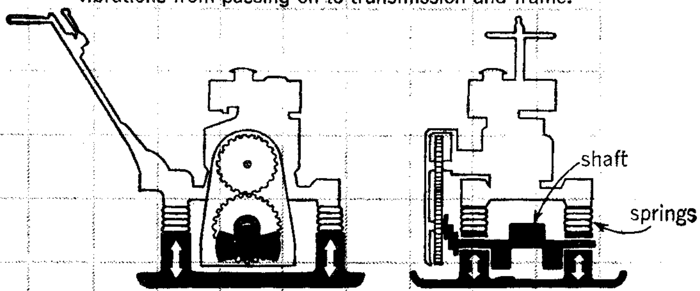

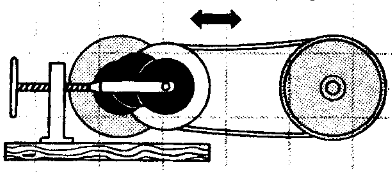

Belt drive can be adjusted for proper tension without need for moving entire base.

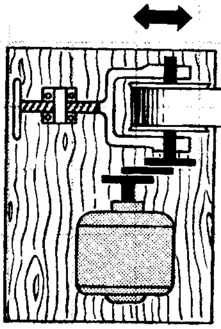

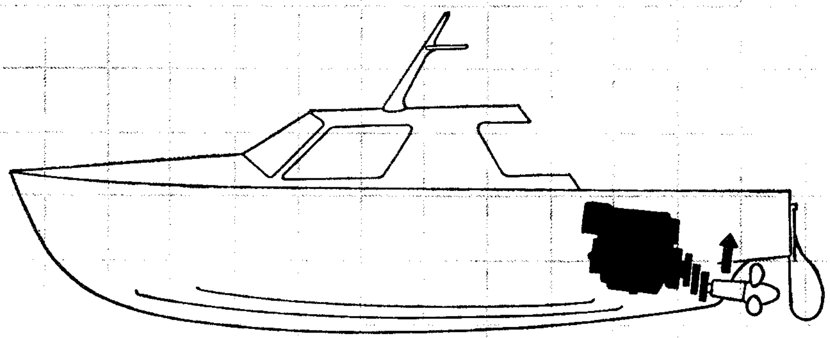

Inboard motor is segregated from propeller shock and vibration and can be mounted higher.

Torque of Slip Couplings

Here are formulas and charts of force, torque and friction conversion-factors for slip couplings form 0.50- to 5.0-inch mean radius.

Douglas C. Greenwood

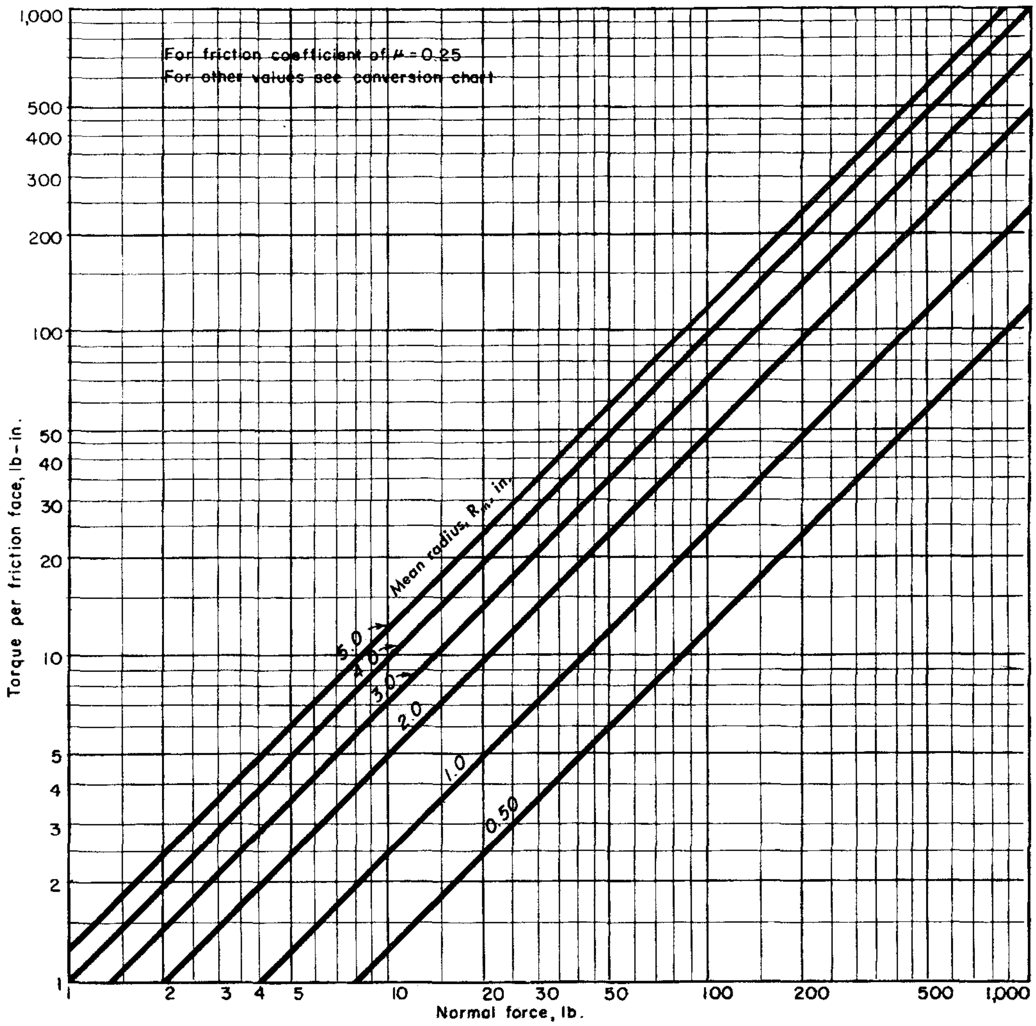

All slip-coupling designs consist, basically, of one member pressing against another. Friction face can be metal or some other material. When torque force exceeds the friction force between pressed-together faces, they slip relative to one another. Usually, pressure is adjustable so driving torque can be varied. Some form of flexible coupling should be mounted on one of the shafts close to the slip coupling.

For each friction face of a flat-disk coupling, torque, force and friction are related in

$$T = \mu F R_m$$

This formula is also true for cone couplings. If pressure is uniform throughout the friction face area the effective mean radius is

$$R_m = 2/3\left(\frac{R_o^3 - R_i^3}{R_o^2 - R_i^2}\right)$$

When the friction face is between mating cones

$$F = \frac{F_a}{\text{Sin } a}$$

If the cones are slipping, this becomes

$$F = \frac{F_a}{\text{Sin } a + \mu \cos a}$$

The face angle for cone couplings can range from about 7 to 30°. Usually it is about $12\frac{1}{2}$°.

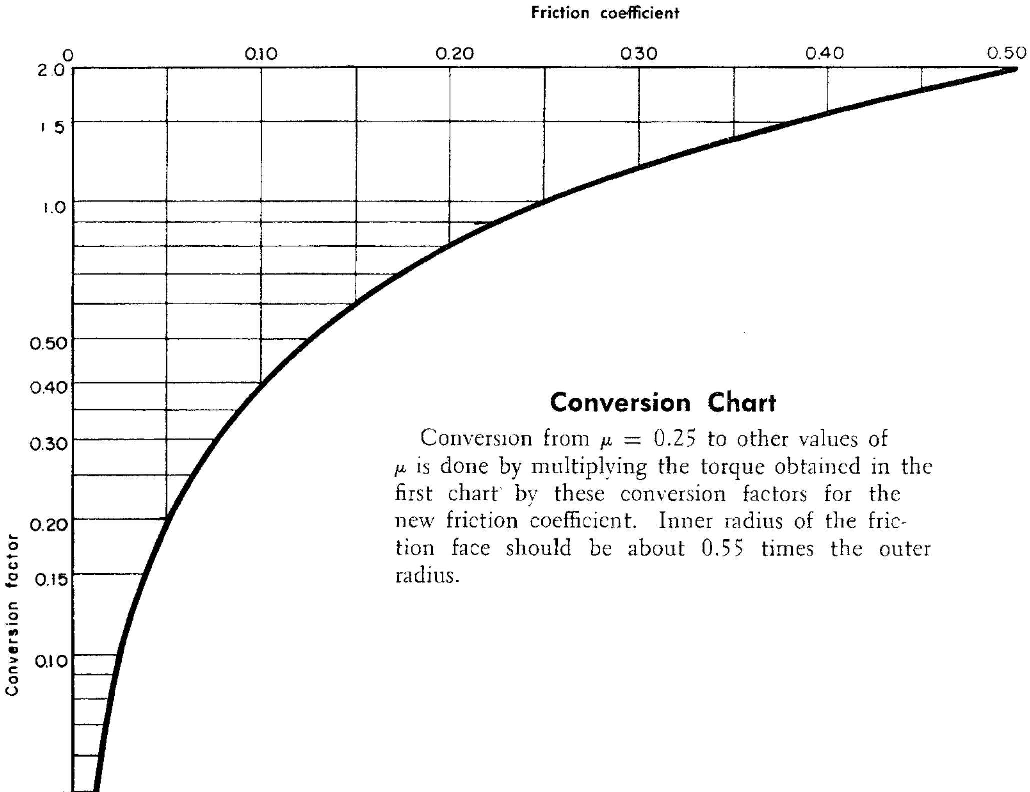
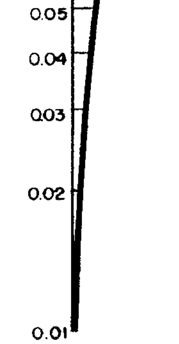

Conversion Chart

Conversion from $\mu = 0.25$ to other values of μ is done by multiplying the torque obtained in the first chart by these conversion factors for the new friction coefficient. Inner radius of the friction face should be about 0.55 times the outer radius.

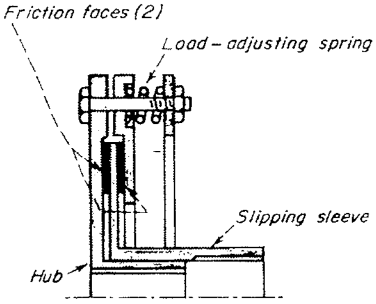

Maximum unit pressure for various friction materials should not be exceeded. While this is not so likely to occur in slip couplings as in clutches, it should nevertheless be checked. Maximum pressures for friction faces are available in most engineering handbooks.

If desirable to stop the drive when slipping occurs, a warning device such as a clacker can be mounted between the two members of the drive—movement of one relative to the other will be audible. An electrical contact similarly mounted can be connected through a slip ring to stop the drive automatically.

Symbols

F = force normal to friction face, lb
F_a = axial force, lb
R_m = mean radius of friction faces, in.
R_o = outer radius of friction faces, in.
R_i = inner radius of friction faces, in.
T = torque, lb-in.
n = number of friction faces
α = cone angle relative to shaft axis
μ = friction coefficient

High-speed Power Couplings

Includes analysis of eight popular types for high-horsepower applications, and stress and spring-rate equations for contoured diaphragms.

N. B. Rothfuss

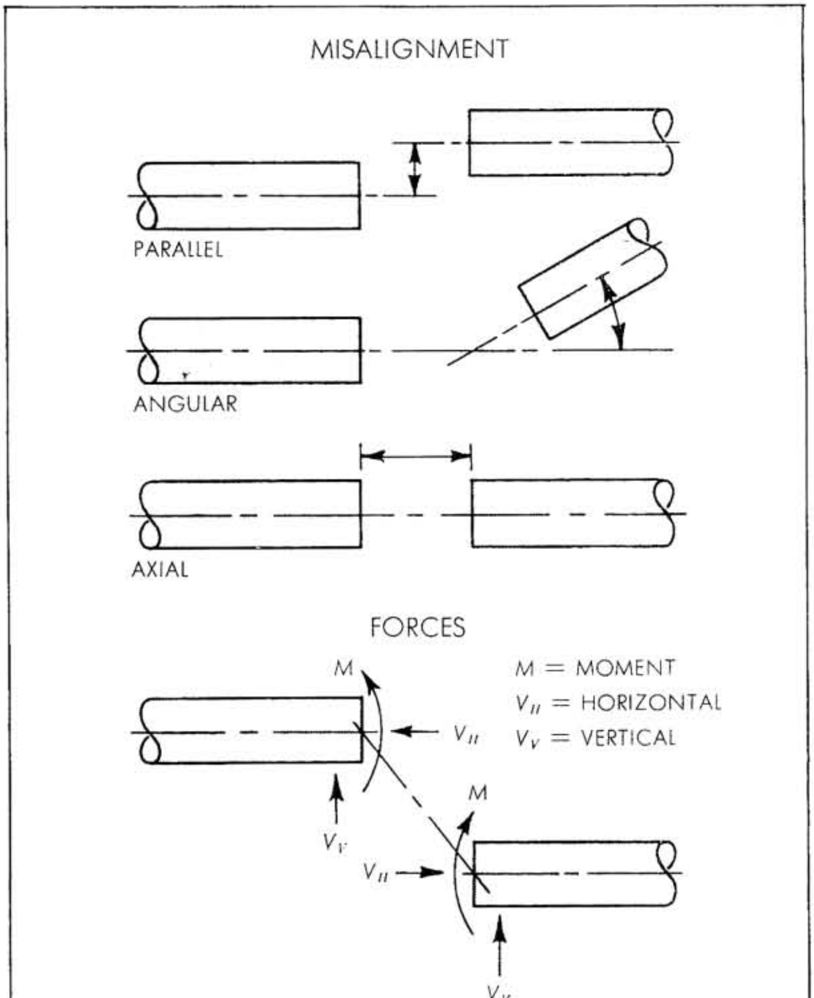

1 . . Types of misalignment and resulting forces. Most couplings can handle two or more types. Selection tables later in article give specific characteristics.

FLEXIBLE couplings are mechanical devices which can efficiently transmit torque and power from a driving to a driven shaft when the shafts are not in alignment. The misalignment can be angular, parallel, or axial end-displacement, Fig 1, or a combination of any two or all three. In addition to initial misalignment, the flexible coupling may be called on to provide protection against shock and vibration or to compensate for the effects of temperature changes, wear of parts, and deflection of support members. Today's couplings frequently must operate at high speeds and with high loads. Misalignments under such conditions become very destructive—not only to the coupled shafts and their components, but also to the coupling itself.

The couplings discussed here are of the rigid type (as distinguished from entirely flexible connectors such as flexible cables). The couplings are capable of rugged duty—1 hp and up. They permit one or more types of misalignment, and their primary function is the transfer of torque (couplings in the instrument category have been covered previously—see Editor's Note at end of article).

The key design criteria for selecting power couplings are covered in detail, and the contoured-diaphragm coupling is featured because it is a relatively new design for which there is little published design and selection data. Equations are included for computing the stresses and spring rates for several specially contoured disks,

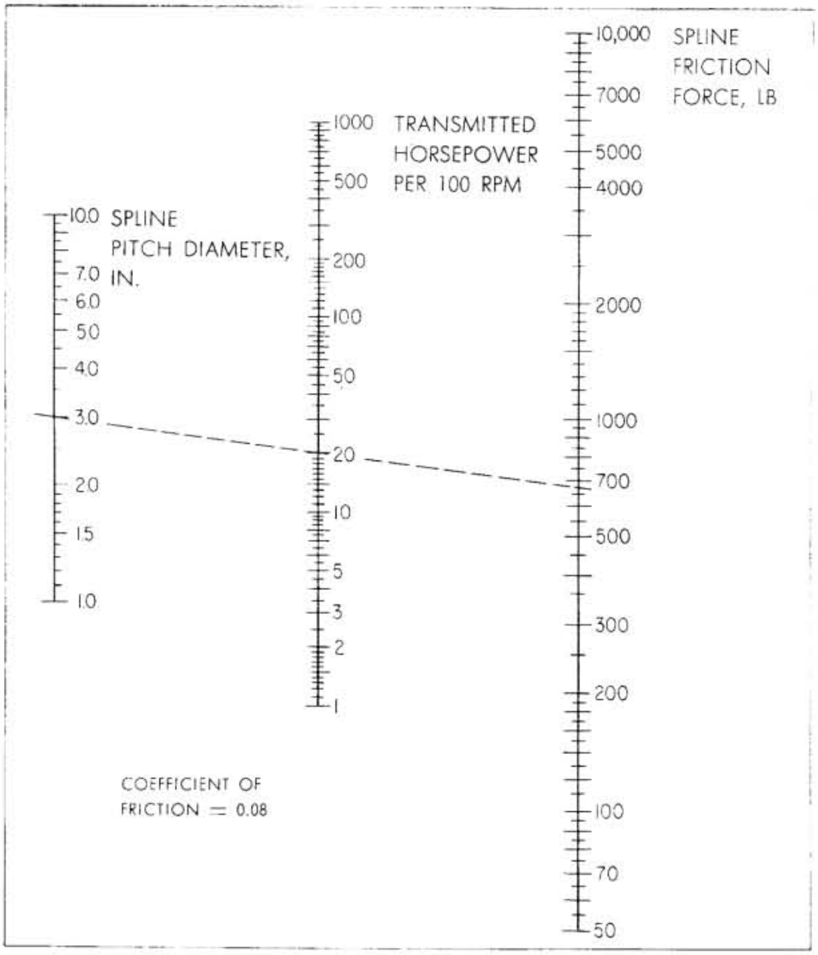

2. . Friction forces in sliding splines

because such disks are finding application in other products such as turbines.

Types of misalignment

Angular and parallel misalignment are usually a result of installation tolerances, movement of supporting structure, and thermal growth and may change while the system is operating. Axial movement or end play is generally a result of thermal growth and system shock and vibration—although installation tolerances, and clearances for pilot diameters, also add to end play.

Some flexible couplings can accommodate up to 2 in. of end play. Usually a coupling generates excessive heat and wears out rapidly if operated at angles higher than its rated capacity.

Misalignment forces

Under misalignment, couplings impose forces and bending moments on input and output shafts, Fig 1. These forces reduce the life of supporting bearings.

Bending moment arises from various causes, depending on the type of coupling employed. With contoured diaphragms, laminated disks and *rubber-tire* elastomeric types, the moment is a function of the spring rate in bending, in units of lb-in./deg. In other words, the coupling requires a certain amount of moment when de-

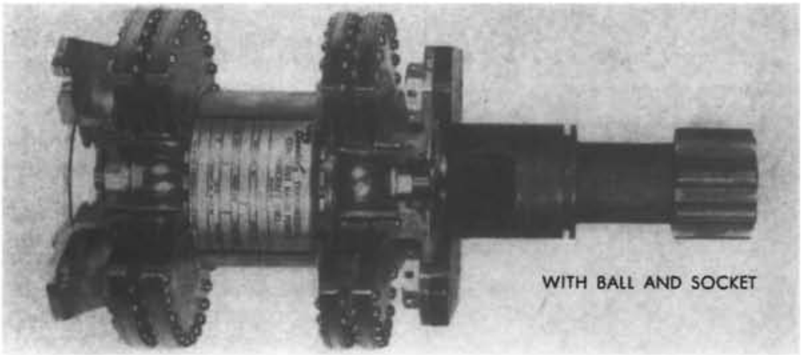

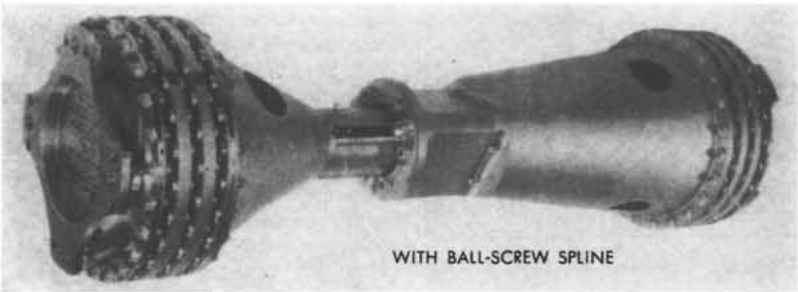

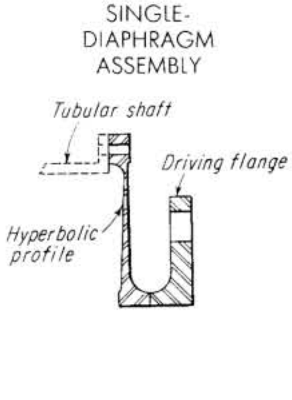

3. . **Contoured - diaphragm** flexible couplings. Diaphragms have hyperbolic profile for improved flexing performflected to a specific number of degrees of misalignment.

Universal joints develop moments by action of the component forces to drive the required horsepower or torque. Gear, chain, and ball-race couplings require moments to move them through the operating angle each revolution. These forces are generated by the coefficient of sliding or rolling friction between the load-carrying surfaces.

Telescoping splines and gear and chain-type couplings depend on sliding, hence can cause very high shearing forces. Contoured-diaphragm couplings, Fig 3, and other flexible metallic and elastomeric couplings usually induce lower forces—but the amount of movement is limited by the magnitude of the bending stresses which are additive to the bending stresses resulting from angular misalignment. If large end play is required when flexible diaphragm couplings are used, intermediate telescoping splines are necessary. For example, Fig 3 also shows a high-speed, high-temperature (550 F) flexible coupling in which a ball spline is used to reduce axial forces from 400 lb to 30 lb.

The vertical shear force, V_V, of a flexible coupling is the sum of its dead weight and the imbalance of the coupling. The imbalance force is determined by using the balance specification in pound-inches in the following formula, which includes shaft speed:

$$V_V(\text{total}) = W + M_r N^2/g$$

where

W = coupling weight, lb
M_r = imbalance, lb-in.
N = shaft speed, rad/sec
g = gravitational constant, in./sec^2

This gives the total V_V. The V_V at each end is half the above value.

The horizontal force, V_H, results from axial or radial movement of the input and output shafts. This movement causes the flexible joint to expand or contract. In the case of a flexible shaft with two axially restrained flexible joints, a spline must be provided to accommodate this expansion or contraction. The horizontal force is developed during the movement and its magnitude depends on the coefficient of friction, torque, and radius of the contacting load members which slide during this axial motion.

The nomograph in Fig 2 gives a quick value of the force, V_H, required to slide a straight-sided spline at various operating conditions of torque and pitch diameter. The coefficient of friction is assumed to be 0.08. For other coefficients, this force must be multiplied by the ratio of actual coefficient of friction to 0.08. Also, to modify the force for involute splines the chart readings should be divided by the cosine of the involute angle.

For example—Find the spline friction force on a spline with a 3-in. pitch diameter which transmits 800 hp at 4000 rpm. Coefficient of friction is 0.11. Solution —hp/100 rpm = 800/40 = 20. From the chart, spline force = 670 lb. Actual force = 670 (0.11)/0.08 = 920 lb.

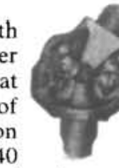

The moment, vertical shear, and horizontal forces are used in estimating the requirements of the supporting bearings. In low-speed high-power systems, the sum of these three forces is usually negligible because the supporting bearings are much larger than necessary, but in high-speed lightweight applications, these forces can add up to a large percentage of the total bearing capacity and must be taken into account.

Speed and load

Couplings are selected by using the maximum operating-torque rating and modifying this rating if the coupling is also to function at maximum operating speed. Centrifugal forces, shock loads, and deflections of load-carrying members also reduce the ratings. Many installations have a wide speed range at the same horsepower rating; therefore the maximum torque capacity is permissible only at minimum speed.

Lubrication

Most couplings and joints—universal, gear, ball-race, chain, and some

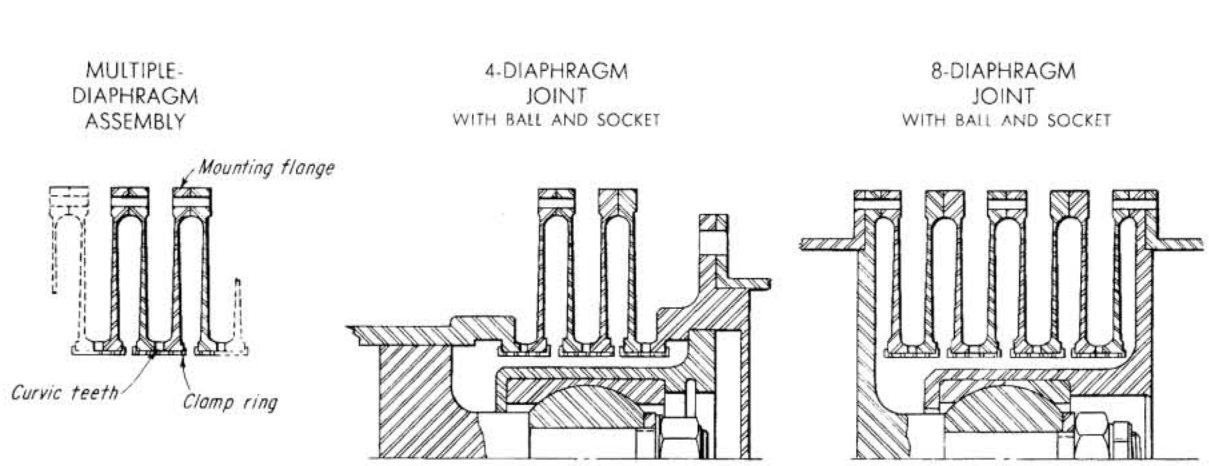

ance and almost-constant stress distribution. Number of diaphragms depends on misalignment requirements.

spring types—depend on relative movement between contacting load surfaces to handle misalignment. This movement is sliding, rolling, or both and always generates heat. A lubricant keeps the coefficient of friction low to avoid excessive heat; otherwise the performance of the coupling is quickly impaired. The friction coefficient of gear couplings operating at high speeds should be less than 0.1 and preferably less than 0.05. Some aircraft and industrial engineers check coupling temperature with special heat-sensitive paper tapes that change color when heated to a specific temperature. They are placed on the surface and the temperature is determined by reading the number on the last element that changed color.

Seals are usually necessary when grease is employed as the lubricant. The seals must also protect the lubricant and internal surfaces from contaminants such as salt, sand, dust, and humidity. If elevated ambient temperatures are encountered seal material selection may be critical.

Containment

In high-speed applications, the failure of the output flexible joint of a shaft system could be catastrophic to personnel or surrounding equipment. Some installations utilize static shrouds or fail guards and other use secondary members which are a part of the rotating assembly. One coupling in Fig 3 incorporates a self-lubricated ball and socket assembly. During normal conditions of misalignment the ball nutates within the socket—but in the event of failure of one of the load-carrying members, the ball will spin within the socket and provide radial restraint. Containment for periods in excess of 25 hr of overrunning has been demonstrated.

Constant velocity ratio

A constant velocity ratio means there is no acceleration or deceleration of the output shaft when the input shaft runs at constant velocity. Without constant ratio, there will be torsional fluctuations that cause vibration and increase the operating stresses. These can damage bearings.

A single universal joint, for example, is not a constant velocity ratio coupling. Most couplings do not produce a theoretically constant velocity —they closely approximate it at small angles of misalignment.

Backlash

Almost all gear, chain, ball-race, and universal joints have both radial and torsional backlash unless the elements are preloaded. Torsional backlash can lead to early deterioration of the joint from fretting or pounding and may affect the performance of other system components. Radial backlash can cause high dynamic forces under varying acceleration conditions.

Torsional spring rate

Torsionally *soft* couplings can be either harmful or advantageous, depending on the type of driving or driven equipment. A soft coupling can improve the system torsional dynamics by absorbing shock and vibration, whereas a torsionally stiff coupling will transmit load at constant velocity ratio during peak transient torques. Gear, chain, universal, and ball-race couplings are generally in the torsionally stiff category; diaphragm and disk couplings can be in either category.

TYPES OF COUPLINGS

High-speed high-power couplings can be classed by the type of flexing member or joint they employ to handle misalignment between shafts. Eight common groupings are

1) Contoured-diaphragm
2) Axial-spring
3) Laminated-disk
4) Universal (Hooke's) joint
5) Ball-race
6) Gear
7) Chain
8) Elastomeric

Contoured-diaphragm couplings

These recent types (Fig 3 and 4), developed by Utica Division of Bendix, are generally for high-torque, high-speed, and high-angle applications. They use one or more thin disks or "diaphragms" which are *contoured* to an almost hyperbolic shape, Fig 3, as contrasted with diaphragms which are parallel-sided or tapered. The contouring 1) provides uniform stress distribution in both torsion and bend-

4. . Double-diaphragm coupling

Falk Corp

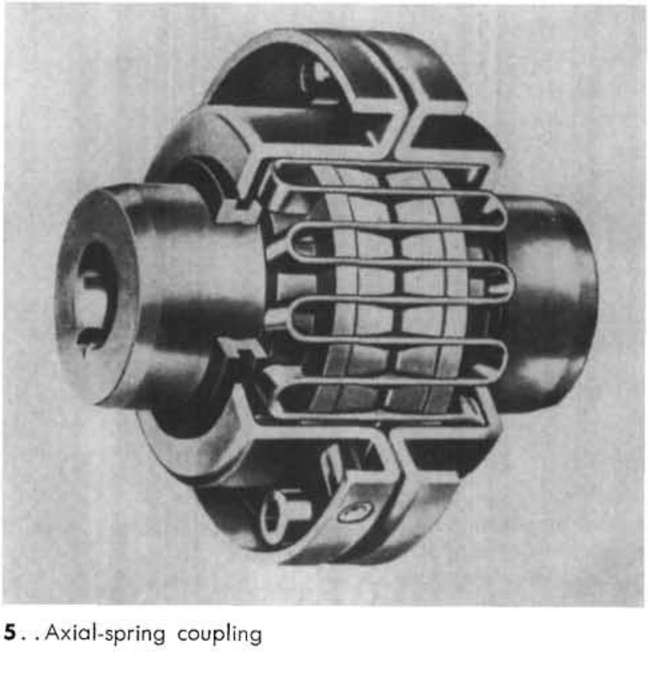

5. . Axial-spring coupling

ing—further discussed in a later section, 2) reduces unnecessary weight, and hence inertia, and 3) permits high flexibility (low spring rate) between misaligned shafts.

The contour blends into a relatively thick rim at the outer diameter and a hub at the inner diameter; the rim and hub then transmit the torque between mating diaphragms or input-output flanges. Torque can be transmitted in either direction of rotation. Since all bending takes place within the profiled area, there are no points of high stress concentration, such as holes or edges, which could lead to early fatigue.

Any number of diaphragms from one to ten can be used. Above eight diaphragms, however, the joint tends to become unstable and a ball and socket joint is provided which restrains the system components from whipping at high speeds. Permissible misaligment per diaphragm is up to 1 deg, and because the diaphragms are in series, the maximum rated angle is the number of diaphragms times the angle per diaphragm. Thus an 8-diaphragm coupling using 1-deg diaphragms is capable of 8-deg continuous operation and 16-deg intermittent or momentary misalignment for a few seconds at a time.

Because there is no rubbing, sliding, or rolling during the torque transmission, lubrication is not required. Speed and load ratings presently range from 2000 to 60,000 rpm, and 20 to 30,000 hp (speeds to 100,000 rpm have been demonstrated in turbine-wheel spin pits).

Both angular and parallel misalignment can be accommodated, ranging up to 10 deg and 0.1 in. respectively. Both are a function of the number of diaphragms and over-all length between input and output diaphragms. Angular and parallel misalignments are not additive. Maximum misalignment values apply to almost all speeds.

Contoured diaphragms provide a true constant velocity ratio at all angles of misalignment. The diaphragms have zero backlash. System torsional, axial, and radial vibrations are neither created nor amplified; hence self-generated noise is negligible. Narrow specifications on balance can usually be met without its being necessary to balance either the component or assembly. By proper selection of materials and surface coatings, these couplings have operated at continuous temperatures up to 900 F.

Axial-spring couplings

These couplings, Fig 5, are generally for high-torque, moderate-speed, and moderate-misalignment applications. They consist of two flanged hubs with specially machined axial slots or grooves which are connected by a flat steel spring wound in the form of an S-shape for the full circumference. Torque is transmitted through each segment or leaf of the spring and misalignment is absorbed by flexing of the spring members. During angular and parallel misalignment operation there is relative motion between the flexing members and their respective grooves, so periodic relubrication is required.

Speed and load ratings range from 100 to 8000 rpm and from 1 to 72,000 hp. Both angular and parallel misalignment can be accommodated, ranging up to 2 deg and 0.1 in., respectively. These maximum misalignment values apply only to the lower speeds.

Although this type of coupling does not produce a theoretically constant velocity ratio, such ratios (and zero backlash) can be approximated by accurate controlling of the spring and groove clearances. Axial movement or end-play capabilities vary from 0.100 to 1.00 in., depending on size. Torsional spring rate is variable and can be specified. System torsional vibrations are effectively reduced by damping action of the coupling.

Laminated-disk couplings

These couplings are generally for high torque, high speed, and moderate angles. They consist of two hubs, one center member, and two laminated-disk assemblies, Fig 6. The disk assemblies are alternately attached with fitted bolts to the flanges and to the rigid center member.

When misaligned, the laminated disks take the form of a wave washer and are the only members subject to fatigue stresses. Torque is transmitted

Thomas Flexible Coupling Co

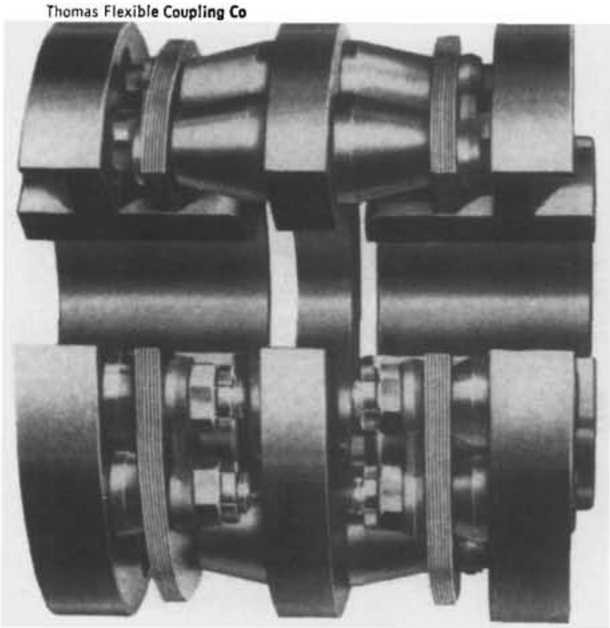

6. . Laminated-disk coupling

Dana Corp

7. . Universal-joint coupling

through the connecting bolts and the deflected disks to the output flange. The number of disks can be varied depending on the horsepower, misalignment, and axial-deflection requirements. Adding to an assembly increases the horsepower capacity but not the misalignment capability because the disks are in parallel and the deflection of each is equal to the total deflection. Period lubrication is not generally required.

The couplings provide almost constant speed ratio and zero backlash. Speed and load ratings range from 500 to 20,000 rpm and from 1 to 4000 hp. Torque ratings are constant at all operating speeds and higher speeds can be attained by special balancing.

Permissible angular and parallel misalignments range to 1.5 deg and 0.10 in., respectively. Both are a function of the over-all span between the input and output flanges. Maximum angular and parallel misalignments are not additive. Torsional spring rate is high.

Universal or Hooke's joint

The modern version of this common type of flexible joint is mostly employed for high-angle, moderate-torque, and moderate-speed applications. It consists of two forks connected by a cross member, Fig 7. The pivot points at each connection oscillate through the particular misalignment angle. Precision needle bearings reduce friction. Periodic lubrication is required.

Although this type of flexible joint will operate at extremely high angles at low speed, it has several limitations. A constant velocity ratio is not produced when there is angular misalignment between input and output shafts. Therefore, the joint introduces torsional accelerations to the system. However, if two joints are used with oriented yokes, and if the input and output centerlines are exactly parallel, the velocity variations will cancel and the velocity ratio will be constant.

Another limitation is that bending moments are introduced during torque transmission which result in high radial forces on the input and output shafts. Also, at high speeds, bearings can wear excessively and lubricant is difficult to contain.

Speed and load ratings range to 8000 rpm and 5000 hp. Angular misalignments up to 45 deg can be accommodated at low speeds, but parallel misalignment is not possible with only one joint.

Zero backlash can be obtained only by using adjustable tapered needle bearings. End play is negligible. Torsional spring rate is high, as it is a function of the bearings and yoke assembly.

Ball-race couplings

This coupling is generally used for high torque, high angle, and moderate speeds. It resembles a universal joint, but employs balls which are located in spherically shaped raceways and maintained in a plane which bisects the two planes at right angles to the input and output shafts, Fig 8. In some designs a ball cage helps retain the balls in the proper position. Periodic lubrication is required.

Speed ratings range to 8000 rpm, and load ratings to 5000 hp. Angular misalignments to 40 deg and higher are possible, but parallel misalignment cannot be accommodated with one joint.

Constant velocity ratio is attained because the balls are located in the bisecting plane. Zero backlash can be accomplished only by preloading. Axial movement or end play can be absorbed by special design. Torsional spring rate is high, as it is a function of the spring rate of the balls and races.

Gear couplings

These couplings are generally for high-torque, moderate-speed applications. They utilize two hubs with gear teeth (actually, the teeth are similar to external splines) which engage and drive through internal teeth of a sleeve, Fig 9. The sleeves are usually made in sections for ease of manufacturing and assembly. In most high-speed gear couplings the external teeth are crowned to 1) reduce friction, 2) increase misalignment capabilities, and 3) attain an almost-constant velocity ratio. Periodic lubrication is required.

Speeds and load ratings usually range from 100 to 25,000 rpm and 10 to 100,000 hp. Angular and parallel misalignments can be accommodated up to 3 deg and 0.030 in. respectively.

Bendix Corp, Bendix Products Div

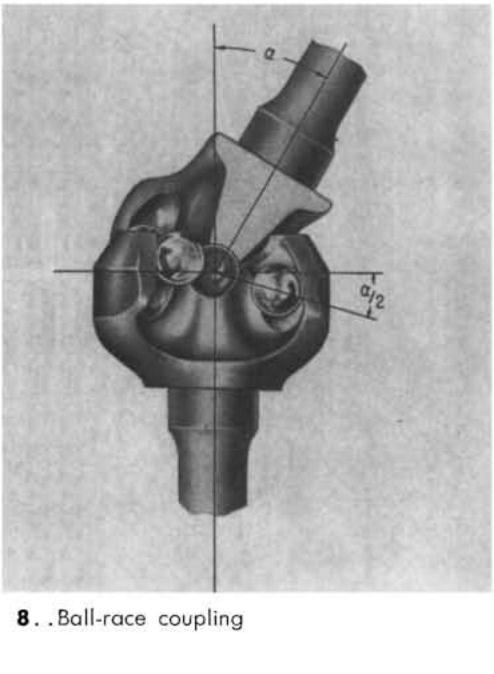

8. . Ball-race coupling

Sier-Bath Gear & Pump Co Inc

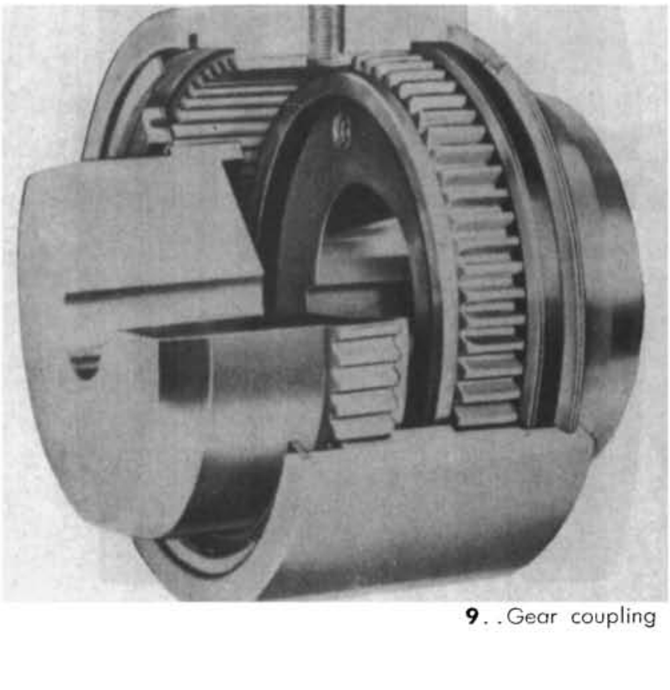

9. . Gear coupling

Maximum misalignments apply to the lower speeds. Negligible backlash is obtained by accurately controlling the tooth spacing and form. Axial movement or end-play capabilities vary from 0.01 to 2.00 in., depending on the length of the internal geared sleeve. Torsional spring rate is high, as it is a function of the spring rate of the gear teeth.

System torsional, axial, and radial vibrations and self-generated noise can be reduced by employing precision gear manufacturing techniques. Gear couplings can be balanced for high-speed, low-angle operation.

Within the past few years some manufacturers have been using a plastic such as nylon for the internally geared outer sleeve. This makes lubrication unnecessary and has been quite successful.

Chain couplings

These couplings are primarily for low-speed, high-torque applications. Several types of chain links are used for connecting the two sprockets. The more popular types are with single or double-strand roller, Fig 10, and with silent chain, Fig 11. Flexibility is provided by the relative motion between sprocket teeth and the chain rollers. Periodic lubrication is generally required.

With double-strand types, one strand usually has standard cylindrical rollers and the second strand spherical rollers. Silent chain couplings have guide links which fit into a groove in one sprocket or between the two sprockets to prevent the chain from moving axially off the connected sprockets.

Speed ratings range from 100 to 6300 rpm; load ratings from 10 to 3000 hp. A protective cover or housing is recommended for operation at high speeds or in high moisture corrosive environments. Both angular and parallel misalignments can be accommodated to 2 deg and 0.030 in., respectively. Both are a function of the over-all length between chain strands. Maximum misalignment values usually apply to the lower speeds and the angular and parallel values are not additive.

Constant velocity and zero backlash can be approximated by accurately controlling the tooth spacing and by properly contouring the chain and sprocket driving members. Axial movement or end play capabilities vary from 0.005 in. to 0.030 in. (approximately) for the double-width chains, and up to 1.00 in. for the single-width chains.

Torsional spring rate is usually high because it is a function of the spring rate of the chain elements and the sprocket teeth. System torsional, axial, and radial vibrations, when misaligned, can be reduced by using precision manufacturing techniques. Operating noise is a function of the clearances, but moderately quiet chain systems are available.

Elastomeric couplings

These rubber-tired couplings, Fig 12, are generally for high-torque, moderate-speed, and moderate-angle applications. They consist of two steel hubs or flanged rims connected by a tire-shaped reinforced-rubber section, either clamped or bonded to the hubs, which transmits the torque. The tire section is split laterally for assembly and disassembly.

Some designs are pressurized with air or liquid to maintain the proper shape. Over-all elasticity varies with internal pressure. For higher speeds (to 6000 rpm) the tire section is replaced with a diaphragm or dish-shaped reinforced rubber member.

During angular and parallel misalignment operation all relative motion is absorbed by the flexing member. No lubrication is needed. Speed ratings range from 10 to 6000 rpm and load ratings from 2 to 4000 hp. Both angular and parallel misalignment can be accommodated, ranging up to 4 deg and 0.125 in. for the tire section and 1 deg and 0.062 in. for the dish section. Constant velocity ratio and zero backlash are approximated by designing for high torsional stiffness. However, a low torsional stiffness or resilience is sometimes an asset, as the coupling will smooth out shock and torsional vibration between driving and driven equipment. Ambient temperatures limited by materials.

SELECTION TABLES

The comparative performance capabilities of the eight types of flexible couplings are listed in Tables I through

Morse Chain Co

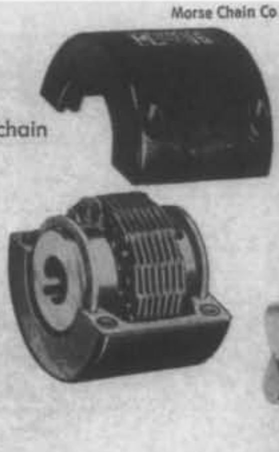

11. . Chain coupling—with silent chain

10. . Chain coupling—with roller chain

Link Belt Co

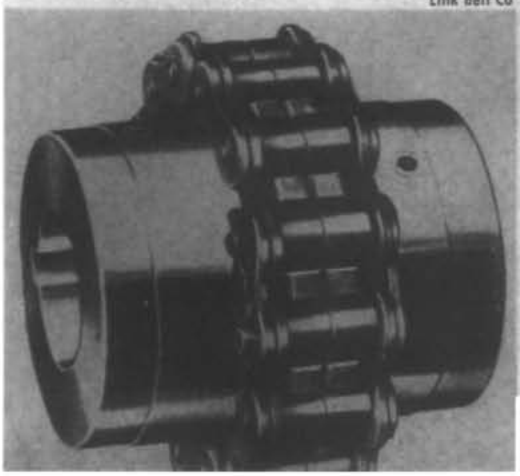

Dodge Manufacturing Corp

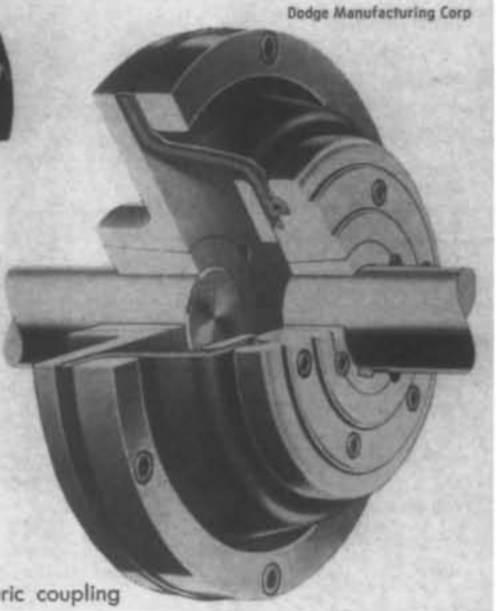

12. . Elastomeric coupling

TABLE I—POWER, SPEED AND MISALIGNMENT CHARACTERISTICS (CONTINUOUS DUTY)

	OPERATING MISALIGNMENT 0.5 TO 1 DEG									OPERATING MISALIGNMENT 1 TO 2 DEG								
	LOW SPEED 1000 to 4000 RPM HP/100 RPM			MODERATE SPEED 4000 TO 7000 HP/100 RPM			HIGH SPEED >7000 HP/100 RPM			LOW SPEED 1000 to 4000 RPM HP/100 RPM			MODERATE SPEED 4000 TO 7000 HP/100 RPM			HIGH SPEED >7000 HP/100 RPM		
TYPE OF COUPLING	**1**	**10**	**100**	**1**	**10**	**100**	**1**	**10**	**100**	**1**	**10**	**100**	**1**	**10**	**100**	**1**	**10**	**100**
CONTOURED DIAPHRAGM	√	√	√	√	√	√	√	√	√	√	√	√	√	√	√	√	√	√
AXIAL SPRING	√	√	√	√	√	√	√	√		√	√		√	√		√		
LAMINATED DISK	√	√	√	√	√	√	√	√	√	√	√		√					
UNIVERSAL JOINT	√	√	√	√	√		√			√	√	√	√	√		√		
BALL-RACE	√	√	√	√	√		√	√		√	√	√	√	√		√	√	
GEAR	√	√	√	√	√	√	√	√	√	√	√	√	√	√	√	√	√	
CHAIN	√	√	√	√	√		√	√		√	√	√	√					
ELASTOMERIC	√	√	√	√	√					√	√	√	√					

III. All are nominal values which may be exceeded by special design. The values shown are guideposts rather than fixed values in the flexible coupling field; in borderline cases, the user should contact the manufacturer.

Table I compares the misalignment capabilities for continuous duty of the couplings on the basis of speed and power requirements. In the 0.5 to 1-deg misalignment section almost every coupling will give satisfactory service. As the misalignment angle is increased, more and more couplings drop out.

Table II compares the functional characteristics of the couplings and is useful to the designer who is seeking a unit with specific operating characteristics.

Table III summarizes the published ratings for each type of coupling. In all cases these conditions are maximum and not additive, in other words,

TABLE II—FUNCTIONAL CHARACTERISTICS

	CONTOURED DIAPHRAGM	AXIAL SPRING	LAMINATED DISK	UNIVERSAL JOINT	BALL-RACE	GEAR	CHAIN	ELASTOMERIC
NO LUBRICATION	√		√					√
NO BACKLASH	√	√	√	see note 1	see note 1			√
CONSTANT VELOCITY RATIO	√	√		see note 2	√	see note 2	see note 2	√
CONTAINMENT	√		see note 1		see note 1			
ANGULAR ONLY	√		√	√	√	√		
AXIAL AND ANGULAR	√		√		√	√	√	√
AXIAL AND PARALLEL	√	√	√			√	√	√
AXIAL, ANGULAR, AND PARALLEL	√	√	√			√	√	√
HIGH TEMPERATURE	√		√					
HIGH ALTITUDE	√		√					
HIGH TORSIONAL SPRING RATE	√		√	√	√	√	√	
LOW BENDING MOMENT	√	√	√	√	√	√	√	√
NO RELATIVE MOVEMENT	√							√

NOTE: 1) Zero backlash and containment can be obtained by special design.
2) Constant velocity ratio at small angles can be closely approximated.

OPERATING MISALIGNMENT 2 TO 5 DEG								
LOW SPEED 1000 to 4000 RPM HP/100 RPM			MODERATE SPEED 4000 TO 7000 HP/100 RPM			HIGH SPEED >7000 HP/100 RPM		
1	10	100	1	10	100	1	10	100
√	√	√	√	√	√	√	√	
√	√	√	√	√		√		
√	√		√	√		√		
√	√	√	√	√		√	√	
√	√	√	√					

OPERATING MISALIGNMENT 5 DEG AND ABOVE								
LOW SPEED 1000 to 4000 RPM HP/100 RPM			MODERATE SPEED 4000 TO 7000 HP/100 RPM			HIGH SPEED >7000 HP/100 RPM		
1	10	100	1	10	100	1	10	100
√	√	√	√	√		√	√	
√	√	√	√			√		
√	√		√			√		
√	√		√			√		

a coupling cannot be operated at the maximum angular and parallel misalignment and at the maximum horsepower and speed simultaneously—although in some cases the combination of maximum angular misalignment, maximum horsepower, and maximum speed would be acceptable.

Contoured-disk Equations

The use of thin parallel-sided disks, or diaphragms, as flexing elements is not new—the literature shows they were used for locomotive couplings in 1922. Contoured disks have been used as turbine wheels to provide uniform stress distribution. Here are equations for determining the form of the contour, and the stresses and spring rates under all conditions of flexing at moderate angles.

Profile equation

The shape of the diaphragm profile has evolved from a constant-thickness

TABLE III—OPERATING CHARACTERISTICS

	CONTOURED DIAPHRAGM	AXIAL SPRING	LAMINATED DISK	UNIVERSAL JOINT	BALL-RACE	GEAR	CHAIN	ELASTOMERIC
SPEED RANGE, RPM	0 to 60,000	0 to 8000	0 to 20,000	0 to 8000	0 to 8000	0 to 25,000	0 to 6300	0 to 6000
HORSEPOWER RANGE, HP/100 RPM	1 to 500	1 to 9000	1 to 100	1 to 100	1 to 100	1 to 2000	1 to 200	0 to 400
ANGULAR MISALIGNMENT, DEG	0 to 8.0	0 to 2.0	0 to 1.5	0 to 45	0 to 40	0 to 3	0 to 2	0 to 4
PARALLEL MISALIGNMENT, IN.	0 to 0.10	0 to 0.10	0 to 0.10	None	None	0 to 0.10	0 to 0.10	0 to 0.10
AXIAL MOVEMENT, IN.	0 to 0.20	0 to 1.0	0 to 0.20	None	Some	0 to 2.0	0 to 1.0	0 to 0.30
AMBIENT TEMPERATURE, F	900	Varies	900	Varies	Varies	Varies	Varies	Varies
AMBIENT PRESSURE, PSIA	Sea level to zero	Varies	Sea level to zero	Varies	Varies	Varies	Varies	Varies

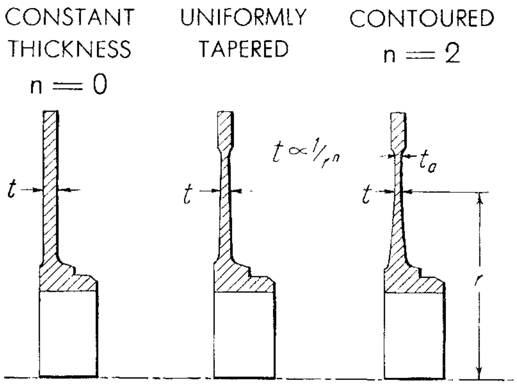

13. . Types of contours for diaphragms. The hyperbolic-type of contour (n=2) is gaining acceptance.

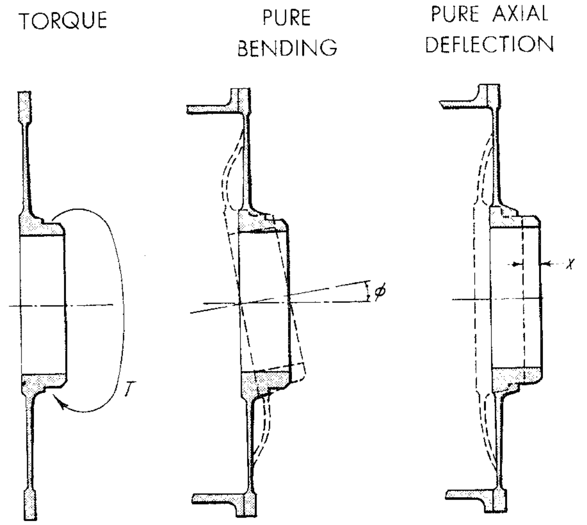

14. . Equations give stresses and spring rates for disks

section—to a uniformly tapered section—and now to the hyperbolic contour. The original contours have proved unsatisfactory for three reasons: First, the bending stress is excessive at the hub, where the diaphragm proper joins the rigid driving shaft or flange. Second, the shear stress is greatest at the hub, which is the area of smallest radius. Third, the effects of stress concentrations due to manufacturing, heat treatment, and attachment methods are greatest at the hub. The resulting combined stress causes early fatigue failures. Furthermore, both earlier forms are inefficient because of the unnecessary increase in shear area with radius and because the excess material thickness at larger radii forces most of the flexing and bending to take place in the hub area.

For a profile with uniform shear stresses and more evenly distributed bending stresses, the shear stress at any radius r is given by the following equation (refer also to the list of symbols on opposite page):

$$S_s = \frac{(T/r)}{A} = \frac{T}{2\pi r^2 t} \quad (1)$$

If the ratio of T/S_s is assumed to be constant (a desirable design goal) the following ratio is constant:

$$k = T/(2\pi S_s) \quad (2)$$

Hence

$$t = k/r^2 \quad (3)$$

Thus it can be seen that a diaphragm designed for constant shear stress will have a thickness varying inversely as the square of the radius.

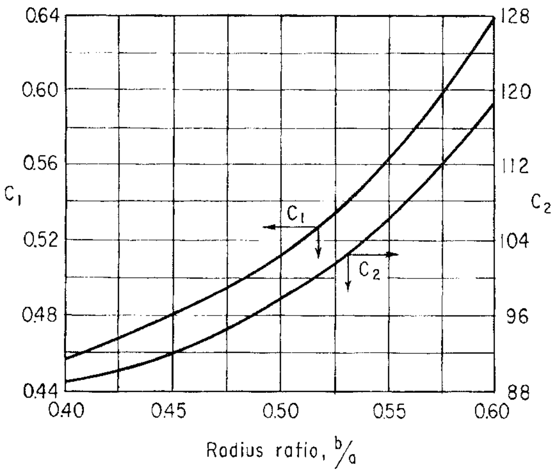

15. . For bending-stress equations

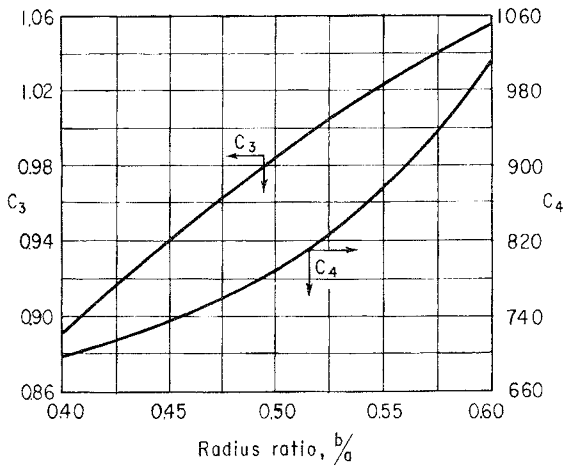

16. . For bending spring rate

TORSIONAL
BUCKLING

subjected to the four types of loading above.

SYMBOLS

A = shear area, in.^{2}
a = major radius of diaphragm profile, in.
b = minor radius of diaphragm profile, in.
C = constants, Fig 15 and 16
E = Young's modulus, psi
G = torsional modulus, psi
K = spring constant, lb/in. or lb-in./deg
N = speed, rpm
r = local radius, in.
S_a = maximum axial stress, psi
S_b = maximum bending stress, psi
S_s = maximum shear stress, psi
S_r = maximum radial centrifugal stress
S_t = maximum tangential centrifugal stress
t = local thickness at radius r, in.
t_a = local thickness at radius a, in.
T = torque, lb-in.
T_B = buckling torque, lb-in.
x = axial deflection, in.
ν = Poisson's ratio, dimensionless
ϕ = bending angle per diaphragm, deg
Z = constant, Fig 17

The bending stresses are lower than those for constant thickness and uniformly tapered configurations, and the point of maximum bending stress is shifted from the hub closer to the rim. The bending stress at the hub is now approximately 60% of the bending stress at the rim, easily accommodating any unavoidable stress concentrations at the hub. The general equation for the profile becomes

$$t = k/r^n \qquad (4)$$

where n is the form factor: $n = 0$ for constant thickness, and $n = 2$ for a hyperbolic type of curve (for a true hyperbolic curve, $n = 1$).

These constants are illustrated in Fig 13. The form based on $n = 2$ has proved satisfactory.

Torque equation

Eq 1, which defines the form of the profile, can be rewritten by substituting a for r to give the maximum torsional shear stress, Fig 14:

$$S_s = \frac{T}{2\pi a^2 t_a} \qquad (5)$$

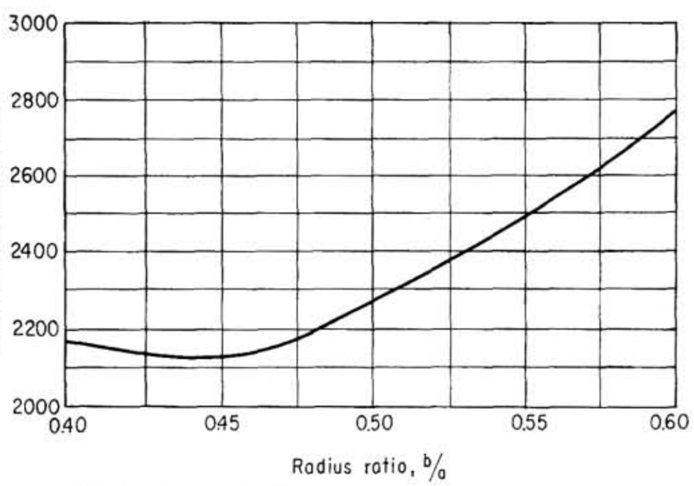

17. . For torque buckling

Bending-stress equation

The stress resulting from bending, S_b, varies from the inner radius b to the outer radius a. At any specific radius it will also vary within practical deflection limits directly with the bending angle ϕ. The maximum bending stress occurs at radius a:

$$S_b = C_1 E t_a \phi / a \qquad (6)$$

See Fig 15 for values of C_1 (and of C_2 for the equation below).

Axial-stress equation

The stress resulting from axial displacement, S_a, varies to a maximum at radius a and is

$$S_a = C_2 G t_a x / a^2 \qquad (7)$$

Radial-stress equation

For high-speed applications, the radial stress, S_r, which is actually the centrifugal stress, should be superimposed on the misalignment stresses S_a and S_b. Maximum S_r occurs at a and is proportional to the square of the peripheral velocity V. Because all diaphragms are very nearly proportional in their radial and axial dimensions and at a constant peripheral velocity, it is generally known that the radial and axial dimensions of a rotating disk can be varied independently without changing the stress at any point in the disk and that the centrifugal stresses can be calculated for one diaphragm and proportioned for others.

The maximum radial stress (at a) is

$$S_r = 2.935\, a^2N^2/10^6 \qquad (8)$$

Tangential-stress equation

A tangential stress, S_t, at the bore imposes a limit on the speed. It can be calculated from

$$S_t = 5.560\, a^2N^2/10^6 \qquad (9)$$

Torsional buckling

The five stress equations, Eq 5 to 9, are usually sufficient for design of contoured disks. Another factor which can be taken into consideration is torsional buckling, T_B. Fig 14 illustrates the result of overloading a diaphragm in torsion. The buckling torque varies not only with the diameter and the thickness ratio but also with the radius ratio and can be calculated from

$$T_B = \frac{\pi E t_a^3 Z}{12(1-\nu^2)} \qquad (10)$$

where T_B is the torque required to start formation of the ripples. Factor Z is a function of b/a, Fig 17.

Spring rates

There are four spring rates to consider: bending, axial, torsional and radial. The radial rate of a diaphragm, however, is extremely high and is therefore neglected.

Bending spring rate, K_b, is the moment in a plane normal to the diaphragm which must be applied to the hub (or rim) of a diaphragm to deflect the rim 1 deg with respect to the hub, its equation is

$$K_b = C_3 \pi E t_a^3 \qquad (11)$$

where C_3 is a function of b/a, see Fig 16.

Axial spring rate, K_a, is the force per inch required to deflect the diaphragm axially:

$$K_a = \frac{C_4 G t_a^3}{a^2} \qquad (12)$$

where C_4 is also obtained from Fig 16.

Torsional spring rate, K_t, is the torque per degree required to cause a rotational deflection of the hub with respect to the rim:

$$K_t = \frac{\pi^2 G a^2 t_a}{90 \log_e (a/b)} \qquad (13)$$

Power capability

The power capability of a contoured diaphragm under *continuous operating misalignment* can be estimated with the nomograph in Fig 18. Assume that it is required that a 5-in. OD coupling with 3-deg misalignment must transmit 500 hp at 6100 rpm. Thus the horsepower per 100 rpm is hp/100 rpm = 500/61 = 8.2.

From the chart, obtain permissible misalignment: 0.5 deg per diaphragm. Hence the number of diaphragms needed is

$$\frac{3 \text{ deg}}{0.5 \text{ deg}} = 6 \text{ diaphragms}$$

The torque and operating angle can be increased by increasing the outer diameter of the diaphragm.

Acknowledgement: The author is indebted to C. B. Gibbons of the Utica Division of the Bendix Corporation for assistance in preparing the equations and curves for contoured flexible diaphragms.

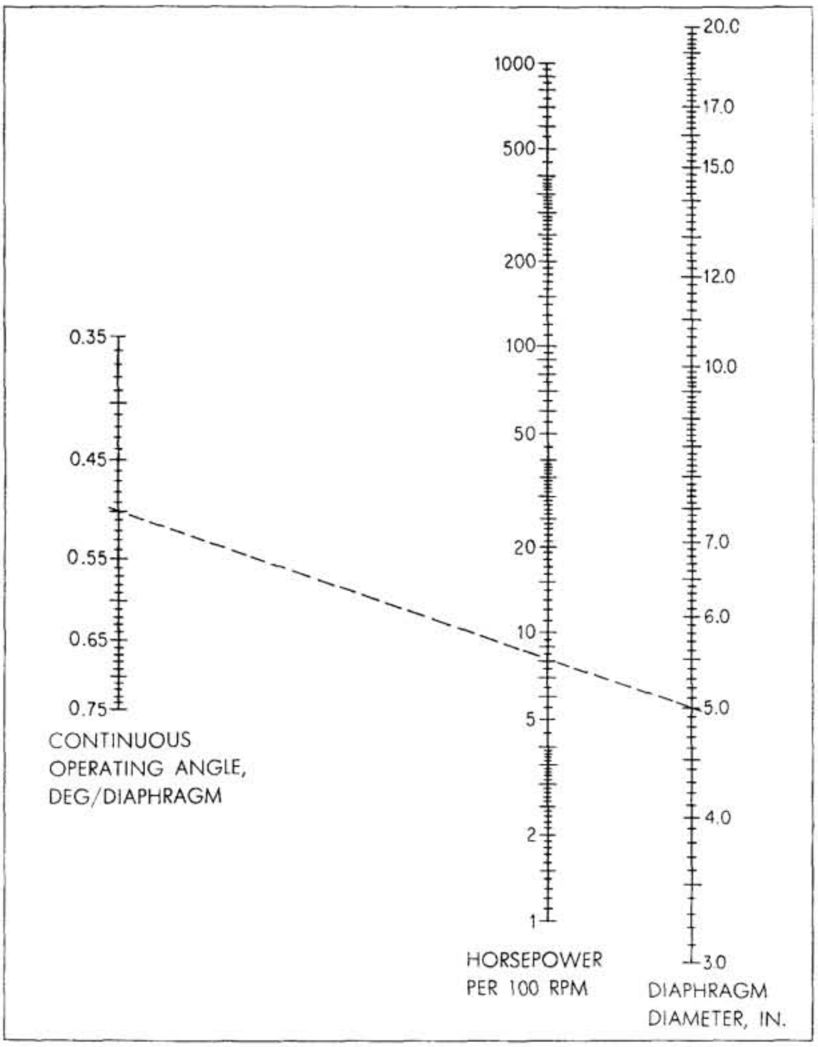

18. . Power vs size and misalignment

Novel Coupling Shifts Shafts

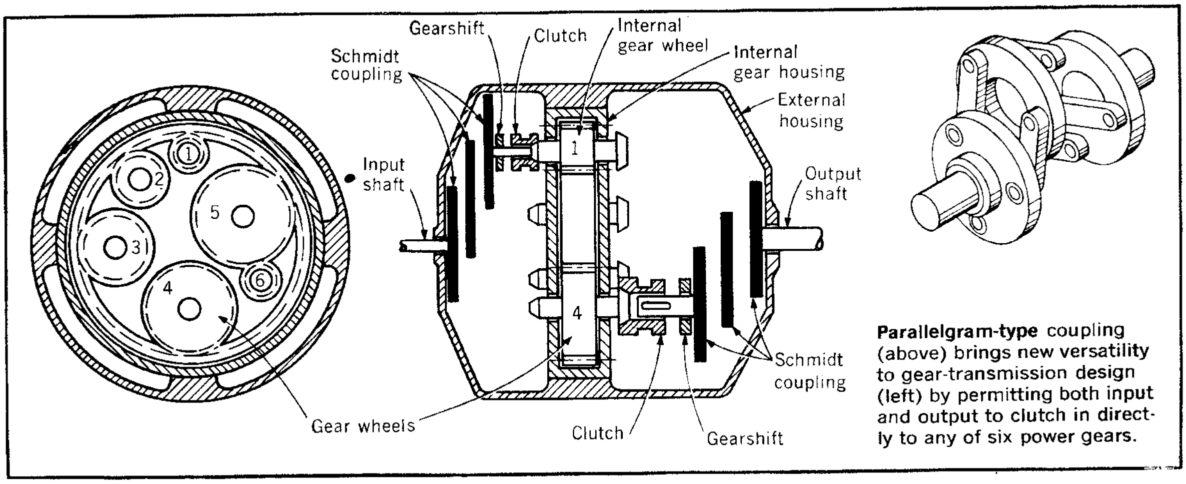

Parallelgram-type coupling (above) brings new versatility to gear-transmission design (left) by permitting both input and output to clutch in directly to any of six power gears.

Schmidt Coupling, Inc., Madison, AL

Novel Coupling Shifts Shafts: to simplify transmission design

A unique disk-and-link coupling that can handle large axial displacement between shafts, while the shafts are running under load, is opening up new approaches to transmission design.

The coupling (drawing, upper right) maintains a constant transmission ratio between input and output shafts while the shafts undergo axial shifts in their relative positions. This permits gear-and-belt transmissions to be designed that need fewer gears and pulleys.

Half as many gears. In the internal-gear transmission above, a Schmidt coupling on the input side permits the input to be "plugged-in" directly to any one of six gears, all of which are in mesh with the internal gear wheel.

On the output side, after the power flows through the gear wheel, a second Schmidt coupling permits a direct power takeoff from any of the same six gears. Thus, any one of 6 x 6 minus 5 or 31 different speed ratios can be selected while the unit is running. A more orthodox design would require almost twice as many gears.

Powerful pump. In the worm-type pump (bottom left), as the input shaft rotates clockwise, the worm rotor is forced to roll around the inside of the gear housing, which has a helical groove running from end to end. Thus, the rotor centerline will rotate counterclockwise to produce a powerful pumping action for moving heavy media.

In the belt drive (bottom right), the Schmidt coupling permits the belt to be shifted to a different bottom pulley while remaining on the same top pulley. Normally, because of the constant belt length, the top pulley would have to be shifted, too, to provide a choice of only three output speeds. With the new arrangement, nine different output speeds can be obtained. □

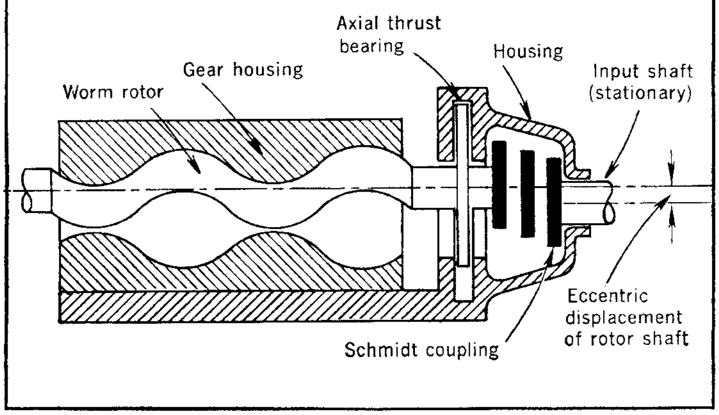

Coupling allows helical-shape rotor to wiggle for pumping purposes.

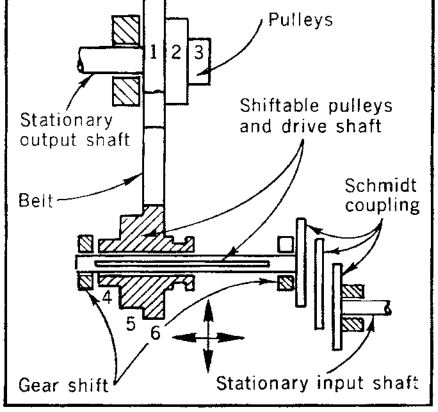

Coupling takes up slack when bottom shifts.

SECTION 5

CLUTCHES

Basic Types of Mechanical Clutches

Sketches include both friction and positive types. Figs. 1-7 are classified as externally controlled; Figs. 8-12 are internally controlled. The latter are further divided into overload relief, over-riding, and centrifugal types.

Marvin Taylor

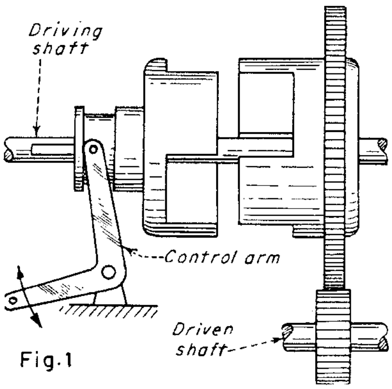

Fig.1

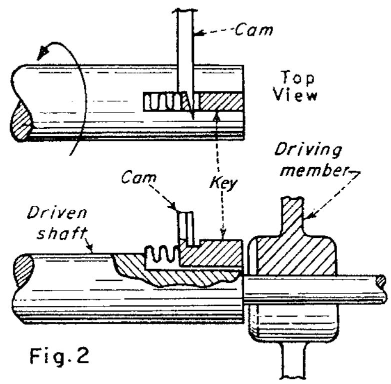

Fig.2

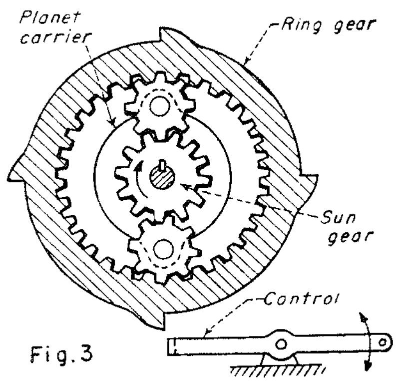

Fig.3

1. JAW CLUTCH. Left sliding half is feathered to the driving shaft while right half rotates freely. Control arm activates the sliding half to engage or disengage the drive. This clutch, though strong and simple, suffers from disadvantages of high shock during engagement, high inertia of the sliding half, and considerable axial motion required for engagement.

2. SLIDING KEY CLUTCH. Driven shaft with a keyway carries freely-rotating member which has radial slots along its hub; sliding key is spring loaded but is normally restrained from engaging slots by the control cam. To engage the clutch, control cam is raised and key enters one of the slots. To disengage, cam is lowered into the path of the key; rotation of driven shaft forces key out of slot in driving member. Step on control cam limits axial movement of the key.

3. PLANETARY TRANSMISSION CLUTCH. In disengaged position shown, driving sun gear will merely cause the free-wheeling ring gear to idle counter-clockwise, while the driven member, the planet carrier, remains motionless. If motion of the ring gear is blocked by the control arm, a positive clockwise drive is established to the driven planet carrier.

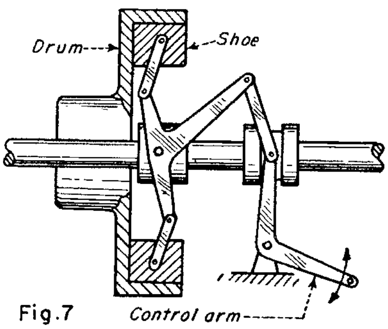

Fig.7

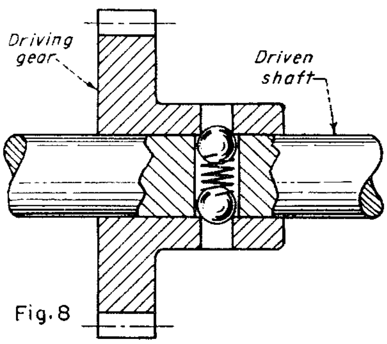

Fig.8

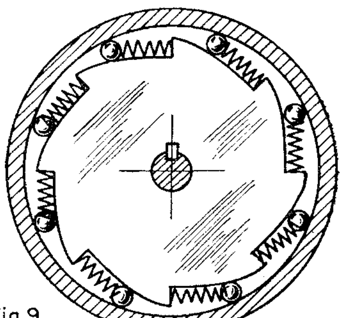

Fig.9

7. EXPANDING SHOE CLUTCH. In sketch above, engagement is obtained by motion of control arm which operates linkages to force friction shoes radially outward into contact with inside surface of drum.

8. SPRING AND BALL RADIAL DETENT CLUTCH. This design will positively hold the driving gear and driven shaft in a given timing relationship until the torque becomes excessive. At this point the balls will be forced inward against their spring pressure and out of engagement with the holes in the hub, thus permitting the driving gear to continue rotating while the driven shaft is stationary.

9. CAM AND ROLLER CLUTCH. This over-running clutch is suited for higher speed free-wheeling than the pawl and ratchet types. The inner driving member has camming surfaces at its outer rim and carries light springs that force rollers to wedge between these surfaces and the inner cylindrical face of the driven member. During driving, self-energizing friction rather than the springs forces the roller to tightly wedge between the members and give essentially positive drive in a clockwise direction. The springs insure fast clutching action. If the driven member should attempt to run ahead of the driver, friction will force the rollers out of a tight wedging position and break the connection.

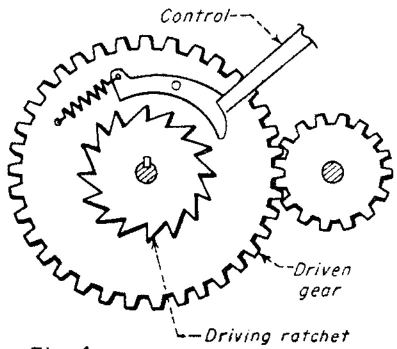

Fig. 4

Fig. 5

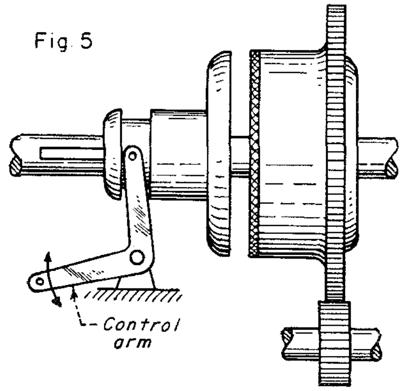

Fig. 6

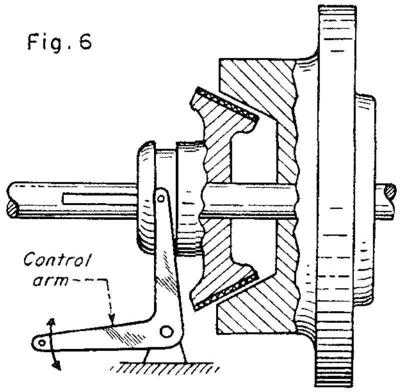

4. PAWL AND RATCHET CLUTCH. (External Control). Ratchet is keyed to the driving shaft; pawl is carried by driven gear which rotates freely on the driving shaft. Raising the control member permits the spring to pull the pawl into engagement with the ratchet and drive the gear. Engagement continues until control member is lowered into the path of a camming surface on the pawl. The motion of the driven gear will then force the pawl out of engagement and bring the driven assembly to a solid stop against the control member. This clutch can be converted into an internally controlled type of unit by removing the external control arm and replacing it with a slideable member on the driving shaft.

5. PLATE CLUTCH. Available in many variations, with single and multiple plates, this unit transmits power through friction force developed between the faces of the left sliding half which is fitted with a feather key and the right half which is free to rotate on the shaft. Torque capacity depends upon the axial force exerted by the control member when it activates the sliding half.

6. CONE CLUTCH. This type also requires axial movement for engagement, but the axial force required is less than that required with plate clutches. Friction material is usually applied to only one of the mating surfaces. Free member is mounted to resist axial thrust.

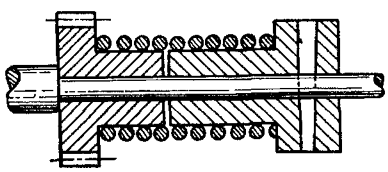

Fig. 10

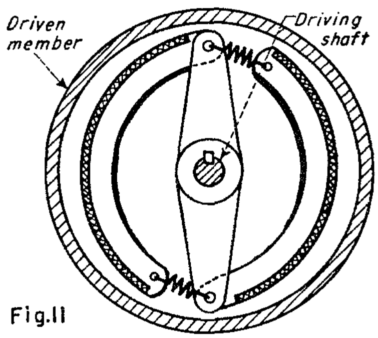

Fig. 11

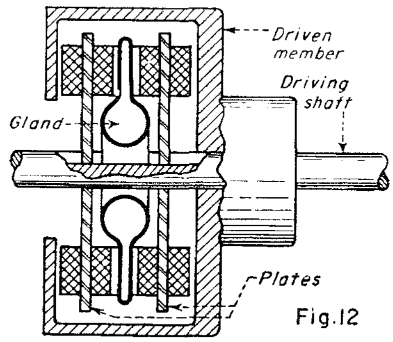

Fig. 12

10. WRAPPED SPRING CLUTCH. Makes a simple and inexpensive uni-directional clutch consisting of two rotating members connected by a coil spring which fits snugly over both hubs. In the driving direction the spring tightens about the hubs producing a self energizing friction grip; in the opposite direction it unwinds and will slip.

11. EXPANDING SHOE CENTRIFUGAL CLUTCH. Similar in action to the unit shown in Fig. 7 with the exception that no external control is used. Two friction shoes, attached to the driving member, are held inward by springs until they reach the "clutch-in" speed, at which centrifugal force energizes the shoes outward into contact with the drum. As the driver rotates faster the pressure between the shoes and the drum increases thereby providing greater torque capacity.

12. MERCURY GLAND CLUTCH. Contains two friction plates and a mercury filled rubber gland, all keyed to the driving shaft. At rest, mercury fills a ring shaped cavity near the shaft; when revolved at sufficient speed, the mercury is forced outward by centrifugal force spreading the rubber gland axially and forcing the friction plates into driving contact with the faces of the driven housing. Axial thrust on driven member is negligible.

Construction Details of Over-Riding Clutches

A. DeFeo

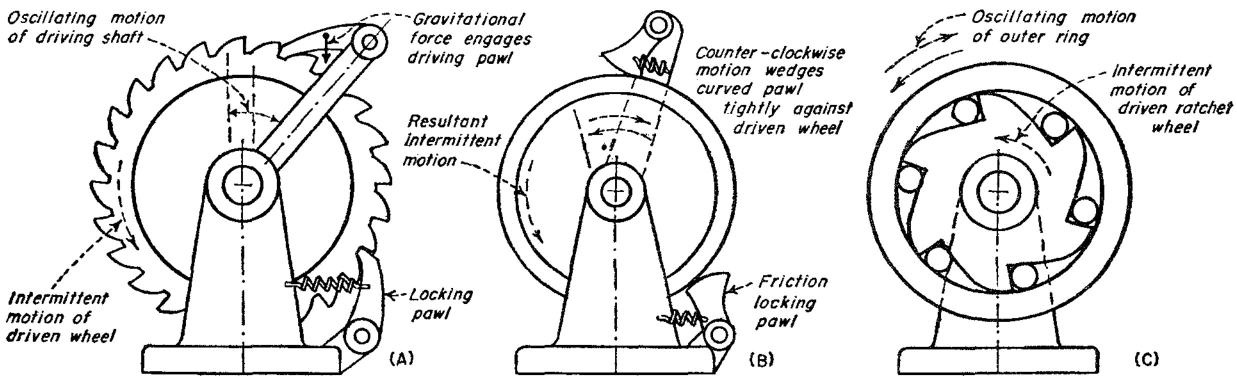

1 Elementary over-riding clutches: (A) Ratchet and Pawl mechanism is used to convert reciprocating or oscillating movement to intermittent rotary motion. This motion is positive but limited to a multiple of the tooth pitch. (B) Friction-type is quieter but requires a spring device to keep eccentric pawl in constant engagement. (C) Balls or rollers replace the pawls in this device. Motion of the outer race wedges rollers against the inclined surfaces of the ratchet wheel.

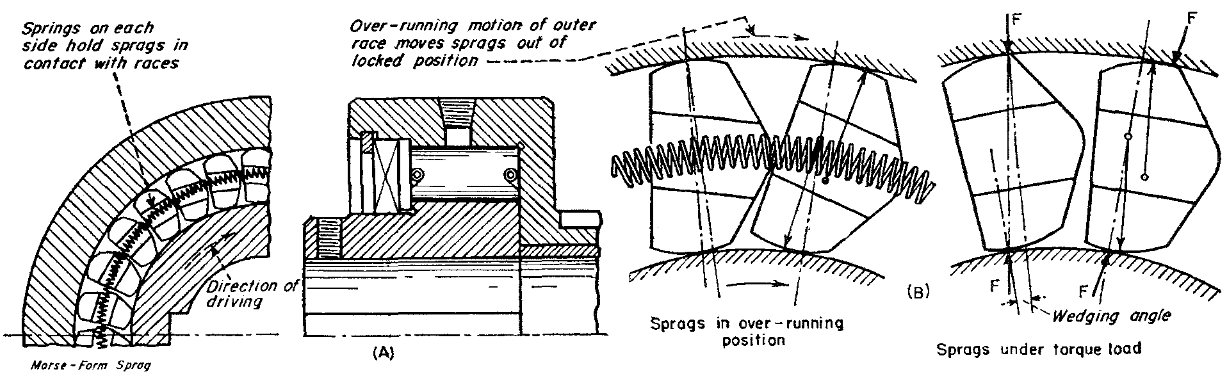

4 With cylindrical inner and outer races, sprags are used to transmit torque. Energizing springs serves as a cage to hold the sprags. (A) Compared to rollers, shape of sprag permits a greater number within a limited space; thus higher torque loads are possible. Not requiring special cam surfaces, this type can be installed inside gear or wheel hubs. (B) Rolling action wedges sprags tightly between driving and driven members. Relatively large wedging angle insures positive engagement.

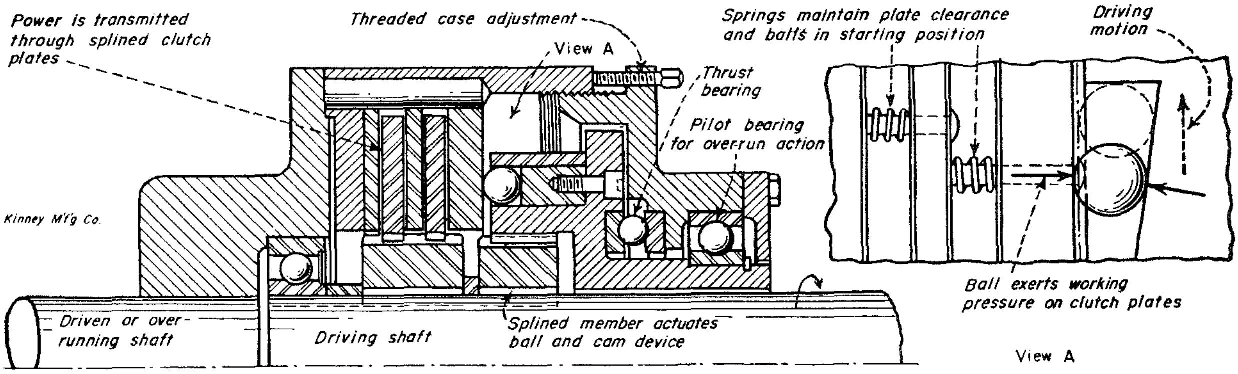

6 Multi-disk clutch is driven by means of several sintered-bronze friction surfaces. Pressure is exerted by a cam actuating device which forces a series of balls against a disk plate. Since a small part of the transmitted torque is carried by the actuating member, capacity is not limited by the localized deformation of the contacting balls. Slip of the friction surfaces determine the capacity and prevent rapid, shock loads. Slight pressure of disk springs insure uniform engagement.

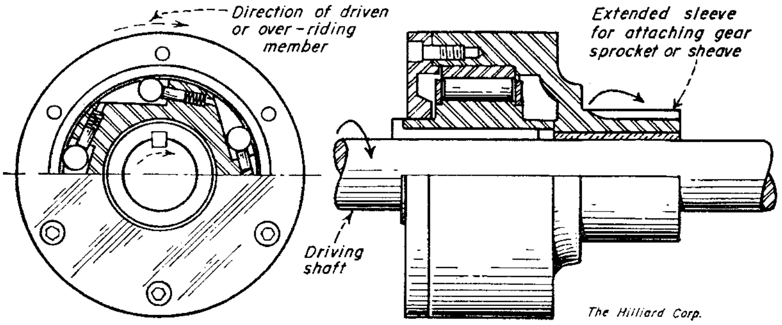

2 Commercial over-riding clutch has springs which hold rollers in continuous contact between cam surfaces and outer race; thus there is no backlash or lost motion. This simple design is positive and quiet. For operation in the opposite direction, the roller mechanism can easily be reversed in the housing.

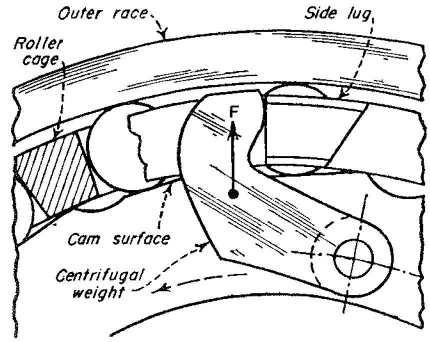

3 Centrifugal force can be used to hold rollers in contact with cam and outer race. Force is exerted on lugs of the cage which controls the position of the rollers.

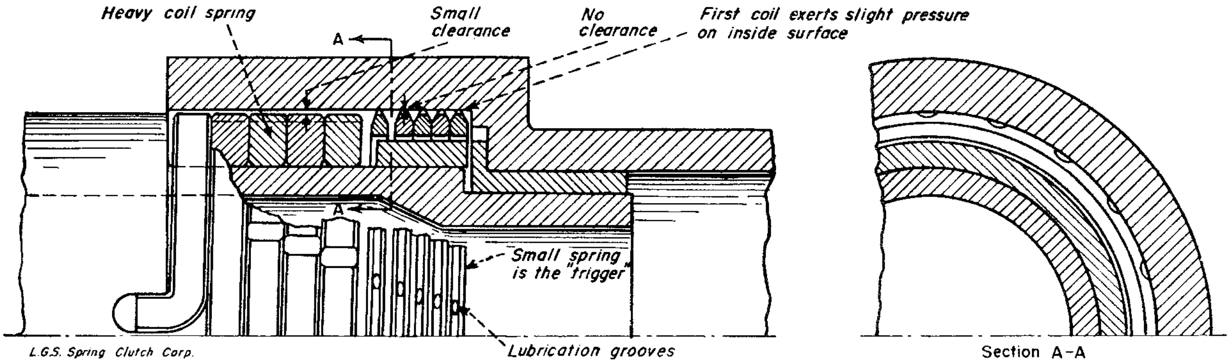

5 Engaging device consists of a helical spring which is made up of two sections: a light trigger spring and a heavy coil spring. It is attached to and driven by the inner shaft. Relative motion of outer member rubbing on trigger causes this spring to wind-up. This action expands the spring diameter which takes up the small clearance and exerts pressure against the inside surface until the entire spring is tightly engaged. Helix angle of spring can be changed to reverse the over-riding direction.

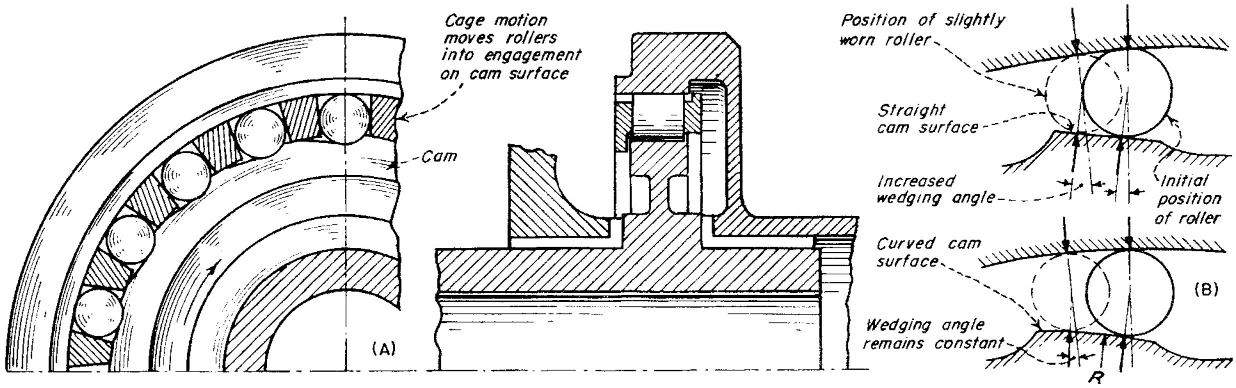

7 Free-wheeling clutch widely used in power transmission has a series of straight-sided cam surfaces. An engaging angle of about 3 deg is used; smaller angles tend to become locked and are difficult to disengage while larger ones are not as effective. (A) Inertia of floating cage wedges rollers between cam and outer race. (B) Continual operation causes wear of surfaces; 0.001 in. wear alters angle to 8.5 deg. on straight-sided cams. Curved cam surfaces maintain constant angle.

Low-Cost Designs for Overrunning Clutches

All are simple devices that can be constructed inexpensively in the laboratory workshop.

James F. Machen

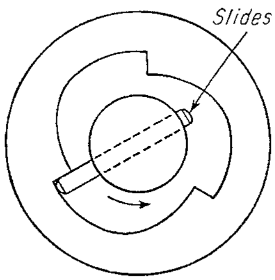

1
Lawnmower type

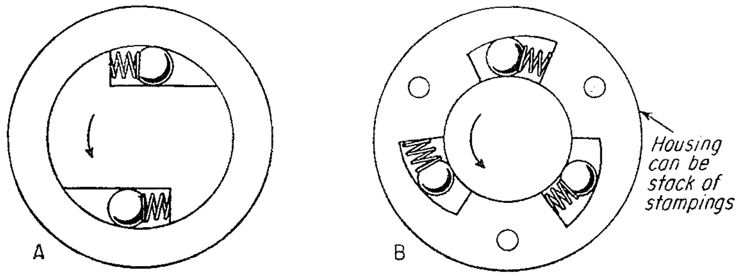

2
Wedging balls or rollers: internal (A); external (B)

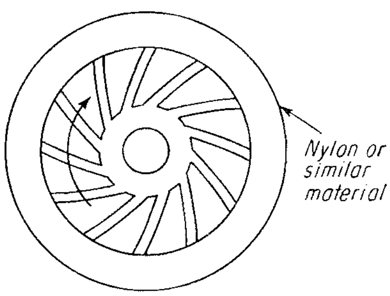

3
Molded sprags
(for light duty)

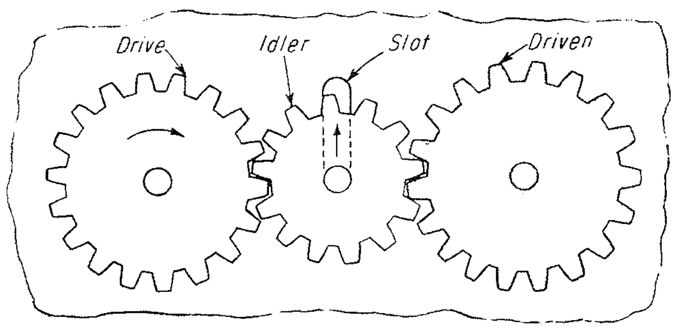

4
Disengaging idler rises in slot when drive direction is reversed

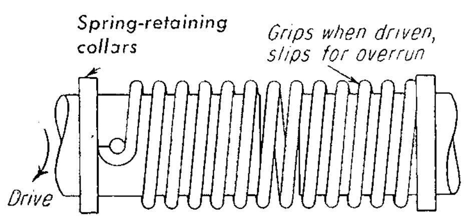

5
Slip-spring coupling

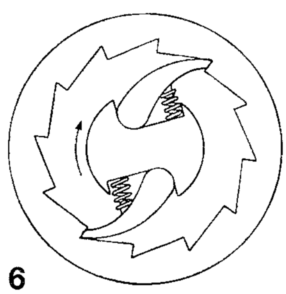

6
Internal ratchet and spring-loaded pawls

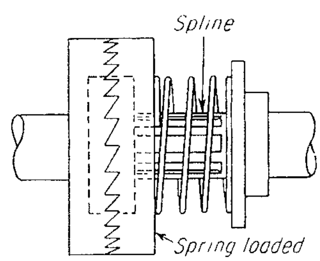

7
One-way dog clutch

(FOR ANGULAR AND AXIAL ADJUSTMENT)

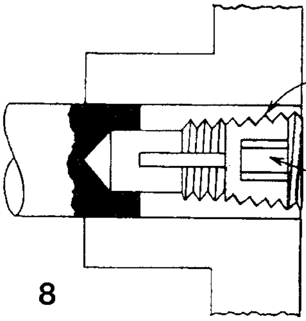

8
Plug jam
(with four axial slots)

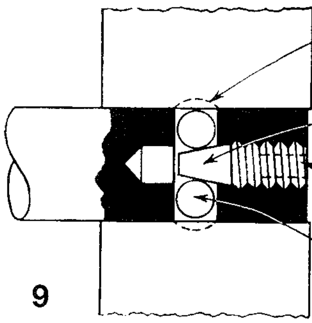

9
Ball jam

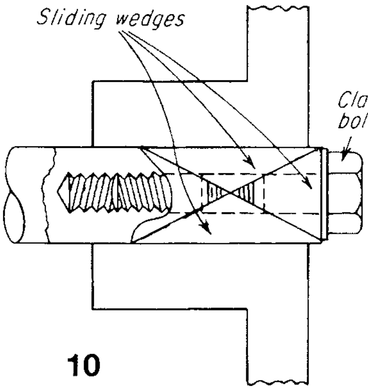

10
Clamped wedges
(for axial adjustment only)

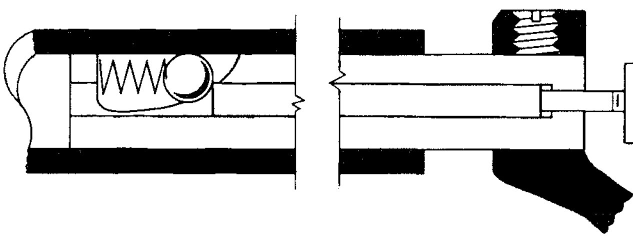

11
One-way slide-lock

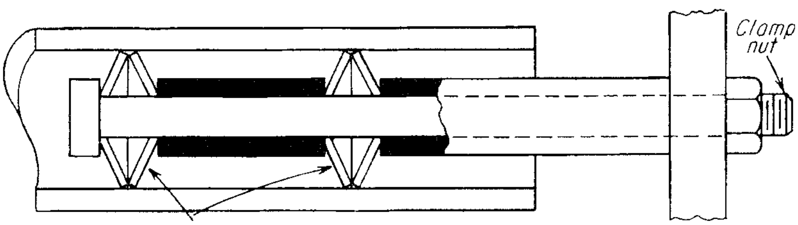

12
Belleville-washer clamp

10 Ways to Apply Overrunning Clutches

These clutches allow freewheeling, indexing, and backstopping applicable to many design problems. Here are some clutch setups.

W. Edgar Mulholland & John L. King JR.

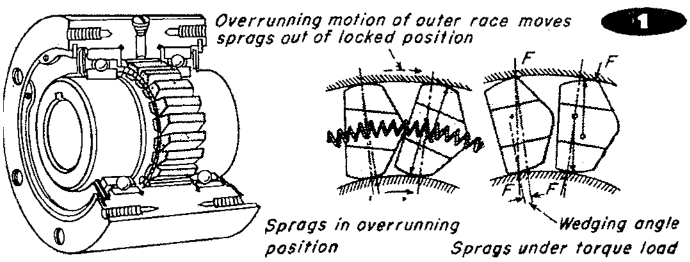

Precision Sprags . . .

act as wedges and are made of hardened alloy steel. In the Formsprag clutch, torque is transmitted from one race to another by wedging action of sprags between the races in one direction; in other direction the clutch freewheels.

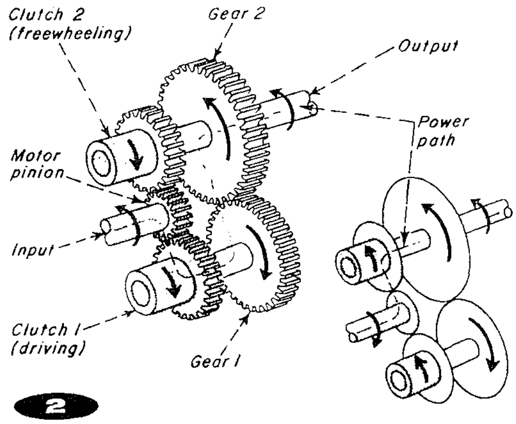

2-Speed Drive—I . . .

requires input rotation to be reversible. Counterclockwise input as shown in the diagram drives gear 1 through clutch 1; output is counterclockwise; clutch 2 over-runs. Clockwise input (schematic) drives gear 2 through clutch 2; output is still counterclockwise; clutch 1 over-runs.

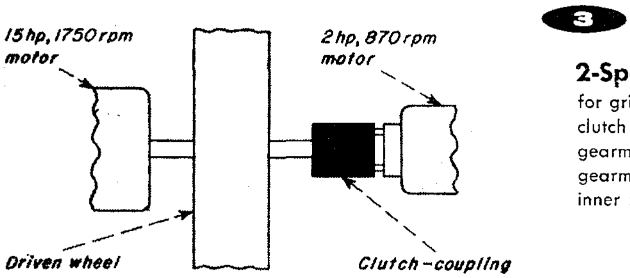

2-Speed Drive—II . . .

for grinding wheel can be simple, in-line design if over-running clutch couples two motors. Outer race of clutch is driven by gearmotor; inner race is keyed to grinding-wheel shaft. When gearmotor drives, clutch is engaged; when larger motor drives, inner race over-runs.

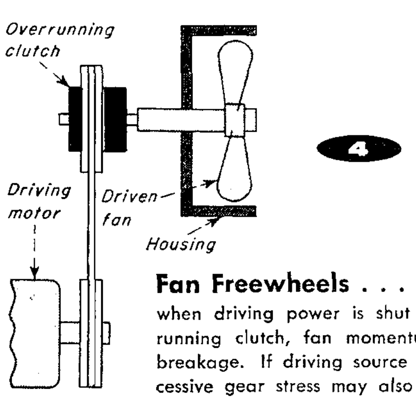

Fan Freewheels . . .

when driving power is shut off. Without over-running clutch, fan momentum can cause belt breakage. If driving source is a gearmotor, excessive gear stress may also occur by feedback of kinetic energy from fan.

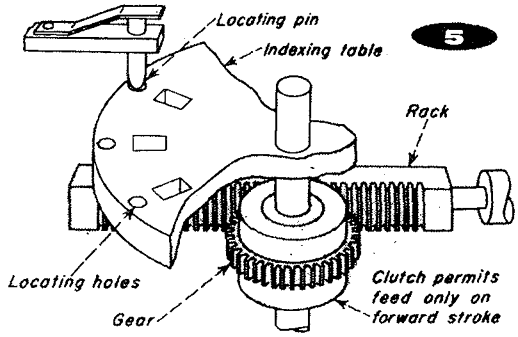

Indexing Table . . .

is keyed to clutch shaft. Table is rotated by forward stroke of rack, power being transmitted through clutch by its outer-ring gear only during this forward stroke. Indexing is slightly short of position required. Exact position is then located by spring-loaded pin, which draws table forward to final positioning. Pin now holds table until next power stroke of hydraulic cylinder

6

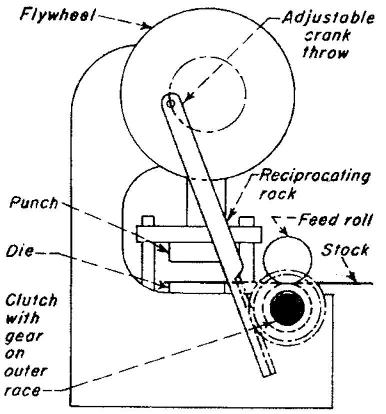

Punch Press Feed . .

is so arranged that strip is stationary on downstroke of punch (clutch freewheels); feed occurs during upstroke when clutch transmits torque. Feed mechanism can easily be adjusted to vary feed amount.

7

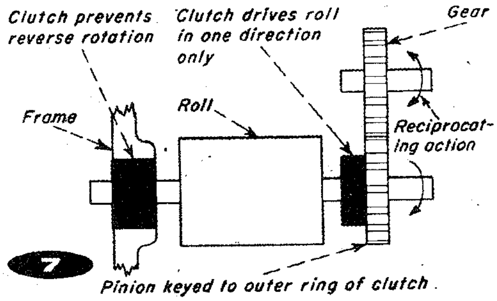

Indexing and Backstopping . . .

is done with two clutches so arranged that one drives while the other freewheels. Application here is for capsuling machine; gelatin is fed by the roll and stopped intermittently so blade can precisely shear material to form capsules.

8

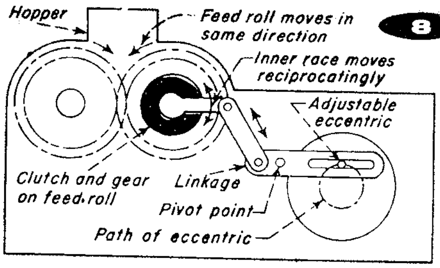

Intermittent Motion . . .

of candy machine is adjustable; function of clutch is to ratchet the feed rolls around. This keeps the material in the hopper agitated.

9

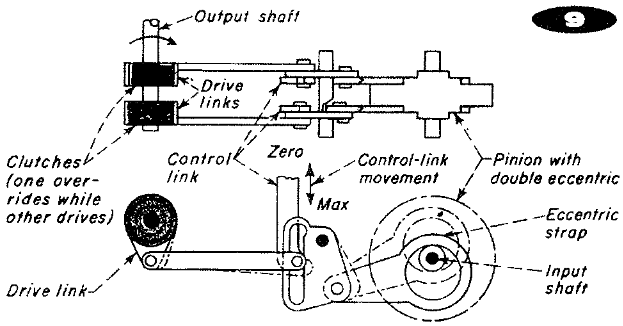

Double-impulse Drive . . .

employs double eccentrics and drive clutches. Each clutch is indexed 180° out of phase with the other. One revolution of eccentric produces two drive strokes. Stroke length, and thus the output rotation, can be adjusted from zero to max by the control link.

10

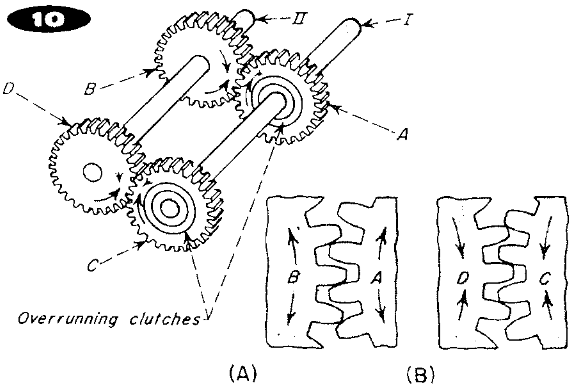

Anti-backlash Device . . .

uses over-running clutches to insure that no backlash is left in the unit. Gear *A* drives *B* and shaft II with the gear mesh and backlash as shown in (A). The over-running clutch in gear C permits gear *D* (driven by shaft II) to drive gear C and results in the mesh and backlash shown in (B). The over-running clutches never actually over-run. They provide flexible connections (something like split and sprung gears) between shaft I and gears *A*, C to allow absorption of all backlash.

6 Ways to Prevent Overloading

These "safety valves" give way if machinery jams, thus preventing serious damage.

Peter C. Noy

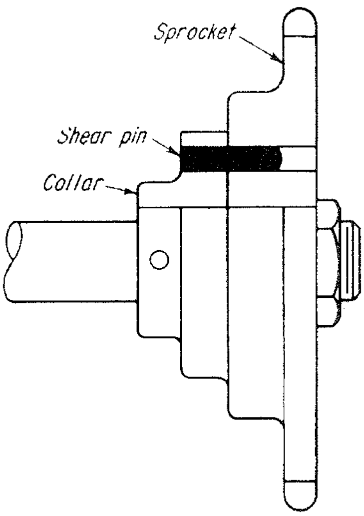

1
SHEAR PIN is simple to design and reliable in service. However, after an overload, replacing the pin takes a relatively long time; and new pins aren't always available.

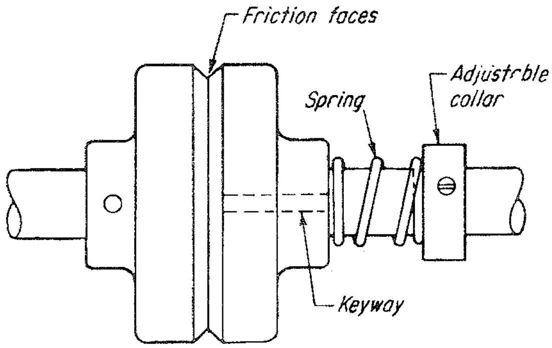

2
FRICTION CLUTCH. Adjustable spring tension that holds the two friction surfaces together sets overload limit. As soon as overload is removed the clutch reengages. One drawback is that a slipping clutch can destroy itself if unnoticed.

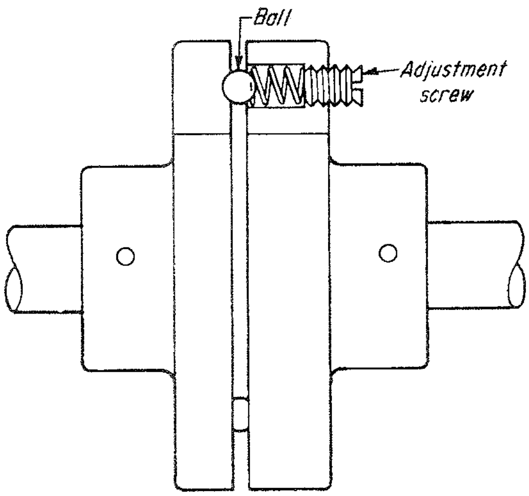

3
MECHANICAL KEYS. Spring holds ball in dimple in opposite face until overload forces the ball out. Once slip begins, wear is rapid, so device is poor when overload is common.

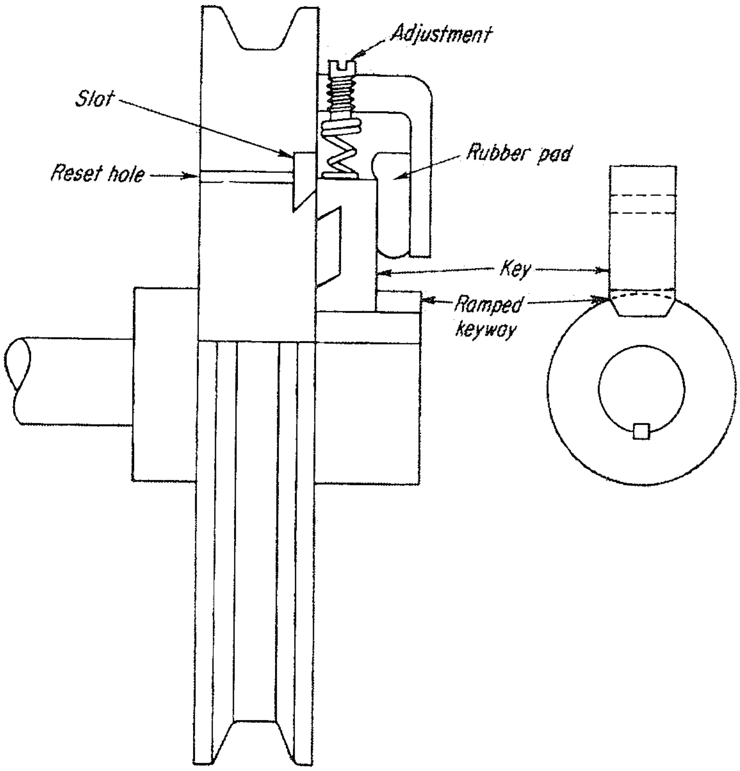

4
RETRACTING KEY. Ramped sides of keyway force key outward against adjustabe spring. As key moves outward, a rubber pad—or another spring—forces the key into a slot in the sheave. This holds the key out of engagement and prevents wear. To reset, push key out of slot by using hole in sheave.

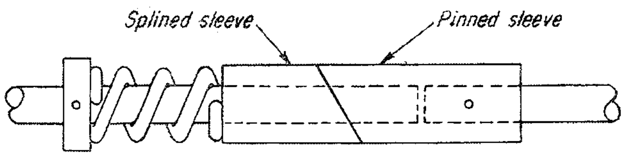

5
ANGLE-CUT CYLINDER. With just one tooth, this is a simplified version of the jaw clutch. Spring tension sets load limit.

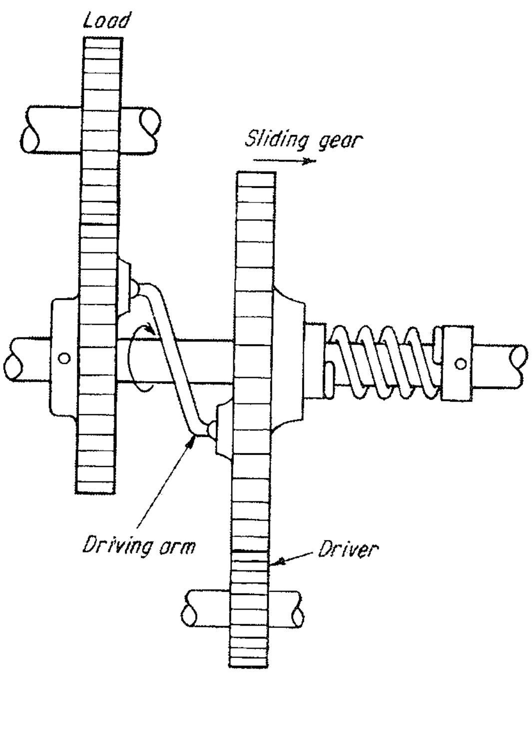

6
DISENGAGING GEARS. Axial forces of spring and driving arm balance. Overload overcomes spring force to slide gears out of engagement. Gears can strip once overloading is removed, unless a stop holds gears out of engagement.

7 More Ways to Prevent Overloading

For the designer who must anticipate the unexpected, here are ways to guard machinery against carelessness or accident.

Peter C. Noy

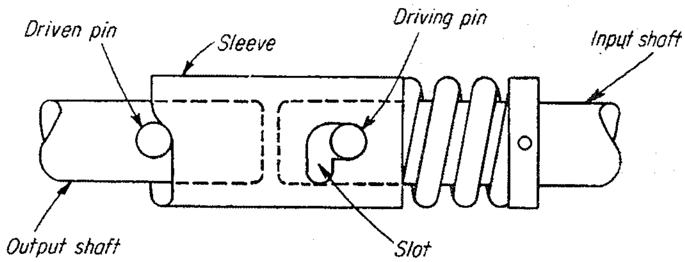

1
CAMMED SLEEVE connects input and output shafts. Driven pin pushes sleeve to right against spring. When overload occurs, driving pin drops into slot to keep shaft disengaged. Turning shaft backwards resets.

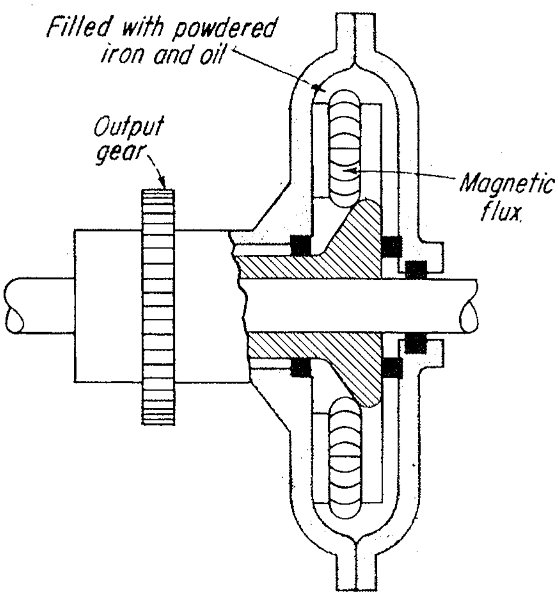

2
MAGNETIC FLUID COUPLING is filled with slurry made of iron or nickel powder in oil. Controlled magnetic flux that passes through fluid varies slurry viscosity, and thus maximum load over a wide range. Slip ring carries field current to vanes.

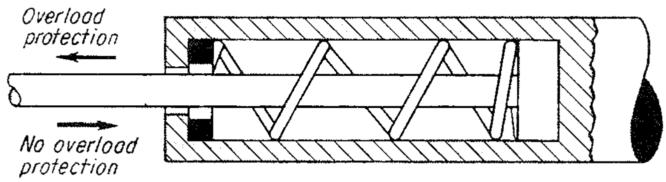

3
SPRING PLUNGER is for reciprocating motion with possible overload only when rod is moving left. Spring compresses under overload.

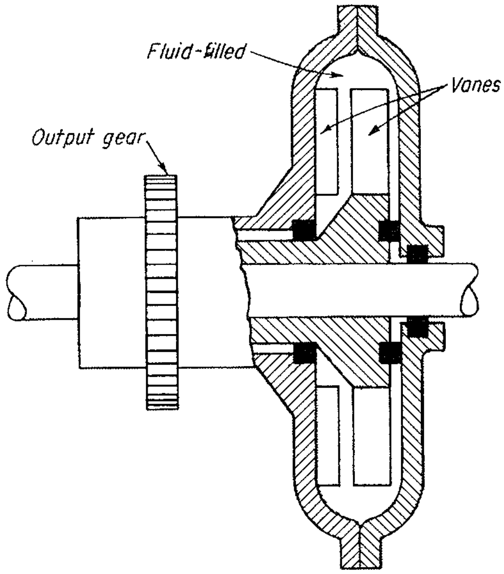

4
FLUID COUPLING. Maximum load can be closely controlled by varying viscosity and level of fluid. Other advantages are smooth transmission and low heat rise during slip.

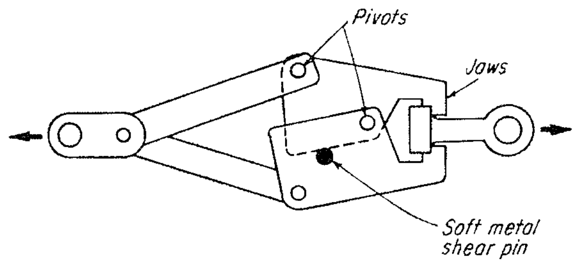

5
TENSION RELEASE. When toggle-operated blade shears soft pin, jaws open to release eye. A spring that opposes the spreading jaws can replace the shear pin.

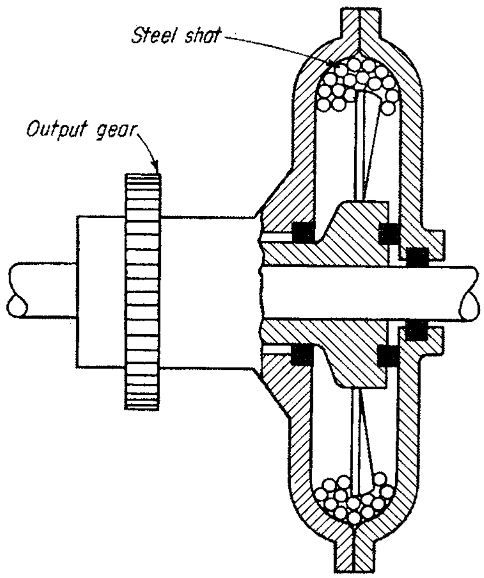

6
STEEL-SHOT COUPLING transmits more torque as speed increases. Centrifugal force compresses steel shot against case, increasing resistance to slip. Adding more steel shot also increases resistance to slip.

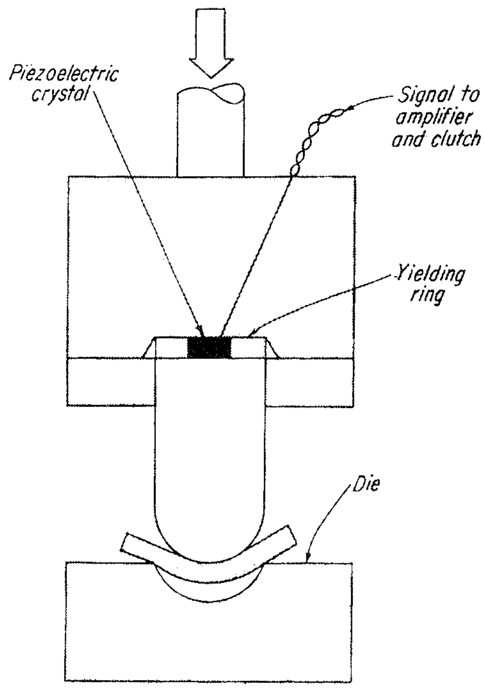

7
PIEZOELECTRIC CRYSTAL sends output signal that varies with pressure. Clutch at receiving end of signal disengages when pressure on the crystal reaches preset limit. Yielding ring controls compression of crystal.

Centrifugal Clutches

These simple devices provide low-cost clutching for machines operating under fast-changing load conditions.

M. F. Spotts

IF you want a practical way of connecting a motor—or any other type of prime mover—to a load when frequent stopping and starting are involved, centrifugal clutches are a good bet. Low in initial cost, centrifugal clutches can save you the expense of buying another form of electric motor, not to mention auxiliary starting equipment. Centrifugal clutches are built in a wide range of sizes and types—all the way from the little gasoline cars run on tracks at funfairs (here the motor disengages at low speed, and as the child presses on the gas pedal the car starts moving) to 500-hp diesel engines.

Other advantages: These clutches are good starters for high-inertia loads. They tolerate a considerable amount of manufacturing variations and are well suited to drives that undergo vibrations and heavy shock loads. Delayed engagements are possible by varying the clutch-spring force, and installation and service costs are low.

A typical centrifugal clutch has a set of shoes that are forced out against the output drum by centrifugal force. The shoes may be loosely held within the drum (Fig 1, next page), but in the more refined designs the shoes are connected to the input member by means of a floating link (Fig 2) or a fixed pivot (Fig 5).

Both attached-shoe designs (Fig 2 and 5) are analyzed here. Until now, however, the design procedure has been basically a graphical one. The design formulas derived here obviate the need for a graphical layout (or the graphical solution can serve as a check).

Floating-link design

The shoe of this type (Fig 2) is supported at the free end H of the floating link BH. End B of the link is attached to the hub of the driving member. The lining contacts the drum of the driven member and covers an angle ϕ, with support H at the midpoint which determines the v and w axes for the shoe. Angle ϕ is large so pressure p between the lining and drum is not constant but varies according to the equation

$$p = p_o \cos(\psi - \theta) \qquad (1)$$

where p_o is the maximum value of the lining pressure located at angle θ to the v-axis. Angle ψ is the angle from the v-axis to the element under consideration.

The pressure on the lining p, when multiplied by the area $br\ d\psi$ of an element of lining, gives the normal force between lining and drum. The component of force parallel to the v-axis is found by multiplying by $\cos\psi$. Eq 1 is substituted for p and the result integrated over the length of the lining, $-\phi/2$ to $\phi/2$, to obtain N_v, the component of normal force parallel to v-axis:

$$N_v = -\int_{-\phi/2}^{\phi/2} pbr \cos\psi\, d\psi$$

$$N_v = -\tfrac{1}{2} brp_o \cos\theta\,(\phi + \sin\phi) \qquad (2)$$

In a similar manner, the total component of normal force N_w parallel to the w-axis is found by multiplying by $\sin\psi$. The integration gives

$$N_w = -\int_{-\phi/2}^{\phi/2} pbr \sin\psi\, d\psi$$

$$N_w = -\tfrac{1}{2} brp_o \sin\theta\,(\phi - \sin\phi) \qquad (3)$$

The accompanying friction forces are

$$F_v = \int \mu pbr \sin\psi\, d\psi = -\mu N_w \qquad (4)$$

$$F_w = -\int \mu pbr \cos\psi\, d\psi = \mu N_v \qquad (5)$$

where μ is the coefficient of friction.

The torque exerted by the shoe is found by multiplying the normal force on the element by μ, and multiplying again by r to give:

Torque equation

$$T = \int_{-\phi/2}^{\phi/2} \mu pbr^2\, d\psi = 2\mu br^2 p_o \cos\theta \sin\frac{\phi}{2} \qquad (6)$$

(Eq 2 to 6 were obtained by G. A. G. Fazekas, "Graphical Shoe-Brake Analysis," Trans. ASME, vol 79, 1957, p 1322.)

The clutch shoe is in equilibrium from the following three forces:

1. An outward radial force consisting of the difference between the centrifugal force F_c on the shoe and the inward force F_s from the springs.
2. Force Q which is the resultant of the previously determined forces N_v, N_w, F_v and F_w.
3. Reaction R which must have a BH direction since this is a two-force member.

When a body with three forces is in equilibrium, the three forces must intersect at a single point. Because R and F_c—F_s intersect at H, force Q must pass through this point also. Fig 3 shows Q passing through H as the resultant of the other two forces

Since Q is also the resultant of the forces arising from p and μ p, the moment made by such forces about H must be zero. This fact is utilized for finding θ, the inclination of the line of maximum pressure. The moment arms about H for p and μp are marked in the figure. Then

$$\int pbrh \sin\psi\, d\psi - \int \mu pbr\,(r - h\cos\psi)\, d\psi = 0$$

The value of the variable p from Eq 1 is substituted, and the resulting expressions are integrated between the limits of $-\phi/2$ and $\phi/2$. The result can be solved for $\tan\theta$ to give:

Line of maximum pressure

$$\tan\theta = \frac{4\mu r \sin\dfrac{\phi}{2} - \mu h\,(\phi + \sin\phi)}{h\,(\phi - \sin\phi)} \qquad (7)$$

When θ is determined, the forces represented by Eq 2 to 5 inclusive can be found and added vectorially as shown in Fig 3. This gives:

Resultant of forces, Q

$$Q = \sqrt{(N_v + F_v)^2 + (N_w + F_w)^2} \qquad (8)$$

Inclination β of force Q

$$\tan\beta = \frac{N_w + F_w}{N_v + F_v} \qquad (9)$$

At low or idling speeds, the shoe is pulled inwardly by the spring force F_s. The outward force F_c on the shoe is equal to:

Centrifugal force

$$F_c = \frac{W}{g}\, r_o\, \omega^2 \qquad (10)$$

where W is the weight of the shoe assumed to be concentrated at radius r_o; ω is the angular velocity, rad/sec, and g is the gravitational constant, 386 in./sec².

As shown in Fig 2, link BH is inclined at angle α to the v-axis. The sine theorem gives equations for:

Forces R and F_c-F_s

$$R = \frac{Q\sin\beta}{\sin\alpha} \qquad (11)$$

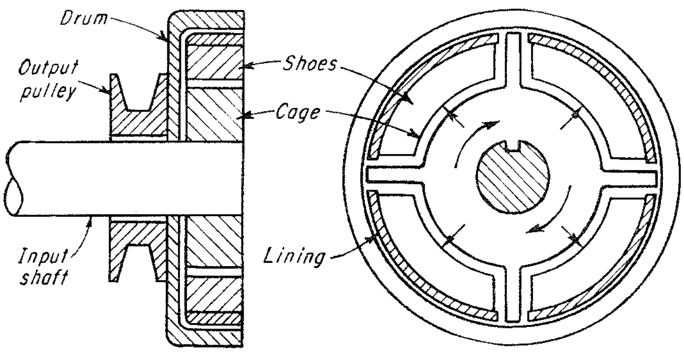

1. Free-shoe centrifugal clutch

SYMBOLS

b = width of lining
F_c = centrifugal force
F_s = spring force
F_v = component along v-axis of friction lining force
F_w = component along w-axis of friction lining force
g = gravitational constant, 386 in./sec²
h = distance from center of rotation to pivot of shoe
hp = transmittable horsepower
M_f = moment of friction forces about fixed pivot
M_n = moment of normal forces about fixed pivot
n = revolutions per minute
N_v = component along v-axis of forces normal to lining
N_w = component along w-axis of forces normal to lining
p = pressure between lining and drum
p_o = maximum lining pressure
Q = resultant of N_v, N_w, F_v and F_w
r = radius of drum
r_o = radius to center of gravity of shoe; outer radius of fixed pivot shoe
r_i = inner radius of fixed pivot shoe
r_p = distance from center of rotation to fixed pivot
R = reaction along floating link
T = torque about center of rotation
W = weight of shoe
α = inclination of floating link with v-axis
β = inclination of resultant Q with v-axis
γ = weight per in.³
θ = inclination of line of maximum pressure with v-axis
μ = coefficient of friction
ϕ = angular extent of lining
ω = angular velocity before slip occurs, radians/sec

$$F_c - F_s = \frac{Q \sin(\alpha - \beta)}{\sin \alpha} \qquad (12)$$

Numerical example

A centrifugal clutch shoe has a radius of 5.25 in. and a width of lining of 2.50 in. Lining pressure is not to exceed 100 psi. Angular length of lining is $\phi = 108$ deg, and the link is at an angle of $\alpha = 48$ deg. The shoe is pivoted at a distance h of 4 in. from the center. Total inward spring force of both springs is 15 lb. Weight of shoe is 3 lb with its center of gravity at a radius of 4.6 in.

As there are linings on the market with a different coefficient of friction, for values of μ of 0.1, 0.2, 0.3, 0.4 and 0.5 find the corresponding values of forces Q, R, and F_c-F_s. Find the torque T, the corresponding slipping rpm, and the horsepower per shoe. Plot the curve for hp vs μ to determine the best value for μ.

Solution

By Eq (7)

$$\tan\theta = \frac{\mu\,[(4)(5.25)(0.80902) - 4(1.88496 + 0.95106)]}{4\,(1.88496 - 0.95106)}$$

$$= 1.511\,\mu$$

By Eq (2)

$$N_v = -(\tfrac{1}{2})(2.5)(5.25)(100)(2.83602)\cos\theta$$
$$= -1861 \cos\theta$$

By Eq (3)

$$N_w = -612.9 \sin\theta$$

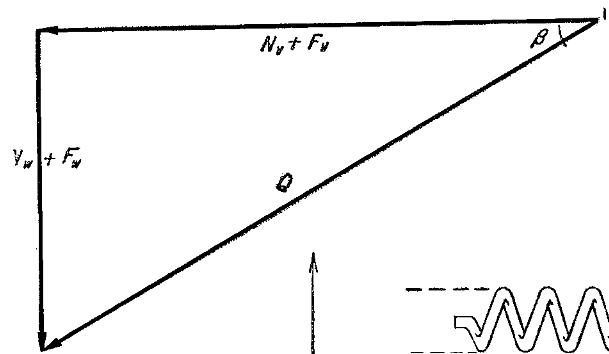

3. Components of resultant force Q

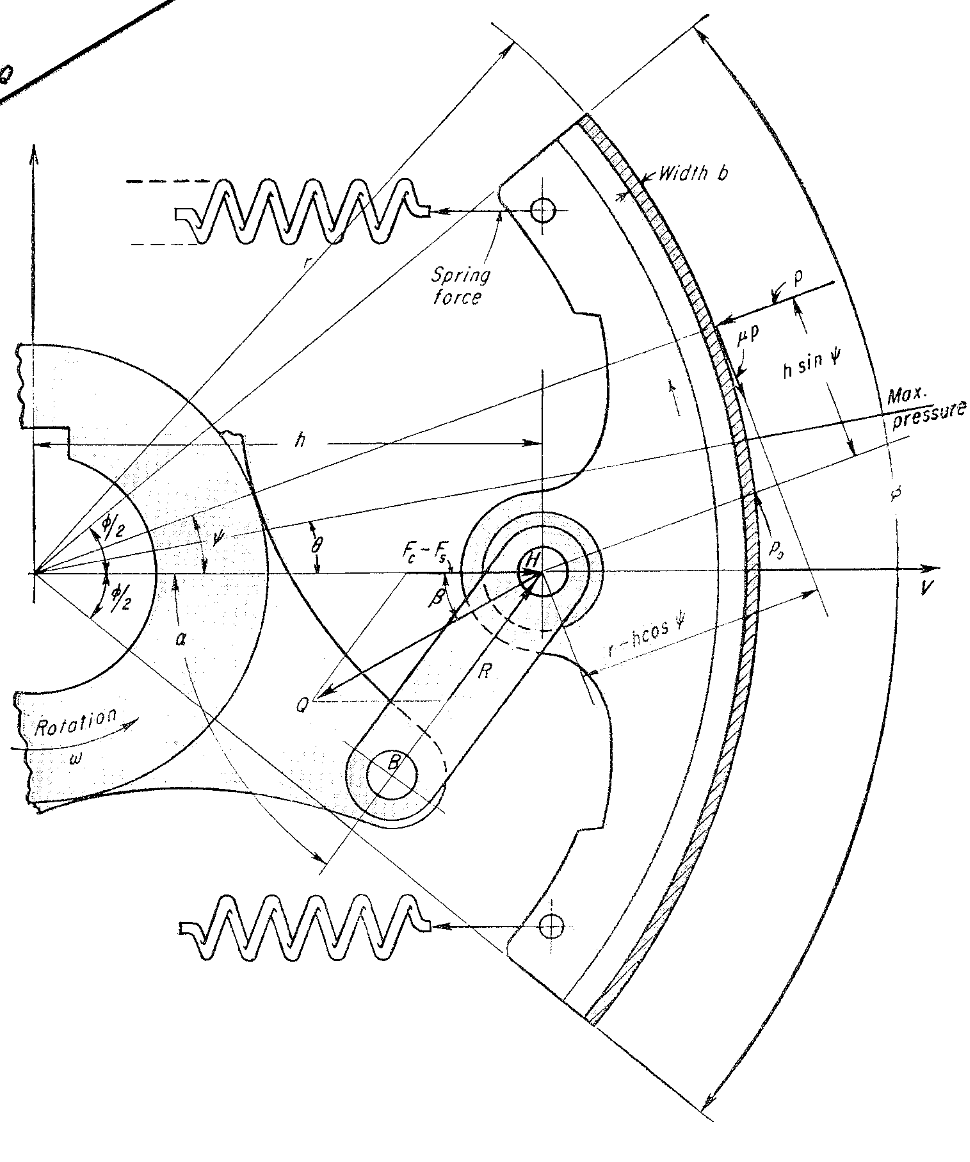

2. Floating-link design

By Eq (6)

$$T = 2\mu\,(2.5)(5.25)^2(100)(0.80902)\cos\theta$$
$$= 11{,}149\mu\cos\theta$$

From Eq (10)

$$\omega = \sqrt{\frac{g\,F_c}{W\,r_o}} = \sqrt{\frac{386\,F_c}{(3)\,4.6}} = 5.29\sqrt{F_c}$$

Then

$$n = \frac{\omega}{2\pi}\,60 = 9.55\omega = 50.5\sqrt{F_c}$$

also

$$hp = \frac{Tn}{63{,}000}$$

The calculations are best carried out in tabular form (see table). Thus, for the case of $\mu = 0.1$

$$\tan\theta = 0.1511$$
$$\theta = 8°\,35.6';\quad \cos\theta = 0.9888$$
$$N_v = -1861\,(0.9888) = -1840.2\ \text{lb}$$
$$N_w = -612.9\,(0.1494) = -91.6\ \text{lb}$$

By Eq 4, 5, and 8

$$F_v = -0.1\,(-91.6) = 9.16\ \text{lb}$$
$$F_w = 0.1\,(-1840.2) = -184.0\ \text{lb}$$
$$Q = \sqrt{(-1840.2+9.16)^2+(-91.6-184.0)^2}$$
$$= 1852\ \text{lb}$$

By Eq 9

$$\tan\beta = \frac{-275.6}{-1831} = 0.15052$$
$$\beta = 8°\,33.6'$$

By Eq 11 and 12

$$R = \frac{1852\,(\sin 8°\,33.6')}{\sin 48°} = 371\ \text{lb}$$

$$F_c - F_s = \frac{1852\sin(48° - 8°\,33.6')}{\sin 48°} = 1583\ \text{lb}$$

$$F_c = 1583 + 15 = 1598\ \text{lb}$$

Thus

$$T = 11{,}149\,(0.1)\,(0.9888) = 1102\ \text{lb-in.}$$
$$n = 50.5\sqrt{1598} = 2019\ \text{rpm}$$

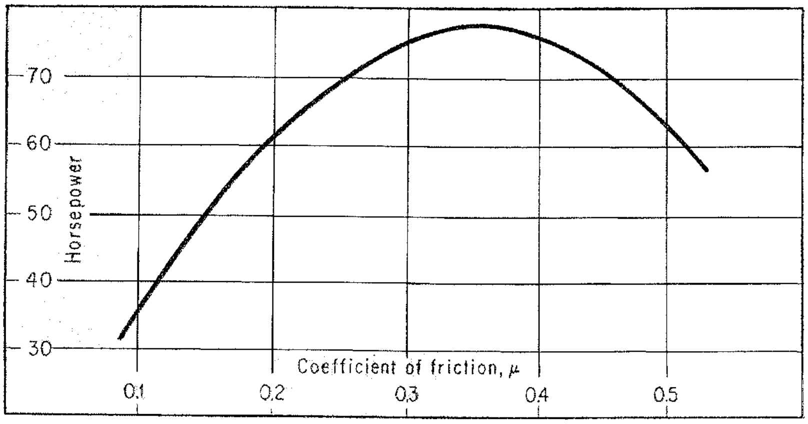

4. Variation of horsepower with coefficient of friction for the floating-link clutch analyzed in the numerical example. Note that best gripping power is obtained with shoe-linings having a coefficient of about 0.35%.

Calculations for various linings

μ	$\tan\theta$	θ	N_v	N_w	F_v	F_w	N_v+F_v	N_w+F_w	$(N_w+F_w)^2$	Q
0.1	0.15112	8°35.6′	−1840.2	−91.6	9.2	−184.0	−1831.0	−275.6	75,960	1852
0.2	0.30225	16°49.0′	−1774.1	−177.3	35.5	−354.8	−1738.6	−532.1	283,130	1818
0.3	0.45337	24°23.3′	−1695.1	−253.1	75.9	−508.5	−1619.2	−761.6	580,030	1789
0.4	0.60449	31° 9.2′	−1592.7	−317.1	126.8	−637.1	−1465.9	−954.2	910,500	1749
0.5	0.75562	37° 4.5′	−1484.9	−369.5	184.7	−742.4	−1300.2	−1111.9	1,236,320	1711

μ	$\tan\beta$	β	R	$\alpha-\beta$	$\sin(\alpha-\beta)$	F_c-F_s	T	F_c	n, rpm	hp
0.1	0.15052	8°33.6′	371	39°26.4′	0.63527	1583	1102	1598	2019	35.3
0.2	0.30605	17° 1.0′	716	30°59.0′	0.51478	1259	2126	1274	1803	60.8
0.3	0.47036	25°11.4′	1024	22°48.6′	0.38768	933	3046	948	1556	75.2
0.4	0.65093	33° 3.7′	1284	14°56.3′	0.25795	607	3817	622	1260	76.3
0.5	0.85518	40°32.2′	1496	7°27.8′	0.12990	299	4448	314	1011	63.2

Small Mechanical Clutches for Precise Service

Clutches used in calculating machines must have: (1) Quick response–lightweight moving parts; (2) Flexibility–permit multiple members to control operation; (3) Compactness–for equivalent capacity positive clutches are smaller than friction; (4) Dependability; and (5) Durability.

Marvin taylor

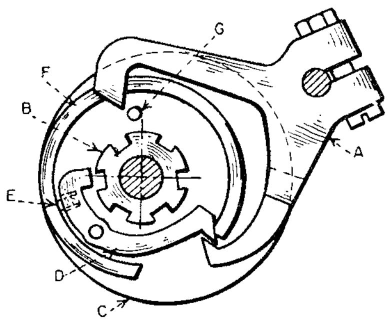

Fig. 1

PAWL AND RATCHET SINGLE CYCLE CLUTCH (Fig. 1). Known as Dennis Clutch, parts *B*, *C* and *D*, are primary components, *B*, being the driving ratchet, *C*, the driven cam plate and, *D*, the connecting pawl carryied by the cam plate. Normally the pawl is held disengaged by the lower portion of clutch arm *A*. When activated, arm *A* rocks counter-clockwise until it is out of the path of rim *F* on cam plate *C* and permits pawl *D* under the effect of spring *E* to engage with ratchet *B*. Cam plate *C* then turns clockwise until, near the end of one cycle, pin *G* on the plate strikes the upper part of arm *A* camming it clockwise back to its normal position. The lower part of *A* then performs two functions: (1) cams pawl *D* out of engagement with the driving ratchet *B* and (2) blocks further motion of rim *F* and the cam plate.

PAWL AND RATCHET SINGLE CYCLE DUAL CONTROL CLUTCH—(Fig. 2). Principal parts are: driving ratchet, *B*, directly connected to the motor and rotating freely on rod *A*; driven crank, *C*, directly connected to the main shaft of the machine and also free on A; and spring loaded ratchet pawl, *D*, which is carried by crank, *C*, and is normally held disengaged by latch *E*. To activate the clutch, arm *F* is raised, permitting latch *E* to trip and pawl *D* to engage with ratchet *B*. The left arm of clutch latch *G*, which is in the path of the lug on pawl *D*, is normally permitted to move out of interference by the rotation of the camming edge of crank *C*. For certain operations block *H* is temporarily lowered, preventing motion of latch *G*, resulting in disengagement of the clutch after part of the cycle until subsequent raising of block *H* permits motion of latch *G* and resumption of the cycle.

PLANETARY TRANSMISSION CLUTCH (Fig. 3). A positive clutch with external control, two gear trains to provide bi-directional drive to a calculator for cycling the machine and shifting the carriage. Gear *A* is the driver, gear *L* the driven member is directly connected to planet carrier *F*. The planet consists of integral gears *B* and *C*; *B* meshing with sun gear *A* and free-wheeling ring gear *G*, and *C* meshing with free-wheeling gear *D*. Gears *D* and *G* carry projecting lugs, *E* and *H* respectively, which can contact formings on arms *J* and *K* of the control yoke. When the machine is at rest, the yoke is centrally positioned so that the arms *J* and *K* are out of the path of the projecting lugs permitting both *D* and *G* to free-wheel. To engage the drive, the yoke rocks clockwise as shown, until the forming on arm *K* engages lug *H* blocking further motion of ring gear *G*. A solid gear train is thereby established driving *F* and *L* in the same direction as the drive *A* and at the same time altering the speed of *D* as it continues counter-clockwise. A reversing signal rotates the yoke counter-clockwise until arm *J* encounters lug *E* blocking further motion of *D*. This actuates the other gear train of the same ratio.

Fig. 2

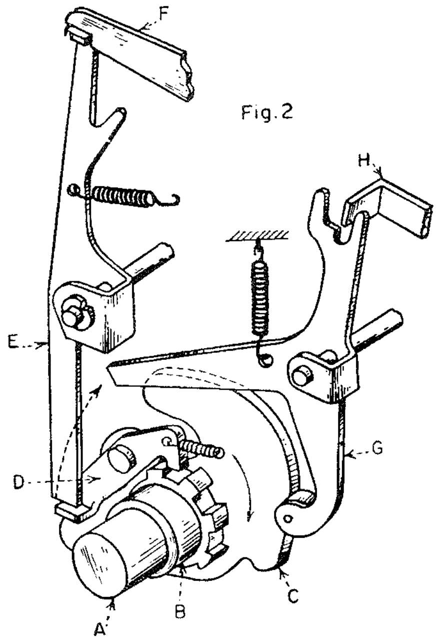

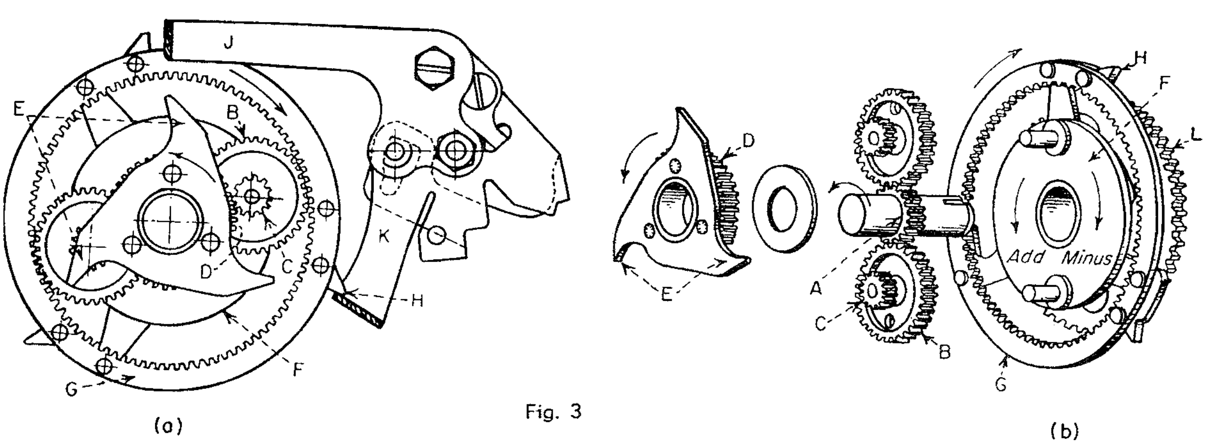

Fig. 3

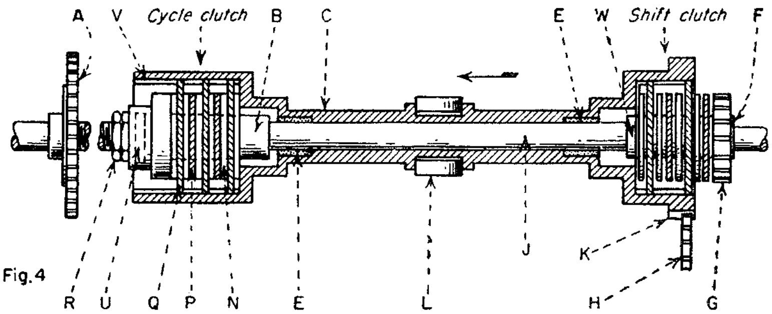

Fig. 4

MULTIPLE DISK FRICTION CLUTCH (Fig. 4). Two multiple disk friction clutches are combined in a single two-position unit which is shown shifted to the left. A stepped cylindrical housing *C* enclosing both clutches is carried by self-lubricated bearing *E* on shaft *J* and is driven by the transmission gear *H* meshing with the housing gear teeth *K*. At either end, the housing carries multiple metal disks *Q* that engage keyways *V* and can make frictional contact with formica disks *N* which, in turn, can contact a set of metal disks *P* which have slotted openings for coupling with flats on sleeves *B* and *W*. In the position shown, pressure is exerted through rollers *L* forcing the housing to the left making the left clutch compact against adjusting nuts *R*, thereby driving gear *A* via sleeve *B* which is connected to jack shaft *J* by pin *U*. When the carriage is to be shifted, rollers *L* force the housing to the right, first relieving the pressure between the adjoining disks on the left clutch then passing through a neutral position in which both clutches are disengaged and finally making the right clutch compact against thrust bearing *F*, thereby driving gear *G* through sleeve *W* which rotates freely on the jack shaft.

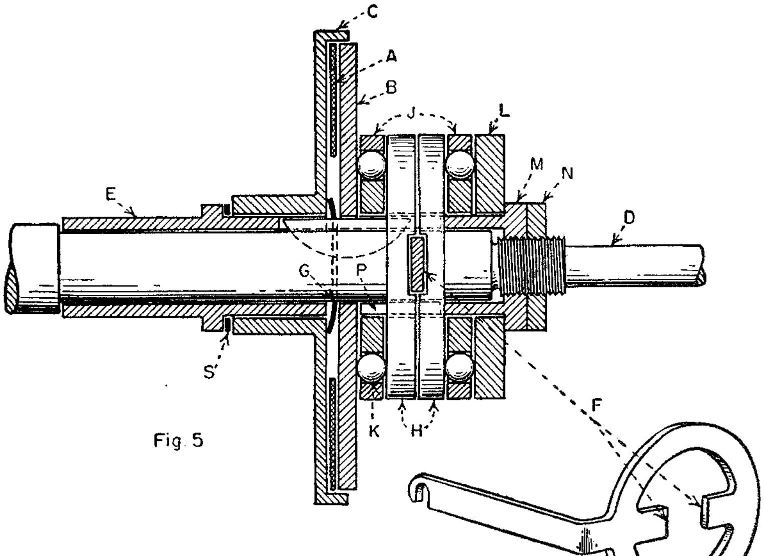

Fig. 5

SINGLE PLATE FRICTION CLUTCH (Fig. 5). The basic clutch elements, formica disk *A*, steel plate *B* and drum *C*, are normally kept separated by spring washer *G*. To engage the drive, the left end of a control arm is raised, causing ears *F*, which sit in slots in plates *H*, to rock clockwise spreading the plates axially along sleeve *P*. Sleeves *E* and *P* and plate *B* are keyed to the drive shaft; all other members can rotate freely. The axial motion loads the assembly to the right through the thrust ball bearings *K* against plate *L* and adjusting nut *M*, and to the left through friction surfaces on *A*, *B* and *C* to thrust washer *S*, sleeve *E* and against a shoulder on shaft *D*, thus enabling plate *A* to drive the drum *C*.

OVERLOAD RELIEF CLUTCH (Fig. 6). This is a simply constructed, double-plate, spring loaded, friction coupling. Shaft *G* drives collar *E* which drives slotted plates *C* and *D* and formica disks *B*. Spring *H* is forced by the adjusting nuts, which are screwed on to collar *E*, to maintain the unit under axial pressure against the shoulder at the left end of the collar. This enables the formica disks *B* to drive through friction against both faces of the gear which is free to turn on the collar, causing output pinion *J* to rotate. If the machine should jam and pinion *J* prevented from turning, the motor can continue running without overloading while slippage takes place between formica plates *B* and the gear.

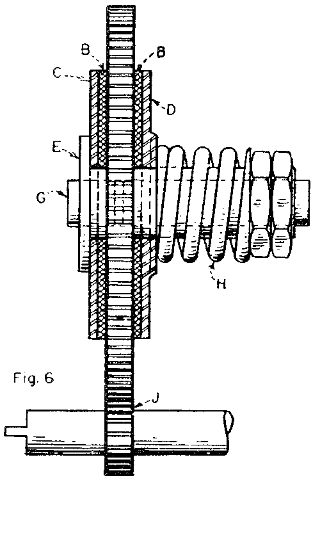

Fig. 6

Serrated Clutches and Detents

L. N. Canick

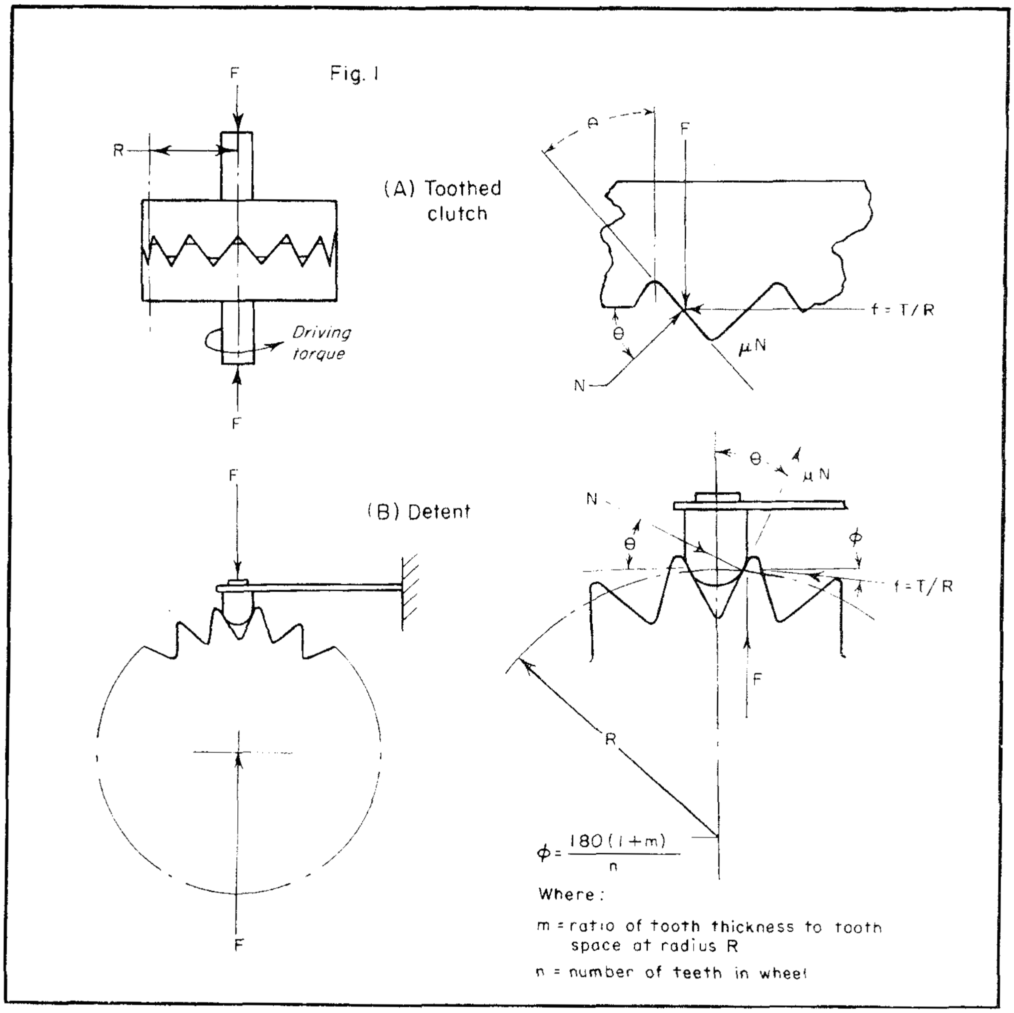

In the design of straight toothed components such as serrated clutches, Fig. 1(A), and detent wheels, Fig. 1(B), the effective pitch radius is usually set by size considerations. The torque transmitting capacity of the clutch, or the torque resisting capacity of the detent wheel, is then obtained by assigning suitable values to the engaging force, tooth angle, and coefficient of friction.

The nomogram, Fig. 2, is designed to be a convenient means for considering the effect of variations in the values of tooth angle and coefficient of friction. For a given coefficient of friction, there is a tooth angle below which the clutch or detent is self-locking and will transmit torque limited only by its structural strength. Where

T = torque transmitted without clutch slip, or torque resisted by detent wheel, lb in.
R = effective clutch, or detent wheel, radius, in.
F = axial, or radial, force, lb
f = tangential force acting at radius R, lb
N = reaction force of driven tooth, or detent, acting normal to tooth face, lb
μ = coefficient of friction of tooth material
θ = see Fig. 1(B)
= angle of tooth face, deg
K = $(1 + \mu \tan \theta)/(\tan \theta - \mu)$

a statement of the conditions of equilibrium for the forces acting on a clutch tooth will lead to the following equation

$$T = R\,F\,K \qquad (1$$

A similar statement of the conditions of equilibrium for the forces acting on a tooth of the detent wheel shown in Fig. 1(B) will lead to the following equation:

$$T = \frac{R\,F}{[(\cos \varphi)/K] - \sin \varphi} \qquad (2)$$

From Eqs (1) and (2), when all other terms have constant values, it is obvious that the required axial force, or the radial force, diminishes as the value of K increases. Dependent upon the values of θ and μ, the value of K can vary from zero to infinity.

The circular nomogram shown in Fig. 2 relates the values of the parameters K, θ, and μ that satisfy the basic equation

$$K = (1 + \mu \tan \theta)/(\tan \theta - \mu)$$

EXAMPLE I. Find the maximum tooth angle for a self-locking clutch, or for which K is infinity, taking the coefficient of friction as 0.4 minimum.

SOLUTION I. Line I through these values for K and μ on the nomogram gives a maximum tooth angle slightly less than 22 deg for the self-locking condition.

EXAMPLE II. Find the minimum value of K to be expected for a clutch having a tooth angle of 30 deg and a coefficient of friction of 0.2 minimum.

SOLUTION II. Line II through these values for θ and μ on the nomogram gives a value for K of 3 approximately.

EXAMPLE III. Find the value of K for a flat-face (θ equals 90 deg) friction clutch, the face material of which has a coefficient of friction of 0.2. Compare its torque transmitting capacity with that of the toothed clutch of Example II.

SOLUTION III. Line III through these values for θ and μ on the nomogram gives a value for K of 0.2.

Torque transmitting capacity of flat-face clutch:

$$T = 0.2\, R\, F$$

Torque transmitting capacity of toothed-clutch:

$$T = 3\, R\, F$$

Thus for equal effective radii and engaging forces, the torque capacity of the toothed-clutch is 3/0.2, or 15, times greater than that of the flat face clutch.

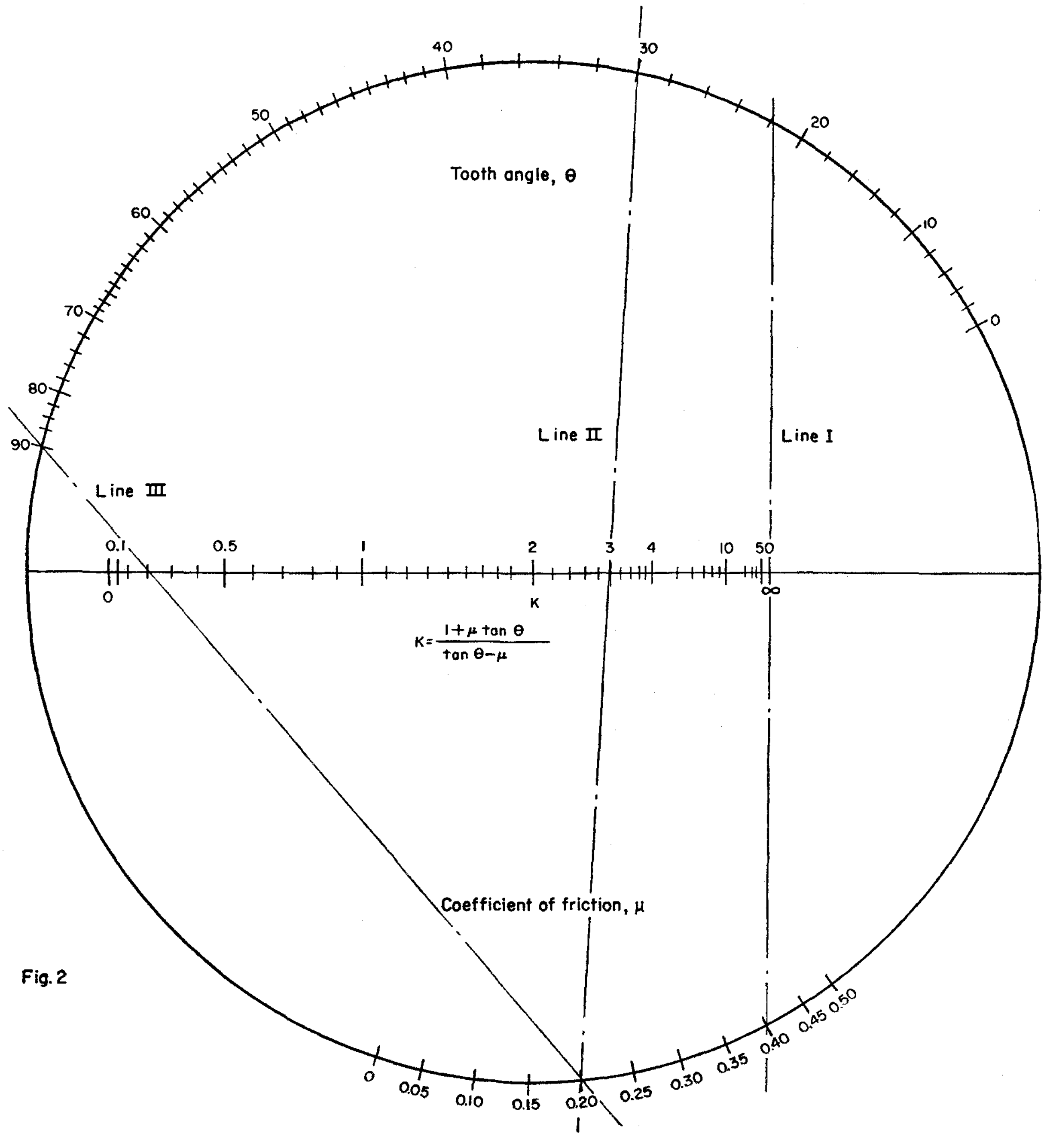

Fig. 2

Spring Bands Grip Tightly to Drive Overrunning Clutch

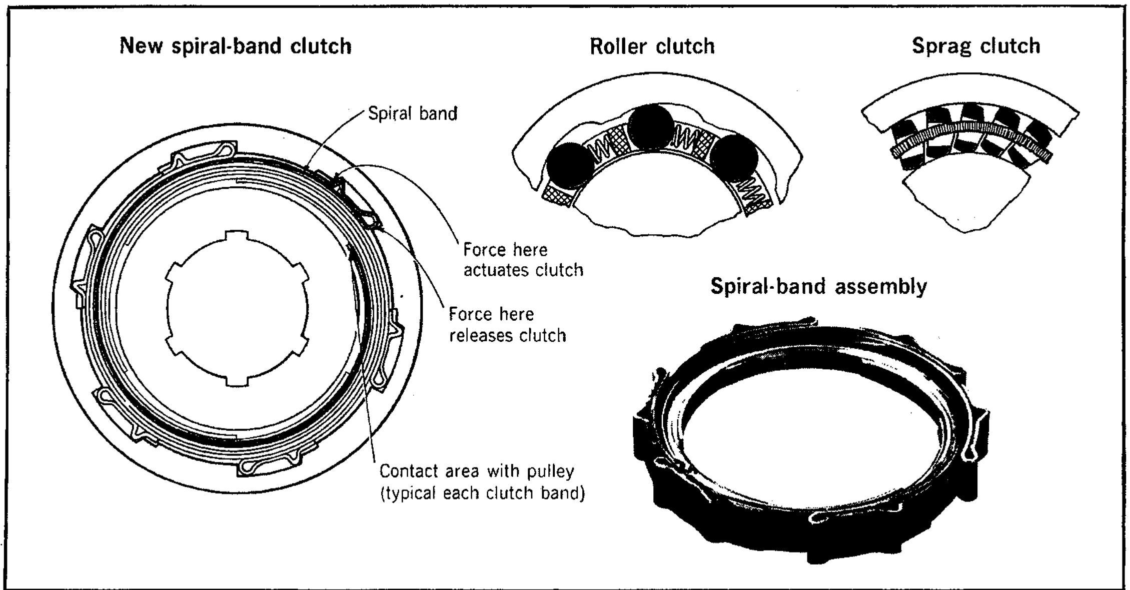

Spiral bands direct force inward as outer ring drives counterclockwise. Roller and sprag types direct force outward.

A new type of overrunning clutch that takes up only half the usual space employs a series of spiral-wound bands instead of the conventional rollers or sprags to transmit high torques. The new design (drawings, above) also simplifies the assembly, cutting costs as much as 40% by eliminating more than half the parts in conventional clutches.

The key to the savings in cost and bulk is the new design's freedom from the need for a hardened outer race. Roller and sprag types must have hardened races because they transmit power by a wedging action between the inner and outer races.

Role of spring bands. Overrunning clutches, including the spiral-band type, slip and overrun when reversed—in drawing above, when outer member is rotated clockwise and inner ring is the driven member.

The new clutch, developed by National Standard Co., Niles, Mich., contains a set of high-carbon spring-steel bands (six in the design illustrated) that grip the inner member when the clutch is driving. The outer member merely serves to retain the spring anchors and to play a part in actuating the clutch. Since it isn't subject to wedging action, it can be made of almost any material, and this accounts for much of the cost saving. For example, in the automotive torque converter in the drawing at right, the bands fit into the aluminum die-cast reactor.

Reduced wear. The bands are spring-loaded over the inner member of the clutch, but they are held and rotated by the outer member. The centrifugal force on the bands thus releases much of the force on the inner member and considerably decreases the overrunning torque. Wear is, therefore, greatly reduced.

The inner portion of the bands fits into a V-groove in the inner member. When the outer member is reversed, the bands wrap, creating a wedging action in this V-groove. This action is similar to that of a spring clutch with a helical-coil spring, but the spiral-band type has very little unwind before it overruns, compared with the coil type. Thus it responds faster.

Edges of the clutch bands carry the entire load, and there is also a compound action of one band upon another. As the torque builds up, each band pushes down on the band beneath it, so each tip is forced more firmly into the V-groove.

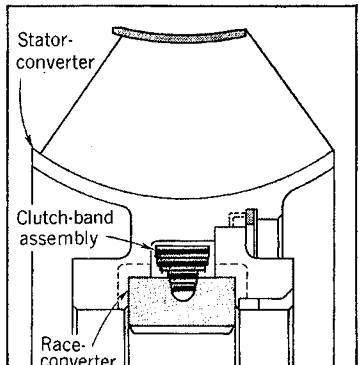

Spiral clutch bands can be bought separately to fit in user's assembly.

National Standard plans to sell the bands as separate components, without the inner and outer clutch members (which the user customarily builds as part of his product). The bands are rated for torque capacities from 85 to 400 ft.-lb. Applications include auto transmissions and starters and industrial machinery. □

Accurate Solution for Disk-Clutch Torque Capacity

Nils M. Sverdrup

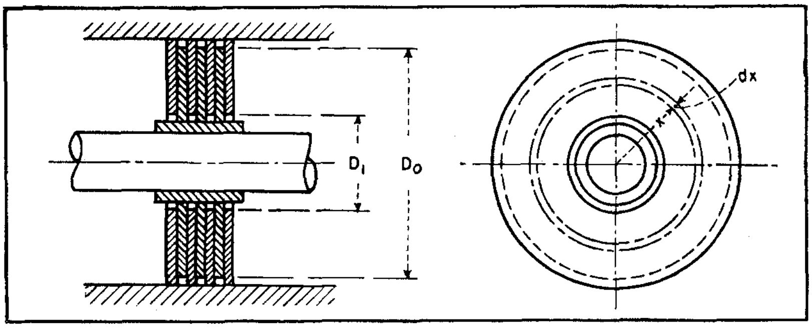

IN COMPUTING TORQUE CAPACITY, the mean radius R of the clutch disks is often used. The torque equation then assumes the following form:

$$T = P\mu Rn \qquad (1)$$

Where

T = torque, in.-lb
P = pressure, lb.
μ = coefficient of friction
R = mean radius of disks, in.
n = no. of friction surfaces

This formula, however, is not mathematically correct and should be used cautiously. The formula's accuracy varies with the ratio D_1/D_0. When D_1/D_0 approaches unity, the error is negligible; but as the value of this ratio decreases, the induced error will increase to a maximum of 33 percent.

By introducing a correction factor, ϕ, Eq (1) can be written

$$T = P\mu Rn\phi \qquad (2)$$

The value of the correction factor can be derived by the calculus derivation of Eq (2).

Sketch above represents a disk clutch with n friction surfaces, pressure between plates being p psi. Inside and outside diameters of effective friction areas are D_1 and D_0 in., respectively. Since the magnitude of pressure on an element of area, dA, at distance x from center is pdA, the friction force is $pdA\mu$ and the moment of this force around the center is $pdA\mu x$.

Integrating within limits $D_1/2$ and $D_0/2$ and multiplying by n friction surfaces, the expression for total torque in in.-lb is obtained.

Hence

$$T = \int_{D^1/2}^{D_0/2} pdA\mu xn \qquad (3)$$

but

$$dA = 2\pi x dx \qquad (4)$$

Substituting in Eq (3)

$$T = \int_{D_1/2}^{D_0/2} p\,(2\pi x dx)\,\mu xn$$

$$= (2/3)\pi p\mu n\left[\left(\frac{D_0}{2}\right)^3 - \left(\frac{D_1}{2}\right)^3\right]$$

$$\text{or} \quad T = 0.262\, p\mu n\,(D_0^3 - D_1^3) \qquad (5)$$

If the total pressure acting on clutch disks be P lb, the expression for pressure per unit area is

$$p = \frac{P}{(\pi/4)\ (D_0^2 - D_1^2)}$$

Substituting this value for p in Eq (5)

$$T = 0.333\ P\mu n\,\frac{D_0^2 + D_0 D_1 + D_1^2}{D_0 + D_1} \qquad (6)$$

Now let

$$\frac{D_1}{D_0} = m \text{ so that, } D_1 = m\,D_0 \qquad (7)$$

Substituting in Eq (6)

$$T = 0.333\ P\mu n D_0 \frac{1 + m^2 + m}{1 + m} \qquad (8)$$

Similarly, by substituting value of D_1 from Eq (7) in Eq (2), and having

$$R = \frac{D_0 + D_1}{4},$$

$$T = P\mu\,\frac{D_0 + m\,D_0}{4}\,n\,\phi$$

or

$$T = 0.25\ P\mu n\phi\ D_0\,(1 + m) \qquad (9)$$

Equating expressions (8) and (9)

$$0.25\ P\mu n\phi\ D_0\,(1 + m) =$$

$$0.333\ P\mu n\ D_0\,\frac{1 + m^2 + m}{1 + m}$$

and solving for ϕ, the result is

$$\phi = 1.333 \times \frac{1 + m^2 + m}{(1 + m)^2} \qquad (10)$$

With various diameter ratios, the values for ϕ were computed and represented in graph herewith. By using this graph and Eq (2), accurate values of torque can be easily determined.

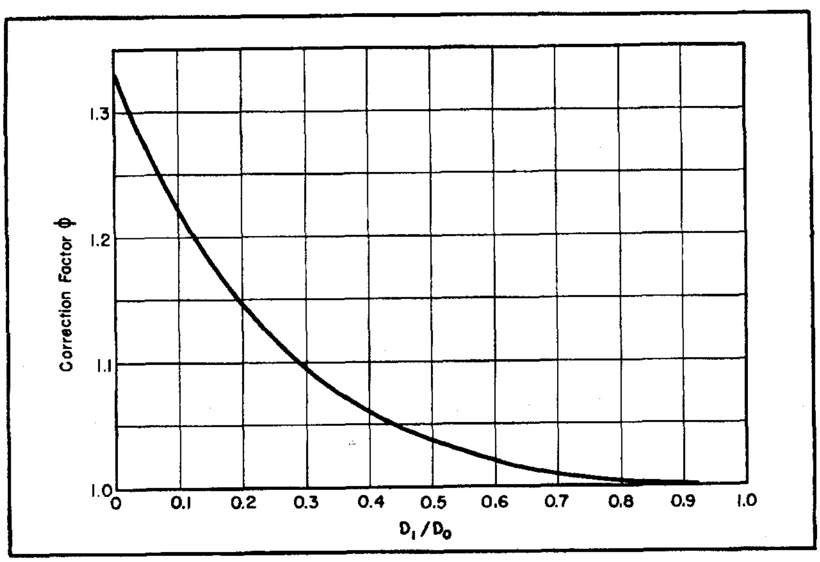

SECTION 6

SEALS & PACKINGS

Rubbing Seals for Oil Retention

David C. Spaulding, JR.

Rubbing seals cover all applications where a positive sliding contact exists between the seal and either the rotating or stationary member. They are limited as to type of operation and speed because of the friction between the contacting surfaces and they should not be used in

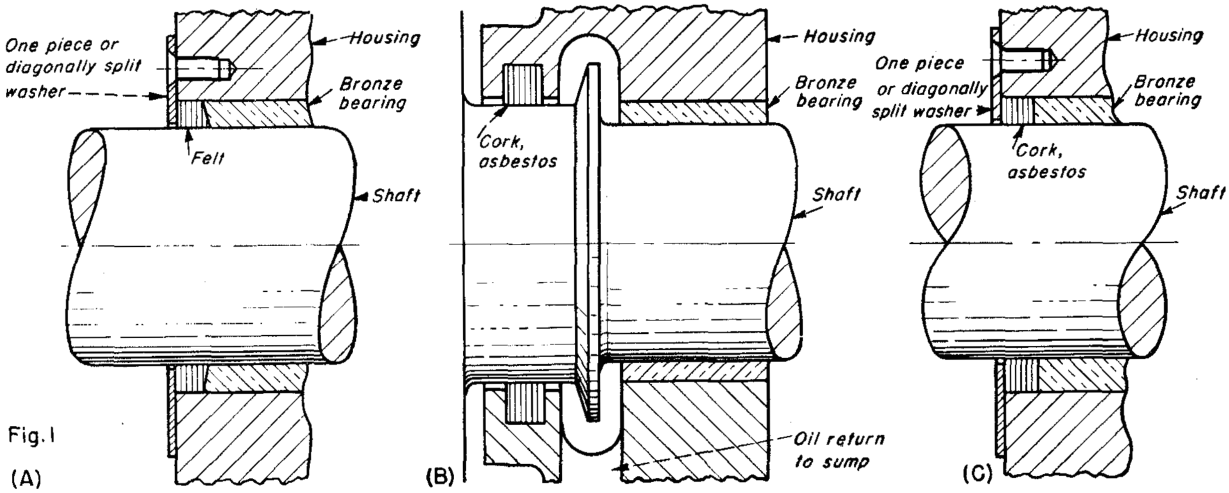

FIG. 1—Rubbing seal for oil lubrication. Felt, cork, asbestos, natural or synthetic rubber or other materials can be used. The natural resiliency of felt provides a close contact between seal and shaft without the excessive pressures often encountered with other types. It also absorbs and retains oil providing for almost constant lubrication. For the retention of felt, design A is recommended, because the tapered sides insure close contact and the removable plate permits easy replacement. (B) and (C) may also be used. Cork and asbestos should be retained as shown in (B). Groove must be straight sided and narrow enough to compress the material slightly to prevent it from turning.

FIG. 2—Bronze or cast iron rings are frequently used to seal bearings. This type of seal is equally effective for reciprocating and rotary motion. Circumferential grooves are cut in the shaft and the rings are compressed and inserted. They bear on the housing effectively sealing in the lubricant.

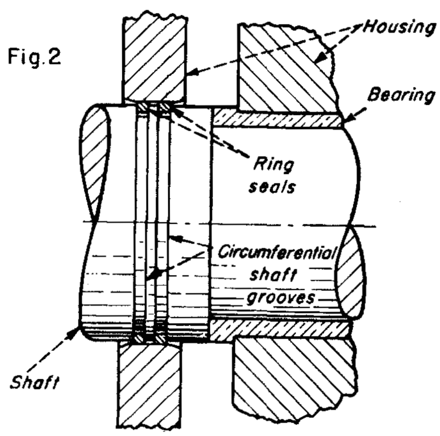

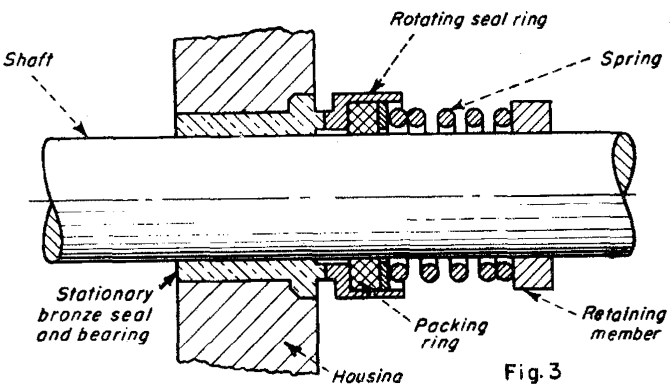

FIG. 3—High pressure and high rotative speeds where leakage is critical use mechanical face type seals. The seal has low total friction, can withstand high misalignment and compensates for wear. Parts of the seal are: stationary seal ring, rotating seal ring, flexible type joint, (diaphragm, bellows, or packing ring) spring, and retaining members. The stationary member can be an integral part of the bearing when a cast bronze sleeve bearing is used. As illustrated, the rotating seal ring, packing spring and retaining member turn with the shaft and the spring keeps the seal ring in contact.

abrasive surroundings. Types that are held against the rotating member by spring pressure can be used where there is a pressure head of fluids within the assembly or on the exterior. For high pressure stuffing box and O-ring type seals are used. O-rings are also used for zero leakage.

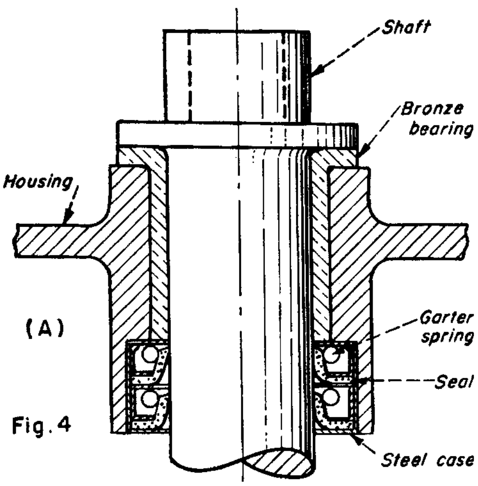

Fig. 4

FIG. 4—Rubbing seals, of the type shown, (A), have widespread use in all types of equipment. The spring tension and sealing ring material may be varied so that a variety of applications can be handled. Small units can be had where the O. D. is the same as the O. D. of the sleeve bearing, (B), thus eliminating the counterboring operation on the housing. The seal may be reversed and used to keep foreign matter out of the assembly. A drain hole may be provided to carry away surplus lubricant. Retention is by press fit on the outside diameter.

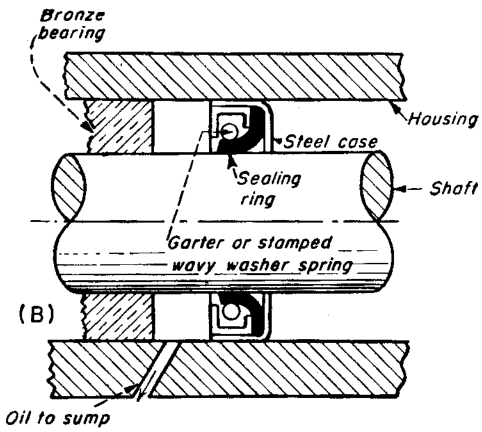

FIG. 5—Rubbing seals of the stuffing box type (A), are used where high pressure are encountered. It can be used for all types of motion and the packing material can be varied depending upon the fluid to be sealed and the application. For rotating motion some leakage is necessary so it cannot be used when permissible leakage is zero. O-rings can also be used for rotary motion if the speed is slow. Special designs use O-ring seals (B), when zero leakage is demanded for either stationary or reciprocating motion.

This ring is made of natural rubber or synthetic rubber depending on the type of solution resistance required. Synthetic rubber, such as buna or neoprene, is resistant to aromatic hydrocarbons, while natural rubber resists the action of alcohol and glycerine.

O-rings can be located either in the shaft or in the housing and any movement or pressure forces the ring to one side, thereby forming a tight seal.

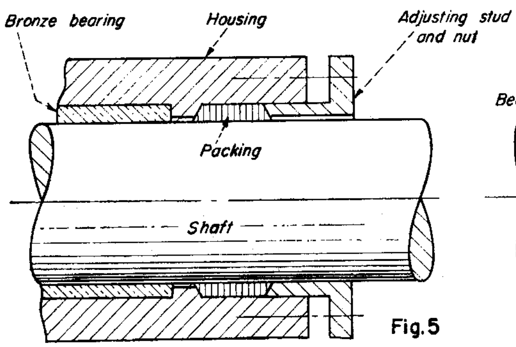

Fig. 5

(A)

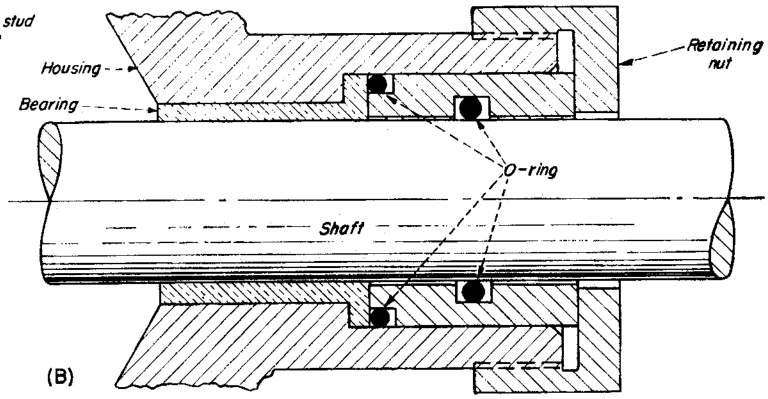

(B)

Non-Rubbing Seals for Oil Retention

David C. Spaulding, JR.

There are two general types of seals: rubbing and non-rubbing. Non-rubbing seals use oil or grease to lubricate mating surfaces and exclude foreign matter by forcing the lubricant out between the bearing surfaces. These seals are not limited by operation or speed since

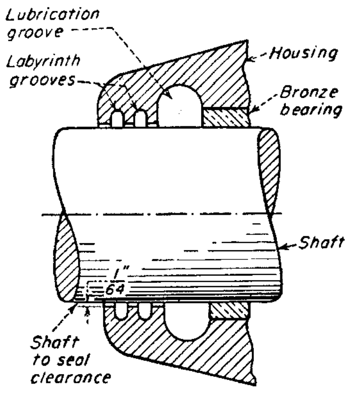

Fig.1

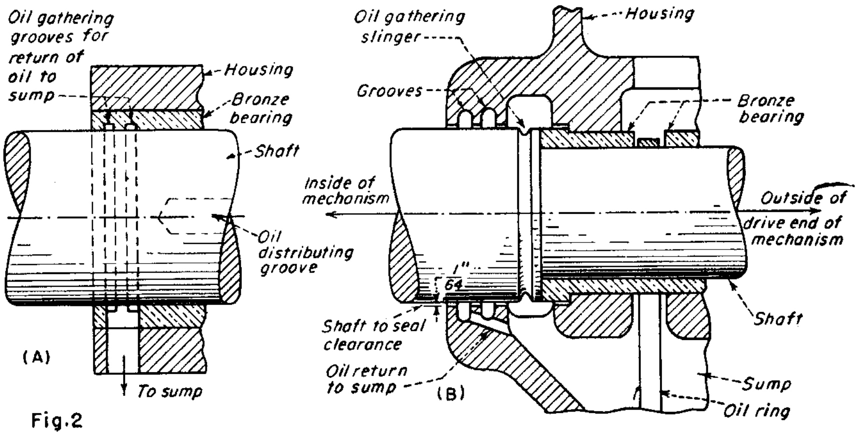

Fig.2

Fig. 1—Non-rubbing seal for grease lubrication. Grooves and housing are filled with grease at assembly or an automatic feed system can be incorporated. Seal offers protection against entrance of foreign matter because of the outward flow of grease through the labyrinth passages. Clearance between shaft and seal is about 1/64 inch.

Fig. 2—Non-rubbing seal for oil lubrication. Grooves can be located in bearing, (A), or in housing, (B). Grooves are connected to an oil return passage leading to a sump in housing. This keeps oil loss to a minimum and maintains a constant supply to the bearing. Design does not prevent entrance of foreign material. Radical clearance between shaft and seal is 1/64 inch.

Fig. 3—Seal for vertical installation. Circular groove picks up lubricant and feeds it to a spiral groove in bearing or shaft. Spiral feeds lubricant to top of bearing. Lubricant runs down between shaft and bearing. Design is effective when the shaft is rotating.

Fig. 4—Similar to Fig. 3 but used for a horizontal installation to reduce leakage of lubricant. Straight groove feeds oil to the bearing. Circular groove collects oil and the spiral groove, located in shaft or bearing, returns it to other end of bearing. Design prevents loss of oil by leakage at outside end.

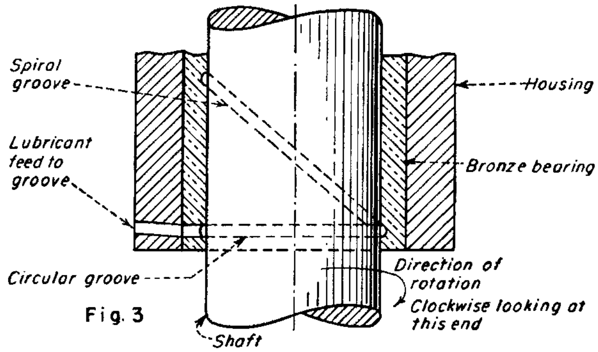

Fig. 3

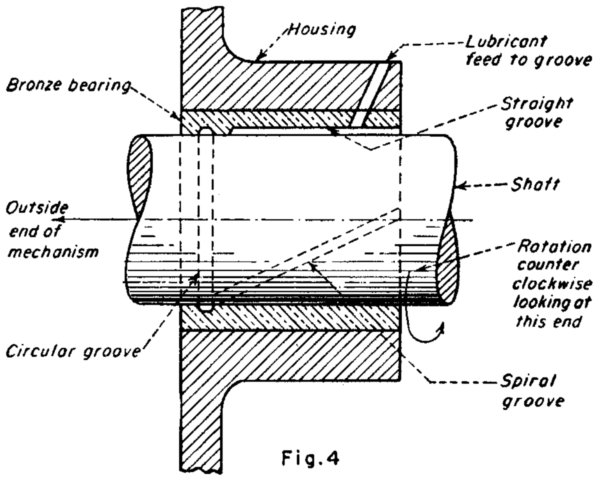

Fig.4

friction is negligible. They are, however, often more expensive than rubbing seals since the shaft, bearing, or housing must be grooved to distribute the lubricant. Distribution over the bearing area is, however, better. Lubricants may be forced-fed or gravity-fed.

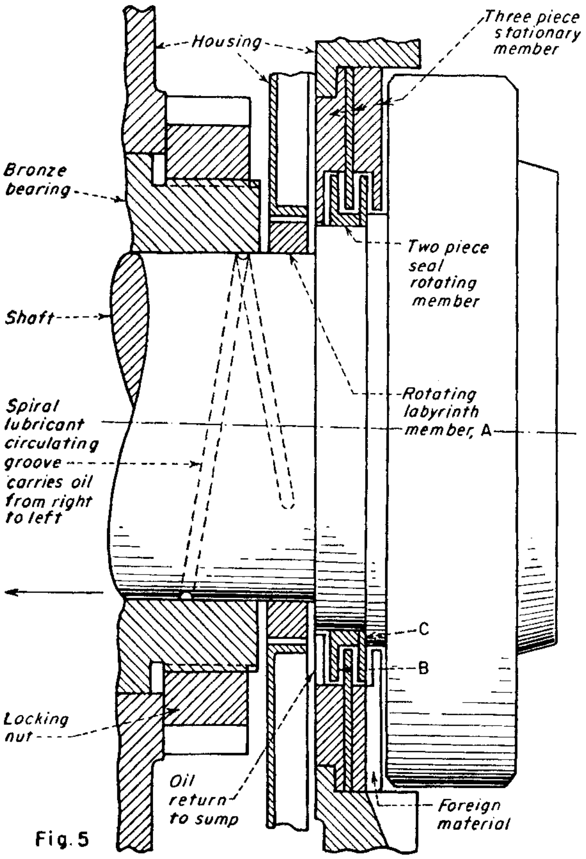

Fig. 5

Fig. 5—Labyrinth seals offer good protection especially at high speeds where the narrow zigzag passage is used in conjunction with centrifugal force. Oil and foreign matter are separated by slinger which limits oil flow past rotating member *(A)*. Inner member *(B)* throws oil back to sump. Member *(C)* throws out foreign matter.

Fig. 6—Non-rubbing seal for oil lubrication. Shaft rotation throws lubricant into the inboard groove *(B)* in the housing and is returned to the oil sump. First slinger *(D)* throws foreign material out of the assembly. Second slinger *(D)* feeds foreign material out through groove *(A)* and hole at *(C)*. Lubricant feeds between shaft and bearing to housing grooves.

Fig. 7—Reservoir type feed for grease lubrication. Grease is distributed in annular groove and feeds through holes in bearing to lubricate the shaft. Foreign matter can be excluded if clean grease is used. Grease will be lost through open bearing ends and assembly must be repacked periodically.

Fig. 8—Reservoir type feed for oil lubrication. Two bearings are used forming an oil reservoir between them. If porous wall type bearings are used oil will saturate and feed through bearings to the shaft. Outward flow of oil prevents entry of foreign material. Reservoir must be periodically refilled with new oil. Bearings are a press fit in the housing.

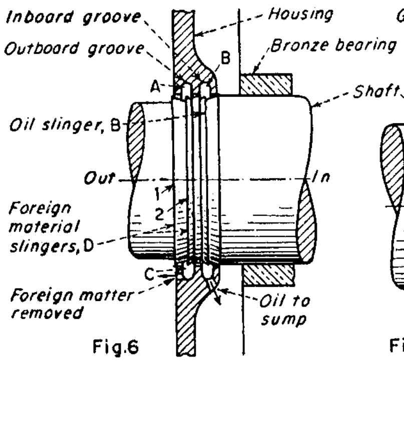

Fig. 6

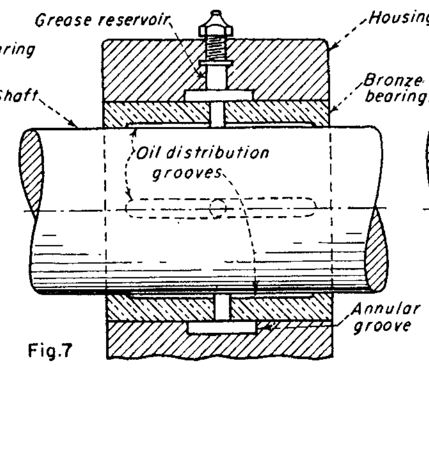

Fig. 7

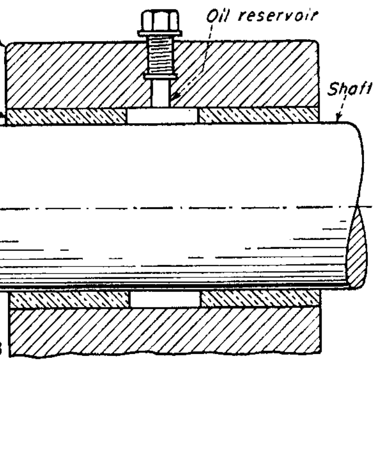

Fig. 8

How to Seal Air Ducts that Separate

These slip joints reseal and realign ducting that is often taken apart. They also take care of expansion, vibration, and joint locations difficult to reach.

James H. LaPointe

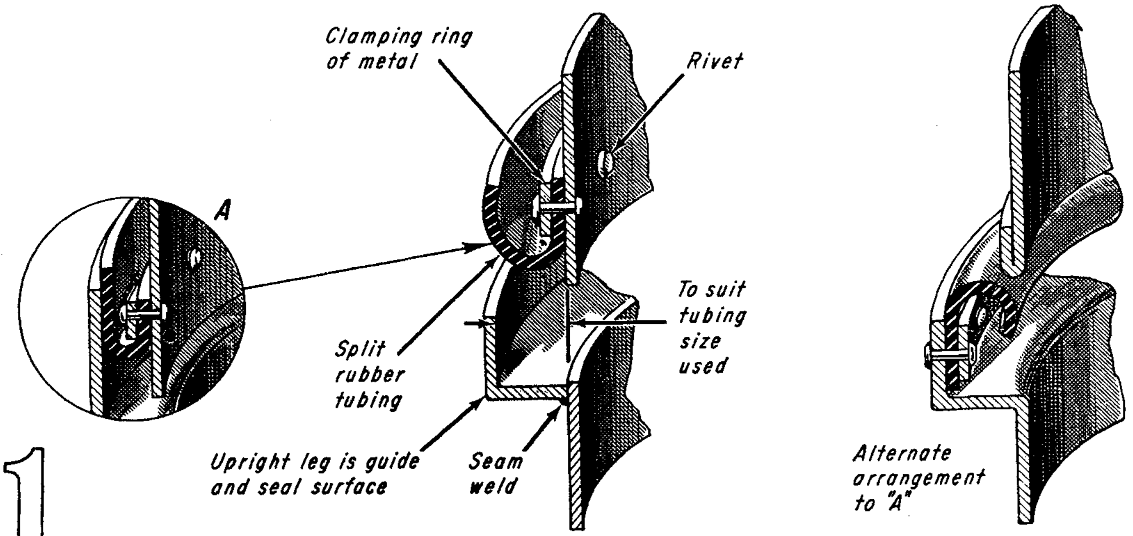

1 SPLIT RUBBER TUBING AND EDGE-ROLLED ANGLE

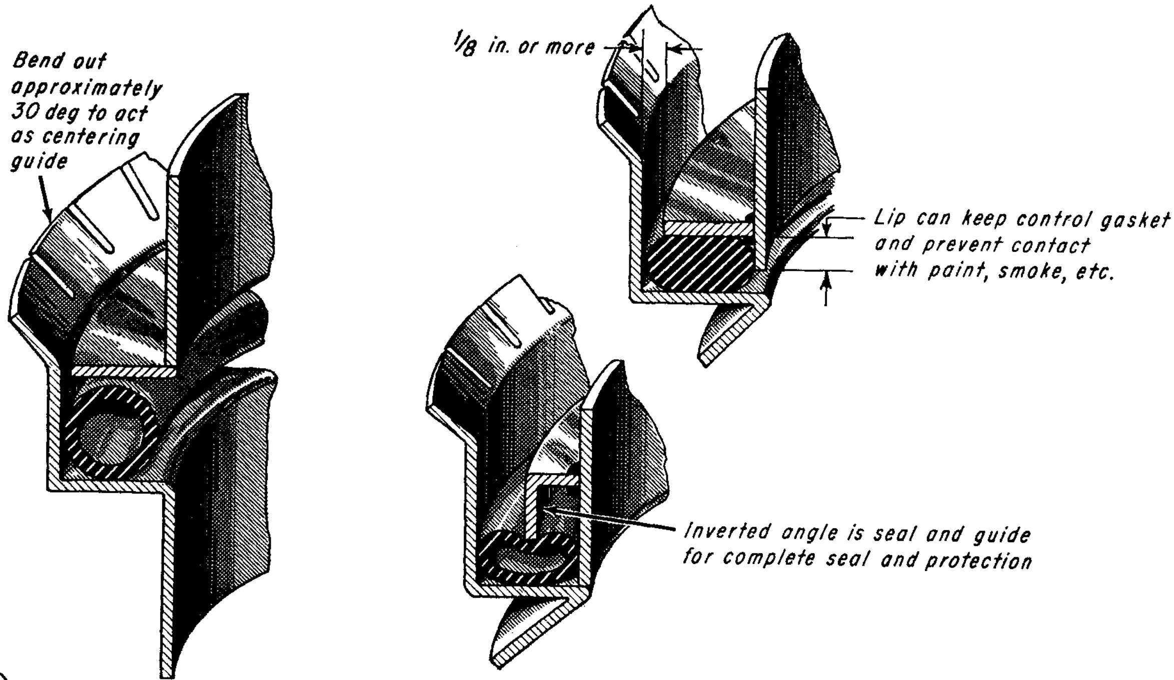

3 PLAIN RUBBER TUBING OR SOLID RING IN COMPRESSION

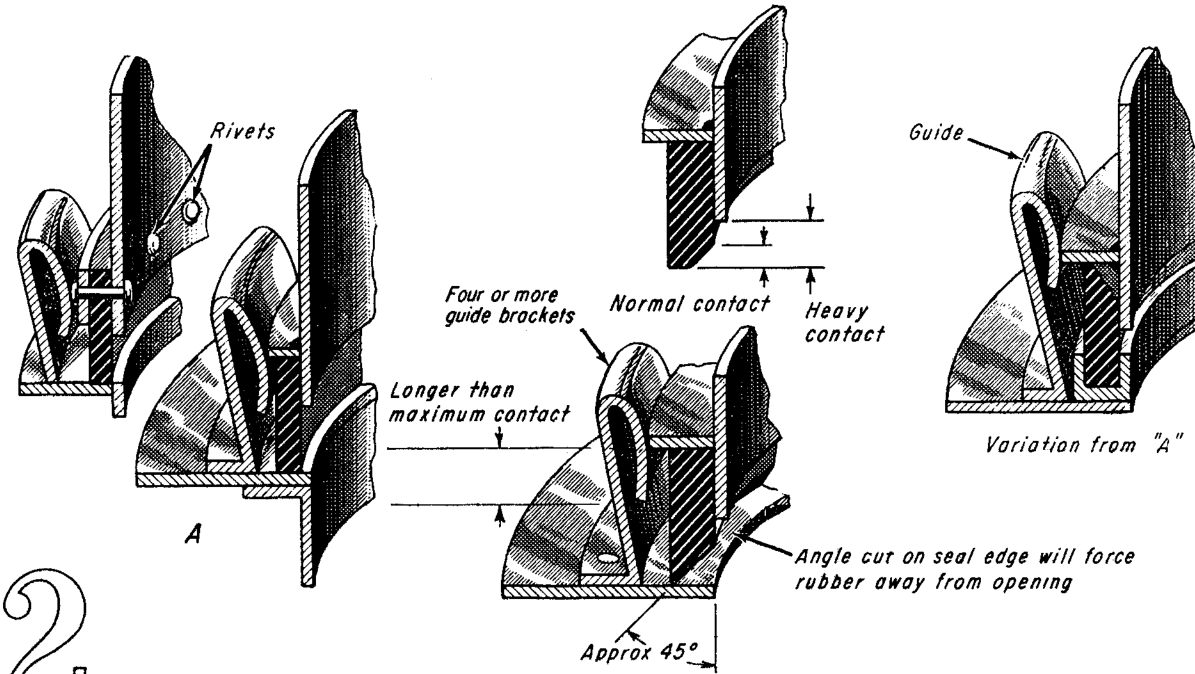

2 FLAT RUBBER AND GUIDE BRACKETS FOR CENTERING

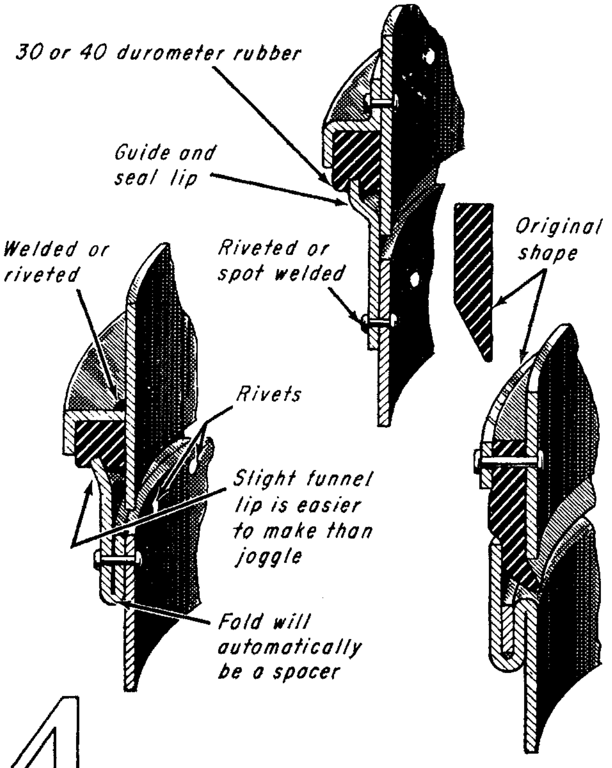

4 CONFINED RUBBER STRIP

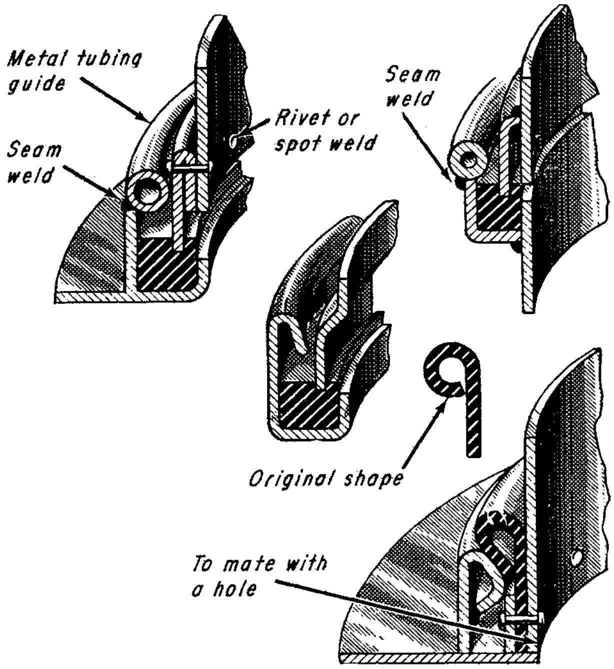

5 METAL TUBING AS GUIDE

More Seals for Ducting that Separates

Six more seals for round ducts and others. Make sure the gasket material can withstand the ducted media.

James H. LaPointe

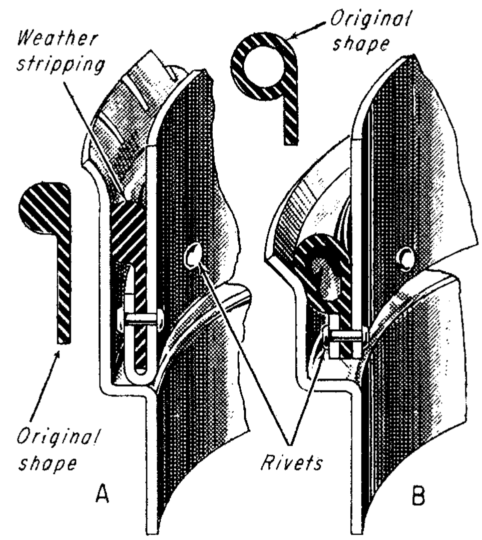

1 WEDGE-GUIDE SEAL

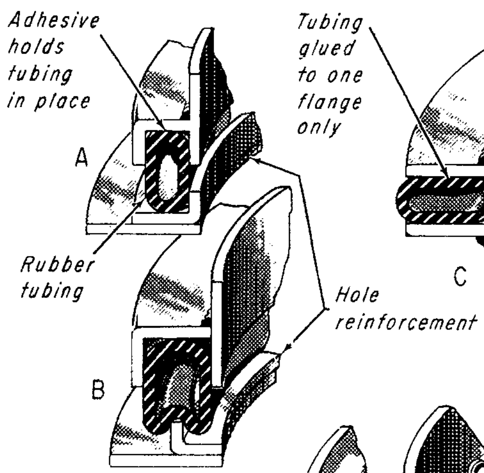

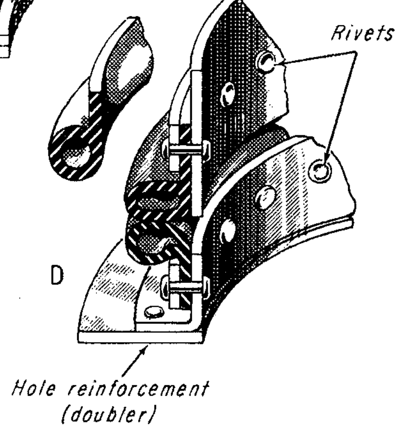

2 NONCENTERING SEALS—RUBBER TUBING

5 ROUND-BAR GUIDE SEALS AND VARIATIONS

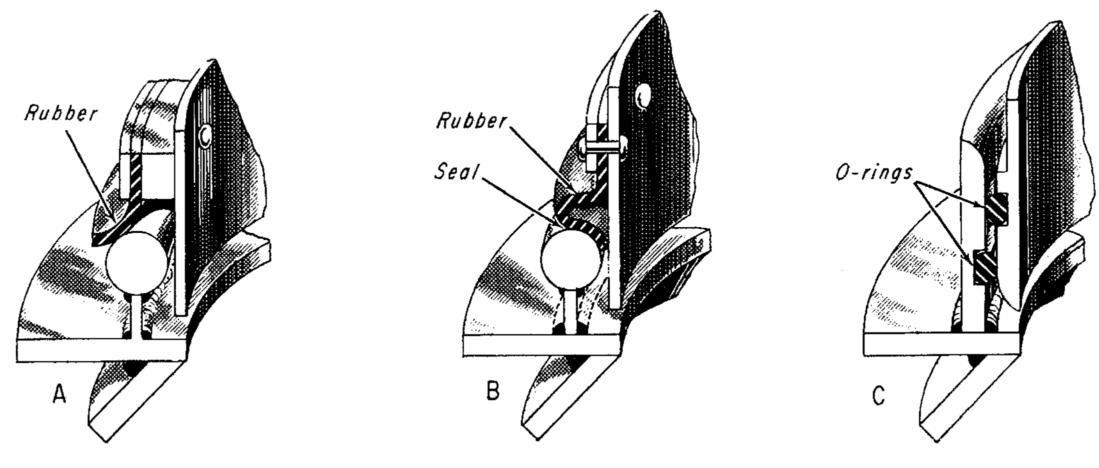

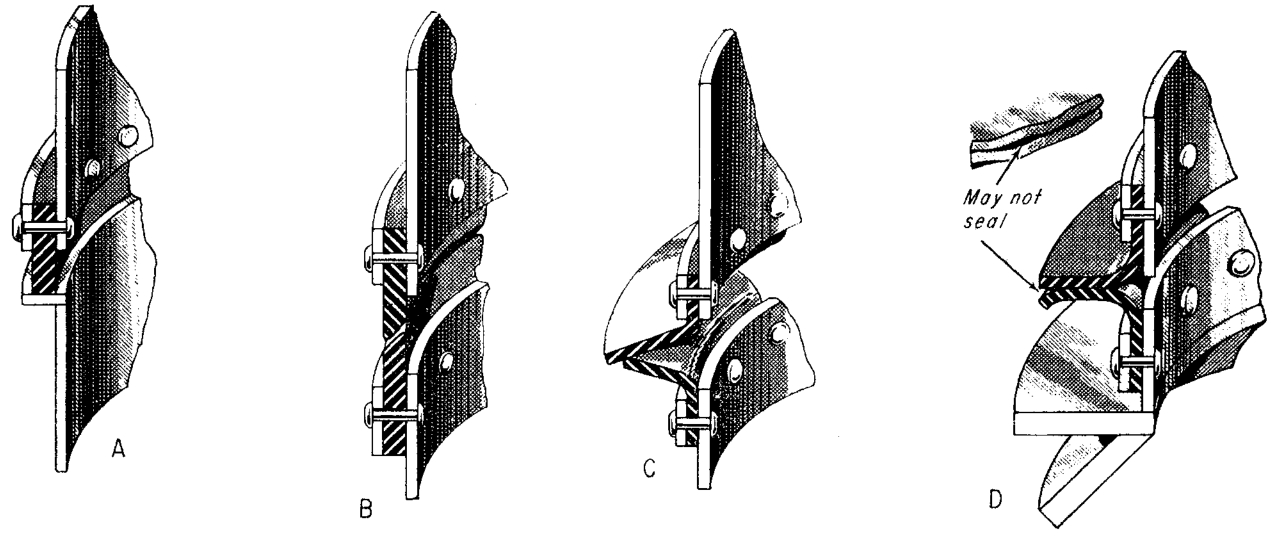

3 NONCENTERING SEALS—FLAT RUBBER

4 SLIP SLEEVES THAT SEAL WITHOUT GASKETS

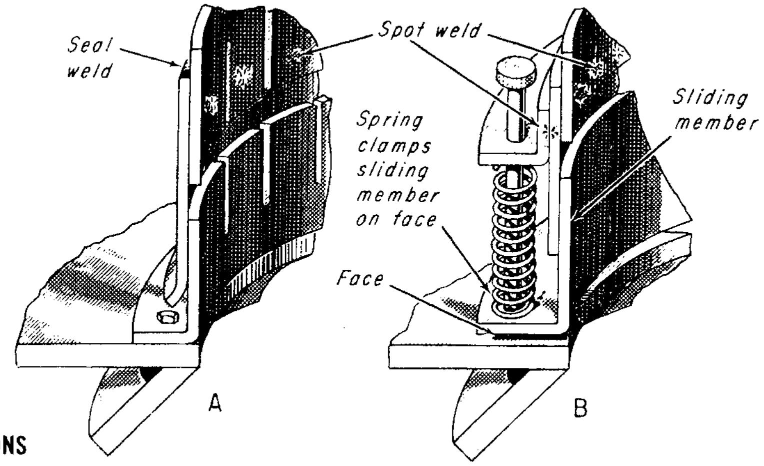

6 METAL TUBING GUIDE AND VARIATIONS

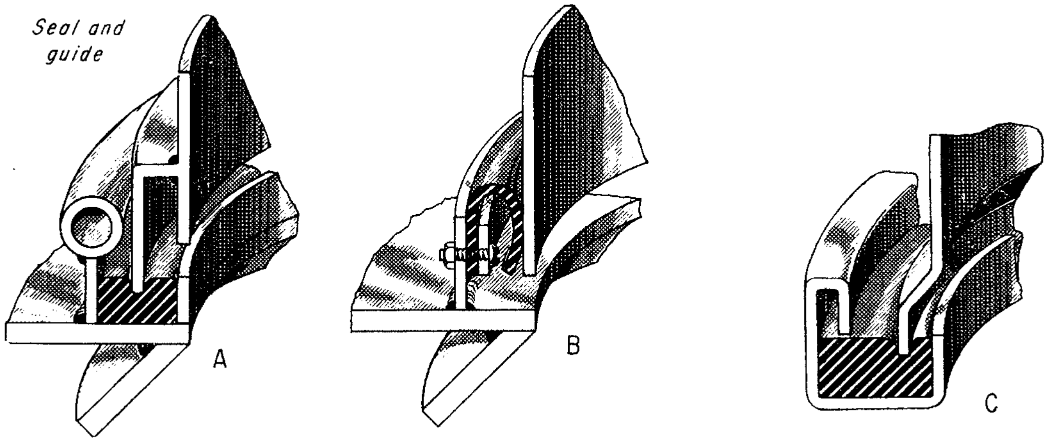

Window Awning Unit Sealing

Illustrated by Robert O. Parmley

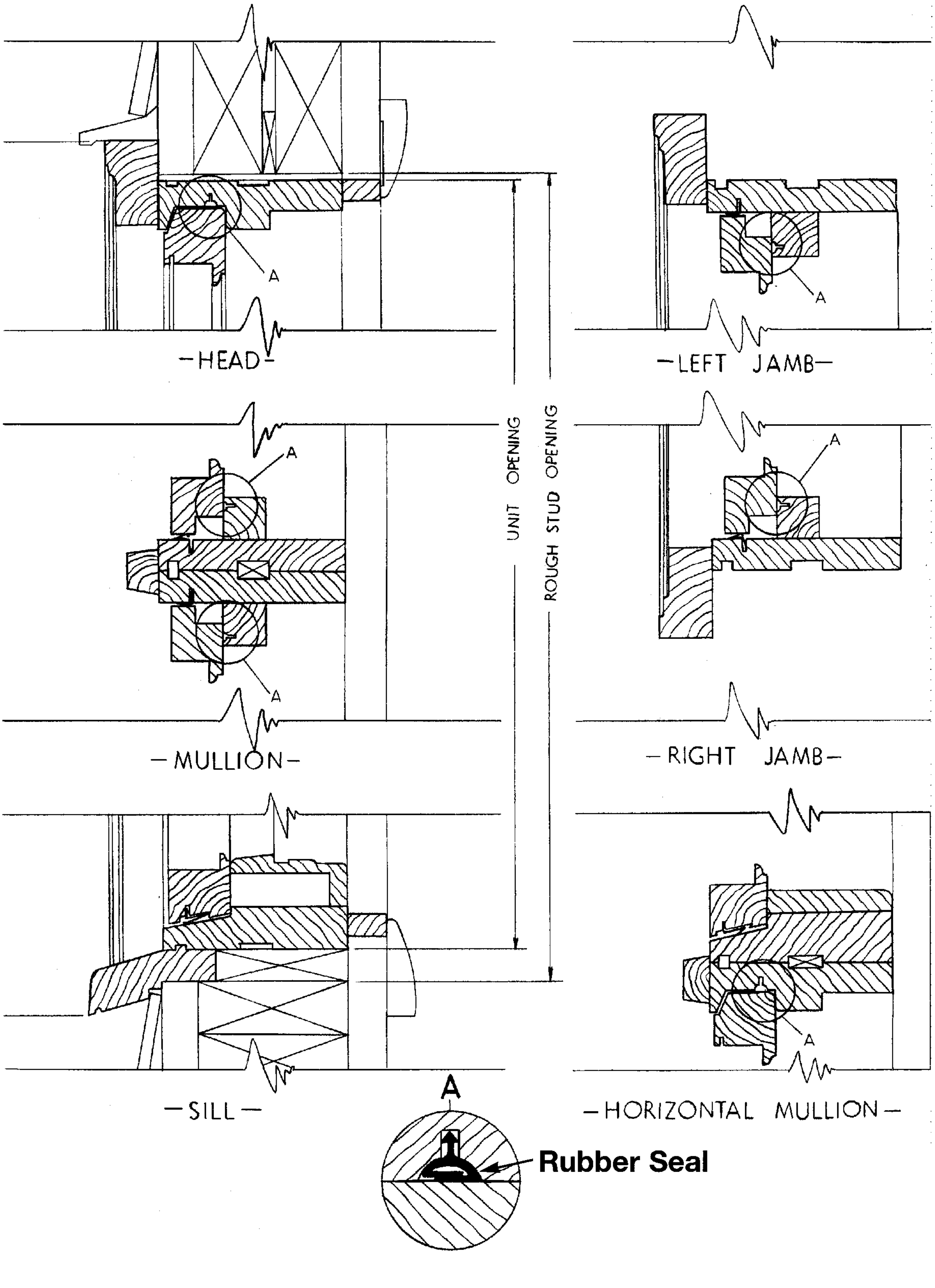

Window Casement Unit Sealing

Illustrated by Robert O. Parmley

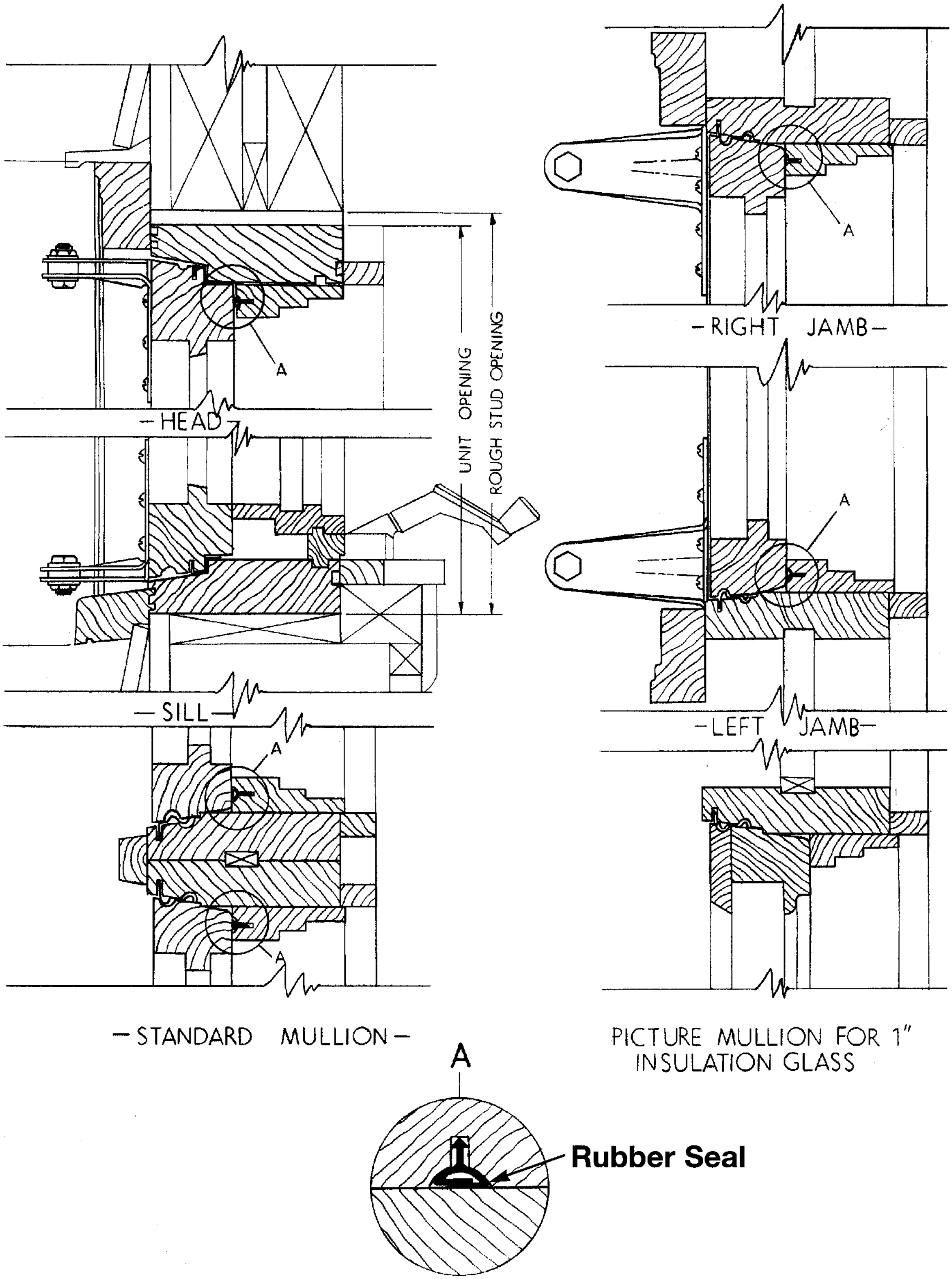

Multiple Seals & Bonding for Dam Retrofittings

Robert O. Parmley

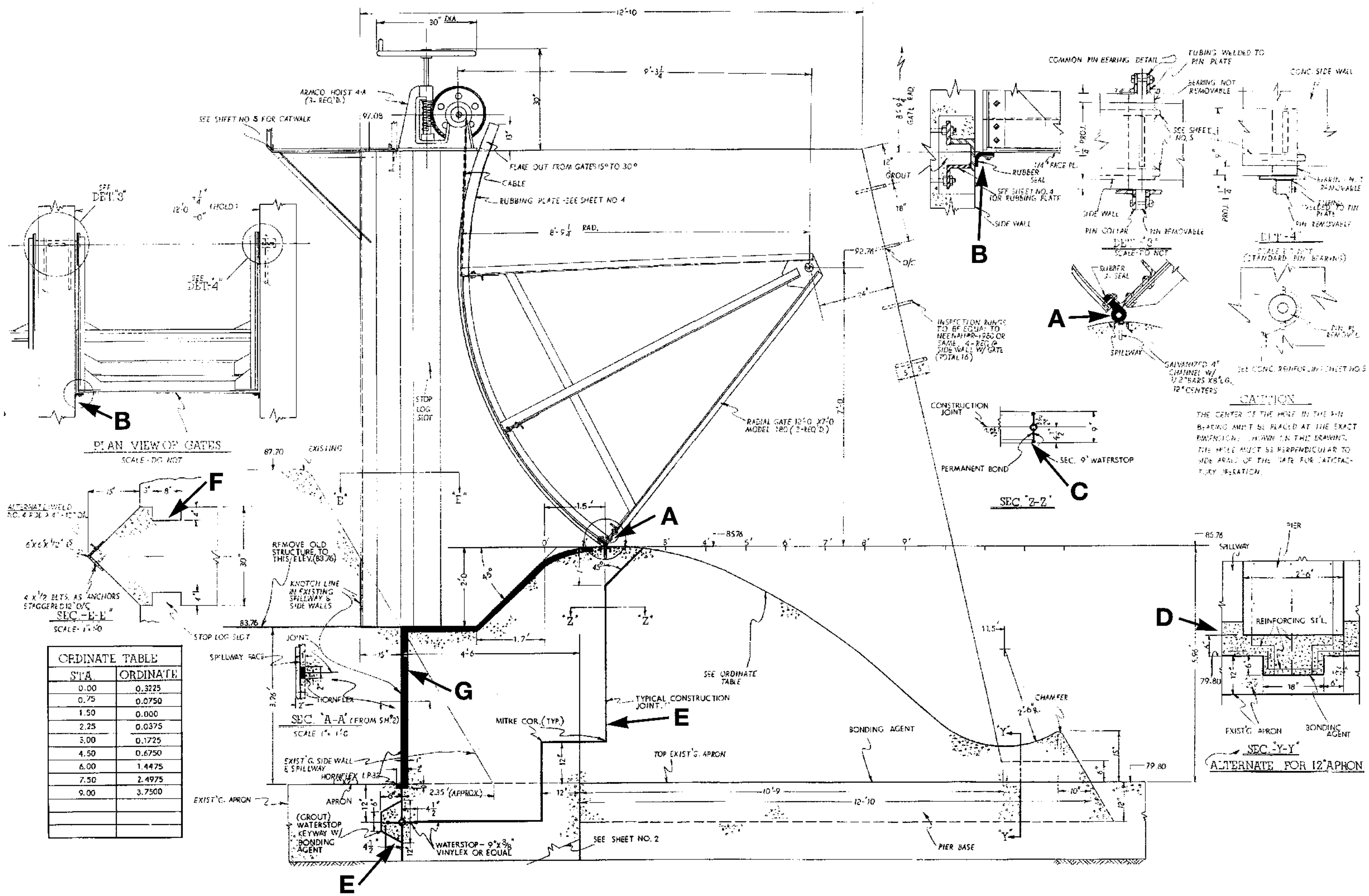

ORDINATE TABLE	
STA.	ORDINATE
0.00	0.3225
0.75	0.0750
1.50	0.000
2.25	0.0375
3.00	0.1725
4.50	0.6750
6.00	1.4475
7.50	2.4975
9.00	3.7500

Engineering drawing detailing the retrofitting of an existing dam with installation of a series of radial gates.

Courtesy: Morgan & Parmley, LTD.

A - Rubber J-seal, anchored at bottom lip or radial gate, forms a positive water seal at top of spillway.

B - Rubber seal strips at each end of radial gate stops water leakage from lake.

C - Construction joint sealed by rubber waterstop permantly encased between adjoining concrete.

D - Apron attachment connected with bonding agent.

E - Grouted keyway, bonding agent and vynil waterstop connects new to old concrete.

F - Keyway for wooden stop logs which originally controlled lake level.

G - Bonding seal at new/old concrete notch line.

SECTION 7

TUBING & PIPE CONNECTIONS

How to Connect Tubing–Cross and Tee Joints

TEE JOINTS

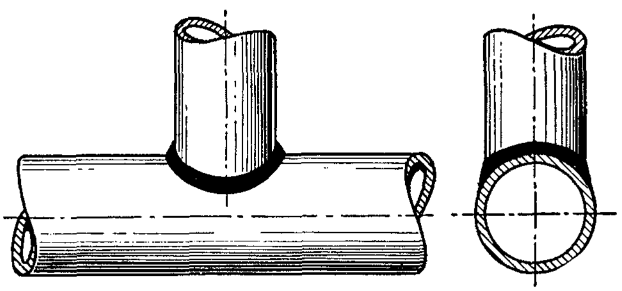

1. Welded joint used for connecting tubes at any angle. Perpendicular member is shaped to fit mating tube.

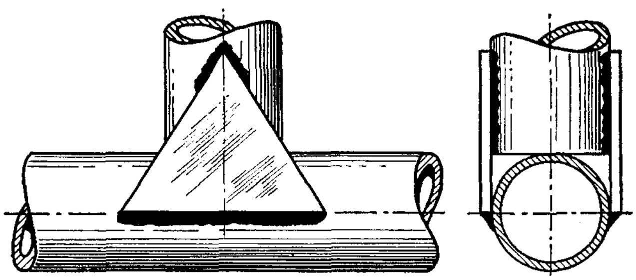

2. Gusset plate makes a reinforced tubing connection. Attachment can be made by means of a weld, rivets or bolts.

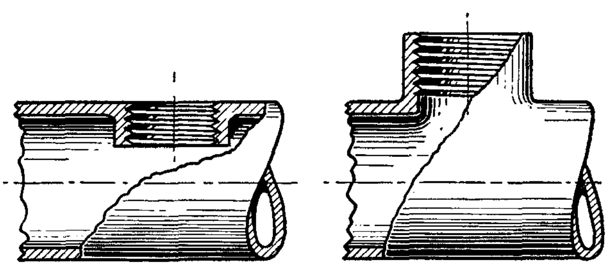

5. Formed flanges simplifies tubing connection. Attachment can be made by using threads or welding operation.

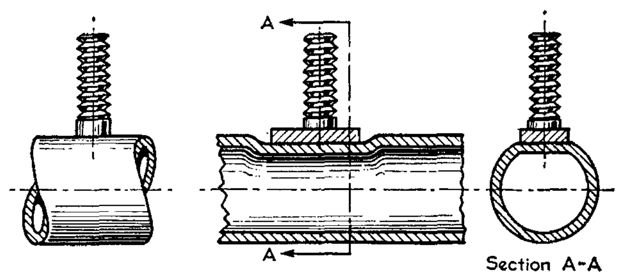

6. Threaded welding studs make a convenient connection. Welding stud to a pad on tubing reinforces joint.

CROSS JOINTS

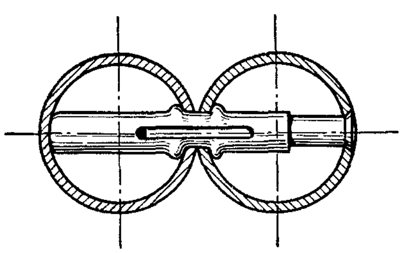

1. Expansion sleeve can be used to join tubes. Split-sleeve is expanded in tubing holes by means of steel drive plug.

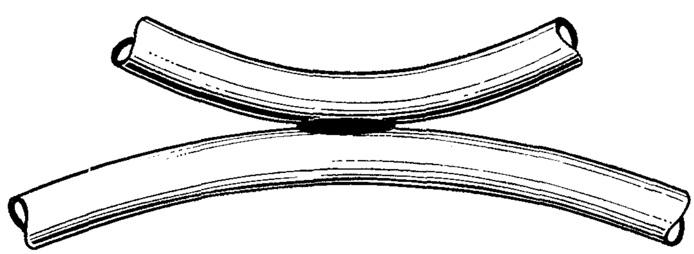

2. Curved tubing used as a cross joint; this can easily be connected by projection welding.

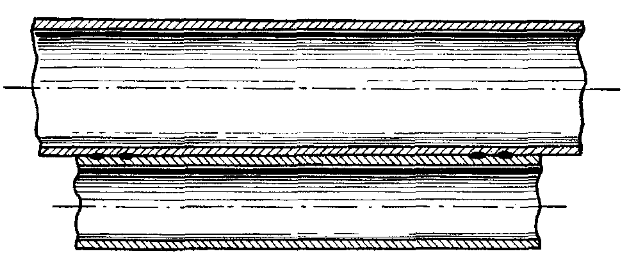

3. Projection welding parallel tubes makes more rigid construction. Air vent tubes can be attached in this way.

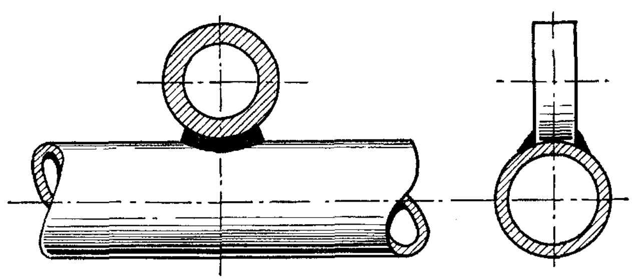

4. Simple guide for other tubing or shafts can be made by projection welding ring to tubing.

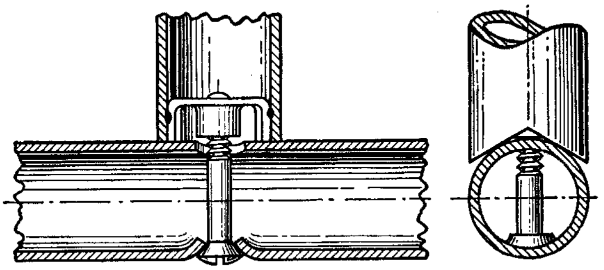

3. Bolted connection is used for racks and frames. Requires a threaded insert and notching the end of joining tube.

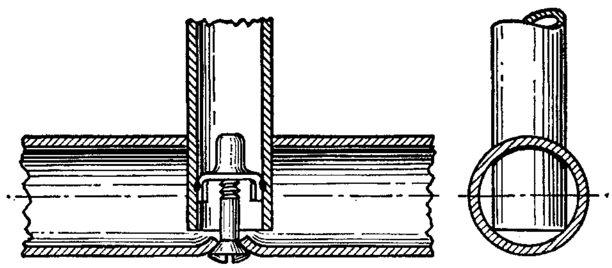

4. Tubes of different sizes can be more rigidly connected by inserting the smaller tube inside the larger one.

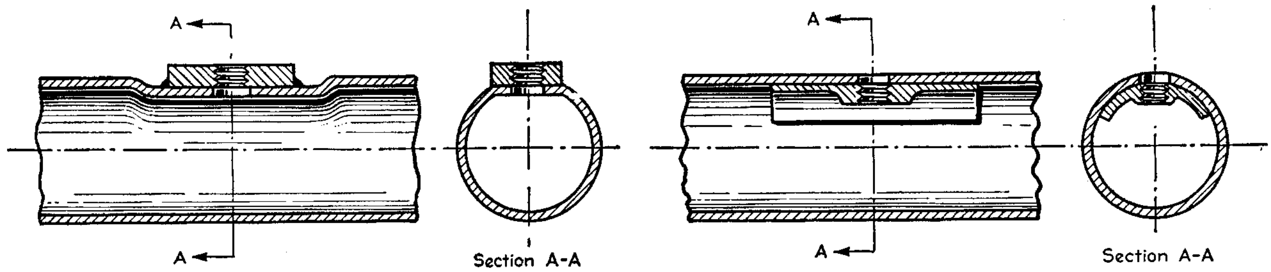

7. Reinforced connection can be made by attaching pads to outside or inside surface. Flattened tubing simplifies the connection for brazing or projection welding. Pads may be threaded either for pipe or screw fitting.

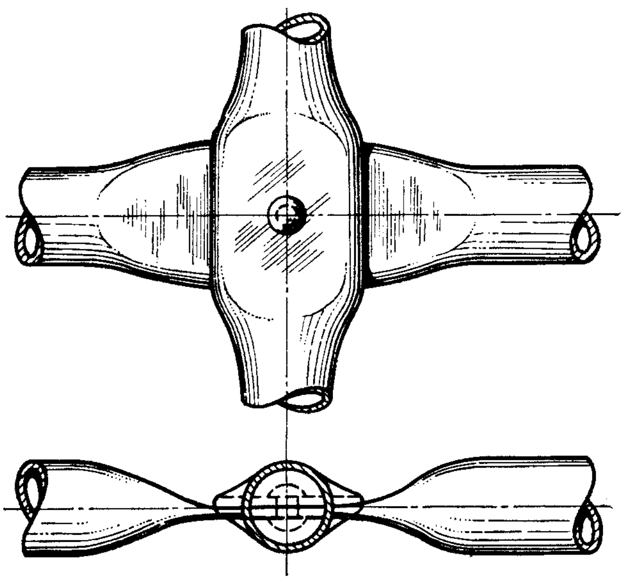

5. Flattened tubing makes joint when tubes intersect in same plane. Connection is welded, riveted or bolted together.

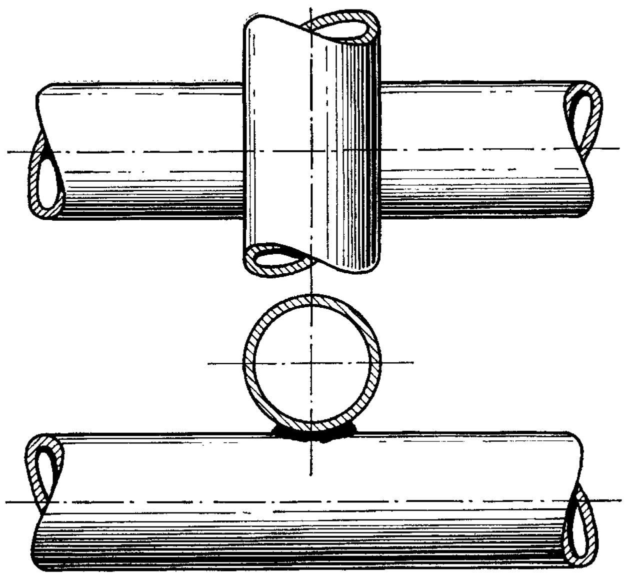

6. Welded connection can be made between tubes in contact. Tubes may cross at any angle.

Different Mechanical Methods for Attaching Tubing

ATTACHMENTS

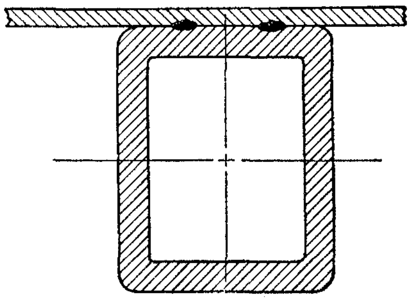

Fig. 1—Welded attachment of plates to tubing by spot or projection welding.

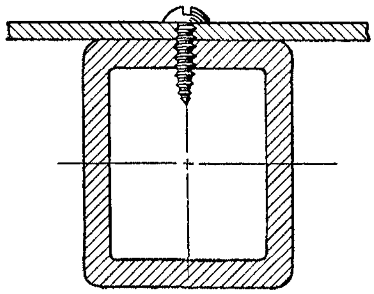

Fig. 2—Self-tapping or drive screws can be used to attach devices to tubing.

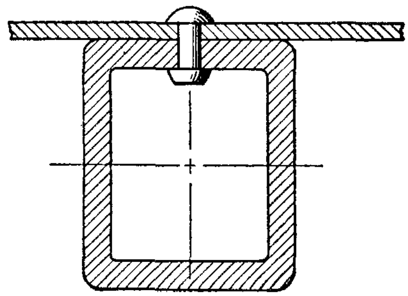

Fig. 3—Blind rivets, mechanical or explosive, can also be used for connection.

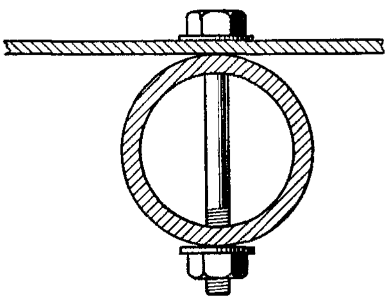

Fig. 4—Bolts or rivets make a rigid connection of plates to tubing.

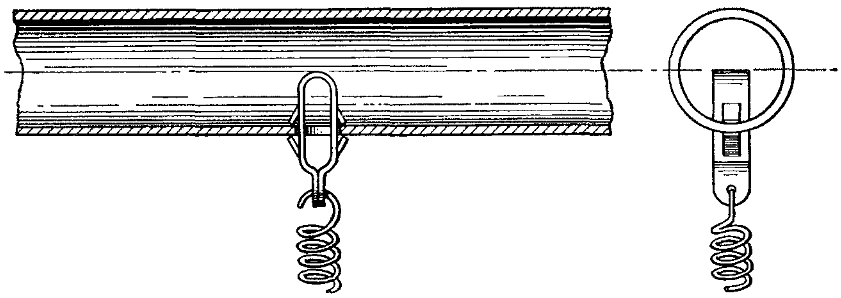

Fig. 5—Clip device is a simple means for holding springs or hangars to tubing. Requires only single hole in tubing and metal prongs lock clip in position.

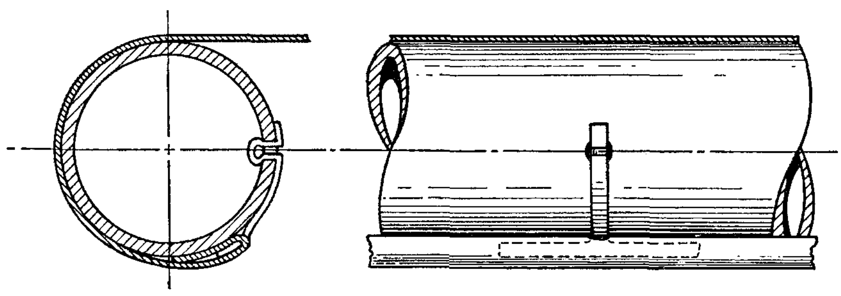

Fig. 6—Fabrics are conveniently fastened to tubing using a metal clip. This clip is inserted into fold of fabric and snapped into hole in tube.

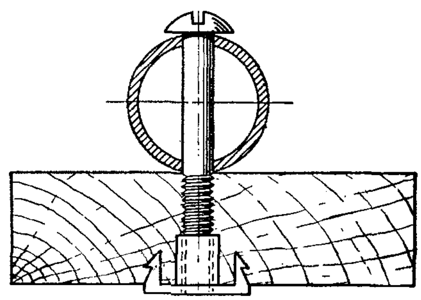

Fig. 7—Wood attachment uses a threaded "T" nut. Prongs hold nut in position.

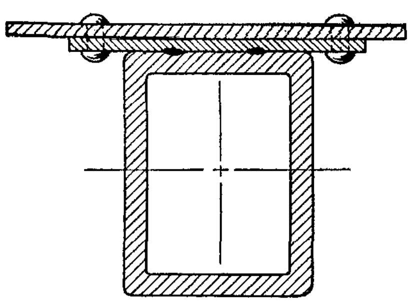

Fig. 8—Fabricated attachment consists of welded strip and riveted joint.

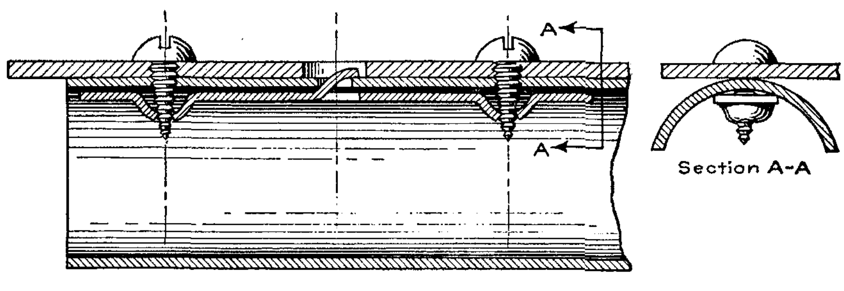

Fig. 9—Threaded clip is held inside tubing by lug and insures a positive connecting device. Clip is used when tubing wall is too thin for screw attachment.

This construction data has been prepared by the Product Development Committee, Formed Steel Tube Insitiute, Cleveland, Ohio

END FITTINGS

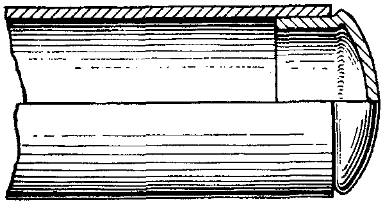

Fig. 10—End plug may be threaded or press-fitted on the OD or ID of tubing.

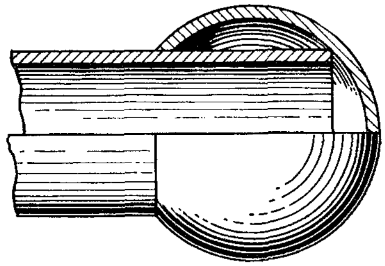

Fig. 11—Ornamental cap may be used to give tubing finished appearance.

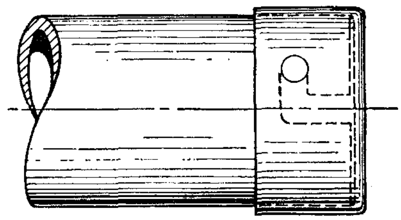

Fig. 12—Detachable cap uses bayonet-type connection for convenient removal.

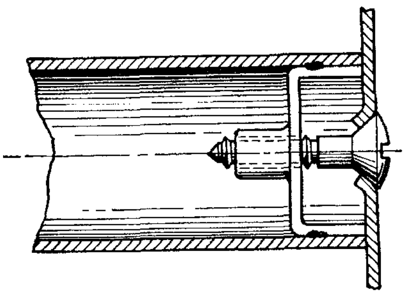

Fig. 13—Threaded insert, welded inside, facilitates the assembly of plates.

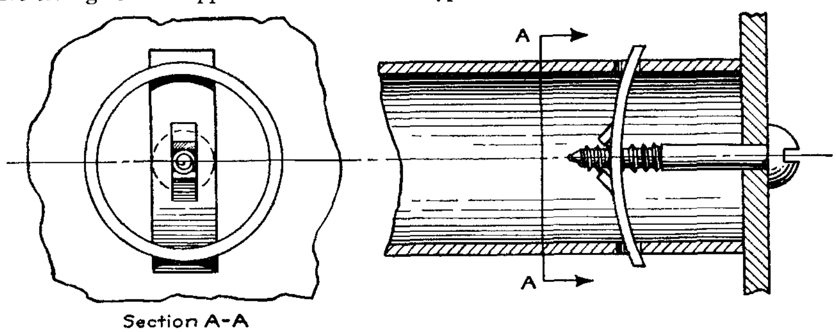

Fig. 14—Spring-steel nut is used for attaching objects to the ends of tubing. Nut requires two slots in the tubing and is held in position by screw.

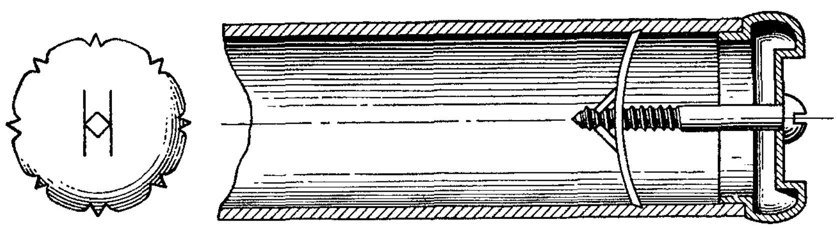

Fig. 15—Arched-nut attachment requires no machining. Nut is first rammed into tube; tightening of screw forces barbs into metal for positive anchorage.

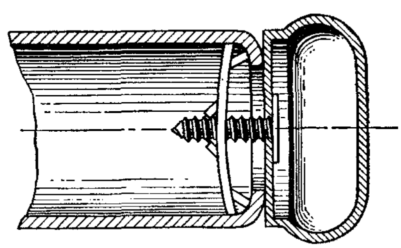

Fig. 16—Rolled-end of tubing simplifies attachment of end fitting.

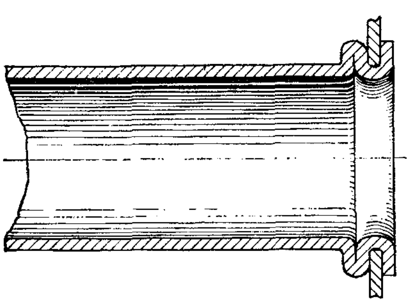

Fig. 17—Roll and press operation can be used to firmly hold tubing in plate.

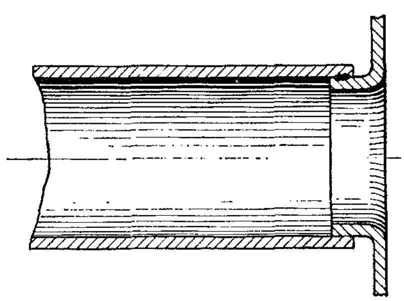

Fig. 18—Formed plate facilitates attachment of tubing by welding or brazing.

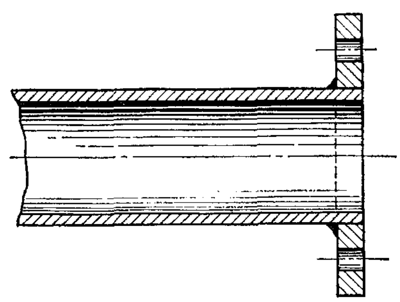

Fig. 19—Flange fitting for piping is made by welding flange to tubing.

Design Hints for Pipe Connections

Robert O. Parmley

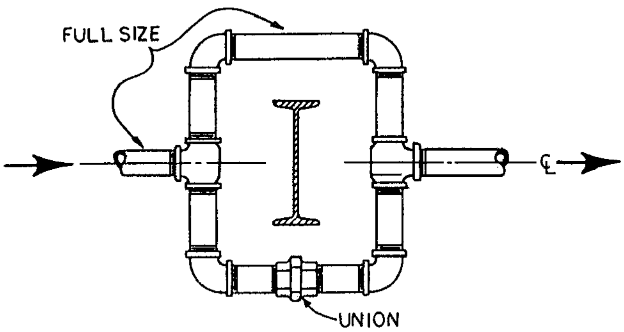

LOOP PRESSURE PIPE AROUND I BEAM

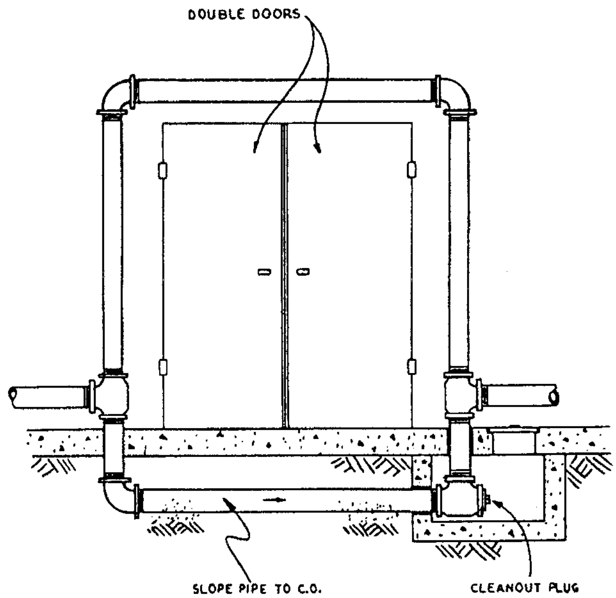

LOOP DRY PIPE AROUND DOOR OPENING

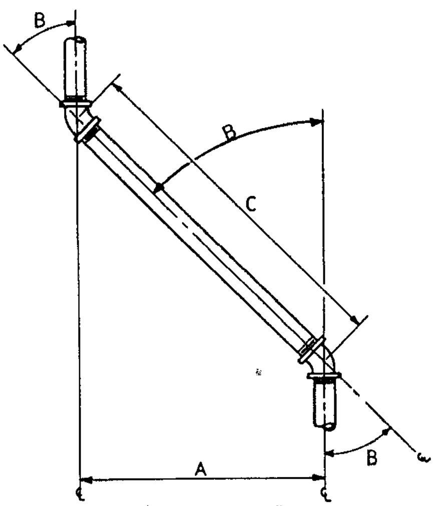

TO FIND "C" MULTIPLY "A" BY CONSTANT FOR ANGLE "B"

B	CONSTANT
$11\frac{1}{4}°$	5.126
$22\frac{1}{2}°$	2.613
30°	2.000
45°	1.414
60°	1.555

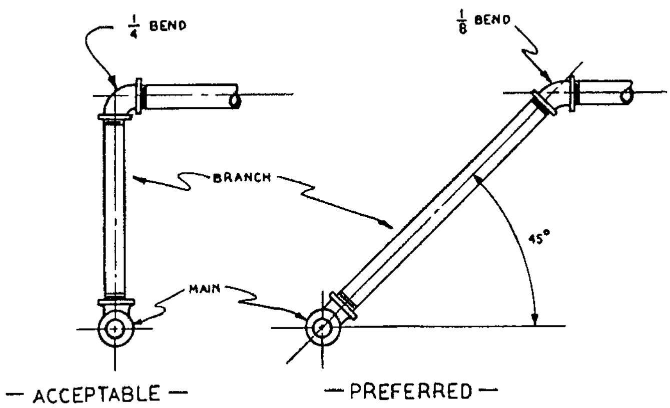

METHODS OF BRANCHING FROM MAIN

Multiple Piping Arrangements in a Wastewater Treatment Facility

Robert O. Parmley

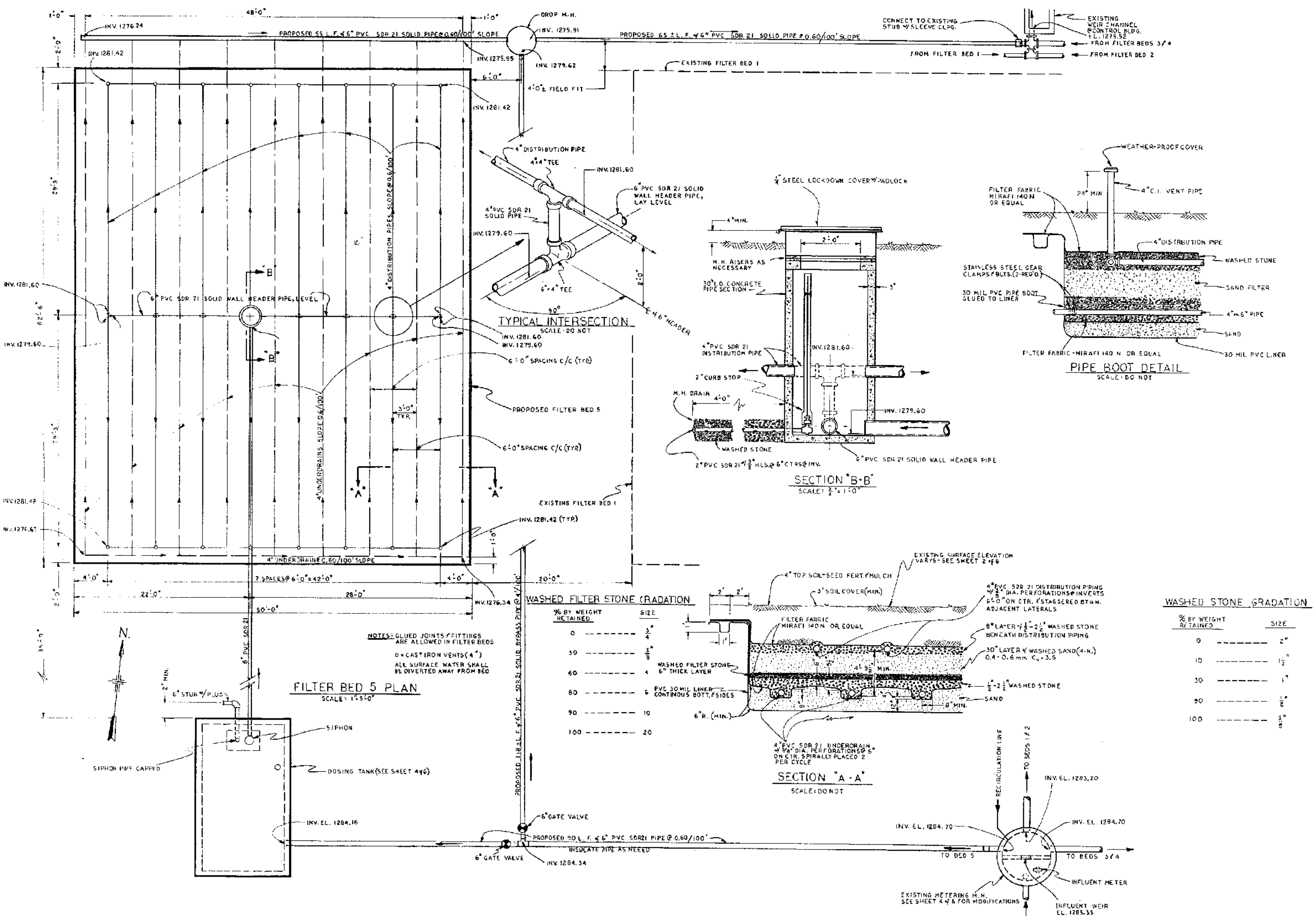

General construction layout for a small wastewater treatment facility; i.e. a sub-surface sand filter system. Note the various piping arrangements and connections throughout the design.

Courtesy: Morgan & Parmley, LTD.

Pumphouse Piping System for Fire Protection Facility

Robert O. Parmley

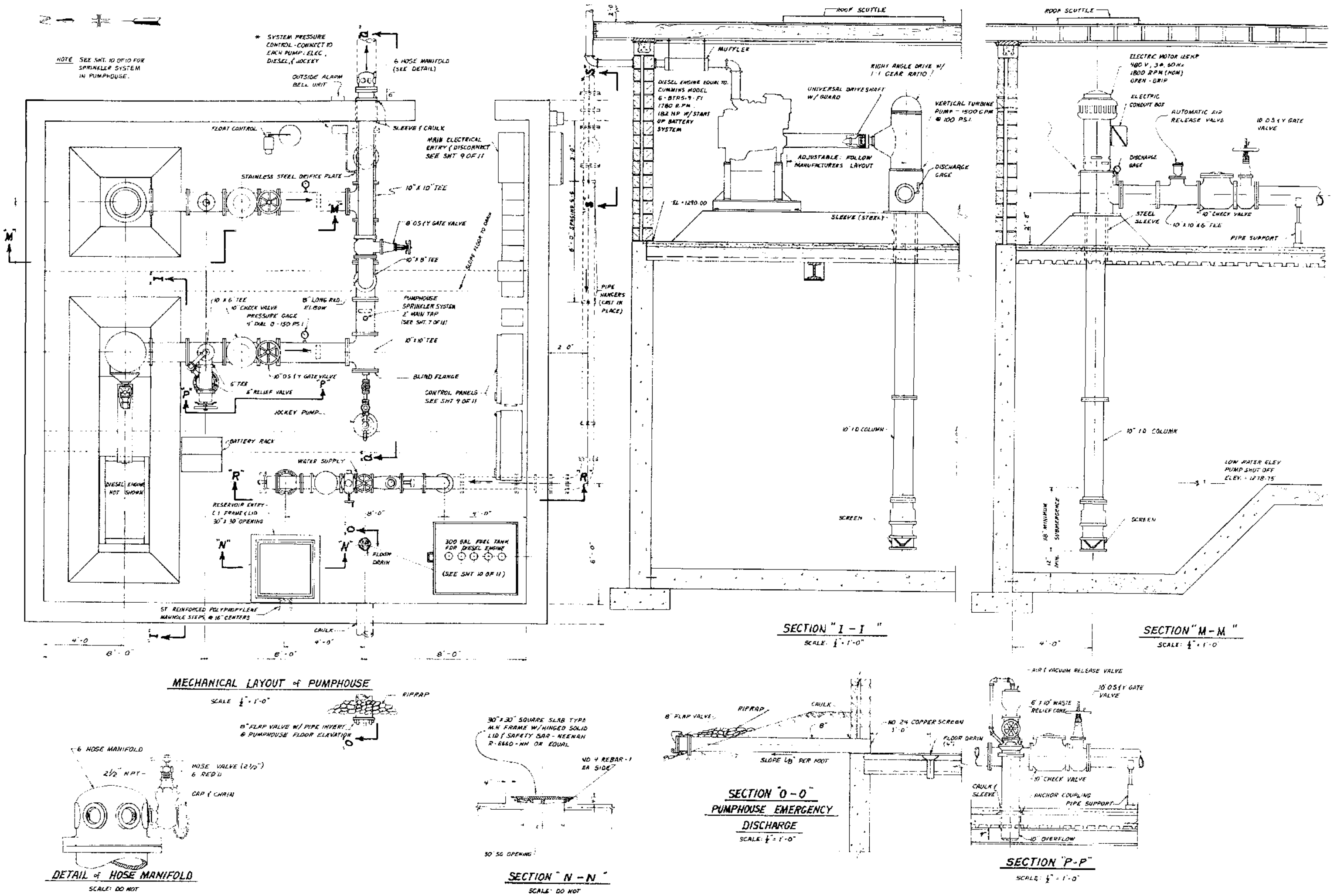

General construction layout for sub-surface fire protection facility. Good example of the variety of pipe connection patterns in a complex facility.

Courtesy: Morgan & Parmley, LTD.

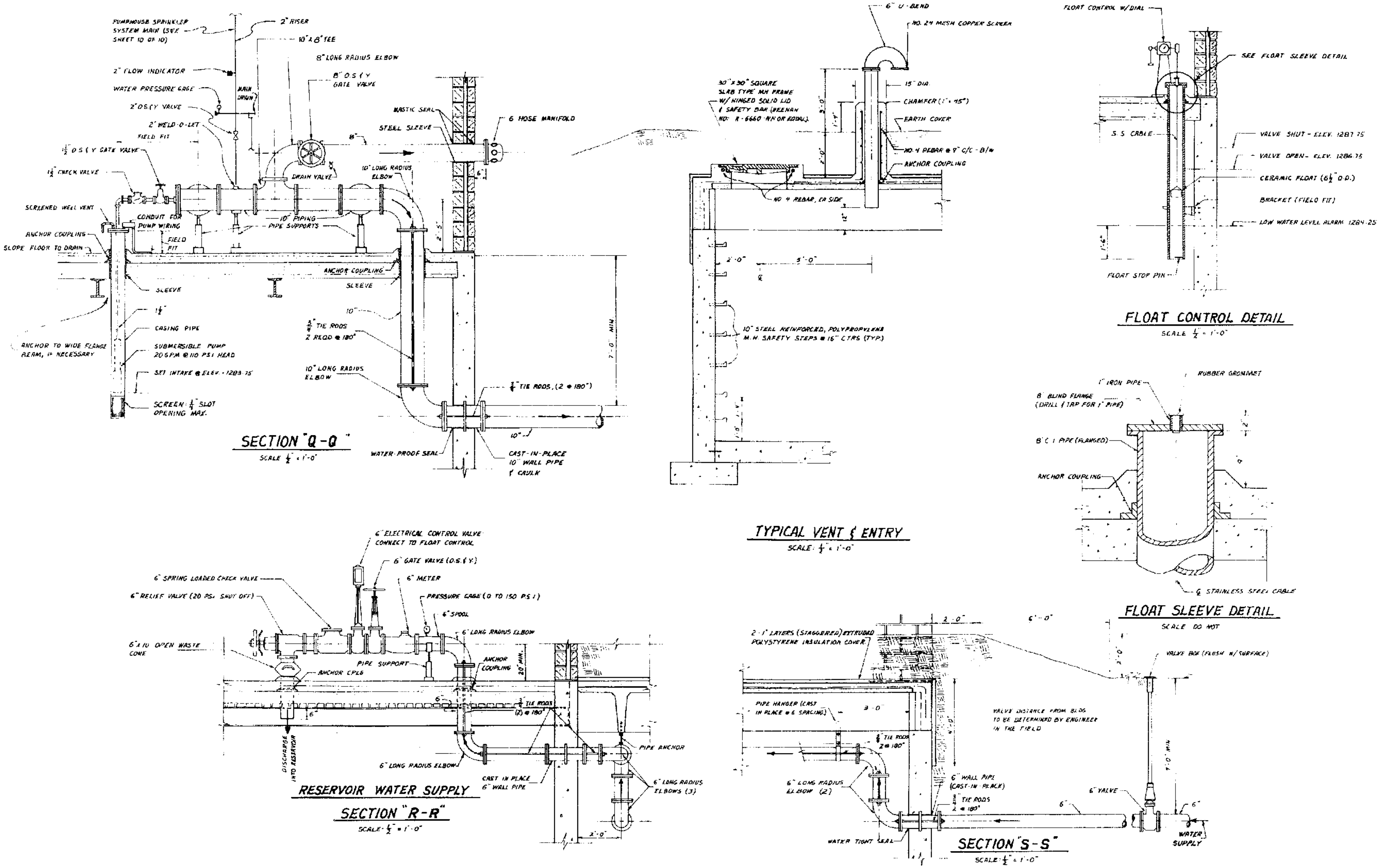

Additional construction details of sub-surface fire protection facility. Piping arrangements and connections show typical employment of standard pipe and fittings.

Courtesy: Morgan & Parmley, LTD.

SECTION 8

BUSHINGS & BEARINGS

Seven Creative Ideas for Flanged Rubber Bushings

They're simple, inexpensive, and often overlooked. Check your design for places where rubber bushings may be a solution to a design problem.

Robert O. Parmley

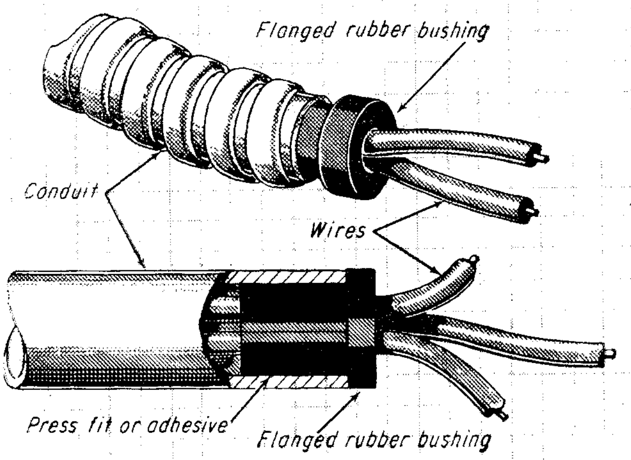

1 Conduit liner

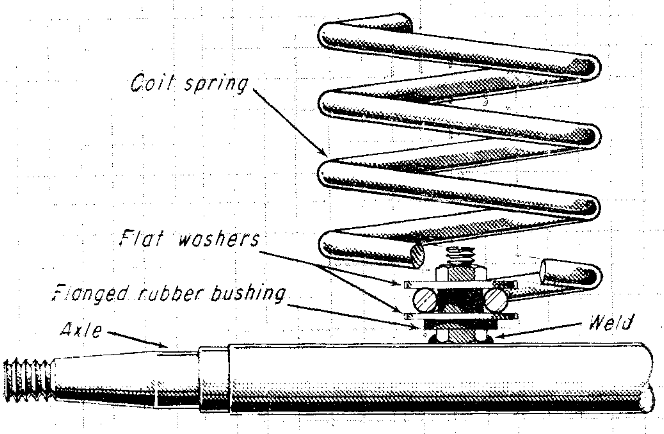

2 Shock absorber

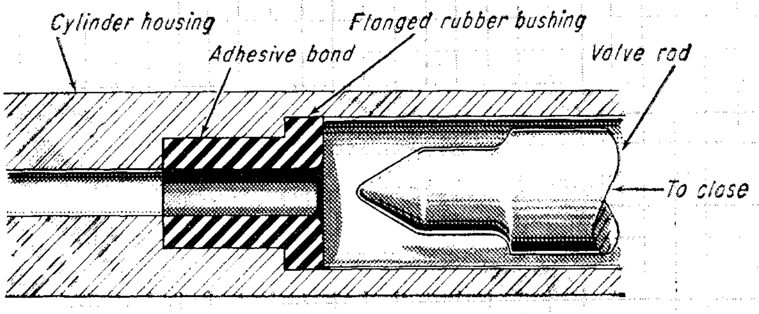

5 Valve seat

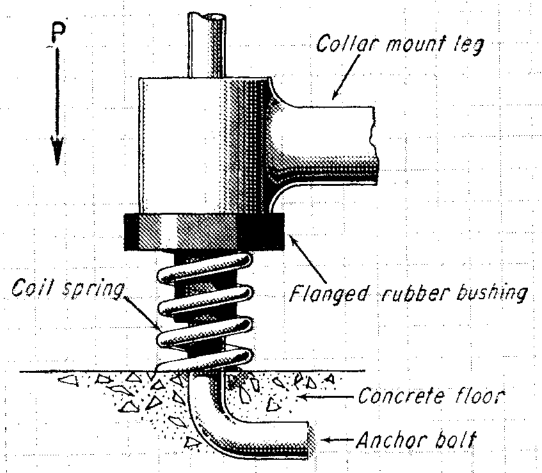

6 Spring support

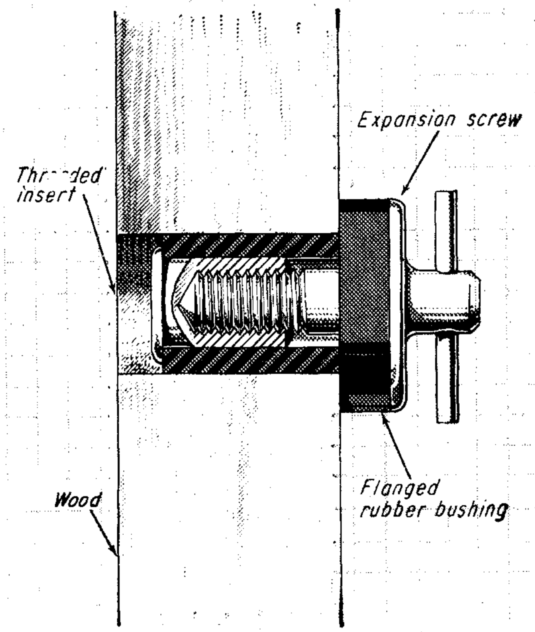

3 Seal expander

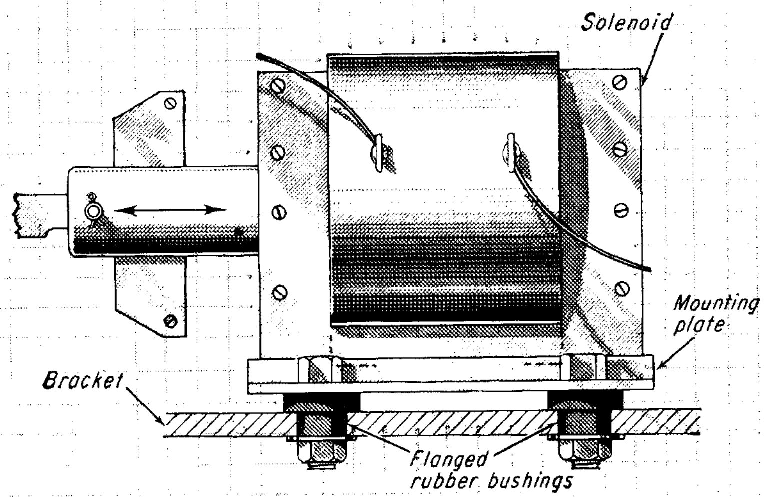

4 Cushion and noise absorber

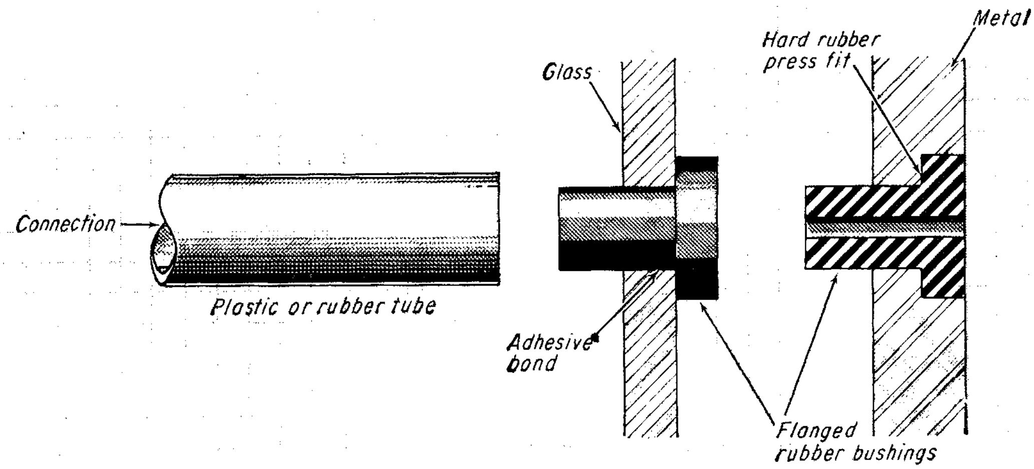

7 Nipple connection

Going Creative with Flanged Bushings

These sintered bushings find a variety of jobs and are available in 88 sizes, from 1/8 inch to 1 5/8 inch internal diameter.

Robert O. Parmley

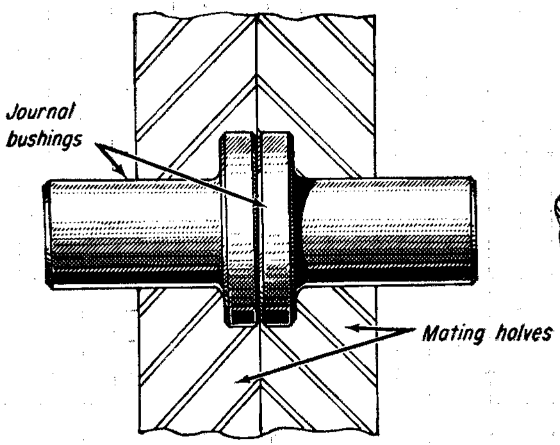

1 **Lock bearings in place**

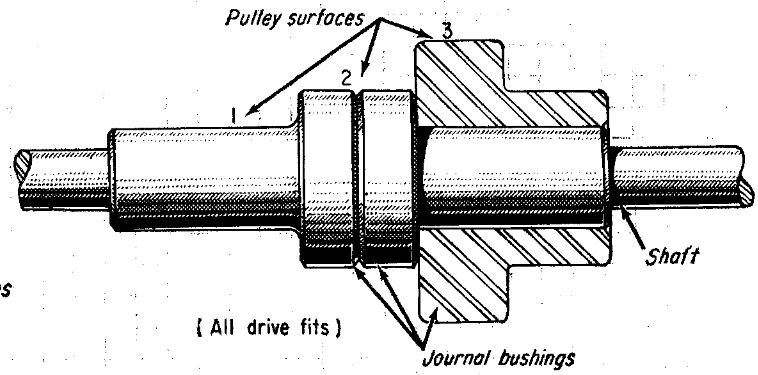

2 **Instant step-pulley**

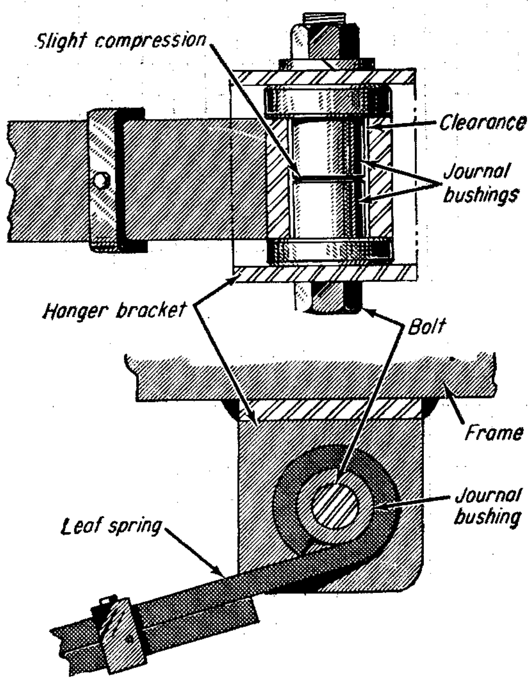

5 **Leaf-spring eye-bearings**

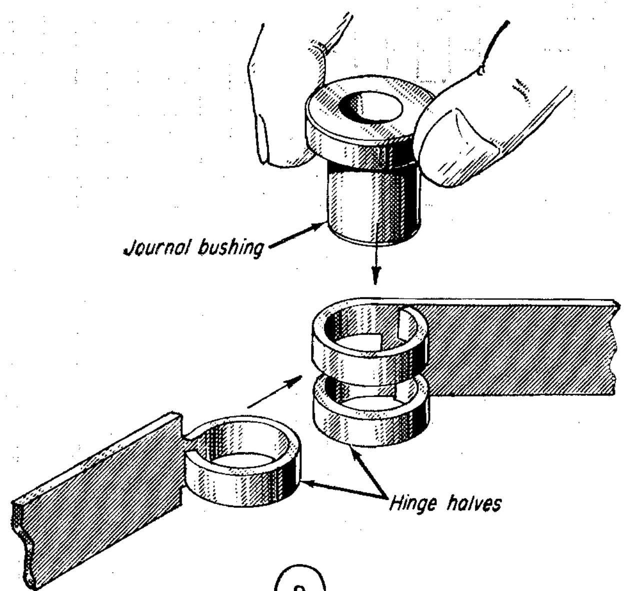

6 **Removable hinge pin**

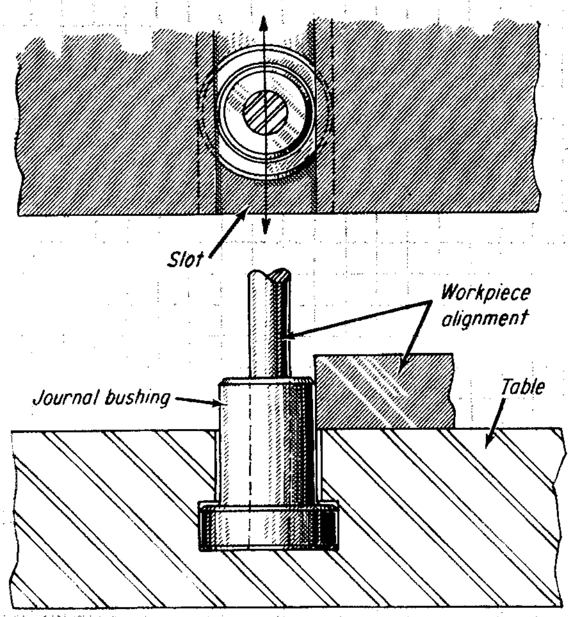

3 **Post or location-pin holder**

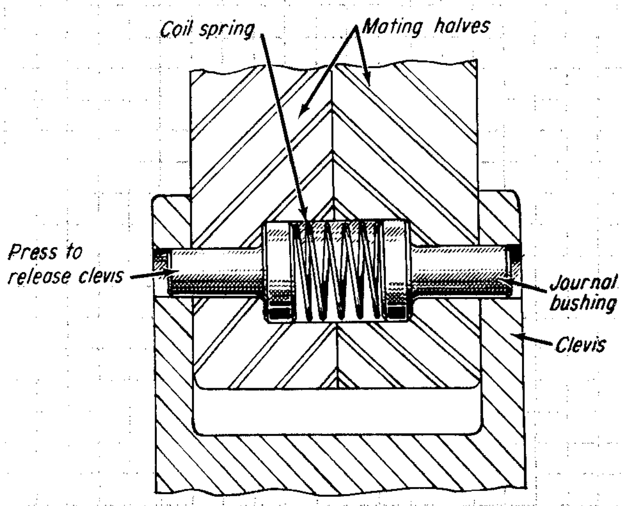

4 **Spring-loaded pins**

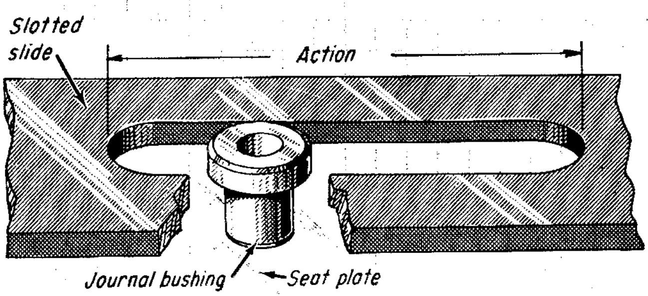

7 **Slider pin is self-lubricating**

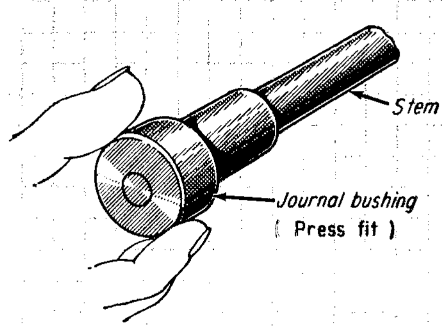

8 **Handle or knob**

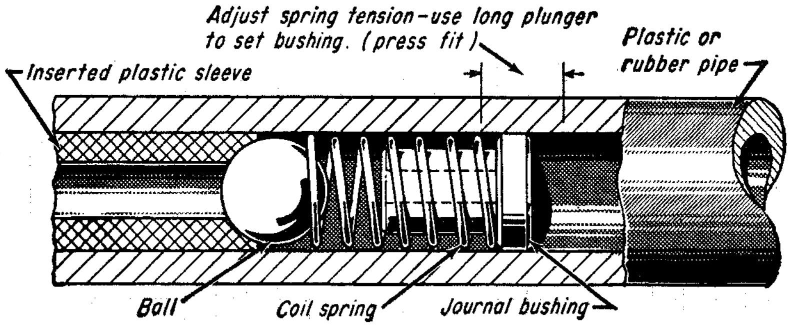

9 Checkvalve

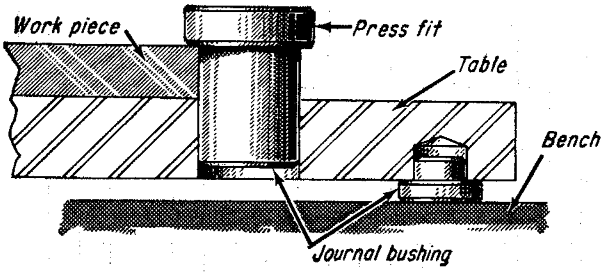

10 Holding fixture, complete with feet

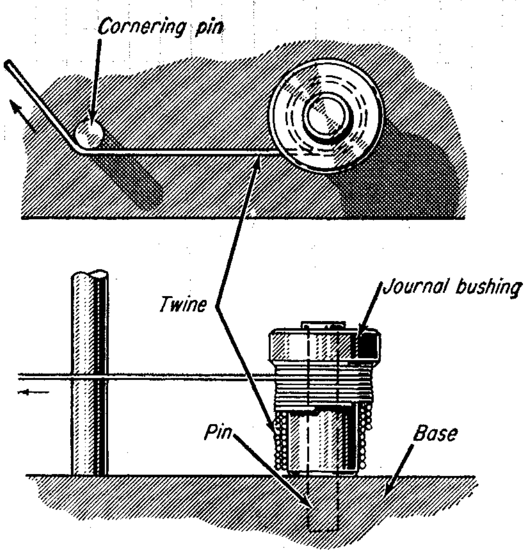

(Press fit in base only)

11 Bobbin

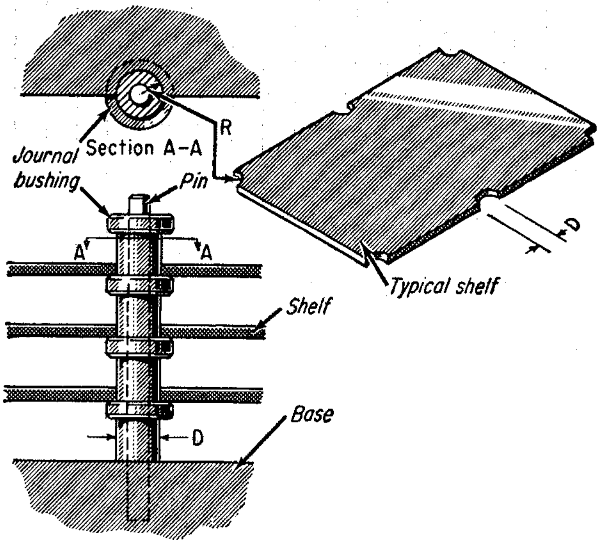

12 Shelf post

How to Calculate Stresses in Press-Fit Bushings

Here is a family of formulas, each helpful for a typical application.

E. H. Schuette

KEY TO FORMULAS

$$A = \frac{b^2 + a^2}{b^2 - a^2}$$

$$B = \frac{b^2}{c^2 - b^2}$$

$$C = \frac{c^2}{c^2 - b^2}$$

$$D = \frac{d^2 + c^2}{d^2 - c^2}$$

E = modulus of elasticity, psi
S = stress, psi
e = interference, in.
μ = Poisson's ratio

Subscripts:
B = bushing
M = matrix metal
S = sleeve
1 = matrix-sleeve interface
2 = sleeve-bushing interface

Assumptions Behind Formulas

Assumption for cases I and II is that the outer bushing-face must deflect to a position coincident with the inner matrix-face. Since pressures on these two faces are equal (one reacting against the other) it is possible to say that matrix deflection minus bushing deflection equals the amount of interference. In cases III and IV, conditions governing analysis are:

1. At any position along the length, an unbalance may exist between internal matrix-pressure and the external bushing-pressure.
2. The total of unbalanced forces up to the given position, over a unit circumferential width, is balanced by total shear force on unit circumferential width of cross-section at that position.
3. Slope of the deflection curve at any position must be related, by rigidity modulus, to shear stress.

With light metals, press-fit bushings greatly increase the strength of bearings and give only a small increase in weight. Many light-metal alloys, however, are sensitive to stress corrosion. Tensile stresses produced by an interference fit should, therefore, be kept to a safe level. Here, beginning on this page, are formulas that will help do this.

The formulas for cases I and II are extensions of the formulas for pressurized, thick-wall cylinders.

In cases III and IV the derived formulas were too long to be of practical value. To simplify them, therefore, 237 specific examples were calculated on an electronic computer. All probable designs were covered. Formulas III and IV, using arbitrary increase of dia c, were developed as a result of the electronic computation, and give results that are 99% accurate.

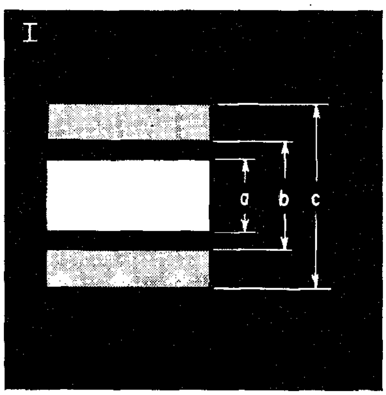

$$S_M = \frac{E_M \frac{e}{b}(B + C)}{(B + C + \mu_M) + \frac{E_M}{E_B}(A - \mu_B)}$$

Matrix metal, bushing . . .
have the form of a cylinder. This formula is an extension of those for thick-walled cylinders with internal pressure.

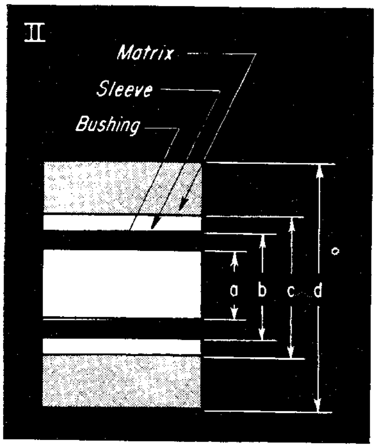

Sleeve between matrix . . .
and bushing complicates formulas. But though lengthy, the formulas involve only simple arithmetic calculations.

$$S_M = p_2 D \qquad S_S = p_1 (B + C) - 2p_2 D$$

$$p_1 = E_M \frac{\frac{e_1}{b}\left[(D + \mu_M) + \frac{E_M}{E_S}(B + C - \mu_S)\right] + \frac{e_2}{b}\left[2\frac{E_M}{E_S}C\right]}{\left[\frac{E_M}{E_S}(B + C + \mu_S) + \frac{E_M}{E_B}(A - \mu_B)\right]\left[(D + \mu_M) + \frac{E_M}{E_S}(B + C - \mu_S)\right] - 4\left[\frac{E_M}{E_S}\right]^2 BC}$$

$$p_2 = E_M \frac{\frac{e_1}{b}\left[2\frac{E_M}{E_S}B\right] + \frac{e_2}{b}\left[\frac{E_M}{E_S}(B + C + \mu_S) + \frac{E_M}{E_B}(A - \mu_B)\right]}{\left[\frac{E_M}{E_S}(B + C + \mu_S) + \frac{E_M}{E_B}(A - \mu_B)\right]\left[(D + \mu_M) + \frac{E_M}{E_S}(B + C - \mu_S)\right] - 4\left[\frac{E_M}{E_S}\right]^2 BC}$$

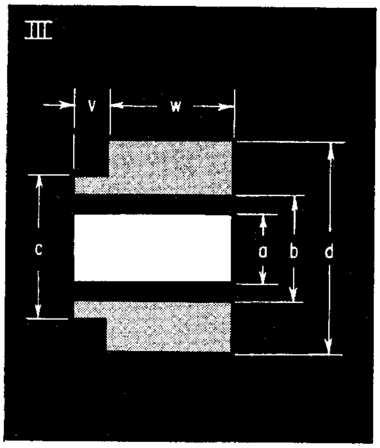

Stepped matrix . . .
causes stresses, pressures and deflections to vary over total length. Formula here derives value of Δc, which gives 99% accurate results when combined with formula for I.

Use formula for case I, substituting $(c+\Delta c)$ for c in $\left(C = \frac{c^2}{c^2 - b^2}\right)$

$$\frac{\Delta c}{b} = \left[\frac{1 + \frac{2a}{b}}{3}\right]\left[\frac{\frac{d-c}{b}}{\frac{d-c}{b} + 1}\right]\left[\frac{\frac{w}{b}}{\frac{w}{b} + \frac{v}{b}}\right]^{1 + \left(\frac{2w}{b}\right)}$$

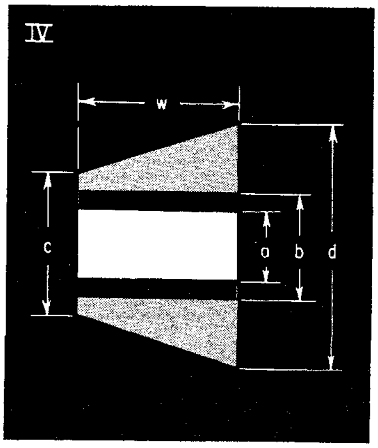

Conical-matrix . . .
formula gives Δc, which is then also incorporated into formula for I, giving same degree of accuracy as III.

Use formula for case I, substituting $(c+\Delta c)$ for c

$$\frac{\Delta c}{b} = \frac{1}{2}\left[\frac{d-c}{b}\right]\left[1 - \frac{(w/b)^2}{(w/b)^2 + 2}\right]$$

When Expandable Bushings are the Answer

They provide the zero clearance of a press fit and the positive drive of a shaft spline or key, yet avoid the disadvantages of precise tolerances and weakening stress concentrations.

Eric Nord

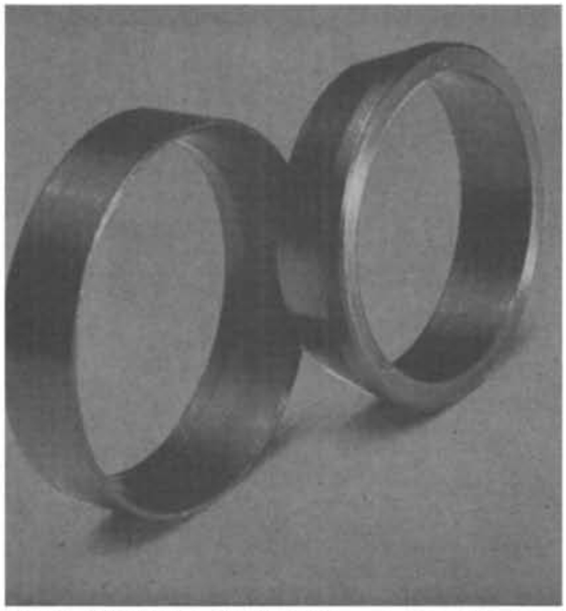

SOLID TAPERED BUSHINGS, made by US Automatic Corp, provide uniform pressure around the circumference; they are used for short bushings.

There are many ways to lock a shaft to its hub. Among them, the lesser known method of expandable bushings have advantages that often make it best choice. It offers an inherent concentricity, rigidity and torque-transmitting ability of a shrink fit plus the liberal tolerances and ease of assembly of a collet-type mounting. Yet it does not require the close tolerances of the press and shrink fit and also does not set up the stress concentrations with notch weaknesses commonly associated with keys, and splines.

Two types of expandable bushings are available—solid and split. Each has its own characteristics and applications.

SOLID TAPERED

These bushings rely on elastic properties of the bushing material to translate axial force into the tightening radial pressure desired. An axial force applied to the outer ring forces it into the mating inner ring; the outer ring expands against the bore of the hub, while the inner ring contracts against the shaft.

Often more than one set of such rings is used in a connection. Here is an approximate equation that we developed for finding theoretical torque for any number of ring sets. It's derived from the action of axial force on the ring elements, neglecting minor frictional forces in the vertical surfaces.

$$T_n = \frac{F_A \gamma}{2}\left[1 - \left(1 - \frac{2\mu}{\tan(\alpha + \theta) + \tan\theta}\right)^n\right]$$

Maximum torque is inversely proportional to the tangent of the ring angle; a smaller ring angle gives greater torque. But there is a limit: the ring angle must be large enough for these rings to be self-releasing for easy disassembly. An angle of 16° 40′ is a good compromise. When this angle is used with a coefficient of friction of

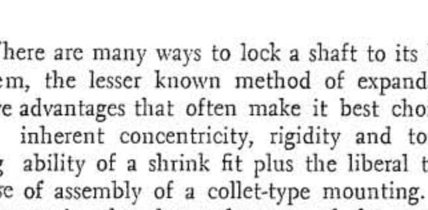

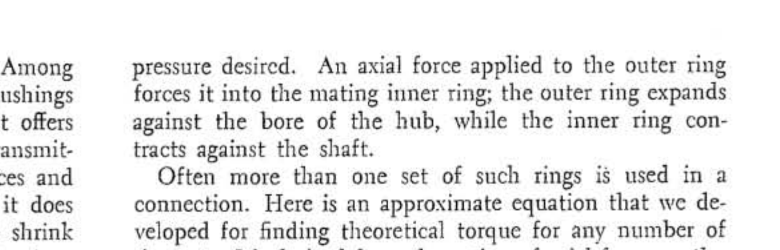

SPLIT TAPERED BUSHINGS, made by Adjustable Bushing Co, North Hollywood, Calif, transmit axial force evenly between rings and can be used for long bushings. Assembly (left) shows direction of forces. Male segments contract to grip shaft, female segments expand against hub bore. Exploded view (right) shows staggered splits in segments.

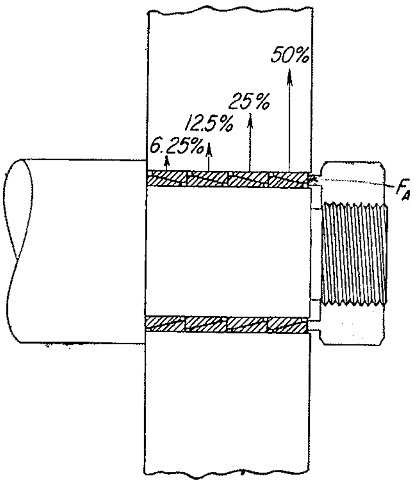

TORQUE TRANSMITTED decreases at a rate of 50% per set in mounts where hub is restrained by a shaft shoulder.

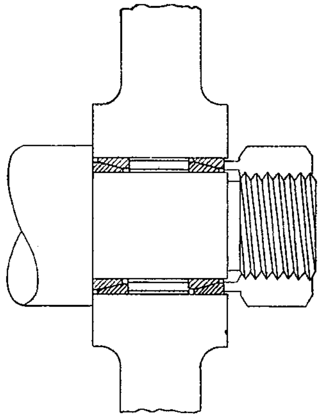

TYPE 1—Shaft shoulder restrains nut during tightening; ring set at end of spacer transmits only half as much torque as set at right.

SYMBOLS

T_n — Theoretical max torque for n ring sets, in.-lb
F_A — Axial force applied after rings are in contact with hub and shaft, lb
r — Radius of shaft, in.
μ — Coefficient of friction
θ — Friction angle ($\tan\theta = \mu$)
α — Ring angle (16° 40′ used in example)
n — Number of ring sets
P_1 — Radial thrust of first ring set, lb
S_c — Compressive stress, psi
D — Shaft diameter, in.

approximately 0.16, the torque equation shows that the first ring set will transmit approximately 50% of the theoretical torque value obtainable with an infinitely large number of ring sets:

$$T_{max} = \frac{F_A r}{2}$$

4 BASIC HUB MOUNTS

When more than one set of rings is used and the hub is restrained by a shoulder (as in diagram above), thrust force declines by 50% in each successive set when the nut is tightened. Only the first set is loaded by the full axial force. This reduction, which results when the rings grip the shaft and hub, makes it advisable to limit the number of ring sets. Type 1, above right, is a more usual design.

When the hub is not restrained by a shoulder, as in Type 2, thrust force acts from both sides when the nut is tightened. Each set transmits 50% of the theoretical maximum torque.

There are two other basic designs: Type 3, which has the same loading as Type 2, but with no axial shift of the hub; and Type 4, with same loading as Type 1, but it has four ring sets instead of two.

Our nomograph, right, based on these 4 types, gives axial load necessary to produce a given torque. For example, a 1-in. shaft that must transmit 3 hp, or 630 lb·in T requires an axial force of approximately 3000 lb in a Type 1 mounting. Types 2 and 3 would require 2400 lb and Type 4, 1500 lb.

Radial thrust of the first outer ring against the hub is given by the equation:

$$P_1 = \frac{F_A}{\tan(\alpha + \theta) + \tan\theta}$$

For values of the ring angle and coefficient of friction given previously, this equation reduces to:

$$P_1 = 1.56\, F_A$$

This radial thrust can be used to determine the allowable compressive stress:

$$S_c = 0.477\, P_1/D^2$$

For hubs with an outside diameter double the shaft of contact pressures of 60% of the working stress is recommended. This working stress should then be divided in a suitable safety factor to give the allowable compression stress. For example, a safety factor of 2 gives 8500 psi for grade 30 cast iron and 17,000 psi for SAE 1020 steel

SPLIT TAPERED

The other version of expandable bushing is one with tapered split rings. With this type, the radial force is acting along the axis–remain constant. They do, however, vary along the circumference, ranging from zero to the split to a maximum opposite the split. Because of the split the bushings are easy to expand and therefore can accommodate broad tolerances in hole size.

This type may be split in two, three or four places to make easier radial expansion, as well as to facilitate assembly in applications where the end of the shaft is inaccessible. Splits can be staggered.

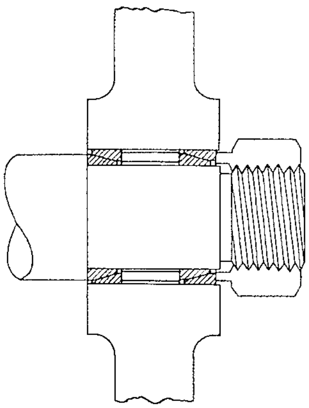

Type 2

TYPE 2—Has no shaft shoulder, so it is free to move axially; thus loading is equal in both ring sets.

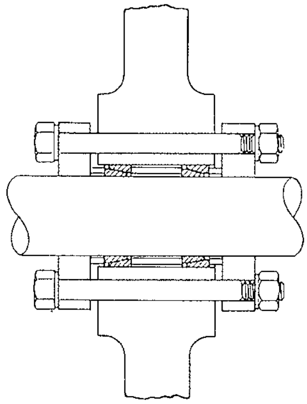

Type 3

TYPE 3—Collet-type mounting; same loading as Type 2, but hub is restrained during tightening.

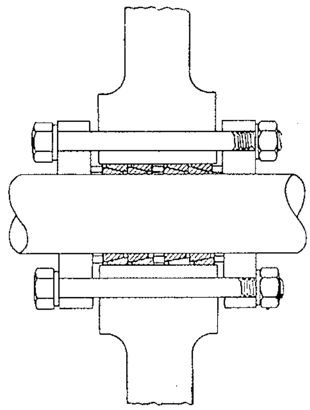

Type 4

TYPE 4—Collet-type mounting; same loading as Type 1, but with four ring sets.

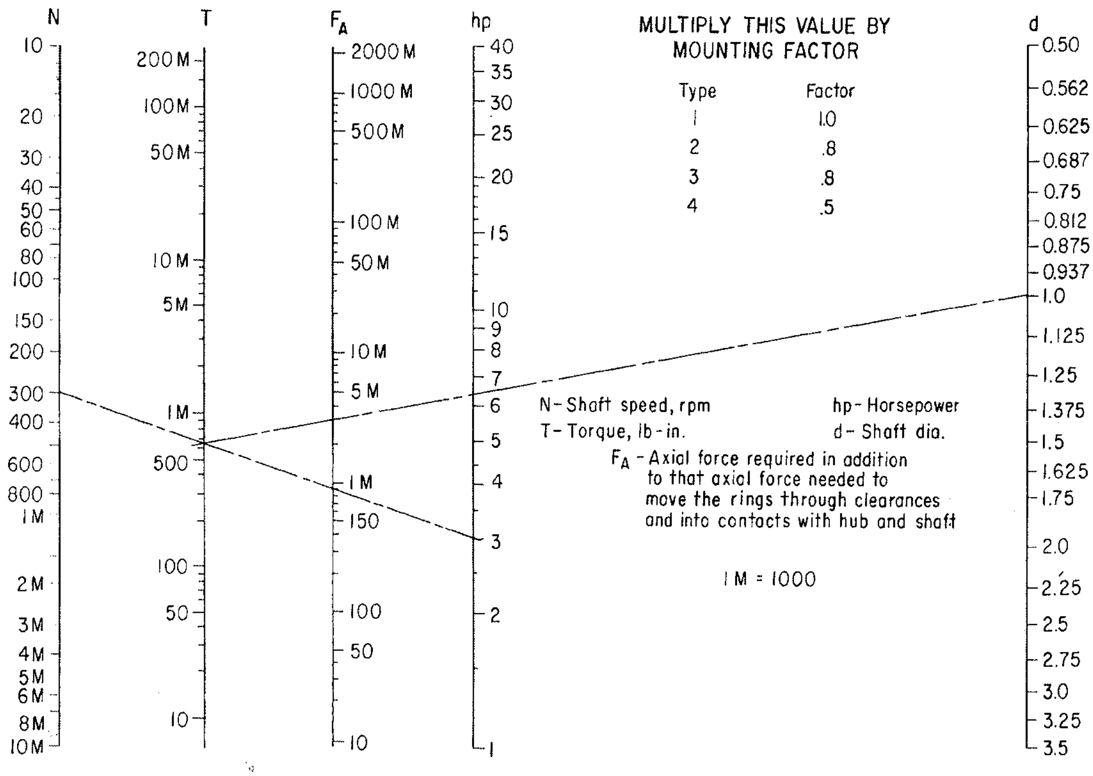

SECTION TORQUE is translated to axial force by this nomograph.

MATERIALS AND FINISHES

Expandable bushings can be made of various metal or nonmetal materials to suit particular requirements. Currently, they are made with:

- Aluminum alloy-2024-T6, anodized per MIL-A-8625
- Sintered-bronze oil impregnated per MIL-B-5687a
- Stainless steel Type 303 passivated
- Carbon steel, B1113, cadmium-plated per QQ-P-416, Type II, Class C
- Nonmetals such as nylon and teflon—these are used as static and dynamic seals in solid tapered bushings;

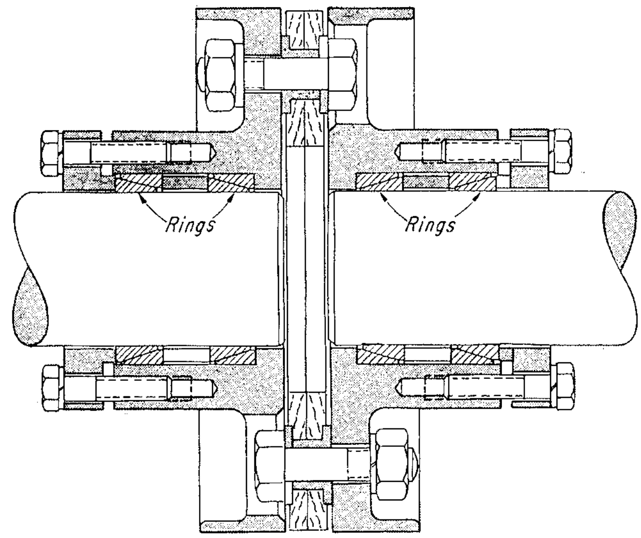

A

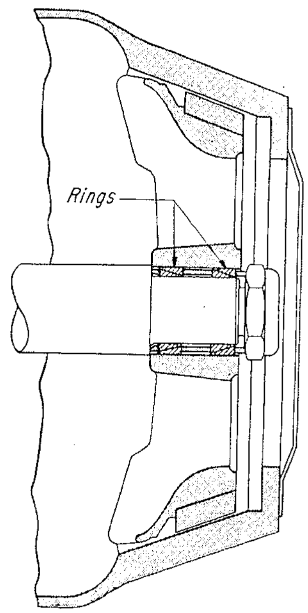

B

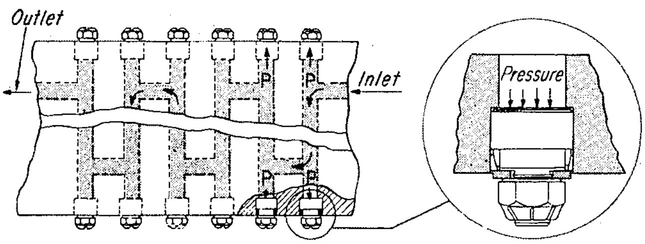

C

Three applications for solid tapered bushings (A) In flexible couplings they eliminate stress concentrations and provide uniform grip; (B) In hoist brake they provide easy assembly in a compact design; (C) In plug seal they give continuous radial-pressure sealing for high-pressure steam-heating plate.

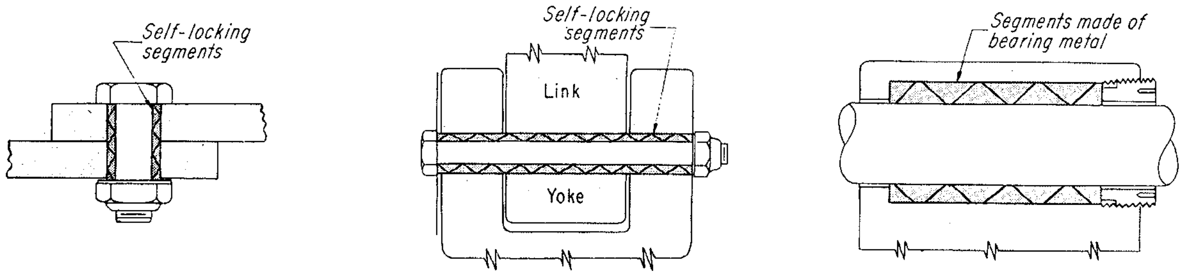

A B C

Three applications for split tapered bushings: (A) structural joints, which are subject to vibrations. Here the bushings provide rigidity in loose-tolerance drilled holes. (B) Link and yoke joints which require relative movement and frequent removal. The bushings give minimum backlash by adjusting the nut for proper fit. (C) plain sleeve bearings can be periodically adjusted for wear by means of screw take-up to maintain precise fit.

stainless steel and carbon steel are also used for sealing solid tapered bushings where high temperatures as well as pressures are involved.

Sleeve Bearing Alignment

R. J. Sollohub

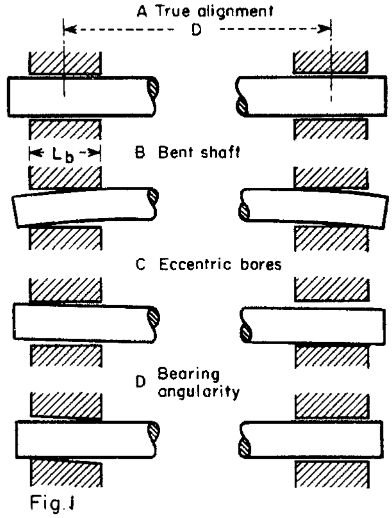

Fig. 1

EXCESSIVE friction losses and bearing failures can be prevented if the basic reasons for tight-running shafts are considered. In many instances, boring or reaming operations at assembly can be omitted without opening up bearing-to-shaft designed clearances.

Three possibilities for shaft-bearing interference are shown in Fig. 1. The most important factor is bearing angularity, although this is the most usually omitted tolerance dimension:

$$C = L_b (\tan \theta + e/2D + S/2)$$

Where C = bearing clearance necessary only to prevent shaft and bearing interference.

L_b = bearing length

Tan θ = bearing angularity as in Fig. 1 (D)

e = Concentricity error, total indicator reading

D = Distance between bearings

S = Shaft runout, in./in.

Angle θ is difficult to measure; it is usually expressed as runout in 0.001 in. per unit diameter on the face of the bearing assembly, or W/D, where W = total indicator reading and D = the diameter swept by the indicator.

EXAMPLE:

Consider a shaft 10 in. between bearings. Total shaft runout is 0.003, or 0.0003 in. per inch of bearing length. Eccentricity of bores is 0.003 in., and W, commonly called wobble, is equal to 0.003 in. on a 5-in. dia. Then:

$$C = \frac{0.003}{5.000} + \frac{0.003}{20} + \frac{0.0003}{2}$$
$$= 0.0006 + 0.00015 + 0.0015$$
$$= 0.0009 \text{ in.}$$

By eliminating all concentricity and shaft runout error, C would be reduced by only 0.0003 in. If only bearing angularity were corrected, the clearance required would be reduced by 0.0006 inches.

The greater the distance between bearings, the less effect concentricity error will have. Shaft runout is pertinent only within the bearing length and is generally easy to maintain. Bearing angularity, however, is harmful regardless of distance between bearings.

In Fig. 2, concentricity is dependent on both endshield and motor frame. Bearing angularity is dependent on squareness of endshield faces and parallelism of motor faces. Thus, the faces of the frame should be machined at the same time on an arbor, and alignment of the machine heads to maintain parallelism is more important than concentricity of bores. Endshield faces should be machined after the bearings have been inserted, by finish boring the bearing or by a qualifying cut locating from the finished bore.

Fig. 3 shows a typical gear train, where parallelism of the two endplates and assembly of the bushings are critical. If the bushings are not machined true and assembled true, alignment will be almost impossible. The OD of the bushing should be turned with a step lead as illustrated, and the bushing should be pressed in square.

Ordinary commercial arbors should not be used to qualify motor-frame rabbets or to turn the OD of bushings. These arbors generally have from 0.001 to 0.0015 in. taper per inch. Step-type arbors ground in 0.0001 in. increments should be used.

REFERENCE:

Sleeve Bearing Alignment by R. J. Sollohub, General Electric Company, Fort Wayne, Ind. Published in *American Machinist*, December 17, 1956, p 151.

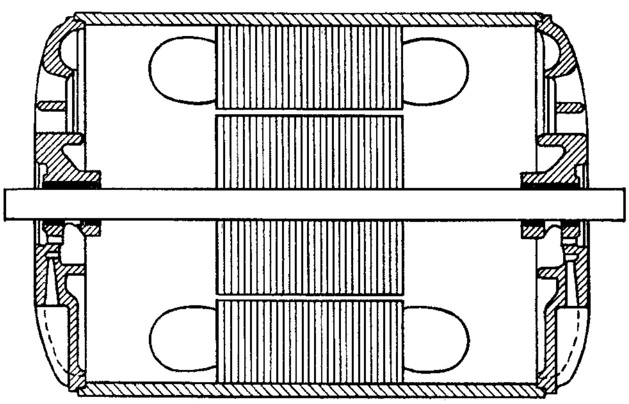
Fig. 2

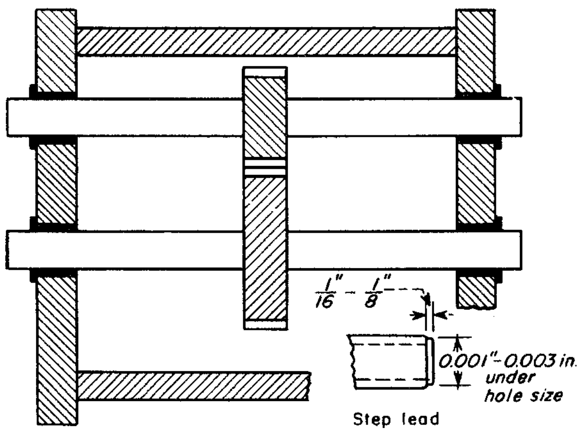

Fig. 3

Getting Better Performance form Instrument Bearings

Military and industrial labs have proved out the value of new surface films and novel designs in making ball bearings run smoother, quieter, and longer.

Nicholas P. Chironis

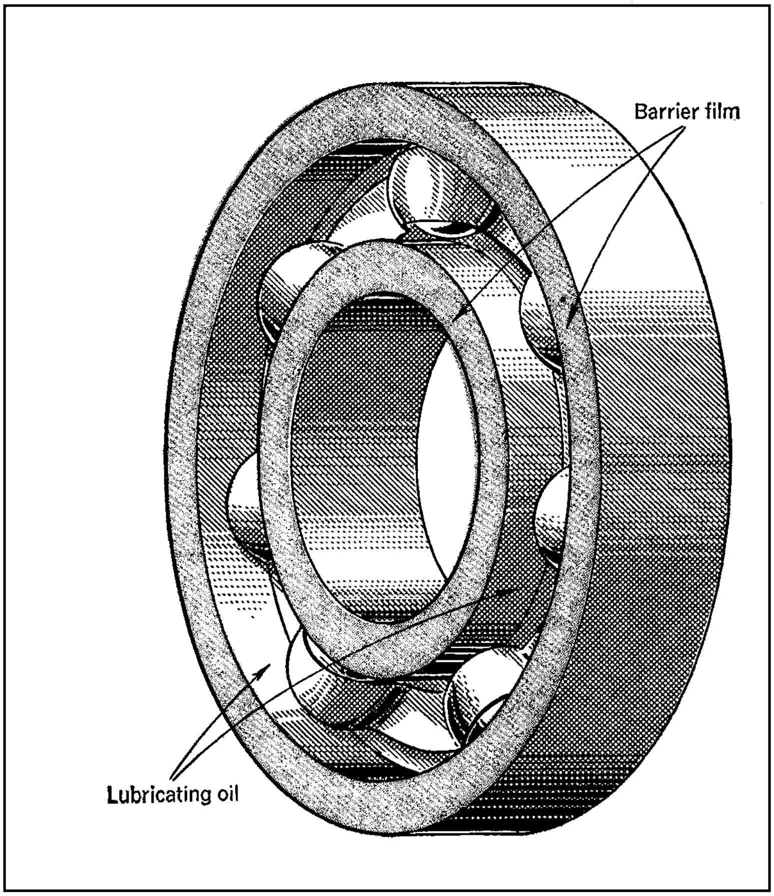

Invisible barrier film, such as a fluorinated methacrylate, prevents migration of lubricant. The Navy is adopting the technique for all instrument motors.

Refinements in both design and operating conditions for instrument ball bearings came to light during last month's Bearing Conference sponsored by Dartmouth College. Out of proof-testing programs at naval and industrial laboratories came such developments as these:

- Barrier films that set up an invisible dike at outer surfaces of bearings (drawing, left) to keep silicone lubricants from migrating.
- Conductive ball bearings that function as circuit components in electromechanical devices to transmit current between stationary and rotating members of an assembly.
- Treatment of bearing surfaces with TCP, the gasoline additive, for a mysteriously effective gain in bearing life and reduction in running torque.
- A new metallic coating process that bonds a highly lubricative film intimately with the metal to which it is applied.
- A square-hole retainer design that prevents adverse torque effects.

Barrier films work. Silicone oils have many virtues as lubricants for servo motors, synchros, and similar units. Especially for their high-temperature stability and excellent low-temperature viscometric properties, they have become first choice in many applications. So the Navy was both surprised and dismayed when service and storage life of its synchros and servo motors proved to be only one-third to one-half of expectation. Some units removed from storage turned out to be totally inoperable.

Study revealed that bearings failed because the small supply of silicone lubricant crept away from their load-carrying area. Changing the type of lubricant was not the answer. A way had to be found to confine sufficient lubricant within the bearings. Shields and seals, often used with grease-lubricated ball bearings, are not effective with oils, and grease could not be used in most instances because of the low torque requirements of instrument applications.

Finally the Navy Research Laboratories hit upon the idea of coating the boundary surfaces of a bearing (drawing, page 45) with a film that has a critical surface tension of wetting below that of the surface to which it is applied and that of the liquid to be retained.

The Navy tested several chemical compositions and found the fluorinated methacrylates, manufactured under various trade names, to be the best type. Use of such barrier films has remarkably extended the operating life of the Navy's instrument motors—from 300 hr. to nearly 4000 hr. The Navy is recommending that the barrier-film technique be employed on all synchros and servo motors purchased by the armed services. It also sees a potential in extending the life expectancy of other components, including rod ends, gears, and pistons.

Narrowing the choice. Miniature Precision Bearings, Inc., Keene, N.H., has tried out materials and techniques for applying barrier films on a commercial level, including blotting, brushing, and spraying. It obtained the best results with the fluorinated methacrylate manufactured by F. W. Nye Co. under the trade name of NYEBAR Type C.

One warning note: Barrier films must be applied under closely controlled conditions because they are readily soluble in commonly-used bearing cleaning solvents.

Conductive ball bearings. A few simple changes in bearing design (drawings below) now make it possible to transmit electric current between the inner and outer rings of a bearing as it rotates. This could previously be done only by adding external slip rings. In the new design, the slip rings are an integral part of the bearings. A plate of precious metal (gold or rhodium) is added to the inner ring, and a contact wire connects the inner and outer rings.

The new bearings that serve as circuit components are being made by Miniature Precision Bearings under license from Federal Mogul Corp. A typical application is in the sensing roll that stops a tape recorder when the tape ends (drawing below, right).

Across the end of the tape is a strip of conductive material that closes the circuit between ends of the roller. Current flows through the top lead, through the inner ring of the left ball bearing to the outer ring, across the conductive strip on the tape through the right ball bearing, and out through the lower lead to a switch.

The conductive bearing can also be used in circuits to ground the rotating members of such tools as hand drills and power saws. Tests by the manufacturer in the 1-amp range show no damage to the bearing by the application of electric currents, a negligible increase in bearing torque because of the addition of the conducting wire, and no problem with electrical resistance traceable to any lubricant tested.

The mystery of TCP. Tricresylphosphate, better known as TCP the gasoline additive, improves the life of bearings and reduces their running torque when it is applied to ring and ball surfaces. But nobody knows exactly why.

Is it the chemical itself that improves the bearing surface, or is it the presence of trace impurities? One researcher has proposed that TCP film degrades in the presence of water and oxygen to form fine phosphoric acid. The acid in turn forms iron phosphate that is effective in reducing sliding friction and running torque.

Whatever the explanation, TCP does work, and effectively too, according to research engineers at Miniature Precision Bearings. In tests with gyro motors, MPB engineers applied TCP to the balls alone, leaving the races uncoated, and reduced by 32% the power required to achieve and maintain synchronous speed. When they also applied TCP to the bearing rings, they reduced power consumption by another 8%. Life tests also showed

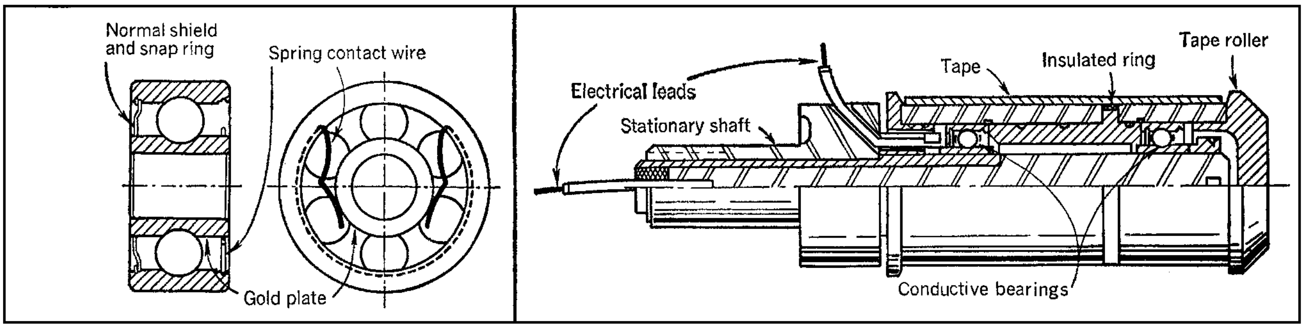

Conductive ball bearing sketched on left can transmit current between inner and outer races without affecting the running torque. When this capability is applied to tape rollers (above, right), current flows through two conductive bearings and across the conductive end of the tape to stop the recorder automatically as the tape runs out.

a marked improvement when TCP was applied.

Discovery of TCP's strange capabilities is credited to MIT's Instrumentation Laboratory at Cambridge, Mass. The process of applying the chemical is simple, though not inexpensive. To produce a one-molecule layer of TCP, parts must be heat-soaked for a long time at 225 F. For MPB's tests, bearings made of AISI 440C were selected because they need only a 72-hr. soak, compared with 360 hr. for parts made of SAE 52100 steel.

TCP works well with lubricating oils and can be used in team with barrier films to improve bearing performance. One word of caution, however, was given to the Bearing Conference by C. H. Hannan, MPB's manager of research: Don't expect TCP to noticeably reduce bearing torques at starting or slow speeds. Benefits seem to be associated with high-speed operation.

Metallic coating. MPB has also acquired rights from Lubrication Sciences, Inc., Mountain View, Calif., for the Dicronite metallic coating process, in which a film of a metallic compound is bonded to a metal surface. MPB is reluctant at this time to disclose the composition of the film.

However, the company says tests show the coating can lubricate better and stand up under higher pressure than any other solid lubricant—and more than twice the pressure that oil can take.

The main purpose of a lubricant in a ball bearing is to prevent metal-to-metal contact; dissipation of heat is a secondary role. If a bearing is highly loaded or if there are impurities on the surfaces of the balls or races, the lubricating film breaks through, and wear begins. Oils can take pressures to around 125,000 psi. With additives, this limit can be raised to about 160,000 psi. Solid lubricants can go still higher, depending on their composition, but they must be cured—heated or baked onto the bearing surface.

MPB says Dicronite is unique in the solid-lubricant field in assuring that the molecules of the metallic coating are bonded directly to the metal substrate. This souping-up of the surface seems to increase life of parts by three to seven times. The lubricating film has a lower coefficient of friction than that of graphite. It is highly resistant to wear and has withstood pressures to 300,000 psi, temperatures from −400 to 900 F in air, and temperatures to 2400 F in vacuum.

The process is conducted under ambient conditions. The workpiece remains at room temperature, therefore experiences no degrading effects when heat-treated parts are involved. Precision of parts can be maintained because thickness of the lubricating film can be specified between 15 and 40 millionths of an inch, with a tolerance of 5 millionths, plus or minus. Because of its simplicity, the process can be applied to parts after they have been assembled.

MPB is already looking into the possibility of using Dicronite on its customers' gear teeth, connecting rods, cam shafts, metering pumps, and speed reduction units. The process has also been tested successfully by NASA in space applications.

Square-hole retainers. Thin-section instrument bearings were originally developed for slow-speed uses, but an increasing number of applications call for high speeds, such as microwave antennas, optical trackers, scanners, and stabilizing devices. This rise in operating speed creates problems.

At higher speeds, ball retainers tend to whirl and squeal as they loop around the piloting race at a substantially higher frequency than that of their own rotation.

The piloting race is the one that makes radial contact with the retainer. Depending on the design, it may be the inner race or the outer one. In either case, the existence of the whirl phenomenon often causes severe damage through random or continuous torque surges.

Tests by Split Ballbearing Div., Lebanon, N.H., indicate that stability of retainers is improved by designing square instead of round pockets in them. As C. A. Griffiths, manager of the company's product engineering department, told the Bearing Conference:

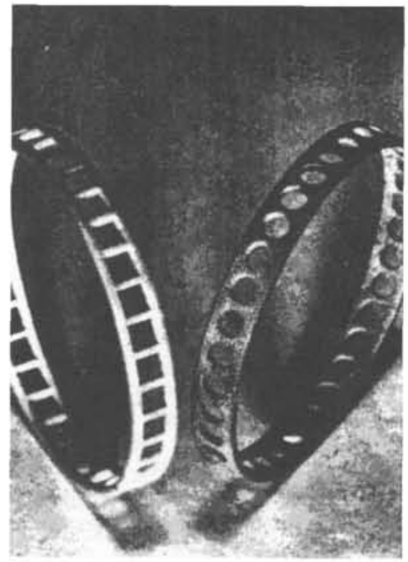

Square-pocket retainer on left cuts down internal vibration in thin-section instrument bearings. It may soon replace the type with round holes.

- Whirl can be reduced or eliminated by cutting down the contact area between the balls and the retainer. The unit pressure increases, so this approach works best when the retainer itself is made of a good bearing material, such as phenolic or bronze.
- In reducing the contact area, the pocket clearance must not be increased, else axial vibration and other excursions will be induced, particularly when heavier machined metallic retainers are used.
- Tight pockets or other design features that restrict the balls are more prone to retainer whirl and should be avoided.
- Square-pocket retainers reduce the contact area to a minimum yet inhibit excursions in any direction (within the standard clearances built into the pockets). In square-hole retainers, no retainer whirl or adverse torque effect was noted in any test so far.

Griffiths also notes that the whirl or squeal frequency is semi-independent of rotation speed. Once a severe whirl mode has been established, the power can be shut off and whirl will continue at the same frequency during most of the coast-down to a stop.

Whirl seemed to occur most often at one or two full harmonic frequencies, but Griffiths was unable to find a predictable relationship.

Which Bearing and Why?

Arnold O. DeHart

The machine designer is faced by a formidable and seemingly endless array of bearing types from which to make a selection that he hopes will do the job in a finished machine. Most of the time, the selection is made the easy way—by choosing from the particular catalogs which happen to be handy in his files. Following this course, he may or may not make the best choice; in any rational design all factors should be weighed before the final selection is made. Rather than competing, each bearing has its own particular advantages and disadvantages and the selection will often be a compromise.

In order to help the designer in this dilemma, a survey of the pertinent selection factors is given in Table 1. This table should help to determine "which" bearing. An examination of the construction and some of the operation features of the bearings should determine the "why".

ROLLING-CONTACT BEARINGS

The term "rolling contact" or "rolling element" is more descriptive than the popular term "antifriction" bearing. True, the starting friction of rolling-contact bearings may be considerably less than the usual hydrodynamic-

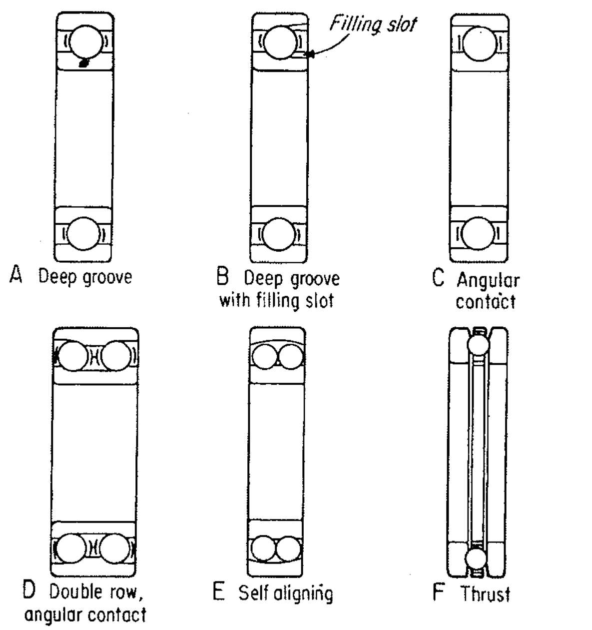

1. BALL BEARINGS with standard deep groove (A) are most versatile. Extra balls (B) increase radial load capacity at expense of high-speed performance and thrust-load capacity. Good thrust- and radial-load performance is given by angular contact design (C). Most high-speed and precision spindles use axially preloaded pairs of these bearings, but the double-row type (D) is simpler to use—preload is built-in at factory. Self-aligning design (E) tolerates much misalignment of housing and shaft but load capacity is reduced due to the high contact stresses that result from the large difference in curvature between the balls and the outer race. The thrust ball bearing, (F), is adaptable to large thrust loads that have almost no radial component. Very large sizes of this bearing are used in gun turrets and large earth moving machinery.

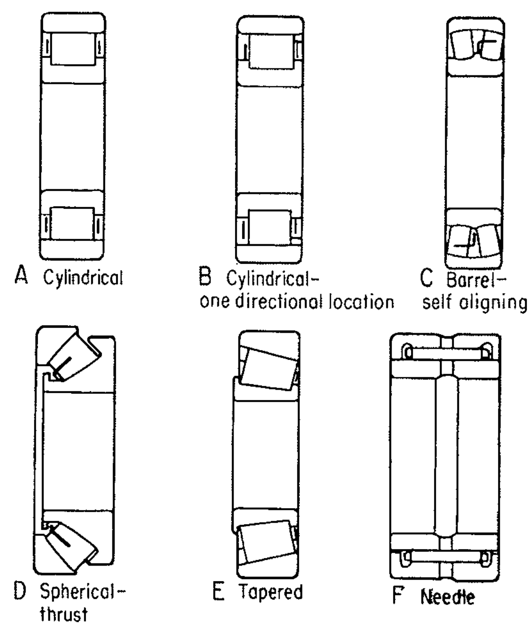

2. ROLLER BEARINGS can support greater loads than ball bearings but are not as versatile as the ball bearing. Cylindrical bearing (A) takes only radial load and permits some axial motion of shaft. Shoulders (B) let bearing withstand light axial loading. Sperical bearing (C) is self-aligning without loss of load capacity. It is best for low-speed use. Barrel-shaped roller in thrust bearing (D) takes large loads with reasonable mis-alignment but available sizes are large. Tapered type (E), usually mounted in pairs, is available in a full range of sizes. Needle bearing (F) takes less space than a standard roller bearing, and where necessary, the needles can be run directly between a hardened shaft and housing. Skewing may be a problem at high speeds, when a separator is used with some loss of load capacity.

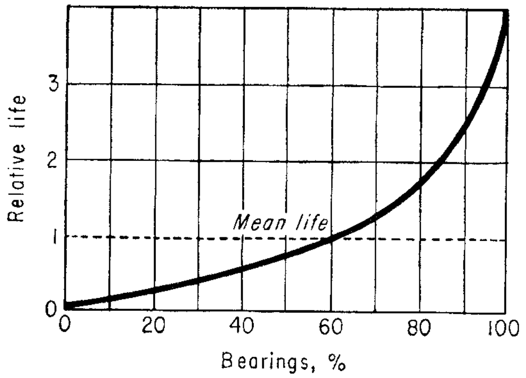

3. VARIATION OF FATIGUE LIFE OF BALL BEARINGS.

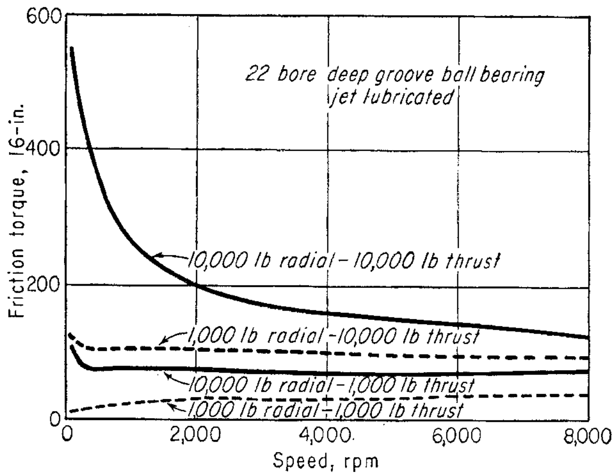

4. EXPERIMENTAL FRICTION-TORQUE CURVES for a ball bearing. These curves differ greatly from those given by the usual formulas. It was observed that changing the bearing geometry, method of lubrication, or separator design can affect the friction markedly. The abrupt drop in torque as the speed increases is probably caused by the building up of a hydrodynamic lubricant film between the rolling elements and the races.

SYMBOLS

A = area, sq in.
A_E = effective area, sq in.
b = width of flow path, in.
c = radial clearance, in.
e = eccentricity, in.
F = friction force, lb
f_S = coefficient of sliding friction
h = film thickness, in.
L = length, in direction of flow, in.
p_O = supply pressure, psi
p = pressure, psi
V = velocity, in. per sec
W = force, lb
ϵ = eccentricity ratio
μ = coefficient of absolute viscosity, lb-sec/sq in.

type bearing; but running friction of these two types is often comparable—the relative values being dependent upon the design and application. And, of course, externally pressurized bearings can be made such that the friction approaches zero as the relative velocity approaches zero. Rolling-contact bearings certainly reduce friction, but they merit the term "antifriction" no more than many other types. Two main types of rolling-contact bearing, ball and roller, are discussed in Figs. 1 and 2.

Bearing Life

The life of rolling-contact bearings is usually limited by fatigue. The actual load-carrying area of the rolling elements is small so that the unit pressures are high. For example, the contact area between a ¾-in.-dia ball and a flat plate may be calculated to be only about 0.00015 sq in. when the force pushing them together is 22 lb. Under these conditions, the maximum calculated compressive stress is 200,000 psi.

What death and taxes are to man, fatigue is to rolling-contact bearings. If a large group of bearings are run until failure and the distribution function of their lives plotted, the curve looks somewhat like Fig. 3. When a bearing is installed in a machine, no one knows where on the curve it lies—the possibility of an early failure is most disturbing. Bearing manufacturers are greatly concerned about early failures and have done considerable work to reduce them.

Rolling-contact-bearing load ratings are determined statistically with actual fatigue tests of a large number of bearings. Some bearing manufacturers give average bearing life, which is known as "B-50" life, while others use a figure called "B-10" life. The B-10 life rating is the life that 90 per cent of the bearings can be expected to exceed at the indicated load. The loads for bearing-life expectancy are listed by the manufacturers. They also give formulas for the calculation of life expectancies at load and speeds other than those which are listed. The manufacturers give much valuable information in their catalogs on proper bearing application and installation. A customer should read and follow the information published there. One manufacturer found that over 95% of all ball-bearing troubles were the result of defective mounting, improper operating conditions, and similar causes that could be detected by visual inspection of the bearing. The manufacturers' recommendations should not be taken lightly; they spend much time, money, and effort in accumulating the experience on which the catalog information is based.

There is one subject, however, on which little information is available—bearing friction. Don't overlook the data in Fig. 4.

Advantages of rolling-contact bearings are that they:

- Maintain accuracy.
- Are relatively insensitive to oil-flow interruption.
- Are insensitive to momentary overloads.
- Have low friction torque under moderate load.
- Can be used without external oil system.

Disadvantages are that they:

- Are large.
- Have low tolerance to dirt and abuse.

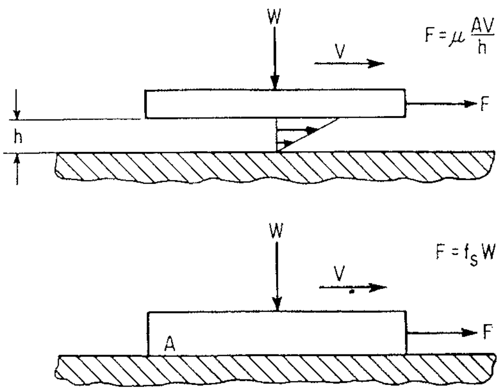

5. **LUBRICATED AND NONLUBRICATED SLIDING.**

Have high noise and vibration levels.
Have unpredictable life (of a single bearing).
Have low tolerance to large dynamic loads.
Are expensive.

Relative ratings based upon specific performance requirements are given in Table 1. This table will help the designer in selecting "which" bearing. Obviously, the large number of special type bearings precludes rating none but the more standard types, and it must be remembered that for a special application there may be bearings of specific design that circumvents the disadvantages of the standard designs.

FLUID-FILM BEARINGS

Fluid-film bearings—known variously as plain bearings, journal bearings, sleeve bearings, sliding bearings, etc.—are the most used and least understood of the bearing types. Viscous fluid friction is substituted for the rolling friction of the rolling-contact bearings or the sliding friction of non-lubricated bearings, Fig. 5. With a fully developed fluid film there is no contact between the parts that have relative motion; it follows that there can be no wear or sliding damage to the surfaces. With a Newtonian fluid, the friction force is given by

$$F = \mu (AV/h)$$

With dry friction, the force is a function of only the applied load and the coefficient of sliding friction

$$F = f_s W$$

Critical examination of these formulas shows that, contrary to popular conception, fluid-film friction can be higher, equal to, or less than dry sliding friction.

The load-carrying capacity of a hydrodynamic bearing is the integral over the effective bearing area of the fluid pressure acting to support the applied load. This pressure that acts to support the load can be generated within the bearing or can be supplied externally.

Self-pressurized Bearings

When the bearing generates its own load-carrying pressure, the methods of generation can be divided roughly

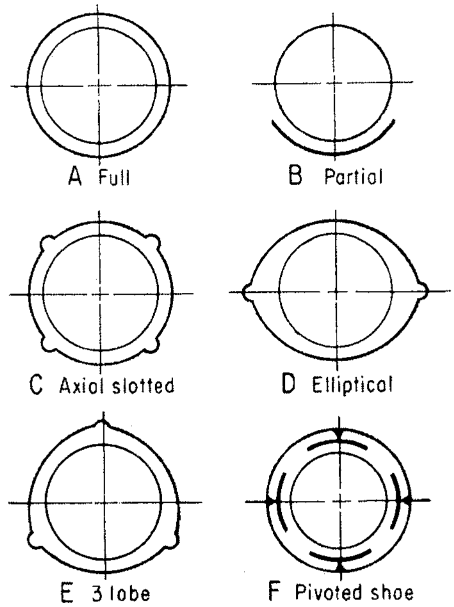

6. **FULL JOURNAL BEARING,** (A) often with an oil groove, is by far the most universally used bearing—today as much as in the day of the Roman chariots. Very high loads can be tolerated, and the bearing operates over a wide range of radial loads and speeds. When the load is nearly unidirectional and the speed is not high, the partial journal bearing (B) can be used. Both the full and the partial journal bearing are unstable at high speeds and light loads. Several designs have improved stability. In the order of increasing stability the bearings are axial slotted (C), elliptical (D), three-lobe (E), and pivoted-shoe bearing (F).

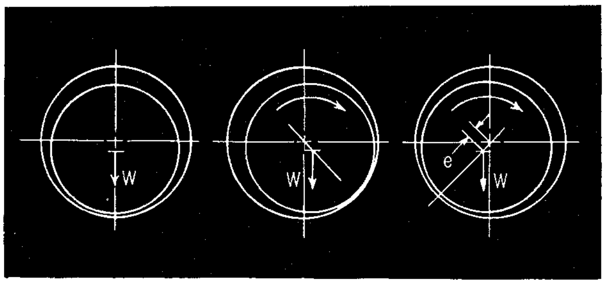

7. **JOURNAL-BEARING OPERATION.**

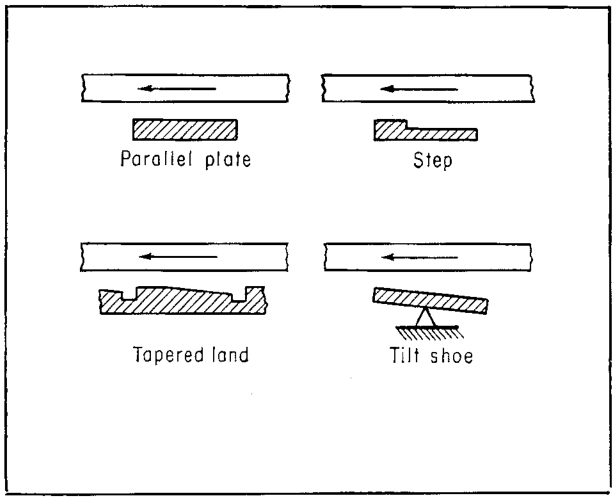

8. **TYPICAL THRUST-BEARING CONFIGURATIONS.**

Table 1-Selection factors for Bearings

Relative rating

- ■ good
- ◩ intermediate
- • poor
- ▬ none
- ☒ does not apply
- □ not available or known

Note: This table is only a general guide-ratings may change when considering special types or treatment

Selection factors	Bearing types: Ball						Roller						Journal						Thrust				External pressure [5]		Gas [5]	
	1a Deep groove	1b Deep groove-fill slot	1c Angular contact	1d 2-row angular contact	1e Self aligning	1f Thrust	2a Cylindrical	2b Cylindrical-locating	2c Barrel	2d Spherical thrust	2e Tapered	2f Needle	6a Full	6b Partial	Axial slotted	6d Elliptical	6e Three-lobed	6f Pivoted shoe	8a Parralel	8b Step	8c Tapered land	8d Tilt shoe	Capillary [6]	Variable flow dam [6]	Pneumostatic	Pneumodynamic
Low starting-friction	◩	◩	◩	◩	◩	◩	◩	◩	◩	◩	◩	◩	•	•	•	•	•	•	•	•	•	•	■	■	■	•
Low running-friction	◩	◩	◩	◩	◩	◩	◩	◩	◩	◩	◩	◩	◩	◩	◩	◩	◩	◩	•	◩	◩	◩	■	◩	■	■
Low noise	•	•	•	•	•	•	•	•	•	•	•	•	■	■	■	■	■	■	■	■	■	■	■	■	■	■
Small dia [1]	•	•	•	•	•	•	◩	◩	◩	◩	◩	■	■	■	■	■	■	◩	•	◩	◩	◩	◩	◩	•	•
Short length [1]	■	■	■	◩	■	■	■	■	■	■	■	◩	◩	◩	◩	◩	◩	◩	■	■	■	◩	◩	◩	•	•
High accuracy	◩	•	■	■	◩	◩	◩	◩	◩	◩	◩	◩	•	•	•	•	•	◩	•	•	•	•	■	■	■	•
Most available	■	■	■	■	■	■	■	■	■	◩	■	■	■	■	•	◩	•	•	■	•	◩	•	•	•	•	•
High radial load [2]	◩	◩	◩	◩	◩	▬	■	■	■	▬	■	▬	■	■	◩	◩	◩	◩	▬	▬	▬	▬	◩	◩	•	•
High thrust load [2]	◩	•	■	■	•	■	▬	•	◩	■	■	▬	▬	▬	▬	▬	▬	▬	•	■	■	■	◩	◩	•	•
High dynamic load [2]	◩	◩	◩	◩	◩	◩	■	■	■	■	■	■	■	◩	◩	◩	•	◩	■	◩	◩	◩	◩	◩	•	•
Tolerate misalignment	◩	◩	◩	•	■	◩	•	•	■	■	•	•	◩	◩	◩	◩	◩	■	◩	◩	◩	■	◩	◩	•	•
Tolerate dirt	◩	◩	◩	◩	◩	◩	◩	◩	◩	◩	◩	◩	■	■	■	■	■	■	■	■	■	■	•	◩	•	•
Low initial cost	◩	◩	◩	◩	◩	◩	◩	◩	◩	◩	◩	◩	■	■	■	◩	◩	•	■	■	■	•	•	•	•	◩
High speed	■	•	■	◩	◩	•	■	■	•	•	•	•	◩	◩	◩	■	■	■	•	■	■	■	■	◩	■	■
High temperature [3]	◩						◩						•												■	◩
Simple lube. system	■	■	■	■	■	■	■	■	■	■	■	■	◩	◩	◩	◩	◩	◩	◩	◩	◩	◩	•	•	•	■
High stability [4]	☒	☒	☒	☒	☒	☒	☒	☒	☒	☒	☒	☒	•	•	◩	■	■	■	■	■	■	■	■	◩	•	•
Easy for designer	■	■	■	■	■	■	■	■	■	■	■	■	■	■	◩	◩	◩	•	■	◩	◩	◩	•	•	•	•

[1] With a given load (raidial or thrust). [2] With a given size. [3] Above 450F. [4] Applies to high-speed fluid-film bearings. [5] Journal or thrust type. [6] Restrictor controlled (liquid).

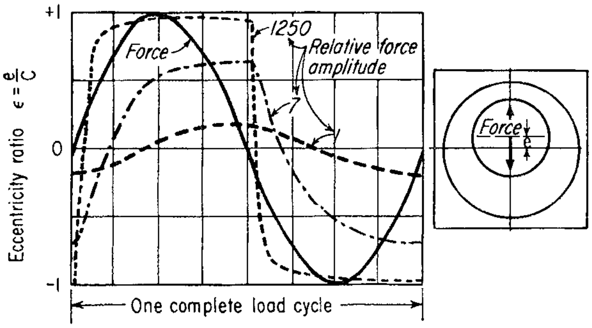

9. ECCENTRICITY RATIO of journal bearing with sinusoidal loading and no rotation.

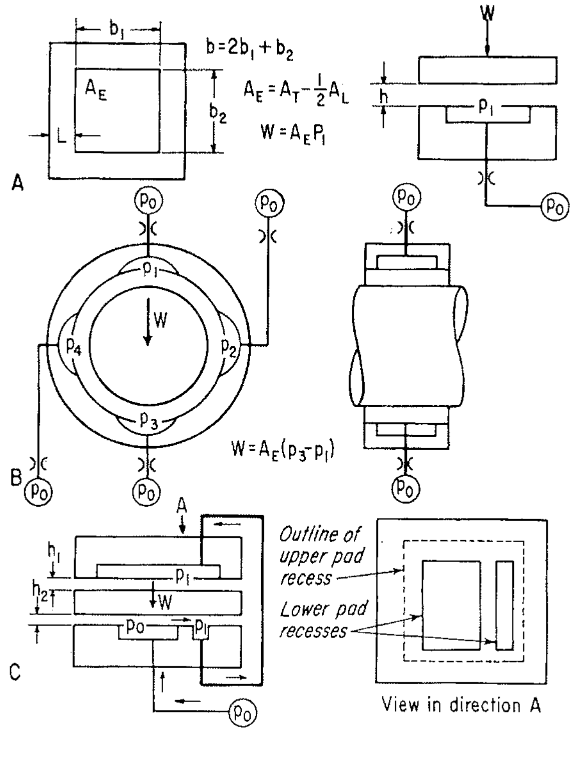

10. EXTERNALLY PRESSURIZED LOAD-LIFT BEARINGS.

as follows into two general classes: Geometry induced, load induced.

Geometry Induced. The most commonly used hydrodynamic bearing is the type in which fluid-film pressure is induced by the effect of geometry. In the journal bearing, the rotating shaft is slightly smaller than the bearings and the load causes it to move off center. This movement causes a converging section to be formed; which, owing to the viscous drag of the lubricant, induces a high-pressure region that supports the load. Journal bearings are generally not "off-the-shelf" items, so there is a wide variety of shapes and designs (probably as many as there are people who have designed bearings). A few of the many possible journal-bearing configurations are shown in Fig. 6.

The operation of a simple cylindrical journal bearing is shown in Fig. 7. When the bearing is at rest, the applied load causes the journal to rest on the bearing surface. When rotation of the journal starts, it first rolls on and then slides against the bearing with only boundary lubrication. Some bearings operate in this manner in service but they require special additives that form tenacious surface films and prevent excessive wear and damage. If possible, such operation is to be avoided. As the journal is driven faster, enough oil may be forced into the converging wedge formed by the clearance of the bearing to lift the journal from the bearing surface. Normal hydrodynamic operation with unidirectional loading now occurs.

Obviously, one of the most critical operating conditions is encountered during start. This is when the bearing wears and scores. Not only must the bearing material be selected to prevent scoring and galling, but attention must also be given to its fatigue resistance, corrosion resistance, and embedability. The selection of a bearing material is often a compromise.

In any complete bearing design, a heat balance must be made to determine whether the temperature rise is excessive. Practically any fluid may be (and probably has been) used for lubrication. The major requirement in a hydrodynamic bearing is that the fluid have sufficient viscosity to support the load. Gases, of course, have some viscosity.

At the moment, there is a great deal of interest in gas-lubricated bearings. Their main advantages are that the lubricant systems can be simpler and the high temperatures do not harm the lubricant. Owing to the lower viscosity, gas load-carrying capacity is less and clearances are smaller than for liquid lubricants–surface finish and geometry must be very good in order to have reasonable operation.

This also applies to the more conventional liquid-lubricated bearings. Equally important is the journal geometry. Quite often journals are found that are not as round as desired. Actual bearing tests have shown that, in highly loaded journal bearings, a repetitive out-of-roundness of only 50 microin. will increase the wear rate by a factor of 10.

The converging geometry that is so helpful in generating the load-carrying pressure in journal bearings is more difficult to obtain for thrust bearings. A great variety of different thrust-bearing geometries is used to produce the load-carrying fluid film. Fig. 8 shows some typical configurations which are commonly used to produce hydrodynamic load-carrying films. It should be noted that parallel thrust washers have no hydrodynamic load-carrying capacity and they rely on boundary lubrication or "thermal wedges" to support loads.

Load Induced. Bearings in this class have load-carrying capacity by virtue of the manner in which the load is applied. "Load-induced" load-capacity can persist only if there is a reversal of the load direction during the loading cycle. The load-carrying capacity arises because a finite amount of time is required to squeeze the fluid from between the two closely fitted surfaces. The fluid can be squeezed out rapidly when the clearance is large, but as the journal approaches the bearing, the thinner clearance space retards the escaping of the fluid and the film is stiffer. Relative motion of a bearing and journal is shown in Fig. 9. Obviously, with good geometry and surface finish, the load-carrying capacity becomes very high—much higher than for comparable unidirectionally loaded bearings.

While "load-induced" or dynamically loaded bearings can support extremely high loads, the bearing material is exposed to cyclic loading which may lead to fatigue failure. Materials then must be selected which have sufficient fatigue strength.

Externally Pressurized Bearings

The load-carrying ability of externally pressurized bearings is not dependent upon either the character of the load or the geometry of the bearing; but rather on an external source of fluid under pressure. This type of bearing has been limited to highly specialized applications but is now finding its way into everyday usage. Indeed, the next great advance in precision tools may be made with externally pressurized bearings. These bearings may take many forms and their application is limited only by imagination.

Their operation can be demonstrated by examination of two common types. A simple type of load lift is shown schematically in Fig. 10A. Assume that the movable plates cannot be tilted but can be displaced vertically. The product of the recess pressure p_1 and the effective area A_E, which is dependent upon the pressure distribution over the entire pad, must be equal to the applied load if the system is to be in static balance. A restriction in the supply line provides a pressure drop which is a function of the flow rate and permits the recess pressure to be lower than the supply pressure. When there is a pressure drop across the restrictor, there must be a flow from the bearing and the loaded member is lifted from the bearing—the amount of lift being proportional to the cube root of the flow rate. The motion of the loaded member is controlled by two restrictors in series; the first being the restrictor in the line and the second being formed between the loaded member and the lands of the bearing. The flow from the recess may be calculated as flow between parallel plates:

$$Q = (bh^3p_1)/(12L\mu)$$

With a fixed supply pressure p_0, the bearing performs like a spring; as the load is applied, the clearance h is reduced to carry the increased load. The bearing is able to carry the greater load because the smaller clearance reduces the flow through the restrictor—the lower the flow through the restrictor, the higher becomes the recess pressure. This action will continue with further increase in load until the member actually contacts the bearing lands and seals off the flow. The recess pressure then becomes equal to the supply pressure and the limit of load-carrying capacity is reached.

An arrangement often used for journal bearings is shown in Fig. 10B. Here, the pressure pads are used on opposite sides of the shaft and the resistance to radial motion of the shaft with load may be made large. In one application, a system was designed in which 20lb of radial force must be exerted to move a 2-in.-dia shaft 1 microin.

Small tubes or orifices are normally used to provide the hydraulic restriction. These restrictors are selected to provide a particular pressure drop at the flow required by the bearing. With the low flow rates encountered in close-clearance bearings, the restrictors become physically so small that plugging with dirt becomes a serious problem. For example, systems have been designed which use 0.004-in.-ID capillary tubing. There are, however, bearing-restrictor systems which minimize the dirt-clogging problem. Most of these function as the variable-dam restrictor shown in Fig. 10C. Here the flow restrictor is between the bearing and journal surfaces—opposite the pad which is being controlled. Another advantage is that the final restrictor design is not dependent upon the diameteral clearance in the bearing. With conventional capillary or orifice-type restrictors, the calculations must include the design clearance and (for critical application) restrictors can be calculated only after the parts have been manufactured and measured.

Advantages that should make pressurized bearings appeal to machine designers are:

Clearance is maintained regardless of speed. Since clearance is always maintained while the bearings are in operation, they do not wear out and bearing material selection ceases to be a problem. Furthermore, the running center of a workpiece is maintained when the part is stopped for gaging.

At zero velocity there is a zero friction. This relationship makes externally pressurized bearings uniquely suited for use in measuring systems and dynamometers. The nature of the viscous friction of externally pressurized bearings prevents "stick-slip" motion often encountered with machine ways.

The recessed areas reduce friction at high speeds. The friction varies directly with the speed, but since most of the friction occurs in the land area this torque is reduced as the land area is reduced.

Highly stable and vibration free. These features are reflected directly in the quality of the parts made on the machine tool.

They are easily designed. The performance characteristics can be readily determined from relatively simple published relationships. Many design variables give designers great freedom in gaining the performance characteristics which they desire.

The main disadvantage of externally pressurized bearing arises from the fact that an external supply of high-pressure fluid along with the usual pumps, filters, pressure regulators, and sumps must be furnished. These are not commercially manufactured items so they must be designed to fit the particular installation.

REFERENCE:

Which Bearing and Why? by Arnold O. DeHart, Senior Research Engineer, Research Laboratories, General Motors Corporation, Warren, Mich. Paper presented at the 1959 Design Engineering Conference, Philadelphia, Pa. Paper No. 59-MD-12.

Formula Found for Predicting the Reliable Like of Bearing

Designers and managing engineers who must make decisions quickly can now confidently predict the useful life of ball and roller bearings and certain electronic components, such as transistors.

Rolling bearings fail in service according to the Weibull distribution. The rated life is taken to be the life that 90% of the bearings will exceed—the L_{10} rating. Up to now, though, engineers have not been able to predict this rating with any confidence until they had a record of failures in a test sample of 30 or more bearing.

John I. McCool, an engineer at SKF Industries Research Laboratory, now shows that the L_{10} life in the Weibull distribution can be accurately projected once three bearings in a batch of 30 have failed. Engineers have noted this third failure, or x_3, but only as a preliminary indication, not as the basis for firm conclusions. Nobody knew statistically how close x_3 was to L_{10}.

Useful findings. McCool's procedure makes it possible to set confidence limits on L_{10} life. It can also quickly indicate significant differences in the L_{10} lives of two groups of bearings. To study the effect of a design change the designer can order tests of two groups of, say bearings, one with the old specifications and one with the new. Each group may contain 30 bearings, but after the third failure the designer can recognize a trend.

The Weibull distribution. For a large number of items (such as bearing and transistors) and failure modes, the fraction F(x) that fails with a life less than x can be expressed by $F(x) = 1 - e^{(-x/\eta)^{\beta}}$ (Eq. 1), where η = scale parameter or characteristic life. And β = shape parameter or Weibull slope.

These two parameters are generally unknown but are presumed to be constant for a particular set of service conditions. Normally these values can be estimated from endurance test results. The 90% reliable life L_{10} is found in terms of η and β by letting $x = L_{10}$ and $F(x) = 0.10$ in eq 1. This gives, $L_{10} = \eta \cdot \left(\log \frac{1}{0.90}\right)^{1/\beta}$

Using x_3 to estimate L_{10} means dispensing with finding η and β. On the average, x_3 will slightly underestimate L_{10} by an amount that depends somewhat on β. Table I shows the factors by which x_3 should be multiplied to give an unbiased estimate of L_{10}.

These factors show that it is not important to know β precisely to estimate L_{10}.

It is shown below, however, that β needs to be known to get confidence limits for L_{10}. A good standard range to use β for rolling bearings is 1.0 to 1.9.

Confidence limits. However, before the engineer uses any statistical estimator, he has to know how often he will be right in his calculations. Table II shows factors for setting confidence limits on L_{10} life.

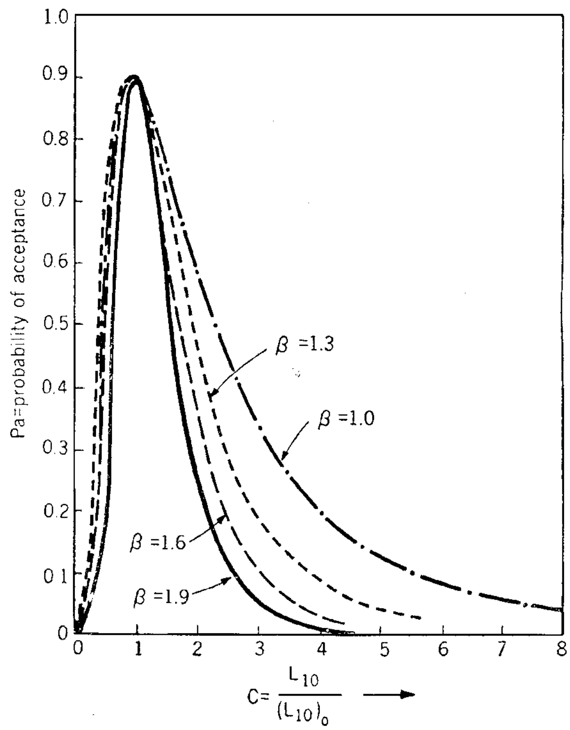

Discriminating ability of test for a specified L_{10} value, 10% significance level, is shown in the graph above.

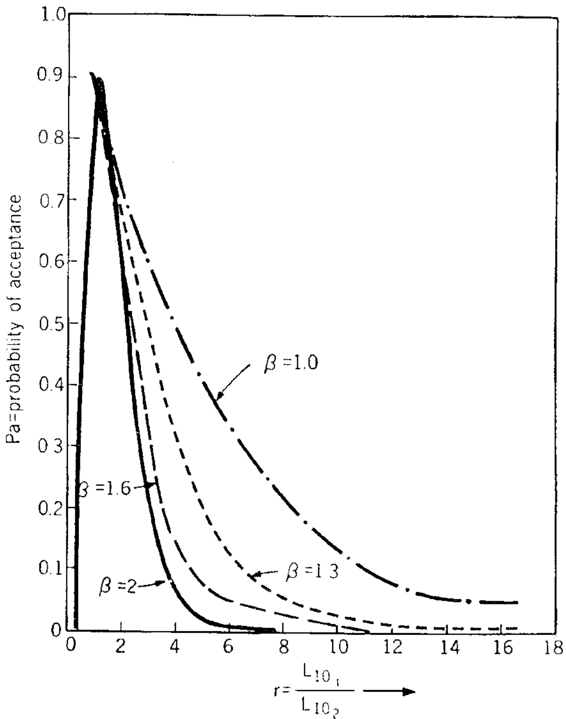

For equality of two L_{10} values—10% significance level—in comparative testing, the curves appear like this.

Rotary-Linear Bearings

Rotary-linear bearing can take a beating from heat and shock. New designs finds first use in steel converter, where heat cause expansion and shaft and jarring blows are applied.

A novel two-directional bearing designed especially for steelmaking equipment may find other uses where the loads are hot and heavy. In this design, a linear inclined bearing causes the bearing housing to roll over the roller bearings (sketch below, right) instead of sliding as in conventional designs.

Because of its demonstrated reliability, this assembly of pillow block and bearing is already being used in steel mills throughout the country. It was designed by Carl L. Dellinger, an engineer with Norma-Hoffmann Bearings Corp., Stamford, Conn., to overcome problems of friction along with thermal expansion.

Hot, heavy load. The prime use of the new design is in the trunnion that supports a steel converter. When 250 tons of molten metal at 3200 F are poured into a converter during the making of steel, the trunnion bearings are subjected to severe punishment by the very hot, very heavy load. The shaft that supports the converter heats up and expands, causing the bearings to slide inside their housings.

The wear caused by this action is bad enough. It means additional power is needed to overcome friction when the shaft is rotated during oxygen lancing operations. Worse yet, however, is the fact that when the sliding surfaces start to gall, the bearing will seize.

One-sided. Only one of the pair of horizontal shafts supporting the converter is equipped with the new bearing assembly. This shaft and bearing take up the expansion. The other shaft is supported by a conventional trunnion bearing.

Both bearings are packed with a lithium-based grease that contains molydisulfide and special extreme-pressure additives to operate in the 200 F temperature inside the bearing. The grease is held in the housing by a Buna N seal that keeps out contaminants.

Heat and shock. As the shafts expand, the spherical roller bearing at the end of one shaft rolls over the enclosed and inclined linear-motion bearings. These linear bearings are tilted 20 deg. from the axis of the shaft center line. Dellinger found that if the lines normal to the roller axis are allowed to intersect above the shaft center line, the housing can withstand greater torsional loads.

In the converter, severe torsional loads are produced during de-sculling operations (knocking out the cooled metal that adheres to the inside of the vessel after steel has been poured out). To remove this encrustation, the converter is rotated until it hits the base plate with the jarring impact of a truck hitting a brick wall. This shock load dislodges the steel, but it punishes the support bearings.

According to Riza E. Murteza,

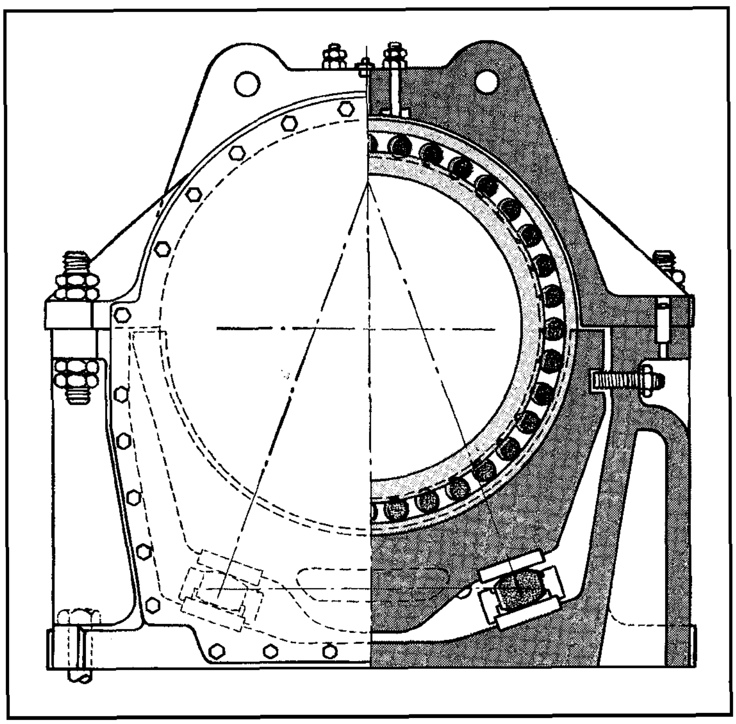

Spherical and linear motion bearings are contained in a sealed housing. The linear bearings are inclined for stability under torsional loading.

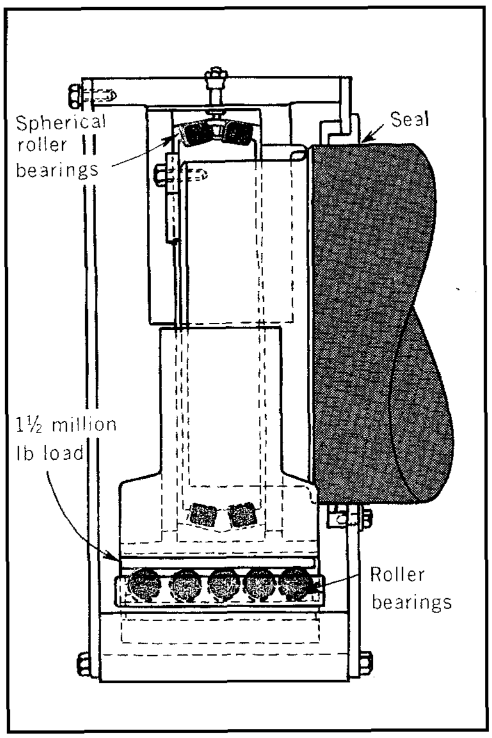

Linear roller bearings take up thermal expansion of shaft and housing, to eliminate sliding.

SECTION 9

LOCKING & CLAMPING

Various Methods of Locking Threaded Members

Locking devises can generally be classified as either form or jam locking. Form locking units utilize mechanical interference or parts whereas the jam type depends on friction developed between the threaded elements. Thus their performance is a function of the torque required to tighten them. Both types are illustrated below.

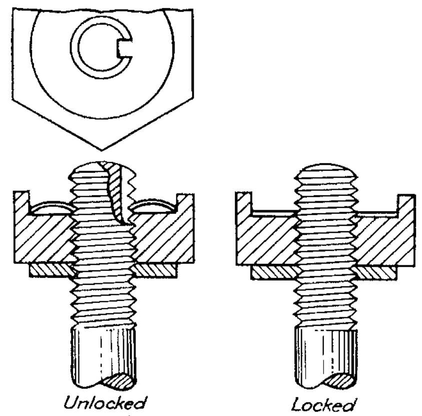

Disk Type Spring

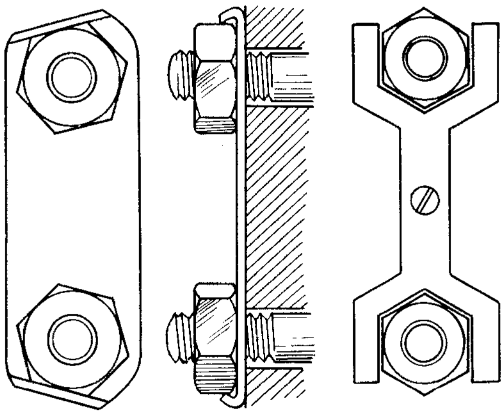
Double Formed Elements

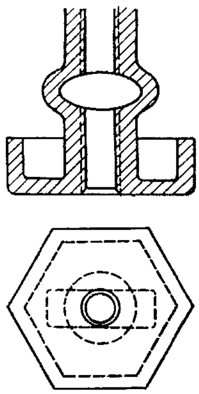
Sheet Metal Nut

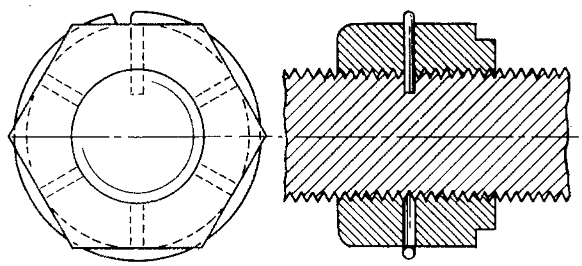
Spring Clip

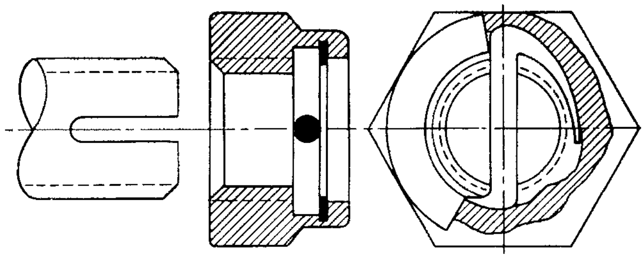
Ratchet Type Nut

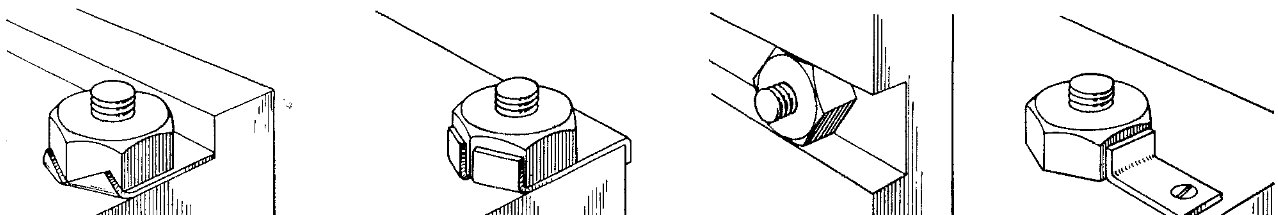
Formed Elements

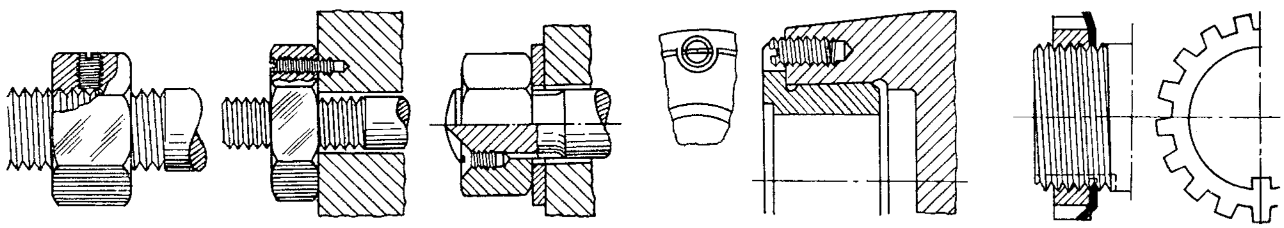

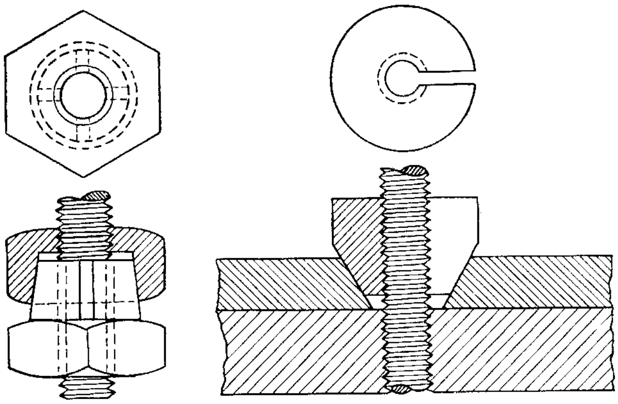

Wedge Action

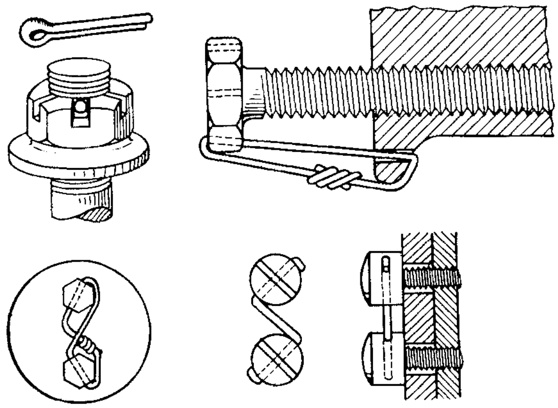

Cotters and Safety Wire

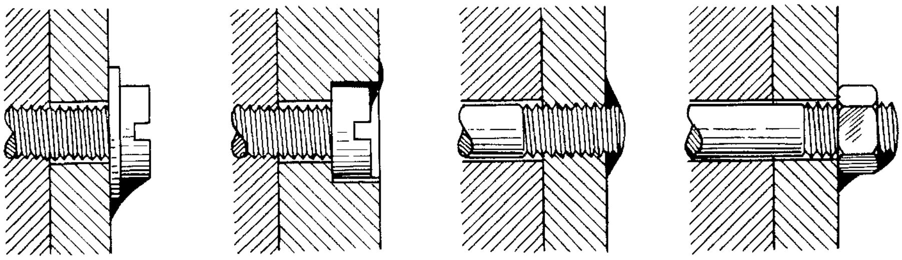

Cement or Solder

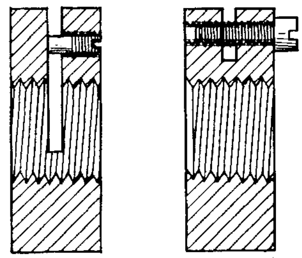

Split Nuts

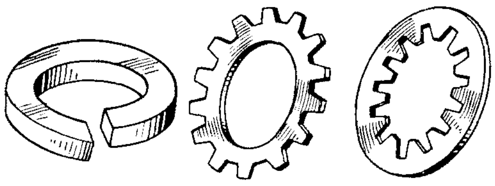

Spring Lock Washers

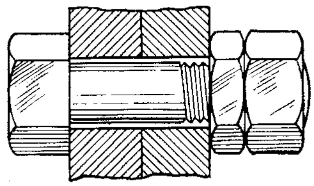

Jam Nuts

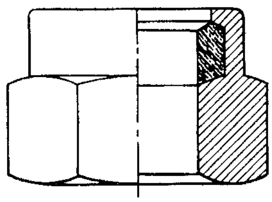

Fiber Inserts

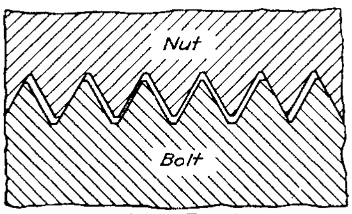

Off-Angle Thread

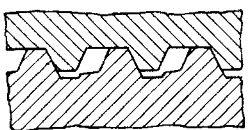

Dardelet (Unlocked)

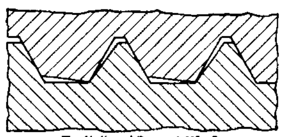

The National Screw & Mfg. Co.
Lock-Thred

Self-Locking Threads

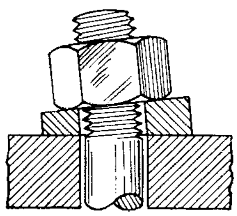

Tapered Washer

Locking-Type Indexing Fingers

These fingers are required in jigs and fixtures, dividing heads, chucks and dial-feed tables to hold parts securely but temporarily in precise relationship.

Federico Strasser

In any indexing device, there are at least three basic parts: a plunger (key, gage, male or movable part), a bushing (female or stationary hole) and a guide for the male part. In the majority of cases, there is also a spring and sometimes also a housing (body).

The actual design of an indexing device varies enormously from one application to the next, and is influenced by several factors—accuracy, production rate and function.

Classification

The basic form of the indexing gage depends primarily upon the kind of immobilization required. Thus, there are three main groups:

1. Locking. The indexing finger must be made inactive positively when the movable member must pass to the next position

2. Automatic bi-directional. The index finger is retracted (lifted) by itself when a certain pre-established load is applied

3. Automatic uni-directional. The same arrangement as in (2) but with the limitation that the mechanism-component may be moved only in one direction (it is locked in the opposite direction)

The shape of the indexing finger may be (in increasing order of accuracy):

1. Steel balls
2. Cylindrical plungers with:
   - semi-spherical point
   - 90° degree taper point
   - cylindrical point
   - tapered point (about 10-20°)

For flat indexing gages, either parallel or tapered points are used, with the tapered design preferred.

Removable indexing keys

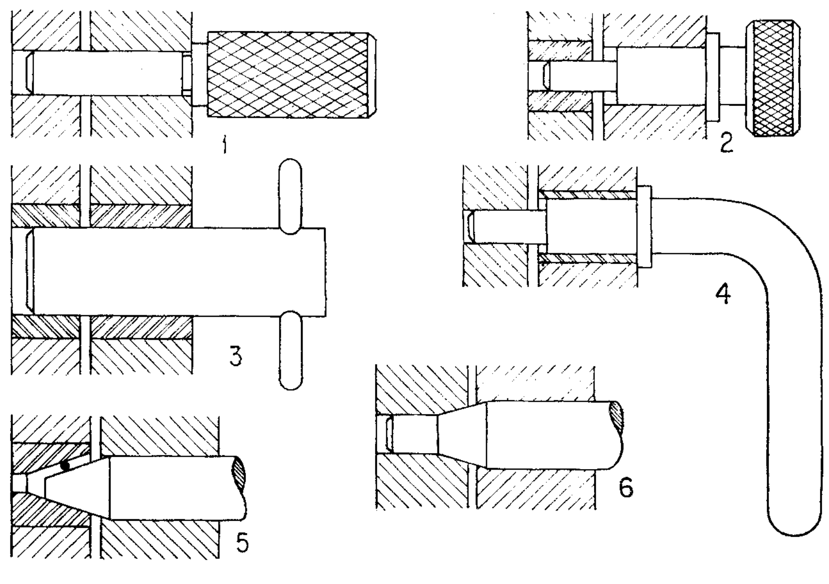

Indexing fingers are usually made from case-hardened steel, and the aligning surfaces must be ground after heat-treatment.

Design principles for numerous indexing devices are given.

Removable indexing keys

These keys offer the advantage of low tooling costs but are slow in use. First, they must be inserted manually before the machining operation. After the operation is completed, the keys must be withdrawn, the work moved to the next station and keys re-inserted.

The simplest design consists of a round plug, provided with a handle (preferably knurled). The cylindrical part is a slip fit in reamed holes in the stationary and the movable member, Fig. 1.

When the two members are not of the same diameter (Fig. 2), the key is stepped

If the mechanism members to be aligned are comparatively soft, it is good practice to use a hardened and ground steel bushing for guiding the indexing gage, increasing accuracy and life. The bushing may be used in either of the toolmembers (Figs. 2 and 4) or in both of them (Fig. 3), according to conditions.

Indexing plungers over 1 in. dia should be hollow, Fig. 3. In this case the handle is a pin put through the head of the gage. Another design consists of bending the protruding part of the gage, (Fig. 4), to 90°, to make a handle. This design is preferred in case of small diameters.

Misalignment

Although cylindrical holes are commonly used for aligning purposes, sometimes toolmakers prefer tapered holes and gages. This design is somewhat objectionable, because any dirt or foreign matter on the gaging surfaces will change the accuracy of alignment, Fig. 5.

The best solution of this problem, but expensive, is a combination of cylindrical and tapered gage ends. In this case, the maximal error (if any) may be only the allowance between the cylindrical hole diameter and the diameter of the cylindrical gage-end, Fig. 6.

Non-removable indexing fingers

These non-removable indexing fingers are preferred for high production tools. In their simplest form the plungers are actuated by a compression spring. For release the plunger is usually pulled out of its seat by means of a suitable handle, which may have any reasonable form, Fig. 7.

If the tool member is thin or soft, the plunger-housing is made as a separate item and a press fit, Fig. 8.

Fig. 9 shows a round indexing gage with a rectangular indexing point. In this case, the shaft must be guided, (prevented from turning radially) while longitudinal movement is effected freely. Therefore, a retaining pin operates in a slot in the housing.

The same indexing task is solved with a flat index gage, Fig. 10. Here a slide is moved in and out by means of a handle.

In the case of movable fixtures (those mounted on lathe faceplates) it is necessary to avoid accidents. For such cases the handle is made in the form of a sleeve (Fig. 11). This design offers another advantage: If the indexing point is too tight in its seat, the gage must be loosened before it can be pulled out. This separation is obviously easier to effect with a large knurled handle bushing than with a mere knob. Furthermore, mounting of the housing is made by means of a threaded portion; however, alignment is insured by means of the shoulder.

In another case (Fig. 12) the housing has a large flange, which is screwed to the body.

The plunger is not always mounted on the interior of the mechanism. If it is mounted from the outside, a threaded, knurled bushing holds the plunger in place. See Fig. 13. Now, the index finger may be removed without dismantling other tool members.

If the index finger is mounted in a part that is too large for axial actuation, the motion may be effected by means of lateral pins (Fig. 14).

The plunger is not always pulled out of the tool-member for making the indexing inactive; sometimes it is pushed in, Fig. 15 Here the bent gage is guided.

Non-removable indexing fingers

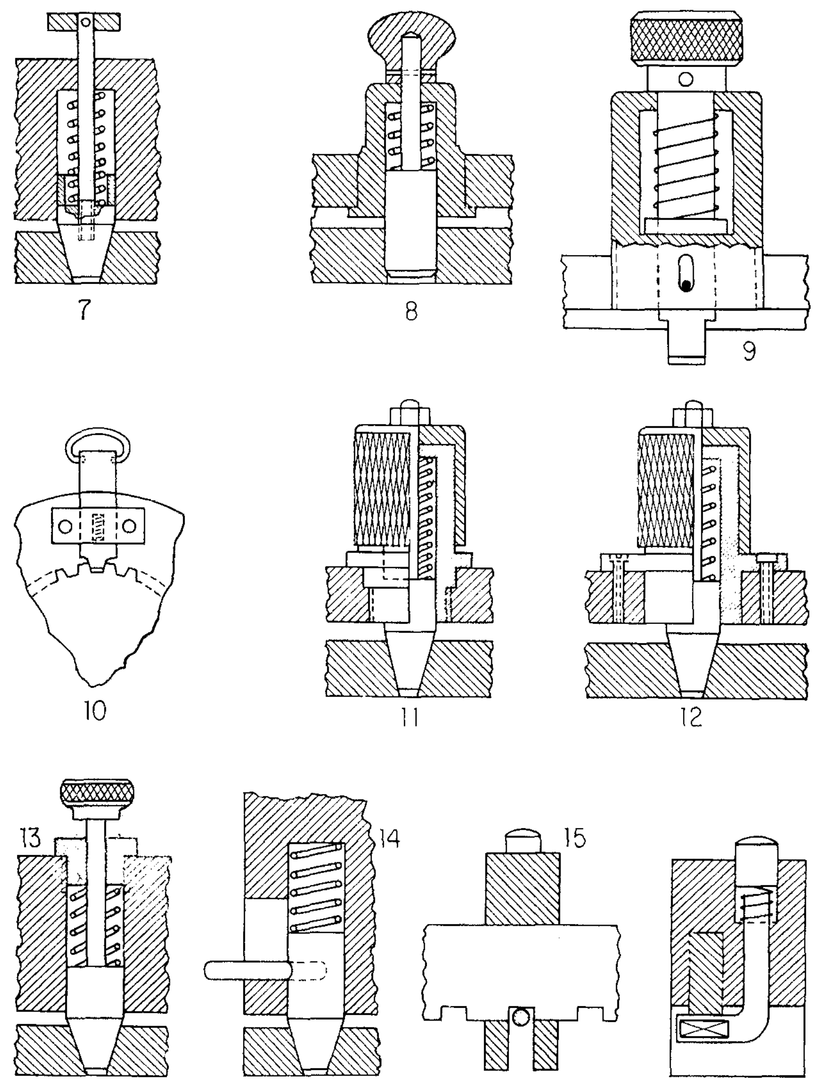

Some indexing fingers must be actuated indirectly; others require a rest position so that the operator need not hold onto them. Here are 14 designs.

Federico Strasser

Removable and non-removable indexing fingers (**AM**—Nov 21, '66, p139) are commonly actuated directly: that is, co-axially with the indexing point. But there are several designs of fingers which are pivoted and indirectly actuated. In such cases the spring may not be co-axial with the indexing plunger. Then, the spring will be located outside of the device, especially when the finger is not round. Here are several examples:

In Fig. 16, the indexing finger consists of a tapered detent on a ball-handled lever. Normally the detent lies in the part to be indexed, being held there by a spring- backed pin. When the lever is pulled up, the mechanism can be indexed.

In the remaining designs, Fig. 17 to 21, the actuating lever is pushed manually or hydraulically to retract the index finger.

To keep out of trouble in such applications, try to foresee potential sources of erratic behavior. For example, in both Figs. 16 and 17, the tool engineer will specify an arc-like pivoting movement of the indexing point to avoid impairing the alignment.

Sometimes the actuating lever is pushed instead of pulled, as in Figs. 18 and 19. Or indirect action may be secured by a handle-operated plunger that is backed by a spring, Fig. 20. When the handle is pushed down, the detent will be lifted out of engagement with the part to be indexed, and when the handle is released the spring will hold the detent in the next notch.

Remote or automatic control can be achieved by hydraulic oil or compressed air. The fluid enters a cylinder and pushes upward a piston connected through a stuffing box to the plunger. When the fluid is released, the spring depresses the plunger, as shown in Fig. 21.

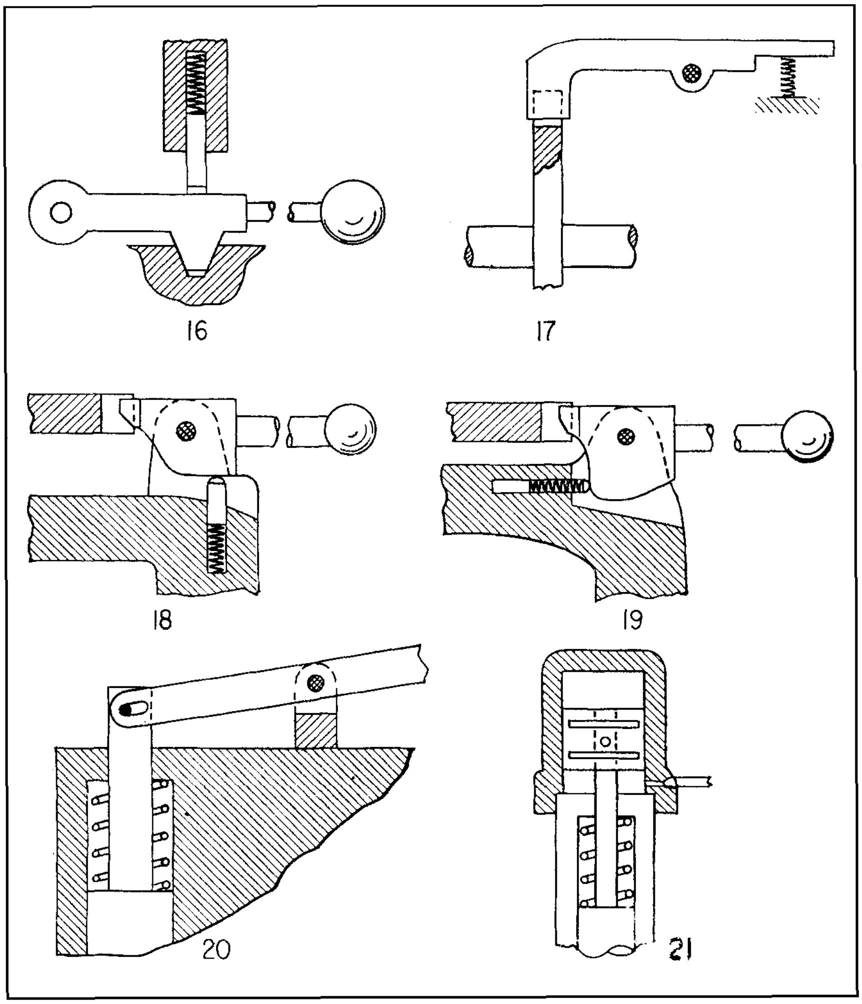

Indexing fingers with rests

So far, the indexing fingers must be held out of engagement by the operator. Sometimes, this is inconvenient or tiring. Therefore a mechanical means of disengaging the finger may be required. There are many ways to accomplish this. Eight examples are shown on page 297.

A very common method is to mill a slot in housing for the finger and drive a pin into a blind hole drilled in the plunger shaft. The pin ordinarily lies in the slot. When the indexing finger is to be made inactive, the knob is pulled out, rotated say 90°, and let go. Now the pin rests on the top of the housing and the plunger can't engage the indexing notch, Fig. 22.

Two other ways of accomplishing the same objective are shown in Fig. 23 and 24. Here the pin engages an appropriate hole drilled to the proper depth

A bayonet lock is always an easy device to use and it's positive. The sleeve handle, Fig. 25, has the bayonet slot cut in it, and a pin is fitted to the housing. This type of finger is engaged or disengaged with a twist of the wrist.

Safe locking of the index finger can be obtained by engaging a spring-backed steel ball into a spherical or notched recess. This design, Fig. 26, requires little effort.

A modification of the wedge idea is the use of a pin in a fast-helix groove. The plunger is prevented from turning, Fig. 27, by a setscrew.

In many cases, a simple eccentric cam (not shown) will lock and unlock the plunger. When a cam can't be placed on the housing head, use a "cam" that acts laterally. In this case a pin in the end of a shaft engages a slot in the plunger and lifts or lowers the latter as the actuating handle is moved.

Racks are a good means for operating heavy plungers. The rack can be cut directly into the plunger body, Fig. 28, while the pinion is operated by the handle.

Our last design, Fig. 29, works without the aid of a spring. In this case the plunger is guided and it is raised or lowered by the knob and screw. The screw is retained in the housing by a pin engaging a circumferential slot.

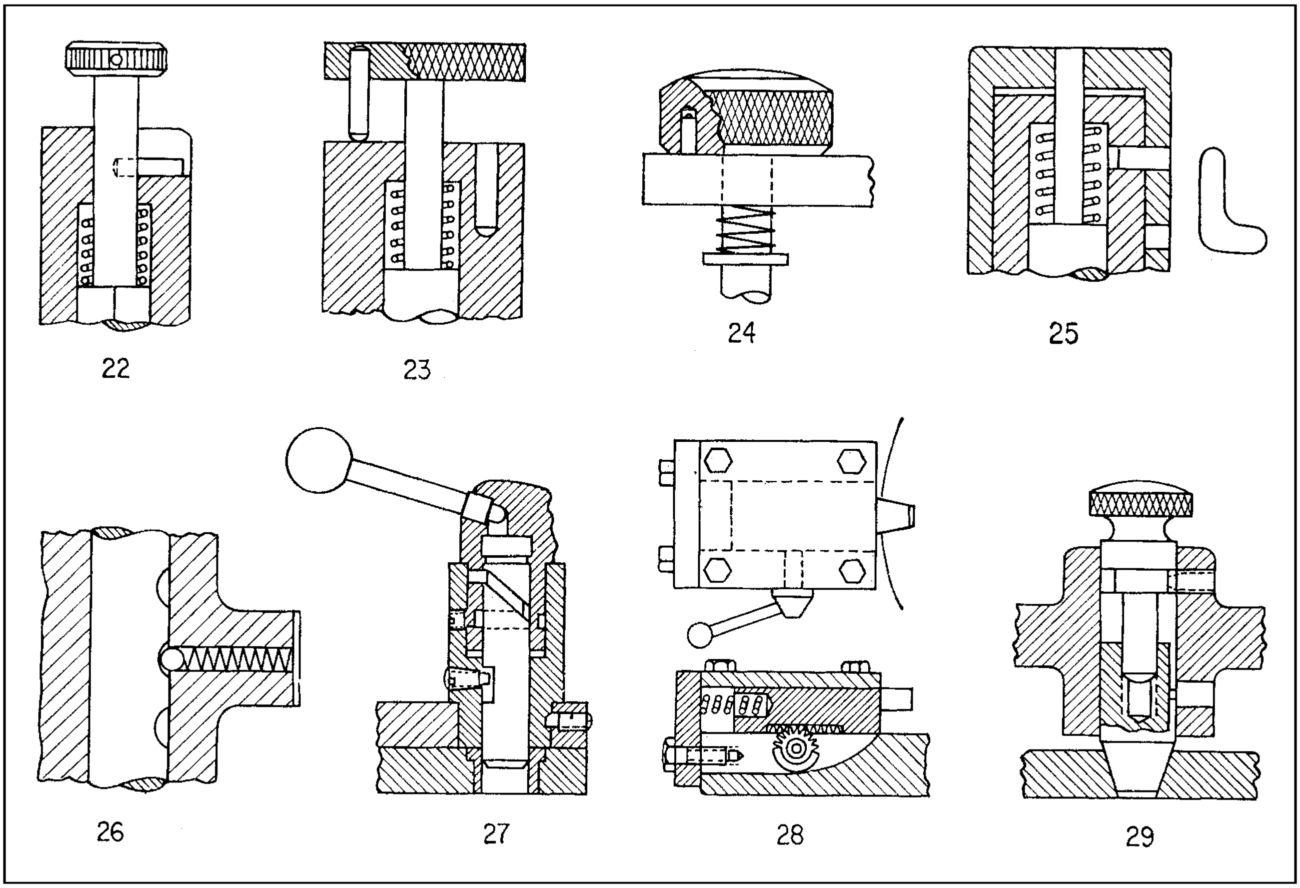

Eight indexing fingers with rest positions: 22—Pin in slot; 23—Pin enters hole in housing; 24—Pin enters knob; 25—Sleeve with bayonet lock; 26—Ball engages recess; 27—Pin in helical groove; 28—Rack-actuated slide and 29—Screw-operated finger

Retaining and Locking Detents

Many forms of detents are used for positioning gears, levers, belts, covers and similar parts. Most of these embody some form of spring in varying degrees of tension, the working end of the detent being hardened to prevent wear.

Adam Fredericks

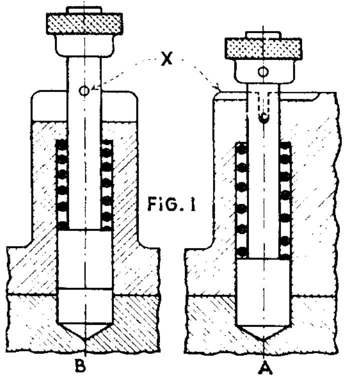

FIG. 1

Fig. 1—Driving plunger, shown in engagement at *A* is pulled out, and given a 90-deg. turn, pin *X* slipping into the shallow groove as shown at *B*, thus disengaging both members.

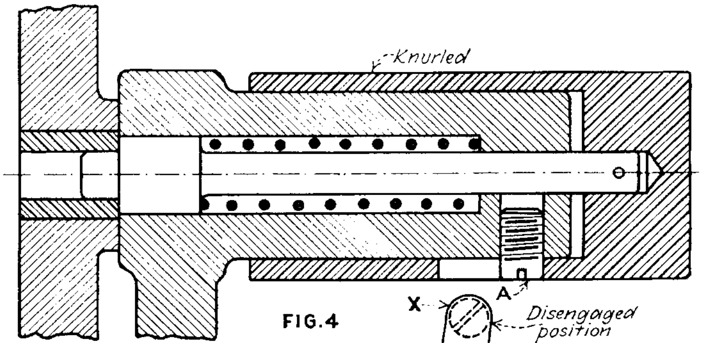

FIG. 4

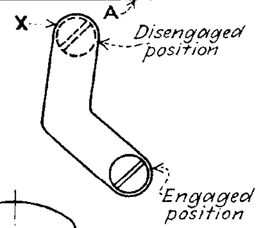

Fig. 4—The plunger is pinned to the knurled handle which is pulled out and twisted, the screw *A* dropping into the locked position at *X* in the bayonet slot.

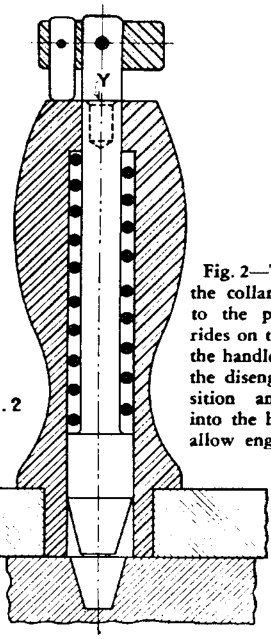

FIG. 2

Fig. 2—The pin in the collar attached to the plunger rides on the end of the handle when in the disengaged position and drops into the hole *Y* to allow engagement.

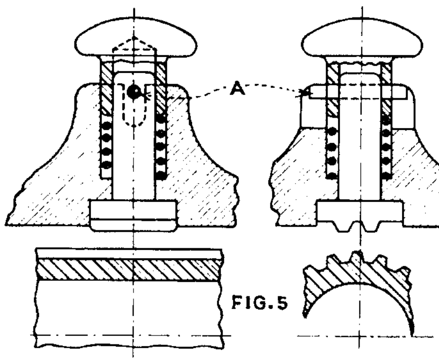

FIG. 5

Fig. 5—In this design, the pin *A* engaging in the slot prevents the plunger from turning. This detent is used as a temporary gear lock which is engaged for loosening a drawback rod through the gear.

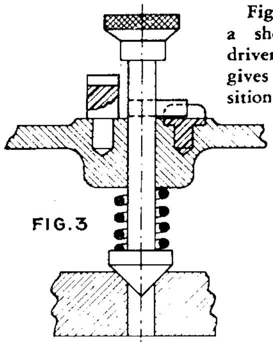

FIG. 3

Fig. 3—A long and a short slotted pin driven into the casting gives two plunger positions.

Fig. 6—An adjustable gear case cover lock. Pushing the door shut, it is automatically latched, while pulling out the knurled knob *A* disengages the latch.

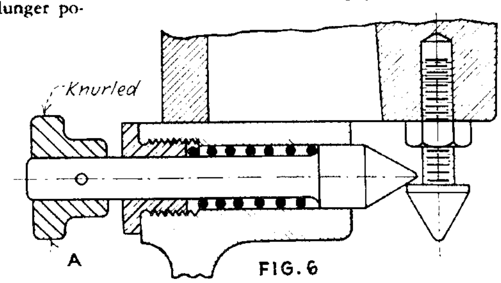

FIG. 6

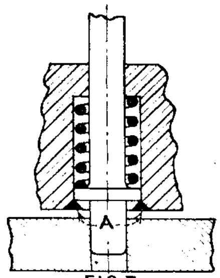

FIG. 7

Fig. 7—In this design the plunger is retained by staking or spinning over the hole at *A*.

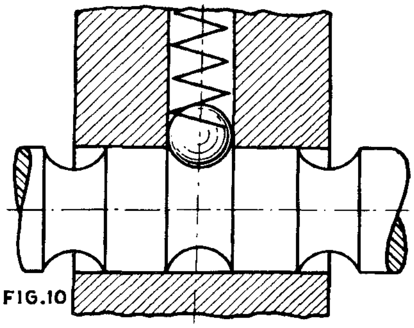

FIG.10

Fig. 10—Another form in which the grooves are cut all around the rod, which is then free to turn to any position.

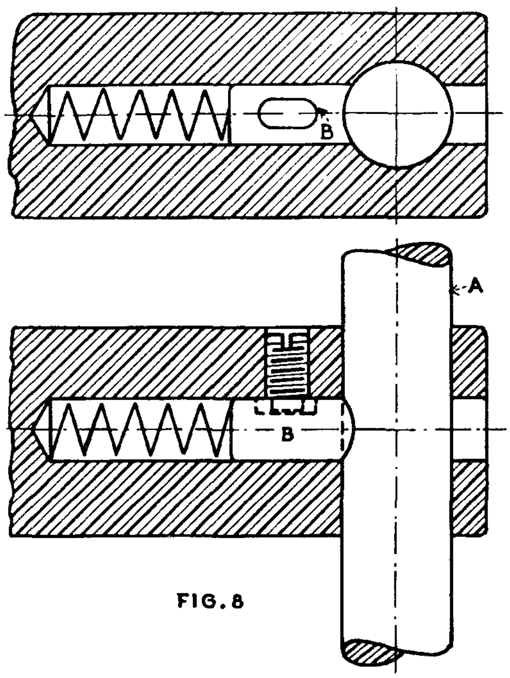

FIG.8

Fig. 8—End of the plunger *B* bearing against the hand lever *A* is concaved and prevented from turning by the dog point setscrew engaging the splined slot. Friction is the only thing that holds the adjustable hand lever *A* in position.

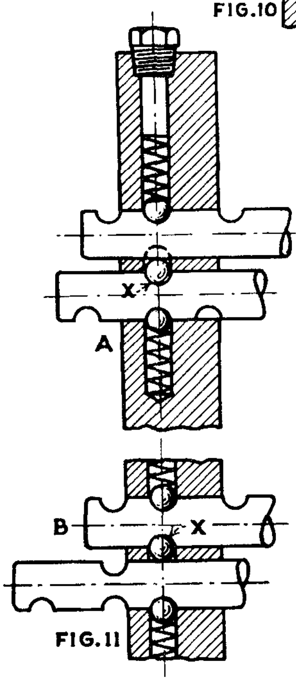

FIG.11

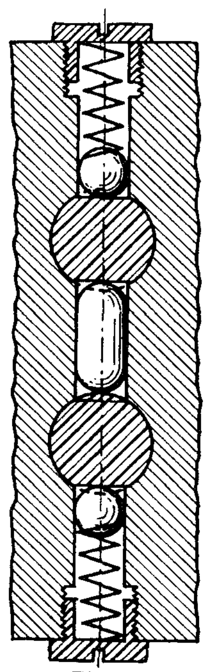

FIG.12

Figs. 11 and 12—Above is shown a double-locking device for gear shift yoke rods. At *A* the neutral position is shown with ball *X* free in the hole. At *B* the lower rod is shifted, forcing ball *X* upwards, retaining the upper rod in a neutral position. The lower rod must also be in neutral position before the upper rod can be moved. To the right is shown a similar design wherein a rod with hemispherical ends is used in place of ball *X*.

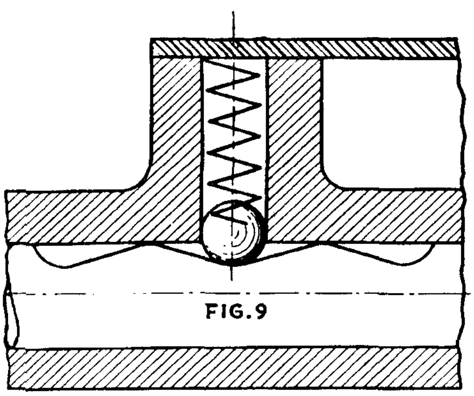

FIG.9

Fig. 9—A spring-backed steel ball makes a cheap but efficient detent, the grooves in the rod having a long, easy riding angle. For economy, rejected or undersized balls can be purchased from manufacturers.

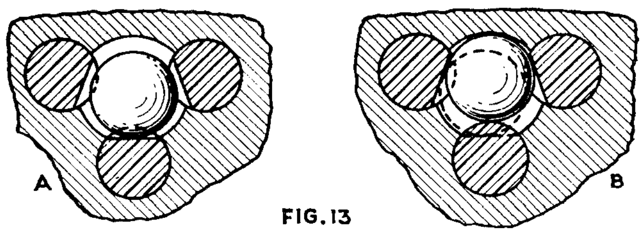

FIG.13

Fig. 13—Without using a spring of any kind, three gear-shifting rods are locked by a large steel ball. At *A*, the neutral position is shown. At *B*, the lower rod has been shifted, forcing the ball upwards, thereby locking the other two rods. The dashed circle shows the position of the ball when the right-hand rod has been shifted.

Snap Fasteners for Polyethylene

It's difficult to cement polyethylene parts together, so eliminate extra cost of separate fasteners with these snap-together designs.

Edger Burns

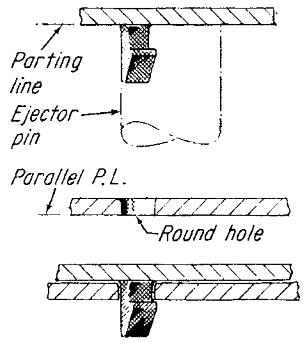

(a) Cored hole

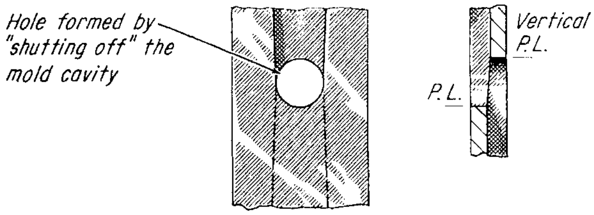

(b) "Shut-off" hole for female snap for different P.L.

1

EJECTOR-PIN of mold is cut to shape of snap. Ejected with the pin, the part is slid off the pin by the operator.

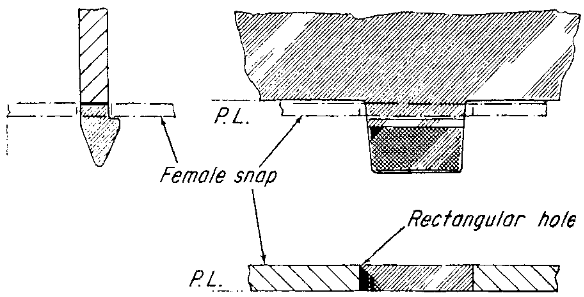

2

WALL-END SNAP is easier to remove from the mold than the ejector-pin snap. The best length for this snap is 1/4 to 1/2 in.

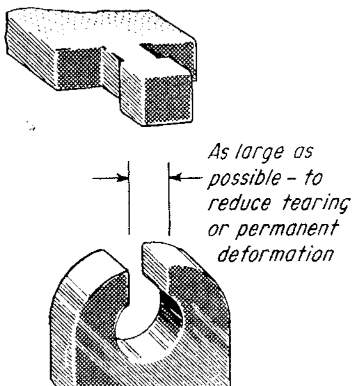

Open snap

5

OPEN SNAP relies on an undercut in the mold and on the ability of the polyethylene to deform and then spring back on ejection.

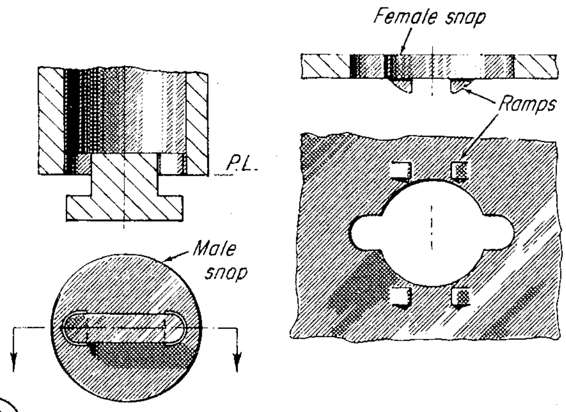

6

T SNAP locks with a 90-deg turn. To prevent this snap from working loose, four small ramps are added to the female part.

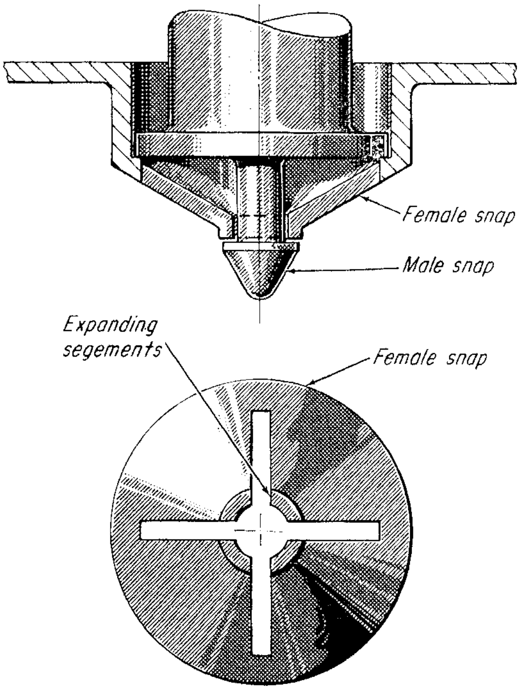

3 **SEGMENTED WALL** of female snap allows a large-headed male snap to enter easily. The snap can not be pulled apart with light loads.

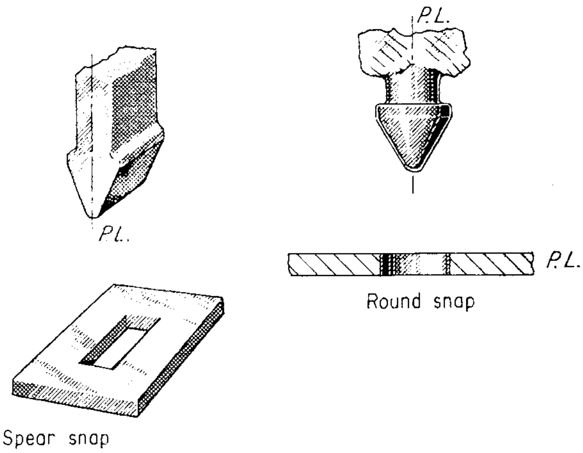

4 **SPEAR AND ROUND** snaps are similar in design to the wall-end snap, but are ideal for assembling small parts to larger ones.

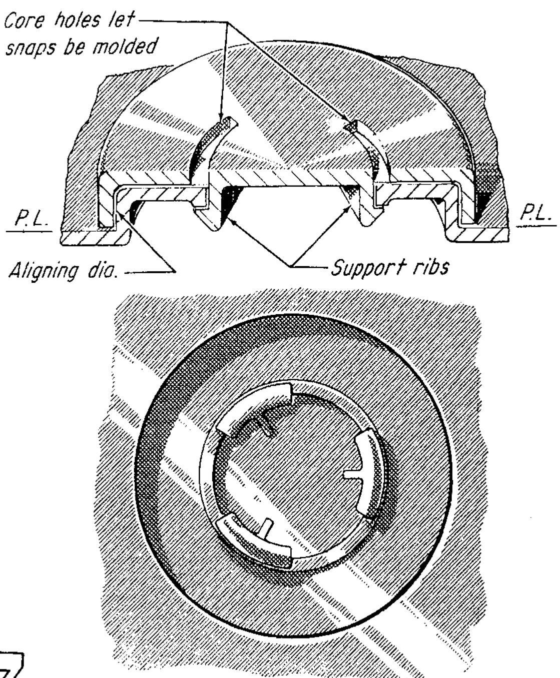

7 **ROTATING** parts can be snapped securely together with three (shown) or two snaps. Mostly for linear polyethylene, it's strong.

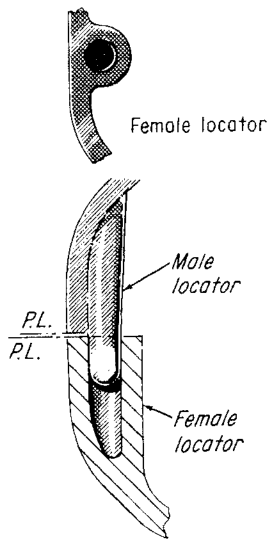

8 **LOCATORS** are not really snaps, but align parts for subsequent eyeleting or riveting or in conjunction with other snaps.

Snap Fasteners for Polystyrene

Here's a low-cost way to join injection-molded polystyrene parts without the use of separate fasteners or solvents.

Edger Burns

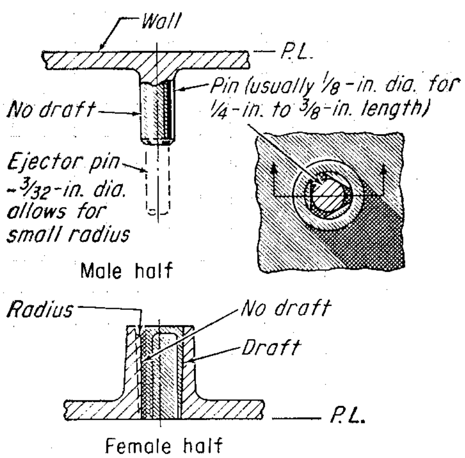

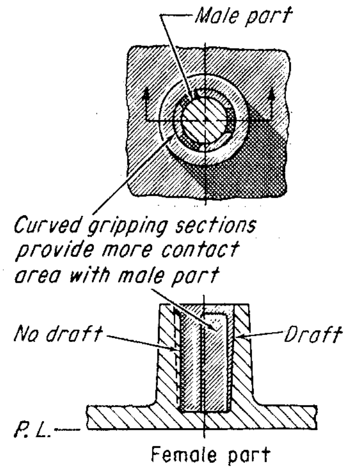

1

TRIANGULAR SNAPS actually depend upon friction, but are strong and easy to assemble. Space several around the parts to be joined. Grip can also be adjusted to suit.

2

CEMENTING SNAP will allow solvent cementing between the male and female members if required, although the snap will hold well without cement. Usually two or more such snaps are positioned around the parts to be joined. Male part is virtually the same as for the triangular snap. Blind, cored hole requires no shutoff.

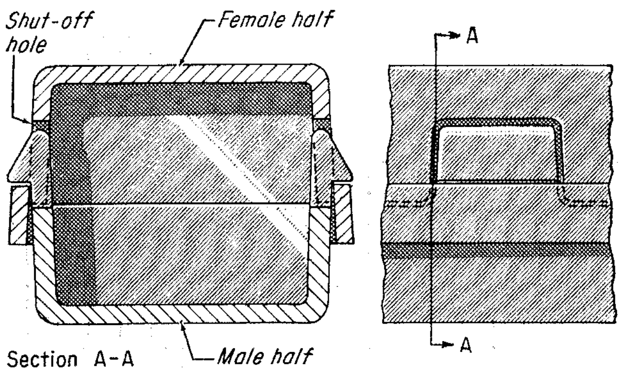

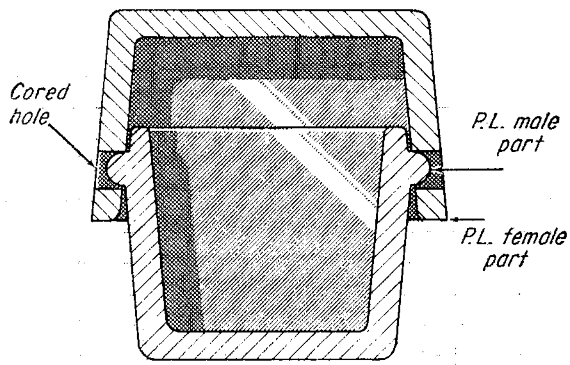

5

BOX SNAP requires a mold shutoff in the female half, large enough to accommodate the male part, which slips behind a shoulder and locks, as shown in the diagram.

6

DETENT SNAPS are ideal whenever a snap has to be frequently undone, and where a tight hold is not required. The detent itself can be a hemispherical bump, or a more elongated shape.

NOTE: *In the following illustrations, the parting line is marked "P.L." It is important in deciding which snap to use and how it should be molded.*

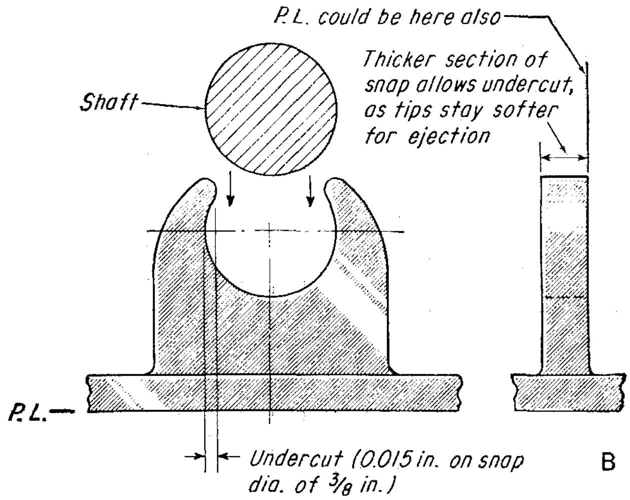

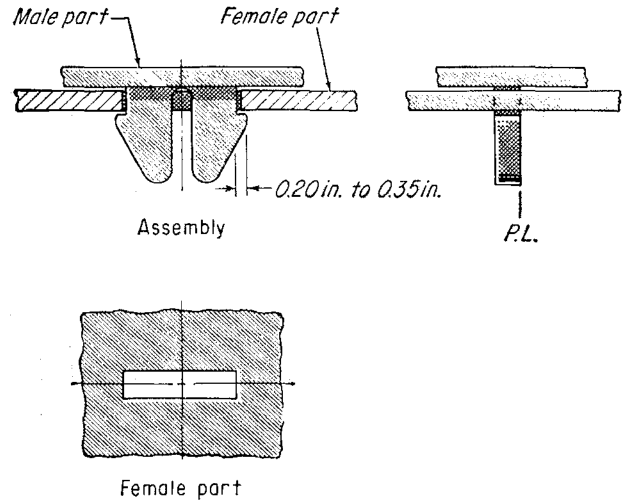

3

OPEN SNAPS have undercuts of about 0.015 in. on a total snap dia of 3/8 in. Despite small undercuts, stiff polystyrene gives good grip. This snap is not suitable for the regular nonimpact polystyrene. If the parting line can be arranged to lie in the other plane, as shown in B, ejection from the mold would be trouble free, thus avoiding excessive scrap.

4

PRONG SNAPS are ideal for snapping small parts onto a larger assembly. The male member is usually on the small part. Slot length in the female part must be designed for maximum holding power, without cracking the prongs on the male member.

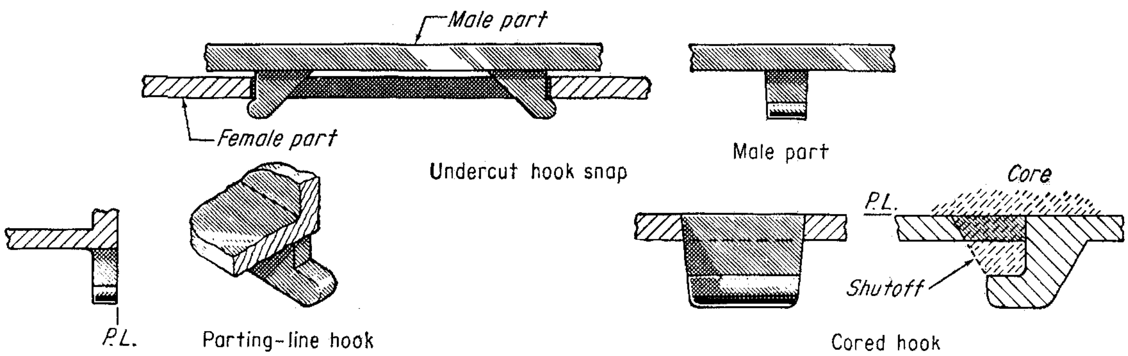

7

HOOK SNAPS. *Undercut hook* snap relies on an undercut in the mold. To prevent polystyrene breakage on ejection from the mold, make the hooks thicker than the other parts – they then retain more heat, stay softer. Since large undercuts cannot be made this way, however, this snap loosens quite easily.

Parting-line hook is much simpler to apply and is easier to design. Choose this snap whenever the parting line can be arranged to be in the plane shown on the drawing. It can be almost any strength and shape desired, and is simple to cut into the mold.

Cored hook requires a core to come down from the other half of the mold, which then produces the inside of the snap. This will leave a hole in the wall to which the hook is attached. Three shutoff surfaces are also required in the mold construction.

Snap-in Access Panels

These doors show in hinges or handles, need only finger holes or prying lips for positioning.

Frank Williams Wood JR

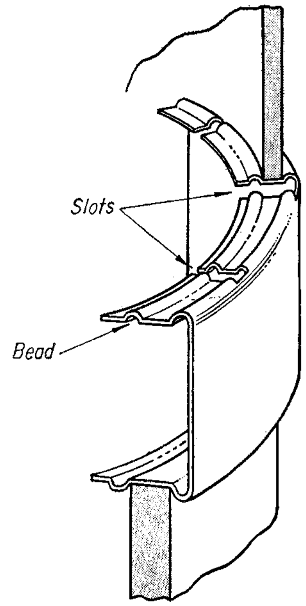

1

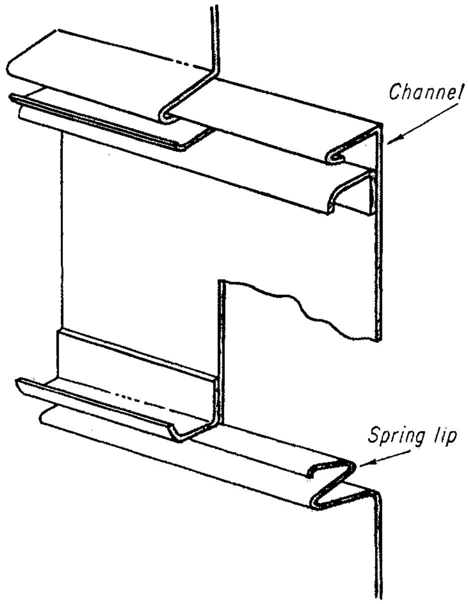

2

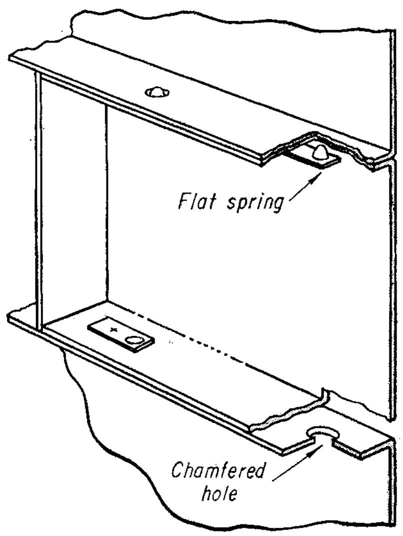

3

1..**BEADED FLANGE** requires panel made of sheetmetal thin enough to flex. Slots are necessary only for curved panels.

2..**DUSTPROOF SEAL** of spring lip is compressed in channel. Should not be used where vibration might loosen it.

3..**FLAT SPRING** holds half-ball or dimple in hole in panel. Chamfer on holes makes action easier.

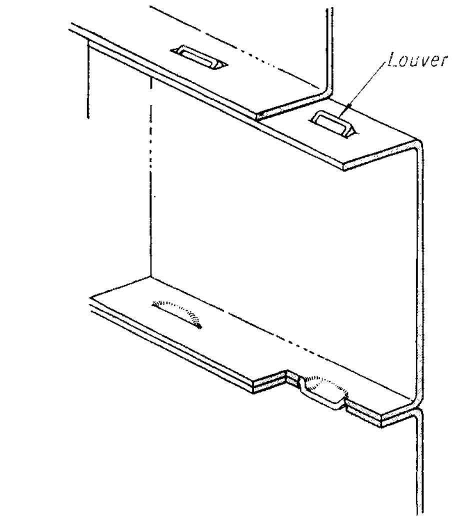

4

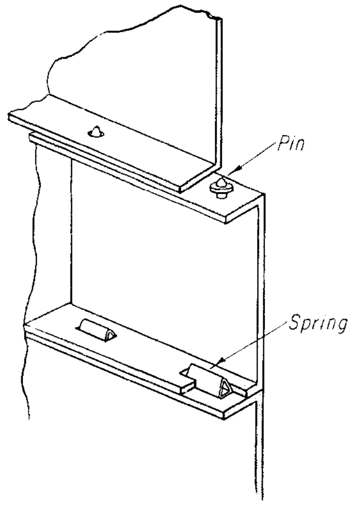

5

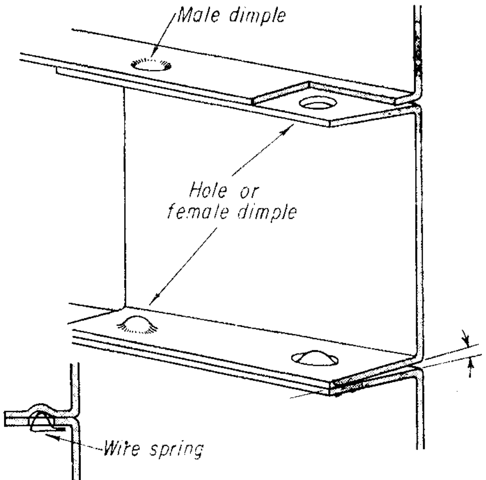

6

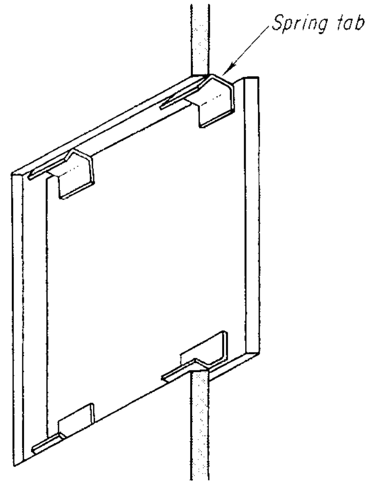

7

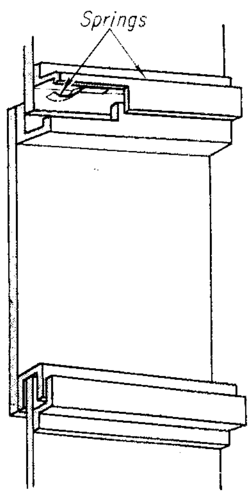

8

4..**LOUVER** fits into slot, which should be longer than the louver for easy alignment, but narrower—for a tight hold.

5..**TWO PINS** or more on top, with matching springs below, keep wide panels from rattling. One pin and a wide spring are enough for narrow panels.

6..**DIMPLES** in cabinet flange fit into corresponding dimples or holes in panel. Wire spring is alternate method. Sloping panel flanges give close fit with less exact dimensions.

7..**SPRING TABS** have slope on front to guide panel into place, and slope on back to hold it there.

8..**MATING CHANNELS** interlock for positive hold. To remove, lift panel against flat springs and swing bottom out and down.

20 Tamper-proof Fasteners

Ways to prevent or indicate unauthorized removal of fasteners in vending machines, instruments, radios, TV sets and other units. Included are positively retained fasteners to prevent loss where retrieval would be difficult.

Federico Strasser

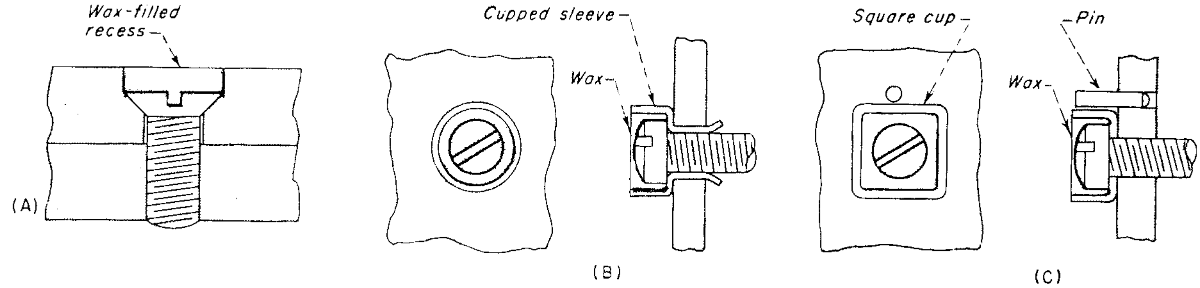

Fig. 1—(A) Wax or other suitable material fills recess above screw. Wax flush with plate hides screw position if surface is painted. (B) Cupped sleeve riveted in screw hole provides cavity for wax when plate is too thin for recessing. (C) Pin prevents rotation of square cup which would allow screw to be removed without disturbing wax.

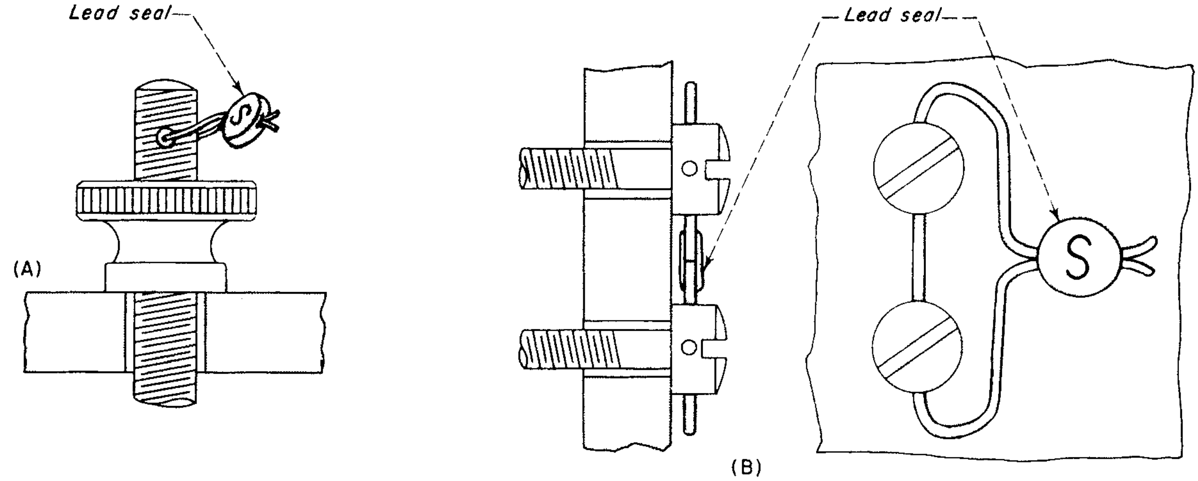

Fig. 2—(A) Lead seal crimped over twisted ends of wire passing through screw allows only limited slackening of nut. (B) Two or more screws strung through heads with wire are protected against unauthorized removal by only one seal. Code or other signet can be embossed on seals during crimping.

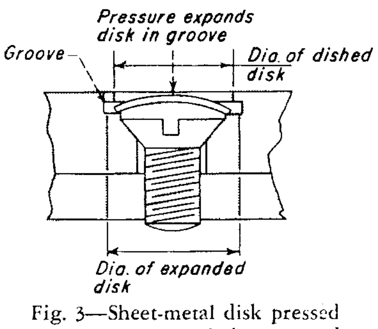

Fig. 3—Sheet-metal disk pressed into groove can only be removed with difficulty and discourages tampering.

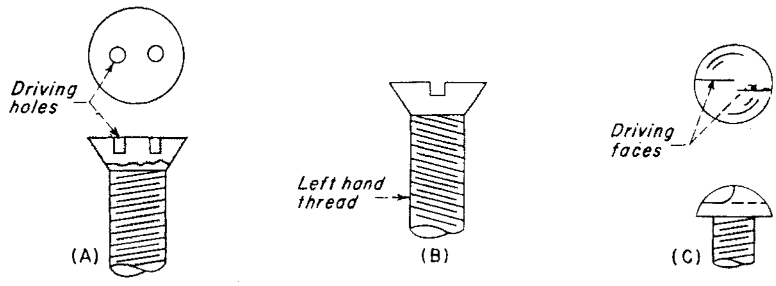

Fig. 4—(A) Spanner-head screws are available in all standard heads and sizes from U.S. manufacturers. Special driver is required for each screw size except ¼-in. dia and above. (B) Left-hand screw thread is sometimes sufficient to prevent unauthorized loosening, or (C) special head lets screw be driven but not unscrewed.

POSITIVELY RETAINED FASTENERS

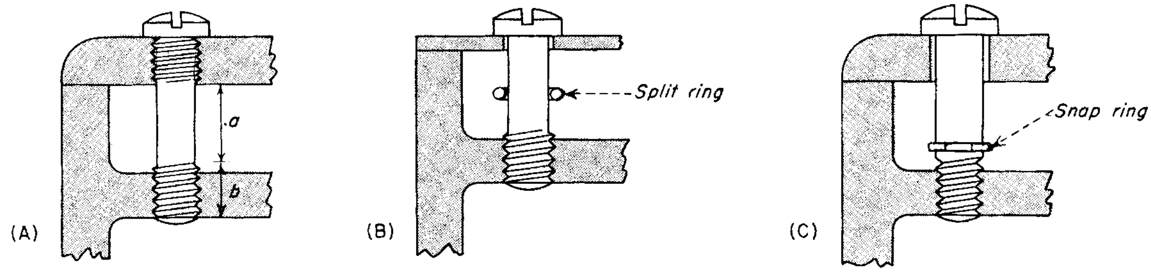

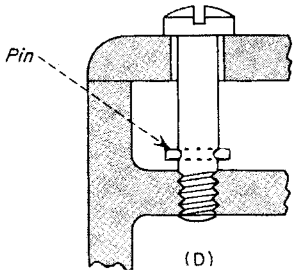

Fig. 5—(A) Tapped cover and casing allows screw (a > b) with reduced shank diameter to be completely unscrewed from casing yet retained positively in cover. For thin sheet-metal covers, split ring on reduced shank (B) is preferable. Snap ring in groove (C) or transverse pin (D) are effective on unreduced shank. Simple and cheap method (E) is fiber washer pushed over thread.

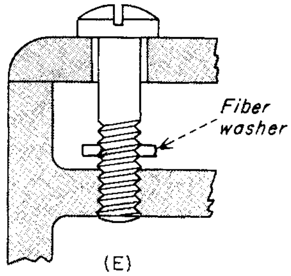

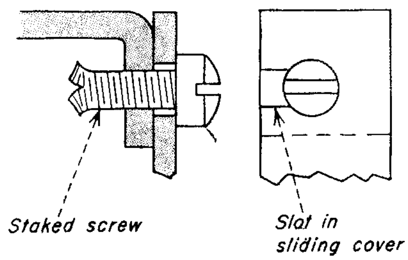

Fig. 6—Open-ended slot in sliding cover allows screw end to be staked or burred so screw cannot be removed, once assembled.

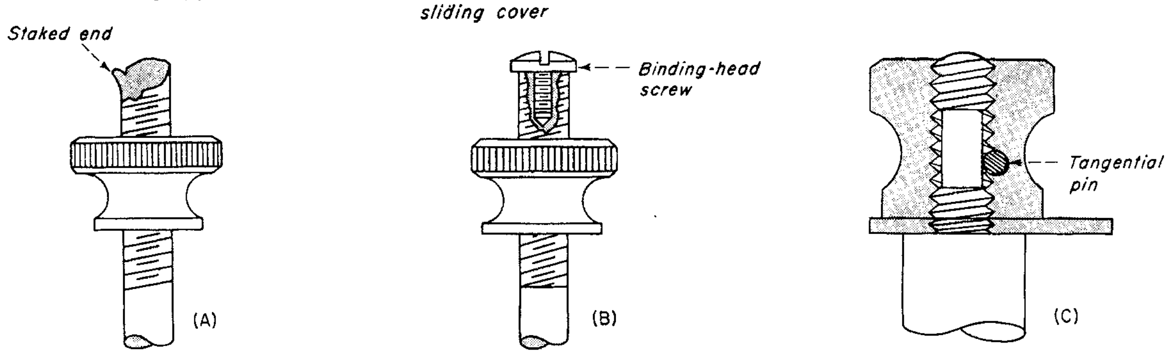

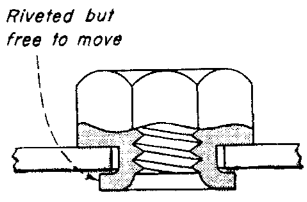

Fig. 7—(A) Nut is retained on screw by staking or similar method but, if removal of nut is occasionally necessary, coaxial binding-head screw (B) can be used. Where screw end must be flush with nut, pin through nut tangential to undercut screw (C) limits nut movement. Rotatable nut (D) or screw (E) should have sufficient lateral freedom to accommodate slight differences in location when two or more screws are used.

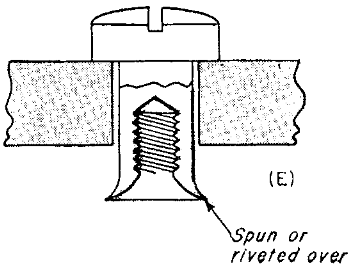

8 Detents for Clevis Mounting

When handles are mounted in clevises they often need to be held in one or more positions by detents. Here are ways to do this.

Irwin N. Schuster

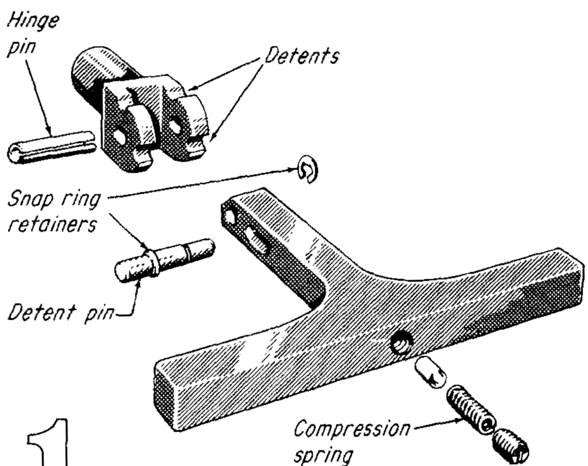

1

CAST OR MILLED clevis features an adjustable tensioning device, which varies the follower load. Handle can be extruded section.

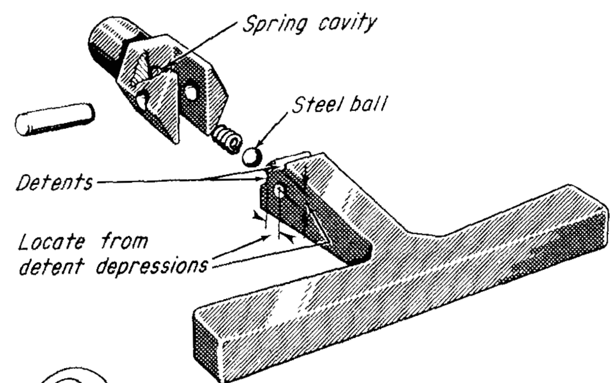

2

CLEVIS MACHINED from hexagonal stock can be drilled to receive a ball detent, which acts in cammed surfaces cast in handle.

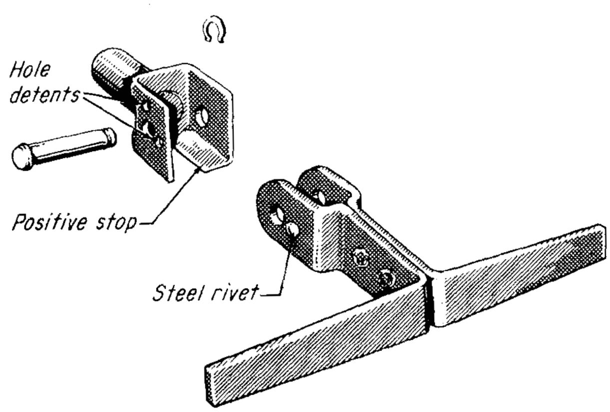

5

WELDED CLEVIS is relieved to improve spring characteristics. Punched holes receive steel rivet head which acts as the detent.

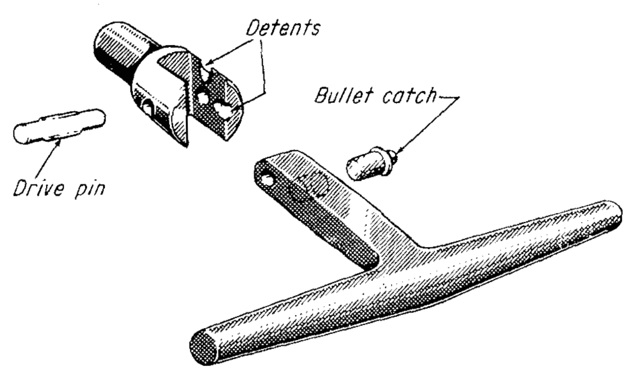

6

CAST HANDLE is drilled to accept a commercial "bullet" catch, which detents in the milled internal surface of the clevis flanges.

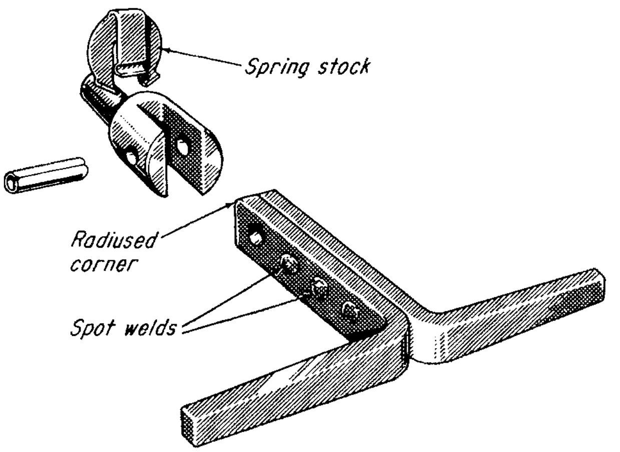

3

STAMPED SPRING snaps onto clevis before final assembly and acts as detent against the flat end and top surfaces of metal handle.

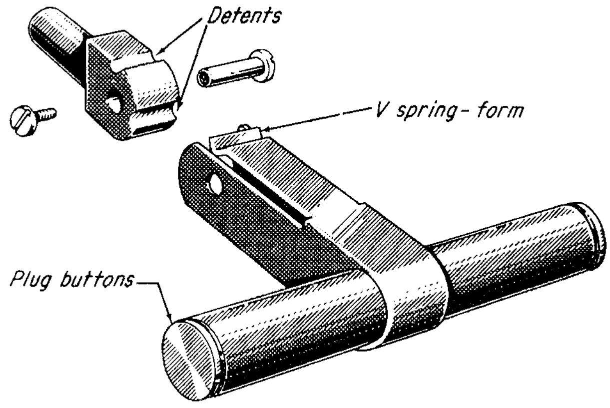

4

TUBE AND SHEETMETAL clevis handle has integral leaf spring which detents in cammed surface of machined shaft head.

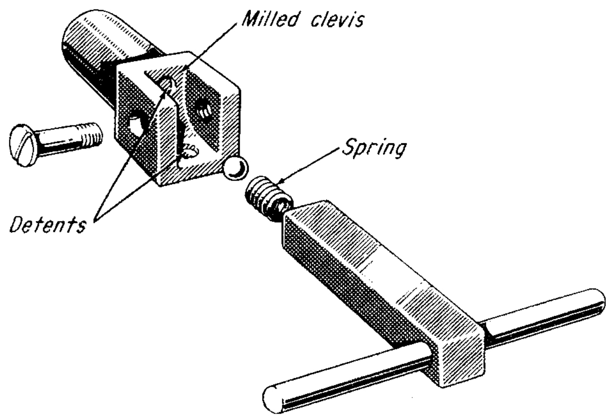

7

MILLED CLEVIS accepts ball-bearing follower, actuated by a spring, which seats against a pivot pin in the bar and rod handle.

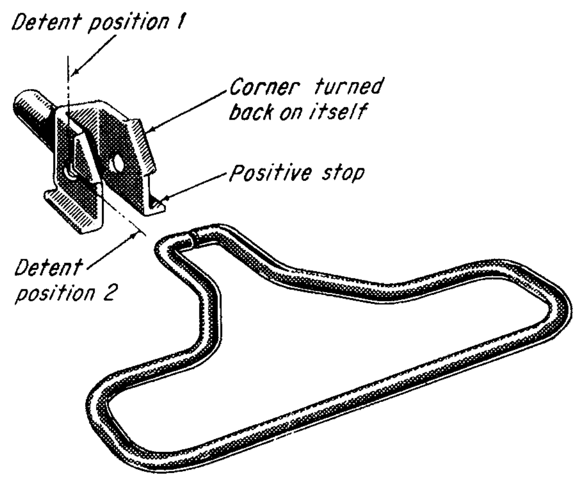

8

WIRE HANDLE acts as spring and follower in sheetmetal clevis, in which cammed surfaces and positive stops are made by bending.

4 Locking Fastener Designs

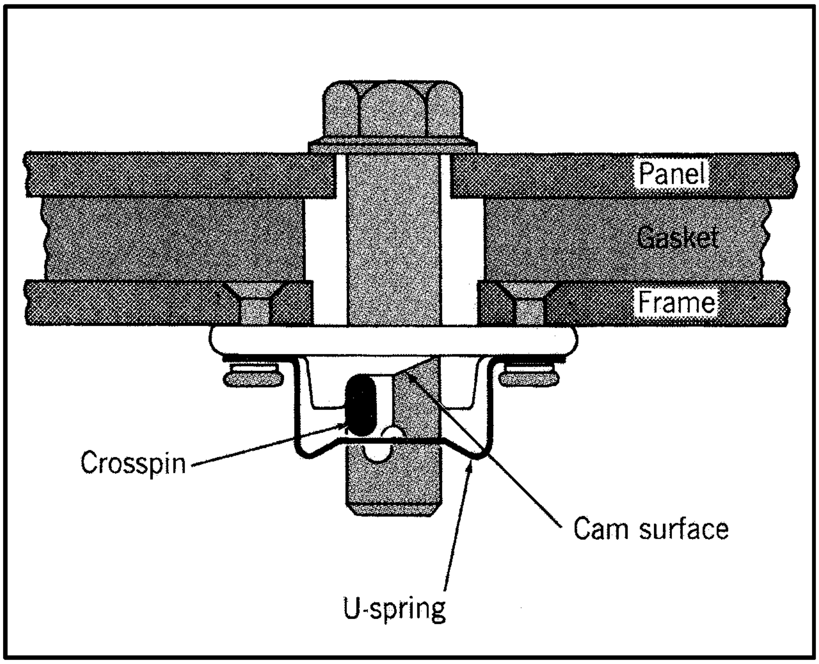

Quick-operating fastener has internal cam action to draw up or release a 300-lb. force with only a quarter-turn of wrench.

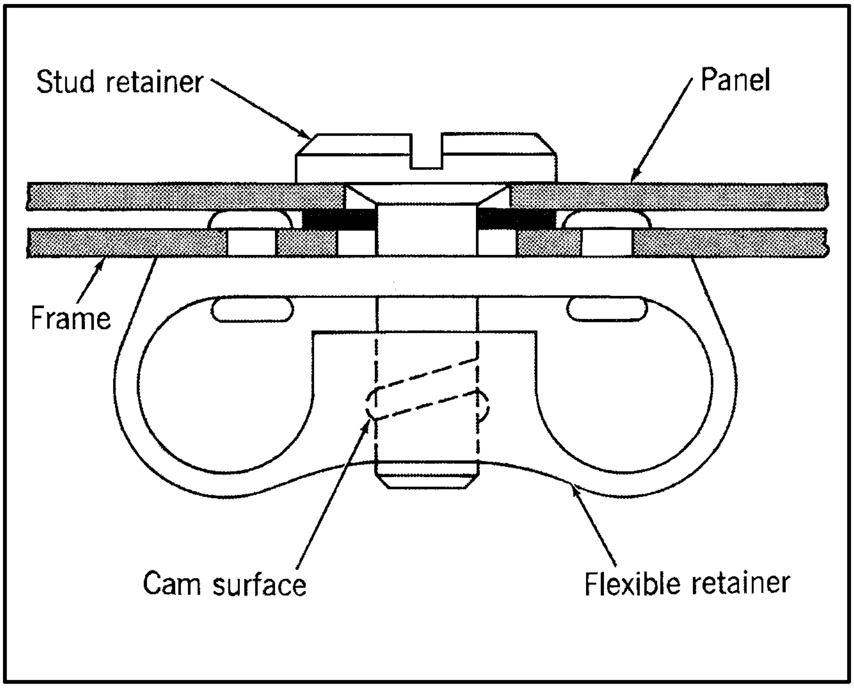

Springy all-plastic quarter-turn fastener with stylish head design can take sharp impact forces and resist corrosion.

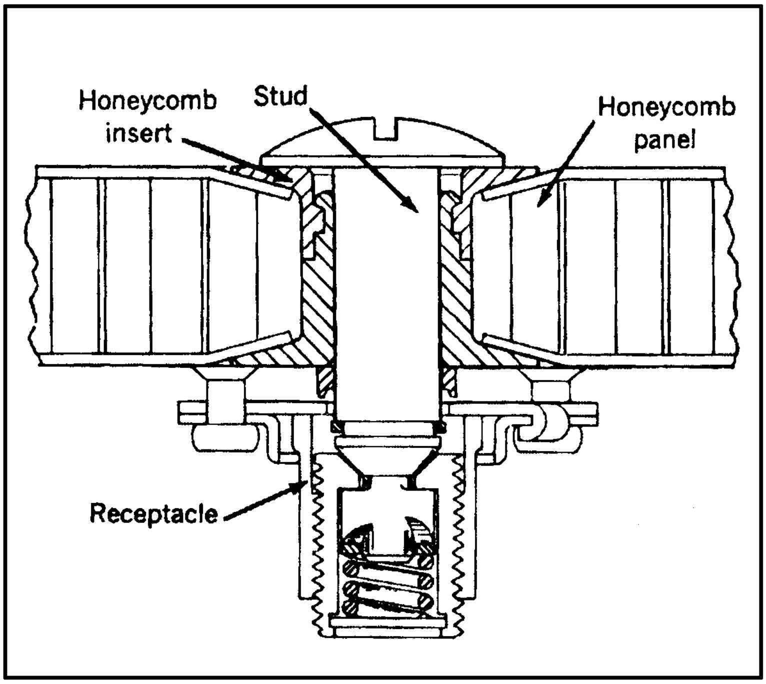

Quarter-turn-fastener concept with through-core bolt makes it easy to attach honeycomb panel to a frame or structure.

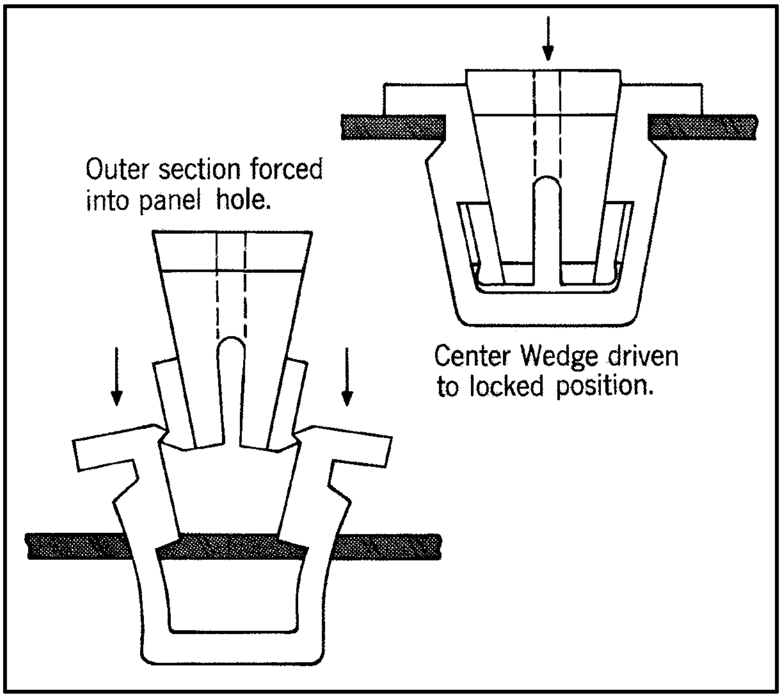

Knock-in fastener can be pushed easily into square-punched hole. Center is then knocked in to make receptacle for screw.

8 Control Mountings

When designing control panels follow this 8-point guide and check for...

Frank William Wood JR

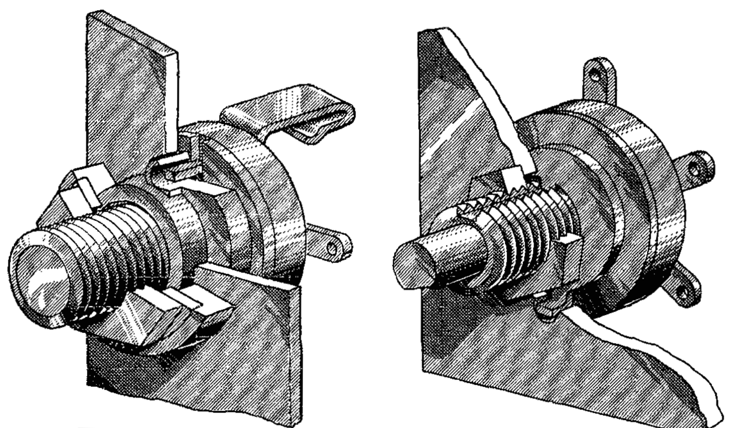

1 ...**LOCKING.** Control will stay fixed in spite of vibration or attempts to force shaft too far. Washer at right has two tabs; one fits in the panel, the other in the control bushing. Left washer has a boss which fits into a cutout in the panel and around a pin projecting from the control body.

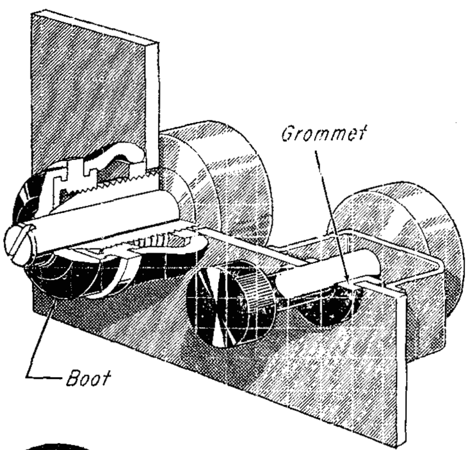

2 ...**SEALING** against dust or water. Boot seals between shaft and bushing and between bushing and panel. With control behind panel rubber grommet seals only one place.

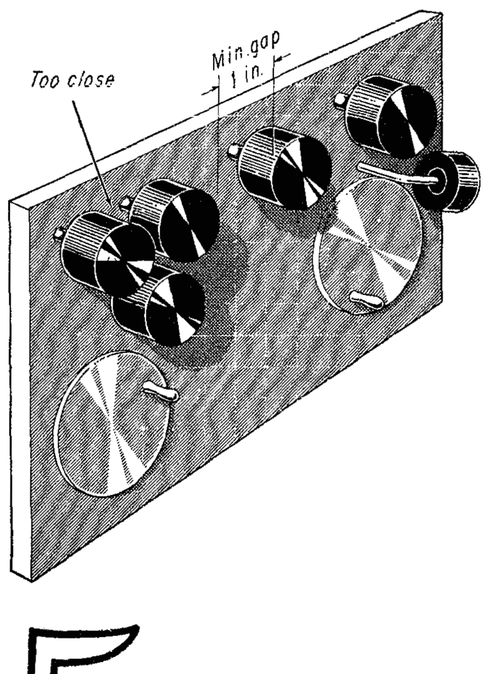

5 ...**HAND-ROOM** at front of the panel. Space knobs at least one inch apart. Extending knob to save space puts it where the operator can bump into it and bend the shaft. Best rule is to keep shaft as short as possible.

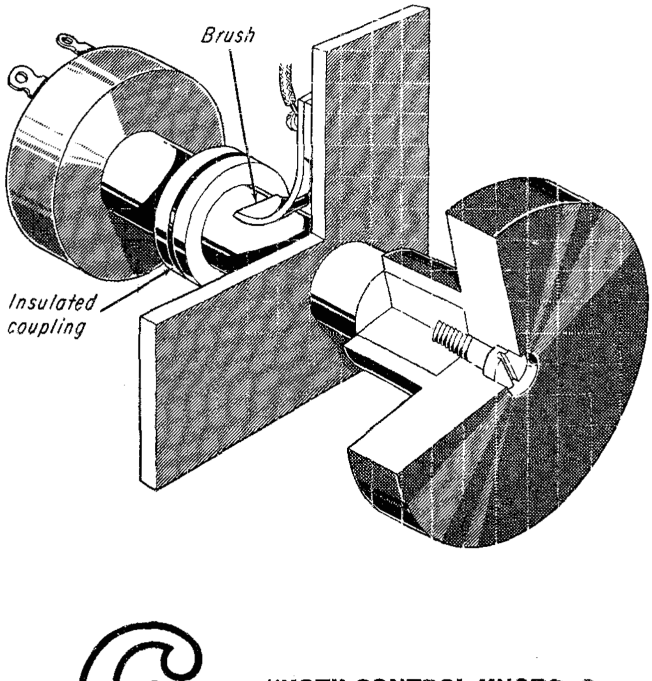

6 ...**"HOT" CONTROL KNOBS.** One approach is to ground them by installing a brush against the shaft. Another solution is to isolate the control by an insulated coupling or a plastic knob having recessed holding screws.

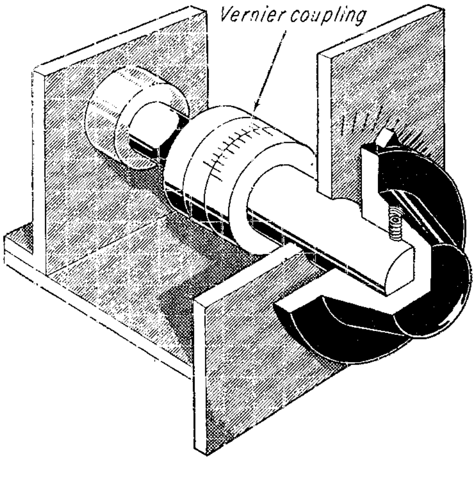

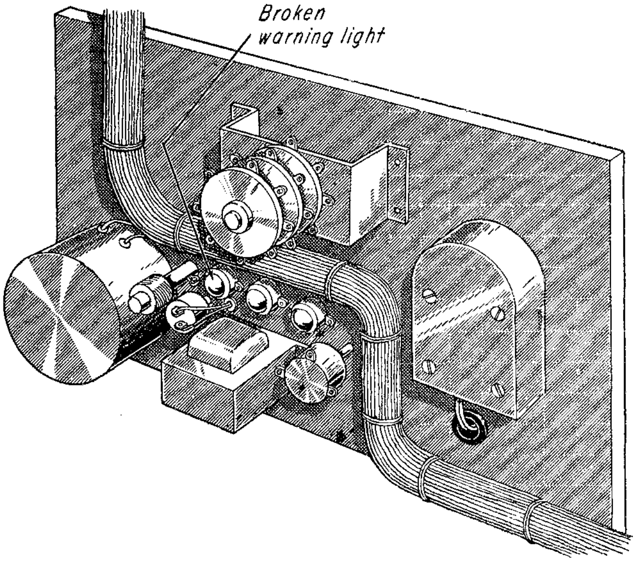

3 . . . **RESETTING** to match controls to panel markings. For crude adjustments a set-screw is enough. Where matching is critical a three-piece vernier coupling permits more accurate calibration.

4 . . . **ACCESSIBILITY** behind the panel. Easy access reduces down time and maintenance costs especially if one man can do most jobs alone. Here, technician can't replace a warning light without dismantling other parts.

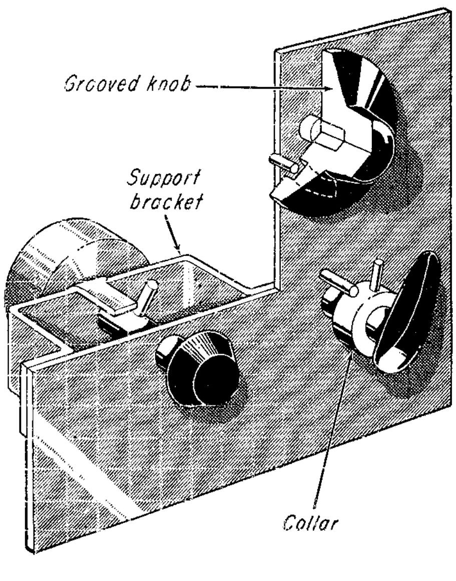

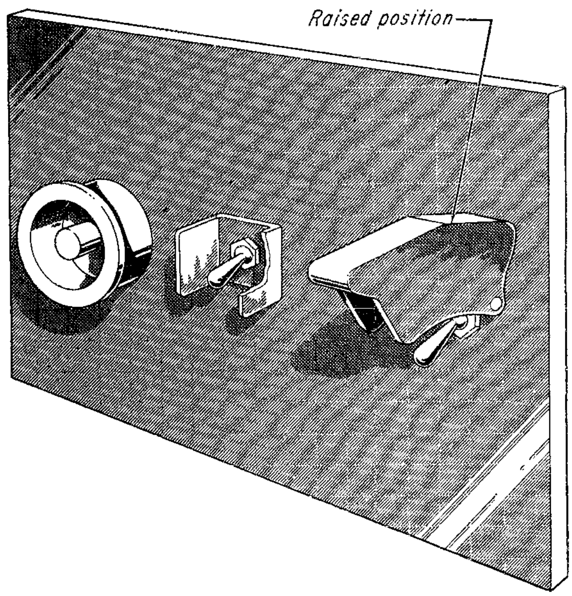

7 . . . **LIMIT STOPS** that are strong enough not to bend under heavy-handed use. Otherwise setting will change when stop moves. Collar and grooved knob permit adjustment; tab on bracket doesn't.

8 . . . **GUARDS** to prevent accidental actuation of switches. Bell-shape guard for push-buttons is just finger-size. U-shape guard separates closely spaced toggle switches, and a swinging guard holds down special ones.

Control-Locks Thwart Vibration and Shock

Critical adjustments stay put—safe against accidental turning or deliberate fiddling with them.

Frank William Wood JR

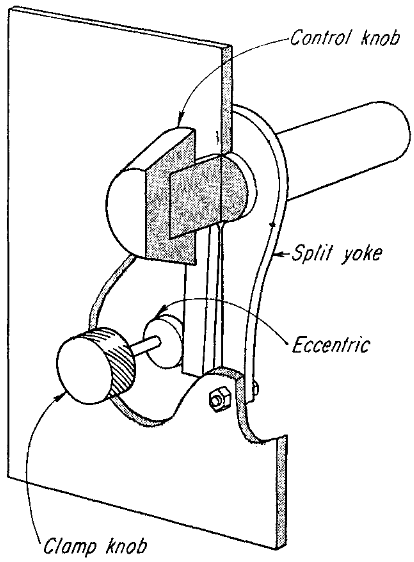

1 . . SPLIT YOKE clamps on shaft when eccentric squeezes ends of yoke together. Knurled knob is handy for constant use, and eliminates need for tool. Another advantage is high torque capacity. But this design needs considerable space on panel.

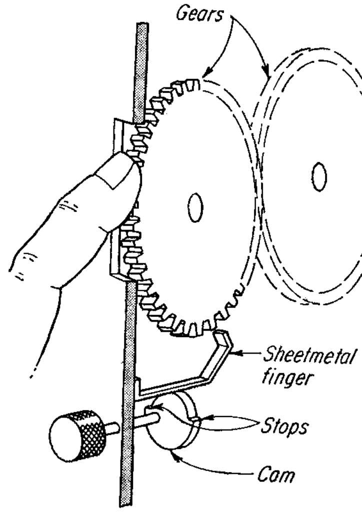

2 . . FINGER springs into place between gear teeth at turn of cam. Although gear lock is ideally suited for right-angle drives, size of teeth limits positioning accuracy.

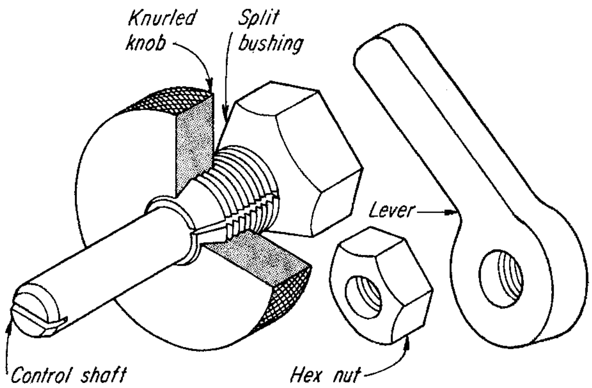

3 . . SPLIT BUSHING tightens on control shaft, because knurled knob has tapered thread. Bushing also mounts control to panel, so requires just one hole. Lever, like knob, does away with tools, but locks tighter and faster. For controls adjusted infrequently, hex nut turns a fault into an advantage. Although it takes a wrench to turn the nut, added difficulty guards against knob-twisters.

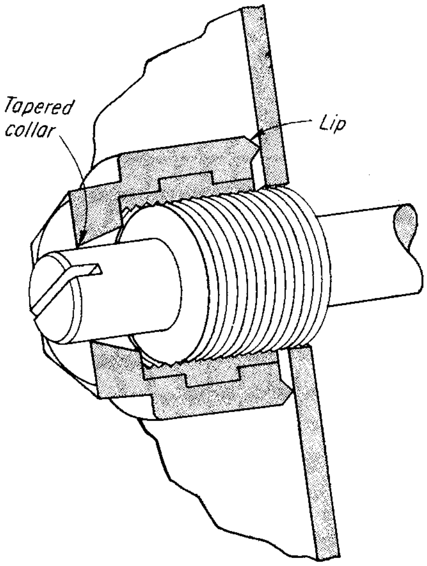

4 . . CONSTANT DRAG of tapered collar on shaft makes control stiff, so it doesn't need locking and unlocking. Compressed lip both seals out dust and keeps molded locking nut from rotating.

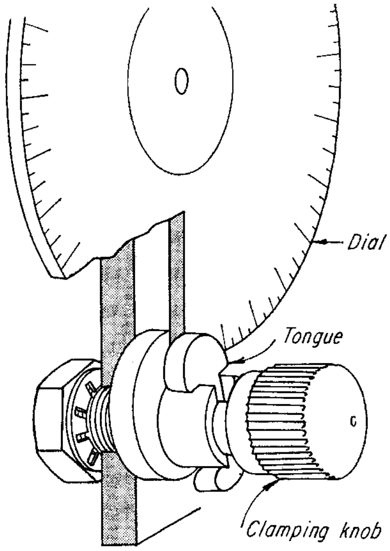

5 . . TONGUE slides in groove, clamps down on edge of dial. If clamp is not tight, it can scratch the face.

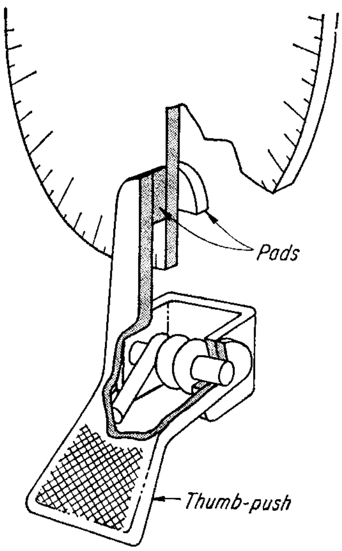

6 . . SPOT-BRAKE clamp is self-locking, which means it takes two hands to make an adjustment, one to hold the clamp open and one to turn the dial.

Low-Cost Latches

These latches cut costs where appearance is a secondary consideration.

L. Kasper

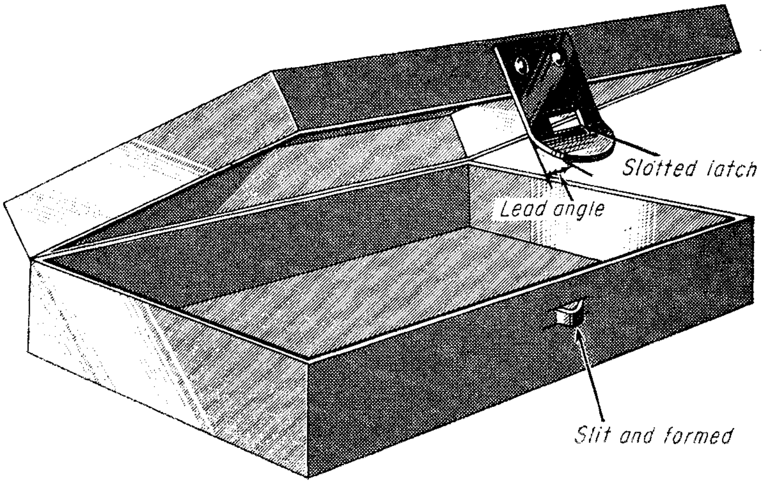

1

SLIT AND FORMED box side depends upon spring action of box metal and latch plate for engagement in latch-plate hole. A box that is too stiff will require a relatively flexible latch plate for ease of operation.

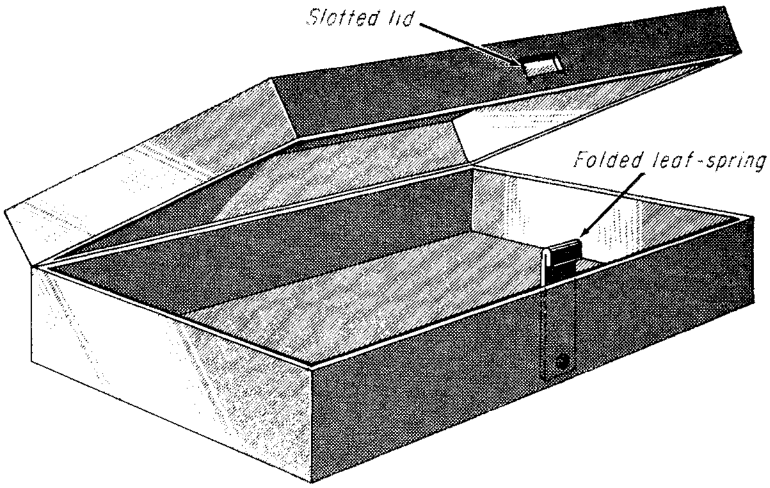

2

FOLDED LEAF-SPRING end is another positive, spring-action latch. Here, however, the leaf spring itself provides spring action – box can be as heavy as desired without interfering with opening or closing. Careful alignment of spring and notch is necessary.

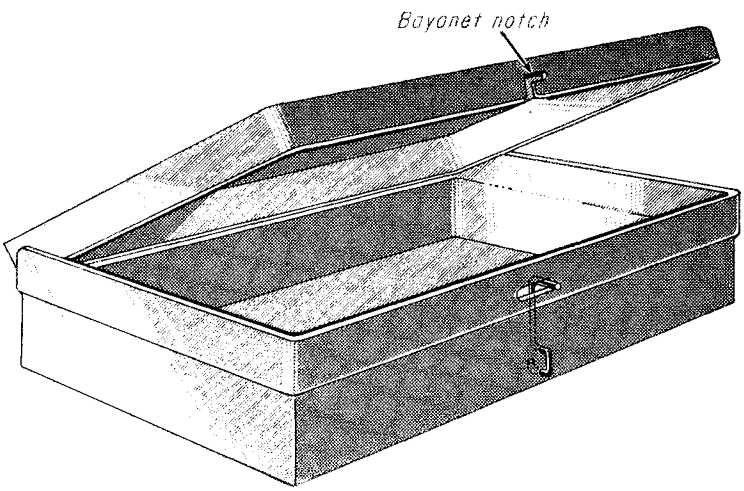

3

BAYONET ACTION of formed-wire spring in lid is again automatic upon closing. Spring must be manipulated for opening unless a lead is deliberately designed into the lid notch so that opening force can overcome holding-force.

4

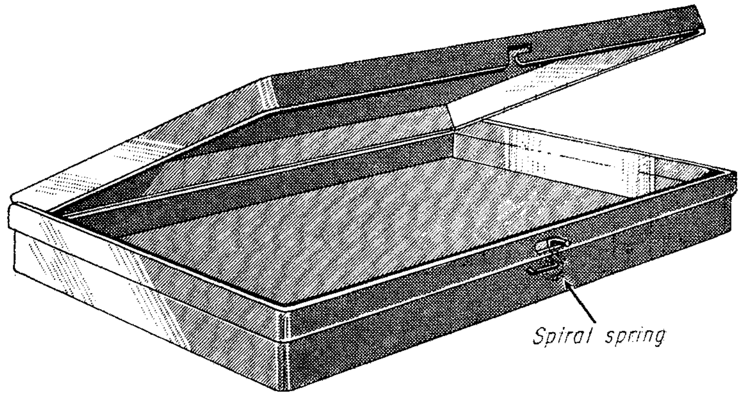

SPIRAL SPRING holds the lid in a manner similar to the previous latch arrangement. Spring action comes from tension windup rather than cantilever and so design is suitable for boxes where a long latch spring is not possible.

5

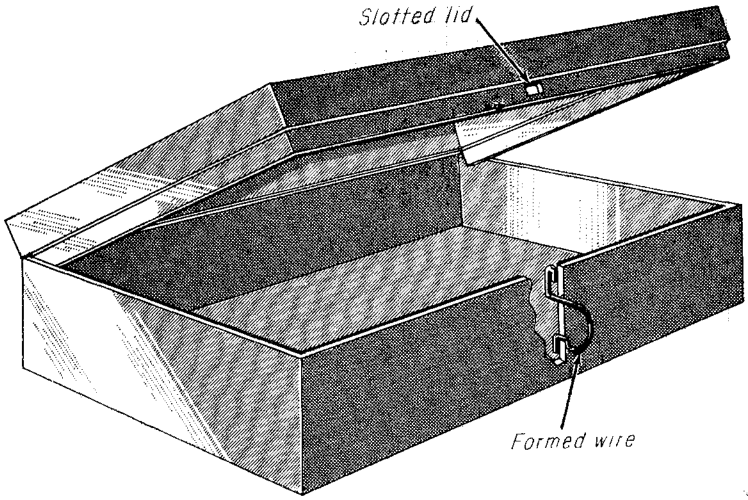

FINGER RING is here provided by forming the spring to do double duty – it not only performs as the latch spring but provides finger hold for withdrawing the box from a narrow shelf or desk drawer. Disadvantage is that protruding spring takes extra space.

6

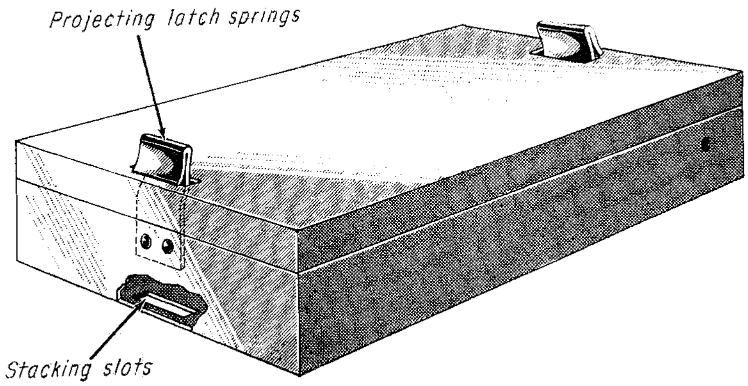

LATCH SPRINGS projecting through the box top provide for stacking by engaging a slot in the bottom of the box above. Several boxes can thus be carried without risk of sliding. The lid can be hinged or completely removable.

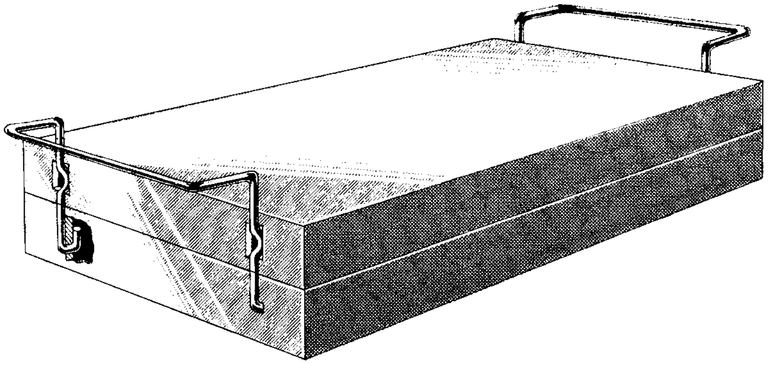

7

LATCH SPRING formed into shape of a handle is suitable for long, narrow boxes. The shape of the handle section permits several boxes to be stacked and carried safely.

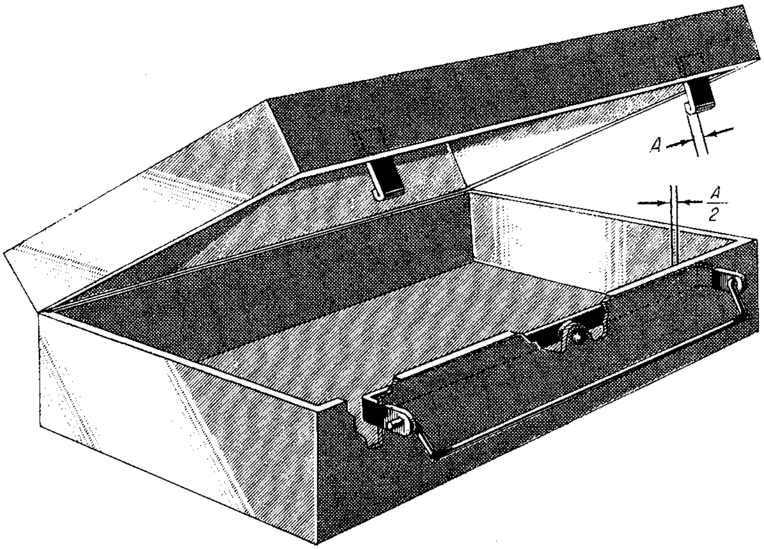

8

CARRYING-HANDLE is attached to the latch spring, which is attached to its center with a spacer between. Press the handle to release the catch.

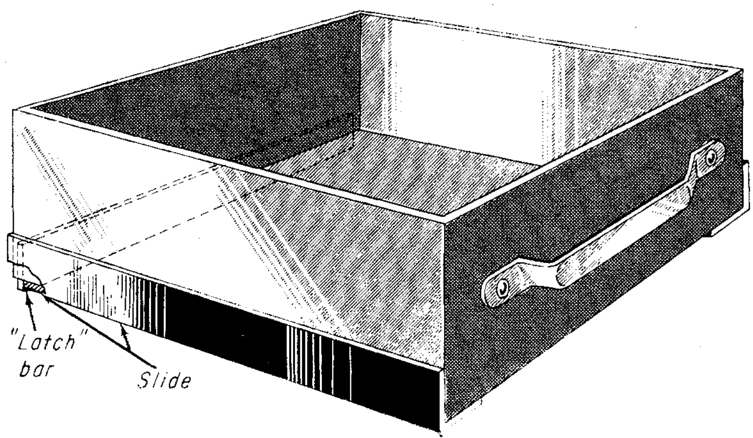

9

LATCH BAR at rear falls into slot when drawer is slid fully in. To withdraw, the box must be raised at the rear by tilting on the front edge. Effect is a self-locking, secret-opening drawer.

10

SWIVEL HANDLE is attached by shoulder screw at pivot point. To withdraw the drawer, tilt the handle about the pivot point until the latch is disengaged from slot in runner.

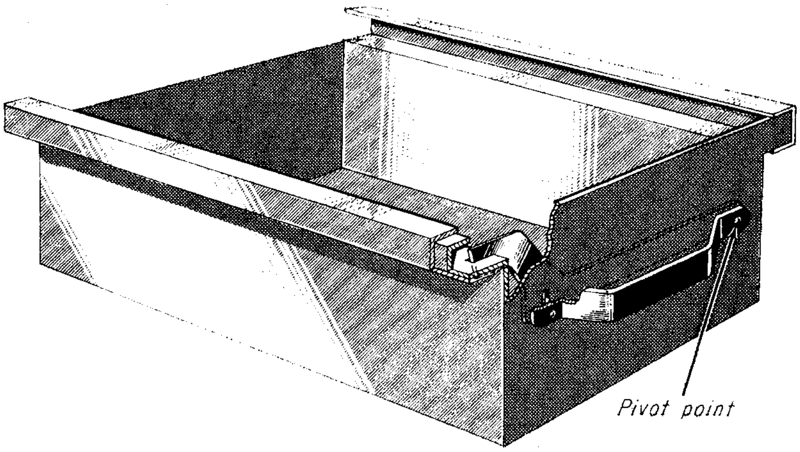

11

DOUBLE-BAYONET notch in one lid snaps over V-spring in other lid to hold box closed. Press spring to open. This type of latch is very suitable for long, narrow boxes.

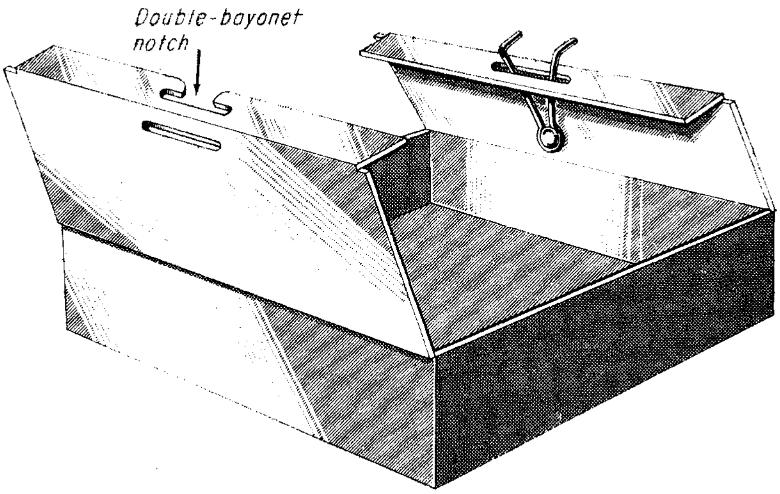

12

NOTCHES are specially shaped to hold cover over instrument housing. Simply lift cover and slide out support legs to remove cover. If fit of legs and slides is made fairly tight, accidental removal or tampering is improbable.

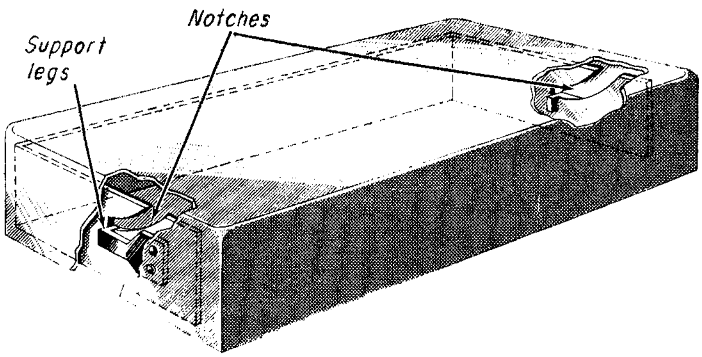

Hinged Lids That Separate

Keyslots, lid grooves, open hooks, sliding pins, and other features let hinged lids be completely removed.

L. Kasper

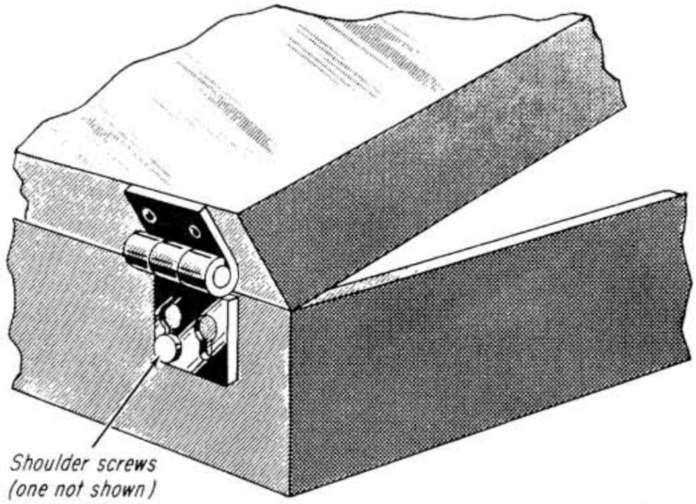

1 **KEYSLOTTING** one leaf of the hinge is a simple way to provide for separation of the lid from the box.

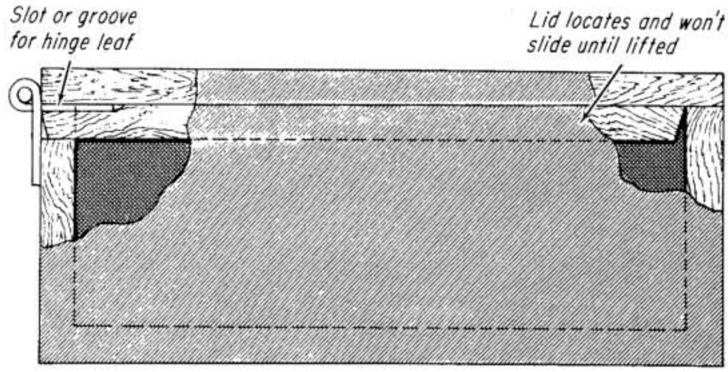

2 **LEAF CAVITY** in lid can be a simple groove. When lid locates against box sides, leaf cannot slip out.

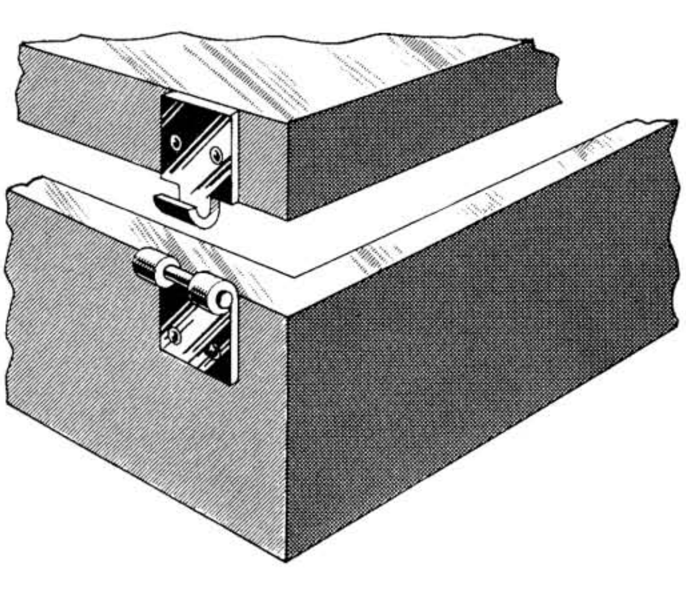

3 **OPEN HOOK** is formed by partly uncurling one leaf. To disassemble the lid it must be opened through 180 deg.

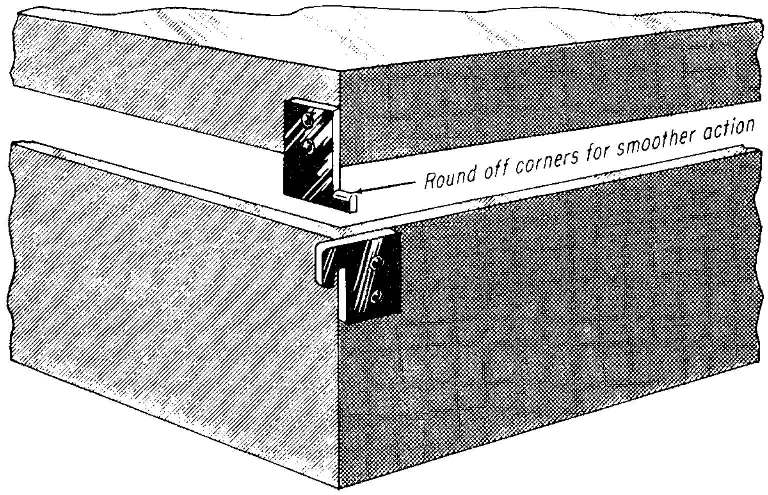

4 **FLAT PLATES** are hook and pin that act as efficient but low-cost hinge for rigid lids. Round off pin corners.

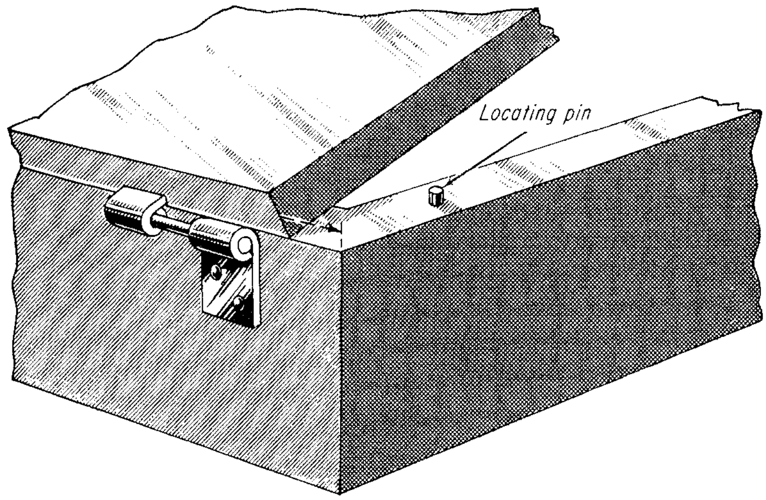

5 **SLIDING PIN** is popular way of making lids separable. Locating pins must be provided if lid does not fit in box.

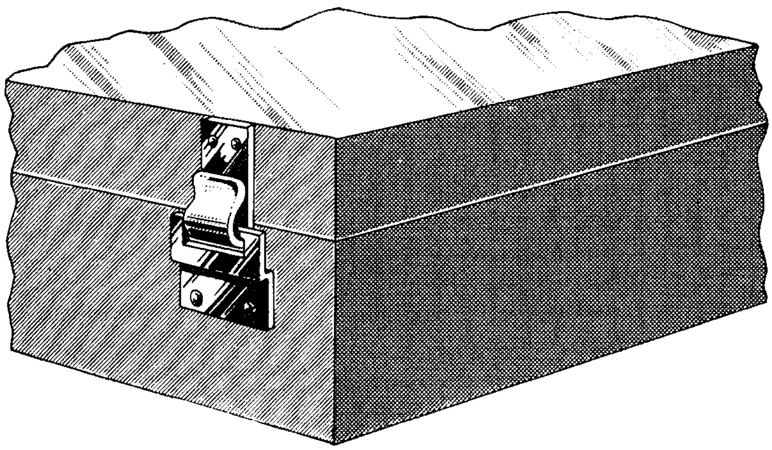

6 **SPRING-TYPE LEAF** must have enough clearance to accept retaining plate thickness unless spring is very light.

Hinge bars, notched lids, spring hing pins and other ways of providing for detachable lids.

L. Kasper

7 **HINGE-BAR AND HOOK** make strong and low-cost hinge, separable when lid is opened through 90 deg.

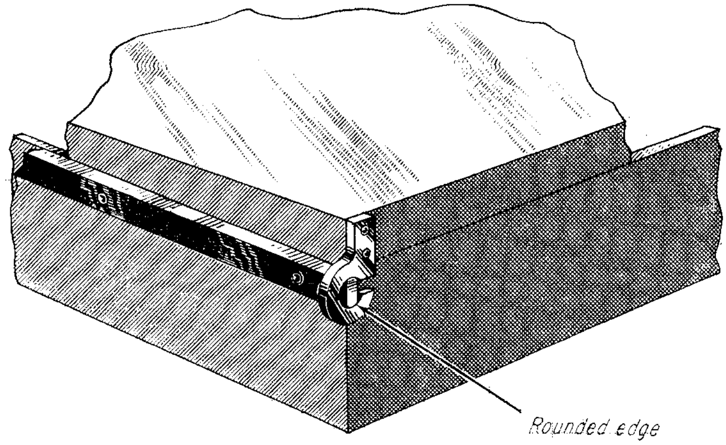

8 **NOTCHED LID** accepts hooked part of hinge plate when lid is opened beyond 90 deg. Only one plate is needed.

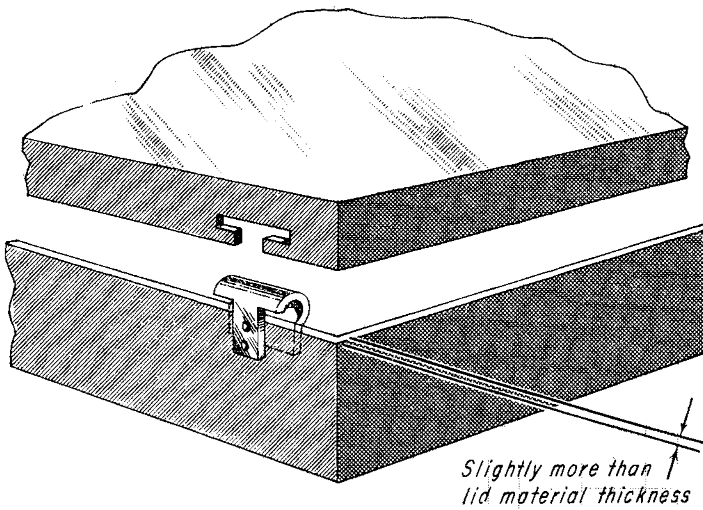

9 **SHOULDER SCREW** in hinge plate needs to be loosened to only slightly more than the thickness of lid to detach it.

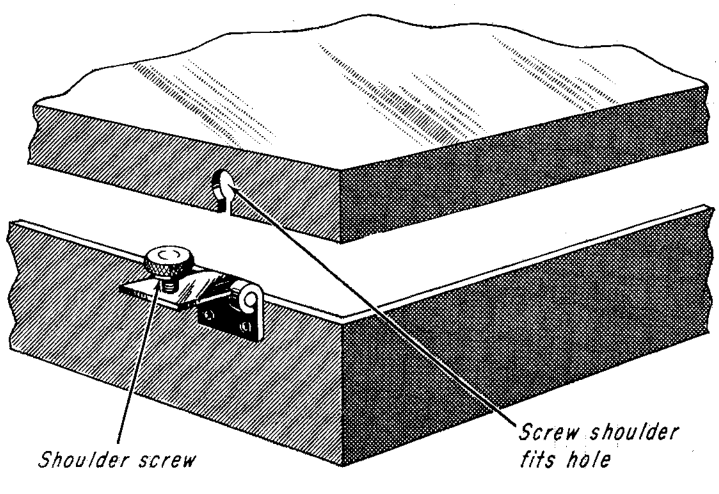

10

LOOPED HINGE PIN is sprung over spacer. When the loop is pulled off the spacer the pin ends retract.

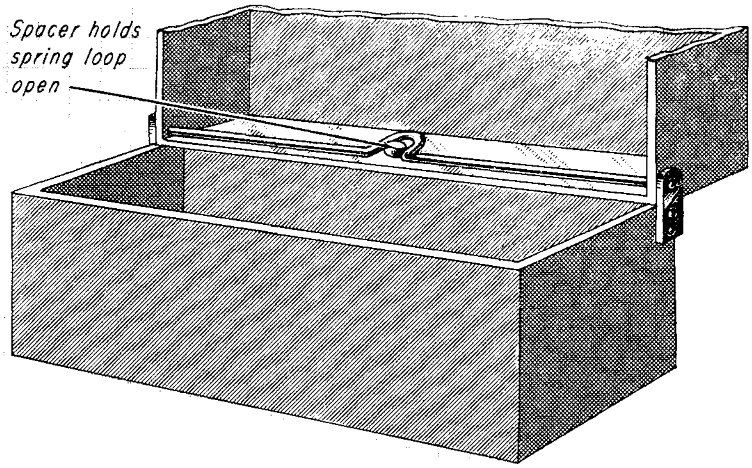

11

HOOKED MEMBER is slipped under pin in position shown. When lid is opened latch can be turned to lock pin.

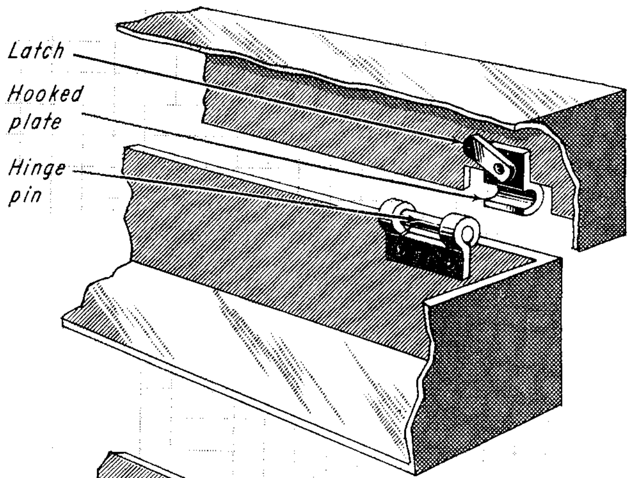

12

HEADED PINS are driven into curled lid edge. Heads are same diameter as the curl. Lid slides when opened 270 deg.

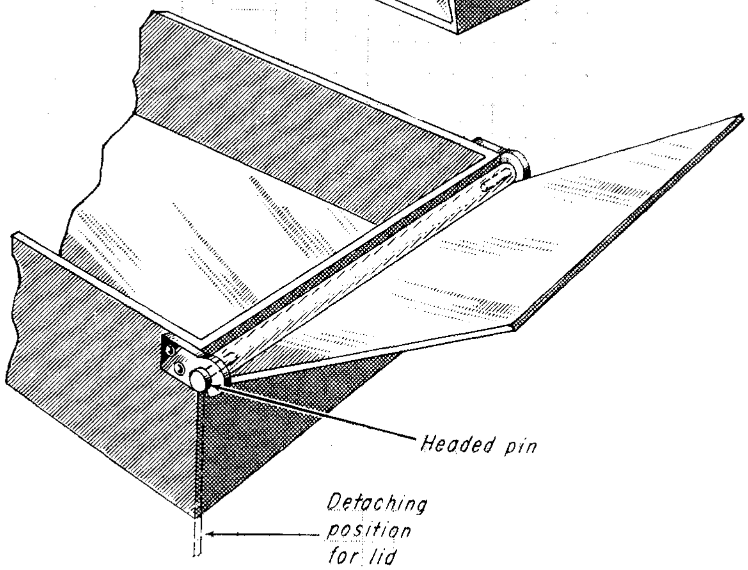

8 Stops for Panel Doors

They protect hinges from overtravel and hold doors in working positions.

Frank William Wood JR

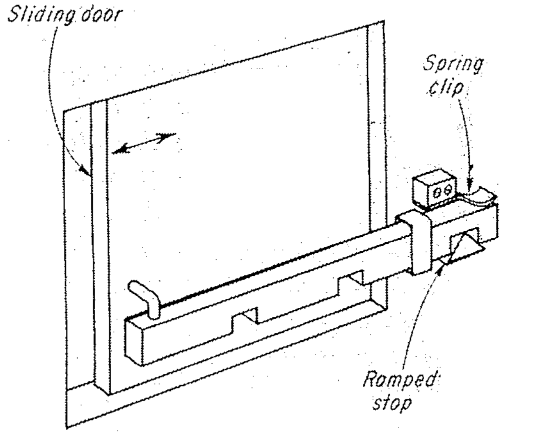

1.
SPRING CLIP presses notched bar down on stop for sliding door.

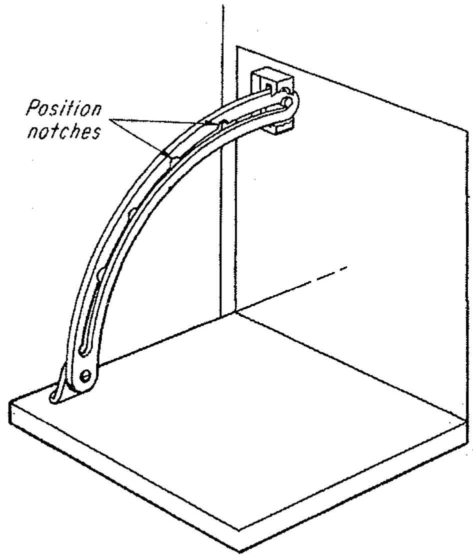

2.
SLOTTED BAR stops when pin jams against end; notches hold drop panel in intermediate positions.

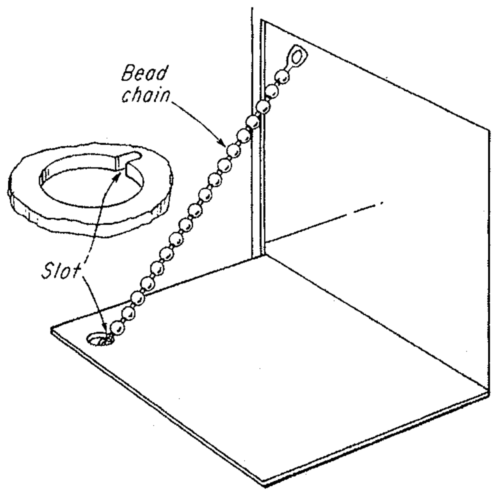

3.
BEADED CHAIN provides as many positions as there are beads. Keyhole slot allows repositioning.

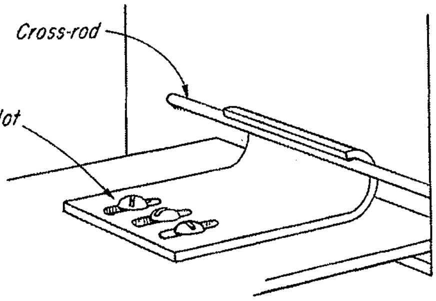

4.
WRAPAROUND back of bar comes to a stop against the cross-rod. Slots permit adjusting bar for different door opening.

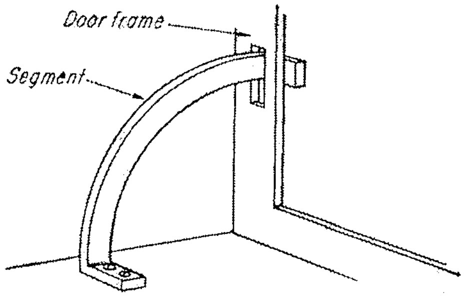

5.
DOG-LEG on end of segment butts against door frame.

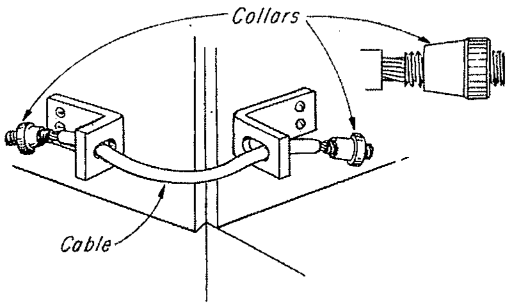

6.
CABLE pulls taut on end collars, which screw back and forth for slight adjustment.

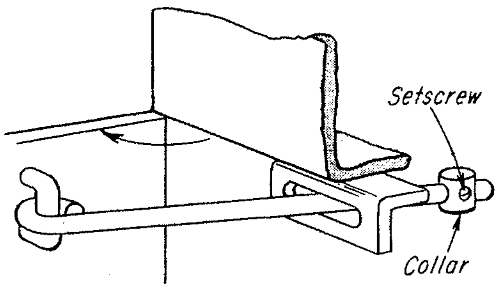

7.
COLLAR slides along rod to adjust stopping point.

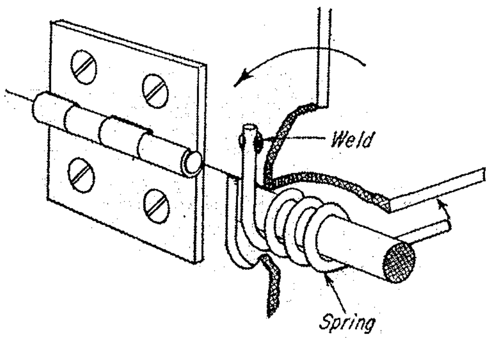

8.
COIL SPRING swings into underside of shelf and cushions door to a soft stop.

Panel-Stops Leave Hands Free

They hold open panel doors while repairs or adjustments are made.

Frank William Wood JR

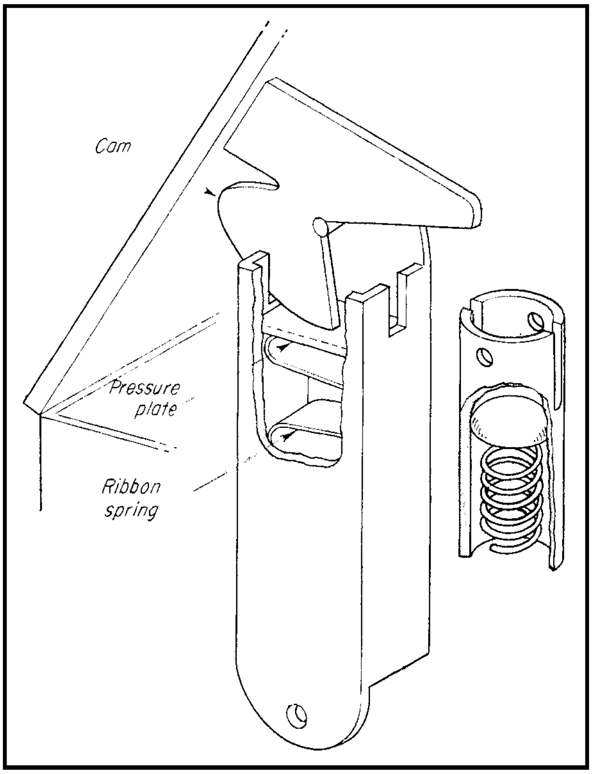

1
CAM rubs on spring-loaded pressure plate. Resulting friction holds panel open at any position. Tubular spring-holder has helical instead of ribbon spring.

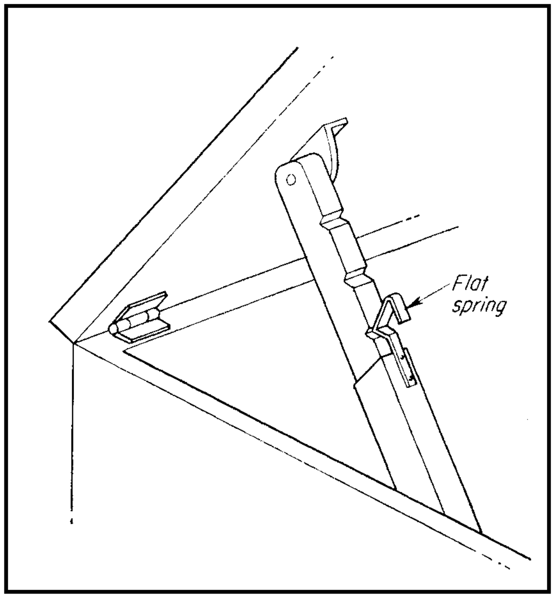

2
NOTCHED BAR catches on flat spring at only a few positions. Serrations increase number of positions. Heavier flat spring holds by friction at any position.

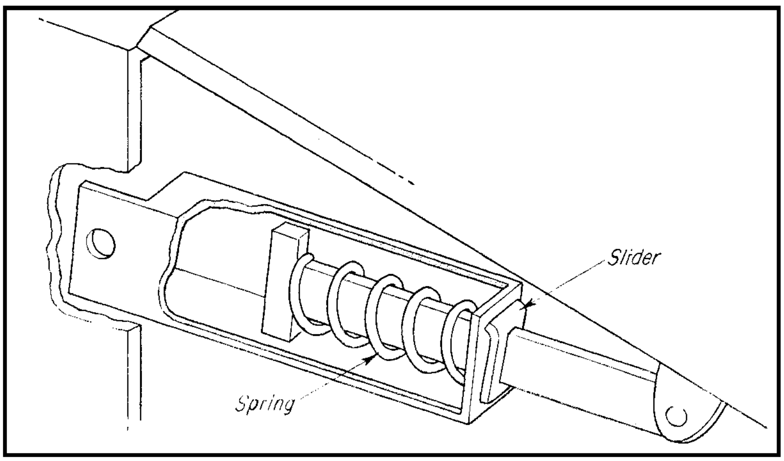

3
SLIDER jams when pulled against spring case, but slides freely after raising the panel slightly releases pressure. Spring holds panel shut.

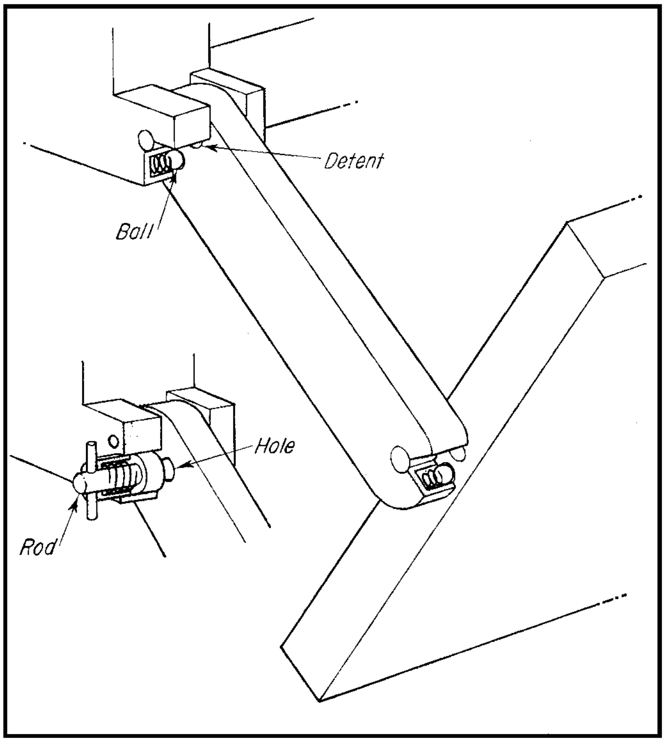

4
DETENTS at both ends of swinging bar cup spring-loaded balls. Rod snaps into holes for more positive hold, but must be pulled out to release. Both methods will hold panel shut.

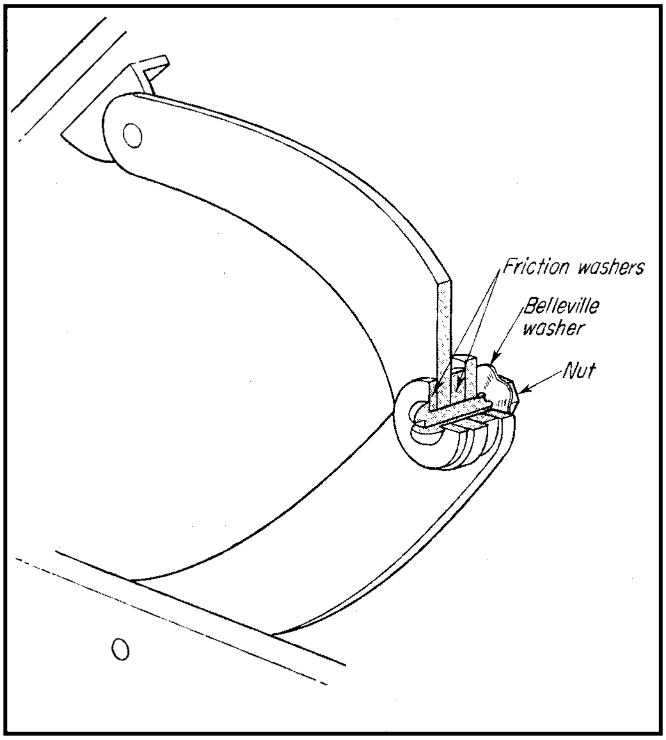

5
FRICTION WASHERS hold panel in any position, but are susceptible to vibration. Tightening down on spring washer adjusts drag for weight of panel. Knurled knob in place of nut allows tightening at desired position.

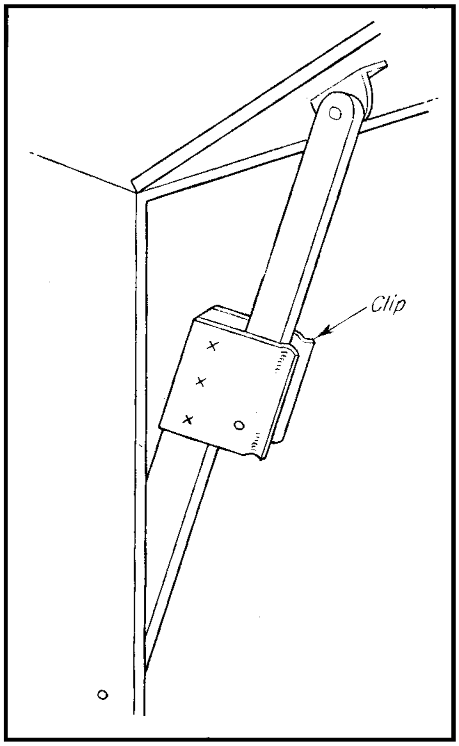

6
CLIP can hold panel door in only one position—open. Push on clip to release.

Better Looking Sheetmetal Joints

Improve their appearance with overlapping beads, backing strip, push-in trim strip, stick-on decals, recessed joints, inverted channels, and painted band.

Frank William Wood JR

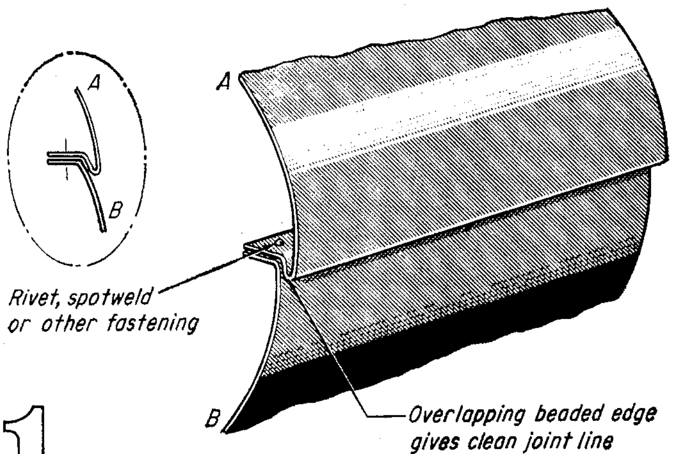

1 OVERLAPPING BEAD

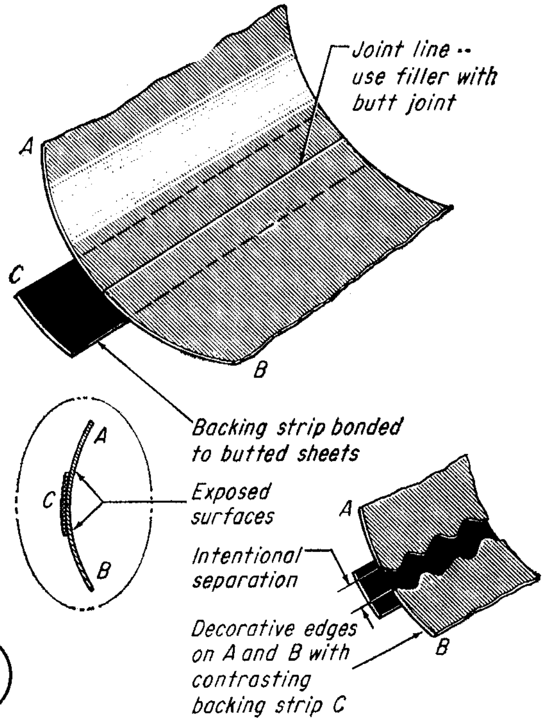

2 BACKING STRIP

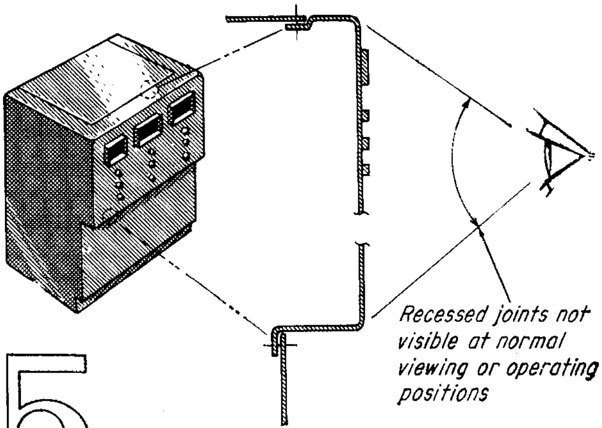

5 RECESSED JOINT

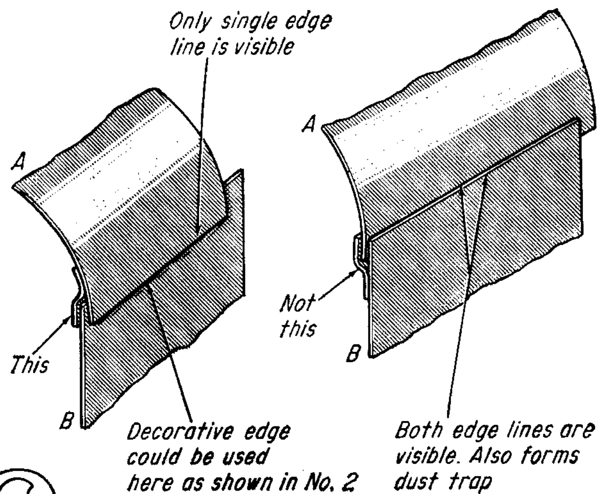

6 INVERTED-CHANNEL JOINT

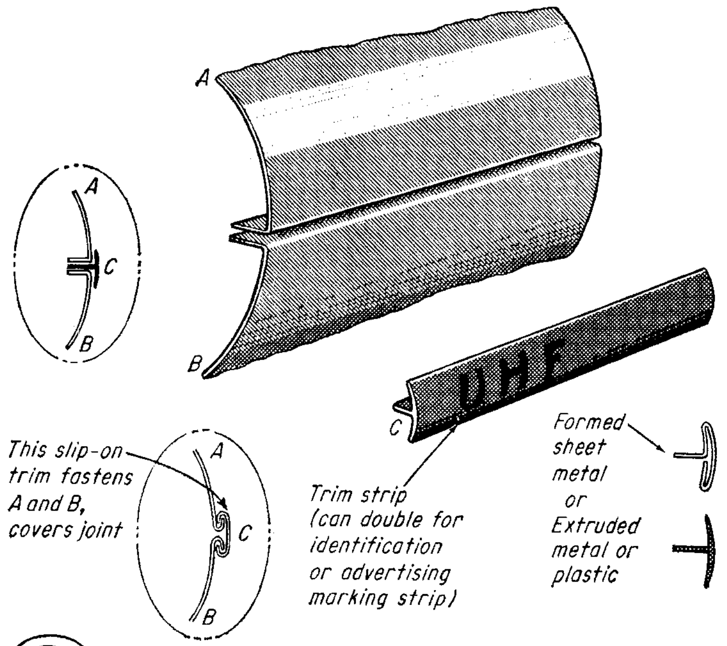

3 TRIM STRIP

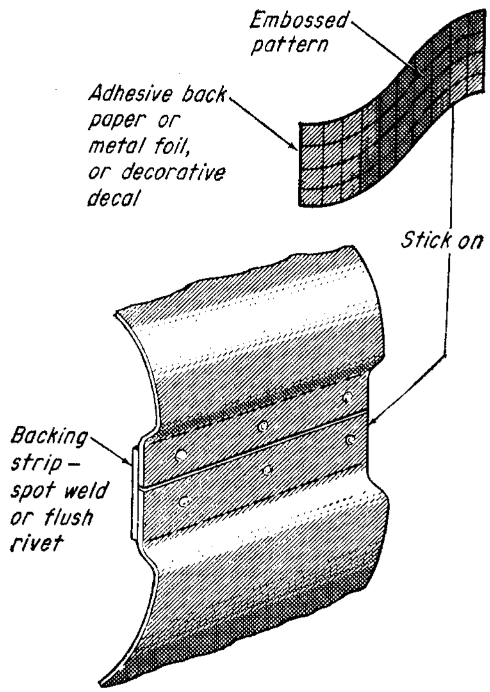

4 DECALCOMANIA STRIPS

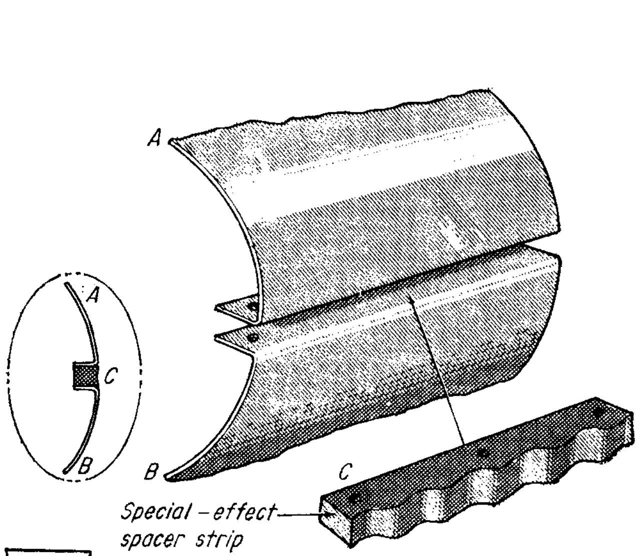

7 SPACER STRIP

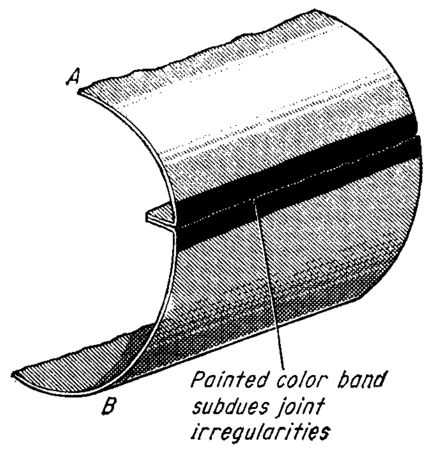

8 PAINTED BAND

8 Interlocking Sheetmetal Fasteners

These eight sheetmetal parts join sheetmetal quickly with the simplest of tools, few screws or bolts.

L. Kasper

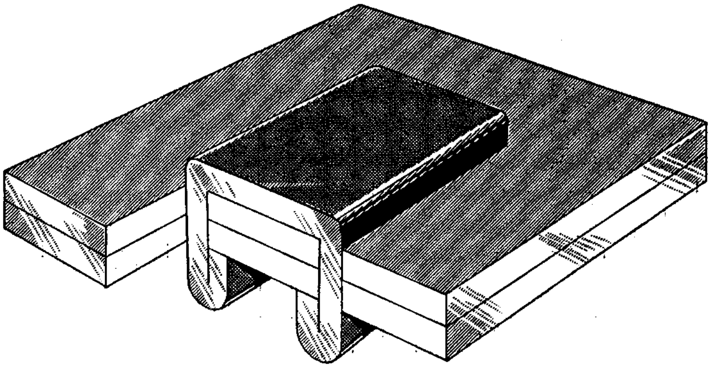

1 **SQUEEZE CLIP** holds two overlapping sheets together. The ends of the clip are pushed through parallel slots, then bent over much like a staple.

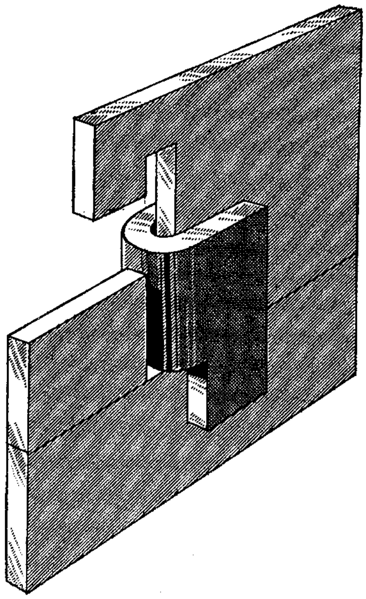

2 **ALIGNING PIECE** slides up out of the way in long slot while butting sheets are being positioned. Afterwards it slips down over lower sheet.

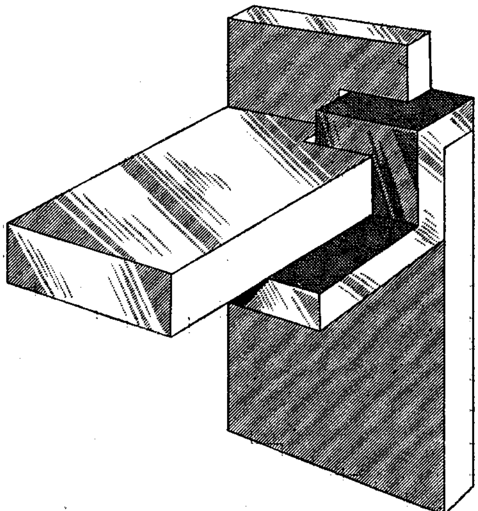

5 **ESS** supports shelf between uprights. By mating with notched edge it acts as a key to keep shelf from sliding back and forth and provides positive location.

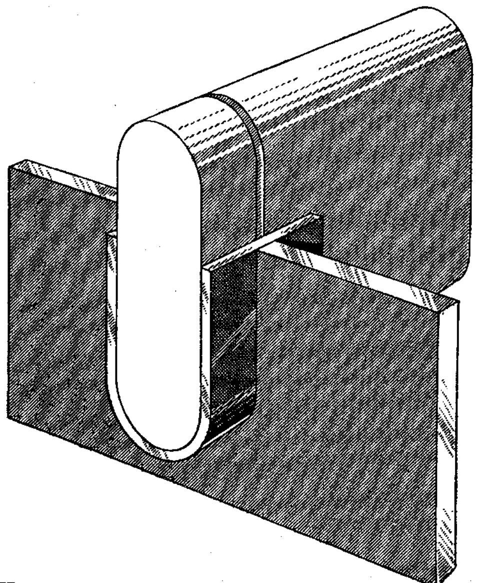

6 **CUP** carries a bar on both sides of divider. Here bars stick up above the top, but deeper cutout will lower them until they are flush or sunk.

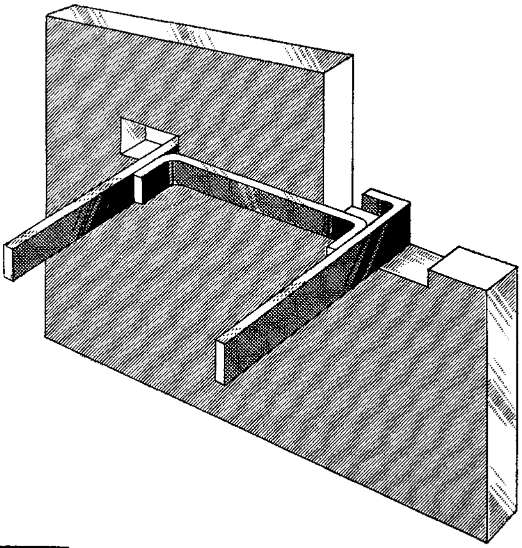

3

BRACKETS provide instantly mobile rack space for boxes. To install or remove, squeeze sides together and push hooked ends through slots.

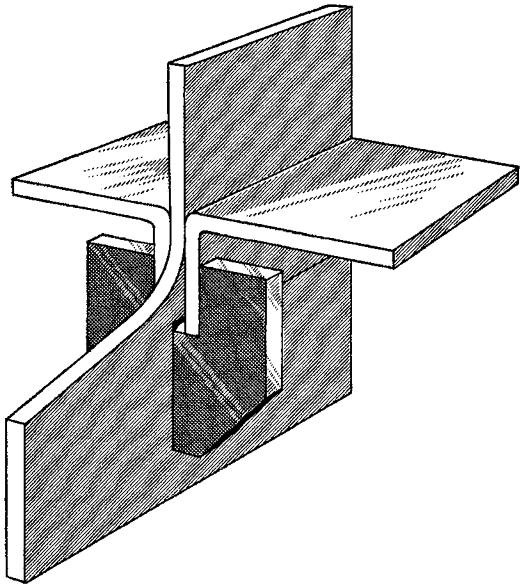

4

FLANGE HOLDER does double duty by holding up shelves on both sides of a partition. Angular corners allow it to fit through small slit when tilted.

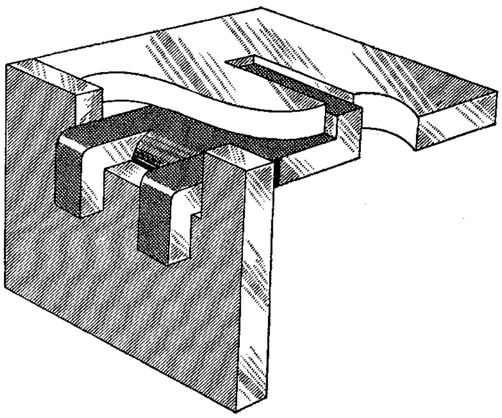

7

CLAW holds top sheet between two end pieces. Tail snaps into slot, then claw is hammered over edge. With notched edge, top is even with sides.

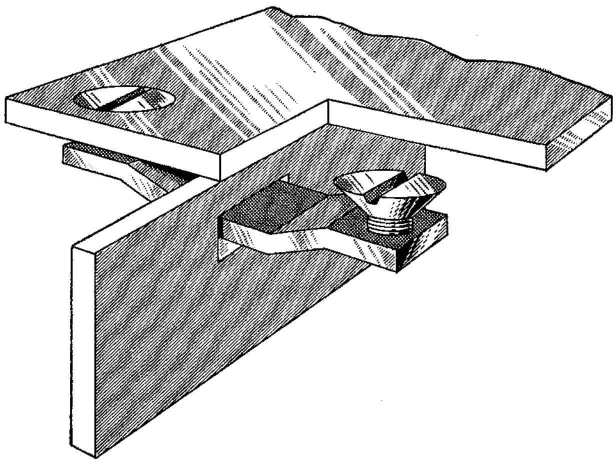

8

BAR clamps divider in place. Extruded holes provide a recess for screws so that they stay flush with upper surface of horizontal sheet.

Lanced Metal Eliminates Separate Fasteners

15 ways in which sheetmetal tabs, ears and lugs can serve to fasten and locate.

Federico Strasser

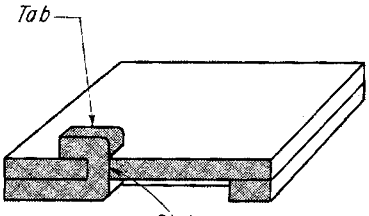

1

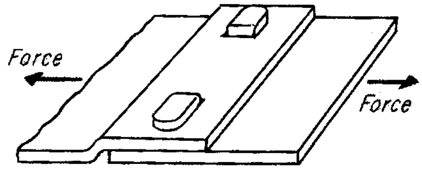

2

BENT-OVER TAB holds together up to four layers of sheetmetal. Designing tabs to stress in shear increases holding strength.

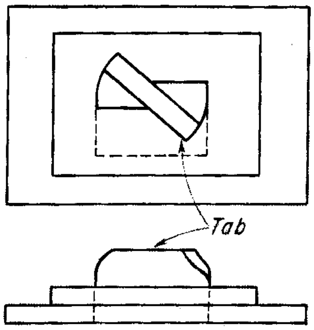

3

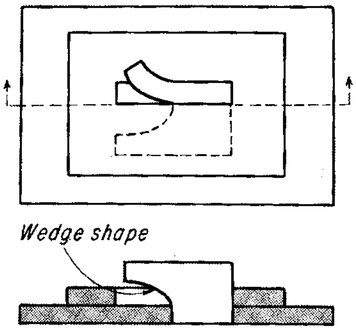

4

TWISTED TAB is less common than bent one. Shaped tab wedges tightly when twisted.

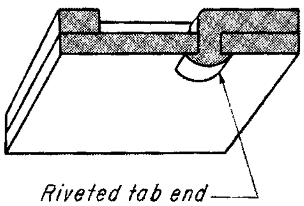

5

WITH THICK STOCK, end of tab can be riveted.

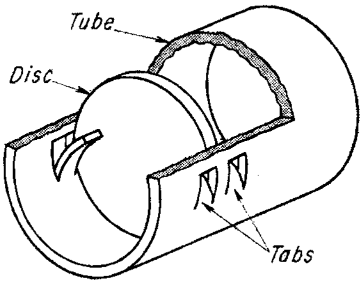

6

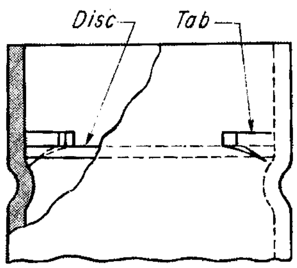

7

THESE TABS both locate and hold disk in tubing. When necking locates disk, tab only holds—again by wedge action.

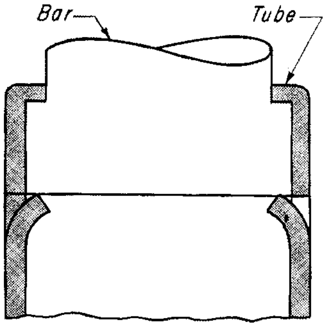

8

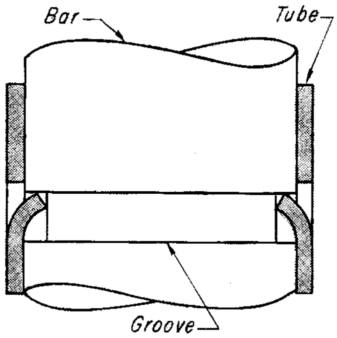

9

LIP AND TABS combine to join round bar and tubing. For longer bars, tabs fit into grooves. Bar can rotate inside tube if tabs are pressed lightly into groove.

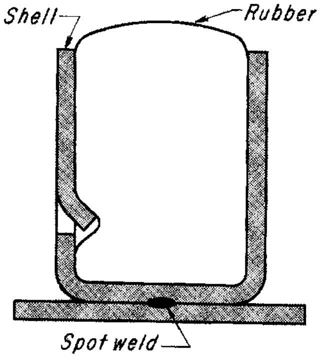

10

LANCED SHELL secures rubber in bumper or instrument foot.

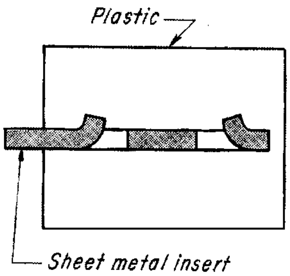

11

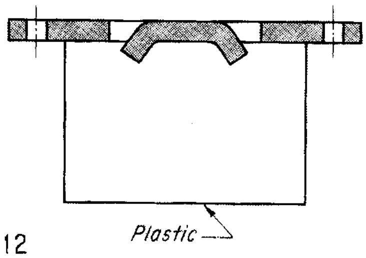

12

METAL REINFORCEMENTS and mounting pads grip plastic better if lanced.

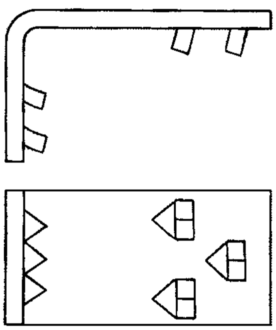
13

CORNER REINFORCEMENT grips wood, plastic or fiber with lanced teeth. Similarly, lanced nameplates or labels attach easily to equipment or instrument panels by pressing into the surface.

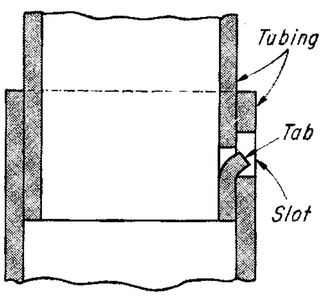

14

INTERLOCKING SLOT and tab connects two pieces of tubing. Joint is permanent if inner tubing has thick wall. If inner tube has thin wall, tab can be depressed and tubes pulled apart if desired.

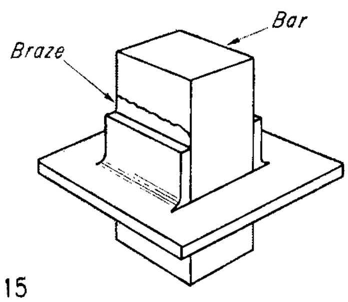

15

LANCED FLAPS provide large contact areas for brazing or soldering sheet-metal fins to bars and pipes. An alternate method for round bars or pipe is an embossed collar around the hole. However, for angular shapes, flaps are easier to make.

Lanced Sheetmetal Parts

Federico Strasser

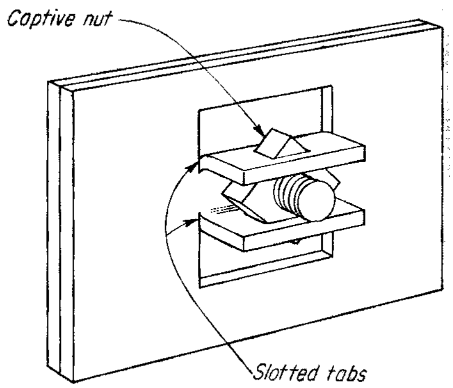

1 CAPTIVE NUT allows blind assembly on panel too thin to tap. Nut is held firmly, cannot get lost.

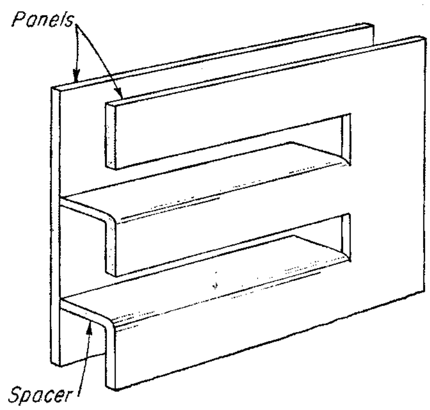

2 SPACERS separate panels with fewer parts and with less weight than extra strips or filler materials.

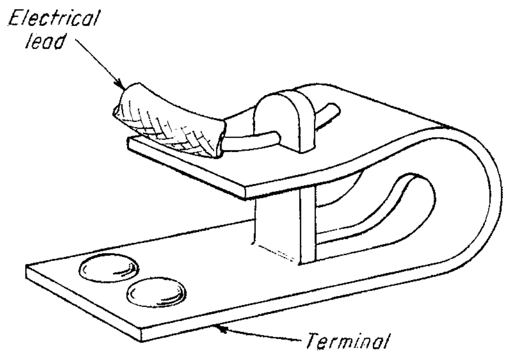

3 TERMINAL made of flat spring stock presses wire lead tightly in lanced tab, yet releases easily.

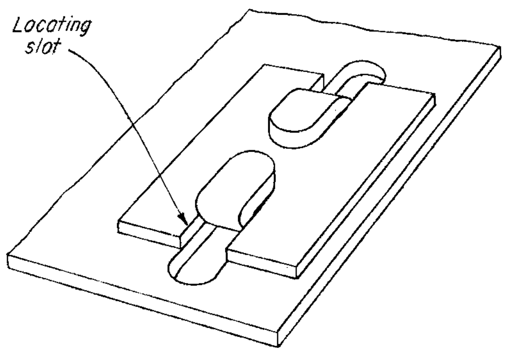

4 TABS fit into slot to align in one direction as well as fasten. Matching tab and slot on other side would align plate in second direction.

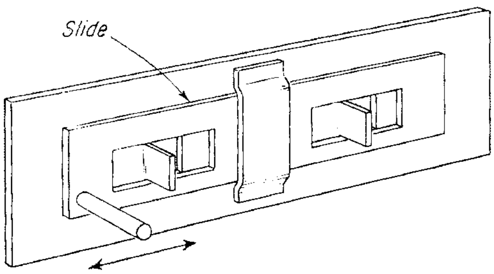

5 SLIDE rides on projecting tabs. At same time, tabs act as limit stops. Length of slot determines how far the slide can travel.

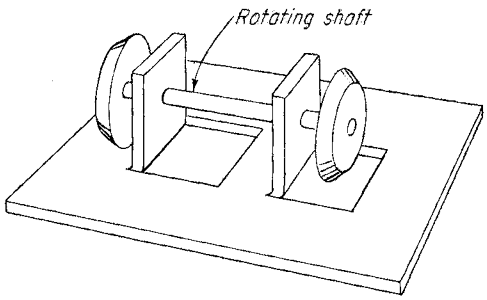

6 RAISED TABS are bearings and supports for rotating shaft in light-duty applications. Tabs will also guide sliding rod or bar. Bent-up end of plate can take place of a tab.

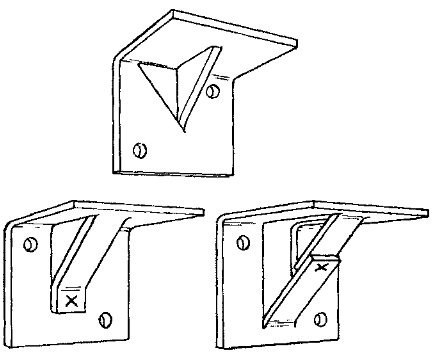

7 REINFORCEMENT RIBS of three different designs all give support for wall bracket, yet retain one-piece construction.

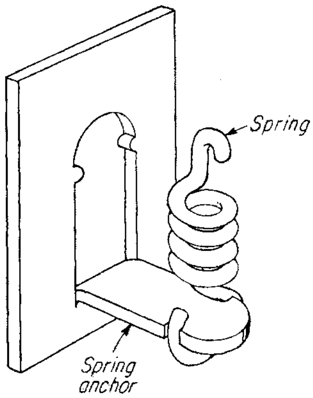

8 SPRING ANCHOR—possible variations: tab with hole, or tab with only one notch for spring that pulls to side.

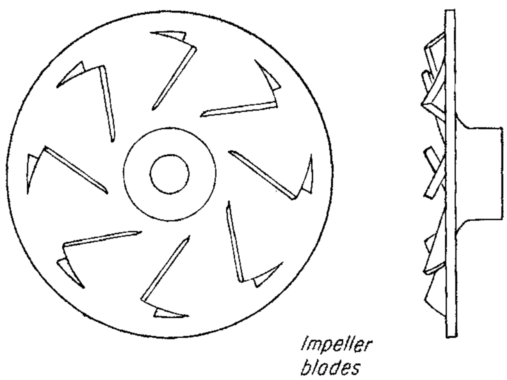

9 LANCED BLADING results in one-piece construction of lightweight cooling fan for small motors.

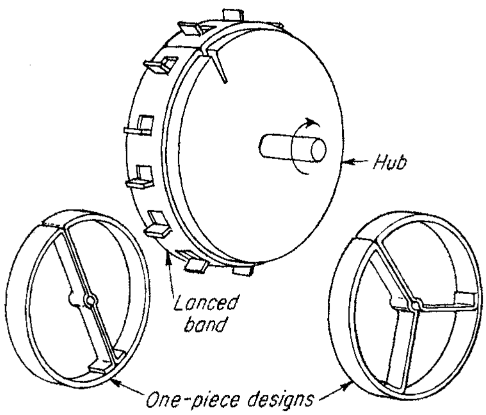

10 CONTINUOUS STRIP is lanced while flat, then cut to length and rolled into a sprocket. Small sketches suggest ways to avoid a separate hub.

Joining Circular Parts without Fasteners

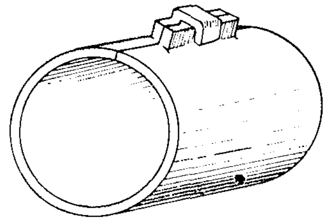

Fig. 1—Fastening for a rolled circular section. Tabs are integral with sheet; one tab being longer than the other, and bent over on assembly.

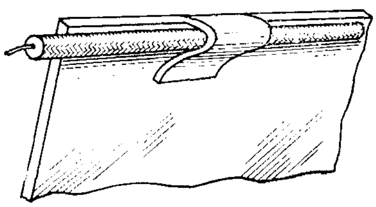

Fig. 5—Similar to Fig. 4 for supporting electrical wires. Tab is integral with plate and crimped over on assembly.

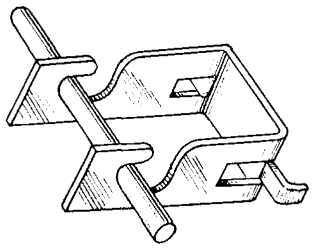

Fig. 6—For supporting of rods or tubes. Installation can be either permanent or temporary. Sheet metal bracket is held by bent tabs.

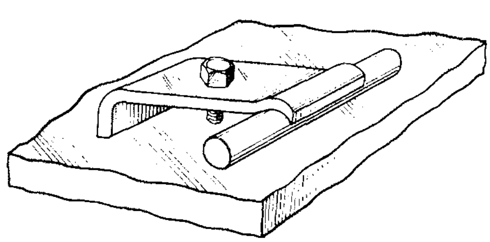

Fig. 7—Embossed sheet metal bracket to hold rods, tubes or cables. Tension is supplied by screw threaded into lower plate.

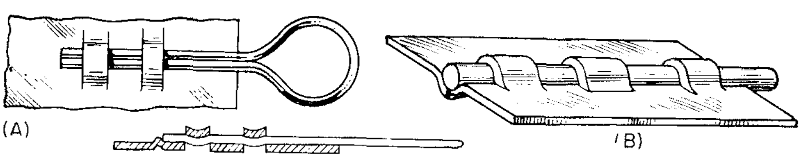

Fig. 10—Plate is embossed and tabs bent over on assembly. If two plates are used having tab edges (B) a piano-type hinge is formed. (A) and (B) can be combined to form a quick release door mechanism. A cable is passed through the eye of the hinge bolt, and a handle attached to the cable.

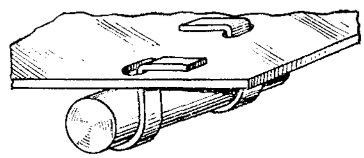

Fig. 11—Rods and tubes can be supported by sheet metal tabs. Tab is wrapped around circular section and bent through plate.

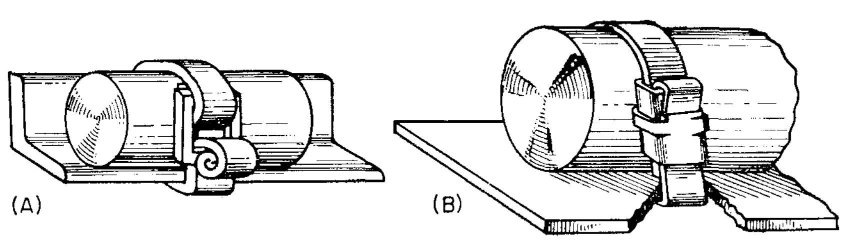

Fig. 14—Strap fastener to hold a circular section tight against a structural shape. Lock can be made from square bar stock (A) or from sheet metal (B) tabbed as shown. Strap is bent over for additional locking. Slotted holes in sheet should be spaced equal to rod dia to prevent tearing.

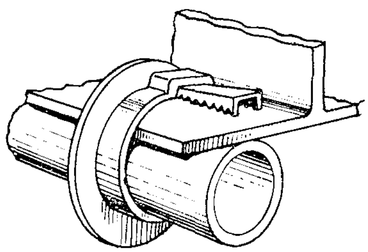

Fig. 15—*C* clamp support usually used for tubing. Serrated wedge is hammered tight; serrations keep wedge from unlocking.

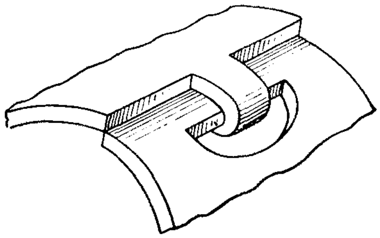

Fig. 2—Similar to Fig. 1 except tube is formed with a lap joint. Tab is bent over and inserted into cut-out on assembly. Joint tension is needed to maintain lock.

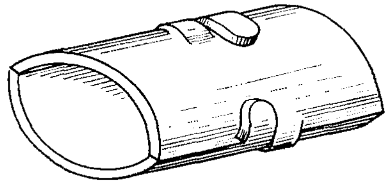

Fig. 3—Tab fastener for elliptical section. Tabs are formed integral with sheet. For best results tabs should be adjacent to each other as shown in sketch above.

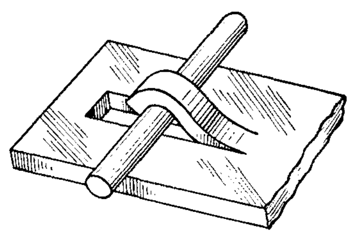

Fig. 4—For supporting rod on plate. Tab is formed and bent over rod on assembly. Wedging action holds rod in place. Rod is free to move unless restrained.

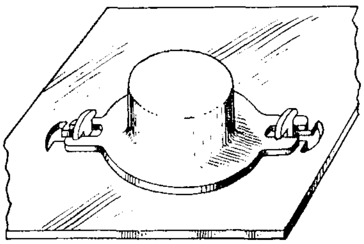

Fig. 8—Fastening of rod to plate. Rod is welded to plate with slotted holes. Tabs in bottom plate are bent on assembly.

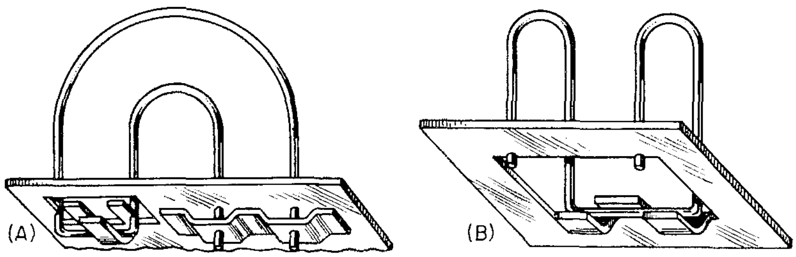

Fig. 9—Tabs and bracket (A) used to support rod at right angle to plate. Bracket can be welded to plate. (B) has rod slotted into place. For mass production, the tabs and slots can be stamped into the sheet. For limited production, the tabs and slots can be hand formed.

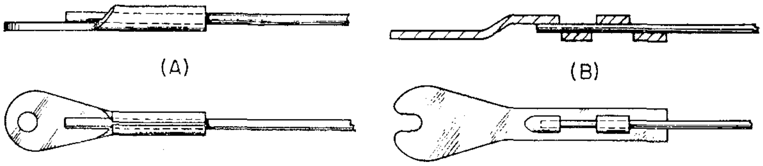

Fig. 12—For connecting wire ends to terminals. Sheet is crimped or tabbed to hold wire in place. Variety of terminal endings can be used. If additional fastening is required, in that parting of the wire and terminal end might create a safety or fire hazard, a drop of solder can be added.

Fig. 13—Spring joins two rods or tubes. Members are not limited in axial motion or rotation except by spring strength.

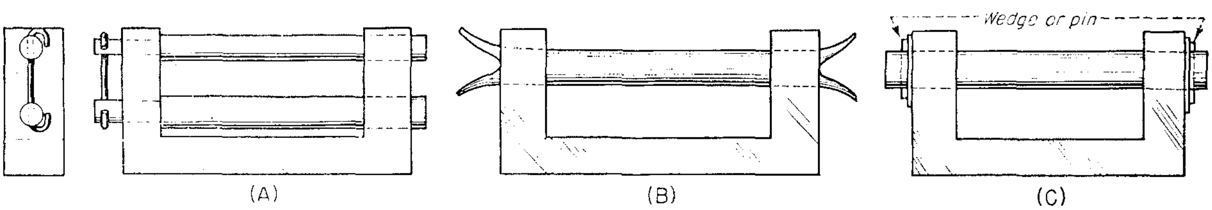

Fig. 16—Methods of locking rods in machine frames. In (A) one end of the rod is machined to a smaller diameter. Shoulder and bent member restrains rod from slipping out of frame. Limited axial and rotational freedom is present.

Split rod in (B) limits axial motion but permits rotation. Rod is split on assembly. Wedge or pin in (C) bear against washers. Axial motion can be restricted but rotation is possible. If rod is to be a roller, bearings can be inserted.

Joining Sheet Metal Parts without Fasteners

Methods of attaching rods, tubing and sheet metal parts in permanent or temporary assemblies without using bolts, screws or rivets.

Erwin Rausch

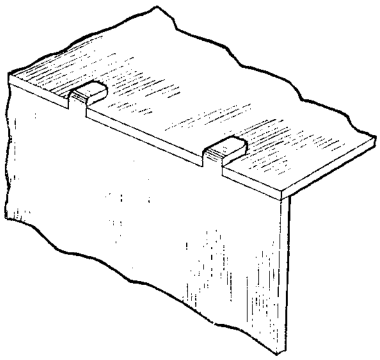

FIG. 1—For butting sheet metal parts at or near a right angle. Two or more tabs are required.

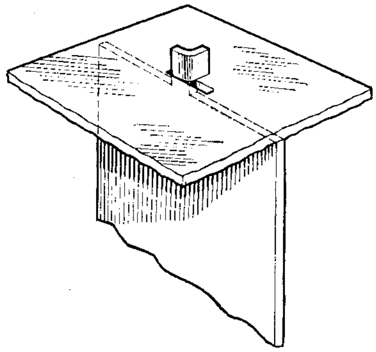

FIG. 2—For applications similar to Fig. 1, but where inaccessibility forbids use of bulky tools.

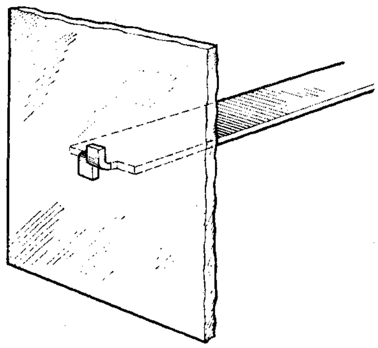

FIG. 3—For use as in Fig. 2, but where greater rigidity is needed.

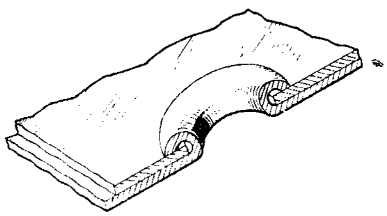

FIG. 4—For permanent attachment of parallel sections. Material must be quarter-hard or softer.

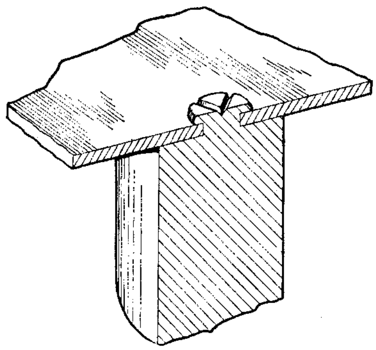

FIG. 5—For positioning shouldered rods in sheet metal. Center-punch as well as "nicking" punch can be used.

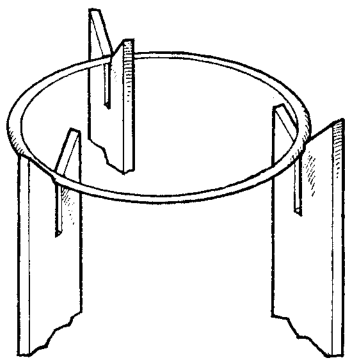

FIG. 6—For temporary support of rods or tubes. Jaws are sprung open during installation and removal.

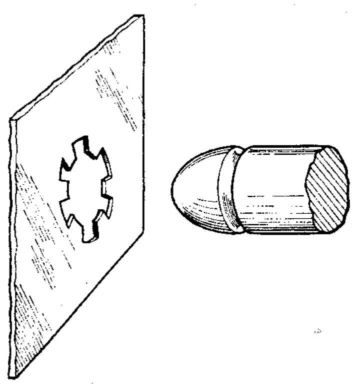

FIG. 7—For semi-rigid attachment. Installation can be permanent or temporary, depending on roundness of rod end and "springiness" of teeth.

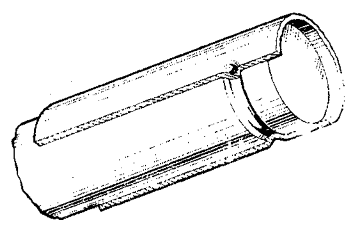

FIG. 8—For permanent location of rod in tube. Dents are made after rod is in place. Axial movement can be obtained by lengthening recess.

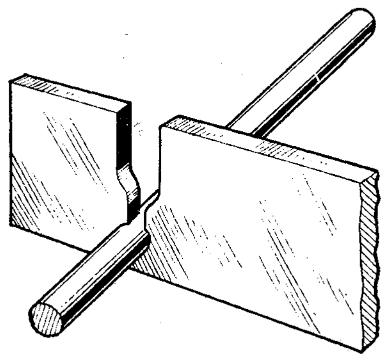

FIG. 9—For temporary positioning of rods in sheet metal. Slots in rod prevent axial movement.

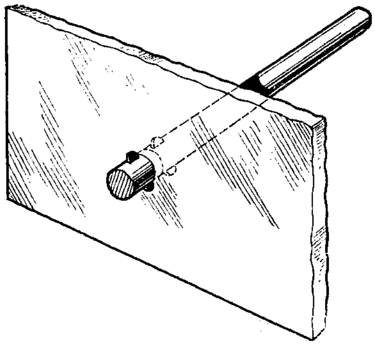

FIG. 10—For permanent assemblies where split forming die can be applied on one or both sides of sheet.

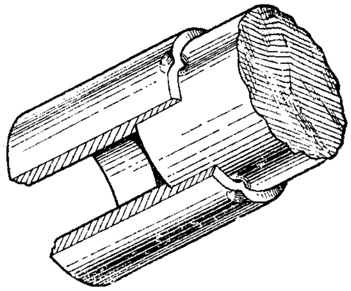

FIG. 11—For attachment of recessed, solid metallic or non-metallic parts in thick-sectioned cylindrical parts.

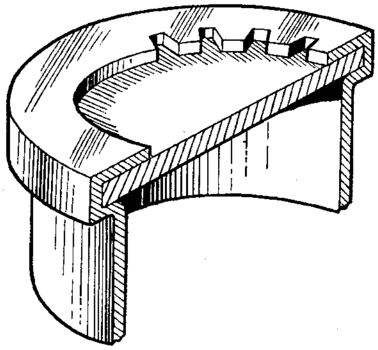

FIG. 12—For closing the end(s) of cylindrical parts. "Toothed" section permits removal of cap, "solid" section does not.

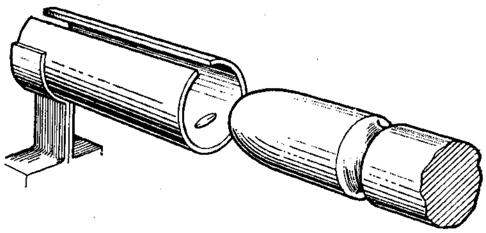

FIG. 13—For bayonet-type electrical fittings. Sleeve and mounting bracket can be modified to suit requirements.

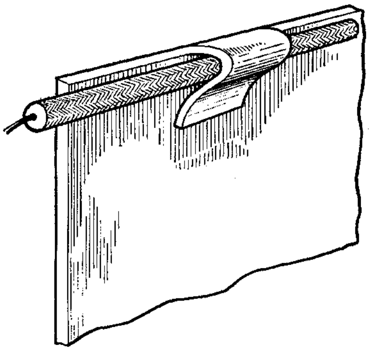

FIG. 14—For supporting electrical conductors.

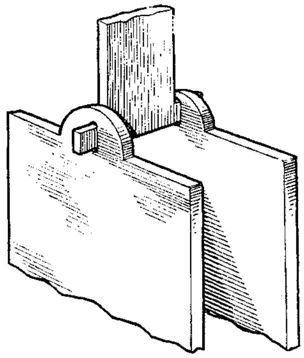

FIG. 15—For permanent assemblies requiring relative movement, but minimum rigidity.

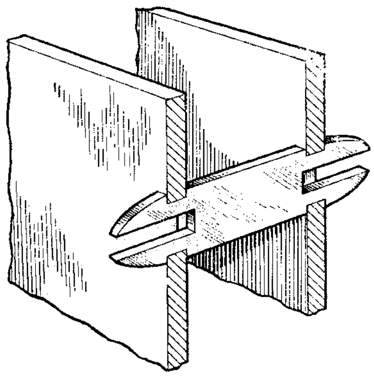

FIG. 16—For temporary use as spacer. Sheet holes can be round or rectangular.

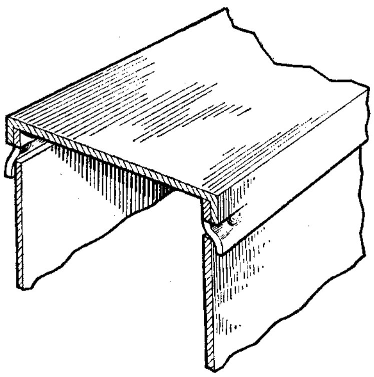

FIG. 17—For attachment of cover to channel or similar assemblies.

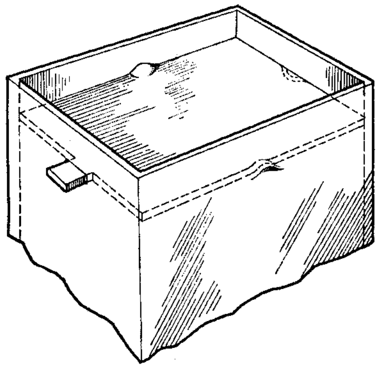

FIG. 18—For recessing sheet metal plates in rectangular housings.

Fastening Sheet-Metal Parts by Tongues, Snaps or Clinching

Detachable and permanent assembly of sheet metal parts without using rivets, bolts or screws.

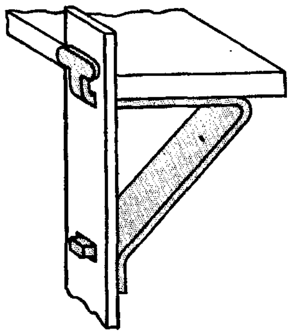

Fig. 1—Supporting bracket formed from sheet metal and having integral tabs. Upper tab is inserted into structure and bent. Ledge weight holds lower tab.

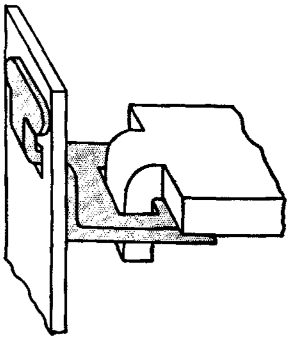

Fig. 2—Supporting bracket similar to Fig. 1 but offering restraint to shelf or ledge. Tabs are integral with sheet metal part and are bent on assembly.

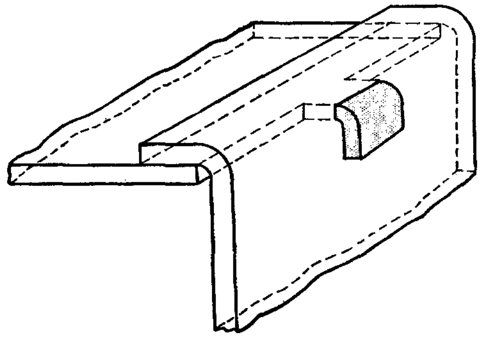

Fig. 3—Supporting ledge or shelf by direct attachment. Tab is integral and bent on assembly. Additional support is possible if sheet is placed on flange and tabbed.

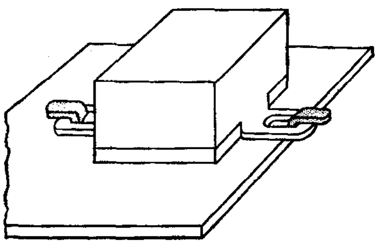

Fig. 7—Box section joined to a flat sheet or plate. Elongated holes are integral with box section and tabs are integral with plate. Design is not limited to edge location.

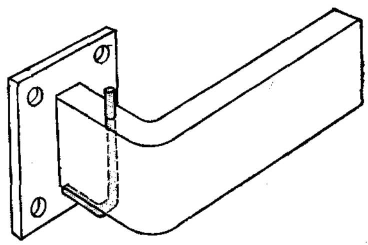

Fig. 8—Bar is joined to sheet metal bracket by a pin or rod. Right angle bends in pin restrict sidewise or rocking motion or bar. Bracket end of pin is peened.

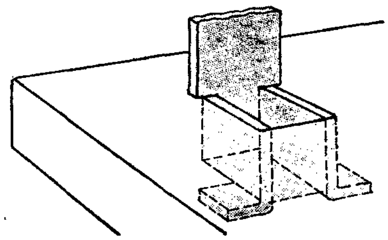

Fig. 9—To support and join sheet metal support at right angle to plate. Motion is restricted in all directions. Bottom surface can be grooved for tabs.

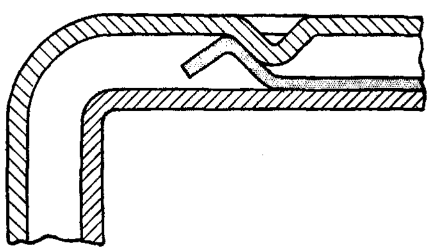

Fig. 13—A spacing method that can be used for circular sections. Formed sheet metal member support outer structure at set distance. Bead centers structure.

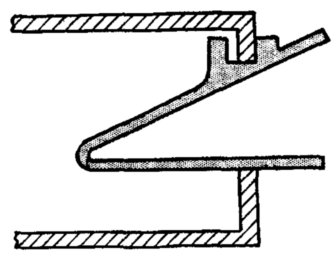

Fig. 14—A removable section held in place by elasticity of material. Design shown is a temporary or a removable cover for an elongated slotted hole in a sheet metal part.

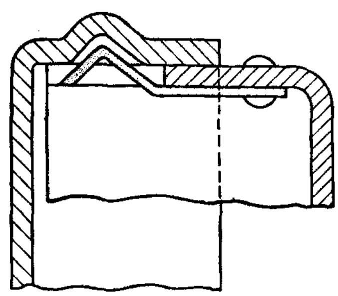

Fig. 15—A cover held in position by bead and formed sheet. Cover is restrained from motion but can be rotated. Used for covers that must be removable.

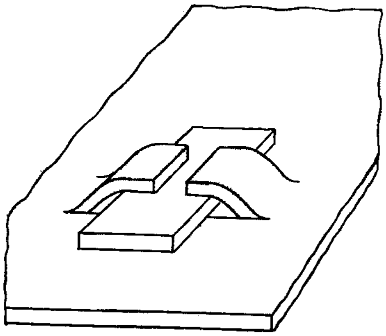

Fig. 4—To support or join a flat sheet metal form on a large plate. Tabs are integral with plate and bent over on assembly. Only side-wise motion is restricted.

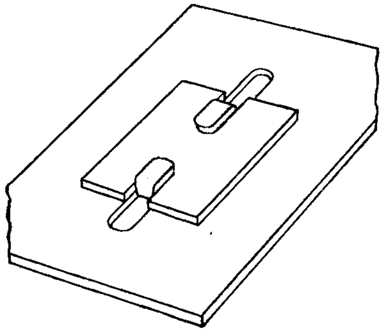

Fig. 5—Similar to Fig. 4 but motion is restricted in all directions. Upper sheet is slotted, and tabs are bent over and into slots on assembly.

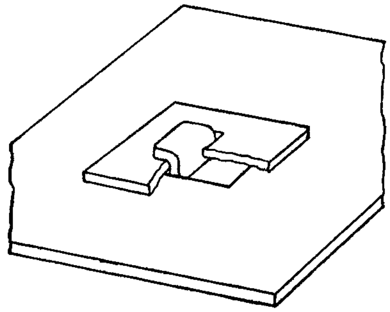

Fig. 6—Single tab design for complete restriction of motion. Upper plate has an elongated hole that matches width and thickness of integral lower plate tab.

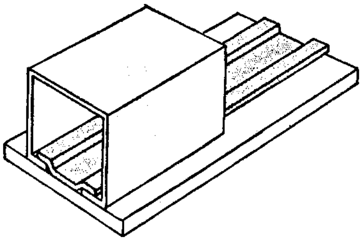

Fig. 10—Channel section spot welded to plate forms bottom surface and joins box section to plate. Channel edges can be crimped or spot welded to restrict motion.

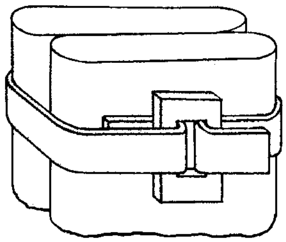

Fig. 11—Sheet metal strap used to join two flat surfaces. Edges of plate are rounded to allow strap to follow contour and prevent cutting of plate by the metal strap.

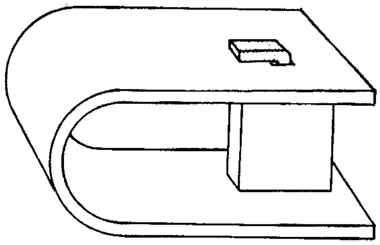

Fig. 12—Sheet metal structures can be spaced and joined by use of a tabbed block. Formed sheet metal U section is held to form by the block as shown.

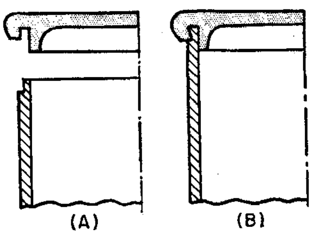

Fig. 16—A non-removable cover design. The vessel is notched as shown in A, and the cover crimped over, B, on assembly. This is a permanent cover assembly.

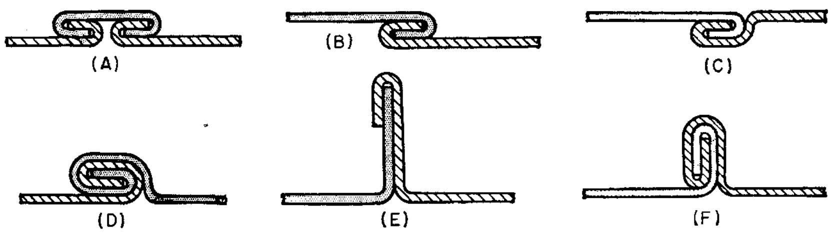

Fig. 17—Six methods of joining two sheet metal parts. These can be temporary or permanent joints. If necessary, joints can be riveted, bolted, screwed or welded for added strength and support. Such joints can also be used to make right angle corner joints on sheet metal boxes, or for attaching top and bottom covers on sheet metal containers.

Retainers for Circuit Boards

These retainers ensure that the board is properly seated and locked against shock and vibration.

Irwin N. Schuster

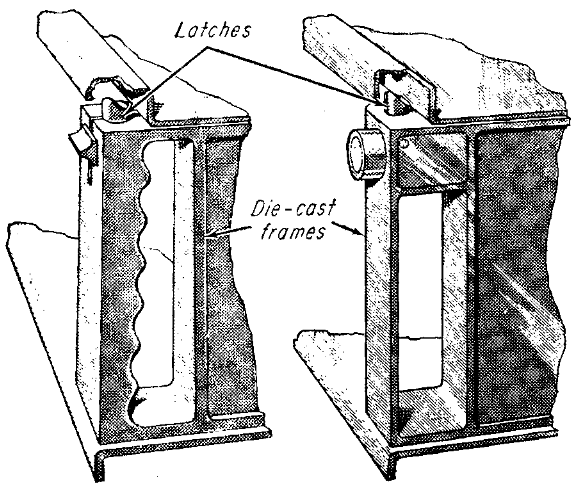

1

SPRING-LOADED LATCHES for large die-cast frames are positive and clean looking. The cost is somewhat high.

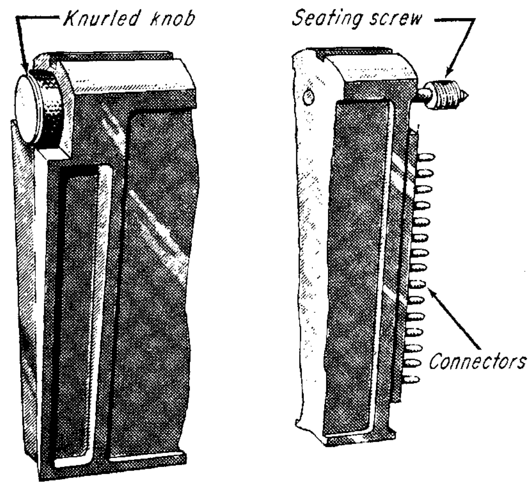

2

TIGHT SEATING is necessary for connectors of the plug and socket type. A screw and a knurled knob aid seating.

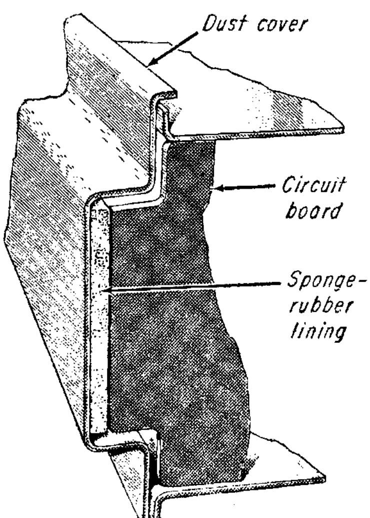

5

DUST COVER, lined with sponge rubber, does double duty – it holds the board in place and helps protect it from shock.

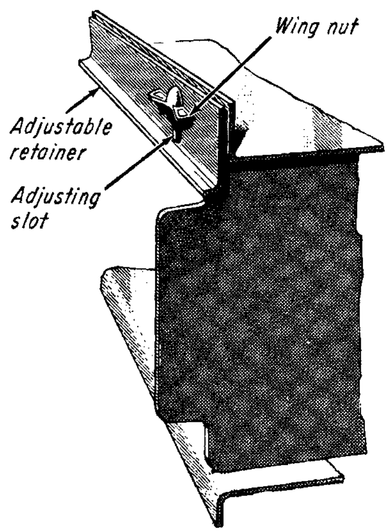

6

ADJUSTABLE PLATES, either flat or formed, are very easy to assemble and hold sliding parts firmly in place.

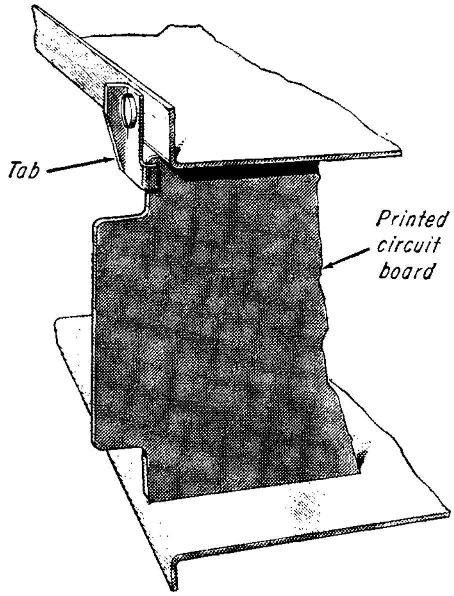

3

SHEETMETAL TABS, pivoting on either a shoulder screw or rivet, are always an efficient, low-cost way to retain parts.

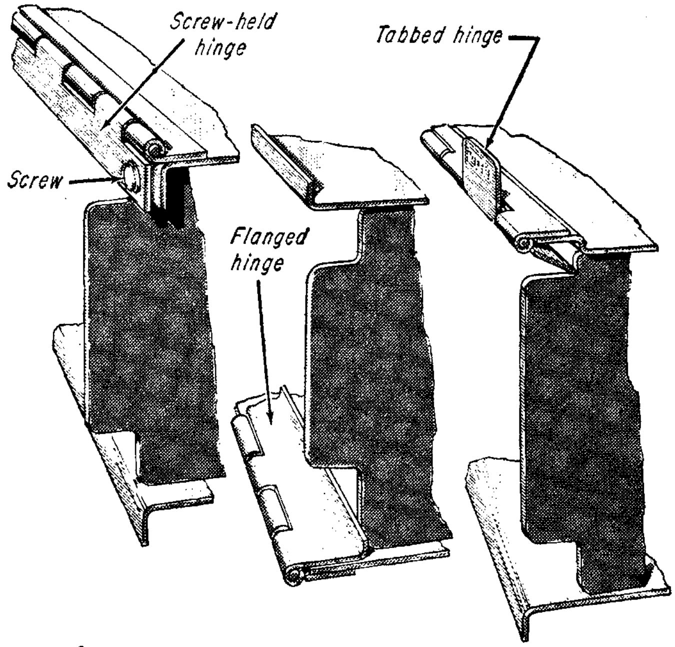

4

HINGES, spring loaded or otherwise modified, provide a variety of suitable means for retaining circuit boards in place.

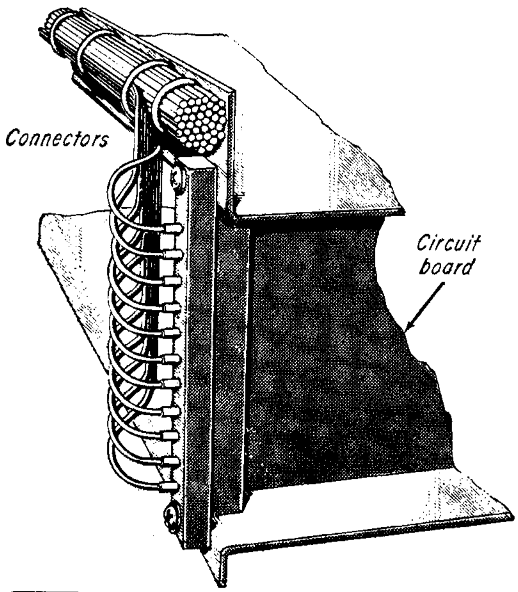

7

FRONT-MOUNTED CONNECTORS do double duty here, providing test points for circuit leads and securing the board.

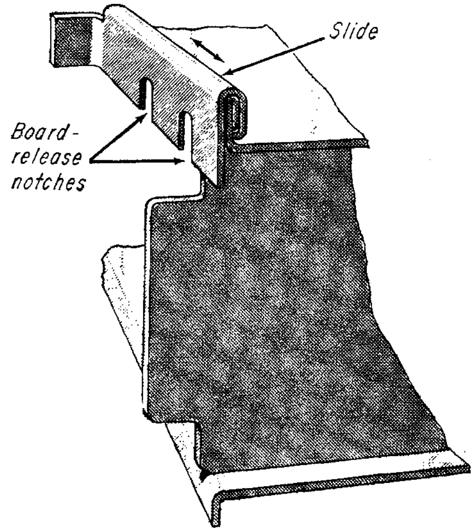

8

NOTCHES in the slide provide entrance and exit gates for circuit boards. Lubrication of the slide may be advisable.

These methods for retaining circuit boards can give you some valuable ideas you can apply to other devices.

Irwin N. Schuster

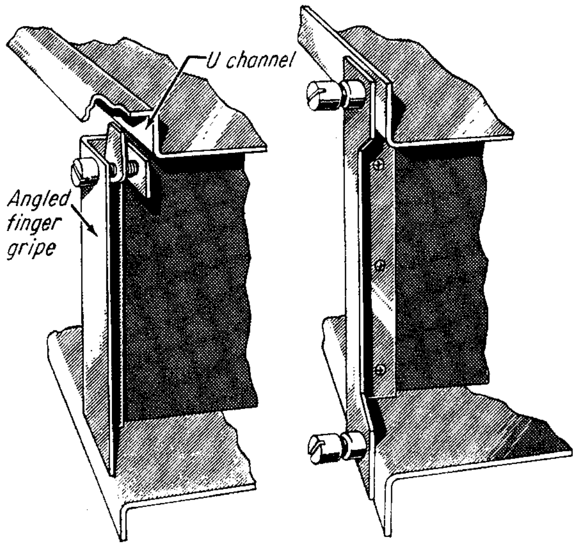

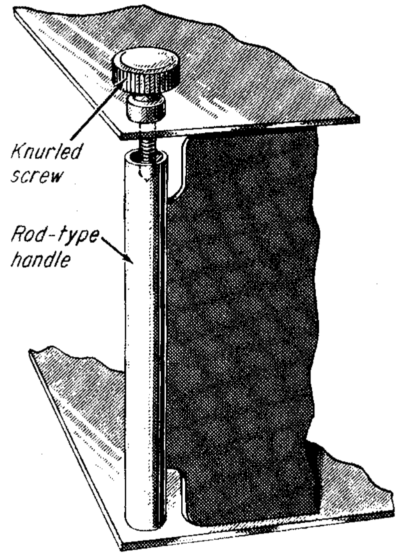

9 **ANGLED HANDLES** fitted with standard hardware parts result in low-cost, yet efficient, slide retainers.

10 **ROD-TYPE HANDLE** can be either solid, with tapped hole for screw, or hollow, with mating dowel-type spring latch.

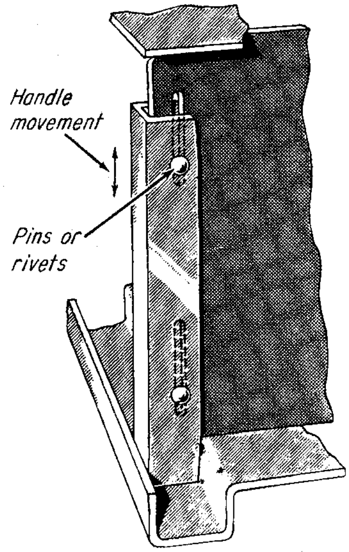

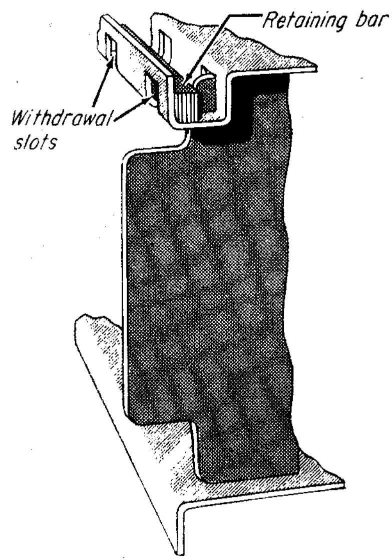

11 **SLIDING HANDLES** can be arranged to fall into locking position when vertical; otherwise they need springs.

12 **SLOTTED U-CHANNEL** not only locates the circuit boards at correct spacings but also accommodates a retaining bar.

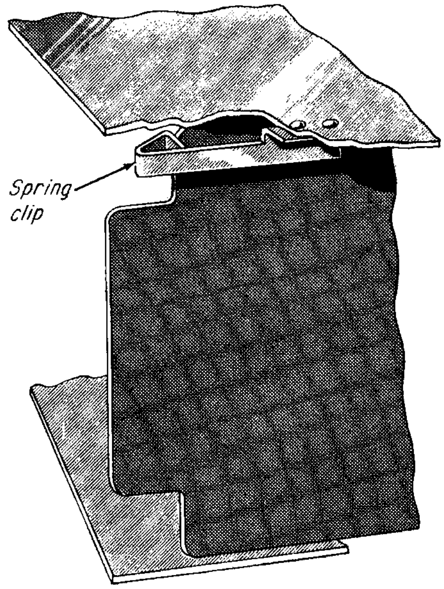

13 **SPRING LATCHES** are always popular for holding parts that must be removed periodically for service.

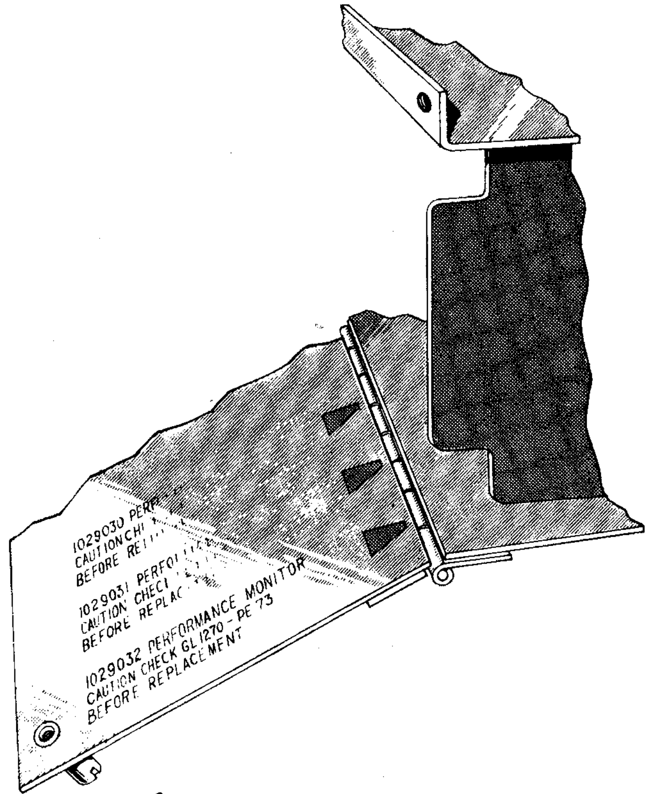

14 **DOUBLE-DUTY COVERS** not only hold units in place but are also ideal locations for operating instructions.

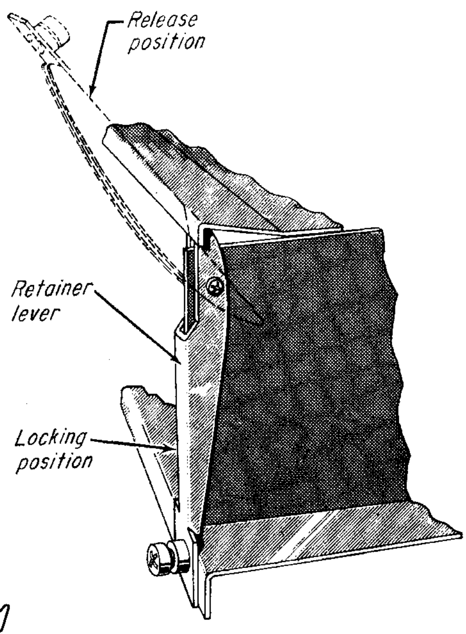

15 **RETAINER LEVERS** jack the boards into and out of the receptacle. Such levers are usually locked in place.

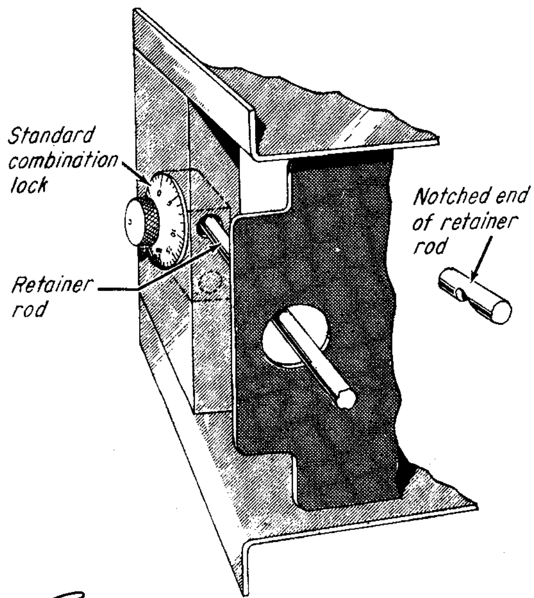

16 **COMBINATION LOCK** and straight, notched bar provide a retaining assembly that is virtually tamperproof.

They allow easy and quick insertion, they guide accurately, and they support the board firmly in place.

Irwin N. Schuster

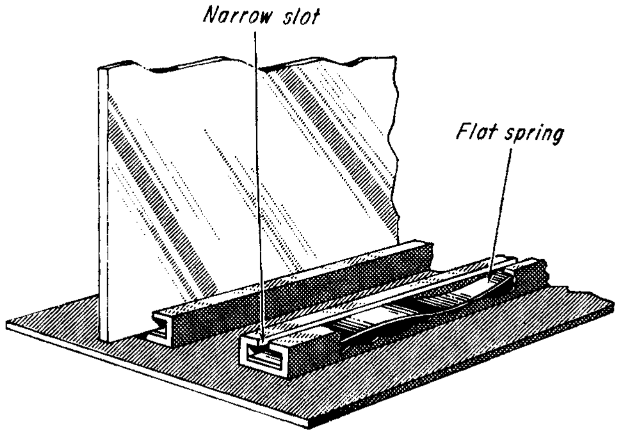

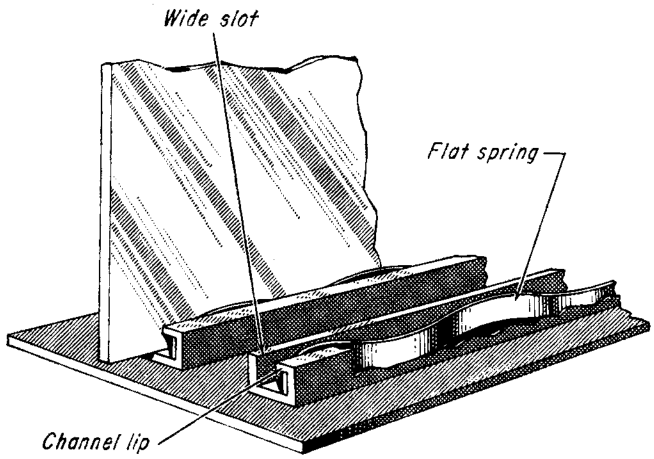

17 **FLAT SPRING** in extruded section provides close limitation for horizontal panel-movement, extreme tolerance vertically.

18 **CHANNEL LIP** allows flat spring to be placed to retain circuit board against channel side and reduce tolerances.

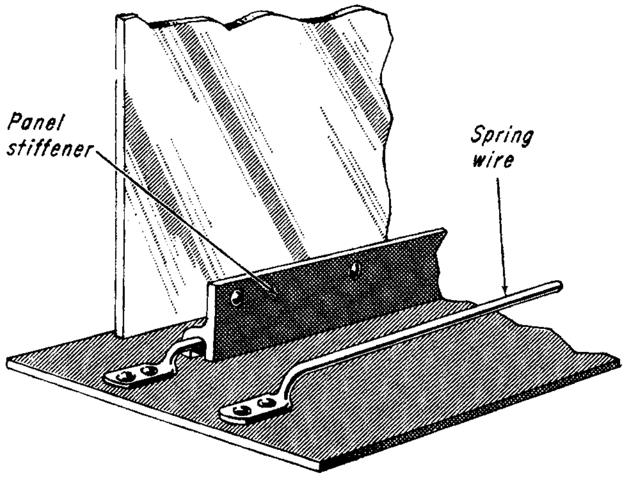

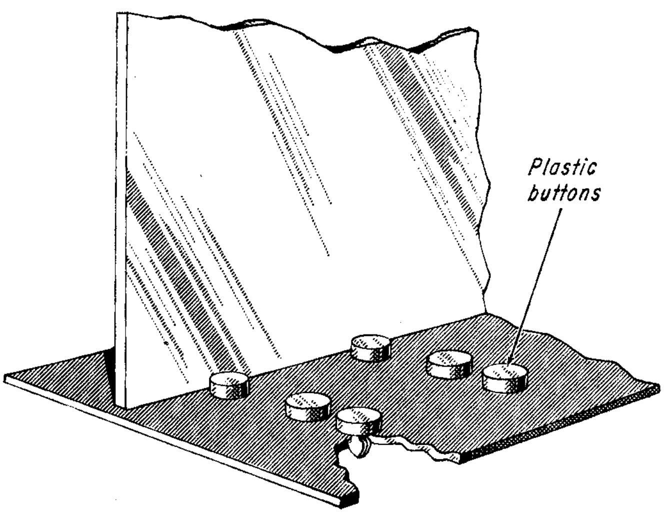

19 **SPRING WIRE** and panel stiffener is a good combination where panel space is not at a premium.

20 **PLASTIC BUTTONS** offer an ultra-simple method of holding panels. The round buttons let panel slide home easily.

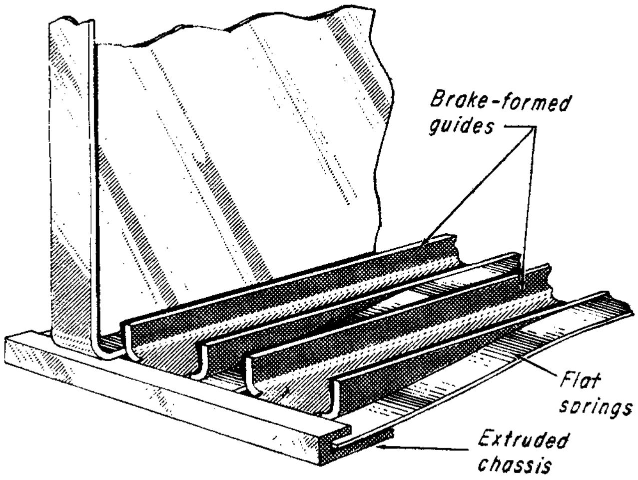

21 **EXTRUDED CHASSIS PARTS,** brake-formed guides, and flat springs allow more tolerance reduction in assembly.

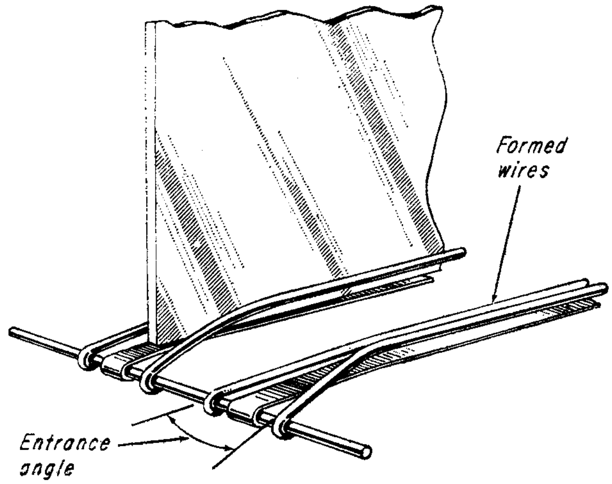

22 **FORMED WIRE** structure lets cooling air through while gripping the circuit board firmly in two planes.

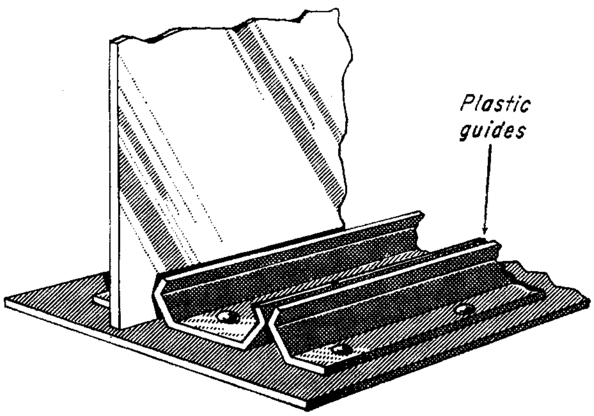

23 **EXTRUDED OR HEAT-FORMED** plastic guides are inexpensive and reduce the chance of shorting to the metal chassis.

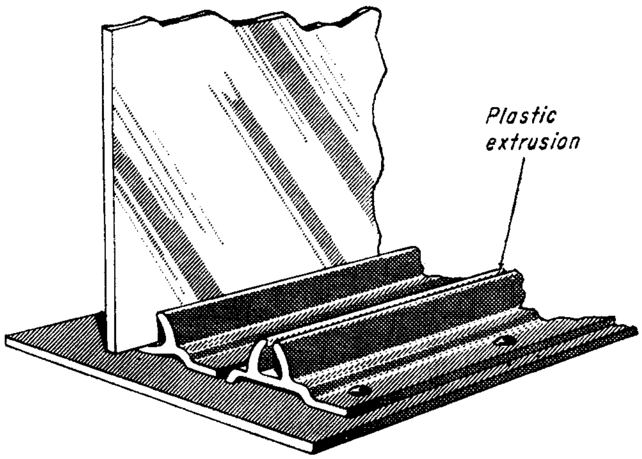

24 **PLASTIC EXTRUSION** here provides its own spring grip to support a light-weight panel in a mild environment.

Printed circuit boards must be easily inserted, accurately guided, and supported firmly in place during service.

Irwin N. Schuster

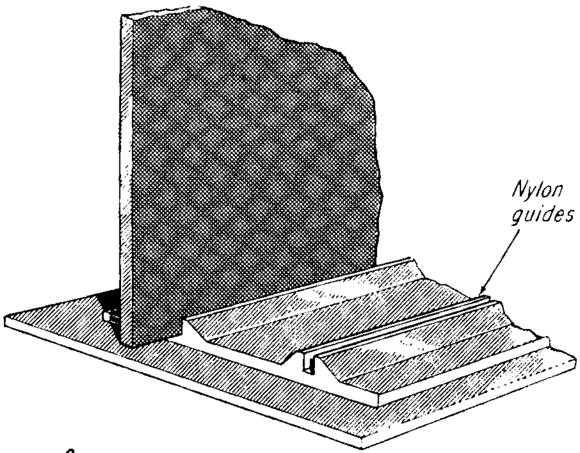

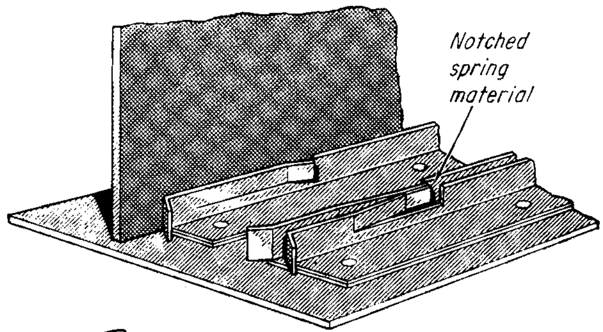

25 **NYLON GUIDES** grip the board along its entire length, lend support, and damp vibration during service.

26 **NOTCHED SPRING MATERIAL** allows wide grooves for ease of alignment when mating with fixed connectors.

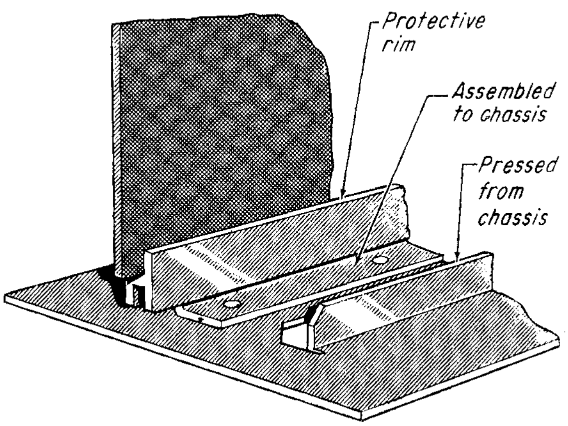

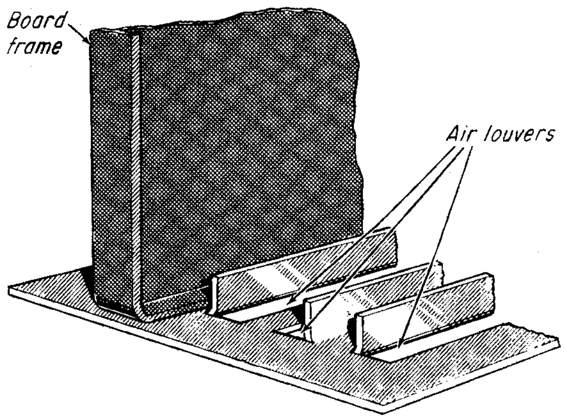

27 **PANEL STIFFENER** and protective rin give excellent service. Guide can b pressed from chassis.

28 **BOARD STIFFENER** requires wide channel in chassis. When channel is pressed from chassis, air louvers are gained.

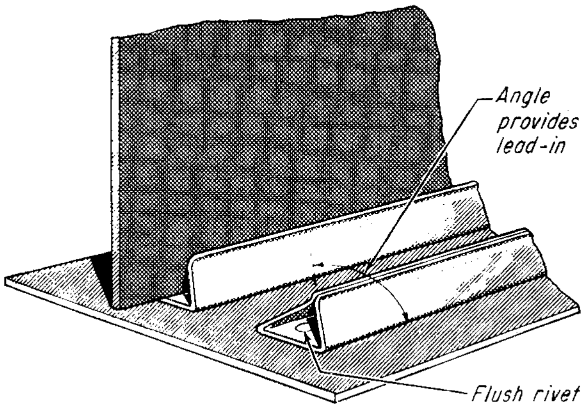

29 **FORMED SHEETMETAL GUIDE** is made of spring material, with the end cut off at an angle to guide the board.

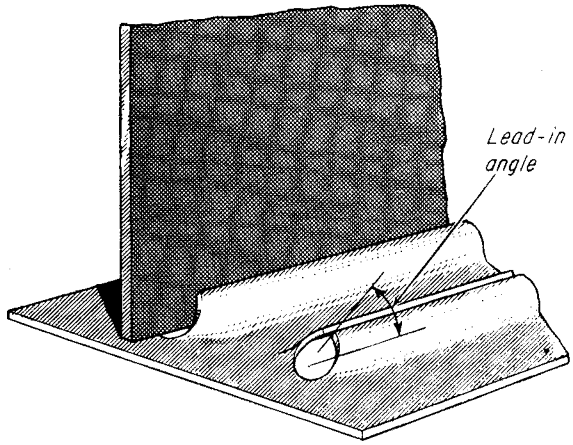

30 **STAMPED-IN** board guide reduces weight of chassis while providing firm board mount. Note lead-in angle.

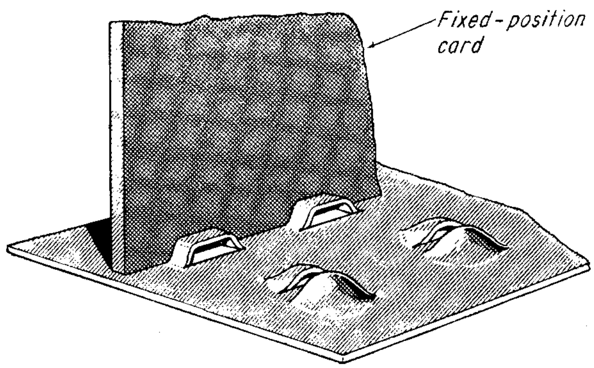

31 **SMALL SECTIONS** stamped in the chassis provide locating guides for cards mounted in fixed positions.

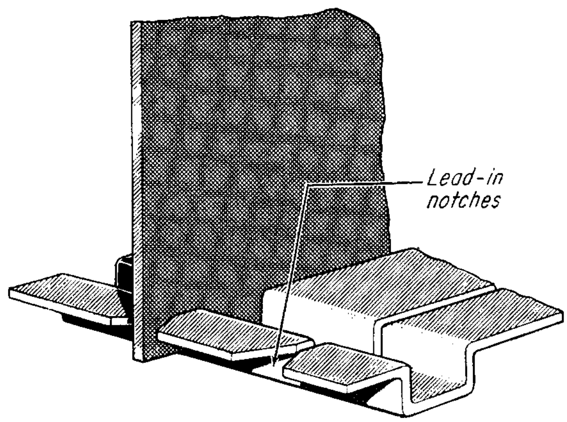

32 **INTEGRAL GUIDE** is ideal when stiff chassis is required and gives excellent lead-in characteristics.

Handles for Printed Circuits

Seven simple designs for making maintenance easier.

Irwin N. Schuster

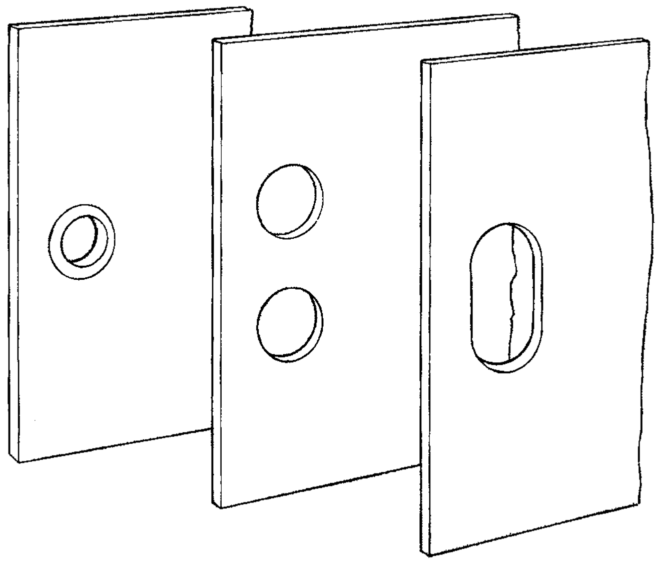

1

PUNCHED OR DRILLED HOLES are adequate if space between boards is sufficient for finger insertion. Grommets may be required in some materials.

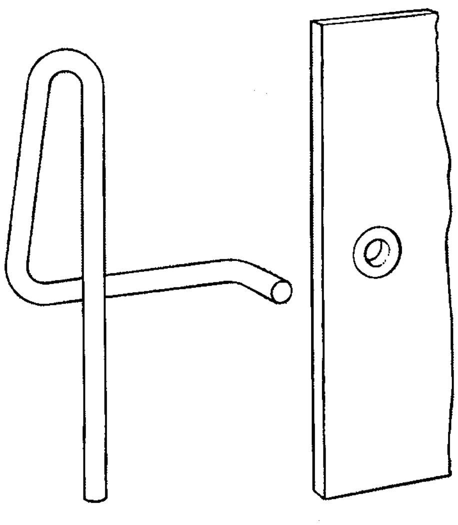

2

SMALL EYELET and removable extractor works well when space and weight are at a premium.

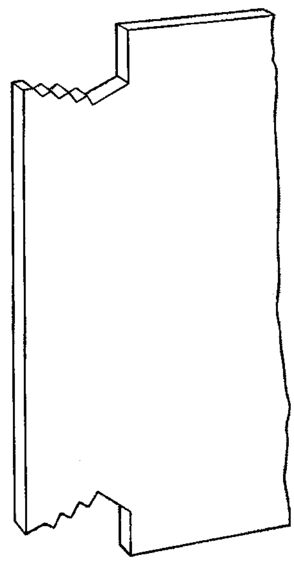

3

SERRATED FINGER GRIPS are often best when spacing of boards is extremely close.

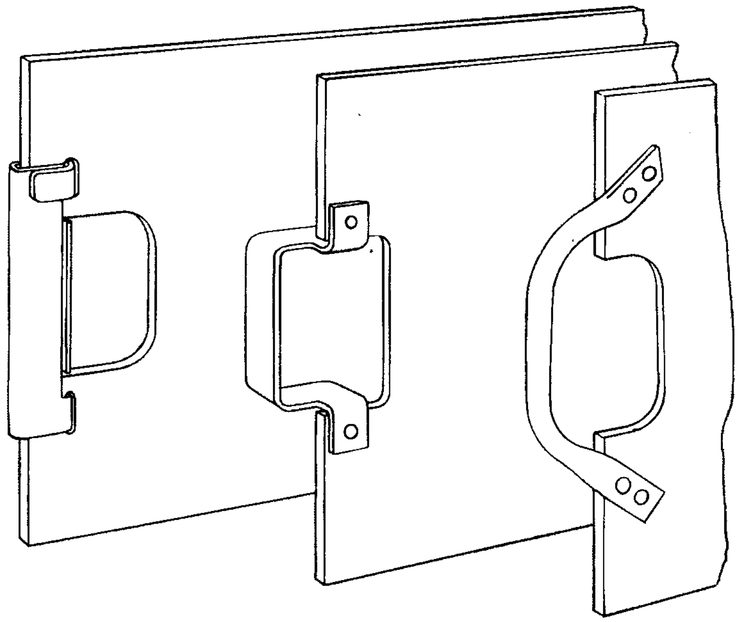

4

INDIVIDUAL HANDLES, tabbed or riveted in place, may be called for on large boards.

5

FORMED BOARDS do double duty when test points and jacks are incorporated into handles.

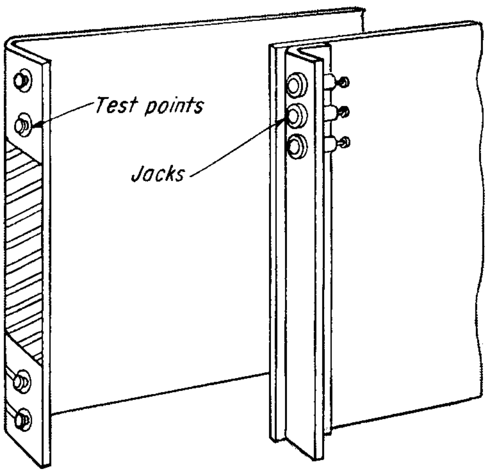

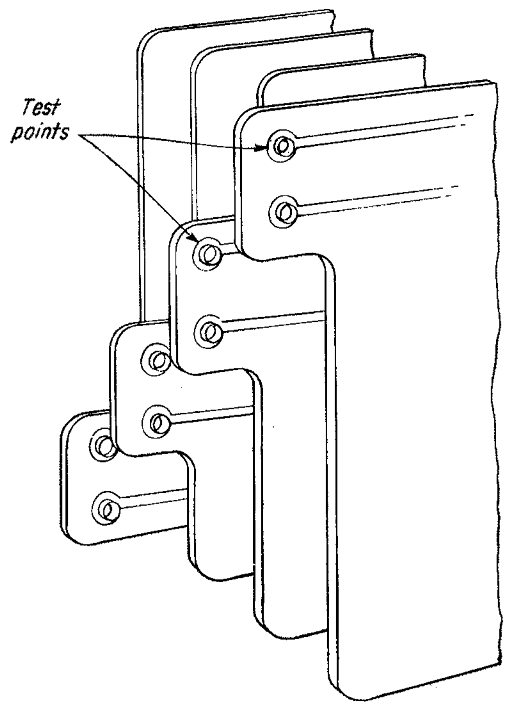

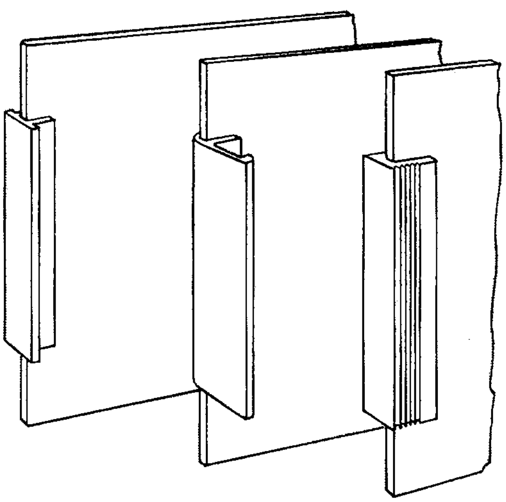

6

EXTRUSIONS staked, crimped or pinned in place form attractive withdrawal aids.

7

STAGGERED POSITIONS of removal tabs give easy access to test points on closely spaced panels.

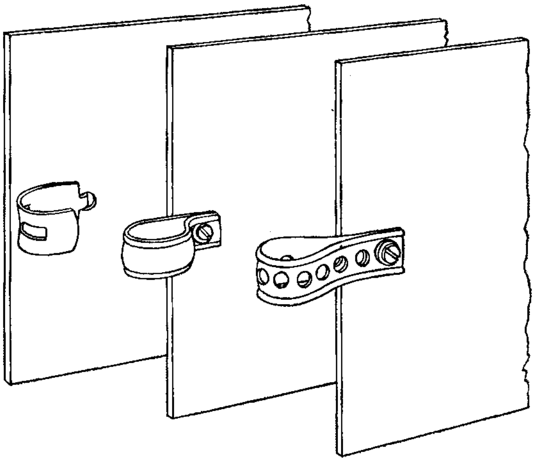

8

CABLE CLAMPS AND STRAPS are readily available in many styles. By using solderable materials, handles can be assembled during component-soldering operation.

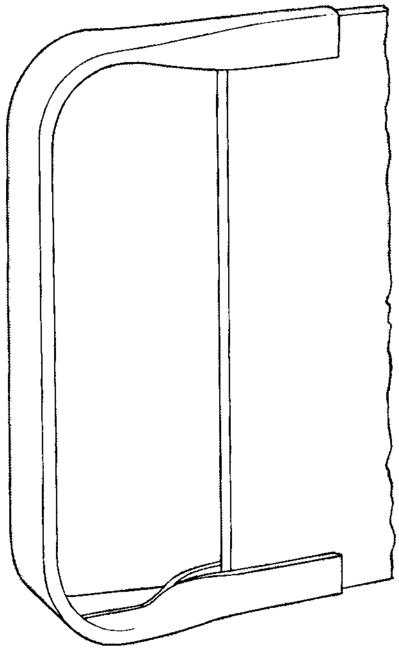

9

MORE COMPLEX SHAPE of sheetmetal handle is often preferred when appearance is an important feature of the design.

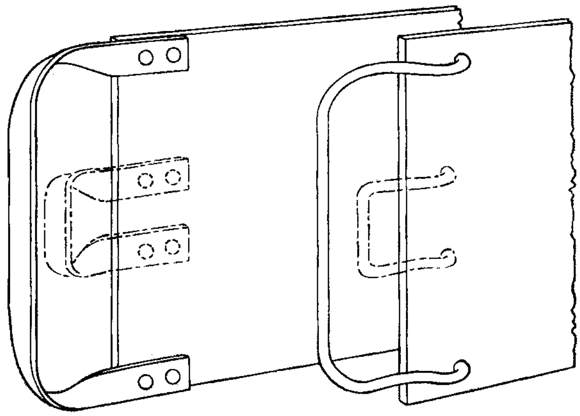

10

WIRE OR SHEETMETAL parts may be easily formed either as full handles or fingergrips.

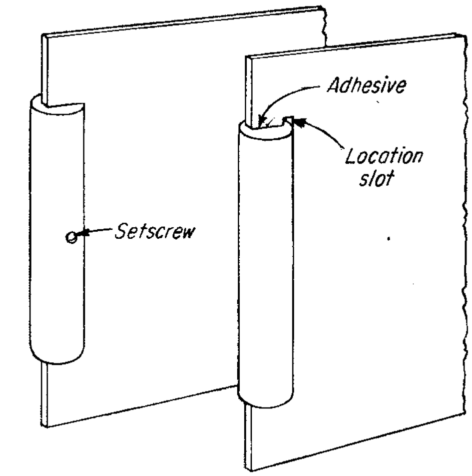

11

SLOTTED ROD, held by either a screw or adhesive, is most suitable when more robust fastening is required.

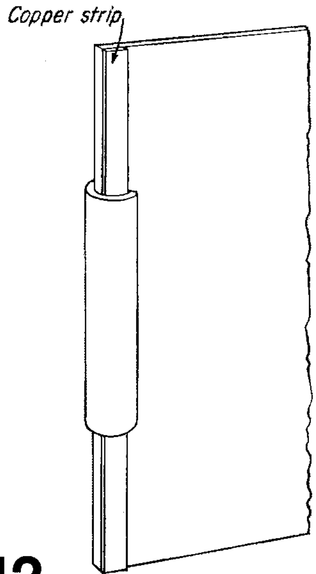

12

SPLIT TUBING can be slipped onto panels and retained by spring effect, or a copper strip can be left to provide a shoulder.

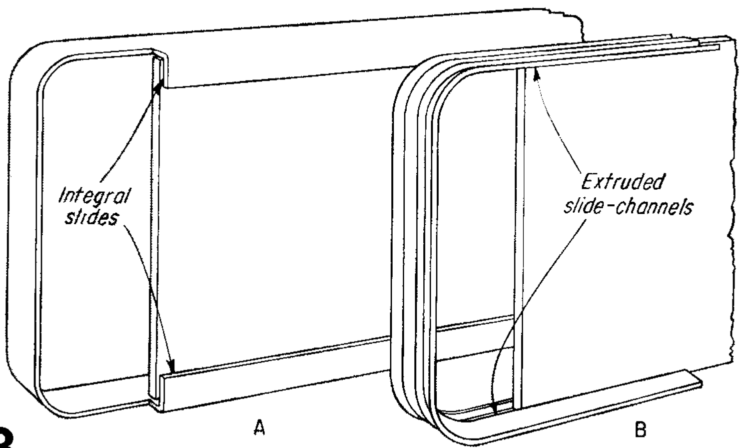

13

BOARD-STIFFENING FRAMES have integral slide surfaces and handles. Method suitable for either press-forming (A) or extrusion (B).

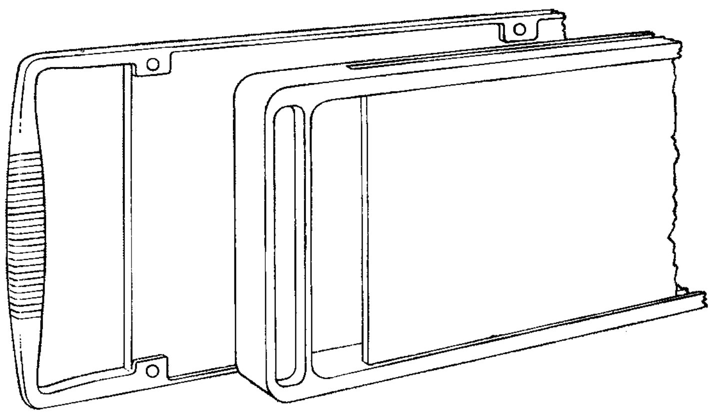

14

DIE-CAST AND MOLDED handles can be provided if needed in quantity large enough to justify added cost of tooling.

Friction Clamping Devices

Bernard J. Wolfe

All types of mechanisms used for gaining mechanical advantage have probably been used in the design of friction clamps. This type of clamp can hold moderately large loads by friction grip on smooth surfaces even of comparatively small area and, in some designs, tightened or released with little effort and movement of the control. In the clamps illustrated here the mechanical advantage is gained by the use of the common devices: lever, toggle, screw, wedge, and combinations of these means.

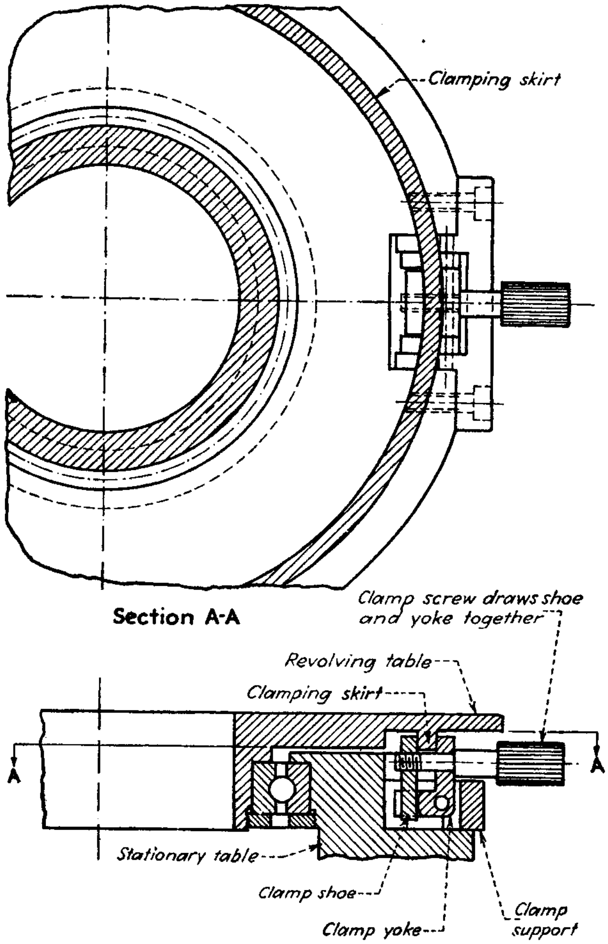

TURN TABLE CLAMP

Clamp assembly floats on pin and does not disturb table setting

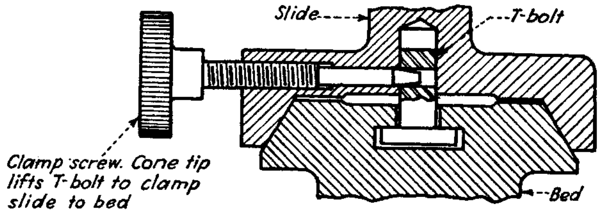

SLIDE CLAMP

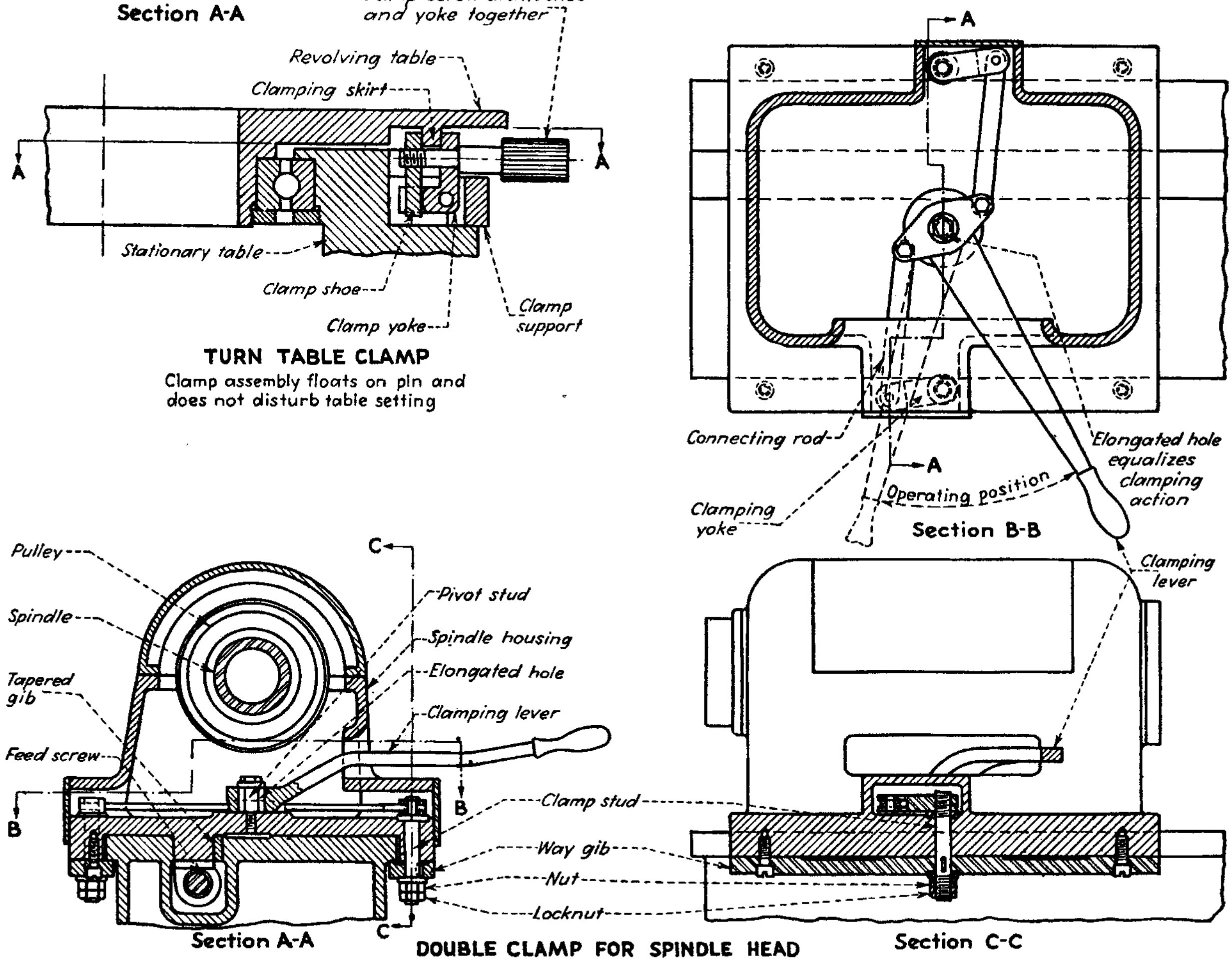

DOUBLE CLAMP FOR SPINDLE HEAD

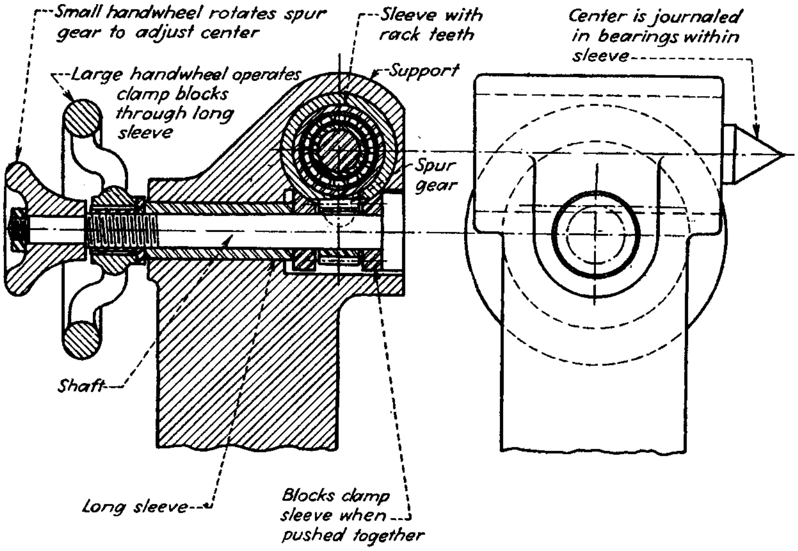

CENTER SUPPORT CLAMP

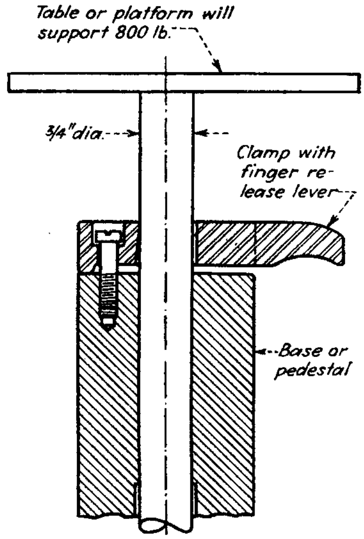

PEDESTAL CLAMP

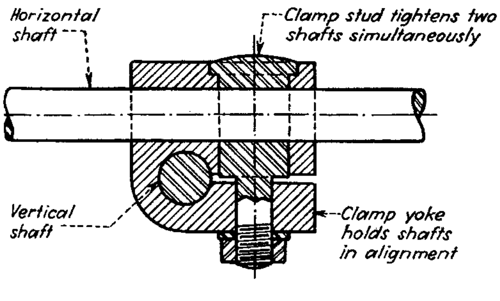

RIGHT ANGLE CLAMP

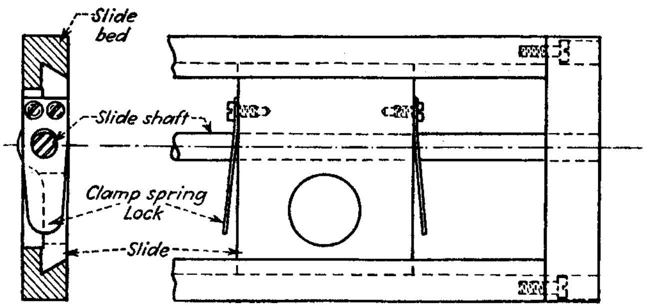

SLIDE CLAMP

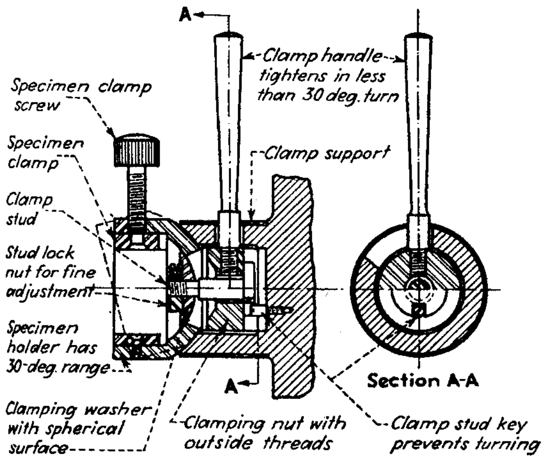

SPECIMEN HOLDER CLAMP

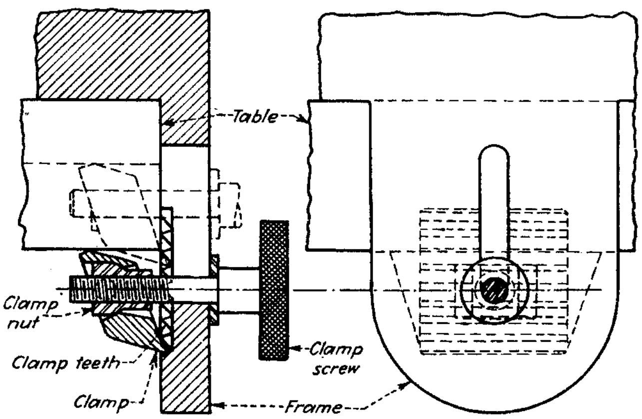

TABLE CLAMP

Clamping Devices for Aligning Adjustable Parts

Methods of clamping parts which must be readily movable are as numerous and as varied as the requirements. In many instances, a clamp of any design is satisfactory, provided it has sufficient strength to hold the parts immovable when tightened. However, it is sometimes necessary that the movable part be clamped to maintain accurate alignment with some fixed part. Examples of this latter-type are described and illustrated.

Louis Kasper

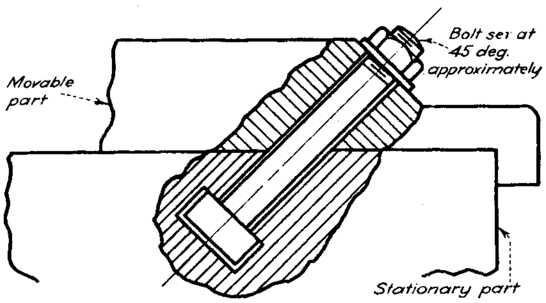

FIG. 1—When nut is tightened, the flange on the edge of the movable part is drawn against the machined edge of the stationary part. This method is effective, but removal of the clamped part may be difficult if it is heavy or unbalanced.

FIG. 2—Lower edge of the bolt head contacts the angular side of locating groove, causing the keys to be held tightly against the opposite side of the groove. This design permits easy removal of the clamped part, but is effective only if the working pressure is directly downward or in a direction against the perpendicular side of the slot.

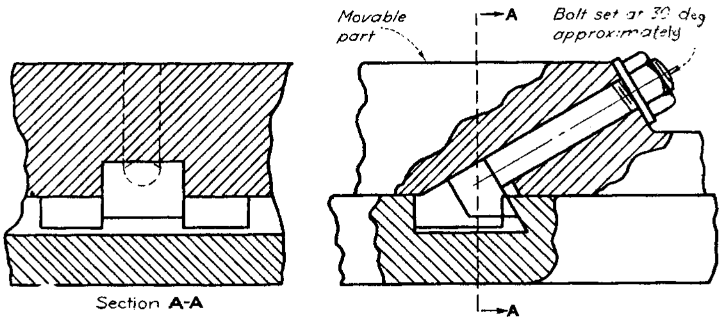

FIG. 3—The movable part is held against one side of the groove while the T-nut is forced against the other side. Removal of the screw permits easy removal of the clamped part. Heavy pressure toward the side of the key out of contact with the slot may permit slight movement due to the springing of the screw.

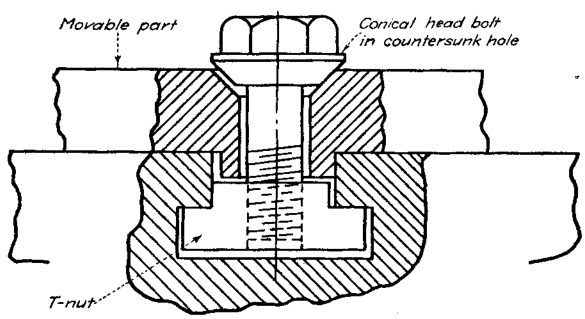

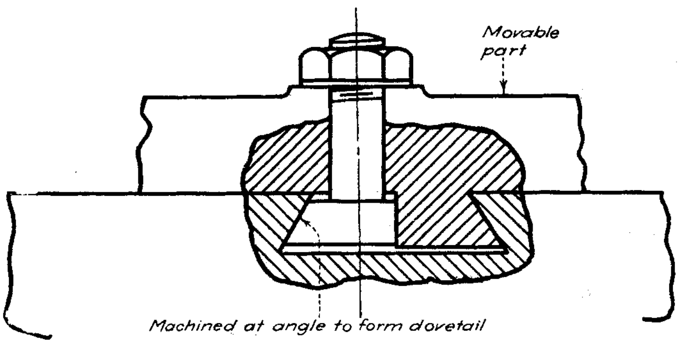

FIG. 4—One side of the bolt is machined at an angle to form a side of the dovetail, which tightens in the groove as the nut is drawn tight. Part must be slid entire length of slot for removal.

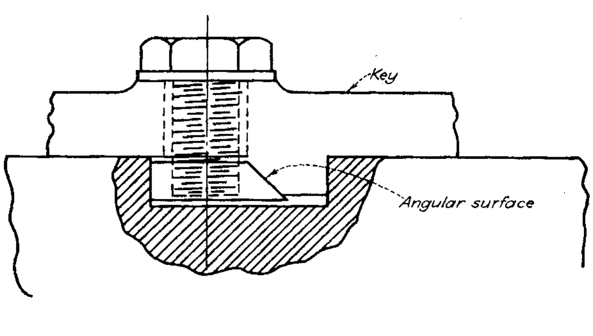

FIG. 5—The angular surface of the nut contacts the angular side of the key, and causes it to move outward against the side of the groove. This exerts a downward pull on the clamped part due to friction of nut against side of groove as nut is drawn upward by the screw.

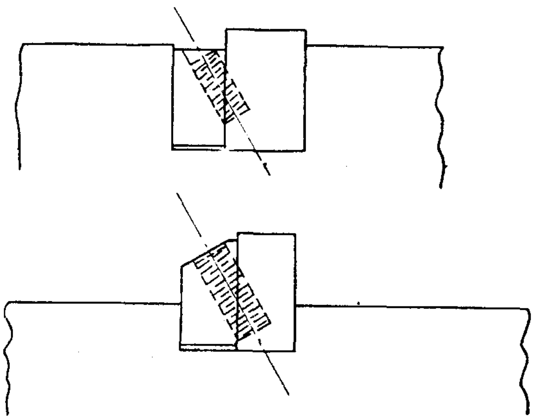

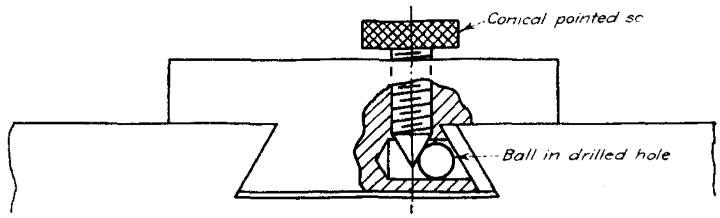

FIG. 8—Screw contact causes the ball to exert an outward pressure against the gib. The gib is loosely pinned to the movable part. This slide can be applied to broad surfaces where it would be impractical to apply adjusting screws through the stationary part.

FIGS. 6 and 7—These designs differ only in depth of the grooves. They cannot withstand heavy pressure in an upward direction but possess the advantage of being applicable to narrow grooves.

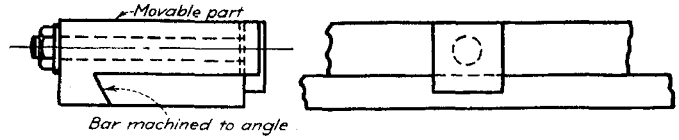

FIG. 10—One edge of a bar is machined at an angle which fits into mating surfaces on the movable part. When the bolt, which passes through the movable part, is drawn tight, the two parts are clamped firmly together.

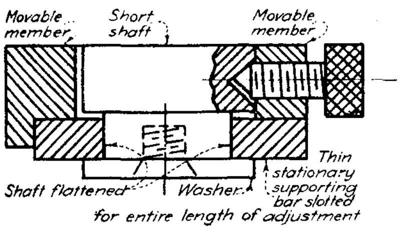

FIG. 9—The movable member is flanged on one side and carries a conical pointed screw on the other side. A short shaft passes through both members and carries a detent slightly out of alignment with the point of the screw. This shaft is flattened on opposite sides where it passes through the stationary member, to prevent its turning when the movable member is removed. A heavy washer is screwed to the under side of the shaft. When the knurled screw is turned inward, the shaft is drawn upward while the movable member is drawn downward and backward against the flange. The shaft is forced forward against the edge of the slot. The upper member may thus be moved and locked in any position. Withdrawing the point of the screw from the detent in the shaft permits removal of the upper member.

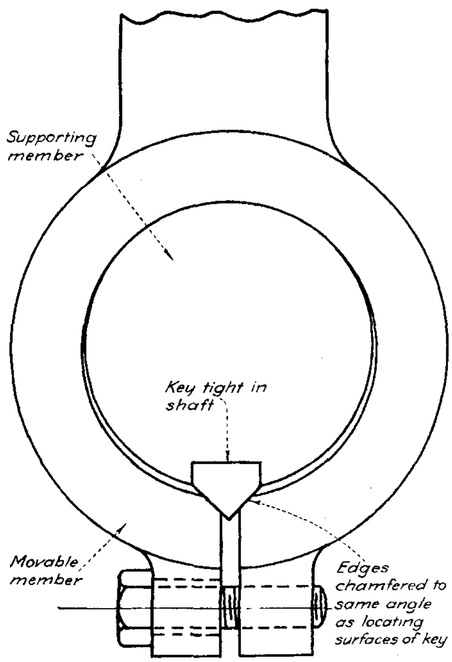

FIG. 11—As the screw is tightened, the chamfered edges of the cut tend to ride outward on the angular surfaces of the key. This draws the movable member tightly against the opposite side of the shaft.

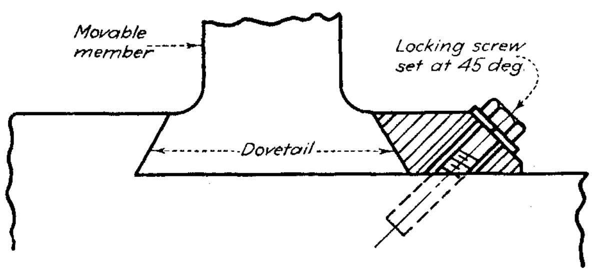

FIG. 12—As the screw is turned, it causes the movable side, which forms one side of the dovetail groove, to move until it clamps tightly on the movable member. The movable side should be as narrow as possible, because there is a tendency for this part to ride up on the angular surface of the clamped part.

How Spring Clamps Hold Workpieces

Here's a review of ways in which spring clamp devices can help you get a grip on things.

Federico Strasser

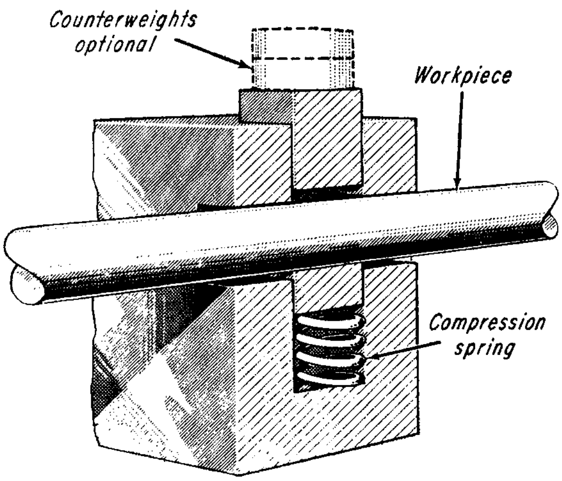

1 **RODS OF DIFFERENT SECTION** can be easily held by this device. Strength of grip can be varied if necessary.

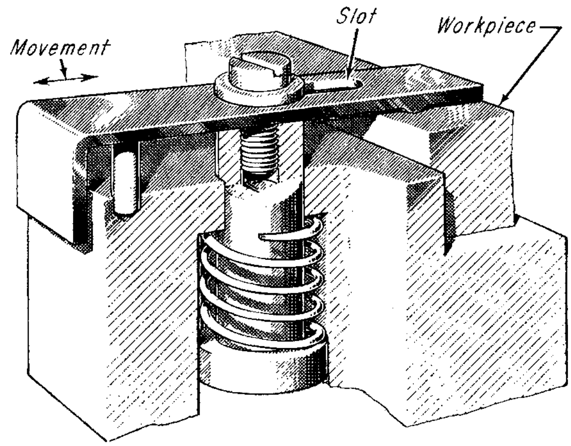

2 **SECOND-CLASS LEVER** gives low clamping forces for parts that are easily marked or require gentle handling.

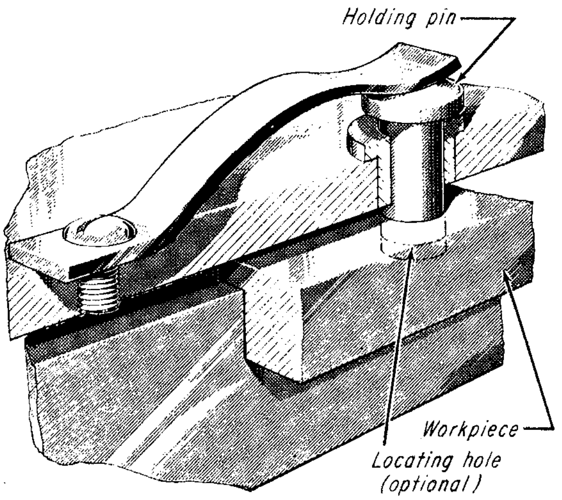

5 **FLAT SPRING ACTS THROUGH PIN** that holds the workpiece in the fixture. This device also positively locates parts.

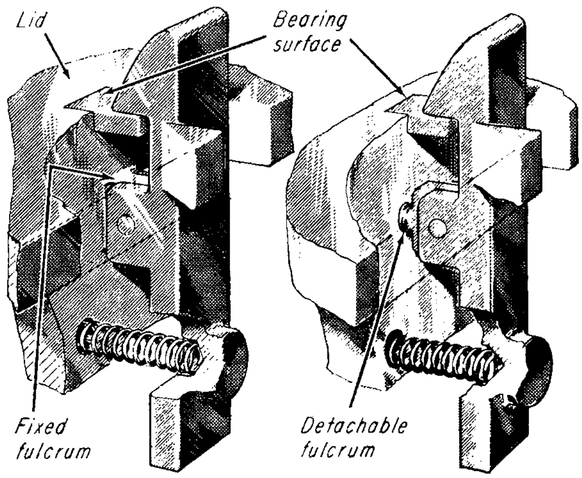

6 **COVER LATCH** is an ideal application for spring and notched lever. Make the fulcrum detachable for ease of repair.

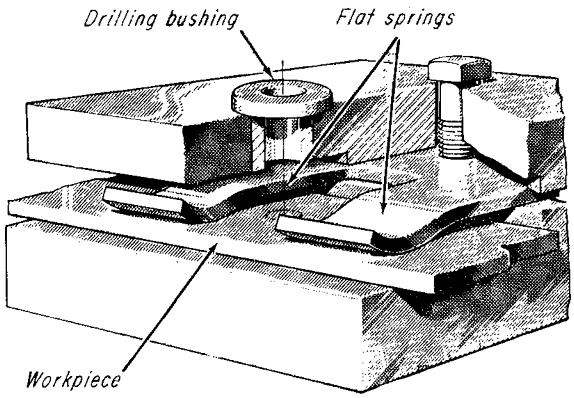

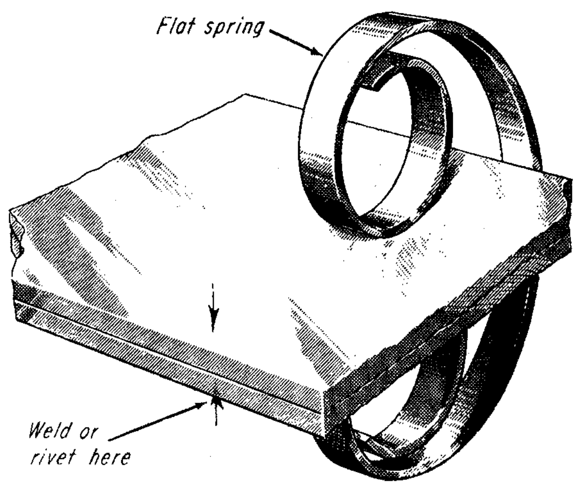

3 **FLAT WORKPIECES** of constant thickness are held with a couple of flat springs attached to the jig table.

4 **SIMPLE CLAMPING FIXTURE** is ideal for holding two flat pieces of material together for either welding or riveting.

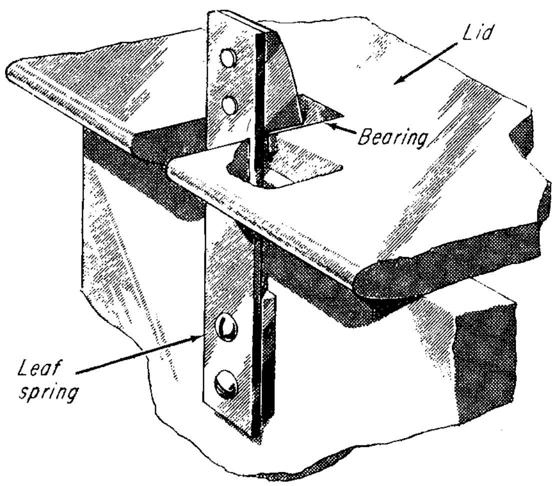

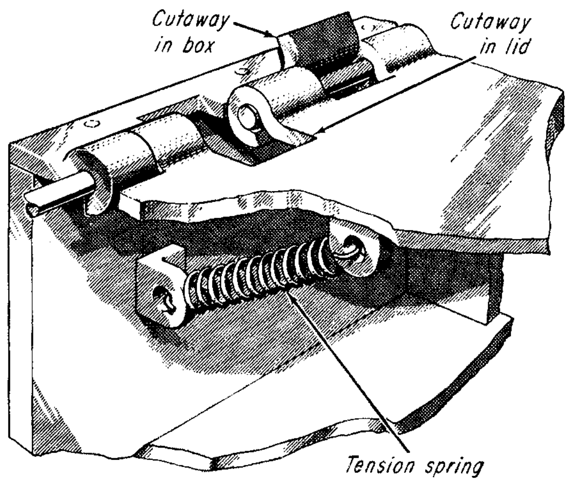

7 **LEAF-SPRING** latch can be fashioned as shown, or the spring itself can be formed to provide its own latching notch.

8 **POSITIVE OPEN-OR-SHUT** lid relies upon a spring. Over-center spring action makes the lid a simple toggle.

SECTION 10

WIRE & CABLE

Wire Locks and Snap Rings for Fastenings

Adam Fredericks

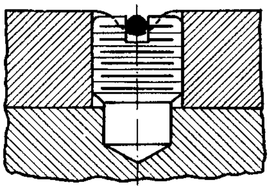

FIG. 1

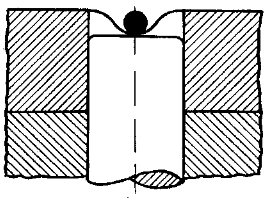

FIG. 2

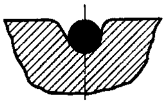

FIG. 3

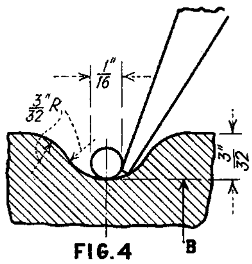

FIG. 4

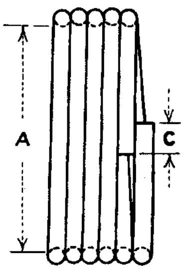

FIG. 5

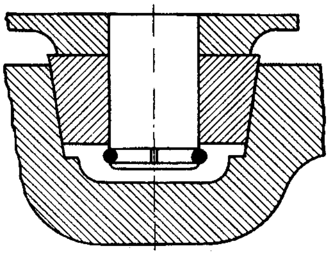

FIG. 6

Frequently considerable savings can be made by the substitution of wire locks or snap rings in place of expensive tapping operations, or to eliminate the necessity of boring holes to two different diameters and grinding shafts to shoulders. Often, screws and lock nuts can also be eliminated.

Wire locks and snap rings can be used only where the loads are radial and thrust loads are light. Spring steel or music wire is usually used for the material. Usually, 1/16-in. diameter wire is sufficiently large. In nearly all of the accompanying illustrations the wire size is shown exaggerated.

Figs. 1 and 2—Two common applications for wire locks to a screw or a pin.

Fig. 3—The two forms of grooves shown here should be avoided, as each offers too much difficulty in snapping off the ring, particularly when the outside or outermost diameter of the wire ring is below the surface of the work.

Fig. 4—Enlarged view of a successful type of groove, the rounded edges permitting the wire to be snapped out with greater facility.

Fig. 5—Wire locks may be made in the form of a close wound spring and successive coils cut off to suit. Diameter *A* should be 1/16-in. smaller than the diameter *B* indicated in Fig. 4. Lap *C* should be 3/16 in. for each 1/16-in. difference between diameters *A* and *B*.

Figs. 6 to 8—Three typical applications of snap rings.

Fig. 9—Spring lock of 3/64-in. wire on a 1/4-in. diameter pin, as used in a well-known universal joint. Once assembled, the spring lock cannot snap out.

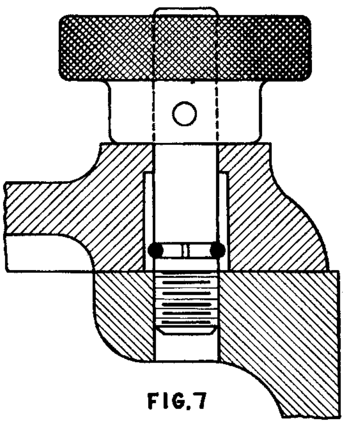

FIG. 7

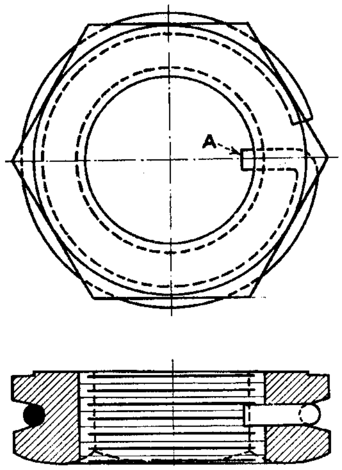

FIG. 10

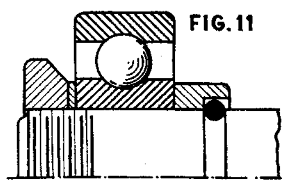

FIG. 11

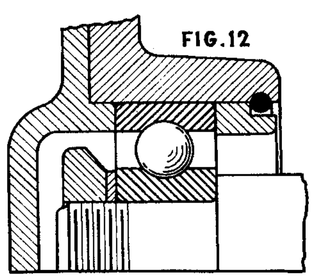

FIG. 12

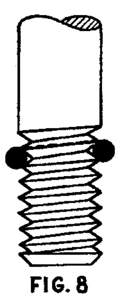

FIG. 8

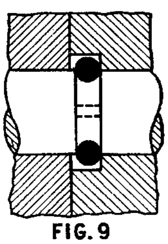

FIG. 9

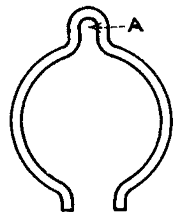

FIG. 13

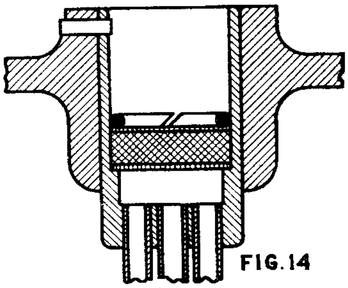

FIG. 14

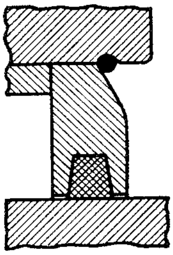

FIG. 15

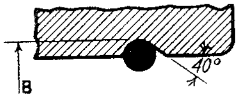

FIG. 16

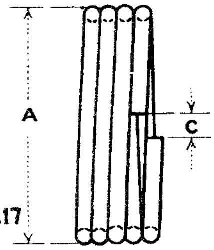

FIG. 17

Fig. 10—A hole in the shaft receives the end *A* of the spring lock. When the position of the nut is changed a new hole must be drilled in the shaft.

Figs. 11 and 12—Typical applications of wire locks.

Fig. 13—Press-formed external wire lock. Loop *A* allows insertion of a wire puller when disassembling.

Fig. 14—Application of a wire lock in a lubricating device to hold the wire mesh screen and felt in place.

Fig. 15 and 16—Felt seal housing held in place by a wire lock, and enlarged view of groove.

Fig. 17—Method of cutting internal lock rings from a close wound spring. Diameter *A* should be $\frac{1}{16}$-in. larger than diameter *B* and gap *C* is $\frac{1}{2}$ in. for each $\frac{1}{16}$-in. difference between diameters *A* and *B*.

Figs. 18 and 19—Wire locks for the felt seal housing of a tapered roller bearing. In Fig. 19 is shown the enlarged view showing the different positions taken by the wire lock for a various of plus or minus $\frac{1}{32}$ in. axially.

Fig. 20—Wire lock, internal, applied to a sheet metal stamping.

Fig. 21—Wire lock in the outer race of an open-end bearing to make it integral.

Fig. 22 to 26—Typical snap ring made of rectangular spring and various applications of snap rings made of rectangular stock, as applied to roller bearings and ball bearings.

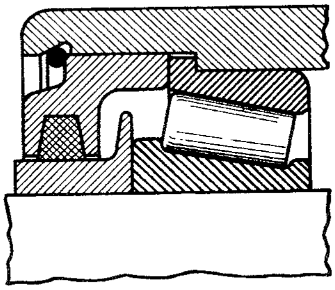

FIG. 18

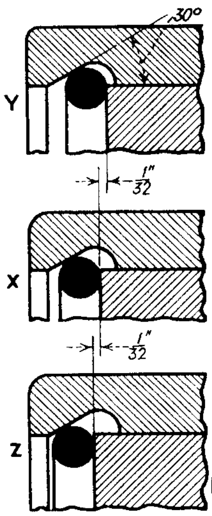

FIG. 19

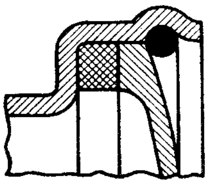

FIG. 20

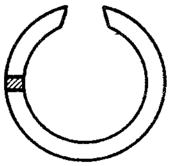

FIG. 22

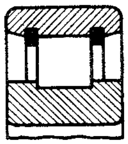

FIG. 24

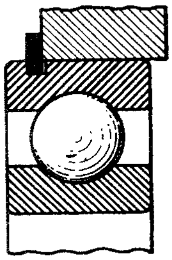

FIG. 25

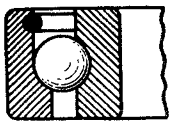

FIG. 21

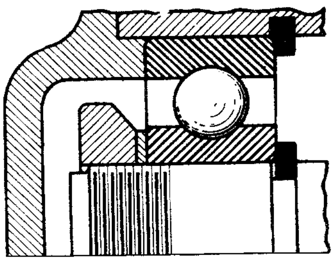

FIG. 23

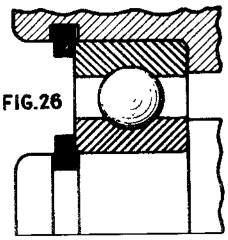

FIG. 26

Applications of Helical Wire Inserts

Originally devised to reduce thread wear and stripping between steel fasteners and soft materials, helical wire inserts are now being used in plastic and wood for similar purposes. Other applications are to prevent galvanic action, act as electrical connectors, and to reduce weight, cost and number of parts needed in an assembly.

Paul E. Wolfe

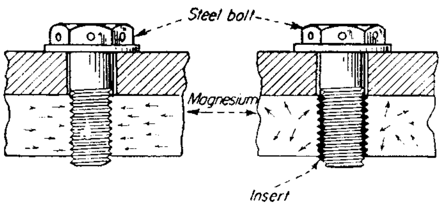

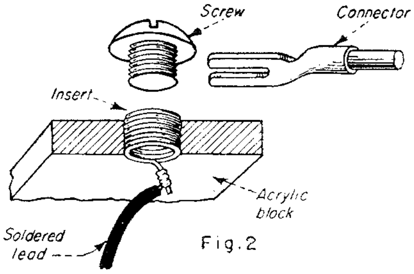

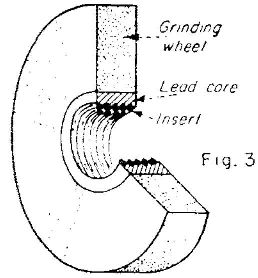

Fig. 1—Galvanic action between steel bolt and magnesium part, (Left), attacks thread causing part failure. Stainless steel insert, (Right), reduces galvanic action to a negligible amount while strengthening threads.

Fig. 2—Insert used as an electrical connection as well as a thread reinforcement. Unit is threaded into plastic and tang is bent to form soldering lug.

Fig. 3—Direct connection of grinding wheel onto a threaded shaft by using a wire insert. Washers and nut are not required thus simplifying assembly.

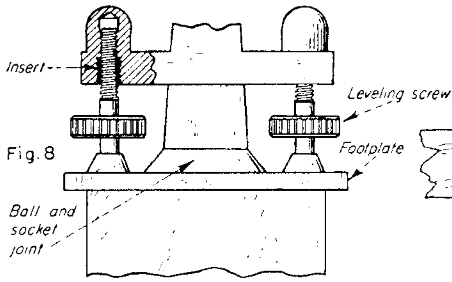

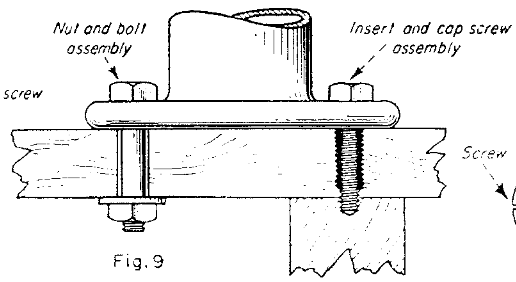

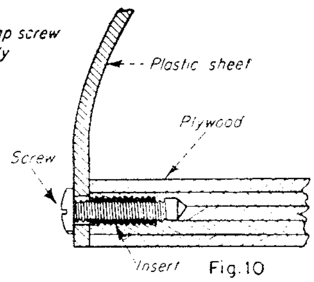

Fig. 8—Wear and backlash can be reduced on adjusting threads. Clamping strength is not needed but intermittent thread travel makes reinforcement desirable.

Fig. 9—Combination of inserts and capscrews permits installation of machinery and other equipment on wood floors and walls. Access to opposite face of the wood is not a factor nor are joists and other obstructions.

Fig. 10—Plastic-to-wood connector. Repeated assembly and disassembly does not affect protected threads in wood or plastic parts.

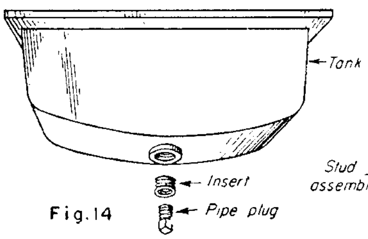

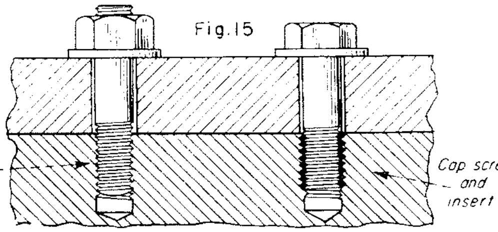

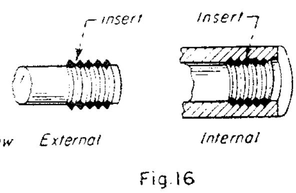

Fig. 14—Seizure and corrosion of pipe threads on compression, fuel and lubricant tanks, pipe lines, fittings, pumps and boilers are prevented by using an insert.

Fig. 15—Stud (Left) transfers thread wear from the tapped hole and into the expendable threads on the stud and nut. Interference fit in the tapped hole is mandatory. Insert (Right) prevents wear and makes stud unnecessary. Lower cost cap screw can be used.

Fig. 16—Thread series can be changed from special to standard, from fine to coarse or vice versa, or corrected in case of a production error by redrilling and retapping. Inserts giving desired thread are then used.

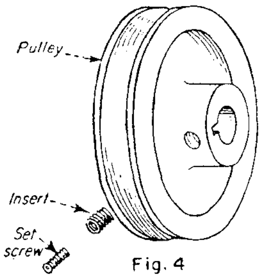

Fig. 4

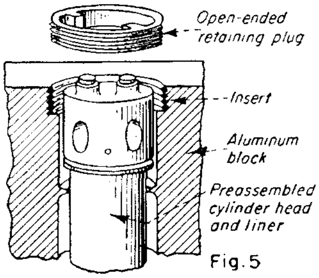

Fig. 5

Fig. 4—Loosening of the set screw by vibration is reduced by using an insert. As pulley is a soft metal die casting set screw tightening often stripped threads.

Fig. 5—Insert withstands combustion thrust of diesel cylinder. It prevents heat seizure and scale on threaded plug making cylinder replacement and servicing easy.

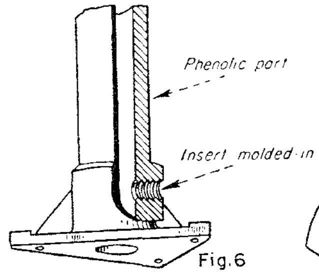

Fig. 6

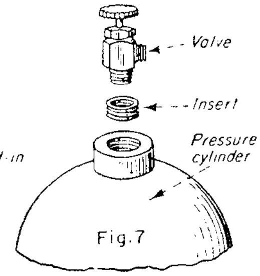

Fig. 7

Fig. 6—Phenolic part insert forms strong thread without tapping and drilling. Insert is resilient, does not crack phenolic or set up local stress concentrations.

Fig. 7—Enlargement of taper pipe threads in necks of pressure vessels, caused by frequent inspection and interchange of fittings, can be minimized.

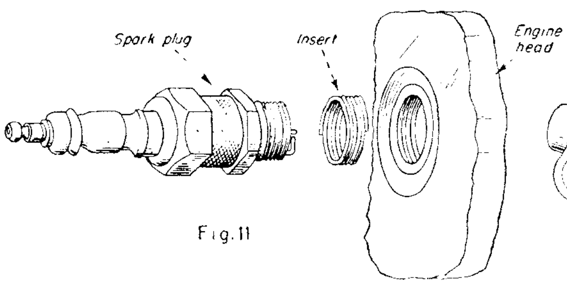

Fig. 11

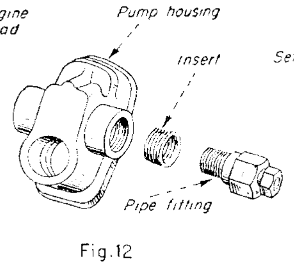

Fig. 12

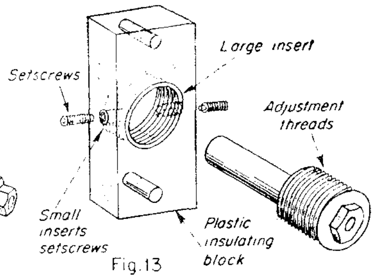

Fig. 13

Fig. 11—Threads are protected from stripping in new aluminum engine heads by inserts. Also can be used to repair stripped spark plug holes in engine heads.

Fig. 12—Insert prevents pipe fittings from peeling chips out of tapped aluminum threads. Introduction of chips into the lines could cause a malfunction.

Fig. 13—Center insert serves as brakeband to lock adjustable bushing. Small inserts keep set screws from stripping plastic when tightened. Also, adjustment threads can not be marred by end of set screw.

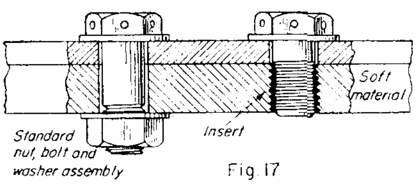

Fig. 17

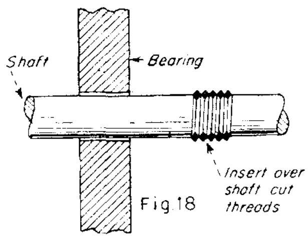

Fig. 18

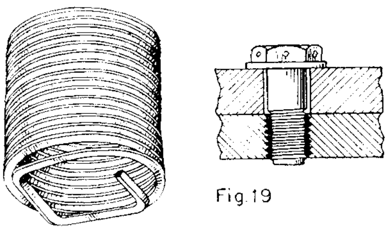

Fig. 19

Fig. 17—Assembly weight may be reduced. Left view shows the standard method of attaching front and mid frame of a compressor. Lockwire is used after assembly is completed. Right view is new method resulting in weight and space economies.

Fig. 18—Assembly of a shaft through a bearing is simplified by adding external insert over cut shaft threads. Machining the full shaft length is also unnecessary.

Fig. 19—Square tang insert—called screw lock—automatically locks the screw so that lock washers, nuts or wires are unnecessary. Insert locks itself into parent material without need for pins, rings, or staking.

Types of Wire Ties for Reinforcing Bars

Typical ties to hold rebars in place during concrete pouring.

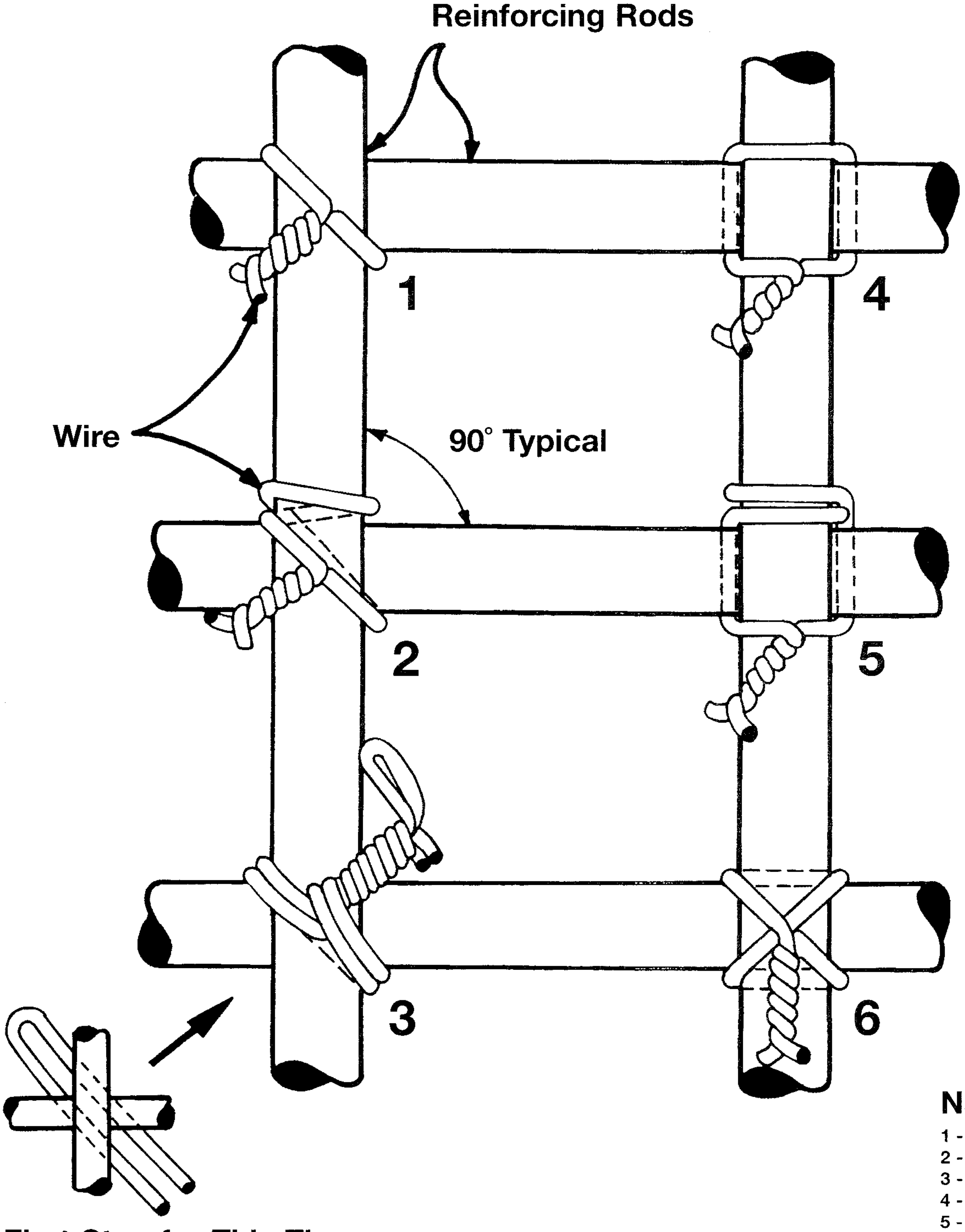

Names of Ties

1 - Simple Tie or Snap Tie
2 - Wall Tie
3 - Double Strung Single Tie
4 - Saddle Tie
5 - Saddle Tie with Twist
6 - Figure-Eight Tie

Source: Standard Handbook of Fastening & Joining, 3rd Edition by Robert O. Parmley

Wire Rope Designs

In designating wire-rope construction, it is customary to state first, the number of strands; second, the number of wires in a strand; third, the kind of center or core whether fiber, hemp, wire strand or wire rope. When wire rope remains in a fixed position (such as in cables for suspension bridges) or where little bending is required, a wire core is desirable. For transmission of motion, flexibility over grooved pulleys is desirable and is secured by thinner wires and hemp or fiber cores.

6 X 7 haulage and guy rope. For use under severe operating conditions.

6 X 19 class wire rope, formerly called standard flexible hoisting rope.

8 X 19 class wire rope, formerly called extra flexible hoisting rope, has somewhat greater flexibility than 6 X 19 rope.

6 X 37 class wire rope, formerly called special flexible hoisting rope. For high-speed use on cranes or where sheaves are small.

a–3 × 7; fiber center.
b–6 × 7; fiber center.
c–7 × 7; wire center.
d–6 × 8; hemp center.
e–6 × 13; hemp center; filler wire.
f–6 × 16; fiber center; filler wire.
g–7 × 19; wire-strand center.
h–6 × 19; fiber center; two stranding operations.
j–6 × 19; hemp center (Seale)
k–6 × 37; fiber center; filler wire.
l–6 × 41; wire-rope center.
m–18 × 7; nonpinning type hoisting rope.
n–6 × 19; flexible wire-rope center. (Seale)
o–6 × 19; hemp center. (Warrington)
p–6 × 19; hemp center; filler wire.
q–8 × 19; hemp center. (Seale)
r–8 × 19; fiber center; filler wire.
s–8 × 19; hemp center. (Warrington)
t–6 × 19; wire-rope center; filler wire.
u–6 × 22; wire-rope center; filler wire.
v–6 × 31; fiber center.
w–8 × 19; fiber center; two stranding operations.
x–6 × 12; one hemp center.
y–6 × 12; seven hemp centers.
z–6 × 37; wire-rope center. (Seale)
aa–6 × 37; fiber center; two stranding operations.
ab–6 × 37; hemp center; three stranding operations.
ac–6 × 24; seven hemp centers.
ad–6 × 42; seven hemp centers; most flexible; called "tiller" or "hand rope."
ae–3 × 37; wire center.
af–Typical wire-rope center.
ag–Typical hemp or fiber center.
ah–Typical strand center.
aj–Steel wires twisted into a single strand of nineteen wires.
ak–Steel wires twisted into a single strand of fifty-one wires.
al–Armored wire rope; 6 × 19; fiber center; sometimes wire center; used under severe hoisting conditions, such as dredging and heavy steam-shovel work.
am–Marline-covered rope; 5 × 19; hemp center; used for ships's rigging and hoisting service where moisture is encountered. (American Chain and Cable Co.)
an–Stone sawing strand; three wires twisted together.
ao,ap–Regular-lay (right and left) wire rope; wires in strands twisted together in one direction and strands twisted in opposite directions.
aq,ar–Lang-lay (right and left) wire rope; wires in strands and strands twisted in the same direction.

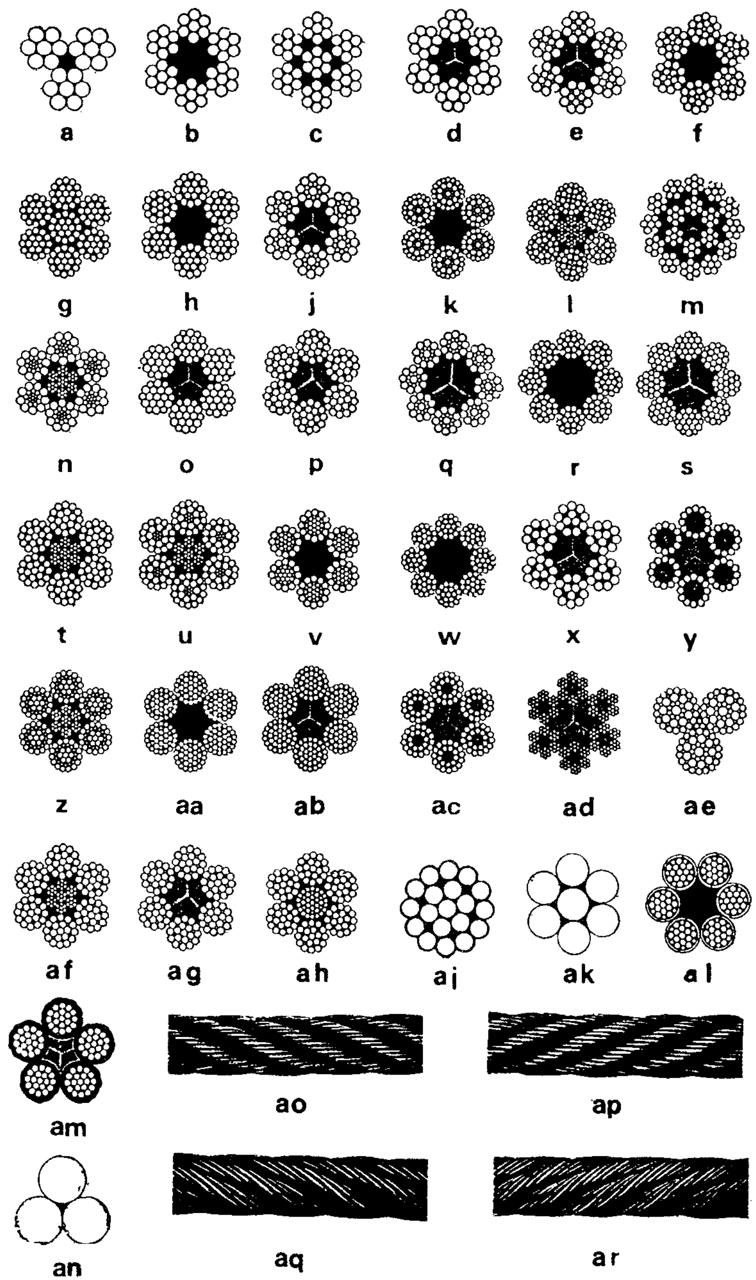

Source: Pictorial Handbook of Technical Devices by Schwarz and grafstein

For Cable Drives–These Design Hints

When gears are too expensive, try a cable drive–low cost, durability and reliability are features

Frank William Wood JR.

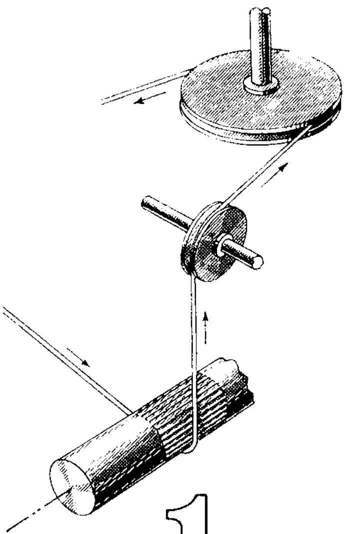

1 **CHANGE OF DRIVE PLANE** from vertical to horizontal is no problem with a cable drive. One or more idlers may be needed—and watch friction.

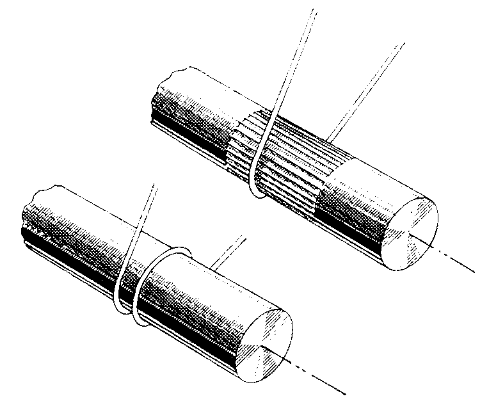

2 **FINE STRAIGHT-KURL** or double-wrapped smooth shaft provides adequate non-slip friction for most drives. Slip occurs before drive is damaged.

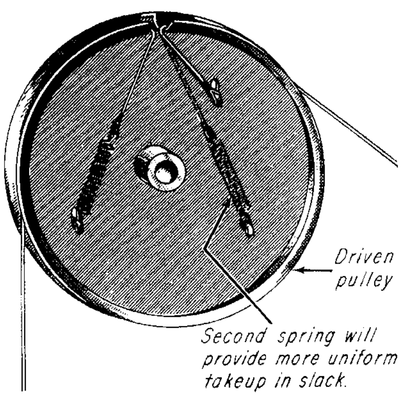

5 **"INSIDE"** location for spring is right on the driven pulley itself. While one spring will often suffice, a second one provides uniformity.

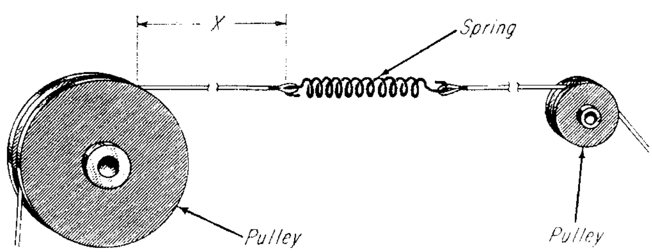

6 **SPRINGS** can be located along any part of the cable, so long as distance X is sufficient to prevent the spring from engaging pulley.

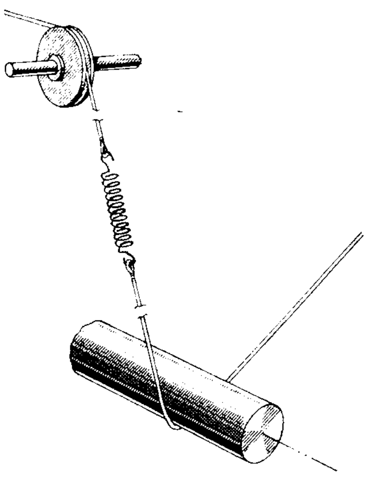

3

BACKLASH in a drive system can be eliminated by using an extension spring preloaded so it won't stretch under normal drive forces.

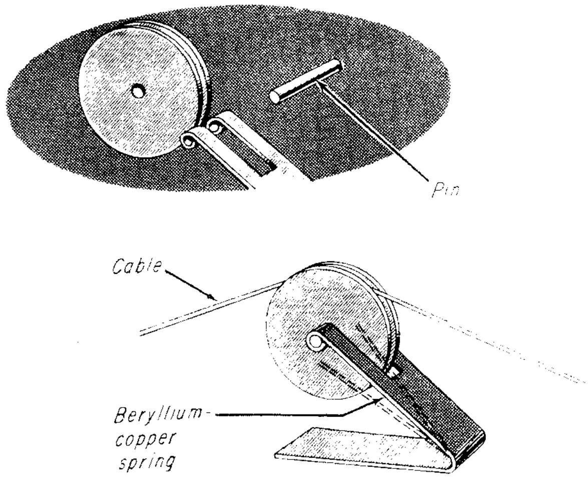

4

"OUTSIDE" location for takeup spring often allows more freedom of design. Beryllium-copper springs need no protective plating.

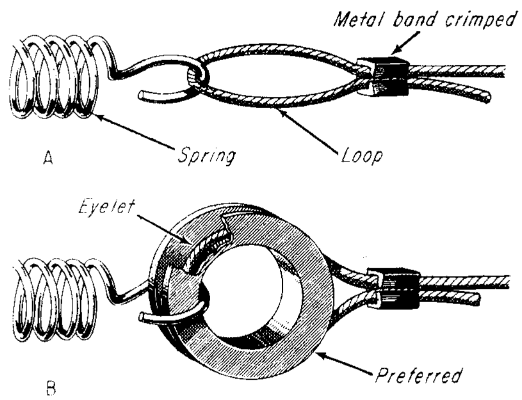

7

SPRING ATTACHMENT to the drive cable should be as secure as possible. Cable loop (A) is good; eyelet (B) causes less cable wear.

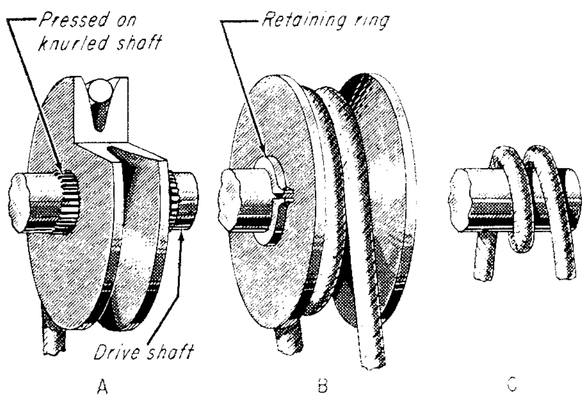

8

PULLEYS of nylon (A) give needed grip, yet slip at unsafe loads. Phenolic pulley (B) is free fit on shaft. Fixed polished shaft (C) adds friction.

Cables Anchor Timber Bridge Abutment

R. O. Parmley

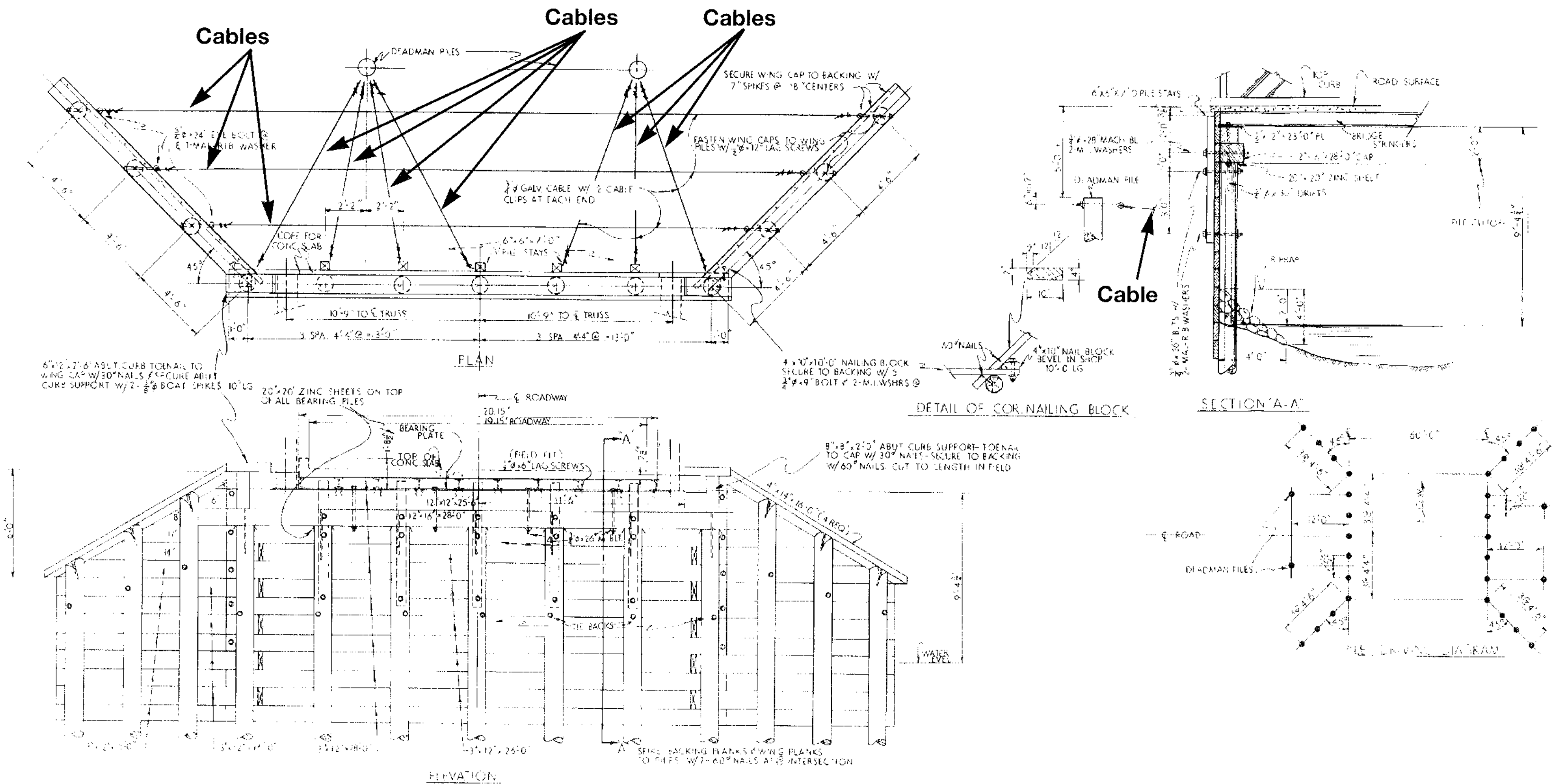

Courtesy: Morgan & Parmley, LTD.

Aerial Cable Installation

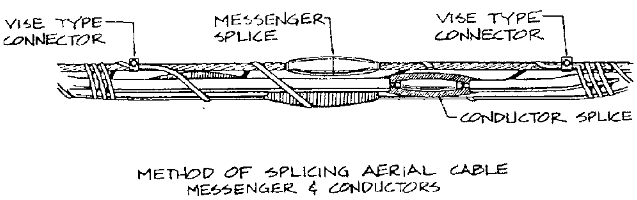

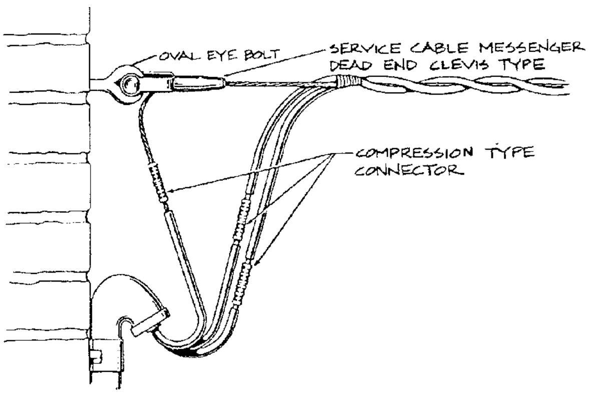

Dead Ending Aerial Service Cable

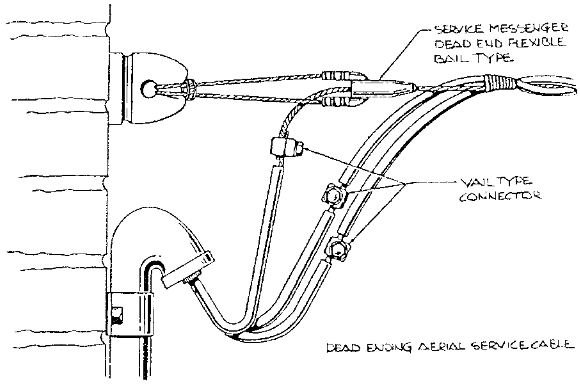

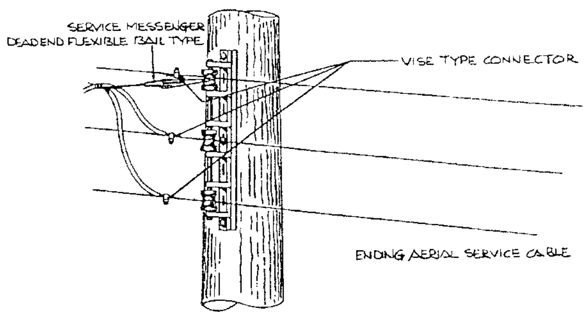

Ending Aerial Service Cable

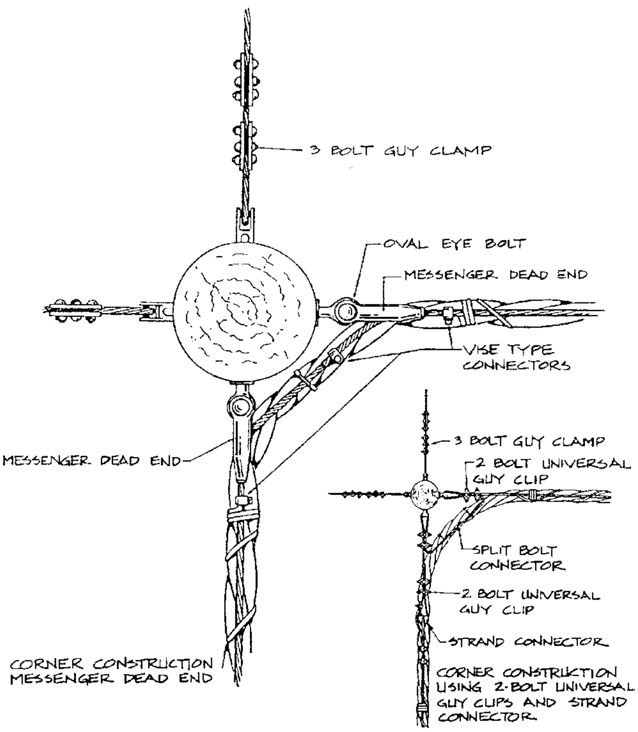

Aerial Cable Corner Construction

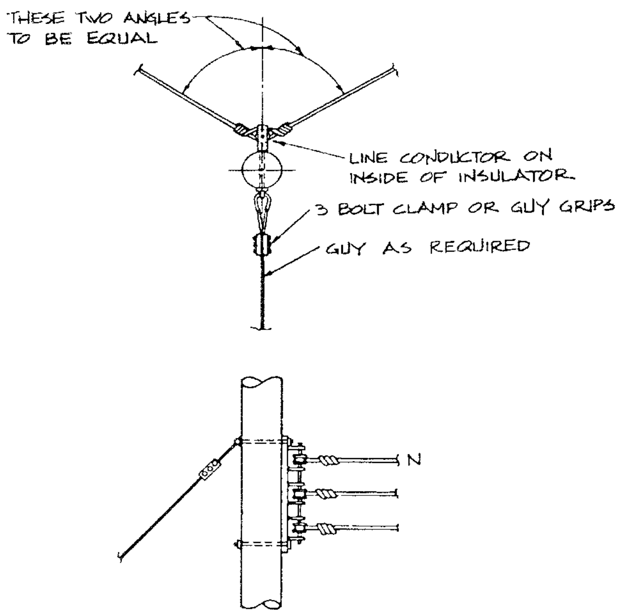

Pole Guy Angle Installation

Source: Standard Mechanical and Electrical Details, by Mueller

Cable Replaces Piston Rod

Long-stroke pneumatic cylinder with wire cable hooked to piston has no piston rod at all.

CYLINDER-and-cable design permits use of pneumatic cylinders in restricted space, since the cable eliminates clearance problems created by the piston rod ordinarily used. The 1.75-in. ID cylinder can be ordered in any length to match the stroke desired. Tol-Air Cable Cylinder operates at 150 psi max and is produced by Tol-O-Matic Inc, Minneapolis.

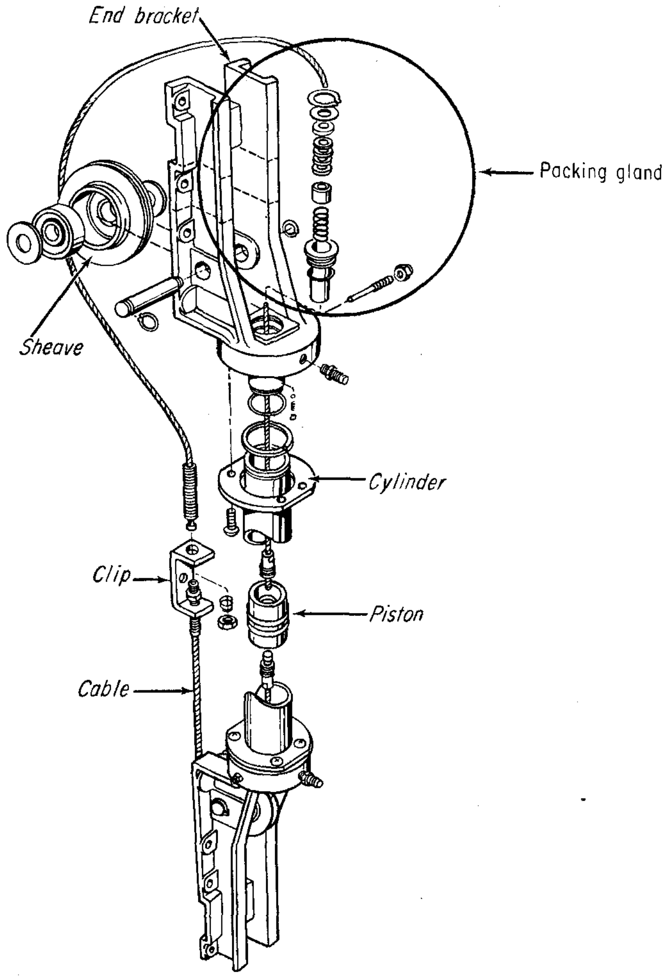

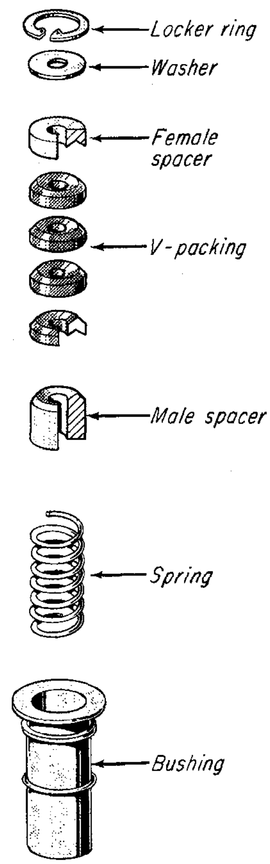

PISTON, CABLES, CLIP form a continuous loop in tension. Piston motion in either direction is transmitted directly to the machine part to which the clip is connected. Standard end brackets are bolted to the flange of a cylinder of the desired length. Cylinder is standard cylinder tubing with a hard-chromed bore to minimize wear. Aluminum end bracket supports cable sheave, packing gland, and air connections. The end brackets can be used with cylinders of any length. Nylon-covered aircraft cable is sealed by V-packings. Swaged, threaded fittings on the cable ends connect to piston and to clip.

SECTION 11

WASHERS

Ideas for Flat Washers

You can do more with washers than you may think. Here are 10 ideas that may save the day next time you need a simple, quick, inexpensive design.

Robert O. Parmley

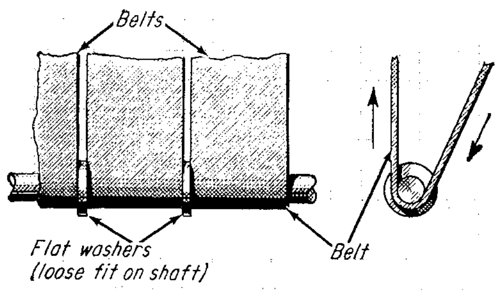

1 Are your belts overlapping? A flat washer, loosely fitted to the shaft, separates them.

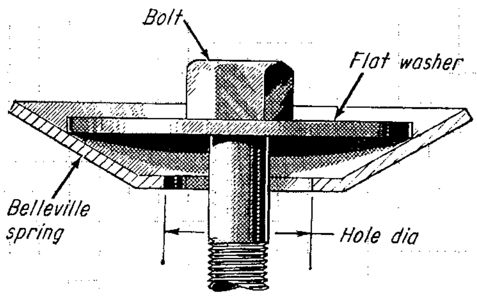

3 Need to hold odd-shaped parts? A flat washer and Belleville spring make a simple anchor.

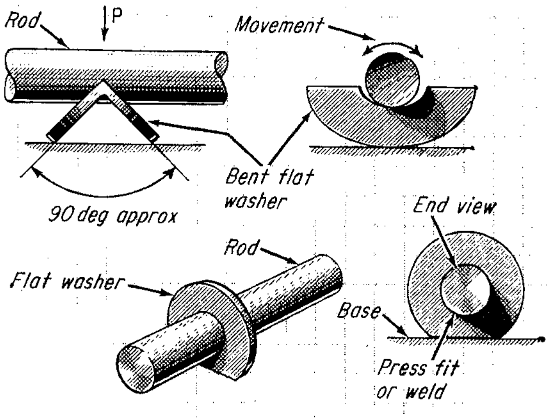

2 How about a rod support? A bent washer permits some rocking; if welded, the support is stable.

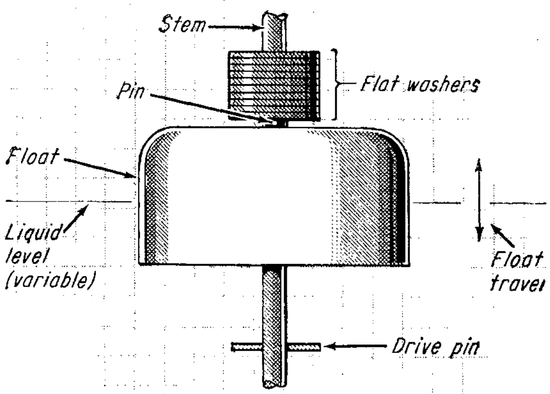

4 Got a weight problem? Adding or subtracting flat washers can easily control float action.

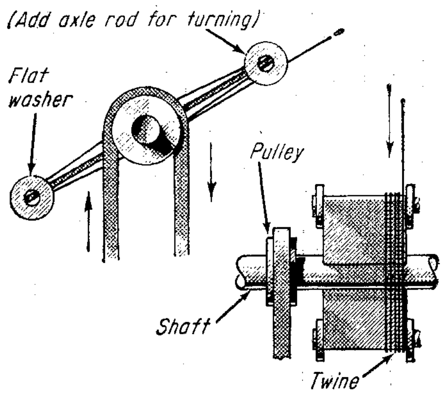

5 How about some simple flanges? Here the washers guide the twine and keep it under control.

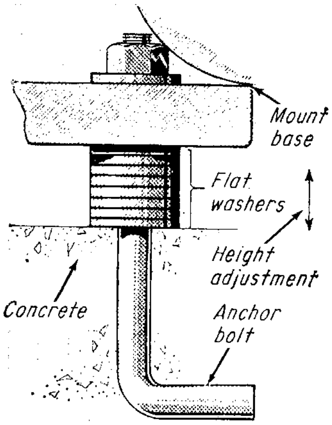

8 Does your floor tilt? Stacked washers can level machines, or give a stable height adjustment.

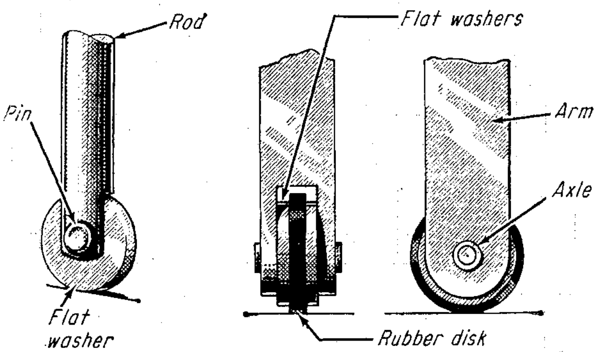

6 Need some wheels? Here flat washer is the wheel. A rubber disk quiets the assembly.

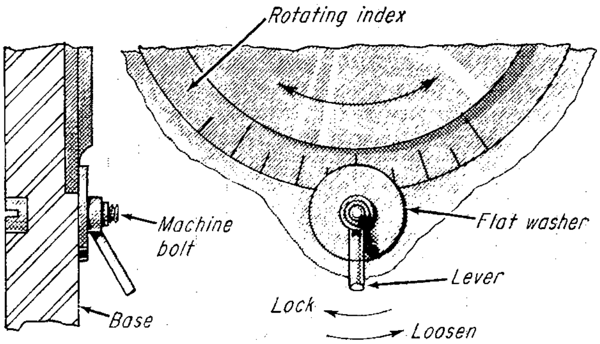

9 Here's a simple lock. A machine bolt, a washer, and a wing or lever nut make a strong clamp.

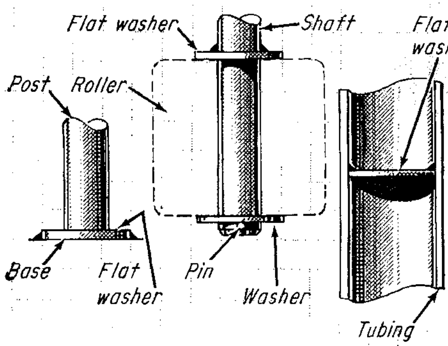

7 Want to avoid machining? Washers can make anchors, stop shoulders, even reduce tubing ID.

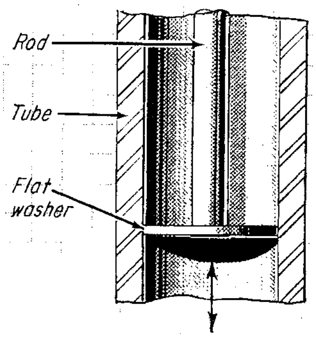

10 Need a piston in a hurry? For light service, tube, rod, and washer will be adequate.

Versatile Flat Washers:
can be used in a variety of unusual applications

Robert O. Parmley

Stiffen machine mount

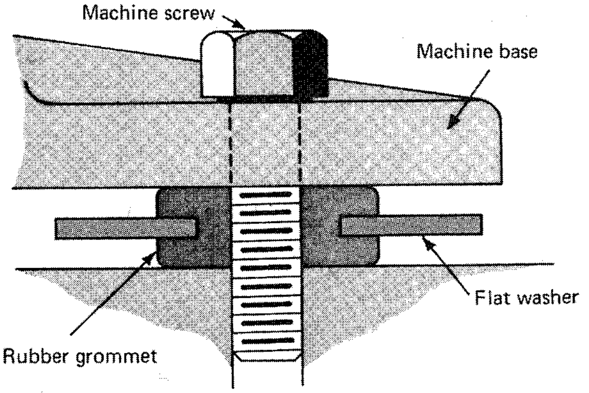

Support a shaft

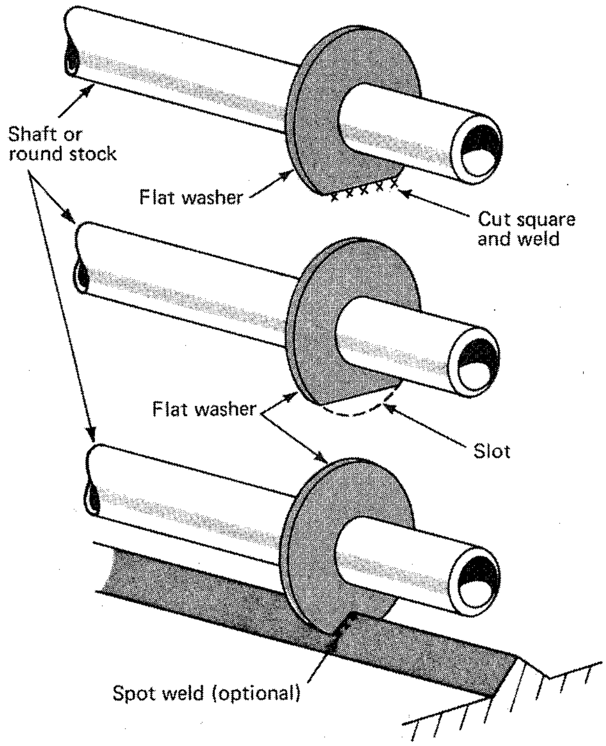

Stabilize a point

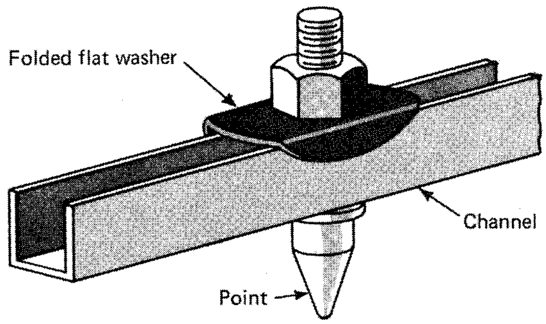

Guide wire or tubing

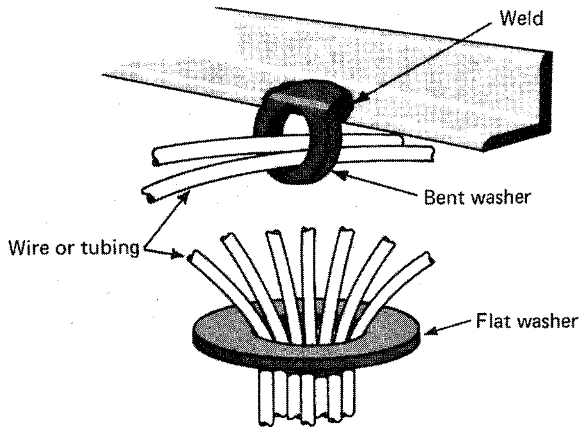

Act as a valve seat

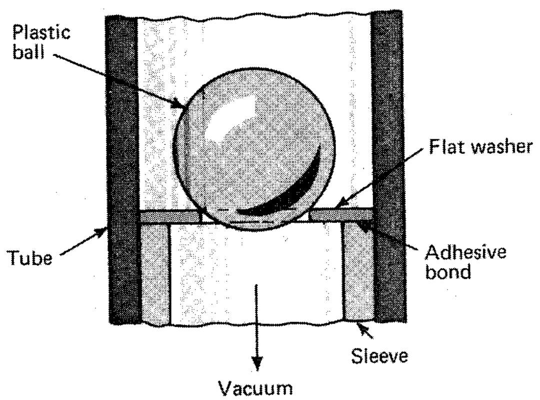

Washers are usually thought of bearing surfaces placed under bolt heads. But they can be used in a variety of ways that could simplify a design or be an immediate fix until a designed part is available.

Reinforce a roller

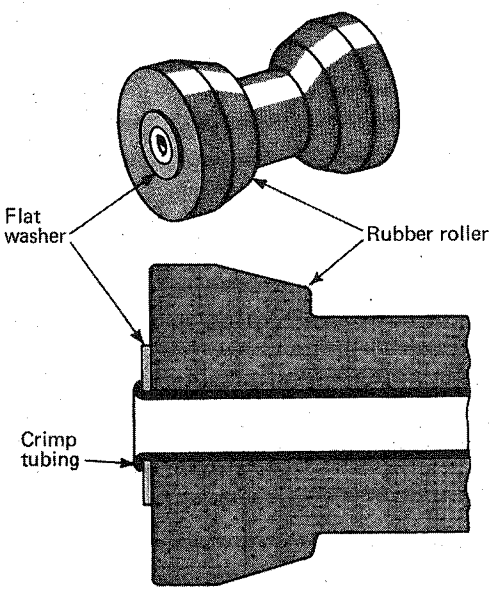

Act as a pulley flange

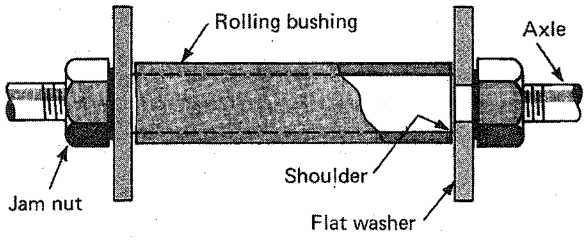

Form a pulley

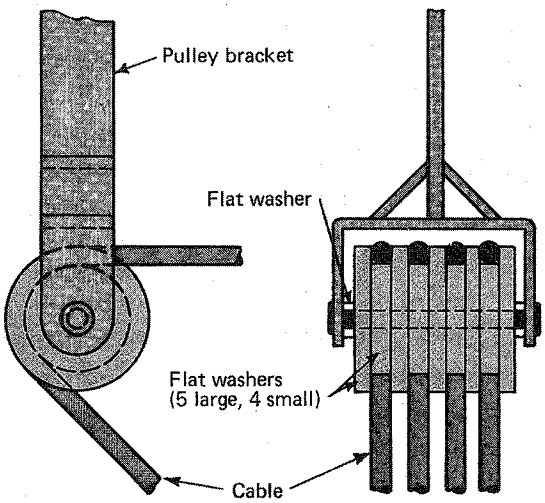

Form a shock absorber

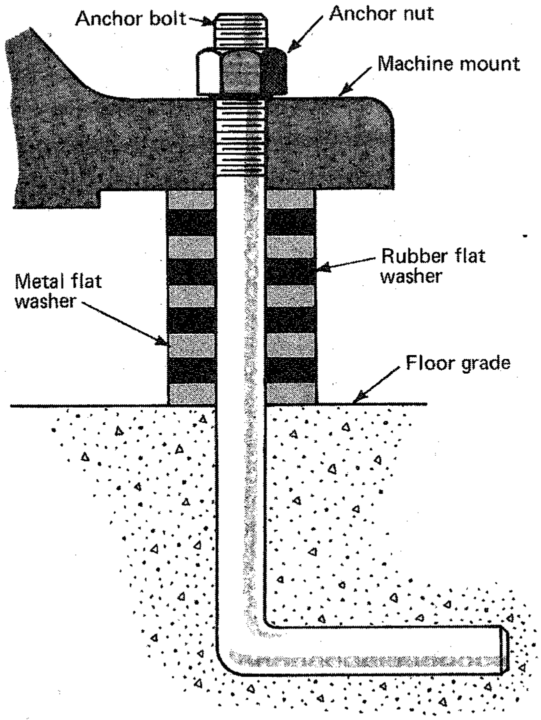

Act as a bearing surface

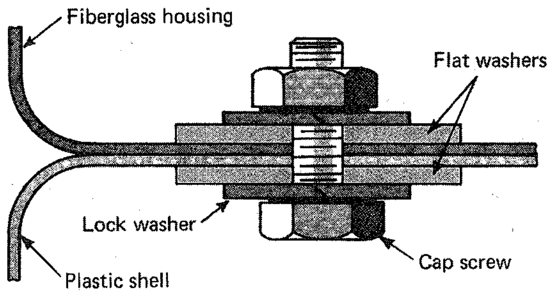

Jobs for Flat Rubber Washers

Rubber washers are more versatile that you think. Here are some odd jobs they can do that may make your next design job easier.

Robert O. Parmley

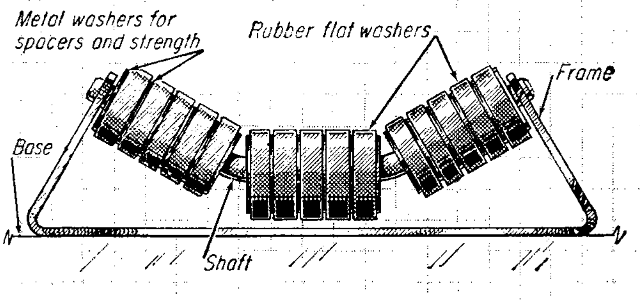

2 Impact absorption idler roller

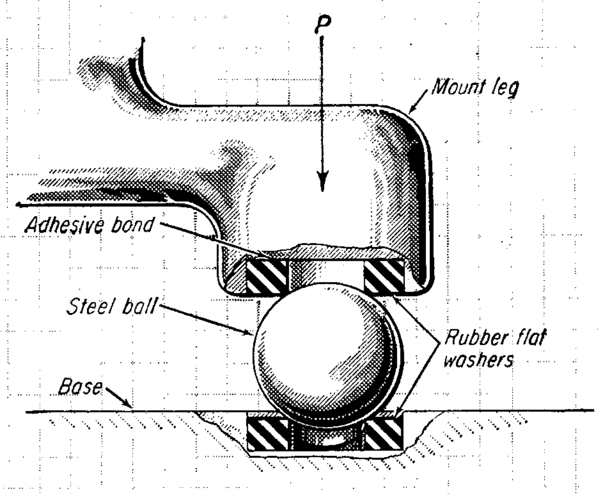

3 Compression mount

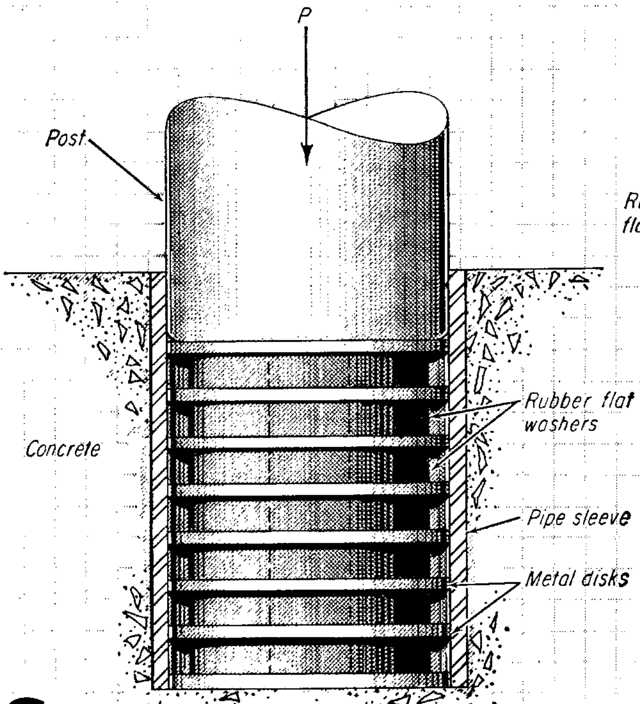

6 Heavy shock load support

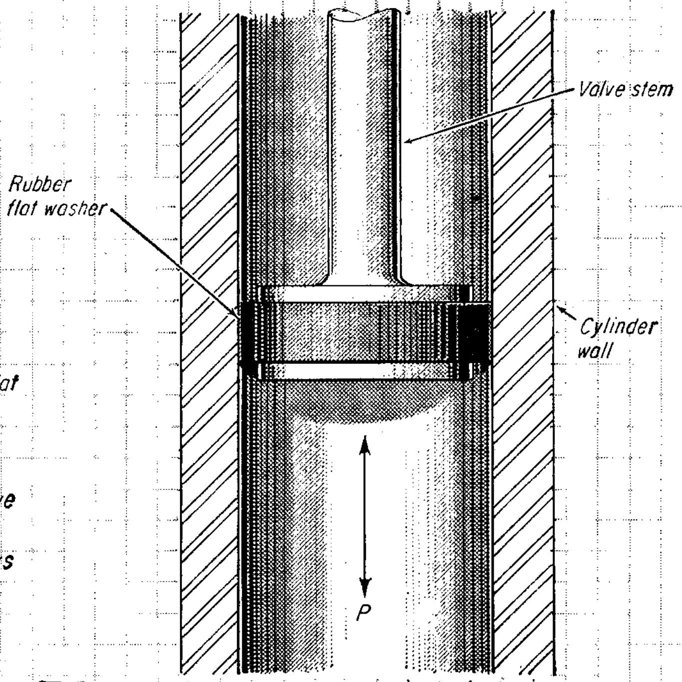

7 Cylinder valve

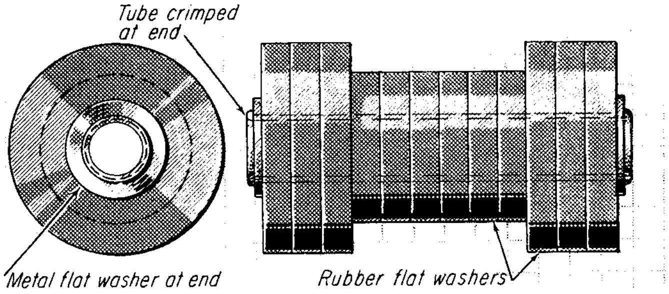

1 Step roller

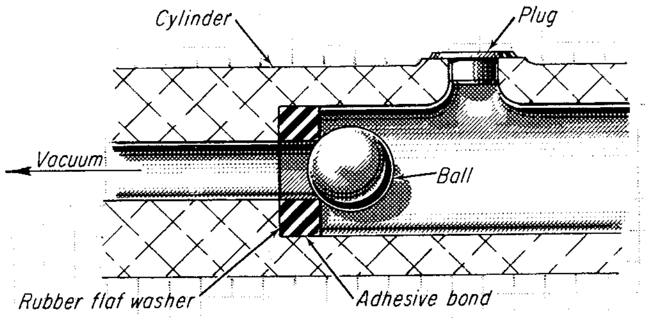

4 Compression ball seat

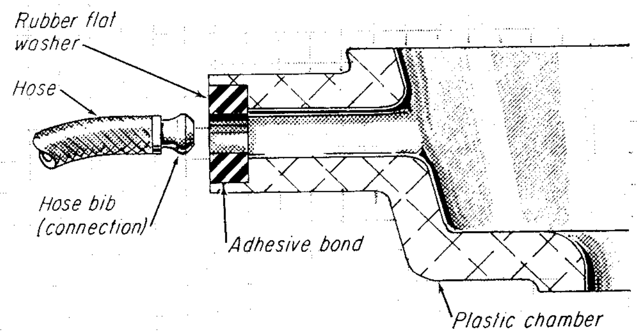

5 Hose bib retainer

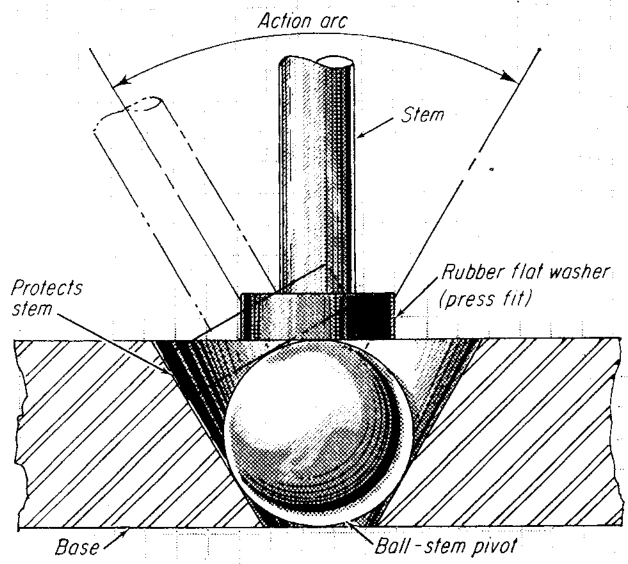

8 Protective bumper

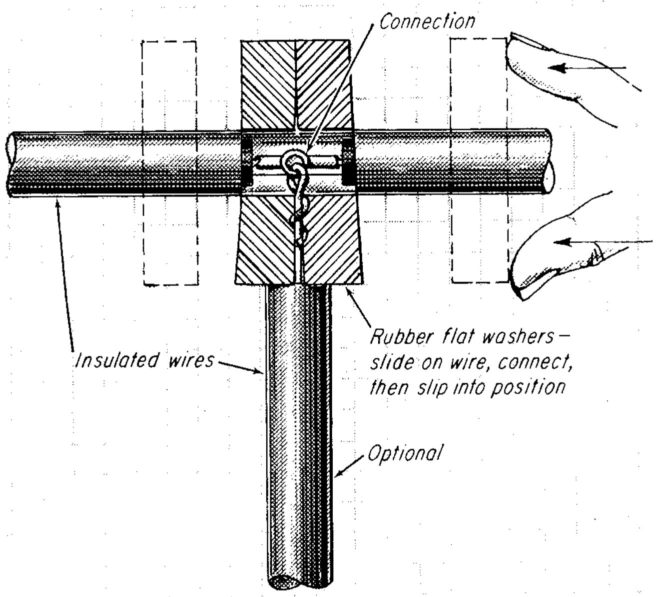

9 Expansion isolator

Take Another Look at Serrated Washers

They're a stock item and come in a variety of sizes. With a little thought they can do a variety of jobs. Here are just eight.

Robert O. Parmley

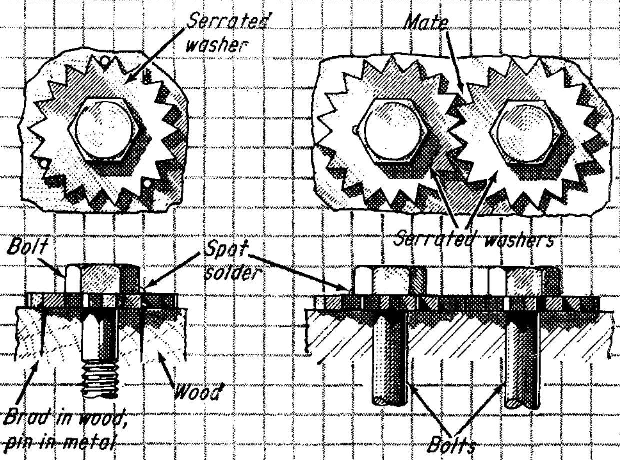

2 Stop rotation of bolts or pins

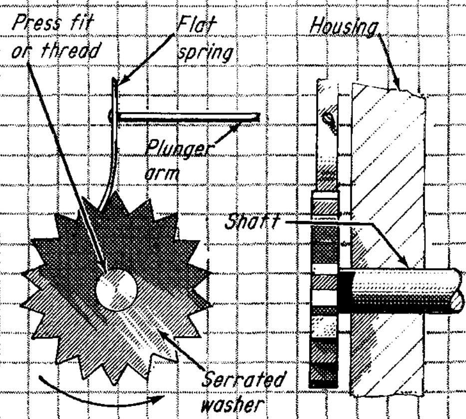

3 Timer gear

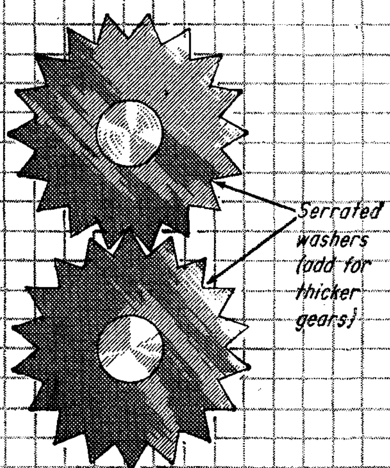

6 Simple gear for light applications

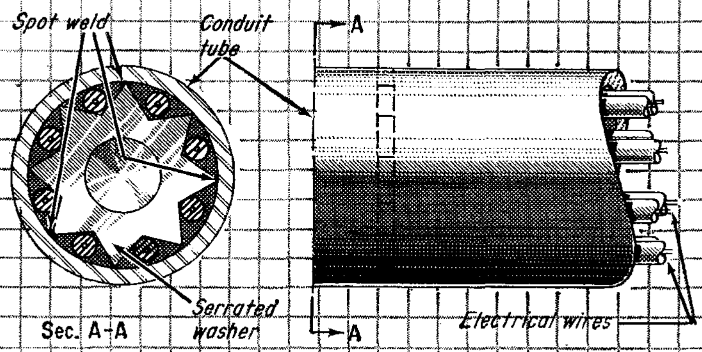

7 Liner to avoid wire twisting

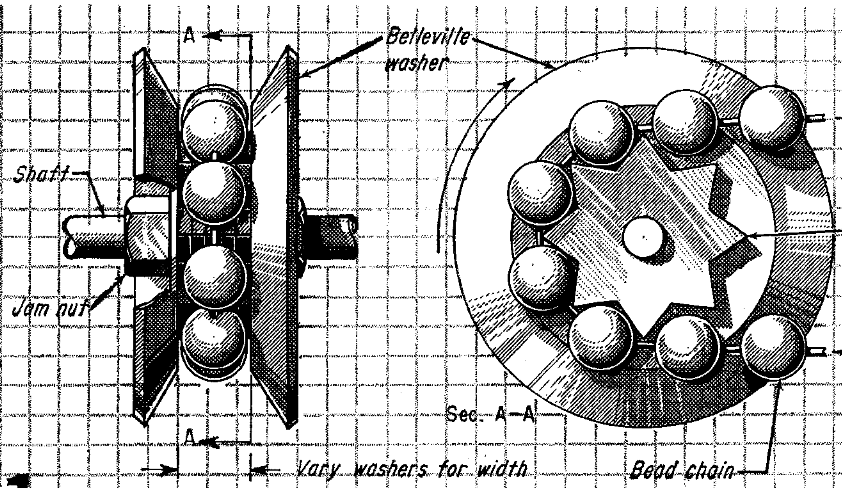

1 Gear or sprocket for bead chain

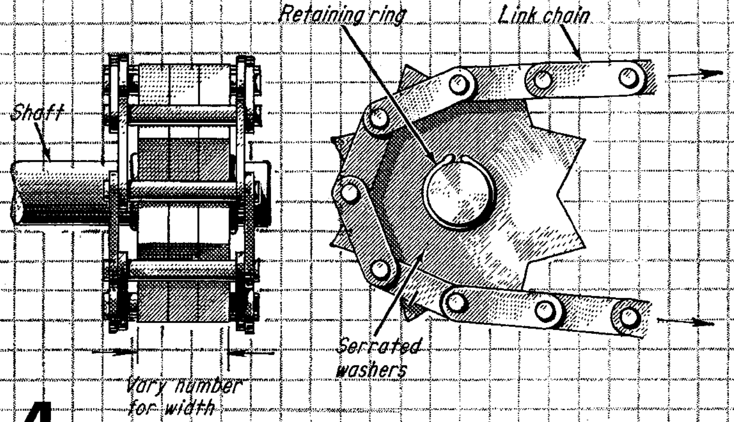

4 Link chain sprockets

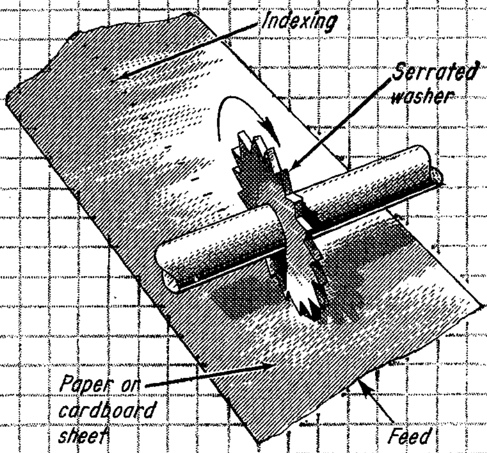

5 Material or paper drive or feeder

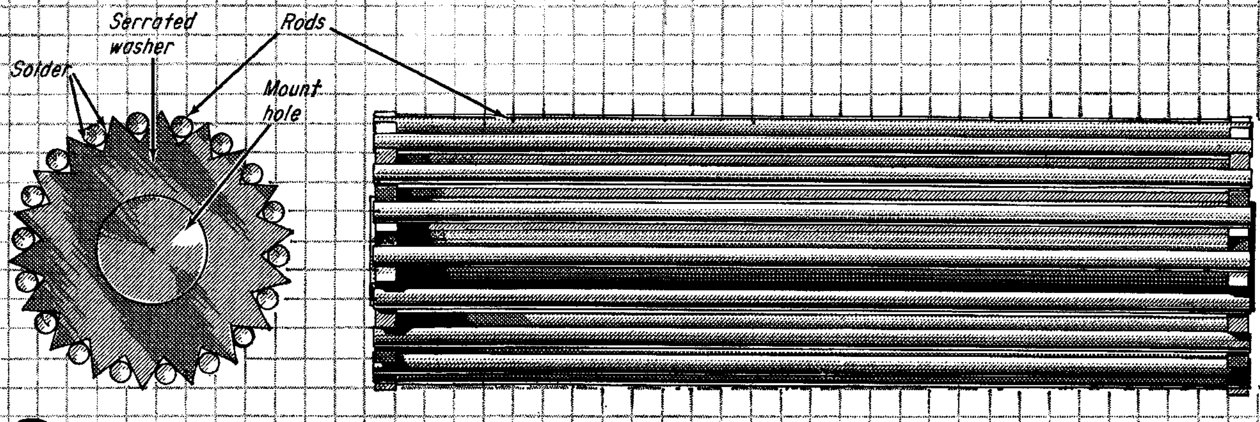

8 End mounting for simple tumbler

Dishwashers Get Busy

Robert O. Parmley

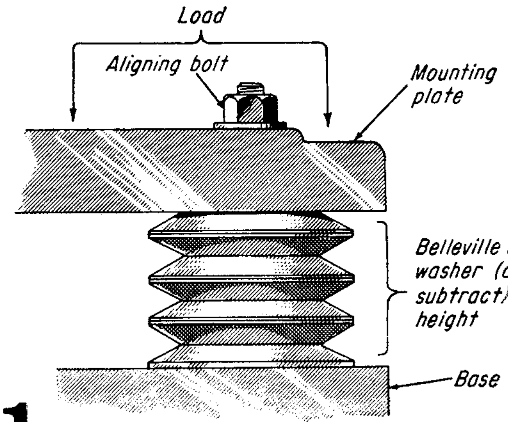

1. HEIGHT ADJUSTMENT

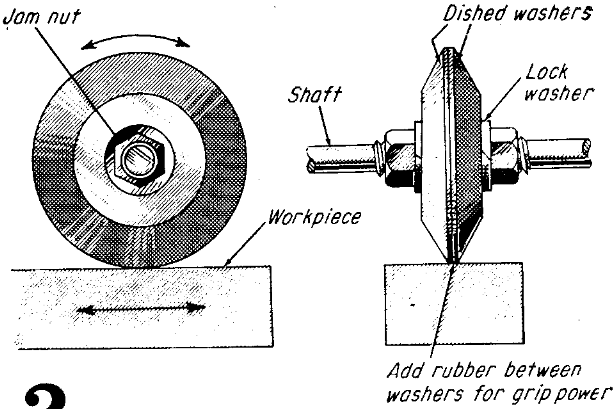

2. GUIDE WHEEL

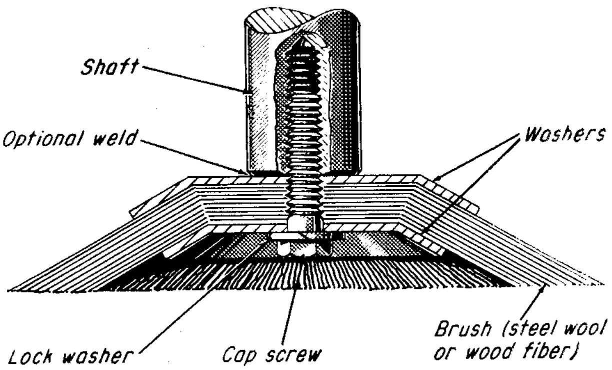

5. BRUSH RETAINER

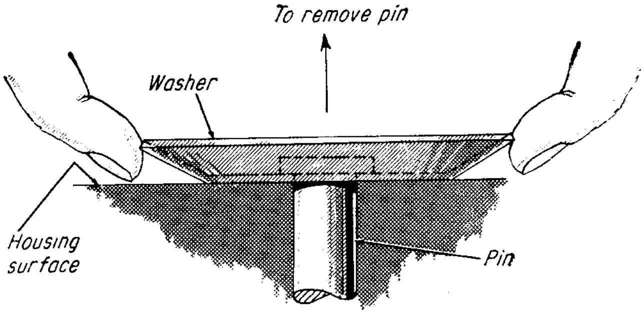

6. EASY PIN REMOVAL

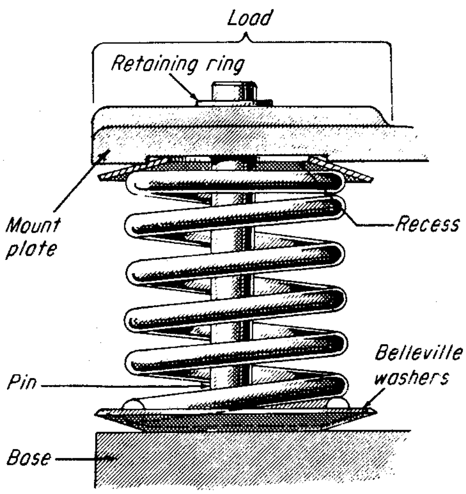

9. COIL SPRING STABILIZER

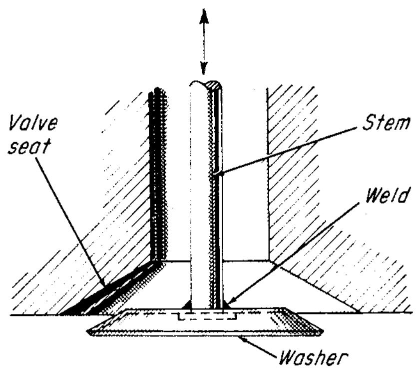

10. SIMPLE VALVE

Let these ideas spur your own design creativity. Sometimes commercial Belleville washers will suit; other wise you can easily dish your own.

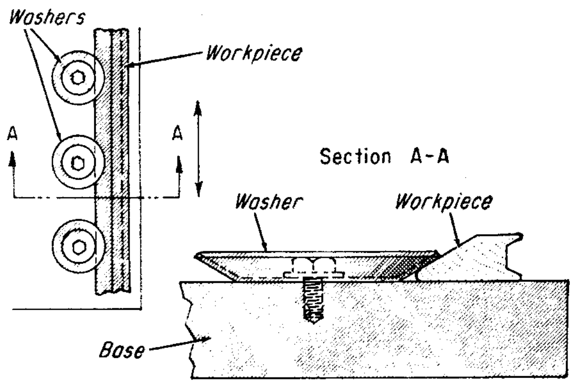

3. ALIGNING BUTTONS will rotate if holding screw is shouldered

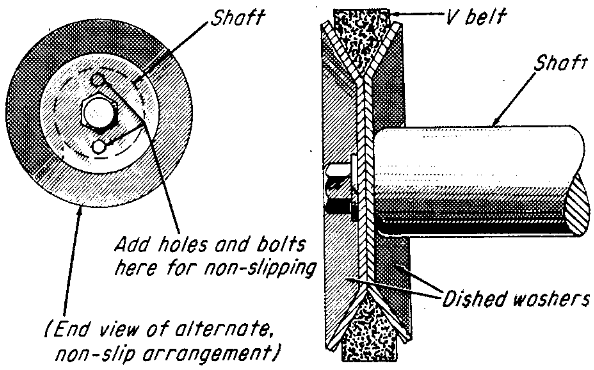

4. V-BELT PULLEY

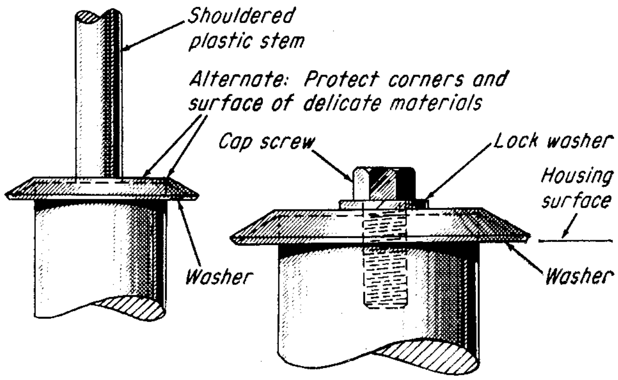

7. END AND CORNER PROTECTION

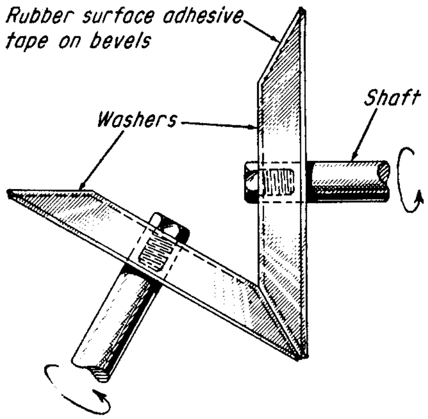

8. SIMPLE BEVEL DRIVE

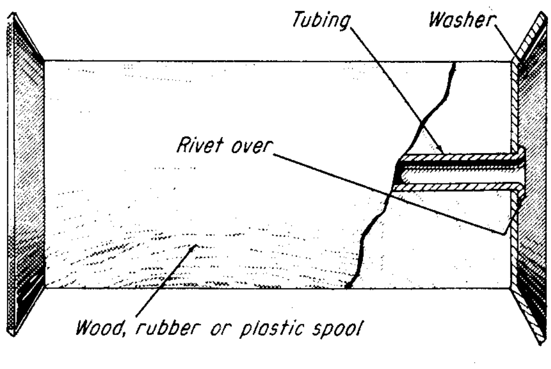

11. FLARED SPOOL-FLANGES

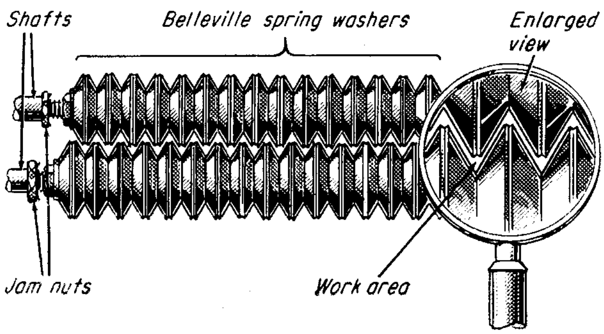

12. CORRUGATING ROLLERS FOR PAPER OR CARDBOARD

Design Problems Solved with Belleville Spring Washers

Robert O. Parmley

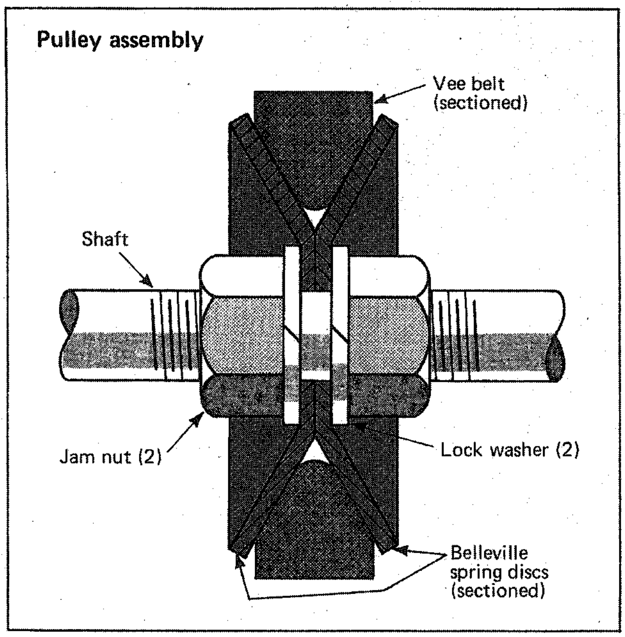

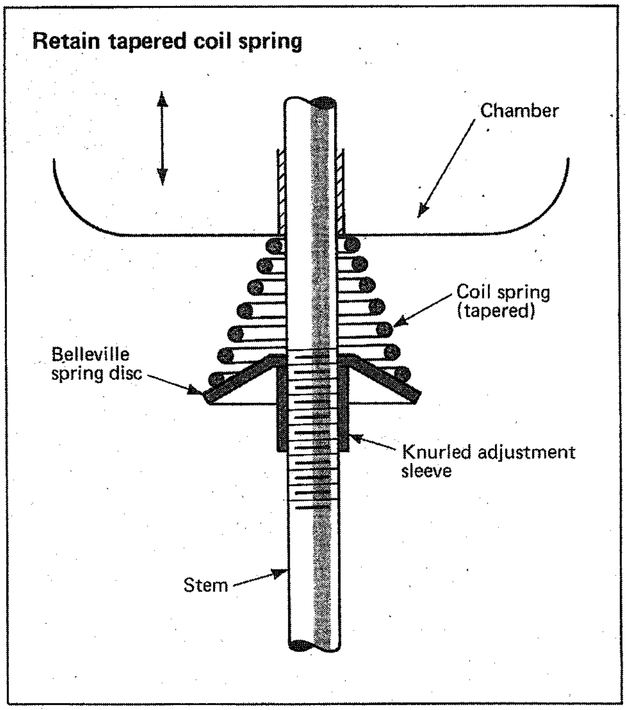

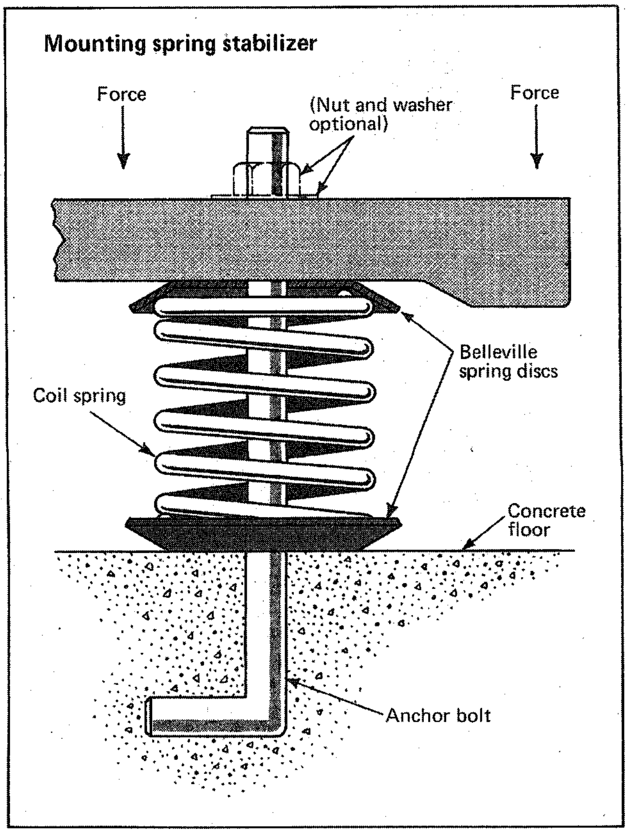

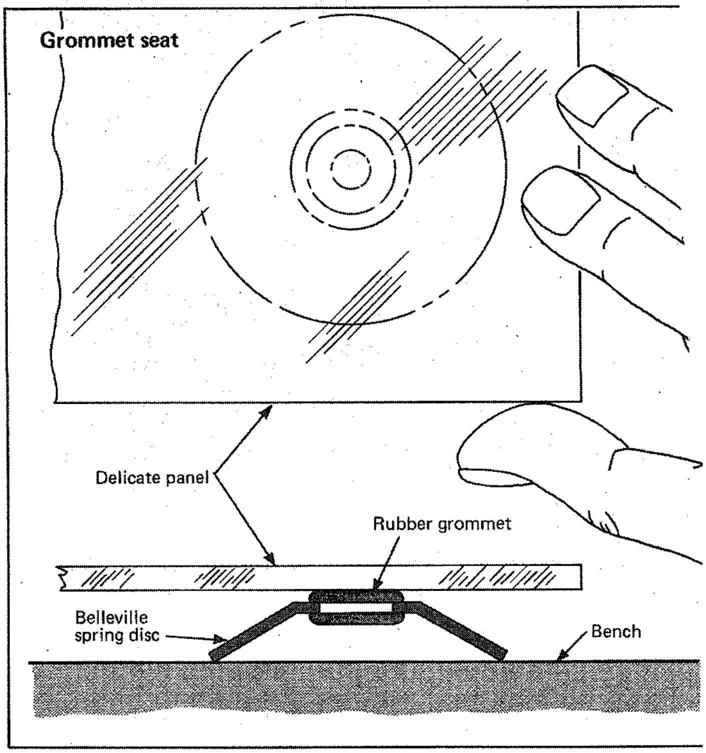

Belleville springs are a versatile component that offer a wide range of applications. There are many places where these components can be used and their availability as a stock item should be considered when confronted with a design problem that requires a fast solution.

Secure anchor bolt

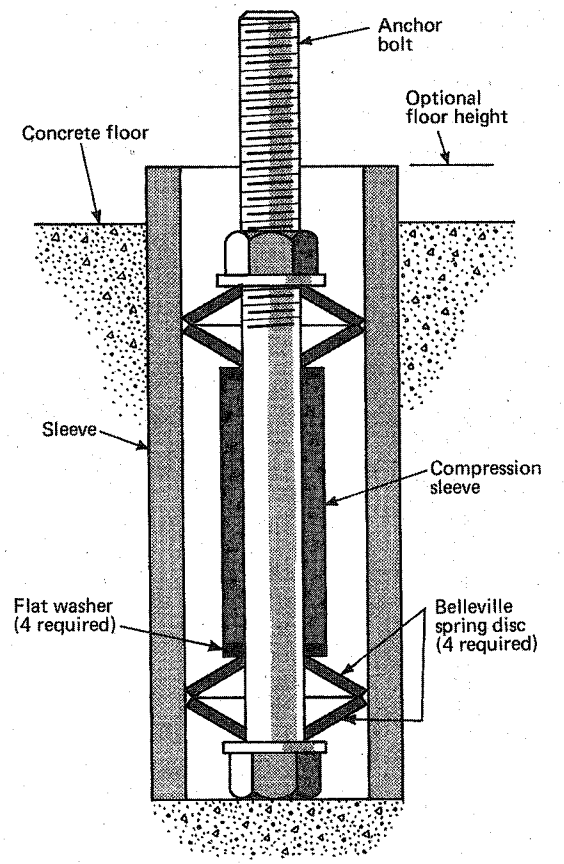

Clamp fixture spring

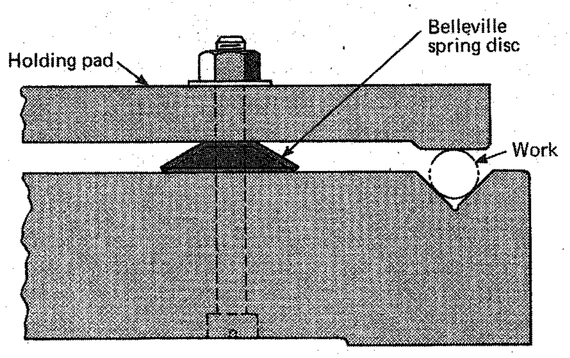

Lock retainer

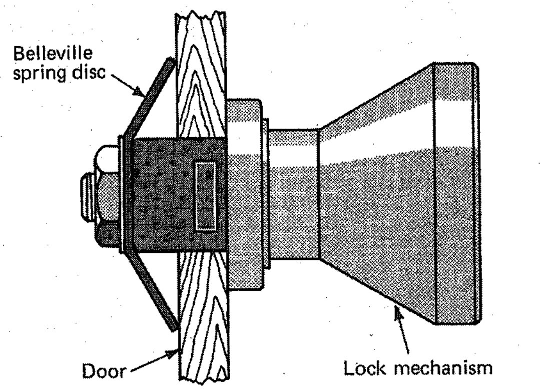

Machine leg spring mounts

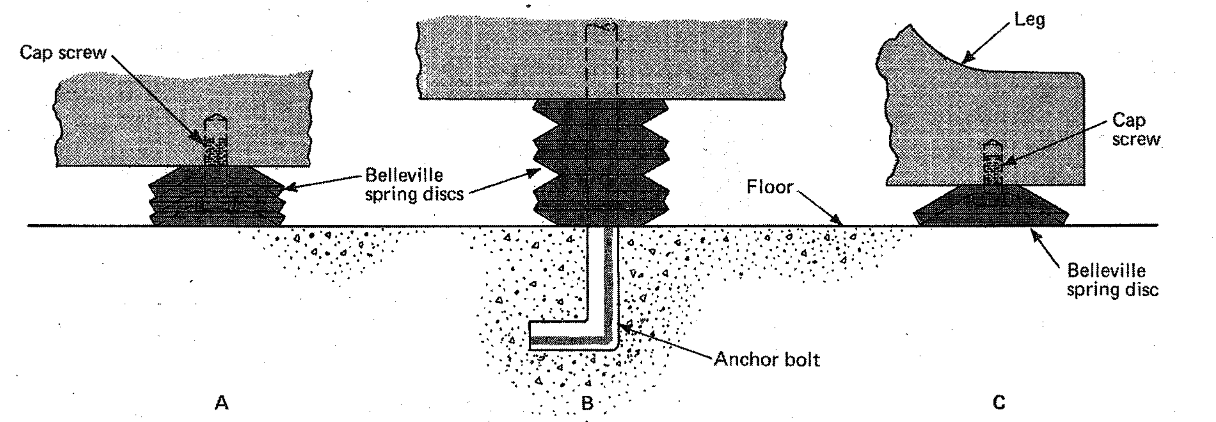

How to Increase Energy Capacity of Belleville Spring Washers

New equations give stress-energy relationships and lead to the unusual arrangement of nesting Bellevilles one inside the other.

H. P. Swieskowski

SINCE 1867, when Julien F. Belleville was issued a patent in Paris for the invention, Belleville springs have never ceased to find wide application. Now, more and more, they are being used to absorb high impact energies. With the arrangements and new design equations given here, you can easily design for maximum energy-absorbing capacity.

Also called *conical disk* springs, Belleville springs are actually no more than conical washers. They are very compact, which leads to first of several advantages:

- They can absorb a large amount of energy at high loads and with a comparatively short working stroke.
- They can return to the system practically all the energy they absorb during the compression or impact stroke. With ring springs, in contrast, approximately 50% of the input energy is dissipated as heat.
- Their load-deflection characteristics can be altered simply by adding or removing individual washers, by stacking washers in various parallel-series combinations, and by nesting them inside larger washers, Fig 1.

Generally speaking, Belleville springs are better suited than helical compression springs where longitudinal space is limited, in other words, where space for solid height is limited and where a helical spring would result in a small index (the ratio of the mean coil diameter to the wire diameter).

Design recommendations

You don't need a maze of nomographs and tables to calculate the impact load a Belleville spring must absorb. With these new design equations, given below, you can predict the amount of induced stress directly. But first, some important findings:

- Nested springs—one washer inside another—require no more space than single springs and reduce the maximum stress by 14%.
- One-parallel-series arrangements of Belleville springs are more efficient energy absorbers than two- or three-parallel

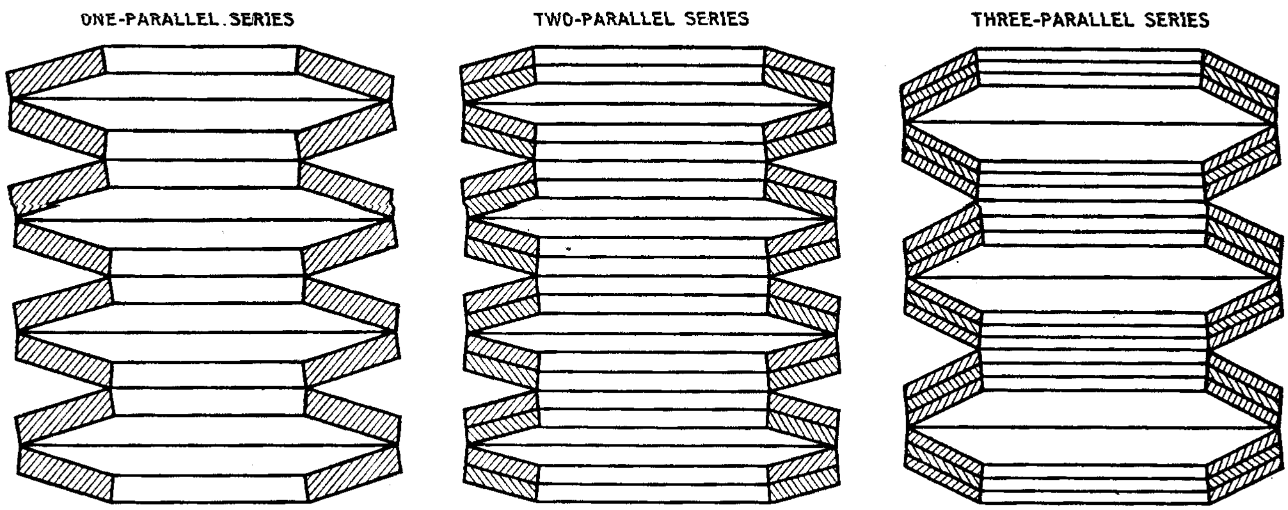

1 . . Four arrangements of Belleville springs. The nested design has highest efficiency for absorbing energy. Contrary to popular opinion, the one-parallel design is more efficient than the two- or three-parallel designs

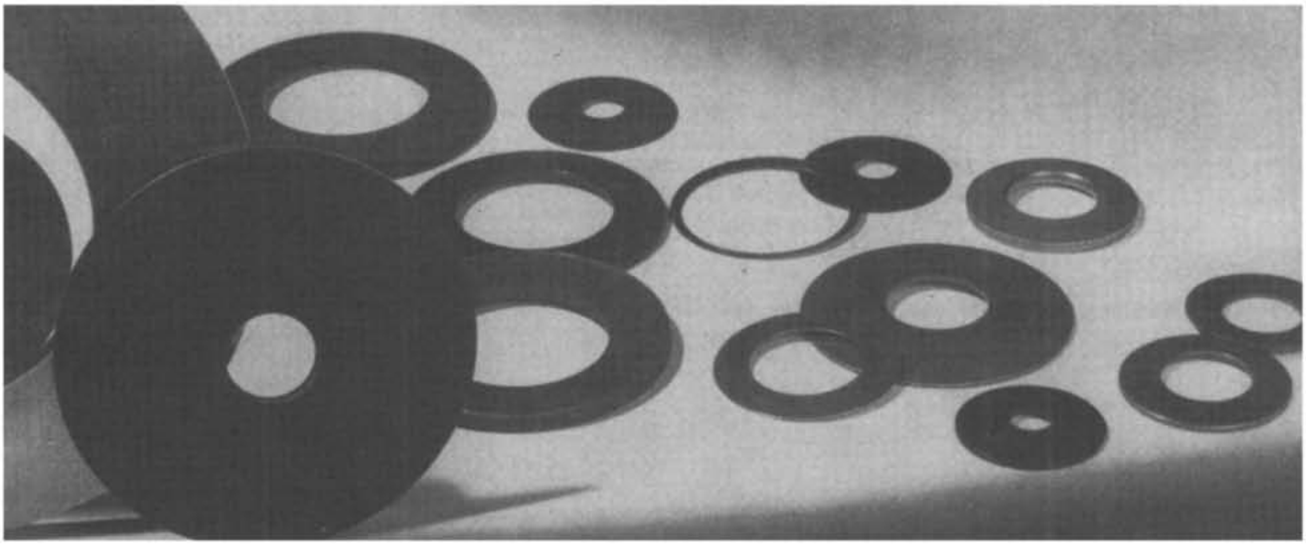

series — contrary to some popular misconceptions. • Final working stress is directly proportional to the square root of the energy capacity and inversely proportional to the outside diameter and square root of the solid height.

One-parallel-series equations

To simplify analysis, it is assumed that the minimum working height is equal to the solid height and that there is no precompression for assembly. Thus the total deflection is

$$F_S = H_F - H_S$$

For symbols, see Box on page 93.

The height-thickness ratio, $B = h/t$, determines the shape of the load-deflection curve. By varying the B values, it is possible to obtain a wide variety of load-deflection curves, Fig 2. The curves are plotted against the deflection in terms of height as the spring washers are com-

NESTED ARRANGEMENT

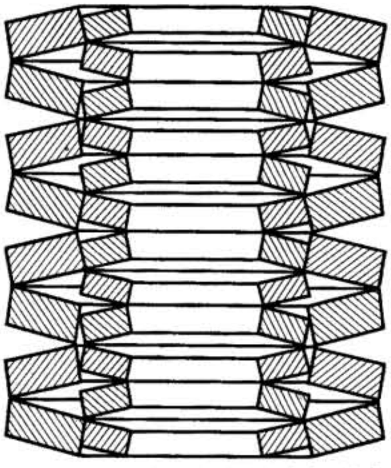

for most ratios of dish height (deflection to flat) to metal thickness.

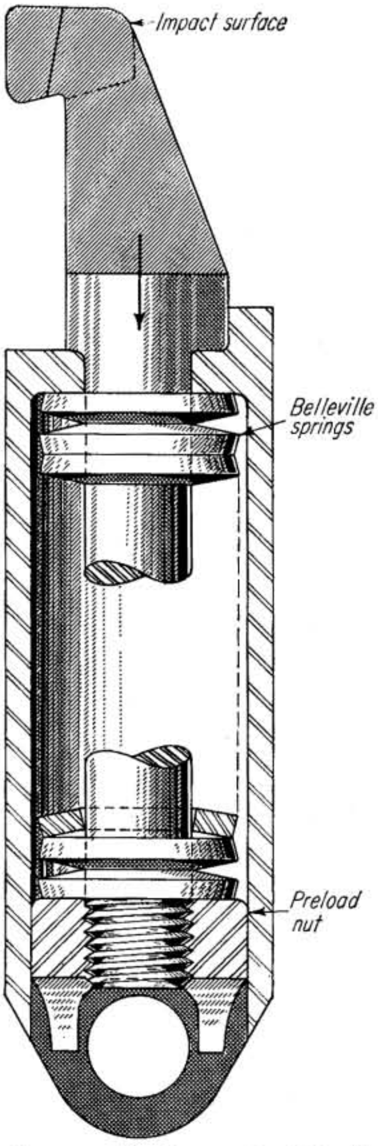

Buffer mechanism with Belleville springs for high-impact energy absorption.

pressed from free height to solid height.

The conventional load and stress formulas for Belleville springs are

Load

$$P = \frac{4EF}{(1-Q^2)\,YD_o^2}\left[\left(h - \frac{F}{2}\right)(h-F)\,t+t^3\right] \qquad (1)$$

Stress

$$S = \frac{4EF}{(1-Q^2)\,YD_0^2}\left[C_1\left(h - \frac{F}{2}\right)+C_2t\right] \qquad (2)$$

where the constants C_1, C_2 and Y are given by the equations

$$Y = \frac{6}{\pi \ln A}\left[\frac{A-1}{A}\right]^2$$

$$C_1 = \left[\frac{A-1}{\ln A} - 1\right]\frac{6}{\pi \ln A}$$

$$C_2 = \frac{3\,(A-1)}{\pi \ln A}$$

The constants can be quickly approximated by means of Fig 3.

The stress equation, Eq 2, gives the value of the compressive stress which occurs on the convex side at the inner diameter. The stress has a maximum value when $F = h$. Hence the maximum (final) stress from Eq 2 is

$$S_S = \frac{4EBt^2}{(1-Q^2)\,YD_o^2}\left(C_1\frac{B}{2} + C_2\right) \qquad (3)$$

The energy stored in one washer compressed from

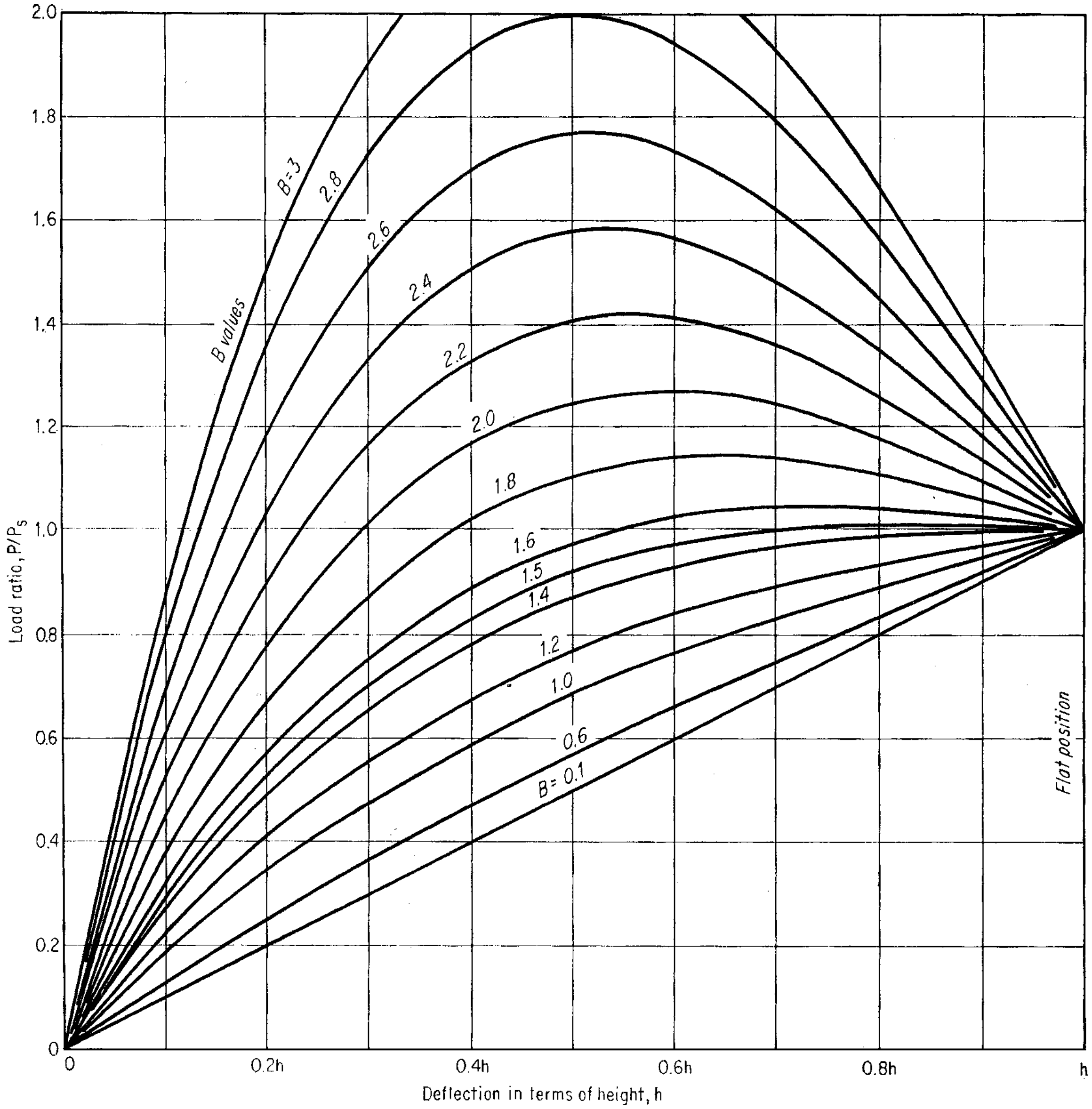

2 . . **LOAD-DEFLECTION CURVES.** The height-thickness ratio, B, determines the shape of the curve.

free height to the flat position is obtained by integration of Eq 1:

$$E_N = \int_o^h P\,dF$$

$$E_N = \frac{4E}{(1-Q^2)\,YD_o^2}\left[\frac{th^4}{8} + \frac{t^3h^2}{2}\right] \qquad (4)$$

For an assembly of N washers in series

$$E_N = \frac{N4E}{(1-Q^2)\,YD_o^2}\left[\frac{th^4}{8} + \frac{t^3h^2}{2}\right] \qquad (5)$$

Keeping in mind that $H_s = Nt$ and $B = h/t$, Eq 5 is rewritten to read

$$E_N = \frac{EH_S\,t^4B^2\,(B^2+4)}{2(1-Q^2)\,YD_o^2} \qquad (6)$$

Combining Eq 3 and 6 gives the relationship between final stress and energy capacity:

$$S_S = \frac{4}{D_o}\left(\frac{2EE_N}{(1-Q^2)H_S(B^2+4)Y}\right)^{1/2}\left(\frac{C_1B}{2} + C_2\right) \qquad (7)$$

For the usual spring materials where $E = 30 \times 10^6$ psi and $Q = 0.3$, the final stress is

$$S_S = \frac{32{,}480}{D_o}\left(\frac{E_N}{H_S(B^2+4)Y}\right)^{1/2}\left(\frac{C_1B}{2} + C_2\right) \qquad (8)$$

For all practical purposes, the stress at solid height, which is the final stress, can be chosen at the permissible stress—the maximum working stress for the spring.

text continued, page 94

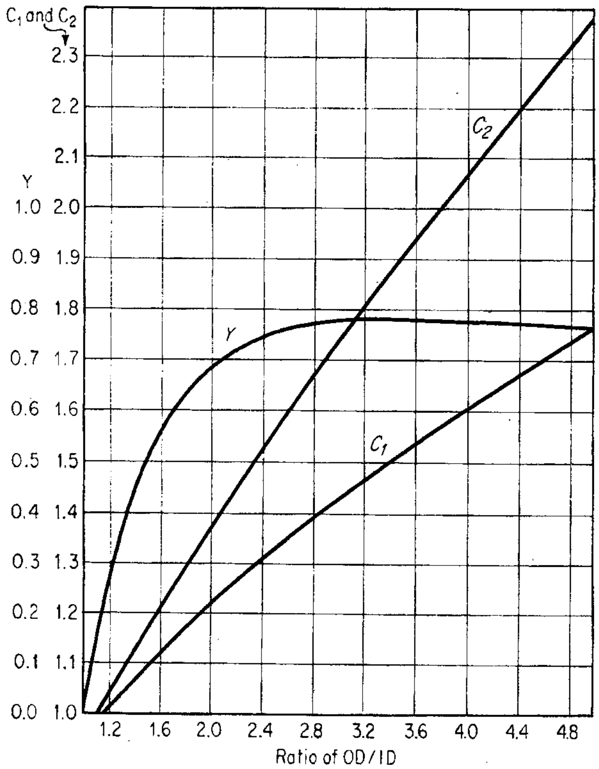

3 . . CONSTANTS for load and stress equations.

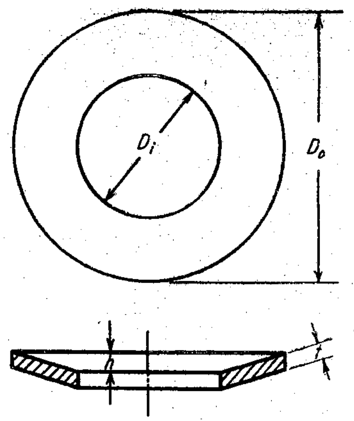

SYMBOLS

General symbols

A = Diameter ratio ($A = D_o/D_i$)
B = Height-thickness ratio ($B = h/t$)
C = Constant; see equations or chart for values of C_1 and C_2
D_i = Inside diameter, in.
D_o = Outside diameter, in.
E = Modulus of elasticity, psi
E_N = Energy capacity, in.-lb
F = Deflection, in.
F_S = Total deflection, in. ($F_S = H_F - H_S$)
h = Dish height, in.
H_F = Free height of spring assembly, in.
H_S = Solid height of spring assembly, in. ($H_S = Nt$)
P = Load, lb
Q = Poisson's ratio
S = Stress, psi
S_S = Final stress, psi
t = Thickness of washer, in.
Y = Constant, see equation or chart for values

For one-parallel series

S'_S Variation index of final stress
E_N^i, S_S^i Energy capacity and final stress of inner spring in nested design, in.-lb, psi
E_N^o, S_S^o Energy capacity and final stress of outer spring in nested design, in.-lb, psi
N = Number of washers in one-parallel series

For two-parallel series

B_2 = Height-thickness ratio
S_{S2} = Final stress, psi
N_2 = Number of parallel units each containing two washers

For three-parallel series

B_3 = Height-thickness ratio
S_{S3} = Final stress, psi
N_3 = Number of parallel units each containing three washers

This is particularly true for critical applications where spring space is limited and loading is of an impact nature. In the design of Belleville springs, a main consideration is to keep the final stress at a safe and reasonable level. Eq 8 shows that the final stress is inversely proportional to the outside diameter and the square root of the solid height; therefore, we make these two values as large as space requirements allow. Doubling the value of the outside diameter (keeping all other variables constant) will result in a 50% reduction in the final stress. A similar increase in the solid height will produce a 30% reduction. Eq 8 further shows that the final stress is directly proportional to the square root of the energy capacity.

The values for the outside diameter, solid height, and energy capacity are usually given within narrow limits for a particular application. The outside diameter is determined by the hole diameter into which the spring must fit. The value of the solid height is dictated by the minimum working height and the energy capacity is prescribed by functional considerations.

The question now remains, what ratios of $A = OD/ID$ and $B = h/t$ will result in the minimum final stress? Visual examination of Eq 8 does not readily show the stress effect of the two ratios. However, by simplifying Eq 8, a series of design curves, Fig 4, is obtained in which the final stress factor is plotted with respect to ratio A. Ratio B acts as a parameter. For this chart, Eq 8 becomes

$$S_S' = \left(\frac{1}{(B^2+4)\,Y}\right)^{1/2}\left(C_1\frac{B}{2} + C_2\right) \qquad \text{(8A)}$$

where S'_S is called the variation index of the final stress.

It can be seen from Fig 5 that the final stress is at a minimum when the diameter ratio $A = 1.7$ for all values of B. Also, for a given B value, the final stress increases at most by 3% in the range $1.5 \leqq A \leqq 2.0$. Therefore, we recommend that the diameter ratio should be kept within the range of 1.5 to 2.0.

Note also from Fig 4 that in the favorable diameter ratio range the final stress increases with increasing values of B. This condition is true except for the height-thickness ratio of $B = 3$, for in the range of $A = 1.5$ to $A = 2.0$, the final stress for $B = 3$ is less than that for smaller B values (of $1 < B \leqq 2$). Belleville washers, however, have been generally designed for energy capacity with B values less than unity because frequently a short work stroke and a high degree of stability are required.

Example 1—One-parallel design

A set of Belleville springs, grouped into a one-parallel series arrangement, are to absorb the recoil of a rifle bolt. The given requirements are:

Outside diameter, $D_o = 0.900$ in.
Solid height, $H_S = 2.035$ in.
Stroke, $F_S = 0.407$ in.
Energy-absorption requirement, $E_N = 100$ in.-lb
Material = alloy steel, AISI 6150

Step 1: Select the diameter ratio. Based on the previous recommendations, a ratio of $A = OD/ID = 1.7$ is chosen. Therefore from Fig 3 (or, for more accuracy, from the equations of the constants):

$$C_1 = 1.15,\ C_2 = 1.26,\ Y = 0.61$$

Step 2: Determine the height-thickness ratio. In this case a stroke of 0.407 is required, which means that

$$B = \frac{h}{t} = \frac{F_s}{H_s} = \frac{0.407}{2.035} = 0.2$$

Step 3: Calculate final working stress from Eq 8:

$$S_s = \frac{32,480}{0.900}\left[\frac{100}{2.035\ (4.04)\ (.61)}\right]^{1/2}\left(1.15\ (0.1) + 1.26\right)$$
$$= 222,000 \text{ psi}$$

Step 4: Calculate the thickness, t. If the stress value of 222,000 psi is acceptable, the thickness t can now be calculated from either Eq 3 or 6.

From Eq 3:

$$t = \left(\frac{S_s\,(1 - Q^2)\;Y\,D_o^2}{4EB\,(C_1\,B/2 + C_2)}\right)^{1/2}$$

$$= \left(\frac{222{,}000\ (.91)\ (.61)\ (.81)}{2(30\times10^6)\ (.2)\ (1.375)}\right)^{1/2} = 0.055 \text{ in.}$$

Step 5: Determine the dish height, h:

$$h = Bt = 0.2(.055) = 0.011 \text{ in.}$$

Step 6: Determine the number of washers:

$$N = \frac{H_S}{t} = \frac{2{,}035}{0.055} = 37$$

The complete design data for this spring are listed in the second column in Table I. The data will be compared later to a nested arrangement.

Variations in stroke

The analysis shows that increased spring travel can be obtained with no corresponding increase in final stress.

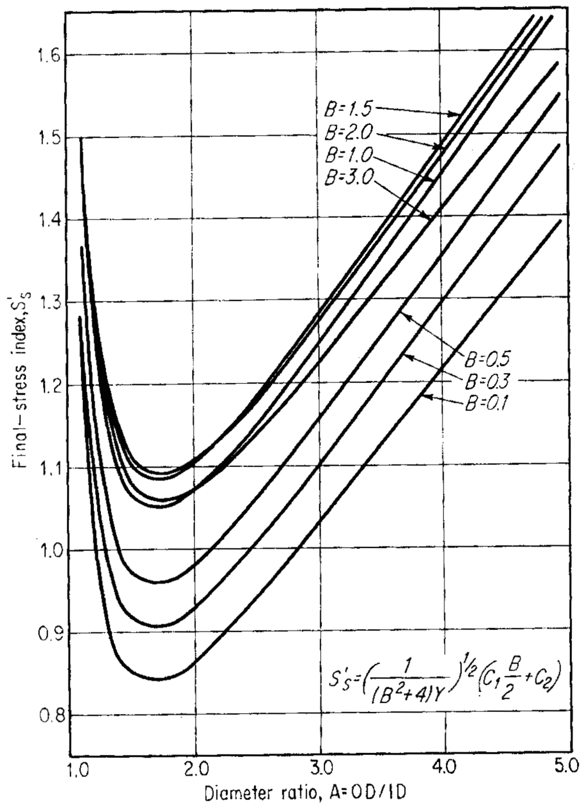

4 . . STRESSES IN one-parallel Bellevilles

Consider the point $A = 2.0$ and $S'_S = 1.07$ in Fig 4. The two curves $B = 1$ and $B = 3$ intersect at this point which means that two spring designs can occupy the same spring space (in other words, with the same H_S and D_o values), and have equal energy capacities and final stresses—however, their total travel, F_S, will be in the proportion of 3 to 1. To illustrate this point, consider the two springs listed in Table II with the same values for:

Outside diameter, D_o = 2.300 in.
Inside diameter, D_i = 1.150 in.
Solid height, H_S = 1.650 in.
Total travel, F_S $\leq$ 3.000 in.
Energy requirement = 342 in. lb.
Material AISI 6150

The two springs have been designed to $B = 1$ and $B = 3$. Final stress and energy capacity of both designs are equal, but the springs differ in total travel and number of washers. The load-deflection diagram for each design is shown in Fig 5. The energy capacities for the springs are represented by the areas under the curves. The areas are equal to each other. Note that there is an energy content common to both designs. The total travel for design B (4.95 in.) is three times that of design A (1.65 in.).

Nested arrangements

Again, to simplify the analysis, it is assumed that there is no diametral clearance between the nested springs. To have a meaningful comparison, both assemblies are designed to the same values for:

- Energy capacity, $E_N = E_N{}^o + E_N{}^i$ (where superscripts o and i pertain to the outer and inner springs, respectively.
- Stroke, F_S
- Solid height, H_S
- Diameter ratio, $A = 1.7$
- Material, AISI 6150
- Outside diameter (the outside diameter of nested arrangement equals the outside diameter of single spring)

For outer spring

$$S_S{}^o = \frac{32{,}480}{D_o}\left(\frac{E_N{}^o}{H_S(B^2+4)Y}\right)^{1/2}\left(C_1\frac{B}{2} + C_2\right) \tag{9}$$

For inner spring

$$S_S{}^i = \frac{55{,}216}{D_o}\left(\frac{E_N{}^i}{H_s(B^2+4)Y}\right)^{1/2}\left(C_1\frac{B}{2} + C_2\right) \tag{10}$$

For efficient design, the stress in the nested arrangement should be equally distributed, thus $S_S{}^o = S_S{}^i$. Therefore Eq 9 and 10 result in

$$E_N{}^o = 2.89\, E_N{}^i \tag{11}$$

From the basic assumption that $E_N = E_N{}^o + E_N{}^i$, and from Eq 11, it follows that

$$E_N = 1.346\, E_N{}^o \tag{12}$$

The relationship between the final stress of the single springs to that of the nested spring is obtained from Eq 8, 9 and 12 as

$$S_S = 1.16 S_S{}^o \tag{13}$$

Therefore, the percentage reduction in final stress, ΔS,

TABLE I.. **SINGLE VS NESTED ARRANGEMENTS**

	ONE-PARALLEL ARRANGEMENT	NESTED ARRANGEMENT	
		OUTER SPRING	INNER SPRING
Thickness, in.	**0.055**	**0.051**	**0.030**
Dish height, in.	**0.011**	**0.0102**	**0.006**
Number of washers	**37**	**40**	**68**
Diameter ratio	**1.7**	**1.7**	**1.7**
Outside diameter, in.	**0.900**	**0.900**	**0.530**
Inside diameter, in.	**0.530**	**0.530**	**0.312**
Height-thickness ratio	**0.20**	**0.20**	**0.20**
Stroke, in.	**0.407**	**0.408**	**0.408**
Solid height, in.	**2.035**	**2.040**	**2.040**
Energy capacity, in.-lb.	**100**	**74**	**26**
Material, AISI	**6150**	**6150**	**6150**
Final stress, psi	**222,000**	**191,000**	**191,000**

that is gained by the substitution of a nested arrangement for a single spring is

$$\Delta S = \left(\frac{S_S - S_S^{\circ}}{S_S}\right) 100 = \frac{S_S - S_S/1.16}{S_S} \cdot 100 = 14\%$$

The stress reduction is constant and applies generally because it is independent of the solid height and outside diameter of the single spring.

Example 2—Nested design

Assume that the final stress of 222,000 psi in the first example is excessive and must be reduced. The use of a nested arrangement will decrease the stress by 31,000 psi to 191,000 psi. A nested arrangement that is equivalent to the first spring in energy and space conditions is easily computed with the aid of Eq 3 and Eq 9 through 13. The design data are listed in Table I.

The solid height and total stroke of the nested design are not exactly equal to those of the single spring because the number of washers in each spring has to be a whole number. However, their differences are negligible, and for comparison purposes the height and stroke are considered equal. Note that the individual energy capacities total 100 in.-lb in Table I.

Other parallel-series arrangements

A comparison is now made of a one-parallel series with two-parallel and three-parallel series. Again, for a valid comparison, all spring assemblies have the same values for energy capacity, stroke, solid height, diameter ratio, material, and outside diameter.

For two spring washers in parallel, the load-deflection formula is

$$P = 2\left\{\frac{4EF}{(1-Q^2)YD_o^2}\left[\left(h - \frac{F}{2}\right)(h-F)\,t + t^3\right]\right\} \qquad (1A)$$

The energy stored in the washers upon compression from free to solid height is

$$E_N = \int_o^h P dF = \frac{8E}{(1-Q^2)YD_o^2}\left[\frac{th^4}{8} + \frac{t^3h^2}{2}\right] \qquad (4A)$$

The energy stored in a two-parallel series, as shown in Fig 1, with N_2 pairs of washers is

$$E_N = \frac{N_2\, 8\, E}{(1-Q^2)YD_o^2}\left[\frac{th^4}{8} + \frac{t^3h^2}{2}\right] \qquad (5A)$$

With the equations $H_s = 2N_2t$ and $B_2 = h/t$, Eq 5A is transformed to

$$E_N = \frac{EH_S t^4 B_2^2\,(B_2^2 + 4)}{2(1 - Q^2)\; Y\; D_o^2} \qquad (6A)$$

Stress at solid height of the two-parallel series is

$$S_{S_2} = \frac{4EB_2t^2}{(1 - Q^2)\; YD_0^2}\left[C_1 \frac{B_2}{2} + C_2\right] \qquad (3A)$$

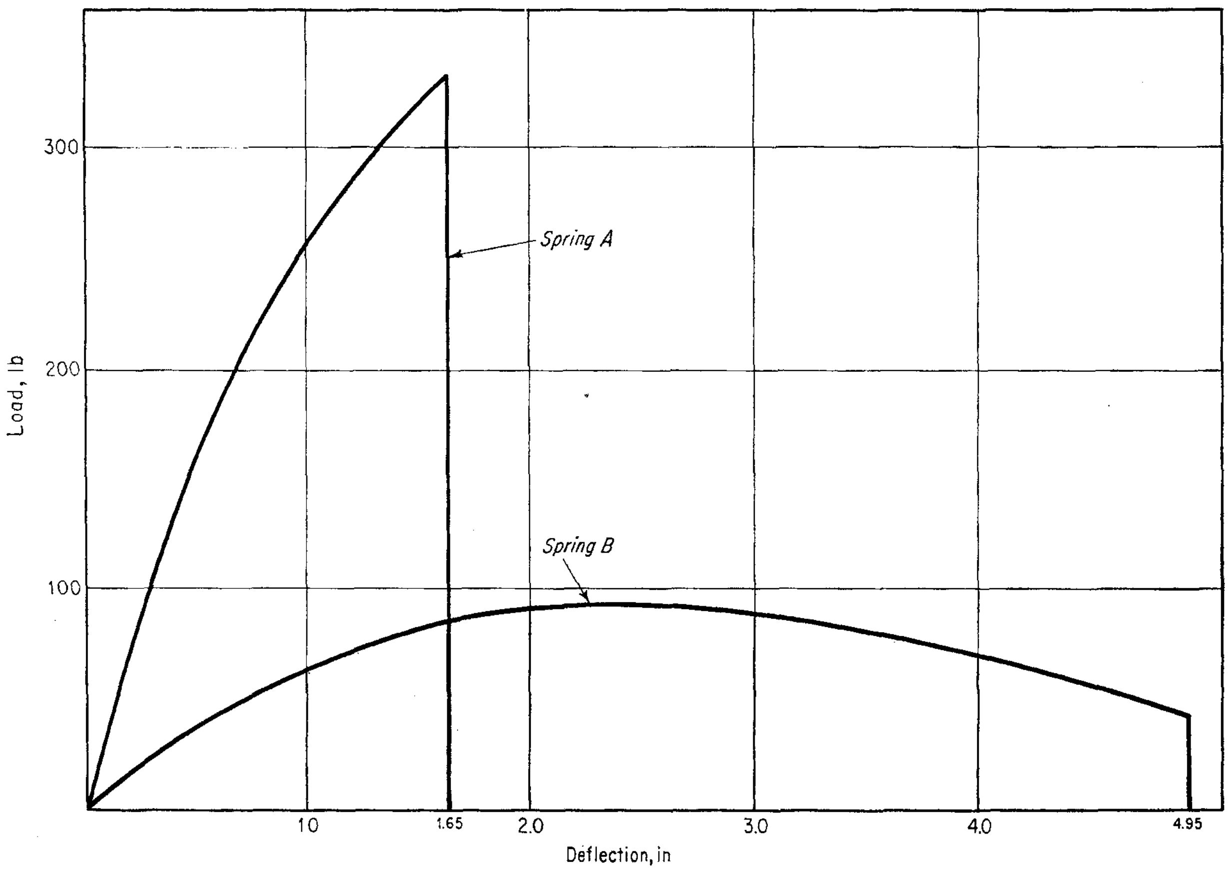

5 . . COMPARISON OF ENERGY CAPACITY. Both springs can absorb equal amounts for a given stress level. Spring A, however, accomplishes the job in one-third the distance required for spring B.

Combining Eq 3A and 6A gives the following expression for the two-parallel series:

$$S_{S2} = \frac{4}{D_o}\left(\frac{2E\,E_N}{(1-Q^2)\,H_S\,(B_2^2+4)\,Y}\right)^{1/2}\left[C_1\frac{B_2}{2}+C_2\right] \quad (7A)$$

The relationship of the final stress of the one-parallel series to the final stress of two-parallel series, obtained from Eq 7 and 7A, is

$$\frac{S_S}{S_{S2}} = \left[\frac{B_2^2+4}{B^2+4}\right]^{1/2}\left[\frac{C_1\frac{B}{2}+C_2}{C_1\frac{B_2}{2}+C_2}\right] \quad (14)$$

From the given condition that both assemblies should have equal strokes, it follows that

$$B_2 = 2B \quad (15)$$

Therefore, Eq 14 is rewritten as

$$\frac{S_S}{S_{S2}} = \left[\frac{B^2+1}{B^2+4}\right]^{1/2}\left[\frac{C_1B+2C_2}{C_1B+C_2}\right] \quad (16)$$

A graph of the stress ratios for one and two-parallel series arrangements are shown in Fig 7. Note that in the practical range of B, ($B \leq 1$), the one-parallel series is more efficient than the two-parallel series. This is particularly true for B values between 0.3 and 0.6 where an 8% stress savings can be realized.

TABLE II..SAME PERFORMANCE — DIFFERENT TRAVEL

	SPRING A	SPRING B
Outside diameter, in.	2.300	2.300
Inside diameter, in.	1.150	1.150
Height, in.	0.055	0.075
Thickness, in.	0.055	0.025
Height-thickness ratio	1.0	3.0
Diameter ratio	2.0	2.0
Number of washers	30	66
Solid height, in.	1.65	1.65
Total travel, in.	1.65	4.95
Final stress, psi	218,000	218,000
Energy capacity, in.-lb.	342	342
Material, AISI	6150	6150

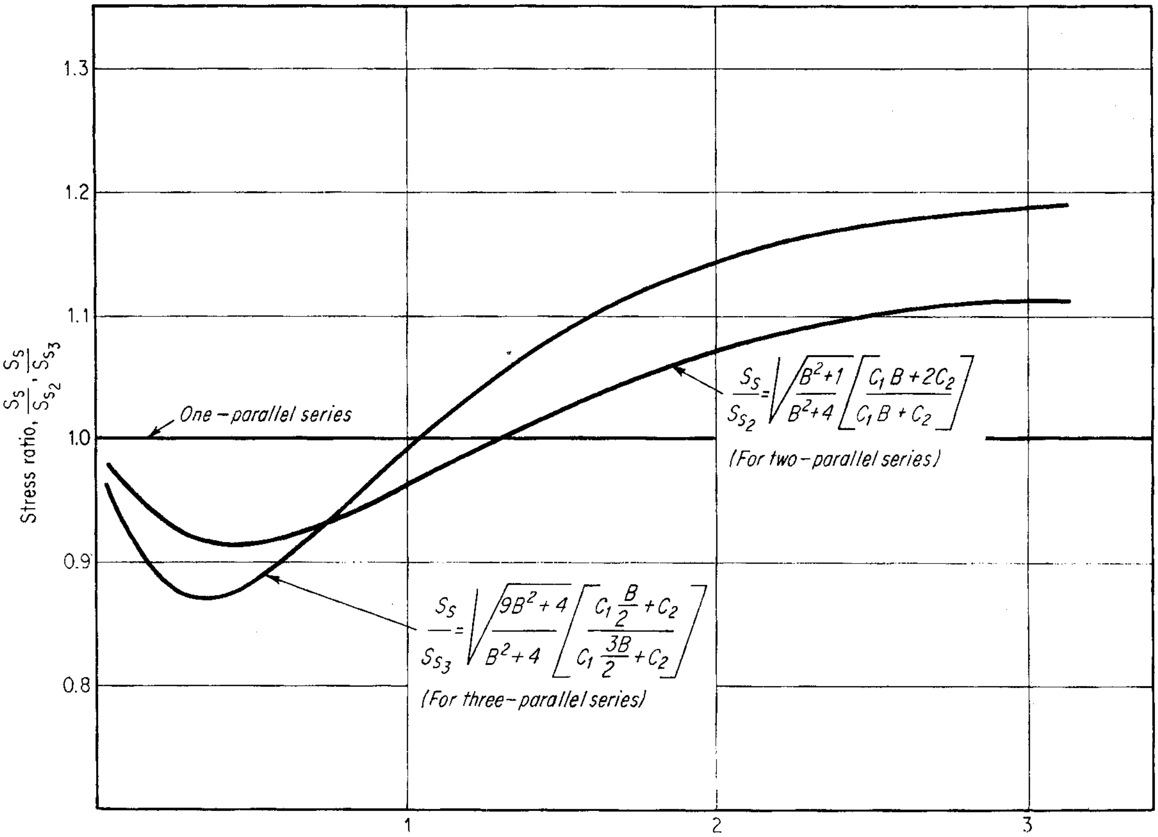

6 . . STRESS COMPARISONS of one-, two- and three-parallel Belleville arrangements. The one-parallel offers better utilization of space in the practical B range of $B = 1$ and under.

Similarly, the final stress of the three-parallel series (shown in Fig 1) is

$$S_{S_3} = \frac{4}{D_o}\left[\frac{2\,E\,E_N}{(1-Q^2)\,H_S\,(B_3^2+4)\,Y}\right]^{1/2}\left[C_1\frac{B_3}{2}+C_2\right] \quad (17)$$

In combination with Eq 7, and the fact that both assemblies have equal strokes, it follows that the ratio of stresses of one-parallel to three-parallel design is

$$\frac{S_S}{S_{S_3}} = \left[\frac{9B^2+4}{B^2+4}\right]^{\frac{1}{2}}\left[\frac{C_1\dfrac{B}{2}+C_2}{C_1\dfrac{3B}{2}+C_2}\right] \quad (18)$$

This equation is also plotted in Fig 6. Note that in the practical B range, the one-parallel series offers a better utilization of spring space than a three-parallel series. For example, two spring assemblies that correspond to the points $B = 0.4$ and $S_S/S_{S3} = 0.87$ (a one-parallel series, with $B = 0.4$, and a three-parallel series, with $B_3 = 1.2$) will have equal strokes and energy capacities and occupy the same space package. The final stress of the one-parallel series, however, will be 13% less. This comparison is shown in Table III.

TABLE III.. **ONE-PARALLEL VS THREE-PARALLEL ARRANGEMENTS**

	ONE-PARALLEL SERIES	THREE-PARALLEL SERIES
Number of individual washers	26	48
Outside diameter, in.	1.87	1.87
Inside diameter, in.	1.10	1.10
Diameter ratio,	1.7	1.7
Height	0.034	0.055
Thickness, in.	0.085	0.046
Height-thickness ratio,	0.4	1.2
Stroke, in.	0.884	0.884
Solid height, in.	2.21	2.21
Energy capacity, in.-lb	600	600
Final stress, psi	305,000	266,000

General load-deflection formulas

Formulas that can be used to good advantage for load-deflection (P/F) calculations are

$$\frac{P}{F} = \frac{4Et^3}{(1-Q^2)\,D_o^2YN} \quad (19)$$

and

$$\frac{P}{F} = \frac{4Et^4}{(1-Q^2)\,D_o^2YH_S} \quad (20)$$

For the usual spring materials where $E = 30 \times 10^6$ psi and $Q = 0.3$, the above equations are reduced to

$$\frac{P}{F} = \frac{132 \times 10^6\,t^3}{D_o^2\,YN} \quad (19A)$$

and

$$\frac{P}{F} = \frac{132 \times 10^6\,t^4}{D_o^2\,Y\,H_S} \quad (20A)$$

The formulas are more convenient to use than Eq 1 and are acceptably accurate for B values less than or equal to unity, where the rate is essentially linear, as can be seen from Fig 2.

Other design recommendations

To simplify the analysis, it was assumed that there was no initial spring compression and also that there was no clearance between minimum operating height and solid height. However, in actual practice, it is recommended that a small precompression be applied to prevent looseness and that clearance be provided to avoid loading to flat position. The two recommendations are easily satisfied by designing for a total energy capacity slightly larger than actually required.

Stress values given by Eq 2 and 8 are localized stresses that occur at the inner diameter and not throughout the entire cross section. Therefore, calculated stress values may at times exceed the yield point of the spring material and yet be permissible.

SEM Applications

N. Dale Long

When a split lockwasher is called for in a screw fastening, a flat washer is invariably necessary. The ways of assembling them illustrated below are strict requirements in military specifications—especially for electronic equipment. Commercial requirements usually vary—depending upon either the designer's decision or product-cost restrictions. For good quality and reliable service, however, the fastening methods shown here can be depended on to pay off.

ASSEMBLY OF FLAT WASHERS AND SPLIT LOCKWASHERS

Flat washers should be placed between . . .

1 Metal surface, whether finished or not, and locking washer	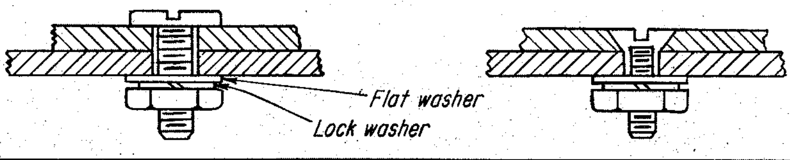
2 Nonmetal surface and locking washer	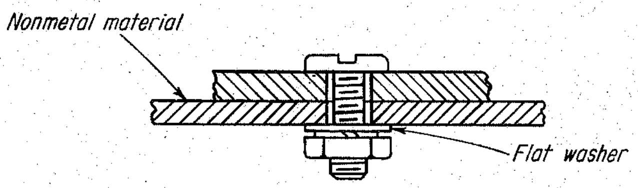
3 Screw head and nonmetal surface	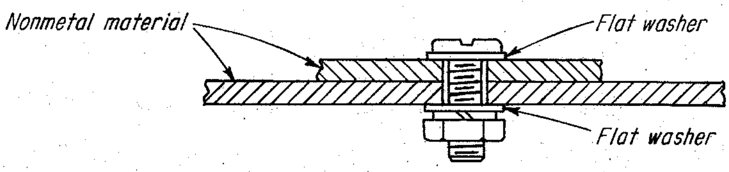
4 Screw head and metal that is 0.032 in. or less thick	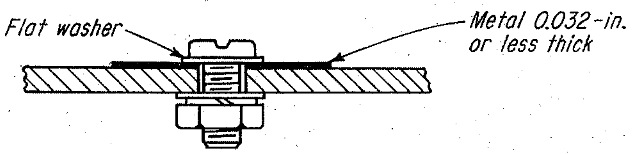
5 Screw head and enlarged or elongated clearance hole	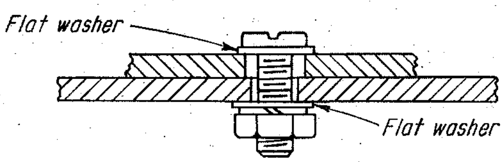
6 Locking washer and enlarged or elongated clearance hole	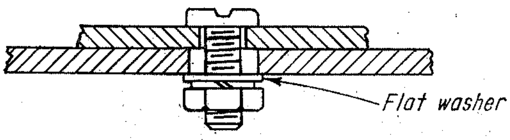

Creative Ideas for Cupped Washers

A standard off-the-shelf item with more uses than many ever considered.

Robert O. Parmley

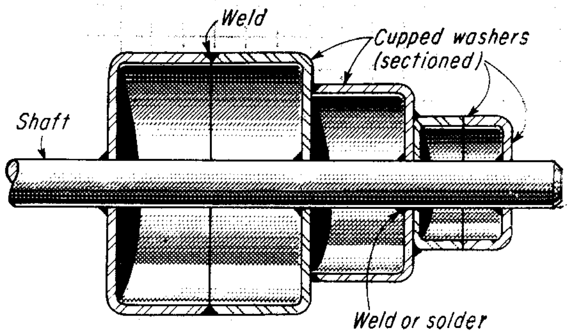

2 Simple step pulley

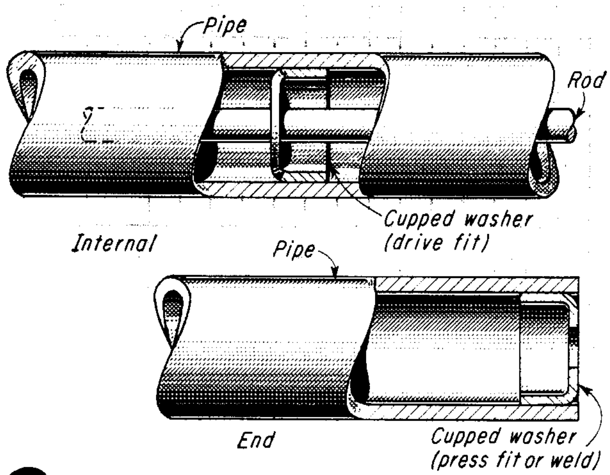

3 Rod aligner and pipe-end bearing

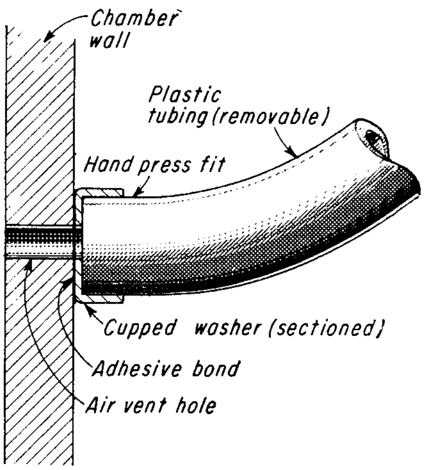

6 Tubing connector

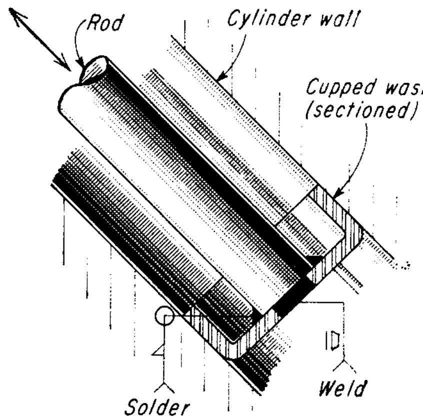

7 Simple piston for cylinder

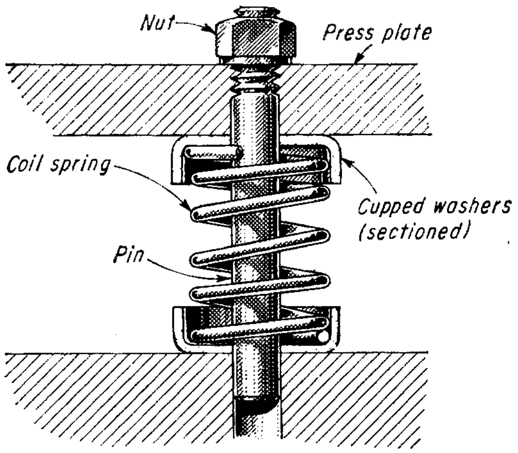

1 Coil spring stabilizer and compression brake

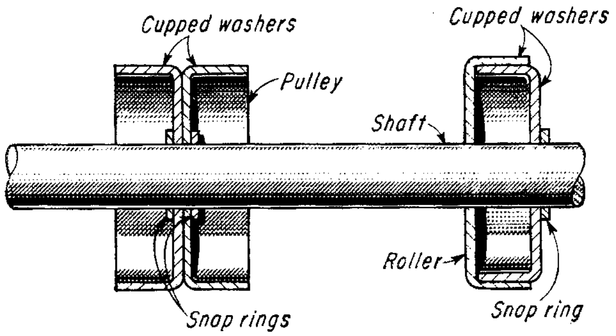

4 Simple pulley and roller

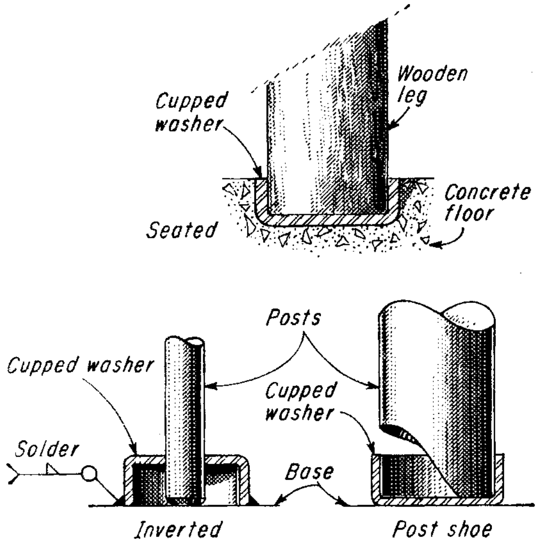

5 Post anchors and supports

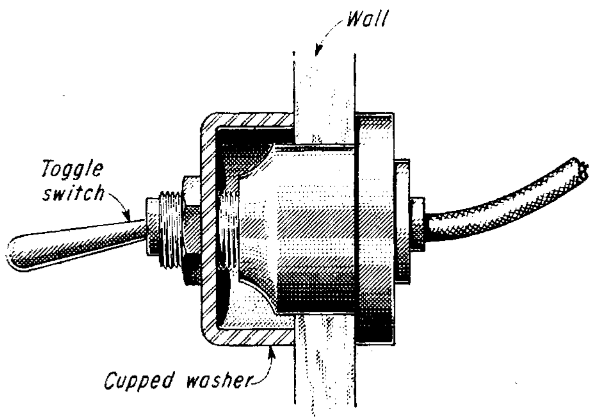

8 Toggle switch housing

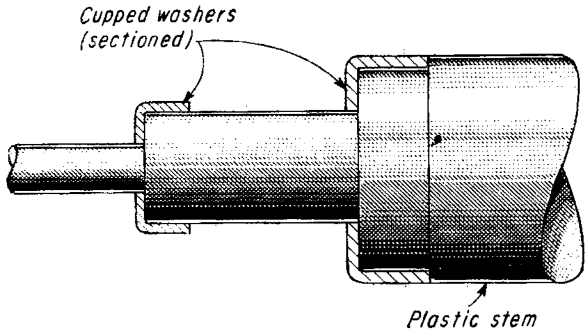

9 Protection for step shoulders

SECTION 12

RETAINING RINGS

Comparisons of Retaining Rings Verses Typical Fasteners

A variety of basic applications show how these rings simplify design and cut costs.

Howard Roberts

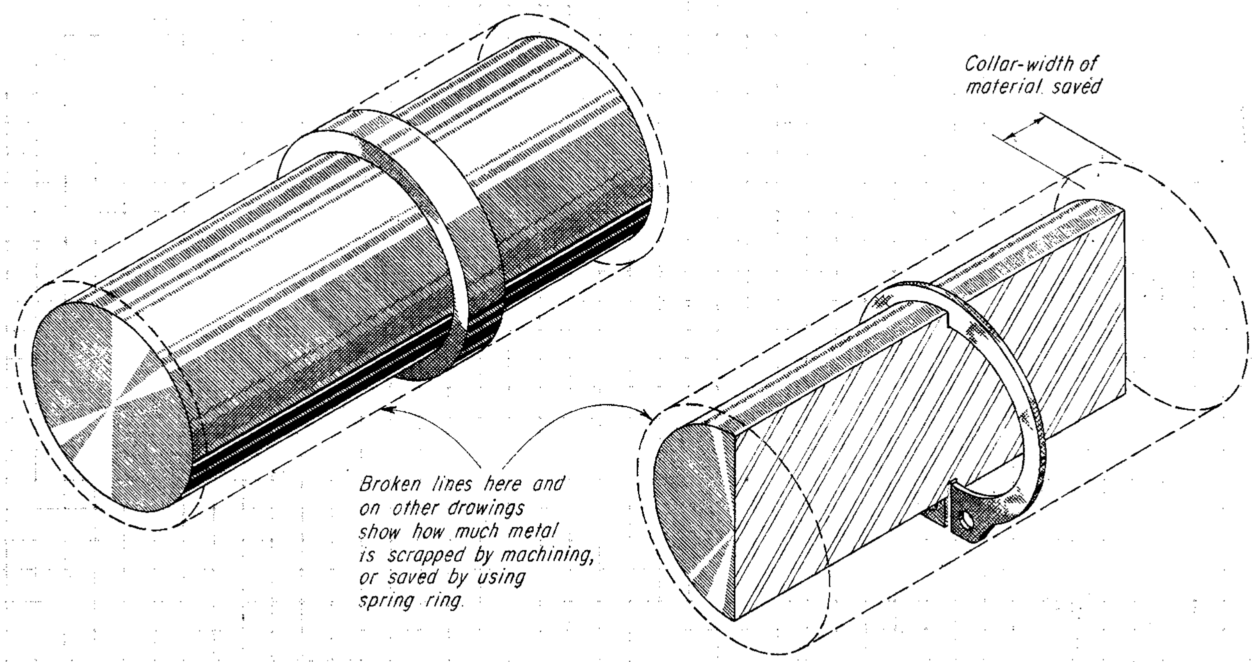

1 **MACHINED SHOULDERS** are replaced with savings in material, tools and time. Grooving for ring can be done during a cut-off, or other machining operation.

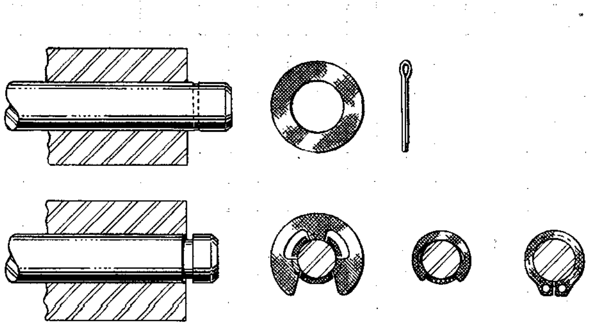

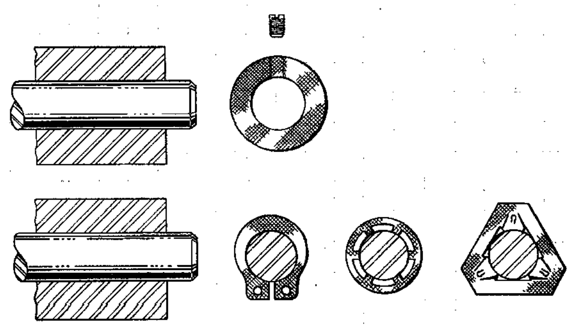

2 **RINGS THAT CAN REPLACE** cotter pin and washer are economical since only one part is required and pin-spreading operation is not needed thus cutting time and costs.

3 **WHEN COLLAR AND SETSCREW** are substituted by ring, risk of screw vibrating loose is avoided. Also, no damage to shaft by screw point occurs – a frequent cause of trouble.

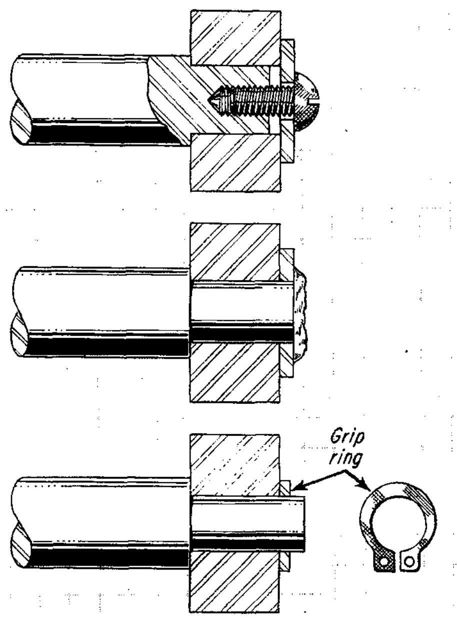

4

RETAIN COMPONENTS on diecastings with a simple-to-use grip ring. Slipped over the end of the shaft, the ring exerts a frictional hold against axial displacement of the shaft.

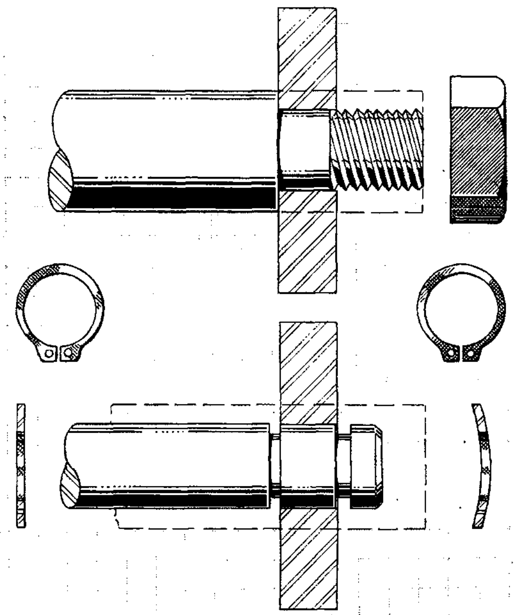

5

SHOULDER AND NUT are replaced by two retaining rings. A flat ring replaces the shoulder, while a bowed ring holds the component on shaft for resilient end-play take-up.

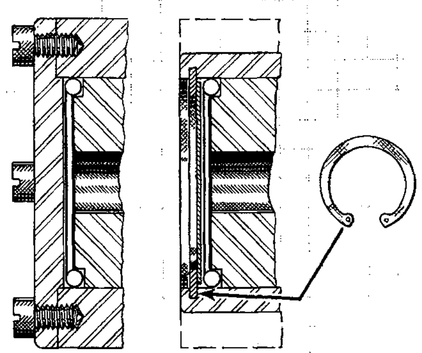

6

COVER-PLATE ASSEMBLY has been redesigned (lower drawing) to avoid use of screws and machined cover-plate. Much thinner wall can be used—no drilling or tapping.

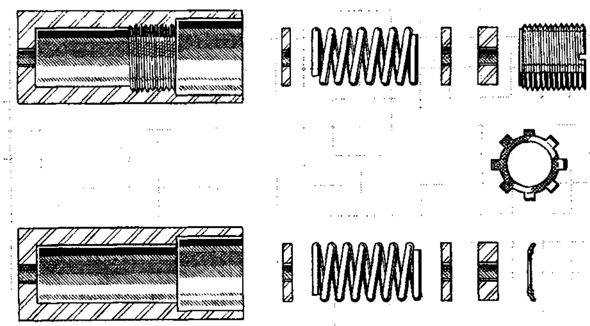

7

THREADED INTERNAL FASTENERS are costly because of expensive internal threading operation. Simplify by substituting a self-locking retaining ring—see lower drawing.

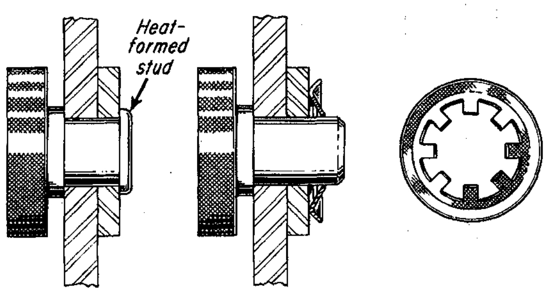

8

HEAT-FORMED STUD provides a shoulder against retained parts but must be scrapped if the parts must be disassembled for service. Self-locking ring can be easily removed.

Retaining Rings Aid Assembly, I

By Functioning as both a shoulder and as a locking device, these versatile fasteners reduce machining and the number and complexity of parts in an assembly.

Robert O. Parmley

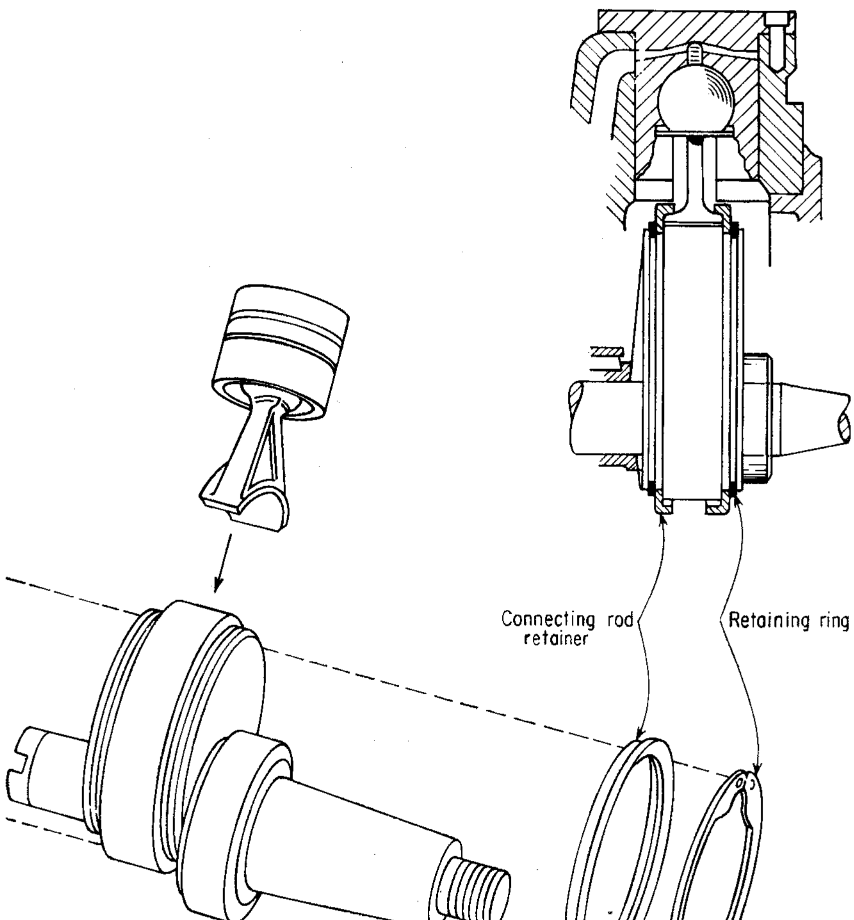

Slow-moving piston of hydraulic motor is assembled to the crank throw by two retainers. These are held in place by two retaining rings that fit into grooves in the crankthrow

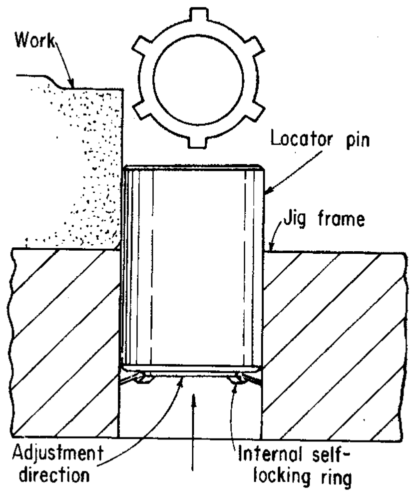

Internal self-locking ring supports a locator. Elevation of the pin may be altered in the entry direction only; the pin won't push down into the frame

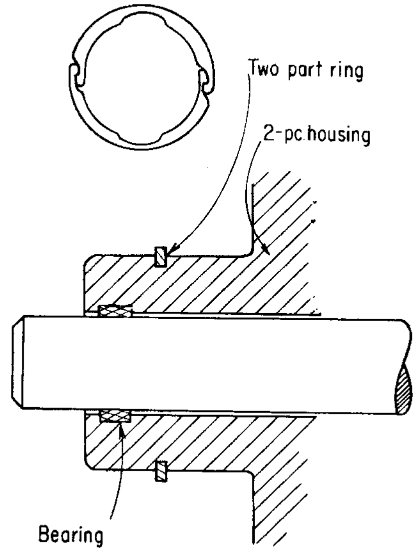

Two-piece interlocking retaining ring serves to hold a two-piece assembly on a rotating shaft, and is more simple than a threaded cap, a couple of capscrews or other means of assembly

Source: American Machinists, June 3, 1968 by permission of Publisher

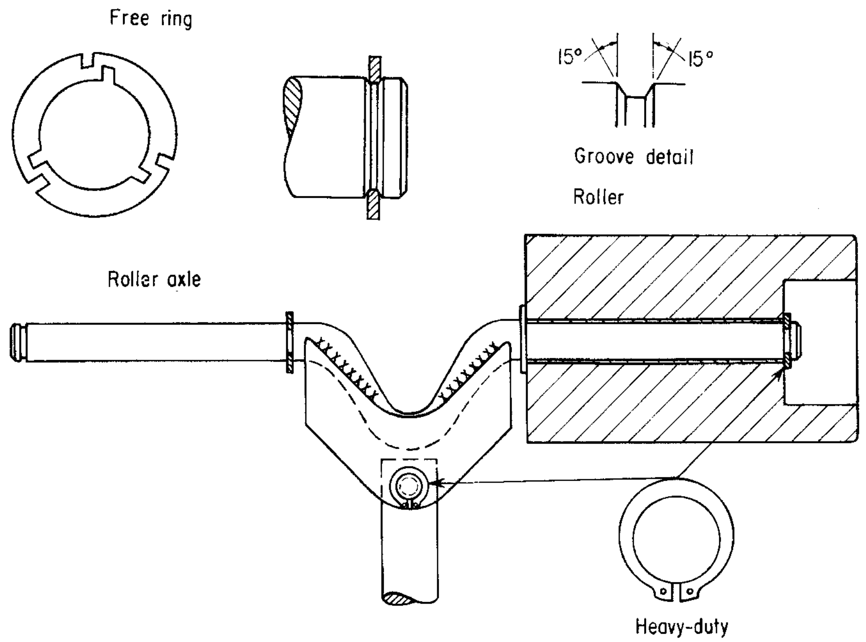

Two types of rings may be used on one assembly. Here permanent-shoulder rings provide a uniform axle step for each roller, without spotwelding or the like. Heavy-duty rings keep the rollers in place

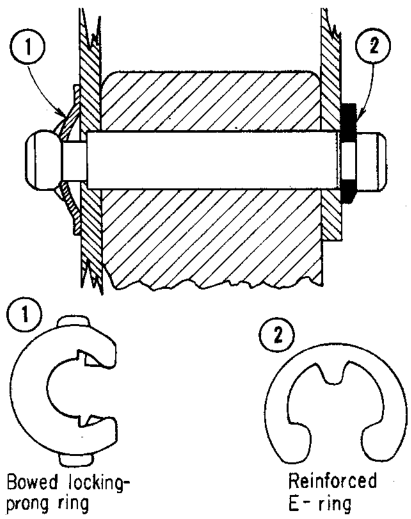

Snug assembly of side members to a casting with cored hole is secured with two rings: 1—spring-like ring has high thrust capacity, eliminates springs, bow washers, etc; 2—reinforced E-ring acts as a retaining shoulder or head. Each ring can be dismantled with a screwdriver

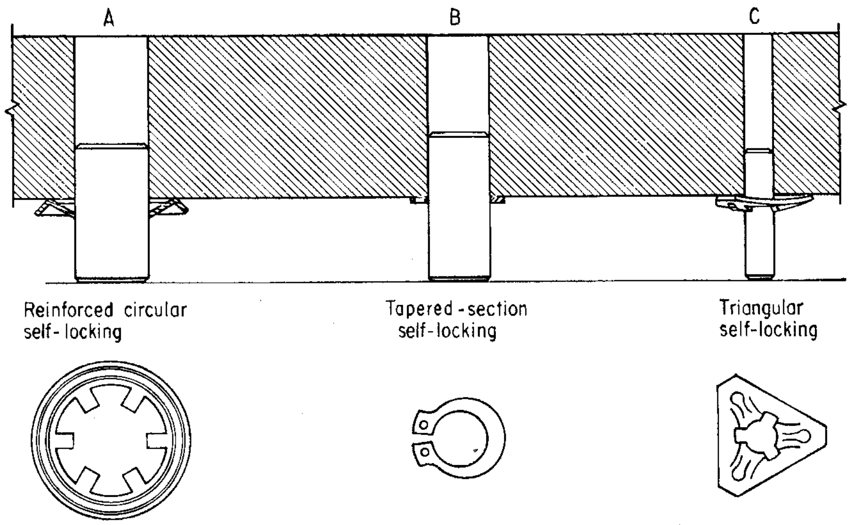

These three examples show self-locking retaining rings used as adjustable stops on support members (pins made to commercial tolerances): A—external ring provides positive grip, and arched rim adds strength; B—ring is adjustable in both directions, but frictional resistance is considerable, and C—triangular ring with dished body and three prongs will resist extreme thrust. Both A and C have one-direction adjustment only

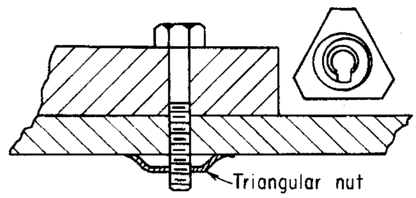

Triangular retaining nut eliminates the need for tapping mounting holes and using a large nut and washer. Secure mounting of small motors and devices can be obtained in this manner

Retaining Rings Aid Assembly, II

Here are eight thought-provoking uses for retaining rings.

Robert O. Parmley

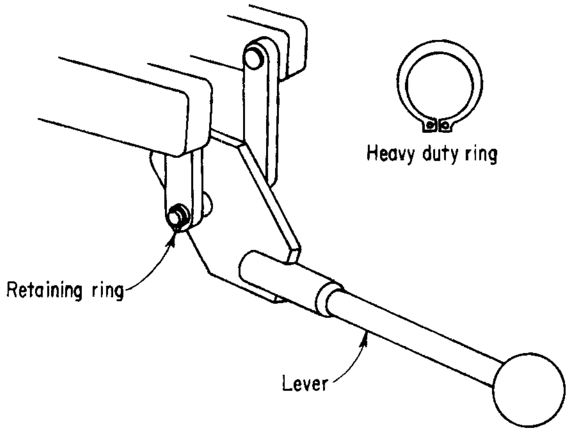

Axial pin for lever is secured with a heavy-duty ring, making a neat, strong assembly

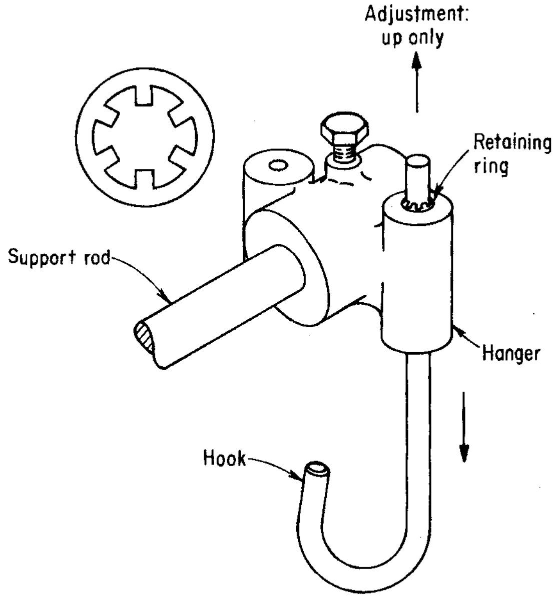

Hanger hook is held at desired height by a self-locking external ring. A multitude of adjustments can be made without trouble

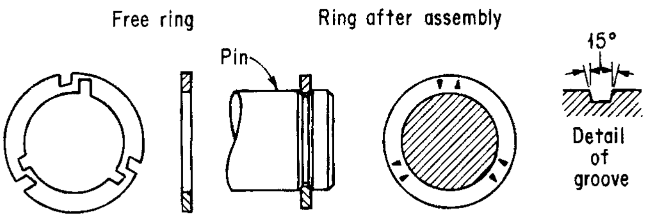

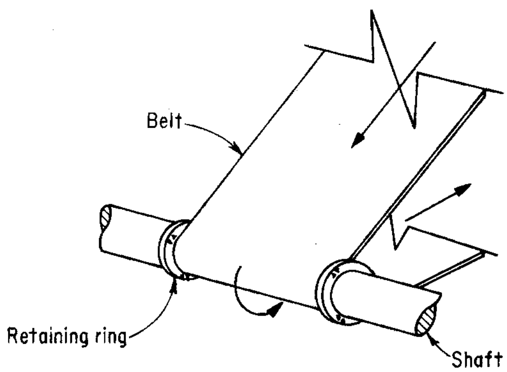

Belt alignment is assured by using permanent shoulder retaining rings. The rings are crimped into the shaft grooves for a permanent, clean, and inexpensive flange. A retainer ring of this type has a high capacity for thrust loads

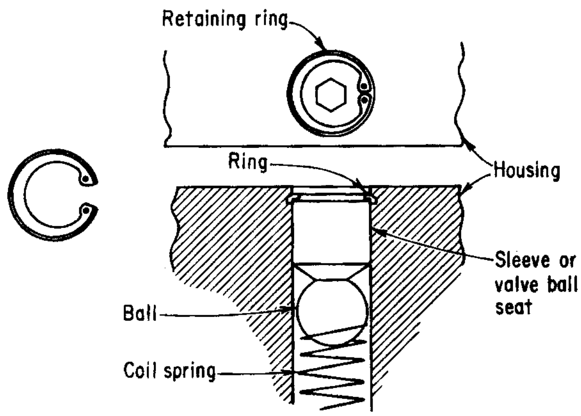

A sleeve or ball seat valve is safely retained by a ring that acts like a wedge in the outer groove. Rigid end-play take-up is provided

Source: American Machinist, Feb. 22, 1971 by permission of publisher.

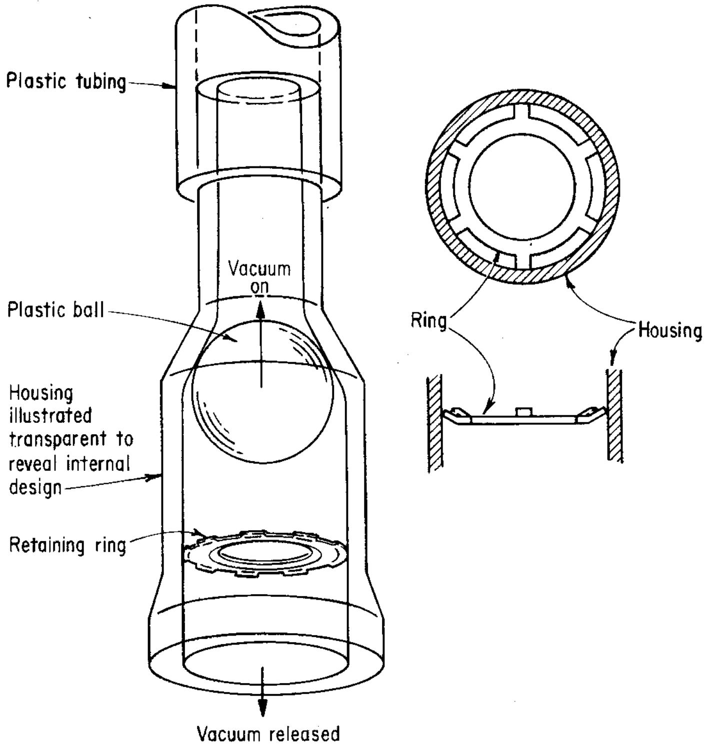

Internal self-locking ring supports the plastic ball valve when the vacuum is released, thus providing a support during the "off" cycle. Air or liquid is released when ball is at rest and exits through the areas between the grip points of the ring, which is adjustable at entry position

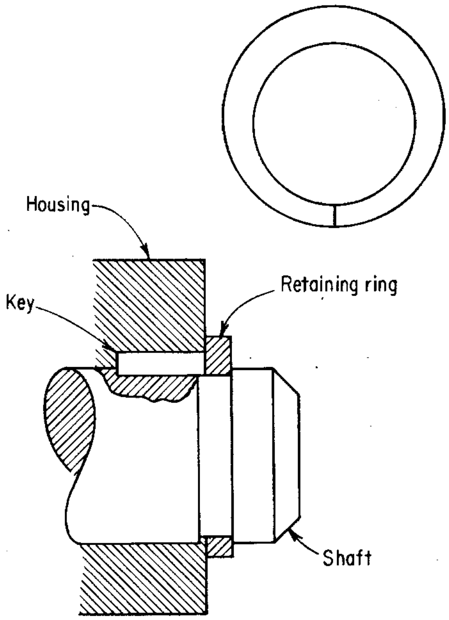

Tamper-proof lock for a shaft in a housing provides location of the shaft and at the same time retains the key. Heavy axial loading and permanent retention of the key are double values in this application

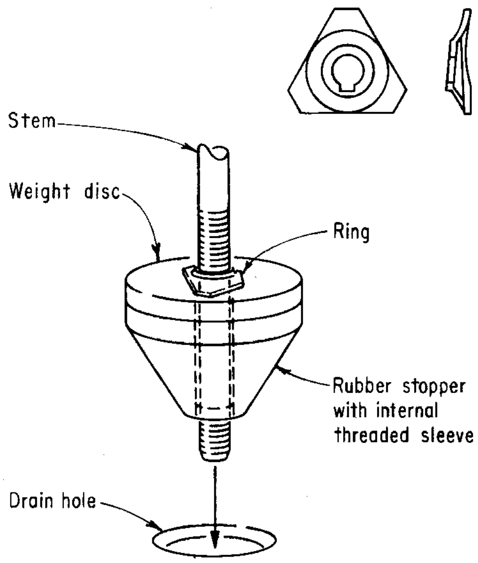

Triangular retainer nut positions and unifies components of the tank drain assembly. The triangular nut eliminates the need for a large standard nut and lockwasher or spring-type component and simplifies the design

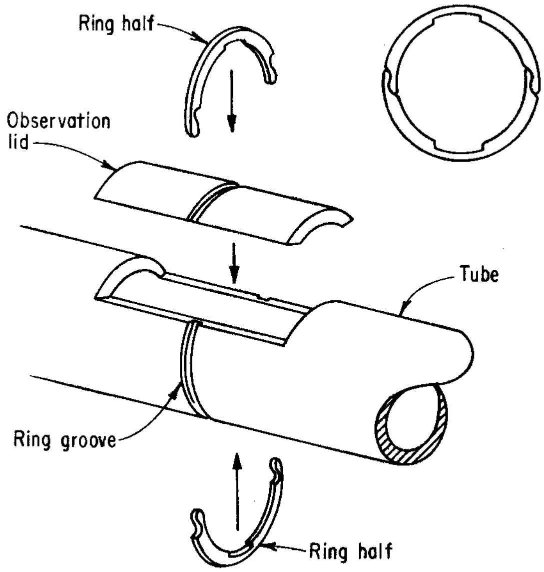

Observation lid on tubing makes it possible to inspect wiring at will. The two-part balanced retainer ring has identical semicircular halves, which are held together by the interlocking prongs at the free ends

Coupling Shafts with Retaining Rings

These simple fasteners can provide an original way around certain design snags. For example, here are eight ways they're used to solve shaft-coupling problems.

Robert O. Parmley

Pin, Sleeve, and Ring

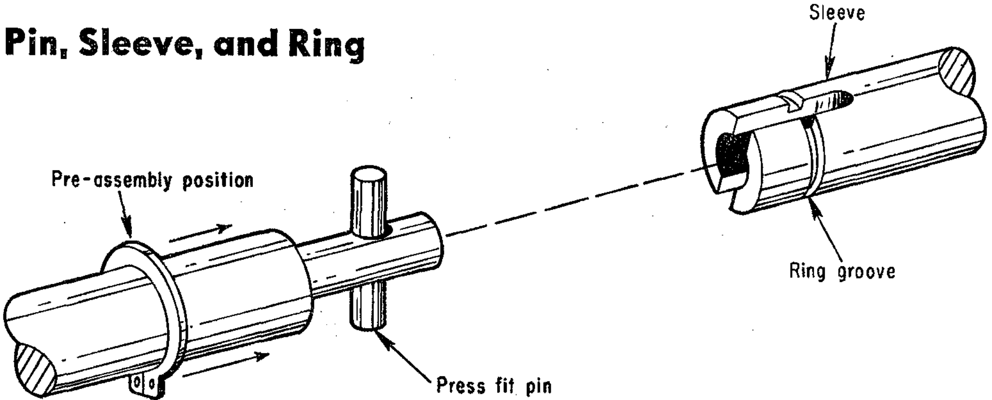

This inexpensive connection is for light torques and moderate loads where accurate positioning is not required. A heavy-duty ring is used to resist high-impact and thrust loads.

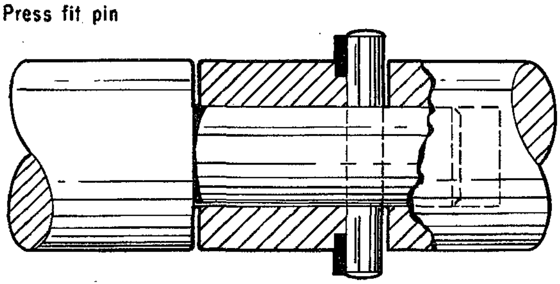

Sleeve, Key, and Ring

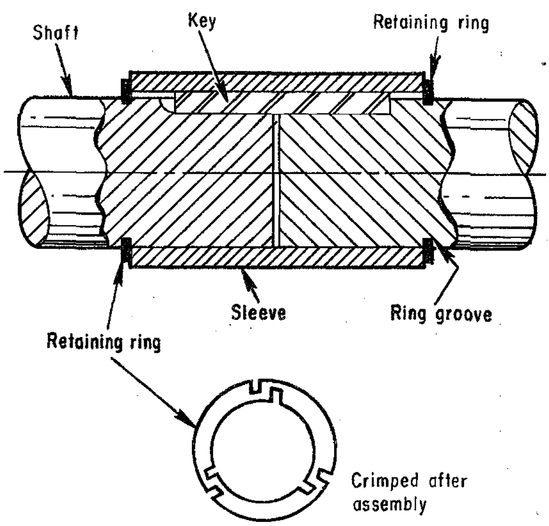

Crimping the retaining ring into the groove produces a permanent, simple, and clean connection. This method is used to avoid machining shoulders in expensive materials, and to permit use of smaller-diameter shafts. When the ring is compressed into a V-shaped groove on the shaft, the notches permanently deform into small triangles, causing a reduction of the inner and outer diameters of the ring. Thus, the fastener tightly grips the groove, and provides a 360-deg shoulder around the shaft. Good torsional strength and high thrust-load capacity is provided by this connection.

Reprinted with Permission from Machine Design, Jan. 19, 1967. A Penton Publication

Two-Shaft Splice

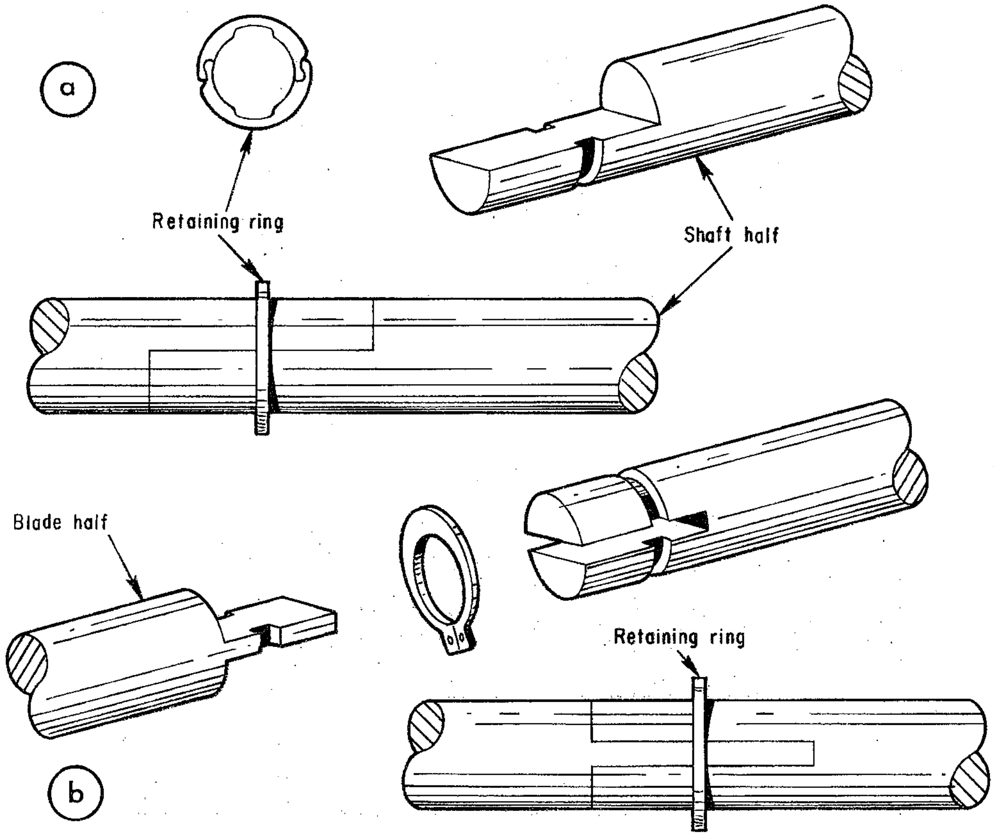

A balanced two-part ring provides an attractive appearance in addition to withstanding high rotational speeds and heavy thrust loads, *a*. The one-piece ring, *b*, secures the shafts in a high-torque capacity design.

End-Flange Connection

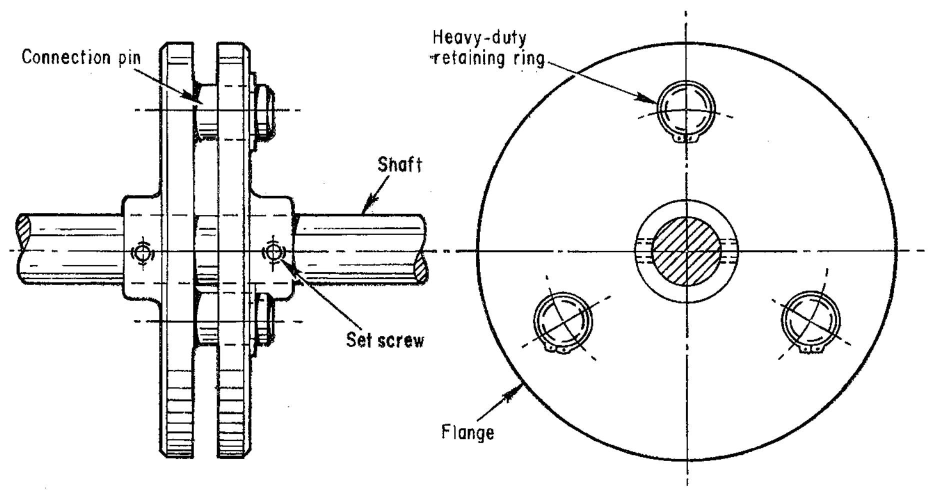

This assembly for heavy-duty service requires minimum machining. Ring thickness should be substantial, and extra ring-section height is desirable.

Collar, Rings, and Threaded Shaft

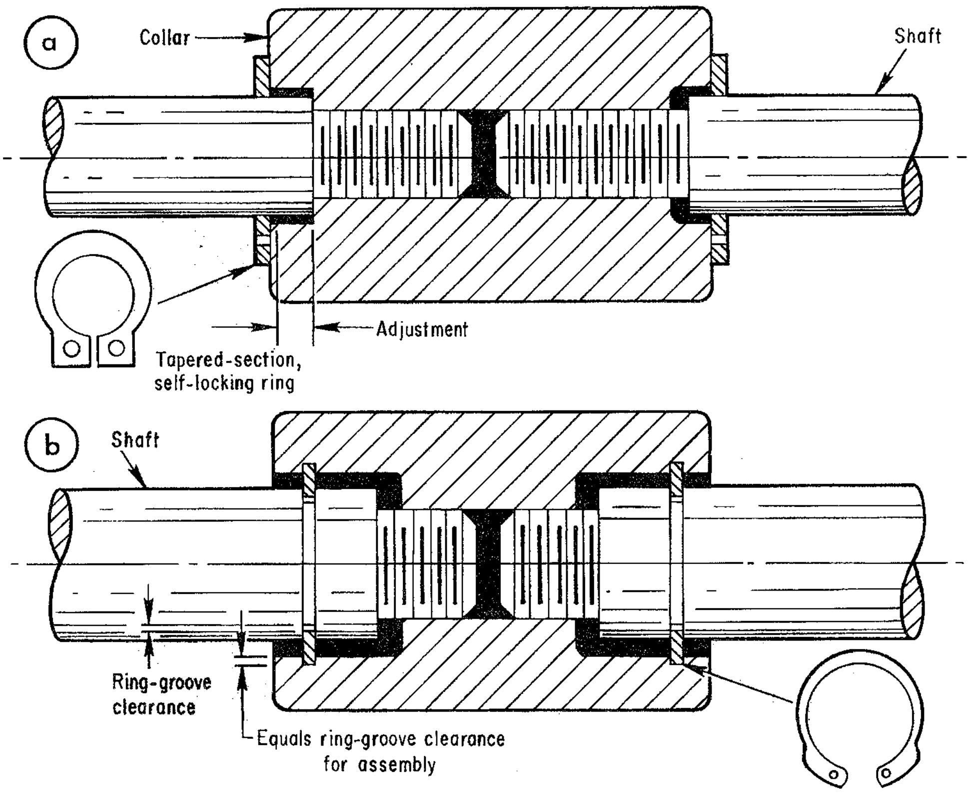

For a connection that requires axial shaft adjustment, the self-locking ring requires no groove, *a*. An alternate solution, *b*, uses an inverted-lug ring seated in an internal groove. Extra ring-section height provides a good shoulder. The ring is uniformly concentric with housing and shaft.

Coupler and Ring

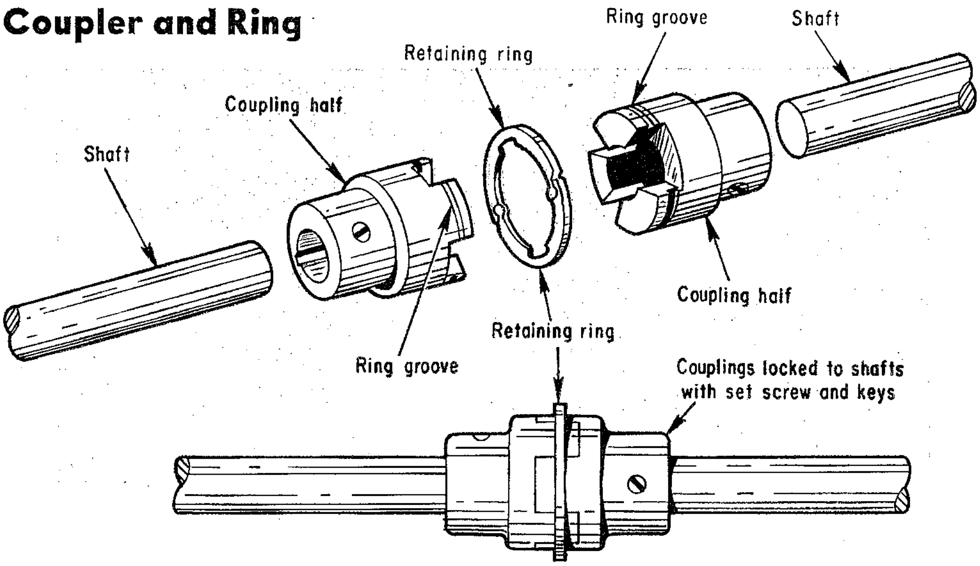

Where attractive appearance is desired in a dependable locking device, this connector and ring can be used.

Slotted Sleeve With Tapered Threads

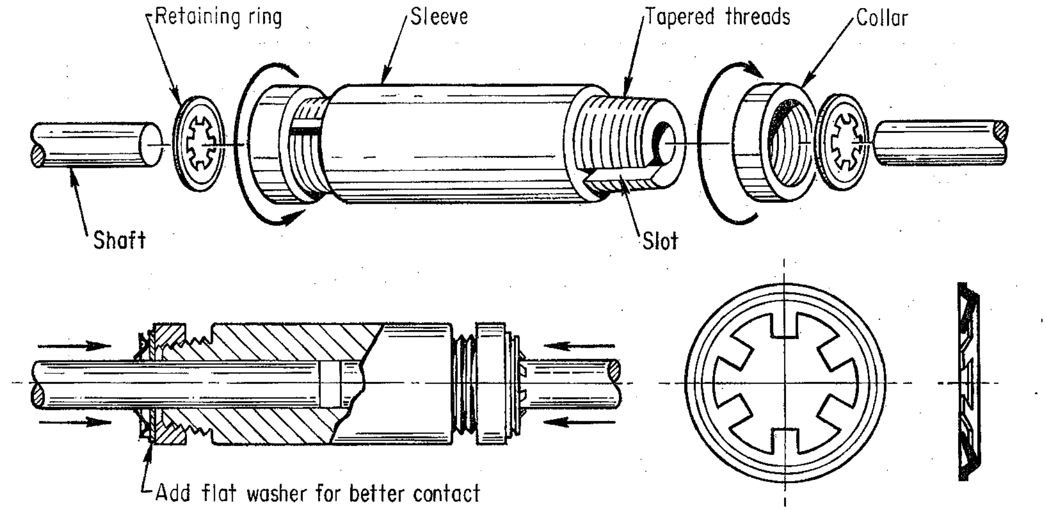

A slotted sleeve with tapered threads connects shafts which cannot be machined. Prongs on the retaining ring provide positive shaft gripping to stop collar movement. The arched rim adds extra strength.

Bossed Coupling and Rings

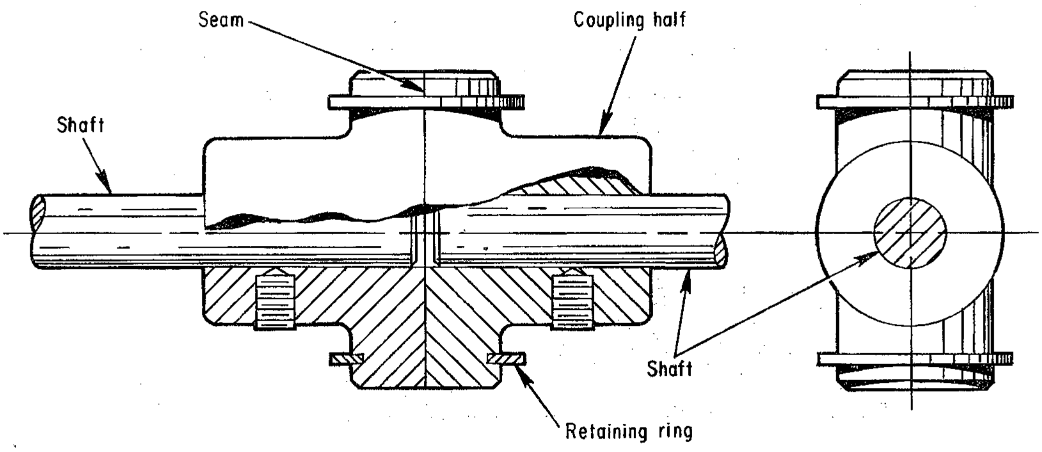

An alternate solution for coupling unmachined shafts uses bossed coupling halves with locking retaining rings.

The Versatile Retaining Ring

A design roundup of some unusual applications of retaining rings.

Robert O. Parmley

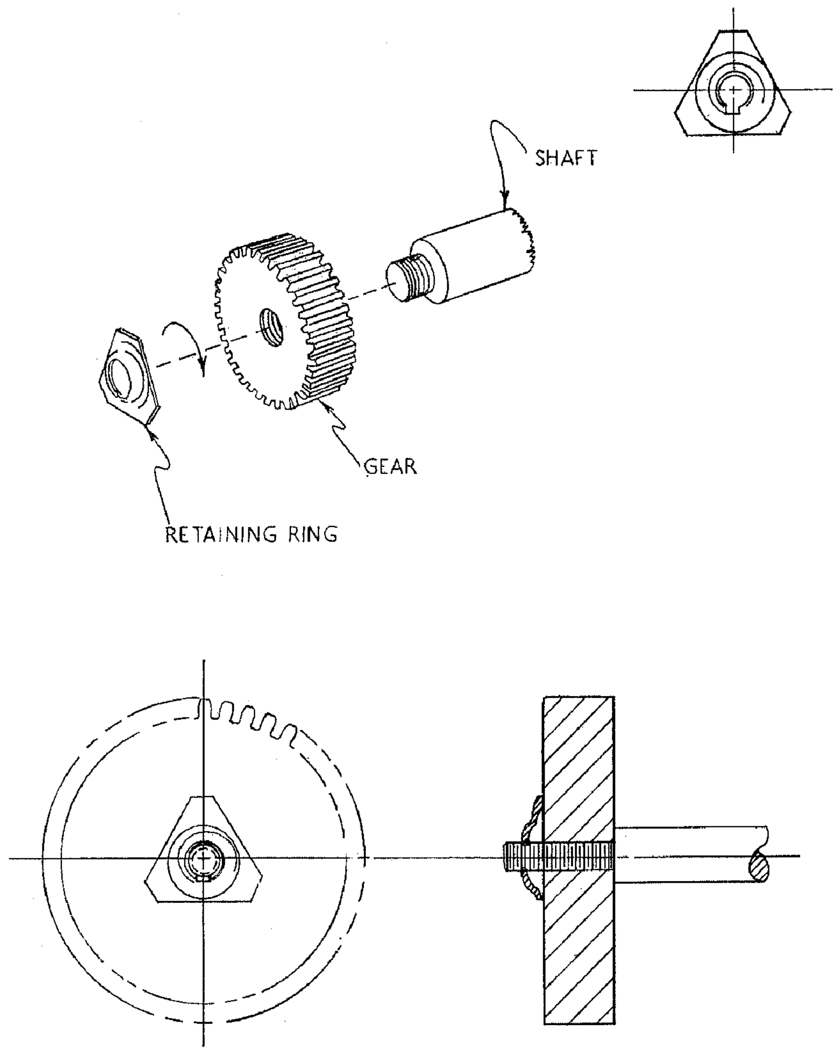

Fig 1 The assembly of a hubless gear and threaded shaft may be accomplished by using a triangular nut retaining component which eliminates the need for a large standard nut and lock washer or other spring type part. The dished body of the triangular nut flattens under torque to lock the gear to the shaft.

Every engineer is familiar with the use of retaining rings in product assembly. Applications for this type of fastening device range from miniature electronic assemblies to heavy duty equipment. In spite of this widespread use, many opportunities for taking advantage of these versatile fastening components often are overlooked. However, when a value engineering approach is taken and the basic function of retaining rings as easily assembled locating and locking devices is kept clearly in mind it will be found that these simple fasteners can provide a unique solution to difficult assembly problems.

This roundup of 8 unusual applications illustrates how different types of retaining rings have been used to simplify assembly and reduce manufacturing costs. The captions under the drawings give the details involved in each case.

The author wishes to acknowledge with appreciation the cooperation he received from the Truarc Retaining Rings Division of Waldes Kohinoor, Inc. in developing these assembly designs.

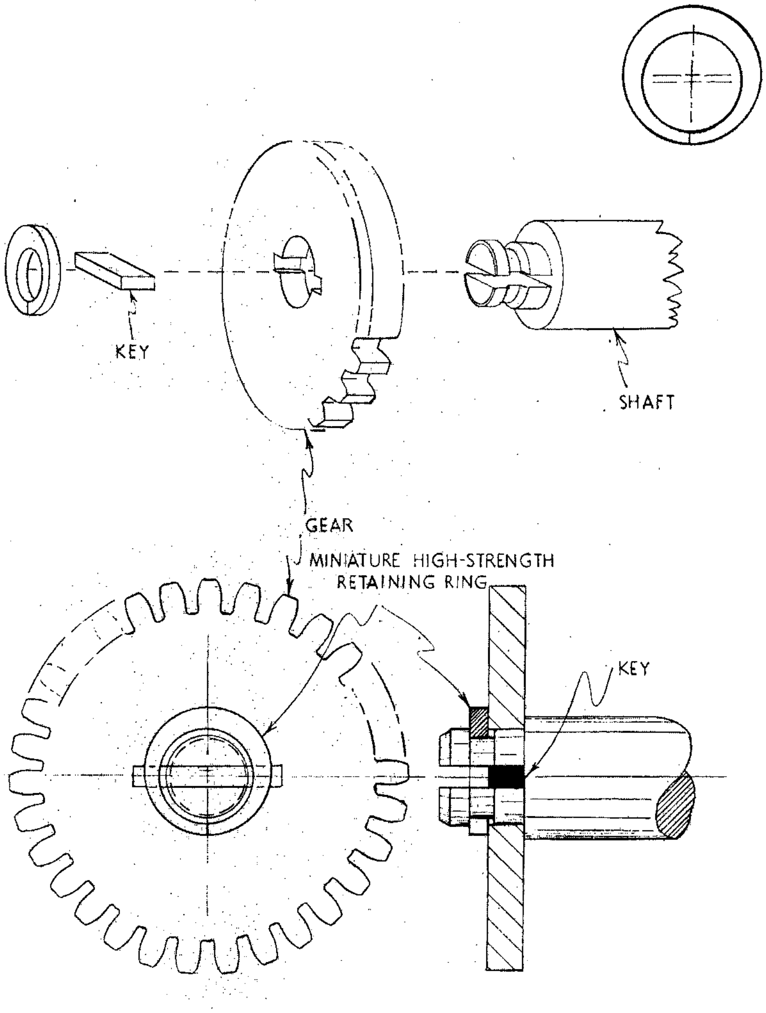

Fig 2 This heavy duty hubless gear and shaft is designed for high torque and end thrusts. The retaining ring seated in a square groove and the key in slot provide a tamper-proof lock. This design is recommended for permanent assemblies in which the ring may be subjected to heavy loads from either or both axial directions. An angled groove can be provided which has one wall cut at a 40° angle to the shaft axis. This will permit the ring to be removed without damage.

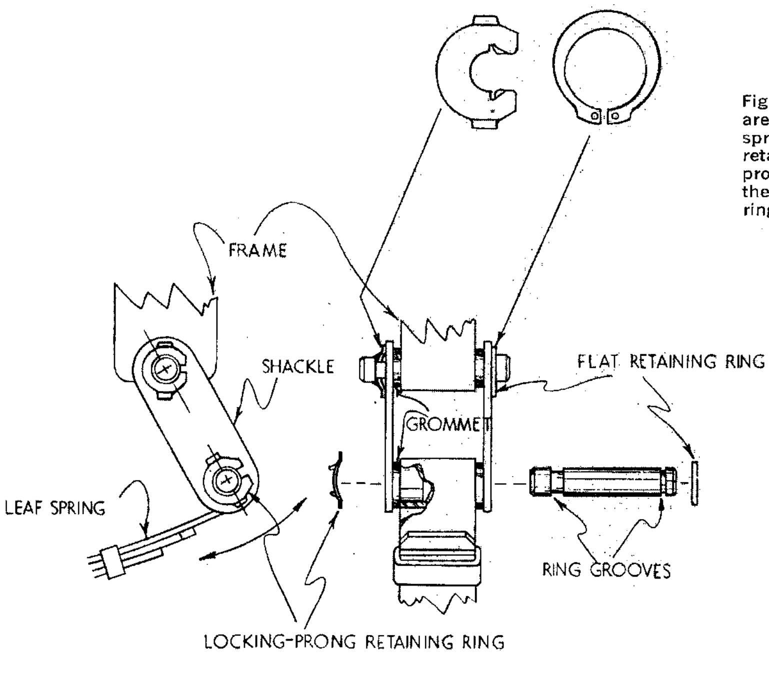

Fig 3 Two different types of retaining rings are used in this application involving a leaf spring and shackle assembly. A locking-prong retaining ring is bowed for tension while the prongs act as fastening elements to secure the pivot bolt. A flat or standard external ring is used as a flange or bolt head.

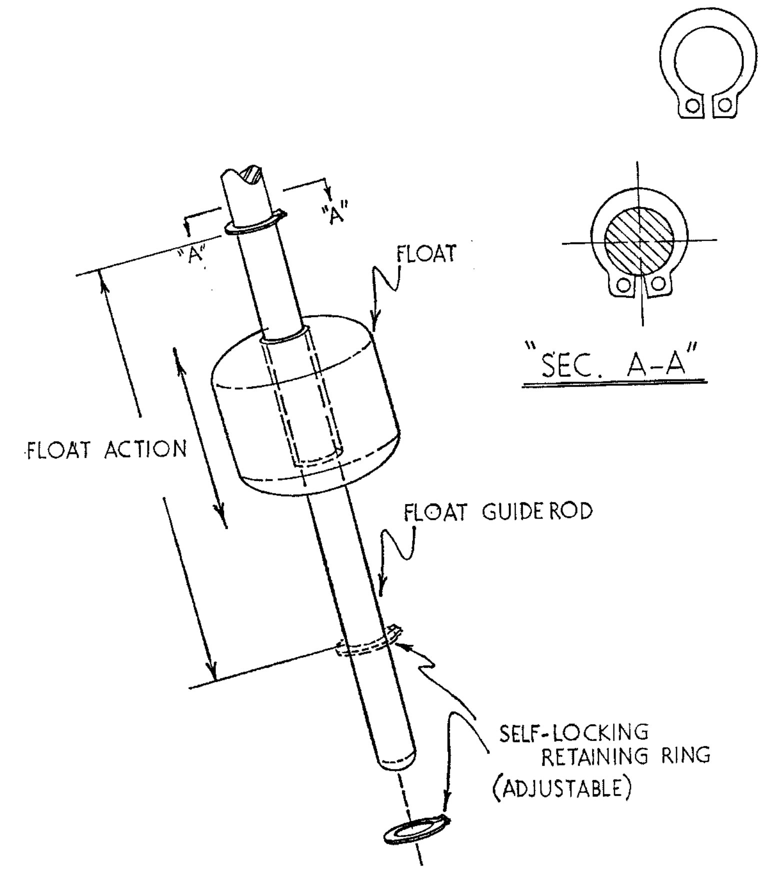

Fig 4 The self-locking retaining rings used in this application provide stops for a float. The rings are adjustable on the guide rod and yet the friction force produced by the heavy spring pressure makes axial displacement from the light weight hollow float impossible.

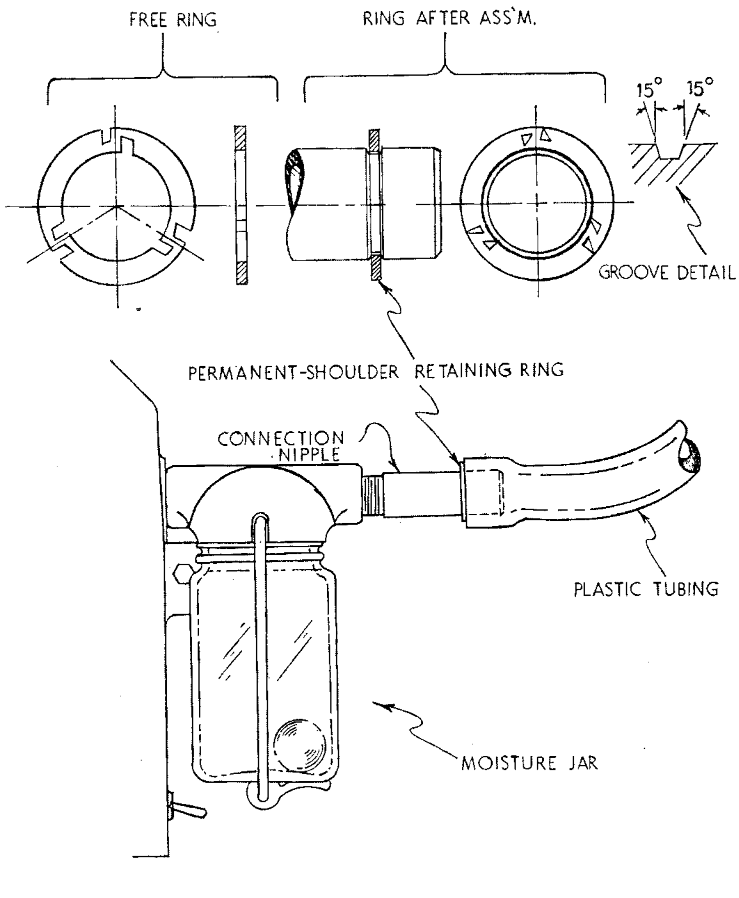

Fig 5 Retaining rings provide a uniform circular shoulder for small diameter parts such as the pipe nipple shown here. In this case the retaining ring shoulder is used as a stop for the plastic tube. The wall thickness of the nipple should be at least three times as thick as the depth of the groove. When assembling the ring in the groove, the nipple should be supported by inserting a mandrel or rod.

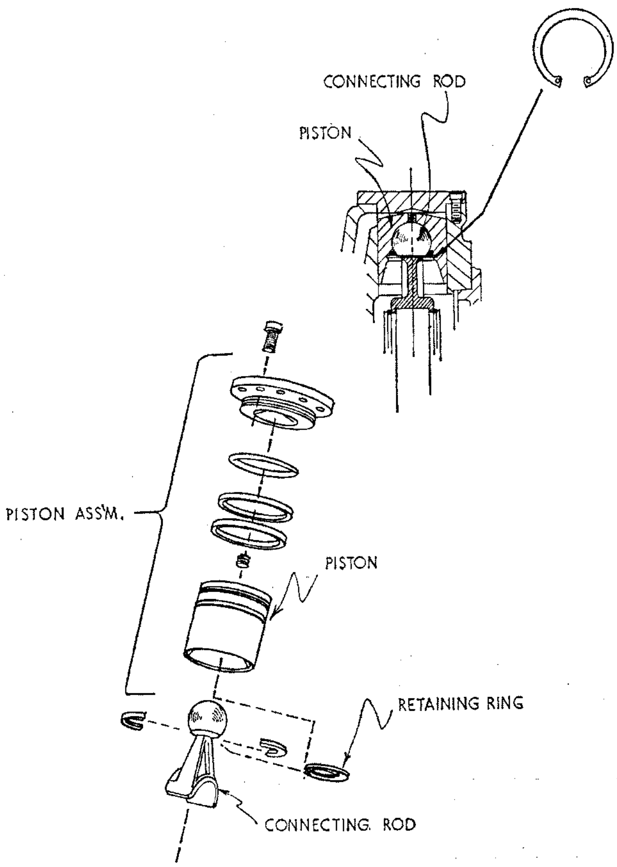

Fig 6 This internal retaining ring is a key part in the assembly of a connecting rod and piston for a hydraulic motor. The ring's lug holes make rapid assembly and disassembly possible when the proper pliers are used. The piston assembly in this case is slow moving and is not subject to heavy cycle loading.

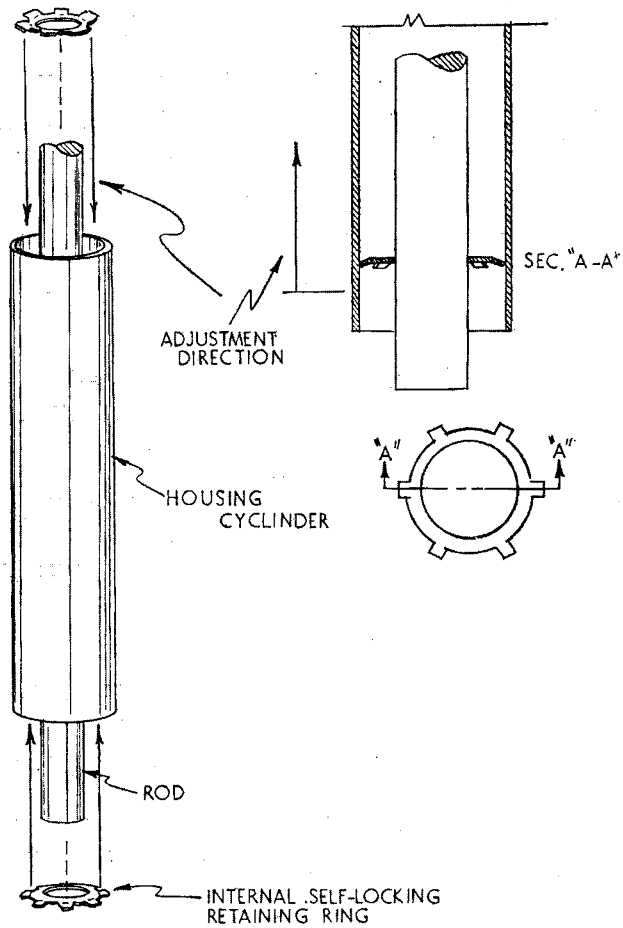

Fig 7 Internal self-locking rings can act as a support carrier when the I.D. of a sleeve or housing cylinder is too large to center and stabilize small rods or conduit. The rings are adjustable in the entry direction only, however, and a sufficient number should be used to secure the rod.

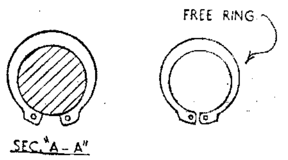

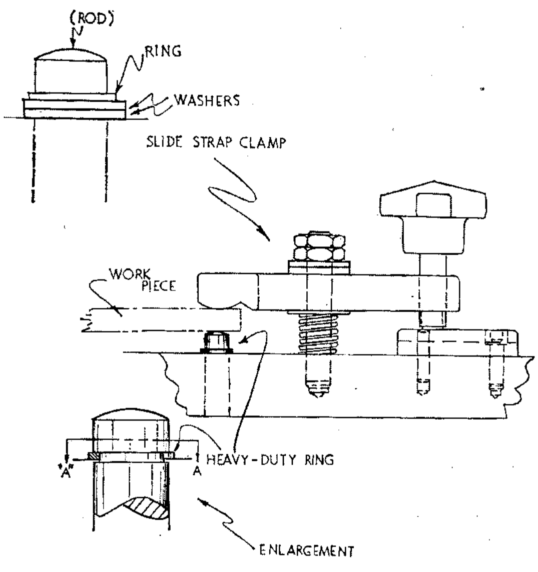

Fig 8 The heavy duty external retaining ring shown here controls the elevation or position of a support post in a holding clamp. This type of ring is ideal for heavy duty applications where extreme loading conditions are encountered. By adding washers under the ring the elevation of the support post can be adjusted as required.

The Multiple-Purpose Retaining Ring

A roundup of ten unusual ways for putting retaining rings to work in assembly jobs.

Robert O. Parmley

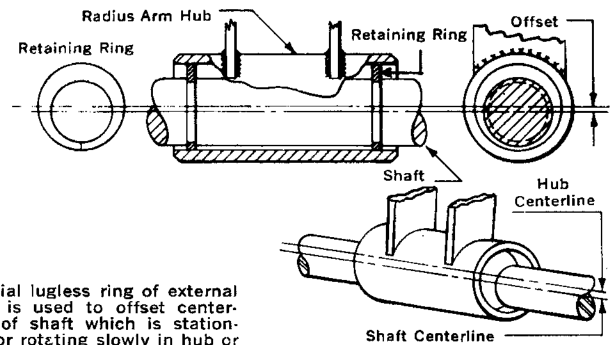

1

Special lugless ring of external type is used to offset centerline of shaft which is stationary or rotating slowly in hub or journal.

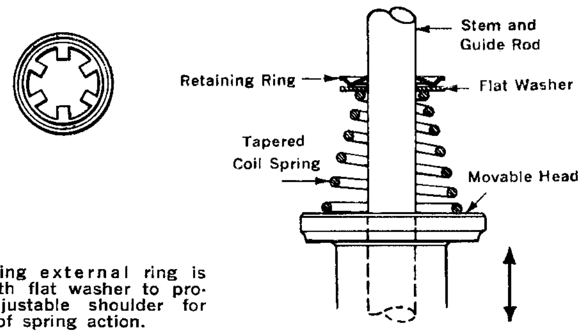

4

Self-locking external ring is used with flat washer to provide adjustable shoulder for control of spring action.

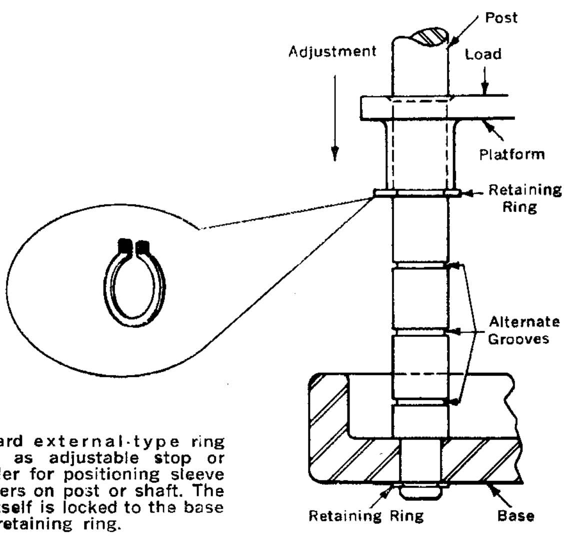

7

Standard external-type ring serves as adjustable stop or shoulder for positioning sleeve members on post or shaft. The post itself is locked to the base by a retaining ring.

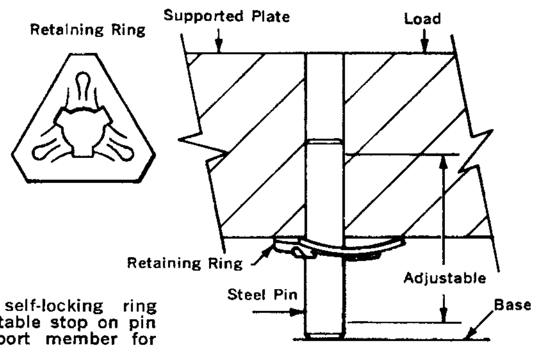

8

Heavy duty self-locking ring acts as adjustable stop on pin used as support member for plate section.

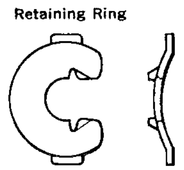

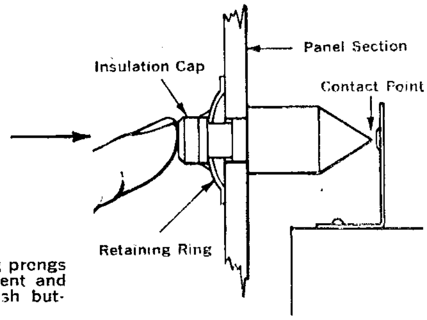

2

Bowed ring with locking prongs acts as fastening element and spring for electrical push button.

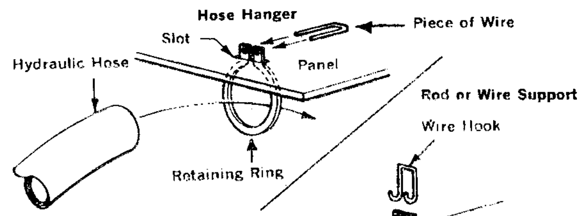

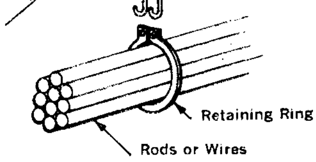

3

Standard external-type rings with holes in lugs for plier assembly provide a practical hanger or support for hose, rods, and wires.

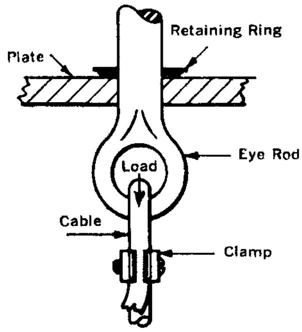

5

Self-locking external ring controls position of eye rod in an adjustable cable hanger arrangement.

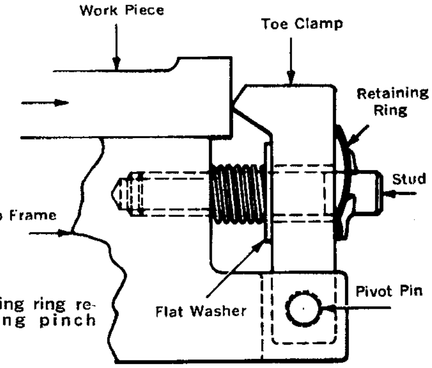

6

Heavy-duty self-locking ring retains stud on swing pinch clamp.

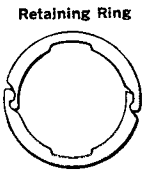

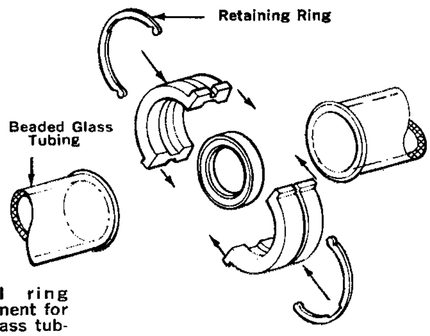

9

Interlocking external ring serves as a locking element for a coupling that joins glass tubing sections.

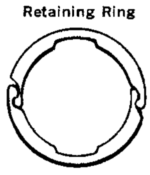

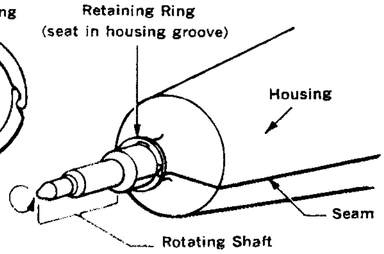

10

Interlocking external ring locks two-piece housing that fits around a rotating shaft.

More Work for Round Retaining Rings

Try this low-cost fastener for locking shafts and other parts. It will also work as a shaft step for bearings and an actuating ring for switches.

Dominic J. Lalera

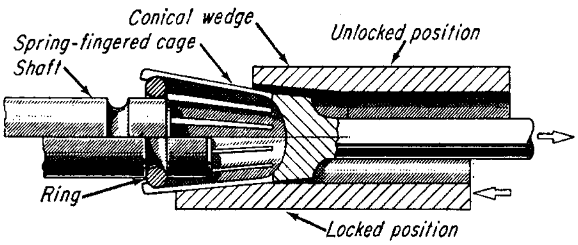

1 **LOCK A SHAFT** by forcing a retaining ring over the groove in the shaft. In locking position, the spring-fingered cage is actuated by the conical wedge.

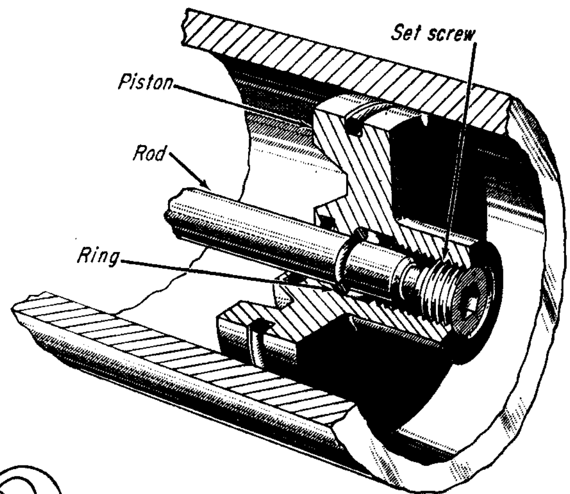

2 **PISTON IS LOCKED** in place on the rod when drawn into place by means of a setscrew. To remove, slide the piston away from the ring, then remove the ring.

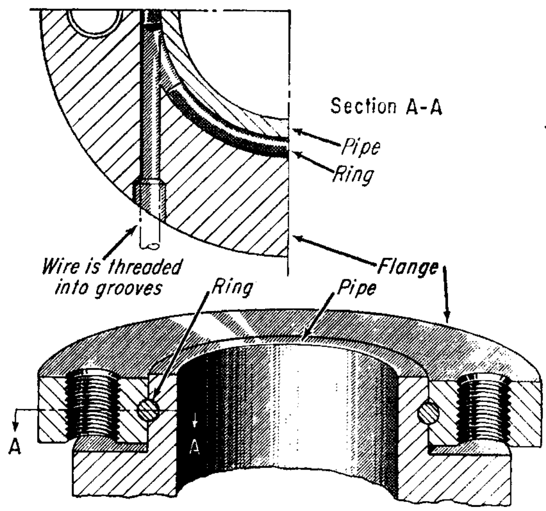

5 **FLANGE ASSEMBLY** is permanently fastened by threading the wire into the mating grooves through the flange. Flange can rotate if wire doesn't protrude.

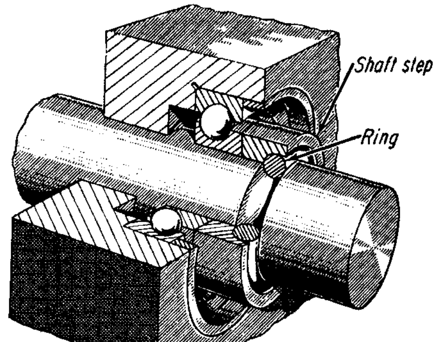

6 **THIS SHAFT STEP** for a rotating bearing is quickly and simply made by grooving the shaft to accept a spring ring. Counterbore the shaft step to mate.

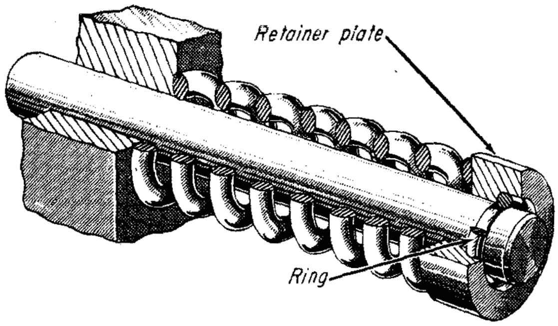

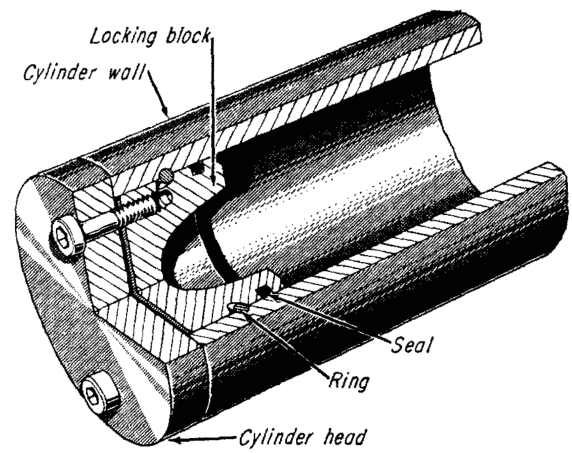

3 **THIS SPRING-HELD** shaft lock is a basic application for retaining rings. The best groove dimensions for round spring rings are readily available from suppliers.

4 **ASSEMBLE CYLINDER HEADS** and similar parts to thin walls by means of a retaining ring and a locking block. Tightening the screws expands the ring.

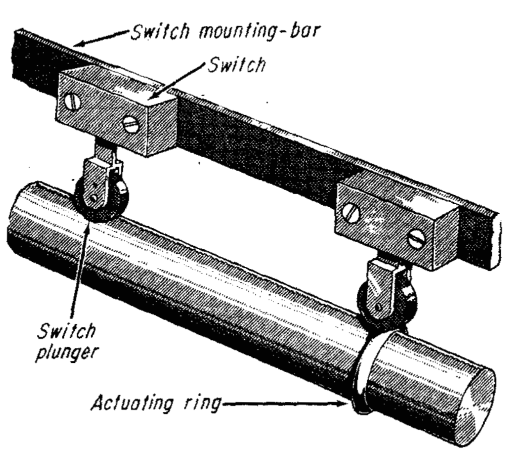

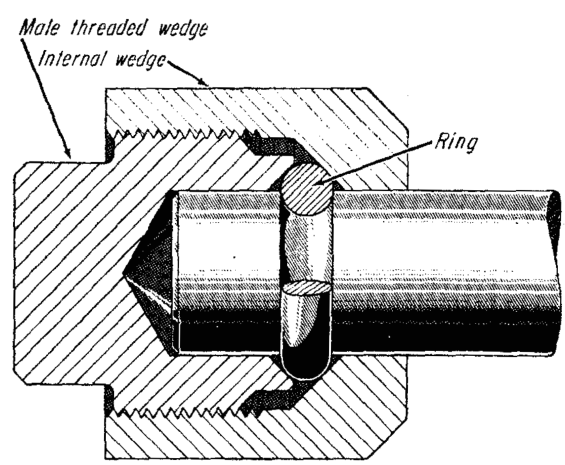

7 **SWITCH ACTUATORS** of round retaining rings offer a simple solution when permanent shaft steps would present assembly problems. Close the ring gap.

8 **THREE-PIECE WEDGE** lets the shaft move freely until the wedge is tightened by screwing it in. The round retaining ring is then forced into the groove.

Energy Absorber Squeezes Rings to Cushion Shocks

A novel shock absorber based on an easily demonstrated but little-known principle handles strains up to 1,000,00 lb. and performs through 100 cycles.

Take a metal clothes hanger and pull it apart until it breaks (assuming you have the super strength needed for this feat). The hanger elongates slightly until it fractures and thus absorbs energy; the amount of energy absorbed is a function of the force exerted and the amount of stretch.

Now, take another hanger and flex it back and forth. During each flex, the metal deforms slightly; it fatigues and eventually breaks.

Although the amount of force applied at any one time during flexing is not much, the total amount of energy absorbed far exceeds that absorbed when the hanger is ruptured by a pure tensile force.

Principle rediscovered. This little-known principle in energy absorption has been applied successfully and with dramatic results to the development of a new shock absorber by Mechanics Research, Inc. (MRI), El Segundo, Calif.

In a recent demonstration (left), MRI sandwiched two soda crackers between weights, each in its own test fixture, and dropped them simultaneously. Baseballs on top of each carriage provided added cracker load.

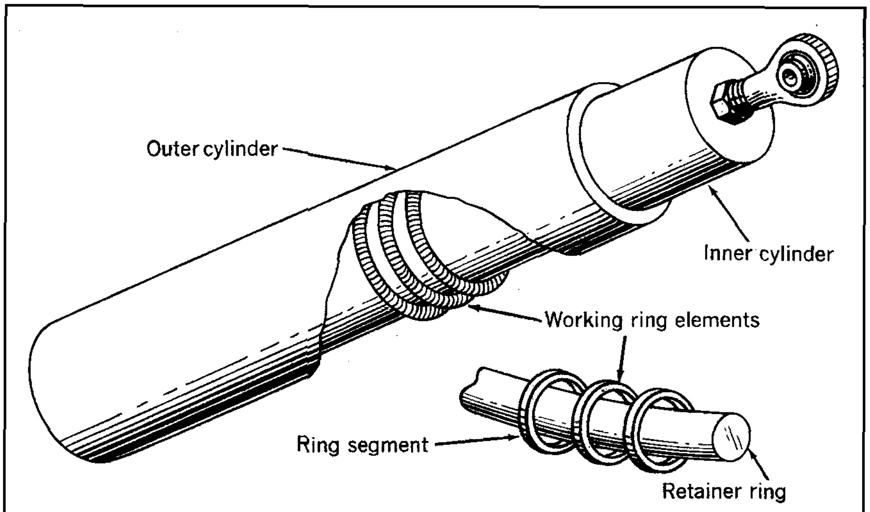

The left carriage struck a plain rigid rod. The cracker, smashed under impact, was sprayed in all directions. The baseball rebounded, springing into the air.

The right carriage, however, struck a novel shock absorber that so effectively absorbs the impact energy that the carriage comes to a smooth stop. The cracker remained intact with nary a crumble, and the baseball did not rebound.

Trapped rings. The new absorbers trap rolling rings (or sometimes tube segments) between concentric tubes under enough interference to strain the metal in the rings beyond its yield point. The interference fit may be only a few thousandths of an inch.

An internal wire ring aligns the small rolling rings at each station. Increasing either the ring wall thickness or the interference increases the energy absorber force. The unit can be designed as either a rotary or linear absorber.

The absorber cannot reset by itself. It needs springs to do so. But it

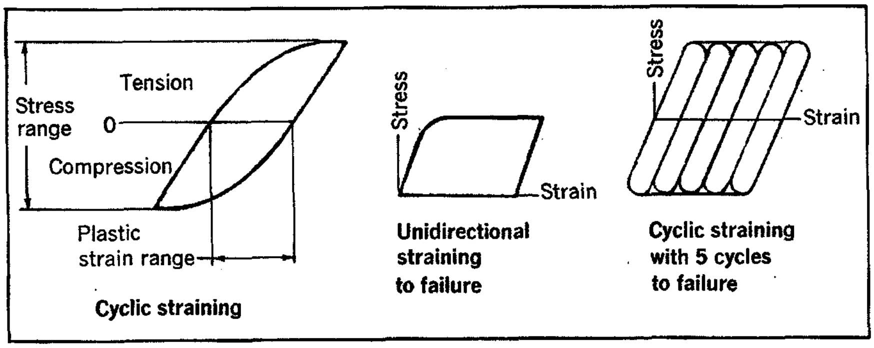

Cyclic plastic straining absorbs more energy than unidirectional straining.

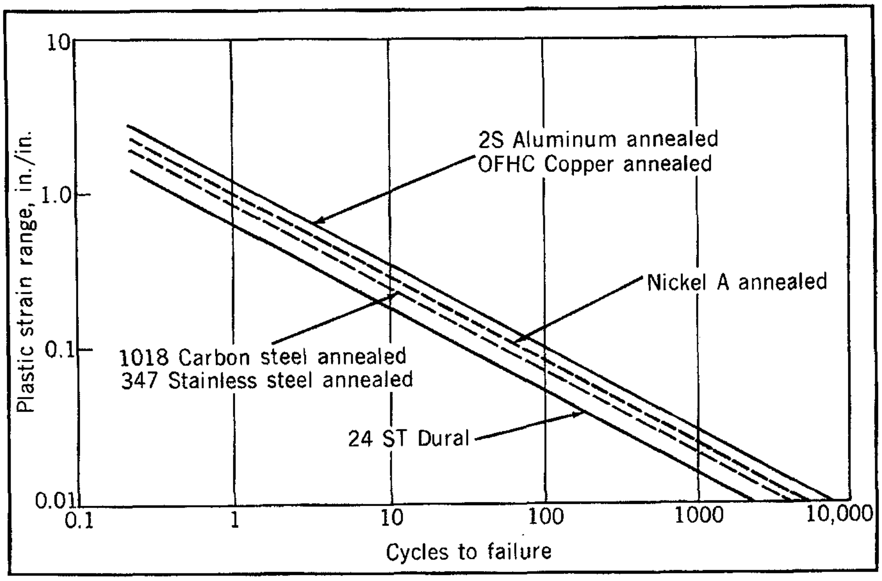

The amount of plastic strain determines the number of cycles to failure.

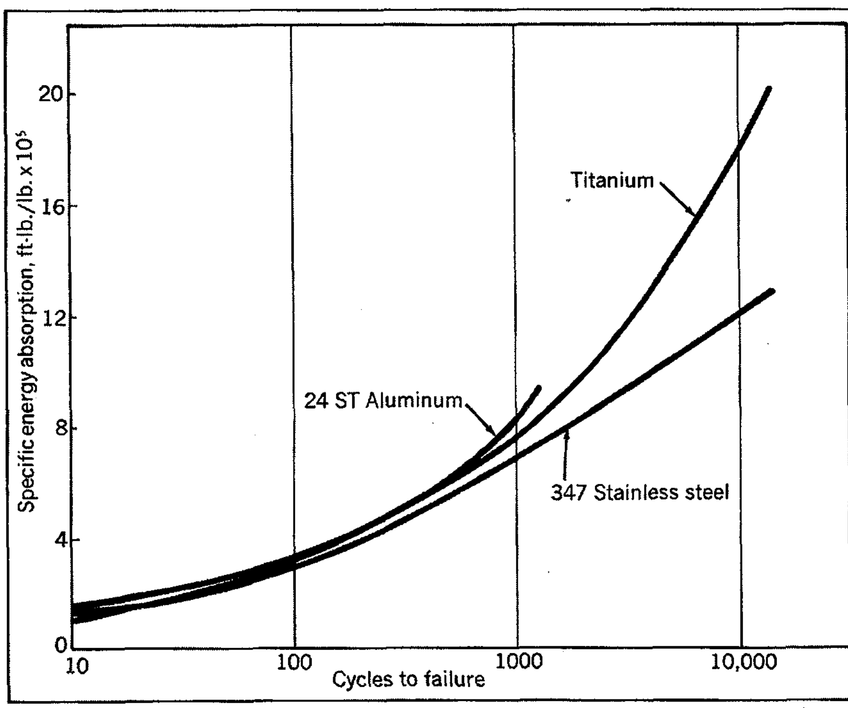

The number of cycles to failure influences total amount of energy absorption.

can be recycled if required and thus fills a need between one-shot systems, such as crushable honeycombs and frangible tubes, and the infinitely reusable devices, such as hydraulic shock absorbers.

Heavyweight capacity. The absorbers can handle forces ranging from 0.01 lb. to 1,000,000 lb., with possible application in automotive safety, spacecraft landers, aircraft seats, and protection from blasts and earthquakes.

All-metal construction avoids the undesirable features of fluids, seals, and elastomers and permits long use in difficult temperature and corrosion environments. Moreover, the load-stroke behavior is relatively insensitive to the effects of temperature and rate.

Cyclic strains. The underlying principle is the cyclic straining of metal in the plastic range. This produces a hysteresis loop (left, top drawing) that stabilizes after a few cycles. Repeated cycling results in almost constant energy absorption per cycle there is eventually fatigue failure.

The specific energy absorption (SEA) for N cycles to failure is about $N^{1/2}$ times the SEA for the one-shot unidirectional straining to failure (middle, top drawing). Thus, an absorber designed to last, say, five cycles to failure (right, top drawing) will be able to absorb $5^{1/2}$ times (roughly 2.24) the SEA for a unidirectional straining.

For example: Suppose the device must handle 1000 cycles (strain cycles) before failure. To do so, the interference fit should cause a plastic strain range of 1.3% (0.013 in./in., left middle chart) to obtain maximum energy absorption of the device.

The amount of SEA for 1000 cycles is about 800,000 ft.-lb./lb. (bottom chart). With a factor of one-half to account for the nonuniform straining in the rings (the curve is for uniform straining), the average SEA would be 400,000 ft.-lb./lb.

Thus, if the rolling rings in the absorber add up to 1 lb., they will absorb the energy of a 4000-lb. force traveling through a foot of stroke 100 times.

Deflections of Perpendicularly Loaded Split Circular Rings

M. M. Lemcoe

FORMULAS FOR THE DEFLECTION of a split uniform circular ring perpendicular to the plane of the ring are given for various positions of the load. Methods of developing those formulas are demonstrated.

In Fig. 1 is shown a split uniform circular ring of radius R, loaded with a force P applied perpendicular to the plane of the ring at the point B. At the point Q, the bending moment M and the twisting moment T due to the load P are respectively:

$$M = P\,R \sin(\beta - \theta) \tag{1}$$

$$T = P\,R\,[1 - \cos(\beta - \theta)] \tag{2}$$

Also, if there were a unit load at the point A, there would be at point Q a bending moment m and a twisting moment t due to that unit load. These are given by the following formula

$$m = R \sin(\alpha - \theta) \tag{3}$$

$$t = R\,[1 - \cos(\alpha - \theta)] \tag{4}$$

From strain energy considerations, the deflection Δ of the point A can be formulated. If E is the modulus of elasticity and G is the shear modulus and if I is the moment of inertia about the neutral axis of a cross-section, and J is the polar moment of inertia of a cross-section, the formula is

$$\Delta = \int_0^{\phi} \frac{M\,m\,R\,d\theta}{E\,I} + \int_0^{\phi} \frac{T\,t\,R\,d\theta}{G\,J} \tag{5}$$

The angle ϕ equals the smaller of angles α or β. Substituting Eqs (1), (2), (3) and (4) into Eq (5) gives:

$$\Delta = P\,R^3 \int_0^{\phi} \left\{ \frac{\sin(\alpha - \theta)\sin(\beta - \theta)}{E\,I} + \frac{[1 - \cos(\alpha - \theta)]\,[1 - \cos(\beta - \theta)]}{G\,J}\, d\theta \right\}$$

From the trigonometric identities

$$\sin(\alpha - \theta)\sin(\beta - \theta) = \tfrac{1}{2}[\cos(\alpha - \beta) - \cos(\alpha + \beta - 2\theta)]$$

$$\cos(\alpha - \theta)\cos(\beta - \theta) = \tfrac{1}{2}[\cos(\alpha - \beta) + \cos(\alpha + \beta - 2\theta)]$$

The formula for $\triangle$ becomes:

$$\begin{aligned}\Delta = {} & \frac{P\,R^3}{2\,E\,I}\left[\int_0^{\phi} \cos(\alpha - \beta)\,d\theta - \int_0^{\phi} \cos(\alpha + \beta - 2\,\theta)\,d\theta\right] \\ & + \frac{P\,R^3}{2\,G\,J}\left[\int_0^{\phi} \cos(\alpha - \theta)\,d\theta - \int_0^{\phi} \cos(\alpha + \beta - 2\,\theta)\,d\theta \right. \\ & \left. + \int_0^{\phi} [1 - \cos(\alpha - \theta)]\,d\theta - \int_0^{\phi} \cos(\beta - \theta)\,d\theta\right]\end{aligned} \tag{6}$$

Integrating Eq (6) gives

$$\begin{aligned}\Delta = {} & \frac{P\,R^3}{E\,I}\left[\frac{\phi\cos(\alpha - \beta)}{2} + \frac{\sin(\alpha + \beta - 2\,\phi) - \sin(\alpha - \beta)}{4}\right] \\ & + \frac{P\,R^3}{G\,J}\left[\frac{\phi\cos(\alpha - \beta)}{2} - \frac{\sin(\alpha + \beta - 2\,\phi) - \sin(\alpha + \beta)}{4} \right. \\ & + \phi + \sin(\alpha - \phi) - \sin\alpha \\ & \left. + \sin(\beta - \theta) - \sin\beta\right]\end{aligned} \tag{7}$$

From Eq (7) formulas can be developed for Δ for various positions of points A and B.

Formulas for various positions of points A and B are given below.

Fig. 1—Split circular ring loaded by a force perpendicular to the ring at point B. The deflection Δ at point A is to be calculated.

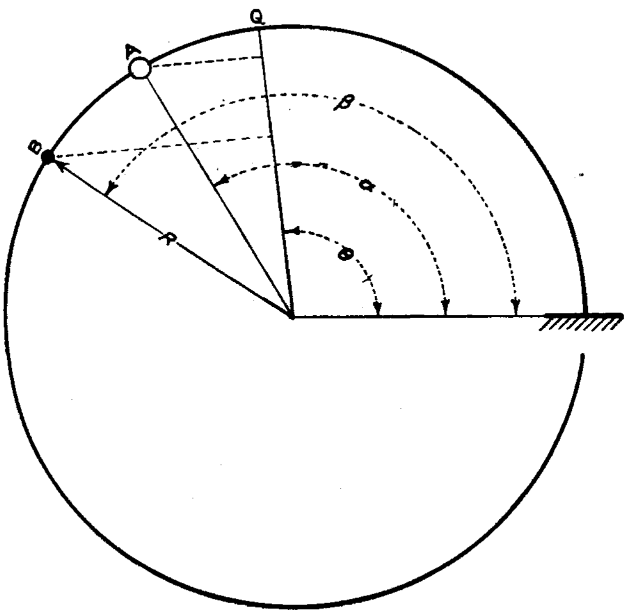

Δ = Deflection at Point A
P = Load at Point B
R = Radius of Ring
E = Modulus of Elasticity
G = Shear Modulus
J = Cross-Section Polar Moment of Inertia
I = Cross-Section Polar Moment of Inertia About Neutral Axis

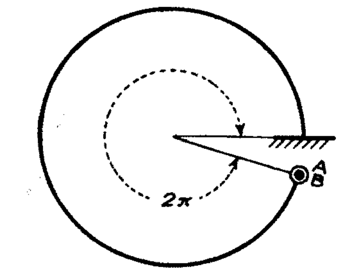

$$\Delta = \pi P R^3 \left(\frac{1}{EI} + \frac{3}{GJ}\right)$$

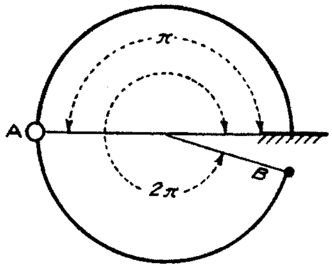

$$\Delta = \frac{\pi P R^3}{2}\left(\frac{-1}{EI} + \frac{1}{GJ}\right)$$

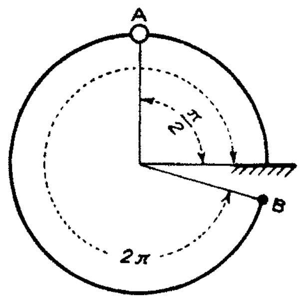

$$\Delta = \frac{P R^3}{2}\left(\frac{-1}{EI} + \frac{\pi - 3}{GJ}\right)$$

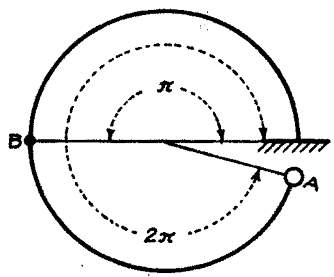

$$\Delta = \frac{\pi P R^3}{2}\left(\frac{-1}{EI} + \frac{1}{GJ}\right)$$

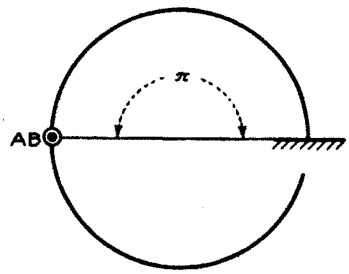

$$\Delta = \frac{\pi P R^3}{2}\left(\frac{1}{EI} + \frac{3}{GJ}\right)$$

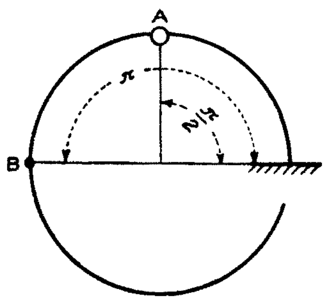

$$\Delta = \frac{P R^3}{2}\left(\frac{1}{EI} + \frac{\pi - 1}{GJ}\right)$$

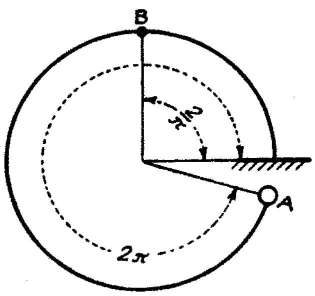

$$\Delta = \frac{P R^3}{2}\left(\frac{-1}{EI} + \frac{\pi - 3}{GJ}\right)$$

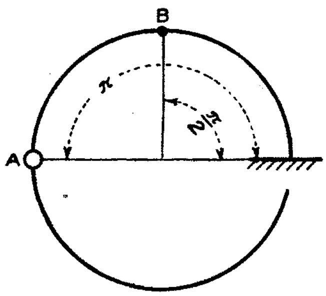

$$\Delta = \frac{P R^3}{2}\left(\frac{1}{EI} + \frac{\pi - 1}{GJ}\right)$$

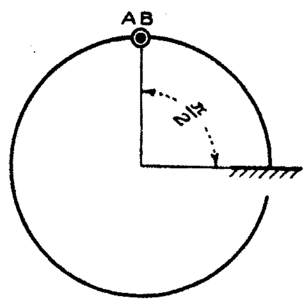

$$\Delta = \frac{P R^3}{2}\left(\frac{\pi}{EI} + \frac{2\pi - 2}{GJ}\right)$$

Improve Design with Retaining Rings

Waldes Kohinoor supplied the retaining rings for the assembly illustrated here. Look at the old design, look at the new design. What did retaining rings do? Well, by changing the design to retaining rings these advantages are achieved:

1) Six beveled rings—one at each end of the three shaft bores—replace 24 hex-head bolts and eliminate drilling and tapping 24 holes in the cast housing.

2) Special gaskets needed to provide a proper seal between the end cap and housing have been replaced by less expensive standard O-rings. Six facing operations on the outside of the casting, required for the gasket seals, have been eliminated. (O-ring grooves are an integral part of the redesigned cover plates.)

3) Twelve external rings—six bowed, six flat—secure the inner races of the bearings. The rings are assembled in grooves machined simultaneously with the shaft cut-off and chamfering operations. They replace six threaded ring nuts and six lock washers and eliminate 12 ground diameters, six threading operations and six keyways on the shaft.

4) Six basic internal rings, installed in grooves machined in the housing, eliminate six machined shoulders and the need for holding close axial tolerances on the bearing bore and end cap.

Reusable following disassembly, the rings are assembled with special pliers, and can be removed for field service.

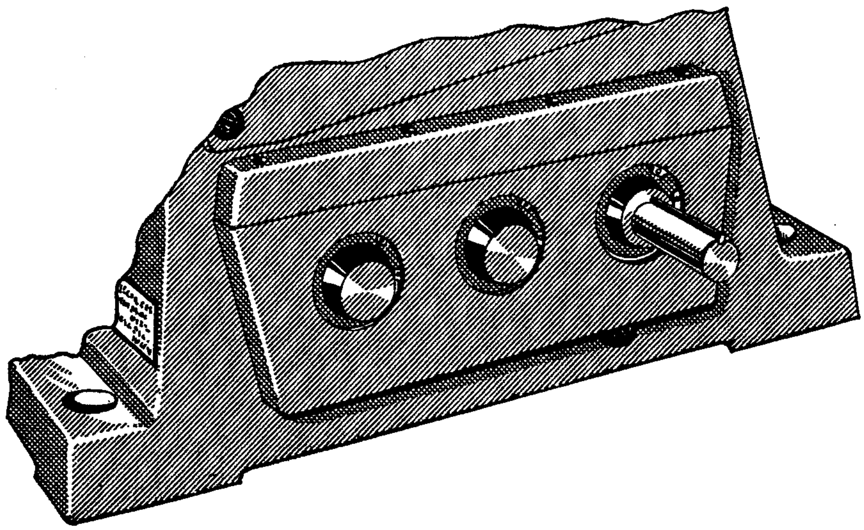

OLD DESIGN

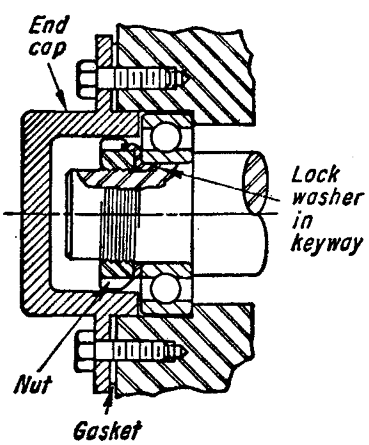

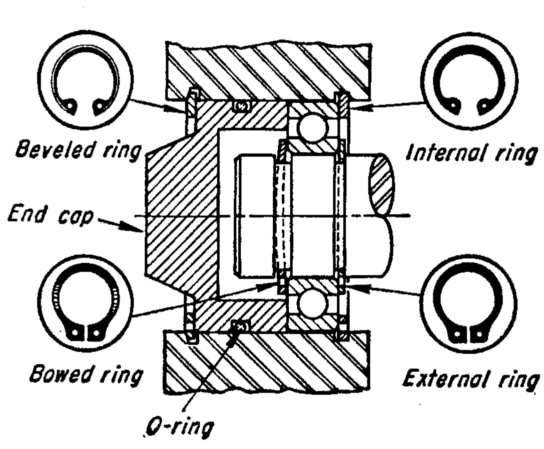

NEW DESIGN

SECTION 13

O-RINGS

8 Unusual Applications for O-Rings

Playing many different roles, O-rings can perform as protective devices, hole liners, float stops, and other key design-components.

Robert O. Parmley

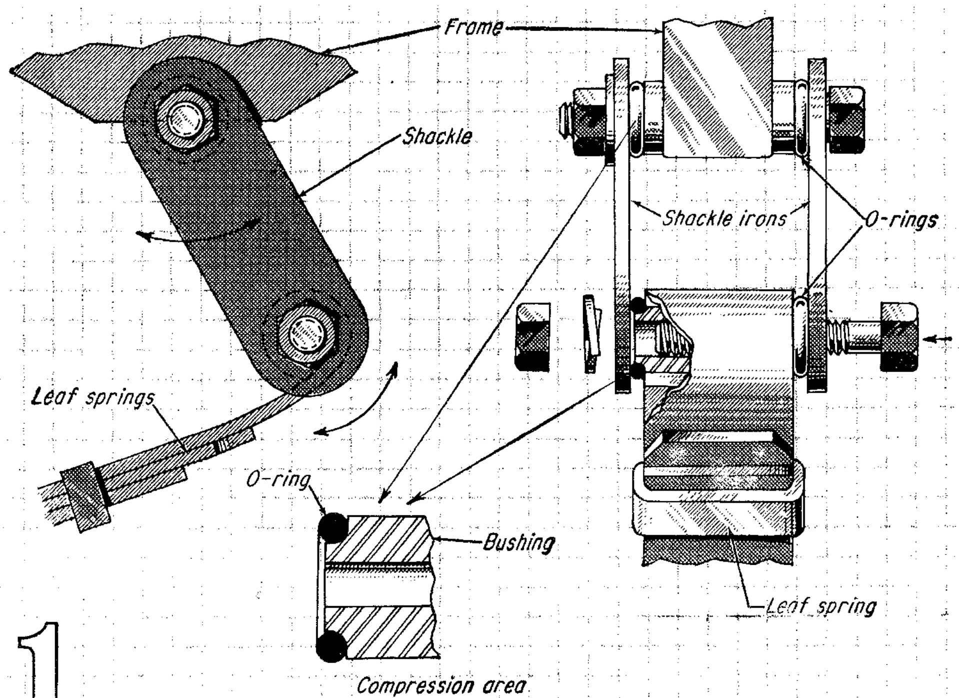

1 PROTECT METAL SURFACES DURING SMALL RELATIVE MOVEMENTS

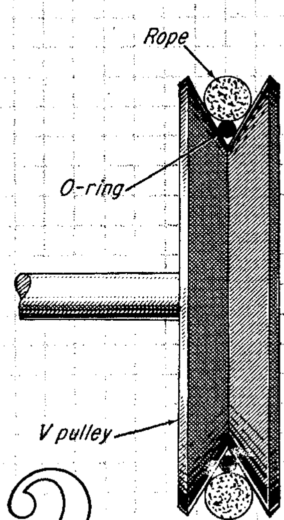

2 CUSHION ROPE IN V-SECTION PULLEY

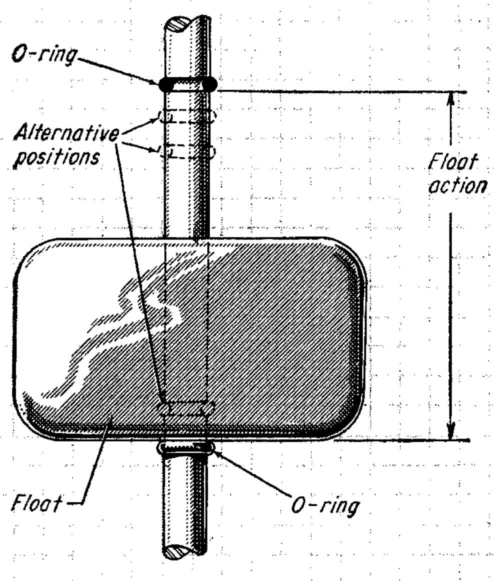

5 QUICKLY ADJUST FLOAT STOP

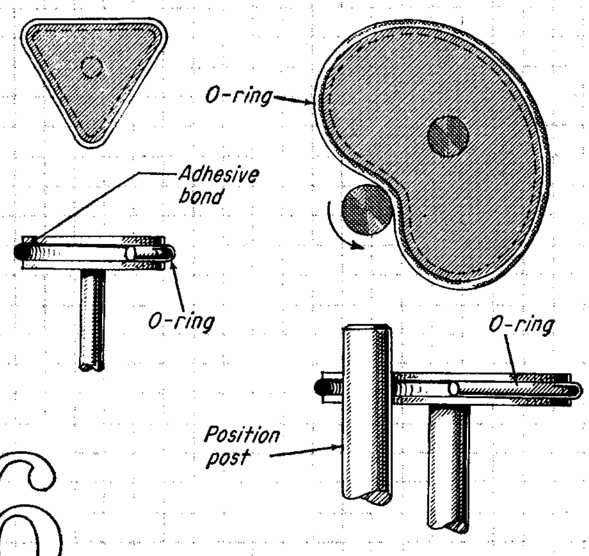

6 O-RINGS CONFORM TO IRREGULAR CONTOURS

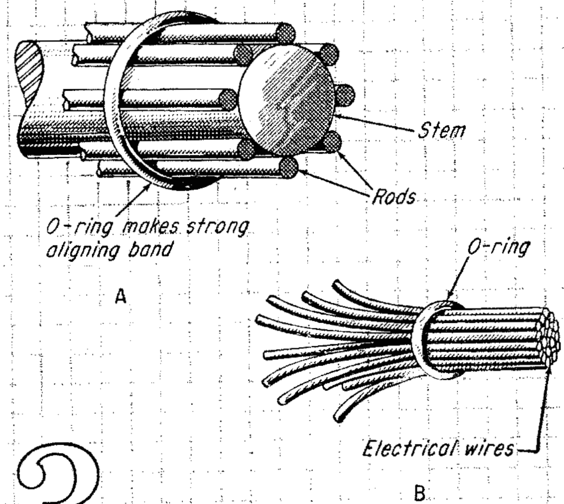

3 RETAIN PARTS (A) OR WIRES (B)

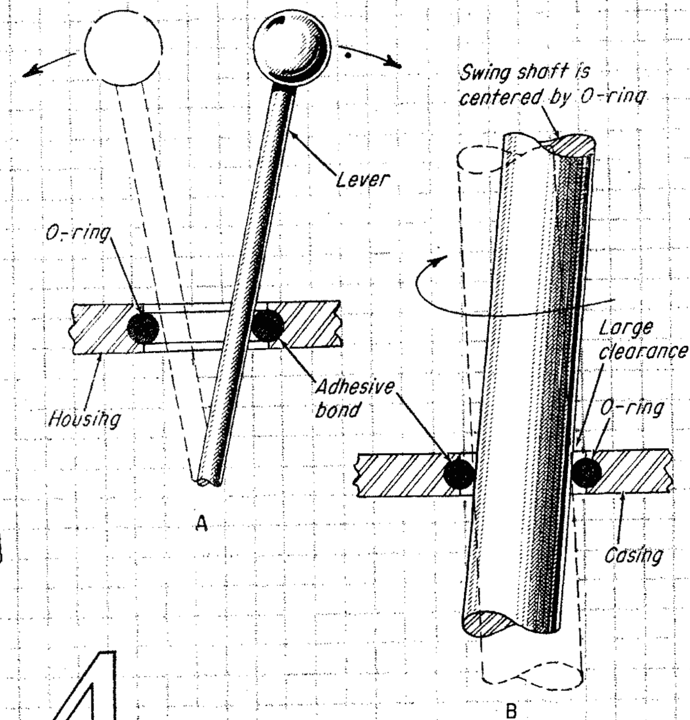

4 LINE HOLES TO CUSHION LEVERS (A) AND STABILIZE SHAFTS IN LARGE HOLES (B)

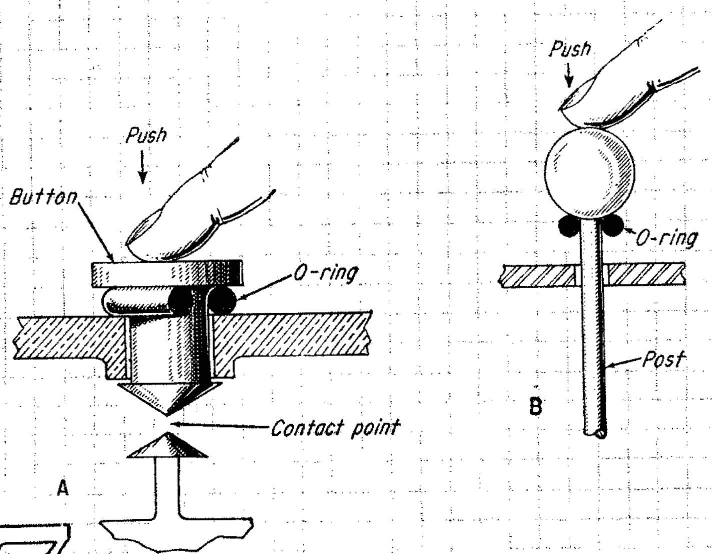

7 CUSHION PRESSURE BUTTONS

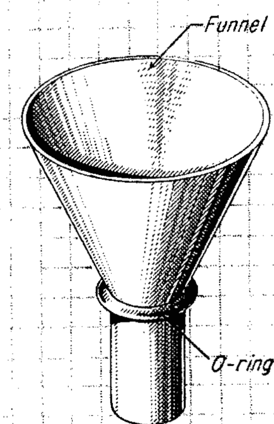

8 SEAL AND CUSHION FUNNEL

16 Unusual Applications for the O-Ring

This handy little component finds a place in pumps, drives, glands, shock-mounts, pivots, knobs, valves and seals.

James F. Machen

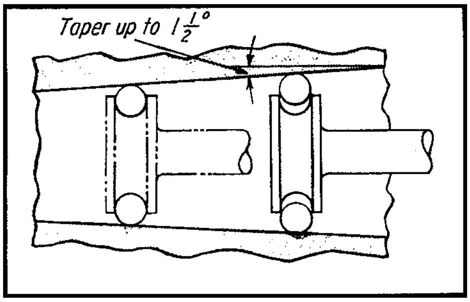

1

Tapered bore . . .
in diecasting, plus loose-fitting O-ring, gives low-cost pump for low-pressure applications. Example: carburetor accelerator-pump.

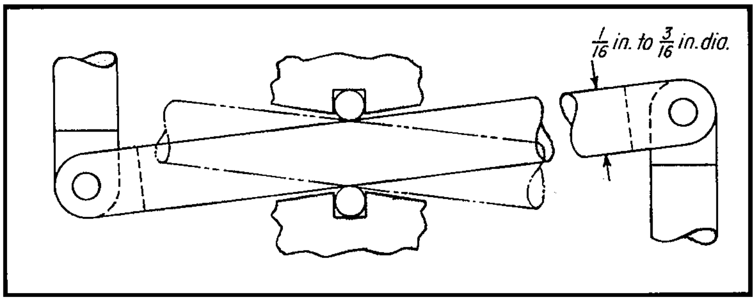

2

Sealed pivot . . .
allows transmittal of multidirectional, mechanical movement to hydraulically or pneumatically isolated system. For high-temperature seals, silicone rubber can often solve the problem—but always guard against excessive "set.'

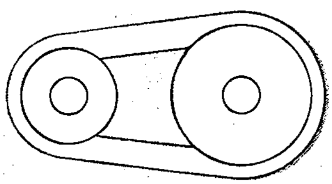

Belt drive

3

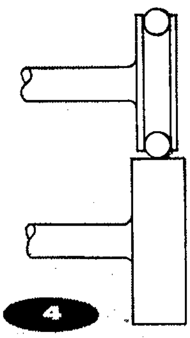

4

Friction drive

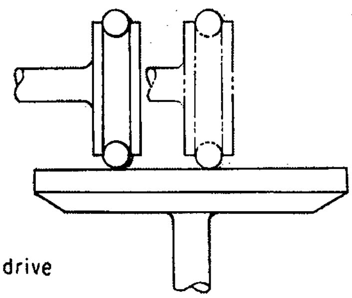

5

Simple drives . . .
utilize not only O-ring but its physical properties also—high friction and elasticity.

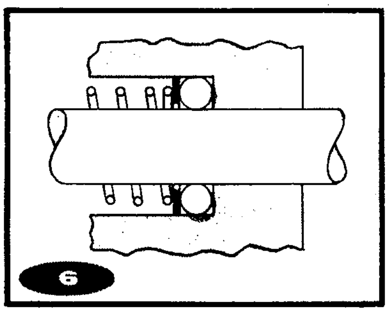

6

Single-ring gland . . .
is ideal for low pressures and high-viscosity fluids. If necessary, another ring may be installed.

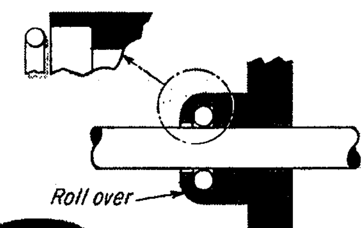

7

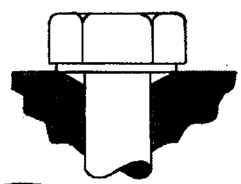

8

Shaft seal . . .
may be held by rolling the thin body-wall over the O-ring. Bolt seal (8) is squeezed into countersink when bolt is tightened. Cross-sectional area of countersink must not be less than that of O-ring since molded rubber is practically incompressible when confined.

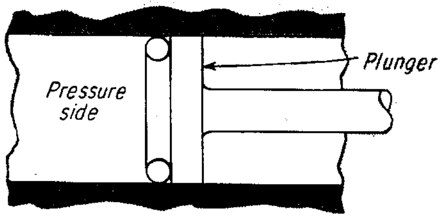

9

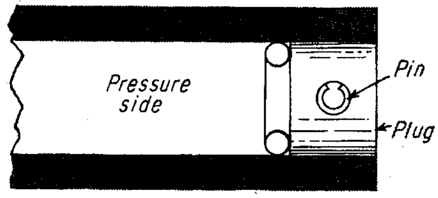

10

One-way pressure . . .
applications require O-ring seals to be supported on pressure side only. Seal may be movable (9) as in grease gun, or static (10) as in pipe plug. Anchor ring to plunger and plug for greater convenience and reliability.

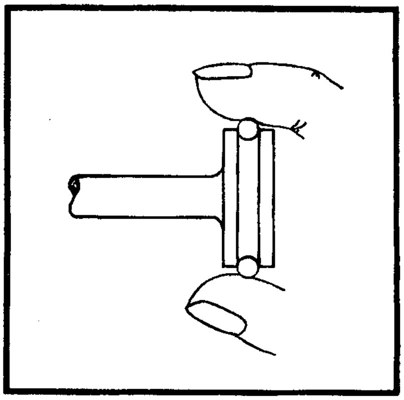

11

Friction grip . . .
on knob not only allows better grip but insulates fingers from heat or electricity. It also improves appearance on both mock-ups and working models.

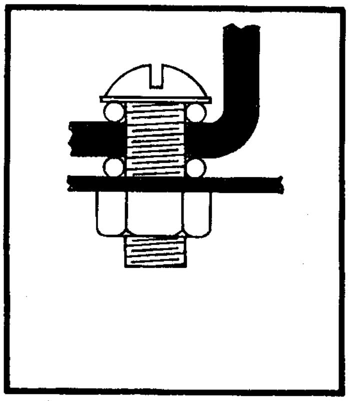

12

Miniature shock-mount . . .
will isolate equipment from vibrations in accordance with behavior of visco-elastic materials

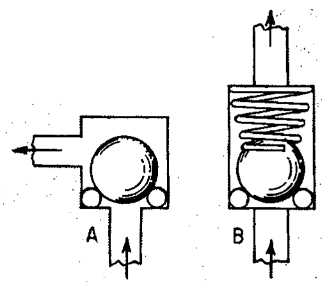

13

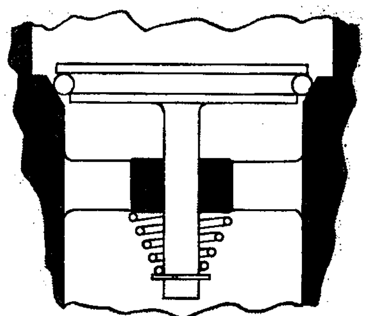

14

Checkvalves . . .
may have ball free (A); or spring-loaded (B). Back pressure will always force ball onto seat provided that gravity first helps locate ball on seat. Heavier-duty checkvalve (14) can be opened to allow back pressure to escape if necessary for shutdown etc.

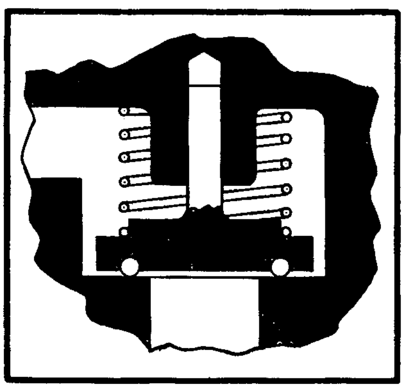

15

High-pressure checkvalve . . .
shown here cannot allow release of back-pressure but could be easily modified to do this by letting valve stem protrude.

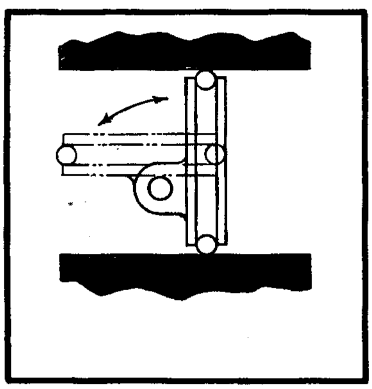

16

Butterfly valve . . .
can become a checkvalve if it is unbalanced; otherwise, it will act as normal two-way valve.

Look at O-Rings Differently

Sure they're seals, but they can also do a variety of other jobs as well as more sophisticated pieces of hardware

Robert O. Parmley

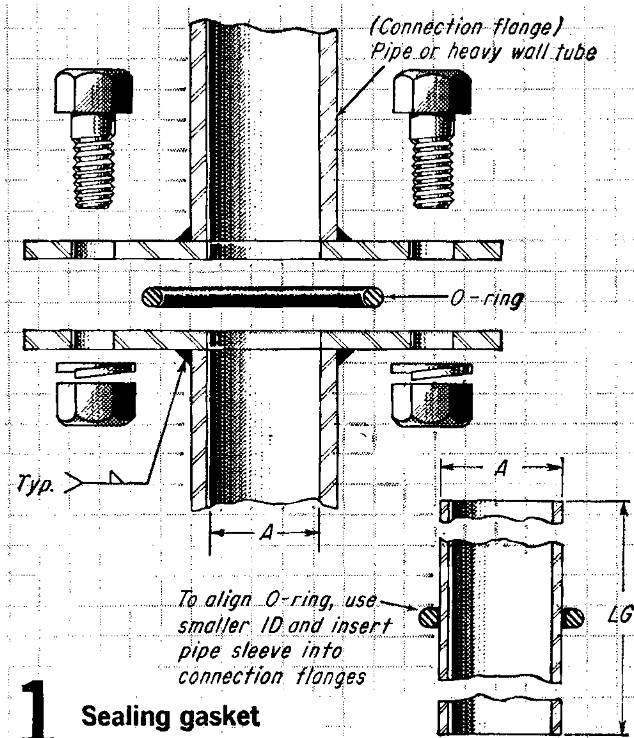

1 Sealing gasket

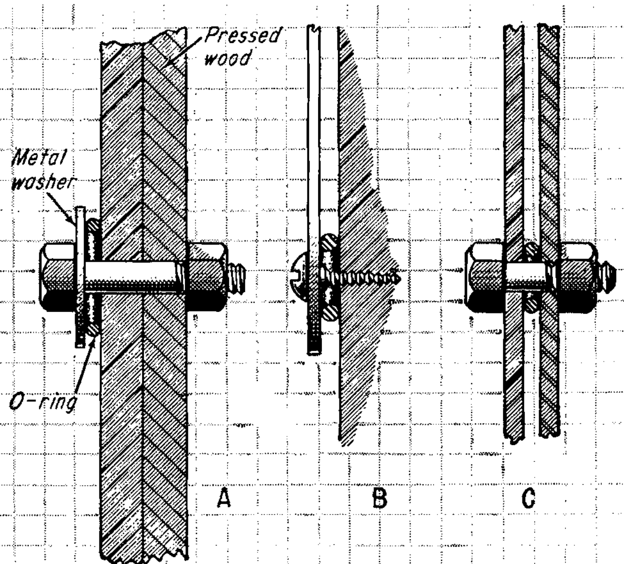

2 Marring protection

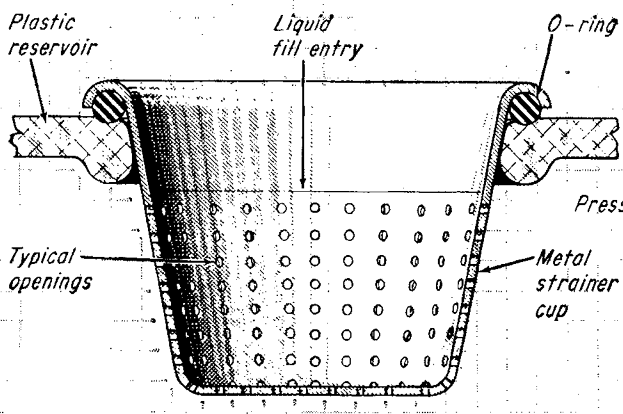

5 Cup rest and strainer seal

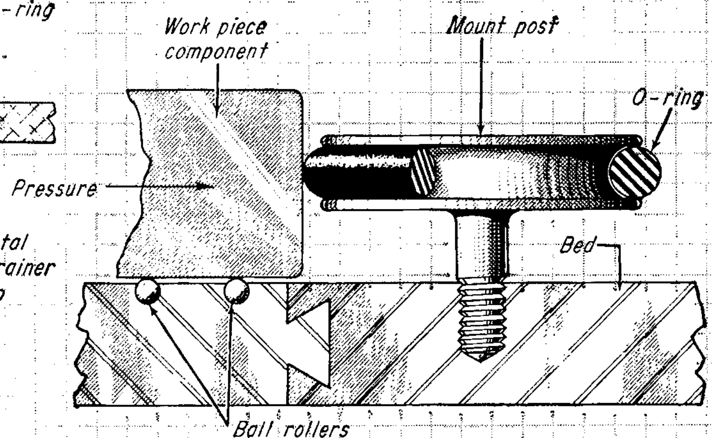

6 Aligning bumper

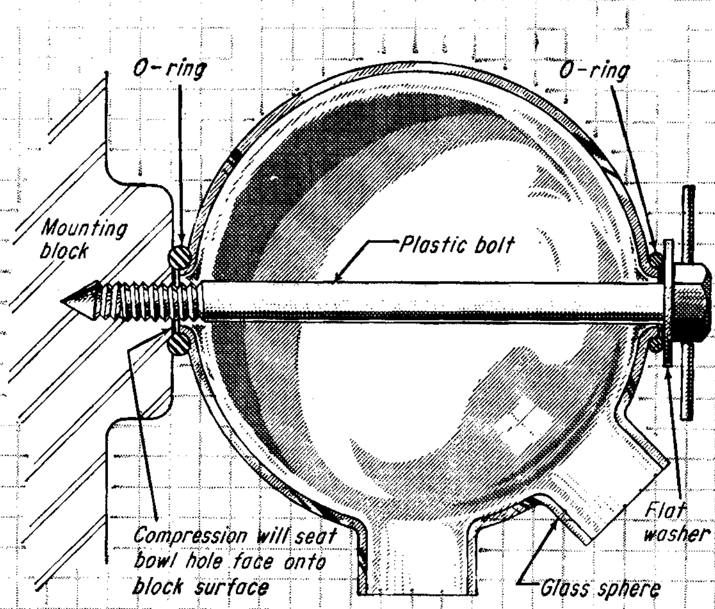

3 Bowl sealing

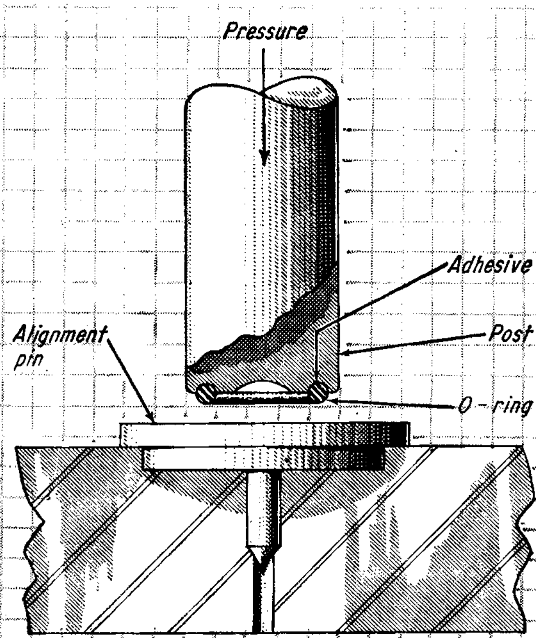

4 Shock absorption

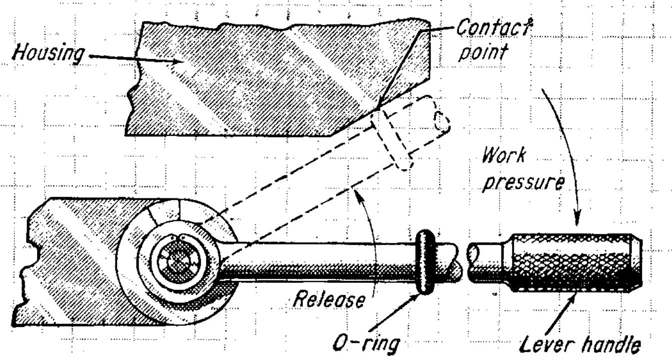

7 Lever stop

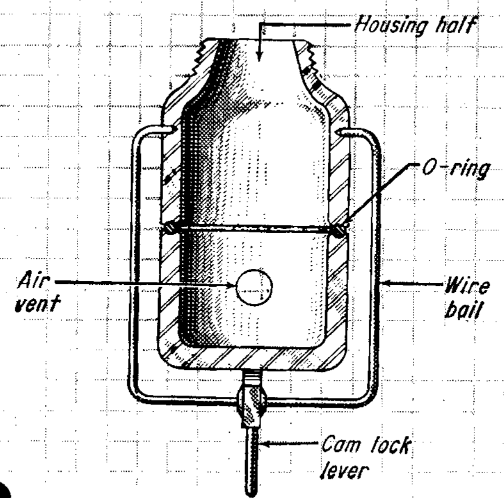

8 Chamber seal

O-Rings Solve Design Problems I

Rubber rings provide for thermal expansion, protect surfaces, seal pipe ends and connections, and prevent slipping.

Robert O. Parmley

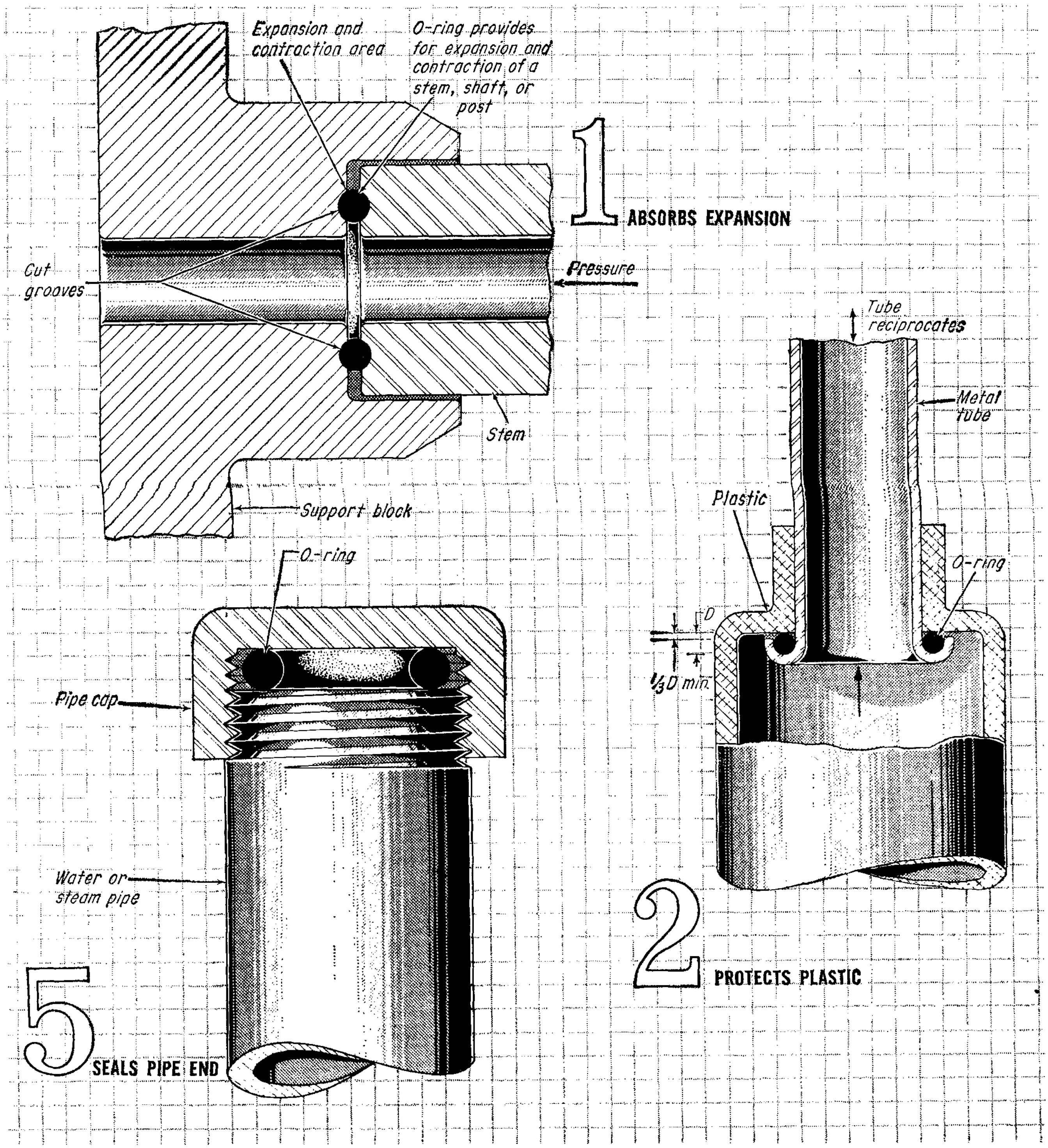

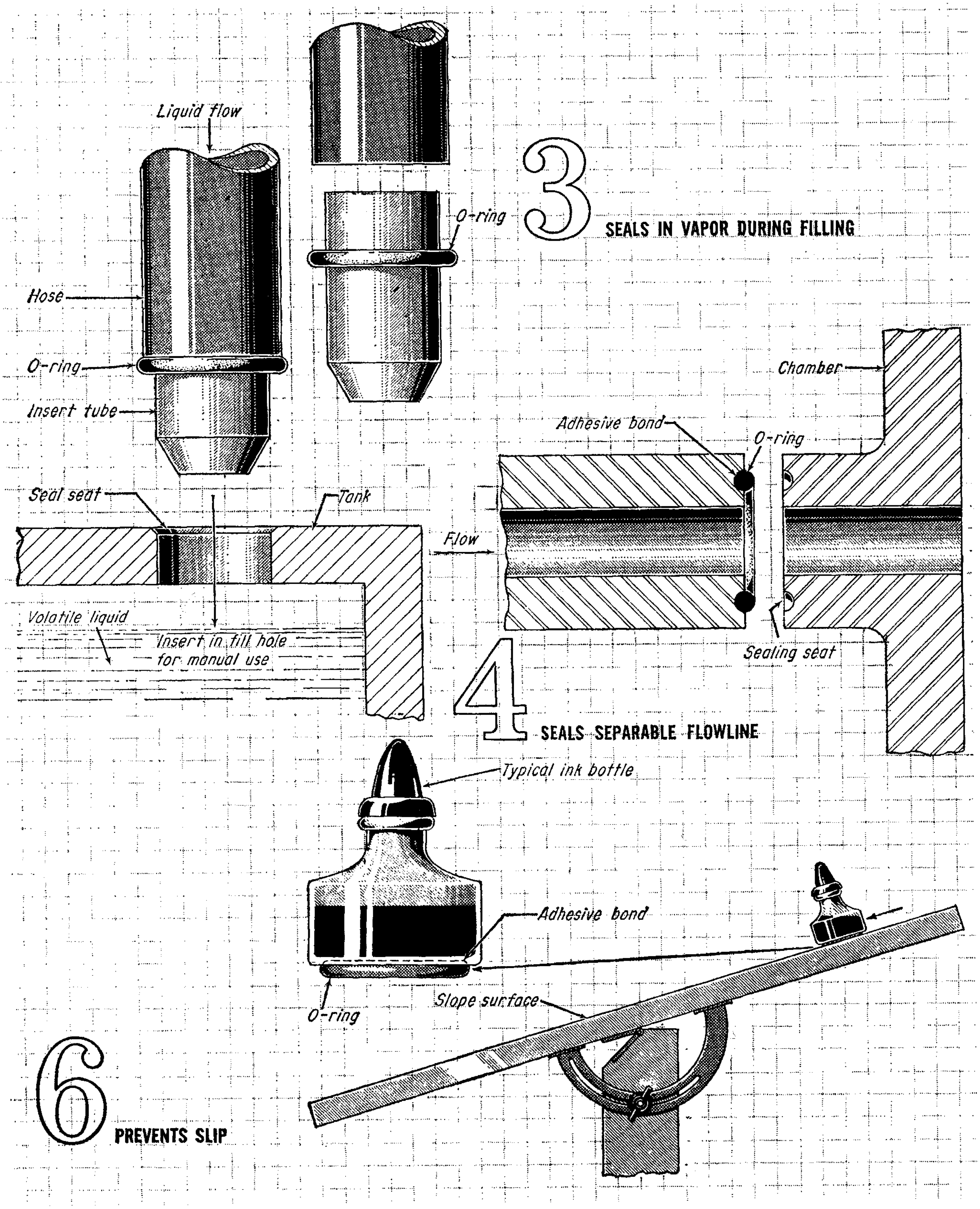
Liquid flow
Hose
O-ring
Insert tube
O-ring
3
SEALS IN VAPOR DURING FILLING
Seal seat
Tank
Volatile liquid
Insert in fill hole
for manual use
Flow
Chamber
Adhesive bond
O-ring
Sealing seat
4
SEALS SEPARABLE FLOWLINE
Typical ink bottle
Adhesive bond
O-ring
Slope surface
6
PREVENTS SLIP

O-Rings Solve Design Problems II

More examples of how rubber rings provide seals for shafts, lids, nozzles, and elbows, and also protect corners, cushion metal surfaces.

Robert O. Parmley

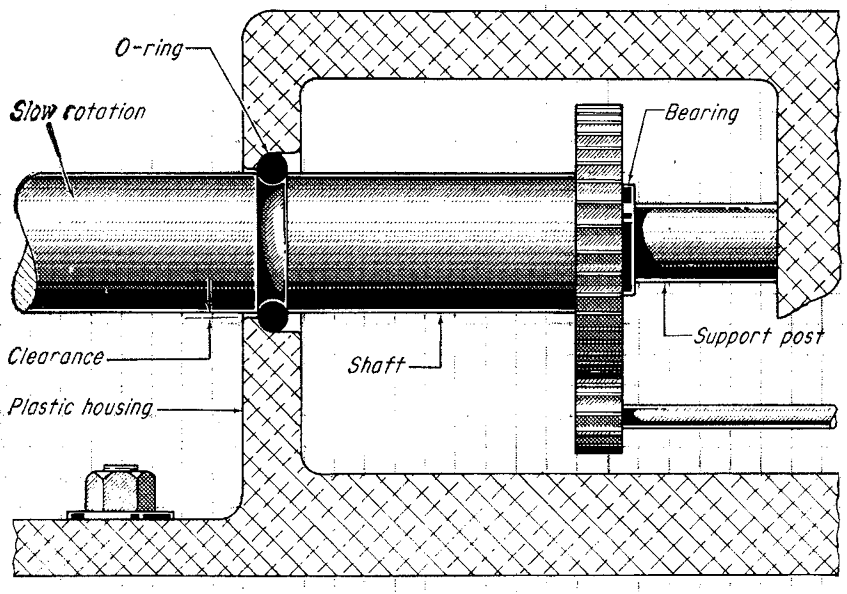

1 SEAL FOR SLOWLY ROTATING SHAFT

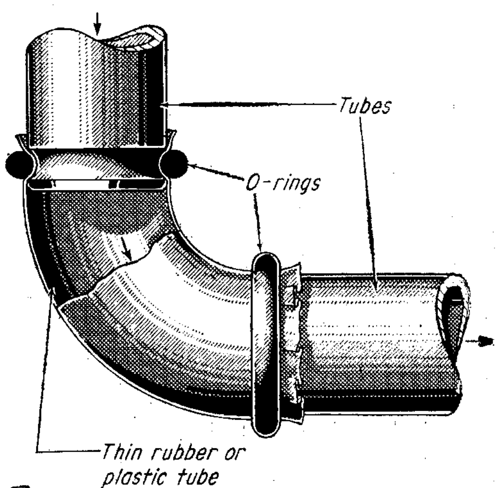

4 RETAINER FOR TUBE-TO-TUBE CONNECTIONS

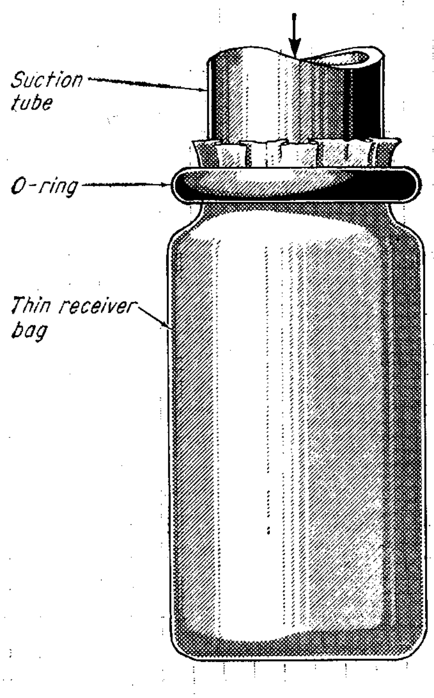

5 CLAMP-BAND FOR SIMPLE BAG ATTACHMENT

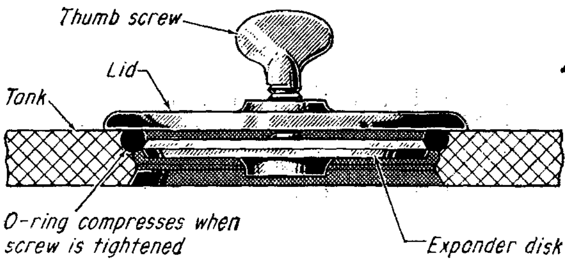

2 LOCKING-SEAL FOR LID ASSEMBLY

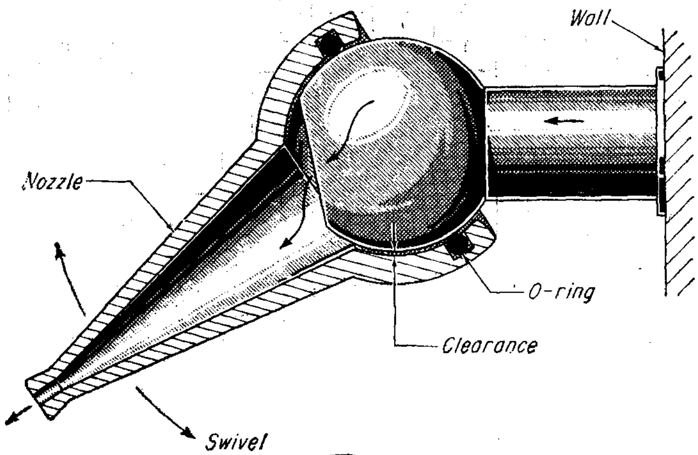

3 LIQUID- OR AIR-NOZZLE SEAL

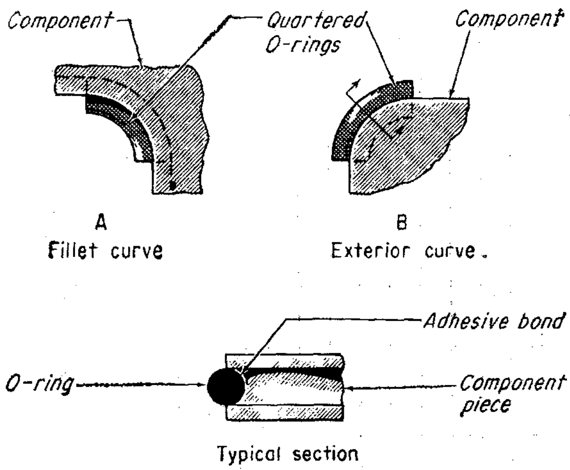

6 PROTECTIVE MOLDING MADE FROM O-RING SEGMENTS

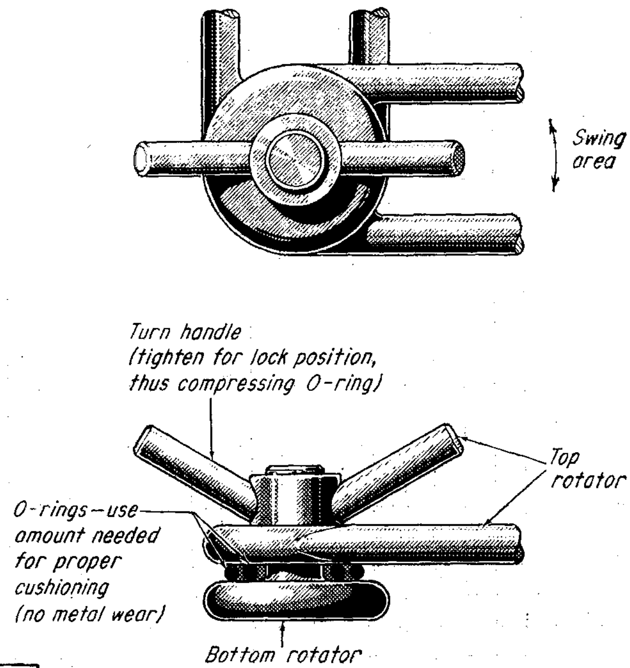

7 CUSHION-RING FOR SWIVEL OR LIGHTWEIGHT ROTATING COMPONENTS

7 More Applications for O-Rings

For an encore to the roundup in the previous issue, O-rings are shown here performing in valves, on guide wheels, and as cushioning etc.

Robert O. Parmley

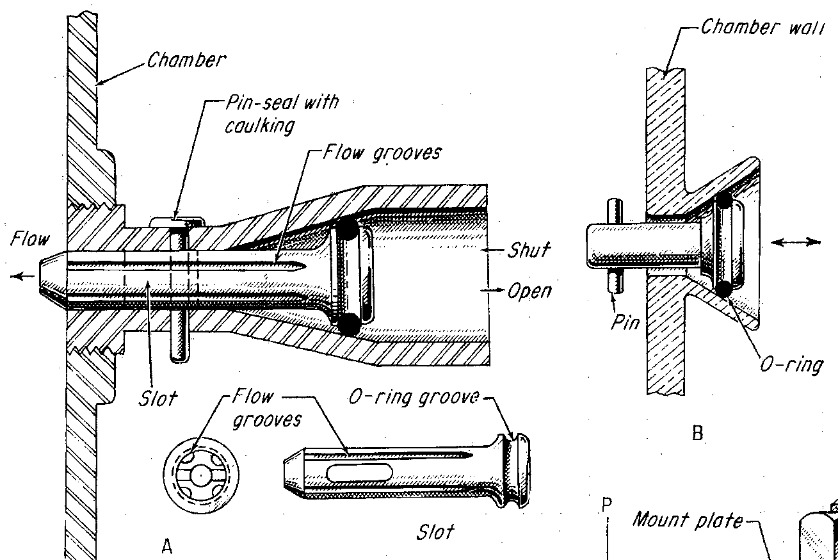

1 **LOW-COST VALVE** has easily changed O-ring, plus flutes for liquid flow, and caulked pin (A). Simpler valve (B) is adequate at less cost.

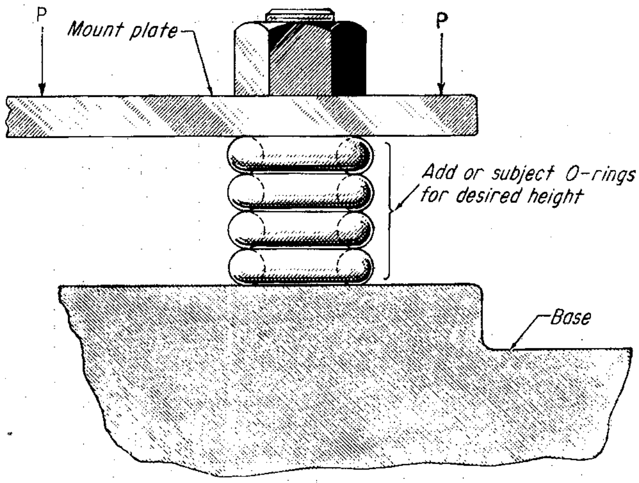

3 **CUSHION-RINGS** for vibration isolation or adjustment are quickly adjustable by merely adding or removing O-rings from the stack.

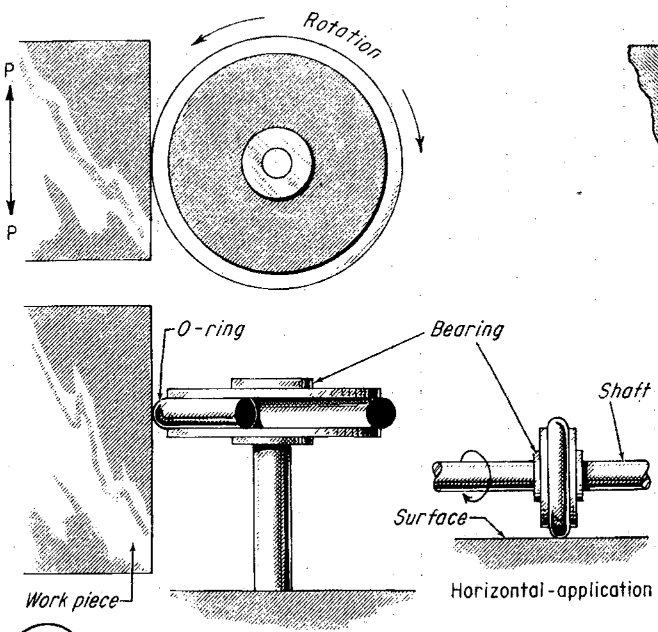

2 **PROTECTED GUIDE WHEELS** are often needed to guide, move, or align work. An O-ring here provides both friction and protection.

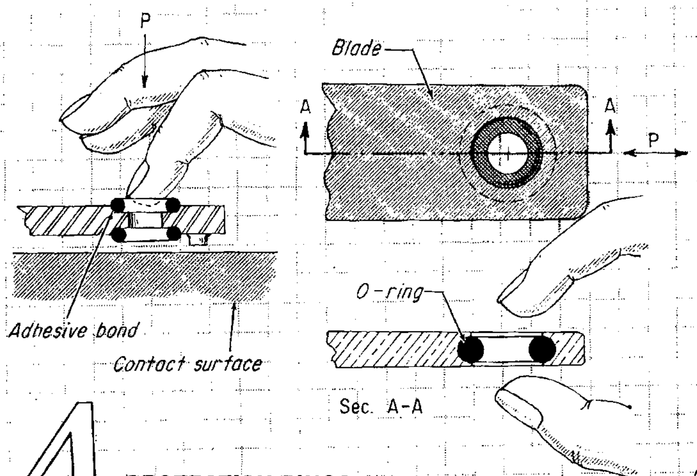

4

PROTECTION RINGS for push-pull or press action insulate against electrical shock, protect fingers against metal edges.

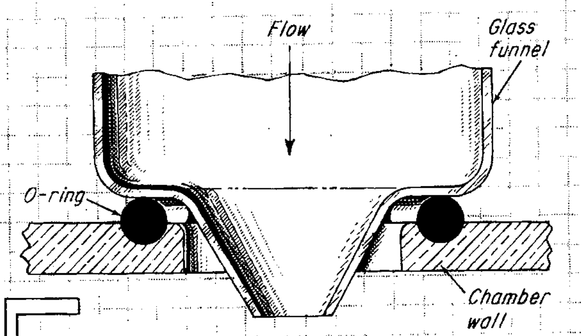

5

REPLACEABLE SEALS protect against spilled acids while cushioning funnels and similar glass apparatus against breakage.

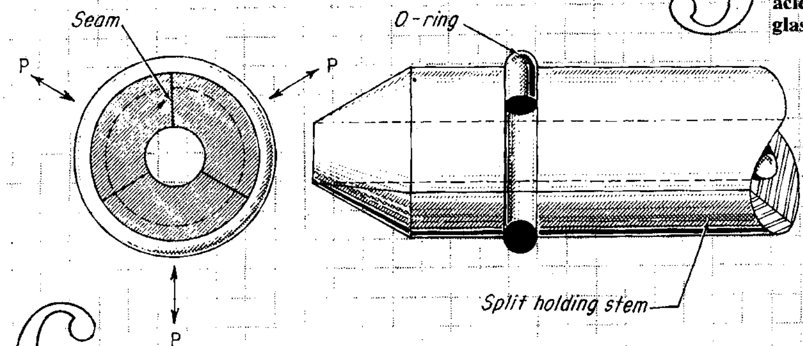

6

SPLIT STEMS can be held firmly with a suitable size O-ring. One or more can be placed at varying positions on the stem.

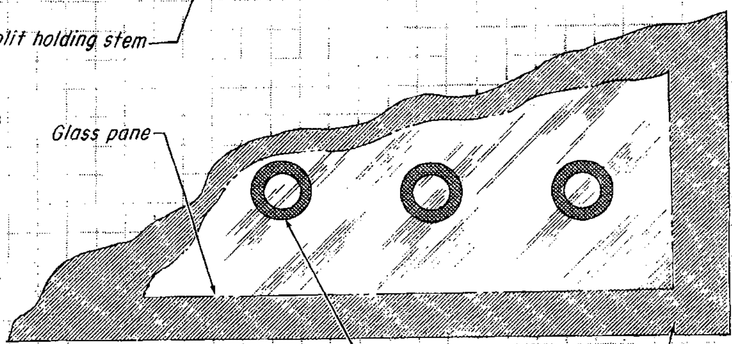

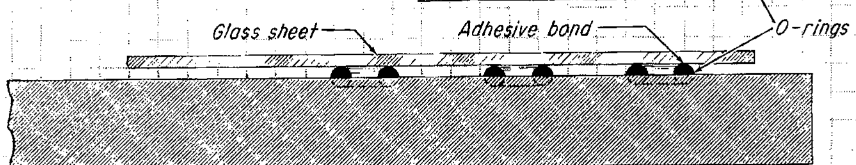

7

WORKING-TABLE FOR GLASS or other delicate materials has O-ring resting pads set into surface at over-all or grouped locations.

Design Recommendations for O-Ring Seals

J. H. Swartz

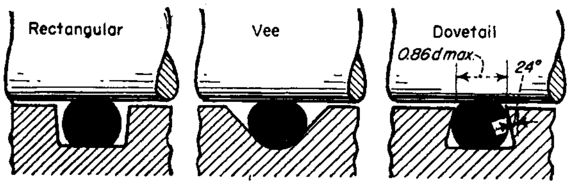

1 Rectangular grooves are recommended for most applications, whether static or dynamic. Slightly sloping sides (up to 5 deg) facilitate machining with form tools. Where practical, all groove surfaces should have the same degree of finish as the rod or cylinder against which the O-ring operates. The Vee type groove is used for static seals and is especially effective against low pressures. The dovetail groove reduces operating friction and minimizes starting friction. The effectiveness of the seal with this groove is critical depending upon: pressure, ring squeeze and angle of undercut. In general, the groove volume should exceed the maximum ring volume by at least 15 percent.

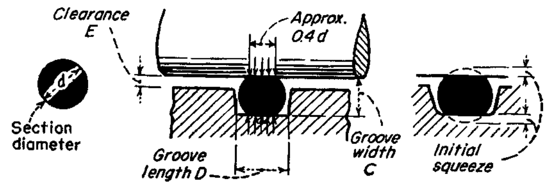

2 To insure a positive seal, a definite initial squeeze or interference of the ring is required. As a rule, this squeeze is approximately 10 percent of the O-ring cross sectional diameter *d*. This results in a ring contact distance of approximately 40 percent under zero pressure and can increase as much as 80 percent of the cross section diameter depending on pressure and composition of the ring. Starting friction can be reduced somewhat by decreasing the amount of squeeze but such a seal would be only moderately effective at pressures above 500 psi. Table I lists the recommended dimensions and tolerances for O-ring grooves for both static and dynamic applications.

EXTERNAL GROOVES

INTERNAL GROOVES

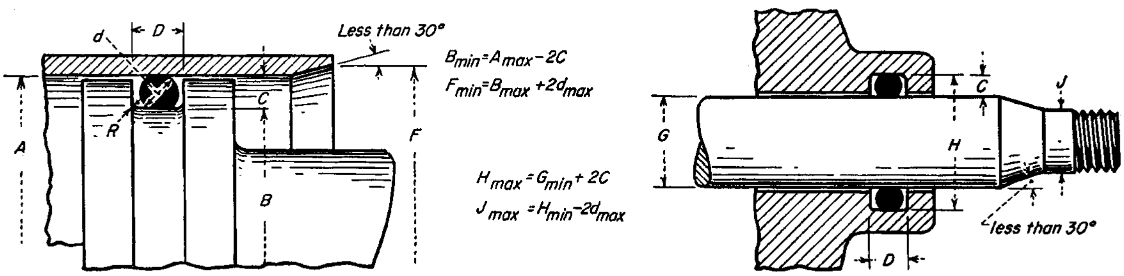

3 On small diameters, to facilitate machining, O-ring grooves should be located on the ram or rod rather than on an inside surface. For larger diameters, grooves can be machined either way. One important factor is that the rubbing surfaces must be extremely smooth. The recommended dimensional data in Table I and listed under dynamic seals should be used for these applications. All cylinders and rods should have a gradual taper to prevent damage to the O-ring during assembly. Equations are listed for calculating limiting dimensions for both external and internal grooves.

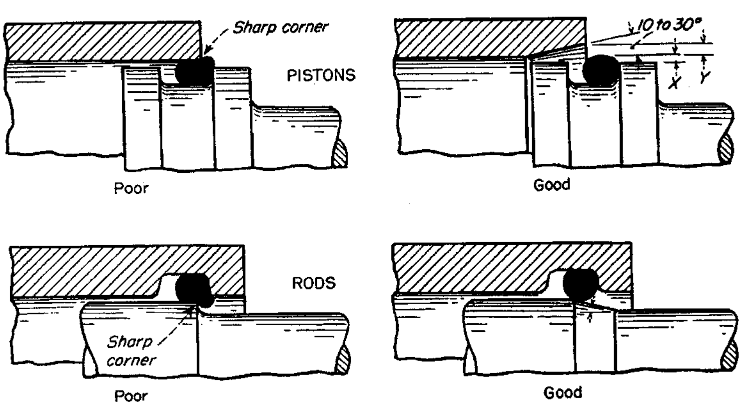

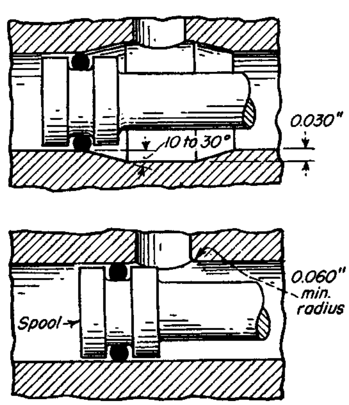

6 To facilitate assembly, all members which slide over O-rings should be chamfered or tapered at an angle less than 30 degrees. An alternative method is to use a generous radius. Such details prevent any possibility of pinching or cutting the O-ring during assembly.

7 Undercut all sharp edges, or cross-drilled ports over which O-rings must pass. While under pressure, rings should not pass over ports or grooves.

Table I—Dimensional Data for Standard AN or J.I.C. O-Rings and Gaskets

Specification AN 6227 or J. I. C. O-Ring Dash Number	Nominal Ring Section Diameter	*d* Actual Section Diameter	For Static Seals: Diametral Squeeze* (minimum)	For Static Seals: *C* Groove Width +0.000 −0.005	For Dynamic Seals: Diametral Squeeze* (minimum)	For Dynamic Seals: *C* Groove Width +0.000 −0.001	*D* Groove Length**	*R* Minimum Radius	2*E* Diametral Clearance (maximum)	Eccentricity (maximum)
1 to 7	1/16	0.070±0.003	0.015	0.052	0.010	0.057	3/32	1/64	0.005	0.002
8 to 14	3/32	0.103±0.003	0.017	0.083	0.010	0.090	9/64	1/64	0.005	0.002
15 to 27	1/8	0.139±0.004	0.022	0.113	0.012	0.123	3/16	1/32	0.006	0.003
28 to 52	3/16	0.210±0.005	0.032	0.173	0.017	0.188	9/32	3/64	0.007	0.004
53 to 88	1/4	0.275±0.006	0.049	0.220	0.029	0.240	3/8	1/16	0.008	0.005
AN 6230 or J. I. C. gaskets 1 to 52	1/8	0.139±0.004	0.022	0.113	——	——	3/16	1/32	0.006	0.003

Note: All dimensions are in inches.
* Diametral squeeze is the minimum interference between O-Ring cross section diameter *d* and gland width *C*.
** If space is limited, the groove length *D* can be reduced to a distance equal to the maximum O-Ring diameter *d* plus the static seal squeeze.

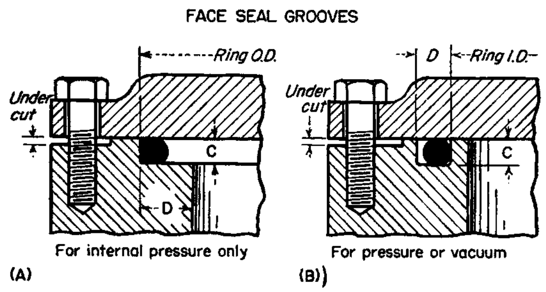

4 For static face seals, two types of grooves are shown. Type (A) is more commonly used because of simpler machining. Groove depths listed in Table I under static seals apply to this application. In high pressure applications where steel flanges are used, slight undercutting of one face (not exceeding 0.010 in.) minimizes possible O-ring extrusion.

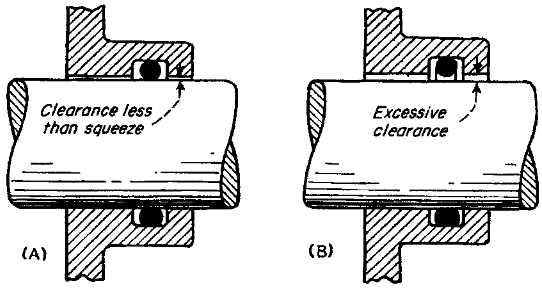

5 Radial clearances should never exceed one-half of the recommended O-ring squeeze even where the pressure does not require the use of a close fit between sliding parts. Under these conditions, if the shaft is eccentric (A), the ring will still maintain its sealing contact. (B) Excessive clearance results in the loss of sealing contact of the O-ring.

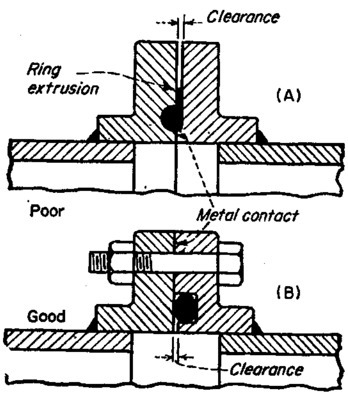

8 Metal-to-metal contact of the inner mating surfaces (A) should be avoided. Clearances should be permitted only on inner surfaces (B).

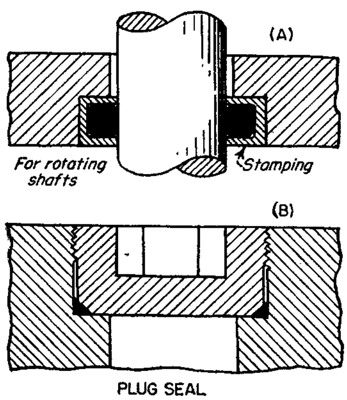

9 Simple stamping (A) pressed in housing is for low speeds and pressures. (B) Chamfered corners of plug makes a recess for an O-ring.

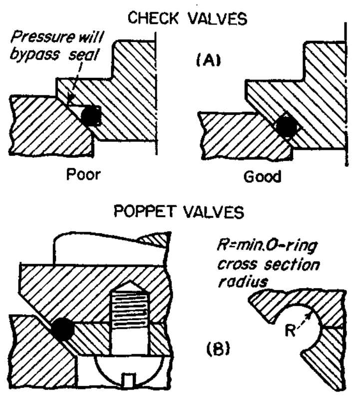

10 Rectangular grooves (A) should be normal to the sealing surface. Special grooves (B) avoid the washout of O-rings during pressure surges.

O-Ring Seals for Pump Valves

Robert O. Parmley

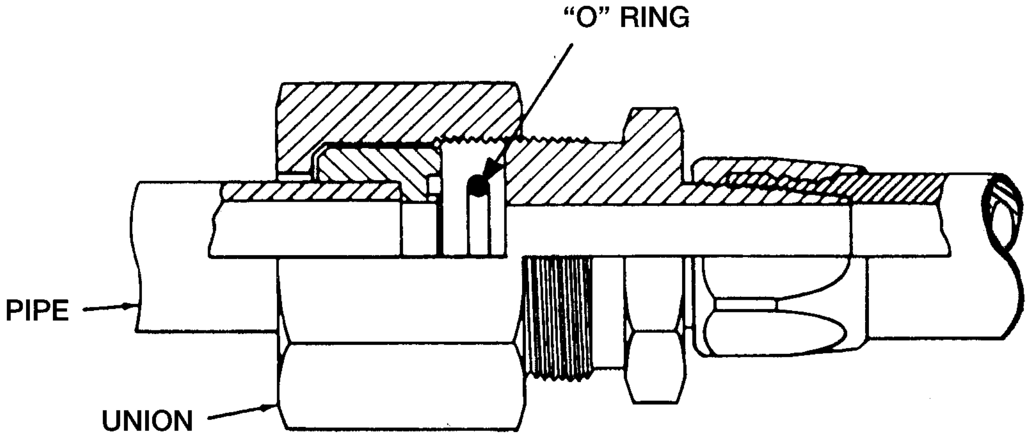

A-Combination Pump Valve

The CPV O-ring seal fitting (a Navy standard) uses an O-ring which is inserted in the packing-gland recess on the face or the union which has been silver-brazed to the end of a pipe. The union and pipe are sometimes called a "tailpiece."

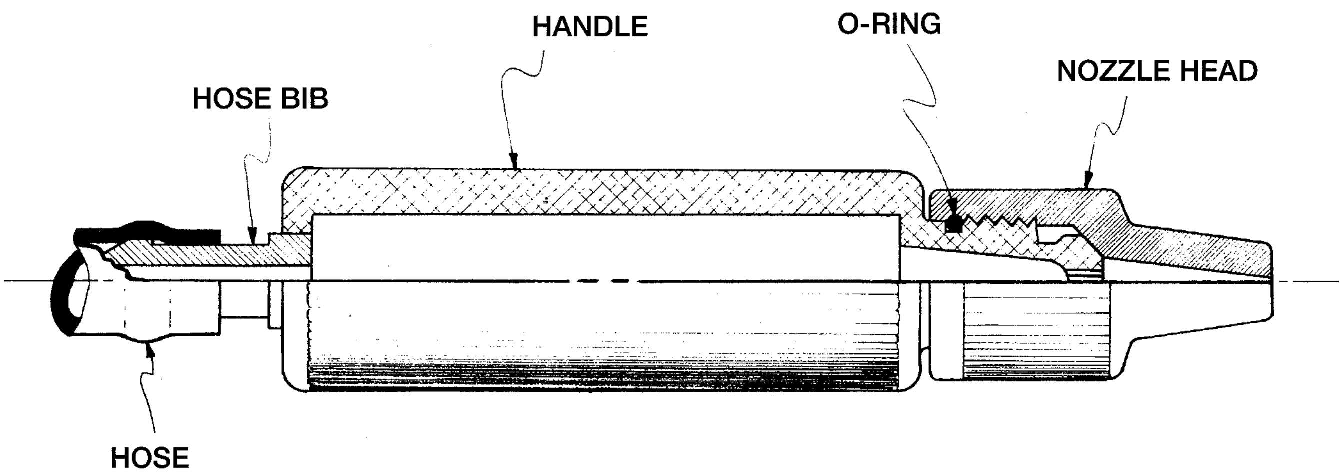

B-Hand-Adjusted Pump Nozzle

The discharge end (nozzle head) of this portable pump unit has the spray adjusted by manually turning the nozzle head. The O-ring maintains a positive, water-tight seal for any adjusted position.

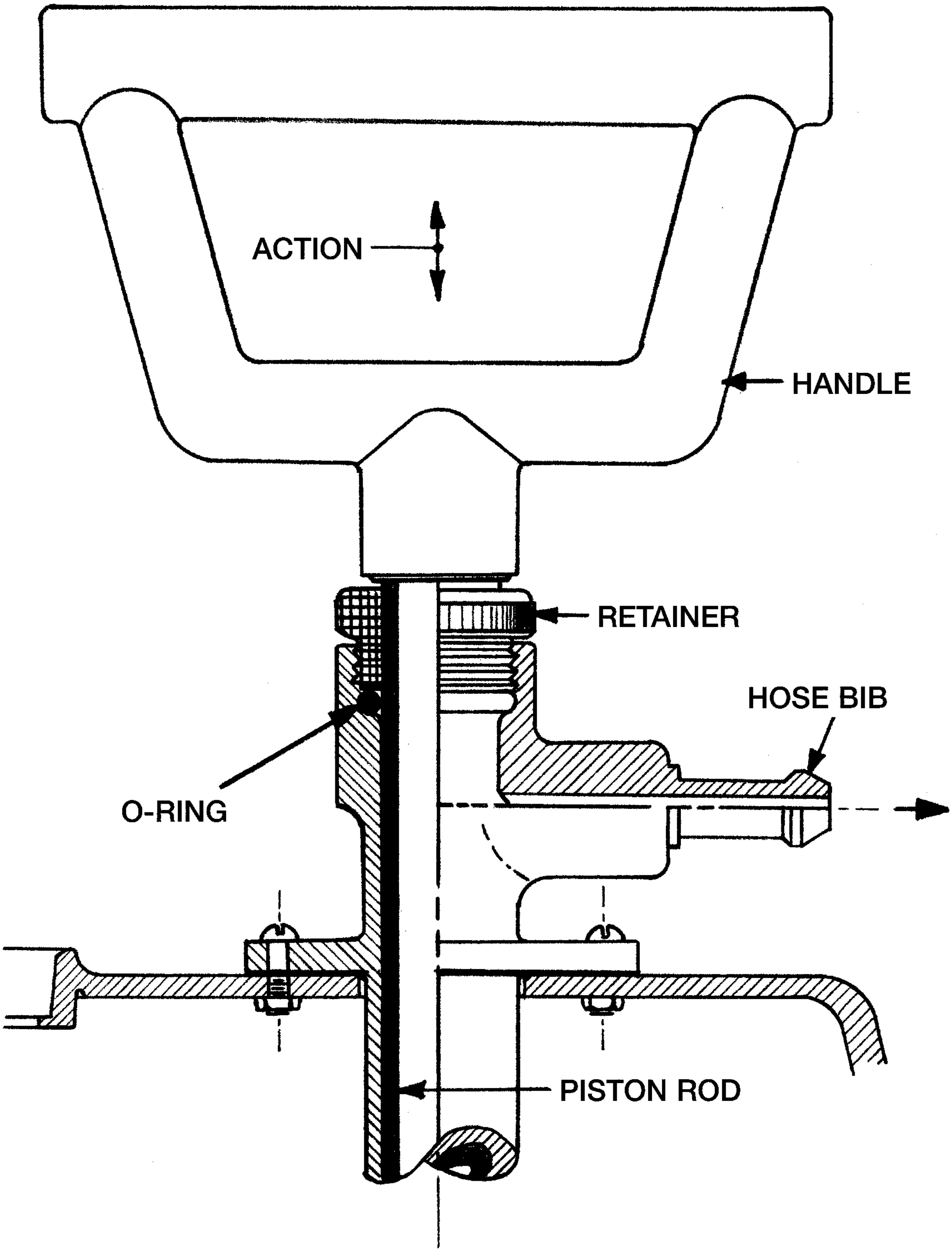

C-Manual Pump Seal

The O-ring, which is seated by the threaded retainer, provides a water-tight seal for the up & down action of the piston rod.

SECTION 14

GROMMETS, SPACERS & INSERTS

A Fresh Look at Rubber Grommets

A small component that's often neglected in the details of a design. Here are eight unusual applications.

Robert O. Parmley

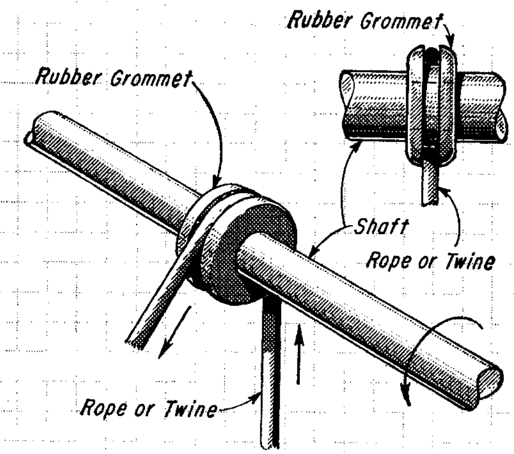

1 Pulley for slow rotation

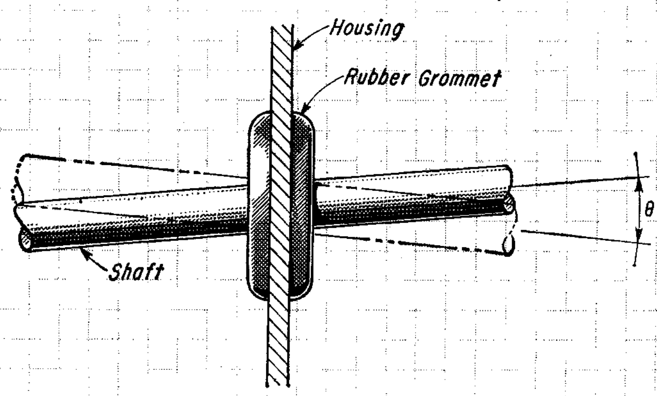

2 Handle shaft misalignment

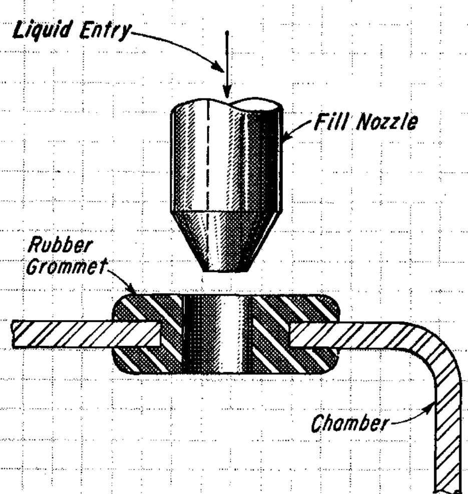

5 Seal for liquid filling

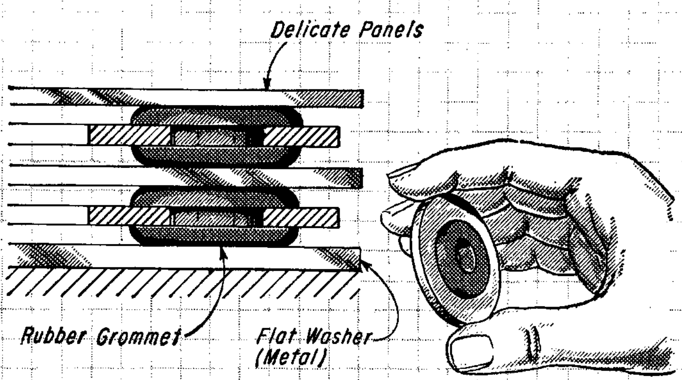

6 Cushioned spacers

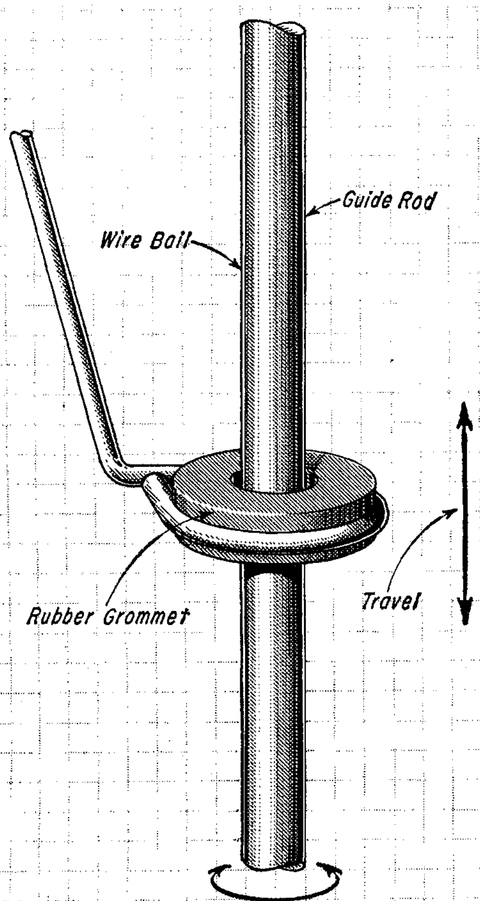

3 Guide liner

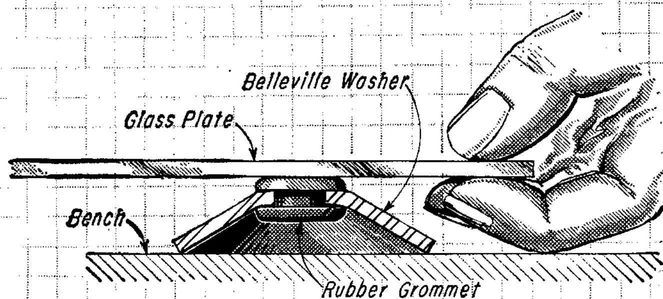

4 Support delicate work plates

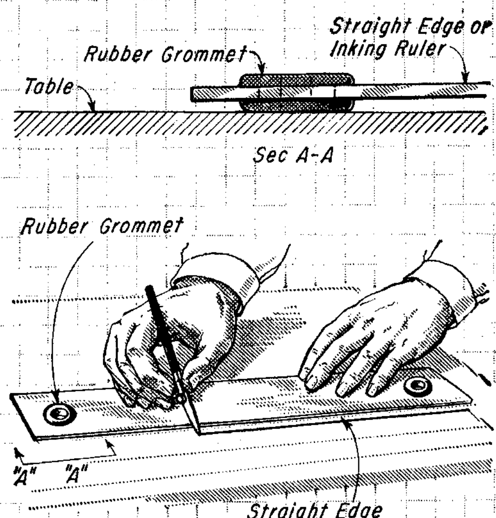

7 Straightedge pads

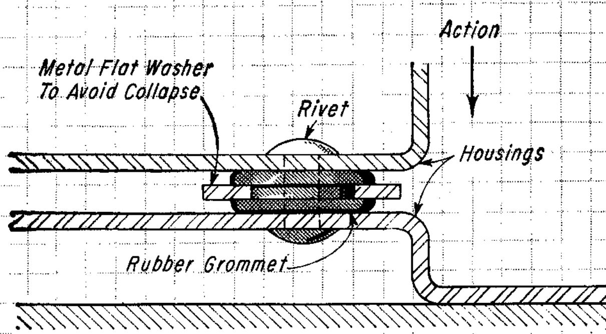

8 Shock absorber

These Spacers are Adjustable

Rubber, metal springs, jackscrews, pivoting bars and sliding wedges allow adjustment after assembly.

Richard A. Cooper

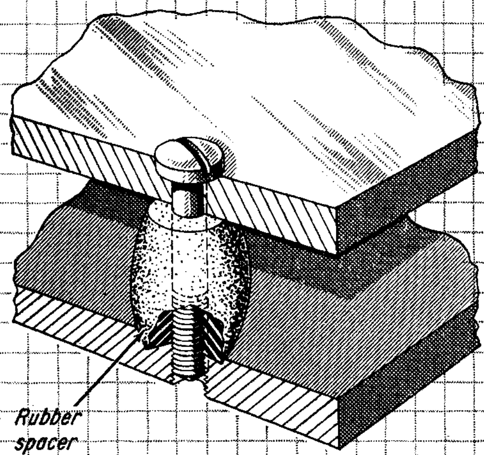

1

TUBULAR RUBBER SPACER is low-cost, efficient device for space adjustment and shock absorption.

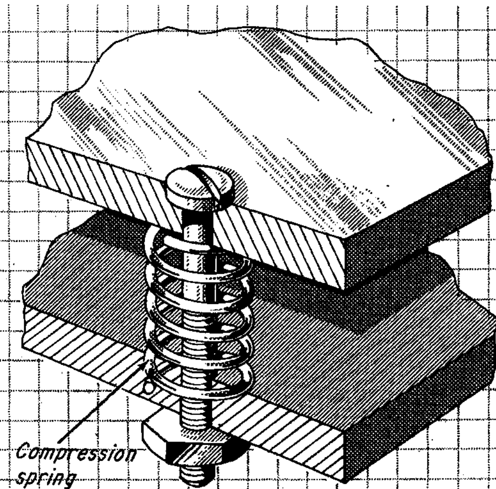

2

COMPRESSION SPRING should be close fit on the adjustment bolt to avoid side deflection of the spring.

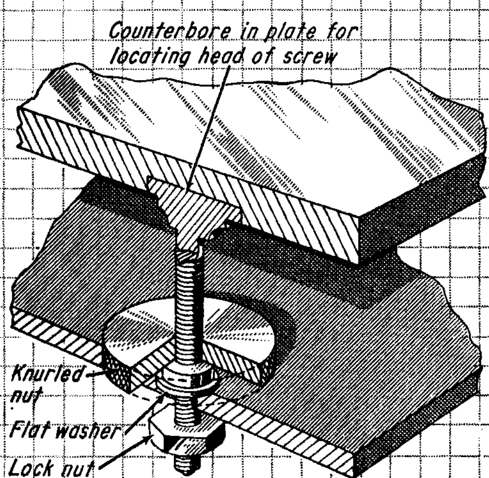

5

JACKSCREW and knurled nut assure accurate adjustment. Here the top piece floats for easy removal.

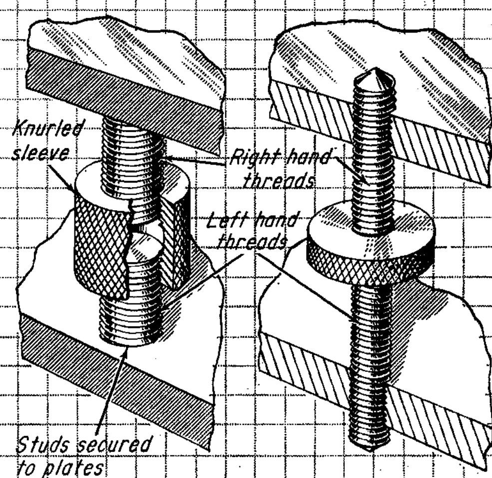

6

OPPOSITE-THREADED STUD device for moving both parts exactly the same distance with one adjustment.

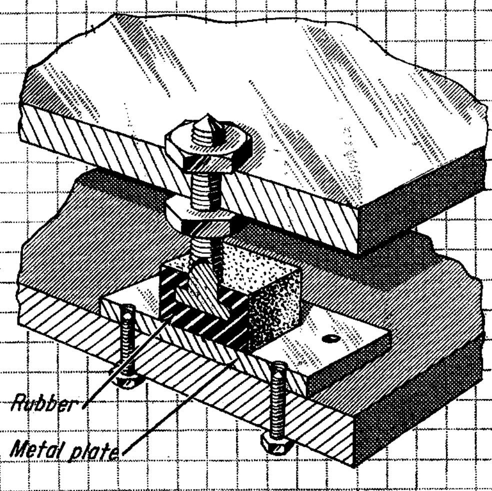

3

RUBBER-SUPPORTED STUD is attached to the metal plate. Support heavy loads with this assembly.

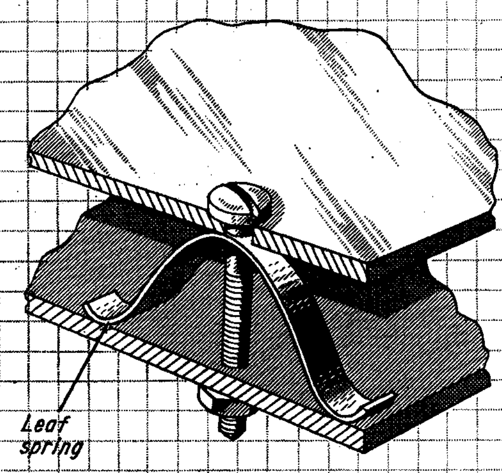

4

LEAF SPRING ends should be turned up to prevent their digging into the bottom part, which could prevent adjustment.

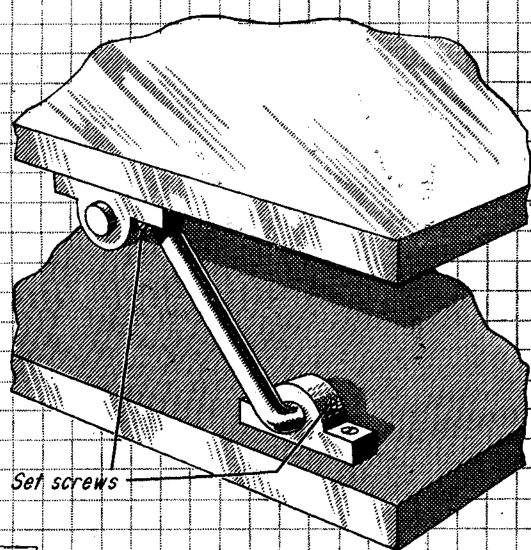

7

PIVOTING BAR allows wide range of adjustment where torque at clamping points is low enough to allow a tight hold.

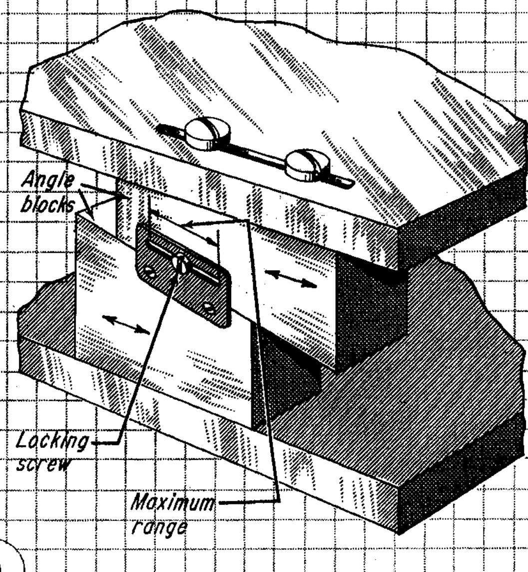

8

SLIDING ANGLE BLOCKS permit great accuracy in simultaneous lateral and vertical adjustment of parts.

Odd Jobs for Rubber Mushroom Bumpers

High energy absorption at low cost is the way mushroom bumpers are usually billed. But they have other uses; here are seven that are rather unconventional.

Robert O. Parmley

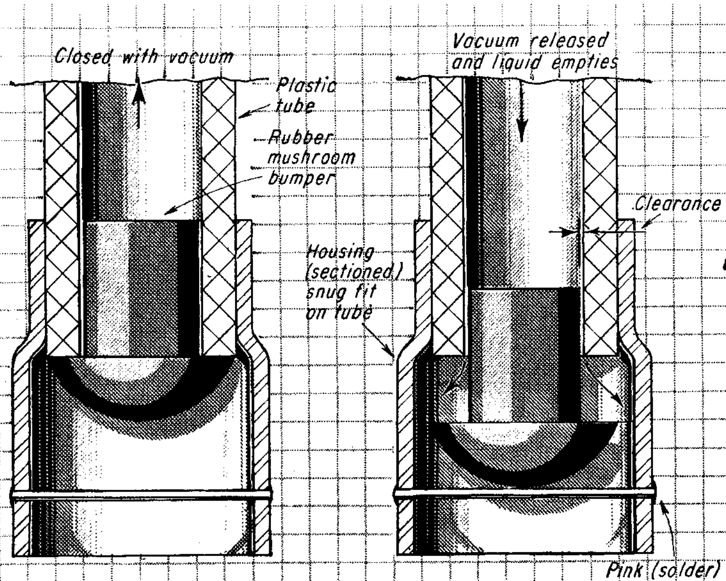

1 **Discharge valve for tubing**

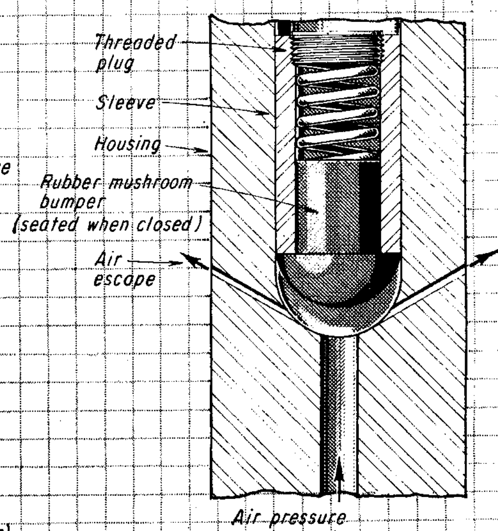

2 **Air pressure valve**

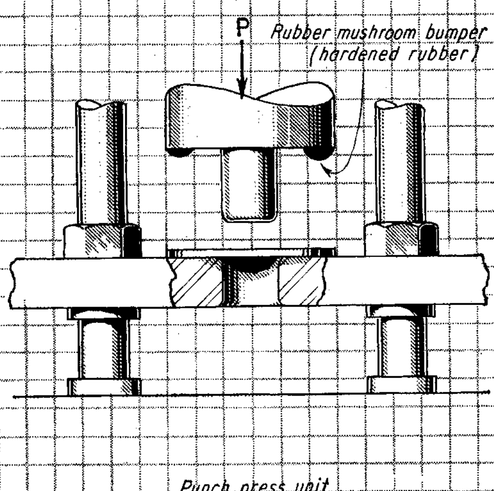

5 **Punching protector**

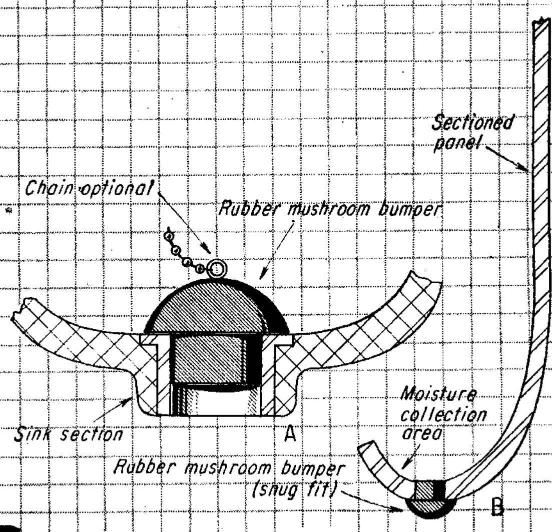

6 **Drain plugs**

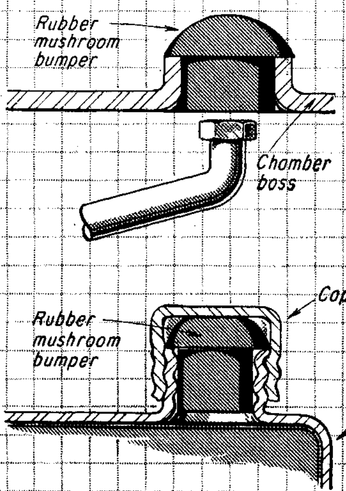

3 Chamber plug

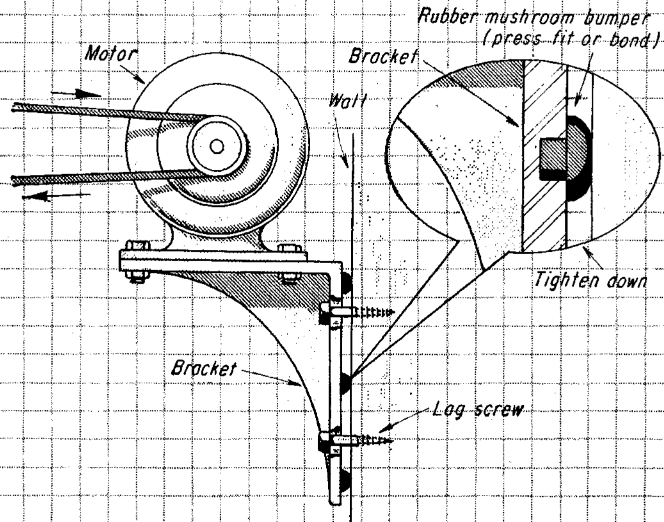

4 Cushion motor vibration

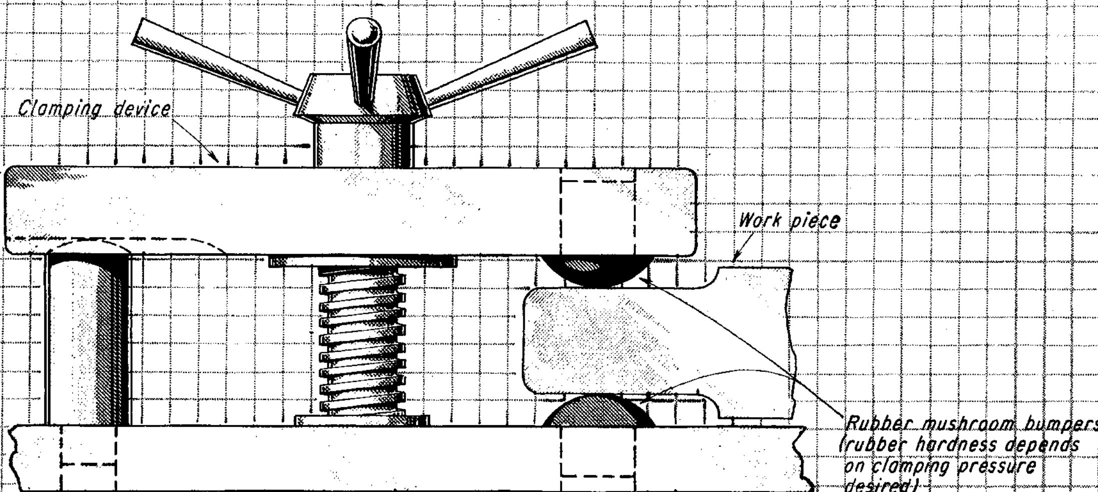

7 Clamp delicate parts

Metal Inserts for Plastic Parts

Plastics are increasingly used in automobiles and appliances and thus a major company compiled these data.

Molded parts should be designed around any inserts that are required. This work is done after the type of compound is selected. Inserts are used for two basic reasons:

1. To add strength to the plastic part or to control shrinkage. Sometimes the purpose is to be decorative or to avoid injuries.
2. To provide an attachment means for the conductance of heat or electricity.

Special means of retention are not necessary for inserts not subject to movement with relation to the molding material. Inserts of round bar stock, coarse diamond knurled and grooved, provide the strongest anchorage under torque and tension. A large single groove, as in Fig. 1, is better than two or more grooves and smaller knurled areas.

Inserts secured by press or shrink fits

Inserts can be secured in the plastic by a press fit or shrink fit. Both methods rely upon shrinkage of the plastic, which is greatest immediately after removal from the mold. The part should be made so that the required tightness is obtained after the plastic has cooled and shrinkage has occurred. The amount of interference required depends on the size, rigidity and stresses to be encountered in service. The hole to receive the mating part should be round and countersunk. In addition, the mating part should be chamfered and filleted to facilitate proper assembly and to eliminate stress concentration.

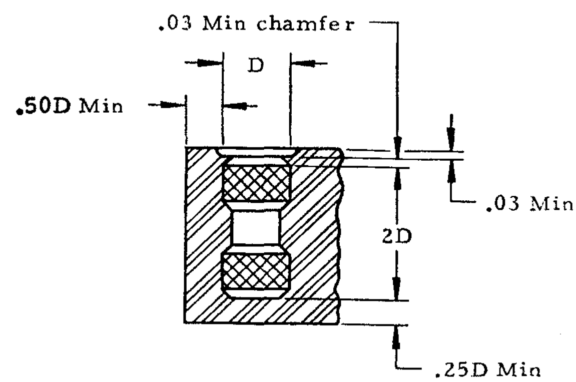

1. Depth of knurling should be about 0.001 in. and a single groove is best

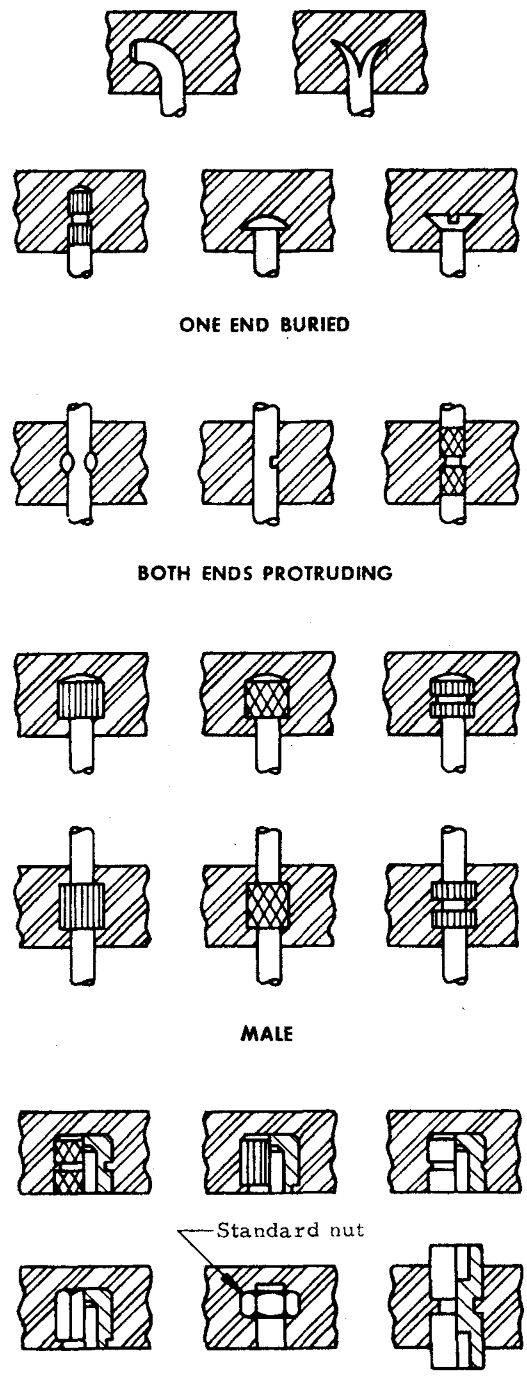

2. Round knurled parts are common inserts

Reprinted with permission from American Machinist, A Penton Media Publication

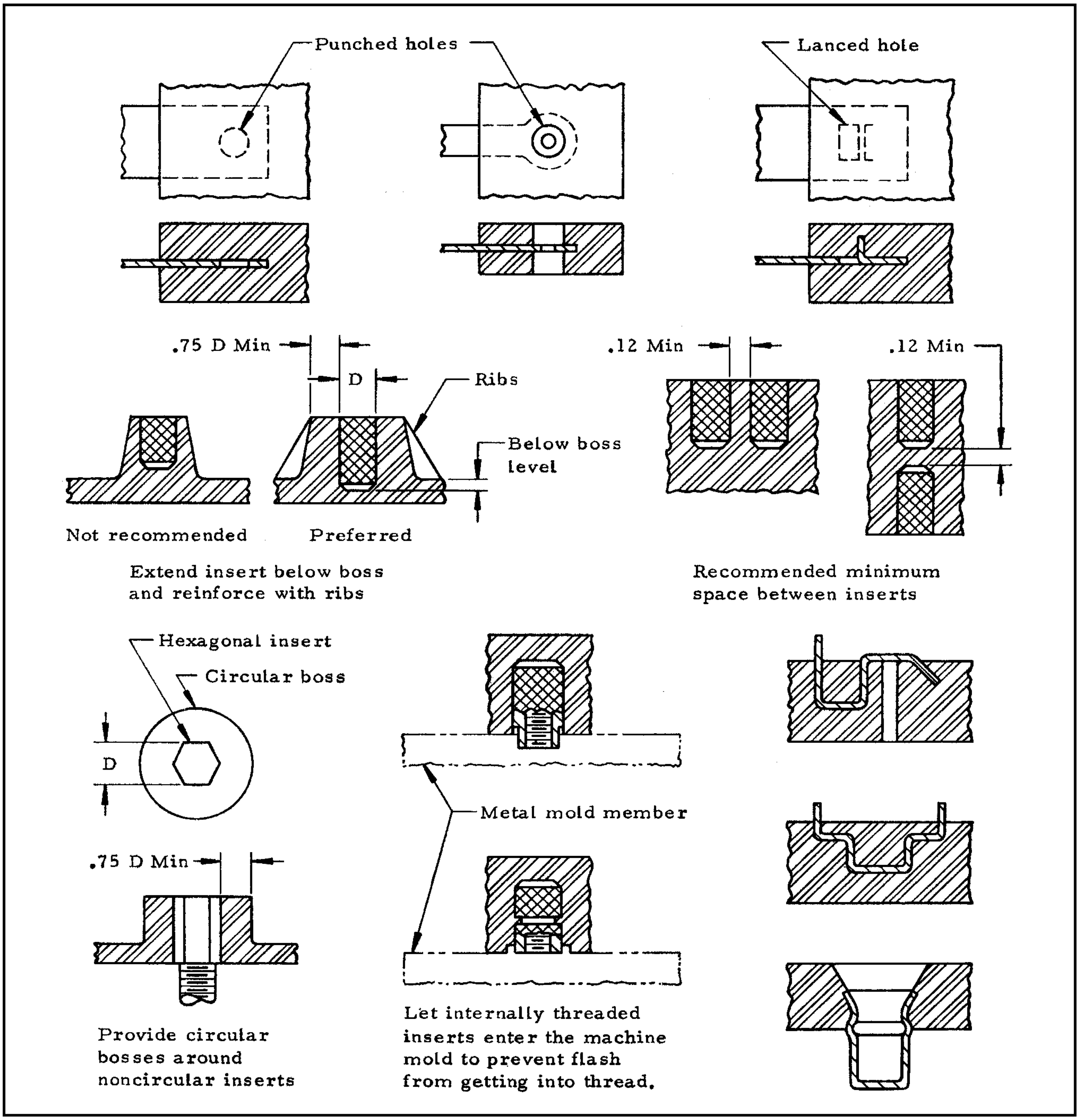

3. Sheet metal and special inserts, as well as knurled inserts, are used to provide connections and closures

How to Select Threaded Inserts

Why use threaded inserts? What types are available? What factors govern their selection? How do you determine whether a particular insert meets the given strength requirements and which one is most economical?

S. H. Davison

When the design calls for lightweight materials like aluminum, magnesium and plastics, threaded holes become a problem because of the low shear strength of these materials. To bolt such components to other machine parts, the threaded holes must be quite deep to develop the required pull-out strength, or they must have a coarse thread to increase shear area.

Further complications arise when the components require frequent disassembly for overhaul or repair; this may give excessive thread wear that will prevent satisfactory thread engagement with the bolt, particularly for high-strength bolts in the fine-thread series; and the depth of engagement needed will require a part so thick as to nullify the lightweight advantage of the material. To overcome these problems, thread inserts of high-strength material are often used.

Inserts available

Three main types of inserts are available:

1. Wire thread inserts are precision coils of diamond-shape stainless steel wire. They line a tapped hole and present a strong, accurate, standard internal thread for the bolt or stud. The OD on these inserts is from 11 to 30% greater than the OD of the internal thread—the lower limit is normally used on the fine-thread inserts specified in aircraft engines. The pull-out strength of wire thread insert depends on shear area of its OD thread.

2. Solid self-tapping inserts require only a drilled hole and counterbore in the part, and are made in two basic forms. (1) A solid self-tapping, self-locking bushing has a 60% external thread approximating the American National form with a uniform OD extending to the first 2 to 2½ threads. These leading threads are slightly truncated to provide the cutting action necessary for self-tapping. Chips flow out through the side hole drilled in the insert wall at the truncated lead threads. (2) A second type has lead threads similar to the pilot threads of a standard tap. These threads progressively flow into truncated threads extending the entire length of the insert—with the exception of the last three threads, which are standard.

In both types, two or three angular slots, depending on the particular design, provide the cutting action for self-tapping.

3. Solid bushings for pre-tapped holes are also made in

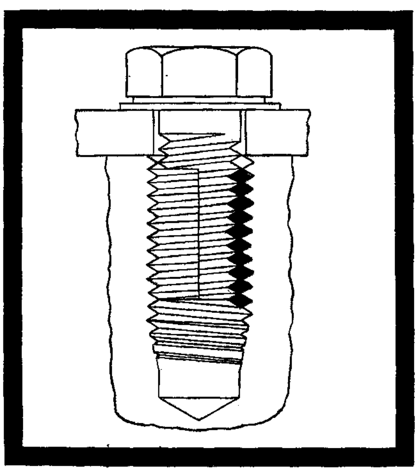

WIRE THREAD INSERTS made of diamond-shape stainless steel wire. Pull-out strength of material depends on ratio of internal to external thread shear area.

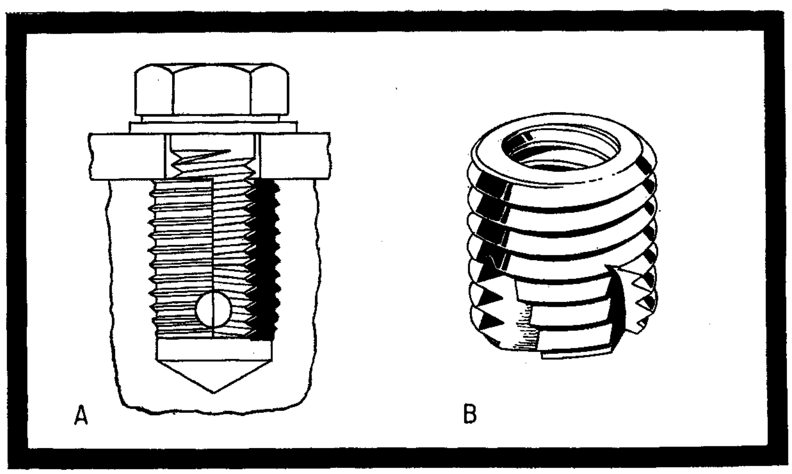

SOLID SELF-TAPPING INSERTS are of two types—(A) chips are removed through the side hole; or (B) with truncated lead threads and two or three angular slots which provide cutting action.

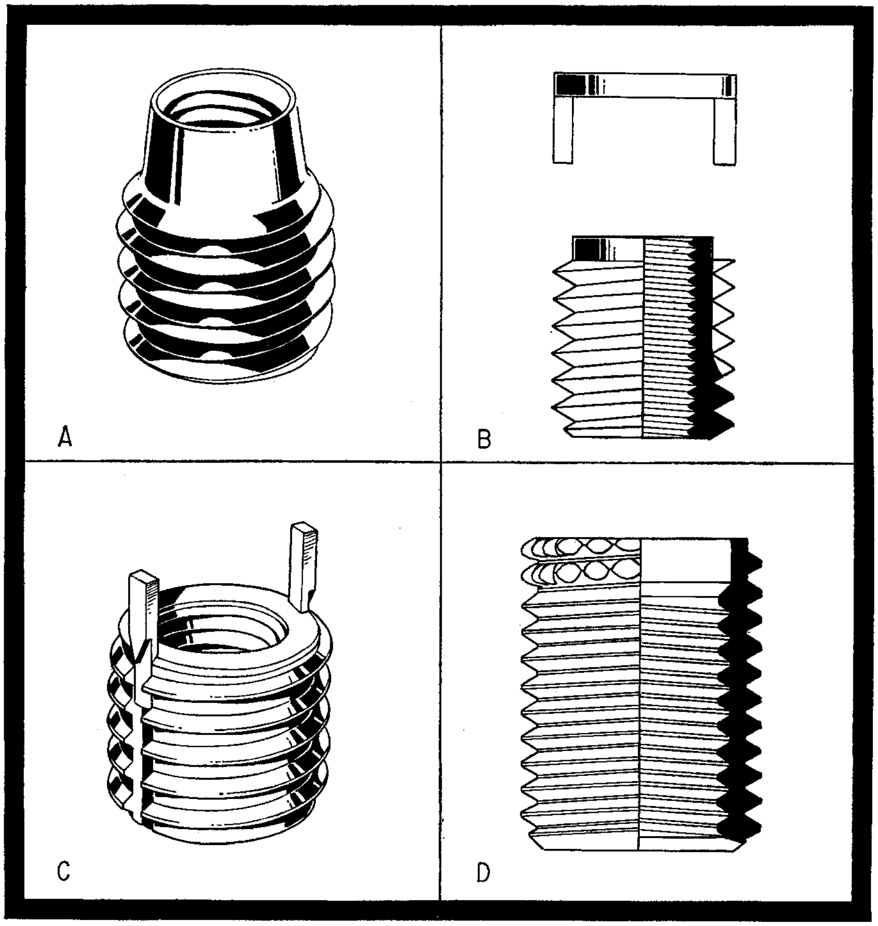

SOLID INSERTS FOR PRE-TAPPED HOLES have many variations. Among the most popular are: (A) modified external threads for interference and locking action; (B) two-piece unit with key ring for locking action; (C) integral keys give locking action; (D) expandable collar with external serrations.

two general types. The first uses modified external threads that form an interference with the parent material, and provide locking action. The second type has many variations, but is characterized by standard external and internal threads, with various types of pins or keys to lock the bushing to the parent material. Some of the most widely used variations are:

A two-piece insert with a locking ring and two keys fits into mating grooves in upper external threads. The ring is pressed into place after the insert is screwed into tapped hole; it cuts through enough threads of parent material to provide a positive lock. A counterbore in the tapped hole is required for the ring, but assembly and replacement can be made with standard tools.

Another solid bushing insert has two integral keys which act as a broaching tool when insert is installed flush with the parent material. Locking pins are pressed into the base of the tapped hole through the grooves in the external thread.

Still another, a solid bushing, has standard internal and external threads and an expandable upper collar with serrations in the outer surface to lock the insert in the parent material.

Factors that affect selection

These factors must be considered in selecting the best type:

- Shear strength of parent material
- Operating temperature
- Load requirement
- Vibratory loads
- Assembly tooling—serviceability and ease of installation
- Relative cost

Shear strength of parent material below 40,000 psi generally calls for threaded inserts. This includes most of the aluminum alloys, all magnesium alloys and plastic materials. But other factors must be considered.

High operating temperature effects the shear strength by reducing strength of the parent material; an insert with a larger shear area may be required.

Bolt loading frequently makes it necessary to use threaded inserts. For example, if the full pull-out strength of a 125,000-psi bolt is required, it is probable that the parent material will need a threaded insert to increase the shear area and thus reduce the effective shear stress.

Vibratory loads may reduce bolt preload, and require a threaded insert to increase the effective shear area. Or vibration may cause creep, galling, and excessive wear, and inserts with both external and internal thread-locking features will be needed.

The pullout capacity of an insert is a function of projected shear area, and should equal the tensile strength of the bolt. This means pull-out strength should be greater than torque-applied tensile strength of the bolt.

In wire thread inserts the projected shear area per coil

RELATIVE EVALUATION—5 TYPES OF THREAD INSERTS

(A—self-tapping insert; B—wire thread insert; C—solid bushing for pre-tapped holes; D—solid bushings for pre-tapped holes and external interference threads; E—self-tapping insert)

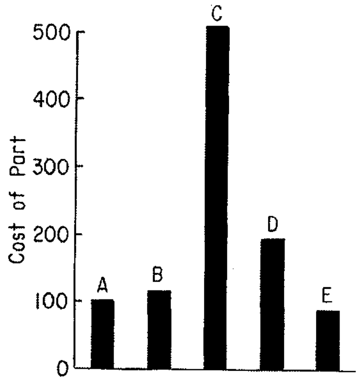

COST OF PART is price quoted for lots of 1000.

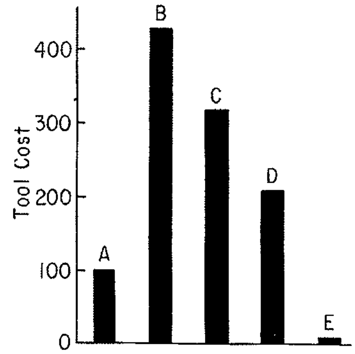

TOOL COST for each type is based on manufacturer's prices for tooling a standard tapping head.

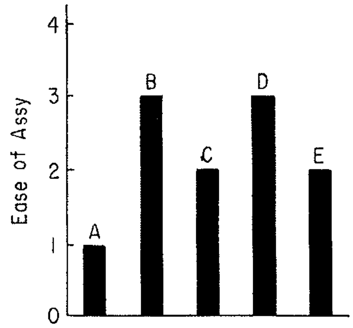

EASE OF ASSEMBLY is a qualitative evaluation.

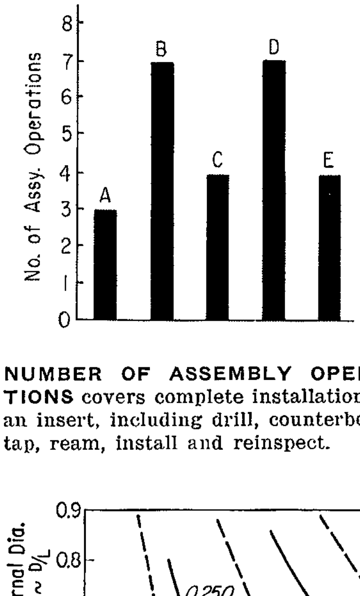

NUMBER OF ASSEMBLY OPERATIONS covers complete installation of an insert, including drill, counterbore, tap, ream, install and reinspect.

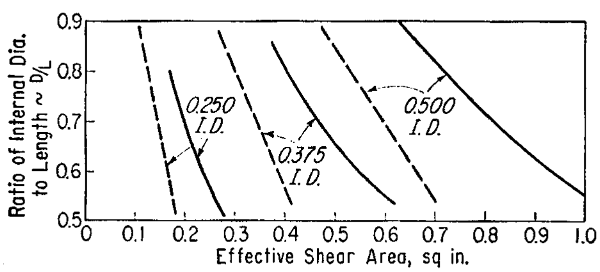

A USEFUL RELATION is effective shear area to D/L ratio. It determines required insert length or pull-out strength. Solid curves are for self-tapping inserts; dotted curves for wire thread inserts.

is relatively small; only way to increase the total projected shear area is to increase the number of coils. On the other hand, in solid and self-tapping inserts the projected shear area can be increased by a larger OD as well as by more threads, while maintaining the same bolt diameter.

One way to determine adequacy of pull-out capacity is to plot the ratio of the internal diameter vs insert length as a function of the effective shear area developed in the parent material. The accompanying curves for three sizes of self-tapping and wire thread inserts were derived from tests in which the insert was pulled out of the parent material. Similar curves could be developed to determine the length needed for any other type of insert.

For example, assume that a $\frac{1}{4}$-28 bolt with an ultimate strength of 5000 lb is to be used in a material with a shear strength of 20,000 psi. The required shear area is 5000 lb/20,000 psi = 0.25 sq in. From the accompanying curves, the D/L ratio is 0.57; insert length, $L = 0.25/0.57 = 0.438$ in.

Similar calculations, using the same curves, can determine whether length of the insert is sufficient to give a required amount of creep resistance: The creep strength of the parent material is substituted for shear strength in the above calculation.

Also, if the insert length is limited, these calculations will give the available pull-out strength, which will vary with shear area of the insert. This analysis can be used to determine either the required length or pull-out strength, and from this, the thickness of the parent material for minimum weight and maximum economy.

Solid threaded bushings often permit using a shorter bolt than for the wire thread insert with limited shear area. With a large number of fasteners in an assembly, weight saving in reduction of parent material is much greater than the small extra weight added by the solid insert.

Other important factors in selecting inserts are assembly tooling, serviceability, relative cost, and ease of installation. These factors have been evaluated in the bar charts prepared by W. Moskowitz of GE's Missile and Space Vehicle Dept, Philadelphia. Data are for five types using 10-32 internal threads. Part of this information is based on estimates of the operating personnel concerning the number of assembly operations, tolerances required during installation, and relative ease of installation.

Flanged Inserts Stabilize Multi-Stroke Reloading Press

E. E. Lawrence, Inventor
Robert O. Parmley, Draftsman

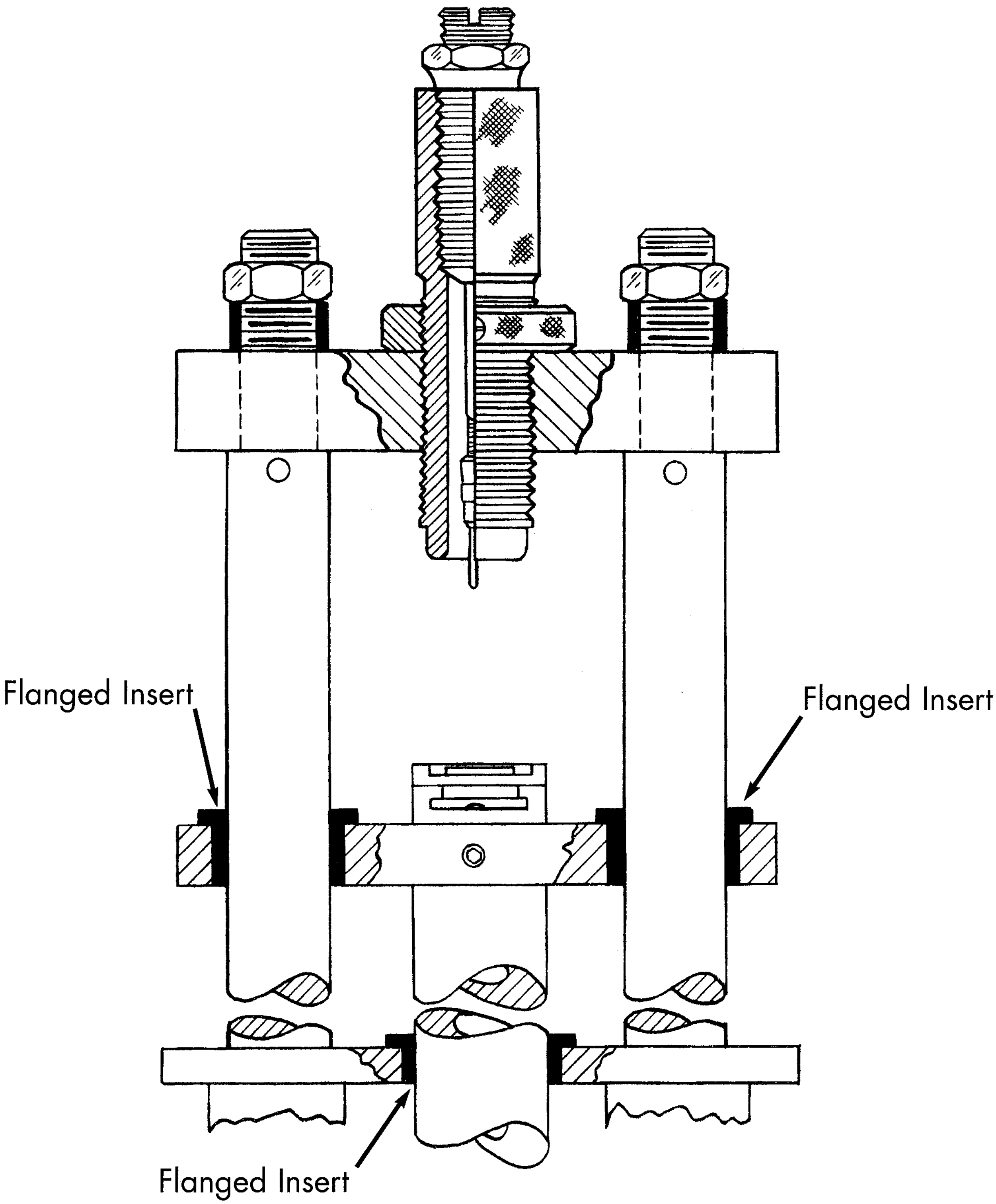

SECTION 15

BALLS

12 Ways to put Balls to Work

Bearings, detents, valves, axial movements, clamps and other devices can all have a ball as their key element.

Louis Dodge

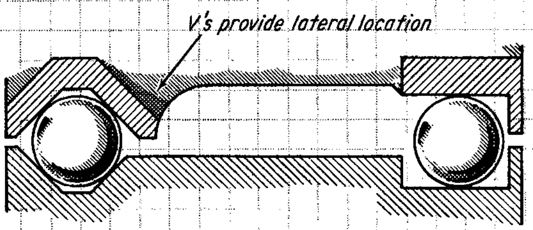

1 BALL-BEARING MACHINE WAY HAS LOW FRICTION.

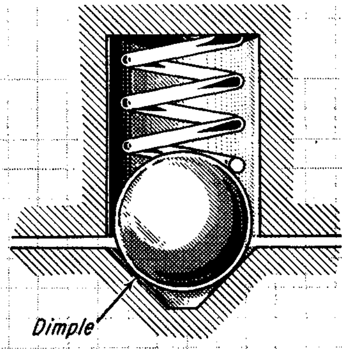

2 DETENT POWER DEPENDS ON SPRING STRENGTH AND DIMPLE DEPTH.

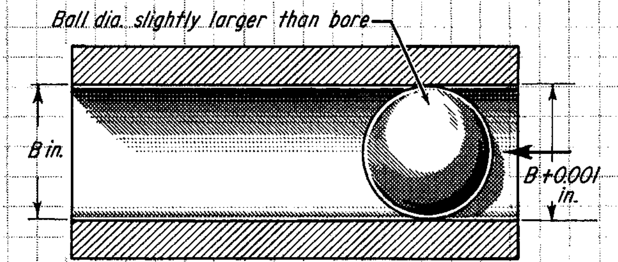

5 BALL ACCURATELY FINISHES BUSHING BORE.

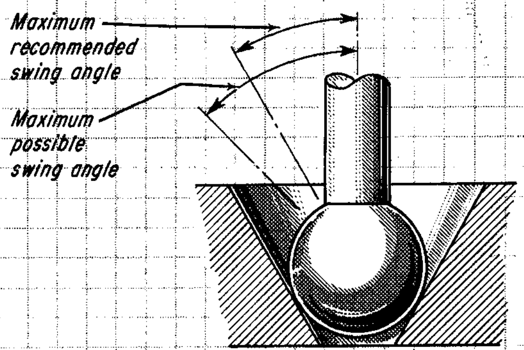

6 BALL SHAFT-END LETS SHAFT SWING.

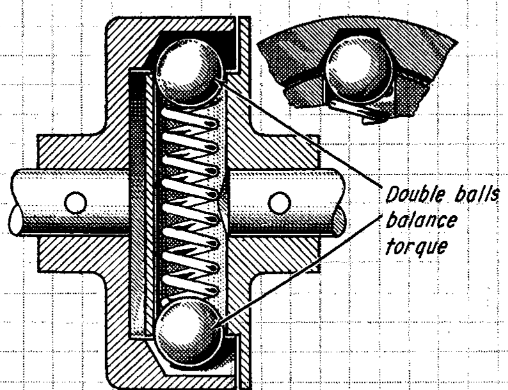

9 CLUTCH HAS LIMITED TORQUE TRANSMISSION.

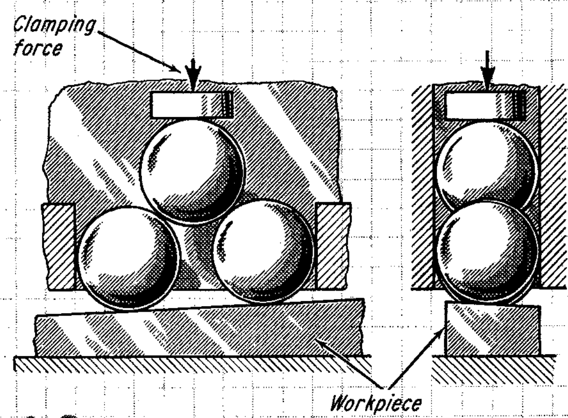

10 CLAMP UNEVEN WORKPIECES.

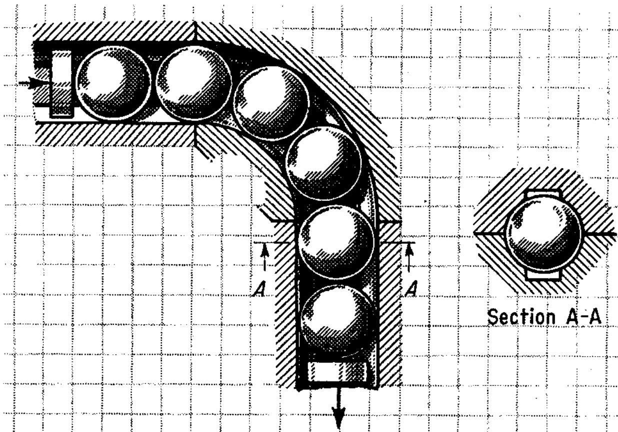

3 TRANSMIT AXIAL FORCE AROUND CURVES.

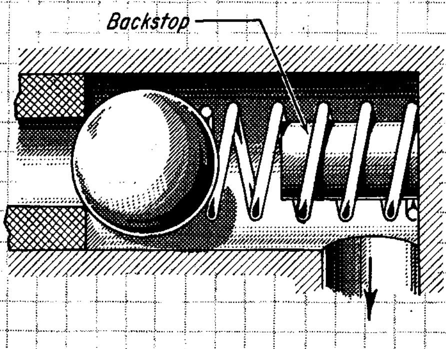

4 CHECK VALVE BACKSTOP IS ADVISABLE.

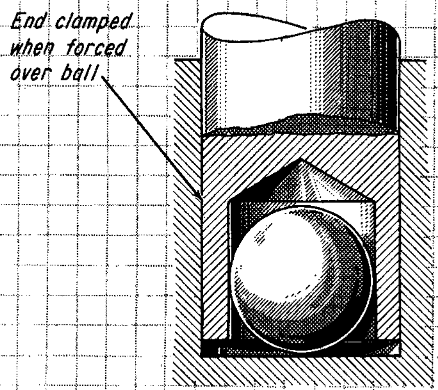

7 BALL-LOCK FASTENS STUD IN BLIND HOLE .

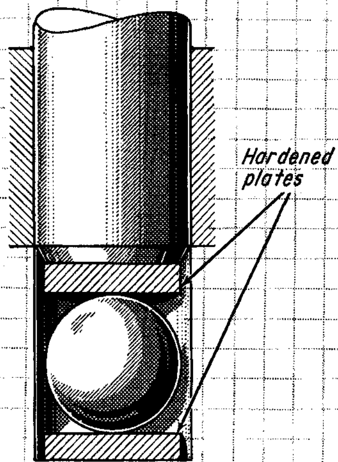

8 THRUST-BEARING TAKES LIGHT LOADS.

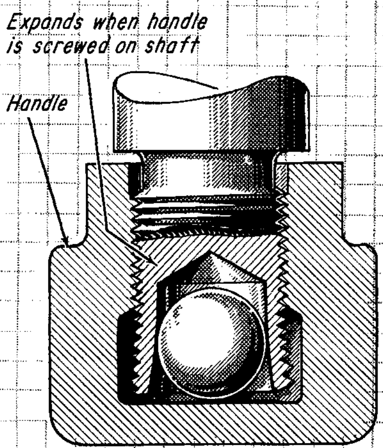

11 BALL-LOCK SECURES HANDLE TO SHAFT.

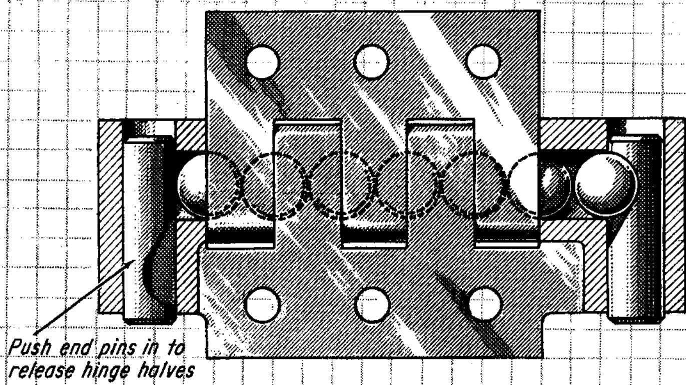

12 HINGE PIN IS SEPARABLE.

How Soft Balls Can Simplify Design

Balls of flexible material can perform as latches, stops for index discs, inexpensive valves and buffers for compression springs.

Robert O. Parmley

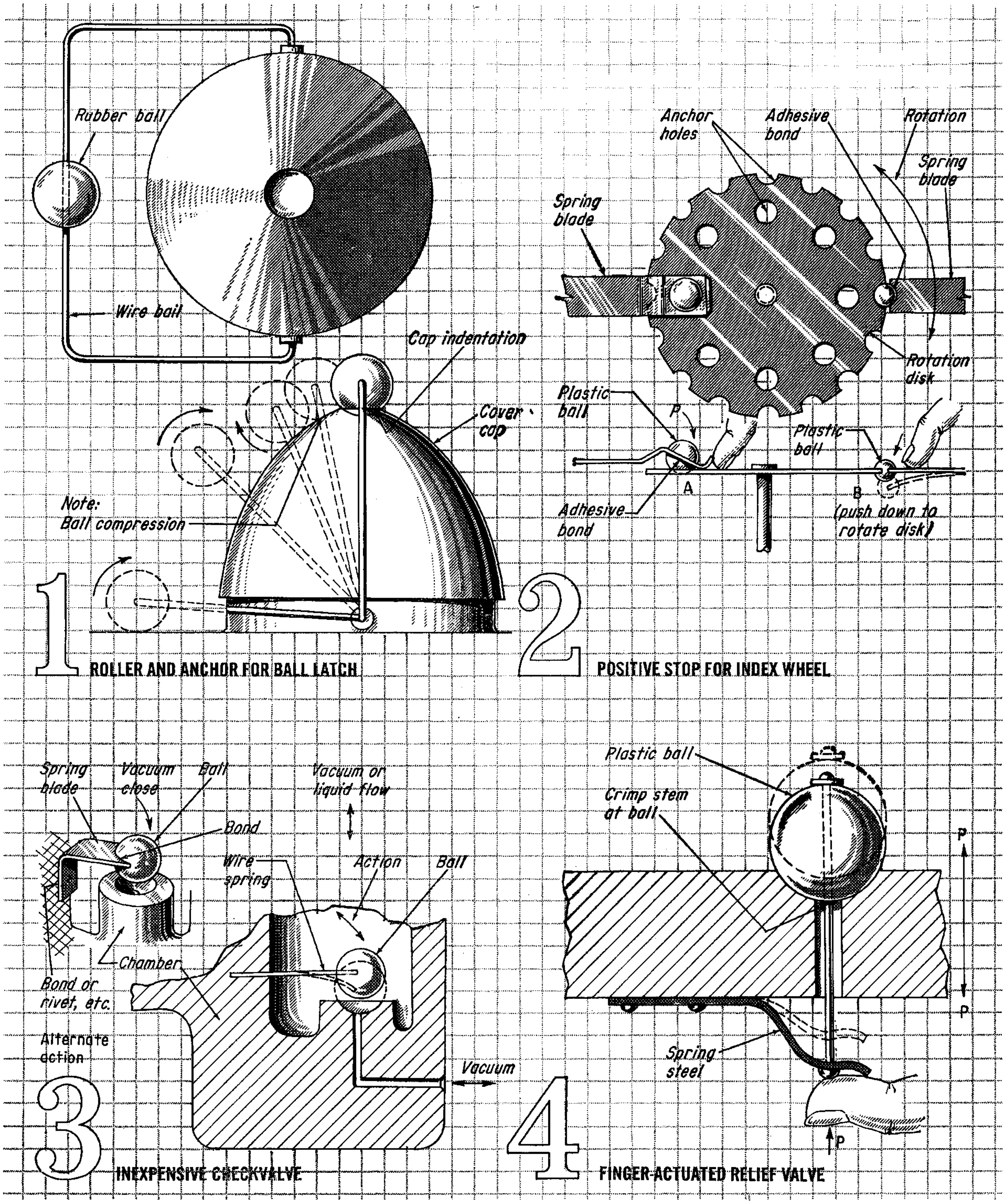

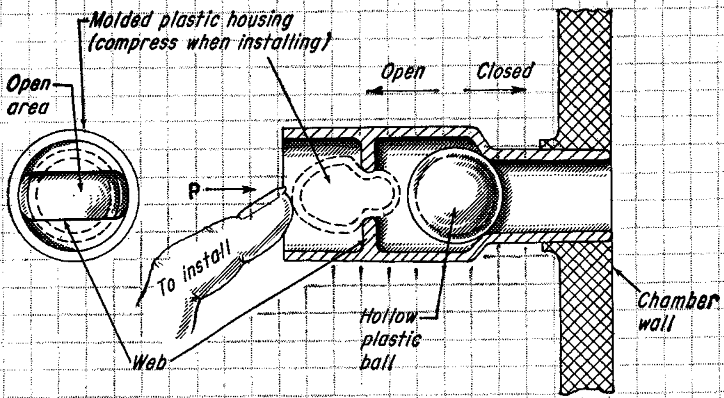

5 CHECKVALVE BALL IS PERMANENTLY INSTALLED

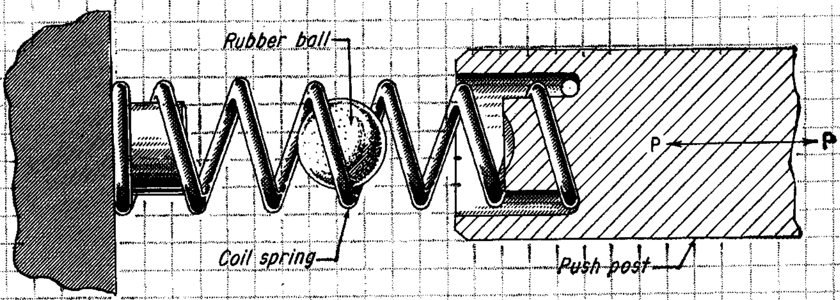

6 SPRING BUFFER FOR COMPRESSION SPRING

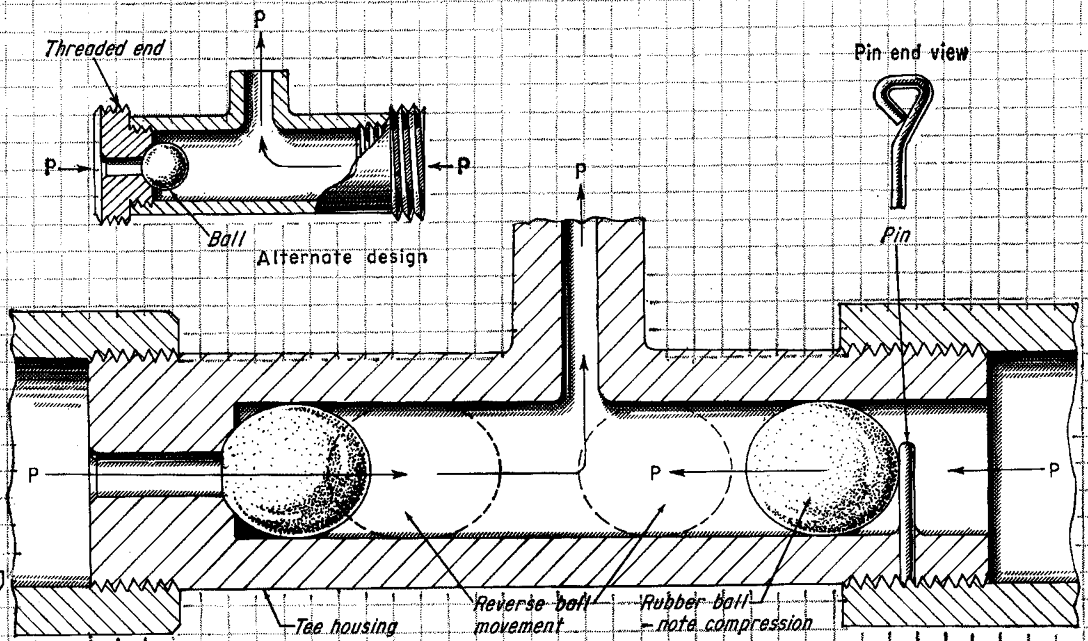

7 TWO-WAY VALVE FOR ALTERNATING PRESSURE

Rubber Balls Find Many Jobs

Plastic and rubber balls, whether solid or hollow, can find a variety of important applications in many designs.

Robert O. Parmley

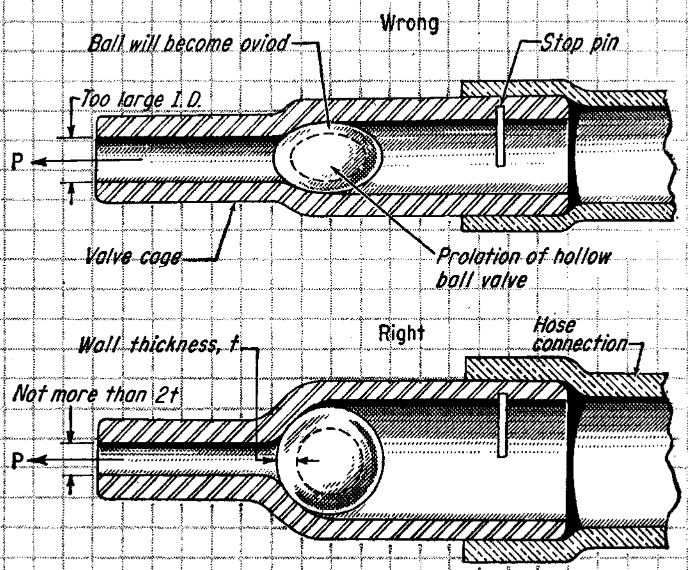

1 **CENTRIFUGALLY MOLDED SPHERES** can be used in efficient, low-cost sealing valves, but avoid ball distortion by making sure that the correct dimensions are applied.

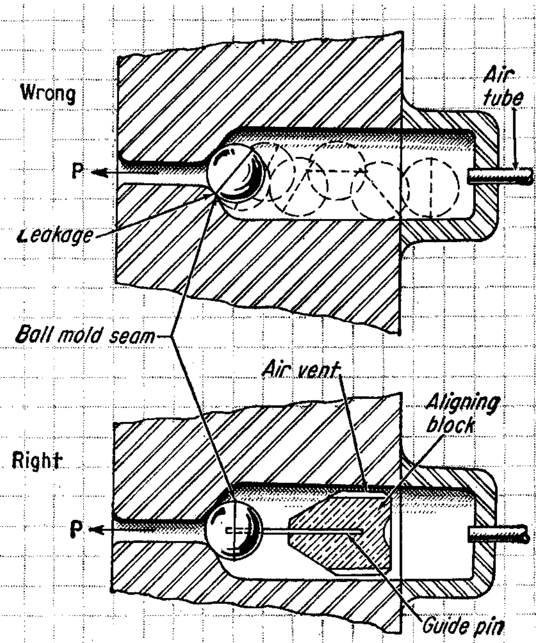

2 **MOLD SEAMS** on solid balls should be held normal to flow line to avoid incomplete seating and consequent leakage.

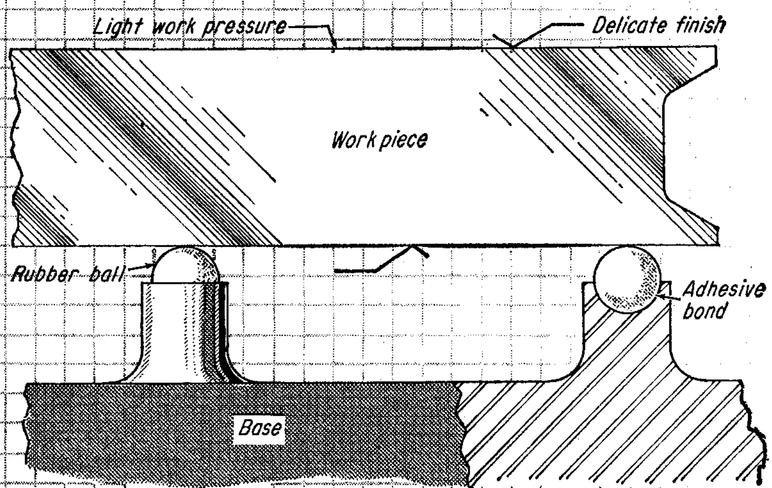

5 **ALIGN DELICATE WORKPIECES** on rubber balls that are bonded into base pillars. Adequate protection of fine finishes is provided, while at the same time friction provides firm grip.

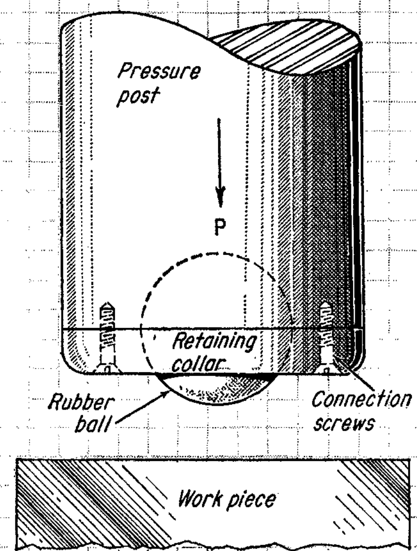

6 **VERTICAL PRESSURE-POST** holds solid ball in easily removed retaining collar. Ball is solid and protects workpiece finishes during assembly operations.

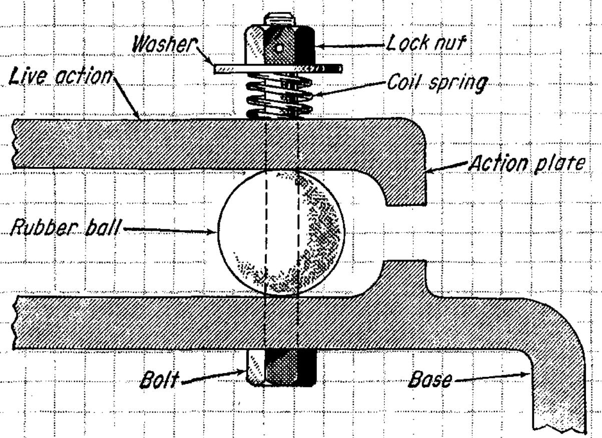

3 **CUSHION PAD AND SHOCK ABSORBER** is easily made for mounting-plates that must either carry dynamic loads or absorb shock forces.

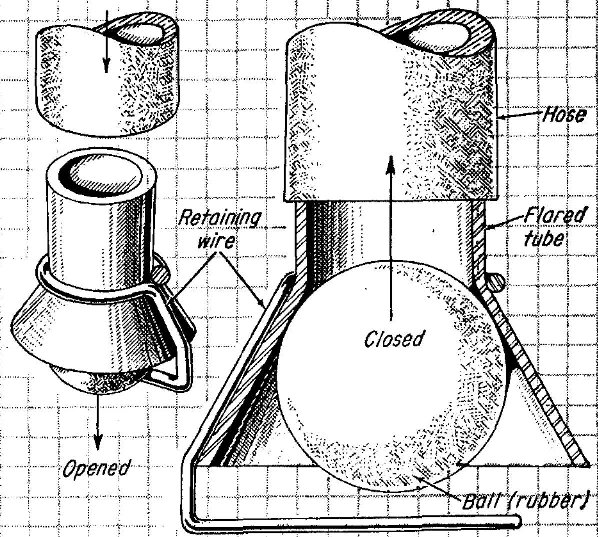

4 **DISCHARGE VALVE** as shown here is an effective way of controlling liquid displacement at the end of hoses where suction would be unwanted or harmful.

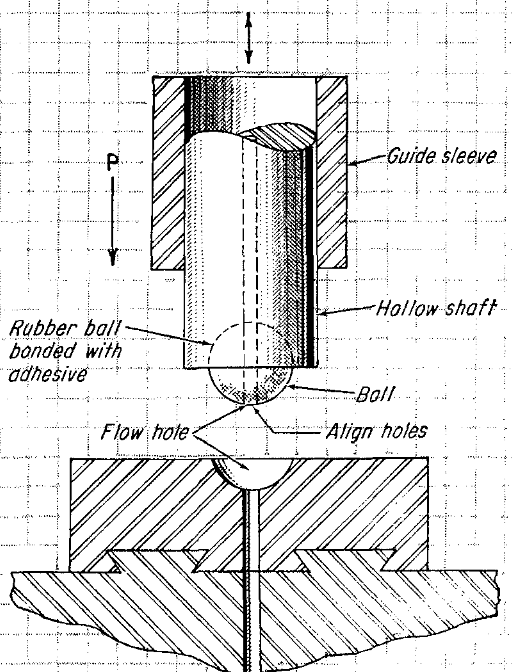

7 **HOLLOW SHAFT-SEAL** embodies adhesive-bonded rubber ball with flow hole. Quick connection of leakproof joint for lubricant or other liquid is gained.

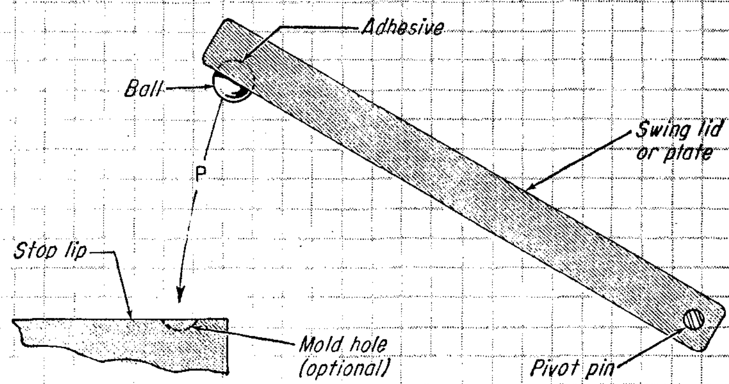

8 **BUMPER STOP** is another example of the simple but effective way a rubber ball can be employed to protect surfaces or parts.

Multiple Use of Balls in Milk Transfer System

Source: Bender Machine Works, Inc. Illustrated by: Robert O. Parmley

Conveying Diagram

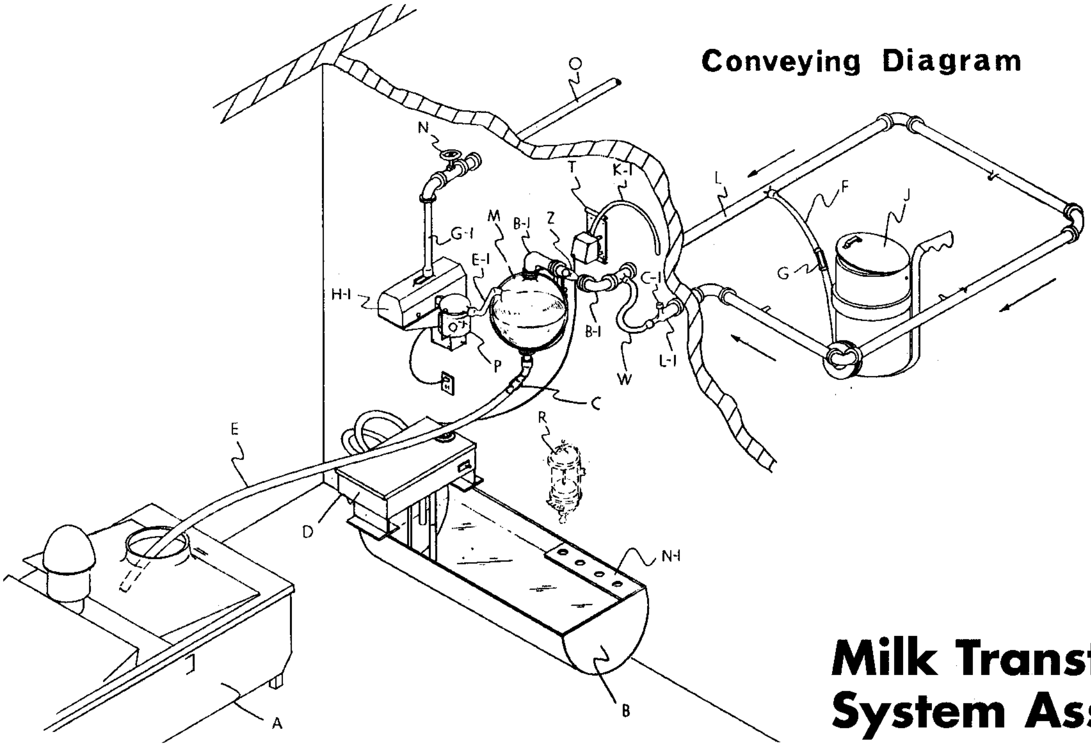

Milk Transfer System Assembly

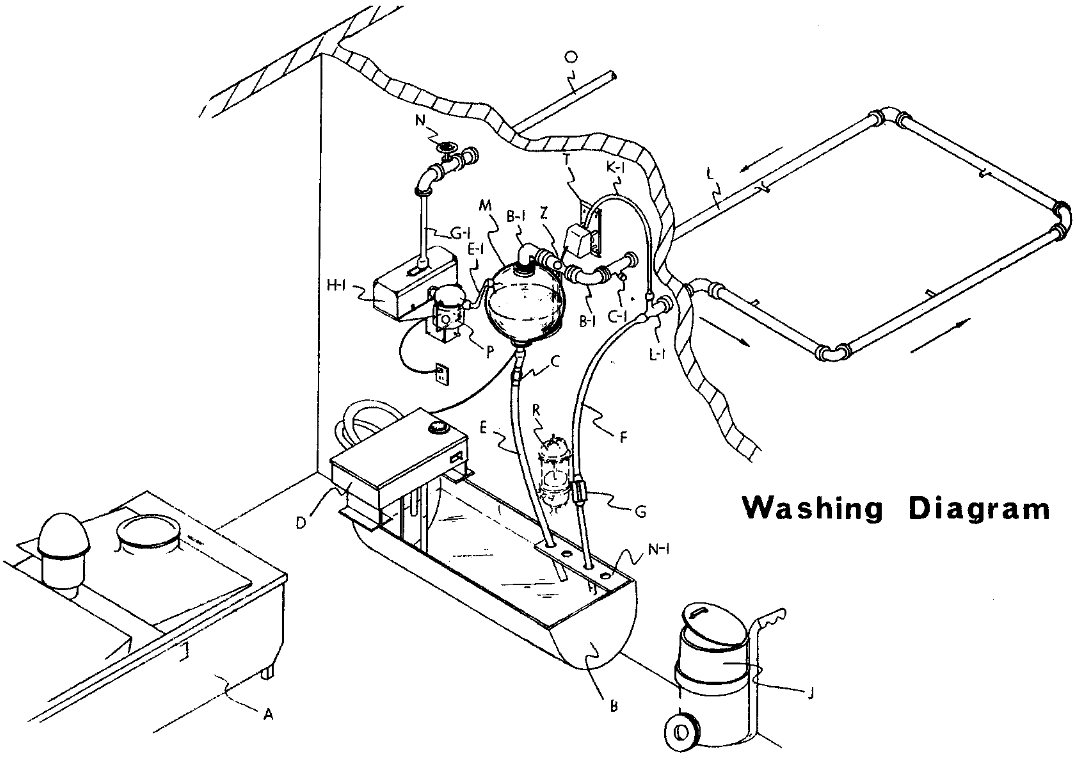

Washing Diagram

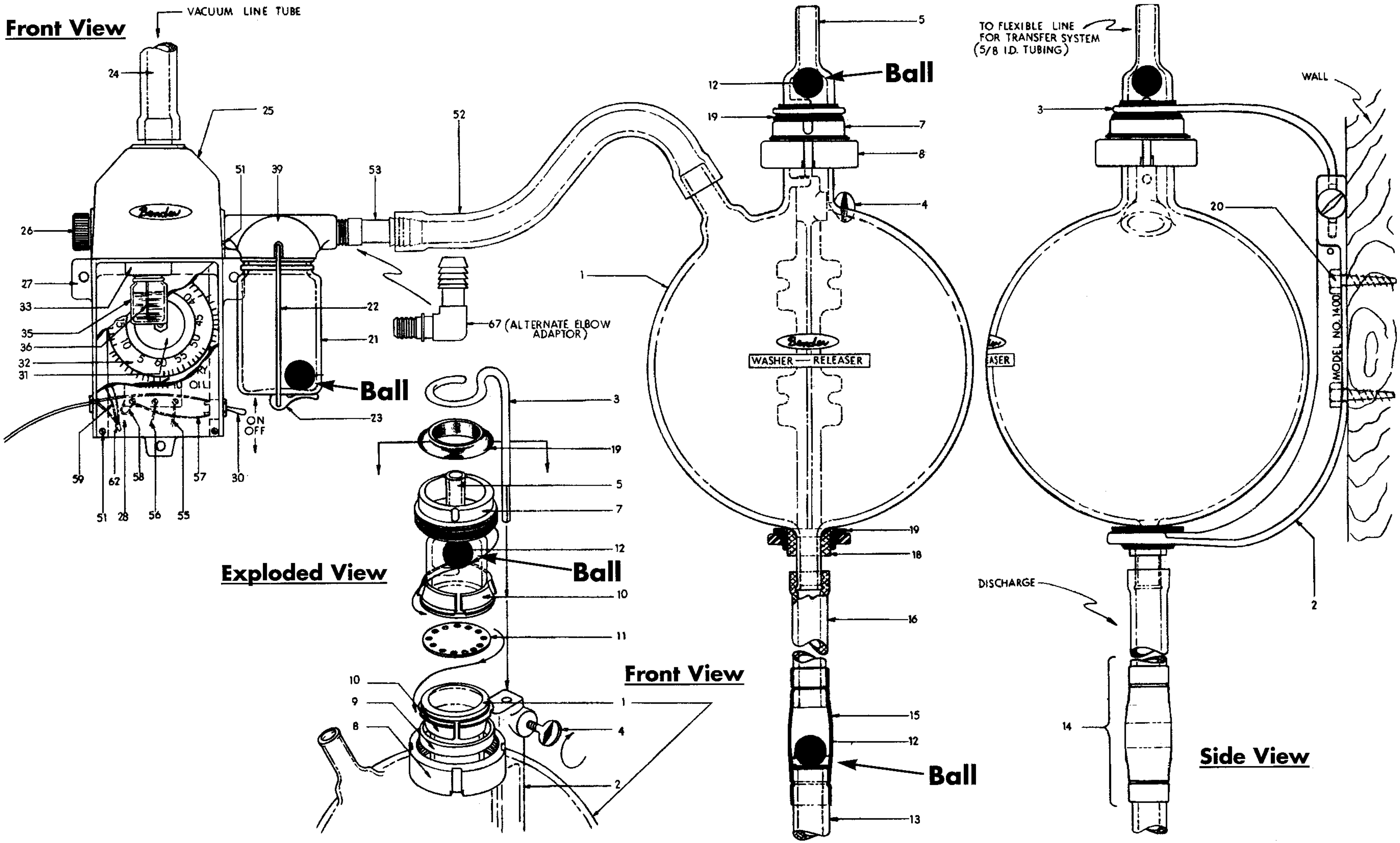

Four plastic balls, located at key positions within the system, act a positive check valves as they respond to the vacuum pulsations.

Use of Balls in Reloading Press

Inventor: E. E. Lawrence Draftsman: R. O. Parmley

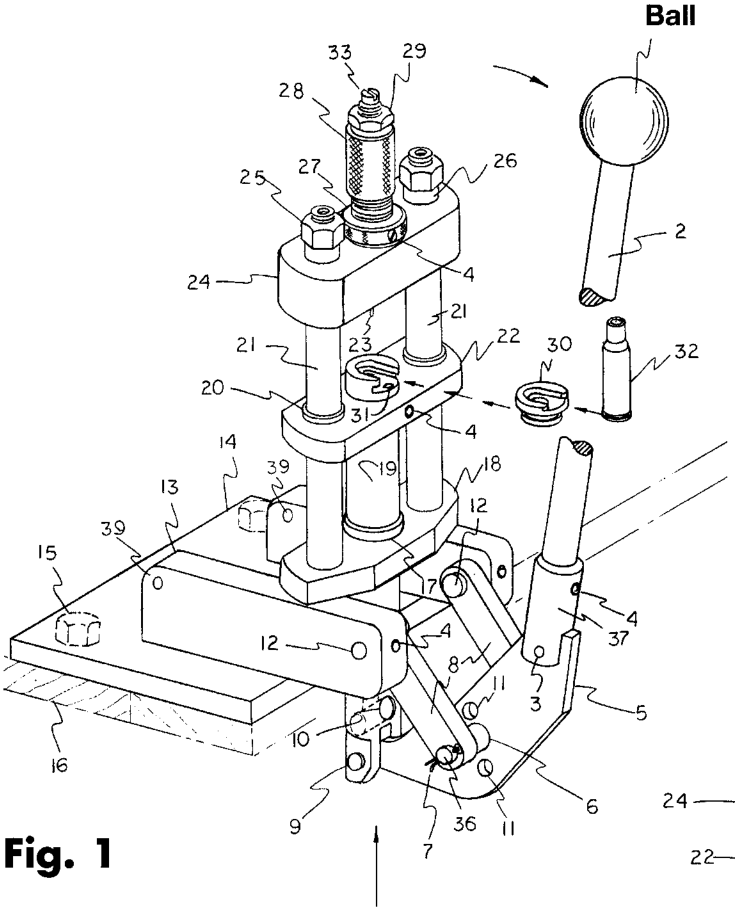

Fig. 1

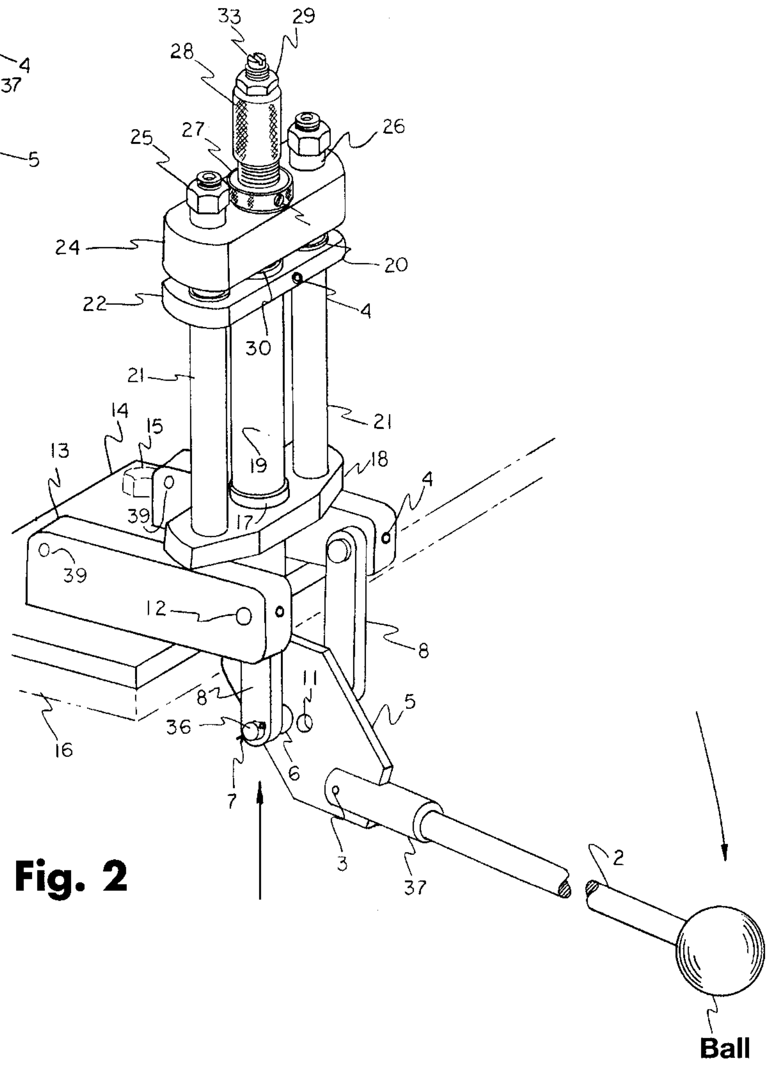

Fig. 2

Fig. 3

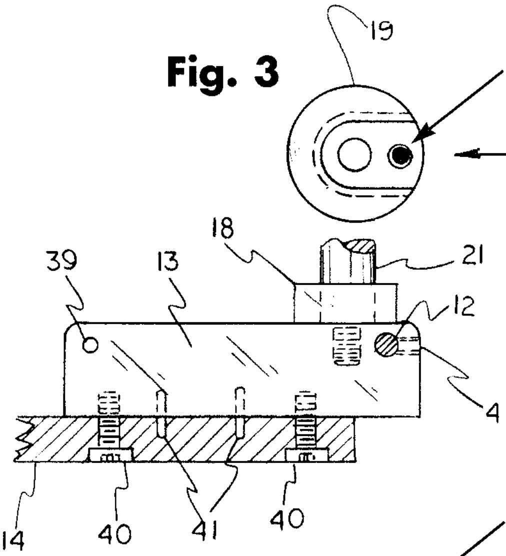

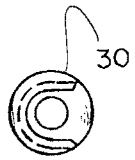

Fig. 4

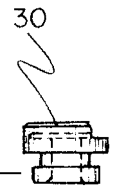

Fig. 5

Fig. 6

Fig. 7

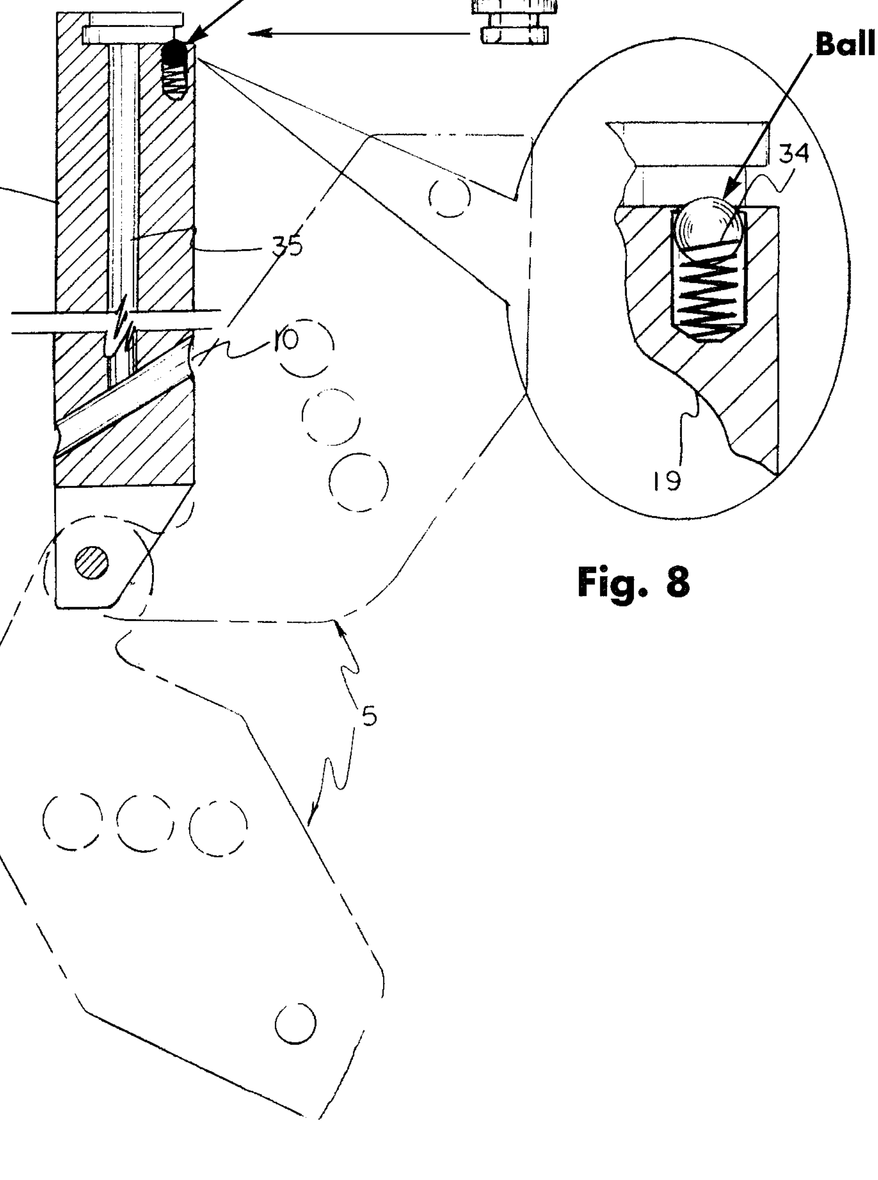

Fig. 8

Nine Types of Ball Slides for Linear Motion

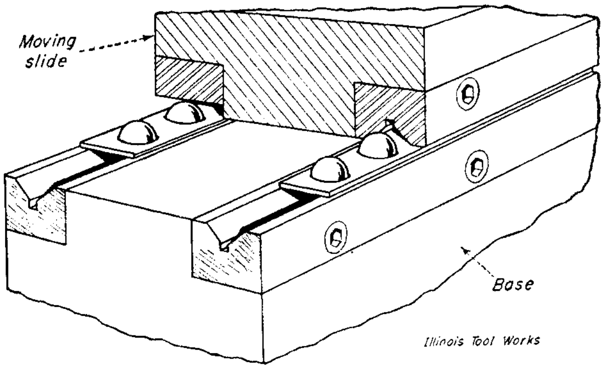

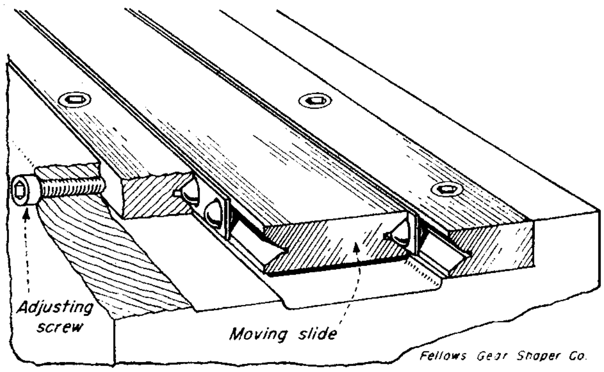

1 V grooves and flat surface make simple horizontal ball slide for reciprocating motion where no side forces are present and a heavy slide is required to keep balls in continuous contact. Ball cage insures proper spacing of balls; contacting surfaces are hardened and lapped.

2 Double V grooves are necessary where slide is in vertical position or when transverse loads are present. Screw adjustment or spring force is required to minimize looseness in the slide. Metal-to-metal contact between the balls and grooves insure accurate motion.

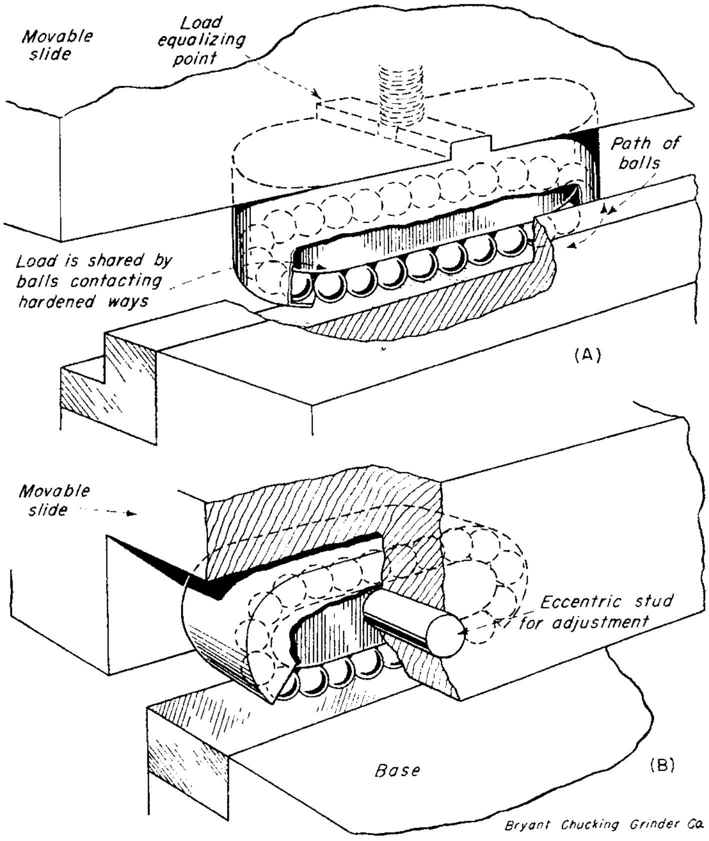

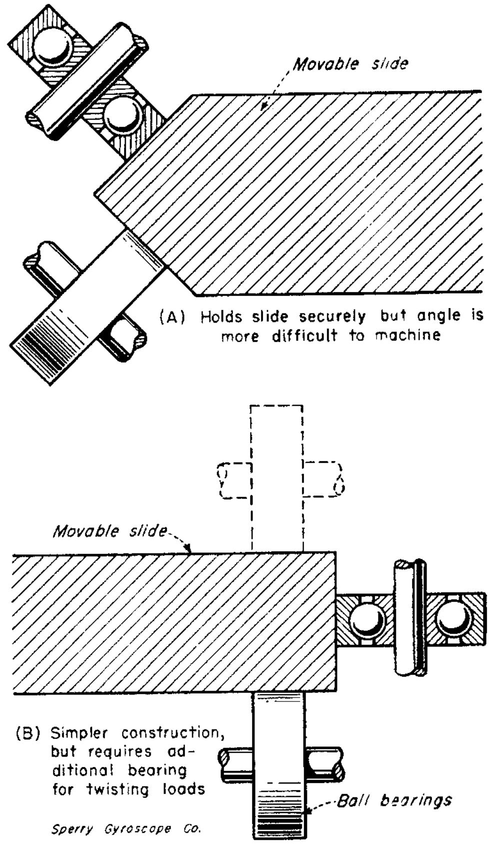

3 Ball cartridge has advantage of unlimited travel since balls are free to recirculate. Cartridges are best suited for vertical loads. (A) Where lateral restraint is also required, this type is used with a side preload. (B) For flat surfaces cartridge is easily adjusted.

4 Commercial ball bearings can be used to make a reciprocating slide. Adjustments are necessary to prevent looseness of the slide. (A) Slide with beveled ends, (B) Rectangular-shaped slide.

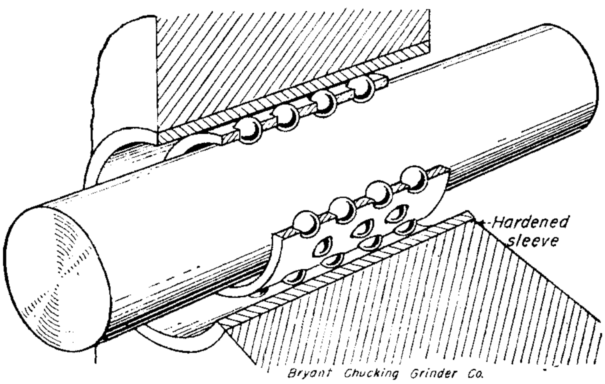

5 Sleeve bearing consisting of a hardened sleeve, balls and retainer, can be used for reciprocating as well as oscillating motion. Travel is limited similar to that of Fig. 6. This type can withstand transverse loads in any direction.

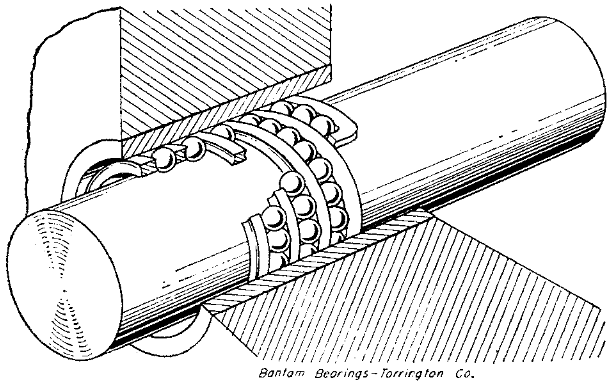

6 Ball reciprocating bearing is designed for rotating, reciprocating or oscillating motion. Formed-wire retainer holds balls in a helical path. Stroke is about equal to twice the difference between outer sleeve and retainer length.

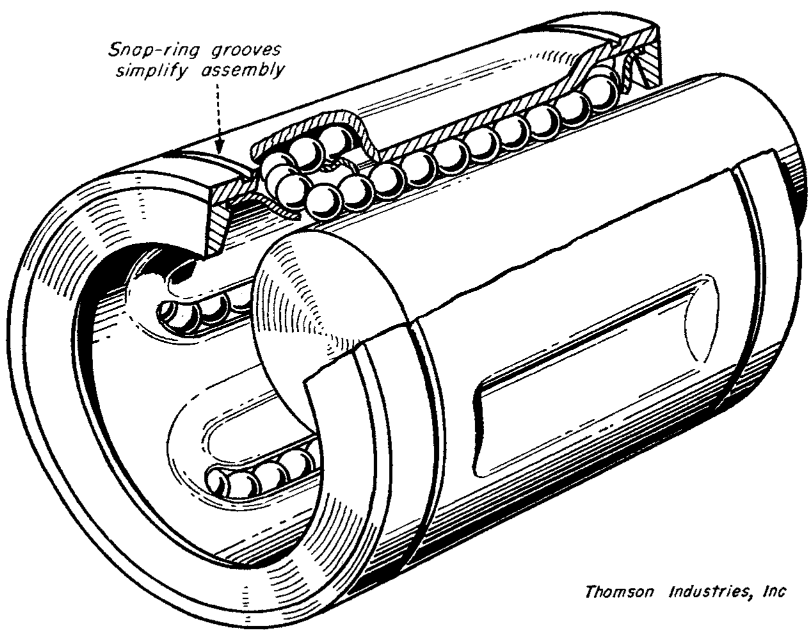

7 Ball bushing with several recirculating systems of balls permit unlimited linear travel. Very compact, this bushing simply requires a bored hole for installation. For maximum load capacity a hardened shaft should be used.

8 Cylindrical shafts can be held by commercial ball bearings which are assembled to make a guide. These bearings must be held tightly against shaft to prevent looseness.

9 Curvilinear motion in a plane is possible with this device when the radius of curvature is large. However, uniform spacing between grooves is important. Circular - sectioned grooves decrease contact stresses.

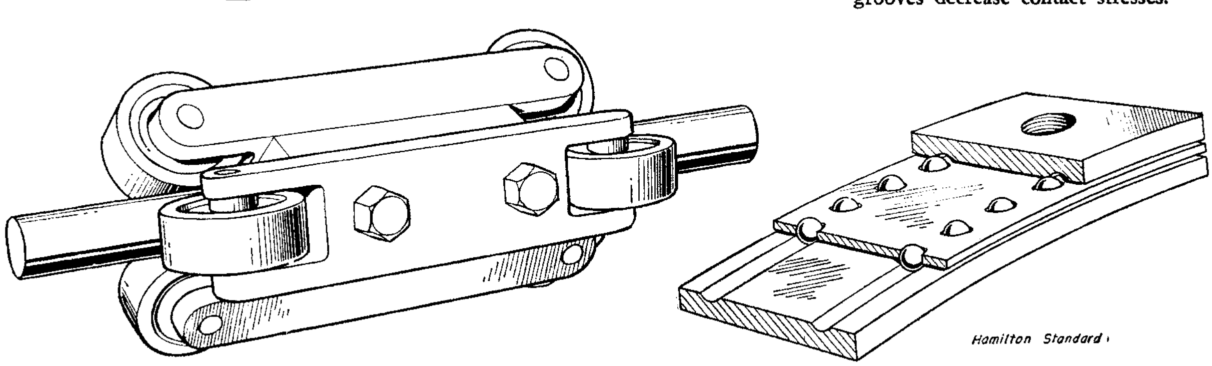

Unusual Applications of Miniature Bearings

R. H. Carter

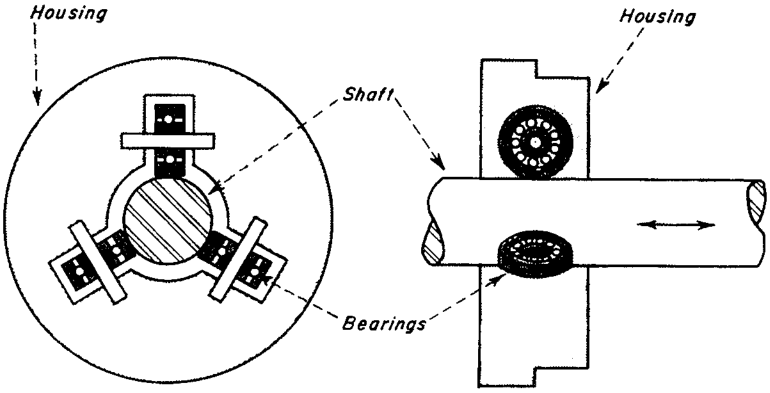

Fig. 1—BALL-BEARING SLIDES. Six miniature bearings accurately support a potentiometer shaft to give low-friction straight line motion. In each end housing, three bearings are located 120 deg radially apart to assure alignment and freedom from binding of the potentiometer shaft.

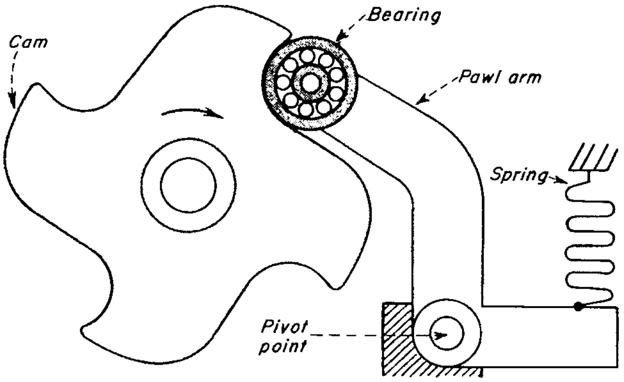

Fig. 2—CAM-FOLLOWER ROLLER. Index pawl on a frequency selector switch uses bearing for a roller. Bearing is spring loaded against cam and extends life of unit by reducing cam wear. This also retains original accuracy in stroke of swing of the pawl arm.

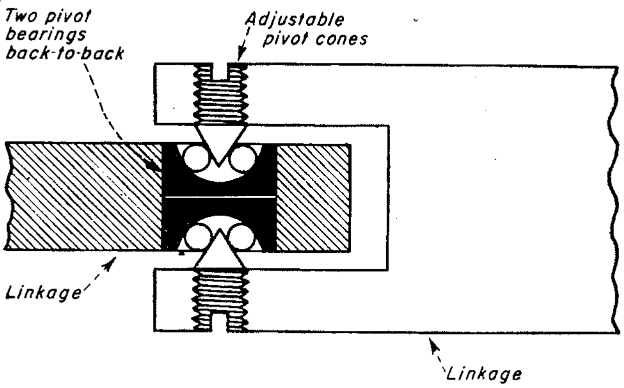

Fig. 3—SEAT FOR PIVOTS. Pivot-type bearings reduce friction in linkages especially when manually operated such as in pantographing mechanisms. Minimum backlash and maximum accuracy are obtained by adjusting the threaded pivot cones. Mechanism is used to support diamond stylus that scribes sight lines on the lenses of gunnery telescopes.

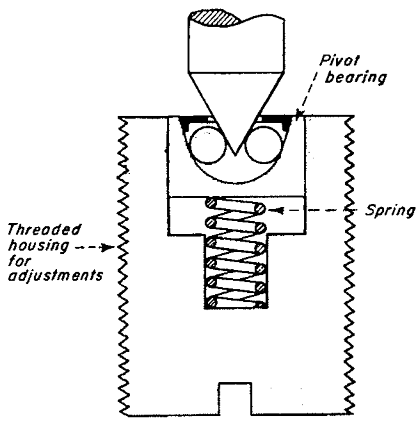

Fig. 4—SHOCK-ABSORBING PIVOT POINT. Bearing with spherical seat resting on spring acts as a pivot point and also absorbs mild shock loads. Used on a recording potentiometer that is temperature controlled. Spring applies uniform load over short distances and gives uniform sensitivity to the heat-sensing element. Close fit of bearing in housing is required.

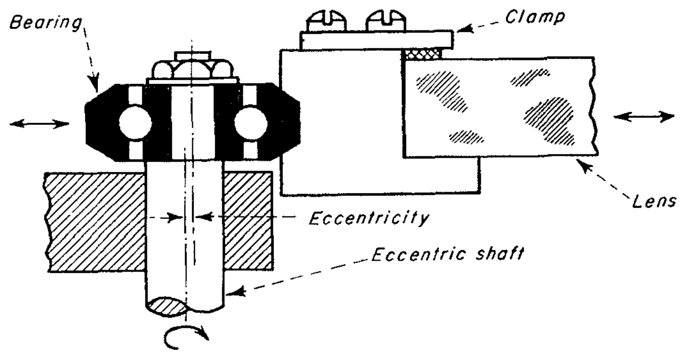

Fig. 5—PRECISE RADIAL ADJUSTMENTS obtained by rotating the eccentric shaft thus shifting location of bearing. Bearing has special-contoured outer race with standard inner race. Application is to adjust a lens with grids for an aerial survey camera.

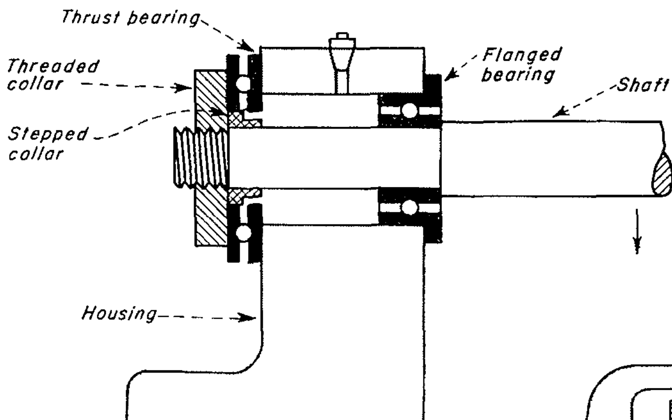

Fig. 6—SUPPORT FOR CANTILEVERED SHAFT obtained with combination of thrust and flanged bearings. Stepped collar provides seat for thrust bearing on the shaft but does not interfere with stationary race of thrust bearing when shaft is rotating.

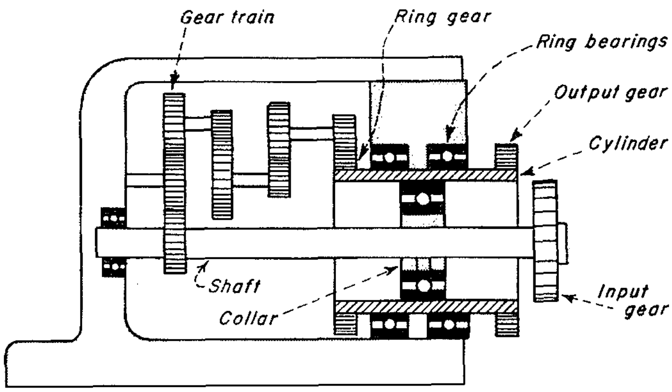

Fig. 7—GEAR-REDUCTION UNIT. Space requirements reduced by having both input and output shafts at same end of unit. Output shaft is a cylinder with ring gears at each end. Cylinder rides in miniature ring bearings that have relative large inside diameters in comparison to the outside diameter.

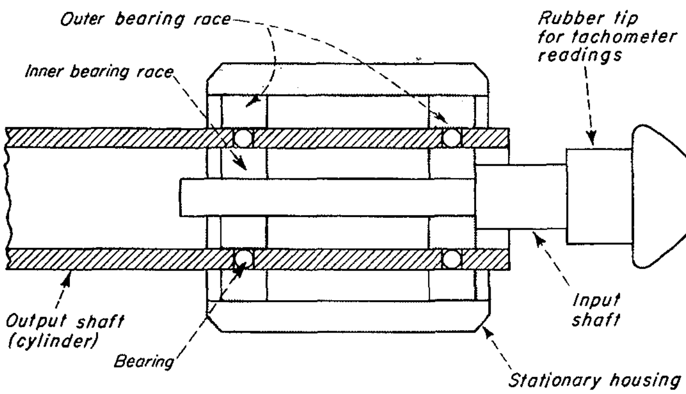

Fig. 8—BEARINGS USED AS GEARS. Manually operated tachometer must take readings up to 6000 rpm. A 10-to-1 speed reduction was obtained by having two bearings function both as bearings and as a planetary gear system. Input shaft rotates the inner race of the inner bearings, causing the output shaft to rotate at the peripheral speed of the balls. Bearings are preloaded to prevent slippage between races and balls. Outer housing is held stationary. Pitch diameters and ball sizes must be carefully calculated to get correct speed reduction.

Rolling Contact Bearing Mounting Units

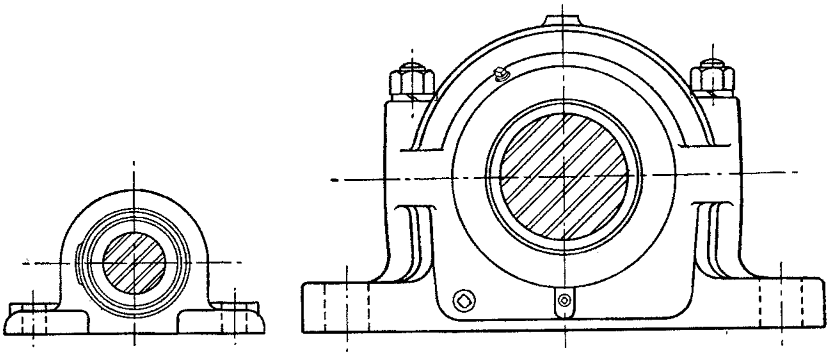

FIG. 1—Pillow blocks are for supporting shafts running parallel to the surface on which they are mounted. Provision for lubrication and sealing are incorporated in the pillow block unit. Assembly and disassembly are easily accomplished. For extremely precise installations, mounting units are inadvisable.

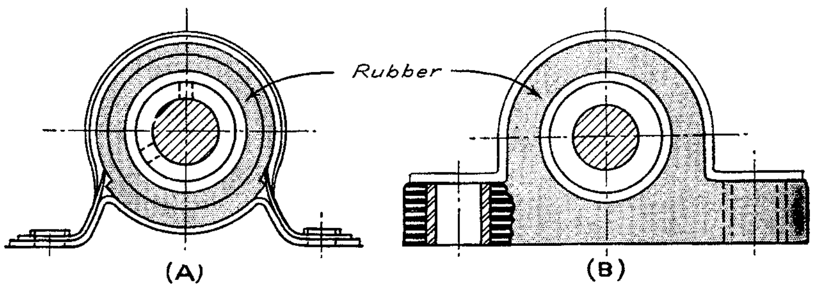

FIG. 2—Pillow blocks can be designed to prevent the transmission of noise to the support. One design (A) consists of a bearing mounted in rubber. The rubber in turn is firmly supported by a steel casing. Another design (B) is made of synthetic rubber. Where extra rigidity is required the synthetic rubber mount can be reinforced by a steel strap bolted around it.

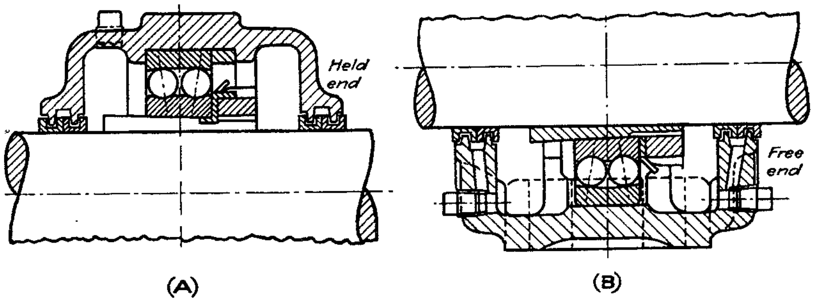

FIG. 3—Changes in the temperature are accompanied by changes in the length of a shaft. To compensate for this change in length, the pillow block (B) supporting one end of the shaft is designed to allow the bearing to shift its position. The pillow block (A) at the other end should not allow for longitudinal motion.

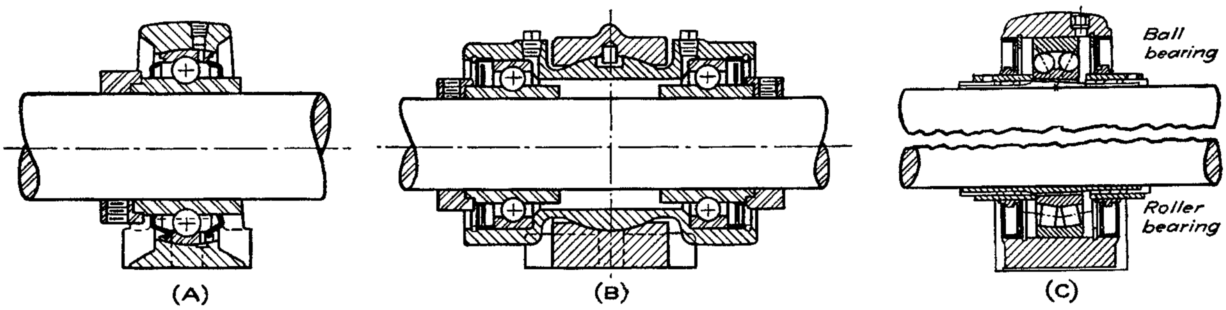

Fig. 4—Compensation for misalignment can be incorporated into pillow blocks in various ways. One design (A) uses a spherical outer surface of the outer race. Design (B) uses a two-part housing. The spherical joint compensates for misalignment. Another design (C) uses a spherical inner surface of the outer race.

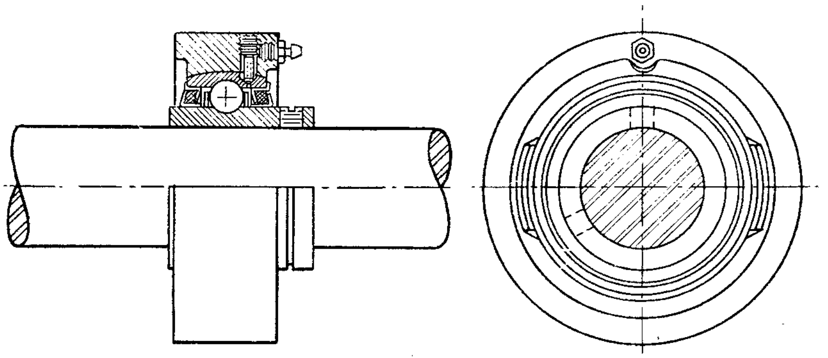

Fig. 5—The cylindrical cartridge is readily adaptable to various types of machinery. It is fitted as a unit into a straight bored housing with a push fit. A shoulder in the housing is desirable but not essential. The advantages of a predesigned and preassembled unit found in pillow blocks also apply here.

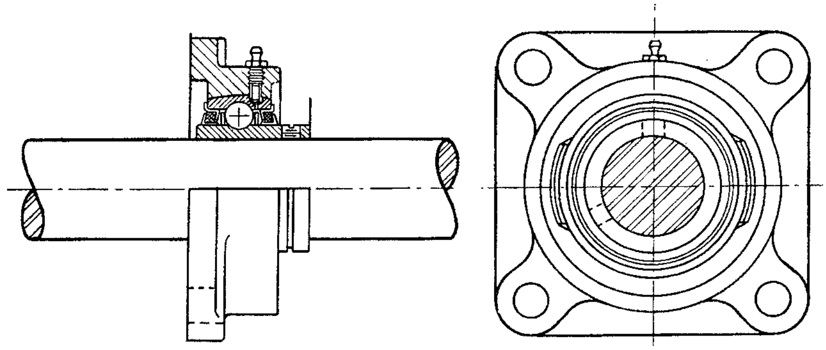

FIG. 6—The flange mounting unit is normally used when the machine frame is perpendicular to the shaft. The flange mounting unit can be assembled without performing the special boring operations required in the case of the cartridge. The unit is simply bolted into the housing when it is being installed.

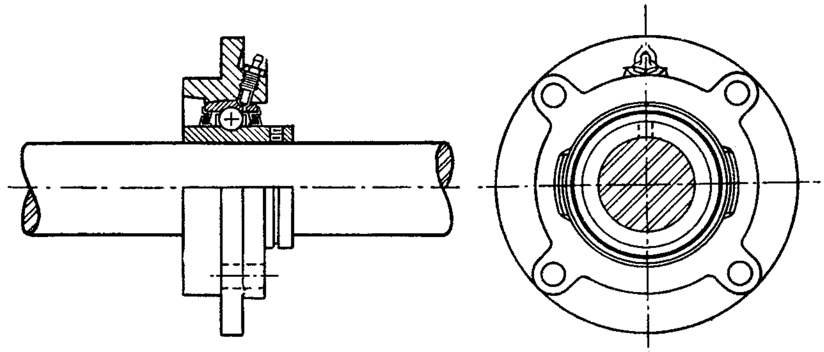

FIG. 7—The flange cartridge unit projects into the housing and is bolted in place through the flange. The projection into the housing absorbs a large part of the bearing loads. A further use of the cylindrical surface is the location of the mounting unit relative to the housing.

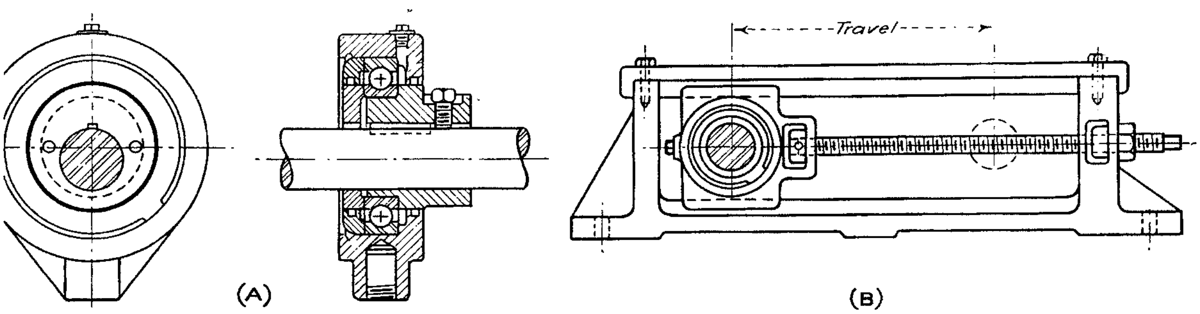

FIG. 8—Among specialized types of mounting units are (A) Eccentrics used particularly for cottonseed oil machinery and mechanical shakers and (B) Take-up units which make possible an adjustment in the position of the shaft for conveyor units. Many other types of special rolling contact bearing mounting units are made.

Eleven Ways to Oil Lubricate Ball Bearings

D. L. Williams

The method by which oil should be applied to a ball bearing depends largely on the surface speed of the balls. Where ball speeds are low, the quantity of oil present is of little importance, provided it is sufficient. Over-lubrication at low speeds is not likely to cause any serious temperature rise. However, as speeds increase, fluid friction due to churning must be avoided. This is done by reducing the amount of oil supplied and by having good drainage from the housing. At very high speeds, with light loads, the oil supply can be limited to a very fine mist.

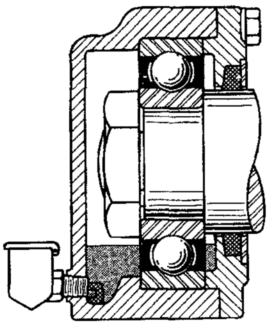

FIG 1

Fig. 1—*Oil Level System.* For moderate speeds, the bearing housing should be filled with oil to the lowest point of the bearing inner race. An oil cup is located to maintain this supply level. Wick acts as a filter when fresh oil is added. This system requires periodic attention.

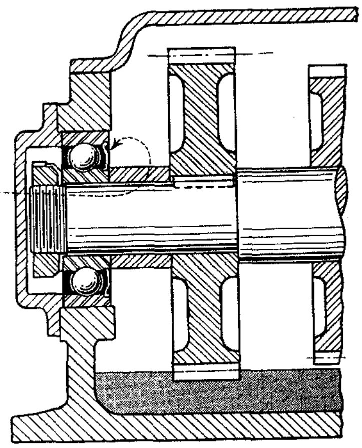

FIG 2

Fig. 2—*Splash Feed* is used where rotating parts require oil for their own lubrication. Splash lubrication is not recommended for high speeds because of possible churning. Bearings should be protected from chips or other foreign material by using a shaft mounted slinger or shielded bearings.

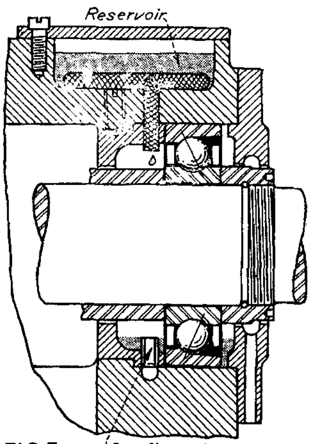

FIG 3

Fig. 3—*Drop Feed.* Oil may be fed in drops using either sight-feed oilers or an overhead reservoir and wick. Drains must be provided to remove excess oil. A short overflow standpipe, serves to maintain a proper oil level. It also retains a small amount of oil even though the reservoir should be empty.

Fig. 4—*Spray Feed.* With higher speeds, definite control of oil fed to bearings is important. This problem is more difficult for vertical bearings because of oil leakage. One method uses a tapered slinger to spray oil into the bearings. Oil flow is altered by the hole diam., the taper and oil viscosity.

FIG 4

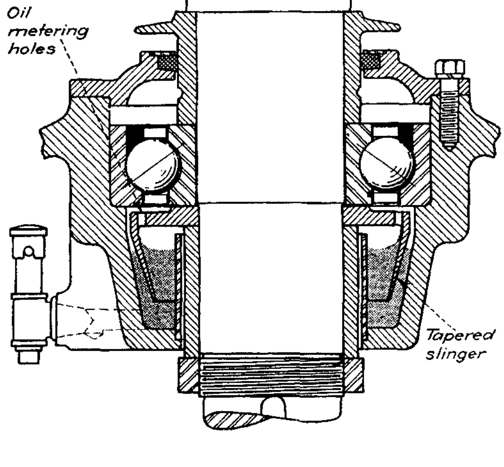

Fig. 5—*Circulating Feed.* Most circulating systems are somewhat complicated and expensive but this is justified by their permanence and reliability. Oil reservoir is attached to the shaft and when rotated, the oil is forced upward where it strikes a scoop, flows through and onto the bearing.

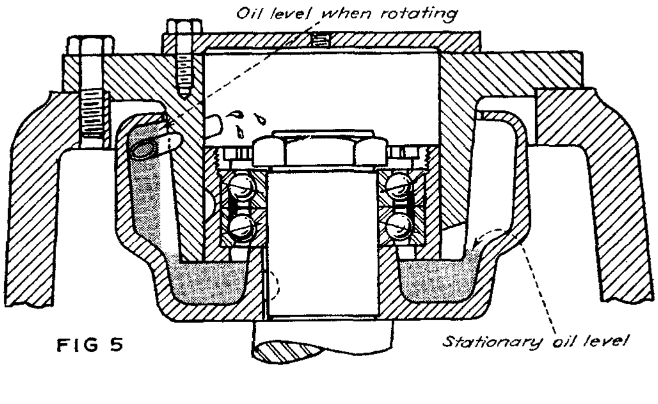

FIG 5

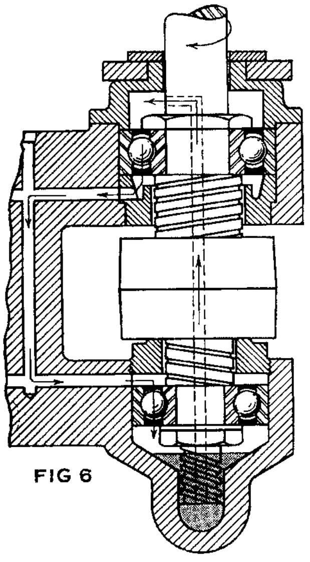

FIG 6

Fig. 6—*Most circulating systems* are used for vertical shaft applications and usually where ball speeds are comparatively high. One system consists of an external screw which pumps the oil upward through the hollow spindle to a point above the top bearings.

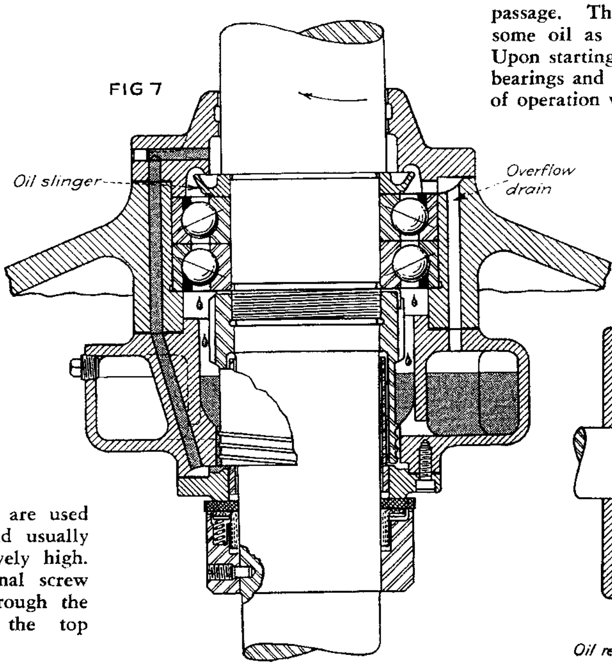

FIG 7

Fig. 7—*Another screw pump application* forces the oil upward through an external passage. The cup-shaped slinger traps some oil as the spindle comes to rest. Upon starting, this oil is thrown into the bearings and avoids a short initial period of operation with dry bearings.

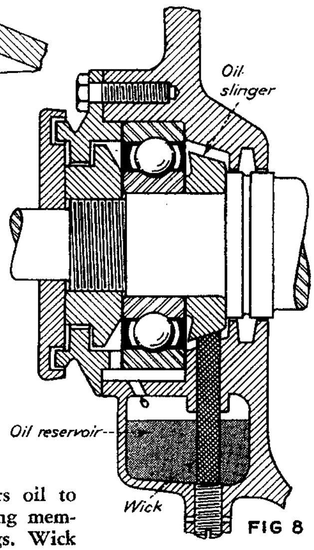

FIG 8

Fig. 8—*Wick Feed* filters and transfers oil to a smoothly finished and tapered rotating member which sprays a mist into bearings. Wick should be in light contact with the slinger or else the wick may become glazed or charred. A light spring is often used for proper wick pressure.

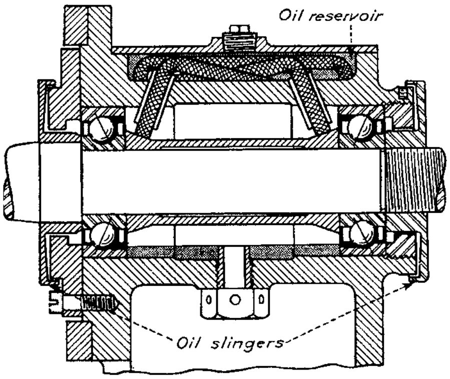

FIG 9

Fig. 9—*Wick feeds* are used in applications of extremely high speeds with light loads and where a very small quantity of oil is required in the form of a fine mist. Slingers clamped on the outside tend to draw the mist through the bearings.

FIG 10

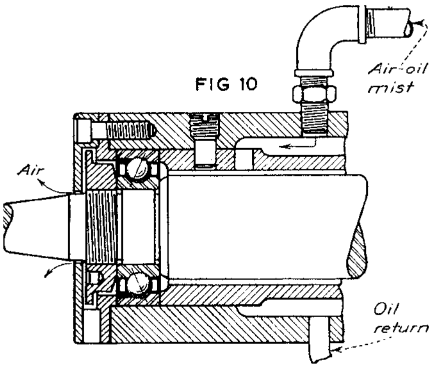

Fig. 10—*Air-Oil Mist.* Where the speeds are quite high and the bearing loads relatively light, the air-oil mist system has proven successful in many applications. Very little oil is consumed and the air flow serves to cool bearings.

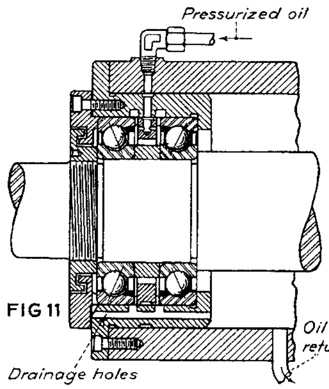

FIG 11

Fig. 11—*Pressure Jet.* For high speeds and heavy loads, the oil must often function as a coolant. This method utilizes a solid jet of cool oil which is directed into the bearings. Here adequate drainage is especially important. The oil jets may be formed integrally with the outer preload spacer.

Ball-Bearing Screw Life

Based on several years of life-load tests, the charts reduce calculation time and increase reliability-analysis.

D. A. Galonska

BALL-BEARING screws are designed individually to meet the specific load, life and space requirements of each application. To simplify such calculations and to provide a higher degree of reliability, a series of tests was conducted which furnished data for the construction of two design charts. With one—a life-load chart—minimum life of ball-bearing screws can now be predicted to within 10 percent. A second chart aids in determining the key dimensions. A numerical problem is included here to illustrate the use of the charts. Also given are rules for selecting the optimum number of balls and circuits in a unit, best materials, hardnesses.

Basic types

Ball-bearing screws are highly efficient units for precision positioning with minimum power, size and cost. With mechanical efficiencies ranging from 90 to 95 percent, ball-bearing screws require only one-third as much torque for the same linear output as conventional Acme thread screws.

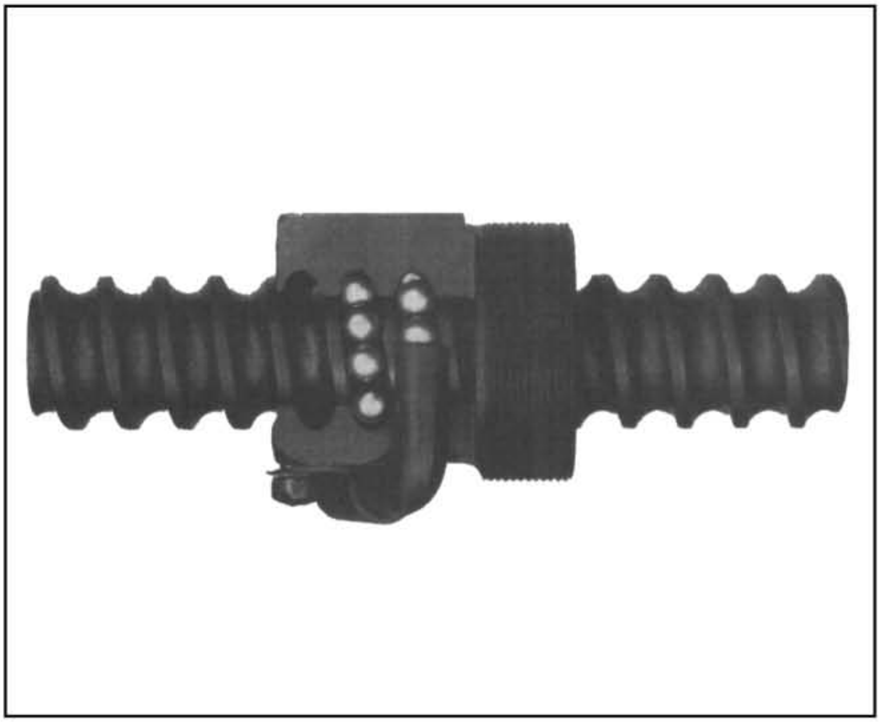

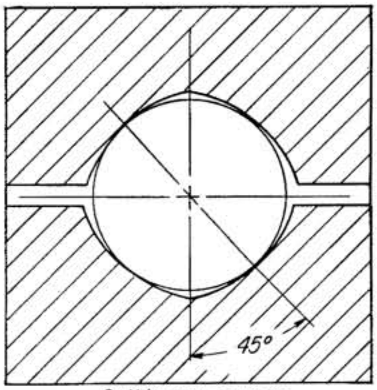

Gothic arc grooves

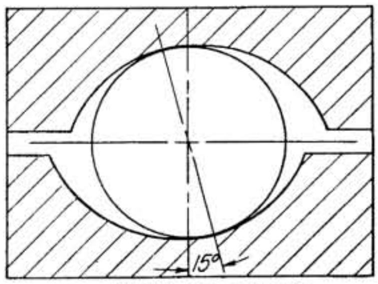

Circle - arc grooves

BASIC BALL-BEARING screw assembly consists of a screw and nut having helical races separated by balls. Two popular types of grooves (right).

The basic unit of a ball-bearing screw assembly consists of a screw and nut having helical races separated by balls. A tubular guide on the nut interrupts the path of the balls, deflects them from the races, and guides them diagonally across the outside of the nut and back to the races. In operation, the rolling balls recirculate continuously through this closed circuit as nut and screw rotate in relation to each other.

The lead of a ball-bearing screw is the distance the nut (or screw) advances for one revolution of the screw (or nut). It is usually expressed as a decimal dimension, but may be given in threads per inch. The ball circle diameter, or pitch diameter, is the diameter of a circle whose radius is the distance from the screw axis to the center of the active bearing balls.

Grooves forming the helical races of ball-bearing screws and nuts may be either of circle arc or Gothic arc cross-section. The Gothic arc groove design minimizes lash by reducing the axial freedom of the assemblies. Also, with this construction, foreign matter entering the grooves is pushed by the balls into the space at the apex. The design of the Gothic arc groove shape is usually based on a 45-degree contact angle, while with circular grooves, the contact angle varies with changes in load, lash, and ball size. The circular groove design, however, may offer a slightly lower frictional loss during operation.

Load-carrying capacity

Load capacity depends on material, hardness, ball and screw diameters and on the number of bearing balls. However, screw and ball diameters are generally limited by the lead specified or space available; hence, to increase the load capacity, it is usually necessary to increase the number of balls. If too many balls or too many turns are designed in a single long circuit, there is a tendency to jam or lock because of the friction caused by the rubbing of adjacent balls rolling in the same direction.

One way to reduce the tendency to jam is to include alternate balls of a smaller diameter. The larger ones serve as bearing balls, the smaller ones as spacers. In this way, adjacent balls rotate in opposite directions, similar to idler gears in a gear train. Obviously this design carries less load for a given space and weight than types in which all the balls are load carriers.

Another method for increasing the number of balls, and thus raising the load-carrying capacity of a ball-bearing nut of given length, is to provide more than one circuit. In a multiple-circuit design, the separate circuits divide the load equally. Also, every ball is a load carrier, and the need for extra nonworking spacer balls is eliminated. Another important advantage is that if one circuit fails, the others can generally carry the load until repairs can be made.

Tests have determined two limiting factors when all balls are to be load carriers:

1. Number of balls in any single circuit should be less than 125.

2. Maximum circuit length should not exceed 3½ turns.

Little is gained by providing more circuits having fewer turns. In one series of tests it was found that the life of nuts having two circuits of 3½ turns each was comparable to that of a nut having five circuits of 1½ turns each.

Load-carrying capacity of ball-bearing screws closely parallels that of conventional ball bearings. Stress levels and impacts on the races determine the life of an assembly. Stress level (load rating) versus number of impacts (or screw revolutions) have been

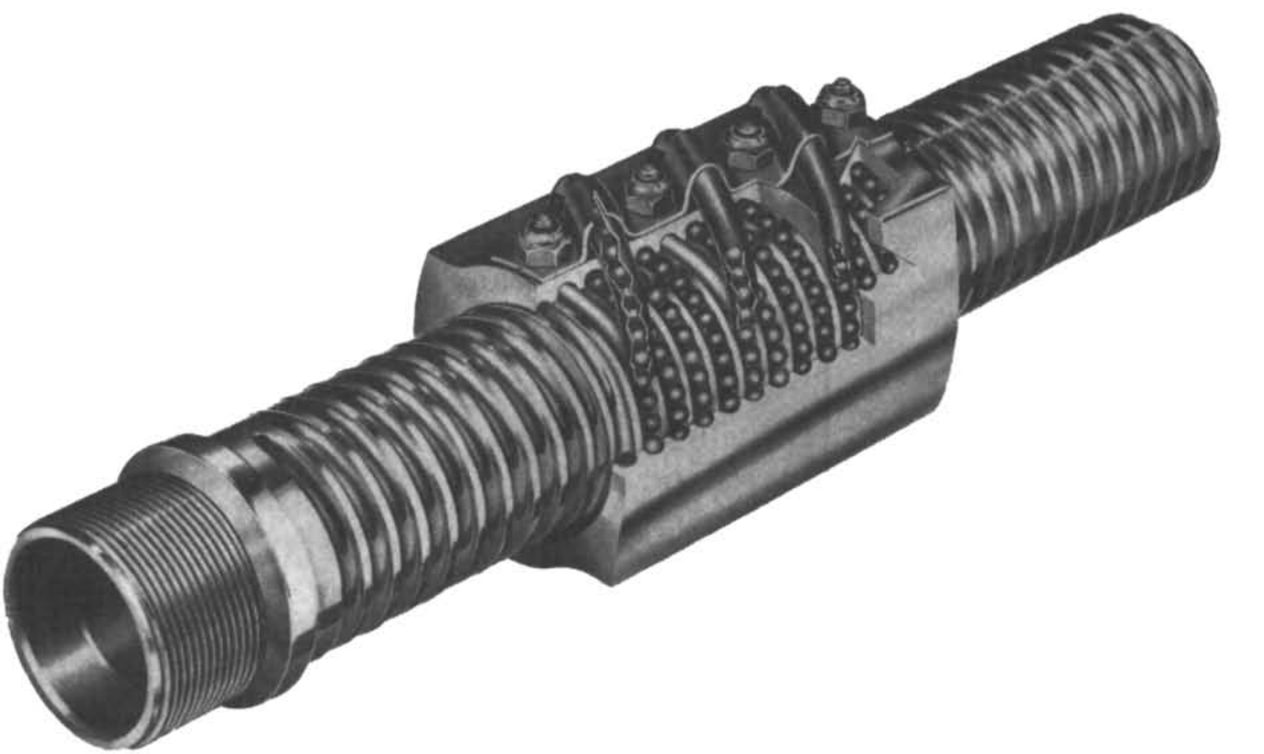

MULTIPLE BALL CIRCUITS increase load-carrying capacity. Each circuit carries equal share of load.

have been determined by laboratory test under simulated service conditions, Fig 1 and 2, pp 52-53. The ratings are specified in terms of one million revolutions. Use of the charts is illustrated in the following problem.

Design problem

Design a ball-bearing screw of minimum size and weight to meet the specifications listed below (see also illustration below). The unit is to operate an aircraft hydraulic locking cylinder. Also given are typical limits on dimensions and load.

Given

- Nut rotated by input drive, but prevented from shifting linearly; screw does the driving.
- Life requirement is 5000 cycles (in both directions).
- Stroke is 5 in. under load in one direction; the screw remains under compression during the return stroke. (Units with strokes as much as 50 ft have been designed and tested.
- Load is 9300 lb in both directions. (Units have been built to provide a thrust of 1,000,000 lb.)
- Ball-circle diameter of pitch dia, D is 1.25 in. (manufacturing limits: min = $\frac{3}{16}$ in.; max ≈ 8 in.)
- Lead = 0.3125 in./rev. (Leads from 0.125 to 1.5 times the pitch diameter are best, although there is no definite top limit.)
- Ball diameter, $d = \frac{7}{32}$ in. The lead specified, as well as the ball-circle diameter, limit the maximum size of the balls because the lands between the grooves must be sufficiently wide to provide adequate support. Also, a portion of the land on the nut is removed by the counterboring required for the ball return system. In this instance, the maximum ball diameter of $\frac{7}{32}$ in. was dictated by experience.

Compute

Total travel = 5 in. stroke in each direction
= 10 in./cycle
= 10 × 5000
= 50,000 in.

rev/in. = 1/0.3125 = 3.2

Total revolutions = 3.2 × 50,000
= 160,000 rev

$$\text{Diameter ratio} = D/d = \frac{1.25}{7/32} = 5.71.$$

(Ideal D/d ratio is between 4 and 8.)

From charts

Number of impacts per revolution for a D/d ratio of 5.71 is 7.8, Fig 2. Impacts are the number of balls that pass one point on the nut in one revolution of the screw. It is best to keep the number of impacts within 5 to 13.6 per revolution. Note from the chart that if the nut were driving, with the screw stationary, the higher diagonal line would be read, resulting in a higher number of impacts.

Multiplying the number of revolutions to be traveled (160,000) by the number of impacts per revolution (7.8), we find the total number of impacts to be 1,248,000. Referring to Fig 1, for this number of impacts and $\frac{7}{32}$ in. dia balls, the load that can be carried per ball is 150 lb. Thus

$$\text{No. of balls required} = \frac{9300}{150} = 62 \text{ balls.}$$

This is less than the maximum of 125 balls per circuit necessary to avoid locking; hence only one circuit is required. If more than 125 balls were required, divide the total by 125 and use the next largest whole number as the number of circuits.

Number of balls per turn is

$$\pi\left(\frac{D}{d}\right) = 5.71\pi = 17.9 \approx 18$$

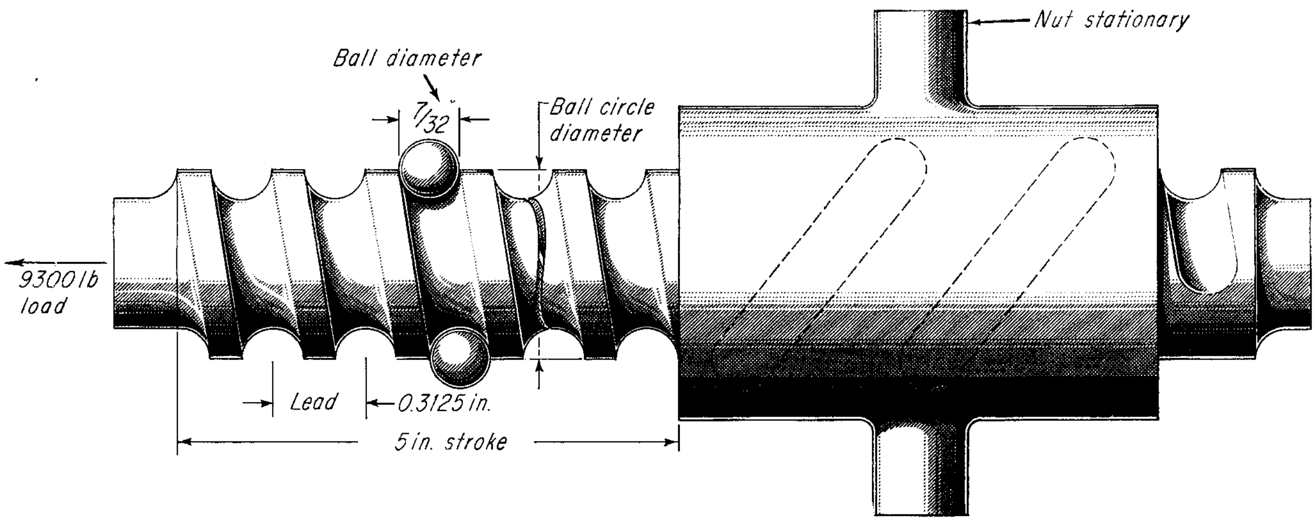

DIMENSIONS for design problem. Nut rotates, but is stationary in a linear direction.

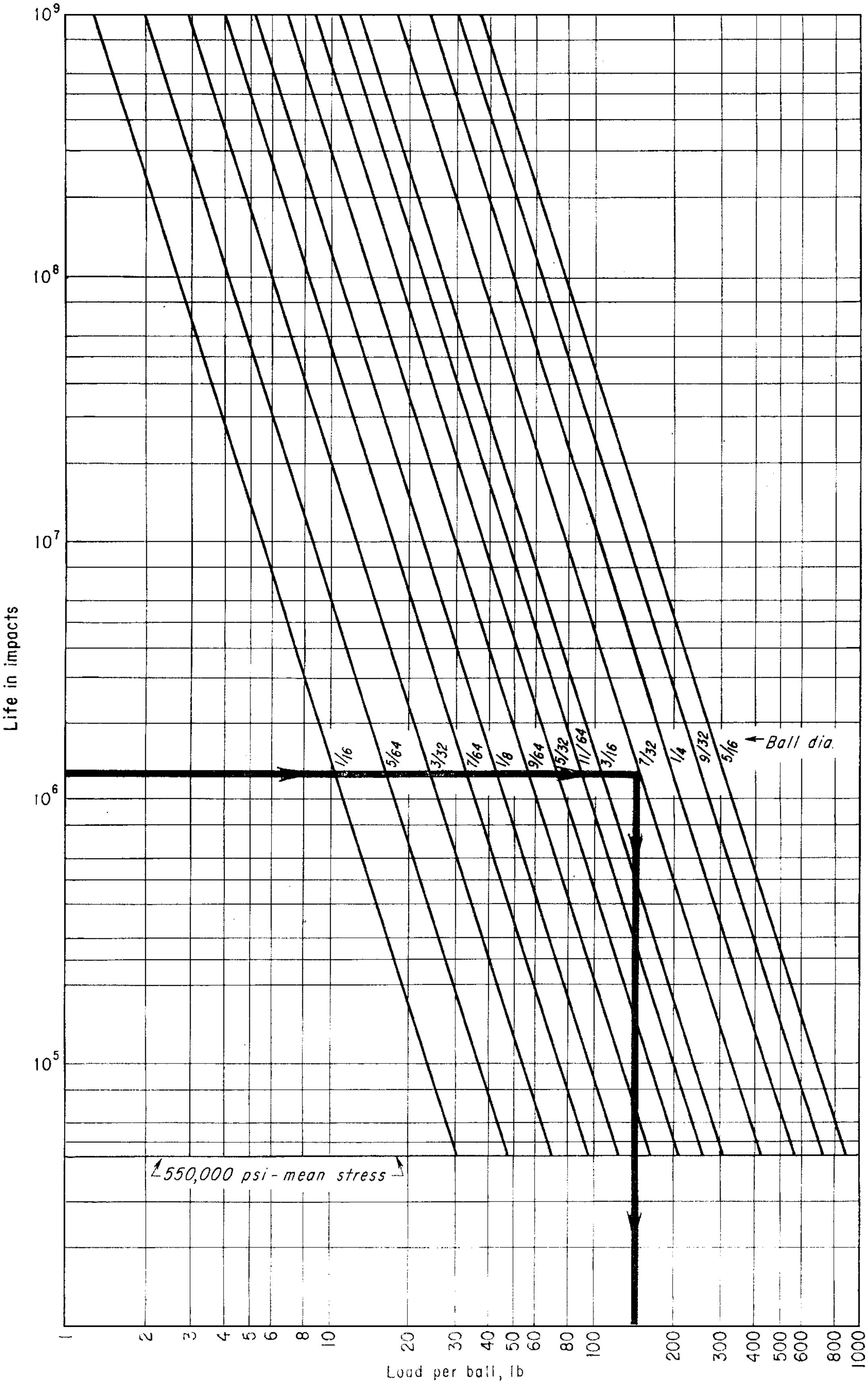

1 • • LIFE-LOAD RELATIONSHIPS for various diameter balls.

Number of turns is

$$\frac{\text{No. of balls}}{\text{No. of balls per turn}} = \frac{62}{18} = 3.44 = 3\tfrac{1}{2}$$

The number of turns determines the minimum length of nut. In general, the minimum nut length can be approximated from the following table:

TOTAL NUMBER OF TURNS	MINIMUM LENGTH OF BALL NUT
$2\frac{1}{2}$	$4\frac{1}{2} \times$ Lead
$3\frac{1}{2}$	$5\frac{1}{2} \times$ Lead
5	$7\frac{1}{2} \times$ Lead
7	$9\frac{1}{2} \times$ Lead
$10\frac{1}{2}$	$13\frac{1}{2} \times$ Lead

Effect of a varying load

In numerous life tests with hardened screws under various load conditions, failures have always been the result of a broken ball. The impact life lines in Fig 1 terminate at the loads which will subject the raceways to a mean stress of 550,000 psi. This is considered to be the maximum static, non-Brinell condition for raceways. Tests have shown that ball-bearing screw assemblies can operate for approximately 44,000 impacts at these loads.

When the operating load changes at a constant rate throughout the stroke, the equivalent constant load can be calculated by taking the root mean cube average of the loads:

$$L = L_1 + \left(\frac{L_2^3 - L_1^3}{2}\right)^{1/3}$$

where L = the equivalent constant load,
L_2 = the higher load
L_1 = the lesser load

Effect of hardness on life

The life-load chart, Fig 1, is based on a minimum raceway hardness of $60R_c$ and a case depth sufficient to support the load throughout the life of the assembly without appreciable spalling. However, it is sometimes impractical or uneconomical to provide such a degree of hardness.

While it is possible to harden very long screws, they will invariably distort as the result of quenching. Straightening of such screws to the required accuracy is difficult and expensive. Hence, a lesser degree of hardness is best for such cases. Also, screws made of stainless steel, such as Armco 17-4PH, are best hardened to between 40 to $45R_c$ by heating to 950 F for 1 hour. This low-temperature heat treatment causes only a minimum of distortion. For lightly loaded, low-cost applications you can

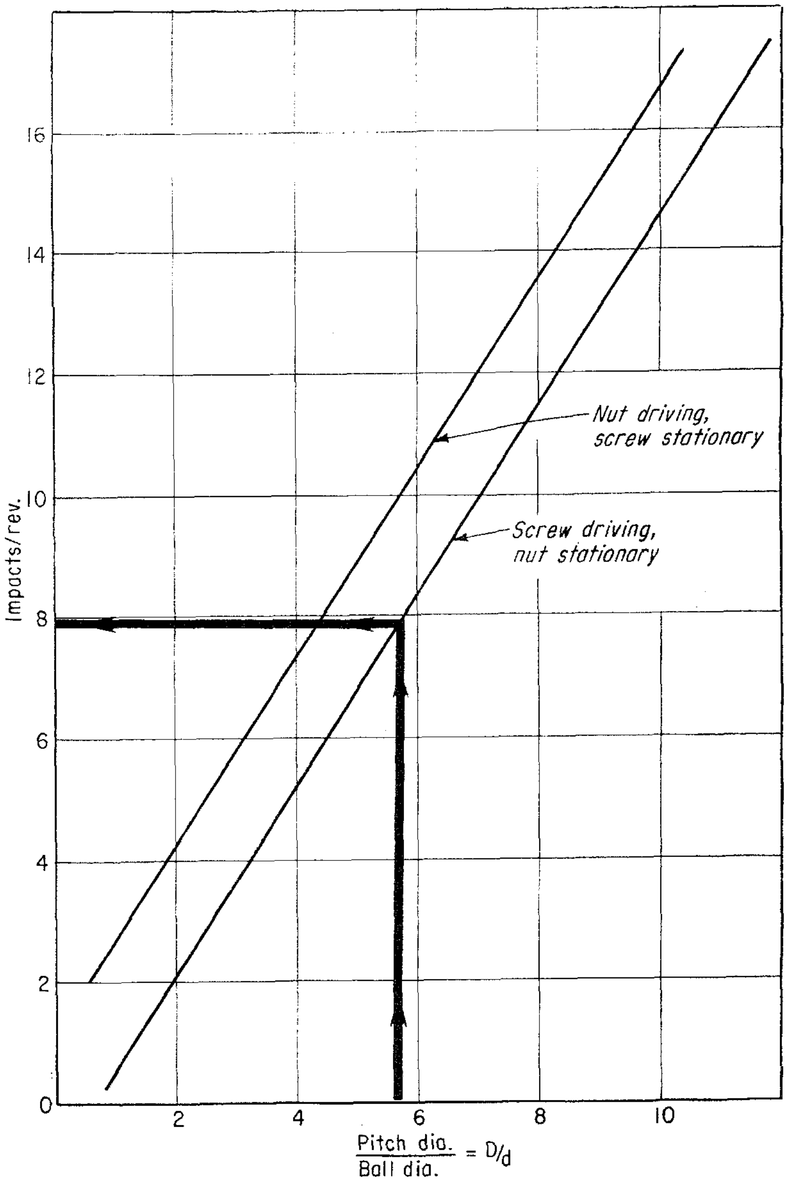

2 • • IMPACTS per revolution versus ratio D/d.

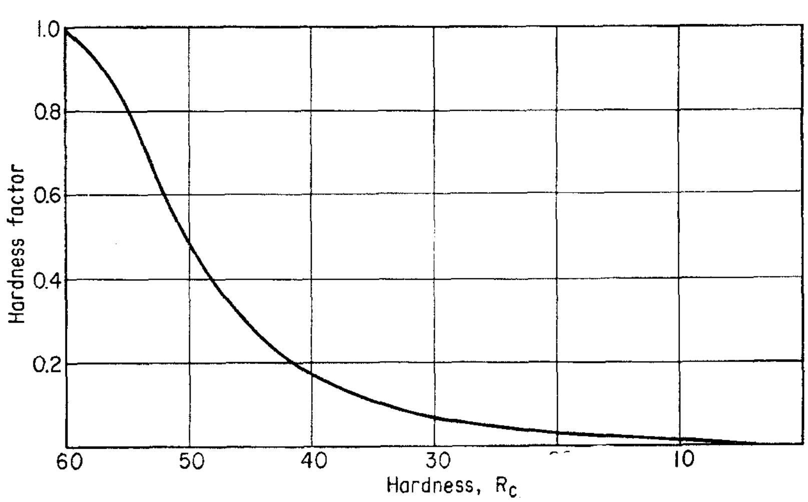

3 • • HARDNESS FACTOR versus Rockwell hardness.

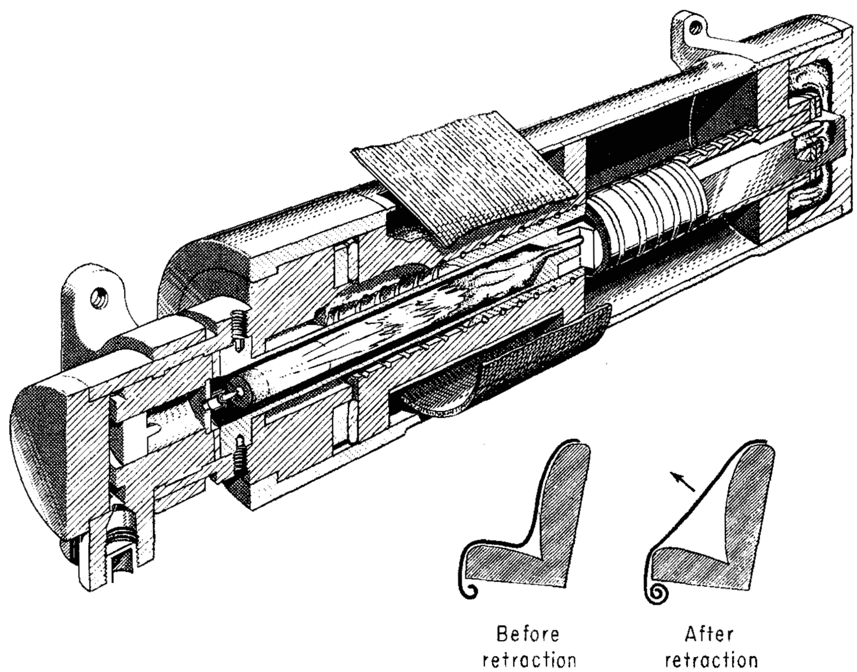

1 Cartridge-operated rotary actuator quickly retracts webbing to forcibly separate a pilot from his seat as the seat is ejected in emergencies. Tendency of pilot and seat to tumble together after ejection prevented opening of chute. Gas pressure from ejection device fires the cartridge in the actuator to force ball-bearing screw to move axially. Linear motion of screw is translated into rotary motion of ball nut. This rapidly rolls up the webbing (stretching it as shown) which snaps the pilot out of his seat. *Talley Industries.*

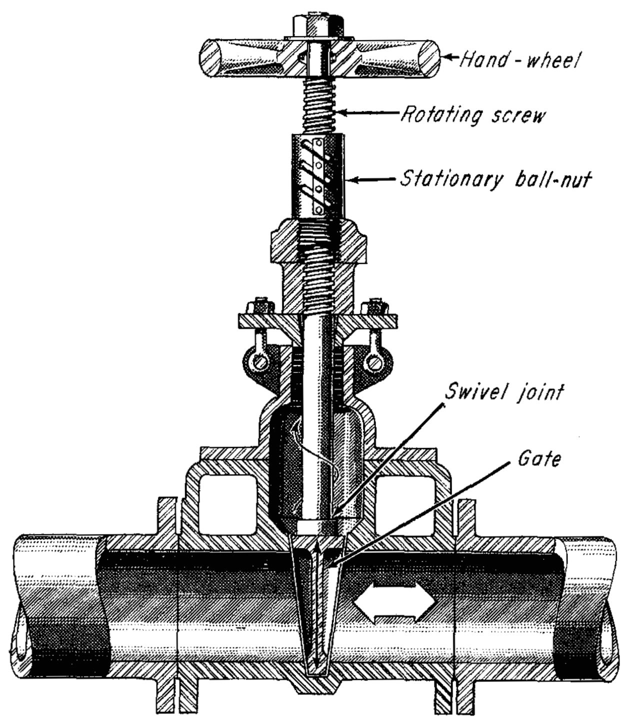

2 Speedy, easily operated, but more accurate control of flow through valve obtained by rotary motion of screw in stationary ball nut. Screw produces linear movement of gate. The swivel joint eliminates rotary motion between screw and gate.

request cold-rolled unheat-treated steel. However, the hardness for such steel is only approximately 27 to 32R_C.

Effect of hardness on the life of ball-bearing screws is shown in Fig 3. Effective load, for determining the life of assemblies, is

$$\text{effective load} = \frac{\text{actual load}}{\text{hardness factor}}$$

Effect of materials on life

The material employed, if properly hardened and compatible, has little effect on the life of a unit. Most ball-bearing screw assemblies produced by Saginaw are made from SAE 4145, 4150, or 6150 steels, that are usually hardened to 60 R_C.

In the chemical and food-processing industries, actuators are generally

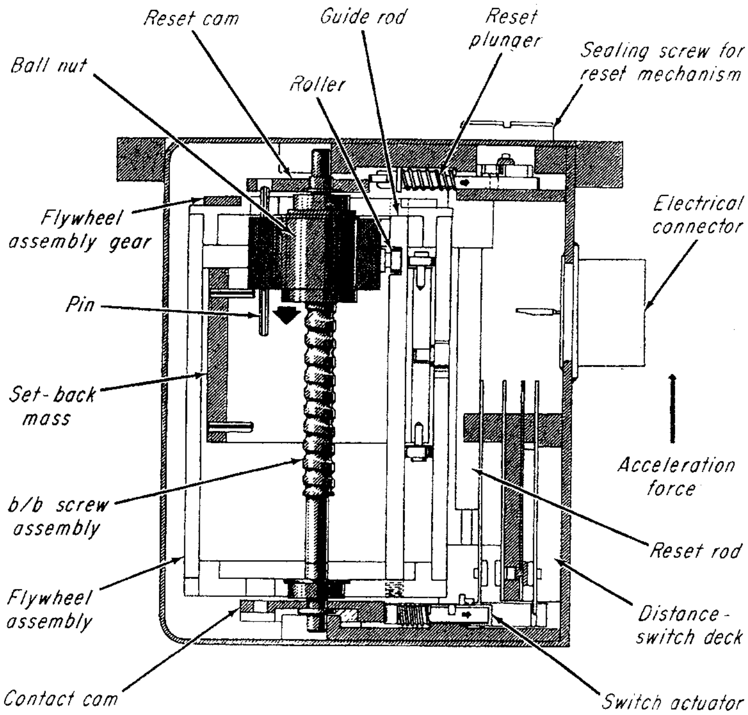

3 Time-delay switching device integrates time function with missile's linear travel. Purpose is to safely arm the warhead. A strict "minimum G-time" 'system may arm a slow missile too soon for adequate protection of own forces; a fast missile may arrive before warhead is fused. Weight of nut, plus inertia under acceleration will rotate the ball-bearing screw which has a fly wheel on the end. Screw pitch is such that a given number of revolutions of flywheel represents distance traveled. *Globe Industries.*

4 Accurate control of piston position in hydraulic actuator for aircraft has ball-bearing screw mounted directly to piston by means of threaded nut. Piston rod is actuated linearly by means of hydraulic pressure applied to ball nut through port A or B. Linear movement produces rotary motion in screw which is attached to no-back braking device. Piston rod, therefore, can be stopped by any linear position by actuating the lever of braking device. Attaching gear train and rotary dial to screw shaft will give direct reading of linear position of piston rod. *Allison Div of General Motors Corp.*

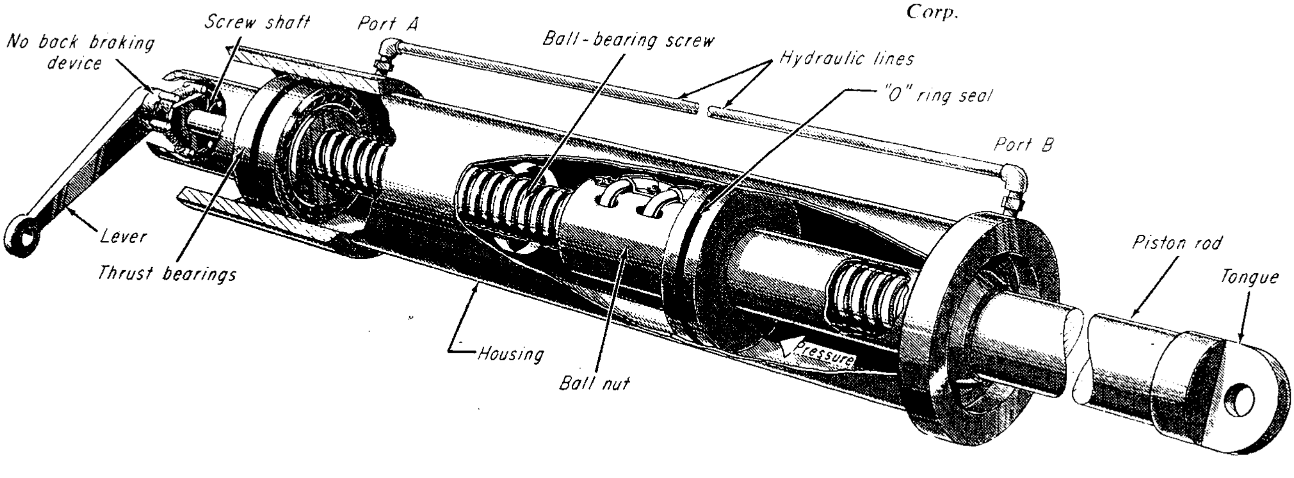

made from corrosion-resistant materials. For high-temperature applications, steels such as the ones listed above are suitable up to about 350 F; AISI Type 440 stainless steel, to 550 F; hot-work tool and die steels, to 800 F; and cobalt-base materials such as Haynes Stellite #25, to 1000 F. The higher temperatures, however, do lower the life of a unit.

Stress on a Bearing Ball

These curves indicate permissible loads when seat is spherical or flat, steel or aluminum.

Jerome E. Ruzicka

COMPRESSIVE STRESS FOR STEEL BALL ON STEEL SEAT
(For aluminum seat, multiply stress by 0.632)

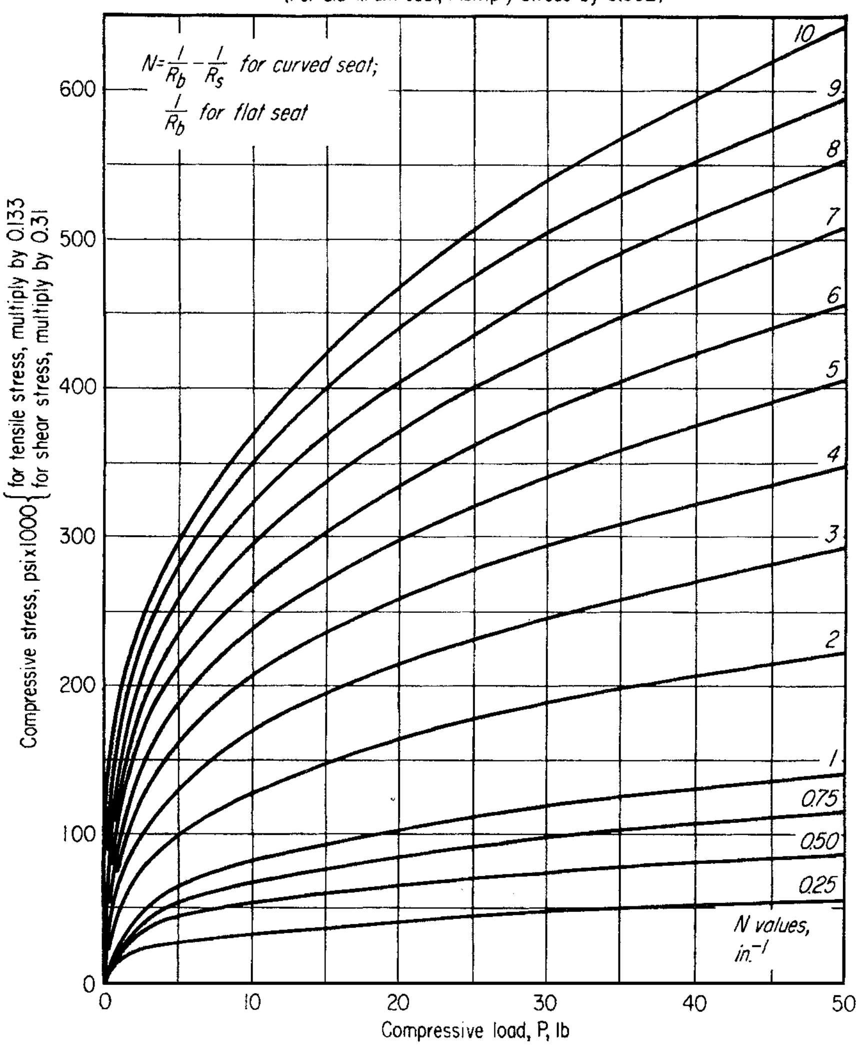

When a design uses steel bearing balls to support a load, it is important to know what stresses result. They are charted on this page. On the continuing page is a diagram that identifies symbols—for applications where the seat is spherical or flat—and also a chart that will help calculate maximum permissible loads.

Symbols used with curves

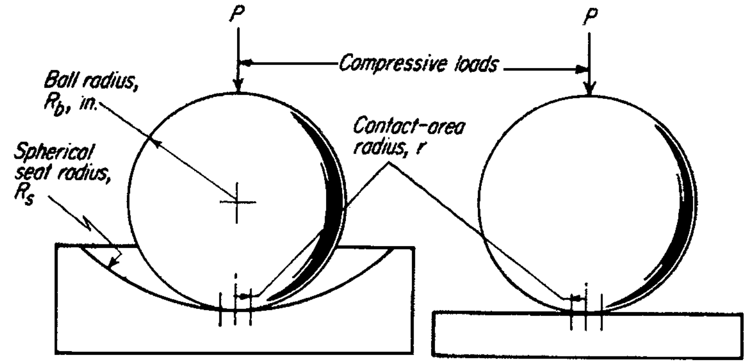

CONTACT RADIUS FOR STEEL BALL ON STEEL SEAT
(For aluminum seat, multiply radius by 1.25)

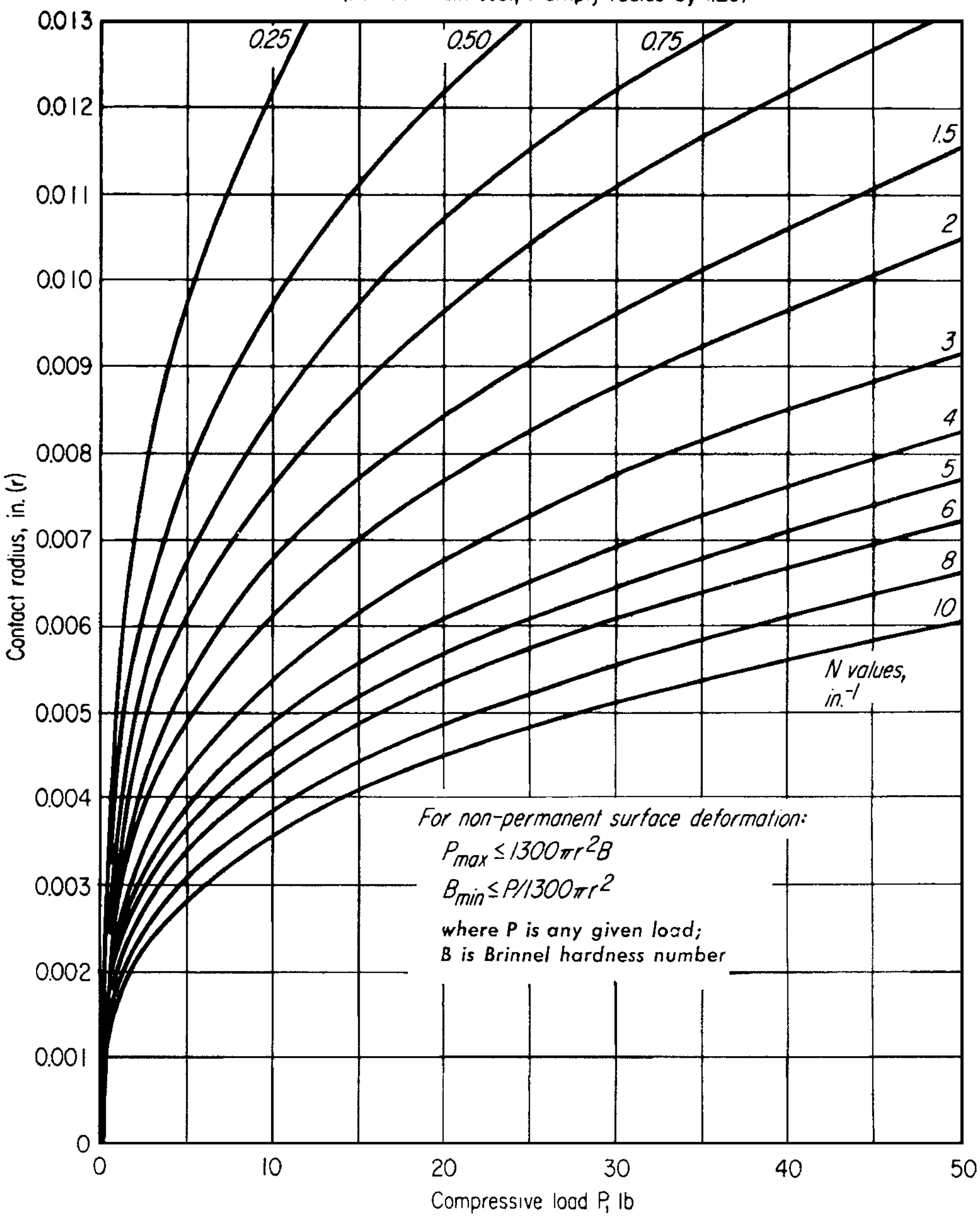

Compute Effects of Preloaded Bearings

The trend is to preload whenever precision and spindle rigidity are desired—and tests now show that preload can increase bearing life.

T. A. Harris

MANY designers are failing to take full advantage of the principles of bearing preload. In fact, there are still some misconceptions in this area. Let us immediately clear up two important points:

- Preloading does *not* necessarily decrease bearing life—in fact, bearings which have been preloaded can definitely last longer, provided they are not over preloaded. Design curves included in this article pinpoint the maximum preload for maximum life.
- Preloading need not be restricted to *ball bearings*. Almost any type of rolling-element bearing assembly — ball, cylindrical, roller, tapered roller, spherical—can gain by preloading.

What is preloading?

Simply stated, preloading is an internal load applied to a bearing assembly while the assembly is in a stationary (unloaded) condition. This static load, of course, is an addition to that imposed by the weight of the shaft and other members of the assembly.

There are two types of preloading —radial and axial:

Radial preloading can be achieved by any one of these methods:

1. Forcing the bearing on a tapered shaft to expand the inner ring and thus take up the clearance (Fig 1A to 1B).
2. Mounting a tapered sleeve on a shaft, and mounting the bearing on to the sleeve (C).
3. Employing an elliptically out-of-round outer ring (D). The ring snaps over a normal inner ring-and-roller set of a cylindrical roller bearing. This provides a selective radial preload in the vicinity of the minor axis and prevents skidding in high-speed, lightly loaded applications.
4. Tightening tapered roller bearings against each other (Fig E and F). Although this is an axial tightening, in effect radial preloading is achieved which improves roller load distribution and increases life.
5. Selecting more interference in the fit between the outer diameter of the bearing and its housing.
6. Heating the outer ring and allowing it to shrink over the rollers after assembly. A line-to-line fit is then required on the shaft and the housing.

Axial preloading, Fig 2, is usually obtained by shifting the inner or outer race of the bearing in the axial direction. This can be done in several ways: by grinding the side of one ring so that it is normally at an offset position in comparison to the other ring,

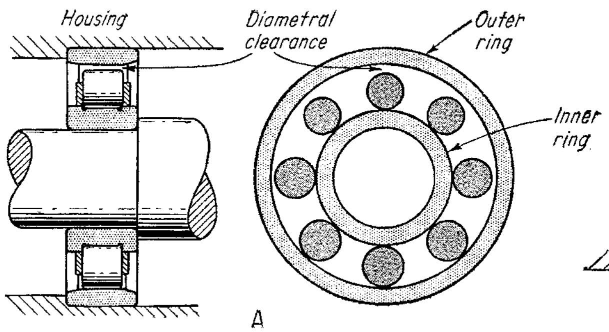

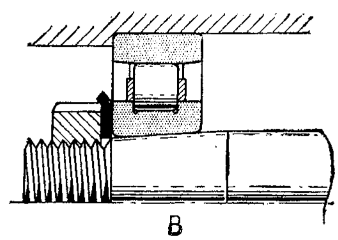

1 A. Diametral (radial) clearance found in most off-the-shelf rolling-element bearings. One object of preloading is to remove this clearance during assembly.
B. Cylindrical roller bearing mounted on tapered shaft to expand inner ring. Such bearings are usually made with a taper on the inner surface of 0.04 in./in.
C. Spherically roller bearing mounted on tapered sleeve to expand the inner ring.
D. Elliptically out-of-round outer ring is snapped over the normally round inner ring of a cylindrical-roller bearing to prevent skidding during high-speed operation.
E. Tapered roller bearings are locked together axially to obtain radial preload.
F. Lightly preloaded tapered roller bearings in the wheel of a mine car.

and then by mounting the bearing in pairs (A to D); by use of shims (E); and by the insertion of spacers in which one spacer is slightly longer than the other (F).

What does preloading do?

Preloading removes the internal clearances that normally exist between the balls (or rollers) and one of the races. In fact, because the result is usually an interference fit between the balls and the races, clearance or play is avoided even under load (up to, of course, a specific point). Thus, preloading:

- **Provides more accurate shaft positioning,** both axially and radially. This is a prime objective for designers of precision tools and mechanisms, such as machine tool spindles, instruments, gyroscopes. Of course, many designers in these fields are already employing preload.
- **Reduces the shaft deflection under load** and improves the assembly stiffness characteristics.
- **Increases the bearing fatigue life,** providing that the assembly is not overpreloaded.
- **Decreases bearing noise** and permits the bearing to take higher shock.
- **Provides system isoelasticity,** in which the deflection in the bearing system is along the line of the external load.

Care must always be taken to avoid excessive preload because this increases the running torque and operating temperature of the bearing and thus significantly reduces bearing life. The following sections give the key equations and charts for accurately predicting the amount of preload a bearing assembly should have. Sample problems are included in most cases.

continued, page 86

2 A. Duplex set with back-to-back angular ball bearings prior to axial preloading. The inner ring faces are ground to provide a specific gap.
B. Same unit as in (A) after tightening axial nut to remove gap. The contact angles will have increased.
C. Face-to-face angular-contact duplex set prior to preloading. In this case it is the outer-ring faces which are ground to provide the required gap.
D. Same set as in (C) after tightening the axial nut. The convergent contact angles increase under preloading.
E. Shim between two standard-width bearings avoids need for grinding the faces of the outer rings.
F. Precision spacers between bearings automatically provide proper preload by making the inner spacer slightly shorter than the outer.

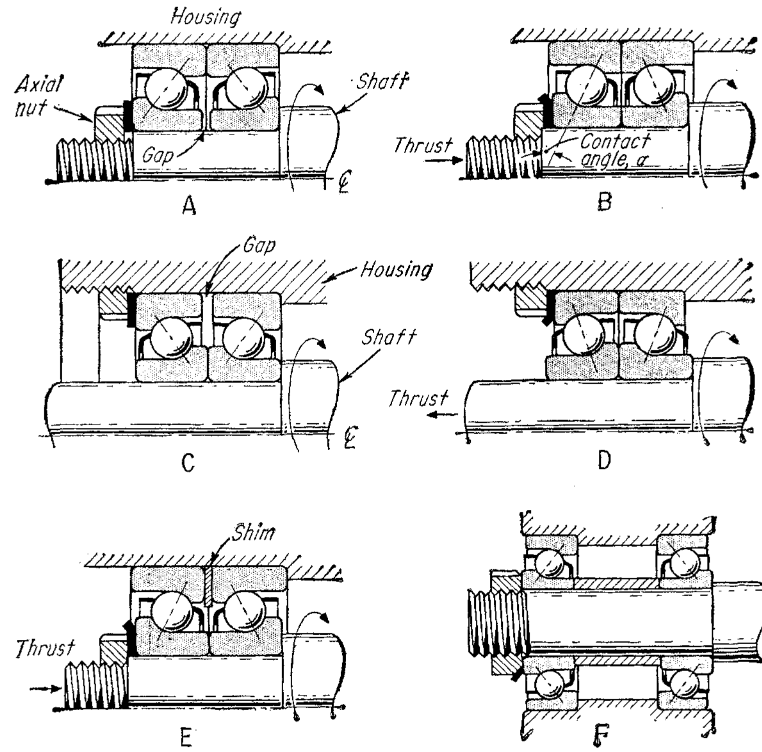

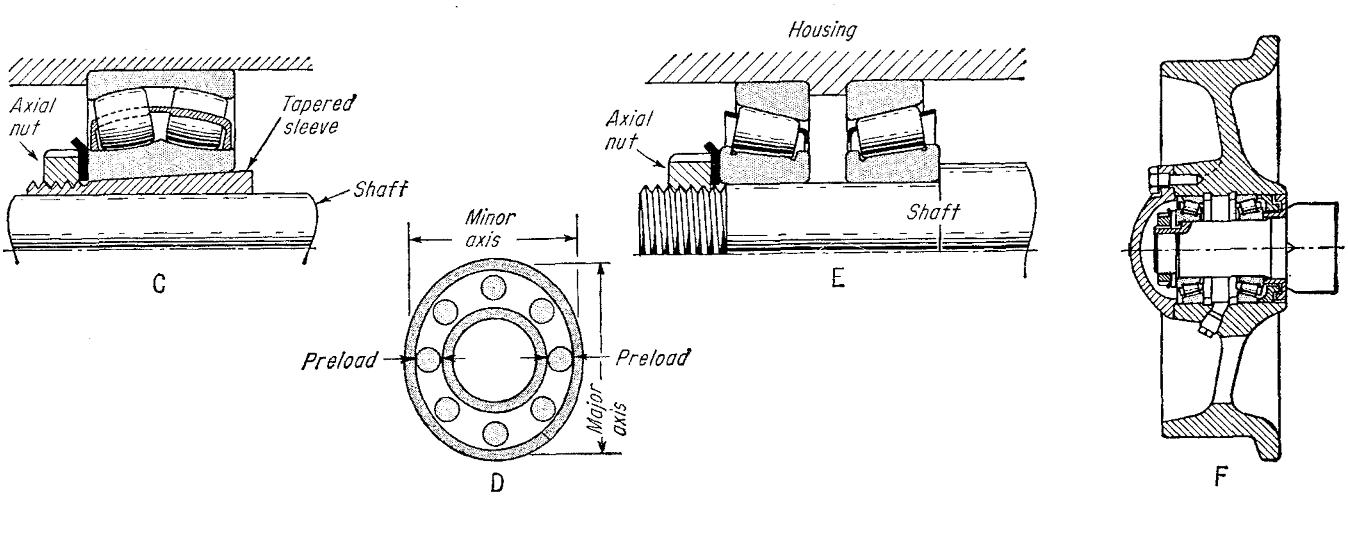

RADIAL PRELOADING

Preload vs bearing life

As stated previously, light preloading increases the bearing fatigue life. Specifically, in the case of radial preloading, the preload extends the circumferential arc of loading (Fig 3), which in turn reduces the maximum load experienced by a ball or roller.

But by how much is the bearing life extended? Most statements on preload are qualitative; quantitative analyses are generally shunned as being too complicated. This was perhaps true in the past. Now, with certain key equations and charts, one can directly come up with accurate estimates as to the amount of preload that is desirable and its effect on bearing life.

First step is to determine the extent of the circumferential zone of rolling element loading. This is obtained by solving Eq 1 and 2 simultaneously for δ, the radial deflection, and ϵ, the projection of the zone of loading on the bearing pitch diameter of symmetry (a numerical problem that follows illustrates the technique):

$$F = ZK\left(\delta - \frac{c}{2}\right)^n J \qquad (1)$$

$$\epsilon = \tfrac{1}{2}\left(1 - \frac{c}{2\delta}\right) \qquad (2)$$

where F is the applied load on the bearing (caused by the load imposed on the shaft from the gearing, belting, rotating mass, etc), Z is the number of balls or rollers, K is the deflection constant defined for most deep-groove ball bearings by Eq 3 and for roller bearings by Eq 4, c is diametral clearance (which is frequently referred to as radial clearance according to Anti-Friction Bearing Manufacturers' Association (AFBMA) terminology), and J is a radial load function given by Fig 4 for ball and roller bearings. The exponent n is 1.5 for ball bearings and 1.1 for roller bearings. For ball bearings

$$K = 1.53 \times 10^7 D^{0.5} \qquad (3)$$

For roller bearings

$$K = 5.28 \times 10^6 L_r^{0.89} \qquad (4)$$

where D is the diameter of the balls and L_r the effective length of the rollers.

You can easily solve Eq 1 and 2 by trial-and-error techniques. Assume a value of ϵ, then pick off J in Fig 4. Next, solve for δ in Eq 1 and use this value in Eq 2 to determine a new value of ϵ, which you then compare against the assumed value. Repeat the process until the difference between the assumed and the calculated values of ϵ is sufficiently small (usually under 0.01).

This value of ϵ will then affect the rating life or L_{10} fatigue life, which is in terms of hours of a radially loaded, rolling bearing in accordance with AFBMA load rating standards given by the equations:

For ball bearings

$$L_{10} = \frac{10^6\lambda}{60N}\left[\frac{C}{F}\right]^3 \qquad (5)$$

For roller bearings

$$L_{10} = \frac{10^6\lambda}{60N}\left[\frac{C}{F}\right]^{\frac{10}{3}} \qquad (6)$$

In the above equations, C is the basic load rating supplied by the bearing catalog, and N the shaft speed. **These equations, however, differ from the often published AFBMA equations in that they contain a life adjustment factor** λ. This factor is obtained from Fig 5 by knowing ϵ, and thus accounts in Eq 5 and 6 for the effect of diametral clearance, both positive and negative, on bearing life.

Generally, in nonpreloaded bearings, the clearances are relatively large and the values for λ quite low, in the 0.7 to 0.9 range (hence it is frequently called a "reduction factor"). But with preloaded bearings, values above 1.0 are readily obtained. In addition, values of ϵ greater than 1 should be avoided to maintain long fatigue life. Good design practice calls for radial preloads which cause ϵ to fall between 0.5 and 1.0. Improved fatigue life is thereby obtained.

Example I—Nonpreloaded life

A single-row deep-groove ball bearing (SKF bearing number 6309 with a loose C3 fit) has a basic dynamic load rating of 9120 lb. This bearing supports a radial load of 2000 lb at a shaft speed of 1000 rpm. According to the catalog, the bearing contains 8 balls of $\frac{11}{16}$ in. diameter. Also, this bearing is listed as having a mean diametral clearance of $c = 0.001$ in. Without any preload, what is the radial deflec-

Symbols

Symbols	Description	Units	Source
B	total groove curvature	—	Eq 14
c	diametral (radial) clearance	in.	bearing mfr or AFBMA tables
C	basic load rating	lb	catalog
d	bearing pitch diameter	in.	catalog
D	ball or roller diameter	in.	catalog
f_i	inner ring groove radius/D	—	bearing mfr.
f_o	outer ring groove radius/D	—	bearing mfr.
F	radial load or preload	lb	bearing application
F_1	axial load on bearing 1	lb	Eq 13 and 15
F_2	axial load on bearing 2	lb	Eq 13 and 15
G	axial deflection constant	—	Fig 9
J	radial distribution integral	—	Fig 4
K	radial deflection constant	—	Eq 3 or 4
L_{10}	rating life (10% failures)	hr	Eq 5 or 6
L_r	effective roller length	in.	catalog
N	shaft speed	rpm	bearing application
T	external thrust load	lb	bearing application
Z	number of balls or rollers	—	catalog
α_0	zero load contact angle	deg	bearing mfr.
α_1	contact angle on bearing 1	deg	Eq 20 and 21
α_2	contact angle on bearing 2	deg	Eq 20 and 21
δ	radial or axial deflection	in.	Radial: Eq 1 and 2 Axial:
δ_p	axial preload deflection	in.	Fig 10
Δ	increase in clearance due to centrifugal force	in.	Eq 11 or 12
ϵ	projection of loading arc on bearing diameter	—	Eq 2
λ	life adjustment factor	—	Fig 5

Note: When source is listed as "bearing mfr.," the data may be found in catalogs.

tion and estimated L_{10} fatigue life?
From Eq 3

$$K = (1.53(10^7)(0.6875)^{0.5} = 1.269 \times 10^7$$

From Eq 1

$$2000 = (8)(1.269)(10^7) \times \left(\delta - \frac{0.001}{2}\right)^{1.5} J$$

$$0.0000197 = (\delta - 0.0005)^{1.5} J \qquad (7)$$

From Eq 2

$$\epsilon = 0.5\left(1 - \frac{0.001}{2\delta}\right) = 0.5\left(1 - \frac{0.0005}{\delta}\right) \qquad (8)$$

Assume a value for ϵ (a good starting point for nonpreloaded bearings is $\epsilon = 0.4$). Use the ϵ value in Fig 4 to determine J, solve for δ in Eq 7, and then solve for ϵ in Eq 8 to see how close it is to the assumed value. This finally yields:

$$\epsilon = 0.402$$
$$\delta = 0.00254 \text{ in.}$$

Now compute the predicted bearing life. At $\epsilon = 0.402$, from Fig 5, $\lambda = 0.9$ and L_{10} from Eq 5 becomes:

$$L_{10} = \frac{(1{,}000{,}000)(0.9)}{(60)(1000)}\left[\frac{9120}{2000}\right]^3 = 1438 \text{ hr}$$

Example II—Preloaded life

Let us now look at what happens when the bearing of the foregoing example (bearing No. 6309) is mounted with a press fit on the shaft and in the housing such that the resultant clearance is 0.0005 in. tight. This provides a light radial preload. What radial deflection and L_{10} fatigue life can now be expected?
From Eq 1

$$2000 = (8)(1.269)(10^7)\left(\delta + \frac{0.0005}{2}\right)^{1.5} J$$

$$0.0000197 = (\delta + 0.00025)^{1.5} J \qquad (9)$$

From Eq 2

$$\epsilon = 0.5\left(1 + \frac{0.0005}{2\delta}\right) = 0.5\left(1 + \frac{0.00025}{\delta}\right) \qquad (10)$$

Solving Eq 9 and 10 with the aid of Fig 4 yields:

$$\epsilon = 0.577$$
$$\delta = 0.0016 \text{ in.}$$

At $\epsilon = 0.577$, from Fig 5, $\lambda = 1.055$. Thus from Eq 5:

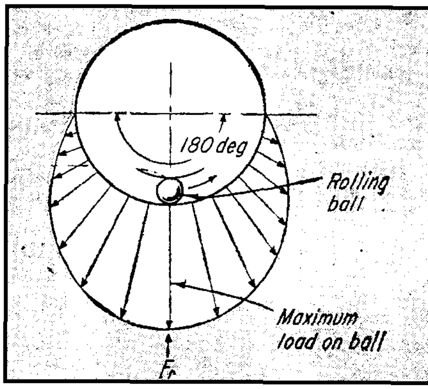

3 Distribution of load among the rolling elements of a radially loaded ball or roller bearing having no diametral clearance (with radial preload). Note that the arc of loading is 180 deg. An unpreloaded bearing would have a much smaller loading arc, fewer of the balls or rollers will be taking up the radial load, and hence the maximum load will be higher (than in a preloaded bearing) which decreases life.

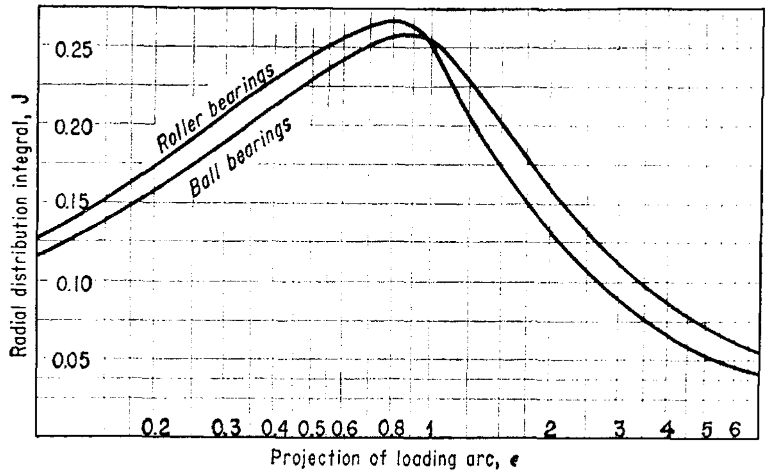

4 **Radial load function J vs the zone of-loading projection, ϵ.** These factors play an important part in computing the change in fatigue life of a ball bearing when preloaded. For best results, design for $0.5<\epsilon<1$.

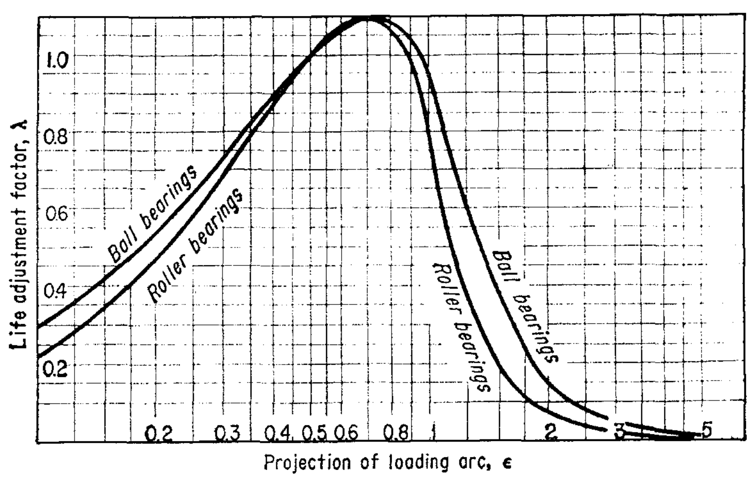

5 **Fatigue-life reduction factor, λ vs ϵ.** Many designers are unaware that this factor should be applied to the standard fatigue equations used in industry to predict the life of roller bearings. To obtain values of 1.0 or over for λ (desirable), factor ϵ should be between 0.5 to 0.9.

$$L_{10} = \frac{(1{,}000{,}000)(1.055)}{(60)(1000)}\left(\frac{9120}{2000}\right)^3$$
$$= 1660 \text{ hr}$$

Hence, this bearing when mounted with 0.0005-in. interference deflects 0.0009 in. less and has a 15% increase in fatigue life.

Equations for high speeds

The previous analysis did not take into consideration the centrifugal force associated with the ball or roller orbital speed. At high cage speeds, the centrifugal force tends to increase the diametral clearance which reduces bearing life. Because this force increases as the square of cage speed, its effect at slow speeds is usually neglected.

The increase in clearance, Δ, caused by centrifugal force can be approximated by the following equations. This calculated value should be added to the value for c used in Eq 1 and 2:

For ball bearings

$$\Delta = 1.07 \times 10^{-9} D^{1.67} d^{0.67} N^{1.33} \times \left[1 \pm \frac{D}{d}\right]^{1.33} \qquad (11)$$

For roller bearings

$$\Delta = 2.38 \times 10^{-12} D^{1.8} L_r^{0.1} d^{0.9} N^{1.8} \times \left[1 \pm \frac{D}{d}\right]^{1.8} \qquad (12)$$

In these equations d is the bearing pitch diameter. Use the minus sign when the inner ring is rotating (as when the shaft is rotating) and the plus sign for outer ring rotation.

For the bearing in Example II (pitch dia = 2.8543 in.), rotating at only 1000 rpm, the increase in clearance from Eq 11 is 0.000008 in.—negligible when compared to the 0.0005 diametral tightness. On the other hand, if the shaft speed is raised to 10,000 rpm, the estimated increase in clearance will be 0.0002 in. which must be subtracted from the preload tightness. Roughly, this will result in a λ factor of 1.03, which will decrease life by about 2.5%. Thus, when designing for a radially preloaded bearing application at other than slow speeds it is necessary to account for the effect of bearing rotational speed.

The clearance in Eq 1 and 2 is that which occurs *after* the bearing is mounted on the shaft and in the housing. When the shaft or housing is other than steel (assuming steel bearings), the effect on clearance of differential expansion due to elevated operating temperatures must be taken.

AXIAL PRELOADING

The most common type of axial preloading occurs in angular contact ball-bearing applications in which duplex bearings are pressed axially against each other to gain increased rigidity against the effect of externally applied thrust load.

The reason for the improvement in rigidity, or *stiffness*, is illustrated by Fig 7 which shows ball-bearing deflection as a function of bearing load. If the bearing can be made to operate to the right of the knee of the curve, ie, if the left-hand portion of the curve could be removed, the subsequent deflection with load can be decreased considerably because the deflection rate diminishes as load increases.

For roller bearings, however, the deflection-load characteristic is nearly linear and there exists no knee to be removed. Consequently roller bearings are rarely preloaded to increase stiffness. Tapered roller bearings, however, require an axial load for proper operation, and in the absence of an applied thrust load this may be effected by applying a light axial preload.

Angular contact ball bearings can be purchased from manufacturers' catalogs to yield specified preloads. The bearings usually have one side face ground down. When such bearings are duplex mounted and locked up against each other as in Fig 6, a specified preload exists according to the difference in width between the inner and outer rings.

For example, SKF angular contact ball bearings which carry the suffix G followed by a code symbol indicate the amount of preload; thus G02 indicates 20 lb and G2 indicates 200 lb preload. Table I (opposite) gives a schedule of preloads supplied by SKF.

However, if you wish to use stand-

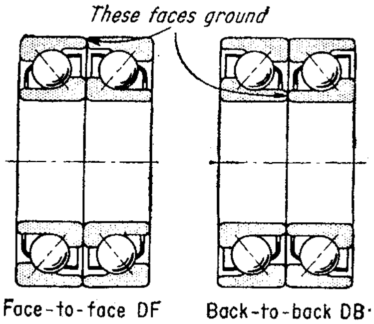

6 Duplex sets of angular contact ball bearings. The back-to-back is the more popular arrangement because the contact angle converges outside the bearing outer ring which provides a high degree of resistance to misaligning forces. Select these bearings when loading is cantilevered or overhung as for pulleys, sheaves. Face-to-face mountings are best when it is desired to dismount spindles and other accessories that are clamped against the inner ring of the bearing—but without relieving the preload of the bearings.

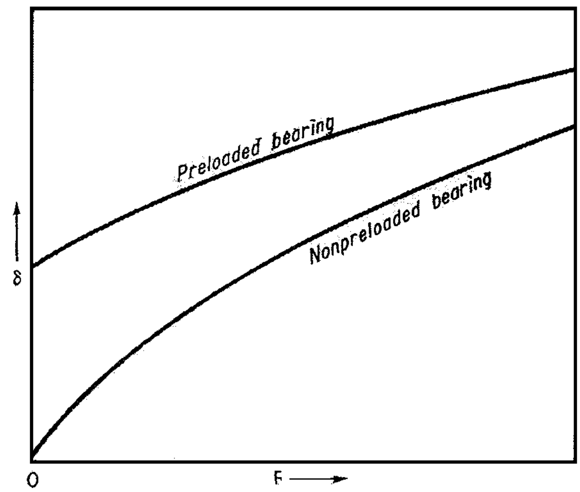

7 Deflection vs load characteristics for ball bearings. As the load increases, the rate of the increase of deflection is slowed, therefore preloading (top line) tends to reduce the bearing deflection under additional loading.

ard bearings, you can use a shim of a width to match the amount that is normally ground off from a preload bearing. Because this amount for a specific preload varies with the bearing type, you must compute this value (see the technique that follows), or you may be able to obtain specific values from the bearing manufacturers.

Computing the grindoff amount

Angular-contact ball bearings that are to be preloaded are usually mounted in pairs in a face-to-face or back-to-back mounting. This mounting may be subjected to an additional, applied thrust load, T. The equilibrium of axial forces requires that

$$T = F_1 - F_2 \qquad (13)$$

where F_1 and F_2 are the thrust loads on bearings 1 and 2, Fig 8. If there is only preload on the bearings (no applied thrust load) then

$$F_1 = F_2.$$

The next important relationship involves the inner and outer raceway groove curvatures, f_i and f_o, which can be obtained from the bearing manufacturers. A constant, B, is then obtained by means of the equation

$$B = f_i + f_o - 1 \qquad (14)$$

The groove curvatures are usually given as a percentage of the ball diameter and fall between 52 to 53% of the ball diameter for most angular-contact bearings.

We now employ two equations to relate the axial deflection, δ, to the axial preload, F:

$$F_j = ZD^2G \times \sin\alpha\left[\frac{\cos\alpha_0}{\cos\alpha} - 1\right]^{1.5} \qquad (15)$$

$$\delta_j = BD\frac{\sin(\alpha - \alpha_0)}{\cos\alpha} \qquad (16)$$

Here, subscript j relates to the specific bearing in question either bearing No. 1 or 2 in a duplex set, α_0 is the initial contact angle (under zero load conditions) and α is the final contact angle.

Values for Z, D, and α_0 in the above equations are easily obtained from catalogs or from the bearing manufacturers. The axial preload, F, is usually known or assumed from the application requirements.

Go to the curve in Fig 9 to obtain a value for G based on the computed value for B (from Eq 14), and to the chart in Fig 10 to obtain other necessary factors as follows:

1. Calculate a constant, t, from the known factors in the first part of Eq 15, by making t equal to

$$t = \frac{F}{ZD^2G} \qquad (17)$$

2. In Fig 10, locate the point of intersection of the line for t and the radial line for α_0. On the curves, the example is $t = 0.01$ and $\alpha_0 = 40$ deg.
3. Swing a radius about the right-hand origin through the located point.
4. At the intersection of this arc and the abscissa line (where $\alpha_0 = 0$) locate the value of δ/BD. In the example $\delta/BD = 0.089$.
5. Align a straight-edge through the intersection of t and α_0 lines such that the straight-edge is parallel to identically numbered markers of the upper and lower $\alpha - \alpha_0$ scales. In the example, locate $\alpha - \alpha_0 = 3.6$ deg.

From the values obtained in steps 4 and 5, you can now quickly determine the axial deflection δ and final contact angle α—without need for further reference to Eq 15 and 16. The amount of grinding required to achieve a given preload is then equal to δ.

Example III—Axial preload on duplex pair

It is desired to obtain an axial preload of 500 lb from a set of duplex angular contact ball bearings. The bearings have 52% inner and outer raceway groove curvatures, an initial contact angle of 40 deg, and a complement of 15 balls of 0.5 in. diameter. How much stock must be ground from the inner ring face of each bearing? From Eq 14:

$$B = 0.52 + 0.52 - 1 = 0.04$$

From Fig 9, for a value of $B = 0.04$, $G = 110{,}000$.

From Eq 17:

$$t = \frac{500}{15 \times (0.5)^2 \times 110{,}000} = 0.0012$$

From Fig 10, $\delta/BD = 0.022$. Hence,

$$\delta_p = (0.022)(0.04)(0.5) = 0.00044 \text{ in.}$$

Subscript p was added to denote that the deflection is due to axial preloading alone.

SKF preload suffixes for bearings
Table I

Bore dia. mm		Light preload		Heavy preload	
Over	Incl.	Lb	Suffix	Lb	Suffix
0	20	20	G 02	100	G 1
20	45	50	G 05	200	G 2
45	80	100	G 1	300	G 3
80	95	100	G 1	400	G 4
95	120	200	G 2	500	G 5
120	150	200	G 2	700	G 7
150	240	300	G 3	900	G 9

Bearings can be ordered with faces of inner ring shaved down to provide a specific preload. Example: To obtain a heavy preload for a 7210 B angular contact bearing, specify 7210 BG 5. This bearing will provide a 500-lb axial preload when clamped in assembly.

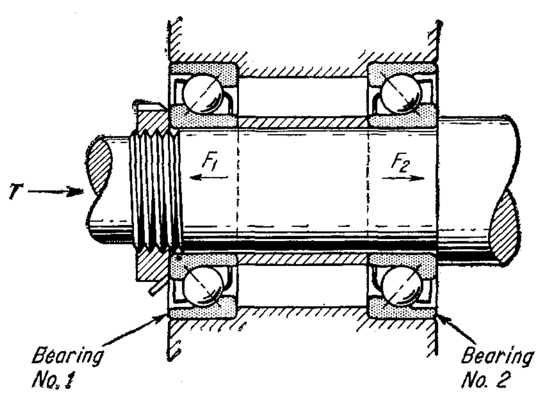

8 **Preloaded set of duplex bearings** subjected to an external thrust load, T. The computation for the resulting deflection is complicated by the fact that the preload at bearing 1 is increased by load T, while the preload at bearing 2 is decreased.

Also from Fig 10, $\alpha - \alpha_0 = 0.9$ deg. Hence,

$$\alpha = 0.9 + 40 = 40.9 \text{ deg}$$

Thus, 0.00044 in. must be removed from the inner ring face of each bearing to obtain 500 lb preload.

Example IV—With external thrust loads

Suppose now that the preloaded duplex bearings of Example III are subjected to external thrust load and it is necessary to obtain the axial deflection (Fig 8). **This complicates the analysis because only one of the two bearings resists this thrust.**

Designating the axial deflection of the bearing set due to the thrust load alone as δ_t, then at bearing 1, the effective axial deflection is $\delta_t + \delta_p$, in which δ_p is the axial deflection due to preloading. Correspondingly, the axial deflection at bearing 2 is $\delta_p - \delta_t$. The latter condition exists as long as bearing 2 is not relieved of all load. Therefore, according to Eq 16:

$$\delta_p + \delta_t = BD \frac{\sin(\alpha_1 - \alpha_0)}{\cos \alpha_1} \quad (18)$$

$$\delta_p - \delta_t = BD \frac{\sin(\alpha_2 - \alpha_0)}{\cos \alpha_2} \quad (19)$$

These two equations can be added together to yield:

$$2\delta_p = BD \left[\frac{\sin(\alpha_1 - \alpha_0)}{\cos \alpha_1} + \frac{\sin(\alpha_2 - \alpha_0)}{\cos \alpha_2} \right] \quad (20)$$

Also, according to Eq 14 and 15:

$$T = ZD^2G \left\{ \sin \alpha_1 \left[\frac{\cos \alpha_0}{\cos \alpha_1} - 1 \right]^{1.5} - \sin \alpha_2 \left[\frac{\cos \alpha_0}{\cos \alpha_2} - 1 \right]^{1.5} \right\} \quad (21)$$

Eq 19 and 20 must be solved simultaneously for the unknown contact angles α_1 and α_2. This procedure is best done on a digital computer; **however, several graphical techniques can be employed in the following manner:**

Example V—Simplified graphical techniques

Determine the axial deflection caused by an external 1000-lb thrust load applied to the preloaded duplex bearing set of Example III.

Establish for each bearing its load-deflection curve caused by preloading alone. This is done by selecting a schedule of loads (from 200 to 1600 lb, Table II), and then by Fig 10 and the method in Example III a series of deflections, δ_j, are obtained.

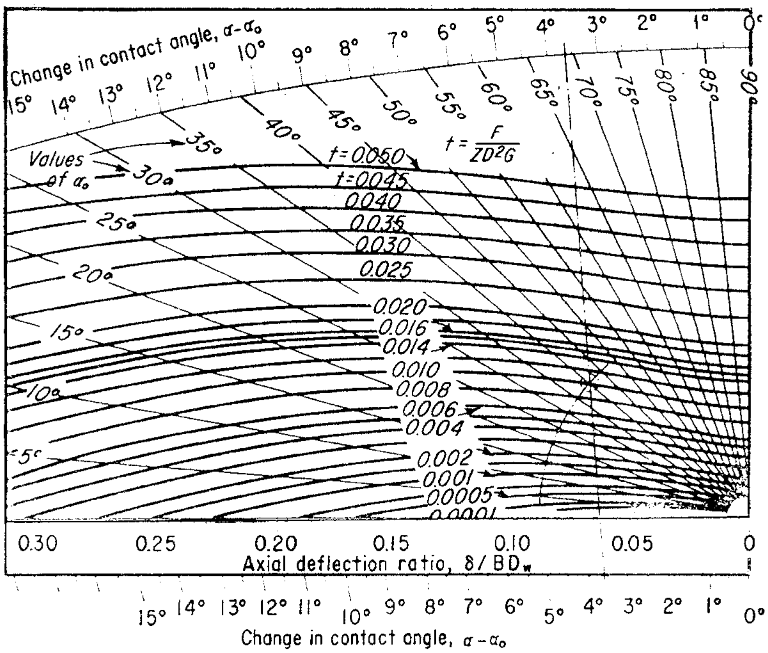

10 **Design chart for computing the axial deflection,** δ, under load, and the resultant change in contact angle α. Dashed lines are for Ex. III.

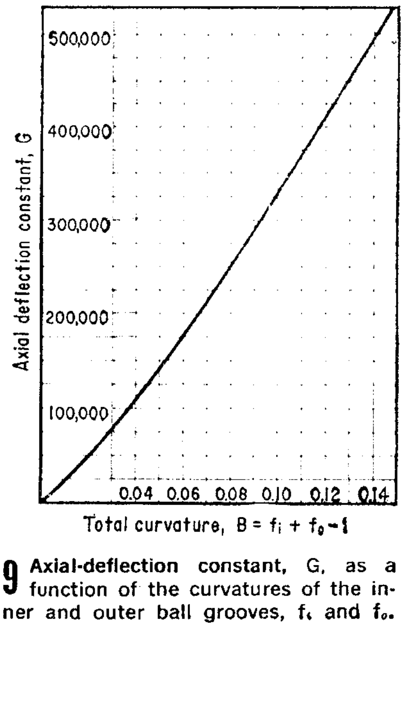

9 **Axial-deflection constant,** G, as a function of the curvatures of the inner and outer ball grooves, f_i and f_o.

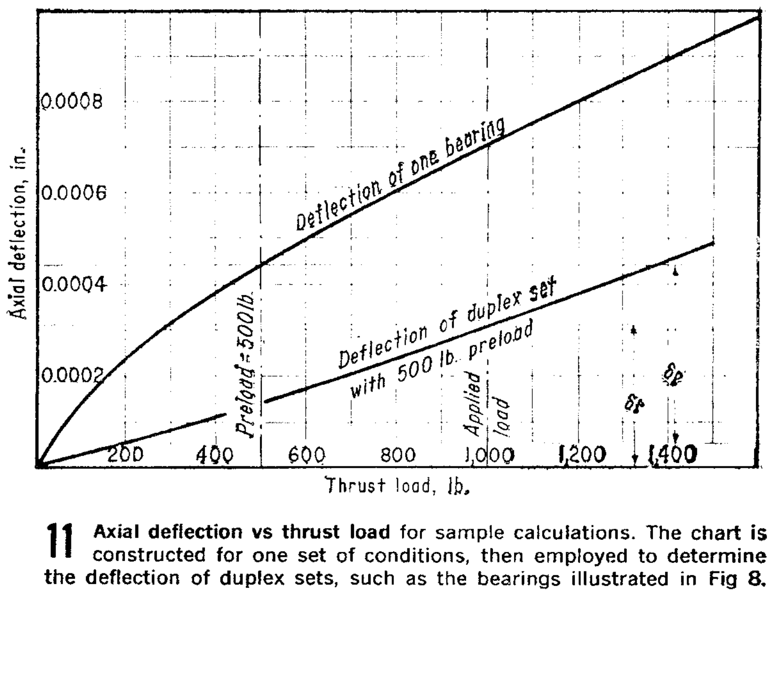

11 **Axial deflection vs thrust load** for sample calculations. The chart is constructed for one set of conditions, then employed to determine the deflection of duplex sets, such as the bearings illustrated in Fig 8.

Now plot the values of δ_j vs F_j (Fig 11). Note that at the preload of 500 lb, δ_p on each bearing is 0.00044 in. This value checks with that of Example III.

Next, with the aid of Fig 11, compute the effect of additional axial deflections caused by external axial thrusts. Thus in Table III, an additional deflection of 0.0001 results in a total deflection of 0.00054 on bearing 1, and 0.00034 on bearing 2. From Fig 11, the corresponding bearing loads are 670 and 340 lb, respectively. These loads act against each other, hence the algebraic sum is T = 670 − 340 = 330 lb.

Finally, plot T versus δ_t on Fig 11. From the latter curve at 1000 lb applied load, the deflection of the duplex bearing set in the loading direction is 0.0003 in. The thrust load on bearing 1 is 1070 lb and on bearing 2, 70 lb. If a single bearing were used to support the 1000 lb load with no help from preloading, the axial deflection would be 0.0007 in.

An approximate — but simpler — graphical method is also available. Note that to relieve the preload on bearing 2 in Example IV, the axial deflection δ_t be equal to the preload deflection δ_p. Therefore on Fig 11, find at $\delta_1 = 2\delta p = 0.00088$, thrust load $T = 1380$ lb. Now at $T = 1380$ lb and $\delta = 0.00044$ in. describe the point on the load-deflection curve of the duplex bearing set at which bearing 2 becomes unloaded. Draw a straight line on Fig 11 between the origin and the point just determined. This straight line approximates the deflection curve of the duplex bearing set. At $T = 1000$ lb find $\delta_t = 0.00033$, which value is practically identical to that previously determined.

In the foregoing examples, the bearings in the duplex set were identical. This condition was picked to simplify the calculations; however, it is sometimes desirable to use duplex bearings which are different in ball complement, ball size, groove curvature, and contact angle. In that case curves of δ_j versus F_j must be determined for each bearing. Thereafter, the calculated procedure is identical.

Triplex bearings

Frequently, two identical angular contact bearings mounted in tandem are reverse-mounted with a third angular contact bearing and preloaded, Fig 12. In this case, Eq 13 becomes:

$$T = 2F_1 - F_2 \qquad (22)$$

The axial deflections in the bearings are given by the equations below:

$$\delta_1 = \delta_{p1} + \delta_t \qquad (23)$$
$$\delta_2 = \delta_{p2} - \delta_t$$

in which δ_{p1} and δ_{p2} are the preload deflections in each bearing. This arrangement can increase bearing stiffness more than a simple duplex mounting. The following example illustrates this condition.

Example V—Three-bearing design

Three angular-contact ball bearings, identical to those of Example III, are mounted with two in tandem and one opposed (Fig 12). The bearings are preloaded to 500 lb. What axial deflection may be expected from an applied thrust load of 1000 lb?

Table II has already given the deflection load for each bearing (this was plotted on Fig 11). The preload in each bearing 1 is 250 lb each and δ_{p1} is 0.00028 in. As before, δ_{p2} is 0.00044 in. The data from Table III is revised to that given in Table IV. Thus the axial deflection is reduced to 0.0002 in. in lieu of 0.0003 in. as calculated for the duplex bearings set. Accordingly, the load on each of bearing 1 is 590 lb and on bearing 2 is 180 lb.

Changes in fatigue life

Will the fatigue life of duplex bearings be increased by axial preload, as was the case with the radially preloaded bearings? According to the AFBMA standard on load rating of ball bearings, the rating life of a thrust-loaded radial ball bearing is given by:

$$L_{10} = \frac{10^6}{60N}\left[\frac{C}{YF}\right]^3 \qquad (24)$$

where Y is the axial load factor supplied in accordance with AFBMA standards by Table V. If more than one bearing is mounted on a shaft, the rating life of the set is given by the following equation:

Load-deflection calculations for the examples
Table II

F_j	$t=\frac{F_j}{ZD^2G}$	$\frac{\delta_j}{BD}$	α_j-α_o	δ_j
200	0.0005	0.012	0.5	0.00024
400	0.0010	0.019	0.8	0.00038
600	0.0015	0.025	1.05	0.00050
800	0.0019	0.029	1.2	0.00058
1000	0.0024	0.034	1.4	0.00068
1200	0.0029	0.039	1.6	0.00078
1400	0.0034	0.044	1.8	0.00088
1600	0.0039	0.049	2.0	0.00098

Table III

δ_t	$\delta_p+\delta_t$	F_1	δ_p-δ_t	F_2	T
0.0001	0.00054	670	0.00034	340	330
0.0002	0.00064	870	0.00024	200	670
0.0003	0.00074	1070	0.00014	100	970
0.0004	0.00084	1290	0.00004	20	1270

Table IV

δ_t	$\delta_{p_1}+\delta_t$	F_1	$2F_1$	δ_{p_2}-δ_t	F_2	T
0.0001	0.00038	400	800	0.00034	340	460
0.0002	0.00048	570	1140	0.00024	200	940
0.0003	0.00058	760	1520	0.00014	100	1420

Y factors — effect of preload on bearing life
Table V

Contact angle, deg	20	25	30	35	40
Y-factor	1.00	0.87	0.76	0.66	0.57

$$L_{10} = \left[\sum_{j=1}^{j=m} L_{10_j}^{-1.1} \right]^{-0.9} \qquad (25)$$

Example VI—Life of a triplex set

Compare the rating life of the duplex bearing set of Example IV with that of the triplex mounting of Example V. The basic load rating of each bearing is 5000 lb and the shaft speed 1000 rpm. The Y factor for a bearing having a 40-deg contact angle is 0.57 (Table V).

Duplex set:

$$L_{10_1} = \frac{10^6}{(60)(1000)} \left[\frac{5000}{(0.57)(1070)} \right]^3$$
$$= 9190 \text{ hr}$$
$$L_{10_2} = \frac{10^6}{(60)(1000)} \left[\frac{5000}{(0.57)(100)} \right]^3$$
$$= 11{,}250{,}000 \text{ hr}$$
$$L_{10} = [L_{10_1}^{-1.1} + L_{10_2}^{-1.1}]^{-0.9}$$
$$= [(9.19 \times 10^3)^{-1.1} + (11.25 \times 10^6)^{-1.1}]^{-0.9}$$
$$L_{10} = 9190 \text{ hr}$$

Triplex set:

$$L_{10_1} = \frac{10^6}{(60)(1000)} \left[\frac{5000}{(0.57)(590)} \right]^3$$
$$= 54{,}800 \text{ hr}$$
$$L_{10_2} = \frac{10^6}{(60)(1000)} \left[\frac{5000}{(0.57)(180)} \right]^3$$
$$= 1{,}929{,}000 \text{ hr}$$
$$L_{10} = [(2)(5.48 \times 10^4)^{-1.1} + (1.929 \times 10^6)^{-1.1}]^{-0.9}$$
$$= 54{,}100 \text{ hr}$$

Thus, the triplex set may have six times longer life than a duplex set. We have already seen that the triplex set yields less deflection under the same load—0.0002 in. as against 0.0003 in. for the duplex bearings. This is a significant gain in bearing design for machine tools, especially if the loads are larger than those chosen for this example. But the main drawback of a triplex set, of course, is that it requires more space, weight and cost.

PRELOADING TO PREVENT SKIDDING

Many modern applications such as aircraft gas turbines rotate at very high speed, 10,000 rpm and above, under light radial loading. This combination of light load and high speed tends to cause skidding, in lieu of rolling, between the bearing inner ring and rolling elements. Skidding, in turn, causes wear of the bearing load-carrying surfaces and results in decreased bearing life.

The cure for the skidding problem is higher specific ball or roller loads; ideally all rolling elements should be loaded. In radial ball bearing applications, this is easily accomplished by applying a light thrust load to the bearing. Also, a light uniform radial preload could eliminate skidding; however, it is mechanically easier to control a simple axial preloading device than it is to control a uniform radial preloading device, especially when the bearings are to operate under elevated temperatures.

When an axial preload cannot be applied, as in cylindrical roller bearings, then one solution is the use of an out-of-round bearing outer ring wherein the major axis is aligned in the direction of radial loading. This has successfully prevented skidding. The roller load distribution becomes concentrated in two areas (Fig 13).

Generally, the amount of out-of-roundness is one order of magnitude larger than the bearing clearance, eg, 0.020 to 0.040 in. as compared to 0.001 in. clearance. To manufacture the out-of-round ring, a circular ring is distorted to the specified condition of out-of-roundness and ground circular. It is then allowed to spring back to its original condition. This process produces an inverted out-of-round ring. The outer ring is, of course, distorted to assemble over the rollers and cause a selective interference fit which is described by the equations below in terms of the roller angular location, ϕ:

When $0 \leq \phi \leq \pm \frac{\pi}{2}$

$$C_k = R \frac{\left[\frac{2}{\pi} - \frac{1}{2} \cos \phi - \frac{1}{2}\phi \sin \phi \right]}{\frac{\pi}{2} - 1} + \frac{C}{2} \qquad (26)$$

When $\pm \frac{\pi}{2} \leq \phi \leq \pi$

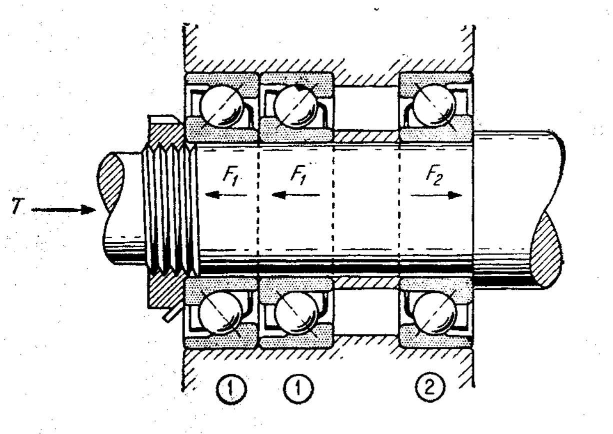

12 Triplex set of angular contact bearings, mounted two in tandem and one opposed. This arrangement provides an even higher axial stiffness and longer bearing life than with a duplex set, but requires more space.

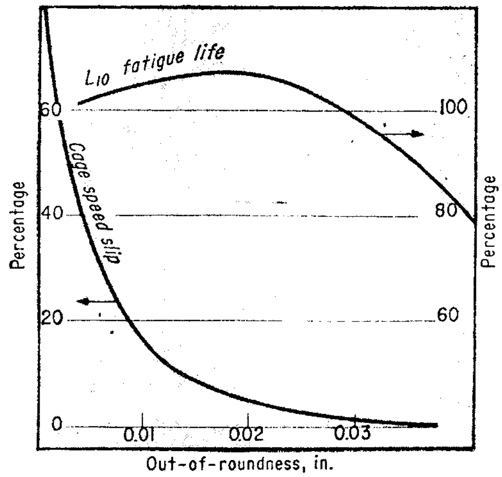

13 Effect of out-of-roundness on slippage of cage and fatigue life. Increasing the out-of-roundness decreases slip, but the fatigue life starts to drop off after a point as evident from the top curve.

$$C_k = R\frac{\left[\frac{2}{\pi} - \frac{1}{2}\cos(\pi-\phi)\right]}{\frac{\pi}{2}-1} - R\frac{\left[\frac{1}{2}(\pi-\phi)\sin(\pi-\phi)\right]}{\frac{\pi}{2}-1} + \frac{C}{2} \quad (27)$$

Where R = out-of-roundness, and C_k = clearance at angular location ϕ_k, (angle ϕ is equal to zero at the position of peak loading, Fig 3), and where the 0 to 180 deg axis is aligned in the radial load direction.

Because the out-of-round outer ring is supported in the housing at virtually two points, 0 and 180 deg, the outer ring is very flexible under roller load. This feature makes the bearing life less sensitive to out-of-roundness than it is to a uniform radial preload. Consequently, it is possible to avoid skidding and yet have satisfactory life.

As the degree of out-of-roundness is increased the cage-speed slip is reduced, (Fig 13), and the L_{10} fatigue life increases but then drops off due to over preloading. Analysis of skidding phenomena is difficult, but SKF has developed an IBM 7090 computer program which estimates the extent of skidding in high-speed roller bearings and further estimates the effectiveness of degrees of outer ring out-of-roundness in minimizing skidding. Bearing users may contract with SKF for the use of the computer program as it pertains to their application.

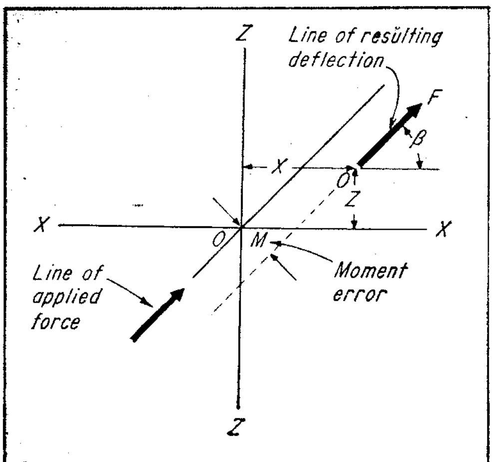

14 Effect of disturbing force F on the center of gravity of spring mass. It is frequently desirable to obtain isoelasticity in bearings in which the displacement in any direction is in line with the disturbing force.

PRELOADING FOR ISOELASTICITY

It is sometimes desirable that the axial and radial yield rates of the bearing and its supporting structures be as nearly identical as possible. In other words, a load in either the axial or radial direction should cause identical deflections (ideally). This necessity for *isoelasticity* in the ball bearings came with the development of the highly accurate, low drift inertial gyros for navigational systems, and for missile and space guidance systems. Such inertial gyros usually have a single degree of freedom tilt-axis and are extremely sensitive to error moments about this axis.

Consider a gyro in which the spin axis, Fig 14, is coincident with the X-axis, the tilt axis is perpendicular to the paper at the origin O, and the center of gravity of the spin mass is located at the intersection of the three coordinate axes. If the spin mass is acted upon by a disturbing force F in the X-Z plane and directed at an oblique angle β to the X-axis, this force will tend to displace the spin mass center of gravity from O to O'. If, as shown by Fig 15, the displacements in the directions of the X and Z axes are not equal, the force F will create an error moment about the tilt axis.

In terms of the axial and radial yield rates of the bearings, the error moment, M, is

$$M = \tfrac{1}{2}F^2(R_z - R_x)\sin 2\beta \quad (28)$$

where the bearing yield rates R_z and R_x are in in./lb of force.

To minimize M and subsequent drift, R_z must be as nearly equal to R_x as possible — a requirement for pinpoint navigation or guidance. Also, from Fig 14 it can be noted that improving the rigidity of the bearing, ie, decreasing R_z and R_x collectively, reduces the magnitude of the minimal error moments achieved through isoelasticity.

What are the best ways for obtaining equal yield rates? In most radial ball bearings, the radial rate is usually smaller than axial rate. This is best overcome by increasing the bearing contact angle which reduces the axial yield rate and increases radial yield rate. You can achieve one-to-one ratios by specifying bearings with contact angles that are 30 deg or higher.

At these high angles, the sensitivity of the axial-to-radial yield-rate ratio to the amount of preload is quite small. It is, however, necessary to preload the bearings to maintain the desired contact angles.

Compact Ball Transfer Units

Masses of ball transfer units in airplane floor make it easy to shove cargo loads in any direction.

Compact ball transfer units roll loads every which way

An improved design of an oft-neglected device for moving loads—ball transfers—is opening up new applications in air cargo planes (photo above) and other materials handling jobs. It can serve in production lines to transfer sheets, tubes, bars, and parts.

Uses of established ball transfer units have been limited largely to furniture (in place of casters) and other prosaic duties. With new design that takes fuller advantage of their multiple-axis translation and instantaneous change of direction, ball transfer units can be realistically considered as another basic type of anti-friction bearing. The improved units are made by General Bearing Co., West Nyack, N.Y.

How they work. Essentially, ball transfers (photo below) are devices that translate omnidirectional linear motion into rolling motion to provide an unlimited number of axes of movement in any given plane. In such a unit, a large main ball rotates on its own center within a housing. This ball is supported by a circular group of smaller balls (drawing below) that roll under load and, in so doing, recirculate within the housing in endless chains.

These units are designed either as "ball up" or as "ball down." In the "ball down" units, design must provide a positive means of recirculating the support balls so they won't fall away under their own weight.

Variations. Many different configurations are available to suit the specific requirements of customers. Balls of carbon steel are most often used, but stainless steel balls are available for uses where corrosion may be a problem. Ball transfer units can be sealed to exclude dirt.

Where loads require that a number of ball transfers must simultaneously contact the load surface, a spring technique has been developed. Each ball transfer (drawing below) is spring-loaded. It starts to deflect when its own rated load is exceeded, allowing other ball transfers to pick up their share of the load. This concept also provides protection against major overloads in any ball transfer unit. □

Main ball shown, 1 in. dia., is supported by 70 smaller balls, hidden.

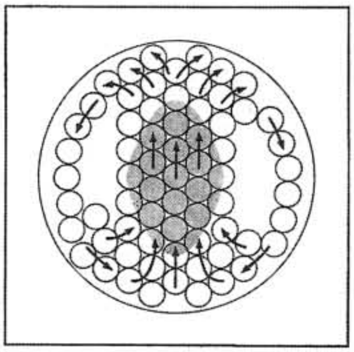

Shaded area seen from above shows load; arrows show ball circulation.

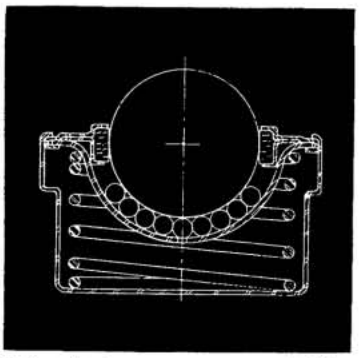

Spring loading assures even distribution of the load on the small balls.

SECTION 16

SPRINGS

12 Ways to Put Springs to Work

Variable-rate arrangements, roller positioning, space saving, and other ingenious ways to get the most from springs.

L. Kasper

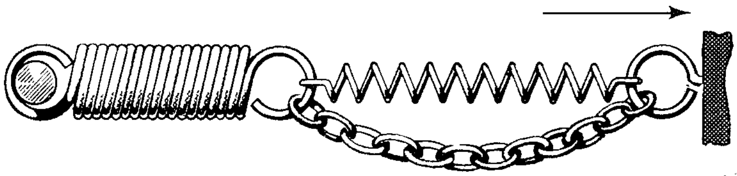

1 VARIABLE RATE with sudden change from light load to heavy load is achieved by limiting the low-rate extension with a spring.

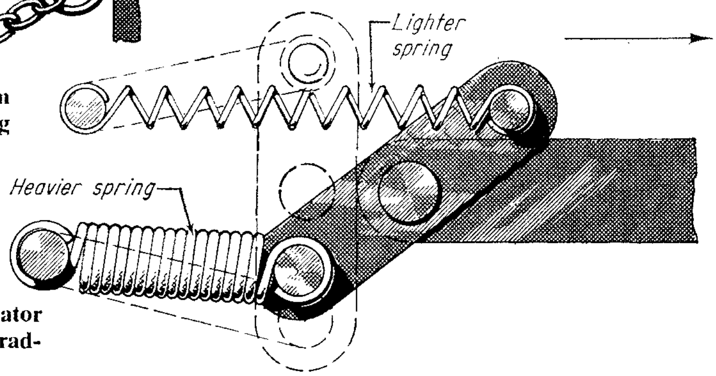

2 DIFFERENTIAL-RATE linkage lets actuator stroke be under light tension at start, then gradually heavier tension.

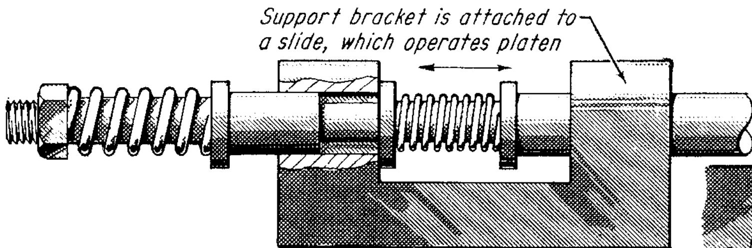

5 COMPRESSING MECHANISM has dual rate for double-action compacting. In one direction pressure is high, in reverse pressure is low.

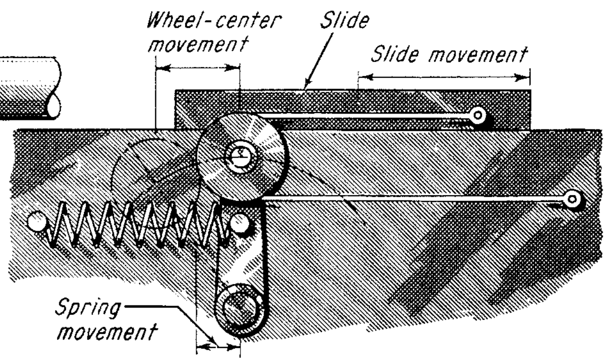

6 SHORT EXTENSION of spring for long movement of slide keeps tension change between maximum and minimum low.

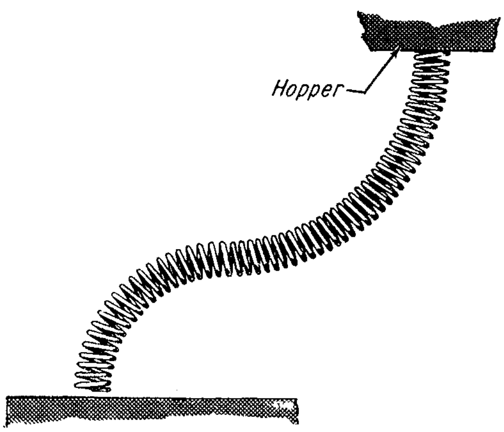

9 CLOSE-WOUND SPRING is attached to a hopper and will not buckle when used as a movable feed-duct for nongranular material.

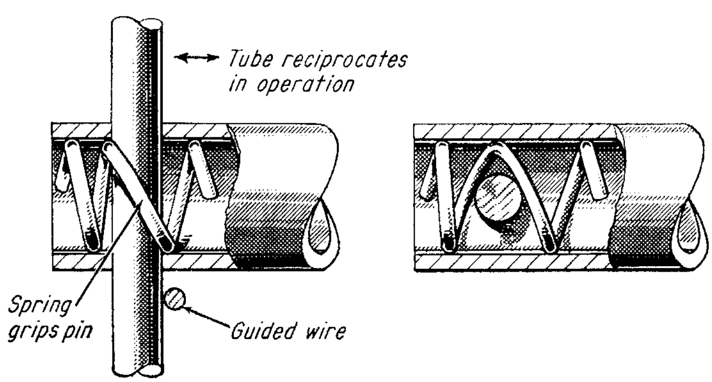

10 PIN GRIP is spring that holds pin by friction against end movement or rotation, but lets pin be repositioned without tools.

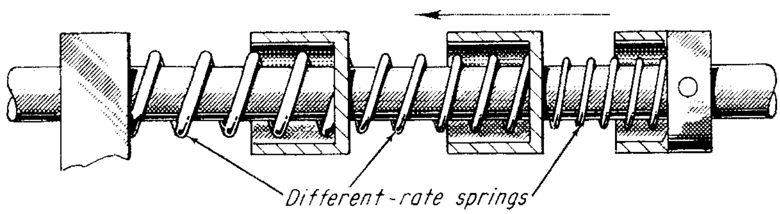

3 **THREE-STEP RATE** change at predetermined positions. The lighter springs will always compress first regardless of their position.

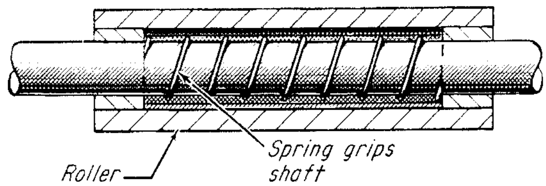

4 **ROLLER POSITIONING** by tight-wound spring on shaft obviates necessity for collars. Roller will slide under excess end thrust.

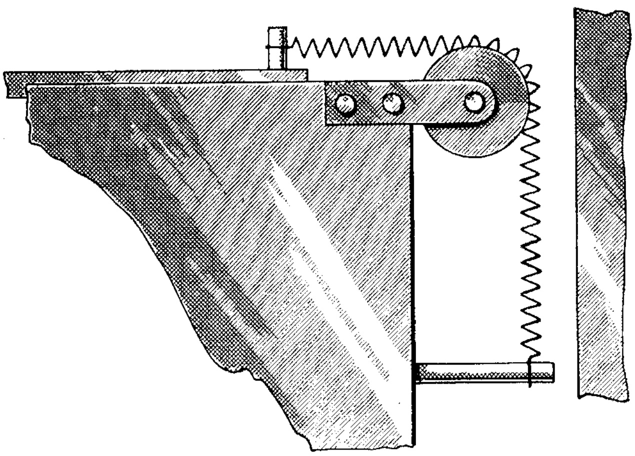

7 **SPRING WHEEL** helps distribute deflection over more coils than if spring rested on corner. Less fatigue and longer life result.

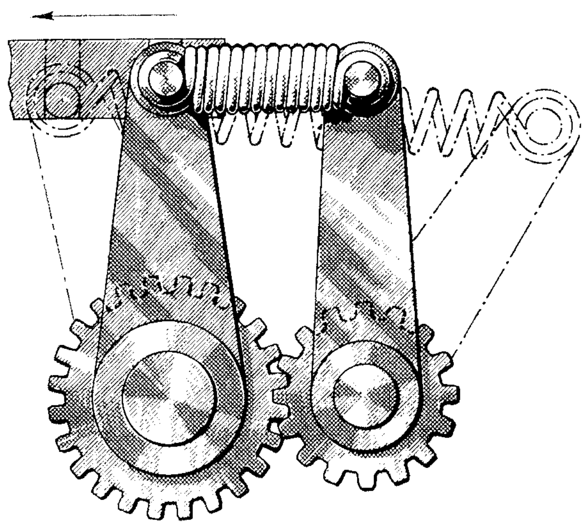

8 **INCREASED TENSION** for same movement is gained by providing a movable spring mount and gearing it to the other movable lever.

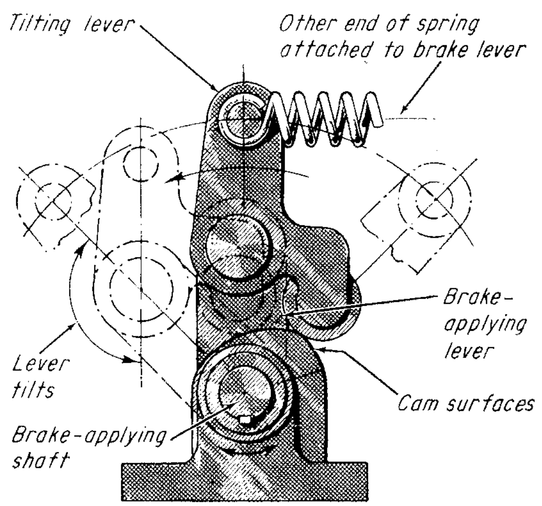

11 **TENSION VARIES** at different rate when brake-applying lever reaches the position shown. Rate is reduced when tilting lever tilts.

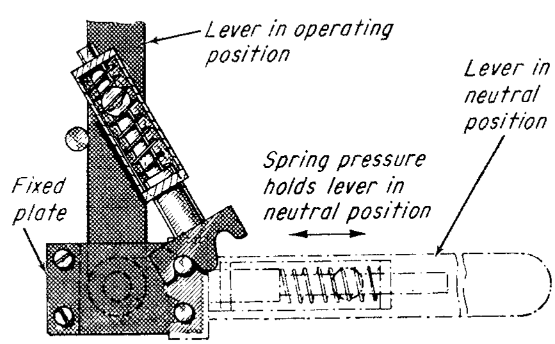

12 **TOGGLE ACTION** here is used to make sure the gear-shift lever will not inadvertently be thrown past neutral.

29 Ways to Fasten Springs

Four pages of ingenious attachments for extension, compression and torsion springs.

Federico Strasser

EXTENSION SPRINGS

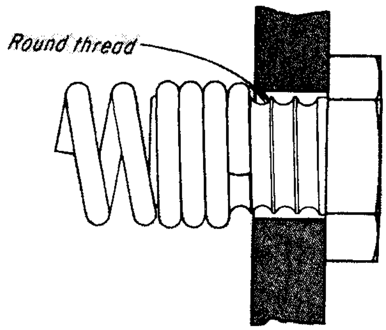

1

Screw fits into spring end.

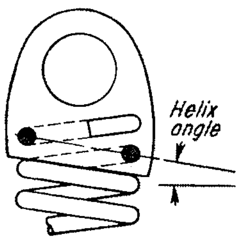

2

Tab with 3 holes engages 1½ spring-coils.

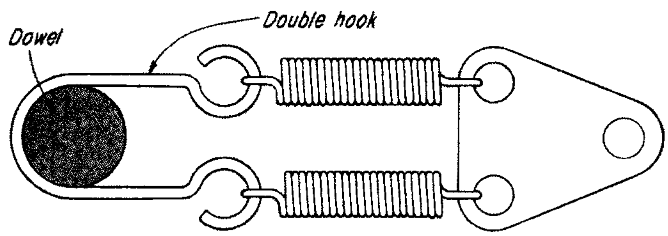

3

Twin-spring setup includes double hook and triangular tab.

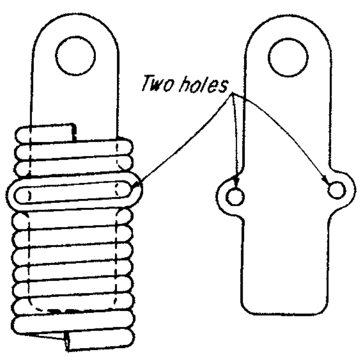

4

Long tab with 2 holes in midsection provides ample adjustment.

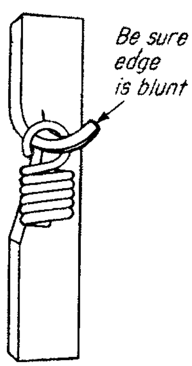

5

Sheetmetal, slit and formed, suspends spring.

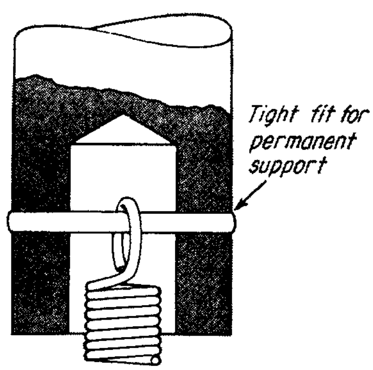

6

Cross-pin holds spring deep in hole.

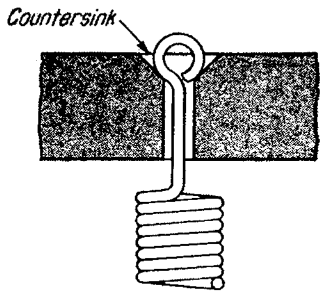

7

Countersunk hole leaves spring free to turn.

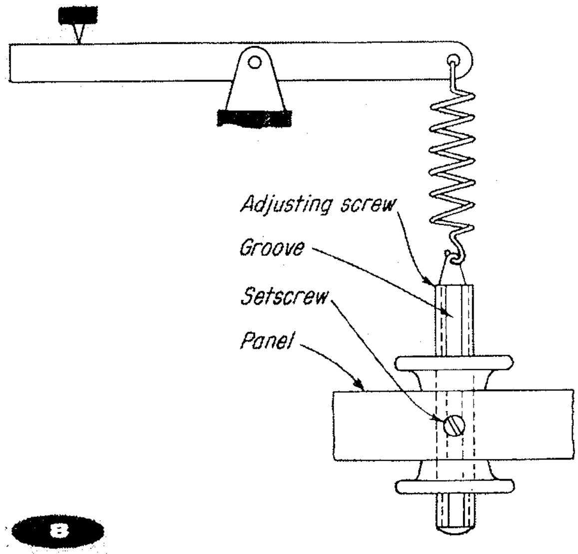

Tension adjustment requires nonrotating screw.

8

COMPRESSION SPRINGS

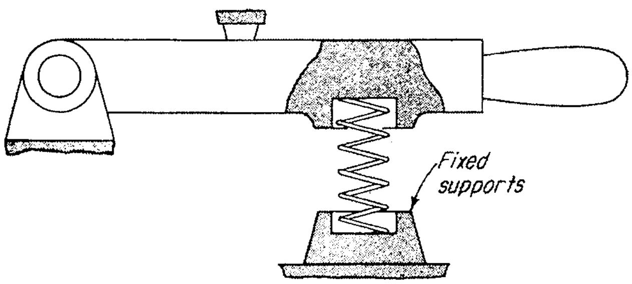

9

Unsupported spring-body must have somewhat more resistance to buckling in fixed supports (9) than pivoted ones (10).

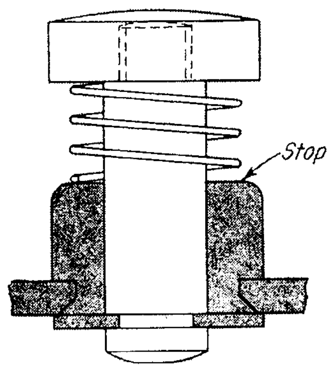

11

Supported springs are exemplified in push button (11) and friction clutch (12).

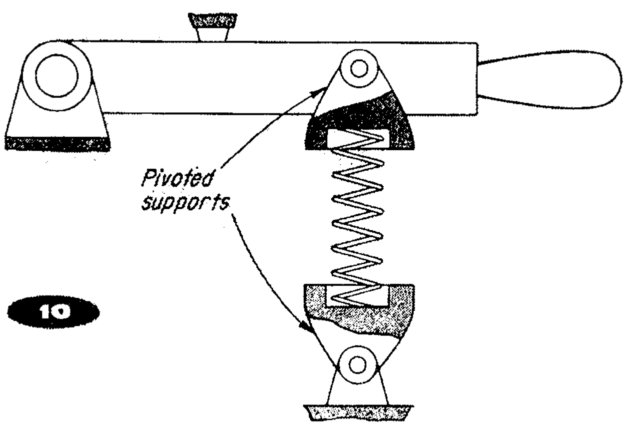

10

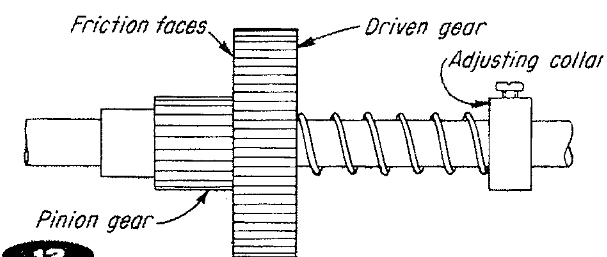

12

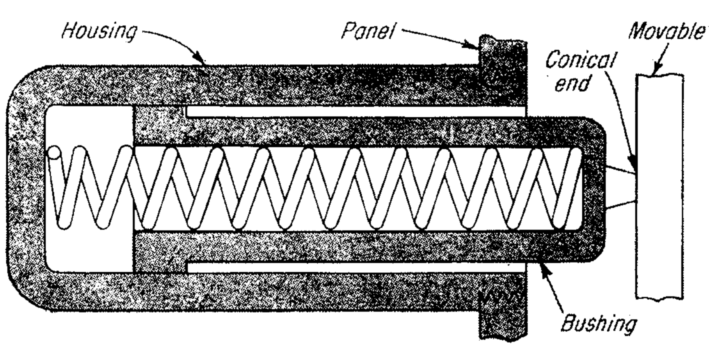

13

Concealed spring is supported externally by closed-end bushing, which also determines amount of compression.

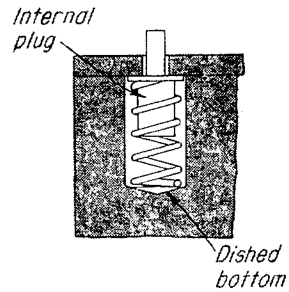

14

Double guidance is exemplified by hole-bottom that centers spring end, and internal plug that supports spring body.

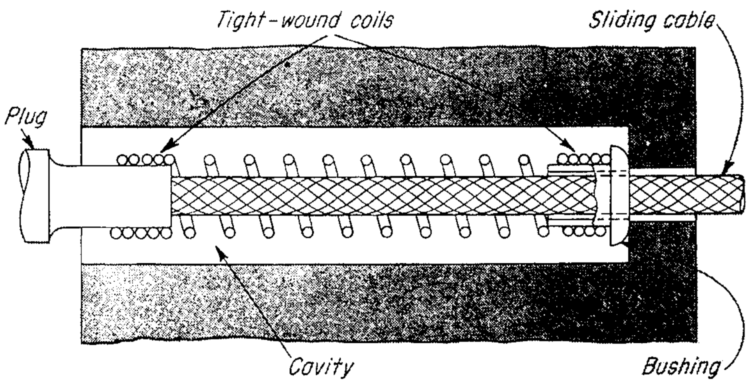

15

Tight-wound end-coils hold switchboard plug bushing—spring absorbs shock when weighted cable snaps entire assembly back into cavity after operator disconnects plug at end of message.

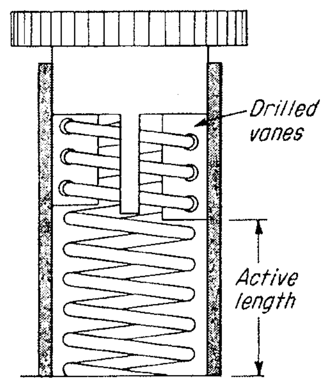

16

Adjustment vanes have holes that match spring pitch. Spring coils threaded through vanes become inactive, thus varying effective spring length.

FLAT TORSION-SPRINGS

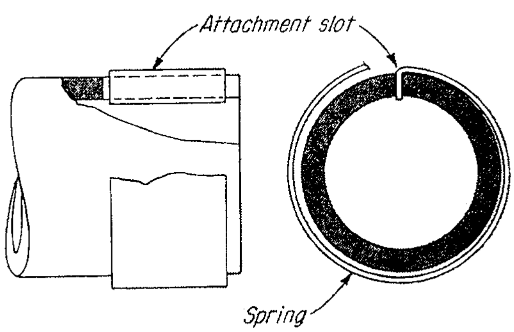

17

Saw-cut slot retains spring positively if slot end is peened over or otherwise closed.

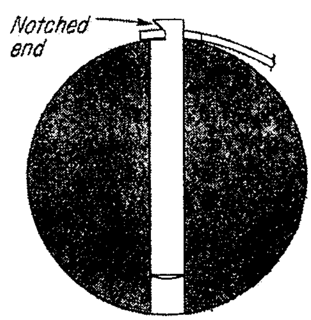

18

Notched dowel provides hook for hole in spring end.

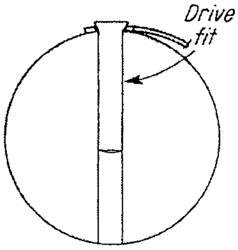

19

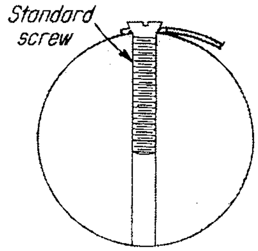

20

Headed drive-pin through spring hole makes disassembly difficult (19). Standard screw (20) eases disassembly.

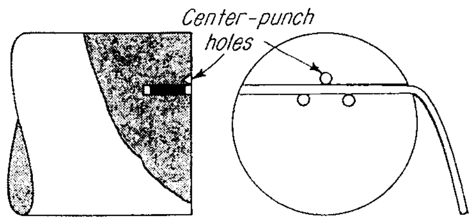

21

Chordal shot in shaft is closed tight by displacing metal with center punch for permanent spring retention.

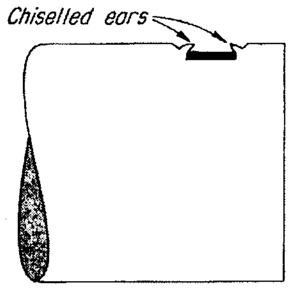

22

Chordal groove holds spring when ears are formed by chiselling or staking after assembly.

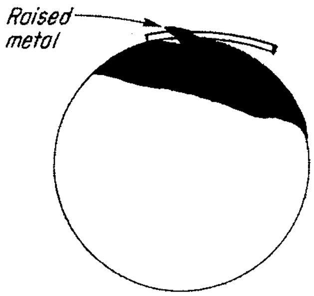

23

Raised metal, produced by staking, provides low-cost yet firm hook on shaft.

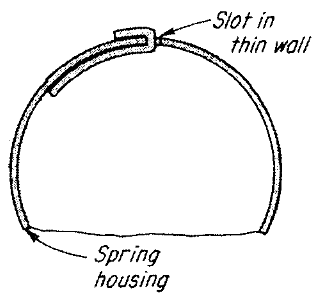

24

Slotted spring-housing is simple, but spring-end can be dangerous if housing revolves and is unprotected.

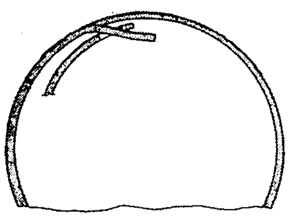

25

Lanced tab avoids hazard of external spring-end but dirt can enter housing.

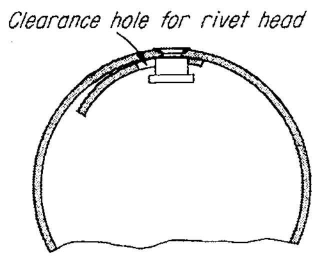

26

Shoulder rivet provides dustproof fastening.

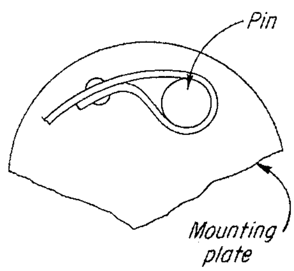

27

Mounting pin on plate may be plain, or headed—for more positive spring retention.

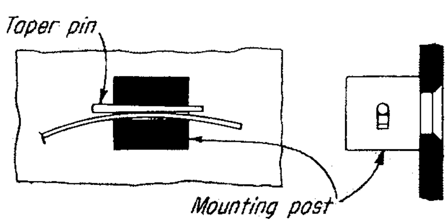

28

Taper pin allows end adjustment of precision, low-torque springs.

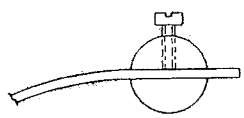

29

Setscrew and slotted post also provides adjustment feature but may be inefficient if spring-end becomes dimpled.

Control Depth Primer Tool Employs Coil Spring

E. E. Lawrence, Inventor
R. O. Parmley, Draftsman

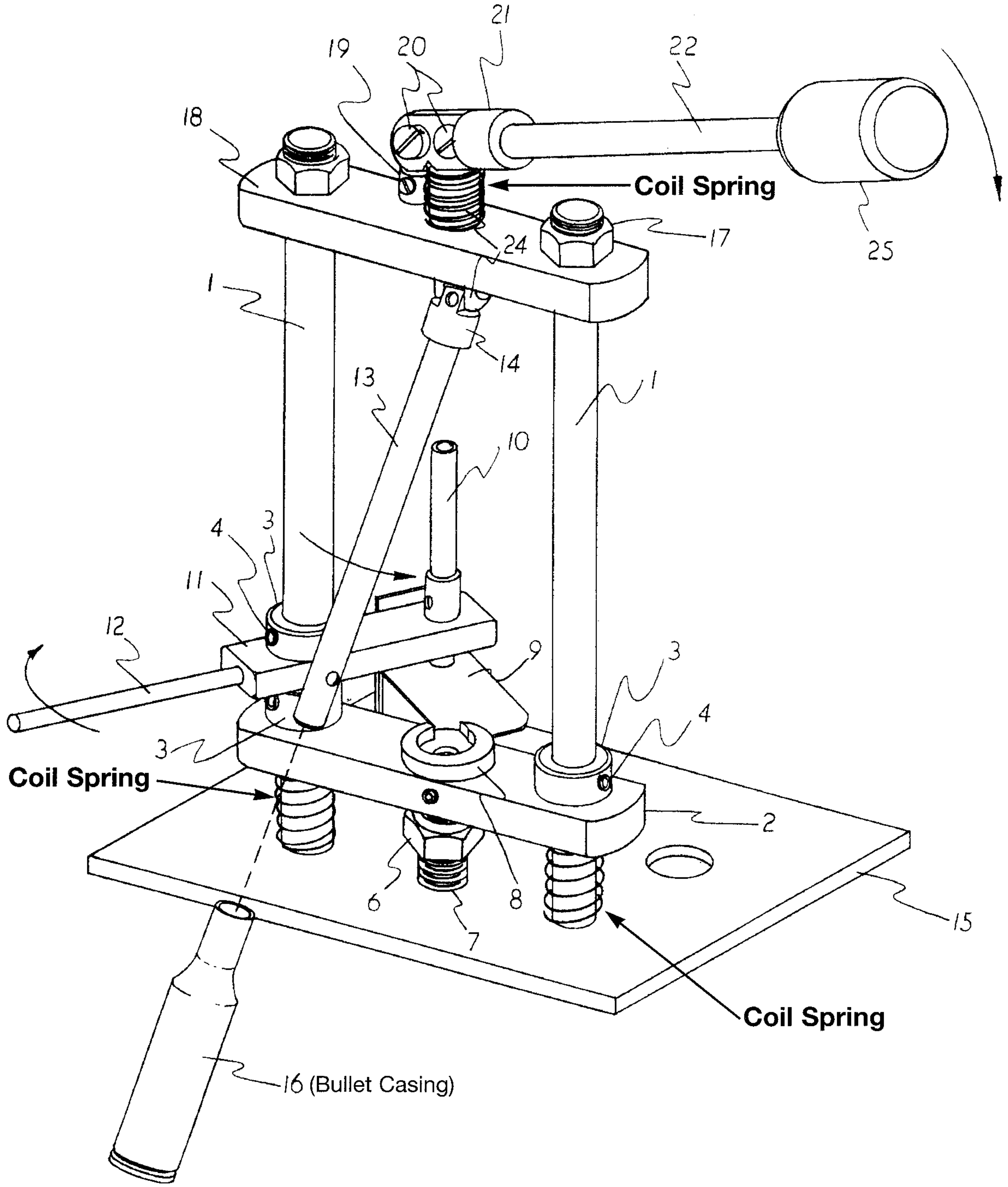

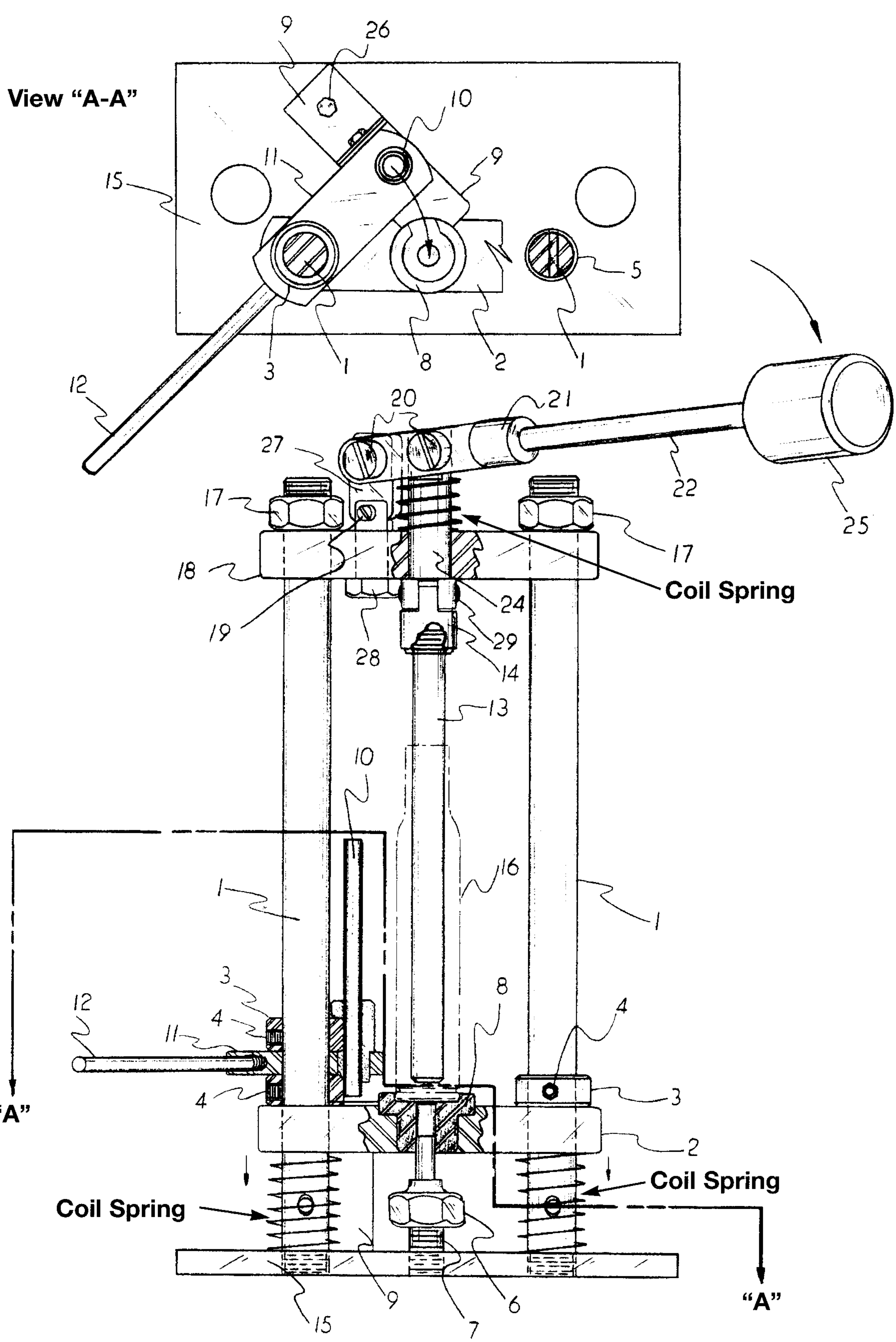
View "A-A"
9
26
10
11
9
15
5
3
1
8
2
1
12
20
21
27
22
25
17
17
18
Coil Spring
24
19
29
28
14
13
10
16
1
1
3
12
4
11
8
4
4
3
"A"
2
Coil Spring
Coil Spring
15
9
7
6
"A"

Multiple Uses of Coil Springs

R. O. Parmley

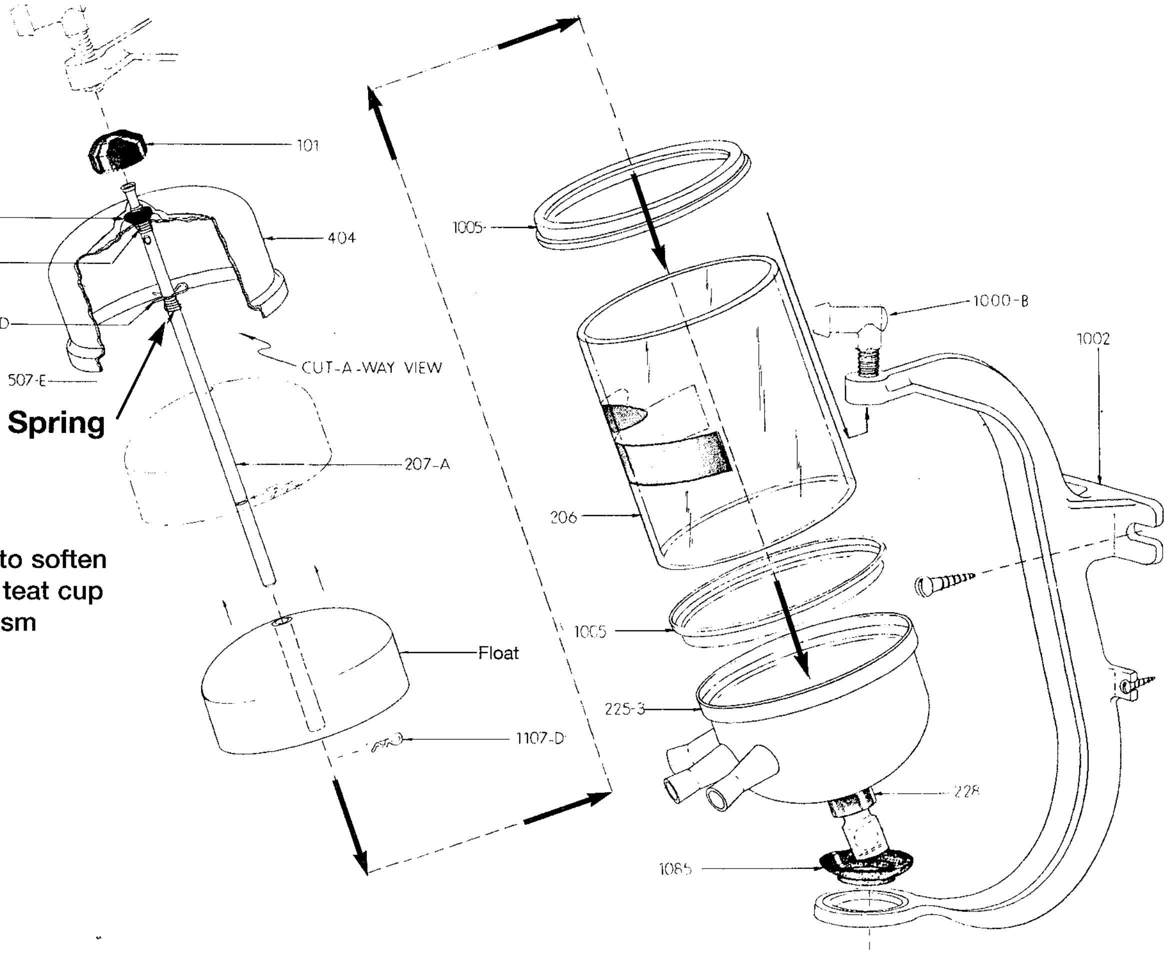

Coil Spring used to soften impact of float in teat cup washing mechanism

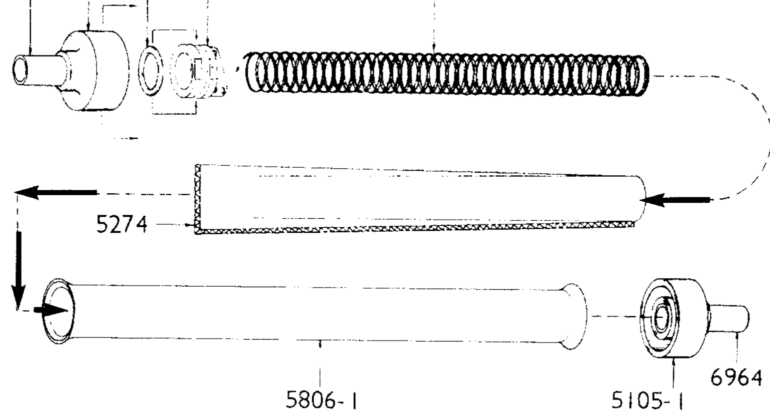

Coil Spring used as reinforcement of filter sock in milk filter assembly

Source: Bender Machine Works, Inc.

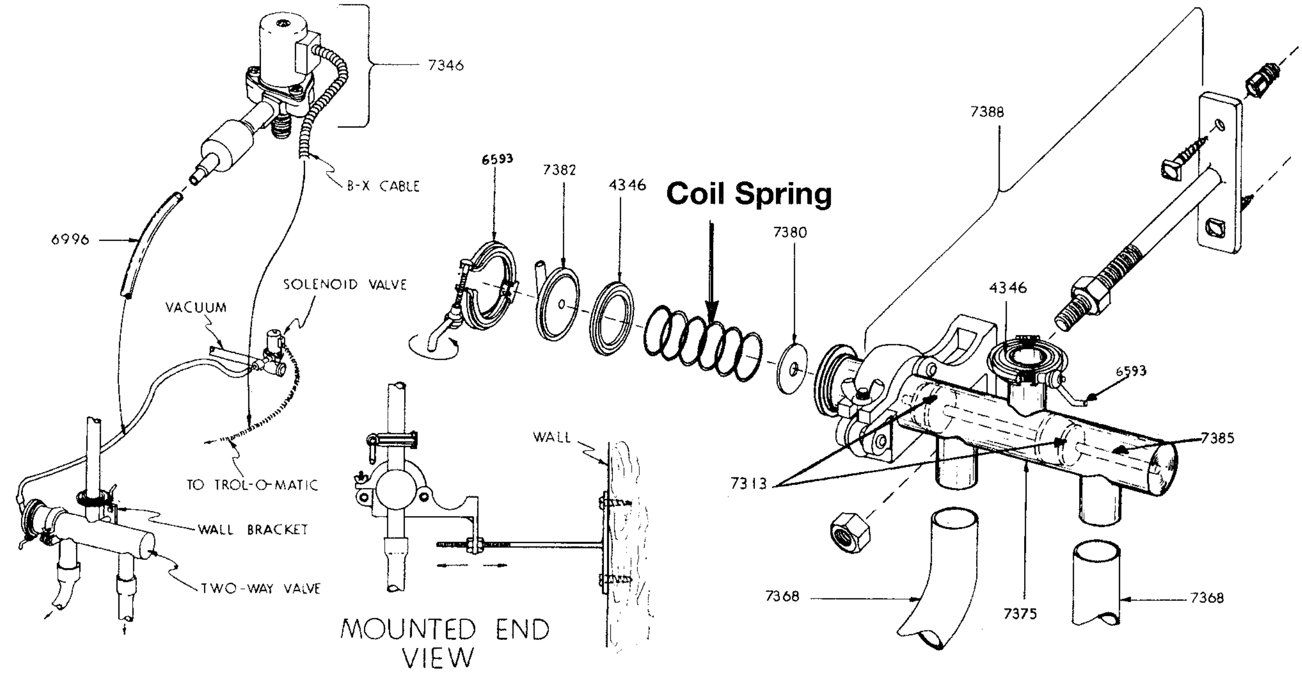

Coil Spring used stabilizing component in two-way valve assembly

Source: Bender Machine Works, Inc.

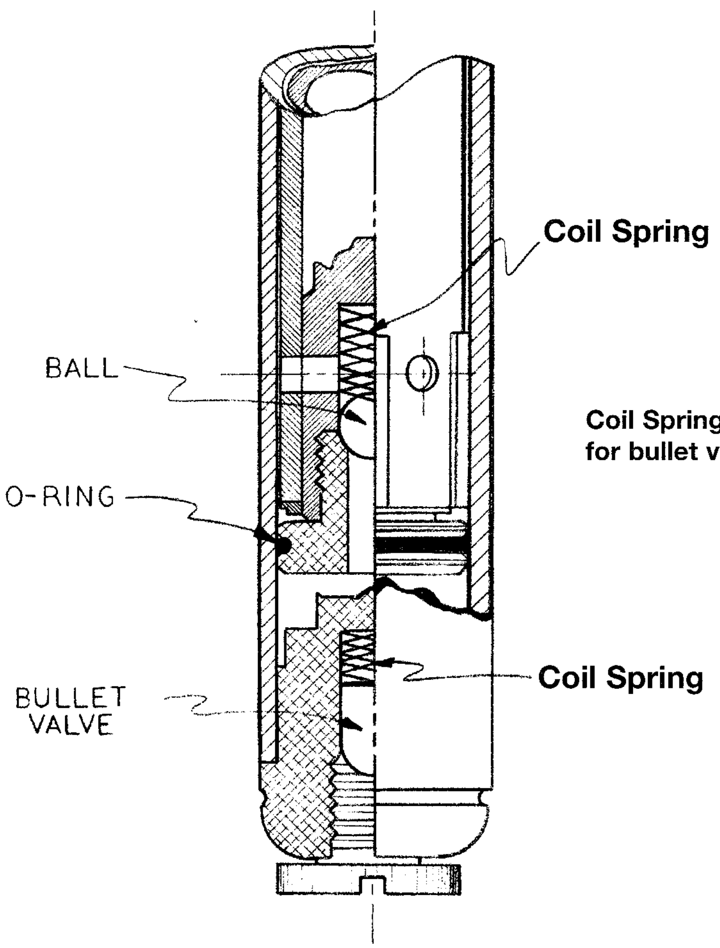

Coil Spring serve as controls for bullet valve and ball valve

Compression Spring Adjustment Methods I

In many installations where compression springs are used, adjustability of the spring tension is frequently required. The methods shown incorporate various designs of screw and nut adjustment with numerous types of spring-centering means to guard against buckling. Some designs incorporate frictional reducing members to facilitate adjustment especially for springs of large diameter and heavy wire.

Henry Martin

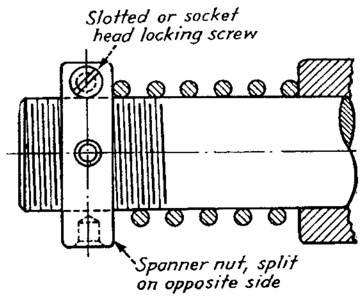

FIG.3

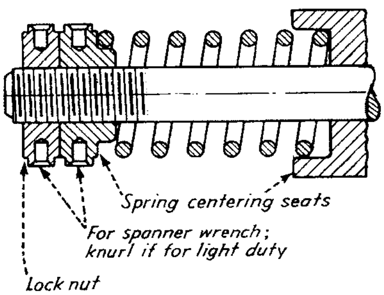

FIG.1

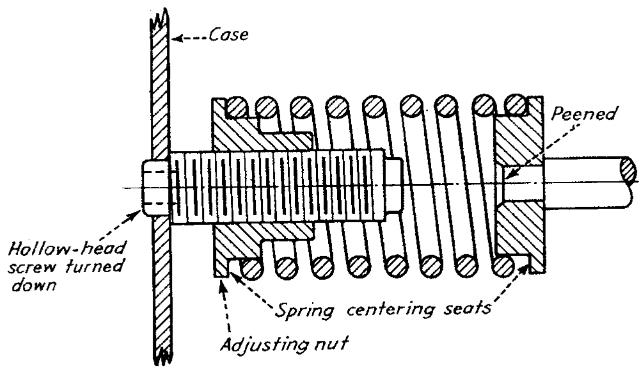

FIG.2

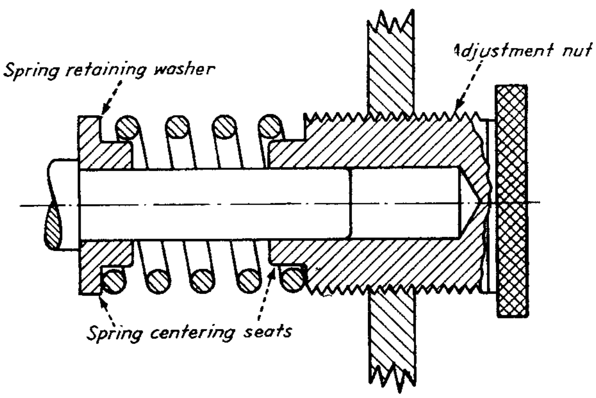

FIG.4

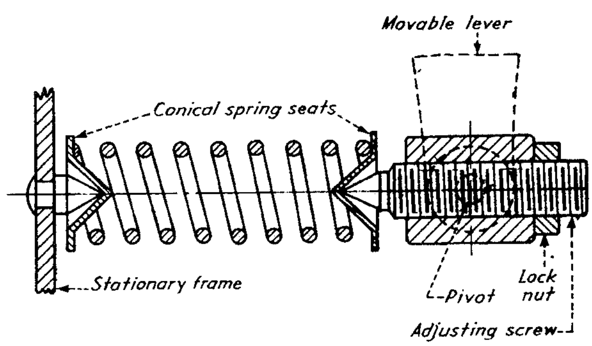

FIG.5

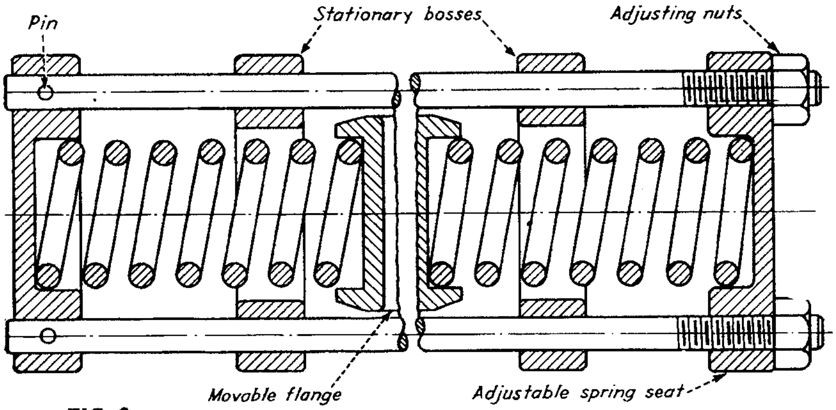

FIG.6

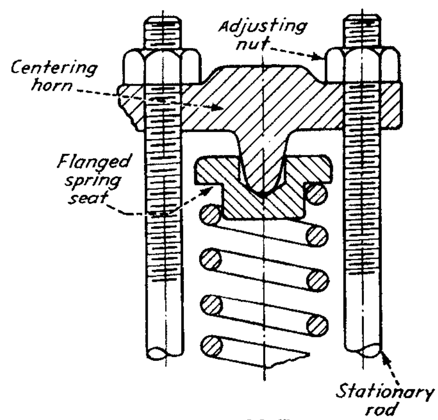

FIG.7

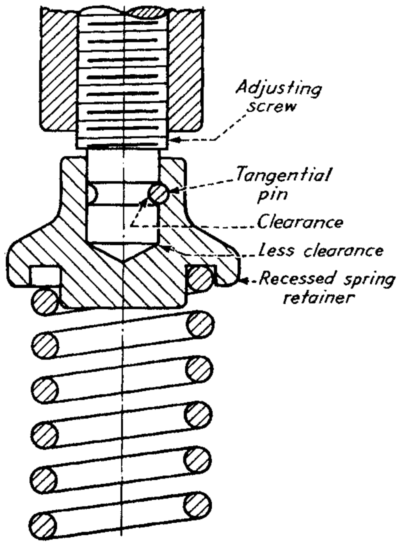

FIG. 8

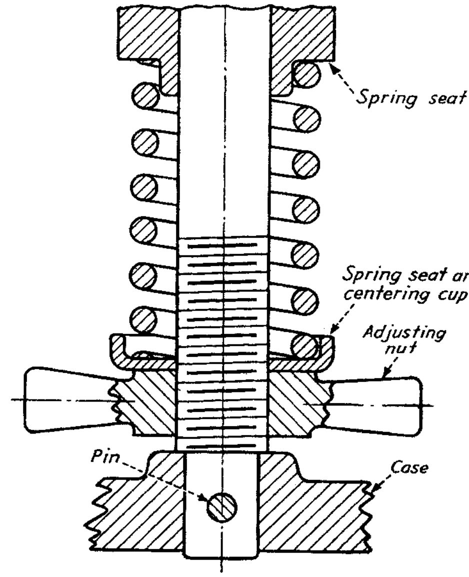

FIG. 9

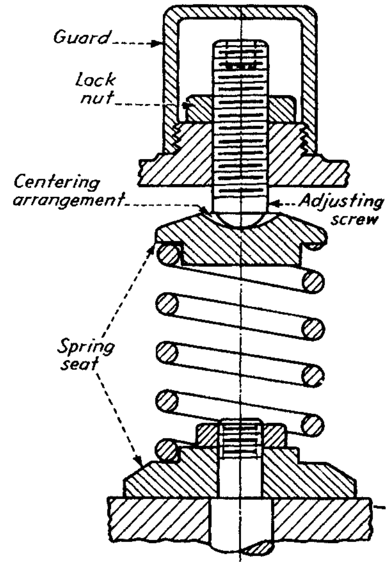

FIG. 10

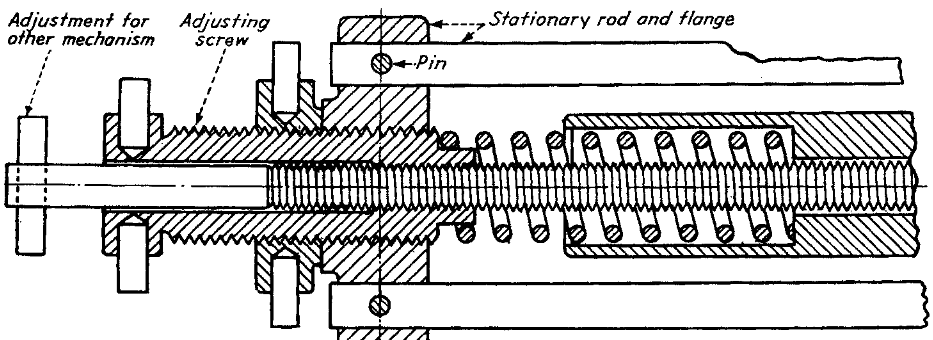

FIG. 11

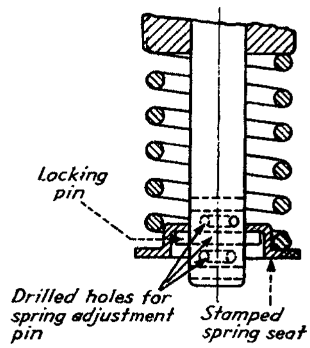

FIG. 12

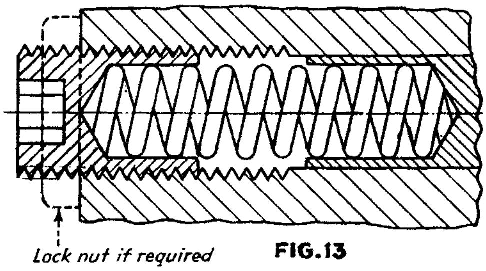

FIG. 13

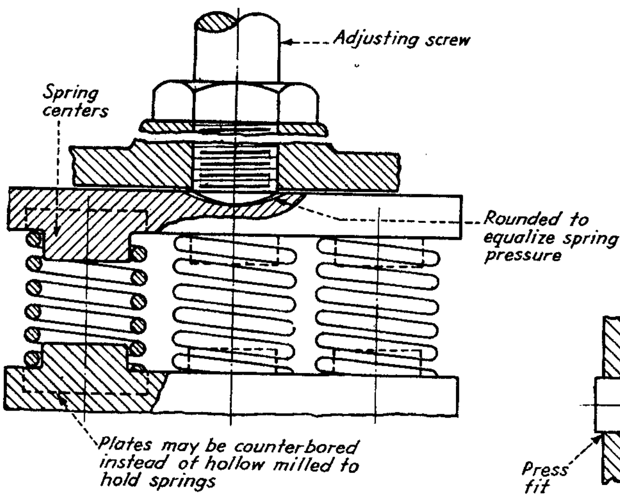

FIG. 14

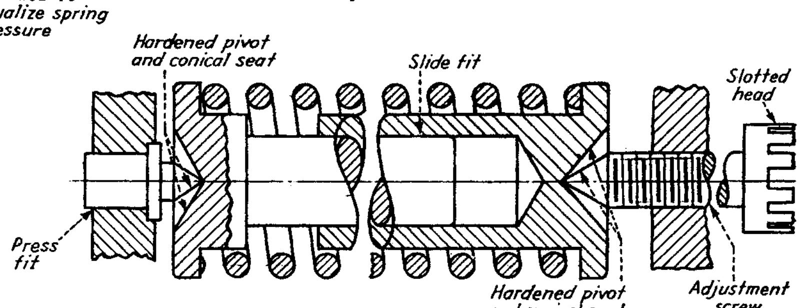

FIG. 15

Compression Spring Adjustment Methods II

In this concluding group of adjustable compression springs, several methods are shown in which some form of anti-friction device is used to make adjustment easier. Thrust is taken against either single or multiple steel balls, the latter including commercial ball thrust bearings. Adjustments of double spring arrangements and other unconventional methods are also illustrated.

Henry Martin

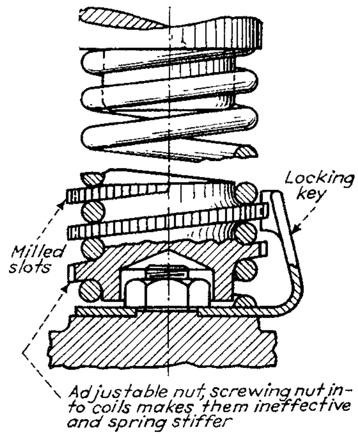

FIG.18

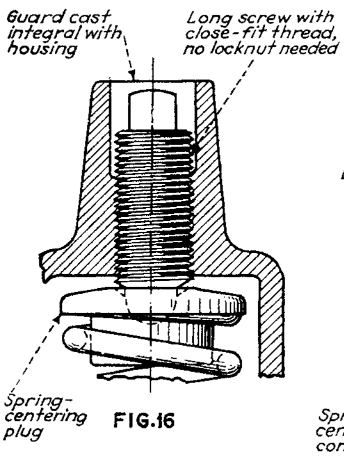

FIG.16

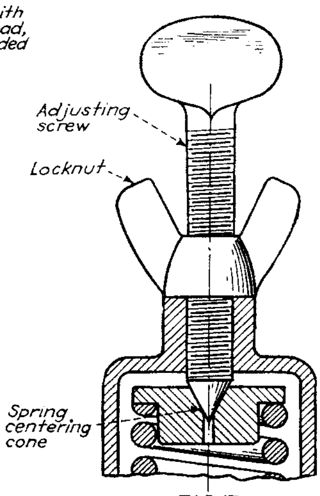

FIG.17

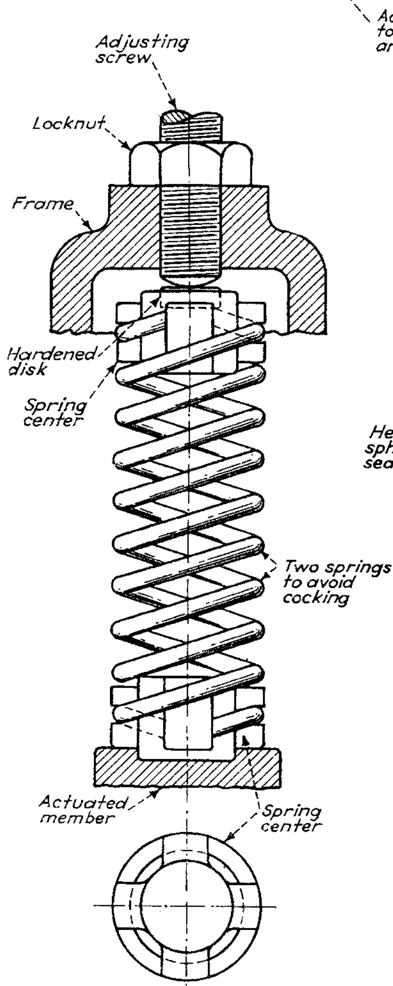

FIG.21

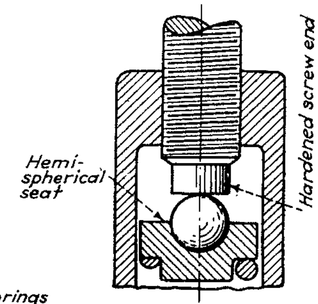

FIG.22

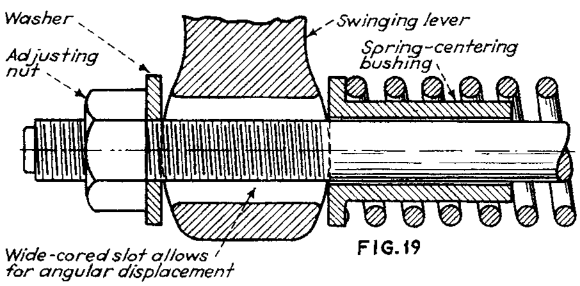

FIG.19

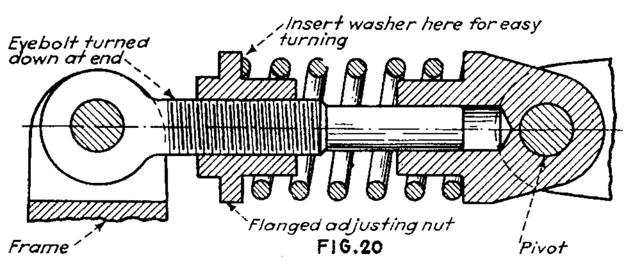

FIG.20

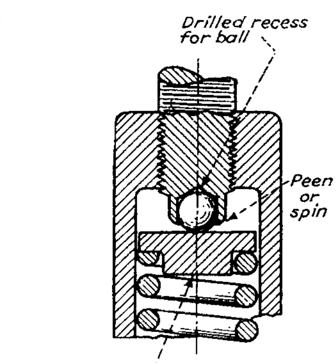

FIG.23

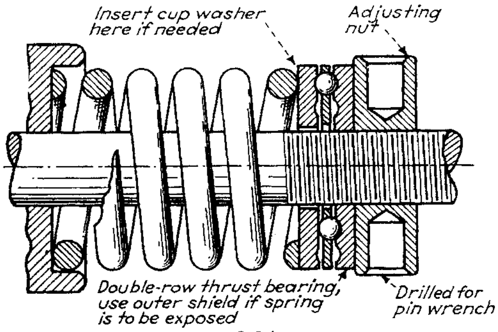

FIG.24

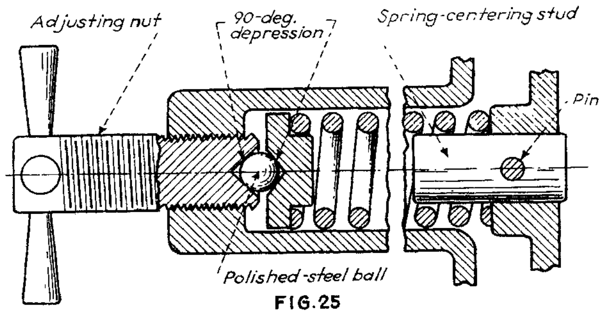

FIG.25

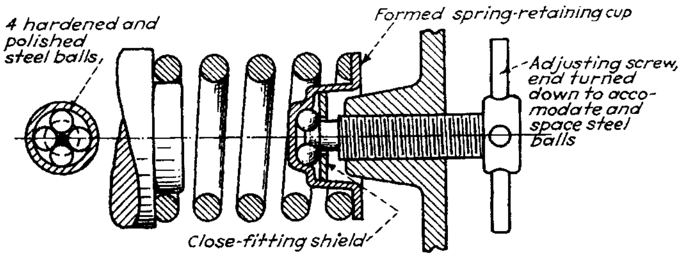

FIG.26

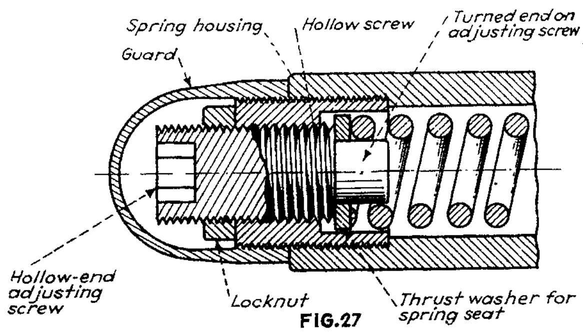

FIG.27

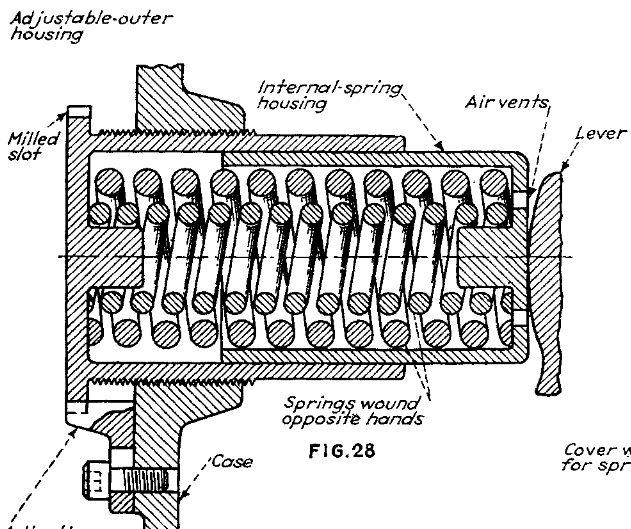

FIG.28

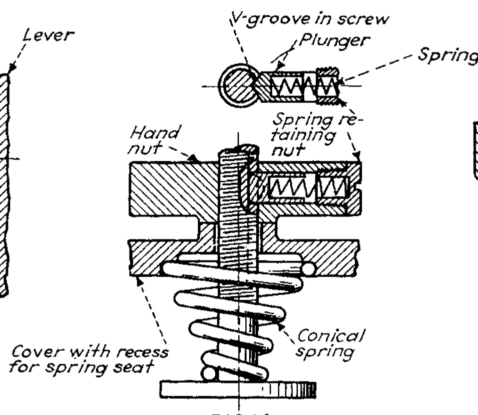

FIG.29

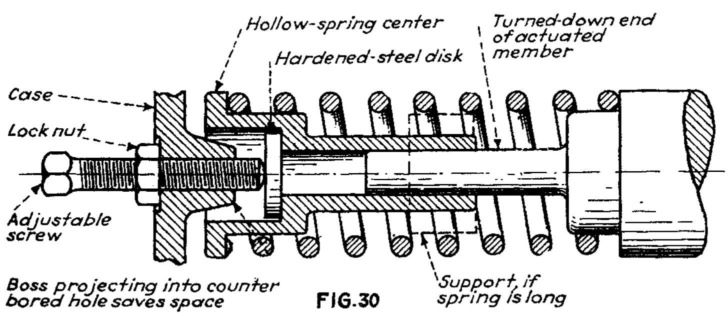

FIG.30

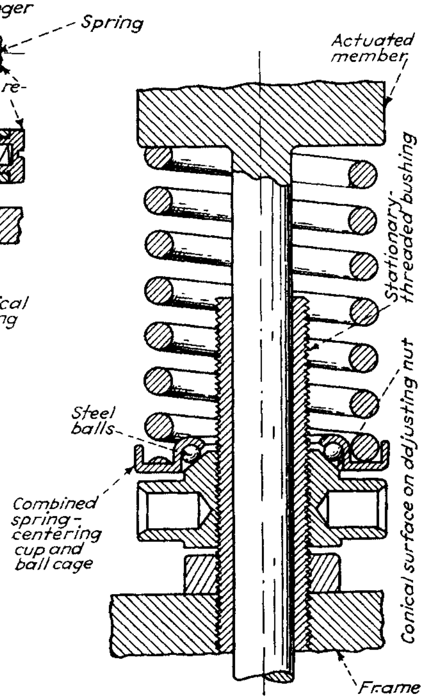

FIG.31

Adjustable Extension Springs

Henry Martin

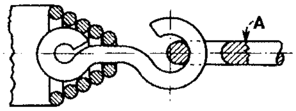

FIG. 1

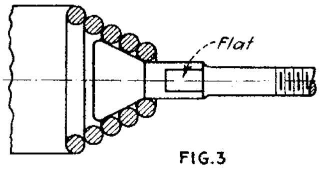

FIG. 3

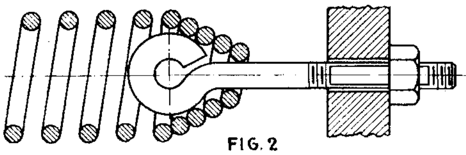

FIG. 2

Design of the end of a tension or extension spring using some form of loop integral with the spring is often unsatisfactory, since many spring failures occur somewhere in the loop, most often at the base of the loop adjacent to the spring body. Use of the accompanying tested methods has reduced breakage and therefore down-time of machinery, especially where adjustability of tension and length is required

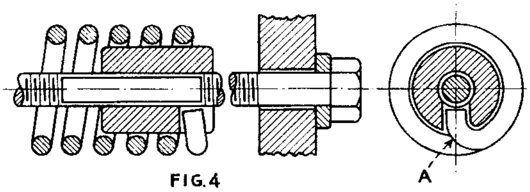

FIG. 4

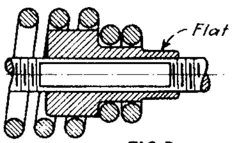

FIG. 5

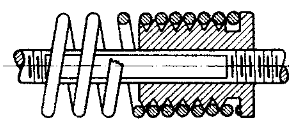

FIG. 7

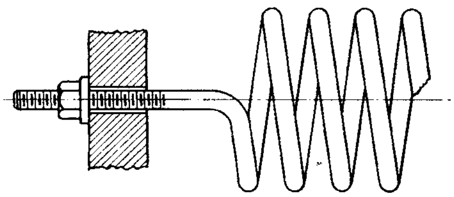

FIG. 6

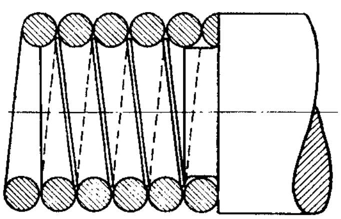

FIG. 8

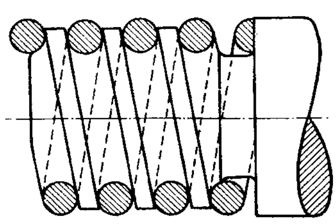

FIG. 9

FIG. 1—Spring-end is tapered about a loop made of larger diameter and somewhat softer wire than that used for the spring. Upper end of wire is also formed into a loop, larger and left open to engage a rod-end or eye-bolt *A*.

FIG. 2—A loop is formed at the end of a soft steel rod threaded at the opposite end for a hex adjusting nut. Ordinary threaded rod-end may be substituted if desired.

FIG. 3—End of adjusting screw is upset in shape of a conical head to coincide with taper of spring-end. Unless initial tension of spring is sufficiently great a wrench flat on stem is provided to facilitate adjustment.

FIG. 4—The last coil of spring is bent inwardly to form hoop *A* which engages slot in nut. Although a neat and simple design, all spring tension is exerted on hook at one point, somewhat off-center of spring axis. Not recommended for heavy loads.

FIG. 5—An improved method over Fig. 4. The nut is shouldered to accommodate two end coils which are wound smaller than the body of spring. Flats are provided for use of wrench during adjustment.

FIG. 6—When wire size permits, the spring end can be left straight and threaded for adjustment. Because of the small size of nut a washer must also be used as shown.

FIG. 7—The shouldered nut is threaded with a coarse V-thread and is screwed into the end of the spring. The point of tangency between the 30-deg. side of thread and wire diameter should be such that the coils cannot pull off. The end of the spring is squared for sufficient friction so that nut need not be held when turning the adjusting screw.

FIG. 8—For close-wound extension springs, end of rod may be threaded with a shallow thread the root of which is the same curvature as that of the spring wire. This form of thread cut with the crests left sharp provides greater engagement contact.

FIG. 9—For more severe duty, the thread is cut deeper than that shown in Fig. 8. The whole spring is close-wound, but when screwed on adjusting rod, the coils are spread, thereby creating greater friction for better holding ability. Spring is screwed against the relieved shoulder of rod.

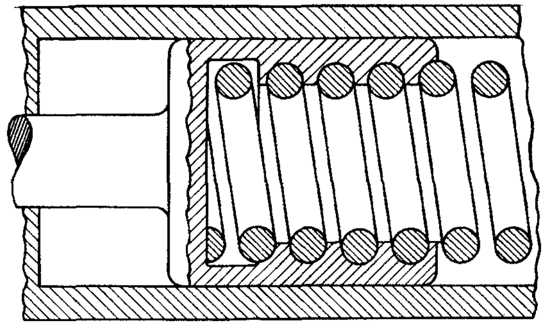

FIG.10

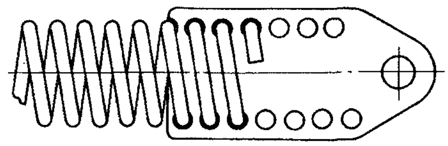

FIG.11

FIG. 10—When design requires housed spring, adjusting rod is threaded internally. Here also, the close-wound coils are spread when assembled. Unless housing bore is considerably larger than shouldered diameter of adjusting rod, or sufficient space is available for a covered spring, methods shown in Figs. 8 or 9 will be less expensive.

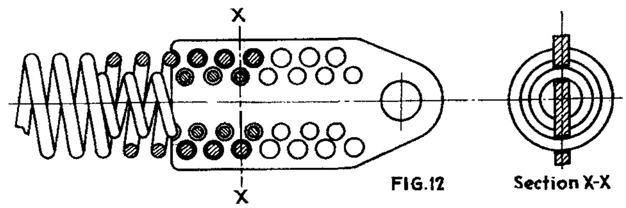

FIG.12 Section X-X

FIG. 11—A thin piece of cold-drawn steel is drilled to exact pitch of the coils with a series of holes slightly larger than spring wire. Three or four coils are screwed into the piece which has additional holes for further adjustment. It will be seen that all coils so engaged are inactive or dead coils.

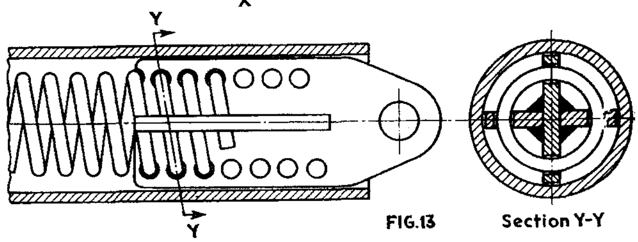

FIG.13 Section Y-Y

FIG. 12—A similar design to that shown in Fig. 11, except that a smaller spring lies inside the larger one. Both springs are wound to the same pitch for ease of adjustment. By staggering the holes as shown, the outer diameter of the inner spring may approach closely that of the inner diameter of the outer spring, thereby leaving sufficient space for a third internal spring if necessary.

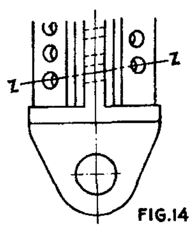

FIG.14

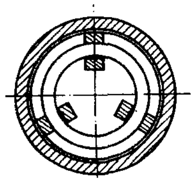

Section Z-Z

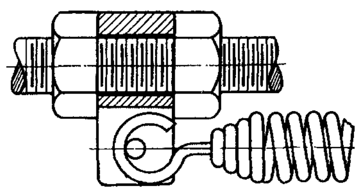

FIG.16

FIG. 13—When the spring is to be guarded, and to prevent binding of the spring attachment in the housing, the end is cross-shaped as shown in the section. The two extra vanes are welded to the solid vane. The location of the series of holes in each successive vane is such as to advance spring at one quarter the pitch.

FIG. 14—This spring end has three vanes and is turned, bored and milled from solid round stock where welding facilities are not convenient. In sufficient quantities, the use of a steel casting precludes machining bar stock. The end with the hole is milled approximately ¼ in. thick for the adjusting member.

FIG. 15—A simple means of adjusting tension and length of spring. The spring anchor slides on a plain round rod and is fastened in any position by a square head setscrew and brass clamping shoe. The eye in the end of the spring engages a hole in the anchor.

FIG. 16—A block of cold-drawn steel is slotted to accommodate the eye of the spring by means of a straight pin. The block is drilled slightly larger than the threaded rod and adjustment and positioning is by the two hex nuts.

FIG. 17—A similar arrangement to that shown in Fig. 16. The spring finger is notched at the outer end for the spring-eye as illustrated in the sectioned end view. In these last three methods, the adjustable member can be made to accommodate 2 or 3 springs if necessary.

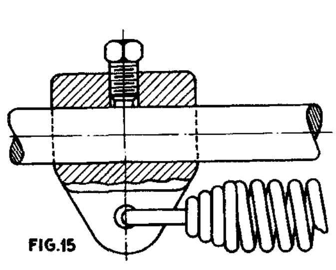

FIG.15

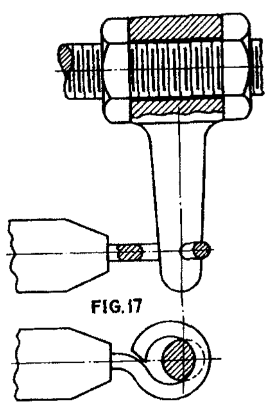

FIG.17

One Spring Returns the Hand Lever

These seven designs need only a single spring—compression, extension, flat or torsion.

L. Kasper

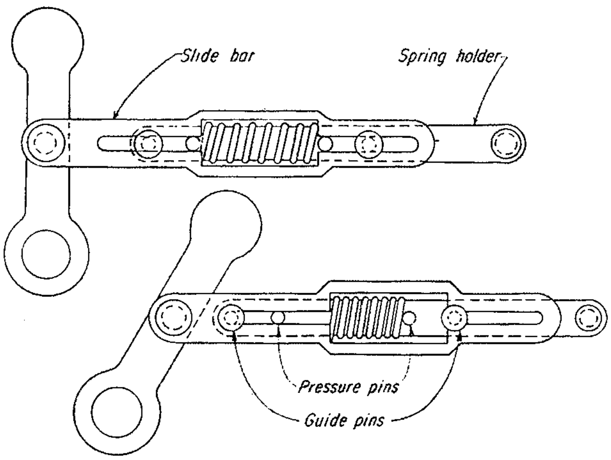

1
SLIDE BAR attached to lever compresses spring against pressure pins in either direction. Guide pins in spring holder hit end of slot to limit movement.

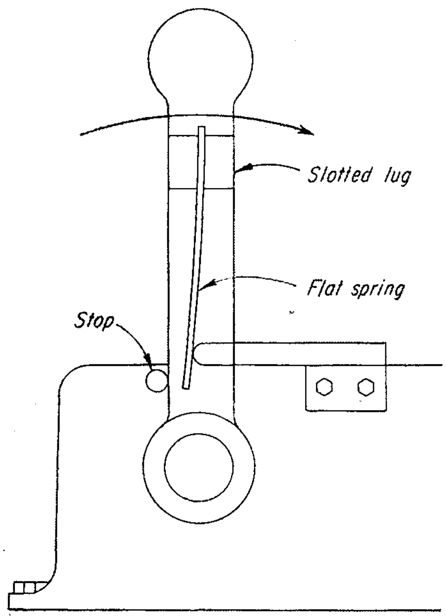

2
FLAT SPRING has initial tension which gives positive return for even a small lever-movement.

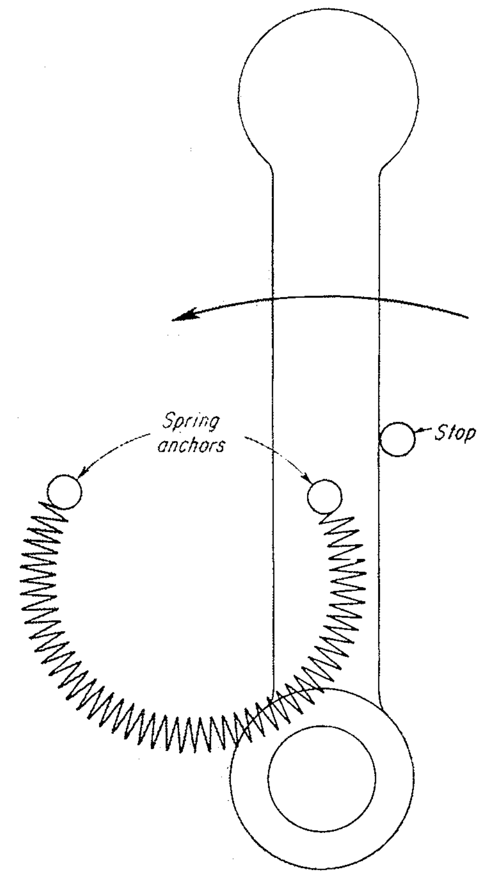

3
CLOSE-WOUND HELICAL SPRING gives almost constant return force. Anchor post for spring also acts as limit stop.

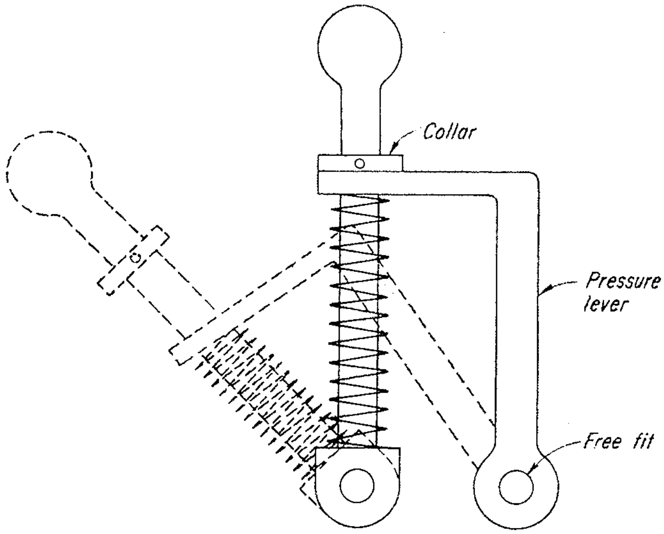

4
PRESSURE LEVER returns hand lever because it rotates on a different center. Collar sets starting position.

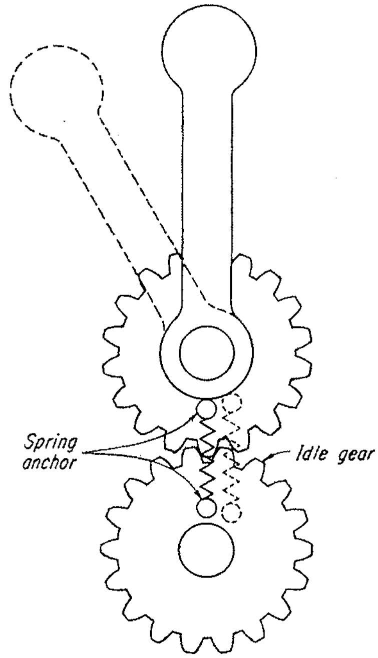

5
GEARS extend spring when lever moves up to 180° in either direction.

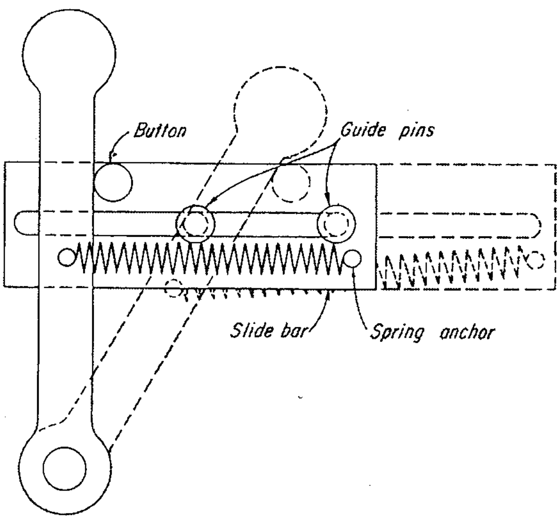

6
SLIDE BAR rides on guide pins as lever pushes it to right. Stretched spring pulls slide bar against lever to return lever to vertical position.

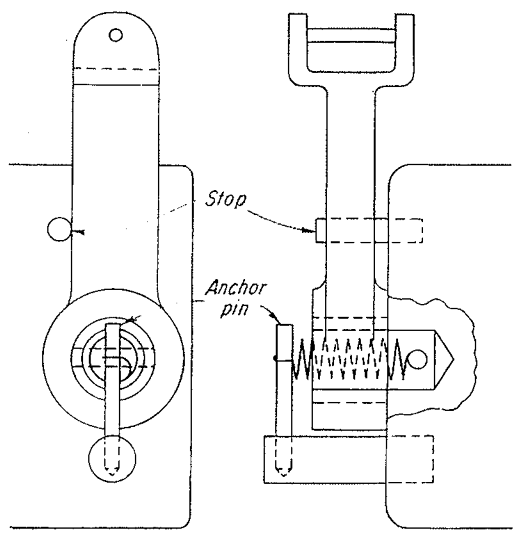

7
OPEN-WOUND HELICAL SPRING extends inside shaft of handle. Coils must be wound in direction of movement so that spring tightens instead of unwinds as lever turns.

6 More One Spring Lever Return Designs

A flat, torsion or helical spring does the job alone.

L. Kasper

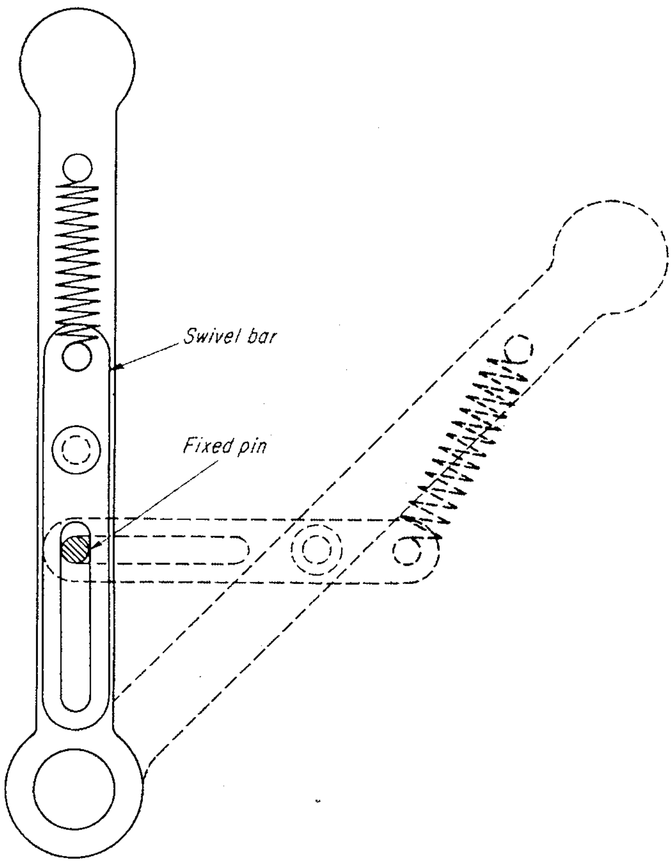

1
SWIVEL BAR, which slides on fixed pin, returns hand lever. Slot in swivel bar is limit stop for movement either way.

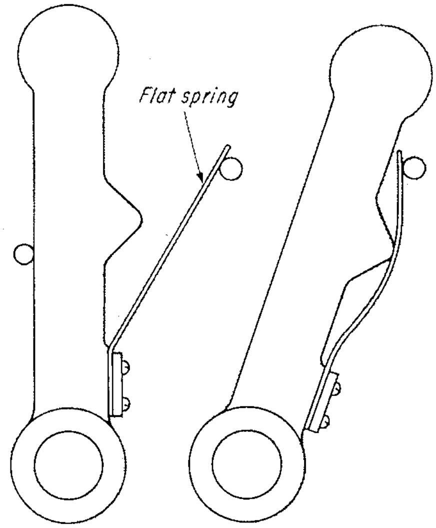

2
HIGHER SPRING RATE, when the projection hits the flat spring, warns operator he's approaching end of travel and assures quick disengagement.

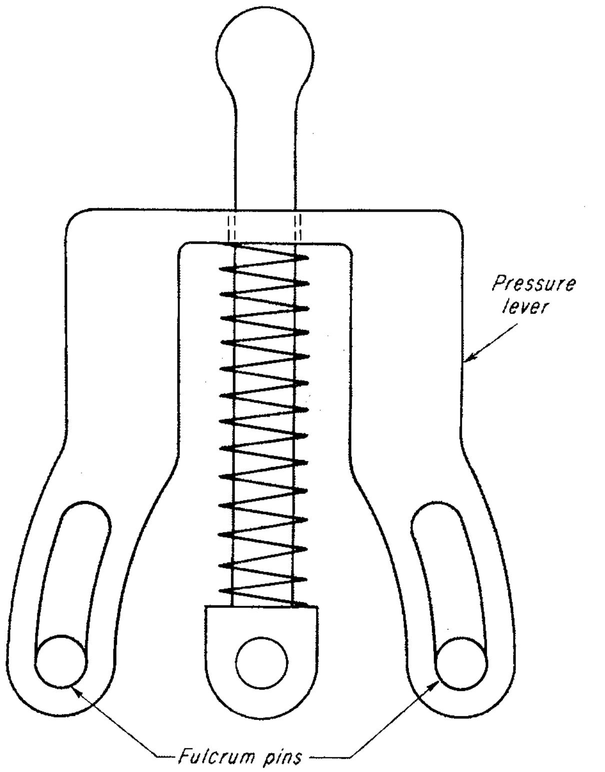

3
DOUBLE PRESSURE-LEVER returns handle to center from either direction by compressing spring. Lever pivots on one pin and comes to stop against the other pin.

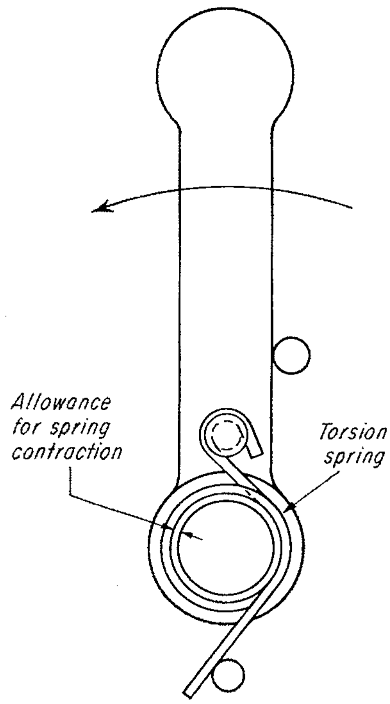

4
TORSION SPRING must have coil diameter larger than shaft diameter to allow for spring contraction during windup.

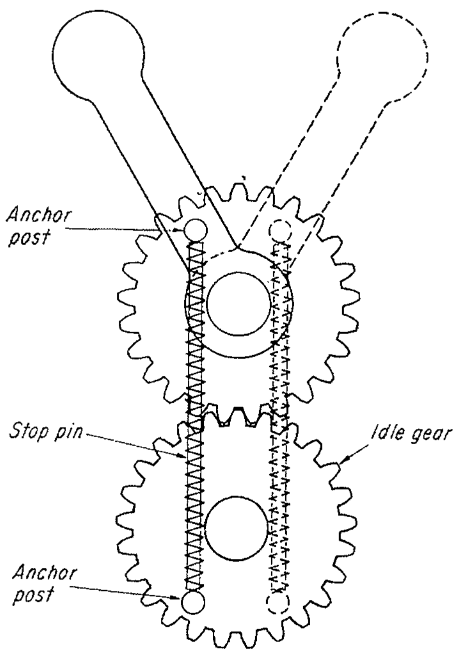

5
LEVER flops to stop because of spring pull. Stop-pins inside springs limit movement.

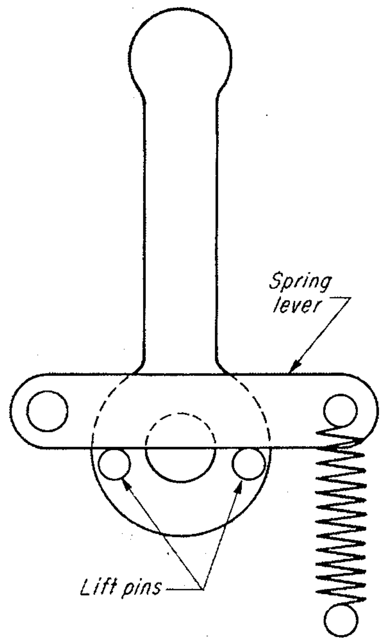

6
SELF-CENTERING HAND LEVER returns to vertical as soon as it's released. Any movement lifts spring lever and creates a righting force.

Springs: How to Design for Variable Rate

Eighteen diagrams show how stops, cams, linkages and other arrangements can vary the load/deflection ratio during extension or compression.

James F. Machen

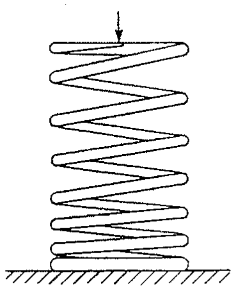

1

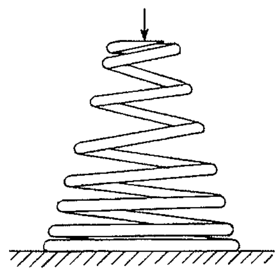

2

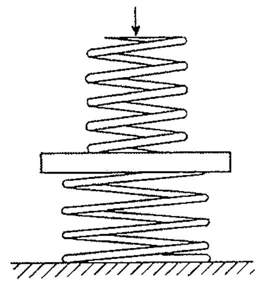

3

WITH TAPERED-PITCH SPRINGS (1), the number of effective coils changes with deflection—the coils "bottom" progressively. Tapered O.D. and pitch (2) combine to produce similar effect except spring with tapered O.D. will have shorter solid height.

IN DUAL SPRINGS one spring closes solid before the other.

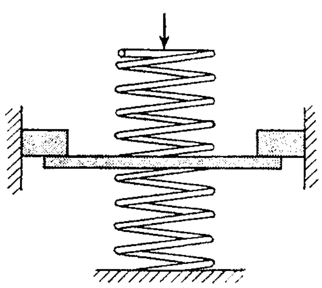

4

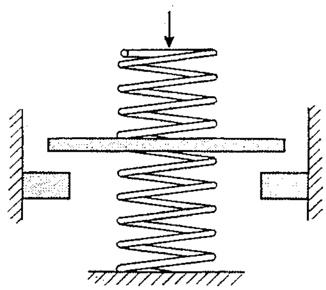

5

STOPS (4, 5) can be used with either compression or extension springs.

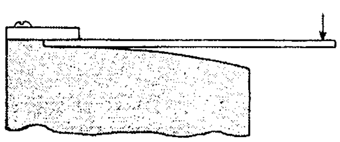

6

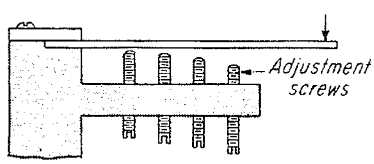

7

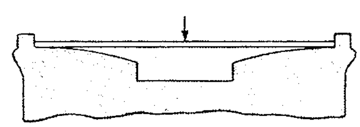

8

LEAF SPRINGS (6, 7, 8) can be arranged so that their effective lengths change with deflection.

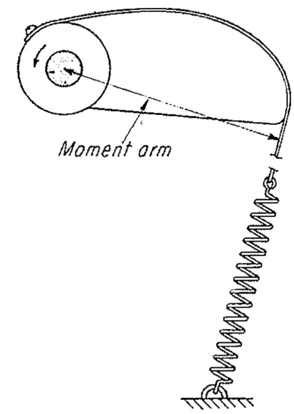

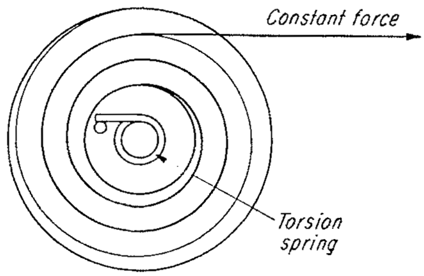

10
TORSION SPRING combined with variable-radius pulley gives constant force.

9
CAM-AND-SPRING DEVICE causes torque relationship to vary during rotation as moment arm changes.

LINKAGE-TYPE ARRANGEMENTS (11, 12) are often used in instruments where torque control or anti-vibration suspension is required.

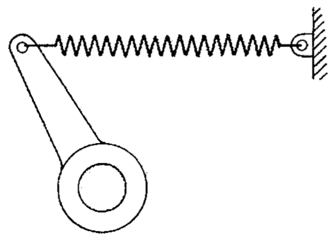

11

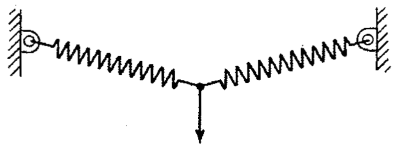

12

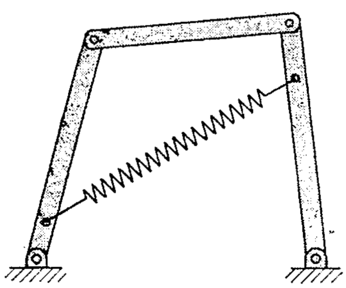

13
4-BAR MECHANISM in conjunction with a spring has a great variety of load/deflection characteristics.

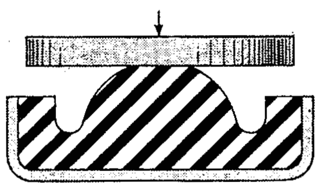

14
MOLDED-RUBBER SPRING has deflection characteristics that vary with its shape.

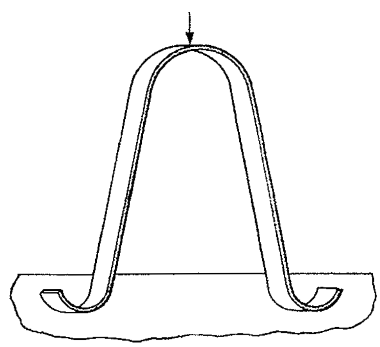

15
ARCHED LEAF-SPRING gives almost constant force when shaped like the one illustrated.

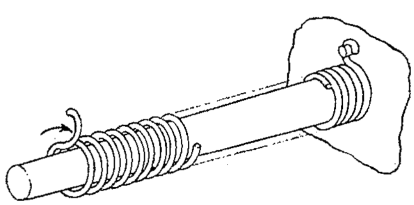

16
TAPERED MANDREL AND TORSION SPRING. Effective number of coils decreases with torsional deflection.

How to Stiffen Bellows with Springs

Rubber bellows are an essential part of many products. Here are eight ways to strengthen, cushion, and stabilize bellows with springs.

Robert O. Parmley

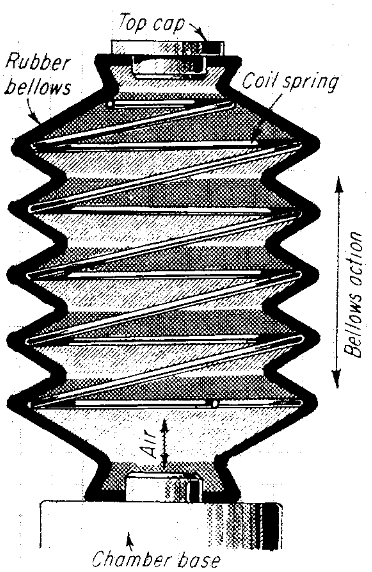

1

INTERNAL COIL SPRING strengthens and adds vertical stability. To install spring, just "corkscrew" it into place.

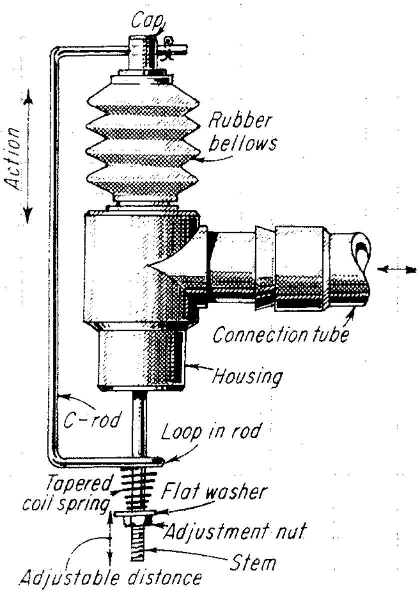

2

CUSHION BELLOWS SUPPORT-ROD with coil spring. Adjustment is provided and bellows are strengthened by this arrangement.

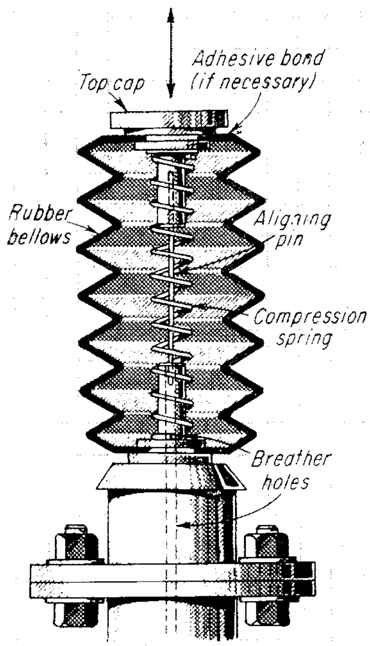

5

COMPRESSION STRENGTH for bellows is best obtained with a coil spring, mounted internally as shown.

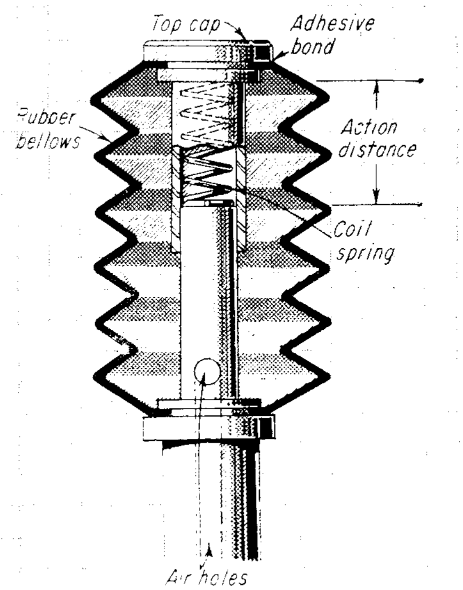

6

INTERNAL RIGIDITY of bellows is here provided by a mating rod and sleeve in which a compression spring is fitted.

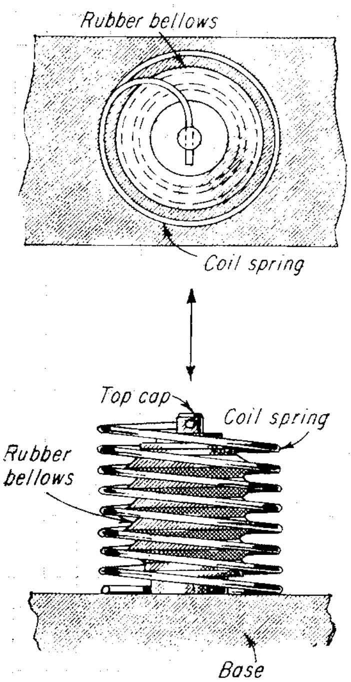

3 **EXTERNAL STABILITY** is provided here, with the added advantage of simple assembly that strengthens bellows, too.

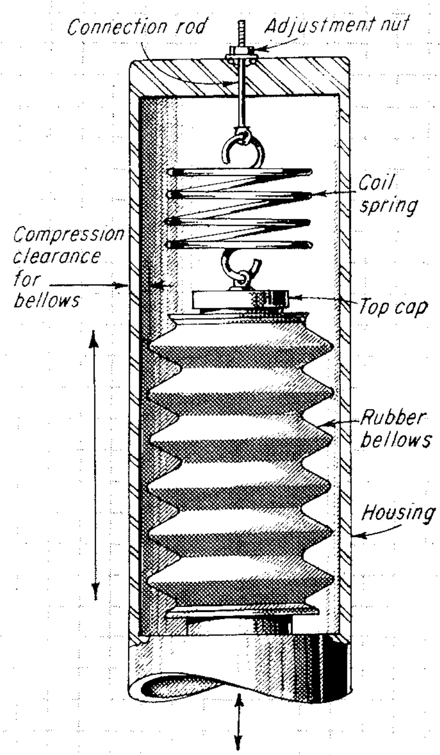

4 **ADJUSTMENT WITH TENSION SPRING** lets bellows be enclosed in casting while adjustment is provided externally.

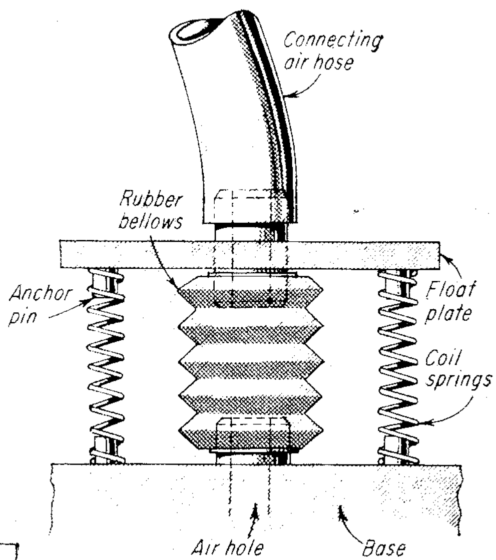

7 **BELLOWS STIFFENER AND STABILIZER** are sometimes combined by means of a platform and four mounting springs.

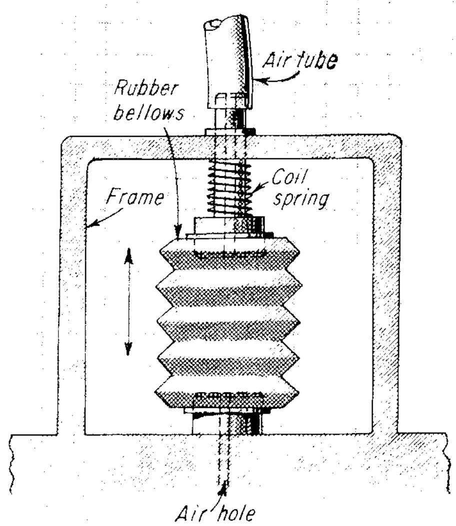

8 **HOUSED STIFFENING UNIT** gives solid mount for hose connection, together with spring action for bellows.

Flat Springs in Mechanisms

These devices all rely on a flat spring for their efficient actions, which would otherwise need more complex configurations.

L. Kasper

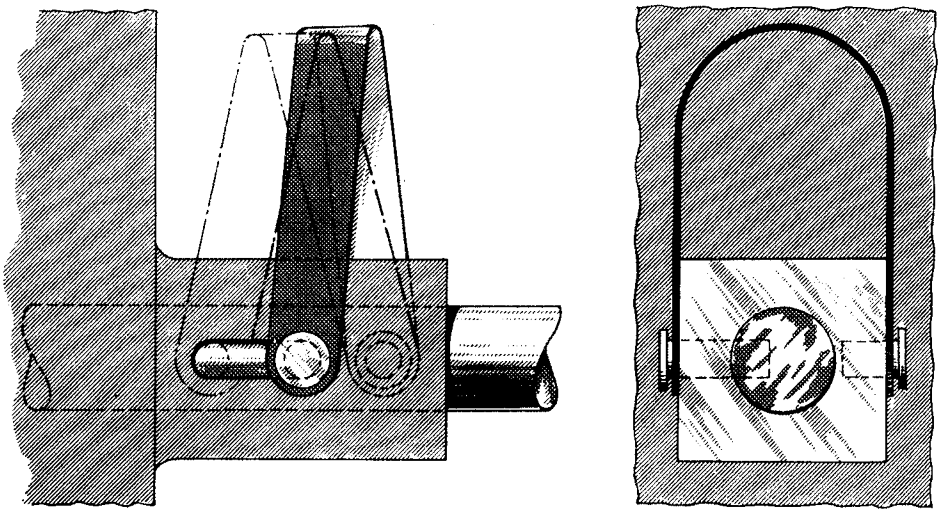

1

CONSTANT FORCE is approached because of the length of this U-spring. Don't align studs or spring will fall.

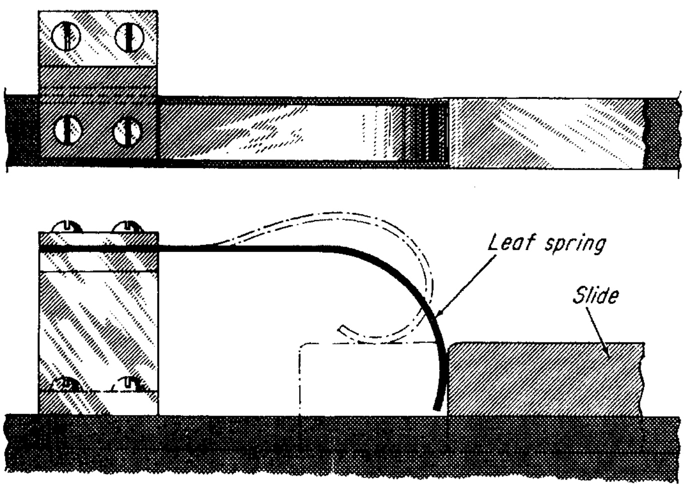

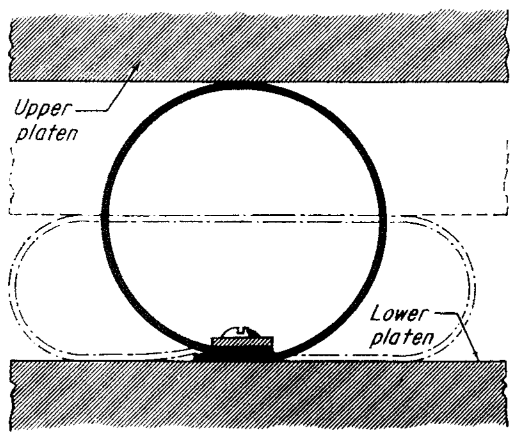

4

SPRING-LOADED SLIDE will always return to its original position unless it is pushed until the spring kicks out.

5

INCREASING SUPPORT AREA as the load increases on both upper and lower platens is provided by a circular spring.

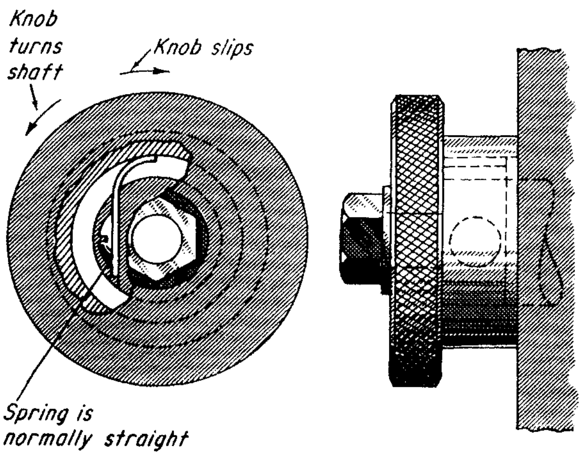

2

FLAT-WIRE SPRAG is straight until the knob is assembled; thus tension helps the sprag to grip for one-way clutching.

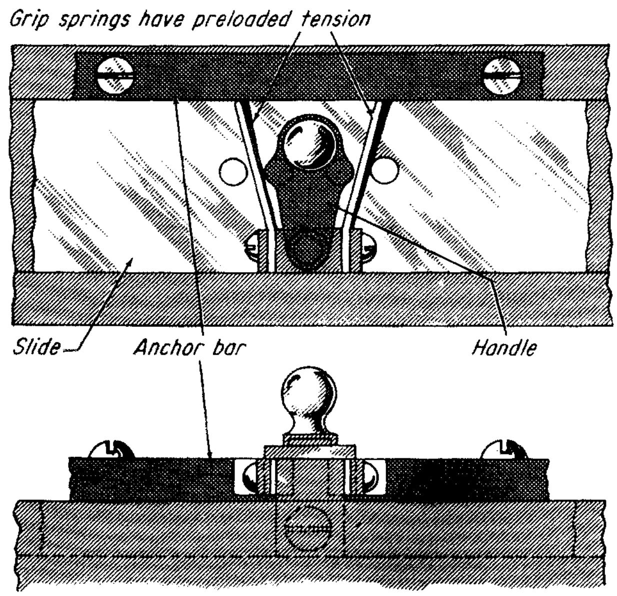

3

EASY POSITIONING of the slide is possible when the handle pins move a grip spring out of contact with the anchor bar.

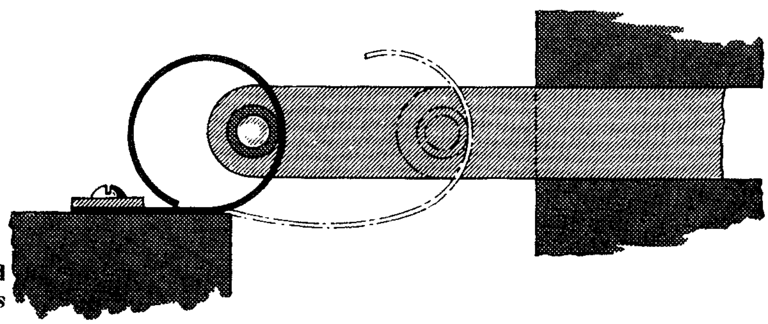

6

CONSTANT TENSION in the spring, and thus force required to activate slide, is (almost) provided by this single coil.

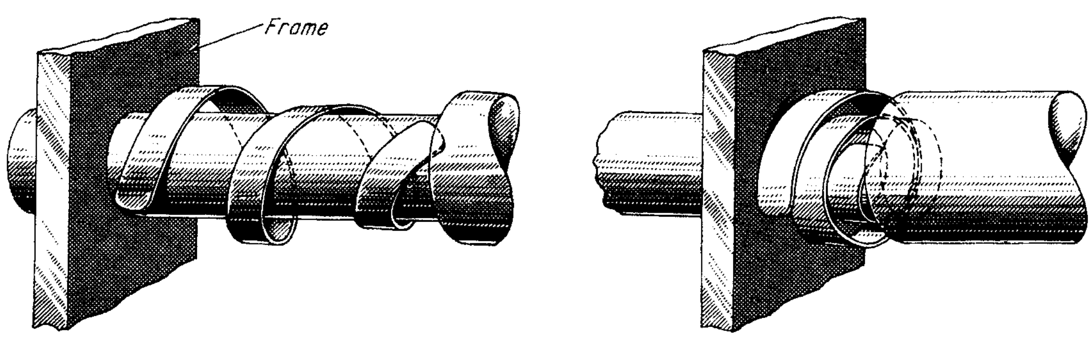

7

VOLUTE SPRING here lets the shaft be moved closer to the frame, thus allowing maximum axial movement.

Flat Springs Find More Work

Five additional examples for the way flat springs perform important jobs in mechanical devices.

L. Kasper

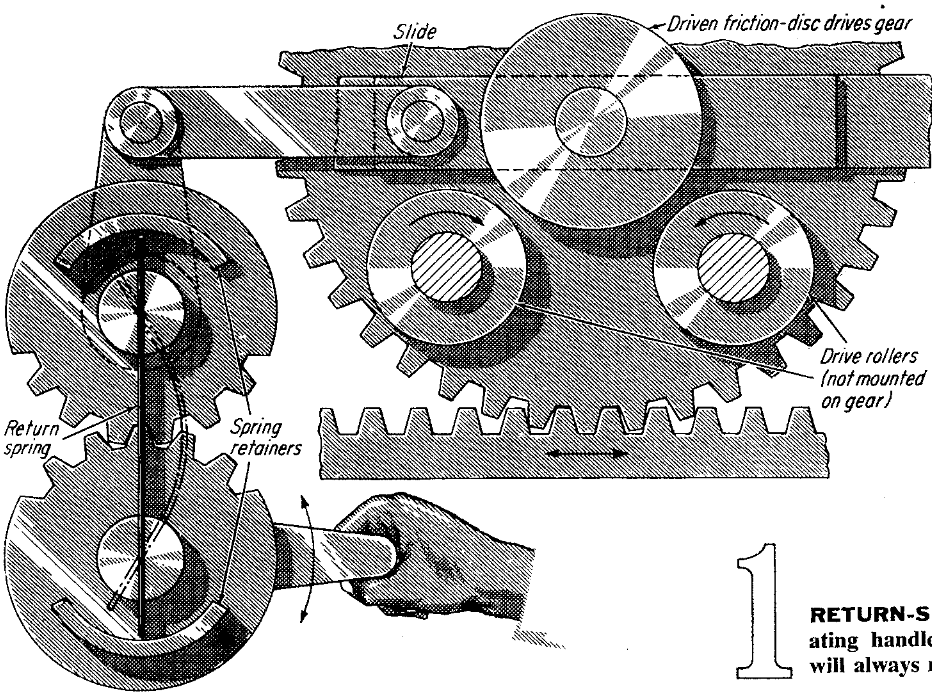

1

RETURN-SPRING ensures that the operating handle of this two-direction drive will always return to the neutral position.

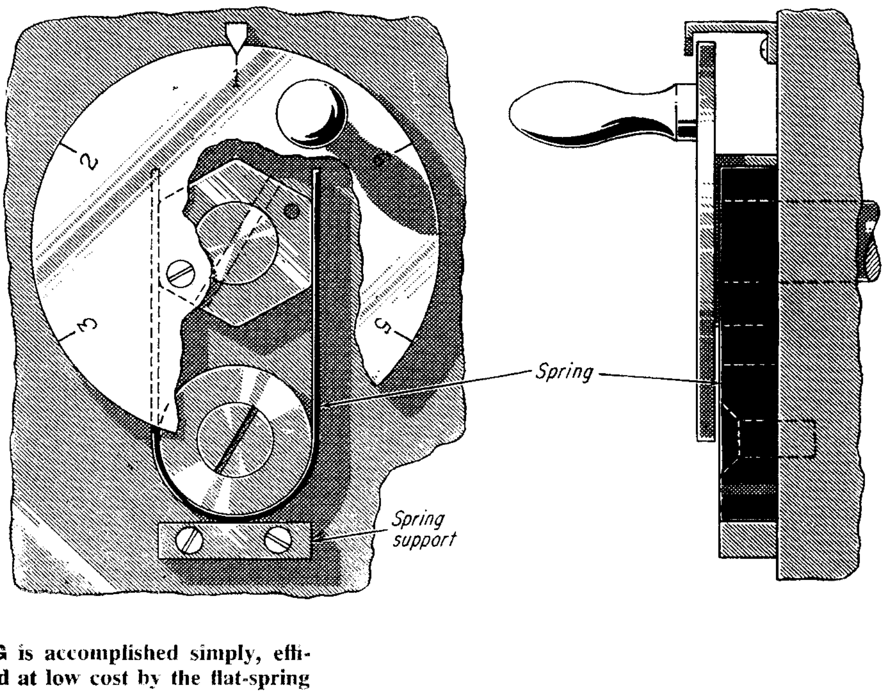

3

INDEXING is accomplished simply, efficiently, and at low cost by the flat-spring arrangement shown here.

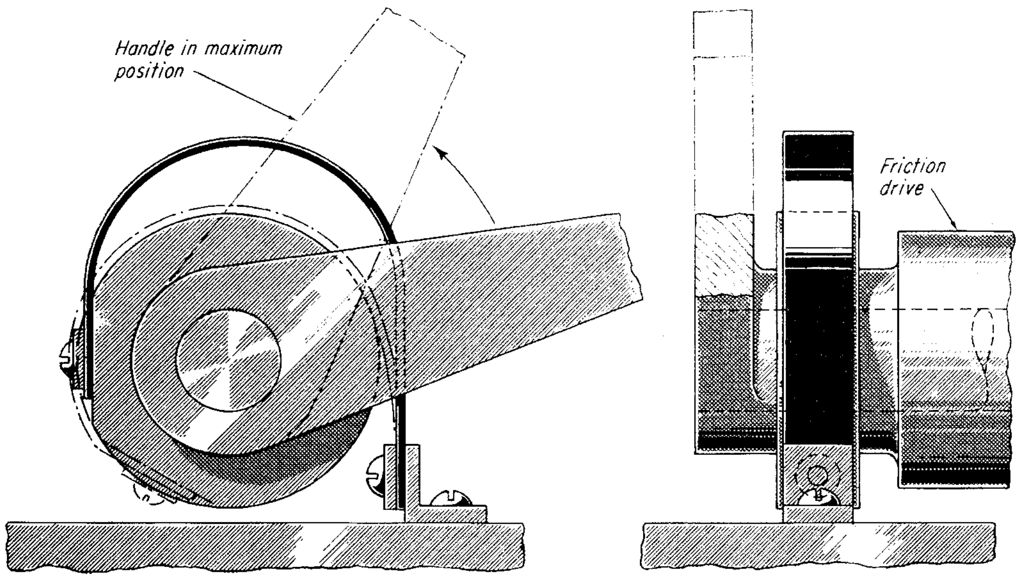

2

SPRING-MOUNTED DISK changes center position as handle is rotated to move friction drive, also acts as built-in limit stop.

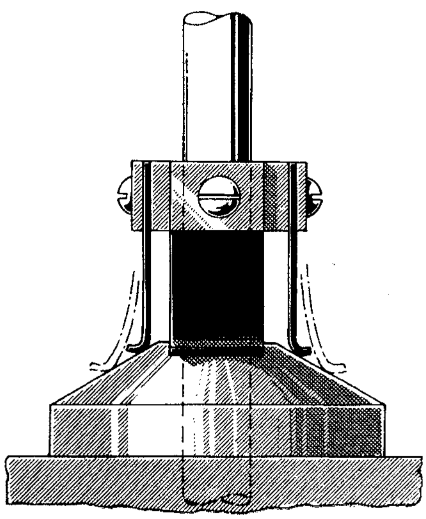

4

CUSHIONING device features rapid increase of spring tension because of the small pyramid angle. Rebound is minimum, too.

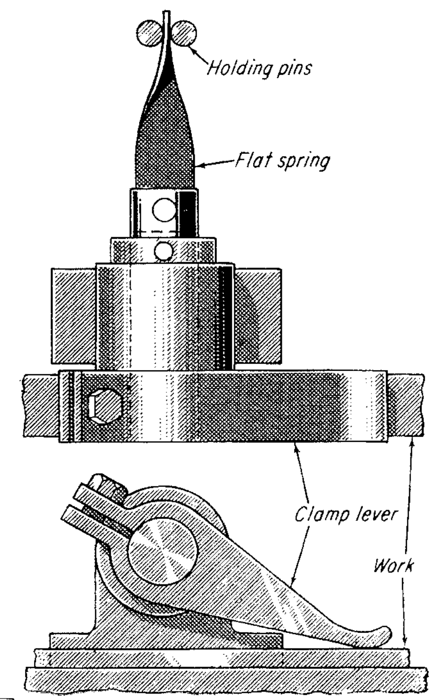

5

HOLD-DOWN CLAMP has flat spring assembled with initial twist to provide clamping force for thin material.

12 Detents for Mechanical Movement

Some of the more robust and practical devices for locating or holding mechanical movements are surveyed by the author.

Louis Dodge

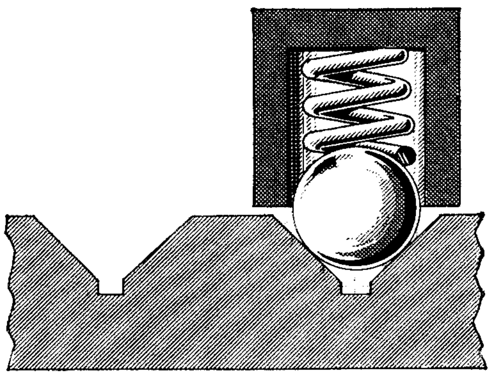

1 FIXED HOLDING POWER IS CONSTANT IN BOTH DIRECTIONS

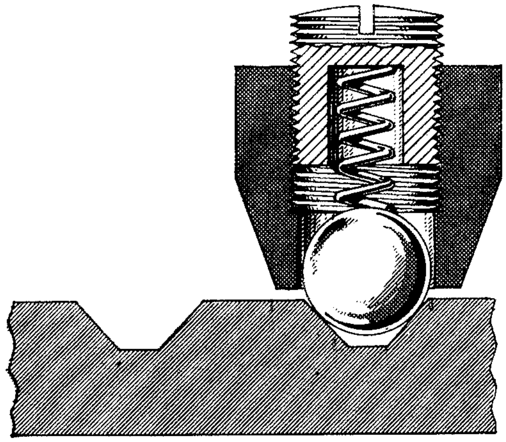

2 ADJUSTABLE HOLDING POWER

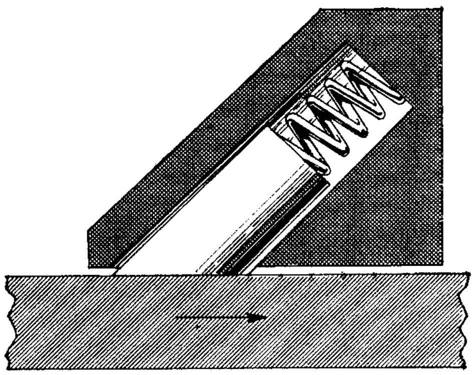

5 WEDGE ACTION LOCKS MOVEMENT IN DIRECTION OF ARROW

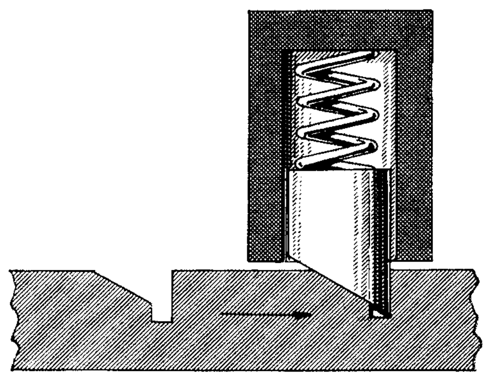

6 NOTCH SHAPE DICTATES DIRECTION OF ROD MOTION

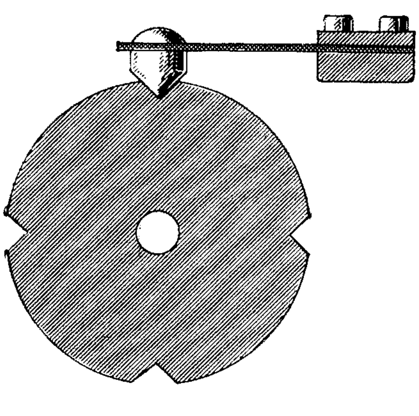

9 LEAF SPRING PROVIDES LIMITED HOLDING POWER

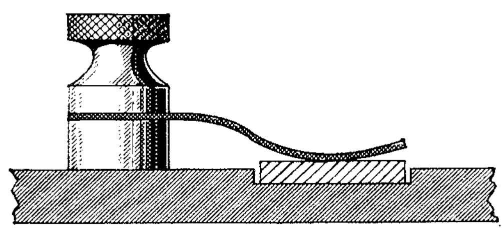

10 LEAF SPRING FOR HOLDING FLAT PIECES

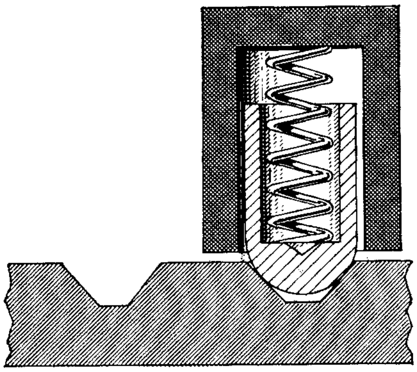

3 DOMED PLUNGER HAS LONG LIFE

Holding power is $R = P \tan \alpha$; for friction coefficient, F, at contact surface $R = P(\tan \alpha + F)$

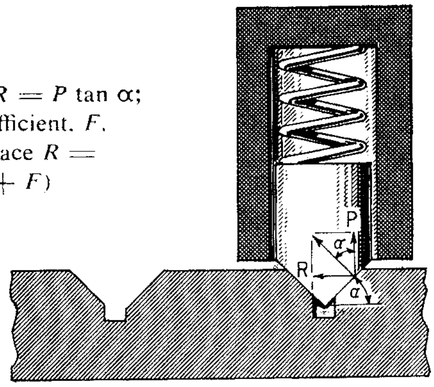

4 CONICAL OR WEDGE-ENDED DETENT

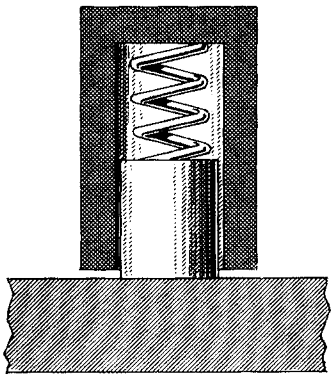

7 FRICTION RESULTS IN HOLDING FORCE

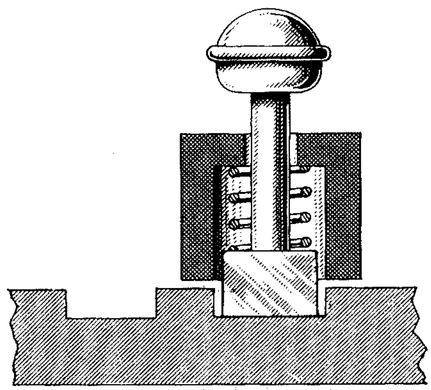

8 POSITIVE DETENT HAS MANUAL RELEASE

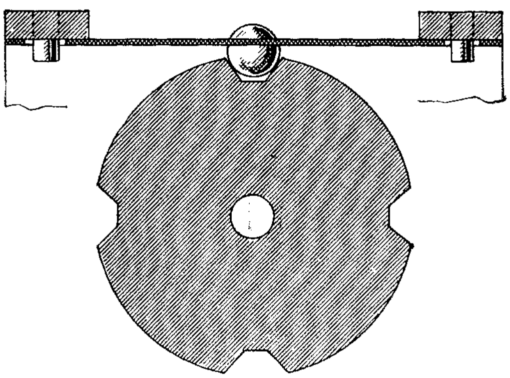

11 LEAF SPRING DETENT CAN BE REMOVED QUICKLY

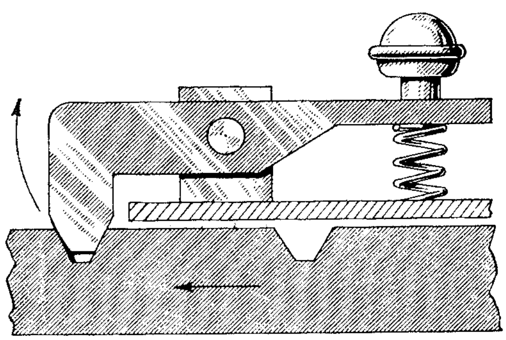

12 AUTOMATIC RELEASE OCCURS IN ONE DIRECTION, MANUAL RELEASE NEEDED IN OTHER DIRECTION

17 Ways of Testing Springs

C. J. McClintock

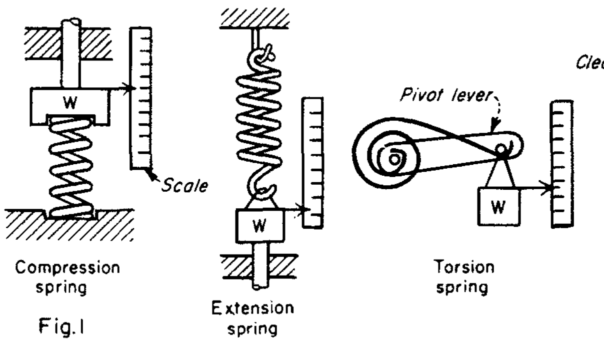

Fig. 1—Dead-weight testing. Weights are directly applied to spring. In the compression spring and the extension spring testers, the test weights are guided in the fixture to prevent buckling. Instead of using a linear scale, the spring deflection can be measured with a dial indicator.

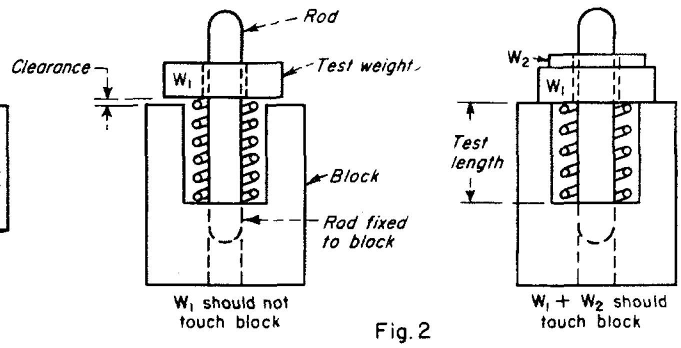

Fig. 2—Ordnance gage incorporates "Go-no-go" principle. Block is bored for specified test length L. Weight W_1 is slightly less than the minimum specified load at L and therefore should not touch block; W_1 plus load tolerance W_2 must touch block for the spring to be acceptable.

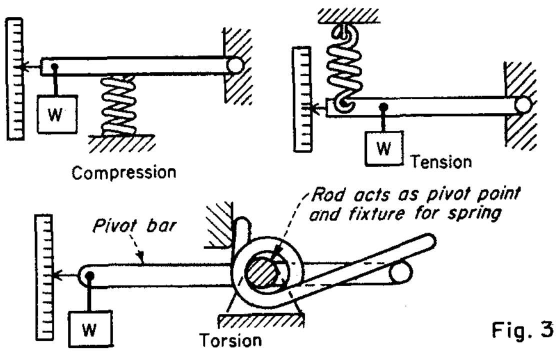

Fig. 3—Pilot-beam testing. Fractional resistance offered to movement of parts is low. These testers are more sensitive than those in which the weight is guided in the fixture. Many of the commercial testers are based on this principle.

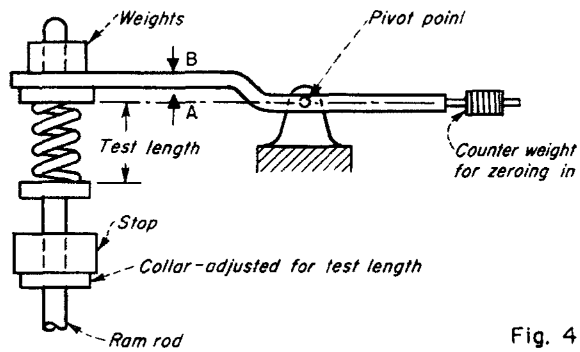

Fig. 4—Zero-gradient beam. Uses refined pivot-beam principle. Ram rod is pushed up with pedal or air cylinder. Beam must not touch contacts A or B. Contacting A indicates spring too weak; B indicates spring too strong.

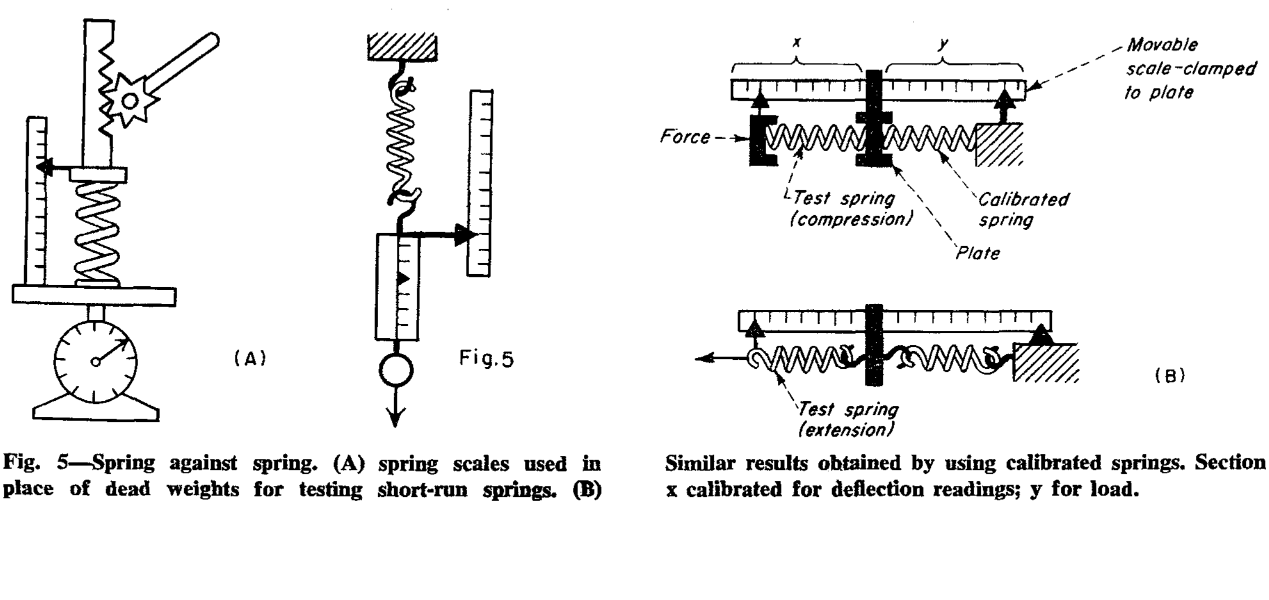

Fig. 5—Spring against spring. (A) spring scales used in place of dead weights for testing short-run springs. (B) Similar results obtained by using calibrated springs. Section x calibrated for deflection readings; y for load.

Spring dimensions are based on calculations using empirical-theoretical equations. In addition, allowances are made for material and manufacturing tolerances. Thus, the final product may deviate to an important degree from the original design criteria. By testing the springs: (1) Results can be entered on the spring drawing, thus including actual performance data; this leads to more realistic future designs. (2) Performance can be checked before assembling spring in a costly unit.

Shown below are 12 ways, Fig. 1 to 5, to quickly evaluate load-deflection characteristics; for more accurate or fully automatic testing, Figs. 6 and 7, describe 5 types of commercial testers.

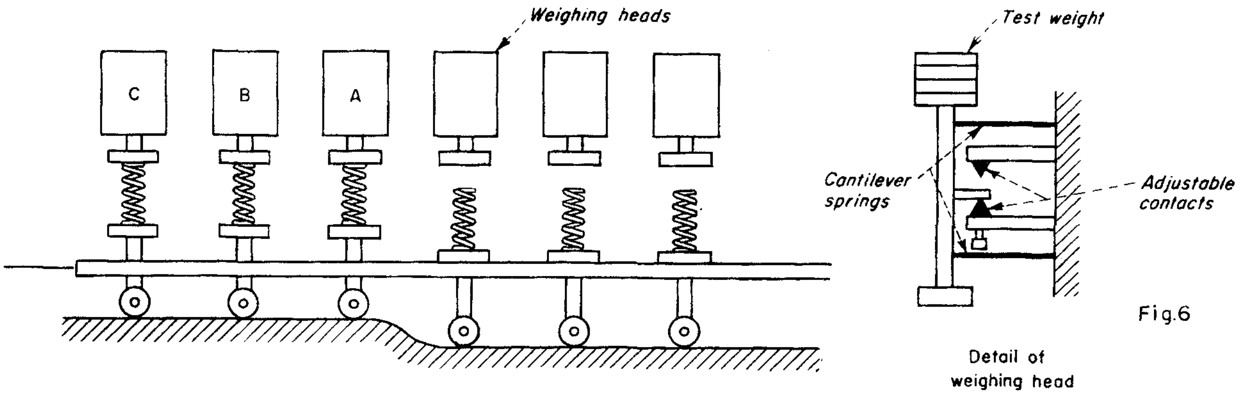

Fig.6

Fig. 6—Fully-automatic testing. Continually moving rotary table with three testing positions. Springs are loaded manually but tested and ejected automatically. Weak springs that allow lower point to make contact are ejected at position A; springs too strong ejected at B. All springs reaching point C are ejected as acceptable.

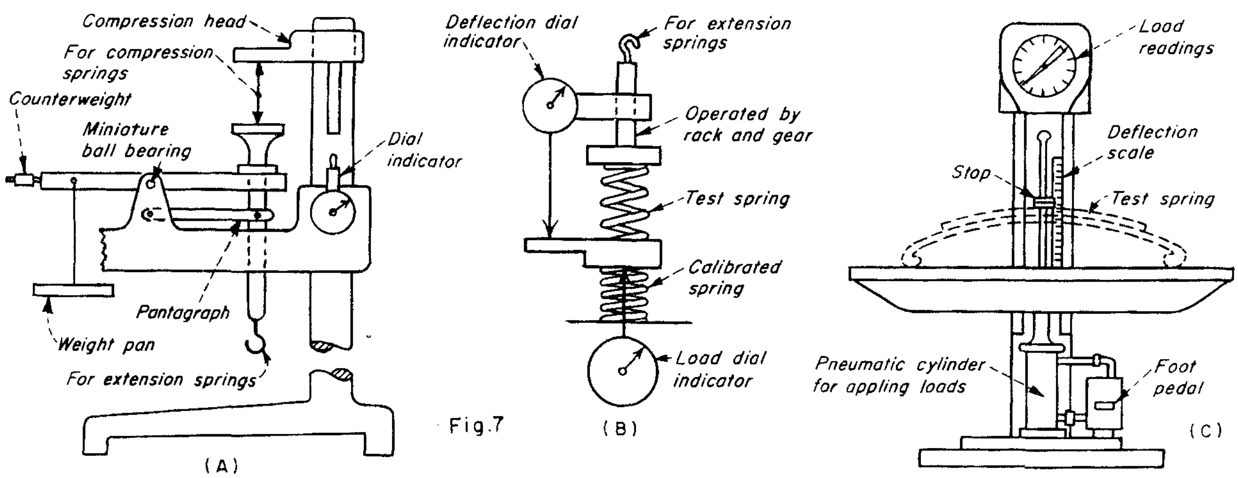

Fig.7

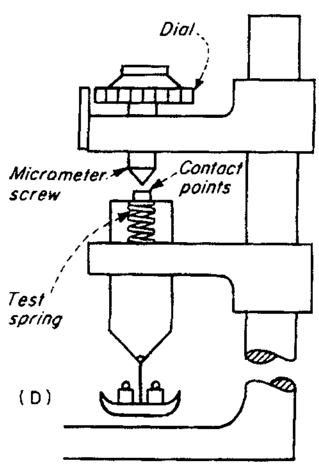

Fig. 7—Commercial testers: (A) Balanced-beam tester uses dead weights for loads. Pantagraph linkage keeps weighing head vertical irrespective of beam movement. Load capacity: 10 lb. Baldwin-Lima-Hamilton Corp. (B) Calibrated spring tester available in several models for testing loads up to 1000 lb. Load applied manually through gear and rack; motor-driven units can be attained for applying heavier loads. Link Engineering Co. (C) Pneumatic-operated tester uses torque bar system for applying loads and a differential transformer for accurately measuring displacements. Wide table permits tests on leaf springs. Load capacity: 2000 lb. Tinius Olsen Testing Machine Co. (D) Electronic micrometer tester has sufficient sensitivity (0.0001 in.) to measure drift, hysteresis and creep as well as load deflection. Adjustments made by large micrometer dial; contact indicated by sensitive electronic circuit. Load capacity: 50 lb. J W Dice Co.

Overriding Spring Mechanisms for Low-Torque Drives

Henry L. Milo, Jr.

Extensive use is made of overriding spring mechanisms in the design of instruments and controls. Anyone of the arrangements illustrated allows an incoming motion to override the outgoing motion whose limit has been reached. In an instrument, for example, the spring device can be placed between

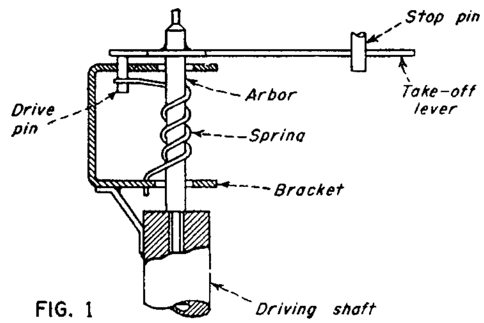

FIG. 1

Fig. 1—Unidirectional Override. The take-off lever of this mechanism can rotate nearly 360 deg. It's movement is limited by only one stop pin. In one direction, motion of the driving shaft also is impeded by the stop pin. But in the reverse direction the driving shaft is capable of rotating approximately 270 deg past the stop pin. In operation, as the driving shaft is turned clockwise, motion is transmitted through the bracket to the take-off lever. The spring serves to hold the bracket against the drive pin. When the take-off lever has traveled the desired limit, it strikes the adjustable stop pin. However, the drive pin can continue its rotation by moving the bracket away from the drive pin and winding up the spring. An overriding mechanism is essential in instruments employing powerful driving elements, such as bimetallic elements, to prevent damage in the overrange regions.

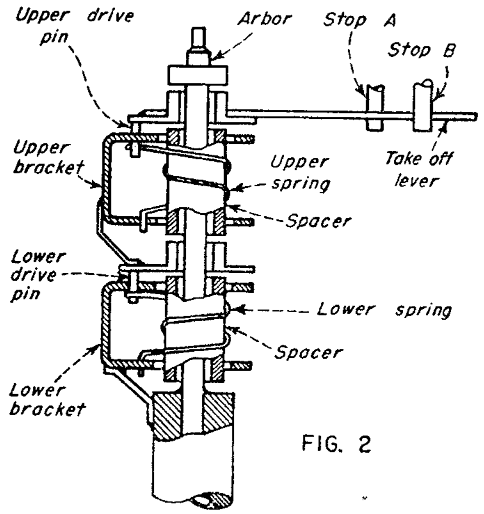

FIG. 2

Fig. 2—Two-directional Override. This mechanism is similar to that described under Fig. 1, except that two stop pins limit the travel of the take-off lever. Also, the incoming motion can override the outgoing motion in either direction. With this device, only a small part of the total rotation of the driving shaft need be transmitted to the take-off lever and this small part may be anywhere in the range. The motion of the driving shaft is transmitted through the lower bracket to the lower drive pin, which is held against the bracket by means of the spring. In turn, the lower drive pin transfers the motion through the upper bracket to the upper drive pin. A second spring holds this pin against the upper drive bracket. Since the upper drive pin is attached to the take-off lever, any rotation of the drive shaft is transmitted to the lever, provided it is not against either stop *A* or *B*. When the driving shaft turns in a counterclockwise direction, the take-off lever finally strikes against the adjustable stop *A*. The upper bracket then moves away from the upper drive pin and the upper spring starts to wind up. When the driving shaft is rotated in a clockwise direction, the take-off lever hits adjustable stop *B* and the lower bracket moves away from the lower drive pin, winding up the other spring. Although the principal uses for overriding spring arrangements are in the field of instrumentatioh, it is feasible to apply these devices in the drives of major machines by beefing up the springs and other members.

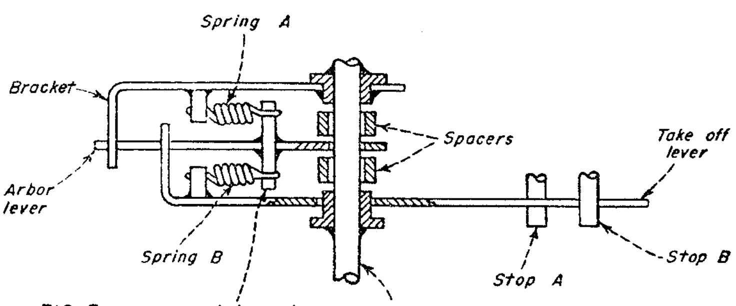

FIG. 5

Fig. 5—Two-directional, 90 Degree Override. This double overriding mechanism allows a maximum overtravel of 90 deg in either direction. As the arbor turns, the motion is carried from the bracket to the arbor lever, then to the take-off lever. Both the bracket and the take-off lever are held against the arbor lever by means of springs *A* and *B*. When the arbor is rotated counterclockwise, the take-off lever hits stop *A*. The arbor lever is held stationary in contact with the take-off lever. The bracket, which is soldered to the arbor, rotates away from the arbor lever, putting spring *A* in tension. When the arbor is rotated in a clockwise direction, the take-off lever comes against stop *B* and the bracket picks up the arbor lever, putting spring *B* in tension.

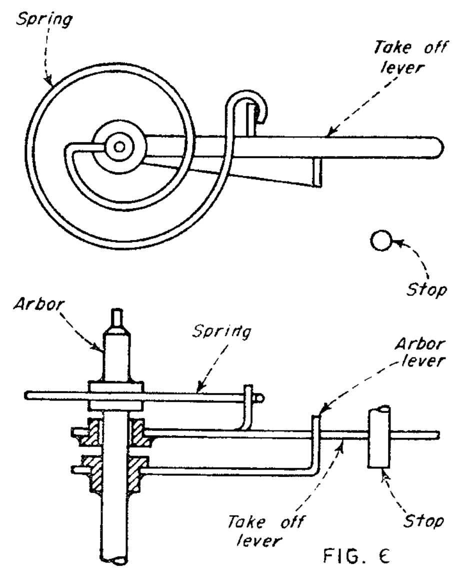

FIG. 6

the sensing and indicating elements to provide overrange protection. The dial pointer is driven positively up to its limit, then stops; while the input shaft is free to continue its travel. Six of the mechanisms described here are for rotary motion of varying amounts. The last is for small linear movements.

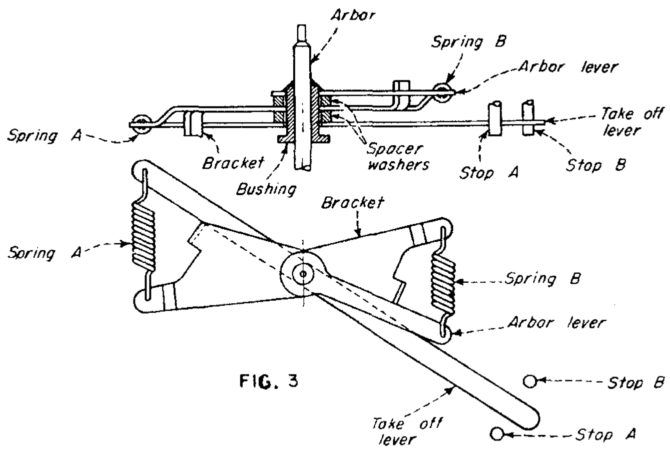

FIG. 3

Fig. 3—Two-directional, Limited-Travel Override. This mechanism performs the same function as that shown in Fig. 2, except that the maximum override in either direction is limited to about 40 deg, whereas the unit shown in Fig. 2 is capable of 270 deg movement. This device is suited for uses where most of the incoming motion is to be utilized and only a small amount of travel past the stops in either direction is required. As the arbor is rotated, the motion is transmitted through the arbor lever to the bracket. The arbor lever and the bracket are held in contact by means of spring *B*. The motion of the bracket is then transmitted to the take-off lever in a similar manner, with spring *A* holding the take-off lever and the bracket together. Thus the rotation of the arbor is imparted to the take-off lever until the lever engages either stops *A* or *B*. When the arbor is rotated in a counterclockwise direction, the take-off lever eventually comes up against the stop *B*. If the arbor lever continues to drive the bracket, spring *A* will be put in tension.

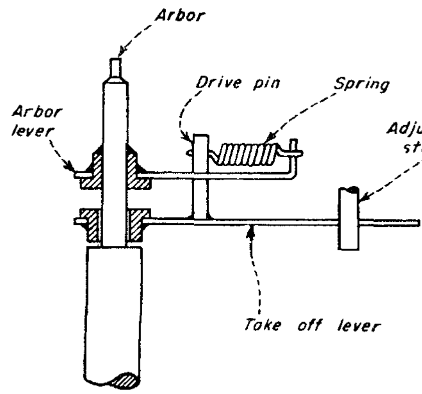

FIG. 4

Fig. 4—Unidirectional, 90 Degree Override. This is a single overriding unit, that allows a maximum travel of 90 deg past its stop. The unit as shown is arranged for over-travel in a clockwise direction, but it can also be made for a counterclockwise override. The arbor lever, which is secured to the arbor, transmits the rotation of the arbor to the take-off lever. The spring holds the drive pin against the arbor lever until the take-off lever hits the adjustable stop. Then, if the arbor lever continues to rotate, the spring will be placed in tension. In the counterclockwise direction, the drive pin is in direct contact with the arbor lever so that no overriding is possible.

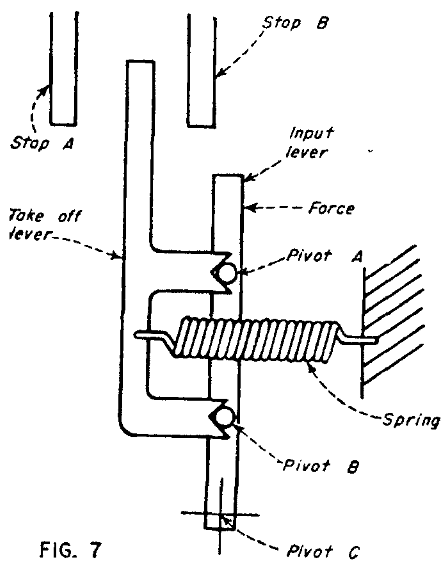

FIG. 7

Fig. 6—Unidirectional, 90 Degree Override. This mechanism operates exactly the same as that shown in Fig. 4. However, it is equipped with a flat spiral spring in place of the helical coil spring used in the previous version. The advantage of the flat spiral spring is that it allows for a greater override and minimizes the space required. The spring holds the take-off lever in contact with the arbor lever. When the take-off lever comes in contact with the stop, the arbor lever can continue to rotate and the arbor winds up the spring.

Fig. 7—Two-directional Override, Linear Motion. The previous mechanisms were overrides for rotary motion. The device in Fig. 7 is primarily a double override for small linear travel although it could be used on rotary motion. When a force is applied to the input lever, which pivots about point *C*, the motion is transmitted directly to the take-off lever through the two pivot posts *A* and *B*. The take-off lever is held against these posts by means of the spring. When the travel is such the take-off lever hits the adjustable stop *A*, the take-off lever revolves about pivot post *A*, pulling away from pivot post *B* and putting additional tension in the spring. When the force is diminished, the input lever moves in the opposite direction, until the take-off lever contacts the stop *B*. This causes the take-off lever to rotate about pivot post *B*, and pivot post *A* is moved away from the take-off lever.

Deflect a Spring Sideways

Formulas for force and stress when a side load deflects a vertically loaded spring.

W. H. Sparing

There are many designs in which one end of a helical spring must be moved laterally relative to the other end. How much force will be required to do this? What deflection will the force cause? What stress will result from combined lateral and vertical loads? Here are formulas that find the answers.

It is assumed that the spring ends are held parallel by a vertical force P (which does not appear in these formulas), and that the spring is long enough to allow overlooking the effect of closed end-turns.

Lateral load for a steel spring

$$Q = \frac{10^6 d^4\ \delta_L}{A n D\,[0.204\,(L-d)^2 + 0.265\,D^2]}$$

where n = number of turns = $(h/d) - 1.2$, D = mean dia in., A = correction factor.

Lateral deflection

$$\delta_L = \frac{AQnD\,[0.204\,(L-d)^2 + 0.265\,D^2]}{10^6 d^4}$$

The correction factor A can never be unity (see chart on continuing page); also P can never be zero. This is because there will always be some vertical deflection, and a side load will always cause a resultant vertical force if the ends are held parallel and at right angles to the original center line.

Combined stress

$$f_c = f\left\{1 + \frac{1}{D}\left[\delta_L + \frac{Q}{P}\,(L-d)\right]\right\}$$

where f = vertical-load stress. Accurate within 10%, these formulas show that the nearer a spring approaches its solid position, the greater the discrepancy between calculated and actual load. This results from premature closing of the end-turns. It is best to provide stops to prevent the spring from being compressed solid. An example shows the combined stress at the stop position may even be higher than the solid stress caused by vertical load only.

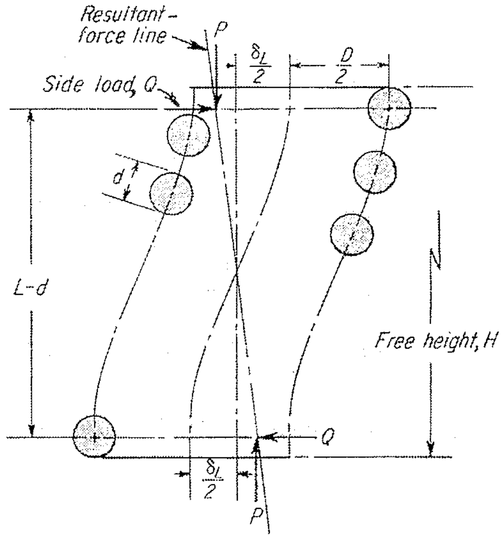

A Working Example

A spring has the following dimensions, in inches:

Outside dia	9
Bar dia (d)	1 15/16
Free height (H)	16 1/2
Solid height (h)	13
Loaded height (L)	14 5/16
Lateral deflection (δ_L)	1 1/2
Stop height	13 3/4

From these dimensions compute values at loaded height and stop height.

	Loaded position	Stop position
D	7.0625	7.0625
n	5.51	5.51
y (vertical deflection)	2.1875	2.75
$H - d$	14.563	14.563
$L - d$	12.375	11.813
$(H - d)/D$	2.06	2.06
$y/(H - d)$	0.150	0.189
A	1.30	1.40
Q	9400 lb	9310 lb

From standard formulas for vertical loads only:

Solid load	36,300 lb
Load at stop	28,500 lb
Stress f when solid	141,500 psi
Stress f at stop	111,200 psi

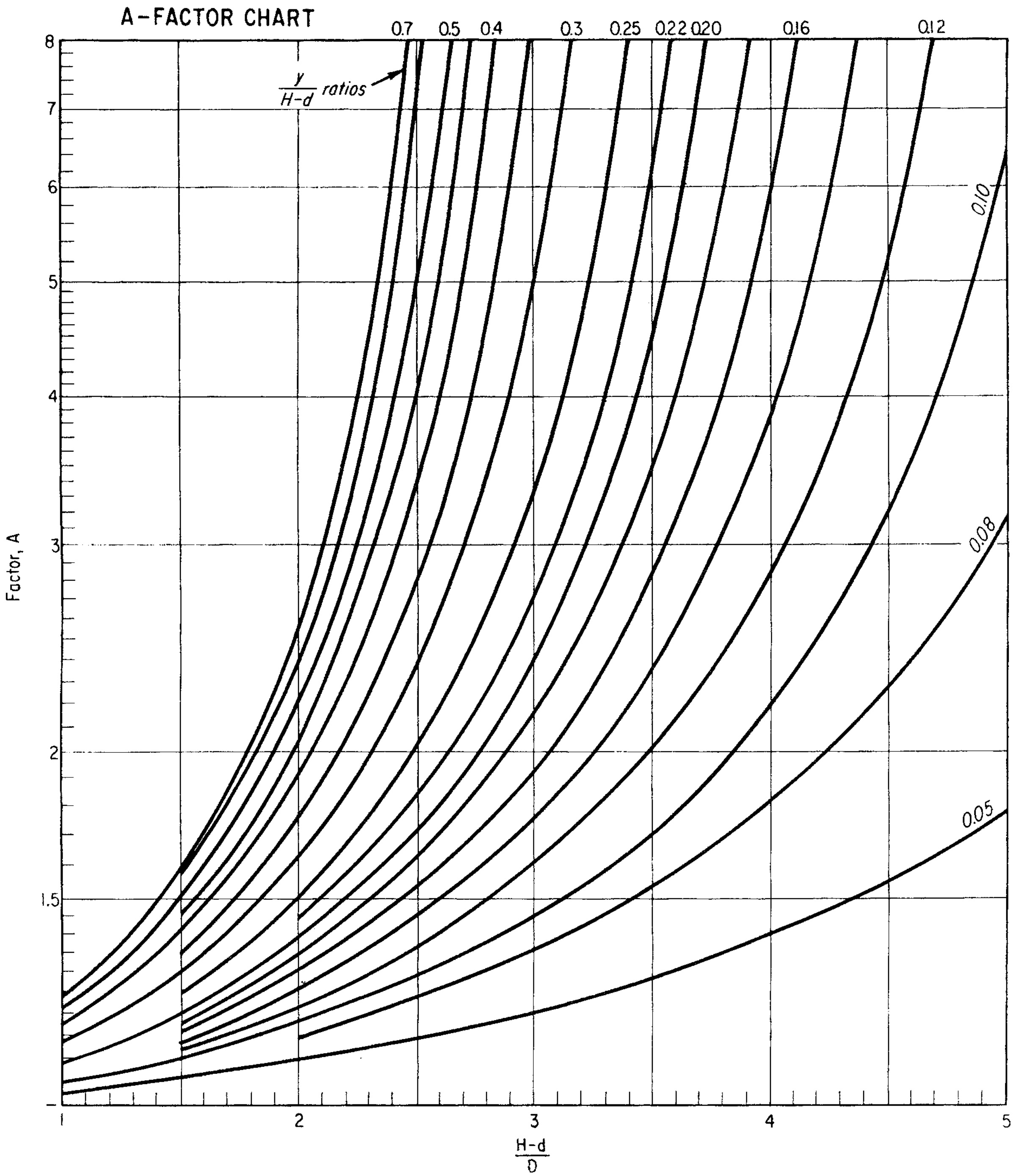

From the combined-stress formula

$$f_c = 111{,}200 \times 1.759$$
$$= 195{,}600 \text{ psi}$$

This stress is so high that settling in service would occur. This particular spring should be redesigned.

Generally, combined stress under the worst condition anticipated should not exceed the solid stress caused by vertical load only. A stop at a reasonable height above solid height is thus desirable—otherwise, spring may have to be modified.

Ovate Cross Sections Make Better Coil Spring

Egg shape proves more efficient that conventional round configuration while also saving space and weight. Analysis also casts light on which materials store energy best.

Nicholas P. Chironis

Almost since helical coil springs were invented, they have conventionally been made of round wire. Few engineers have been aware that round wire does not perform as efficiently as it should, and that other cross sections often used in helical springs, such as square or rectangular wire, give even poorer results.

Now, however, the proposal of a new cross-sectional shape of wire to bring out the best performance in a coil spring is focusing attention on this aspect of spring design. According to H. O. Fuchs, a Stanford Univ. professor, the ideal cross section, based on fatigue tests, is a blend of a circle with an ellipse (drawing).

Such egg-shaped wire, Fuchs contends, can store more elastic energy than the conventional round wire in a spring taking up the same space. Thus, less spring weight is needed to absorb or store a given amount of energy. Moreover, an egg-shaped or "stress-equalized" spring wire will have a higher resonant frequency than a round wire and will be less subject to flutter.

Egg-shaped wire for coil springs is not especially costly to make. Whatever the cross-sectional shape, the wire is, in smaller diameters, drawn through dies with an opening of the desired shape or, in larger diameters, roll-formed to any configuration.

Anti-surge auxiliary. Fuchs, working with John G. Schwarzbeck, a consulting engineer, has also developed an auxiliary coil spring (drawing, page 87) that gives anti-surge protection without requiring any more space than the main spring takes up.

The turns of the auxiliary coil interlace with those of the main stress-equalized spring, which is modified by flattening of its rounded surfaces. As the turns of the larger coil move together during compression, they are frictionally engaged by the turns of the bumper, or anti-surge, spring. Being more flexible, the auxiliary spring contracts as a unit, taking up the surge energy by bending to a slightly smaller radius.

Stress peaks. In conventional coil springs with circular cross section, efficiency is curtailed by stress peaks at points on surfaces of the coil turns during deflection of the spring. At the inside of the coil, for example, direct shearing stresses augment the torsional stresses while the shorter metal fibers are twisted through the same angle as the longer fibers at the outer side of the turn. Thus, total stresses are higher at the inner side than at the outer side of the coil.

In a round wire, the increased stress at the inside of the turn is approximately $1.6/C$ times the average surface stress, where C is the spring index, equal to the mean coil diameter divided by the wire diameter. A spring index of 5, therefore, means there is about 30% greater peak stress at the inside of the coil turn, over and above the average surface stress.

Moreover, spring efficiency is proportional to the square of the permissible stress. So the efficiency of such a spring in fatigue loading, where maximum stress range is the determining factor, is only 60% of the efficiency of the same spring in static loading, where average stress is the determining factor.

Differing curvature. In the egg-shaped cross section, the curvature on the inside of a coil turn is sharper than that on the outside. The difference between the two curvatures is calculated to equalize substantially the stresses produced on the surfaces of the coil during axial deflection. The centroid of the cross section is toward the outside of the midpoint between the inner and outer surfaces.

Overall length and width dimensions of the egg-shaped cross section are approximately related to the coil's inner and outer diameters by the expression:

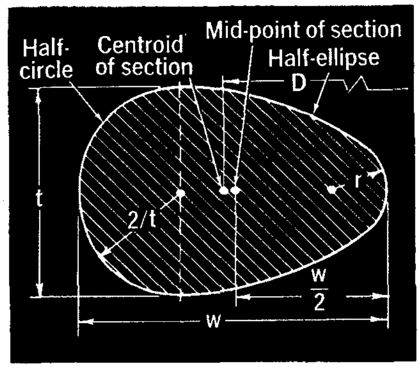

Circle blends with ellipse to equalize stresses during flexing in new wire shape.

$$\frac{w}{t} = 1 + \frac{1.2}{c}$$

where

w = overall length of the section in a radial direction normal to the coil axis

t = overall width thickness of the section in a direction parallel to the coil axis

$c = \dfrac{D_o + D_i}{2w}$

D_o = outer diameter of coil

D_i = inner diameter of coil

The exact equation for the w/t ratio is a much more involved relationship, but the error in use of the above approximate relationship is slight (graph, page 88). For design purposes, it is important to know the relationship between the radii of inner and outer curvatures:

$$\frac{t}{2r} - 1 = 2\left(\frac{w}{t} - 1\right)$$

where $\frac{t}{2r} - 1$

defines the "egginess" of the oval section. When $t = r$, the egginess will, of course, be zero. For the section shown in the drawing (above and right), $t = 0.6$, $r = 0.15$, and $w = 0.9$, which works out to an egginess of 1.

Fuchs has also worked out the four other formulas needed to design an egg-shaped spring:

Stress equation

$$S/P = 2.55D/wt^2$$

Load-deflection equation

$$P/f = Gt^4[2.1(w/t) - 1.1]/8ND^3$$

Area of section

$$A = \pi wt/4$$

Coil diameter to centroid

$$D = 0.5(D_o + D_i) + 0.152(w-t)$$

where A = area of cross section, D = coil diameter (of centroid of section), f = deflection, G = shear modulus, N = number of active coils, P = load, S = maximum shear stress.

Which material is best? For optimum energy absorption, it is important also to employ materials that can absorb and pack kinetic energy in the smallest space possible. The key factor in energy absorption is the specific resilience, R, of the material (energy stored per unit mass). Fuchs found this factor best determined from the equations:

$$R_o = \sigma^2/2E$$

and

$$R_1 = \tau^2/2E$$

depending on the type of stressing, normal or shear. The permissible stress in tension or shear is σ or τ respectively; the corresponding modulus of elasticity is E or G.

Fortunately for the designer, the stresses in springs are either predominantly normal, as in bending, or predominantly shear, as in torsion; there is no need to be concerned about intermediate cases and triaxial states of stress. Fuchs defines R as energy stored per unit volume, mainly to dodge the nuisance of working with pounds force and pounds mass. The units of R are inch-pounds per cubic inch or lb./in.^{2}.

Results. Comparing materials, using values of permissible stresses recommended in the SAE Manual on Helical Springs, Fuchs calculated the apparent values of resilience with the moduli given there (table above).

Some interesting results emerged from Fuchs' calculations. For example, there is a big difference in resilience between music wire and some of the steels favored by aerospace designers, such as alloy steel and 302 stainless. In torsion or compression springs, the resilience of music wire is almost double that of 302 stainless.

The high values for compression springs are due to the existence of beneficial self-stresses. According to Fuchs, in those helical torsion springs (stressed in bending) that are cold-wound from small wire, beneficial self-stresses also exist but are less effective. In the hot-wound 0.50-in. alloy steel spring, the self-stresses induced by coiling are removed by heat-treating.

The much higher apparent resilience that can be obtained from the material in compression springs explains why weight can be saved by replacing an extension spring by a pair of long "hooks" that compress a spring between their inner ends when the outer ends are pulled apart (drawing right).

Permissible stresses. The table also illustrates the fact that the level of permissible design stresses is much more important in springs than in structural members. That's because the weight of a spring will be inversely proportional to the square of the stress.

In music wire and in hard-drawn stainless, the decrease in diameter from 0.10 to 0.05 in. corresponds to an increase in permissible stress of about 13%, but to an increase in resilience of about 28%. The dependence on the square of the stress also explains why springs were among the first products that utilized the stress increase that was made possible by shot peening.

Steel, according to Fuchs, is hard to beat as a spring material. Any competing material will have to be evaluated on the basis of specific resilience. Aluminum alloys, whose moduli of elasticity and density are about one-third that of steel, will save weight only if their permissible stresses exceed one-third of the corresponding stresses for steel. Glass fiber, which has even lower value of modulus and of density, seems to be worthy of serious consideration only for special applications, according to Fuchs.

Fuchs also warns that because hollow sections are theoretically more efficient than are solid sections, many engineers are frequently tempted to make springs out of tubes instead of bars and wires.

This approach, he says, is reasonable for springs that must only maintain a static load, but it will not work for springs in fatigue service, because it is too difficult to shotpeen the inside of small, straight hollow sections and impossible to shotpeen the inside of a coiled tube.

And, if the surfaces are not shotpeened, the permissible stress is so much less that it results in a weight increase instead of a weight saving.

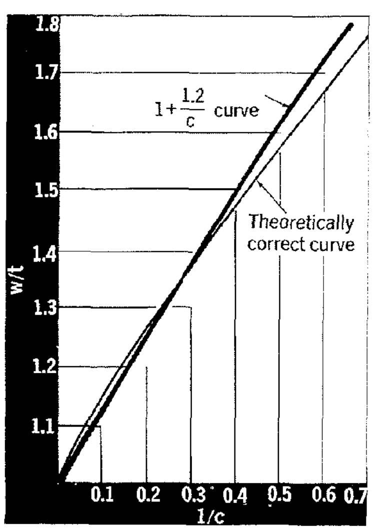

Comparing the resilience of spring materials

Material	Modulus, lb./in.^{2} x 10^6 E	Modulus, lb./in.^{2} x 10^6 G	Diameter, in.	Torsion springs σ, ksi	Torsion springs R_0, psi	Compression springs τ_1, ksi	Compression springs R_1, psi	Tension springs τ_2, ksi	Tension springs R_2, psi
Alloy steel (hot-wound)	29	11	0.50	155	410	146	985	106	515
Music wire (cold-wound)	30	11.5	0.10	212	750	154	1030	114	565
			0.05	240	960	174	1320	128	710
302 stainless hard-drawn (cold-wound)	25.5	10	0.10	148	430	106	560	91	415
			0.05	170	565	123	755	105	550
Phosphor bronze (cold-wound)	15	6.2	0.10	90	270	70	395	55	245
			0.05	98	320	76	460	60	290

Variants of coil springs

Stress-equalized spring can have...

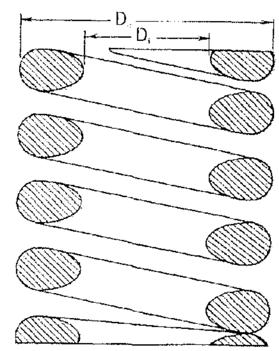

...interwound anti-surge spring...

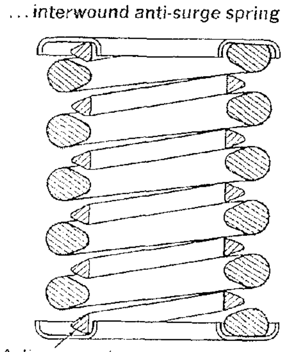

Anti-surge spring

...and various degrees of egginess

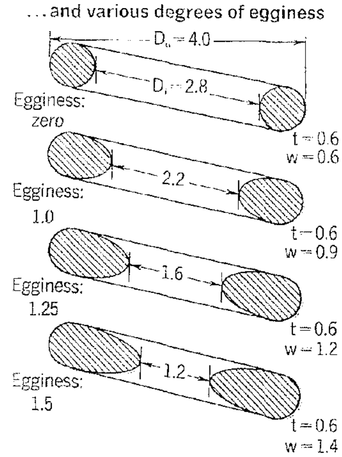

Unusual Uses for Helical Wire Springs

Haim Murro

SPRING BELTING (left). For low power transmission at high speeds. Allows a certain amount of variation in the center distance and absorbs inertia forces. Spring ends can be joined smoothly by using a smaller internal spring as shown on the following page.

ELECTRICAL FITTING (right). An inexpensive lamp or fuse socket which insures proper contact even when subject to moderate vibration. Small threaded parts also can be joined in this same way.

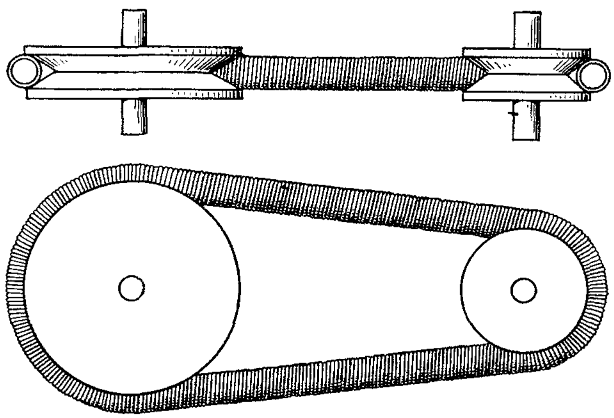

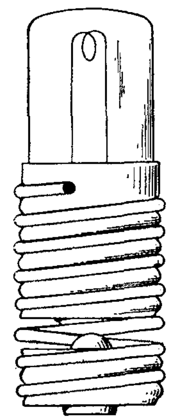

SCREW THREAD INSERTS (left). Wire with diamond cross section. For tapped holes in light alloys and plastics. Are made of stainless steel for corrosion-free threads. Can be used to renew worn-out tapped threads.

ROTATING TYPE OIL SEAL (right). Uses helical wire spring to exert a radial force on the packing. Friction is kept to a minimum and efficiency is high even at high shaft speeds.

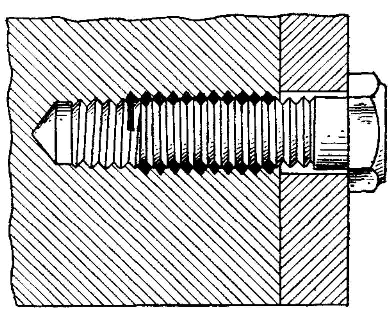

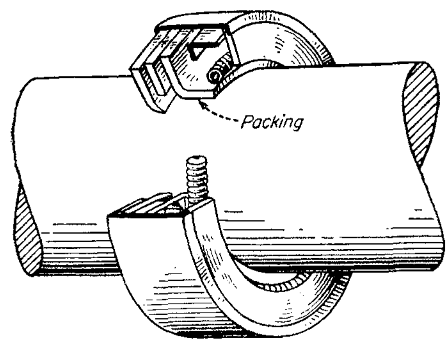

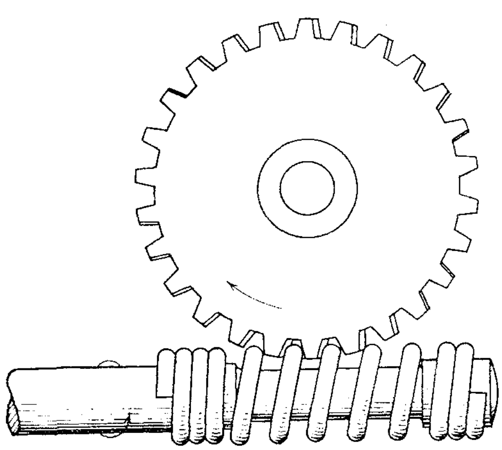

WORM GEARING. Used on low power transmissions. Allows a certain amount of misalignment between worm and wheel. Wheels are best made from laminated plastics.

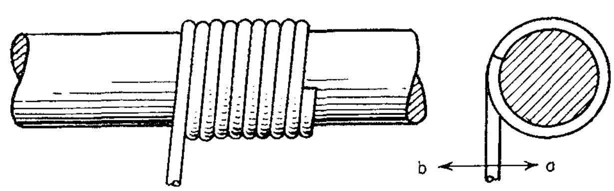

FRICTION RATCHET. Spring rotates shaft when pulled in the *a* direction, but turns freely on the shaft when pulled in the opposite or *b* direction.

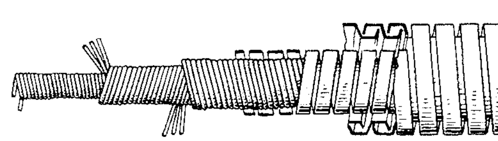

FLEXIBLE SHAFT. Inner springs serves as shaft, outer one as a casing. For single direction of rotation unless shaft consists of two or more springs wound in opposite directions.

A selection of practical applications that are characterized by the functions served in each case by the helical wire spring. The spring rate property is put to use in most cases, but not in the axial loading sense that represents the more common applications for which these types of springs are employed in industrial products.

SENSITIVE STICK (left). Round conductor bar is mounted within a spring fastened to insulators to serve as an electrical switch. Deflecting the spring laterally completes the circuit. Can operate relays or alarm and can be made with intermediate insulators where considerable length is required.

THREAD MEASURING GAGE (right). Dimension *d* allows calculating the effective dia of thread. Pressing the loops releases the bolt to be unscrewed. Can be used on fluted parts like thread taps.

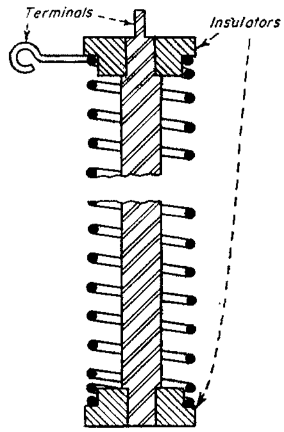

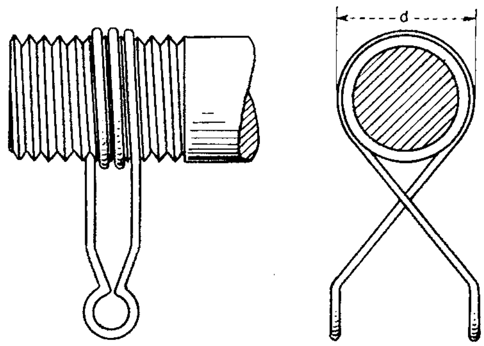

FLEXIBLE CHUTE (left). For feeding small articles from hoppers to automatic machines. Spring can be wound in different shapes as required by the articles being handled.

TUBING REINFORCEMENT (right). Gives plastic or rubber tubing added rigidity as well as protection against mechanical damage. Can be cast inside rubber as shown in lower sketch.

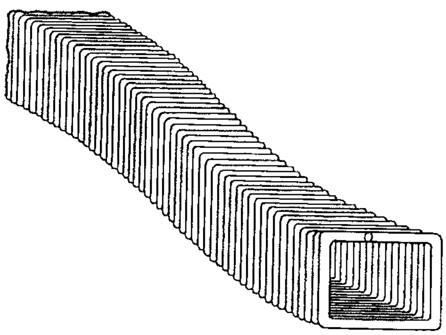

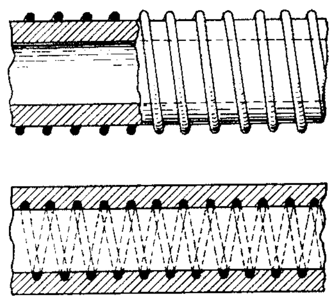

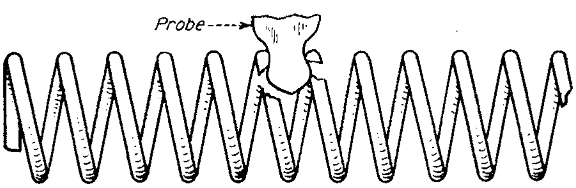

ELECTRICAL CONNECTION for small, light products like hearing aids uses a special probe that is easily inserted between coils of spring which is a conducting material.

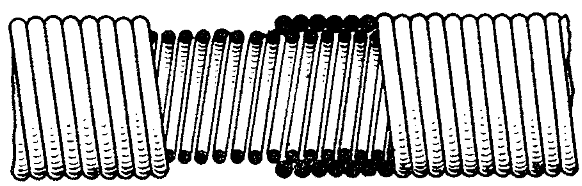

SMALL SPRING connects ends of larger spring with a thread-like action. Useful where external projection cannot be tolerated, like the spring-belting on opposite page.

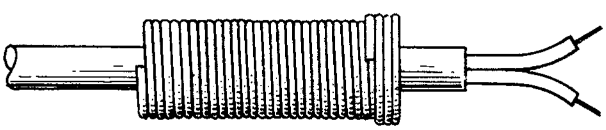

SHIELD FOR ELECTRICAL WIRE AND CABLE. Provides wear resistant covering for wires and protection against physical damage.

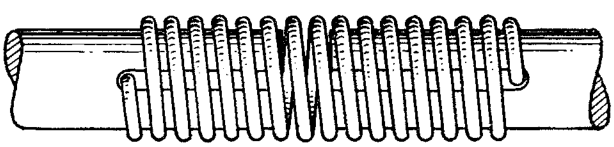

SMALL DIAMETER SHAFT COUPLINGS. Allows for some misalignment and can be used with shafts or unequal diameters. For single direction of rotation only.

Optimum Helical Springs

How do you go about designing a spring with least weight or volume? Not sure? Neither were some of experts—until these formulas were derived.

Henry Swieskowski

AT Springfield Armory we have frequently been confronted with space, cost, and weight limitations in spring design. The formulas that I present here go well beyond the current literature in these respects. They also tell you what you can do to further reduce the weight or size of the spring. Separate sets of formulas treat the following three load requirements:

Case 1—When the spring must provide a specific load at the assembled height. All retainer-type springs are in this class, and this is the most common spring problem.

Case 2—When the spring must provide a specific amount of energy during its working stroke. The stroke is the distance from assembled height to fully compressed height. This requirement is called for with springs whose function is to stop a moving mass or to accelerate a resting mass.

Case 3—When the spring must provide a specific final load at the fully compressed height. This requirement frequently occurs in the design of latches and linkages.

Because minimum values are sought, the analysis considers spring ends as being plain; in other words, there are no inactive coils (a prominent spring manufacturer has recently warned that most designers unnecessarily call for square-and-ground spring ends and thus add to the cost of the spring). However, the formulas can be modified in applications where the spring ends are squared or ground.

The analyses are based on the following conventional formulas (see also the list of symbols on next page):

Load-deflection formula

$$\frac{P}{F} = \frac{Gd^4}{8\,D^3 N} \tag{1}$$

Final-stress formula

$$S_2 = \frac{8\,DP_2}{\pi d^3} \tag{2}$$

Stroke formula

$$s = F_2 - F_1 \tag{3}$$

Energy formula

$$E = s\left[\frac{P_2 + P_1}{2}\right] \tag{4}$$

SYMBOLS

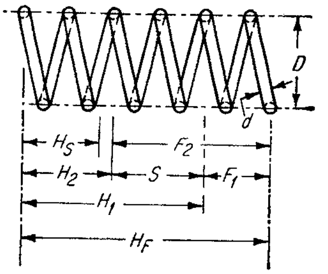

C = spring index; $C = D/d$
d = wire diameter, in.
D = mean coil diameter, in.
E = energy capacity, in.-lb.
F_1 = initial deflection, in.
F_2 = final deflection, in.
G = modulus of torsion, lb/in.^{2}
H_1 = assembled height, in.
H_2 = minimum compressed height, in.
H_F = free height, in.
N = number of active coils
P_1 = load at assembled height, lb
P_2 = load at minimum compressed heigth, lb
R = load-deflection rate, lb/in.; $R = P/F$
s = stroke, in.; $s = H_1\text{-}H_2$
S_2 = stress at minimum compressed height, psi
V = volume of spring material, in.^{3}
W = weight of spring material, lb
ρ = density of spring material, lb/in.^{3}

Volume formula

$$V = \frac{\pi^2 d^2 DN}{4} \qquad (5)$$

Formulas for the three cases are derived below, with related charts and numerical examples to simplify the design procedure.

Case 1—Minimum spring volume for given initial load, P_1

Combining Eq 1,2,3 and 5 yields the relationship between the volume of spring material and the basic spring parameters:

$$V = \frac{\pi^2 sd^6 G}{4\,(\pi d^3 S_2 D - 8P_1 D^2)} \qquad (6)$$

Substituting the value of the spring index, $C = D/d$, into Eq 6 gives:

$$V = \frac{\pi^2 sD^4 G}{4C^3\,(\pi S_2 D^2 - 8P_1 C^3)} \qquad (7)$$

To determine which values of spring index produce minimum spring material, Eq 7 is differentiated with respect to C and set equal to 0.

$$16\, P_1 C^3 - \pi S_2 D^2 = 0 \qquad (8)$$

This equation now leads to the following design formulas:

Spring index for a minimum volume spring (by solving for C):

$$C = \left[\frac{\pi D^2 S_2}{16\, P_1}\right]^{1/3} \qquad (9)$$

Wire diameter for a minimum volume spring (by solving for d):

$$d = \left[\frac{16\, P_1 D}{\pi S_2}\right]^{1/3} \qquad (10)$$

Minimum volume for given initial load (by substituting Eq 9 into Eq 7):

$$V_{\min} = \frac{8s\, P_1 G}{S_2^2} \qquad (11)$$

Thus, for a given mean coil diameter, you can design the spring to have minimum volume by selecting the spring index according to Eq 9 or the wire diameter according to Eq 10.

The relationship is made clear in the illustration at right. This is a plot of Eq 7 with the mean coil diameter D acting as a parameter by assuming the values 0.2 0.5, 0.9 and 1.4 in. For each D value, there is a C value that leads to minimum spring volume.

Example 1—Design a spring to have minimum material-volume with the following requirements:

Initial load, P_1 = 15 lb
Mean coil diameter, D = 1.02 in.
Stroke, s = 1.16 in.
Final stress, S_2 = 100,000 psi
G (steel) = 11.5 × 10^6 psi

Step 1—Calculate min volume, Eq 11

$$V_{\min} = \frac{8(1.16)\,(15)\,(11.5\times 10^6)}{10^{10}} = 0.16 \text{ in.}^3$$

Step 2—Find the wire size, Eq 10

$$d = \left[\frac{16\,(15)\,(1.02)}{\pi 10^5}\right]^{1/3} = 0.092 \text{ in.}$$

Step 3—Solve for the number of active coils, Eq 5

$$N = \frac{4\,(0.16)}{\pi^2\,(0.092)^2\,(1.02)} = 7.5$$

Step 4—Calculate the active solid height

Solid height, $H_s = (N + 1)\, d = 8.5\,(.092) = 0.782$ in.

For practical design allow a 10% clearance between solid height and minimum-compressed height. Hence

$H_2 = 1.1 H_s = 0.860$ in.

$H_1 = H_2 + s = 0.860 + 1.16 = 2.020$ in.

Step 5—Now compute the load-deflection rate to determine the free height, Eq 1

$$R = \frac{(11.5\times 10^6)\,(0.092)^4}{8\,(1.02^3)\,7.5} = 12.9 \text{ lb/in.}$$

Thus

$$F_1 = \frac{P_1}{R} = \frac{15.0}{12.9} = 1.163 \text{ in.}$$

Free height

$H_F = H_1 + F_1 = 2.020 + 1.163 = 3.183$ in.

Case 2—Minimum spring volume for required energy capacity, E

The volume of spring material is obtained by combining Eq 1 to 5:

$$V = \frac{\pi^2 s^2 d^6 G}{8D\,(\pi s\, S_2\, d^3 - 8ED)} \qquad (12)$$

With the aid of the spring ratio $C = D/d$, Eq 12 becomes:

$$V = \frac{\pi^2 s^2 D^4 G}{8C^3\,(\pi s\, S_2 D^2 - 8EC^3)} \qquad (13)$$

Differentiating with respect to C and letting $dV/dC = 0$, results in

$$16EC^3 - \pi s\, S_2 D^2 = 0 \qquad (14)$$

As in Case 1, we obtain the following design formulas:

Spring index for minimum volume:

$$C = \left[\frac{\pi D^2 s\, S_2}{16E}\right]^{1/3} \qquad (15)$$

Wire diameter for minimum volume:

$$d = \left[\frac{16ED}{\pi s\, S_2}\right]^{1/3} \qquad (16)$$

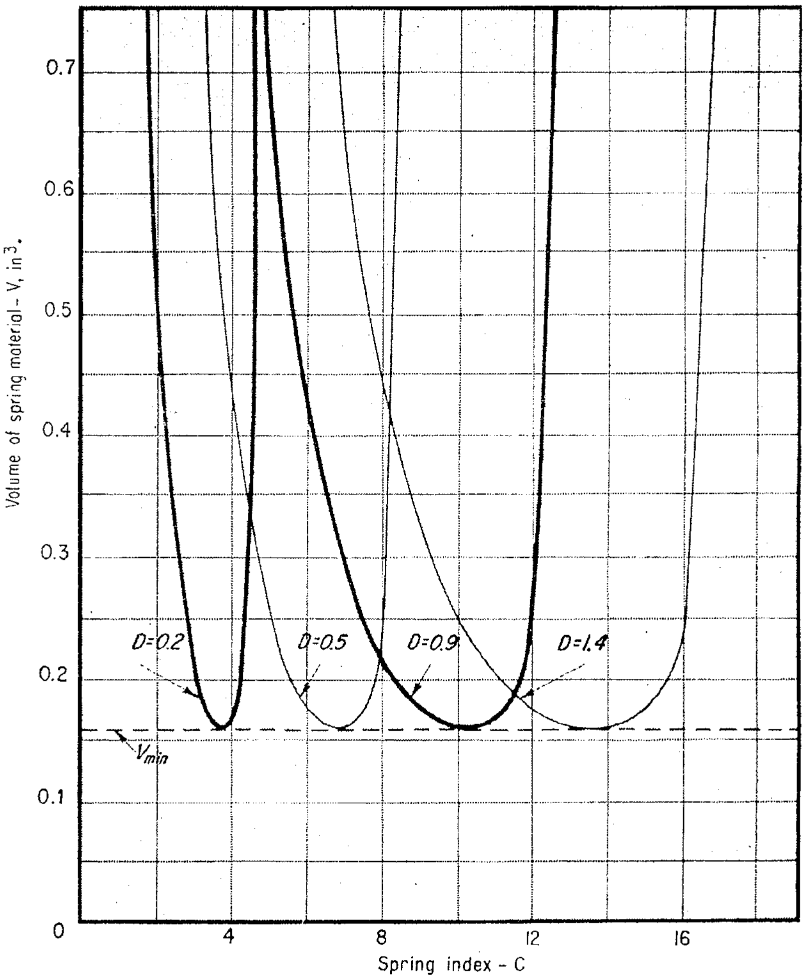

2. Variations in volume for springs of different diameters. Note that there is an optimum value of spring index for each case. A slight shift in the C-value chosen by the designer boosts the spring weight.

Minimum volume for given energy requirement

$$V_{\min} = 4EG/S_2^2 \qquad (17)$$

Thus, V_{min} is independent of the mean coil diameter when d is chosen in accordance with Eq 16. Eq 17 shows the interesting result that V_{min} is also independent of the stroke, s.

Case 3—Minimum spring volume and required final load, P_2

A slightly different approach is taken in the analysis of minimum volume and final load. Here it is the total deflection, F_2, rather than the stroke, s, that is the important parameter.

Combining Eq 1, 2, and 5 yields the surprising result:

$$V = \frac{2F_2 G P_2}{S_2^2} \qquad (18)$$

In other words, the volume for this case is independent of the mean coil diameter, D, and spring index, C. Thus, when the requirements for F_2, G, P_2 and S_2, are given, equal spring volumes are obtained regardless of the values chosen for the coil diameter and spring index.

Example 2—Design a minimum-volume spring with the following requirements:

Final load, $P_2 = 50$ lb
Mean coil diameter, $D = 0.95$ in.
Total deflection, $F_2 = 1.0$ in.
Final stress, $S_2 = 80{,}000$ psi
Modulus of torsion, $G = 11.5\times10^6$

Actually, from the above requirements, only one solution is possible.

Step 1—Compute the minimum volume, Eq 18:

$$V_{\min} = \frac{2(1)\,(50)\,(11.5)\,(10^6)}{(80{,}000)^2}$$

$$= 0.18 \text{ in.}^3$$

Step 2—Find the wire diameter, Eq 2:

$$d = \left[\frac{8(0.95)\,(50)}{80{,}000\,\pi}\right]^{1/3} = 0.115 \text{ in.}$$

Step 3—Calculate the number of coils, Eq 1:

$$N = \frac{(11.5)\,(10^6)\,(0.115)^4\,(1.0)}{8\,(0.95)^3\,(50)} = 5.9$$

Step 4—Determine the active solid height

$$H_s = (N+1)\,d$$
$$= 6.9\,(0.115) = 0.794 \text{ in.}$$

Again let the minimum compressed height be increased by a 10% clearance:

$$H_2 = 1.1H_S$$
$$= 1.1\,(.794) = 0.873 \text{ in.}$$
$$H_F = H_2 + F_2$$
$$= .873 + 1.000 = 1.873 \text{ in.}$$

Designing for minimum weight

Although the findings were in reference to minimum spring volume, you can apply the equations equally as well to minimum spring weight by relating the spring weight, W, to the density of spring material, ρ, in the following manner:

For required initial load

$$W_{\min} = \rho\left[\frac{8s\,P_1\,G}{S_2^2}\right]$$

For required energy capacity

$$W_{\min} = \rho\left[\frac{4EG}{S_2^2}\right]$$

For required final load

$$W_{\min} = \rho\left[\frac{2F_2\,P_2\,G}{S_2^2}\right]$$

When springs are ground or squared

The study considered spring ends as being open and not ground. For other end conditions, the minimum spring volume will be greater by an amount:

For squared ends (closed ends):

$$V_{\min} = \tfrac{1}{2}\pi^2\,d^2\,D$$

For ground ends:

$$V_{\min} = \tfrac{1}{4}\pi^2\,d^2\,D$$

Machined Helical Springs
Gives More Precise Performance

The traditional coil spring, made by winding a wire around a mandrel, is today confronted by a new contender—a square-section helical spring machined from solid metal and ground to close tolerances like other mechanical components.

Machined springs have always appealed to designers for the limited number of applications where precise requirements are more important than cost. But regardless of cost, most methods of manufacturing machined springs were painfully slow and somewhat unpredictable.

A new method of precision-grinding helical elements may get around the earlier handicaps that have discouraged interest among designers. This technique has been worked out by J. Soehner Div. of Kinemotive Corp., Lynbrook, N. Y.

Assuring precision. Even with improved productivity of the manufacturing line, the machined springs won't compete on price with the conventionally wound helical coils. But the spring designer is often confronted with rigid requirements as to the spring rate (the load-deflection rate) or the coil-expansion rate (when the spring must serve as a friction brake). Sometimes, too, the spring must be assembled very precisely with other mechanical components so all work as a team in a common function.

In such cases, conventional springs have shortcomings that are more important than price.

Soehner's technique is keyed to the development of special automatic grooving equipment that speeds up manufacture without sacrificing precision. This equipment can grind precision-squared helical coils, with slots that can be very narrow if necessary. In one application, Soehner succeeded in grinding slots only 0.015 in. wide by 0.250 in. deep in tubular stock.

Integral designs. Soehner's springs usually are ground from premachined and hardened stock in sizes ranging from 0.125 in. to 6 in. OD and with load capacities from a few grams to more than 1000 lb. Any material that can be machined is stock for Soehner's grinding wheels, including such metals as Ni-Span-C and Inconel X750.

The designer gains freedom from

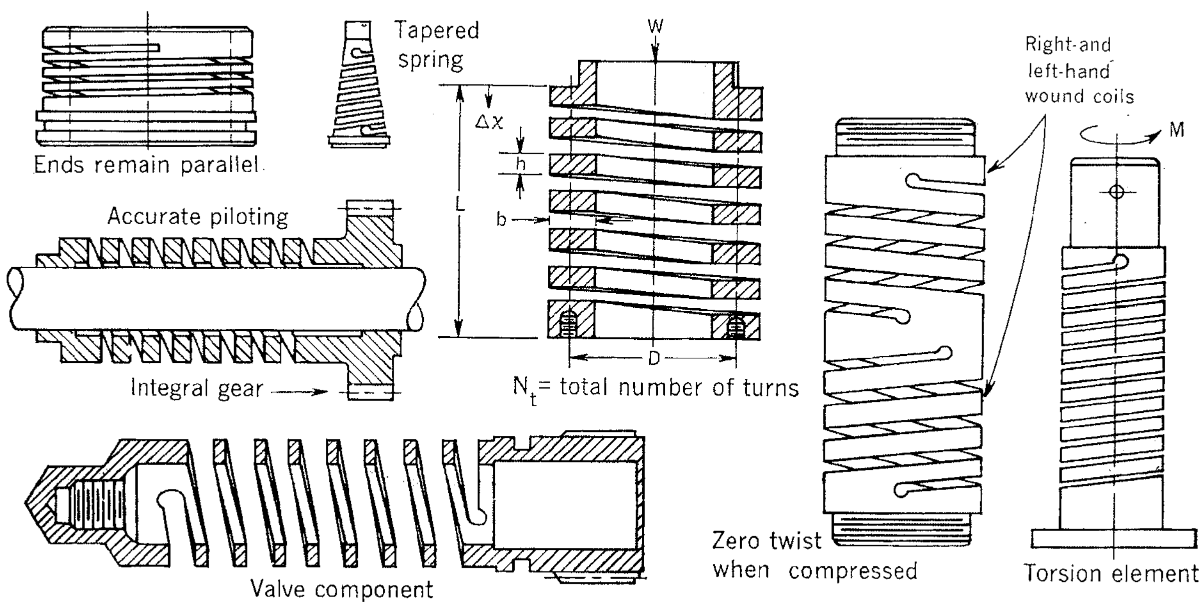

Spring can now be designed as an integral part of another component or to perform a multiple function in a machine.

routine limitations when coils are ground instead of wound. For example, an entire subassembly can be machined from one solid piece. Springs can be machined integrally with gears, valve seats, threaded ends, piloting surfaces, tapered coils, and right- and left-hand coils in series.

Even with maximum care in design, a spring may not perform precisely according to formula. Soehner finds that its machined springs can be reground as needed to meet ultra-precise requirements. The spring assembly can be measured for spring rate and other performance specifications and then remounted on the grinder for modification. Regrinding of a few ten-thousandths of an inch from the spring's outer diameter, coil width, or coil height will bring the rate precisely to the specified measurement.

British formulas. Most U.S. formulas for helical springs were derived originally from springs that are wound from coil. Such formulas employ a curvature factor to allow for stresses induced in the wire when it is wound. For machined square-coil springs, however, Soehner finds that formulas developed by the British Standards Institute provide more accurate designs. These formulas make use of "stiffness factors," μ, and λ, that in turn vary with the b/h ratio of the coil cross section. Specifically, for compression and extension springs:

Axial spring rate, K_x:

$$K_x = \frac{W}{\Delta x} = \frac{\mu G b^2 h^2}{D^3 (N_t - 1)}$$

Shear stress, S_s:

$$S_s = \frac{\lambda W (D+b)(b+h)}{b^2 h^2}$$

where W=axial load, lb; G=shear modulus, psi; N_t = number of turns; and where dimensions D, b and h are defined in the middle drawing, bottom of facing page.

Values of μ and λ are given in the chart below. The machined springs also can provide a torque or load at right angles to the spring axis:

Torsional spring rate, $K\theta$:

$$K_\theta = \frac{M}{\Delta\theta} = \frac{Ehb^3}{2400\, DN_t}$$

Fiber stress:

$$S_f = \frac{6M}{hb^2}$$

where M= torque, in.-lb.; $\Delta\theta$=angular deflection (twist), deg.; E= Young's modulus, psi; and S=fiber stress, psi.

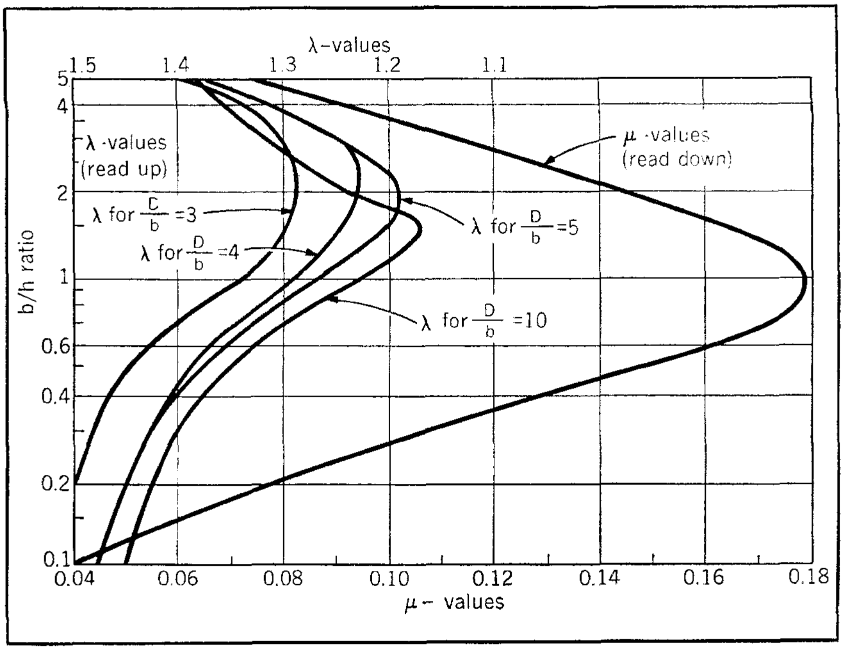

Stiffness factors μ and λ are shown for various wire cross-section ratios.

Pneumatic Spring Reinforcement

Robert O. Parmley, P.E.

A typical pneumatic spring is basically a column of trapped air or gas which is configured within a designed chamber to utilize the pressure of said air (or gas) for the unit's spring support action. The compressibility of the confined air provides the elasticity or flexibility of the pneumatic spring.

There are many designs of pneumatic springs which include: hydro-pneumatic, pneumatic spring/shock absorber, cylinder, piston, constant-volume, constant mass and bladder types. The latter, bladder type, is one of the most basic designs. This type of pneumatic spring is generally composed or rubber or plastic membranes without any integral reinforcement. See Figure 1.

A cost-effective method to reinforce the bladder membrane is to utilize a steel coil spring for external support. Figure 2 illustrates the conceptual design. Proper sizing of the coil spring is necessary to avoid undue stress and pinching of the membrane during both the flexing action and rest phase.

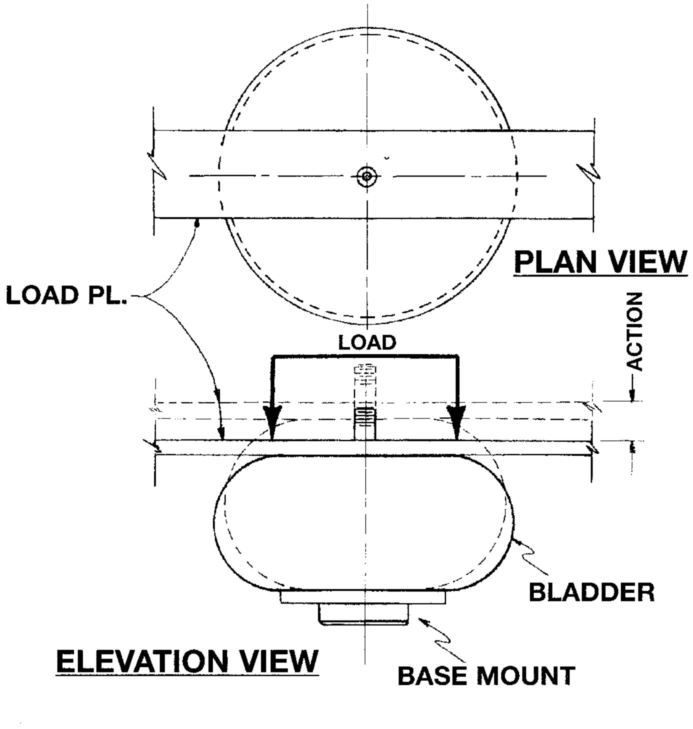

Figure 1

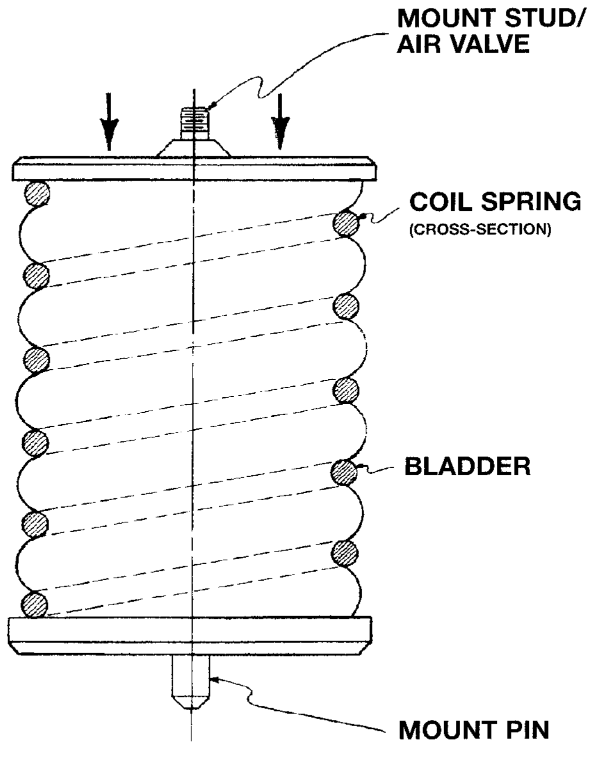

Figure 2

Nonlinear Springs

Two forms of nonlinear systems offer improved working characteristics in a wide range of applications. Design equations are given for each.

William A. Welch

MANY of today's products that use spring systems will function better if a nonlinear type is employed in place of one of the usual linear springs. But nonlinear systems require more complex analyses—nonlinearity is a dirty word to some engineers—and frequently designers stick to their familiar linear-spring types, even when they know better.

Why the increased interest in nonlinearity? Nonlinear springs, as you know, have a force-deflection rate (spring rate) which increases—or sometimes decreases—with deflection, Fig 1. Such springs can out-perform the linear types in two classes of applications:

1) Shock-absorbing springs—as in automotive applications, aircraft landing gear, fragile product packaging, dynamic stops for machines.

2) Periodic motion mechanisms—as in feed mechanisms, sorting machines, sequence controls (such as springs for valves, latches, escapements), reciprocating tools.

Let us see why nonlinearity is useful in such applications. A suspension system for a vehicle is a good example of the first class of applications. It must ease road shocks over a wide range of speeds. The effective vertical impact velocity will be essentially a function of vehicle speed, but the shock attenuation is related to the ratio of impact velocity to system natural frequency. Therefore, it is desirable to have the system frequency increase with the impact velocity. This is obtainable with a nonlinear spring system. Similar conditions prevail in aircraft landing gear where the spring system must be soft on ordinary landings, yet stiffen rapidly under shock loads during emergency landings or when there is a sudden down draft. Such conditions occur also in packaging. Examples of the second class

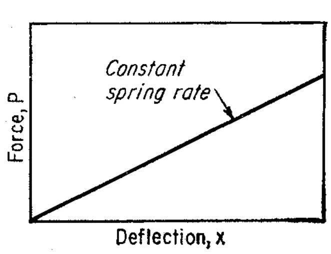

Linearity in springs

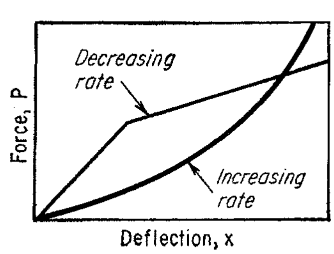

Nonlinearity

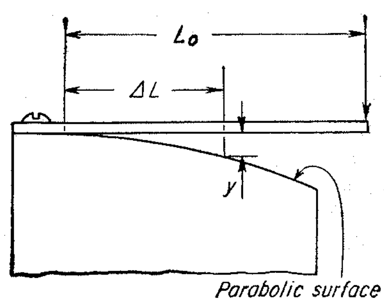

Cantilever non-linear leaf spring

1. Spring rate k is the amount of deflection produced by a load P. Hence k = P/x. For most springs, the spring rate is constant, giving a straight-line (linear) curve

Symbols

a = displacement at transition for bi-linear system, in.
C = non-linearity parameter, dimensionless, which describes the rapidity of the change of the spring rate, k, with changes in deflection
E = elastic modulus, psi
F = harmonic force amplitude, lb
I = cross section moment of inertia, $in.^4$
k = spring rate, lb/in.
L = free length, in.
m = mass, inch-pound-second units
P = spring force, lb
t = time, sec
x = displacement, in.
x' = velocity, in./sec
x'' = acceleration, in./sec^2
y = ordinate of spring abutment, in.
z = abcissa of spring abutment, in.
ω = circular natural frequency, rad/sec

of application are the vibrating conveyors and sorters, Fig 2. Such machines are tuned, by proper choice of springs, to the operating frequency of the drive motor. The problem is how to maintain such tuning when the speed of the feeder, and hence the operating frequency is varied. This is usually done by adjusting the spring rate or the mass—or by designing a nonlinear system to remain "in tune" over a range without adjustment.

Equations of nonlinearity systems

Couple a spring to a mass and you have a vibratory system. If the spring is linear (force exactly proportional to displacement), behavior of the system is described by the very tractable differential equation:

$$mx'' + kx = 0$$

(See list of symbols above.)

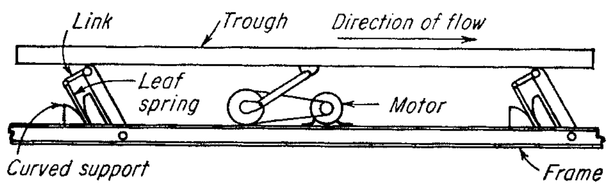

2. Application of cantilever leaf spring with curved support to a reciprocating conveyor. This arrangement enables the driven load to operate close to resonance over a range of motor speeds. It is desirable to vibrate at resonance, or close to it, to obtain large amplitudes for feeding and thus avoid the need for a much larger motor.

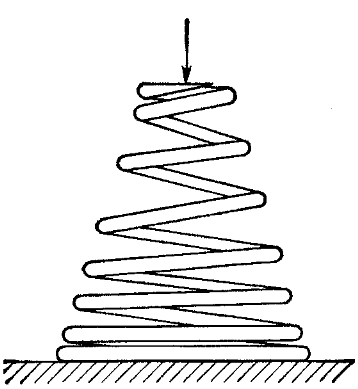

Tapered O D spring

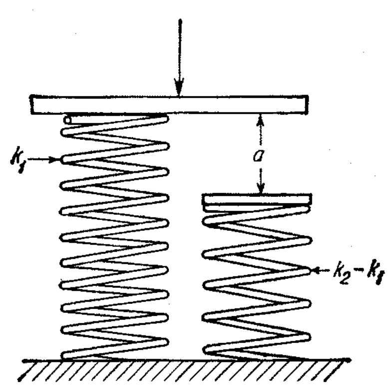

Dual helical springs

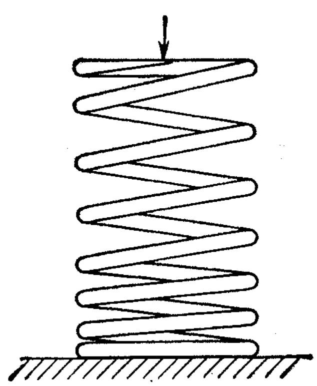

Tapered-pitch spring

on a force-deflection chart. Others may have an increasing or decreasing spring rate, and the rate may change abruptly or smoothly. This is done in various ways.

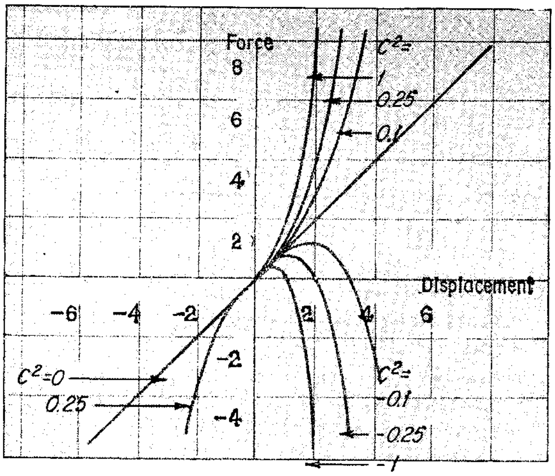

3. **Pick the degree of nonlinearity.** A value $C^2 = 0$ gives zero nonlinearity (i.e., a linear spring). Generally, a high value (much over $C^2 = 1$) is desired.

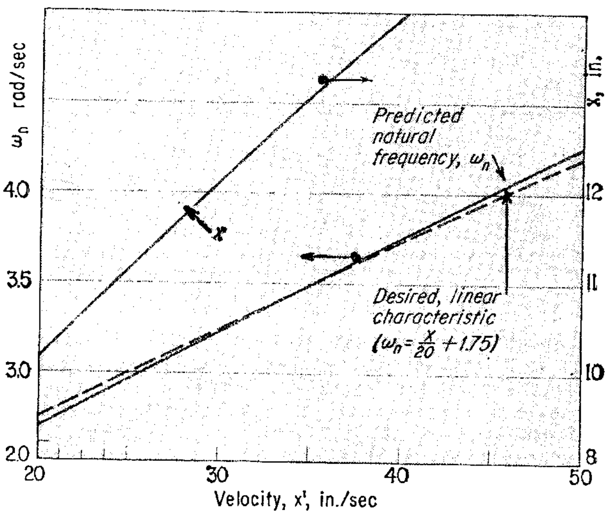

4. **Computed natural frequency,** ω_n, **for the cubic force spring is compared to the desired frequency (broken line.) Note how closely the behavior is approximated.**

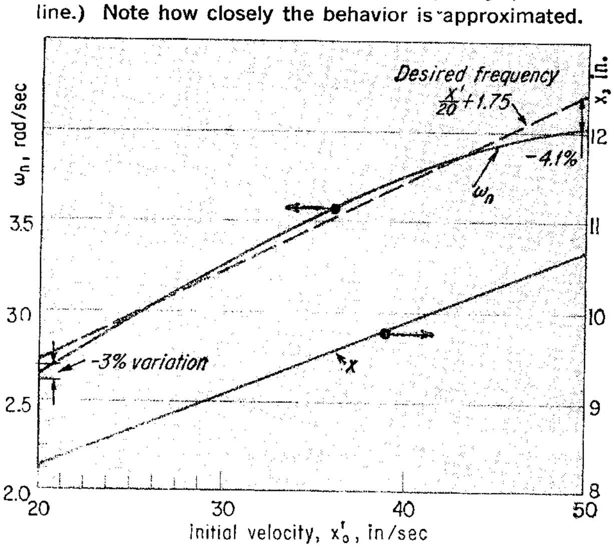

5. **An example of how a bi-linear spring is almost as good as a nonlinear type.** Maximum derivation from specification is only about 4% which benefits tuning.

All manner of useful characteristics are easily derived from this simple relationship: natural frequency, displacement and velocity at any instant, response to dynamic loads, and accelerations. However, if the spring is not linear, the motion is not a simple harmonic but a cantankerous one indeed.

No general solutions are known for the equations of nonlinear systems. Only a few successful approximate solutions have been developed for special cases. The most useful one is the solution which produces a spring force in the form of a cubic curve:

$$P = k\,(x \pm C^2 x^3) \qquad (1)$$

The dynamic equation for this nonlinear system is

$$x''m + k\,(x \pm C^2 x^3) = F \cos \omega t \qquad (2)$$

Here, k is the basic spring rate at zero displacement (actually, at the beginning of the deflection), and C^2 is the parameter describing the nonlinearity, Fig 3. The known approximate solution of Eq 2 gives the all-important design formula:

$$\omega = \left(\frac{k}{m}\right)^{1/2} \left(1 \pm \frac{3C^2 x^2}{4}\right)^{1/2} \qquad (3)$$

With this equation you can approximate any spring rate characteristic you may be seeking. When the C^2 term in this equation is positive the spring stiffens and the natural frequency increases with increasing deflection. The opposite is true with a negative C^2 term.

This equation can be applied directly to the solution of two types of applications.

Rate varying with amplitude

To design a nonlinear system with a specified natural frequency at a particular amplitude:

1) Estimate the required k from the expression $\omega = (k/m)^{\frac{1}{2}}$ for a linear system.

2) Obtain the corresponding C value from the equation:

$$C^2 = \frac{4\,(\omega^2 m - k)}{3\,k\,x^2} \qquad (3a)$$

Or you may assume a value of C which reflects the required degree of nonlinearity. In this case use

$$k = \frac{\omega^2 m}{1 + \dfrac{3\,C^2 x^2}{4}} \qquad (3b)$$

This procedure will suffice for problems in which the amplitude is known, such as a mechanism driven by a crank. Several trials may be needed to obtain a practical combination of k and C^2; the design procedure for a spring with the required characteristic is given later.

Rate varying with impact velocity

When the system natural frequency must have a specified relation to maximum velocity, or impact velocity, a more complex solution is necessary. Typically, this requirement occurs in shock attenuating systems. By equating the stored energy of the spring to the kinetic energy of the mass at impact, it can be shown that

$$C^2 x^4 + \left[2 - \frac{3}{2}\left(\frac{x'\,C}{\omega}\right)^2\right] x^2 - 2\left(\frac{x'}{\omega}\right)^2 = 0 \qquad (4)$$

The solution of x from Eq 4 is substituted back into Eq 3b to find k. Roots can be found quickly by means of the Remainder Theorem and synthetic division (*PE*—Nov 26 '62, p 135). Because ω is not a linear function of the velocity, a specified relation can only be satisfied at two specific points. A good approximation can be attained, however, as shown in the example below, where the deviation is about 2%.

Example: Find the initial spring rate for an oscillating feed system, Fig 2, which must have a natural frequency which varies with the linear feed velocity. Specifically it is desired to have the frequency vary with velocity according to the straight-line relationship of

$$\omega = \frac{x'}{20} + 1.75 \text{ rad/sec}$$

The velocity, x', is expected to vary between 20 and 50 in./sec. The mass of the system is $m = 10$ in-lb-sec units.

The value of C^2 is tentatively selected as 30.

Evaluating Eq 4, for the average value of $x' = 35$ ips

$$30x^4 + \left[2 - \left(\frac{(3)(1225)(30)}{2\,(12.25)}\right)x^2\right] - \frac{(2)(1225)}{12.25} = 0$$

$$30x^4 - 4500x^2 - 200 = 0$$

$$x = 12.25 \text{ in.}$$

Also, for a value of $x' = 35$,

$$\omega = \frac{35}{20} + 1.75 = 3.5 \text{ rad/sec}$$

Substituting the x and ω values into Eq 3b gives

$$k = \frac{12.25\,(10)}{1 + \frac{3\,(30)(150)}{4}} = 0.0363 \text{ lb/in.}$$

Natural frequency can now be verified by substituting x and k into Eq 3.

Note in Fig 4 that if we plot natural frequency and displacement values for the specified range of x', we obtain a natural frequency which does vary almost linearly with velocity.

Bilinear systems

Another form of nonlinear system, which is sometimes more convenient to use, is the bilinear system, Fig 1. In this case, the spring force is

$$P = k_1 x \quad \text{from} \quad x = 0 \text{ to } x = a$$

and

$$P = k_1 a + k_2\,(x - a)$$

from $x = a$ to x_{max}

The motion of the system can be treated as two separate harmonic motions connected by the condition that their velocities are equal at $x = a$. If a is chosen smaller than the minimum amplitude, all motions of the system in operation will be nonlinear. Both the ratio ω_2/ω_1 and the value of a determine how the system natural frequency varies with amplitude or velocity.

The procedure for design is:

1) Select k_1 from the expression

$$\omega_1 = \sqrt{\frac{k_1}{m}}$$

This is the system frequency for all amplitudes smaller than a.

2) Compute the amplitude and natural frequency for several velocities, using Eq 5 and 6 below.

If necessary, adjust the parameters until a good match with desired characteristics is obtained. Increasing the ratio ω_2/ω_1 will increase the slope of frequency vs velocity.

Amplitude of the bilinear system is

$$x = \frac{x'_0}{\omega_2} \cos\left[\sin^{-1} \frac{a\omega_1}{x'_0}\right] + a \tag{5}$$

Natural frequency is

$$\omega = \frac{\pi}{2\left[\frac{1}{\omega_1} \sin^{-1}\left(\frac{a\omega_1}{x'_0}\right) + \frac{\pi}{\omega_2}\right]} \tag{6}$$

Example: Find the two spring rates for a bilinear system with: $m = 10$ in.-lb-sec units, $\omega_2/\omega_1 = 25$, $x'_0 = 20$ ips min $= 50$ ips max, $\omega_1 = 0.5$ rad/sec.

For $x'_0 = 35$ ips, from Eq 5 and 6, $a = 6.7$ in.

$$\omega = \frac{\pi}{2\left[\frac{1}{0.5} \sin^{-1}\left(\frac{3.35}{35}\right) + \frac{\pi}{12.5}\right]}$$

$$= 3.56 \text{ rad/sec}$$

$$x = \frac{35}{12.5} \cos\left(\sin^{-1} \frac{3.35}{35}\right) + 6.7 = 9.49 \text{ in.}$$

$$k_1 = \omega_1^2 m = 0.25\,(10) = 2.5 \text{ lb/in.}$$

$$k_2 = \omega_2^2 m = 156.25(10) = 1562.5 \text{ lb/in.}$$

The values of ω and x are plotted in Fig 5 for the specified range of x_0'. Maximum error is about 4%.

Cantilever-spring design

A popular method of obtaining the nonlinear spring characteristic is to have a cantilever spring, Fig 1, operate over a curved supporting surface (usually a parabolic surface). The surface reduces progressively the free length of the cantilever as the load increases. This stiffens the spring with deflection.

The change in free length is

$$\Delta L = L_0 - \left[\frac{3EI}{k + 3kC^2x^2}\right]^{1/3} \tag{7}$$

Taking z and y as the coordinates of the supporting surface (where $z = \Delta L$):

$$y = \frac{P}{6EI}\,[z^3 - 3\,(L_0 - z)^2 z + 2\,(L_0 - z)] \tag{8}$$

The bilinear spring can be any of the usual types of springs, arranged so that one of two springs engages the mass when $x = a$, Fig 1. In such an arrangement, the spring constant of the second portion, k_2, is the sum of the two spring rates acting together.

Friction-Spring Buffers

Here's a new way of teaming springs to dissipate kinetic energy in rapid, high-impact, reciprocating mechanisms.

Dr. Karl W. Maier

HERE is a new friction shock absorber that can successfully absorb rapid reciprocating forces with a high damping efficiency. The device is actually an assembly of two metal springs—so simple in construction that it might prompt you to say, "Why didn't I think of that?" It can, however, be classified as a new machine element, and as such has received a US patent.

The *Coil-cone Buffer,* as it is called (Fig 1), is well suited to high-speed reciprocating mechanisms where, in addition to a cushioning action, the application calls for high damping and a continuous and rapid withdrawal of kinetic energy. Such applications include:

- **Automatic guns, to damp impact and recoil.** One version of the buffer (in production for two years) is cushioning the impact of the bolts in an automatic rifle. Another type is undergoing tests at Springfield Armory as an external recoil mechanism for an automatic gun installed in aircraft.
- **Power-actuated fastening and demolition tools** to damp the recoil and ease the operation of the tool.
- **Suspension and cushioning systems of heavy vehicles,** such as freight-protection devices in railroad cars, and damping-buffers in trucks, farm equipment and construction machinery.
- **Rapid-actuating valves** to damp severe surges in the valve springs and increase spring life.

A new spring arrangement

The friction unit of the device has two coil springs in a nested arrangement—an inner *support spring* and an outer *brake spring,* Fig 2.

The support spring is a typical helical spring made of round steel wire. Thus it has a high stiffness in the radial direction. The brake spring, on the other hand, is coiled from a wire of triangular cross section and cut into single brake coils to facilitate radial expansion of its coils.

The outside of the brake coils is ground cylindrically to fit snugly into a tubular housing which acts as the shock absorber body. It is this wall which acts as a friction surface.

The plane of contact between brake coils and support spring is inclined toward the axis of the device by a desired camming angle α. **When the support spring is compressed axially, it forces the brake coils outward to press against the friction surface of the housing.**

The buffer assembly

To complete the friction-buffer assembly, the nested-spring unit of Fig 2

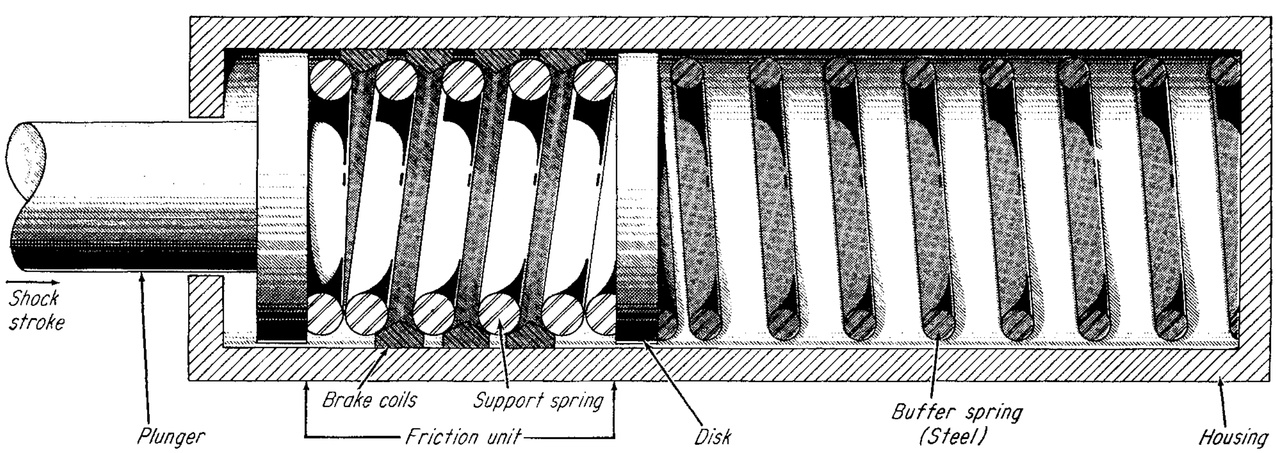

1. Friction buffer assembly contains two spring systems in series. The buffer spring takes most of the deflection during impact, while the friction unit, installed ahead of the buffer spring, absorbs most of the impact energy.

is installed between 1) a resilient buffer spring supported at the closed end of the housing and 2) an axially movable plunger for transmission of external forces (Fig 1).

Camming angles of 30 and 36 deg have been found to be practical choices. With an angle of $\alpha = 30$ deg, tests have shown that a brake coil will receive a radial expansion force about 3.5 times the axial force. Therefore a very high axial braking force is generated between the brake coils and inner wall of the buffer housing.

The relationship between the inner support spring, the brake coils, and the housing wall is such that the coils of the inner spring cannot be compressed to its solid height. The axial force is propagated through the friction assembly in zigzag fashion, from inner coil, to outer coil, to inner coil, etc.

During the compression stroke, the buffer force, P_n, at the plunger is much higher than the force felt by the buffer spring, P_0. For example, the force-deflection diagram, Fig 3, shows buffer units plotted with one, two, or three brake coils. For the unit with three brake coils ($n = 3$), P_3 is about three times P_0. But during the rebound, or extension stroke, P_3 is reduced to about one-third of P_0. This means that the device returns only one-ninth of the energy absorbed during its compression stroke. This amount, however, is sufficient to return the plunger to its original, extended position.

The friction unit, installed ahead of the buffer spring, acts as a force multiplier or force reducer, depending on the direction of motion. Considering its relatively small size, the friction

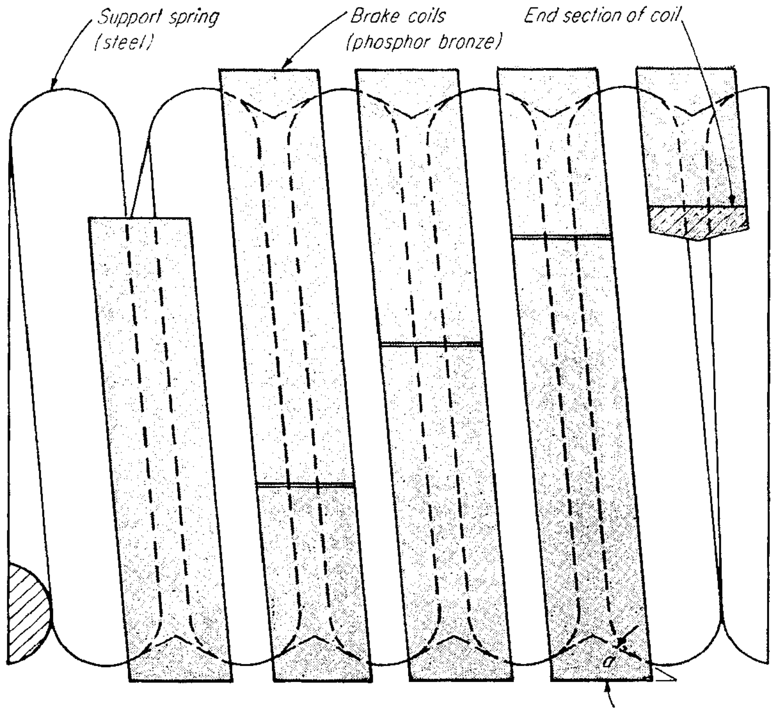

2. Nested spring friction unit of the buffer assembly has segmented brake coils which expand radially when a support spring is compressed axially under impact. Phosphor bronze coils are employed for better friction characteristics. The damping efficiency of the unit is at its highest when the surfaces of the housing wall are dry; however, the unit operates well in the lubricated condition. The number of brake coils contained in the unit influences the amount of energy that can be absorbed. This is illustrated in the force-deflection diagram on the following page.

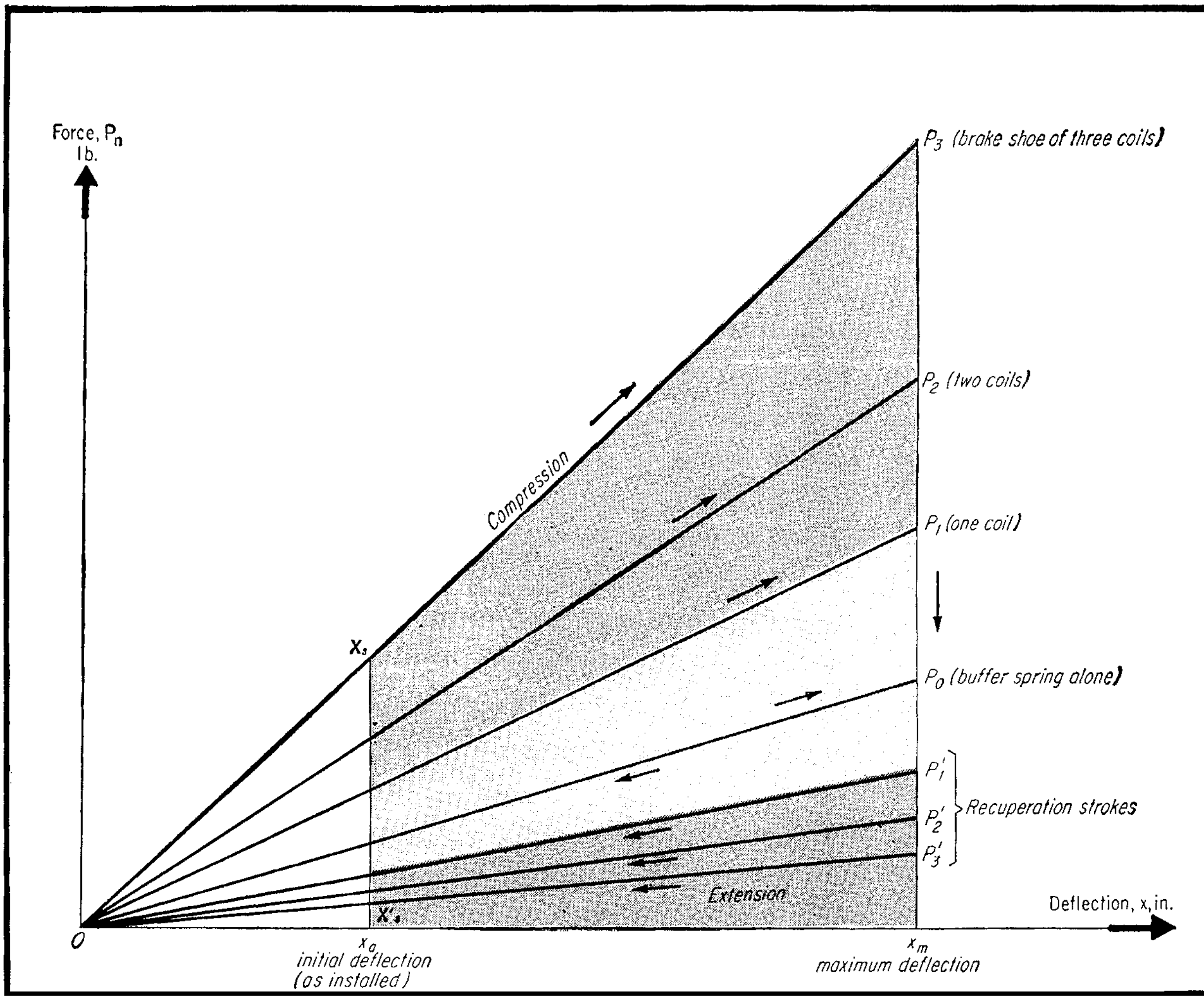

3. Force-deflection characteristics of nested-spring friction buffers. Curves are shown of three different assemblies having one, two or three brake coils. The compression stroke for a three-coil unit is line OP_3; its rebound (extension) stroke is P'_3O. Hence the kinetic energy dissipated by the device is quite large—area $x_3P_3P'_3x'_3$ shown in color and obtained by subtracting area $x_ax'_3P'_3x_m$ from area $x_ax_3P_3x_m$. For a one-coil buffer, the dissipated energy area is shown shaded. Note also the curve for the buffer spring if used alone. It does not dissipate any energy because the recuperation stroke closely coincides with the compression stroke OP_0, and thus the energy is returned during rebound.

unit does a quite remarkable job.

The plunger stroke of the buffer unit is practically identical with the stroke of the buffer spring because the friction unit hardly changes its length during operation. Since the buffer spring can be chosen at will, it permits the development of long-stroke buffers, the stroke being as high as the solid height of the buffer or better.

Energy capacity per unit volume

This factor, also called the volume efficiency, is the ratio of the energy absorbed to the cylindrical volume occupied by the buffer assembly when compressed solid (which includes the buffer spring and friction unit). Very high energy capacities are obtainable in the range of 300 to 600 in.-lb/in.^{3}.

Competitive devices

The all-metal construction of the buffer makes it a rugged device capable of operating without maintenance in the dry or lubricated condition. When lubricated, its damping efficiency drops somewhat. However, there is practically no wear on the friction surfaces and thus the devices have long wear life. The major components are coil springs which can be produced by a spring manufacturer at low cost as compared to machining of parts from solid stock.

Other types of damping buffers have these limitations:

• **Ring springs** have only a limited stroke (15% of solid height), limited damping (60% max)—and they are quite expensive to manufacture.

• **Metal-rubber devices** are even more limited in energy capacity, damping and life.

• **Hydraulic buffers** are more expensive in manufacture and may also require maintenance. Also, they are not easily installed in small spaces.

New Equations Simplify Belleville Spring Design

Research has reduced complex mathematics to easy calculations that help designers to select best dimensions.

Nicholas P. Chironis

As spring designs go, the Belleville is an old-timer—it was patented back in 1835 by Julien Belleville, a French engineer—but it seems to be just coming into its own. Many applications are cropping up in the aerospace and automotive industries, and the way has now been paved for still wider use.

Equations and graphs worked out by Gerhard Schremmer of the Rochester Institute of Technology (Rochester, N.Y.) enable a designer to make sure a Belleville is properly proportioned, without going through complex mathematics.

As Schremmer reported at the annual meeting of the American Society of Mechanical Engineers, the new equations and test data make it possible to predict accurately the endurance strength of a Belleville and to determine its optimum dimensions for a given load.

Packed with power. A Belleville spring is no more than a coned disk (drawing right), and some designers and manufacturers refer to Bellevilles as disk springs, cone-disk springs, or "Belleville washers."

Whatever name the Belleville goes by, the spring's most appealing feature is its ability to provide a very high spring force with a very small deflection. According to Union Spring & Mfg. Co., the Belleville accomplishes this while packed into about one-quarter the space that a helical spring needs (drawing below).

Moreover, by stacking Bellevilles in various arrangements, a designer can obtain various load-deflection characteristics.

Failure points. Schremmer of Rochester Tech says designers have long been calculating Bellevilles on the erroneous assumption that the stress to worry about is the maximum compressive stress at the upper inner edge of the spring, point *A* in drawing on facing page.

Recent tests by Schremmer and others have proved that fatigue failure—and in most dynamic applications, fatigue is the problem—originates somewhere in the lower surface. Depending on the dimensions, and also somewhat on the deflection, either the inner or the outer edge (points *B* or *C*) is more involved in damaging stresses.

Although the stress at *B* or *C* is less than that at *A*, it is more responsible for fatigue behavior, because it is a tensile stress. Schremmer, therefore, derived equations for tensile stresses at points *B* and *C*:

$$S_B = \frac{4Et\delta}{D_o^2 C_3(1-\mu)}\left[C_4\left(\frac{h}{t}-\frac{\delta}{2t}\right)-\frac{1}{2}\right]$$

$$S_C = \frac{4Et\delta}{D_o^2 C_1(1-\mu)}\left[C_2\left(\frac{h}{t}-\frac{\delta}{2t}\right)-\frac{1}{2}\right]$$

where:

D_o = outside diameter
E = modulus of elasticity
h = height of unloaded Belleville
r_i = inner radius
r_o = outer radius
t = thickness
μ = Poisson's ratio (0.3 for most metals)
δ = spring deflection during use

and where:

$$C_1 = 1 - \frac{r_i}{r_o} \qquad C_2 = \frac{1}{\ln\frac{r_o}{r_i}} - \frac{1}{C_1}$$

$$C_3 = C_1\left(\frac{r_i}{r_o}\right) \qquad C_4 = \frac{1}{\ln\frac{r_o}{r_i}} - \frac{r_1/r_o}{C_1}$$

In addition to the equations, Schremmer developed a graph (right) from experimental data that helps determine the decisive point of the spring, dependent on the ratios h/t and D_i/D_o. The tests covered a wide range of Belleville spring sizes, thicknesses, and deflections. In the central range of the graph, either point *B* or point *C* may be dominant.

This ambiguity is caused by the natural scattering of fatigue strength and also somewhat by the influence of the actual deflections. In other words, the smaller the initial deflection due to the preload, the higher the probability of failure at point *B* rather than that at point *C*.

Enduring the stresses. Based on 3600 fatigue tests on Belleville springs made of 50 Cr V4, a chrome-vanadium steel similar to SAE 6150, Schremmer was able also to plot a series of endurance-strength diagrams. In these applications, a Belleville spring undergoes continuing changes in stress from a maximum-stress value to a minimum-stress value, as when under cyclic loading. To get the endurance-strength diagrams, Schremmer employed the equation for S_B and S_C for whichever stress was critical, and the Wei-

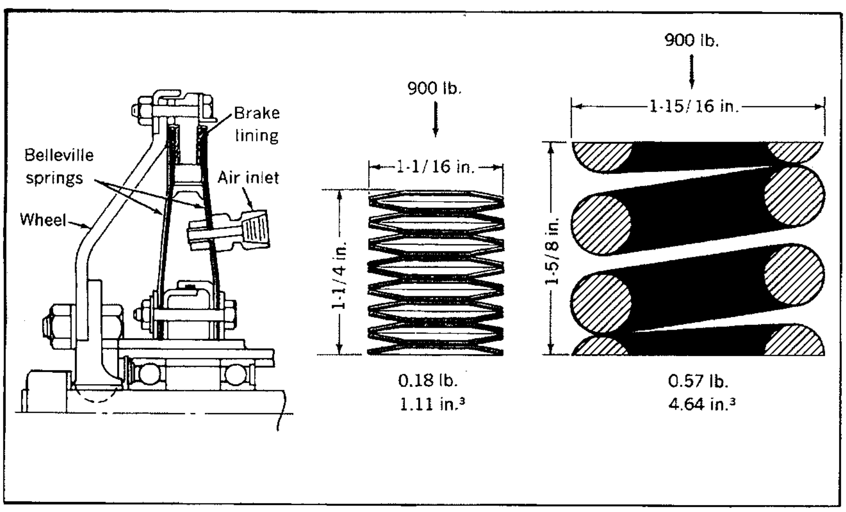

Bellevilles stack compactly (center), compared to equivalent helical spring on right, easing problem of design when space is at a premium, as in brake at left.

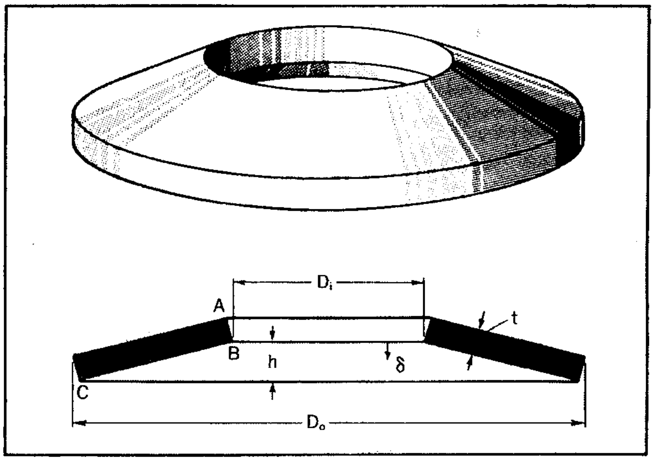

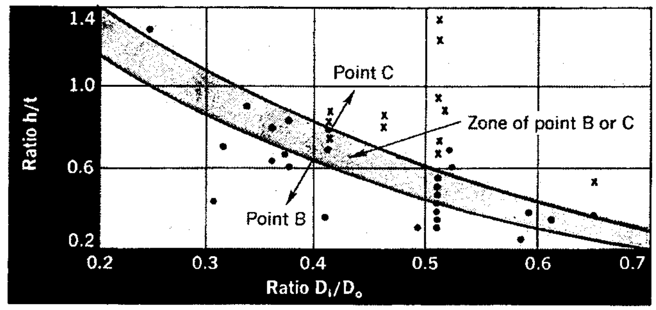

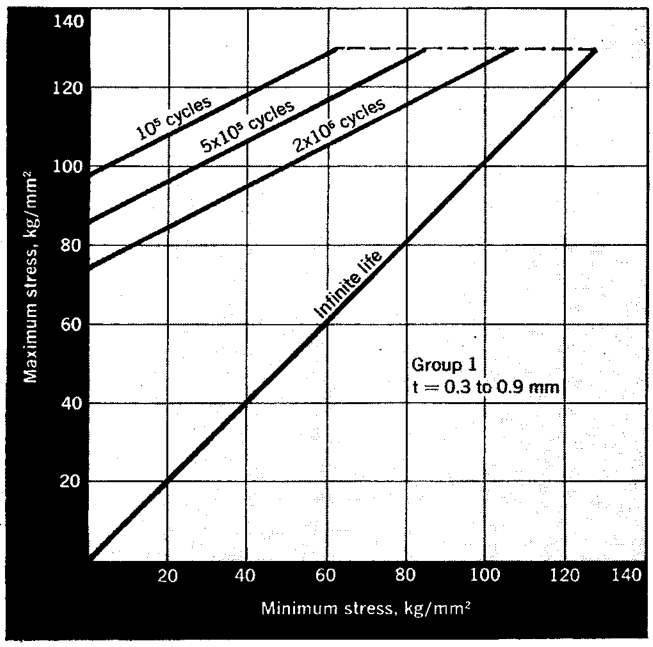

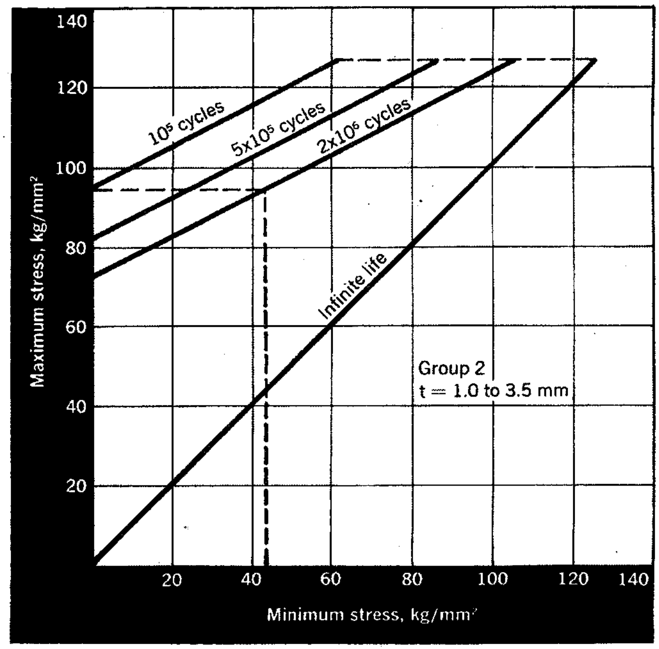

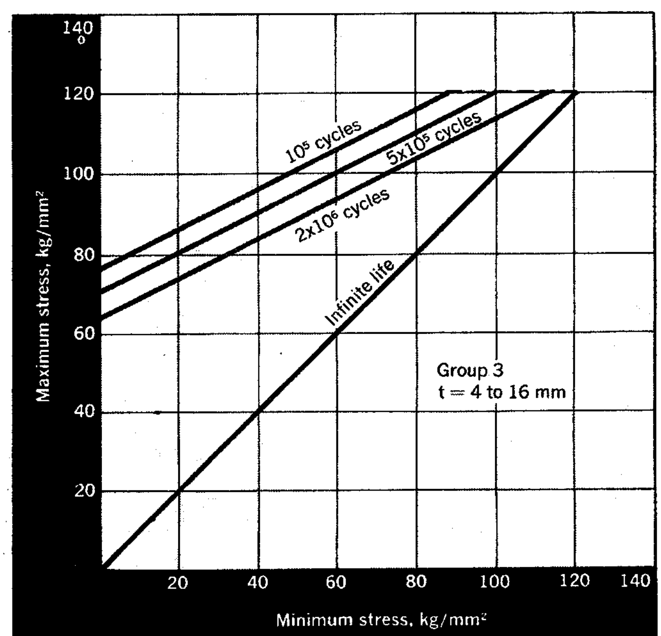

Fatigue life of dynamically loaded Belleville spring can be predicted accurately by use of new test data and equations. In drawing at top left, potential fatigue failure is narrowed down to point B or point C when ratios of height to thickness and inside diameter to outside diameter are known (chart at top right). Until now, the trouble spot has been assumed to be the top of the inside lip, point A. The other three charts on this page show endurance-strength curves for three groups of thicknesses, leading to a finding of the maximum number of loading cycles permissible for an application, based on a 99% confidence level. The right-angled dashed line in the middle chart at right illustrates how to use the curves. If you compute the minimum and maximum stresses that occur during operation, using the equations given on the facing page, you can pick the permissible number of operating cycles directly off the chart. For example, a Belleville spring that undergoes a stress variation from 44 to 94 kg/mm^2 will probably last for 2 million cycles.

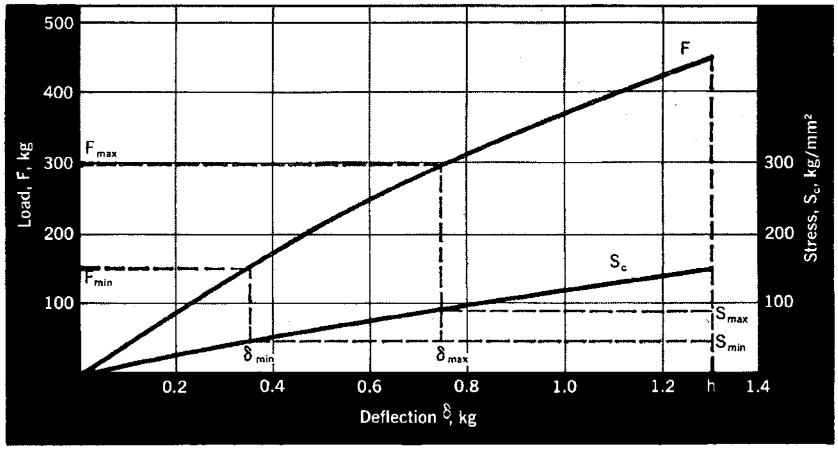

Plotting load-deflection curve, F, and stress-deflection curve, S_C, gives the safe stress ranges, a valuable guide in design of reliable Belleville springs.

bull statistical method to evaluate the points on the curves.

With these methods, three groups of data were obtained (graphs, page 117) for three groups of thicknesses with a 99% probability of survival. The diagrams give figures for 10^5, $5x10^5$ and $2x10^6$ cycles. The diagonals can be considered as infinite-life lines, and a certain amount of interpolation can be done between the $2x10^6$ lines and the diagonals.

Design for longevity. With the charts, it is now possible to design Bellevilles for indefinite life spans (above $2x10^6$ cycles). For example, suppose a Belleville spring has dimensions of: D_o=45 mm (1.77 in.), D_i=22.5 mm, t=1.75 mm, h=1.3 mm. Then, h/t=0.74, and D_o/D_i=2. The spring is preloaded with a force F_{min}=155 kg (343 lb.). Four steps lead to the maximum permissible load, F_{max}, to assure indefinite life:

Step 1—Determine the load-deflection curve. Some spring manufacturers provide such data; otherwise the engineer may employ the equation below and calculate the loads for four equal-spaced deflections at δ=0.25, 0.50, 0.75, 1.0.

$$F = \frac{4Et^3\delta}{\alpha D_o^2(1-\mu)}\left[\left(\frac{h}{t}-\frac{\delta}{t}\right)\left(\frac{h}{t}-\frac{\delta}{2t}\right)+1\right]$$

where the value of α is

$$\alpha = \frac{1}{\pi}(1-R)^2 \Big/ \left[\frac{1+R}{1-R}-\frac{2}{\ln R^{-1}}\right]$$

$$\text{and } R = \frac{r_1}{r_o}$$

Plot the resulting load-deflection curve for the F and δ values.

Step 2—With the given values of h/t=0.74 and D_o/D_i=2 (or D_i/D_o=0.5), determine with the aid of the chart (middle) that it is the stress at point C that controls fatigue failure.

Step 3—Now employ the above equation for S_c to solve for S_c at the four deflection points. Plot the values in the load-deflection chart (top, page 117).

Step 4—The deflection at $F_{min.}$= 155 kg is picked off from the chart as being δ_{min}=0.325 mm=0.25h. The stress at this deflection is S_{min}= 45 kg/mm² (64,000 psi). For t=1.75 mm, the chart for group 2 is valid. Employing S_{min}=45 kg/mm², obtain from the chart the maximum allowable stress, S_{max}=94 kg/mm². Going back to the load-deflection curve with S_{max}, and knowing that δ_{max}=0.74 mm gives a maximum-load value of F_{max}=300 kg (663 lb).

Thus the spring may be loaded between 155 and 300 kg for an indefinite number of times. Moreover, if Schremmer's theories are correct, there is a probability of 99% that there will not be any fatigue failure.

In his tests, Schremmer used up to eight single-stacked springs. The tests were made with a sinusoidal-motion loading applied at approximately 30 cps. The center guide rods were hardened, ground, lubricated.

Schremmer recommends that Bellevilles be made of chrome vanadium, with dimension ratios of approximately D_i/D_o=0.50 to 0.588 and h/t=0.6 to 0.7. These ratios will give a maximum energy-absorption capacity for a minimum space.

New Springs Do More Jobs

By shaping the coil of the familiar Neg'ator springs, you can change at will its constant-load level or gradient.

Nicholas P. Chironis

RECENT developments in prestressed coil springs and spring motors now make it possible to select or adjust the constant-force or constant-torque levels in an application—and even obtain a negative spring gradient in which the force decreases with deflection.

These unusual spring characteristics, developed by Norman E. Sindlinger and his R & D group at the Hunter Spring Div of Ametek in Hatfield, Pa, were obtained by modifying the shapes of Neg'ator springs (a trade name of Ametek). The new constant-force types are interesting to designers of devices that require a way to select or dial a desired load level—as in orthopedic traction devices, X-ray heads, and machine counterbalances for tool interchangeability.

The new negative-gradient types are also being studied for overcenter devices (as in the computer window discussed later in the article) and for long-deflection retraction devices, where the design calls for controlled decrease in force during either extension or retraction. For instance, a negative-gradient spring can reduce acceleration and prevent a jarring stop when a retracted mechanism nears the full-return position.

Spring motors. The key factor that changes a strip of spring steel into a Neg'ator spring is the curvature built into the spring by prestressing during the manufacturing process. Thus a Neg'ator strip, when allowed to relax into its newly acquired natural position, will form a tight coil. If the coil is slipped over a pencil and its end pulled linearly, the coil will resist the pull with a constant force, regardless of the length extended, because the force required to uncoil the spring at any position is a constant.

The spring also can easily be arranged to produce torque, thus functioning as a motor. In the "type-B motor," the spring is coiled on a storage drum that is free to rotate. The outer end of the spring is then extended, secured to, and reverse-wound on a larger output drum. Release of the output spool at any degree of wind-up permits the material to revert to its natural curvature by returning to the smaller drum. This imparts rotation to the output drum, and the torque produced can be held almost constant during the entire cycle.

Because of the constantly decreasing radius, or lever arm, as the material runs off the output drum, a constant-force spring will produce a spring motor with a slightly positive gradient. However, a constant output torque is maintained in the type-B motor by varying the incremental stresses introduced during forming, so the force exerted at the periphery of the output coil will increase during run-down. It was this approach that led to the negative gradient springs.

Varying output. The linear spring force produced by a prestressed coil spring is

$$P = \frac{Ebt^3}{26.4R_n^2}$$

where P = load; E = modulus of elasticity, psi; b = width of material, in.; t = thickness of material, in. and R_n = natural radius of curvature, in.

From this we see that load is directly proportional to width, thus any change in the width of the band will vary the load proportionately. Thus, by shaping the bands, springs and spring motors can deliver selective constant or controllable torques of any simple mathematical variation. Several shapes have been tried —the stepped-width, the tapered-width, and even a spring with sinusoidally varying width. Another configuration that appears to have good practical value is the double-tapered shape.

Stepped-width springs. These are best for applications that require a selection of discrete loads with constant-force output over a finite working stroke. They have built-in steps to provide load changes (see photo on previous page), and several relatively long working strokes, each with a constant force output. Thus, one spring can deliver a choice of different loads without involved mechanisms or the need to couple independently acting springs.

This type can also be mounted as a motor in which the torque output varies in steps. The motor spring in Fig 1 has five separate widths, each representing a discrete torque with an effective deflection of x turns. Thus, in use for orthopedic traction or as a counterbalance, the weight of vertical equipment can be varied by changing attachments.

Single-tapered springs. The Neg'ator spring is one of the few springs that can produce a negative gradient (decreasing load with increasing deflection, Fig 2) without need for an auxiliary linkage system. Usually, the negative gradient is obtained by heat setting or by varying the bending radius during the coiling operation. This produces negative gradients of up to 2 to 1. The new way is to taper the spring width.

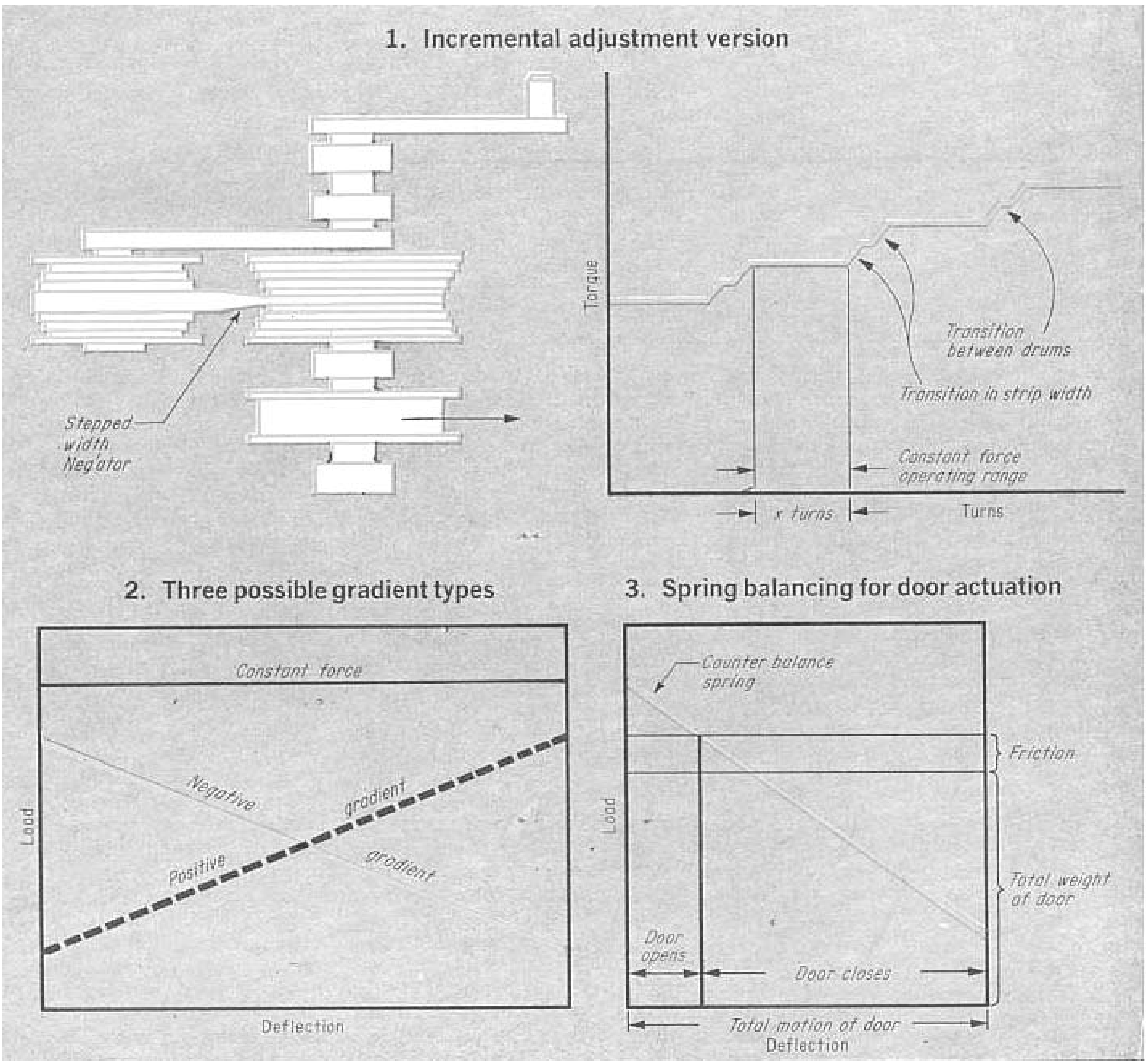

A recent application of the negative-gradient tapered spring is the counter-balancing of vertically rising access doors in computer cabinets. The main requirement here is that the doors never be left partially open —they should always be either fully open or fully closed. The spring is mounted so that its maximum force output slightly overbalances the weight of the door and the friction in slides. When the door is raised above the balance point, the spring will finish the job of opening, Fig 3. At any position below the balance point, the door will slide closed, with the decreasing spring force keeping it from slamming.

Dual-tapered spring motors. Two tapered spring bands in a spring motor device produce a still wider variety of output characteristics. By changing the direction of coil winding, the individual spring moments are either cumulative or opposing. Both versions produce selective constant-torque levels.

In the cumulative-gradient type, Fig 4, positive-gradient and negative-gradient springs are wound on their respective storage drums so that the resulting moment is the graphical sum of both characteristics. If the gradients are identical and output shafts are locked together, the sum of the moments of each spring remains constant as both springs are deflected.

If one spring is offset by prewinding or unwinding relative to the other spring, a new sum of the moments of the individual springs re-

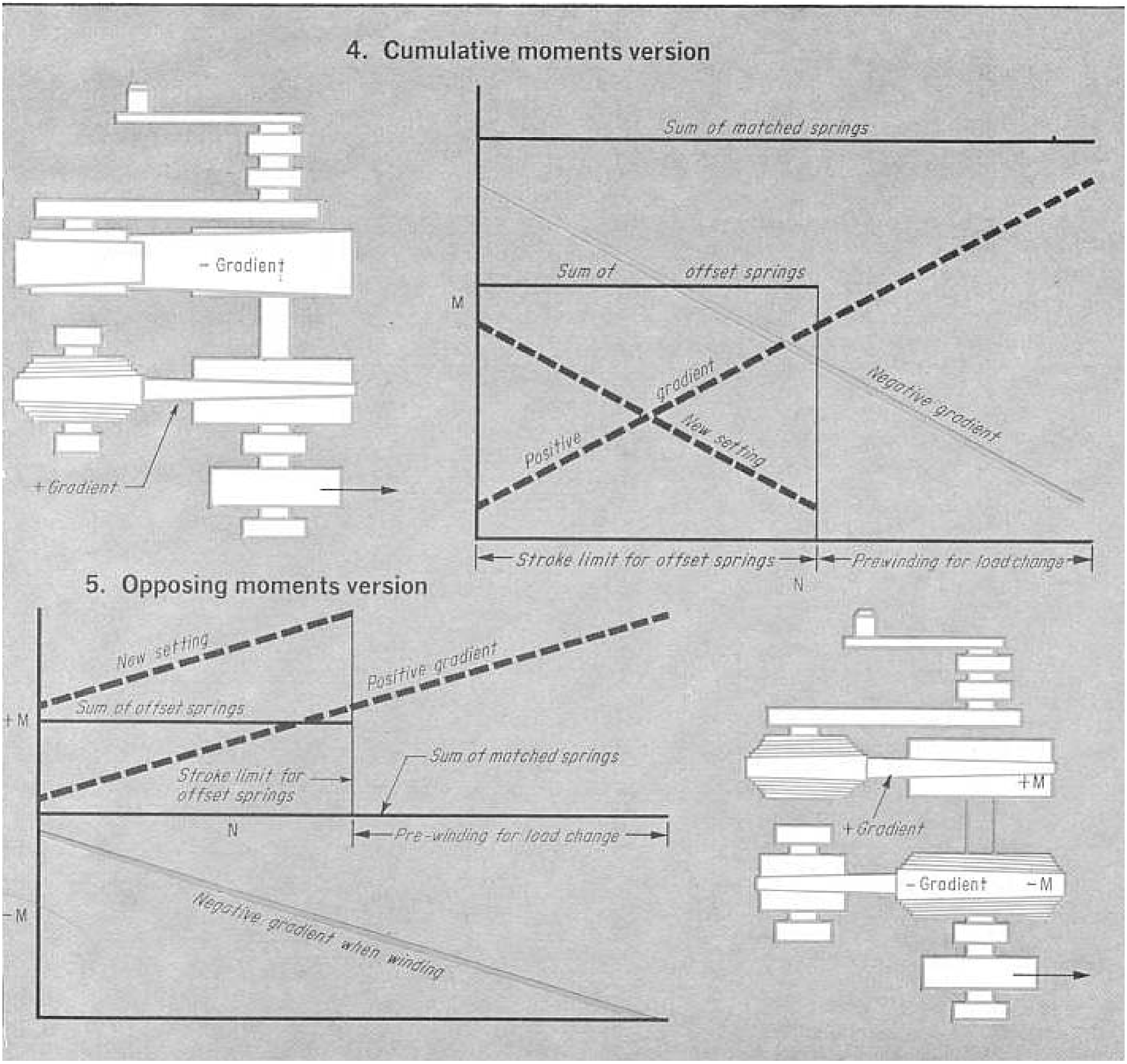

sults, and this remains constant as both springs are deflected. However, the offset decreases the available stroke.

In the opposing-gradient type, one spring winds up on one output drum while another spring unwinds from the other, Fig 5. Thus, one opposes withdrawal of the cable while the other assists. When the spring moments are equal zero output force is obtained and the force range is limited only by the size of the device (see the torque diagram).

Load settings. The simplest way to adjust the output torque of spring motors with stepped-width or dual-tapered springs is to couple a clutch between the output drum and cable pulley. The output cable can then be declutched from the system, rotated to its new position, and once again engaged to transmit the new torque level to the system. The clutch maybe a simple slip or positive engagement type.

If it is necessary, however, that the output shaft remain loaded by the spring during torque adjustment, one of these more sophisticated mechanisms can be employed:

- **Orbiting the storage drum about the output drum** (Fig 6) has the least system hysteresis as it involves no gearing, and it is the simplest and lowest in cost. Actual operating volume requirements are lower than for the other two systems, but total volume requirements are greatest, since clearance must be provided for the storage drum to rotate entirely around the output drum.
- **Revolving the system around a set of spur gears** when making the adjustment (Fig 7) requires less over-all space. This method, however, introduces significant backlash.
- **Coupling a differential gear train to the system** provides good space economy (Fig 8), but it is the most expensive system of the three.

In any of these systems, Sindlinger suggests that an acceleration-sensitive brake or other means of limiting velocity be incorporated in case the spring is accidentally released during torque adjustment. Also, the systems can be easily equipped with load-indicating devices that sense the built-up diameter of the spring coil wrapped on one of the drums.

6. Rotating storage-drum type

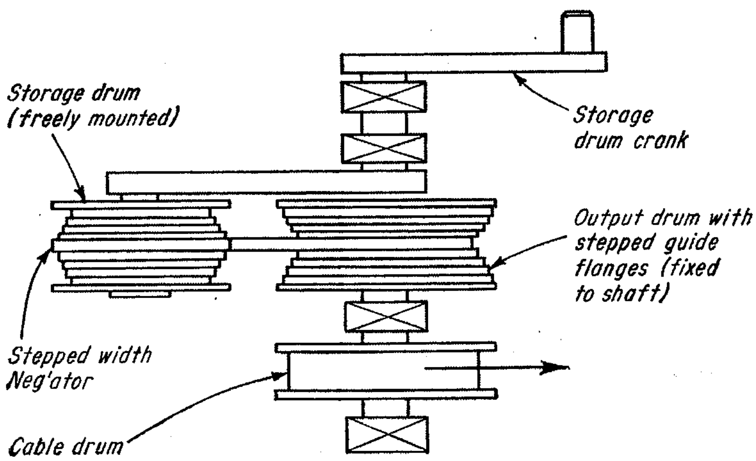

7. Orbital output-drum type

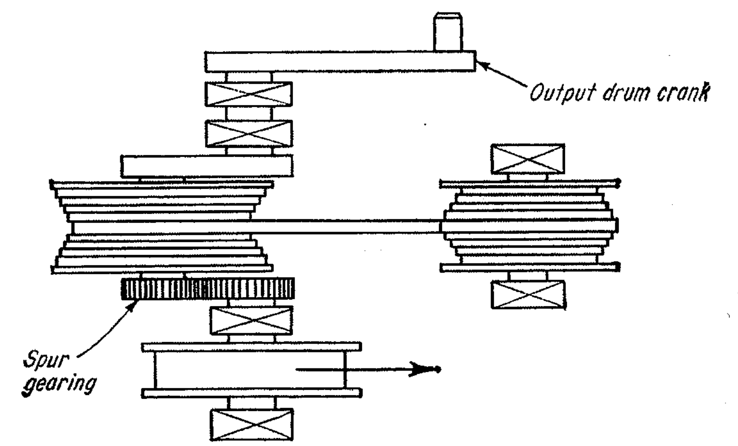

8. Planetary gear type

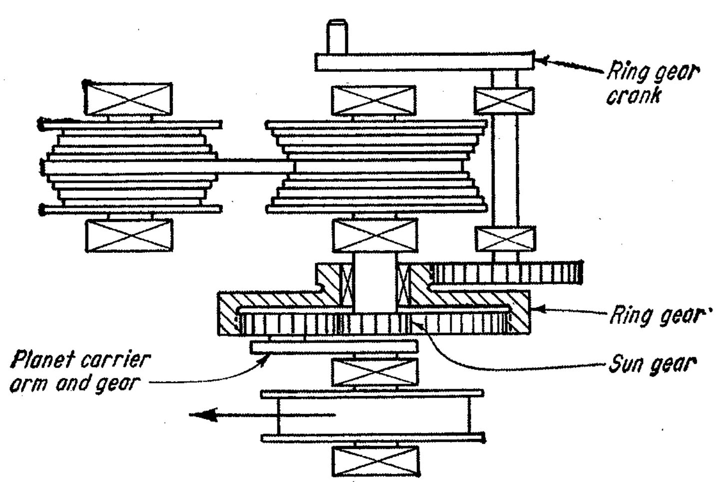

SECTION 17

PINS

Slotted Spring Pins Find Many Jobs

Assembled under pressure, these fasteners provide powerful gripping action to locate and hold parts together.

Robert O. Parmley

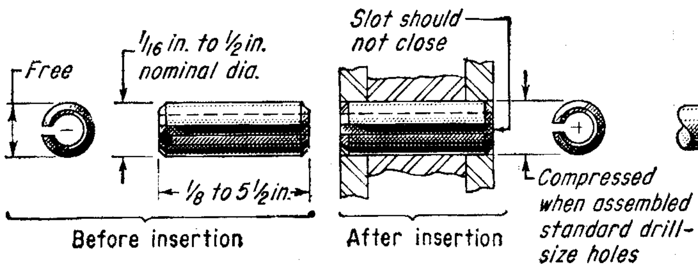

1 **PINNING PARTS** is basic function

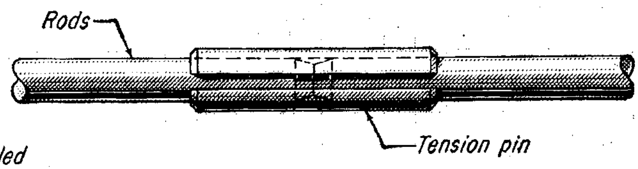

2 **GRIP-SLEEVE** action provides external splice

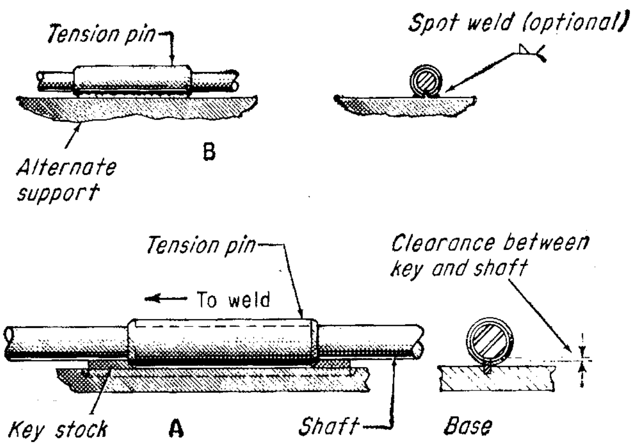

5 **LOW-COST SHAFT SUPPORT** is keyed (A), or spot welded (B)

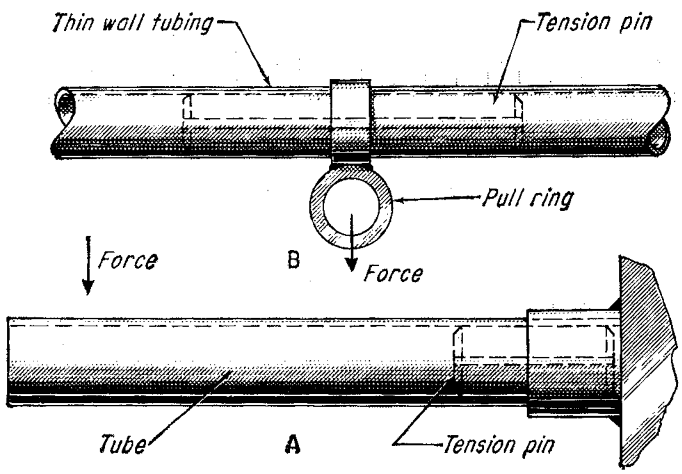

6 **THIN-WALL TUBING IS STRENGTHENED** by tension pin at high stress position

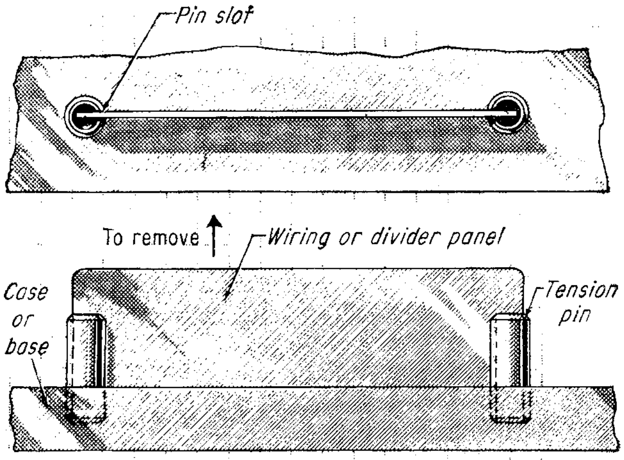

3 THIN PANELS
are inexpensively supported

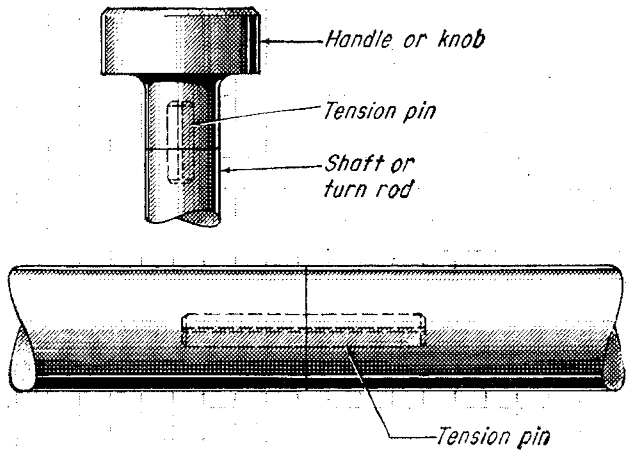

4 LOW-TORQUE SHAFT
connection, or knob assembly

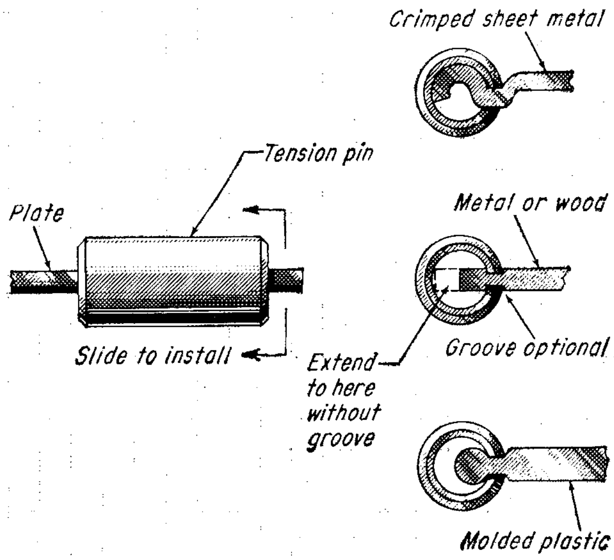

7 PROTECT PROJECTING LIPS

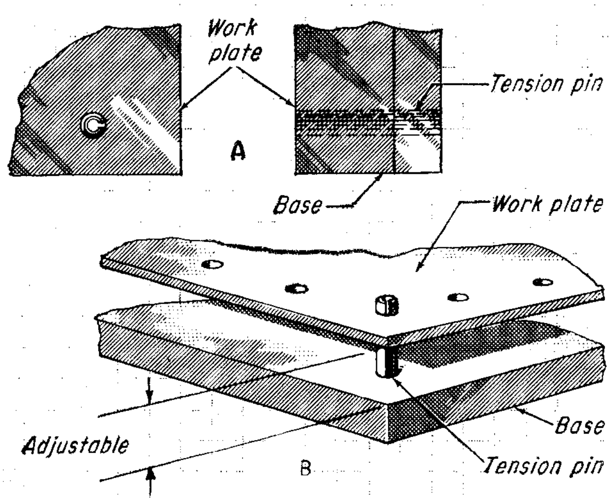

8 SUPPORT POSTS
locate (A), provide adjustment (B)

8 Unusual Jobs for Spring Pins

Be sure you get top value from these versatile assembly devices. These examples show how.

Andrew J. Turner

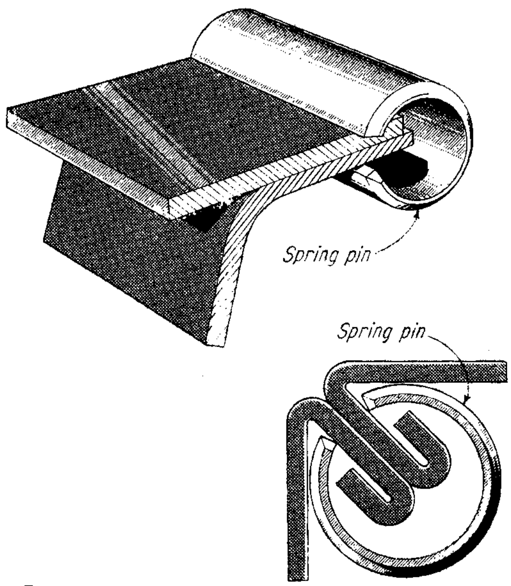

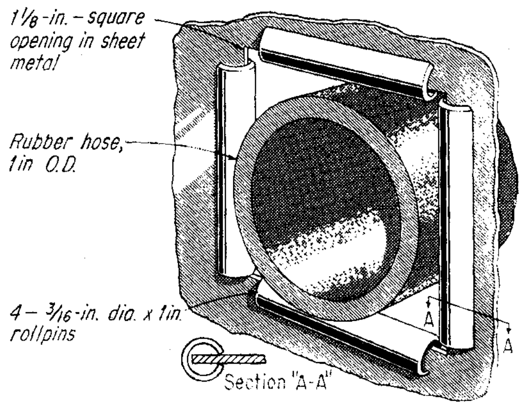

1

SLOT IN PIN does duty as anchoring device, holding two pieces together. Fastening can be either permanent or temporary. Parts can be metal or non-metal.

2

PROTECT HYDRAULIC tubing or electrical wires touching sharp edges of castings by clipping pins over the edges of the hole. Its size is only slightly reduced.

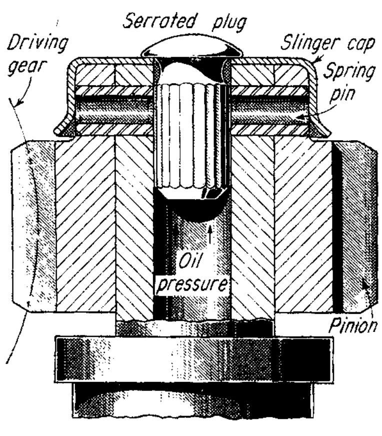

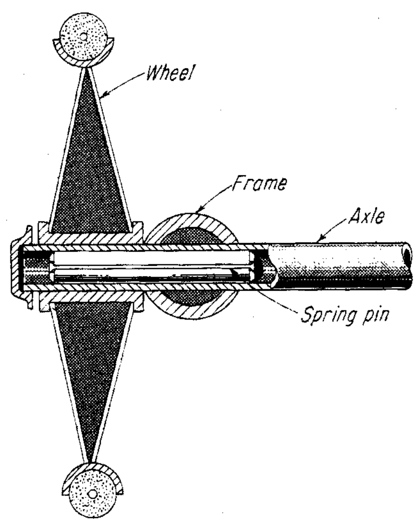

5

LUBRICANT PASSAGE is combined with retaining pin for gear. Also, slinger ring not only performs functionally but improves appearance too.

6

STIFFEN LIGHT-DUTY structures such as tubular axles with spring pins; they are simple to install and add considerable strength to the assembly.

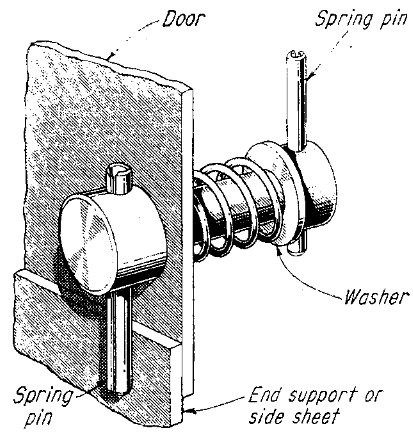

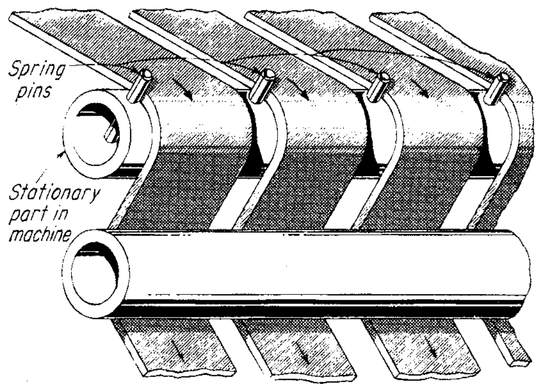

3 **TWO PINS SERVE AS HANDLE** and latch. This low-cost assembly replaces an expensive forged handle and a fabricated-metal latch-piece.

4 **AS BELT GUIDES,** spring pins eliminate molded spacers, or costly machined grooves for spacer rings which would otherwise be needed.

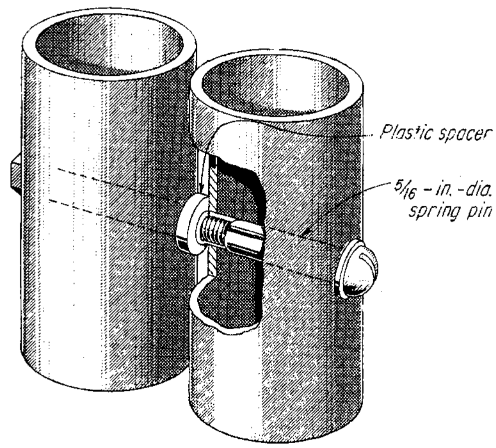

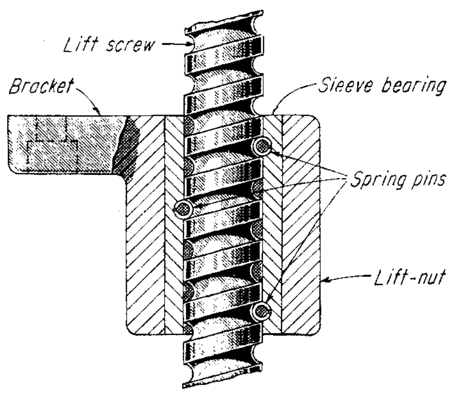

7 **HARDENED STEEL SLEEVE** for pivot-screw gives durability to legs of folding table illustrated here, while keeping costs competitively low.

8 **LOW-COST THREAD** in lift-nut can be made by fitting spring pins at correct pitch-positions as shown. Rotate the pins to reduce wear.

8 More Spring Pin Applications

Some additional ways that these fasteners, assembled under pressure, can grip and locate parts. They can even valve fluids.

Robert O. Parmley

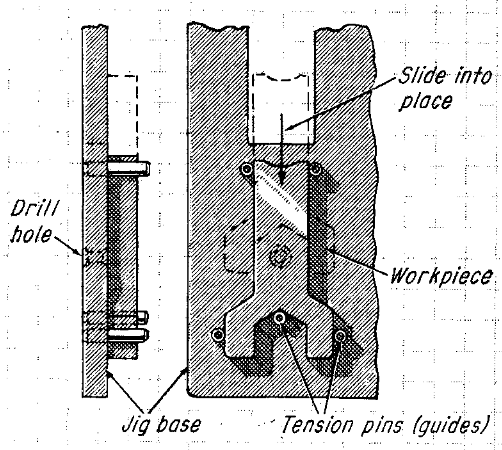

1 **LOCATE WORKPIECES** with this inexpensive jig

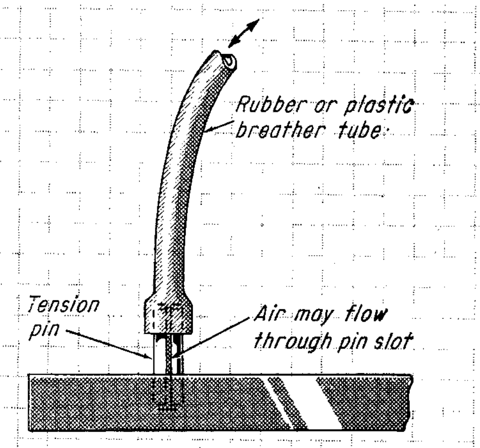

2 **FLEXIBLE BREATHER TUBE** is enclosed to prevent swinging and to keep it away from moving machine parts

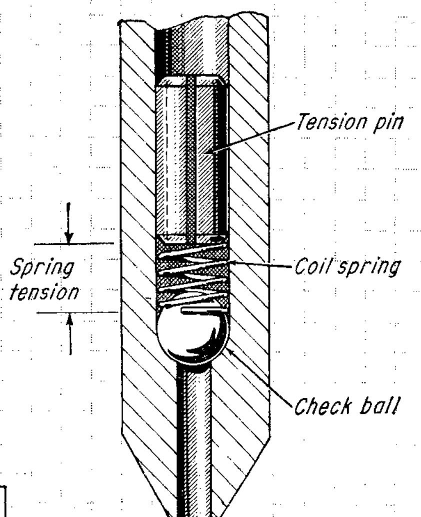

4 **CHECK-VALVE** spring retainer allows maximum flow, is easily adjustable

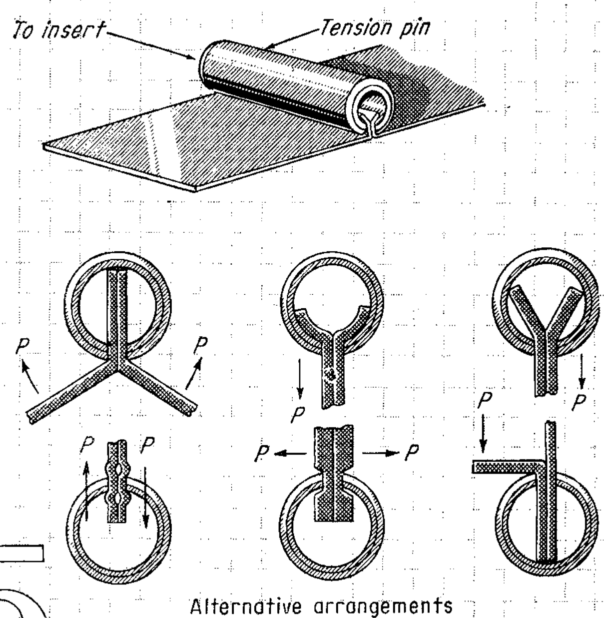

5 **HOLD FLATS** together for gluing

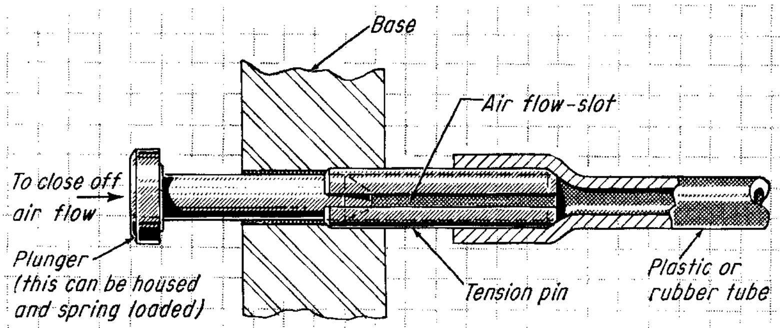

3 **AIR VALVE** is simple yet effective

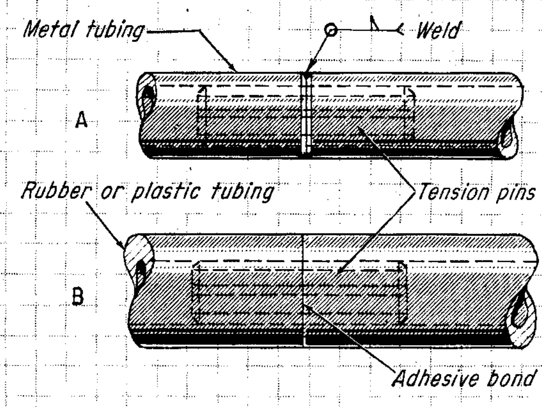

7 **ALIGN TUBING** for bonding or reinforce for strength with internal pin

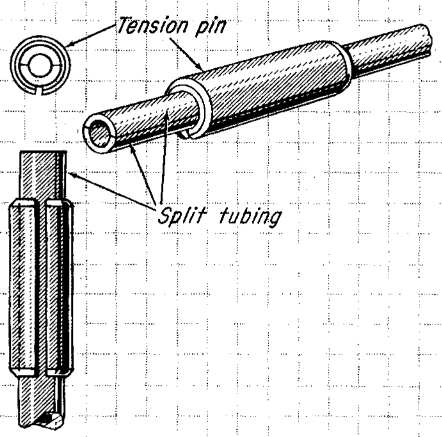

6 **SPLIT TUBING IS HELD** with tension pin sleeve

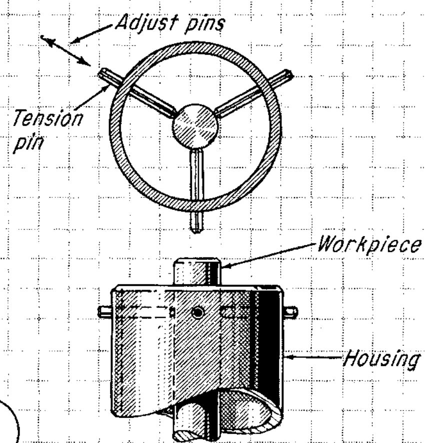

8 **CONCENTRIC OR ECCENTRIC POSITIONING** is quickly adjustable

8 Electrical Jobs for Spring Pins

Put these handy assembly devices to work as terminals, connectors, actuators, etc.

Andrew J. Turner

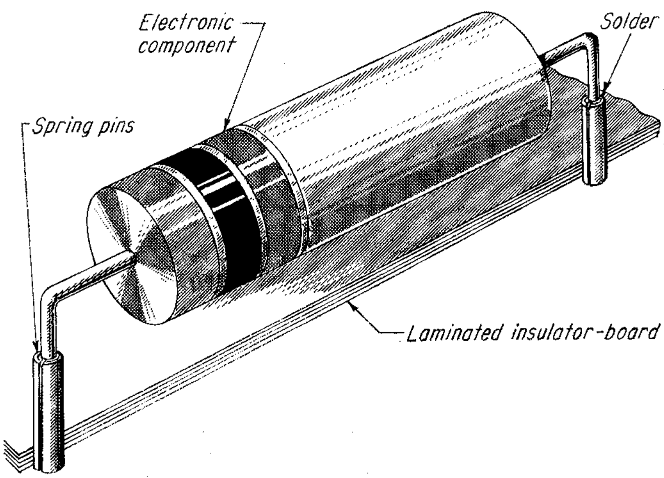

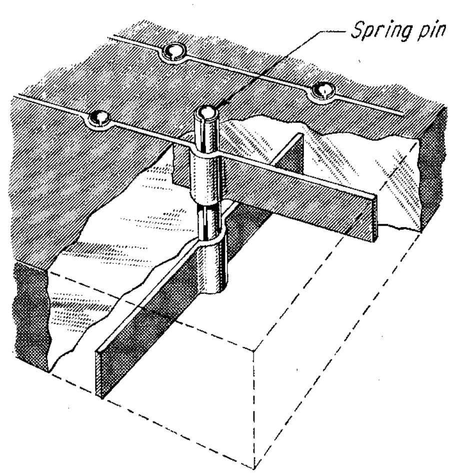

1

LOW-COST TERMINALS are made by assembling two 1/16-in.-dia tin-dipped Rollpins into phenolic board. The board should be about 3/32 in. thick.

2

AS ELECTRICAL CONNECTORS in "patchboard" circuits, spring pins have ample conductivity. Select various circuits by removing or inserting pins.

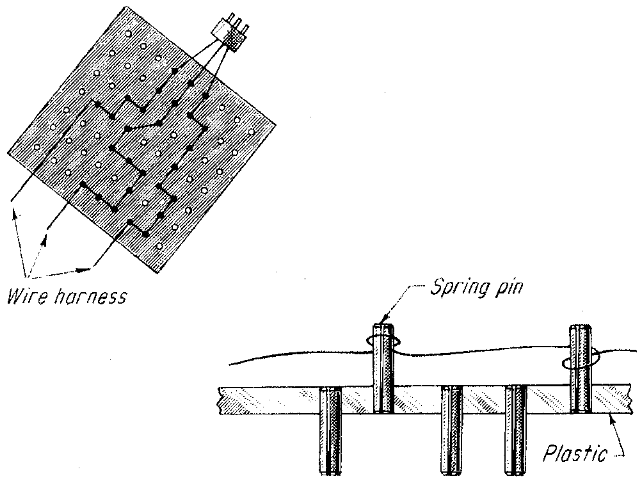

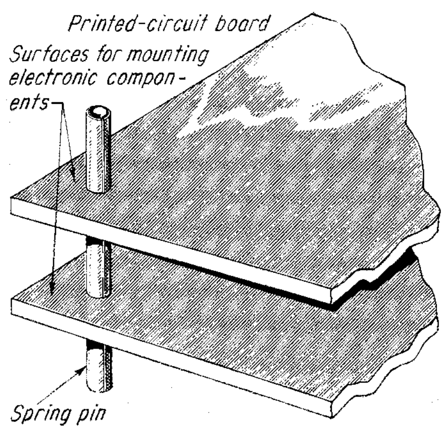

5

FORMING FIXTURE for wire harnesses is quickly adjusted when different harness-shapes are needed. Plastic sheet has pin holes on ¼-in. centers.

6

STAND-OFFS for printed-circuit boards can be spring pins. Select a pin long enough to ensure adequate spacing between the boards.

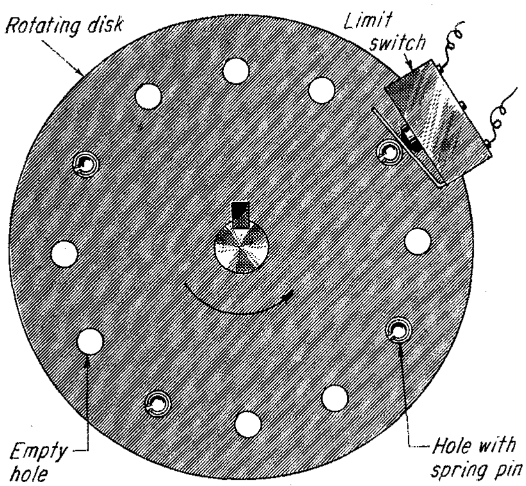

3 **SWITCH ACTUATORS** can be quickly relocated in rotating disk if spring pins are employed. Hard steel of pin gives excellent wear resistance.

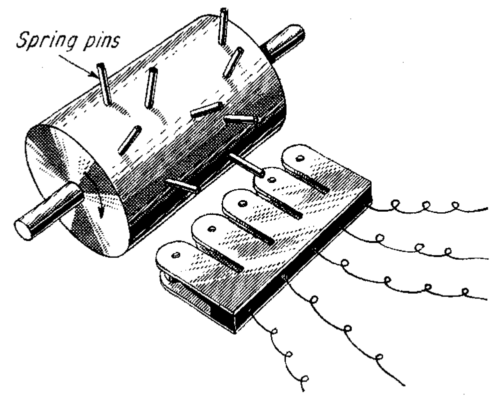

4 **DRUM-MOUNTED ACTUATORS** function in similar way to spring-pin actuators in Fig. 3. Protruding length of pins may be critical, but is easily adjusted.

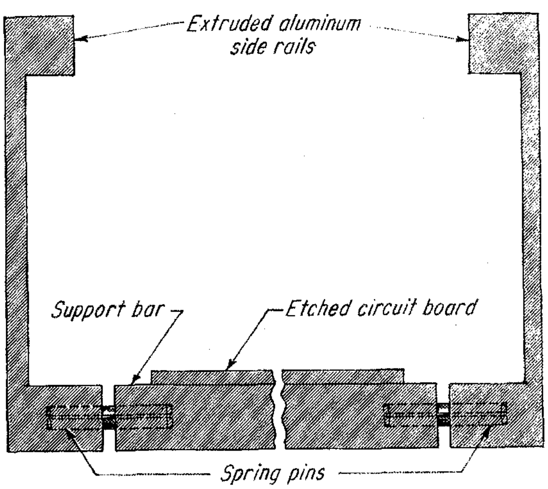

7 **SUPPORT BARS** in electronic units can be easily and quickly installed into the sliding chassis with spring pins. Close tolerances are not needed.

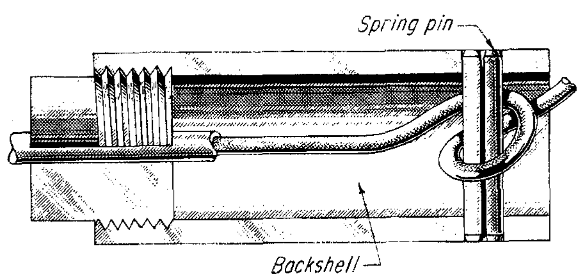

8 **STRAIN RELIEF** for wire in electrical connectors will not slip during assembly. Loop wire then fill shell with potting compound to seal wire in place.

Uses of Split Pins

Ten examples show how these pins simplify assembly of jigs and fixtures. The pins are easily removed.

Robert O. Parmley

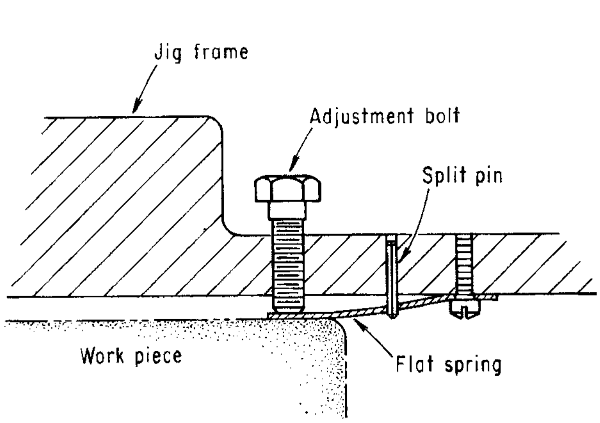

1. Prevention of spring slippage

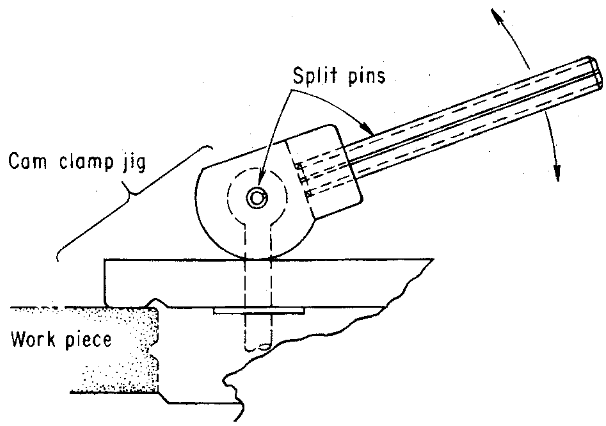

2. Cam pivot and handle

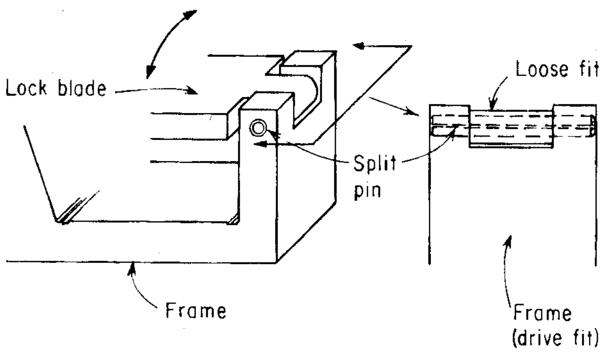

3. Clamp pivot

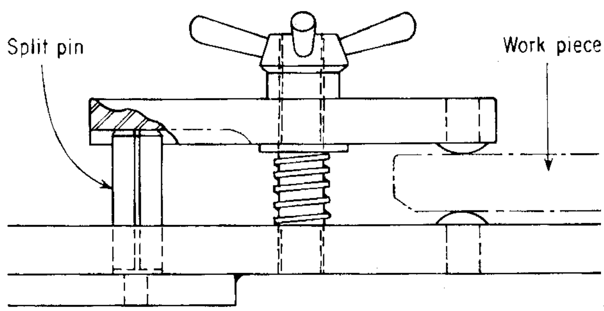

4. Support post

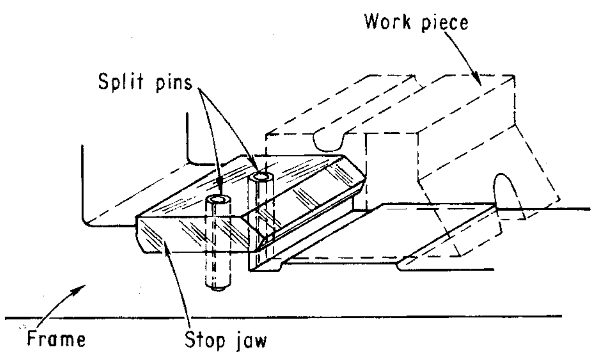

5. Anchor for stop jaw

Source: American Machinist, March 25, 1968. Reprinted by permission of publisher.

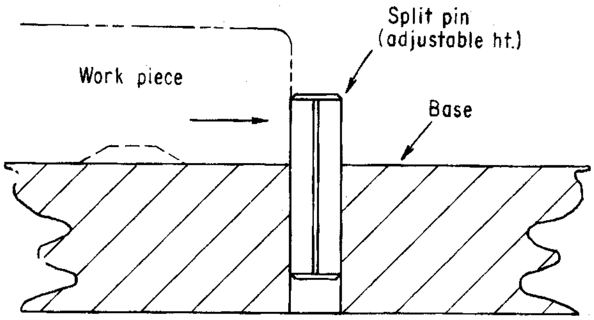

6. Locator or stop pin

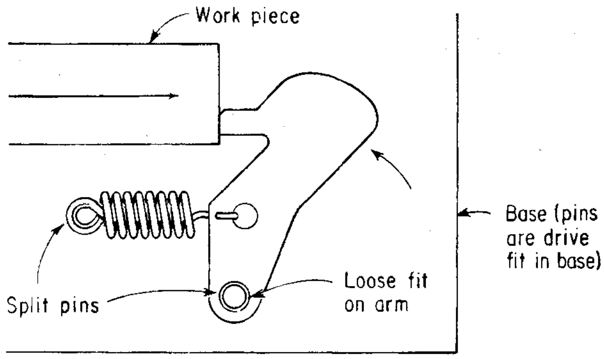

7. Spring anchor and arm pivot

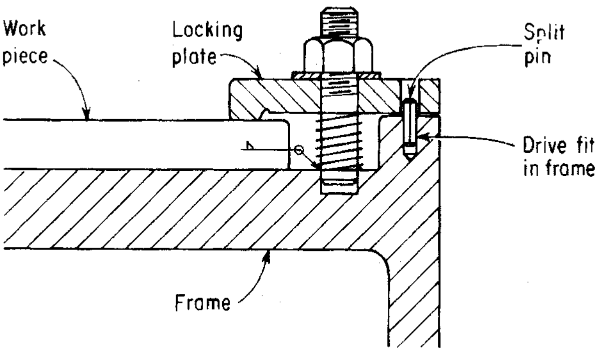

8. Stabilizer for locking plate

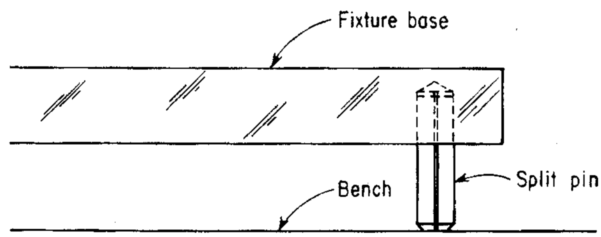

9. Support for post leg

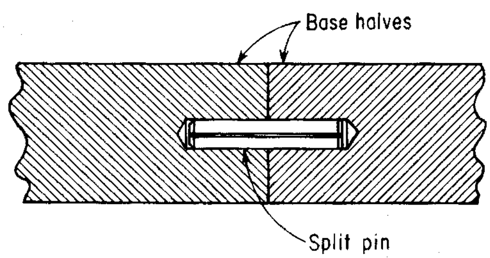

10. Dowels for fixture base

Slotted tubular pins are intended to be forced into their locations; free diameter should be larger than hole diameter so the pin exerts radial force all along its mounting hole to resist axial motion when properly mounted. Maximum compression is controlled by the amount of gap when the pin is free. When it acts as a pivot, the hole through the pivoting member should be a free fit (see figures 7 and 8) so the pin will not be worked loose from its anchor hole. These pins may be made of heat-treated carbon steel, corrosion-resistant steel, or beryllium-copper.

Design Around Spiral-Wrapped Pins

Coil, rolled, or spiral-wrapped pins come in a wide range of lengths and diameters. Their applications are limitless; here are eight.

Robert O. Parmley

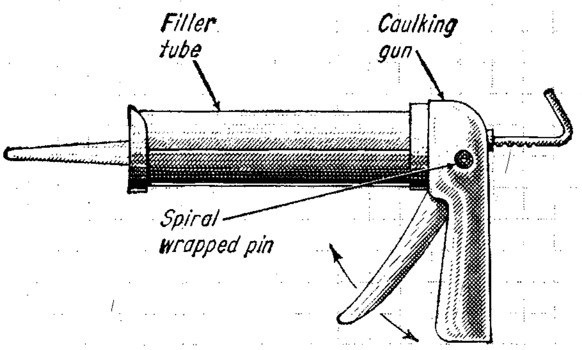

2 Pivot. Pin is a drive fit in the handle housing, and acts as a pivot for trigger

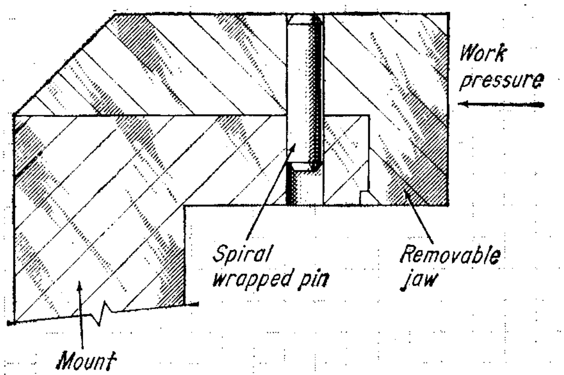

3 Dowel. Here, the dowel acts as a locator anchor pin that can be removed and reused

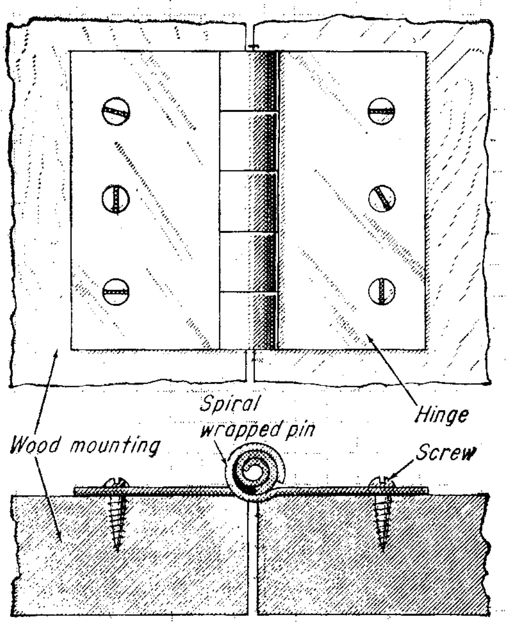

6 Hinge pins. If hole size in both members is different hinge will be free moving; if the hole size is the same in both members a friction hinge is the result

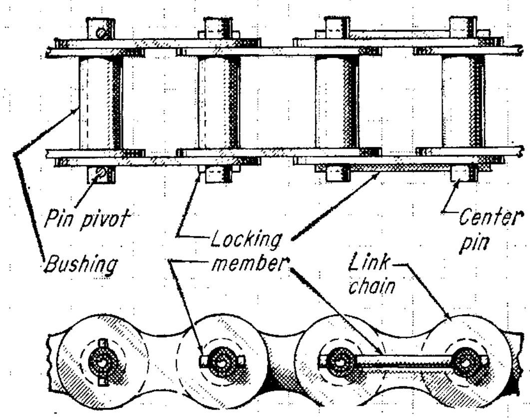

7 Link chain connection. Pins are used as pivot or locking members. An advantage: Both types are removable and reusable

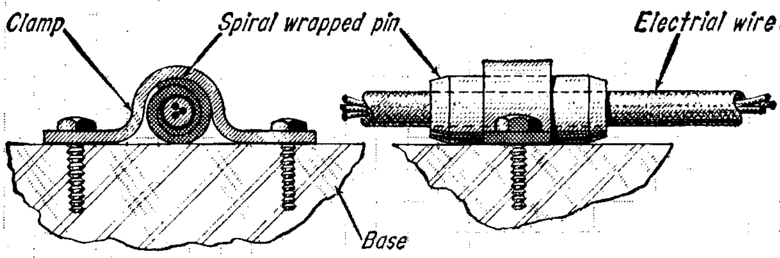

1 Wire gripper. As clamp is tightened in place, pin coils, and secures the wire

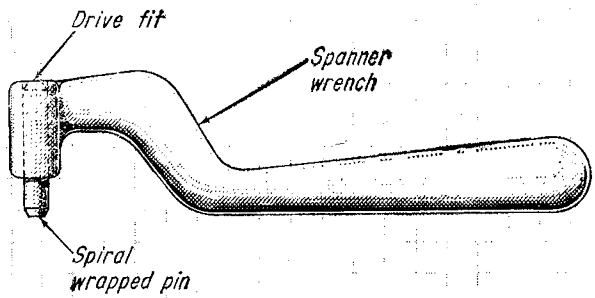

4 Wrench pin. Coil construction permits pin to fit holes with large tolerances

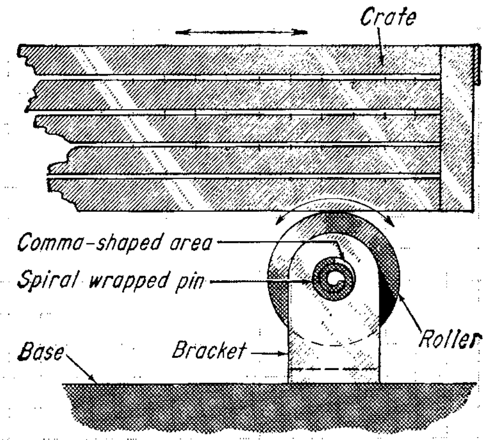

5 Lubricated shaft for work roller. Comma-shaped area of the spiral wrapped pin forms an oil reservoir for the roller

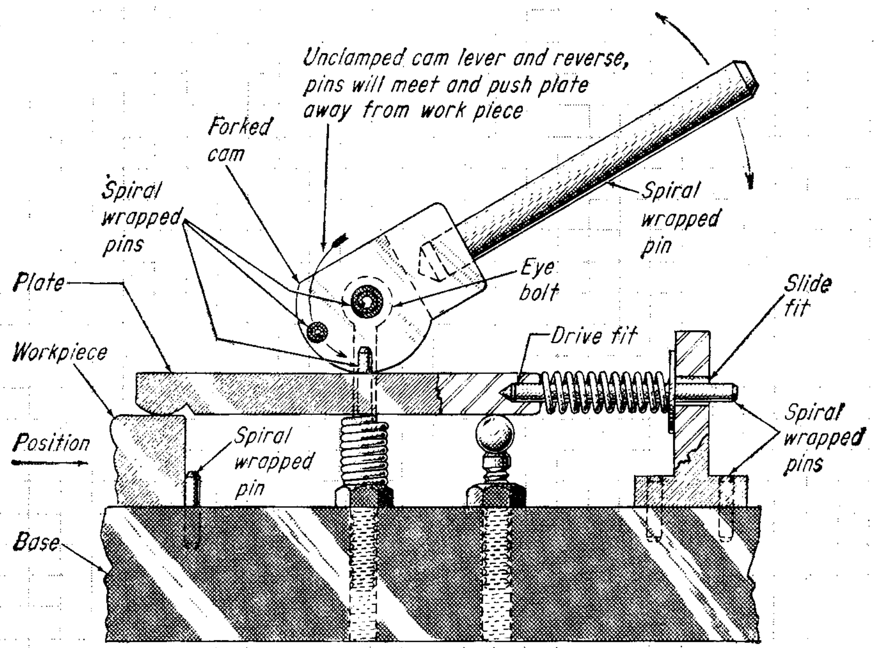

8 Pivot, stop, locator, handle, and anchor are typical applications in the design of a clamp. The pins are drive or slide fits, and can be removed and reused if the clamp position must be changed

A Penny-Wise Connector – The Cotter Pin

They're simple, inexpensive and make excellent electrical connectors. Why not consider cotter pins the next time you need one?

Robert O. Parmley

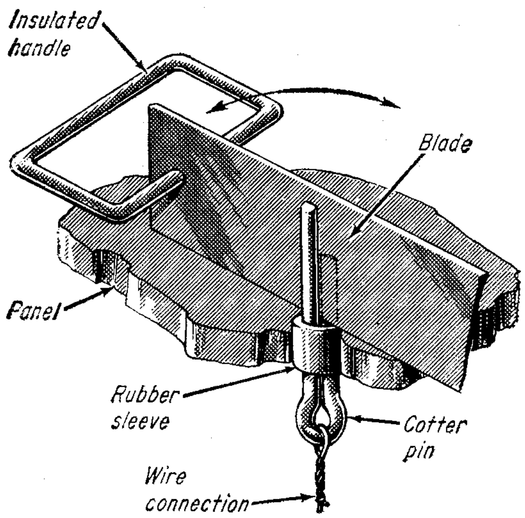

1 **Knife blade connector**

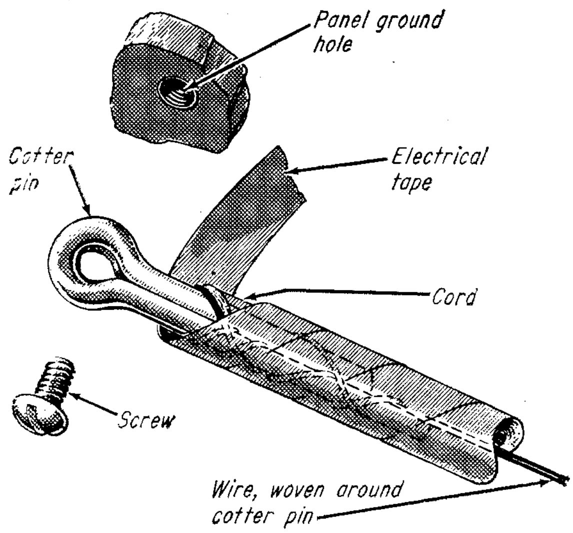

3 **End mounting connection**

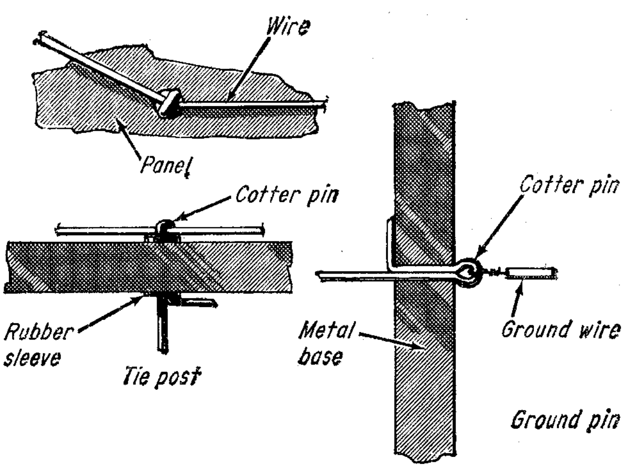

2 **Tie post and ground connections**

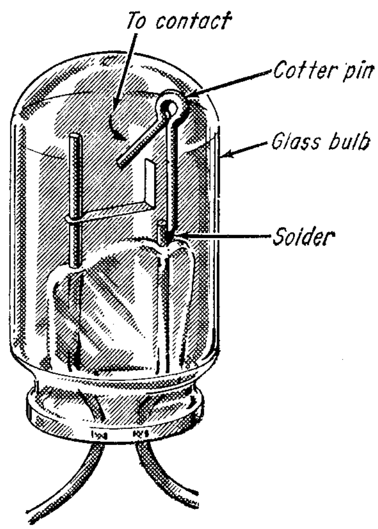

4 **Glow switch**

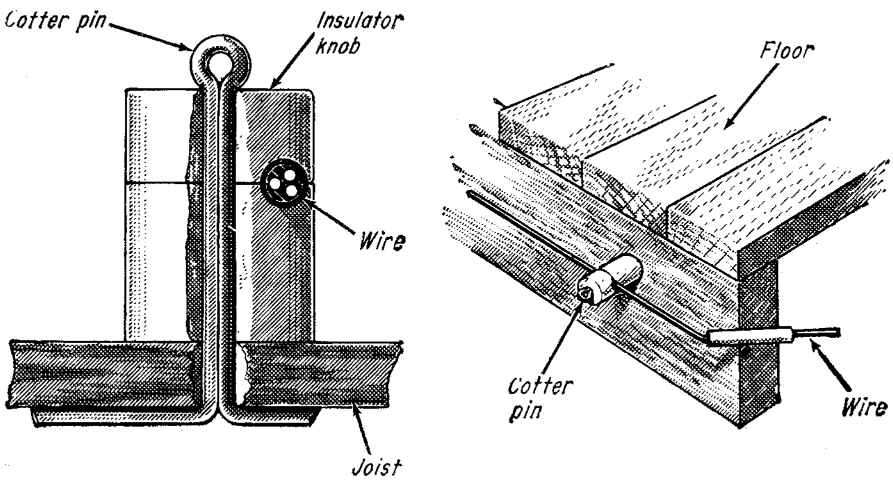

5 Knob anchor pin

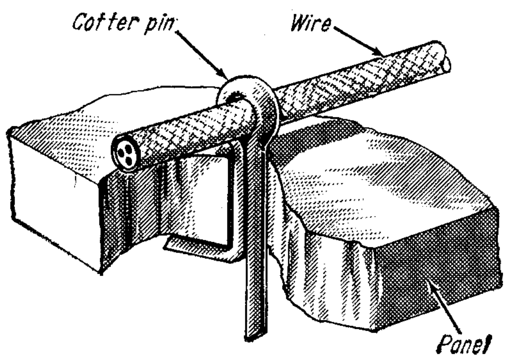

6 Wire eyelet

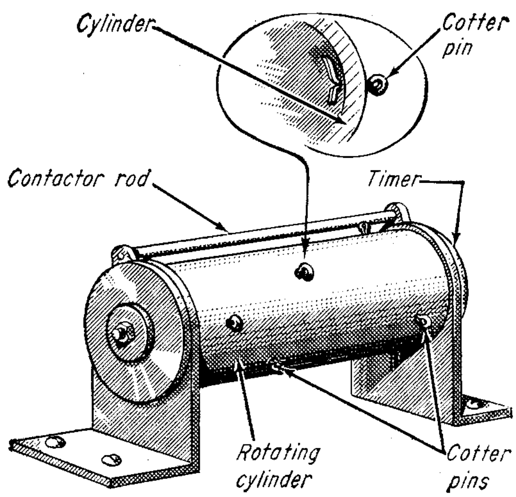

8 Cylinder contactor

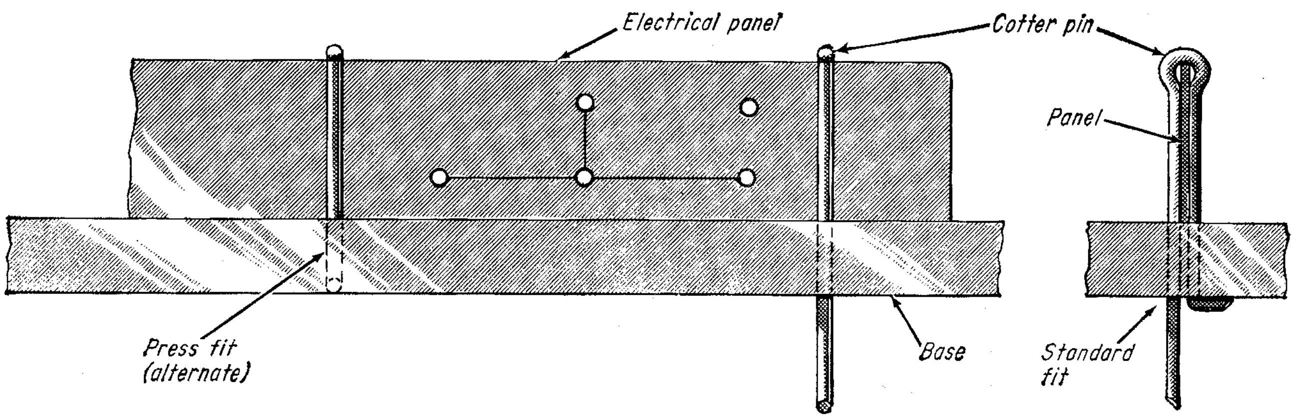

7 Electrical panel stabilizer

Alternates for Doweled Fasteners

Some simple ways to fasten or locate round or flat parts without having to use dowels or other pins.

Federico Strasser

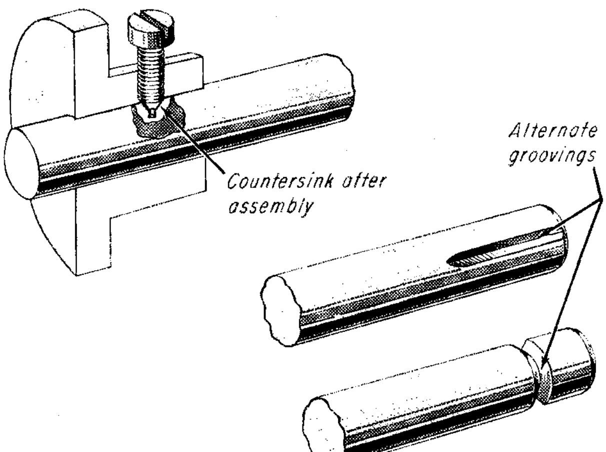

1 **SETSCREW** through hub of wheel or other circular part is superior to a dowel when angular adjustment must be made—note alternate groovings.

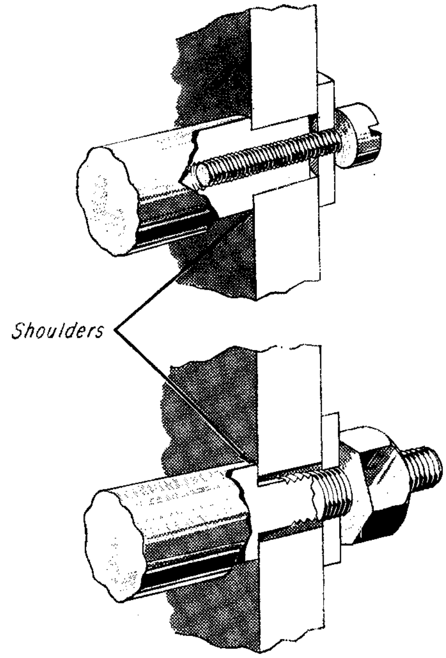

2 **SHOULDER** on shaft lets gear or disk be held at end of shaft. Two alternative ways are shown—a dowel would not be too practical here.

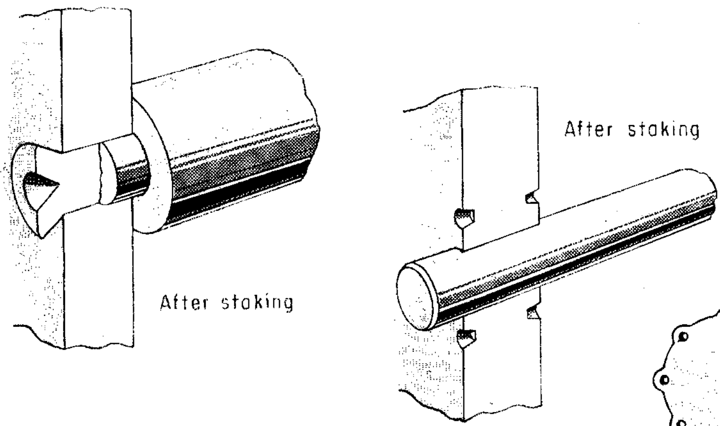

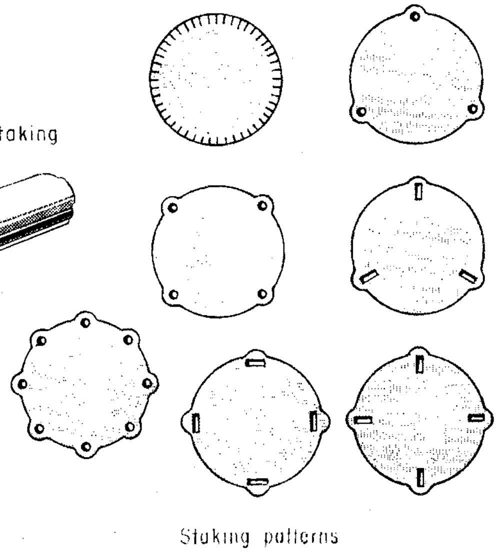

Staking patterns

5 **STAKING** either the shaft or the attached part is ideal for light loads. Various stake patterns are shown—staking can be done either by hand or by machine (PE—Sep 4 '61, page 354). Two advantages of this method of fastening parts onto shafts are low cost and assembly speed.

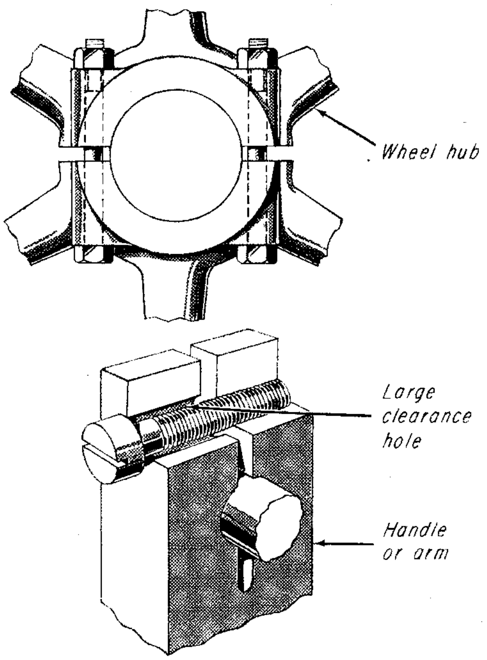

3

PRESSURE JOINTS are best when large composite wheels or similar parts are to be fastened to their shafts with only one or two screws.

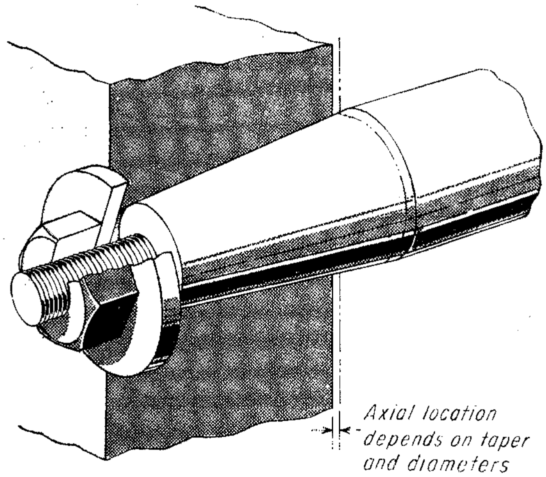

4

TAPERED JOINTS are ideal when no clearance can be allowed between hub and shaft. Dowelling would be impracticable because of fit.

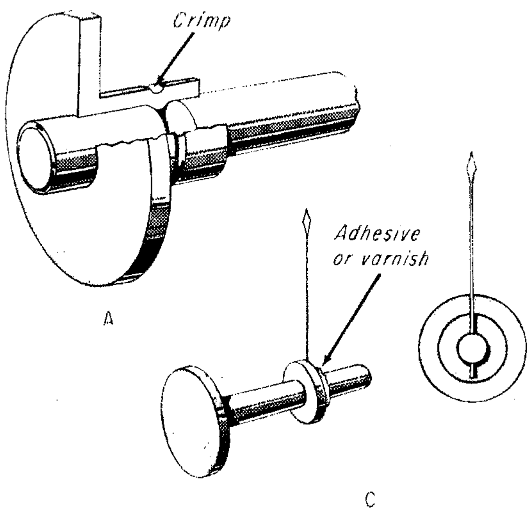

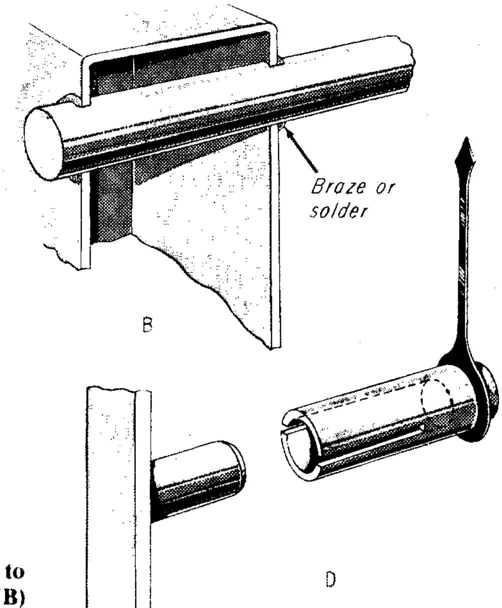

6

PERMANENT FASTENINGS of parts assembled to shafts are crimped (A); soldered, brazed or welded (B) or adhesive-held (C). Non-permanent fastening of small indicator-pointer is best achieved by providing simple push fit (D). If positive location is required here, dimple hub after assembly.

6 More Alternates for Doweled Fastenings

These simple but effective methods fasten or locate round and flat plates without dowels or other pins.

Federico Strasser

1 **TORQUE LIMITERS** are necessary in many cases where a doweled fastening would be useless. If shaft load becomes excessive a low-cost means of providing for its disengagement is to have a spring-loaded ball mounted externally (A) or internally (B).

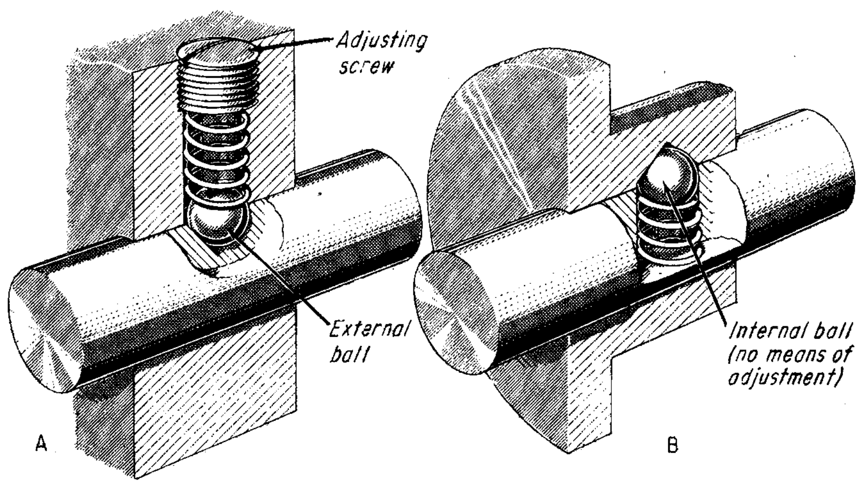

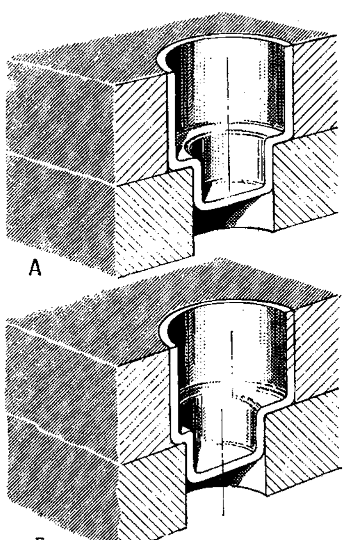

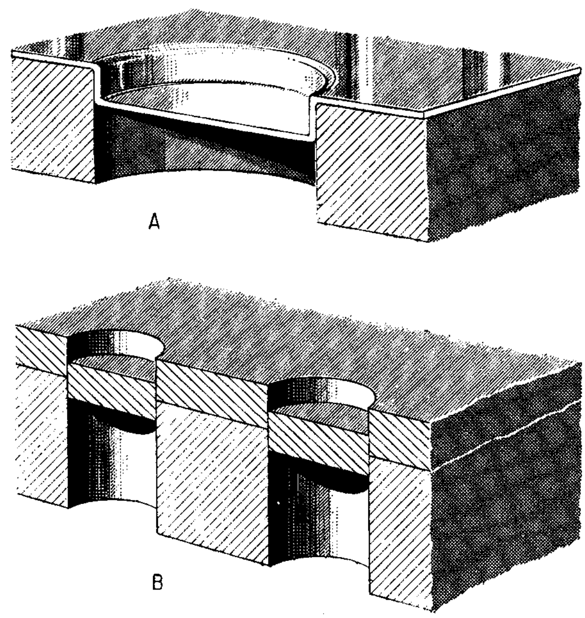

3 **SHEET METAL "DOWELS"** can be used where location of two parts is needed without precise hole location. Cup is drawn after assembly.

4 **SELF-DOWELING** part can be sheet metal (A) or other thin-material part (B). Merely emboss or punch slug halfway through to locate in hole.

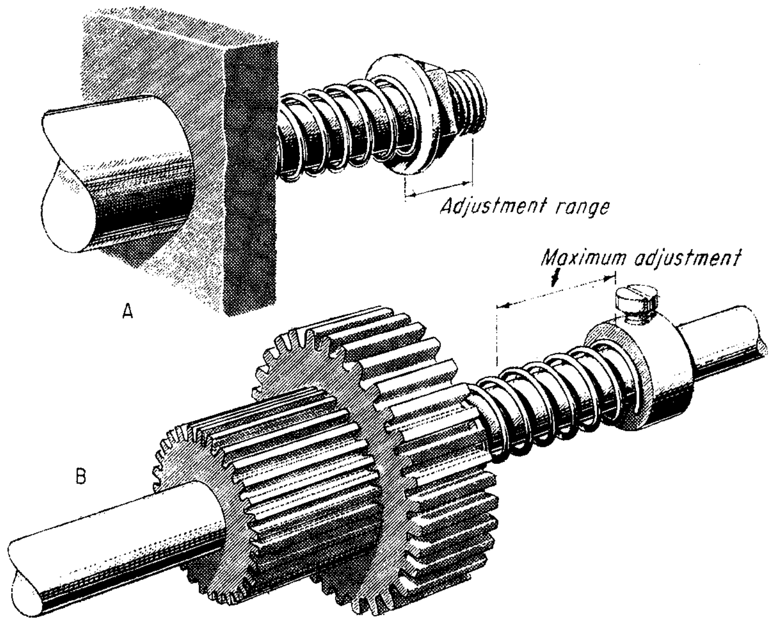

2

BASIC FRICTION-CLUTCH can also provide for disengagement when torque exceeds a safe value. There is basically no difference between collared shaft (A) and ringed shaft (B), but adjustment of tension in collared shaft is limited by amount of threading on end of shaft.

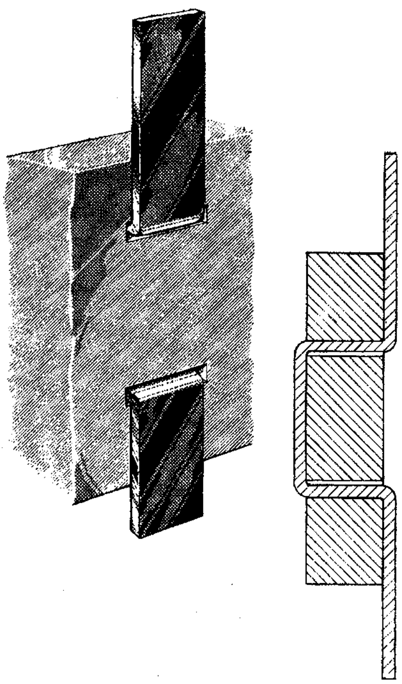

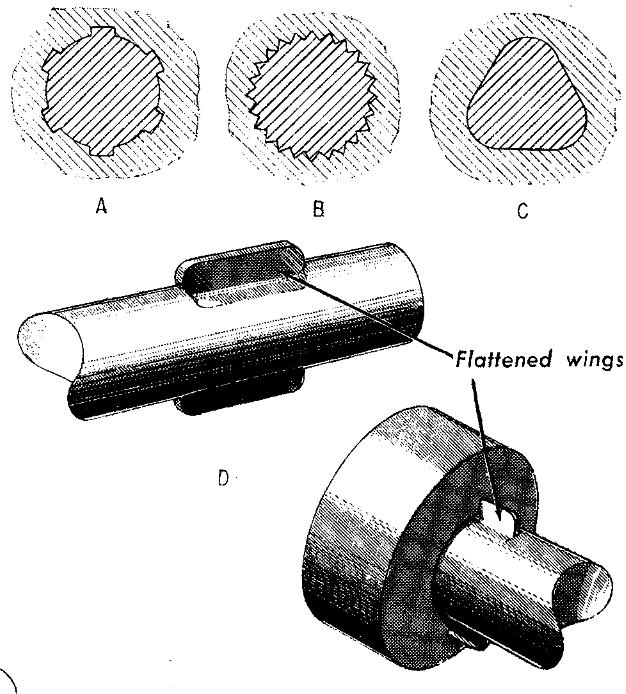

5

FOLDED ASSEMBLIES eliminate the need for pins or other locating fasteners. Illustrated is a terminal mounted on insulating plates.

6

SPLINES such as square (A) and involute (B) are often the best way to locate and hold hubs. Don't overlook simpler methods shown at C and D.

SECTION 18

CAMS

Generating Cam Curves

It usually doesn't pay to design a complex cam curve if it can't be easily machined–so check these mechanisms before starting your cam design.

Preben W. Jensen

IF you have to machine a cam curve into the metal blank without using a master cam, how accurate can you expect it to be? That depends primarily on how precisely the mechanism you use can feed the cutter into the cam blank. The mechanisms described here have been carefully selected for their practicability. They can be employed directly to machine the cams, or to make master cams for producing others.

The cam curves are those frequently employed in automatic-feed mechanisms and screw machines. They are the circular, constant-velocity, simple-harmonic, cycloidal, modified cycloidal, and circular-arc cam curve, presented in that order.

Circular cams

This is popular among machinists because of the ease in cutting the groove. The cam (Fig 1A) has a circular groove whose center, A, is displaced a distance a from the cam-plate center, A_0, or it may simply be a plate cam with a spring-loaded follower (Fig 1B).

Interestingly, with this cam you can easily duplicate the motion of a four-bar linkage (Fig 1C). Rocker BB_0 in Fig 1C, therefore, is equivalent to the motion of the swinging follower in Fig 1A.

The cam is machined by mounting the plate eccentrically on a lathe. The circular groove thus can be cut to close tolerances with an excellent surface finish.

If the cam is to operate at low speeds you can replace the roller with an arc-formed slide. This permits the transmission of high forces. The optimum design of such "power cams" usually requires time-consuming computations, but charts were published re-

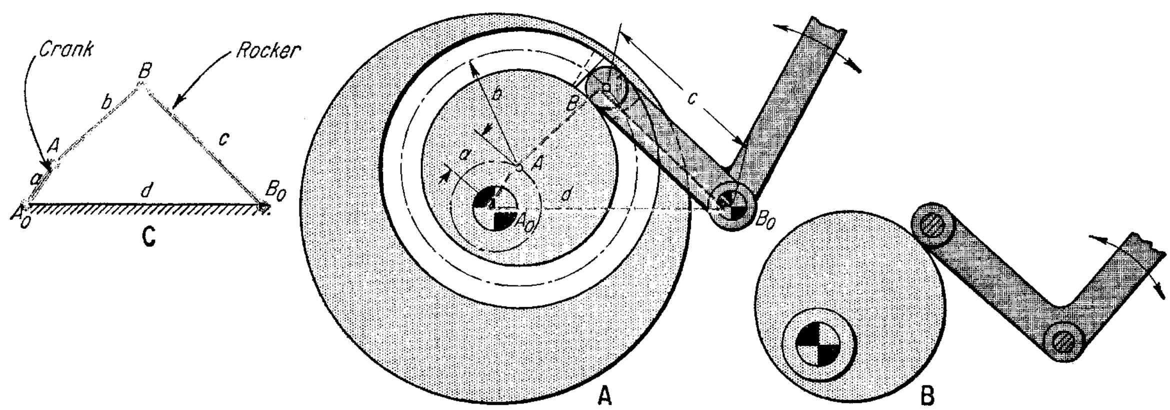

1. Circular cam groove is easily machined on turret lathe by mounting the plate eccentrically onto the truck. Plate cam in **(B)** with spring load follower produces same output motion. Many designers are unaware that this type of cam has same output motion as four-bar linkage **(C)** with the indicated equivalent link lengths. Hence it's the easiest curve to pick when substituting a cam for an existing linkage.

cently (see Editor's Note at end of article) which simplify this aspect of design.

The disadvantage (or sometimes, the advantage) of the circular-arc cam is that, when traveling from one given point, its follower reaches higher speed accelerations than with other equivalent cam curves.

Constant-velocity cams

A constant-velocity cam profile can be generated by rotating the cam plate and feeding the cutter linearly, both with uniform velocity, along the path the translating roller follower will travel later (Fig 2A). In the case of a swinging follower, the tracer (cutter) point is placed on an arm equal to the length of the actual swinging roller follower, and the arm is rotated with uniform velocity (Fig 2B).

Simple-harmonic cams

The cam is generated by rotating it with uniform velocity and moving the cutter with a scotch yoke geared to the rotary motion of the cam. Fig 3A shows the principle for a radial translating follower; the same principle is, of course, applicable for offset translating and swinging roller follower. The gear ratios and length of the crank working in the scotch yoke control the pressure angles (the angles for the rise or return strokes).

For barrel cams with harmonic motion the jig in Fig 3B can easily be set up to do the machining. Here, the barrel cam is shifted axially by means of the rotating, weight-loaded (or spring-loaded) truncated cylinder.

The scotch-yoke inversion linkage (Fig 3C) replaces the gearing called for in Fig 3A. It will cut an approximate simple-harmonic motion curve when the cam has a swinging roller follower, and an exact curve when the cam has a radial or offset translating roller follower. The slotted member is fixed to the machine frame *1*. Crank *2* is driven around the center *0*. This causes link *4* to oscillate back and forward in simple harmonic motion. The sliding piece *5* carries the cam to be cut, and the cam is rotated around the center of *5* with uniform velocity. The length of arm *6* is made equal to the length of the swinging roller follower of the actual cam mechanism and the device adjusted so that the extreme positions of the center of *5* lie on the center line of *4*.

The cutter is placed in a stationary spot somewhere along the centerline of member *4*. In case a radial or offset translating roller follower is used, the sliding piece *5* is fastened to *4*.

The deviation from simple harmonic motion when the cam has a swinging follower causes an increase in acceleration ranging from 0 to 18% (Fig 3D), which depends on the total angle of oscillation of the follower. Note that for a typical total oscillating angle of 45 deg, the increase in acceleration is about 5%.

Cycloidal motion

This curve is perhaps the most desirable from a designer's viewpoint because of its excellent acceleration characteristic. Luckily, this curve is comparatively easy to generate. Before selecting the mechanism it is worthwhile looking at the underlying theory of the cycloids because it is possible to generate not only cycloidal motion but a whole family of similar curves.

The cycloids are based on an offset sinusoidal wave (Fig 4). Because the radii of curvatures in points *C*, *V*, and *D* are infinite (the curve is "flat" at these points), if this curve was a cam groove and moved in the direction of line *CVD*, a translating roller follower, actuated by this cam, would have zero acceleration at points *C*, *V*, and *D* no matter in what direction the follower is pointed.

Now, if the cam is moved in the direction of *CE* and the direction of motion of the translating follower is lined perpendicular to *CE*, the acceleration of the follower in points *C*, *V*, and *D* would still be zero.

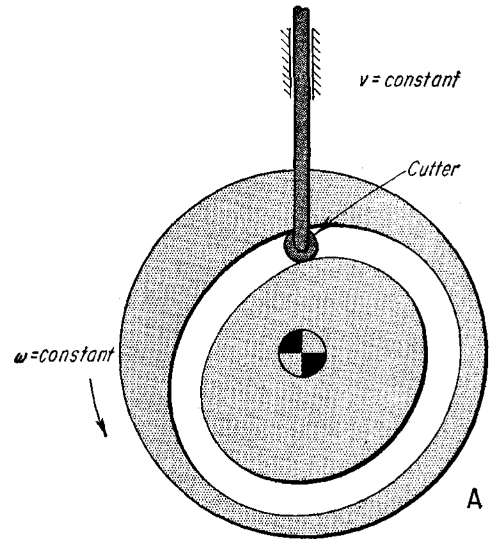

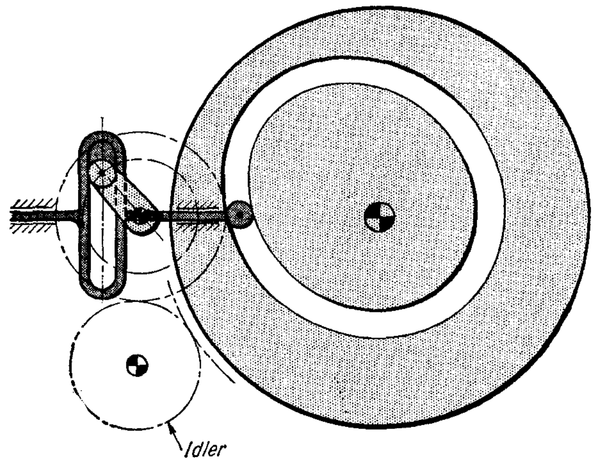

3. **For producing simple harmonic curves: (A)** Scotch yoke device feeds cutter while gearing arrangement rotates cam; **(B)** truncated-cylinder slider for

2. **Constant-velocity** cam is machined by feeding the cutter and rotating the cam at constant velocity. Cutter is fed linearly **(A)** or circularly **(B)**, depending on type of follower.

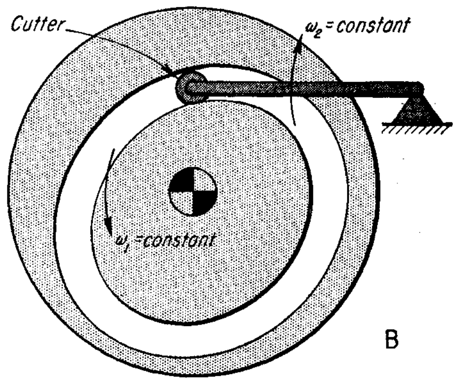

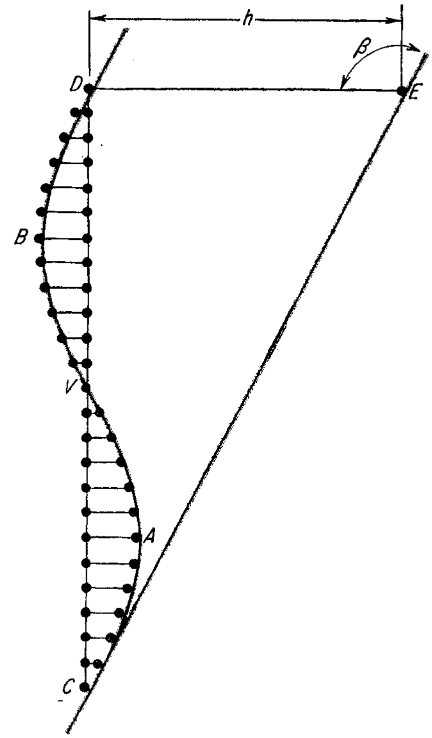

4. **Layout of a cycloidal curve.**

This has now become the basic cycloidal curve, and it can be considered as a sinusoidal curve of a certain amplitude (with the amplitude measured perpendicular to the straight line) superimposed on a straight (constant-velocity) line.

The cycloidal is considered the best *standard* cam contour because of its low dynamic loads and low

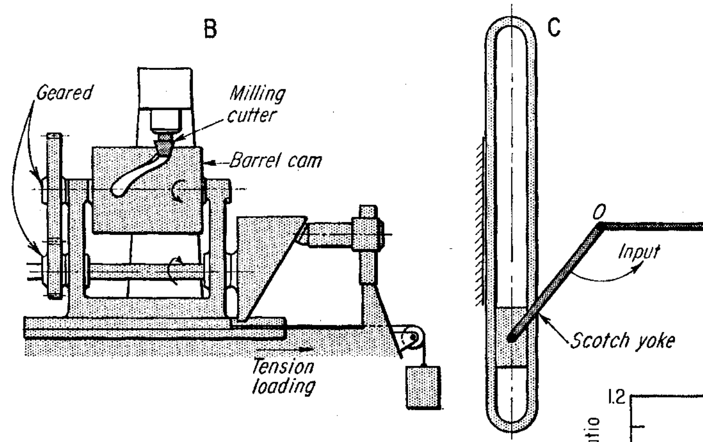

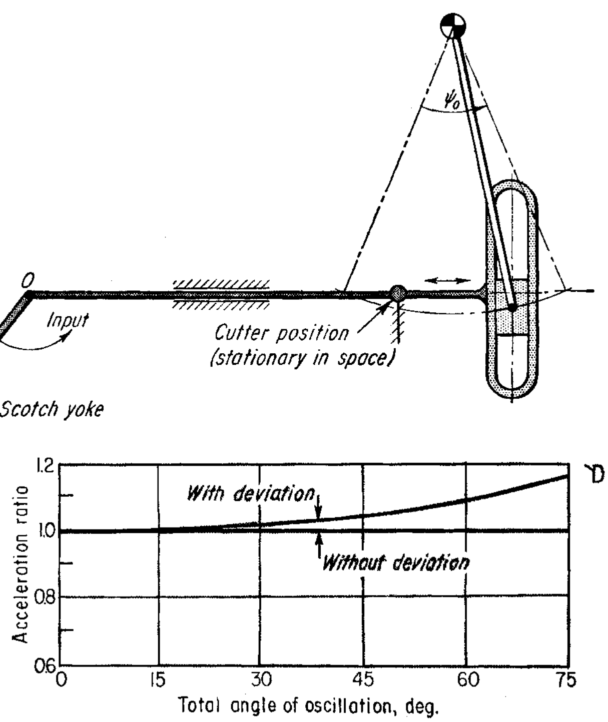

cylindrical cam; **(C)** scotch-yoke inversion linkage for avoiding gearing; **(D)** increase in acceleration when translating follower is replaced by swinging follower.

shock and vibration characteristics. One reason for these outstanding attributes is that it avoids any sudden change in acceleration during the cam cycle. But improved performances are obtainable with certain modified cycloidals.

Modified cycloids

To get a modified cycloid, you need only change the direction and magnitude of the amplitude, while keeping the radius of curvature infinite at points *C*, *V*, and *D*.

Comparisons are made in Fig 5 of some of the modified curves used in industry. The true cycloidal is shown in the cam diagram of *A*. Note that the sine amplitudes to be added to the constant-velocity line are perpendicular to the base. In the Alt modification shown in *B* (after Hermann Alt, German kinematician, who first analyzed it), the sine amplitudes are perpendicular to the constant-velocity line. This results in improved (lower) velocity characteristics (see *D*), but higher acceleration magnitudes (see *E*).

The Wildt modified cycloidal (after Paul Wildt) is constructed by selecting a point *w* which is 0.57 the distance $T/2$, and then drawing line *wp* through *yp* which is midway along *OP*. The base of the sine curve is then constructed perpendicular to *yw*. This modification results in a maximum acceleration of 5.88 h/T^2, whereas the standard cycloidal curve has a maximum acceleration of 6.28 h/T^2. This is a 6.8% reduction in acceleration.

(It's quite a trick to construct a cycloidal curve to go through a particular point *P*—where *P* may be anywhere within the limits of the box in *C*—and with a specific slope at *P*. There is a growing demand for this type of modification, and a new, simple, graphic technique developed for meeting such requirements will be shown in the next issue.)

Generating the modified cycloidals

One of the few devices capable of generating the family of modified cycloidals consists of a double carriage and rack arrangement (Fig 6A).

The cam blank can pivot around the spindle, which in turn is on the movable carriage *I*. The cutter center is stationary. If the carriage is now driven at constant speed by the lead screw, in the direction of the arrow, the steel bands 1 and 2 will also cause the cam blank to rotate. This rotation-and-translation motion to the cam will cause a spiral type of groove.

For the modified cycloidals, a second motion must be imposed on the cam to compensate for the deviations from the true cycloidal. This is done by a second steel band arrangement. As carriage *I* moves, the bands 3 and 4 cause the eccentric to rotate. Because of the stationary frame, the slide surrounding the eccentric is actuated horizontally. This slide is part of carriage *II*, with the result that a sinusoidal motion is imposed on to the cam.

Carriage *I* can be set at various angles β to match angle β in Fig 5B and C. The mechanism can also be modified to cut cams with swinging followers.

Circular-arc cams

Although in recent years it has become the custom to turn to the cycloidal and other similar curves even when speeds are low, there are many purposes for which

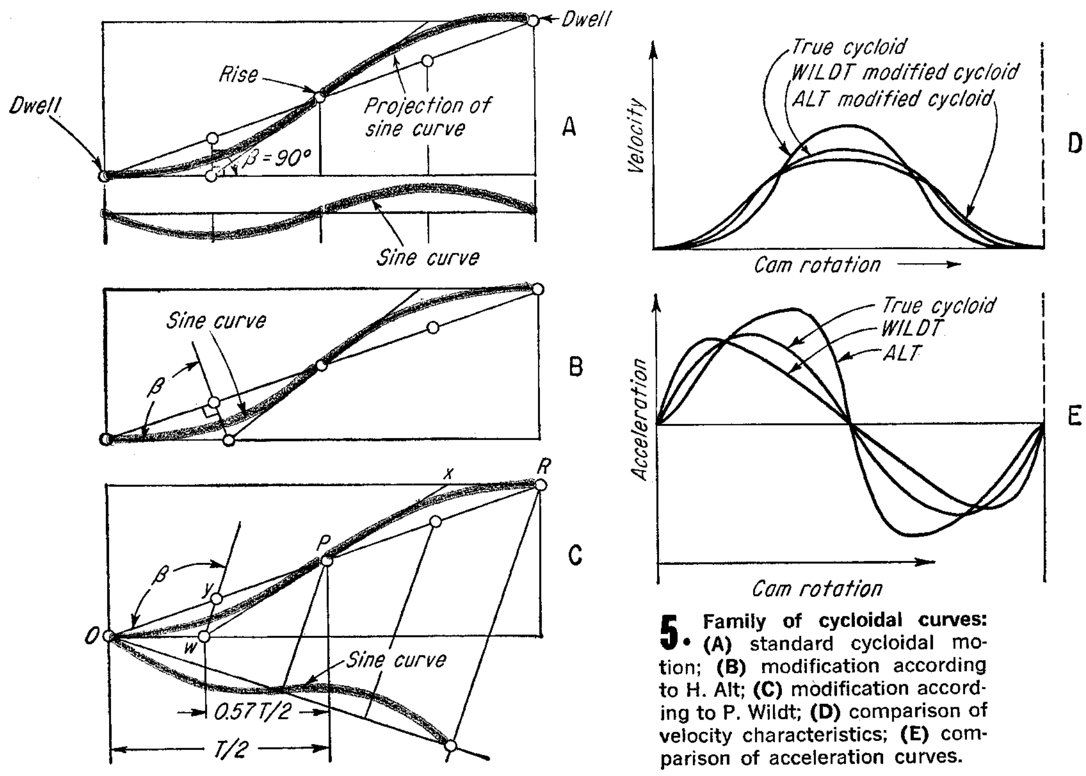

5. Family of cycloidal curves: **(A)** standard cycloidal motion; **(B)** modification according to H. Alt; **(C)** modification according to P. Wildt; **(D)** comparison of velocity characteristics; **(E)** comparison of acceleration curves.

circular-arc cams suffice. Such cams are composed of circular arcs, or circular arcs and straight lines. For comparatively small cams the cutting technique illustrated in Fig 7 produces good accuracy.

Assume that the contour is composed of circular arc *1-2* with center at O_2, arc *3-4* with center at O_3, arc *4-5* with center at O_1, arc *5-6* with center at O_4, arc *7-1* with center at O_1, and the straight lines *2-3* and *6-7*. The method involves a combination of drilling, lathe turning, and template filing.

First, small holes about 0.1 in diameter are drilled at O_1, O_3, and O_4, then a hole is drilled with the center at O_2 and radius of r_2. Next the cam is fixed in a turret lathe with the center of rotation at O_1, and the steel plate is cut until it has a diameter of $2r_5$. This takes care of the larger convex radius. The straight lines *6-7* and *2-3* are now milled on a milling machine.

Finally, for the smaller convex arcs, hardened pieces are turned with radii r_1, r_3, and r_4. One such piece is shown in Fig 7B. The templates have hubs which fit into the drilled holes at O_1, O_3, and O_4. Now the arc *7-1*, *3-4*, and *5-6* are filed, using the hardened templates as a guide. Final operation is to drill the enlarged hole at O_1 to a size that a hub can be fastened to the cam.

This method is frequently better than copying from a drawing or filing the scallops away from a cam where a great number of points have been calculated to determine the cam profile.

Compensating for dwells

One disadvantage with the previous generating devices is that, with the exception of the circular cam, they cannot include a dwell period within the rise-and-fall cam

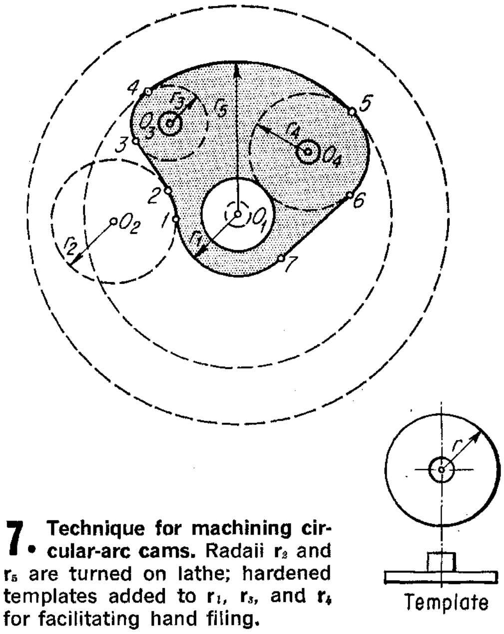

7. Technique for machining circular-arc cams. Radaii r_2 and r_5 are turned on lathe; hardened templates added to r_1, r_3, and r_4 for facilitating hand filing.

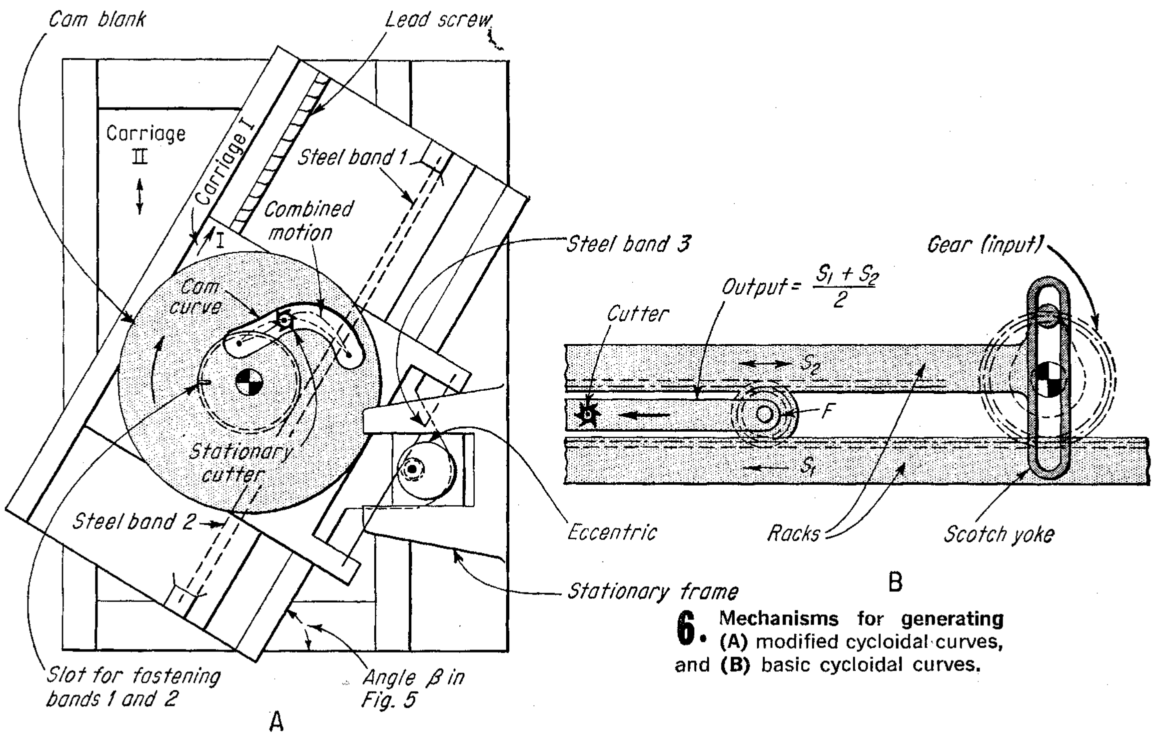

6. Mechanisms for generating (A) modified cycloidal curves, and (B) basic cycloidal curves.

cycle. The mechanisms must be disengaged at the end of rise and the cam rotated in the exact number of degrees to where the fall cycle begins. This increases the inaccuracies and slows down production.

There are two devices, however, that permit automatic machining through a specific dwell period: the double-geneva drive and the double eccentric mechanism.

Double-genevas with differential

Assume that the desired output contains dwells (of specific duration) at both the rise and fall portions, as shown in Fig 8A. The output of a geneva that is being rotated clockwise will produce an intermittent motion similar to the one shown in Fig 8B—a rise-dwell-rise-dwell . . . etc, motion. These rise portions are distorted simple-harmonic curves, but are sufficiently close to the pure harmonic to warrant use in many applications.

If the motion of another geneva, rotating counterclockwise as shown in (C), is added to that of the clockwise geneva by means of a differential (D), then the sum will be the desired output shown in (A).

The dwell period of this mechanism is varied by shifting the relative position between the two input cranks of the genevas.

The mechanical arrangement of the mechanism is shown in Fig 8D. The two driving shafts are driven by gearing (not shown). Input from the four-star geneva to the differential is through shaft *3;* input from the eight-station geneva is through the spider. The output from the differential, which adds the two inputs, is through shaft *4.*

The actual device is shown in Fig 8E. The cutter is fixed in space. Output is from the gear segment which rides on a fixed rack. The cam is driven by the motor which also drives the enclosed genevas. Thus, the entire device reciprocates back and forth on the slide to feed the cam properly into the cutter.

Genevas driven by couplers

When a geneva is driven by a constant-speed crank, as shown in Fig 8D, it has a sudden change in acceleration at the beginning and end of the indexing cycle (as the crank enters or leaves a slot). These abrupt changes can be avoided by employing a four-bar linkage with coupler in place of the crank. The motion of the coupler point C (Fig 9) permits smooth entry into the geneva slot.

Double eccentric drive

This is another device for automatically cutting cams with dwells. Rotation of crank A (Fig 10) imparts an oscillating motion to the rocker C with a prolonged dwell at both extreme positions. The cam, mounted on the rocker, is rotated by means of the chain drive and thus is fed into the cutter with the proper motion. During the dwells of the rocker, for example, a dwell is cut into the cam.

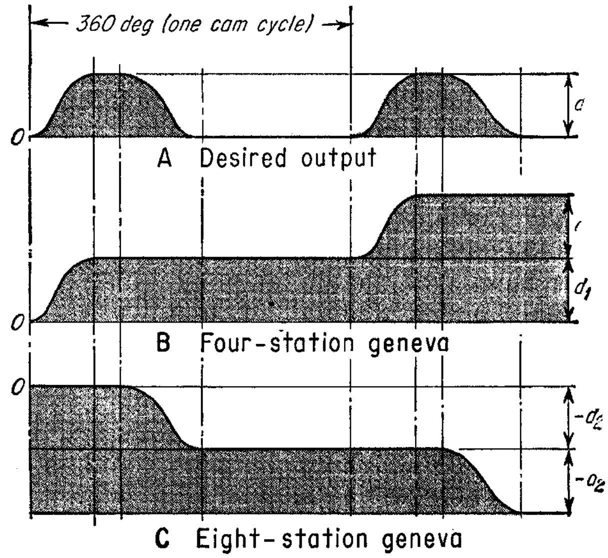

8. **Double genevas with differential** for obtaining long dwells. Desired output characteristic **(A)** of cam is obtained by adding the motion **(B)** of a four-station geneva to that of **(C)** eight-station geneva. The mechanical arrangement of genevas with a differential is shown in **(D)**; actual device is shown in **(E)**. A wide variety of output dwells **(F)** are obtained by varying the angle between the driving cranks of the genevas.

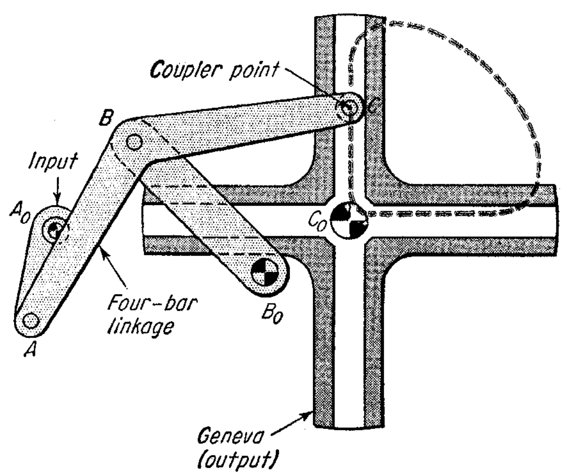

9. **Four-bar coupler mechanism** for replacing the cranks in genevas to obtain smoother acceleration characteristics.

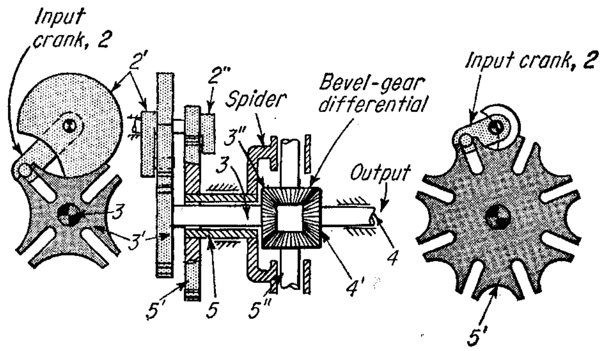

D Double geneva with differential

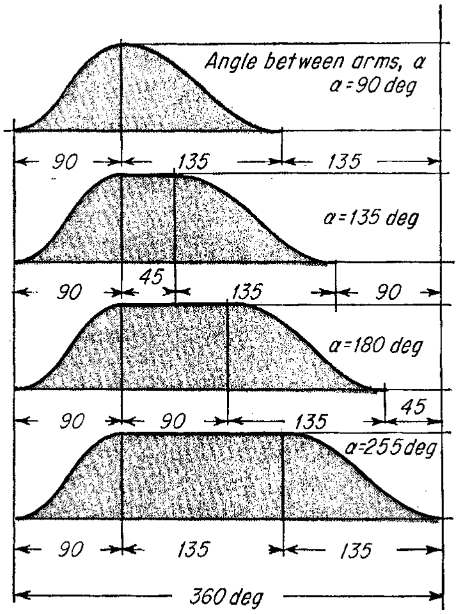

F Various dwell resultants

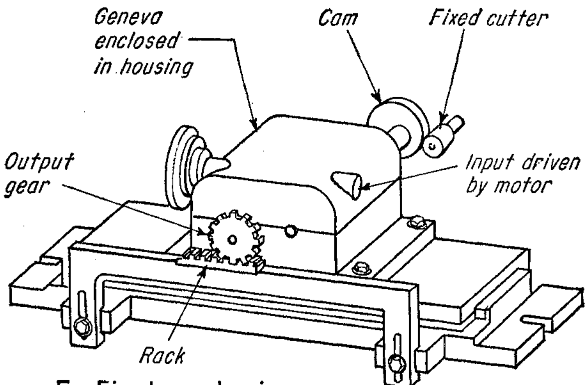

E Final mechanism

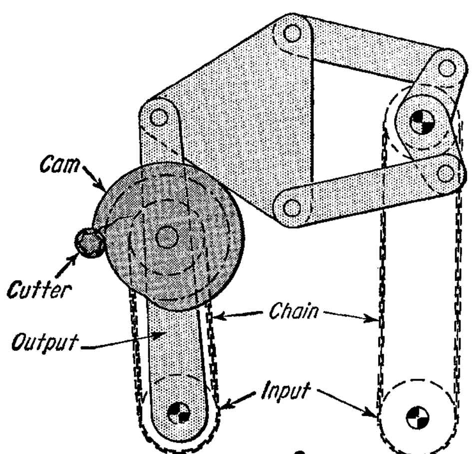

C

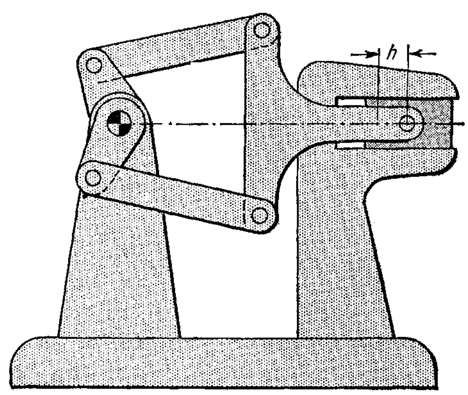

B

10. **Double eccentric drive** for automatically cutting cams with dwells. Cam is rotated and oscillated, with dwell periods at extreme ends of oscillation corresponding to desired dwell periods in cam.

Balance Grooved Cams

A quick analytical method for computing the rim cut needed to balance a cam, and a layout method for refining the results.

R. F. Koen

SYMBOLS

A = area of segment, in.^{2}
C = constant = $1.5D/R_r$
d = depth of cam groove, in.
D = cam follower diameter, in.
E = unbalance moment, in.^{3}
F = centrifugal force, lb
g = gravitational constant, 32 ft/sec^2
h = radial width of periphery balance cut at specific cam angle, in.
L = perpendicular distance from vertical axis of cam to center of area segment
M = mass, lb-sec^2/in.
n = speed of rotating body, rpm
r_{max} = maximum radius of cam groove, in.
r_1 = radius of groove centerline on lighter side, in.
r_2 = radius of groove centerline on heavier side (diametrically opposite to r_1) in.
R_r = radius to rim, in.
R_c = radius to center of balance cut ($R_c = R_r - h/2$)
T = thickness of cam, in.
V = velocity, in./sec
W = weight of body, lb
y_1 = feed-in dimension (radial displacement of cam follower) on lighter side of cam (from cam displacement tables), in.
y_2 = feed-in dimension on heavier side of cam, in.
ρ = density of cam material, lb/in.^{3}

WHEN a machine is redesigned to increase its productivity, the first approach is to boost its operating speed. What you invariably run up against, however, is the possiblity of destructive vibrations induced by unbalance or by velocity changes in the rotating parts. Frequently the culprits are cams—common machine elements —which create direct or indirect forces.

Direct forces are those induced by the cam profile in accelerating the cam follower. We are not concerned here with profile design (see Editor's Note for articles on this subject) but with indirect forces developed by the inherent unbalance of the cam, in particular, a grooved cam. When the groove is machined, Fig 1, the plate becomes unbalanced with respect to rotation about the center, point *O*. The solution recommended here is to nullify the unbalance by removing a portion of the rim. This "balance cut" (shown in color) is machined to the same depth as the depth of the groove—or the plate can be cast without the undesirable rim sector.

Equations are presented here which determine, approximately, the varying radial width of the cut, *h*. A layout procedure is included for checking the amount of balance error that will remain if the original layout for the balance cut is followed through. A tabular method then pinpoints the additional modifications the original cut requires. The result is an accurately balanced cam, as attested by the performance of dozens of cams we have machined and then checked with balancing instruments.

There are no restrictions as to the

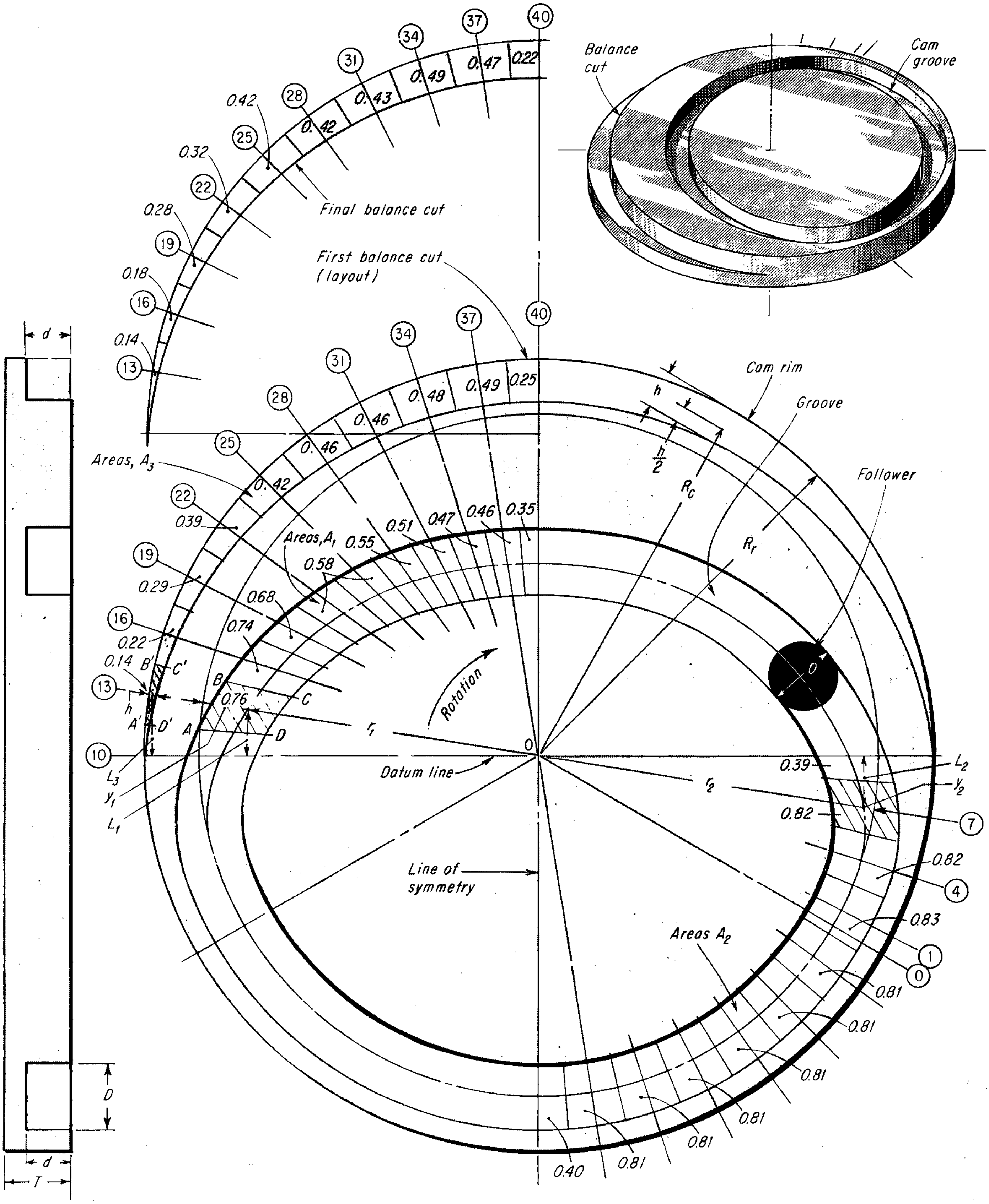

1 . . GROOVE CAM WITH FIRST AND FINAL BALANCE-CUT LAYOUTS.

type of cam curve that can be used with this method. However, as stated above, the method is directly applicable to groove cams only. Plate cams —those with the cam profile on the rim—cannot be balanced in the same manner (by simply removing material from the rim) because this will obviously obliterate part of the working profile. Lead inserts and drilled balance holes are employed for this purpose and it is likely that they can be accurately located by suitably modifying the method given here. Such a modification is presently under study.

In applying this method it is assumed that:

1) The balance cut on the rim of the cam is relatively small and therefore the difference between the rim radius, R_r, and the radius to the center of the balance cut will be small.

2) The section to be cut can be considered a series of straight lines.

3) The difference between the diameter of the cam follower and the width of the groove at the section cut is insignificant.

Empirical equations

For static equilibrium, the summation of moments around O must be equal to zero; hence

$$r_1 D + R_r h - r_2 D = 0 \qquad (1)$$

See Box on page 64 for definition of symbols. From Eq 1, the radial depth of the balance cut, h, is

$$h = \frac{D(r_2 - r_1)}{R_r} \qquad (2)$$

If y is the cam-follower radial displacement given in cam-displacement tables—or the feed-in dimension for machining the groove—then on the lighter side of the cam (the side where the groove is closest to the cam center):

$$r_1 = r_{max} - y_1$$

and on the heavier side (diametrically opposite the lighter side):

$$r_2 = r_{max} - y_2$$

Substituting these values into Eq 2 results in

$$h = \frac{D}{R_r}(y_1 - y_2) \qquad (3)$$

However, Eq 3 has been based on a two-dimensional analysis. It does not take into consideration moments either above or below the plane where the bottom of the cut is made (which is at the same level as the bottom of the groove). By comparing the h values of correctly balanced cams with the h values obtained from Eq 3 it was found that the measured h values were approximately 50% greater than the calculated values. Hence Eq 3 is modified to read:

$$h = \frac{1.5D}{R_r}(y_1 - y_2) \qquad (4)$$

The ratio $1.5D/R_r$ is constant for any given cam; hence letting

$$C = 1.5D/R_r \qquad (5)$$

then

$$h = C(y_1 - y_2) \qquad (6)$$

Layout method

The advantage of employing Eq 6 is that you can directly and quickly determine the h values from the cam displacement tables. These h values usually provide suitably balanced cams. For more critical applications, however, the layout procedure below will produce more accurately balanced cams. We have checked the results of the method with our balancing machines. This method is applied after the y values from the displacement table and the h values from Eq 6 are determined. Referring to Fig 1:

1) Locate the datum line. This line (line 10-0) is perpendicular to the line of maximum unbalance (in the case of Fig 1, the line of symmetry).

2) Lay out equal angular segments on the cam groove and on the rim balance cut.

3) Measure the area of each segment by a planimeter (areas A_1, A_2, and A_3).

4) Locate the center of each area by construction.

5) Measure the perpendicular distances to the centers from the datum line (distances L_1, L_2, and L_3).

6) Sum up the area moments on the balanced and unbalanced sides of the cam (ΣA_1L_1, ΣA_2L_2 and ΣA_3L_3).

7) Check for balance. If rim cut is of proper dimensions then the following equation holds true:

$$\Sigma A_2L_2 - \Sigma A_1L_1 = \Sigma A_3L_3$$

8) If this equation is not satisfied then constant C must be modified as follows:

$$C_1 = C\left(\frac{A_2L_2 - A_1L_1}{A_3L_3}\right) \qquad (7)$$

9) Compute new h values by employing the equation

$$h_1 = C_1(y_1 - y_2) \qquad (8)$$

A more accurate balance cut can now be made by using these new values for h. Before actually machining the cut, the new balance curve can be plotted on the cam and then checked by repeating the above procedure. This can lead to a still more accurate balance; however, cams cut to first-generation h_1 values have proved highly satisfactory.

Design example

A shop layout drawing of an actual cam with $D = 1.002$ in., $R_r = 5.875$ in., and $d = 0.687$ in. is shown in Fig 2. It is to be made of meehanite ($\rho = 0.260$ lb/in.^{3}). Cam speed n is equal to 400 rpm. The cam displacement diagram is shown above the layout drawing. Cam displacement values are given in Table I.

From Eq 5

$$C = 1.5(1.002)/5.875 = 0.255$$

1) Determine the y-values per Table I. Values for only half the cam in this example need to be determined

TABLE I. . CAM DISPLACEMENT DATA

POSITION	ANGLE		DISPLACEMENT, IN.
0	0	240	0.000
1	3	237	0.001
2	6	234	0.006
3	9	231	0.020
4	12	228	0.045
5	15	225	0.085
6	18	222	0.139
7	21	219	0.207
8	24	216	0.286
9	27	213	0.374
10	30	210	0.467
11	33	207	0.560
12	36	204	0.653
13	39	201	0.746
14	42	198	0.838
15	45	195	0.928
16	48	192	1.018
17	51	189	1.106
18	54	186	1.192
19	57	183	1.276
20	60	180	1.358
21	63	177	1.438
22	66	174	1.515
23	69	171	1.589
24	72	168	1.660
25	75	165	1.728
26	78	162	1.792
27	81	159	1.853
28	84	156	1.909
29	87	153	1.962
30	90	150	2.010
31	93	147	2.056
32	96	144	2.096
33	99	141	2.132
34	102	138	2.163
35	105	135	2.189
36	108	132	2.211
37	111	129	2.228
38	114	126	2.241
39	117	123	2.248
40	120	120	2.250

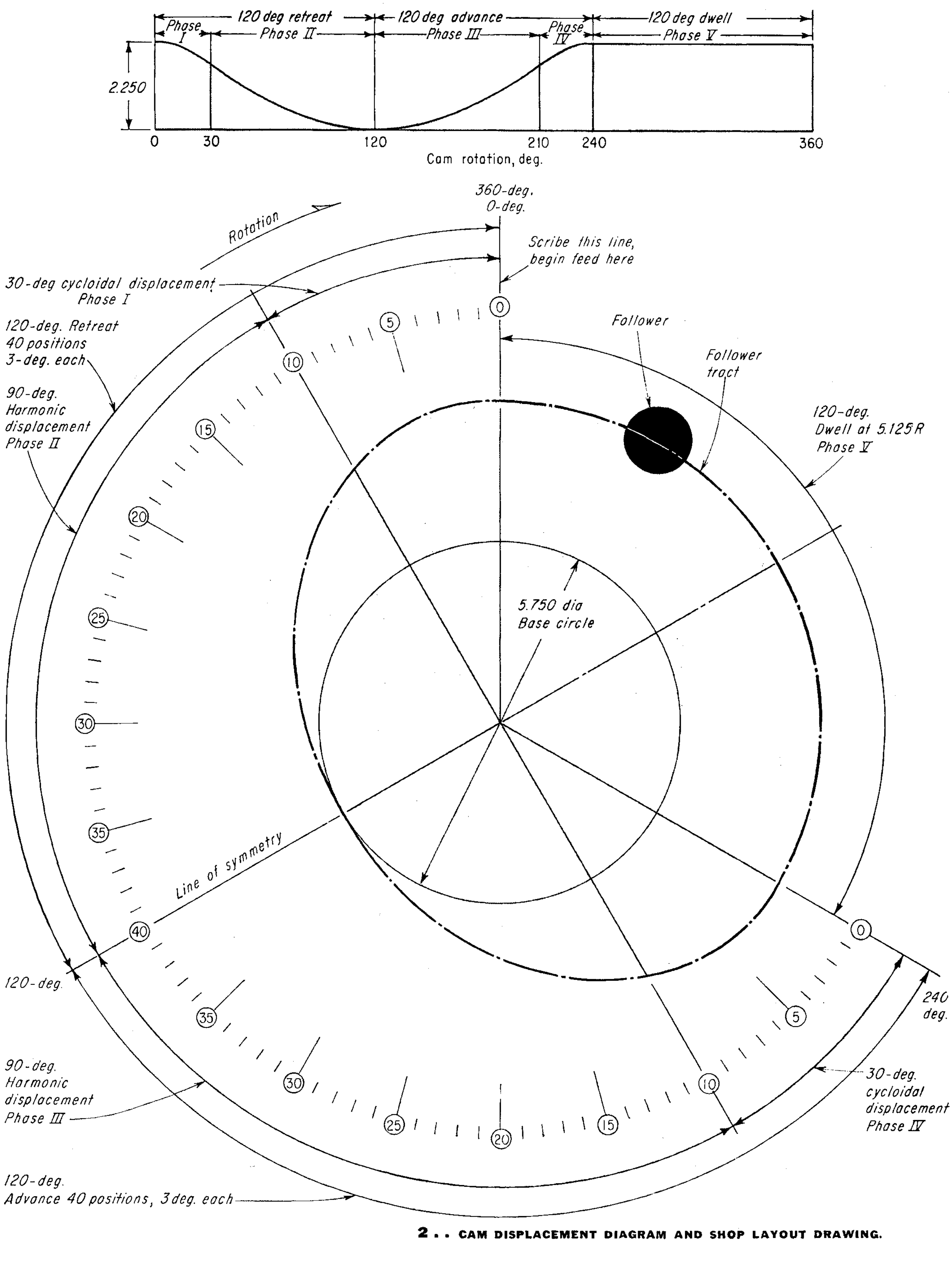

2 . . CAM DISPLACEMENT DIAGRAM AND SHOP LAYOUT DRAWING.

TABLE II. . BALANCING-ERROR ANALYSIS

1	2	3	4	5	6	7	8	9	10
	Computing the balancing cut					For displacement groove			
Cam position	Displacement, y_1 (from Table I)	Opposite position number	Displacement, y_2 (from Table I)	Unbalance $y_1 - y_2$	Balance cut, h	Area A_1	Distance L_1	Product A_1L_1	Area A_2
40	2.250	–	0	2.250	0.574	0.35	2.90	1.015	0.40
37	2.228	–	0	2.227	0.568	0.46	2.89	1.330	0.81
34	2.163	–	0	2.163	0.552	0.47	2.84	1.335	0.81
31	2.056	–	0	2.056	0.524	0.51	2.75	1.403	0.81
28	1.909	–	0	1.909	0.487	0.55	2.62	1.441	0.81
25	1.728	–	0	1.728	0.441	0.58	2.41	1.399	0.81
22	1.515	–	0	1.515	0.386	0.58	2.13	1.235	0.81
19	1.276	1	0.001	1.275	0.325	0.68	1.75	1.190	0.83
16	1.018	4	0.045	0.973	0.248	0.74	1.28	0.948	0.82
13	0.746	7	0.207	0.539	0.137	0.76	0.68	0.516	0.83

$\Sigma A_2L_2 = 11.812$

because the cam is symmetrical about the centerline. Diametrically opposite positions, however, do not have identical displacement values. Diametric displacement values can be determined from Table I as follows:

Position 13 (39 deg of cam):
$y_1 = 0.746$ in.
Position 7(39 + 180 = 219 deg of cam):
$y_2 = 0.207$ in.

Record the difference $(y_1 - y_2)$ in column 5 of Table II.

2) Calculate the h values per Eq 6. For example, the depth of the balance cut at position 13 is

$$h = 0.255(0.746 - 0.207) = 0.137 \text{ in.}$$

Hence multiply the values in column 5 by 0.255 to obtain column 6. If a diametrically opposite side falls between two cam displacement positions then the exact displacement value is determined by interpolation.

3) Locate the line of maximum unbalance. This will be where the h value is maximum—in this problem at position 40. The datum line, or *vertical axis,* as it is called, will be perpendicular to the line of maximum unbalance.

4) Lay out equal angular segments—both on the cam groove and on the rim balance cut.

5) Measure each area segment with a planimeter on the cam groove and on the balance cut. Record these values in Table II, columns 7, 10 and 13. Thus, for position 13: $A_1 = 0.76$, $A_2 = 0.83$, $A_3 = 0.14$ in.^{2}

6) Locate the center of each measured area by construction. Measure normal distances from area center to vertical axis and record in Table II. For position 13: $L_1 = 0.68$, $L_2 = 0.77$, $L_3 = 0.90$ in.

7) Multiply each area segment by its distance value. For example, position 13: $A_1L_1 = (0.76)(0.68) = 0.516$ in.^{3}

8) Sum up each column of AL values. Thus

$$\Sigma A_1L_1 = 11.812$$
$$\Sigma A_2L_2 = 26.399$$
$$\Sigma A_3L_3 = 15.367$$

9) Check for balance. Determine the magnitude of unbalance force at the operating speed of the cam. If the cam speed is relatively slow, and so develops small unbalance forces in operation, it may not be advisable to go to the expense of making a balance cut. Without a balance cut, the error, E, is equal to

$$E_{\text{unbalanced}} = \Sigma A_2L_2 - \Sigma A_1L_1 = 26.399 - 11.812 = 14.587 \text{ in.}^3$$

With a balance cut the error is

$$E_{\text{balanced}} = \Sigma A_2L_2 - \Sigma A_1L_1 - \Sigma A_3L_3 = 26.399 - 11.812 - 15.367 = 0.780$$

The basic equation for centrifugal force is

$$F = \frac{MV^2}{R}, \text{ lb}$$

Converting to in.-lb-rpm units

$$F = \frac{W(2\pi Rn)^2}{32.2(12)(3600)R} = 28.416 \times 10^{-6}\,(WRn^2)$$

Weight W of a sector is equal to $Ad\rho$. Also R can be replaced by L. Since error $E = AL$, the equation for the centrifugal force due to the summation of the unbalanced masses becomes

$$F = 28.416 \times 10^{-6}(d\rho n^2)E = (28.416)(10^{-6})(0.687)(0.260)(400)^2E$$

$$F = 0.81E$$

Without a balance cut the centrifugal force will be

$$F_{\text{unbalanced}} = (0.81)(14.587) = 11.8 \text{ lb}$$

With a balance cut

$$F_{\text{balanced}} = (0.81)(0.780) = 0.63 \text{ lb}$$

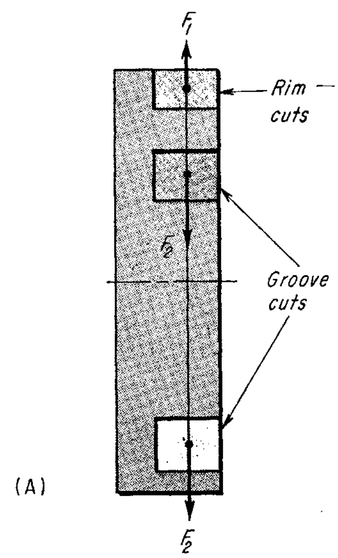

3 . . FOR PERFECT BALANCE, rim cut must be same depth

11	12	13	14	15	16	17	18	19	20
For opposite groove		For balancing cut			Final corrected balancing cut				
Distance L_2	Product A_2L_2	Area A_3	Distance L_3	Product A_3L_3	Unbalanced y_1-y_2	Balanced cut, h_1	Area A_3	Distance L_3	Product A_3L_3
5.12	2.045	0.25	5.58	1.395	2.250	0.544	0.22	5.59	1.230
5.06	4.100	0.49	5.53	2.710	2.227	0.539	0.47	5.53	2.600
4.87	3.943	0.48	5.33	2.560	2.163	0.523	0.49	5.33	2.610
4.56	3.700	0.46	5.08	2.340	2.056	0.498	0.43	5.02	2.108
4.15	3.360	0.46	4.55	2.095	1.909	0.462	0.42	4.55	1.980
3.63	2.940	0.42	4.00	1.680	1.728	0.418	0.42	4.00	1.680
3.01	2.439	0.39	3.38	1.320	1.515	0.367	0.32	3.38	1.082
2.33	1.935	0.29	2.59	0.751	1.275	0.309	0.28	2.59	0.725
1.58	1.298	0.22	1.77	0.390	0.973	0.235	0.18	1.77	0.318
0.77	0.639	0.14	0.90	0.126	0.539	0.130	0.14	0.90	0.126
$\Sigma A_1L_1=26.399$			$\Sigma A_3L_3=15.367$						$\Sigma A_3L_3=14.459$

10) Correct the initial balance-cut layout. With a balance cut on the rim, the unbalance force is only 0.63 lb. Because this force is small it is probably not necessary to make a correction in the C value and recalculate the h value. The correction is computed, however, for illustration purposes. From Eq 7:

$$C_1 = 0.255\left(\frac{26.399 - 11.812}{15.367}\right)$$

$$C_1 = 0.242$$

11) Recalculate the h values per corrected constant C. Example, for position 13, the previous value of $h = 0.137$ in column 5 will be replaced by the value

$$h_1 = 0.539(0.242) = 0.130$$

This is entered into column 17.

12) Lay out the new rim balance cut. Use corrected h values.

13) Determine new values for A_3 and L_3. These are entered into columns 18, 19 and 20. Thus

$$\Sigma A_3L_3 = 14.459$$

The final balance cut is shown at top of Fig 1.

14) Recheck for balance

$$\Sigma A_2L_2 - \Sigma A_1L_1 - \Sigma A_3L_3 = 0$$

$$26.399 - 11.812 - 14.459 = 0.128 \text{ (unbalanced)}$$

The recheck for balance still does not yield perfect results; however, inaccuracies in methods of measurement to determine balance values easily account for this small unbalance. The centrifugal force will be

$$F = 0.81(0.128) = 0.01 \text{ lb.}$$

Because the balance cut is made on the rim to the exact depth of the cam groove, the cam is dynamically as well as statically balanced. For example, in Fig 3A, a balance cut made to the depth of the cam groove places the centrifugal force, F_1, due to the balance cut in the same normal plane as the unbalance force, F_2, due to the groove. There is no dynamic couple acting on the shaft.

If, however, the balance cut is made the full width of the cam blank, as in (B), the centrifugal force F_1, due to the balance cut, and the centrifugal force F_2 acting at the midpoint of the groove will not line up. This produces a dynamic couple $F_2\,(T - d)2$.

The cam in (B) is statically but not dynamically balanced.

The machining of a balance cut is simplified by the fact that a radius usually can be found which will pass through most of the h points. If this is possible, the cam can be chucked off-center on a lathe and machined quite simply. If one radius does not suffice the balance cut can be made on a cam miller in a manner similar to the machining of the cam groove.

A full-width balance cut, Fig 3B, is sometimes made to facilitate machining; for example, a cut can be made with a band saw on a scribed line. In such cases, Eq 5 should be modified to read

$$C = \frac{1.5\,Dd}{R_rT}$$

The cam, of course, will not be dynamically balanced.

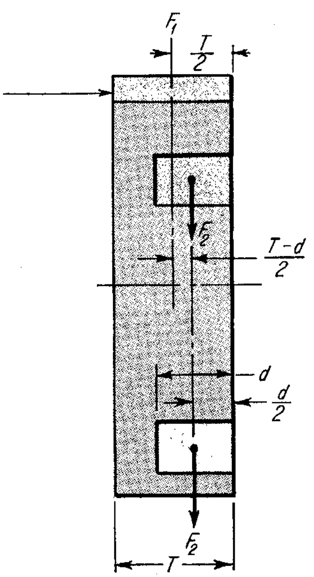

(B)

as groove. Full-width rim-cut causes unbalance moments.

Computer and N/C Simplifies Cam Design

Complex, "exotic" cam curves can now be confidently specified without tedious calculations. And numerical control assures accurate machining of the chosen contours.

Nicholas P. Chironis

New technique produces wide variety of shapes, including barrel and cup cams.

A fast computer in tandem with a specially designed numerical-control converter is opening up new versatility in cam design. No longer need the designer fear—and shun—the complex, "exotic" cam curves in favor of the older and more familiar ones.

The more complex curves entail long, tedious calculations to plot a series of coordinates for the contours. Moreover, machining such contours is slow and expensive unless numerical control can be used.

Making it easy. With the equipment and design procedure developed by Cam Technology, Inc., Elmsford, N.Y., a Cam Tech engineer can take a cam drawing (photos left) and read off the desired displacement requirements of the follower. He punches the dimensional data into the computer, plus the type of cam curve he judges best for the application, and out comes a long punched tape completely designing the cam.

This paper tape is fed into the special N/C converter, which can be wheeled up to operate any standard high-precision jig borer and jig grinder. With this technique, mathematically precise contours and unusual cam configurations have been made to tolerances in the ten-thousandths of an inch.

The function of a cam, of course, is to displace a follower by a specified linear or angular distance while the cam itself rotates a specific amount. Simple as this may seem, the variety of possible cam types and profiles is almost endless. Each design engineer, though, has his own preferences.

To simplify the drawing specifications, Theodore Weber, Cam Tech's president, set up the computer-converter system to solve a cam problem in three phases: (1) operational requirements, (2) cam profile selection, and (3) linkage conversion.

Operational specifications. The first item is simply the designer's basic requirements, relating the displacement of a point in the follower linkage to camshaft rotation.

In the drawing (p 52), a machine part must move a distance y while the cam rotates an angle θ. This motion is pictured in linearized form as moving a plunger vertically the distance y.

For most cams, only the coordinates of the beginnings and ends of

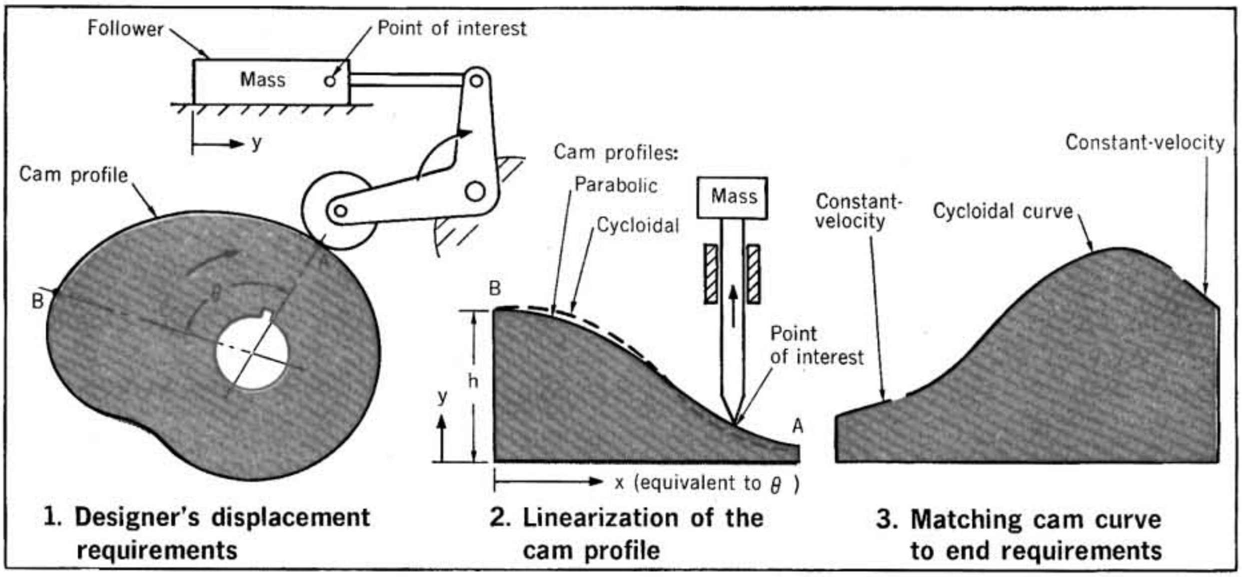

segments need be given, such as the location of the points A and B. For "function" type cams, in which a certain mathematical relationship between input and output must be maintained, the equation or equations governing this relationship must also be specified.

Curve selection. Many curves can be employed to move the plunger for the portion of the cam profile, A—B. Some are common, some are less known. To the eye they look the same—but they produce very different dynamic effects on the follower. One curve may cause high acceleration forces, another may induce an abrupt change in acceleration, and still another may cause dangerous vibrations.

Cam Tech programmed into the computer dozens of cam curves, so the designer need only specify the type of curve he prefers. Moreover, all the curves have been converted into more involved generalized forms to fit any type of slope termination. A cycloid curve, for example, can be asked to match, with ease, constant-velocity portions (drawing, above).

Linkage conversion. The conversion of linearized data to the specialized linkage arrangement that a designer may require involves even more complex calculations than those for the cam profile itself. The endless variety of linkage arrangements between cam and point of application would seem to make the computerization of such a conversion a hopeless task.

However, experience has shown that the vast majority of linkages fall into one of four classifications: the three shown in the drawing below as Types A, B, and C and the connecting-rod type in the drawing above.

Many seemingly unrelated types of follower linkage will fall into one of the above categories. For instance, if a flat face on the follower-arm branch pushes the curved surface on a slider (Type D), it is only necessary to complete the circle of that curved surface to note that this shape comes under Type B. Similarly, a curved face that pushes a straight face on the slider (Type E) falls under Type C.

Further transformations are necessary when the follower diameter is not also a feasible cutter diameter. The follower may, for instance, be flat, or the contour may be specified at the cam surface. Parallel-curve transformation is then used to define a feasible cutter path.

Pick a curve. Cams are often the limiting factor in determining how fast a machine can be operated continuously. A poorly selected profile can produce high dynamic loads and vibration at high speeds that

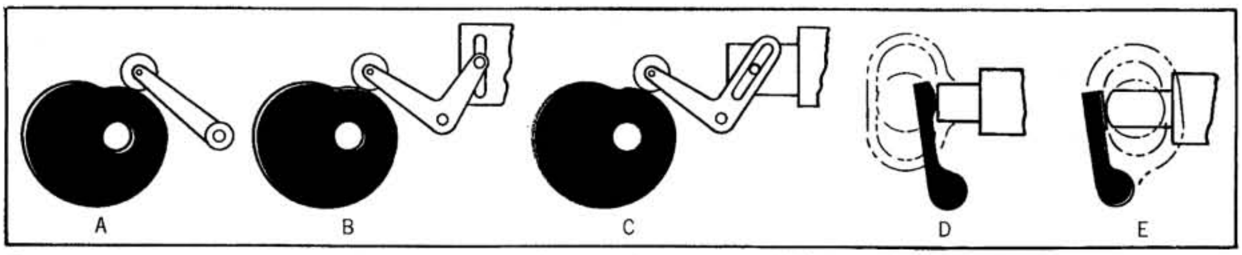

Computer must transform basic curve into desired follower-linkage system. Majority of linkages fall into these types.

can literally rip any machine apart.

Parabolic curve. This will produce the lowest maximum acceleration. Its equation, for the first half of the follower motion, y, is:

$$y = 2h\left(\frac{\theta}{\beta}\right)^2$$

where h = maximum rise of follower, in.
θ = cam-angle rotation for follower displacement, y
β = total cam-angle rotation

The shape of its acceleration is rectangular (drawing, below) with an abrupt change from positive acceleration to negative acceleration (deceleration). This change, sometimes called "infinite jerk," can induce transient shock waves that are especially destructive if there is any looseness in the system.

The parabolic curve, therefore, should be limited to low-speed application. It is still specified by some machine tool builders, but it is Weber's recommendation that this curve be avoided whenever possible.

Simple harmonic curve. This is both easy to calculate and to construct graphically. It eliminates the midpoint transient of the parabolic (at a cost of a 23% higher acceleration), but it unfortunately also produces an abrupt change in acceleration in the beginning and end of its cycle. With the new computer techniques, fewer designers should be calling for this type of curve. Its equation is:

$$y = \frac{h}{2}\left[1 - \cos\left(\frac{\pi\theta}{\beta}\right)\right]$$

The cubic curve shown in the diagram also suffers from an abrupt change in the ends of the cycle.

Cycloidal curve. This is a favorite among many designers because it has no abrupt changes in acceleration and gives low vibration, noise, and shock. Many designers formerly shunned this curve because it called for a higher degree of machining accuracy than did those previously described. To a mathematician, its equation reveals its inherent complexity:

$$y = h\left[\frac{\theta}{\beta} - \frac{1}{2}\sin\left(\frac{2\pi\theta}{\beta}\right)\right]$$

Third harmonic curve. This is a curve derived by Weber that can be tailored to operate below the natural frequency of the follower system and thus can avoid resonance. It is actually a modified cycloidal curve, obtained by introducing a small third-harmonic component in the cycloidal curve to reduce the peak acceleration to 1.28 times the parabolic peak (the cycloidal peak acceleration is about 1.57 times that of the parabolic peak). Its equation is:

$$y = h\left[\frac{\theta}{\beta} - \frac{15}{32\pi}\sin\left(\frac{2\pi\theta}{\beta}\right) - \frac{1}{96\pi}\sin\left(\frac{6\pi\theta}{\beta}\right)\right]$$

This curve is Weber's favorite. It produces smaller dynamic loads than the cycloidal curve (drawing) and smaller vibration amplitudes than all other curves except the cycloidal.

Still other curves are preferred by some engineers, including the so-called "3-4-5" polynomial:

$$y = h\left[10\left(\frac{\theta}{\beta}\right)^3 - 15\left(\frac{\theta}{\beta}\right)^4 + 6\left(\frac{\theta}{\beta}\right)^5\right]$$

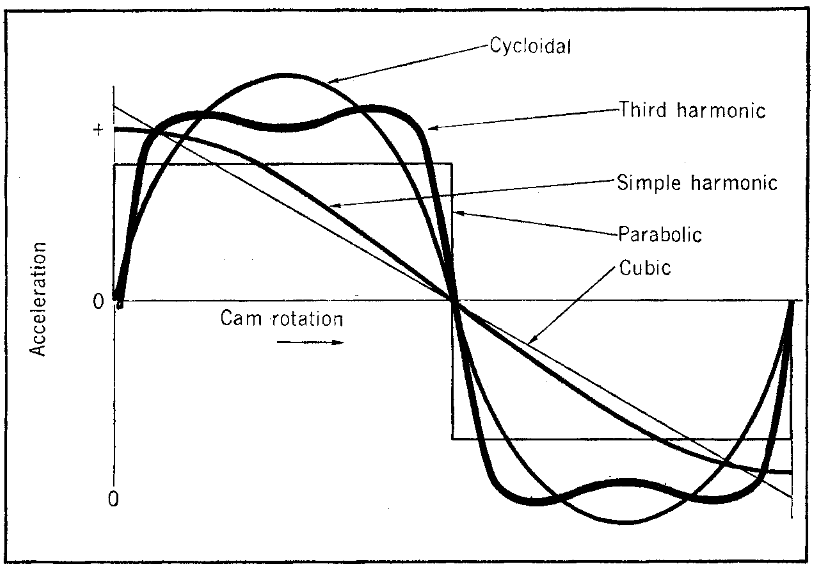

Analysis of five types of cam profile shows that the parabolic, long favored by machine designers for its low maximum-acceleration values, produces an abrupt change in acceleration. So do the cubic and simple harmonic profiles. The cycloidal is smooth, but the little-known third harmonic performs still better.

Special N/C controllers. To obtain the needed accuracy for cam fabrication, Weber had to develop his own N/C control center.

Most digital N/C types move from point to point in small steps, with a feedback system that rounds off the error. The analog N/C's produce a smoother curve, but they do not have the accuracy of the digital types.

Weber, therefore, was forced to design a special hybrid system combining the smoothness of the analog system with the accuracy of the digital system. This control system, working in a team with Weber's computer, typically processes one information datum each tenth of a degree, or 3600 data points per complete cam revolution. These data are processed at a rate of five per second, compared with approximately one per second for most N/C systems.

Theory of Envelopes: Cam Design Equations

These profile and cutter-coordinate equations for six types of cam accept any lift requirements. Included are details on applying the envelope theory to other types.

Dr. Roger S. Hanson & Frederic T. Churchill

ANALYTICAL determinations of cam profiles and cutter coordinates are usually subordinated to graphical techniques because of the voluminous calculations required. In recent years, with the widespread use of high-speed computing equipment, these calculations need no longer be a deterrent. When high-speed, heavy-inertia loads or accurate positioning are design requirements, the designer now has a choice between the analytical approach and the graphical. He is limited only by the ability of present-day machine tools to reproduce the

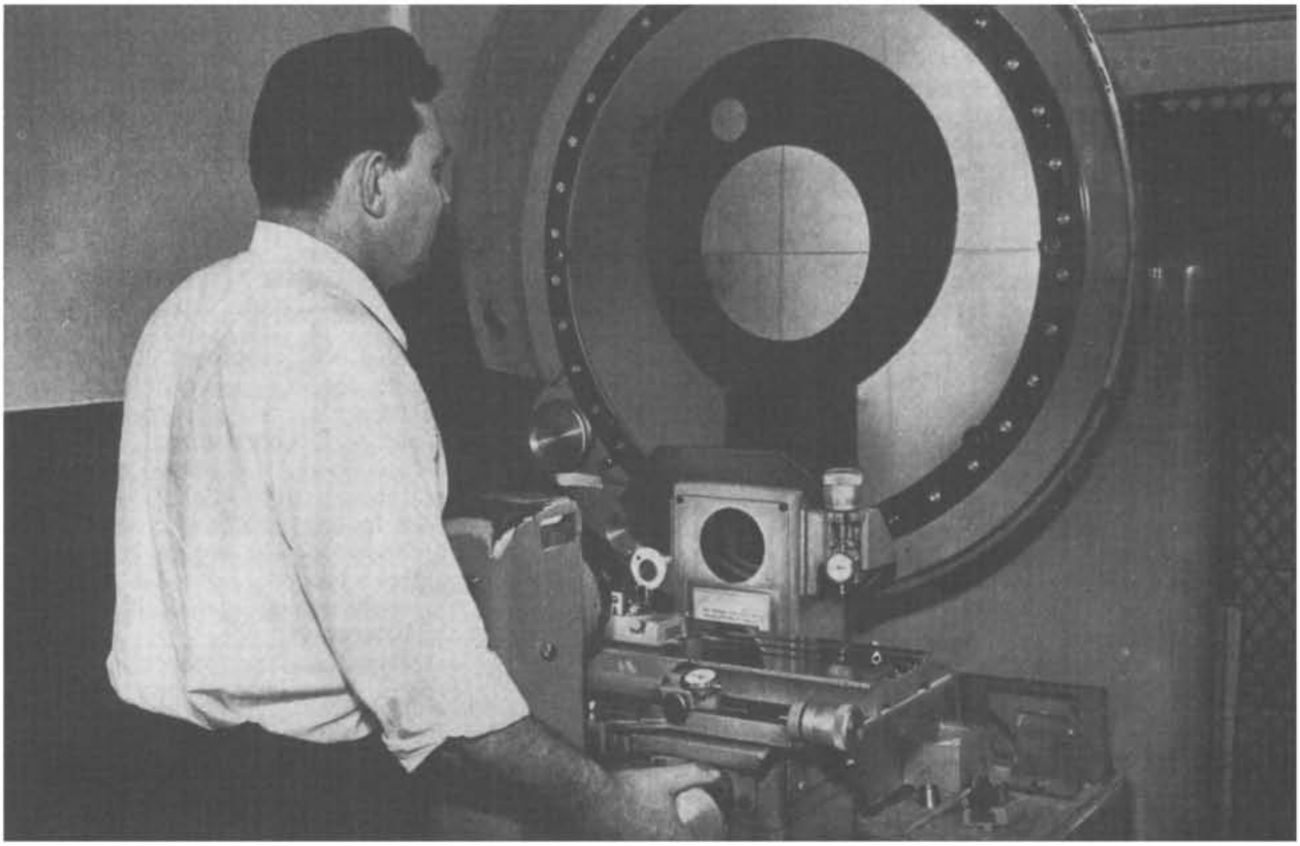

SHADOWGRAPH CHECKS CAM ACCURACY TO ± 0.0005 IN. MAGNIFICATION 10X.

accurate specifications he has made for the cam profile.

The theory of envelopes has not been employed to any extent in cam design—yet it is a powerful analytical tool. The theory is illustrated here and then applied to the development of profile and cutter-coordinate equations for the six major types of cams:

Flat-face follower cams

- Swinging in-line follower
- Swinging off-set follower
- Translating follower

Roller-follower cams

- Translating follower
- Translating off-set follower
- Swinging follower

The design equations for these cams (the profile and cutter-coordinate equations) are in a form that accepts any profile curve—such as the cycloidal or harmonic curve—or any other desired input-output relationship. The cutter-coordinate equations are *not* a simple variation of the profile equations, because the normal line at the point of tangency of the cutter and the profile does not continually pass through the cam center. We had need for accurate cutter equations in the case of a swinging flat-face follower cam. The search for the solution led us to employ the theory of envelopes. A detailed problem of this case is included to illustrate the use of the design equations which, in our application, provided coordinates for cutting cams to a production tolerance of ± 0.0002 in. from point to point, and 0.002-in. total over-all deviation per cam cycle.

The question will come up whether computers are necessary in solving the design equations. Computers are desirable, and there are many outside services available. Calculations by hand or with a desk calculator will be time consuming. In many applications, however, the manual methods are worth while when judged by the accuracy obtainable. The designer will undoubtedly develop his own short cuts when applying the manual methods.

Application to visual grinding

The design equations offered here can also be put to good advantage in visual grinding. Magnification is limited by the definition of the work blank projected on the glass screen. On a particular visual grinder, the definition is good at a magnification of 30X, although provision is made for 50X. Using Mylar drawing film for the profile, which is to be fixed to the ground-glass screen, a 30X drawing or chart of portions of the cam profile can be made. Best results are obtained by locating the coordinate axis zero near the curve segment being drawn and by increasing the number of calculated points in critical regions to ½ or ¼-deg increments for greater accuracy. (Interpolation between points specified in 2-deg intervals by means of a French curve, for example, suffers in accuracy.) This procedure facilitates checking a cam with a fixture employing a roller, because the position of the roller follower can be specified simultaneously with the profile point coordinates.

The real limitation in visual grinding is the size of ground-glass field and the limited scope of blank profile which can be viewed at one time. If 30X is the magnification for good definition, and the screen is 18 in., the maximum cam profile which can be viewed at one time is $18/30 = 0.60$ in. If the layout is drawn 30 times size and a draftsman can measure ± 0.010 in., the error in drawing the chart is $0.010/30 = \pm 0.0003$ in. In addition, the coordination of chart with cam blank,

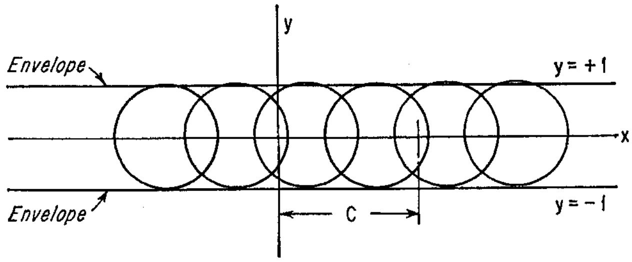

1A . . LINEARLY MOVING CIRCLES

The theory of envelopes is a topic in calculus not always taught in college courses. It is illustrated here by two examples, before we proceed to apply to it cam design.

The envelope can be defined this way: If each member of an infinite family of curves is tangent to a certain curve, and if at each point of this curve at least one member of the family is tangent, the curve is either a part or the whole of the envelope of the family.

Linearly moving circle

As the first example of envelope theory, consider the equation

$$(x - c)^2 + (y)^2 - 1 = 0 \tag{1}$$

This represents a circle of radius 1 located with its center at $x = c$, $y = 0$. As c is varied, a series of circles are determined—the family of circles governed by Eq 1 and illustrated in Fig 1A.

Eq 1 can be rewritten

$$f(x, y, c) = 0 \tag{2}$$

It is shown in calculus that the slope of any member of the family of Eq 2 is

$$\frac{dy}{dx} = -\frac{\left(\dfrac{\partial f}{\partial x}\right)}{\left(\dfrac{\partial f}{\partial y}\right)} \tag{3}$$

$$\frac{\partial f}{\partial x}\,dx + \frac{\partial f}{\partial y}\,dy = 0 \tag{4}$$

This may be written

$$\frac{\partial f}{\partial x}\frac{dx}{dc} + \frac{\partial f}{\partial y}\frac{dy}{dc} = 0 \tag{5}$$

This slope relation holds true for any member of the family. If another curve (the envelope) is tangent to the member of the family at a single point, its slope likewise satisfies Eq 5.

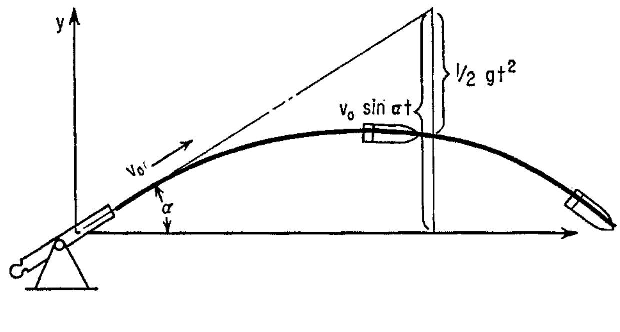

1B . . SHELL TRAJECTORY

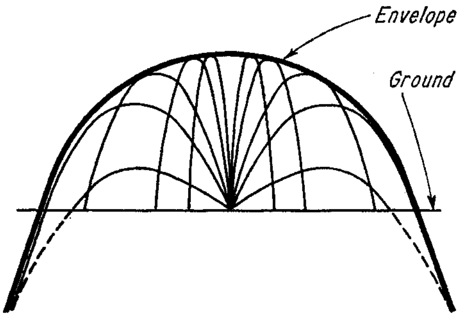

1C . . PARABOLIC ENVELOPE OF TRAJECTORIES

It is also shown in calculus that the total differential of Eq 2 is

$$df = \frac{\partial f}{\partial x}dx + \frac{\partial f}{\partial y}dy + \frac{\partial f}{\partial c}dc = 0 \tag{6}$$

or

$$\frac{\partial f}{\partial x}\frac{dx}{dc} + \frac{\partial f}{\partial y}\frac{dy}{dc} + \frac{\partial f}{\partial c} = 0$$

From Eq 5 and 6, the general equation for the envelope is

$$\frac{\partial f(x,y,c)}{\partial c} = 0 \tag{7}$$

The envelope may be determined by eliminating the parameter c in Eq 7 or by obtaining x and y as functions of c. (The point having the coordinates at x and y is a point on the envelope, and the entire envelope can be obtained by varying c.)

Returning to Eq 1 and applying Eq 7 gives

$$\frac{\partial f(x,y,c)}{\partial c} = 2(x-c)\left(\frac{-\partial c}{\partial c}\right) + \frac{\partial y^2}{\partial c} - 0 = 0$$
$$= 2(x-c)(-1) + 0 - 0 = 0$$

Therefore $x = c$. Substituting this into Eq 1 gives $y = \pm 1$. Thus the lines $y = +1$ and $y = -1$ are the envelopes of the family of Eq 3. This, of course, is evident by inspection of Fig 1.

Shell trajectories

As a second example of envelope theory, consider the envelope of all possible trajectories (the range envelope) of a gun emplacement. If the gun can be fired at any angle α in a vertical plane with a muzzle velocity v_o, Fig 1B, what is the envelope which gives the maximum range in any direction in the given vertical plane? Air resistance is neglected.

The equation of the trajectory is

$$y = x \tan \alpha - \frac{gx^2}{2v_o^2}(1 + \tan^2 \alpha) \tag{8}$$

where v_o = muzzle velocity
t = time
g = gravitational constant

Eq 8 is derived as follows:

$$y = v_o \sin \alpha t - \tfrac{1}{2}gt^2 \tag{9}$$

where

$$t = \frac{x}{v_x} = \frac{x}{v_o \cos \alpha} \tag{10}$$

Substituting this value of t into Eq 9 gives

$$y = \frac{v_o \sin \alpha x}{v_o \cos \alpha} - \tfrac{1}{2}g\left(\frac{x}{v_o \cos \alpha}\right)^2 \tag{11}$$

which can be readily put in the form of Eq 8.

Rewriting Eq 8 so that all factors are on one side of the equation:

$$f(x,y,\alpha) = x \tan \alpha - \frac{gx^2}{2v_o^2}(1 + \tan^2 \alpha) - y = 0 \tag{12}$$

Thus

$$\frac{\partial f(x,y,\alpha)}{\partial \alpha} = x \sec^2 \alpha\left(1 - \frac{gx \tan \alpha}{v_o^2}\right) = 0 \tag{13}$$

Solving Eq 13 for $\tan \alpha$ gives

$$\tan \alpha = \frac{v_o^2}{gx}$$

Eliminating the parameter α by substituting this value of $\tan \alpha$ into Eq 8 yields the envelope of the useful range of the gun,

$$y = \frac{v_o^2}{2g} - \frac{gx^2}{2v_o^2} \tag{14}$$

which is a parabola, pictured in Fig 1C.

SYMBOLS

b = y-intercept of straight line
c = linear-distance parameter
e = offset of flat-face or roller follower
f = function notation
g = gravitational constant
$H = r_b + r_f + L$
$J = [(r_b + r_f)^2 - e^2]^{1/2}$
L = lift of follower
$M = \phi - \theta + \Psi$
m = general slope of straight line
$N = \theta - \phi - \Psi$
r_a = distance between pivot point of swinging follower and cam center
r_b = radius of base circle of cam
r_c = radius of cutter
R_c = radius vector from cam center to cutter center. Employed in conjunction with ω
r_f = radius of roller follower
r_r = length of roller-follower arm
t = time
v_o = initial (muzzle) velocity
x, y = rectangular coordinates of cam profile, or of circle or parabola in examples on envelope theory
x_c, y_c = cutter coordinates to produce cam profile
$\frac{d}{dx}$ = total derivative with respect to x
$\frac{\partial}{\partial x}$ = partial derivative with respect to x
α = angle of muzzle inclination in trajectory problem; also angle between x-axis and tangent to cutter contact point
β = maximum lift angle for a particular curve segment = θ_{max}
ω = angular displacement of cutter center, referenced to zero at start of cam profile rise. Employed in conjunction with R_c.
ϵ = angular displacement of cutter, referenced to x-axis, with the cam considered stationary (for specifying polar cutter coordinates); $\epsilon = \tan^{-1}(y_c/x_c)$; also $\epsilon = \omega$ when rise begins at x-axis as in Fig. 7.
θ = cam angle of rotation
ϕ = angular rotation or lift of the follower, usually specified in terms of θ
Ψ = angle between initial position of face of swinging follower, and line joining center of cam and pivot point of follower (a constant)
λ = maximum displacement angle of follower arm

the condition of the machine, and the operator's degree of skill all add some error. In a particular segment, the operator can grind ±0.0003 in., but when the chart and work piece are moved to the next profile segment they must be properly coordinated to take advantage of the grinder's skill and to prevent discontinuities that can affect seriously the dynamic characteristics of the cam.

FLAT-FACE FOLLOWERS

The theory of envelopes is now applied to finding the design equations for cams with flat-face followers. In general:

1) Choose a convenient coordinate system—both rectangular and polar coordinates are given here.
2. Write the general equation of the envelope, involving one variable parameter.
3) Differentiate this equation with respect to the variable parameter and equate it to zero. The total derivative of the variable usually suffices (in place of the partial derivative).
4) Solve simultaneously the equations of steps 2 and 3 either to eliminate the parameter or to obtain the coordinates of the envelope as functions of the parameter.
5) Vary the parameter throughout the range of interest to generate the entire cam profile.

Flat-face in-line swinging follower

Flat-face swinging-follower cams are of the in-line type, Fig 2, if the face, when extended, passes through the pivot point. The initial position of the follower before lift starts is designated by angle ψ. This angle is a constant and can be computed from the equation

$$\Psi = \sin^{-1} \frac{r_b}{r_a}$$

where

r_a = distance between cam center and pivot point measured along x-axis

r_b = radius of base circle of cam

The angular rotation or "lift" of the follower, ϕ, is the output motion. It is usually specified as a function of the cam angle of rotation, θ. Thus θ is the independent variable and ϕ the dependent variable.

A well-known analytical technique is to assume the cam is stationary and the follower moving around it. Varying θ and ϕ and maintaining ψ constant produces a family of straight lines that can be represented as a function of x, y, θ, ϕ. Since ϕ is in turn a function of θ, essentially there is

$$f(x,y,\theta) = 0 \qquad (15)$$

This is the form of Eq 2. Thus to obtain the envelope of this family, which is the required cam profile, one solves simultaneously Eq 15, and

$$\frac{\partial f(x,y,\theta)}{\partial \theta} = \frac{df}{d\theta} = 0 \qquad (16)$$

The first step is to write the general form of the equation of the family. We begin with

$$y = mx + b \qquad (17)$$

Where b is the y-intercept and m the slope. In this case, m is equal to

$$m = -\tan(\phi - \theta + \Psi) \qquad (18)$$

Hence

$$y = -\tan(\phi - \theta + \Psi)x + b \qquad (19)$$

Also

$$x = r_a \cos\theta$$
$$y = r_a \sin\theta$$

Solving for b results in

$$b = r_a[\sin\theta + \cos\theta \tan(\phi - \theta + \Psi)] \qquad (20)$$

Therefore

$$f(x,y,\theta) = y + \tan(\phi - \theta + \Psi)(x - r_a\cos\theta) - r_a\sin\theta = 0 \qquad (21)$$

This equation is in the form of Eq 15. It is now differentiated with respect to θ:

$$\frac{df}{d\theta} = \tan(\phi - \theta + \Psi)r_a\sin\theta + (x - r_a\cos\theta)[\sec^2(\phi - \theta + \Psi)]\left(\frac{d\phi}{d\theta} - 1\right) - r_a\cos\theta = 0 \qquad (22)$$

For simplification in notation, let

$$M = \phi - \theta + \Psi$$

The rectangular coordinates of a point on the cam profile corresponding to a specific angle of cam rotation, θ, are then obtained by solving Eq 21 and 22 simultaneously. The coordinates are

$$x = r_a\left[\cos\theta + \frac{\cos(\theta + M)\cos M}{\frac{d\phi}{d\theta} - 1}\right] \qquad (23)$$

$$y = r_a\left[\sin\theta + \frac{\cos(\theta + M)\cos M}{\frac{d\phi}{d\theta} - 1}\right] \qquad (24)$$

As mentioned previously the desired lift equation, ϕ, is usually known in terms of θ. For example, in a computer a cam must produce an input-output relationship of $\phi = 2\theta^2$. In other words, when θ rotates 1 deg, ϕ rotates 2 deg; when θ rotates 2 deg, ϕ rotates 8 deg, etc. Then

$$\phi = 2\theta^2$$

and

$$\frac{d\phi}{d\theta} = 4\theta$$

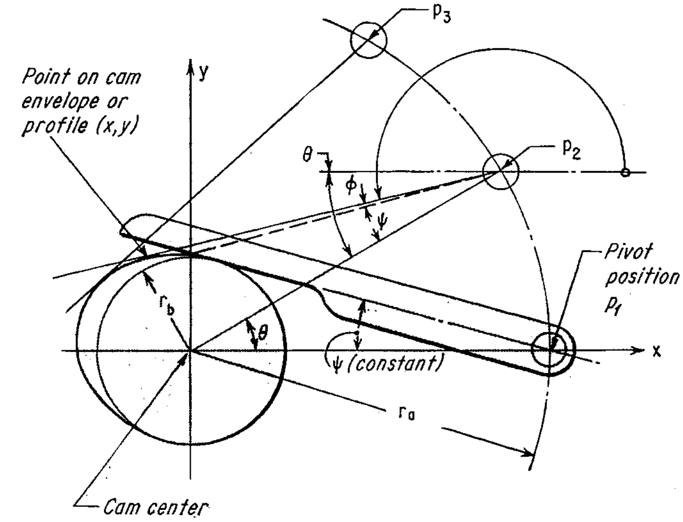

2 . . Flat-face swinging-follower cam with line of follower face extending through pivot point.

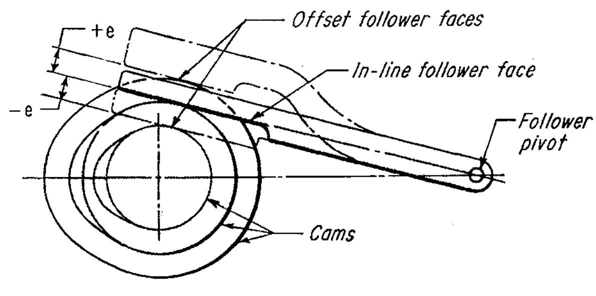

3 . . Two types of offset flat-face follower.

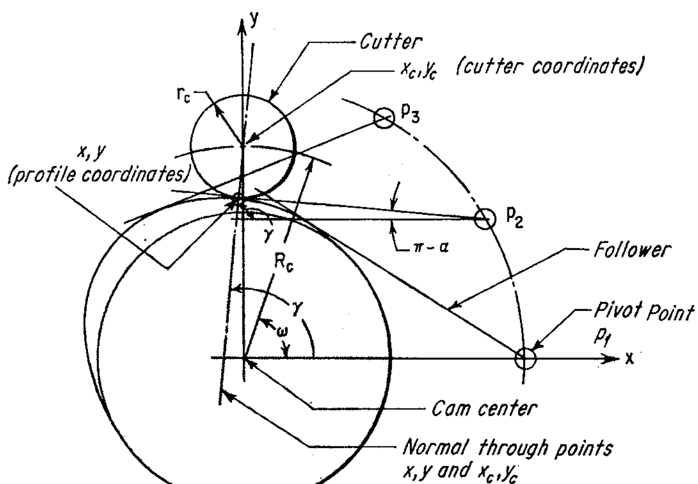

4 . . Cutter coordinates for flat-face swinging follower.

Substituting the value of ϕ into the equation for m, and the value of $d\phi/d\theta$ into Eq 23 and 24 gives x and y in terms of θ.

Where the lift equation must also meet certain velocity and acceleration requirements (as is the more common case), portions of analytical curves in terms of ϕ, such as the cycloidal or harmonic curves, must be used and matched with each other. A detailed cam design problem of an actual application is given later to illustrate this technique.

Offset swinging follower

The profile coordinates for a swinging flat-faced follower cam in which the follower face is not in line with the follower pivot, Fig 3, are

$$x = r_a\left[\cos\theta + \frac{\cos(\theta+M)}{\frac{d\phi}{d\theta}-1}\cos M\right] + e\sin M \quad (25)$$

$$y = r_a\left[\sin\theta + \frac{\cos(\theta+M)}{\frac{d\phi}{d\theta}-1}\sin M\right] + e\cos M \quad (26)$$

where e = the offset distance between a line through the cam pivot and the follower face. Distance e is considered positive or negative, depending on the configuration. In other words, the effect of e in Eq 25 and 26 is to increase or decrease the size of the in-line follower cam. When $e = 0$, Eq 25 and 26 simplify to Eq 23 and 24.

Cutter coordinates

For cam manufacture, the location of the milling cutter or grinding wheel must be specified in rectangular or polar coordinates—usually the latter.

The rectangular cutter coordinates for the in-line swinging follower, Fig 4, are

$$x_c = x + r_c\sin M \quad (27)$$

$$y_c = y + r_c\cos M \quad (28)$$

where

x, y = profile coordinates (Eq 23 and 24)

r_c = radius of cutter

The polar coordinates are

$$R_c = (x_c^2 + y_c^2)^{1/2} \quad (29)$$

$$\omega = 90° - (\Psi + \epsilon) \quad (30)$$

$$\epsilon = \tan^{-1}\frac{y_c}{x_c} \quad (31)$$

where

ϵ = angular displacement of the cutter with respect to the x axis, and with the cam stationary.

ω = angular displacement of the cutter center referenced to zero at the start of the cam profile rise, for cam specification purposes and convenience in machining.

The angles, ω, and the corresponding distances, R_c, are subject to adjustment to bring these values to even angles for convenience of machining. This will be illustrated later in the cam design example.

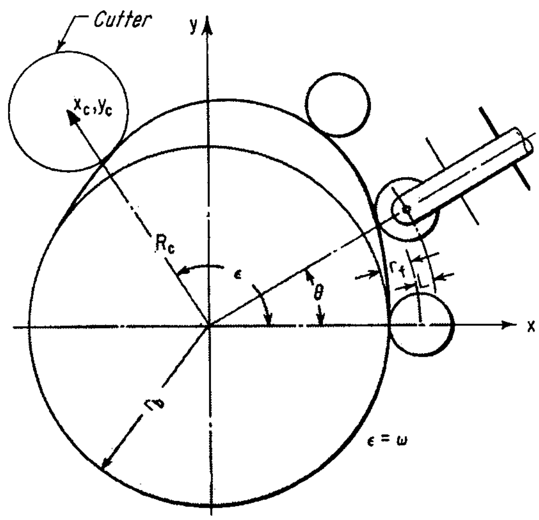

5 . . **Radial cam** with flat-face follower.

For offset swinging follower, the rectangular coordinates of the cutter are

$$x_c = x + r_c\sin M \quad (32)$$

$$y_c = y + r_c\cos M \quad (33)$$

and the polar cutter coordinates are

$$R_c = (x_c^2 + y_c^2)^{1/2} \quad (34)$$

$$\epsilon = \tan^{-1}\frac{y_c}{x_c} \quad (35)$$

Flat-face translating follower

The follower of this type of flat-face cam moves radially, Fig 5. The general equation of the family of lines forming the envelope is

$$y = mx + b$$

where

$m = \cos\theta$

L = lift of follower

$x = (r_b + L)\cos\theta$

$y = (r_b + L)\sin\theta$

$b = (r_b + L)/\sin\theta$

Hence

$$y = \frac{r_b + L - x\cos\theta}{\sin\theta} \quad (36)$$

Therefore

$$f(x,y,\theta) = y\sin\theta + x\cos\theta - (r_b + L) = 0 \quad (37)$$

and

$$\frac{df}{d\theta} = y\cos\theta - x\sin\theta - \frac{dL}{d\theta} = 0 \quad (38)$$

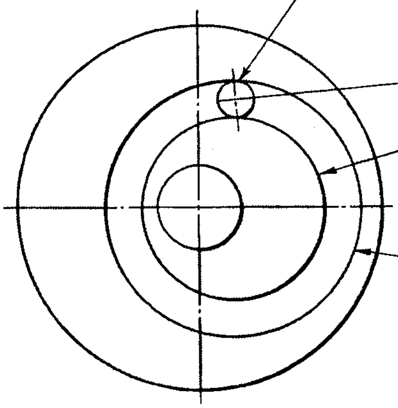

6 . . **Positive-action cam** with double envelope.

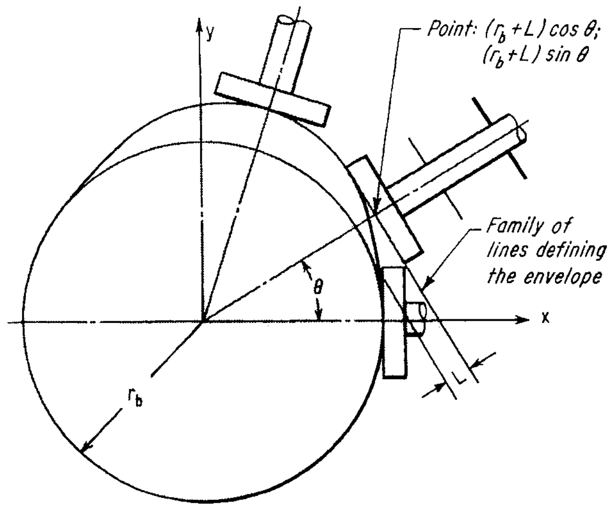

7 . . **Radial cam** with roller follower.

The profile coordinates are (by solving simultaneously Eq 37 and 38):

$$x = (r_b + L)\cos\theta - \frac{dL}{d\theta}\sin\theta \qquad (39)$$

$$y = (r_b + L)\sin\theta + \frac{dL}{d\theta}\cos\theta \qquad (40)$$

where L is usually given in terms of the cam angle θ (similar to ϕ for the swinging follower).

The rectangular coordinates are

$$x_c = x + r_c\cos\theta \qquad (41)$$

$$y_c = y + r_c\sin\theta \qquad (42)$$

Polar coordinates of profile points are obtained by squaring and adding Eq 39 and 40:

$$R^2 = x^2 + y^2$$

$$R = \left[(r_b + L)^2 + \left(\frac{dL}{d\theta}\right)^2\right]^{1/2} \qquad (43)$$

Cutter coordinates in polar form are obtained by squaring and adding Eq 41 and 42.

$$R_c = \left[(r_b + L + r_c)^2 + \left(\frac{dL}{d\theta}\right)^2\right]^{1/2} \qquad (44)$$

$$\omega = \tan^{-1}\frac{y_c}{x_c}$$

$$= \tan^{-1}\left[\frac{(r_b + L + r_c)\sin\theta + \dfrac{dL}{d\theta}\cos\theta}{(r_b + L + r_c)\cos\theta - \dfrac{dL}{d\theta}\sin\theta}\right]$$

ROLLER FOLLOWERS

In determining the profile of a roller-follower cam by envelope theory, two envelopes are mathematically possible—one the inner, profile envelope and the other an outer envelope. If a positive-action cam is to be constructed, Fig 6, both envelopes are applicable, since they constitute the slot in which the roller follower would be constrained to move to give the desired output motion.

The equations for three types of roller-follower cams are derived below.

Translating roller follower

The radial distance, H, to the center of the follower for this type of cam, Fig 7, is equal to:

$$H = r_b + r_f + L$$

where

r_f = radius of the follower roller

r_b = base circle radius

L = lift = $L(\theta)$

The general equation of the envelope is

$$(x - H\cos\theta)^2 + (y - H\sin\theta)^2 - r_f^2 = 0 \qquad (45)$$

The profile coordinates are (by applying $d/d\theta = 0$ and solving for y and x):

$$y = \frac{x\left[H\sin\theta - \dfrac{dL}{d\theta}\cos\theta\right] + H\dfrac{dL}{d\theta}}{H\cos\theta + \dfrac{dL}{d\theta}\sin\theta} \qquad (46)$$

and

$$x = H\cos\theta \pm \frac{r_f}{\left[1 + \left(\dfrac{H\sin\theta - \dfrac{dL}{d\theta}\cos\theta}{H\cos\theta + \dfrac{dL}{d\theta}\sin\theta}\right)^2\right]^{1/2}} \qquad (47)$$

where

$$\frac{dL}{d\theta} = \frac{dH}{d\theta}$$

Here the plus-minus ambiguity may be resolved by examining $\theta = 0$ when $x = r_b$. At this point

$$H = r_b + r_f$$

$$\frac{dH}{d\theta} = \frac{dL}{d\theta} = 0$$

and

$$x = r_f + r_b \pm r_f$$

Only the negative sign is meaningful in the above equation; thus the negative sign in Eq 47 establishes the inner envelope, and the plus sign the outer envelope, which in this case is discarded.

The final equation for y can be computed by substituting Eq 47 into 46.

Rectangular coordinates of the cutter are

$$x_c = x + \frac{r_c}{r_f}(H\cos\theta - x) \qquad (48)$$

$$y_c = y + \frac{r_c}{r_f}(H\sin\theta - y) \qquad (49)$$

Polar coordinates of the cutter are

$$R_c = (x_c^2 + y_c^2)^{1/2} \qquad (50)$$

$$\epsilon = \tan^{-1}\frac{y_c}{x_c} \qquad (51)$$

Swinging roller follower

This type of cam is illustrated in Fig 8. Angle ψ is equal to

$$\Psi = \cos^{-1}\frac{r_r^2 + r_a^2 - (r_b + r_f)^2}{2r_a r_r} \qquad (52)$$

The general equation of the family is

$$[x - r_a\cos\theta + r_r\cos N]^2 + [y - r_a\sin\theta + r_r\sin N]^2 - r_f^2 = 0 \qquad (53)$$

where

$$N = \theta - \phi - \Psi$$

The profile coordinates are (by the method outlined for the translating roller follower):

$$y = \frac{x\left[r_a\sin\theta - r_r\left(1 - \dfrac{d\phi}{d\theta}\right)\sin N\right]}{r_a\cos\theta - r_r\left(1 - \dfrac{d\phi}{d\theta}\right)\cos N} \qquad (54)$$

and

$$x = r_a\cos\theta - r_r\cos N \pm \frac{r_f}{\left[1 + \left(\dfrac{r_a\sin\theta - r_r\left(1 - \dfrac{d\phi}{d\theta}\right)\sin N}{r_a\cos\theta - r_r\left(1 - \dfrac{d\phi}{d\theta}\right)\cos N}\right)^2\right]^{1/2}} \qquad (55)$$

Referring to the $\pm$ sign, the negative sign gives the actual cam profile; the positive sign produces an outer envelope. The equation for y can be computed by substituting Eq 55 into 54.

The rectangular cutter coordinates are:

$$x_c = x + \frac{r_c}{r_f}(x_f - x) \qquad (56)$$

$$y_c = y + \frac{r_c}{r_f}(y_f - y) \qquad (57)$$

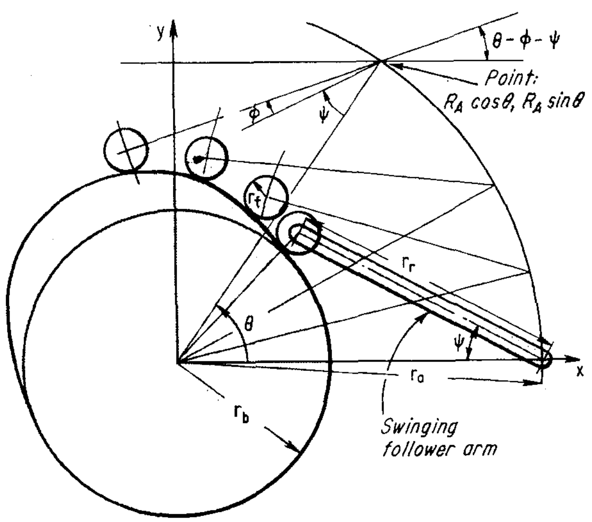

8 . . Swinging roller-follower cam.

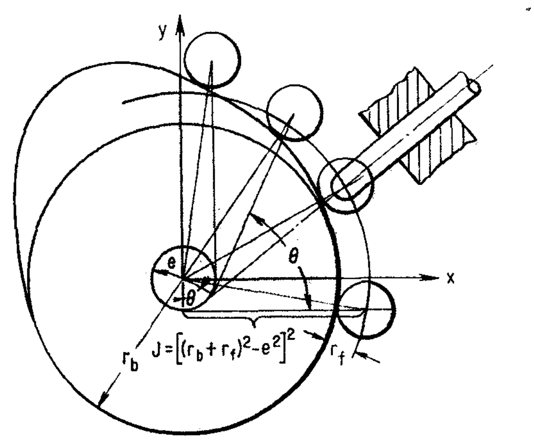

9 . . Offset radial-roller cam.

where x_f and y_f, the coordinates to the center of cutter, are equal to

$$x_f = r_a \cos\theta - r_r \cos N$$
$$y_f = r_a \sin\theta - r_r \sin N$$

The polar cutter coordinates are

$$R_c = (x_c^2 + y_c^2)^{1/2} \qquad (58)$$

$$\epsilon = \tan^{-1}\frac{y_c}{x_c} \qquad (59)$$

Translating offset roller follower

The roller follower of this type of cam, Fig 9, moves radially along a line that is offset from the cam center by a distance *e*.

The general equation of the envelope is

$$[x - e\sin\theta - (J + L)\cos\theta]^2 + [y + e\cos\theta - (J + L)\sin\theta]^2 - r_f^2 = 0 \qquad (60)$$

where

$$J = [(r_b + r_f)^2 - e^2]^{1/2}$$

The profile coordinates are (by applying $d/d\theta = 0$, and solving for y and x):

$$y = \frac{x\left[(J+L)\sin\theta - \left(e + \frac{dL}{d\theta}\right)\cos\theta\right] + (J+L)\frac{dL}{d\theta}}{(J+L)\cos\theta + \left(e + \frac{dL}{d\theta}\right)\sin\theta} \qquad (61)$$

$$x = e\sin\theta + (J+L)\cos\theta \pm \frac{r_f}{\left[1 + \left(\dfrac{(J+L)\sin\theta - \left(e + \frac{dL}{d\theta}\right)\cos\theta}{(J+L)\cos\theta + \left(e + \frac{dL}{d\theta}\right)\sin\theta}\right)^2\right]^{1/2}} \qquad (62)$$

Here again the negative sign of the plus-minus ambiguity is physically correct. The plus sign produces the outer envelope.

Final equation for y can be obtained by substituting Eq 62 into 61.

The rectangular cutter coordinates are

$$x_c = x + \frac{r_c}{r_f}(x_f - x) \qquad (63)$$

$$y_c = y + \frac{r_c}{r_f}(y_f - y) \qquad (64)$$

where

$$x_f = e\sin\theta + (J + L)\cos\theta$$
$$y_f = -e\cos\theta + (J + L)\sin\theta$$

The polar cutter coordinates are the same as Eqs 58 and 59.

NUMERICAL EXAMPLE

The design specification

We have recently applied the cam equations to the design of a flat-faced swinging follower with face in line with the follower pivot. The follower oscillates through an output angle, λ, with a dwell-rise-fall-dwell motion.

The angular displacement of the follower arm is specified by portions of curves which can be expressed as mathematical functions of the angle of rotation of the cam. The specified angular motion of the arm consists of a half-cycloidal rise from the dwell, followed by half-harmonic rise and fall, and then by a half-cycloidal return to the dwell, as shown in Fig 10. Each region is 31.5 deg; the total cycle is completed in 126 deg.

Also included are the general shape of the follower velocity and acceleration curves, which result from: 1) the choice of curves, 2) the stipulation that the cam angle of rotation, β, for each curve segment be equal, and 3) the stipulation that the angular velocity at the matching points of the curves be the same for both curves. The cam is to rotate in the counterclockwise direction. It is to be specified by polar coordinates, R_c, ω, in 1-deg increments.

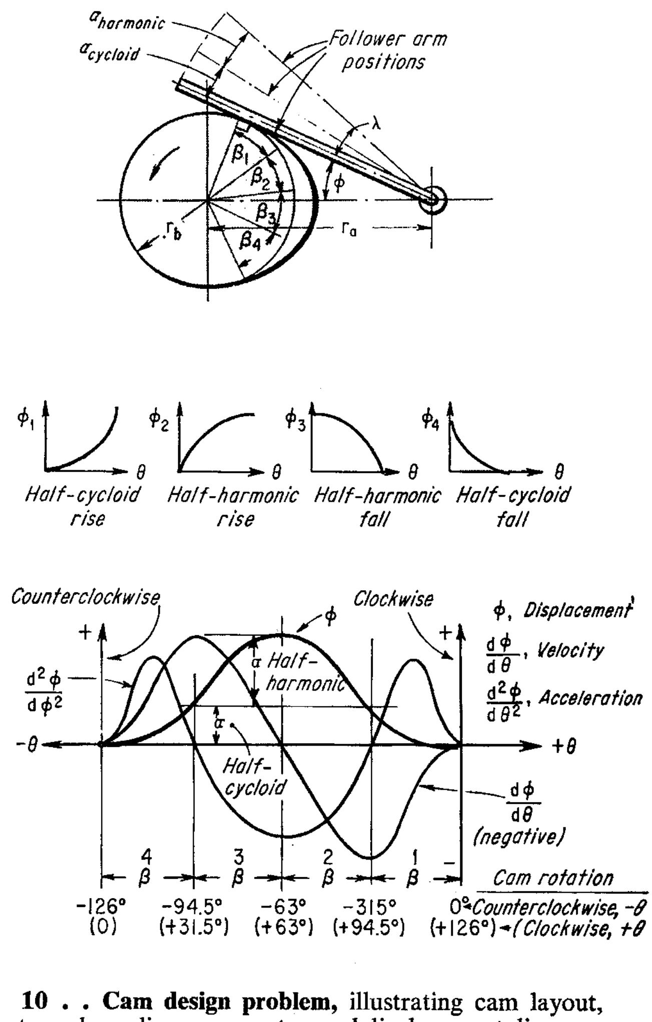

10 . . Cam design problem, illustrating cam layout, top, phase diagrams, center, and displacement diagram.

The equations of angular displacement for the four regions, or curve segments are

Rising—region 1 (half-cycloid)

$$\phi_1 = \alpha_C\left[\frac{\theta_1}{\beta_1} - \frac{1}{\pi}\sin\left(180° \times \frac{\theta_1}{\beta_1}\right)\right]$$

Rising—region 2 (half-harmonic)

$$\phi_2 = \alpha_C + \alpha_H \sin\left(90° \times \frac{\theta_2}{\beta_2}\right)$$

Falling—region 3 (half-harmonic)

$$\phi_3 = \alpha_C + \alpha_H \cos\left(90° \times \frac{\theta_3}{\beta_3}\right)$$

Falling—region 4 (half-cycloid)

$$\phi_4 = \alpha_C\left[1 - \frac{\theta_4}{\beta_4} - \frac{1}{\pi}\sin\left(180° \times \frac{\theta_4}{\beta_4}\right)\right]$$

where

λ = maximum displacement angle of follower arm = 2.820,997,8 deg

α_C = half-cycloidal angle of displacement of follower = 1.240,958,6 deg

α_H = half-harmonic angle of displacement of follower = 1.580,039,2 deg

β = θ maximum = maximum lift angle for a particular curve segment = −31.5 deg

θ = cam angle, degree of counterclockwise rotation, or in a negative direction

$\phi = f(\theta)$ = instantaneous angle of displacement of the follower

Subscripts:

1 = half-cycloidal, rising

2 = half-harmonic, rising

3 = half-harmonic, falling

4 = half-cycloidal, falling

Also given are:

r_a = 3.25 in.

r_b = 1.1758 in.

Ψ = 21.209,369,3 deg

For illustrative purposes, however, the computations are rounded to four decimal places.

Solution

Eq 23 and 24 will give the x and y coordinates of the profile. The derivative, $d\phi/d\theta$, is also the angular velocity of the follower.

The computations for locating the profile when θ = −40 deg are presented below. All angles are in degrees:

$$\phi_{-40°} = \alpha_C + \alpha_H\left(\sin 90° \times \frac{\theta_2}{\beta_2}\right)$$

$$= 1.2406 + 1.5800\left[\sin 90\left(\frac{-(40 - 31.5)}{-31.5}\right)\right]$$

$$= 1.8908 \text{ deg}$$

$$\frac{d\phi}{d\theta} = \frac{\pi}{2}\frac{\alpha_H}{\beta_2}\left(\cos 90\frac{\theta_2}{\beta_2}\right)$$

$$= -0.0718$$

$$M = \phi - \theta + \Psi = 1.8909 - (-40) + 21.2094$$

$$= 63.1002 \text{ deg}$$

From Eq 23:

$$x_{-40°} = 3.25\left[\cos(-40) + \frac{\cos(63.1002-40)\cos(63.1002)}{(-0.718-1)}\right]$$

$$= 1.2278 \text{ in.}$$

Similarly, from Eq 24:

$$y = 0.3983 \text{ in.}$$

The cutter coordinates are obtained by means of Eq 27 through 31, and

$$x_c = x + r_c \sin M$$

$$= 1.2278 + 1.5 \sin 63.1002 = 2.5655 \text{ in.}$$

$$y_c = y + r_c \cos M$$

$$= 1.0769 \text{ in.}$$

$$R_c = (x_c^2 + y_c^2)^{1/2} = [2.5655^2 + 1.0769^2]^{1/2}$$

$$= 2.7823 \text{ in.}$$

$$\epsilon = \tan^{-1}\frac{1.0796}{2.5655} = 22.7713 \text{ deg}$$

$$\omega = 90 - (\Psi + \epsilon)$$

$$= 90 - (21.2094 + 22.7713) = 46.0193 \text{ deg}$$

Cams and Gears Team Up in Programmed Motion

Pawls and ratchets are eliminated in this design, which is adaptable to the smallest or largest requirements; it provides a multitude of outputs to choose from at low cost.

Theodore Simpson

A new and extremely versatile mechanism provides a programmed rotary output motion simply and inexpensively. It has been sought widely for filling, weighing, cutting, and drilling in automatic and vending machines.

The mechanism, which uses overlapping gears and cams (drawing below), is the brainchild of mechanical designer Theodore Simpson of Nashua, N. H.

Based on a patented concept that could be transformed into a number of configurations, PRIM (Programmed Rotary Intermittent Motion), as the mechanism is called, satisfies the need for smaller devices for instrumentation without using spring pawls or ratchets.

It can be made small enough for a wristwatch or as large as required.

Versatile output. Simpson reports the following major advantages:

- Input and output motions are on a concentric axis.
- Any number of output motions of varied degrees of motion or dwell time per input revolution can be provided.
- Output motions and dwells are variable during several consecutive input revolutions.
- Multiple units can be assembled on a single shaft to provide an almost limitless series of output motions and dwells.
- The output can dwell, then snap around.

How it works. The basic model

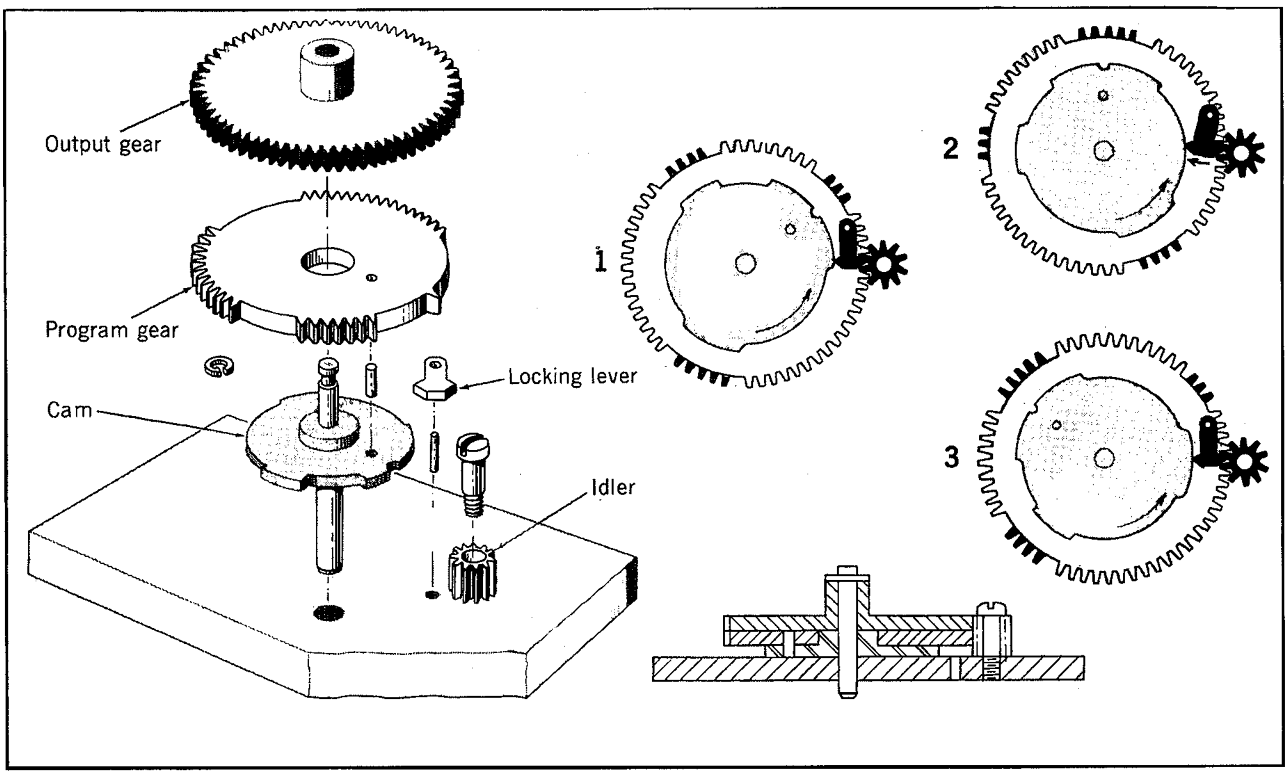

Basic intermittent-motion mechanism, at left in drawings, goes through the rotation sequence as numbered above.

(drawing, below left) repeats the output pattern, which can be made complex, during every revolution of the input.

Cutouts around the periphery of the cam give the number of motions, degrees of motion, and dwell times desired. Tooth sectors in the program gear match the cam cutouts.

Simpson designed the locking lever so one edge follows the cam and the other edge engages or disengages, locking or unlocking the idler gear and output. Both program gear and cam are lined up, tooth segments to cam cutouts, and fixed to the input shaft. The output gear rotates freely on the same shaft, and an idler gear meshes with both output gear and segments of the program gear.

As the input shaft rotates, the teeth of the program gear engage the idler. Simultaneously, the cam releases the locking lever and allows the idler to rotate freely, thus driving the output gear.

Reaching a dwell portion, the teeth of the program gear disengage from the idler, the cam kicks in the lever to lock the idler, and the output gear stops until the next program-gear segment engages the idler.

Dwell time is determined by the space between the gear segments. The number of output revolutions does not have to be the same as the number of input revolutions. An idler of a different size would not affect the output, but a cluster idler with a matching output gear can increase or decrease the degrees of motion to meet design needs.

For example, a step-down cluster with output gear to match could reduce motions to fractions of a degree, or a step-up cluster with matching output gear could increase motions to several complete output revolutions.

Snap action. A second cam and a spring are used in the snap-action version (drawing below). Here, the cams have identical cutouts.

One cam is fixed to the input and the other is lined up with and fixed to the program gear. Each cam has a pin in the proper position to retain a spring; the pin of the input cam extends through a slot in the program gear cam that serves the function of a stop pin.

Both cams rotate with the input shaft until a tooth of the program gear engages the idler, which is locked and stops the gear. At this point, the program cam is in position to release the lock, but misalignment of the peripheral cutouts prevents it from doing so.

As the input cam continues to rotate, it increases the torque on the spring until both cam cutouts line up. This positioning unlocks the idler and output, and the built-up spring torque is suddenly released. It spins the program gear with a snap as far as the stop pin allows; this action spins the output.

Although both cams are required to release the locking lever and output, the program cam alone will relock the output—a feature of convenience and efficient use.

After snap action is complete and the output is relocked, the program gear and cam continue to rotate with the input cam and shaft until they are stopped again when a succeeding tooth of the segmented program gear engages the idler and starts the cycle over again.

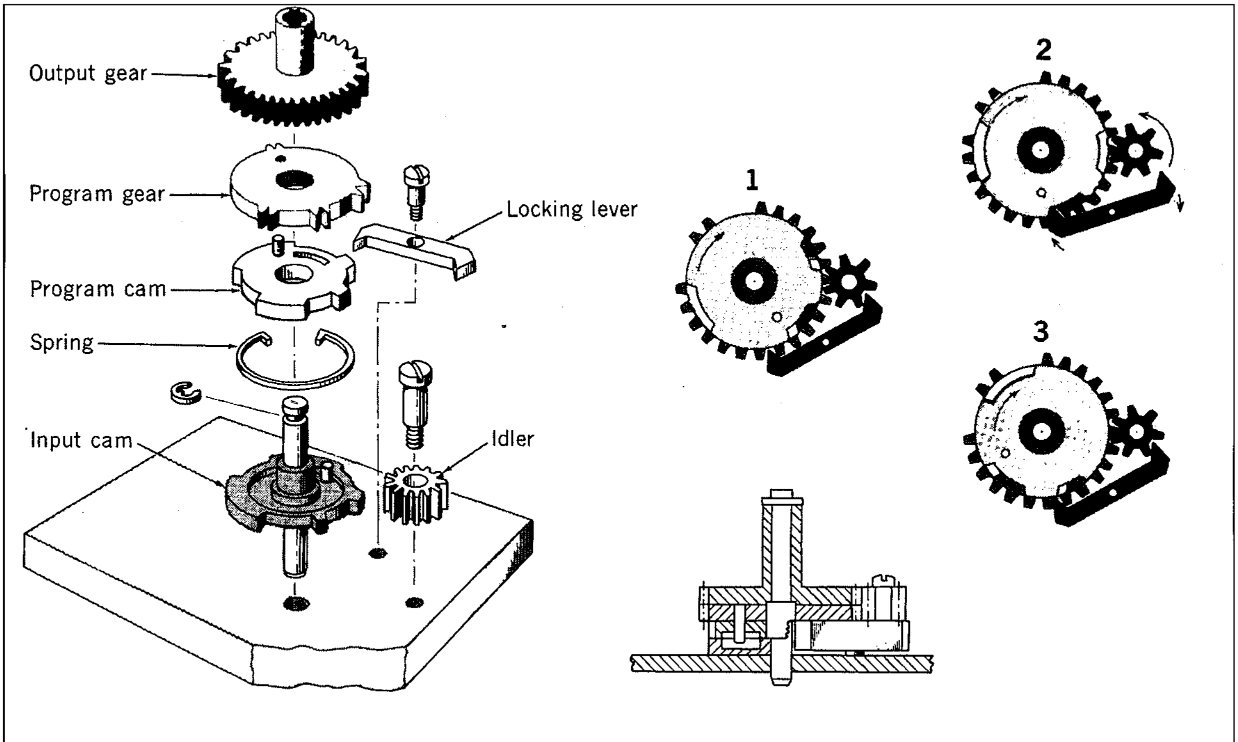

Snap-action version, with a spring and with a second cam fixed to the program gear, works as shown in numbered sequence.

Minimum Cam Size

Whether for high-accuracy computers or commercial screw machines–here's your starting point for any can design problem.

Preben W. Jensen

THE best way to design a cam is first to select a maximum pressure angle—usually 30 deg for translating followers and 45 deg for swinging followers—then lay out the cam profile to meet the other design requirements. This approach will ensure a minimum cam size.

But there are at least six types of profile curves in wide use today—constant-velocity, parabolic, simple harmonic, cycloidal, 3-4-5 polynomial, and modified trapezoidal—and to design the cam to stay within a given pressure angle for any given curve is a time-consuming process. Add to this the fact that the type of follower employed also influences the design, and you come up with a rather difficult design problem.

You can avoid all tedious work by turning to the unique design charts presented here (Fig 5 to 10). These charts are based on a construction method (Fig 1 to 4) developed in Germany by Karl Flocke back in 1931 and published by the German VDI as Research Report 345. Flocke's method is practically unknown in this country—it does not appear in any published work. It is repeated here because it is a general method applicable to any type of cam curve or combination of curves. With it you can quickly determine the minimum cam size and the amount of offset that a follower needs—but results may not be accurate in that the points of max pressure angle must be estimated.

The design charts, on the other hand, are applicable only to the six types of curves listed above. But they are much quicker to use and provide more accurate results.

Also included in this article are

Symbols

e = offset (eccentricity) of cam-follower centerline with camshaft centerline, in.

R_b = base radius of cam, in.

R_f = roller radius, in.

R_{min} = minimum radius to pitch curve, in.; $R_{min} = R_b + R_f$

R_{max} = maximum radius to pitch curve, in.

y = linear displacement of follower, in.

y_{max} = prescribed maximum cam stroke, in.

L_f = length of swinging follower arm, in.

α = pressure angle, deg—the angle between the cam-follower centerline and the normal to the cam surface at the point of roller contact

β = cam angle rotation, deg

ϕ_o = angle of oscillation of swinging follower, deg

τ = slope of cam diagram, deg

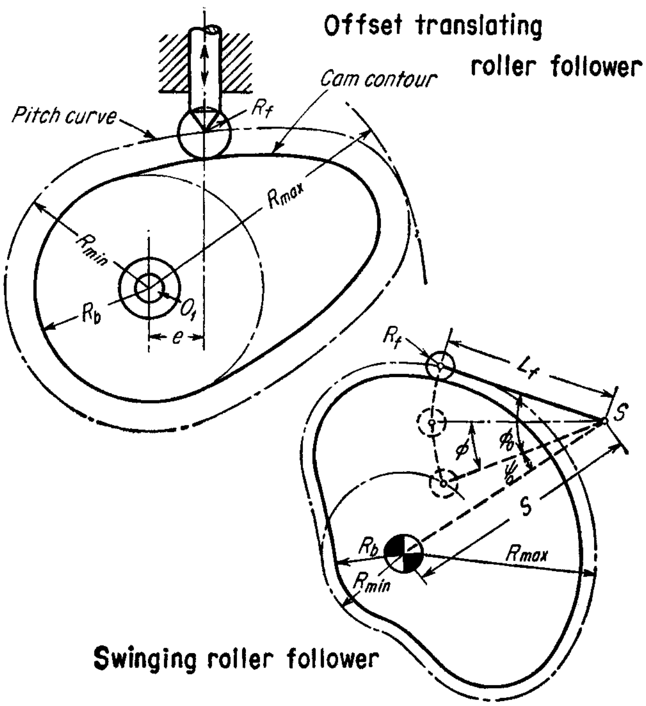

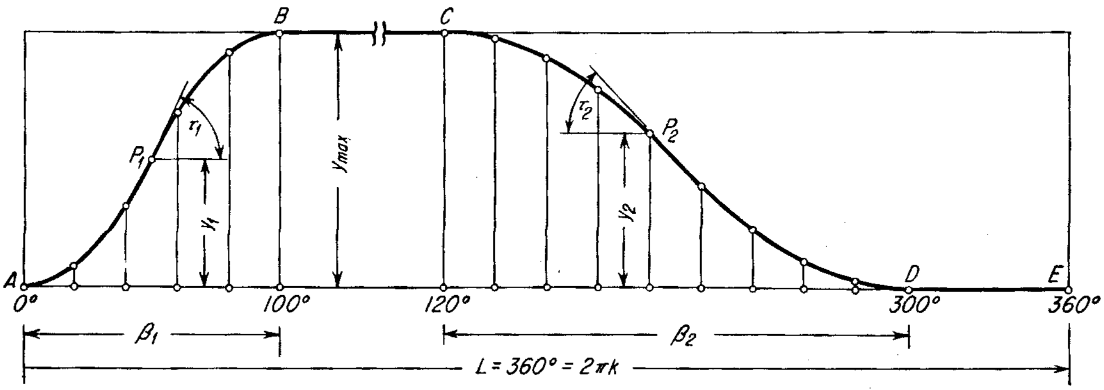

1. Cam diagram

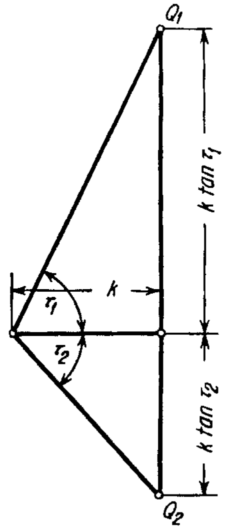

2. Slope analysis

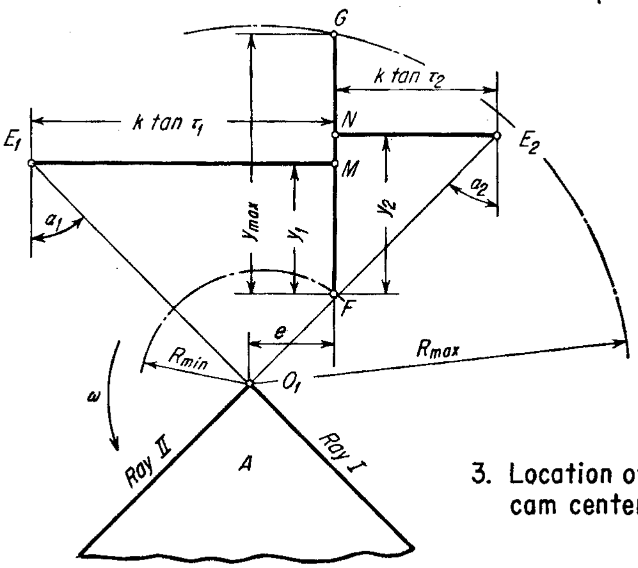

3. Location of cam center

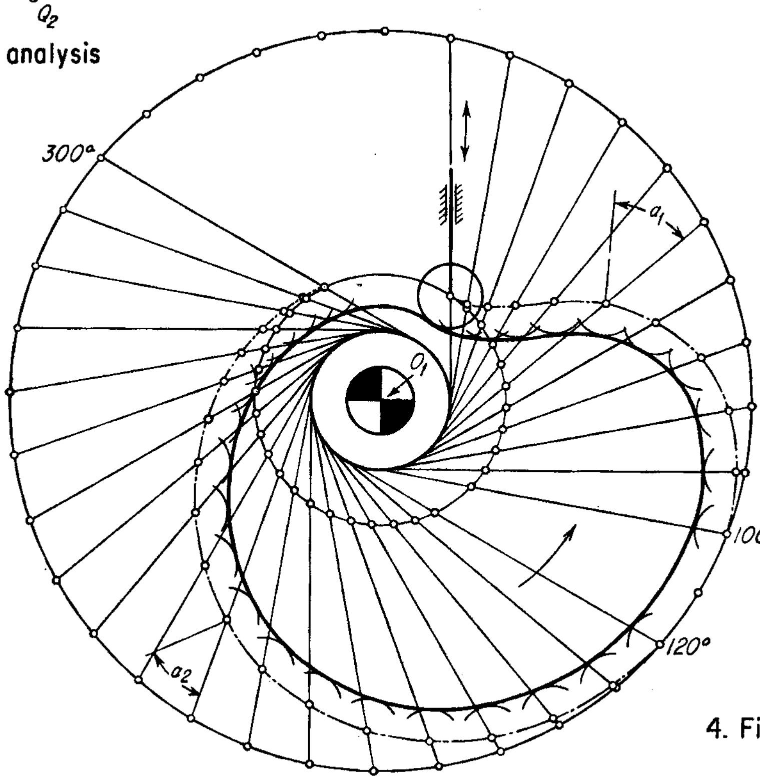

4. Final cam shape

eight mechanisms for reducing the pressure angle when the maximum permissible pressure angle must be exceeded for one reason or another.

Why the emphasis on pressure angle?

Pressure angle is simply the angle between the direction where the follower wants to go and the direction where the cam wants to push it. Pressure angles should be kept small to reduce side thrusts on the follower. But small pressure angles increase cam size which in turn:

- Increases the size of the machine.
- Increases the number of precision points and cam material in manufacturing.
- Increases the circumferential speed of the cam which leads to unnecessary vibrations in the machine.
- Increases the cam inertia which slows up starting and stopping times.

Translating followers

Flocke's method for finding the minimum cam size—in other words e, R_{min} and R_{max} (see list of symbols) —is as follows:

In Fig 1

1. Lay out the cam diagram (time-displacement diagram) as the problem requires. Type of curve to be employed—parabolic, harmonic, etc—depends upon the requirements. Cam rise is during portion of curve *AB;* cam return, during *CD.*
2. Choose points of maximum slope during rise and return (points P_1 and P_2). The maximum pressure angle will occur near, or sometimes at, these points.
3. Measure slope angles τ_1 and τ_2.
4. Measure the length, L, in inches corresponding to 360 deg.
5. Calculate k:

$$k = \frac{L}{2\pi}$$

In Fig 2

1. Lay out k and angles τ_1, τ_2. This locates points Q_1 and Q_2.
2. Measure $k(\tan \tau_1)$ and $k(\tan \tau_2)$.

In Fig 3

1. Lay out vertical line, FG, equal to total displacement, y_{max}.
2. Lay out from point F, the displacements y_1 and y_2 (at points P_1 and P_2). This locates points M and N.
3. Lay out $k(\tan \tau_1)$ to left of M to obtain point E_1. Similarly k tan τ_2 to right from N locates E_2 (for CCW rotation of cam).
4. At points E_1 and E_2 locate the desired (usually maximum permissible) pressure angles of points P_1 and P_2. These angles are designated as α_1 and α_2.
5. The lines define the limits of an area A. Any cam shaft center chosen within this area will result in pressure angles at points P_1 and P_2 which will be equal to or less than the prescribed angles α_1 and α_2. If the cam shaft center is chosen anywhere along Ray I, the pressure angle at E_1 will be exactly α_1 (and similarly along Ray II for α_2). Thus, if O_1, the intersection of these two rays, is chosen as the cam center, the layout will provide the desired pressure angles for both rise and return.
6. The construction results in an offset roller follower whose eccentricity, e, is measured directly on the drawing. Radii R_{min} and R_{max} are also measured directly on the drawing. The actual cam shape is drawn to scale in Fig 4.

Design charts

The above procedure, however, does not ensure that the pressure angle is not exceeded at some other point. *Only for some cases of parabolic motion will the maximum pressure angle occur at the point of maximum slope.* Thus the same procedure has to be repeated for numerous points during the rise and return motions. The six charts (Fig 5 to 10) developed by the author avoid the need for repetitive construction. Also, for cases where the cam size has already been chosen, the charts provide the maximum pressure angle during rise and return motions.

The scale of all the charts assumes that the stroke is equal to one unit. Hence, if $y_{max} = 1$ in. then the scales can be read off directly in inches.

Design problem

All charts, Fig 5 to 10, show construction for the case where cam rotation during cam rise and fall respectively is $\beta_1 = 25$ deg and $\beta_2 = 80$ deg; total stroke, $y_{max} = 2$ in; max

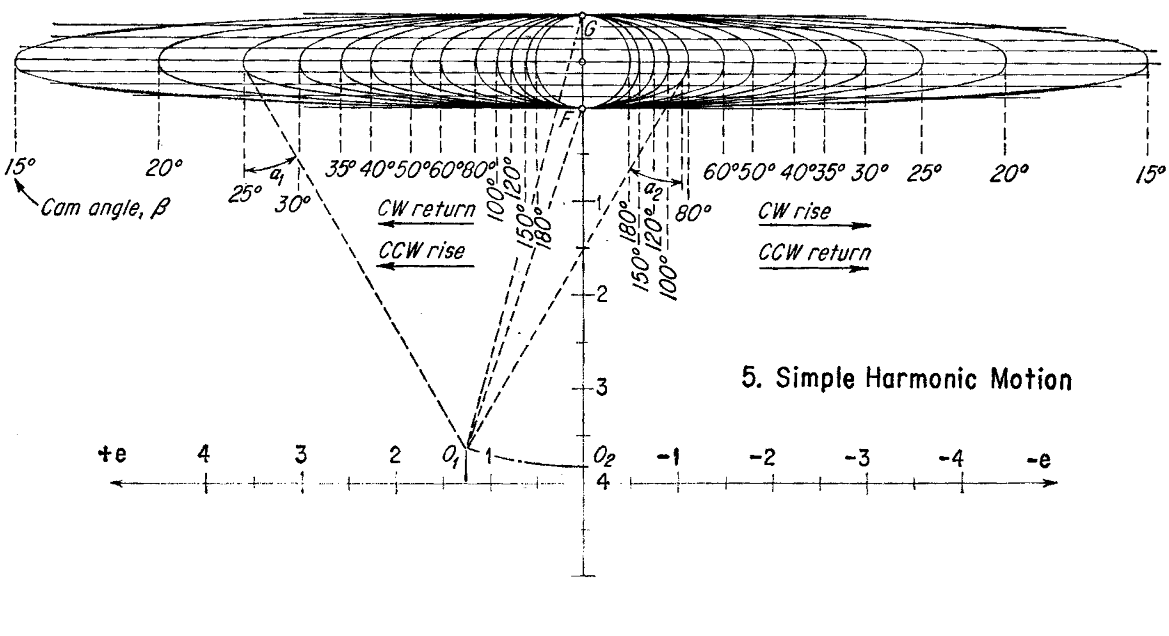

5. Simple Harmonic Motion

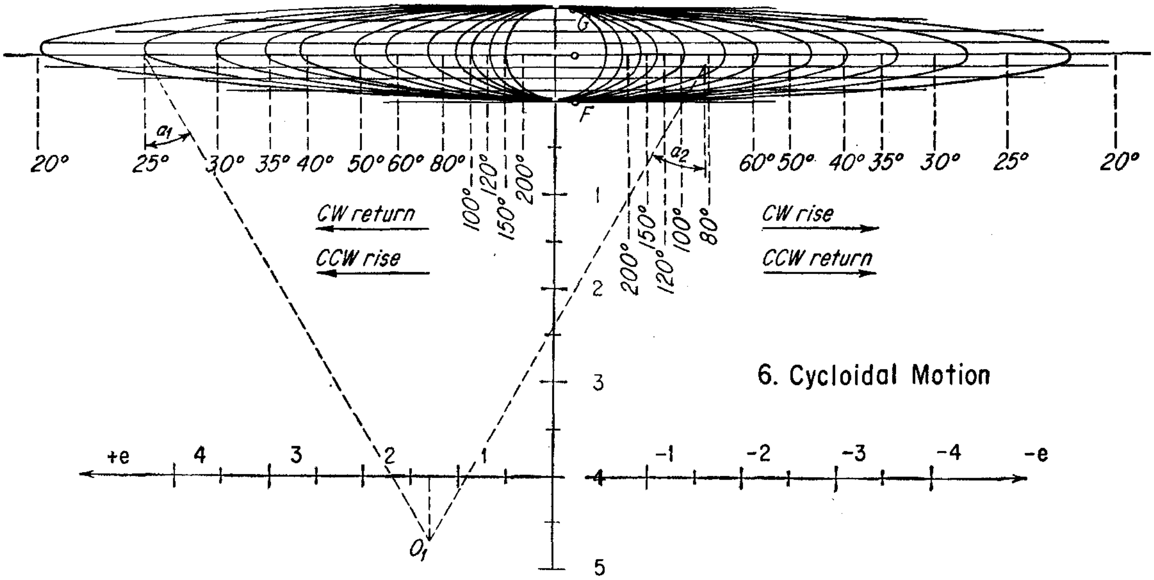

6. Cycloidal Motion

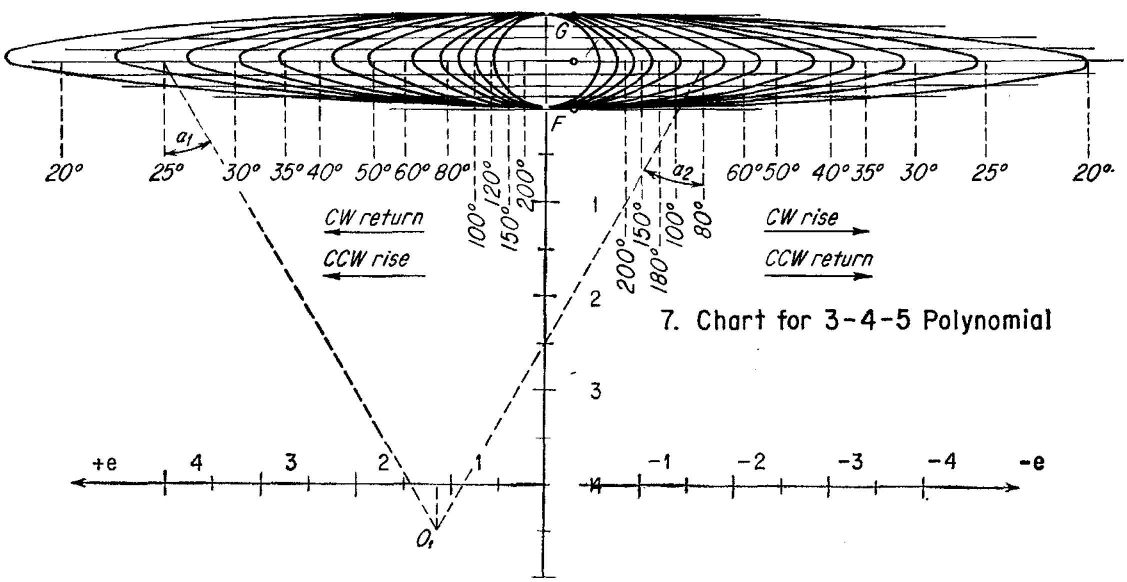

7. Chart for 3-4-5 Polynomial

pressure angle during rise, $\alpha_1 = 30$ deg; during return, $\alpha_2 = 30$ deg. The cam rotates counterclockwise (CCW). Assume simple harmonic motion (Fig 5).

Construction

1. Because rotation is CCW, go to the left of center for the rise stroke, and to the right for the return stroke, as noted on the chart. Thus go to the $\beta = 25$ deg curve and layout angle $\alpha_1 = 30$ deg *tangent* to the curve. Lay out α_2 tangent to the $\beta = 80$ deg curve.

2. The point where the two lines intersect locates the cam shaft center O_1.

3. Read down to the e scale to obtain the required eccentricity. Hence $e = (1.23)(2) = 2.46$ in. (multiply by 2 because $y_{max} = 2$ in.).

4. Distance O_1F is R_{min}. To obtain its scale value, swing an arc from F to locate O_2. Hence $R_{min} = (3.85)(2) = 7.7$ in.

5. Distance $O_1G = R_{max} = (4.83)(2) = 9.66$ in.

All dimensions required to construct the minimum cam size are now known. You can also determine what part of the stroke the maximum pressure angle will occur at by noting the points of tangency of the α_1 and α_2 lines to the 25-deg and 80-deg curves. Extend these points horizontally to the FG line. Thus the max pressure angle occurs $\frac{7}{16}$ of the stroke upward during rise, and $\frac{11}{16}$ of the stroke downward during return.

If you want to know the pressure angle, say at a point one quarter of the stroke during rise, go upward one quarter of the distance from F to G, then to the left to intersect the 25 deg curve. Connect this point of intersection to O_1. The angle that this new line makes with the vertical will be the requested pressure angle.

For parabolic cams

The procedure is slightly different here (Fig 9). The elongated curves are pointed at the ends. Thus the lines for pressure angles α_1 and α_2 are not tangent to the curve for the numerical

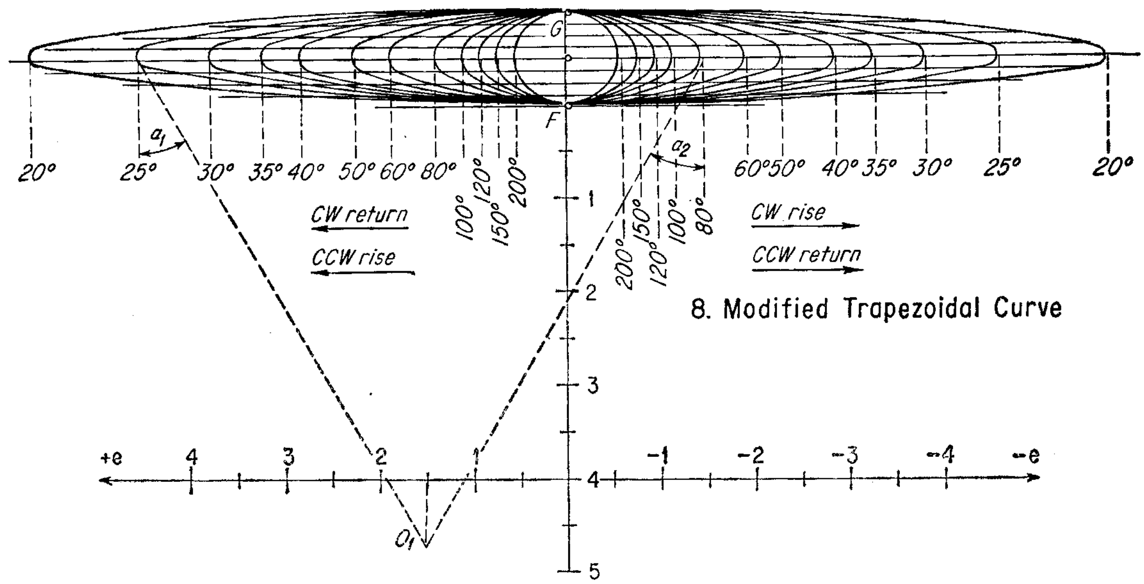

8. Modified Trapezoidal Curve

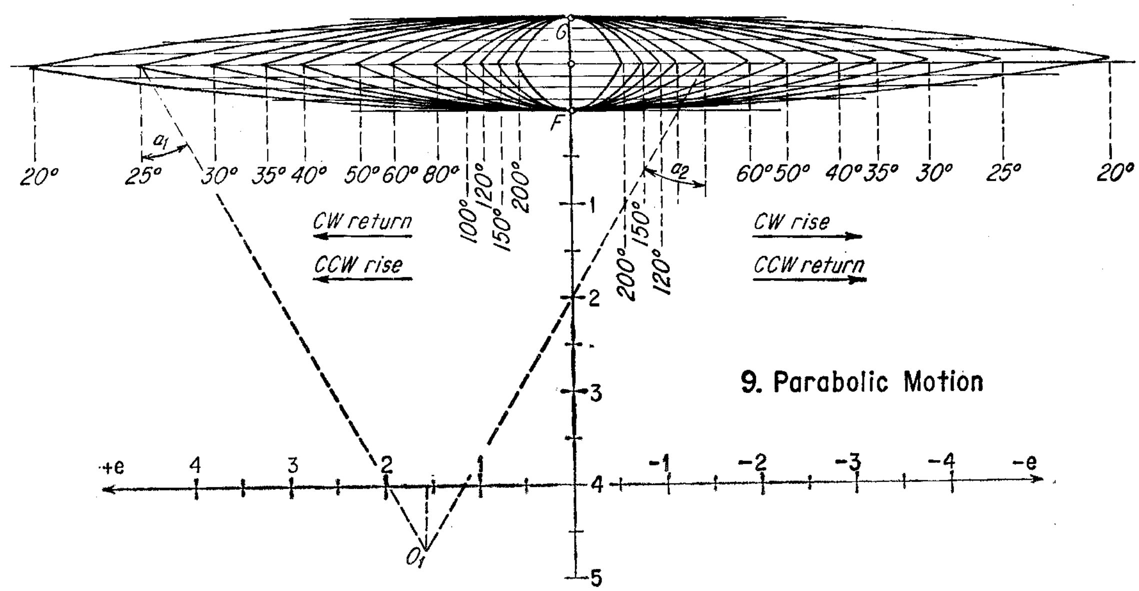

9. Parabolic Motion

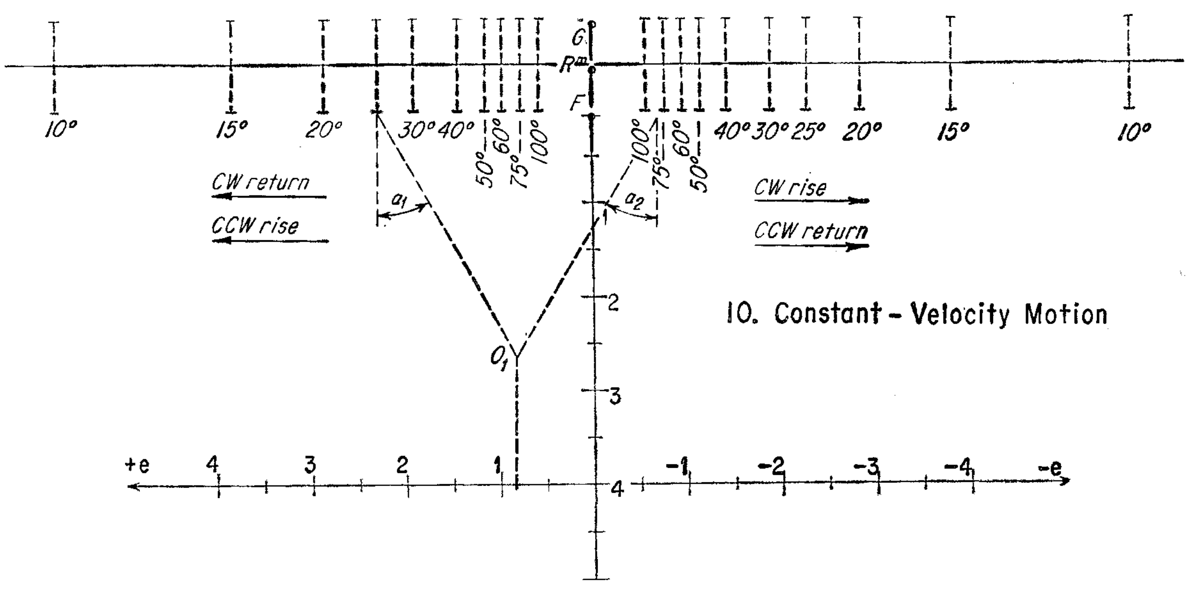

10. Constant - Velocity Motion

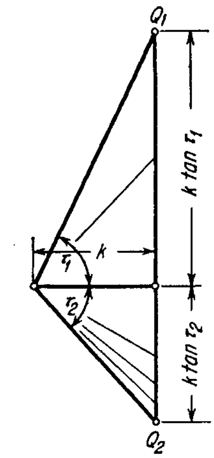

12. Slope analysis

Comparison of Cam Sizes

Type of cam	Max radius, R max	Eccentricity, e
Constant velocity	3.65	0.8
Parabolic motion	5.90	1.58
Simple harmonic motion	4.80	1.24
Cycloidal motion	5.90	1.58
3-4-5 Polynomial	5.65	1.48
Modified trapezoidal	5.90	1.57
Double harmonic motion	5.85	1.60

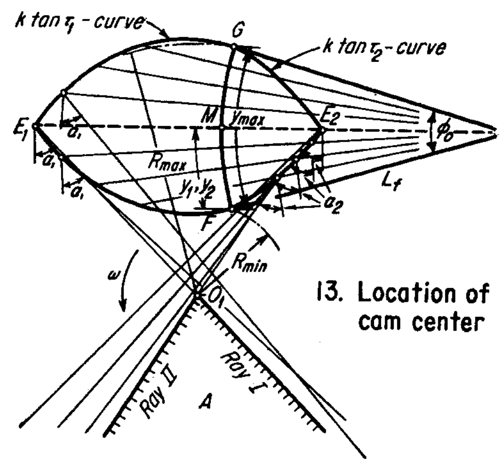

13. Location of cam center

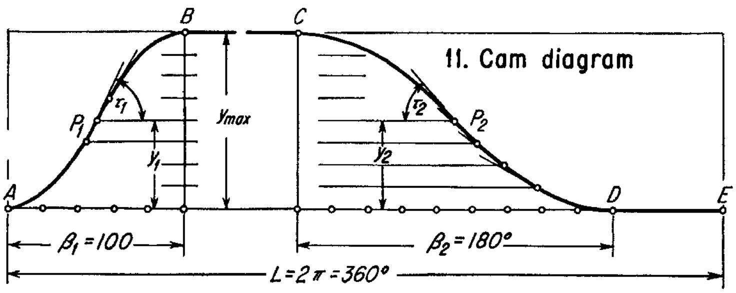

11. Cam diagram

conditions given (but in some cases the lines may be).

For constant velocity cams

The elongated curves for this type of motion become vertical lines (Fig 10). Use the lower points of these lines for laying out a_1 and a_2, as shown by the dashed lines.

Comparison of cam sizes

A comparison of the required cam sizes for the six types of cam contours is given at the top of this page. Note that the constant-velocity curve requires the smallest cam size.

Swinging followers

Cams with swinging followers require a construction technique similar to the Flocke method described previously.

Assume that a cam diagram is given (Fig 11). Also known are the length of follower arm, L_f, and the angle of arm oscillation during rise and fall, ϕ_o. The length of the circular arc through which the roller follower swings must be equal to y_{max} in Fig 11. (See p. 69 for an illustration of a swinging follower cam.)

The construction technique, illustrated in Fig 11, 12 and 13, is as follows:

1. Divide the ordinate of the cam diagram into equal parts (8 in this case).
2. Select points along the divisions and find the slope angles at the points. The procedure is shown only for points P_1 and P_2, but it should be repeated for other points.
3. Calculate $k = L/(2\pi)$. In Fig 12, lay off k and angles τ_1 and τ_2. Obtain $k(\tan \tau_1)$ and $k(\tan \tau_2)$.
4. In Fig 13 lay off L_f (from S to F) and divide ϕ_o into 8 equal parts.
5. Lay out y_1 and y_2 as shown (in this case y_1 and y_2 are equal).
6. If cam rotation is away from pivot point S (counterclockwise in this case) lay off $ME_1 = k \tan \tau_1$ to the left of point M, and $ME_2 = k \tan \tau_2$ to the right of point M. (Reverse directions for clockwise rotation of cam.)
7. Lay out a_1 and a_2 at E_1 and E_2. Repeat procedure for other points as shown. Now choose the lowest line from both ends to obtain an area, A, which is the farthest area possible from F. This results in Ray I and Ray II. If a cam shaft center is chosen anywhere within this area, the maximum pressure angle will not be exceeded, either during rise or return.
8. If O_1 is chosen, the maximum pressure angles during rise will occur at the middle of the stroke because Ray I is determined from E_1, which in turn corresponds to the middle of the stroke. Note that the maximum pressure angle for the return stroke will occur when the follower moves back ⅞ of the stroke because Ray II originates from a point ⅞ of angle ϕ_o measured downward from the top.

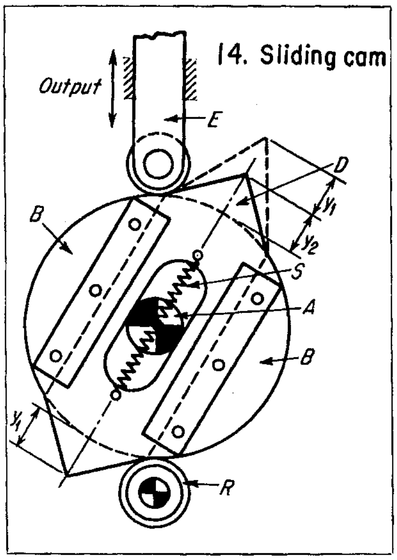

14. Sliding cam

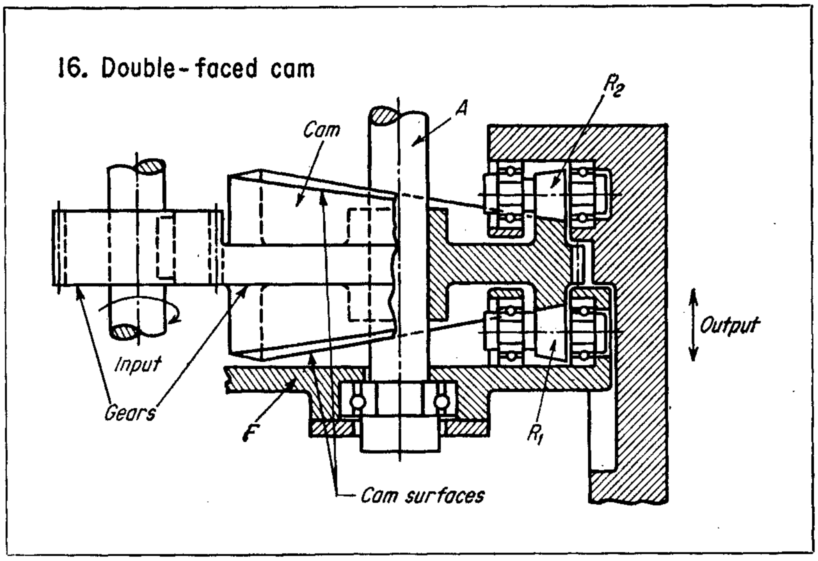

16. Double-faced cam

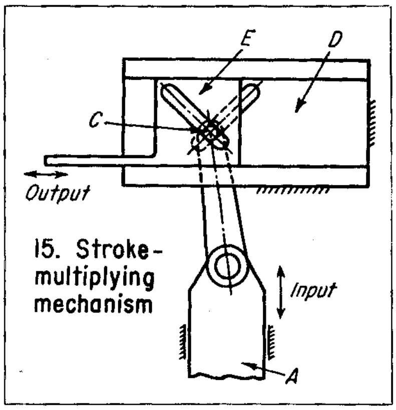

15. Stroke-multiplying mechanism

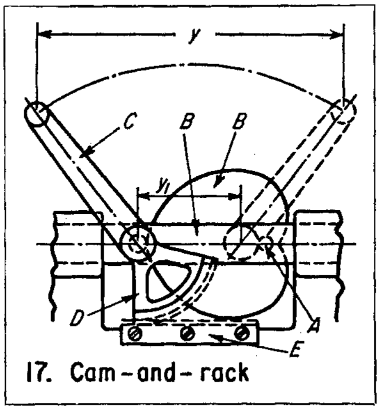

17. Cam-and-rack

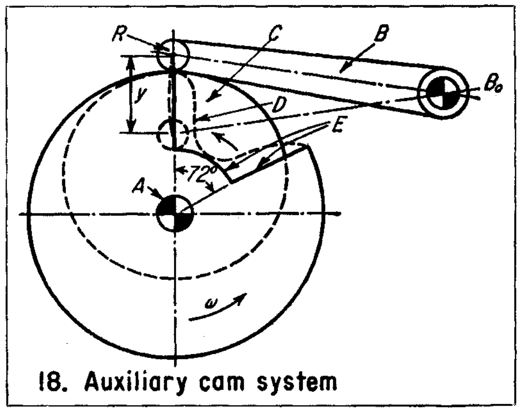

18. Auxiliary cam system

When the pressure angles are too high to satisfy the design requirements, and it is undesirable to enlarge the cam size, then certain devices can be employed to reduce the pressure angles:

Sliding cam, Fig 14—This device is used on a wire-forming machine. Cam *D* has a rather pointed shape because of the special motion required for twisting wires. The machine operates at slow speeds, but the principle employed here is also applicable to high-speed cams.

The original stroke desired is $(y_1 + y_2)$ but this results in a large pressure angle. The stroke therefore is reduced to y_2 on one side of the cam, and a rise of y_1 is added to the other side. Flanges *B* are attached to cam shaft *A*. Cam *D*, a rectangle with the two cam ends (shaded), is shifted upward as it cams off stationary roller *R*, during which the cam follower *E* is being cammed upward by the other end of cam *D*.

Stroke multiplying mechanism, Fig 15—This device is employed in power presses. The opposing slots, one in a fixed member *D* and the second in the movable slide *E*, multiply the motion of the input slide *A* driven by the cam. As *A* moves upward, *E* moves rapidly to the right.

Double-faced cam, Fig 16 — This device doubles the stroke, hence reduces the pressure angles to one-half their original values. Roller R_1 is stationary. When the cam rotates, its bottom surface lifts itself on R_1, while its top surface adds an additional motion to the movable roller R_2. The output is driven linearly by roller R_2 and thus is approximately the sum of the rise of both surfaces.

Cam-and-rack, Fig 17—This device increases the throw of a lever. Cam *B* rotates around *A*. The roller follower travels at distances y_1, during which time gear segment *D* rolls on rack *E*. Thus the output stroke of lever *C* is the sum of transmission and rotation giving the magnified stroke *y*.

Cut-out cam, Fig 18—A rapid rise and fall within 72 deg was desired. This originally called for the cam contour, *D*, but produced severe pressure angles. The condition was improved by providing an additional cam *C* which also rotates around the cam center *A*, but at five times the speed of cam *D* because of a 5:1 gearing arrangement (not shown). The original cam is now completely cut away for the 72 deg (see surfaces *E*). The desired motion, expanded over 360 deg (since 72 x 5 = 360), is now designed into cam *C*. This results in the same pressure angle as would occur if the original cam rise occurred over 360 deg instead of 72 deg.

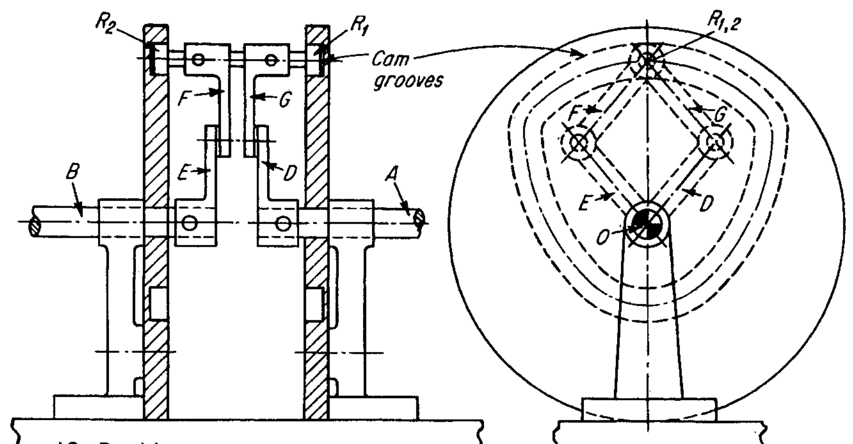

19. Double cam-groove system

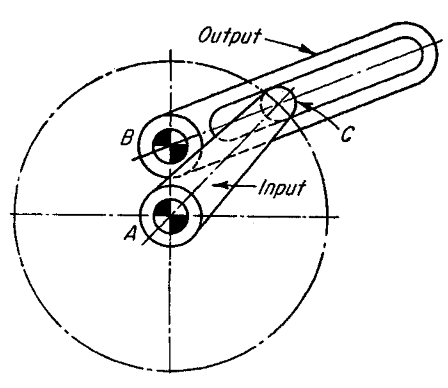

20. Whitworth quick-return

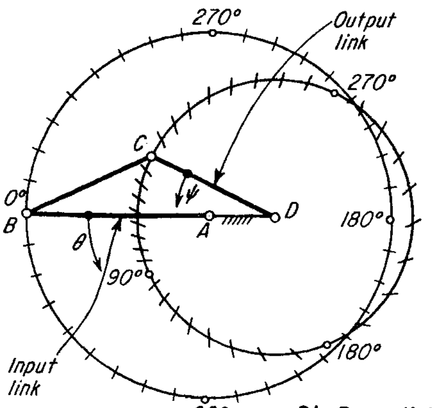

21. Drag link

22. Modification of original cam shape

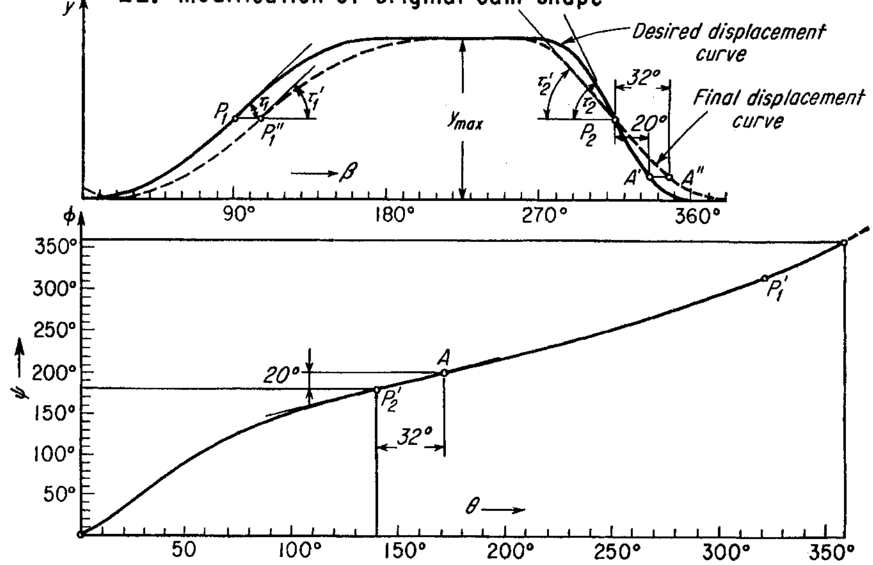

Double-cam mechanism, Fig 19—If you were to increase the cam speed at the point of high-pressure angles, and change the contour accordingly, the pressure angle would be reduced. The device in Fig 19 employs two cam grooves to change the input speed A to the desired varying-speed output in shaft B. Shaft B then becomes the cam shaft to drive the actual cam (not shown). If the cam grooves are circular about point O then the output will be a constant velocity. Distance OR therefore is varied to provide the desired variation in output.

Whitworth quick return mechanism, Fig 20—This is a simpler way of imparting a varying motion to the output shaft B. However, the axes, A and B, are not colinear.

Drag link, Fig 21—This is another simple device for varying the output motion of shaft D. Shaft A rotates with uniform speed. The construction in Fig 22 shows how to modify the original cam shape to take full advantage of the varying input motion provided by shaft D. The construction steps are as follows (the desired displacement curve is given at the top of Fig 22, with the maximum pressure angle designated as τ_2):

1. Plot the input vs output diagram (θ vs ψ) for the linkage illustrated in Fig 21.
2. Find the point with the smallest slope, P_2.
3. Pick any point A on the tangent to P'_2 and measure the corresponding angles to P'_2 (32 deg and 20 deg).
4. Go 20 deg to the right of P_2 in the cam diagram to locate A'. Also locate A by going 32 deg to the right of P_2 as shown. Point A' is on the final cam shape. Repeat this procedure with more points until you obtain the final curve. The pressure angle at P_2 is thus reduced from τ_2 to τ_2'.

Spherical Cams: Linking Up Shafts

European design is widely used abroad but little-known in the U.S. Now a German engineering professor is telling the story in this country, stirring much interest.

Anthony Hannavy

Problem: to transmit motion between two shafts in a machine when, because of space limitations, the shaft axes may intersect each other. One answer is to use a spherical-cam mechanism, unfamiliar to most American designers but used in Europe to provide many types of motion in agricultural, textile, and printing machinery.

Recently, Prof. W. Meyer zur Cappellen of the Institute of Technology, Aachen, Germany, visited the U. S. to show designers how spherical-cam mechanisms work and how to design and make them. He and his assistant kinematician at Aachen, Dr. G. Dittrich, are in the midst of experiments with complex spherical-cam shapes and with the problems of manufacturing them.

Fundamentals. Key elements of spherical-cam mechanism (above Fig. 1) can be considered as being posi-

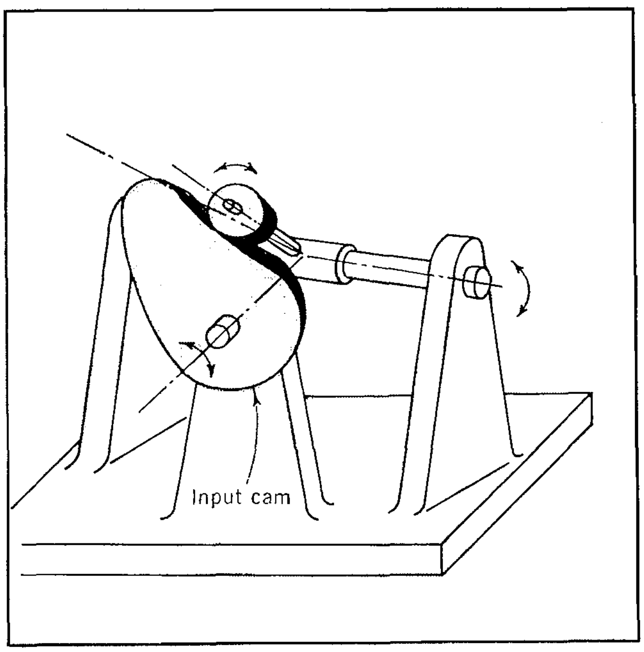

3 Spherical mechanism with radial follower

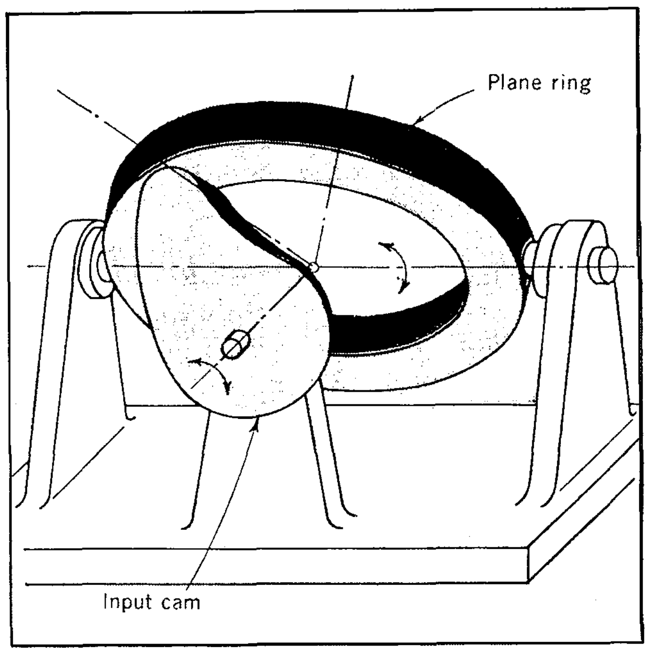

4 Cam mechanism with flat-faced follower

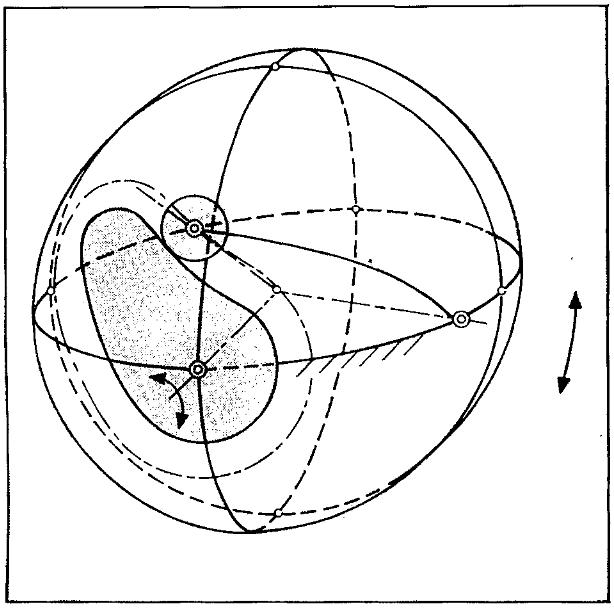

Radial roller follower shown on a sphere

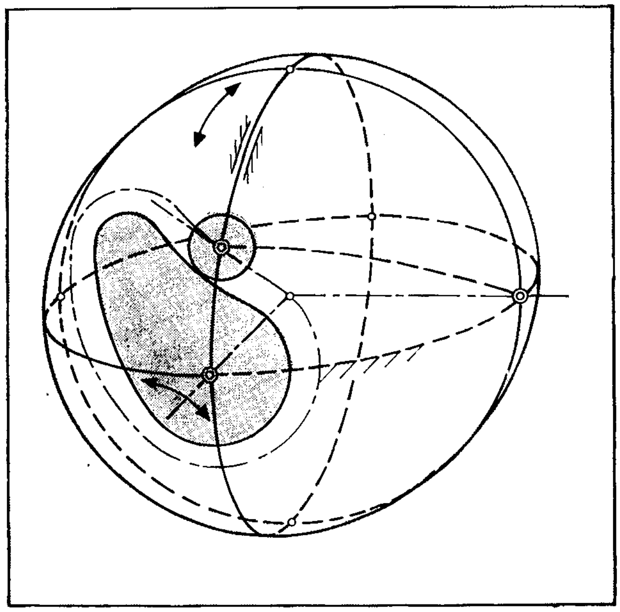

Mechanism with radial roller follower shown on a sphere

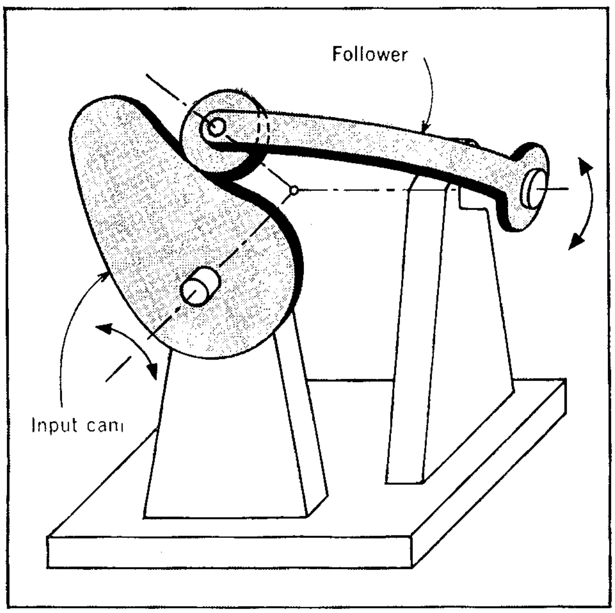

1 Spherical cam mechanism with radial follower

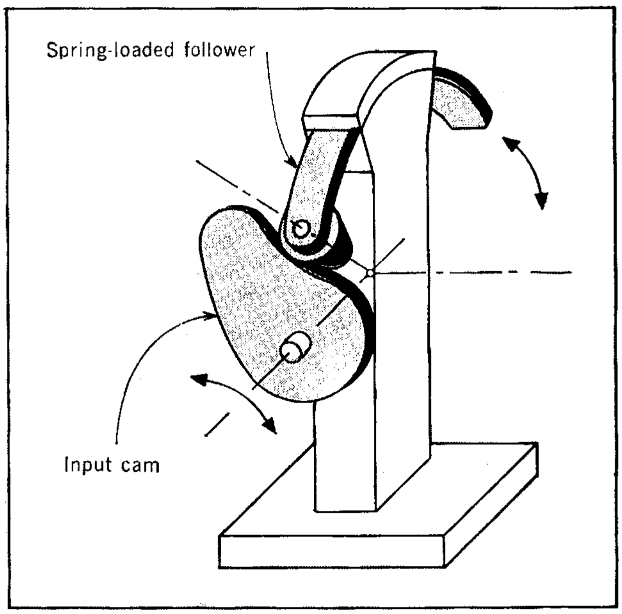

2 Cam mechanism with rocking roller follower

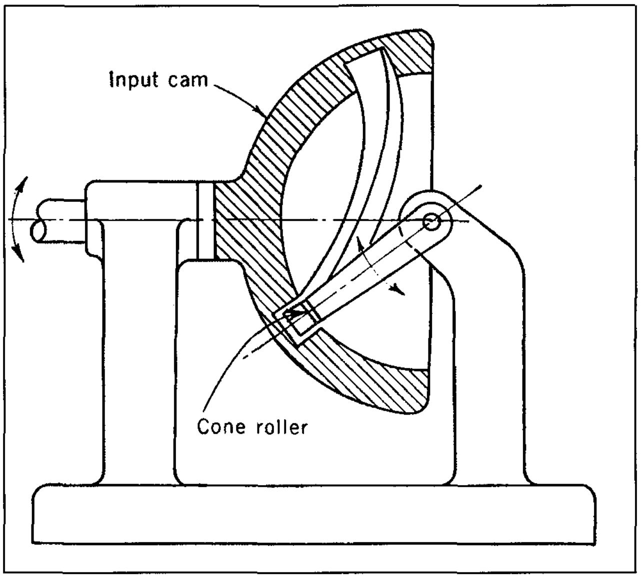

5 Hollow-sphere cam mechanism

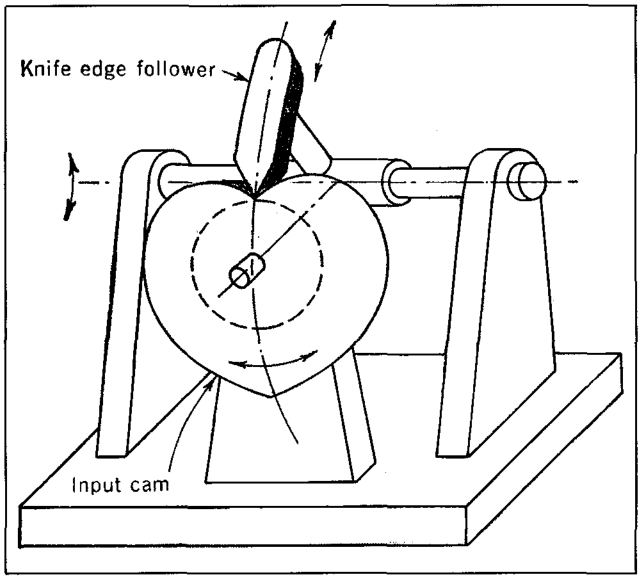

6 Mechanism with Archimedean spiral; knife-edge follower

tioned on a sphere. The center of this sphere is the point where the axes of rotation of the input and follower cams intersect.

In a typical configuration in an application (Fig. 1), the input and follower cams are shown with depth added to give them a conical roller surface. The roller is guided along the conical surface of the input cam by a rocker, or follower.

A schematic view of a spherical-cam mechanism (above Fig. 2) shows how the follower will rise and fall along a linear axis. In the same type of design (Fig. 2), the follower is spring-loaded. The designer can also use a rocking roller follower (Fig. 3) that oscillates about an axis that, in turn, intersects with another shaft.

These spherical-cam mechanisms using a cone roller have the same output motion characteristics as spherical-cam designs with non-rotating circular cone followers or spherically-shaped followers. The flat-faced follower in Fig. 4 rotates about an axis that is the contact face rather than the center of the plane ring. The plane ring follower corresponds to the flat-faced follower in plane kinematics.

Closed-form guides. Besides having the follower contained as in Fig. 2, spherical-cam mechanisms can be designed so the cone roller on the follower is guided along the body of the input cam. For example, in Fig. 5, the cone roller moves along a groove that has been machined on the spherical inside surface of the input cam. However, this type of guide encounters difficulties unless the guide is carefully machined. The cone roller tends to seize.

Although cone rollers are recommended for better motion transfer between the input and output, there are some types of motion where their use is prohibited.

For instance, to obtain the motion diagram shown in Fig. 6, a cone roller would have to roll along a surface where any change in the concave section would be limited to the diameter of the roller. Otherwise there would be a point where the output motion would be interrupted. In contrast, the use of a knife-edge follower theoretically imposes no limit on the shape of the cam. However, one disadvantage with knife-edge followers is that they. unlike cone followers, slide and hence wear faster.

Manufacturing methods. Spherical cams are usually made by copying from a stencil. In turn, the cam-shaped tools can be copied from a stencil. Normally the cams are milled, but in special cases they are ground.

Three methods for manufacture are used to make the stencils:

- Electronically controlled point-by-point milling.
- Guided-motion machining.
- Manufacture by hand.

However, this last method is not recommended, because it isn't as accurate as the other two.

Tailored Cycloid Cams:
German Method

The cycloid cam is becoming the best all-around performer, but the problem is knowing how to fit it to specific machines requirements.

Nicholas P. Chironis

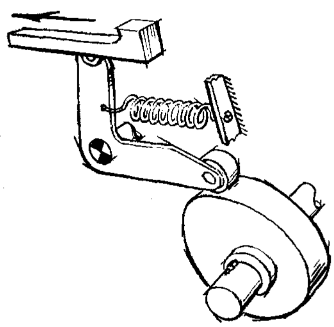

IT'S quite a trick to construct a cycloid curve to go through any point P within a cam diagram, *with a specific velocity at P* (Fig 1, opposite).

There is a growing demand for this type of modification because cam designers are turning more and more to the cycloid curve to meet most automatic machine requirements. They like the fact that a cycloid cam produces no abrupt change in acceleration and so induces the lowest degree of vibration, noise, shock, and wear. A cycloid cam also induces low side-thrust loads on a follower and requires small springs. However, the mathematical computations to tailor such cams become quite complex and the cycloid is all too often passed over for one of the more easily analyzed cams.

Recently, a well-known mechanism analyst at University of Bridgeport, Professor Preben W. Jensen, began a careful study through German cam design methods and came up with three graphical techniques for tailoring a cycloid cam, one of which solves the problem stated above. In an exclusive interview with PRODUCT ENGINEERING, Prof Jensen outlined the three common problems and the construction methods for solving them. He also provided the velocity and acceleration formulas for the cycloid, including the key relationship for keeping the maximum accelerations of the cam followers to a minimum. Specifically, the three types of tailoring are:

1) To have the cam follower start at point A, pass through P with a certain slope (velocity) and then proceed to point B—the entire motion to have cycloidal characteristics which includes zero acceleration slopes (smoothly starting velocities) at points A and B, Fig 1. (A cam diagram is actually a displacement record of the motion of a follower as it rises from point A to B during a specific rotation of the cam from line A to A'. Distance A-A' may be 180 deg or any other portion of the full rotation of the cam.)

2) To have the cam follower start with cycloid motion from point A, meet smoothly a constant velocity portion of the cam line (P_1-P_2 in Fig 2), and then continue on with cycloid motion to point B.

3) Given some other cam curve (curve AB in Fig 3), to return the follower to its starting point with cycloid motion (curve BMD).

Going through any point

This is the first of the modifications. The method of construction is:

Step 1. Draw a line DE with the given slope at P in Fig 1B.

Step 2. Divide AP into a number of equal parts, say 6—the larger the number of parts into which the line divided, the higher the degree of accuracy of the method. From the mid-point M of line AP, draw a line to D. This gives a distance C_1.

Step 3. Calculate radius R_1 from the relationship

$$R_1 = \frac{2C_1}{\pi}$$

(The derivation of the above equation is beyond the scope of this article.)

Step 4. Draw a quarter circle with R_1 as its radius and divide it into 3 equal parts. By dropping perpendiculars, obtain distance y_1 and y_2.

Step 5. Lay out distances y_1, y_2, and R_1, as shown in the diagram. The points so determined are points on the modified cycloid.

The other part of the displacement curve from P to B is determined in exactly the same way with the aid of the other small diagram in which R_2 is the radius.

The acceleration curve resulting from this displacement curve (determined by the method shown later) is continuous.

Going through constant velocity

In this second modification, constant velocity motion is required from P_1 to P_2. With the same method as described previously, AP_1 and P_2B are connected with a modified cycloid, as shown in Fig 2, and again an acceleration curve is obtained which is continuous.

Slowing down from given curve

Suppose that the first part of the cam, curve AB in Fig 3, must employ a different type of cam contour. How do you retract the follower smoothly to D using the cycloid curve so as to have continuous acceleration?

Solution: Connect B with D and draw the tangent to the curve given at B. Divide BD into equally spaced parts, with midpoint at M. Choose the line of maximum slope FME. This slope determines the maximum velocity during the return of the follower. The rest of the construction is carried out exactly as in the first case.

Velocity and acceleration equations

For a given rotation of the cam (distance θ in Fig 4) the equation for a tailored cycloid which gives the distance y that the follower will move is:

$$y = h\left[\frac{\theta_m}{\beta} - \frac{1}{2\pi}\sin\left(2\pi\frac{\theta_m}{\beta}\right)\right] \quad (1)$$

where distance θ_m is computed from the equation

$$\theta_m = \theta + \frac{\beta}{2\pi}\left(\frac{\tan\delta}{\tan\gamma}\right)\sin\left(2\pi\frac{\theta}{\beta}\right)$$

and where

γ = direction of amplitude for the superimposed sine wave; ie, the angle of 'distortion' of the cycloid. For example, in Fig 4, when $\gamma = 90$ deg, then $\theta_m = \theta$ and you have a pure cycloid curve.

δ = angle of slope for the line connecting A and B

θ = portion of cam rotation, deg (or inches when measured on diagram)

β = time for total lift, deg (or inches)

h = total follower movement, in.

$$T = \frac{60}{N}\left(\frac{\beta}{360}\right)$$

N = rpm of cam

Dimensions θ, θ_m and y are also in inches on the cam layout. Although Fig 4 shows P at the midpoint of B, the equations hold true for other cases

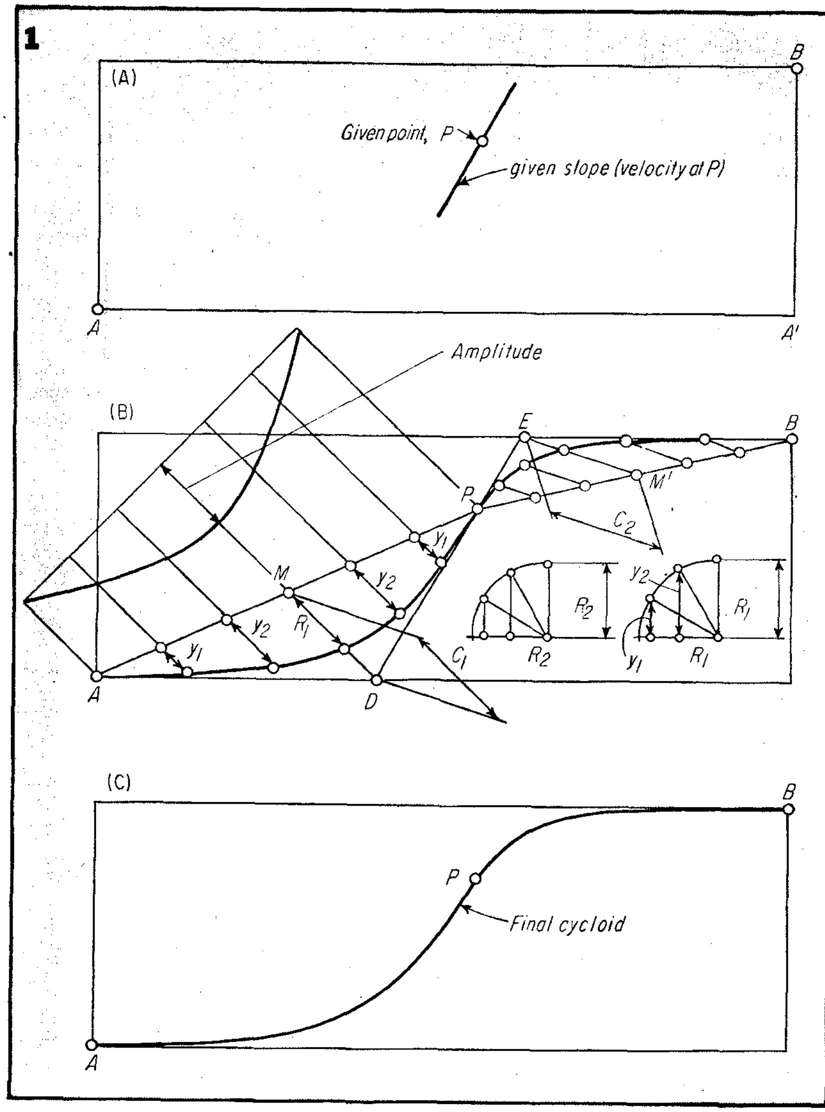

Technique for modifying a cycloid cam so that its follower speeds up smoothly to a specific velocity (slope at P) after extending a certain distance (to point P).

In the modification below, the cam follower is designed to move with a constant velocity during a portion of its stroke (line P_1P_2), as in cutting operations.

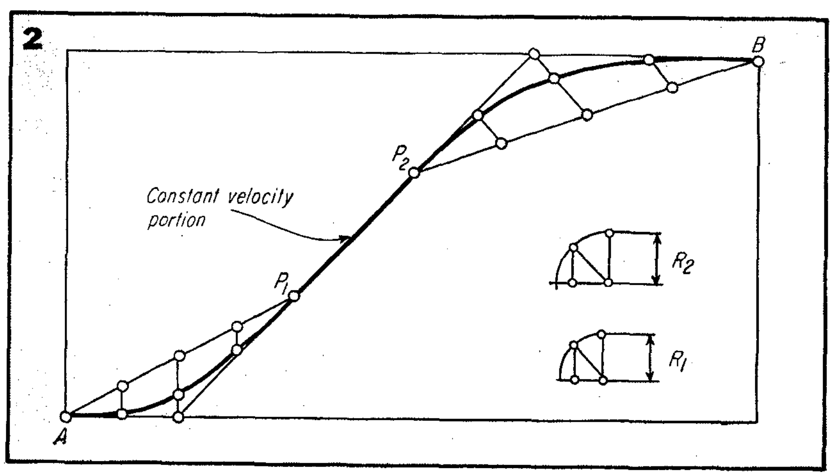

by proper modification of the value for T.

Velocity equation

$$V = \frac{h}{T}\left[\frac{1 - \cos\left(2\pi\frac{\theta}{\beta}\right)}{1 - \frac{\tan\delta}{\tan\gamma}\cos\left(2\pi\frac{\theta}{\beta}\right)}\right] \quad (2)$$

where V = follower velocity, in./sec

Acceleration equation

$$A = \frac{h}{T^2}\left[\frac{2\pi(1-K)\sin\left(2\pi\frac{\theta}{\beta}\right)}{\left[1 - K\cos\left(2\pi\frac{\theta}{\beta}\right)\right]^3}\right] \quad (3)$$

where $K = \tan\delta/\tan\gamma$

The stroke h and cam rotation β are usually fixed by the basic requirements of the problem. Therefore, the maximum acceleration, A, will depend upon K. There is one value of K which will give the lowest possible maximum value of acceleration. This optimum K value is

$$K_{optimum} = 1 - \tfrac{1}{2}\sqrt{3} = 0.134 \quad (4)$$

Comparison of cam curves

For the above optimum value of K the following minimum values of maximum acceleration are obtained:

For the best tailored cycloid cam

$$A_{max} = 5.89\frac{h}{T^2} \quad (5)$$

For a standard cycloid cam

$$A_{max} = 6.28\frac{h}{T^2} \quad (6)$$

For a parabolic cam

$$A_{max} = 4.00\frac{h}{T^2} \quad (7)$$

For a simple harmonic cam

$$A_{max} = 4.93\frac{h}{T^2} \quad (8)$$

Although the parabolic and simple-harmonic cams have lower acceleration maximums than the cycloids, their accelerations go through what is commonly referred to a "jerk," which is an abrupt change in acceleration (in these cases, from positive to negative values, see Fig 5).

Design example

A cam rotates with N = 200 rpm, the stroke of the follower is h = 2.0 in., and the corresponding cam shaft rotation is β = 60 deg. Determine the displacement, velocity, and acceleration curves for a best tailored cycloid having the lowest maximum acceleration.

Solution: In Fig 6 an arbitrary scale is chosen for the abscissa, namely that β = 60 deg has a length of 4 in. The stroke is laid out to scale (but establishing the stroke at a different scale would not change the procedure). Points A and B represent the start and end of the lift, respectively.

Angle δ is found from:

$$\tan\delta = \frac{h}{T} = \frac{2.00}{4.00} = 0.5$$

Because the lowest maximum acceleration is wanted, K = 0.134. Hence

$$\tan\gamma = \frac{\tan\delta}{K_{optimum}} = \frac{0.5}{0.134} = 3.73$$

$$\tan\gamma = 75 \text{ deg}$$

Referring again to Fig 6, P is the midpoint of AB, and AP is divided into 6 equal parts. Point D is situated so that line 3-D makes an angle of γ = 75 deg with the horizontal. This line indicates the direction of the amplitude of the sine wave which is superimposed on AP. The displace-

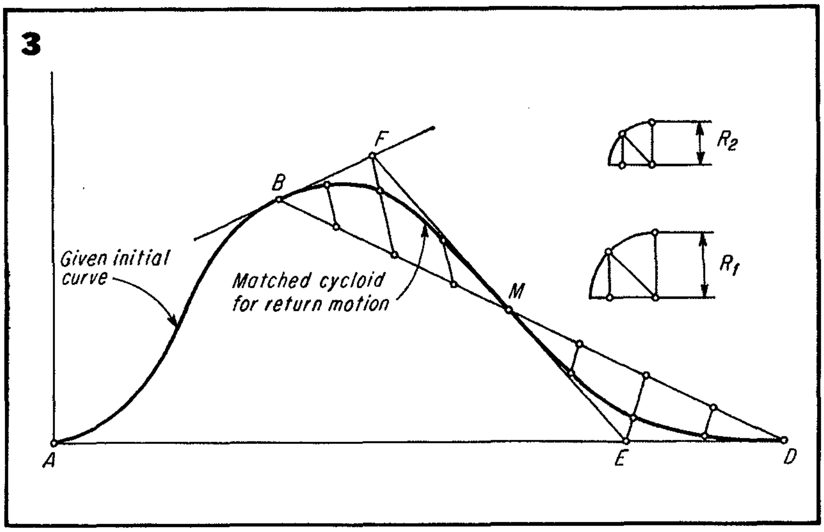

3. Graphical technique for slowing down the follower at the end of its work stroke (point B) and returning it to its initial position by means of the cycloid curve.

4. Basic cycloid curve (below) with factors which play a key role in finding its velocity and acceleration equations. When γ = 90 deg, the curve is a pure cycloid.

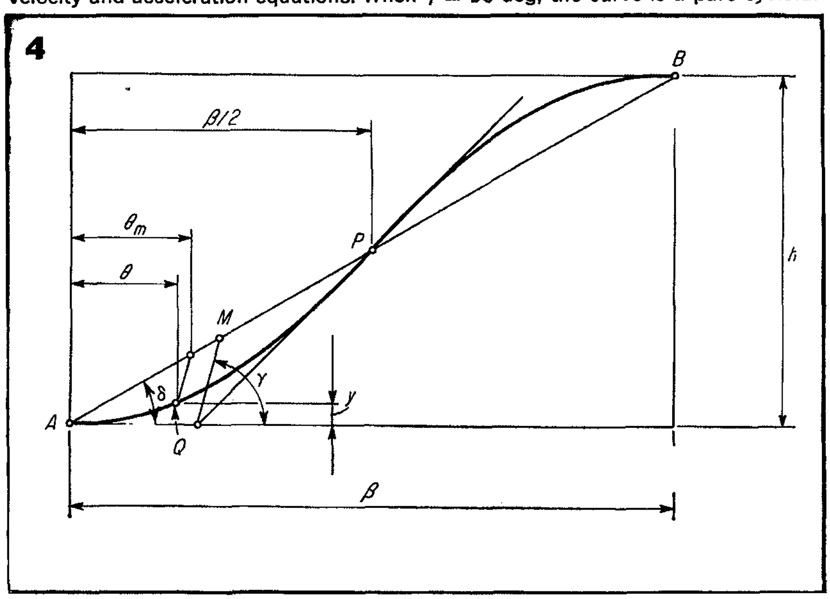

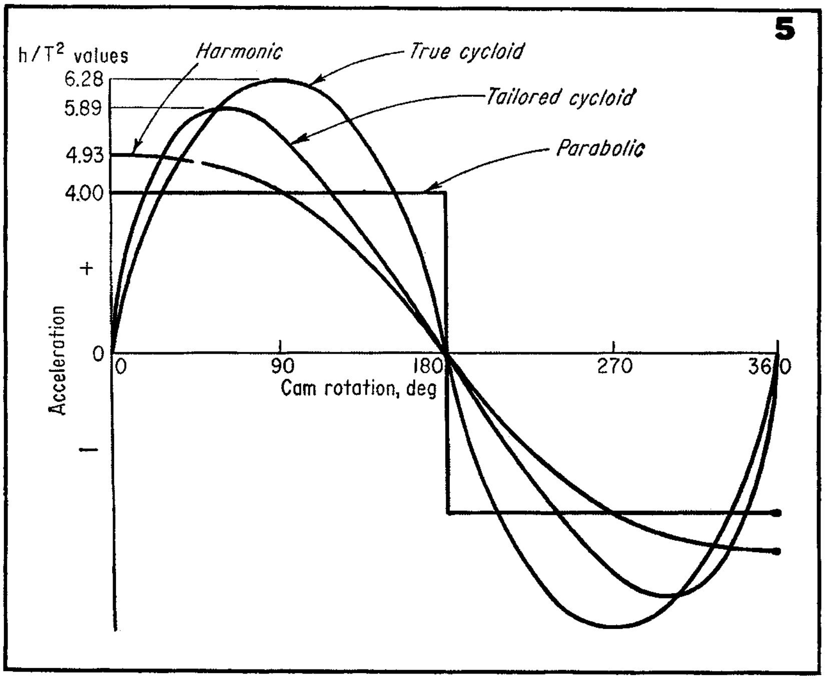

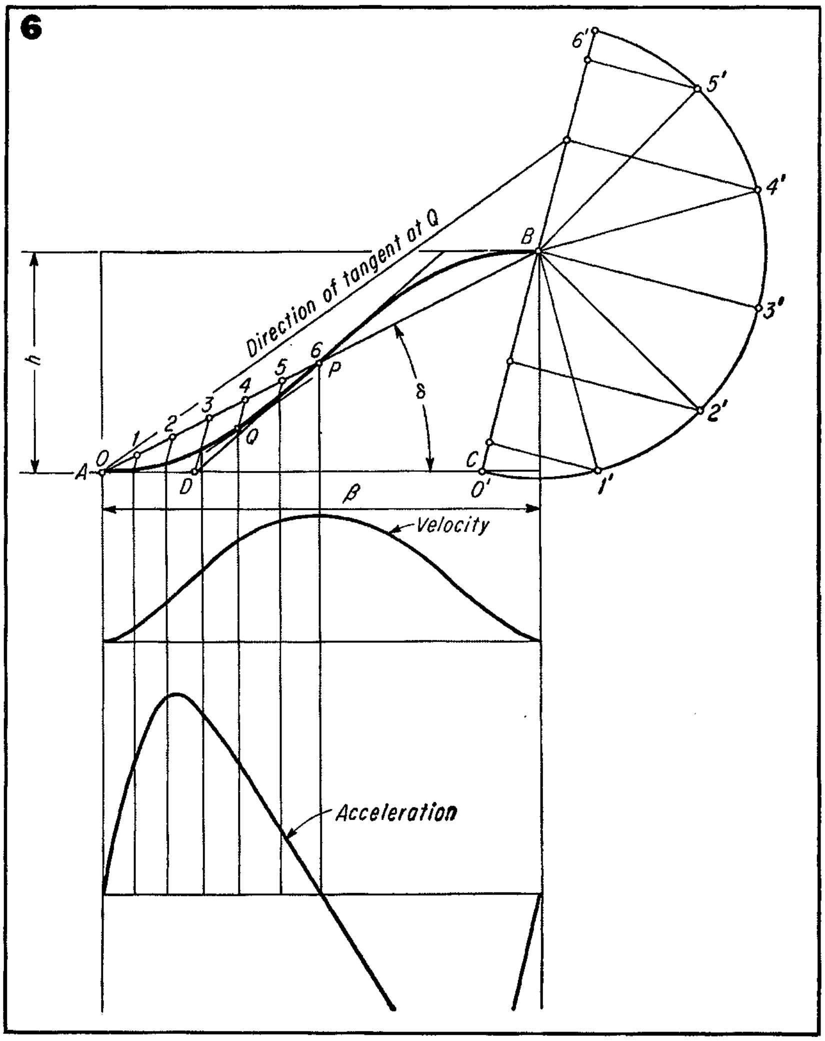

ment curve can now be drawn (the curve from 6 to B is congruent with the curve from A to 6).

The velocity at any point can be found from Eq 2, but can also be found graphically the following way:

Through B, draw line BC parallel to 3-D. With BC as radius, a half circle is drawn and divided into six equal parts. Now to find the velocity at point Q, draw a perpendicular from 4′ on BC and connect the point of intersection with A. This line is parallel to the tangent at Q. The procedure is repeated for the remaining points and the velocity curve is obtained.

To calculate the velocity at point Q by means of Eq 2, the value of θ for this point, is not $\theta = \beta/3$, but $\theta = 0.315\beta$ (see Fig 4). Hence

$$T = \frac{60}{N}\left[\frac{\beta}{360}\right]$$

$$= \frac{60(60)}{200(360)} = 0.05 \text{ sec}$$

and from Eq 2:

$$V = \frac{2.0}{0.05}\left[\frac{1 - \cos[2\pi(0.315)]}{1 - \left(\frac{0.5}{3.73}\right) \times \cos[2\pi(0.315)]}\right]$$

$$V = 56.3 \text{ in./sec}$$

The acceleration is found from Eq 3:

$$A = \frac{2(2\pi)(1 - 0.134)\sin 113.5°}{0.05^2(1 - 0.134\cos 113.5°)^3}$$

$$= 3320 \text{ in./sec}^2$$

The maximum acceleration, however, is more easily found from Eq 5:

$$A_{\text{max (optimum)}} = 5.89\,\frac{2}{0.05^2}$$

$$= 4710 \text{ in./sec}^2$$

It is also of interest to notice that the maximum pressure angle of the modified cycloid is lower than that of the true cycloid. The angle for the modified curve can be measured from Fig 6 as approximately 41 deg. For a true cycloid it would be 45 deg.

5. Comparison of acceleration curves for four popular types of cam curves. The harmonic and parabolic curves have undesirable abrupt changes at 0 and 180 deg, respectively.

6. Construction details for finding the displacement, velocity and acceleration curve for a tailored cycloid cam.

Modifications and Uses for Basic Types of Cams

Edward Rahn

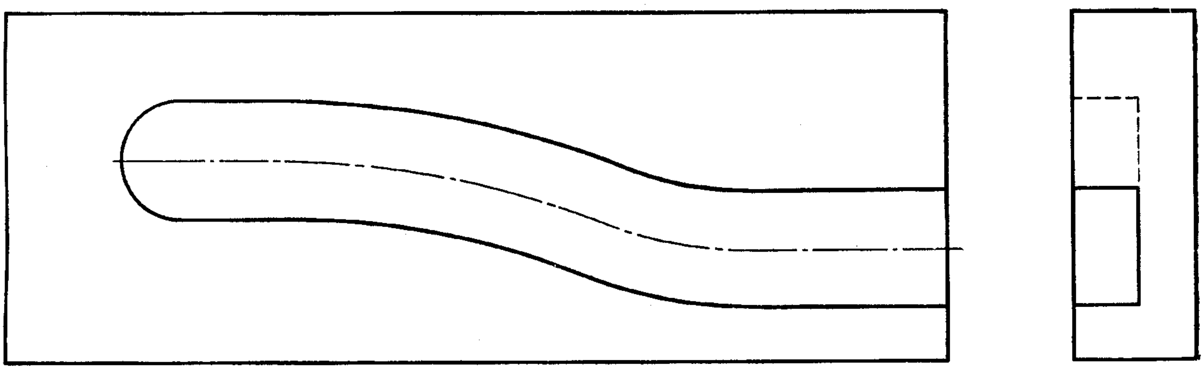

FLAT PLATE CAM—Essentially a displacement cam. With it, movement can be made from one point to another along any desired profile. Often used in place of taper attachments on lathes for form turning. Some have been built in sections up to 15 ft. long for turning the outside profile on gun barrels. Such cams can be made either on milling machines or profiling machines.

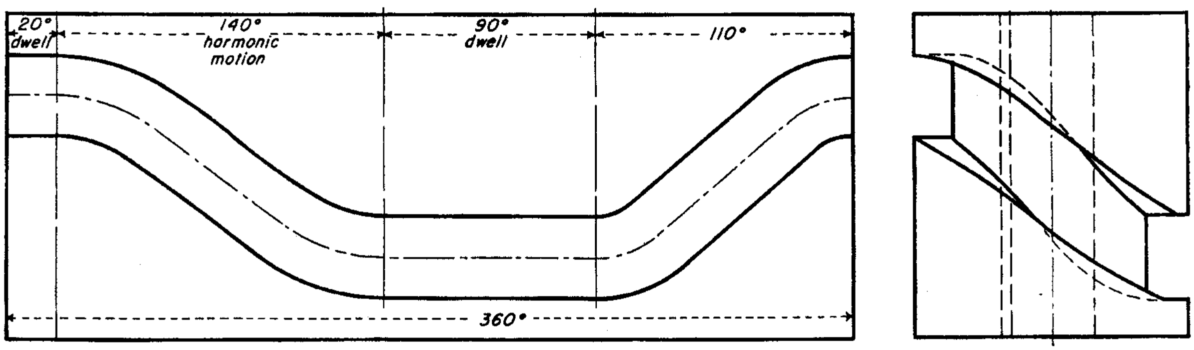

BARREL CAM—Sometimes called a cylindrical cam. The follower moves in a direction parallel to the cam axis and lever movement is reciprocating. As with other types of cam, the base curve can be varied to give any desired movement. Internal as well as external barrel cams are practical. A limitation: internal cams less than 11 in. in diam. are difficult to make on cam millers.

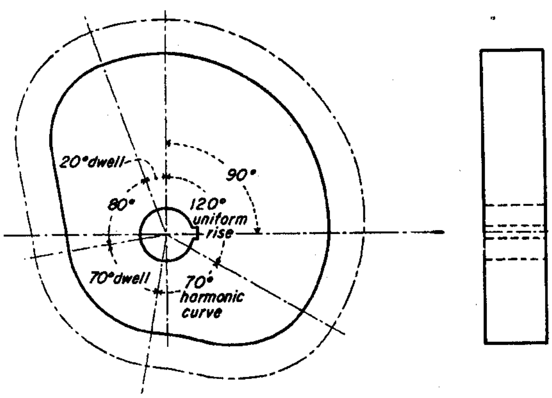

NON-UNIFORM FACE CAM—Sometimes called a disk cam. Follower can be either a roller, hexagon or pointed bar. Profile can be derived from a straight line, modified straight line, harmonic, parabolic or non-uniform base curve. Generally, the shock imposed by a cam designed on a straight line base curve is undesirable. Follower usually is weight loaded, although spring, hydraulic or pneumatic loading is satisfactory.

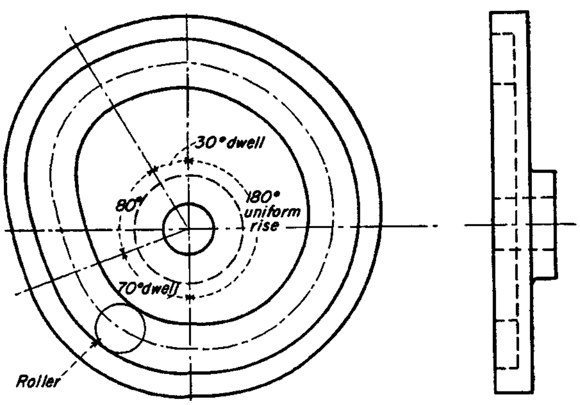

BOX CAM—Gives positive movement in two directions. A profile can be based on any desired base curve, as with face cams, but a cam miller is needed to cut it; whereas with face cams, a band saw and disk grinder could conceivably be used. No spring, pneumatic or hydraulic loading is needed for the followers. This type cam requires more material than for a face cam, but is no more expensive to mill.

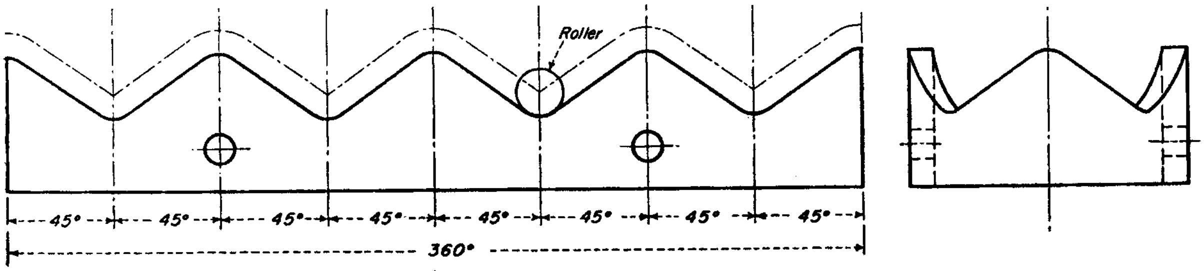

SIDE CAM—Essentially a barrel cam having only one side. Can be designed for any type of motion, depending on requirements and speed of operation. Spring or weight loaded followers of either the pointed or roller type can be used. Either vertical or horizontal mounting is permissible. Cutting of the profile is usually done on a shaper or a cam miller equipped with a small diameter cutter, although large cams 24 in. in diameter are made with 7-in. cutters.

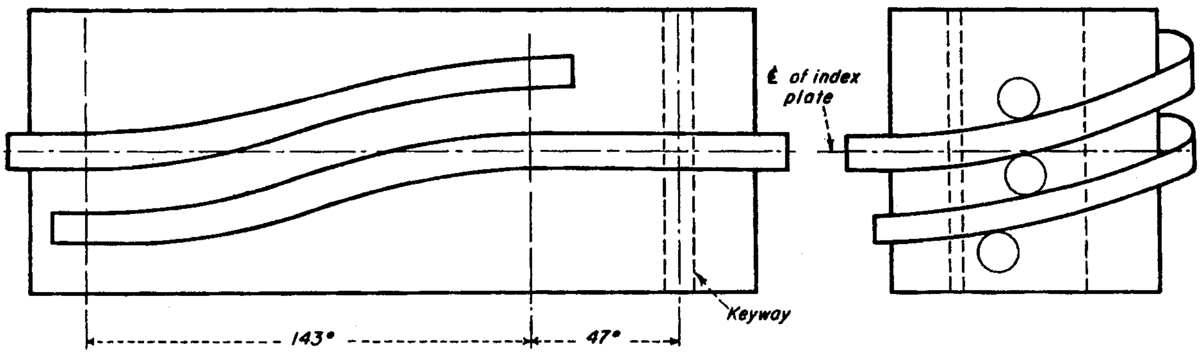

INDEX CAM—Within limits, such cams can be designed for any desired acceleration, deceleration and dwell period. A relatively short period for acceleration can be alloted on high speed cams such as those used on zipper-making equipment on which indexing occurs 1,200 to 1,500 times per minute. Cams of this sort can also be designed with four or more index stations.

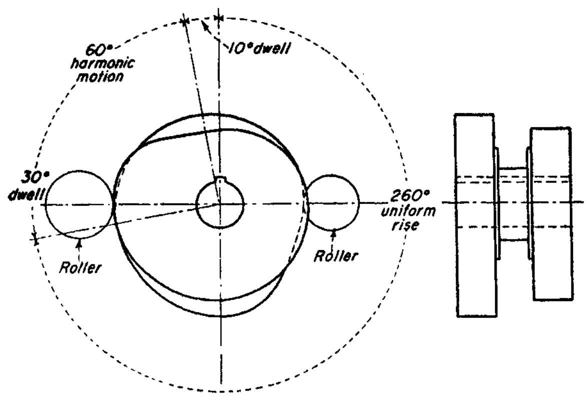

DOUBLE FACE CAM—Similar to single face cam except that it provides positive straight line movement in two directions. The supporting fork for the rollers can be mounted separately or between the faces. If the fork fulcrum is extended beyond the pivot point, the cam can be used for oscillatory movement. With this cam, the return stroke on a machine can be run faster than the feed stroke. Cost is more than that for a box cam

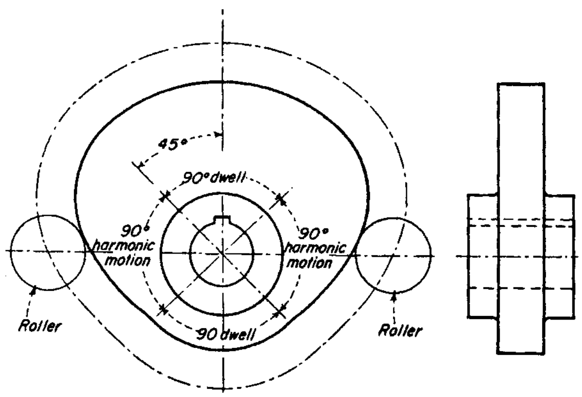

SINGLE-FACE CAM WITH TWO FOLLOWERS—Similar in action to a box or double face cam except flexibility is less than that for the latter type. Cam action for feed and return motions must be the same to prevent looseness of cam action. Used in place of box cams or double face cams to conserve space, and instead of single face cams to provide more positive movement for the roller followers.

SECTION 19

THREADED COMPONENTS

Getting the Most From Screws

Special jobs often call for special screw arrangements; here are some examples of how this busy fastener can perform.

Federico Strasser

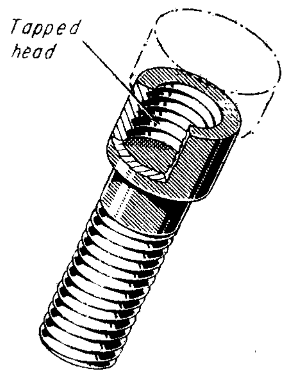

1 TAPPED HEAD LETS EXTENSIONS BE ADDED.

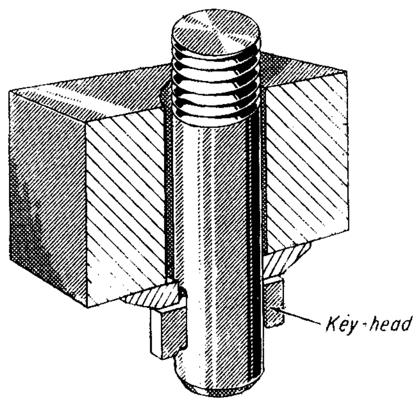

2 KEY-TYPE HEAD PROVIDES QUICK-RELEASE FEATURE.

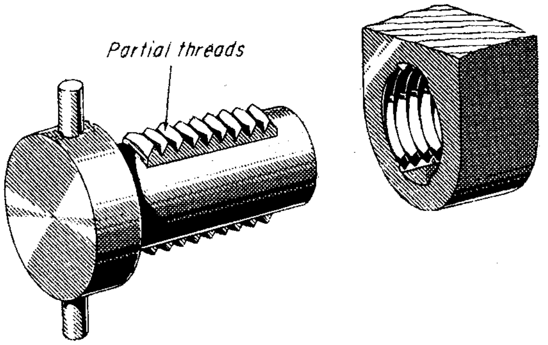

4 PARTIAL THREADS ASSEMBLE FAST, DON'T WORK LOOSE.

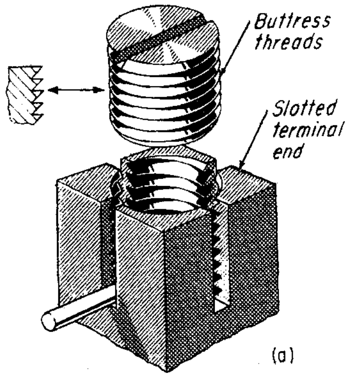

5 BUTTRESS THREADS PREVENT (a) radial forces from opening slotted ends; otherwise (b) a reinforcing sleeve is needed.

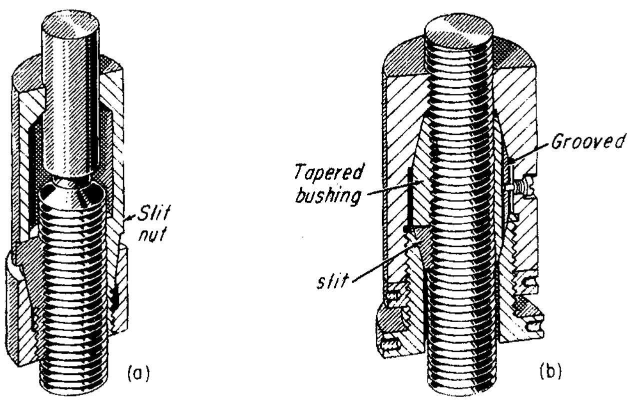

7 SLIT NUT (a) and tapered bushing (also slit) (b) allows backlash-free adjustment.

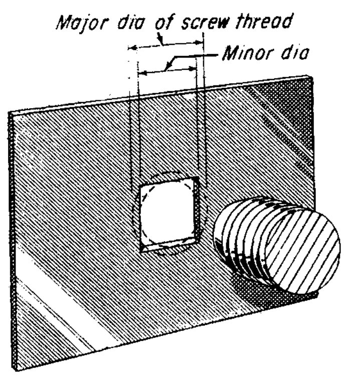

8 SQUARE HOLE for light metal or plastic substitutes well for threaded holes.

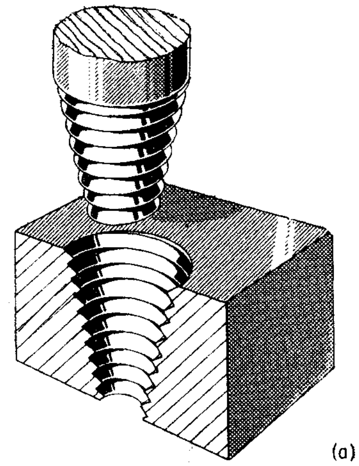

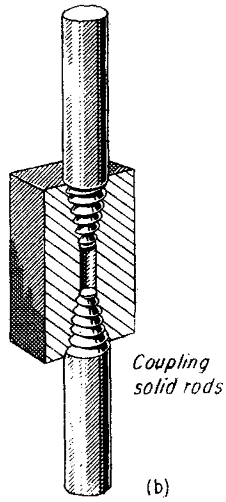

3 TAPERED SCREWS ASSEMBLE AND RELEASE FAST, BUT WORK LOOSE EASILY.

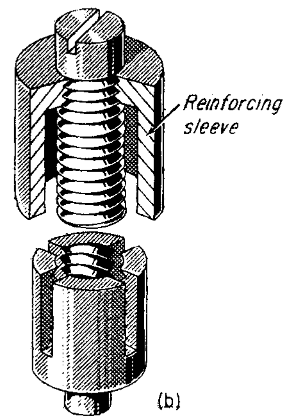

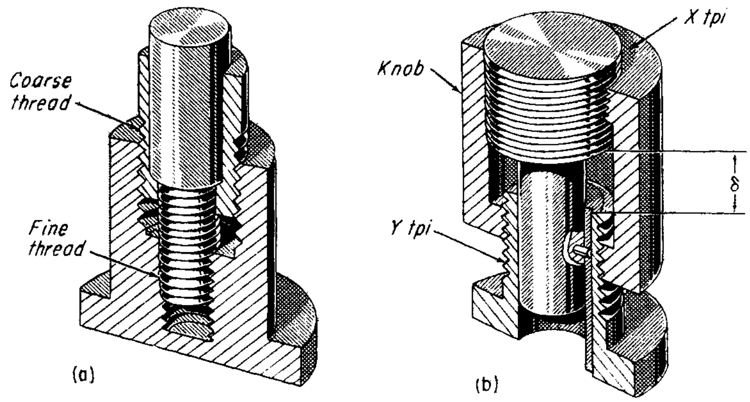

6 DIFFERENTIAL THREADS PROVIDE (a) extra tight fastening or (b) extra small relative movement, δ, per revolution of knob.

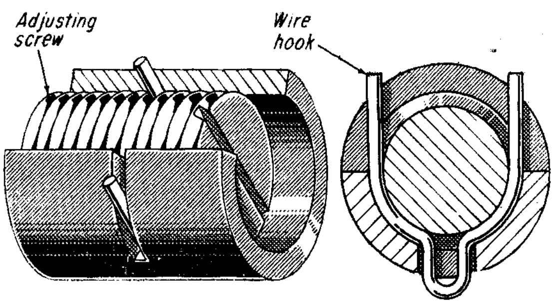

9 WIRE HOOK provides single-thread grip for low-cost device.

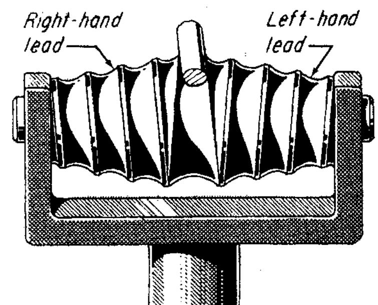

10 DOUBLE SCREW for wire guide or follower always leads wire to center.

How to Provide for Backlash in Threaded Parts

These illustrations are based on two general methods of providing for lost motion or backlash. One allows for relative movement of the nut and screw in the plane parallel to the thread axis; the other method involves a radial adjustment to compensate for clearance between sloping faces of the threads on each element.

Clifford T. Bower

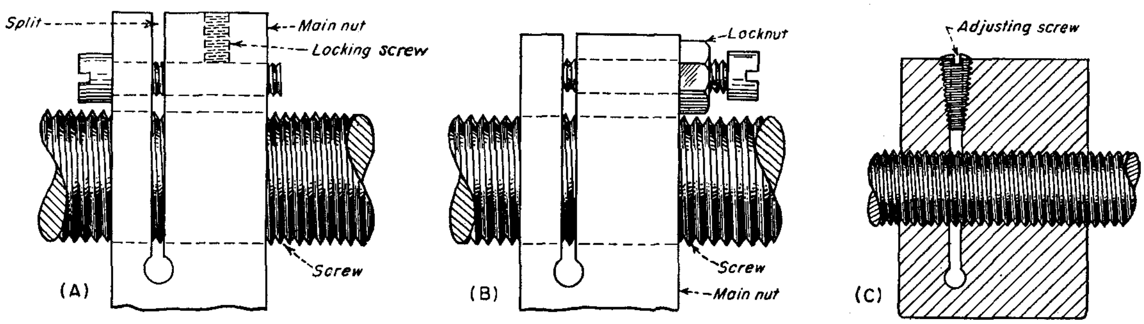

THREE METHODS of using slotted nuts. In *(A)*, nut sections are brought closer together to force left-hand nut flanks to bear on right-hand flanks of screw thread and vice versa. In *(B)*, and *(C)* nut sections are forced apart for same purpose.

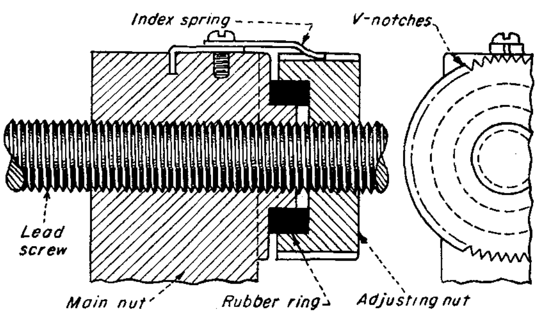

AROUND THE PERIPHERY of the backlash-adjusting nut are "v" notches of small pitch which engage the index spring. To eliminate play in the lead screw, adjusting nut is turned clockwise. Spring and adjusting nut can be calibrated for precise use.

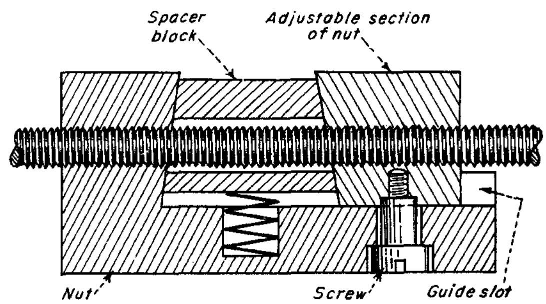

SELF-COMPENSATING MEANS of removing backlash. Slot is milled in nut for an adjustable section which is locked by a screw. Spring presses the tapered spacer block upwards, forcing the nut elements apart, thereby taking up backlash.

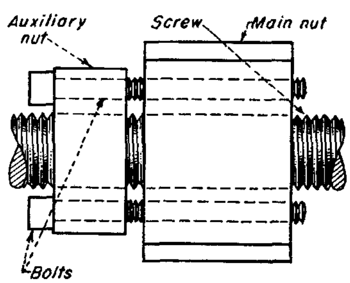

MAIN NUT is integral with base attached to part moved by screw. Auxiliary nut is positioned one or two pitches from main nut. The two are brought closer together by bolts which pass freely through the auxiliary nut.

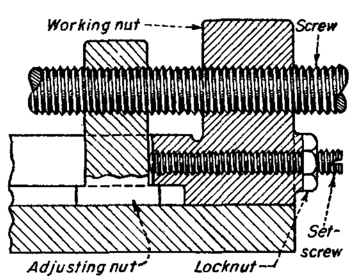

ANOTHER WAY to use an auxiliary or adjusting nut for axial adjustment of backlash. Relative movement between the working and adjusting nuts is obtained manually by the set screw which can be locked in place as shown.

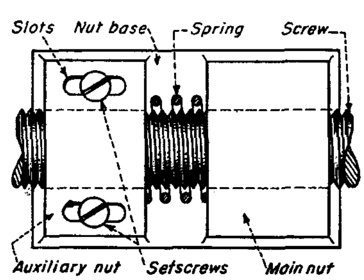

COMPRESSION SPRING placed between main and auxiliary nuts exerts force tending to separate them and thus take up slack. Set screws engage nut base and prevent rotation of auxiliary nut after adjustment is made.

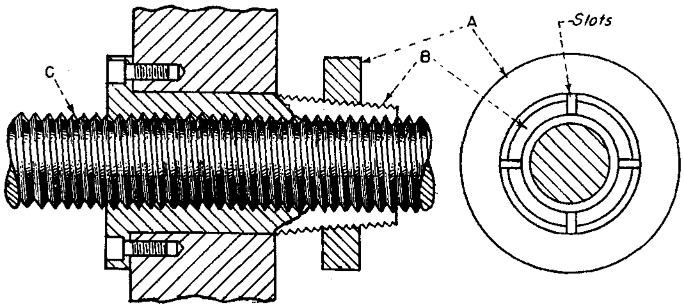

NUT *A* IS SCREWED along the tapered round nut, *B*, to eliminate backlash or wear between *B* and *C*, the main screw, by means of the four slots shown.

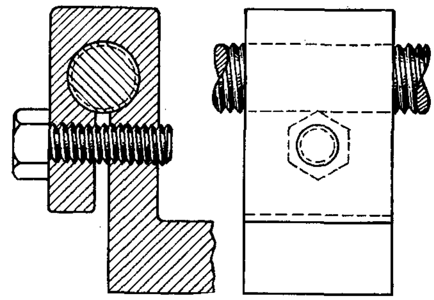

ANOTHER METHOD of clamping a nut around a screw to reduce radial clearance.

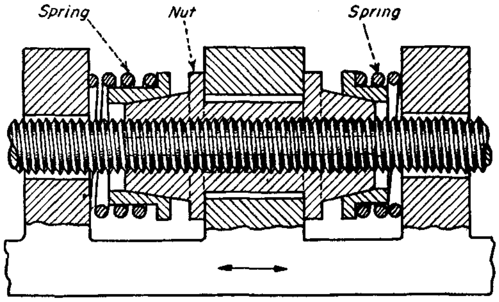

AUTOMATIC ADJUSTMENT for backlash. Nut is flanged on each end, has a square outer section between flanges and slots cut in the tapered sections. Spring forces have components which push slotted sections radially inward.

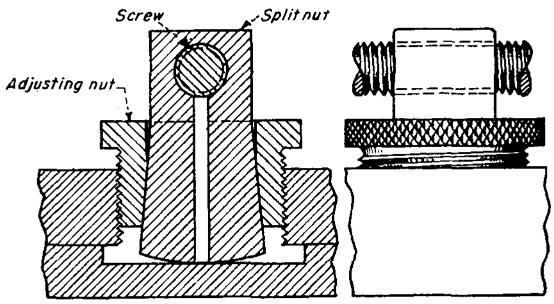

SPLIT NUT is tapered and has a rounded bottom to maintain as near as possible a fixed distance between its seat and the center line of the screw. When the adjusting nut is tightened, the split nut springs inward slightly.

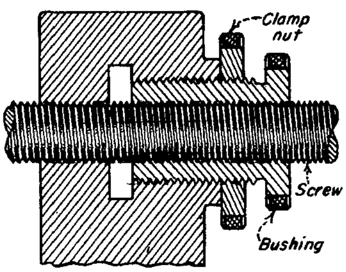

CLAMP NUT holds adjusting bushing rigidly. Bushing must have different pitch on outside thread than on inside thread. If outer thread is the coarser one, a relatively small amount of rotation will take up backlash.

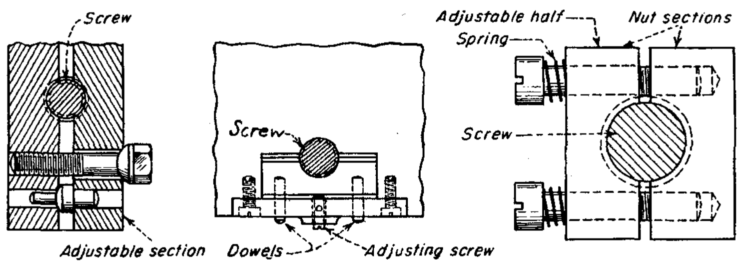

TYPICAL CONSTRUCTIONS based on the half nut principle. In each case, the nut bearing width is equal to the width of the adjustable or inserted slide piece. In the sketch at the extreme left, the cap screw with the spherical seat provides for adjustments. In the center sketch, the adjusting screw bears on the movable nut section. Two dowels insure proper alignment. The third illustration is similar to the first except that two adjusting screws are used instead of only one.

7 Special Screw Arrangements

How differential, duplex, and other types of screws can provide slow and fast feeds, minute adjustments, and strong clamping action.

Louis Dodge

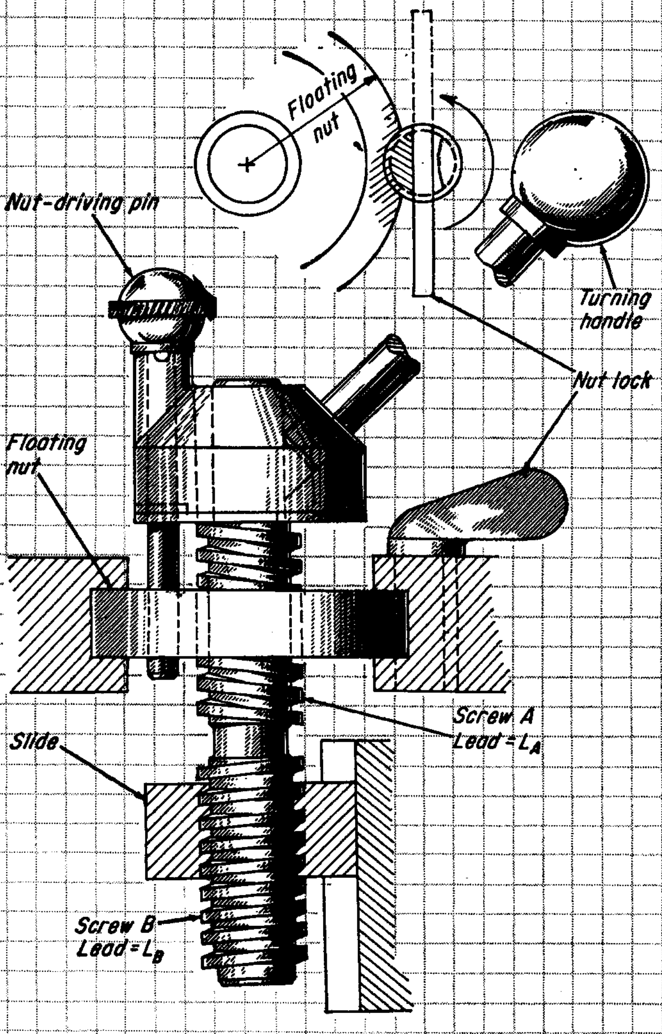

1 **RAPID AND SLOW FEED.** With left- and right-hand threads, slide motion with nut locked equals L_A plus L_B per turn; with nut floating, slide motion per turn equals L_B. Get extremely fine feed with rapid return motion when threads are differential.

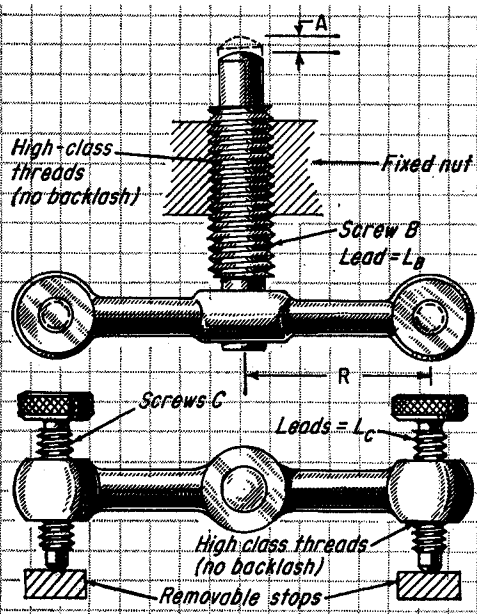

2 **EXTREMELY SMALL MOVEMENTS.** Microscopic measurements, for example, are characteristic of this arrangement. Movement A is equal to $N(L_B \times L_C)/2\pi R$, where N equals number of turns of screw C.

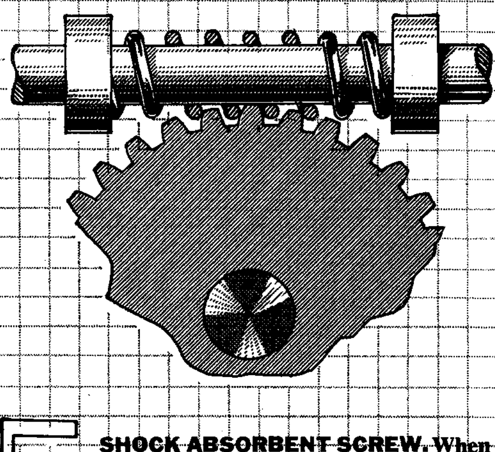

5 **SHOCK ABSORBENT SCREW.** When springs coiled as shown are used as worm drives for light loads, they have the advantage of being able to absorb heavy shocks.

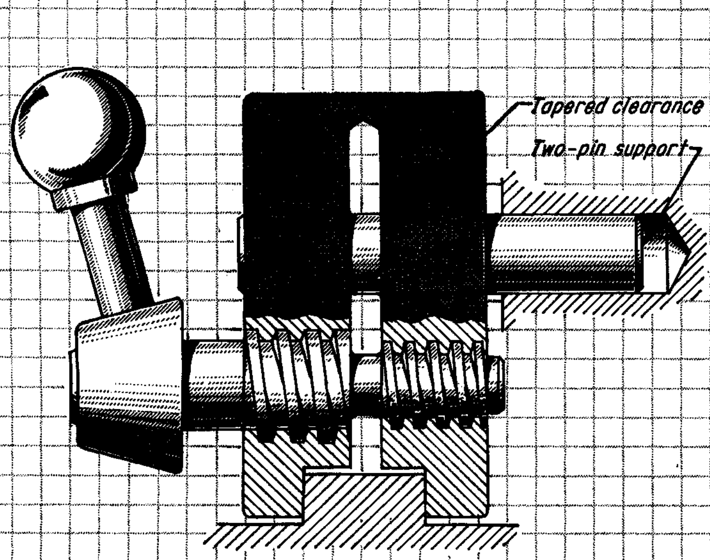

3

DIFFERENTIAL CLAMP. This method of using a differential screw to tighten clamp jaws combines rugged threads with high clamping power. Clamping pressure, $P = Te/[R(\tan\phi + \tan\alpha]$, where T = torque at handle, R = mean radius of screw threads, ϕ = angle of friction (approx. 0.1), α = mean pitch angle of screw, and e = efficiency of screw (generally about 0.8).

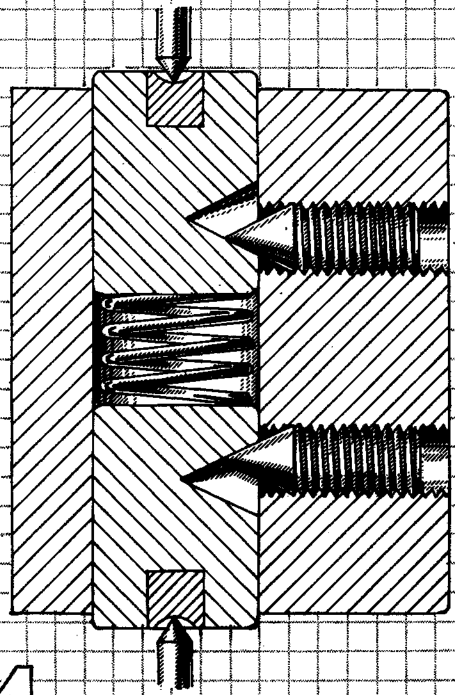

4

BEARING ADJUSTMENT. This screw arrangement is a handy way of providing for bearing adjustment and overload protection.

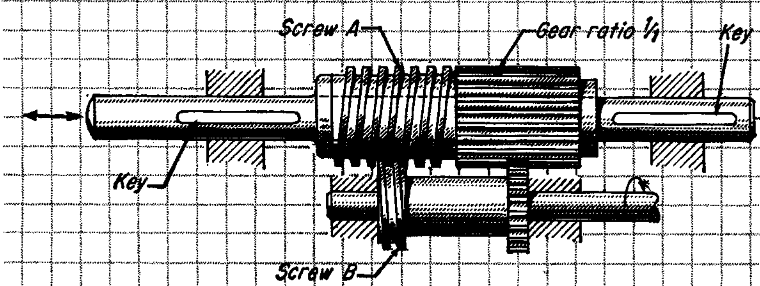

6

HIGH REDUCTION of rotary motion to fine linear motion is possible here. Arrangement is for low forces. Screws are left and right hand. $L_A = L_B$ plus or minus a small increment. When $L_B = 1/10$ and $L_A = 1/10.05$ the linear motion of screw A will be 0.05 in. per turn. When screws are the same hand, linear motion equals $L_A + L_B$.

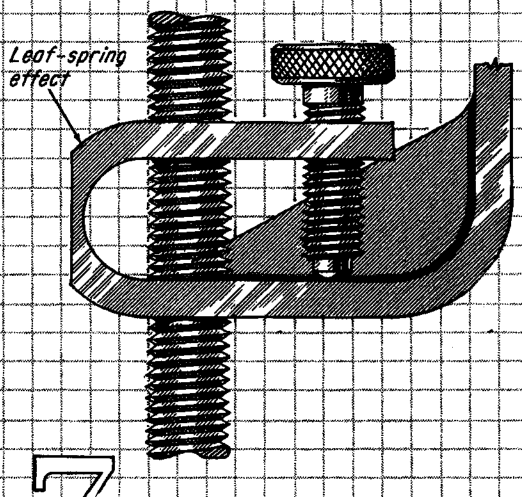

7

BACKLASH ELIMINATION. The large screw is locked and all backlash is eliminated when the knurled screw is tightened — finger torque is sufficient.

20 Dynamic Applications for Screw Threads

Have you forgotten how simply, and economically, screw threads can be made into dynamic members of a linkage? Here are some memory-joggers, plus suggestions for simplified nuts, threads and nut guides.

Kurt Rabe

You need a threaded shaft, a nut . . . plus some way for one of these members to rotate without translating and the other to translate without rotating. That's all. Yet these simple components can do practically all of the adjusting, setting, or locking used in design.

Most such applications have low-precision requirements. That's why the thread may be a coiled wire or a twisted strip; the nut may be a notched ear on a shaft or a slotted disk. Standard screws and nuts right off your supply shelves can often serve at very low cost.

Here are the basic motion transformations possible with screw threads (Fig 1):

- transform rotation into linear motion or reverse (A),
- transform helical motion into linear motion or reverse (B),
- transform rotation into helical motion or reverse (C).

Of course the screw thread may be combined with other components: in a 4-bar linkage (Fig 2), or with multiple screw elements for force or motion amplification.

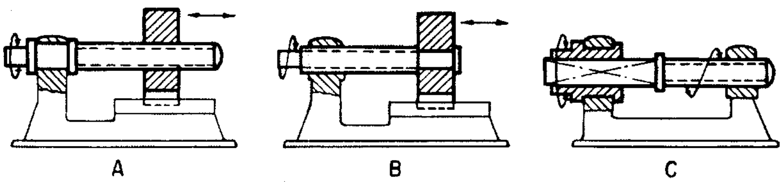

1 MOTION TRANSFORMATIONS of a screw thread include: rotation to translation (A), helical to translation (B), rotation to helical (C). Any of these is reversible if the thread is not self-locking (see screw-thread mathematics on following page—thread is reversible when efficiency is over 50%).

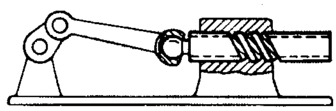

2 STANDARD 4-BAR LINKAGE has screw thread substituted for slider. Output is helical rather than linear.

A Review of Screw-Tread Mathematics

a — friction angle, $\tan a = f$
r — mean radius of thread $= \frac{1}{2}$ (root radius + outside radius), in inches
l — lead, thread advance in one revolution, in.
b — lead angle, $\tan b = 1/2\pi r$, deg
f — friction coefficient
P — equivalent driving force at radius r from screw axis, lb
L — axial load, lb
e — efficiency
c — half angle between thread faces, deg

SQUARE THREADS:

$$P = L \tan (b \pm a) = L \frac{(1 \pm 2\pi r f)}{(2\pi r \mp fl)}$$

Where upper signs are for motion opposed in direction to L. Screw is self-locking when $b \leqq a$.

$$e = \frac{\tan b}{\tan (b + a)} \quad \text{(motion opposed to } L\text{)}$$

$$e = \frac{\tan (b - a)}{\tan b} \quad \text{(motion assisted by } L\text{)}$$

V THREADS:

$$P = L \frac{(l \pm 2\pi r f \sec c)}{(2\pi r \mp lf \sec c)}$$

$$e = \frac{\tan b\,(1 - f \tan b \sec c)}{(\tan b + f \sec c)} \quad \text{(motion opposed to } L\text{)}$$

$$e = \frac{\tan b - f \sec c}{\tan b\,(1 + f \tan b \sec c)} \quad \text{(motion assisted by } L\text{)}$$

For more detailed analysis of screw-thread friction forces, see Marks *Mechanical Engineers' Handbook*, McGraw-Hill Book Co.

Rotation to Translation

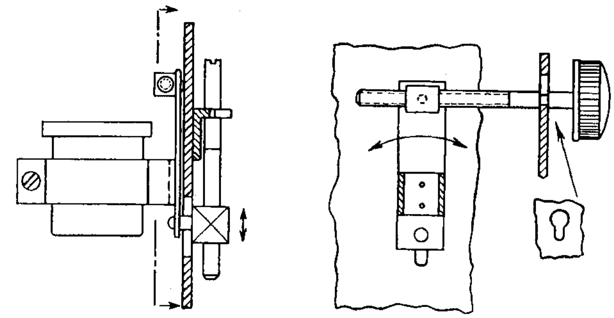

3 TWO-DIRECTIONAL LAMP ADJUSTMENT with screwdriver to move lamp up and down. Knob adjust (right) rotates lamp about pivot.

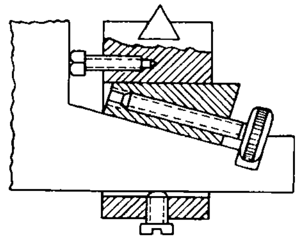

4 KNIFE-EDGE BEARING is raised or lowered by screw-driven wedge. Two additional screws locate the knife edge laterally and lock it.

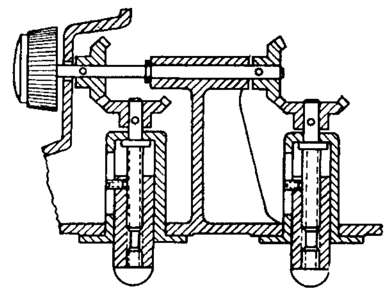

5 SIDE-BY-SIDE ARRANGEMENT of tandem screw threads gives parallel rise in this height adjustment for projector.

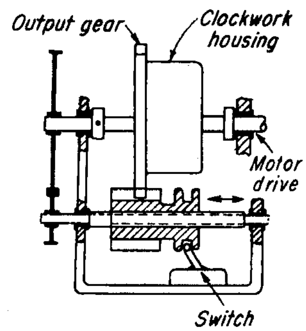

6 AUTOMATIC CLOCKWORK is kept wound tight by electric motor turned on and off by screw thread and nut. Note motor drive must be self-locking or it will permit clock to unwind as soon as switch turns off.

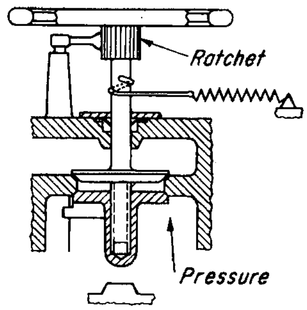

7 VALVE STEM has two oppositely moving valve cones. When opening, the upper cone moves up first, until it contacts its stop. Further turning of the valve wheel forces the lower cone out of its seat. The spring is wound up at the same time. When the ratchet is released, spring pulls both cones into their seats.

A Review of Screw-Tread Mathematics Continued

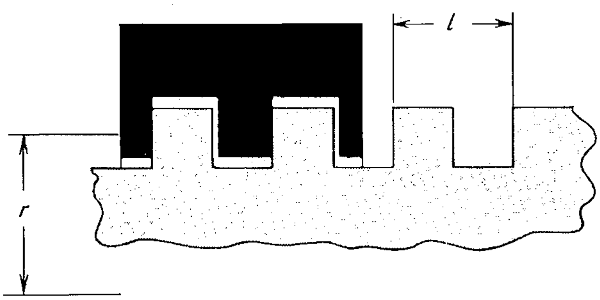

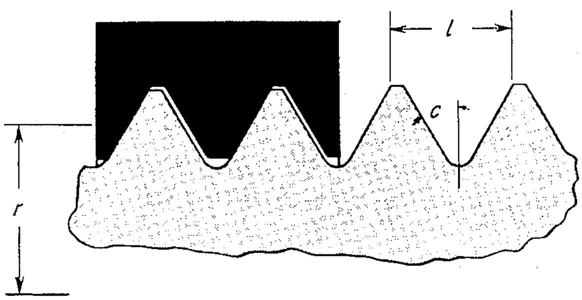

Translation to Rotation

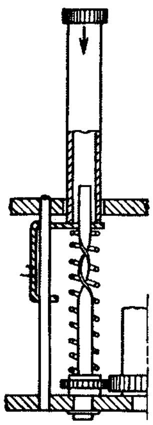

8 A METAL STRIP or square rod may be twisted to make a long-lead thread, ideal for transforming linear into rotary motion. Here a push-button mechanism winds a camera. Note that the number of turns or dwell of output gear is easily altered by changing (or even reversing) twist of the strip.

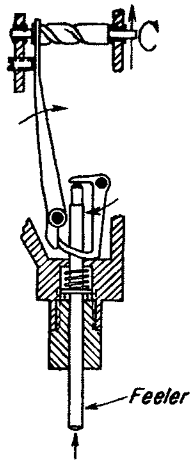

9 FEELER GAGE has its motion amplified through a double linkage and then transformed to rotation for dial indication.

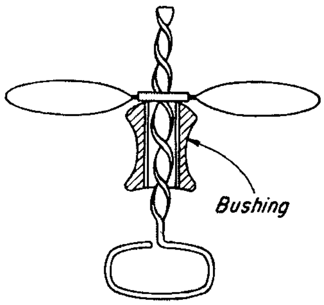

10 THE FAMILIAR flying propeller-toy is operated by pushing the bushing straight up and off the thread.

Self-Locking

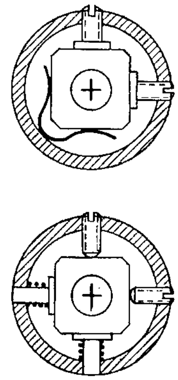

11 HAIRLINE ADJUSTMENT for a telescope, with two alternative methods of drive and spring return.

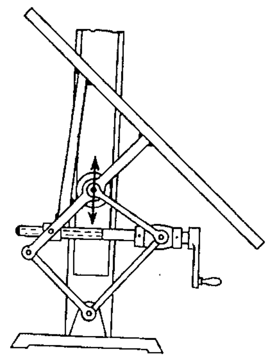

12 SCREW AND NUT provide self-locking drive for a complex linkage.

Double Threading

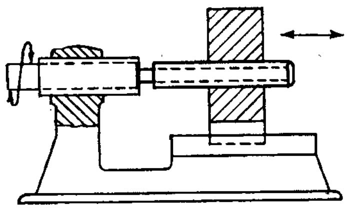

13 DOUBLE-THREADED SCREWS, when used as differentials, provide very fine adjustment for precision equipment at relatively low cost.

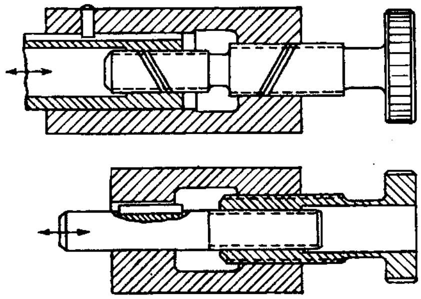

14 DIFFERENTIAL SCREWS can be made in dozens of forms. Here are two methods: above, two opposite-hand threads on a single shaft; below, same hand threads on independent shafts.

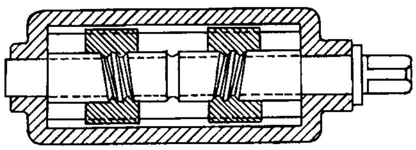

15 OPPOSITE-HAND THREADS make a high-speed centering clamp out of two moving nuts.

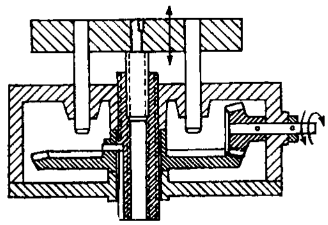

16 MEASURING TABLE rises very slowly for many turns of the input bevel gear. If the two threads are 1½—12 and ¾—16, in the fine-thread series, table will rise approximately 0.004 in. per input-gear revolution.

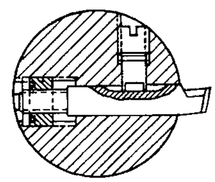

17 LATHE TURNING TOOL in drill rod is adjusted by differential screw. A special double-pin wrench turns the intermediate nut, advancing the nut and retracting the threaded tool simultaneously. Tool is then clamped by setscrew.

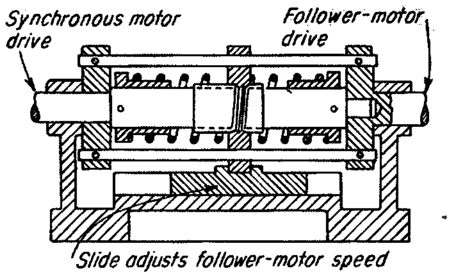

18 ANY VARIABLE-SPEED MOTOR can be made to follow a small synchronous motor by connecting them to the two shafts of this differential screw. Differences in number of revolutions between the two motors appear as motion of the traveling nut and slide so an electrical speed compensation is made.

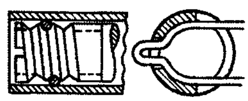

19 (left) **A WIRE FORK** is the nut in this simple tube-and screw design.

20 (below) **A MECHANICAL PENCIL** includes a spring as the screw thread and a notched ear or a bent wire as the nut.

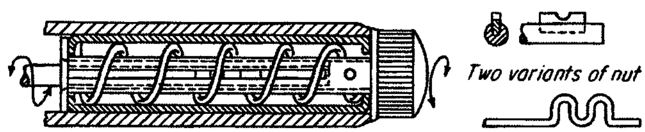

EDITOR'S NOTE: For other solutions to adjusting, setting, and locking problems in translating motion, see:

10 Ways to Employ Screw Mechanisms, May 26 '58, p 80. Shows applications in terms of three basic components—actuating member, threaded device, and sliding device.

5 Cardan-gear Mechanisms. Sep 28 '59, p 66. Gearing arrangements that convert rotation into straight-line motion.

5 Linkages for Straight-line Motion, Oct 12 '59, p 86. Linkages that convert rotation into straight-line motion.

Preloading of Bolts

For optimum tension-bolt design, the bolts must be preloaded to a specific amount. Here are charts which quickly give the data you need.

Bernie J. Cobb

1.. PRELOAD VS AXIAL LOAD RELATIONSHIPS

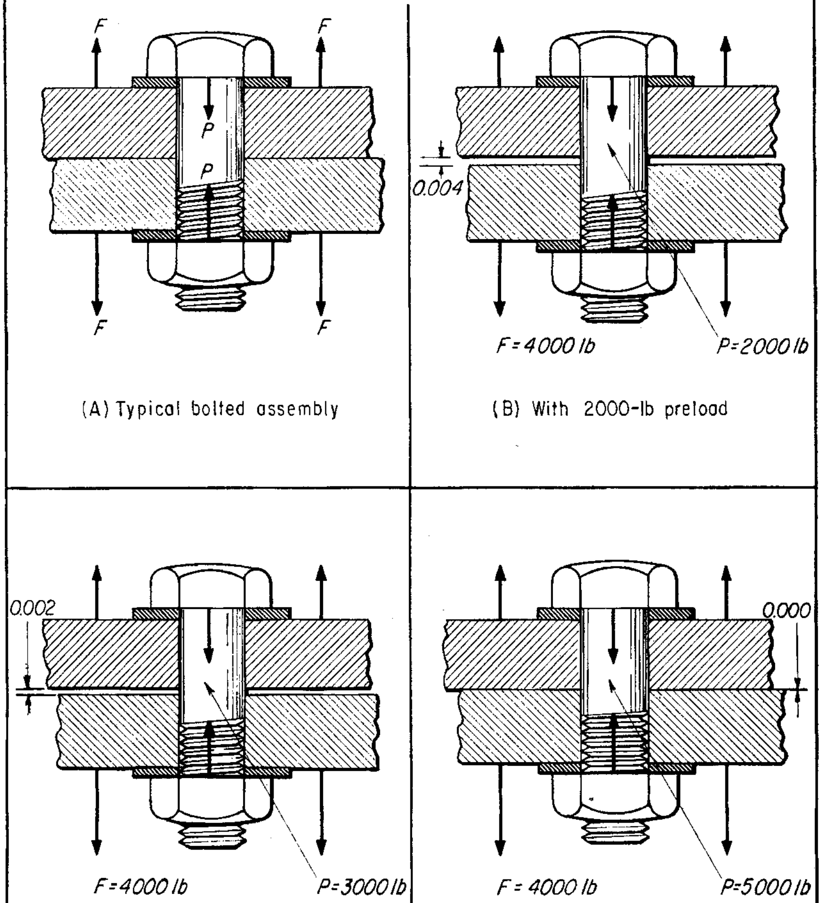

(A) Typical bolted assembly

(B) With 2000-lb preload

(C) With 3000-lb preload

(D) With 5000-lb preload

THE rule is, always tighten a bolted assembly to the maximum permissible preload. The benefits are twofold: 1) You extend the fatigue life, by reducing or eliminating fluctuations in stress. 2) You can design a smaller, lighter, less costly assembly for a given tensile load.

Although other methods have been published for computing the necessary data, the design charts offered here are both accurate and simple to use. They show a direct relationship for the four key factors: bolt diameter, bolt strength, tightening torque, and preload. When any two of these factors are given, the charts produce the other two.

The stress equation on which the charts are based is derived from the currently accepted maximum strain theory. The data in these charts have simplified critical problems in missile design and have been successfully applied to the design of solid propellant rocket motors, where the bolts must absorb the blow-off load exerted by internal pressure of the motor against the nozzle and igniter, maintain a positive pressure on the gasket between the flanges, and be as lightweight as possible.

How preload works

A bolted unit is shown in Fig 1. The bolt is tightened (in A) to produce a preload, *P*. The applied axial load, *F*, may be the result of internal pressure (the plates may then represent flanges), or of external loads (one of the plates may be a bracket, the other a machine frame).

If a tightening torque is applied to the nut to provide a 2000-lb preload, as in B, and if the applied load varies from zero to a maximum of 4000 lb, the bolt will experience a cyclic load change of 2000 lb which will contribute to fatigue failure. There will also be a separation between plates of, say, 0.004 in. (This is a function of bolt diameter and material.)

If the preload is increased to 3000 lb, as in C, the load variations will be reduced to 1000 lb, which will increase fatigue life and reduce plate separation under load by 50%, to 0.002 in. If the preload is now increased to 5000 lb, as in D, there will be no separation of the plates under load, and the load variations will be reduced to zero. Fatigue failure should not occur.

The important information to know in the above analysis is the maximum preload that can be safely applied to a particular bolt, and how much tightening torque must be applied to obtain the maximum preload.

Maximum preload

A value accepted by many designers and recommended by Kent (*Mechanical Engineer's Handbook*, 12th ed), is that the prestress must not exceed 80% of the bolt-proof strength. The resulting 20% margin of safety allows for variations in applied torque and for the friction forces that may occur. Proof strength is defined as 85% of

SYMBOLS

d_p = Pitch diameter of screw threads, in.
d_r = Minor diameter of screw threads, in.
D = Mean bearing diameter of nut, in.
m = $\dfrac{\tan(\beta + \phi)}{\cos\alpha}$
N = Reaction force normal to helix, lb
F = Applied axial load in bolt, lb
P = Maximum permissible preload, lb
S = Combined bolt stress, psi
S_t = Tensile stress, psi
S_s = Combined stress, psi
T = Applied tightening torque to bolt head, in.-lb
α = One half of thread profile angle, deg
β = Helix angle of thread, deg
ϵ = Poisson's ratio (0.3 for steel)
μ = Coefficient of friction between threads
v = Coefficient of friction between nut and washer on bearing surface
ϕ = Friction angle, deg, $\tan\phi = \mu$

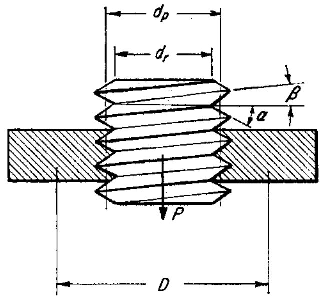

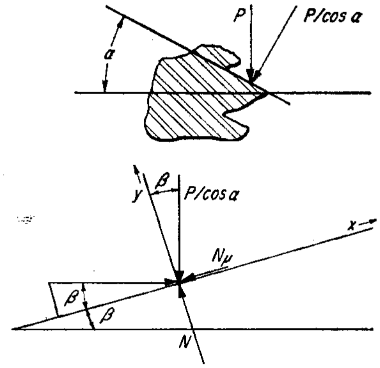

DERIVATION OF DESIGN EQUATIONS

Load-torque ratio

The summation of forces, left, acting on a thread along the x and y axis are

$$F\cos\beta - \sin\beta\,(P/\cos\alpha) - N\mu = 0$$

$$N - \cos\beta\,(P/\cos\alpha) - F\sin\beta = 0$$

Combining these equations and substituting tan ϕ for μ results in

$$\frac{F}{P} = \frac{\tan(\phi+\beta)}{\cos\alpha} = m$$

The torque acting on the bolt is

$$T = \frac{1}{2}Fd_p + \frac{1}{2}PDv,\quad \frac{P}{T} = \frac{2}{Dv + m\,d_p}$$

Stress-torque ratio

For pure tension and torsion in the bolt

$$S_t = \frac{P}{A} = \frac{4P}{\pi\,d_r^2},\quad S_s = \frac{16\,T}{\pi\,d_r^3}$$

Since the torque on the bolt shank $T = Fd_p/2$, and $F = Pm$, then

$$S_s = \frac{8\,P\,m\,d_p}{\pi\,d_r^3},\quad \frac{S_s}{S_t} = 2\,m\,\frac{d_p}{d_r}$$

To combine these stresses, the maximum strain theory by Saint-Venant is employed which states that elastic failure occurs when the deformation normal to any plane in the body reaches a value equal to the strain at the yield stress in pure tension:

$$S = \frac{1}{2}\left[(1-\epsilon)\,S_t + (1+\epsilon)(S_t^2 + 4\,S_s^2)^{1/2}\right] \qquad (1)$$

To obtain a solution for S, the values for S_t and S_s must first be calculated. If S is greater than the yield strength of the material, then S_t or S_s must be reduced, or failure may likely occur. The yield strength in shear is usually about 60% of the tensile yield, or $S_s = 0.6S$. To modify Eq 1 so that the above relationship holds true when there is pure torsion (when $S_t = 0$), a correction factor, C, must be employed. Hence, from Eq 1 with $\varepsilon = 0.3$ and $S_t = 0$:

$$\frac{S_s}{0.6} = \frac{1}{2}\left[(1+0.3)\,\sqrt{4\,(C\,S_s)^2}\right],\ C = 1.3$$

Eq 1 now becomes

$$S = \frac{1}{2}\left[(1-\epsilon)\,S_t + (1+\epsilon)\,(S_t^2 + 6.76\,S_s^2)^{1/2}\right]$$

Substituting values for S_t, S_s/S_t, and $\varepsilon = 0.3$, and dividing by T gives

$$\frac{S}{T} = \frac{0.89 + 1.66\sqrt{1 + (5.2\,m\,d_p/d_r)^2}}{d_r^2\,(\nu D + m\,d_p)} \qquad (2)$$

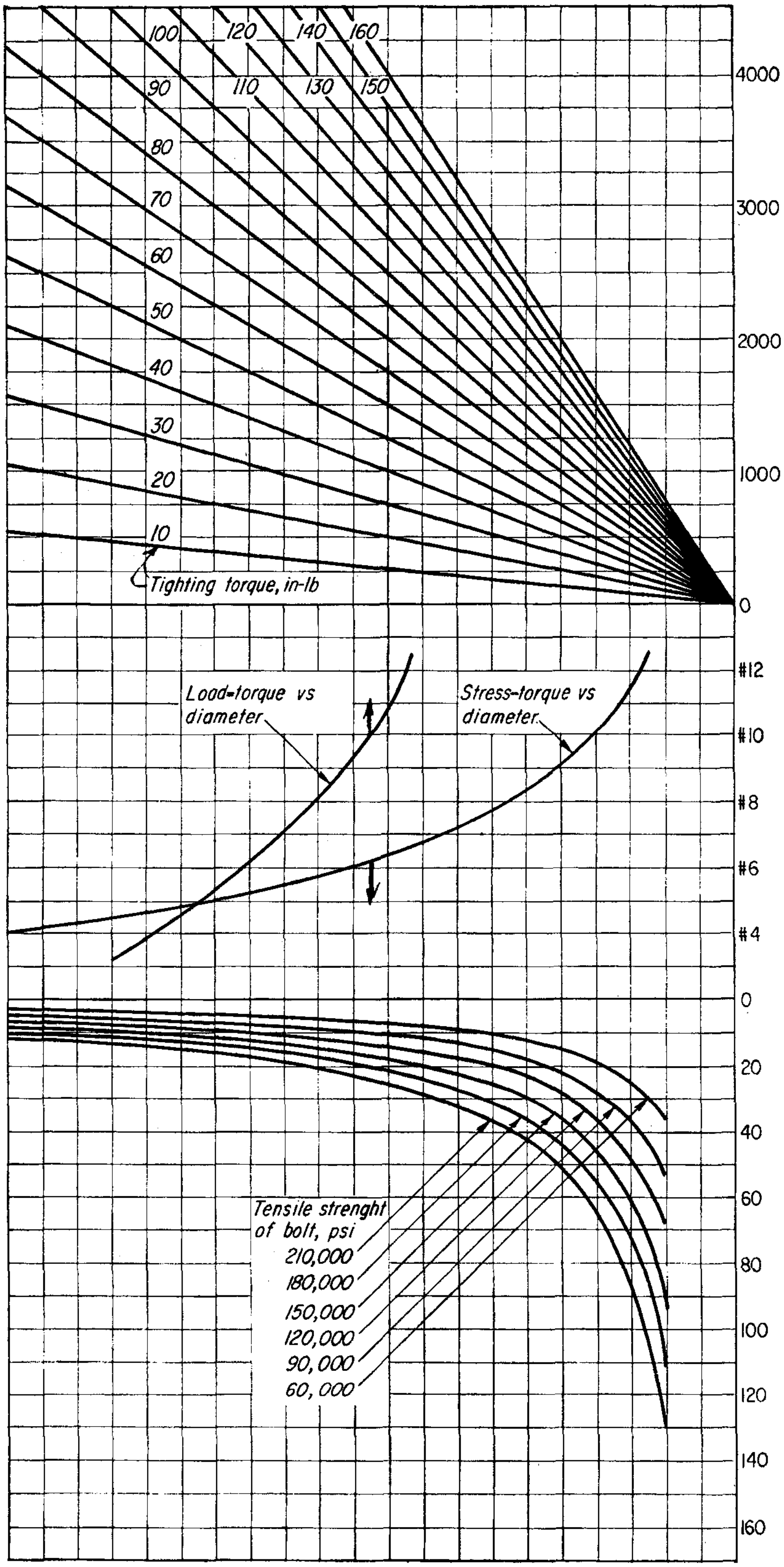

2. . FOR BOLT SIZES, #4 TO #12.

the ultimate (tensile) strength of the bolt, which results in a maximum permissible prestress of 80 × 85 = 68%, or roughly two thirds, of the tensile strength. However, a value of only 60% of the tensile strength was used in the charts to compensate for certain deviations, which will be explained later.

An ideal limit suggested by some researchers is that the bolt be tightened to its yield point and then slightly loosened. The drawback here is that the yield point of the bolt cannot be determined with any reasonable degree of accuracy.

Equations

The equations which form the basis of the analysis and related design curves are as follows:

Stress-torque ratio:

$$\frac{S}{T} = \frac{0.89+1.66\sqrt{1+(5.2md_p/d_r)^2}}{d_r^2\,(vD+md_p)}$$

Preload-torque ratio:

$$\frac{P}{T} = \frac{2}{vD + md_p}$$

where

$$m = \frac{\tan(\beta+\phi)}{\cos\alpha}$$

Design curves

The most common bolt applications utilize steel bolts and nuts, unlubricated (as received from the manufacturer). For this type of application, values of 0.14 for collar friction ν, and 0.12 for thread friction μ, are reasonable and were used to plot the curves. The curves are plotted for fine threads but may be used for coarse

BOLT CANDIDATES FOR PROBLEM I

BOLT DIAMETER, IN.	TIGHTENING TORQUE, IN.-LB
1/4	180
5/16	225
3/8	275
7/16	320
1/2	360

and extra-fine threads with only small error. When the recommended tightening torque from the curves for a specific bolt size is applied to coarse threads instead of fine, the prestress will be somewhat higher, probably on the order of 10%; when applied to extra-fine threads, it will be somewhat less, again probably on the order of 10%. For critical applications, the formula can be used to make calculations which can be checked from the curves.

The three groups of curves, Fig 2, 3, and 4, are for bolt sizes ranging from #4 to #12, from ¼-in. to ½-in. diameter and from ½-in. to 1-in. diameter, respectively. In each group the top family of curves is for the preload-torque ratio and the bottom family for the stress-torque ratio. The center curves act as pivot points.

Problem I—bolt selection

The design requirement is to select a bolt that can successfully sustain a 4000-lb axial load. Here are the steps to follow:

1) Make the preload equal to the anticipated axial load. Hence, $P = F$. (The preload can also be made larger than the anticipated axial load.)

2) Select several bolt sizes in the size range expected, then check tensile-strength and tightening-torque requirements. For example, choose a bolt of ⅜-in. diameter. This calls for use of the curves, Fig 3, to the right. From the column for ⅜-in. bolt diameter, read across to the load-torque line, then pivot upward to intersect the 4000-lb load line, as shown by the arrows. A reading of the radial torque line at this point gives a tightening-torque value of 275 in.-lb.

3) Return to the ⅜-in. bolt diameter and read across to the stress-torque line, then pivot downward to intersect

TENSILE LOAD, LB	BOLT STRENGTH, PSI
4000	Over 210,000
4000	180,000
4000	120,000
4000	90,000
4000	60,000

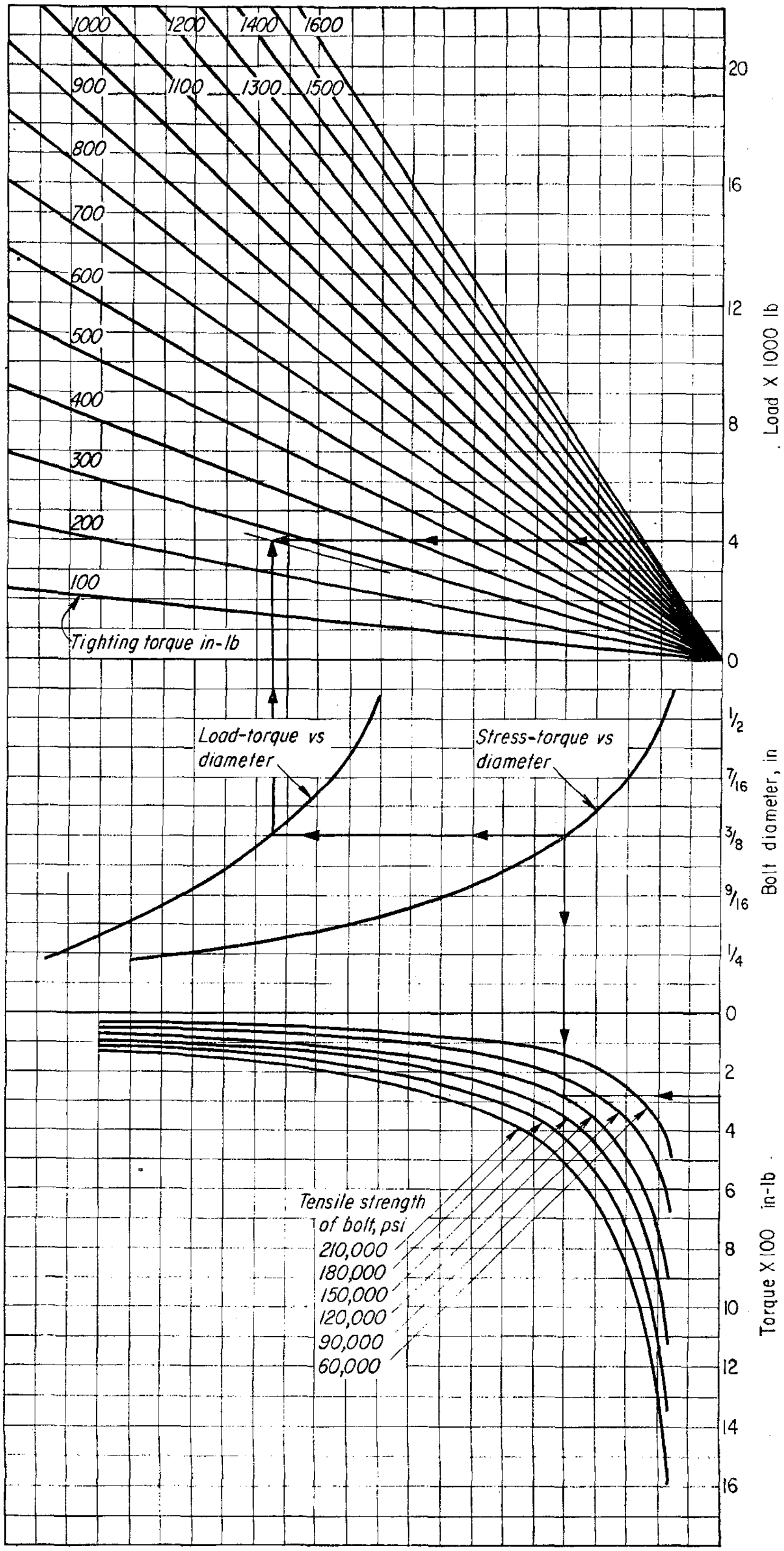

3. . FOR BOLT DIAMETERS, ¼ IN. TO ½ IN.

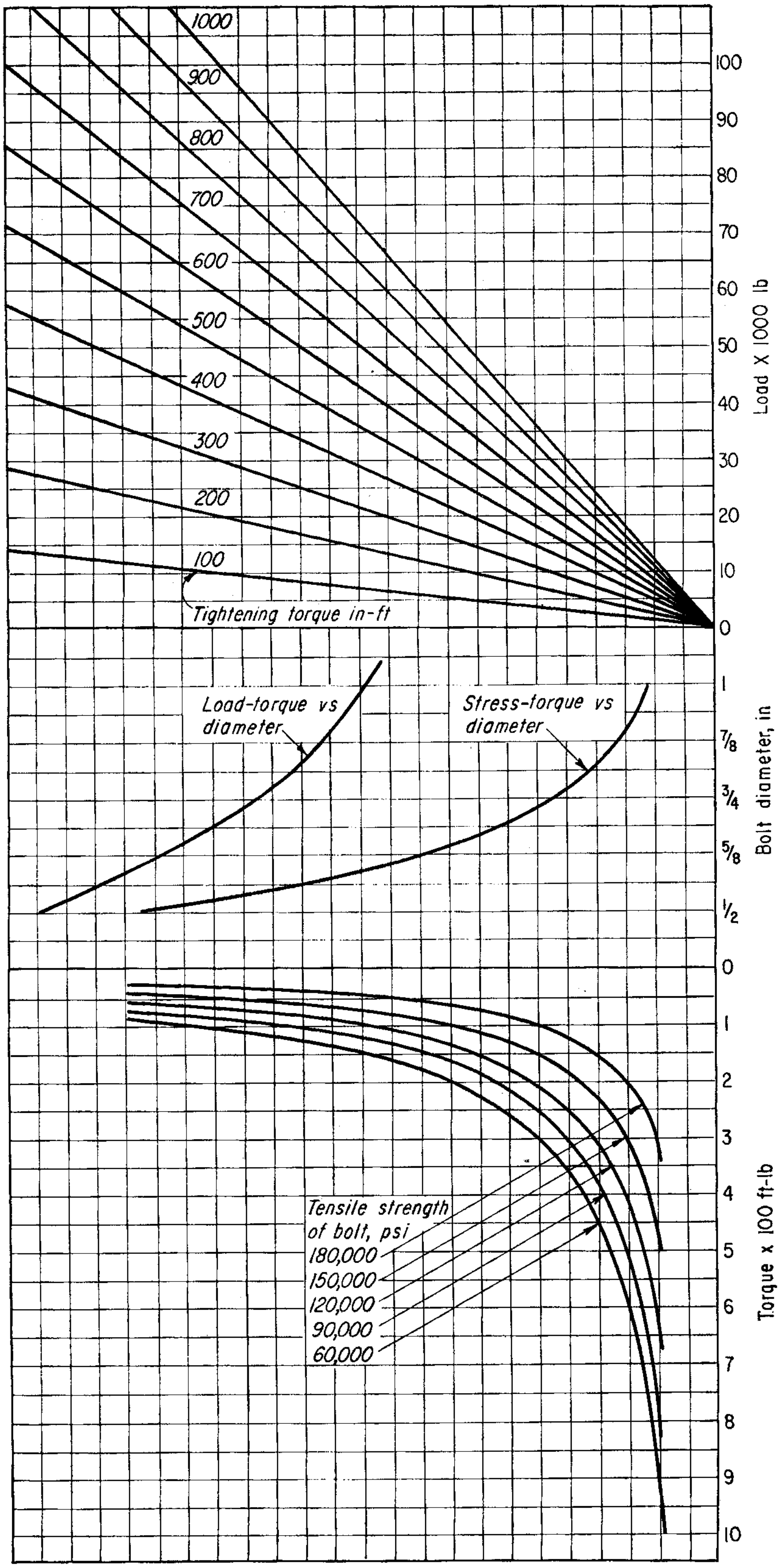

4..FOR BOLT DIAMETERS, ½ IN. TO 1 IN.

a line drawn from the 275 in.-lb. point. At this intersection the tensile strength is 120,000 psi. This is the material-strength requirement for the bolt.

4) The procedure is repeated for other bolt sizes and the results are listed in the table, p 64, in order of bolt size. All the bolts, with the exception of the ¼-in. bolt, will satisfy the requirements of absorbing a 4000-lb axial load without stress fluctuations or plate separation. The smaller bolts require higher-strength material but may be better for lightweight design.

Problem II—a check on accuracy

Use the equations to determine the tightening torque and required material strength for a ¾-16 UNF-2 bolt that is subjected to a 20,000-lb force.

Bolt pitch = 1/16 in., d_r (from tables) = 0.6718, d_p = 0.7029, D = 0.9375, μ = 0.12, v = 0.14, α = 30 deg.

$$\text{Sin } \beta = \frac{1}{16\pi\,(0.7029)} = 0.0283$$

$$\beta = 1°\,37'$$

$$\tan \phi = 0.12 \quad \text{or } \phi = 6°\,50'$$

$$m = \frac{\tan\,(1°\,37' + 6°\,50')}{\cos 30°}$$

$$= \frac{0.14856}{0.86603} = 0.17154$$

$$T = \frac{P}{2}\,(vD + md_p)$$

$$T = \frac{20{,}000}{2}\,[(0.9375)\,(0.14) + (0.7029)\,(0.17154)]$$

$$T = 2518 \text{ in.-lb.} = 210 \text{ ft-lb}$$

Substituting values of T, m, d_p, d_r, μ and D in Eq 2, p 63, and combining:

$$\frac{S}{2518} = \frac{0.89 + 1.66\sqrt{1 + 5.2\,(0.180)^2}}{(0.451)\,(0.131 + 0.121)}$$

$$\frac{S}{2518} = \frac{0.89 + 2.34}{(0.451)\,(0.252)} = 70{,}000 \text{ psi}$$

$$S = 70{,}000 \text{ psi}$$

For 60% prestress, the tensile strength of the material should be:

$$S_t = \frac{70{,}000}{0.60} = 116{,}667 \text{ psi}$$

From the curves on page 66, for ¾-in. bolt and 20,000-lb load:

T = 210 ft-lb; S_t = 120,000 psi.

For **reprint** of above article, just check 709 on one of the Reader Service cards found in this issue.

World of Self-Locking Screws

Screws and bolts with self-locking ability are making the scene on more products because of today's emphasis on safety and reliability.

Frank Yeaple

Self-locking ability in fasteners is definitely in. The fear of costly lawsuits stemming from a fastener's loss of clamp load is making manufacturers of products spend a little more time and money to assure joint reliability. Hence design engineers have a freer hand in selecting locknuts and lockscrews.

Last month's issue contained a roundup of proprietary types of locknuts. Locknuts are generally cheaper than lockscrews, and fewer special parts (the locknuts) need to be stocked to handle original and replacement parts. But because lockscrews mate with a standard nut, they can provide a better guarantee that the locking system will be retained even when the original nut is lost.

This roundup of self-locking screws and bolts includes many novel thread forms that are competing for the job of maintaining a tight joint under adverse conditions. Also included are special shank and head designs and the use of plastic inserts and anaerobics to improve self locking characteristics.

Variable pitch threads. A screw thread with an oscillating pitch distance can increase and decrease between maximum and minimum values to provide a high resistance to self loosening from shock and vibration. The Leed-Lok prevailing-torque screw (Fig 1), available from National Lock Fasteners Division of Keystone Consolidated Industries (Rockford, Ill.), uses the varying pitch to induce interference on the flanks of the threads. The locking threads need not be produced along the entire length of the screw, but only at desired points. For example, the pitch for a ½-20 thread may vary as follows: 0.047, 0.050, 0.047. This significantly increases turning friction but does not deform the mating threads beyond their elastic limit.

Tilted threads. Another way to induce interference is by deflecting and slightly deforming the threads during the thread

1. Leed-lok threads

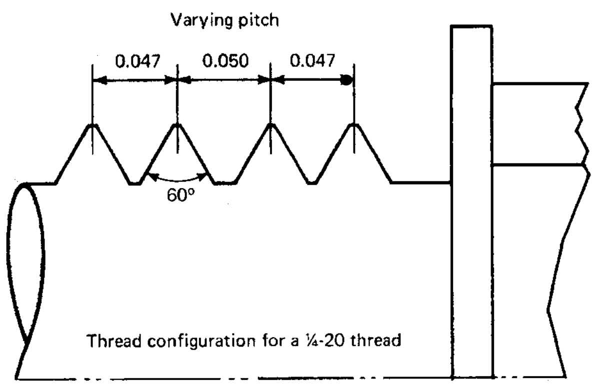

2. E-Lok threads

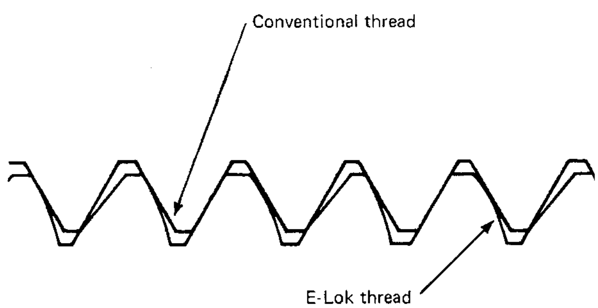

3. Vibresist threads

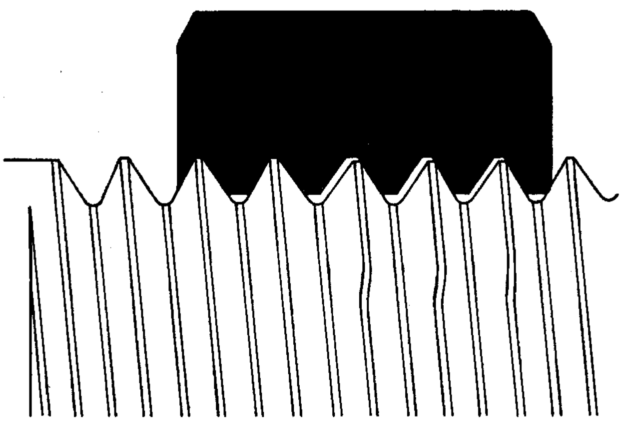

4. Tru-Flex threads

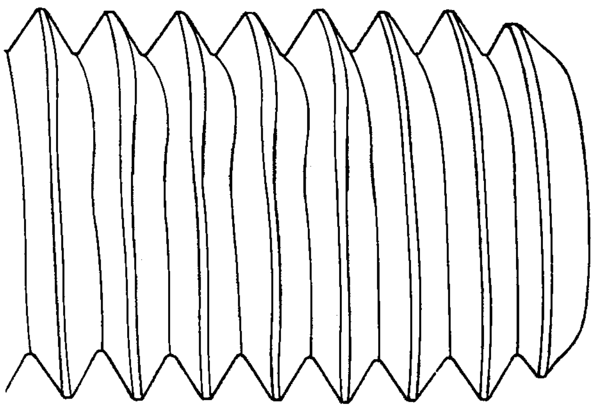

5. Orlo threads

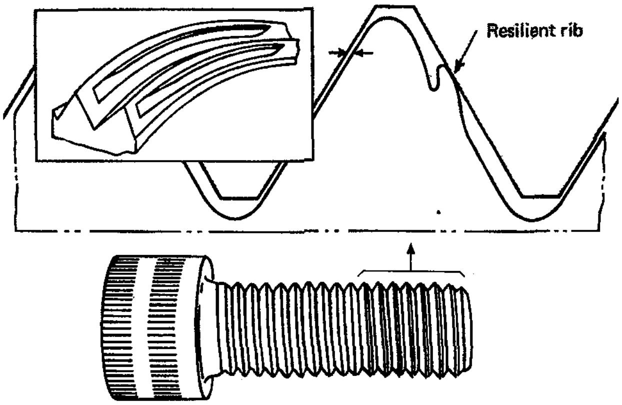

6. Spiralock threads

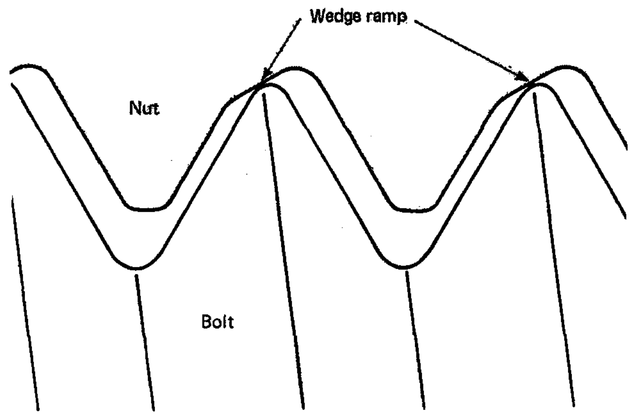

rolling process when the screws are made. Employed by the Everlock Division (Troy, Mich) of Microdot on its E-Lok screws (Fig 2), the process deflects the 60-deg thread form a certain amount (about 10 deg) from the normal to the screw axis. In general, every two tilted threads are followed by two straight (normal) threads over the chosen length of screw.

Partially offset threads. In this method, portion of each thread is deformed parallel to the thread helix axis (Fig 3). As an example, Vibresist screws produced by Russell, Burdsall, & Ward (Mentor, Ohio) provide a consistent prevailing torque, slight or substantial as required. The mating internal threads wedge between the offset screw threads. Spring action is reinforced, and because locking, here as with the other altered-thread types, depends on the elasticity of metal, the screw does not lose its grip at elevated temperatures. The locking threads can be specified adjacent to the head for locking in tapped holes, along the middle of the thread length for locking in tapped holes and near the screw end for locking with standard nuts.

Screws with somewhat similarly deformed threads are offered by Cleveland Cap Screw (division of SPS Technologies, Cleveland, Ohio) on its Tru-Flex screws (Fig 4). In the process, threads near the end of the screw are specially deformed for a circumference of less than 180 deg of arc. When meshed with conventional female threads, the locking threads are repositioned from root to crest to induce a resisting torque. It was found that reshaping several threads within a 180-deg arc of the fastener circumference would provide ample prevailing torque with only minute changes in pitch diameter.

Resilient rib thread. The Orlo thread (Fig 5) has a cold-formed resilient rib on the non-pressure flank of the thread, either part way or continuously around. When a screw with Orlo threads is assembled into a threaded part, the ribs are compressed like springs to force the screw's pressure flanks against the mating threads, and this will increase resistance to rotational forces from vibration or shock. The spring-like action of the rib threads permits the screw to be reused effectively. Orlo threads are available on screws by Holo-Krome Co (West Hartford, Conn)., and Pioneer Screw & Nut (Elk Grove Village, Ill).

Wedge-ramp roots. This internal thread form, called Spiralock (Fig 6), is applied to locknuts and tapped holes to provide locking characteristics to standard bolts. The key innovation is the addition of a 30-deg ramp to the roots of conventional 60-deg threads. When the bolt is seated, the crest of the bolt thread is pulled up tight against the ramp and is wedged firmly with positive metal-to-metal contact that runs the entire length of the nut or tapped hole. The special thread form, in fact, allows wide latitude in bolt tolerances. Spiralock™ locknuts are available from the Greer and the Kaynar divisions of Microdot (Greenwich, Conn.); taps for producing the thread may be obtained from Detroit Tap and Tool Co. (Warren, Mich.)

Threads with special wedge-ramp roots also have been applied to screws. In the Lok-thred form (Fig 7), available from Lock Thread Corporation and National Lock Fasteners (Rockford, Ill.), the thread of the screw itself performs the locking action. This male thread is shallow, with ample radii and a wide root pitched at a

7. Lok-Thred threads

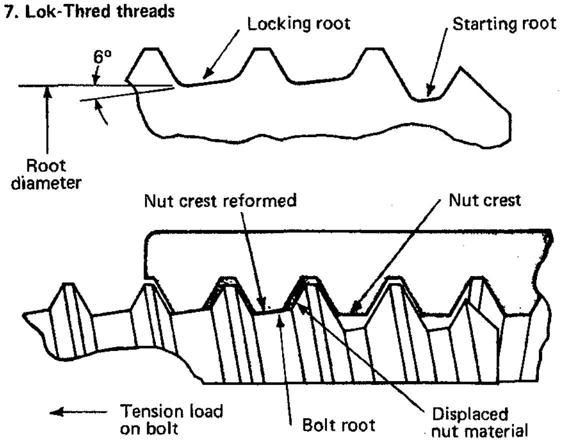

8. Lamcolok threads

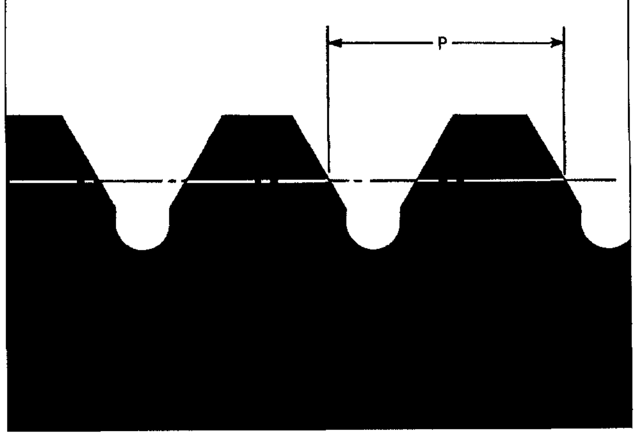

9. Powerlok threads

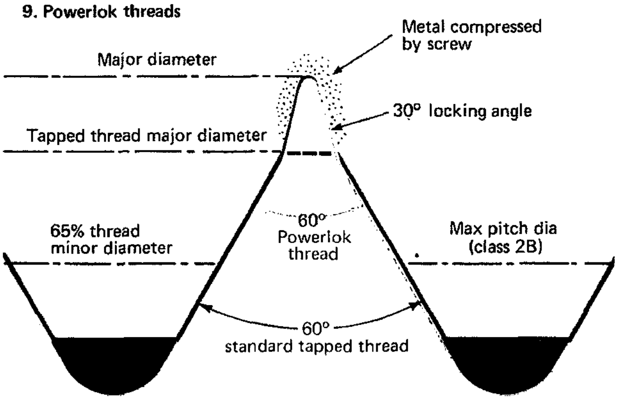

10. Chexoff threads

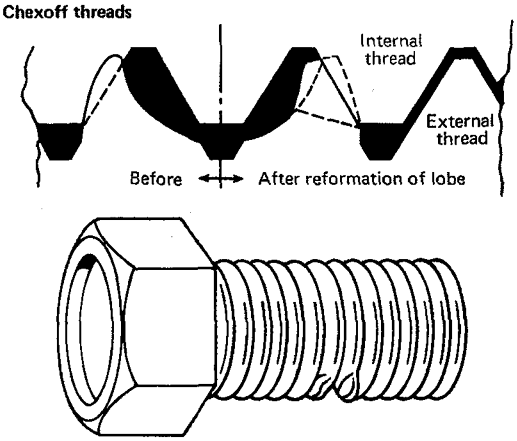

locking angle. These locking roots converge toward the head. A Lok-Thred bolt enters an ordinary tapped hole freely for a few turns, then meets resistance when the bolt root contacts and, by swaging, reforms the nut threads to a perfect fit about the wedge-like locking roots of the bolt. In service, much of the clamp load is carried on the tapered roots, which wedge against the nut crest to lock securely as the work load increases. Bolts which have this type of wedge root thread have a larger root diameter than ordinary threads, which gives strength in tension, torsion and shear, as well as increased endurance limits.

Locking roots. A self-locking thread based on flank interference with standard internal thread flanks (Fig 8) provides a clamping force and holding torque that remains constant. Developed by Lamson & Sessions (Cleveland, Ohio), the Lamcolock thread design can be rolled on almost any bolt or screw. It employs a recessed full-radius root and a decreased major diameter giving the thread a wide, squat look. The decreased major diameter provides room for material to flow into the root recesses, thus averting possible galling.

Locking crests. The locking ability of Powerlok screws (Fig 9) is enhanced through the combination of a novel 60 deg - 30 deg thread form and a tri-lobular thread body section. Locking action is developed at the outermost radius of the torque arm of the screw body, whereas most locking screws develop their resistance at lesser radius points. The deeper thread form of the Powerlok geometry, along with a slight increase in the major diameter of the thread as compared to equivalent size conventional screws, also adds to the locking ability. Basically, the nut-thread metal is elastically deformed in the compressed areas created by the 30-deg portion of the thread. Powerlok screws are available from several fastener manufacturers, including Continental Screw Co (New Bedford, Mass.), Midland Screw Co. (Chicago, Ill.), Central Screw Division of Microdot, and Elco Industries (Rockford, Ill.).

Resilient bulges. By deforming several threads on one side of the Chexoff screw to form lobes (Fig 10), controlled thread interference is induced when the screw is threaded. Available from Central Screw Co, (Des Plaines, Ill.), the special screws with lobes create a wedge-like effect by exerting pressures on the opposite side of the mating threads. The lobes may all be located on the same line or else staggered in order to provide considerable periphery pressures.

In another design, Deutsch Fasteners Corp. induces a resilient bulge on one side of the bolt (Fig 11) that increases in a similar manner the frictional contact between mating threads on the opposite side of the bolt. The bulge is formed by the interference action of a precision ball, pressed into a hole drilled close to the minor diameter of the threads during manufacture.

Sine-wave threads. In another approach to improving the locking characteristics of bolts, Valley-Todeco, Inc. (Sylmar, Calif), has developed its Sine-Lok interference-type thread (Fig 12) for use on the upper regions of a bolt, normally consisting merely of a straight shank. The lower portion of the bolt has conventional threads. During assembly, the bolt shank,

11. Resilient-bulge threads

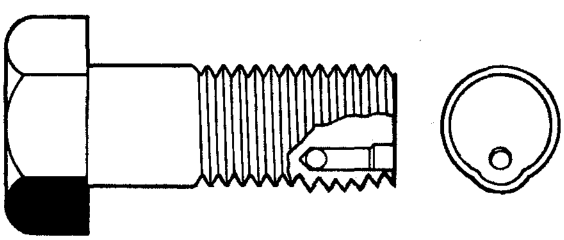

12. Sine-Lok bolt shank

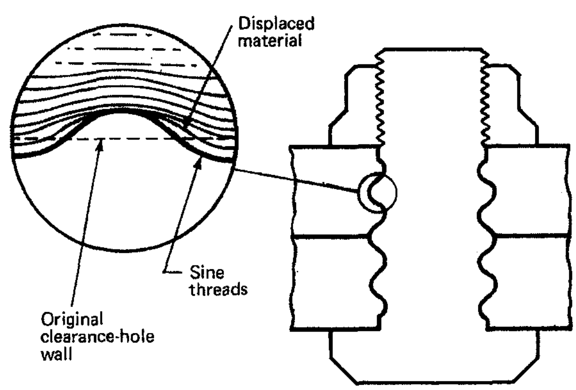

13. Taper-Lok shank

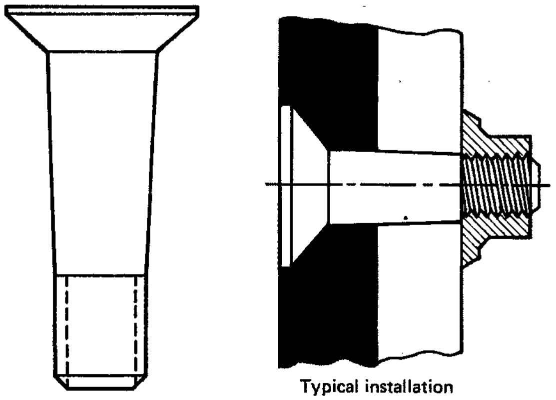

14. Uniflex head

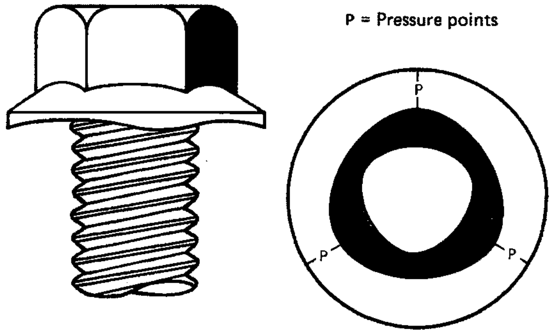

which has a series of modified sine waves, is threaded through the clearance holes of the two parts being assembled, instead of simply being pushed through. The sine wave threads displace the material of the clearance-hole wall into their roots. The protruding, threaded end of the bolt is then tightened by a standard nut. The bolt thus gets a double threading action that helps prevent loosening.

Tapered shank. Another way to increase the shank's grip of the parts being assembled together is to provide a slight taper to the shank, as shown in the Taper-Lok screw by Voi-Shan Division of VSI Corp. (Pasadena, Calif.). (Fig 13). Although only 0.25 in. per linear foot, the taper provides a controlled interference fit that compresses the material of the joint elastically around the hole to induce an excellent preload condition.

Head-grip screws. Many new head shapes for screws are designed to increase resistance to vibrational loosening in joints. The Uniflex head (Fig 14), developed by Continental Screw Co. (New Bedford, Mass) to complement the company's line of trilobular thread-rolling screws, has a washer-like, undulating head-bearing surface. When the surface, which has three alternate high-and-low areas, is tightened against the joint being assembled, the relieved areas are aligned with potential stress points at the lobes of the trilobular screw thread. As a result of this bearing-area relief, thread engagement is increased and bolt loosening noticeably resisted.

High locking power and clamping force are provided with Tensilock screws available from Eaton Corporation (Massilon, Ohio) (Fig 15). The screw head has a concentric circle of 24 embedded, carburized teeth, with an outer concentric groove that permits flexing of the head to occur. The Durlok fastener available from SPS Technology's Cleveland Cap Screw (Cleveland, Ohio) also has ratchet-like teeth around the periphery of the bearing surface (Fig 16). To limit depth of penetration and marring of the mating surface, the serrations are encircled by a smooth outer bearing area.

Lockscrews with the toothed portion of the head furnished in the form of a preassembled washer include the Melgrip screw by Elco Industries (Rockford, Ill) (Fig 17), and Sems screws available from a number of manufacturers, including Shakeproof Division of Illinois Tool (Elgin, Ill), National Lock Fasteners (Rockford, Ill.), and Central Screw (Fig 18). Melgrip's locking effectiveness results from the mating serrations on the underside of the bolt head and top of the washer surface, coupled by the bidirectional gripping teeth on the periphery of the washer which embed into the joint material. Thus, the washer cannot skid or score.

Sems screws are available in a vast variety of washer types to provide spring tensioning for improved loosening resistance, as well as to bridge oversized holes or insulate and protect material surfaces.

Nylon-pellet insert. Self-locking screws that use a resilient nylon insert in the threaded section to develop a

15. Tensilock head

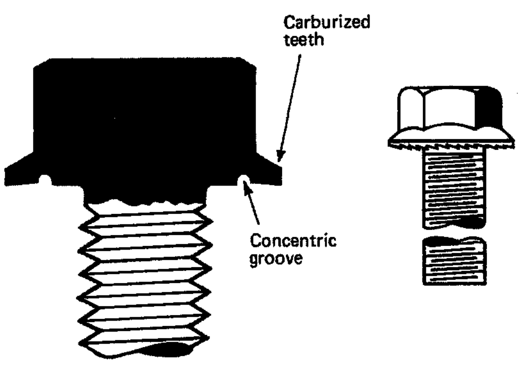

16. Durlok head

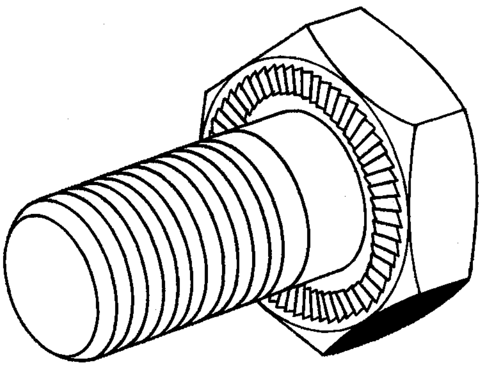

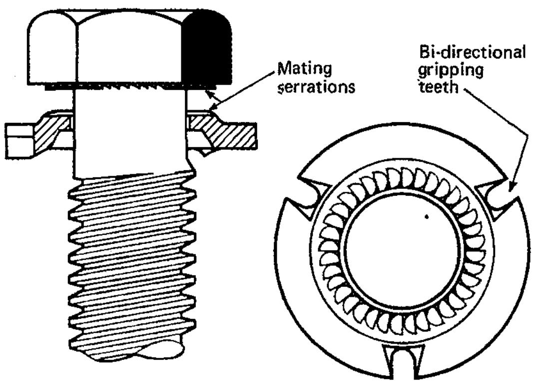

17. Melgrip washer-head

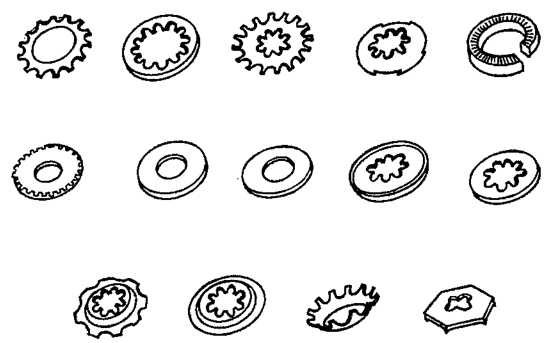

18. Sems washer types

prevailing-torque locking action (Fig 19) have been a familiar product for a number of years. The nylon pellet, press-fitted into the screw, projects slightly beyond the crest of the thread. Once the threads are engaged, the screw is held in position by lateral pressure. The pellet technique can be applied also to nuts and studs. Screws with nylon-pellet inserts are available from Nylok Fastener Division of USM Corp. (Paramus, N.J.) and ND Industries, Inc. (Troy, Mich.).

Nylon fused patch. Another effective and well-established way to help a screw resist loosening is by use of a plastic locking patch that is fused on a dimensionally controlled area of the screw threads, shown in Fig 20. This nylon patch is thickest in the center and feathers-out along the edge to provide a gradual engagement of the locking patch as it encounters mating threads. As the mating threads fully engage the patch, the nylon is compressed to build up a resistance to turning at the right in the figure, and a strong metal-to-metal contact between threads at the left. This type of screw is available from the Esna Division of Amerace Corp. (Union, N.J.), Long-Lok Fasteners Corp. (Cincinnati, Ohio), Holo-Krome Co., (West Hartford, Conn.), and the Unbrako Division of SPS Industries (Jenkintown, Pa.)

Adhesive thread locking. Epoxy and anaerobic adhesives and stiffly viscous fluids have become popular for turning low-cost plain bolts and nuts into lock fasteners. Epoxy, which is a two-part adhesive, is applied in the form of alternating strips or microcapsules to the threaded fastener. Once applied, the epoxy (or one of the anaerobics) remains dormant on the fastener (Fig 21) until a cure is activated by engagement with a mating thread. The curing process for most of the chemical adhesives may continue for days, although by the twelfth hour a good bond has generally been achieved. The adhesive technique, however, does not offer reusability capabilities. Screws with preapplied adhesives are available from ND Industries, (Troy, Mich.), Cleveland Cap Screw (Cleveland, Ohio) and Camcar Division of Textron (Rockford, Ill). Or you can buy your own.

Highly viscous fluid coatings, such as Vibra-Tite available from ND Industries (Troy, Mich.) and Oakland Corp., offer a compromise by making the parts adjustable as well as improving self-locking. The user can apply it from a bottle with a brush applicator, like glue. Vibra-Tite, however, is not an adhesive, so its primary usage is not to provide a heavy-duty locking capability; but it does permit the fastener to be assembled, disassembled or adjusted.

Prevailing torque. Remember that most self-locking screws rely on friction in one form or another to hold fast against axial or transverse vibration. Transverse vibration is most difficult to protect against because accelerating forces can cause momentary slip at a microscopic level, eventually loosening the thread. Lab and field tests are recommended.

19. Nylon-pellet screw

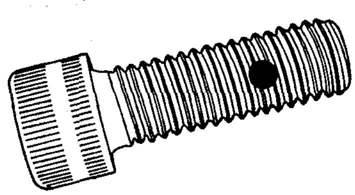

20. Nylon locking-patch screw

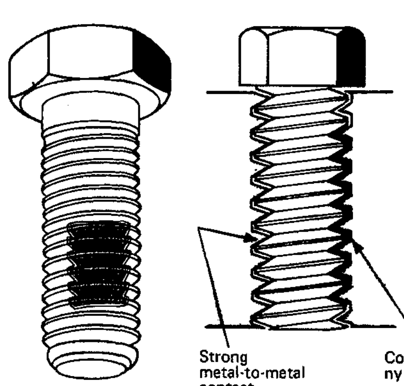

21. Adhesive-lock screw

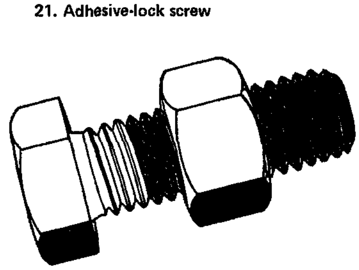

Unconventional Thread Form Holds Nut to Bolt During Severe Vibrations

Wedge shape at root of nut creates metal-to-metal contact over mating thread length. The result is a firmer grip.

When subjected to high transverse vibrations, fasteners tend to loosen with all the undesirable consequences that follow. Engineers at Microdot Inc. (Troy, Mich.) say they have solved the problem. Their solution: a new thread that resists vibrations more effectively than others now available.

Known as Spiralock, the thread is being used in a free-spinning, flanged nut, to eliminate internal self-loosening, the cause of walk-off. The thread form incorporates a wedge ramp at the root of the thread. This wedge ramp is created by widening a portion of the normal thread angle at its root.

Hold tight. When torque is applied, the crests of the mating fastener are pulled against the wedge ramp to form metal-to-metal contact over the entire length of the spiral path of mating threads. Such contact prevents the fastener from loosening under severe vibration conditions.

According to Microdot designers, the fastener works effectively because under clamp load the air space between the mating threads is eliminated. Air space, which is normal in free-spinning fasteners, is the cause of internal self-loosening, they contend.

With such fasteners, the diametrical tolerances needed on both the male and female threads frequently create air spaces of 0.018 in. The average air space is 0.010 in. and the minimum air space needed for assembly is 0.0025 in.

Thus, when any assembly using a regular free-spinning nut is subjected to transverse vibration, the air space allows the mated thread flanks to move laterally and the nut walks-off. Laboratory tests at Microdot on a Junkers vibration testing machine compared performance of Spiralock with other nuts.

Nuts of various sizes were tightened to 75% of proof load on standard nuts and then subjected to high amplitude vibration. In every case, the test engineers say, the bolt failed from metal fatigue before the nut loosened. All bolts and nuts used in the test were SAE grade 8.

When comparing Spiralock nuts to prevailing torque nuts several differences should be kept in mind, the designers say. Under normal vibration conditions, both Spiralock and prevailing torque nuts retain an acceptable amount of initial clamp load when tightened to 75% proof load. Under high vibrations the new wedged thread retains a higher percentage of initial clamp load than a prevailing torque nut.

However, initial clamp load must be achieved for Spiralock to be effective. In applications where there can be no assurance of achieving initial clamp load or if it can be lost due to brinelling, the new nut should not be used, the designers warn.

Where it can be used, though, the Spiralock offers important benefits to manufacturers. It is free-spinning, reusable, and speeds assembly time. Above all, its ability to withstand high vibration or cyclic transverse loading qualify it for high-vibration applications, it is said.

Typical free-spinning flanged lock nut

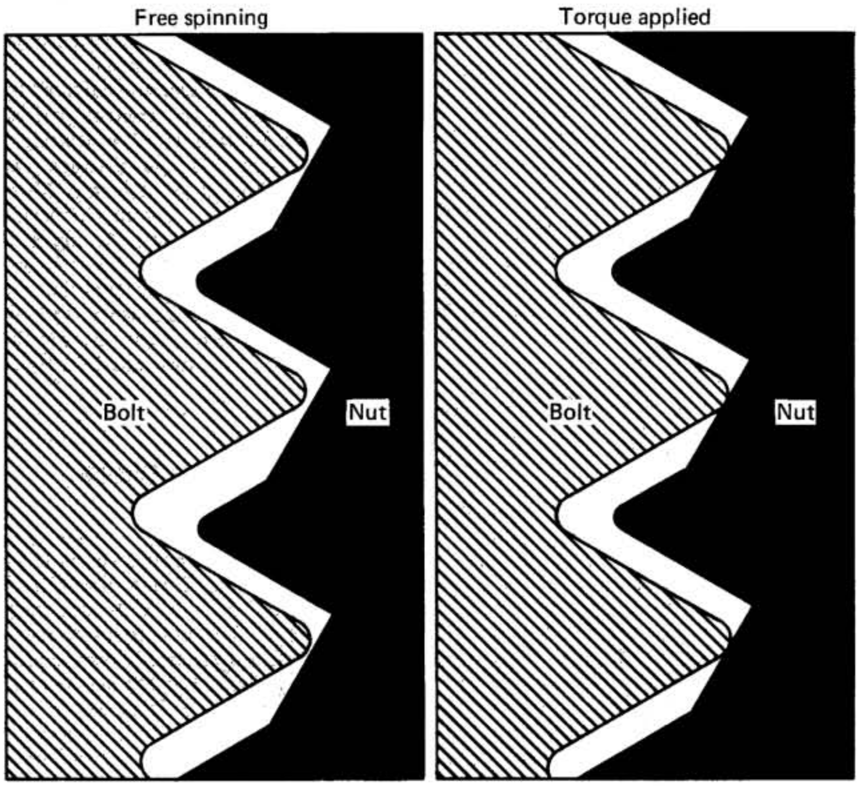

Widened angle at thread root forms wedge. Bolt remains free-spinning until torque is applied. Then bolt threads contact wedge, eliminate air space and prevent lateral movement.

SECTION 20

FASTENING & JOINING

Fastening Studs and Pins to Plates

Ten removable and five permanent methods for fastening studs that provide pivots for linkages, act as stop pins, or register of parts in assembly.

D. Mascio

REMOVABLE ASSEMBLIES

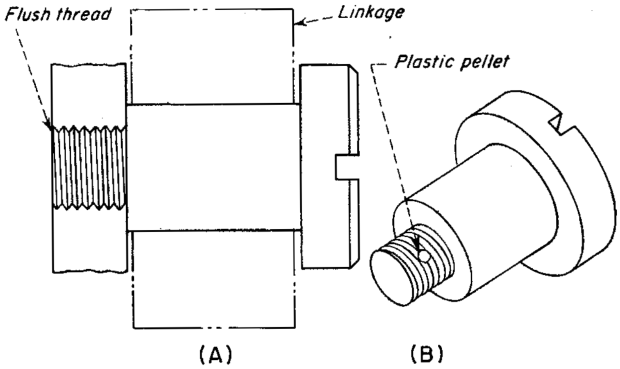

Fig. 1—(A) Shoulder screw in threaded hole may have slotted head. Thickness of mounting plate should be at least equal to thread diameter—especially if design does not allow thread to protrude or to be cut flush. (B) Loosening of screw can be prevented by having plastic pellet inserted into body of thread, or patented, self-locking threads.

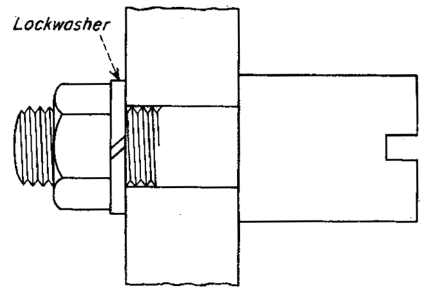

Fig. 2—Shoulder screw in unthreaded hole requires nut and washer. Plate can be any thickness. Loosening of screw is prevented by lock washer or by using a lock nut.

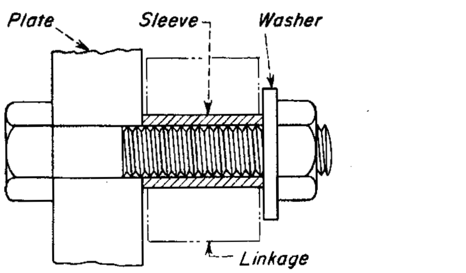

Fig. 3—Standard bolt and nut can be used to hold movable linkage by using sleeve to prevent binding when screw is tightened..

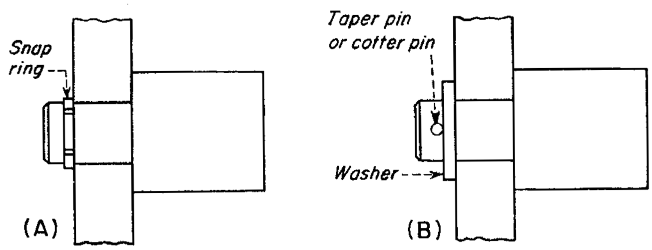

Fig. 4—Where end play is permissible, stud can be retained by (A) unthreaded shoulder pin and snap ring; (B) washer and cotter or taper pin. Wedging effect of taper pin prevents end play if pin is properly located.

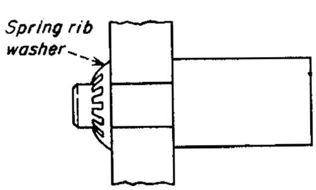

Fig. 5—Quick assembly is obtained with spring rib washer but slippage may occur with high loads. Also stud is difficult to disassemble.

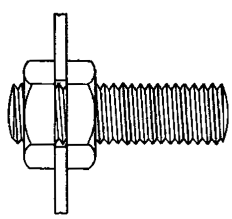

Fig. 6—Threaded rod provides for axial adjustment in sheet metal assemblies by clamping plate between two nuts (usually lock nuts).

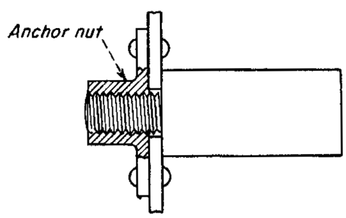

Fig. 7—Anchor nut enables shouldered stud to thread into thin sheet metal when only one side of plate is accessible.

REMOVABLE ASSEMBLIES

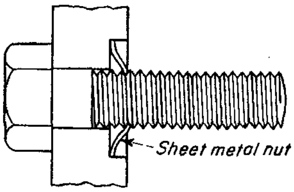

Fig. 8—Sheet metal nut and standard screw make simple fastening for small mechanism assemblies. Nut can be recessed.

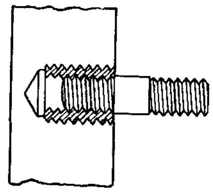

Fig. 9—Inserts with tapped hole provide seat in plastic or soft metal for standard stud threaded on both ends. Inserts are retained in plate by various patented methods.

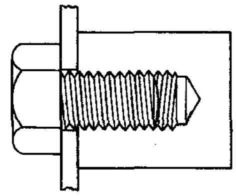

Fig. 10—Stud with tapped hole is retained in thin sheet metal with standard screw. Hole can be tapped all the way through.

PERMANENT ASSEMBLIES

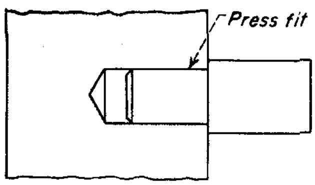

Fig. 11—(A) Shoulder stud is pressed into hole in plate. Holding power can be improved by using brazing ring or (B) having groove pressed on the shank by licensed manufacturers.

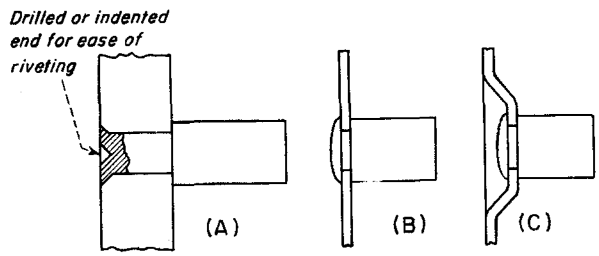

Fig. 12—(A) Riveted shoulder stud in clearance hole is center drilled for ease of riveting. Plate countersunk for flush riveting. (B) Riveting over sheet metal will not be flush unless (C) metal is indented.

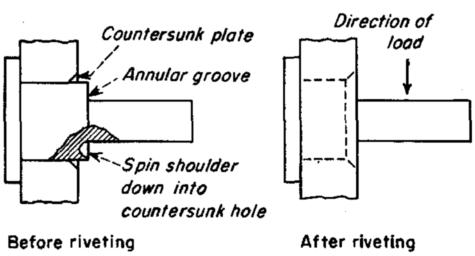

Fig. 13—Stepped-up stud does not reduce shear area at junction of pin and shoulder (as in Fig. 12 A). Therefore, for same pin diameter shear strength is higher. Also, when stud is used as a stop pin, head of stud resists shock loads which may cause stud in Fig 12 (A) to pull out.

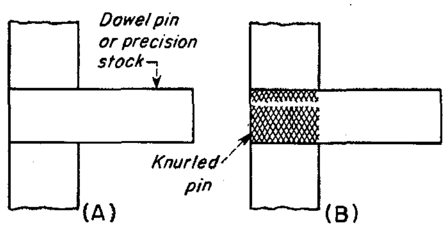

Fig. 14—(A) Press-fitted dowel pins can be used for small sizes up to $\frac{3}{8}$ in. dia.—precision stock for larger diameters. Press fit is also obtained with knurled pin (B) or with patented items such as grooved pins, slotted tubular pins, spirally rolled pins.

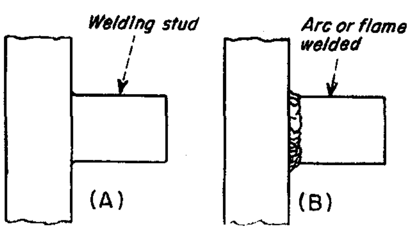

Fig. 15—(A) Special studs for welding allow dissimilar metals to be welded, which is frequently impossible with resistance welding. Special gun for welding creates little heat, therefore no distortion. (B) Flame welded studs have fillet around bottom.

16 Ways to Align Sheets and Plates with One Screw

Federico Strasser

Two Flat Parts

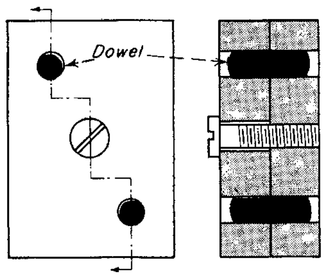

1 Dowels . . .
accurately align two plates, prevent shear stress in fastening screw. Two pins are necessary because screw can not act as aligning-pin.

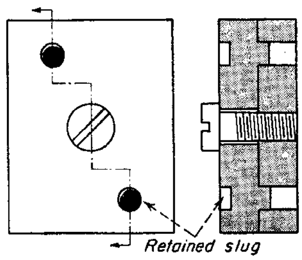

2 Retained slugs . . .
act as pins, perform same function as dowels; are cheaper but not as accurate.

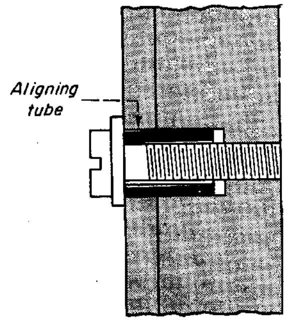

3 Aligning tube . . .
fits into counterbored hole through both parts. Screw clearance must be provided in tube.

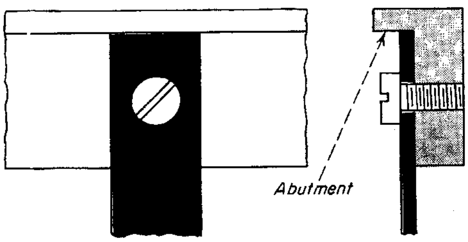

4 Abutment . . .
provides positive, cheap alignment of rectangular part.

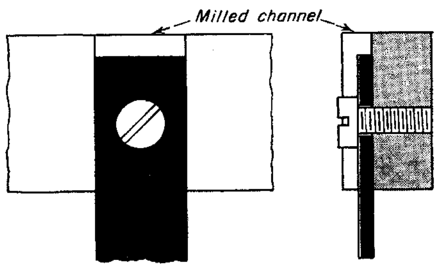

5 Matching channel . . .
milled in one part gives more efficient alignment than abutment in preceding method.

Formed Stampings Assembled with Flat Parts

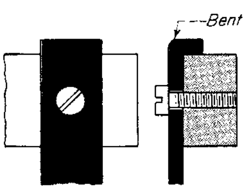

6 Bent flange . . .
performs similar function as abutment, but may be more suitable where machining or casting of abutment in large part is not desirable or practical.

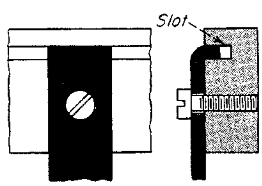

7 Narrow slot . . .
receives flange or leg on sheet metal part, allows it to be mounted remote from edge of other part.

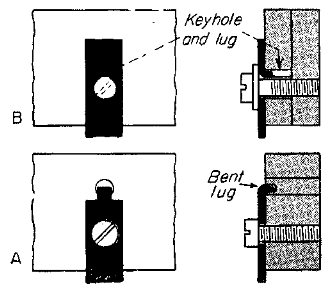

8 Bent lug . . .
(A) fits into hole, aligns parts simply and cheaply; or (B) lug formed by slitting clearance hole in sheet metal keys parts together at keyhole.

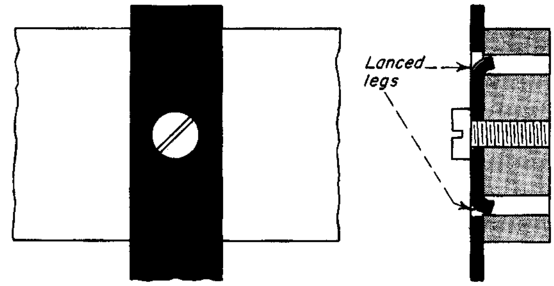

9 Two legs . . .
formed by lancing, align parts in manner similar to retained slugs in method 2, but formed legs are only an alternative for sheet too thin to partially extrude slug.

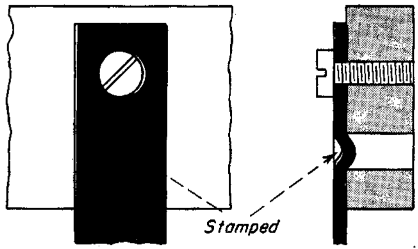

10 Aligning projection . . .
formed by slitting and embossing is good locating method, but allows a relatively large amount of play in the assembly.

Flat Parts and Bars

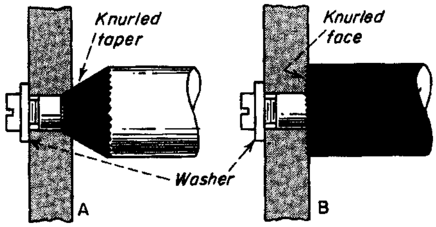

11 Knurled end . . .
of round bar (A) has taper which digs into edge of hole when screw is tightened; this gives accurate angular location of bar or sheet. (B) Radial knurling on shoulder is even more positive.

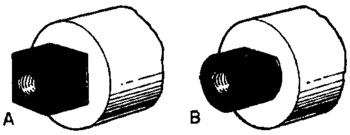

12 Noncircular end . . .
on bar may be square (A) or D-shaped (B) and introduced into a similarly-shaped hole. Screw and washer hold parts together as before.

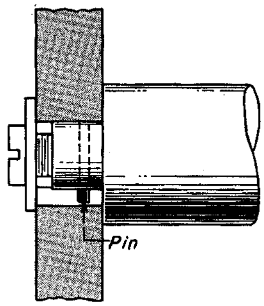

13 Transverse pin . . .
in rod end fits into slot, lets rod end be round but nonrotatable.

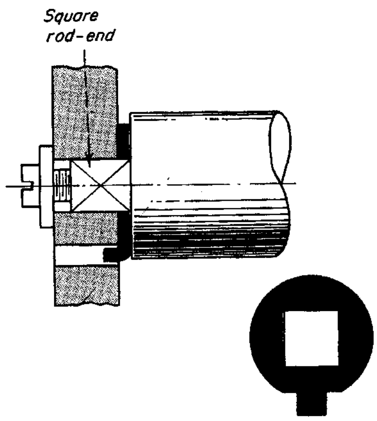

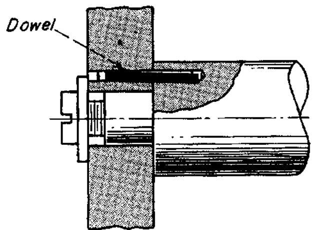

15 Dowel . . .
is simple, efficient method of preventing rotation if rod dia is big enough.

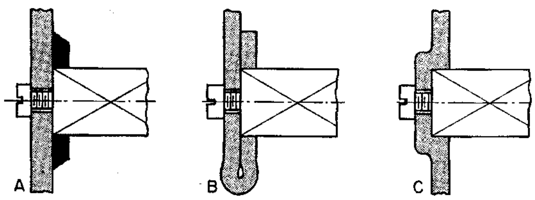

14 Washer over square rod end . . .
has leg bent to fit in small hole. Washer hole is square, preventing angular movement when all three parts are assembled and fastened with screw and washer.

16 Double sheet thickness . . .
allows square or hexagonal locating-hole for shaft end to be provided in thin sheet. Extra thickness can be (A) welded (B) folded or (C) embossed.

For Better Grip-Longer Holes in Sheetmetal

In Steel or brass, depth of a threaded hole should be at least half its width, and in zinc or aluminum the right ratio is 2/3. If the metal is too thin, here's what to do.

Federico Strasser

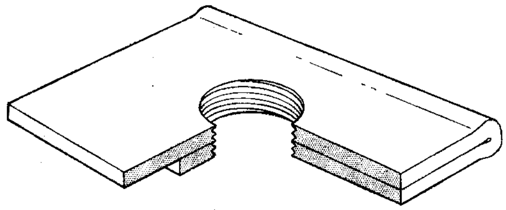

1

BENT-OVER SHEET doubles depth of holes near edge. Sometimes one more bend, for triple depth, is possible.

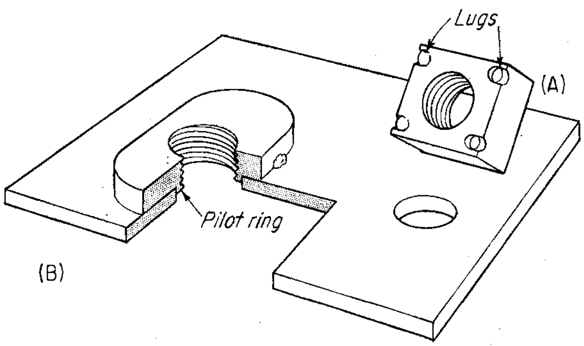

2

PROJECTION-WELDING fuses lugs on nut (A) to sheet. Flanged nut (B) for spotwelding has pilot rim to locate it on hole.

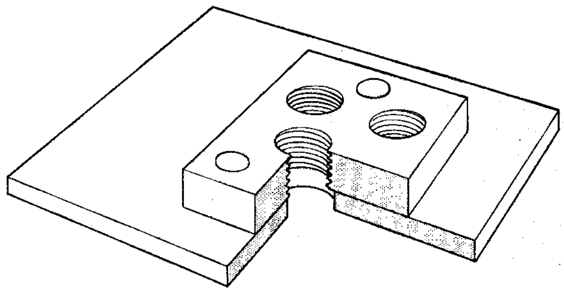

3

PATCH OF SHEET or plate, for a longer thread, serves holes away from edge; needs at least two rivets or welds to keep it from turning. Larger pieces cover group of holes.

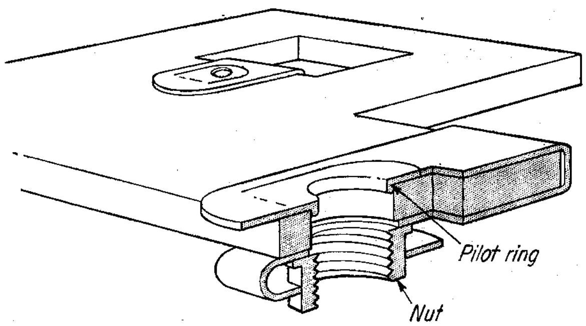

4

CLIP slips over edge of sheet, and positions on hole when pilot rim springs into place. Extra cutout next to hole allows installation away from edge.

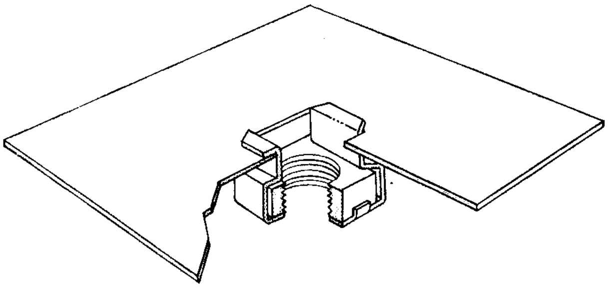

5

FLOATING NUT snaps into square hole and allows misalignment of bolt. If the thread strips, replacement is easy.

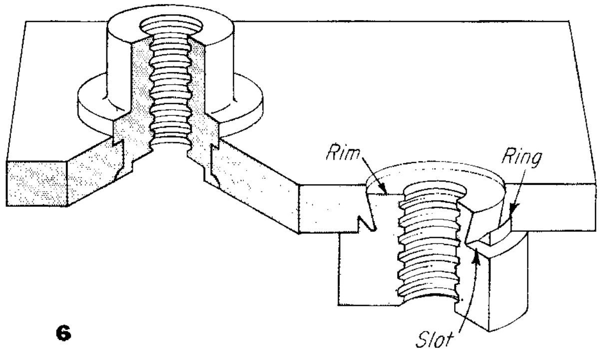

6

STAKED NUT fits in relieved hole. Relieving nut makes it easier to stake. Squeeze on clinch nut forces sheet to flow under tapered rim. Slots in ring keep nut from turning.

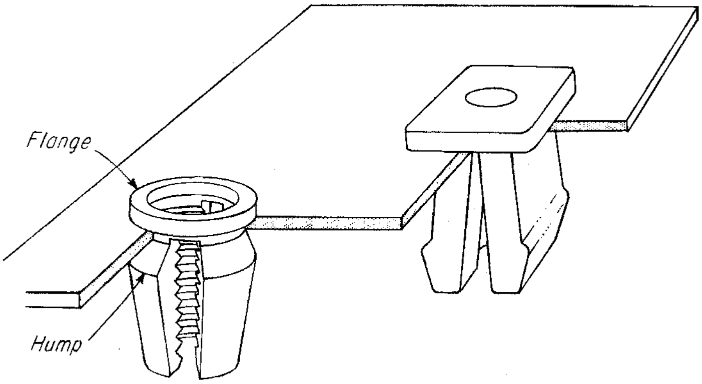

7

TAPPED HOLE snaps into sheet and grips it between flange and hump. Screw forces prongs apart so hump presses even harder on sheet. Slot digs into side of hole to prevent turning. Another version sits flush.

Square-shape plastic grommet, which doubles as insulator, cannot turn in square hole. Screw must make its own threads in smooth grooves, as it wedges grommet tightly in place.

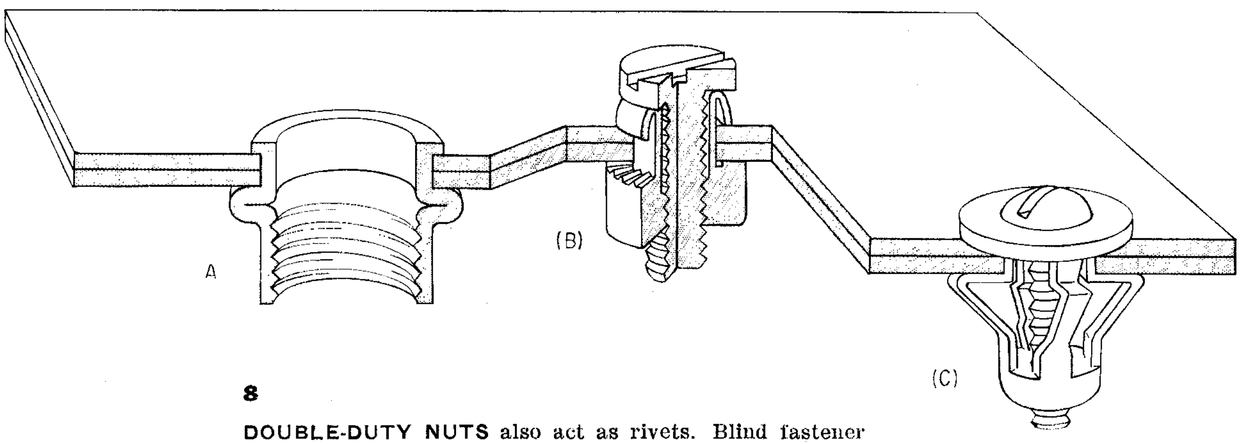

8

DOUBLE-DUTY NUTS also act as rivets. Blind fastener (A) requires special tools; other blind fastener (C) doesn't. Nut (B) bites into sheet when screw tightens down on neck, and bends it over.

Bolts Get Help Against Shear

Especially when they are loose, clamping bolts or screws encounter side loads they weren't meant to carry. Here are ways to stop bending and to align parts as well.

Federico Strasser

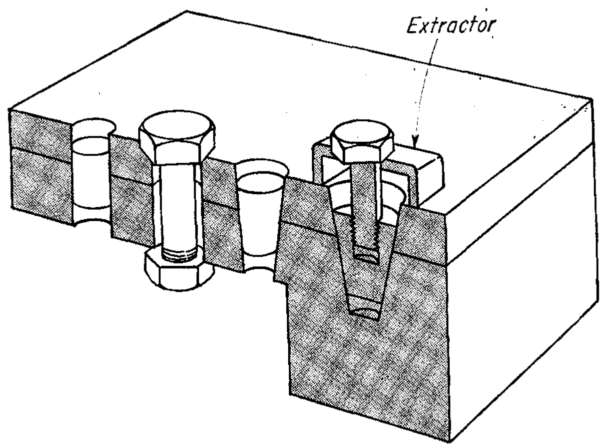

DOWEL PINS hold against small loads at temporary or semi-permanent joints. For joints taken apart more often, use tapered pins; they come out easier. Where a dowel pin fits in a blind hole, it can't be knocked out so must be drilled and tapped to take an extractor. Fancier types carry a threaded rod on top which sticks out of the hole. As a nut is tightened down on it, the pin lifts out.

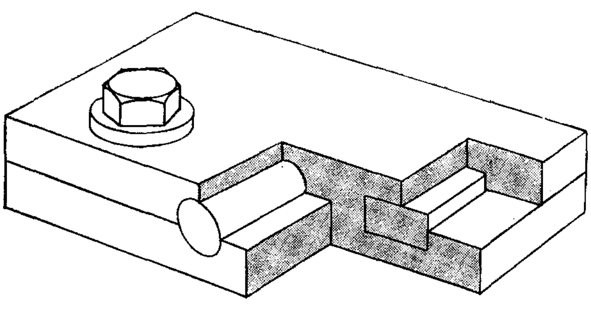

KEY is pin laid flat between two parts. Although round pin is easier to install than the rectangular key, it lets parts shift when the bolts loosen even slightly.

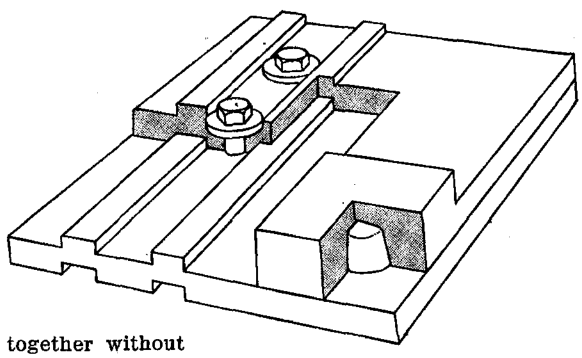

RIBS lock extruded or formed sheets together without further preparation. On cast or molded parts, integral boss fits into hole which is either molded or drilled.

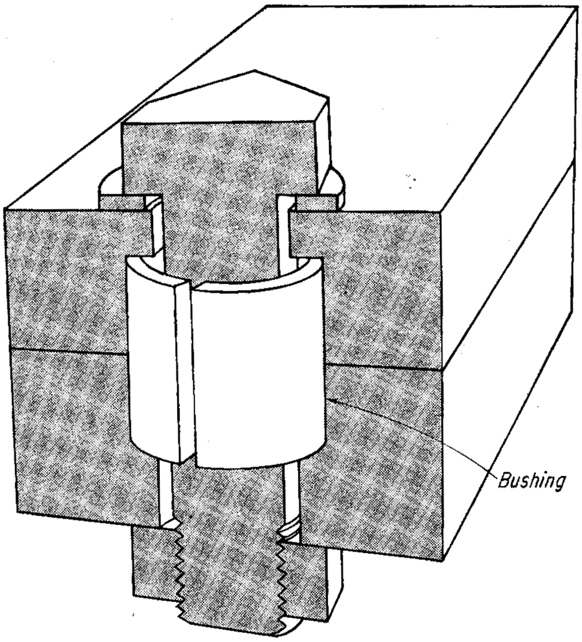

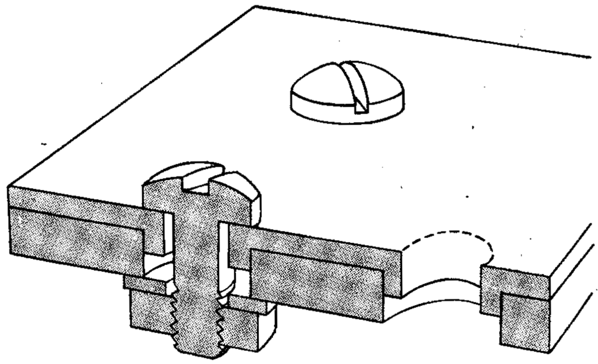

BUSHING is split so that it fits tightly yet doesn't need a reamed hole as a dowel does. Solid bushing replaces it when high side loads would compress a split bushing.

BOSS on extruded hole becomes a built-in bushing when used to locate and hold a sheetmetal part.

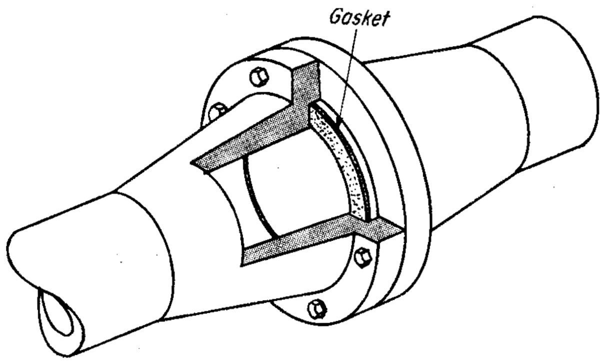

RABBET takes high loads and gives precision fit. Here rabbet also locates gasket between pipe flanges.

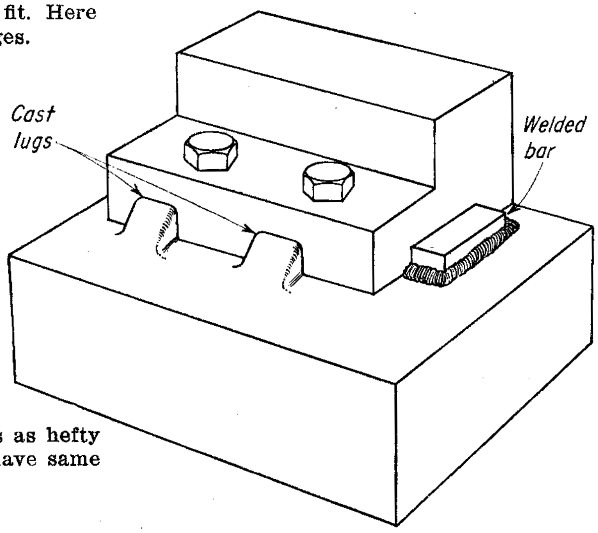

CAST LUGS or welded bars provide shoulders as hefty as a more expensive recess would, but don't have same clean look.

10 Ways to Conceal Fasteners

How to improve appearance of instrument panels by hiding screw heads.

Frank William Wood JR

The appearance of an otherwise good-looking instrument panel is often spoiled by screw heads distributed in an uneven pattern across the panel surface. The following designs illustrate methods of improving appearance by subduing and concealing fasteners. In some cases, applications of these designs will not only improve appearance but also will reduce fabricating and assembly costs. Sometimes you get tamper protection as well.

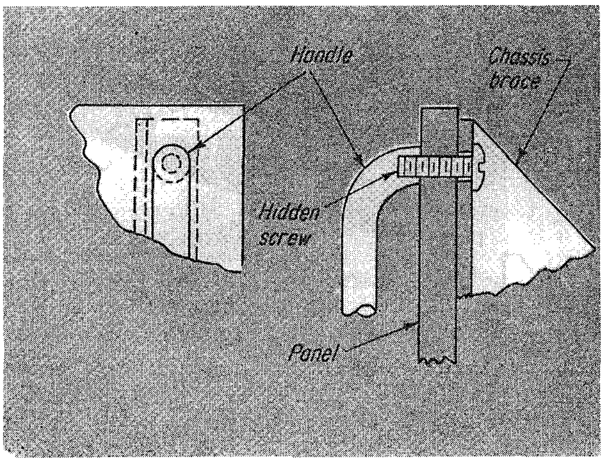

1 DOUBLE-DUTY SCREW attaches chassis to panel, is concealed by handle . A bonus is reduced fabrication and assembly time.

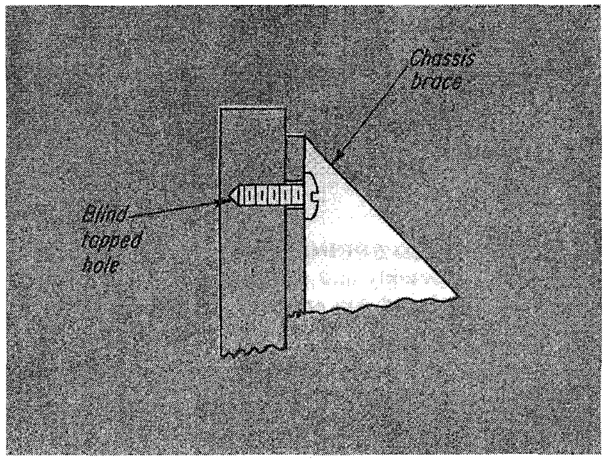

2 BLIND HOLE in panel conceals screw. This method is best suited for thicker panels, when adequate depth can be obtained without close tolerances.

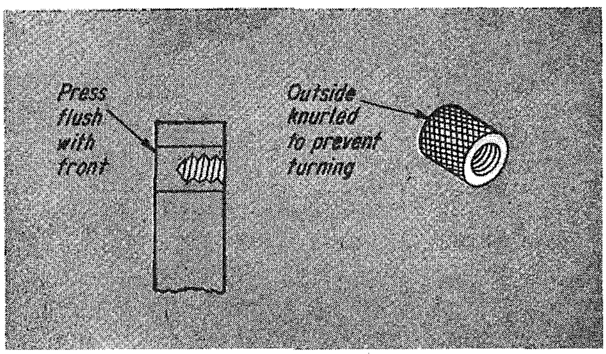

3 TAPPED INSERT pressed into panel is sometimes more economical than blind-tapped panel.

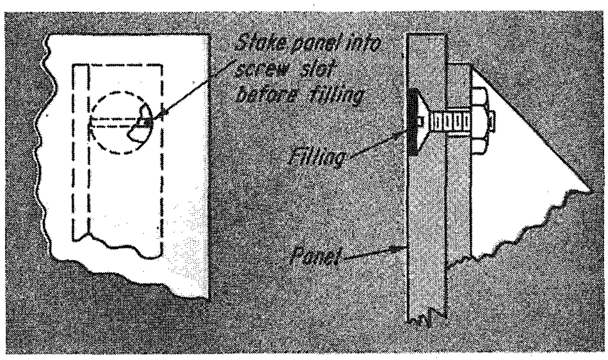

4 RECESSED SCREW HEAD is concealed with an epoxy resin before panel finish is applied. To prevent loosening of screw, the panel should be threaded. This thread, in conjunction with staking, locks the screw securely in position.

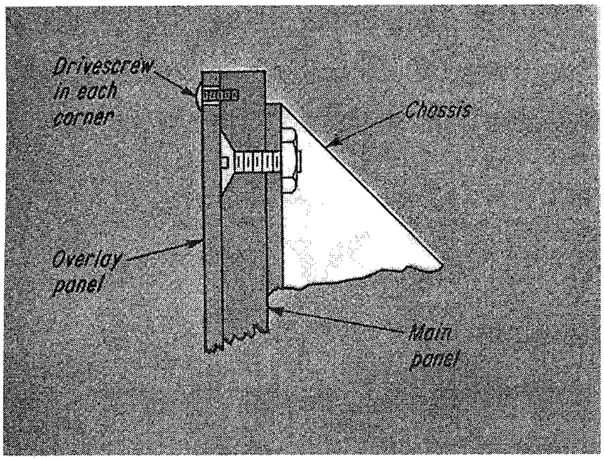

5 "OVERLAY" PANEL conceals all front-panel hardware. Overlay panel offers no support for components and in many cases is attached with pressure-sensitive adhesive. All markings and nomenclature for controls can be carried by this panel.

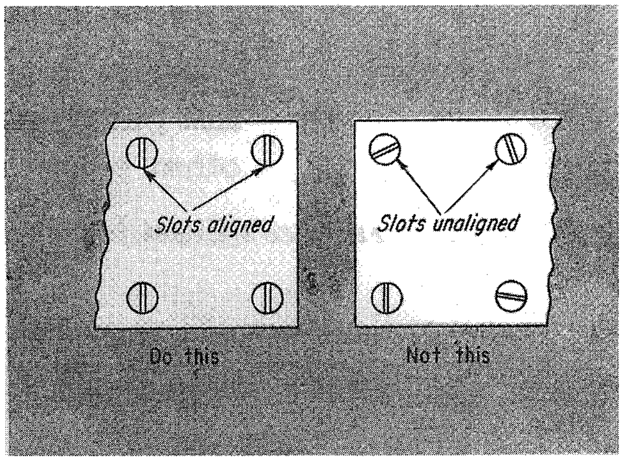

6 ORIENT SCREW-HEAD SLOTS in same direction to subdue detracting appearance of screw heads.

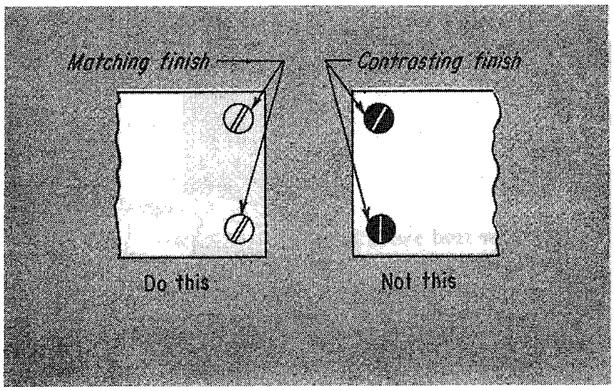

7 MATCHING HARDWARE FINISH to that of the panel effectively subdues hardware appearance. A familiar example of this is the black oxide finish commonly used on panel-meter screws.

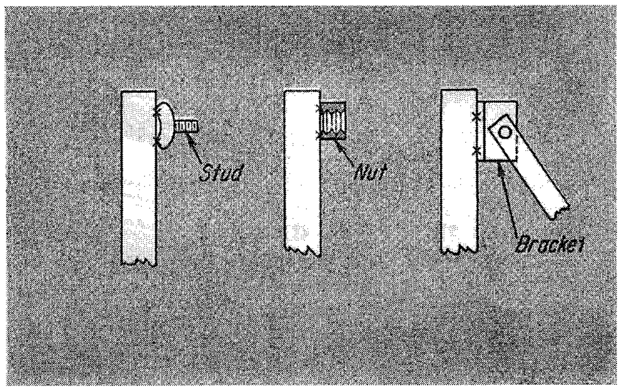

8 SPOT-WELDED STUDS AND NUTS are commercially available for use on steel panels. Or, alternatively, special brackets can be used.

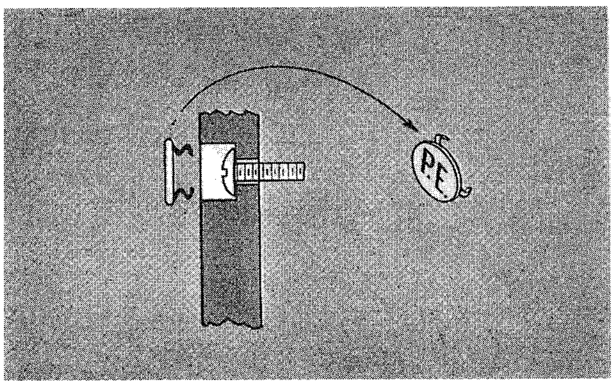

9 SNAP-IN "PLUG BUTTON" fits into counterbored recess to conceal screw head and also provide corporate or product identity.

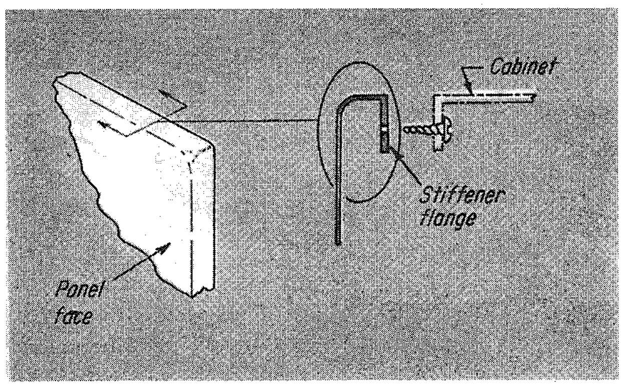

10 SHEETMETAL STIFFENER FLANGES can be integral, as shown here, or separate when panel material cannot be formed. Sheetmetal screws hold panel.

Attaching Motors to Instrument Gearheads

Methods include servoclamps, screws, pins, adapter plates and half-rings, plus an eccentric mounting.

Frank William Wood JR

Instrument gearheads are increasingly useful in complex servo equipment where space is at a premium. Motors to drive the gearheads are usually mounted in line with them and must be reliably and economically attached. Sketches show some of the various methods possible. The method chosen for a particular design is determined by configuration of the motor, the type of input plate on the gearhead, or a combination of both.

Installation should be simple—it should not require disassembly of gearhead; connection should not loosen under vibration or shock, should not increase diameter of gearhead, should provide adjustment in high-precision requirements, and should provide necessary environmental protection at point of attachment (keep dust, moisture, etc., from entering gearhead). Backlash adjustment is also a desirable feature to include.

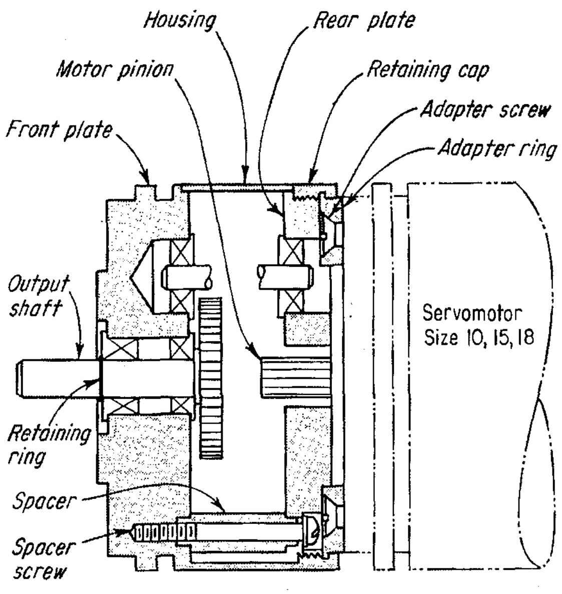

1 TYPICAL GEARHEAD and motor using "plate construction" gearhead.

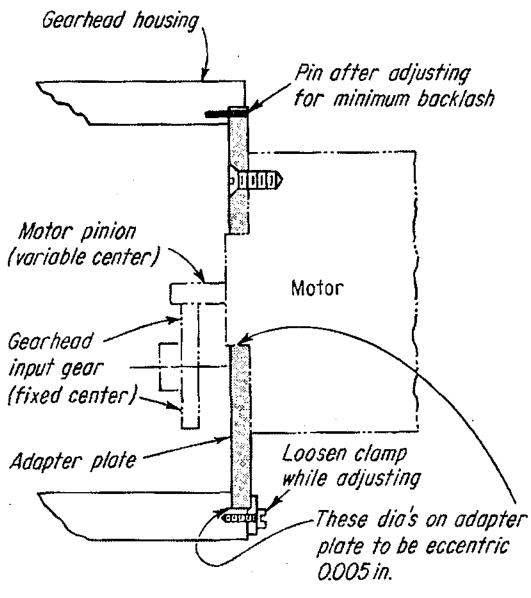

2 MOTOR IS MOUNTED on eccentrically bored adapter plate to permit backlash adjustment. By rotating adapter plate, backlash can be reduced to minimum between motor pinion and gearhead input gear.

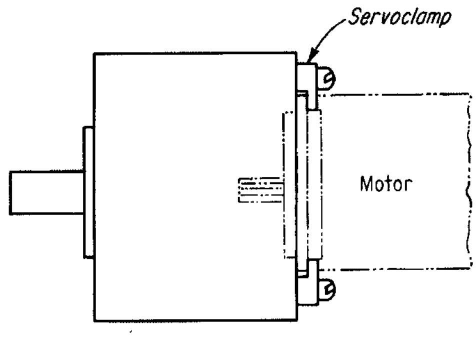

3 STANDARD SERVOCLAMP

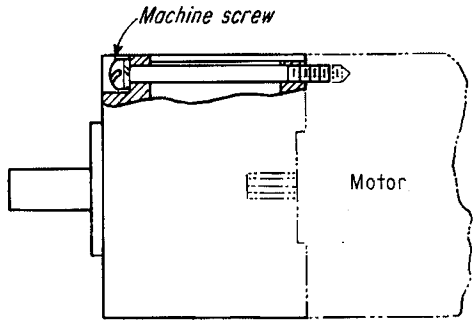

4 BOLT THROUGH GEARHEAD INTO MOTOR

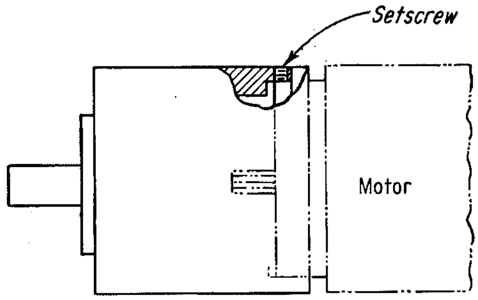

5 SETSCREW THROUGH HOUSING SIDE-CLAMP TO MOTOR

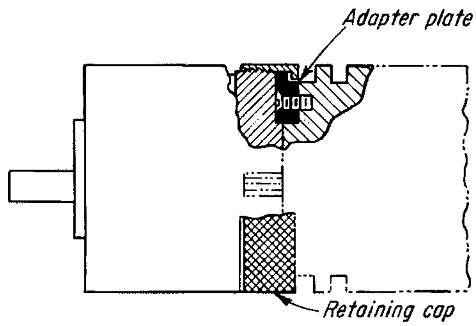

6 ADAPTER PLATE AND RETAINING CAP

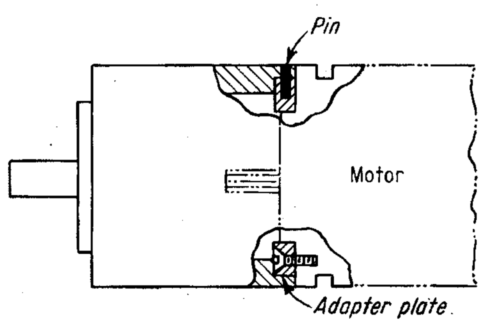

7 PIN THROUGH HOUSING SIDE INTO ADAPTER PLATE

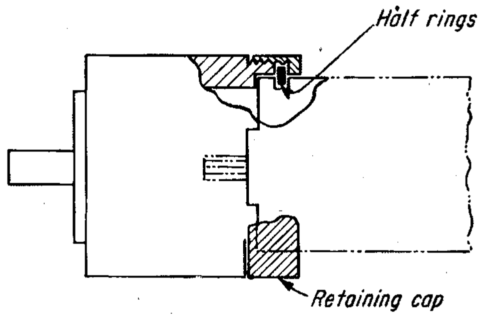

8 TWO HALF-RINGS AND RETAINING CAP

Fastening Precision Gear-Plates

Don't waste high-precision gears; design their mounts to provide accurate alignment even with unskilled assembly. Aim for rigidity too. Here are some "tricks of the trade."

Frank William Wood JR

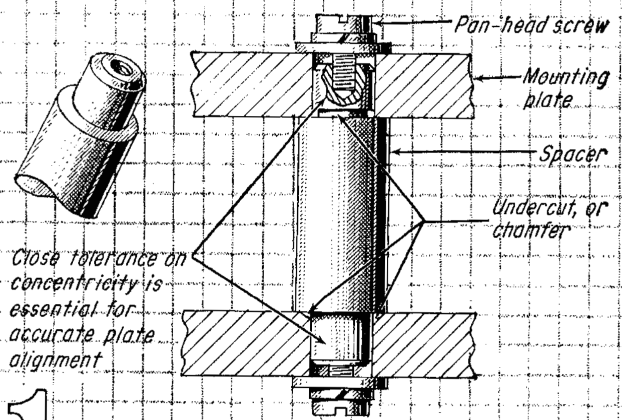

1 **SHOULDERED SPACERS** are good when accurately made.

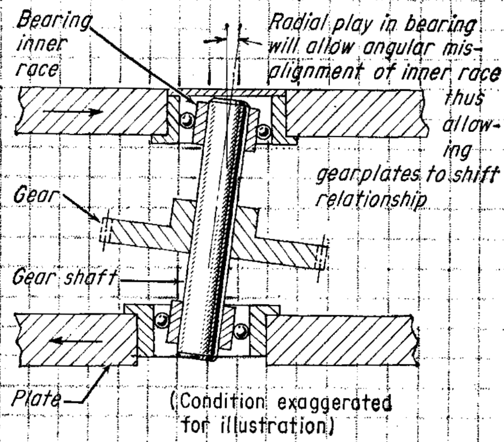

2 **DON'T RELY** on shafts for alignment.

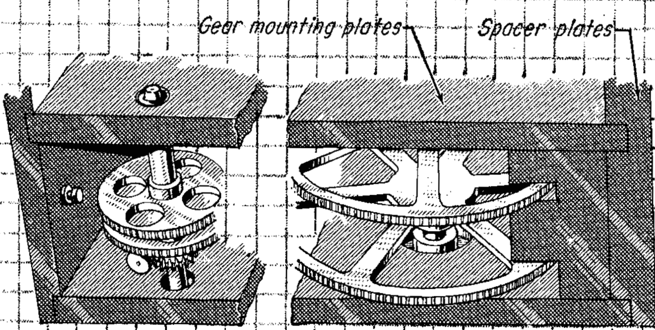

5 **PLATES SUPPORTED AND REGISTERED** in grooves support heavy loads, but precision production requirements make method expensive.

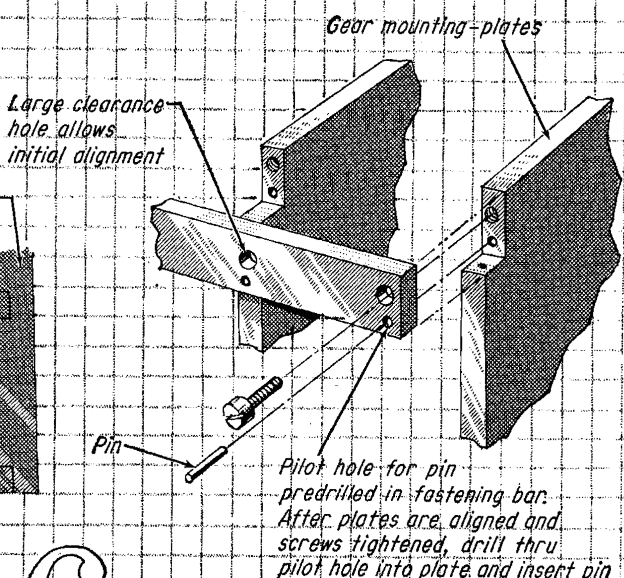

6 **ALIGNMENT PINS** ensure constant accuracy of alignment even after disassembly and re-assembly.

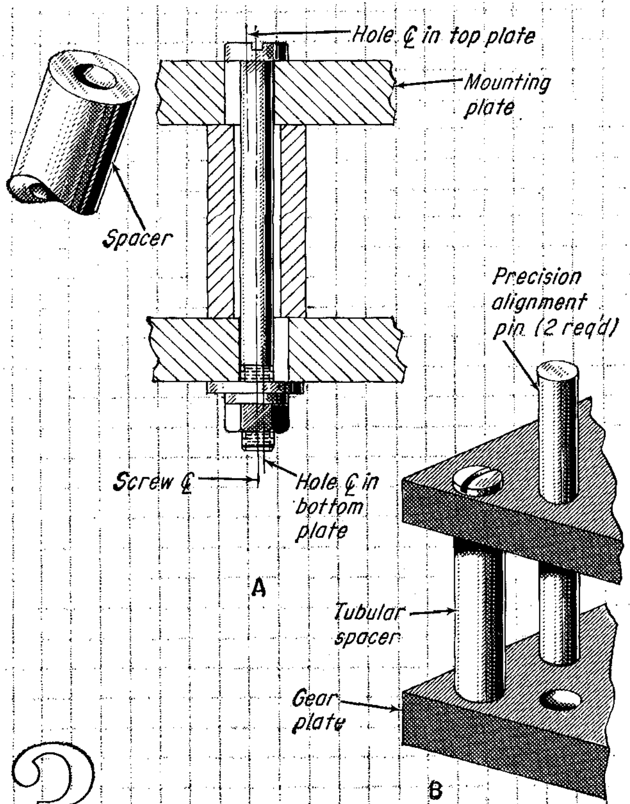

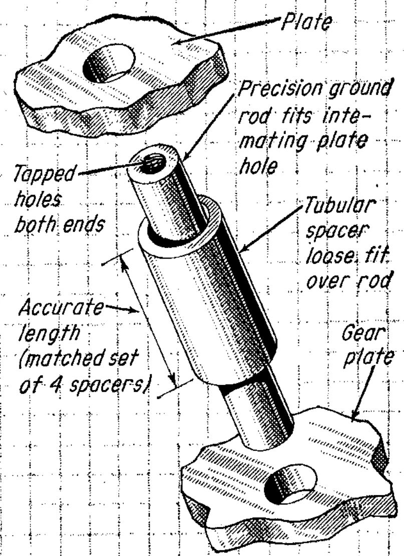

3 TUBULAR SPACERS
(with through bolt) need alignment pins.

4 PRECISION-GROUND ROD
and matched-length spacers ensure parallel alignment.

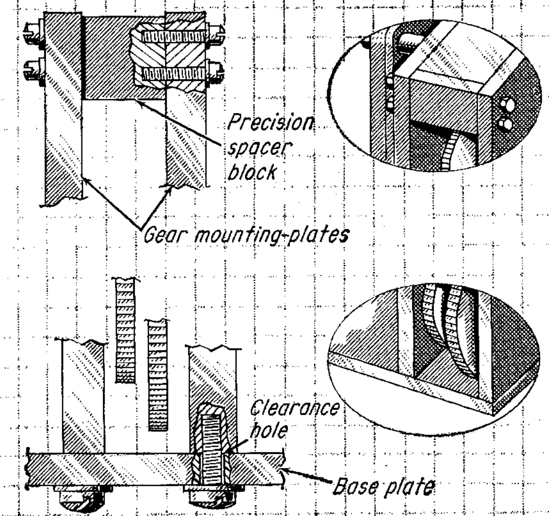

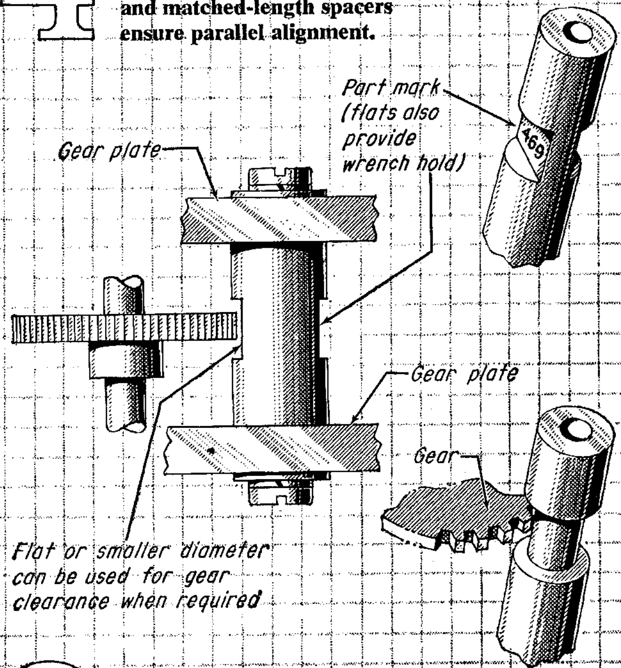

7 SPACER BLOCKS
between mounting-plates make assembly tough to align. Base-plate removal also leaves mounting plates supported on one end only.

8 AUXILIARY FEATURES
on spacers increase cost but are sometimes necessary.

Bonding Sheet Metal with Adhesive

Tabs, lugs, rivets, folds, and other reinforcing methods should always accompany adhesive when the bonded parts are metal.

Federico Strasser

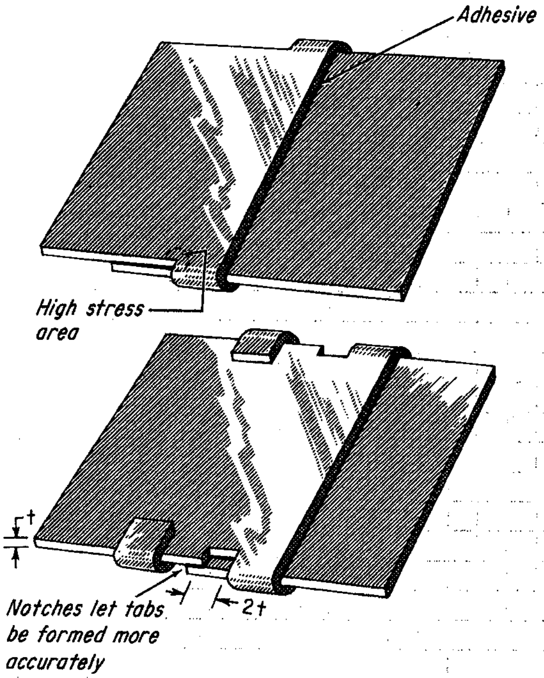

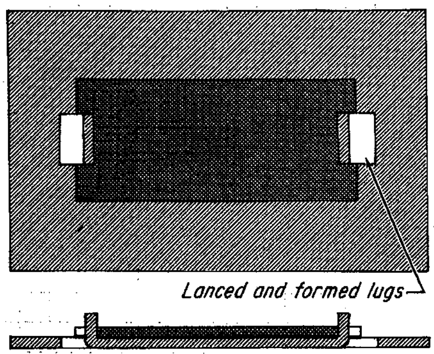

1 TABS ADD PEEL STRENGTH.

4 SLOTS HERE ALLOW MAXIMUM JOINT STRENGTH.

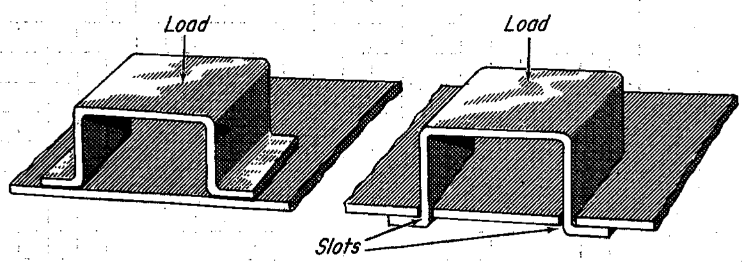

Not recommended

Best design

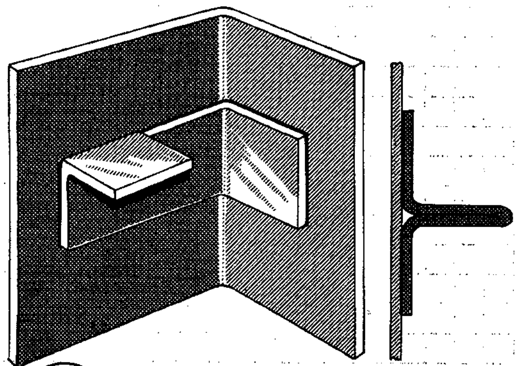

6 INCREASED BOND AREA GIVES MORE SHEAR STRENGTH BUT NO MECHANICAL AID.

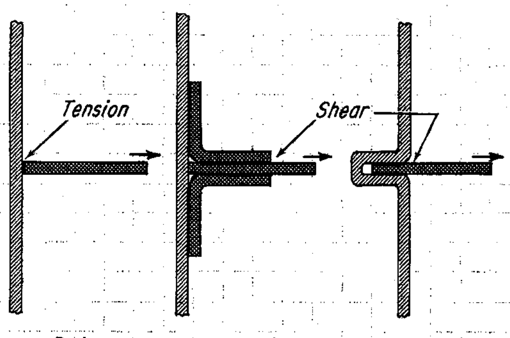

Bad

Good

7 ADHESIVE IS STRONGER IN SHEAR, PROVIDE FOR THIS IN DESIGN.

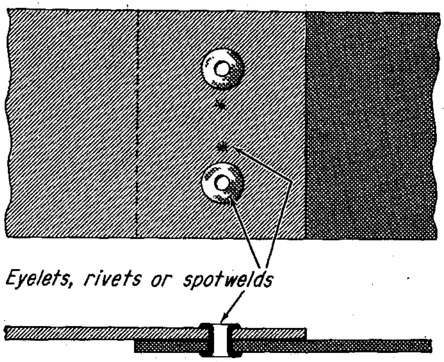

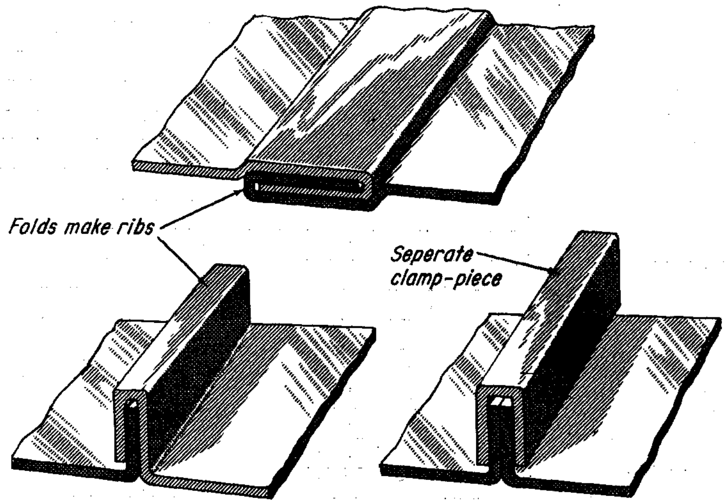

2 RIVETS OR SPOT WELDS ADD PEEL AND SHEAR STRENGTH.

3 FOLDS ARE SELF-CLAMPING; RIBS ADD RIGIDITY.

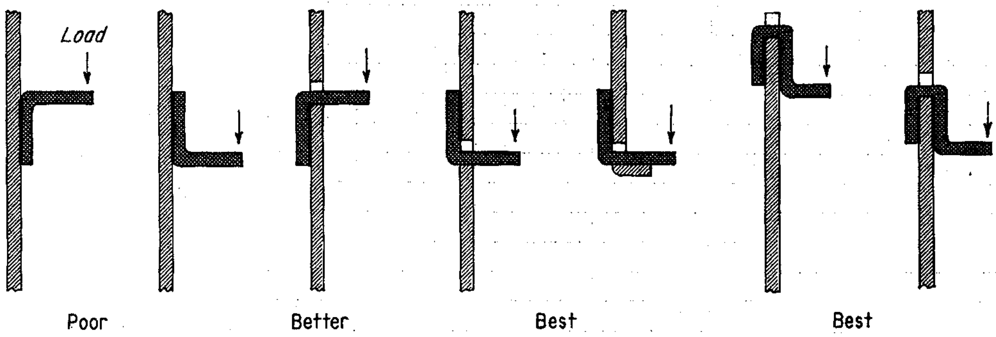

5 MECHANICAL SUPPORT FOR BONDED BRACKETS RELIEVES STRESS IN ADHESIVE.

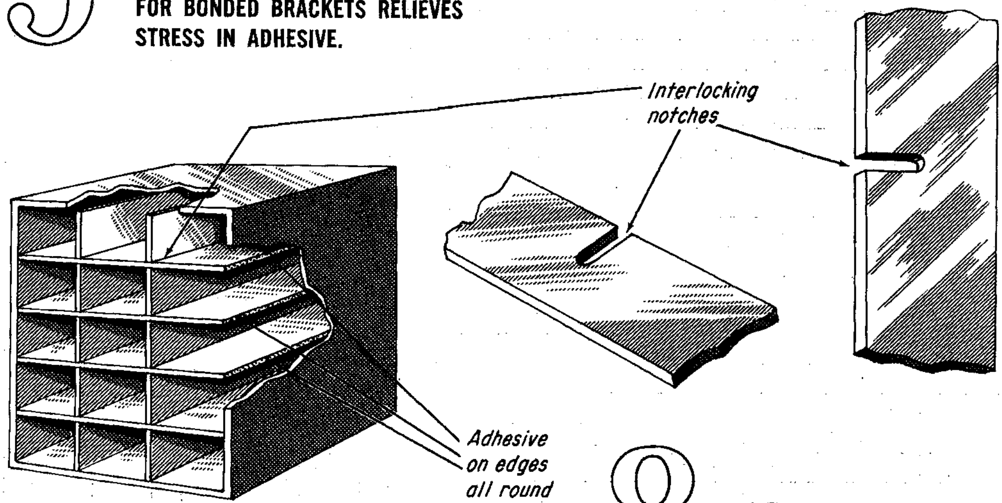

8 INTERLOCKING NOTCHES LET STRUCTURES SUPPORT THEMSELVES.

7 Ways to Assemble with Adhesives

Adhesives have come into their own now, so why not use them to greater advantage in mechanical and electrical assemblies?

Eugene J. Amitrani

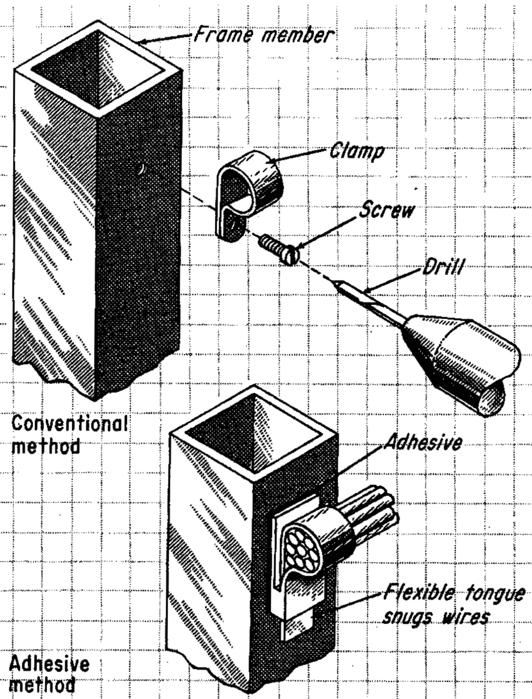

1 **CABLE CLAMP OF NEW DESIGN** uses adhesive as a fastening method. Conventional clamps can be fastened in the same manner.

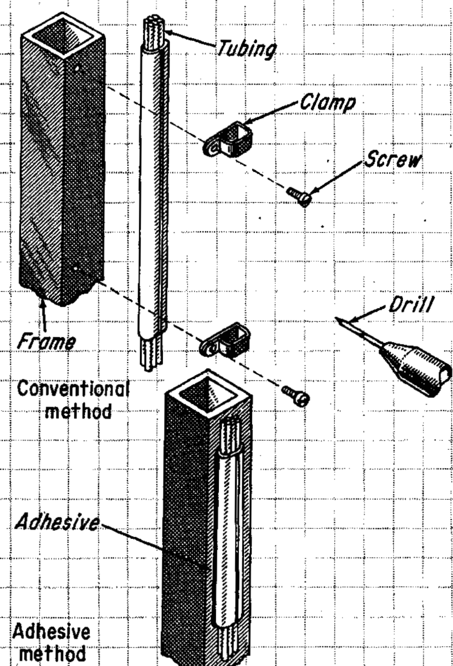

2 **TUBING ASSEMBLED TO FRAME** members does not require the use of screws and clamps when adhesive is used for the job.

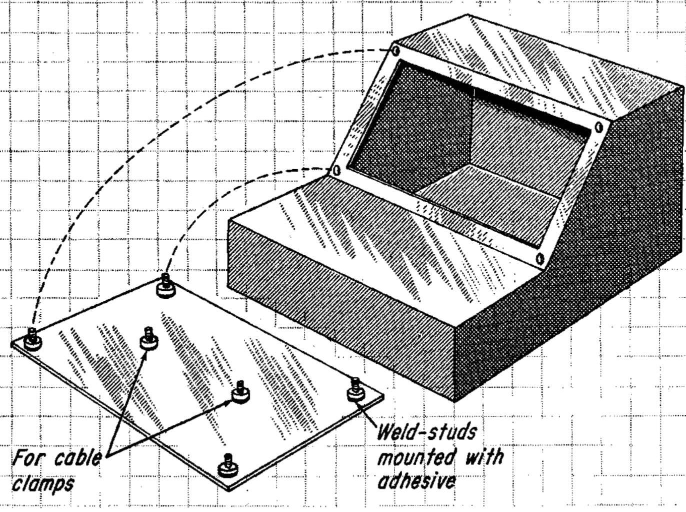

5 **PANEL FINISH IS NOT MARRED** by using adhesive to mount studs. Welded studs spoil finish on panel outer surface.

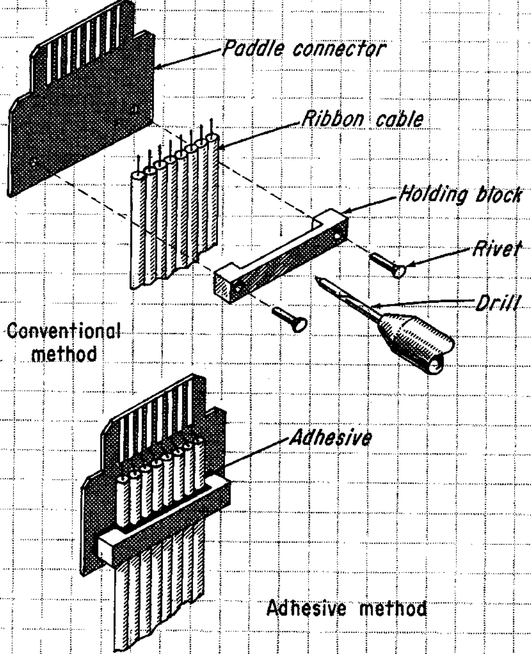

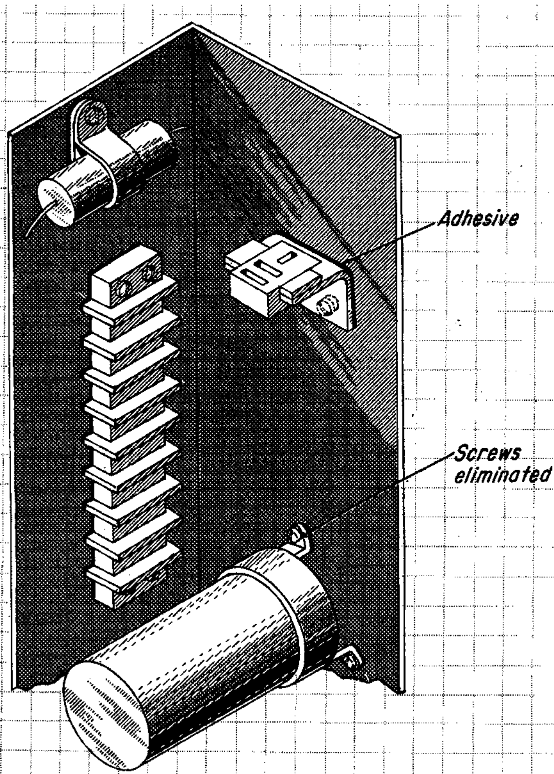

3 **SAVE RIVETS AND TIME** by using adhesive to fasten ribbon cable to connector-board. Dissassembly is not easy, though.

4 **SCREWS AND LOCKWASHERS** shown by dotted lines in sketch can be eliminated by using adhesive to attach components.

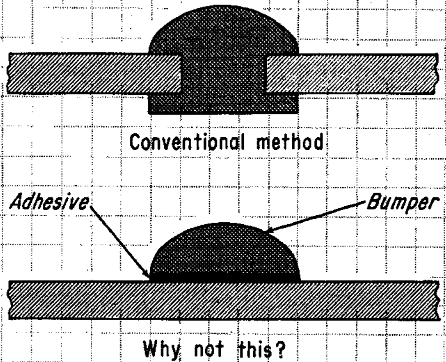

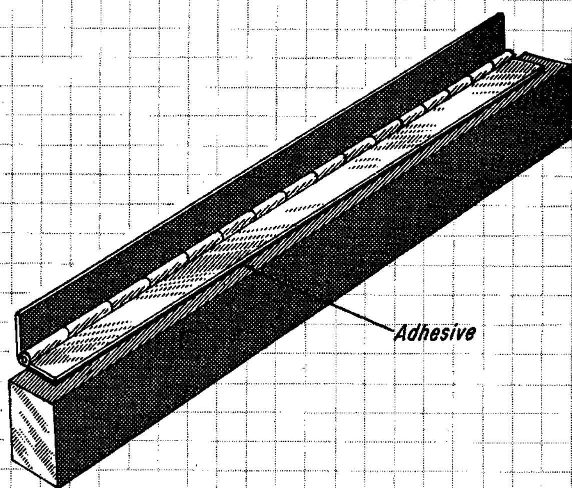

6 **RUBBER BUMPERS** usually need to be specially shaped and fitted into a hole in the component. Adhesive can simplify such assemblies.

7 **PIANO HINGES** are frequently used in instrument cases. Adhesive saves both hardware and time spent in making sure alignment is accurate.

Glass-to-Metal Joints

Five ways of joining glass and metal to keep thermal stresses to safe levels.

Robert H. Dalton

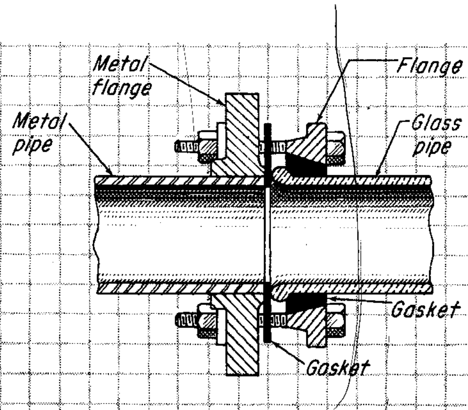

1 Glass pipe joined to metal flange; gaskets distribute clamping stresses

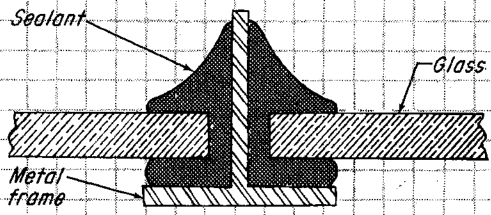

4 Flexible sealant retains glass to metal frame under light loads

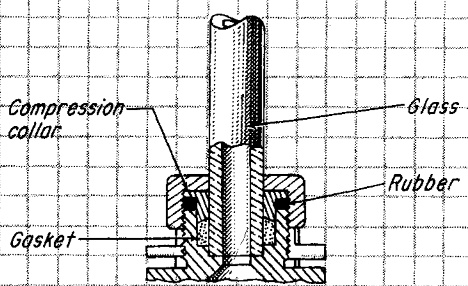

2 Clamp for gage glass for low-pressure boiler permits axial movement

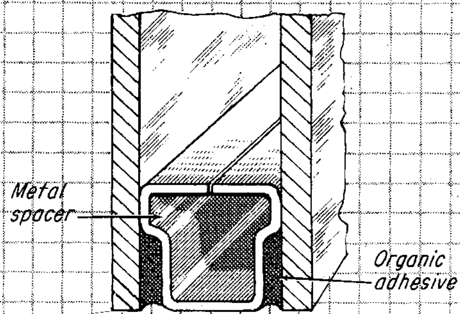

5 Double-glazed window bonded to metal spacer forms rigid structure

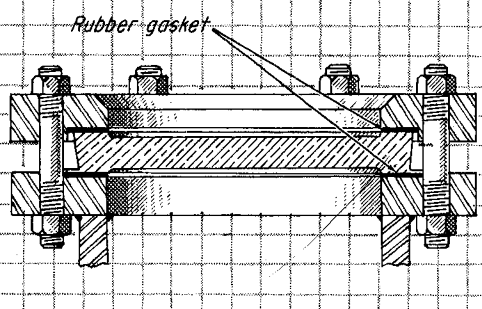

3 Window for high-pressure service requires flexible gaskets

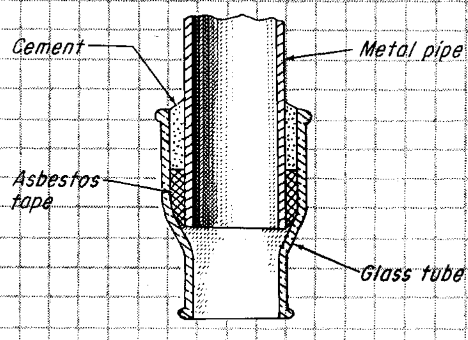

6 Cement combined with asbestos tape joins glass and metal pipe

Fused glass

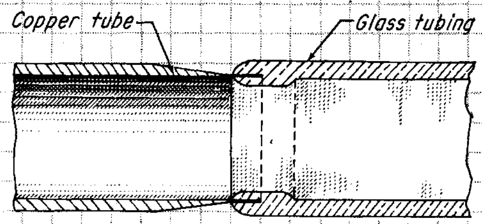

7 Housekeeper seal uses thin wedge of metal to minimize stresses at joint

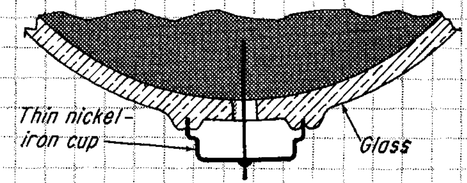

8 Saled-beam lamp has thin flexible metal cap fused to glass

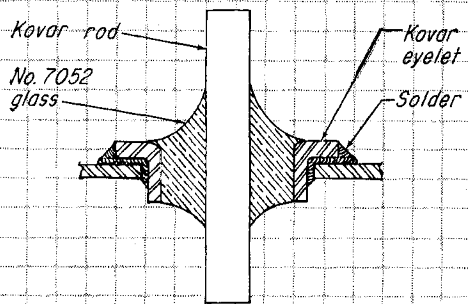

9 Hermetic seal matches expansion rate of rod and glass to reduce stress

Solder glass

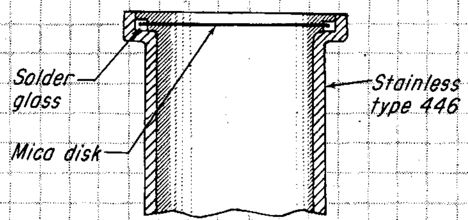

10 Low-melting solder glass minimizes heat damage to mating parts

Metallized glass

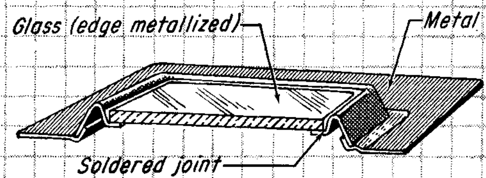

11 Metallized edge of glass window is soldered to flexible metal frame

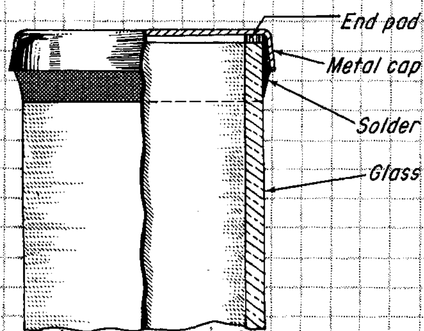

12 Thin metal cap soldered to large-area metallized glass surface

Simplifying Assemblies with Spring-Steel Fasteners

Since annealed spring steel can be stamped, twisted, or bent into any desirable shape and then heat-treated to develop spring characteristics, it can be designed for multiple functions in addition to that of fastening. Shown below are 16 ways in which spring-steel fasteners can be used to. . . . .

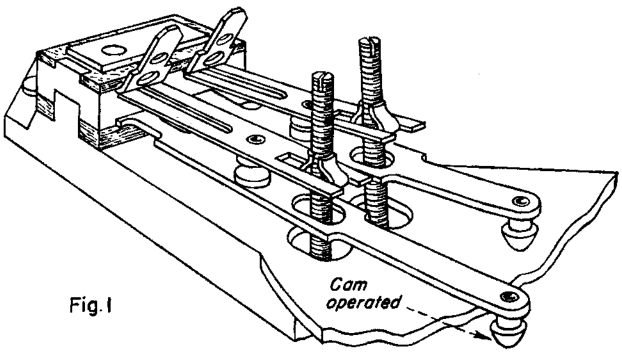

Fig. 1

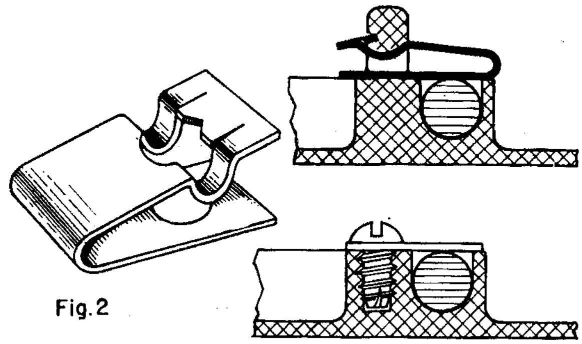

Fig. 2

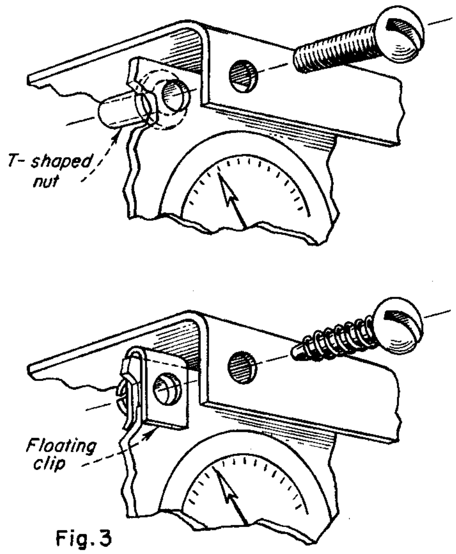

Fig. 3

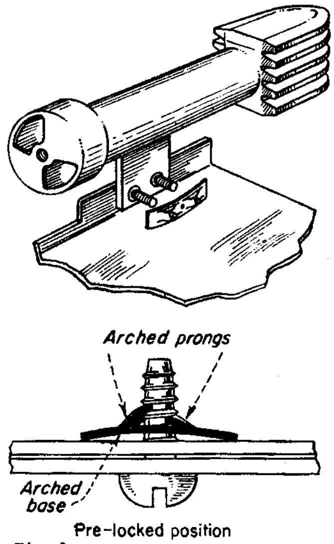

Fig. 4

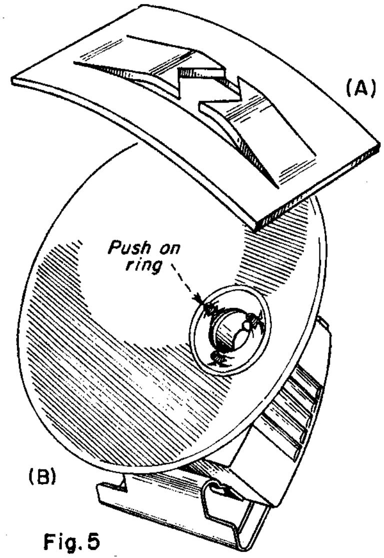

Fig. 5

FIG. 1—Multiple-purpose flat spring has stamped hole helically formed to accept adjusting screw. Replaces a locknut, bushing with internal threads and spring blade. Screw adjusts gap of contacts thus changing duration of current flow. Application: thermostatic timing control unit of an automatic beverage percolator.

FIG. 2—Spring-steel clip firmly holds stud of control knob while allowing it to turn freely on its bearing surface. Clip is removed by merely compressing spring arms and pulling off stud. Replaces screw and machined plate.

FIG. 3—Floating clip, which snaps in place by hand, reduces hole misalignment problems by permitting sufficient shift of mounting holes to offset normal manufacturing tolerances of main parts. Replaces welded T-shape nuts.

FIG. 4—Twin-hole nut removes need for hand wrench in hard-to-reach location and replaces two nuts and lockwashers. Combined force of arched prongs and base when nut is compressed creates high resistance to vibration loosening. Application: gas burner assembly of an automatic household clothes dryer heating unit.

FIG. 5—Push-on nuts (A) easily press over studs, rivets, tubing and other unthreaded parts. Their steel prongs securely bite into smooth surfaces under load. Application: (B) triple-hole push-on ring on a flash bulb reflector.

FIG. 6—Previous method of assembling desk calendar (A) required seven parts: wire guide, spring clip, plate, two bolts and two nuts. Multi-purpose spring clip (B) replaces above although using same retaining principle.

compensate for hole or part misalignment; prevent vibration loosening; eliminate parts; speed assembly; permit fastener removals; lock on unthreaded studs; and permit blind installations.

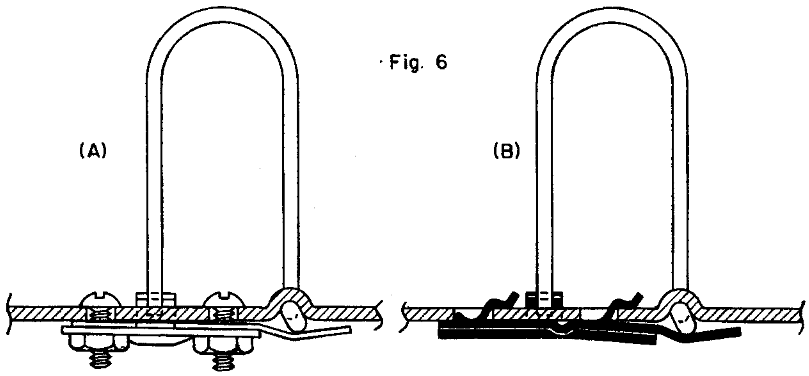

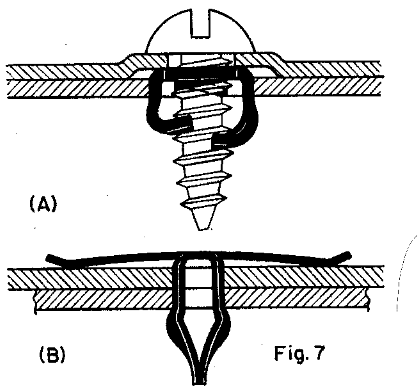

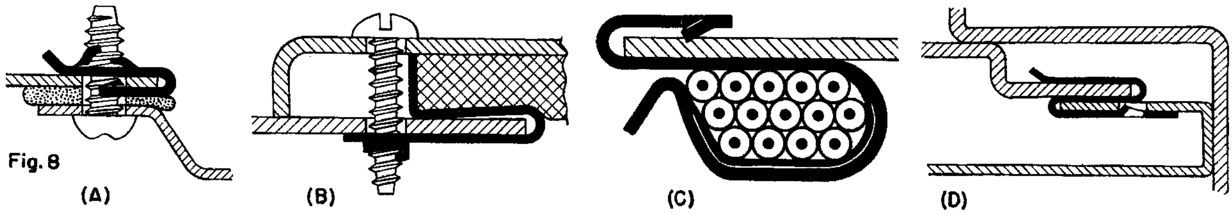

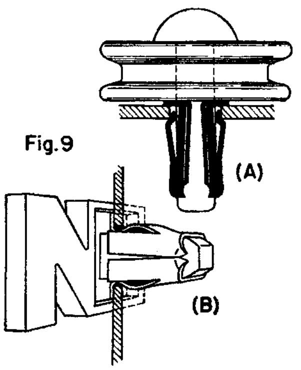

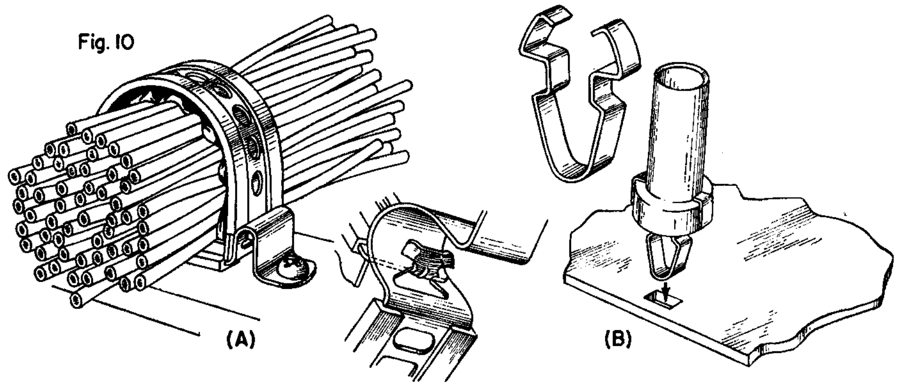

FIG. 7—Expansion-type fastener permits blind installation where access is from one side of an assembly only. Insertion of screw (A) spreads fastener arms apart thus producing a wedging effect in the hole. Dart-type fastener (B) can be quickly snapped in place; one common application is attaching molding trim strips to auto panels.

FIG. 8—End clips pressed by hand on panel edges have barbed retaining leg which either bites into the metal or snaps into a mounting hole. Applications: (A) sheet metal screw and J-clip with arched prongs compresses insulating material between panels; (B) bent leg of clip acts as spacer between two panels to support sheet of insulating material; (C) barbed-leg-clip retains wires without need for mounting hole; (D) S-clip spring-steel fastener secures removable panel in inaccessible position.

FIG. 9—Tubular-type fastener has cam-like prongs which spring out after insertion to hold fastener in position. Applications: (A) radio dial pulley; (B) attaching automotive name plate to panel.

FIG. 10—Special-function fasteners for quick assembly and disassembly of components. (A) Wire harness clamp using torque and slot principle; (B) dart-shaped clip for attaching coils and other parts to electronic chassis.

Spring-Steel Fasteners

This is the first of a series of articles on special fasteners. Future articles will cover cold-formed and quick-operating fasteners, plus new fastening ideas.

Ted Black

Spring-steel fasteners are versatile and low in cost. The steel is bent, twisted, and pierced, sheared and drawn into almost any desired shape to form a one-piece fastener that combines the functions of several ordinary fastening components, reducing fastening costs.

Spring clips are a major class of spring-steel fasteners and are particularly useful as light-duty fasteners. They are self-retaining units, needing only a hole, flange or panel edge to clip to. Their inherent springiness makes them resistant to loosening by vibration, and tolerant of tolerance buildup and misalignment.

The field of application of spring clips is a broad one, including automobiles, home appliances, hi-fi and electronic equipment, toys, aircraft and office equipment.

Dart type spring clips (Fig 1) have hips that engage within a hole to fasten two sheets or panels. Dart clips are popular for fastening printed-circuit boards and nameplates. Other shapes fasten cables, tubes and wires.

An advantage of dart clips is easy removability; therefore, minimum disassembly damage. Their retention power can be varied by changing the length and thickness of the clip legs.

Stud-gripper spring clips (Fig 2) are designed to grip unthreaded studs, pins, rivets and tubes. The studs can be of circular cross section, as is usually the case, or of square or D cross section.

Generally, the stud gripper has two or more prongs that permit the clip to be forced down on a stud. Such grippers resist removal. Any back pressure against the clip causes the prong to bite deeper into the stud.

Some stud grippers use a split tubular sleeve to grip the unthreaded stud or rivet. Such clips provide a secure lock, yet allow panels to be separated for service.

Cap push-on stud grippers are used on

1. Dart clips

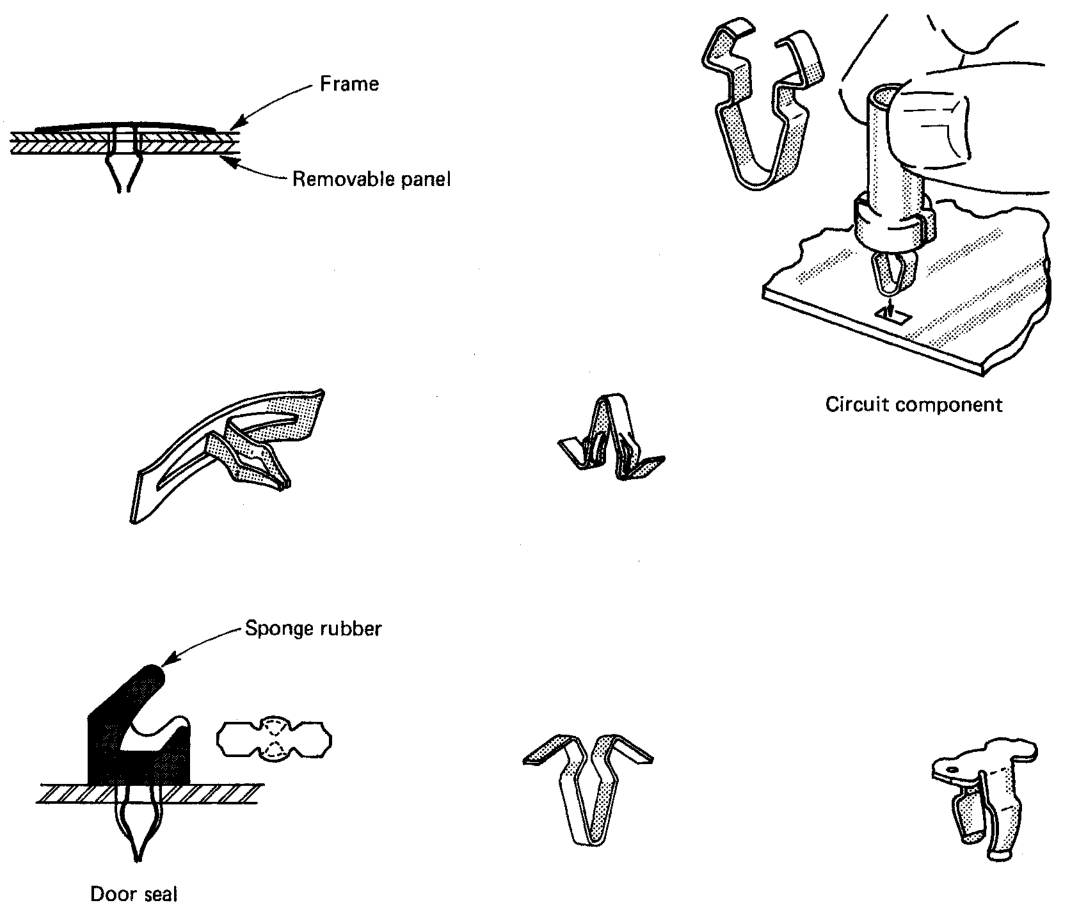

2. Stud grippers

Push-on type

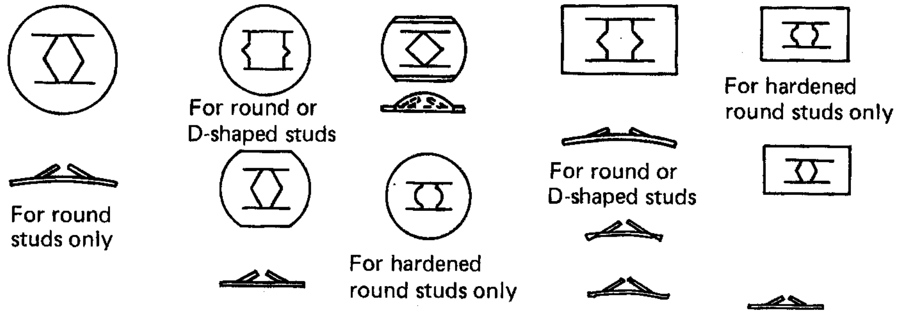

Ball-stud type

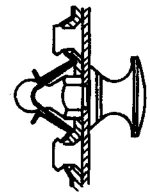

Tubular type

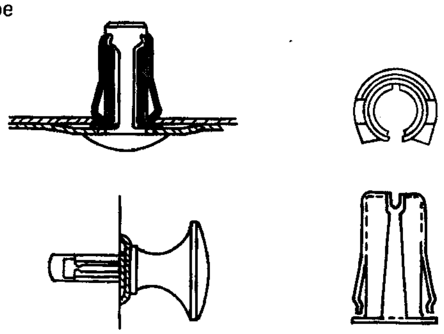

Cap type

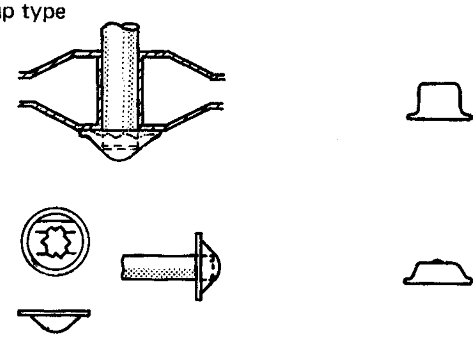

3. Cable, wire and tube clips

Cable clips

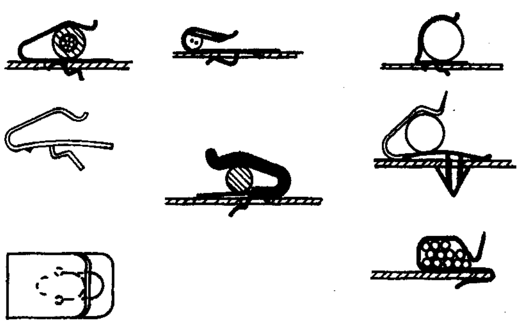

U-clips

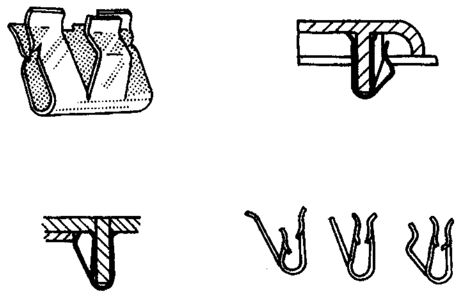

S-clips

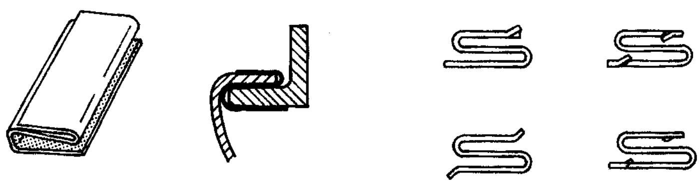

D-clips

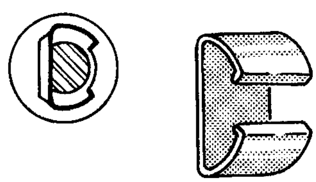

axles, shafts or rods, or as stud-end covers. Quickly installed, they eliminate the need for special machining or threading operations or cotter keys.

Wire and tube clips (Fig 3) are designed to grip into a hole or plate, or retain a wire or tube. They can be employed on existing parts and assemblies without a design change.

U-shape clips are used for assembling cover panels or as inexpensive hinge retainers. S-shape clips can clamp onto a part while clamping a panel or a flange of a component. C-shape clips provide a compression action that can hold plastic knobs firmly to steel shafts and permit them to be easily removed.

Spring-steel nuts (Fig 4) are single-thread engaging locknuts stamped into various convenient shapes. Available designs include flat, arched-back nuts; W-shape nuts with turned-up ends; self-retained, self-locking nuts; single-thread nuts for use in cavities; high-torque nuts with out-of-phase threads to increase vibration resistance; and nuts that cut their own threads into diecast metal or molded plastic studs.

Some spring-steel locknuts have threads in which the thread-engaging portion is helically formed in true relation to the pitch of the screw thread. These nuts have straight sides and hexagonal shapes for easy handling and positive rundown. Also useful are spring nuts designed to retain a shiftable nut to provide rivetless retention of nuts on plates (Fig 5).

4. Spring-steel nuts

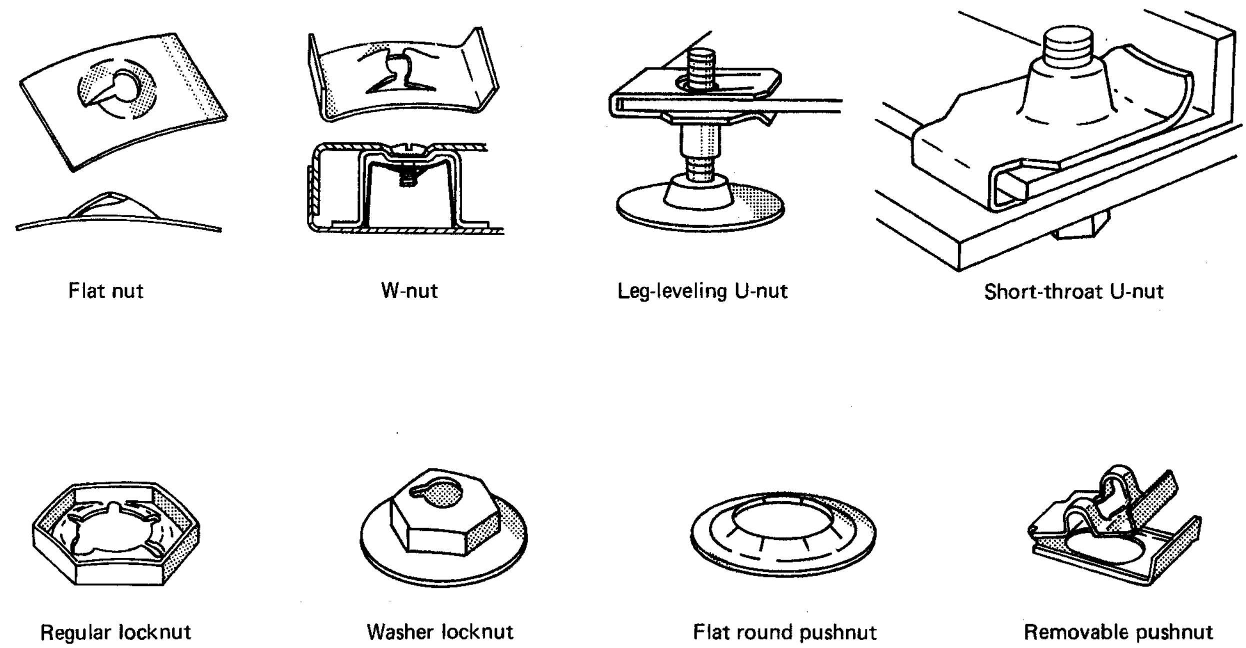

5. Clip-on nuts and nut retainers

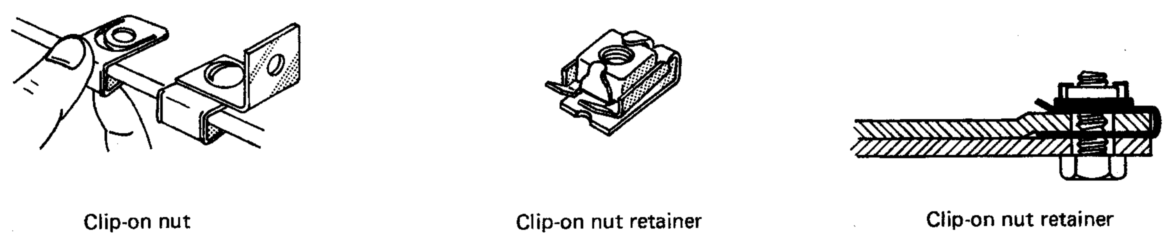

Snap Fasteners for Polyethylene Parts

It's difficult to cement polyethylene parts together, so eliminate extra cost of separate fasteners with these snap-together designs.

Edger Burns

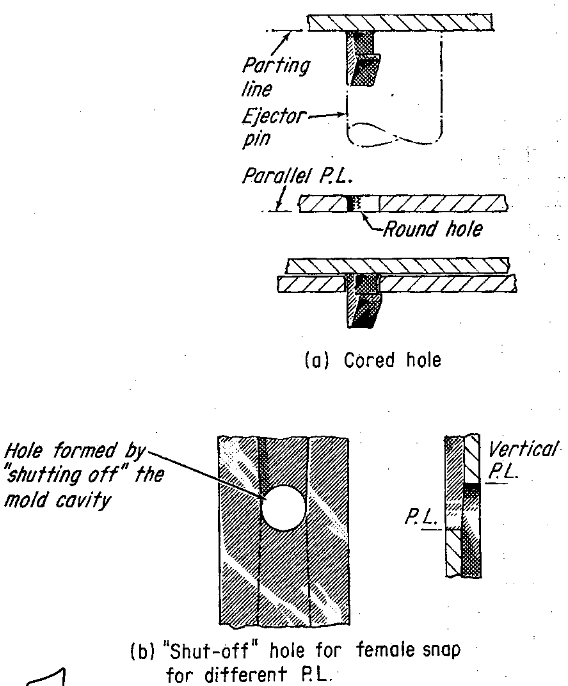

1 **EJECTOR-PIN** of mold is cut to shape of snap. Ejected with the pin, the part is slid off the pin by the operator.

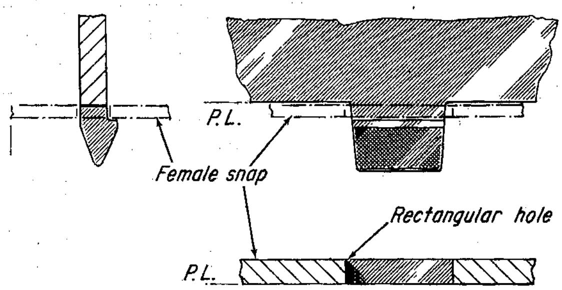

2 **WALL-END SNAP** is easier to remove from the mold than the ejector-pin snap. The best length for this snap is 1/4 to 1/2 in.

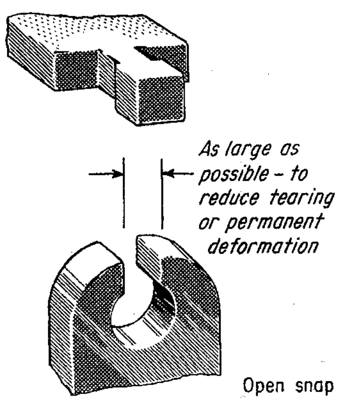

3 **OPEN SNAP** relies on an undercut in the mold and on the ability of the polyethylene to deform and then spring back on ejection.

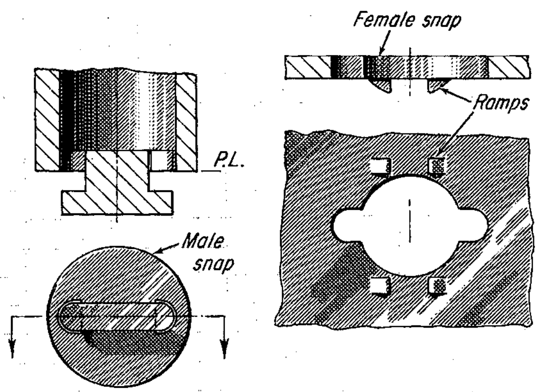

4 **T SNAP** locks with a 90-deg turn. To prevent this snap from working loose, four small ramps are added to the female part.

Plastic Snap-Fit Design Interlocks in Unique and Useful Ways

Snap-on caps and latches are deceptively simple, but were evolved using good engineering design. Here's a recent study.

In response to the often-heard suggestion that snap fits are not dependable because they have a tendency to pop out, Dr. William W. Chow of the University of Illinois in Urbana has developed (and presented in an ASME paper) an analytic method for predicting snap-in and snap-out forces. His conclusion is that a well-designed snap fit cannot be easily pulled out, and has certain advantages over other methods.

For example, a screw fit can vibrate loose, a press fit depends on friction and strain to hold, and a sonic weld is permanent.

The snap fit is a simple mechanical interlock whose pull-out force can be hundreds of times larger than the push-in force. It takes careful selection of the slope of the bevel on both the entering lip and the withdrawal lip. The extreme is a cap or latch that snaps on easily, but locks on permanently—like a fish hook.

We asked Chow how he solved the design problems. He said he first examined the simplest case of a cantilever-type snap with zero friction. Next, the same snap was analyzed with the effect of friction. The results then were generalized to cover all kinds of snaps.

The calculation. Assuming zero friction (μ=zero) the snap-in force is related to the spring rate of the snap by the tangent of the lead angles and the interference (see accompanying cantilever drawing as an example).

With zero friction, snap-in force $F_i = F_s \tan\alpha$, or $K\ i \tan\alpha$. Snap-out force $F_o = F_s \tan\beta$, or $K\ i \tan\beta$, where:

μ = coefficient of friction
F_s = snap force, the force that reduces i to zero
i = interference
K = spring rate of the snap
α = lead angle
β = return angle

The smaller the lead angle, the easier it is to assemble the snap. The smaller the return angle, the less force is needed to disassemble the snap. When the return angle is 90 deg, the snap is self-locking. When the return angle is greater than 90 deg, the interference is a barb.

With friction, the tangent term becomes a more complex function of the lead angle, α, and the coefficient of friction, μ:

$$\text{Force } F_i = F_s \frac{(\sin\alpha + \mu\cos\alpha)}{(\cos\alpha - \mu\sin\alpha)}$$

$$\text{Force } F_o = F_s \frac{(\sin\beta + \mu\cos\beta)}{(\cos\beta - \mu\sin\beta)}$$

The analysis also applies to hollow cylinder snaps and distortion snaps, but the spring rate has to be figured accordingly. Spring rate of a snap is defined as the snap force, F_s, that is required to reduce the interference to zero, divided by the interference. The spring rate for a hollow cylinder snap, K_{cyl}, is the total force in the radial direction, F_r, divided by the increase in radius, i_{rad}.

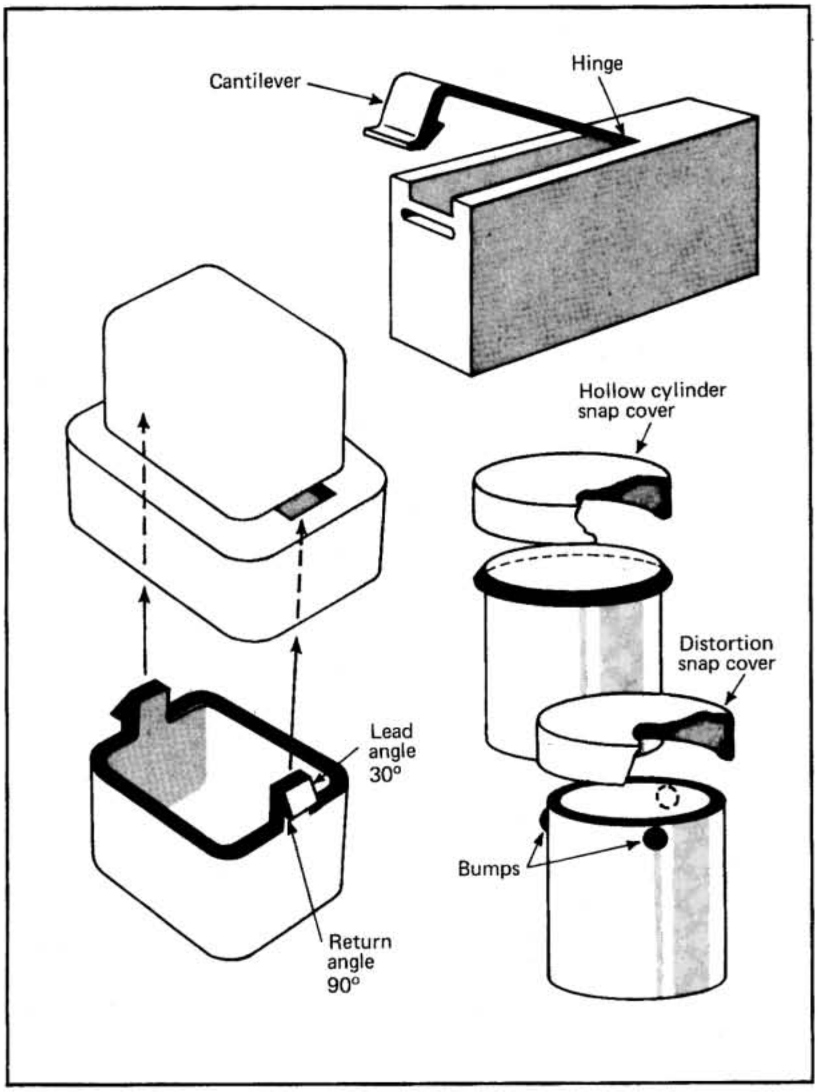

These snap-fit designs are typical of what can be done using the accompanying calculation techniques. The example worked out is for simple cantilever

$$K_{cyl} = \frac{F_r}{i_{rad}}$$

Snap-in snap-out forces. The next drawing shows examples of cylindrical snaps. The distortion-type lid is a variation of the hollow cylinder snap, and mates with a smaller cylinder with three bumps. The spring rate, K_{dist} is three times the force at each bump, F_b, divided by the interference at the bump, i_{bump}:

$$K_{dist} = \frac{3F_b}{i_{bump}}$$

The product of K and i gives the snap force, and the product of the snap force and the tangent of the lead angles gives the snap-in and snap-out forces.

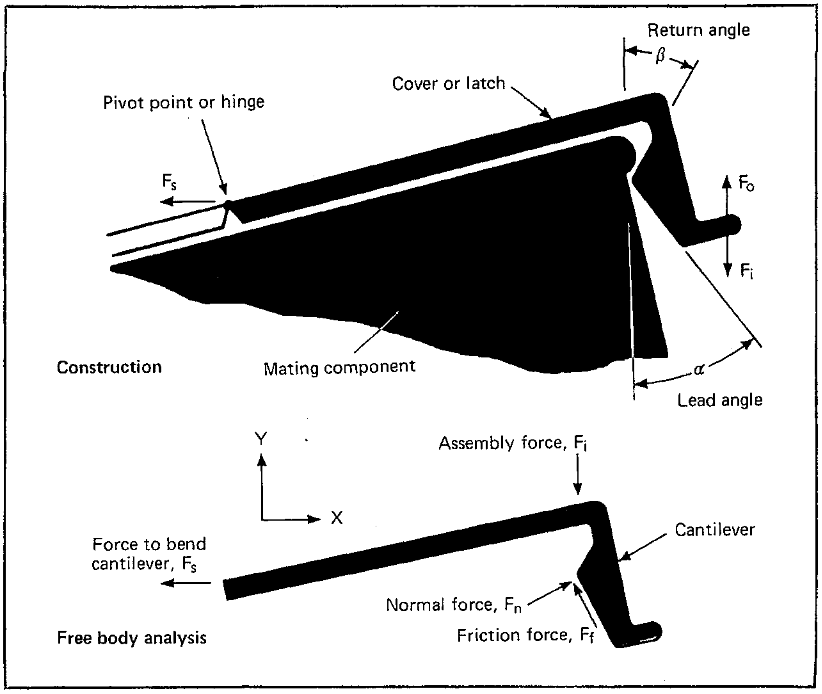

Cantilever design with hinge is simplest configuration for mathematical analysis

Basic stress-strain equations for snap-fit elements

	Spring rate, K	Stress, σ	Strain, ϵ	Allowed interference, i
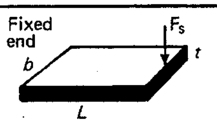 Fixed end, F_s, b, t, L — Uniform cantilever	$\frac{Eb}{4}\left(\frac{t}{L}\right)^3$	$\frac{3Eit}{2L^2}$	$\frac{3it}{2L^2}$	$\frac{2S_y L^2}{3Et}$
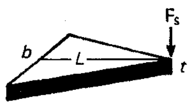 F_s, b, L, t — Tapered cantilever	$\frac{Eb}{6}\left(\frac{t}{L}\right)^3$	$\frac{Eit}{L^2}$	$\frac{it}{L^2}$	$\frac{S_y L^2}{Et}$
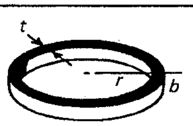 t, r, b — Thin-wall cylinder	$2\pi Eb\left(\frac{t}{r}\right)$	$\left(\frac{i}{r}\right)E$	$\frac{i}{r}$	$\frac{S_y r}{E}$

Typical snap-in and snap-out forces are in the range of 2.5 to 250 Newtons (about 0.50 to 55 lb). Interferences are usually between 0.25 to 2.5 mm (about 0.010 to 0.100 in.). If: the coefficient of friction is 0.15; the lead angle is 30 deg; the interference is 1 mm; and the spring rate is 5000 N/m; then the equation shows that snap-in force is 3.98 Newtons.

The table lists some approximate spring rates for three simplified spring geometries: a uniform cantilever; a tapered cantilever; and a thin-walled hollow cylinder.

Referring to the free body drawing of the cantilever: force acting at the interference consists of a normal component, F_n, and a tangent component, F_f(friction). Since all the forces meet at one point, the summation of moments and forces equals zero: $M = 0$; and $F = F_n + F_s + F_n + F_f = 0$.

F_i = snap-in force

F_s = snap force, the force needed to reduce interference to zero

F_n = normal force at the interference

F_f = friction force at the interference $= \mu F_n$

Consider the x-component:

$$F_n \cos\alpha - F_f \sin\alpha - F_s = 0$$

$$F_n = \frac{F_s}{\cos\alpha - \mu \sin\alpha}$$

Consider the y-component:

$$F_n \sin\alpha + F_i = 0$$

$$F_i = F_n (\sin\alpha + \mu\cos\alpha)$$

Combine the x and y, and we're back to:

$$F_i = F_s \frac{(\sin\alpha + \mu\cos\alpha)}{(\cos\alpha - \mu\sin\alpha)}$$

$$F_o = F_s \frac{(\sin\beta + \mu\cos\beta)}{(\cos\beta - \mu\sin\beta)}$$

And, if friction is considered negligible, $F_i = F_s \tan\alpha$; and $F_o = F_s \tan\beta$.

Widely applicable. Snap fits for plastic are common in closures for fill pipes, bottles, container walls, and other applications where positive closure is needed but tools aren't readily available.

Cap and plug manufacturers such as Caplugs/Protective Closures (Buffalo, N.Y.), Niagara Plastics (Erie, Pa.), Clover (Tonawanda, N.Y.), Sinclair & Rush (St. Louis, Mo.), and Heyco (Kenilworth, NJ), employ the principles in many products they offer.

Caplugs, for example, features internal beads in certain of its cap closures, so that they snap into place and hold against vibration. Jim Rooney, president of Niagara Plastics, points out that a popular material is low-density polyethylene.

Fasteners that Disconnect Quickly

Ideal for linkages, these quick-disconnect designs can simplify installation and maintenance because no tools are needed.

Frank W. Wood JR.

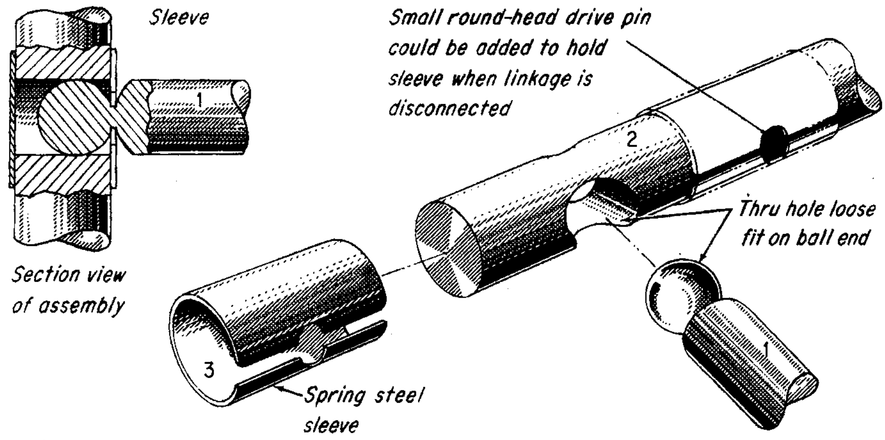

1

BALL JOINT **and spring sleeve provide snug universal motion when hole in center of sleeve snaps over base diameter of ball. Ball diameter must always be less than that of the mating arm.**

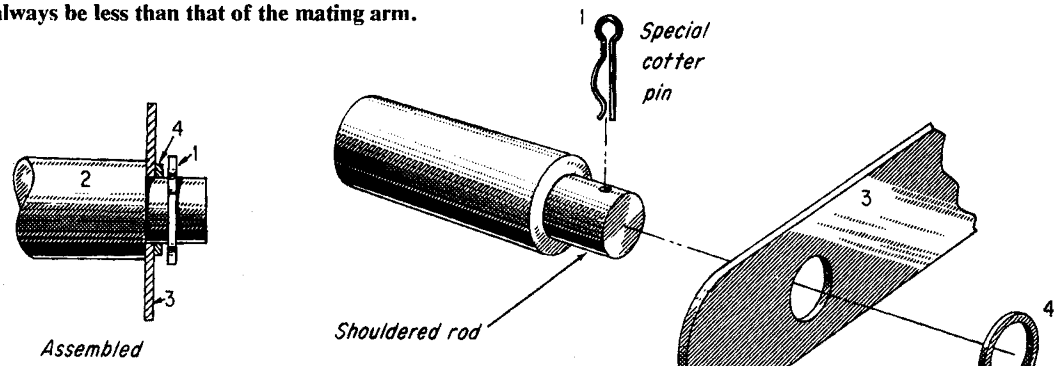

3

SPECIAL COTTER PIN **can be removed more easily than conventional cotter pins. Although limited by rod diameter, pin is reusable. Light-duty applications only are recommended.**

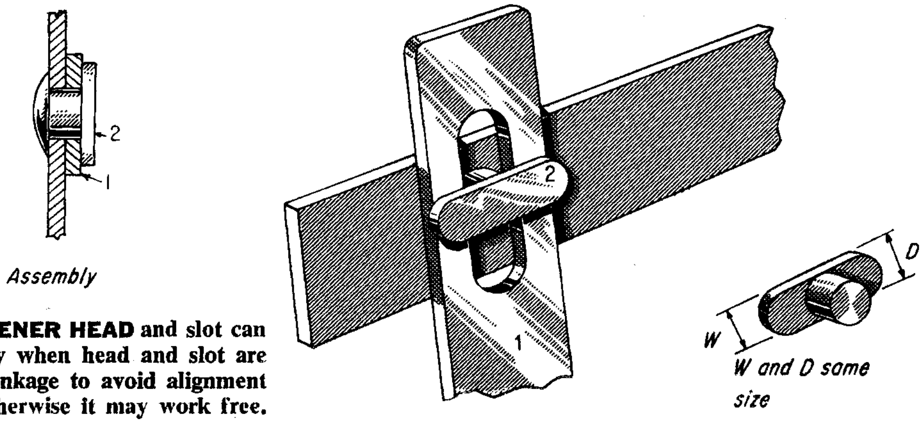

5

ELONGATED FASTENER HEAD **and slot can be disconnected only when head and slot are aligned. Phase the linkage to avoid alignment of slot and head; otherwise it may work free.**

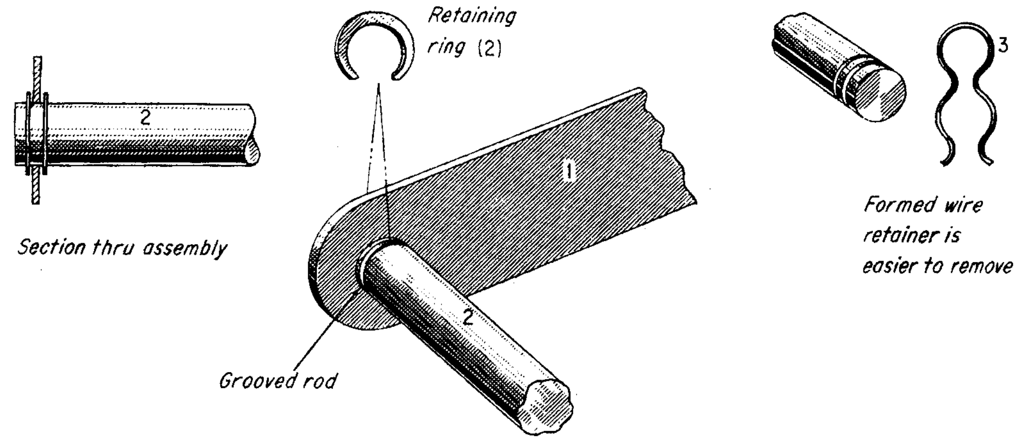

2

GROOVED ROD and retaining rings, while not having the freedom of motion of previous design, are simple and inexpensive to make. Double grooves are usually necessary.

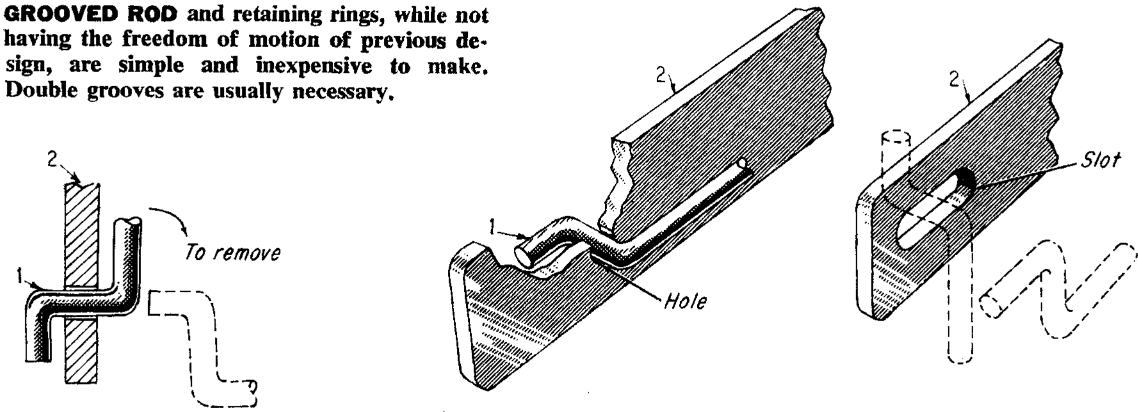

(A) (B)

4

FORMED ROD in hole or slot allows disassembly only when the rod is free to be manipulated out of the arm. Slot design has play, which may or may not be advantageous.

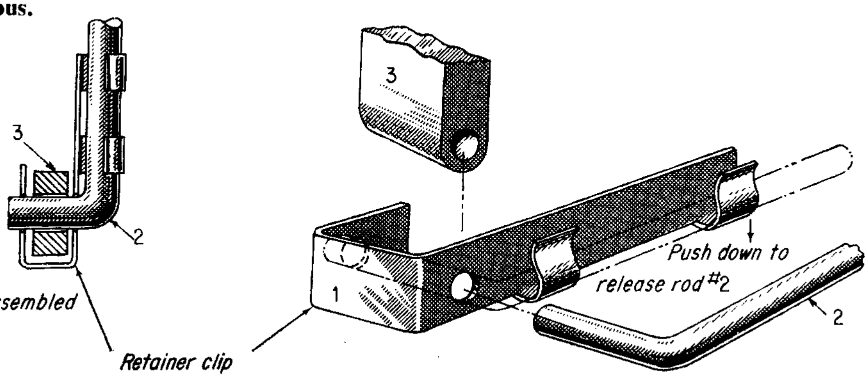

6

RETAINER CLIP and formed rod are ideal when production quantities are high enough to warrant tooling costs necessary for clip. But the clip is relatively easy to make.

More Quick-Disconnect Linkages

These methods of fastening linkage arms allow them to be disassembled without tools. Snap slides, springs, pins, etc, are featured.

Frank W. Wood JR.

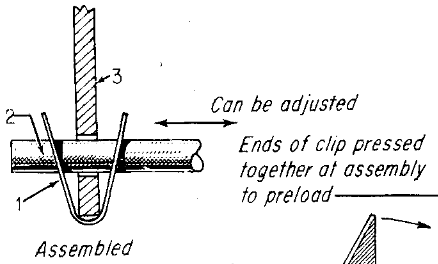

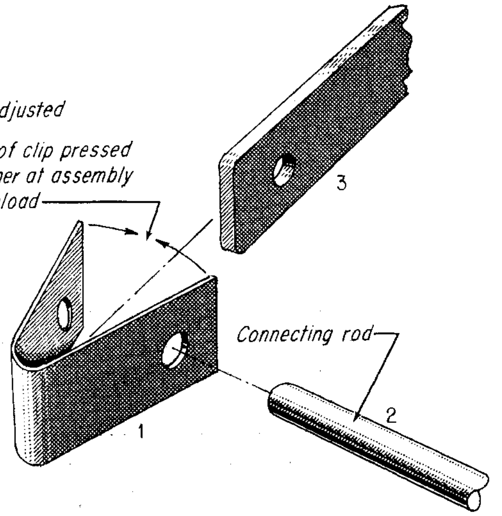

1 **PRELOADED FLAT SPRING** lets the connecting rod be adjusted merely by squeezing the end of the clip together to remove grip. This fastening is not recommended for insulated rods.

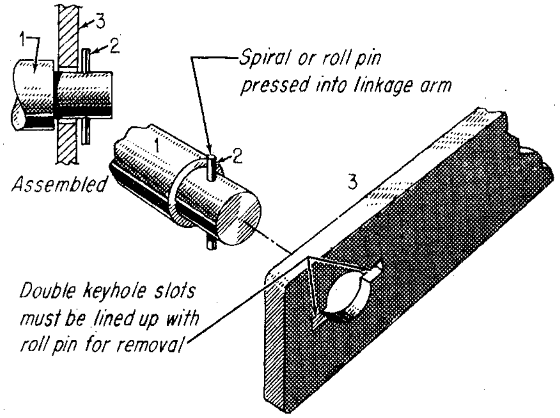

3 **SPECIAL PIN AND DOUBLE KEYHOLE** comprise a bayonet type of fastening – reliable only when pinned rod won't turn during operation, when alignment may let pinned arm work free.

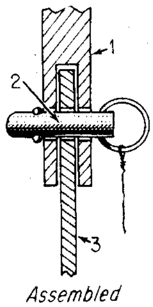

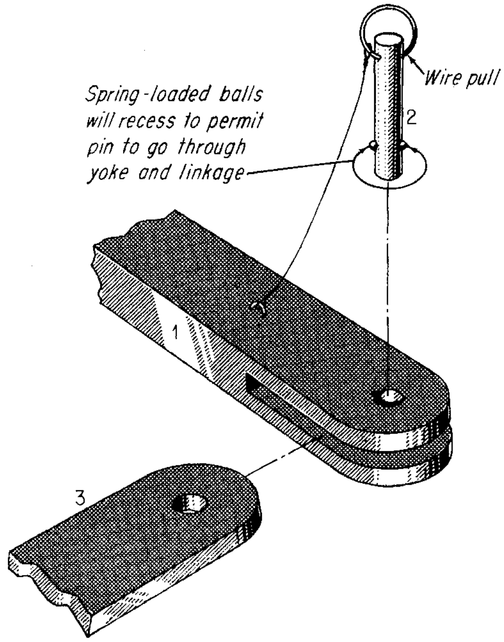

5 **YOKE AND SPRING DETENT PIN** together make a common fastening method for many mechanisms. It's sometimes wise to tie pin to a member so that the pin will not be lost.

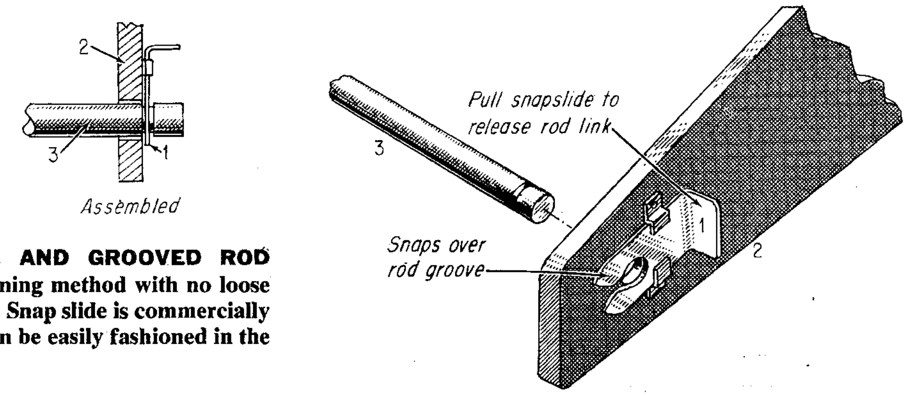

2 **SNAP SLIDE AND GROOVED ROD** provide a fastening method with no loose parts to handle. Snap slide is commercially available, or can be easily fashioned in the model room.

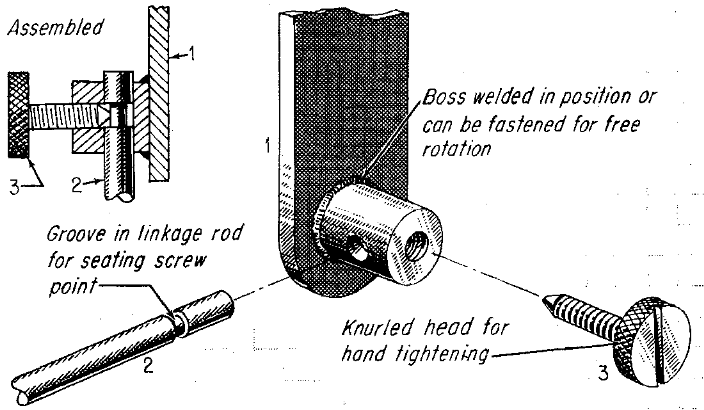

4 **GROOVED ROD AND CLAMP SCREW** will not allow relative movement between rod and other linkage member unless the boss is free to rotate on its arm.

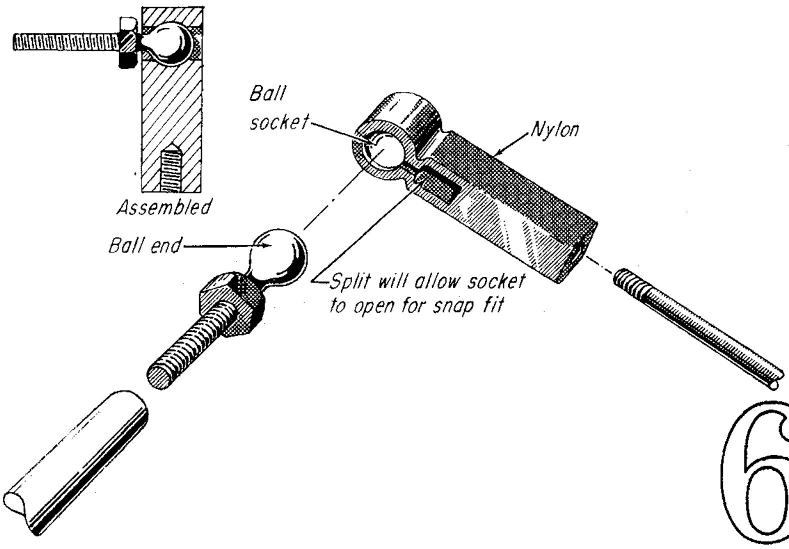

6 **NYLON ROD COUPLER** allows typical ball-and-socket freedom combined with the self-lubricating properties of nylon. If load becomes excessive, the nylon will yield, preventing damage to linkage.

8 Dentents for Clevis Mounting

When handles are mounted in clevises they often need to be held in one or more positions by detents. Here are ways to do this.

Irwin N. Schuster

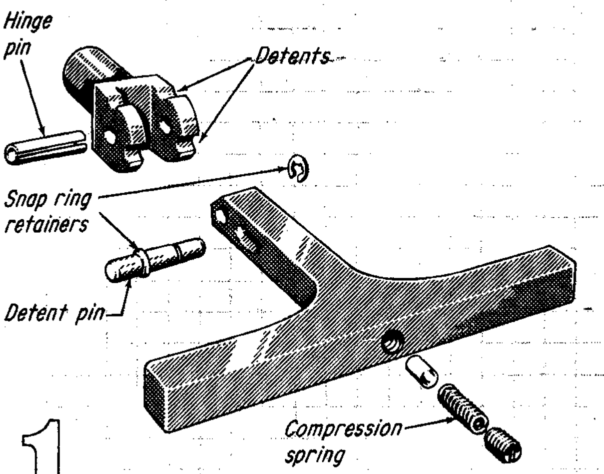

1

CAST OR MILLED clevis features an adjustable tensioning device, which varies the follower load. Handle can be extruded section.

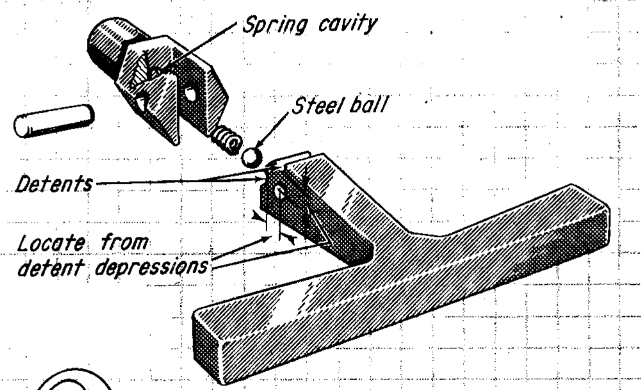

2

CLEVIS MACHINED from hexagonal stock can be drilled to receive a ball detent, which acts in cammed surfaces cast in handle.

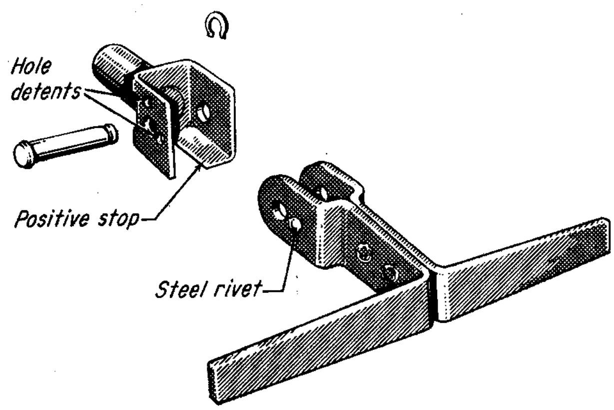

5

WELDED CLEVIS is relieved to improve spring characteristics. Punched holes receive steel rivet head which acts as the detent.

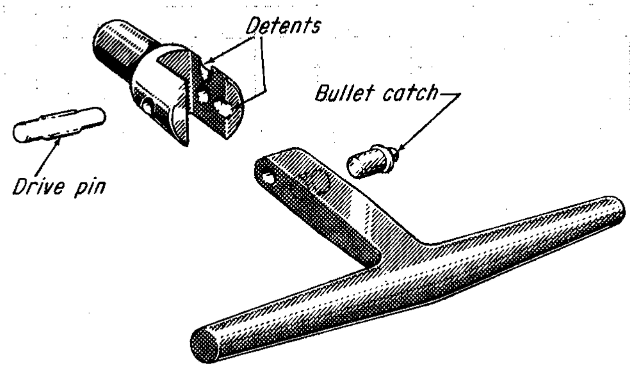

6

CAST HANDLE is drilled to accept a commercial "bullet" catch, which detents in the milled internal surface of the clevis flanges.

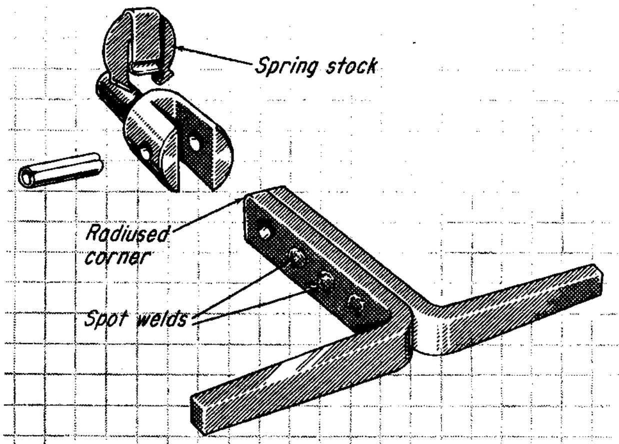

3

STAMPED SPRING snaps onto clevis before final assembly and acts as detent against the flat end and top surfaces of metal handle.

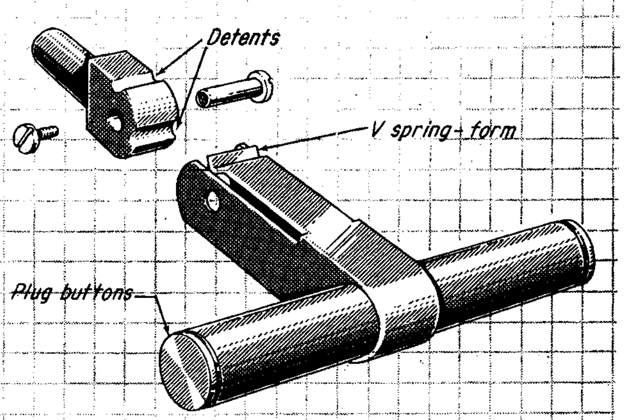

4

TUBE AND SHEETMETAL clevis handle has integral leaf spring which detents in cammed surface of machined shaft head.

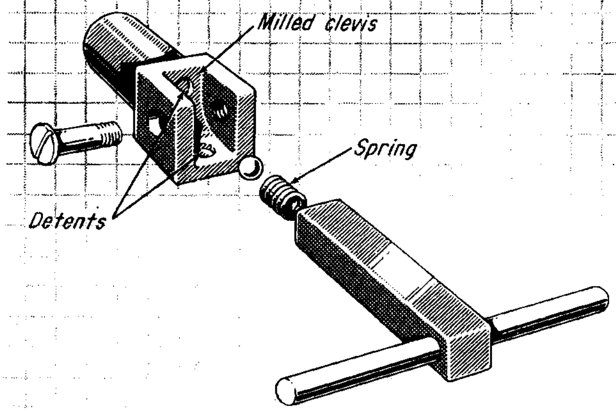

7

MILLED CLEVIS accepts ball-bearing follower, actuated by a spring, which seats against a pivot pin in the bar and rod handle.

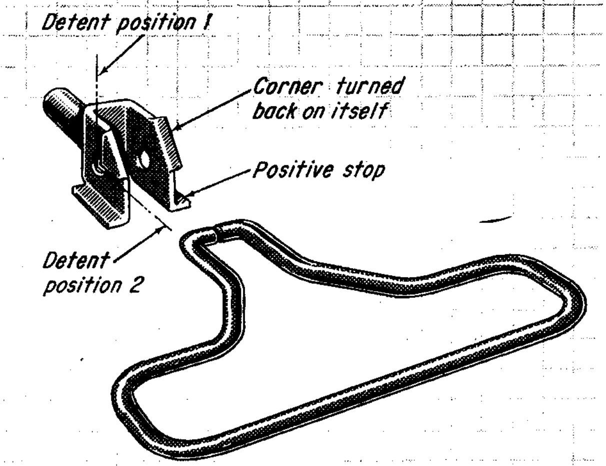

8

WIRE HANDLE acts as spring and follower in sheetmetal clevis, in which cammed surfaces and positive stops are made by bending.

8 Control Mountings

When designing control panels follow this 8-point guide and check for...

Frank W. Wood JR.

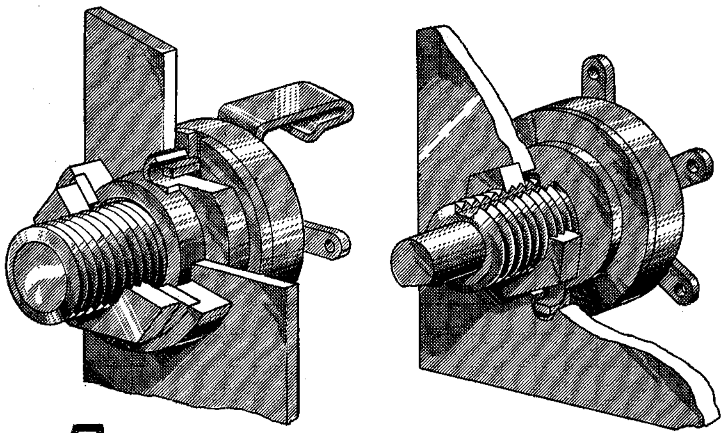

1 ... **LOCKING.** Control will stay fixed in spite of vibration or attempts to force shaft too far. Washer at right has two tabs; one fits in the panel, the other in the control bushing. Left washer has a boss which fits into a cutout in the panel and around a pin projecting from the control body.

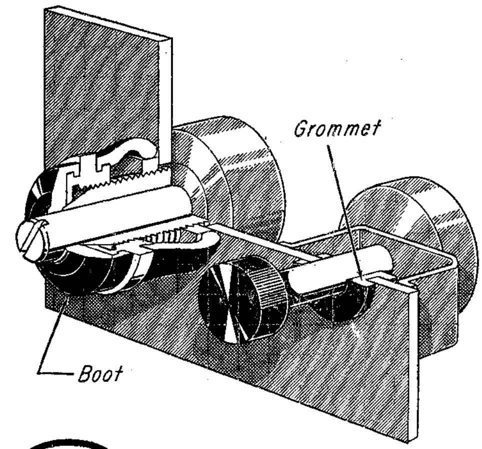

2 ... **SEALING** against dust or water. Boot seals between shaft and bushing and between bushing and panel. With control behind panel rubber grommet seals only one place.

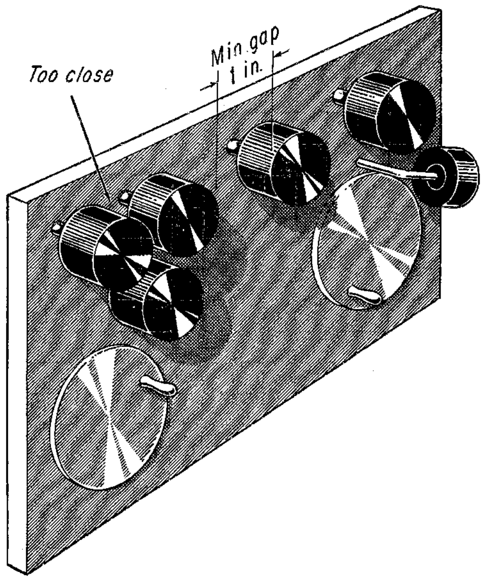

5 ... **HAND-ROOM** at front of the panel. Space knobs at least one inch apart. Extending knob to save space puts it where the operator can bump into it and bend the shaft. Best rule is to keep shaft as short as possible.

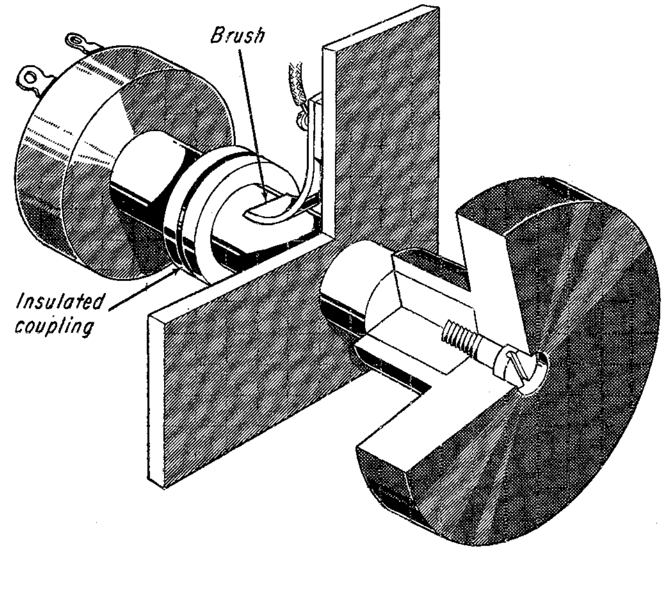

6 ... **"HOT" CONTROL KNOBS.** One approach is to ground them by installing a brush against the shaft. Another solution is to isolate the control by an insulated coupling or a plastic knob having recessed holding screws.

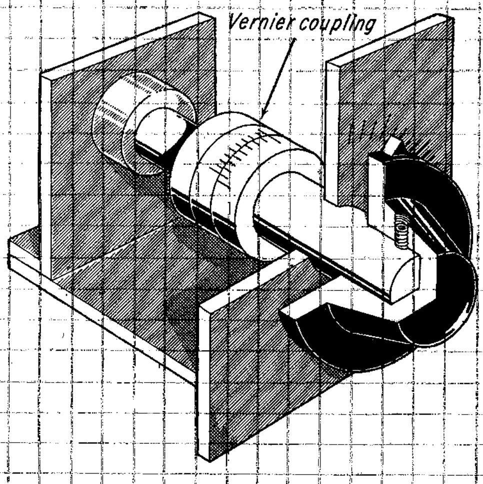

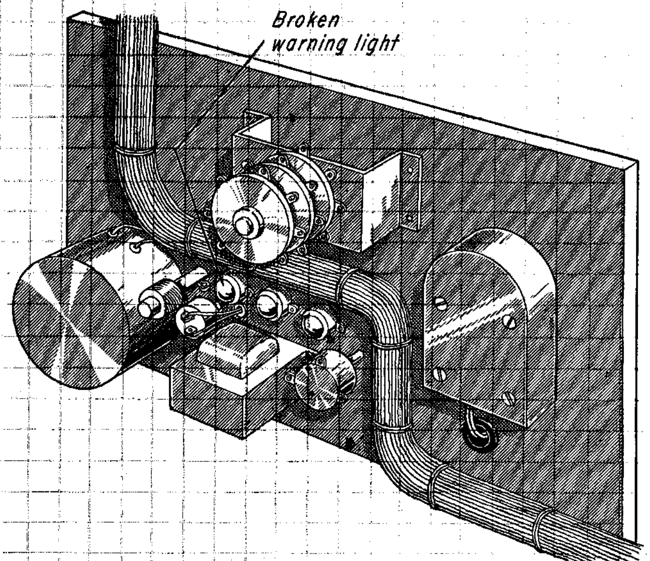

3 ... **RESETTING** to match controls to panel markings. For crude adjustments a set-screw is enough. Where matching is critical a three-piece vernier coupling permits more accurate calibration.

4 ... **ACCESSIBILITY** behind the panel. Easy access reduces down time and maintenance costs especially if one man can do most jobs alone. Here, technician can't replace a warning light without dismantling other parts.

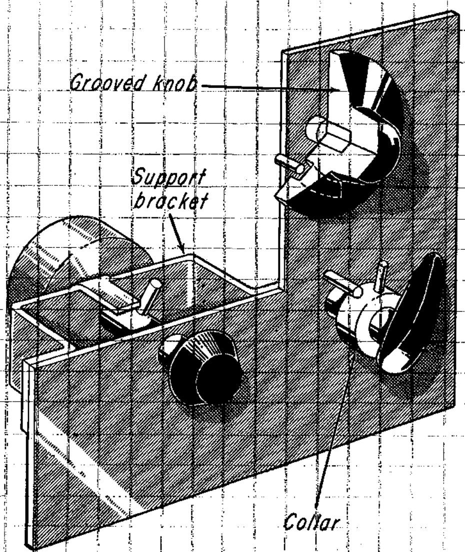

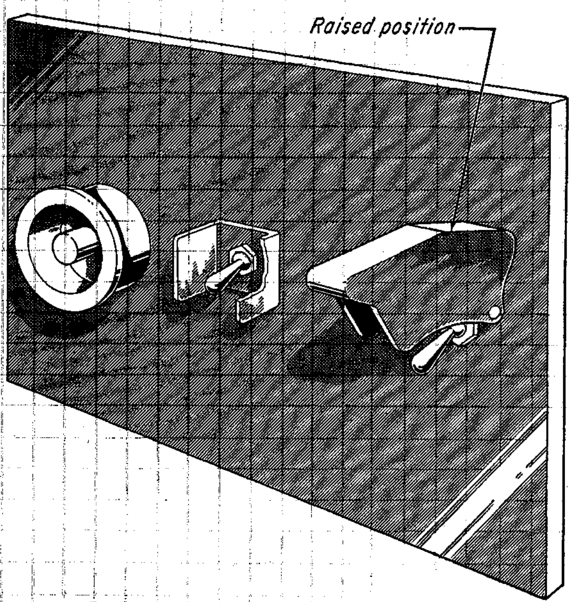

7 ... **LIMIT STOPS** that are strong enough not to bend under heavy-handed use. Otherwise setting will change when stop moves. Collar and grooved knob permit adjustment; tab on bracket doesn't.

8 ... **GUARDS** to prevent accidental actuation of switches. Bell-shape guard for push-buttons is just finger-size. U-shape guard separates closely spaced toggle switches, and a swinging guard holds down special ones.

18 Ways to Join Honeycomb Panels

A design guide to aid selection among mid-panel and panel-rib joints, spar-panel intersections, and edge-member attachments.

Frank J. Filippi & Boris Levenetz

Ever-increasing use of honeycomb-sandwich structures in many different products, including missiles, has revealed a lack of basic design information for these structures. The designer's problem is always: What is the best way to join panels without sacrificing much of their strength?

There are two basic approaches to joint design: The pictorial design approach, used extensively; and the analytic design approach, used less because of lack of time. The pictorial design procedure is mainly concerned with optimizing one type of structure such as honeycomb sandwich. Analytic design seeks to achieve the best load transfer at the lightest weight, irrespective of the type of structure necessary to accomplish the transfer. In this digest the pictorial approach is presented. In any joint design, however, productibility is the major factor influencing final selection. The design engineer must recognize that his skills are currently at the mercy of the production engineer who must reduce the design to a producible article at a reasonable cost.

MID-PANEL JOINT

A mid-panel joint must be designed to carry bending, shear, compression, and tension loads. The shear loads require connection of the panel cores, since the core is the only element able to transmit shear forces perpendicular to the panel. For applications not involving shear loads, joining the cores is not mandatory, but is very desirable for joint stabilization. The ideal joint would have cores and faces welded together, providing necessary ties for proper load transfer. It can not, however, be produced because of inaccessibility of the core for welding. A producible and analytically satisfactory joint, Fig. 1, shows the joint before the welding operation as prepared for joining. The now-accessible core is welded to the web, the joint is closed, and a fusion weld picks up the faces and web. The addition of the web guarantees a good shear joint for the core, while the thickened facing compensates for the loss in strength from the fusion welding operation. Although some deformation of the core is encountered, good shear transfer is still possible.

Much of the brazed honeycomb sandwich manufactured today is made from precipitation-hardenable stainless steels. As a result of heat treatment, these steels exhibit a net growth averaging 0.004 in. per in. Unfortunately, the fact that this growth is neither consistent nor exactly predictable results in dimensional discrepancies of the heat-treated parts. Machining a panel edge before welding gives a measure of compensation for erratic growth and should be considered as necessary design practice along at least two adjacent edges of any precipitation-hardenable steel sandwich.

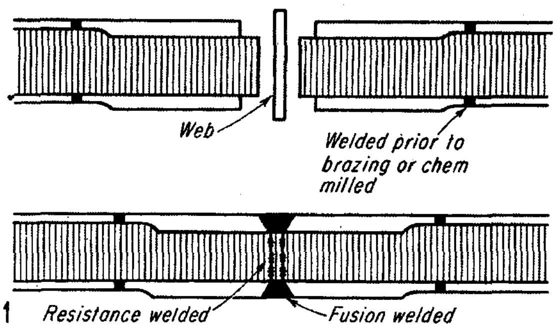

1

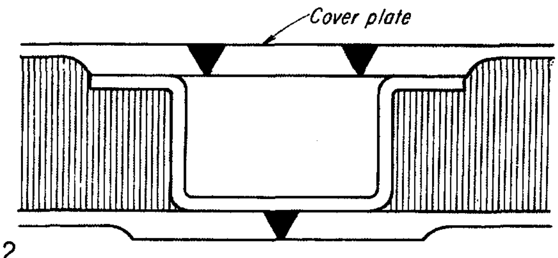

2

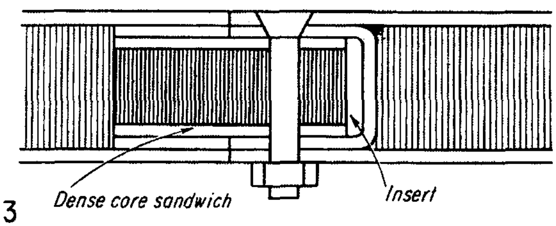

3

Where welding access is from one side only, the joint

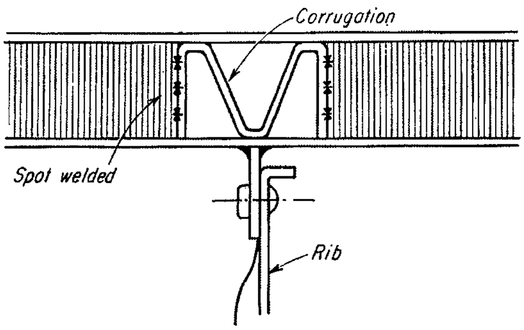

4

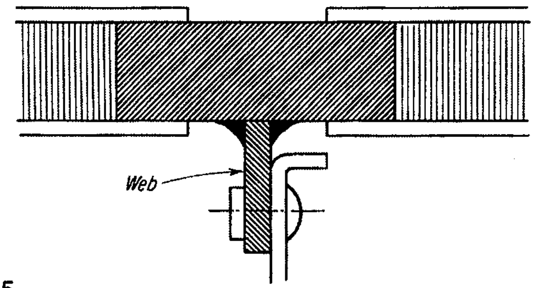

5

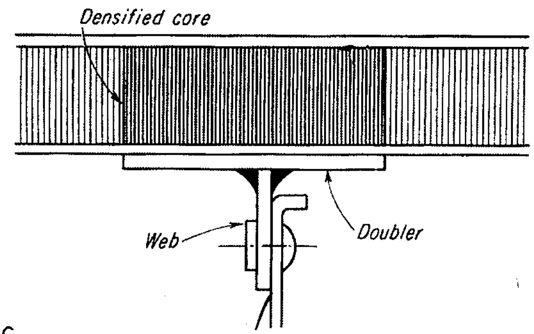

6

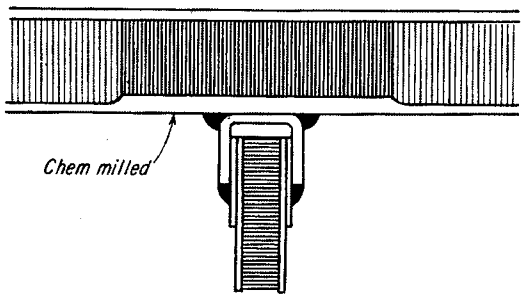

7

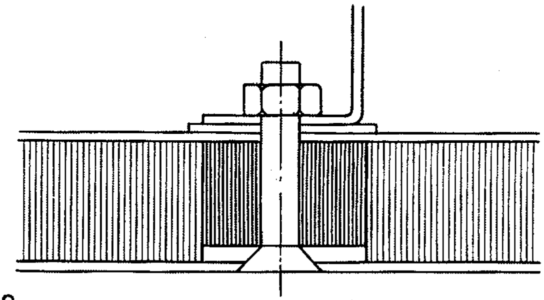

8

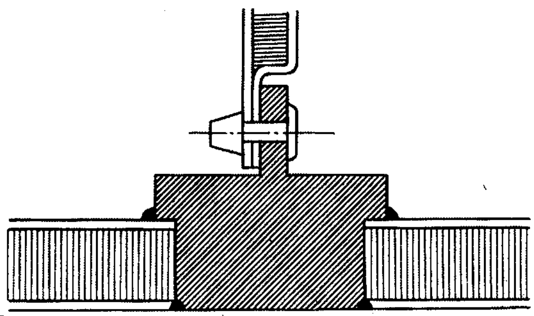

9

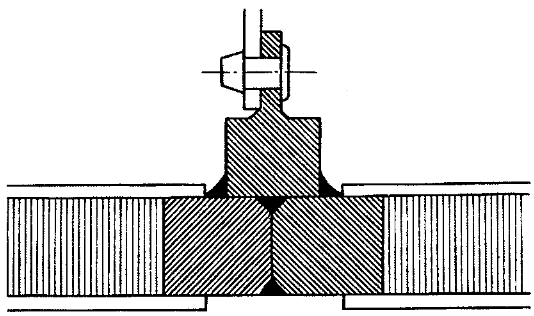

10

becomes more cumbersome. A solution is presented in Fig. 2 that is satisfactory except for the incumbent weight penalty. The panels are brazed with the edge members extended beyond the net part size and trimmed to final size. Within limits, growth compensation is possible with this joint. Welding the cover plate to the panels as the last operation completes the joint.

A mechanical joint, admittedly heavier yet, is shown in Fig. 3. Essentially a tongue-and-groove joint, the tongue portion is a sandwich bar of densified core, its faces designed to carry the longitudinal loads of the panels. The bar may be mechanically attached, or brazed in place as shown. The mating portion of the joint is brazed with a U-channel edge member through which the mechanical attachment is made.

PANEL-RIB JOINT

The panel-rib joint must maintain the integrity of the original panel and transfer any additional loads, in most cases a shear-flow, from the rib into the panel, where this load is distributed between both faces. Fig. 4 shows a

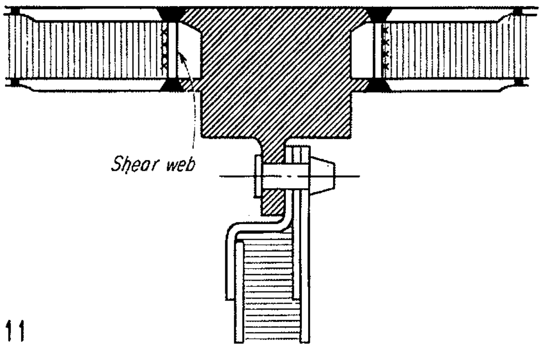

11

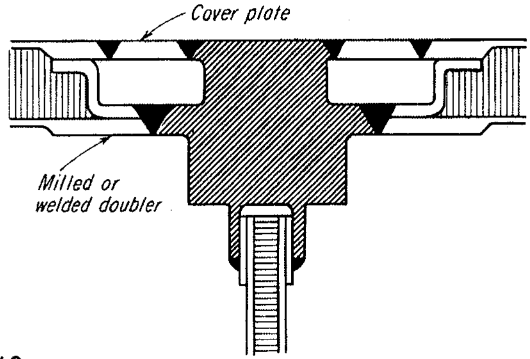

12

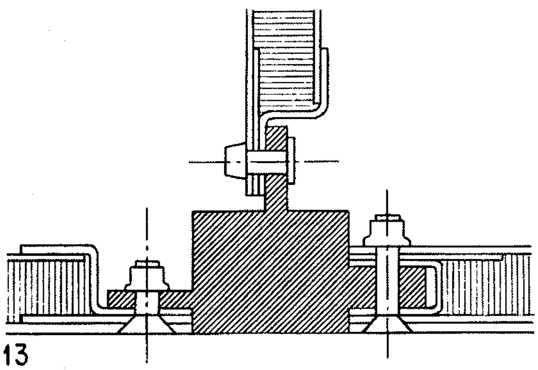

13

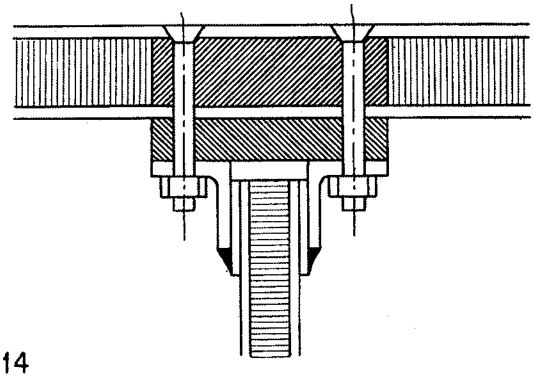

14

joint which theoretically would meet these requirements. The corrugation transfers the rib loads into the outer face of the panel and also makes a link between the honeycomb cores. This joint is plainly difficult to produce because of the accessibility and welding problems. The solution shown in Fig. 5 would be easy to make but extremely inefficient because of the discontinuity of the faces.

The design in Fig. 6 meets design requirements and is producible. It is best to make the brazed joint without the web, then attach it by subsequent welding. The panel then becomes essentially flat, greatly simplifying the braze fixturing and production sequence. The doubler shown on the drawing may be seamwelded, brazed, or chemically milled as an integral part of the facing. A variation of this design, Fig. 7, shows attachment of a honeycomb sandwich rib to the panel. The U-channel is welded to both pieces to effect the joint with a minimum of manufacturing problems.

A mechanical joint, if acceptable for the application, is quite simple, as shown in Fig. 8. The rib is directly attached to a densified core insert which provides reinforcement for the countersink and for the bolt-crushing forces. The doubler between rib flange and panel provide better distribution of compression and shear loads.

SPAR-PANEL INTERSECTION

The function of this joint is to transmit shear loads from the panels into the spar and to assist the spar in carrying the bending loads by loading an effective width of the panel in tension or compression. The theoretical joint in Fig. 9 incorporates all necessary elements for correct load transfer. Unfortunately, the unreasonable welding requirements make it almost impossible to produce with current knowledge. The production people would prefer to make the joint as shown in Fig. 10. The limitation of this design is the inability to satisfactorily vary the spar cross-section as loading changes.

A good design is one that incorporates an independently produced spar to which the panels are welded, Fig. 11. A shear web is introduced between the sandwich and the spar as previously discussed before the elements are welded together. This layout shows a honeycomb sandwich spar web riveted to the spar caps with high-shear rivets. If welding from one side only is necessary a method similar to one previously described (4) is applicable, as shown in Fig. 12. The shear transfer is over the short flange of the edge member and cap flange which must have the rigidity to take the shear load in bending. The cover plate takes forces only in the plane of the outer facing sheet.

Again reverting to a mechanical joint, Fig. 13 is a composite of two types of panel connection to the spar cap. The double joint takes all kinds of loads effectively, while the single joint is able to take shear perpendicular to the panel and loads in the panel of the outer panel facing only. Another interesting variation of a mechanical spar joint enables a simplified approach to joining the

(12)—**Pivoted Joints** . . . Method at left is satisfactory for low-cost consumer products where some binding can be tolerated until the joint works in. The one shown second from the left is perhaps best, because there is some small clearance between the rivet head and the wall.
(13)—**Washers** . . . If a metallic section is to be assembled to a softer material, a washer may be necessary to provide the necessary rigidity for clinching action. The soft material should be outside with the washer under the rivet head. For conventional assemblies either way is practical.
(14)—**Tight Joints** . . . Since blind rivets exert considerable gripping force when clinched, the joint shown second from left is impractical. Conversely, either of examples in which a single rivet is employed may prove as satisfactory as the one with multiple rivets.
(15)—**Multiple Assemblies** . . . One, two or more components or sections can be riveted to a base or panel with a single rivet, provided they can be mounted from the front, or the base section is accessible from the rear or underneath.
(16)—**Straps and Clamps** . . . A blind rivet can be used to assemble straps, clamps, and similar members around a component. Allowance must be made for the squeezing action on the clamp.
(17)—**Housings and Panels** . . . Of the many ways to construct a housing or panel, the ones shown here are perhaps the most common. Examples: left —a double-channel section forming the joint to which the panels are assembled and riveted; center —a back-up stringer with a finishing strip inserted between mating panels; right—a base angle with riveted panels and a finishing strip between the gap. In selecting the design, consider cost, appearance, strength and thermal expansion.
(18)—**Weatherproof Joints** . . . It's difficult to produce a pressure-tight riveted joint, but reasonably moisture resistant, weather-tight assemblies have been evolved.
(19)—**Extruded Sections** . . . Blind riveting is common, because of the limited access and clearances in most extruded sections. Rigidity of the joint at right is far greater than that at left. Setting against unsupported internal projections is seldom recommended.
(20)—**Compressible Materials** . . . Compressible materials do not provide a firm base for the setting action, and the rivet may tear through. Use of a formed sleeve or bushing, or a washer and back-up plate can solve this problem.
(21)—**Tubing** . . . For maximum rigidity, the rivet should not extend through both walls of tubular members. The rivet will set blind against the curved inner wall section, or the tubing can be flattened to increase the contact area.
(22)—**Plastic Members** . . . Preferably, the rivet should be set against a metallic rather than a plastic member. However, the rivets are being set successfully against many molded and extruded plastics, which resist setting pressure without cracking.
(23)—**Blind Holes or Slots** . . . Clinching the rivet against the side of a blind hole or into and against a milled slot, intersecting hole, or internal cavity is possible because of the clinching action of the rivet.

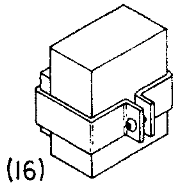

STRAPS AND CLAMPS

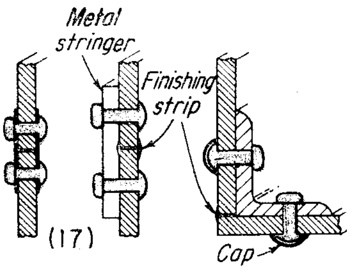

HOUSINGS AND PANELS

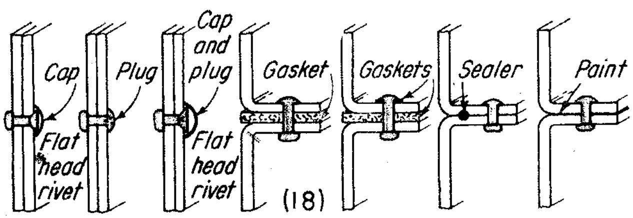

Good Good Very Good Good Very Good Good

WEATHERPROOF JOINTS

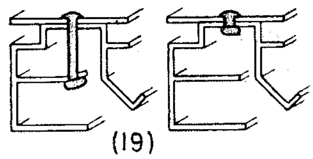

Unsatisfactory Good

EXTRUSIONS

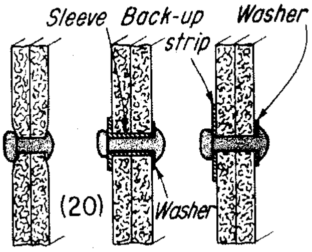

Unsatisfactory Good Good

COMPRESSIBLE MATERIALS

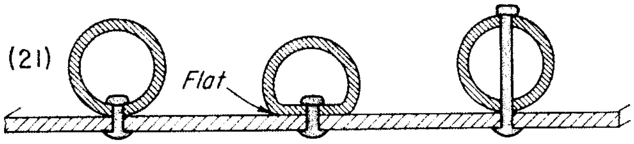

Good Good Unnecessary

TUBING

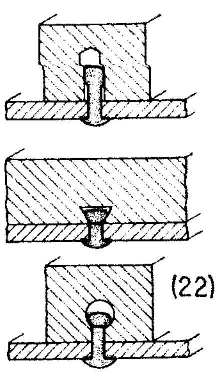

BLIND HOLES AND SLOTS

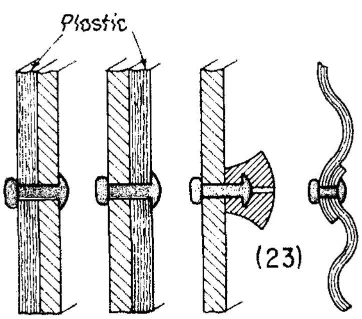

Depends on Material Good Good

PLASTICS

12 Ways to Anchor Heavy Machines

Machine design is not really finished until anchoring and leveling methods have been decided. Here's a selection from which to choose.

Louis Dodge

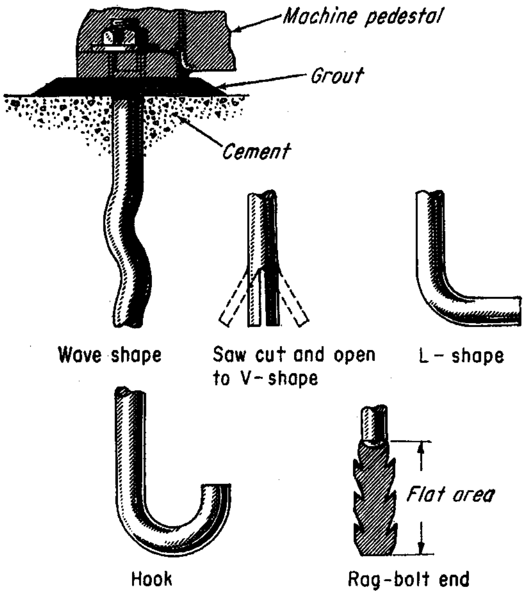

1. ANCHOR BOLT AND ALTERNATIVE ENDS

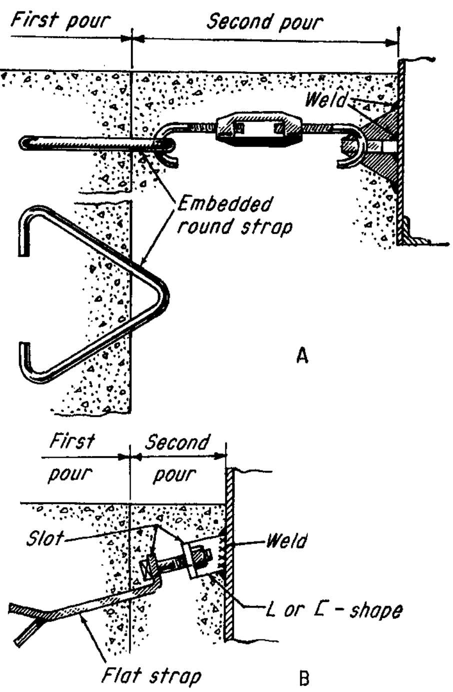

7. TURNBUCKLE ANCHOR (A). ADJUSTMENT-BOLT ANCHOR (B).

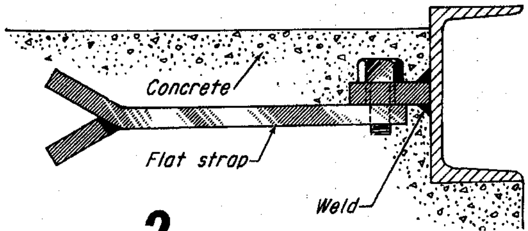

2. ANCHOR STRAP

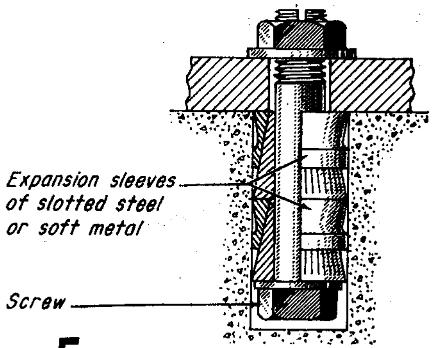

5. EXPANSIUN-SLEEVES

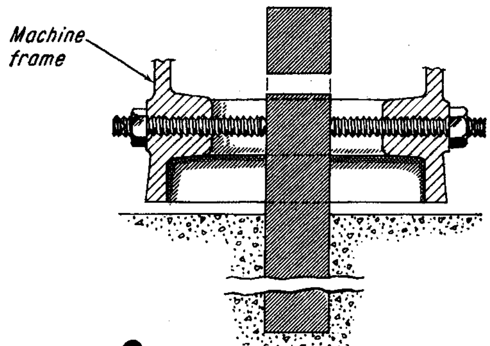

8. LATERAL-ALIGNMENT ANCHOR

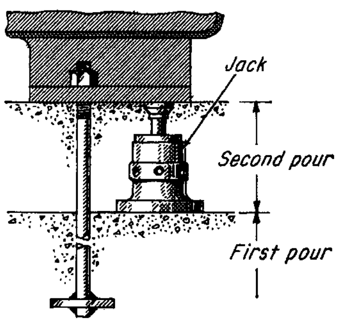

10. ALIGNING JACK AND ANCHOR BOLT

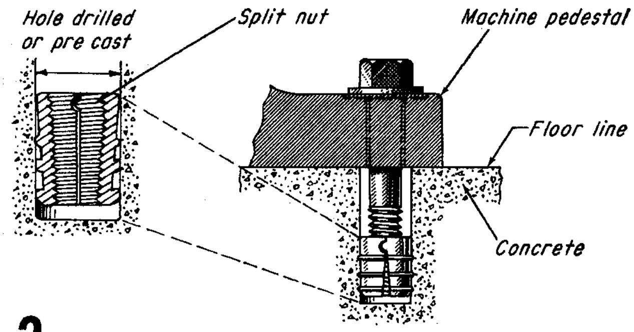

3. SPLIT ANCHOR-NUT WITH WEDGE ACTION

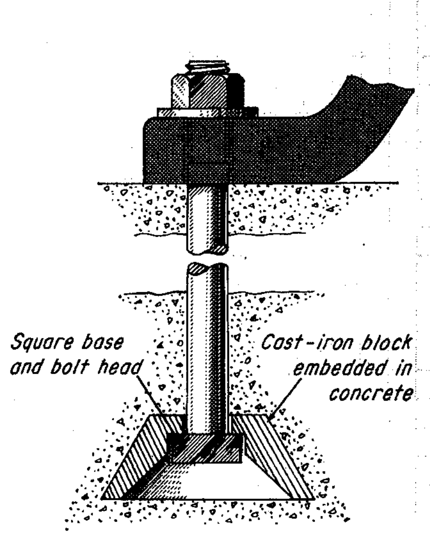

4. EMBEDDED ANCHOR BLOCK

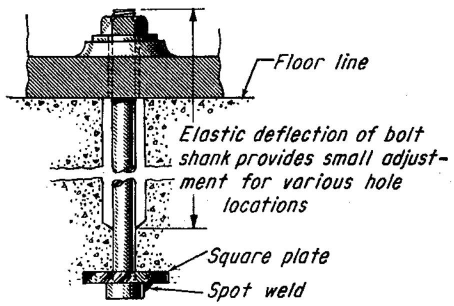

6. ANCHOR BOLT FOR LOCATION ADJUSTMENT

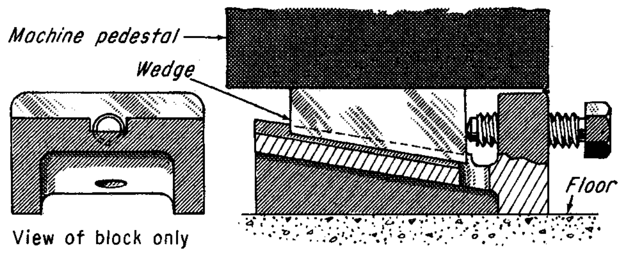

9. WEDGE-BLOCK LEVELING

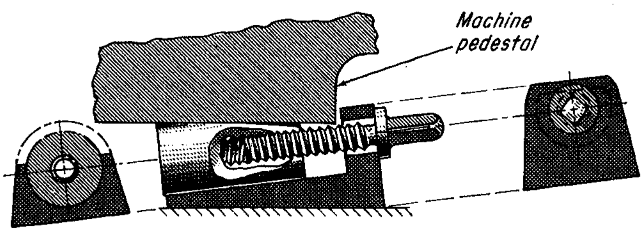

11. CYLINDRICAL WEDGE BLOCK FOR UNEVEN OR SLOPING FLOORS

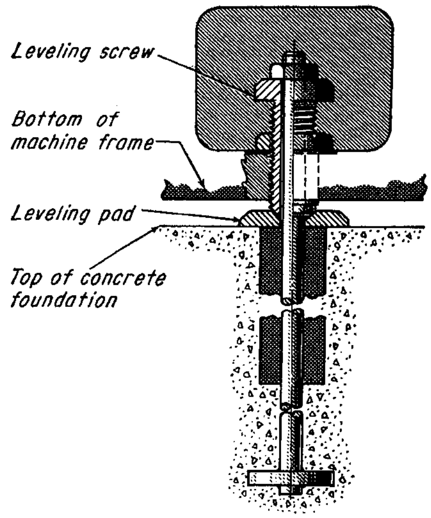

12. LEVELING SCREW WITH ANCHOR BOLT

Design Details of Blind Riveted Joints

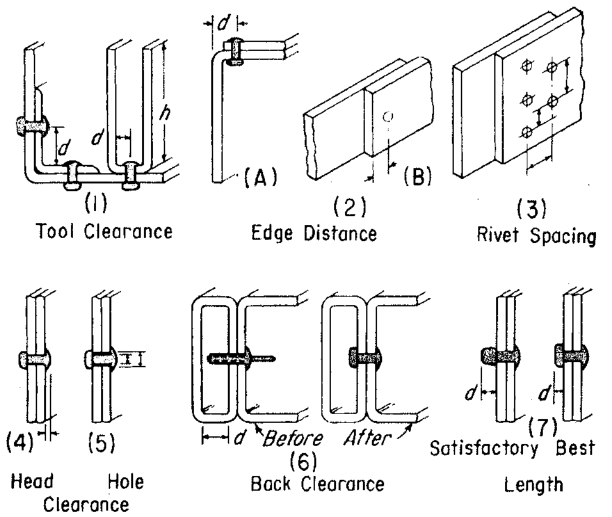

CLEARANCES AND ALLOWANCES

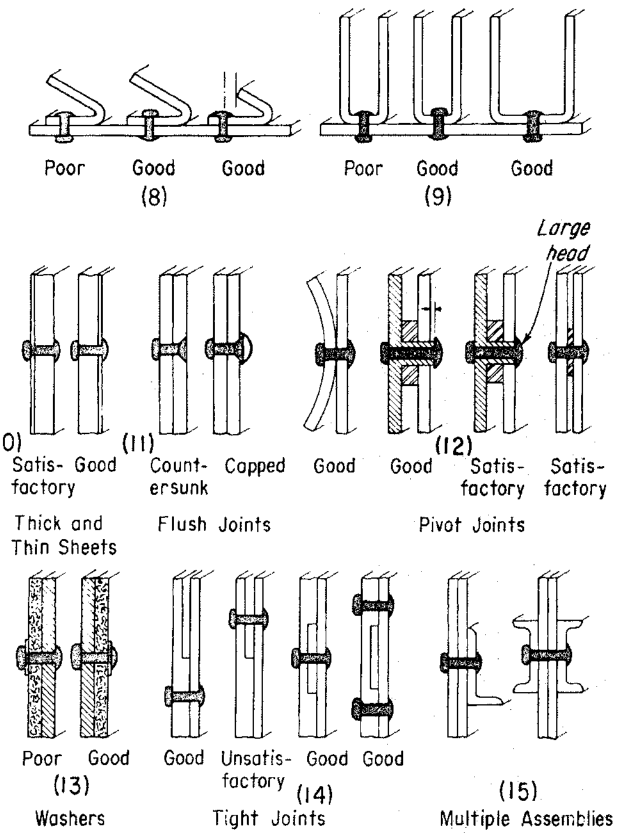

GENERAL DESIGN PRACTICE

Clearances and Allowances

(1)—**Tool Clearance . . .** Minimum allowable distance from a wall or projection to the rivet-hole centerline is critical, should be checked against tool specifications. Depth of a channel or cylindrical section likewise limits the application if the rivet is inserted as shown. However, tool extensions can often be employed, and the nosepiece of the tool can be extended by as much as an inch.

(2)—**Edge Distance . . .** From the standpoint of joint strength, the recommended distance from the rivet centerline to the edge of a sheet should not be less than twice the rivet diameter. If joint strength is secondary, this dimension can be greatly reduced. Example: the rivet functions only to hold a bracket or component in position.

(3)—**Rivet Spacing . . .** This also is a function of application and strength requirements.

(4)—**Head Clearance . . .** Standard head dimensions vary with rivet size. Height and diameter can readily be determined from specification sheets. Frequently, the work can be countersunk, or the joint designed to prevent interference with mating sections.

(5)—**Hole Clearance . . .** Permissible clearance depends on whether the fastener grips the wall or clinches underneath. In the latter case, oversized holes are less critical, and one does not depend on wall constriction to prevent breakout.

(6)—**Back Clearance . . .** Distance from flat of the head to end of the unclinched rivet determines the required back clearance—not dimensions after setting. These values should take into account the maximum combined material thicknesses.

(7)—**Rivet Length . . .** There is a delicate balance between joint thickness, mandrel-head dimensions, the cold-working properties of the rivet material and, of course, the shank diameter of a blind rivet. On the other hand, one length can be used for a wide range of panel thicknesses. For any use beyond the tabulated data, actual limitations should be determined by test.

General Design

(8)—**Angles and Formed Sections . . .** Avoid obstructions to the tool, which should set flush on the work. Thus, the "poor" joint requires a special offset tool, may still be inaccessible. Reverse the rivet and set from the other side, or reduce the length of the angular section.

(9)—**Channel Sections . . .** For adequate tool clearance, set from the underside of the channel or widen the section. A tool extension may be used to reach inside the section, but makes the tool somewhat more awkward to handle.

(10)—**Thick and Thin Sheets . . .** If there's a choice, it's best to set the rivet against the thicker material. Rivets of this type can be set against 0.030 in. and thinner aluminum stock.

(11)—**Flush Joints . . .** A truly flush surface can be obtained only by countersinking the outer wall or plate. Dimpling generally is not recommended because of the possibility of the rivet not fully "bottoming" and setting against the hole edge. A smooth, watertight, but not completely flush surface is obtained by countersinking and capping the rivet.

(12)—**Pivoted Joints** . . . Method at left is satisfactory for low-cost consumer products where some binding can be tolerated until the joint works in. The one shown second from the left is perhaps best, because there is some small clearance between the rivet head and the wall.

(13)—**Washers** . . . If a metallic section is to be assembled to a softer material, a washer may be necessary to provide the necessary rigidity for clinching action. The soft material should be outside with the washer under the rivet head. For conventional assemblies either way is practical.

(14)—**Tight Joints** . . . Since blind rivets exert considerable gripping force when clinched, the joint shown second from left is impractical. Conversely, either of examples in which a single rivet is employed may prove as satisfactory as the one with multiple rivets.

(15)—**Multiple Assemblies** . . . One, two or more components or sections can be riveted to a base or panel with a single rivet, provided they can be mounted from the front, or the base section is accessible from the rear or underneath.

(16)—**Straps and Clamps** . . . A blind rivet can be used to assemble straps, clamps, and similar members around a component. Allowance must be made for the squeezing action on the clamp.

(17)—**Housings and Panels** . . . Of the many ways to construct a housing or panel, the ones shown here are perhaps the most common. Examples: left —a double-channel section forming the joint to which the panels are assembled and riveted; center —a back-up stringer with a finishing strip inserted between mating panels; right—a base angle with riveted panels and a finishing strip between the gap. In selecting the design, consider cost, appearance, strength and thermal expansion.

(18)—**Weatherproof Joints** . . . It's difficult to produce a pressure-tight riveted joint, but reasonably moisture resistant, weather-tight assemblies have been evolved.

(19)—**Extruded Sections** . . . Blind riveting is common, because of the limited access and clearances in most extruded sections. Rigidity of the joint at right is far greater than that at left. Setting against unsupported internal projections is seldom recommended.

(20)—**Compressible Materials** . . . Compressible materials do not provide a firm base for the setting action, and the rivet may tear through. Use of a formed sleeve or bushing, or a washer and back-up plate can solve this problem.

(21)—**Tubing** . . . For maximum rigidity, the rivet should not extend through both walls of tubular members. The rivet will set blind against the curved inner wall section, or the tubing can be flattened to increase the contact area.

(22)—**Plastic Members** . . . Preferably, the rivet should be set against a metallic rather than a plastic member. However, the rivets are being set successfully against many molded and extruded plastics, which resist setting pressure without cracking.

(23)—**Blind Holes or Slots** . . . Clinching the rivet against the side of a blind hole or into and against a milled slot, intersecting hole, or internal cavity is possible because of the clinching action of the rivet.

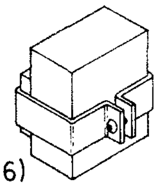

(16)

STRAPS AND CLAMPS

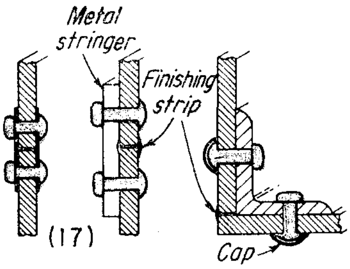

(17)

HOUSINGS AND PANELS

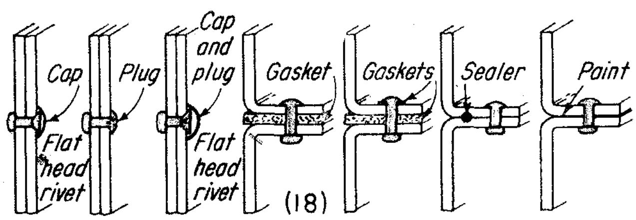

(18)

Good Good Very Good Good Very Good Good

WEATHERPROOF JOINTS

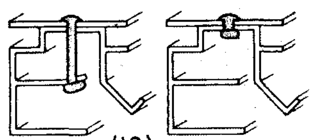

(19)

Unsatisfactory Good

EXTRUSIONS

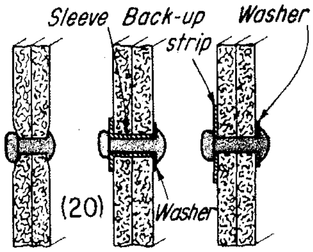

(20)

Unsatisfactory Good Good

COMPRESSIBLE MATERIALS

(21)

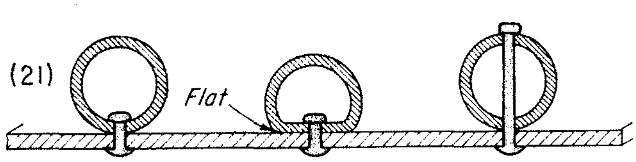

Good Good Unnecessary

TUBING

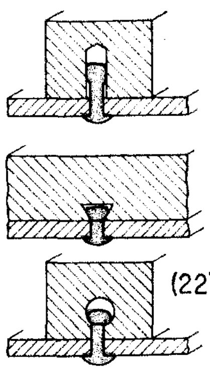

(22)

BLIND HOLES AND SLOTS

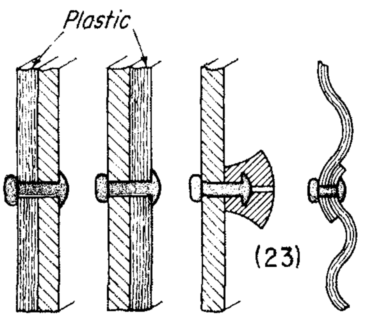

(23)

Depends on Material Good Good

PLASTICS

SECTION 21

DESIGN HINTS

Design Hints for Mechanical Parts

How to avoid close tolerances, and otherwise improve parts, where accurate assembly is necessary.

Federico Strasser

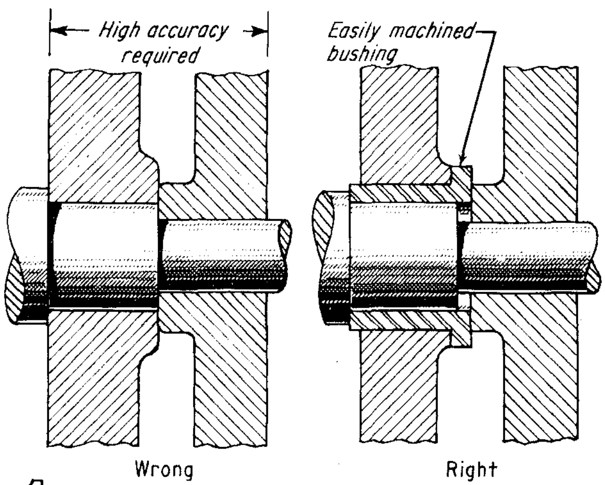

1 **BUSHING FACE** is much easier to machine than the hub of a large part such as a flywheel or heavy gear.

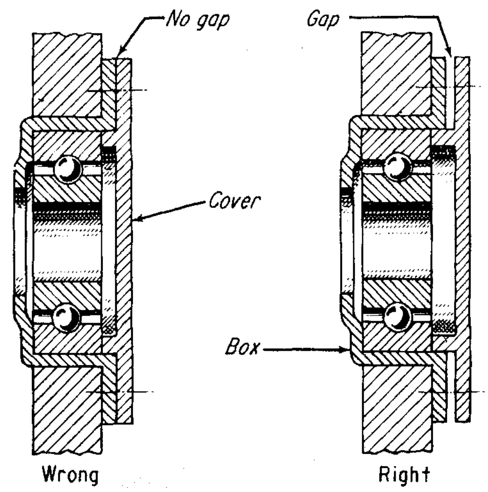

2 **HOLD-DOWN COVER** for bearing should have a take-up gap between the cover flange and the bearing box.

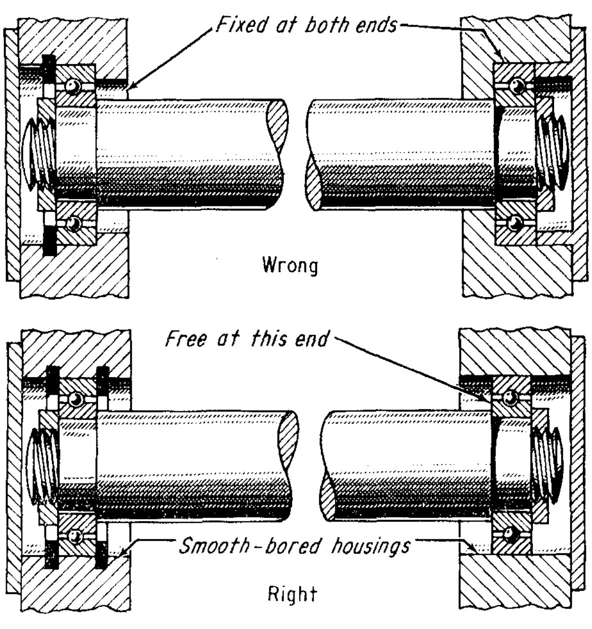

5 **SMOOTH-BORED HOUSINGS** shown on right let one bearing move when shaft length changes because of expansion.

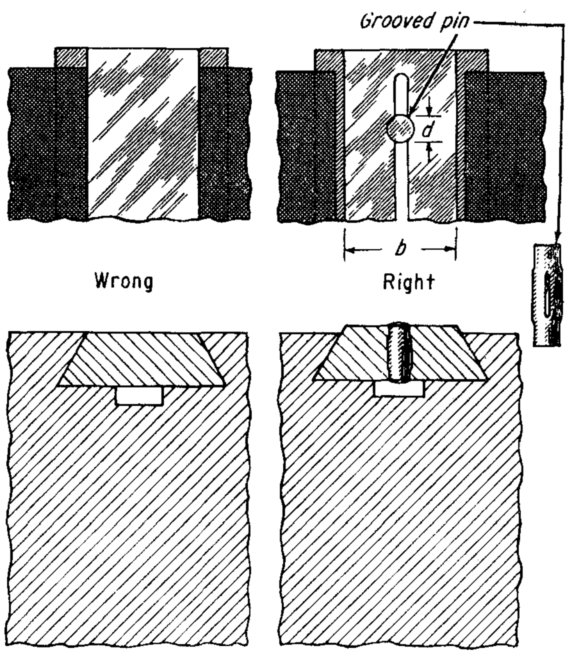

6 **DOVETAILED** parts that are to be a tight fit are best provided with a slot and grooved pin where d equals $b/3$ to $b/4$.

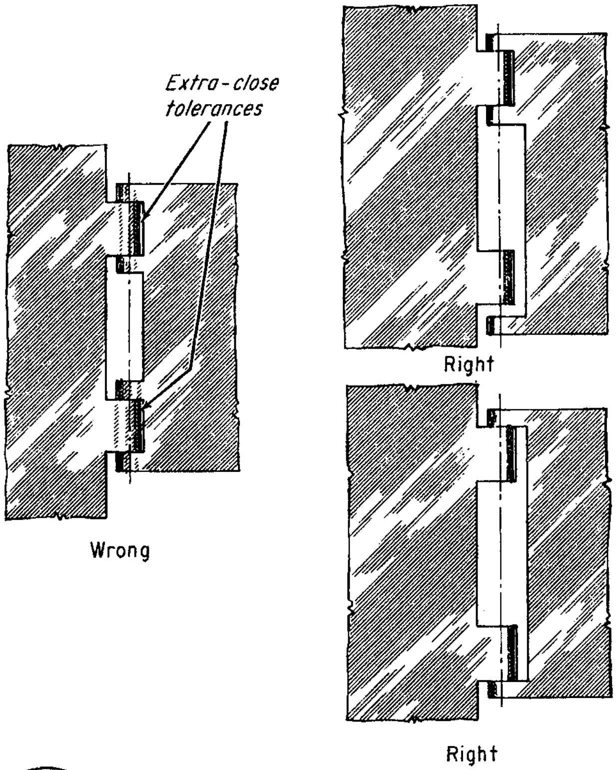

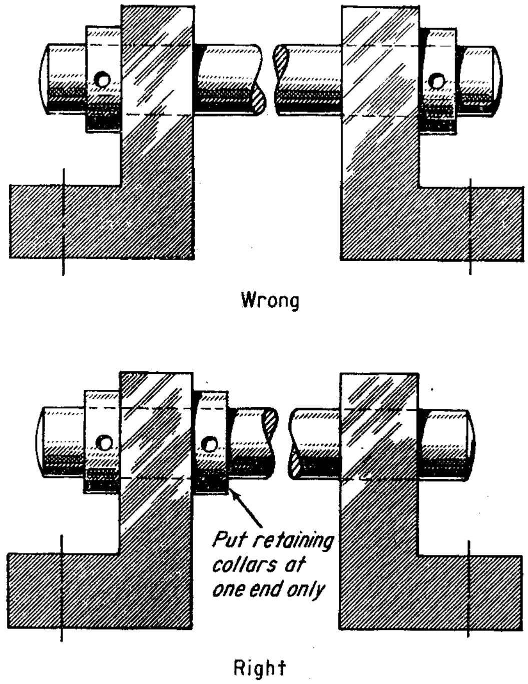

3 **HINGE MOUNTINGS** of the design shown on the left will entail extremely close tolerances. Let one end float.

4 **COLLARS** that retain the axial position of journal bearings should be placed at one end only to accommodate expansion.

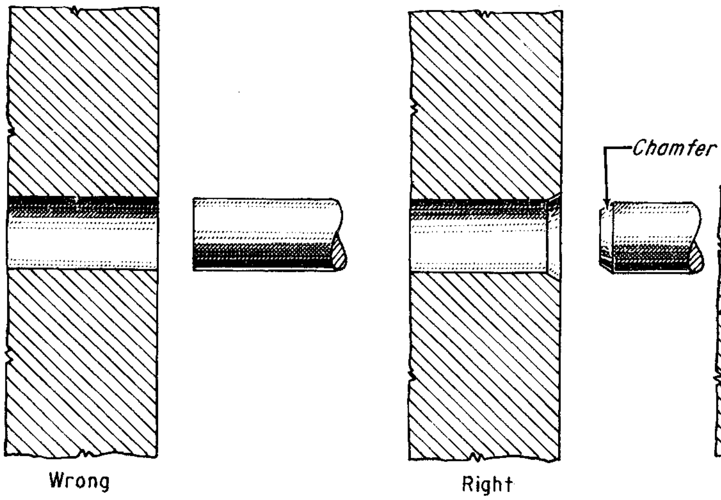

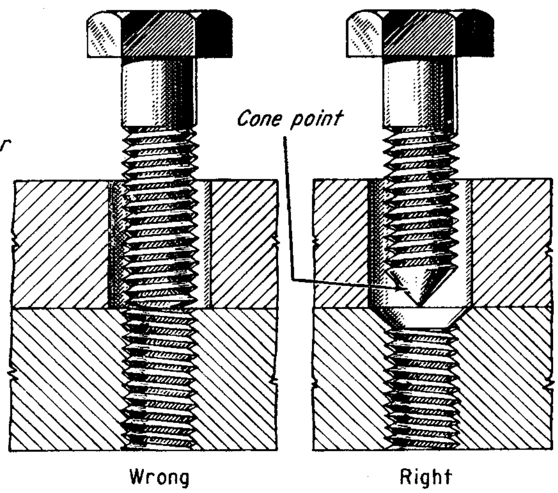

7 **CHAMFER** on pins and shafts that must be driven into holes is advisable if entry is to be clean and easy.

8 **CONE POINT** on screw and corresponding chamfer on internal thread ensures quick engagement in blind thread.

Designing for Easier Machining

Flat working surfaces, bushings, single fits and other features simplify setups, speed machining reduce tool replacement, and save material.

Federico Strasser

FLATS PROVIDE DRILLING SURFACES.

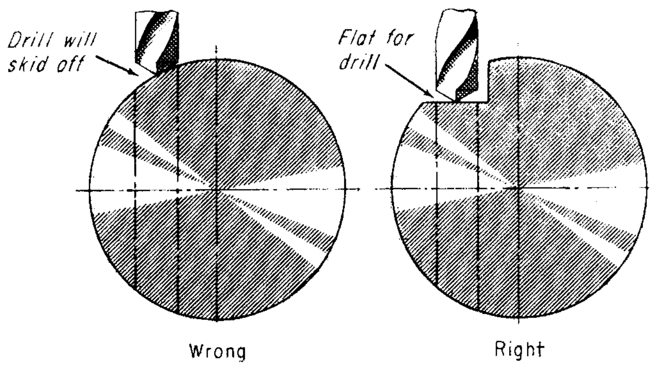

1

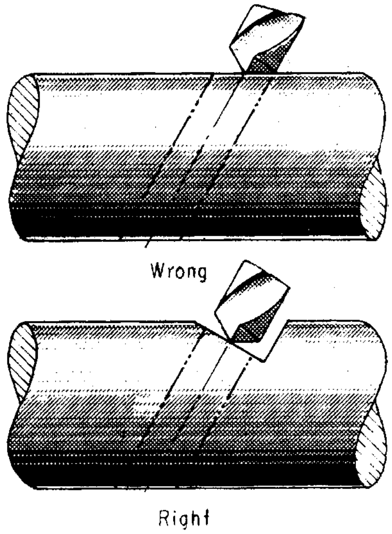

2

3

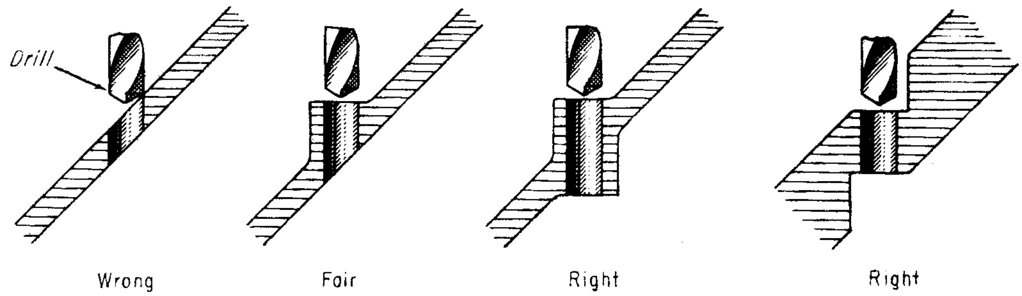

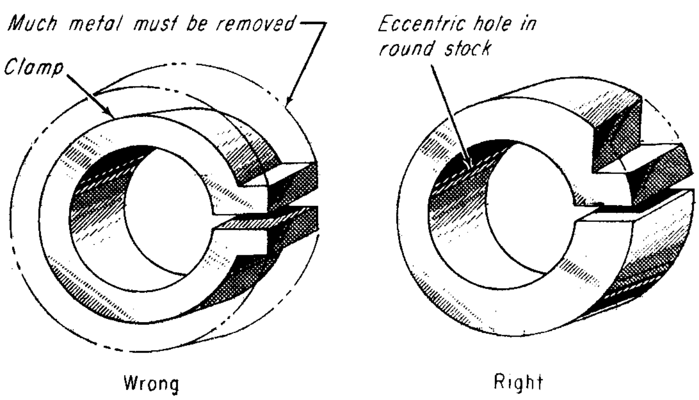

4 ECCENTRIC HOLE LETS MATERIAL BE SAVED.

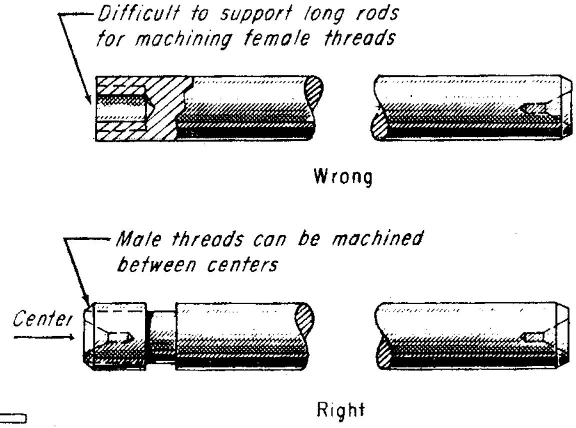

5 MALE THREADS ARE BEST ON LONG RODS.

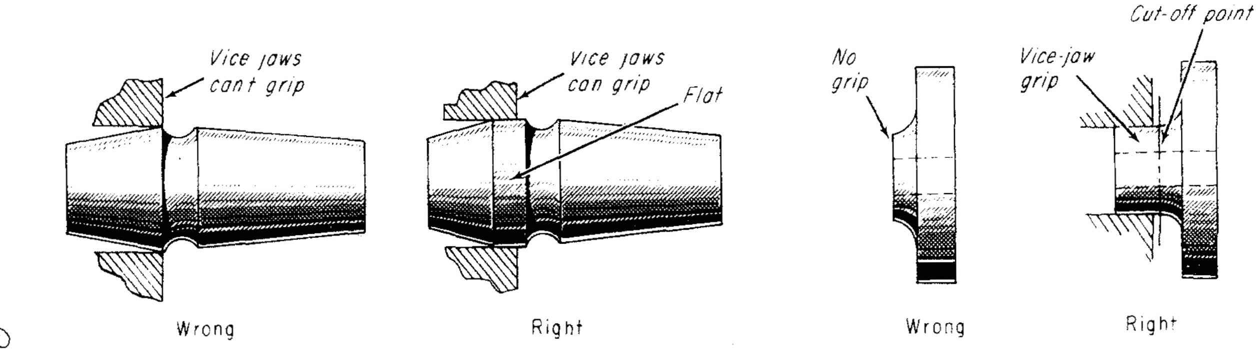

6 **PROVIDE GRIPPING SURFACES WHEN MACHINING IS TO BE DONE.**

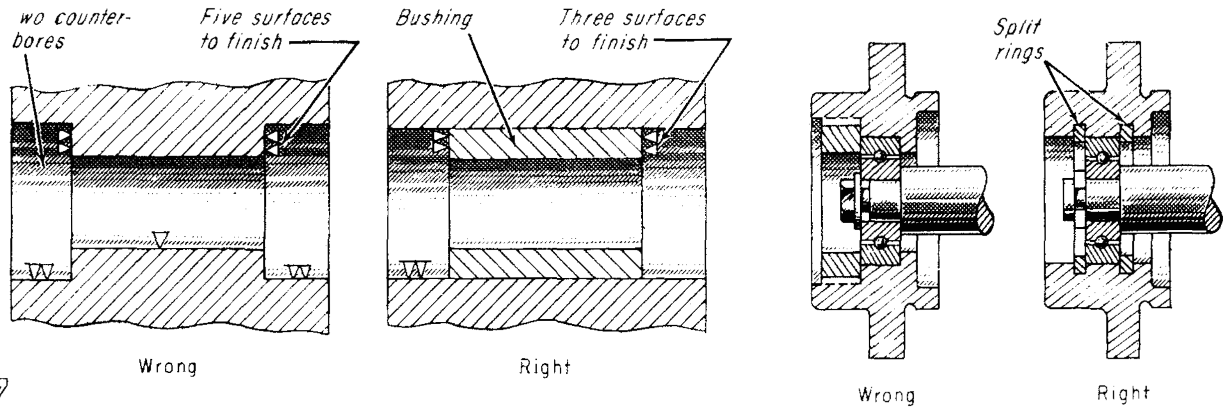

7 **BUSHINGS REDUCE MACHINING COSTS AND AID STANDARDIZATION . . . SPLIT RINGS ALSO GIVE GOOD RESULTS.**

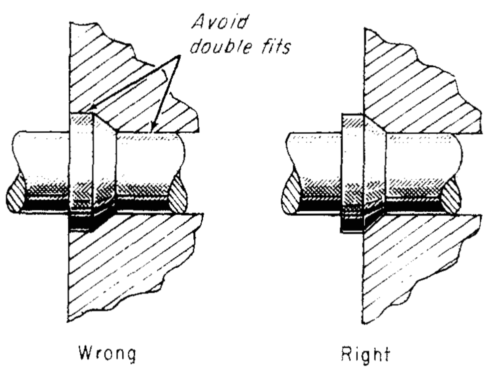

8 **SINGLE FITS ALLOW TIGHTER TOLERANCES.**

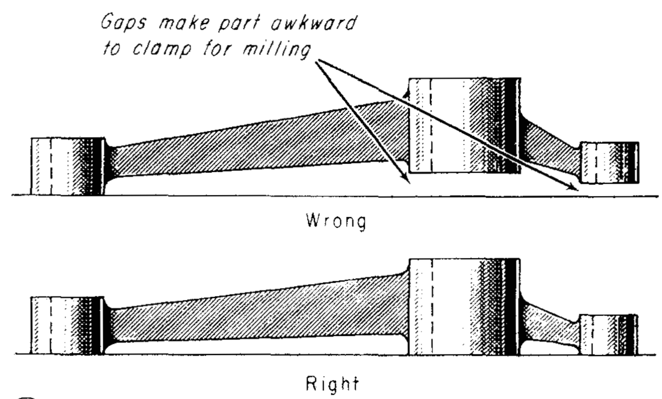

9 **KEEP SURFACES ON SAME PLANE FOR BETTER CLAMPING.**

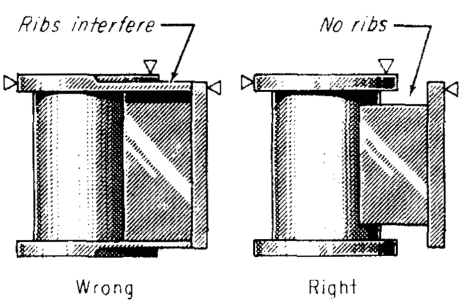

10 **DON'T LET RIBS INTERFERE WITH MACHINING.**

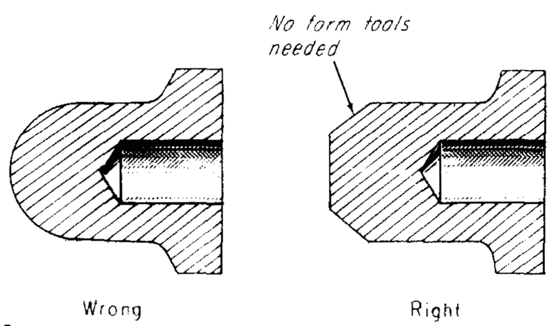

11 **DON'T CALL FOR CONTOURS THAT NEED SPECIAL FORM CUTTERS.**

How to Design for Heat Treating

To prevent cracking and warping in heat treated parts, avoid abrupt changes of workpiece contours.

Federico Strasser

The ideal shape for a part that is to be heat treated is a shape in which every point of any section or surface receives and gives back the same amount of heat with the same speed. Such a shape, of course, does not exist, but it is the designer's task to come as near to it as possible. To do this, keep the workpiece body simple, uniform, and symmetrical. For example, the first figures below show how changes in cross section must be made gradually to minimize stress concentrations during heat treatment. The other figures show further specific ways to keep out of trouble when subjecting parts to heat treatment. Holes, for example, should be correctly located.

1

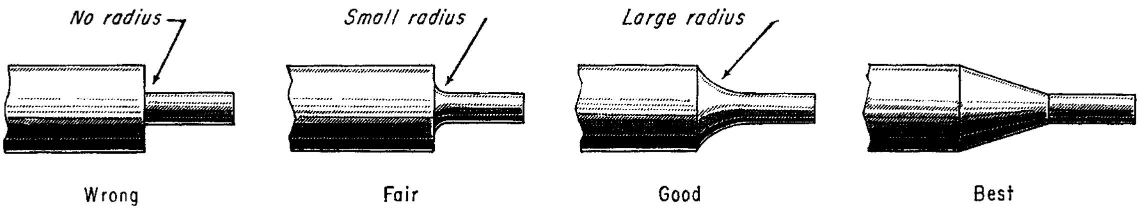

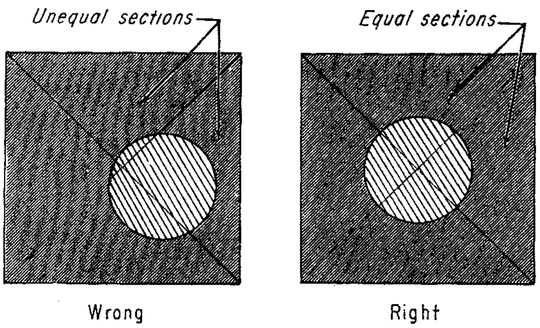

2

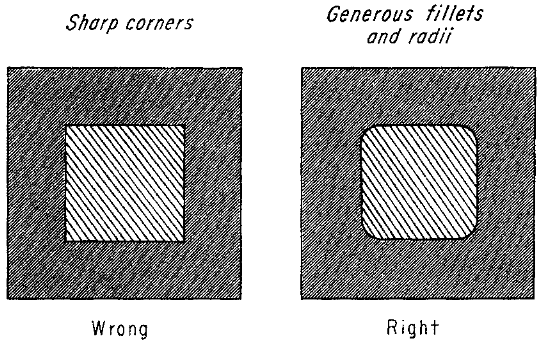

3

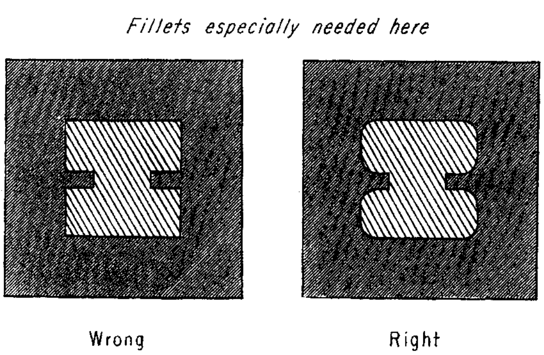

4

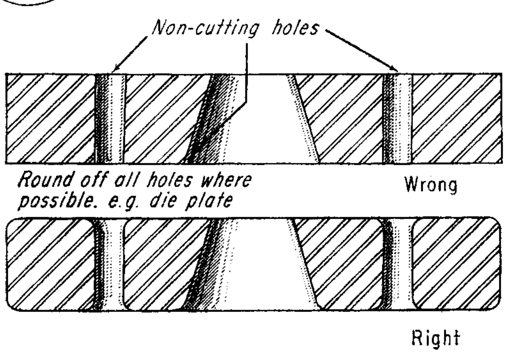

5

6

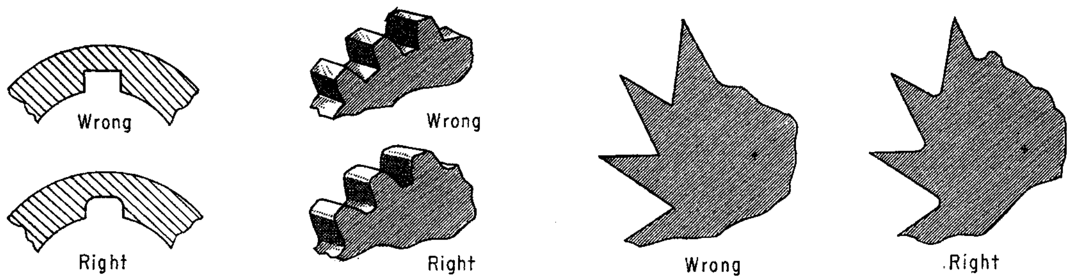
Wrong
Right
Wrong
Right
Wrong
Right
Wrong
Right

7

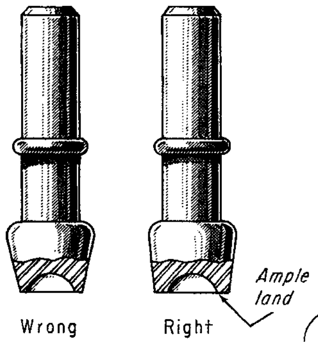
Ample land
Wrong
Right

8

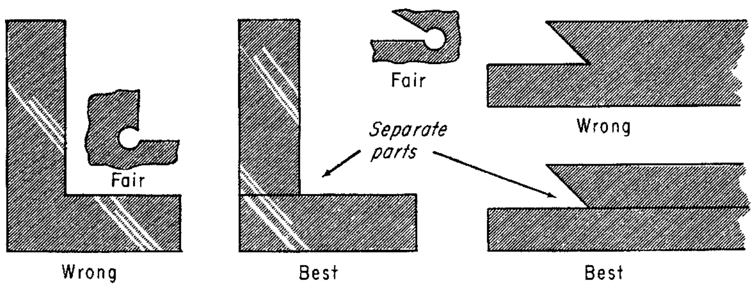
Fair
Fair
Separate parts
Wrong
Best
Wrong
Best

9

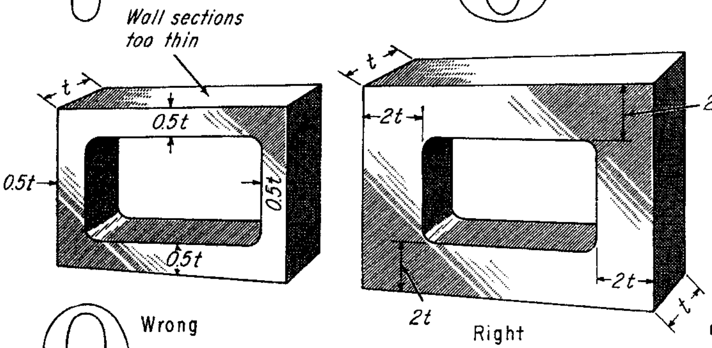
Wall sections too thin
t
0.5t
0.5t
0.5t
0.5t
Wrong
t
2t
2t
2t
2t
t
Right

10

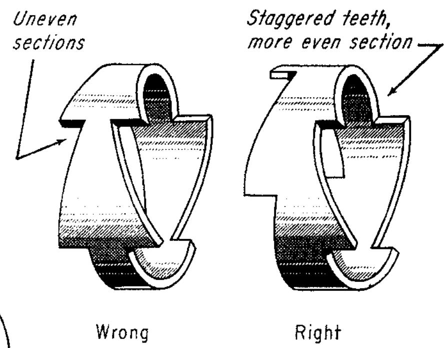
Uneven sections
Staggered teeth, more even section
Wrong
Right

11

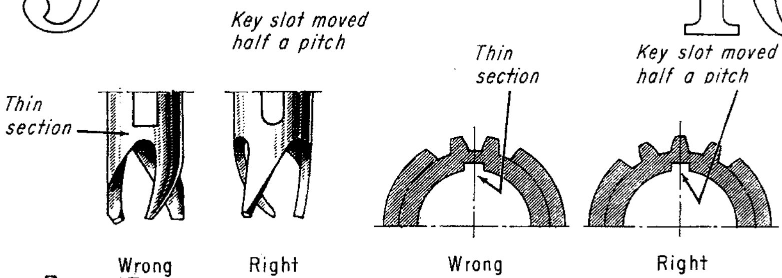
Key slot moved half a pitch
Thin section
Wrong
Right
Thin section
Key slot moved half a pitch
Wrong
Right

12

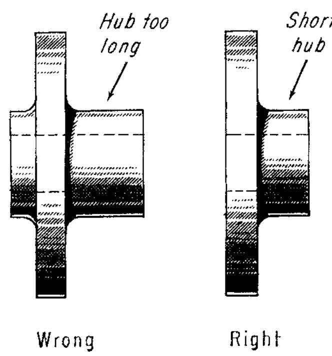
Hub too long
Short hub
Wrong
Right

More Design Hints for Heat Treating

Watch out for faulty designs such as thin sections, blind holes, unbalanced slots, and other weaknesses that can cause cracking and warping in heat-treated parts. Follow these how-to tips.

Federico Strasser

Nearly all serious failures of hardened steel parts are caused by internal stresses. Avoiding sudden changes of section is one good way to ensure balanced heating and cooling, the secret of success in all heat treating. Some other good design tips, which supplement those in our last issue, are illustrated.

1

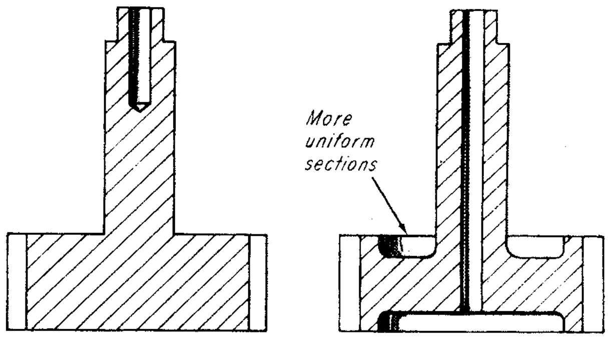

Wrong Right

2

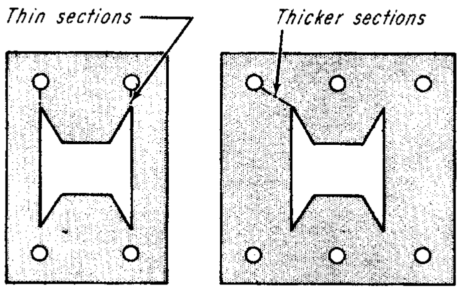

Wrong Right

3

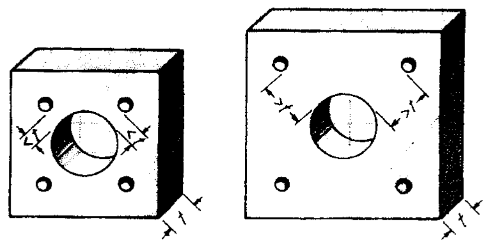

Wrong Right

4

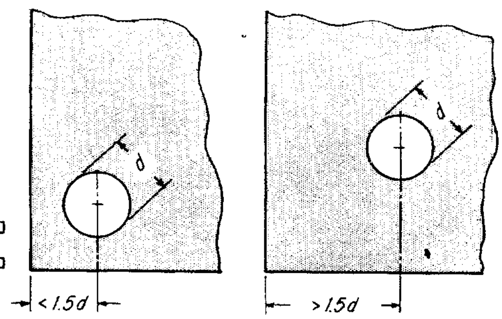

5

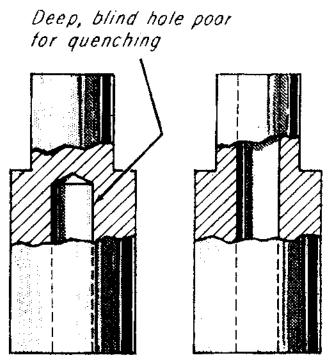

Wrong Right

6

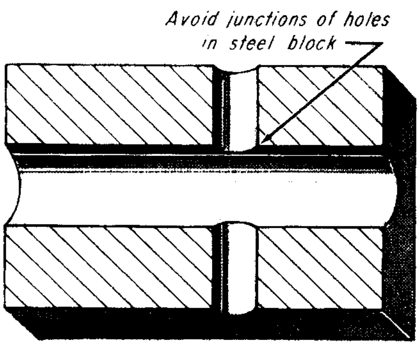

7

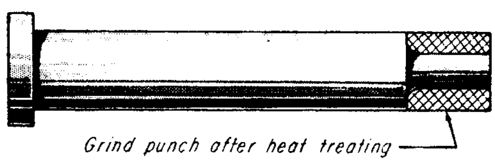

8

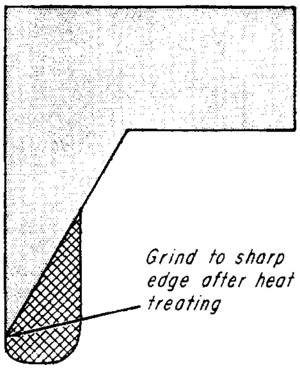

9

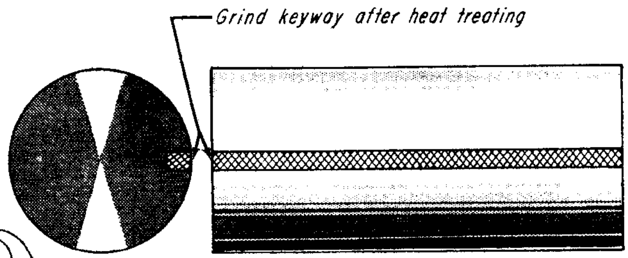

10

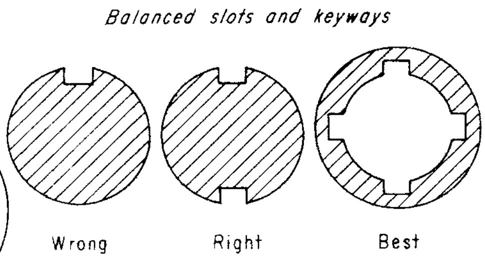

11

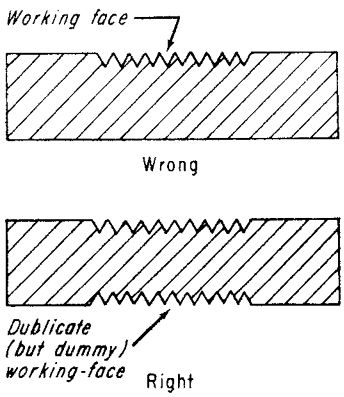

12

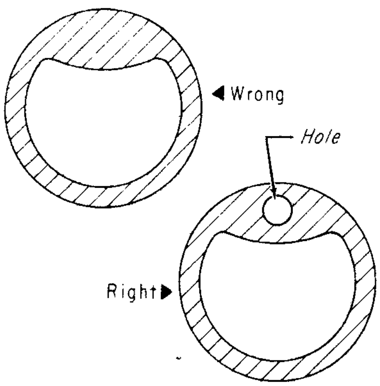

13

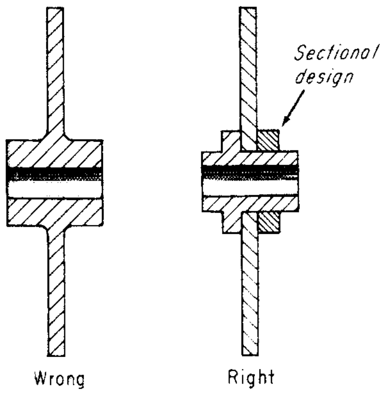

14

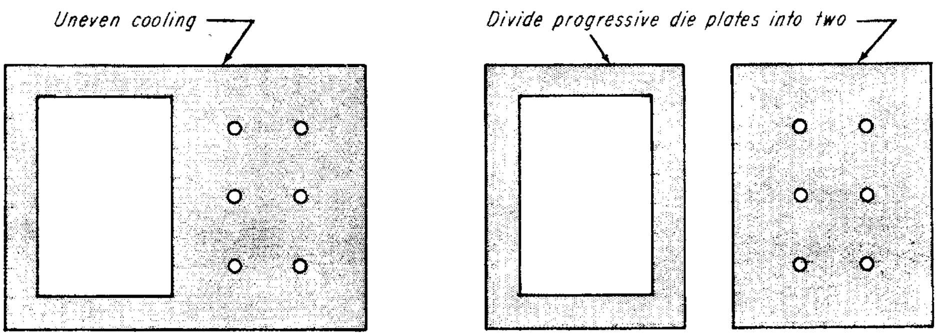

How to Design for Better Assembly

Small but important details of mechanical parts make all the difference between mediocre and superior design.

Federico Strasser

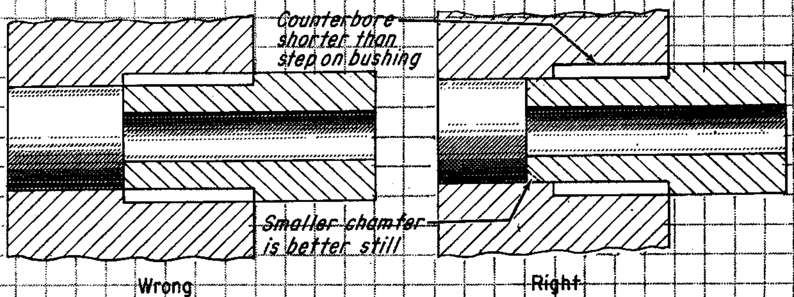

1 **LONG BUSHINGS** are easier to assemble when they have different OD's, but make sure the counterbore is shorter than the step.

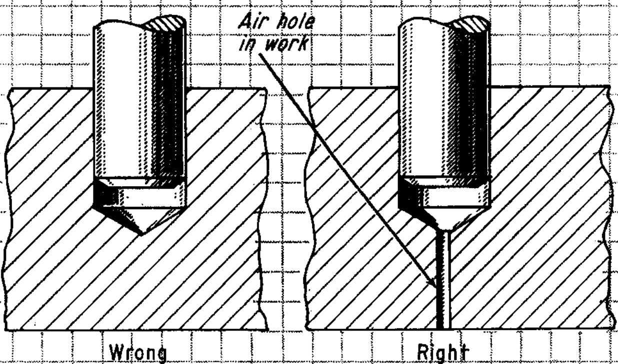

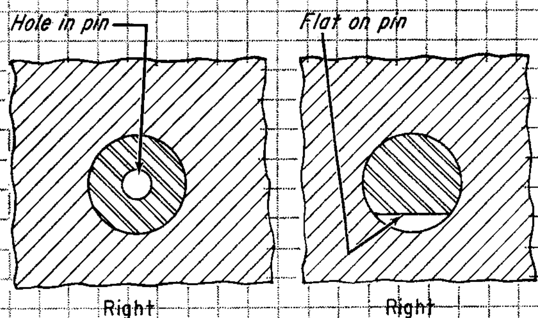

3 **AIR-RELIEF HOLES** and channels in dowels prevent air compression from hindering assembly. Also hole allows entry for extraction punch.

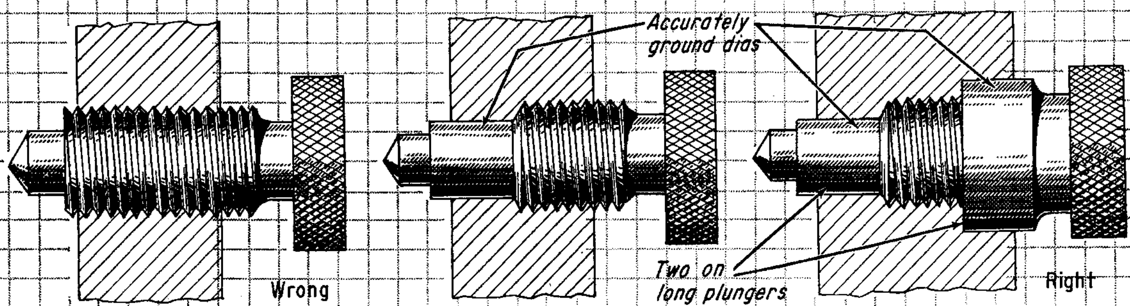

6 **ALIGNING DIAMETERS** should be provided on threaded plungers. Never rely on the thread for accurate concentric alignment of plunger.

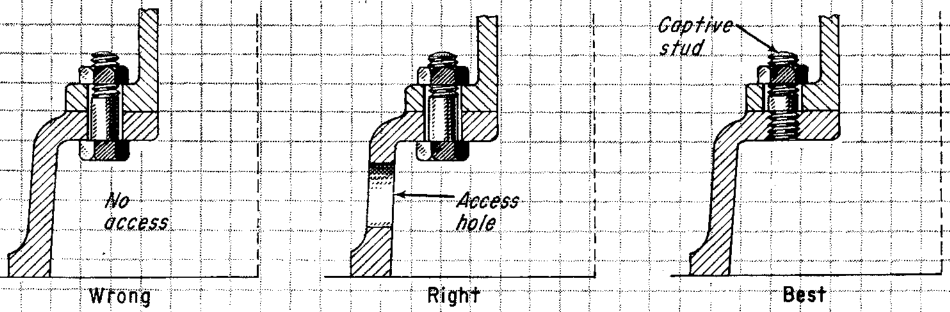

2 **ACCESS HOLES** or studs should always be provided in assemblies where bolt heads would be impossible or difficult to reach with a wrench.

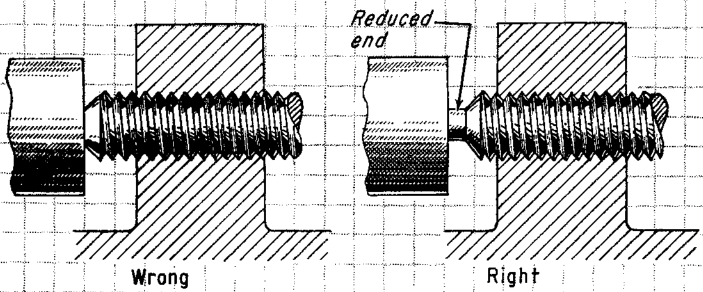

4 **PRESSURE SCREWS** should have reduced ends to prevent expansion of the threads, which would make removal of the screws difficult.

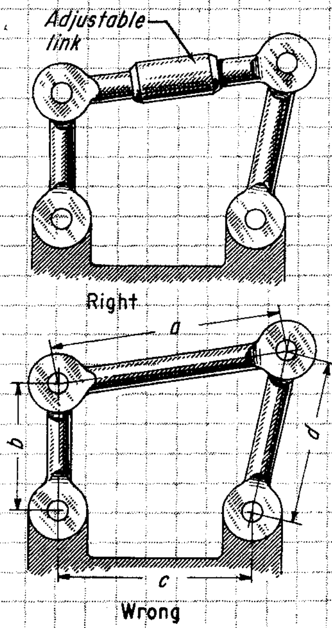

5 **ADJUSTABLE LINK** is necessary here where dimension *a* must be exact; otherwise dimensions *b*, *c*, *d* must have excessively close tolerances.

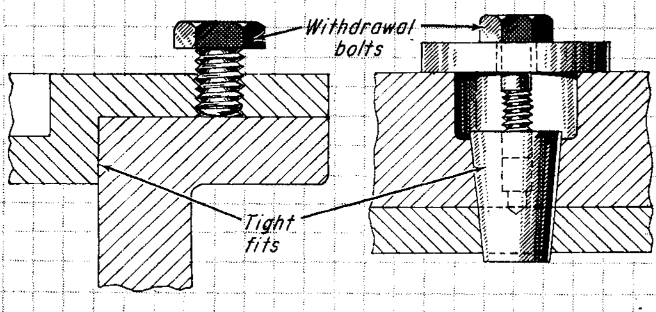

7 **WITHDRAWAL BOLTS** make disassembly easier when tight fits are required between two parts that can not otherwise be separated safely.

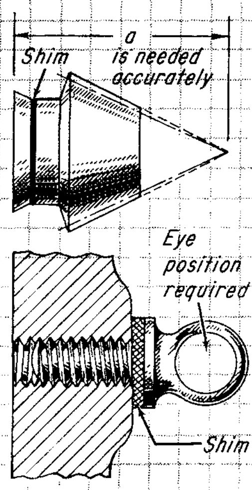

8 **SHIMS** for bevel gears or threaded eyebolts are necessary where dimension *a* and the angular position of the eye are important to the design.

Designing with Ribs and Beads

The reinforcing member, stop, or spacer in your present design may be superfluous. An embossed rib or bead may do the job better, and at the same time save weight and add strength.

Federico Strasser

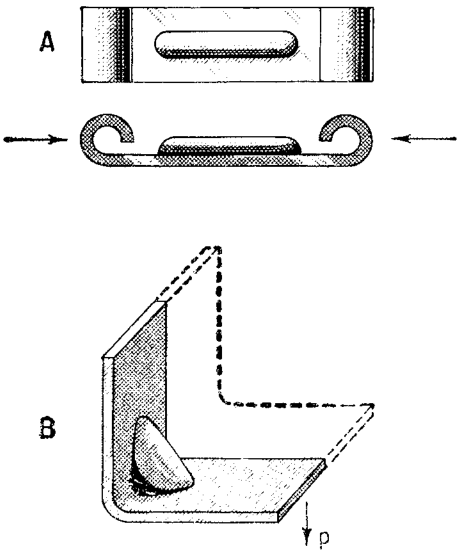

2 Stiffening. A stiffening rib (A) can increase strength 4 to 6 times in a component subject to buckling loads. An embossed corner rib (B) reduces bracket cross section as well as weight by 50%.

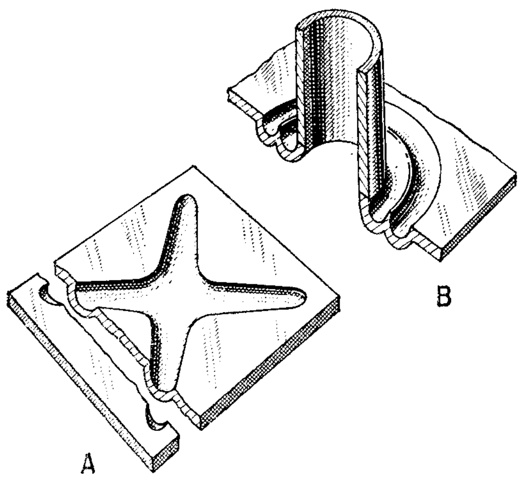

3 Stress relieving. Internal stresses caused by cold-working and heat-treating can be relieved by an "X" rib (A). Round ribs (B) compensate for cooling stresses after welding heavy to light sections.

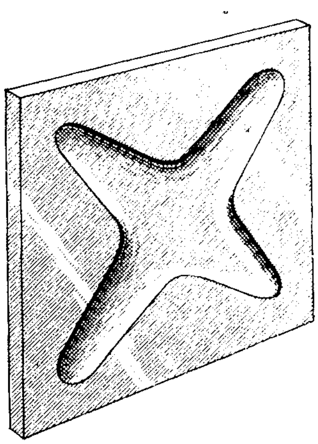

6 Noise reduction. Vibration-induced noise in large panels can be reduced by a rib. The rib changes the panel frequency.

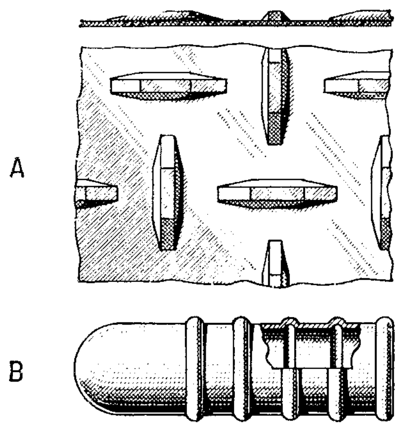

7 Safety. An embossed rib on a flat metallic surface such as a floor (A) gives a slip-proof surface even when oily. An embossed pattern on handles and wheels (B) can eliminate operator hand slippage.

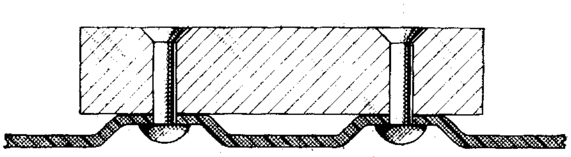

1 Spacers. A rib can create a small distance between workpieces without any additional parts. The distance can be held to a close tolerance by simple machining.

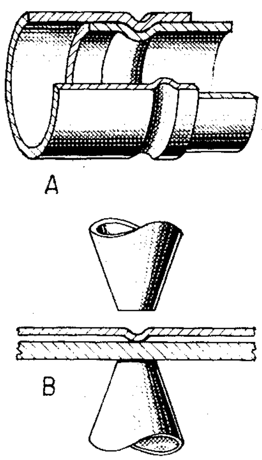

4 Permanent assemblies. In hollow assemblies, an inward or outward bead (A) forms a firm, permanent joint. In sheetmetal assemblies, small embossed beads (B) in the thinner member aid in welding.

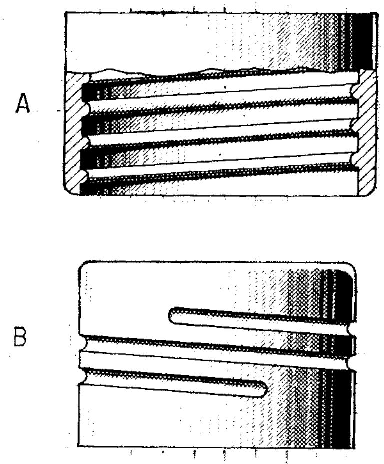

5 Temporary assemblies. In thin-walled round parts such as bulb bases, sockets, flashlight reflectors, small caps and other parts the rounded threads are embossed so a temporary union can be made.

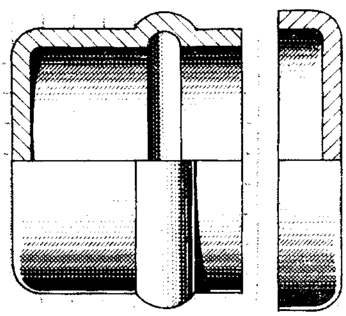

8 Stops. A bead formed on a rounded part is one way to align and position a matching component quickly and accurately.

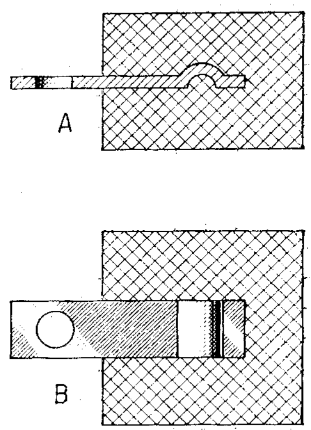

9 Anchors. Sheetmetal parts that are inserted in a plastic molding can be ribbed or dimpled to increase the resistance of the part being pulled from the molding.

Design Machined Parts Properly

Ample clearances, level surfaces, square entrances, and other important details improve parts that are to be milled, ground, and broached.

Federico Strasser

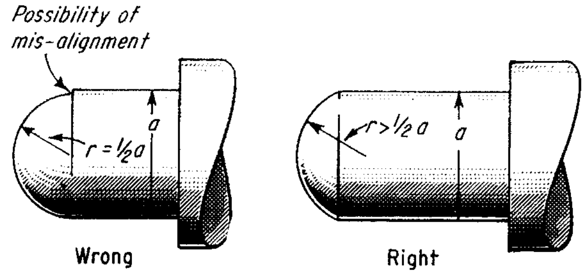

1 KEEP RADII LARGE ON ROUNDED ENDS.

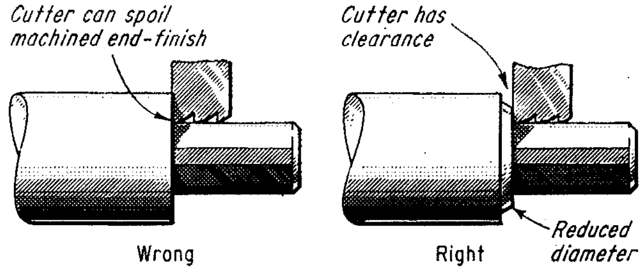

2 LEAVE CLEARANCE FOR MILLING CUTTERS.

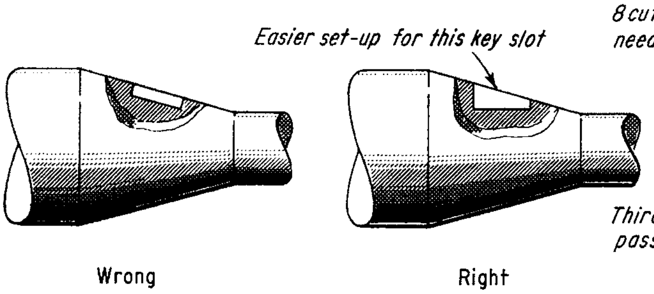

3 MILL KEYSLOTS PARALLEL TO SHAFT AXIS.

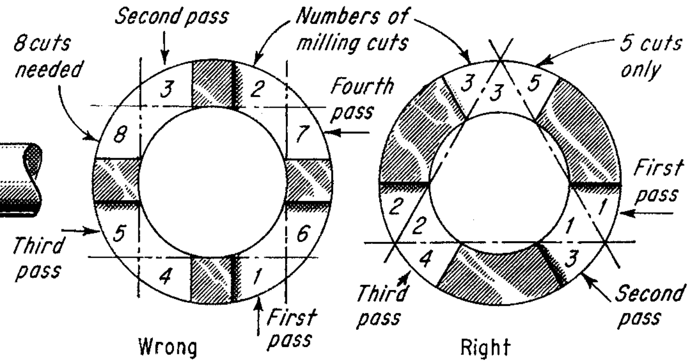

4 AN ODD NUMBER OF SLOTS REQUIRES FEWER MILLING CUTS.

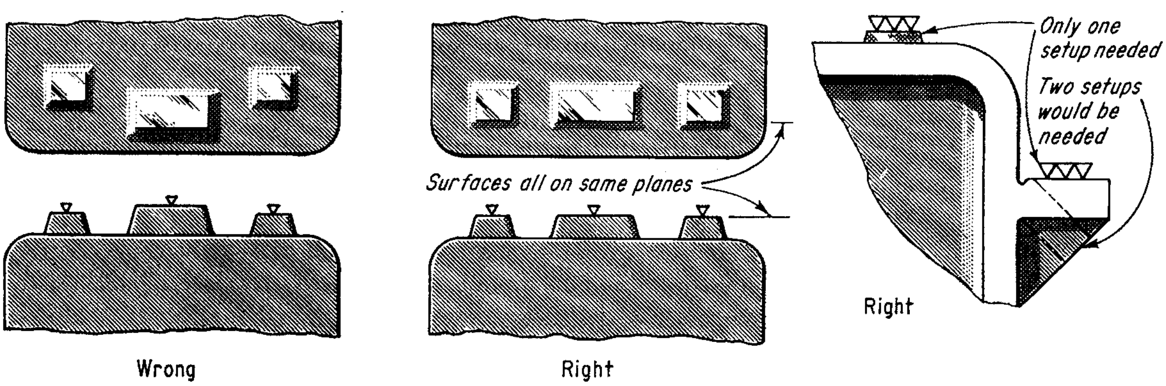

5 SURFACES TO BE FINISHED SHOULD BE ON SAME PLANE...
...OR AT LEAST PARALLEL.

Innovative Detents

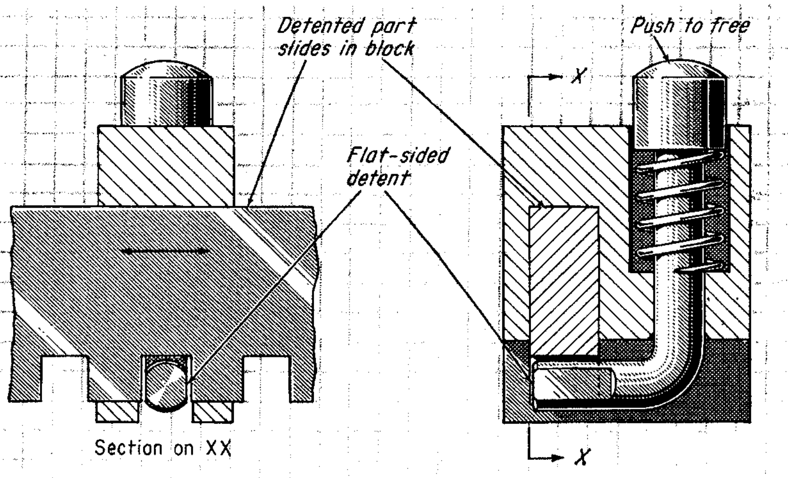

POSITIVE DETENT HAS PUSH-BUTTON RELEASE FOR STRAIGHT RODS

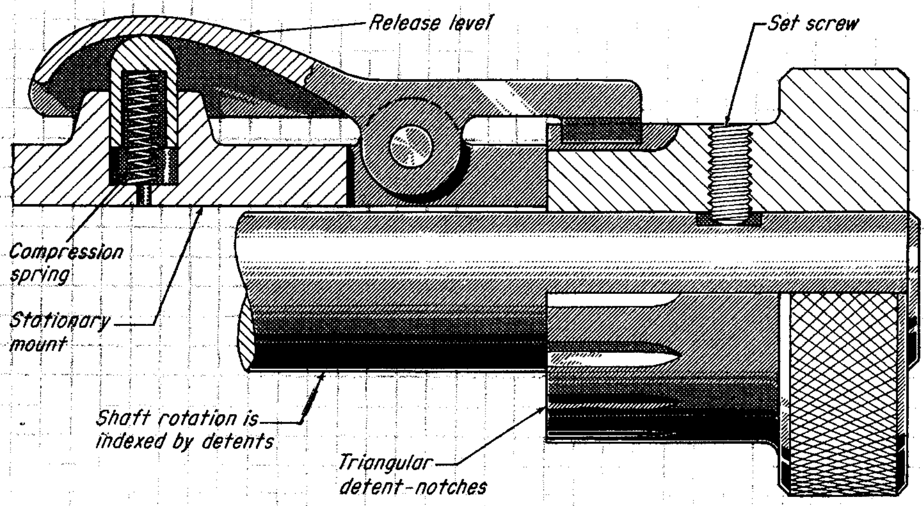

AXIAL DETENT FOR POSITIONING OF ADJUSTMENT KNOB WITH MANUAL RELEASE

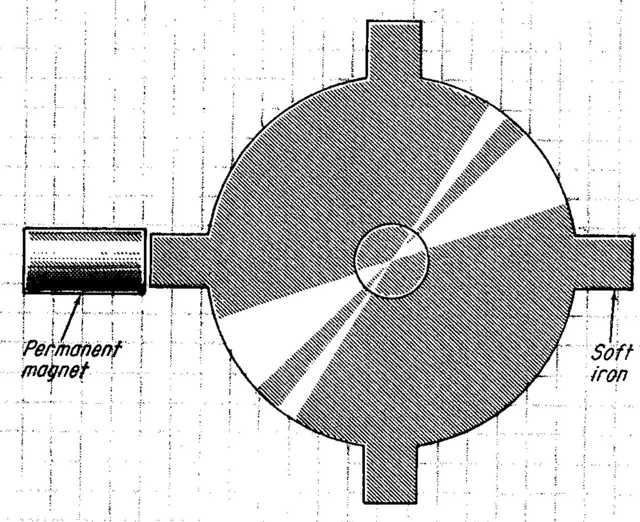

MAGNETIC DETENT

Cleaner Lines for Control Cabinets

How to improve the appearance of consoles and similar functional cabinets with divider strips, concealed catches, recesses, baffles, and trim.

F. W. Wood

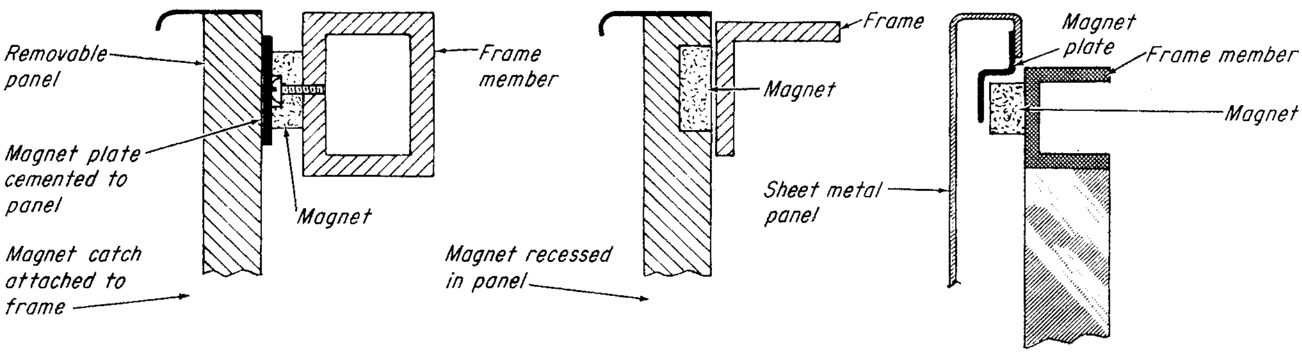

1

CONCEALED CATCHES permit a clear, uncluttered exterior panel appearance. Catches not requiring close alignment are preferable.

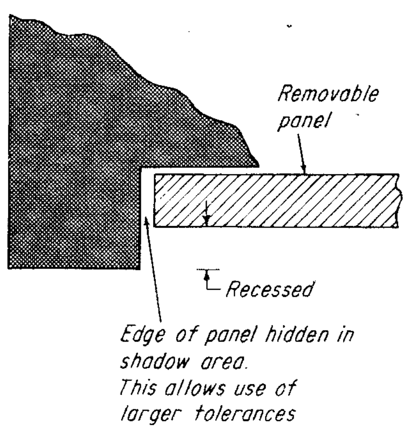

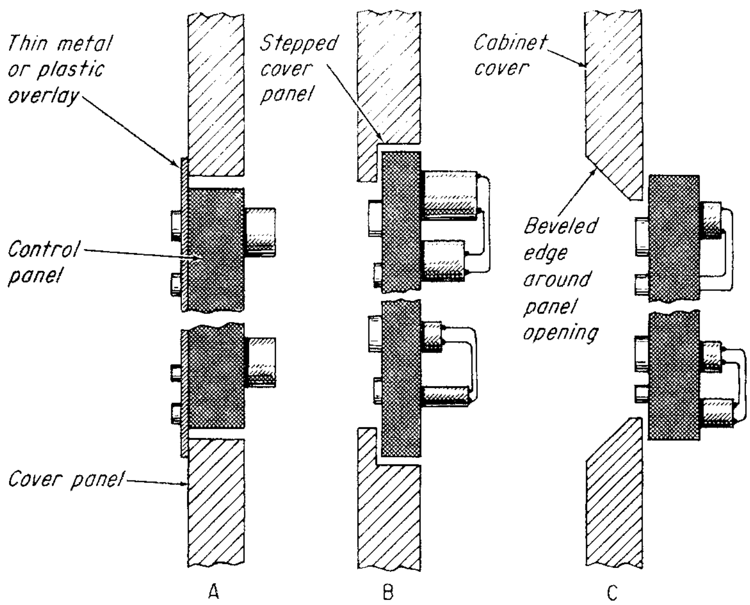

3

RECESSING provides a "shadow" area round the panel and effectively subdues any out-of-squareness of the panel or adjacent surfaces.

4

OVERLAY JOINTS are particularly useful for hiding unsightly joint lines around control panels — you can see only one line around the panel.

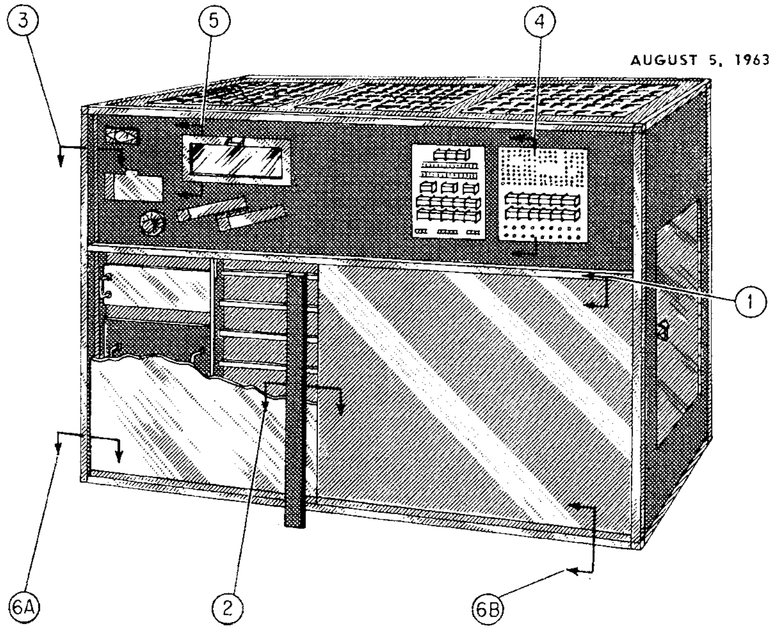

ALL THE DESIGN FEATURES described here are applied to various parts of the data-processing console shown in artist's conception.

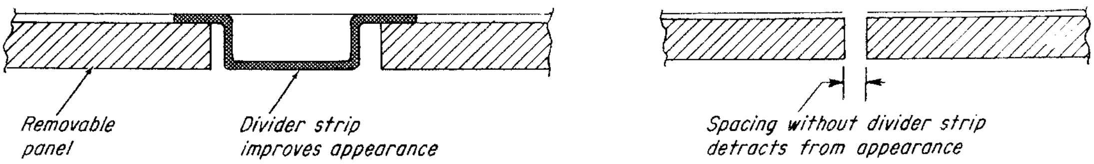

2

DIVIDER STRIP between two removable panels overcomes the need for a tight butt joint. Contrasting-finish styling is also possible.

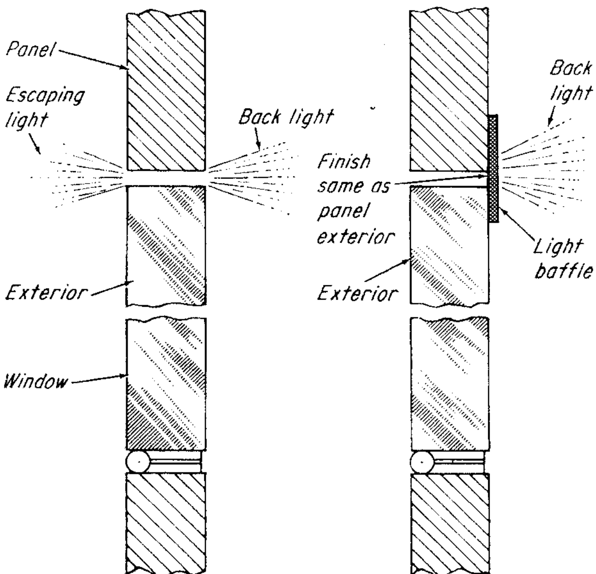

5

LIGHT BAFFLES behind all hinging or sliding windows prevent back-lighting from emphasizing bad fits. Baffle and panel color should be the same.

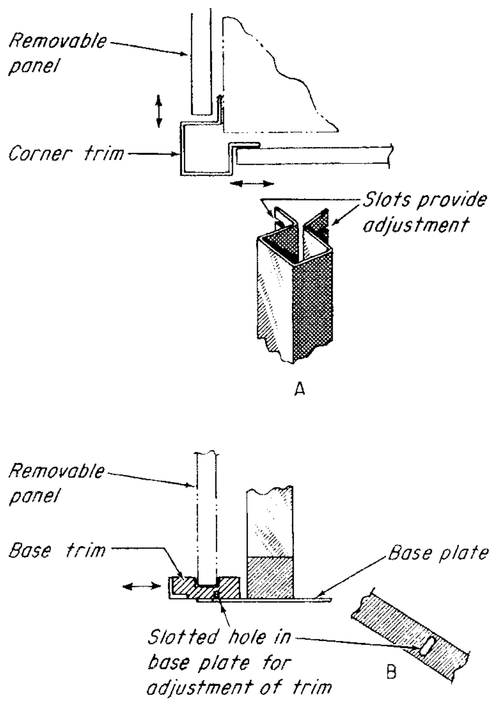

6

ADJUSTABLE TRIM gives illusion of a good fit between non-squared panels and frames. Open-ended slots provide for easy assembly.

Flexure Devices for Economic Action

Advantages: Often simpler, friction and wear are virtually nil, no lubrication.
Disadvantages: Limited movement, low force capacity.

James F. Machen

1

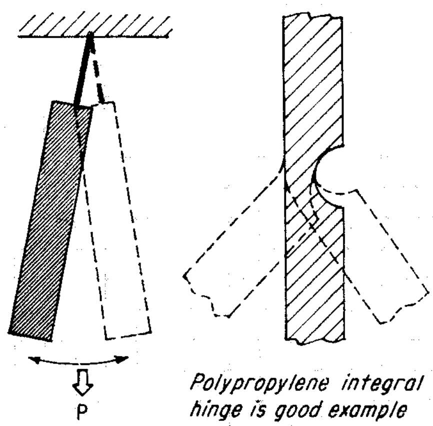

BASIC FLEXURE connection (single-strip pivot) eliminates need for bearing in oscillatory linkages such as relay armatures

2

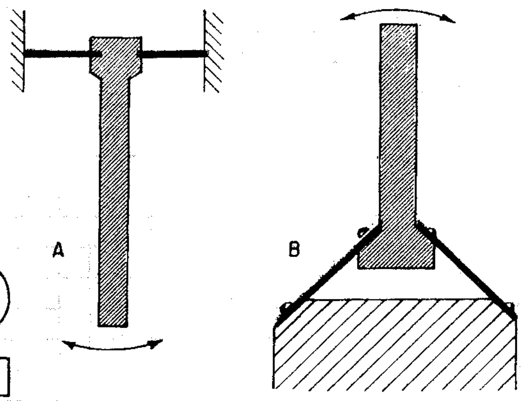

TWO EXAMPLES of two-strip pivots

5

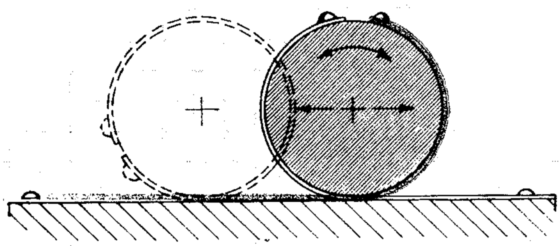

"RACK AND PINION" equivalent of rolling pivots

6

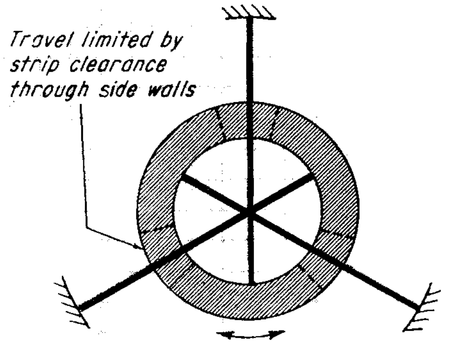

120° Y CROSS-STRIP pivot holds center location to provide frictionless bearing with angular spring rate

9

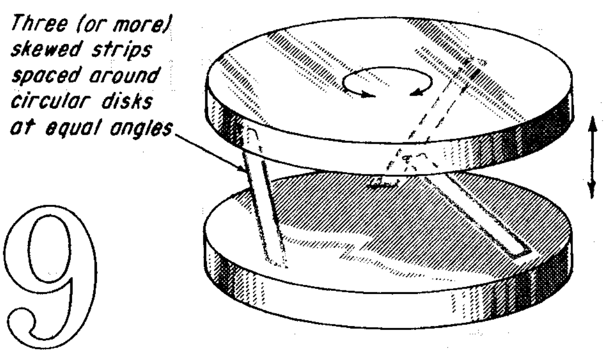

SKEWED STRIP converts angular motion into linear motion or vice versa

10

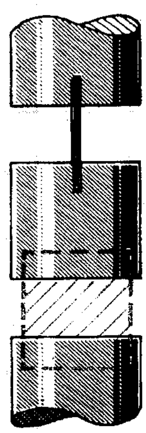

LIGHT-DUTY UNIVERSAL JOINT is ideal for many sealed instrument actions

3

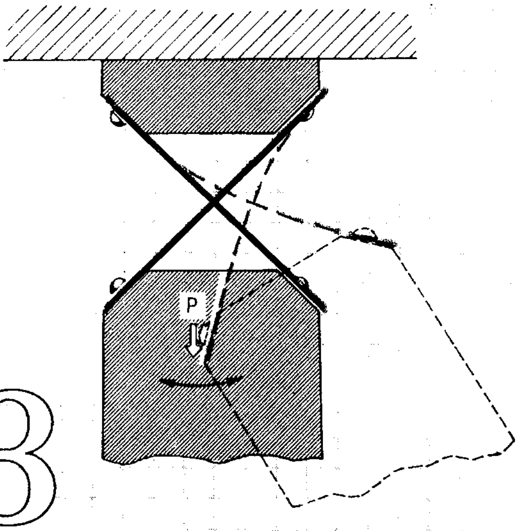

CROSS-STRIP PIVOT combines flexibility with some load-carrying capacity

4

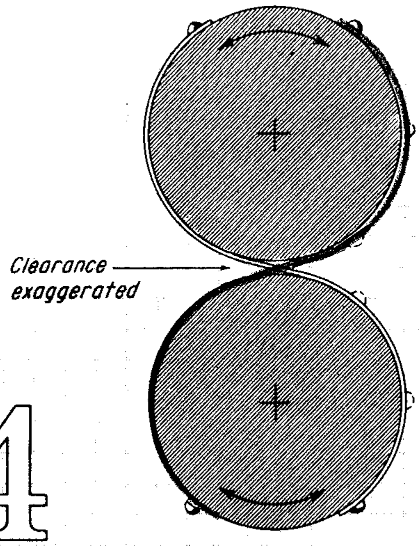

CROSS-STRIP ROLLING PIVOT maintains "geared" rolling contact between two cylinders — different diameters give "gear" ratio

7

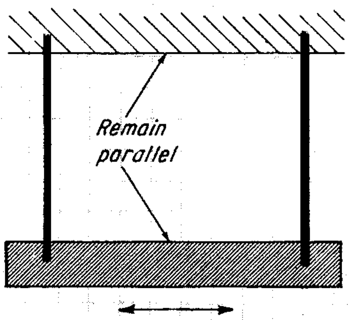

PARALLEL-MOTION linkage has varying spacing

8

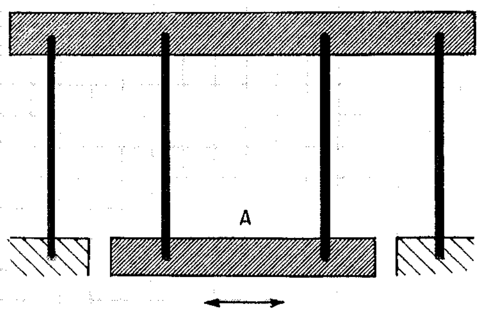

IN THIS PARALLEL-MOTION linkage, platform A remains level and its height does not change with sideways oscillation

11

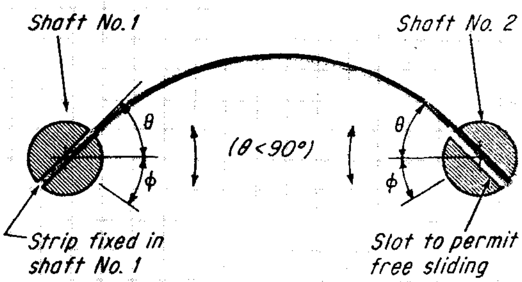

FLEXURE TRANSMITS equal but opposite, low-torque, angular motion between parallel shafts

12

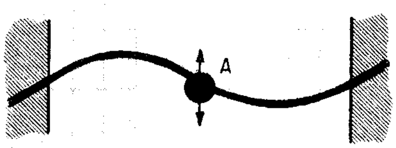

SINE SPRING, straight line mechanism lets point A move in approximately a straight line for short distances.

Isolating Machines from Vibration

Here is a selection of resilient pads, spring and rubber mounts, as they are commonly arranged to absorb vibrations.

Louis Dodge

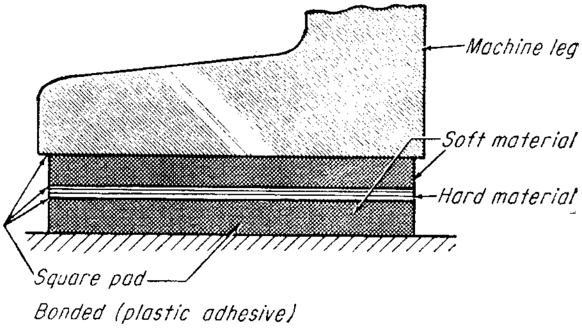

1 SQUARE PADS AND PLAIN FOOTING

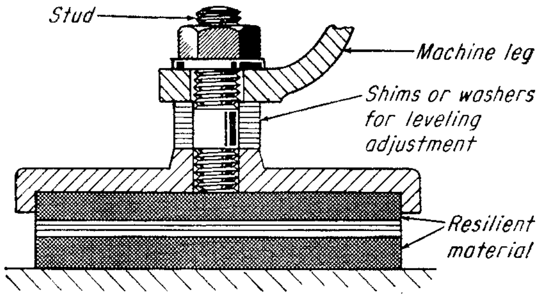

2 ROUND PADS AND SHIMMED FOOTING

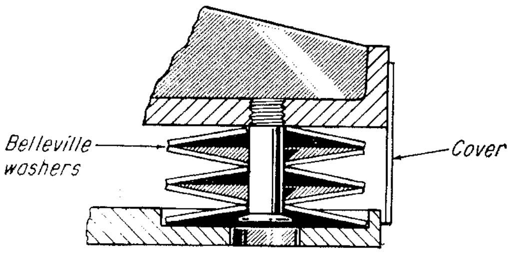

5 BELLEVILLE SPRING MOUNT
(STIFFNESS VARIES WITH NUMBER OF WASHERS)

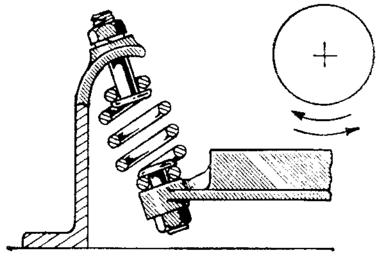

6 SUSPENSION-SPRING
(FOR SMALL, HIGH-SPEED MACHINERY)

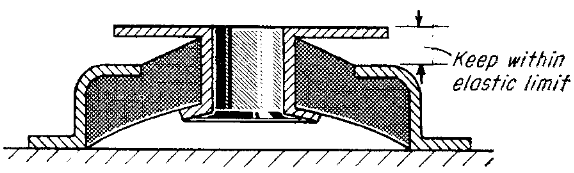

Limited deflection

8 HOW FOUNDATIONS ARE ISOLATED

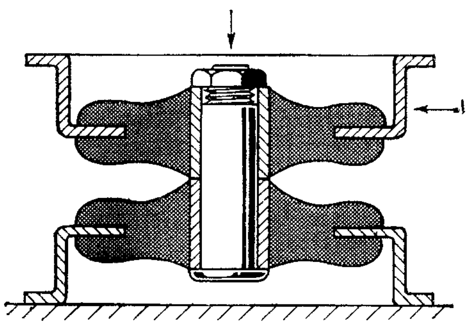

Lateral and vertical loads

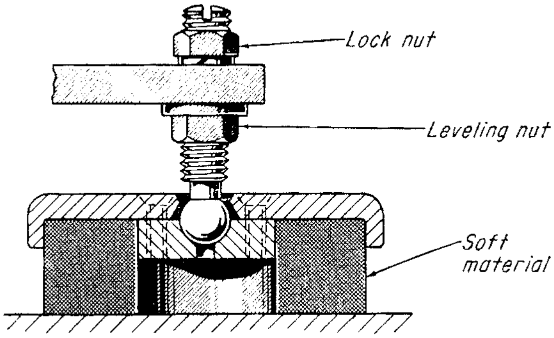

3 LEVELING SCREW FOR UNEVEN FLOORS

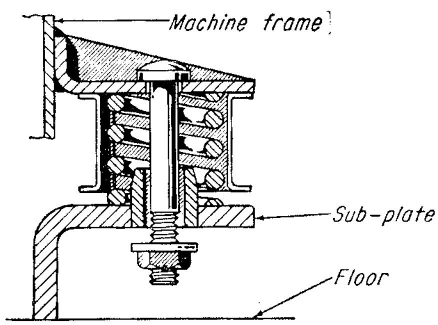

4 COIL SPRING MOUNT —AVOID RESONANCE FREQUENCIES

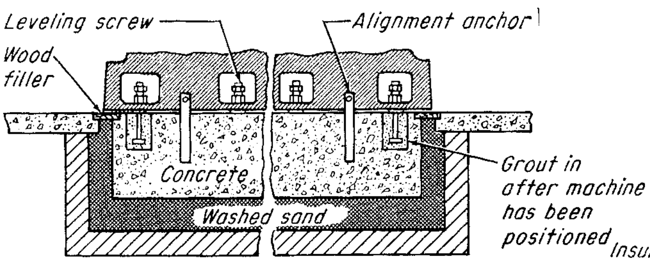

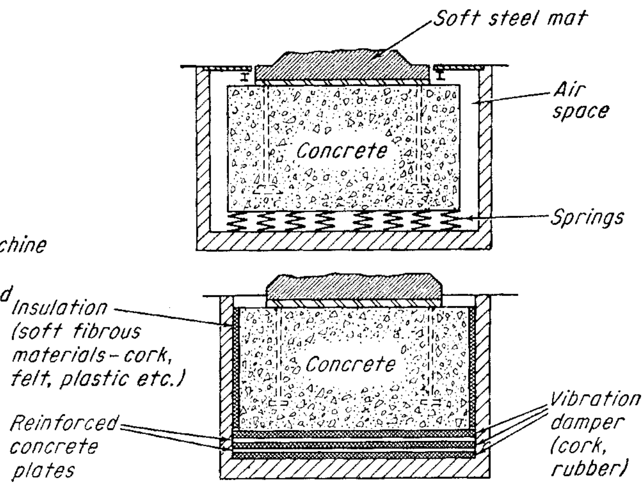

7 RUBBER BUSHING MOUNTS HAVE HIGH DAMPING FACTOR

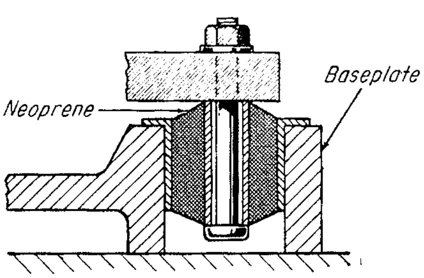

Vertical deflection

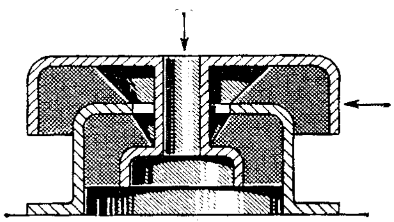

Equal static deflection for vertical and horizontal loads

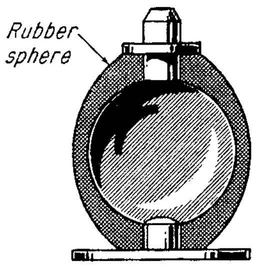

Rubber plus pneumatic resilience

Types of Mounts for Vibration Isolation

Thomas R. Finn

TRANSMISSION OF VIBRATION from a machine or motor to the supporting structure can be reduced by using special mountings. Vibrations may be caused by an unbalanced rotor or reciprocating elements of a machine. By flexibly supporting the vibrating member, the disturbance can be greatly absorbed by the resilient mounting.

For most effective vibration isolation, the mounting should be very soft so that its natural frequency is low in comparison to the frequency of the disturbance. As a rule, the disturbing frequency should always be greater than 2.5 times the natural frequency of the mounted system. For *simple linear vibrations,* the natural frequency of the supported mass f_n can be determined by the static deflection of the springs or mount. This is expressed by:

$$f_n = 188 \div \sqrt{d} \text{ (in cpm)}$$

There are many commercial mounts available. Most of these devices utilize rubber for resiliency; this rubber is most often stressed in shear to obtain larger static deflection for a given thickness. Where greater load capacity (per unit volume) is required, rubber in compression is used.

An unrestrained body mounted on four resilient mounts, has six modes of vibration and consequently six natural frequencies.

For single-degree translational motion of a body which is supported on more than one mount, the stiffness of each unit should be in proportion to the weight supported. Besides motion in the vertical plane, the natural frequency in the horizontal plane should be also calculated. For the lowest natural frequency of the system, mountings should be loaded close to the maximum rating given.

In applying vibration mounts, three factors are important: (1) keep mounts far apart for better stability; (2) mounts should be in a plane which passes through the center of gravity of the suspended mass; (3) use of hold-down screws or snubbers to limit large motions.

STRIP-TYPE ISOLATORS

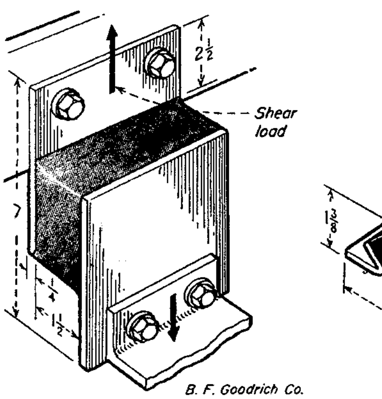

Fig. 1—Rated at 80 lb/linear in. with a shear deflection of 1 in., this type has a compression rating of 250 lb/linear in. at 5/16 in. deflection. Requires drilling and cutting to proper length.

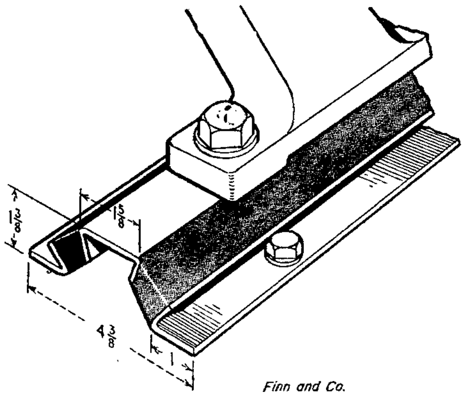

Fig. 2—This mount has ratings from 40 to 105 lb/linear in. and deflects ¼ in. Rubber is stressed in shear and compression. As a result, the load deflection curve is non-linear, which prevents resonance.

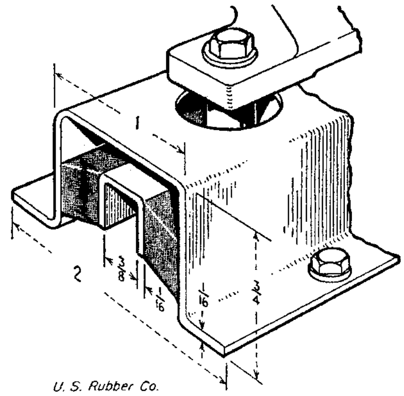

Fig. 3—Channel-type mounting comes in two basic sizes: small, for vertical loads up to 95 lb (illustrated); large, for loads to 420 lb. Lengths are 1 to 7 in. Can be inverted for overhead suspensions.

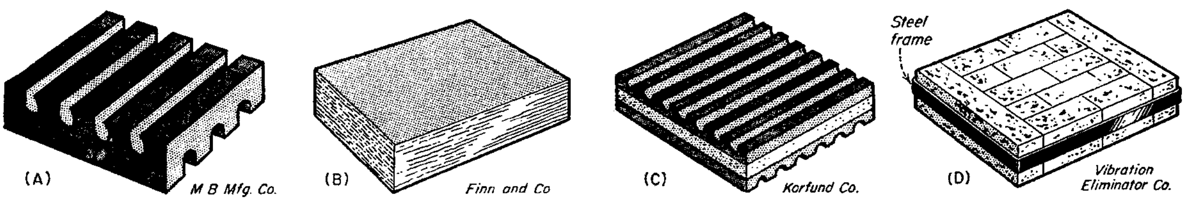

Fig. 4—For heavy, flat base, equipment several materials are available for vibration isolation; these are most effective where very high frequencies and disturbing sound are to be reduced. Sheets of felt, cork, and rubber are most commonly used. (A) *Isomode* pads of neoprene are 5/16 in. thick and are used at loadings of from 10 to 60 psi. Maximum deflected height is ¼ in.; several layers can be used. (B) *Vibrapad* consisting of alternate layers of cotton duck and rubber, ⅝ in. thick, is used for loads up to 200 psi. (C) *Elasto-rib* is a combination of cork and ribbed-rubber which is rated up to 35 psi. Minimum thickness is 1 in. (D) Natural cork plates are held by a steel frame. Thickness ranges from 1 to 4 in. and widths up to 24 inches

INDIVIDUAL MOUNTS

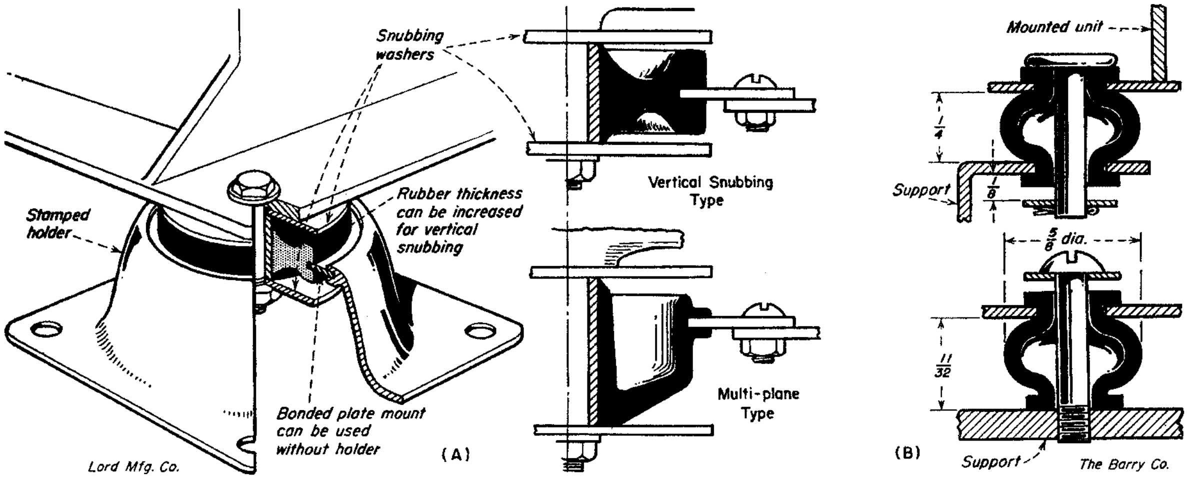

Fig. 5—(A) Axial ratings of this standard series are: 1 to 90 lb at deflections of 1/16 or ⅛ in. Mounting is about twice as stiff radially as compared to the axial direction. For loads up to 310 lb, the rubber is solid. (B) Small mount is rated from 1/3 to 3 lb per unit. Isolates vibrations as low as 900 cpm in all directions. Attachment is simplified by punched or tapped holes.

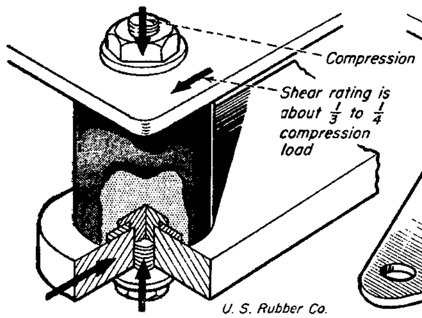

Fig. 6—Stud-type pads are simple to attach and rated in compression from 2 to 270 lb, but limited to applications of shear and compression forces. Pads with tapped holes are made for cap screws.

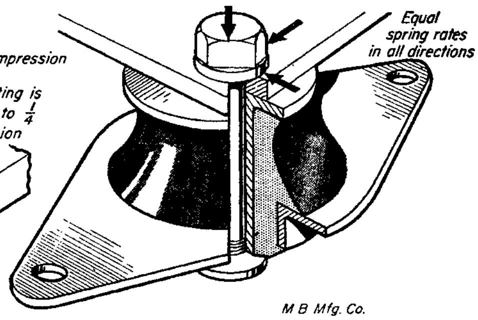

Fig. 7—Mounts are rated at 150 to 2,670 lb at 0.15 in. deflection. The natural frequency is about 490 cpm. Sleeve ID varies from 0.437 to 1.00 in. and the overall height is from 1.75 to 4.00 in.

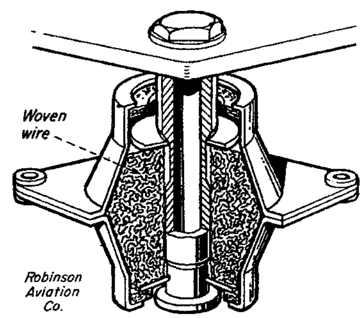

Fig. 8—All metal mount for extreme temperature conditions. Woven wire is used for resilient element. With a varying spring rate, it has good damping effects. Unit load ratings are from 2 to 25 lb.

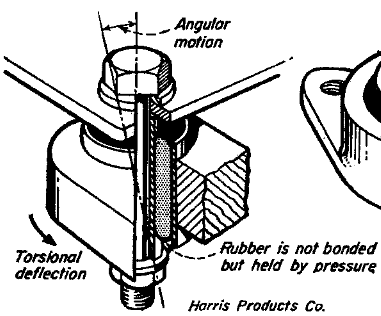

Fig. 9—Specially designed, this mount is widely used in automotive industry. Besides axial and radial resiliency, it is used for torsional and angular motion.

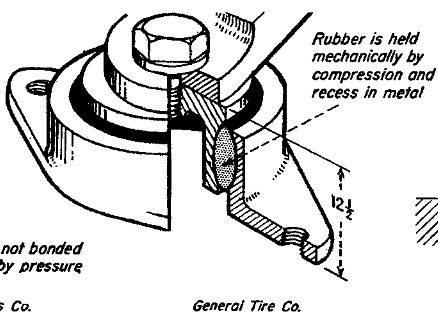

Fig. 10—For heavy loads, rolling joint is useful in applications where alignment is important. Normal ratings range from 125 to 1,500 lb at 0.24 in. deflection.

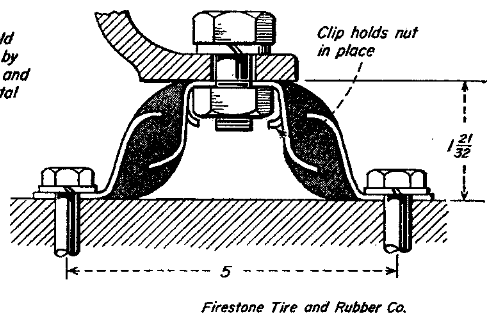

Fig. 11—Metal reinforced rubber pads are designed for loads of 250 to 1,700 lb. All pads have the same overall dimensions. Attaching bolts are: ½, ⅝ or ¾ inch.

Printed-Circuit Guides

They allow easy and quick insertion, they guide accurately, and they support the board firmly in place.

Irwin N. Schuster

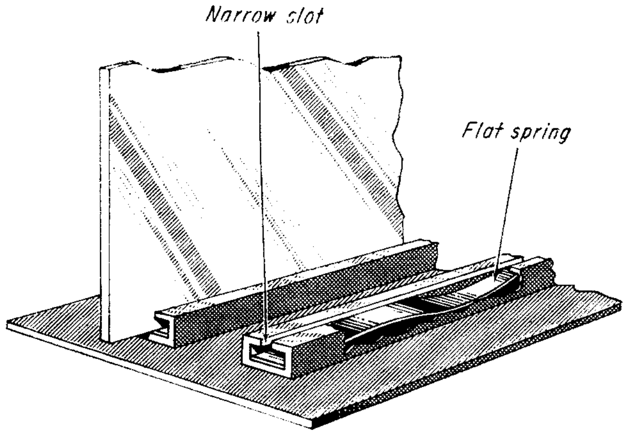

1 **FLAT SPRING** in extruded section provides close limitation for horizontal panel-movement. extreme tolerance vertically.

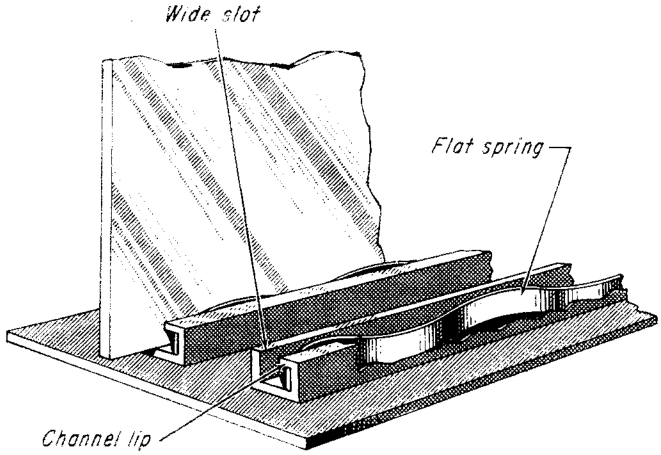

2 **CHANNEL LIP** allows flat spring to be placed to retain circuit board against channel side and reduce tolerances.

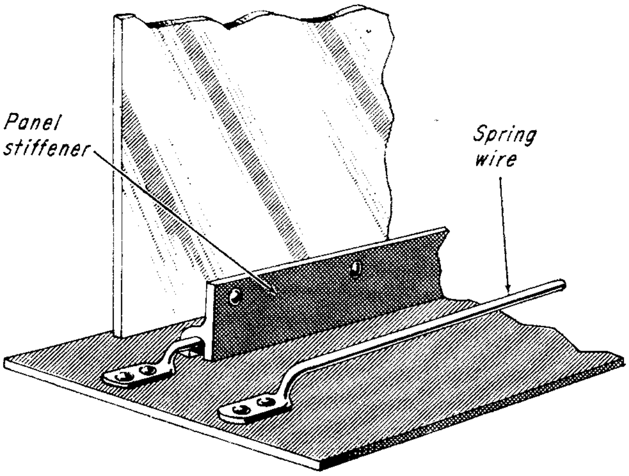

3 **SPRING WIRE** and panel stiffener is a good combination where panel space is not at a premium.

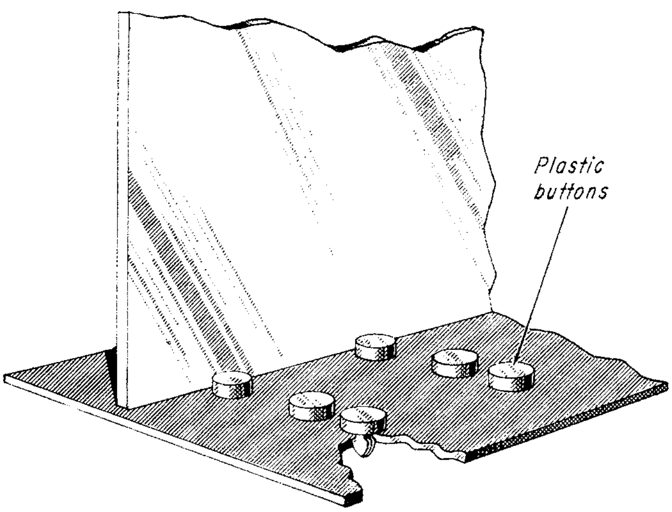

4 **PLASTIC BUTTONS** offer an ultra-simple method of holding panels. The round buttons let panel slide home easily.

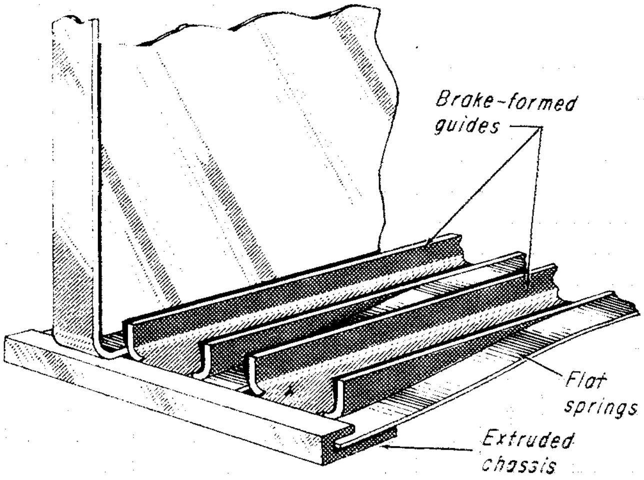

5 **EXTRUDED CHASSIS PARTS,** brake-formed guides, and flat springs allow more tolerance reduction in assembly.

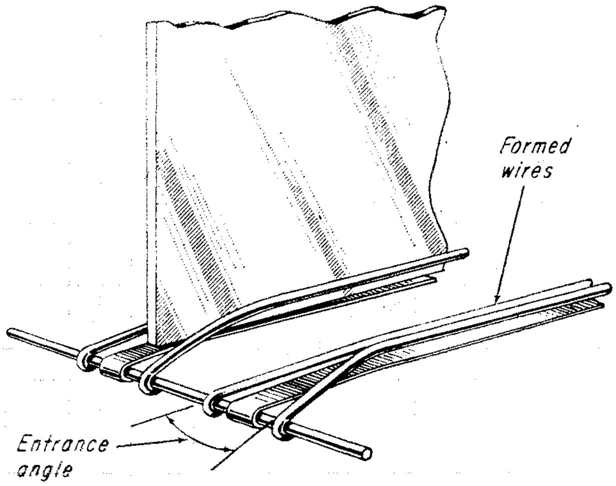

6 **FORMED WIRE** structure lets cooling air through while gripping the circuit board firmly in two planes.

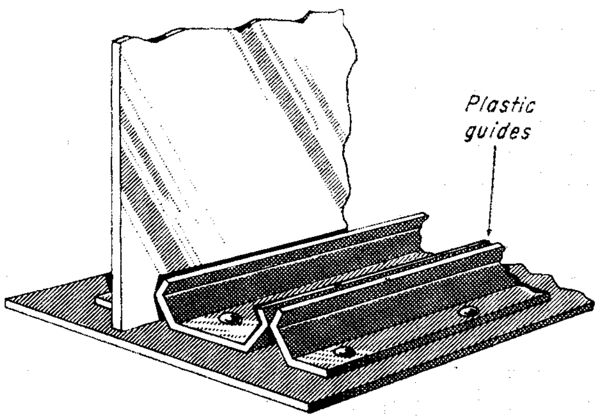

7 **EXTRUDED OR HEAT-FORMED** plastic guides are inexpensive and reduce the chance of shorting to the metal chassis.

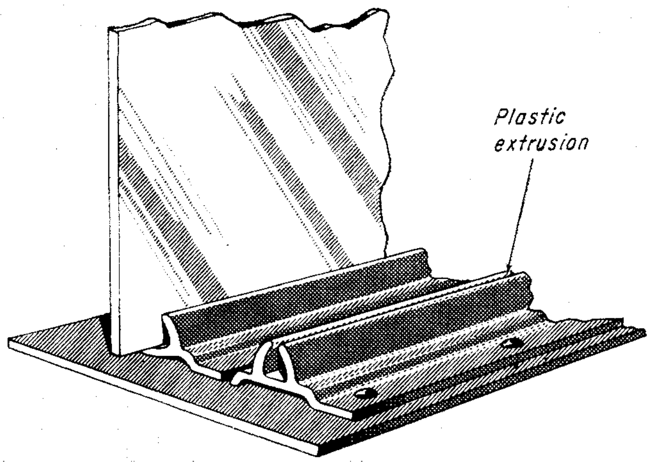

8 **PLASTIC EXTRUSION** here provides its own spring grip to support a light-weight panel in a mild environment.

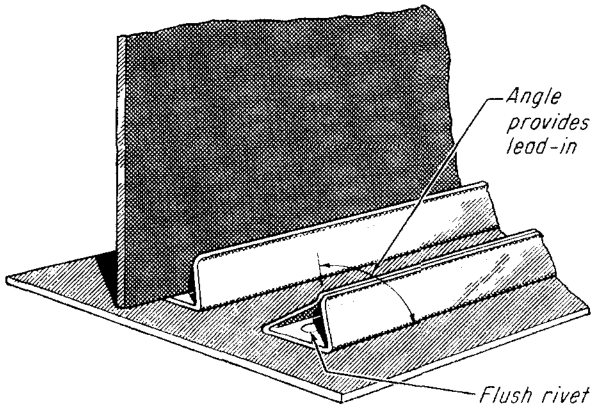

9 **FORMED SHEETMETAL GUIDE** made of spring material, with the end c off at an angle to guide the board.

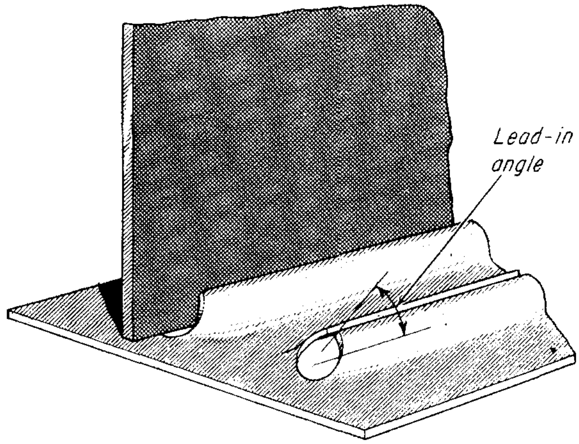

10 **STAMPED-IN** board guide reduces weight of chassis while providing firm board mount. Note lead-in angle.

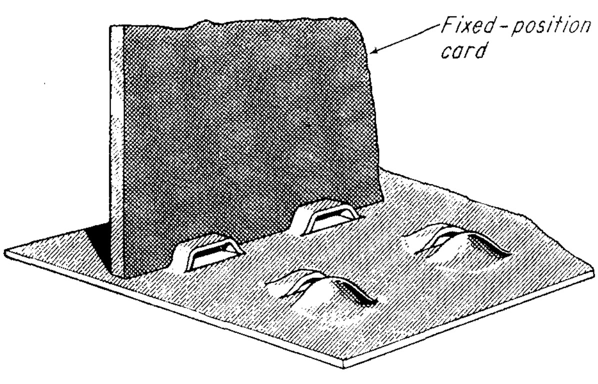

11 **SMALL SECTIONS** stamped in the chassis provide locating guides for cards mounted in fixed positions.

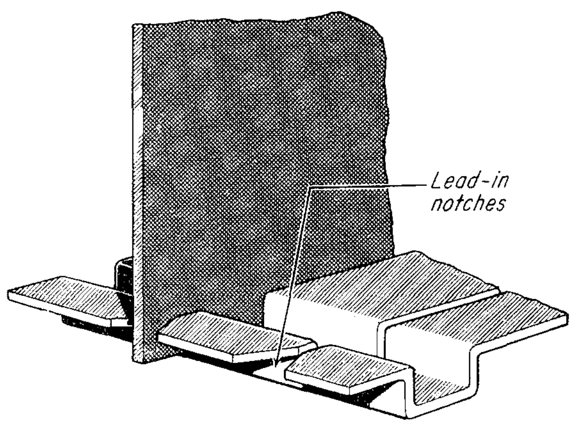

12 **INTEGRAL GUIDE** is ideal when stiff chassis is required and gives excellent lead-in characteristics.

Hinges, Panels and Doors

Here are some low cost ways to avoid spoiling the appearance of your equipment with hinges that show.

Frank W. Wood

1

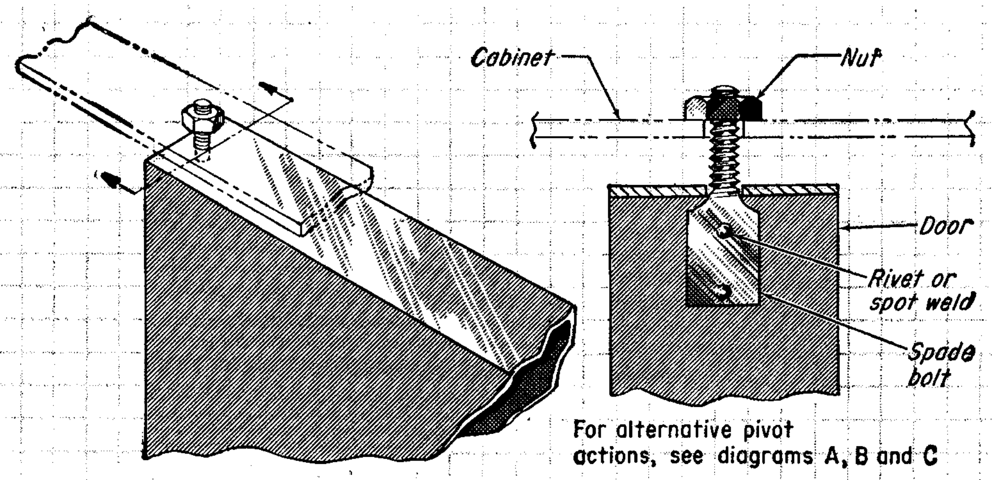

SPADE BOLT AND STANDARD HARDWARE

2

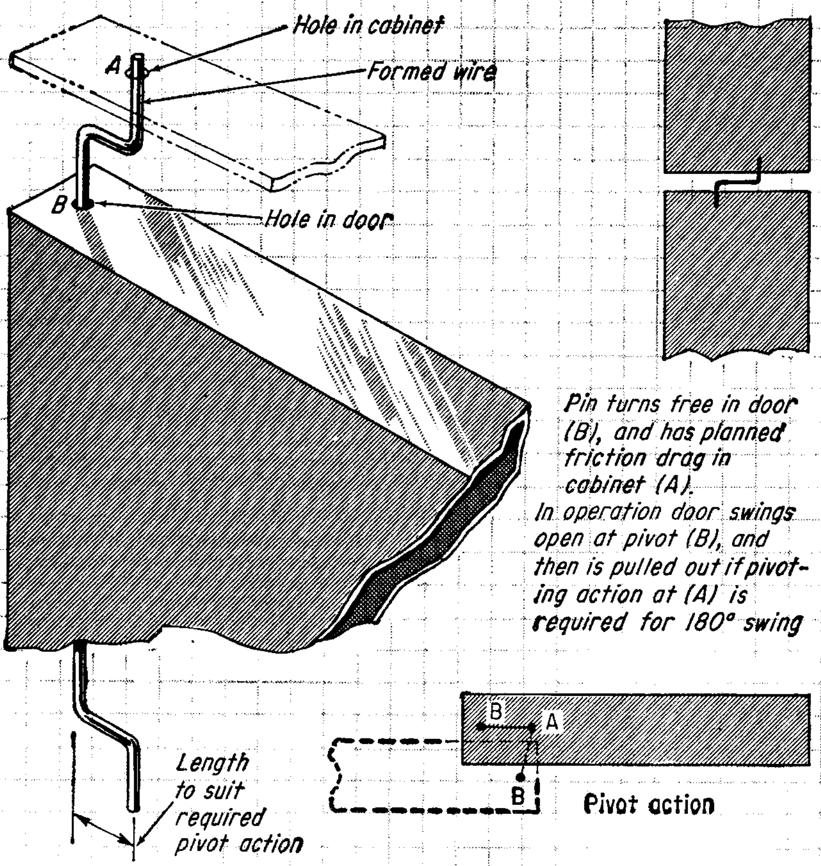

FORMED WIRE FOR DOUBLE HINGE ACTION

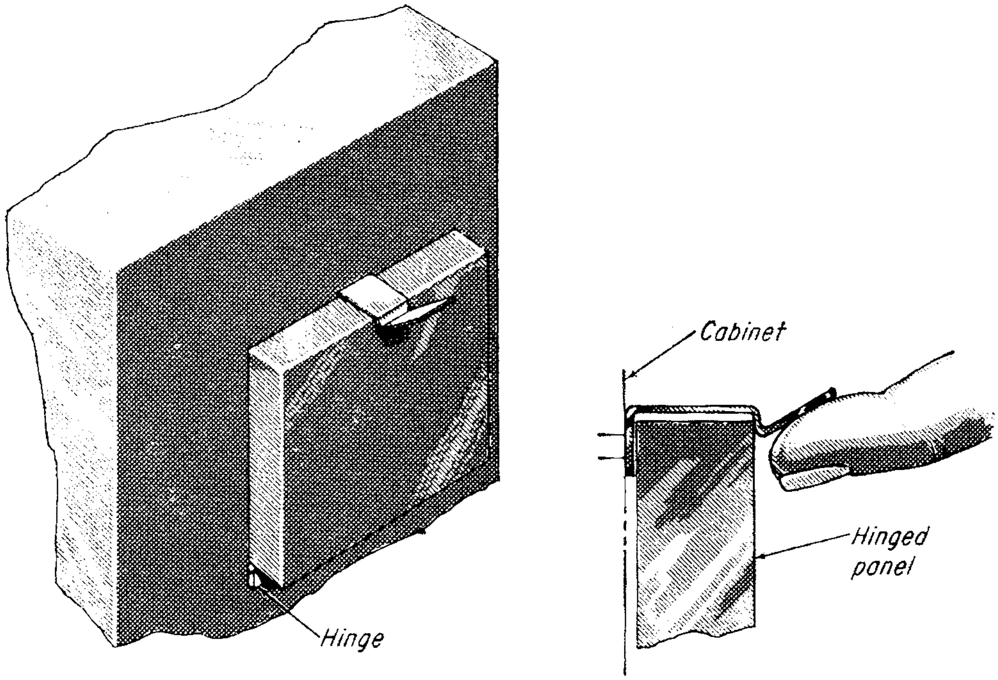

3

EXPOSED CATCH provides an easy-to-make and lower-cost catch if the appearance of the external fastener is not objectionable.

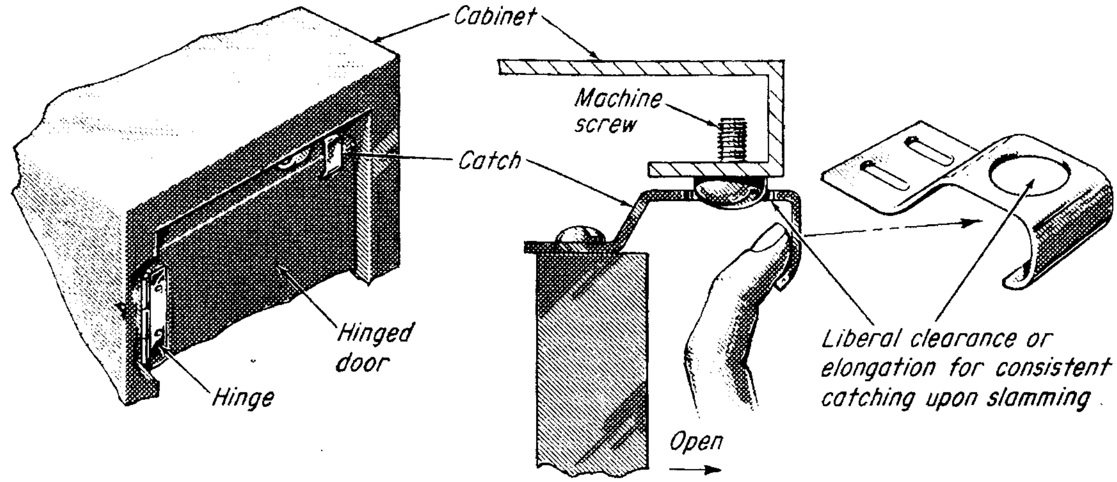

4

HEAVY DUTY CATCH, held by a machine screw, will retain hinged assemblies weighing several hundred pounds. Good initial alignment is advisable.

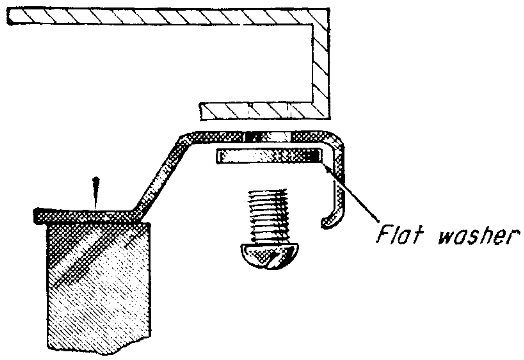

5

CATCH DOUBLES AS SHIPPING LOCK when the screw is removed and a large washer is added between the screw head and the catch.

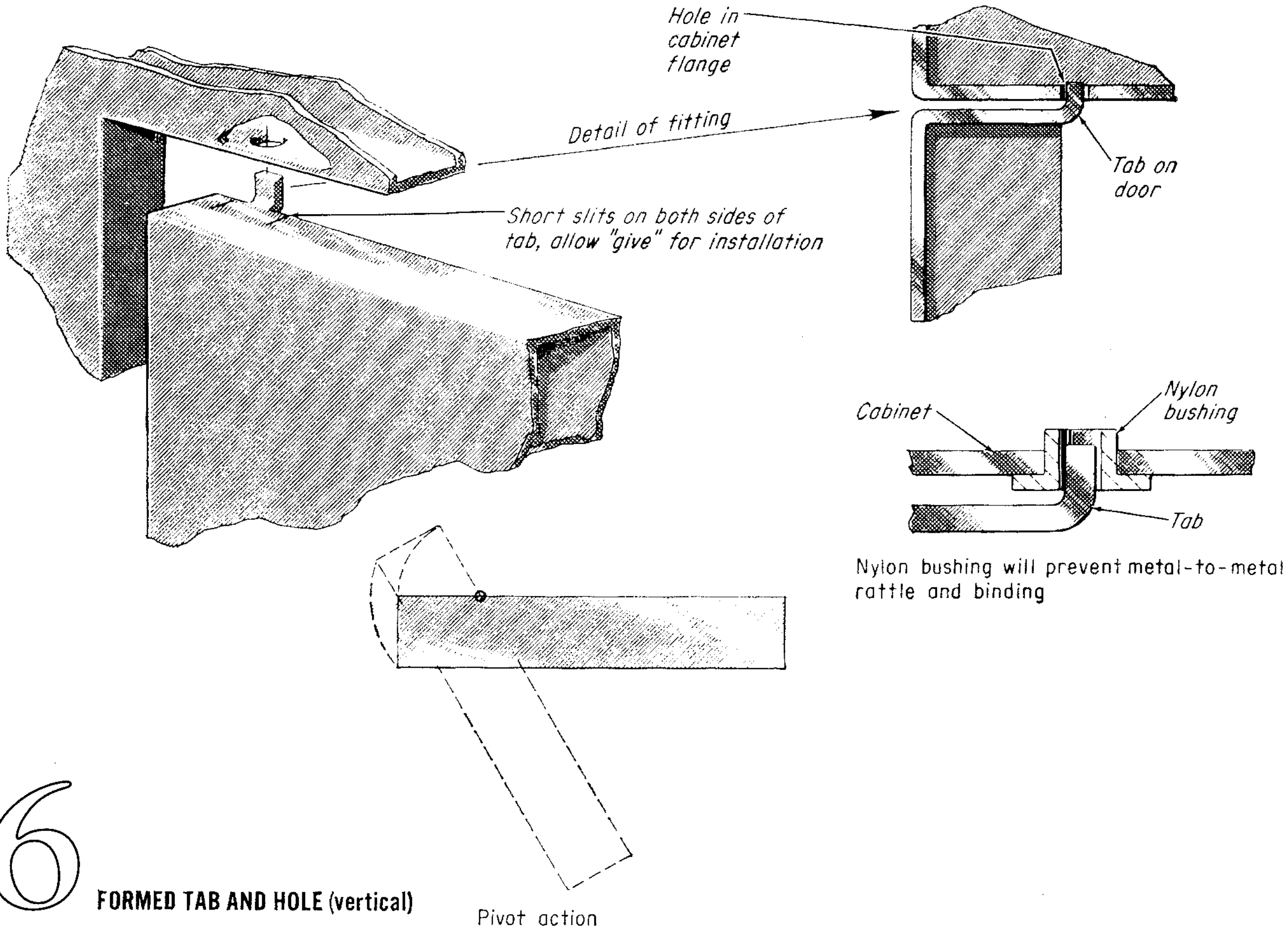

6 FORMED TAB AND HOLE (vertical)

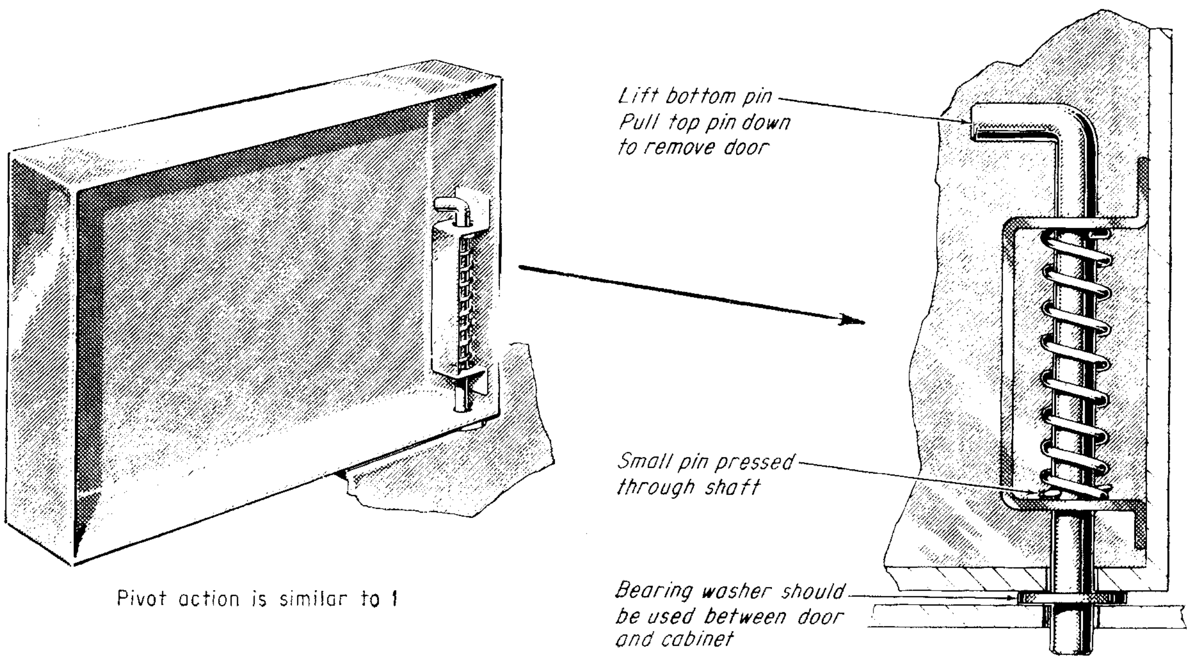

7 HANDLE PIN AND SPRING

Plastic Hinges

They'll cut costs and improve your product. You can clamp them, snap them, or otherwise locate them with their molded-in shapes.

Irwin N. Schuster

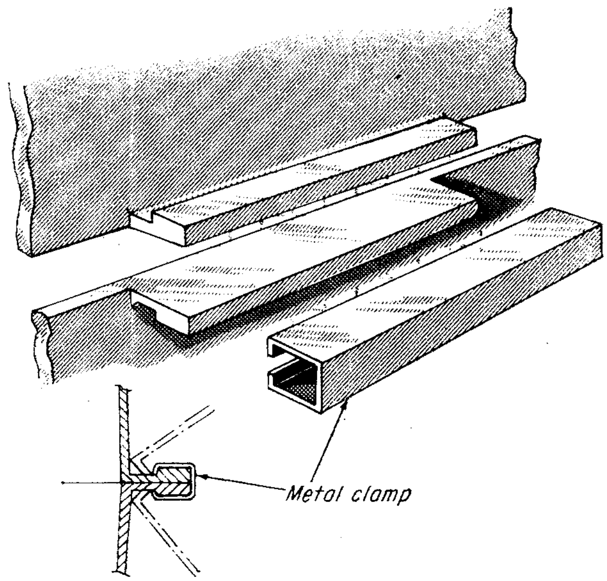

1

Rigid metal section, slipped onto molded tabs, clamps them together. Plastic material is either polypropylene or polyethylene.

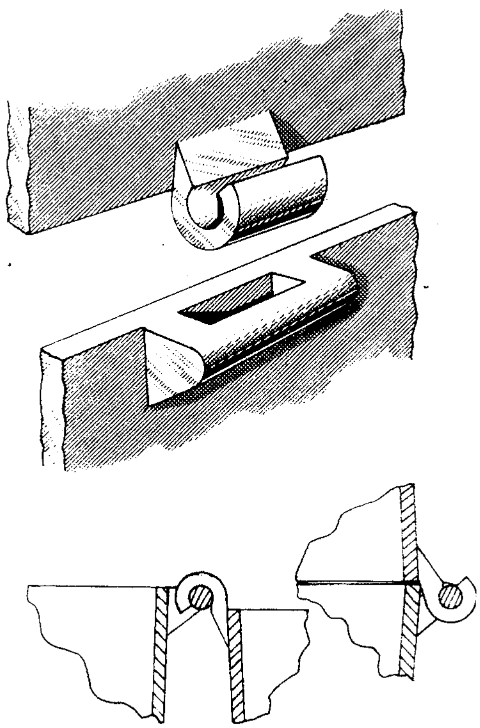

4

Soft plastic hinge is snapped over pin in full open position, giving maximum strength when top is closed; is best for containers with top handle.

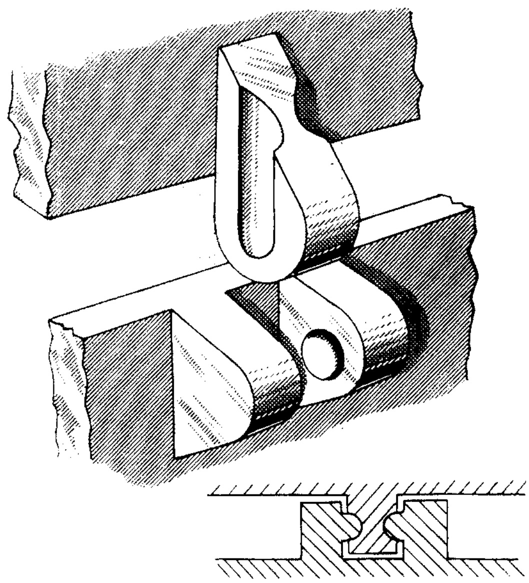

5

Assembled similar to number four, this hinge is fully moldable with no undercuts and can be disassembled only when fully open.

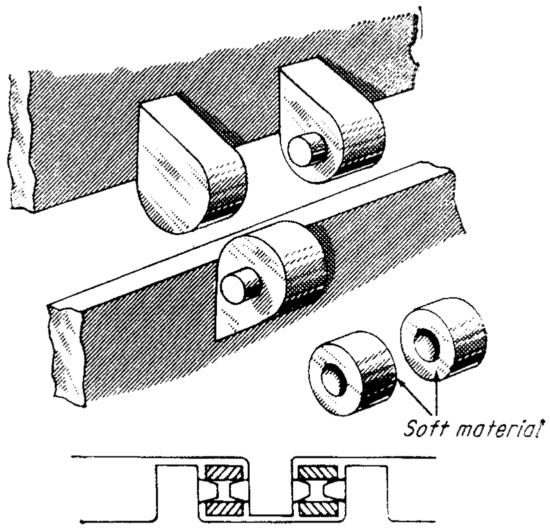

2

Soft plastic tubing sections are snapped onto nipples between both halves of this hard-plastic hinge as they are assembled together.

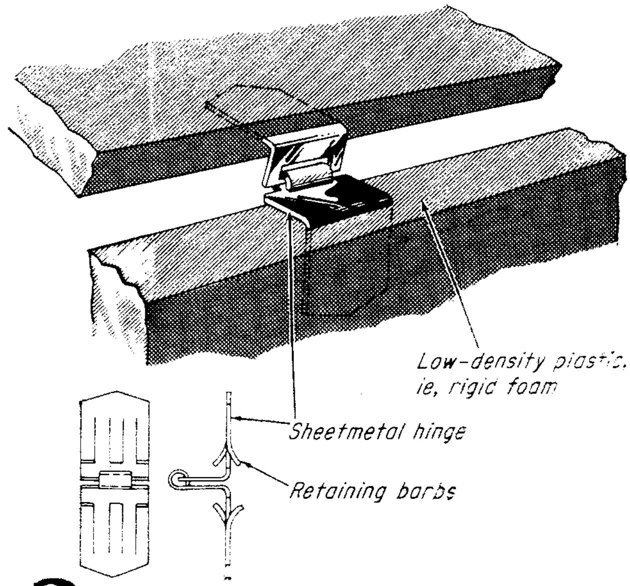

3

Stamped metal hinge with formed retaining barbs penetrates into locating depressions in rigid foam parts. Hinge costs little, performs well.

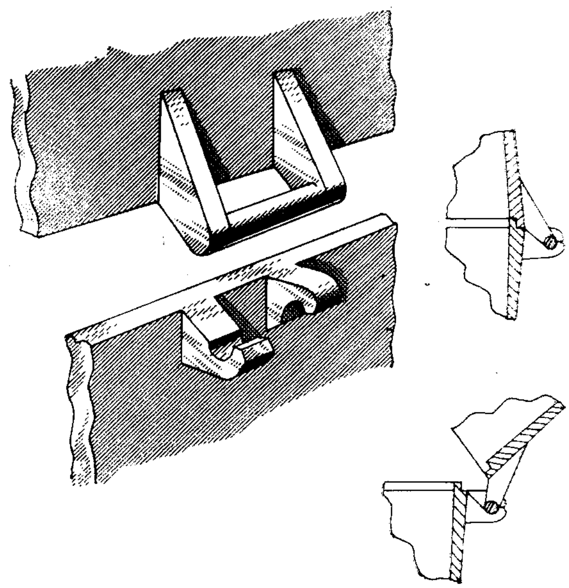

6

This hinge must be used in pairs, unless three lower tabs are molded. Snapped in from the back, pin cannot be removed when top is closed.

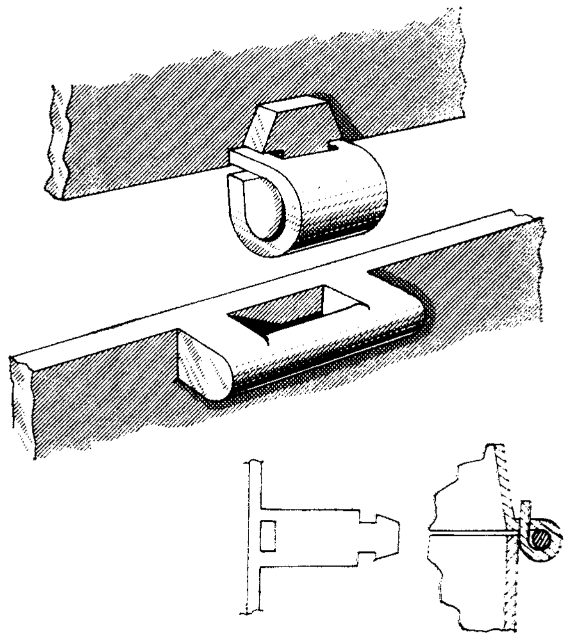

7

This strap, mating into itself, can loop around a molded pin, metal rings, or other closed sections, giving more security than a snap-on arrangment.

Pivots Do Many Jobs

Simple, easy, and inexpensive, pivots can eliminate play in machine tools as well as scientific and measuring instruments. Here are some ideas on how to make them, where to apply them.

Maurice Conklin

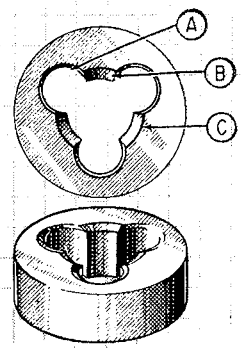

Making a pivot

3 In soft metals like brass a female locating recess with contact limited to three constrained areas can be made by drilling three holes (A), a center hole (B), and countersinking (C) around them.

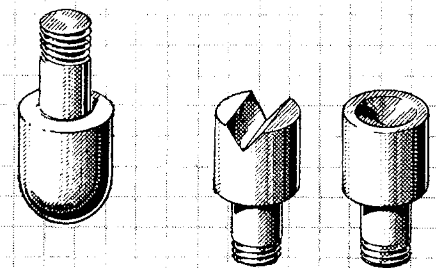

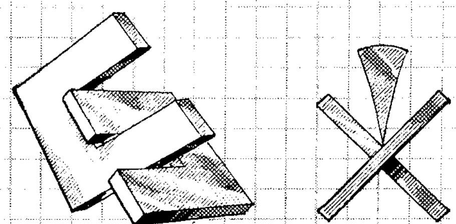

1 Round-tipped leg, V-slot, or conical hole pivots can be machined with threaded shanks for easy installation and adjustment on a part.

4 Sheetmetal squared U-sections can be crossed to form a knife-edge support with an infinitely sharp corner at the bottom of the Vee making a pivot point.

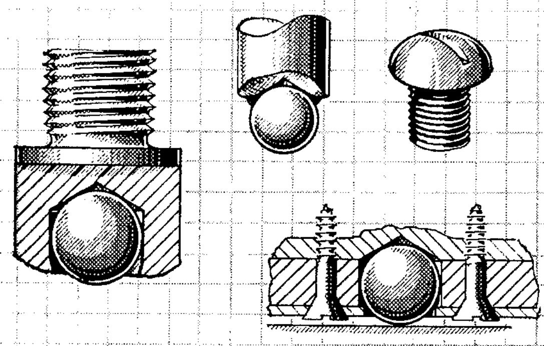

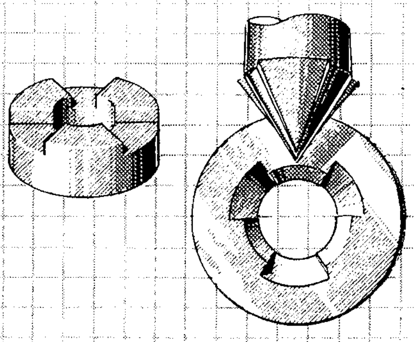

2 Balls used as feet can be peened into a sleeve, soldered or held by a clip. A round-headed screw can be a suitable substitute for the ball.

5 A similar reduced-area contact is made by milling segments around a hole either plain or countersunk, or a three-ribbed punch tip can form a countersink leaving the remaining area to make contact.

Applying a pivot

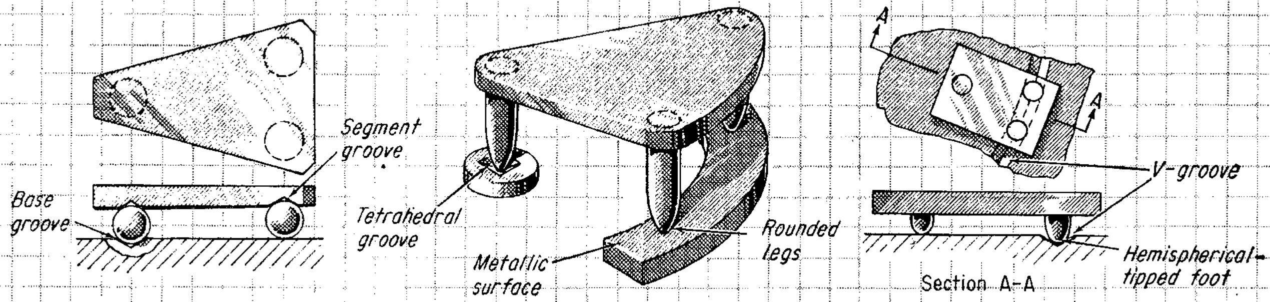

6 Need to turn through an arc? A ball set into a drilled spot on the base and segment does the trick. The outer two balls slide on the base and being set in the segment, support the outer end. Another way is to set the rounded tip of one leg in a tetrahedral pocket and let the other legs slide on a metallic surface. A third method is to place two hemispherical-tipped feet into and accurately grooved V-section, the third foot slides.

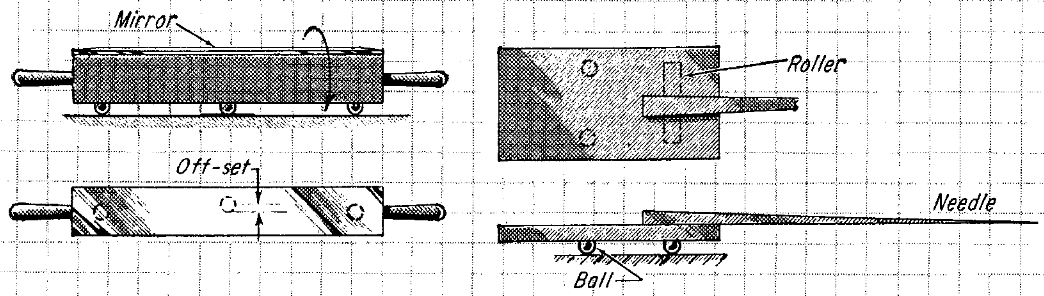

7 Need to measure material thickness? How about a block with three balls, one off-center. When a thin piece of metal is slipped under the off-centered ball, the block tips. Top face of the block is a mirror, part of an optical level to indicate thickness. Another method used to measure filament thickness has two balls and a roller. The filament is slipped between the balls and under the roller, rise of the needle gives thickness.

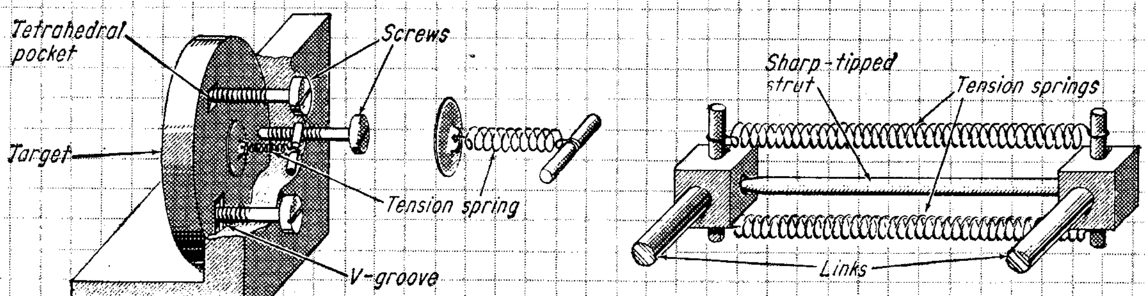

8 Need to support a mirror or other target? It's simple with a central tension spring and three ball-tipped screws. One screw end fits into a tetrahedral pocket, the second in a V-groove, the third on the flat surface. The target can now be positioned accurately with no force other than gravity. Another approach is to support two links with tension springs and strut. The tension spring eliminates backlash and holds the assembly together; the sharp tipped strut permits free pivoting of the mirror or target attached to the links.

Dimensions for Hand Grip

To get maximum advantage from knobs and handles, use the size suggested in these sketches.

Frank William Wood JR.

KNOBS

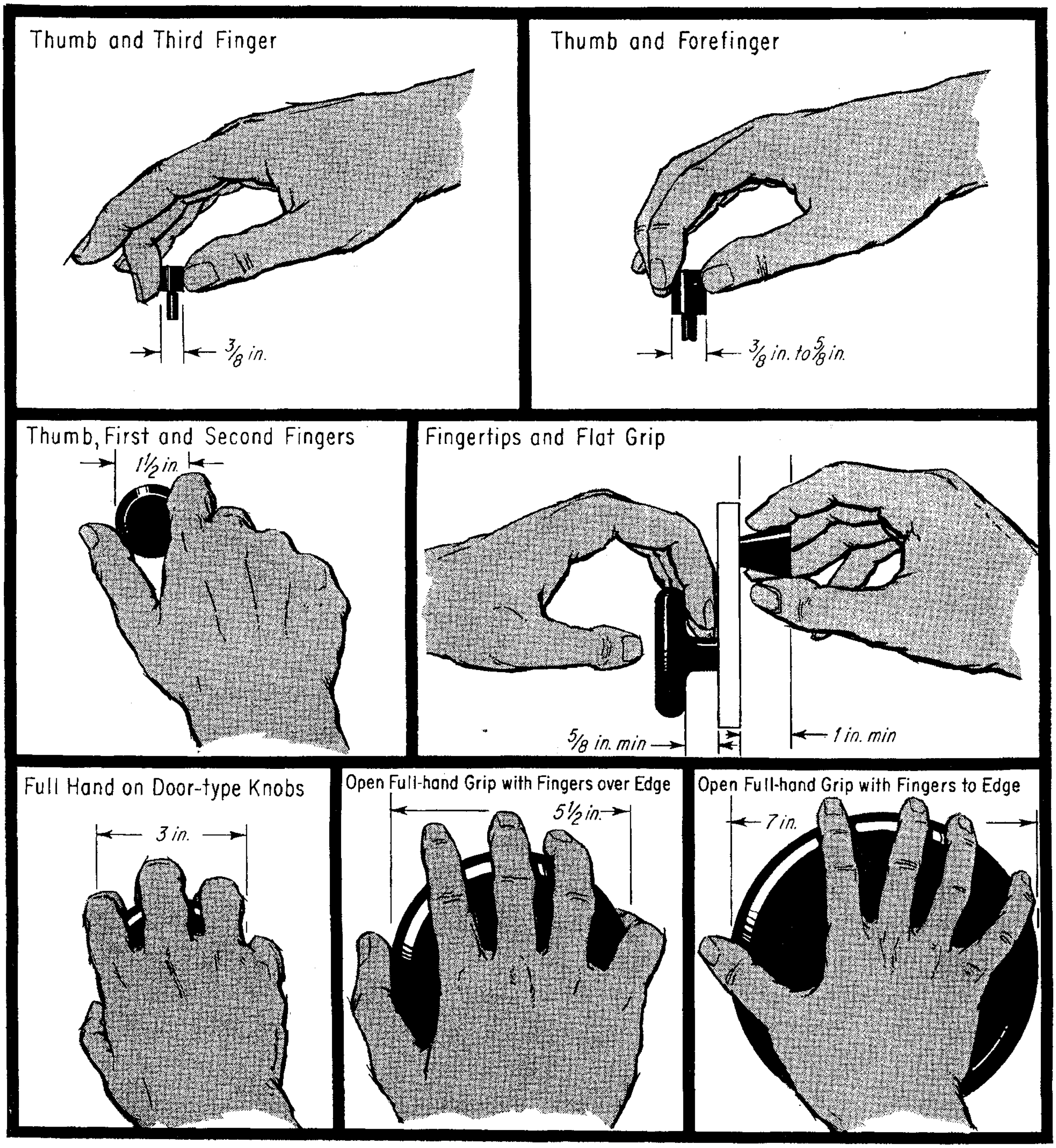

HANDLES

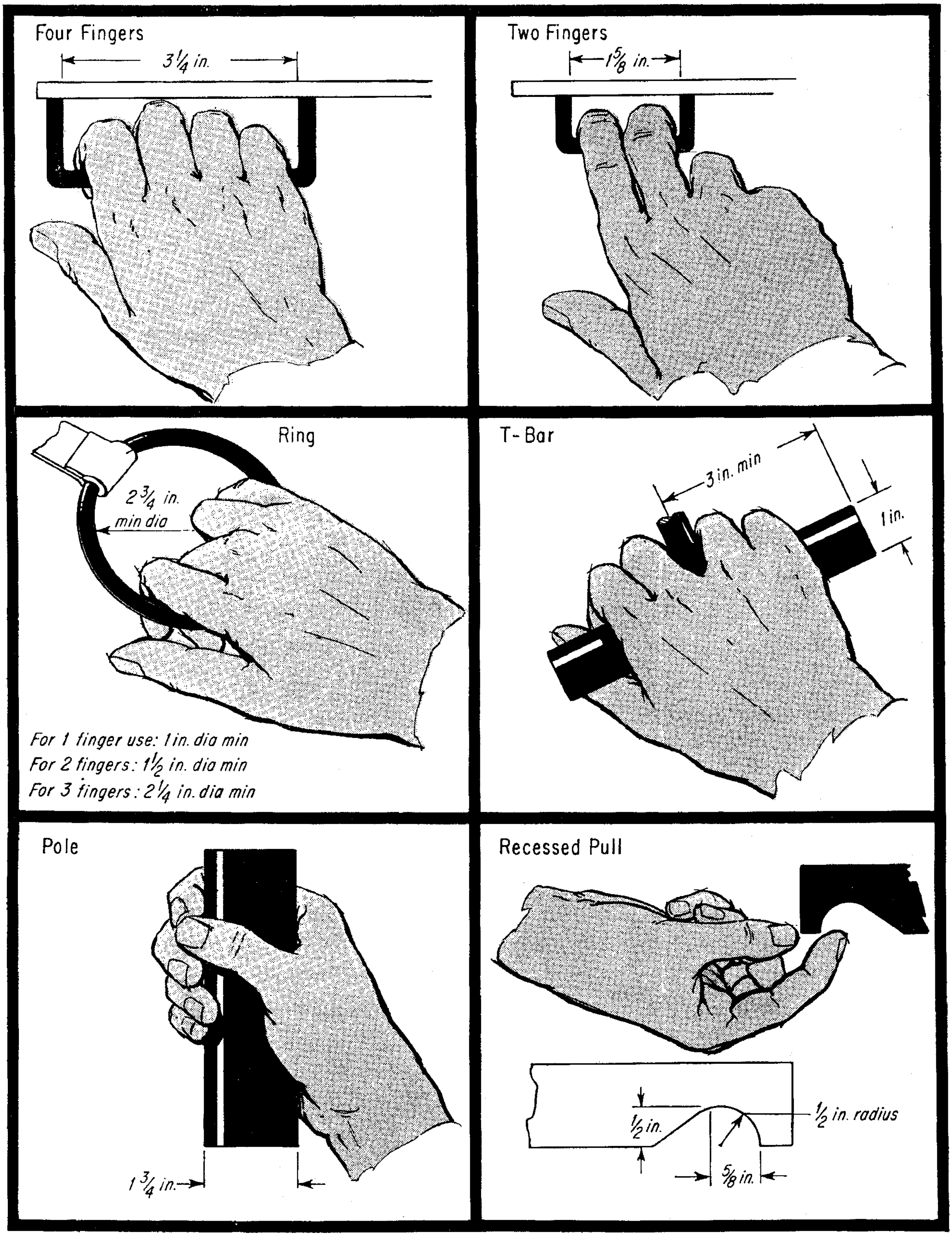
Four Fingers
3 1/4 in.
Two Fingers
1 5/8 in.
Ring
2 3/4 in. min dia
For 1 finger use: 1 in. dia min
For 2 fingers: 1 1/2 in. dia min
For 3 fingers: 2 1/4 in. dia min
T-Bar
3 in. min
1 in.
Pole
1 3/4 in.
Recessed Pull
1/2 in.
1/2 in. radius
5/8 in.

Thirteen Ways to Use Metallic Bellows

Sketches serve two purposes: 1) Illustrate unique as well as typical applications; 2) Show how the movement of bellows can be transferred to other elements.

E. Perry Cumming

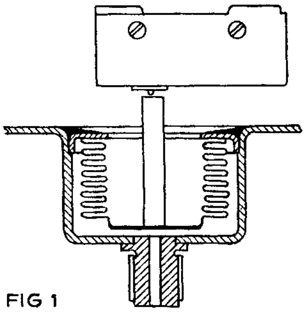

FIG 1

ACTUATE GAGES and switches. Pressures can be as high as 2,000 psi. Maximum value should exist when the bellows is near free-length.

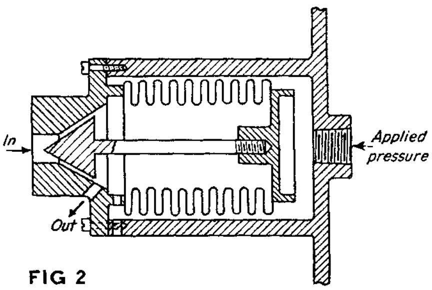

FIG 2

FLOW CONTROL. Variations in pressure adjust needle in flow valve. Also shows how bellows can be packless seals for valve stems and shafts.

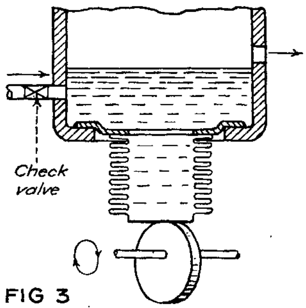

FIG 3

METERING DEVICE. Dispensing machines can use bellows as constant or variable displacement pump to measure and deliver predetermined amounts of liquids.

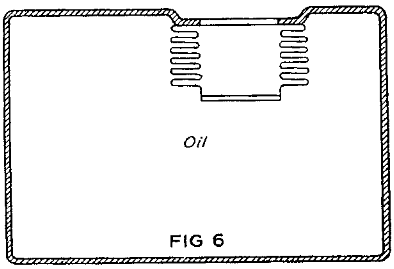

FIG 6

ABSORB EXPANSION OF FLUIDS OR GASES. Transformer (above) uses bellows to absorb increases in volume of oil caused by thermal expansion. Single controls of this type can operate from —70 to 250 F or from 0 to 650 F.

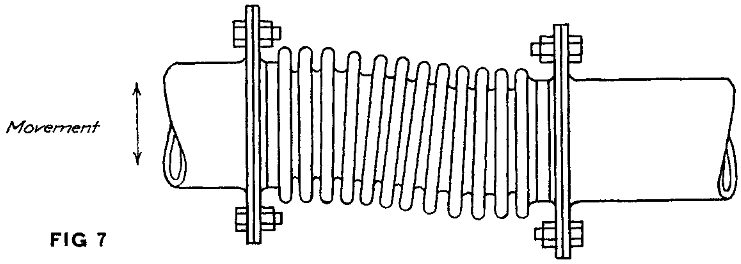

FIG 7

FLEXIBLE CONNECTOR. Suitable for wide range of applications from instruments to jet engines and large piping. Bellows absorb movement caused by thermal expansion, isolate vibration and noise as well as permit misalignment of mating elements. Wide variety of sizes and materials are now possible. Units are now in use from ¼ to 72 inches in diameter, made from such materials as brass, phosphor bronze, beryllium copper and stainless steel.

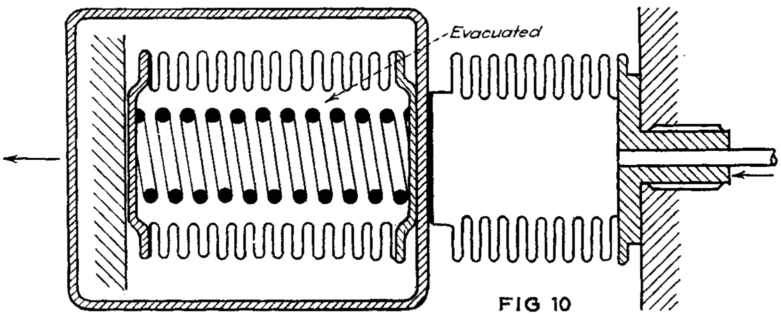

FIG 10

PRESSURE COMPENSATOR. Effect of ambient pressure can be eliminated in a pressure measuring system by matching the area of a pressure bellows with that of an aneroid and combining the two into a single assembly. Errors caused by ambient pressure can be held to a max of one percent. Present materials permit aneroid operation from —70 to 450 F.

FIG 11

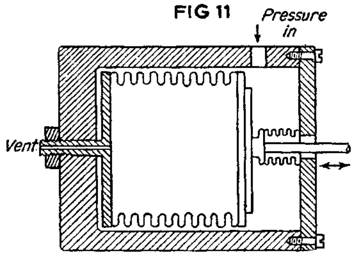

PRESSURE MOTOR. Similar to Fig. 2. Bellows used instead of piston and cylinder arrangement. Eliminates effects of leakage and friction. Long stroke can be provided with sensitive response.

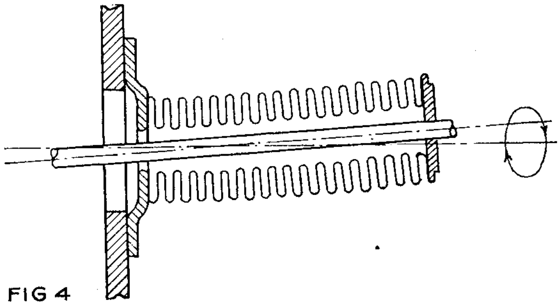

FIG 4

FLEXIBLE COUPLING. Bellows can transmit torque through oblique shafts with negligible amount of backlash or can be used to transmit circular motion through the wall of a sealed container as shown above.

FIG 5

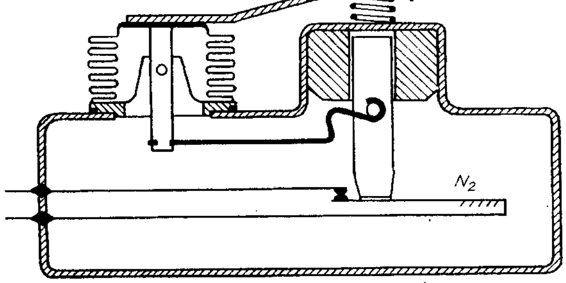

HERMETIC SWITCH. Bellows provide a gas tight flexible member through which motion can be transmitted into a sealed assembly. Flexibility and long life are important characteristics of these elements.

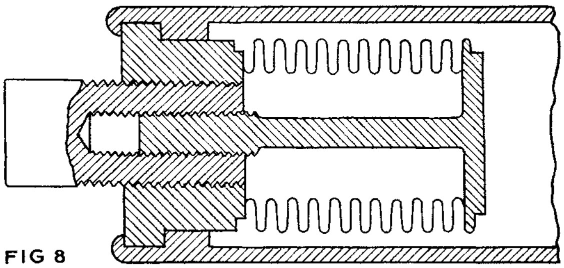

FIG 8

SEALED ADJUSTMENT. Accurately calibrated adjustments inside sealed instruments are possible by means of single or compound threads. To meet varied installation requirements, bellows are available with ends prepared for ring or disk end plates of standard or special design. These plates are fastened by brazing or welding techniques.

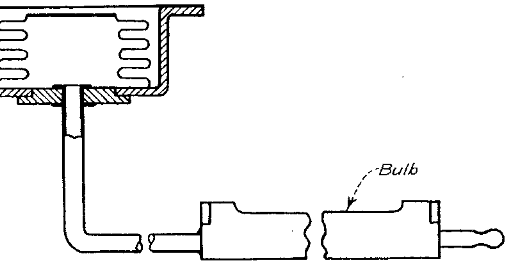

FIG 9

VAPOR PRESSURE THERMOSTAT. Small dia bellows offer large movement over a relatively small, adjustable temperature range. Can be filled so as to be unaffected by over-runs in temperature. Compensation for changes in ambient temperature is unnecessary whether this temperature is above or below the value selected for control purposes.

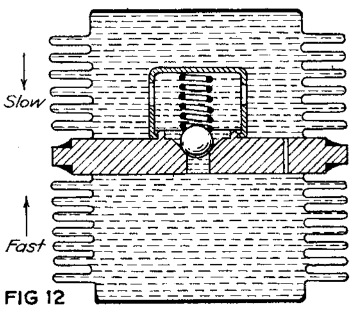

FIG 12

TIME DELAY MECHANISM. A check valve and proper size bleed hole between two liquid filled bellows allows fast motion in one direction and slow motion in the other direction.

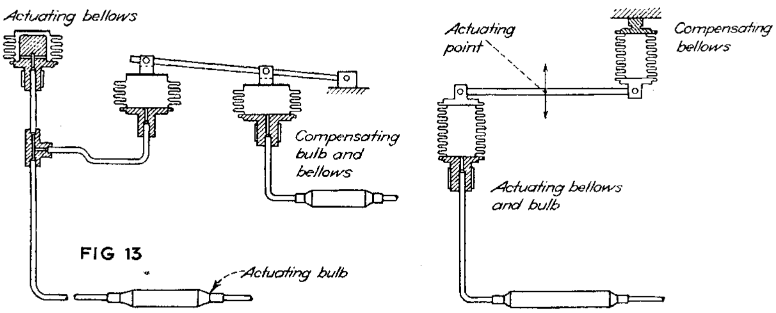

FIG 13

AMBIENT TEMPERATURE COMPENSATION. Two methods are shown. The left one uses two bellows in the actuating system. One is driven by the compensating assembly and correctly positions the actuating bellows as ambient temperature changes. The other method uses a floating lever whose mid-point is positioned by both the actuating and compensating bellows.

Frictional Supports for Adjustable Parts

L. Kasper

Frictional supports permitting relative longitudinal and rotational adjustment between a rod and a clamping member have wide application because of their simplicity of design and the ease and rapidity with which they can be adjusted. Possibilities of design are endless, as indicated by the accompanying group of designs. Illustrations include types having slight and strong resistance to friction, types in which the frictional resistance can be varied to suit conditions, types that have greater resistance in one direction than the other, and types that have positive detents for certain positions. The sketches are self-explanatory.

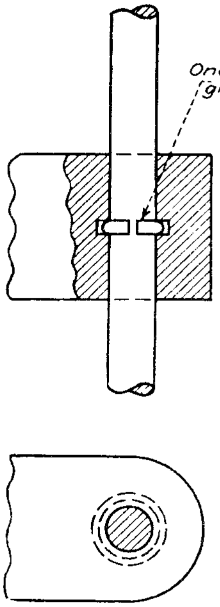

FIG. 1

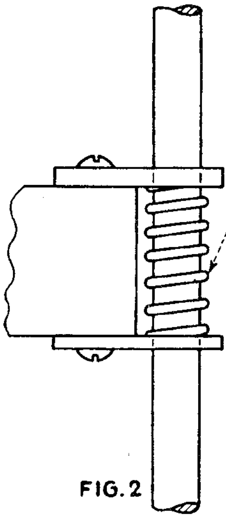

FIG. 2

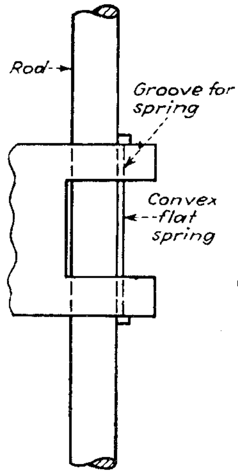

FIG. 3

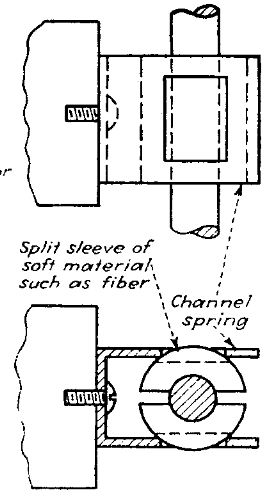

FIG. 4

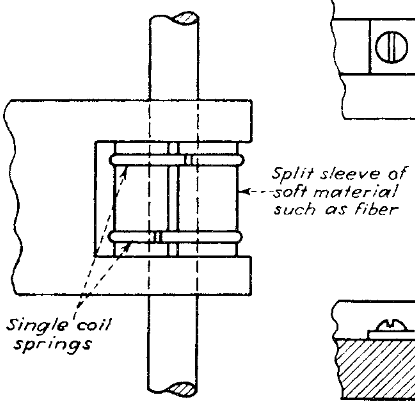

FIG. 5

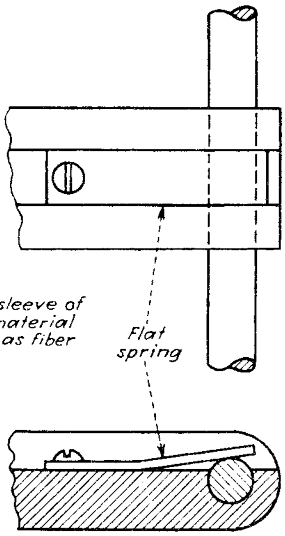

FIG. 6

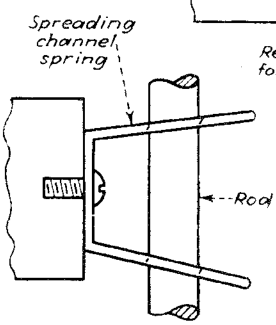

FIG. 7

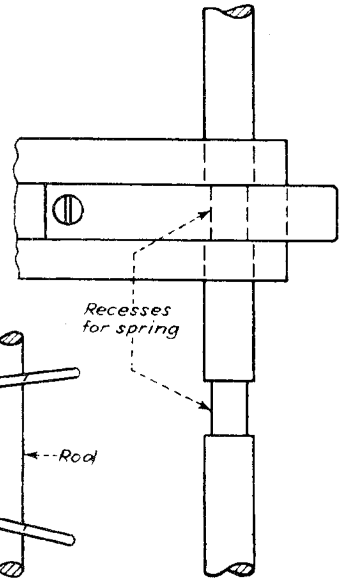

FIG. 8

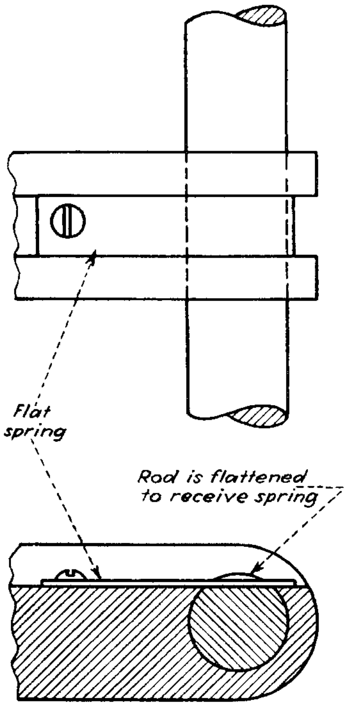

FIG. 9

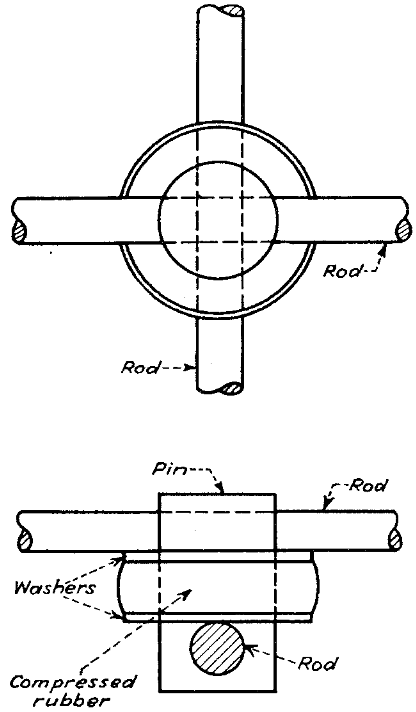

FIG. 10

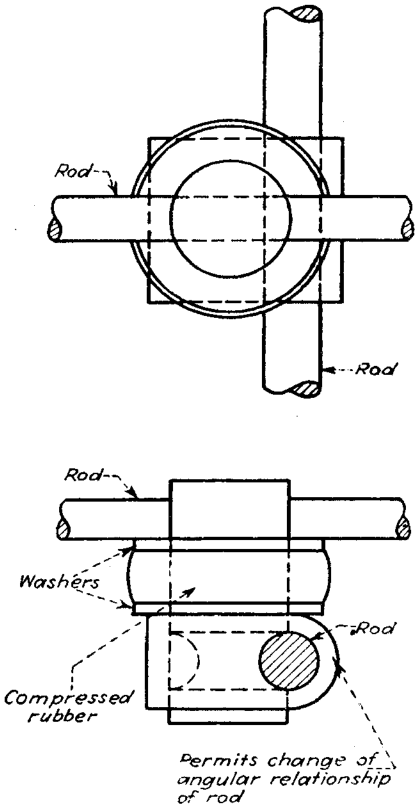

FIG. 11

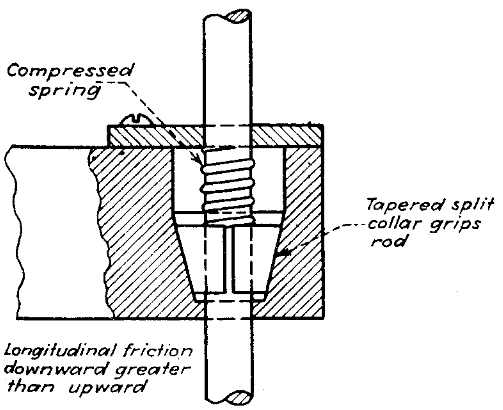

FIG. 12

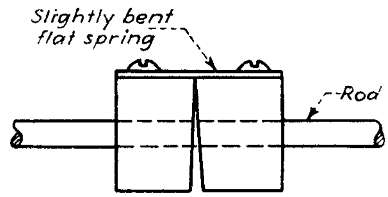

FIG. 13

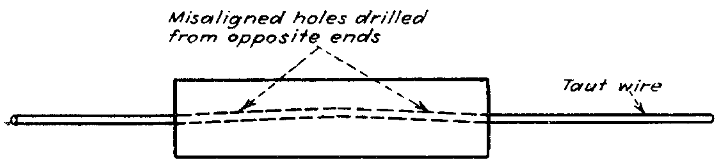

FIG. 14

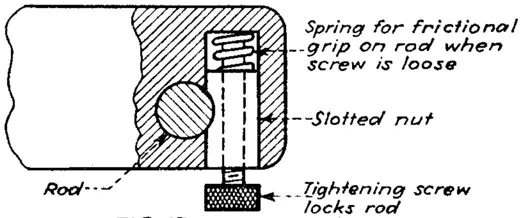

FIG. 15

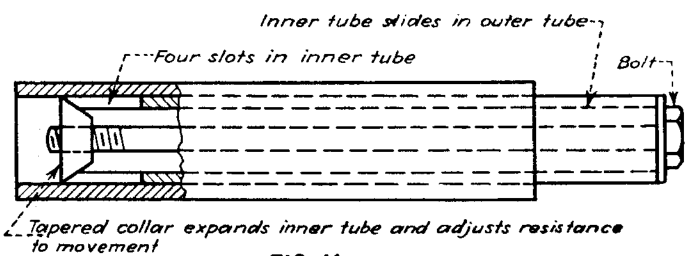

FIG. 16

Building Strength into Brackets

They must meet specific requirements–stability, light weight, and the like. Here's your guide.

S. Warren Kaye

For stability, a good bracket must be able to carry load in three directions at right angles to each other—vertical, fore and aft, and sideways. Besides being able to withstand regular acceleration and operating loads, it must often be rugged enough to avoid damage from handling and accidental loads—for example, if it is stepped on, or used as a handhold, as in aircraft and missiles.

Space Age requirements also point up the frequent need to minimize weight of brackets. One way to do this is to place the equipment they support as near as possible to suitable attachment points on the basic structure. (Sometimes, in fact, by a minor rearrangement, such as shifting a stiffener or frame, the equipment can be attached directly to the structure, and the bracket eliminated.)

Other general rules for designing brackets: Avoid tension loads on riveted joints, do not combine rivets and bolts in the same local area; avoid using aluminum bolts in tension wherever possible; in a rivet pattern, avoid smaller rivets in the outer row; and don't overload first rivet or first row of rivets.

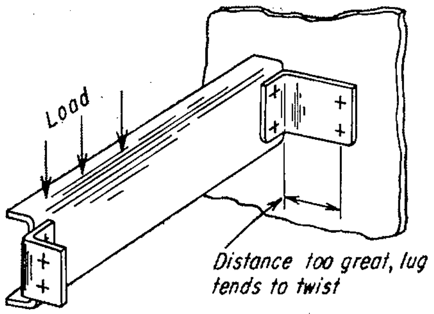

Poor design

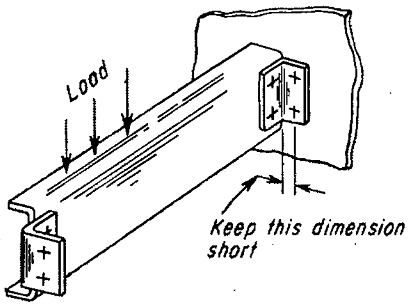

Improved design

1 MOUNTING LUGS should be either kept short or have rivet locations that reduce twisting.

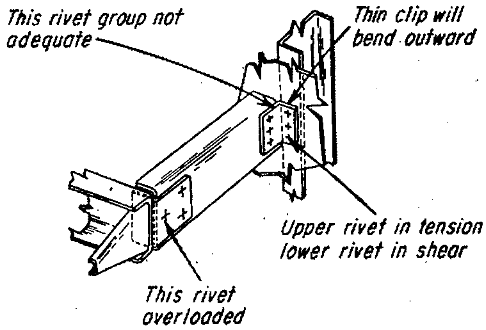

Poor design

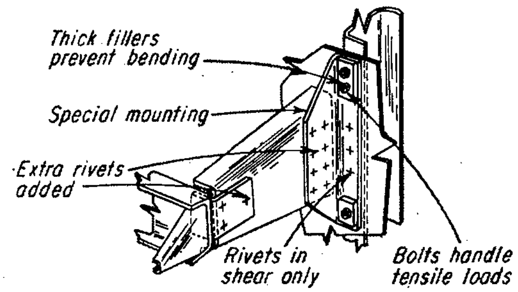

Improved design

2 SPECIAL MOUNTING is best for cantilever bracket where large moments cause high tensile stress at mounting. If possible, design a one-piece bracket.

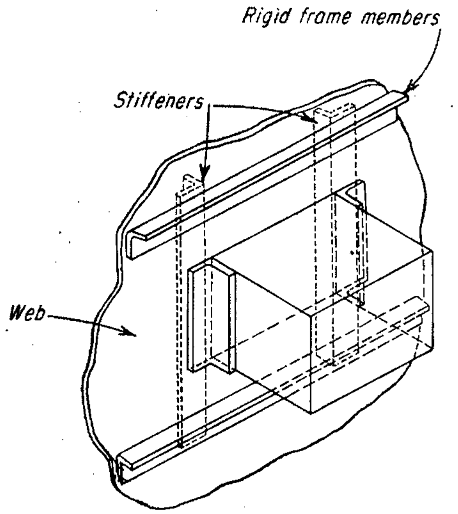

3 STIFFENERS carry moment loads to rigid frame, prevent unsupported web from "oilcanning."

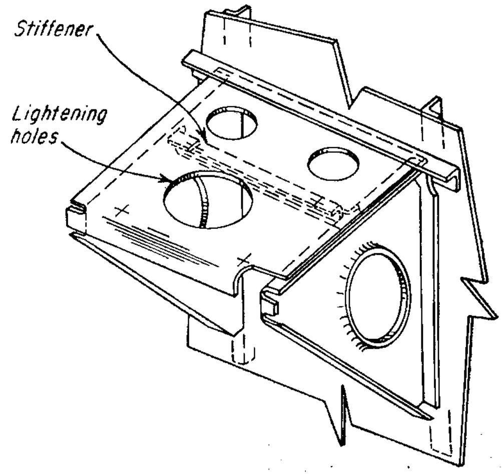

4 SHELF SHEET can be thinner and lighter if stiffeners are provided. Lightening holes are flanged where possible.

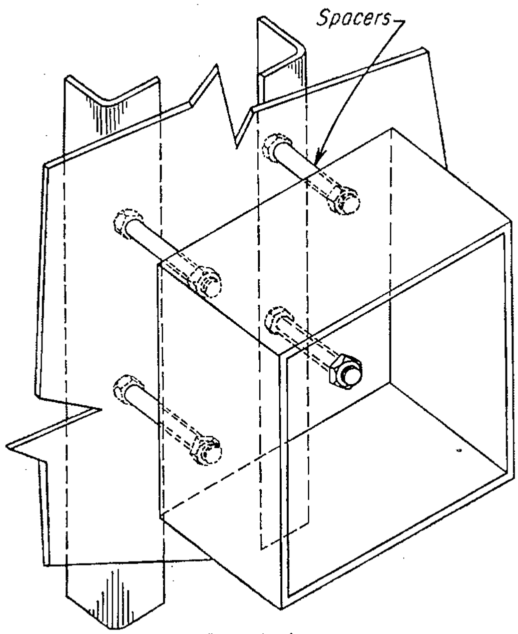

Poor design

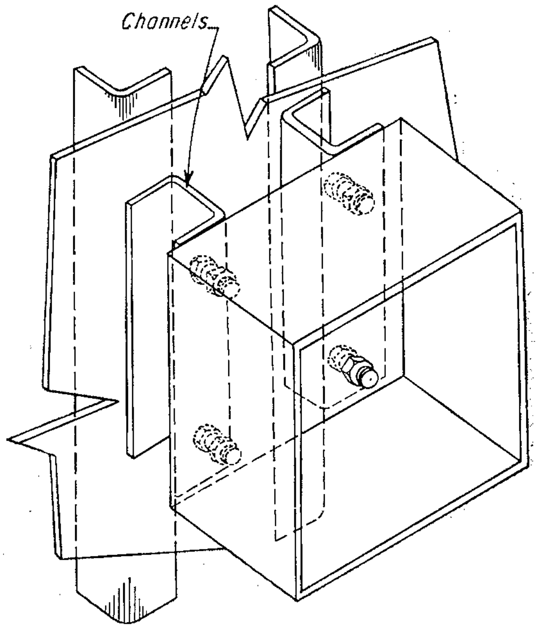

Improved design

5 CHANNELS are best for spacing mounted equipment from attachment wall. Channel thickness must be sufficient to withstand bending from side loads. If necessary, extra stiffening should be provided.

Adhesive Applicators for High-Speed Machines

THE METHODS OF APPLYING LIQUID ADHESIVES that are illustrated here include rotary applicators on movable axes and otherwise movable between adhesive pick-up position and applying position, endless belt applicators, applicators in the form of moving daubers, plates, and the like, reciprocating dies exuding measured quantities of cement, and spray nozzles. All of these mechanisms are used or are applicable on production machines such as for making pasteboard boxes or cartons, pasting labels or envelopes, and making shoes or other products involving the use of liquid adhesives.

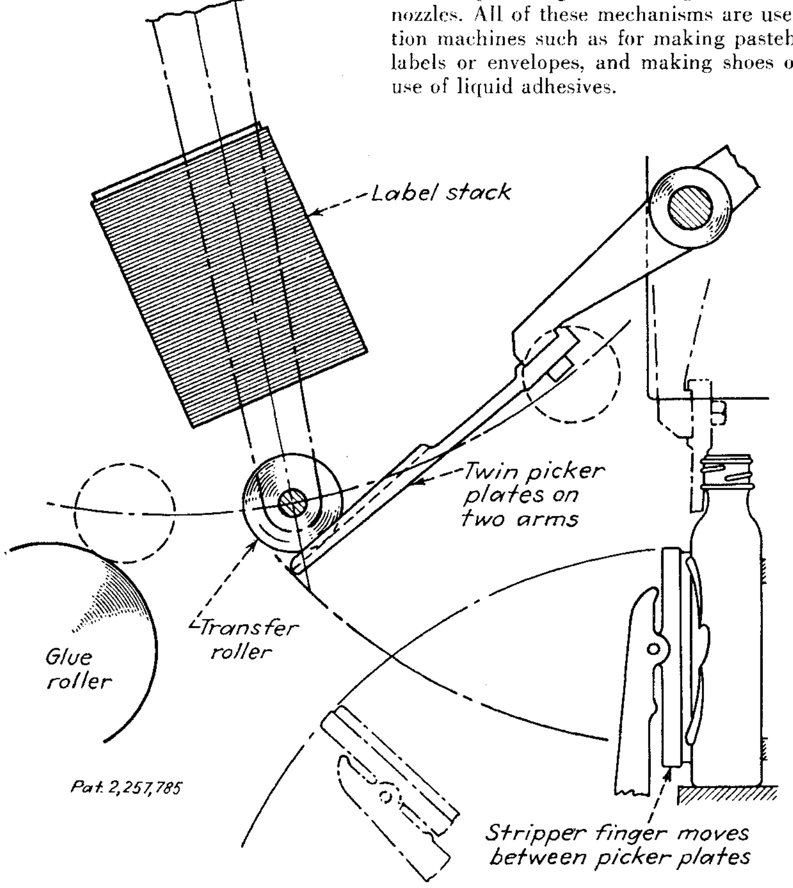

FIG. 1 – *Bottom label is spread with glue by two abutting glue-coated picker plates, which separate during contact with label stack, then carry label to bottle*

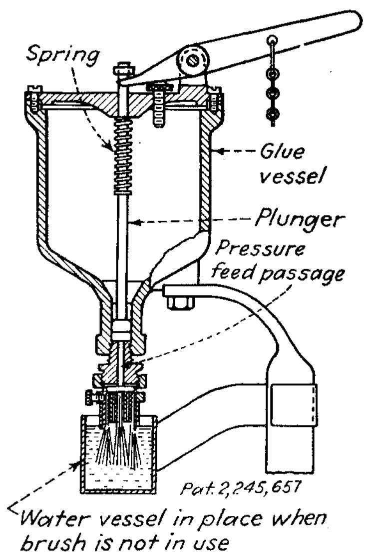

FIG. 3–*Brush applicator is fed through passages between bristle tufts by spring operated plunger*

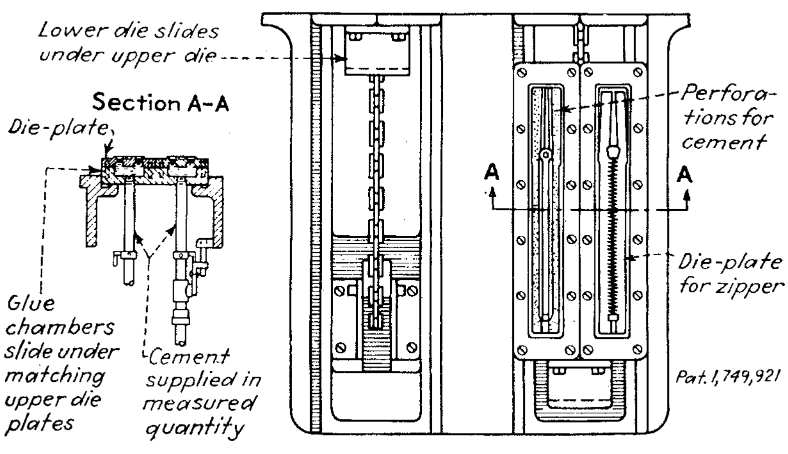

FIG. 2 – *Measured quantities of cement are forced through perforations in specially designed upper and lower die plates, which are closed hydraulically over zippers. Lower die only is shown*

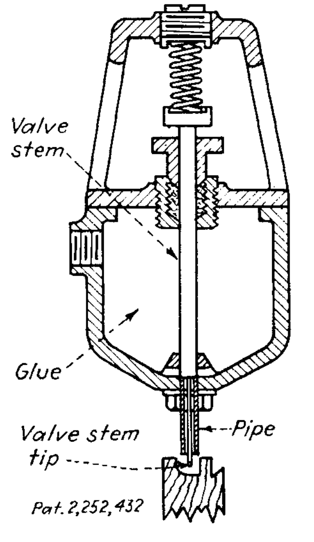

FIG. 4–*Shoulder on valve stem in glue chamber retains glue until pressure on tip opens bottom valve*

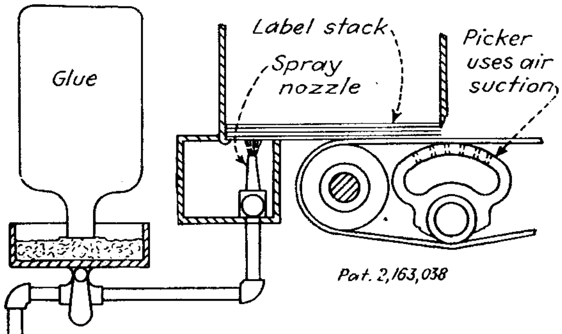

FIG. 5 – *Glue is applied to envelopes by means of spray nozzle*

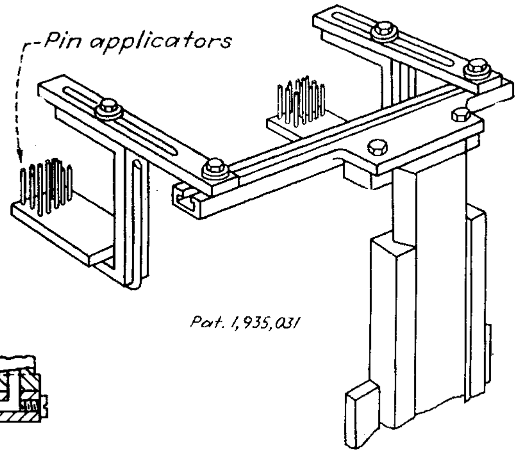

FIG. 8 – *Pin applicators reciprocate vertically, first immersing in glue, then contacting underside of carton flaps in desired pattern*

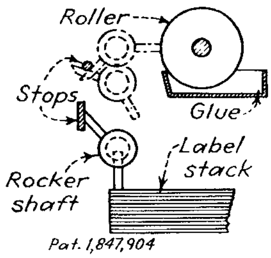

FIG. 6 – *Rocker shaft on rack, which is moved vertically by sector gear, carries glue on contact bar from roll to label stack*

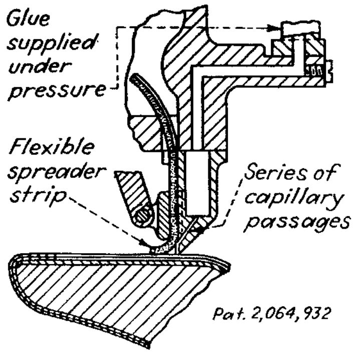

FIG. 7 – *Glue is extruded through nozzle on work*

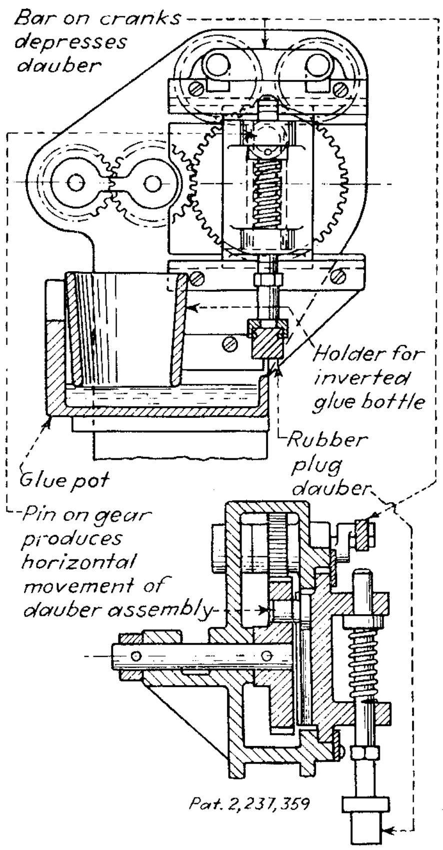

FIG. 10 – *Dauber assembly is moved horizontally between glue pot and work by eccentric pin on gear. Vertical movements are produced by crank operated bar over dauber shaft*

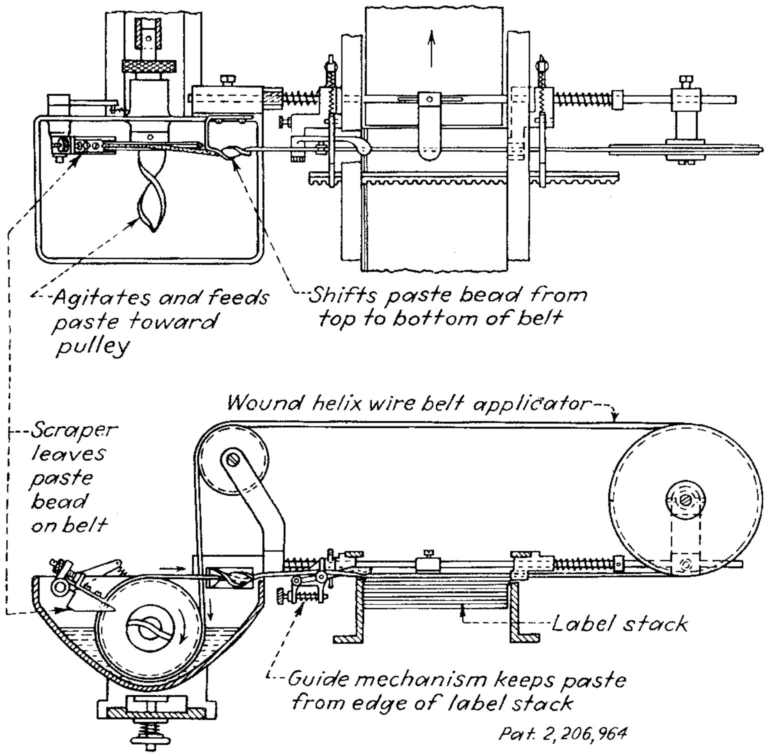

FIG. 9 – *Paste belt applicator passes around pulley in pastepot and slides over label stack*

7 Basic Hoppers for Parts

Hoppers, feeding single parts to an assembly station, speed up many operations. Reviewed here are some devices that may not be familiar to all design engineers.

Peter C. Noy

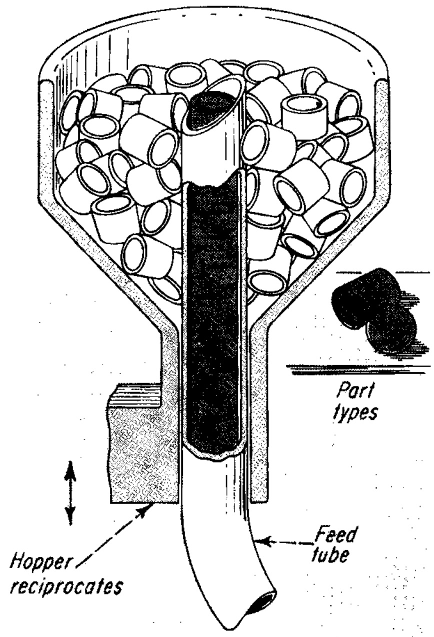

1

Reciprocating feed . . .

for spheres or short cylinders is perhaps the simplest feed mechanism. Either the hopper or the tube reciprocates. The hopper must be be kept topped-up with parts unless the tube can be adjusted to the parts level.

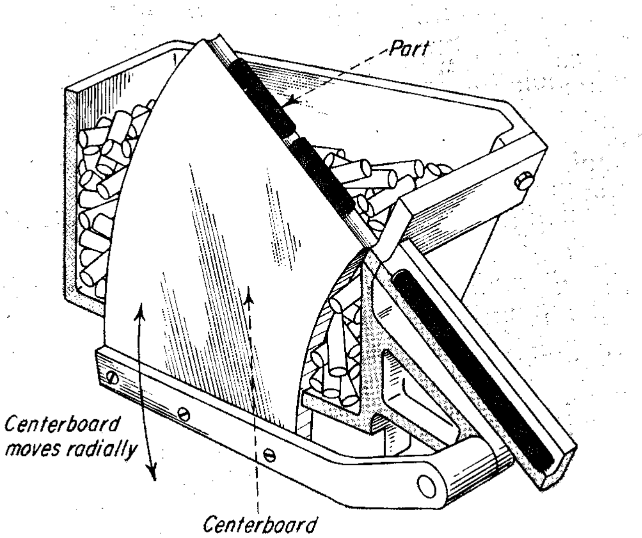

2

Centerboard selector . . .

is similar to reciprocating feed. The centerboard top can be milled to various section shapes to pick up moderately complex parts. It works best, however, with cylinders too long to be fed with the reciprocating hopper. Feed can be continuous or as required.

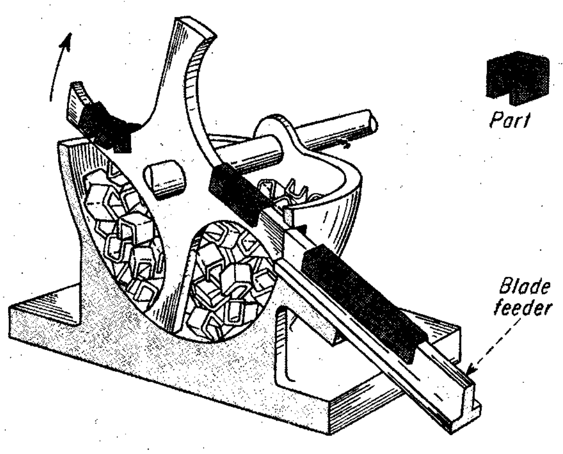

3

Rotary centerblades . . .

catch small U-shaped parts effectively if their legs are not too long. Parts must also be resilient enough to resist permanent set from displacement forces as blades cut through pile of parts. Feed is usually continuous.

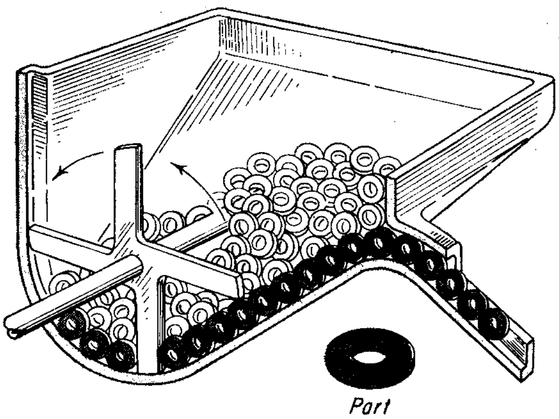

4

Paddle wheel . . .

is effective for disk-shaped parts if they are stable enough. Thin, weak parts would bend and jam. Such designs must be avoided if possible—especially if automatic assembly methods will be employed. *(See pp. 150, 151.)*

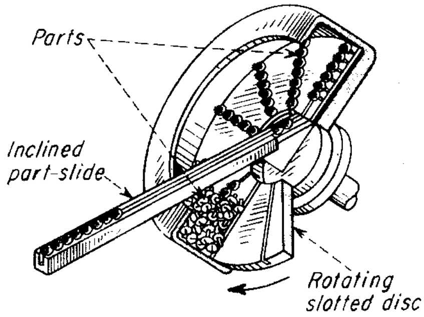

5

Rotary screw-feed . . .

handles screws, headed pins, shouldered shafts and similar parts. In most hopper feeds, random selection of chance-orientated parts necessitates further machinery if parts must be fed in only one specific position. Here, however, all screws are fed in the same orientation (except for slot position) without separate machinery.

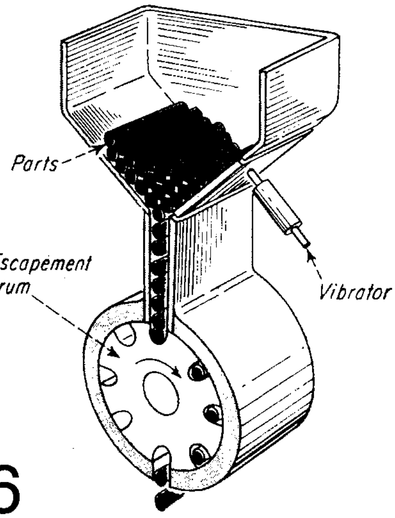

6

Long-cylinder feeder . . .

is a variation of the first two hoppers. If the cylinders have similar ends, the part can be fed without pre-positioning, thus assisting automatic assembly. *(See pp. 150, 151.)* A cylinder with differently shaped ends requires extra machinery to orientate the part before it can be assembled.

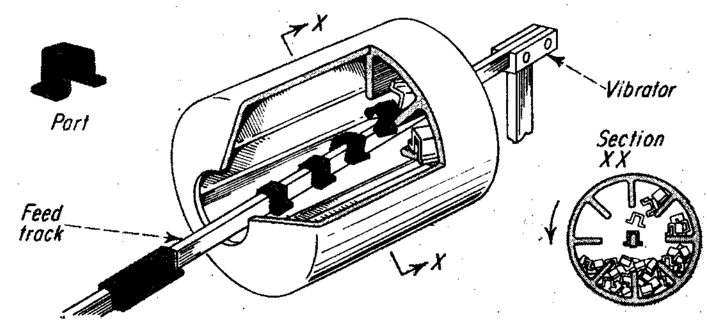

7

Barrel hopper . . .

is most useful if parts tend to tangle. The parts drop free of the rotating-barrel sides. By chance selection some of them fall onto the vibrating rack and are fed out of the barrel. Parts should be stiff enough to resist excessive bending because the tumbling action can subject parts to relatively severe loads. The tumbling sometimes helps to remove sharp burrs.

SECTION 22

MECHANISMS

Machinery Mechanisms

Selected from industrial and automatic machinery, many of these 41 mechanisms have never appeared in American literature. A diverse grouping—with the very well-known omitted.

Professor Preben W. Jensen

REVERSING MECHANISMS

Double-link reverser

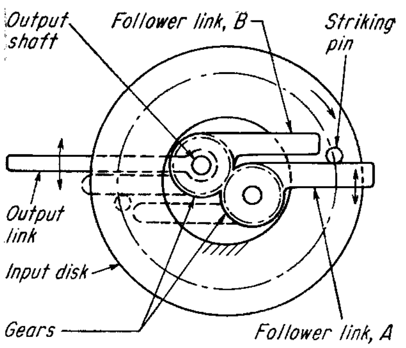

Automatically reverses the output drive every 180-deg rotation of the input. Input disk has press-fit pin which strikes link A to drive it clockwise. Link A in turn drives link B counterclockwise by means of their respective gear segments (or gears pinned to the links). The output shaft and the output link (which may be the working member) are connected to link B.

After approximately 180 deg of rotation, the pin slides past link A to strike link B coming to meet it—and thus reverses the direction of link B (and of the output). Then after another 180-deg rotation the pin slips past link B to strike link A and start the cycle over again.

Toggle-link reverser

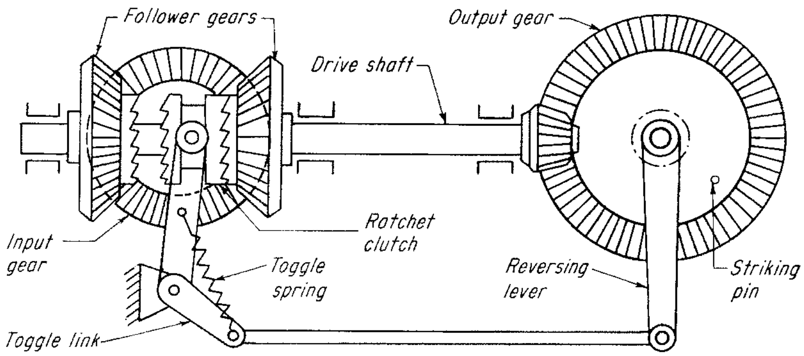

This mechanism also employs a striking pin—but in this case the pin is on the output member. The input bevel gear drives two follower bevels which are free to rotate on their common shaft. The ratchet clutch, however, is spline-connected to the shaft—although free to slide linearly. As shown, it is the right follower gear that is locked to the drive shaft. Hence the output gear rotates clockwise, until the pin strikes the reversing level to shift the toggle to the left. Once past its center, the toggle spring snaps the ratchet to the left to engage the left follower gear. This instantly reverses the output which now rotates counterclockwise until the pin again strikes the reversing level. Thus the mechanism reverses itself every 360-deg rotation of the input.

Modified-Watt's reverser

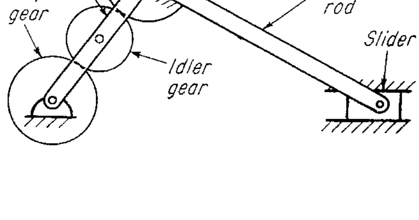

This is actually a modification of the well-known Watt crank mechanism. The input crank causes the planet gear to revolve around the output gear. But because the planet gear is fixed to the connecting rod it causes the output gear to continually reverse itself. If the radii of the two gears are equal then each full rotation of the input link will cause the output gear to oscillate through same angle as rod.

INTERMITTENT MECHANISMS

Rapid-transfer geneva

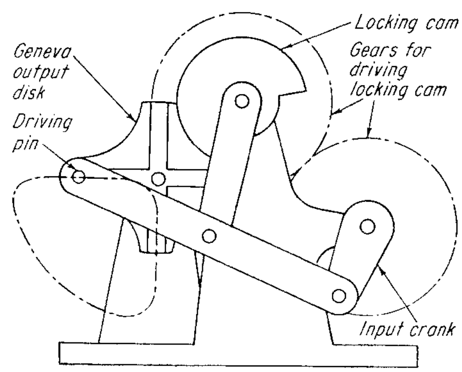

The coupler point at the extension of the connecting link of the 4-bar mechanism describes a curve with two approximately straight lines, 90 deg apart. This provides a good entry situation in that there is no motion in the geneva while the driving pin moves deeply into the slot — then there is an extremely rapid index. A locking cam which prevents the geneva from shifting when it is not indexing, is connected to the input shaft through gears.

Long-dwell geneva

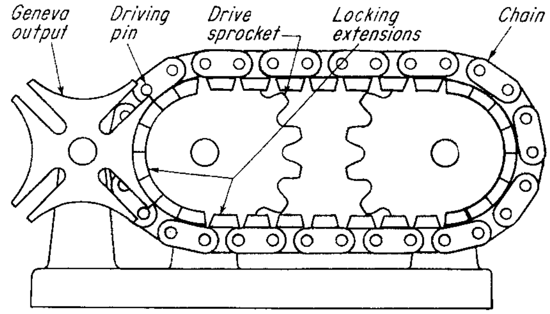

This arrangement employs a chain with an extended pin in combination with a standard geneva. This permits a long dwell between each 90-deg shift in the position of the geneva. The spacing between the sprockets determines the length of dwell. Note that some of the links have special extensions to lock the geneva in place between stations.

Modified motion geneva

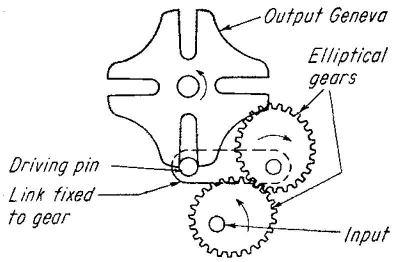

With a normal geneva drive the input link rotates at constant velocity, which restricts flexibility in design. That is, for given dimensions and number of stations the dwell period is determined by the speed of the input shaft. Use of elliptical gears produces a varying crank rotation which permits either extending or reducing the dwell period.

DWELL MECHANISMS

Epicyclic dwell mechanism

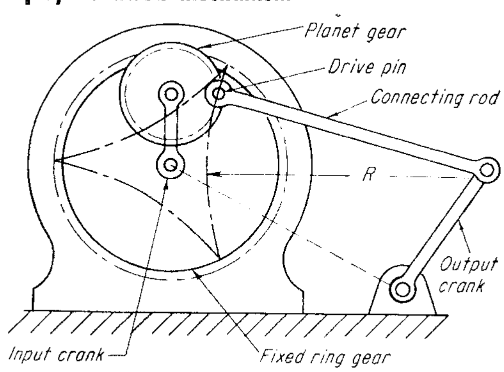

Here the output crank pulsates back and forth with a long dwell at the extreme right position. Input is to the planet gear by means of the rotating crank. The pin on the gear traces the epicyclic three-lobe curve shown. The right portion of the curve is almost a circular arc of radius R. If the connecting rod is made equal to R, the output crank comes virtually to a standstill during a third of the total rotation of the input. The crank then reverses, comes to a stop at left position, reverses, and repeats dwell.

Cam-worm dwell mechanism

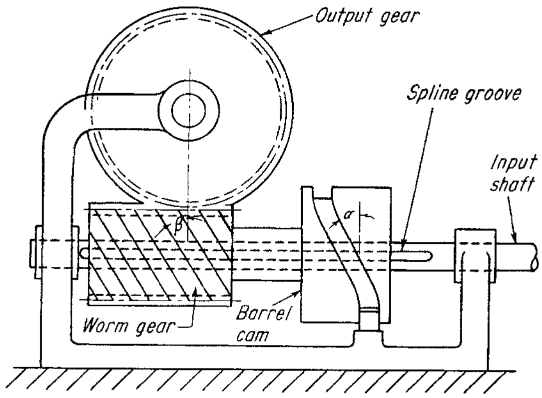

Without the barrel cam, the input shaft would drive the output gear by means of the worm gear at constant speed. The worm and the barrel cam, however, are permitted to slide linearly on the input shaft. Rotation of the input shaft now causes the worm gear to be cammed back and forth, thus adding or subtracting motion to the output. If barrel cam angle α is equal to the worm angle β, the output comes to a stop during the limits of rotation illustrated, then speeds up to make up for lost time.

Cam-helical dwell mechanism

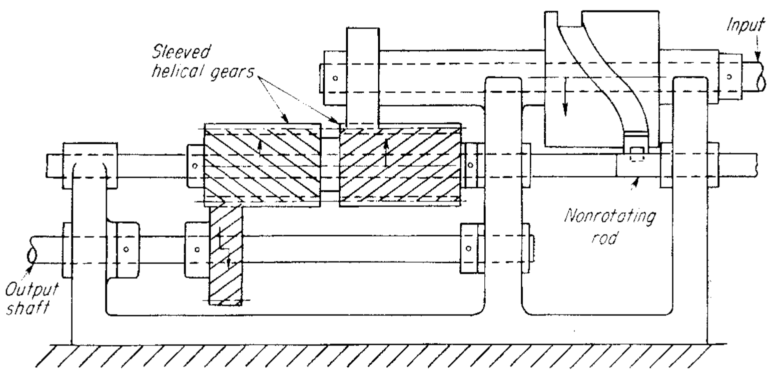

When one helical gear is shifted linearly (but prevented from rotating) it will impart rotary motion to the mating gear because of the helix angle. This principle is used in the mechanism illustrated. Rotation of the input shaft causes the intermediate shaft to shift to the left, which in turn adds or subtracts from the rotation of the output shaft.

Cam-roller dwell mechanism

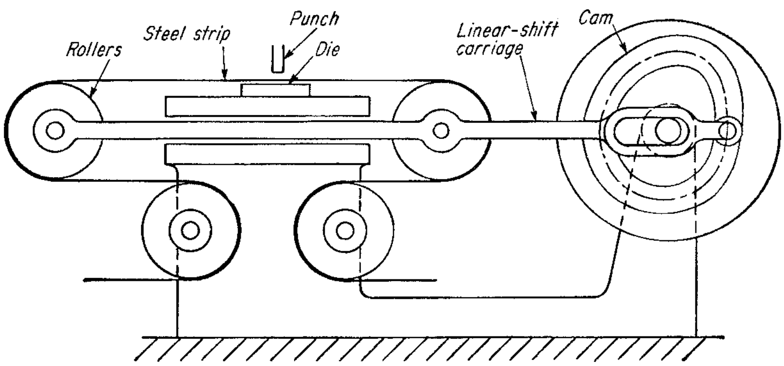

A steel strip is fed at constant linear velocity. But at the die station (illustrated), it is desired to stop the strip so that the punching operation can be performed. The strip passes over movable rollers which, when shifted to the right, cause the strip to move to the right. Since the strip is normally fed to the left, proper design of the cam can nullify the linear feed rates so that the strip stops, and then speeds to catch up to the normal rate.

Double-crank dwell mechanism

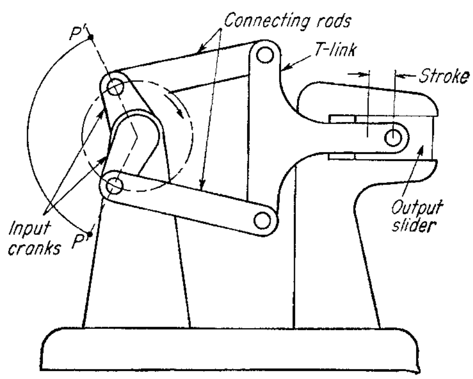

Both cranks are connected to a common shaft which also acts as the input shaft. Thus they always remain a constant distance apart from each other. There are only two frame points—the center of the input shaft and the guide for the output slider. As the output slider reaches the end of its stroke (to the right), it remains practically at standstill while one crank rotates through angle *PP'*. Used in textile machinery for cutting.

6-Bar dwell mechanism

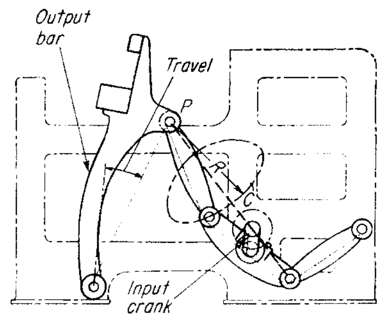

Rotation of the input crank causes the output bar to oscillate with a long dwell at the extreme right position. This occurs because point *C* describes a curve that is approximately a circular arc (from *C* to *C'*) with center at *P*. The output is practically stationary during that portion of curve.

Three-gear drive

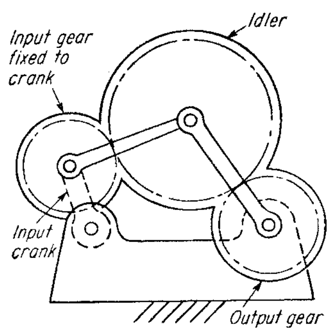

This is actually a four-bar linkage combined with three gears. As the input crank rotates it takes with it the input gear which drives the output gear by means of the idler. Various output motions are possible. Depending on proportions of the gears, the output gear can pulsate, or come to a short dwell—or even reverse briefly.

ADJUSTABLE-OUTPUT MECHANISMS

Linkage motion adjuster

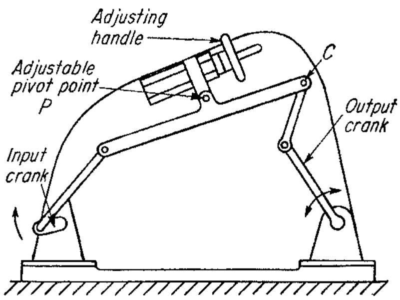

Here the motion and timing of the output link can be varied *during operation* by shifting the pivot point of the intermediate link of the 6-bar linkage illustrated. Rotation of the input crank causes point *C* to oscillate around the pivot point *P*. This in turn imparts an oscillating motion to the output crank. Shifting of point *P* is accomplished by a screw device.

Cam motion adjuster

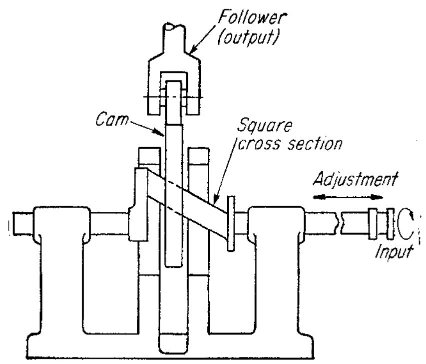

The output motion of the cam follower is varied by linearly shifting the input shaft to the right or left during operation. The cam has a square hole which fits over the square cross section of the crank shaft. Rotation of the input shaft causes eccentric motion in the cam. Shifting the input shaft to the right, for instance, causes the cam to move radially outward, thus increasing the stroke of the follower.

Double-cam mechanism

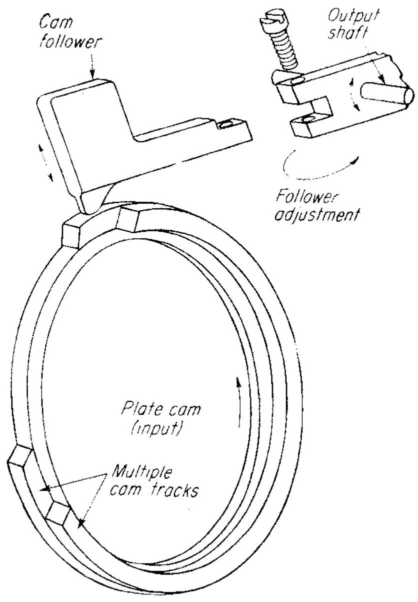

This is a simple but effective technique for changing the timing of a cam. The follower can be adjusted in the horizontal plane but is restricted in the vertical plane. The plate cam contains two or more cam tracks.

Valve stroke adjuster

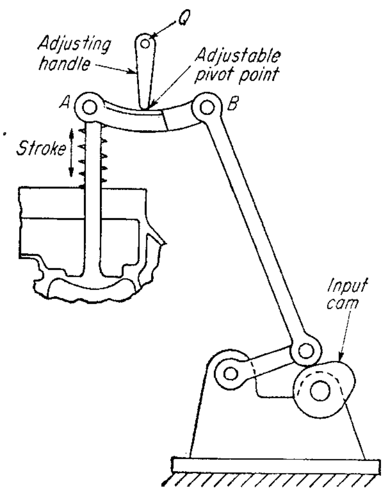

This mechanism adjusts the stroke of valves of combustion-engines. One link has a curved surface and pivots around an adjustable pivot point. Rotating the adjusting link changes the proportion of strokes of points *A* and *B* and hence of the valve. The center of curvature of the curve link is at point *Q*.

3-D mechanism

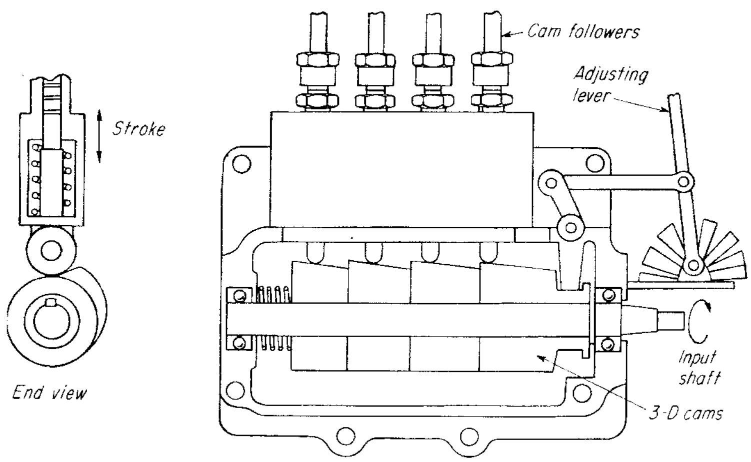

Output motions of four followers are varied during the rotation by shifting the quadruple 3-D cam to the right or left. Linear shift is made by means of adjustment lever which can be released in any of the 6 positions.

Piston-stroke adjuster

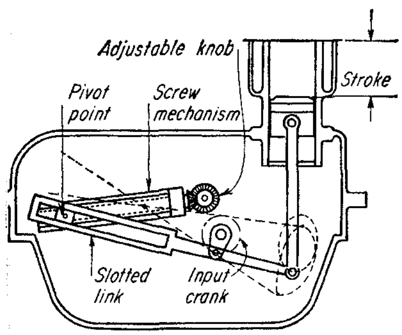

The input crank oscillates the slotted link to drive the piston up and down. The position of the pivot point can be adjusted by means of the screw mechanism even while the piston is under full load.

Shaft synchronizer

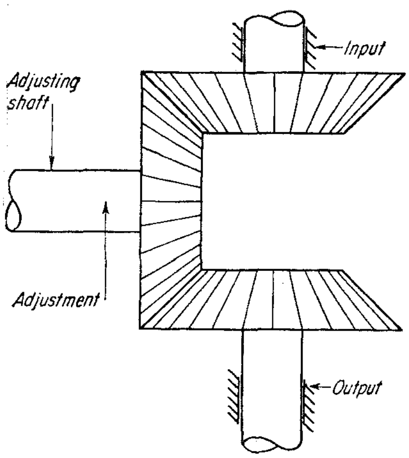

Actual position of the adjusting shaft is normally kept constant. The input then drives the output by means of the bevel gears. Rotating the adjusting shaft in a plane at right angle to the input-output line changes the relative radial position of the input and output shafts, used for introducing a torque into the system while running, synchronizing the input and output shafts, or changing the timing of a cam on the output shaft.

Eccentric pivot point

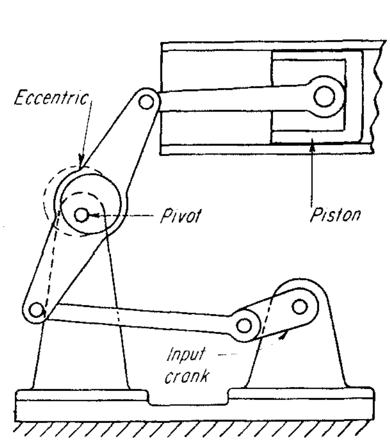

Rotation of the input crank reciprocates the piston. The stroke depends on position of the pivot point which is easily adjusted, even during rotation, by rotating the eccentric shaft.

FORCE AND STROKE MULTIPLIERS

Typewriter drive

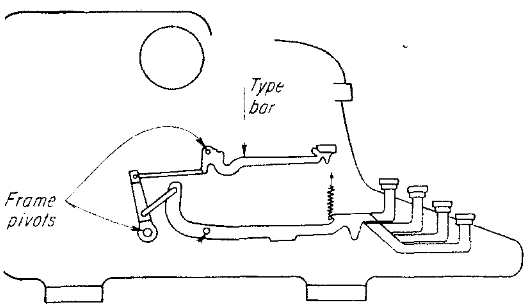

Multiplies the finger force in a typewriter, thus producing a strong hammer action at the roller from a light touch. There are three pivot points attached to the frame. Arrangement of the links is such that the type bar can move in free flight after a key has been struck. The mechanism illustrated is actually two four-bar linkages in series. In certain typewriters, as many as four 4-bar linkages are used in a series.

Double-toggle puncher

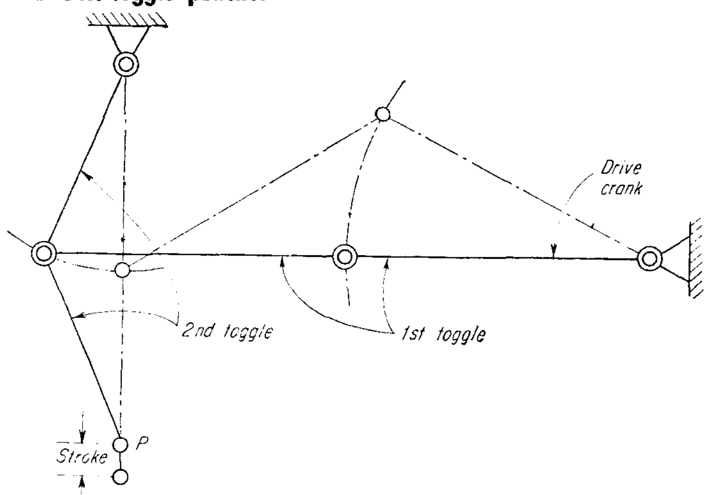

The first toggle keeps point *P* in the raised position even though its weight may be exerting a strong downward force (as in a heavy punch weight). When the drive crank rotates clockwise (driven, say, by a reciprocating mechanism), the second toggle begins to straighten to create a strong punching force.

Pulley drive

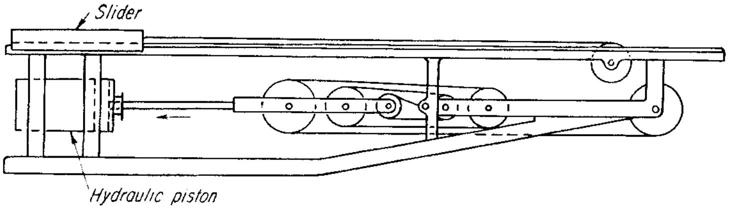

A simple arrangement which multiplies the stroke of a hydraulic piston, causing the slider to propel rapidly to the right for catapulting.

ANGLE MULTIPLIERS

Wide angle oscillator

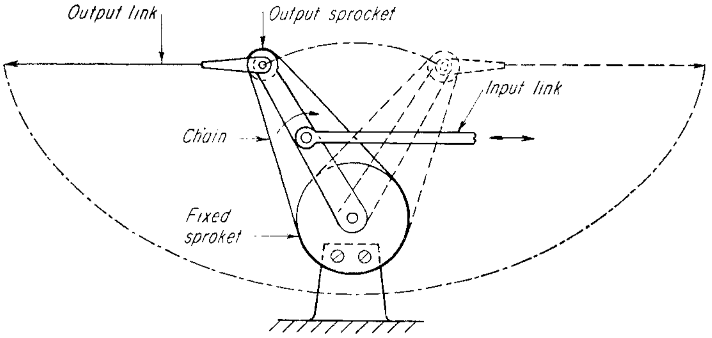

Motion of the input linkage is converted into a wide angle oscillation by means of the two sprockets and chain in the diagram illustrated. An oscillation of 60 deg is converted into 180-deg oscillation.

Gear-sector drive

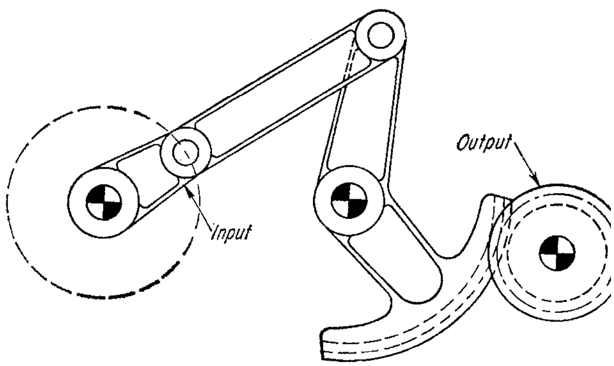

This is actually a four-bar linkage combined with a set of gears. A four-bar linkage usually can get no more than about 120-deg maximum oscillation. The gear segments multiply the oscillation in inverse proportion to the radii of the gears. For the proportions shown, the oscillation is boosted 2½ times.

Angle-doubling drive

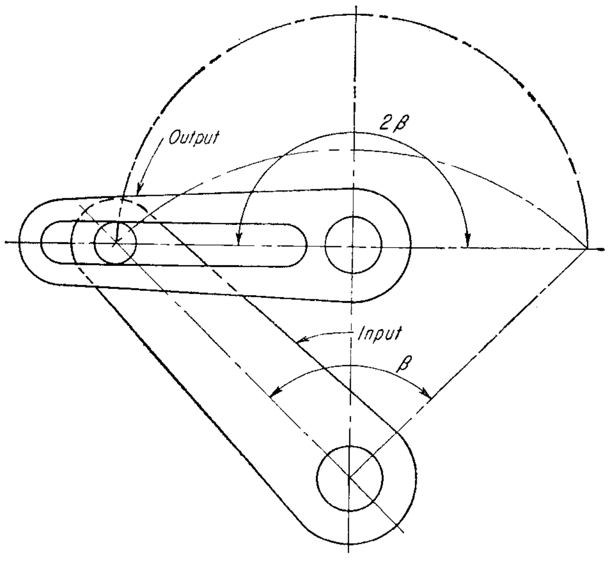

Frequently it is desired to enlarge the oscillating motion β of one machine member into an output oscillation of, say, 2β. If gears are employed, the direction of rotation cannot be the same unless an idler gear is used, in which case the centers of the intput and output shafts cannot be too close. Rotating the input link clockwise causes the output to also follow in a clockwise direction. For a particular set of link proportions, distance between the shafts determines the gain in angle multiplication.

Gear-rack drive

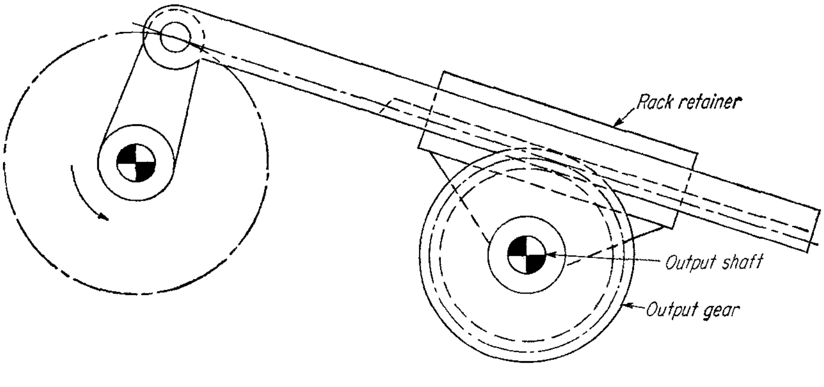

This mechanism is frequently employed to convert the motion of an input crank into a much larger rotation of the output (say, 30 to 360 deg). The crank drives the slider and gear rack, which in turn rotates the output gear.

Chain drive

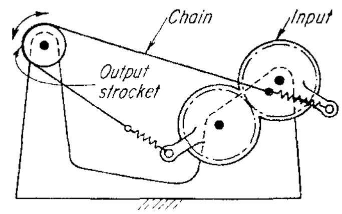

Springs and chains are attached to geared cranks to operate a sprocket output. Depending on the gear ratio, the output will produce a specified oscillation, say two revolutions of output in each direction for each 360 deg of input.

Linkage-train drive

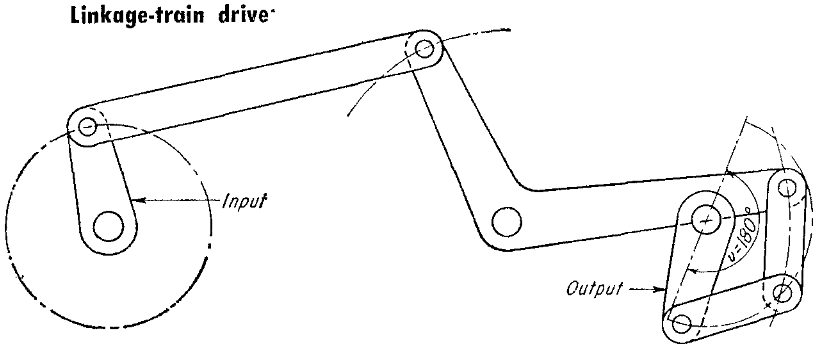

Arranging linkages in series can increase the angle of oscillation. In the case illustrated the oscillating motion of the L-shaped rocker is the input for the second linkage. Final oscillation is 180 deg.

ROTARY TO LINEAR-MOTION MECHANISMS

Linear reciprocator

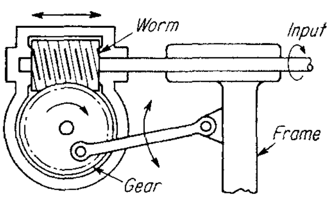

The objective here is to convert a rotary motion into a reciprocating motion that is *in line* with the input shaft. Rotation of the shaft drives the worm gear which is attached to the machine frame by means of a rod. Thus input rotation causes the worm gear to draw itself (and the worm) to the right—thus providing a back and forth motion. Employed in connection with a color-transfer cylinder in printing machines.

Disk and roller drive

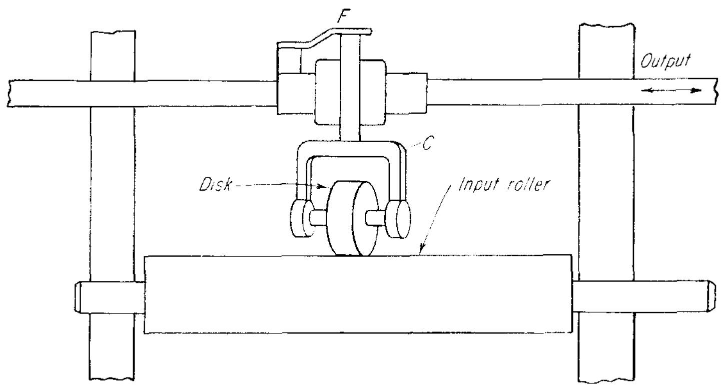

Here a hardened disk, riding at an angle to an input roller, transforms the rotary motion into linear motion *parallel to the axis of the input*. The roller is pressed against the input shaft with the help of a flat spring, *F*. Feed rate is easily varied by changing the angle of the disk. Arrangement can produce an extremely slow feed with a built-in safety factor in case of possible jamming.

Bearings and roller drive

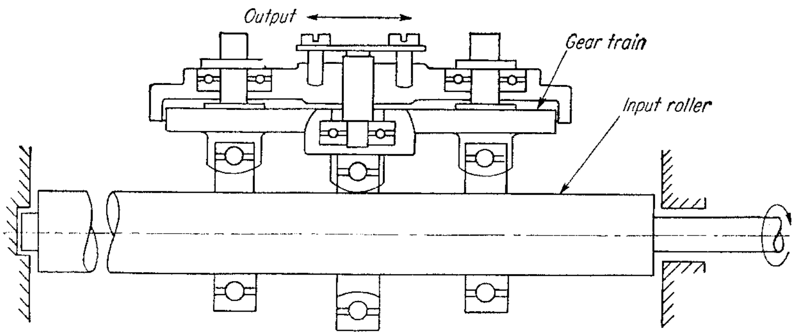

Similar to the previous one, this arrangement avoids large Hertzian stresses between disk and roller by employing three ball bearings in place of the single disk. The inner races of the bearings make contact on one side or the other. Hence a gearing arrangement is required to alternate the angle of the bearings. This arrangement also reduces the bending moment on the shaft.

Reciprocating space crank

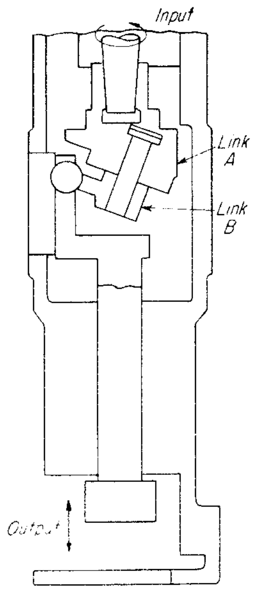

Rotary input causes the bottom surface of link *A* to wobble in reference to the center line. Link *B* is free of link *A* but restrained from rotating by the slot. This causes the output member to reciprocate linearly. Employed for filing machine.

Sinusoidal reciprocator

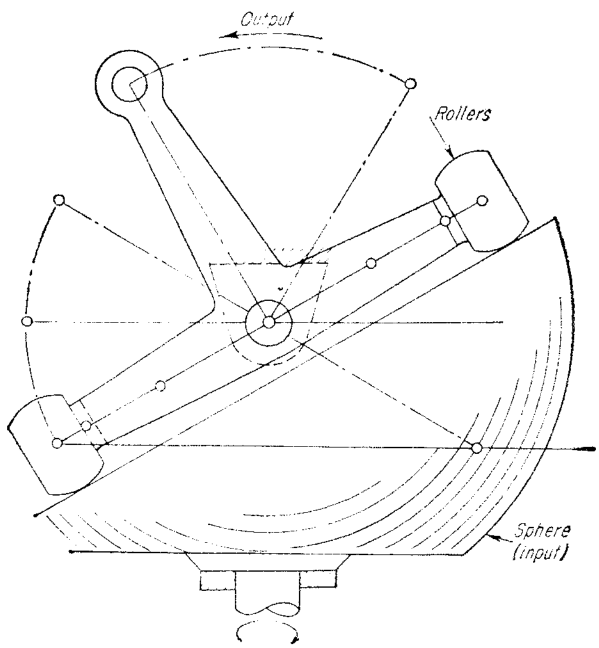

This transforms rotary motion into a reciprocating motion in which the oscillating output member is in the same plane as the input shaft. The output member has two arms with rollers which contact the surface of the truncated sphere. Rotation of the sphere causes the output to oscillate.

Cross-bar reciprocator

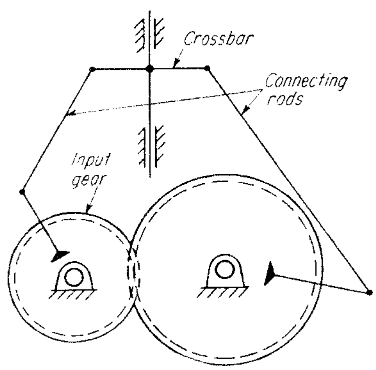

Although complex-looking, this device has been successful in high speed machines for transforming rotary motion into a high-impact linear motion. Both gears contain cranks connected to the cross bar by means of connecting rods.

Two-speed reciprocator

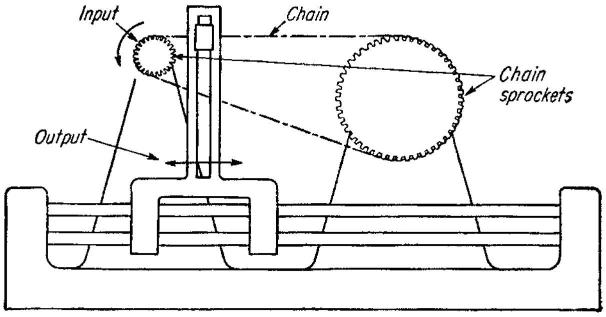

A drive pin, fastened to a chain, rides in a vertical slot to reciprocate a carriage in a horizontal direction. Velocity in both directions is constant and depends on the angle of slope that the chain makes with the vertical slot. Thus, velocity to the left is higher than to the right because the top of the chain is horizontal.

PARALLEL LINK MECHANISMS

Parallel link feeder

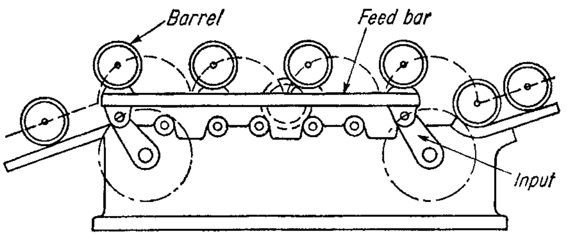

One of the cranks is the input, the other follows to keep the feeding bar horizontal. Employed for moving barrels from station to station.

Parallelogram linkage

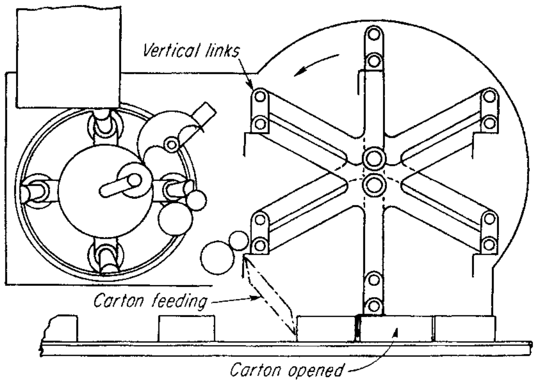

All seven short links are kept in a vertical position while rotating. The center link is the driver. This particular application feeds and opens cartons, but the device is capable of many diverse applications.

Parallel link driller

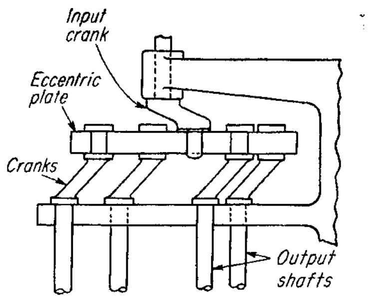

For powering a group of shafts. The input crank drives the eccentric plate. This in turn rotates the output cranks, all of which are of the same length and rotate at the same speed. Gears would require more room between shafts and are usually more expensive.

Parallel plate driver

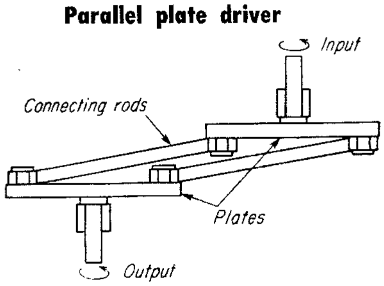

Here again, the input and output rotate with the same angle of relationship. The position of the shafts, however, can vary to suit other requirements without affecting the input-output relationship between shafts.

Slider-Crank Mechanisms

New equations and computer-tabulated values of velocities, accelerations, and forces reduce computation time an errors.

Professor Merl D. Creech

THE slider crank—an efficient mechanism for changing reciprocating motion to rotary—is widely used in engines, pumps, automatic machinery, and machine tools. The crank is a special case of the basic four-bar kinematic chain in which one of the four bars is of infinite length, ie, the motion of a point moving along a straight line is equivalent to the rotation of the same point about a center at infinity.

To design a slider-crank mechanism for high-speed operation, it is necessary to calculate the varying angular velocities and accelerations of the connecting rod and the linear accelerations of the slider to determine the maximum inertia forces acting on the system. Such time-consuming calculations frequently lead to errors.

The equations developed here for finding such factors are in a more streamlined form than is generally available. They have been programmed on a computer to obtain a set of design tables. Tabulations are carried to four significant figures and accurate interpolation is possible when required. Two numerical examples illustrate the use of the tables.

Derivation of equations

The effect of the angular acceleration of the crankshaft on the angular velocities and accelerations of the connecting rod and the acceleration of the slider is quite small. Hence it is assumed to be zero in the derivation.

From the geometry of the system in Fig 1 (see also

1.. Slider-crank mechanism

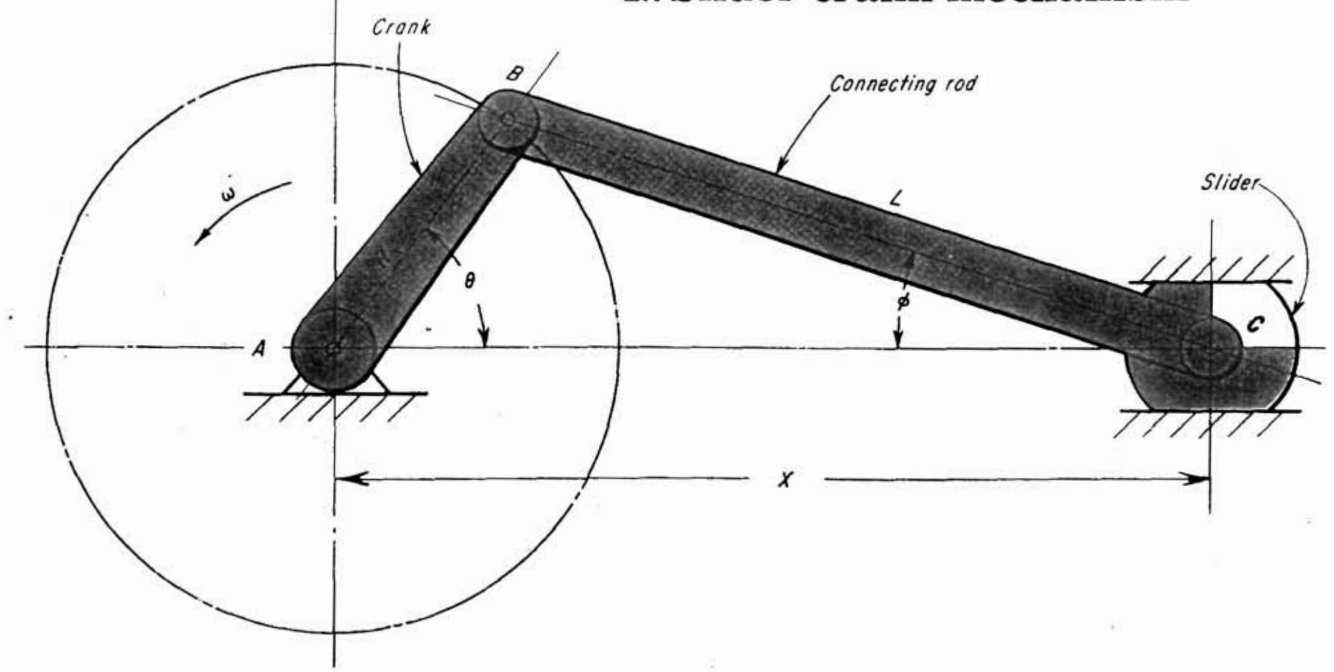

list of symbols), the relationship between θ and ϕ is

$$R \sin \theta = L \sin \phi \qquad (1)$$

and

$$x = R \cos \theta + L \cos \phi \qquad (2)$$

Differentiating Eq 1 with respect to time gives

$$\theta'(R/L) \cos \theta = \phi' \cos \phi \qquad (3)$$

Also from Eq 1 we can write

$$(R/L)^2 \sin^2 \theta = \sin^2 \phi = 1 - \cos^2 \phi \qquad (4)$$

Solving for $\cos \phi$ gives

$$\cos \phi = \left[1 - \left(\frac{R}{L}\right)^2 \sin^2 \theta\right]^{1/2} \qquad (5)$$

Since $\omega = \theta'$, Eq 3 and 5 can be combined to give

Angular velocity of the connecting rod

$$\phi' = \omega \left[\frac{(R/L) \cos \theta}{[1 - (R/L)^2 \sin^2 \theta]^{1/2}}\right] \qquad (6)$$

Now, differentiating Eq 2 with respect to time

$$\frac{x'}{L} = -\theta'\left(\frac{R}{L}\right) \sin \theta - \phi' \sin \phi \qquad (7)$$

Substituting Eq 1 into Eq 7 gives

Linear velocity of the piston

$$\frac{x'}{L} = -\omega\left[1 + \frac{\phi'}{\omega}\right]\left(\frac{R}{L}\right) \sin \theta \qquad (8)$$

Differentiating Eq 3 with respect to time

$$-(\theta')^2\left(\frac{R}{L}\right) \sin \theta + \theta''\left(\frac{R}{L}\right) \cos \theta = \phi'' \cos \phi - (\phi')^2 \sin \phi \qquad (9)$$

SYMBOLS

L = length of connecting rod
R = crank length; radius of crank circle
x = distance from center of crankshaft, A, to wrist pin, C
x' = slider velocity (linear velocity of point C)
x'' = slider acceleration
θ = crank angle measured from dead center (when slider is fully extended)
θ' = crank angular velocity = $d\theta/dt$
θ'' = crank angular acceleration = $d^2\theta/dt^2$
ϕ = angular position of connecting rod; $\phi = 0$ when $\theta = 0$
ϕ' = connecting-rod angular velocity = $d\phi/dt$
ϕ'' = connecting-rod angular acceleration = $d^2\phi/dt^2$
ω = constant crank angle velocity

Since $\omega = \theta'$ = constant and $\theta'' = 0$, the values of $\cos \phi$ from Eq 5, $\sin \theta$ from Eq 1, and ϕ' from Eq 6 are substituted into Eq 9 to give

Angular acceleration of the connecting rod

$$\phi'' = \frac{\omega^2(R/L) \sin \theta[(R/L)^2 - 1]}{[1 - (R/L)^2 \sin^2 \theta]^{3/2}} \qquad (10)$$

Next, differentiating Eq 7 with respect to time

$$\frac{x''}{L} = -\theta''\left(\frac{R}{L}\right) \sin \theta - (\theta')^2\left(\frac{R}{L}\right) \cos \theta - \phi'' \sin \phi - (\phi')^2 \cos \phi \qquad (11)$$

Substituting the value of ϕ' from Eq 6, $\sin \phi$ from Eq 4, $\cos \phi$ from Eq 5 and ϕ'' from Eq 10 into Eq 11 gives

Slider acceleration

$$\frac{x''}{L} = -\omega^2\left(\frac{R}{L}\right)\left[\cos \theta + \frac{\phi''}{\omega^2} \sin \theta + \frac{\phi'}{\omega} \cos \theta\right] \qquad (12)$$

Dynamic forces

The resultant force, F_R, acting on the connecting rod, Fig 2, is due to the angular and linear accelerations, ϕ'' and x'' respectively. The effect of gravity on the connecting rod is small in comparison to these dynamic forces and can be neglected. Thus, resultant force (see Symbols in Fig 3) is equal to

$$F_R = Mr\phi'' + Mx'' \sin \phi \qquad (13)$$

The moments acting on the connecting rod are

$$F_R d = MK^2\phi'' + Mrx'' \sin \phi \qquad (14)$$

where

$$K^2 = I_C/M \qquad (15)$$

Hence the distance of the resultant, F_R, from point C is equal to

$$d = \frac{K^2\phi'' + rx'' \sin \phi}{r\phi'' + x'' \sin \phi} \qquad (16)$$

The signs of the terms in the above equations are correct for counterclockwise rotation of the crank shaft and for values of θ in the first quadrant.

There are also dynamic forces in the longitudinal direction (along the line of centers, BC). The resultant longitudinal force, F_L, can be written as

$$F_L = Mr(\phi')^2 - Mx'' \cos \phi \qquad (17)$$

Tabulated values

From considerations of symmetry it is necessary only to tabulate the values of the velocities and accelerations for values of θ from 0 deg to 180 deg. But there is always the problem of signs—to avoid error, check with Fig 3, which shows the directions of the acceleration and velocity of the connecting rod and slider for clockwise and counterclockwise rotation of the crank.

Table I gives the relationship between the design equations and the values tabulated in Tables II to VII. These values, grouped under R/L ratios of 0.2, 0.3, 0.4, 0.5, 0.6 and 0.7, will handle most applications that may arise and the designer can always interpolate between values if necessary.

Example I—reciprocating engine

Stroke of engine = 7.2 in.
Connecting-rod length = 12.0 in.

2.. Dynamic forces on connecting rod

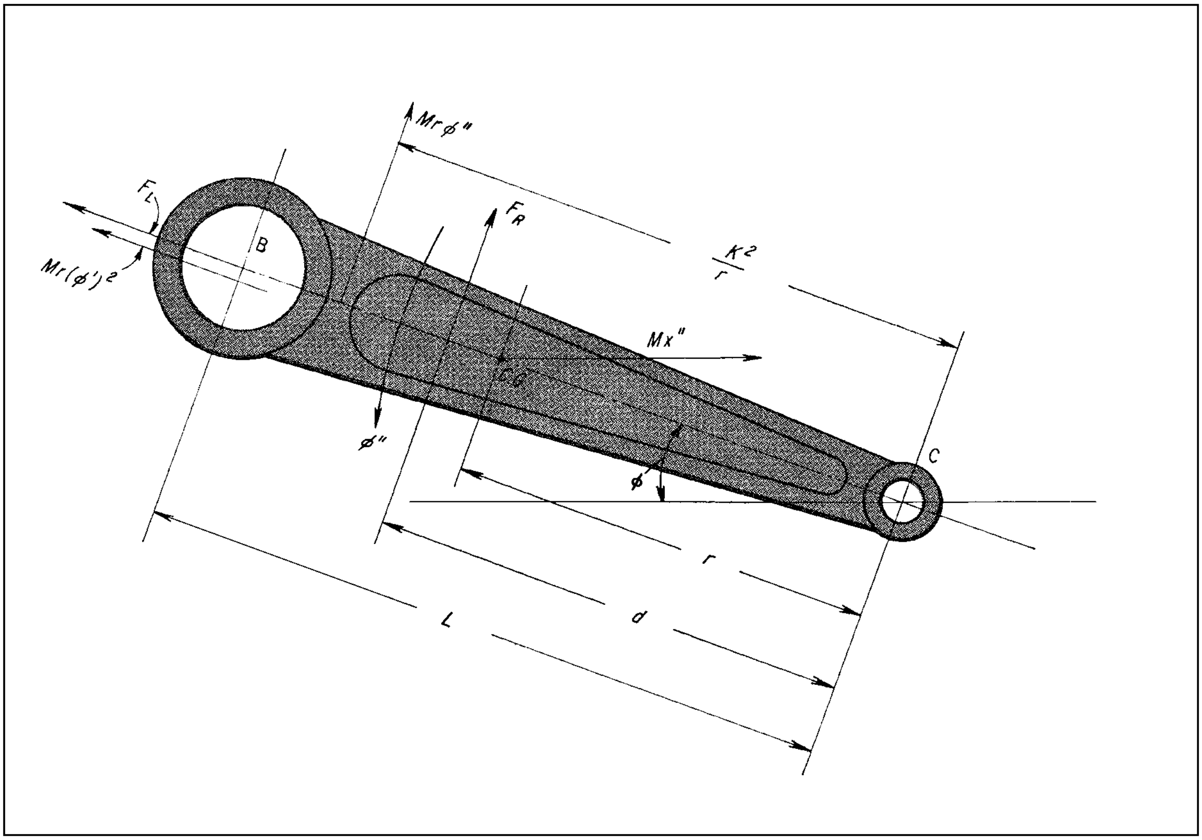

Connecting-rod weight = 8.106 lb.

Center of mass of connecting rod = 6.4 in. from center of wrist pin.

Moment of inertia about the center of wrist pin = 1.1088 in.-lb-sec².

Part A: Find the direction, magnitude, and location of the inertia forces acting on the connecting rod when the crank is 35 deg from top dead center and the engine speed is 2400 rpm.

$$R/L = 3.6/12 = 0.30$$

$$\omega = \frac{(2400)(2\pi)}{60} = 251.33 \text{ rad/sec}$$

The following values of the required parameters are found from Table III for $\theta = 35$ deg:

$$\phi = 9.908 \text{ deg}, \quad \phi'/\omega = 0.2495, \quad \phi''/\omega^2 L = -0.1638, \quad x'/\omega L = -0.2150, \quad x''/\omega^2 L = 0.2789$$

Using these tabulated values, the following terms are calculated:

TABLE I.. Relation between equations and tabulated values

CONNECTING ROD	SYMBOL	EQ. NO.	COLUMN	SLIDER	SYMBOL	EQ. NO.	COLUMN
ANGULAR DISPLACEMENT	ϕ	5	2	LINEAR DISPLACEMENT	x	2	—
ANGULAR VELOCITY	ϕ'/ω	6	3	LINEAR VELOCITY	$x'/\omega L$	8	4
ANGULAR ACCELERATION	ϕ''/ω^2	10	5	LINEAR ACCELERATION	$x''/\omega^2 L$	12	6

3.. Directions of velocities and accelerations

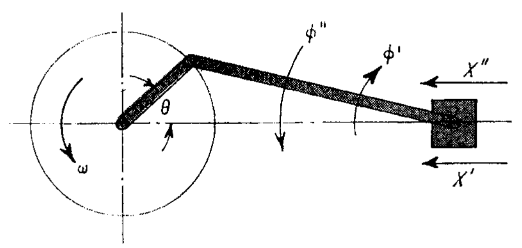

(A) $0 < \theta < 90°$

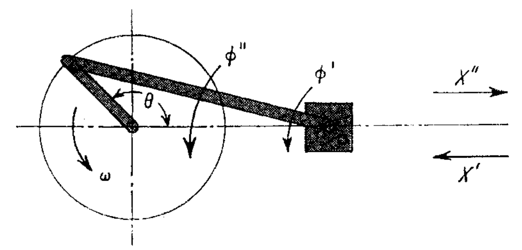

(B) $90° < \theta < 180°$

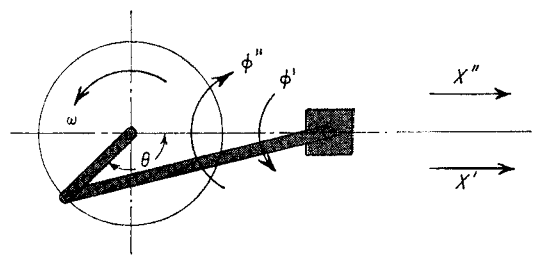

(C) $180° < \theta < 270°$

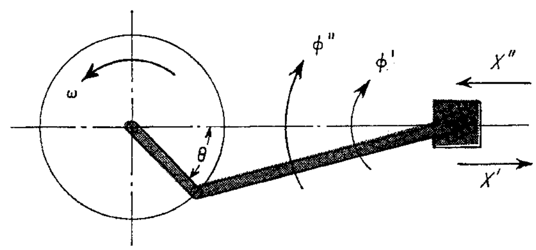

(D) $270° < \theta < 360°$

Counterclockwise rotation

Clockwise rotation

SYMBOLS

d = distance of resultant F_R from C
F_R = resultant of forces
I_C = moment of inertia of connecting rod about C
K = radius of gyration from C
M = mass of connecting rod
r = distance of center of gravity from C

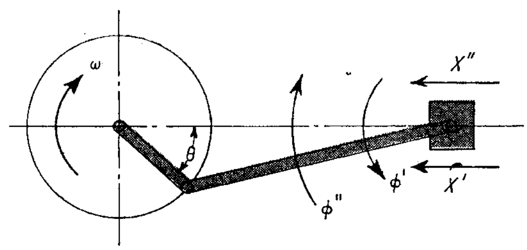

(A) $270° < \theta < 360°$

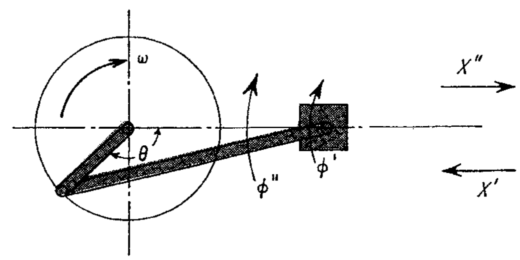

(B) $180° < \theta < 270°$

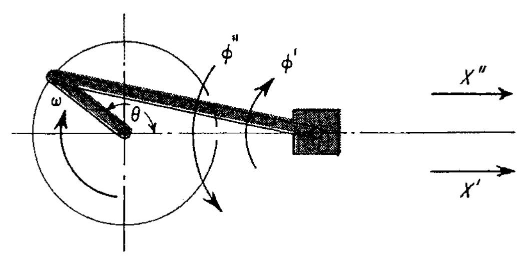

(C) $90° < \theta < 180°$

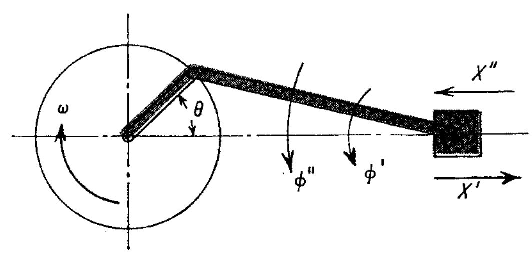

(D) $0° < \theta < 90°$

TABLE II

$R/L=0.2$

θ, deg	ϕ, deg	ϕ'/ω	$\chi'/\omega L$	ϕ''/ω^2	$\chi''/\omega^2 L$
0	0.000	0.2000	–0.0000	0.0000	0.2400
5	0.998	0.1993	–0.0209	–0.0167	0.2386
10	1.990	0.1971	–0.0416	–0.0334	0.2346
15	2.967	0.1934	–0.0618	–0.0499	0.2280
20	3.922	0.1884	–0.0813	–0.0661	0.2188
25	4.848	0.1819	–0.0999	–0.0820	0.2073
30	5.739	0.1741	–0.1174	–0.0975	0.1936
35	6.587	0.1649	–0.1336	–0.1123	0.1780
40	7.386	0.1545	–0.1484	–0.1265	0.1606
45	8.130	0.1429	–0.1616	–0.1399	0.1418
50	8.812	0.1301	–0.1731	–0.1524	0.1219
55	9.429	0.1163	–0.1829	–0.1638	0.1012
60	9.974	0.1015	–0.1908	–0.1740	0.0800
65	10.443	0.0859	–0.1968	–0.1830	0.0586
70	10.832	0.0696	–0.2010	–0.1904	0.0374
75	11.138	0.0528	–0.2034	–0.1963	0.0166
80	11.359	0.0354	–0.2039	–0.2006	–0.0036
85	11.492	0.0178	–0.2028	–0.2032	–0.0228
90	11.536	0.0000	–0.2000	–0.2041	–0.0408
95	11.492	–0.0178	–0.1957	–0.2032	–0.0576
100	11.359	–0.0354	–0.1900	–0.2006	–0.0730
105	11.138	–0.0528	–0.1830	–0.1963	–0.0870
110	10.832	–0.0696	–0.1748	–0.1904	–0.0994
115	10.443	–0.0859	–0.1657	–0.1830	–0.1104
120	9.974	–0.1015	–0.1556	–0.1740	–0.1200
125	9.429	–0.1163	–0.1448	–0.1638	–0.1282
130	8.812	–0.1301	–0.1333	–0.1524	–0.1352
135	8.130	–0.1429	–0.1212	–0.1399	–0.1410
140	7.386	–0.1545	–0.1087	–0.1265	–0.1458
145	6.587	–0.1649	–0.0958	–0.1123	–0.1497
150	5.739	–0.1741	–0.0826	–0.0975	–0.1528
155	4.848	–0.1819	–0.0691	–0.0820	–0.1552
160	3.922	–0.1884	–0.0555	–0.0661	–0.1571
165	2.967	–0.1934	–0.0417	–0.0499	–0.1584
170	1.990	–0.1971	–0.0279	–0.0334	–0.1593
175	0.998	–0.1993	–0.0140	–0.0167	–0.1598
180	0.000	–0.2000	–0.0000	–0.0000	–0.1600

TABLE IV

$R/L=0.4$

θ, deg	ϕ, deg	ϕ'/ω
0	0.000	0.4000
5	1.997	0.0987
10	3.982	0.3949
15	5.942	0.3885
20	7.863	0.3794
25	9.732	0.3678
30	11.536	0.3536
35	13.263	0.3366
40	14.898	0.3171
45	16.429	0.2949
50	17.843	0.2701
55	19.126	0.2428
60	20.267	0.2132
65	21.255	0.1814
70	22.078	0.1476
75	22.728	0.1122
80	23.198	0.0756
85	23.483	0.0380
90	23.578	0.0000
95	23.483	–0.0380
100	23.198	–0.0756
105	22.728	–0.1122
110	22.076	–0.1476
115	21.255	–0.1814
120	20.267	–0.2132
125	19.126	–0.2428
130	17.843	–0.2701
135	16.429	–0.2949
140	14.898	–0.3171
145	13.263	–0.3366
150	11.536	–0.3536
155	9.732	–0.3678
160	7.863	–0.3794
165	5.942	–0.3885
170	3.982	–0.3949
175	1.997	–0.3987
180	0.000	–0.4000

TABLE III

$R/L=0.3$

θ, deg	ϕ, deg	ϕ'/ω	$\chi'/\omega L$	ϕ''/ω^2	$\chi''/\omega^2 L$
0	0.000	0.3000	–0.0000	0.0000	0.3900
5	1.498	0.2990	–0.0340	–0.0238	0.3876
10	2.986	0.2958	–0.0675	–0.0476	0.3804
15	4.453	0.2907	–0.1002	–0.0713	0.3685
20	5.889	0.2834	–0.1317	–0.0949	0.3520
25	7.283	0.2741	–0.1615	–0.1182	0.3314
30	8.626	0.2628	–0.1894	–0.1412	0.3069
35	9.908	0.2495	–0.2150	–0.1638	0.2789
40	11.118	0.2342	–0.2380	–0.1857	0.2478
45	12.247	0.2171	–0.2581	–0.2068	0.2143
50	13.286	0.1981	–0.2753	–0.2269	0.1789
55	14.225	0.1775	–0.2894	–0.2455	0.1423
60	15.058	0.1553	–0.3002	–0.2626	0.1051
65	15.776	0.1317	–0.3077	–0.2776	0.0680
70	16.374	0.1069	–0.3120	–0.2905	0.0317
75	16.844	0.0811	–0.3133	–0.3008	–0.0032
80	17.184	0.0545	–0.3116	–0.3083	–0.0361
85	17.389	0.0274	–0.3070	–0.3129	–0.0667
90	17.457	0.0000	–0.3000	–0.3145	–0.0943
95	17.389	–0.0274	–0.2907	–0.3129	–0.1189
100	17.184	–0.0545	–0.2793	–0.3083	–0.1403
105	16.844	–0.0811	–0.2663	–0.3008	–0.1585
110	16.374	–0.1069	–0.2518	–0.2905	–0.1735
115	15.776	–0.1317	–0.2361	–0.2776	–0.1856
120	15.058	–0.1553	–0.2194	–0.2626	–0.1949
125	14.225	–0.1775	–0.2021	–0.2455	–0.2019
130	13.286	–0.1981	–0.1843	–0.2269	–0.2069
135	12.247	–0.2171	–0.1661	–0.2068	–0.2099
140	11.118	–0.2342	–0.1477	–0.1857	–0.2118
145	9.908	–0.2495	–0.1291	–0.1638	–0.2126
150	8.626	–0.2628	–0.1106	–0.1412	–0.2127
155	7.283	–0.2741	–0.0920	–0.1182	–0.2124
160	5.889	–0.2834	–0.0735	–0.0949	–0.2117
165	4.453	–0.2907	–0.0551	–0.0713	–0.2111
170	2.986	–0.2958	–0.0367	–0.0476	–0.2105
175	1.493	–0.2990	–0.0183	–0.0238	–0.2101
180	0.000	–0.3000	–0.0000	–0.0000	–0.2100

TABLE V

$R/L=0.5$

θ, deg	ϕ, deg	ϕ'/ω
0	0.000	0.5000
5	2.497	0.4986
10	4.980	0.4948
15	7.435	0.4871
20	9.846	0.4769
25	12.199	0.4636
30	14.477	0.4472
35	16.665	0.4275
40	18.747	0.4045
45	20.704	0.3780
50	22.521	0.3479
55	24.178	0.3144
60	25.658	0.2773
65	26.946	0.2370
70	28.024	0.1937
75	28.879	0.1478
80	29.498	0.0998
85	29.874	0.0503
90	30.000	0.0000
95	29.874	–0.0503
100	29.498	–0.0998
105	28.879	–0.1478
110	28.024	–0.1937
115	26.946	–0.2370
120	25.658	–0.2773
125	24.178	–0.3144
130	22.521	–0.3479
135	20.704	–0.3780
140	18.747	–0.4045
145	16.665	–0.4275
150	14.477	–0.4472
155	12.199	–0.4636
160	9.846	–0.4769
165	7.435	–0.4871
170	4.980	–0.4943
175	2.497	–0.4986
180	0.000	–0.5000

$\chi'/\omega L$	ϕ''/ω^2	$\chi''/\omega^2 L$
−0.0000	0.0000	0.5600
−0.0488	−0.0293	0.5563
−0.0969	−0.0588	0.5454
−0.1437	−0.0884	0.5273
−0.1887	−0.1182	0.5023
−0.2312	−0.1483	0.4708
−0.2707	−0.1786	0.4332
−0.3067	−0.2090	0.3900
−0.3386	−0.2393	0.3420
−0.3662	−0.2692	0.2901
−0.3892	−0.2984	0.2351
−0.4072	−0.3264	0.1782
−0.4203	−0.3525	0.1205
−0.4283	−0.3762	0.0633
−0.4314	−0.3968	0.0079
−0.4297	−0.4136	−0.0447
−0.4237	−0.4261	−0.0931
−0.4136	−0.4338	−0.1367
−0.4000	−0.4364	−0.1746
−0.3833	−0.4338	−0.2064
−0.3642	−0.4261	−0.2321
−0.3430	−0.4136	−0.2517
−0.3204	−0.3968	−0.2658
−0.2968	−0.3762	−0.2748
−0.2726	−0.3525	−0.2795
−0.2481	−0.3264	−0.2806
−0.2237	−0.2984	−0.2791
−0.1994	−0.2692	−0.2756
−0.1756	−0.2393	−0.2708
−0.1522	−0.2090	−0.2653
−0.1293	−0.1786	−0.2597
−0.1069	−0.1483	−0.2543
−0.0849	−0.1182	−0.2494
−0.0633	−0.0884	−0.2454
−0.0420	−0.0588	−0.2425
−0.0210	−0.0293	−0.2406
−0.0000	−0.0000	−0.2400

TABLE **VI**

$R/L = 0.6$

θ, deg	ϕ, deg	ϕ'/ω	$\chi'/\omega L$	ϕ''/ω^2	$\chi''/\omega^2 L$
0	0.000	0.6000	−0.0000	0.0000	0.9600
5	2.997	0.5985	−0.0836	−0.0336	0.9537
10	5.980	0.5941	−0.1661	−0.0678	0.9349
15	8.933	0.5867	−0.2464	−0.1031	0.9036
20	11.841	0.5761	−0.3234	−0.1401	0.8599
25	14.683	0.5622	−0.3961	−0.1793	0.8040
30	17.457	0.5447	−0.4634	−0.2212	0.7363
35	20.129	0.5235	−0.5243	−0.2661	0.6572
40	22.685	0.4982	−0.5778	−0.3143	0.5674
45	25.104	0.4685	−0.6230	−0.3657	0.4679
50	27.363	0.4343	−0.6592	−0.4199	0.3601
55	29.438	0.3952	−0.6857	−0.4762	0.2461
60	31.306	0.3511	−0.7021	−0.5332	0.1283
65	32.941	0.3021	−0.7081	−0.5888	0.0100
70	34.320	0.2485	−0.7039	−0.6405	−0.1049
75	35.419	0.1906	−0.6900	−0.6853	−0.2123
80	36.219	0.1291	−0.6672	−0.7202	−0.3079
85	36.706	0.0652	−0.6367	−0.7424	−0.3880
90	36.869	0.0000	−0.6000	−0.7500	−0.4500
95	36.706	−0.0652	−0.5587	−0.7423	−0.4926
100	36.219	−0.1291	−0.5146	−0.7202	−0.5163
105	35.419	−0.1906	−0.4691	−0.6853	−0.5229
110	34.320	−0.2485	−0.4237	−0.6405	−0.5154
115	32.941	−0.3021	−0.3795	−0.5888	−0.4971
120	31.306	−0.3511	−0.3372	−0.5332	−0.4717
125	29.438	−0.3952	−0.2973	−0.4762	−0.4422
130	27.363	−0.4343	−0.2600	−0.4199	−0.4112
135	25.104	−0.4685	−0.2255	−0.3657	−0.3806
140	22.685	−0.4982	−0.1935	−0.3142	−0.3519
145	20.129	−0.5235	−0.1640	−0.2661	−0.3258
150	17.457	−0.5447	−0.1366	−0.2212	−0.3029
155	14.688	−0.5622	−0.1110	−0.1793	−0.2836
160	11.841	−0.5761	−0.0870	−0.1401	−0.2678
165	8.933	−0.5867	−0.0642	−0.1031	−0.2556
170	5.980	−0.5941	−0.0423	−0.0678	−0.2469
175	2.997	−0.5985	−0.0210	−0.0336	−0.2417
180	0.000	−0.6000	−0.0000	−0.0000	−0.2400

$\chi'/\omega L$	ϕ''/ω^2	$\chi''/\omega^2 L$
−0.0000	0.0000	0.7500
−0.0653	−0.0328	0.7450
−0.1297	−0.0658	0.7301
−0.1924	−0.0995	0.7053
−0.2526	−0.1341	0.6710
−0.3093	−0.1697	0.6274
−0.3618	−0.2066	0.5750
−0.4094	−0.2446	0.5145
−0.4514	−0.2839	0.4467
−0.4872	−0.3240	0.3726
−0.5163	−0.3644	0.2936
−0.5383	−0.4046	0.2112
−0.5531	−0.4434	0.1273
−0.5606	−0.4798	0.0440
−0.5609	−0.5123	−0.0366
−0.5543	−0.5395	−0.1120
−0.5415	−0.5601	−0.1803
−0.5231	−0.5730	−0.2397
−0.5000	−0.5773	−0.2887
−0.4731	−0.5730	−0.3268
−0.4433	−0.5601	−0.3540
−0.4116	−0.5395	−0.3709
−0.3788	−0.5123	−0.3786
−0.3457	−0.4798	−0.3786
−0.3129	−0.4434	−0.3727
−0.2808	−0.4046	−0.3623
−0.2497	−0.3644	−0.3492
−0.2199	−0.3240	−0.3343
−0.1914	−0.2839	−0.3193
−0.1642	−0.2446	−0.3046
−0.1382	−0.2066	−0.2910
−0.1133	−0.1697	−0.2789
−0.0895	−0.1341	−0.2687
−0.0664	−0.0995	−0.2606
−0.0439	−0.0659	−0.2547
−0.0219	−0.0328	−0.2512
−0.0000	−0.0000	−0.2500

TABLE **VII**

$R/L = 0.7$

θ, deg	ϕ, deg	ϕ'/ω	$\chi'/\omega L$	ϕ''/ω^2	$\chi''/\omega^2 L$
0	0.000	0.7000	−0.0000	0.0000	1.1900
5	3.497	0.6986	−0.1036	−0.0313	1.1826
10	6.981	0.6945	−0.2060	−0.0634	1.1604
15	10.438	0.6875	−0.3057	−0.0971	1.1234
20	13.851	0.6775	−0.4016	−0.1334	1.0719
25	17.207	0.6641	−0.4923	−0.1731	1.0045
30	20.487	0.6471	−0.5765	−0.2171	0.9225
35	23.672	0.6261	−0.6529	−0.2665	0.8254
40	26.740	0.6004	−0.7201	−0.3222	0.7132
45	29.668	0.5696	−0.7769	−0.3848	0.5865
50	32.427	0.5331	−0.8221	−0.4548	0.4459
55	34.988	0.4901	−0.8544	−0.5318	0.2933
60	37.316	0.4401	−0.8730	−0.6146	0.1314
65	39.376	0.3827	−0.8772	−0.7005	−0.0354
70	41.131	0.3179	−0.8669	−0.7851	−0.2009
75	42.543	0.2459	−0.8424	−0.8622	−0.3573
80	43.579	0.1678	−0.8050	−0.9248	−0.4956
85	44.213	0.0851	−0.7567	−0.9659	−0.6073
90	44.427	0.0000	−0.7000	−0.9802	−0.6861
95	44.213	−0.0851	−0.6380	−0.9659	−0.7293
100	43.579	−0.1678	−0.5737	−0.9248	−0.7387
105	42.543	−0.2459	−0.5099	−0.8622	−0.7196
110	41.131	−0.3179	−0.4487	−0.7851	−0.6797
115	39.376	−0.3827	−0.3916	−0.7005	−0.6270
120	37.316	−0.4401	−0.3394	−0.6146	−0.5686
125	34.988	−0.4901	−0.2924	−0.5318	−0.5098
130	32.427	−0.5331	−0.2504	−0.4548	−0.4539
135	29.668	−0.5696	−0.2130	−0.3848	−0.4035
140	26.740	−0.6004	−0.1798	−0.3221	−0.3592
145	23.672	−0.6261	−0.1501	−0.2665	−0.3214
150	20.487	−0.6471	−0.1235	−0.2171	−0.2899
155	17.207	−0.6641	−0.0994	−0.1731	−0.2643
160	13.851	−0.6775	−0.0772	−0.1334	−0.2441
165	10.438	−0.6875	−0.0566	−0.0971	−0.2289
170	6.981	−0.6945	−0.0371	−0.0634	−0.2183
175	3.497	−0.6986	−0.0184	−0.0313	−0.2120
180	0.000	−0.7000	−0.0000	−0.0000	−0.2100

$$\phi' = (251.33)(0.2495) = 62.68 \text{ rad/sec}$$
$$\phi'' = (251.33)^2(0.1638) = 10{,}347 \text{ rad/sec}^2$$
$$x' = (12)(251.33)(0.2150) = 648.4 \text{ in./sec}$$
$$x'' = (12)(63{,}167)(0.2789) = 211{,}380 \text{ in./sec}^2$$

$$Mr\phi'' = \left(\frac{8.106}{386}\right)(6.4)(10{,}347) = 1391 \text{ lb}$$

$$\sin\phi = 0.1719; \quad \cos\phi = 0.9851$$

$$Mx'' \sin\phi = \left(\frac{8.106}{386}\right)(211{,}380)(0.1719) = 763.2 \text{ lb}$$

Substituting these values into Eq 13 gives

$$F_R = 1391 + 763 = 2154 \text{ lb}$$

Substituting into Eq 16

$$d = \frac{(1.109)(10{,}347)+(763.2)(6.4)}{2154} = 7.59 \text{ in.}$$

$$Mr(\phi')^2 = (0.021)(6.4)(62.68)^2 = 528.1 \text{ lb}$$
$$Mx'' \cos\phi = (4439)(0.9851) = 4373 \text{ lb}$$

Substituting into Eq 17

$$F_L = 528 + 4373 = 4901 \text{ lb}$$

Part B: Find the bending and tensile stresses caused by the inertia forces.

The connecting rod, Fig 4, is assumed to be a trapezoidal steel bar of rectangular cross section of constant thickness, t, with a width of 3 in. at the crank pin and a width of 2 in. at the wrist pin end. Also, density of steel $\rho = 0.28$ lb/in.^{3}

Let A = constant = $\rho t/g$ = (0.28)(0.965)/386 = 0.0007 lb-sec^2/in^5. Also from Fig 4

$$h = 2 + y/12$$

Then $$I_C = A\int_0^{12} hy^2\,dy$$

$$= 0.0007\left[\frac{2y^3}{3} + \frac{y^4}{48}\right]_0^{12}$$

$$I_C = 1.109 \text{ in.-lb-sec}^2$$

and $$K^2 = \frac{1.109}{0.021} = 52.8 \text{ in.}^2$$

Referring to the load diagram in Fig 4, the connecting rod can be considered as a simply supported beam loaded with a distributed varying load W. The load W at any point y is

$$W = A\int h\,(y\phi'' + x'' \sin\phi)\,dy$$

$$A\int\left(2y\phi'' + \frac{y^2}{12}\phi'' + 2x'' \sin\phi + \frac{y}{12}x'' \sin\phi\right)dy$$

The reaction R_C is

$$R_C = F_R(L - d)/L$$

The bending moment at any point z is

$$M_b = -zR_C + A\int_0^z\left[2y\phi'' + \frac{y^2}{12}\phi'' + 2x'' \sin\phi + \frac{y}{12}x'' \sin\phi\right](z-y)\,dy$$

Perform the indicated integration:

$$M_b = -zR_C + A\left[\frac{z^3}{3}\phi'' + \frac{z^4}{144}\phi'' + z^2x'' \sin\phi + \frac{z^3}{72}x'' \sin\phi\right]$$

The maximum bending moment occurs where $dM_b/dz = 0$. Hence, differentiating the above equation gives

$$\frac{dM_b}{dz} = 0 = -R_C + A\left[z^2\phi'' + \frac{z^3}{36}\phi'' + 2zx'' \sin\phi + \frac{z^2}{24}x'' \sin\phi\right]$$

Factor z is the distance from C to the point of maximum bending moment. To determine the crank angle at which point the maximum bending moment occurs, values for the resulting force, F_R, and the moment of the resulting force, F_Rd, about the wrist pin are tabulated in Table VIII for 30-deg increments of θ. (This requires repeating the calculations in Part A for every 30 deg, hence the value of the design tables.) The maximum moment occurs at $\theta = 240$ deg.

Using the appropriate values for this angle gives

$$\frac{R_C}{M\omega^2} = \frac{F_R}{M\omega^2}\left[\frac{12-d}{12}\right]$$

$$= (2.288)\left[\frac{12-7.76}{12}\right] = 0.8084$$

Therefore

$$R_C/\omega^2 = \left(\frac{8.106}{386}\right)(0.8084) = 0.0169$$

From which

$$z^3 + 39.47z^2 + 166.77z - 3326.1 = 0$$

This cubic equation has three real roots, only one of which is positive. The two negative roots have no physical meaning in this case. Solving the cubic equation results in

$$z = 6.862$$

This value of the root is substituted into the bending moment equation to find the maximum bending moment in the connecting rod when the angle $\theta = 240$ deg from the top dead center:

$$M_b = 4540 \text{ in.-lb.}$$

At the section where the bending moment is maximum

$$h = 2 + 0.569 = 2.569 \text{ in.}$$
$$I = 0.965\,(2.569)^3/12 = 1.363 \text{ in.}^4$$

Bending stress equals

$$S_b = \frac{M_bh}{2I} = \frac{(4540)(1.284)}{1.364}$$

$$S_b = 4270 \text{ psi}$$

Example II—mechanical press

Stroke = 16 in.; connecting rod = 26.67 in. When crank is 25 deg from the bottom dead center, Fig 5, the torque exerted by flywheel on crankshaft is 7500 ft-lb. Thus $R/L = 0.3$, and $F_t = 7500\,(12)/8 = 11{,}250$.

4.. Load and bending-moment analysis

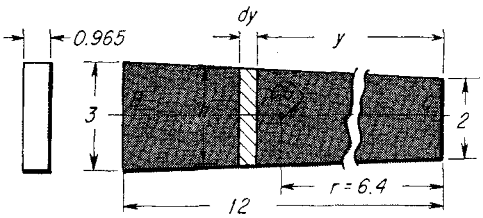

(A) Simplified section of connecting rod

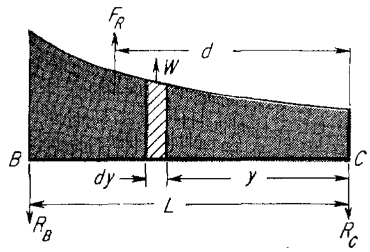

(B) Load diagram

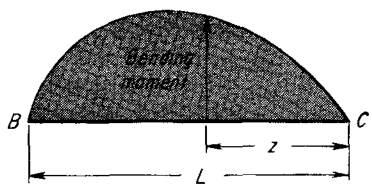

(C) Bending moment diagram

TABLE **VIII.. Dynamic forces for $R/L = 0.3$**

θ	ϕ	ϕ''/ω^2	$\chi''/L\omega^2$	$F_R/M\omega^2$	d	$F_R d/M\omega^2$
30	8.626	0.1412	+0.3069	1.4567	7.53	10.97
60	15.058	0.2626	+0.1050	2.0081	7.95	15.96
75	16.844	0.3007	−0.0032	1.9137	8.26	15.81
90	17.457	0.3145	−0.0943	1.6730	8.60	14.40
120	15.058	0.2626	−0.1949	1.0723	9.30	9.97
150	8.626	0.1412	−0.2127	0.5208	9.61	5.00
180	0.000	0.0000	−0.2100	0.0000	..	0.00
210	8.626	0.1412	+0.2127	1.2871	7.70	9.91
240	15.058	0.2626	+0.1949	2.2883	7.76	17.75
270	17.457	0.3145	+0.0943	2.3524	7.98	18.78
285	16.844	0.3008	+0.0032	2.0361	8.24	15.95
300	15.058	0.2626	−0.1050	1.3525	8.72	11.76
330	8.626	0.1412	−0.3068	0.3511	11.16	3.92

5.. Forces on punch press

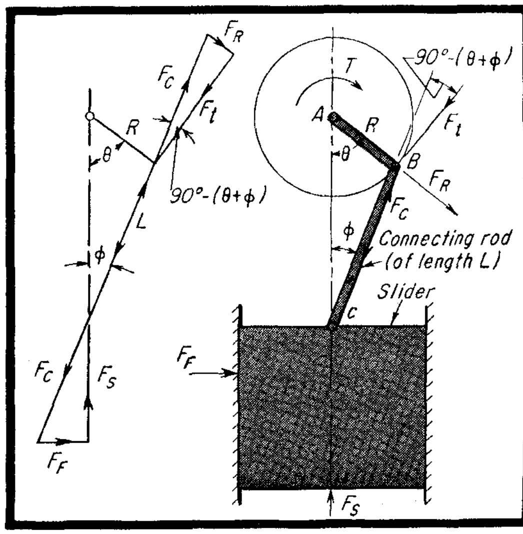

From Table III $\phi = 7.283$ deg; hence $\phi + \theta = 32.283$ deg. The forces exerted by the slide and connection are

$$F_s = \frac{F_t \cos\phi}{\sin(\theta + \phi)} \qquad F_C = \frac{F_t}{\sin(\theta + \phi)}$$

Hence

$$F_s = \frac{(11{,}250)(0.9919)}{0.5341} = 20{,}900 \text{ lb.}$$

$$F_C = \frac{11{,}250}{0.5341} = 21{,}100 \text{ lb.}$$

The radial force on the crank pin is

$$F_R = \frac{F_t \cos(\theta + \phi)}{\sin(\theta + \phi)}$$

$$F_R = \frac{(11{,}250)(0.8454)}{0.5341} = 17{,}800 \text{ lb.}$$

The force of the slide against the frame is

$$F_F = \frac{F_t \sin\phi}{\sin(\theta + \phi)}$$

$$F_F = \frac{(11{,}250)(0.1268)}{0.5341} = 2675 \text{ lb.}$$

The value for the side thrust is useful in estimating the wear rate of the guides.

Now, assuming the press makes three working strokes per minute, its angular speed is

$$\omega = 3(2\pi)/60 = 0.3142 \text{ rad/sec}$$

From Table III, the relative angular velocity, ϕ', of the connecting-rod knuckle to its bearing is

$$\phi' = (0.3142)(0.2741) = 0.0861 \text{ rad/sec}$$

The relative angular velocity of the crank pin to its bearing (at point B) is

$$\theta' + \phi' = 0.3142 + 0.0861 = 0.4003 \text{ rad/sec}$$

These velocities are then used to estimate the wear life of the knuckle and crank-pin bearings.

Torque Factors for Slide Crank Mechanisms

Alexander Hammer

THE ACCOMPANYING TABLE gives values of a factor f_t for determining torque imposed on a crankshaft by a force acting on a crosshead in the direction of stroke.

P = force on piston or crosshead, lb.
θ = crank position, from head end dead center, deg
β = connecting rod angle corresponding to θ, deg
P_l = force on connecting rod, lb
$P_l = P/\cos\beta$, lb
l = connecting rod length, in.
r = crank radius, in.
k = l/r = ratio of length of connecting rod to radius of crank
a = perpendicular distance from centerline of connecting rod to center of crank shaft, in.
$a = r\sin(\theta + \beta)$, in.
T = torque on crankshaft, lb in.
f_t = factor from accompanying table for specific k and crank angle θ
$T = P_l a = (P/\cos\beta)\, r\sin(\theta + \beta)$

$$= Pr\left[\frac{\sin\theta\cos\beta + \cos\theta\sin\beta}{\cos\beta}\right] \qquad (1)$$

since $\dfrac{r}{kr} = \dfrac{\sin\beta}{\sin\theta}$, then $\sin\beta = \dfrac{\sin\theta}{k}$

and $\sqrt{1 - \cos^2\beta} = \sin\theta/k$

or $\cos\beta = \sqrt{k^2 - \sin^2\theta}/k$

substituting these values of $\sin\beta$ and $\cos\beta$ in Eq (1), there results

$$T = Pr\left[\sin\theta\left(1 + \frac{\cos\theta}{\sqrt{k^2 - \sin^2\theta}}\right)\right] \qquad (2)$$

substituting f_t for the expression contained in the brackets of Eq (2), there results

$$T = Prf_t \qquad (3)$$

Values of f_t are given in the accompanying table for k ratios ranging from 3.0 to 5.0.

PROBLEM: Find torque on crankshaft resulting from a force of 150 lb on crosshead, when crank radius is 3 in., connecting rod length is 12 6 in., and crank angle is 40 deg from head end dead center?

SOLUTION:

$l = 12.6$, $r = 3$, $k = l/r = 12.6/3 = 4.2$

From Table, for k equal to 4.2 and θ equal to 40 deg, f_t is 0.7614, then

$T = Prf_t = 150 \times 3 \times 0.7614 = 342.63$ lb in.

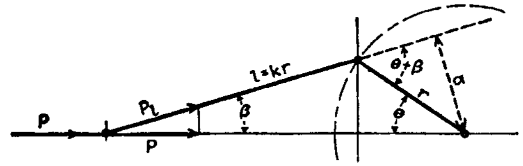

Tangential Factors f_t

Crank angle deg.	Ratio of Length of Rod to Length of Crank $l/r = k$									
	3.0	3.1	3.2	3.3	3.4	3.5	3.6	3.7	3.8	3.9
0	0.0000	0.0000	0.0000	0.0000	0.0000	0.0000	0.0000	0.0000	0.0000	0.0000
5	0.1161	0.1152	0.1143	0.1135	0.1127	0.1120	0.1113	0.1106	0.1100	0.1094
10	0.2308	0.2289	0.2272	0.2255	0.2240	0.2226	0.2212	0.2199	0.2187	0.2175
15	0.3425	0.3397	0.3372	0.3348	0.3326	0.3304	0.3284	0.3266	0.3248	0.3231
20	0.4499	0.4463	0.4430	0.4399	0.4370	0.4343	0.4317	0.4293	0.4269	0.4247
25	0.5516	0.5473	0.5434	0.5397	0.5362	0.5329	0.5298	0.5268	0.5240	0.5214
30	0.6464	0.6415	0.6370	0.6328	0.6288	0.6250	0.6215	0.6181	0.6150	0.6120
35	0.7331	0.7278	0.7228	0.7182	0.7138	0.7097	0.7058	0.7021	0.6987	0.6954
40	0.8108	0.8052	0.7999	0.7949	0.7903	0.7859	0.7818	0.7779	0.7743	0.7708
45	0.8786	0.8728	0.8673	0.8622	0.8575	0.8530	0.8488	0.8448	0.8410	0.8375
50	0.9358	0.9300	0.9245	0.9194	0.9147	0.9102	0.9060	0.9021	0.8983	0.8948
55	0.9820	0.9763	0.9710	0.9661	0.9615	0.9572	0.9532	0.9494	0.9458	0.9424
60	1.0168	1.0115	1.0066	1.0020	0.9977	0.9937	0.9900	0.9864	0.9831	0.9799
65	1.0402	1.0355	1.0311	1.0270	1.0232	1.0196	1.0162	1.0131	1.0101	1.0073
70	1.0525	1.0485	1.0448	1.0413	1.0380	1.0350	1.0322	1.0295	1.0270	1.0246
75	1.0539	1.0508	1.0479	1.0451	1.0426	1.0402	1.0380	1.0359	1.0339	1.0321
80	1.0452	1.0430	1.0410	1.0391	1.0374	1.0357	1.0342	1.0328	1.0314	1.0301
85	1.0269	1.0258	1.0247	1.0238	1.0229	1.0221	1.0213	1.0206	1.0199	1.0192
90	1.0000	1.0000	1.0000	1.0000	1.0000	1.0000	1.0000	1.0000	1.0000	1.0000
95	0.9655	0.9666	0.9676	0.9686	0.9695	0.9703	0.9711	0.9718	0.9725	0.9732
100	0.9245	0.9266	0.9286	0.9305	0.9323	0.9339	0.9354	0.9369	0.9382	0.9395
105	0.8779	0.8810	0.8840	0.8867	0.8892	0.8916	0.8938	0.8959	0.8979	0.8998
110	0.8269	0.8309	0.8346	0.8381	0.8413	0.8444	0.8472	0.8499	0.8524	0.8548
115	0.7724	0.7771	0.7815	0.7856	0.7894	0.7930	0.7964	0.7995	0.8025	0.8053
120	0.7153	0.7206	0.7255	0.7300	0.7343	0.7383	0.7421	0.7457	0.7490	0.7522
125	0.6563	0.6620	0.6673	0.6722	0.6768	0.6811	0.6851	0.6889	0.6925	0.6959
130	0.5963	0.6021	0.6076	0.6126	0.6174	0.6219	0.6261	0.6300	0.6337	0.6373
135	0.5356	0.5415	0.5469	0.5520	0.5568	0.5612	0.5655	0.5694	0.5732	0.5767
140	0.4748	0.4804	0.4857	0.4907	0.4953	0.4997	0.5038	0.5077	0.5113	0.5148
145	0.4140	0.4194	0.4243	0.4290	0.4334	0.4375	0.4414	0.4450	0.4485	0.4518
150	0.3536	0.3585	0.3630	0.3673	0.3712	0.3750	0.3785	0.3819	0.3850	0.3880
155	0.2937	0.2979	0.3019	0.3056	0.3091	0.3124	0.3155	0.3184	0.3212	0.3238
160	0.2342	0.2377	0.2410	0.2441	0.2470	0.2498	0.2523	0.2548	0.2571	0.2593
165	0.1752	0.1779	0.1804	0.1828	0.1851	0.1872	0.1892	0.1911	0.1929	0.1946
170	0.1166	0.1184	0.1201	0.1218	0.1233	0.1247	0.1261	0.1274	0.1286	0.1298
175	0.0582	0.0591	0.0600	0.0608	0.0616	0.0623	0.0630	0.0637	0.0643	0.0649
180	0.0000	0.0000	0.0000	0.0000	0.0000	0.0000	0.0000	0.0000	0.0000	0.0000

Crank angle deg.	4.0	4.1	4.2	4.3	4.4	4.5	4.6	4.7	4.8	4.9	5.0
0	0.0000	0.0000	0.0000	0.0000	0.0000	0.0000	0.0000	0.0000	0.0000	0.0000	0.0000
5	0.1089	0.1083	0.1078	0.1073	0.1069	0.1064	0.1060	0.1056	0.1052	0.1049	0.1045
10	0.2164	0.2154	0.2144	0.2135	0.2125	0.2117	0.2109	0.2101	0.2093	0.2086	0.2079
15	0.3215	0.3199	0.3185	0.3171	0.3157	0.3145	0.3133	0.3121	0.3110	0.3099	0.3089
20	0.4227	0.4207	0.4188	0.4170	0.4153	0.4136	0.4121	0.4106	0.4091	0.4078	0.4064
25	0.5189	0.5165	0.5143	0.5121	0.5101	0.5081	0.5062	0.5044	0.5027	0.5011	0.4995
30	0.6091	0.6064	0.6038	0.6014	0.5991	0.5968	0.5947	0.5927	0.5907	0.5888	0.5870
35	0.6923	0.6893	0.6865	0.6838	0.6813	0.6788	0.6765	0.6743	0.6722	0.6701	0.6682
40	0.7675	0.7644	0.7614	0.7586	0.7559	0.7533	0.7509	0.7486	0.7463	0.7442	0.7421
45	0.8341	0.8309	0.8279	0.8250	0.8222	0.8196	0.8171	0.8147	0.8124	0.8102	0.8081
50	0.8915	0.8883	0.8853	0.8824	0.8797	0.8771	0.8746	0.8722	0.8700	0.8678	0.8657
55	0.9392	0.9361	0.9332	0.9305	0.9278	0.9253	0.9230	0.9207	0.9185	0.9164	0.9144
60	0.9769	0.9741	0.9714	0.9688	0.9664	0.9641	0.9619	0.9598	0.9577	0.9558	0.9540
65	1.0046	1.0021	0.9997	0.9974	0.9953	0.9932	0.9912	0.9894	0.9876	0.9859	0.9842
70	1.0224	1.0202	1.0182	1.0163	1.0145	1.0127	1.0111	1.0095	1.0080	1.0065	1.0051
75	1.0303	1.0287	1.0271	1.0256	1.0242	1.0228	1.0215	1.0203	1.0191	1.0180	1.0169
80	1.0289	1.0278	1.0267	1.0257	1.0247	1.0238	1.0229	1.0220	1.0212	1.0204	1.0197
85	1.0186	1.0180	1.0175	1.0169	1.0164	1.0160	1.0155	1.0151	1.0147	1.0143	1.0139
90	1.0000	1.0000	1.0000	1.0000	1.0000	1.0000	1.0000	1.0000	1.0000	1.0000	1.0000
95	0.9738	0.9744	0.9749	0.9754	0.9759	0.9764	0.9769	0.9773	0.9777	0.9781	0.9785
100	0.9407	0.9418	0.9429	0.9440	0.9449	0.9459	0.9468	0.9476	0.9484	0.9492	0.9499
105	0.9015	0.9032	0.9048	0.9063	0.9077	0.9090	0.9103	0.9116	0.9127	0.9139	0.9150
110	0.8570	0.8592	0.8612	0.8631	0.8649	0.8667	0.8683	0.8699	0.8714	0.8729	0.8742
115	0.8080	0.8105	0.8129	0.8152	0.8174	0.8194	0.8214	0.8233	0.8251	0.8268	0.8284
120	0.7551	0.7580	0.7607	0.7632	0.7657	0.7680	0.7702	0.7723	0.7743	0.7762	0.7781
125	0.6991	0.7022	0.7051	0.7078	0.7105	0.7130	0.7154	0.7176	0.7198	0.7219	0.7239
130	0.6406	0.6438	0.6468	0.6497	0.6524	0.6550	0.6575	0.6599	0.6621	0.6643	0.6664
135	0.5801	0.5833	0.5863	0.5892	0.5920	0.5946	0.5971	0.5995	0.6018	0.6040	0.6061
140	0.5181	0.5212	0.5242	0.5270	0.5297	0.5322	0.5347	0.5370	0.5393	0.5414	0.5435
145	0.4549	0.4578	0.4607	0.4633	0.4659	0.4683	0.4706	0.4729	0.4750	0.4770	0.4790
150	0.3909	0.3936	0.3962	0.3986	0.4009	0.4032	0.4053	0.4073	0.4093	0.4112	0.4130
155	0.3263	0.3287	0.3310	0.3331	0.3352	0.3371	0.3390	0.3408	0.3425	0.3442	0.3457
160	0.2614	0.2634	0.2652	0.2670	0.2688	0.2704	0.2720	0.2735	0.2749	0.2763	0.2776
165	0.1962	0.1977	0.1992	0.2006	0.2019	0.2032	0.2044	0.2055	0.2067	0.2077	0.2088
170	0.1309	0.1319	0.1329	0.1338	0.1348	0.1356	0.1364	0.1372	0.1380	0.1387	0.1394
175	0.0654	0.0660	0.0665	0.0670	0.0674	0.0679	0.0683	0.0687	0.0691	0.0694	0.0698
180	0.0000	0.0000	0.0000	0.0000	0.0000	0.0000	0.0000	0.0000	0.0000	0.0000	0.0000

Mechanisms for Producing Specific Types of Motions

Sigmund Rappaport

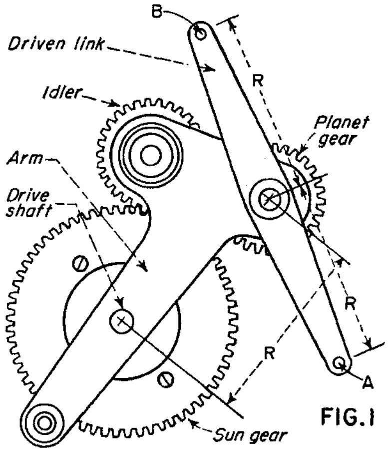

FIG. 1

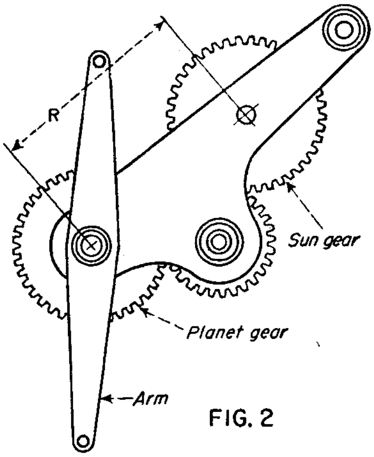

FIG. 2

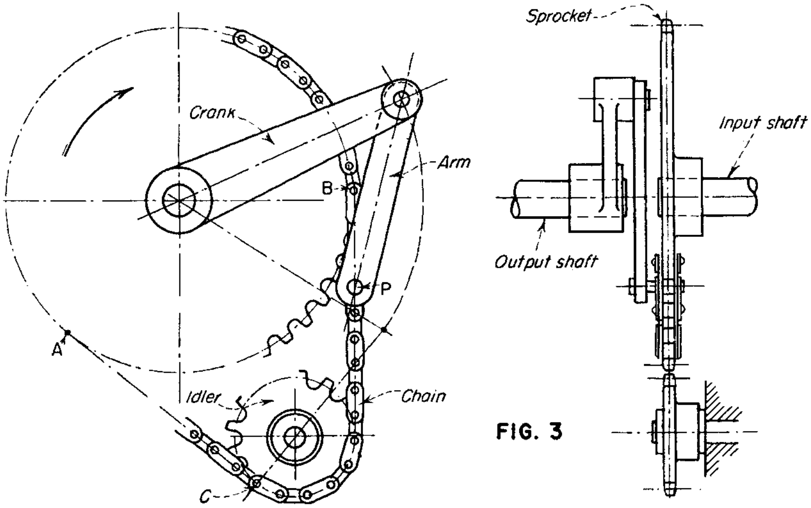

FIG. 3

Straight Line Motion

FIG. 1—No linkages or guides are used in this modified hypocyclic drive which is relatively small in relation to the length of its stroke. The sun gear of pitch diameter D is stationary. The drive shaft, which turns the T-shaped arm, is concentric with this gear. The idler and planet gears, the latter having a pitch diameter of $D/2$, rotate freely on pivots in the arm extensions. Pitch diameter of the idler is of no geometrical significance, although this gear does have an important mechanical function. It reverses the rotation of the planet gear, thus producing true hypocyclic motion with ordinary spur gears only. Such an arrangement occupies only about half as much space as does an equivalent mechanism containing an internal gear. Center distance R is the sum of $D/2$, $D/4$ and an arbitrary distance d, determined by a particular application. Points A and B on the driven link, which is fixed to the planet, describe straight-line paths through a stroke of $4R$. All points between A and B trace ellipses, while the line AB envelopes an astroid.

Parallel Motion

FIG. 2—A slight modification of the mechanism in Fig. 1 will produce another type of useful motion. If the planet gear has the same diameter as that of the sum gear, the arm will remain parallel to itself throughout the complete cycle. All points on the arm will thereby describe circles of radius R. Here again, the position and diameter of the idler gear are of no geometrical importance. This mechanism can be used, for example, to cross-perforate a uniformly moving paper web. The value for R is chosen such that $2\pi R$, or the circumference of the circle described by the needle carrier, equals the desired distance between successive lines of perforations. If the center distance R is made adjustable, the spacing of perforated lines can be varied as desired.

Intermittent Motion

FIG. 3—This mechanism, developed by the author and to his knowledge novel, can be adapted to produce a stop, a variable speed without stop or a variable speed with momentary reverse motion. Uniformly rotating input shaft drives the chain around the sprocket and idler, the arm serving as a link between the chain and the end of the output shaft crank. The sprocket drive must be in the ratio N/n with the cycle of the machine, where n is the number of teeth on the sprocket and N the number of links in the chain. When point P travels around the sprocket from point A to position B, the crank rotates uniformly. Between B and C, P decelerates; between C and A it accelerates;; and at C there is a momentary dwell. By changing the size and position of the idler, or the lengths of the arm and crank, a variety of motions can be obtained. If in the sketch, the length of the crank is shortened, a brief reverse period will occur in the vicinity of C; if the crank is lengthened, the output velocity will vary between a maximum and minimum without reaching zero.

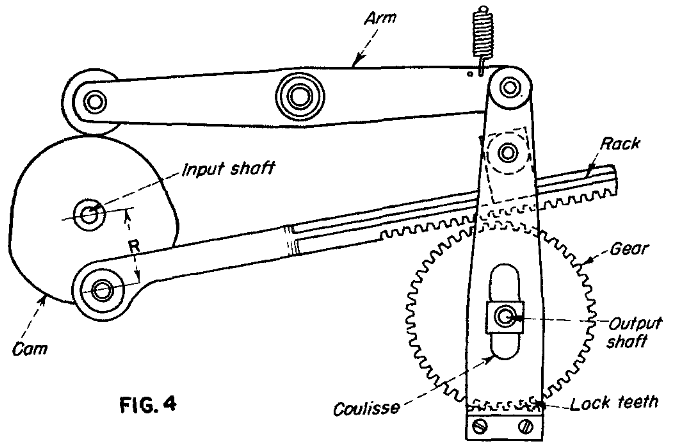

FIG. 4

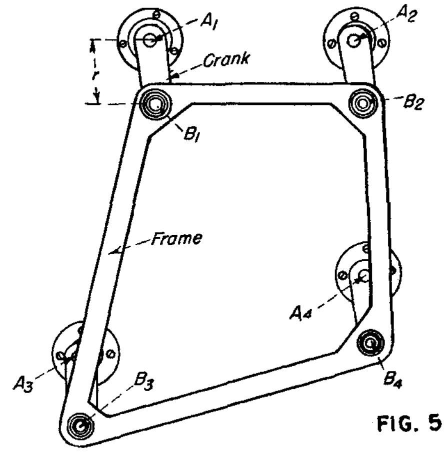

FIG. 5

Intermittent Motion

FIG. 4—An operating cycle of 180 deg motion and 180 deg dwell is produced by this mechanism. The input shaft drives the rack which is engaged with the output shaft gear during half the cycle. When the rack engages, the lock teeth at the lower end of the coulisse are disengaged and, conversely, when the rack is disengaged, the coulisse teeth are engaged, thereby locking the output shaft positively. The change-over points occur at the dead-center positions so that the motion of the gear is continuously and positively governed. By varying R and the diameter of the gear, the number of revolutions made by the output shaft during the operating half of the cycle can be varied to suit requirements.

Rotational Motion

FIG. 5—The absence of backlash makes this old but little used mechanism a precision, low-cost replacement for gear or chain drives otherwise used to rotate parallel shafts. Any number of shafts greater than two can be driven from any one of the shafts, provided two conditions are fulfilled: (1) All cranks must have the same length r; and (2) the two polygons formed by the shafts A and frame pivot centers B must be identical. The main disadvantage of this mechanism is its dynamic unbalance, which limits the speed of rotation. To lessen the effect of the vibrations produced, the frame should be made as light as is consistent with strength requirements.

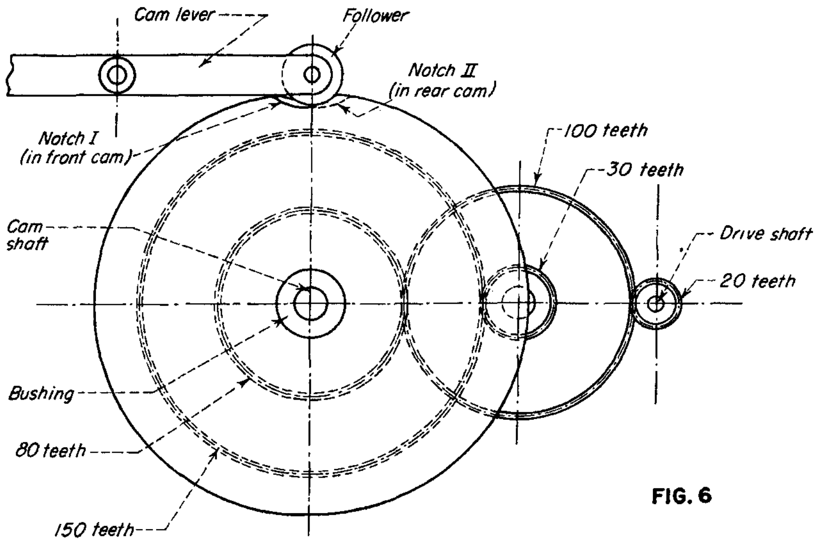

FIG. 6

Fast Cam-Follower Motion

FIG. 6—Fast cam action every n cycles when n is a relatively large number, can be obtained with this manifold cam and gear mechanism. A single notched cam geared $1/n$ to a shaft turning once a cycle moves relatively slowly under the follower. The double notched-cam arrangement shown is designed to operate the lever once in 100 cycles, imparting to it a rapid movement. One of the two identical cams and the 150-tooth gear are keyed to the bushing which turns freely around the cam shaft. The latter carries the second cam and the 80-tooth gear. The 30- and 100-tooth gears are integral, while the 20-tooth gear is attached to the one-cycle drive shaft. One of the cams turns in the ratio of 20/80 or 1/4; the other in the ratio 20/100 times 30/150 or 1/25. The notches therefore coincide once every 100 cycles (4×25). Lever movement is the equivalent of a cam turning in a ratio of 1/4 in relation to the drive shaft. To obtain fast cam action, n must be broken down into prime factors. For example, if 100 were factored into 5 and 20, the notches would coincide after every 20 cycles.

Traversing Mechanisms Used on Winding Machines

The seven mechanisms shown below are used on different types of yarn and coil winding machines. Their fundamentals, however, may be applicable to other machines which require similar changes of motion. Except for the lead screw as used, for example on lathes, these seven represent the operating principles of all well-known, mechanical types of traversing devices.

E. R. Swanson

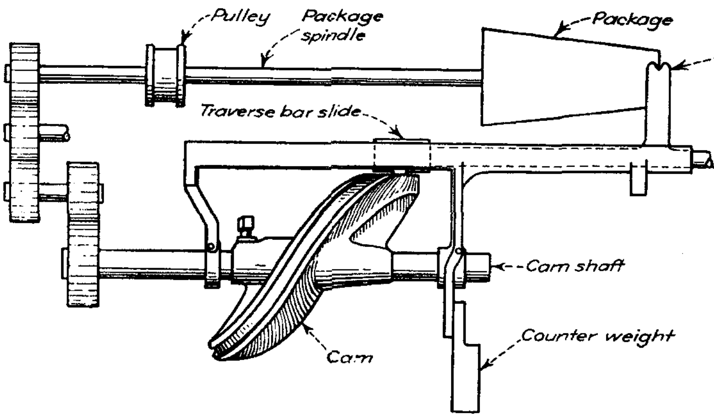

FIG. 1. Package is mounted on belt driven shaft on this precision type winding mechanism. Cam shaft imparts reciprocating motion to traverse bar by means of cam roll that runs in cam groove. Gears determine speed ratio between cam and package. Thread guide is attached to traverse bar. Counterweight keeps thread guide against package.

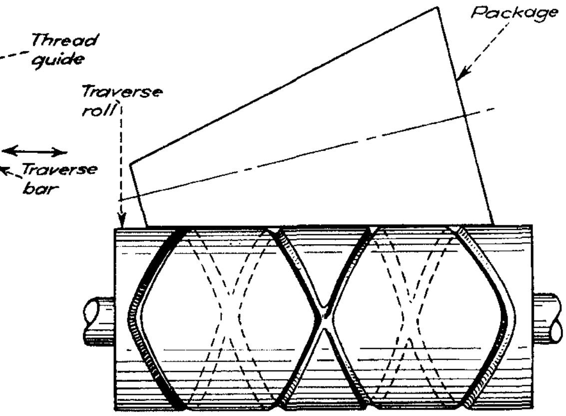

FIG. 2. Package is friction-driven from traverse roll. Yarn is drawn from the supply source by traverse roll and is transferred to package from the continuous groove in the roll. Different winds are obtained by varying the grooved path.

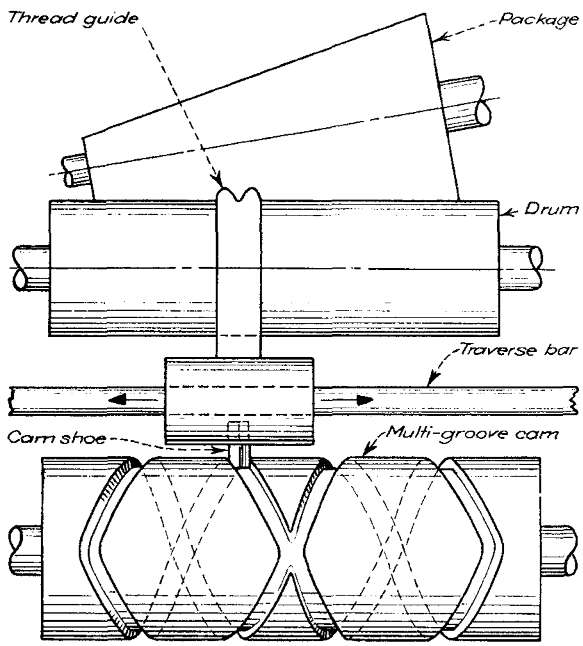

FIG. 4. Drum drives package by friction. Pointed cam shoe which pivots in the bottom side of the thread guide assembly rides in cam grooves and produces reciprocating motion of the thread guide assembly on the traverse bar. Plastic cams have proved quite satisfactory even with fast traverse speeds. Interchangeable cams permit a wide variety of winds.

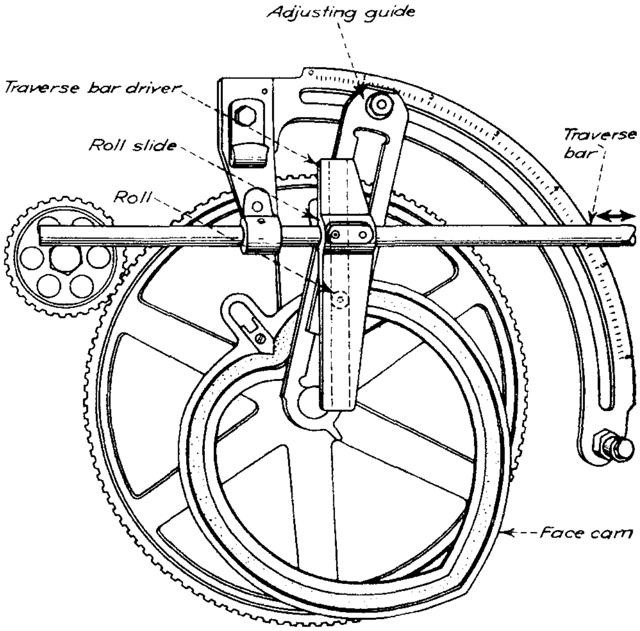

FIG. 5. Roll that rides in heart-shaped cam groove engages slot in traverse bar driver which is attached to the traverse bar. Maximum traverse is obtained when adjusting guide is perpendicular to the driver. As angle between guide and driver is decreased, traverse decreases proportionately. Inertia effects limit this type mechanism to slow speeds.

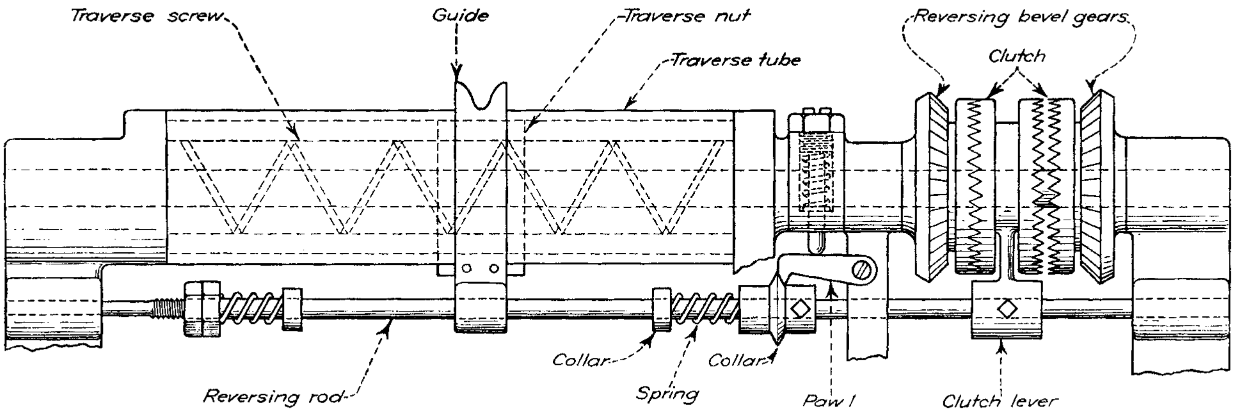

FIG. 3. Reversing bevel gears which are driven by a common bevel gear, drive the shaft carrying the traverse screw. Traverse nut mates with this screw and is connected to the yarn guide. Guide slides along the reversing rod. When nut reaches end of its travel, the thread guide compresses the spring that actuates the pawl and the reversing lever. This engages the clutch that rotates the traverse screw in the opposite direction. As indicated by the large pitch on the screw, this mechanism is limited to low speeds, but permits longer lengths of traverse than most of the others shown.

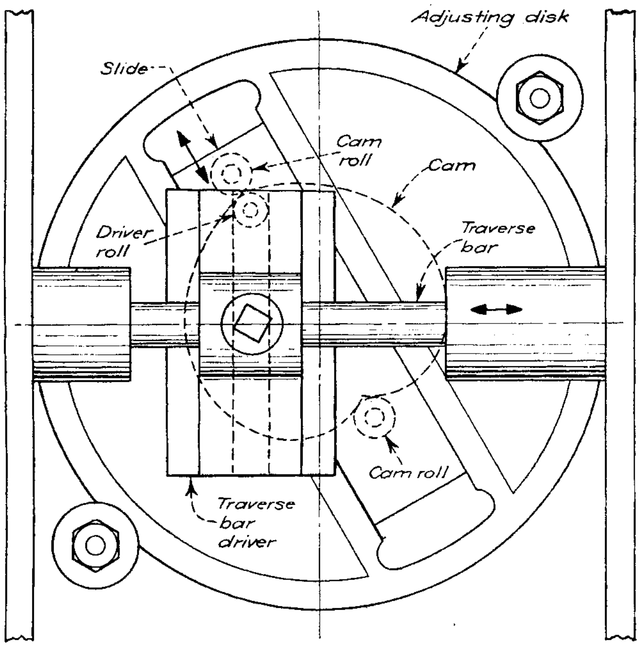

FIG. 6. Two cam rolls that engage heart shaped cam are attached to the slide. Slide has a driver roll that engages a slot in the traverse bar driver. Maximum traverse (to capacity of cam) occurs when adjusting disk is set so slide is parallel to traverse bar. As angle between traverse bar and slide increases, traverse decreases. At 90 deg traverse is zero.

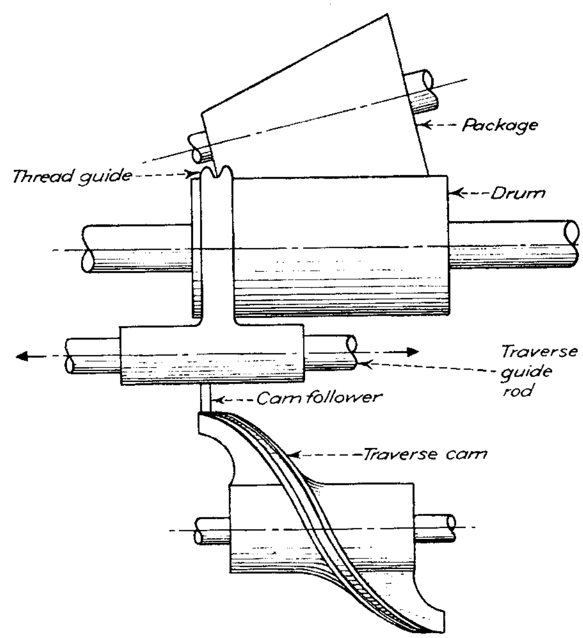

FIG. 7. Traverse cam imparts reciprocating motion to cam follower which drives thread guides on traverse guide rods. Package is friction driven from drum. Yarn is drawn from the supply source through thread guide and transferred to the drum-driven package. Speed of this type of mechanism is determined by the weight of the reciprocating parts.

Mechanisms for Providing Intermittent Rotary Motion

Eleven ways of converting uniform angular motion to intermittent angular motion and an explanation of two indirect ways to get this conversion.

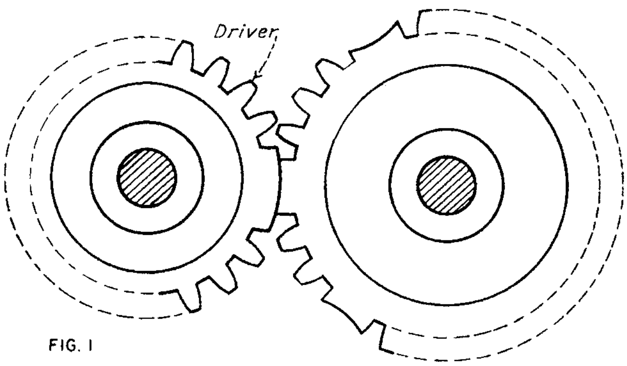

FIG. 1

EXTERNAL TIMING GEARS

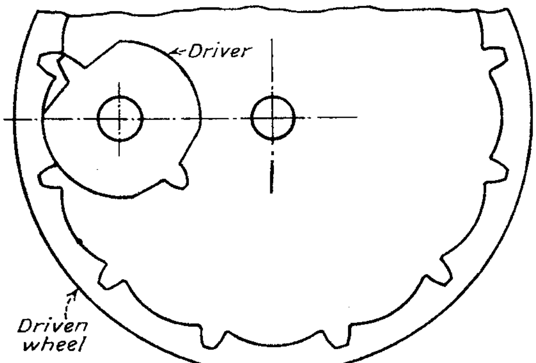

FIG. 2

INTERNAL TIMING GEARS.

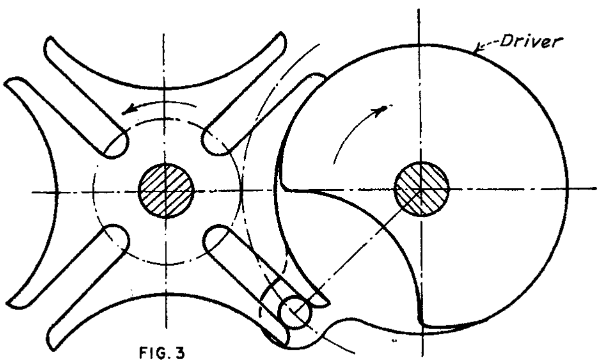

FIG. 3

EXTERNAL GENEVA MECHANISM. Operation is smoother than timing gears. Practical number of slots is from 3 to 18. Duration of dwell is more than 180 deg of driver rotation.

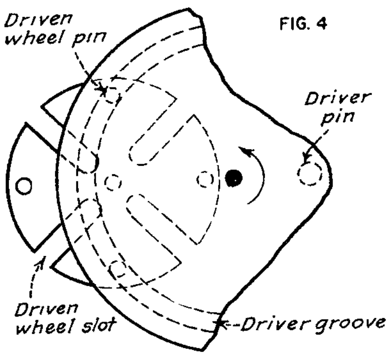

FIG. 4

EXTERNAL GENEVA MECHANISM. Difference from mechanism of of Fig. 3 lies in method of locking. Driver grooves lock driven wheel pins during dwell. During movement, driver pin mates with driven wheel slot.

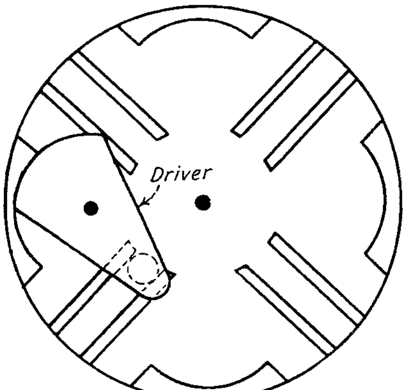

FIG. 5

INTERNAL GENEVA MECHANISM. Driver and driven wheel rotate in same direction. Duration of dwell is more than 180 deg of driver rotation.

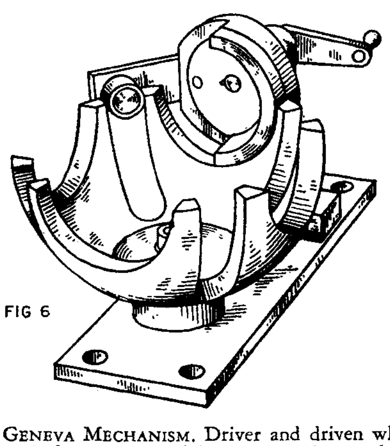

FIG 6

SPHERICAL GENEVA MECHANISM. Driver and driven wheel are on perpendicular shafts. Duration of dwell is exactly 180 deg of driver rotation.

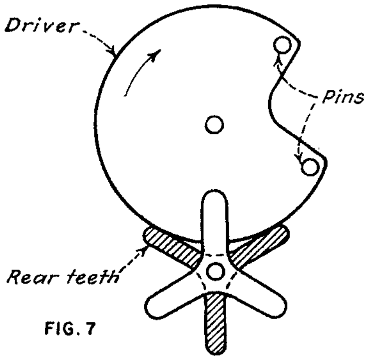

FIG. 7

INTERMITTENT COUNTER MECHANISM. One revolution of driver advances driven wheel 120 degrees. Driven wheel rear teeth locked on cam surface during dwell.

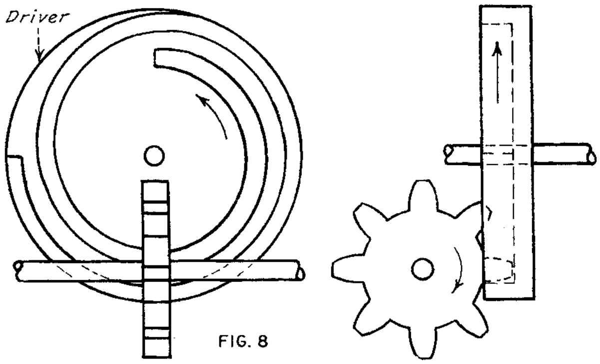

FIG. 8

SPIRAL AND WHEEL. One revolution of spiral advances driven wheel 1 tooth. Driven wheel tooth locked in driver groove during dwell.

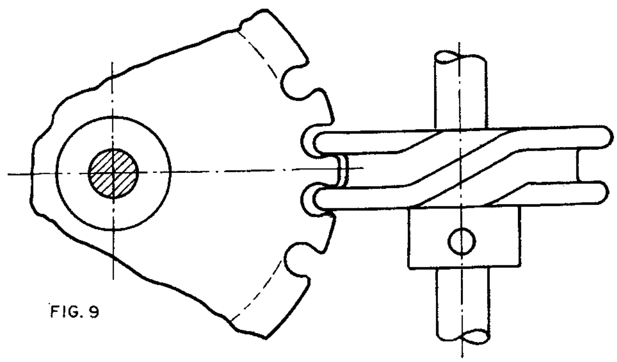

FIG. 9

SPECIAL WORM AND WHEEL. Spiral of Fig. 8 is replaced by special worm.

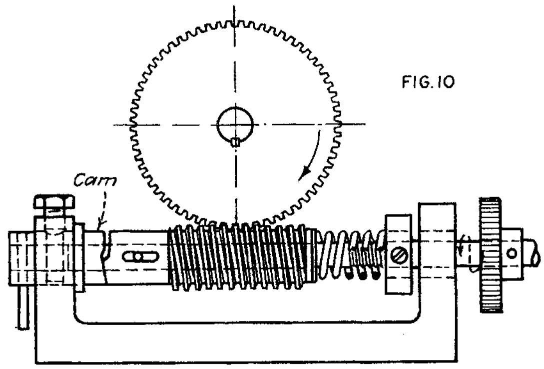

FIG. 10

WORM, CAM AND WHEEL. Standard worm and cam replace special worm of Fig. 9.

FIG. 11

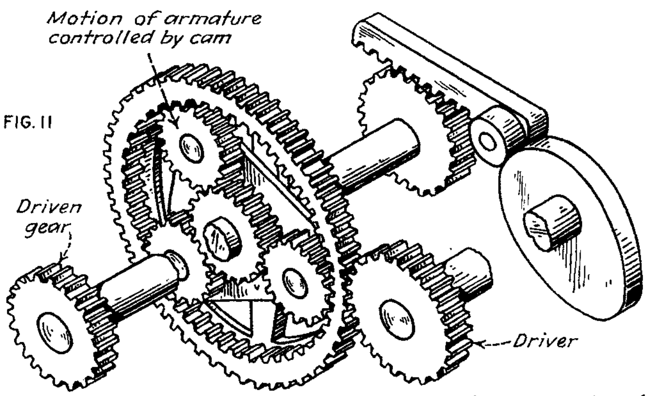

SPECIAL PLANETARY GEAR MECHANISM. Principle of relative motion of mating gears illustrated in Fig. 10 can be applied to spur gears in planetary system. Motion of normally fixed planet centers produces intermittent motion of sum gear.

THE CONVERSION of a uniform rotation to an intermittent rotation need not be performed in a single step. Two ways in which this can be carried out in two steps are:

1. Conversion of uniform rotation to reciprocating motion followed by conversion of reciprocating motion to intermittent motion.

2. Conversion of uniform rotation to angular oscillation followed by conversion of angular oscillation to intermittent rotation.

Fig. 11—Courtesy G. J. Tarbourdet, ASME paper No. 48-SA-18.

Intermittent Movements and Mechanisms

SEVERAL RECENTLY PATENTED mechanisms for producing intermittent motion are included in this group of devices. Many of the simpler and well-known mechanisms such as the common ratchet and pawl with its many modifications, escapements, numerous variations of the Geneva mechanisms and timed electrical contactors have been intentionally omitted in favor of the more ingenious combinations of mechanisms for accomplishing intermittent motion under unusual conditions.

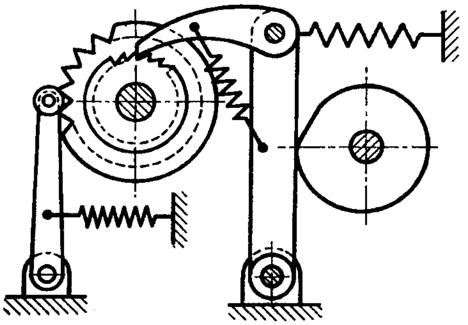

FIG. 1– CAM DRIVEN RATCHET

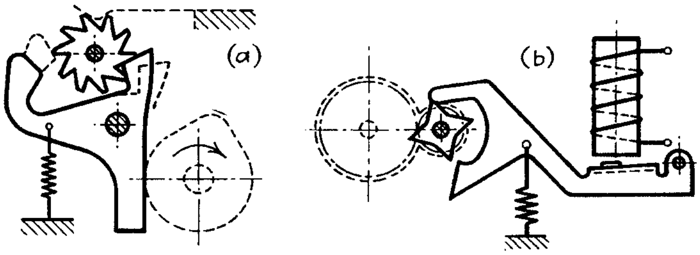

FIG. 3– (a) CAM OPERATED ESCAPEMENT ON A TAXIMETER
(b) SOLENOID OPERATED ESCAPEMENT

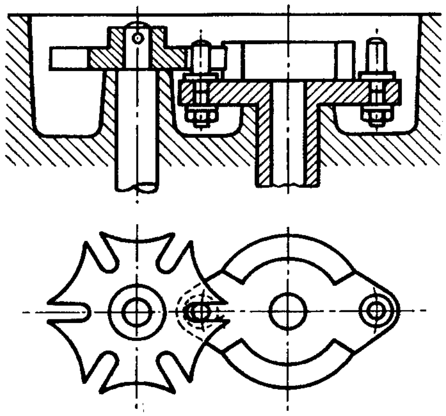

FIG. 2– SIX-SIDED MALTESE CROSS AND DOUBLE DRIVER GIVES 3:1 RATIO

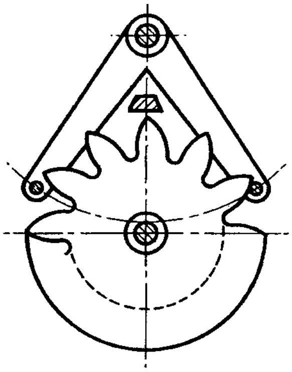

FIG. 4– ESCAPEMENT USED ON AN ELECTRIC METER

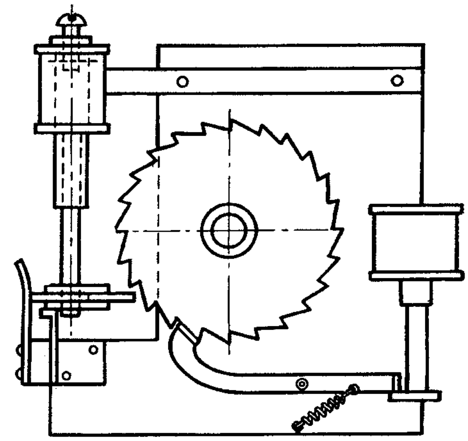

FIG. 5– SOLENOID-OPERATED RATCHET WITH SOLENOID RESETING MECHANISM. A SLIDING WASHER ENGAGES TEETH

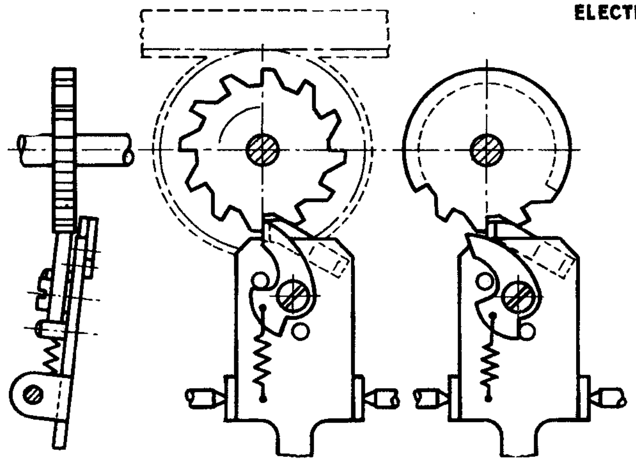

FIG. 6– PLATE OSCILLATING ACROSS PLANE OF RATCHET GEAR ESCAPEMENT CARRIES STATIONARY AND SPRING HELD PAWLS

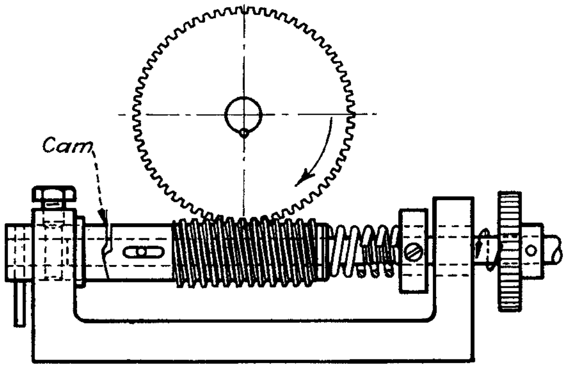

FIG. 7– WORM DRIVE COMPENSATED BY CAM ON WORK SHAFT, PRODUCES INTERMITTENT MOTION OF GEAR

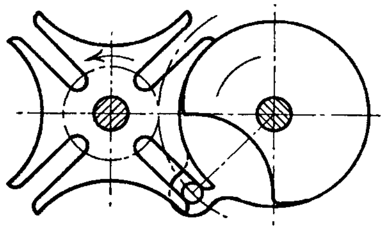

FIG. 8- GENEVA MECHANISM

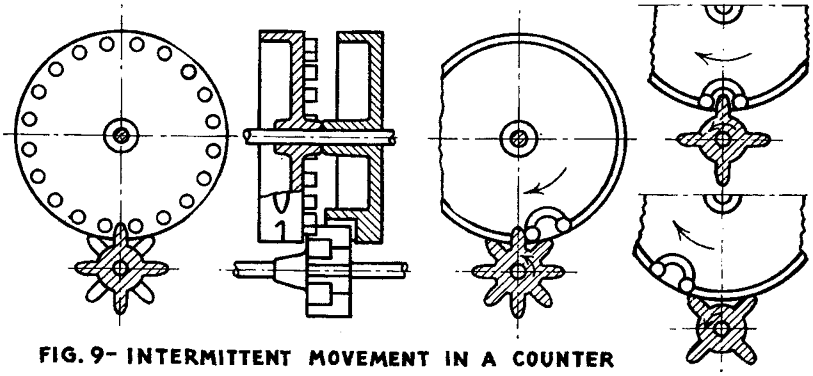

FIG. 9- INTERMITTENT MOVEMENT IN A COUNTER

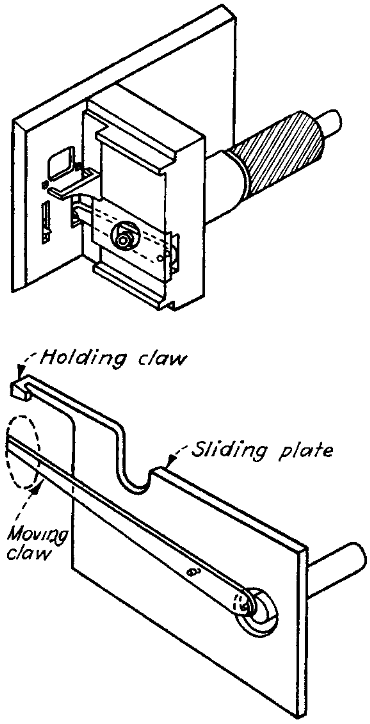

FIG. 10-MOTION PICTURE FILM MOVEMENTS FEATURING SIMPLICITY, FEW OPERATING PARTS, QUIETNESS

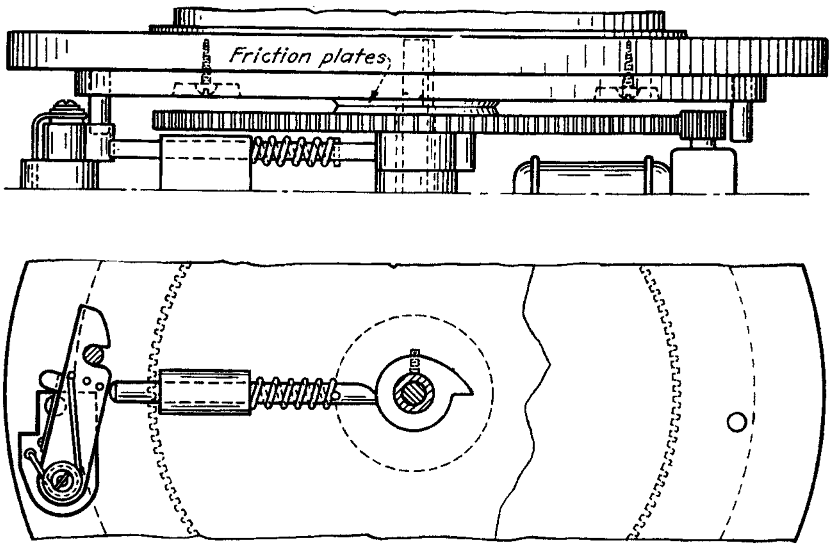

FIG. 11-DISPLAY SIGN MOVEMENT DEPENDS ON FRICTION AND USES A CAM-OPERATED LOCKING MECHANISM. ELECTRICALLY-OPERATED LOCKING MECHANISM HAS ALSO BEEN WORKED OUT BY MEANS OF TIMED-ELECTRIC CONTACTS AND MOTOR-DRIVEN LOCK PARTS

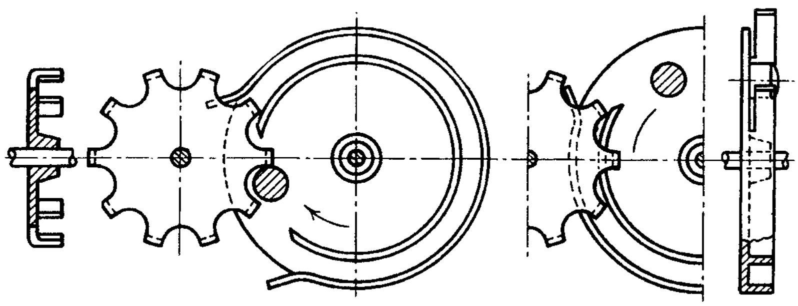

FIG. 12-MODIFICATION OF THE GENEVA MECHANISM

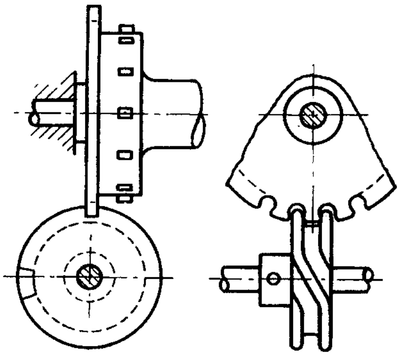

FIG. 13- SIMPLE WORM GEAR MECHANISM

Friction Devices for Intermittent Rotary Motion

W. M. Halliday

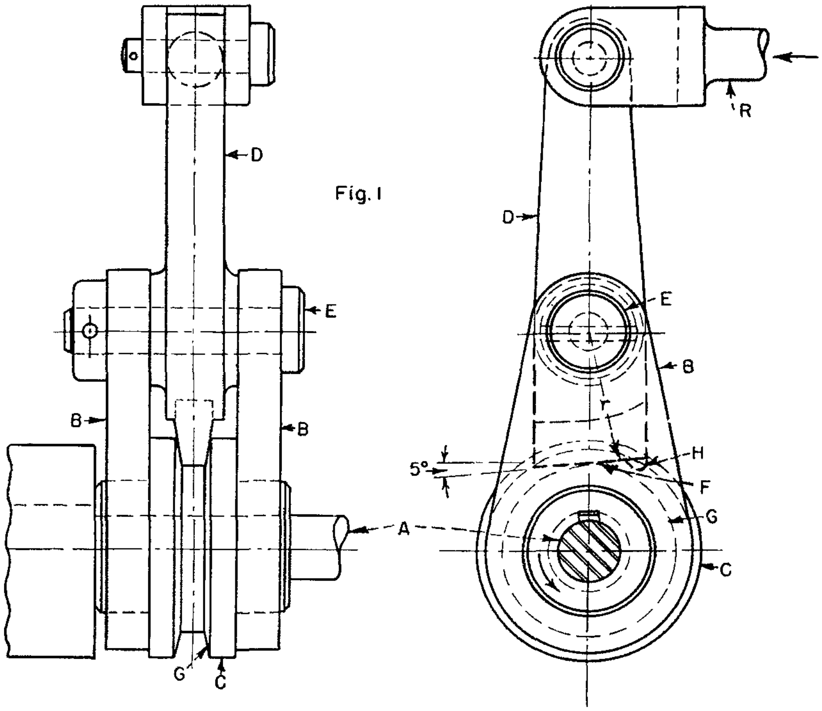

FIG. 1—WEDGE AND DISK. Consists of shaft A supported in bearing block J; ring C keyed to A and containing an annular groove G; body B which can pivot around the shoulders of C; lever D which can pivot about E; and connecting rod R driven by an eccentic (not shown). Lever D is rotated counterclockwise about E by the connecting rod moving to the left until surface F wedges into groove G. Continued rotation of D causes A, B and D to rotate counterclockwise as a unit about A. Reversal of input motion instantly swivels F out of G, thus unlocking the shaft which remains stationary during return stroke because of friction induced by its load. As D continues to rotate clockwise about E, node H, which is hardened and polished to reduce friction, bears against bottom of G to restrain further swiveling. Lever D now rotates with B around A until end of stroke.

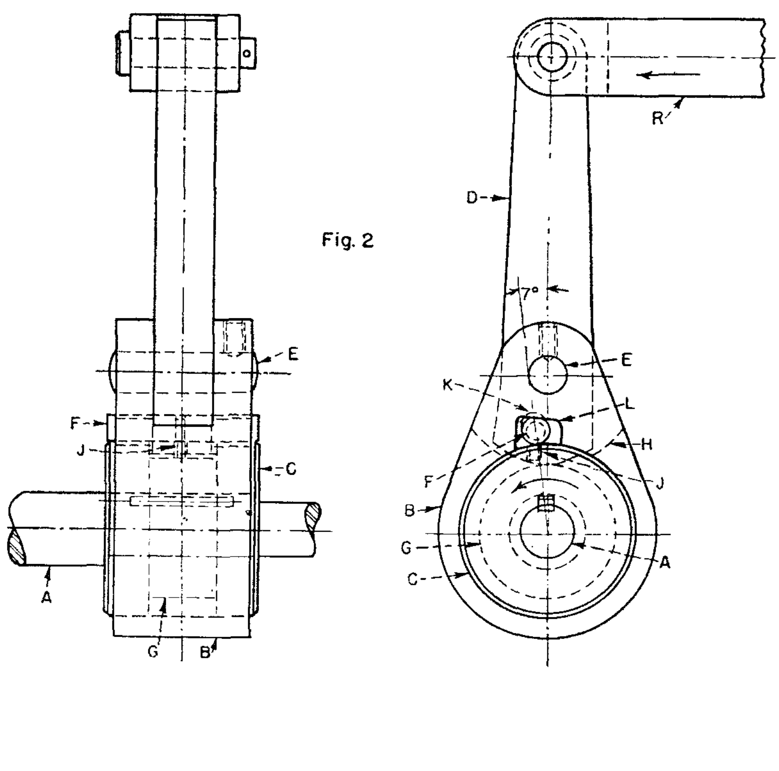

FIG. 2—PIN AND DISK. Lever D, which pivots around E, contains pin F in an elongated hole K which permits slight vertical movement of pin but prevents horizontal movement by means of set screw J. Body B can rotate freely about shaft A and has cut-outs L and H to allow clearances for pin F and lever D, respectively. Ring C, which is keyed to shaft A, has an annular groove G for clearance of the tip of lever D. Counterclockwise motion of lever D actuated by the connecting rod jams pin between C and the top of cut-out L. This occurs about seven degrees from the vertical axis. A, B and D are now locked together and rotate about A. Return stroke of R pivots D around E clockwise and unwedges pin until it strikes side of L. Continued motion of R to the right rotates B and D clockwise around A while the uncoupled shaft remains stationary because of its load.

Friction devices are free from the common disadvantages inherent in conventional pawl and ratchet drives such as: (1) noisy operation; (2) backlash needed for engagement of pawl; (3) load concentrated on one tooth of the ratchet; and (4) pawl engagement dependent on an external spring.

The five mechanisms presented here convert the reciprocating motion of a connecting rod into intermittent rotary motion. The connecting rod stroke to the left drives a shaft counterclockwise; shaft is uncoupled and remains stationary during the return stroke of connecting rod to the right.

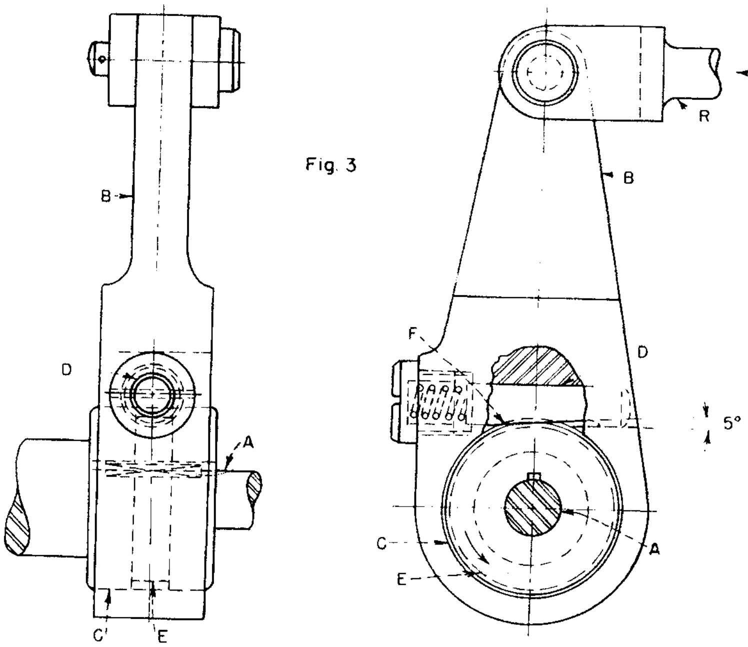

FIG. 3—SLIDING PIN AND DISK. Counterclockwise movement of body B about shaft A draws pin D to the right with respect to body B, aided by spring pressure, until the flat bottom F of pin is wedged against annular groove E of ring C. Bottom of pin is inclined about five degrees for optimum wedging action. Ring C is keyed to A and parts A, C, D and B now rotate counterclockwise as a unit until end of connecting rod's stroke. Reversal of B draws pin out of engagement so that A remains stationary while body completes its clockwise rotation.

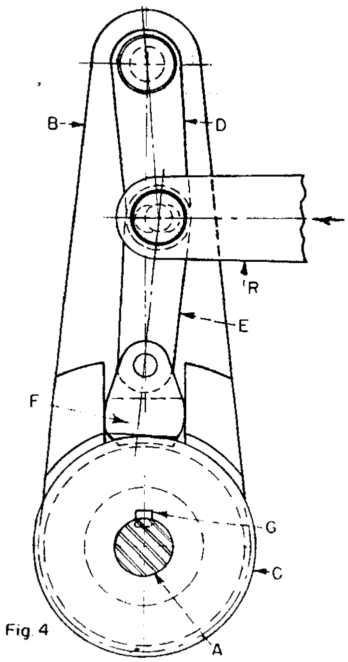

FIG. 4—TOGGLE LINK AND DISK. Input stroke of connecting rod R to the left wedges block F in groove G by straightening toggle links D and E. Body B, toggle links and ring C which is keyed to shaft A, rotate counterclockwise together about A until end of stroke. Reversal of connecting rod motion lifts block, thus uncoupling shaft, while body B continues clockwise rotation until end of stroke.

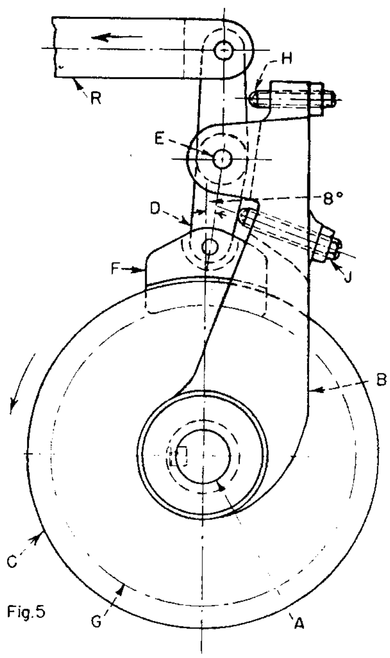

FIG. 5—ROCKER ARM AND DISK. Lever D, activated by the reciprocating bar R moving to the left, rotates counterclockwise on pivot E thus wedging block F into groove G of disk C. Shaft A is keyed to C and rotates counterclockwise as a unit with body B and lever D. Return stroke of R to the right pivots D clockwise about E and withdraws block from groove so that shaft is uncoupled while D, striking adjusting screw H, travels with B about A until completion of stroke. Adjusting screw J prevents F from jamming in groove.

Basic Types of Variable Speed Friction Drives

Haim Murro

THESE DRIVES are used to transmit both high torque, as on power spindle presses, and low torque, as in laboratory instruments. All perform best if used to reduce and not to increase speed. All friction drives have a certain degree of slip due to imperfect rolling of the friction members, but by correct design this slip can be held constant, resulting in constant speed of the driven member. Variations in load should be compensated by inertia masses on the driven end. Springs or similar elastic members can be used to keep the friction parts in constant contact and exert the force necessary to create the friction. In some cases, gravity will take place of such members. Specially made friction materials are generally recommended, but leather or rubber are often satisfactory. Normally only one of the friction members is made or lined with this material, while the other is metal.

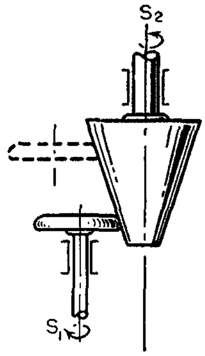

Fig. 1

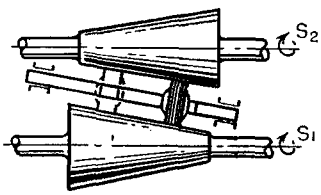

Fig. 2

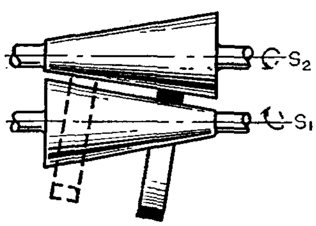

Fig. 3

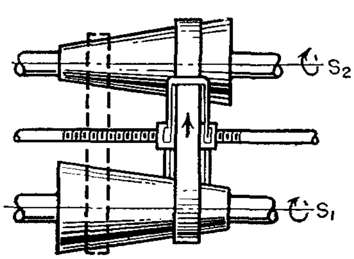

Fig. 4

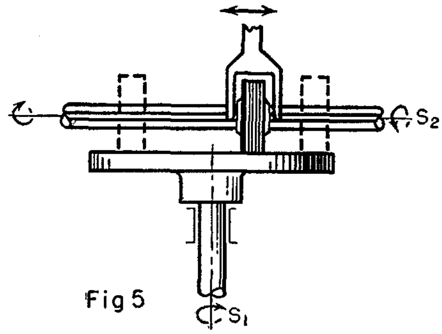

Fig 5

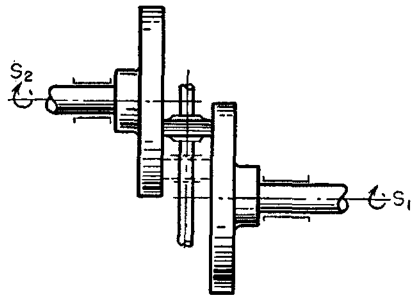

Fig. 6

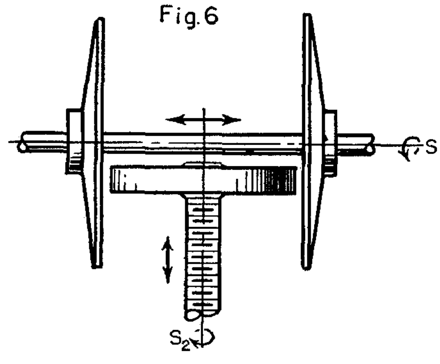

Fig. 7

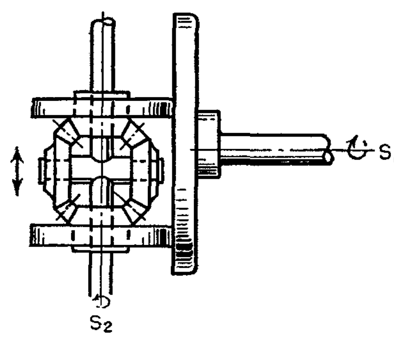

Fig. 8

Fig. 1—Cone and roller drive. Speed varies in accordance with axial position of roller on the cone and its operating diameter.

Fig. 2—Two cones and a free spinning roller that can be moved along the surfaces of the cones.

Fig. 3—Two cones and a free endless leather belt between them. The belt is shifted between cone faces to obtain the desired speed ratio.

Fig. 4—Two cones belted by a flat movable belt. Two metal fingers position belt along faces of the cones.

Fig. 5—A disk and roller drive. Roller is moved radially on the disk. Speed ratio depends upon the operating diameter of disk. Direction of relative rotation of shafts is reversed when roller is moved past the center of the disk as indicated by dotted lines.

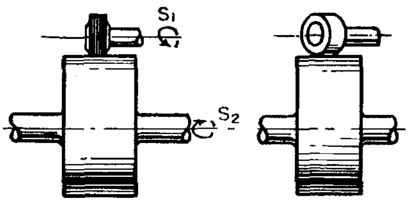

Fig. 9

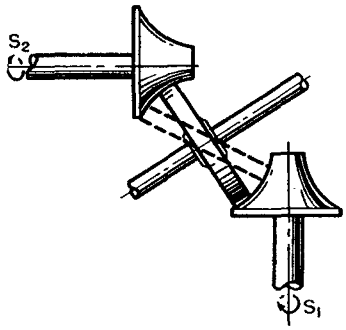

Fig. 10

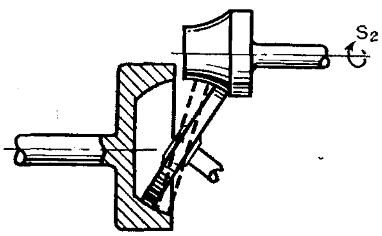

Fig. 11

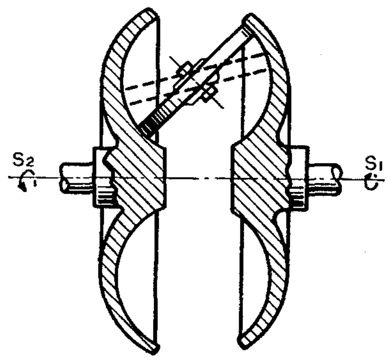

Fig. 12

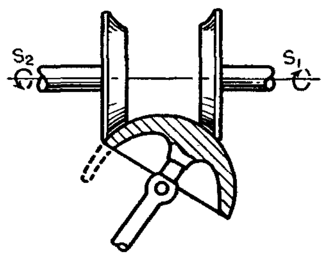

Fig. 13

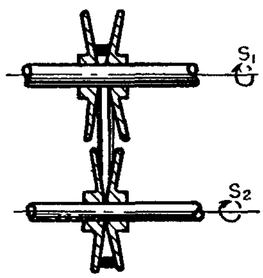

Fig. 14

Fig. 6—Two disks and a free spinning roller, movable between them. Change of speed will be fast, because the operating diameters of the disks change in an inverse ratio.

Fig. 7—Two disks mounted on same shaft and a roller mounted on a threaded spindle. Contact of roller can be changed from one disk to the other to change direction of rotation. Rotation will be accelerated or decelerated with movement of the screw.

Fig. 8—Disk and two differential rollers. Rollers and their bevel gears are free to rotate on shaft, S_2. Other two bevel gears are free to rotate on pins connected by S_2. Good for high reduction and accurate adjustment of speed. S_2 will have the differential speed of the two rollers. Differential assembly is movable across face of disk.

Fig. 9—Drum and roller. Change of speed is effected by skewing the roller relative to the drum.

Fig. 10—Two spherical cones on intersecting shafts and a free roller.

Fig. 11—Spherical cone and groove with a roller. Suitable when small adjustments in speed are desired.

Fig. 12—Two disks with torus contours and a free rotating roller.

Fig. 13—Two disks with a spherical free rotating roller.

Fig. 14—Split pulleys for V belts. Effective diameter of belt grip can be adjusted by controlling distance between two parts of pulley.

Speed Control for Small Mechanisms

Friction devices, actuated by centrifugal force, automatically keep speed constant regardless of variation of load or driving force.

Federico Strasser

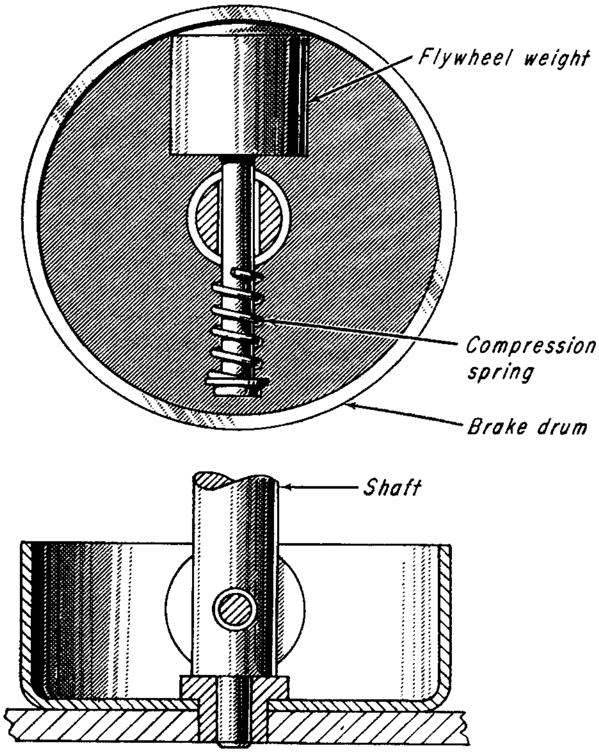

1

WEIGHT counterbalanced by a spring brakes the shaft when rotation speed becomes too high. Braking area is small.

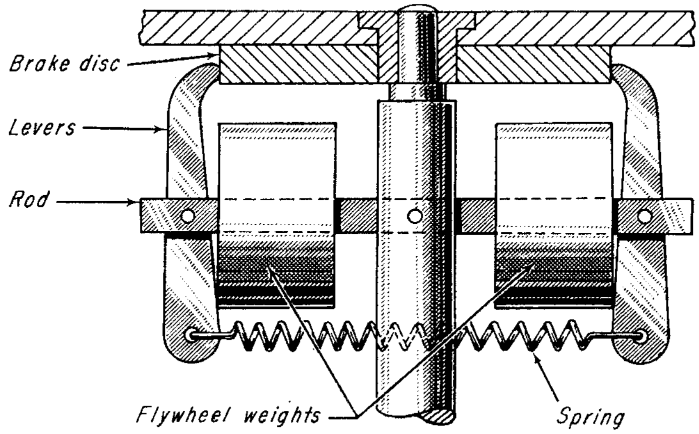

2

WEIGHT-ACTUATED LEVERS make this arrangement suitable where high braking moments are required.

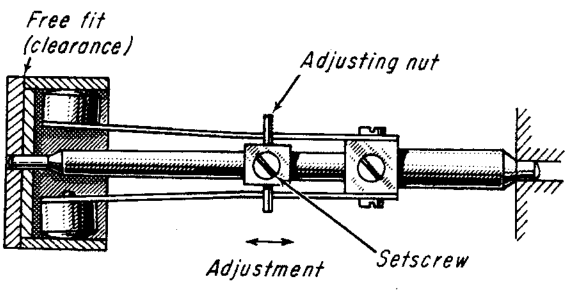

5

ADJUSTMENT of speed at which this device starts to brake is quick and easy. Adjusting nut is locked in place with setscrew.

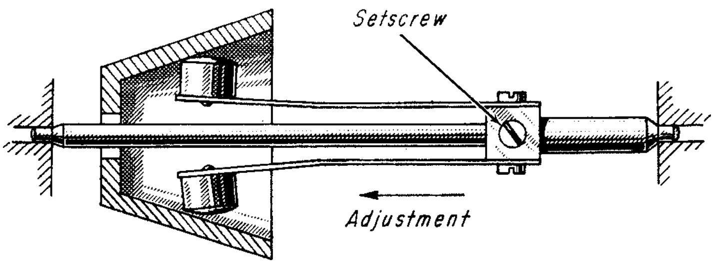

6

TAPERED BRAKE DRUM is another way of providing for varying speed-control. The adjustment is again locked.

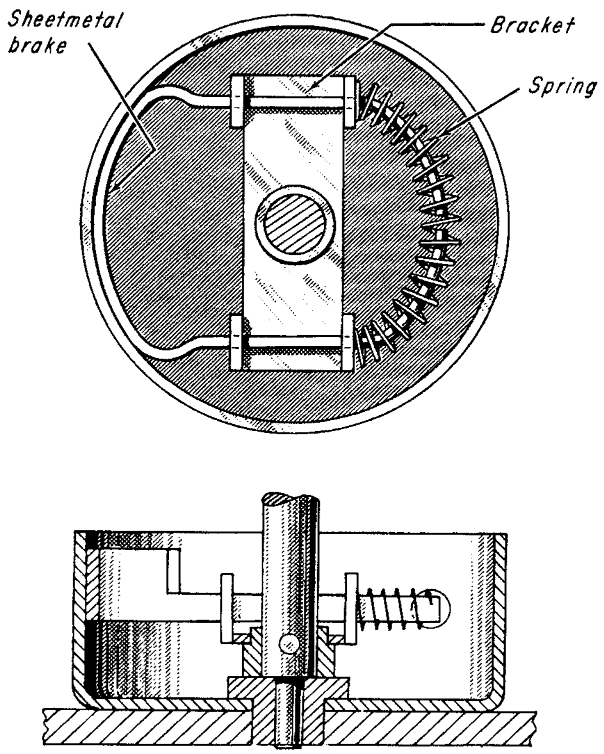

3

SHEETMETAL BRAKE provides larger braking area than previous design. Operation is thus more even and cooler.

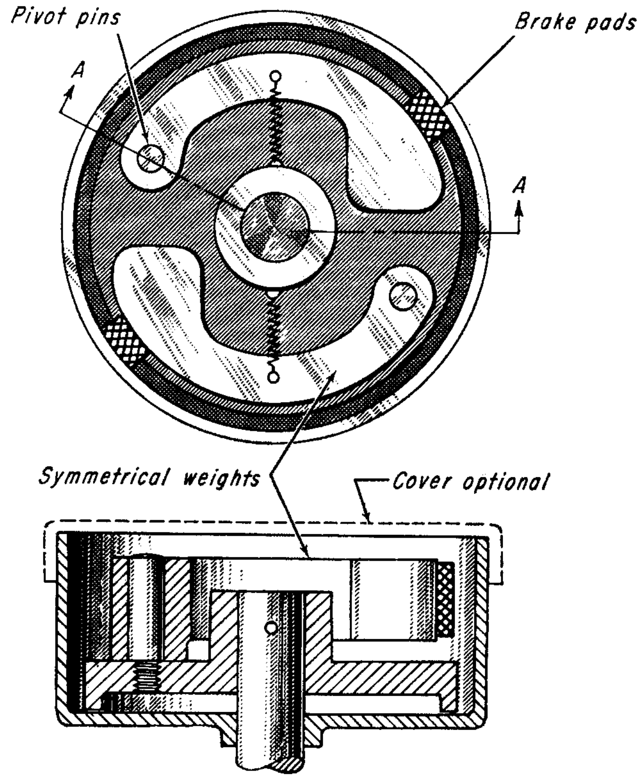

Section A-A

4

SYMMETRICAL WEIGHTS give even braking action when they pivot outward. Entire action can be enclosed.

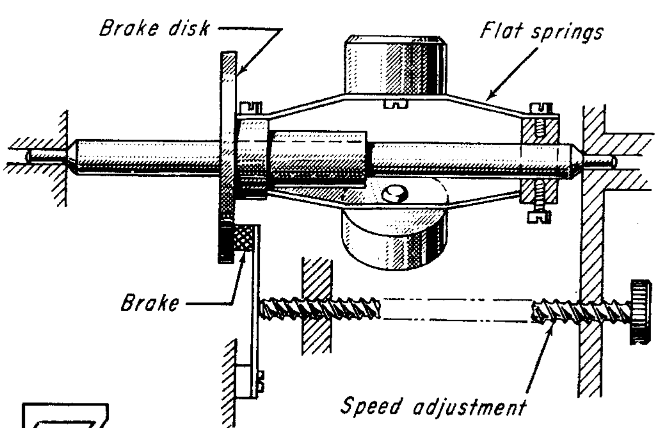

7

THREE FLAT SPRINGS carry weights that provide brake force upon rotation. Device can be provided with adjustment.

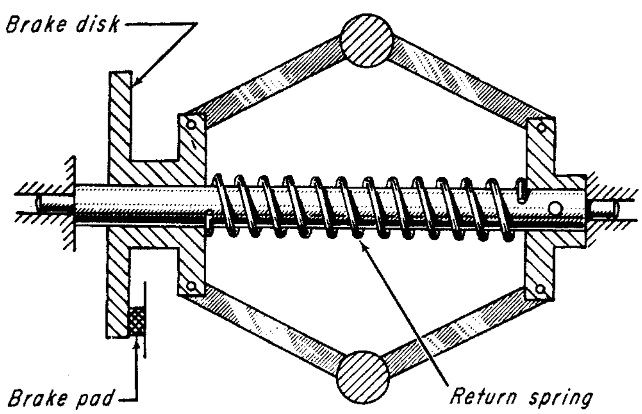

8

TYPICAL GOVERNOR action of swinging weights is utilized here. As in the previous device, adjustment is optional.

Mechanical Devices for Automatically Governing Speed

Speed governors, designed to maintain speeds of machines within reasonably constant limits irrespective of loads, may depend for their action upon centrifugal force or cam linkages. Other types may utilize pressure differentials and fluid velocities as their actuating media. Examples of these governing devices are illustrated.

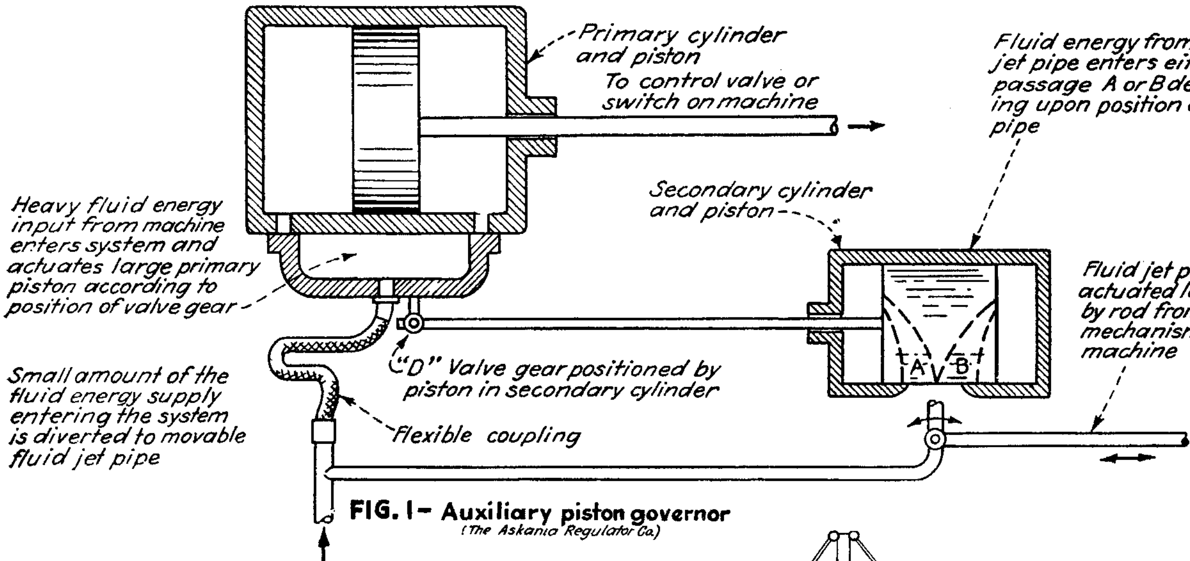

FIG. 1– Auxiliary piston governor
(The Askania Regulator Co.)

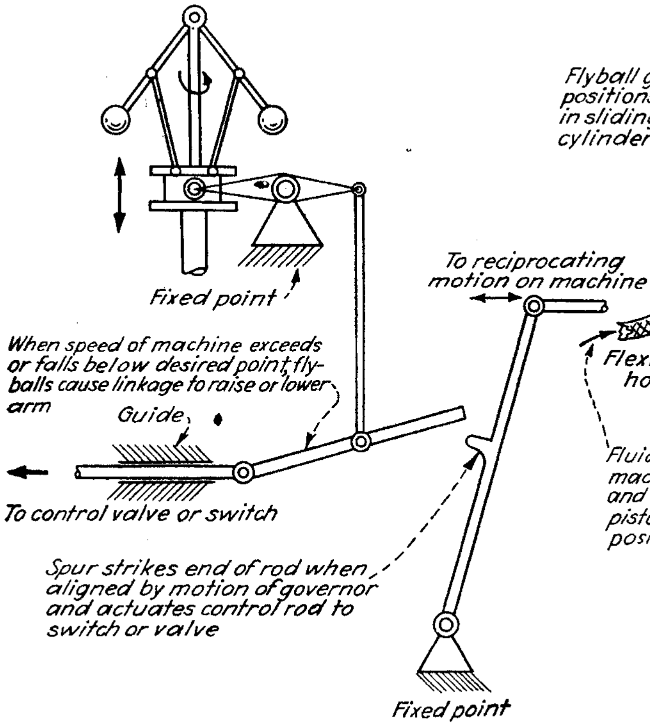

FIG. 2– Hit-and-miss governor

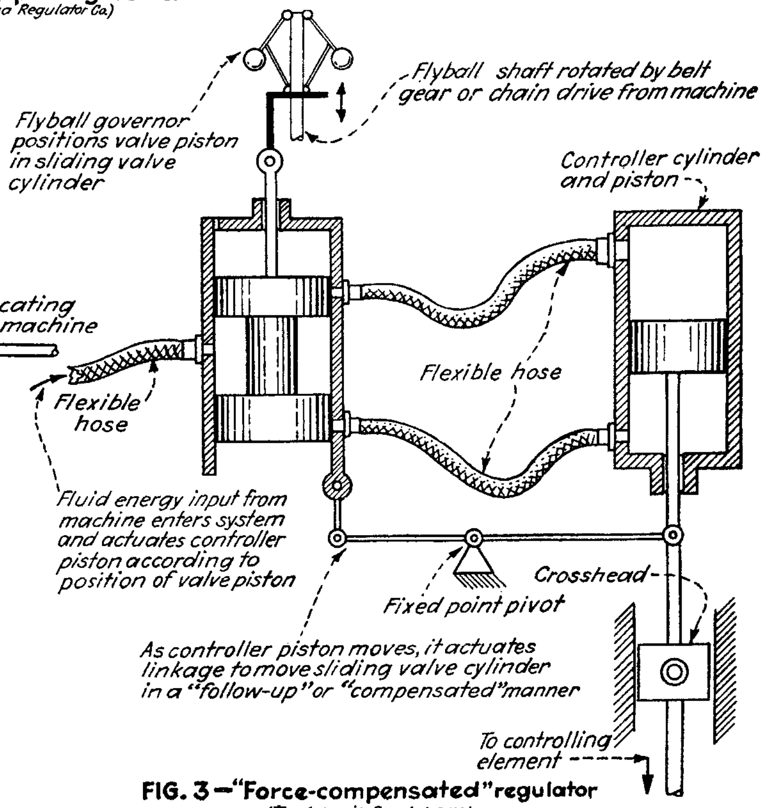

FIG. 3–"Force-compensated" regulator
(The Askania Regulator Co.)

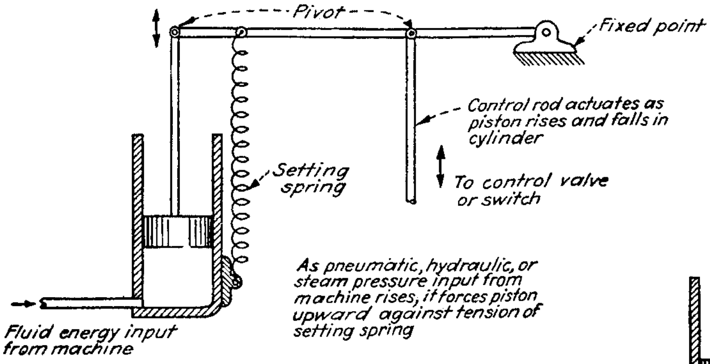

FIG. 4— Pressure-actuated governor

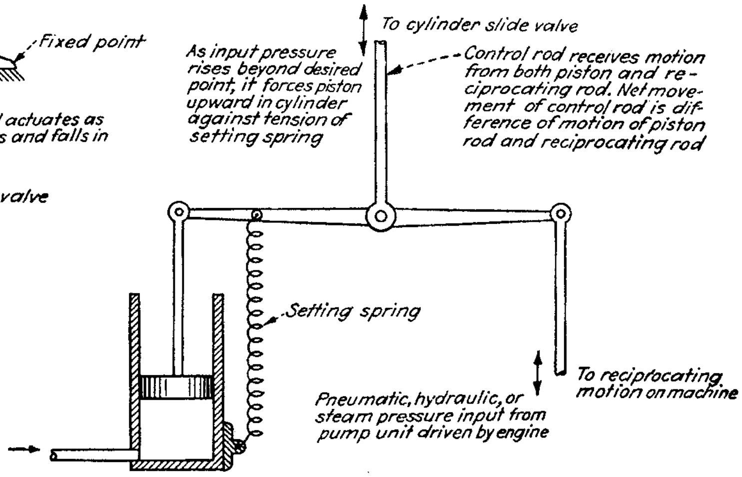

FIG. 5— Varying differential governor

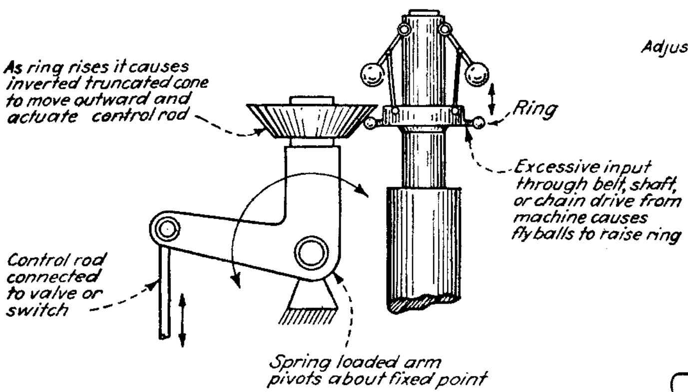

FIG. 6— Centrifugal governor

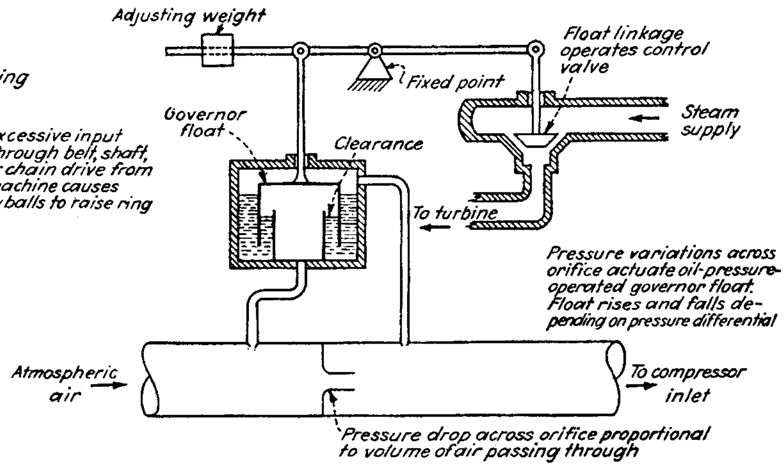

FIG. 7— Constant volume governor

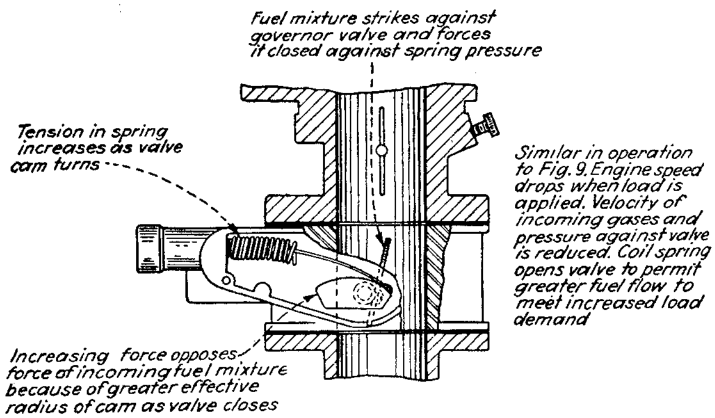

FIG. 8— Velocity-type governor (coil spring)

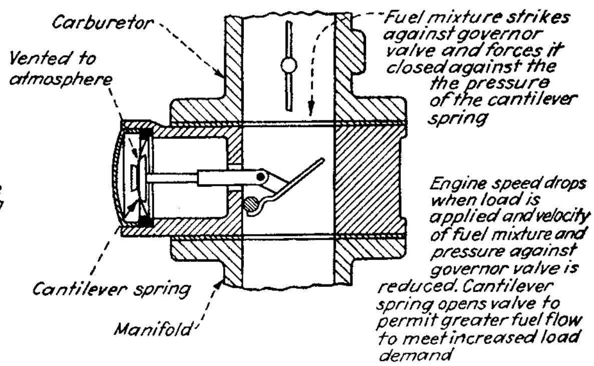

FIG. 9— Velocity-type governor (cantilever spring)

Accelerated and Decelerated Linear motion Elements

John E. Hyler

When ordinary rotary cams cannot be conveniently applied, the mechanisms here presented, or adaptations of them, offer a variety of interesting possibilities for obtaining either acceleration or deceleration, or both

FIG. 1—Slide block moves at constant rate of reciprocating travel and carries both a pin for mounting link *B* and a stud shaft on which the pinion is freely mounted. Pinion carries a crankpin for mounting link *D* and engages stationary rack, the pinion may make one complete revolution at each forward stroke of slide block and another in opposite direction on the return—or any portion of one revolution in any specific instance. Many variations can be obtained by making the connection of link *F* adjustable lengthwise along link that operates it, by making crankpin radially adjustable, or by making both adjustable.

FIG. 2—Drive rod, reciprocating at constant rate, rocks link *BC* about pivot on stationary block and, through effect of toggle, causes decelerative motion of driven link. As drive rod advances toward right, toggle is actuated by encountering abutment and the slotted link *BC* slides on its pivot while turning. This lengthens arm *B* and shortens arm *C* of link *BC*, with decelerative effect on driven link. Toggle is spring-returned on the return stroke and effect on driven link is then accelerative.

FIG. 3—Same direction of travel for both the drive rod and the driven link

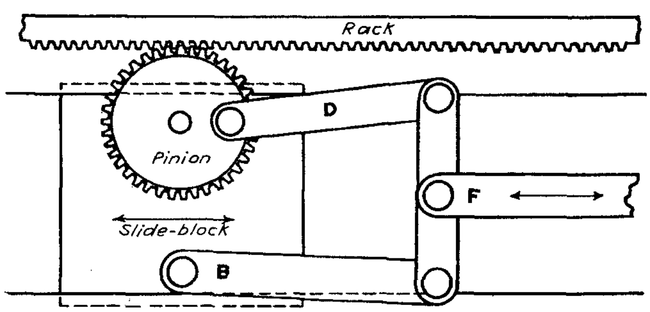

FIG. 1

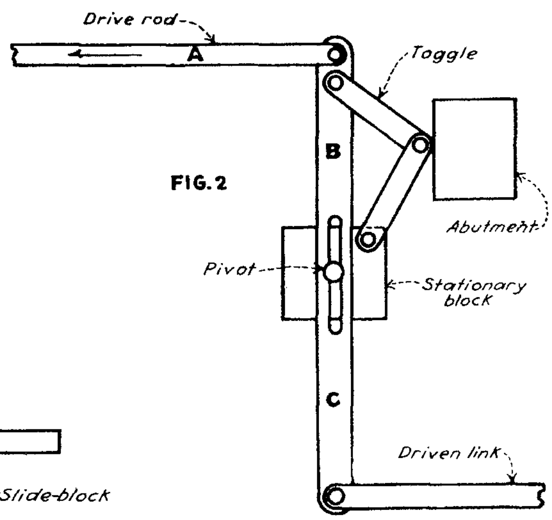

FIG. 2

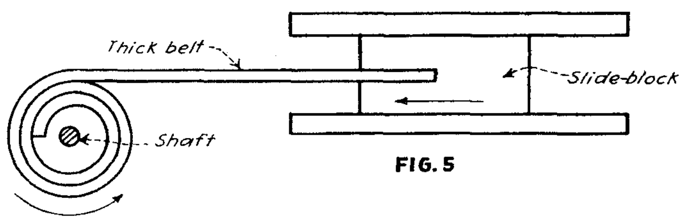

FIG. 5

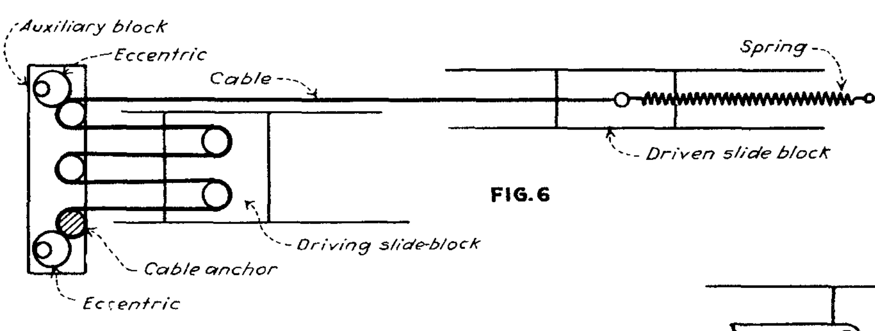

FIG. 6

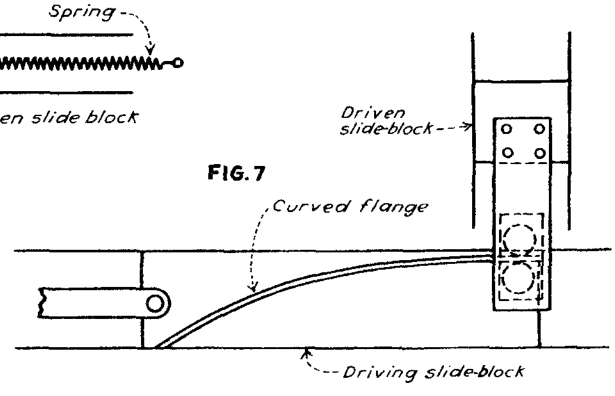

FIG. 7

is provided by this variation of the preceding mechanism. Here, acceleration is in direction of arrows and deceleration occurs on return stroke. Accelerative effect becomes less as toggle flattens.

Fig. 4—Bellcrank motion is accelerated as rollers are spread apart by curved member on end of drive rod, thereby in turn accelerating motion of slide block. Driven elements must be spring-returned to close system.

Fig. 5—Constant-speed shaft winds up thick belt, or similar flexible member, and increase in effective radius causes accelerative motion of slide block. Must be spring- or weight-returned on reversal.

Fig. 6 — Auxiliary block, carrying sheaves for cable which runs between driving and driven slide blocks, is mounted on two synchronized eccentrics. Motion of driven block is equal to length of cable paid out over sheaves resulting from additive motions of the driving and the auxiliary blocks.

Fig. 7—Curved flange on driving slide block is straddled by rollers pivotally mounted in member connected to driven slide block. Flange can be curved to give desired acceleration or deceleration, and mechanism is self-returned.

Fig. 8—Stepped acceleration of the driven slide block is effected as each of the three reciprocating sheaves progressively engages the cable. When the third acceleration step is reached, the driven slide block moves six times faster than the drive rod.

Fig. 9—Form-turned nut, slotted to travel on rider, is propelled by reversing screw shaft, thus moving concave roller up and down to accelerate or decelerate slide block.

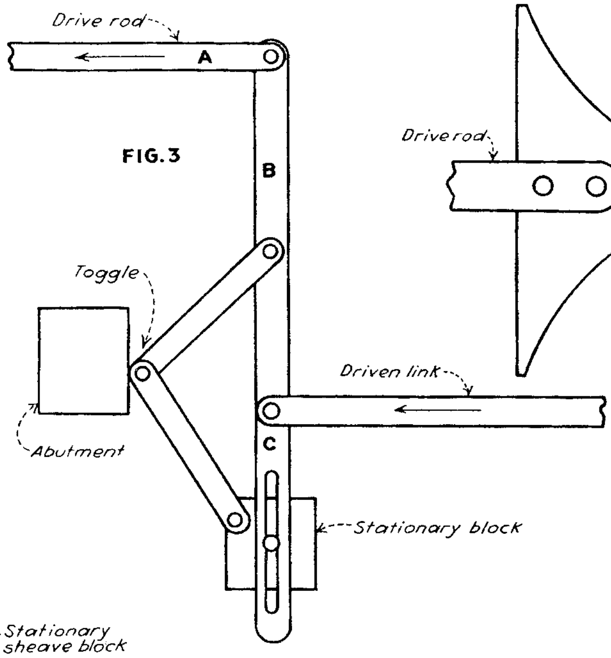

FIG. 3

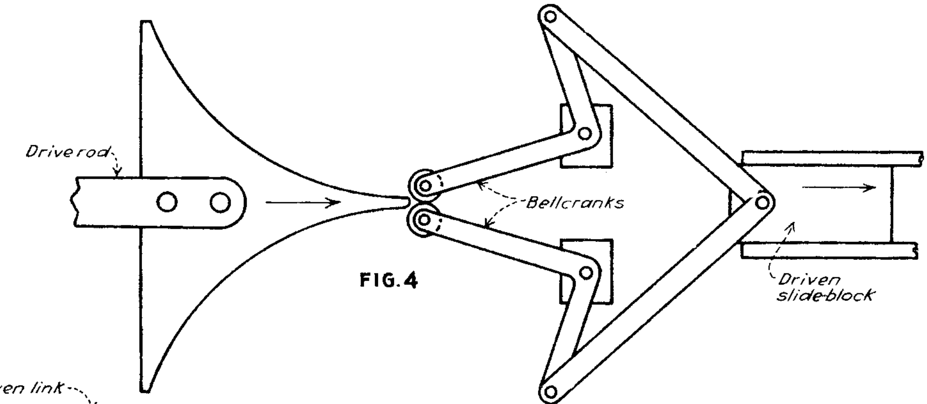

FIG. 4

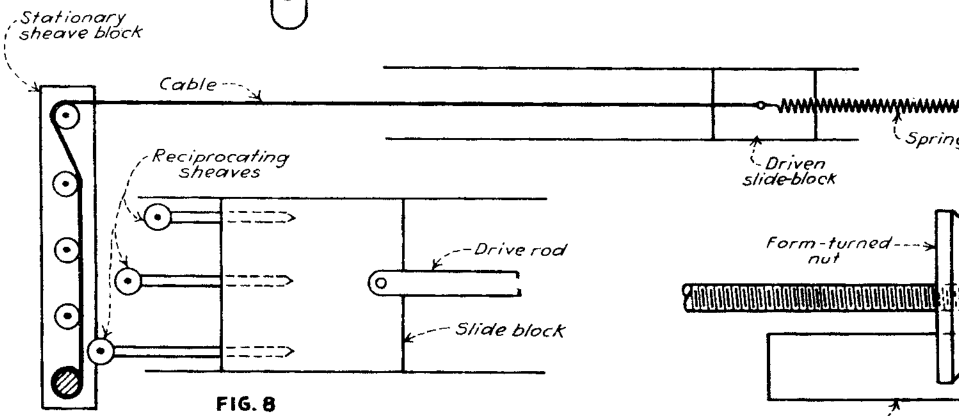

FIG. 8

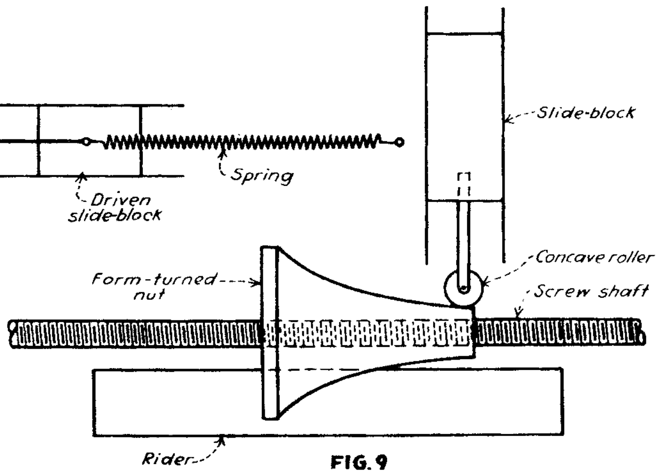

FIG. 9

How to Prevent reverse Rotation

Wedges, ratchet-and-pawl arrangements, internal pins, friction pads, and sliding key action can protect mechanisms form torque feedback.

L. Kasper

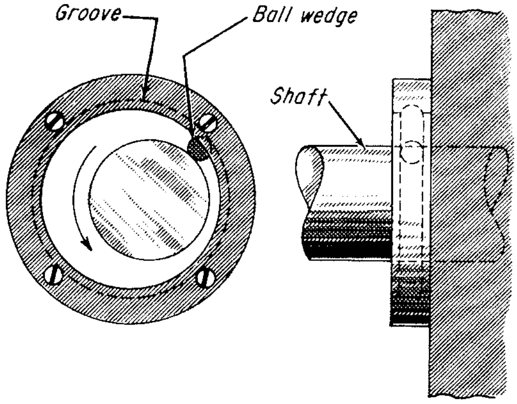

1 **INTERNALLY GROOVED** ring is located eccentrically with the rotating shaft. Ball wedges if shaft reverses direction of rotation.

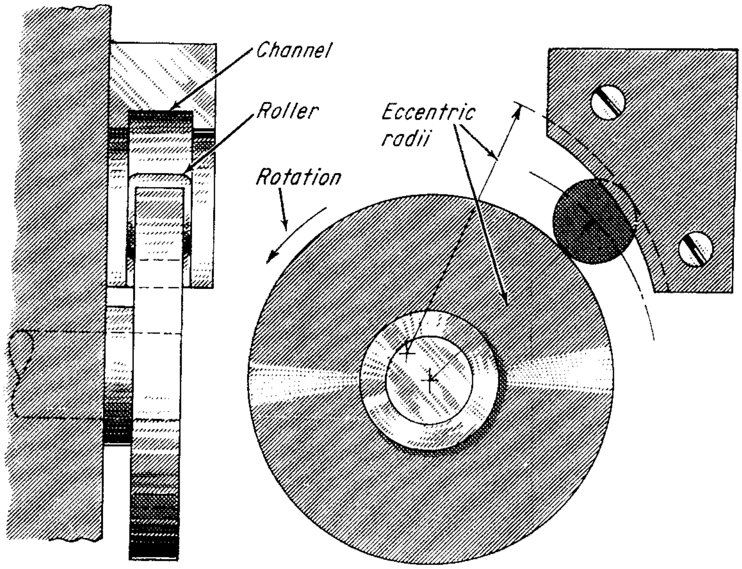

2 **ROLLER WEDGES** when direction of rotation is reversed as in previous device. For vertical shafts, hold roller in place with a spring.

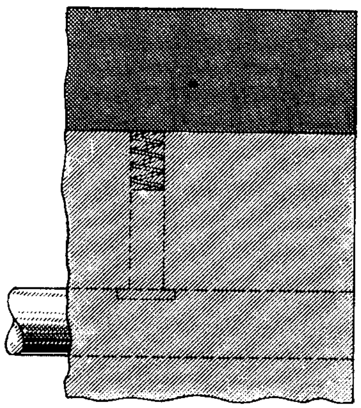

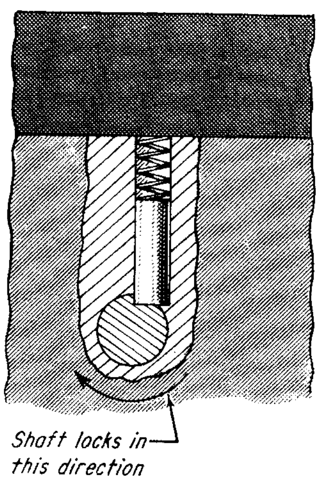

5 **SPRING-LOADED PIN** device is applicable when no part of the shaft is exposed. Blacklash here can be equal to almost one revolution.

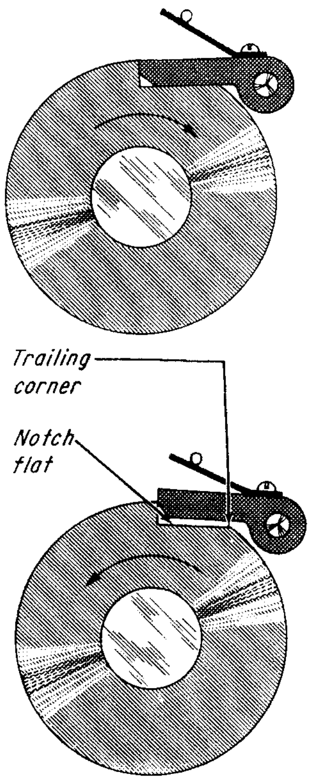

3 **SINGLE-TOOTH RATCHET** has special pawl, shaped to avoid annoying sound. The notch corner engages pawl before it can hit the flat.

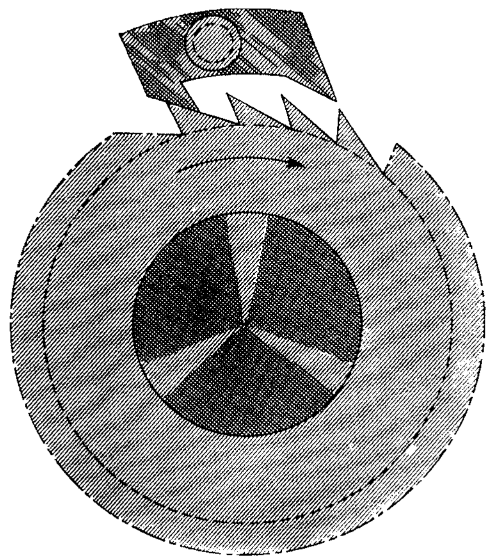

4 **SWINGING PAWL** will operate silently in any position. As one pawl tooth leaves the ratchet, the other tooth engages at about half depth.

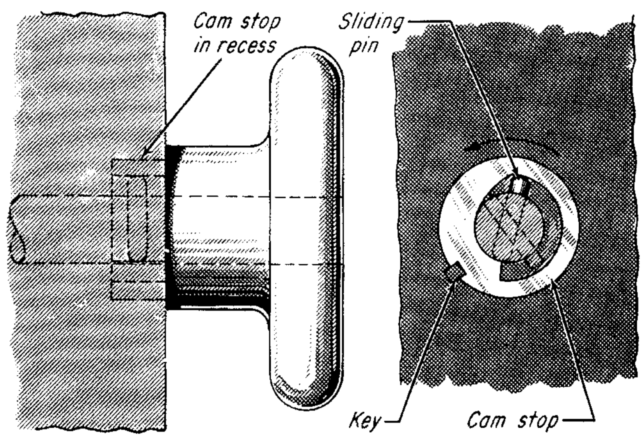

6 **SLIDING PIN** is moved into position (during normal rotation) to prevent reverse rotation. Key the cam stop into housing.

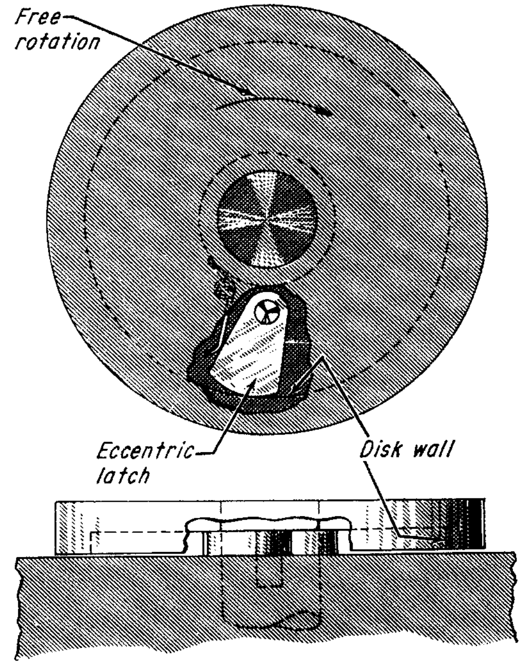

7

ECCENTRIC LATCH allows shaft to rotate in one direction; attempted reversal immediately causes latch to wedge against disk wall.

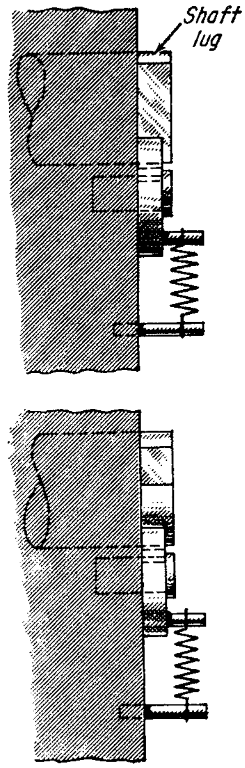

8

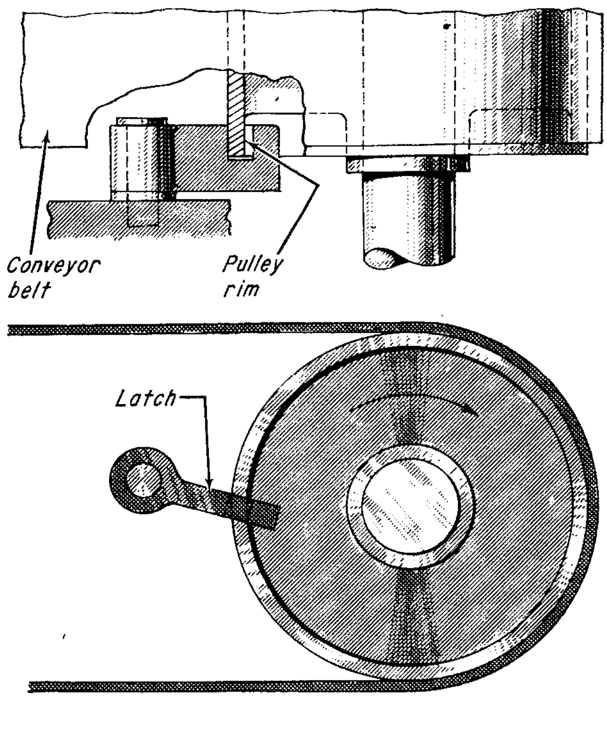

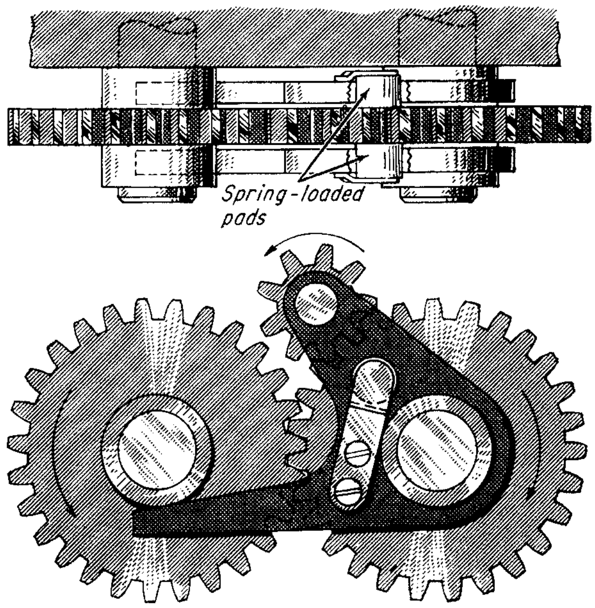

10

LATCH ON RIM of pulley is free only when rotation is in direction shown. This arrangement is ideal for conveyor-belt pulleys.

11

SPRING-LOADED FRICTION PADS contact the right gear. Idler meshes and locks gear set when rotation is reversed.

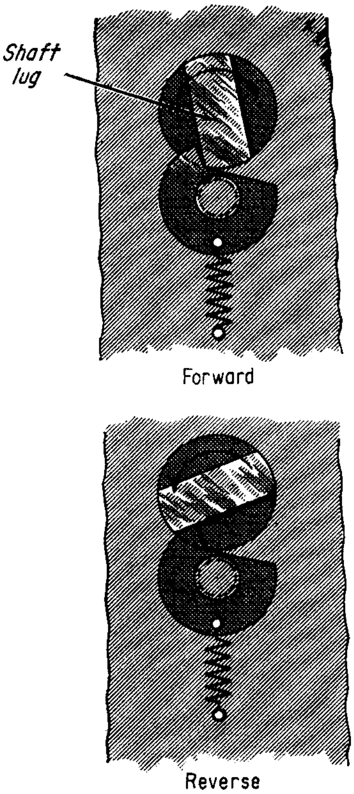

LUG ON SHAFT pushes the notched disk free during normal rotation. Disk periphery stops lug to prevent reverse rotation.

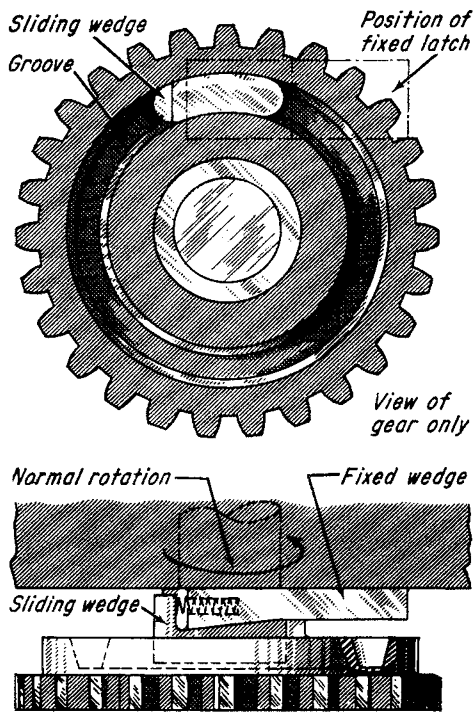

9

FIXED WEDGE AND SLIDING WEDGE tend to disengage when the gear is turning clockwise. The wedges jam in reverse direction.

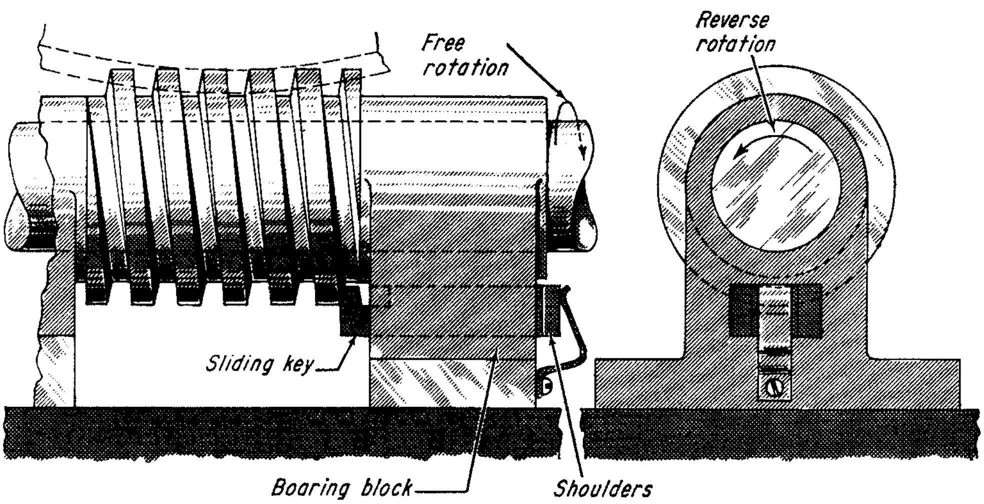

12

SLIDING KEY has tooth which engages the worm threads. In reverse rotation key is pulled in until its shoulders contact block.

Automatic Stopping Mechanisms for Faulty Machine Operation

Many machines, particularly automatically operated production machines, may damage themselves or parts being processed unless they are equipped with devices that stop the machine or cause it to skip an operation when something goes wrong. The accompanying patented mechanisms show principles that can be employed to interrupt normal machine operation: Mechanical, electrical or electronic, hydraulic, pneumatic, or combinations of these means. Endless varieties of each method are in use.

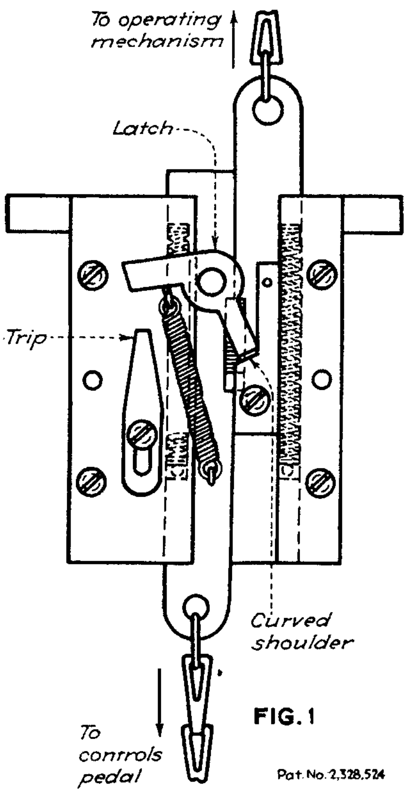

FIG. 1

Pat. No. 2,328,524

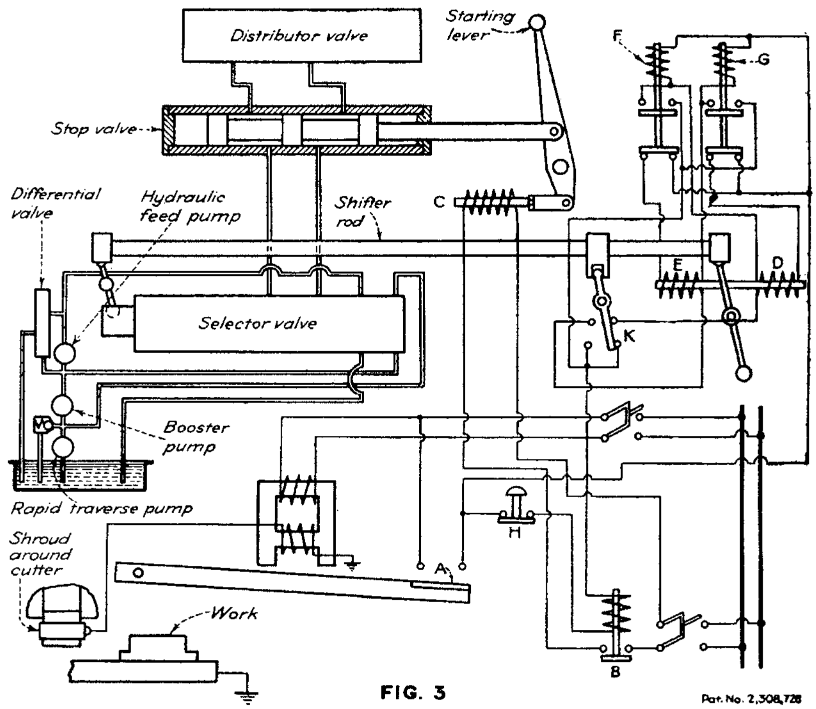

FIG. 3

Pat. No. 2,308,728

Fig. 1—Repetition of machine cycle is prevented if pedal remains depressed. Latch carried by left slide pushes right slide downward by means of curved shoulder until latch is disengaged by trip member.

FIG. 2

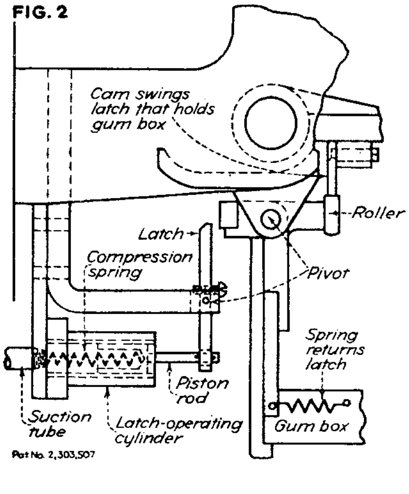

Pat No. 2,303,507

Fig. 2—Gumming of suction picker and label carrier when label is not picked up by the suction, is prevented by insufficient suction on latch-operating cylinder, caused by open suction holes on picker. When latch-operating cylinder does not operate, gum box holding latch returns to holding position after cyclic removal by cam and roller, thus preventing gum box and rolls from rocking to make contact with picker face.

Fig. 3—Damage to milling cutter, work or fixtures is prevented by shroud around cutter, which upon contact closes electric circuit through relay, thus closing contact *A*. This causes contact *B* to close, thus energizing relay *C* to operate stop valve, and closes circuit through relay *D*, thus reversing selector valve by means of shifter rod so that bed travel will reverse on starting. Simultaneously, relay *F* opens circuit of relay *E* and closes a holding circuit that was broken by the shifter lever at *K*. Relay *G* also closes a holding circuit and opens circuit through relay *D*. Starting lever, released by push button *H*, releases contact *A* and returns circuit to normal. If contact is made with shroud when bed travel is reversed, interchange *D* and *E*, and *F* and *G* in above sequence of operations.

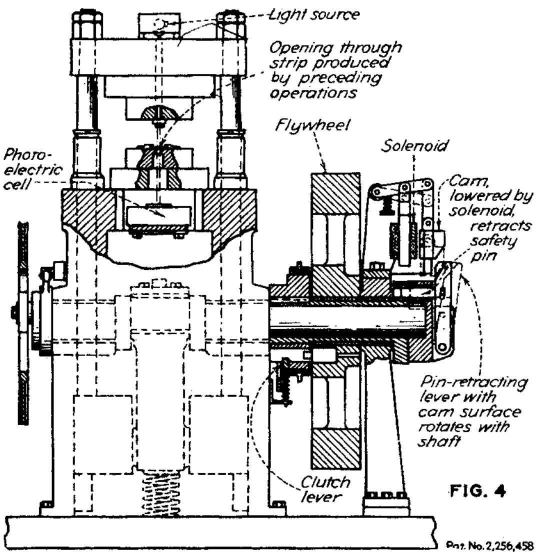

FIG. 4

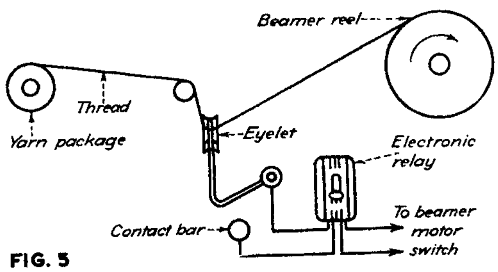

FIG. 5

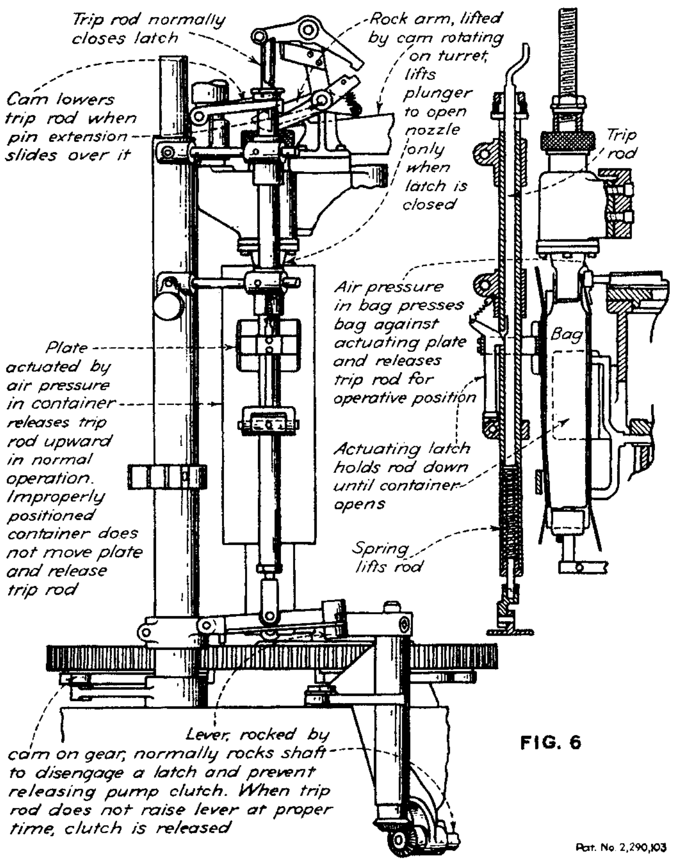

FIG. 6

Fig. 4—High-speed press is stopped when metal strip advances improperly so that hole punched in strip fails to match with opening in die block to permit passage of light beam. Intercepted light beam to photo-electric cell results in energizing solenoid and withdrawal of clutch pin.

Fig. 5—Broken thread permits contact bar to drop, thereby closing electronic relay circuit, which operates to stop beamer reeling equipment.

Fig. 6—Nozzle on packaging machine does not open when container is not in proper position.

Fig. 7—Obstruction under explorer foot of wire-stitching machine prevents damage to machine by raising a vertical plunger, which releases a latch lever so that rotary cam raises lever that retains clutch operating plunger.

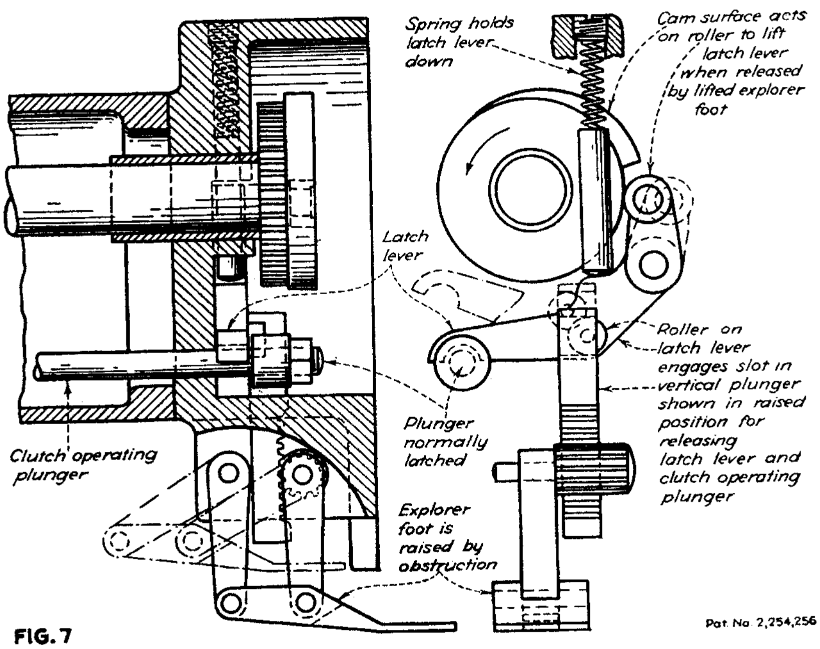

FIG. 7

Automatic Stop Mechanisms Protect Machines and Work

This group of stop mechanisms includes types and applications for machines in different fields. Such devices, which prevent automatic machines form damaging themselves or the work passing through them, make use of mechanical, electrical, hydraulic, and pneumatic principles. Typical mechanisms illustrated prevent excess speed, miswearing, jamming of toggle press and foodcanning machines, operation of printing presses when the paper web breaks, improper feeding of wrapping paper, and uncoordinated operation of glass-making machines.

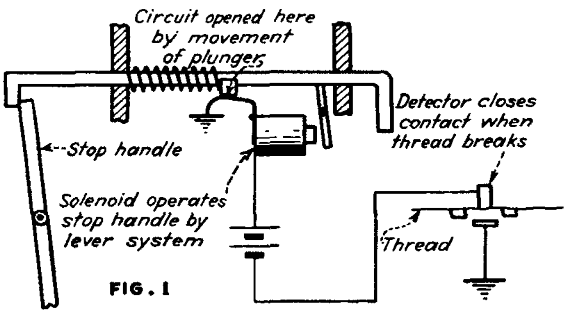

FIG. 1

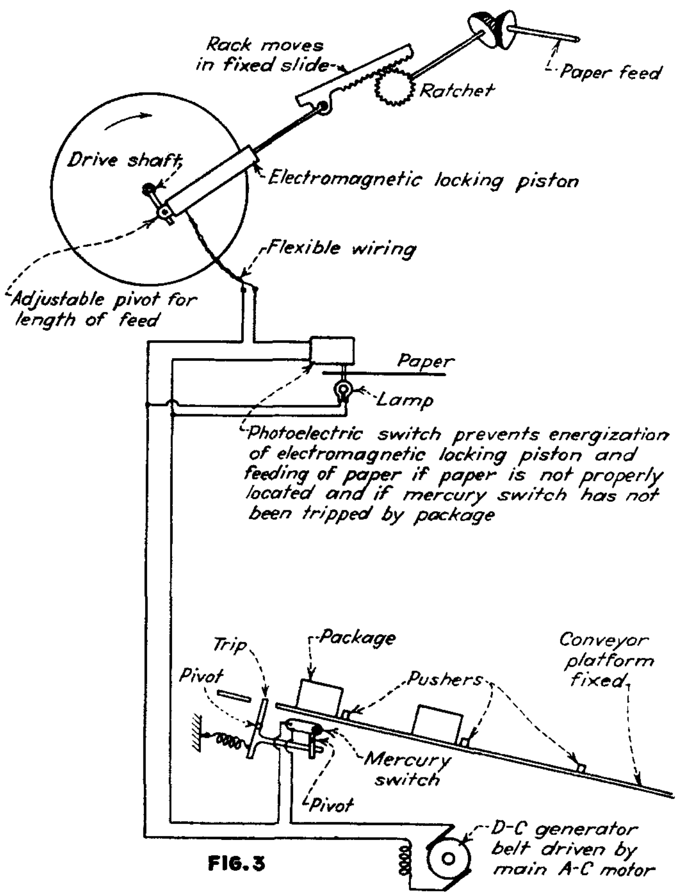

FIG. 3

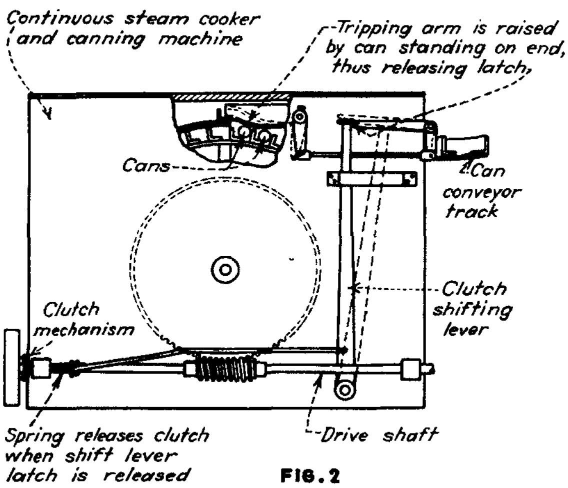

FIG. 2

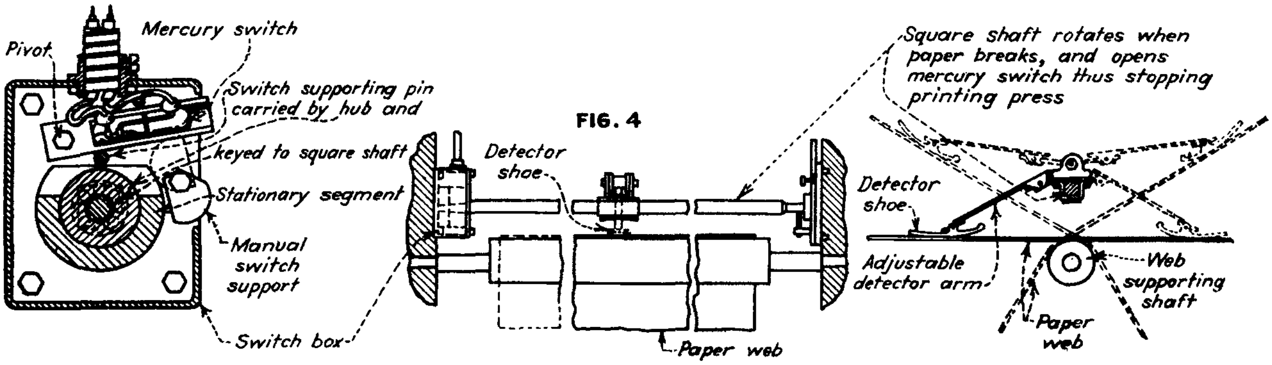

FIG. 4

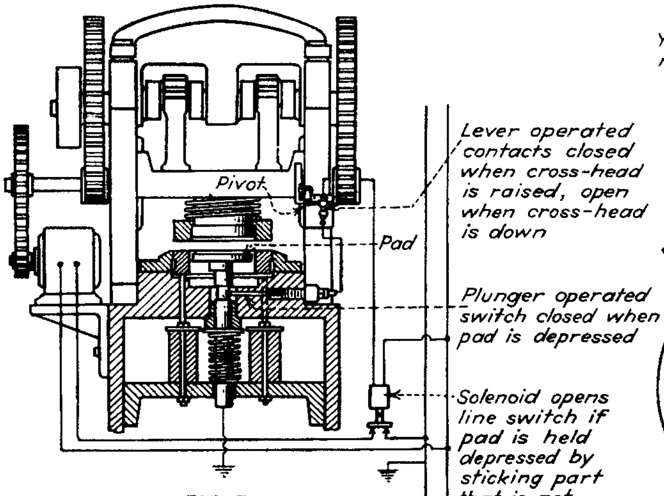

FIG. 5

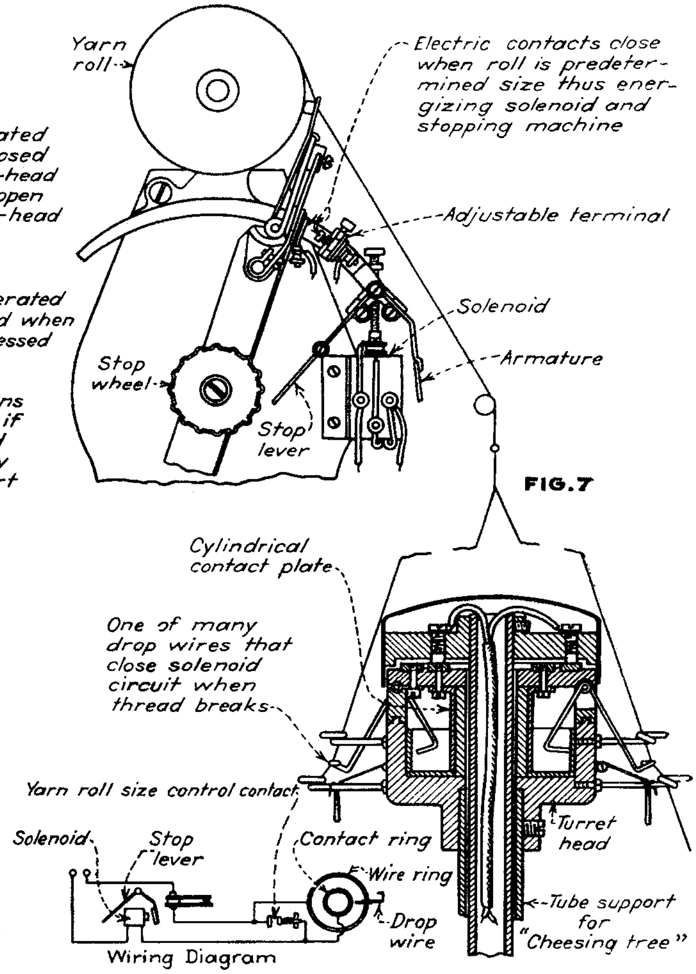

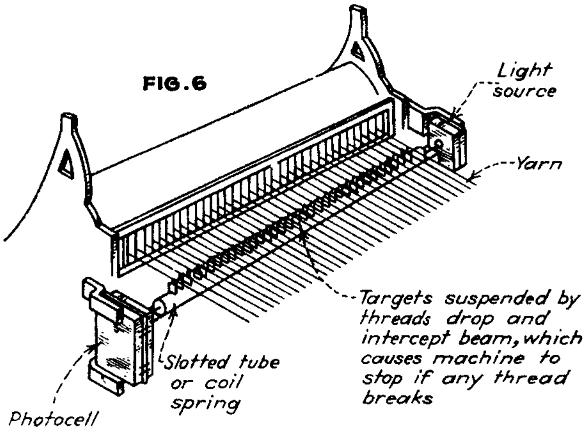

FIG. 6

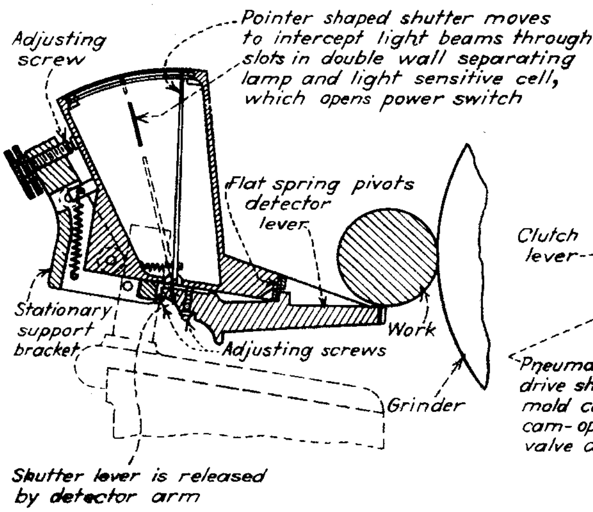

FIG. 8

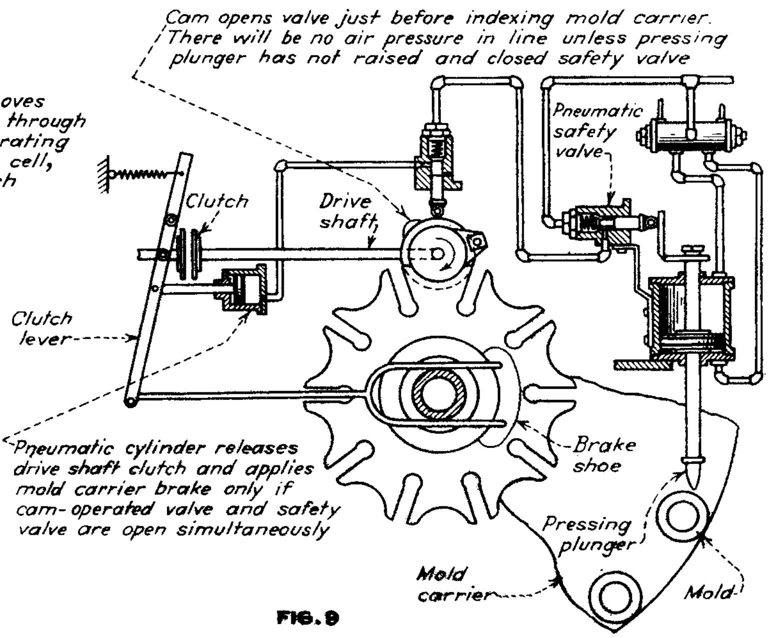

FIG. 9

Mechanical Automatic Stop Mechanisms

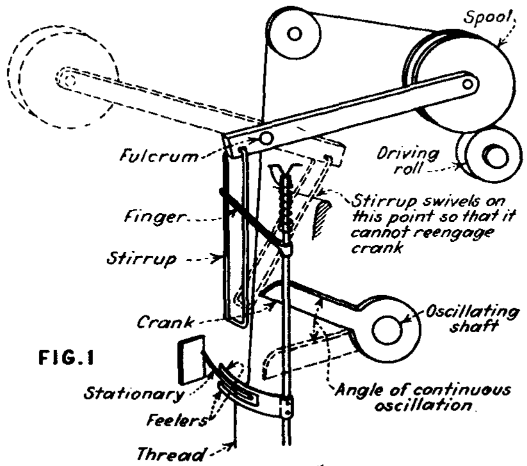

FIG. 1

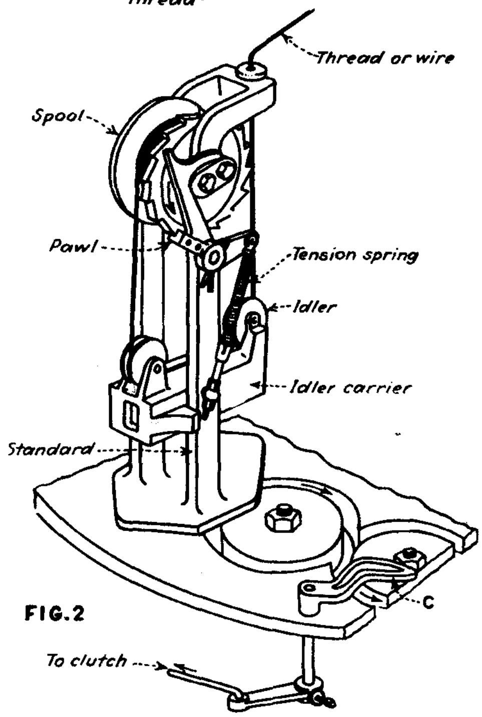

FIG. 2

FIG. 1—A mechanism used on the Barber-Colman spooler. When thread breaks the feelers are released and the spiral spring causes the spindle with finger to rotate. Latter throws the stirrup into the path of the oscillating crank, which on its downward stroke throws the spool into the position shown dotted, the stirrup then being thrown out of the path of the oscillating crank.

FIG. 2—Mechanism used with variations on tubular braiding machines. When braiding, tension on the wire or thread lifts the idler carrier which thereby releases the pawl from the ratchet on spool flange and allows the spool to turn and unwind. When machine stops the tension on wire is decreased allowing the idler carrier to fall so that the pawl can engage the ratchet. If wire breaks while the machine is running the unsupported idler carrier falls to the base of the standard and when the standard arrives at the station in the raceway adjacent to the cam *C*, the lug *L* on idler carrier strikes the cam *C*, rotating it far enough to disengage a clutch on the driving shaft, thereby stopping the machine.

FIG. 3—When thread breaks the stop drops and intercepts reciprocating bar. On the next counter-clockwise oscillation of the eccentric arm the bar *B* is raised. A feature of this design is that it permits the arm *B* to move up or down independently for a limited distance.

FIG. 4—Schematic diagram of mechanism to cause bobbin changer to operate. If contact arm does not slip on bobbin the lever *A* will rotate to the position shown. But if contact with bobbin center slips, as it will do if the bobbin is empty.

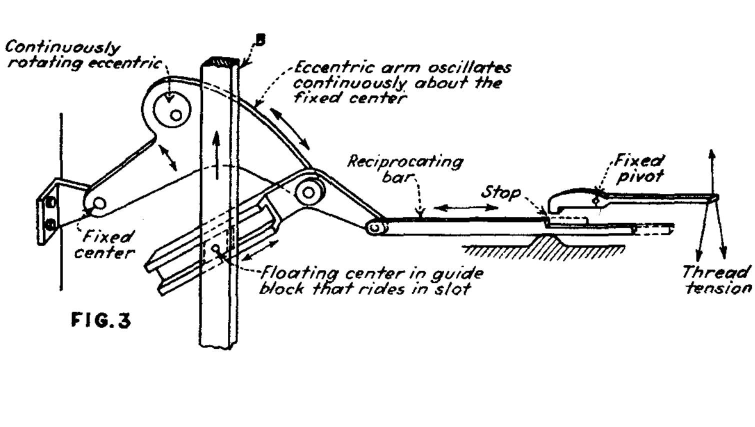

FIG. 3

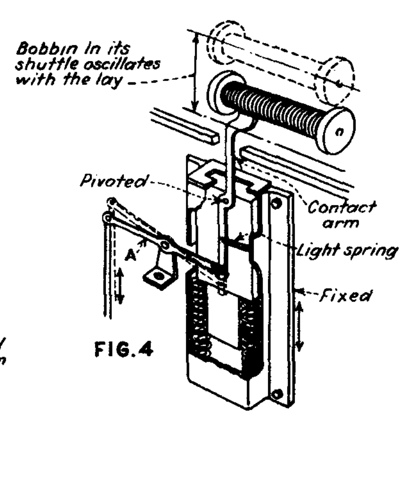

FIG. 4

Designs shown here diagrammatically were taken from textile machines, braiding machines and packaging machines. Possible modifications of them to suit other applications will be apparent.

lever A will not rotate to position indicated by dashed line, thereby causing bobbin changer to come into action.

Fig. 5—Simple type of stop mechanism for limiting the stroke of a reciprocating machine member. Arrows indicate the direction of movements.

Fig. 6—When the predetermined weight of material has been poured on the pan, the movement of the scale beam pushes the latch out of engagement, allowing the paddle wheel to rotate and thus dump the load. The scale beam drops, thereby returning the latch to the holding position and stopping the wheel when the next vane hits the latch.

Fig. 7—In this textile machine any movement that will rotate the stop lever counter-clockwise will bring it in the path of the continuously reciprocating shaft. This will cause the catch lever to be pushed counter-clockwise and the hardened steel stop on the clutch control shaft will be freed. A spiral spring then impels the clutch control shaft to rotate clockwise, which movement throws out the clutch and applies the brake. Initial movement of the stop lever may be caused by the breaking of a thread, a moving dog, or any other means.

Fig. 8—Arrangement used on some package loading machines to stop machine if a package should pass loading station without receiving an insert. Pawl finger F has a rocking motion obtained from crankshaft, timed so that it enters the unsealed packages and is stopped against the contents. If the box is not filled the finger enters a considerable distance and the pawl end at bottom engages and holds a ratchet wheel on driving clutch which disengages the machine driving shaft.

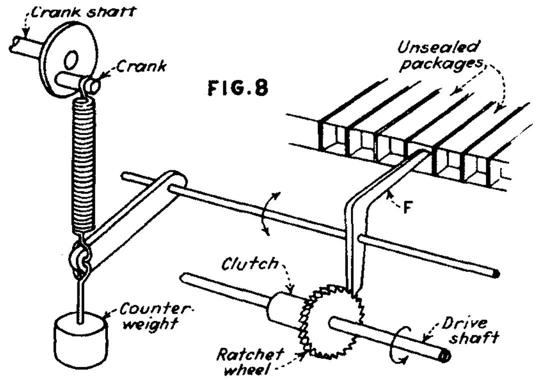

FIG. 8

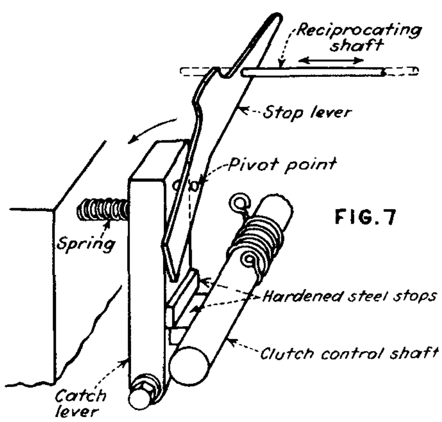

FIG. 7

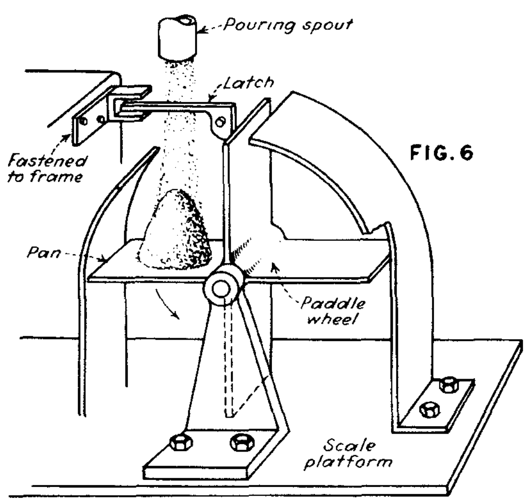

FIG. 6

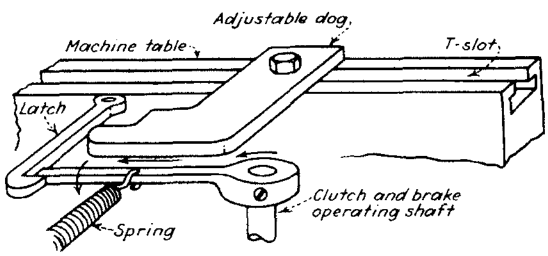

FIG. 5

Automatic Feed Mechanisms for Various Materials

Design of feed mechanisms for automatic or semi-automatic machines depends largely upon such factors as size, shape, and character of materials or parts being fed into a machine, and upon the type of operations to be performed. Feed mechanisms may be merely conveyors, may give positive guidance in many instances, or may include tight holding devices if the parts are subjected to processing operations while being fed through a machine. One of the functions of feed mechanism is to extract single pieces from a stack or unassorted supply of stock or, if the stock is a continuous strip of steel, roll of paper, long bar, and the like, to maintain intermittent motion between processing operations. All of these conditions are illustrated in the accompanying feed mechanisms.

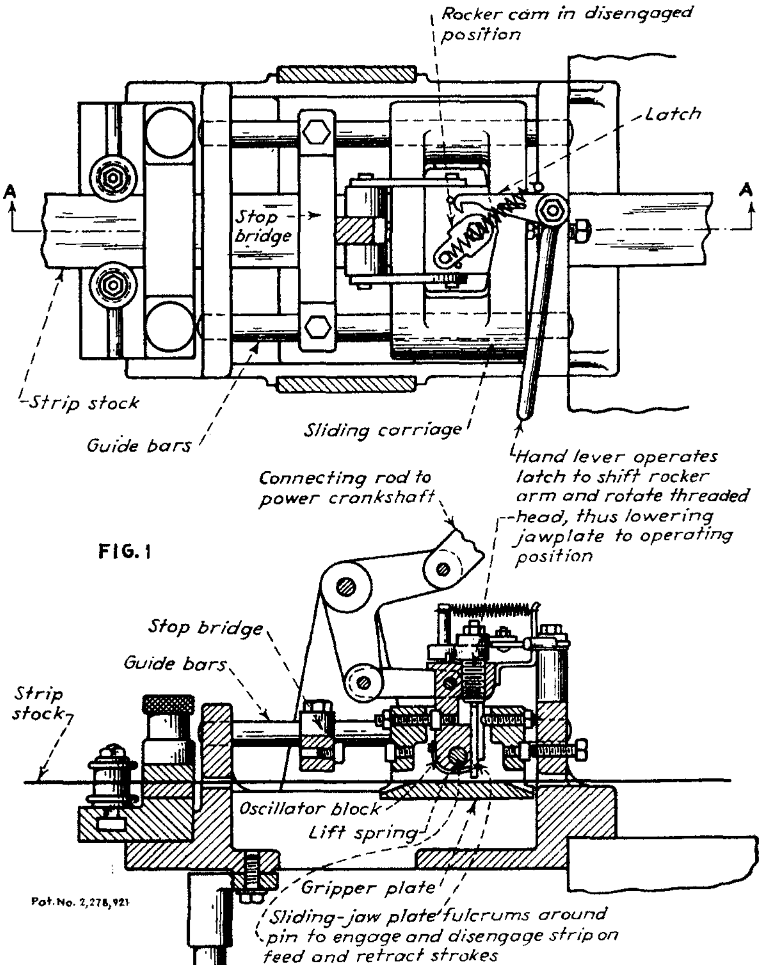

FIG. 1

Section A-A

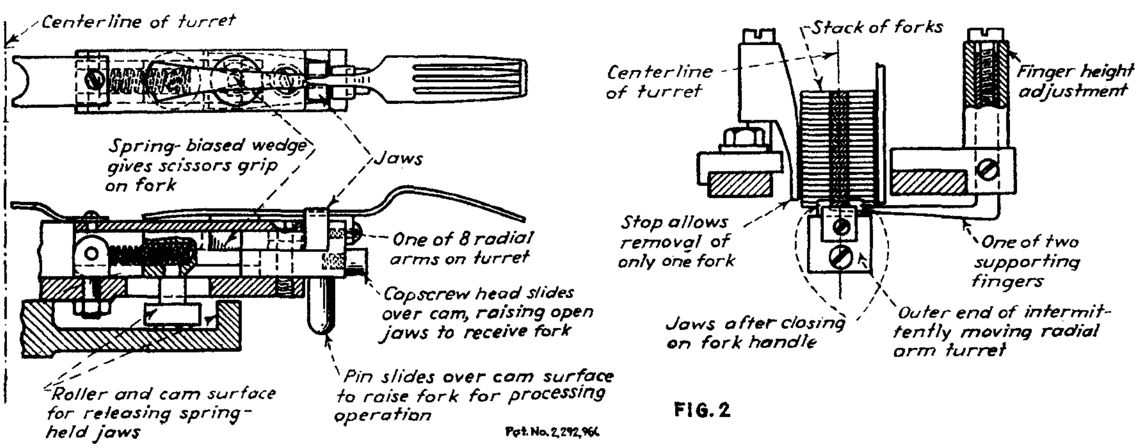

FIG. 2

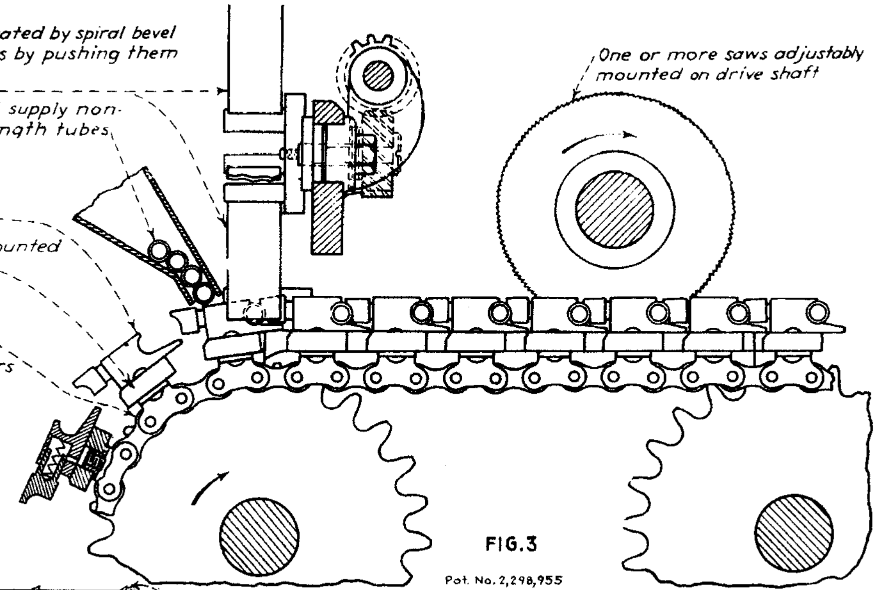

FIG.3
Pat. No. 2,298,955

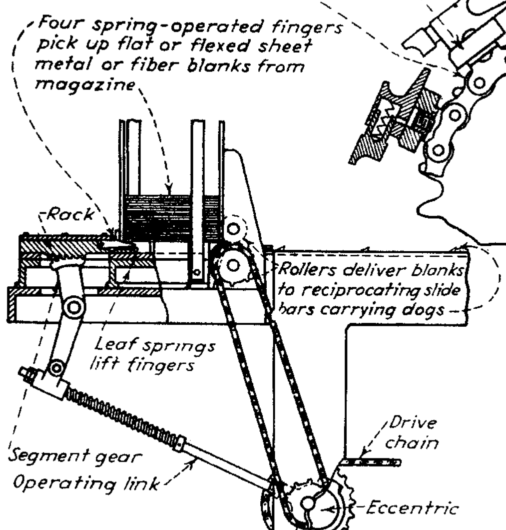

FIG.4
Pat. No. 2,270,871

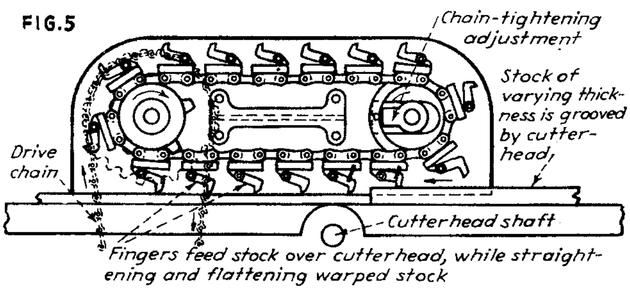

FIG.5

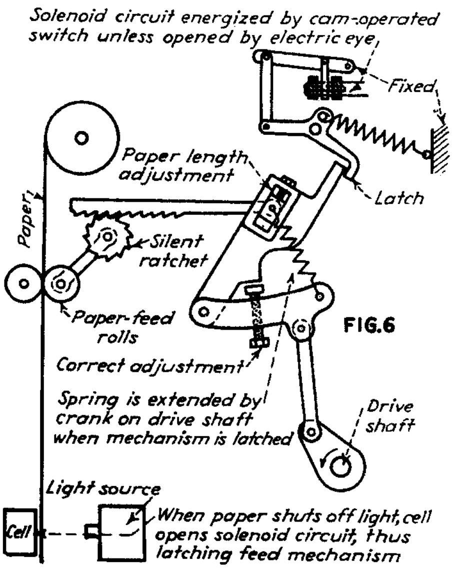

FIG.6

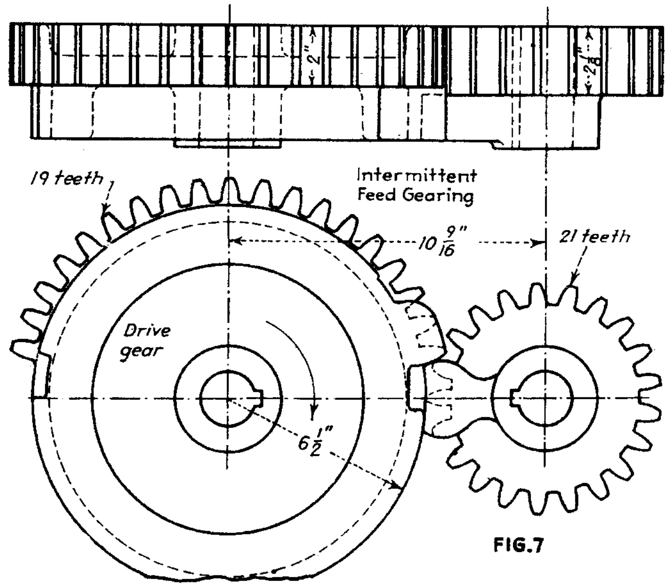

FIG.7

Automatic Safety Mechanisms for Operating Machines

THE most satisfactory automatic guard mechanisms for preventing injury to machine operators are those that have been designed with the machine. When properly designed they (1) do not reduce visibility, (2) do not impede the operator, (3) do not cause painful blows on the operator's hand in avoiding serious injury, (4) are safe with respect to wear in the safety mechanism, (5) are sensitive and instantaneous in operation, and (6) render the machine inoperative if tampered with or removed.

Safety devices range from those that keep both hands occupied with controls away from the work area to guards that completely inclose the work during operation of the machine and prevent operation of the machine unless so protected. The latter might include the "electric eye," which is the activating means of one of the mechanisms illustrated.

FIG. 1

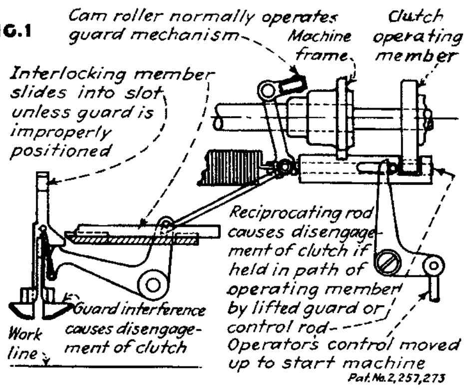

FIG. 2

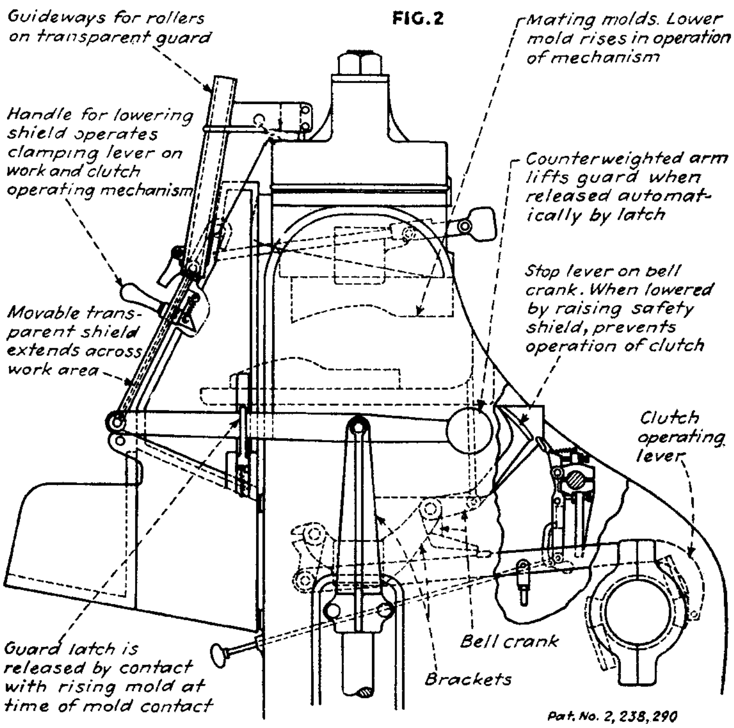

FIG. 3

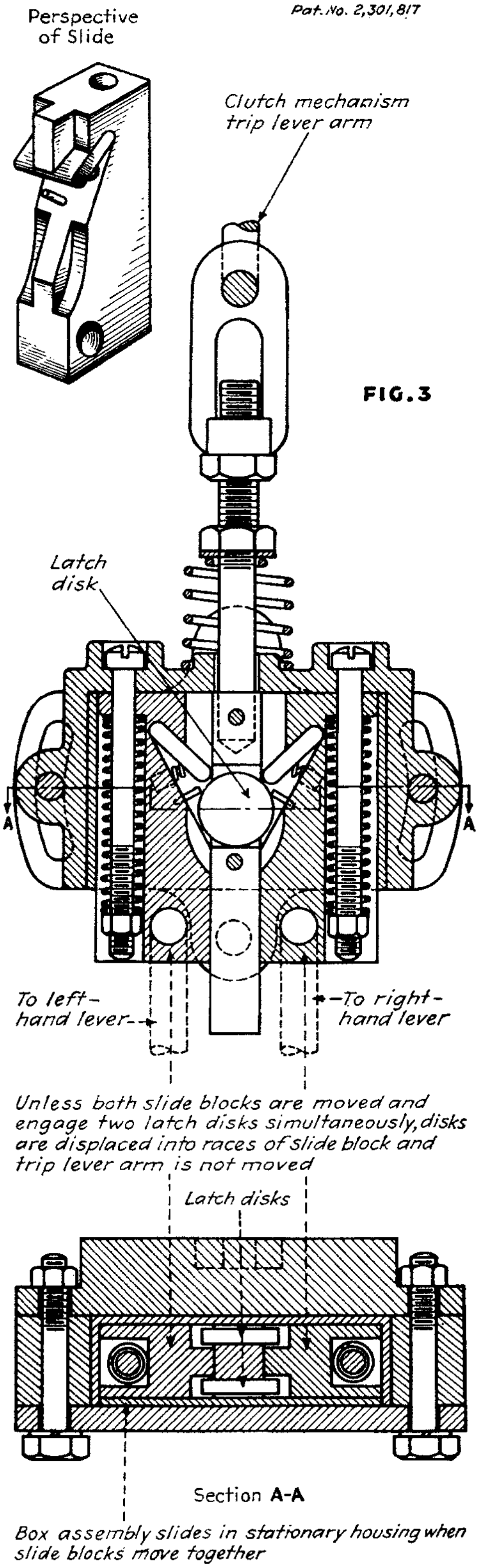

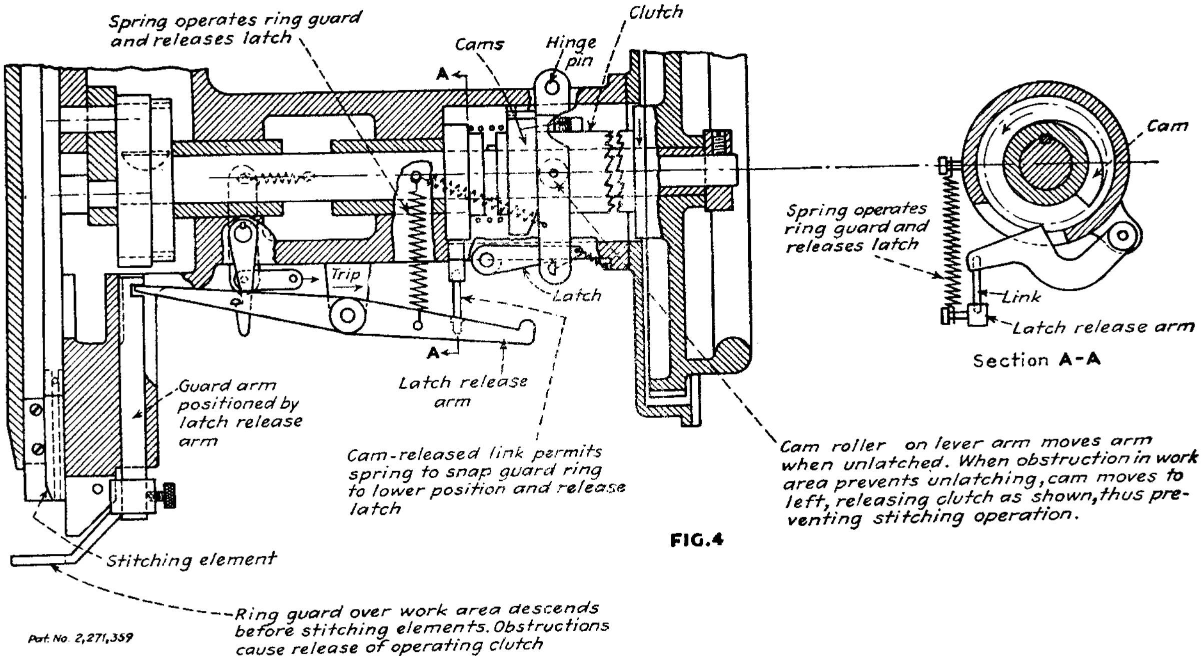

FIG.4

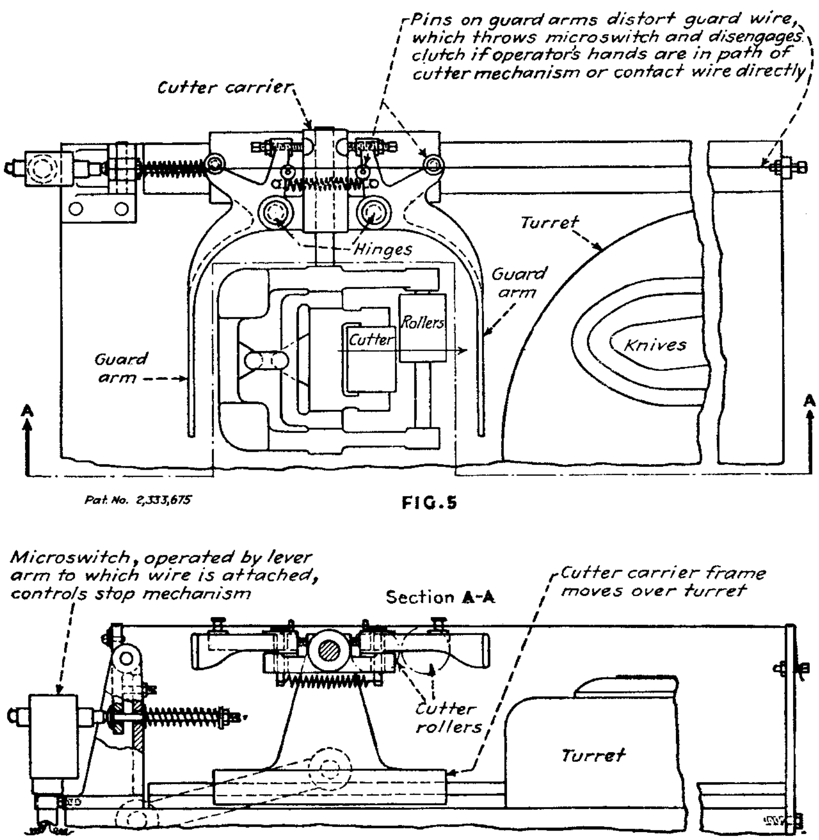

FIG.5

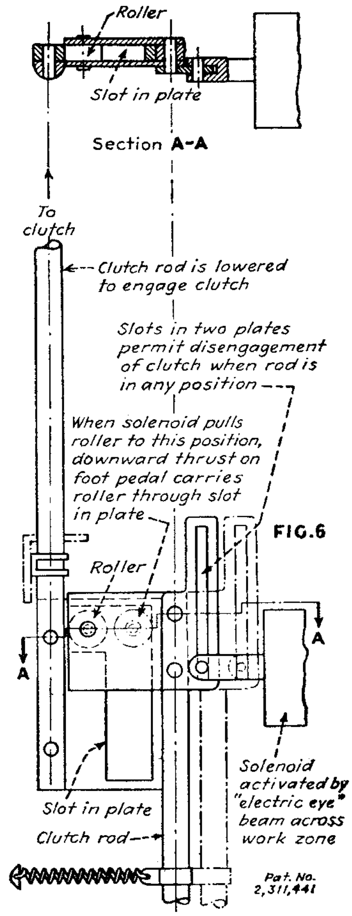

FIG.6

Mechanisms Actuated by Air or Hydraulic Cylinders

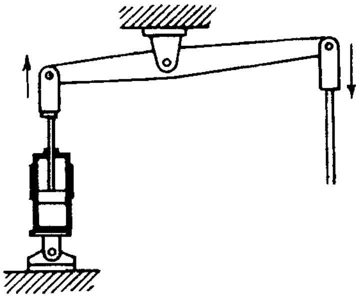

Fig. 1—Cylinder can be used with a first class lever.

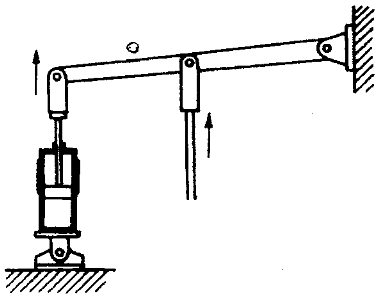

Fig. 2—Cylinder can be used with a second class lever.

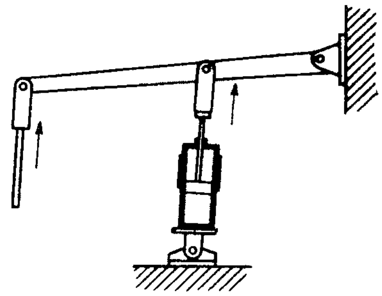

Fig. 3—Cylinder can be used with a third class lever.

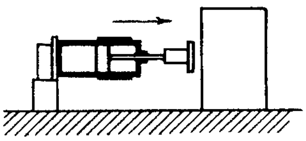

Fig. 4—Cylinder can be linked up directly to the load.

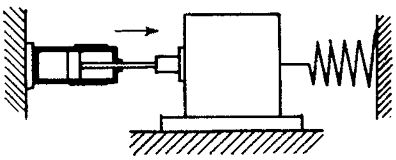

Fig. 5—Spring reduces the thrust at the end of the stroke.

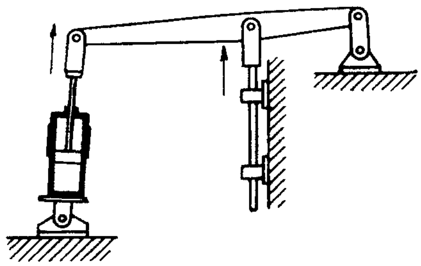

Fig. 6—Point of application of force follows the direction of thrust.

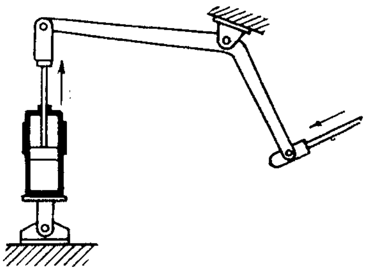

Fig. 7—Cylinder can be used with a bent lever.

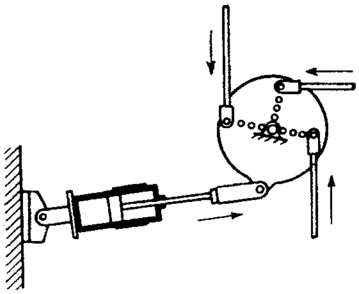

Fig. 8—Cylinder can be used with a trammel plate.

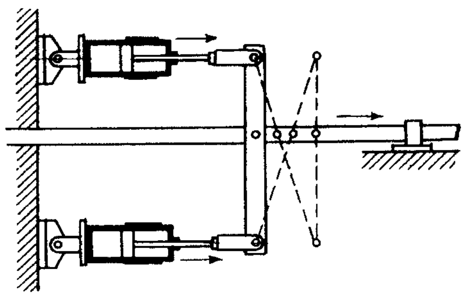

Fig. 9—Two pistons with fixed strokes position load in any of four stations.

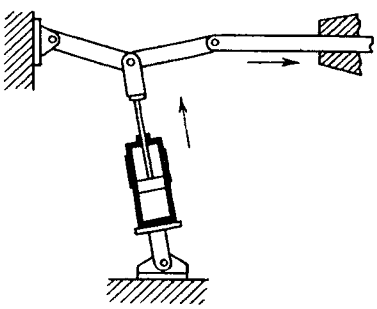

Fig. 10—A toggle can be actuated by the cylinder.

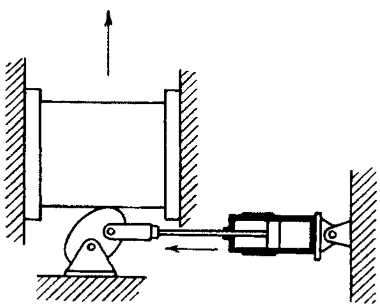

Fig. 11—The cam supports the load after completion of the stroke.

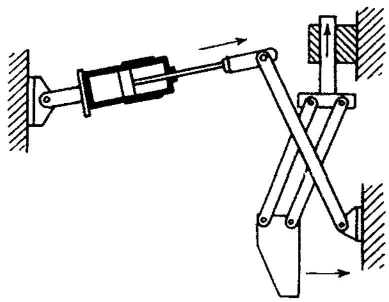

Fig. 12—Simultaneous thrusts in two different directions are obtained.

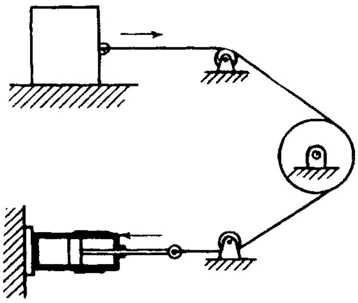

Fig. 13—Force is transmitted by a cable.

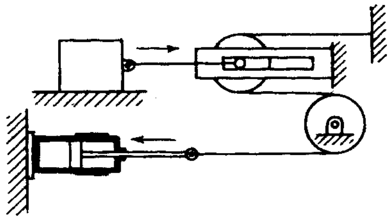

Fig. 14—Force can be modified by a system of pulleys.

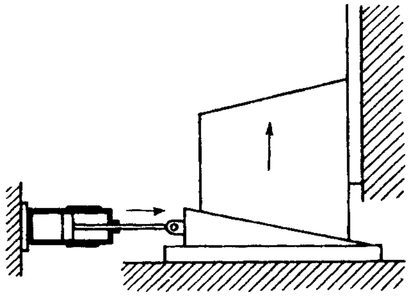

Fig. 15—Force can be modified by wedges.

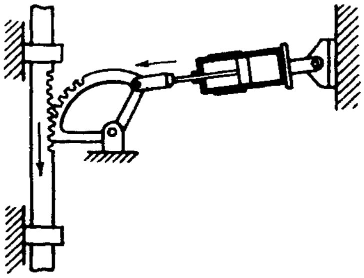

Fig. 16—Gear sector moves rack perpendicular to stroke of piston.

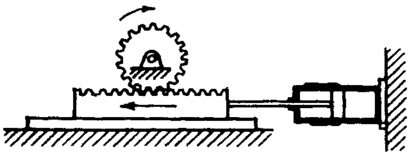

Fig. 17—Rack turns gear sector.

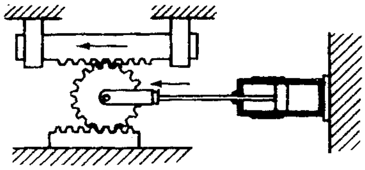

Fig. 18—Motion of movable rack is twice that of piston.

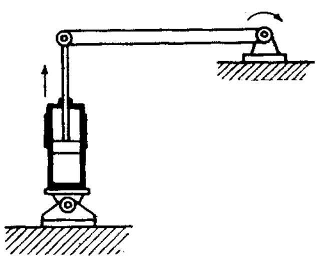

Fig. 19—Torque applied to the shaft can be transmitted to a distant point.

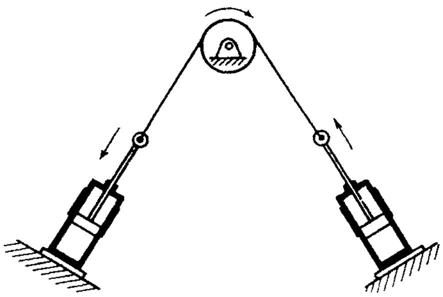

Fig. 20—Torque can also be applied to a shaft by a belt and pulley.

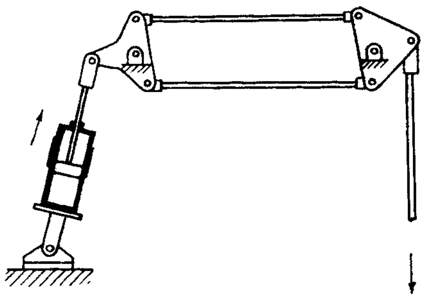

Fig. 21—Motion is transmitted to a distant point in the plane of motion.

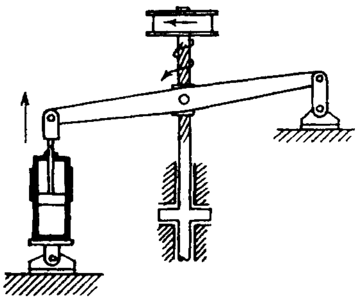

Fig. 22—A steep screw nut produces a rotation of shaft.

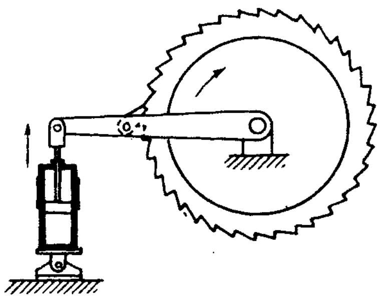

Fig. 23—Single sprocket wheel produces rotation in the plane of motion.

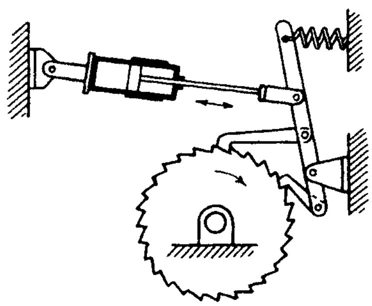

Fig. 24—Double sprocket wheel makes the rotation more nearly continuous.

Piston-Actuated Mechanisms

They are also hydraulic to mechanical transducers. Output–stroke, force, speed–can be altered by a variety of methods.

Louis Dodge

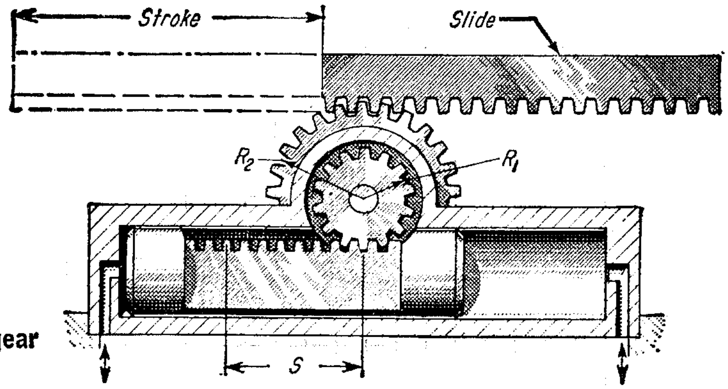

2 Slide stroke, force, and speed depend on gear cluster ratio

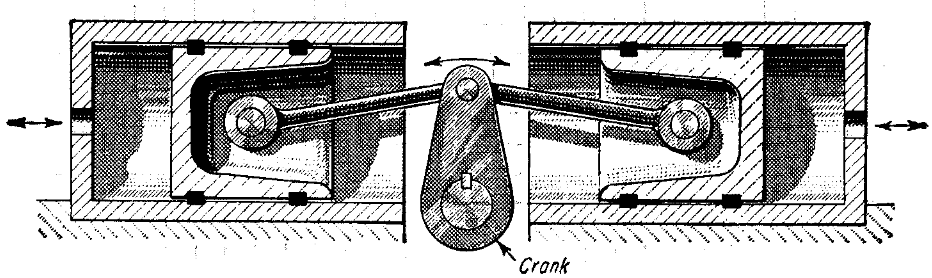

4 Rotary motion by alternately activated pistons

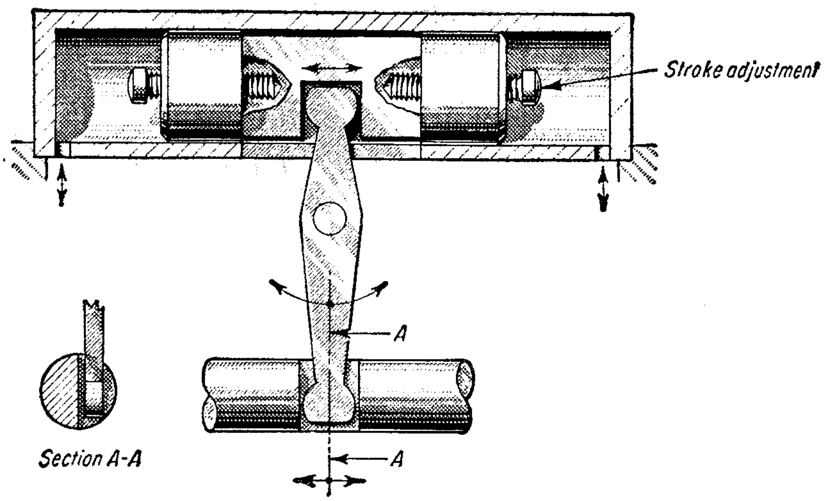

6 Oscillating motion with stroke adjustment

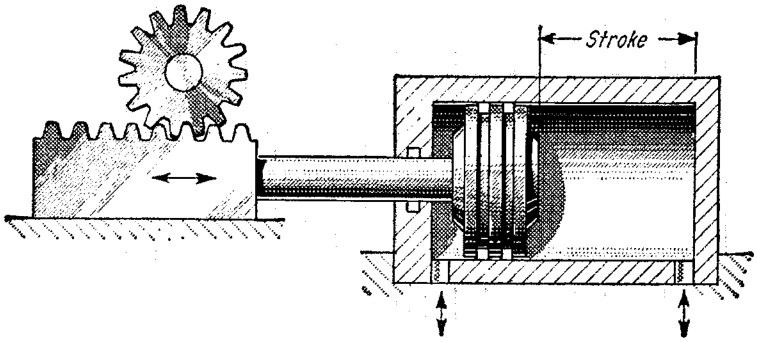

1 Simple rack and pinion converter

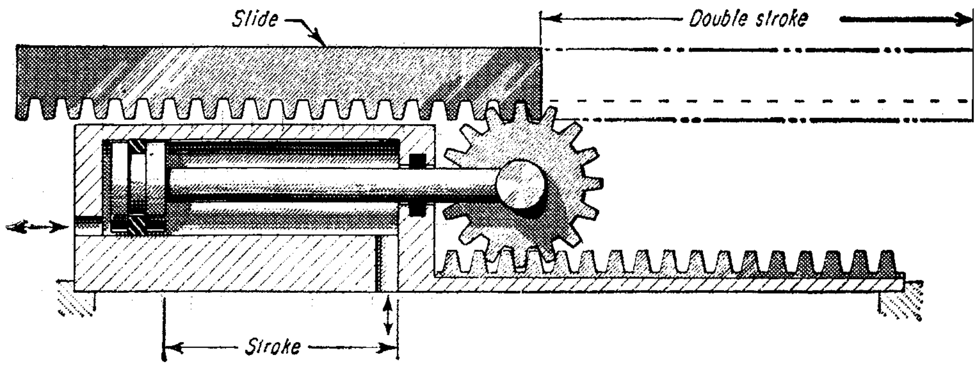

3 Gear can double speed and stroke, halve force

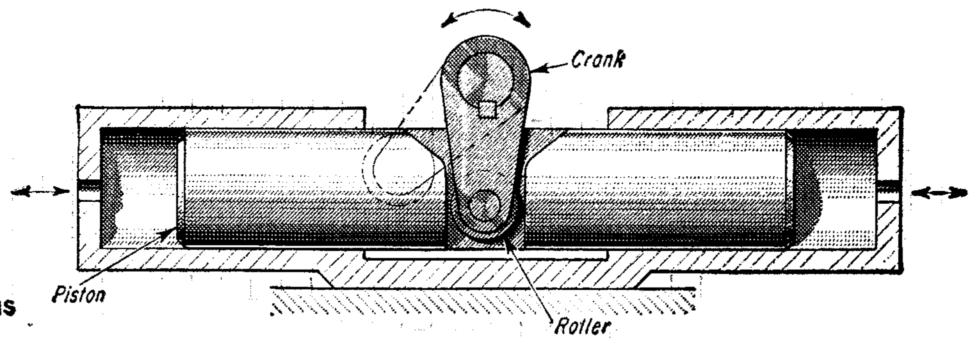

5 Rotary motion without transverse load on pistons

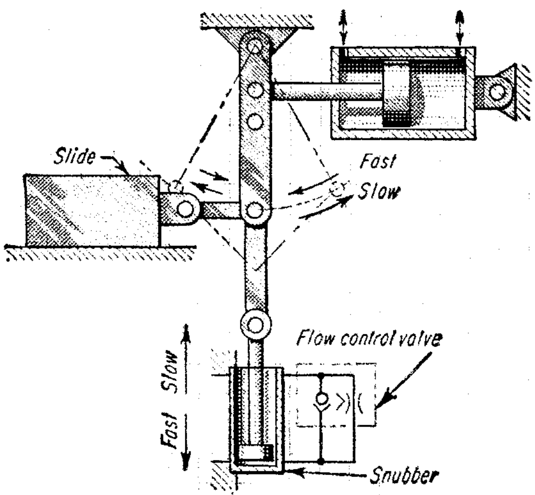

7 Two-speed slider from single piston

Computing Mechanisms I

Analog computing mechanisms are capable of virtually instantaneous response to minute variations in input. Basic units, similar to the types shown, are combined to form the final computer. These mechanisms add, subtract, resolve vectors, or solve special or trigonometric functions. Other computing mechanisms for multiplying, dividing, differentiating or integrating ore presented on the next page.

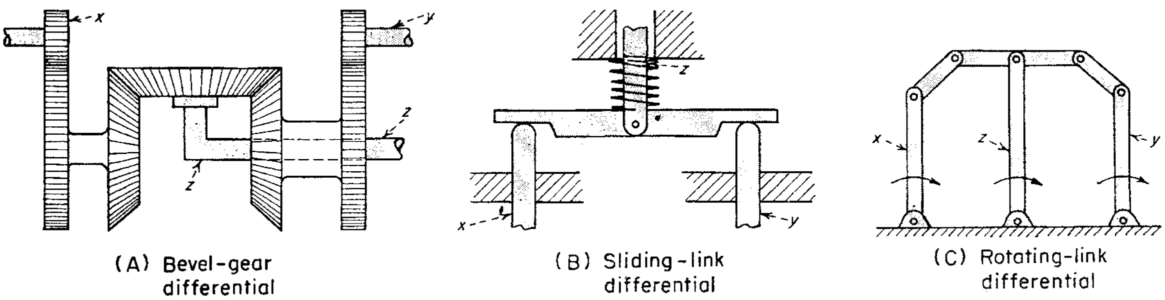

Fig. 1—ADDITION AND SUBTRACTION. Usually based on the differential principle; variations depend on whether inputs: (A) rotate shafts, (B) translate links, (C) angularly displaced links. Mechanisms solve equation: $z=c\ (x\pm y)$, where c is scale factor, x and y are inputs, and z is the output. Motion of x and y in same direction results in addition; opposite direction—subtraction. Nineteen additional variations are illustrated in "Linkage Layouts by Mathematical Analysis," Alfred Kuhlenkamp, Product Engineering, page 165, August 1955.

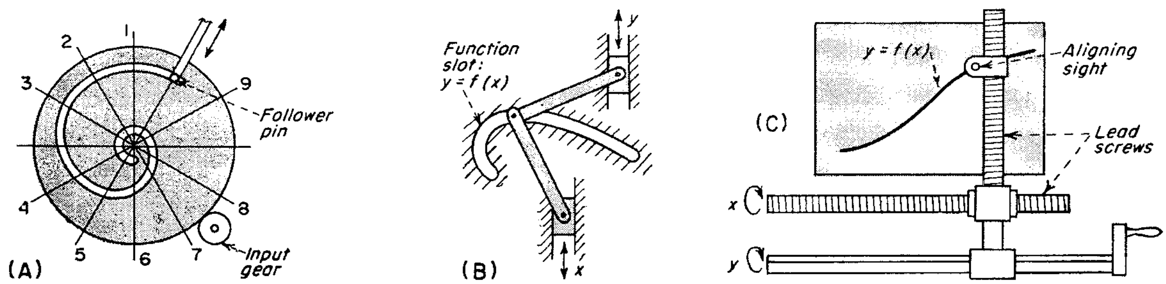

Fig. 2—FUNCTION GENERATORS mechanize specific equations. (A) Reciprocal cam converts a number into its reciprocal. This simplifies division by permitting simple multiplication between a numerator and its denominator. Cam rotated to position corresponding to denominator. Distance between center of cam to center of follower pin corresponds to reciprocal. (B) Function-slot cam. Ideal for complex functions involving one variable. (C) Input table. Function is plotted on large sheet attached to table. Lead screw for x is turned at constant speed by an analyzer. Operator or photoelectric follower turns y output to keep sight on curve.

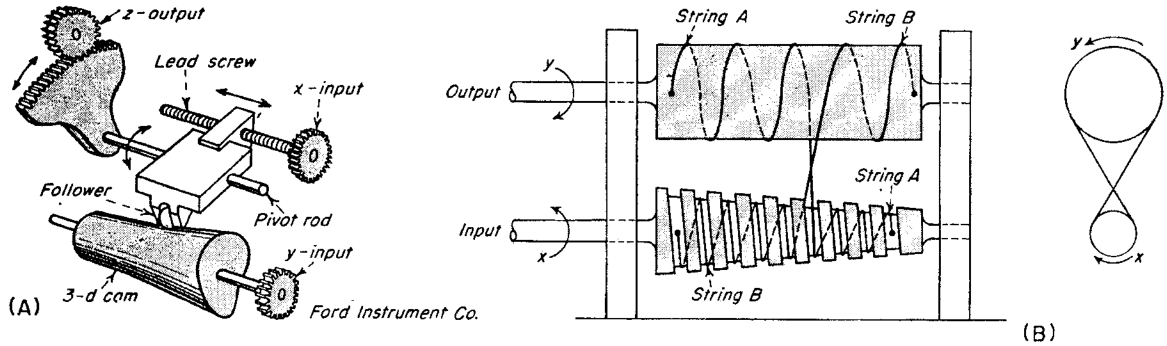

Fig. 3—(A) THREE-DIMENSIONAL CAM generates functions with two variables: $z=f\ (x,\ y)$. Cam rotated by y-input; x-inputs shifts follower along pivot rod. Contour of cam causes follower to rotate giving angular displacement to z-output gear. (B) Conical cam for squaring positive or negative inputs: $y=c\ (\pm x)^2$. Radius of cone at any point is proportional to length of string to right of point; therefore, cylinder rotation is proportional to square of cone rotation. Output is fed through a gear differential to convert to positive number.

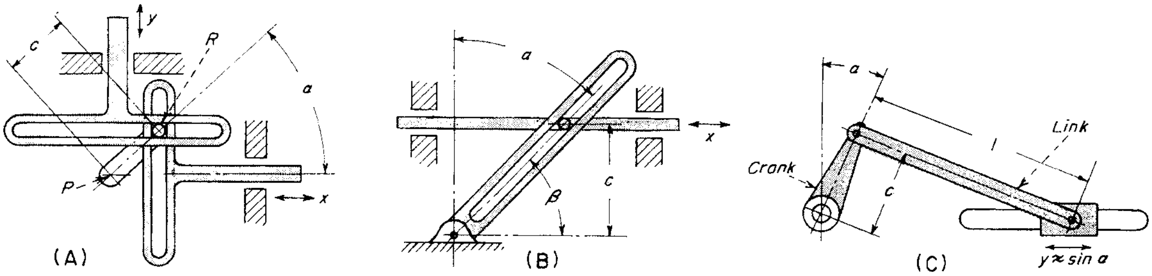

Fig. 4—TRIGONOMETRIC FUNCTIONS. (A) Scotch-yoke mechanism for sine and cosine functions. Crank rotates about fixed point *P* generating angle α and giving motion to arms: $y = c \sin \alpha$; $x = c \cos \alpha$. (B) Tangent-cotangent mechanism generates: $x = c \tan \alpha$ or $x = c \cot \beta$. (C) Eccentric and follower is easily manufactured but sine and cosine functions are approximate. Maximum error is: $e \max = l - \sqrt{l^2 - c^2}$; error is zero at 90 and 270 deg. *l* is the length of the link and *c* is the length of the crank.

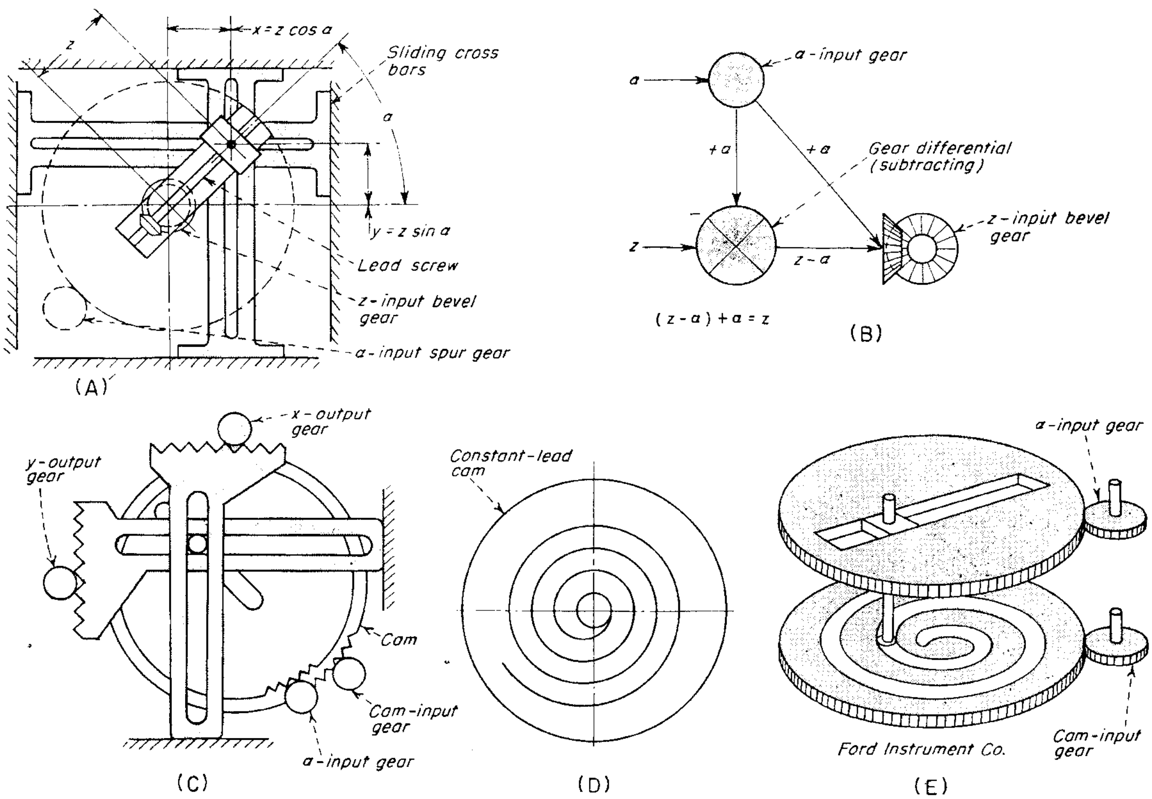

Fig. 5—COMPONENT RESOLVERS for obtaining x and y components of vectors that are continuously changing in both angle and magnitude. Equations are: $x = z \cos \alpha$, $y = z \sin \alpha$ where z is magnitude of vector, and α is vector angle. Mechanisms can also combine components to obtain resultant. Input in (A) are through bevel gears and lead screws for z input, and through spur gears for α-input. Compensating gear differential (B) prevents α-input from affecting z-input. This problem solved in (C) by using constant-lead cam (D) and (E).

Computing Mechanisms II

Several typical computing mechanisms for performing the mathematical operations of multiplication, division, differentiation, and integration of variable functions. Analog computing mechanisms for adding and subtracting, for resolving vectors, and for trigonometric functions, are discussed in Part I.

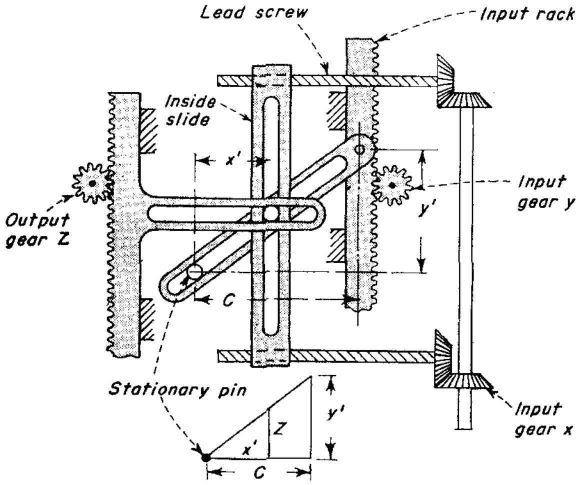

Fig. 1 (A)

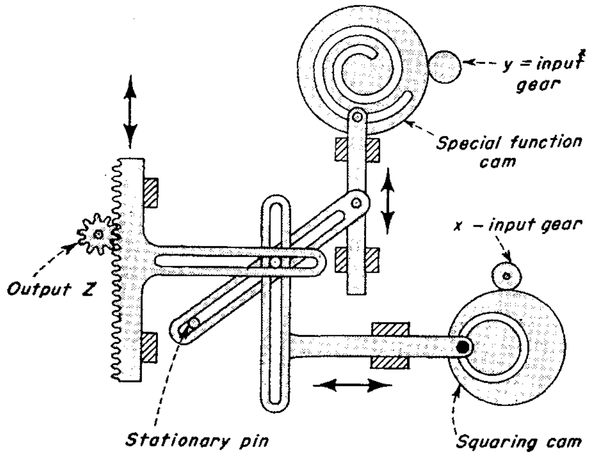

Fig. 2 (A)

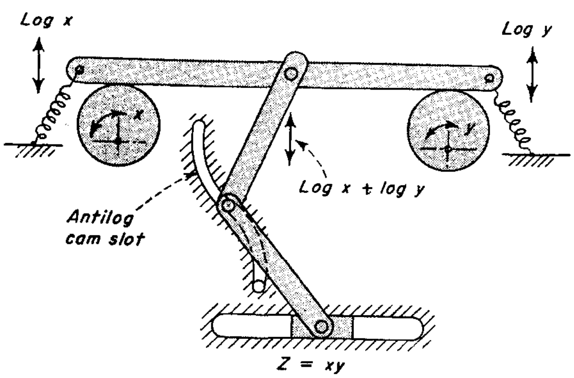

Fig. 1 (B)

Fig. 1—MULTIPLICATION OF TWO TABLES x and y usually solved by either: (A) Similar triangle method, or (B) logarithmic method. In (A), lengths x' and y' are proportional to rotation of input gears x and y. Distance c is constant. By similar triangles: $z/x=y/c$ or $z=xy/c$, where z is vertical displacement of output rack. Mechanism can be modified to accept negative variables. In (B), input variables are fed through logarithmic cams giving linear displacements of log x and log y. Functions are then added by a differential link giving $z=\log x + \log y=\log xy$ (neglecting scale factors). Result is fed through antilog cam; motion of follower represents $z=xy$.

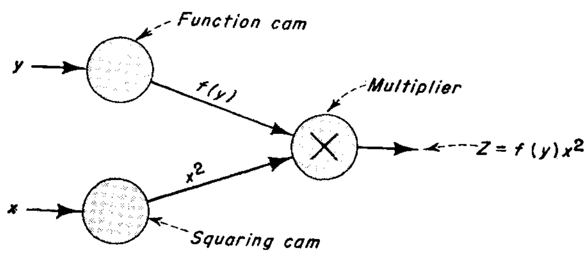

Fig. 2 (B)

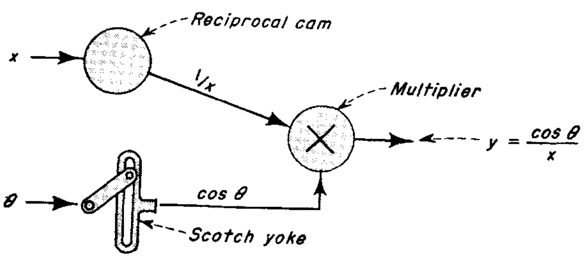

Fig. 2 (C)

Fig. 2—MULTIPLICATION OF COMPLEX FUNCTIONS can be accomplished by substituting cams in place of input slides and racks of mechanism in Fig. 1. Principle of similar triangles still applies. Mechanism in (A) solves the equation: $z=f(y)\,x^2$. Schematic is shown in (B). Division of two variables can be done by feeding one of the variables through a reciprocal cam and then multiplying it by the other. Schematic in (C) shows solution of $y=\cos \theta/x$.

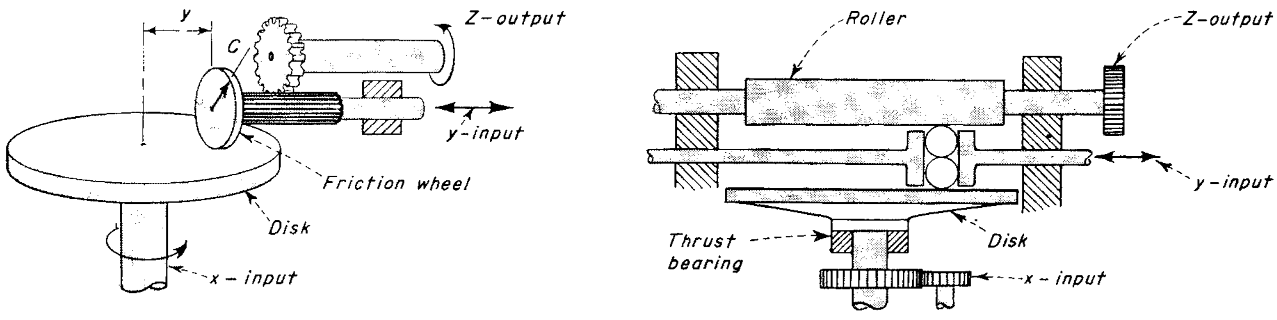

(A) (B)

Fig. 3—INTEGRATORS are basically variable speed drives. Disk in (A) is rotated by x-input which, in turn, rotates the friction wheel. Output is through gear driven by spline on shaft of friction wheel. Input y varies the distance of friction wheel from center of disk. For a wheel with radius c, rotation of disk through infinitesmal turn dx causes corresponding turn dz equal to: dz=(1/c) y dx. For definite x revolutions, total z revolutions will be equal to the integral of (1/c) y dx, where y varies as called for by the problem. Ball integrator in (B), gives pure rolling in all directions.

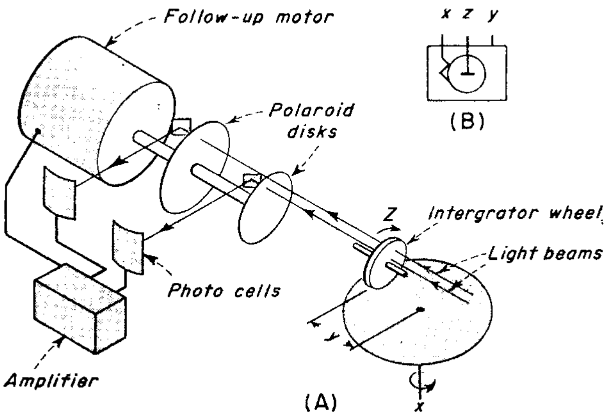

Fig. 4—FOLLOW-UP MOTOR avoids slippage between wheel and disk of integrator in Fig. 3 (A). No torque is taken from wheel except to overcome friction in bearings. Web of integrator wheel is made of polaroid. Light beams generate current to amplifier which controls follow-up motor. Symbol at upper right corner is schematic representation of integrator. For more information see, "Mechanism," by Joseph S. Beggs, McGraw-Hill Book Co., N. Y., 1955.

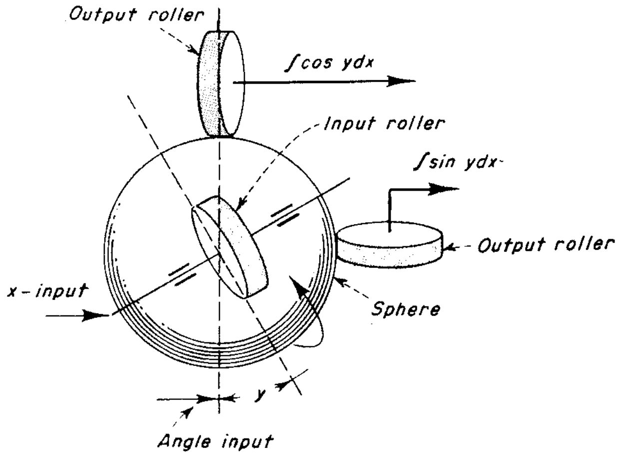

Fig. 5—COMPONENT INTEGRATOR uses three disks to obtain x and y components of a differential equation. Input roller x spins sphere; y input changes angle of roller. Output rollers give integrals of components paralleling x and y axes. Ford Instrument Company.

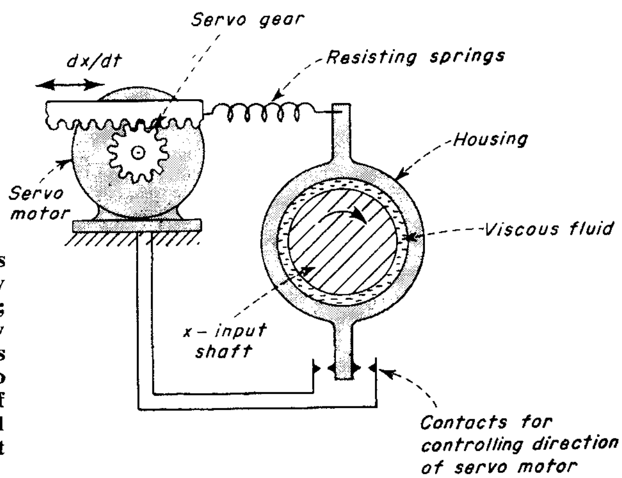

Fig. 6—DIFFERENTIATOR uses principle that viscous drag force in thin layer of fluid is proportional to velocity of rotating x-input shaft. Drag force counteracted by spring; spring length regulated by servo motor controlled by contacts. Change in shaft velocity causes change in viscous torque. Shift in housing closes contacts causing motor to adjust spring length and balance system. Total rotation of servo gear is proportional to dx/dt. From "Mechanical Computing Mechanisms," Reid and Stromback, Product Engineering, October 1949 page 126.

Eight Paper-Feed Mechanisms

In a world of reports, forms and memos, a prime need is to keep paper moving. Here are some ways that do the job for single sheets or continuous strips.

Frank William Wood JR & Vernal Huffines

SINGLE-SHEET FEEDERS

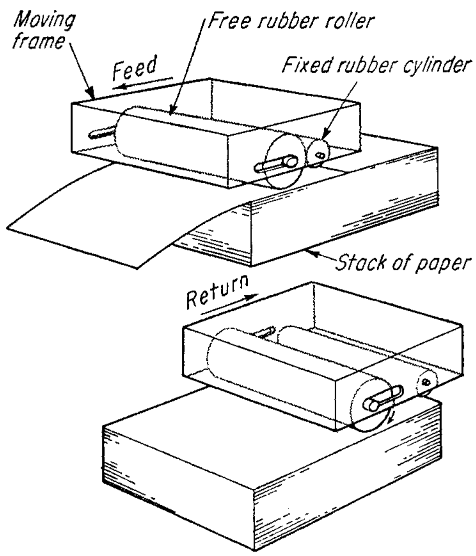

1

FREE ROLLER rides in slot. During feed it jams against the fixed cylinder and grips top sheet of paper. Return motion of frame transfers free roller to opposite end of slot, where it's free to roll back over paper.

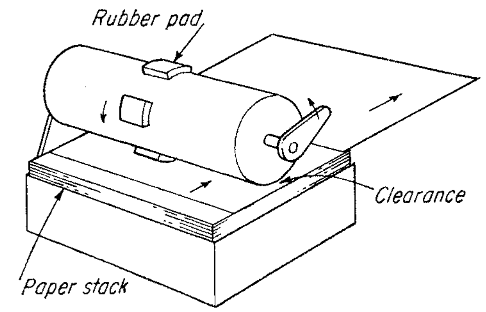

2

RUBBER PADS on rotating cylinder kick out one sheet per pad every revolution. Constant-force spring under paper-holder maintains proper clearance between paper and cylinder. Spacing of pads and the cylinder speed determine feed rate.

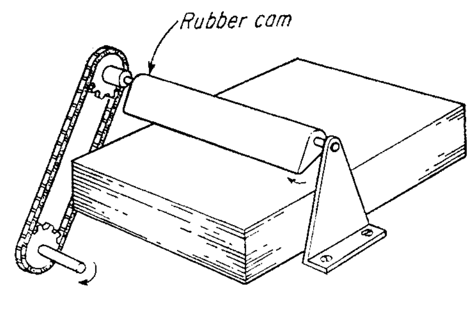

3

RUBBER CAM feeds one sheet each revolution. Constant-force spring under paper table keeps correct clearance. By correct timing, two or more cams in a stack will deliver different sheets in sequence. As with all single-sheet feeders, paper must be smooth enough to slide off pile.

CONTINUOUS-STRIP FEEDERS

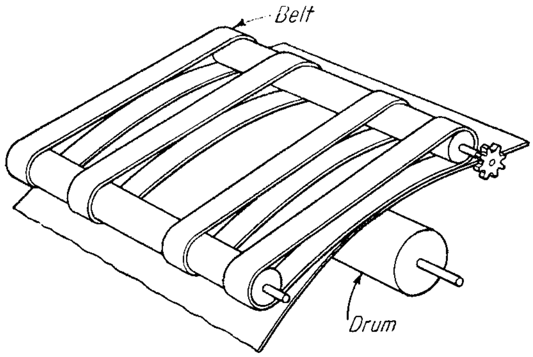

4

BELTS pressing against drum allow paper to slip and stay in alignment.

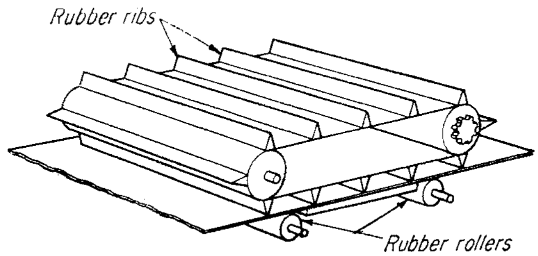

5

RIBBED BELT is another type of feed that allows paper to slip.

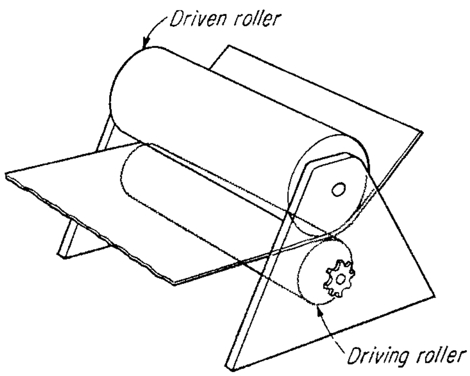

6

FRICTION ROLLERS are the commonest, cheapest way to feed paper in continuous strips.

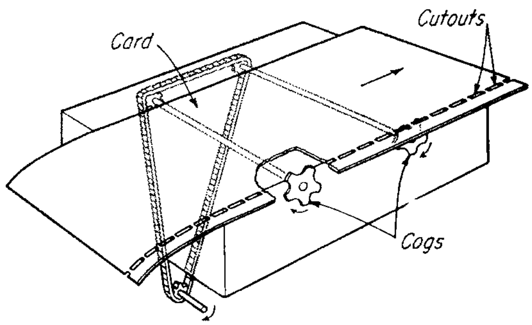

7

COGS fit in perforations to give positive feed with no slipping.

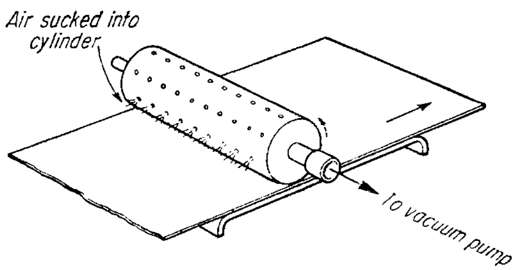

8

VACUUM PUMP sucks air in through the holes, holding paper against the cylinder. Intermittent operation of vacuum keeps paper from wrapping around cylinder.

How to Collect and Stack Die Stamping

When you're called upon to design a way to collect die stampings as they come from the press, do you shopping here for ideas.

Federico Strasser

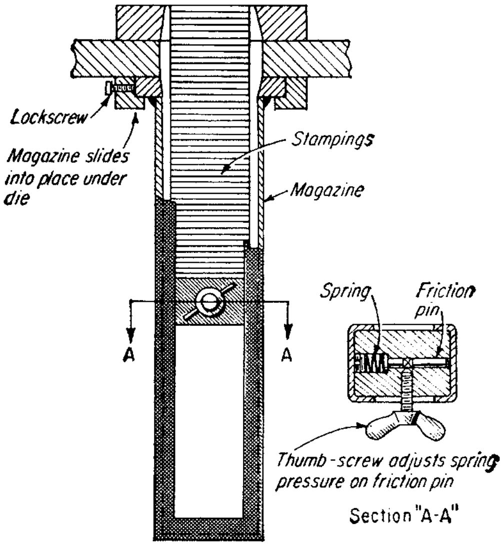

1. SLIDING MAGAZINE

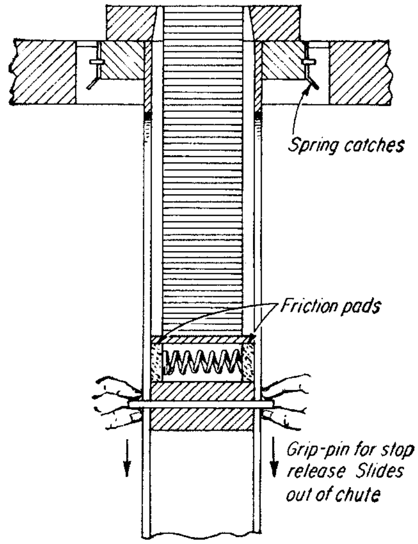

2. HANGING MAGAZINE

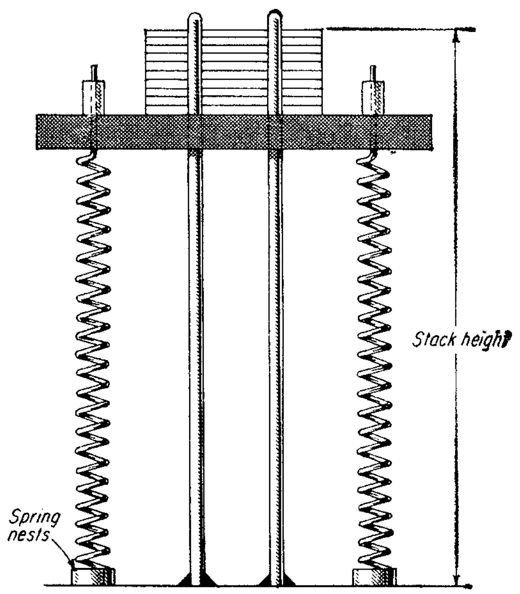

3. SPRINGS — stack height is constant when stamping weight divided by spring rate equals stamping thickness

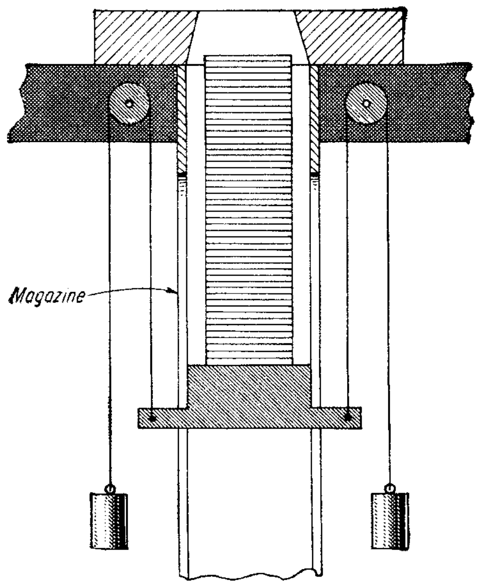

4. COUNTERBALANCE METHOD does not need high stacking friction as in first two methods shown above

DIRECT STACKING WITH BACK PRESSURE. FRICTION DRAGS, SPRINGS, AND COUNTERBALANCE WEIGHTS PROVIDE BACK PRESSURE TO ALLOW SMOOTH STACKING IN FIRST FOUR METHODS

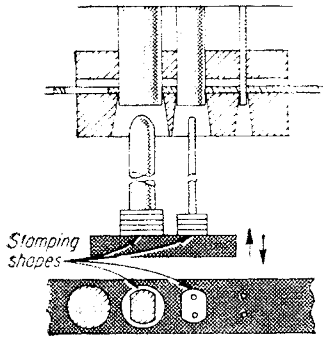

5. PEGGED MAGAZINE lets stampings be stacked by gravity, guided by hole in stamping

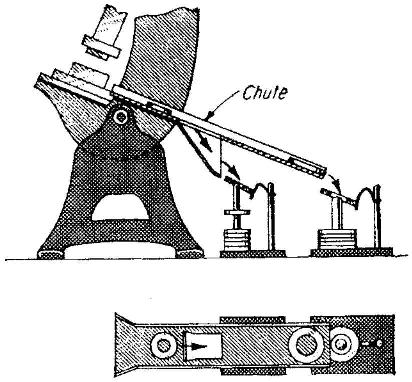

6. CHUTED STACKING WITH PEGGED MAGAZINE "sieves" stampings from two-stage die

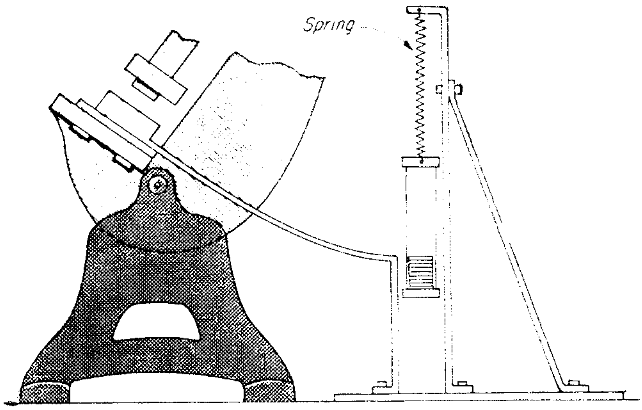

7. CHUTED STACKING WITH SPRING-SUSPENDED MAGAZINE

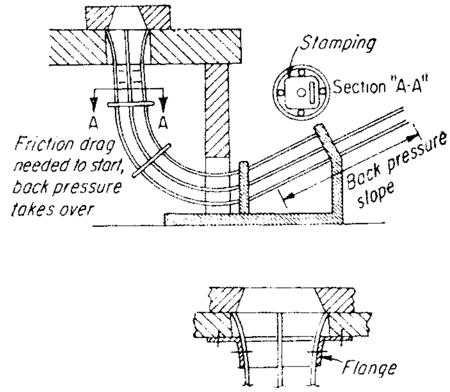

8. RODS FORM CHUTE

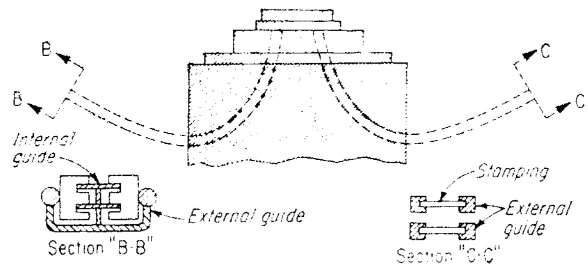

9. SPECIAL SHAPES ARE CHUTED IN CORRECT ORIENTATION

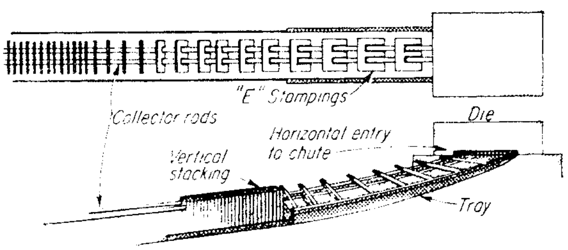

10. E-STAMPINGS ARE CHUTED FROM HORIZONTAL TO VERTICAL STACKING ON RODS

Sort, Feed, or Weigh Mechanisms

Sooner or later, you may be faced with the need to design such devices for your plant. These 19 selections are easily modified to suit your product.

Nicholas P. Chironis

ORIENTING DEVICES

Orienting short, tubular parts

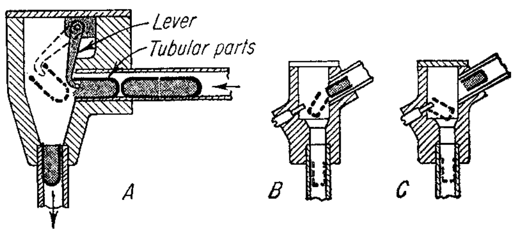

Here's a common problem: Parts come in either open-end or closed-end first; you need a device which will orient all the parts so they feed out facing the same way. In (A), when a part comes in open-end first, it is pivoted by the swinging lever so that the open end is up. When it comes in closed-end first, the part brushes away the lever to keel over head-first. Fig B and C show a simpler arrangement with pin in place of lever.

Orienting dish-like parts

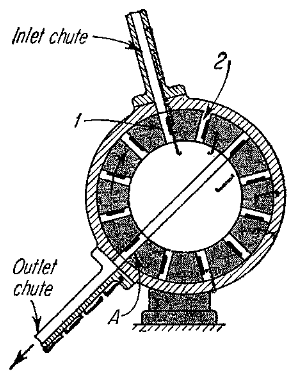

Part with open-end facing to the right (part 1) falls on to a matching projection as the indexing wheel begins to rotate clockwise. The projection retains the part for 230 deg to point *A* where it falls away from the projection to slide down the outlet chute, open-end up. An incoming part facing the other way (2) is not retained by the projection, hence slides *through* the indexing wheel so that it, too, passes through the outlet with the open-end up.

Orienting pointed-end parts

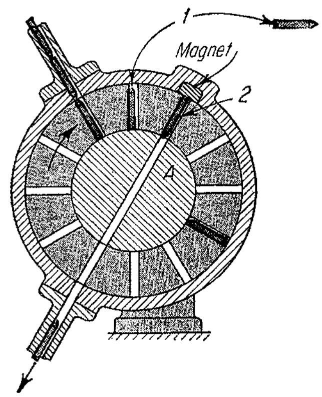

Main principle here is that the built-in magnet cannot hold on to a part as it passes by if the part has its pointed end facing the magnet. Such a correctly oriented part (part 1) will fall through the chute as the wheel indexes to a stop. An incorrectly oriented part (part 2) is briefly held by the magnet until the indexing wheel continues on past the magnet position. The wheel and the core with the slot must be made of nonmagnetic material.

Orienting U-shaped parts

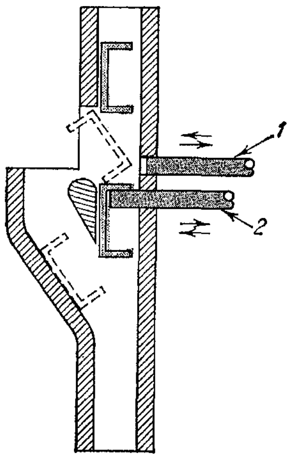

Key to this device is two pins which reciprocate one after another in the horizontal direction. The parts come down the chute with the bottom of the U facing either to the right or left. All pieces first strike and rest on pin 2. Pin 1 now moves into the passage way, and if the bottom of the U is facing to the right, the pin would kick over the part as shown by the dotted lines. If on the other hand the bottom of the U had been to the left, motion of pin 1 would have no effect, and as pin 2 withdrew to the right, the part would be allowed to pass down through the main chute.

Orienting cone-shaped parts

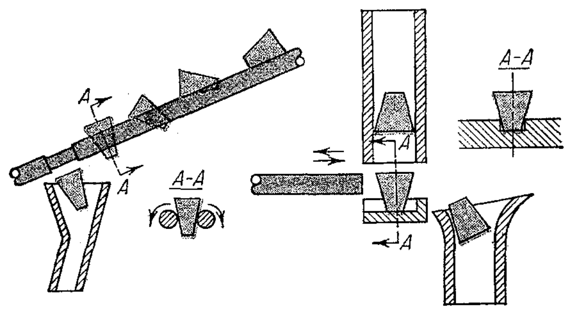

Regardless of which end of the cone faces forward as the cones slide down the cylindrical rods, the fact that both rods rotate in opposite directions causes the cones to assume the position shown in section A-A (left). When the cones reach the thinned-down section of the rods, they fall down into the chute as illustrated.

In the second method of orienting cone-shaped parts (right), if the part comes down small end first, it will fit into the recess. The reciprocating rod, moving to the right, will then kick the cone over into the exit chute. But if the cone comes down with its large end first, it sits on top of the plate (instead of inside the recess), and the rod merely pushes it into the chute without turning it over.

Orienting stepped-disk parts

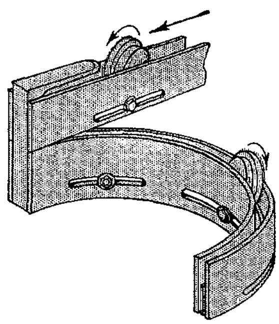

Parts rolling down the top rail to the left drop to the next rail which has a circular segment. The parts, therefore, continue to roll on in the original direction but their faces have now been rotated 180 deg. The idea of dropping one level may seem over simplified, but it avoids the use of camming devices which is the more common way of accomplishing this job.

SIMPLE FEEDING DEVICES

Feeding a fixed number of parts

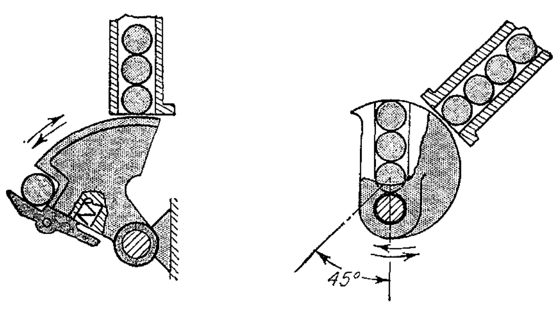

The oscillating sector picks up the desired number of parts, left diagram, and feeds them by pivoting the required number of degrees. The device for oscillating the sector must be able to produce dwells at both ends of the stroke to allow sufficient time for the parts to fall in and out of the sector.

The circular parts feed down the chute by gravity, and are separated by the reciprocating rod. The parts first roll to station 3 during the downward stroke of the reciprocator, then to station 1 during the upward stroke; hence the time span between parts is almost equivalent to the time it takes for the reciprocator to make one complete oscillation.

The device in (B) is similar to the one in (A), except that the reciprocator is replaced by an oscillating member.

One-by-one separating device

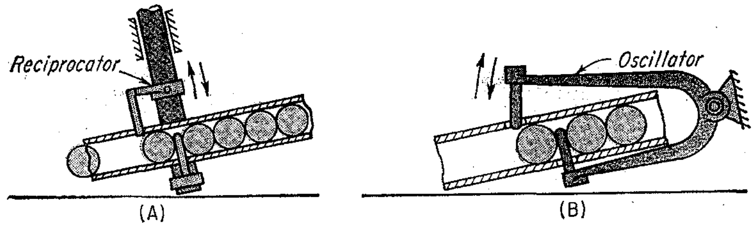

Mixing different parts together

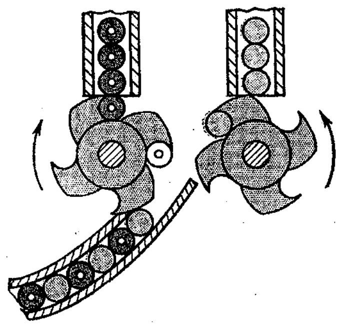

Two counter rotating wheels form a simple device for alternating the feed of two different workpieces.

Pausing until actuated

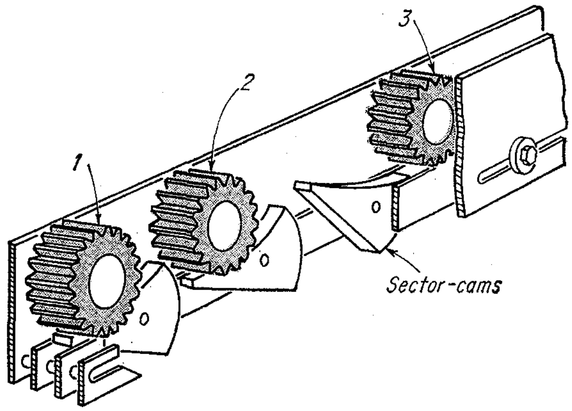

Each gear in this device is held up by a pivotable cam sector until the gear ahead of it moves forward. Thus, gear 3, rolling down the chute, kicks down its sector cam but is held up by the previous cam. When gear 1 is picked off (either manually, or mechanically), its sector cam pivots clockwise because of its own weight. This permits gear 2 to move into the place of gear 1—and frees cam 2 to pivot clockwise. Thus, all gears in the row move forward one station.

SORTING DEVICES

In the simple device (A) the balls run down two inclined and slightly divergent rails. The smallest balls, therefore, will fall into the left chamber, the medium-size ones into the middle-size chamber, and the largest ones into the right chamber.

In the more complicated arrangement (B) the balls come down the hopper and must pass a gate which also acts as a latch for the trapdoor. The proper-size balls pass through without touching (actuating) the gate. Larger balls, however, brush against the gate which releases the catch on the bottom of the trapdoor, and fall through into the special trough for the rejects.

Sorting balls according to size

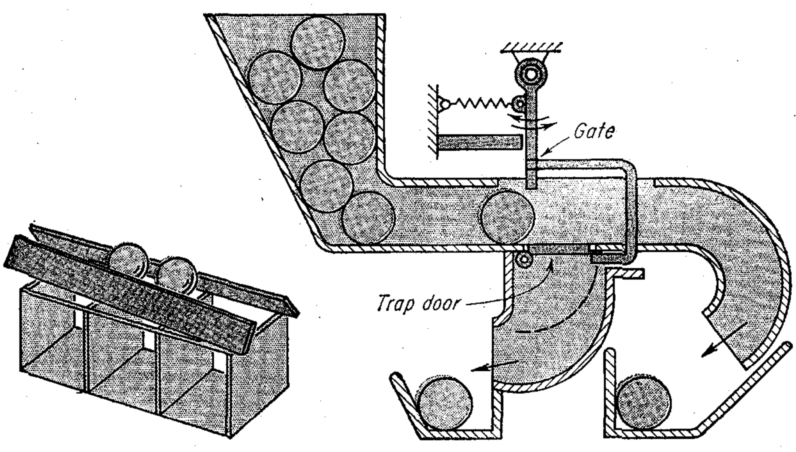

Sorting according to height

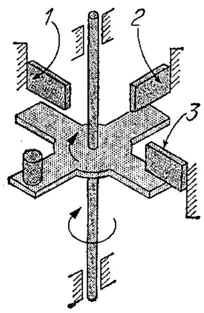

This is a simple device in which an assembly worker can place the workpiece on a slowly rotating cross-platform. Bars 1, 2, and 3 have been set at decreasing heights beginning with the highest bar (bar 1), and the lowest bar (bar 3). The workpiece is therefore knocked off the platform at either station 1, 2, or 3 depending on its height.

WEIGHT-REGULATING ARRANGEMENTS

By varying the vibration amplitudes

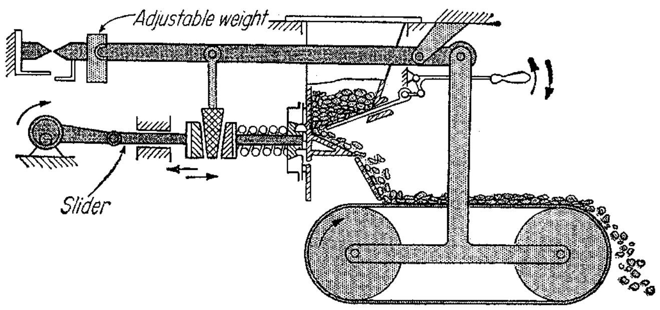

The material in the hopper is fed to a conveyor by means of vibration actuated by the reciprocating slider. The pulsating force of the slider passes through the rubber wedge and on to the actuating rod. The amplitude of this force can be varied by moving the wedge up or down. This is done automatically by making the conveyor pivot around a central point. As the conveyor becomes overloaded, it pivots clockwise to raise the wedge which reduces the amplitudes—and the feed rate of the material.

Further adjustments in feed rate can be made by shifting the adjustable weight or by changing the speed of the conveyor belt.

By linkage arrangement

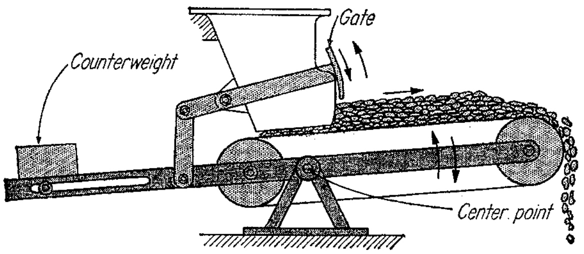

The loose material comes down the hopper and is fed to the right by the conveyor system which can pivot about the center point. The frame of the conveyor system also actuates the hopper gate, so that if the material on the belt exceeds the required amount the conveyor pivots clockwise and closes the gate. The position of the counterweight on a frame determines the feed rate of the system.

By electric-eye and balancer

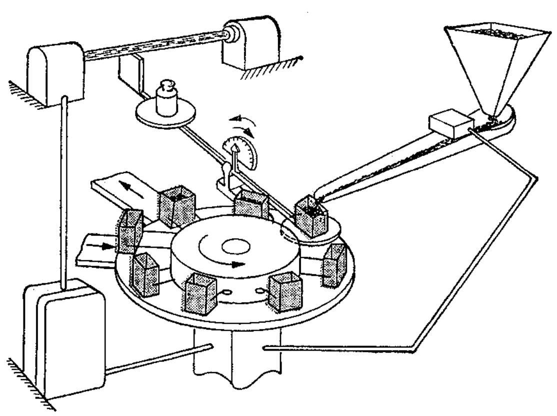

The indexing table automatically comes to a stop at the feed station. As the material drops into the container, its weight pivots the screen upward to cut off the operation of the photocell relay. This in turn shuts the feed gate. Reactuation of the indexing table can be automatic after a time interval, or by the cutoff phase of the electric eye.

EDITOR'S NOTE: The above material is based on the book *"Mechanism,"* by C. H. Kohevnikov; published in Russian, Moscow, 1965.

Spring Motors & Typical Associated Mechanisms

MANY applications of spring motors in clocks, phonographs, motion picture cameras, rotating barber poles, game machines and other mechanisms offer practical ideas for adaptation to any mechanism in which operation for an appreciable length of time is desirable. While spring motors are usually limited to comparatively small power applications where other sources of power are unavailable or impracticable, they may also be useful for intermittent operation requiring

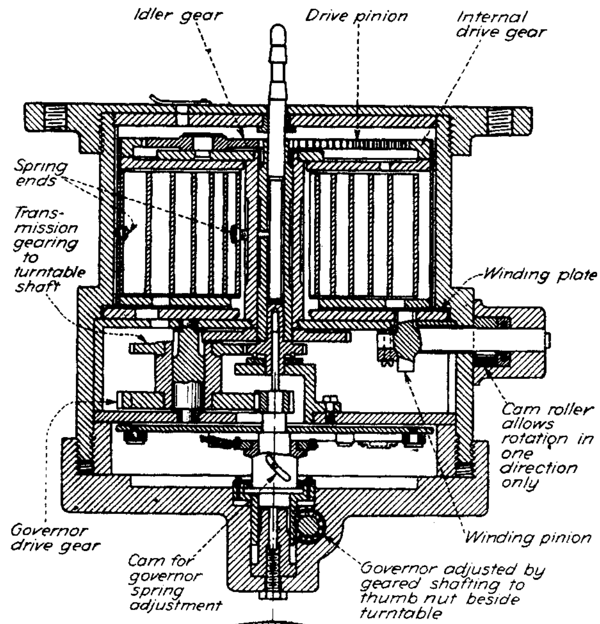

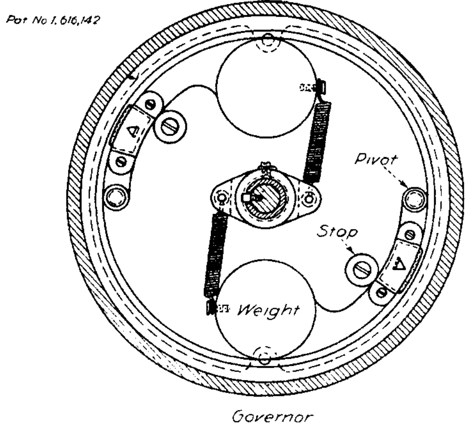

FIG. 2

FIG. 1

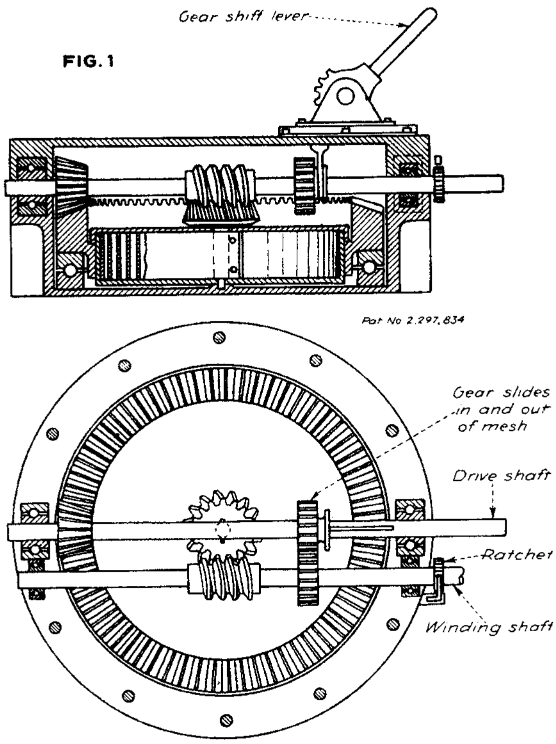

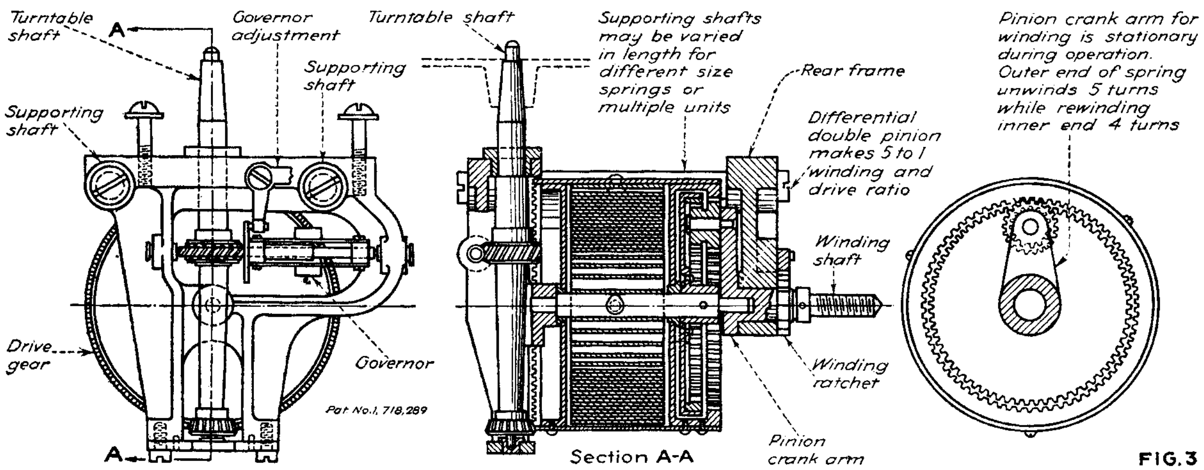

FIG. 3

comparatively high torque or high speed, using a low power electric motor or other means for building up energy.

The accompanying patented spring motor designs show various methods of transmission and control of spring motor power. Flat-coil springs, confined in drums, are most widely used because they are compact, produce torque directly, and permit long angular displacement. Gear trains and feed-back mechanisms hold down excess power so that it can be applied for a longer time, and governors are commonly used to regulate speed.

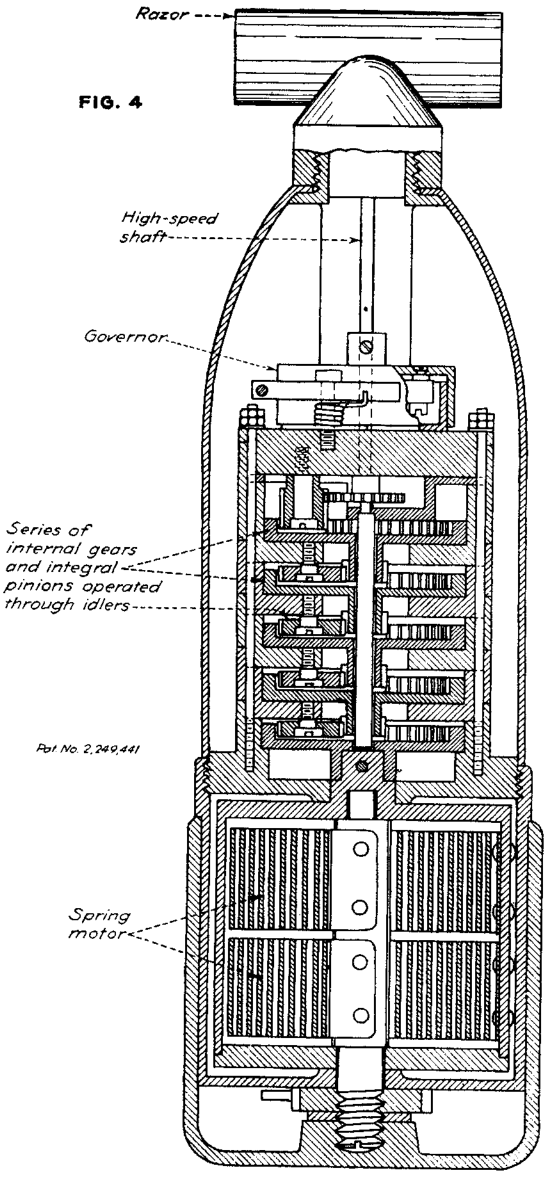

FIG. 4

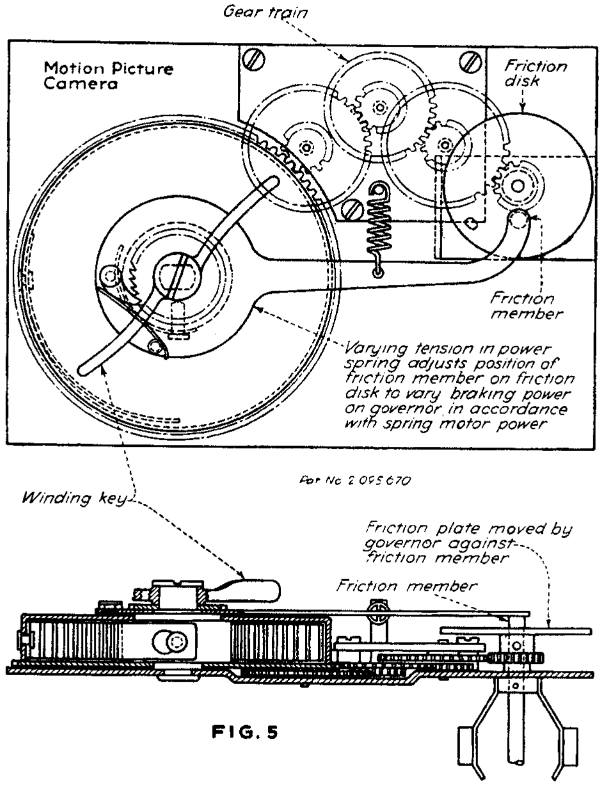

FIG. 5

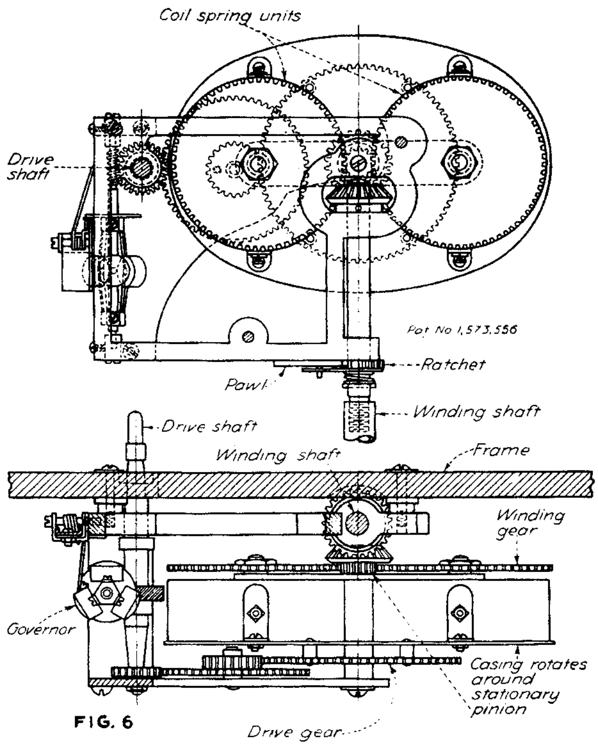

FIG. 6

6 Escapement Mechanisms

Federico Strasser

Escapements, a familiar part of watches and clocks, can also be put to work in various control devices, and for the same purpose—to interrupt the motion of a gear train at regular intervals.

Each escapement shown here contains an energy absorber. Whether balance wheel or pendulum, it allows the gear train to advance one tooth at a time, locking the wheel momentarily after each half-cycle. Energy from the escape wheel is transferred to the escapement by the advancing teeth, which push against the locking surfaces (pallets).

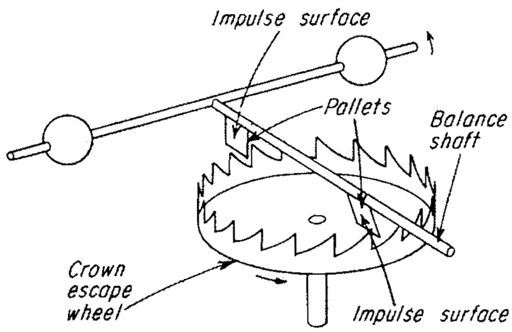

1 VERGE. Pallets are alternately lifted and cleared by diametrically opposed teeth on escape wheel, thus rocking balance shaft. One pallet or the other is always in contact with a tooth of the escape wheel.

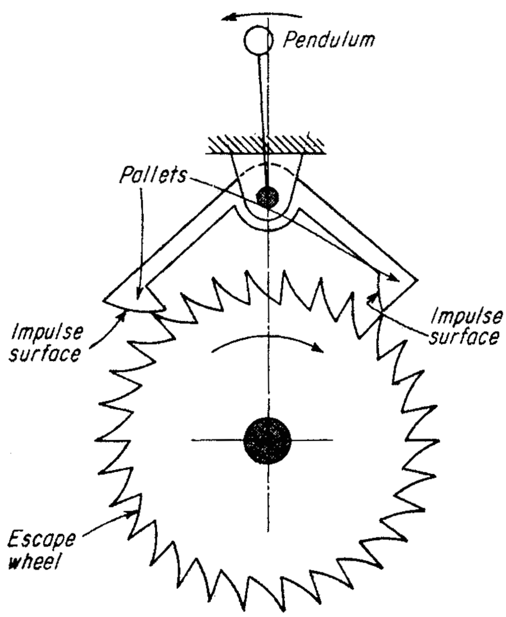

2 ANCHOR—RECOIL. As pendulum swings to one side, pallet engages tooth of escape wheel. When wheel is gripped, it recoils slightly. Pendulum starts in opposite direction by push of wheel transmitted through pallet. As pendulum swings to other side, the other pallet engages escape-wheel tooth, recoils, and repeats cycle.

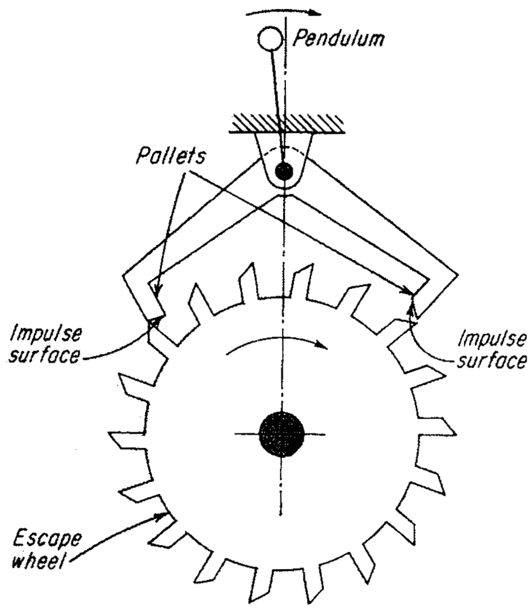

3 ANCHOR—DEAD BEAT. For greater accuracy, recoil escapement is modified by changing angle of impulse surfaces of pallets and teeth so that recoil is eliminated. The teeth of escape wheel fall "dead" upon pallets; as pendulum completes its swing, escape wheel does not turn backward.

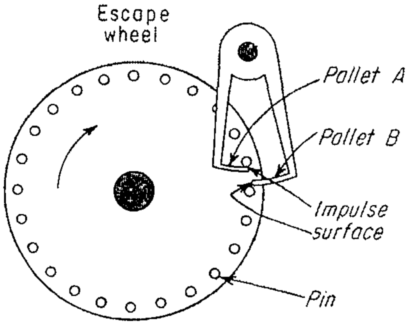

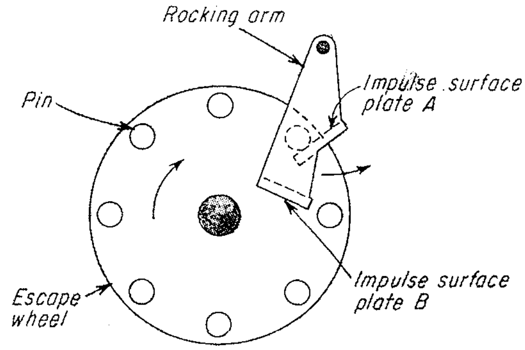

4 PIN WHEEL. Pallet A is about to unlock escape wheel. Pin will give a push to pallet A while sliding down impulse surface. As pendulum continues to swing, pallet B will stop pin, thus locking escape wheel. After pendulum reverses direction and swings toward dead center, pallet B releases wheel and receives an impulse from pin.

5 LANTERN WHEEL. Escape wheel is stopped when pin hits plate A of pallet, attached to rocking arm. As arm swings to right, pin pushes against impulse surface of plate until pin is clear. Escape wheel then turns freely until pin is stopped by plate B of pallet. Arm starts back toward left, receiving impulse from pin until latter clears plate.

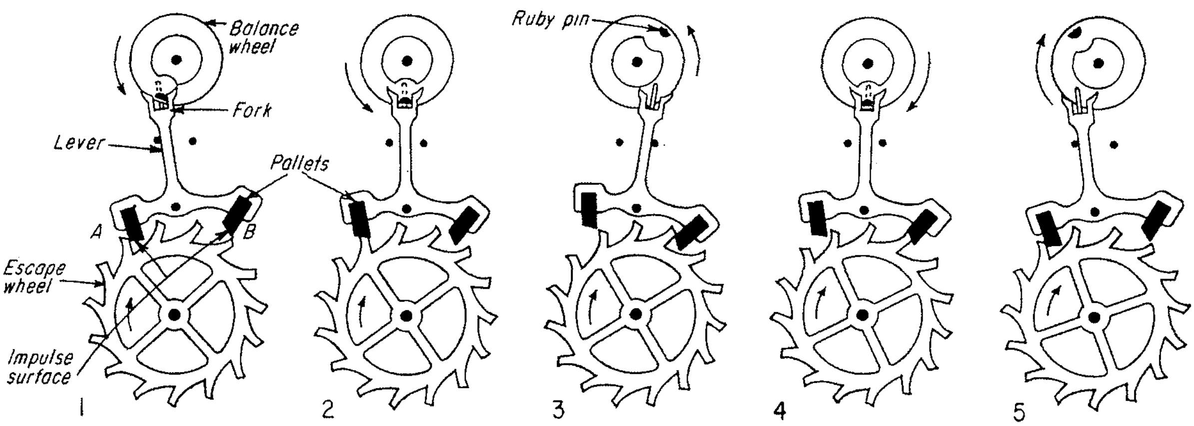

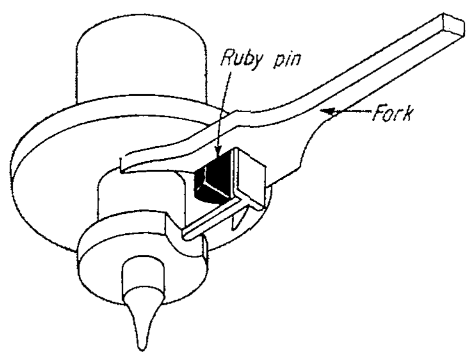

6 MUDGE'S LEVER. As balance wheel swings counterclockwise (1), the ruby pin enters fork of lever and pushes it to the right. The lever releases tooth of escape wheel, which starts turning and gives a tiny push (2) to impulse surface of pallet A. This is transmitted to balance wheel through fork and ruby pin. Balance wheel continues rotating counterclockwise (3) while lever swings to right and pallet B stops the escape wheel by engaging tooth. When balance wheel reaches its hairspring's limit, it reverses direction and re-enters fork (4). Ruby pin pushes lever to left, and receives impulse when escape wheel starts to move. Balance wheel continues clockwise until it reaches opposite limit of its hairspring. Lever continues moving to left until it again stops escape wheel (5) and awaits return of ruby pin. Another view of Mudge's lever is given in (6). This escapement is very precise because of the small portion of each half-cycle that escape wheel and balance wheel are in contact. Friction drag is at a minimum.

7 More Escapement

Another selection of these ingenious mechanical components for use in control systems.

Federico Strasser

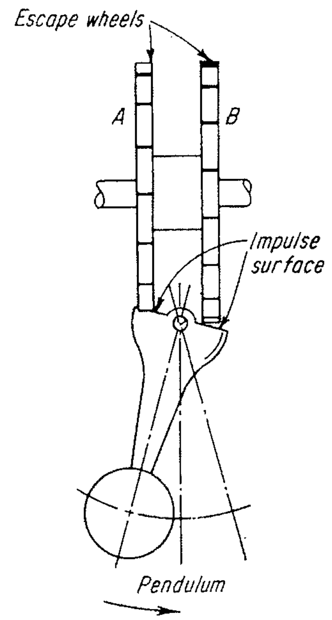

2 DOUBLE RATCHET. Two escape wheels are mounted on a common axis and pinned together so teeth are aligned with a half-pitch distance between them. Drawing shows pendulum in its extreme left position, with its impulse surface locking a tooth of the escape wheel *A*. As pendulum starts to right, escape wheels start to turn, imparting a push to the pendulum. As it approaches its extreme right position, pendulum again stops the escape wheels, by engaging a tooth on wheel *B*, then receives a second impulse as it starts toward the left.

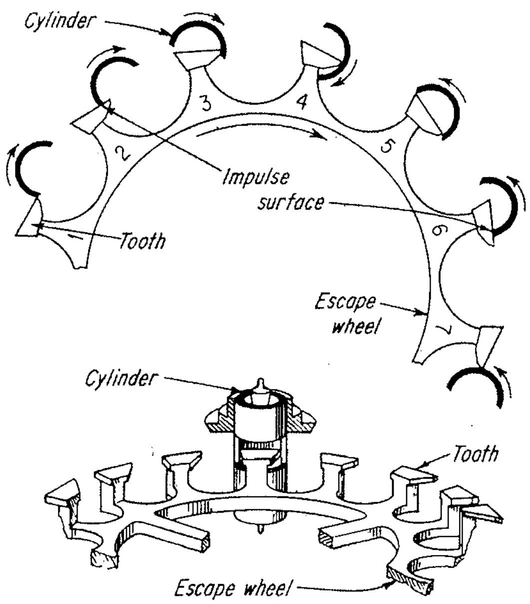

1 CYLINDER. Tooth of escape wheel and cylinder (balance-wheel shaft) are shown in seven positions. Tooth has been locked (1) and is about to enter cycle. Tooth is providing impulse (2) by sliding action along cylinder lip. Escape wheel is locked while cylinder rotates clockwise (3) to its limit (4), then starts back (5). As tooth starts forward, impulse is again imparted (6) to cylinder lip. Second tooth is locked (7) during period of backswing.

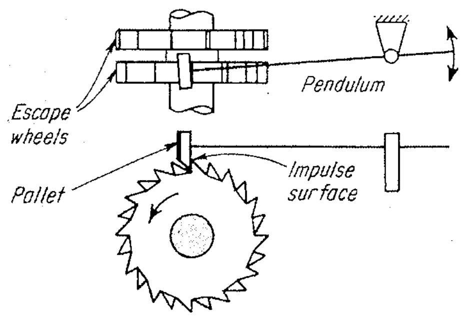

3 HIGH-SPEED DOUBLE RATCHET. Same principle as in 2, but used with a small-mass pendulum. Speeds to 50 beats per second can be obtained.

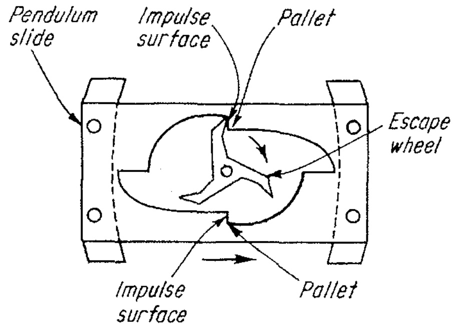

4 THREE-LEGGED. The three teeth of escape wheel work alternately upon top and bottom pallets. Top pallet is shown being driven to right. When tooth clears pallet, escape wheel will turn until tooth engages bottom pallet. When pendulum slide starts back toward left, bottom pallet will receive push from escape wheel, until tooth clears pallet.

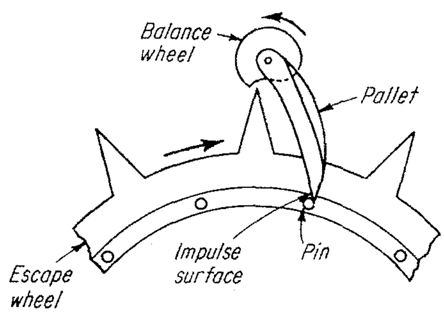

5 DUPLEX. Single pallet of balance wheel is shown receiving impulse from pin of escape wheel. As balance wheel rotates counterclockwise, tooth of escape wheel clears notch, permitting escape wheel to turn clockwise. Next tooth of escape wheel is stopped by balance wheel until balance wheel reaches limit, reverses direction, and pallet swings back to position shown. Escapement receives but one impulse per cycle.

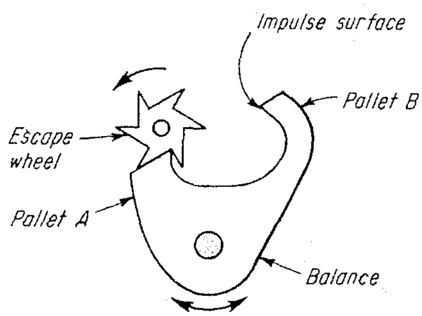

6 STAR WHEEL. Dead-beat escapement in which pallets alternately act upon diametrically opposed teeth. Illustration shows balance in extreme clockwise position with escape wheel locked. Balance starts turning counterclockwise, releasing escape wheel. At other extreme, pallet *B* locks escape wheel for a moment before direction of balance is again reversed and push is imparted.

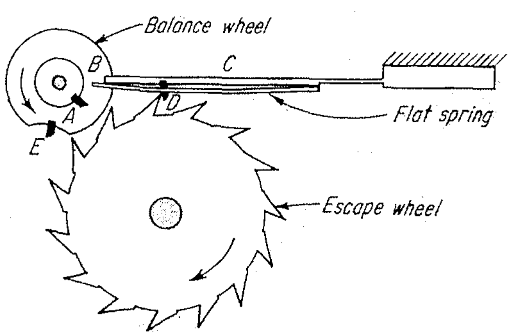

7 CHRONOMETER. As balance wheel turns counterclockwise, jewel *A* pushes flat spring *B* and raises bar *C*. Tooth clears jewel *D* and escape wheel turns. A tooth imparts push to jewel *E*. As jewel *A* clears flat spring, jewel *D* returns to position and catches next tooth. On return of balance wheel (clockwise), jewel *A* passes flat spring with no action. Thus, escapement receives a single impulse per cycle.

Design Hints for Mechanical Small Mechanisms

How to avoid close tolerances, and otherwise improve parts, where accurate assembly is necessary.

Federico Strasser

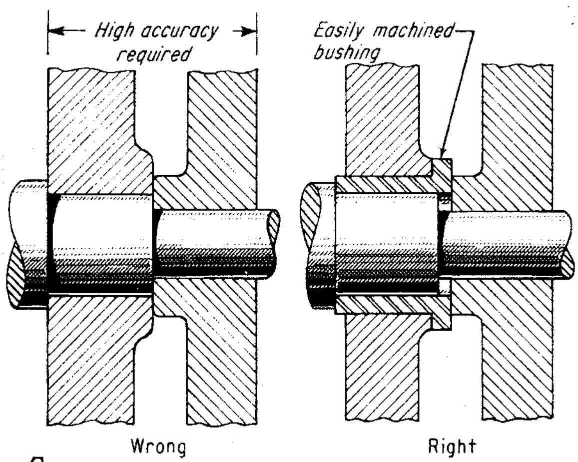

1 **BUSHING FACE** is much easier to machine than the hub of a large part such as a flywheel or heavy gear.

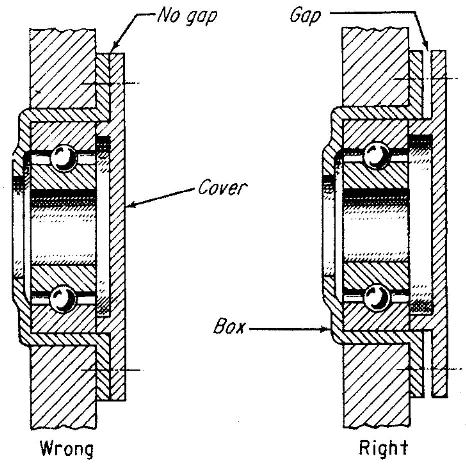

2 **HOLD-DOWN COVER** for bearing should have a take-up gap between the cover flange and the bearing box.

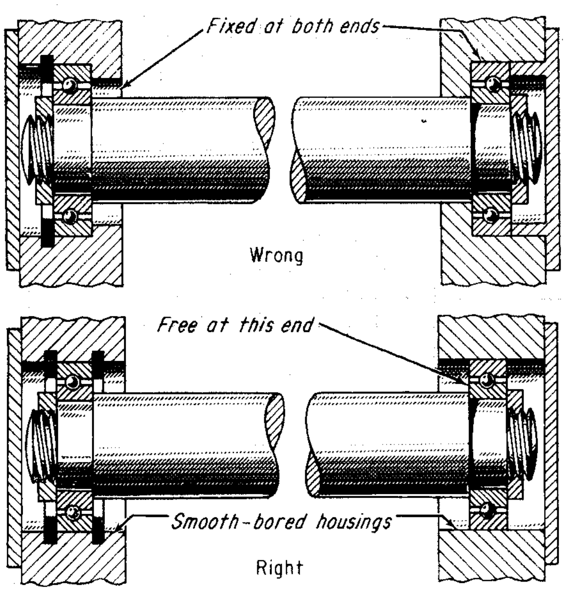

5 **SMOOTH-BORED HOUSINGS** shown on right let one bearing move when shaft length changes because of expansion.

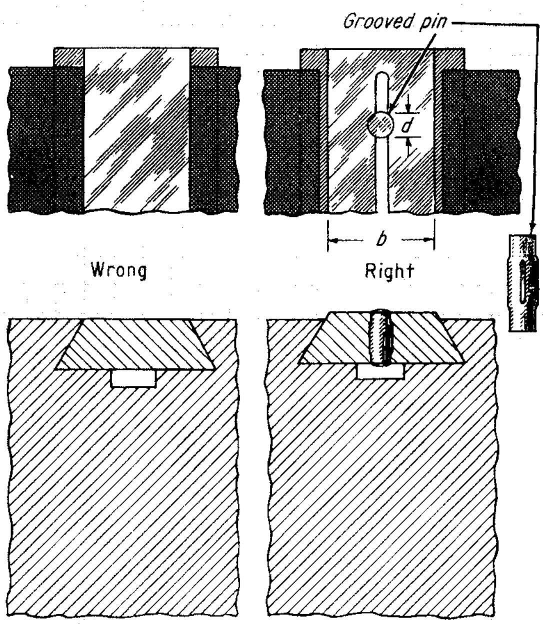

6 **DOVETAILED** parts that are to be a tight fit are best provided with a slot and grooved pin where d equals $b/3$ to $b/4$.

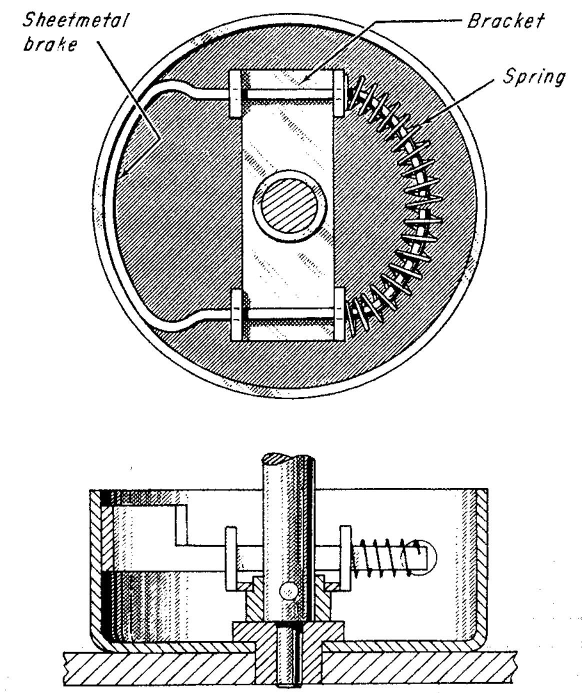

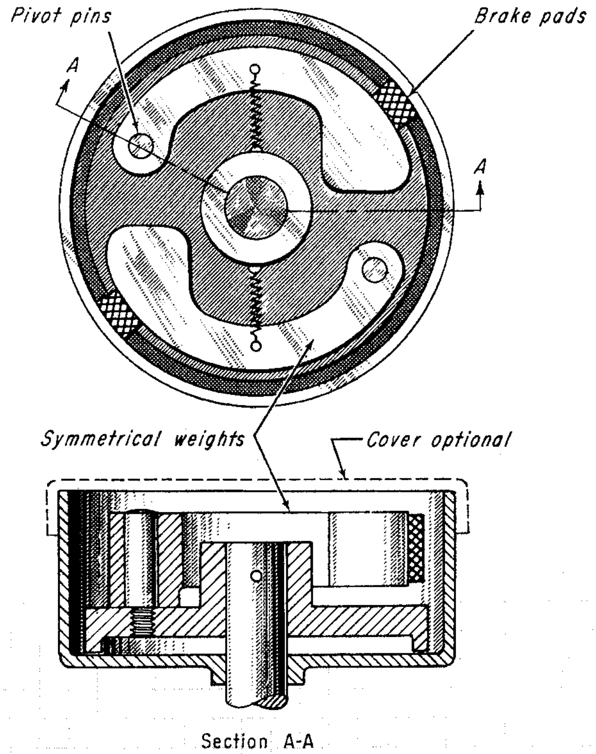

3

SHEETMETAL BRAKE provides larger braking area than previous design. Operation is thus more even and cooler.

4

SYMMETRICAL WEIGHTS give even braking action when they pivot outward. Entire action can be enclosed.

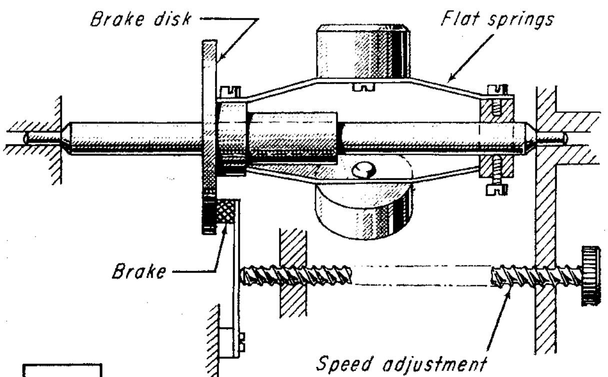

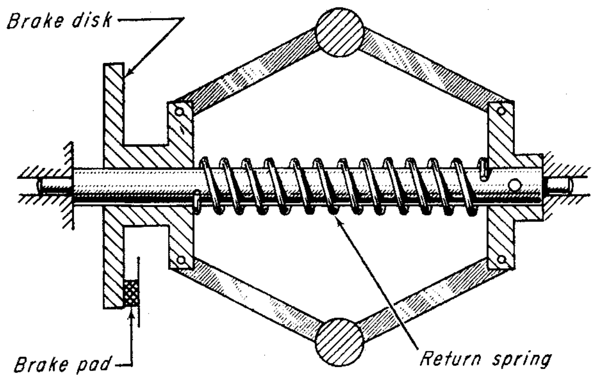

7

THREE FLAT SPRINGS carry weights that provide brake force upon rotation. Device can be provided with adjustment.

8

TYPICAL GOVERNOR action of swinging weights is utilized here. As in the previous device, adjustment is optional.

SECTION 23

LINKAGE

8 Basic Push-Pull Linkages

These arrangements are invariably the root of all linkage devices.

Frank William Wood JR.

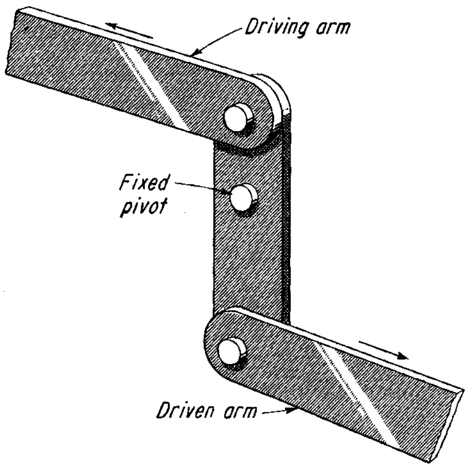

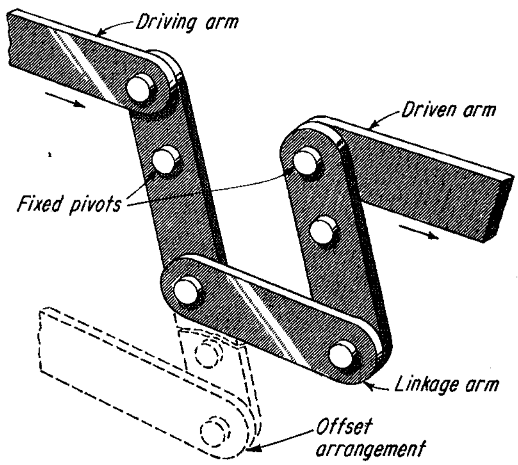

1 **FIXED PIVOTS** on arm lengths are located to control ratio of input and output movements of this push-pull-actuated linkage. Mechanism can be either flat bars or round rods of adequate thickness to prevent bowing under compression.

2 **PUSH-PULL LINKAGE** for same direction of motion can be obtained by adding linkage arm to previous design. In both cases, if arms are bars it might be best to make them forked rather than merely flatted at their linkage ends.

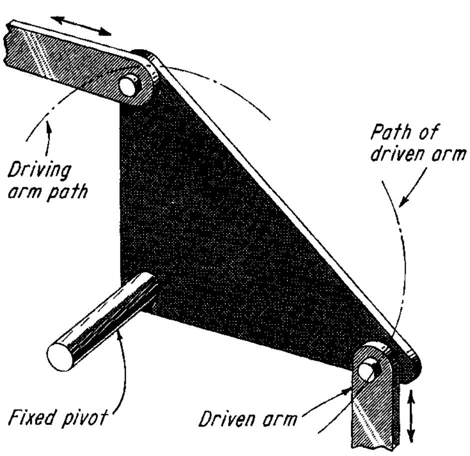

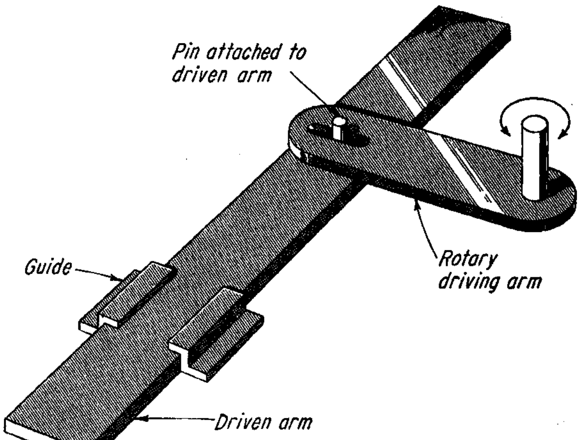

5 **VERTICAL OUTPUT MOVEMENT** from horizontal input is gained with this push-pull linkage. Although the triangular-shaped plate could be substituted by an L-shaped arm, the plate gives greater freedom of driving- and driven-arm location.

6 **FOR LIMITED STRAIGHT-LINE** 2-direction motion use this rotary-actuated linkage. Friction between the pin and sides of slot limit this design to small loads. A bearing on the pin will reduce friction and slot wear to negligible proportions.

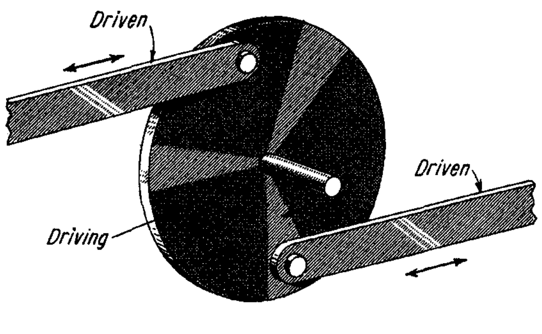

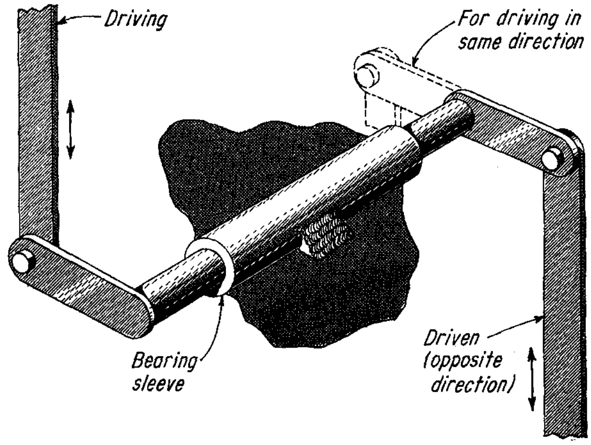

3 **ROTARY-ACTUATED LINKAGE** gives opposite direction of motion and can be obtained by using 3-bar linkage with pivot point of middle link located at midpoint of arm length. Disk should be adequately strengthened for heavy loads.

4 **SAME-DIRECTION MOTION** is given by this rotary-actuated linkage when end arms are located on the same sides; for opposite-direction motion, locate the arms on opposite sides. Use when a crossover is required between input and output.

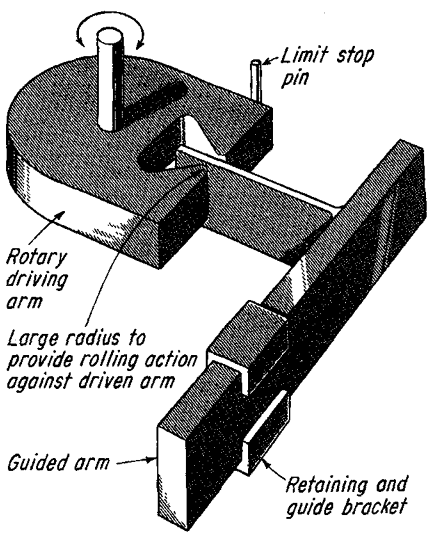

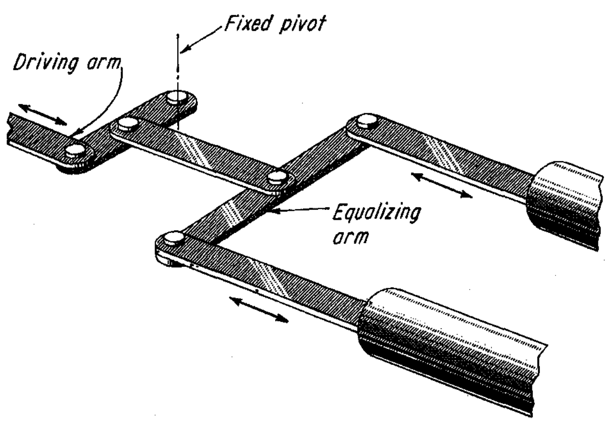

7 **THIS ROTARY-ACTUATED** linkage for straight-line 2-direction motion has rotary driving arm with a modified dovetail opening that fits freely around a flat sheet or bar arm. Driven arm reciprocates in slot as rotary driving arm is turned.

8 **EQUALIZING LINKAGE** here has an equalizing arm that balances the input force to two output arms. This arrangement is most suitable for air or hydraulic systems where equal force is to be exerted on the pistons of separate cylinders.

5 Linkages for Straight-Line Motion

These devices convert rotary to straight-line motion without the need for guides.

Sigmund Rappaport

1

Evans' linkage . . .
has oscillating drive-arm that should have a maximum operating angle of about 40°. For a relatively short guide-way, the reciprocating output stroke is large. Output motion is on a true straight line in true harmonic motion. If an exact straight-line motion is not required, however, a link can replace the slide. The longer this link, the closer does the output motion approach that of a true straight line—if link-length equals output stroke, deviation from straight-line motion is only 0.03% of output stroke.

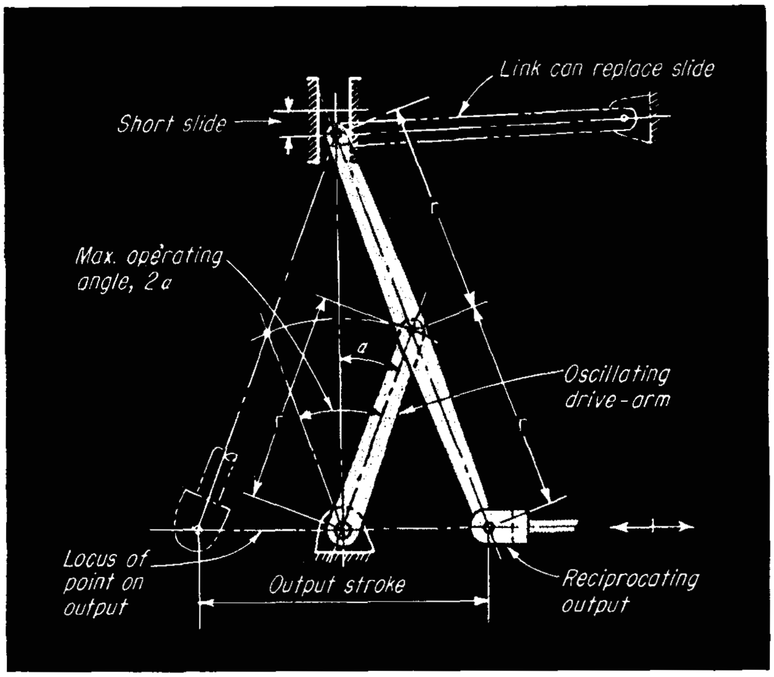

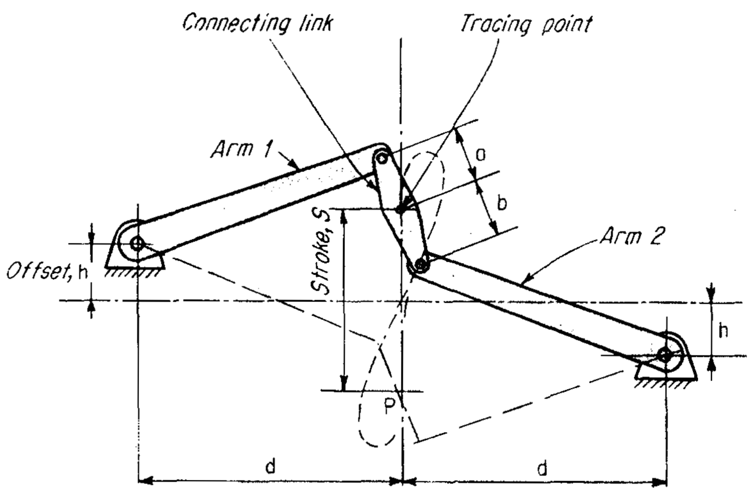

2

Simplified Watt's linkage . . .
generates an approximate straight-line motion. If the two arms are equally long, the tracing point describes a symmetrical figure 8 with an almost straight line throughout the stroke length. The straightest and longest stroke occurs when the connecting-link length is about ⅔ of the stroke, and arm length is 1.5S. Offset should equal half the connecting-link length. If the arms are unequal, one branch of the figure-8 curve is straighter than the other. It is straightest when a/b equals (arm 2)/(arm 1).

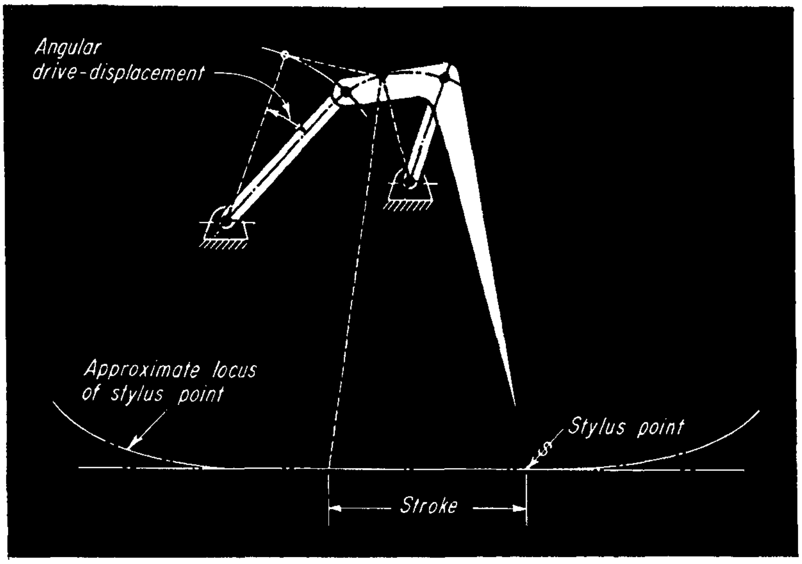

3

Four-bar linkage . . .
produces approximately straight-line motion. This arrangement provides motion for the stylus on self-registering measuring instruments. A comparatively small drive-displacement results in a long, almost-straight line.

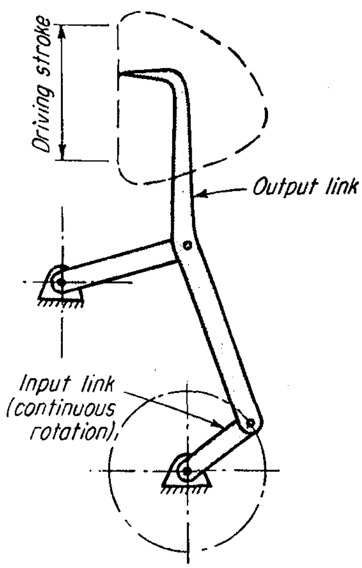

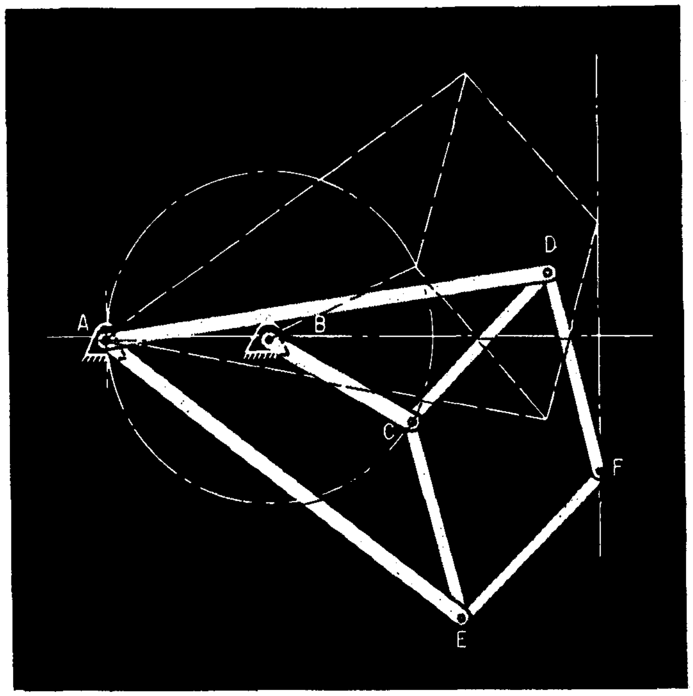

4

D-drive . . .
results when linkage arms are arranged as shown here. Output-link point describes a path resembling the letter *D*, thus it contains a straight portion as part of its cycle. Motion is ideal for quick engagement and disengagement before and after a straight driving-stroke. Example, the intermittent film-drive in movie-film projectors.

5

The "Peaucellier cell" . . .
was first solution to the classical problem of generating a straight line with a linkage. Its basis: within the physical limits of the motion, AC x AF remains constant. Curves described by C and F are, therefore, inverse; if C describes a circle that goes through A, then F will describe a circle of infinite radius—a straight line, perpendicular to AB. The only requirements are: *AB*=*BC*; *AD*=*AE*; and CD, *DF*, *FE*, *EC* are all equal. The linkage can be used to generate circular arcs of large radius by locating *A* outside the circular path of C.

10 Ways to Change Straight-Line Direction

Arrangements of linkages, slides, friction drives and gears that can be the basic of many ingenious devices.

Federico Strasser

Linkages

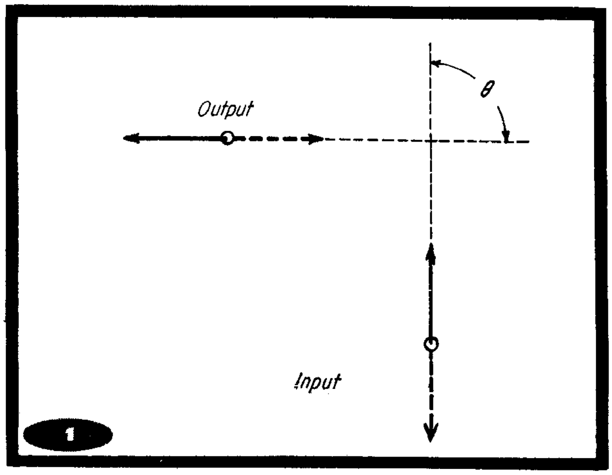

Basic problem (θ is generally close to 90°)

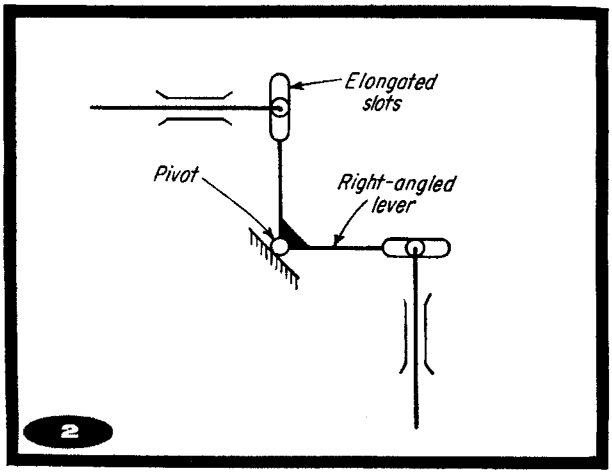

Slotted lever

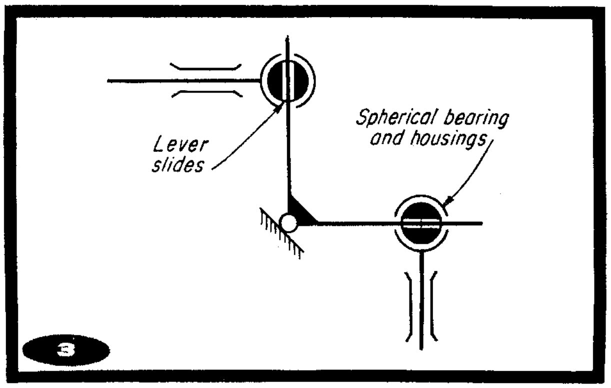

Spherical bearings

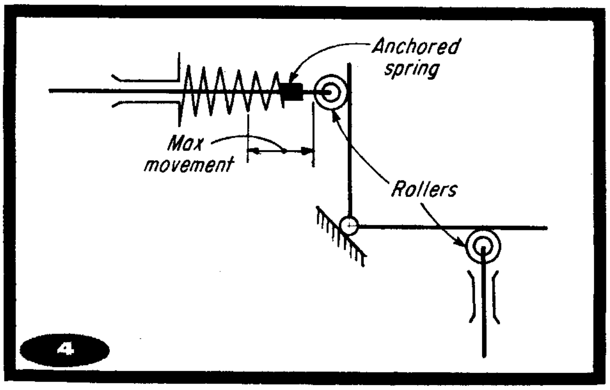

Spring-loaded lever

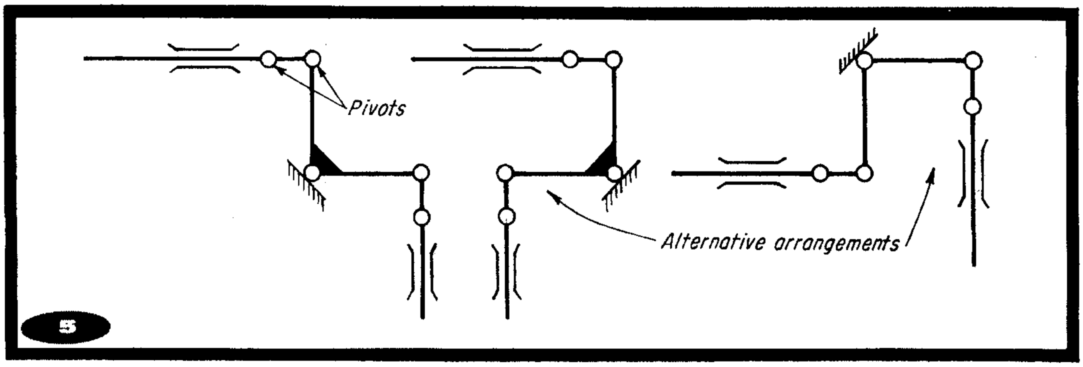

Pivoted levers with alternative arrangements

Guides

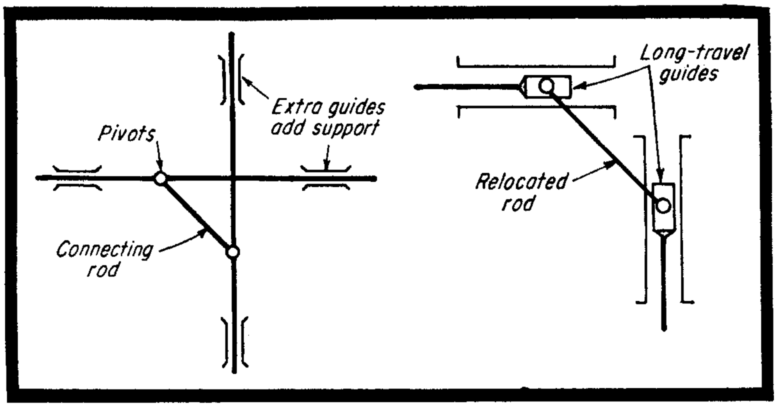

6

Single connecting rod (left) is relocated (right) to get around need for extra guides

Friction Drives

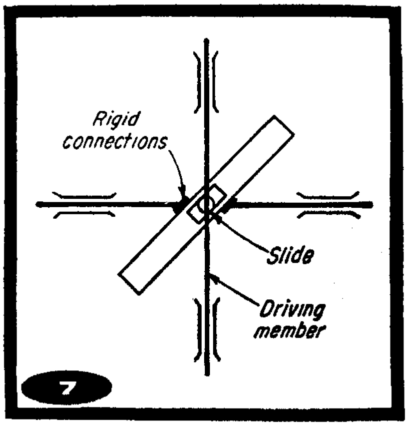

Inclined bearing-guide

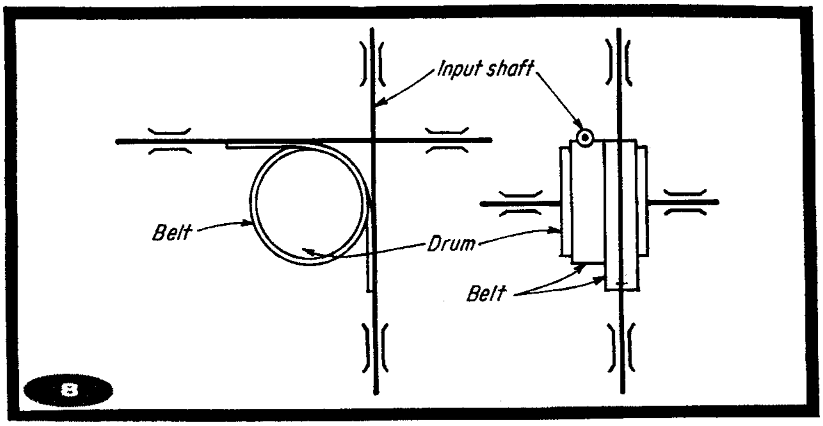

Belt, steel band, or rope around drum, fastened to driving and driven members; sprocket-wheels and chain can replace drum and belt

Gears

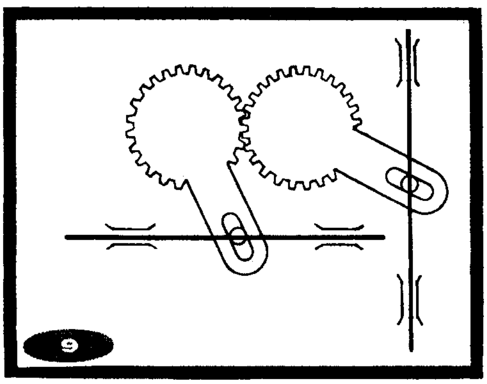

Matching gear-segments

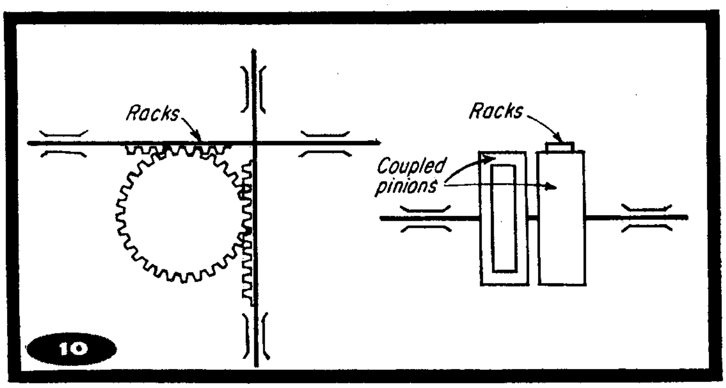

Racks and coupled pinions (can be substituted by friction surfaces for low-cost setup)

9 More Ways to Change Straight-Line Direction

These devices, using gears, cams, pistons, and solenoids, supplement similar arrangements employing linkages, slides, friction drives, and gears, shown.

Federico Strasser

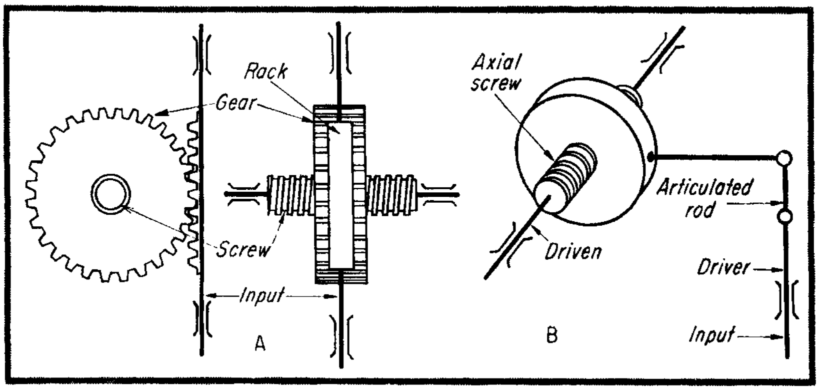

1

Axial screw with rack-actuated gear (A) and articulated driving rod (B) are both irreversible movements, i.e. driver must always drive.

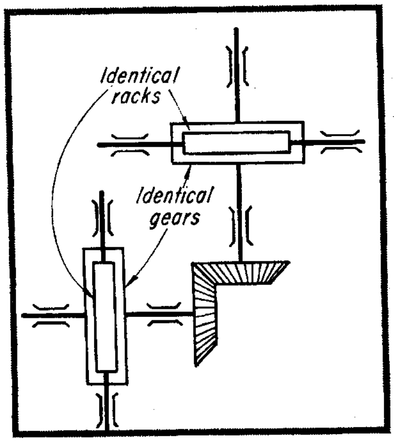

2

Rack-actuated gear with associated bevel gears is reversible.

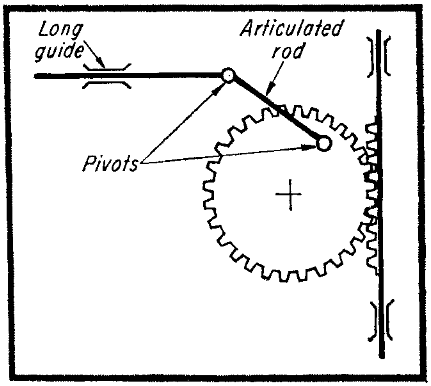

3

Articulated rod on crank-type gear with rack driver. Action is restricted to comparatively short movements.

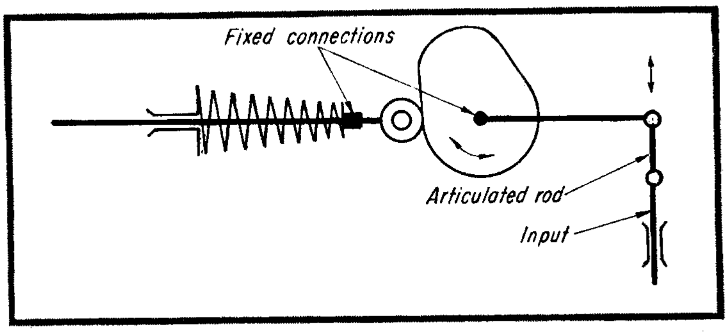

4

Cam and spring-loaded follower allow input/output ratio to be varied according to cam rise. Movement is usually irreversible.

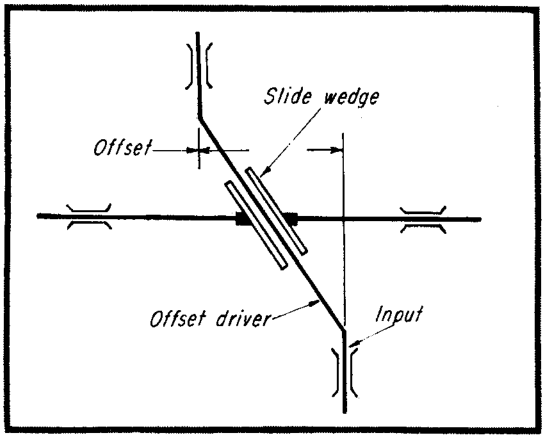

5

Offset driver actuates driven member by wedge action. Lubrication and low coefficient of friction help to allow max offset.

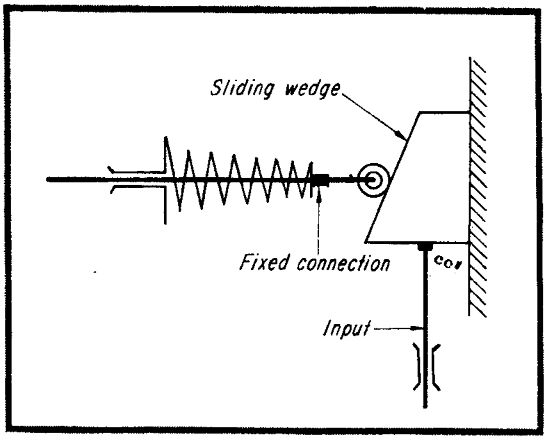

6

Sliding wedge is similar to previous example but requires spring-loaded follower; also, low friction is less essential with roller follower.

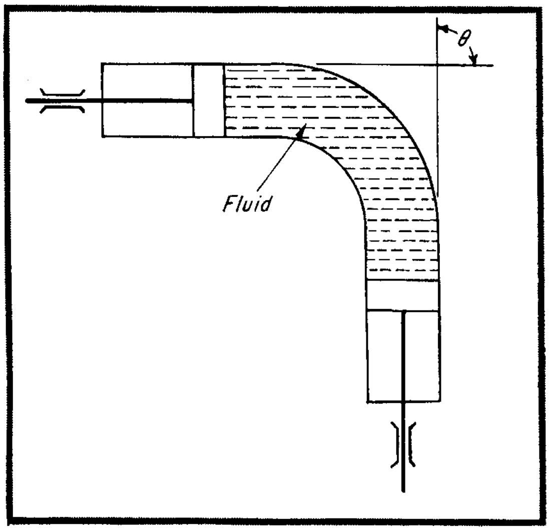

7

Fluid coupling is simple, allows motion to be transmitted through any angle. Leak problems and accurate piston-fitting can make method more expensive than it appears to be. Also, although action is reversible it must always be a compressive one for best results.

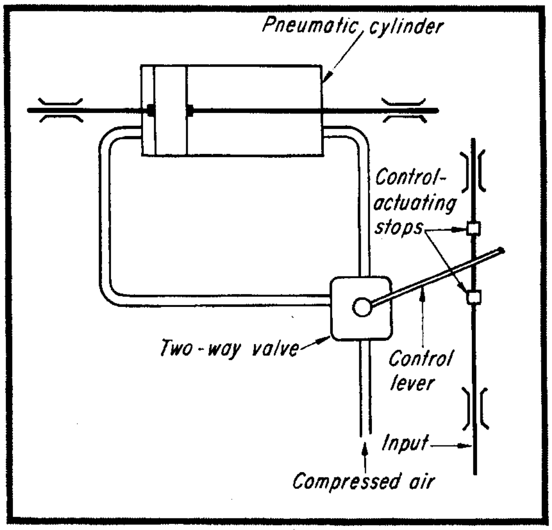

8

Pneumatic system with two-way valve is ideal when only two extreme positions are required. Action is irreversible. Speed of driven member can be adjusted by controlling input of air to cylinder.

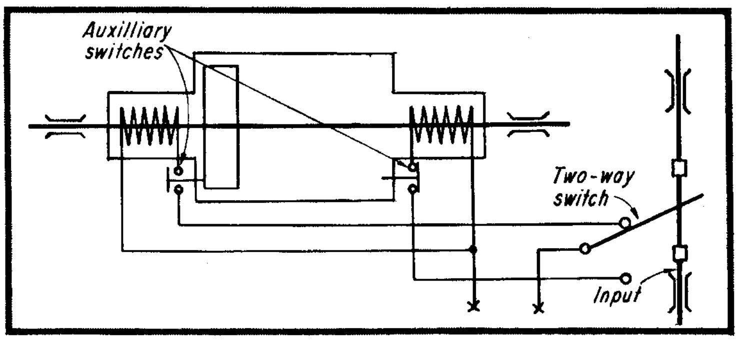

9

Solenoids and two-way switch are here arranged in analogous device to previous example. Contact to energized solenoid is broken at end of stroke. Again, action is irreversible.

Shape of Pin-Connected Linkages

For symmetrical arrangements with 4 or 5 links.

Philip O. Potts & R. T. Liddicoat

Freely hanging conveyor-parts, special-purpose suspensions and hinged linkages are examples of some mechanical arrangements that can be analyzed quickly by the chart on the continuing page. It has been designed specifically to find the equilibrium shape of 4- or 5-member assemblies (sketched below). When their weights, link lengths, and spans are changed, their angles α and β will change too.

The chart finds these angles for various combinations of weights, spans, or link lengths. It plots the equations:

$$n = 2 \sin \alpha + 2 \sin \beta$$
$$m = 1 + (2 \sin \alpha + 2 \sin \beta)$$
$$\frac{\tan \alpha}{\tan \beta} = \frac{2W_2}{W_1} + 1$$
$$\frac{\tan \alpha}{\tan \beta} = \frac{Q_2}{Q_1} + 1$$

These are for a practical range of n and m, W and Q, up to 90° and 70° for α and β respectively. The equations are derived from the geometry of the mechanism and a "virtual work" principle, and where the tangent curves and sine curves intersect are values for α and β.

Since equations for the two linkages are similar, any tangent curve holds for a value of Q_2/Q_1 that is twice W_2/W_1, and any sine curve holds for a value of n that is one less than m.

Example: In a 4-link system, the span is $3L$; W_2 loads are twice W_1. Follow the sine curve for $n = 3$, and the tangent curve for $W_2/W_1 = 2$. They intersect at $\alpha = 73°$, $\beta = 33°$. If the system had 5 links, the same angles would be read for a span length of $4L$ and a load ratio of $Q_2/Q_1 = 4$.

Results can also be determined in reverse—if a certain shape or position of a linkage is needed, the necessary loading or span to give required angles can be read directly from the chart. Also, the linkages may be oriented in any direction as long as links are in tension and loads are perpendicular to span. Forces produced by other means than gravity may be substituted for weights.

Link weight may either be neglected or assumed added into W or Q: n is any positive quantity between 0 and 4; m is any positive quantity between 1 and 5.

Equilibrium shape . . .
of hanging, pin-connected linkages depends on weight ratio and link-lengths. Symmetrical weights, and equi-length links in relation to span length are assumed in analytic method described here.

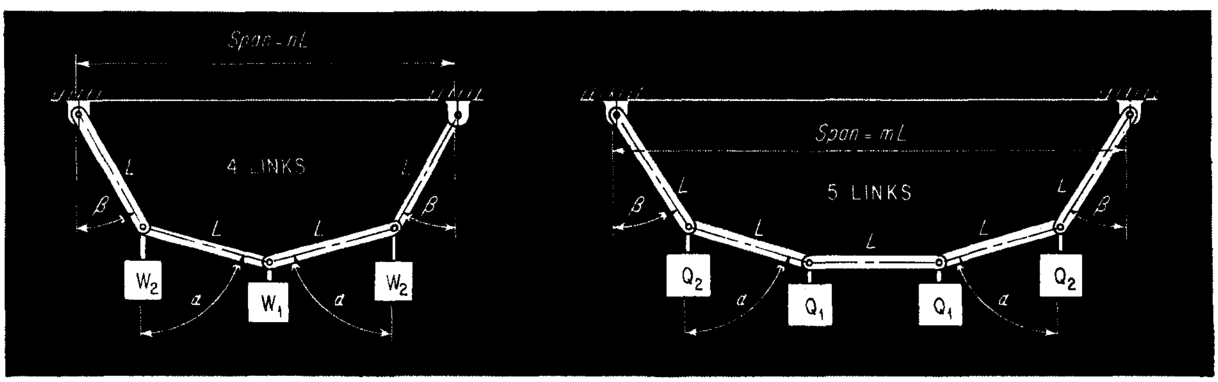

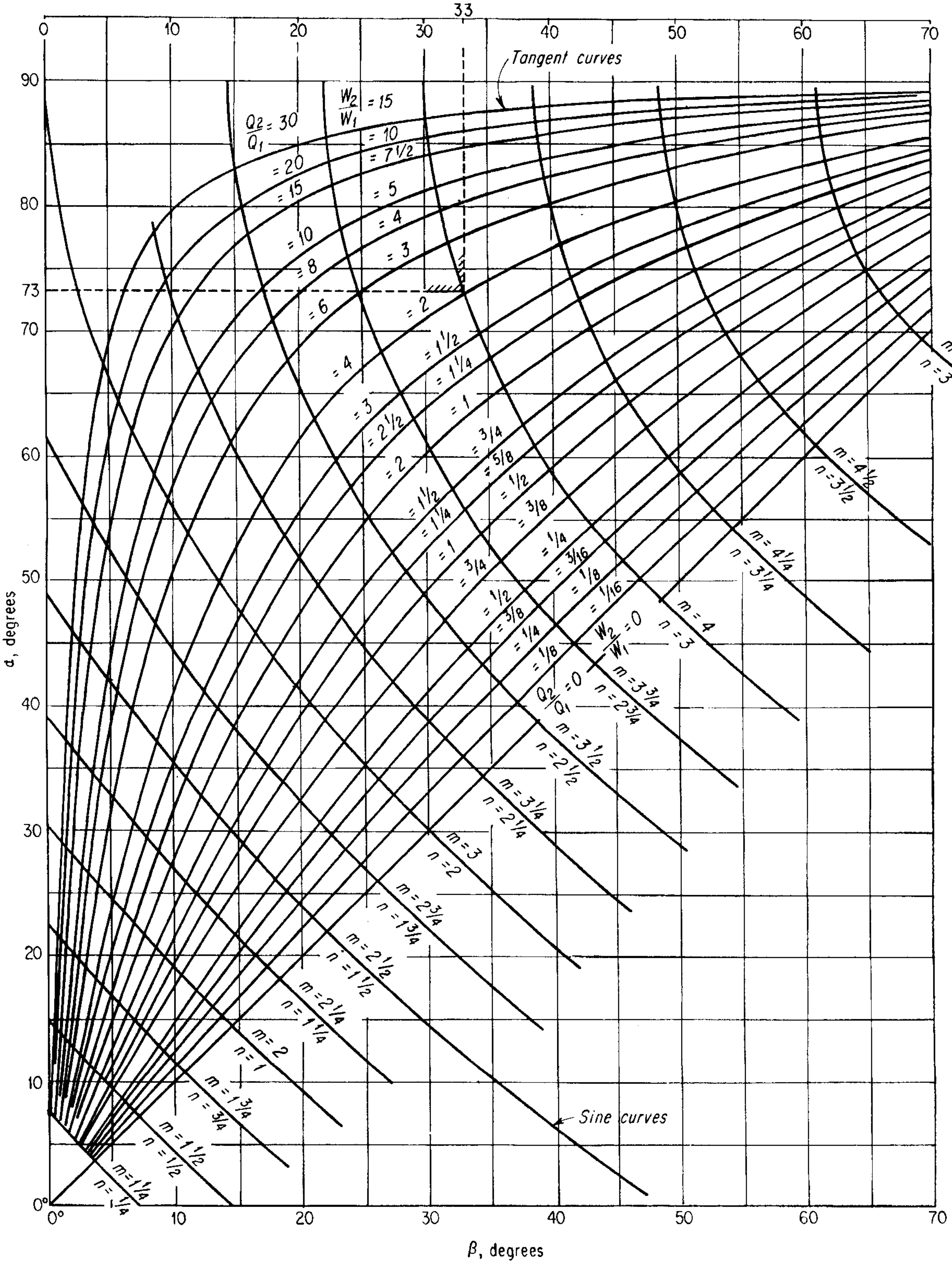

Tangent curves
Sine curves
Q2/Q1 = 30
W2/W1 = 15
W2/W1 = 0
Q2/Q1 = 0
α, degrees
β, degrees
33
73

Seven Popular Types of Three-Dimensional Drives

Main advantage of three-dimensional drives is their ability to transit motion between nonparallel shafts. They can also generate other types of helpful motion. With this roundup are descriptions of industrial applications.

Dr. W. Meyer Zur Capellen

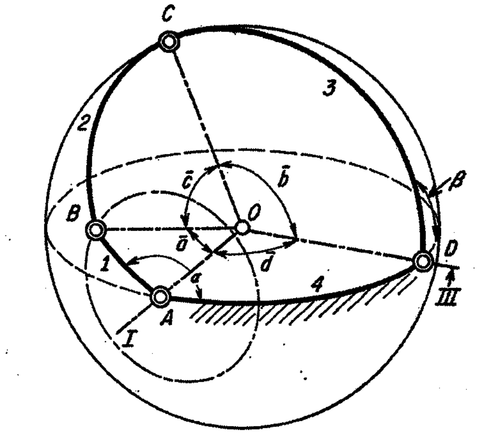

The Spherical Crank

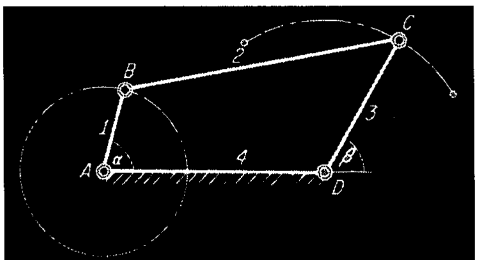

4-Bar Linkage

1 spherical crank drive

This type of drive is the basis for most 3-D linkages, much as the common 4-bar linkage is the basis for the two-dimensional field. Both mechanisms operate on similar principles. (In the accompanying sketches, α is the input angle, and β the output angle. This notation has been used throughout the article.)

In the 4-bar linkage, the rotary motion of driving crank *1* is transformed into an oscillating motion of output link 3. If the fixed link is made the shortest of all, then you have a double-crank mechanism, in which both the driving and driven members make full rotations.

In the spherical crank drive, link *1* is the input, link *3* the output. The axes of rotation intersect at point *O*; the lines connecting *AB*, *BC*, *CD* and *DA* can be thought of as part of great circles of a sphere. The length of the link is best represented by angles *a*, *b*, *c* and *d*.

2 spherical-slide oscillator

The two-dimensional slider crank is obtained from a 4-bar linkage by making the oscillating arm infinitely long. By making an analogous change in the spherical crank, you can obtain the spherical slider crank shown at right.

The uniform rotation of input shaft I is transferred into a nonuniform oscillating or rotating motion of output shaft III. These shafts intersect at an angle δ corresponding to the frame link *4* of the spherical crank. Angle γ corresponds to length of link *1*. Axis II is at right angle to axis III.

The output oscillates when γ is smaller than δ; the output rotates when γ is larger than δ.

Relation between input angle α and output angle β is (as designated in skewed Hook's joint, below)

$$\tan \beta = \frac{(\tan \gamma)(\sin \alpha)}{\sin \delta + (\tan \gamma)(\cos \delta)(\cos \alpha)}$$

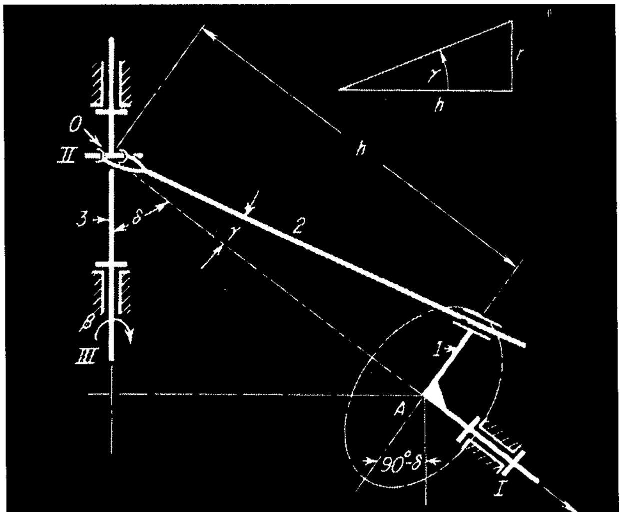

Spherical-Slide Oscillator

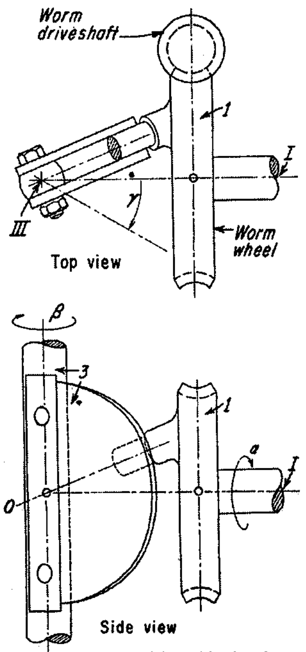

Washing-Machine Mechanism

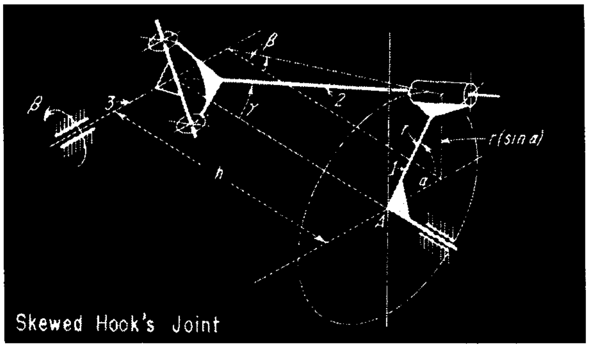

Skewed Hook's Joint

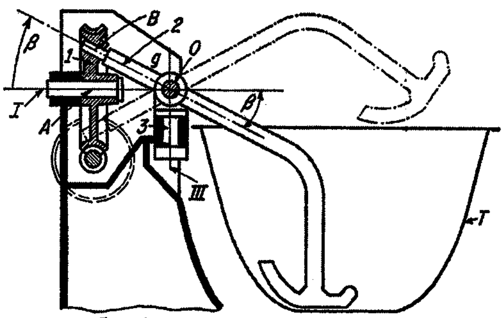

Dough- Kneading Mechanism

3 skewed hook's joint

This variation of the spherical crank is often used where an almost linear relation is desired between input and output angles for a large part of the motion cycle.

The equation defining the output in terms of the input can be obtained from the above equation by making $\delta = 90°$. Thus $\sin \delta = 1$, $\cos \delta = 0$, and

$$\tan \beta = \tan \gamma \sin \alpha$$

The principle of the skewed Hook's joint has been recently applied to the drive of a washing machine (see sketch at left).

Here, the driveshaft drives the worm wheel *1* which has a crank fashioned at an angle γ. The crank rides between two plates and causes the output shaft III to oscillate in accordance with the equation above.

The dough-kneading mechanism at right is also based on the Hook's joint, but utilizes the path of link 2 to give a wobbling motion that kneads dough in the tank.

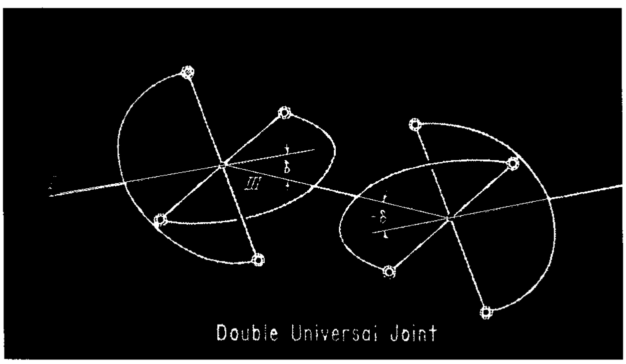

Double Universal Joint

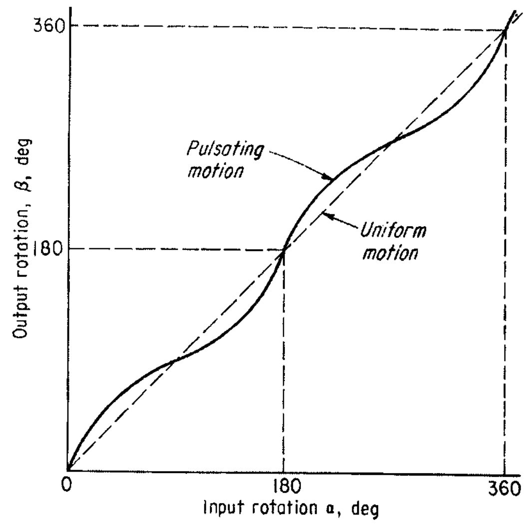

Input-output relationship

4 the universal joint

The universal joint is a variation of the spherical-slide oscillator, but with angle $\gamma = 90°$. This drive provides a totally rotating output and can be operated as a pair, as shown above.

Equation relating input with output for a single universal joint, where δ is angle between connecting link and shaft I:

$$\tan \beta = \tan \alpha \cos \delta$$

Output motion is pulsating (see curve) unless the joints are operated as pairs to provide a uniform motion.

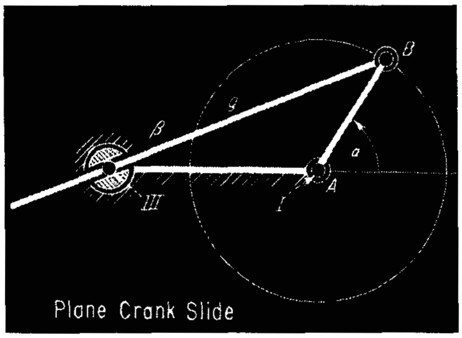

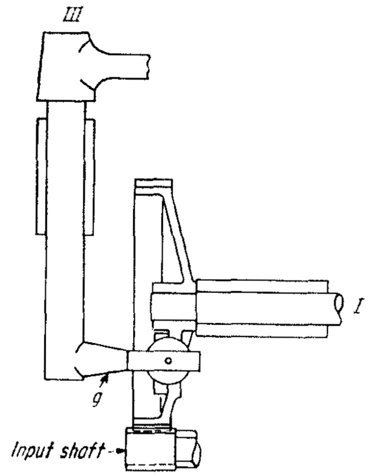

Agitator Mechanism

5 the 3-D crank slide

The three-dimensional crank slide is a variation of a plane crank slide (see sketch), with a ball point through which link g always slides, while a point B on link g describes a circle. A 3-D crank is obtained from this mechanism by making output shaft III not normal to the plane of the circle; another way is to make shafts I and III nonparallel.

A practical variation of the 3-D crank slide is the agitator mechanism (right). As input gear I rotates, link g swivels around (and also lifts) shaft III. Hence, vertical link has both an oscillating rotary motion and a sinusoidal harmonic translation in the direction of its axis of rotation. The link performs what is essentially a screw motion in each cycle.

6 the elliptical slide

The output motion, β, of a spherical slide oscillator, p23-12, can be duplicated by means of a two-dimensional "elliptical slide." The mechanism has a link g which slides through a pivot point D and is fastened to a point P moving along an elliptical path. The ellipse can be generated by a Cardan drive, which is a planetary gear system with the planet gear half the diameter of the internal gear. The center of the planet, point M, describes a circle; any point on its periphery describes a straight line, and any point in between, such as point P, describes an ellipse.

There are certain relationships between the dimensions of the 3-D spherical slide and the 2-D elliptical slide: $\tan\gamma/\sin\delta = a/d$ and $\tan\gamma/\cot\delta = b/d$, where a is the major half-axis, b the minor half-axis of the ellipse, and d is the length of the fixed link DN. The minor axis lies along this link.

If point D is moved within the ellipse, a completely rotating output is obtained, corresponding to the rotating spherical crank slide.

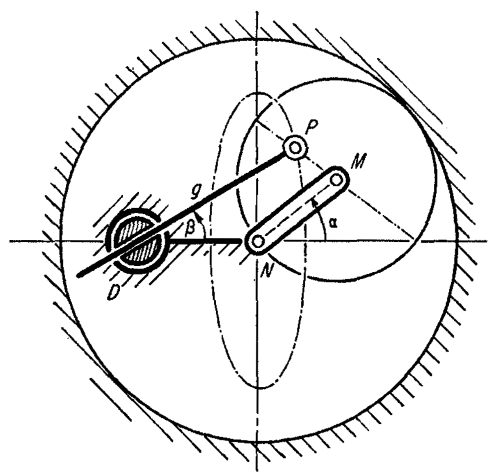

The Elliptical Slide

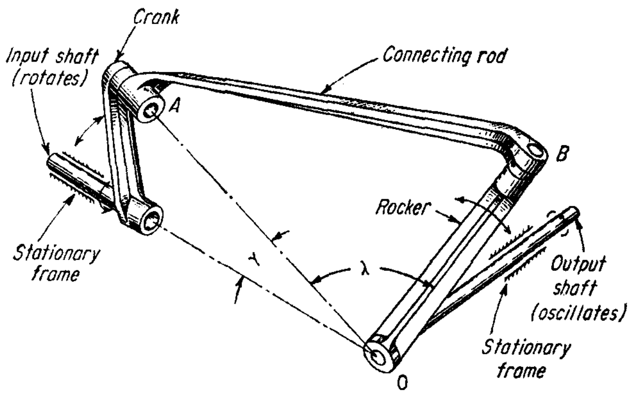

(A) Basic Configuration

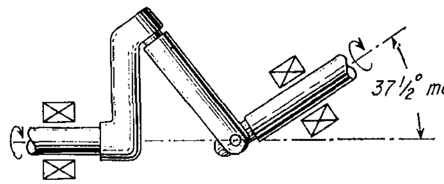

(B) Its Inversion

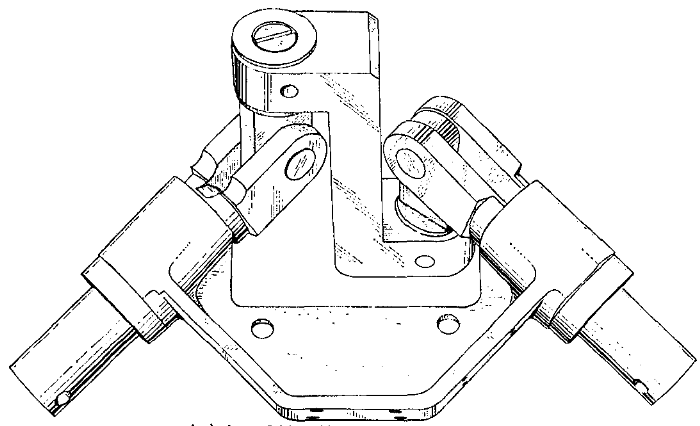
(C) As a 90° Uniform Motion Transmitter

7 the space crank

One of the most recent developments in 3-D linkages is the space crank shown in (A) see also PE—"Introducing the Space Crank—a New 3-D Mechanism," Mar 2 '59. It resembles the spherical crank discussed on page 76, but has different output characteristics. Relationship between input and output displacements is:

$$\cos\beta = (\tan\gamma)(\cos\alpha)(\sin\beta) - \frac{\cos\lambda}{\cos\gamma}$$

Velocity ratio is:

$$\frac{\omega_o}{w_i} = \frac{\tan\gamma\sin\alpha}{1 + \tan\gamma\cos\alpha\cot\beta}$$

where ω_o is the output velocity and ω_i is the constant input velocity.

An inversion of the space crank is shown in (B). It can couple intersecting shafts, and permits either shaft to be driven with full rotations. Motion is transmitted up to 37½° misalignment.

By combining two inversions, (C), a method for transmitting an exact motion pattern around a 90° bend is obtained. This unit can also act as a coupler or, if the center link is replaced by a gear, it can drive two output shafts; in addition, it can be used to transmit uniform motion around two bends.

Transmission Linkages for Multiplying Short Motions

THE ACCOMPANYING SKETCHES show typical mechanisms for multiplying short linear motions, usually converting the linear motion into rotation. Although the particular mechanisms shown are designed to multiply the movements of diaphragms or bellows, the same or similar constructions have possible applications wherever it is required to obtain greatly multiplied motions. These patented transmissions depend on cams, sector gears and pinions, levers and cranks, cord or chain, spiral or screw feed, magnetic attraction, or combinations of these devices.

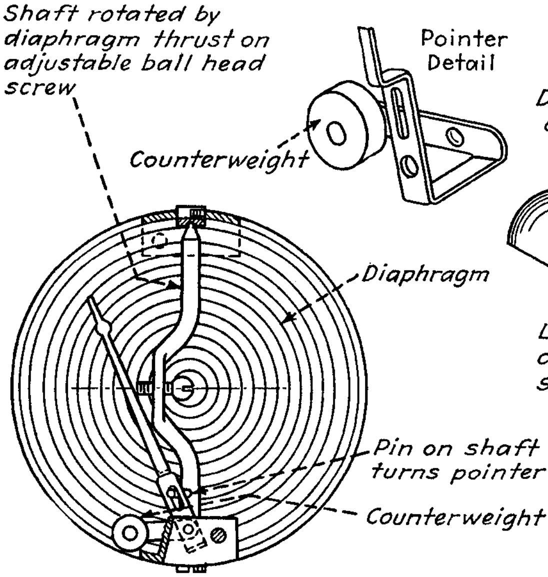

FIG. 1 – *Lever type transmission in pressure gage*

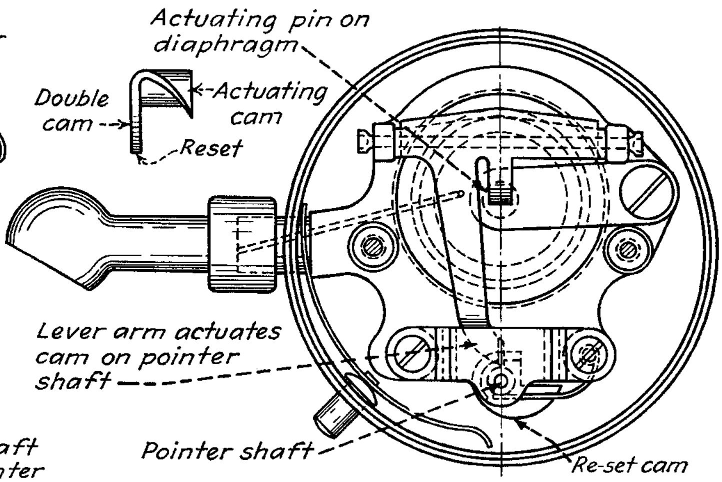

FIG. 2 – *Lever and cam drive for tire gage*

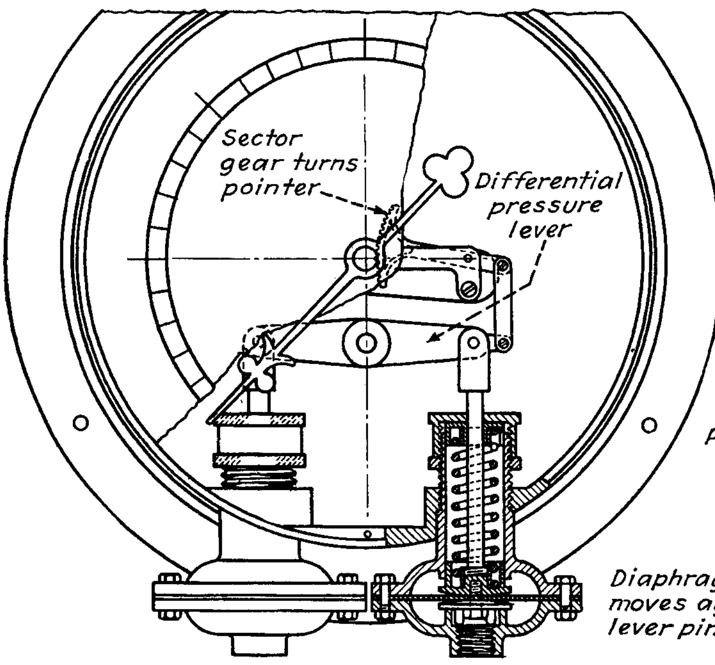

FIG. 3 – *Lever and sector gear in differential pressure gage*

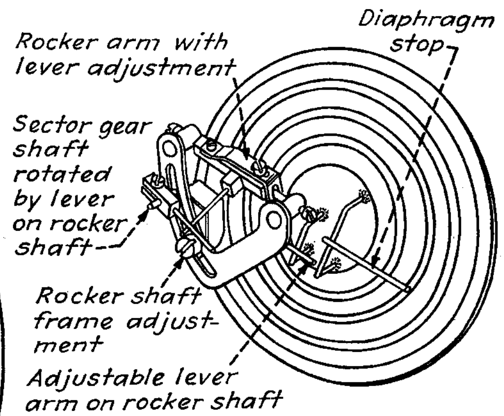

FIG. 4 – *Sector gear drive for aircraft airspeed indicator*

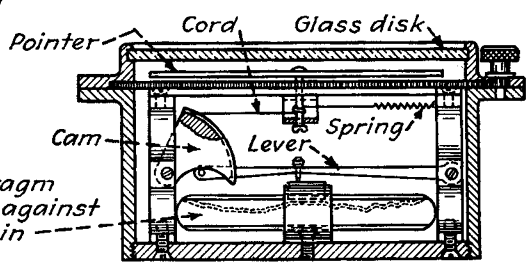

FIG. 5 – *Lever, cam and cord transmission in barometer*

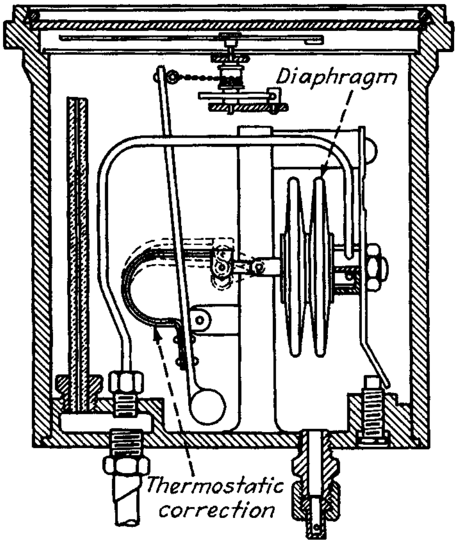

FIG. 6 – *Link and chain transmission for rate of climb instrument*

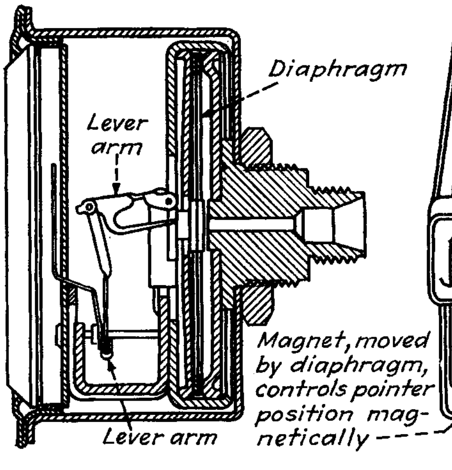

FIG. 7 – *Lever system in automobile gasoline tank gage*

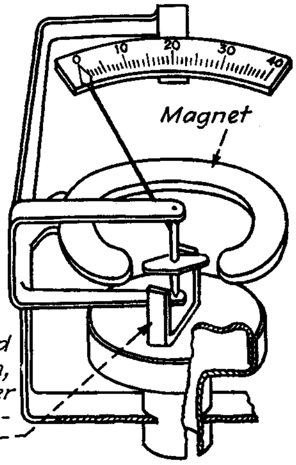

FIG. 8 – *Interfering magnetic fields for fluid pressure measurement*

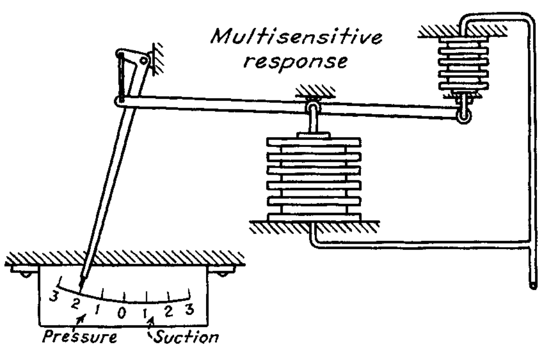

FIG. 9 – *Lever system for atmospheric pressure variations*

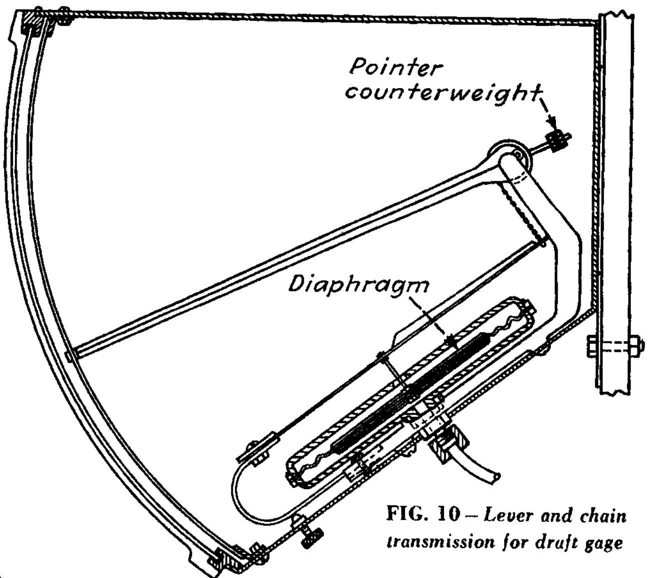

FIG. 10 – *Lever and chain transmission for draft gage*

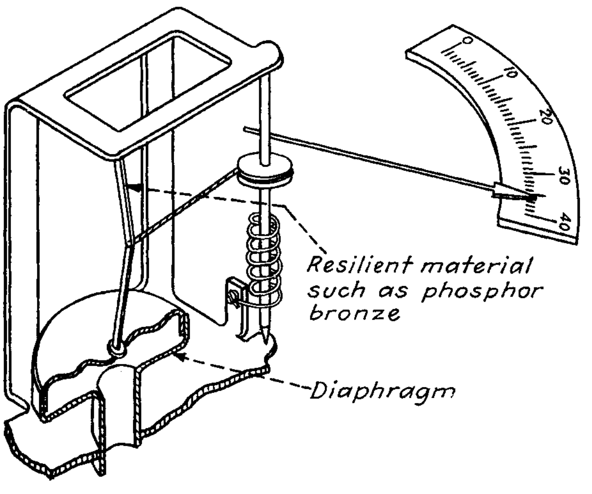

FIG. 11 – *Toggle and cord drive for fluid pressure instrument*

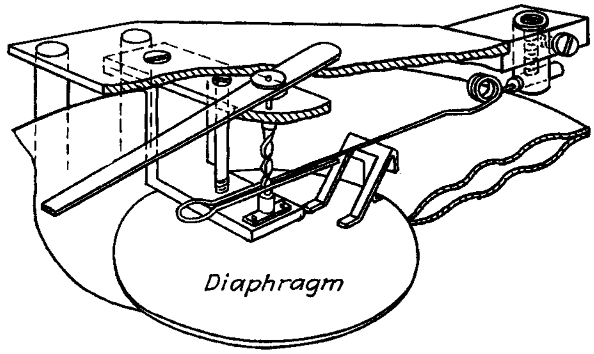

FIG. 12 – *Spiral feed transmission for general purpose instrument*

Power Thrust Linkages and Their Applications

POWERED STRAIGHT LINE MOTION over short distances is applicable to many types of machines or devices for performing specialized services. These motions can be produced by a steam, pneumatic or hydraulic cylinder, or by a self-contained electric powered unit such as the General Electric Thrustors shown herewith. These Thrustors may be actuated manually by pushbuttons, or automatically by mechanical devices or the photo-electric relay as with a door opener. These illustrations will suggest many other arrangements.

Fig. 1—Transfer motion to distant point.

Fig. 2—Double throw by momentary applications.

Fig. 3—Trammel plate divides effort and changes directions of motion.

Fig. 4—Constant thrust toggle. Pressure is same at all points of throw.

Fig. 5—Multiplying motion, 6 to 1, might be used for screen shift.

Fig. 6—Bell crank and toggle may be applied in embossing press, extruder or die-caster.

Fig. 7—Horizontal pull used for clay pigeon traps, hopper trips, and sliding elements with spring or counterweighted return.

Fig. 8—Shipper rod for multiple and distant operation as series of valves.

Fig. 9—Door opener. Upthrust of helical racks rotates gear and arm.

Fig. 10—Accelerated motion by shape of cam such as on a forging hammer.

Fig. 11—Intermittent lift as applied to lifting pipe from well.

Fig. 12—Straight-line motion multiplied by pinion and racks.

Fig. 13—Rotary motion with cylindrical cam. Operates gate on conveyor belt.

Fig. 14—Thrust motions and "dwells" regulated by cam.

Fig. 15—Four positive positions with two Thrustors.

Fig. 16—Toggle increasing thrust at right angle.

Fig. 17—Horizontal straight-line motion as applied to a door opener.

Fig. 18—Thrusts in three directions with two Thrustors.

Fig. 19—Fast rotary motion using step screw and nut.

Fig. 20—Intermittent rotary motion. Operated by successive pushing of operating button, either manually or automatically.

Fig. 21—Powerful rotary motion with worm driven by rack and pinion.

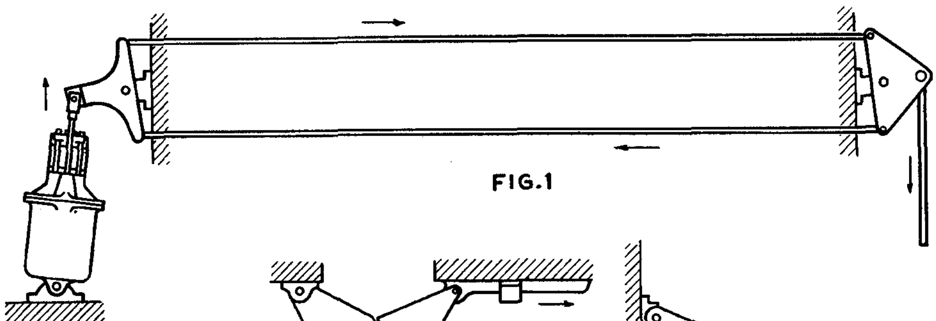

FIG.1

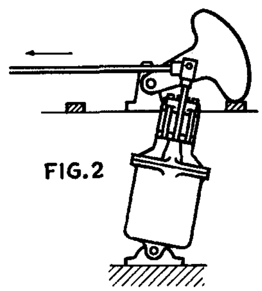

FIG.2

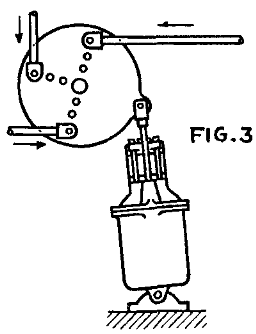

FIG.3

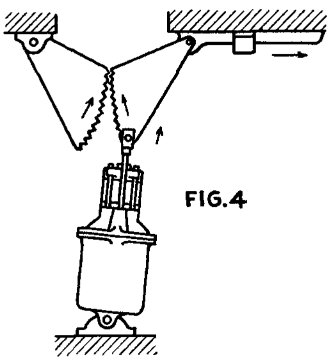

FIG.4

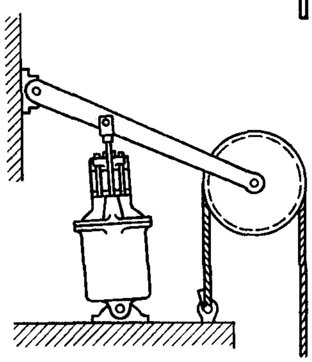

FIG.5

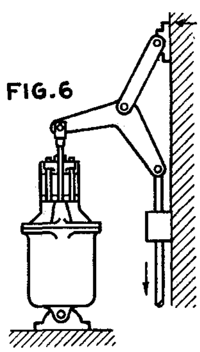

FIG.6

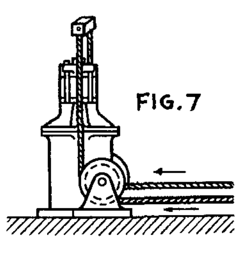

FIG.7

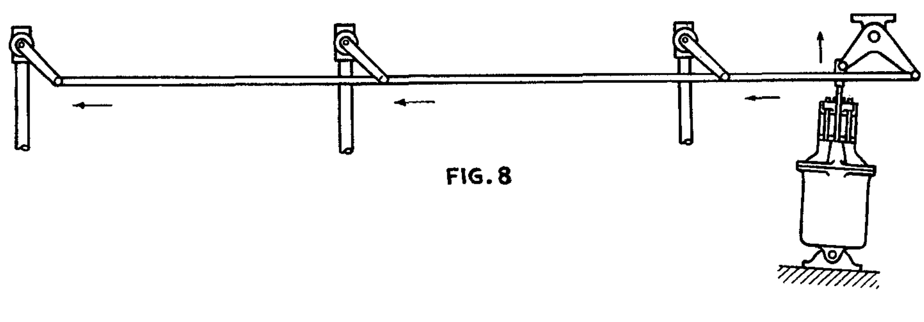

FIG.8

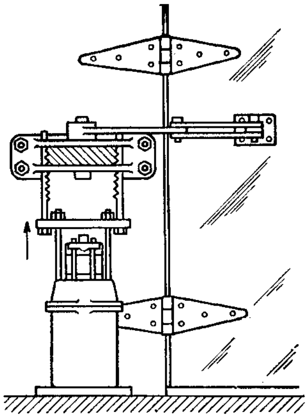
FIG.9

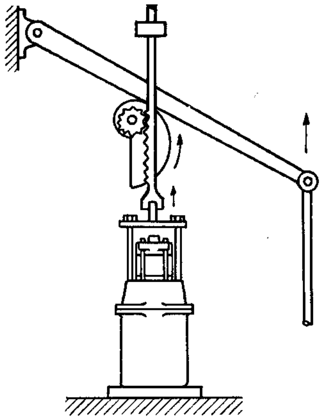
FIG.10

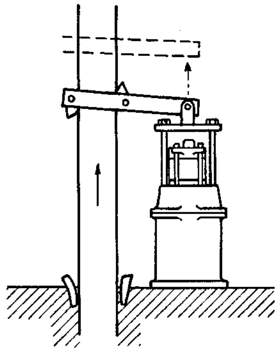
FIG. 11

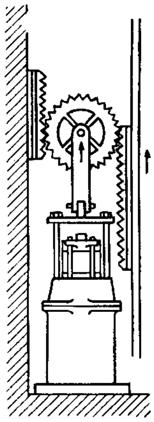
FIG.12

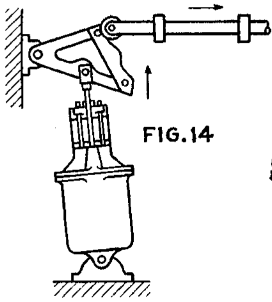
FIG.14

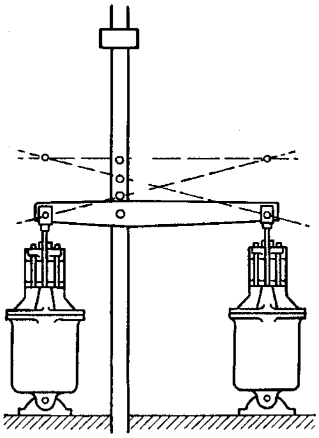
FIG.15

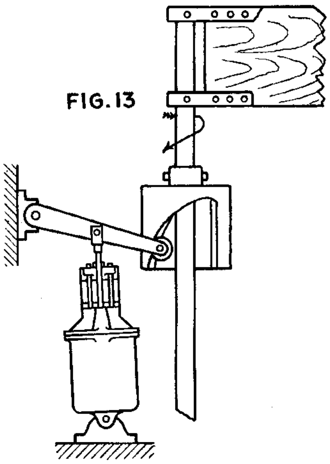
FIG.13

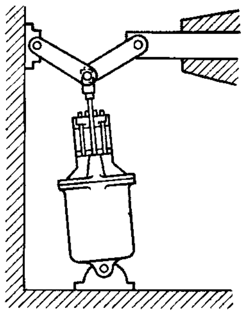
FIG.16

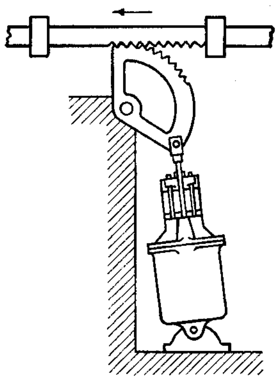
FIG.17

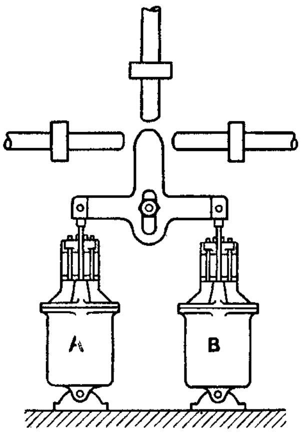

FIG.18

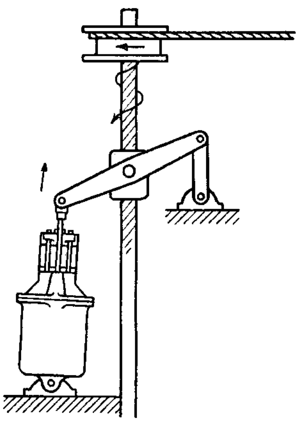
FIG.19

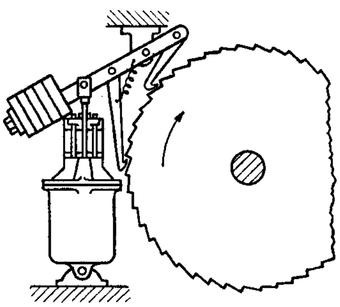
FIG.20

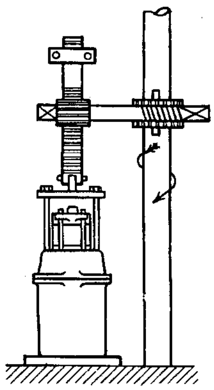
FIG.21

Toggle Linkage Applications in Different Mechanisms

Thomas P. Goodman

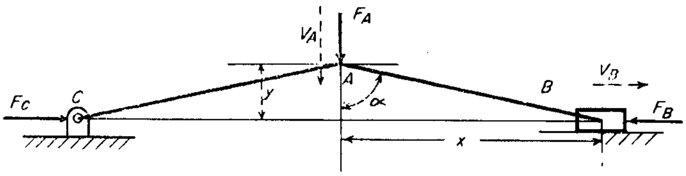

Fig. 1 Mechanical advantage $= \frac{F_B}{F_A} = \frac{1}{2}\frac{x}{y} = \frac{1}{2}\,\mathrm{Tan}\,\alpha = \frac{V_A}{V_B}$

MANY MECHANICAL LINKAGES are based on the simple toggle which consists of two links that tend to line-up in a straight line at one point in their motion. The mechanical advantage is the velocity ratio of the input point A to the output point B: or V_A/V_B. As the angle α approaches 90 deg, the links come into toggle and the mechanical advantage and velocity ratio both approach infinity. However, frictional effects reduce the forces to much less than infinity although still quite high.

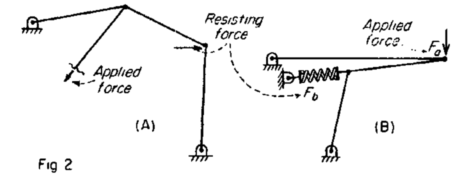

Fig 2

FORCES CAN BE APPLIED through other links, and need not be perpendicular to each other. (A) One toggle link can be attached to another link rather than to a fixed point or slider. (B) Two toggle links can come into toggle by lining up on top of each other rather than as an extension of each other. Resisting force can be a spring force.

HIGH MECHANICAL ADVANTAGE

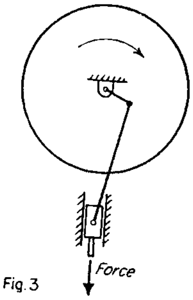

Fig. 3

IN PUNCH PRESSES, large forces are needed at the lower end of the work-stroke, however little force is required during the remainder. Crank and connecting rod come into toggle at the lower end of the punch stroke, giving a high mechanical advantage at exactly the time it is most needed.

COLD-HEADING RIVET MACHINE is designed to give each rivet two successive blows. Following the first blow (point 2) the hammer moves upward a short distance (to point 3), to provide clearance for moving the workpiece. Following the second blow (at point 4), the hammer then moves upward a longer distance (to point 1). Both strokes are produced by one revolution of the crank and at the lowest point of each stroke (points 2 and 4) the links are in toggle.

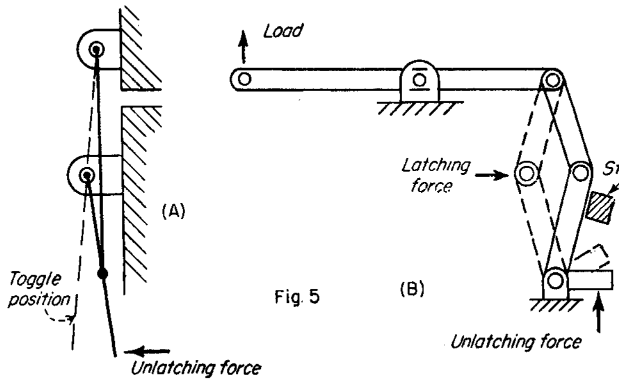

Fig. 5

LOCKING LATCHES produce a high mechanical advantage when in the toggle portion of the stroke. (A) Simple latch exerts a large force in the locked position. (B) For positive locking, closed position of latch is slightly beyond toggle position. Small unlatching force opens linkage.

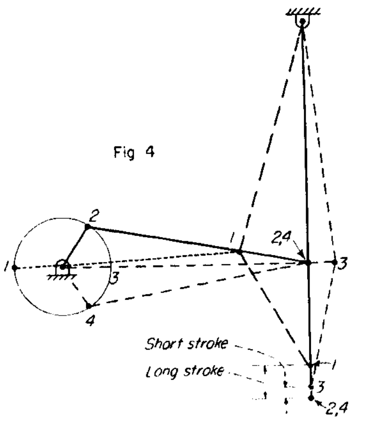

Fig 4

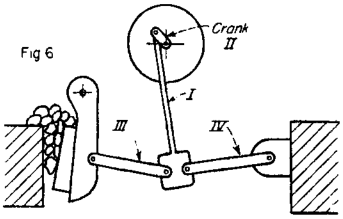

Fig 6

STONE CRUSHER uses two toggle linkages in series to obtain a high mechanical advantage. When the vertical link I reaches the top of its stroke, it comes into toggle with the driving crank II; at the same time, link III comes into toggle with link IV. This multiplication results in a very large crushing force.

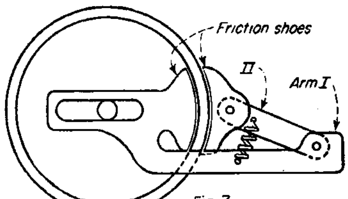

Fig 7

FRICTION RATCHET is mounted on a wheel; light spring keeps friction shoes in contact with the flange. This device permits clockwise motion of the arm I. However, reverse rotation causes friction to force link II into toggle with the shoes which greatly increases the locking pressure.

HIGH VELOCITY RATIO

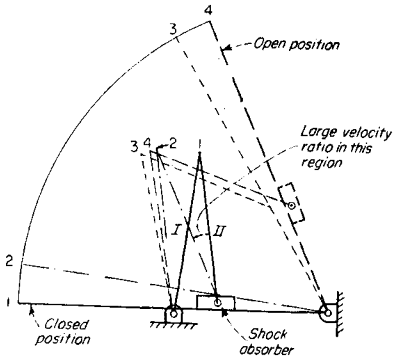

Fig. 8

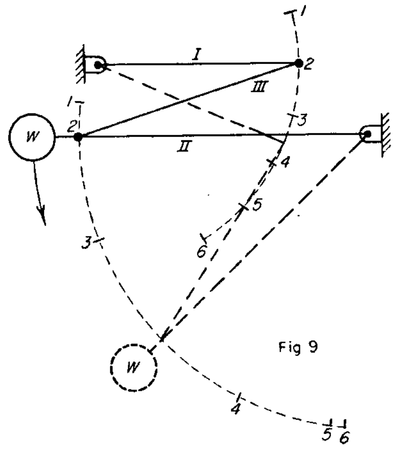

Fig 9

DOOR CHECK LINKAGE gives a high velocity ratio at one point in the stroke. As the door swings closed, connecting link I comes into toggle with the shock absorber arm II, giving it a large angular velocity. Thus, the shock absorber is more effective retarding motion near the closed position.

IMPACT REDUCER used on some large circuit breakers. Crank I rotates at constant velocity while lower crank moves slowly at the beginning and end of the stroke. It moves rapidly at the mid stroke when arm II and link III are in toggle. Falling weight absorbs energy and returns it to the system when it slows down.

VARIABLE MECHANICAL ADVANTAGE

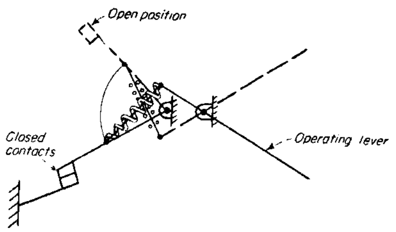

Fig 10

TOASTER SWITCH uses an increasing mechanical advantage to aid in compressing a spring. In the closed position, spring holds contacts closed and the operating lever in the down position. As the lever is moved upward, the spring is compressed and comes into toggle with both the contact arm and the lever. Little effort is required to move the links through the toggle position; beyond this point, the spring snaps the contacts closed.

Fig 12

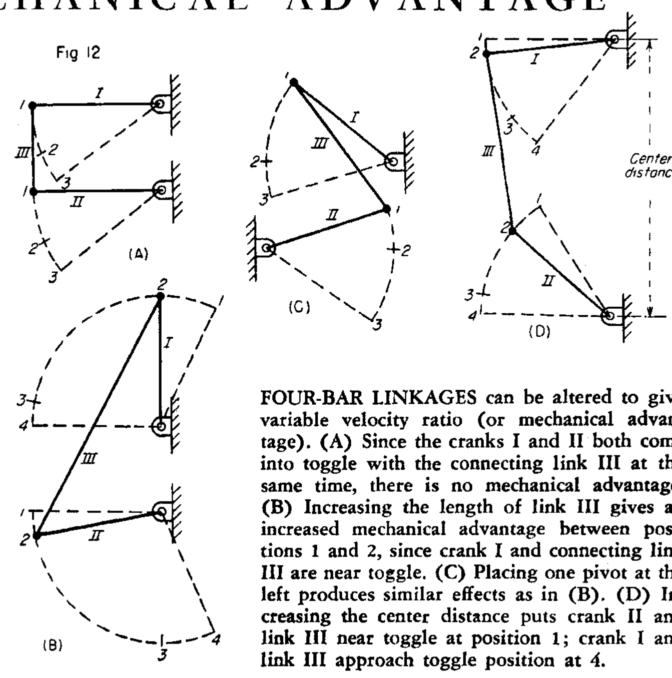

FOUR-BAR LINKAGES can be altered to give variable velocity ratio (or mechanical advantage). (A) Since the cranks I and II both come into toggle with the connecting link III at the same time, there is no mechanical advantage. (B) Increasing the length of link III gives an increased mechanical advantage between positions 1 and 2, since crank I and connecting link III are near toggle. (C) Placing one pivot at the left produces similar effects as in (B). (D) Increasing the center distance puts crank II and link III near toggle at position 1; crank I and link III approach toggle position at 4.

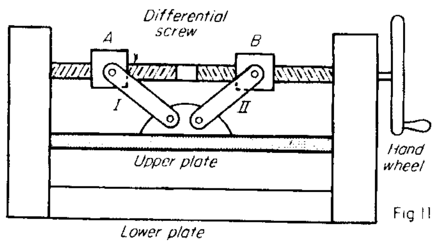

Fig 11

TOGGLE PRESS has an increasing mechanical advantage to counteract the resistance of the material being compressed. Rotating handwheel with differential screw moves nuts *A* and *B* together and links I and II are brought into toggle.

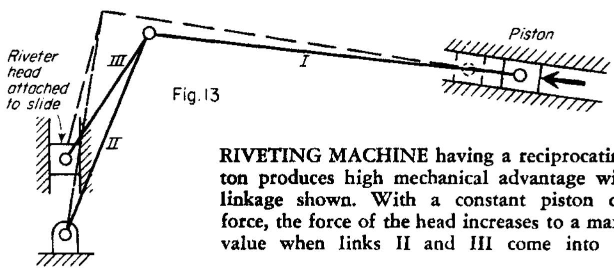

Fig.13

RIVETING MACHINE having a reciprocating piston produces high mechanical advantage with the linkage shown. With a constant piston driving force, the force of the head increases to a maximum value when links II and III come into toggle.

When Linkages Need Harmonic Analysis

Feeding the working equation into a computer provided the handy table that accompanies this article. Now you'll find it easier to perform the harmonic analysis needed for efficient crank-and-rocker mechanisms.

Dr. Ferdinand Freudenstein & K. Mohan

The proportions of linkages can be determined readily enough by graphical methods. But when you have to know how these proportions affect the higher harmonics and inertia forces, complex analytical methods are very useful.

Equations for harmonic analysis of the general crank-and-rocker linkage were developed (by author Freudenstein) in *Journal of Applied Mechanics*, Dec '59, p 673. Those equations established procedures for the calculation of various coefficients and terms needed to determine whether a given mechanism has significant overtones.

But those equations still require considerable computations. Because crank-and-rocker mechanisms are important in the design of high-speed machinery, we carried the work a step further by programing on an IBM 650 computer the following:

Working equation for output angle:

$$\psi = K + \sum_{m=1}^{\infty} \frac{(-\tan\frac{1}{2}u)^m}{(-m)} \sin m\,\phi - \frac{C_0}{4} \sin u \cos\phi -$$

$$\sum_{m=1}^{\infty} \frac{\sin u}{4m} (C_{m-1} - C_{m+1}) \cos m$$

It was with this equation that we obtained the table that accompanies this article.

The rotation of rocker or output link (see diagram) has been expressed as a Fourier Series in terms of the input-crank rotation angle ϕ, and the proportions of the linkage are given in terms of a design parameter u. This parameter is the maximum value of the "pressure angle," which in the diagram is the absolute value of angle BCD

SYMBOLS

A_G = acceleration of gyro
a_m = amplitude of mth sine series term, radians
b_m = amplitude of mth cos series term, radians
c_m = amplitude of mth harmonic of rocker motion, radians
d_m = amplitude ratio, mth to 1st harmonic of rocker motion
f_m = amplitude ratio, mth to 1st harmonic of slider-crank motion
F_{max} = maximum inertia force, lb
C = variables defined by equations
K = a constant in the Fourier Series
α = variable defined by equations
u = pressure angle, degrees
R_ψ = maximum output rotation, degrees
ϕ = input angle (drive crank)
ψ = output angle (driven link)
r_p = pitch radius of gear in example, in.

Subscripts, 1, 2, 3 . . . m refer to the order number of the harmonic; for example, mth harmonic; note that m is also used as a factor in the equations. Angular values, shown in radians, can be converted to degrees by multiplying by 57.3.

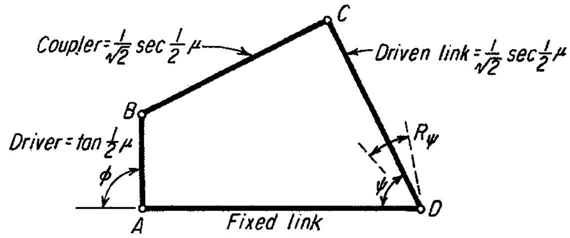

Crank-and-Rocker Mechanism for High-Speed Operation

Harmonics of certain crank-and-rocker linkages

m	a_m	b_m	c_m	d_m	f_m
Case 1: $u = 5$, $R\psi = 7.073315$					
1	0.043660	−0.043641	0.061733	1.000000	0.000000
2	−0.000953	0.000000	0.000953	0.015437	0.015427
3	0.000028	−0.000014	0.000031	0.005022	0.000000
4	−0.000001	0.000000	0.000001	0.000012	0.000004
5	....	....	....	....	....
6	....	....	....	....	....
Case 2: $u = 10$, $R\psi = 14.160203$					
1	0.087490	−0.087131	0.123479	1.000000	0.000000
2	−0.003827	0.000000	0.003827	0.030993	0.030944
3	0.000223	−0.000111	0.000249	0.002017	0.000000
4	−0.000015	....	0.000015	0.000121	0.000030
5	0.000001	....	0.000001	0.000008	....
6	....	....	....	....	....
Case 3: $u = 15$, $R\psi = 21.274683$					
1	0.131650	−0.130551	0.185405	1.000000	0.000000
2	−0.008666	0.000000	0.008666	0.046741	0.046531
3	0.000760	−0.000375	0.001000	0.005394	0.000000
4	−0.000075	0.000000	0.000075	0.000405	0.000101
5	0.000008	−0.000003	0.000008	0.000043	....
6	−0.000001	0.000000	0.000001	0.000005	....
Case 4: $u = 20$, $R\psi = 28.431708$					
1	0.176330	−0.173616	0.247458	1.000000	0.000000
2	−0.015546	0.000000	0.015546	0.062823	0.062318
3	0.001827	−0.000892	0.002000	0.008082	0.000000
4	−0.000242	0.000000	0.000242	0.000978	0.000242
5	0.000034	−0.000012	0.000036	0.000145	0.000000
6	−0.000005	0.000000	0.000005	0.000020	0.000002
Case 5: $u = 25$, $R\psi = 35.647729$					
1	0.221690	−0.216365	0.309774	1.000000	0.000000
2	−0.024573	0.000000	0.024573	0.079326	0.078367
3	0.003632	−0.001750	0.004000	0.012913	0.000000
4	−0.000604	0.000000	0.000604	0.001950	0.000479
5	0.000107	−0.000038	0.000114	0.000368	0.000000
6	−0.000020	0.000000	0.000020	0.000065	0.000005
Case 6: $u = 30$, $R\psi = 42.941404$					
1	0.267950	−0.258654	0.372423	1.000000	0.000000
2	−0.035898	0.000000	0.035898	0.096390	0.094741
3	0.006413	−0.003037	0.007071	0.018987	0.000000
4	−0.001289	0.000000	0.001289	0.003461	0.000843
5	0.000276	−0.000096	0.000292	0.000784	0.000000
6	−0.000062	0.000000	0.000062	0.000166	0.000013

m	a_m	b_m	c_m	d_m	f_m
Case 7: $u = 35$, $R\psi = 50.334529$					
1	0.315300	−0.300351	0.435460	1.000000	0.000000
2	−0.049707	0.000000	0.049707	0.114153	0.111509
3	0.010448	−0.004843	0.011489	0.026384	0.000000
4	−0.002471	0.000000	0.002471	0.005674	0.001364
5	0.000623	−0.000210	0.000657	0.001509	0.000000
6	−0.000164	0.000000	0.000164	0.000377	0.000027
Case 8: $u = 40$, $R\psi = 57.853304$					
1	0.363970	−0.341265	0.498935	1.000000	0.000000
2	−0.066237	0.000000	0.066237	0.132757	0.128740
3	0.016072	−0.007244	0.017607	0.035289	0.000000
4	−0.004387	0.000000	0.004387	0.008793	0.002077
5	0.001277	−0.000408	0.001414	0.002834	0.000000
6	−0.000388	0.000000	0.000388	0.000778	0.000052
Case 9: $u = 45$, $R\psi = 65.530207$					
1	0.414210	−0.381196	0.562920	1.000000	0.000000
2	−0.085785	0.000000	0.085785	0.152392	0.146547
3	0.023689	−0.010303	0.025826	0.045879	0.000000
4	−0.007359	0.000000	0.007359	0.013073	0.003019
5	0.002439	−0.000724	0.002646	0.004700	0.000000
6	−0.000842	0.000000	0.000842	0.001496	0.000091
Case 10: $u = 50$, $R\psi = 73.406779$					
1	0.466310	−0.419839	0.627463	1.000000	0.000000
2	−0.108723	0.000000	0.108723	0.173274	0.164957
3	0.033799	−0.014039	0.036592	0.058318	0.000000
4	−0.011821	0.000000	0.011821	0.018839	0.004227
5	0.004410	−0.001190	0.004472	0.007127	0.000000
6	−0.001714	0.000000	0.001714	0.002732	0.000149
Case 11: $u = 55$, $R\psi = 81.538039$					
1	0.520570	−0.456870	0.692620	1.000000	0.000000
2	−0.135496	0.000000	0.135496	0.195628	0.184075
3	0.047024	−0.018417	0.050498	0.072908	0.000000
4	−0.018359	0.000000	0.018359	0.026507	0.005737
5	0.007646	−0.001824	0.007810	0.011277	0.000000
6	−0.003317	0.000000	0.003317	0.004789	0.000232
Case 12: $u = 60$, $R\psi = 90.00000$					
1	0.577350	−0.491515	0.758235	1.000000	0.000000
2	−0.166667	0.000000	0.166667	0.219810	0.204012
3	0.064150	−0.023280	0.068242	0.090001	0.000000
4	−0.027778	0.000000	0.027778	0.036635	0.007592
5	0.012830	−0.002619	0.013115	0.017890	0.000000
6	−0.006173	0.000000	0.006173	0.008141	0.000345

PROPORTIONS OF CRANK-AND-ROCKER LINKAGES

Case	u	AB/AD	BC/AD = CD/AD
1	5	0.04366	0.707836
2	10	0.08749	0.709887
3	15	0.13165	0.713282
4	20	0.17633	0.718091
5	25	0.22169	0.724385
6	30	0.26795	0.732164
7	35	0.31530	0.741499
8	40	0.36397	0.752602
9	45	0.41421	0.765473
10	50	0.46631	0.780324
11	55	0.52057	0.797297
12	60	0.57735	0.816604

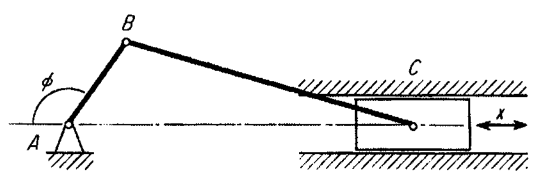

In-Line Slider Crank

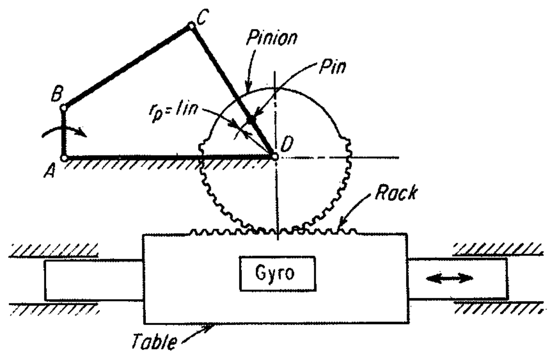

Crank-and-Rocker For Gyro Shake Table

minus 90°. The ideal pressure angle is zero, but in practice it is held to within a prescribed limit. Values of u from 5 to 60° in increments of 5 are given in the table with the corresponding values of R_ψ, the maximum output rotation in degrees.

The other terms in the working equation are defined by the following mathematical relationships, and they determine the various amplitudes and ratios shown in the table.

Equation for 1st harmonic

$\alpha = \sin u$; $\alpha_2 = \frac{1}{4}\alpha^2$; $\alpha_4 = 3/64\,\alpha^4$; $\alpha_6 = 5/512\,\alpha^6$; $\alpha_8 = 35/(128)^2\,\alpha^8$

$$
\begin{aligned}
C_8 &= \alpha_8 \ldots \\
C_6 &= \alpha_6 + 8C_8 \ldots \\
C_4 &= \alpha_4 + 6C_6 - 20C_8 \ldots \\
C_2 &= \alpha_2 + 4C_4 - 9C_6 + 16C_8 \ldots \\
C_o &= 1 + C_2 - C_4 + C_6 - C_8 \ldots \\
C_m &= (m \text{ odd}) = 0
\end{aligned}
$$

The working equation for output angle can be expressed in the following forms:

$$\psi = K + \sum_{m=1}^{\infty} (a_m \sin m\phi + b_m \cos m\phi)$$

$$\psi = K + \sum_{m=1}^{\infty} c_m \sin (m\phi + \phi_m)$$

which give us the following:

$$\psi = K + c_1 \sum_{m=1}^{\infty} d_m \sin (m\phi + \phi_m)$$

where

$$
\begin{aligned}
a_m &= (-\tan\tfrac{1}{2}u)^m/(-m) \\
b_1 &= -\tfrac{1}{4}\sin u\,(2C_o - C_2) \\
b_m\,(m \text{ even}) &= 0 \\
b_m\,(m \text{ odd}) &= \frac{-\sin u}{4m} = (C_{m-1} - C_{m+1}) \\
c_m &= \sqrt{a^2{}_m + b^2{}_m};\ \cos\phi_m = a_m/c_m \\
d_m &= c_m/c_1
\end{aligned}
$$

In-line slider-crank mechanism

Equation above for the first harmonic can be compared with the corresponding equation in the harmonic analysis of an in-line slider-crank mechanism (diagram above) taken from *Engineering Dynamics—Vol IV—Internal Combustion Engines*, by C. B. Biezeno and R. Grammel, translated by M. P. White, Blackie and Son Ltd, London, p 6, Eq (5) and (6):

$$X = X_o + e_1 \sum_{m=1}^{\infty} f_m \sin m\phi$$

where X is the slider displacement and e_1 and f_m correspond to c_1 and d_m in the equation for the first harmonic.

The value of the link length ratio AB/BC for the in-line

HARMONIC ANALYSIS OF HIGH-SPEED MACHINERY

■ What is meant by "harmonic analysis"? It covers determination of resonant speeds, the severity of passing through various speed ranges (including resonant speed), and magnitude of the inertia forces. Such analysis will tell you how to design for efficient operation at high speeds and how to avoid undue resonance disturbances.

To determine these factors it is useful to express the motion in a Fourier Series—in other words, to express it in a series of harmonics of the form:

$$Y = K + a_1 \sin(\omega t + \phi_1) + a_2 \sin(2\,\omega t + \phi_2) + \cdots + a_m \sin(m\omega t + \phi_m) + \cdots$$

Here, Y represents the motion to be analyzed, K = a constant, a_m = amplitude of mth harmonic, ω = angular velocity, t = time—so that ωt represents ϕ, an angular displacement as a function of time. The term $a_1 \sin(\omega t + \phi_1)$ is the first harmonic or fundamental The other terms are the higher harmonics (like overtones in the musical field.

The harmonics of a given motion are used in the determination of the significance of resonant speeds and the corresponding inertia forces, which are proportional to the second derivative of Y. Higher harmonics are often neglected, as sometimes in connecting-rod motion of internal combustion engines. For complex motions as in crank-and-rocker mechanisms, the higher harmonics must be evaluated because the resulting amplitudes can be of greater significance. In these higher harmonics the associated critical speed is usually taken to be $m\omega t$, radians/sec. In some high-speed cam applications, harmonics as high as the 20th have been considered significant. ■

slider-crank should be identical to the link length ratio AB/BC for the crank-and-rocker. On this basis the tabular data include values for d_m and f_m which can be used to compare these ratios for the two types of mechanisms.

For small values of the maximum pressure angle u, the in-line slider-crank has practically the same value of harmonic amplitudes as the crank-and-rocker for even harmonics; but the slider-crank values are slightly lower.

As pressure angle increases, the slider-crank values become progressively lower than crank-and-rocker values. Thus, at a pressure angle of 30°, d_2 and f_2 differ by approximately 1.7%; while at 60° the difference is approximately 8%.

The ratio of 2nd to 1st harmonic amplitude, and 3rd to 1st harmonic amplitude can be significant in high-speed operation, as the following ratios show:

$$d_2\,(30°) = 9.639\% \qquad d_2\,(60°) = 21.981\%$$
$$d_3\,(30°) = 1.90\% \qquad d_3\,(60°) = 9.0\%$$

As a guide, it would seem reasonable to limit the maximum pressure angle to 30° or less in high-speed applications, and to 45° or less for moderate speeds; also 60° usually can be useful eventually only in low-speed and light-duty instrument drives.

The range R_ψ is approximately proportional to the pressure angle with the "constant" of proportionality varying between 1.41 and 1.50. The ratios d_m, c_m, amplitudes and the link length ratio AB/AD also appear to be approximately linear with the pressure angle—at least sufficiently so for qualitative estimates. Accurate values, however, can be calculated from the table.

Example

Analyze the harmonics of a shake table (sketch, p 49) for testing gyroscopes and other devices. The proportions of the crank-and-rocker are selected for high-speed operation with maximum pressure angle of 25°, the input crank rotates at 10 rps, and the gyro weighs 8 oz. Find:

(1) Proportions of the linkage;

(2) Inertia force of the gyro due to the 2nd harmonic, compared with the 1st harmonic;

(3) Amplitude of the first three harmonics of the table motion.

SOLUTION

(1) From the table, a 25° pressure angle corresponds to Case 5. The proportions are $AB/AD = 0.22169$; $BC/ADCD/AD = 0.724385$. If fixed link AD is 10 in., the driving crank AB is 2.217 in.; the coupler BC and the driven link CD are 7.244 in. each.

(2) The inertia force is equal to the mass of the gyro multiplied by its acceleration, and gyro acceleration is equal to pitch radius r_p of the gear multiplied by its angular acceleration. For the mth harmonic the gyro acceleration is

$$A_G = r_p \frac{d^2}{dt^2}\left[c_m \sin\,(m\phi + \phi_m)\right]$$

$$A_G = r_p\, m^2\, c_m \left(\frac{d\phi}{dt}\right)^2 \sin\,(m\phi + \phi_m)$$

Therefore maximum inertia force F_{max} due to mth harmonic is:

$$F_{max} = \left[\frac{\text{gyro weight (lb)}}{g\left(\frac{\text{in}}{\text{sec}^2}\right)}\right] \times \left[r_p\, m^2\, c_m \left(\frac{d\phi}{dt}\right)^2\right] \text{lb.}$$

If $g = 386$ in./sec², gyro weight $= 0.5$ lb, $r_p = 1$ in.,

$$\left(\frac{d\phi}{dt}\right) = 10 \times 2\pi \frac{\text{rad}}{\text{sec.}}$$

$$F_{max} = \frac{0.5}{386} \times 1 \times (20\pi)^2 \times m^2\, c_m$$

Taking m and c_m from the table gives:

1st harmonic $m = 1$; $c_m = 0.309774$; $F_{max} = 1.587$ lb.
2nd harmonic $m = 2$; $c_m = 0.024573$; $F_{max} = 0.503$ lb

$$\text{Ratio 2nd to 1st harmonic} = \frac{0.503}{1.587} \times 100 = 31.7\%$$

(3) From the table for Case 5, the amplitudes of the first harmonics are given in the c_m column as:

$c_1 = 0.309774$; $c_2 = 0.023573$; $c_3 = 0.00400$ radians

Ratio of higher harmonics to the 1st harmonic can also be obtained from the d_m column. For example,

Ratio of amplitude of 2nd to 1st: $(d_2) = 0.079326 = 7.9\%$

Ratio of amplitude of 3rd to 1st: $(d_3) = 0.012913 = 1.3\%$

The significance of these values depends upon the particular design requirements, as well as the number of decimal places you want to use.

ACKNOWLEDGEMENTS: The authors are indebted to the Electronic Research Laboratories of Columbia University for having made available their computational facilities and to Mr. Sy Newman for programing help on the IBM 650 computer.

Four-Bar Linkages and Typical Industrial Applications

All mechanisms can be broken down into equivalent four-bar linkages. They can be thought of as the basic mechanisms and are useful in many mechanical operations.

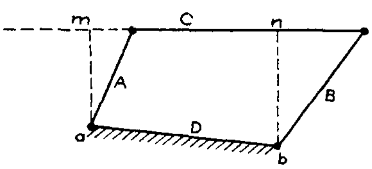

FOUR-BAR LINKAGE—Two cranks, a connecting rod and a line between the fixed centers of the cranks make up the basic four-bar linkage. Cranks can rotated if A is smaller than B or C or D. Link motion can be predicted.

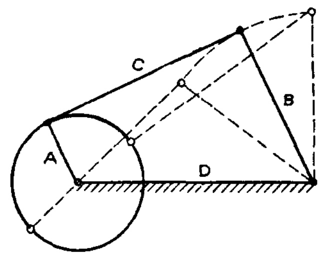

CRANK AND ROCKER — Following relations must hold for operation: $A+B+C>D$; $A+D+B>C$; $A+C-B<D$, and $C-A+B>D$.

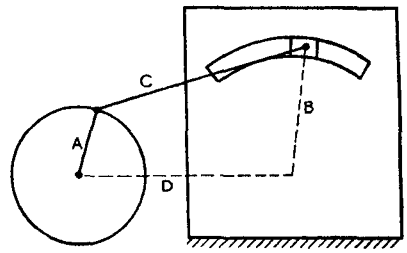

FOUR-BAR LINK WITH SLIDING MEMBER—One crank replaced by circular slot with effective crank distance of B.

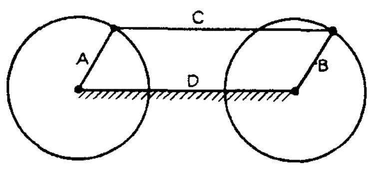

PARALLEL CRANK FOUR-BAR—Both cranks of the parallel crank four-bar linkage always turn at the same angular speed but they have two positions where the crank cannot be effective. They are used on locomotive drivers.

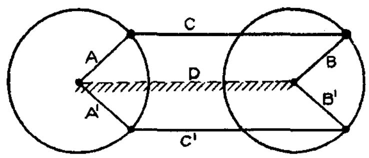

DOUBLE PARALLEL CRANK—This mechanism avoids dead center position by having two sets of cranks at 90 deg advancement. Connecting rods are always parallel. Sometimes used on driving wheels of locomotives.

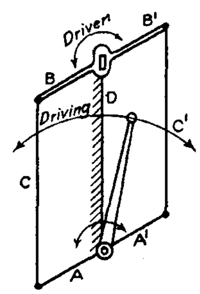

PARALLEL CRANKS—Steam control linkage assures equal valve openings.

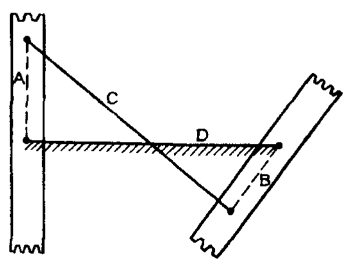

NON-PARALLEL EQUAL CRANK—The centrodes are formed as gears for passing dead center and can replace ellipticals.

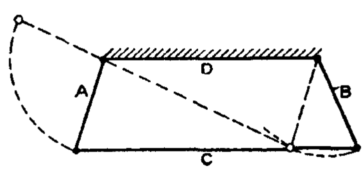

SLOW MOTION LINK—As crank A is rotated upward it imparts motion to crank B. When A reaches dead center position, the angular velocity of crank B decreases to zero. This mechanism is used on the Corliss valve.

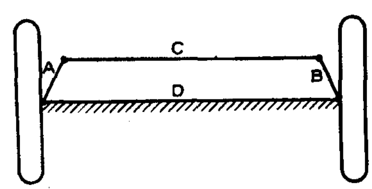

TRAPAZOIDAL LINKAGE—This linkage is not used for complete rotation but can be used for special control. Inside moves through larger angle than outside with normals intersecting on extension of rear axle in cars.

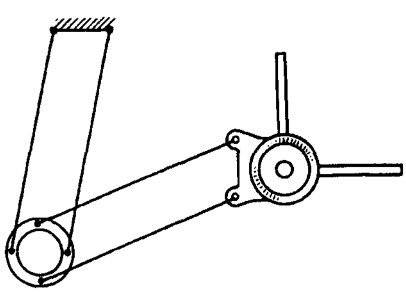

DOUBLE PARALLEL CRANK MECHANISM—This mechanism forms the basis for the universal drafting machine.

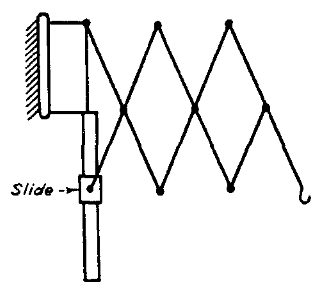

ISOSCELES DRAG LINKS—"Lazy-Tong" device made of several isosceles links; used for movable lamp support.

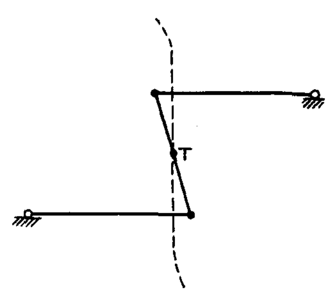

WATT'S STRAIGHT-LINE MECHANISM—Point T describes line perpendicular to parallel position of cranks.

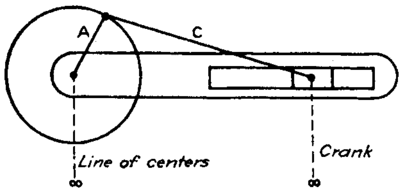

STRAIGHT SLIDING LINK—This is the form in which a slide is usually used to replace a link. The line of centers and the crank B are both of infinite length.

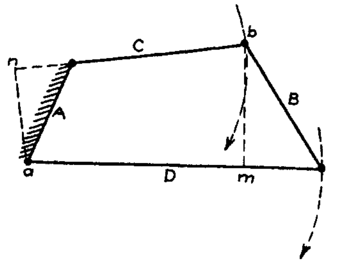

DRAG LINK—This linkage used as the drive for slotter machines. For complete rotation: $B>A+D-C$ and $B<D+C-A$.

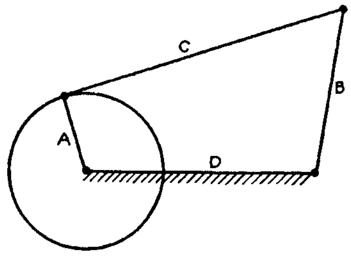

ROTATING CRANK MECHANISM—This linkage is frequently used to change a rotary motion to swinging movement.

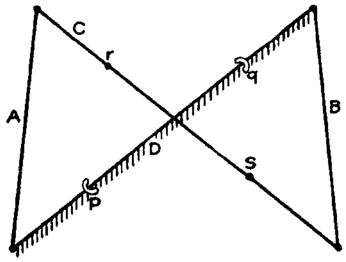

NON-PARALLEL EQUAL CRANK—If crank A has uniform angular speed, B will vary.

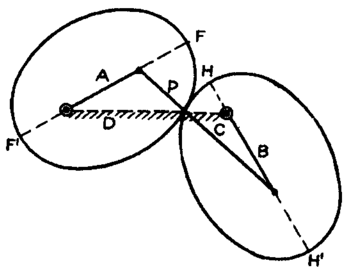

ELLIPTICAL GEARS—They produce same motion as non-parallel equal cranks.

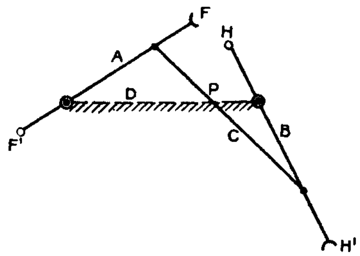

NON-PARALLEL EQUAL CRANK—Same as first but with crossover points on link ends.

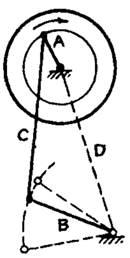

TREADLE DRIVE—This four-bar linkage is used in driving grindwheels and sewing machines.

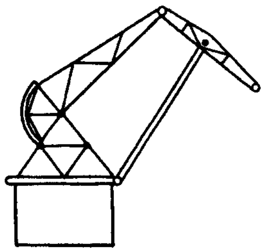

DOUBLE LEVER MECHANISM—Slewing crane can move load in horizontal direction by using D-shaped portion of top curve.

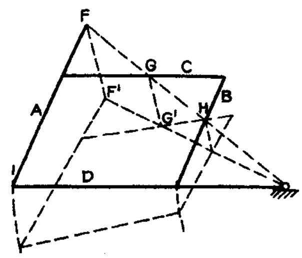

PANTOGRAPH—The pantograph is a parallelogram in which lines through F, G and H must always intersect at a common point.

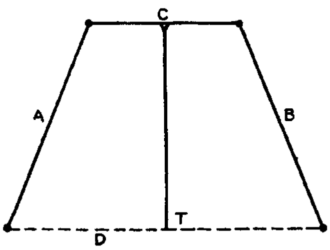

ROBERT'S STRAIGHT-LINE MECHANISM—The lengths of cranks A and B should not be less than 0.6 D; C is one half D.

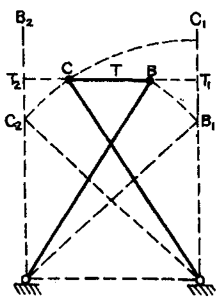

TCHEBICHEFF'S—Links made in proportion: $AB=CD=20$, $AD=16$, $BC=8$.

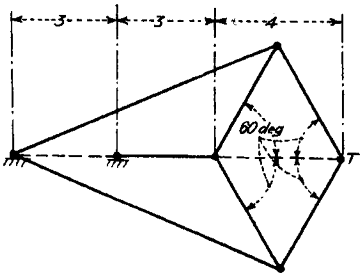

PEUCELLIER'S CELL — When proportioned as shown, the tracing point T forms a straight line perpendicular to the axis.

Four-Bar Power Linkages

With large forces or high speeds, the transmission angle becomes highly important. These new German charts simplify design.

J. Volmer & Preben W. Jensen

THE most common function of a four-bar linkage is transforming rotary motion into oscillating motion. Frequently, in such applications, a large force must be transmitted, or force must be converted at high speed. it is then that a factor called the *force-transmission angle* becomes of paramount importance.

The force-transmission angle, angle μ in Fig 1, is comparable to the pressure angle in cams. For best results, μ should be as close to 90 deg as possible during the entire rotation of the crank. This will reduce bending in the linkages and will produce the most favorable force-transmission conditions. (When μ becomes small, a large force is required to drive the rocker arm, and the force fluctuations increase.)

The charts presented here make it easier to find the best force-transmission linkage in a wide range of possible selections. Four examples show how to apply the charts to a number.

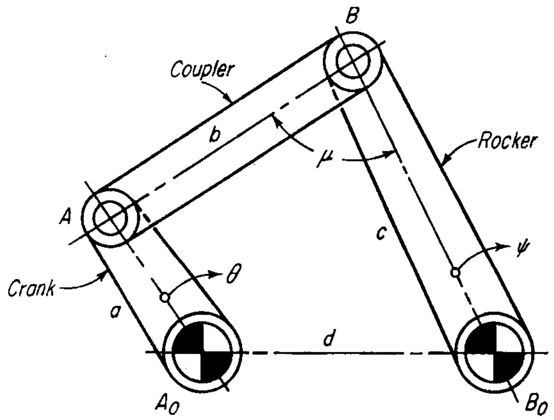

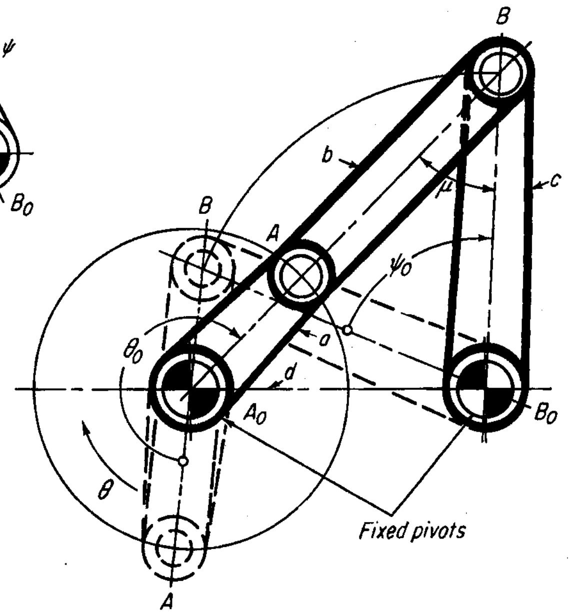

1. Four-bar linkage, (above) when operating as power-driving crank-and-rocker mechanism, should be designed with the force-transmission angle μ as close to 90 deg as possible. Sketch at right shows its two dead-center positions with input and output requirements defined by θ_0 and ψ_0, respectively.

Layout techniques

For finding family of linkages which meet θ_0 and ψ_0 requirements. Pin B of the linkages will lie somewhere along arc LE — but only one linkage of each family will have optimum transmission angle.

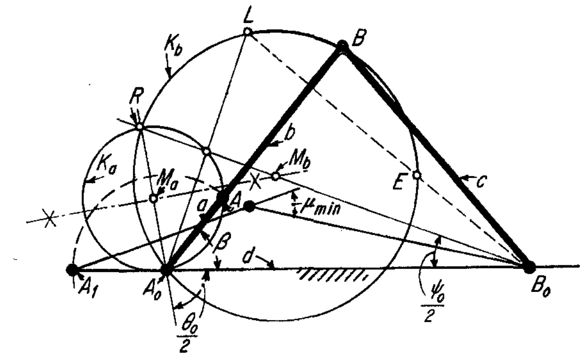

2. Where θ_0 is less than 180 deg.

3. Where θ_0 is greater than 180 deg.

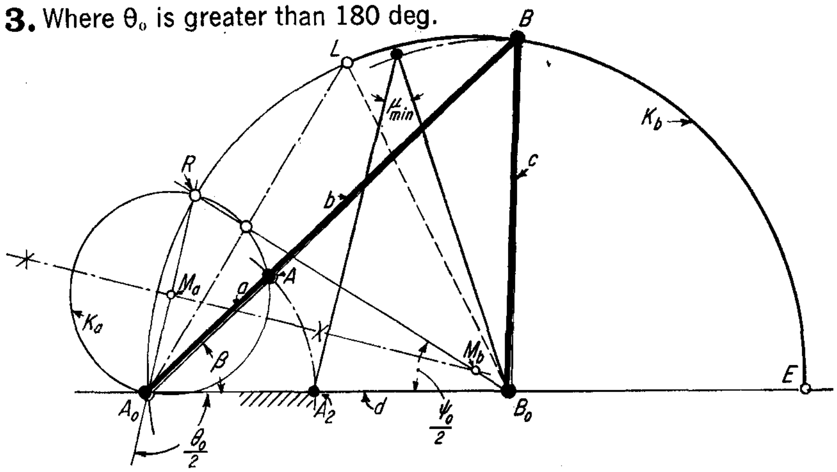

The linkage family

When a four-bar power linkage is designed to operate, for example, as a quick-return mechanism, angular displacement of the output link (the rocker) is usually prescribed in relationship to that of the input link (the crank). These angles are measured from the dead-center positions of the rocker (where the rocker reverses its direction of rotation). Thus, in Fig 1, ψ_0 is the angle between the two dead-center positions of the rocker, and θ_0 is the corresponding angle of the crank. Both angles are measured clockwise from the *inside* dead-center position, where crank and coupler are superimposed, to the outside dead-center position.

When values are given for ψ_0 and θ_0, and for the distance between centers, A_0B_0, a family of linkages that meets these conditions can be evolved by a graphical method developed some years ago by H. Alt. His method, illustrated in Fig 2, is the first phase of the design procedure:

1) Lay out the line of centers, A_0B_0.

2) Construct angles $\theta_0/2$ with center at A_0 and $\psi_0/2$ with center at B_0. Both angles are measured in the same direction. This locates point R.

3) Draw M_aM_b, the perpendicular bisector of A_0R. Locate point M_b.

4) Draw circles K_a and K_b through point R with M_a and M_b as centers, respectively.

5) On circle K_b make $RL = A_0R$ and connect point L with B_0 to locate point E on circle K_b.

6) Choose any point on the circular arc LE as point B, which is the center of the moving joint. This will be one of a family of linkages.

7) Construct line A_0B to intersect circle K_a. This locates crank pivot point A, thus defining all dimensions of the required four-bar linkage.

This method, however, stops short of determining which of all possible mechanisms obtained from the construction is the best power linkage.

Transmission angles

The question is, which linkage, from the above family, has μ_{min} closest to 90 deg. Since angle μ can be either smaller or larger than 90 deg, it is useful to define it as the angle between AB and BB_0—or between the extension of line AB and BB_0. Thus μ is always taken as $\mu \leqq 90$ deg. For example, if $\mu = 120$ deg, it is taken as $\mu = 60$ deg; a linkage in which μ varies from 75 deg to 120 deg ($\mu_{min} = 60$ deg) is more desirable than a linkage where μ varies from 45 deg to 90 deg ($\mu_{min} = 45$ deg).

The design charts

Previous investigations carried out by the first-mentioned author, J. Vol-

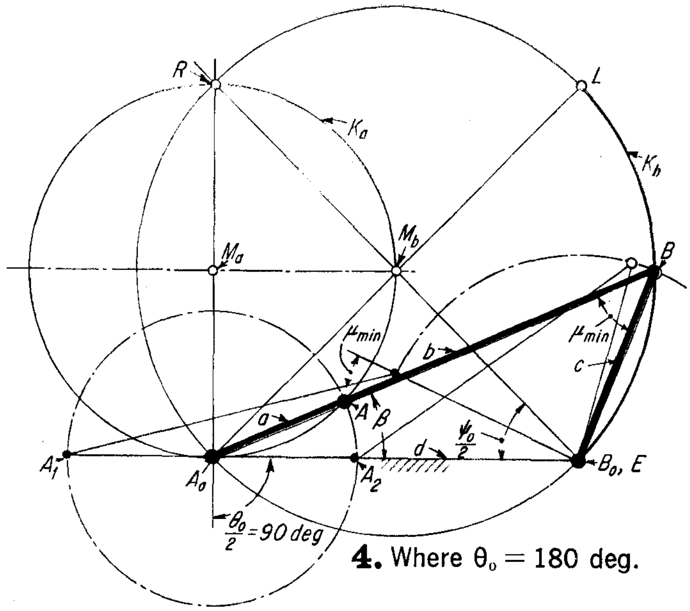

4. Where $\theta_0 = 180$ deg.

5. Where $\theta_0 = \psi_0 + 180$ deg.

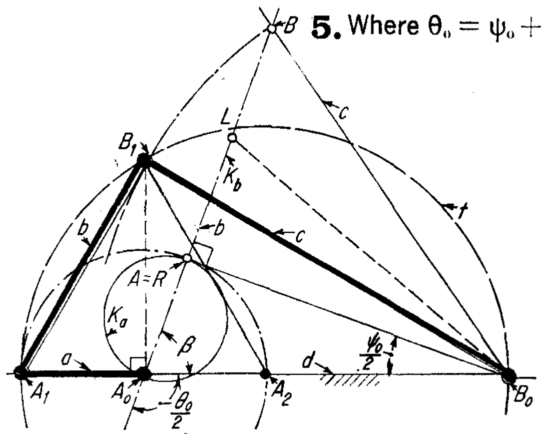

mer, have shown how to find the crank positions where μ is minimum. For $\theta_0 < 180$ deg, μ_{min} occurs when crank pin A is at A_1 (see Fig 2); for $\theta_0 > 180$ deg when A is at A_2, see Fig 3; when $\theta_0 = 180$ deg the minima of μ at A_1 and A_2 are equal (see Fig 4). The linkage with $\theta_0 = 180$ deg is called a centric crank-and-rocker mechanism.

Recently the second author, Preben W. Jensen, showed that among the family of linkages with given angles θ_0 and ψ_0, the optimum linkage can be determined with the aid of a chart originally published by H. Alt in *Verein Deutscher Ingenieure,* Vol 85 (1941) p 69. Alt's chart, however, was not very exact. It has now been corrected and also completed for the whole range of angles θ_0 and ψ_0. The chart is shown in Fig 7.

Here is how to use the chart to find the linkage with the largest μ_{min} value from the linkage family in Fig 2:

For the given values of θ_0 and ψ_0, find the value for angle β from the chart (dashed lines). Angle β = angle AA_0B_0. This locates point B and thus defines the mechanism. Read also the value for max μ_{min} (solid lines). No better minimum transmission angle can be obtained for the given conditions—every other linkage for the same dead-center angles possess a lower value of μ_{min}.

Interpolation can be employed between the curves for β and μ_{min}. However, when more accurate values for β are needed, use the equations (by assuming values for β and d):

$$\frac{a}{d} = -\frac{\sin\dfrac{\psi_0}{2}\cos\left(\dfrac{\theta_0}{2}+\beta\right)}{\sin\left(\dfrac{\theta_0}{2}-\dfrac{\psi_0}{2}\right)}$$

$$\frac{b}{d} = \frac{\sin\dfrac{\psi_0}{2}\sin\left(\dfrac{\theta_0}{2}+\beta\right)}{\cos\left(\dfrac{\theta_0}{2}-\dfrac{\psi_0}{2}\right)}$$

$$c^2 = (a+b)^2+d^2-2(a+b)d\cos\beta$$

where $a = AA_0$, $b = AB$, $c = BB_0$, and $d = A_0B_0$.

The design chart in Fig 6 is for the special case where $\theta_0 = 180$ deg, and the chart in Fig 9 for the design of a slider crank mechanism. The following examples illustrate use of the three charts.

Example I—Typical design

The dead-center position construction for $\theta_0 = 160$ deg and $\psi_0 = 40$ deg is shown in Fig 2. From the chart in Fig 7 find $\beta = 50.5$ deg and max $\mu_{min} = 32$ deg. Although there is no linkage with more favorable force transmission characteristics, a linkage with such a low minimum value of transmission angle is not capable of running at high speeds or transmitting great forces.

Example II—When $\theta_0 = \psi_0 + 180$ deg

When θ_0 and ψ_0 are chosen so that $\theta_0 = \psi_0 + 180$ deg at the dead-center position construction, then angle A_0RB_0 becomes a right angle, and circle K_b degenerates into the line A_0R. Fig 5 shows the construction for $\theta_0 = 220$ deg and $\psi_0 = 40$ deg. For all linkages within this family, the crankpin center A coincides with point R, and line A_0R extended beyond point L is the locus of point B, where $A_0R = RL$. Therefore, angle β is useless for finding the optimum linkage.

To obtain this linkage, locate A, ($A_1 A_0 = A_0A$). Draw circle t, with A_1B_0 as the diameter, to intersect with a line from A_0 perpendicular *to* A_0B_0. This locates point B_1. The required optimum linkage is $A_0A_1B_1B_0$. Angle $A_2B_1B_0 = \max \mu_{min}$. All mechanisms of this family lie on the diagonal dashed line in the chart, Fig 7. For this example, the chart shows that max $\mu_{min} = 30$ deg, and that $\beta = 70$ deg.

Example III—Centric linkage design

The centric four-bar linkage where the crank angle rotates 180 deg between the two dead center positions ($\theta_0 = 180$ deg) provides the greatest amplitudes ψ_0 of the rocker with most favorable transmission angle. However, Fig 7 is not applicable for this case because it indicates that $\beta = 0$ deg for any desired rocker angle ψ_0. This means that the length of crank and rocker must be zero—a solution without practical significance. Thus, a second chart, Fig 6, is used. For example, if a total rocker displacement of $\psi_0 = 90$ deg is required, a mechanism with $\mu_{min} = 40$ deg will be constructed with angle of $\beta = 23$ deg, and a mechanism with $\mu_{min} = 30$ deg with an angle of $\beta = 35$ deg. The dead-center position construction for this mechanism is shown in Fig 4. Here, other conditions can also be prescribed, for instance, a desired length of crank, rocker, or coupler.

Example IV—Slider-crank mechanism

For $\psi_0 = 0$ deg, the four-bar linkage degenerates into the slider-crank mechanism. Instead of the rocker angle ψ_0 the stroke, s, of the slider is used. The construction is as follows (see Fig 8):

1) Draw line A_0B_0 perpendicular to the direction of stroke.

2) Construct angle $\theta_0/2$ and a line parallel to A_0B_0 with distance $s/2$ as shown. This locates point R.

3) Draw M_aM_b, the perpendicular bisector of A_0R.

4) Draw, through R, circle K_a and K_b about M_a and M_b as centers.

5) The line parallel to A_0B_0 at distance s intersects circle K_b at points L and E. Arc LE on circle K_b is the locus of point B. Point A is on circle K_a in line with A_0B.

For example, suppose a ratio of 4:5 of the crank angles is required for a quick-return mechanism. This ratio provides a dead-center angle of $\theta_0 = 160$ deg and $\theta'_0 = 200$ deg (160:200 = 4:5). As in the case of the crank-and-rocker mechanism, there is a whole family of slider-crank mechanisms fulfilling this condition. Here, the optimum mechanism will be the one whose transmission angle is closest to 90 deg when the crank is perpendicular to the direction of stroke. To find this optimum linkage use the $\psi_0 = 0$ deg ordinate in the chart of Fig 7. Thus, for $\theta_0 = 160$ deg, the chart gives $\beta \approx 76$ deg, which permits completion of the construction in Fig 8 (angle β locates point B on arc LE). The chart also gives max $\mu_{min} = 43$ deg. If the supplementary angle, $\theta'_0 = 200$ deg, is used the construction provides the same linkage because the chart shows $\beta' = 104$ deg, which is the supplement of angle β. (The $c = b$ line in Fig 6 gives points for a linkage with equal coupler and rocker links).

Because an exact value for angle β cannot be found at the ordinate of the chart, a third chart, Fig 9, has

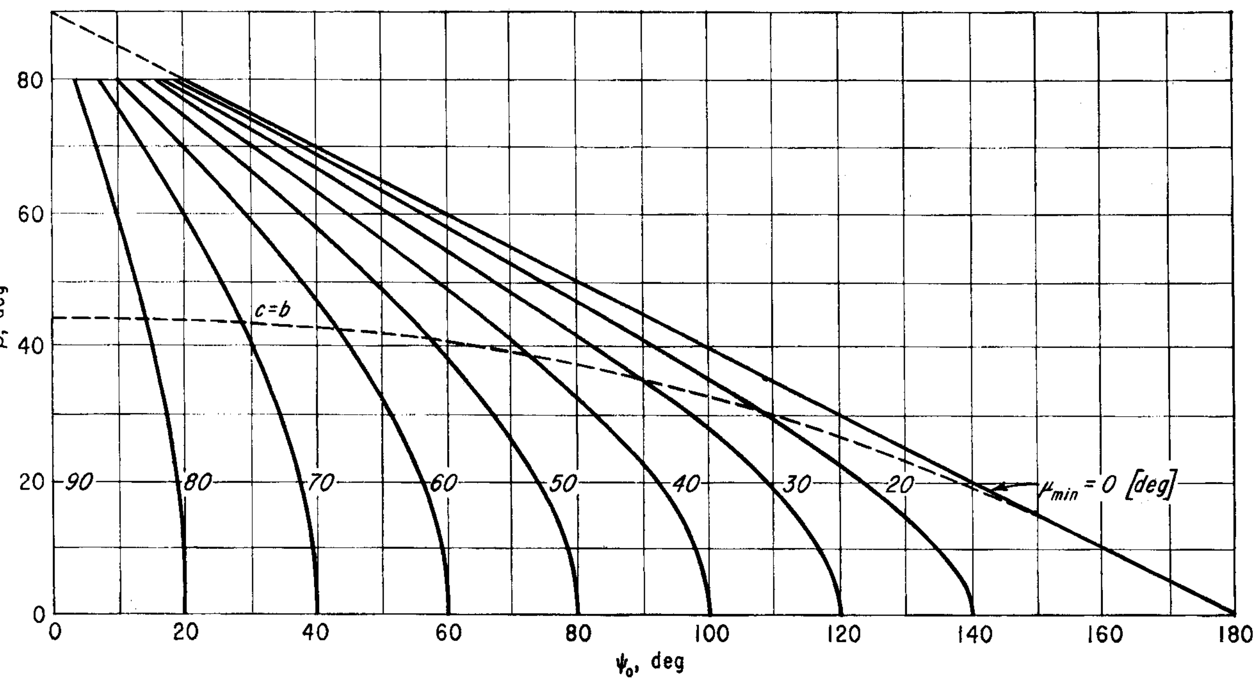

6. Optimum transmission angle — where $\theta_0 = 180$ deg.

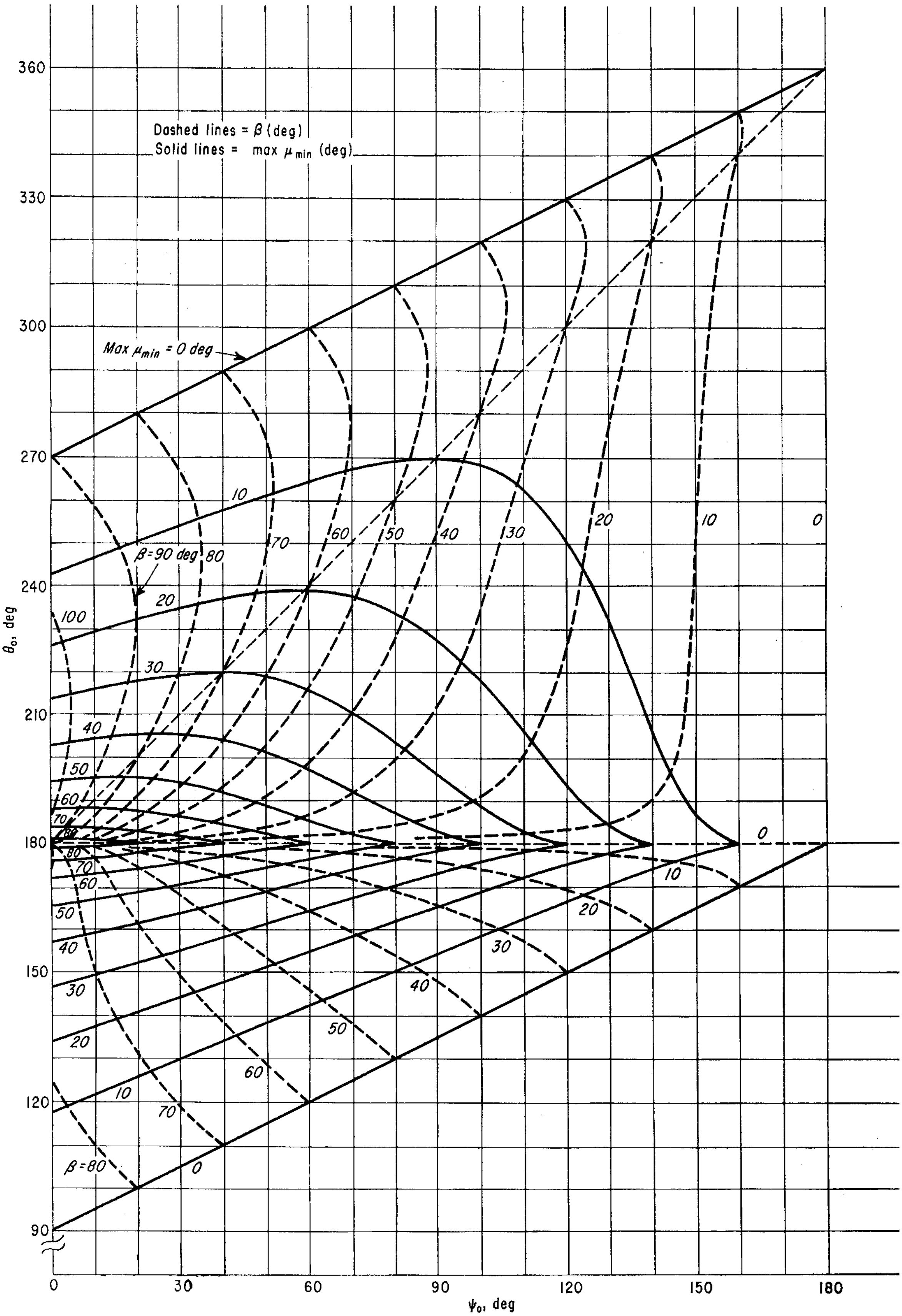

7. Optimum transmission angles — general case.

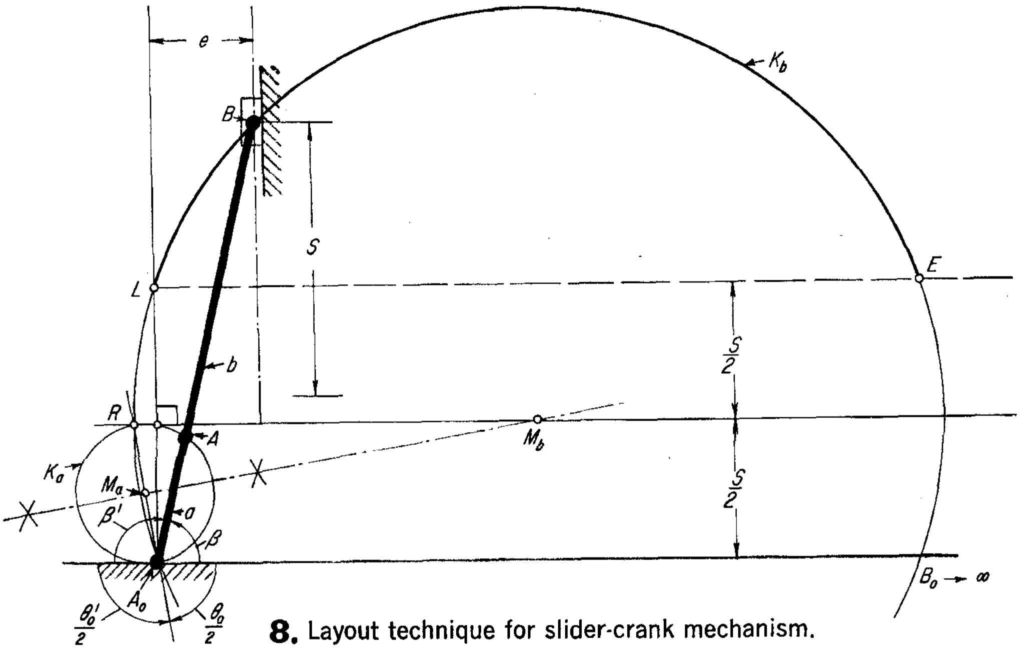

8. Layout technique for slider-crank mechanism.

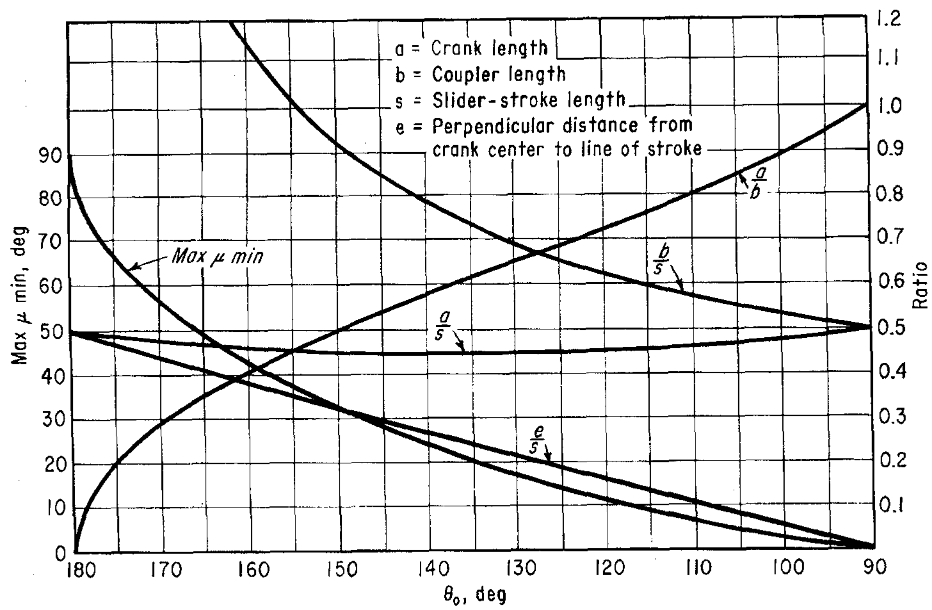

9. Design chart for slider-crank mechanism.

been developed to provide greater accuracy. Here max μ_{min} is plotted as a function of θ_0, along with ratios a/s, b/s, e/s, and a/b. For the desired angle of $\theta_0 = 160$ deg, max $\mu_{min} = 43$ deg, $a/s = 0.465$, $b/s = 1.150$, $a/b = 0.406$, and $e/s = 0.378$. Instead of using angle β in Fig 8, draw a line from point A_0 perpendicular to A_0B_0 at a distance e—obtained from the ratio e/s—to locate point B on circle K_b. The line connecting A_0 and B intersects circle K_a at crank pin center, A, and the optimum slider-crank mechanism for the prescribed ratio of 4:5 is completely defined.

5 Graphic Methods for Designing Four-Bar Linkages

This roundup covers the four-bar linkages that can generate a path approximating a straight line. The methods permit rapid solution of general configurations to fit space requirements, and they simplify mathematical solutions that find precise dimensions.

Erwin P. Pollitt

The classical problem here is to find a four-bar linkage that will generate a straight-line motion. Such linkages are used extensively in mechanical design, in place of cams and gears. Specific applications involve computers, instruments, counterweights and simple translators of rotary motion. Their preference over cams and gears depends upon analysis of their advantages and disadvantages. The advantages are simplicity, negligible friction (and wear), low inertia, economy, and stability in performance. The disadvantages are limited range, approximation of the desired motion, bulkiness, limited control over velocity and acceleration, and the fact that they are relatively difficult to design.

In general, linkages are designed by mathematical or graphical methods. In either case the characteristic problem is that of selecting from a large number of dimensional constants a particular set that will fit the specified space requirements and tolerances. The approach to the problem must be synthetic and approximate, instead of analytical and exact. The five graphical methods presented here offer a practical approach for determining the general configuration. Then, if necessary, mathematical methods can be applied to get the best out of the linkage with respect to the number of precision points and magnitude of deviation from the straight line.

Linkages developed by the five graphical methods have these characteristics:

Method A—These give a tracer point with nearly infinite radius of curvature.

Method B—Easiest to construct, but have a limited range characterized by two precision points.

Method C—Relatively harder to construct, but offer greater accuracy—up to five precision points.

Method D—These are the most accurate—up to six precision points. This is the limit because the equation of motion of a point is generally of the sixth order.

Method E—Offer four precision points, but can be adapted to more than four.

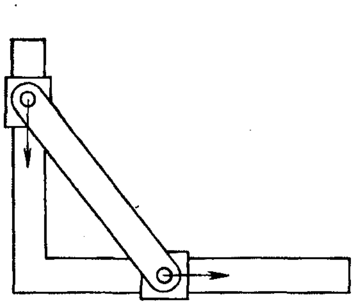

Method A

Synthesis of a Linkage Equivalent to Elliptical Trammel

Approach to solution: **the component of the mechanism containing the point which performs the rectilinear motion is used as the coupler of the linkage; two points on this component are selected as the moving pivots, and the exact—or approximate—center of curvature of their path is made the fixed crank pivot.**

The path of the tracer point of the linkage obtained has an infinite, or nearly infinite radius of curvature.

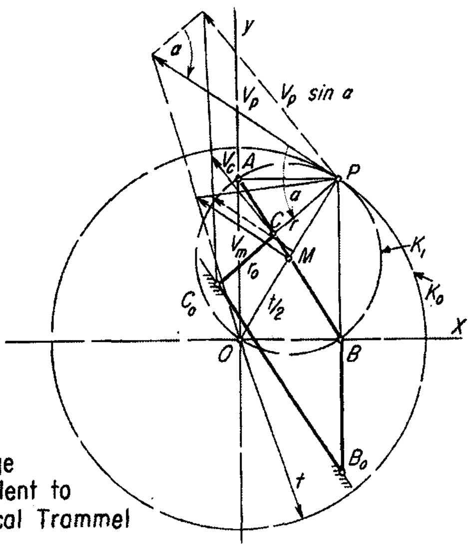

Linkage Equivalent to Elliptical Trammel

1

The bar is constrained at points A and B to move along the x and y-line. In the linkage the bar is made the coupler. Point B is made one moving pivot, and an arbitrarily chosen point C on the bar the second moving pivot. Crank BB_o, in the design position, is made perpendicular to the x-line, and as long as possible so that B moves approximately along this line while the center of curvature C_o of the point C on the trammel is selected as the second fixed pivot. Point A is then the tracer point.

The center of curvature C_o of point C must lie on a line through C and the instantaneous center of rotation P of AB which is found as the intersection of the normals through A and B to y and x respectively.

The radius of curvature CC_o can be calculated, or solved graphically by the use of Euler-Savary's theorem in the form:

$$\frac{V_p \sin \alpha}{V_c} = \frac{r_o}{r_o - r}$$

where V_p is the velocity of the change of position of the instantaneous center, the angle between the tangent to the centrodes at the instantaneous center and the ray C_oP. V_c the velocity of point C of the moving system, $r = CP$, and $r_o = C_oP$.

The velocity of any point of the moving system, for instance, velocity V_m of the midpoint M of AB, is arbitrarily selected, and V_c determined. The fixed centrode of the trammel is the circle K_o with O, the intersection point of x and y, as center, and $OP = t$, the length of bar AB as radius; the moving centrode is the circle K_1 through P and O, with M, the midpoint of AB as center and $t/2$ as radius. The velocity V_p is determined from the consideration that the motion of the bar is equivalent to rolling of the moving centrode on the fixed centrode. V_p is therefore the velocity of this rolling motion, of the point of circle K_1 with which the instantaneous center coincides.

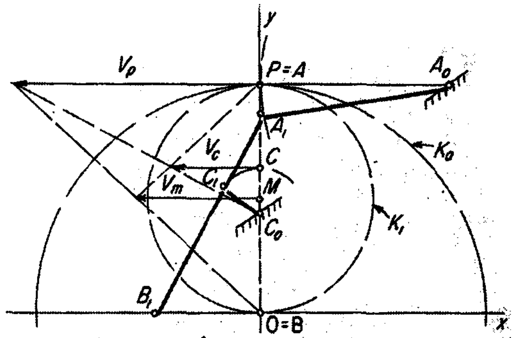

Thompson's Indicator Linkage

2

A special case of Fig 1 is the Thompson indicator mechanism shown here. It is widely used in radio sets for indicating the tuned frequency. To determine the linkage, the position of bar AB is chosen so that it coincides with the y-axis; then point A, which coincides with instantaneous center P, is made one moving pivot; and the fixed pivot A_o is located on the perpendicular to y through A. The center C_o of the curvature of the path of an arbitrarily selected moving pivot point C on line AB must also lie on the y-axis. Balance of the procedure is same as Fig. 1.

Having assumed the magnitude of vector V_m of center M of K_1 the vector V_p sin α can now be constructed. A line drawn through the end points of the vectors V_c and V_p sin α and the intersection of this line with CP determines point C_o.

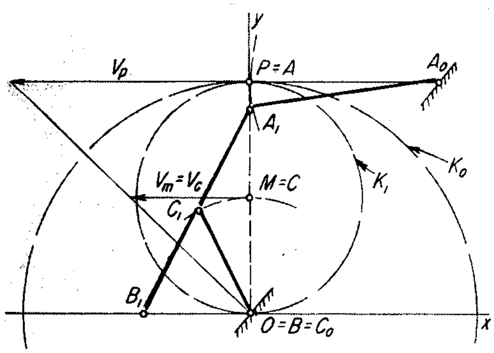

Evan's Linkage

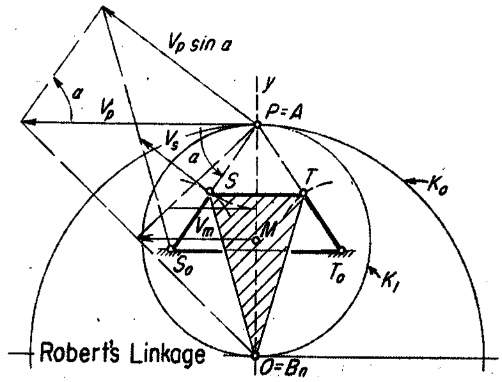

Robert's Linkage

3
This is a second variation where point C coincides with center point M of bar AB; and C_o coincides with points O and B. Here, again, path of A approximates the y-axis, and path of B approximates the x-axis.

4
Here is a third variation of this group, with the moving crank centers symmetrical to AB, which again coincides with the y-axis.

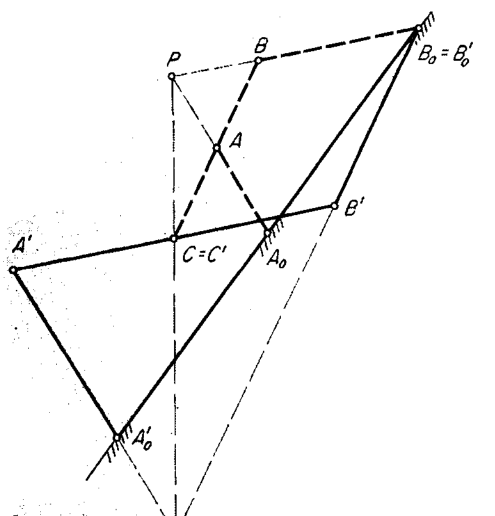

Watt's Linkage

5
By Robert's Law additional linkages can be found such that a point of their coupler performs a path identical to the path of a point of the coupler of a given linkage. In this linkage, A'_oA' and B'_oB' are so related to Evan's linkage that tracer point C' of the coupler of this linkage corresponds to the coinciding tracer point of C of the Evan's coupler. The fixed pivot, B'_o, coincides with B_o, and the fixed link $A'_oB'_o$ has the same direction as the fixed link A_oB_o of the Evan's linkage. Coupler A'B' passes through C and is parallel to BB_o, while crank $B'B'_o$ is parallel to AB. Other similarities in the geometry are also apparent. This linkage is similar to Watt's linkage used extensively in steam engines.

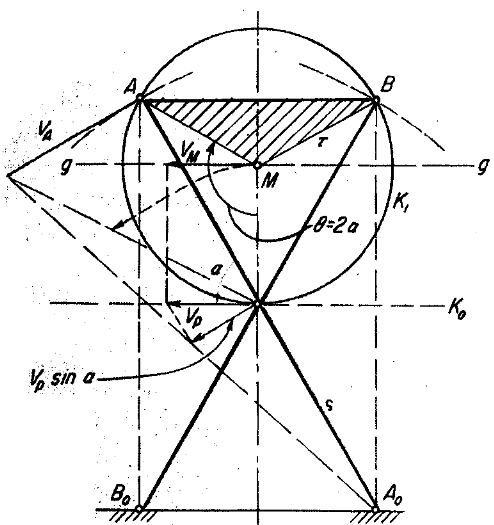

Cycloidal Linkage

6
Center M of circle K_1 rolling on a straight line K_o generates a straight-line motion along line g-g parallel to K_o. The contact point of the circle K_1 and line K_o is the instantaneous center P. K_o is the fixed centrode and K_1 the moving centrode. The motion of point M is approximated by a coupler link whose tracer point coincides with M, and whose moving pivots AB coincide in the shown position with two points on the periphery of the rolling circle which are symmetrical to the normal line to K_o through M. The centers of curvature, A_o, B_o, of the path of these two points are selected as the fixed pivots of the cranks, and they are determined as previously. The velocity V_p is equal to velocity V_m. The path of points A and B are cycloids whose radius of curvature may be calculated as follows: $\rho = 4r \sin \theta/2$; where r is radius of the rolling circle, and θ is its angle of rotation. The cycloidal linkage is used extensively in the textile industry.

Method A

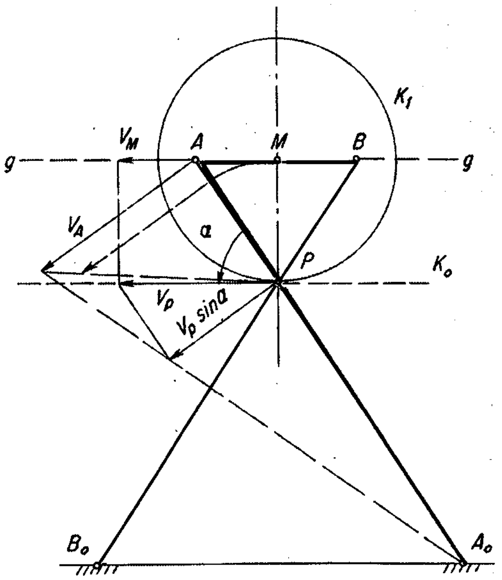

Tchebisheff's Linkage

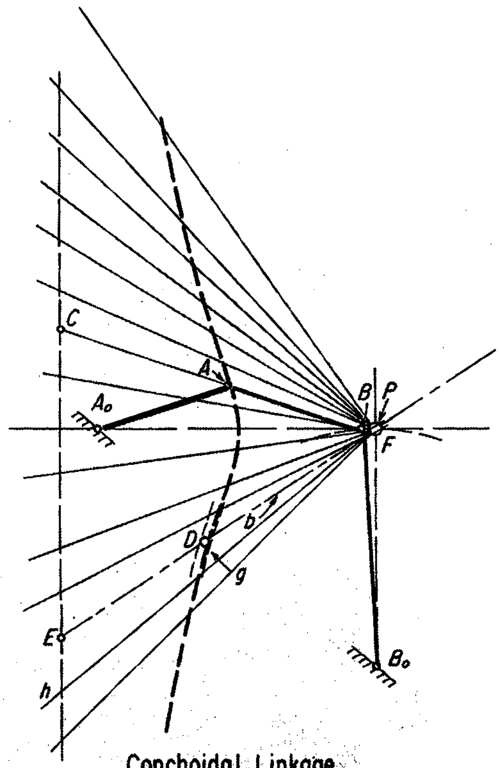

Conchoidal Linkage

7
This is a modification of the previous linkage, with moving crank centers selected so as to coincide with two points inside the periphery located at equal distances from center of the rolling circle. One linkage of this type became known as Tchebisheff's linkage, characterized by a high degree of approximation to straight-line motion of the center point of its coupler.

8
The conchoid is the locus of points *D* on rays connecting all points of a generating straight line *h* with a focus *F* and having equal distance from the straight line. If the motion of a straight bar *b* is so constrained that the bar passes in all positions through the focus *F* (by means of a pivoted slide *P*); and point *D*, fixed on the bar, moves along a conchoidal groove *g*, another point, *E*, of the bar will describe the generating straight line *h*. Portions of this motion of point *E* are approximated by a linkage—A_oA, BB_o. A_o is the center of curvature of the conchoid at its apex, and A_oA is equal to its radius of curvature. *AB* is made equal to the distance between focus and apex of the conchoid, and crank BB_o is made as long as possible. Link *AB* is extended, and the distance between *B* and its end-point *C* is made equal to the distance between focus and generating line of the conchoid. Point *C* then describes an approximately straight-line path in the vicinity of the apex of the conchoid, and is used as tracer point.

To summarize characteristics of the above linkages, the path of the tracer point of the symmetrical linkages, Figs 4, 6 and 7, has an infinite radius of curvature. In the linkages of Figs 1, 2, 3 and 8, the corresponding radius of curvature approaches infinity as the length of the arbitrarily assumed crank is increased. In Fig 5 the tracer of the midpoint of the coupler will have an infinite radius of curvature when the linkage is in its antisymmetrical position, provided the cranks have equal lengths.

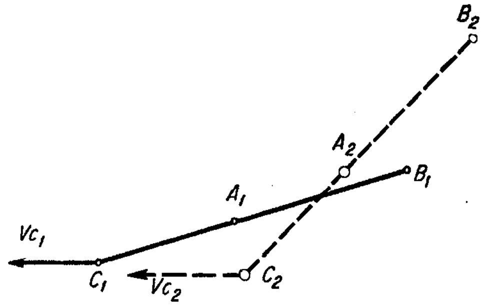

Method B

Synthesis of a Linkage Which Moves a Coupler Point Through Two Given Positions Such That Its Velocities in These Positions Are Collinear

Approach to solution: **two positions of the moving crank, A_1 B_1, A_2 B_2 are arbitrarily selected; the locus of the instant center of those link configurations is constructed consistent with the velocity requirements and the selected coupler positions.**

In the linkage obtained the path of the tracer point has two precision points and its tangents are collinear.

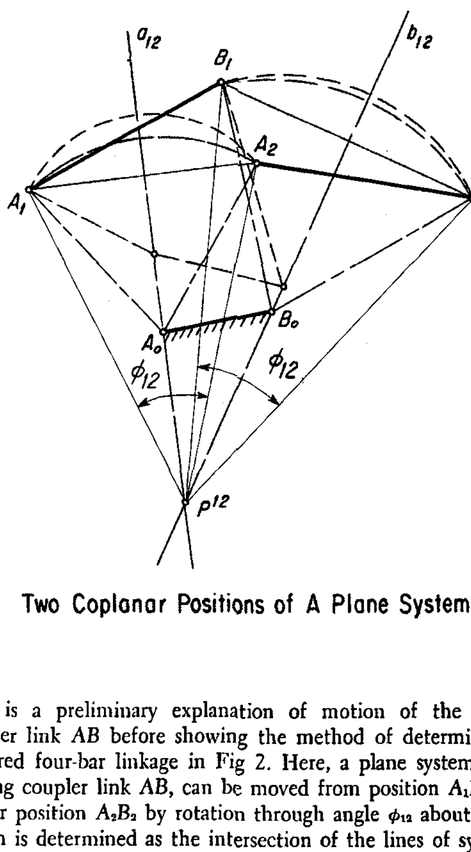

Two Coplanar Positions of A Plane System

1

This is a preliminary explanation of motion of the essential coupler link AB before showing the method of determining the required four-bar linkage in Fig 2. Here, a plane system S, containing coupler link AB, can be moved from position A_1B_1 to coplanar position A_2B_2 by rotation through angle ϕ_{12} about pole P^{12} which is determined as the intersection of the lines of symmetry, a_{12} and b_{12}, through distances A_1—A_2 and B_1—B_2, respectively. Pole P^{12} is a point common to the two positions of AB and the reference plane. This movement of AB can be accomplished by a four-bar linkage as follows: Connect coupler point A to any pivot point A_o on line a_{12}, and coupler point B to any point B_o on line b_{12}. A_oB_o is chosen so direction of the velocities of one point of coupler AB is collinear. Thus its path approaches a straight line.

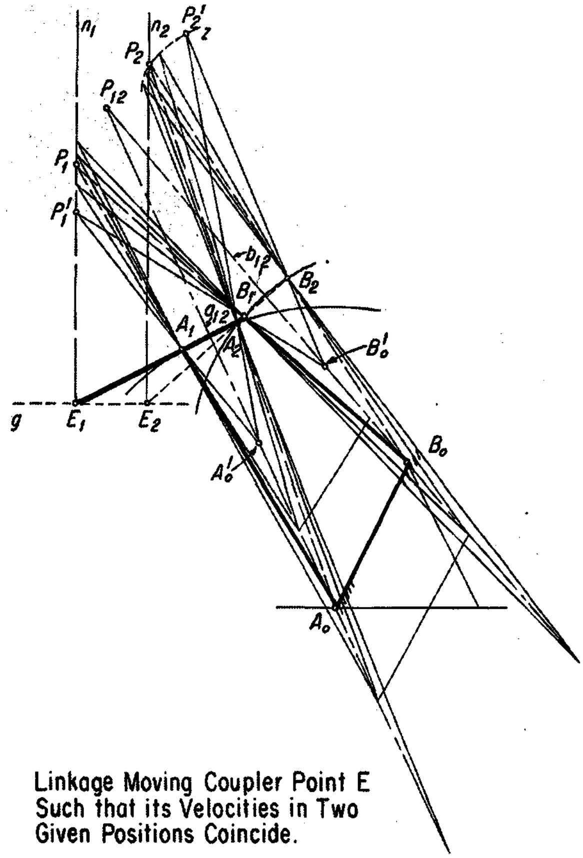

Linkage Moving Coupler Point E Such that its Velocities in Two Given Positions Coincide.

2

Two positions A_1B_1, A_2B_2 of a coupler link AB are so selected that the positions E_1, E_2 of the third point E of the coupler lie on the straight line g, representing the approximate path which point E is required to travel. This line is direction of the velocities of E in its positions E_1, E_2. The instantaneous centers, relative to the reference plane, of the coupler in positions $A_1B_1E_1$, $A_2B_2E_2$ must lie on the normals n_1 and n_2 to g through E_1 and E_2. Also, the instantaneous centers must lie on the point of intersection of the lines A_oA_1, B_oB_1, and A_oA_2, B_oB_2, respectively, where A_o and B_o denote the yet unknown crank centers. Crank center A_o must also lie on the line of symmetry a_{12} of A_1A_2, crank center B_o, on the line of symmetry b_{12} of B_1B_2. If a point P'_1 on n_1 is assumed to be the instantaneous center for link position A_1B_1, the corresponding crank centers would be A'_o, B'_o, determined by the intersection of lines P'_1A_1 with a_{12} and P'_1B_1 with b_{12} respectively. The intersection point P'_2 of the lines A'_oA_2 and B'_oB_2 determines the corresponding instantaneous center of A_2B_2. P'_2 represents one point of the locus z of all possible instantaneous centers of system position $E_2A_2B_2$ for which the instantaneous center of system position $E_1A_1B_1$ lies on line n_1. The intersection point of this curve z with n_2 gives the instantaneous center P_2 of the link position $E_2A_2B_2$, which satisfies the requirement concerning direction of velocity of point E_2 and is used to construct the desired crank centers A_o, B_o. The path of point E_1 is nearly straight for a considerable distance past the positions E_1, E_2, so that the linkage is usable through a considerable range.

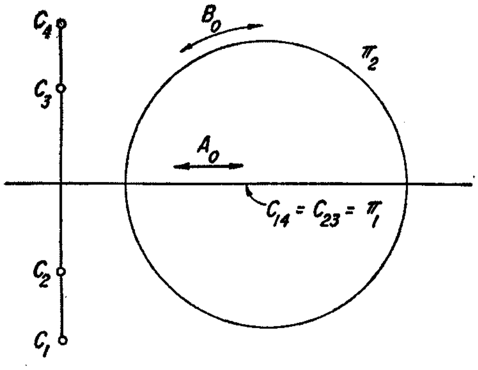

Method C

Synthesis of a Linkage by Means of Burmester's Focal Curves

Approach to solution (in its simplest form): two pairs of positions (C_1 C_4, C_2 C_3) of a coupler point, lying on a straight line and having a common bisector C_{14} are chosen; a degenerated curve of Burmester's centers is selected so as to coincide with this bisector; the crank pivots are found by determining the poles of rotation of the coupler.

In the linkage obtained, path of the tracer point has up to five precision points.

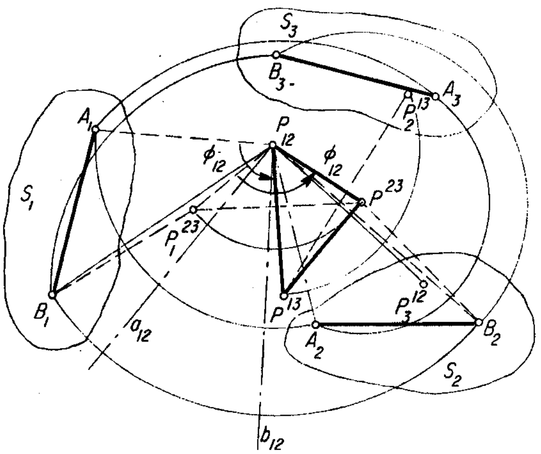

Three Coplanar Positions of a Plane System–the Pole Triangle

1

For an understanding of these methods it is first necessary to establish a certain relationship between congruent points of these coplanar positions of the plane system, their poles and angles of rotation.

For three coplanar positions S_1, S_2, S_3, there exist three poles of rotation P^{12}, P^{13}, P^{23}, forming the pole triangle which lies in the reference plane. The pairs of poles, P^{12} and P^{13}, are common to S_1S_2, S_1S_3 and the reference plane, respectively. Point P_1^{23} in the system S_1 is congruent to pole P^{23} and is found by rotating triangle $A_2B_2P^{23}$ about P^{12} until A_2B_2 coincides with A_1B_1. The angle of rotation from S_1 to S_2 is $P_1^{23}P^{12}P^{23}$, designated as ϕ_{12}.

Analogous relations apply to the points P_2^{13} congruent to P^{13} in system S_2, and P_3^{12} congruent to P^{12} in system S_3.

$\angle P_1^{23}P^{12}P^{23} = \phi_{12}$ $\quad$ $\angle P_1^{23}P^{13}P^{23} = \phi_{13}$

$\angle A_1P^{12}A_2 = \phi_{12}$ $\quad$ $\angle A_1P^{13}A_3 = \phi_{12}$

$\angle A_1P^{12}A_0 = \frac{1}{2}\phi_{12}$ $\quad$ $\angle A_1P^{13}A_0 = \frac{1}{2}\phi_{13}$

$\angle B_1P^{12}B_0 = \frac{1}{2}\phi_{12}$ $\quad$ $\angle B_1P^{13}B_0 = \frac{1}{2}\phi_{13}$

$\angle A_1P^{12}A_0 = \angle B_1P^{12}B_0$ $\quad$ $\angle A_1P^{13}A_0 = \angle B_1P^{13}B_0$

$\angle P_1^{23}P^{12}A_1 = \alpha$

$\angle P^{13}P^{12}A_0 = \alpha$

$\angle P_1^{23}P^{13}A_1 = \beta$

$\angle P^{12}P^{13}A_0 = \beta$

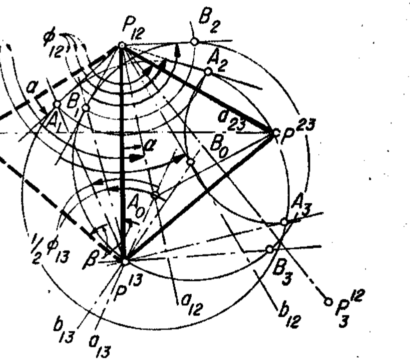

Three Coplanar Positions of a Plane System-relation between Pole Triangle and System Points

2

The three congruent points, A_1, A_2, A_3, lie on a circle whose center is A_0 at the intersection of lines of symmetry—a_{12}, a_{13}, and a_{23}. These lines of symmetry pass through their associated poles of rotation. Center point A_0 can be found without determining A_2 and A_3 from the noted angle relations. Angle $P_1^{23}P^{12}A_1$ must be equal to angle $P^{13}P^{12}$ A_0, and angle $P_1^{23}P^{13}A_1$ must be equal to angle $P^{12}P^{13}A_0$.

Conversely the point A_1 associated with any point A_0 can be found by the same angle relationships. Corresponding angular relations exist between B_1, B_2, B_3, and Center B_0.

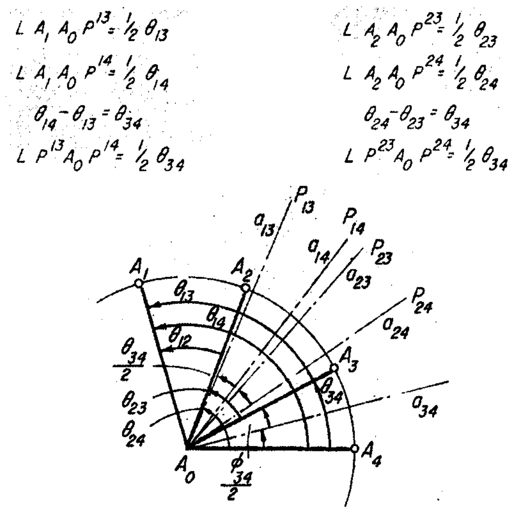

Four coplanar positions of a plane system-relation between the center point and the poles of rotation

3
To go one step further, if four coplanar positions S_1, S_2, S_3, S_4 of the moving system S are given, there exist six poles of rotation and twelve points in the system which are congruent to these poles. To determine the fixed pivots of a four-bar linkage capable of moving the system through these four system positions, two points in the moving system must be found whose congruent points in these four positions lie on a circle. Relationship between such points, A_1, A_2, A_3, A_4, and corresponding poles is shown. The center A_0 lies on the intersection of bisectors a_{13}, a_{14}, a_{23}, a_{24} of the angles $A_1A_0A_3$, $A_1A_0A_4$, $A_2A_0A_3$ and $A_2A_0A_4$. But poles P^{13}, P^{14}, P^{23} and P^{24} must also lie on these bisectors. From these angle relations it follows that the angles $P^{13}A_0P^{14} = P^{23}A_0P^{24}$, and $P^{13}A_0P^{23} = P^{14}A_0P^{24}$.

Thus, a point of reference plane at equal angles from any pair of poles with one common digit, is the center point of a circle called Burmester center—with four congruent points.

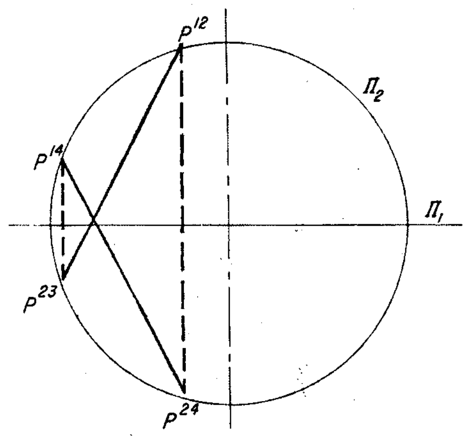

Focal curve consisting of a straight line and a curve

5
For certain pole positions the focal curve assumes very simple shapes. For example, if pairs of associated poles—P^{13}, P^{23}, P^{14}, P^{24}—are symmetrical to a straight line, the focal curve degenerates into straight line π_1 and circle π_2 through the four poles.

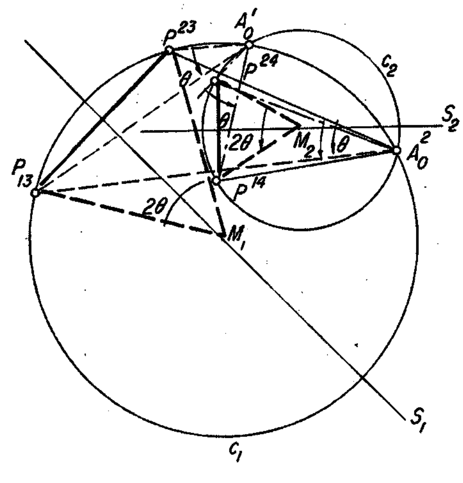

Construction of focal curve

(b)

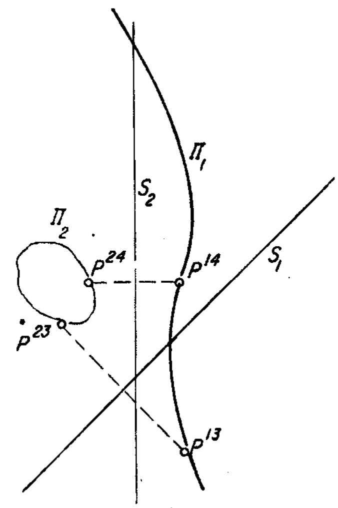

(a)

Typical focal curve

4
The locus of all such points is a plane curve of the third order, called a Focal Curve, see (a), and the Focal Curve which is the locus of all centerpoints associated with four system positions is called the centerpoint curve. It can be shown that this curve passes through all six poles, and can be constructed by selecting two pair of poles whose indices have one common digit—for example, P^{13}—P^{23}, P^{14}—P^{24}—and drawing a circle through each pair of poles such that the radii of these circles are proportional to the distance between the poles of a pair; the points of intersection of the two circles, A^1_0, A^2_0, are points of the focal curve. The radius of the crank circle associated with each center point, and the location of the congruent points can be found by the angular relations illustrated in Fig 2, p 42.

When four system positions are selected in such a manner that four congruent positions of a point of the system lie on a straight line, and for these system positions the centerpoint curve is constructed, any two points on the curve can be selected as the centers of the cranks of the desired four-bar linkage.

Method C continued

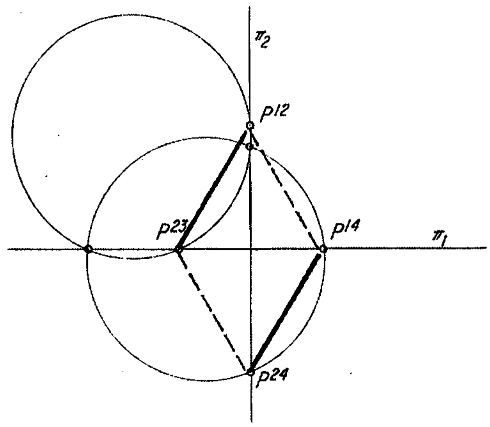

Focal Curve Consisting of Two Straight Lines

6

If the lines connecting associated poles constitute opposite sides of a rhombus, the focal curve degenerates into the diagonals π_1, π_2 of this rhombus and they are perpendicular to one another.

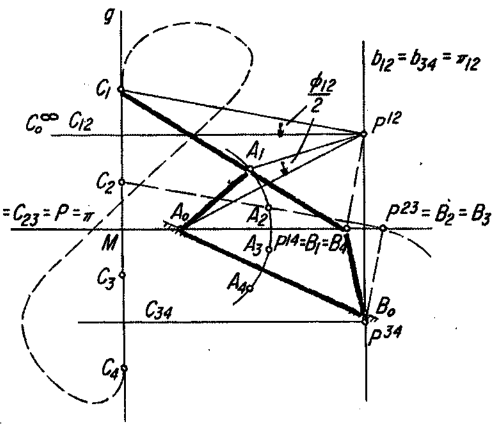

Construction of Linkage by Use of Center Point Curve Consisting of Two Straight Lines

8

This is another example of the use of the simplified shape of the centerpoint curve for the design of a linkage. As in the preceding example, four positions, C_1-C_4, C_2-C_3, on the line g of the coupler point C are selected so that they are symmetrical to the normal p. Furthermore, the positions B_1B_4 and B_2B_3 of moving point B are selected so that they coincide, respectively with one another, and also lie on line p. In this case P^{14} coincides with B_1B_4, P^{23} coincides with B_2B_3.

The poles P^{12}, P^{34} must be the intersection points of line symmetry c_{12} of C_1C_2 and c_{34} of C_3C_4 with lines of symmetry b_{12}, b_{34} of B_1B_2, B_3B_4. By choosing this configuration, pole quadrangle becomes a rhombus; consequently centerpoint curve consists of the lines of symmetry p; centerpoint B_0 can be selected anywhere on b_{12}; centerpoint A_0, anywhere on p. Position A_1 of moving point A, which must lie on the line B_1C_1, can again be found by using angle relations of Fig 2, by making angle $A_1P^{12}A_0 = \frac{1}{2}\phi_{12}$. Conversely, movable pivot point A may be selected anywhere on the coupler, and centerpoint A_0 determined in an analogous manner.

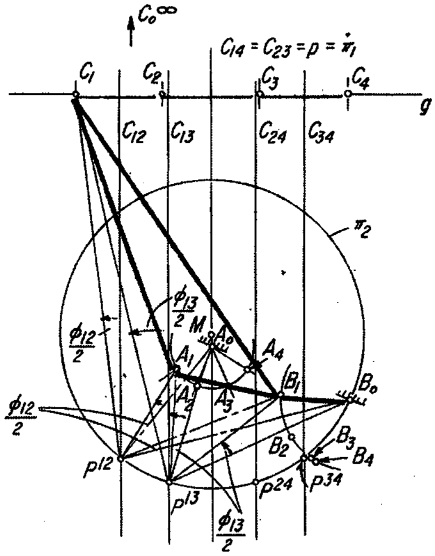

Construction of Linkage by Use of Center Point Curve Consisting of Straight Line and Circle

7

In designing a linkage by the use of the centerpoint curve it is convenient to select the system positions in such a manner that advantage is taken of the possible simplifications shown above. This is achieved here with four congruent points on a straight line chosen in such a way that C_1, C_4 and C_2, C_3 are symmetrical relative to the perpendiculars, p to g. Then the poles P^{12}, P^{13}, P^{24}, P^{34} must lie on the lines of symmetry, c_{12}, c_{13}, c_{24}, c_{34}, which are, respectfully, also symmetrical to p. Poles P^{12}, P^{13} are arbitrarily chosen on c_{12}, c_{13}, and poles P^{24}, P^{34} are placed symmetrical to them, relative to p on c_{24}, c_{34}, respectfully.

The centerpoint curve for this pole configuration is line π_1, coinciding with p, and the circle π_2, through the four poles. The crank center A_0 is selected anywhere on π_1. The position A_1 of the moving pivot A is determined by the angle relations noted on Fig 2, p 42, and Fig 3, p 43.

A ray through P^{12} is drawn, making the angle $C_1P^{12}C_2 = \frac{1}{2}\phi_{12}$ with line $P^{12}A_0$, and another ray is drawn through P^{13}, making the angle $C_1P^{12}C_3 = \frac{1}{2}\phi_{13}$ with line $P^{13}A_0$. The intersection point of these two rays determines the position A_1 of the moving pivot A and the length of crank A_1A_0. Crank center B_0 is selected anywhere on the circle π_2, and B_1 is determined by an analogous method as was used to determine A_1.

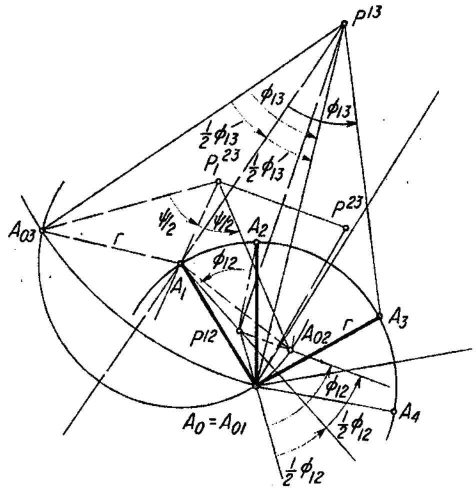

Relation Between Circle Point and Poles of Rotation

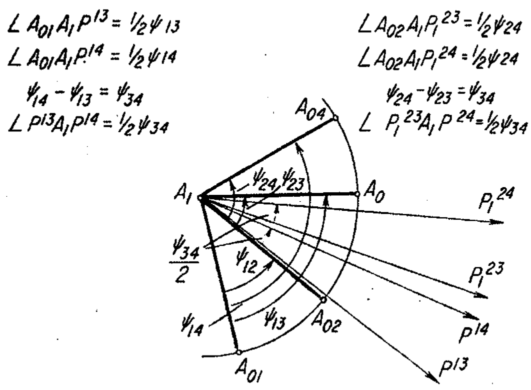

Four Coplanar Positions of a Plane System-Regulation between Circle Point and Poles of Rotation

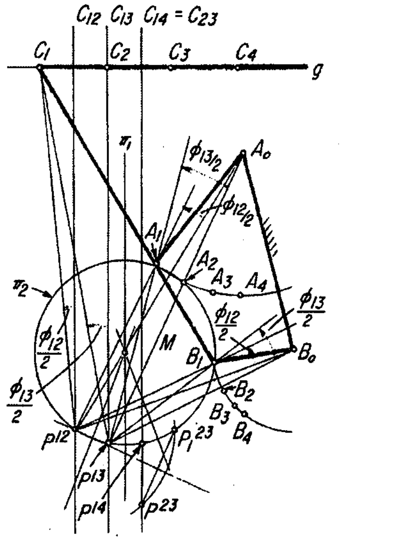

Construction of Linkage by Use of Circle Point Curve Consisting of Straight Line and Circle

9

To each point of the centerpoint curve which lies in the reference plane and is the locus of all possible fixed pivots of cranks capable of moving the plane system through four prescribed coplanar positions, there is a corresponding moving pivot in the moving plane to which the crank must be attached. The relation between these points, called circle points, and the poles is illustrated here. This relation can also be used for designing linkages for generating approximately straight line motions.

Consider the systems S rotated back about the poles P^{12}, P^{13}, P^{14} to starting position S_1 from three positions, S_2, S_3, S_4. Then the points which in these system positions coincide with the center point will also rotate about the poles and since their distance from the movable pivot remains unchanged, they must also lie on a circle with the movable pivot, the circle point, as center.

This figure shows three congruent positions, A_1, A_2, A_3, of movable point A which lie on a circle with radius r, and A_o, the centerpoint, as center. Poles P^{12}, P^{13}, P^{23} are assumed to lie anywhere on the bisectors of the angles $A_1A_oA_2$, $A_1A_oA_3$, $A_2A_oA_3$. When system from position S_2 is rotated about P^{12} back into position, S_1 (held fixed in the reference plane), the point which in system position, S_2, coincides with A_o ($=A_{o1}$) will go into position A_{o2}, which is symmetrical to A_o relative to the line A_1P^{12}. When system from position S_3 is rotated back about pole P^{13}, so as also to come into coincidence with S_1, the point which in system S_3 coincided with A_o comes into position A_{o3}, which is symmetrical to A_o with respect to the line A_1P^{13}. Both points, A_{o2} and A_{o3}, lie on a circle with A_1 as center and r as radius. Pole P^{23}, through rotation about P^{12} and P^{13} respectively, goes into its congruent position P_1^{23}. Since the distance of point P_1^{23} from the points, A_{o2} and A_{o3}, is equal to distance $P^{23}A_o$, the congruent point P_1^{23}, of pole P^{23}, must lie on the line of symmetry through the points $A_{o2}A_{o3}$, which also passes through A_1.

10

The locus of all circle points is also a focal curve which can be constructed in an analogous manner as the centerpoint curve, except that different pole points must be used as shown here. This relationship is analogous to Fig 3, illustrating the relationship of centerpoint to poles of rotation.

11

The circle point curve can also be used for designing a linkage for generating an approximately straight-line coupler motion. Again, by proper selection of the poles of rotation it is possible to obtain a degenerated form of the focal curve to simplify construction. Four positions of a moving system are chosen so that four congruent points of the system lie on a straight line, and their distances, C_1C_2, C_2C_3, and C_3C_4 are equal. In this case, pole P^{12} must lie on the line of symmetry c_{12} of C_1C_2; pole P^{13} on the line of symmetry c_{13} of C_1C_3 and passing through C_2, and both P^{14}, P^{23} on the line of symmetry $c_{14} = c_{23}$. For the circle point curve to degenerate into a circle and straight line (as in Fig. 5), P^{12}, P_1^{23} and P^{13}, P^{14}, respectively, must be symmetrical to a straight line. This line must be the line of symmetry π_1 of the lines c_{13},c_{14}, on which the poles P^{13}, P^{14}, respectively, lie. Therefore, P^{12} and P_1^{23} must also be symmetrical to line $P^{12}P^{13}$. If P^{12} is arbitrarily chosen on c_{12}, P_1^{23} is located symmetrical to P^{12} relative to line π_1. P^{23} is found on c_{23} by making the distance $P^{12}P^{23}$ equal to $P^{12}P_1^{23}$. Then P^{13} is determined as the point of intersection of the line of symmetry of $P^{23}P_1^{23}$ with line c_{13}, and P^{14} is the point on c_{14} which is symmetrical to p^{13} with respect to π_1. The line π_1 and the circle π_2 through $P^{12}P^{13}P^{14}P_1^{23}$ whose center, M, must also lie on π_1 are the two branches of the circle point curve of system position, $C_1A_1B_1$. The points A_1 and B_1 are chosen on π_2 so that they lie on a straight line passing through the tracer point C_1. The fixed crank centers A_o and B_o are found by considerations analogous to Fig 2, p 42. A ray is drawn through P^{12} which makes angle $\phi_{12}/2$ with A_1P^{12}. Another ray is drawn through P^{13} which makes angle $\phi_{13}/2$ with A_1P^{13}. Crank center A_o is the point of intersection of these two rays. Crank center B_o is determined in an analogous manner.

By proper selection of the positions of the poles of rotation, the circle point and centerpoint curves described above offer the simplest means for the application of Burmester's method to design of four-bar linkages.

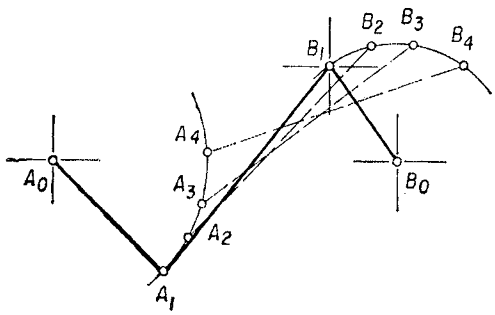

Method D

Burmester's Method for Determining, in a Given Linkage, a Coupler Point Which Performs an Approximately Straight-Line Motion

Approach to solution: four positions of a four-bar linkage (A_1B_1—A_4B_4) are chosen; the properties of the pole triangle and of the circle point curves of points at infinity of the coupler are used.

The path of the tracer point obtained has four precision points.

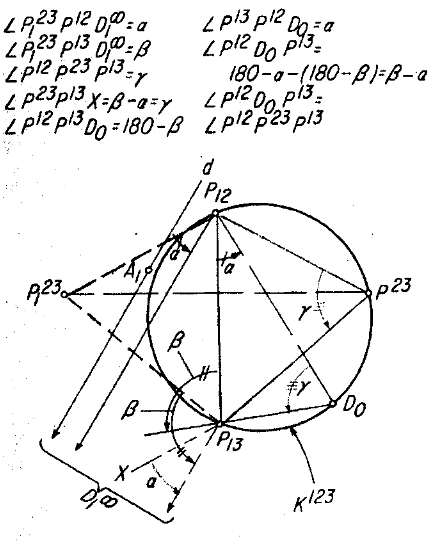

Three coplanar positions of a plane system—location of the center points of system points at infinity.

a

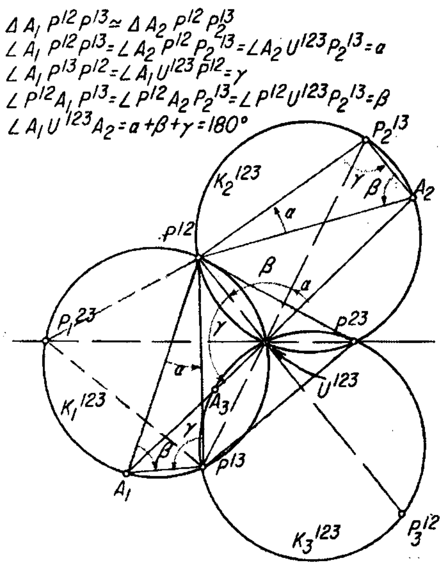

Three coplanar positions of a plane system—location of three congruent points, relative to the pole triangle, lying on a straight line.

b

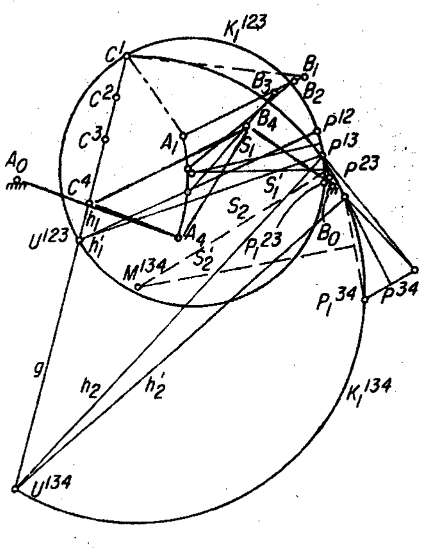

Four coplanar positions of a plane system—location of four congruent points lying on a straight line.

c

Since there are an infinite number of linkages capable of moving a system through four given positions in such a manner that four congruent points of the system lie on a straight line, it is possible to reverse the problem. That is, find a coupler point in a given linkage such that its four congruent positions line on a straight line. In the method developed by Burmester for solving this problem the angle relations of Fig 2, on p 42, are applied. The straight line is considered a circle with infinitely faraway center point.

If point A_1 in the system S_1—see (a) above—moves along a straight line d to infinity, then the rays $P^{12}D_1$, $P^{13}D_1$ through the infinitely faraway point D_1 at infinity become parallel. The center point D_o associated with D_1 is constructed as in Method C, Fig 2, p 42, by making angle $P_1^{23}P^{12}D_1$ = angle $P^{13}P^{12}D_o$, and angle $P_1^{23}P^{13}D_1$ = angle $P^{12}P^{13}D_o$. If this procedure is applied to all infinitely faraway points of system S_1, S_2, S_3, it is evident that all center points associated with the points at infinity of the moving system lie on the circle k^{123} through $P^{12}P^{13}P^{23}$ in the reference plane.

Conversely, by the previously established to the relationship between circle point and centerpoint, the circle points associated with the center points at infinity, of the reference plane, must lie on the circles —see (b) above—k_1^{123} through $P^{12}P^{13}P_1^{23}$ in system S_1; k_2^{123} through $P^{12}P^{23}P_2^{13}$ in system S_2; k_3^{123} through $P^{13}P^{23}P_3^{12}$ in system S_3. If three congruent points, $A_1A_2A_3$, of the system lie on these circles, their centerpoint must be at infinity and the three points must therefore lie on a straight line. If two of these circles k_1^{123}, k_2^{123}, their intersection point U^{123}, and the triangles $A_1P^{12}P^{13}$, $A_2P_2^{13}P^{12}$, are considered, it is noted that the sum of the angle $A_1U^{123}P^{12}$ and $A_2U^{123}P^{12}$ is 180°, and that the straight line A_1A_2 must pass through point U^{123}. From these geometric relations it must be concluded that three circles intersect at U^{123} and that a straight line carrying three concruent points A_1, A_2, A_3 must pass through this point.

Now if four coplanar positions—see (c) —of the systems S_1, S_2, S_3, S_4, are given, the pole triangles P^{12} P^{13} P_1^{23} and P^{14} P^{24} P_1^{34} for S_1 S_2 S_3, and S_1, S_3, S_4, are determined, together with their centers of height U^{123}, U^{134}. The line connecting these two centers of height is the only line which carries four congruent positions of a point of the system. The position point, C_1, of the tracer point of the coupler is determined as the intersection point of the line U^{123}, U^{134} with the circle k_1^{123}. Center M^{123} and circle k_1^{134} center M^{134}. The linkage with the coupler point at C_4 is shown at position S_4.

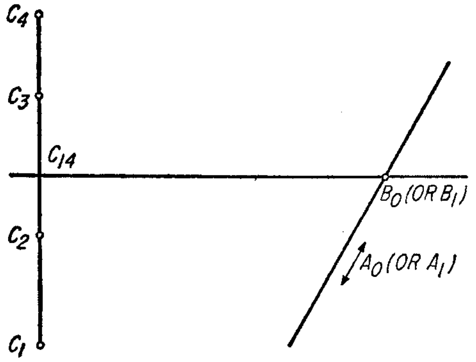

Method E

Synthesis of the Linkage by Point Position Reduction

Approach to solution (in the simplest form): four positions (C_1-C_4) of a coupler point lying on a straight line are chosen. The position of one fixed crank pivot B_o or one position of pivot B_1 is selected on the bisector of two coupler point positions; the other pivots are determined by considering motion of selected pivot relative to coupler.

In the linkage obtained, the path of the tracer point has up to six precision points.

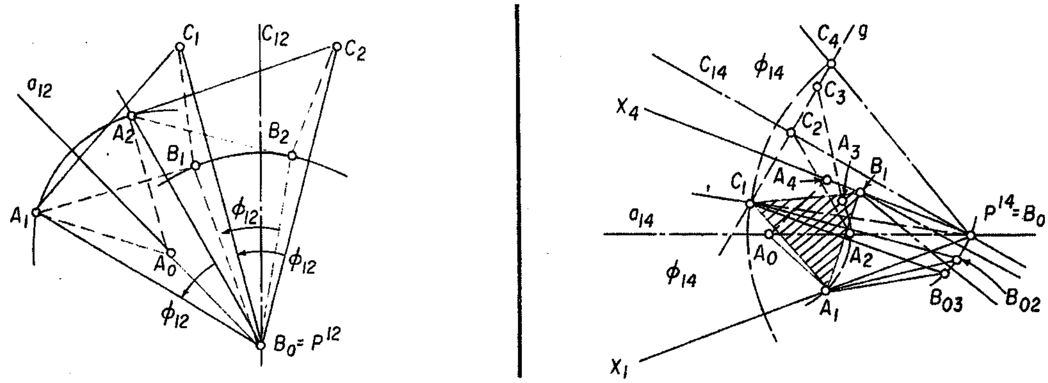

a Method of point position reduction – one pole coinciding with fixed crank pivot, four precision points b

1 This method, developed by Kurt Hain of the West German Federal Research Institute of Agriculture, is based on selecting the poles of rotation of the moving system in such a manner that one of them coincides with either the fixed or the moving pivot of the crank. Through this choice of one pole of rotation, relatively simple graphical solutions are possible and up to six precision points can be obtained.

This principle is illustrated in (a) above, where A_1C_1 and A_2C_2 are two positions of the line connecting the moving pivot A with the tracer point C. The fixed pivot A_o must lie on the bisector a_{12} of A_1 and A_2; the pole P^{12} must lie on the intersection of a_{12} and the bisector c_{12} of C_1 and C_2. The fixed pivot B_o is selected so as to coincide with P^{12}; consequently, A_oB_o lies on a_{12}. Positions B_1 and B_2 of the second movable pivot must lie on a circle with B_o as center. Triangles $A_1B_1C_1$ and $A_2B_2C_2$ must be congruent.

The application of the method is shown in (b) above for four points of coincidence, C_1 to C_4, with the straight line g of the path of tracer point C of the coupler. The pole P^{14} is selected anywhere on the bisector c_{14}, of the points C_1, C_4 and is assumed to coincide with the crank center B_o; then P^{14} must also lie on the bisector a_{14} of the yet unknown positions A_1, A_4 of the moving pivot A, which must also pass through the fixed pivot A_o of the second crank.

Furthermore, angle $A_1P^{14}A_4$ must be equal to angle $C_1P^{14}C_4$ ($= \phi_{14}$), and distance A_1C_1 must be equal to A_4C_4. If two rays—X_1B_o, X_4B_o—are drawn to make angle ϕ_{14}, and an arc of any radius is drawn with B_o as center, the intersection points A_1, A_4 of the arc with the rays will fulfill this requirement (triangles $A_1C_1B_o$ and $A_4C_4B_o$ being congruent) and also determine the distance AC. The crank positions, A_1 to A_4, must follow one another in the same sequence as the corresponding positions of point C if the path of the motion of point C between the four selected positions also must be approximately straight. To determine position of the moving pivot B, the circle point to B_o, a relationship is considered which is analogous to that shown in Fig. 9, on p 45. Consider the motion of crank BB_o relative to A_1C_1, with the yet unknown point B_1 as fulcrum. In each of the system positions A_2C_2, A_3C_3, there is a point which coincides with B_o. If A_2C_2, A_3C_3, are rotated so as to come into coincidence with A_1C_1 these points will assume the positions B_{o2}, B_{o3}; these points are determined by making triangle $A_1C_1B_{o2}$ congruent to triangle, $A_2C_2B_o$, and triangle $A_1C_1B_{o3}$ congruent to triangle $A_3C_3B_o$. In these rotations the distances of B_{o2} and B_{o3} from B_1 remain equal to BB_o. This means that B_o must lie on a circle with B_1 as center. B_1 is then found as intersection of B_oB_{o2}, B_1 is then found as intersection of $B_{o2}B_{o3}$, $B_{o2}B_{o3}$, respectively.

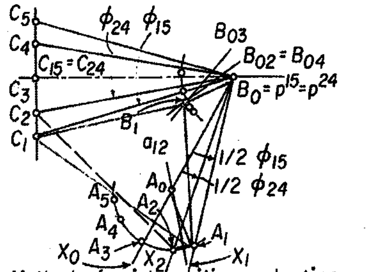

Method of point position reduction – two poles coincide with fixed crank pivot, five precision points.

2

Since both radius and position of the fixed pivots of the second crank were arbitrarily chosen, this method can be expanded to the synthesis of linkages with five precision points. The five points shown are chosen symmetrical to point C_3 so that the lines c_{15}, c_{24} coincide with the normal through C_3 to line g. Both poles, P^{15} and P^{24}, which must lie on this line, are assumed to coincide with B_o. A ray B_oX_o is drawn on which the yet unknown second crank center A_o is assumed to lie. The balance of the construction is analogous to Fig 1 (b) above.

Four-Bar Linkage Proportions

Given two points, a function of the length of stroke you want, this handy chart quickly and accurately locates the other two. You find the proportions of all four-bars without cumbersome mathematical or graphical methods.

Preben W. Jensen

Proportions of 4-bar linkages for straight-line motions are usually determined by graphical methods. Then, the precision points in the required straight line are checked by mathematical methods, where necessary. But graphical methods, although simpler than a purely mathematical solution, can be quite complicated. The late Dr Kurt Rauh, professor of kinematics at the Technical Institute, Aachen, Germany, conceived the chart shown on next page, which simplifies graphical determination.

The chart is based on two circles, one having twice the diameter of the other. The smaller, called the Cardan circle, rotates inside the larger one; at the same time the center of the Cardan circle serves as a hub around which all of the space on the chart radiates.

Fig 2, p 79, shows the behavior of typical points on the chart during this rotation. The center, M, of the Cardan circle, describes a circular path around center, W, of the large circle; all points on the circumference of the Cardan circle describe straight-line paths at different angles through W. All other points, whether inside or outside the Cardan circle, describe elliptical paths.

The diagram shows the elliptical paths of two arbitrary points, E_1 and E_2. Portions of these elliptical paths have been replaced by circular arcs, and the centers of curvature, K_1 and K_2, found. Note that these centers are on an extension of the lines PE_1 and PE_2, where P is the common pole of the two circles.

If E_1K_1 and E_2K_2 are taken as two links in a 4-bar linkage with K_1 and K_2 as stationary points, points E_1 and E_2 will be the coupler points describing circular arcs which, within a certain range, approximate the elliptical paths.

If these coupler points are connected to W on the circumference of the Cardan circle, this point will describe the desired straight line as long as points E_1 and E_2 move on those parts of the circular arcs that

1 . . PROPORTIONS OF 4-BAR LINKAGES are determined with this special chart—made up of two separate systems. One finds coupler points; other finds stationary points. For coupler points, read figures from circles and rays. For stationary points, read figures from ovals and curved rays.

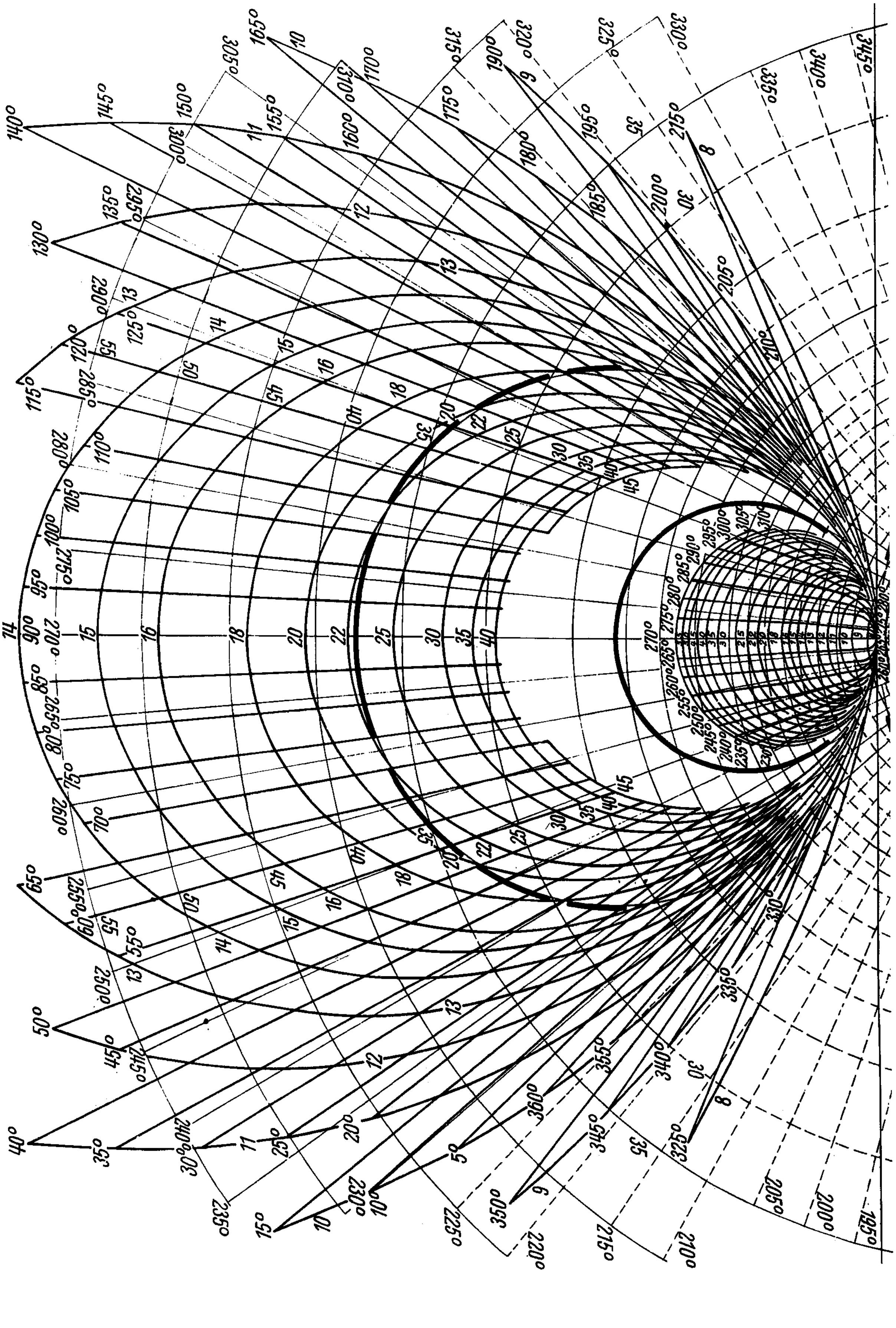

For coupler points, turn this way

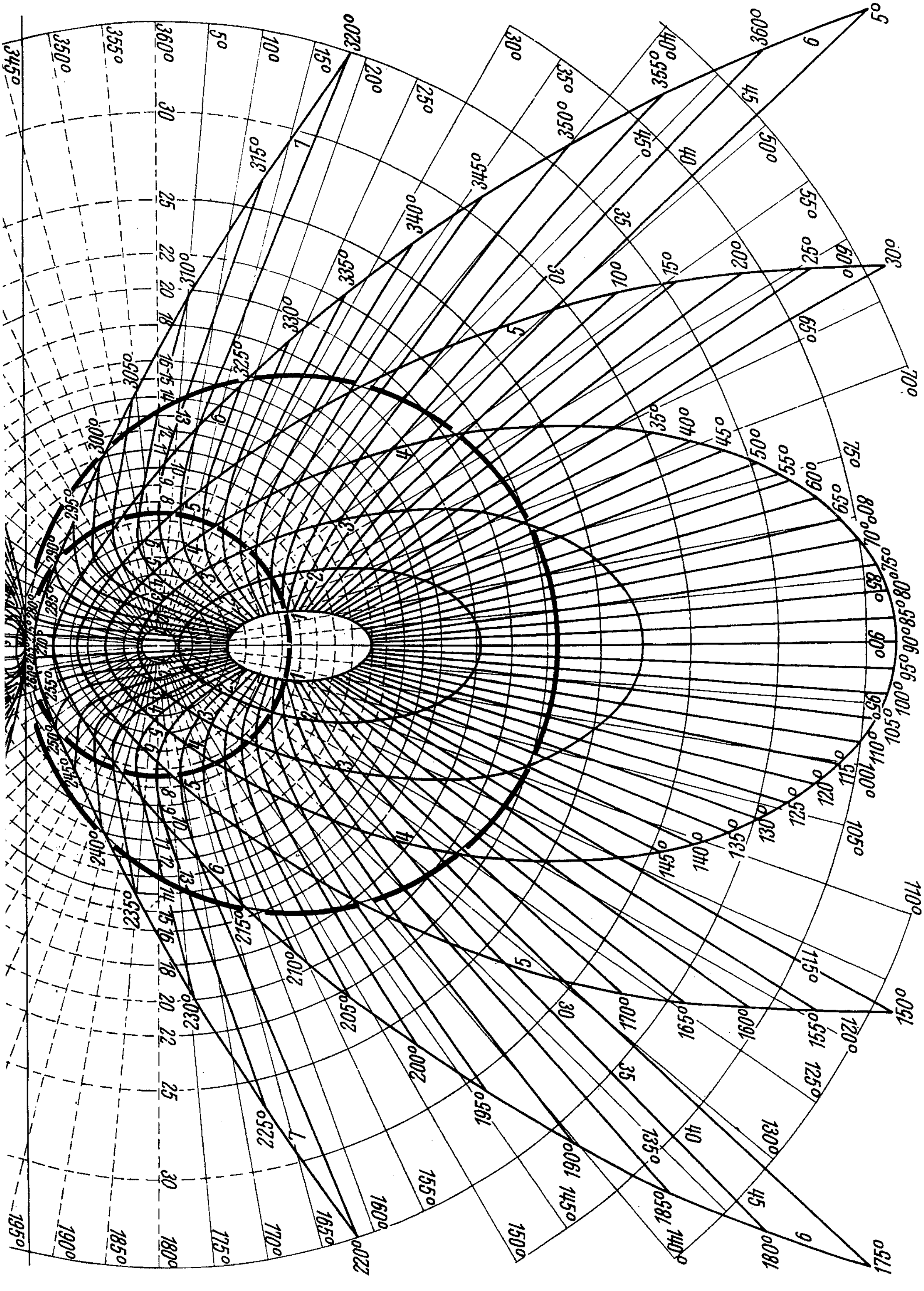

For stationary points, turn this way

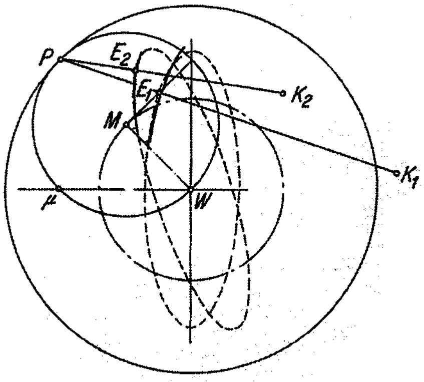

2 . . **PATHS OF TYPICAL POINTS** during rotation of Cardan circle. Here, circular arcs have been drawn replacing parts of the elliptical paths of E_1 and E_2. K_1 and K_2 are centers of curvature of these arcs.

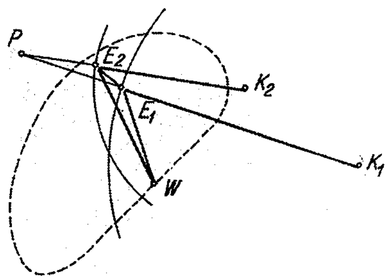

3 . . **ACTUAL LINKAGE** determined in Fig 2 causes point W to describe the desired straight-line path during part of its complete path which is shown by dotted line.

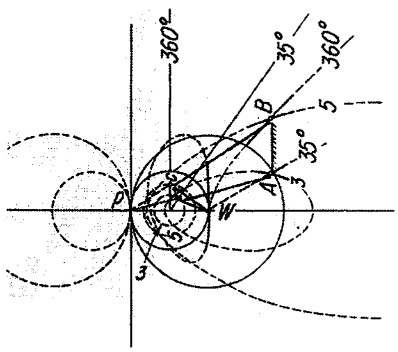

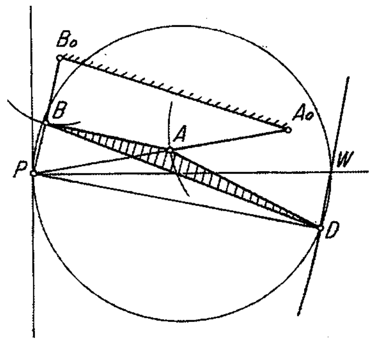

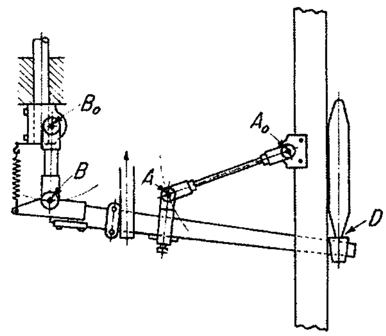

4 . . **POINTS FOUND** from special chart produce desired straight-line motion. Points A and B are arbitrary; points D and C determined from chart.

5 & 6 . . **WEAVING MECHANISM** (right) is designed to fit points (left) determined by the chart. A_0 and B_0 are chosen to give required length of travel for point D; A and B are found from chart. Note that D travels at slight angle from vertical.

closely approximate the elliptical paths they replace. The complete path described by coupler point W is shown dotted in Fig 3 together with the 4-bar linkage that produces it. This linkage results from the arbitrary selection of points E_1 and E_2 and the development of centers K_1 and K_2 from the chart.

How the Chart Works

The chart has been constructed so that you can find the coupler points corresponding to two given stationary points (centers of curvature) or vice versa. Here is how:

Concentric with the Cardan circle is a system of circles that are divided by rays at 5° intervals. The intersections represent possible coupler points. A companion system of ovals, divided by curved rays at 5° intervals, represents the possible fixed points (centers of curvature). To use the chart, start with whichever pair of points, coupler or fixed, are predetermined. Then locate these points in the appropriate system; the corresponding points will be located at the same-numbered intersections in the other system. When the coupler points thus determined are connected to a point on the Cardan circle, this point will produce straight-line motion through point W.

Solving a Sample Problem

In Fig 4, straight-line motion is desired at point W. Stationary points A and B are selected as shown. A falls on the intersections of oval 3 and curved ray 35°; thus corresponding coupler point D is at the intersection of circle 3 and ray 35°. Similarly, B falls at intersection of oval 5 and curved ray 360°; its coupler point, C, at intersection of circle 5 and ray 360°.

Coupler points D and C are connected to W on the circumference of the Cardan circle, which will then describe the desired straight line as shown. The best approximation of a straight line is obtained when the coupler points are connected to W or points near it. The straight-line portion of the path described by W is in a vertical direction. When C and D are connected to other points on the Cardan circle, the straight-line portion will go through W at an angle to the vertical, depending upon distance of the chosen point

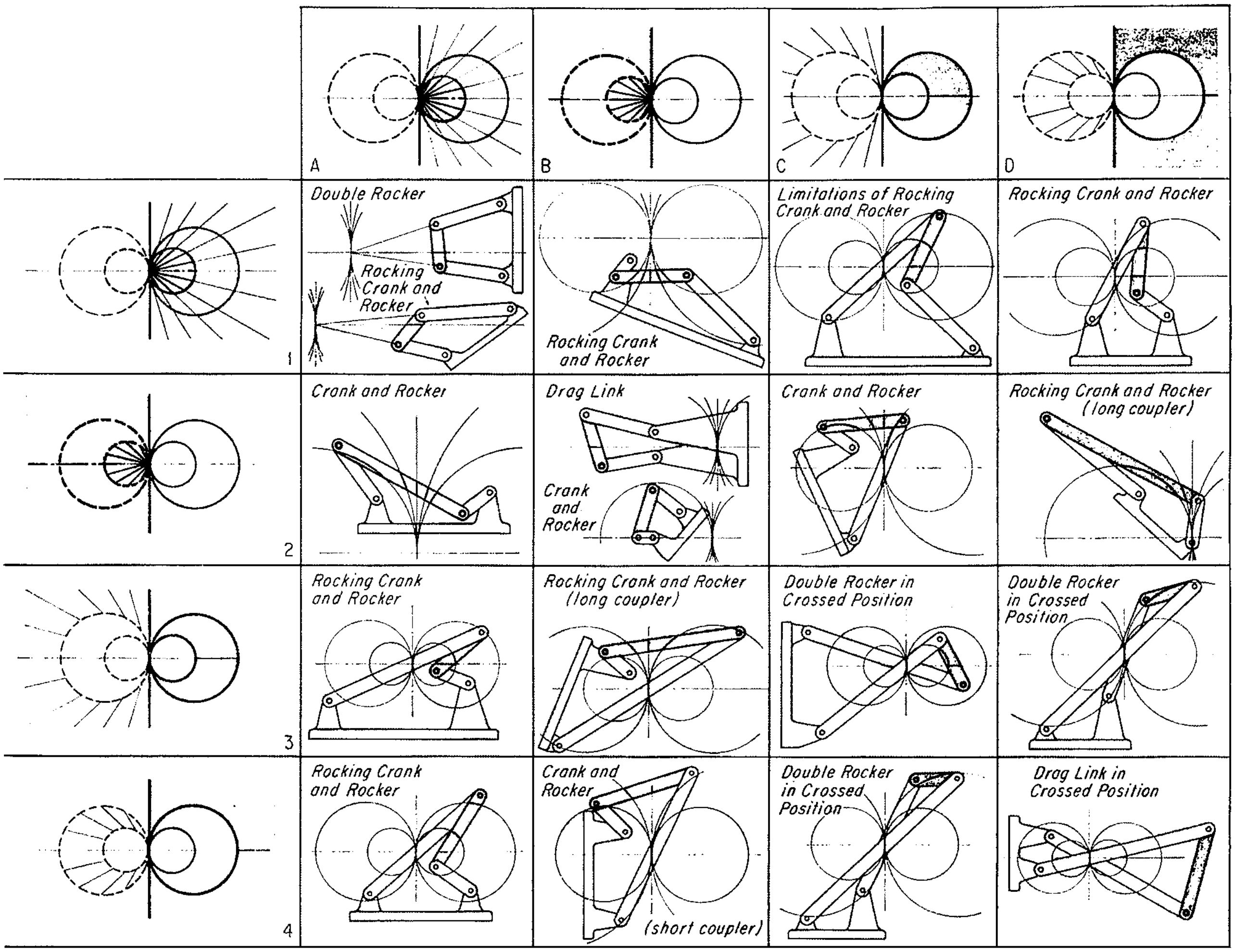

7 . . **A VARIETY OF MECHANISMS** can be produced by choosing points from different parts of the chart. In each case, colored coupler is produced when one point is taken from colored area in first column and other from colored area in top row.

from W. Thus any desired direction of travel is possible in theory. However, there is this limitation: the further the chosen point is from W, the less accurate the approximation of straight-line motion.

This effect is more clearly shown in Fig 5, which gives another 4-bar linkage proportioned from the chart. In this case points A_0 and B_0 are centers of curvature for coupler points A and B, which are connected to tracer point D. A_0 and B_0 are predetermined points on the machine; A and B are found from the chart.

The straight-line portion of the coupler path described by point D goes through W at an angle as shown. A typical application of this 4-bar linkage is the weaving mechanism (Fig 6), used in the textile industry. Proportions for this mechanism are determined from the sample 4-bar linkage determined in Fig 5.

Wide Variety Possible

Coupler points for a 4-bar linkage can fall anywhere on the chart, depending upon the type of mechanism required. Fig 7 shows diagrammatically the wide variety of mechanisms that may be determined from the chart The relation of the coupler points to their corresponding centers of rotation to the Cardan circle determines the type of mechanism. For example, if both coupler points fall within the Cardan circle on the right-hand side of the chart, the type of mechanism will be 1A. On the other hand, if both coupler points fall on the left-hand side of the chart, the type of mechanism will be 2B. However, any combination of these is possible, as can be seen from the diagrams.

SECTION 24

FABRICATION TIPS

Design of Screw-Machine Products

If designers of screw machine products will follow practical 'standards' for certain features, they won't affect function but will save plenty.

S. A. Cappon & Herbert A. Eichstaedt

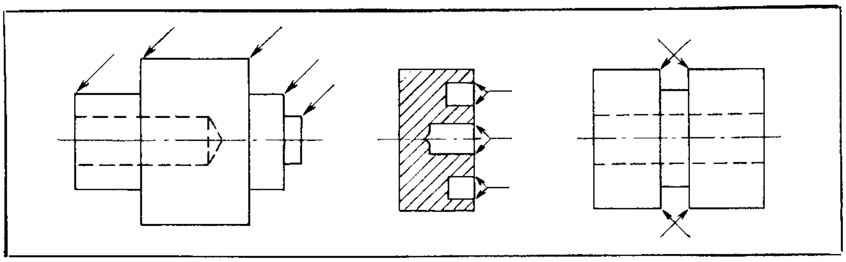

Fig. 1. Corners should be dimensioned as liberally as possible. A practical drawing note is: "break corners 0.010 in. by 45°"

There are several aspects of drafting practice that need special attention when screw-machine products are involved. These details are often neglected, or the parts designer does not understand what is practical. From long association with such problems, we recommend the following "rules."

1. Sharp corners and corner breaks

External corners. Never specify "Sharp Corners." These do not exist. Corners must be dimensioned. (See sketches in Fig. 1.) A drawing note that is practical, economical, and permits easy machining at minimum cost is: "break corners 0.010 in. x 45°." If sharper corners are needed, specify them; for example, "0.002-in. R max." This is as close to a sharp corner as can be obtained. Remember that to achieve this optimum sharpness, considerable cost is incurred.

Breaking a corner as suggested ".010 in. x 45°" is sometimes expressed as "max. R allowed:" This is costlier than an actual chamfer, because it is necessary to blend the radius with a diameter or a face.

The sharp-corner condition in Fig. 2 A must also be dimensioned. Although an external feature, it is equivalent to an internal corner. A practical dimension is: "0.010 in. x 45°", or possibly "max. 0.010R".

Use an undercut if possible. Thus, a theoretically sharp corner is achieved. This feature is necessary when the smaller diameter must be ground and

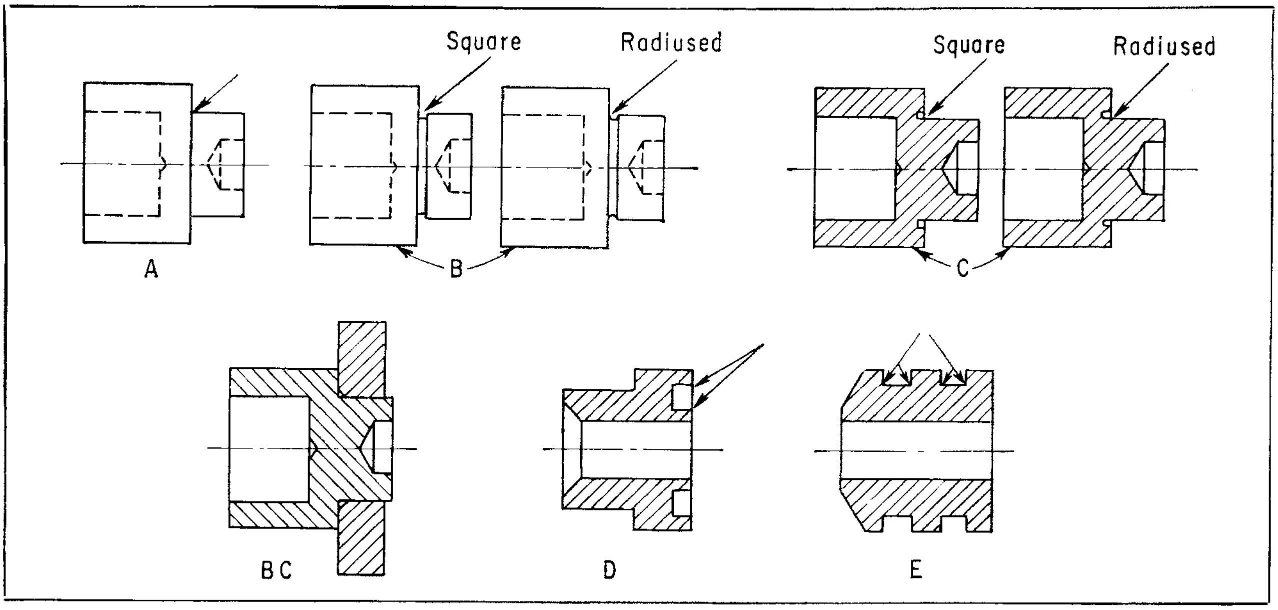

Fig. 2. Undercuts are often given a radius to avoid crack development in heat treatment

grinding relief is required, or a mating part must fit flush against the shoulder face. The relief shown in Fig. 2 B is easy to machine, because it can be established by a cut-off blade or flat tool bit from the cross-slide, which is easier than Fig. 2 C. Dimensioning of such an undercut for a minimum cost is: "0.062 in. wide x 0.015 in. deep."

A square-corner undercut, Fig. 2 B or Fig. 2 C, is sometimes changed to a radiused undercut, particularly if there is concern about crack development after the product undergoes heat treatment.

The condition in Fig. 2 D has only one solution. To achieve minimum cost, the dimensions for such a sharp corner should not be less than "0.008 in. x 45°," or 0.008 in. R. Anything smaller results in excessive tool sharpening and downtime.

In the cases shown in Figs. 2 B and 2 C, if there is an assembly problem with a mating part that has to be flush with the shoulder face, an internal chamfer on the mating part will overcome some of the problems.

Internal corners. Here again there's no such thing as a sharp corner. The most economical dimension for the sketches that are shown in Fig. 3 is not less than 0.010 in. x 45°.

The condition shown in Fig. 3 B can be resolved from an economical standpoint with a dimension not less than 0.010 in. x drill-point angle (standard 118° or special angle).

Further variations of this condition are shown in Fig. 3 C and 3 D. For an economical dimensioning 0.010 in. x 45° is recommended. To establish Fig. C 3, a recessing tool with the above corner break can easily be ground. For Fig. 3 D trepanning blades ground in the same manner will achieve these results (0.010 in. x 45°).

If a sharper corner is required for Fig. 3 C, a blade-type tool will be needed. Both the tool and a reamer will require frequent regrinding, but a 0.003 in. R can be obtained if necessary. Similarly, for Fig. 3 D blade-type tools and end-cutting counterbore-reamers can be used.

In the cases shown in Fig. 3 C and 3 D, a ½° to 2° angle is recommended for the sides of the recesses. This provides a natural tool relief at withdrawal.

If corner sharpness requirements are 0.005 in. or less in Fig. 4 A, use one of the alternatives, Fig. 4 D or Fig. 4 E. The dimensioning of such undercuts for practical and economical reasons should be "0.062 in. wide x 0.015 in. deep."

The radius-type undercut is more desirable and depends on what other operations are required on the part. However, the drawing should specify 0.062 in. wide x 0.015 in. deep and allow optional selection of a square corner or a radius relief.

The conditions shown so far should not be considered as "undercuts." They are merely "reliefs" to satisfy "sharp corner" situations. Although like undercuts in nature, they are not true undercuts.

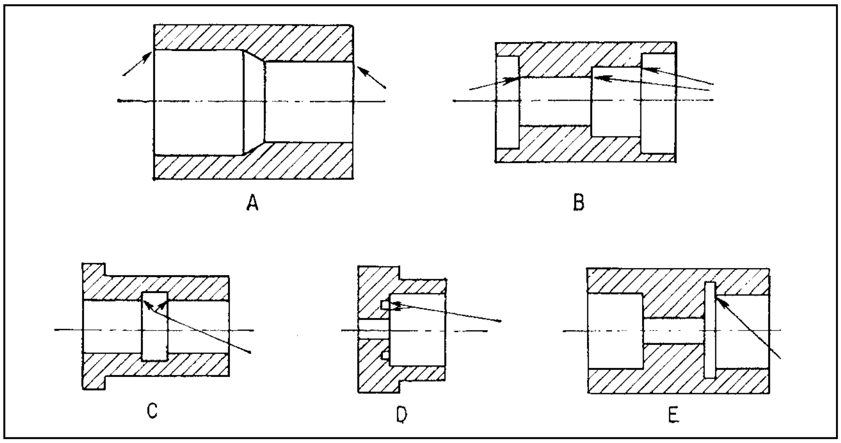

Fig. 3. Internal corners should be dimensioned "0.010 in. by 45°." In examples C, D and E, a side wall angle in the recesses of ½ to 2° is helpful for tool clearance. The same applies to Fig. 4 B and C

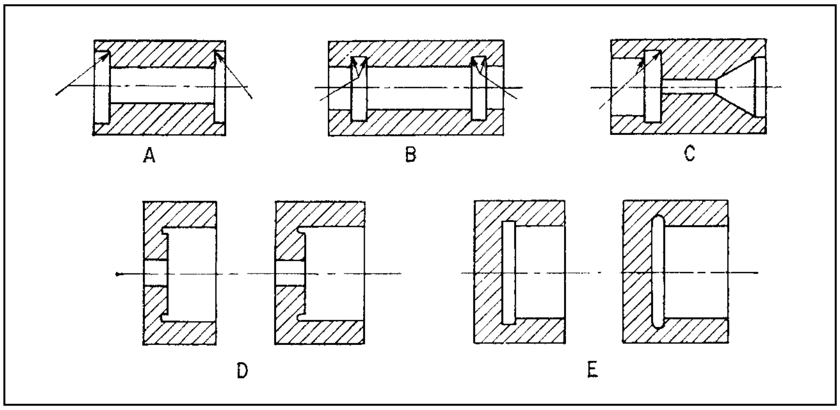

Fig. 4. Corners may be dimensioned as an 0.010 in. fillet or radius, or 0.010 in. x 45°. Radius under cuts, examples D and E, are preferable to those with a square corner

Design of Screw-Machine Products (continued)

Our previous installment showed you how to dimension corner breaks for practical production. Now, we give you similar 'standard practices' for burrs of various kinds.

S. A. Cappon & Herbert A. Eichstaedt

Rules for screw-machine part design

- Cut threads can't be machined closer than 2 threads from a shoulder.
- Deep blind holes (tapped) require space for chips.
- Specify cut off burrs. Don't say "Small cut off burr permitted."
- Design product so standard bars, shapers, and tolerances can be used.
- Investigate pre-shaped forms.
- Use standard threads and holes. Avoid special tooling expenses.
- Extra close tolerances are expensive. Diameters are held closer than lengths.
- Specify materials with maximum machinability characteristics.
- Specify corner breaks and radii.

2. Burrs

Through proper tooling, burrs can be minimized or eliminated. Certainly it is necessary to apply "standards" regarding burrs that will result in the most economical method of producing the screw product.

To understand the problem better, we should first know something about the kinds of burrs produced, and their nature. We can consider a burr, except the external cut-off type, to be nothing more than displaced (and deposited) metal, or metal not removed by the tool during the cutting process.

Cut-off burrs

External burrs. If an external cut-off burr is permitted, the drawing should specify it. If the size of the burr must be limited, then indicate the dimension as shown at A, Fig. 5.

If burr is allowed on the OD but a size cannot be given, at least the direction should be indicated, as shown at B, Fig. 5.

When hexagonal stock is used, a burr is generated during the forming process, but removal of this burr is expensive. To minimize the burr and even to eliminate it in some cases, provide a chamfer on each side of the part section that retains the original stock shape (square, hexagon, etc.). See Fig. 5 C. Also, indicate specifically whether these burrs are allowed or not.

Generally speaking, to avoid generating external burrs it is necessary to provide chamfers or radiuses whenever you have intersecting surfaces.

Internal burrs. Such defects are generated when cutting off into a hole. As shown in A, Fig. 6, a burr will always be generated at the point shown. This defect is detrimental if the part must slide over a mating part. Also, gaging will be difficult.

If permitted from a functional standpoint, allow a generous chamfer as at B, Fig. 6. This feature can be established through a recessing operation before the part is cut off. In such cases a burr will be generated but it cannot be detrimental to assembly or gaging. And if this is the case, specify on the drawing that a burr is allowed.

Another application of the above idea occurs when the part must be cut off into a tapped

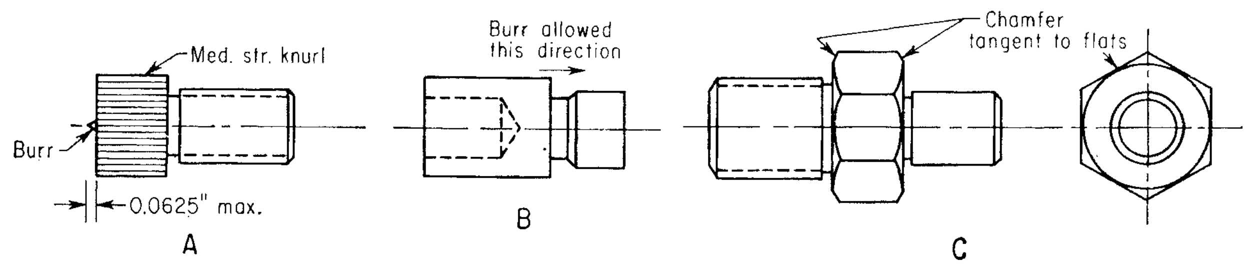

Fig. 5. External burrs should be dimensioned, as at A, controlled in direction as at B, or removed by chamfering

hole. In addition to a chamfer for relocation of an acceptable burr, it is also important to allow for an ample recess for chip accumulation.

Intersecting surfaces 1, as at Fig. 6 C, will generate burrs. If such burrs are permitted, define them accurately on the drawing. Also clarify the permitted direction of the burr. Such instructions facilitate the method of production. Or, if permissible, avoid square shoulders on points 1.

Secondary operations like cross drilling, milling, tapping, etc. produce heavy burrs. Fig. 7 A shows a typical case.

If a slot is milled, Fig. 7 B, and a burr is permitted on the OD, that fact should be specified. Then the shop will produce the part with either a cutter rotating towards the outside, or will try to have a milling cutter travel from the center of the part to the outside (if a radius is not allowed on the bottom of the slot).

If a burr is not allowed on the OD or only a very small one, and none on the inside, offer an optional V-groove at the bottom of the slot, Fig. 7 C. This groove permits accumulation of a burr, while maintaining a clean OD, avoiding another operation.

In fact, there are some special cases. For example:

1. Avoid performing any operation on a threaded area. In designing a part, this can sometimes be avoided. See Fig. 7 D.

2. In broaching a blind hole, heavy burrs are generated. Provide enough depth for the hole prior to broaching. Otherwise, production of the part will involve excessive tool cost. ■

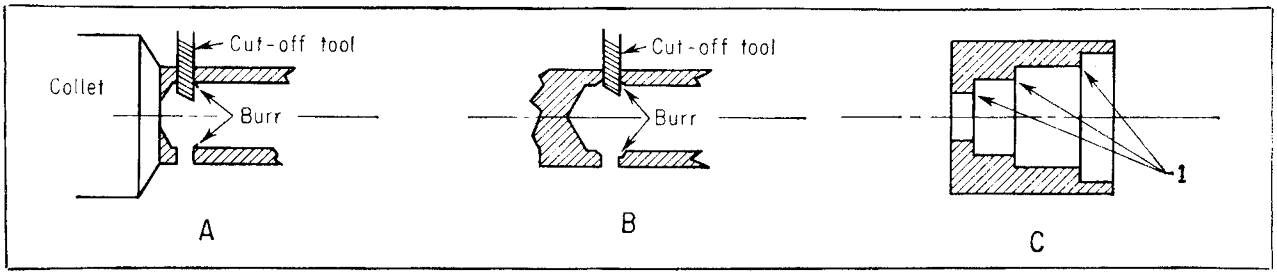

Fig. 6. Internal burrs can be minimized by forethought to such matters as tool shape or providing recesses or radii

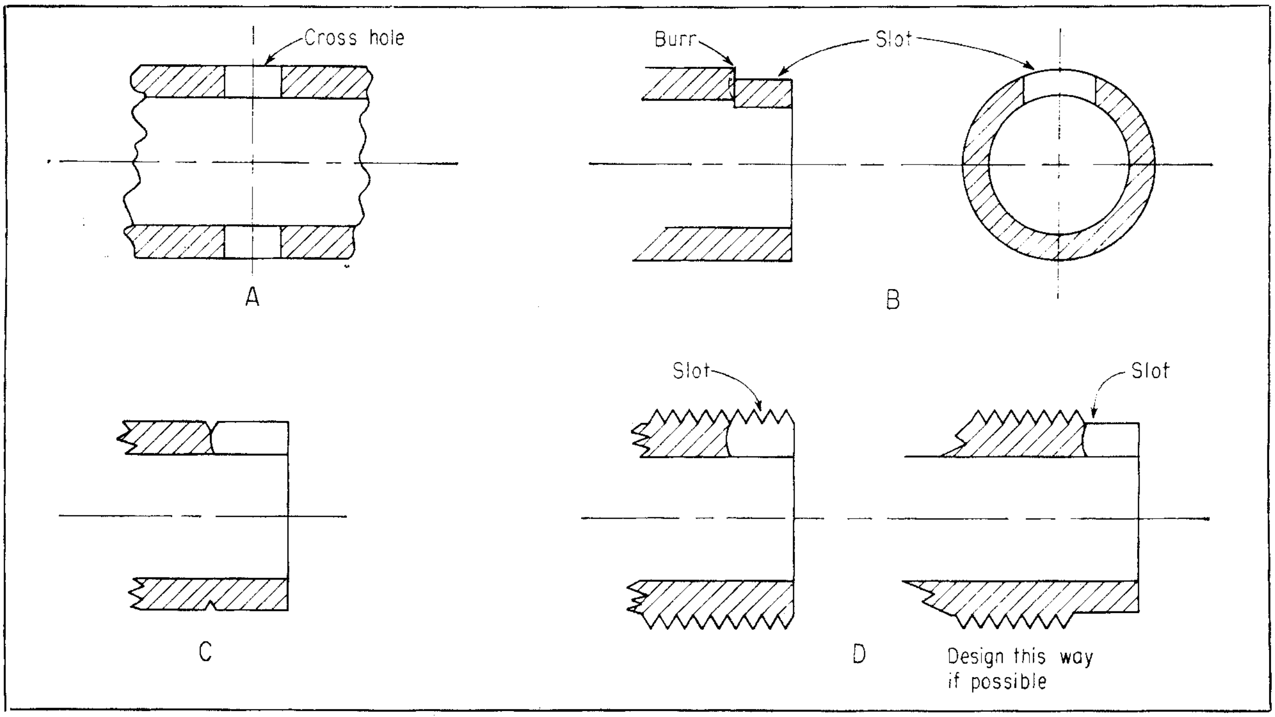

Fig. 7. Slots and crossholes can produce heavy unwanted burrs. A groove as at C or a turned down section as at D will avoid burrs that interfere with assembly

Design of Screw-Machine Products (continued)

The previous installment showed you how to handle burrs for various parts. Here we give you practical information on another area important to cost reduction.

S. A. Cappon & Herbert A. Eichstaedt

4. Dimensioning and finish

In addition to the standards established by large companies and associations, there are a few points that need emphasis:

(a) In dimensioning a screw product be guided by the probable gaging problems. As a rule, if the part can be easily gaged, it can also be easily manufactured.

(b) Use decimal dimensions. Standardize the block reference for tolerances as follows:

Two decimals	±0.010 in.
Three decimals	±0.005 in.
Angle dim.	±1°
Finish spec.	125 mu-in. RMS

Unless otherwise specified

(c) 'Unless otherwise specified'. Call out closer tolerances only when absolutely necessary. The most economical way is to complete the part in one operation. In this case, normal inside and outside operations can qualify the part to ±0.002 in. on diameters, but not recesses or total length. Any closer limits may require second operations, and this could make the cost of the product excessive.

Surface finish should be realistically related to function. If the finish specified is 125 microinches RMS, the screw-products manufacturer must tool up for 63 microinches RMS (or one-half the spec). Also think in terms of gaging the part or checking the finish. Sketch A in Fig. 8 shows an impossible condition, both internally and externally.

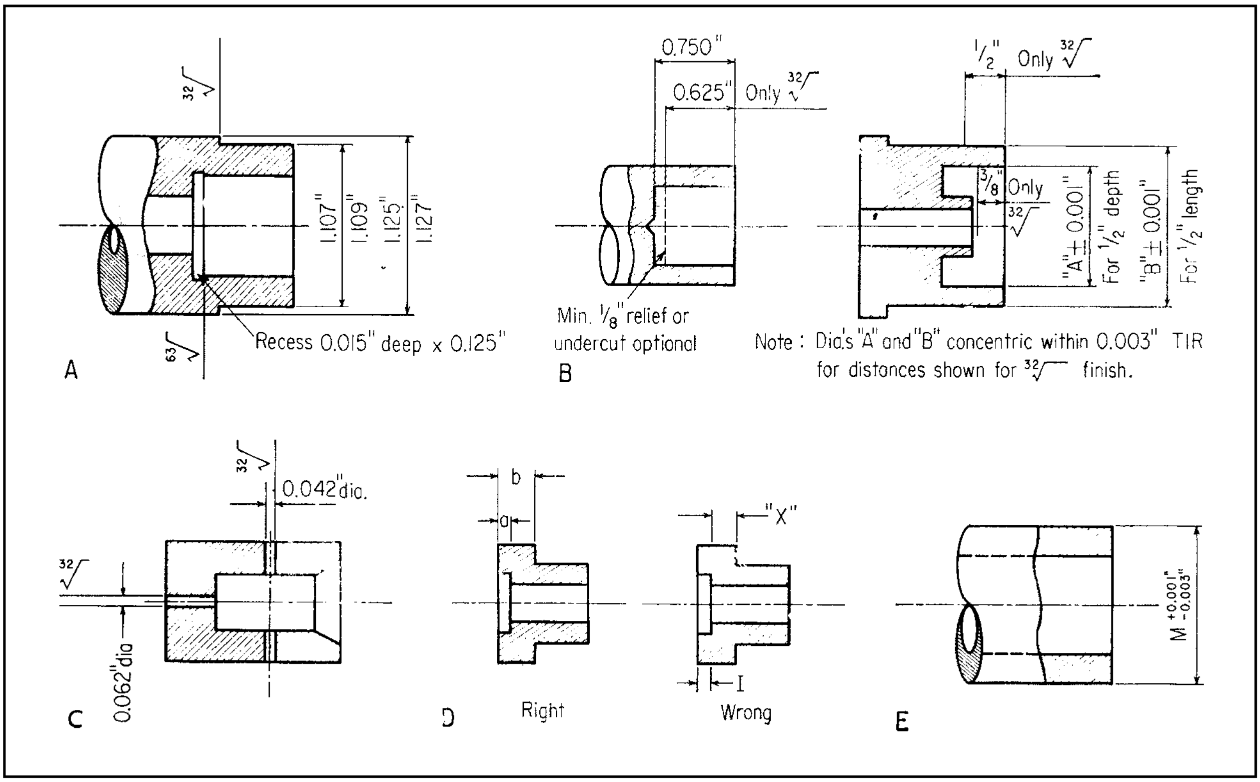

Fig. 8. Dimensioning is important to production of desired finish and ability to gage the part

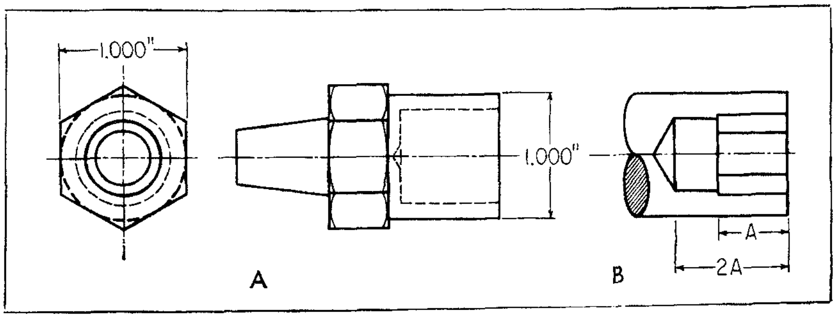

Fig. 10. The 1.000-in. dimension may not clean up to a cylinder. (left). Always allow sufficient chip clearance when broaching a hole

If a hole is blind, the specified finish cannot go all the way to the bottom. The first of the sketches at B, Fig. 8, shows a suitable specification. When special finish is required for a specific length, that length should be dimensioned. The same considerations apply to special close tolerances on diameter or concentricity.

Another situation difficult to measure and to produce is shown at C, Fig. 8. By sectioning a part one can measure the finish, but the result is not conclusive, nor is it accurate, for all parts in a batch or run.

(d) 'Special situations'. These should be avoided. In most cases, dimensioning can be done so that internal features are not tied together. Sketches at D, Fig. 8 show the right and wrong ways. By proper balancing of limits for dimensions *a* and *b*, one can determine what is required for dimension *X*.

Sometimes close limits must be held in one direction but not in the other (See Sketch E, Fig. 8). On the plus side only 0.001 in. from the nominal can be used, but on the minus side one can take advantage of 0.003 in. This is important, for it more or less indicates the functional aspect of dimension M.

If the part is to be plated or heat treated, or both, then the dimensions that are specified must be identified. The best method of dimensioning is to show dimensions "before" and "after."

In the case of a tapered part (Fig. 9), one of the circled dimensions must be omitted. For ease in gaging, it is preferable to leave out angle V. Otherwise, be guided by functional aspects.

(e) Concentricity between various diameters (internal and external) can be expected within 0.004 in. TIR, except when it relates to stock diameter. Closer limits can be obtained if necessary.

The degree of concentricity, perpendicularity, and parallelism required of the part should be amply described as a note rather than by symbols.

(f) Miscellaneous. When a part is made from hex or any multilateral stock, beware of an outside diameter that must be equal to the distance between opposite flats (See Sketch A, Fig. 10). Because of stock tolerances between flats, this diameter may not come out as a continuous circle at all points.

A broached hexagonal hole is established by first drilling a hole of a specific depth. In the case of a blind hole, allow enough extra depth for chips or burrs (Sketch B, Fig. 10). As a rule of thumb, allow additional depth equal to the broached depth. The diameter of the drilled hole should leave only minimum stock.

Do not specify "no concavity or convexity allowed" on a drawing. Give a specific figure: "Concavity (or convexity) to be within 0.003 in.

Tool clearance

On internal or external surfaces, where a straight shoulder or face must be established, tool clearance is important, particularly at withdrawal. In such cases the external face or the sides of a recess should be dimensioned so that a ½ to 2° clearance angle is provided.

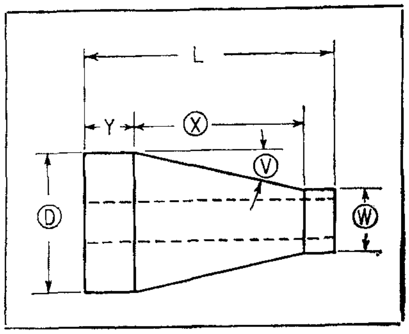

Fig. 9. Taper is customarily written as the difference between diameters divided by the distance between them, or 'total taper.' Taper can also be written as the angle measured from the centerline

This will achieve two things. First, the tool will have a natural clearance, so that at the end of its travel and at the moment of withdrawal it is completely relieved from the work. And toolmarks are avoided.

When long operations, like facing, cutoff, or deep-hole drilling, are required, indicate by notes whether steps are permitted. If steps will not interfere with the function of the part, mention the dimensions of the steps in the notes or put them on the print. A step of 0.005 in. is sometimes beneficial.

Design of Screw-Machine Products (continued)

To conclude the current series, the authors discuss the precautions that you should observe in relation to blind holes, undercuts, threads and material specifications.

S. A. Cappon & Herbert A. Eichstaedt

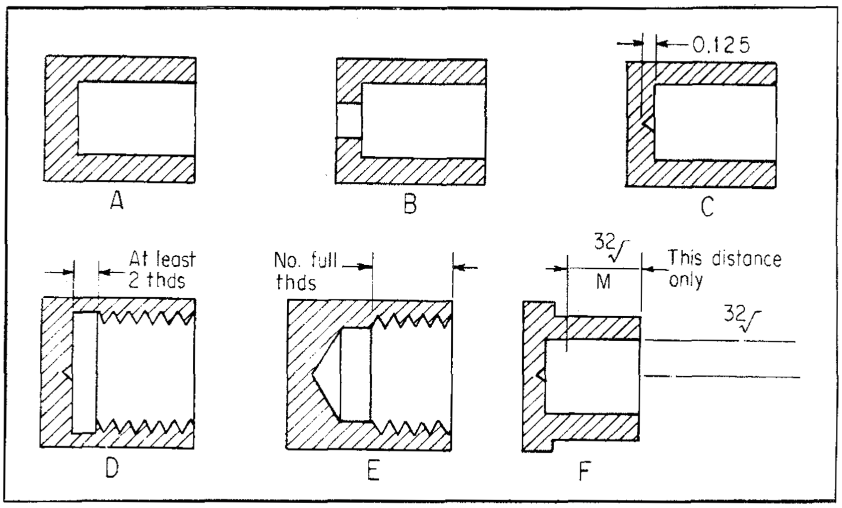

Fig. 11. Blind holes should allow a drill point, preferably at least 0.125 in. If the hole must be tapped a recess two threads wide minimizes important burrs. If a drilled hole is tapped, E, show the number of usable threads

5. Flat-bottom holes

Flat-bottom holes are of two kinds: (1) a plain flat-bottom blind hole, and (2) a 2-step hole with a squared corner on the bottom of larger hole, as shown at A and B, Fig. 11.

The conditions and suggestions regarding the corner itself have been discussed under "sharp corners." If possible, however, use an angle, preferably a standard drill-point.

For a plain flat-bottom blind hole, a drill point should be allowed as shown in sketch C, Fig. 11, preferably 0.125 in. deep.

Do not insist that the bottom of the hole be perpendicular to the hole wall. Also don't ask for excessively fine surface finish.

Limit tapping depth and surface-finish requirements to a set distance from the bottom of the hole. A recess solves this problem. If the hole is tapped the recess should be equivalent to two threads. See Sketch D, Fig. 11. But a recess is not the "final answer." Another solution is shown in Sketch E, Fig. 11, but here the distance to the bottom of the hole should be 2½ threads at least.

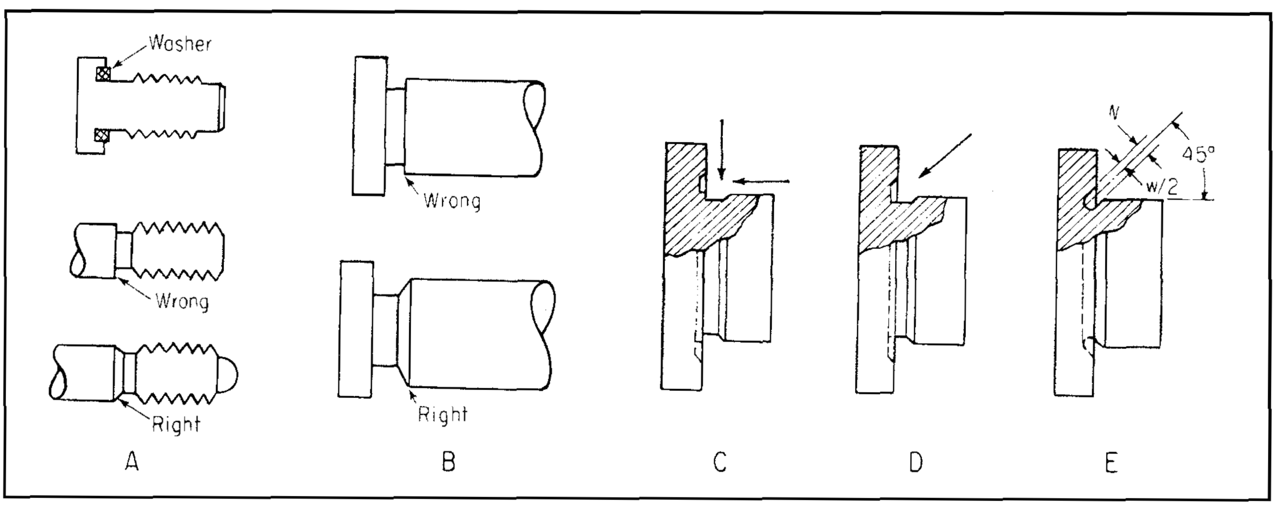

Fig. 12. Undercuts are used for many purposes. Use a chamfer as shown at B. Angular undercuts D and E should be avoided if possible

If a special surface finish is required, see "Dimensioning." Sketch F shows depth M for the required surface finish, starting at least ⅛ in. from the bottom. If this much relief interferes with the function of the part, allow at least 0.032 in.

6. Undercuts

Undercuts are used for a large variety of purposes:

(a) Thread relief (internal or external)

(b) As a substitute for a sharp corner (internal or external)

(c) Broach relief

(d) Grinding relief

(e) Assembly relief

(f) Burnishing relief

Also, some undercuts are used in special applications. Examples: (1) an undercut for a packing or flue washer, Sketch A, Fig. 12, or (2) an undercut required in bearing races for shield grooves.

It is difficult to standardize dimensions for undercuts, except in the case of a thread (internal or external). Here the width of the undercut equals 2 to 2½ threads, and depth equals the depth of the thread at least. Whenever possible, specify a chamfered undercut rather than a straight one. (See B, Fig. 12).

An angular undercut, internal or external, is difficult to produce and should be avoided whenever possible. Usually when the need for such an undercut exists, a relief is required in both directions.

A typical undercut in both directions is shown at C, Fig. 12. This undercut can be established with two separate tools.

Sketch D, however, shows an angular undercut that must be machined with a special attachment, and sometimes obtained as a second operation. If a second operation is used, a burr will develop. Thus additional cost is incurred.

If an angular undercut is necessary due to some functional requirement of the part, then apply it as shown in Sketch E. Give the 45° angle, and specify width W and the maximum or minimum depth required.

If an undercut is primarily a manufacturing aid, or relief, the only one that must have a specific dimension is thread relief (external or internal). All others can vary in size, type and direction. Therefore they can be left entirely to the discretion of the screw-products manufacturer by an option on the drawing.

Any limitations as to size, kind and direction should be stated on the drawing. Also, if a relief or undercut is permitted, it should not be less than 0.032 in. wide by 0.005 in. deep.

7. Materials

There are several aspects of materials that must be specified on the print:

(a) Analysis. Obviously the analysis of the product material is closely related to its function or the methods of manufacture. You should note whether the material should be of welding quality, or cold forming quality if it is to be crimped or heat-treated if certain strength requirements are mandatory.

(b) Specify stock size. For example, if you specify a diameter equal to stock size, you let the supplier know that you will accept standard stock surface imperfection.

(c) Imperfections. If on sulphurized steels you require the part to be free of surface seams, pipes or impurities, then so specify. In this case larger stock will be required to allow removal of the layer of stock containing these blemishes.

(d) End use. In the case of stainless steel parts, indicate on print the end use of part. Thus the supplier is advised that proper annealing may be required. In case of aluminum it is important to specify the end use of the part. This will indicate what analysis and temper should be supplied.

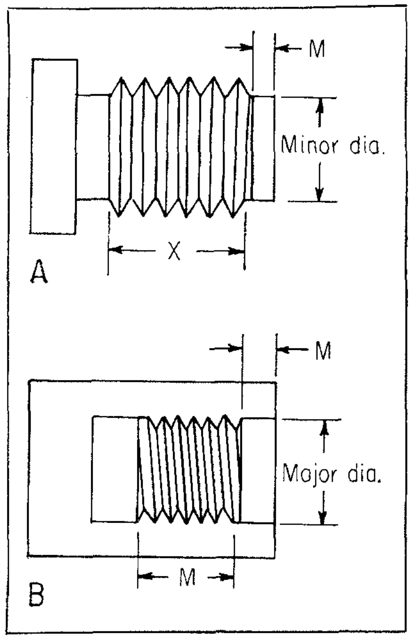

Fig. 13. Always dimension thread length X. The pilot or clearance M may be marred by the threading tool and is less than the minor diameter or the major diameter

(e) Stock shape. If the geometry of the part will allow use of tubing, specify if tubing is objectionable.

(f) Material treatment. Be specific in the case of carbon or alloy steels to state whether use of HR material is objectionable.

8. Threads

The usable length of thread should be dimensioned in all cases, unless the end of the thread runs into an undercut.

Sometimes a pilot is provided ahead of the thread (internally or externally). In this case, make sure that either the pilot diameter M is less than the root diameter of the thread or specify on print that area M can be marred by the threading tool. See sketches A and B, Fig. 13.

Design of Screw-Machine Products (continued)

Supplementary information has been developed on dimensioning of screw-machine parts.

S. A. Cappon

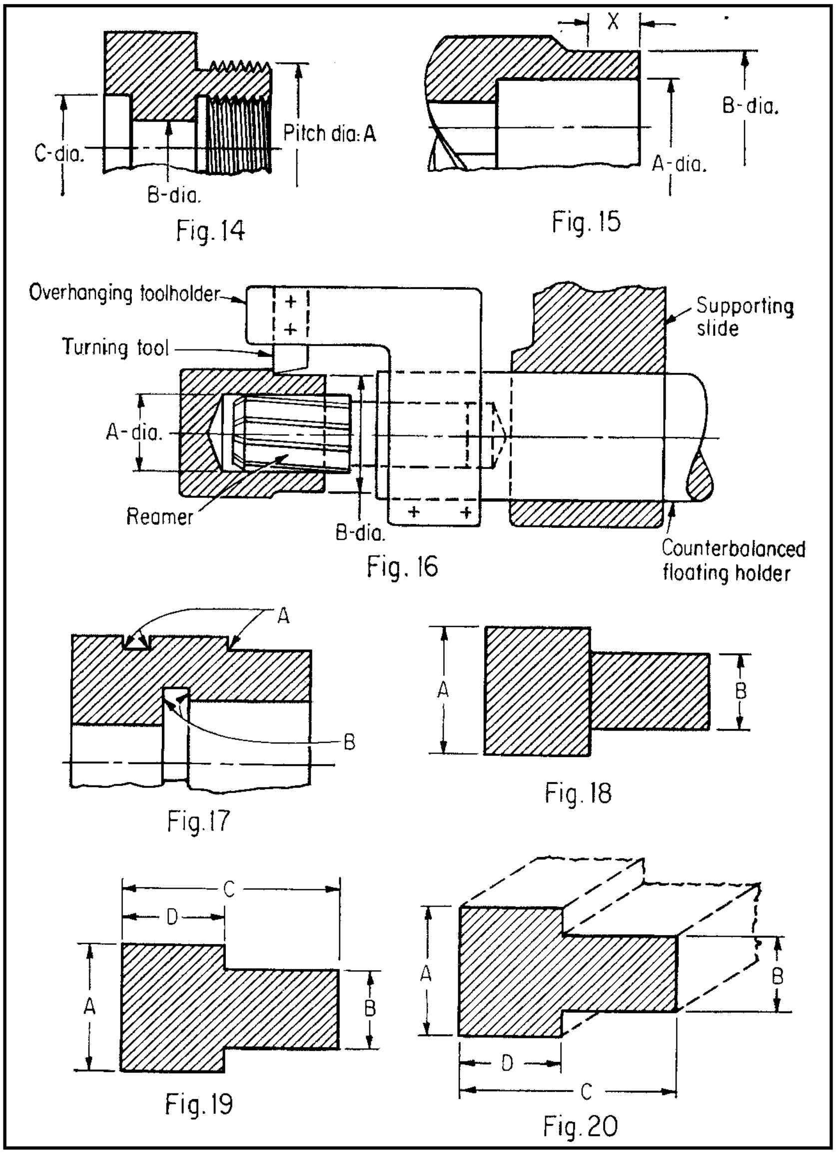

Concentricity-Eccentricity

Both of these features represent relationships between circular surfaces of a part: A concentricity notation designates surfaces that must have a common center within certain close limits.

An eccentricity notation is the distance between centers of one or more circular surfaces with its respective tolerance.

Fig. 14 shows a part for which we will assume a close concentricity between two diameters, say within 0.004 TIR. Let us relate counterbore diameter C and pitch diameter *A* in this manner. For good reasons, this part will be produced on an automatic with the threaded end out. A second operation will be required to machine the counterbore diameter C, using diameter B as a pilot. Obviously the concentricity specifications will be met easily in this case. In fact, any screw machine should maintain a 0.004 in. TIR between circular surfaces on parts with a 1:1 ratio of diameter and length. And special tooling will hold a closer concentricity limit.

Often a concentricity requirement does not extend for the entire length of a surface. This situation is seldom noted on the part-drawing as it should be. A suitable method is shown in Fig. 15. Possibly a note should be added to identify that X is being related to the concentricity between diameters A and B.

A drawing properly dimensioned with respect to such features provides an understanding of the functional characteristics of the part. In turn, functional aspects govern the manufacturing method and tooling.

Zero concentricity can be obtained between diameters A and B, Fig. 16. For this job it is possible to use a counterbalanced floating reamer holder with an overhanging turning tool and holder to cut diameter B.

Proper dimensioning of surfaces perpendicular to the part axis represents a chance for real economies. If perpendicularity is not functional, as at A and B, Fig. 17, consider allowing a slight angle, say ½° at least. Thus, a natural tool clearance is provided and surfaces A and B are established with minimum tool wear and are entirely unmarred. If, however, a specific perpendicularity is needed, then it should be so specified, even if a second operation appears essential.

Centerlines

It is often difficult to determine whether a dimension is a diameter or not. For example, in Fig. 18, if the note "dia" does not appear alongside of dimension A, it will be difficult to prove that A and B are truly diameters. A drawing should not leave anything to interpretation. Proper dimensioning avoids ambiguities and misunderstandings.

Perhaps the customary interpretation of Fig. 19 might be that A and B are diameters while C and D are lengths. However, a second possible interpretation is that the sketch represents a cross section of an extruded shape, Fig. 20. By adding a centerline, Fig. 21, we definitely and correctly identify A and B as diameters and C and D as lengths.

However, there is still a possibility for misunderstanding. Only by showing centerlines properly can we clearly define the part. The use of two centerlines, Fig. 22, now shows us that A, B and D are diameters and C is a length dimension.

Now suppose we consider Fig. 23 without centerlines. We can interpret the dimensions as:

(a) The part is an extruded shape as above.

(b) Diameters A and C are eccentric to each other.

(c) A is a diameter; B and D are lengths, and C is a truncated diameter.

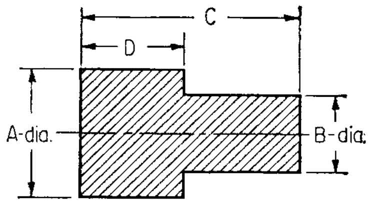

Fig. 21

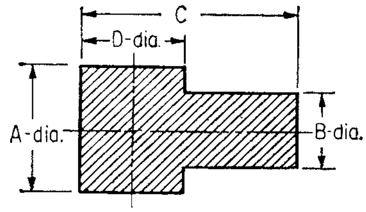

Fig. 22

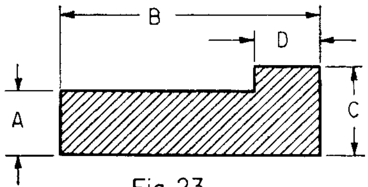

Fig. 23

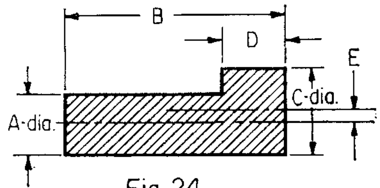

Fig. 24

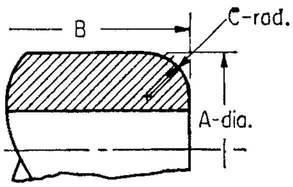

Fig. 25

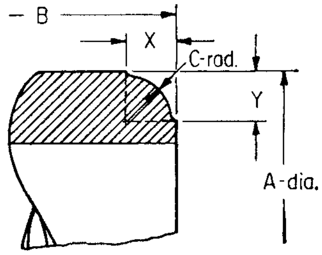

Fig. 26

With centerlines properly shown the sketch does not allow for misinterpretation.

In Fig 24 the note "dia" appears where a diameter is the case and also dimension E is introduced to show the amount of eccentricity.

A symbol, ø, can be used in place of "dia" to indicate diameter, but diameters must be properly identified along with clearly defined centerlines.

Radii

Consideration should be given to radii. For instance in Fig. 25, if one wants a perfect blend, the radius C must be tangent to A and B. But if this blend is not necessary or functional, it should be replaced with a generous chamfer, to reduce manufacturing cost.

Good appearance is the only valid reason for a radiused corner. Only occasionally does a radius ease assembly or avoid damage to mating surfaces; for example, an outer bearing race. The race is normally ground on the OD and face after heat treatment, and grinding stock is left on these surfaces. Fig. 26 shows a method of dimensioning such surfaces, with the expectation that radus C will blend with the ground surfaces.

Facing Tools for Chuckers

When the tools feeds along an arc for facing cuts, special attention must be paid to the effect of cross-arm rotation on operating rake and relief angles.

Warren A. Phinney

If you don't know what's going to happen to the rake and relief angles when the cutting tool is feeding along an arc, you may get poor tool performance, and you may even have smashups if the relief angle becomes negative.

One way to avoid the smashups, at least, is to locate the tip of the tool on an arc passing through the center of the workpiece. But this method causes large changes in operating rake and relief angles during long facing cuts, and these changes may force the use of undesirably small lip angles which compromise tool performance and prevent the use of disposable toolbits.

There is, however, a better method for cuts that do not go all the way to the center of the work. With the method described here, relatively long facing cuts can be made without introducing large changes in operating rake and relief angles.

This method can be used to advantage for short facing cuts because it reduces the number of tool blocks required for parts of various diameters and enables one facing tool block to handle various diameters without reshimming of tool holders for height or resetting of toolholder back-up screws for projection height.

Nomenclature:

R1 is radius of max diameter cut.
R2 is radius of min diameter cut.
R3 is distance from center of work spindle to axis of swinging cross-arm.
R4 (to be determined) is the distance from the axis of swinging cross-arm to tool tip.
A is axis of work spindle.
B is axis of swinging cross-arm.
AB is distance from axis of work spindle to axis of swinging cross-arm and is equal to R3.
Δ (to be determined) is maximum change in operating rake and relief angles during the course of the cut.

Layout method

1. Lay out points A and B.
2. Draw circles and arcs, as indicated, for R1, R2, R1-R2, and R3.
3. Locate point C at intersection of arcs R3 and R1-R2, and project line AC to point D, the position of the tool tip at the largest diameter cut.
4. Similarly, locate point E and project line EA to point F, the position of the tool tip at the smallest diameter cut.
5. About point B, draw arc DF, the path of the tool tip as it moves through the cut. This also checks steps 3 and 4. For counterclockwise spindle rotation, the outline of the toolbit may be drawn in at this time. For inverted tools (clockwise spindle rotation), refer to step 8.
6. Observe that the operating rake and relief angles are equal at D and F. To determine the maximum change (Δ) in these angles, proceed as follows:
7. Construct line BG perpendicular to and bisecting line AE and intersecting arc AE at point H.
8. Construct line HJ perpendicular to AB and intersecting arc AE at H and arc DF at K. The outline of the toolbit at K may be drawn at this time. Angle AKH is Δ, the maximum change in operating rake and relief angles.

Note that, if the tool is inverted for

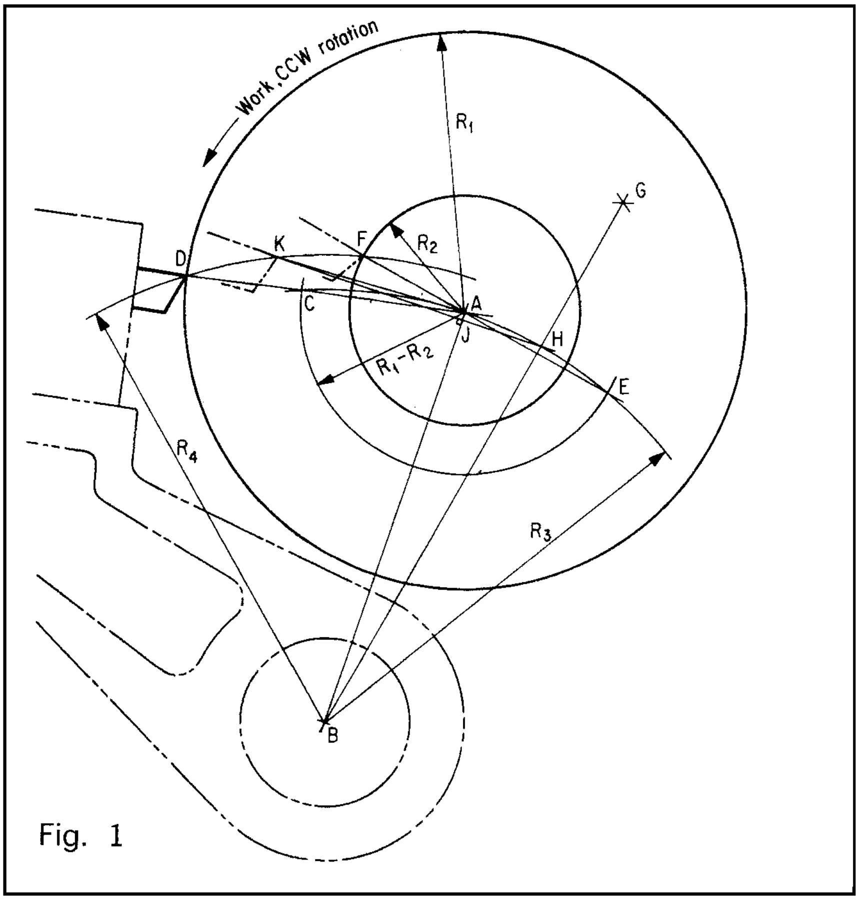

Fig. 1

clockwise spindle rotation, operating relief at K will be less than at D and F. For this condition, the basic tool alignment may be drawn in at point K rather than at point F and the change in rake and relief angles checked at points D and F rather than at point K. This will avoid introducing, during the cut, operating relief angles less than the angles provided on the toolbit or toolholder.

Mathematical method

Tool tip location:

$$(1)\ R4 = \sqrt{AB^2 + R1 \times R2}$$

Change in rake and relief angles for tool tip feeding along R4:

$$(2)\ \Delta = \sin^{-1}\frac{AB}{R4} - \cos^{-1}\frac{R1 + R2}{2R4}$$

Change in rake and relief angles for tool tip feeding along R3:

$$(3)\ \Delta = \cos^{-1}\frac{R2}{2AB} - \cos^{-1}\frac{R1}{2AB}$$

Note that, for clockwise spindle rotation, a component of tool motion is opposed by work rotation. Conversely, for counterclockwise spindle rotation, a component of tool motion is in the direction of work rotation, so climb-cutting conditions may exist. Make sure that the feed works are suitable for these conditions.

Examples of use

This method was developed because of the need to face a 10-in.-OD by 5½-in.-ID flywheel rim on a chucking lathe with a rotating cross-arm axis located 14¾ in. from the work-spindle centerline. Allowing ⅛ in. for tool approach and overtravel:

$$R1 = 5\tfrac{1}{8}$$
$$R2 = 2\tfrac{5}{8}$$
$$R3 = AB = 14.75$$

$$\begin{aligned}(1)\ R4 &= \sqrt{AB^2 + R1 \times R2}\\ &= 15.199\end{aligned}$$

$$\begin{aligned}(2)\ \Delta &= \sin^{-1}\frac{AB}{R4} - \cos^{-1}\frac{R1 + R2}{2R4}\\ &= \sin^{-1}\frac{14.750}{15.199}\\ &\quad -\cos^{-1}\frac{5.125 + 2.625}{2 \times 15.199}\\ &= \sin^{-1} 0.9704 - \cos^{-1} 0.2449\\ &= 76°01' - 75°14'\\ &= 0°47'\end{aligned}$$

Had the tool tip been located conventionally on an arc passing through the center of the work spindle, the change in operating rake and relief angles would have been:

$$\begin{aligned}(3)\ \Delta &= \cos^{-1}\frac{R2}{2AB} - \cos^{-1}\frac{R1}{2AB}\\ &= \cos^{-1}\frac{2.625}{2 \times 14.750}\\ &\quad - \cos^{-1}\frac{5.125}{2 \times 14.750}\\ &= \cos^{-1} 0.08898\\ &\quad - \cos^{-1} 0.17372\\ &= 84°54' - 80°0'\\ &= 4°54'\end{aligned}$$

In round numbers, the change in operating rake and relief angles was reduced from 5 deg to 1 deg.

To clarify the change in operating rake and relief angles for alternate (not successive) tool tip locations, Fig. 2 shows the tool tip stationary and the arc of work-center travel moving relative to the toolbit instead of, as in Fig. 1, the toolbit moving relative to the work center. In addition, the ratio of the work radii relative to AB is increased, perhaps beyond practical limits.

The change in operating rake and relief angles is equal to the angle originating at the tool tip and subtending the arc A to A2. It can also be seen that, if the tool tip is positioned as shown at D2 and D3, the change in operating rake and relief angles increases as compared with that for position D.

To minimize the change in operating rake and relief angles occurring during the course of the cut and to equalize operating rake and relief angles at the beginning and end of the cut, it is necessary to calculate side BD, equal to R4, of triangle ABD by Equation (1). Then the change in operating rake and relief can be found with Equation (2).

To calculate the change in operating rake and relief angles for a tool tip located on an arc passing through the center of work, refer to Fig. 3, where A to N is the circular arc of work-center travel relative to the tool tip. The change in rake and relief angles is found with Equation (3). ■

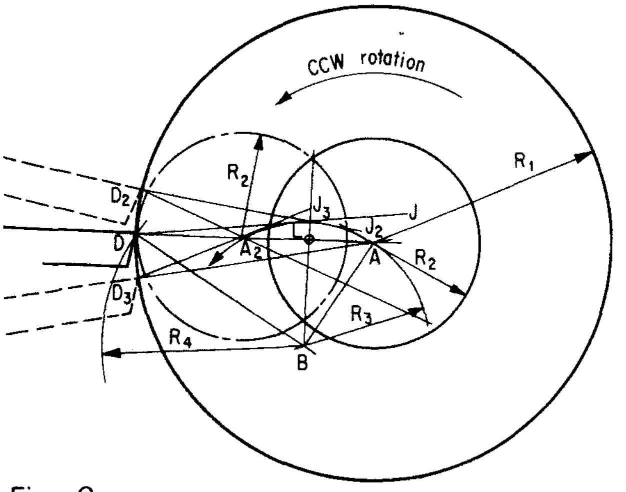

Fig. 2

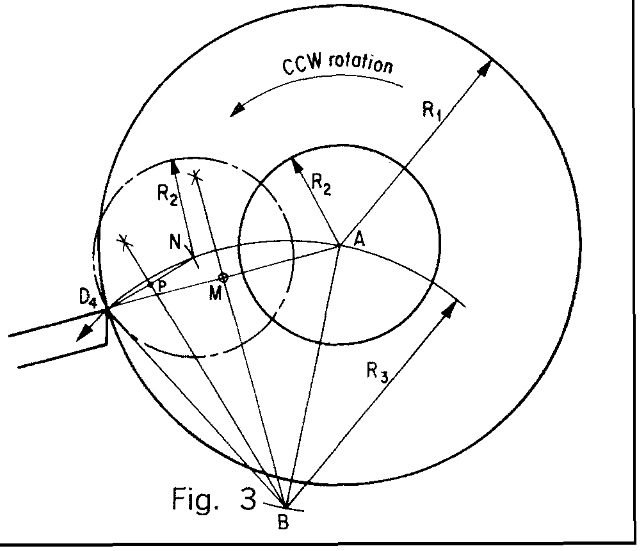

Fig. 3

Shaving-Tool Corrections

I. Zorich

NOMENCLATURE:

c = step on work
d_1 = smallest work dia shaved
d = any work dia for which tool step is to be corrected
D = dia of supporting roller
R = Distance from work center to roller center
p = tool travel past center
X = depth of tool to be corrected
y = length of cutting edge to form profile
$Z = c - \Delta Z$
ΔZ = vertical tool movement of tool edge, when floating toolholder passes center by distance p
α = top rake angle
β = clearance angle
ψ = angle between tool top rake and a line drawn from intersection of top rake with work diameter to center of work

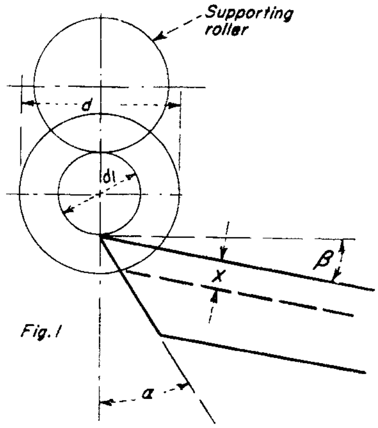

Fig. 1

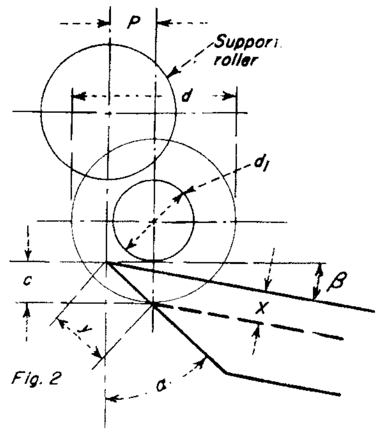

Fig. 2

FORMULAS
For Fig 2

$$c = \frac{d - d_1}{2}$$

$$p = c \times \tan \alpha$$

$$y = \frac{c}{\cos \alpha}$$

$$X = y \times \sin 90° - (\alpha + \beta)$$

$$= y \times \cos (\alpha + \beta)$$

$$= c \times \frac{\cos (\alpha + \beta)}{\cos \alpha} \quad \text{.......... (3)}$$

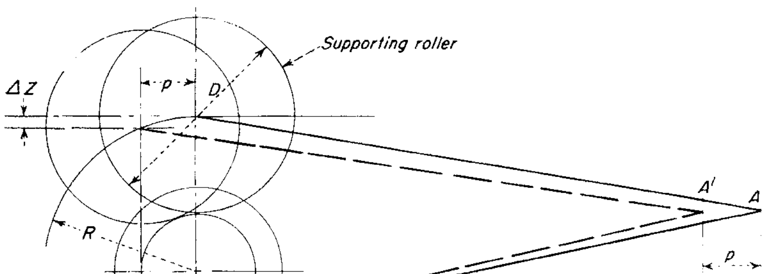

Fig. 3

For Fig 3

$$Z = c - \Delta Z \qquad p = c \times \tan \alpha$$

$$\Delta Z = R - \sqrt{R^2 - p^2}$$

$$= R - \sqrt{R^2 - c^2 (\tan \alpha)^2}$$

$$Z = c - R + \sqrt{R^2 - c^2 (\tan \alpha)^2}$$

$$X = \frac{Z \times \cos (\alpha + \beta)}{\cos \alpha}$$

$$= \left[c - R + \sqrt{R^2 - c^2 (\tan \alpha)^2}\right] \times \frac{\cos (\alpha + \beta)}{\cos \alpha} \quad \text{.......... (4)}$$

Shaving operations are finding increased use on automatics and turret lathes. The edge of the shaving tool is always on a vertical line with the center of the supporting roller. Here are the formulas for shaving-tool tool corrections for three conditions:

CONDITION 1—The edge of the shaving tool and center of the supporting roller just reach the center of the work, Fig 1.

Formulas for tool correction are:

$$X = \frac{d \sin (\alpha - \psi) \cos (\alpha + \beta)}{2 \sin \alpha} \quad (1)$$

$$\sin \psi = \frac{d_1}{d} \sin \alpha \quad \text{........} (2)$$

CONDITION 2—Edge of the shaving tool and centerline of the supporting roller pass the center of the work but the tool step cutting the other diameter just reaches the center of the work, Fig 2. The toolholder is nonfloating.

CONDITION 3—The setup in Fig 3 is the same as in Fig 2, except that the toolholder is floating. Here A is the position when the edge of the shaving tool reaches work center and A' is the position when the center is passed and the tool step reaches the center at the other diameter.

EXAMPLE (Fig 3):

What is the dimension of step X when $c = 0.25$, $R = 2$, $\alpha = 15°$ and $\beta = 5°$?

$$X = \left[0.25 - 2 + \sqrt{4 - 0.0625(\tan 20°)^2}\right] \times \frac{\cos 20°}{\cos 15°}$$

$$= 0.224$$

Under certain material and cutting conditions:

$$(\tan \alpha)^2 = \text{a constant } K_1$$

$$\frac{\cos (\alpha + \beta)}{\cos \alpha} = \text{constant } K_2$$

Then:

$$X = \left[c - R + \sqrt{R^2 - c^2 \times K_1}\right] \times K_2$$

Draw-Die Radius

Ferenc Kuchta

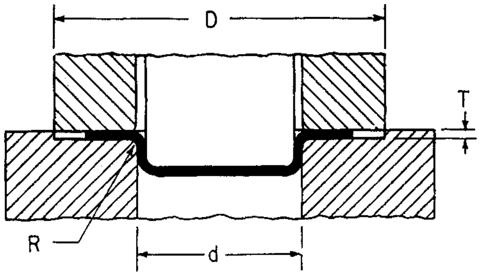

$R = 0.8\sqrt{(D-d)\,T}$

where D = blank diameter, in.

Tolerance for $R = \pm 0.005$ in.

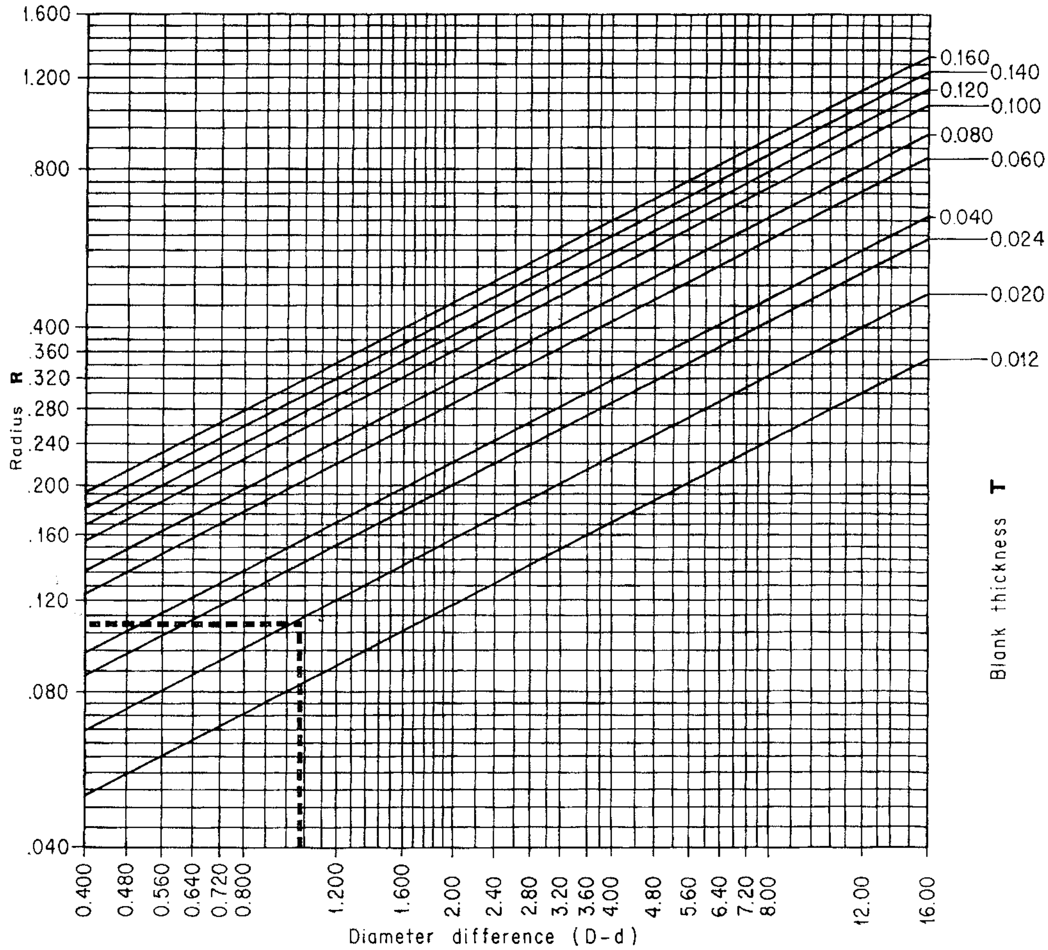

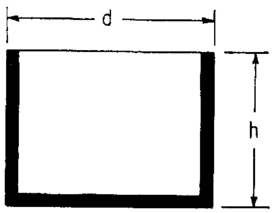

Example:

$d = 1.00$, $h = 0.75$, $T = 0.020$

$D = \sqrt{d^2 + 4dh} = 2.00$

$D-d = 1$

$R = 0.110 \pm 0.005$

Rules for Drawing Round Shells

Courtesy Dayton Rodgers Manufacturing Company

IN metal-stamping work, the expression "drawing" describes an operation in which a flat sheet or metal blank is formed into a shell or cup of fairly uniform thickness. In producing round shells without flange, the factors that govern the possible height of single-operation drawing of a shell are:

1. Ratio of height to diameter of shell
2. Ductility of the material
3. Corner radius

When drawing a round shell (without flange) in one operation, the maximum ratio of height divided by diameter may vary between ¼ and a possible ¾, depending on the corner radius and ductility of the material. A generous corner radius helps to secure greater height in one operation, while too small a corner radius may cause the shell to fracture at the radius. Soft, ductile material will permit drawing to a greater height in one operation.

Ductility of materials is measured as percent elongation in 2 in. or percent reduction of area. In general, materials such as deep-drawing steel, annealed sheet steel (SAE 1005 - 1015), dead-soft cold - rolled strip steel (SAE 1010-1020), some stainless steels (304, 410, 420 and 430), soft-temper aluminum (2SO, 3SO and 53SO), soft-temper brass and copper will allow drawing to a maximum height in one operation. Other less ductile materials may require one or more pre-cupping operations; that is, additional drawing dies for gradually reducing the blank to the diameter required, and possibly annealing between operations.

Corner radius of the shell has a considerable effect on the possible height of single-operation drawing. Corner radius should, when possible, be specified at a minimum of four times thickness of material when the height of the shell exceeds one-third of the diameter. When a smaller radius is specified, additional drawing or flattening operations may be

Draw-Reduction Ratios for Round Shells

(Without Flange)

Shell height = inside height of shell
Shell diameter = inside diameter of shell plus one thickness of material

Height-Dia. Ratio	% Reduction of Dia.	Blank-Draw Ratio	Height-Dia. Ratio	% Reduction of Dia.	Blank-Draw Ratio	Height-Dia. Ratio	% Reduction of Dia.	Blank-Draw Ratio
.01	2.0	1.02	.48	41.5	1.70	.95	54.4	2.194
.02	3.8	1.03	.49	41.9	1.72	.96	54.5	2.201
.03	5.5	1.05	.50	42.3	1.73	.97	54.7	2.208
.04	7.1	1.07	.51	42.7	1.745	.98	54.9	2.216
.05	8.7	1.09	.52	43.1	1.758	.99	55.1	2.224
.06	10.2	1.11	.53	43.5	1.770	1.00	55.3	2.231
.07	11.5	1.13	.54	43.8	1.780	1.05	56.2	2.28
.08	13.0	1.15	.55	44.2	1.790	1.10	57.0	2.32
.09	14.3	1.16	.56	44.5	1.800	1.15	57.8	2.37
.10	15.4	1.18	.57	44.8	1.810	1.20	58.5	2.41
.11	16.6	1.20	.58	45.1	1.820	1.25	59.2	2.45
.12	17.8	1.21	.59	45.4	1.830	1.30	59.9	2.49
.13	18.8	1.23	.60	45.8	1.840	1.35	60.5	2.53
.14	19.9	1.24	.61	46.0	1.850	1.40	61.0	2.56
.15	21.0	1.26	.62	46.4	1.862	1.45	61.6	2.60
.16	21.9	1.28	.63	46.7	1.873	1.50	62.2	2.64
.17	22.8	1.29	.64	47.0	1.885	1.55	62.7	2.68
.18	23.7	1.31	.65	47.3	1.898	1.60	63.2	2.72
.19	24.6	1.32	.66	47.6	1.910	1.65	63.7	2.76
.20	25.5	1.34	.67	47.8	1.920	1.70	64.2	2.79
.21	26.3	1.35	.68	48.1	1.930	1.75	64.6	2.83
.22	27.1	1.37	.69	48.4	1.940	1.80	65.1	2.86
.23	27.8	1.38	.70	48.7	1.950	1.85	65.5	2.90
.24	28.6	1.40	.71	49.0	1.960	1.90	65.9	2.93
.25	29.3	1.41	.72	49.2	1.970	1.95	66.3	2.97
.26	30.0	1.43	.73	49.5	1.980	2.00	66.7	3.00
.27	30.7	1.44	.74	49.8	1.990	2.05	67.0	3.03
.28	31.3	1.45	.75	50.0	2.000	2.10	67.4	3.06
.29	31.9	1.47	.76	50.2	2.010	2.15	67.8	3.10
.30	32.6	1.48	.77	50.5	2.020	2.20	68.1	3.13
.31	33.2	1.49	.78	50.7	2.030	2.25	68.4	3.16
.32	33.8	1.51	.79	51.0	2.040	2.30	68.7	3.20
.33	34.4	1.52	.80	51.2	2.050	2.35	69.0	3.23
.34	35.0	1.53	.81	51.4	2.060	2.40	69.3	3.26
.35	35.5	1.55	.82	51.6	2.070	2.45	69.6	3.29
.36	36.0	1.56	.83	51.8	2.080	2.50	69.9	3.32
.37	36.5	1.57	.84	52.1	2.090	2.55	70.2	3.35
.38	37.0	1.58	.85	52.4	2.100	2.60	70.4	3.38
.39	37.5	1.60	.86	52.6	2.110	2.65	70.7	3.41
.40	38.0	1.61	.87	52.8	2.120	2.70	70.9	3.44
.41	38.5	1.62	.88	53.0	2.130	2.75	71.2	3.47
.42	39.0	1.63	.89	53.2	2.140	2.80	71.5	3.50
.43	39.4	1.65	.90	53.4	2.150	2.85	71.7	3.53
.44	39.8	1.66	.91	53.6	2.160	2.90	71.9	3.56
.45	40.2	1.67	.92	53.8	2.170	2.95	72.1	3.58
.46	40.7	1.68	.93	54.0	2.178	3.00	72.2	3.60
.47	41.1	1.69	.94	54.2	2.185			

How to use table: Divide height of shell by diameter; find corresponding ratio in col. 1; Percent reduction is given in col. 2 (use to determine number of reductions required); Blank-draw-ratio is given in col. 3 (blank-draw ratio times shell diameter equals blank diameter approximately).

required. In no case should the corner radius be less than thickness of material for a one-operation draw.

When the ratio of "height divided by diameter" exceeds 5/8, it will be necessary in most cases to reduce the flat blank to the finished shell by using two or more draw dies of proportionately decreasing diameters. In some cases, one or more annealing operations will be necessary between first and finish draw operations. The necessity of annealing depends to a large extent on the workability of the metal being drawn.

Determination of the number of reductions necessary to draw a shell with ratios (height divided by diameter) greater than 5/8 cannot be done by hard and fast rules. In general, for ductile materials, with generous corner radius in the shell, the requirements are:

1. Height equals 5/8 to 1 1/8 times the diameter of the shell—two reductions will be required.
2. Height equals 1 1/8 to 2 times the diameter of the shell—three reductions will be required.
3. Height equals 2 to 3 times the diameter of the shell—four reductions will be required.

It may be necessary to anneal the shell when more than two reductions are required. When corner radius is less than four thicknesses of material, add one or two flattening dies and operations, depending on corner radius desired.

For less-ductile materials, it is more difficult to predict the number of operations required. In general, the measure of ductility of the material (percent of elongation or percent reduction of area) will determine the maximum reduction possible in one operation.

Finish of edge depends on the "height divided by diameter" ratio and on the material being drawn. For relatively shallow shells where the "height divided by diameter" ratio is not over 1/3, it is possible to produce an edge within commercial tolerances without requiring finishing operations. That is, the height and uniformity of the edge depends on the size of blank used. For higher shells it is not possible to do this, and one of the following finishing operations will be required:

1. Flange trim and finish draw (Fig. 1).
2. Pinch trim (Fig. 2).
3. Machine trim (Fig. 3).
4. Wedge or "shimmy"-die trim (not suitable for small quantities).

A "Draw Reduction Table" offers a simple means of determining percent of draw reduction and flat-blank diameter. By dividing the inside shell height by the mean shell diameter, a height-diameter ratio is obtained. Find this ratio in Col. I of the table. Directly opposite in Col. II find the percent of reduction of diameter (a measure of the amount of cold-working to be done in drawing the flat blank into a shell). Directly opposite in Col. III, find the Blank-Draw ratio. Multiply the mean shell diameter by this factor to obtain the approximate flat blank diameter.

It must be understood that this table can only be used with round straight-sided shells or cups. Shells or cups with flanges must be investigated by other methods. Care must be used when attempting to predict the number of operations required to produce a flanged shell or cup.

EDGE-TRIMMING METHODS

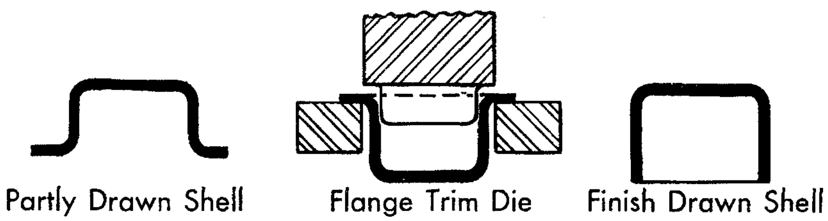

Fig. 1—**FLANGE TRIM AND FINISH DRAW.** This method is satisfactory for most shells, particularly diameters greater than 2 in. Only one additional die—a trimming die—is required.

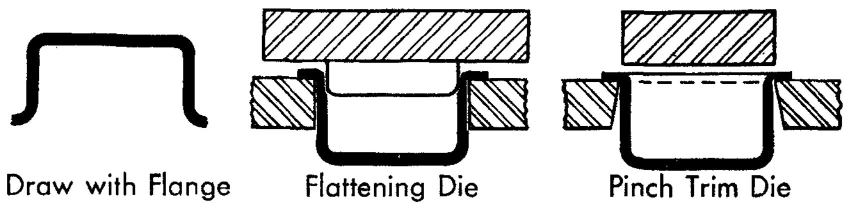

Fig. 2—**PINCH TRIM DIE.** This method will produce a shell with uniform height, but the inside edge is considerably rounded. The flange must be flattened to a sharp corner, which will require one or two dies.

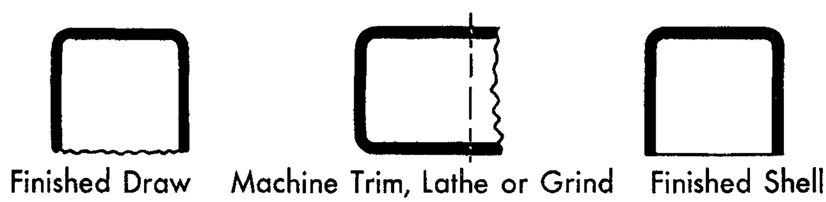

Fig. 3—**MACHINE OR BOX TRIM.** Tooling cost is generally low, but this method is slow. The best-appearing edge is produced, and sometimes this method is the only practical one.

Tonnage for Air Bends

Capacity ratings of press brakes are based in air bends in which dies do not strike solidly on the metal. All pressure is used in forming–none in coining or squeezing.

Roy F. Dehn

Air-bend dies produce a bend with an inside radius approximately 15% or 5/32 of the die opening.

This means that less than an 8-times die opening must be used if a smaller radius is desired—requiring higher tonnage.

Press ratings are based on die openings of 8 times the material thickness up to about ⅝ in. plate. Die openings up to 10 or 12 times are used for forming heavier thicknesses of plate.

If the die opening is too large, an excess amount of metal is drawn into the die, causing a curve to form in the metal each side of the point radius.

If the metal is formed over a die opening less than 8 times the plate thickness, there is danger of fracturing the metal in the heavier thicknesses, unless a small amount of preheat is applied.

Effective width of die opening

When the punch radius is equal to or less than the material thickness, the effective width of die opening to use with the tonnage table, page 99, is die width *W*.

When the punch radius is greater than the plate thickness, the effective width of die opening to use with the tonnage table is 2 times *X* shown on sketch.

Pressure per foot

Check tonnage required from table to be sure it is within the capacity of the machine, making allowance for coining and drawing forces required on other than air-bend dies.

Bending pressure is proportional to the ultimate strength of the material for the same thickness and die opening.

The inside radius of a bend is approximately 5/32 of the die opening and is about the same for varying thicknesses of material bent on the same die set.

Heavier thicknesses of plate contain higher carbon content in order to maintain full ultimate strength. This results in more bending fractures which can be reduced by 10 or 12 times die opening or the use of special flanging steel.

High tensile steel plates are usually formed over 10 to 12 times die opening.

The manufacturers of special steels usually recommend the radius of die opening to use with their materials.

Bends across grain will show less breakage than when bent in line with the grain of the plate, especially in the thicker plates.

It helps to avoid cracks by rounding the edges of thick plates at each end of the bend, on the outside of the bend.

Approximate spring back:

Low carbon steel, 1° to 2°
0.40 to .50 carbon steel, 3° to 4°
Spring steel annealed, 10° to 15°

The same size of press brake, as formerly used for bends of 8 times plate thickness in mild steel, is suitable for 12-times bends in the popular low-alloy steels.

If less flange width is required, a smaller die opening must be considered, and this will affect the tonnage rating needed.

Forming practice

Material bent on too wide a die opening may not come square. Rehitting with dies set closer in trying to square up the bend frequently overloads the press. The forming of channel or offset bends may require more than six times the load needed for a single right angle bend in the same material.

Effective width of die opening

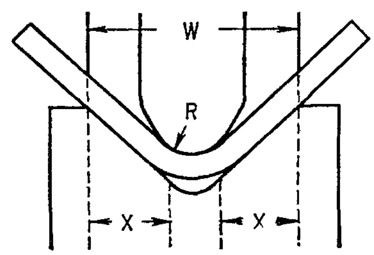

To adjust a mechanical press brake ram and bed parallel under load follow these three steps:

1. With the eccentrics on bottom center, adjust right hand pitman or screw (or pitman with drive motor) 0.015 in. or 0.025 in. above left-hand end.
2. Run both screws down together until left hand end bottoms in die and stalls adjusting motor.
3. Release adjusting clutch on cross shaft and run right hand screw down until it stalls.

Ram and bed are then parallel under pressure and it is only necessary to back up adjustment for the thickness of the material.

Another method is to use a short test piece under each end of the press, adjusting until equal results are obtained on both ends. Use wide enough test pieces so that the unit pressure will not be high enough to indent the dies. Another method is to start with a shallow bend and run the adjustment down between strokes, until the desired angle is formed. However, one must check for equal angles at both ends of the bend.

Dies should preferably be of a closed height so that the adjusting screws project about one to three inches.

If a load is put on one end of the press so that it is substantially performed by one pitman, it should be limited to half the press capacity to avoid overloads.

Tons pressure per foot for 90° air bends in mild steel

Thickness of metal		Width of vee die opening – Inches																									
Inches	Gauge	1/4	3/8	1/2	5/8	3/4	1	1 1/4	1 1/2	2	2 1/2	3	4	5	6	7	8	9	10	11	12	13	14	16	18	20	22
.036	20	3	1.7	1.1																							
.048	18	5	**3**	2.2	1.7	1.3																					
.060	16	9	5.5	**3.8**	2.8	2.2	1.5																				
.075	14		9	6.3	**4.7**	3.5	2.5	1.8																			
.105	12			13	10	8	5.6	4.1	3.2																		
.135	10				18	14	**9.5**	7	5.5	4																	
3/16						25	19	14	**11**	7	5.5	4															
1/4							38	29	22	**15**	11	8.5	6														
5/16								48	38	26	**19**	15	10	7.5													
3/8									60	41	30	**24**	16	12	9												
1/2										80	60	46	**32**	23	18	15	10										
5/8												78	55	**40**	30	24	20	15									
3/4													85	63	**48**	40	32	25	21								
7/8														95	74	58	**48**	43	35	30							
1															105	85	70	**64**	56	53	40	36					
1 1/8																118	95	82	**73**	68	62	55					
1 1/4																	126	109	94	86	**80**	74	64				
1 3/8																		138	119	106	93	**84**	78	69			
1 1/2																			148	132	118	104	**96**	82	75		
1 5/8																					141	130	120	**101**	86	80	
1 3/4																						155	144	123	**105**	92	87
2																							188	171	148	**129**	116

Underlined tonnages are for minimum vee die openings recommended

This chart for mild steel of 55,000 to 65,000 psi

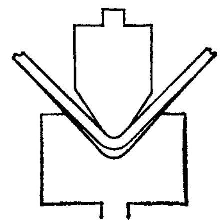

Tons pressure per foot for mild steel 90° air bend

Tonnage vs Stroke of Press Brakes

This chart can be used to check the capacity of press brakes, because it shows tonnage available at different points in the stroke.

Roy F. Dehn

Data are based on a die opening width *W*, and are correct for the usual proportions of width of die opening to material thickness.

Distance *A* is punch travel required to make the bend, and equals 40% of die width *W*. Full tonnage to make the bend is required at 0.7 *A* above bottom, where *W*, or width of die opening = 8 or more. Also, under these conditions, 0.7 *A* = 0.28 *W*.

Problem:

What length of 3/8 in. mild steel plate can be bent on a 320-ton brake with a 5-in. stroke?

Solution:

A 3-in. die opening would normally be used. Therefore the height above bottom for full tonnage = 3 × 0.28 = 0.84 in.

Percentage of stroke above bottom stroke = 0.084 ÷ 5 = 16.8%.

Enter the chart at 16.8% of stroke above bottom stroke and draw a dash line to the stroke-capacity curve.

Drop down a dash line and read the tonnage available at 16.8% of stroke equals 1.3 times full capacity, or 1.3 × 320 = 416 tons.

From the chart "Tonnage for air bends," (**AM**—March 28, '66, p99) find that the pressure to bend 3/8-in. plate in a 3-in. wide die equals 24 tons per foot.

Then, 416 ÷ 24 = 17 ft, or maximum length of air bend that can be made on the 320-ton brake, using 3/8-in. mild steel plate.

This value would have to be adjusted upward or downward for other materials.

If alloy-steel plate is to be bent on extra-wide die openings, consult the press-brake manufacturer with regard to the limiting effect of the available flywheel energy.

This chart may be used also for work to be done on mechanical press brakes rated with a bottom stroke capacity equal to 150% of mid-stroke capacity. ■

Tonnage vs stroke

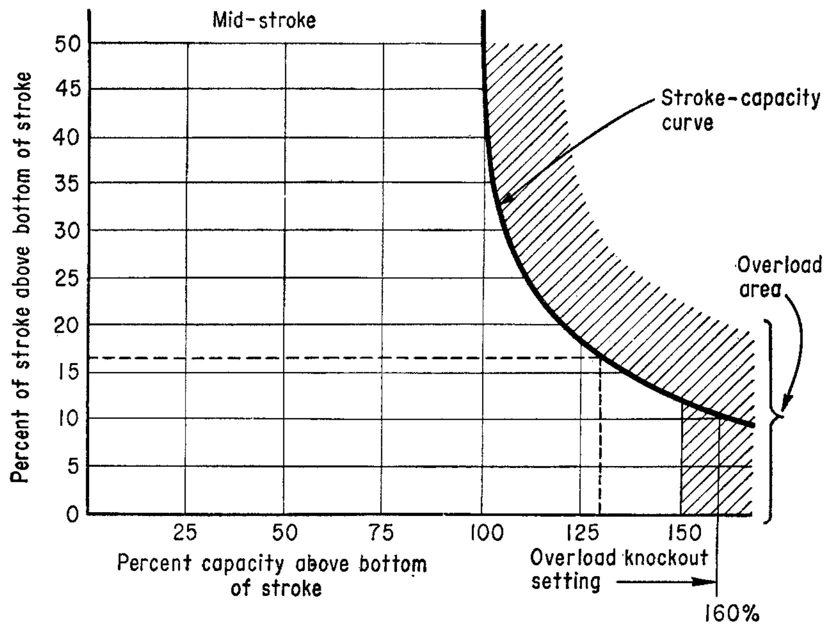

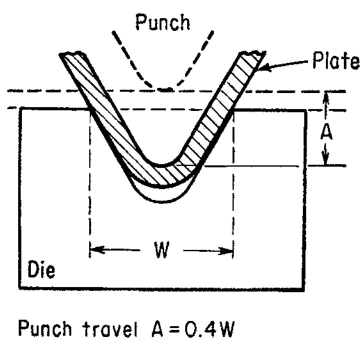

Punch travel A = 0.4W

Bend work diagram

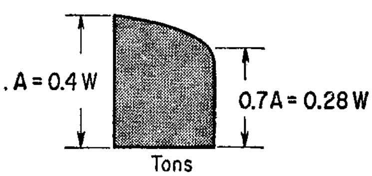

A = distance punch travels

Tonnage Chart for Various Bend Angles

Roy F. Dehn

The chart published earlier (**AM**—March 28, '66, p99) gives the tonnage per foot to produce 90° air bends in various plate thicknesses and using various die openings. In many cases, however, material must be bent to less than a 90° bend angle, and then the accompanying chart provides a means of estimating the tonnage in relation to that required for a 90° air bend.

Example: What is the percentage of tonnage for a 90° bend that is required to bend plate to an inside bend angle of 175°?

According to the tabulation, the percentage is 50%. Now cross check this by using the curve AEP.

Solution:

Follow the 175° inside bend angle to the right until the dash-line extension cuts curve AEP. Drop down to the scale for 100% air bend tonnage, and read that 50% of that tonnage is required. If the full 90° bend in 2 in. plate requires 171 tons per foot, a 175° bend will require 50% of it, or 85 tons per foot. ■

Tonnage vs bend angle

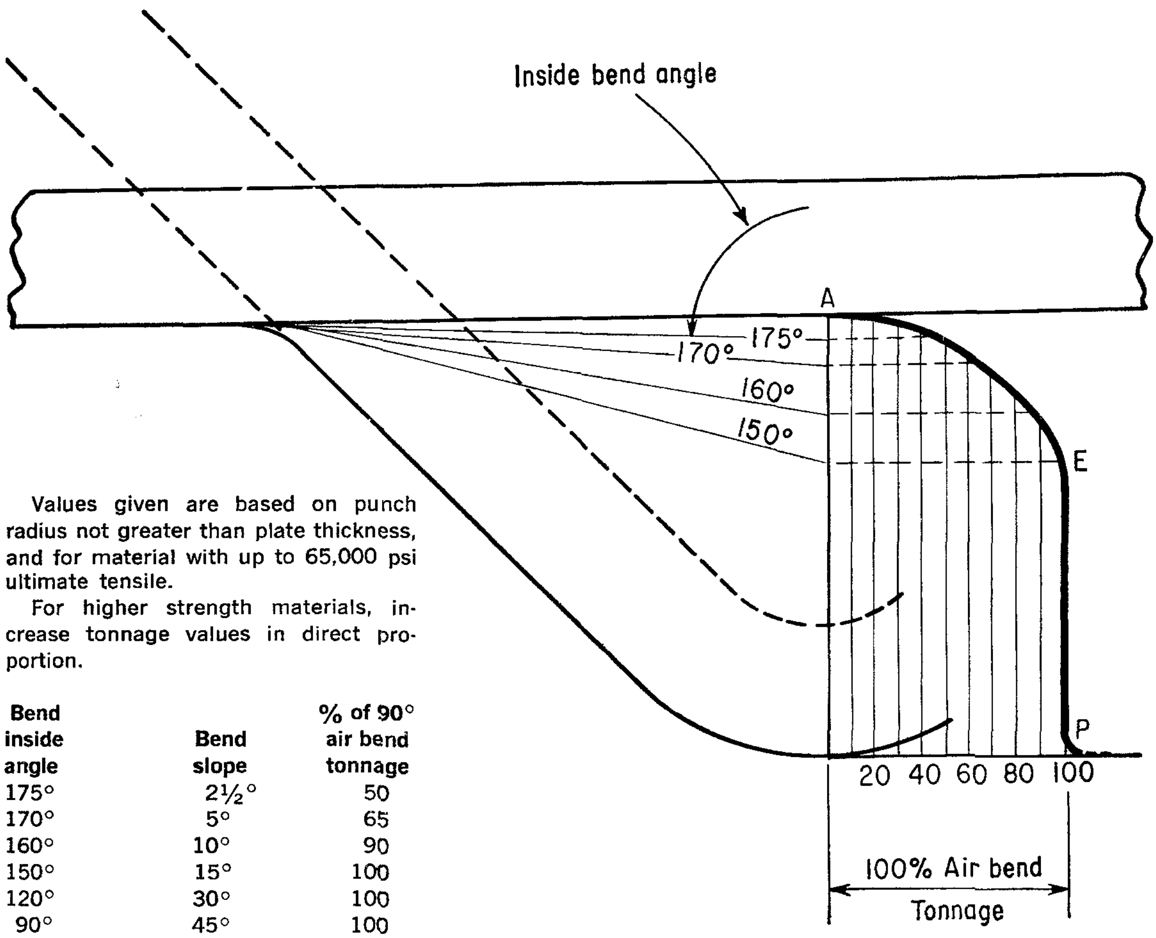

Values given are based on punch radius not greater than plate thickness, and for material with up to 65,000 psi ultimate tensile.

For higher strength materials, increase tonnage values in direct proportion.

Bend inside angle	Bend slope	% of 90° air bend tonnage
175°	2½°	50
170°	5°	65
160°	10°	90
150°	15°	100
120°	30°	100
90°	45°	100

Press Tools for Bending

Don R. King

Selection of a suitable method is the initial step in designing press tools for parts that require bending. Often, for a given shape, there are several possible methods. To select the one best suited to your job, we give here schematic drawings of press tools to serve as a reference guide. These are classified according to standard arrangements to produce basic bend configurations. Notes under each sketch give the advantages and disadvantages of the particular design.

In most cases, the bend is shown as accomplished at the last station of a progressive die, in order to indicate the relationship of cut off. Of course, the construction may apply to intermediate stations, where the bend includes only part of the strip, or is turned parallel to the direction of feed. Dimensions "x" on certain sketches are likely to be critical in respect to part dimensions. They should be checked for limitations of die wall thickness or space.

RIGHT-ANGLE BENDS

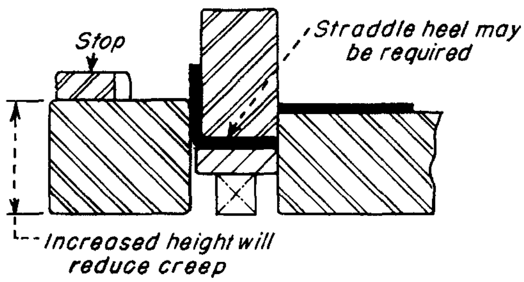

No. 1
- Good location and alignment
- Inclined ejection possible
- Slight tendency for part to creep
- No scrap waste

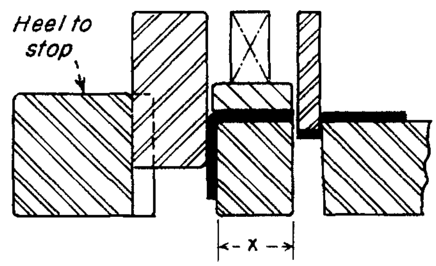

No. 2
- Good location and alignment
- Inclined ejection preferred
- Scrap slug wasted
- No creep if other punches are engaged
- Large spring space needed in punch holder

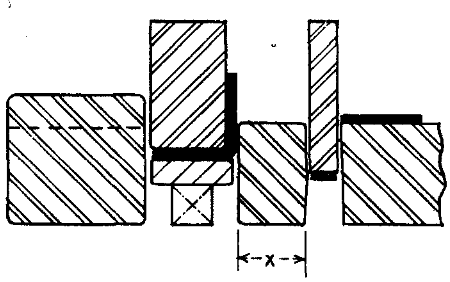

No. 3
- Alignment may depend on stock fit in stripper
- Push-through ejection is possible
- Some tendency to creep
- Scrap slug wasted
- Long cut-off punch required

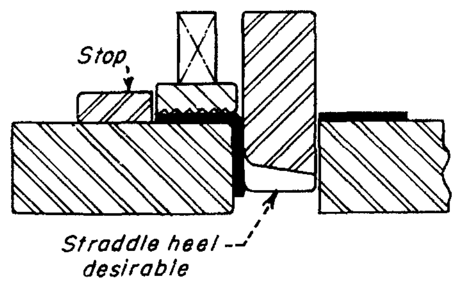

No. 4
- Inclined ejection required
- Tendency to creep
- No scrap waste
- Punch sharpening more difficult than other designs
- Large spring space needed in punch holder

RIGHT-ANGLE BENDS . . . continued

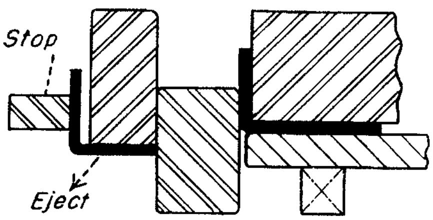

No. 5
Requires inverted pierce and notch operations
No creep if other punches are engaged
No scrap loss
Good ejection

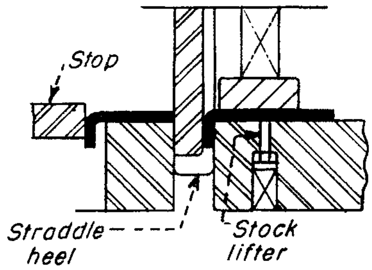

No. 6
For bends with short legs only
No creep if other punches are engaged
No scrap loss
More difficult to resharpen
Large spring space needed in punch holder

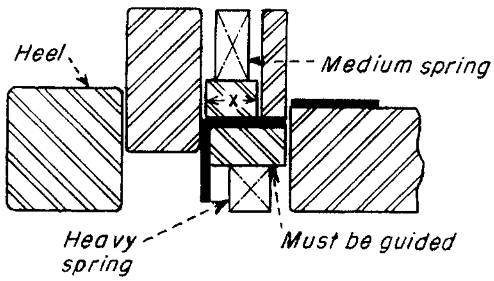

No. 7
More complicated and costly than other designs
Eliminates scrap slug, when forming downward is necessary
No creep occurs

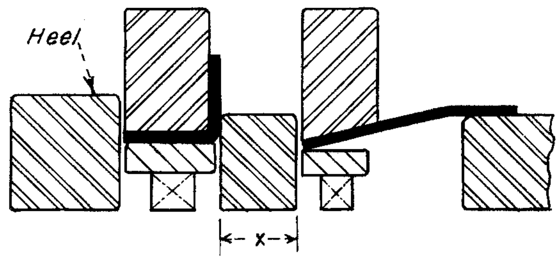

No. 8
Limited to thin material and short forming travel
Eliminates scrap slug, when inside form-up is necessary

ACUTE-ANGLE BENDS

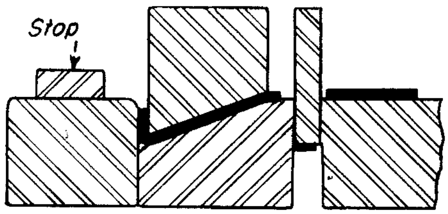

No. 9
Not suited to parts of all proportions
Resharpening die may cause difficulty
Scrap slug is wasted
Distortion of stock and creep are possible

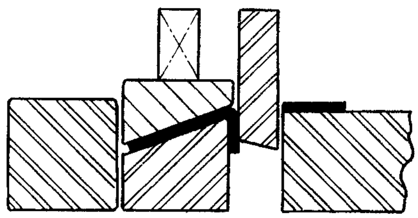

No. 10
Suitable only for moderately acute angles
No scrap waste
Some distortion of stock is likely

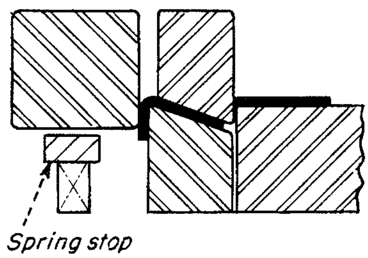

No. 11
No scrap waste
Not suited to parts of all proportions
Resharpening may cause some difficulty
Distortion of stock and creep are likely

ACUTE-ANGLE BENDS . . . continued

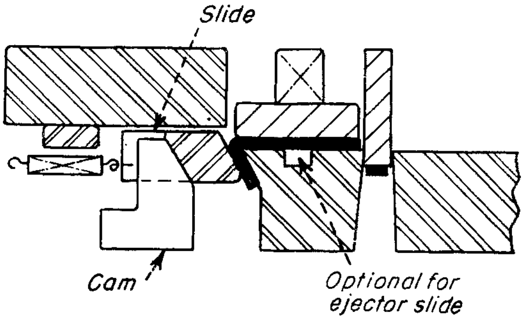

No. 12
- Widest adaptability
- Good-quality bends are produced
- More costly than other dies
- Inversion of design is possible

OBTUSE-ANGLE BENDS

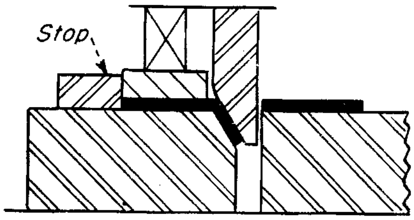

No. 13
- Inclined ejection is required
- Some difficulty in resharpening
- Special backup heel may be needed
- Large spring space required in punch holder

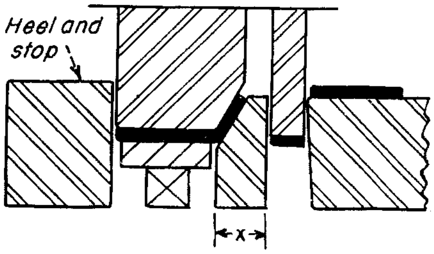

No. 14
- Inclined ejection is desirable
- Scrap slug wasted
- Some difficulty in resharpening

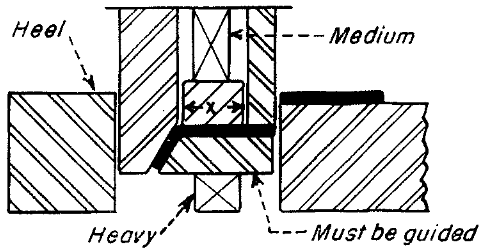

No. 15
- More complicated and costly than other designs
- Scrap slug is eliminated when form down is necessary

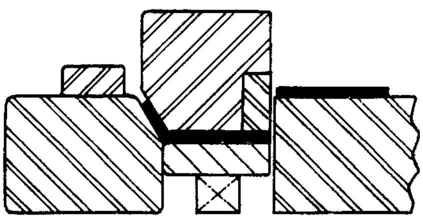

No. 16
- Good-quality bends produced on short legs and sharp corners
- Stock distortion occurs on long legs or when angle is close to 90°

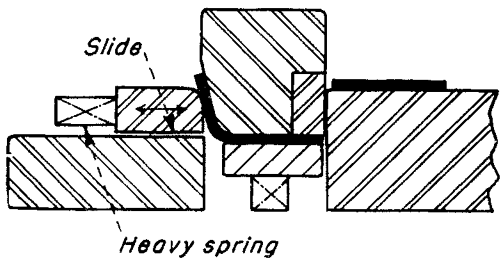

No. 17
- Desirable design when bend radius is large, because follow wiper minimizes stock out of control
- Usually unsuited to angles greater than 120°

OBTUSE-ANGLE BENDS — Continued

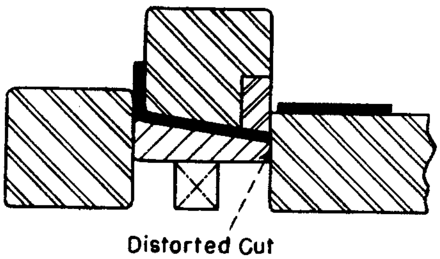

No. 18
Good design only when angle is close to 90°
Bends of good quality produced regardless of leg length or radius

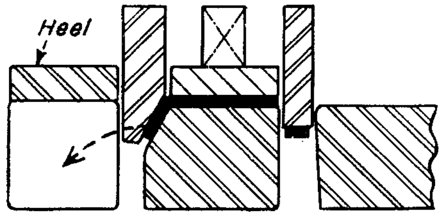

No. 19
Good-quality bends when legs are short
Push-through ejection is possible
Scrap slug is wasted
Large spring space needed in punch holder

CHANNELS

No. 20
Good location and alignment of bends
Inclined ejection is desirable
Scrap slug is wasted
Long cutoff punch is required

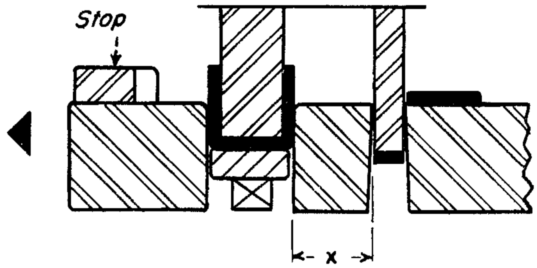

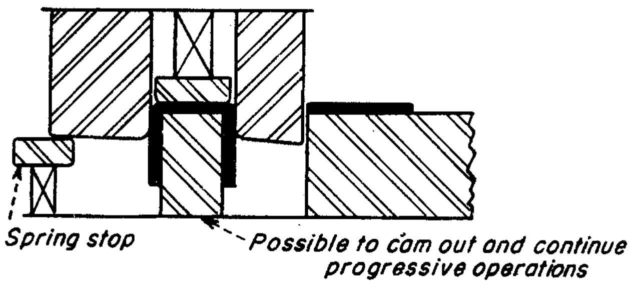

No. 21
Good design for cross-transfer operation
Inclined ejection is desirable
Large spring space needed in punch holder

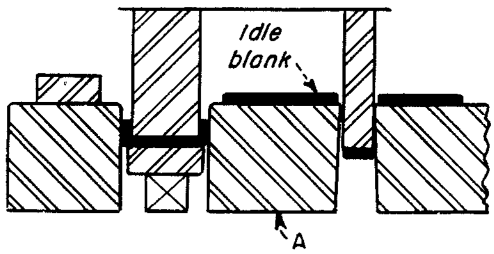

No. 22
Same notes as for No. 20 above
Introducing an idle station avoids thin die wall

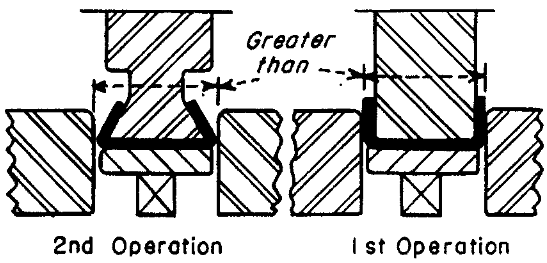

ACUTE CHANNELS

No. 23
Good quality bends are produced
Special ejection requirements must be met, but inversion may help
Cross-transfer or cut-and-carry progressive operation may be employed
Closely fitted guides or nest are required on 2nd operation

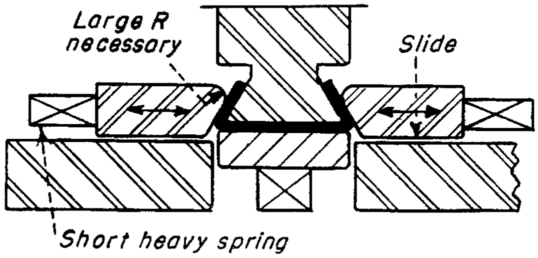

ACUTE CHANNELS — continued

No. 24
- Good quality bends produced; even 90° bends in springy material
- Not used for heavy stock or extreme acute angles
- Special ejection means are required

WINGED CHANNELS

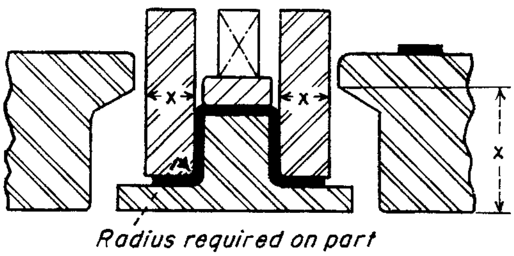

No. 25
- Limited to small parts
- Fair-quality bends produced, but wings will not be square unless spanked
- Large spring space may be required in punch holder

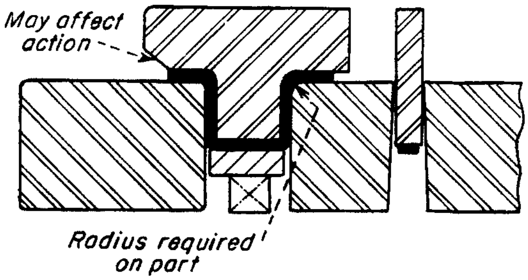

No. 26
- Bends usually of poor quality, but die cost is low
- Distortion remains from "slip forming" unless straightened by spanking
- Not suited to parts of all proportions

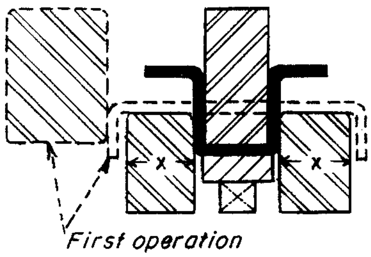

No. 27
- Bends of best quality produced
- Two operations are required; these may be cross-transfer or cut-and-carry progressive

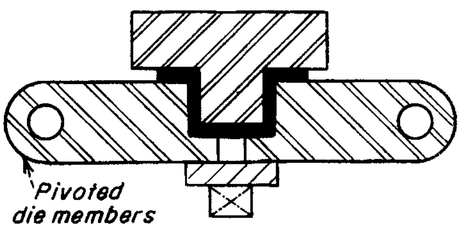

No. 28
- Bends of fair quality
- Do not use for heavy stock
- Die more difficult to construct, but useful for odd angles

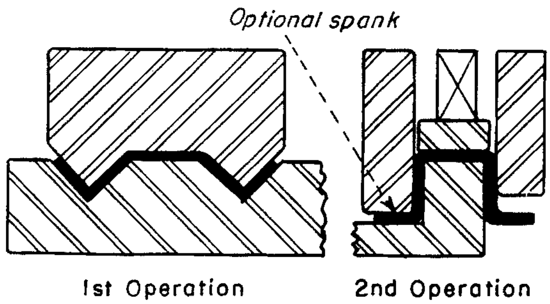

No. 29
- Fair quality bends
- Useful for odd wing angles
- Inversion of design is possible
- Die may be cross-transfer or cut-and-carry progressive type

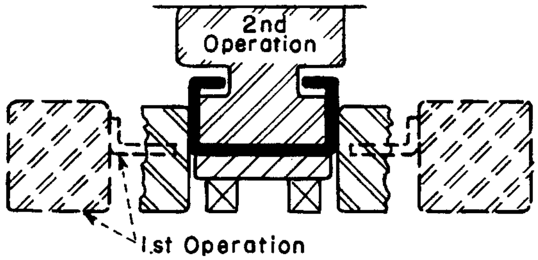

RETURN FLANGES

No. 30
- Two operations are required, but method produces good-quality bends
- Special ejection means required, but inversion may aid ejection
- Piece may be cross transferred or made in cut-and-carry progressive die

Z-BENDS AND OFFSETS

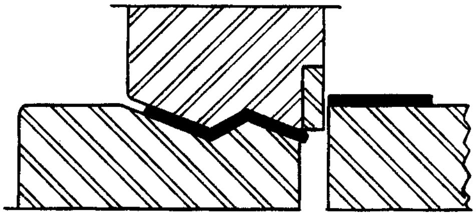

No. 31
- Good quality bends on small offset
- Low die cost

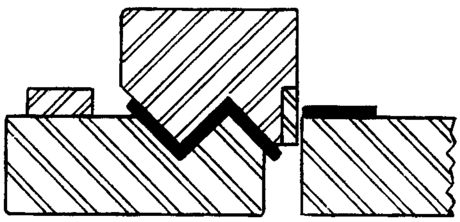

No. 32
- Fair quality bends
- Slippage of stock will cause some variation in bend location
- Die is low in cost

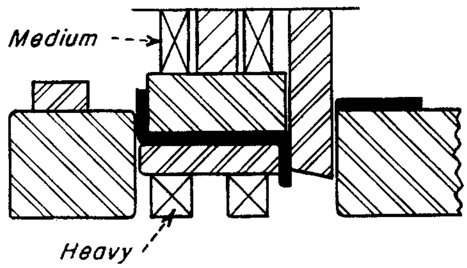

No. 33
- Good quality bends produced
- Slight tendency to creep is minimized by balancing spring pressures
- Large spring space required
- Pads must be guided

END HOOKS

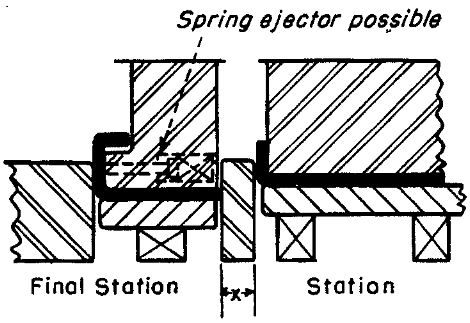

No. 34
- Good quality bends
- Special ejection requirements
- Inverted piercing and notching required

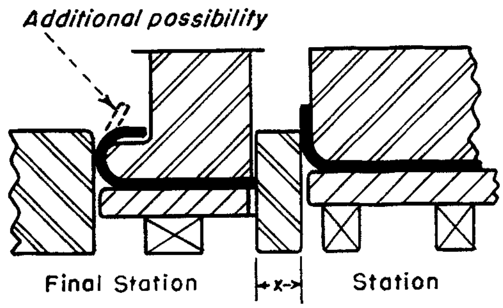

No. 35
- Notes same as at left, except that slight distortion of bend radius may occur

Wing Bending methods

Tangent and stretch bending methods and folding techniques are opening up new economies in making sheet-metal products by wrap-around instead of multi-panel construction.

Edward P. Schneider

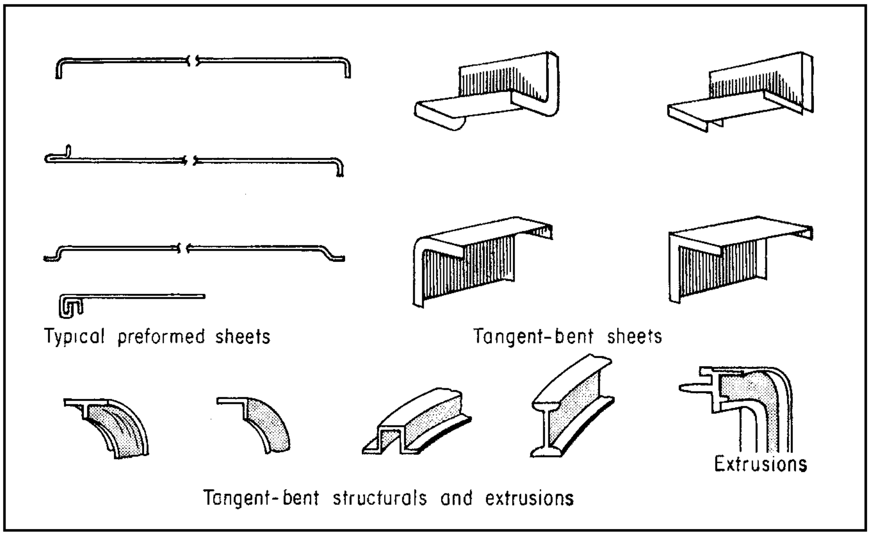

1. These preformed sheets and tangent-bent parts are only a few of the many shapes that lend themselves to wrap-around construction of products

Wing-type and stretch-bending equipment are used in the metal working industry for the production folding, tangent bending, and stretch bending of preformed sheet stock, bars, tubes, structurals, and extrusions with sections like those shown in Fig. 1. The greatest proportion of these jobs is done on the tangent bender due to the capabilities of the machine, its relatively high production rate, and the quality of work attainable.

Material—Use of wing-type and stretch bending machinery involves processing parts made from various grades of these materials:

(1) Low carbon steel
(2) Stainless steel
(3) Drawing-quality steel
(4) Copper and brass
(5) Aluminum
(6) Magnesium (in heated dies)

Material properly selected and prepared for bending operations meets these conditions:

(1) Sufficient elongation
(2) Preform section design suitable for proper dies and insert support during bending.
(3) More complicated preform designs can be supported by mandrels, or mechanically actuated die inserts during bending.
(4) A preformed section properly dimensioned for the tangent bending process is illustrated in Fig. 2. In this typical section, as dimensioned, it is understood that mill tolerance of +0.005 in., −0.003 in. metal thickness (MT) is acceptable.

The bending methods illustrated are normally used for making up to 90° metal folds or radius bends in flat or preformed metal.

Metal folding is a wing-type bending method by which comparatively sharp bends are made in flat or preformed sheet metal to produce cabinet shells and parts with sheer or well-defined corners. Where preformed material is processed through a metal-folding operation, corner notching is utilized so that no side flange upsetting or stretching is done, as in the case of tangent bending.

Tangent bending is a metal-forming process in which flat or preformed material is precision-bent to a specified radius. This type of bending is accomplished by a controlled rocking movement of a straight block-type 'rocker die' around a properly positioned 'radius die.' The bending takes place in small, progressive increments, always at the tangent point of rocker die application. At this tangent point the material is confined so tightly between the die elements that each stage of progressive metal movement causes continuous flow into a wrinkle-free bend.

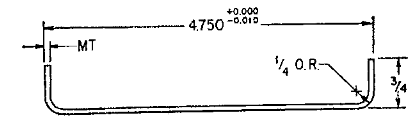

2. Tangent-bent parts should be dimensioned to the outside of the form

The rocker die component in a properly designed tangent bending die does not merely slide around the bend to set the metal down; its movement with respect to the material being processed is positively controlled by mechanical means.

The bending methods illustrated are normally used for making up to approximately 100° bends in flat or preformed metal. Variations in design of a product and the bending machine result in bends up to 180° for the wing-type bending methods shown in Figs. 5 and 6 on special applications.

The pivot point in each of the four bending methods shown corresponds to the swing center of the bender wing in a properly designed and efficiently maintained setup.

For either of the fold-action bending methods in Figs. 3 and 4, the pivot point is exactly in line with the top surfaces of clamp and wing dies, and is at a distance of MT (or slightly less) from the nose of the radius die.

Right angle bend—fold action

This wing-type bending, or folding method, Fig. 3, is usually employed in leaf-type sheet metal bending brakes or plain wing type folding machines where a 'sharp' corner is desired. Although the nose on the radius die may be machined to get a small inside radius in a fold, actual production will check between MT and 2 MT inside radius.

For 'sharp' folds in sheet metal having inside radius = MT (or less) it is always advisable to consider coining them on a press brake.

Radius bend—fold action

Technically this is the same action, Fig. 4, as utilized in Fig. 3, differing mainly in that a greater uniformity of forming from end to end of the bend is possible. This method of fold-action radius bending requires a much greater overbending allowance as well as a means of checking the unwinding of the bend when the bender wing swings down.

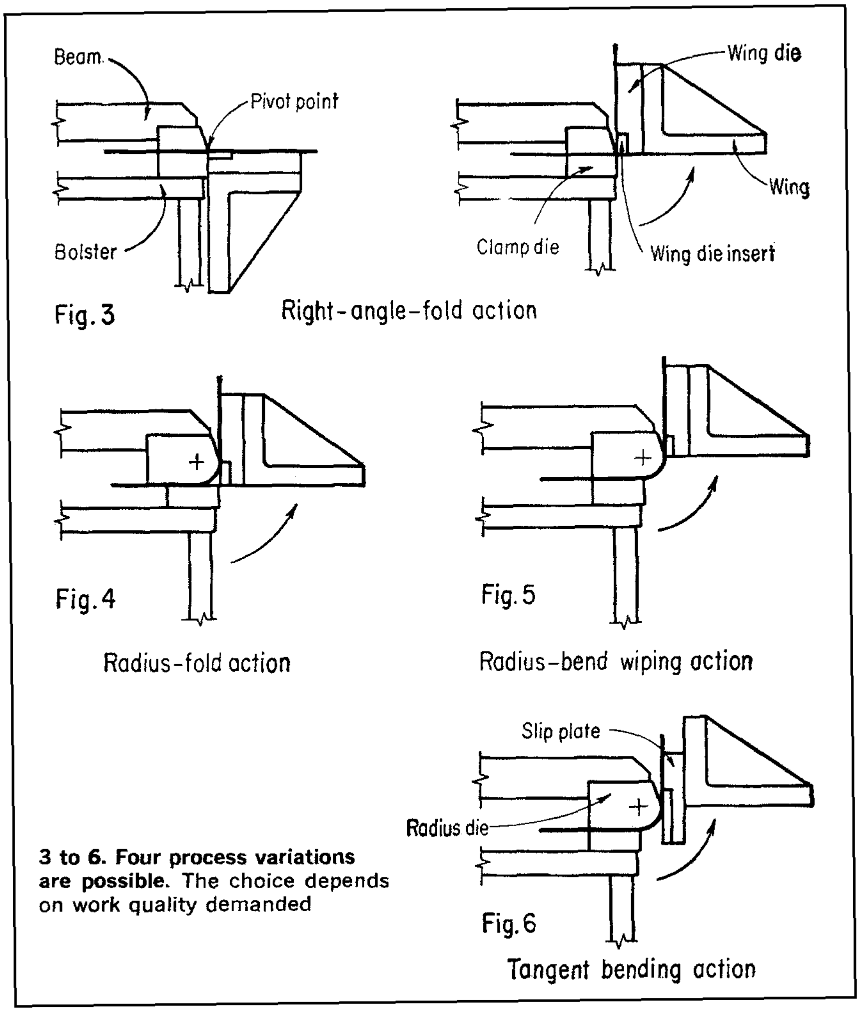

3 to 6. Four process variations are possible. The choice depends on work quality demanded

Radius bend—wipe action

In this type of wing-action radius bending, Fig. 5, the pivot point, or wing swing center, corresponds exactly with the center of the radius on the nose end of the radius die.

The wing die pushes the part metal against the radius die and skids on the outer surface of the bend area as the bender wing swings up. This action 'wipes' a bend in the part metal. Overbend requirements are less and more positively predicted in this method of radius bending of flat sheet metal than in bending methods described under Figs. 4 and 6. The wiping pressure is readily varied by shimming or spring loading the wing die to give desired setting effect to the bend as it is made.

Radius bend—tangent bending action

In this type of wing-action radius bending, the pivot point, or wing swing center corresponds exactly with the center of the radius on the nose end of the die.

Die space distances are at standard 3-place decimal dimensions, plus 0 000 in., minus 0.002 in., for:

(1) Bolster to pivot point, vertical direction.

(2) Pivot point vertically to beam in clamping position

(3) Pivot point horizontally away from wing to beam

In this method of wing-type bending, the rocker die applies canti-lever-beam type bending forces to the material in progressive increments, always tangent to the radius die during the completion of a bend.

Normally there is no skidding of a rocker die on part material as a tangent bend is made or as bender wing returns. This feature makes the process ideal for bending precoated or pre-finished stock.

Spring-Back Control

Don R. King

The problem of springback occurs in almost every bending operation. Even with dead-soft materials, springback may become serious where accuracy of the bend is required.

The pressure-pad type of wiped bend, Fig 1, is usually considered superior, but it is not always the complete answer. A point often overlooked is the rather high pad pressure required. This may be difficult to obtain unless a cushion is available in the press.

Standard formulas will give the approximate holding pressure, but in all cases the die should be tried out in "slow motion". If at any point in the bending stroke, a separation can be detected between the stock and the punch, more spring is needed. A relief angle on the punch, as shown, and a tight wiper setting are of some help.

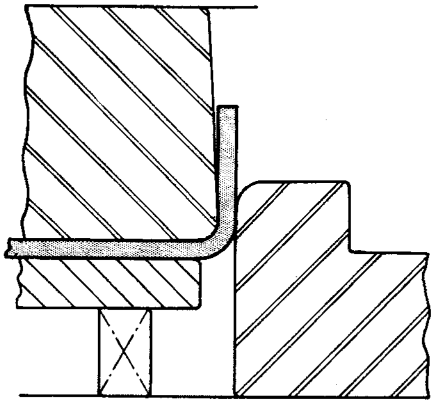

FIG 1

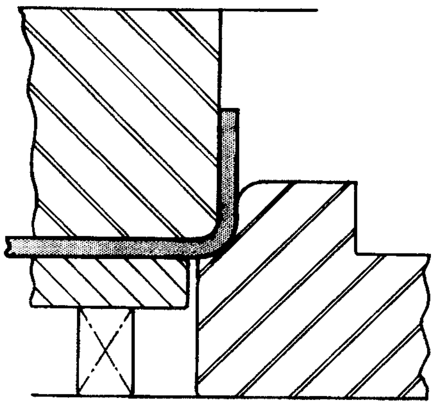

FIG 2

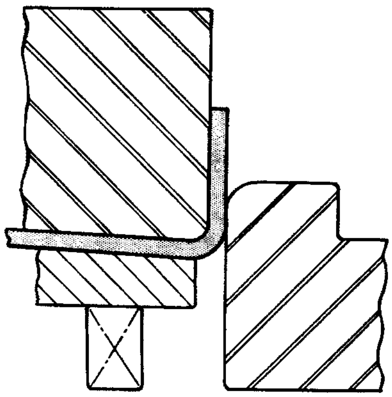

FIG 3a

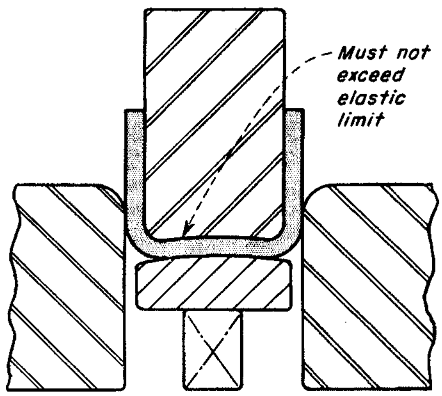

FIG 3b

"SPANKING" THE BEND

Another means of giving a more definite "set" to the material is illustrated in Fig 2. Here "spanking" of the bend area occurs at the bottom of the stroke. Careful stroke adjustment is required to prevent abnormally high pressures. Some improvement may be gained by altering the spanking radius to reduce the area of contact, but this partially defeats the purpose, and does not set the entire bend area.

One of the most satisfactory control methods is shown in Fig 3*a*. Here the pad and punch are constructed on an angle to compensate for the amount of springback. Uniformity of bends is good and not affected by the press stroke. As applied to channels, Fig 3*b*, this method is limited to combinations of channel width and material thickness that will not be permanently overformed by the compensation.

The usual explanation offered for the superiority of the pressure-pad, wiped-type of bend is that the material is ironed or stretched. It seems doubtful that the friction involved can produce stretching, and ironing mostly takes place after the bend is complete. A more likely explanation is that the wiper block or the entire die yields, and after passing tangency of the bend, re-

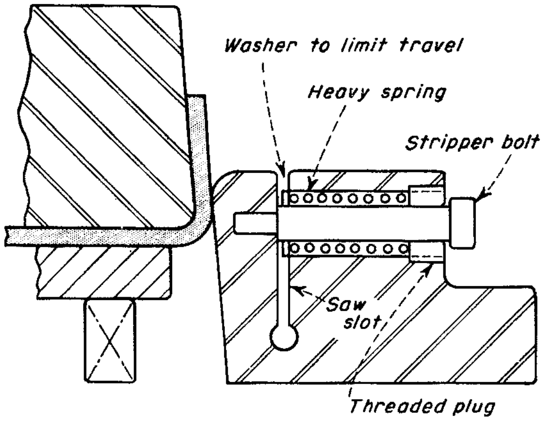

FIG 4

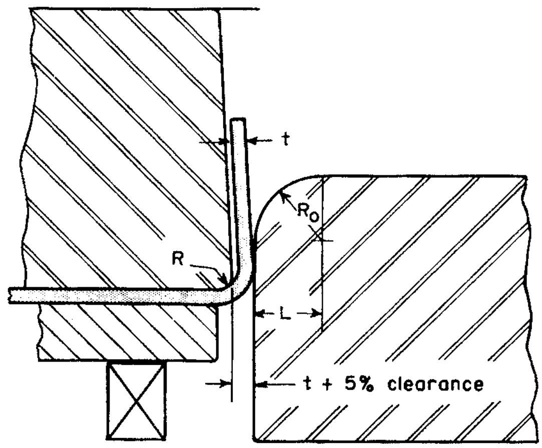

FIG 5

covery takes place and produces a small amount of overbending.

Extension of this reasoning led to the construction shown in Fig 4. Controlled movement of the wiper is introduced by means of springs and stops. The amount of movement required is very small. A few thousandths past tangency will correct a considerable angle of springback, and the simple spring-hinged wiper will be satisfactory in most cases. On light material, auxiliary springs may not be required.

Until now, we have considered only cases where the wiper is closely fitted, with stock clearance only, and have ignored the wiper-nose radius, as it has little effect under this condition. In Fig 5, a small clearance is provided between wiper and punch, in addition to stock thickness, and the wiper radius (actually length L) plays an important part in controlling spring back. When length L is in proper proportion, a small amount of "air bending" takes place at some point in the bending cycle. This is added to the formed bend, resulting in an overbend sufficient to counteract springback. The amount of overbend increases with an increase in L. It is also affected by the clearance, but it is easier to maintain this at about 5% of stock thickness and alter the nose radius. Exact dimensions will usually have to be determined by experiment. For a starting point, Table 1 shows the approximate dimension that will produce a slight overbend.

When the bend radius is large in proportion to stock thickness, the wiper radius becomes rather large. If space is limited, the nose contour shown in Fig 6 may be substituted. With this arrangement, L may be about 60% of the dimension for a plain radius.

table 1 . . LENGTH OF L TO OVERBEND

BEND RADIUS	LENGTH L
R = Sharp	4 t
R = ½ t	6 t
R = t	10 t
R = 2 t	15 t

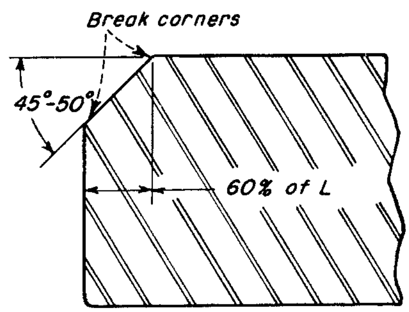

FIG 6

Control of U-Shaped Bends

Bernard K. H. Bao

Long U-shaped pieces are often troublesome to make when close tolerances are required across the bends. Various corner-setting means are used in die design to compensate for spring back. And usually strip-stock tolerances are required in production.

The method described in this article, in the author's opinion, is the most efficient way to control spring back when the inside bending radius is less than three times the stock thickness. Stock with a close thickness tolerance is not required. Regular sheet-stock tolerance is satisfactory in piece-part production. It is also possible to overbend a piece 2° to 3° when required.

The set corner on the die block is ground with a radius $R + t$ and is stopped at $\frac{1}{2}t$, as shown in Fig. 1. For soft and ¼ hard CRS or aluminum, the punch is made square (without back taper) for a 90° bend. Back taper is allowed on the punch side when overbend is required. Clearance between punch, die and pad is made to maximum stock thickness ($t_{max.}$) In calculating the dimension h, use minimum stock thickness. A nomograph, page 157 simplifies the calculation of h.

A regular rubber stamp, as shown in Fig. 2, may be used to show detailed dimensions of the set corner. Dimensions are filled in after all calculations are made.

Usually it is difficult to hold a close-tolerance bend in one bending operation for a part as shown in Fig. 3. For example, a piece with a large radius (say 8 to 10 times stock thickness) on one side and a smaller bending radius (say less than 3 times stock thickness) on the other side. By using the set corner described, it is possible to bend this part in one operation. The punch face and pad are ground at an angle to compensate for the spring back of the longer leg, Fig. 4. For the shorter leg the punch side is ground with a back taper to over-bend the shorter leg for the amount needed.

Punch radius R' for the longer leg usually is smaller than R on the finished part. It may be calculated* once the angle of spring back is determined by tryout.

*Refer to BAO Stamping Calculator sold by **BAO Slide Co**, P.O. Box 7902, Chicago 80, Ill.

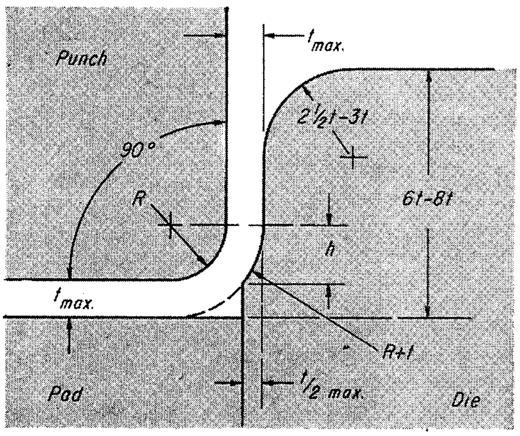

Fig.1

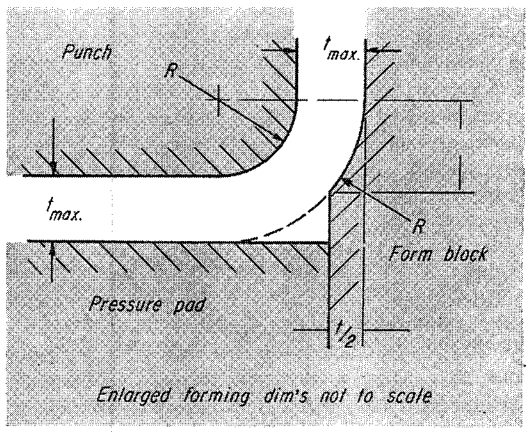

Fig.2

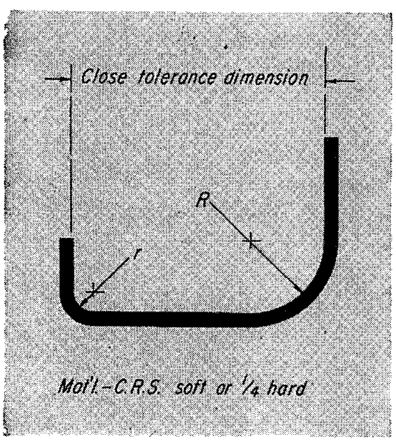

Fig.3

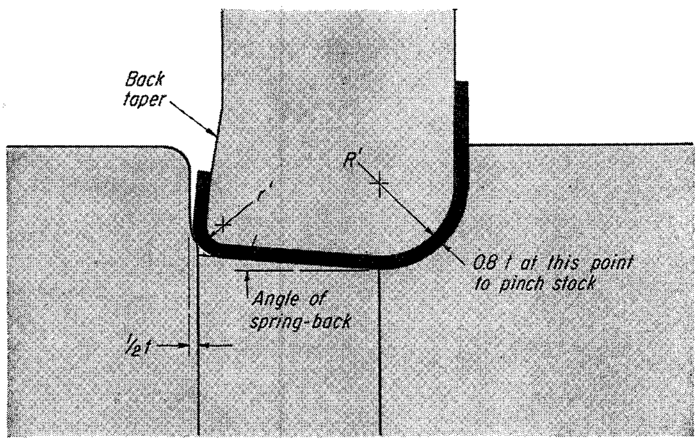

Fig.4

Determining die block dimension "h"

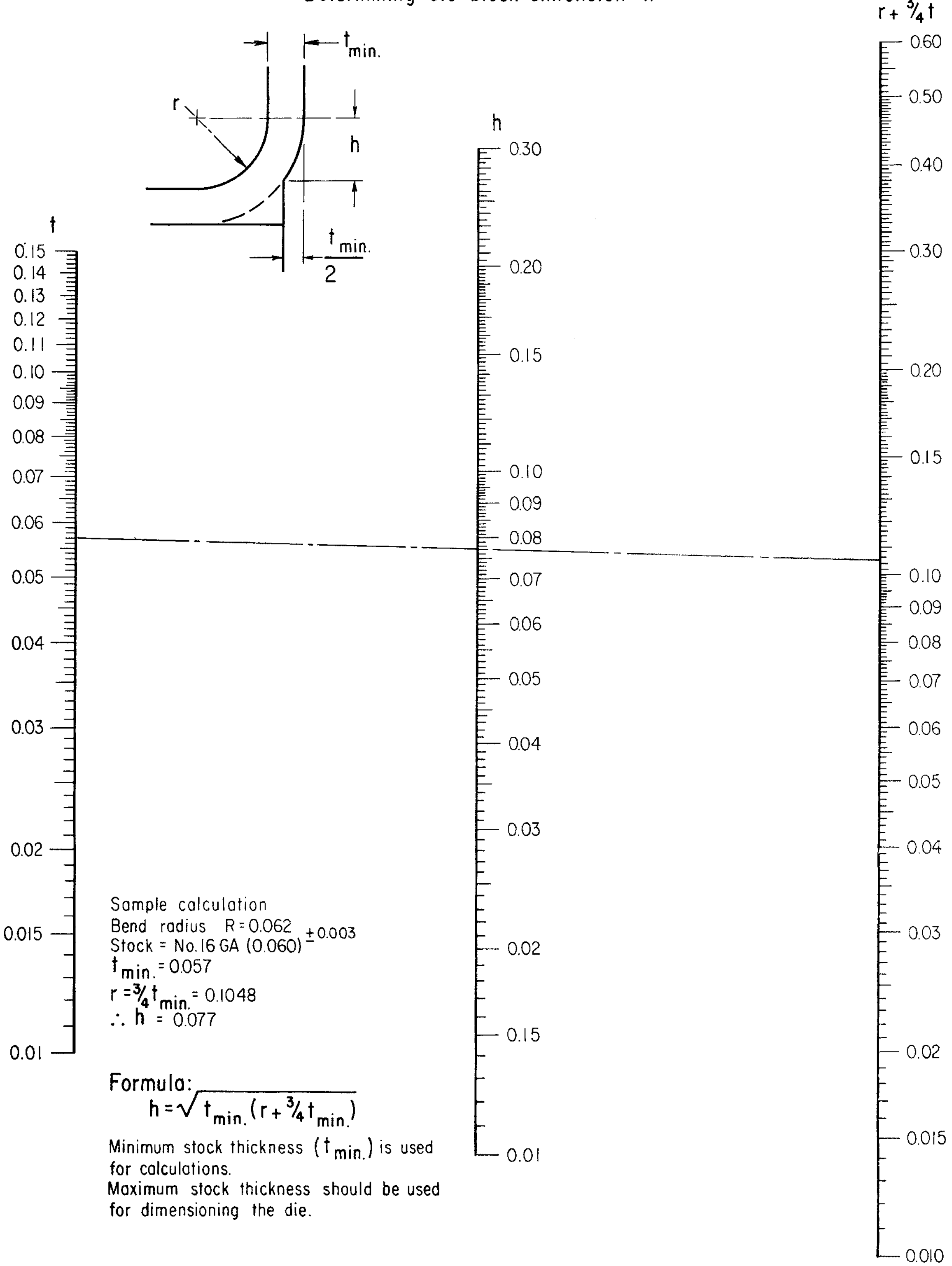

Sample calculation
Bend radius R = 0.062
Stock = No. 16 GA (0.060) ± 0.003
$t_{min.} = 0.057$
$r = \frac{3}{4} t_{min.} = 0.1048$
$\therefore h = 0.077$

Formula:

$$h = \sqrt{t_{min.}\left(r + \frac{3}{4} t_{min.}\right)}$$

Minimum stock thickness ($t_{min.}$) is used for calculations.
Maximum stock thickness should be used for dimensioning the die.

SECTION 25

INNOVATIVE VALVING

Types of Valves Used in Hydraulic Transmissions

Valves are the nerve center of hydraulic circuits. In machine tools, they provide reversal of motion, dwell and throttling action, sequence control, and relief of oil pressure. Some of the common forms of these valves are illustrated. Data and illustrations supplied from Socony-Vacuum Oil Company publication "Hydraulic Systems."

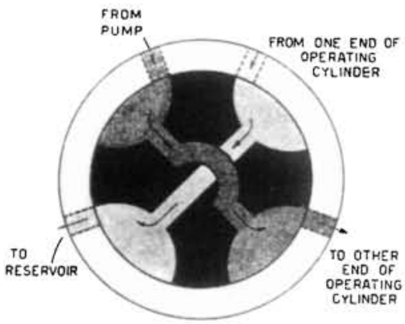

Fig. 1—Schematic diagram of rotary reversing valve. Oilways in an oscillating cylindrical plug register with ports which connect both the main oil line from the pump and the discharge line to the reservoir with either end of the operating cylinder. When oil is directed from the pump to one end of the operating cylinder, oil in the other end of the cylinder is discharged through the reversing valve to the reservoir. One position of the reversing valve shown.

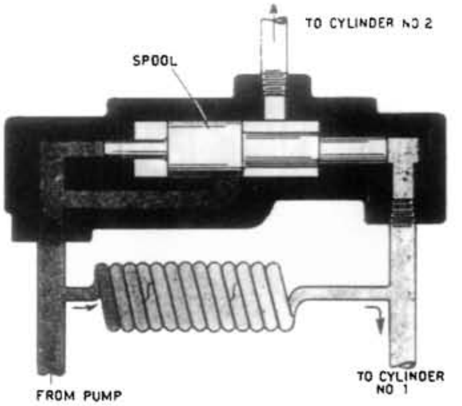

Fig. 2—Sequence control valve. Some machines are designed so that one series of motions must be completed before another series can start. This type valve prevents the flow of oil to No. 2 operating cylinder until the motion in No. 1 cylinder has been completed. Both ends of the freely floating spool are under oil pressure. The end exposed to pump pressure is smaller than the end exposed to pressure from No. 1 cylinder. From the pump, oil flows through a coil of tubing which slightly restricts the oil flow.

Pressure in No. 1 cylinder and on No. 1 end of the valve spool is less than the pump pressure, and this difference on the ends of the valve shifts the spool towards the low pressure side. Flow of oil to No. 2 cylinder is prevented. When motion in No. 1 cylinder is completed, oil no longer flows through the coil. Pressure on both sides of the valve is equalized. Full pump pressure now acts on the large end of the spool, and the spool shifts to admit oil to No. 2 cylinder.

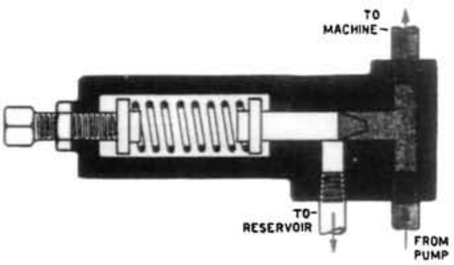

Fig. 3 - Spring-loaded relief valve. This valve is placed in the pump discharge line to permit oil to escape from the line to the reservoir when the amount of oil delivered by a constant-discharge pump is more than is needed. High pressure overcomes the compression of the spring, lifts the valve from its seat, and by-passes the oil until the pressure drops below the compression adjustment of the spring.

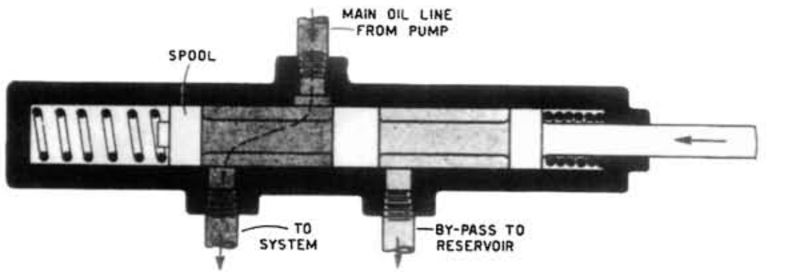

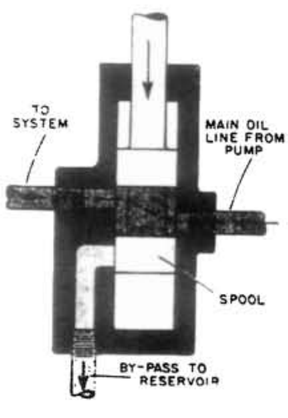

Fig. 4—Stop valves usually placed in the main oil line from the pump are operated manually or by cams. They are designed to stop the machine at a predetermined point. When the spool is shifted to a stop position, the flow of oil is interrupted and machine motion halted. While the machine is idling, the oil is by-passed at low pressure to the reservoir thereby reducing power costs. The machine is restarted either manually by the operator, or by cams which move the valve to a new position.

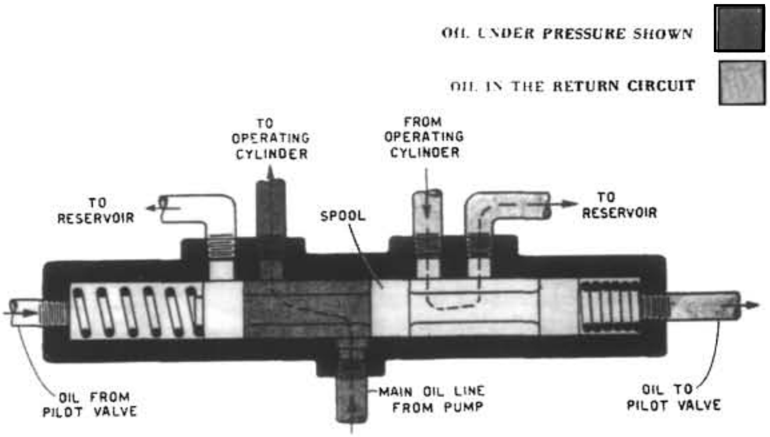

Fig. 5—Reversing valve. This valve directs oil flow in and out of either end of an operating cylinder. A separate pilot valve, Fig. 6, controls the oil pressure. The reversing-valve spool maintains a central position and floats between two springs. Pilot valve action moves the spool. When the spool is at one end of the valve, oil under pressure flows from the pump through the valve into one end of the operating cylinder, and at the same time, oil in the other end of the operating cylinder is discharged into the reservoir.

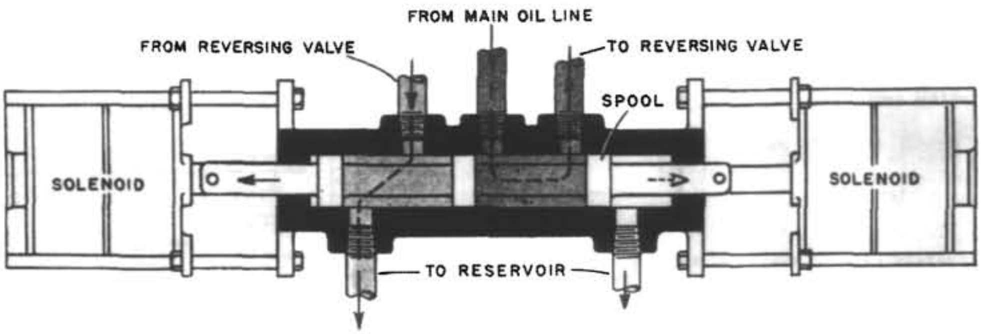

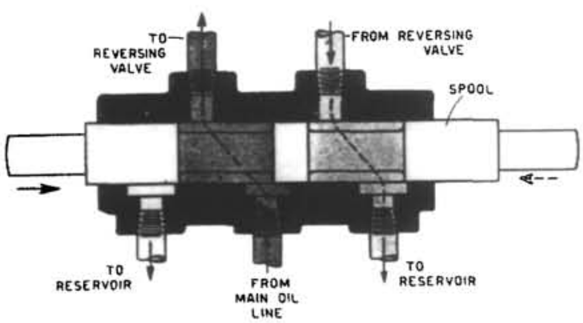

Fig. 6—Pilot valve. (above and left) Spools of these valves are thrown by cams or dogs, or may be moved magnetically by solenoids. Oil pressure from the pump is directed alternately to both ends by means of a reversing valve. Fig. 5.

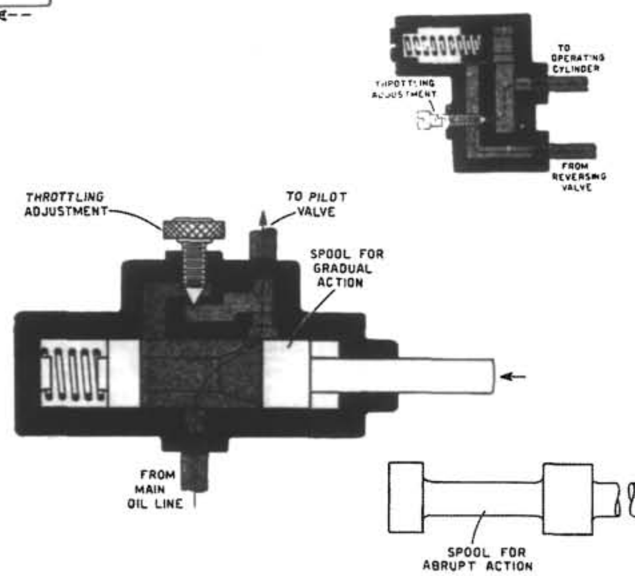

Figs. 7 and 8—Dwell and throttling valves. These spring-loaded valves are actuated by cams or oil pressure. Cam action moves the spool and shuts off this free oil delivery, permitting only a restricted oil flow through throttling adjustment. In the pilot valve line, this valve delays action of the reversing valve and permits a period of dwell at the end of the stroke of the operating piston. The change from free to restricted flow may be abrupt or gradual, depending upon the spool employed. In pressure actuated valves, Fig. 8, the valve is normally held closed by the spring. Delivery of oil is restricted by a throttling adjustment as long as the valve is closed. When flow is reversed, oil pressure lifts the valve and permits free delivery of the oil.

8 Ways to Make a Poppet Valve

Low seat forces can keep a tight seal—even for metal-to-metal seating.

Dominic J. Lapera

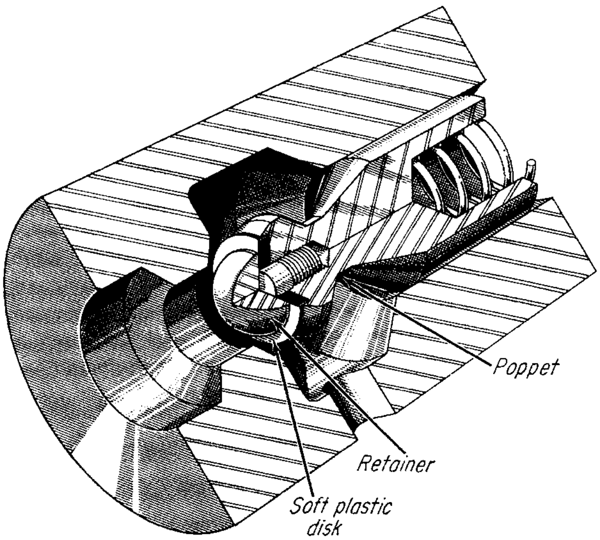

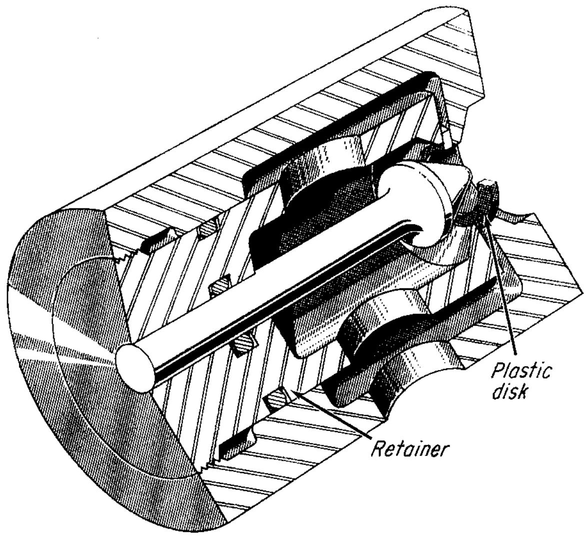

1 **CAPTIVE DISK** keeps bubble-tight seal when spring pushes it against conical seat in valve body. This, the most common design, is often found in checkvalves. It gives reliable service.

2 **CONICAL STEM** bears against sharp corner of soft plastic disk. Concentric retainer, which screws into the valve body, holds disk in place which is located by recess in body.

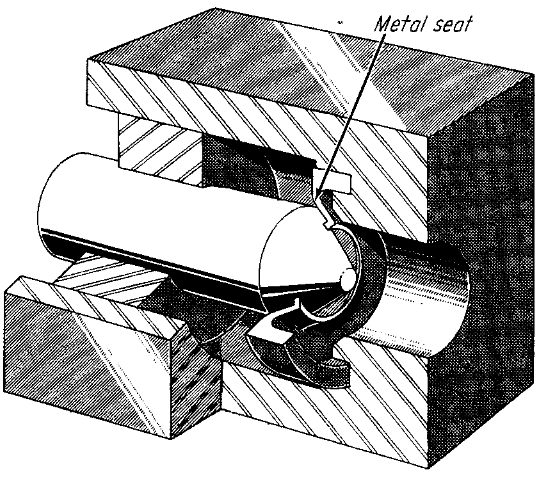

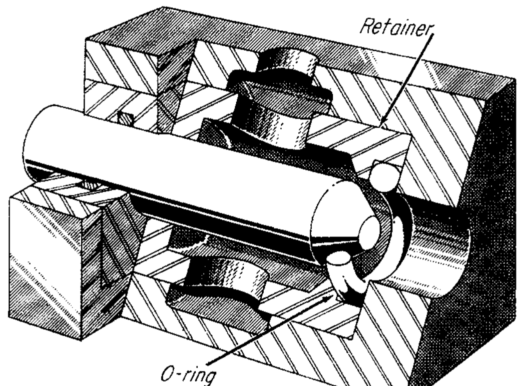

5 **FLEXIBLE METAL SEAT** can stand higher temperatures than plastic, but because flexing takes up some irregularities, it doesn't require the high seat loads normal with metal-to-metal valves.

6 **O-RING SEAT** will open at same pressure as consistently as much more expensive valves. However, cracking pressure must be quite high when compared to pressure at the normally rated flow.

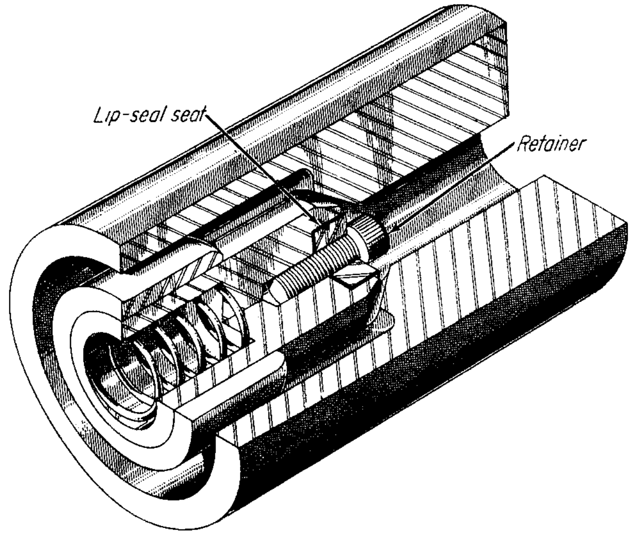

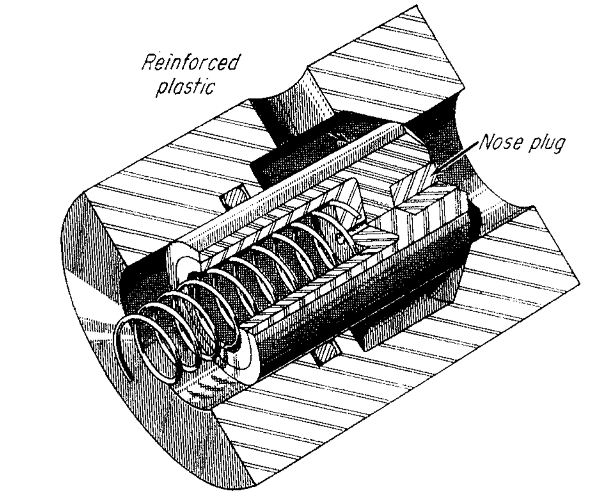

3 **LIP-SEAL SEAT** requires smallest force to be bubble-tight. Large forces flatten lip, so design works best when differential across seat is low. Example is a relief valve where fluid pressure opposes spring force.

4 **PLASTIC POPPET** cannot stand shock loading. Accurate machining for a good seal is easy because poppet guide and seat are in the same piece. Best angle between cone and seat is 20 to 30°.

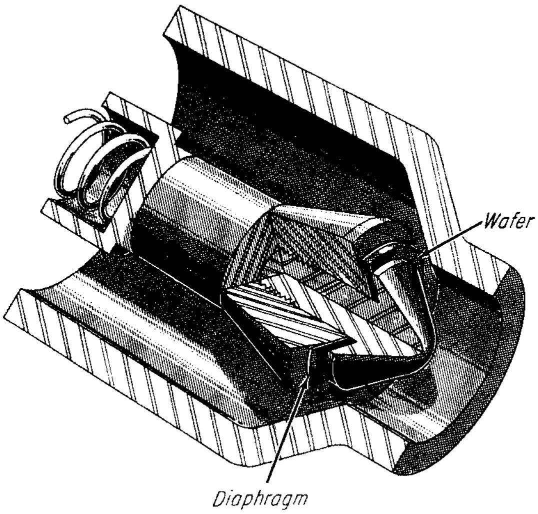

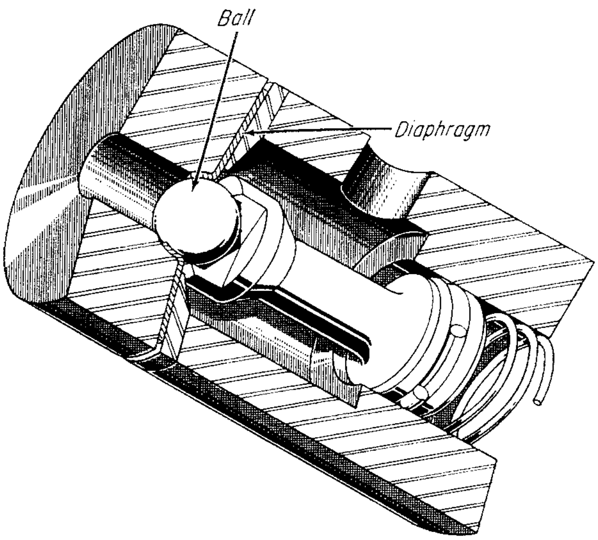

7 **METAL DIAPHRAGM** backs up seat wafer and presses it to contour of the cone. This compensates for irregularities common on large valves. Wafer must be thin enough not to wrinkle when deformed.

8 **BALL** forces plastic diaphragm against spherical seat. Vent will keep pressure from building up behind the ball which is not a force-fit in socket. Spring strength determines cracking pressure.

Weirs Replace Gate Valves

Simplify control of wastewater flows to treatment facilities.

Robert O. Parmley

The original metering manhole (Fig. 1) distributed wastewater flows to three separate treatment facilities and were hydraulically controlled daily by manually adjusting gate valves. Since flows to each treatment facility were not identical, the operator had problems maintaining proper hydraulic loading. Attempts were made to alternate discharges, but the influent wastewater quantities varied which resulted in a significant unbalance to the treatment components.

Solution: Modify the metering manhole by removing the three gate valves and replacing each with a weir box. Refer to Figures 2 and 3 for general arrangement.

Since two treatment facilities were designed to each receive 40% of the wastewater and one only 20% of the flow, the two former weir boxes would have to be capable of discharge twice the volume of the third. This ratio was achieved by making five identical v-notch weirs. Two were placed on two weir boxes and only one on the third. Refer to Figures 4, 5 and 6 for the exploded views of these assemblies. Note that the throats of weirs must be placed at the same elevation.

This arrangement insures accurate distribution, cost-effective design, low maintenance and trouble-free operation.

Figure 1

Plan view of original metering manhole

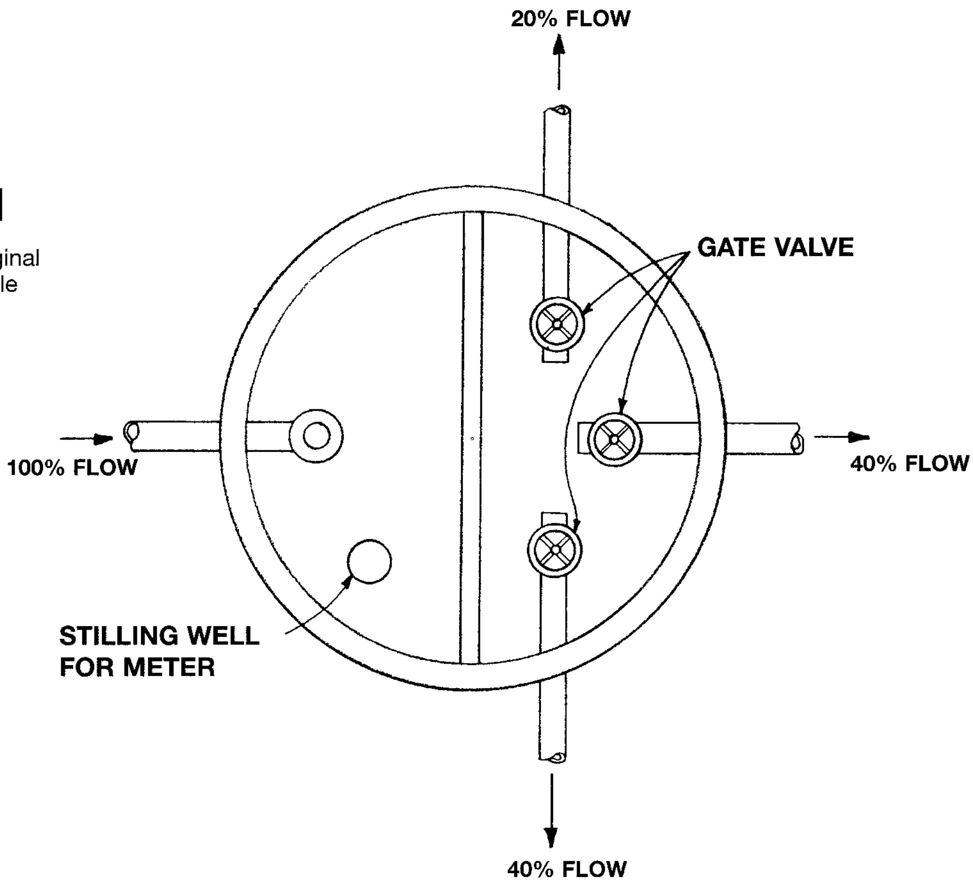

Plan View of Original Metering Manhole

Figure 2

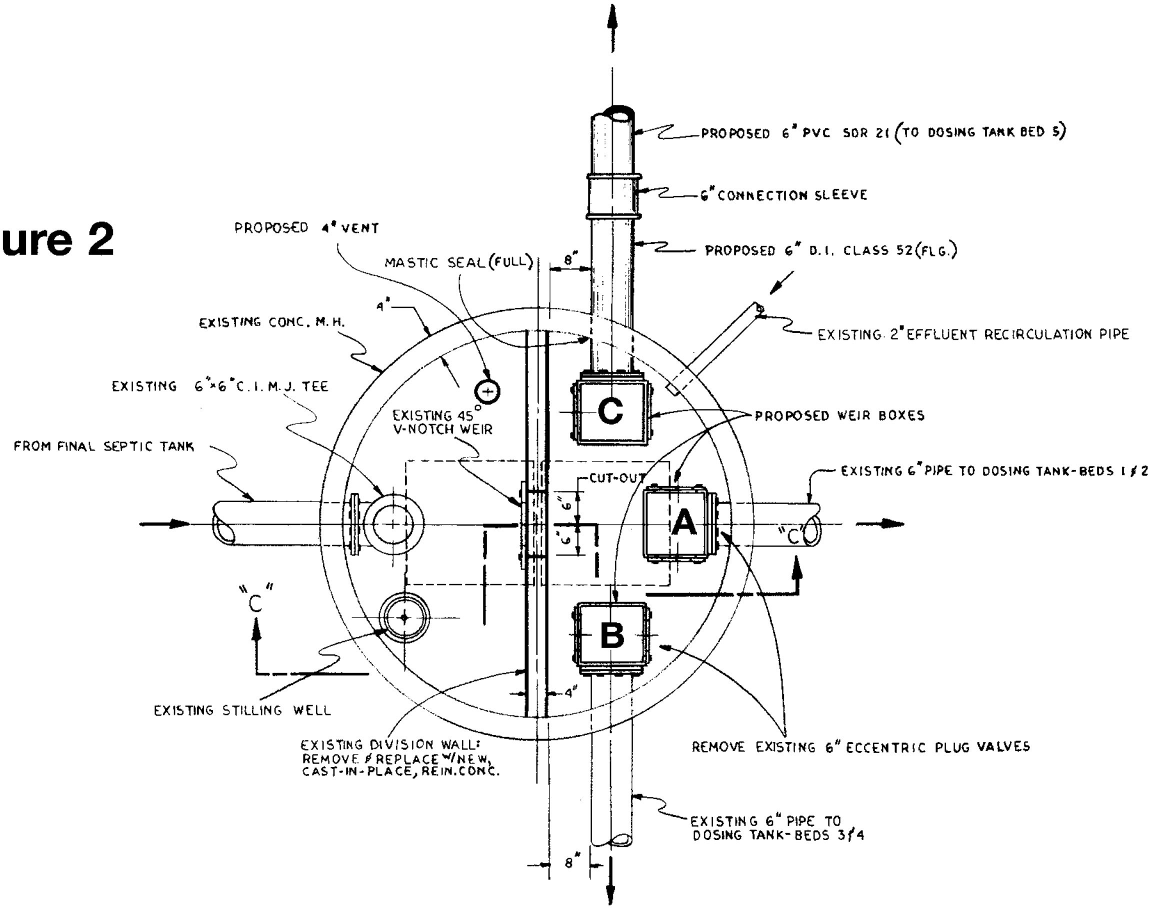

PLAN VIEW-EXISTING METERING MANHOLE W/MODIFICATIONS

Figure 3

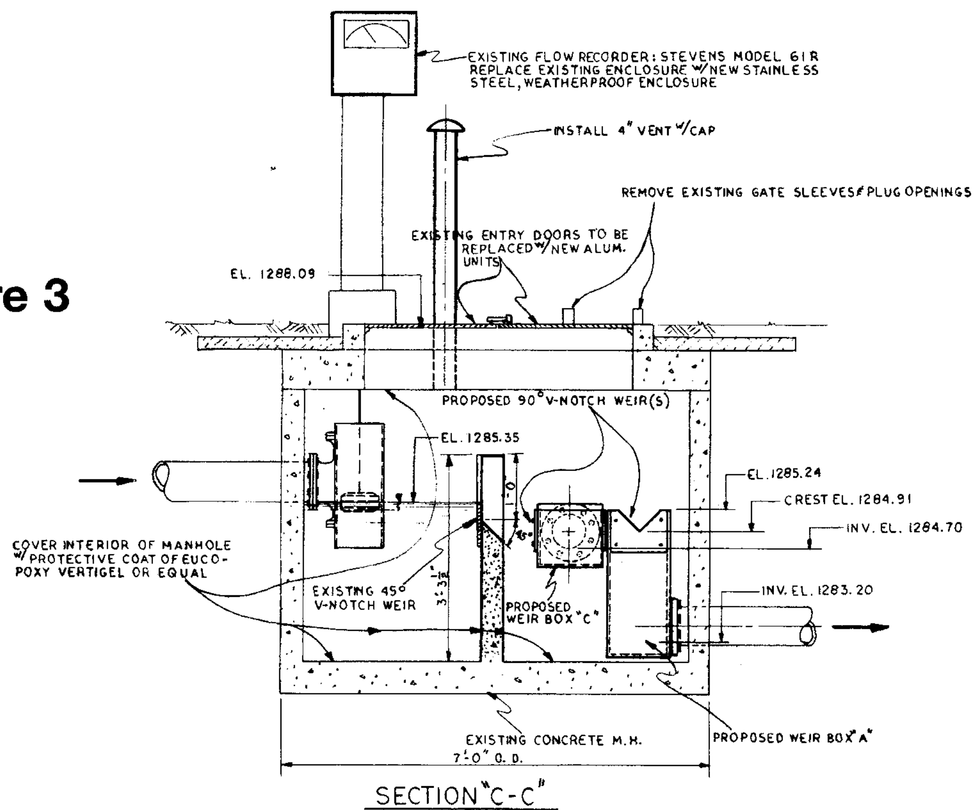

SECTION "C-C"

Drawings Courtesy of Morgan & Parmley, LTD.

Figure 4

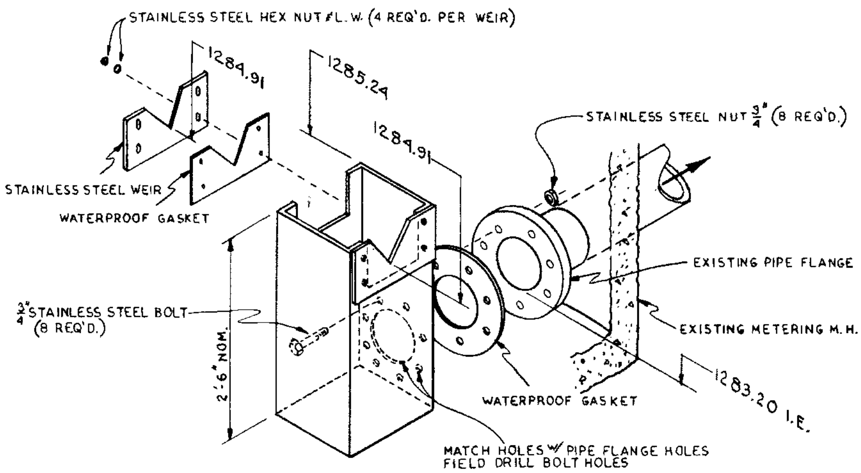

Exploded View of Weir Box @ Discharge "A"

Figure 5

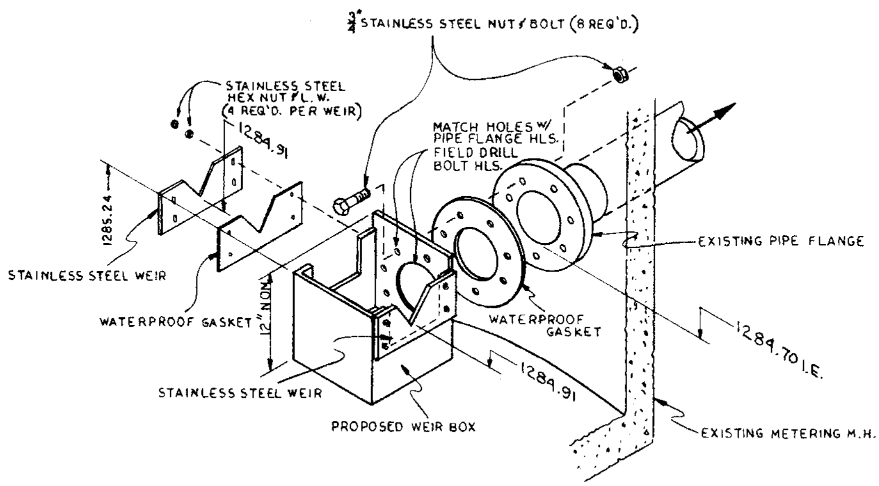

Exploded View of Weir Box @ Discharge "B"

Figure 6

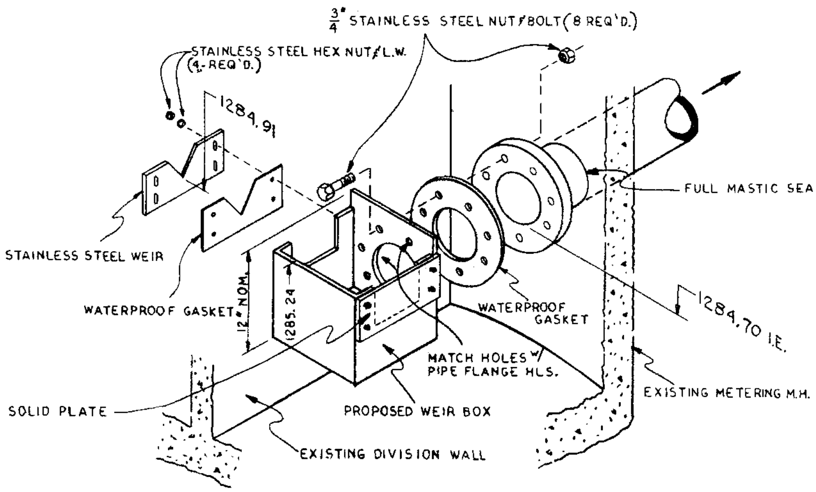

Exploded View of Weir Box @ Discharge "C"

Drawings Courtesy of Morgan & Parmley, LTD.

Siphon Serves as Regulating Valve

Robert O. Parmley

The previous article described the distribution of wastewater to three sperate treatment facilities. Prior to final treatment, the wastewater is temporarily stored in a dosing tank. Refer to Figure 1 for an overall schematic layout.

The final treatment process consists of a sub-surface rapid sand filter. This type of treatment functions best by alternating cycles, i.e. dosing/ resting. As an alternative to regulating valving and complex electronic controls, a simple, automatic siphon was selected. This mechanism, too, is cost-effective, low maintenance, and provides reliable trouble-free operation.

Figure 1

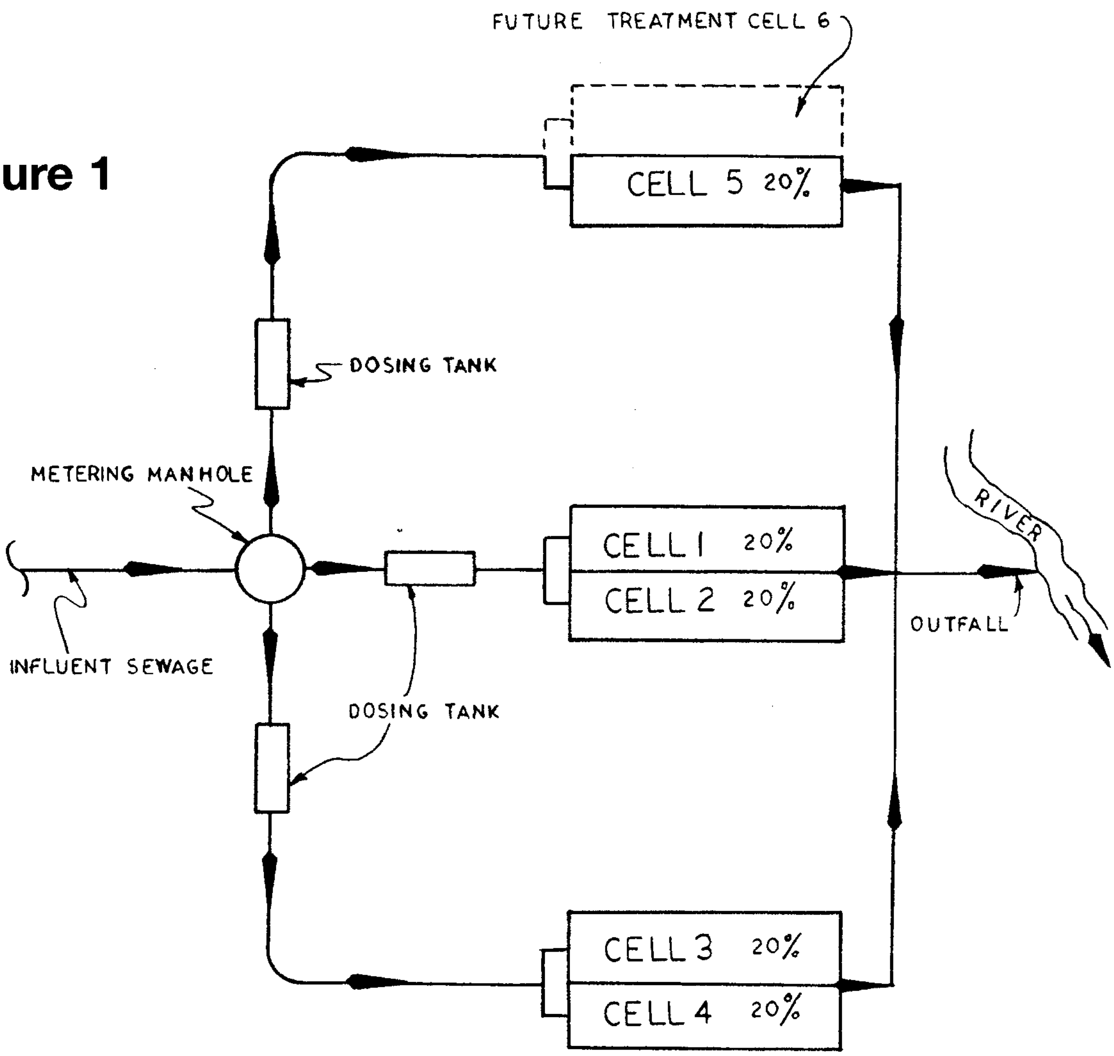

Schematic of Wastewater Treatment Facility

Figure 2

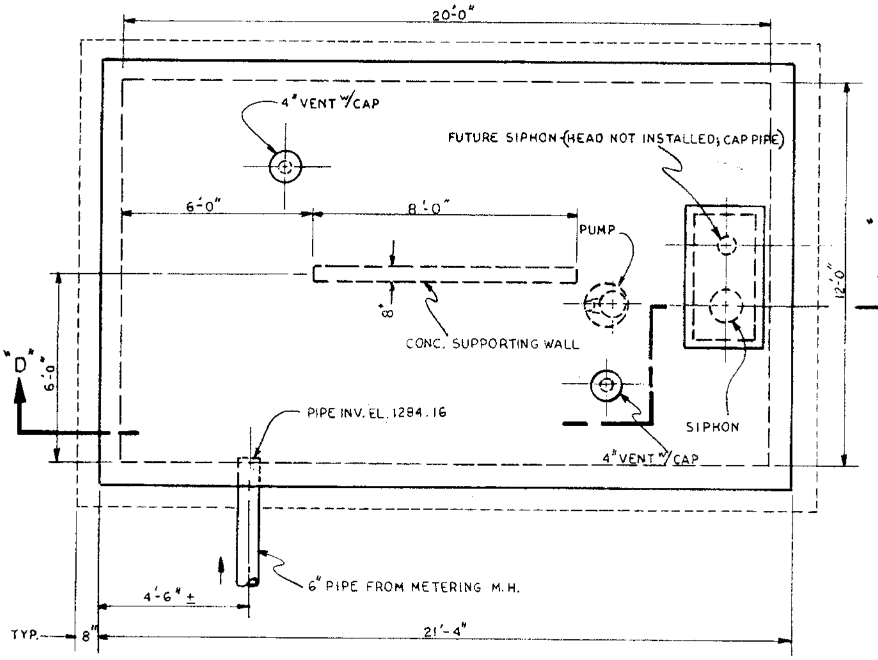

Plan View - Dosing Tank

Figure 3

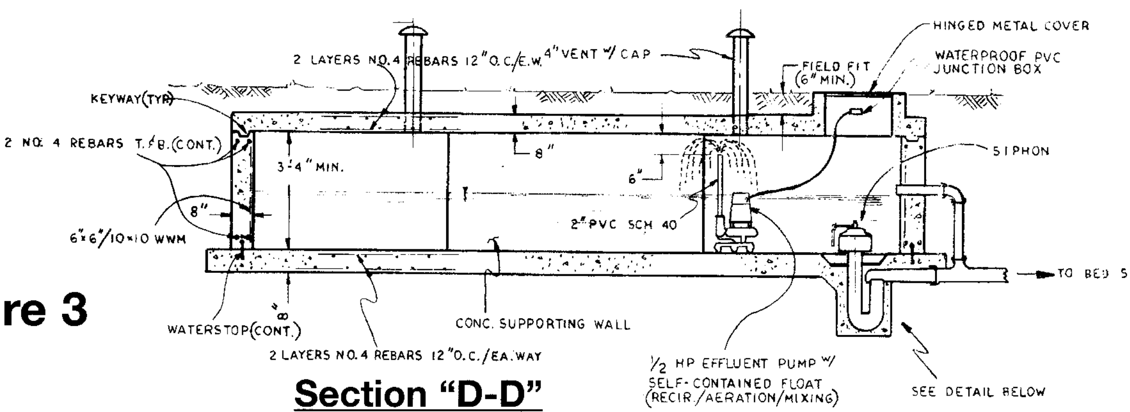

Section "D-D"

Figure 4

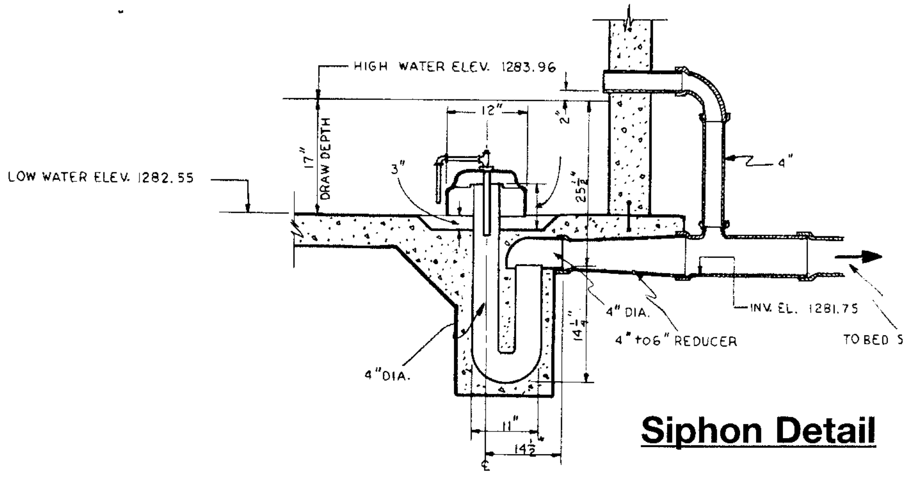

Siphon Detail

Triple-Duty Valve

One valve meters propellant, loads and fires BB shot in CO_2 powered handgun.

GAS-OPERATED pistol uses CO_2 cartridge in the handle to fire 0.177 BB's. The cartridge is screwed up against a puncture pin which pierces the sealed cap and channels the gas into the manifold. A metering orifice is used to reduce gas flow during the time the valve is opened. Gas flow and the amount of gas used are controlled by the spring-loaded valve and piston assemblies which also feed the BB's into the barrel.

With a CO_2 cartridge installed in the pistol, gas flows through the hollow puncture pin, filter, and metering orifice into the manifold valve chamber. The gas pressure, A, holds the piston against the elevator and the valve tightly against its seat on the rear of the piston. This restricts the gas to the manifold chamber.

When the trigger is pulled the elevator is raised until the nose of the piston contacts the cam face of the elevator, B. Gas pressure drives the piston and valve forward, camming the elevator up until the BB in the elevator is in line with the barrel. At this point the forward motion of the valve stem is arrested by the valve retainer. The piston continues forward, unseating the valve, C, and the gas is released from the manifold chamber. The gas passes through the hollow piston and drives the BB down the barrel.

The pressure in the manifold chamber drops to atmospheric as the metering orifice limits the flow of CO_2. The piston spring, assisted by the spring-loaded cam on the elevator, retracts the piston where it closes off the valve. The manifold chamber is sealed and gas passing through the metering orifice builds up pressure. The descending elevator aligns with the ready magazine and another BB is pushed into the elevator. The pistol is loaded and ready to fire.

Metered gas flow conserves gas and permits over 100 shots with one 8.5 gr CO_2 cylinder. Average velocity of 375 fps is maintained during the usable life of the cylinder. Capacity of pistol is 150 BB shots with 5 at a time channeled into a ready-to-fire magazine. The Daisy CO_2 100 semi-automatic pistol is produced by the Daisy Manufacturing Co, Rogers, Arkansas.

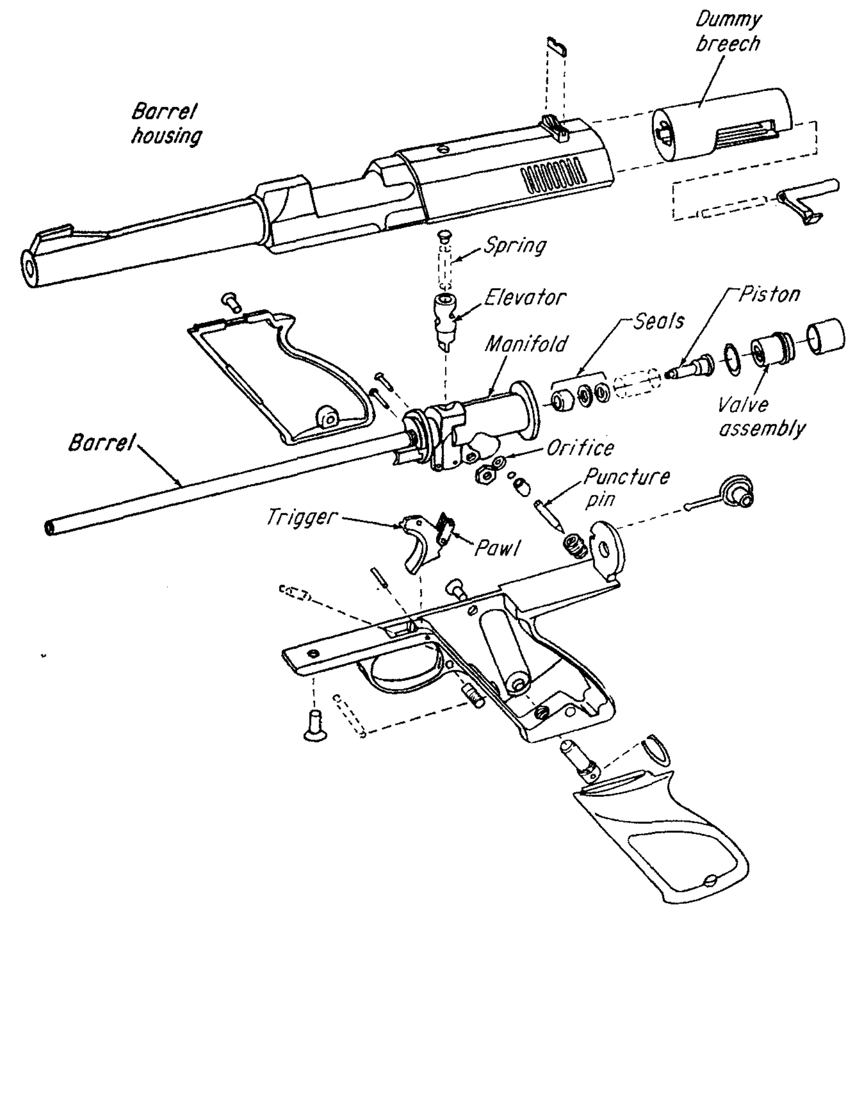

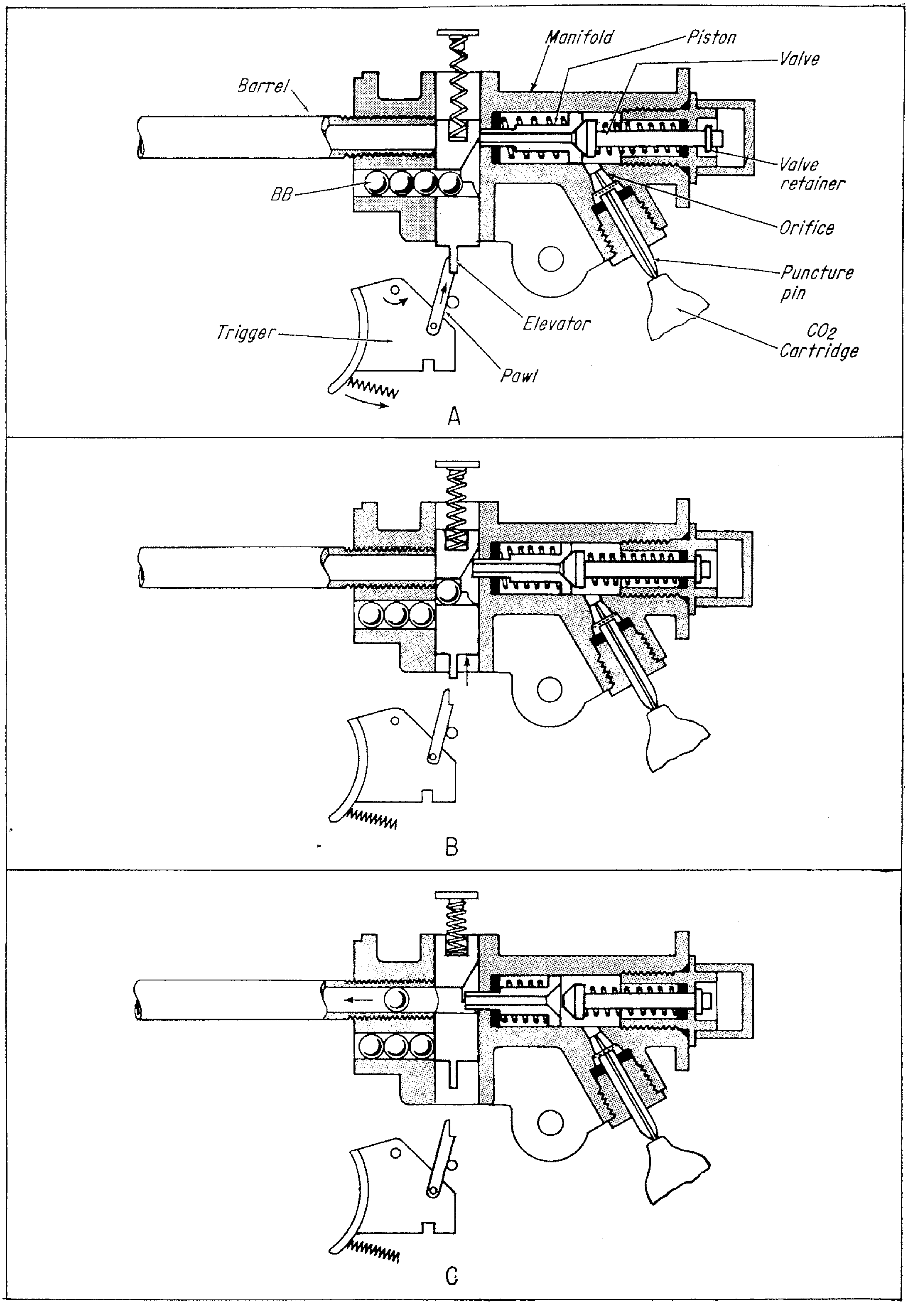

Manifold
Piston
Valve
Barrel
Valve retainer
BB
Orifice
Puncture pin
Elevator
Trigger
CO_2 Cartridge
Pawl
A
B
C

Flow Regulator Valve

Robert O. Parmley

This simple, self-cleaning device is designed to deliver a continuous quantity or flow of liquid over a relatively broad range of pressure. The controlling component is a precision engineered, flexible orifice which adjusts its opening area inversely to the active pressure. When flow pressures are below the threshold point, the flexible component responds as a fixed orifice. However, when pressures are encountered above the threshold level the inserts commences to distort or restrict thus reducing the orifice area and thereby maintaining the desired flow.

These regulators are widely used in various mechanisms, including: water systems, fire protection facilities, medical devices, filling equipment, drinking fountains, filtering units, fan coils, cooling tanks and similar systems.

Refer to Figure 1, which illustrates an inexpensive installation in a municipal pumphouse. It was incorporated into the interior piping design to protect a public potable well from being over pumped. In the event of a major fire or main break, the distribution system pressure would be significantly reduced thereby normally allowing the well pump to produce a larger delivery. This condition would result in a greater drawdown of the (cone of influence) pumping level, well below the well screen top, and air would be introduced into the system. The flow regulator, shown in Figure 1, avoids this adverse condition.

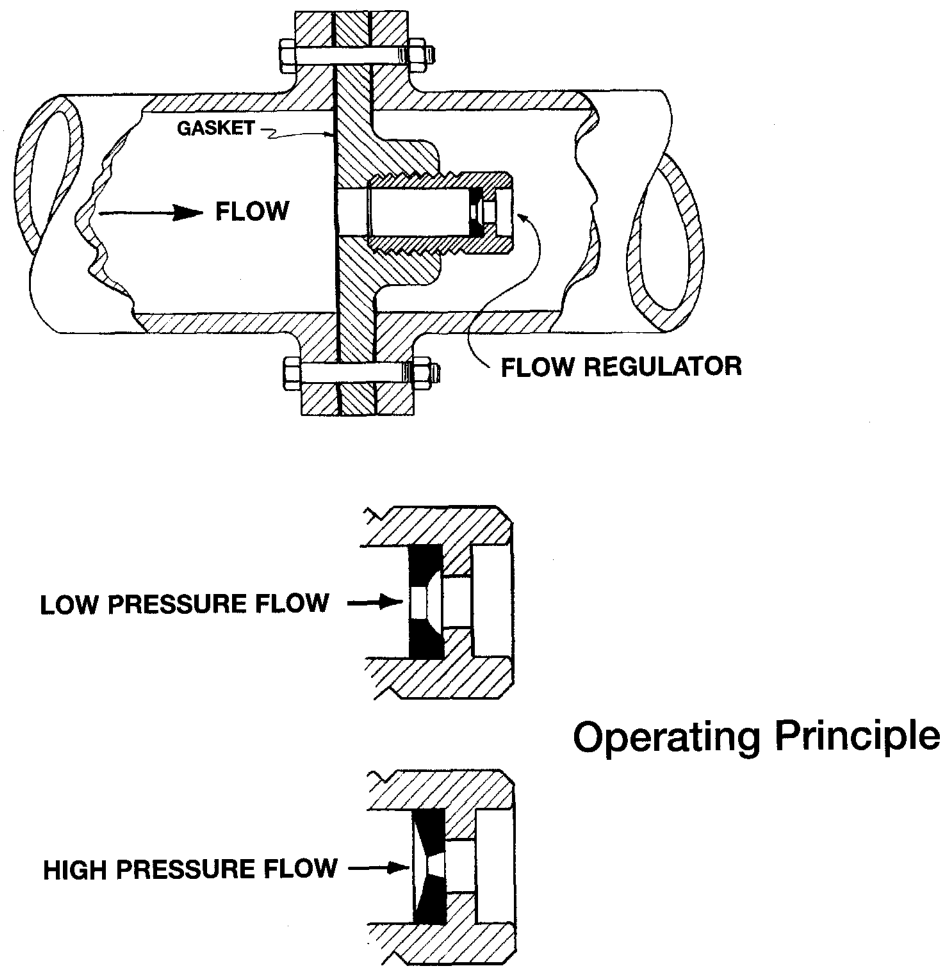

Figure 1

Fuel Injection Systems–Secondary Problems

Vapor suppression and idle fuel metering are two stumbling blocks to perfect fuel delivery. Here are several ways to overcome these problems.

Gerald Bloom

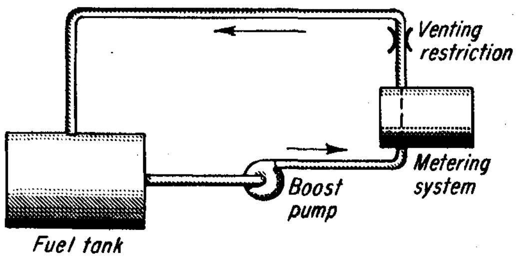

VENTED PRESSURIZED SYSTEM. Boost pump supplies fuel under pressure to the metering pump; unused fuel returns to tank through restriction which maintains pressure. Recirculated fuel helps cool the metering pump, which, in turn, helps reduce vapor formation.

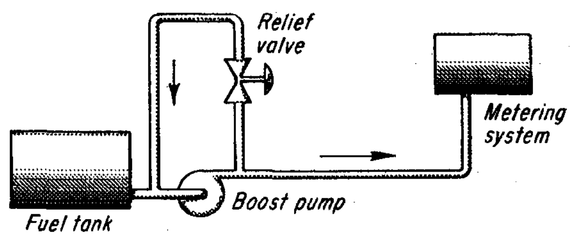

UNVENTED PRESSURIZED SYSTEM. Boost pump pressure is set high enough to condense all vapors, which eliminates loss of fuel constituents, but fuel cooling is lost. The boost pump should be kept as close as possible to tank to minimize inlet pressure drop and negative head.

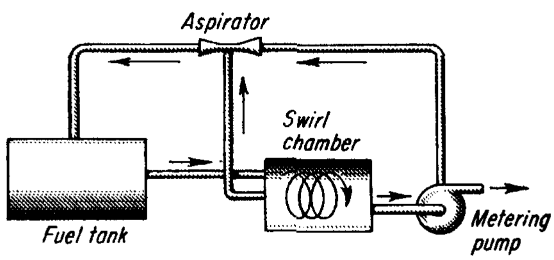

ASPIRATOR SYSTEM. Fuel is drawn from tank by metering pump suction. Then it spins in the swirl chamber where liquid and vaporized fuel separate by centrifugal force. Vapor is drawn off by low pressure generated by return flow through aspirator. System is very inexpensive.

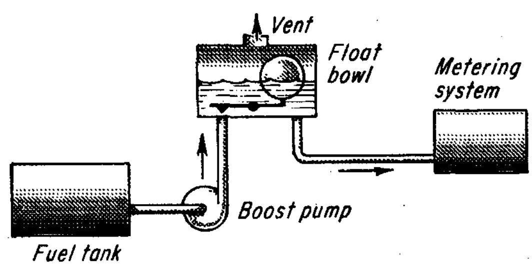

FLOAT BOWL. Fuel is pumped to the float bowl as in a normal automotive carburetor. Fuel vapor vents to the atmosphere where the more volatile elements of the fuel are lost. System is considered excellent for ground and marine applications, but can't handle altitude problems.

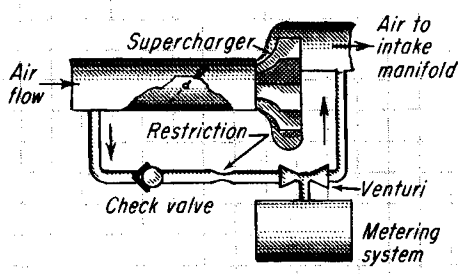

AIR-SIGNAL BIASING. Though unusal requirement is for enrichment at idle, some engines do not scavenge cylinders and need to lean the fuel. Here, the pressure differential at idle opens a check valve, air flows through venturi, sending a reduced pressure signal to the system.

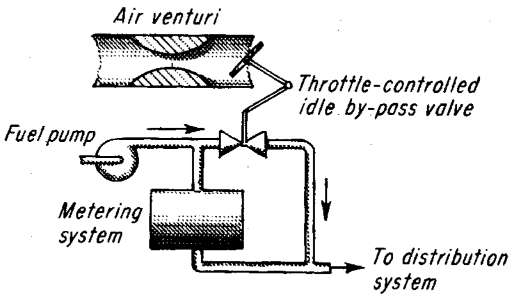

IDLE BY-PASS. Venturi pressure drop in mass-flow metering system is too low to give a usable signal at idle. So, main metering system is by-passed by a throttle-connected valve which meters fuel at supply pump pressure to maintain a proper idling speed and eliminate engine stalling.

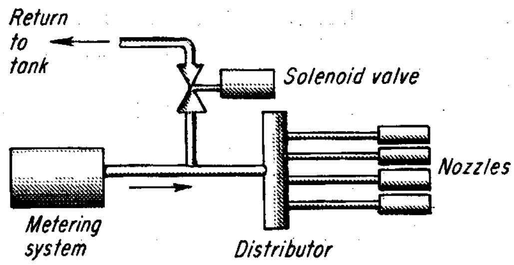

MOTORING CUT-OFF. When wheels drive engine, ideally fuel should be shut-off. This is done by opening by-pass solenoid valve, which prevent fuel line pressure from building up enough to open nozzles. Solenoid is energized by throttle piston and engine speed or intake manifold vacuum.

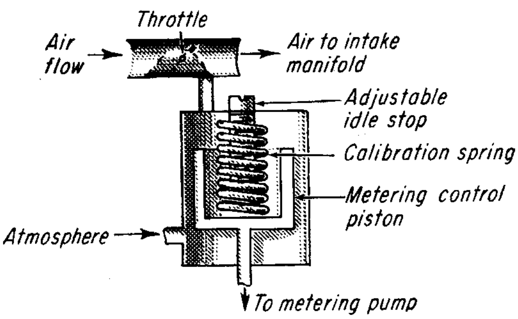

IDLE STOP. Speed-density system requiring idle enrichment can be designed with a fixed stop (shims or adjustable screw) to prevent control piston from going to zero output position. A spring as the idle stop permits leaning out when wheels drive as in driving downhill.

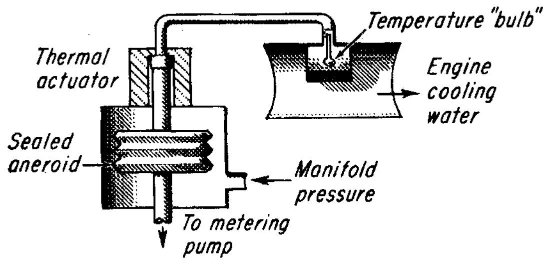

COLD ENRICHMENT. To provide extra fuel for a cold engine, metering system is set rich. As engine coolant warms, thermal actuator gradually leans the fuel/air mixture. Another method uses a temperature-sensitive switch to feed fuel directly into the intake manifold of the engine.

SECTION 26

PUMPS

Pumps . . . Major Classes and Types

One of man's oldest aids, the pump today ranks second only to the electric motor as the most widely used industrial machine. Anything that will flow is pumped–from highly volatile ether to thick muds and sludges. moltem metals and liquids at 1000 F, or higher, pose few real problems for modern pumps.

Though the origin of pumps is lost in antiquity, we do know that crude pumping devices provided water for ancient Egypt, China, India, Greece and Rome. Today the U.S. alone draws more than 200 billion gallons each day from its water resources and pumps move almost every drop. Of this total, an impressive 80 billion gallons is said to be industry's share.

To meet these demands we find an almost confusingly large variety of available pumps. They range from tiny adjustable displacement units to giants handling well over 100,000 gallons per minute. Number of designs soars into the hundreds, some differing in elements as small as packing glands, some in the entire principle of operation.

It's neither possible nor desirable to cover every variation in a concise practice practical handbook or manual. So we've made a highly selective choice of widely used industrial pumps of all classes and types – the pumps you're likely to run into in your work. And we've stuck to units using mechanical means to move liquid from one point to another, putting aside for a time such devices as ejectors, hydraulic rams, etc.

So you'll find the important facts about industrial pumping in easy-to-read form in the following pages. Put them to work improving the effectiveness of your pumping operations.

CLASS	TYPE		IMPORTANT GENERAL FACTS
CENTRIFUGAL	Volute		The majority of centrifugal pumps built in the U.S. today are volute type. They are available as horizontal or vertical pumps, single- or multistage for wide flow ranges
	Diffuser		Diffuser-type centrifugals find many uses as multistage high-pressure units. Originally more efficient than volute-type pumps, today efficiency of both types is about equal
	Mixed-flow		Mixed-flow centrifugal pumps are ideal for low-head large-capacity applications. Usually vertical, they have a single-inlet impeller. Some horizontal units are built
	Axial-flow		Axial-flow units, often called propeller pumps, develop most of their head by lifting action of vanes, are usually vertical, and best suited for low heads, large capacities
	Turbine or regenerative		For clear liquids, turbine pumps, either horizontal or vertical, fill a need between other centrifugal and usual rotary designs. They are low- to medium-capacity,high-head
ROTARY	Gear	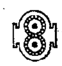	Gear pumps consist of two or more gears (spur, single- or double-helical teeth), while vane pumps have a series of vanes, blades or buckets turned by a single rotor. This rotary class also includes lobe or shuttle-block designs
	Vane		
	Cam-and-piston		Cam-and-piston rotaries, like most types in this class, are positive-displacement units, giving steady discharge flow. Along with screw-type pumps, and related designs, they handle a wide range of nonabrasive viscous liquids
	Screw		
RECIPROCATING	Direct-acting	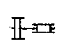	Old standbys for years, direct-acting steam pumps now are available in many designs for handling cold or hot water, oil, and a wide range of industrial liquids of many types
	Power		Power pumps are driven from outside through a crankshaft or other device. Capacities range from very low to medium flows, at pressures up to 15,000 psi, or higher
	Crank-flywheel		Crank-and-flywheel pumps are one form of reciprocating power pump, so designated to distinguish them from power pumps using, for example, an eccentric as drive mechanism

Source: The following 25 pages are reprinted with permission of Power Magazine, The McGraw-Hill Companies.

classes and types in use today

	Centrifugal		Rotary	Reciprocating		
	Volute and diffuser	Axial flow	Screw and gear	Direct-acting steam	Double-acting power	Triplex
Discharge flow	Steady	Steady	Steady	Pulsating	Pulsating	Pulsating
Usual max. suction lift, ft	15	15	22	22	22	22
Liquids handled	Clean, clear; dirty, abrasive; liquids with high solids content		Viscous, nonabrasive	Clean and clear		
Discharge pressure range	Low to high		Medium	Low to highest produced		
Usual capacity range	Small to largest available		Small to medium	Relatively small		
How increased head affects:						
Capacity	Decrease		None	Decrease	None	None
Power input	Depends on specific speed		Increase	Increase	Increase	Increase
How decreased head affects:						
Capacity	Increase		None	Small increase	None	None
Power input	Depends on specific speed		Decrease	Decrease	Decrease	Decrease

DEFINITIONS

PUMPING is the addition of energy to a liquid to *move it from one point to another*

CENTRIFUGAL PUMPS employ centrifugal force to develop a pressure rise for moving a liquid

ROTARY PUMPS use gears, vanes, pistons, screws, cams, segments, etc, in a fixed casing to produce steady positive displacement of a liquid

RECIPROCATING PUMPS use pistons, plungers, diaphragms or other devices to positively displace a given volume of liquid during each stroke of the unit

IMPELLER is the rotating element in a centrifugal pump through which liquid passes and by means of which energy is imparted to the liquid

CASING of a centrifugal pump is the housing surrounding the impeller. It contains the bearings for supporting the shaft on which impeller mounts

LIQUID PISTON OR PLUNGER of a reciprocating pump is the moving member that contacts the liquid and imparts energy to it

SINGLE-STAGE centrifugal pump is one in which total head is developed by one impeller

MULTISTAGE centrifugal pump is one having two or more impellers acting in series in one casing

Pumps . . . *major classes and types*

The world of pumps can be extremely confusing to newcomers—and even to some oldtimers. Diagram, *left*, is designed to clear up much of the mystery and confusion surrounding pump *classes* and *types*. You might call it your road map to the world of pumps. Based on often-used standard classifications, it incorporates a number of useful facts that are a big help in pump selection and application.

Three classes of pumps find use today—*centrifugal, rotary* and *reciprocating*. Note that these terms apply only to the mechanics of moving the fluid, not to the service for which the pump is designed. This is important, because many pumps are built and sold for a specific service, and in the complex problem of finding which has the best design details we may overlook the basic problems of class and type.

Each classification is further subdivided into a number of different types, diagram *left*. For example, under the rotary classification we have cam, screw, gear and vane pumps. Each is a particular type of rotary pump.

To go one step further, let's take a brief look at a fuel-oil pump in wide use today. It is a rotary three-screw type available with rotors of a number of different materials and four means of balancing axial thrust.

The last two items are important *details* in pump application; first two are keys to classification of the unit. The Hydraulic Institute recommends that the standard classification be considered as applying to type only, leaving the builder to use the details he has developed or standardized for that type of pump. So in selecting a pump we often find we must compare, detail for detail, a number of makes. Broad breakdown in diagram comes in handy then.

Our next consideration is a wide statement of the general characteristics of a given class of pumps. Table, *above left*, does just this for us.

For example, if we want to handle relatively small capacities of clean, clear liquids at high head, we can refer to the table. In any problem of this type we must remember that suction lift should not exceed recommended limit. Capacity in gallons per minute (gpm) determines pump size and influences classification. Nature of fluid is also involved, as is pump construction. Head is a big factor.

Table shows a reciprocating pump is suitable for the general conditions we have in mind—small capacity, high head, clean, clear liquids. Then, depending on job needs, we may choose a piston or plunger type, direct-acting, crank-and-flywheel, or power type. It may be simplex, duplex, triplex, or have a larger number of cylinders.

Once we've settled these items we're ready to study valve details, materials, drives, etc. In general, you'll find that pump details are greatly influenced by job requirements. Thus the particular arrangement of a centrifugal pump may depend as much on piping, space and working conditions as on any other existing factors. Drive chosen for the pump may be fixed by the pump speed, plant heat balance, power supply available or cost of a particular fuel in the area. But again, these are details, to be decided after we find a pump suitable for the hydraulic conditions we must meet. And the key to meeting the hydraulic conditions is the right class and type of pump.

Where two or more different units meet hydraulic needs, we must go one step further and decide which pump is best for the installation. We may want or need low first cost, long life or maximum operating economy. Normally we do not find all in one package. So we must decide which is most important and go ahead from there.

Getting the right pump is much like coming to a fork in the road. Our map tells us which way to turn. Once on the right road all we need do is watch our route markers. The next 29 pages do just that for you in the world of pumps.

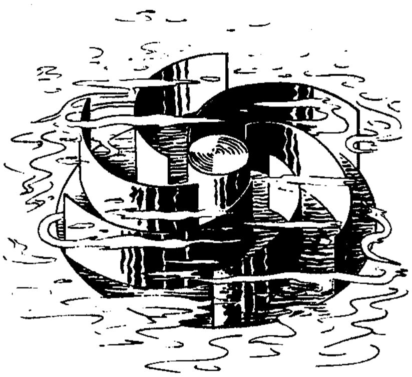

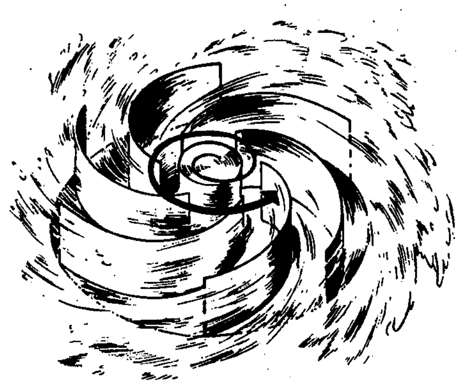

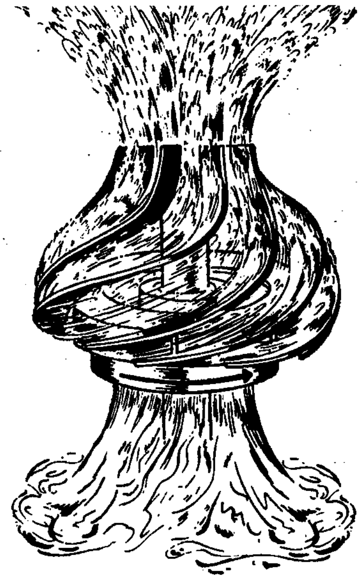

CENTRIFUGAL

As a boy you probably whirled around your head a bucket on the end of a rope, just like the little guy in the three sketches above. As you recall, the water stayed in the bucket just as long as you kept it turning at a fair speed. The force that kept the water in the bucket is at work in centrifugal pumps.

Imagine an impeller at rest in water, *above left*. This is like the lad's bucket before he starts whirling it. Now rotate the impeller, *middle sketch*. Water will fly out from between the blades just as it would squirt out of the whirling bucket if it had a hole in the bottom.

The force causing the water to leave the impeller (or the bucket) is *centrifugal force* and that's where pumps of this class get their name. They depend on centrifugal action even though details differ, as we'll see later.

Going back to the middle sketch, as the impeller throws out liquid, more rushes into the center where the lowest pressure exists, and where a suction pipe is normally fitted. This liquid too is thrown out, is followed by more, and we have the steady discharge characteristic of centrifugals.

Once the liquid is being thrown from the impeller we must guide it to its destination. Otherwise we've accomplished little more than make a big splash.

By putting the impeller in a casing we can change flow from haphazardly outward to controlled movement in the direction we want. With vanes like those of the deepwell pump in the righthand sketch we can even turn the flow upward. A casing, with or without vanes, acts something like a hose attached to the bottom of the boy's bucket.

The result is a workable pump for imparting energy to a liquid at one point to cause it to move to another.

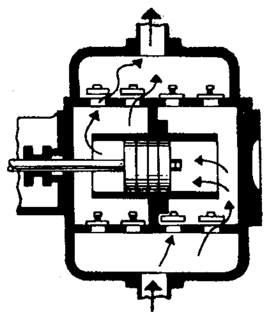

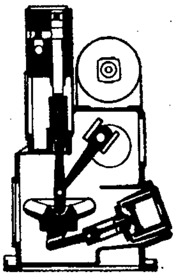

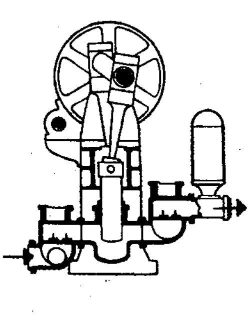

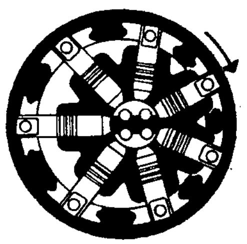

RECIPROCATING

Long of major importance in the pumping field, reciprocating units today are finding many new uses, particularly in the fields of metering and proportioning, and where extremely high pressures are needed.

Direct-acting steam pumps, *top left*, have two sets of valves in the liquid end. When the piston moves to the left as shown, liquid is drawn in through the righthand set of suction valves and liquid previously drawn into the cylinder is discharged through the upper left set of discharge valves. This is a double-acting pump, liquid being discharged on every stroke. The actual arrangement of the valves differs in various designs.

Power pumps, *top right and lower left*, have a number of different arrangements for suction and discharge valves. In these two single-acting units, liquid is drawn into the cylinder during one stroke of the plunger. On the next stroke, the plunger forces liquid through the discharge valves into the pump outlet.

Radial-piston pumps, *lower right*, one of many relatively recent designs, have their pistons attached to an outer ring whose center of rotation can be changed. Moving the ring to an eccentric position produces suction and discharge through valves in the center of the pump. Reversing the direction of ring rotation reverses liquid flow. A large number of other designs are discussed later.

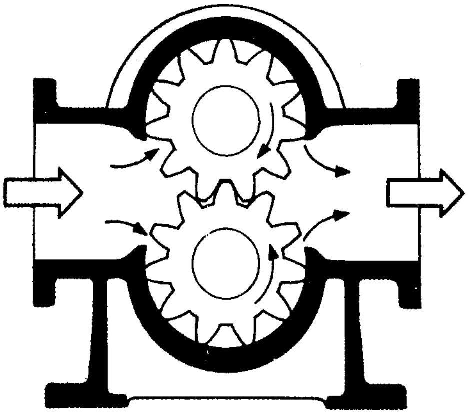

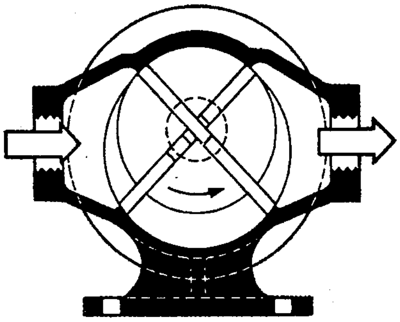

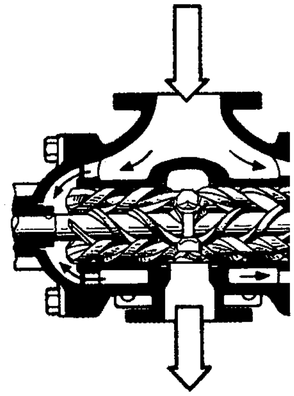

ROTARY

Like reciprocating pumps but unlike centrifugals, most rotary pumps are positive-displacement units — that is a given quantity of liquid is discharged for each revolution of the shaft. Like the centrifugal pump, flow is usually steady, without large pressure pulsations.

Rotary gear pumps, *above left*, have two or more gears in a casing and during rotation the liquid fills the spaces between the gear teeth on the suction side. From there it is carried around and squeezed out as the teeth mesh on the other side of the pump.

Sliding-vane rotary pumps, *above center*, are built in a number of different designs. In the type shown, the vanes move in and out of the rotor, which is set off-center in the casing. When the rotor turns counterclockwise, liquid flows into the cavity formed by rotor bottom and casing wall.

As the rotor turns, it brings the next vane into position to trap the liquid in the cavity. Further rotation forces the liquid around and out the discharge opening of the pump. The vanes are held against the inner wall of the casing by centrifugal force produced by rapid rotation of the rotor.

Screw pumps, *above right*, draw the liquid into one or both ends of the rotor or rotors, where it is trapped in the pockets formed by the threads. It is moved along to the discharge point much like a nut on a thread. Screw-type rotary pumps may have one, two or three screws. When only a single screw is used, liquid enters at one end, is discharged at the other. The screw runs in a double-threaded helix. Clearance is an important factor in many rotary-pump designs that are used today.

Later, pp 88, we'll discuss the large number of other rotary-pump designs used for a variety of industrial services.

How pumps work

OTHER PUMPING PRINCIPLES

Some of the most interesting recent design developments are in pumps for process and nuclear-energy applications. To handle liquid metals, for example, we now have electromagnetic pumps, in which electrical energy is applied directly.

Electromagnetic pumps include the Faraday type for ac or dc power, the ac linear-induction design (a modification of this is called the Einstein-Szilard pump) and the electromagnetic centrifugal. These, and other similar designs, represent new approaches to the problem of moving a liquid from one point to another.

Among older ideas for moving liquids there are, of course, the familiar air lift, hydraulic rams, and the Humphrey pump. Here, however, we stick to common mechanical methods.

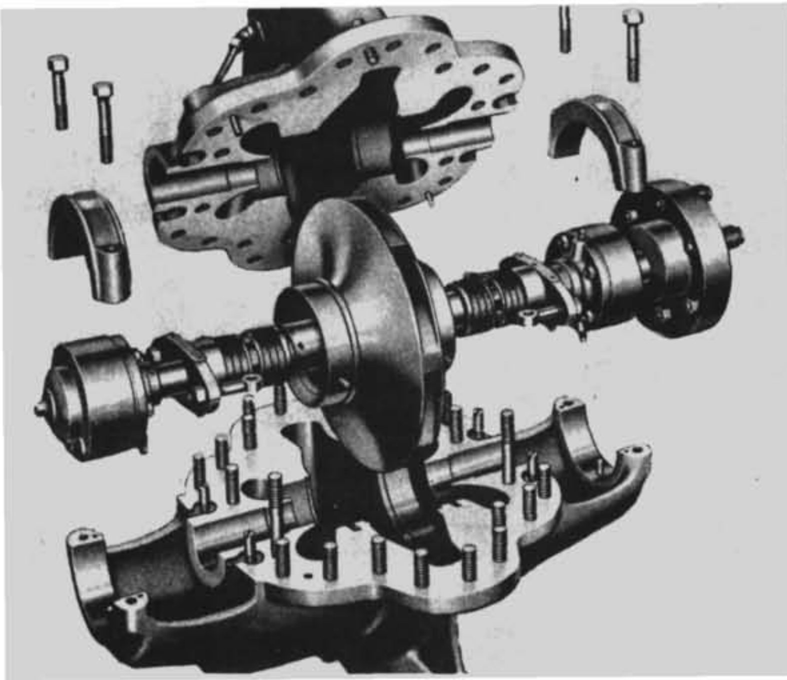

SINGLE-STAGE general-purpose pump has horizontally split casing, water-sealed stuffing boxes, cast-iron double-suction casing. The impeller is made of bronze

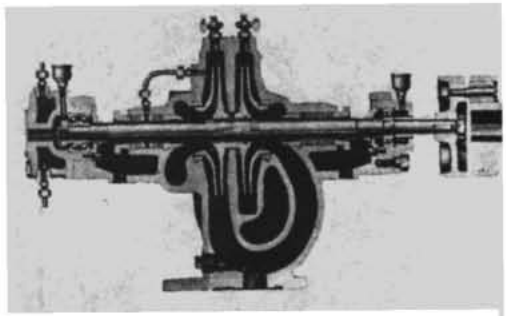

TWO-STAGE horizontally split pump has opposed impellers, ball-type bearings

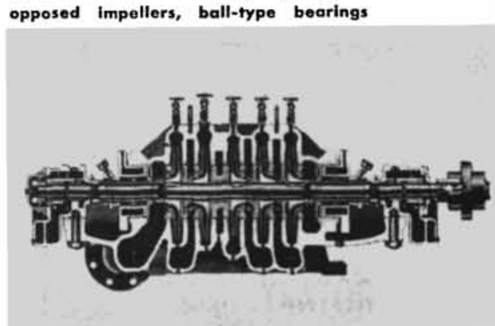

MULTISTAGE single-suction opposed-impeller pump for continuous heavy duty

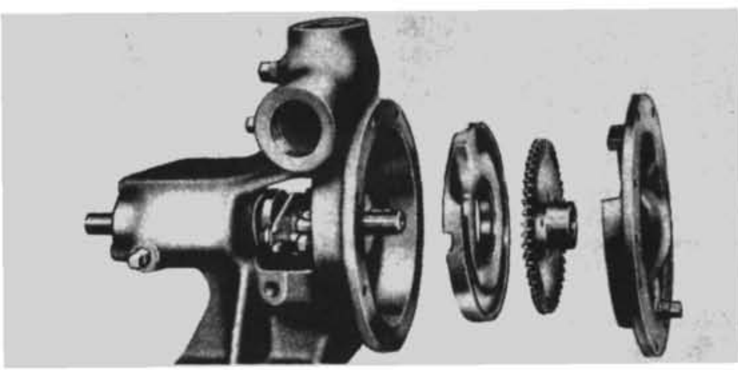

HORIZONTAL TURBINE PUMP, single stage, is self-venting to prevent vapor binding. Units like this are built with standard stuffing boxes, or with a mechanical seal

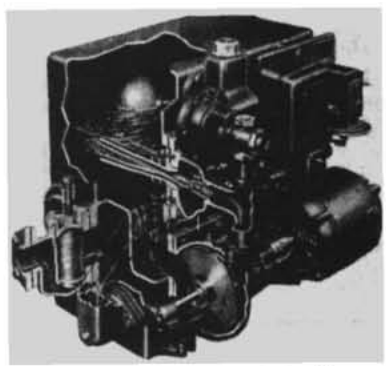

ENCLOSED-TYPE non-overload impeller on stainless-steel shaft for vacuum service

Centrifugal pumps

Earlier we saw how modern pumps are classified and typed. Now we're ready to take a closer look at centrifugal pumps – the most widely used units.

Illustrations on these two pages are a small sampling of today's designs. Study shows that though all come under one broad classification, intended application is a major factor in impeller and casing design, materials used, and other mechanical and hydraulic features. For these reasons we find pump builders stressing ultimate use somewhat more than classification and type.

Thus centrifugal pumps are termed boiler-feed, general-purpose, sump, deep-well, refinery (hot oil), condensate, vacuum (heating), process, sewage, trash, circulating, self-priming, sanitary, bait, booster, paper stock, chemical, fire, jet, sand, slurry, ash, glass, stoneware, submersible, tail-water, etc. In general, each has specific features of design and materials recommended by the builder for the particular service. This makes selection and application easier.

Another subdivision grows out of broad structural features. Thus we find horizontal and vertical units, close-coupled designs, single- and double-suction impellers, horizontally split casings and barrel casings, etc. Correct evaluation of all these variations is one of the big jobs in selecting a pump.

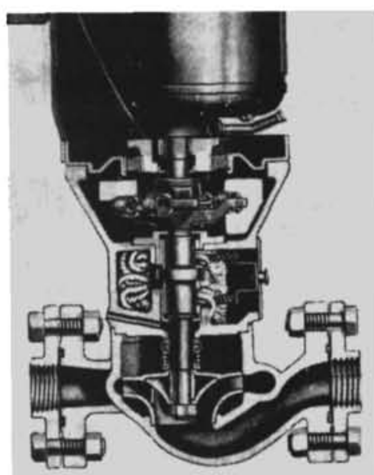

SINGLE-STAGE pump with sleeve bearings and mechanical seal for hot-water uses

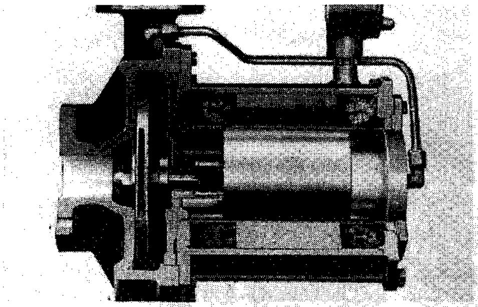

SEAL-LESS leakproof combined motor-pump has no stuffing boxes, uses no lubricant

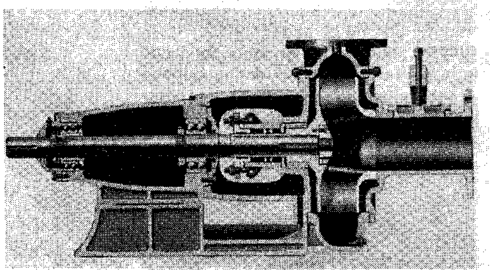

NON-CLOGGING PUMP: 2-bladed impeller, ball bearings, removable suction cover

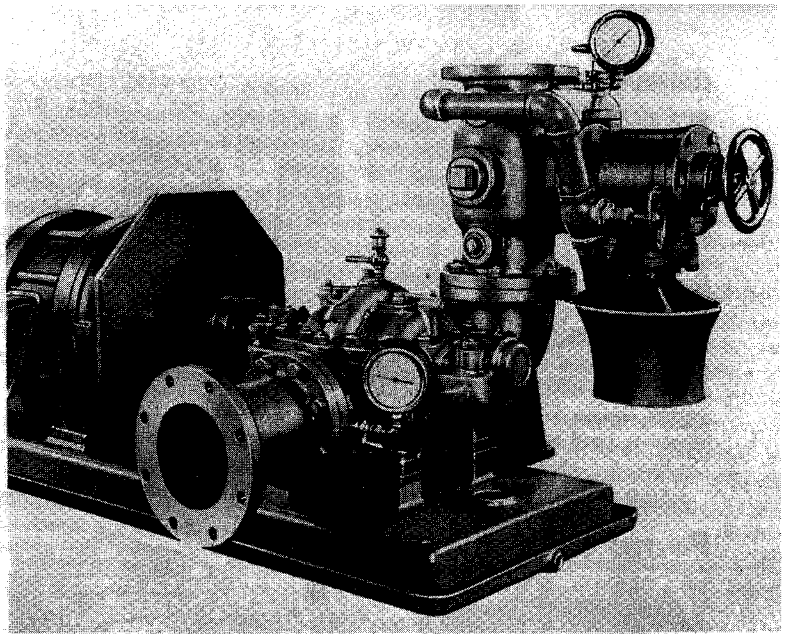

SUCTION SIDE of a single-stage fire pump, complete with motor and fittings. Pumps and fittings for this service are laboratory tested before underwriters' approval

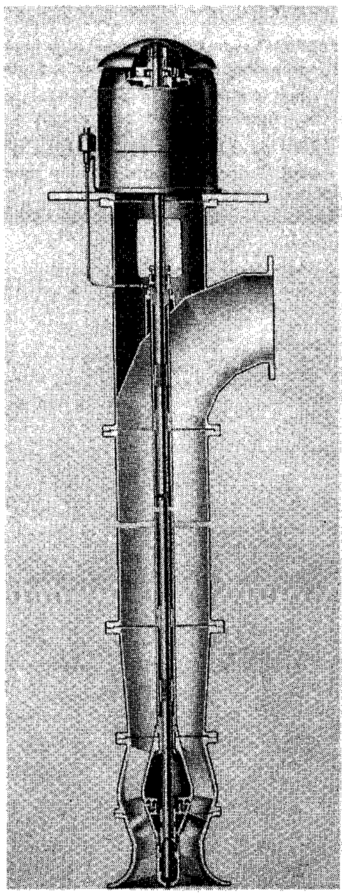

MIXED-FLOW vertical pump may be either water or oil lubricated, depending on job

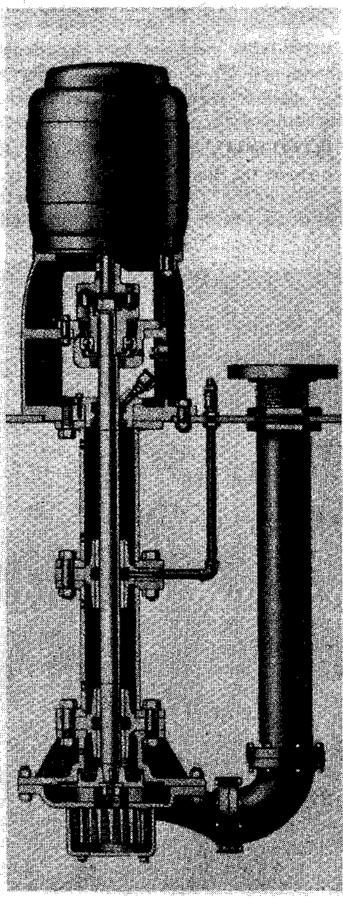

VERTICAL single-stage unit has semi-open impeller, ball and sleeve shaft bearings

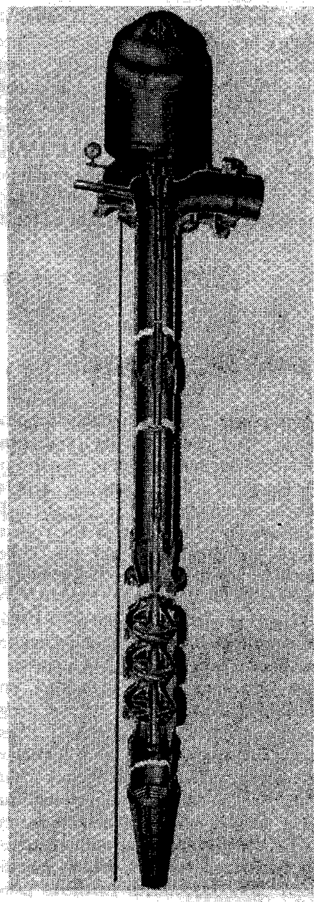

WATER-LUBRICATED vertical pump: semi-open impellers, open line-shaft bearings

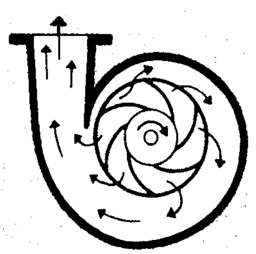

VOLUTE converts velocity energy of the liquid into static pressure (read in psi)

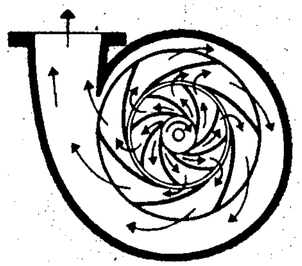

DIFFUSER changes flow direction, aids in converting velocity energy to pressure

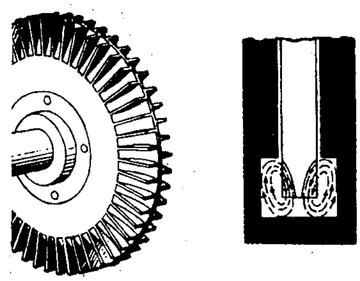

TURBINE pump adds energy to the liquid in a number of impulses during rotation

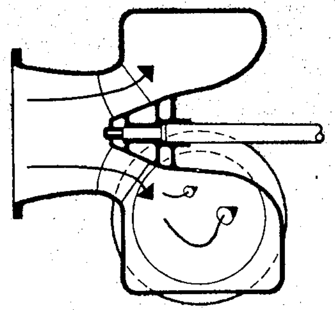

MIXED-FLOW units use both centrifugal force and lift of vanes on the liquid

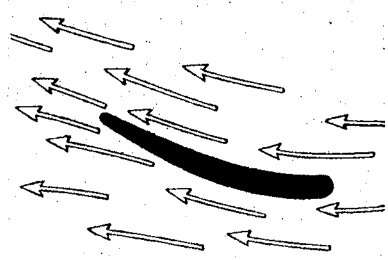

PROPELLER pump develops most of its head by propelling action of vanes on liquid

Pump action

In volute-type pumps the impeller discharges into a progressively expanding spiral casing, proportioned to gradually reduce liquid velocity. Thus velocity energy is changed to pressure head in the volute.

Stationary guide vanes surround the runner in a diffuser-type pump. These gradually expanding passages change the direction of liquid flow and convert velocity energy to pressure head.

Liquid in a turbine pump is picked up by the impeller's vanes and whirled at a high velocity for nearly one revolution in an annular channel in which the impeller turns. Energy is added to the liquid in a number of impulses, so it enters the discharge at high velocity.

Mixed-flow pumps develop their head partly by centrifugal force and partly by the lift of the vanes on the liquid. Propeller pumps develop most of their head by the propelling or lifting action of the vanes on the liquid.

Specific speed

Specific speed is an index of pump type, using the capacity and head obtained at the point of maximum efficiency. It determines the general profile or shape of the impeller. In numbers, specific speed is the rpm at which an impeller would run if reduced in size to deliver 1 gpm against a total head of 1 ft.

Impellers for high heads usually have low specific speed; impellers for low heads have high specific speed.

As diagram, *right*, shows, each impeller design has a specific-speed range for which it is best adapted. These ranges are approximate, without clear-cut divisions between them. Chart gives general relations between impeller shape, efficiency and capacity.

Suction limitations of different pumps bear a relation to the specific speed. The Hydraulic Institute publishes charts giving recommended specific speed limits for various cond'tions.

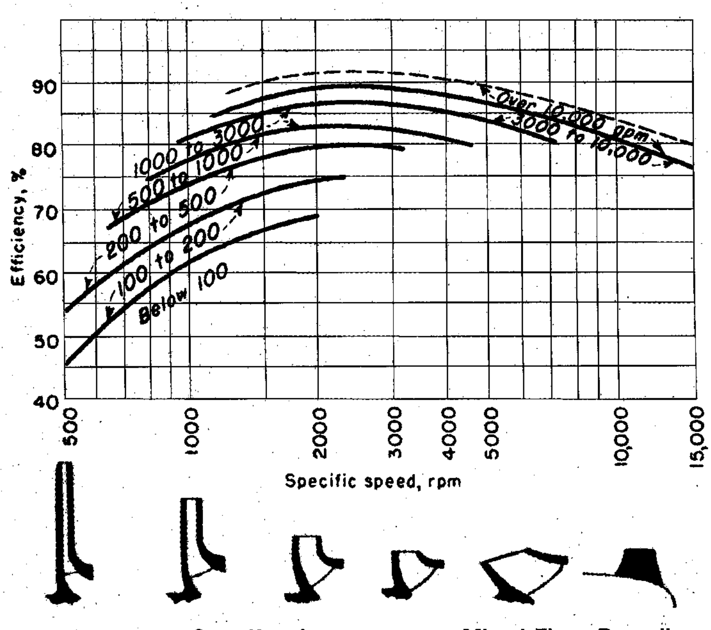

SPECIFIC SPEED is approximately related to impeller shape and efficiency, as shown by these curves. There is no sharp dividing line between various impeller designs

Impellers

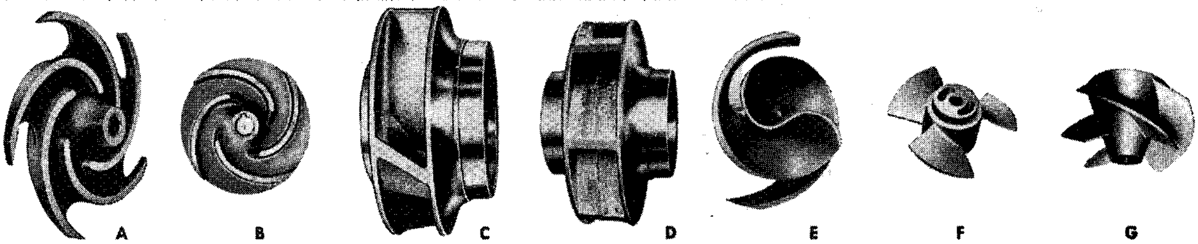

Besides being classified according to specific speed, an impeller is also typed as to how the liquid enters, its vane details, and use for which it is intended.

Open impellers, *A*, have vanes attached to a central hub with relatively small shrouds. *Semi-open, B,* have a shroud, or wall, on only one side. *Closed* impellers, *C* and *D*, have shrouds on both sides to enclose liquid passages. *Single* or *end-suction* units, *C*, have liquid inlet on one side; in *double-suction* type, *D*, liquid enters both sides. *E, F* and *G* are *paper-stock, propeller and mixed-flow* designs.

Casings

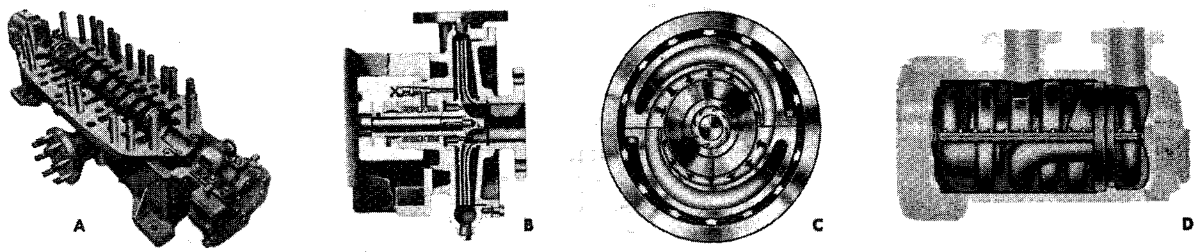

Centrifugal-pump casings may be split *horizontally, A, vertically, B,* or *diagonally* (at an angle other than 90 deg).

Horizontally split casings are also termed *axially* split. Both suction and discharge nozzles are normally in lower half of casing; upper half lifts for easy inspection. Vertically split casings are also called *radially* split. They're used in close-coupled or frame-mounted end-suction designs.

Barrel casings, C and *D*, are used on high-pressure diffuser and volute pumps. Inner casing fits in outer barrel. Discharge pressure acting on inner case provides seal.

Wearing rings

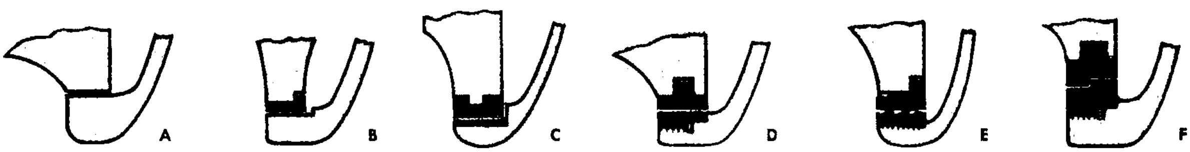

To prevent costly wear of casing and impeller at the running joint, wearing rings, also called casing rings, are installed. Where these rings are removable, as they usually are, they can be replaced at a fraction of the cost of a new impeller or pump casing that might otherwise be needed.

Seal *A* is a plain flat joint. Similar joint, *B*, has a flat ring mounted on the pump casing. At *C* the ring fits into a casing groove; impeller has a similar ring.

In designs *D, E,* and *F*, rings are fitted to both casing and impeller. Form varies with pressure, service, etc.

Bearings

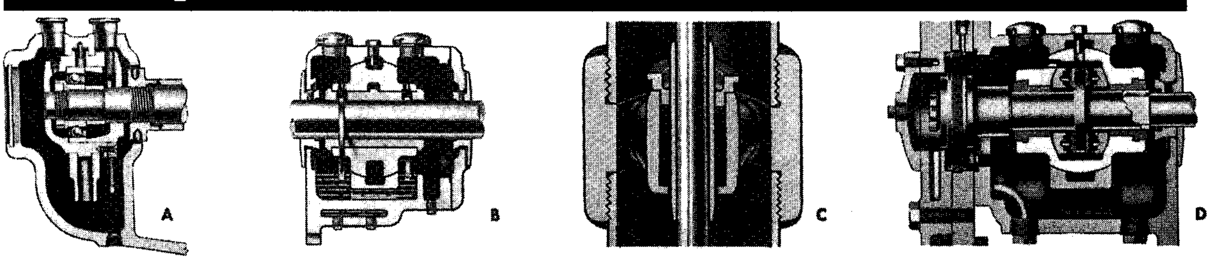

Practically every type of bearing has been used in centrifugal pumps. Today, *ball, sleeve* and *Kingsbury* bearings find most common use. Many pumps are available with more than one type of bearing to meet different needs.

Ball bearings, *A*, may be of single- or double-row type. Spherical roller bearings are widely used for large shafts.

Sleeve bearings, *B* and *C*, may be either horizontal or vertical. In the latter, water is often the lubricant.

Kingsbury thrust bearings, *D*, find use in larger pumps. Design resembles that used in other rotating machinery.

Shaft and interstage sleeves

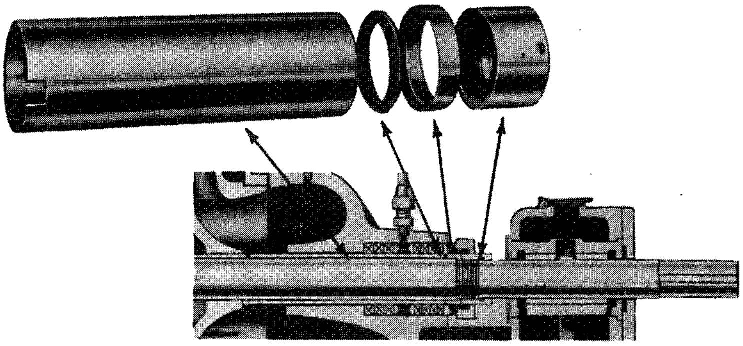

Sleeves protect shaft against corrosion, erosion and wear affecting its strength. Many forms are used on large pumps but on small ones sleeve is often left off to cut hydraulic and stuffingbox losses. Shaft is then made of a metal that is sufficiently corrosion- and wear-resistant for satisfactory life.

Interstage sleeves guard multistage pump shafts. In some, long hub on impeller replaces interstage sleeve.

Lantern rings

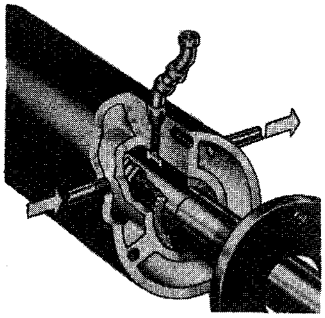

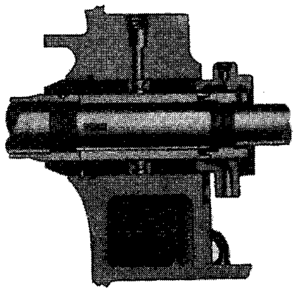

These are used to prevent air leakage into pump when running with a suction lift and to distribute sealing liquid uniformly around annular space between box core, shaft-sleeve surface.

Also called seal cages and waterseal rings, they receive liquid under pressure from pump or independent source.

Grease sometimes serves as sealing medium when clear liquid isn't available or can't be used (sewage pumps).

Stuffing boxes

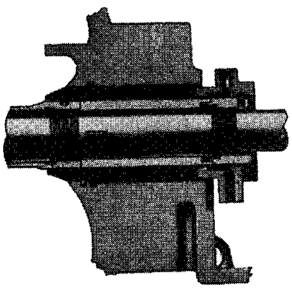

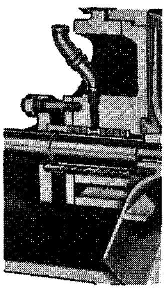

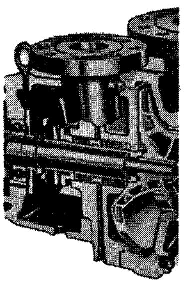

Stuffing box stops air leaking into casing when pressure is below atmospheric; holds leakage out of casing to a minimum when pressure is above.

Sketches show solid-packed box, which has no lantern rings; two injection designs, which do. On pumps handling hot liquids, or having high stuffing-box pressures, box is often water-jacket cooled. In some, coolant and pumped liquid mix.

Mechanical seals

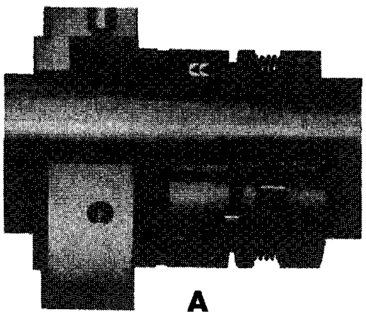

A

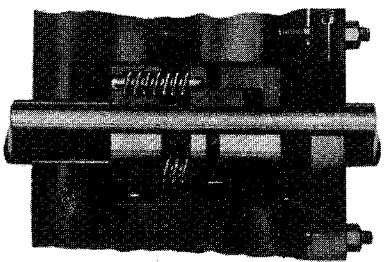

B

Mechanical seals in wide variety serve where leakage is objectionable. They also find use where stuffing-boxes can't give adequate leak protection.

Sealing surfaces are perpendicular to pump shaft and usually comprise two polished lubricated parts running on each other. Though not guaranteed leakproof, leakage is usually nil.

Outside type, *A*, is used where gritty liquids or leakage retained in stuffing box would be undesirable. *Inside*, *B*, finds much use for volatile liquids.

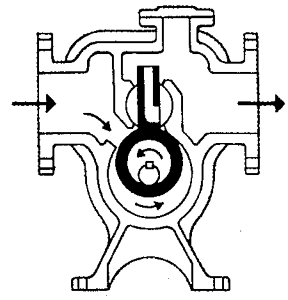

CAM-AND-PISTON

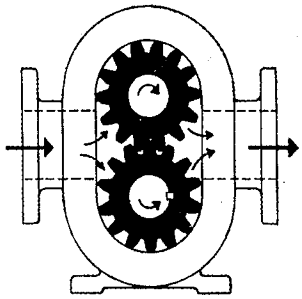

EXTERNAL-GEAR

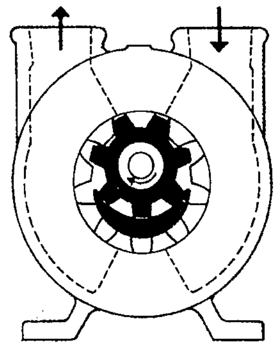

INTERNAL-GEAR

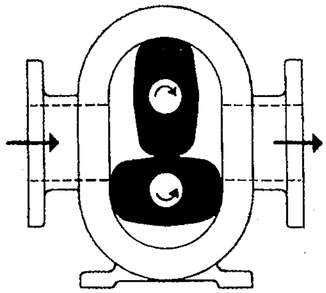

TWO-LOBE

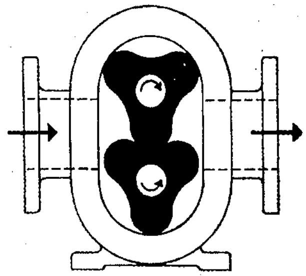

THREE-LOBE

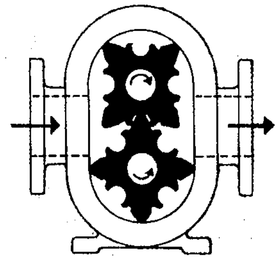

FOUR-LOBE

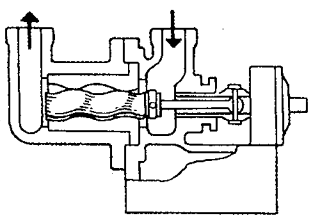

SINGLE-SCREW

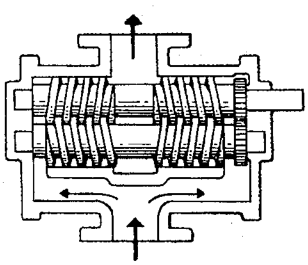

TWO-SCREW

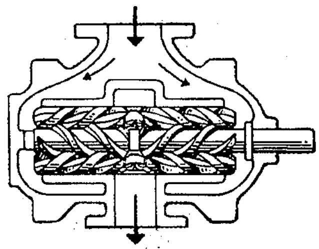

THREE-SCREW

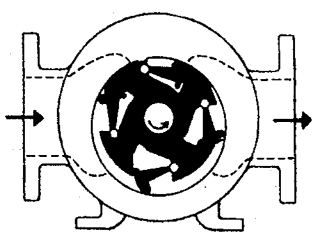

SWINGING-VANE

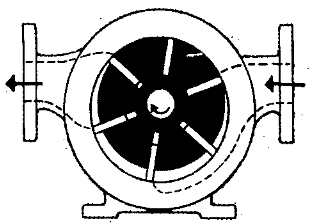

SLIDING-VANE

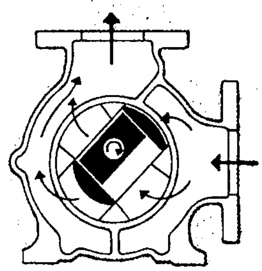

SHUTTLE-BLOCK

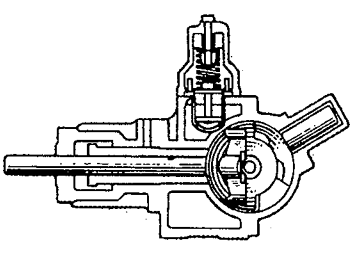

UNIVERSAL-JOINT

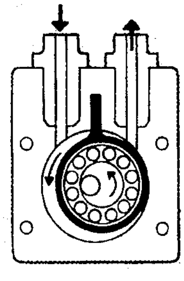

ECCENTRIC IN FLEXIBLE CHAMBER

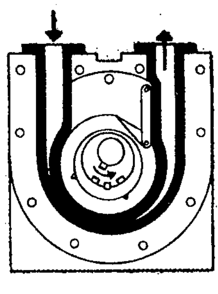

FLEXIBLE-TUBE

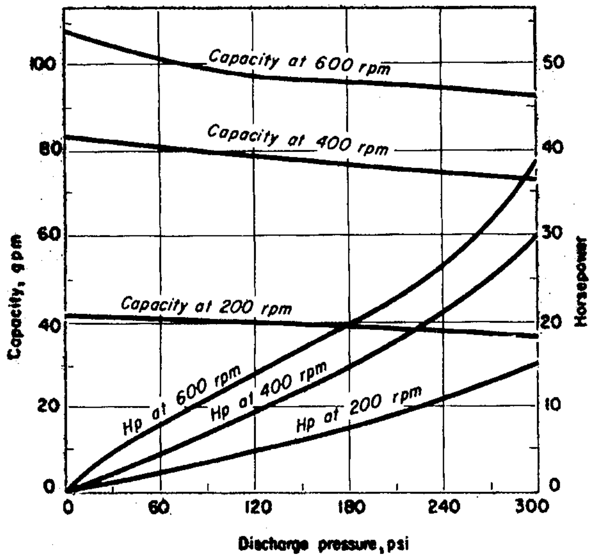

CAPACITY and horsepower performance curves of a gear-type rotary pump handling heavy fuel oil. Note the flat H-Q curves

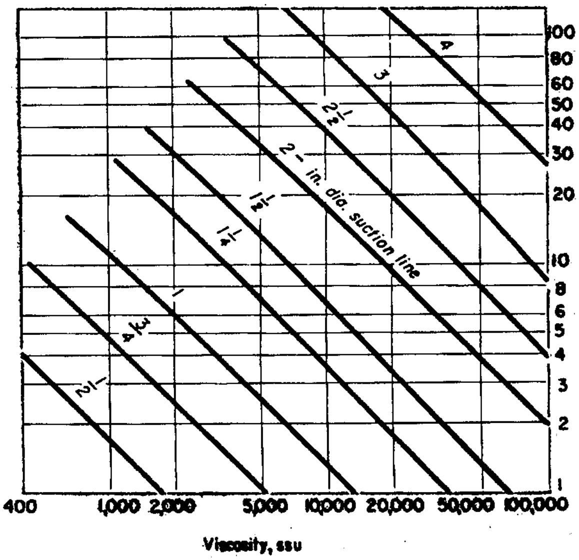

RECOMMENDED SIZE of suction piping for viscous liquids in 10 ft of straight pipe with two elbows and one gate valve

Rotary pumps

Rotary pumps, usually positive-displacement units, consist of a fixed casing containing gears, vanes, pistons, cams, segments, screws, etc, operating with minimum clearance. Instead of "throwing" liquid as in a centrifugal, rotaries trap it, pushing it around the closed casing, much like reciprocating pumps. But unlike a piston pump, a rotary discharges a smooth flow.

Fifteen designs, *left*, illustrate a few of the devices chosen to move fluids from one point to another. Often thought of as viscous-liquid pumps, rotaries are by no means confined to this service alone. They'll handle any liquids from A to Z, if free of hard solids. And hard solids can be handled if steam jacketing will melt them. As with centrifugals, materials and drives vary with job, liquid, etc.

Cam-and-piston pumps, also called rotary-plunger type, consist of an eccentric with a slotted arm at its top. Shaft rotation causes eccentric to trap liquid in casing, discharges it through slot to outlet.

External-gear pumps are the simplest rotary type. Liquid first fills the spaces between gear teeth as they separate on suction side, is then carried around and squeezed out as the teeth mesh. Gears may have spur, single- or double-helical teeth. Some designs have drilled idler to cut internal thrust.

Internal-gear pumps have one rotor with internally cut teeth meshing with an externally cut gear idler. Crescent-shaped partition, to prevent liquid from passing back to suction side, may or may not be used.

Lobular pumps resemble the gear-type in action, have two or more rotors cut with two, three, four or more lobes on each rotor, synchronized for positive rotation by external gears.

Single-screw pumps have a spiraled rotor turning eccentrically in an internal-helix stator or liner. Rotor is metal while helix is hard or soft rubber.

Two- and three-screw pumps have one or two idlers, respectively. Flow is between the screw threads along the axis of the screws. Opposed screws may be used to eliminate end thrust.

Swinging-vane pumps have a series of hinged vanes which swing out as the rotor turns, trapping liquid and forcing it out the discharge pipe.

Sliding-vane pumps use vanes that are thrown against casing bore when rotor turns. Liquid trapped between two vanes is carried around and forced out the discharge.

Shuttle-block pump has a cylindrical rotor turning in a concentric casing. In the rotor is a shuttle block and piston reciprocated by an eccentrically located idler pin, producing suction and discharge.

Universal-joint pump has a stub shaft in free end of rotor supported in a bearing at about 30 deg with the horizontal. Opposite end of rotor is fixed to drive shaft. When rotor revolves, four sets of flat surfaces open and close for a pumping action of four discharges per revolution.

Eccentric in flexible chamber produces pumping action by squeezing the flexible member against pump housing to force liquid out discharge.

Flexible-tube pump has a rubber tube squeezed by a compression ring on an adjustable eccentric. Pumps of this design are built single- and 2-stage.

Characteristic curves, ***above left,*** for a typical rotary gear pump show the flat H-Q relation obtainable. Displacement of a rotary varies directly as speed, except as capacity may be affected by viscosity and other factors. Thick liquids may limit pump capacity at higher speeds because they can't flow into casing fast enough.

Slip or loss in capacity through clearances between the casing and rotating element, assuming a constant viscosity, varies as pressure increases. For example, in above curves, capacity at 0 discharge pressure is 108 gpm. But at 300 psi and same speed, capacity is 92 gpm. Difference is slip.

Power input to a rotary increases with liquid viscosity; efficiency decreases. This is true, of course, with other classes of pumps. But since rotaries find wide use for viscous liquids, it is wise to use the chart, ***above right,*** for sizing suction lines to prevent excessive friction loss.

SINGLE-ACTING vertical-type power pump has pinion shaft for driving crankshaft

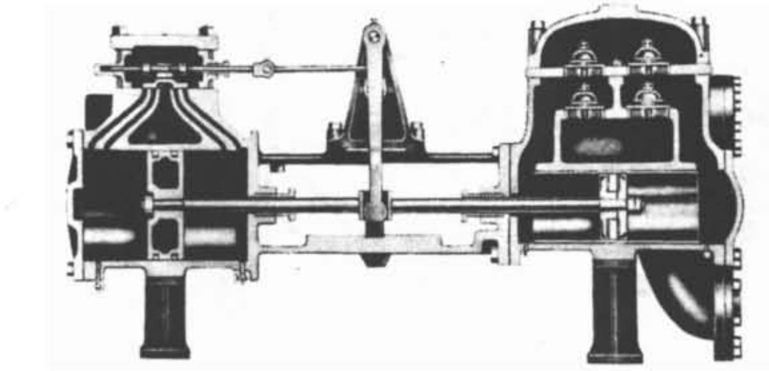

DIRECT-ACTING horizontal duplex piston pump. Steam end is at left, liquid end is at right. Piston-rod motion shifts steam valve for admission and exhaust of the steam

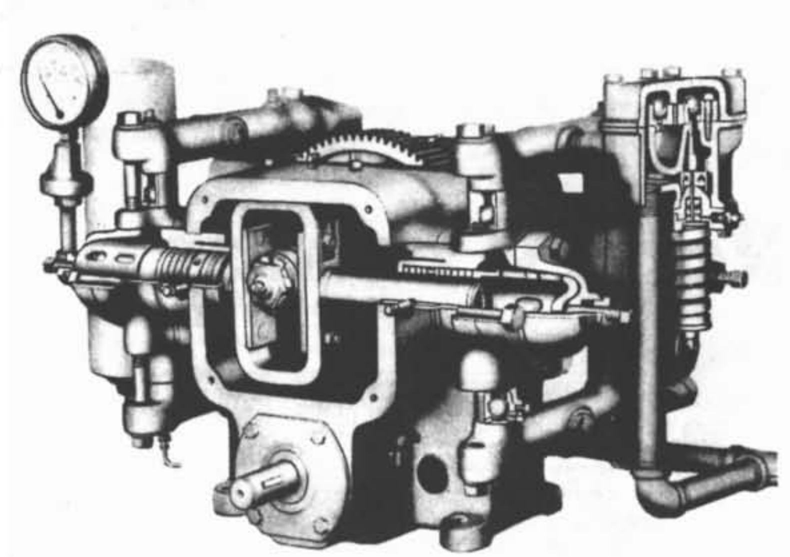

QUADRUPLEX horizontal-plunger power pump for high pressures is motor driven through pinion and gear. Each Scotch yoke drives two plungers. Pump valves are the ball type

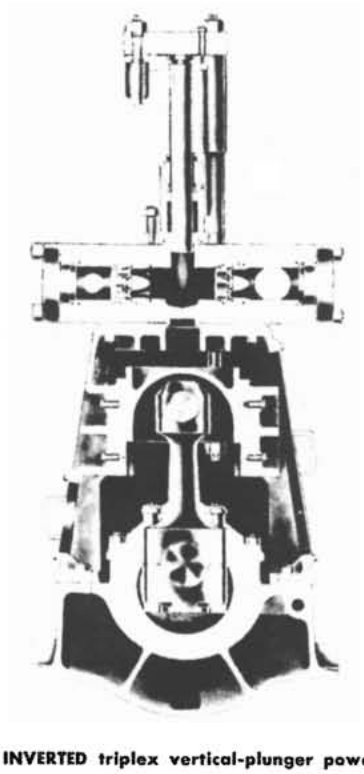

INVERTED triplex vertical-plunger power pump for high-pressure job applications

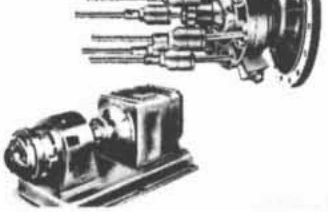

ROTARY-PLUNGER single-acting pump unit has five or seven plungers in a circle

Reciprocating pumps

The 13 pumps on these two pages are but a few of the many reciprocating types in regular use today. But you will find shown here most of the major designs.

Reciprocating pumps, unlike centrifugals, p 80, are more often classed according to type, rather than use. Perhaps this is because their ultimate use is less clearly defined than for centrifugal pumps. While certain applications for this type, like fuel-oil pumping, are declining, others, like boiler and chemical feeding, are rising.

Biggest recent developments are in non-geared higher speed power pumps – both large and small units. Adjustable displacement pumps, also called metering and proportioning or controlled-volume, are being improved every year to give wider capacity ranges, greater accuracy, easier control.

Power pumps, always of importance in the marine field for boiler feed are finding some new berths in stationary plants for the same service where loads justify them. And if pressures in super-pressure plants rise, it is likely that power-type reciprocating pumps will be used for boiler feed. Of course, much depends on new developments in the design of centrifugal pumps.

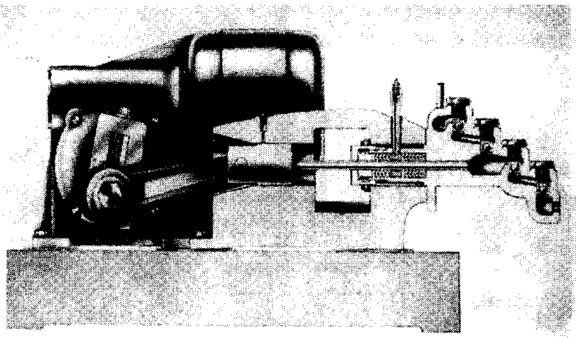

CONTROLLED-VOLUME plunger pump has screw adjustment of stroke length. Change of crankpin position alters capacity of pump

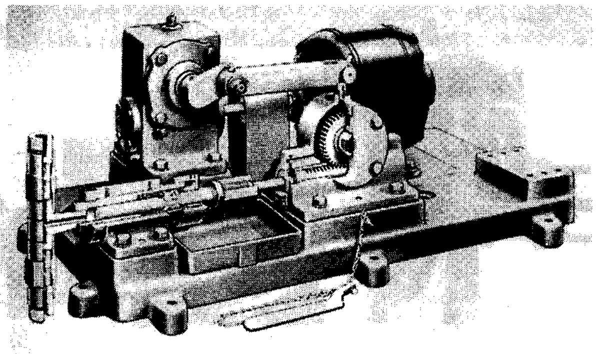

METERING and proportioning plunger pump has lost-motion type of coupling for adjusting stroke length and capacity of pump

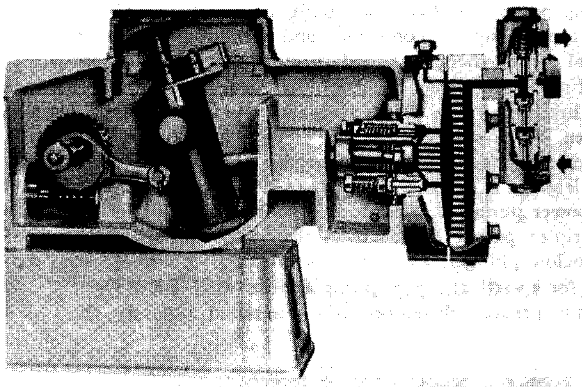

PISTON-DIAPHRAGM unit for controlled-volume pumping has oil for actuation of diaphragm which pumps the liquid handled

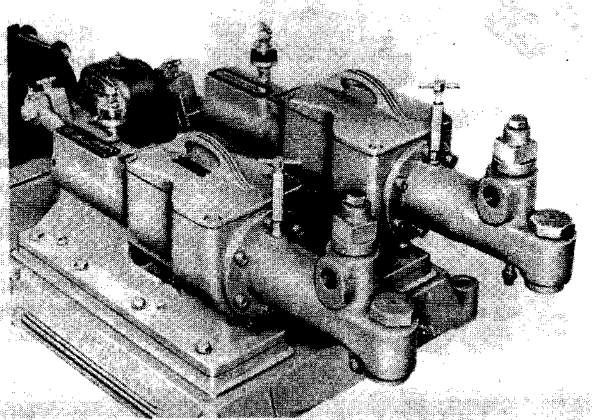

DUPLEX plunger-type feeder pump has micrometer adjustment of stroke length by means of variation of the crankpin position

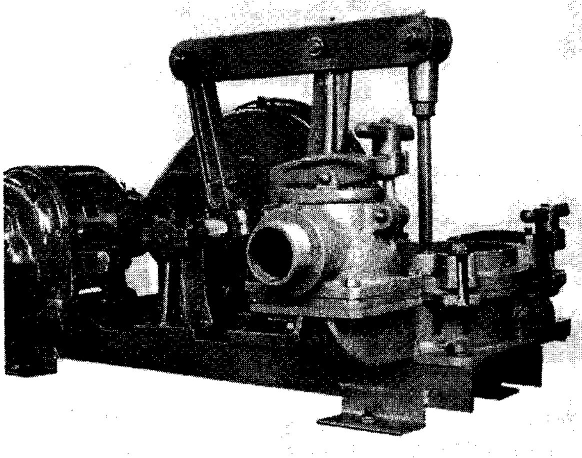

DIAPHRAGM pump with ball suction and discharge valves is built with stationary or movable base, is motor driven through beam

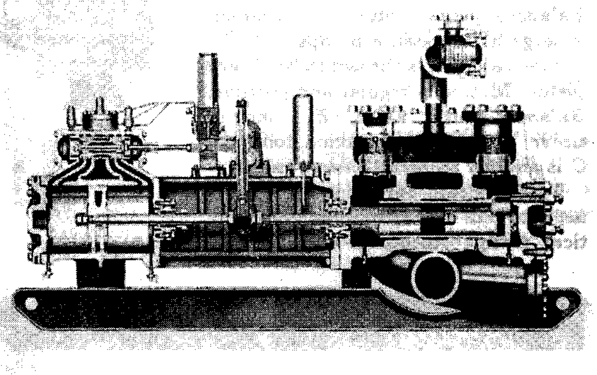

DUPLEX STEAM slush pump has divided-cylinder pot-type liquid end with suction manifold at the bottom of the liquid cylinder

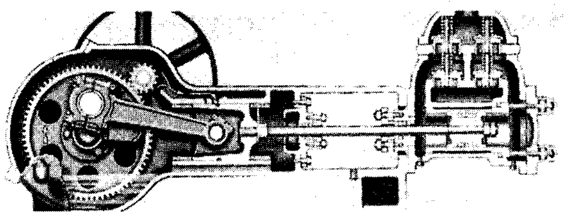

HORIZONTAL SIMPLEX power pump is driven by pinion geared to crankshaft, has disk-type suction, discharge valves, air dome

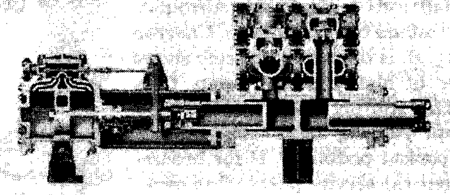

HORIZONTAL DUPLEX outside-end-packed pot-valve-type plunger pump: the plungers shown are attached together by the tie rods

Liquid ends for direct-acting and power pumps

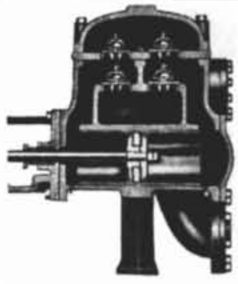
A

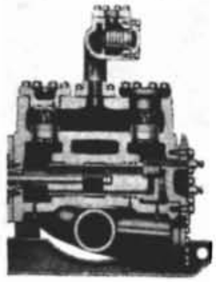
B


C

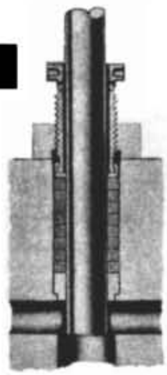
D

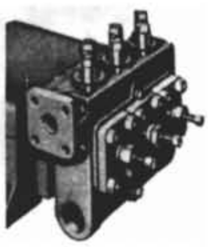
E

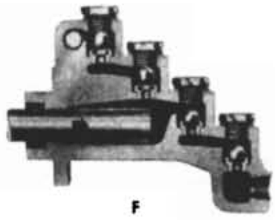
F

G

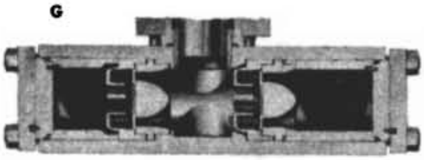

Reciprocating-pump liquid ends are built in a large number of designs for various liquids, service conditions and pressures. Shown above are a few typical arrangements for modern pumps.

Direct-acting steam pump, *A*, often has *valve-plate* liquid end with removable discharge-valve decks. Cup-type packing for liquid piston is also shown. *Valve-pot* type, *B*, has valve chambers closed by individual covers. *Outside-packed* plunger pump, *C*, has its valves in pots—all packing leakage is external where it can be seen.

Vertical power pump, *D*, has plunger packing at cylinder top, while horizontal triplex pump, *E*, has it in the usual location with valves above and below plunger. At *F*, valves are in step arrangement. Another design for a vertical triplex pump appears at *G*. Liquid-end design is a function of pressure developed, liquid handled, capacity, etc.

Steam ends direct-acting pumps

Flat or 'D' slide valves find use for steam pressures of 200 psi and less Balanced piston valves are common in large high-pressure pumps.

Flat valve, *A*, is thrown by auxiliary piston. Motion is regular and positive. *Balanced-piston valve*, *B*, runs in sleeve, has minimum friction, long life. *C* is another *balanced-piston* valve.

Typical steam-valve linkage, *D*, connects to rod. Steam-end design of vertical pumps resembles those shown.

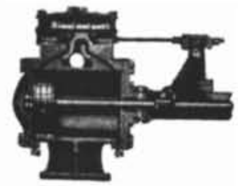
A

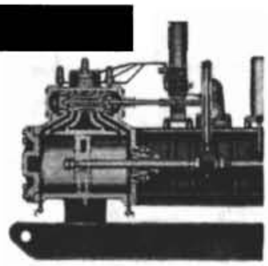
B

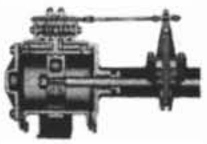
C


D

Packing

Packing is any material used to control leakage between a moving and stationary part in a pump. Flexible, and usually soft, it is expendable.

Simple piston-rod stuffing box, *A*, has several rings of square packing. On small rods a single nut surrounds gland, instead of studs shown. *Chevron* packing, *B*, is often used. Sketch shows plunger of high-pressure pump. *C* is a jacketed stuffing box.

Piston packing takes many forms. *Duck-packed* piston, *D*, is for bronze-fitted general-service pump. *Cup* packing, *E*, is standard for oil pumps. *Solid rubber rings*, *F*, are also popular.

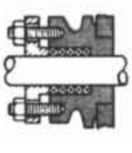
A

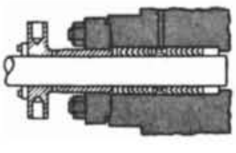
B

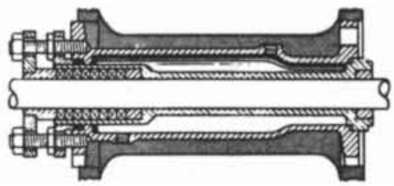
C

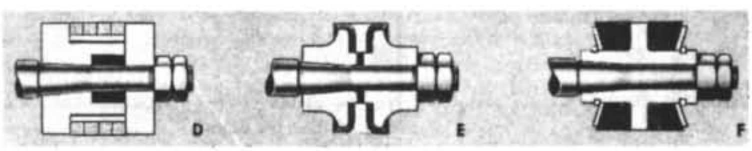
D E F

Liquid valves for direct-acting and power pumps

A

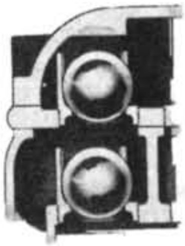

B

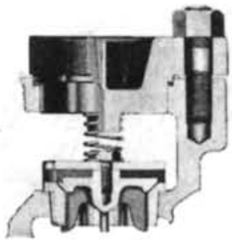

C

D

As a general rule, stem-guided disk valves are used for low-pressure jobs, wing-guided (flat- or bevel-faced) for moderate pressures, and bevel-faced wing for high pressures. But much depends on liquid, etc.

Flat disk, A, has inclined ribs in seat to direct liquid so it rotates disk slightly at each stroke. *Ball valve, B,* often finds use where free opening for thick liquid is desired. Cage guides ball during its rise and fall. Seat is circular and completely open. *Wing-guided* valve, *C,* for thick gritty liquids, can be fitted with renewable rubber inserts for wings. Another design, *D,* for high-pressure clear liquids, has renewable seats.

Low-pressure valve, *E,* and *high-pressure* valve, *F,* for thick liquids are alloy-steel with synthetic inserts for all ordinary services. Special materials are used where corrosive liquids are to be handled. Double-ported ring-type valves, *G,* p 92, are popular in large power pumps.

E

F

Cushion chambers and pressure alleviators

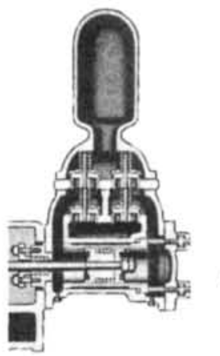

A

B

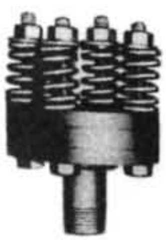

C

Suction and *discharge cushion chambers* smooth liquid flow. Discharge chamber, *A,* is often built as part of pump while suction chamber may be part of pump or in adjacent piping.

Pressure alleviators, *B* and *C,* find use with high-pressure power pumps to absorb shock from sudden stopping of liquid. They usually consist of a spring-loaded plunger operating in a stuffingbox. Liquid does not escape from piping system during surges.

Variable-capacity devices

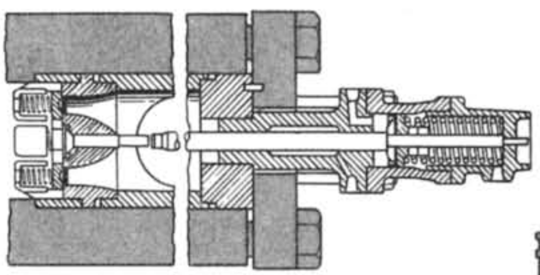

A

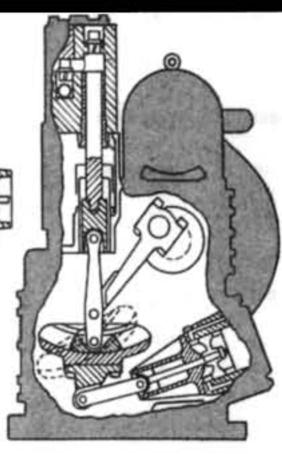

B

There seems no end to devices for varying capacity of small reciprocating pumps. A few appear on pp 90-91. For large power pumps, however, not so many variations exist perhaps because of the lesser number of designs.

Suction-valve unloader, A, gives a quick but gradual reduction in liquid delivery from full to zero flow in not more than one-half revolution of pump. It increases liquid delivery in same way, is pneumatically actuated.

Stroke-transformer, B, can automatically or manually vary plunger motion from zero to maximum stroke. Output is infinitely controllable.

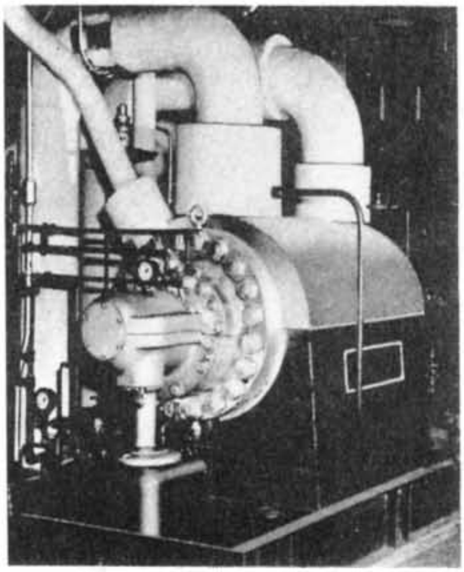

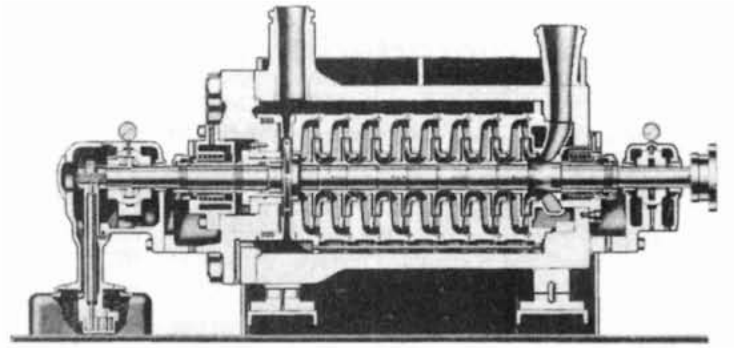

High-pressure boiler feed

The modern double-case barrel-type centrifugal pump is today's answer for pressures approaching 6000 psi and temperatures to 1000 F. In the common 2600-psi range, units of this type run at about 3600 rpm, have up to 12 stages. The first superpressure plant uses two pumps of this type in series, with heaters between. Note how vertically split inner assemblv is housed in casing.

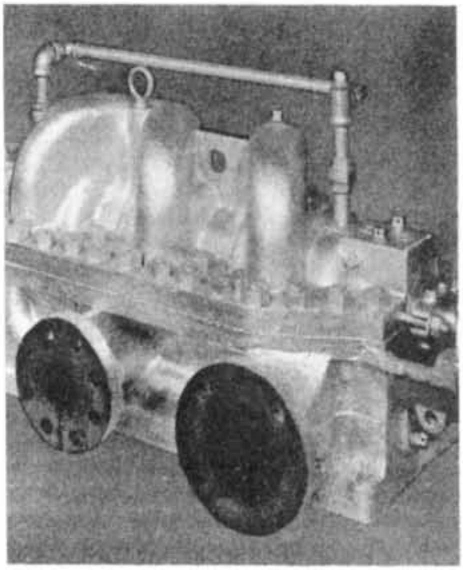

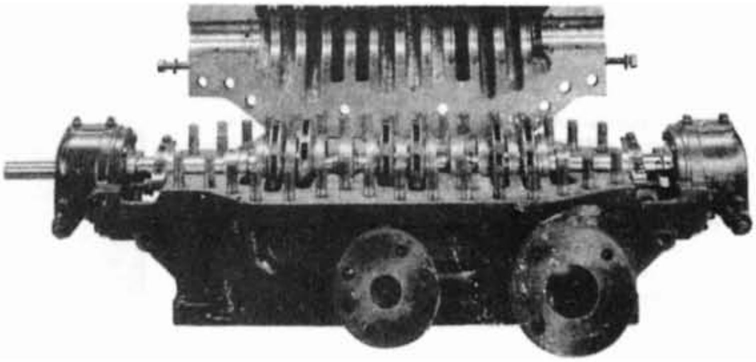

Medium- and high-pressure boiler feed

Horizontal split-case diffuser-type pumps with about six stages are common for 3600-rpm duty at pressures to 1600 psi. Some thinking today sees these units applied up to 2500 psi, but that is in the future. Design shown is 6-stage with back-to-back impellers in groups of two for better hydraulic balance. A big advantage of this type of pump is easy removal of top for maintenance.

Pump applications

Any attempt to list every possible application of pumps is almost certain to run aground because editors, being human, might overlook important jobs like pumping goldfish, apples, oranges, eggs and beer.

So these two pages, and the following four, give a necessarily selective cross section of pump classes and types *on the job*. There lies the ultimate goal of pump designers and builders—a product that performs a given service at the best over-all cost with minimum operating and maintenance needs. To secure these results the pump must be suited to the job, installed correctly, operated and maintained as the builder recommends. For now, let's take a quick look at application.

Pump class, type, drive and materials are among the major factors in unit selection. While generalizations are often dangerous, studies of a large number of modern installations show that industrial and service establishments throughout the U. S. use centrifugals for about 60% of their jobs, reciprocating for about 22%, rotary for about 12% and deepwell for about 6%. About 86% of the centrifugals have motor-drive, 44% of reciprocating, 96% of rotary and 95% of deepwell. Steam engines, turbines and internal-combustion engines drive about 13% of the centrifugals. Steam is outstanding for reciprocating units, driving almost half of those in use.

While these statistics are helpful from an over-all viewpoint, they serve merely as a guide to what industry is doing today. For help with a specific installation, the text and illustrations on these six pages will lead you through the maze of classes and types toward a sound answer.

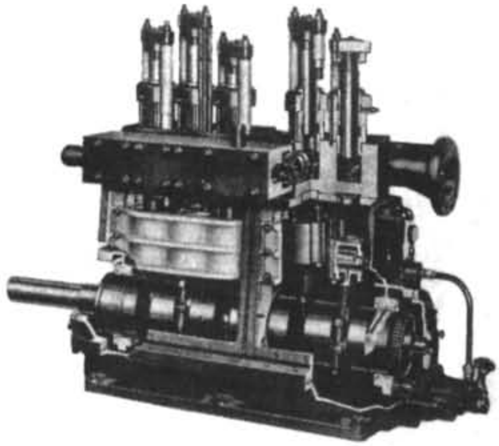

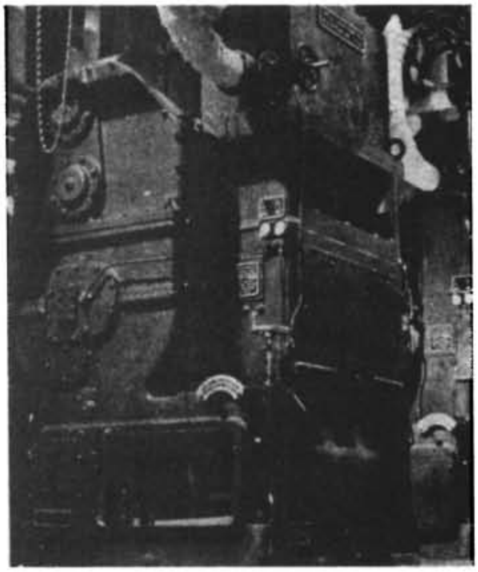

Power reciprocating for boiler feed

At pressures over about 250 psi where load is variable, power reciprocating pumps find application. They are also used for desuperheater feed in this pressure range. Vertical quintuplex units like that above are popular in feed service because they are easy to control automatically in stepless straight-line fashion from 0 to 100% of rated capacity. Use is now on the upswing.

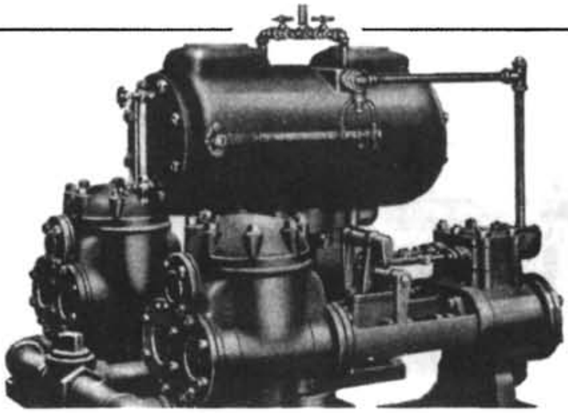

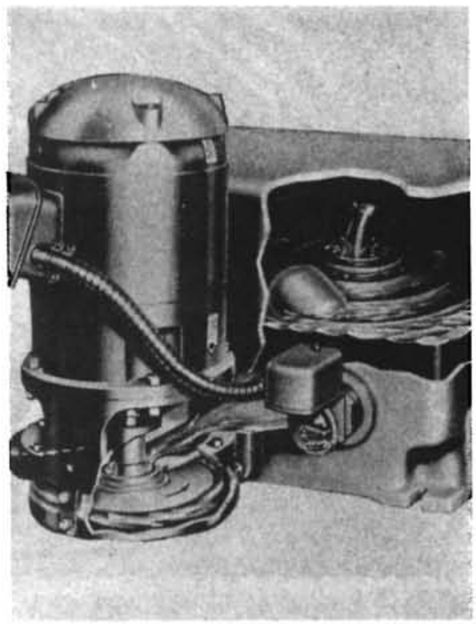

Low-pressure boiler feed

Direct-acting pumps, with or without receiver, find use in smaller low-pressure boiler installations. Simple, rugged and economical, they give outstanding service. Though not always classed as feed pumps, centrifugal condensation sets, *right,* are extremely popular in heating and similar installations. Compact and efficient, they handle wide temperature, pressure, capacity ranges.

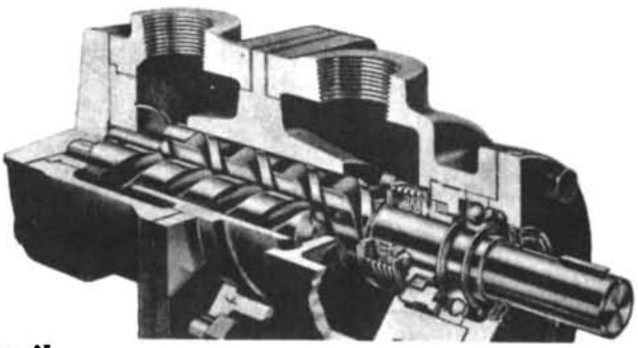

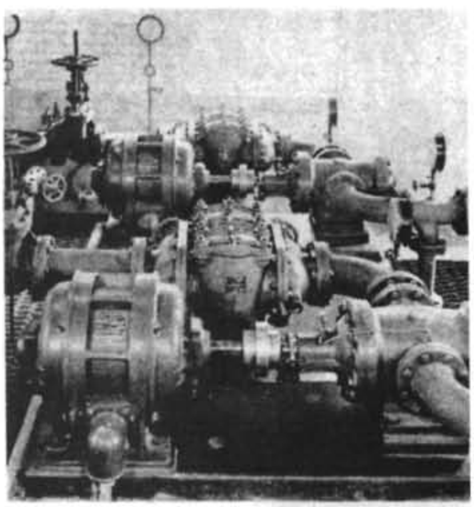

Fuel oil

Screw and gear pumps are the modern units for fuel-oil pumping but direct-acting steam pumps still do the job in some plants. Screw pump shown handles up to 80 gpm at continuous pressures of 275 psig, intermittent to 325 psig. Pumps of this type find many other uses besides fuel-oil pumping, including lubrication, booster, circulating, governing and elevator jobs.

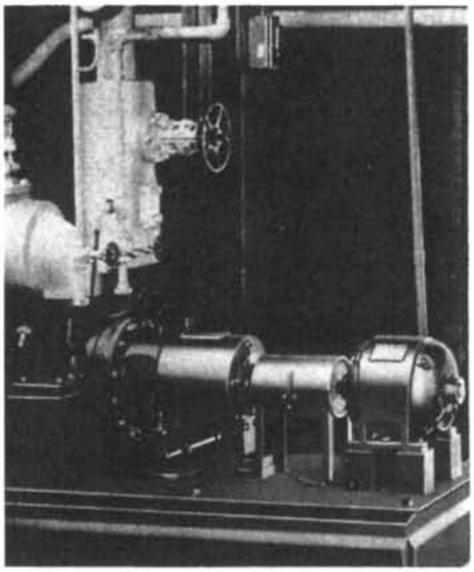

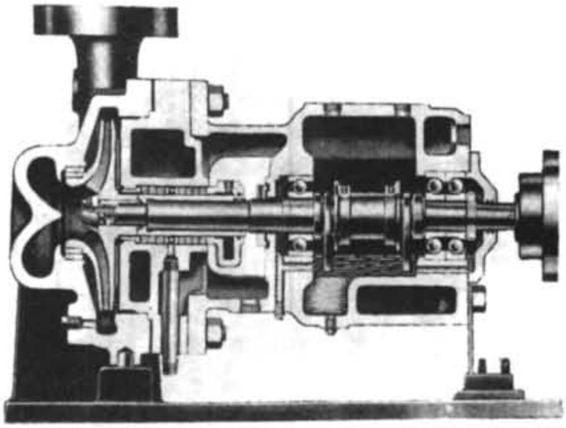

Heater drains, condensate

Handling condensate from hotwells, heater drains and other sources may impose severe operating conditions on a pump. In condenser service, suction head is low, liquid is near the boiling point, suction seal is a minimum and load changes wide. Usual centrifugal condensate pumps have one to four stages, special sealing and balancing features. Unit shown is single-stage.

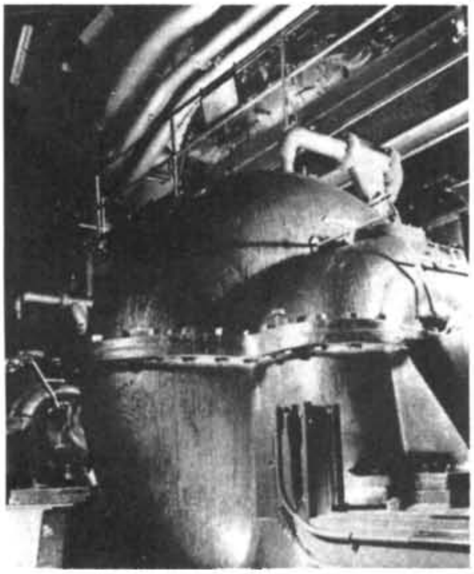

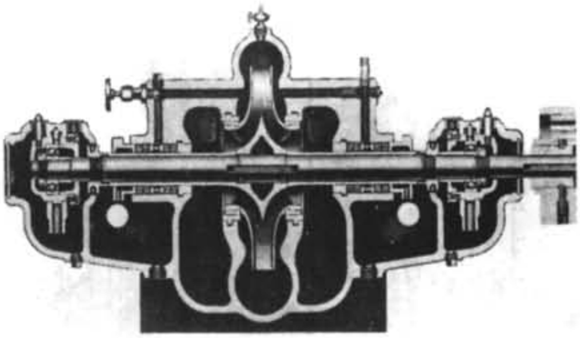

Cooling water

Whether tremendous, like the 55,000-gpm unit at left, or tiny as those on a small air conditioner, cooling-water pumps have some common traits. They are usually single-stage, standard-fitted, split-case. In the larger capacities they are often horizontal units, though many vertical designs are also used, both large and small. Their duty is seldom severe; operation is trouble-free.

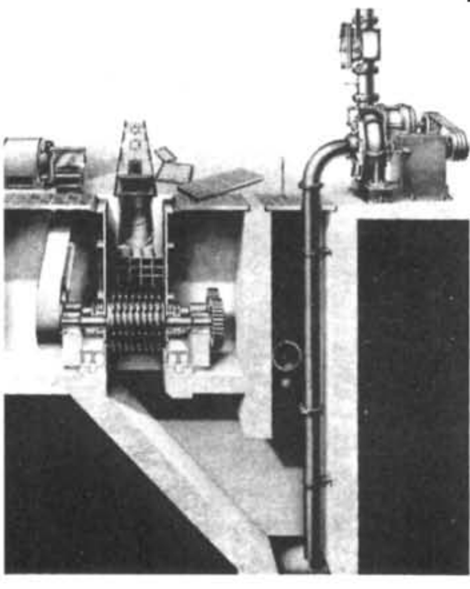

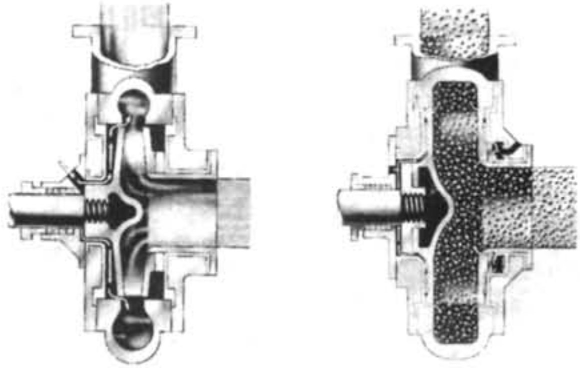

Handling ash, abrasive solids

In contrast to cooling-water service, handling abrasive solids of any kind imposes many special problems on a pump. Rubber-lined units with special seals, as shown, are one good answer for ashes, sand, etc. Other designs include packingless types, flat-blade impellers and special arrangements for suction inlet. While the pump is important, so are other system details.

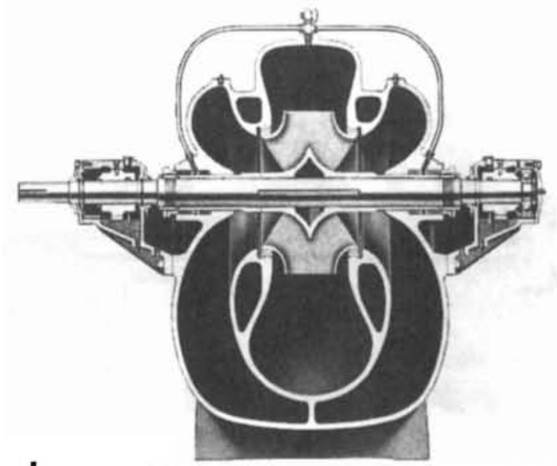

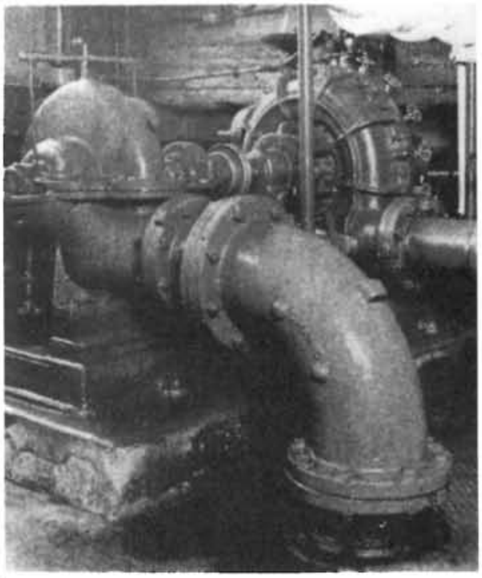

General purpose

This term applies to all classes of pumps, but centrifugal designs in this category perhaps outnumber all others. Usual meaning of term is a pump to handle clear cool liquids at ambient or moderate temperatures. Often single-stage, these units may be split-case, and are standard-fitted pumps equally good for a number of services. Some handle liquids with solids.

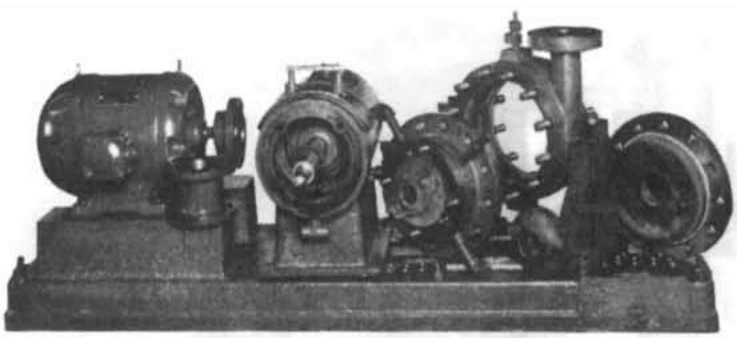

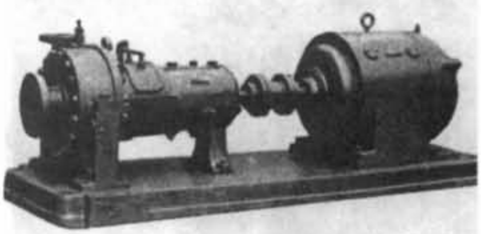

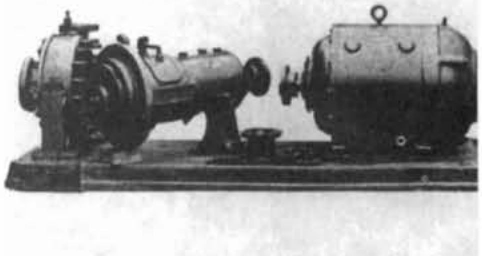

General process work

In recent years engineers have developed special process-pump designs featuring accessibility, good efficiency and long life. Some designs are available as part of a standard line whereas others are made up to suit the particular service conditions for a specific job. As these illustrations show, ease of maintenance is a prime consideration; complete disassembly is simple.

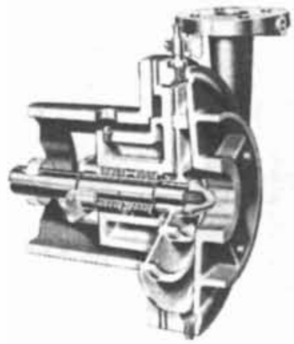

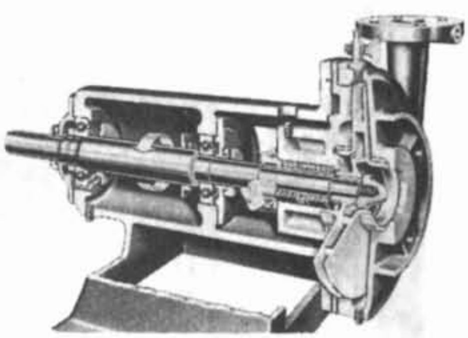

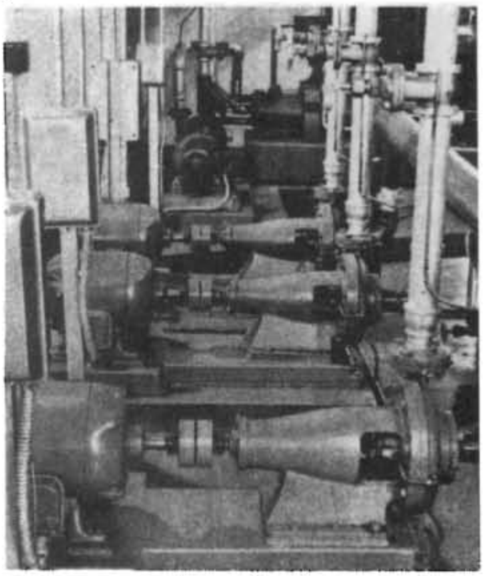

Chemical process

Outwardly resembling the general process pump, units designed for chemical service may differ markedly in materials, stuffing boxes, seals, etc. Usual aim is to produce a single pump line that comes as close as possible to being able to serve all process needs in the chemical industry. Usual units are horizontal, with radially split casings. They can handle a wide range of chemical liquids.

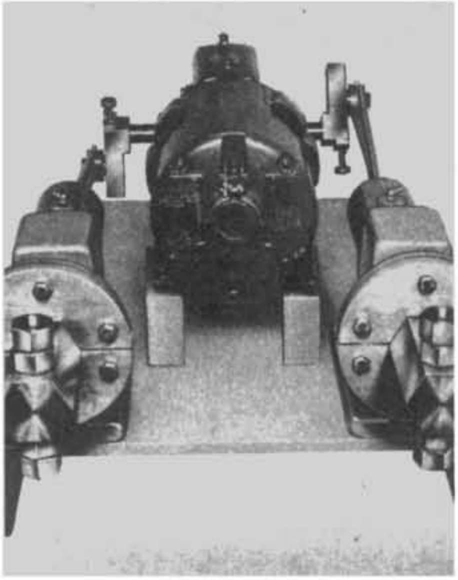

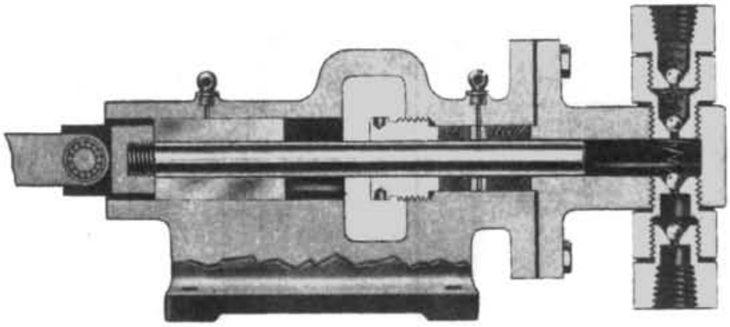

Chemical feed

Requiring easy adjustment of capacity, chemical-feed pumps are built in a large number of different designs. Unit shown has its reciprocating pumping elements arranged for accessibility. Suction and discharge valves are ball type.

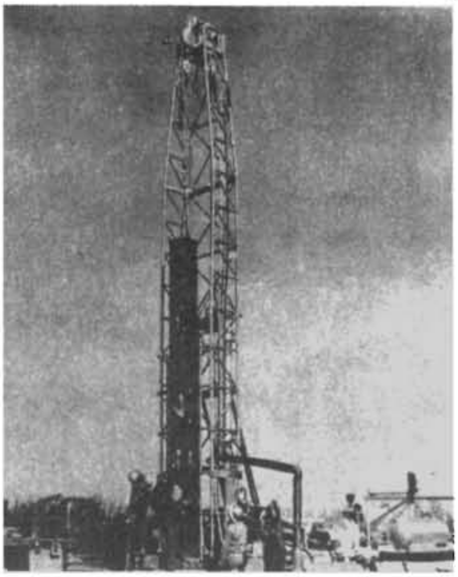

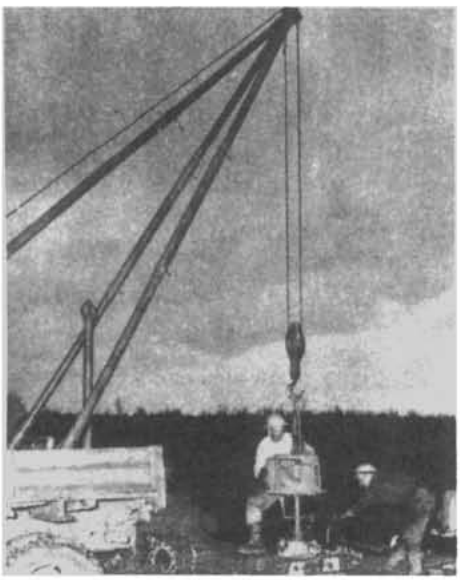

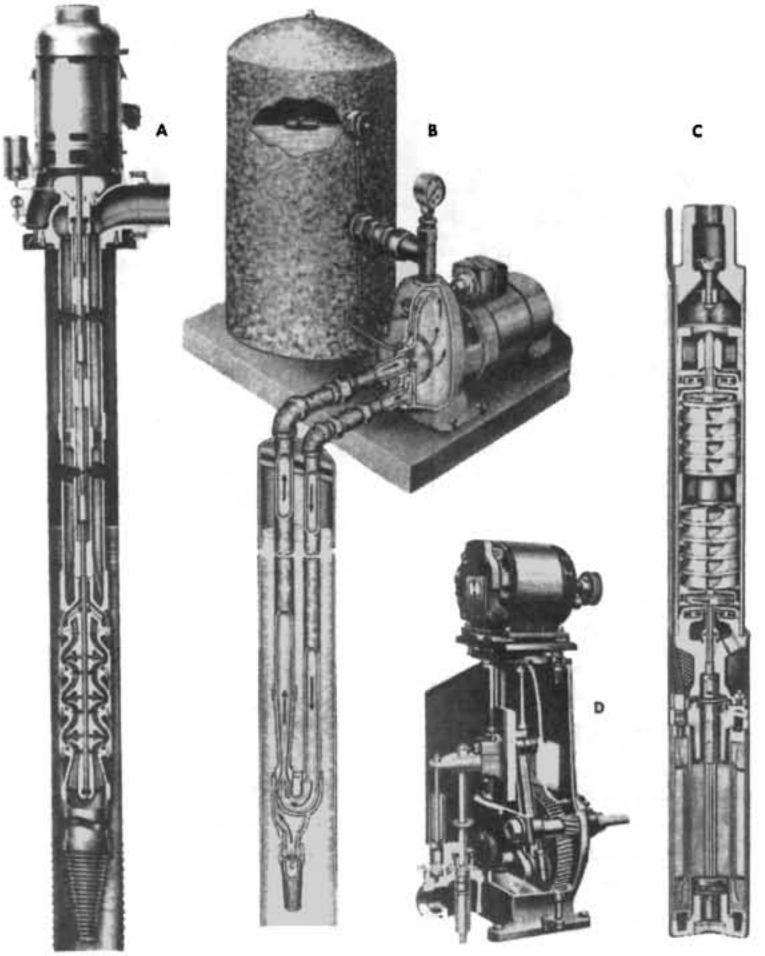

Well-water supply

Water, like gold, is where you find it. Often this is deep in the earth. So we find many designs for this service. *Deepwell* pump, *A*, often called a *turbine* pump, is a multi-stage diffuser unit. *Jet pumps*, *B*, bypass a portion of their discharge to an ejector nozzle at the suction screen where it helps improve flow into pump. *Submersible*, *C*, has motor in well. *D* is *plunger* pump.

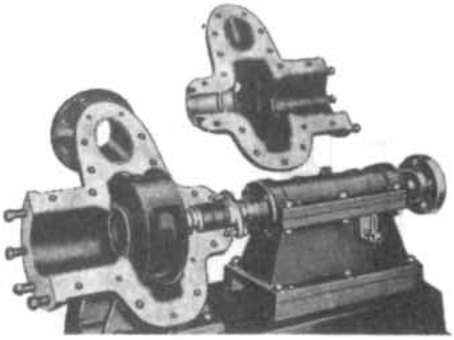

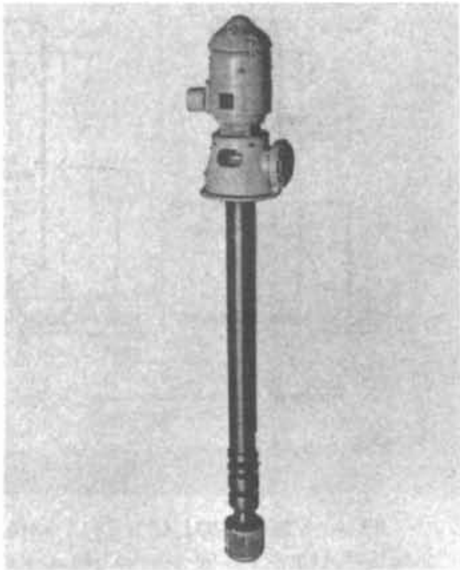

Sewage and sump

Centrifugal pumps for sewage usually have special non-clogging impellers and a casing that is easily opened for unit inspection, ***above right.*** Sump pumps, *left* and *extreme right,* may be portable or permanent, depending on needs of the installation. Impeller is almost always the non-clogging type to prevent solids from catching in it. Automatic control is practically universal.

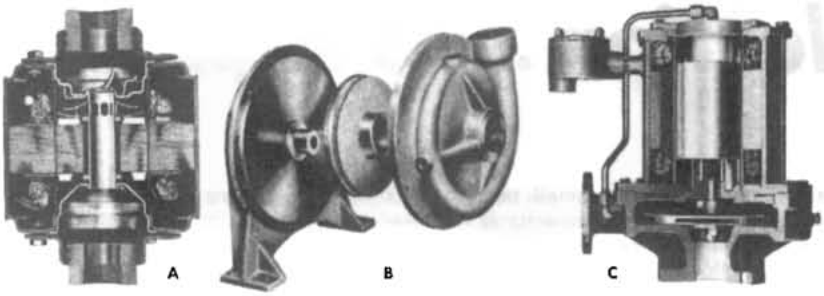

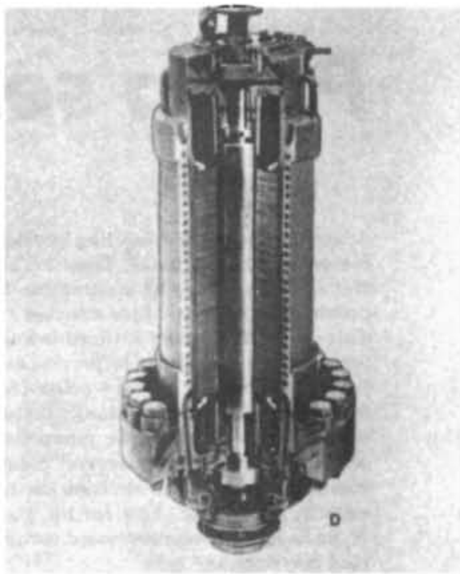

New and special services

Developed in '30s for hot-water circulation, and later refined for chemical and nuclear-power jobs, canned pumps are now strongly bidding for industrial jobs where leak-free service and minimum maintenance are essential. Unit *A* is fractional hp, goes right in pipe. *B* has axial air-gap motor, is built in 10-hp and smaller sizes. *C* is chemical unit, *D* one for nuclear-energy service.

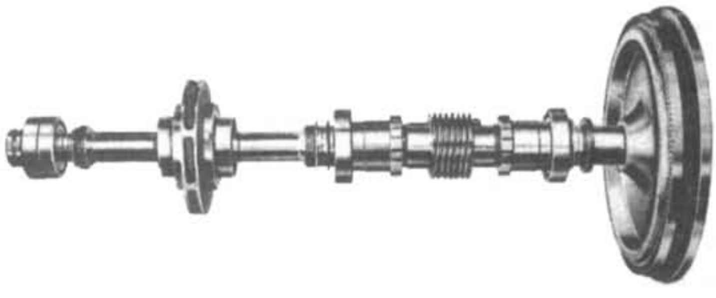

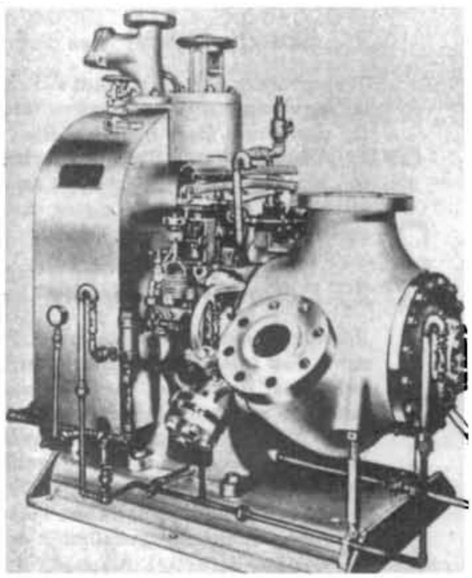

High-pressure services

Where quick starts, compact installation and steam drive are desirable, as in certain boiler-feed applications, petroleum refining, etc, the high-pressure turbine-driven type shown above has many uses. It consists of a single-stage impeller near one end of the shaft; at the other end is a velocity-staged turbine wheel. Single shaft produces a compact unit easy to install and operate.

Typical piping hookups for pumps serving industrial loads

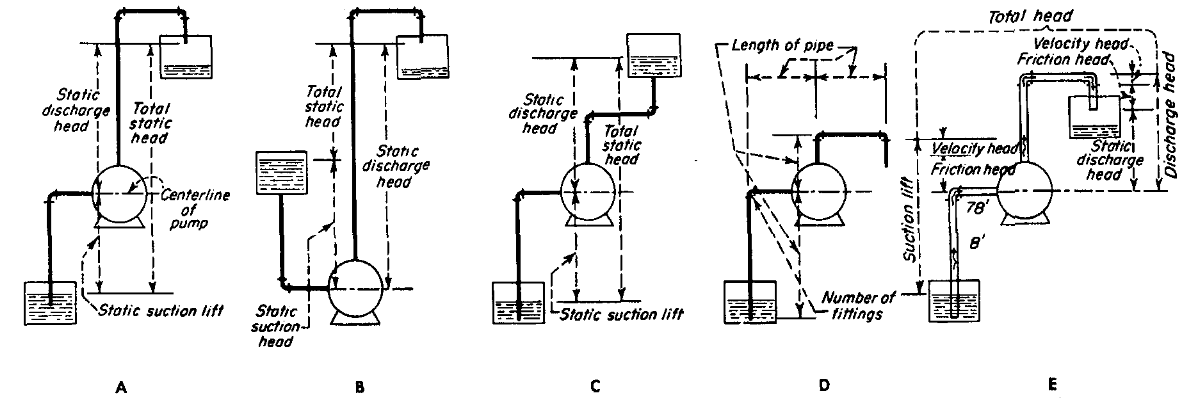

Pump selection . . . 5 steps to

Selecting a pump is much like buying a hat—you have three major decisions to make. These are *size, type* and *best buy.* But of course choosing a pump can be a far more complex problem, especially where unusual or difficult liquid conditions are met. Steps outlined below have proven suitable for typical general-purpose, process and similar applications. Selection of other types — boiler-feed, condensate-return, hydraulic-system, etc. — usually involves analysis of factors not directly related to the pump itself. For example, you might have to compute several plant heat balances before you can make a firm decision on boiler-feed pump type, capacity, drive, etc., best for the existing conditions. Some of these factors were discussed earlier; others are too complex for coverage here.

1 Sketch layout (see diagrams above)

Trying to pick a pump without a sketch of the system layout is like a miner trying to work without his lamp. You're in the dark from start to finish. Base sketch on actual job, as planned. Show all piping, fittings, valves, equipment, etc. Mark length of pipe runs of sketch. Be sure to include all vertical lifts. Where piping is complex, an isometric sketch is often extremely helpful.

2 Determine capacity (see Table I)

Job conditions fix capacity required. For example, maximum steam flow from the exhaust of a turbine, along with steam conditions, determines the minimum amount of cooling water at a given temperature. Seasonal changes, safety factor desired, etc., influence actual capacity chosen. Where demand is unknown and must be estimated, Table I is a big help in indicating typical ranges to be expected. It does *not,* however, give exact values because there can be wide variations from one installation to another. Except for small pumps and those for metering and proportioning, capacity is expressed in gallons per minute (gpm).

3 Figure total head (see Tables II, III)

Diagrams above show various heads in typical pumping systems. Definitions, *facing page,* will help you understand the meanings of various terms. If a pump handles 500 gpm of water through 86 ft of 6-in. suction pipe, diagram above right, and there is one medium-radius elbow having a resistance equal to 14 ft of straight pipe, total equivalent length of suction pipe is $86 + 14 = 100$ ft. Friction loss from Table II is 1.7 ft of water per 100 ft of pipe. Velocity head is almost 0.5 ft and static suction lift is 8 ft. Hence, suction lift is $8 + 1.7 + 0.5 = 10.2$ ft. **Discharge head is found in a similar way, using discharge pipe size, length of runs and fittings in the line. Total head is the sum of suction lift and discharge head. Where we have a static suction head, as in the second hookup from the left, we subtract suction head from discharge head to obtain the total head. Always have pump manufacturer check your head calculations. Then you'll be certain the pump is suitable.**

4 Study liquid conditions

Up to this point we've determined but two requirements our pump must meet — head and capacity. Now we come to characteristics of the liquid and their effect on pump selection. Liquid heavier than water (specific gravity greater than 1) takes more horsepower to be moved from one point to another; lighter liquids require less power. Liquid temperature and vapor pressure fix the net positive suction head needed for satisfactory operation. Unless you are thoroughly experienced with this phase of pump selection, it is best to have the manufacturer check suction conditions. Viscosity of liquid affects horsepower, head and

DEFINITIONS

STATIC SUCTION LIFT is vertical distance, ft, from supply level to pump centerline; pump above supply.

STATIC SUCTION HEAD: same as static suction lift, but pump is below supply level.

STATIC DISCHARGE HEAD is vertical distance, ft, from pump centerline to point of free delivery.

TOTAL STATIC HEAD is vertical distance, ft, from supply level to discharge level.

FRICTION HEAD is pressure, in ft of liquid, needed to overcome resistance of pipe, fittings.

SUCTION LIFT is static suction head plus suction friction head and velocity head.

SUCTION HEAD is static suction head minus suction friction head and velocity head.

DISCHARGE HEAD is static discharge head plus discharge friction head and velocity head.

TOTAL HEAD is sum of suction lift and discharge head. Where there is suction head, total head is difference between discharge and suction heads.

NOTE: Some engineers use *dynamic suction lift, dynamic discharge head* and *total dynamic head* instead of terms above. While the word *dynamic* helps express idea of motion, ie, head when liquid is flowing, the simpler terms are favored.

I: TYPICAL WATER REQUIREMENTS

Usual buildings*			Cities and towns	
Fixture	Cold, gpm	Hot, gpm	Population	Total**, gpm
Water-closet flush valve	45	0	1000	800
Water-closet flush tank	10	0	2000	1200
Urinals, flush valve	30	0	3000	1500
Urinals, flush tank	10	0	4000	1700
Lavatories	3	3	5000	2000
Shower, 4-in. head	3	3	6000	2200
Shower, 6-in. and larger	6	6	8000	2700
Needle bath	30	30	9000	2900
Shampoo spray	1	1	10,000	3100
Baths, tub	5	5	20,000	5100
Kitchen sink	4	4	40,000	8700
Pantry sink, ordinary	2	2	50,000	11,000
Pantry sink, large bibb	6	6	60,000	13,000
Slop sinks	6	6	100,000	19,000
Wash trays	3	3	150,000	28,000
Laundry tray	6	6	180,000	33,000
Garden-hose bibb	10	0	200,000	37,000

*Approximate maximum flow from fixtures: to obtain maximum *probable* flow, multiply maximum possible flow by a usage factor based on previous experience.

**Total includes water for domestic supply and fire protection. Where city or town is predominantly industrial, a greater flow will probably be required.

better results

capacity, as well as class of pump chosen. Here, again, your best bet is the manufacturer. Liquid pH influences pump materials, p 85, while solids affect mechanical construction.

5 Choose class and type

Studying the layout, like trying on a hat, tells us what *size* (capacity and head) pump we need. This furnishes our first lead as to what class of pump is suitable. For example, where high-head small-capacity service is required, table p 77, shows that a reciprocating pump would probably be suitable. Reviewing the liquid characteristics furnishes another clue to class because exceptionally severe conditions may rule out one or another right at the start. Sound economics dictates choosing the pump that provides the lowest cost per gallon pumped over the useful life of the unit.

Operating factors deserving recognition when deciding on class include type of service (continuous or intermittent), running-speed preferences (high-speed pumps often cost less), future load expected and its effect on pump head, possibility of parallel or series hookup, and many others peculiar to a given job. These factors deserve as much study as head and capacity; they're just as important.

Once you know class and type you're ready to check these in a rating table, p 104, or a rating chart as on p 87. As you can see, the table lists pump capacity, head, horsepower, etc. Where required capacity and head, or both, falls between two tabulated values, it is usual practice to choose a pump to meet the next larger condition where this is not too far from the existing job conditions. Otherwise, another make or type of pump may have to be used.

One important fact to keep in mind is that many large pumps are custom-built for a given plant or application. Under these conditions the pump manufacturer performs most of the steps listed above, basing his design on information supplied by the engineer on the job.

II: PIPE FRICTION LOSS FOR WATER

(Wrought-iron or steel Schedule 40 pipe in good condition)

Dia, in.	Flow, gpm	Velocity, ft per sec	Velocity head, ft of water	Friction loss, ft of water per 100 ft pipe
2	50	4.78	0.355	4.67
2	100	9.56	1.42	17.4
2	150	14.3	3.20	38.0
2	200	19.1	5.68	66.3
2	300	28.7	12.8	146
4	200	5.04	0.395	2.27
4	300	7.56	0.888	4.89
4	500	12.6	2.47	13.0
4	1000	25.2	9.87	50.2
4	2000	50.4	39.5	196
6	200	2.22	0.0767	0.299
6	500	5.55	0.479	1.66
6	1000	11.1	1.92	6.17
6	2000	22.2	7.67	23.8
6	4000	44.4	30.7	93.1
8	500	3.21	0.160	0.424
8	1000	6.41	0.639	1.56
8	2000	12.8	2.56	5.86
8	4000	25.7	10.2	22.6
8	8000	51.3	40.9	88.6
10	1000	3.93	0.240	0.497
10	3000	11.8	2.16	4.00
10	5000	19.6	5.99	10.8
10	7500	29.5	13.5	24.0
10	10,000	39.3	24.0	42.2
12	2000	5.73	0.511	0.776
12	5000	14.3	3.19	4.47
12	10,000	28.7	12.8	17.4
12	15,000	4[illegible] 0	28.7	38.4
12	20,000	[illegible]7.3	51.1	68.1

III: RESISTANCE OF FITTINGS AND VALVES

(Length of straight pipe, ft, giving equivalent resistance)

Pipe size, in.	Std ell	Med-rad ell	Long-rad ell	45-deg ell	Tee	Gate valve, open	Globe valve, open	Swing check, open
1	2.7	2.3	1.7	1.3	5.8	0.6	27	6.7
2	5.5	4.6	3.5	2.5	11.0	1.2	57	13
3	8.1	6.8	5.1	3.8	17.0	1.7	85	20
4	11.0	9.1	7.0	5.0	22	2.3	110	27
5	14.0	12.0	8.9	6.1	27	2.9	140	33
6	16.0	14.0	11.0	7.7	33	3.5	160	40
8	21	18.0	14.0	10.0	43	4.5	220	53
10	26	22	17.0	13.0	56	5.7	290	67
12	32	26	20.0	15.0	66	6.7	340	80
14	36	31	23	17.0	76	8.0	390	93
16	42	35	27	19.0	87	9.0	430	107
18	46	40	30	21	100	[illegible].2	500	120
20	52	43	34	23	110	2.0	560	134
24	63	53	40	28	140	14.0	680	160
36	94	79	60	43	200	20.0	1000	240

Typical centrifugal-pump rating table

Size	Gpm	Total head, ft: 10	15	20	25	30
2C	100			1000-.8	1060-1.0	1150-1.2
	150			1070-1.2	1150-1.5	1240-1.7
	200				1290-2.1	1360-2.4
3CS	150	750-.53	850-.78	950-1	1030-1.2	1100-1.5
	200		950-1.1	1010-1.4	1100-1.7	1170-2
	250			1170-1.9	1190-2.3	1260-2.6
	300					1400-3.5
3CL	200	690-.63	800-.95	910-1.3	1010-1.6	1110-2.05
	300	870-1.2	950-1.6	1000-1.9	1100-2.4	1170-2.8
	400			1200-3.1	1230-3.7	1290-4.1
	500					1490-5.8
4C	400	750-1.3	850-1.8	940-2.4	1040-3	1120-3.7
	600			1080-4	1170-4.6	1210-5.5
	800					1400-8.4
1¼D	25		617-.21	707-.03	778-.40	845-.51
	50		680-.37	760-.49	865-.63	900-.76
	75			856-.78	916-.94	980-1.1
	100					
	125					
	150					
2DL	150		820-.93	850-1.1	930-1.35	990-1.6
	200			970-1.8	1040-2.1	1080-2.3
	250					
	300					

Example: 1080-4 indicates pump speed is 1080 rpm; actual input required to operate pump is 4 hp.

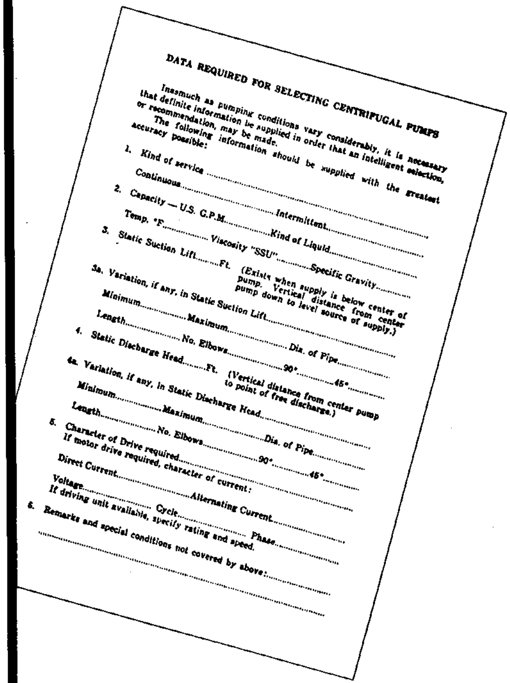

DATA REQUIRED FOR SELECTING CENTRIFUGAL PUMPS

Inasmuch as pumping conditions vary considerably, it is necessary that definite information be supplied in order that an intelligent selection, or recommendation, may be made.

The following information should be supplied with the greatest accuracy possible:

1. Kind of service ....
Continuous..............................Intermittent..............................
2. Capacity — U.S. G.P.M..............Kind of Liquid..............................
Temp, °F.............. Viscosity "SSU"..............Specific Gravity..............
3. Static Suction Lift.........Ft. (Exists when supply is below center of pump. Vertical distance from center pump down to level source of supply.)
3a. Variation, if any, in Static Suction Lift..............................
Minimum..............Maximum..............................
Length..............No. Elbows..............Dia. of Pipe..............
4. Static Discharge Head.........Ft. (Vertical distance from center pump to point of free discharge.) 90°..............45°..............
4a. Variation, if any, in Static Discharge Head..............................
Minimum..............Maximum..............................
Length..............No. Elbows..............Dia. of Pipe..............
5. Character of Drive required..............90°..............45°..............
If motor drive required, character of current:
Direct Current..............................
Voltage..............Alternating Current..............................
If driving unit available, specify rating and speed. Cycle.............. Phase..............
6. Remarks and special conditions not covered by above:..............................
....

Other considerations in choosing pumps

Our previous two pages outline usual steps in choosing a pump for typical industrial services. There are cases, however, where selection is better made by the pump builder.

Estimating data sheets, *above right,* are available from manufacturers to aid you in making a complete statement of conditions a new pump must meet. When sending such an estimate to a manufacturer it is wise to include a clear free-hand sketch of the installation.

While the sheet shown is for a centrifugal pump, forms for reciprocating and rotary estimates resemble this closely. Having the manufacturer select your pump insures getting the right unit, *provided* you supply the information he needs.

Net positive suction head is often listed on estimate sheets and must be entered to give a complete picture of pumping conditions. This term gives pressure available or required to force a given flow, gpm, into the impeller, cylinder or casing of a pump. For uniformity, npsh is stated as feet of liquid equivalent to required pressure in psi over and above vapor pressure of liquid at pumping temperature.

Every pump has its individual required npsh characteristics which the manufacturer can plot on a performance curve. Npsh at any point on the curve is head in feet of liquid pumped equivalent to pressure in psi required to force liquid into the pump. Values shown by pump manufacturer are based on tests and are regularly corrected to the centerline of the pump.

As engineer in charge of plant services you must locate the pump and design the suction piping so available npsh is equal to or greater than npsh required by pump. Curves, *right,* give vapor pressure of water at different temperatures. They also give conversion factors for changing flow from lb per hour to gpm. Both are useful in planning.

Pipe sizes for lines where flow demand is likely to change or resistance may increase over a period of years require careful study. If sized only on basis of today's demands or resistance, we may find that what was once an economical installation becomes a money-waster.

Complete Analysis. Though not all jobs warrant it, a piping system can be completely analyzed for present and future operations by using pump characteristic and system-head curves like those on p 86. But instead of plotting one system-head curve, a series, one for each operating condition, is plotted. Study of these will show just what we may expect from a given pump today, tomorrow, and five or more years from now. This is a job for the engineer in the plant and it deserves more attention than it usually receives.

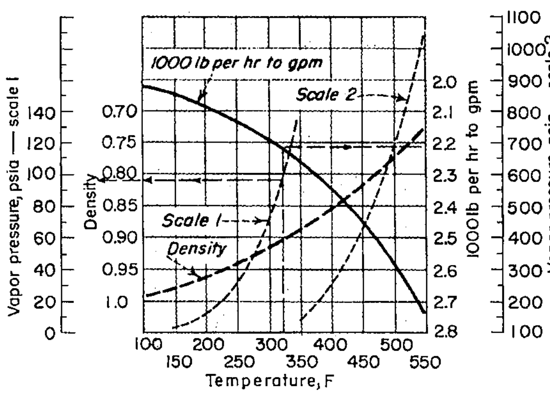

SIX SELF-PRIMING PUMPS

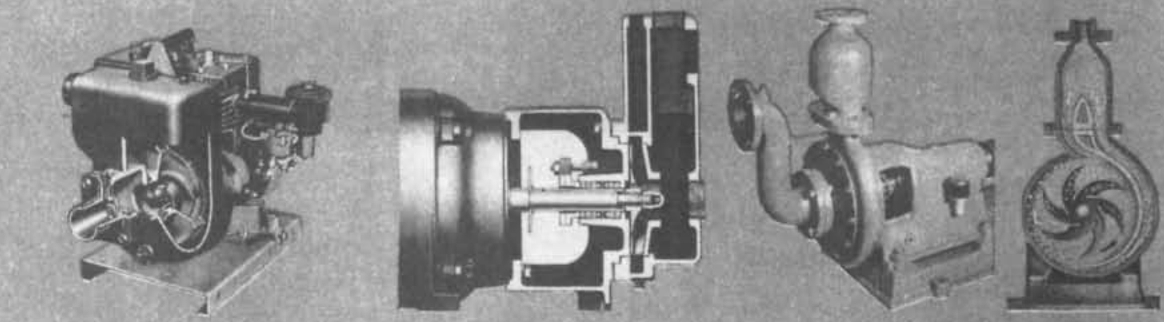

DIFFUSER priming method here does not return liquid to suction side of the pump

DOUBLE VOLUTE recirculates liquid-vapor mixture during prime, separates vapor

AIR SEPARATOR and two discharge ports in pump give priming action in this unit

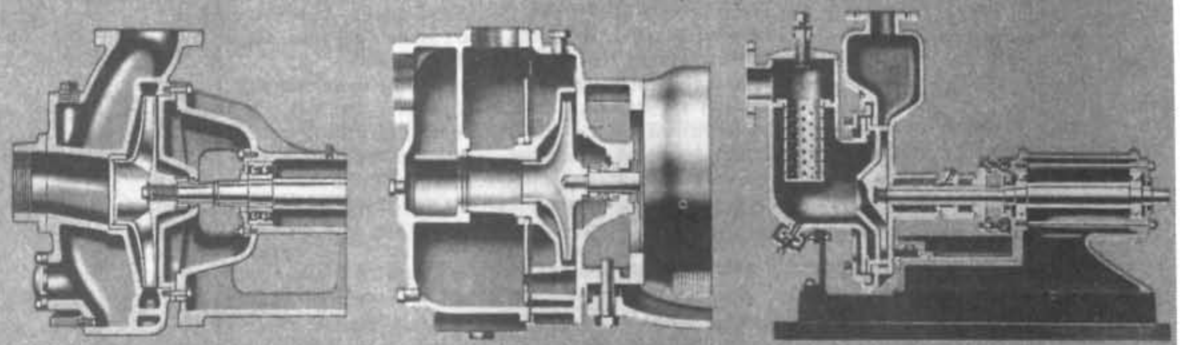

PRIMING CHAMBER in this unit surrounds straight-in suction; no valves are used

LIQUID flows into lower volute and out upper volute during priming in this unit

SLOTS in impeller vanes permit air to be entrained by priming liquid in this pump

EIGHT AUXILIARY PRIMING METHODS

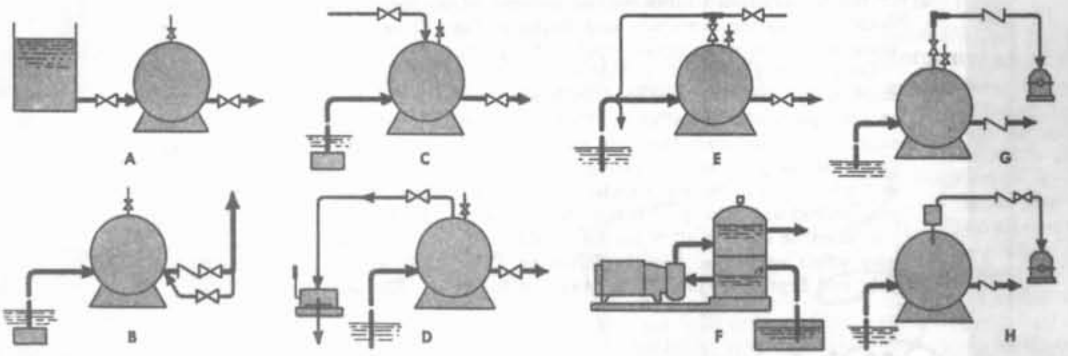

Priming pumps

Positive-displacement pumps — reciprocating and rotary — are self-priming for total suction lifts to about 28 ft. when in good condition. But with long suction lines, high lifts or other abnormal conditions, they must be primed.

Centrifugal pumps are not self-priming; on a suction lift they must be primed. Either special self-priming units may be used or auxiliary priming equipment may be installed.

Illustrations at top of this page show six modern self-priming units. Designs vary from one maker to another, but a liquid reservoir of some type on the discharge is common. It holds priming liquid and serves as an air separator. Other designs have a liquid reservoir on both suction and discharge, liquid being circulated from discharge to suction on prime. Automatic valves or hydraulic action stop circulation after pump primes. Some pumps circulate liquid continuously.

Auxiliary equipment for pump priming includes ejectors, vacuum pumps, etc., used in hookups like those sketched.

With a flooded suction, *A*, open casing air-vent petcocks and then slowly open suction gate valve. Incoming liquid pushes air from casing. Bypass around discharge check valve, *B*, permits using liquid in discharge line. Foot valve, *C*, holds water in suction line, is augmented by auxiliary supply. Separate pump, *D*, draws air from casing for priming. Or an ejector, *E*, does same job. Priming tank, *F*, holds supply of liquid large enough to establish flow through pump on starting. Vacuum pumps, *G* and *H*, are manually and automatically controlled to prime the main pump.

Find How Much Horsepower to Pipe Liquids

Charts give answers for flow from 50 to 100,000 gpm for pipe-roughness ratios of 0.02 to smooth.

Douglas C. Greenwood

The charts on these two pages will make it easier to design pumps and other equipment for handling liquid flowing in pipes.

First, it is often helpful to know the theoretical horsepower required to raise the liquid to various heads. This is obtained from the horsepower-gpm charts. They are plotted for a 10-ft head of water: For other heads, multiply hp by $H/10$ where H is the revised head; for other liquids, multiply by the corresponding specific gravity.

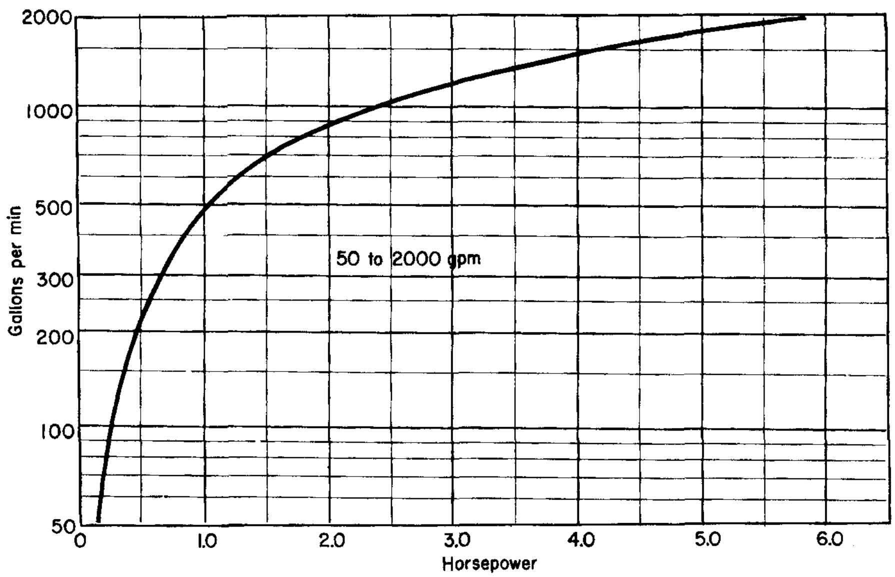

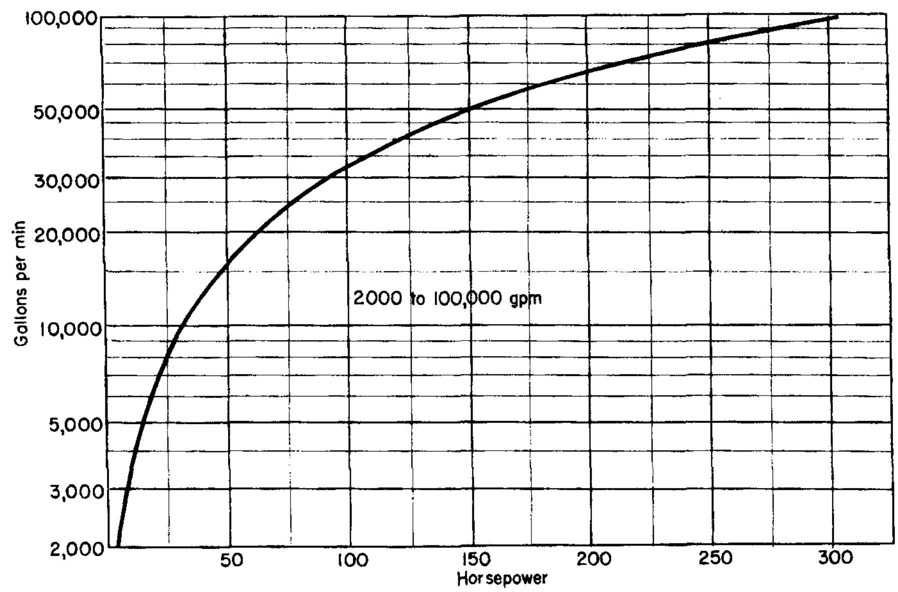

Hp-gpm Chart . . . shows how much hp is required to pump water against a 10-ft head. Full-pipe flow is assumed.

SYMBOLS

G = flow rate, gpm
H_1 = head loss, ft
L = length of pipe, ft
P = pressure, psi
R = Reynold's number $= 0.0833\, Vd/\nu$
V = velocity, fps
d = pipe dia, in.
f = friction factor
w = fluid density, lb per cu ft
r = relative roughness of pipe $= \epsilon/d$
ϵ = effective height of roughness particle, in.
ν = kinematic viscosity, ft^2/sec

Next, for practical results friction losses must be accounted for. These vary and should be known for each individual case.

Much used in liquid-flow calculations is the Darcy formula

$$H_1 = f\,\frac{6LV^2}{d32.16}$$

which can be modified, if velocity is in gpm, to

$$H_1 = 0.0312 f\,\frac{LG^2}{d^5}\,w$$

or for head loss in psi units

$$P = 0.000217 f\,\frac{LG^2}{d^5}\,w$$

Practical values of f vary from about 0.01 to 0.06 depending on pipe smoothness and dia. For laminar flow, $f = 64.4/R$. The flow chart gives f for various values of R and pipe roughness. Values ϵ for various pipes are: 0.00006 in. for smooth drawn tubing; 0.0018 in. for wrought iron; 0.01 in. for cast iron. Curves for relative roughness values of 0.0005 to 0.01 are plotted. Most of these lie in the transition zone between laminar flow and complete turbulence.

Fluid-flow Chart . . .

gives friction for various pipe conditions and values of Reynold's Number.

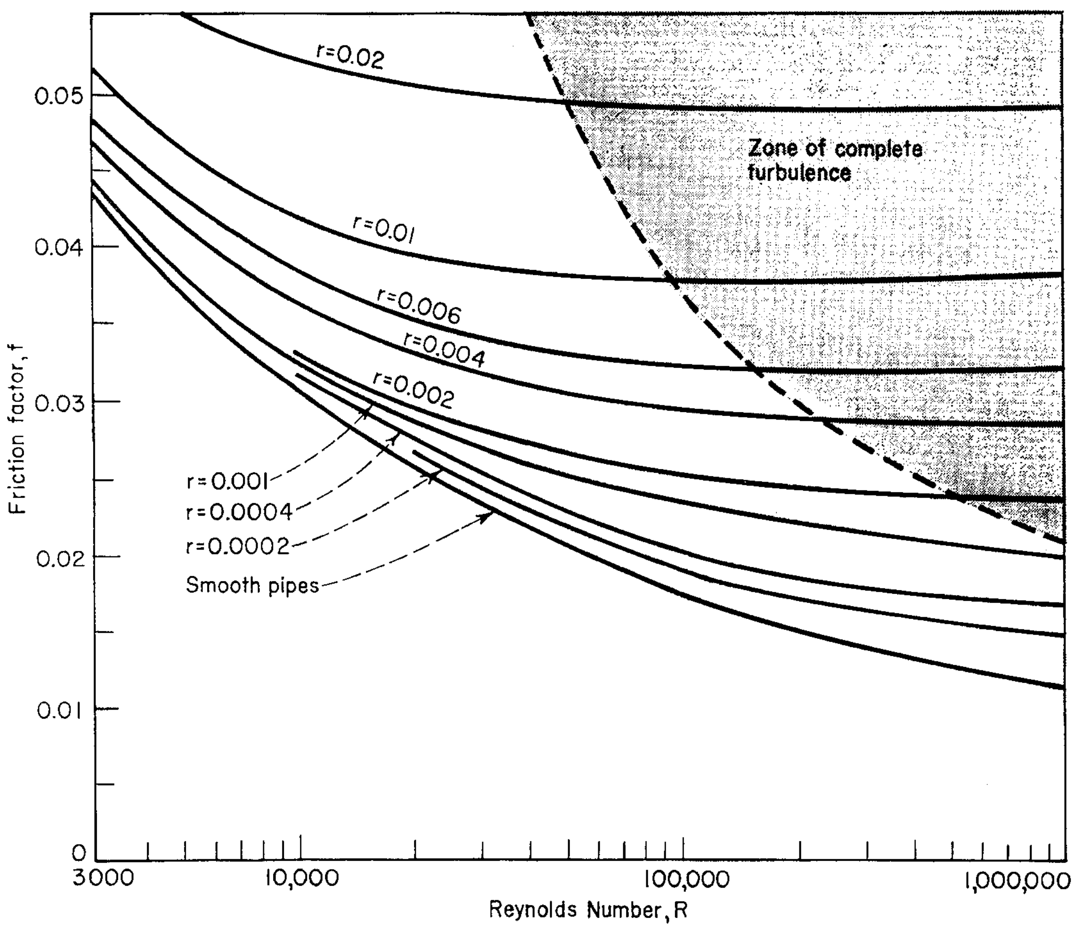

SECTION 27

CREATIVE ASSEMBLIES

10 Ways to Amplify Mechanical Movements

How levers, membranes, cams, and gears are arranged to measure, weigh, gage, adjust, and govern.

Federico Strasser

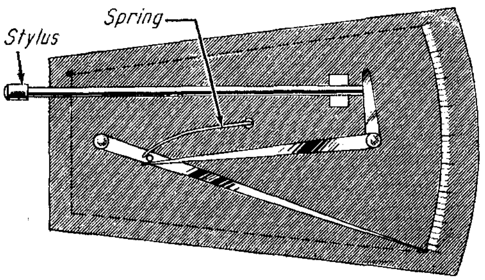

1 **HIGH AMPLIFICATION** for simple measuring instruments is provided by double lever action. Accuracy can be as high as 0.0001 in.

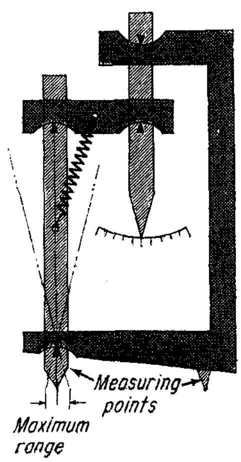

2 **PIVOTED LEVERS** allow extremely sensitive action in comparator-type measuring device shown here. The range, however, is small.

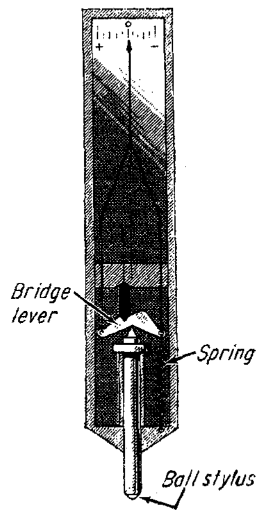

3 **ULTRA-HIGH AMPLIFICATION,** with only one lever, is provided in the Hirth-Minimeter shown here. Again, the range is small.

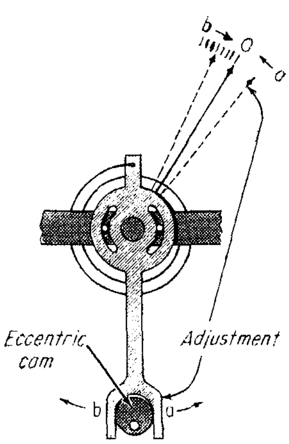

7 **FOR CLOSE ADJUSTMENT,** electrical measuring instruments employ eccentric cams. Here movement is reduced, not amplified.

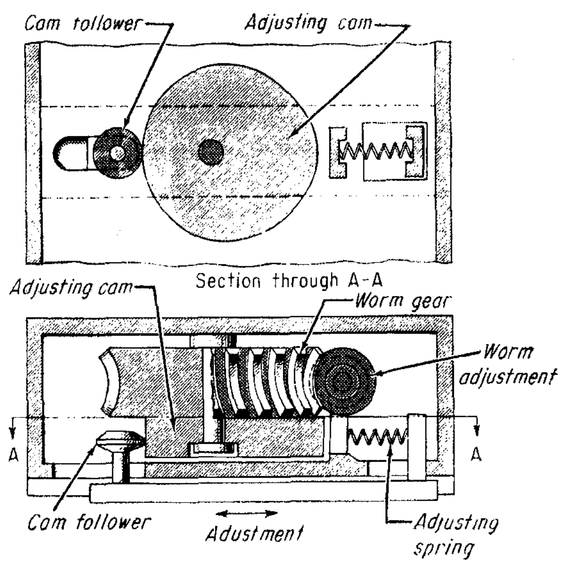

8 **MICROSCOPIC ADJUSTMENT** is achieved here by employing a large eccentric-cam coupled to a worm-gear drive. Smooth, fine adjustment result.

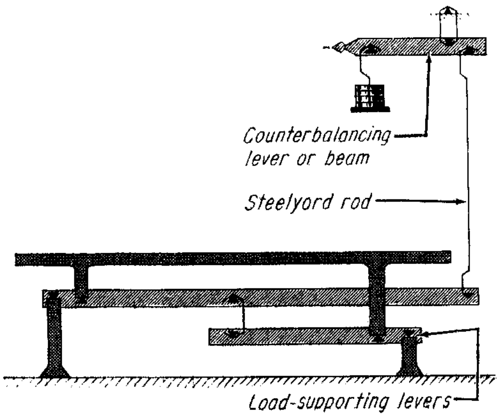

4

LEVER - ACTUATED weigh-scale needs no springs to maintain balance. The lever system, mounted on knife edges, is extremely sensitive.

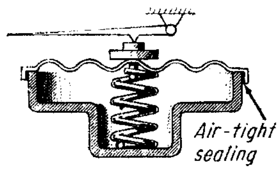

5

CAPSULE UNIT for gas-pressure indicators should be provided with a compression spring to preload the membrane for more positive action.

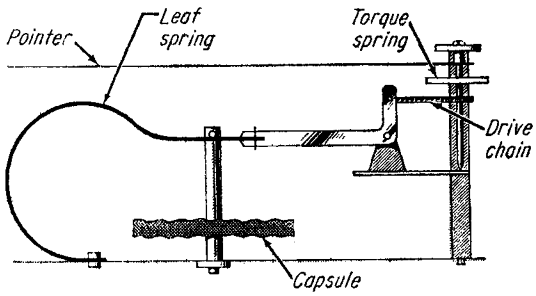

6

AMPLIFIED MEMBRANE MOVEMENT can be gained by the arrangement shown here. A small chain-driven gear links the lever system.

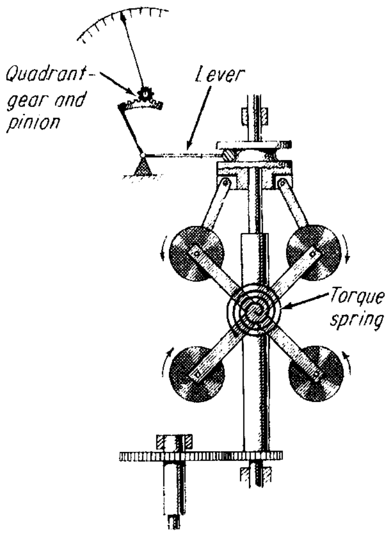

9

QUADRANT-GEAR AND PINION coupled to an L-lever provide ample movement of indicator needle for small changes in governor speed.

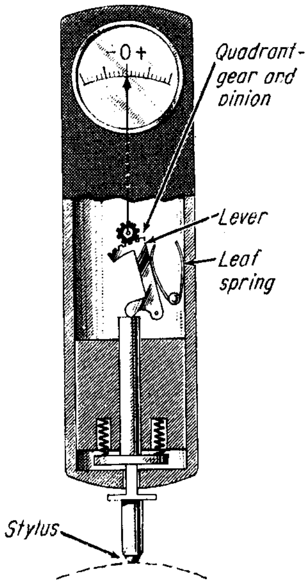

10

COMBINATION LEVER AND GEARED quadrant are used here to give the comparator maximum sensitivity combined with ruggedness.

10 Ways to Amplify Mechanical Action

Levers, wires, hair, and metal bands are arranged to give high velocity ratios for adjusting and measuring.

Federico Strasser

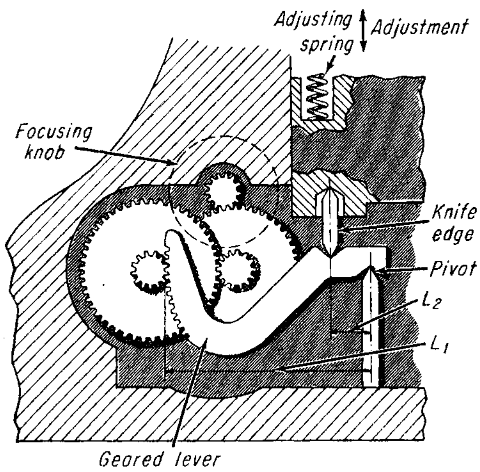

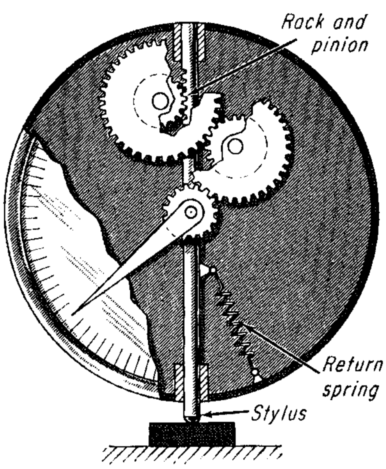

1 **LEVER AND GEAR** train amplify the microscope control-knob movement. Knife edges provide frictionless pivots for lever.

2 **DIAL INDICATOR** starts with rack and pinion amplified by gear train. The return-spring takes out backlash.

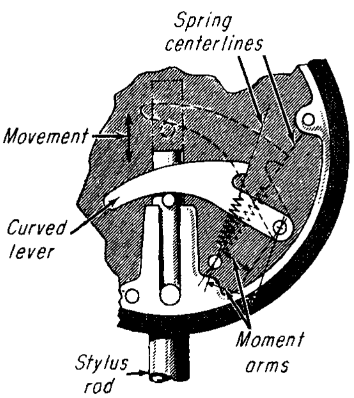

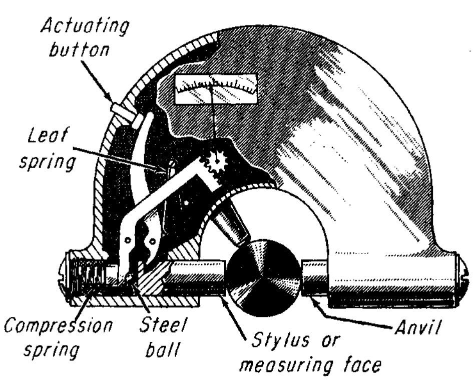

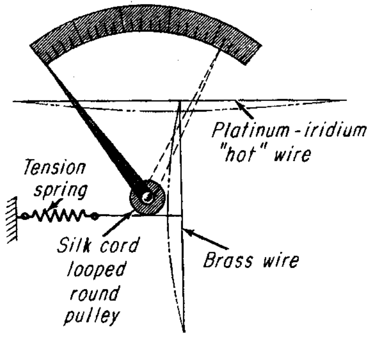

3 **CURVED LEVER** is so shaped and pivoted that the force exerted on the stylus rod, and thus stylus pressure, remains constant.

4 **ZEISS COMPARATOR** is provided with a special lever to move the stylus clear of the work. A steel ball greatly reduces friction.

5 **"HOT-WIRE" AMMETER** relies on the thermal expansion of a current-carrying wire. A relatively large needle movement occurs.

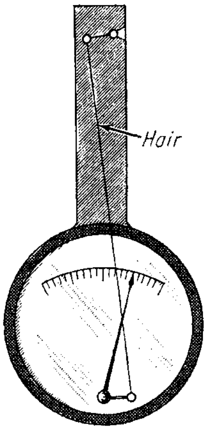

6 **HYGROMETER** is actuated by a hair. When humidity causes expansion of the hair, its movement is amplified by a lever.

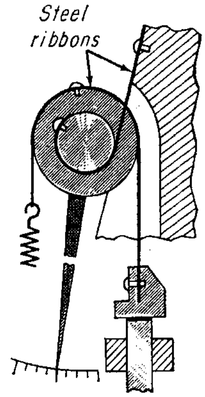

7 **STEEL RIBBONS** transmit movement without the slightest backlash. The movement is amplified by differences in diameter.

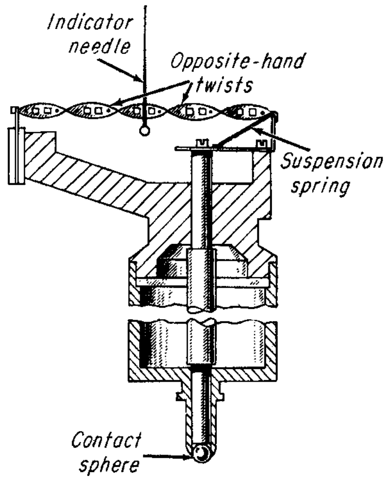

8 **METAL BAND** is twisted and supported at each end. Small movement of contact sphere produces large needle movement.

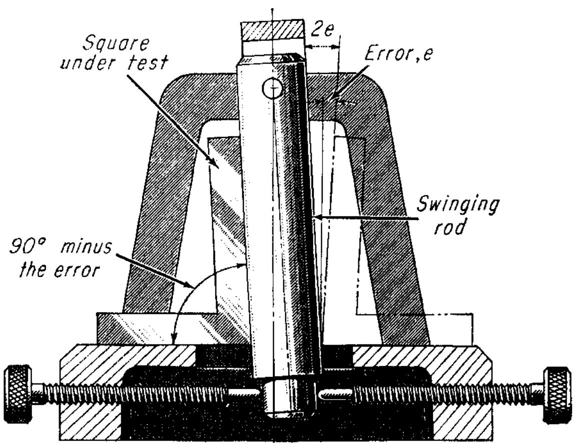

9 **ACCURACY** of 90° squares can be checked with a device shown here. The rod makes the error much more apparent.

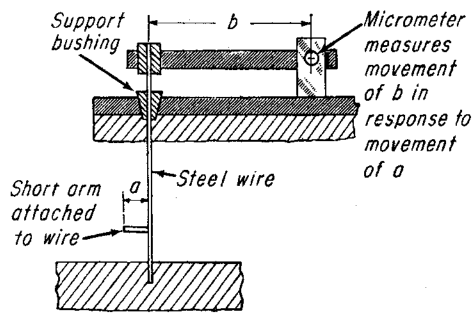

10 **TORSIONAL** deflection of the short arm is transmitted with low friction to the longer arm for micrometer measurement.

How to Damp Axial and Rotational Motion

Fluid-friction devices include two hydraulic and two pneumatic actions; swinging-vane arrangements dissipate energy and govern speed.

Frederico Strasser

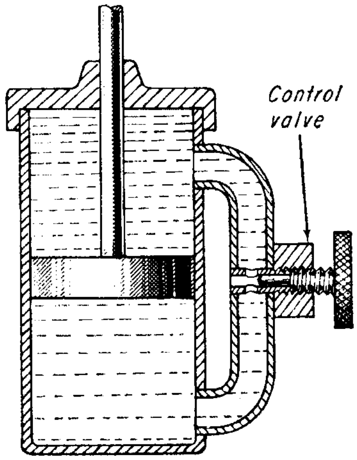

1 **ADJUSTABLE BYPASS** between the two sides of the piston controls speed at which fluid can flow when piston is moved.

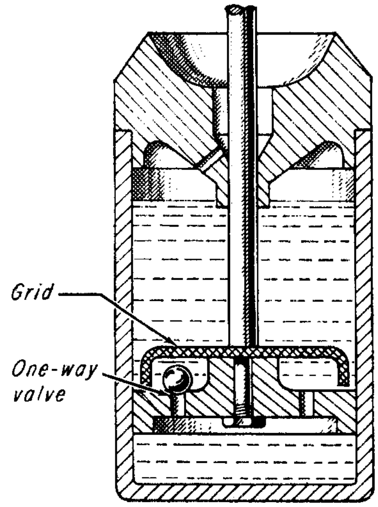

2 **CHECK VALVE** in piston lets speed be controlled so that the piston moves faster in one direction than in the other.

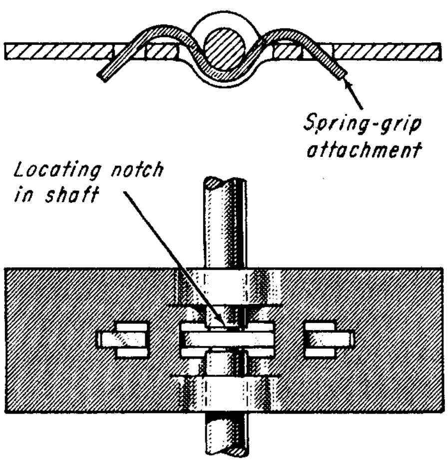

5 **ROTATING VANES** are resisted by the air as they revolve. Make allowance for sudden stops by providing a spring.

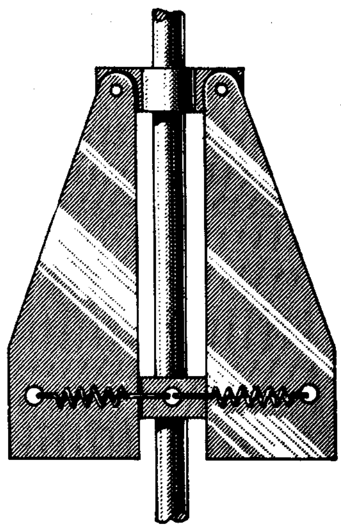

6 **SWINGING VANES** create increased wind drag as centrifugal force opens them to a larger radius.

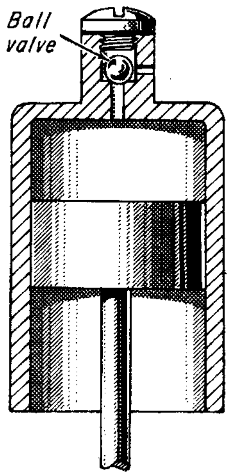

3 **PNEUMATIC CHECK VALVE** acts in manner similar to that of previous device. Vertical position, of course, is necessary.

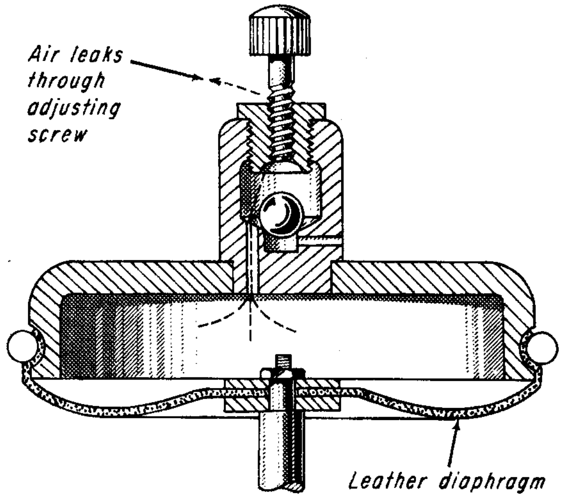

4 **FLEXIBLE DIAPHRAGM** controls short movements. Speed is fast in one direction, but greatly slowed in return direction.

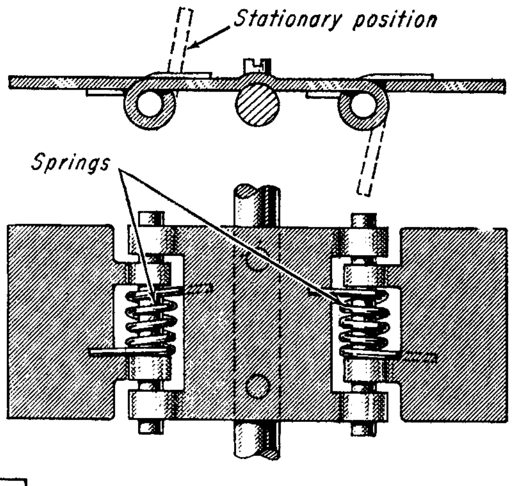

7 **VANE AREA INCREASES** when the spring-loaded vanes swing out. Forces differ for motion into or against the wind.

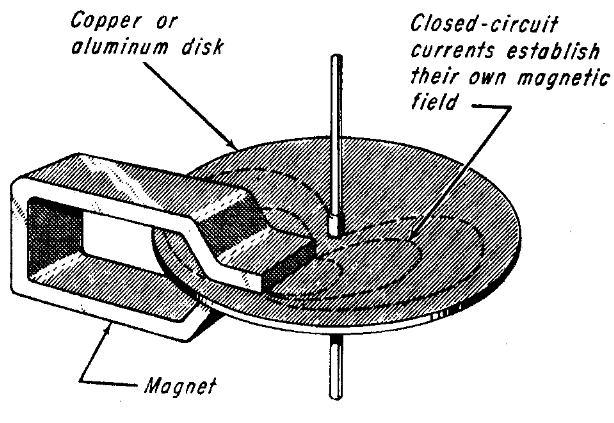

8 **EDDY CURRENTS** are induced in disk when it is moved through a magnetic field. Braking is directly proportional to speed.

8 Snap-Action Devices

A further selection of basic arrangements for obtaining sudden motion after gradual buildup of force.

Peter C. Noy

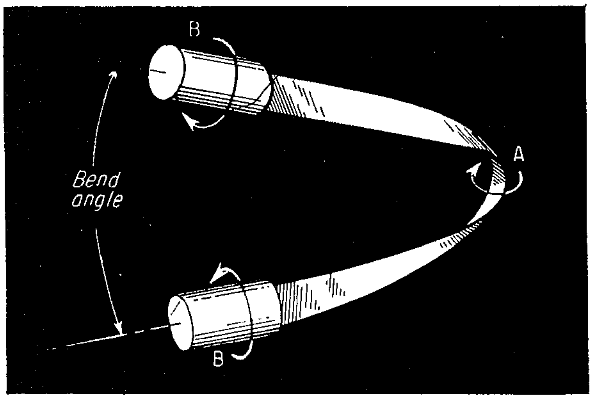

1

Torsion ribbon . . .
bent as shown will turn "inside out" at A with a snap action when twisted at *B*. Design factors are ribbon width and thickness, and bend angle.

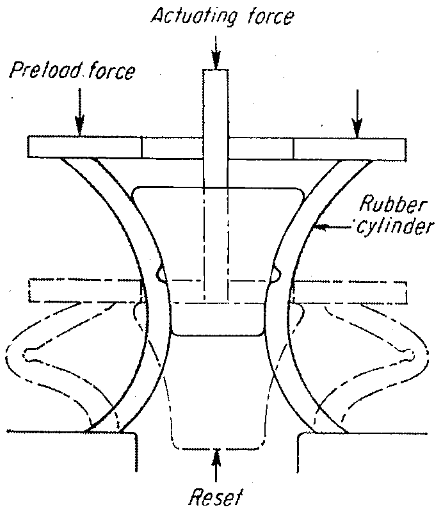

2

Collapsing cylinder . . .
has elastic walls that may be deformed gradually until their stress changes from compressive to bending with the resultant collapse of the cylinder

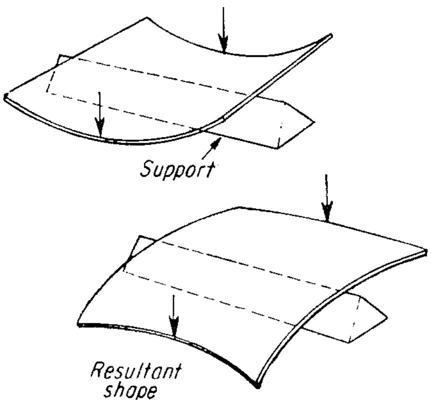

3

Bowed spring . . .
will collapse into new shape when loaded as shown. "Push-pull" type of steel measuring tape illustrates this action; the curved material stiffens the tape so that it can be held out as a cantilever until excessive weight causes it to collapse suddenly.

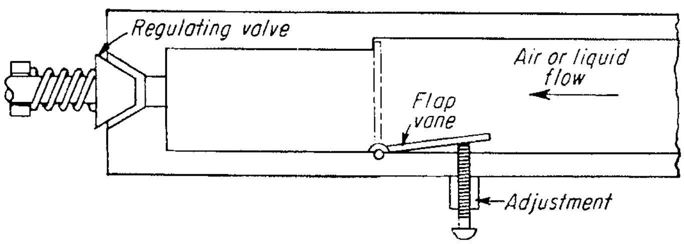

4

Flap vane . . .
is for air or liquid flow cutoff at a limiting velocity. With a regulating valve, vane will snap shut (because of increased velocity) when pressure is reduced below a certain value.

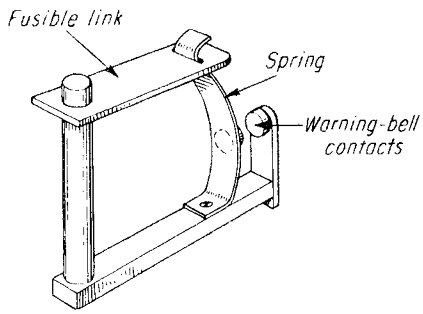

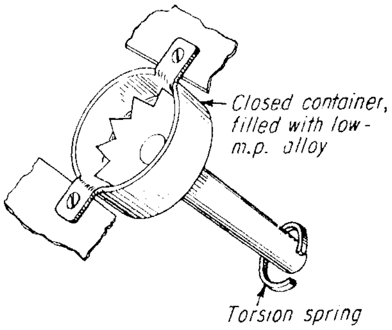

5

Sacrificing link . . .
is used generally where high heat or chemically corrosive conditions would be hazardous —if temperature becomes too high, or atmosphere too corrosive, link will yield at whatever conditions it is designed for. Usually the device is required to act only once, although a device like the lower one is quickly reset but restricted to temperature control.

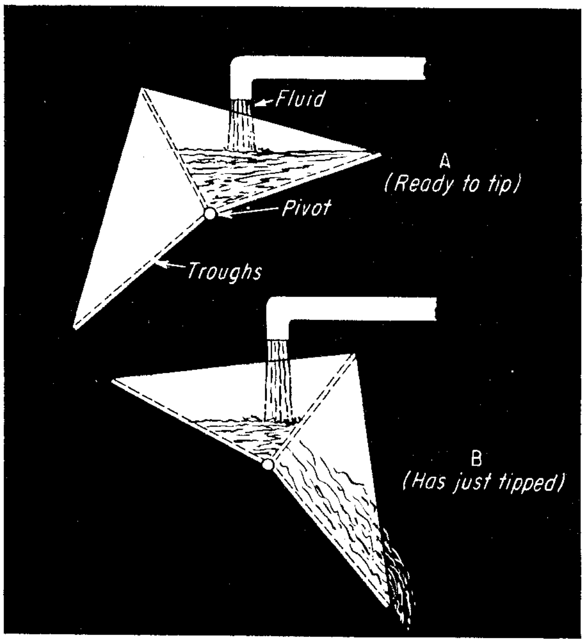

6

Gravity-tips . . .
although slower acting than most snap mechanisms, can be called snap mechanisms because they require an accumulation of energy to trigger an automatic release. Tipping-troughs used to spread sewage exemplify arrangement shown in A, once overbalanced, action is fast.

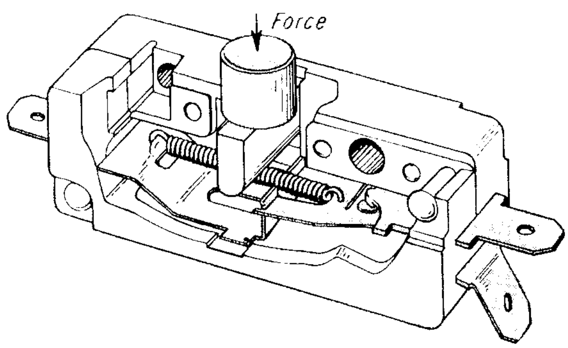

7

Overcentering tension . . .
spring combined with pivoted contact-strip is one arrangement among many similar ones used in switches. Arrangement shown here is somewhat unusual, since the actuating force bears on the spring itself.

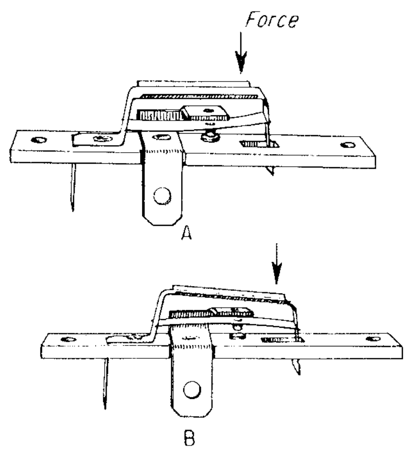

8

Overcentering leaf-spring . . .
action is also the basis for many ingenious snap-action switches used for electrical control. Sometimes spring action is combined with the thermostatic action of a bimetal strip to make the switch respond to heat or cold either for control purposes or as a safety feature.

Make Diaphragms Work for You

Diaphragms have more uses than you think. Here's a display of applications that simple fabric-elastomer diaphragms can handle economically and with a minimum of design problems

John F. Taplin

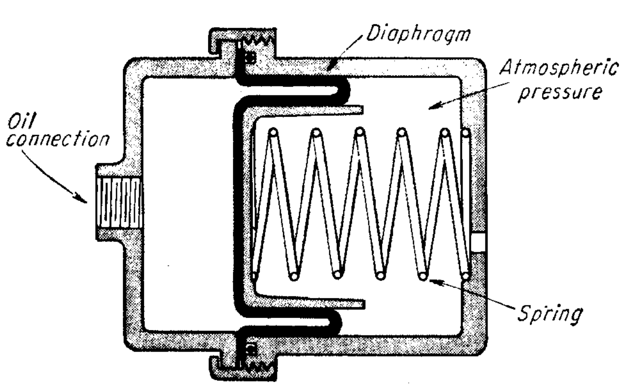

2 Expansion compensator for liquid-filled systems handles thermal expansion of the liquid as well as any system losses.

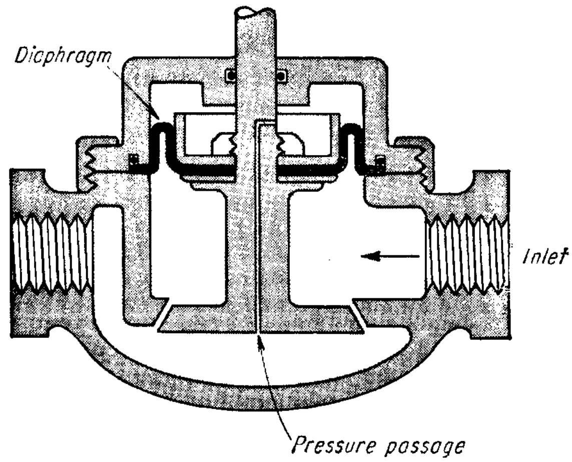

3 A balanced valve uses a fabric-elastomer diaphragm to hydrostatically balance the valve poppet as well as the valve head.

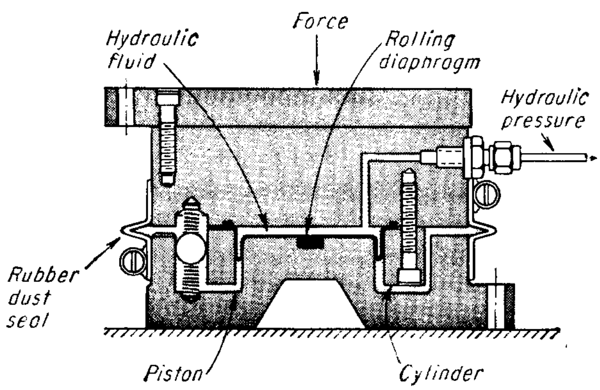

6 A force-balance load cell converts the weight or force of any object into an accurate reading at a remote point.

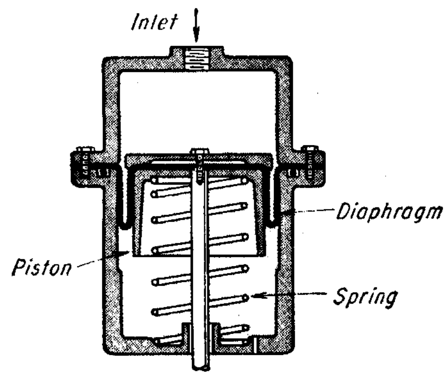

7 Linear actuator converts gas or fluid pressure into a linear stroke without leakage or break-out friction effects.

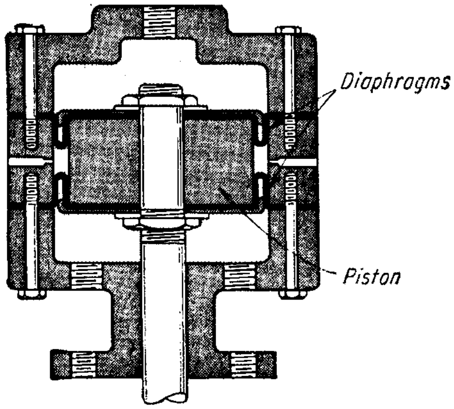

1 Double-acting actuator provides for thrust in either direction by placing two diaphragm assemblies back to back.

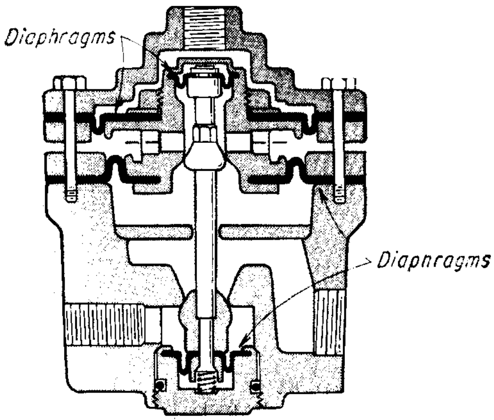

4 Regulating valve controls the value of air pressure by means of a diaphragm-balanced valve and two control diaphragms.

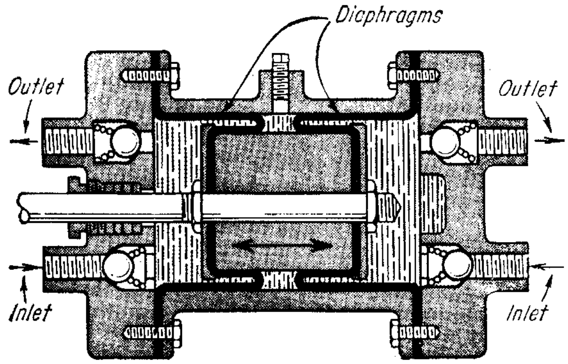

5 Double-acting pump has two diaphragms to give smooth and continuous flow of fluid to equipment at a safe working pressure.

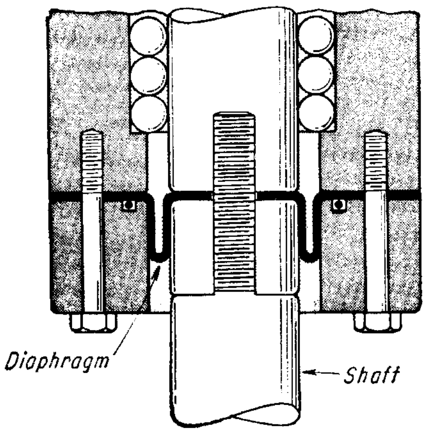

8 Shaft seal uses lubricant pressure to force the sidewall of the diaphragm to roll against the shaft and housing.

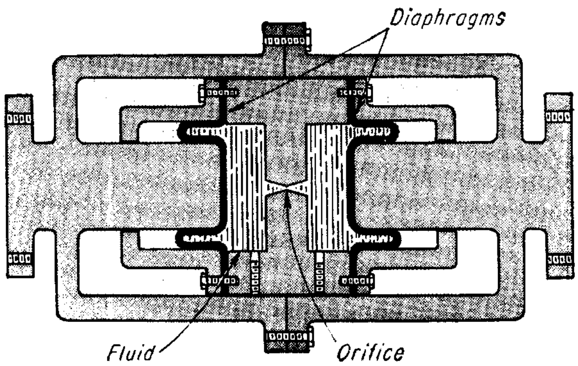

9 Damping mechanism prevents abrupt or sudden motion in a machine. Damping amount is controlled by orifice size.

Control-Locked Thwart Vibration and Shock

Critical adjustments stay put–safe against accidental turning or deliberate fiddling with them.

Frank William Wood JR.

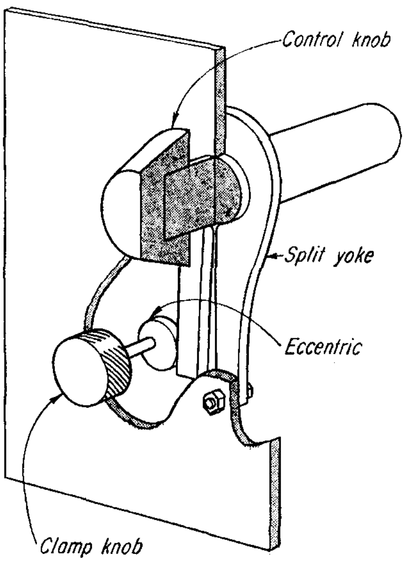

1.. SPLIT YOKE clamps on shaft when eccentric squeezes ends of yoke together. Knurled knob is handy for constant use, and eliminates need for tool. Another advantage is high torque capacity. But this design needs considerable space on panel.

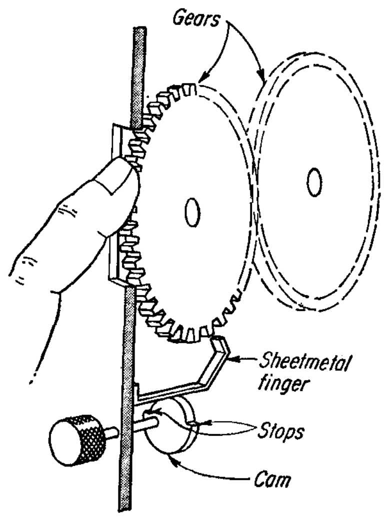

2.. FINGER springs into place between gear teeth at turn of cam. Although gear lock is ideally suited for right-angle drives, size of teeth limits positioning accuracy.

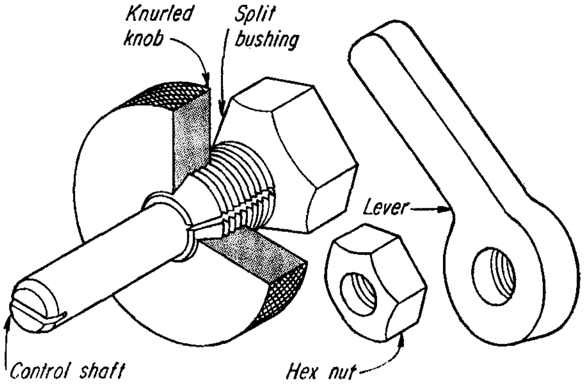

3.. SPLIT BUSHING tightens on control shaft, because knurled knob has tapered thread. Bushing also mounts control to panel, so requires just one hole. Lever, like knob, does away with tools, but locks tighter and faster. For controls adjusted infrequently, hex nut turns a fault into an advantage. Although it takes a wrench to turn the nut, added difficulty guards against knob-twisters.

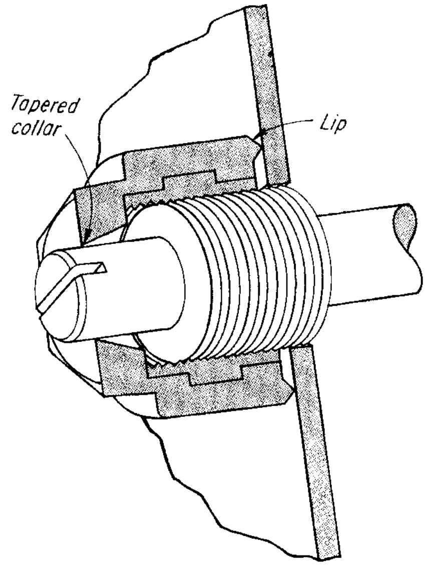

4 . . CONSTANT DRAG of tapered collar on shaft makes control stiff, so it doesn't need locking and unlocking. Compressed lip both seals out dust and keeps molded locking nut from rotating.

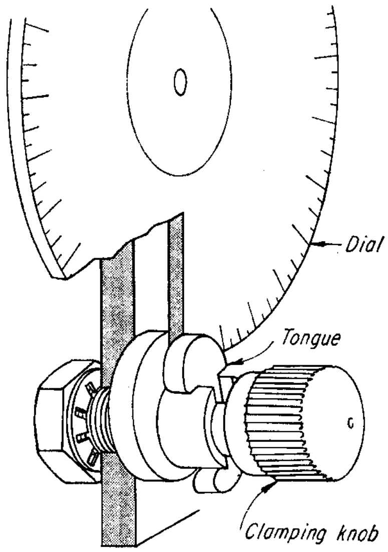

5 . . TONGUE slides in groove, clamps down on edge of dial. If clamp is not tight, it can scratch the face.

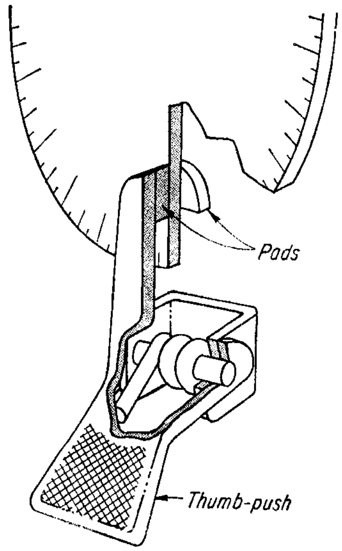

6 . . SPOT-BRAKE clamp is self-locking, which means it takes two hands to make an adjustment, one to hold the clamp open and one to turn the dial.

Liquid Level Mechanisms – Indicators and Controllers

Means of determining liquid level, detection of changes in liquid level, transmission of indicated levels, or warnings of changes beyond set limits; and means of using level changes for level control, or control of other conditions such as temperature and pressure, have been accomplished by numerous mechanisms. The most popular devices employ floats or pressure measurement with instruments such as the U-tube manometer, bourdon tube, and bellows.

The methods shown here are largely indicating methods or simple devices for automatic control of liquid level although they can conceivably be applied to control other conditions such as temperature and pressure. Methods using electric resistance of a column of liquid and measurement of pressure changes by means of piezo-electric crystals are not shown. Patent No. 2,162,180 describes a method involving determination of change in air pressure when a measured volume of air is introduced into a tank.

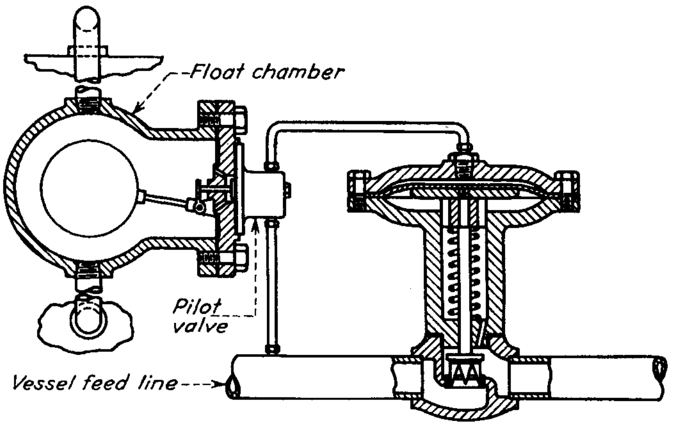

Fig. 1-Float and Lever- Operated Pilot Valve

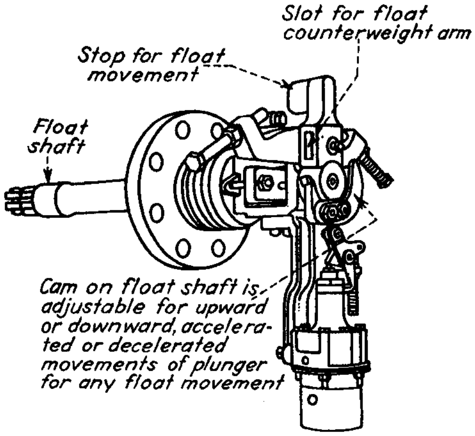

Fig. 2-Float and Cam-Operated Pilot Valve

Fig. 3-Pump-Type Lever Indicator

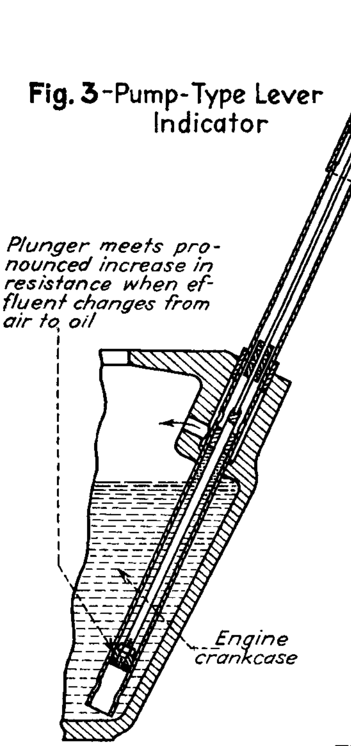

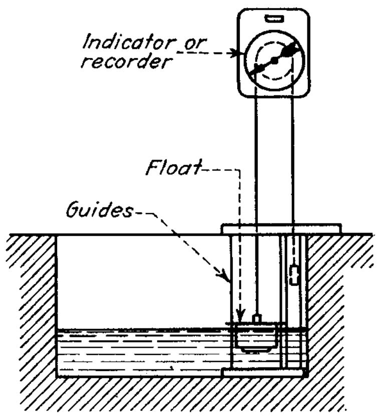

Fig. 4-Float and Pulley Indicator

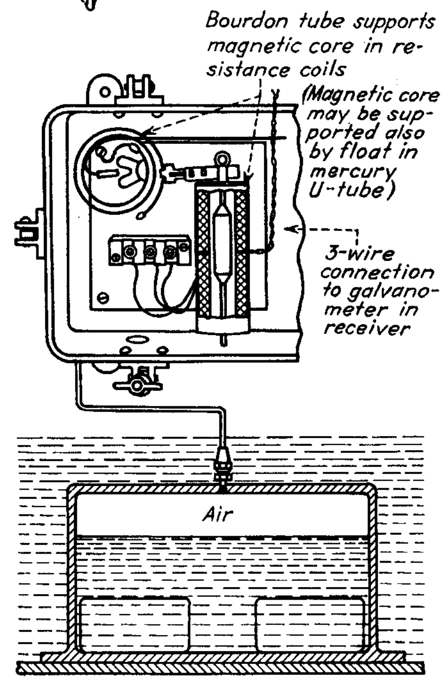

Fig. 5-Pressure Dome Indicator

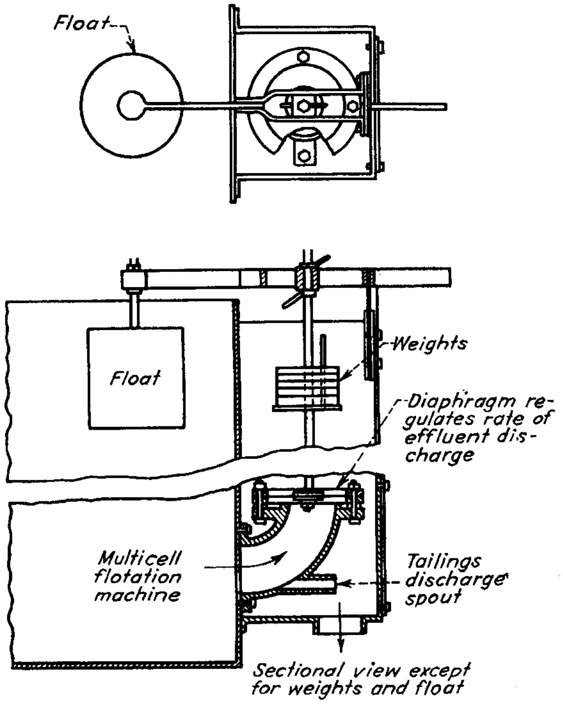

Fig. 6-Float Control of Discharge

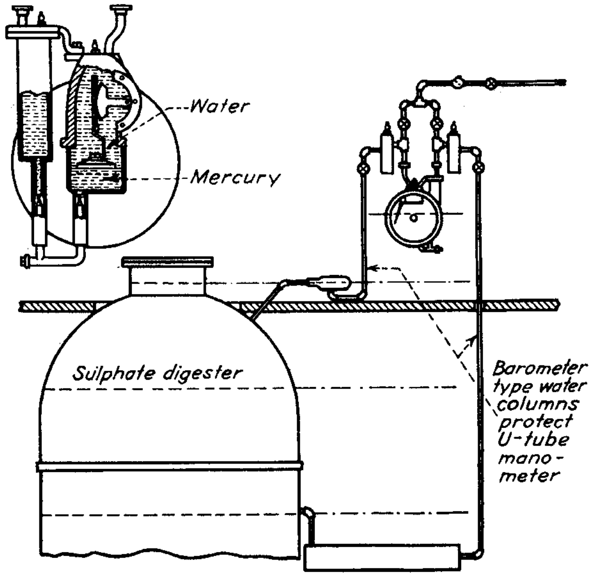

Fig.7-U-Tube Manometer with Water Columns

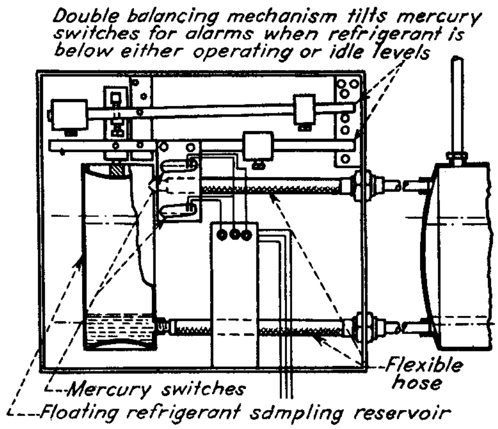

Fig.10-Refrigerant Balance

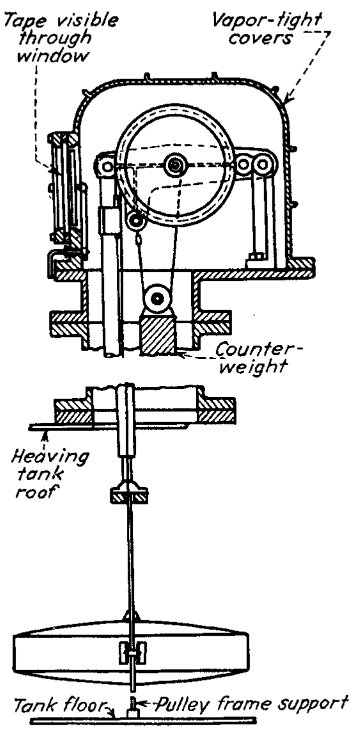

Fig. 8-Tank Roof Indicator

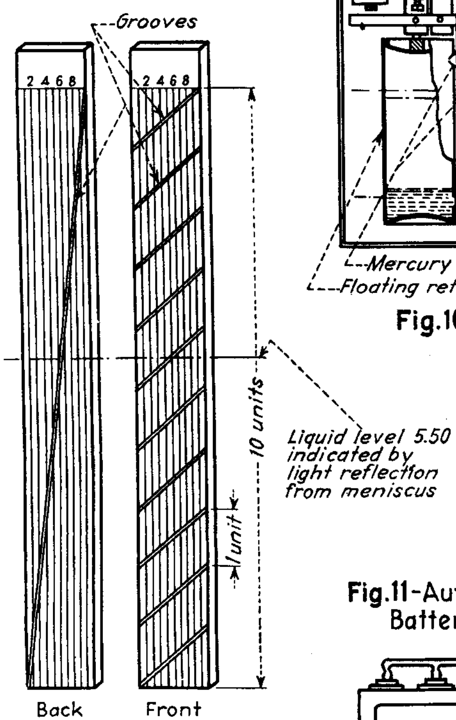

Fig.9-Dip Stick Indicator

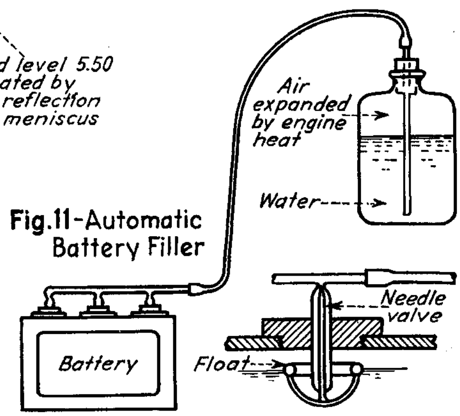

Fig.11-Automatic Battery Filler

Liquid Level Indicators and Controllers

Thirteen different systems of operation are shown. Each one represents at least one commercial instrument. Some of them are available in several modified forms.

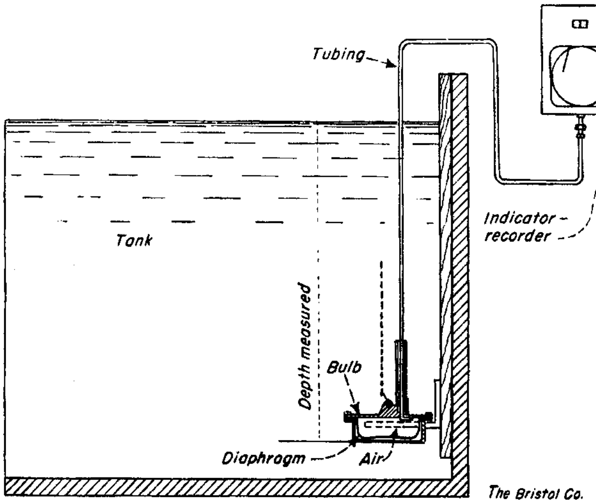

DIAPHRAGM ACTUATED INDICATOR. Can be used with any kind of liquid, whether it be flowing, turbulent, or carrying solid matter. Recorder can be mounted above or below the level of the tank or reservoir.

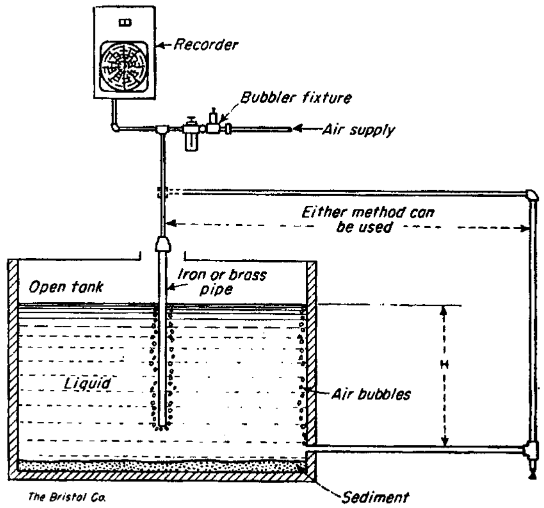

BUBBLER TYPE RECORDER measures height *H*. Can be used with all kinds of liquids, including those carrying solids. Small amount of air is bled into submerged pipe. Gage measures pressure of air that displaces fluid.

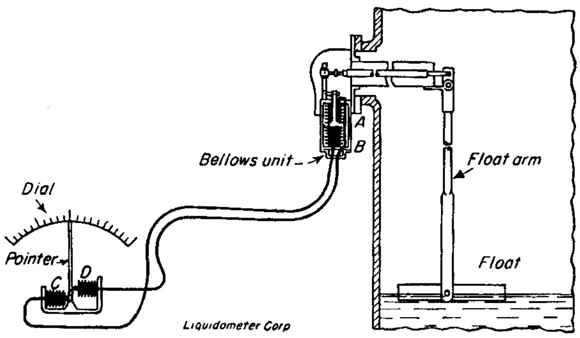

BELLOWS ACTUATED INDICATOR. Two bellows and connecting tubing are filled with incompressible fluid. Change in liquid level displaces transmitting bellows and pointer.

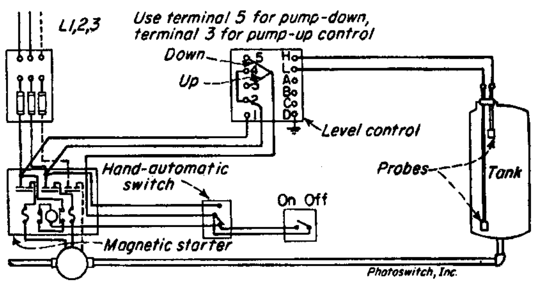

ELECTRICAL TYPE LEVEL CONTROLLER. Positions of probes determine duration of pump operation. When liquid touches upper probe, relay operates and pump stops. Through auxiliary contacts, lower probe provides relay holding current until liquid drops below it.

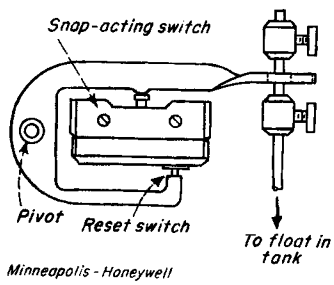

FLOAT-SWITCH TYPE CONTROLLER. When liquid reaches predetermined level, float actuates switch through horseshoe-shape arm. Switch can operate valve or pump, as required.

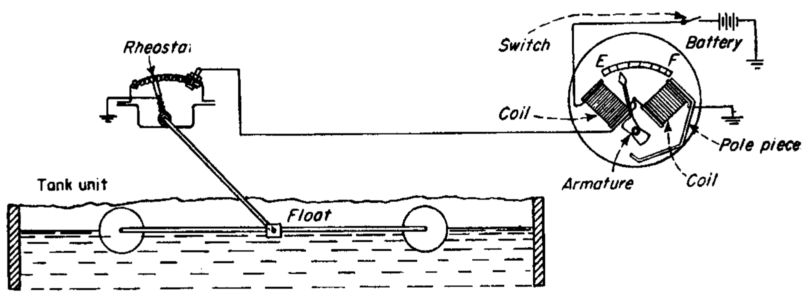

AUTOMOTIVE TYPE LIQUID LEVEL INDICATOR. Indicator and tank unit are connected by a single wire. As liquid level in tank increases, brush contact on tank rheostat moves to the right, introducing an increasing amount of resistance into circuit that grounds the "F" coil. Displacement of needle from empty mark is proportional to the amount of resistance introduced into this circuit.

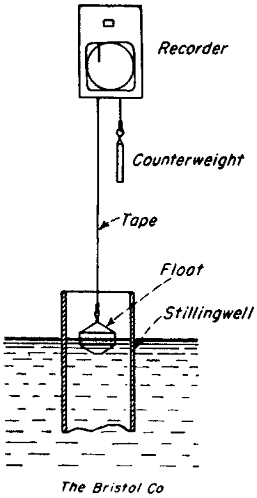

FLOAT TYPE RECORDER. Pointer can be attached to a calibrated float tape to give an approximate instantaneous indication of fluid level.

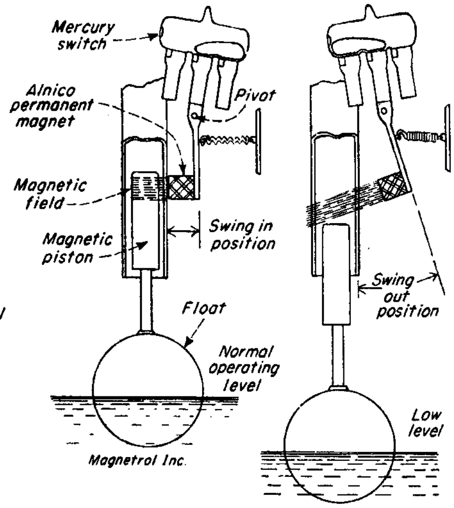

MAGNETIC LIQUID LEVEL CONTROLLER. When liquid level is normal, common-to-right leg circuit of mercury switch is closed. When level drops to predetermined level, magnetic piston is drawn below the magnetic field.

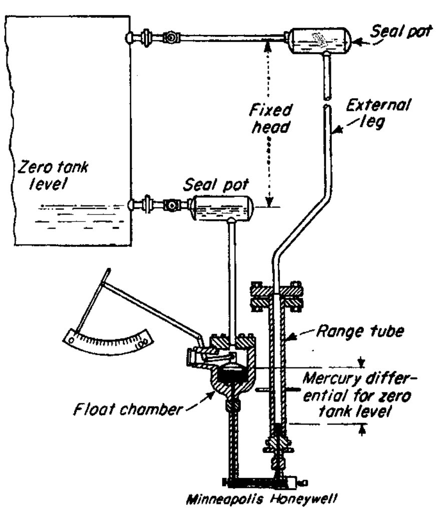

DIFFERENTIAL PRESSURE SYSTEM. Applicable to liquids under pressure. Measuring element is mercury manometer. Mechanical or electric meter body can be used. Seal pots protect meter body.

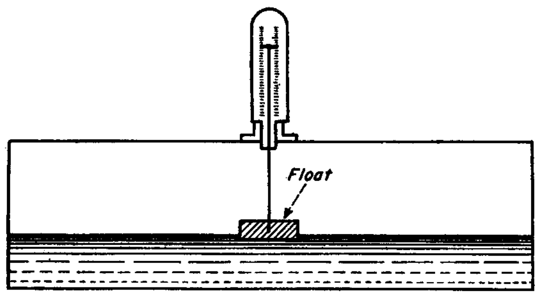

DIRECT READING FLOAT TYPE GAGE. Inexpensive, direct-reading gage has dial calibrated to tank volume. Comparable type as far as simplicity is concerned has needle connected through a right-angle arm to float. As liquid level drops, float rotates the arm and the needle.

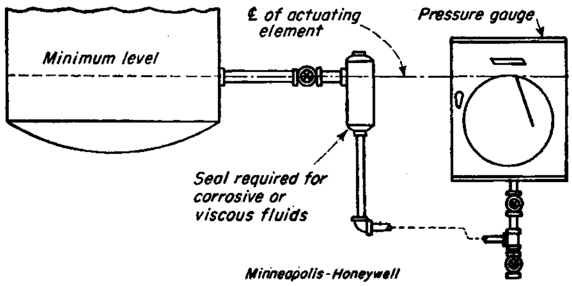

PRESSURE GAGE INDICATOR for open vessels. Pressure of liquid head is imposed directly upon actuating element of pressure gage. Center line of the actuating element must conincide with the minimum level line, if the gage is to read zero when the liquid reaches the minimum level.

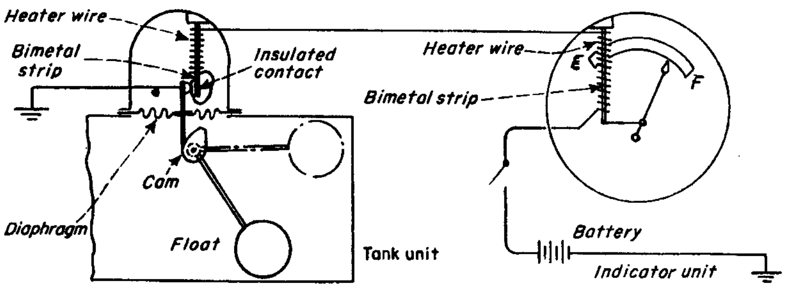

BIMETALLIC TYPE INDICATOR. When tank is empty, contacts in tank unit just touch. With switch closed, heaters cause both bimetallic strips to bend. This opens contacts in tank and bimetals cool, closing circuit again. Cycle repeats about once per sec. As liquid level increases, float forces cam to bend tank bimetal. Action is similar to previous case, but current and needle displacement are increased.

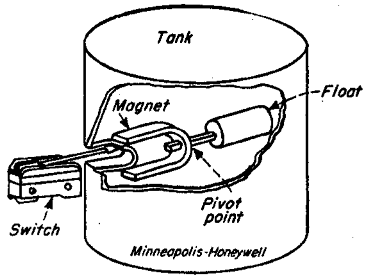

SWITCH ACTUATED LEVEL CONTROLLER. Pump is actuated by switch. Float pivots magnet so that upper pole attracts switch contact. Tank wall serves as other contact.

Hangers Put Up by Hand

No tools needed to install these hangers made of wire, rod or bar-stock.

L. Kasper

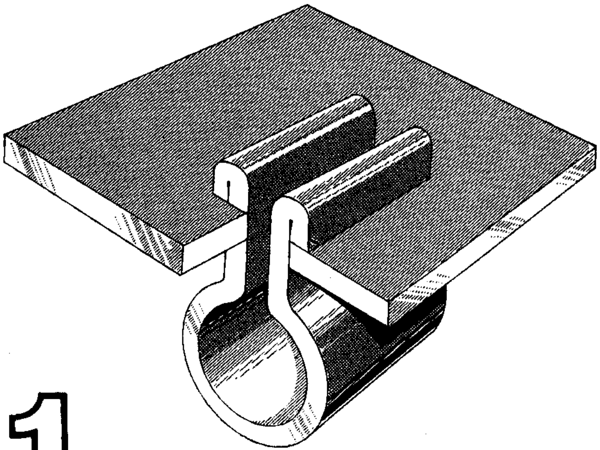

1

CLIP is most secure when tubing of right size helps keep it spread. To install, hook one side over edge of slot and spring in other side.

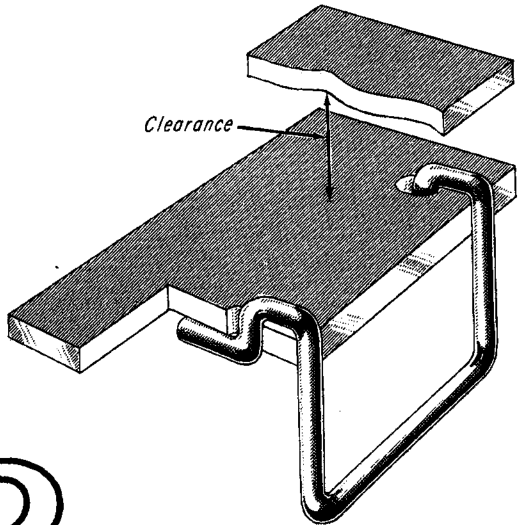

2

EDGE HANGER doesn't have to be sprung, but requires enough clearance above holes so that ends can be pushed down through.

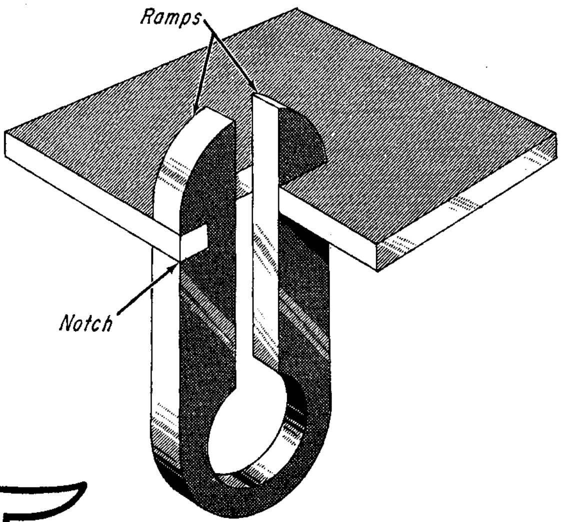

5

RAMPS cam split end together as hanger is pushed into slot. Ends spread again when notches engage sheet.

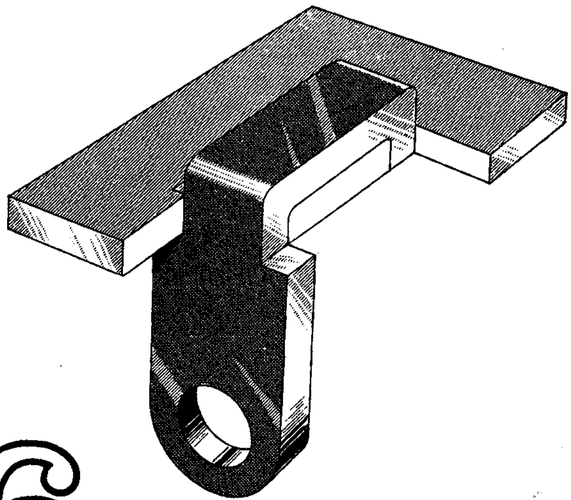

6

L-SHAPE can be inserted blind from below. Small end enters large slot first, then tilts over into smaller, close-fitting slot.

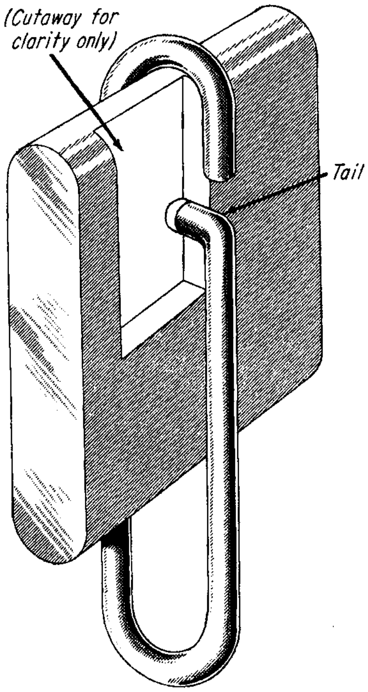

3

LOOP hooks over bar and is held secure by short tail which snaps into hole drilled through the side.

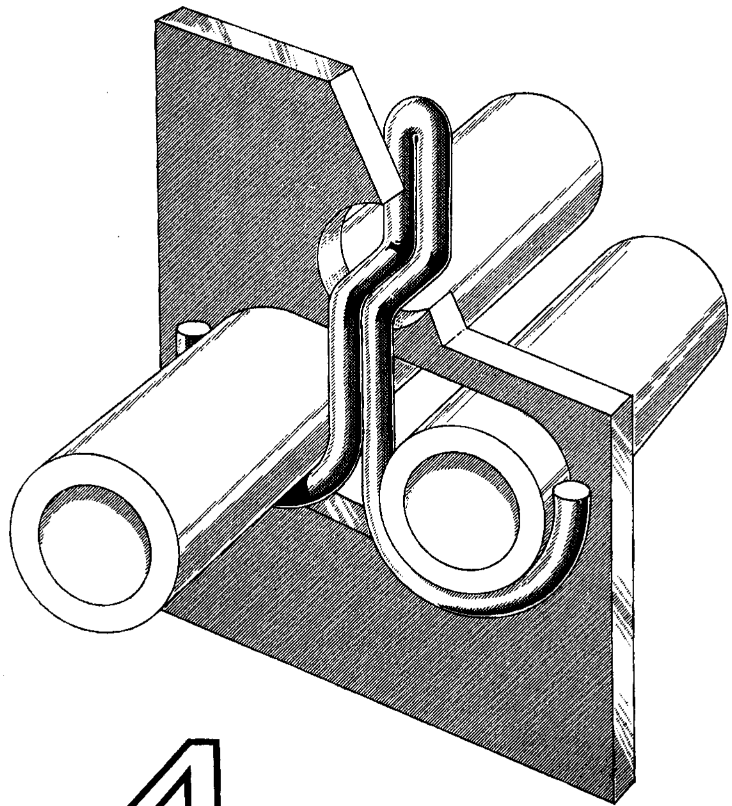

4

DOUBLE HANGER supports two tubes as they pass through divider. While tubes are in place hanger can't come out.

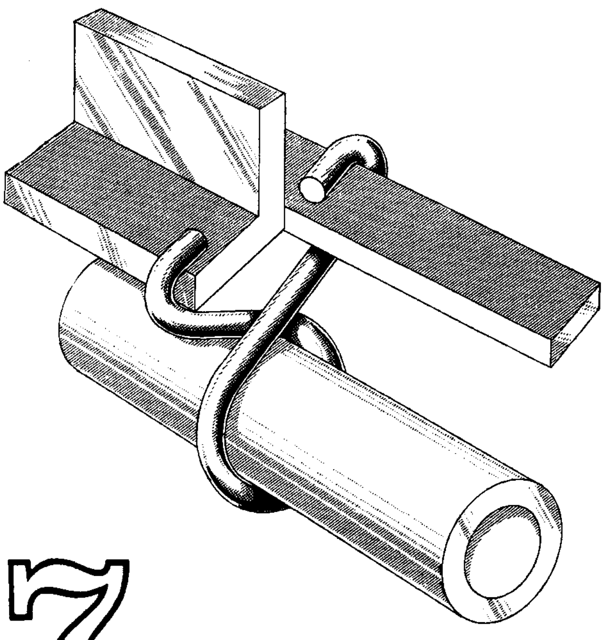

7

COIL grips edges of T- or I-section or flat bar. Spreading the ends wraps wire tightly around tubing to prevent vibration.

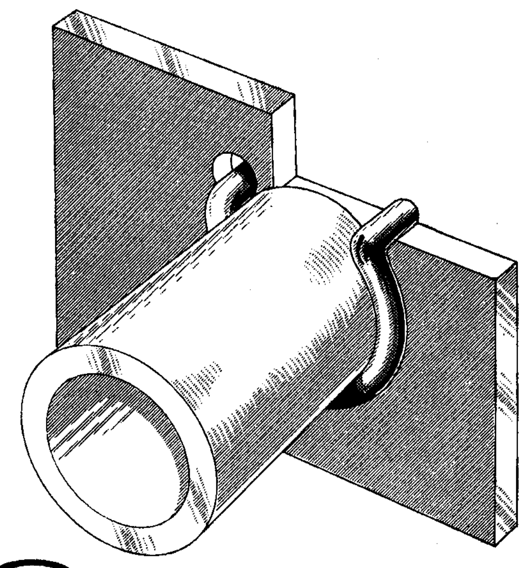

8

END PIECE supports pipe between walls of any thickness. First spring it over pipe, then slide it along pipe into holes.

Assemble Sheetmetal with Sheetmetal

These sheetmetal parts join sheetmetal quickly with the simplest of tools.

L. Kasper

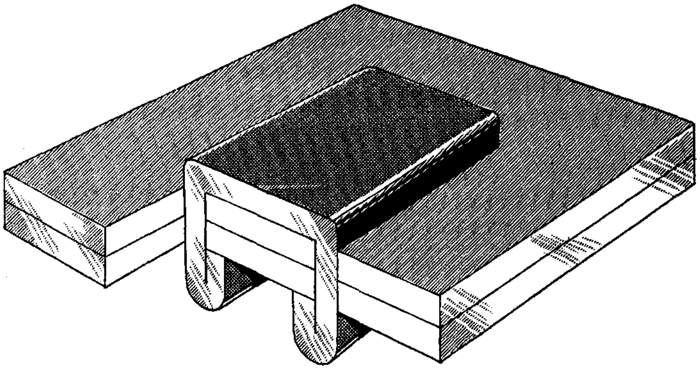

1 **SQUEEZE CLIP** holds two overlapping sheets together. The ends of the clip are pushed through parallel slots, then bent over much like a staple.

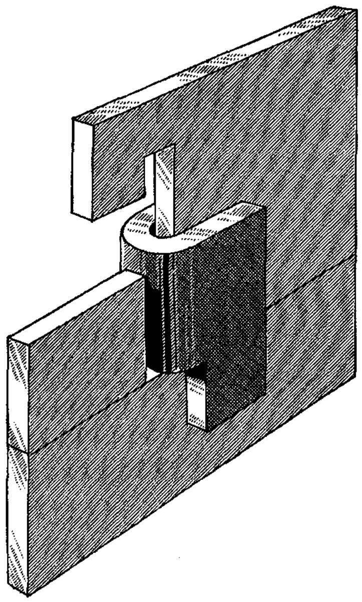

2 **ALIGNING PIECE** slides up out of the way in long slot while butting sheets are being positioned. Afterwards it slips down over lower sheet.

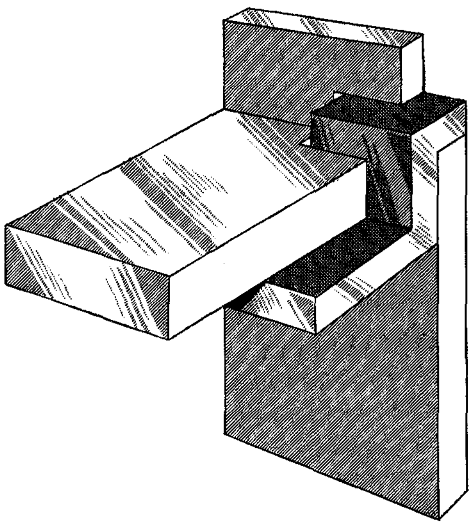

3 **ESS** supports shelf between uprights. By mating with notched edge it acts as a key to keep shelf from sliding back and forth. and provides positive location.

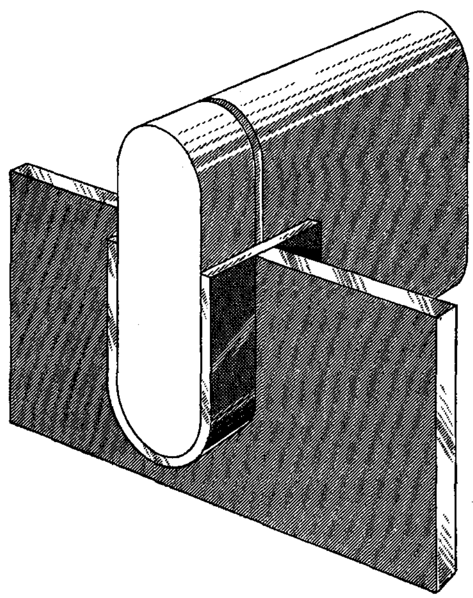

4 **CUP** carries a bar on both sides of divider. Here bars stick up above the top, but deeper cutout will lower them until they are flush or sunk.

Devices for Indexing or Holding Mechanical Movements

Louis Dodger

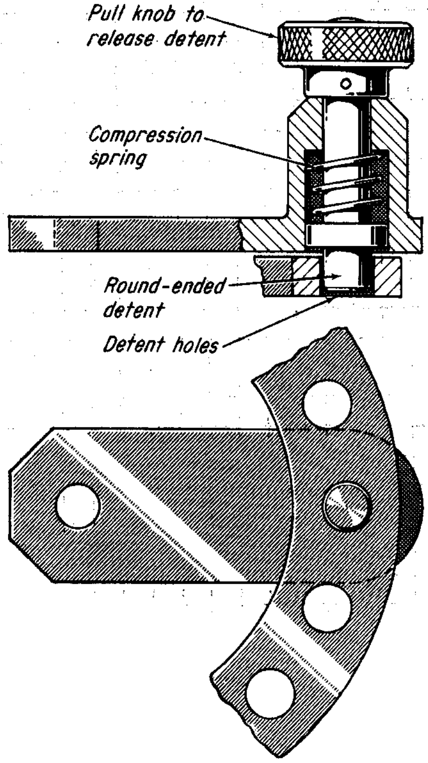

1

AXIAL POSITIONING (INDEXING) BY MEANS OF SPACED HOLES IN INDEX BASE

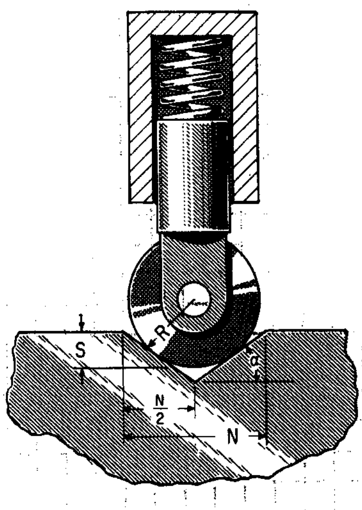

3

ROLLER DETENT POSITIONS IN A NOTCH:

RISE, $S = \frac{N \tan \alpha}{2} - R \times \frac{1-\cos}{\cos \alpha}$

ROLLER RADIUS, $R = \left(\frac{N \tan \alpha}{2} - S\right)\left(\frac{\cos \alpha}{1-\cos \alpha}\right)$

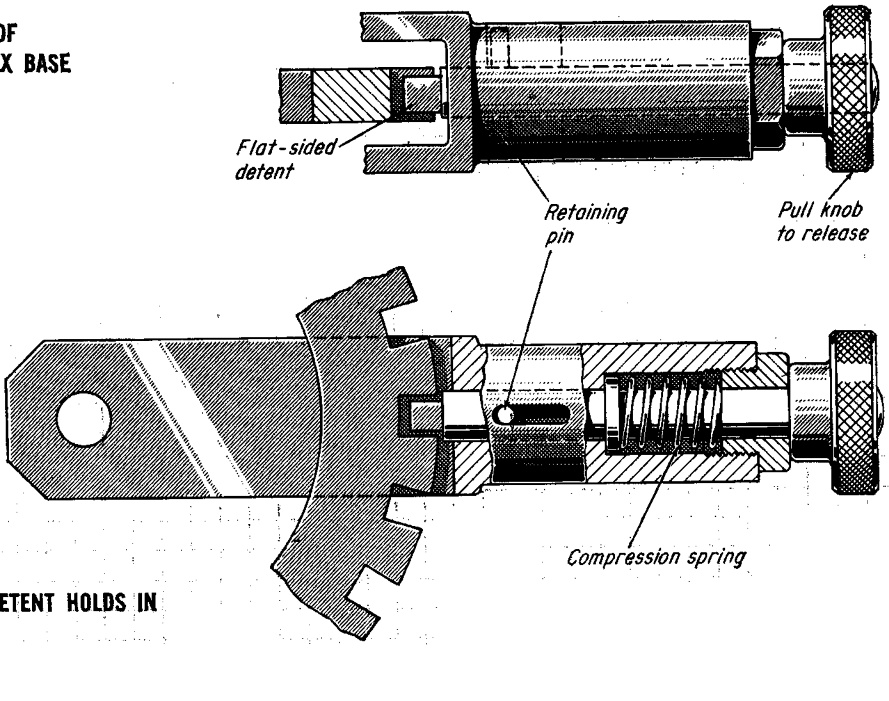

2

RADIALLY ARRANGED DETENT HOLDS IN SLOTTED INDEX BASE

Slashes Errors with Sensitive Balance

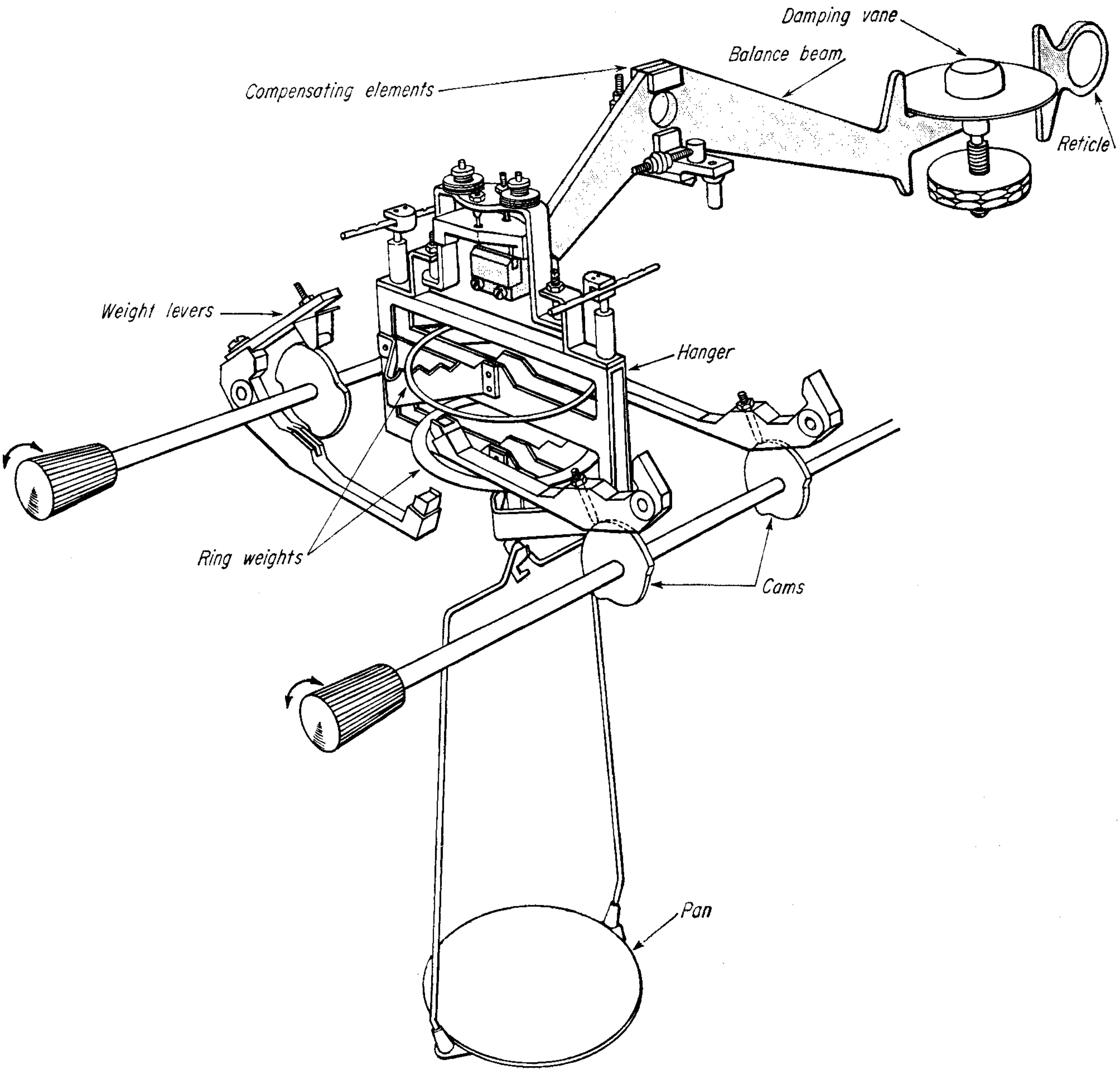

SENSITIVITY OF BALANCE is independent of temperature fluctuations. To keep the center of gravity constant, two temperature-sensitive elements are riveted to aluminum-alloy balance beam, bridging a slot which is directly over the balance point. Their coefficient of expansion compensates for beam deflection caused by variations in temperature.

Enclosed in a cylindrical canister at the rear of the balance beam is a vane that damps its movement, preventing oscillation. The hanger at the front of the scale carries sets of ring weights which are lifted by cam-operated levers. The shafts on which the cams are mounted are connected to the mechanical readout.

The scale in effect weighs by subtraction since it is balanced, when empty, by all the ring weights resting on the hanger. To weigh an unknown, the ring weights are lifted from the hanger. The sum of the raised weights is shown on the mechanical counter, which displays the first three digits. The complete total is displayed by the mechanical plus the optical system that projects through the reticle.

Rotary Piston Engine

Warren Ogren, Inventor
Robert Parmley, Draftsman

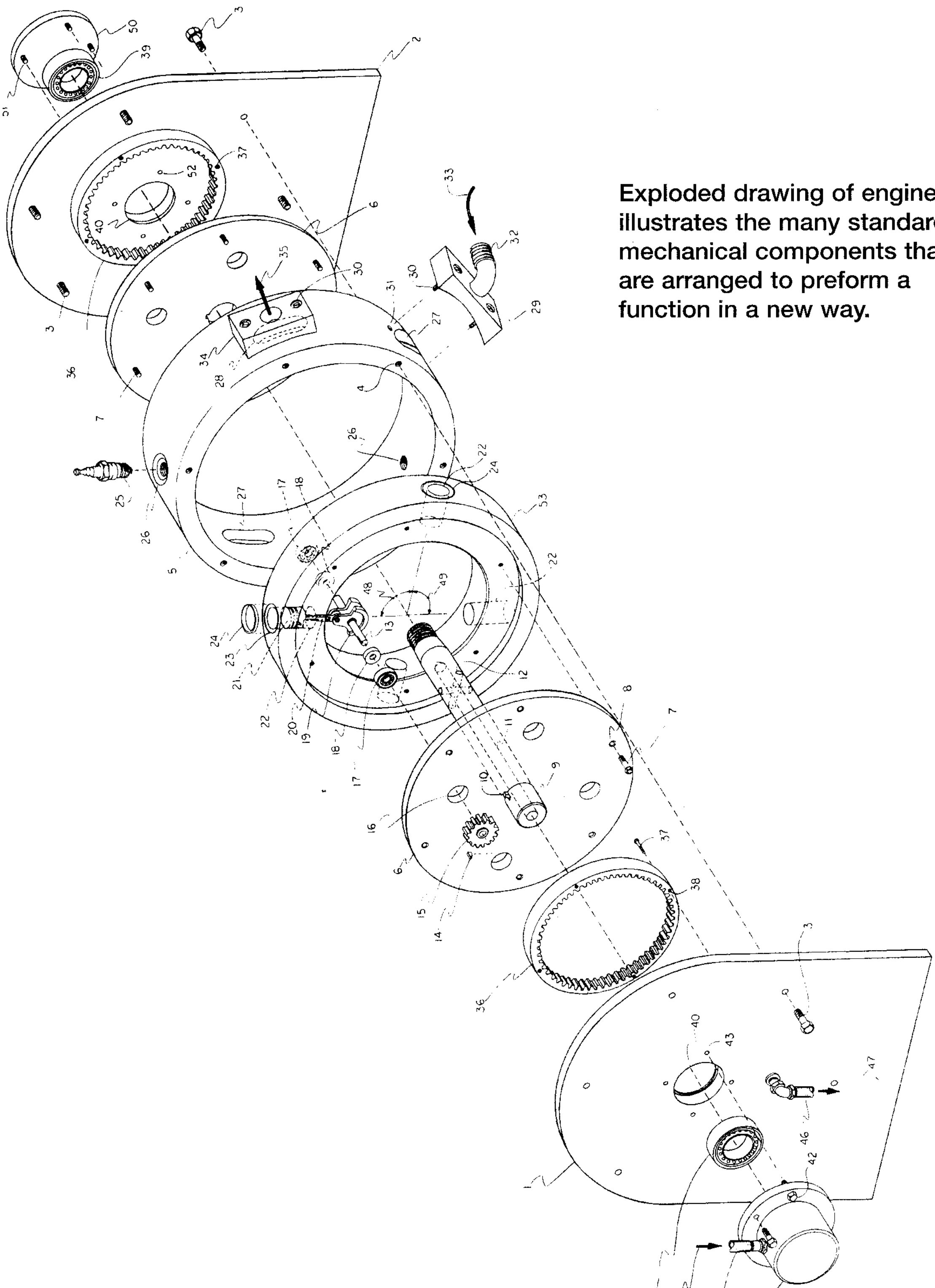

Exploded drawing of engine illustrates the many standard mechanical components that are arranged to preform a function in a new way.

End View of Rotary Piston Engine

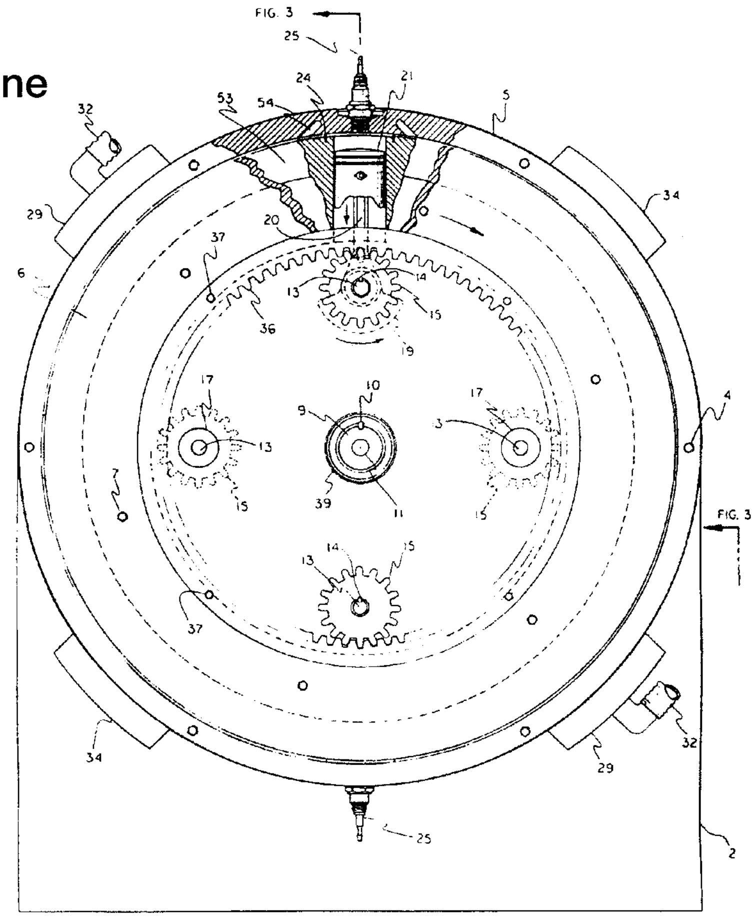

Figure 2

Cut-Away View of Rotary Piston Engine

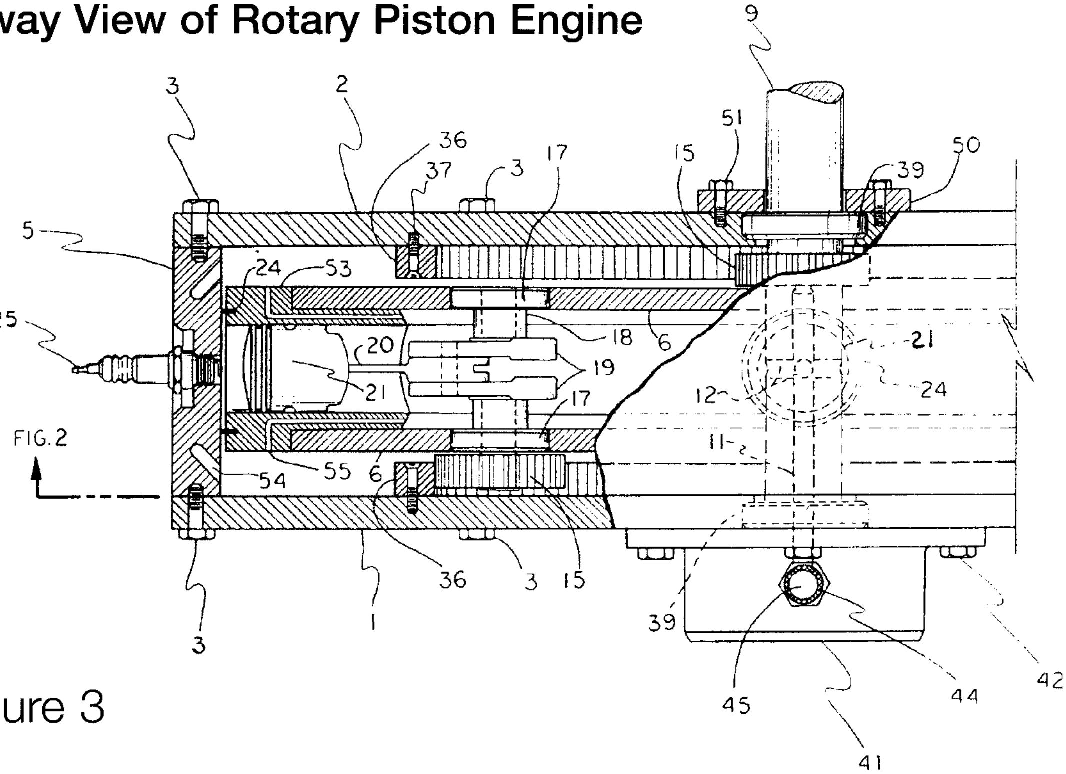

Figure 3

SECTION 28

DESIGN FORMULAS

Volume and CG Equations

The list covers 55 shapes, many of which are the result of drilled holes, bosses, and fillets in machined and cast parts

E. W. Jenkins

CYLINDERS

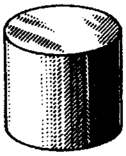

1. . Cylinder

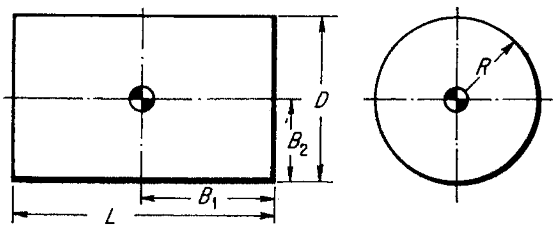

$$V = \frac{\pi}{4} D^2L = 0.7854D^2L$$

$$B_1 = L/2$$
$$B_2 = R$$

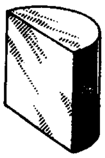

2. . Half cylinder

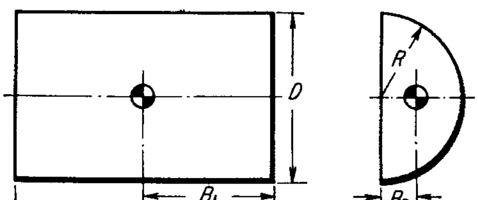

$$V = \frac{\pi}{8} D^2L = 0.3927D^2L$$

$$B_1 = L/2$$
$$B_2 = \frac{4R}{3\pi} = 0.4244R$$

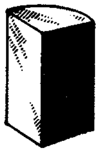

3. . Sector of cylinder

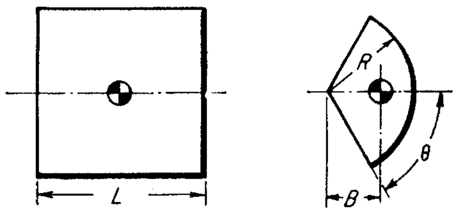

$$V = \theta R^2L \qquad B = \frac{2R\sin\theta}{3\theta}$$

4. . Segment of cylinder

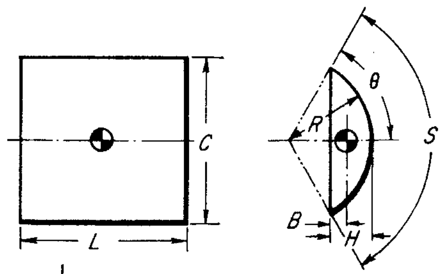

$$V = LR^2\left(\theta - \frac{1}{2}\sin 2\theta\right)$$

$$V = 0.5L\,[RS - C\,(R - H)]$$

$$B = \frac{4R\sin^3\theta}{6\theta - 3\sin 2\theta}$$

$$S = 2R\theta$$
$$H = R\,(1 - \cos\theta)$$
$$C = 2R\sin\theta$$

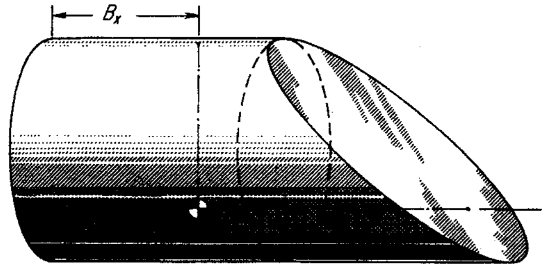

VOLUME equations are included for all cases. Where the equation for the CG (center of gravity) is not given, you can easily obtain it by looking up the volume and CG equations for portions of the shape and then combining values. For example, for the shape above, use the equations for a cylinder, Fig 1, and a truncated cylinder, Fig 10 (subscripts C and T, respectively, in the equations below). Hence taking moments

$$B_x = \frac{V_C B_C + V_T(B_T + L_C)}{V_C + V_T}$$

or

$$B_x = \frac{\left(\frac{\pi}{4} D^2 L_C\right)\left(\frac{L_C}{2}\right) + \frac{\pi}{8} D^2 L_T\left(\frac{5}{16} L_T + L_C\right)}{\frac{\pi}{4} D^2 L_C + \frac{\pi}{8} D^2 L_T}$$

$$B_x = \frac{L_C^2 + L_T\left(\frac{5}{16} L_T + L_C\right)}{2L_C + L_T}$$

In the equations to follow, angle θ can be either in degrees or in radians. Thus θ (rad) $= \pi\theta/180$ (deg) $=$ 0.01745 θ (deg). For example, if $\theta = 30$ deg in Case 3, then $\sin\theta = 0.5$ and

$$B = \frac{2R\,(0.5)}{3\,(30)\,(0.01745)} = 0.637R$$

Symbols used are: B = distance from CG to reference plane, V = volume, D and d = diameter, R and r = radius, H = height, L = length.—*Nicholas P. Chironis*

5. . Quadrant of cylinder

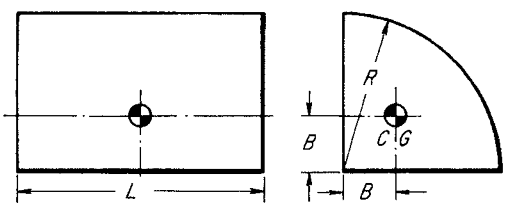

$$V = \frac{\pi}{4} R^2 L = 0.7854 R^2 L \qquad B = \frac{4R}{3\pi} = 0.4244R$$

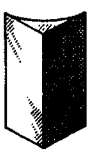

6. . Fillet or spandrel

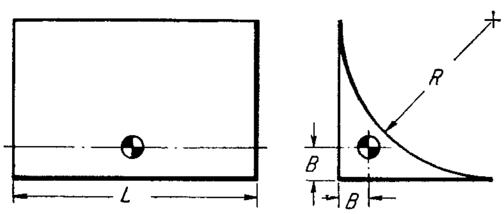

$$V = \left(1 - \frac{\pi}{4}\right) R^2 L = 0.2146 R^2 L$$

$$B = \frac{10 - 3\pi}{12 - 3\pi} R = 0.2234R$$

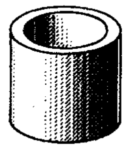

7. . Hollow cylinder

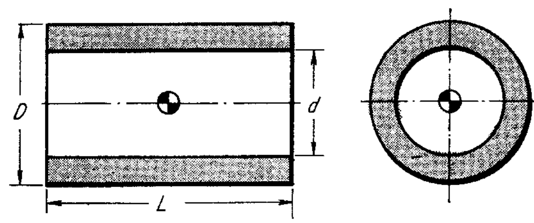

$$V = \frac{\pi L}{4} (D^2 - d^2)$$

CG at center of part

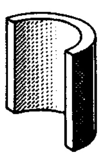

8. . Half hollow cylinder

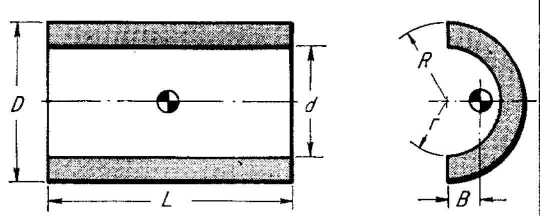

$$V = \frac{\pi L}{8} (D^2 - d^2)$$

$$B = \frac{4}{3\pi}\left[\frac{R^3 - r^3}{R^2 - r^2}\right]$$

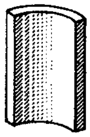

9. . Sector of hollow cylinder

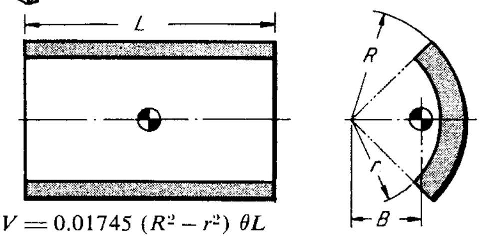

$$V = 0.01745\,(R^2 - r^2)\,\theta L$$

$$B = \frac{38.1972\,(R^3 - r^3)\sin\theta}{(R^2 - r^2)\,\theta}$$

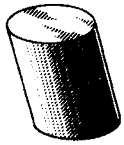

12. . Oblique cylinder (or circular hole at oblique angle)

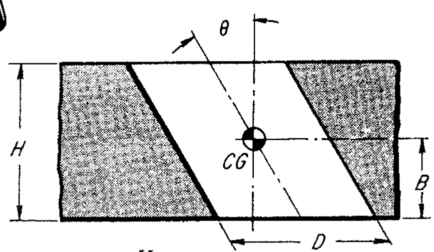

$$V = \frac{\pi}{4} D^2 \frac{H}{\cos\theta} = 0.7854 D^2 H \sec\theta$$

$$B = H/2 \qquad r = \frac{d}{2}$$

10. . Truncated cylinder (with full circle base)

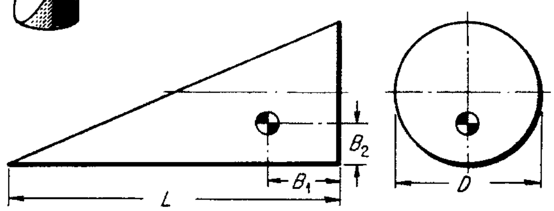

$$V = \frac{\pi}{8} D^2 L = 0.3927 D^2 L$$

$$B_1 = 0.3125L$$

$$B_2 = 0.375D$$

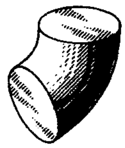

13. . Bend in cylinder

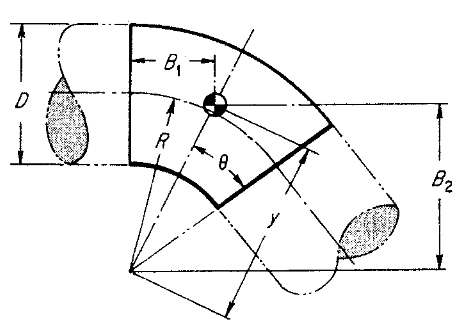

$$V = \frac{\pi^2}{360} D^2 R\theta = 0.0274 D^2 R\theta$$

$$y = R\left[1 + \frac{r^2}{4R^2}\right]$$

$$B_1 = y\tan\theta$$

$$B_2 = y\cot\theta$$

11. . Truncated cylinder (with partial circle base)

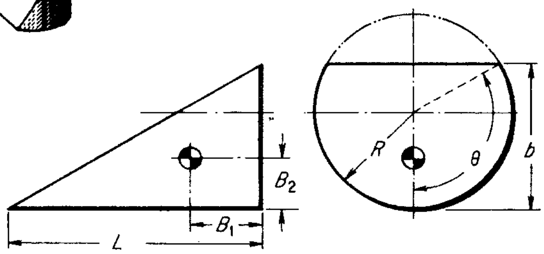

$$b = R\,(1 - \cos\theta)$$

$$V = \frac{R^3 L}{b}\left[\sin\theta - \frac{\sin^3\theta}{3} - \theta\cos\theta\right]$$

$$B_1 = \frac{L\left[\dfrac{\theta\cos^2\theta}{2} - \dfrac{5\sin\theta\cos\theta}{8} + \dfrac{\sin^3\theta\cos\theta}{12} + \dfrac{\theta}{8}\right]}{\left[1 - \cos\theta\right]\left[\sin\theta - \dfrac{\sin^3\theta}{3} - \theta\cos\theta\right]}$$

$$B_2 = \frac{2R\left[-\dfrac{\theta\cos\theta}{2} + \dfrac{\sin\theta}{2} - \dfrac{\theta}{8} + \dfrac{\sin\theta\cos\theta}{8} - N\right]}{\left[\sin\theta - \dfrac{\sin^3\theta}{3} - \theta\cos\theta\right]}$$

where $N = \dfrac{5\sin^3\theta}{6} - \dfrac{\sin^3\theta\cos\theta}{12}$

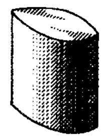

14. . Curved groove in cylinder

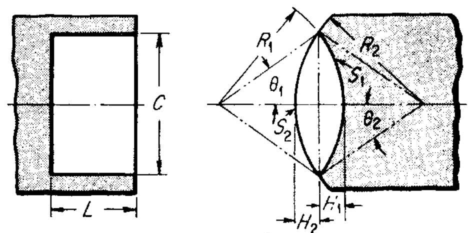

$$\sin\theta_1 = \frac{C}{2R_1} \qquad \sin\theta_2 = \frac{C}{2R_2} \qquad S = 2R\theta$$

$$H_1 = R_1\,(1 - \cos\theta_1) \qquad H_2 = R_2\,(1 - \cos\theta_2)$$

$$V = L\left[R_1^2\left(\theta_1 - \frac{1}{2}\theta_1\sin 2\theta_1\right) + R_2^2\left(\theta_2 - \frac{1}{2}\theta_2\sin 2\theta_2\right)\right]$$

Compute CG of each part separately

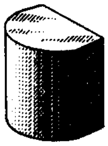

15. . Slot in cylinder

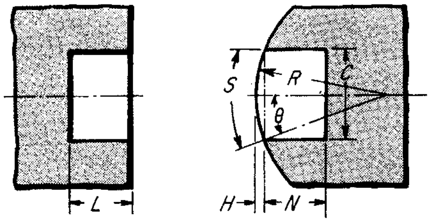

$H = R\,(1 - \cos\theta)$ $\quad \sin\theta = \dfrac{C}{2R}$ $\quad S = 2R\theta$

$V = L\left[CN + R^2\left(\theta - \frac{1}{2}\sin 2\theta\right)\right]$

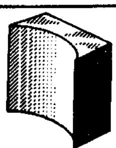

16. . Slot in hollow cylinder

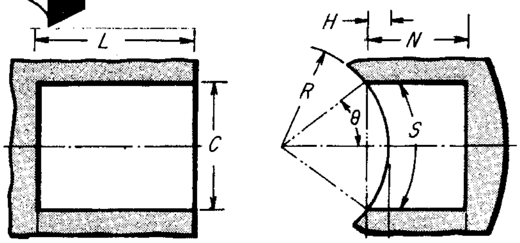

$S = 2R\theta$ $\quad \sin\theta = \dfrac{C}{2R}$ $\quad H = R\,(1 - \cos\theta)$

$V = L\left[CN - R^2\left(\theta - \frac{1}{2}\sin 2\theta\right)\right]$

$V = L\left(CN - 0.5\,[RS - C\,(R - H)]\right)$

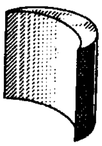

17. . Curved groove in hollow cylinder

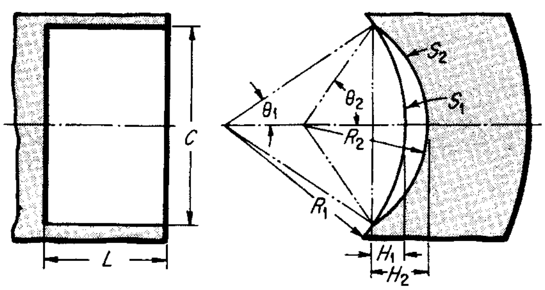

$\sin\theta_1 = \dfrac{C}{2R_1}$ $\quad \sin\theta_2 = \dfrac{C}{2R_2}$ $\quad S = 2R\theta$

$H_1 = R_1\,(1 - \cos\theta_1)$ $\quad H_2 = R_2\,(1 - \cos\theta_2)$

$V = L\left(\left[R_2^2\left(\theta_2 - \frac{1}{2}\sin 2\theta_2\right)\right] - \left[R_1^2\left(\theta_1 - \frac{1}{2}\sin 2\theta_1\right)\right]\right)$

$V = \frac{L}{2}\left(\left[R_2S_2 - C\,(R_2 - H_2)\right] - \left[R_1S_1 - C\,(R_1 - H_1)\right]\right)$

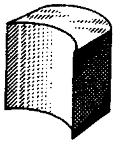

18. . Slot through hollow cylinder

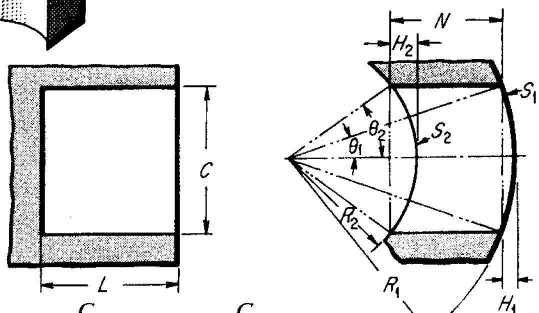

$\sin\theta_1 = \dfrac{C}{R_1}$ $\quad \sin\theta_2 = \dfrac{C}{R_2}$ $\quad S = 2R\theta$

$H_1 = R_1\,(1 - \cos\theta_1)$ $\quad H_2 = R_2\,(1 - \cos\theta_2)$

$V = L\left(CN + \left[R_1^2\left(\theta_1 - \frac{1}{2}\sin 2\theta_1\right)\right] - \left[R_2\left(\theta_2 - \frac{1}{2}\sin\theta_2\right)\right]\right)$

$V = L\left(CN + 0.5\,[R_1S_1 - C\,(R_1 - H_1)] - 0.5\,[R_2S_2 - C\,(R_2 - H_2)]\right)$

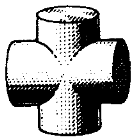

19. . Intersecting cylinder (volume of junction box)

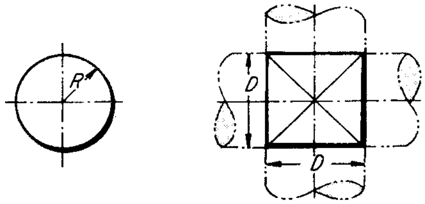

$V = D^3\left(\frac{\pi}{2} - \frac{2}{3}\right) = 0.9041D^3$

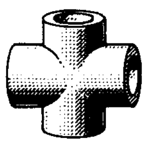

20. . Intersecting hollow cylinders (volume of junction box)

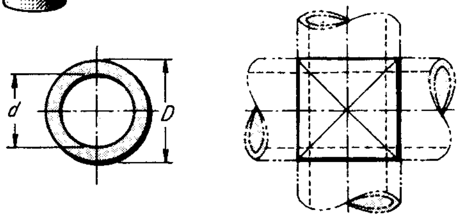

$V = \left(\frac{\pi}{2} - \frac{2}{3}\right)(D^3 - d^3) - \frac{\pi}{2}\,d^2\,(D - d)$

$V = 0.9041\,(D^3 - d^3) - 1.5708\,d^2\,(D - d)$

21. . Intersecting parallel cylinders

$(M<R_1)$

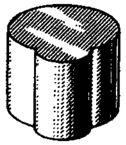

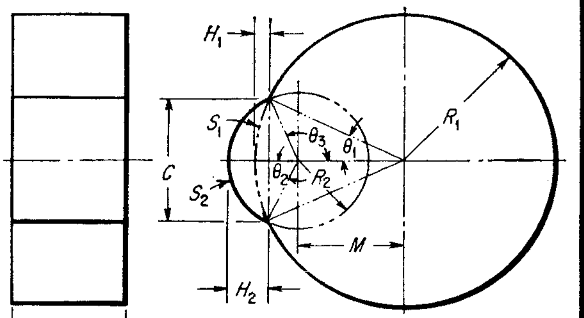

$$\theta_2 = 180° - \theta_3 \qquad \cos\theta_3 = \frac{R_2^2 + M^2 - R_1^2}{2MR_2}$$

$$\cos\theta_1 = \frac{R_1^2 + M^2 - R_2^2}{2MR_1} \qquad H_1 = R_1\,(1-\cos\theta_1) \qquad S_1 = 2R_1\theta_1$$

$$V = L\left(\pi R_1^2 + \left[R_2^2\left(\theta_2 - \frac{1}{2}\sin 2\theta_2\right)\right] - \left[R_1^2\left(\theta_1 - \frac{1}{2}\sin 2\theta_1\right)\right]\right)$$

22. . Intersecting parallel cylinders

$(M>R_1)$

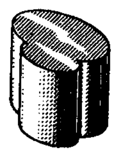

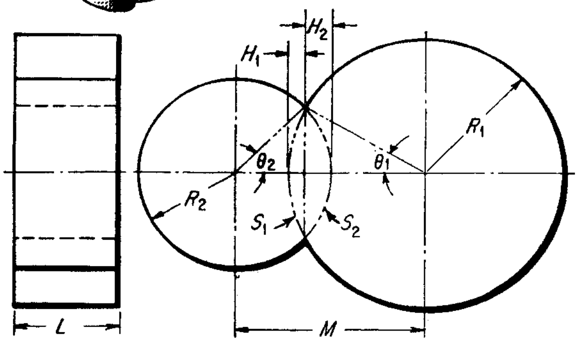

$$H_1 = R_1\,(1-\cos\theta_1) \qquad S_1 = 2R_1\theta_1 \qquad \cos\theta_1 = \frac{R_1^2 + M^2 - R_2^2}{2MR_1}$$

$$V = L\left(\left[\pi\,(R_1^2 + R_2^2)\right] - \left[R_1^2\left(\theta_1 - \frac{1}{2}\sin 2\theta_1\right)\right] - \left[R_2^2\left(\theta_2 - \frac{1}{2}\sin 2\theta_2\right)\right]\right)$$

SPHERES

23. . Sphere

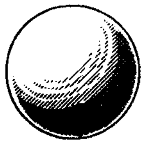

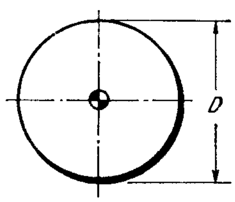

$$V = \frac{\pi D^3}{6} = 0.5236D^3$$

24. . Hemisphere

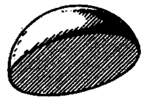

$$V = \frac{\pi D^3}{12} = 0.2618D^3$$

$$B = 0.375R$$

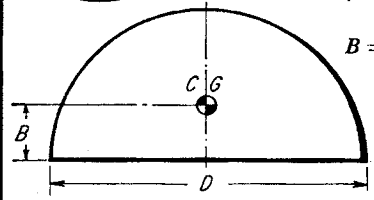

25. . Spherical segment

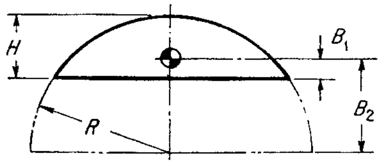

$$V = \pi H^2\left(R - \frac{H}{3}\right)$$

$$B_1 = \frac{H\,(4R-H)}{4\,(3R-H)}$$

$$B_2 = \frac{3\,(2R-H)^2}{4\,(3R-H)}$$

26. . Spherical sector

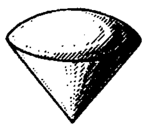

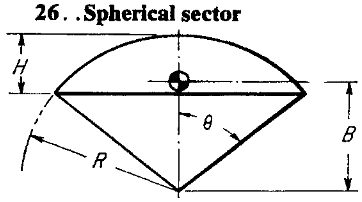

$$V = \frac{2\pi}{3}R^2H = 2.0944R^2H$$

$$B = 0.375\,(1+\cos\theta)\,R = 0.375\,(2R-H)$$

27. . Shell of hollow hemisphere

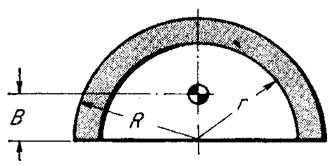

$$V = \frac{2\pi}{3}\,(R^3 - r^3) \qquad B = 0.375\left(\frac{R^4 - r^4}{R^3 - r^3}\right)$$

28. . Hollow sphere

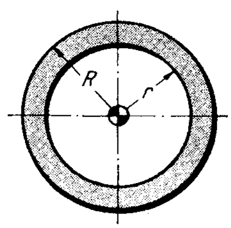

$$V = \frac{4\pi}{3}\,(R^3 - r^3)$$

29. . Shell of spherical sector

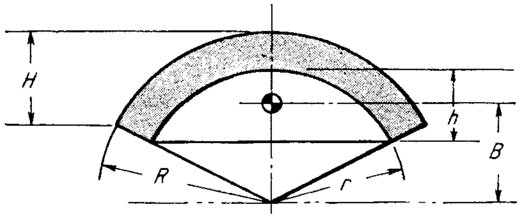

$$V = \frac{2\pi}{3}\,(R^2H - r^2h)$$

$$B = 0.375\left\{\frac{[R^2H\,(2R - H)] - [r^2h\,(2r - h)]}{R^2H - r^2h}\right\}$$

30. . Shell of spherical segment

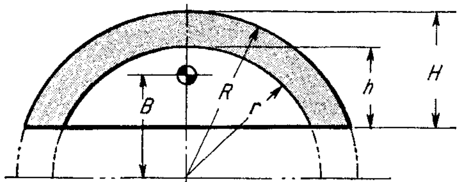

$$V = \pi\left[H^2\left(R - \frac{H}{3}\right) - h^2\left(r - \frac{h}{3}\right)\right]$$

$$B = \frac{3}{4}\left[\frac{\left(R - \frac{H}{3}\right)\frac{H^2\,(2R - H)^2}{3R - H} - \left(r - \frac{h}{3}\right)\frac{h^2\,(2r - h)^2}{3r - h}}{H^2\left(R - \frac{H}{3}\right) - h^2\left(r - \frac{h}{3}\right)}\right]$$

31. . Circular hole through sphere

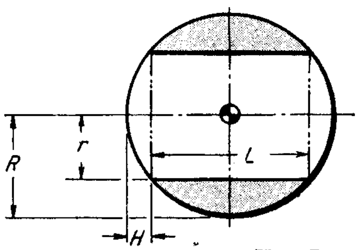

$$V = \pi\left[r^2L + 2H^2\left(R - \frac{H}{3}\right)\right] \qquad H = R - \sqrt{R^2 - r^2} \qquad L = 2(R - H)$$

32. . Circular hole through hollow sphere

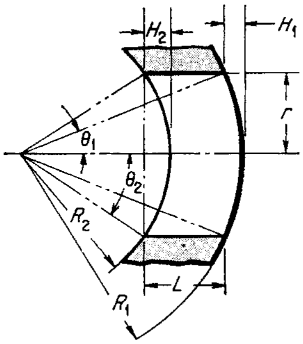

$$V = \pi\left\{r^2L + H_1\left(R_1 - \frac{H_1}{3}\right) - H_2^2\left(R_2 - \frac{H_2}{3}\right)\right\}$$

$\sin\theta_1 = r/R_1 \qquad \sin\theta_2 = r/R_2 \qquad H = R\,(1 - \cos\theta)$

33. . Spherical zone

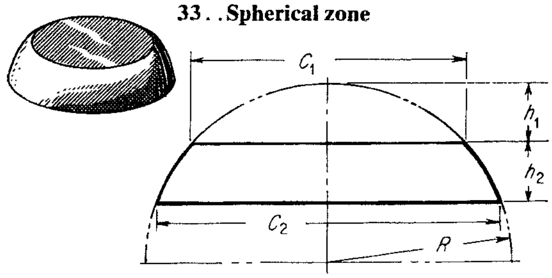

$$V = \pi\left\{\left[H^2\left(R - \frac{H}{3}\right)\right] - \left[h_1^2\left(R - \frac{h}{3}\right)\right]\right\}$$

$$V = \frac{\pi h_2}{6}\left[\frac{3}{4}\,C_1^2 + \frac{3}{4}\,C_2^2 + h_2^2\right]$$

34. . Conical hole through spherical shell

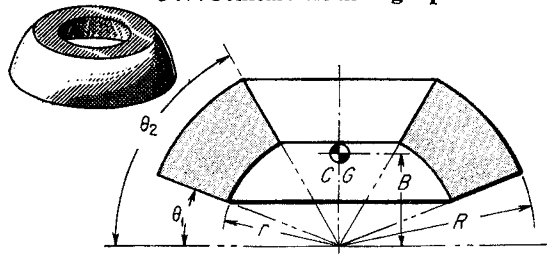

$$V = \frac{2\pi}{3}\,(R^3 - r^3)\,(\sin\theta_2 - \sin\theta_1)$$

$$B = \frac{0.375\,(R^4 - r^4)\,(\sin\theta_2 + \sin\theta_1)}{R^3 - r^3}$$

RINGS

35. . Torus

36. . Hollow torus

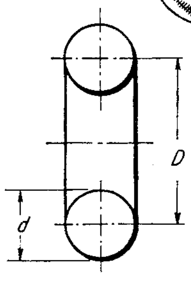

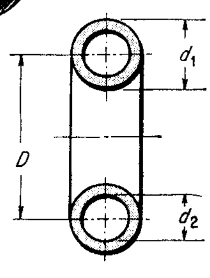

$$V = \frac{1}{4}\,\pi^2d^2D = 2.467d^2D \qquad V = \frac{1}{4}\,\pi^2D\,(d_1^2 - d_2^2)$$

37. . Bevel ring

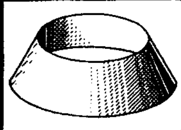

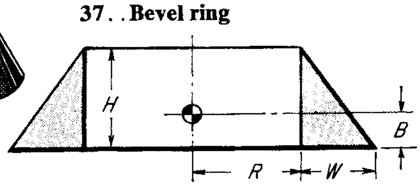

$$V = \pi\left(R + \frac{1}{3}\,W\right)WH \qquad B = H\left[\frac{\frac{R}{3} + \frac{W}{12}}{R + \frac{W}{3}}\right]$$

38. . Bevel ring

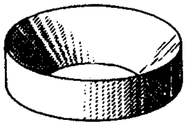

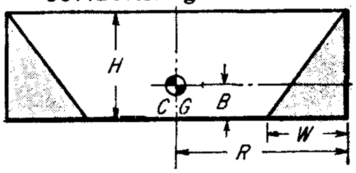

$$B > \frac{H}{3}$$

$$V = \pi\left(R - \frac{1}{3}W\right)WH \qquad B = H\left[\frac{\frac{R}{3} - \frac{W}{12}}{R - \frac{W}{3}}\right]$$

39. . Quarter torus

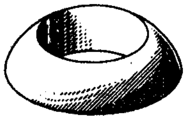

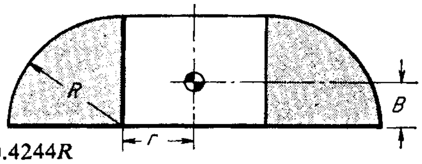

$$B < 0.4244R$$

$$V = \frac{\pi^2 R^2}{2}\left(r + \frac{4R}{3\pi}\right) = 4.9348R^2\,(r + 0.4244R)$$

$$B = \frac{4R}{3\pi}\left[\frac{r + \frac{3R}{8}}{r + \frac{4R}{3\pi}}\right] = \frac{0.4244Rr + 0.1592R^2}{r + 0.4244R}$$

40. . Quarter torus

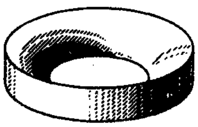

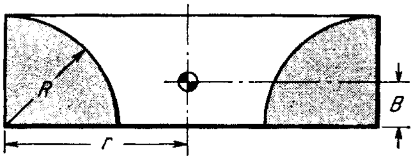

$$V = \frac{\pi^2 R^2}{2}\left[r - \frac{4R}{3\pi}\right] \qquad B = \frac{4R}{3\pi}\left[\frac{r - \frac{3R}{8}}{r - \frac{4R}{3\pi}}\right]$$

41. . Curved shell ring

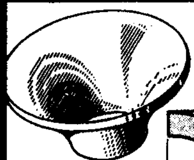

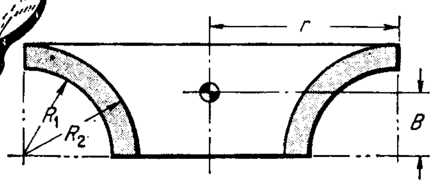

$$V = 2\pi\left\{r - \frac{4}{3\pi}\left[\frac{R_2^3 - R_1^3}{R_2^2 - R_1^2}\right]\right\}\frac{\pi}{4}\,(R_2^2 - R_1^2)$$

$$B = \frac{4}{3\pi}\left[\frac{R_2^3\left(r - \frac{3}{8}R_2\right) - R_1^3\left(r - \frac{3}{8}R_1\right)}{(R_2^2 - R_1^2)\left\{r - \frac{4}{3\pi}\left[\frac{R_2^3 - R_1^3}{R_2^2 - R_1^2}\right]\right\}}\right]$$

42. . Curved shell ring

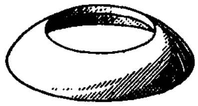

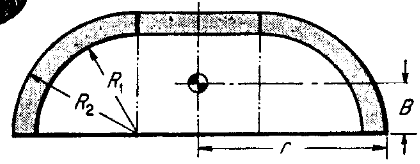

$$V = \frac{\pi^2}{2}\left[r(R_2^2 - R_1^2) + \frac{4}{3\pi}\,(R_2^3 - R_1^3)\right]$$

$$B = \frac{2}{\pi}\left[\frac{\frac{2r}{3}\,(R_2^3 - R_1^3) + \frac{1}{4}\,(R_2^4 - R_1^4)}{r(R_2^2 - R_1^2) + \frac{4}{3\pi}\,(R_2^3 - R_1^3)}\right]$$

43. . Fillet ring

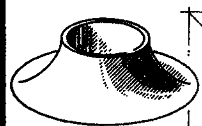

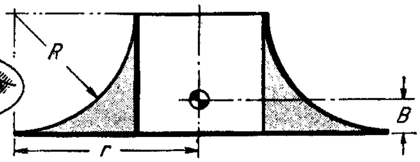

$$V = 2\pi R^2\left[\left(1 - \frac{\pi}{4}\right)r - \frac{R}{6}\right]$$

$$B = R\left[\frac{\left(\frac{5}{6} - \frac{\pi}{4}\right)r - \frac{R}{24}}{\left(1 - \frac{\pi}{4}\right)r - \frac{R}{6}}\right]$$

44. . Fillet ring

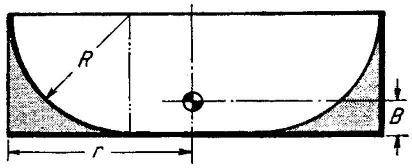

$$V = 2\pi R^2\left[\left(1 - \frac{\pi}{4}\right)r - \left(\frac{5}{6} - \frac{\pi}{4}\right)R\right]$$

$$B = R\left[\frac{\left(\frac{5}{6} - \frac{\pi}{4}\right)r - \left(\frac{19}{24} - \frac{\pi}{4}\right)R}{\left(1 - \frac{\pi}{4}\right)r - \left(\frac{5}{6} - \frac{\pi}{4}\right)R}\right]$$

45. . Curved-sector ring

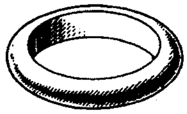

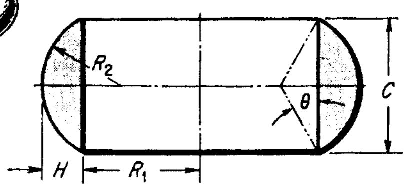

$$V = 2\pi R_2^2 \times \left[R_1 + \left(\frac{4\sin 3\theta}{6\theta - 3\sin 2\theta} - \cos\theta\right)R_2\right]\left[\theta - 0.5\sin 2\theta\right]$$

MISCELLANEOUS

46. . Ellipsoidal cylinder

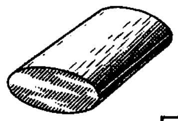

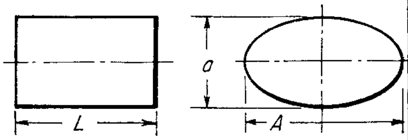

$$V = \frac{\pi}{4} AaL$$

47. . Ellipsoid

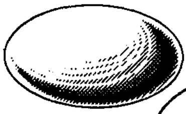

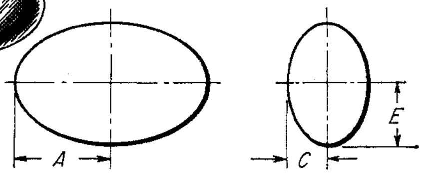

$$V = \frac{4}{3} \pi ACE$$

48. . Paraboloid

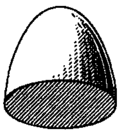

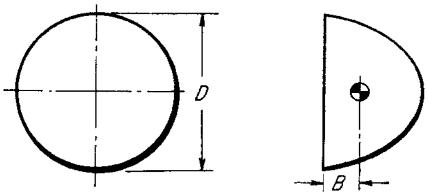

$$V = \frac{\pi}{8} HD^2 \qquad B = \frac{1}{3} H$$

49. . Pyramid (with base of any shape)

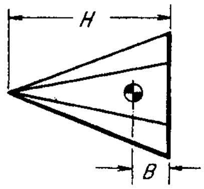

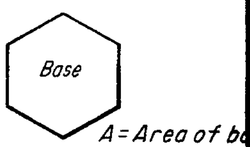

$$V = \frac{1}{3} AH \qquad B = \frac{1}{4} H$$

50. . Frustum of pyramid (with base of any shape)

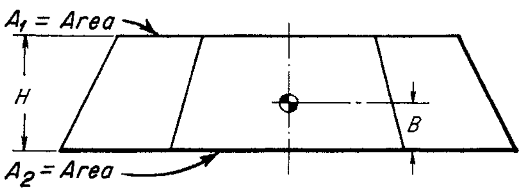

$$V = \frac{1}{3} H (A_1 + \sqrt{A_1 A_2} + A_2)$$

$$B = \frac{H (A_1 + 2\sqrt{A_1 A_2} + 3A_2)}{4 (A_1 + \sqrt{A_1 A_2} + A_2)}$$

51. . Cone

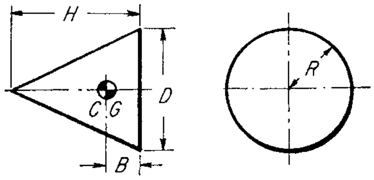

$$V = \frac{\pi}{12} D^2 H$$

$$B = \frac{1}{4} H$$

52. . Frustum of cone

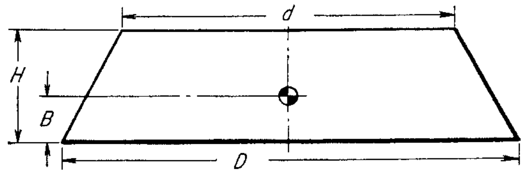

$$V = \frac{\pi}{12} H (D^2 + Dd + d^2)$$

$$B = \frac{H (D^2 + 2Dd + 3d^2)}{4 (D^2 + Dd + d^2)}$$

53. . Frustum of hollow cone

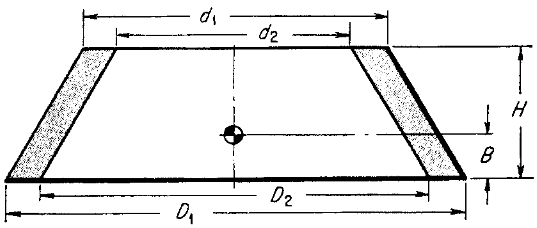

$$V = 0.2618H [(D_1^2 + D_1 d_1 + d_1^2) - (D_2^2 + D_2 d_2 + d_2^2)]$$

54. . Hexagon

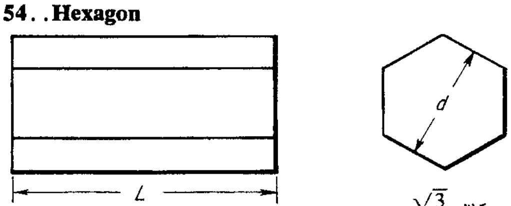

$$V = \frac{\sqrt{3}}{2} d^2 L$$

$$V = 0.866 d^2 L$$

55. . Closely packed helical springs

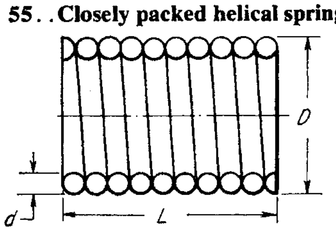

$$V = \frac{\pi^2 dL}{4} (D - d)$$

$$V = 2.4674 (D - d)$$

Common Area of Intersection Circle

Here's a fast method that will give quick, preliminary estimates.

L. E. Iversen

■ If you're given the radii of two intersecting circles and the distance between their centers, you can calculate their approximate common area quickly by means of this graph and formula.

Instead of solving many equations of considerable length (which you must do for exact area), all you do is select a constant, K, from the graph, subtract it from 1, and multiply by the area of one of the circles (see symbols).

To find K, use the ratio of radii $\frac{R}{r}$ for the abscissa, and ratio of distance between centers to one radius $\frac{c}{r}$ as the ordinate.

EXAMPLE Find area common to two circles with radii of 2 in. and 3 in., whose centers are 1.75 in. apart.

SYMBOLS

C = distance between centers

r, R = radii of circles

$A_R = K\pi R^2$ = partial area of circle R with no area common to circle r

$A_R = \pi r^2$ = total area of circle r, including area common to circle R

$A_C = (1 - K)\ \pi R^2$ = area common to both circles

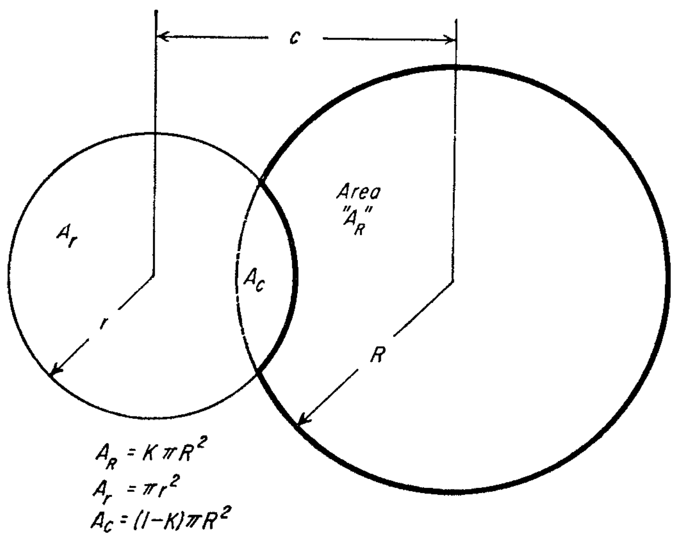

Let $r = 2.0$, $R = 3.0$, $c = 1.75$

$$\text{Then, } \frac{c}{r} = \frac{1.75}{2.0} = 0.875$$

$$\frac{R}{r} = \frac{3}{2} = 1.5$$

From the graph, K approximates 0.66 and

$$A_c = (1 - 0.66)\,\pi\,(3)^2 = 9.6 \text{ sq in.}$$

The graph is separated into four regions indicated by shaded and open areas: K's for common areas of intersecting circles fall within the rectangular, central portion. Points falling within upper left portion (outside the rectangle) indicate the circles do not intersect. Along the line, $K = 1$, circles are tangent; points in lower right or left portions indicate one circle is completely within the other.

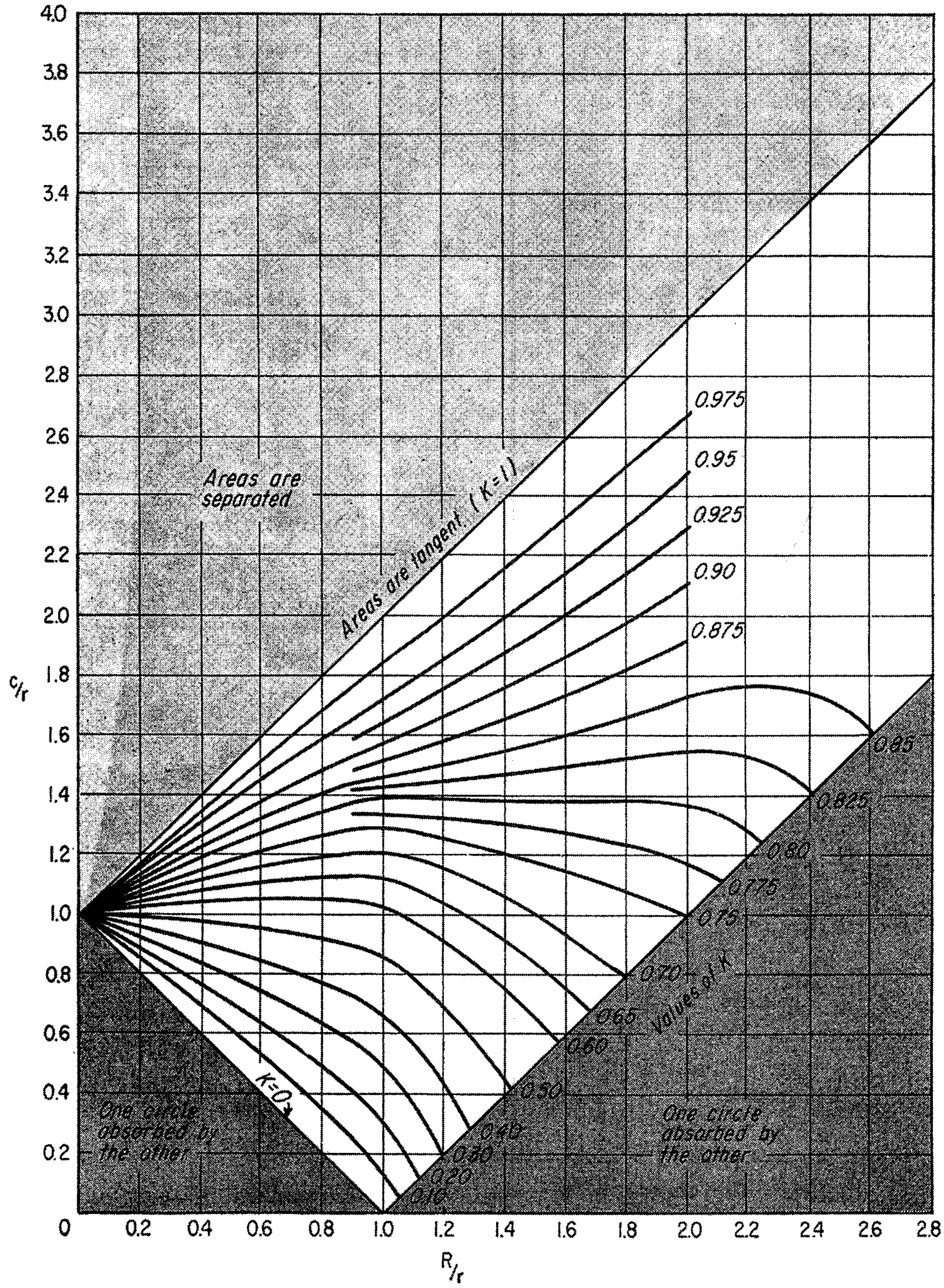

Compound Angles

D. E. Sweet

Attempts to derive formulas and tables for accurate computation of compound angles can be discouraging. Each case is usually presented in a manner such that it is often easier to consider each problem separately. There is one case, however, that can be standardized to the extent that formulas and tables can be a big help. An example is shown in Fig. 1. Here an angle is to be relieved down and away: it could be found on a cutting tool (for example, a counterbore blade).

Because the "down" and "away" angles are usually arbitrarily selected, the tables and charts given will aid the computation for the true angle. For convenience in using the table and chart, the "down" angle is designated as the "tipping angle" and the "away" angle as the "turning angle." The case angle A is tipped to angle ϕ and then turned to angle α; the resultant angle is the true angle or T.

In the table, constants are given for combinations of "tip" and "turn" angles from 5° to 45°. There are two constants for each combination, namely, constant 1 and constant 2.

To determine the true angle (using table)

Rule: multiply constant 1 by the tangent of the case angle A and *add* constant 2. The result of this addition is the tangent of the true angle.

If it is necessary to compute constants for tip-turn angles not given in the table, they can be found in these formulas:

Constant 1 = $\cos \alpha \div \cos \phi$
Constant 2 = $\sin \alpha \tan \phi$

Example: Case angle $A = 29°$, tip and turn angles = 5°. What is the true angle T?

Tan 29° = 0.55431; constant 1 = 1.0000; constant 2 = 0.00762. Then tan $T = 1 \times 0.55431 + 0.00762 = 0.56193$.

$T = 29° 20'$.

CONSTANT TABLE

TIP ANGLES ϕ	CONSTANT	TURN ANGLES α 5°	10°	15°	20°	25°	30°	35°	40°	45°
5°	1	1.0000	0.9886	0.9696	0.9433	0.9098	0.8693	0.8223	0.7690	0.7098
	2	.00762	.01519	.02264	.02992	.03697	.04374	.05018	.05624	.06186
10°	1	1.0115	1.0000	0.9808	0.9542	0.9203	0.8794	0.8318	0.7779	0.7180
	2	.01537	.03062	.04563	.06031	.07452	.08816	.10114	.11334	.12468
15°	1	1.0313	1.0195	1.0000	0.9728	0.9383	0.8966	0.8480	0.7931	0.7320
	2	.02335	.04653	.06935	.09164	.11324	.13397	.15369	.17223	.18947
20°	1	1.0601	1.0480	1.0279	1.0000	0.9645	0.9216	0.8717	0.8152	0.7525
	2	.03172	.06320	.09420	.12448	.15382	.18198	.20876	.23395	.25736
25°	1	1.0992	1.0866	1.0658	1.0368	1.0000	0.9555	0.9038	0.8452	0.7802
	2	.04064	.08097	.12069	.15948	.19707	.23315	.26746	.29974	.32973
30°	1	1.1503	1.1372	1.1153	1.0851	1.0465	1.0000	0.9459	0.8845	0.8165
	2	.05032	.10025	.14943	.19746	.24400	.28867	.33115	.37111	.40825
35°	1	1.2161	1.2022	1.1792	1.14715	1.1064	1.0572	1.0000	0.9352	0.8632
	2	.06103	.12159	.18123	.23948	.29592	.35010	.40162	.45008	.49512
40°	1	1.3004	1.2856	1.2609	1.2267	1.1831	1.1305	1.0693	1.0000	0.9230
	2	.07313	.14571	.21717	.28699	.35462	.41955	.48129	.53936	.59333
45°	1	1.4088	1.3927	1.3660	1.3289	1.2817	1.2247	1.1584	1.0833	1.0000
	2	.08749	.17365	.25882	.34202	.42262	.5000	.57358	.64279	.70711

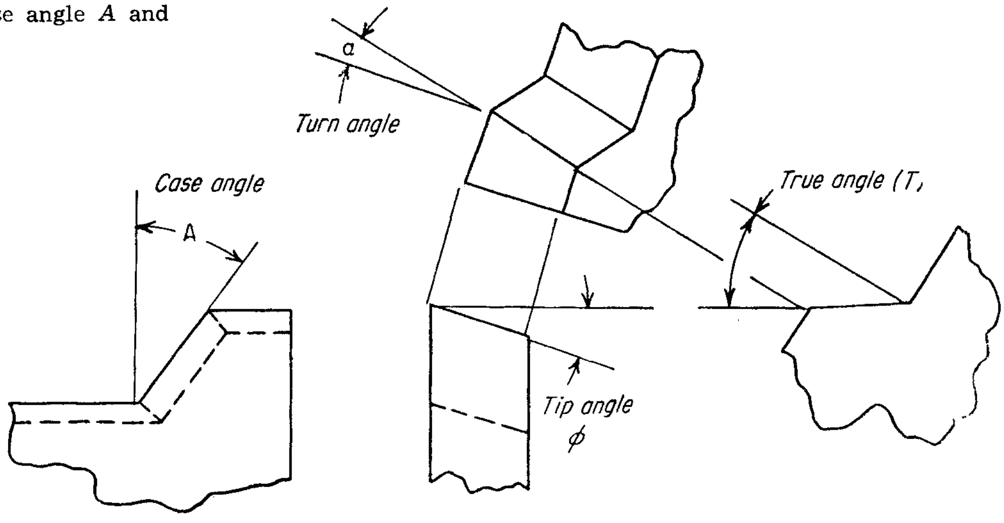

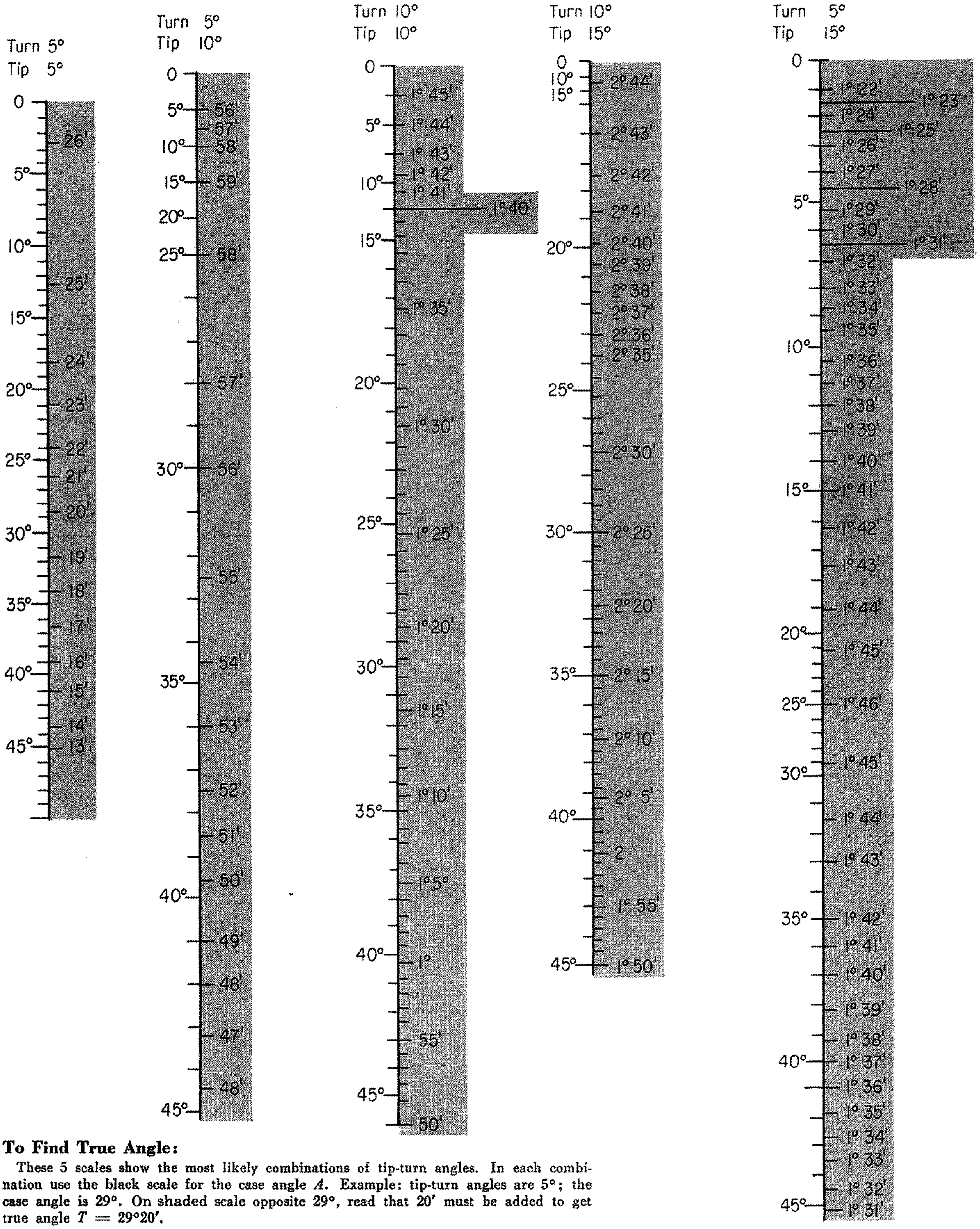

To Find True Angle:

These 5 scales show the most likely combinations of tip-turn angles. In each combination use the black scale for the case angle *A*. Example: tip-turn angles are 5°; the case angle is 29°. On shaded scale opposite 29°, read that 20′ must be added to get true angle $T = 29°20'$.

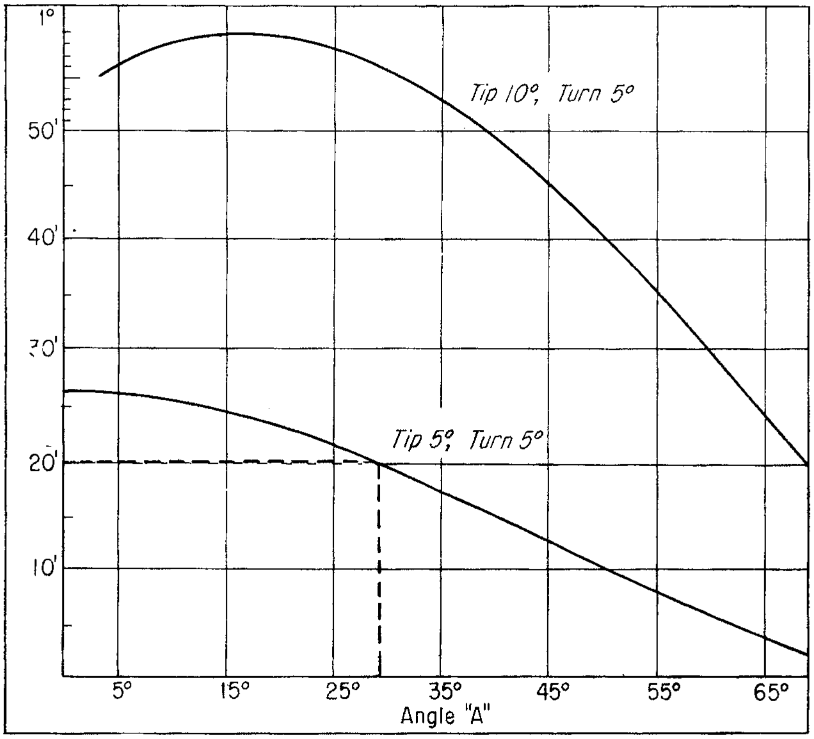

Graphical Solution of True Angle This chart is laid out with two curves for tip-turn angle combinations. Example: case angle $A = 29°$, tip and turn angles are 5°. Follow construction lines to see that 20′ must be added to angle $A = 29°$, to get true angle $T = 29°20'$.

Proof

Given θ, α and ϕ

To Find T

Solution:

$$AC = 1 = AB'$$
$$CB = \tan\theta = B'C$$
$$B'C' = \sin\phi = CD$$
$$B'C'' = \cos\alpha\,(B'C + CE)$$
$$CE = \tan\alpha\; CD$$
$$B'C'' = (\tan\theta + \tan\alpha\sin\phi)\times\cos\alpha$$
$$= \tan\theta\cos\alpha + \frac{\sin\alpha}{\cos\alpha}\times\cos\alpha\sin\phi$$
$$= \tan\theta\cos\alpha + \sin\alpha\sin\phi$$
$$AC' = \cos\phi = A'C''$$
$$\tan T = \frac{B'C''}{A'C''}$$
$$= \frac{\tan\theta\cos\alpha + \sin\alpha\sin\phi}{\cos\phi}$$
$$= \tan\theta\left(\frac{\cos\alpha}{\cos\phi}\right) + \sin\alpha\tan\phi$$
$$\text{Constant } 1 = \frac{\cos\alpha}{\cos\phi}$$
$$\text{Constant } 2 = \sin\alpha\tan\phi$$

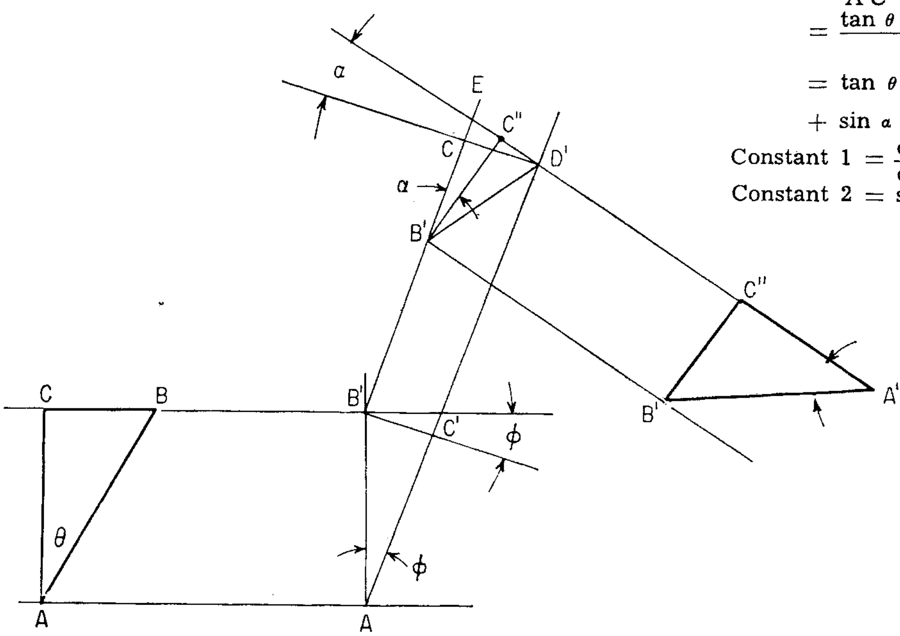

Calculation of Dihedral Angles

William W. Johnson

FORMULAS DEVELOPED by spherical trigonometry can be used to determine the angles required in constructing sheet metal products such as hoppers. Ten principal and five check equations are listed later for determining all the angles required in detailing the hoppers, and verifying the calculations. Ordinarily, only the first five of the principal equations are required but the attachments or supporting structure may necessitate the use of the next five.

Referring to Fig. 1(*A*) *M* and *N* represent two transparent planes which meet at their common intersection *OC*. Fig. 1(B) is another view of these planes. The angle *C* in the spherical triangle *ABC* is measured by the plane angle between tangents to *AC* and *BC*.

These tangents intersect radii *OA* and *OB* produced in *K* and *L*. Therefore, the numerical measure of the angle between the tangents to the great circles of a sphere at their points of intersection is the numerical measure of a spherical angle, and also the dihedral angle between the planes *M* and *N*.

The elements involved are defined as follows.

Given data:

A = angle between plane M and plane of reference;
B = angle between plane N and plane of reference;
c = angle in plane of reference between its intersections with the planes M and N

Data which can be computed:

C = dihedral angle between planes M and N
b = angle in M, between its intersection with N and plane of reference;
a = corresponding angle in plane N;
m = angle in plane of reference between its intersections with M and a plane normal to the plane of reference through the intersection of the planes M and N:
n = corresponding angle between intersections of N and the same normal plane;
$m + n = c$;
ψ = angle in normal plane between its intersection with reference plane and the intersection of planes M and N
φ = angle between plane M and the same normal plane;
θ = angle between plane N and the normal plane.
$\Phi + \theta = C$

A horizontal plane may be chosen for the reference plane. If this is done, the plane normal to plane of reference is vertical.

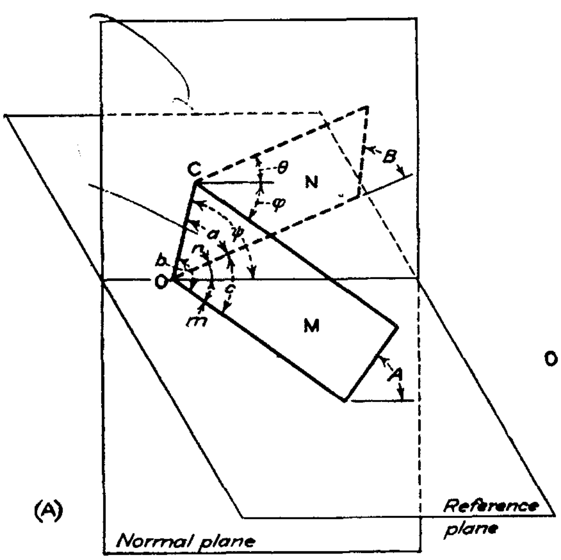

Fig. 1—Planes and angles used in the principal and check equations are defined in (A). These are used in (B) to develop the spherical triangle ABC.

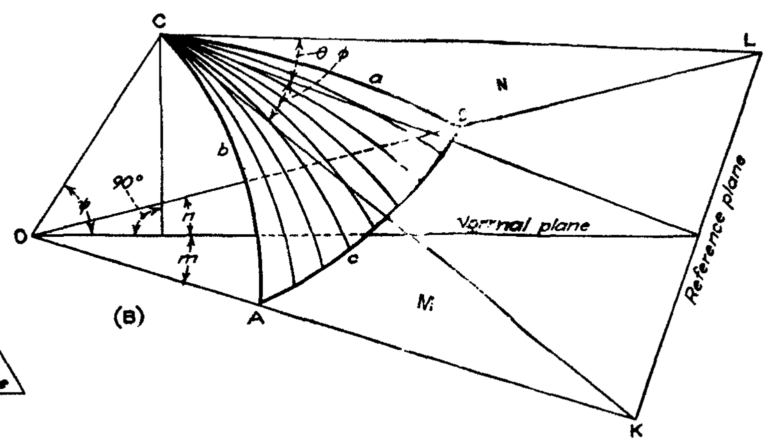

FORMULAS

$$\cos C = -\cos A \cos B + \sin A \sin B \cos c. \qquad (1)$$

This formula can be modified for logarithmic computation by the use of an auxiliary angle x.

Letting $$\cot x = \tan B \cos c \qquad (2)$$

Then $$\cos C = \frac{\sin (A - x) \cos B}{\sin x} \qquad (3)$$

$$\sin a = \frac{\sin c \sin A}{\sin C} \qquad (4)$$

$$\sin b = \frac{\sin c \sin B}{\sin C} \qquad (5)$$

$$\sin \psi = \sin b \sin A = \sin a \sin B$$
$$\tan m = \tan b \cos A$$
$$\tan n = \tan a \cos B$$
$$\cot \Phi = \tan A \cos b$$
$$\cot \Theta = \tan B \cos a$$

Table I—Sign Convention for Trigonometric Functions

Quadrant	Angles, deg	sin	cos	tan	cot	sec	csc
I	0–90	+	+	+	+	+	+
II	90–180	+	−	−	−	−	+
III	180–270	−	−	+	+	−	−
IV	270–360	−	+	−	−	+	−

CHECK FORMULAS

$$\tan\tfrac{1}{2}(a - b) = \sin\tfrac{1}{2}(A - B) \csc\tfrac{1}{2}(A + B) \tan(\tfrac{1}{2}c) \qquad (I)$$
$$\tan\tfrac{1}{2}(a + b) = \cos\tfrac{1}{2}(A - B) \sec\tfrac{1}{2}(A + B) \tan(\tfrac{1}{2}c) \qquad (II)$$
$$\cot(\tfrac{1}{2}C) = \cos\tfrac{1}{2}(a + b) \sec\tfrac{1}{2}(a - b) \tan\tfrac{1}{2}(A + B) \qquad (III)$$

$$\tan \varphi = \frac{\tan m}{\sin \psi} \qquad (IV)$$

$$\tan \Theta = \frac{\tan n}{\sin \psi}$$

In applying these equations, the algebraic signs must conform to Table I.

SAMPLE PROBLEM

The outline of a hopper is shown in Fig. 2. Fig. 3 gives the development of the sides. This problem presents as many difficulties as are likely to occur in practice. Below is given the computation of the angles pertaining to the intersection of the sides M and N of the hopper. The lower horizontal plane is taken as the plane of reference. The pitch angles A and B are first computed from the given dimensions.

$$\tan A = \frac{41.625}{7.750} \qquad \tan B = \frac{41.625}{28.814}$$
$$\log \tan A = 0.7300525 \qquad \log \tan B = 0.1597416$$
$$A = 79° \, 27' \, 11'' \qquad B = 55° \, 18' \, 27''$$

Since the angle of the corner is given as 45 deg,

$$c = 135 \text{ deg.}$$

The dihedral angle C at the intersection of the sides

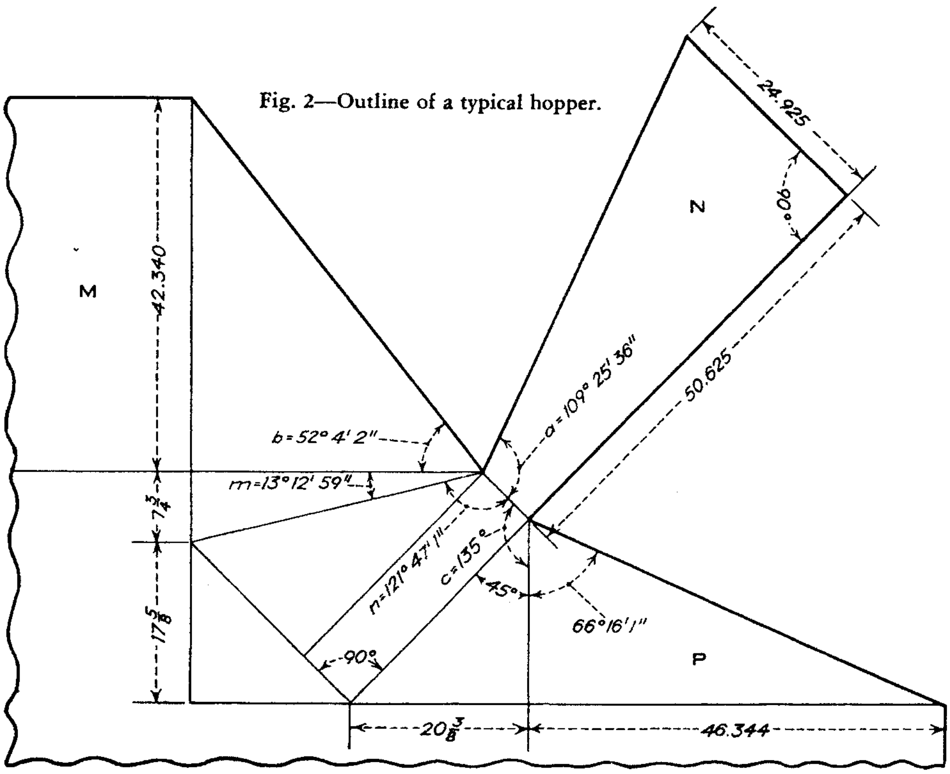

Fig. 2—Outline of a typical hopper.

M and N is found from Eqs. (2) and (3):

Since log tan $(E) = 0.1597416$ and log cos $(c) = 9.8494850$,
log cot $(x) = 0.0092266$
Thus, $x = 135° 36' 31''$ and
$(A - x) = -56° 9' 20''$
Using Eq. 3 and log sin $x = 9.8448227$,
log cos $C = 9.8297891$ or
$C = 132° 30' 46''$

Next, the angles a and b at which the sides M and N must be cut are found by Eqs. (4) and (5):

log sin $a = 9.9745431$
$a = 109° 25' 36''$
log sin $b = 9.8969296$
$b = 52° 4' 2''$

To check, use Eqs. (I), and (III), first finding $\frac{1}{2}(A + B)$ and $\frac{1}{2}(A - B)$ by addition and subtraction:

$\frac{1}{2}(A + B) = 67° 22' 49''$
$\frac{1}{2}(A - B) = 12° 4' 22''$

Thus,
log $\sin\frac{1}{2}(A - B) = 9.3204661$,
log $\csc\frac{1}{2}(A + P) = 0.0347617$, and
log $\tan\frac{1}{2}c = 0.3827757$.

Adding these three,
log $\tan\frac{1}{2}(a - b) = 9.7380035$ or
$\frac{1}{2}(a - b) = 28° 40' 47''$.

Similarly,
log $\cos\frac{1}{2}(A - B) = 9.9902868$,
log $\sec\frac{1}{2}(A + B) = 0.4149709$, and
log $\tan\frac{1}{2}c = 0.3827757$.

Adding,
log $\tan\frac{1}{2}(a + b) = 0.7880334$, and
$\frac{1}{2}(a + b) = 80° 44' 49''$

Solving simultaneously,
$a = 109° 25' 36''$ and
$b = 52° 4' 2''$.

Therefore,
log $\cos\frac{1}{2}(a + b) = 9.2062731$,
log $\sec\frac{1}{2}(a - b) = 0.0568439$, and
log $\tan\frac{1}{2}(A + B) = 0.3302131$.

From Eq. III, log $\cot(\frac{1}{2}C) = 9.6433301$ or
$\frac{1}{2}C = 66° 15' 23''$ and
$C = 132° 30' 46''$.

The angles a and b are identified in Fig. 3 showing the development of the hopper on the plane of reference. The corresponding angles at the other intersection, or corner of the hopper, can be determined by a similar process.

The dihedral angle formed by the intersection of the sides N and P are:

angle $C_1 = 140° 34' 20''$.

The cut angles for the sides N and P are:

angle $a_1 = 90°$. angle $b_1 = 66° 16' 1''$.

The pitch angle for the side P is $63° 55' 7''$. (See Fig. 3).

When the slopes of the sides M and N, and hence a and b are equal, and $c = 90°$, the required equations then become:

$$-\cos C = \cos^2 A \tag{1}$$

and

$$\sin a = \frac{\sin A}{\sin C} \tag{4 \& 5}$$

Fig. 3—Development of sides of hopper of Fig. 2.

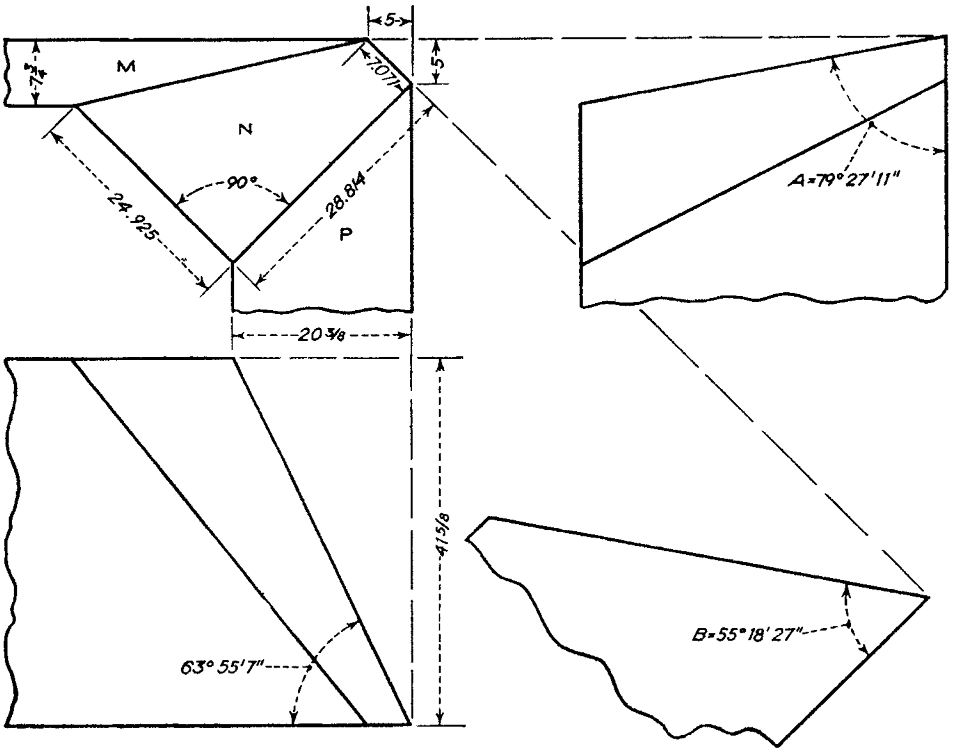

Frustums of Cones

Ronald L. Wakelee

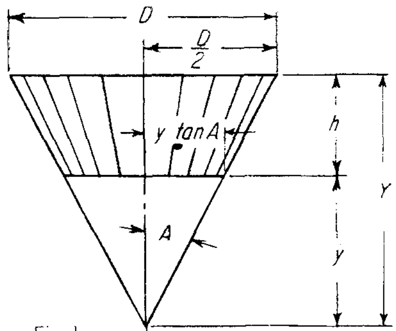

Fig. 1

Frustrum of
Right circular cone

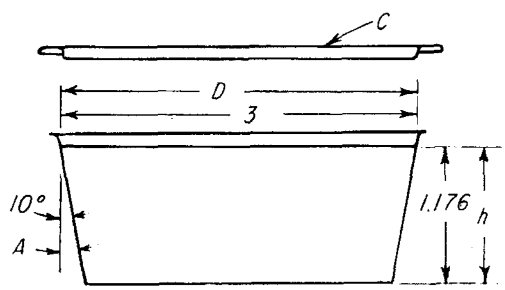

Fig. 2

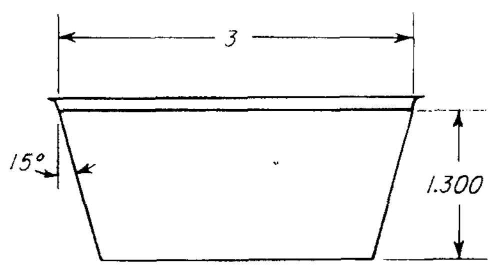

Fig. 3

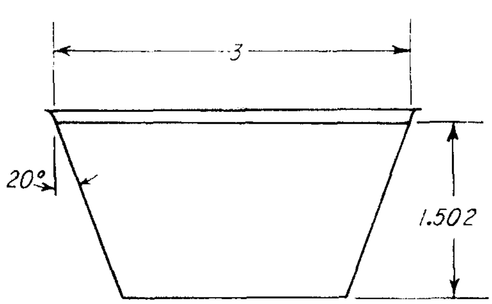

Fig. 4

Efficient solution of problems relating to frustums of cones may be hampered for lack of quantity A, Fig. 1. This quantity does not appear in the conventional formula for the volume of a frustrum:

$$V = 0.2618\, h\, (D^2 + Dd + d^2)$$

Quantity A, Fig. 1, was needed for solution of a problem involving thin-wall containers of frustrum shape. The customer wished to pack a standard volume in a container with a pleasing profile or side wall angularity.

Selection of can, profile starts with certain known factors: Volume V to be packed, open-end diameter D, and an approximate ratio of $D/h = 2\frac{1}{2}$, or $h = 0.4\, d$ as suggested by customer. If possible a standard packer's can end is selected. In this case D is taken as 3. The problem is to find the exact value of h.

First step is to draw up tentative can profiles, Figs. 2, 3, 4, of equal volume, which must be 7.218 cu in. Note that side angularity A is 10°, 15°, and 20° for the three profiles. The value of h in each case is calculated from the formula 7, page 312:

$$h = \frac{D - \sqrt[3]{D^3 - 7.64\, V \tan A}}{2 \tan A}$$

The customer-selected profile is shown in Fig. 2. Here $D = 3$, $A = 10°$ and $V = 7.218$ cu in. By substituting these values in equation 7, $h = 1.176$.

Bottom diameter d of the container is easily found from the formula:

$$\begin{aligned} d &= D - 2 \tan A \times h \\ &= 3 - (2 \tan 10° \times 1.176) \\ &= 3 - (2 \times 0.17633 \times 1.176) \\ &= 2.585 \end{aligned}$$

Length of Material for 90 Degree Bends

As shown in Fig. 1, when a sheet or flat bar is bent, the position of the neutral plane with respect to the outer and inner surfaces will depend on the ratio of the radius of bend to the thickness of the bar or sheet. For a sharp corner, the neutral plane will lie one-third the distance from the inner to the outer surface. As the radius of the bend is increased, the neutral plane shifts until it reaches a position midway between the inner and outer surfaces. This factor should be taken into consideration when calculating the developed length of material required for formed pieces.

The table on the following pages gives the developed length of the material in the 90-deg. bend. The following formulas were used to calculate the quantities given in the table, the radius of the bend being measured as the distance from the center of curvature to the inner surface of the bend.

1. For a sharp corner and for any radius of bend up to T, the thickness of the sheet, the developed length L for a 90-deg. bend will be

$$L = 1.5708\left(R + \frac{T}{3}\right)$$

2. For any radius of bend greater than $2T$, the length L for a 90-deg. bend will be

$$L = 1.5708\left(R + \frac{T}{2}\right)$$

3. For any radius of bend between $1T$ and $2T$, the value of L as given in the table was found by interpolation.

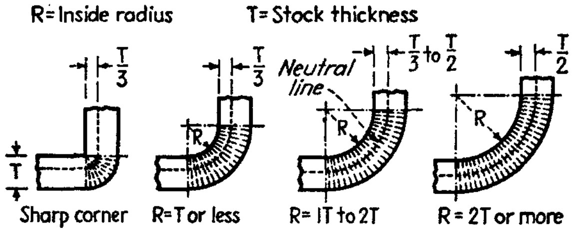

Fig. 1.

The developed length L of the material in any bend other than 90 deg. can be obtained from the following formulas:

1. For a sharp corner or a radius up to T:

$$L = 0.0175\left(R + \frac{T}{3}\right) \times \text{degrees of bend}$$

2. For a radius of $2T$ or more:

$$L = 0.0175\left(R + \frac{T}{2}\right) \times \text{degrees of bend}$$

For double bends as shown in Fig. 2, if $R_1 + R_2$ is greater than B:

$$X = \sqrt{2B(R_1 + R_2 - B/2)}$$

With R_1, R_2, and B known:

$$\cos A = \frac{R_1 + R_2 - B}{R_1 + R_2}$$

$$L = 0.0175(R_1 + R_2)A$$

where A is in degrees and L is the developed length.

If $R_1 + R_2$ is less than B, as in Fig. 3,

$$Y = B \operatorname{cosec} A - (R_1 + R_2)(\operatorname{cosec} A - \operatorname{cotan} A)$$

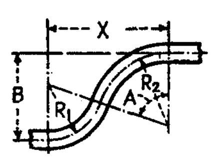

Fig. 2.

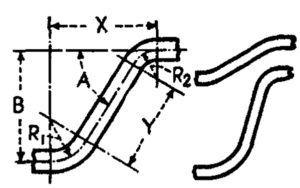

Fig. 3.

The value of X when B is greater than $R_1 + R_2$ will be

$$X = B \cot A + (R_1 + R_2)(\operatorname{cosec} A - \operatorname{cotan} A)$$

The total developed length L required for the material in the straight section plus that in the two arcs will be

$$L = Y + 0.0175(R_1 + R_2)A$$

To simplify the calculations, the table on this page gives the equations for X, Y, and the developed length for various common angles of bend. The table on following pages gives L for values of R and T for 90-deg. bends.

EQUATIONS FOR *X*, *Y*, AND DEVELOPED LENGTHS

Angle A, deg.	X	Y	Developed length
15	$3.732B + 0.132(R_1 + R_2)$	$3.864B - 0.132(R_1 + R_2)$	$3.864B + 0.130(R_1 + R_2)$
22½	$2.414B + 0.199(R_1 + R_2)$	$2.613B - 0.199(R_1 + R_2)$	$2.613B + 0.194(R_1 + R_2)$
30	$1.732B + 0.268(R_1 + R_2)$	$2.000B - 0.268(R_1 + R_2)$	$2.000B + 0.256(R_1 + R_2)$
45	$B + 0.414(R_1 + R_2)$	$1.414B - 0.414(R_1 + R_2)$	$1.414B + 0.371(R_1 + R_2)$
60	$0.577(B + R_1 + R_2)$	$1.155B - 0.577(R_1 + R_2)$	$1.155B + 0.470(R_1 + R_2)$
67½	$0.414B + 0.668(R_1 + R_2)$	$1.082B - 0.668(R_1 + R_2)$	$1.082B + 0.510(R_1 + R_2)$
75	$0.268B + 0.767(R_1 + R_2)$	$1.035B - 0.767(R_1 + R_2)$	$1.035B + 0.542(R_1 + R_2)$
90	$R_1 + R_2$	$B - R_1 - R_2$	$B + 0.571(R_1 + R_2)$

8 Simple Methods to Measure Moment of Inertia

Oscillating and "falling weight" setups combine with simple formulas to give accurate answers for complex shapes.

Bernard Brenner

Moment of inertia is generally difficult to find when one or more of the following conditions exist: Body shape is irregular; material density is unknown; parts must be disassembled before precise dimensions can be found. The experimental methods shown here handle all such cases with sufficient accuracy for most engineering work. Only requirements: measurements of weight and time; and simple dimensions.

SYMBOLS

D = dia, in.
d = distance, in.
f = friction torque, oz-in.
g = gravity, in./sec^2
J = inertia of test body about symmetry axis, oz-in.-sec^2
J_r = reference inertia, oz-in.-sec^2
k = torsional spring constant, oz-in./radians
L = length of pendulum, in.
R = radius, in.
T = period of oscillation (or time of weight fall), sec
W = weight of test body, oz
W_c = connecting-rod weight, oz
W_r = reference weight, oz

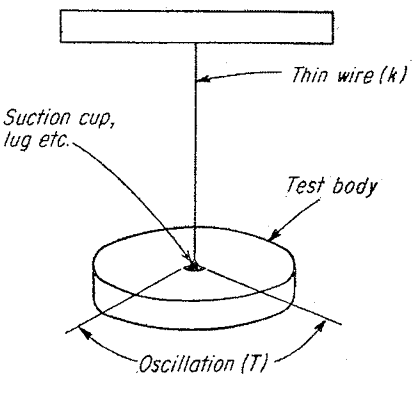

1—Torsional Pendulum (when k is known)

$$J = \frac{kT^2}{4\pi^2}$$

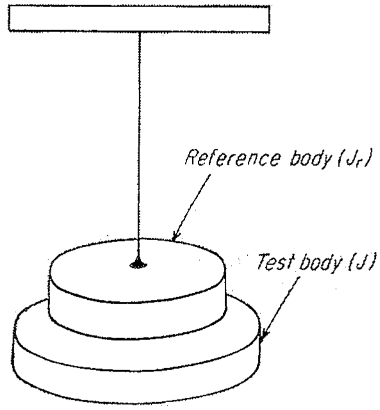

2—Torsional Pendulum (k is unknown)
T_1 is period with J_r only
T_2 is period with J_r and J together

$$J = J_r\left[\left(\frac{T_2}{T_1}\right)^2 - 1\right]$$

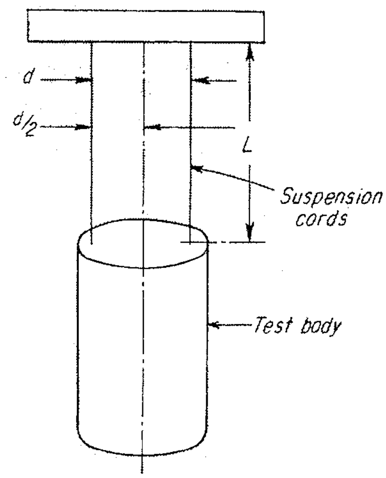

3—Bifilar Suspension (suspension cords must be highly flexible)

$$J = \frac{W d^2 T^2}{16 \pi^2 L}$$

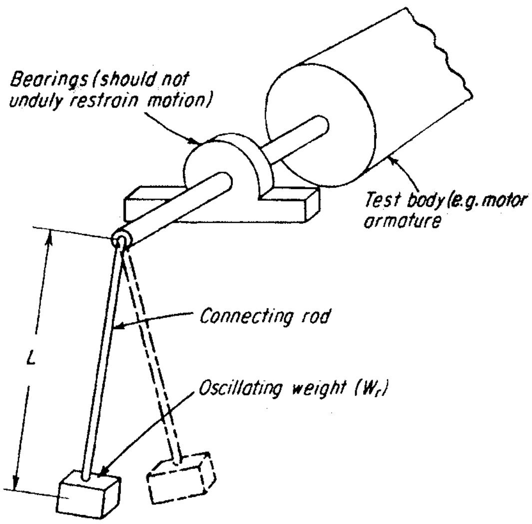

4—Pendulum (connecting-rod weight relatively light)

$$J = W_r L\left(\frac{T^2}{4\pi^2} - \frac{L}{g}\right)$$

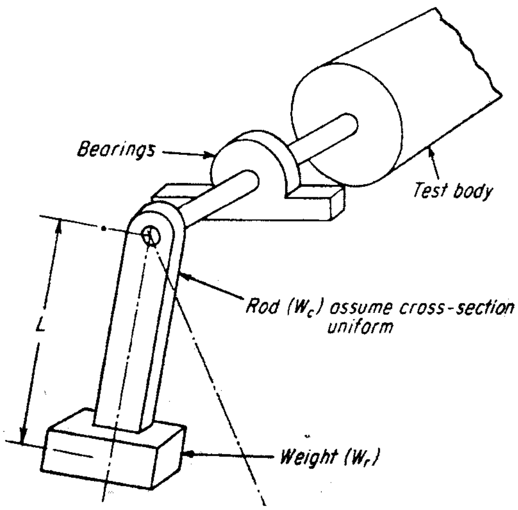

5—Pendulum (connecting-rod weight appreciable)

$$J = L\left[\frac{T^2}{4\pi^2}\left(W_r + \frac{W_c}{2}\right) - \frac{L}{g}\left(W_r + \frac{W_c}{3}\right)\right]$$

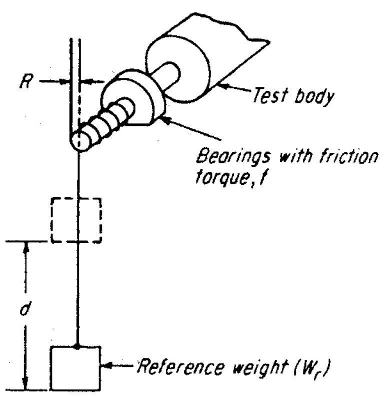

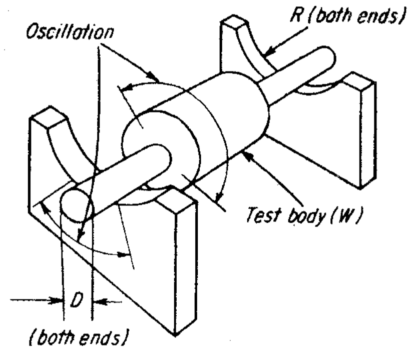

6—Rocker

$$J = \frac{WD^2T^2}{16\pi^2 R}$$

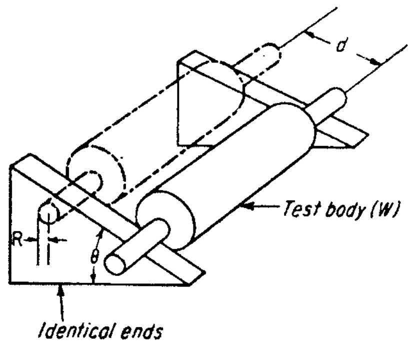

7—Inclined Plane

Body rolls d in. from rest (without slipping) in t seconds.

$$J = \frac{WR^2t^2}{2d}\sin\theta$$

8—Falling Weight

Weight W_r starts from rest and travels d in. in T sec. Frictionless:

$$J = W_r R^2\left(\frac{T^2}{2d} - \frac{1}{g}\right)$$

With shaft friction f:

$$J = W_r R^2\left(\frac{T^2}{2d} - \frac{1}{g}\right) - \frac{RT^2 f}{2d}$$

Friction Wheel Drives Designed for Maximum Torque

Analysis of forces present in a friction wheel drive. Development of a design for drives that can be utilized to protect machines from excessive load torques.

Rudolf Kroener

DURING THE POST WAR YEARS, as a consequence of the general scarcity of leather, rubber, and metals, in Germany efforts were made to replace belt drives and gear drives with friction wheel drives. The satisfactory results obtained are ascribed to:

1. Ability to manufacture a facing material having a high coefficient of friction. Cellulose type of materials have been developed possessing coefficients of friction ranging up to 0.5. When compared with materials having friction coefficients ranging from 0.15 to 0.2, the new materials offer an opportunity to reduce bearing pressures 60 to 70 percent.
2. Development of designs in which the contact or normal force between the friction wheels is varied automatically with changes in load torque of the driven machine. These designs make it possible to apply friction wheel drives to serve as disconnect clutches for limiting the transmission of torque before it becomes excessive.

When the faces of two friction wheels are pressed together, and where

μ = coefficient of friction of the materials in contact
P = radial force pressing the wheels together, lb
T = force transmitted tangentially to the wheels at their point of contact without slip, lb
r = radius of driving wheel, in.
n = speed of driving wheel, rpm
H = horsepower transmitted by the friction wheel drive

$$T = \mu P \tag{1}$$

$$H = \frac{r\,n\,T}{63{,}025} \tag{2}$$

Since the radial force P is equal and opposite to the force exerted by the wheels on their supporting bearings, it is evident that for constant values of T the bearing pressures increase as the coefficient of friction decreases. Low coefficients of friction, therefore, are conducive to resultant power loss and bearing wear.

In a friction wheel drive where the wheel centers are adjusted and fixed to obtain a radial force sufficient to transmit a desired torque, the bearing pressure remains at a constant value regardless of variations in the transmitted torque. When the load torque varies to a large extent, such an arrangement compares unfavorably with gear drives and belt drives, since in such drives the bearing pressures vary with the torque transmitted.

This disadvantage is overcome in types of friction drives in which the driving wheel is mounted on a swinging center.

The swing drive shown in Fig. 1 is designed to change the radial pressure P simultaneously and automatically with variations in load torque. In this arrangement the motor is fastened to a sub-base. The sub-base is free to swing on an axle at the right side. The opposite side of the base is supported by a spring. The driving friction wheel is pushed upward by the spring to maintain contact with the driven wheel. The driven wheel is mounted on a non-adjustable center.

When the torque load on the driven

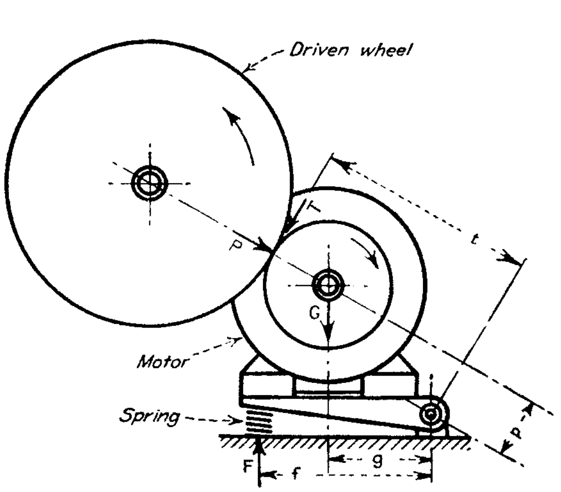

Fig. 1—Friction drive in which swing base is supported by a spring and axle.

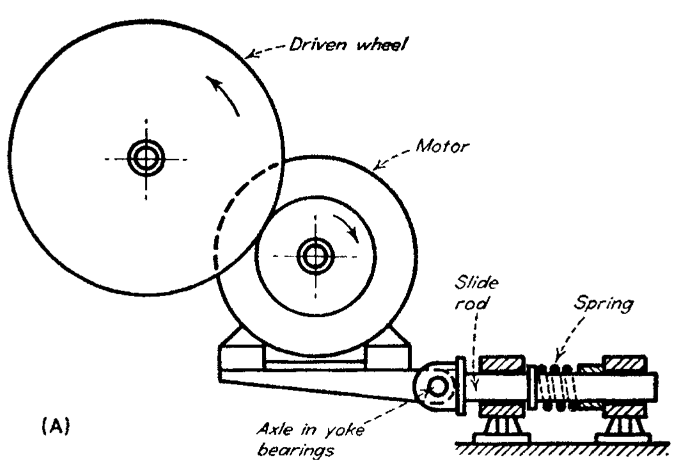

Fig. 2—(A) General arrangement of a maximum torque friction wheel drive with horizon-

wheel changes for any reason, the state of equilibrium is disturbed. The effect of an increase in torque load, until slipping occurs, is to cause the driving wheel to roll back or down on the driven wheel thus further compressing the spring. The spring force is thus increased, which results in an increased radial force P and an increase in the transmitted torque. Where

F = spring force, lb
f = horizontal distance from center of axle to line of spring force, in.
p = perpendicular distance from line of wheel centers to center of axle, in.
G = resultant of motor weight, driving wheel weight, and subbase weight, referred to axis of the motor, lb
g = horizontal distance from center of axle to vertical line passing through axis of motor, in.
t = perpendicular distance from tangent through point of contact of wheel faces to center of axle, in.

then to satisfy conditions of equilibrium

$$Gg - Ff - Pp + Tt = 0 \tag{3}$$

and the spring force F is found by substituting in Eq (3) the value of P as given by Eq (1), or

$$F = \frac{Gg + T[t - (p/\mu)]}{f} \tag{4}$$

In the design shown in Fig. 1, the extent to which the radial pressure P may build up, until slipping occurs, in response to increasing load torque is not limited. Excessive load torques may damage the friction facings, the driven machine, or the motor.

Any of many safety devices such as slip clutches, shear pins or keys, and breaking bolts, of course, can be used to protect the driven machine from excessive overloads. Fuses, overload relays, and thermal cut out devices can also be installed to protect the motor. Such protective devices are not necessary, however, when the friction wheel drive is designed to perform as a maximum torque clutch in which contact at the wheel faces ceases when a predetermined value of load torque is exceeded.

In the friction wheel drive shown in Fig. 2 (A), the drive motor M is fastened to a swing plate, one side of which is supported on an axle. This axle is free to turn in yoke bearings on the ends of rods that are free to slide in fixed bearings. The spring F is compressed between a shoulder and a spacer on each slide rod.

In this arrangement, an increase in load torque on the driven wheel causes the tangential force T to increase, which in turn causes the driving wheel to ride at a lower position on the face of the driven wheel.

As the driving wheel drops to a lower position, the cosine of the angle included between the line of centers of the axle and motor and the horizontal centerline of the slide rods increases, thus compressing the spring F and increasing the contact force P. With an increasing load torque, the driving wheel will finally fall away from the driven wheel.

At the instant of last contact of the two wheels, the spring has its maximum compression. The maximum torque that the arrangement shown in Fig. 2 (A) can transmit, therefore, depends upon the spring rate of the spring.

The geometrical relations present in the drive shown in Fig. 2 (A) when operating under a normal load and under maximum load are shown in Figs. 2 (B) and (C), respectively. For normal load conditions, the notations for dimensions and angles carry the subscript 1; for maximum load conditions they carry the subscript 2. The geometrical relations existing are.

At a normal load,

$$a_1 = (R + r)\cos\beta_1$$
$$h_1 = g - (R + r)\sin\beta_1$$
$$b_1 = \sqrt{s^2 - h_1^2}$$
$$p_1 = s\sin(\alpha_1 - \beta_1)$$
$$t_1 = r + s\cos(\alpha_1 - \beta_1)$$
$$c_1 = a_1 + b_1$$
$$\sin\alpha_1 = \frac{h_1}{s} = \frac{g - (R + r)\sin\beta_1}{s}$$

At maximum load,

$$\alpha_2 = \beta_2$$
$$a_2 = (R + r)\cos\beta_2$$
$$h_2 = g - (R + r)\sin\beta_2$$
$$b_2 = \sqrt{s^2 - h_2^2} = h_2/\tan\beta_2$$
$$p_2 = s\sin(\alpha_2 - \beta_2) = 0$$
$$t_2 = r + s\cos(\alpha_2 - \beta_2) = r + s$$
$$c_2 = a_2 + b_2$$
$$\sin\alpha_2 = \sin\beta_2 = g/(R + r + s)$$

Where

F = spring force or horizontal component of the reaction load exerted by the axle, lb
N = vertical component of the reaction load exerted by the axle, lb

the relations that satisfy conditions of equilibrium are

$$Gb + Tt - Pp = 0 \tag{5}$$
$$P\cos\beta - T\sin\beta = F \tag{6}$$
$$P\sin\beta + G + T\cos\beta = N \tag{7}$$
$$\sqrt{N^2 + F^2} = S \tag{8}$$
$$T = \mu P \tag{9}$$

Substituting Eq (9) in Eq (6)

$$T_2\left(\frac{\cos\beta_2}{\mu} - \sin\beta_2\right) = F_2 \tag{10}$$

The spring force F_2 required to maintain sufficient radial pressure P_2 to transmit a maximum horsepower H_2 from Eqs (2) and (10) is then

$$F_2 = \frac{63{,}025\,H_2}{rn}\left(\frac{\cos\beta_2}{\mu} - \sin\beta_2\right) \tag{11}$$

by similar analysis

$$F_1 = \frac{63{,}025\,H_1}{rn}\left(\frac{\cos\beta_1}{\mu} - \sin\beta_1\right) \tag{11A}$$

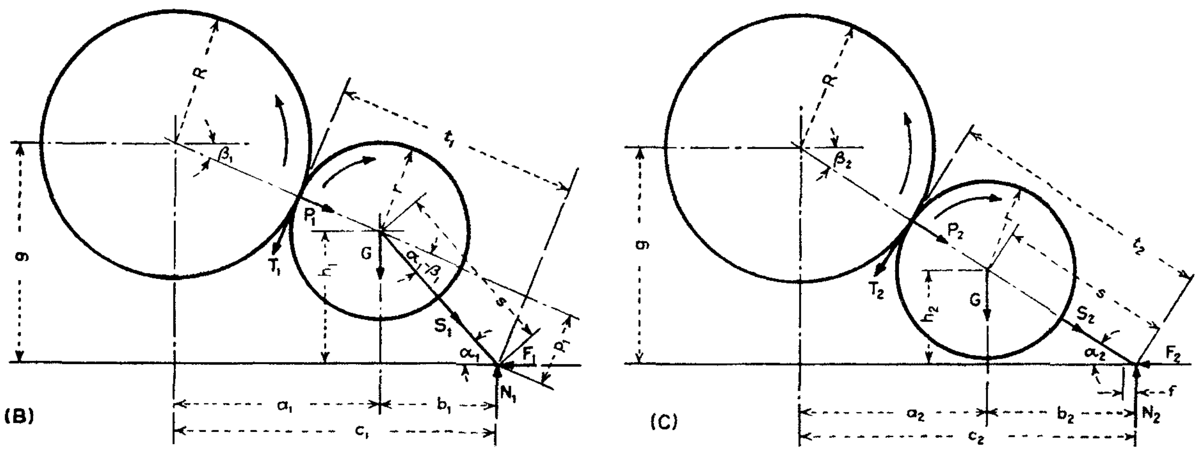

tal slide rods and compression springs. (B) Geometrical relation of parts under normal driving conditions. (C) Geometrical relation of parts under maximum torque driving conditions.

Radii of Gyration for Rotating Bodies

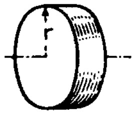	Solid cylinder about its own axis	$R^2 = \frac{r^2}{2}$
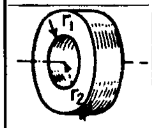	Hollow cylinder about its own axis	$R^2 = \frac{r^2_1 + r^2_2}{2}$
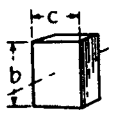	Rectangular prism about axis through center	$R^2 = \frac{b^2 + c^2}{12}$
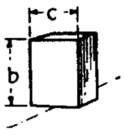	Rectangular prism about axis at one end	$R^2 = \frac{4b^2 + c^2}{12}$
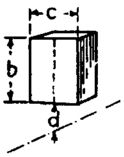	Rectangular prism about outside axis	$R^2 = \frac{4b^2 + c^2 + 12bd + 12d^2}{12}$

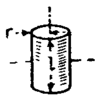	Cylinder about axis through center	$R^2 = \frac{l + 3r^2}{12}$
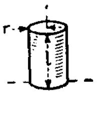	Cylinder about axis at one end	$R^2 = \frac{4l^2 + 3r^2}{12}$
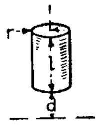	Cylinder about outside axis	$R^2 = \frac{4l^2 + 3r^2 + 12dl + 12d^2}{12}$
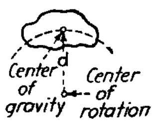	Any body about axis outside its center of gravity $R^2_1 = R^2_0 + d^2$ where R_0 = radius of gyration about axis through center of gravity R_1 = radius of gyration about any other parallel axis d = distance between center of gravity and axis of rotation	

APPROXIMATIONS FOR CALCULATING MOMENTS OF INERTIA

Name of Part	Moment of Inertia
Flywheels (not applicable to belt pulleys)	Moment of inertia equal to 1.08 to 1.15 times that of rim alone
Flywheel (based on total weight and outside diameter)	Moment of inertia equal to two-thirds of that of total weight concentrated at the outer circumference
Spur or helical gears (teeth alone)	Moment of inertia of teeth equal to 40 per cent of that of a hollow cylinder of the limiting dimensions
Spur or helical gears (rim alone)	Figured as a hollow cylinder of same limiting dimensions
Spur or helical gears (total moment of inertia)	Equal to 1.25 times the sum of that of teeth plus rim
Spur or helical gears (with only weight and pitch diameter known)	Moment of inertia considered equal to 0.60 times the moment of inertia of the total weight concentrated at the pitch circle
Motor armature (based on total weight and outside diameter)	Multiply outer radius of armature by following factors to obtain radius of gyration: Large slow-speed motor .... 0.75–0.85 Medium speed d-c or induction motor ..... 0.70–0.80 Mill-type motor 0.60–0.65

WR^2 OF SYMMETRICAL BODIES

For computing WR^2 of rotating masses of weight per unit volume ρ, by resolving the body into elemental shapes. See page 208 for effect of WR^2 on electric motor selection.

Note: ρ in pounds per cubic inch and dimensions in inches give WR^2 in lb.-in. squared.

1. Weights per Unit Volume of Materials.

Material	Weight, Lb. per Cu. In.
Cast iron	0.260
Cast-iron castings of heavy section *i.e.*, flywheel rims	0.250
Steel	0.283
Bronze	0.319
Lead	0.410
Copper	0.318

2. Cylinder, about Axis Lengthwise through the Center of Gravity.

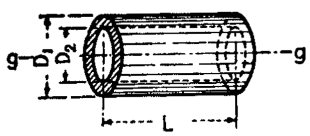

$$\text{Volume} = \frac{\pi}{4} L(D^2_1 - D^2_2)$$

(*a*) For any material:

$$WR^2 = \frac{\pi}{32} \rho L(D^4_1 - D^4_2)$$

where ρ is the weight per unit volume.

(*b*) For cast iron:

$$WR^2 = \frac{L(D^4_1 - D^4_2)}{39.2}$$

(*c*) For cast iron (heavy sections):

$$WR^2 = \frac{L(D^4_1 - D^4_2)}{40.75}$$

(*d*) For steel:

$$WR^2 = \frac{L(D^4_1 - D^4_2)}{36.0}$$

3. Cylinder, about an Axis Parallel to the Axis through Center of Gravity.

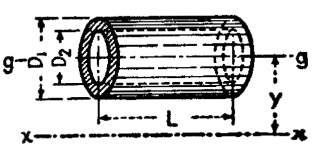

$$\text{Volume} = \frac{\pi}{4} L(D^2_1 - D^2_2)$$

(*a*) For any material:

$$WR^2_{x-x} = \frac{\pi}{4} \rho L(D^2_1 - D^2_2) \left(\frac{D^2_1 + D^2_2}{8} + y^2\right)$$

(*b*) For steel:

$$WR^2_{x-x} = \frac{(D^2_1 - D^2_2)L}{4.50} \left(\frac{D^2_1 + D^2_2}{8} + y^2\right)$$

4. Solid Cylinder, Rotated about an Axis Parallel to a Line that Passes through the Center of Gravity and Is Perpendicular to the Center Line.

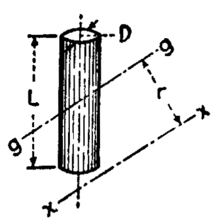

$$\text{Volume} = \frac{\pi}{4} D^2L$$

(*a*) For any material:

$$WR^2_{x-x} = \frac{\pi}{4} D^2L\rho \left(\frac{L^2}{12} + \frac{D^2}{16} + r^2\right)$$

(*b*) For steel:

$$WR^2_{x-x} = \frac{D^2L}{4.50} \left(\frac{L^2}{12} + \frac{D^2}{16} + r^2\right)$$

5. Rod of Rectangular or Elliptical Section, Rotated about an Axis Perpendicular to and Passing through the Center Line.

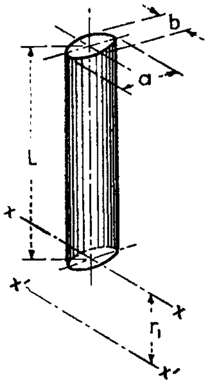

For rectangular cross sections:

$$K_1 = 1/12; \qquad K_2 = 1$$

For elliptical cross sections:

$$K_1 = \frac{\pi}{64}; \qquad K_2 = \frac{\pi}{4}$$

$$\text{Volume} = K_2abL$$

(*a*) For any material:

$$WR^2_{x'-x'} = \rho abL\left\{K_2\left[\frac{L^2}{3} + r_1(r_1 + L)\right] + K_1a^2\right\}$$

(*b*) For a cast-iron rod of elliptical section ($\rho = 0.260$):

$$WR^2_{x'-x'} = \frac{abL}{4.90}\left[\frac{L^2}{3} + r_1(r_1 + L) + \frac{a^2}{16}\right]$$

6. Elliptical Cylinder, about an Axis Parallel to the Axis through the Center of Gravity.

$$\text{Volume} = \frac{\pi}{4}abL$$

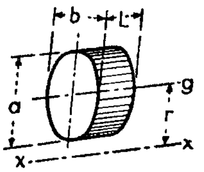

(*a*) For any material:

$$WR^2_{x-x} = \rho\frac{\pi}{4}abL\left(\frac{a^2 + b^2}{16} + r^2\right)$$

(*b*) For steel:

$$WR^2_{x-x} = \frac{abL}{4.50}\left(\frac{a^2 + b^2}{16} + r^2\right)$$

7. Cylinder with Frustum of a Cone Removed.

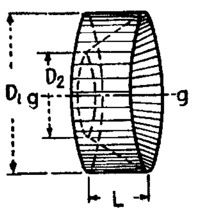

$$\text{Volume} = \frac{\pi L}{2(D_1 - D_2)}\left[\frac{1}{3}(D^3{}_1 - D^3{}_2) - \frac{D^2}{2}(D^2{}_1 - D^2{}_2)\right]$$

$$WR^2_{g-g} = \frac{\pi\rho L}{8(D_1 - D_2)}\left[\frac{1}{5}(D^5{}_1 - D^5{}_2) - \frac{D_2}{4}(D^4{}_1 - D^4{}_2)\right]$$

8. Frustum of a Cone with a Cylinder Removed.

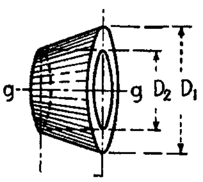

$$\text{Volume} = \frac{\pi L}{2(D_1 - D_2)}\left[\frac{D_1}{2}(D^2{}_1 - D^2{}_2) - \frac{1}{3}(D^3{}_1 - D^3{}_2)\right]$$

$$WR^2_{g-g} = \frac{\pi\rho L}{8(D_1 - D_2)}\left[\frac{D_1}{4}(D^4{}_1 - D^4{}_2) - \frac{1}{5}(D^5{}_1 - D^5{}_2)\right]$$

9. Solid Frustum of a Cone.

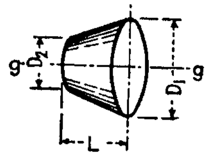

$$\text{Volume} = \frac{\pi L}{12}\frac{(D^3_1 - D^3_2)}{(D_1 - D_2)}$$

$$WR^2_{g-g} = \frac{\pi\rho L}{160}\frac{(D^5_1 - D^5_2)}{(D_1 - D_2)}$$

10. Chamfer Cut from Rectangular Prism Having One End Turned about a Center.

Distance to center of gravity, where $A = R_2/R_1$ and $B = C/2R_1$

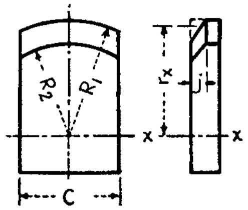

$$r_x = \frac{jR^3{}_1B}{\text{volume} \times (1 - A)}\left[\frac{1}{3}(A^3 - 3A + 2) + \frac{B^2}{3}\left(1 - A - A\log_e\frac{1}{A}\right) + \frac{3}{40}\frac{B^4}{A}(A^2 - 2A + 1) + \frac{5}{672}\frac{B^6}{A^3}(3A^4{}_1 - 4A^3 + 1)\cdots\right]$$

$$\text{Volume} = \frac{jR^2{}_1B}{(1 - A)}\left\{(A^2 - 2A + 1) + \frac{B^2}{3}\left[\log_e\frac{1}{A} - (1 - A)\right] + \frac{1}{40}\frac{B^4}{A^2}(2A^3 - 3A + 1) + \frac{1}{224}\frac{B^6}{A^4}(4A^5 - 5A^4 + 1) + \cdots\right\}$$

$$WR^2{}_{x-x} = -\frac{\rho jR^4{}_1B}{6(1 - A)}\left\{(A^4 - 4A + 3) + B^2(A^2 - 2A + 1) + \frac{9}{10}B^4\left[\log_e\frac{1}{A} - (1 - A)\right] + \frac{5}{56}\frac{B^6}{A^2}(2A^3 - 3A^2 + 1) + \cdots\right\}$$

11. Complete Torus.

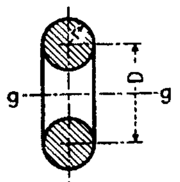

$$\text{Volume} = \pi^2 Dr^2$$

$$WR^2_{g-g} = \frac{\pi^2\rho Dr^2}{4}(D^2 + 3r^2)$$

12. Outside Part of a Torus.

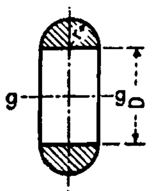

$$\text{Volume} = 2\pi r^2\left(\frac{\pi D}{4} + \frac{2}{3}r\right)$$

$$WR^2_{g-g} = \pi\rho r^2\left[\frac{D^2}{4}\left(\frac{\pi D}{2} + 4r\right) + r^2\left(\frac{3\pi}{8}D + \frac{8}{15}r\right)\right]$$

13. Inside Part of a Torus.

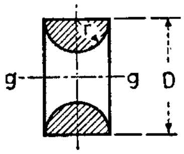

$$\text{Volume} = 2\pi r^2 \left(\frac{\pi D}{4} - \frac{2}{3} r\right)$$

$$WR^2_{g-g} = \pi \rho r^2 \left[\frac{D^2}{4}\left(\frac{\pi D}{2} - 4r\right) + r^2 \left(\frac{3\pi}{8} D - \frac{8}{15} r\right)\right]$$

14. Circular Segment about an Axis through Center of Circle.

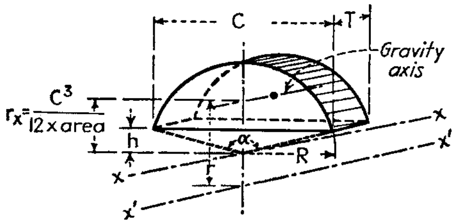

$$\alpha = 2 \sin^{-1} \frac{C}{2R} \text{ deg.}$$

$$\text{Area} = \frac{R^2\alpha}{114.59} - \frac{C}{2}\sqrt{R^2 - \frac{C^2}{4}}$$

(*a*) Any material:

$$WR^2_{x-x} = \rho T \left[\frac{R^4\alpha}{229.2} - \frac{1}{6}\left(3R^2 - \frac{C^2}{2}\right)\frac{C}{2}\sqrt{R^2 - \frac{C^2}{4}}\right]$$

(*b*) For steel:

$$WR^2_{x-x} = \frac{T}{3.534}\left[\frac{R^4\alpha}{229.2} - \frac{1}{6}\left(3R^2 - \frac{C^2}{2}\right)\frac{C}{2}\sqrt{R^2 - \frac{C^2}{4}}\right]$$

15. Circular Segment about Any Axis Parallel to an Axis through the Center of the Circles. (Refer to 14 for Figure.)

$$WR^2_{x'-x'} = WR^2_{x-x} + \text{weight } (r^2 - r^2_x)$$

16. Rectangular Prism about an Axis Parallel to the Axis through the Center of Gravity.

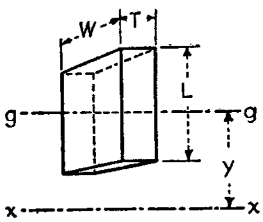

$$\text{Volume} = WLT$$

(*a*) For any material:

$$WR^2_{x-x} = \rho WLT \left(\frac{W^2 + L^2}{12} + y^2\right)$$

(*b*) For steel:

$$WR^2_{x-x} = \frac{WLT}{3.534}\left(\frac{W^2 + L^2}{12} + y^2\right)$$

17. Isosceles Triangular Prism, Rotated about an Axis through Its Vertex.

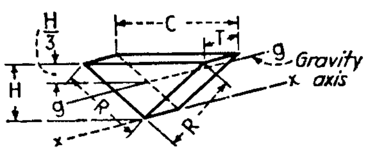

$$\text{Volume} = \frac{CHT}{2}$$

$$WR^2_{x-x} = \frac{\rho CHT}{2}\left(\frac{R^2}{2} - \frac{C^2}{12}\right)$$

18. Isosceles Triangular Prism, Rotated about Any Axis Parallel to an Axis through the Vertex.

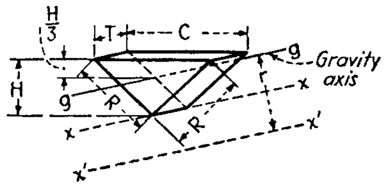

$$\text{Volume} = \frac{CHT}{2}$$

$$WR^2_{x'-x'} = \frac{\rho CHT}{2}\left(\frac{R^2}{2} - \frac{C^2}{12} - \frac{4}{9}H^2 + r^2\right)$$

19. Prism with Square Cross Section and Cylinder Removed, along Axis through Center of Gravity of Square.

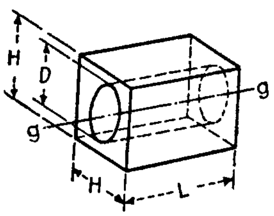

$$\text{Volume} = L\left(H^2 - \frac{\pi D^2}{4}\right)$$

$$WR^2_{g-g} = \frac{\pi \rho L}{32}(1.697H^4 - D^4)$$

20. Any Body about an Axis Parallel to the Gravity Axis, When WR^2 about the Gravity Axis Is Known.

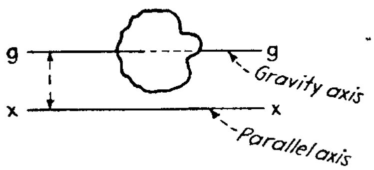

$$WR^2_{x-x} = WR^2_{g-g} + \text{weight} \times r^2$$

21. WR^2 of a Piston, Effective at the Cylinder Center Line, about the Crankshaft Center Line.

$$WR^2 = r^2 W_p\left(\frac{1}{2} + \frac{r^2}{8L^2}\right)$$

where r = crank radius
L = center-to-center length of connecting rod
W_p = weight of complete piston, rings, and pin

22. WR^2 **of a Connecting Rod, Effective at the Cylinder Center Line, about the Crankshaft Center Line.**

$$WR^2 = r^2\left[W_1 + W_2\left(\frac{1}{2} + \frac{r^2}{8L^2}\right)\right]$$

where r = crank radius
L = center-to-center length of connecting rod
W_1 = weight of the lower or rotating part of the rod $= [W_R(L - L_1)]/L$
W_2 = weight of the upper or reciprocating part of the rod $= W_R L_1/L$
$W_R = W_1 + W_2$, the weight of the complete rod
L_1 = distance from the center line of the crank-pin to the center of gravity of the connecting rod

23. Mass Geared to a Shaft.—The equivalent flywheel effect at the shaft in question is

$$WR^2 = h^2(WR^2)'$$

where h = gear ratio
$= \dfrac{\text{r.p.m. of mass geared to shaft}}{\text{r.p.m. of shaft}}$
$(WR^2)'$ = flywheel effect of the body in question about its own axis of rotation

24. Mass Geared to Main Shaft and Connected by a Flexible Shaft.—The effect of the mass $(WR^2)'$ at the position of the driving gear on the main shaft is

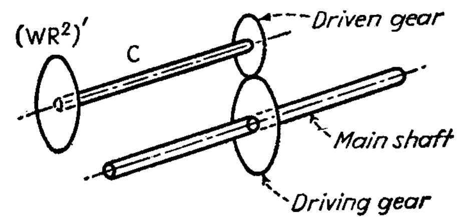

$$WR^2 = \frac{h^2(WR^2)'}{1 - \dfrac{(WR^2)'f^2}{9.775C}}$$

where h = gear ratio
$= \dfrac{\text{r.p.m. of driven gear}}{\text{r.p.m. of driving gear}}$
$(WR^2)'$ = flywheel effect of geared-on mass
f = natural torsional frequency of the shafting system, in vibrations per sec.
C = torsional rigidity of flexible connecting shaft, in pound-inches per radian

25. Belted Drives.—The equivalent flywheel effect of the driven mass at the driving shaft is

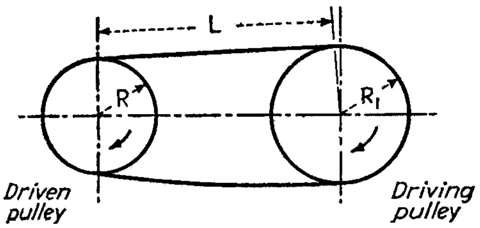

$$WR^2 = \frac{h^2(WR^2)'}{1 - \dfrac{(WR^2)'f^2}{9.775C}}$$

where $h = R_1/R$
$= \dfrac{\text{r.p.m. of pulley belted to shaft}}{\text{r.p.m. of shaft}}$
$(WR^2)'$ = flywheel effect of the driven body about its own axis of rotation
f = natural torsional frequency of the system, in vibrations per sec.
$C = R^2AE/L$
A = cross-sectional area of belt, in sq. in.
E = modulus of elasticity of belt material in tension, in lb. per sq. in.
R = radius of driven pulley, in in.
L = length of tight part of belt which is clear of the pulley, in in.

26. Effect of the Flexibility of Flywheel Spokes on WR^2 of Rim.—The effective WR^2 of the rim is

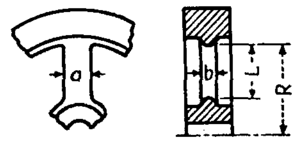

$$WR^2 = \frac{(WR^2)'}{1 - \frac{(WR^2)'f^2}{9.775C}}$$

where $(WR^2)'$ = flywheel effect of the rim
f = natural torsional frequency of the system of which the flywheel is a member, in vibrations per sec.
C = torque required to move the rim through one radian relative to the hub

$$C = \frac{12_g Eka^3bR}{L^2}\left(\frac{L}{3R} + \frac{R}{L} - 1\right)$$

where g = number of spokes
E = bending modulus of elasticity of the spoke material
$k = \pi/64$ for elliptical, and $k = 1/12$ for rectangular section spokes

All dimensions are in inches.

For cast-iron spokes of elliptical section:

$$E = 15 \times 10^6 \text{ lb. per sq. in.}$$

$$C = \frac{ga^3bR \times 10^6}{0.1132L^2}\left(\frac{L}{3R} + \frac{R}{L} - 1\right)\frac{\text{lb.-in.}}{\text{radians}}.$$

Note: It is found by comparative calculations that with spokes of moderate taper very little error is involved in assuming the spoke to be straight and using cross section at mid-point for area calculation.

TYPICAL EXAMPLE

The flywheel shown below is used in a Diesel engine installation. It is required to determine effective WR^2 for calculation of one of the natural frequencies of torsional vibration. The anticipated natural frequency of the system is 56.4 vibrations per sec.

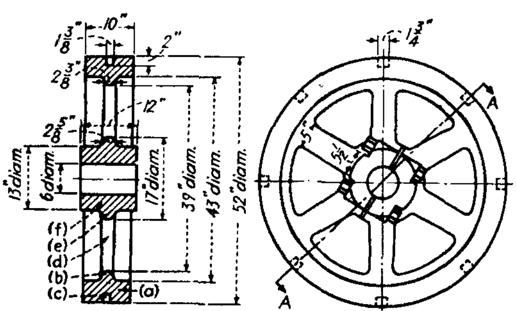

Section A-A

Note: Since the beads at the ends of the spokes comprise but a small part of the flywheel WR^2, very little error will result in assuming them to be of rectangular cross section. Also, because of the effect of the clamping bolts, the outer hub will be considered a square equal to the diameter. The spokes will be assumed straight and of mid-point cross section.

Part of fly wheel	Formula	WR^2
(a)	2c	$\frac{10[(52)^4 - (43)^4]}{40.75} = 955{,}300$
(b)	2b	$\frac{2.375[(43)^4 - (39)^4]}{39.2} = 67{,}000$
(c)	16a neglecting $\left(\frac{W^2 + L^2}{12}\right)$	$-0.250 \times 1.75 \times 2 \times 1.375(25)^2 \times 8 = -6{,}000$
		Total for rim = 1,016,300 lb.-in. squared
(d)	5b	$6 \times \frac{5.25 \times 2.5 \times 11}{4.90}\left[\frac{(11)^2}{3} + 8.5(8.5+11) + \frac{(5.25)^2}{16}\right] = 36{,}800$
(e)	2b	$\frac{2.625[(17)^4 - (13)^4]}{39.2} = 3{,}700$
(f)	19	$\frac{\pi \times 0.250 \times 12}{32}[1.697 \times (13)^4 - (6)^4] = 13{,}900$
		Total for remainder of flywheel = 54,400 lb.-in. squared

From formula (26)

$$C = \frac{6 \times (5.25)^3 \times 2.5 \times 19.5 \times 10^6}{0.1132 \times (11)^2}\left(\frac{11}{3 \times 19.5} + \frac{19.5}{11} - 1\right) = 2{,}970 \times 10^6 \frac{\text{lb.-in.}}{\text{radians}}$$

and $$WR^2 = \frac{1{,}016{,}300}{1 - \frac{1{,}016{,}300 \times (56.4)^2}{9.775 \times 2{,}970 \times 10^6}} + 54{,}400$$

$$= \underline{1{,}197{,}000} \text{ lb.-in. squared}$$

SECTION 29

STRUCTURAL DATA

Stress in Preloaded Bolts

Two computational aides–a formula that combines tensile and shear stresses, and a table of design stresses for bolt materials.

A. G. Hopper & G. V. Thompson

1. Forces in a bolted assembly

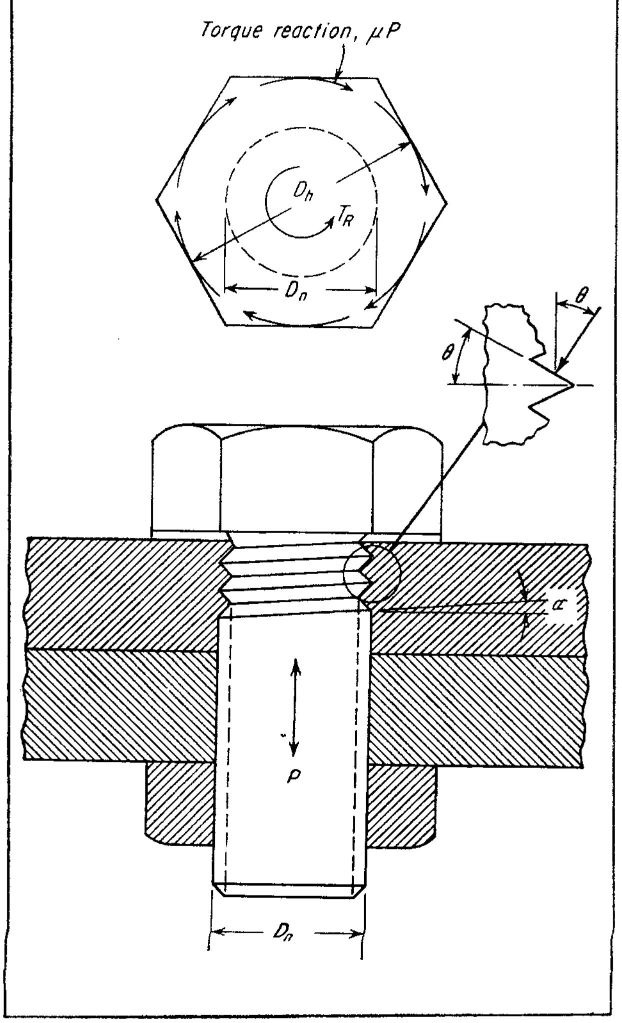

WHEN a bolt is tightened by applying torque to the bolt head or nut, shearing stresses develop simultaneously with the normal tensile stresses. For some reason, most authors omit consideration of these shearing stresses—yet it is the resulting combined stresses that should determine your design limit.

Here is a way to combine the stresses, as well as a list of recommended design stress values for steel bolts. There is also a design chart which gives the required data within minutes, and three sample problems to illustrate the selection of a proper bolt size by this method. One of the problems is based on new ASME data on pressure-vessel design.

But first, a word about the two criteria which form the basis for the equations and design method. We have found from experience that:

- Stresses are best combined by means of the maximum shear theory of failure—this is now being followed by the ASME Boiler and Pressure Vessel Code.
- Largest average stress intensity across the bolt section, produced by the preload or service, should be limited to two-thirds of the minimum yield strength of the material at the operating temperature (see Table I, p 83, for our compiled list of bolt materials).

With these two well-founded assumptions we can develop the formula and the charts for the solution of bolt-selection problems. Several examples are given, including the design of bolts to prevent a gasket from blowing out in a cylinder or pressure vessel.

Bolt load

If the forces in a screw are analyzed by considering the developed helix to be an inclined plane, the following equation is obtained (see *Design of Machine Elements*, 3rd Edition (1961), M. F. Spotts, Prentice-Hall):

$$T = r_t P\left[\frac{\cos\theta\tan\alpha + \mu}{\cos\theta - \mu\tan\alpha} + \left(\frac{r_c}{r_t}\right)\mu\right] \qquad (1)$$

For standard screws the helix angle α is small and θ is *half the thread angle (see Symbols p 82, and Fig 1). The* value for the coefficient of friction is always difficult to determine. However, assuming a value of $\mu = 0.15$ fairly accurate results can be obtained under a variety of condi-

SYMBOLS

A = Cross sectional area
α = Helix angle
D = Average of mean pitch and minor diameters of external thread, in.
D_N = Nominal diameter, in.
D_h = Distance across flats of bolt head or nut, in.
θ = One-half the thread angle
μ = Coefficient of friction
n = number of threads per in.
P = Load, lb
r = Radius or radial genetrix, in.
r_t = Pitch radius of thread, in.
r_c = Collar radius or moment arm to frictional force on nut or bolt head, in.
S = Stress intensity, psi
S_{av} = Average stress intensity (the design stress to be determined), psi
σ = Normal stress, psi
T = Applied torque, (ft-lb in the design charts)
T_R = Residual torque, in.-lb
τ = Shear stress, psi

tions. Therefore, for screws with the standard 60-deg thread, the following torque-load relation holds true:

$$T = 0.2 D_N P \tag{2}$$

Normal stress

The average tensile stress normal to the bolt section (Fig 2) is

$$\sigma = \frac{P}{A} = \frac{4P}{\pi D^2} \tag{3}$$

Here D is taken as the average of the mean pitch and minor diameters of the external thread.

Residual torque

The residual torque on the bolt, T_R, is the break-away torque necessary to turn the bolt under load a minute amount. This torque can be determined by examining a free body at the bearing face of the nut or bolt head (Fig 1). The force of friction, μP, can be conservatively taken as acting at a moment arm of ½ D_h. Hence:

$$T_R = \tfrac{1}{2} D_h \mu P \tag{4}$$

When torque is applied to the preloaded bolt, about 50% of the applied torque is dissipated, overcoming friction on the bearing face of the nut or bolt head. An additional 40% of the applied torque is wasted by friction on the contact flanks of the threads. The remaining 10% represents useful torque-producing bolt tension.

The torque predicted by Eq 4 is somewhat conservative, as can be noted by using Eq 2 to eliminate P from Eq 4. Thus when:

$$P = \frac{T}{0.2 D_N}$$

and $\mu = 0.15$

then $$T_R = 0.375 \left[\frac{D_h}{D_N} \right] T \tag{5}$$

For most bolts, D_h/D_N is about 1.5. Hence:

$$T_R = 0.5625\ T \tag{6}$$

This is 12-½% higher than the rule-of-thumb value of T_R = 0.5T, commonly used in shops.

Shear stresses

Shearing stresses resulting from the residual torque can be determined by the relation for a twisted shaft:

text continued, page 84

2. Tensile and shear stresses across the bolt

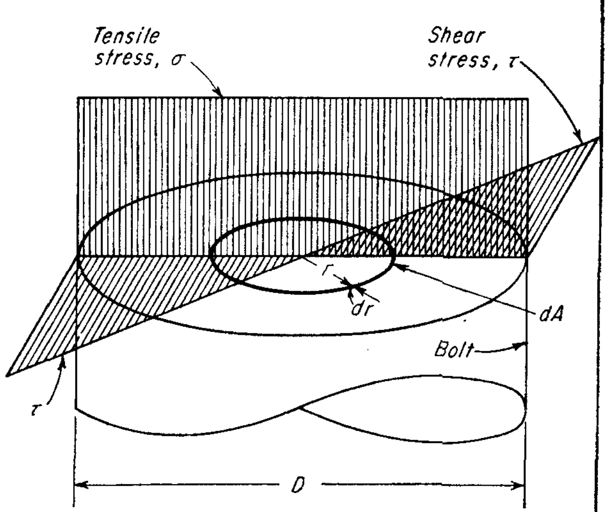

3. Mohr's circle for combining stresses

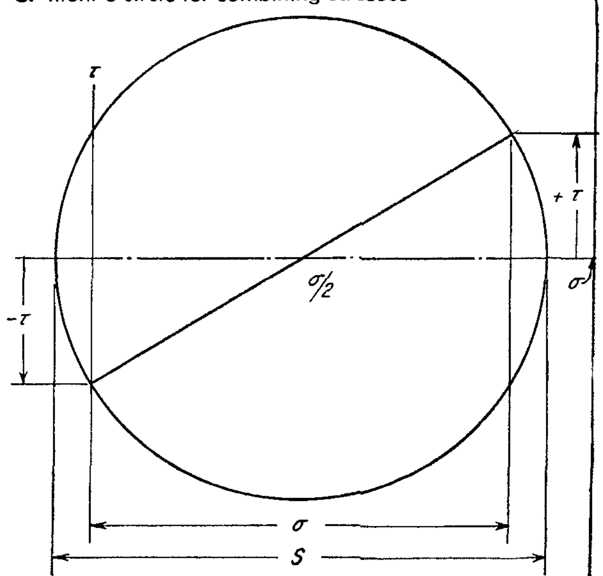

Table I — Strength of Bolting Materials

Material	ASTM Designation	Grade	Nominal Composition	Condition	Size, in. (inclusive)	Minimum Tensile Strength, psi	Minimum Yield Strength, psi
Carbon Steel	SA 261	BO	Fe-.56C-1Mn		All	100,000	75,000
	SA 307	B	Fe		All	55,000	11,000
	SA 325		Fe-.3C-.3Mn		Up to 1½	105,000	77,000
	"		"		Over 1½ to 3	90,000	55,000
Low Alloy Steel							
Type 501	SA 193	B5	5 Cr-½ Mo		Up to 2½	100,000	80,000
AISI 4140 4142 4145	SA 193	B7	1 Cr-.2 Mo		"	125,000	105,000
	SA 193	B14	1 Cr-.3 Mo-V		"	125,000	105,000
	SA 193	B16	1 Cr -.5 Mo-V		"	125,000	105,000
	SA 320	L7	1 Cr-.2 Mo		Up to 2½	125,000	105,000
AISI 4140 4142 4145	SA 320	L9	3.5 Ni		"	125,000	105,000
AISI 2317	SA 320	L10	3.5 Ni		Up to 4	70,000	40,000
	SA 320	L43	2Ni-.8Cr-.25Mo		"	125,000	105,000
	SA 354	BB	Heat	Quenched, Tempered	¼ to 2½	105,000	83,000
	SA 354	BC	Treatable	"	¼ to 2½	125,000	109,000
	SA 354	BD	Carbon Steel	"	¼ to 1½	150,000	125,000
Stainless Steel							
Type 416	SA 193	B6	12 Cr		Up to 4	110,000	85,000
Type 321	"	B8T	18 Cr-8 Ni	Solution Heat Treat	All	75,000	30,000
Type 347	"	B8C	18 Cr-8 Ni	"	All	75,000	30,000
Type 304	"	B8	18 Cr-8 Ni	"	All	75,000	30,000
Type 316	"	B8M	18 Cr-10 Ni-2Mo	"	All	75,000	30,000
Type 410	"	B6	12 Cr	—	Up to 4	110,000	85,000
Ni-Moly	SB 335		58 Ni-28 Mo-5 Fe	Annealed	5/16 to 1½	115,000	46,000
	SB 336		54 Ni-16 Mo-15.5 Cr	Annealed	Over 1½ to 3½	110,000	46,000
Monel	SB 164	A, B	Ni-2.5 Fe-2 Mn	Annealed	All	70,000	25,000
	SB 164	A	"	Hot Fin.	Up to 2⅛	80,000	40,000
	"	B	"	"	Up to 3	75,000	35,000
	SB 164	A	"	Cold Drawn Str. Rel.	Up to 3½	84,000	50,000
	SB 164	A	"	Cold Drawn Str. Equal.	½ to 3½	90,000	70,000
	"	B	"	Cold Drawn As Drawn	Up to 3	85,000	50,000
Inconel	SB 166		Ni-15.5 Cr-8 Fe	Annealed	All	80,000	35,000
	SB 166		Ni-15.5 Cr-8 Fe	Hot Fin.	½ to 3	90,000	40,000
Aluminum	SB 211	Al	A1-4.5 Cu	2014-T6	Up to 6½	65,000	55,000
	SB 211	Al	A1-4 Cu-1.5 Mg	2024-T4	Up to 6½	62,000	40,000
	SB 211	Al	A1-1 Mg	6061-T6	Up to 8	42,000	35,000
Copper	SB 12		Cu	SOFT	Up to 3	30,000	10,000
	SB 98	A, D	Cu-3 Si	SOFT	All	52,000	15,000
	"	A, D	Cu-3 Si	¼ HARD	All	55,000	24,000
	"	A, D	Cu-3 Si	½ HARD	Up to 2	70,000	38,000
	SB 98	B	Cu-2 Si-1½ Zn	SOFT	All	40,000	12,000
	SB 98		Cu-2 Si-1½ Zn	Bolt Temper	Up to ½	85,000	55,000
	"		"	Bolt Temper	Over ½ to 1	75,000	45,000
	"		"	Bolt Temper	Over 1 to 1½	75,000	40,000
Alum. Bronze	SB 150	Alloy No. 1	92 Cu-8Al		Up to ½	80,000	40,000
	"	Alloy No. 1	"		Over ½ to 1	75,000	37,500
	"	Alloy No. 1	"		Over 1	72,000	35,000
	SB 150	Alloy No. 2	Cu-10A1-5 Ni-2.5 Fe		½ to 1	100,000	50,000
	"	Alloy No. 2	"		Over 1 to 2	90,000	45,000
	"	Alloy No. 2	"		Over 2 to 4	85,000	42,000
	SB 150	Alloy No. 3	Cu-7Al-2.5 Fe		Up to ½	80,000	40,000
	"	Alloy No. 3	"		Over ½ to 1	75,000	35,000
	"	Alloy No. 3	"		Over 1 to 2	70,000	32,000

$$\tau = \frac{T_R r}{J} = \frac{16\mu P\, D_h r}{\pi D^4} \tag{7}$$

Eq 7 shows that the shearing stress will vary from zero at the bolt axis to a maximum at the outside diameter.

Combined stresses

If the maximum shear theory is accepted as the criterion for incipient yielding, the stress intensity at any point can be readily evaluated by considering Mohr's circle (Fig 3):

$$S = 2\sqrt{\left(\frac{\sigma}{2}\right)^2 + \tau^2} \tag{8}$$

Substituting Eq 3 and 7 into Eq 8, the stress intensity becomes

$$S = \frac{32\mu P\, D_h}{\pi D^4}\sqrt{\left(\frac{D^2}{8\mu D_h}\right)^2 + r^2} \tag{9}$$

Average stress intensity

The stress intensity across the bolt section can now be determined by means of the following integral:

$$S_{av} = \frac{1}{A}\int_o^{D/2} S\, da \tag{10}$$

where, in an annular element as shown in Fig 2, the elemental area, dA, is $2\pi r\, dr$ and the area, A, is $\pi D^2/4$. Hence:

$$S_{av} = \frac{8}{D^2}\int_o^{D/2} S\, r\, dr \tag{11}$$

Substituting the value of the stress intensity, S, at any point, Eq 9, into Eq 11 yields

$$S_{av} = \frac{256\mu P\, D_h}{\pi\, D^6}\int_o^{D/2} r\sqrt{r^2 + \left(\frac{D^2}{8\mu D_h}\right)^2}\, dr \tag{12}$$

which integrates to

$$S_{av} = \frac{P}{6\pi\mu^2\, D_h^2 D^3}\left[(D^2 + 16\mu^2\, D_h^2)^{3/2} - D^3\right] \tag{13}$$

The average stress intensity can also be written as a function of the applied torque by solving for P in Eq 2 and substituting into Eq 13. Therefore, for applied torque in in.-lb and a coefficient of friction of 0.15, the design stress limit becomes

$$S_{av} = \frac{37T}{\pi D_N\, D_h^2 D^3}\left[(D^2 + 0.36\, D_h^2)^{3/2} - D^3\right] \tag{14}$$

Eq 2 and 13 are plotted in Fig 4 and 5 by using dimensions for unified coarse thread series bolts from ¼ in. to 3 in. dia inclusive. **Note that the torque in the charts is in ft-lb.** Fig 4 is for bolts to ⅞-in. dia; Fig 5 for bolts 1-in. to 3-in. dia. In some cases, a particular bolt size may appear in more than one curve —the 1-in. size, for example, appears in three places. The coefficient of friction is taken as 0.15. Experiments indicate that these graphs can also be used for fine threads because the friction forces in Eq 1 will change by less than 2.5%. The torque scales cover the range from 0 to 12,000 ft-lb.

Watch for cases where excellent lubrication of the bolt is attained (μ = 0.1 or less), because a reduction in the coefficient of friction will cause greater bolt load (or stress) for a given applied torque. In such cases, go to the equations directly, as shown in sample problem II.

To make a conservative estimate of the bolt stresses, the lowest possible coefficient of friction should be selected. Conversely, to make a conservative estimate of the bolt preload, the highest possible coefficient of friction should be selected.

Example I—From the design charts

Given—A bolt is to be preloaded to 15,000 lb to avoid separation of the bolted plates during impact loads. Bolt material is a nickel-molybdenum steel with a minimum yield point of 46,000 psi (from Table I). Using a figure of two-thirds the yield strength gives a design limit of 30,667 psi. Assume average friction conditions; hence $\mu = 0.15$.

To find—What bolt diameter should be selected and how much tightening torque should be applied to the nut of the bolt to obtain the required initial load.

The bolt-load scale in Fig 4 goes only to 5000 lb; hence, use Fig 5. Note that there are two bolt-load scales, each relating to a group of curves. Read down from the 15,000-lb bolt-load to the 30,000-psi curve.

This intersection point directly gives the required bolt size—1-in. dia. Now move to the torque scale to the left and read: 250 ft-lb. This is the required tightening torque to obtain the preload.

Example II—From the formulas

How much tightening torque must be exerted on the nut of a ½-20 UNF, carbon steel bolt to obtain a 5000-lb preload? In this case the surfaces are smooth and well lubricated and the coefficient of friction is estimated to be 0.08. Determine also the resulting stresses in the bolt.

The helix angle, α, can be calculated from

$$\tan\alpha = \frac{1}{2\pi n r_t}$$

and angle θ = 30 deg for V-threads.

Average value of the pitch diameter, for a ½-20 UNF-bolt with class 2A fit, from "American Standard Unified Screw Threads (ASA B1.1-1960)," is 0.464 in. Hence $r_t = 0.232$ in.

From Mark's *Handbook*, 4th ed, p 899, value for $D_h = 0.8125$ in.

As previously stated, $r_c \approx ½\ D_h$. Thus $r_c = 0.406$. Also, we know that $\theta = 30$ deg. Hence, from Eq 1 the required tightening torque is: $T = 310$ in.-lb.

Average stress intensity is calculated from Eq 13 by employing value of $D = 0.4507$ in. (obtained from ASA B1.1):

$$S_{av} = 33{,}811 \text{ psi}$$

Multiplying this value by 3/2 gives the required minimum yield point of the material: 50,717 psi. From the carbon steel materials, either SA 261 or 325 will satisfy this requirement.

Turn the page now for a table and formula for selecting the proper bolt preload in a gasketed cylinder head or pressure vessel.

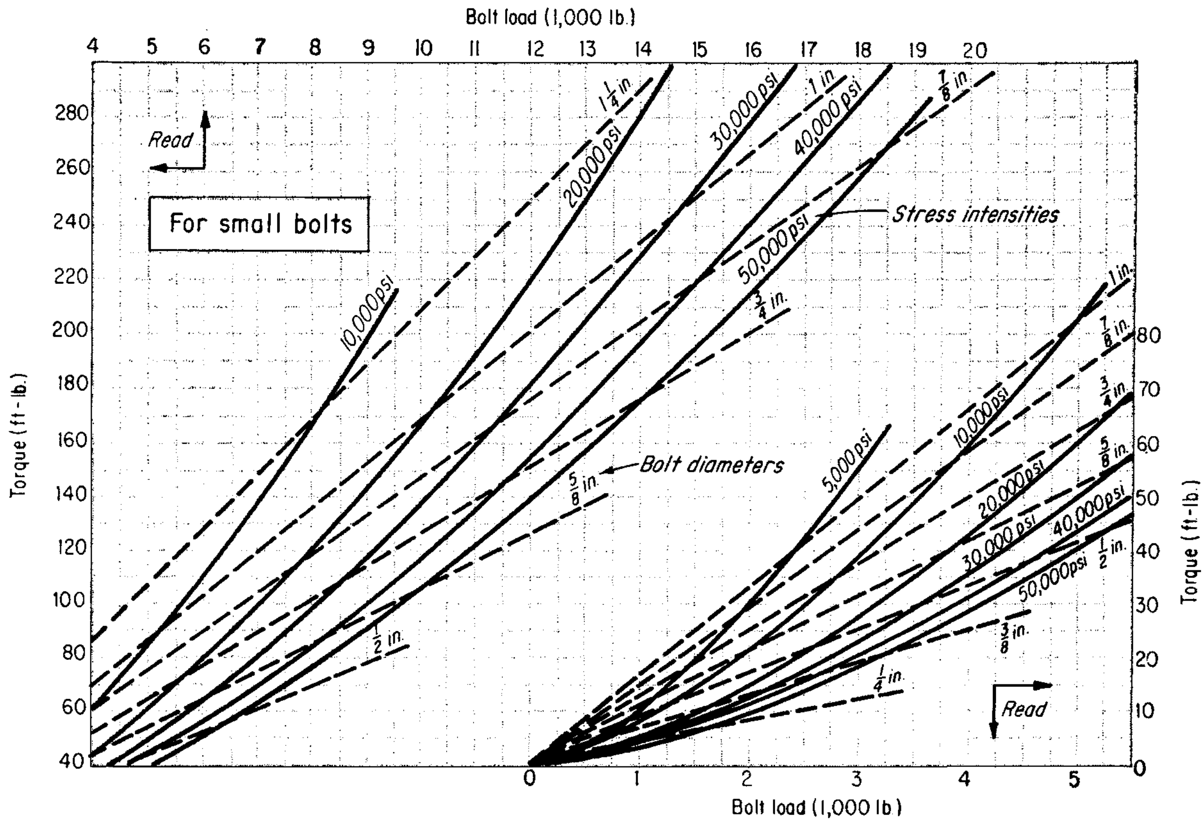

4 & 5. Tightening torque vs bolt load

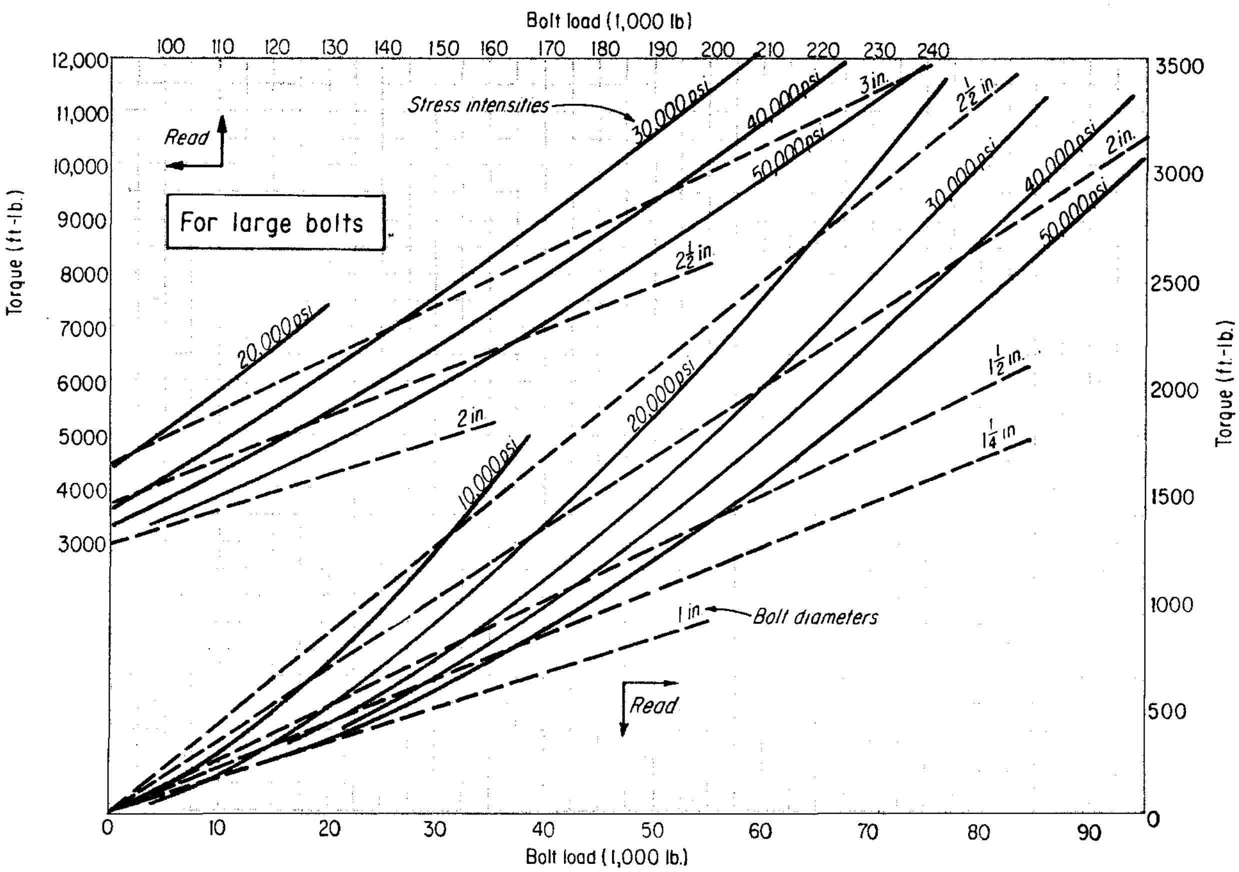

Stresses in Curved Bars

These equations quickly give the stress concentration factors and true bending stresses for a wide variety of cross-sections.

W. H. Sparing & R. P. Radwill

BARS with curvatures ranging from large-radius arcs to sharp-angle bends are common components in machines and products. Yet many designers are hazy about how to evaluate the true stresses when such bars are subjected to bending loads.

An analytical method for determining such stresses has been developed by S. Timoshenko in his book *Strength of Materials—Part I* (Van Nostrand, Princeton, NJ, 1956). We have verified the accuracy of Timoshenko's method by subjecting various curved bars to bending loads and measuring the strains in the fibers with electric strain gages. The measurements indicate close agreement with theory—even when the cross sections are complex and the bend radius is much smaller than the height of the section being tested.

Timoshenko's method, however, requires evaluation of an integral relating to the cross section of the bar. Integration can be cumbersome. Hence, in addition to presenting his method as a series of step-by-step equations, we have tabulated the solution of the integral for 12 common geometric shapes. Three problems are included to illustrate the use of the equations.

Curved-bar theory

In a straight bar, Fig 1, during bending the fibers are elongated on the convex side and shortened on the concave side. Those on the neutral axis remain at their original length. The strains of compression and tension fibers equidistant from the gravity axis are equal in magnitude because the elemental lengths between two plane sections before bending are equal. Strain is determined as the quotient of the length of deformation divided by the original length.

In a curved bar, Fig 2, the deformations at equidistant points above and below the neutral axis are equal, but the elemental lengths between two radial sections vary. Thus the strains due to bending for compression and tension fibers equidistant from the neutral axis are not equal. Specifically, the elemental arc at the concave surface is minimum and the deformation is maximum. Therefore, the strain on this surface is maximum.

To meet the condition of equilibrium on a cross section, the neutral axis (the axis where there is no stress) cannot coincide with the gravity axis. The neutral axis shifts toward the concave surface, so that the summation of the distributed normal forces on the cross section is equal to zero.

The key equation in curved bar analysis is given below. It gives the location of the neutral surface with respect to the center of curvature for any cross section (refer to Fig 3 and to the list of symbols):

$$r = \frac{A}{\displaystyle\int_A \frac{dA}{v}} \tag{1}$$

where

$$dA = L\,dv$$

For a rectangle, p 64, dimension r becomes

$$r = \frac{A}{b \ln(c/a)} \tag{2}$$

Starting with Eq 1, the procedure and equations for determining the bending stress with the stress concentration due to the curvature are as follows:

Distance e between center-of-gravity and neutral axes, Fig 2, is obtained from the equation

$$e = R - r \tag{3}$$

where the value for R is known or calculated from the relationship $R = a + d$, and the value for r is obtained from Eq 1 for the particular cross section.

Factor d is the distance from the base of the section

1 . . STRAIGHT-BAR STRESS DISTRIBUTION. Fibers equidistant from neutral axis are equally stressed.

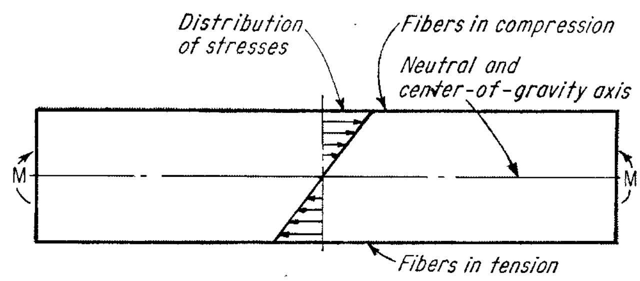

to its gravity axis. (It is calculated as shown in Problem II). Hence

$$h_B = d - e \tag{4}$$

and

$$h_A = h - d + e \tag{5}$$

The *true* bending stress—the normal bending stress with the additional stress concentration—on the concave surface is

$$\sigma_B = \frac{M h_B}{Aea} \tag{6}$$

and on the convex surface is

$$\sigma_A = \frac{M h_A}{Aec} \tag{7}$$

The *nominal* bending stress—*without* the stress concentration—can be obtained from the familiar expression

$$S_B = \frac{M}{Z_B} \qquad S_A = \frac{M}{Z_A} \tag{8}$$

where Z is the section modulus equal to

$$Z_B = I_{CG}/d \qquad Z_A = I_{CG}/(h-d) \tag{9}$$

and where

$$I_{CG} = I_{xx} - Ad^2 \tag{10}$$

The stress concentration factor is the ratio of σ_B/S_B or σ_A/S_A. Usually the first of these factors will be greater than unity, and the other less than unity. The factor that is greater than unity is usually of greatest interest.

To simplify the analysis of curved bars, twelve of the most common shapes are illustrated on the next page with equations for the integral which appears in the denominator of Eq 1.

Problem I—Rectangular curved bar

Given—Rectangular-section bar, Fig 2, with these dimensions in inches: $h = 2½$, $b = 1¼$, $R = 1¾$, $a = ½$

Solution—From the geometry of the figure

$A = 3.125$ in.^{2}; $d = h/2 = 1.250$ in.

$h-d = 1.250$ in.; $I_{CG} = 1.628$ in.^{4}; $Z_B = 1.302$ in.^{3}

From Eq 2

$$r = \frac{3.125}{1.25 \ln (3/0.5)} = 1.395 \text{ in.}$$

text continued, next page

SYMBOLS

- a = Inner radius of curvature, in.
- A = Area of section, in.^{2}
- b = Width of section, in.
- c = Outer radius of curvature, in.
- d = Distance from base of section to gravity axis, in.
- e = Distance of the neutral axis from gravity axis, in.
- h = Height of section, in. ($h = h_B + h_A$)
- h_B = Distance from inner radius of curvature to neutral axis, in.
- h_A = Distance from neutral axis to outer radius of curvature, in.
- I_{xx} = Moment of inertia about the base of section, in.^{4}
- I_{CG} = Moment of inertia about the center of gravity of section, in.^{4}
- L = Length of differential area, in. (see fig 3)
- ln = Natural logarithm (to base 2.718)
- M = Bending moment with respect to gravity axis, in.-lb
- r = Distance from center of curvature to neutral axis, in.
- R = Distance from center of curvature to gravity axis, in. ($R = a + d$)
- S_B = Nominal bending stress, lower fiber, psi
- S_A = Nominal bending stress, upper fiber, psi
- v = Distance from center of curvature to a differential area (dA) of the section, in.
- Z_B = Section modulus, lower fiber, in.^{3}
- Z_A = Section modulus, upper fiber, in.^{3}
- σ_B = Bending stress with stress concentration at the concave surface, psi
- σ_A = Bending stress with stress concentration at the convex surface, ps

2 . . CURVED-BAR GEOMETRY. Neutral axis does not coincide with center-of-gravity axis.

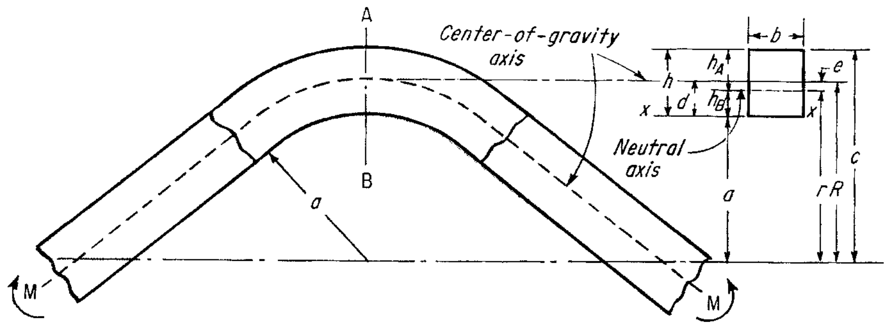

3 . . ELEMENTAL SECTION of curved bar with varying cross section.

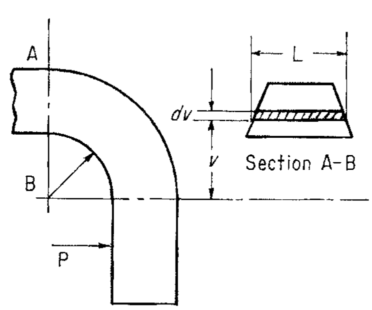

RECTANGLE

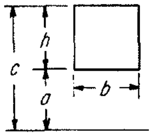

$$\int \frac{dA}{v} = b \ln \frac{c}{a}$$

TRAPEZOID

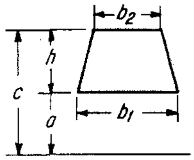

$$\int \frac{dA}{v} = \left[\frac{b_1 c - b_2 a}{h} \ln \frac{c}{a}\right] - (b_1 - b_2)$$

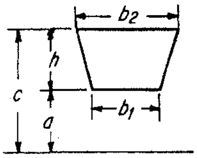

$$\int \frac{dA}{v} = \left[\frac{b_1 c - b_2 a}{h} \ln \frac{c}{a}\right] + (b_2 - b_1)$$

TRIANGLE

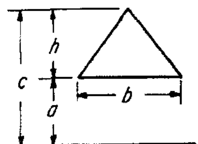

$$\int \frac{dA}{v} = \left[\frac{bc}{h} \ln \frac{c}{a}\right] - b$$

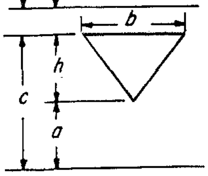

$$\int \frac{dA}{v} = b - \left[\frac{ba}{h} \ln \frac{c}{a}\right]$$

CIRCLE

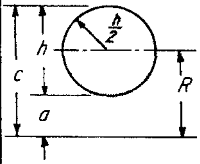

$$\int \frac{dA}{v} = 2\pi\left[R - \left(R^2 - \frac{h^2}{4}\right)^{1/2}\right]$$

SEMI-CIRCLE

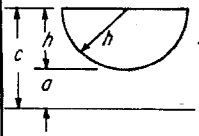

$$\int \frac{dA}{v} = 2h + \pi c - \frac{\pi}{45}(\theta + \beta)(c^2 - h^2)^{1/2}$$

where:

$$\theta = \arc\tan \frac{c - h}{(c^2 - h^2)^{1/2}}\text{, deg}$$

$$\beta = \arc\tan \frac{h}{(c^2 - h^2)^{1/2}}\text{, deg}$$

SEMI-CIRCLE

When $h < a$

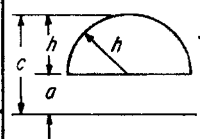

$$\int \frac{dA}{v} = a\pi - 2h - \frac{\pi}{45}(\theta - \beta)(a^2 - h^2)^{1/2}$$

$$\theta = \arc\tan \frac{a + h}{(a^2 - h^2)^{1/2}}\text{, deg}$$

$$\beta = \arc\tan \frac{h}{(a^2 - h^2)^{1/2}}\text{, deg}$$

When $a < h$

$$\int \frac{dA}{v} = a\pi - 2h + 2(h^2 - a^2)^{1/2} \ln\left[\frac{a + h + (h^2 - a^2)^{1/2}}{a + h - (h^2 - a^2)^{1/2}}\right]$$

When $a = h$ $\quad \int \frac{dA}{v} = 1.1416h$

From Eq 3, 4, and 5

$e = 1.750 - 1.395 = 0.355$ in.
$h_B = 1.250 - 0.355 = 0.895$ in.
$h_A = 1.250 + 0.355 = 1.605$ in.

From Eq 6 and 7

$$\sigma_B = \frac{0.895M}{3.125 \times 0.355 \times 0.500} = 1.614M$$

$$\sigma_A = \frac{1.605M}{3.125 \times 0.355 \times 3.00} = 0.482M$$

From Eq 8

$$S_B = S_A = \frac{M}{1.302} = 0.768M$$

Therefore the magnitude of the stress concentration factor is $\sigma_n/s_n = 1.614/0.768 = 2.10$

Problem II—C-clamp

The C-clamp at right has a contant cross section around the ⅜-in. radius curvature. The stress concentration factor due to the curvature will remain constant, but the nominal stress will vary directly as the bending moment. Therefore, the maximum bending stress including stress concentration will occur at the inner fiber of a section (section A-B) taken vertically through the center of the radius.

A systematic approach to determine the area, neutral axis, and moment of inertia of section A-B is tabulated with the illustration. These properties are obtained by adding and subtracting rectangles. For computing the moment of inertia, each rectangle is taken from the base line x—x. This method is especially convenient when calculating machines are used in the numerical work. Thus from the table: $\Sigma A = 0.2265$; $\Sigma I_{xx} = 0.0574$.

The nominal vertical bending stress in tension and compression is now calculated. Subscripts A and B refer to the outer and innner fibers, respectively.

$d = 0.0911/0.2265 = 0.402$ in.
$h - d = 0.875 - 0.402 = 0.473$ in.
$R = 0.375 + 0.402 = 0.777$ in.
$I_{CG} = 0.0574 - (0.0911)(0.402)^2 = 0.0208$ in.^{4}
$Z_B = 0.0208/0.402 = 0.052$ in.^{3}
$Z_A = 0.0208/0.473 = 0.044$ in.^{3}
$M = 300 \times 2.527 = 760$ lb-in.

QUARTER-CIRCLE

$$\int \frac{dA}{v} = h + \frac{\pi c}{2} - \frac{\pi}{90}(\theta + \beta)(c^2 - h^2)^{1/2}$$

where:

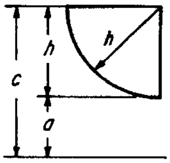

$$\theta = \arctan \frac{c - h}{(c^2 - h^2)^{1/2}}\text{, deg}$$

$$\beta = \arctan \frac{h}{(c^2 - h^2)^{1/2}}\text{, deg}$$

QUARTER-CIRCLE

When $h < a$

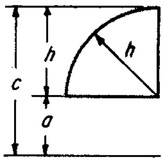

$$\int \frac{dA}{v} = \frac{a\pi}{2} - h - \frac{\pi}{90}(\theta - \beta)(a^2 - h^2)^{1/2}$$

When $a < h$

$$\int \frac{dA}{v} = \frac{a\pi}{2} - h + (h^2 - a^2)^{1/2} \ln \left[\frac{a + h + (h^2 - a^2)^{1/2}}{a + h - (h^2 - a^2)^{1/2}}\right]$$

When $a = h$

$$\int \frac{dA}{v} = 0.5708h$$

where:

$$\theta = \arctan \frac{a + h}{(a^2 - h^2)^{1/2}}\text{, deg}$$

$$\beta = \arctan \frac{h}{(a^2 - h^2)^{1/2}}\text{, deg}$$

REVERSE-FILLET

$$\int \frac{dA}{v} = \left[h \ln \frac{c}{a}\right] - h - \frac{\pi}{2}c + \frac{\pi}{90}(\theta + \beta)(c^2 - h^2)^{1/2}$$

Where

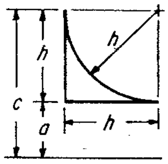

$$\theta = \arctan \frac{c - h}{(c^2 - h^2)^{1/2}}\text{, deg}$$

$$\beta = \arctan \frac{h}{(c^2 - h^2)^{1/2}}\text{, deg}$$

REVERSE-FILLET

When $h < a$

$$\int \frac{dA}{v} = \left[h \ln \frac{c}{a}\right] - \frac{a}{2}\pi + h + \frac{\pi}{90}(\theta - \beta)(a^2 - h^2)^{1/2}$$

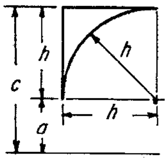

$$\theta = \arctan \frac{a + h}{(a^2 - h^2)^{1/2}}\text{, deg}$$

$$\beta = \arctan \frac{h}{(a^2 - h^2)^{1/2}}\text{, deg}$$

When $a < h$

$$\int \frac{dA}{v} = \left[h \ln \frac{c}{a}\right] + h - \frac{\pi}{2}a - (h^2 - a^2)^{1/2} \ln \left[\frac{a + h + (h^2 - a^2)^{1/2}}{a + h - (h^2 - a^2)^{1/2}}\right]$$

When $a = h$

$$\int \frac{dA}{v} = 0.1223h$$

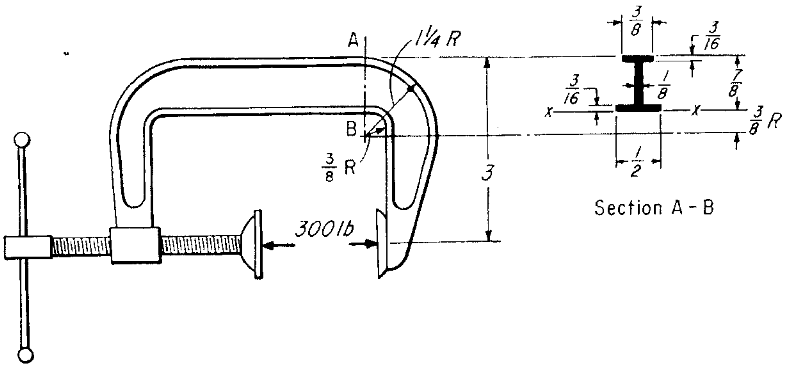

CROSS-SECTION PROPERTIES

RECTANGLE	AREA, A	d	$A \times d$	I_{xx}
$^3/_8 \times ^7/_8$	+0.3281	0.4375	+0.1436	+0.0837
$^3/_8 \times ^3/_{16}$	+0.0703	0.0938	+0.0066	+0.0008
$^1/_4 \times ^{11}/_{16}$	−0.1719	0.3438	−0.0591	−0.0271
Summation, Σ	=0.2265		=0.0911	=0.0574

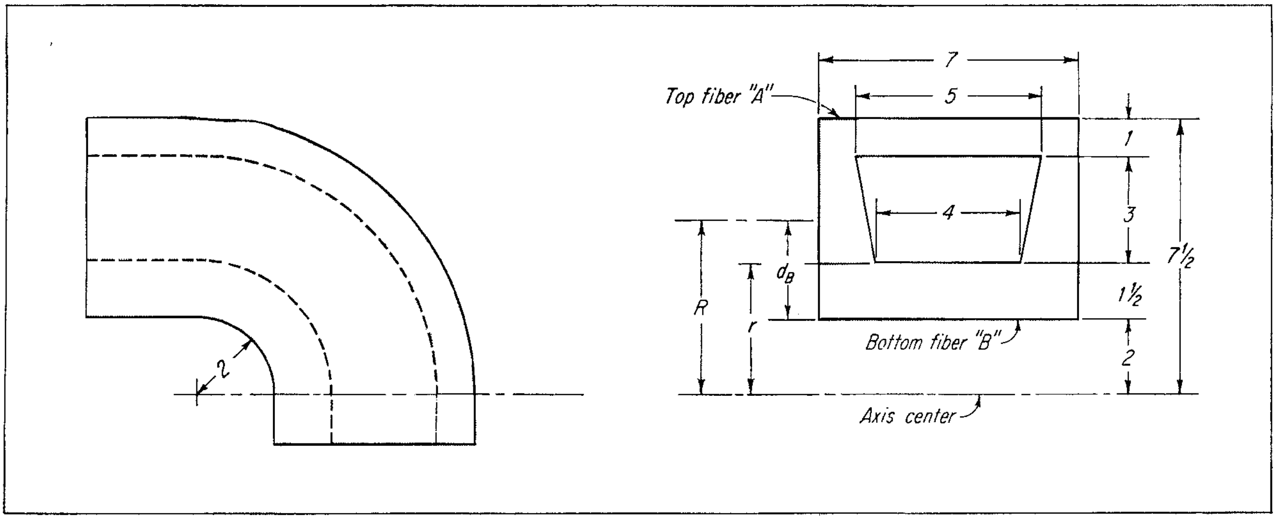

HOLLOW CURVED BEAM (for Problem III)

Thus the nominal stresses are

$S_A = 760/0.044 = 17{,}300$ psi (compression)
$S_B = 760/0.052 = 14{,}600$ psi (tension)

To compute the effect of the bend, section A-B is divided into three rectangles—lower, center, and top. The bend integral for a rectangle is calculated for each:

Lower rectangle

$$\int \frac{dA}{v} = \frac{1}{2}\left(\ln \frac{9/16}{3/8}\right) = 0.2027 \text{ in.}$$

Inner rectangle

$$\int \frac{dA}{v} = \frac{1}{8} \ln\left(\frac{1\,1/16}{9/16}\right) = 0.0795 \text{ in.}$$

Upper rectangle

$$\int \frac{dA}{v} = \frac{3}{8} \ln\left(\frac{1\,1/4}{1\,1/16}\right) = 0.0611 \text{ in.}$$

Sum of the integrals = 0.3433 in. Hence

$$r = \frac{A}{\int \frac{d_A}{v}} = \frac{0.2265}{0.3433} = 0.660 \text{ in.}$$

$$\begin{aligned} e &= 0.777 - 0.660 = 0.117 \text{ in.} \\ h_B &= 0.402 - 0.117 = 0.285 \text{ in.} \\ h_A &= 0.473 + 0.117 = 0.590 \text{ in.} \end{aligned}$$

The corrected (true) bending stresses are then

$$\sigma_B = \frac{(760)\,(0.285)}{(0.227)\,(0.117)\,(0.375)} = 21{,}700 \text{ psi (tension)}$$

$$\sigma_A = \frac{(760)\,(0.590)}{(0.227)\,(0.117)\,(1.250)} = 13{,}500 \text{ psi (compression)}$$

Thus the nominal bending stress in tension should be multiplied by a factor of 21,700/14,600 = 1.49 to obtain the true bending stress in tension. Also, the true compression stress in bending is 13,500/17,300 = 0.78 of the nominal value. Hence, it is reduced by 22%. These figures indicate that stress concentration must be considered to avoid large errors in evaluating curved-bar bending stress, especially when hardened material or fatigue loading is involved.

Problem III—Hollow sections

Frequently hollow irregular sections, above, are employed as machine members. From the geometry of the section (calculated as described in Problem II): $A = 25.00$ in.^{2}, $d = 2.585$ in., $R = 4.585$ in., $I_{CG} = 85.03$ in.^{4}, $z_B = 32.89$ in.^{3}

Outer rectangle

$$\int \frac{d_A}{v} = 7 \ln \frac{7.5}{2.0} = 9.252 \text{ in.}$$

Inner trapezoid

$$\int \frac{d_A}{v} = \left(\frac{4 \times 6\frac{1}{2} - 5 \times 3\frac{1}{2}}{3}\right)\left(\ln \frac{6\frac{1}{2}}{3\frac{1}{2}}\right) + (5 - 4)$$
$$= 2.754 \text{ in.}$$

$$r = \frac{25.00}{9.252 - 2.754} = 3.847 \text{ in.}$$

$$\begin{aligned} e &= 4.585 - 3.847 = 0.738 \text{ in.} \\ h_B &= 2.585 - 0.738 = 1.847 \text{ in.} \end{aligned}$$

$$\sigma_B = \frac{1.847\, M}{(25.00\,(0.738)\,(2.000)} = 0.0501\, M$$

$$s_B = M/32.89 = 0.0304\, M \text{ (tension)}$$

Stress concentration factor is 0.0501/ 0.0304 = 1.65.

Stresses Around Holes

Stress-concentration factors for plates with single and multiple holes. You'll find them indispensable for actual problems.

William Griffel

1. Beams subjected to bending

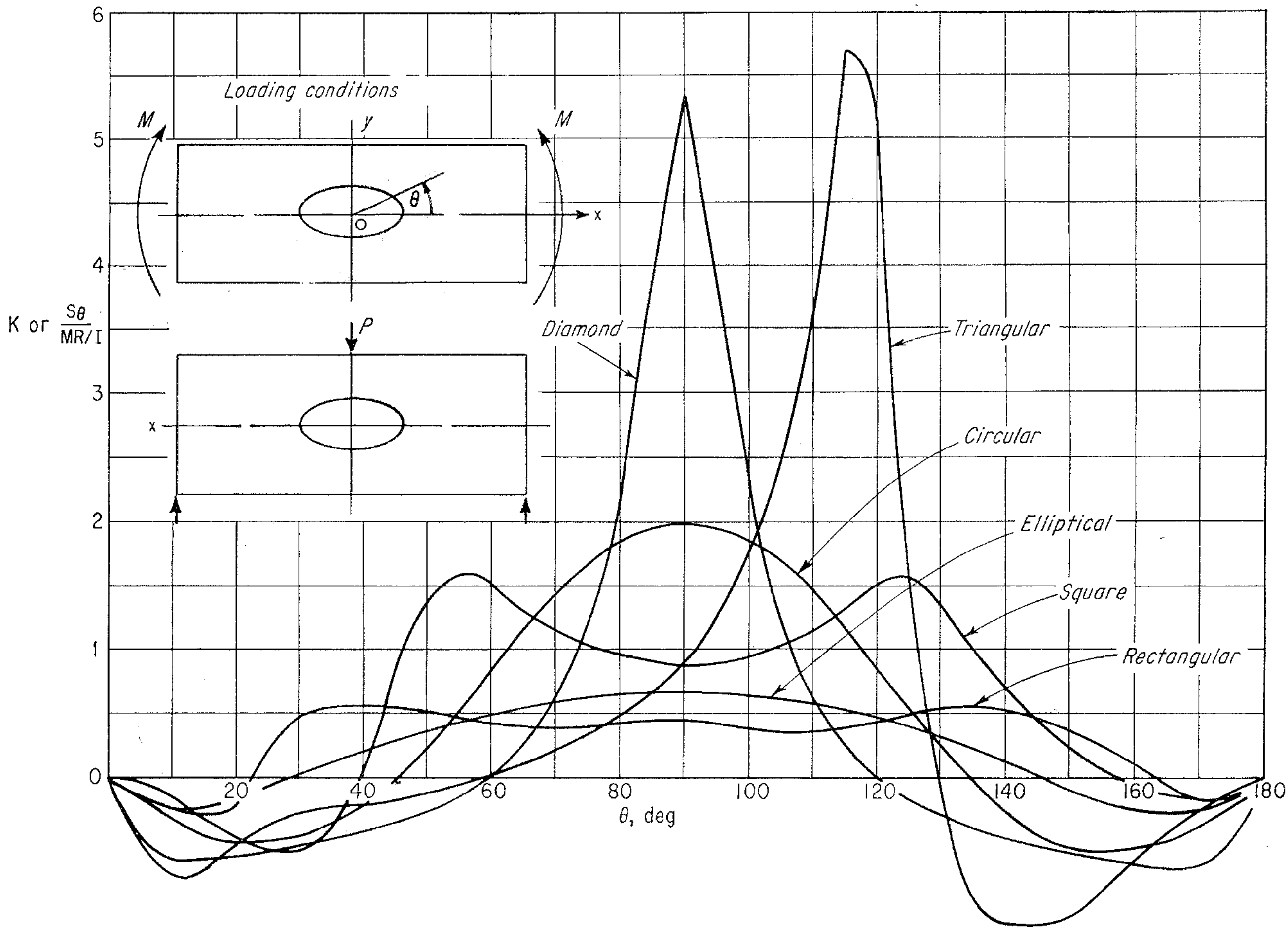

IF you use plates and beams as machine members you doubtless know that stress tends to concentrate at the holes. You may have found that this "bunching up" of stress can cause failure at loadings that are normally considered safe. Stress concentration is also a problem when parts are subjected to shock and vibration, to repeated or alternating stresses, and to extreme temperature conditions.

It is quite a simple matter to predict the actual stress around holes if you know the *stress concentration factor* (K). This factor varies according to these conditions:

1) type of hole (circular, elliptical, square, diamond, triangular, or rectangular)

2) grouping of holes (if there are more than one)

3) type of loading (tension, bending, combined stresses)

The data presented in this series cover a wide range of such conditions. Much of the data is based on theory and experimental work by the Russian scientist G. N. Savin. An English translation of his book, *Stress Concentration Around Holes,* is now available from Pergamon Press.

The first article in this series ("Plates with holes,"* Sept 16 '63, p98) covered plates under tension and plates with multi-row holes. This article presents data on plates under pure bending (simple beam and cantilever), plates under combined loading, and the effect of large bales, edge holes, and multiple holes in narrow strips. Subsequent articles will cover plates under cylindrical, spherical, and twisting loading, and round plates with multiple holes.

SIMPLE-BEAM LOADING

Here we have a case of pure bending resulting from applied moments at the ends of the plate or from the plate being loaded as a simple beam (Fig 1). The data, theoretically, are for an "infinite" plate, but this should not restrict applications because tests have shown that a hole does not appreciably affect the stresses at a distance of more than a few diameters from its edge. Specifically, a distance of five diameters from the hole center can be regarded as an infinite distance, and the data will provide a good approximation to cases where the hole diameter is $\frac{1}{5}$ or less of the total width of the plate. Note that the x axis coincides with the neutral axis of the plate.

For a plate without a hole and subjected to bending,

* Product Engineering

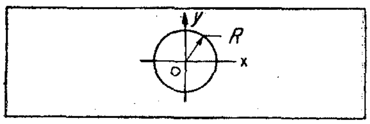

Circular hole

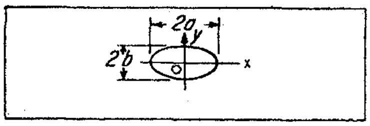

Elliptical hole a/b = 3

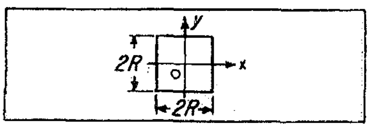

Square hole

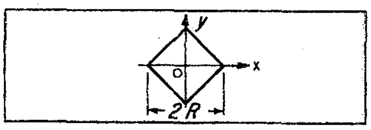

Diamond hole

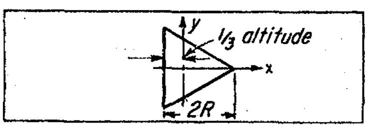

Triangular hole

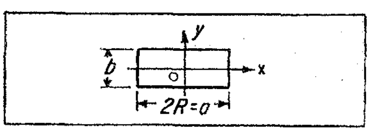

Rectangular hole a/b = 3.2

Symbols

a, b = dimensions of elliptical or rectangular holes, in.

c = distance from neutral axis to outer fiber, in.

d = distance from center of hole to cantilever support, in.

I = moment of inertia of transverse cross section of the plate about the neutral axis through its cross section, $in.^4$

K = stress concentration factor, dimensionless

L = length of beam, in.

$m = (a - b)/(a + b)$

M = applied moment, lb-in.

P = applied load, lb

Q = factor for designating distances between holes

R = size constant. For an elliptical hole, $R = \frac{1}{2}(a + b)$; for a circle, R = radius; for other types of holes, see dimensions of the holes on the applicable charts

r = radial distance to point of stress, in.

S_{max} = actual maximum stress, including effect of stress concentrations, psi

S_θ = tangential stress along contour of a hole at a point located by angle θ, psi

θ = angle which locates point of tangential stress, deg the stress can be calculated from the well known basic formula

$$S = \frac{Mc}{I} \tag{1}$$

Now, let us see how the type of hole affects the stress equations.

Elliptical hole

The equation for the tangential stress along the contour of an elliptical hole is

$$S_\theta = \frac{MR}{I}\left[\frac{(1+m-2m^2)\sin\theta+(m-1)\sin 3\theta}{1+m^2-2m\cos 2\theta}\right] \tag{2}$$

where

a = semi axis along the x axis, in.
b = semi axis along the y axis, in.
$m = (a - b)/(a + b)$
R = constant characterizing the size of the hole in. For an ellipse, $R = \frac{1}{2}(a + b)$
S_θ = tangential stress along the contour of the hole at a point located by θ where θ is measured counterclockwise from the x axis.

The curve in Fig 1 is for an ellipse with 3:1 axis proportions. These proportions are most commonly employed. Factor m then equals ½, and Eq 3 reduces to

$$S_\theta = \frac{MR}{I}\left[\frac{4\sin\theta - 2\sin 3\theta}{5 - 4\cos 2\theta}\right] \tag{3}$$

The maximum value of S_θ occurs at 90 deg, in which

2. Cantilever beams with holes

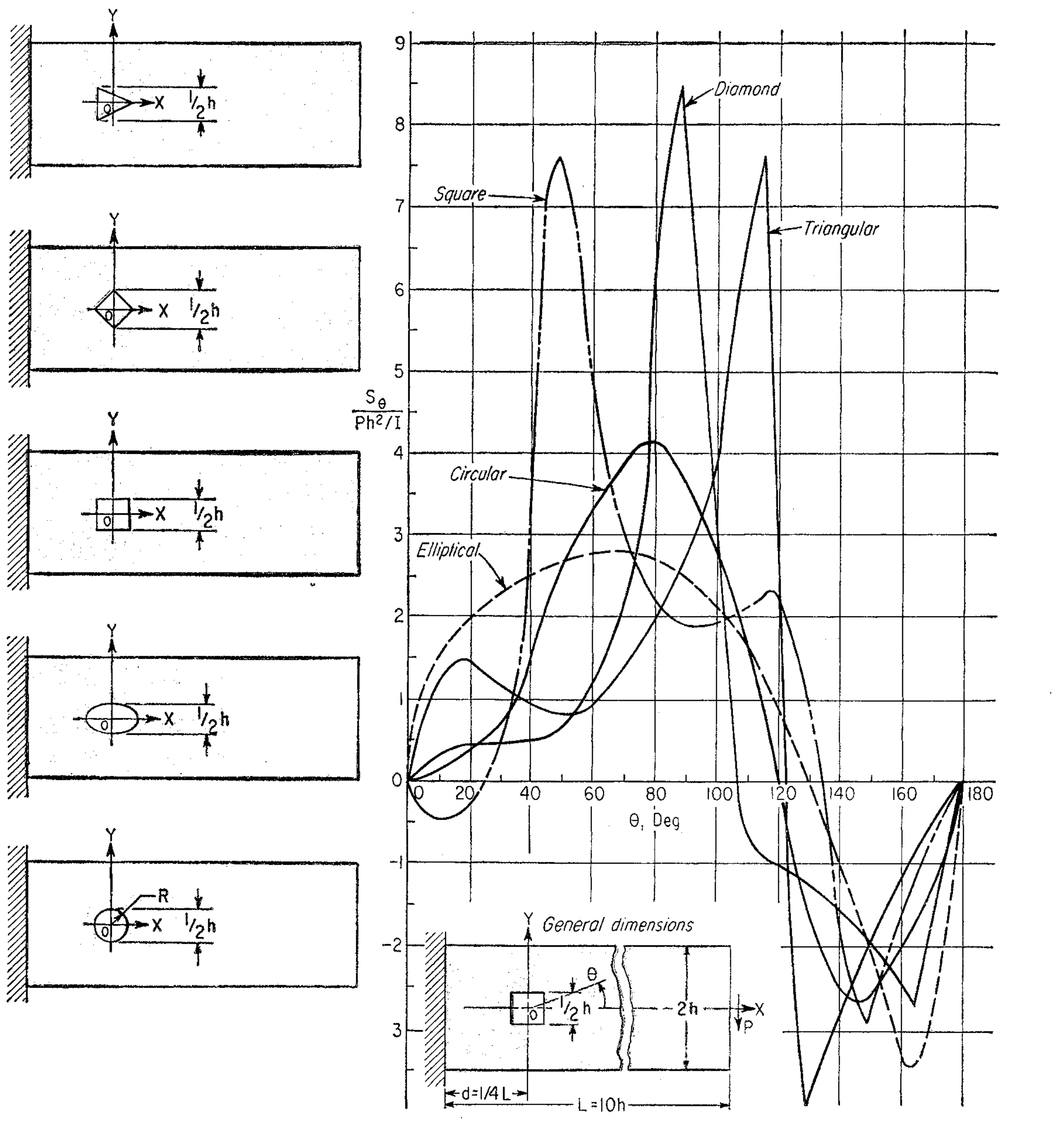

case Eq 4 reduces to

$$S_{max} = \frac{Mb}{I}\left(1 + \frac{b}{a}\right) = \frac{4Mb}{3I} \tag{4}$$

If $b = 0$ but $a \neq 0$, as in the case of a slit along the o-x axis of length $2a$, $S_\theta = 0$. This means that a slit of length 2a parallel to the neutral axis of the strip (or beam) will not cause any stress concentration in the investigated plate.

If $a = 0$ and $b \neq 0$, as in the case of a slit of length $2b$ along the y axis, S_θ will be very large and the material will plastically deform or crack.

Circular hole

In this case $a = b$ and $m = 0$ in Eq 3. Thus

$$S_\theta = \frac{MR}{I}[\sin\theta - \sin 3\theta] \tag{5}$$

where R = radius of the circular hole.

Square hole

The equation for S_θ is

$$S_\theta = \frac{MR}{I}\left[\frac{14\sin\theta - 12\sin 3\theta - 2\sin 5\theta}{15 + 12\cos 4\theta}\right] \tag{6}$$

where $2R$ = length of a side of the square.

Diamond hole

This case is actually that of a square rotated 45 deg. The stress equation is as follows:

3. Plates subjected to combined loading (in x and y directions)

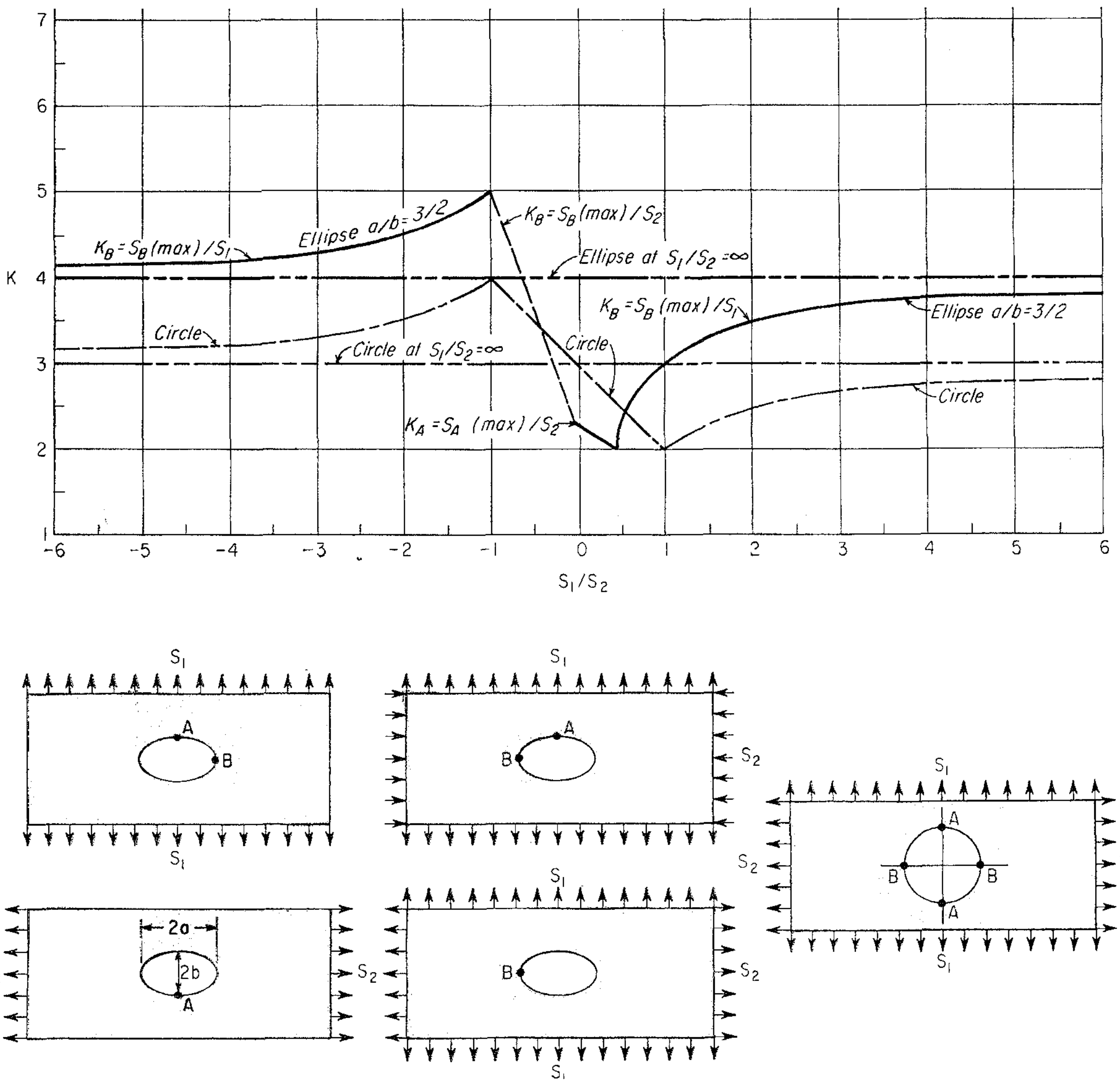

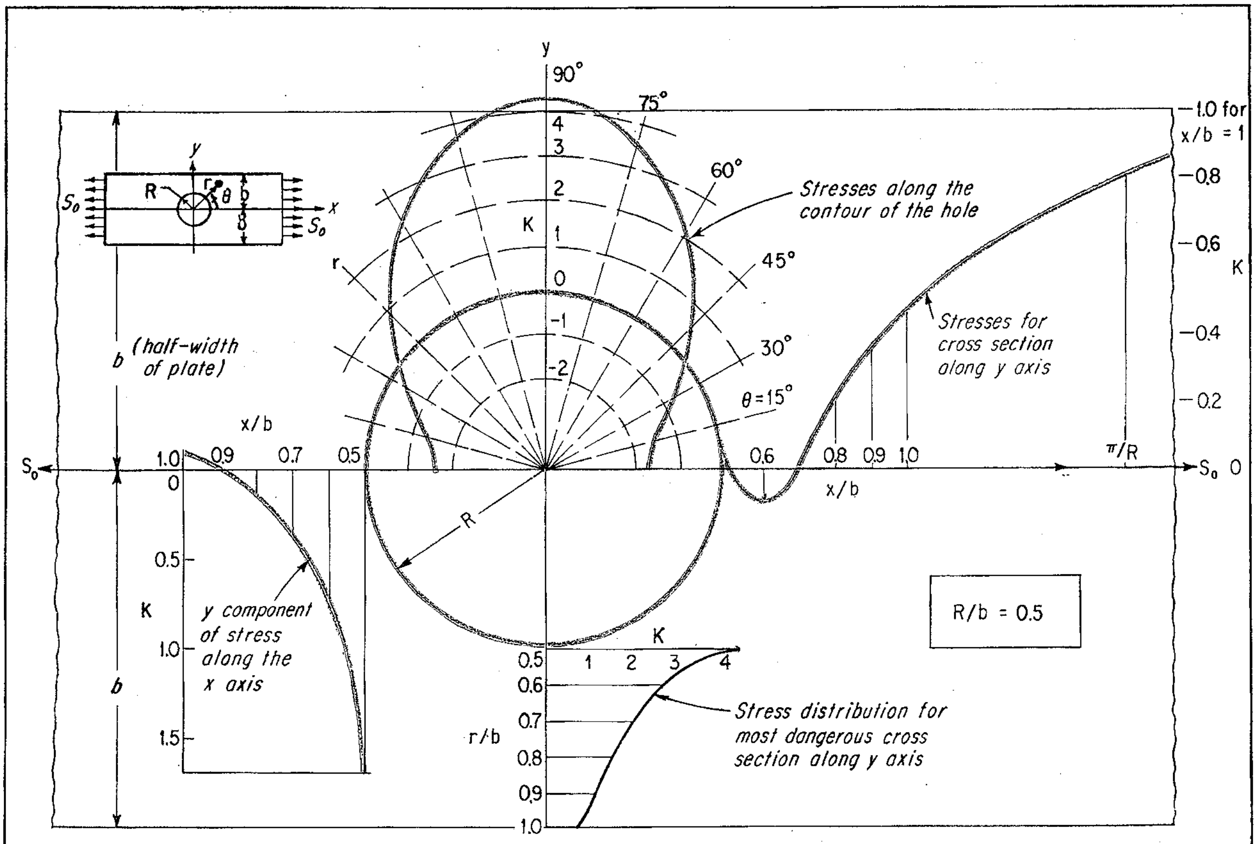

4. Stress distribution in plates with large holes

$$S_\theta = 2\,\frac{MR}{I}\left[\frac{\sin\theta - 6\sin 3\theta + \sin 5\theta}{15 - 12\cos 4\theta}\right] \quad (7)$$

where $2R$ = length of a diagonal.

Triangular hole

This is the case of an equilateral triangle with the y axis through its center of gravity (at one-third the altitude)

$$S_\theta = 3\,\frac{MR}{I}\left[\frac{\sin\theta - 3\sin 3\theta + \sin 4\theta}{13 - 12\cos 3\theta}\right] \quad (8)$$

where $2R$ = height of the triangle.

Rectangular hole

This is the special case where $a/b = 3.2/1$

$$S_\theta = \frac{MR}{I} \times$$

$$\left[\frac{1228\sin\theta - 490\sin 3\theta - 112\sin 5\theta - 48\sin 7\theta}{1825 - 1580\cos 2\theta + 720\cos 4\theta + 480\cos 6\theta}\right] \quad (9)$$

where $2R = a$.

There is a good agreement of the theoretical data in Fig 1 with photoelastic experimental findings. In the case of circular holes, for example, Savin has found that the curve gives satisfactory results even when the diameter of the circular hole amounts to as much as ⅗ the width of the plate.

Sample problem—diamond hole

Consider a plate 14 in. high x 0.25 in. thick, with a diamond hole at its center. Diagonal $2R$ = 4 in. Applied moment M = 25,000 in. lb:

$$I = 0.25\,(14 - 4)^3/12 = 20.8 \text{ in.}^4$$

From the curve in Fig 1, the maximum value of K is 5.35. Hence

$$S_{max} = K\,\frac{MR}{I} = \frac{5.35\,(25{,}000)\,(7)}{20.8} = 12{,}900 \text{ psi}$$

Off-centered axes

If the center of the hole is not situated on the neutral axis of the beam (or plate) but at a distance d from it, as shown below, the problem will be reduced to: a)

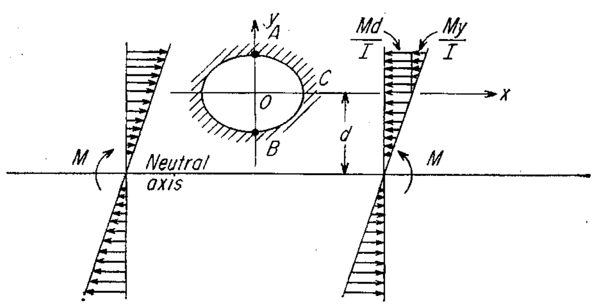

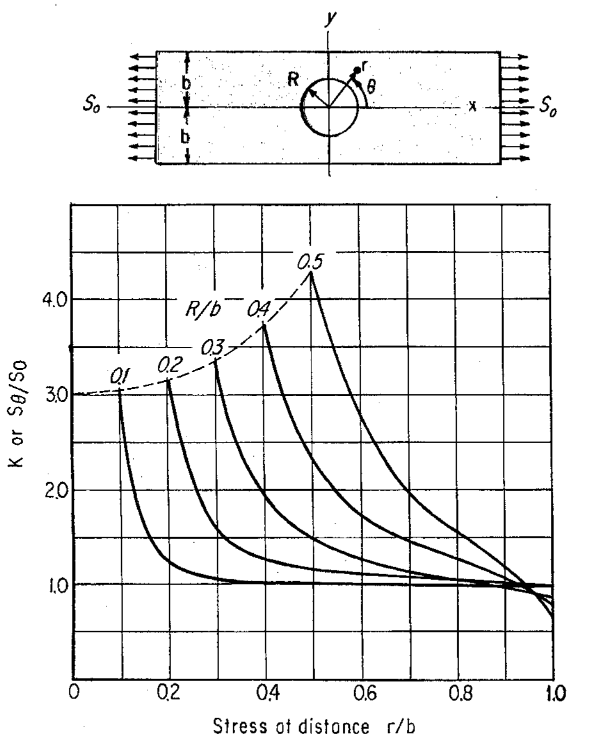

5. Stress distribution in plates with various hole sizes

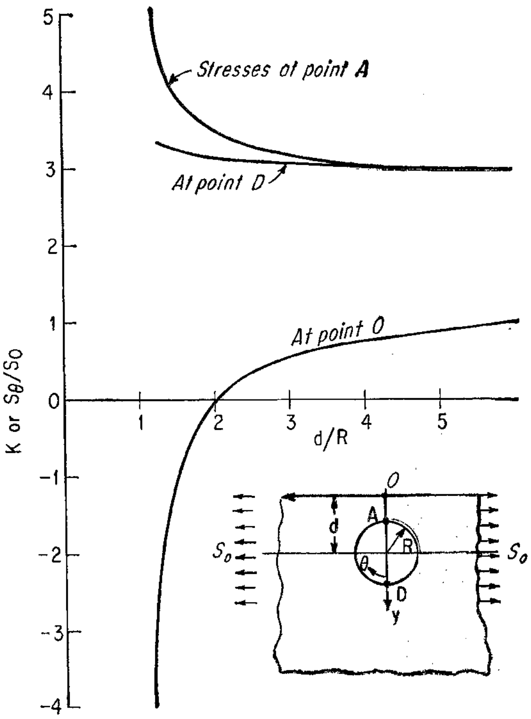

6. Effect of edge holes

calculation of tension in the direction of the neutral axis by the stresses $S = Md/I$, and b) pure bending of the plate with a hole the center of which is in the neutral axis, $S_x = My/I$. Thus for an elliptical hole the stress at point A is

$$S_\theta = \frac{M}{I}\left[(b+d) + \frac{b}{a}(b+2d)\right]$$

If $d = 0$

$$S_\theta = \frac{Mb}{I}\left[1 + \frac{b}{a}\right]$$

which is the same as Eq 4.

The stress at point B:

$$S_\theta = \frac{M}{I}\left[(d-b) + \frac{b}{a}(2d-b)\right]$$

The stress at point C:

$$S_\theta = \frac{Md}{I}$$

CANTILEVER BENDING

This is the case of a cantilever rigidly supported at one end (Fig 2) with length L, height $2h$, and transverse load P applied at the free end. The hole center is on the bar axis (x axis) and is at a distance d from the fixed end. The effect of the hole shape now follows:

Elliptical hole

The stress distribution around an elliptical hole of semiaxis a and b (Fig 2) can be determined by the following equation

$$S_\theta = -\frac{P(L-d)}{I} \times \left[\frac{(1+m-2m^2)\sin\theta + (m-1)\sin 3\theta}{1-2m\cos 2\theta + m^2}\right] - \frac{P}{I}\left[\frac{[2h^2+R^2(m^2-1)]\sin 2\theta + R^2(1-m)\sin 4\theta}{1-2m\cos 2\theta + m^2}\right] \quad (10)$$

where $m = \dfrac{a-b}{a+b}$

$$R = \frac{a+b}{2}$$

Comparing Eq 10 with Eq 4, it can be seen that the first part of Eq 10 shows the stress due to bending moment $M = -P(L\text{-}d)$, while the second part characterizes the influence of the transverse force P.

Circular hole

The equation for the stress is obtained from Eq 10 by letting $a = b$; therefore, $m = 0$ and $R =$ radius of the circular hole:

$$S_\theta = -\frac{PR\,(L-d)}{I}(\sin\theta - \sin 3\theta)$$

$$-\frac{P}{I}\,[(2h-R^2)\sin 2\theta + R^2 \sin 4\theta] \quad (11)$$

Photoelastic investigations by Savin of the stress distribution in a cantilever containing circular holes showed that:

- Eq 11 is applicable to fairly large diameters of circular holes—as large as half of the plate height.
- The stress S_θ along the contour of the hole is highest at the top point of the hole contour (in the zone of tension).
- The stress on the outside contour of the beam is higher than the corresponding stress on the contour of the hole.
- The most dangerous cross-sections appear to be the parts of the plate that are not weakened by the hole and at the point where the beam (plate) is built in.
- The principal normal stresses occur in the cross section where the beam is supported.
- If the cantilever has two holes, the influence of each hole on the stress along the beam axis extends to a distance not much larger than one hole diameter from the hole center. This state appears to be the result of the redistribution of stresses due to presence of second hole.

Square hole

$$S_\theta = -\frac{PR\,(L-d)}{I}\left[\frac{14\sin\theta - 12\sin 3\theta - 2\sin 5\theta}{3\,(5+4\cos 4\theta)}\right] - \quad (12)$$

$$\frac{P}{I}\left[\frac{(14.4h^2 - 7.4R^2)\sin 2\theta + 12R^2\sin 4\theta + 2R^2 \sin 6\theta}{3\,(5+4\cos 4\theta)}\right]$$

where $2R$ = length of one side of the square.

Diamond hole

$$S_\theta = -\frac{2PR\,(L-d)}{I}\left[\frac{\sin\theta - 6\sin 3\theta + \sin 5\theta}{3\,(5-4\cos 4\theta)}\right] - \quad (13)$$

$$\frac{P}{I}\left[\frac{(216h^2 - 78.5R^2)\sin 2\theta + 84R^2 \sin 4\theta - 14R^2 \sin 6\theta}{21\,(5-4\cos 4\theta)}\right]$$

where $2R$ = length of the diagonal of the diamond.

Triangular hole

$$S_\theta = -\frac{3PR\,(L-d)}{I}\left[\frac{\sin\theta - 3\sin 3\theta + \sin 4\theta}{13-12\cos 3\theta}\right]$$

$$-\frac{P}{I}\left[\frac{\left(12h^2 - \frac{29}{3}R^2\right)\sin\theta + 6\,(3h^2 - R^2)\sin 2\theta}{13-12\cos 3\theta}\right]$$

$$-\frac{P}{I}\left[\frac{9R^2\sin 4\theta - 3R^2 \sin 5\theta}{13-12\cos 3\theta}\right] \quad (14)$$

where $2R$ = height of hole.

Special cases

To permit comparison of the influence of various types of holes on the stress distribution, the stresses along the contour of the holes have been calculated for the can-

7. Effect of twin holes

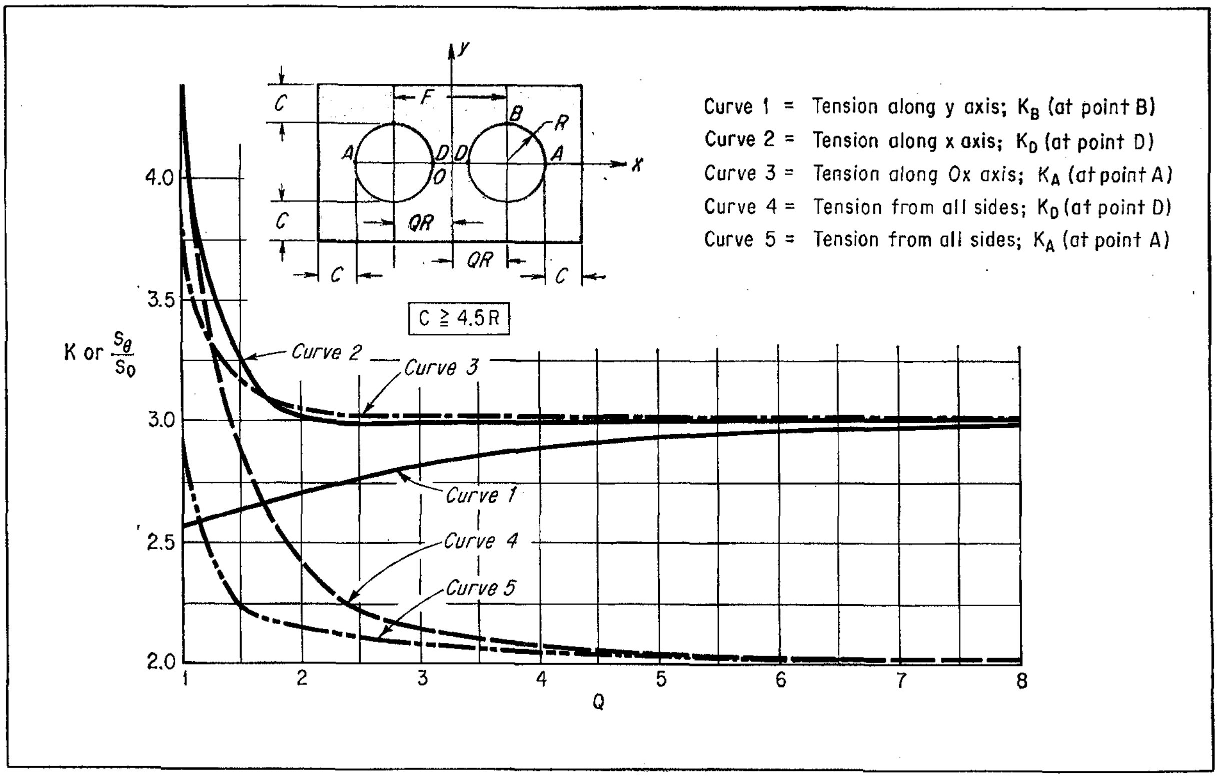

tilever bar with the following dimensions: height of beam $= 2h$, $d = \frac{1}{4}L$, $L = 10h$, and maximum dimension of the hole in y axis = one quarter of beam height (or $\frac{1}{2}h$). Constant R was determined from these given conditions, and the results plotted in Fig 2.

COMBINED LOADING

This group covers combined tension or compression in two perpendicular directions (Fig 3). For ease of calculation, it is more convenient to solve separately the stress states for the individual uniaxial stresses and to obtain the sought solution of the biaxial stress state by superposition of separate solutions.

If equal tensile or compressive stresses are acting in two perpendicular directions, the stress concentration at the edge of a circular hole can be found by using Lame's formula for thick cylinders. On the basis of this theory the tensile stress S_θ in a tangential direction at the edge of a small hole is

$$S_{\theta(\max)} = 2\,S_o \qquad (15)$$

where S_o = nominal stress (the stress that will occur if the stress concentration around the hole is ignored), psi. This means a small circular hole causes the stress in the case under consideration to be doubled.

It was found previously (Eq 3 in the first article) that for simple tension

$$S_{\theta(\max)} = 3\,S_o \qquad (16)$$

Comparing Eq 15 and 16, it can be concluded that for a case of simple tension a compressive stress S_c exists in which

$$S_c = -S_o \qquad (17)$$

This stress acts in a tangential direction at points B in Fig 3. Then, by the principle of superposition, Eq 15 is obtained from Eq 16 and 17. This approach also gives the solution to the case of the circular hole (Fig 3). The tangential stress at points B at the edge of the hole is equal to $3\,S_1 - S_2$, and at points A is equal to $3\,S_2 - S_1$. When $S_2 = -S_1$, which is in the case of pure shear, the maximum stress at point B is

$$S_{B\,(\max)} = 3\,S_1 - (-S_1) = 4\,S_o$$

For points A

$$S_{A\,(\min)} = 3\,S_2 - S_1 = -4\,S_1$$

This means that in the case of twisting of a thin circular tube (which can be treated as a plate), a small circular hole produces a high stress concentration in which the maximum tensile stress at the edge of the hole becomes four times as large as the shearing stress uniformly distributed over the ends of the tube. This also happens in a solid shaft under torsion having holes in a radial direction, such as oil ducts in crankshafts.

The variation in K versus S_1/S_2 is shown in Fig 3 for an elliptical hole of dimension $a/b = 3/2$, and also for a circular hole.

EFFECT OF LARGE HOLES

If the hole is large in comparison to the width of the plate, specifically if the hole diameter is larger than 1/5 the plate width, then the plate width does influence the stress distribution to a significant amount.

The plate under consideration (Fig 4) has a width $2b$, with b its center on the axis of symmetry of the strip. The hole radius $= R$, and the plate is loaded with a uniform tensile stress S_o.

The equations for stresses in finite-width plates are very involved, so only the plotted results are summarized in Fig 4 and 5. Fig 4 shows the stress distribution with a circular hole of size $R/b = 0.5$; ie, the hole diameter

8. Twin holes spaced at various distances

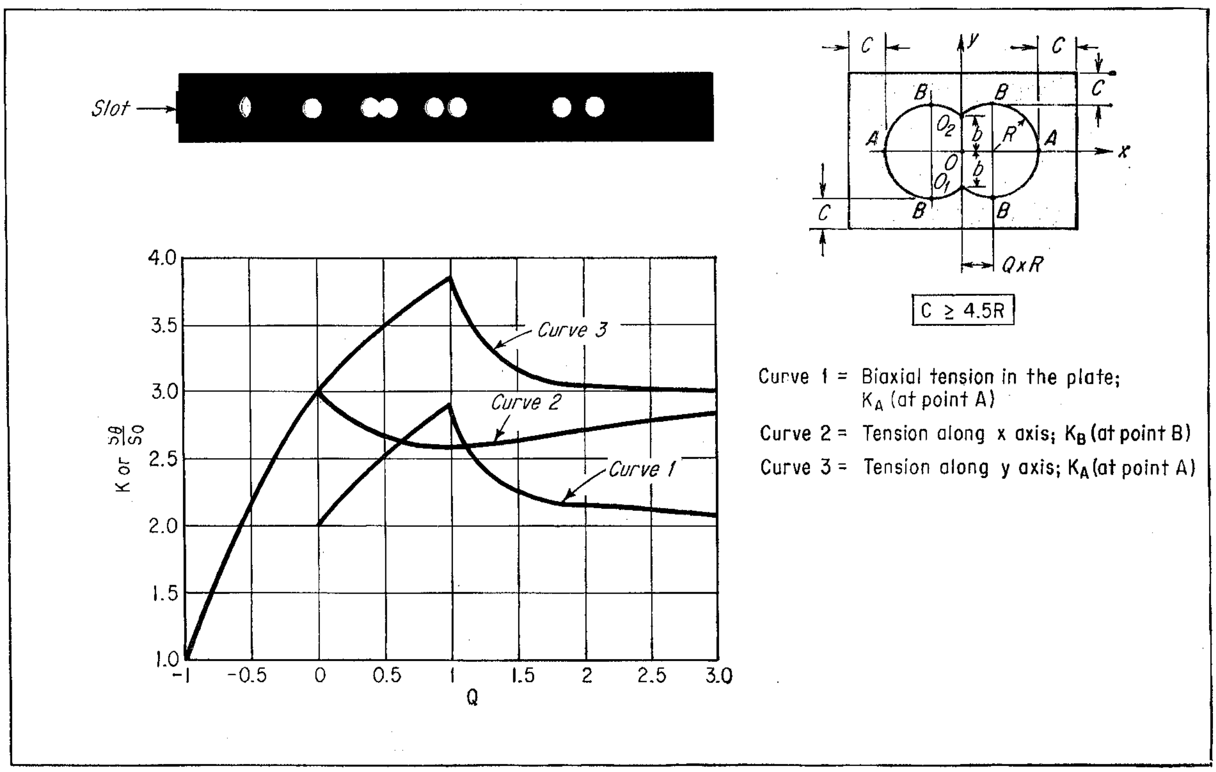

is half the plate width. Fig 5 gives the stress concentration factor $K = S_\theta/S_o$ for various hole sizes at various distances r/b from the hole center where r is the radial distance. In all cases, $\theta = \pi/2$, which is the most critical case. The dashed line gives the increase in stress concentration with increase in relative hole size R/b. Note that the stress concentration coefficient increases rapidly with the increasing radius of hole; thus, for $R/b = 0.5$ the stress coefficient equals $K = 4.32$, while for $R/b = 0$, $K = 3.0$.

It is usual to accept accuracies of up to 6% in stress analysis. On this basis, the data for infinite plates can be applied to plates of finite dimensions, provided that the ratio of the diameter to plate width is not less than 0.2; in other words, the data holds for widths at least five times the hole diameter. This conclusion also applies to cases of pure bending stresses.

EDGE HOLES

This is the case where the plate is large in comparison to the hole diameter, and the hole is at a close proximity to one edge (Fig 6). Specifically the hole is at a distance d from the edge; angle θ in this case is measured counterclockwise from point D at the hole edge. The plate is under tension loading.

The stresses along the hole boundary are

$$S_\theta = S_o\,(1 + 2\cos 2\theta)$$

Values of K at points O, A, and D are given in Fig 6 for various values of d/R.

SINGLE-ROW HOLES

Double holes

First of these cases involves two equal holes of radius R (Fig 7). The stress state around these holes is determined for the cases where there is:

- Tension S_o in the y direction only (curve 1, Fig 7).
- Tension S_o in the x direction only (curves 2, 3).
- Tension S_o in both direction (curves 4,5).

The distance of the holes from the y axis is given by means of constant, Q.

Thus a hole is designated as being at a distance Q x R from the y-axis. Specifically, if F = distance between hole center lines, then $Q = F/2R$.

Here again the solution for the biaxial uniform stress state was obtained by superposition of the solutions for single-axis stress states. The maximum stress S_θ along the contour of the holes will be at points A and D (curves 4,5). This holds true whether the tensile stress, S_o, is applied along the two axes, or it is applied in the direction of the x axis only (curves 3 and 2).

If the plate is under tension S_o in the direction of the y axis, the maximum stress will be at the points in which θ differs little from 90 deg, ie, at points situated very near to point B (curve 1). The values of S_θ in Fig

9. Infinite number of holes—loading in x direction

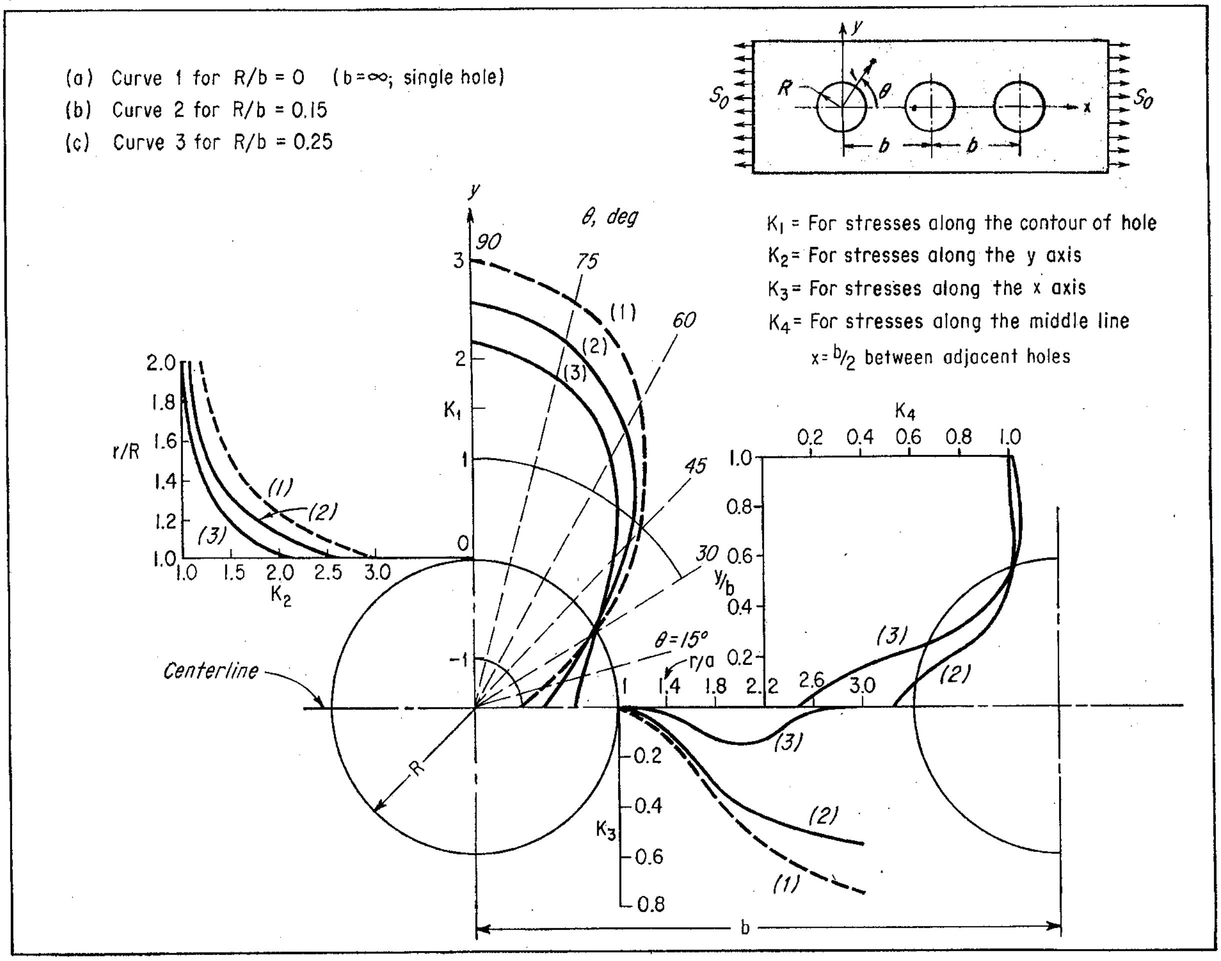

7 permit numerical evaluation of the influence of the holes on each other.

Within the accuracy of up to 6% the following can be said for almost all cases of tensile stresses along the x and y axes, and also for biaxial tensile force:

- For $Q = 3$, where the center distance between the holes is equal to three diameters, the stress S_o along the contour of the holes will be equal to that prevailing when there is only one hole.
- The results obtained for infinite plates can be applied to calculations in the case of plates of finite sizes perforated by two holes, provided that points A and B are at a distance of at least $4.5R$ from the edge.

Overlapping holes

The plate under consideration (Fig 8) contains two overlapping holes. The final contour therefore is actually one hole consisting of two equal circular areas. It is assumed that the contour of the hole is free of external forces and that the stresses are either biaxial, or uniaxial along the x or y axis.

Factor Q, which when multiplied by the radius R locates the arc centers, is plotted against S_θ/S_o. The resulting shapes of the holes are illustrated. Note that the holes do not intersect until $Q<1$. For $Q = 1$, the holes just touch; for $Q = 0$, the holes blend into one circular hole; for $Q = -1$ the hole has become a slot of length $2b$ along the y axis.

Since the equations are quite involved, only the results are summarized in the form of the three curves in Fig 8. Curve 1 gives the stress concentration factor at points A for biaxial tension in the plate ($S_\theta/S_o = K_A$). Curve 2 is for uniaxial stress when tension is applied along the x axis. Here the points B are the points of interest. Curve 3 is for when tension is applied along the y axis. Points A are then the points of interest.

Infinite number of holes

The charts in Fig 9 and 10 are for cases where there are more than two holes in a row. Fig 9 is when the tensile loading is along the x axis, and Fig 10 when it is along the y axis. Distance b in these figures denotes the distance between hole centers; R is the hole radius and r locates the point of interest.

In Fig 9, values of $S_\theta/S_o = K_1$ give the stresses along the contour of the hole; $S_y/S_o = K_2$ for stresses along the y axis; $S_r/S_o = K_3$ for stresses along the x axis, and $S_x/S_o = K_4$ for stresses along the centerline of the holes.

The size of the hole relative to spacing between holes is R/b. Two curves, $R/b = 0.15$ and $R/b = 0.25$, are plotted for each stress concentration factor K and compared to the case of a single circular hole.

10. Infinite number of holes—loading in y direction

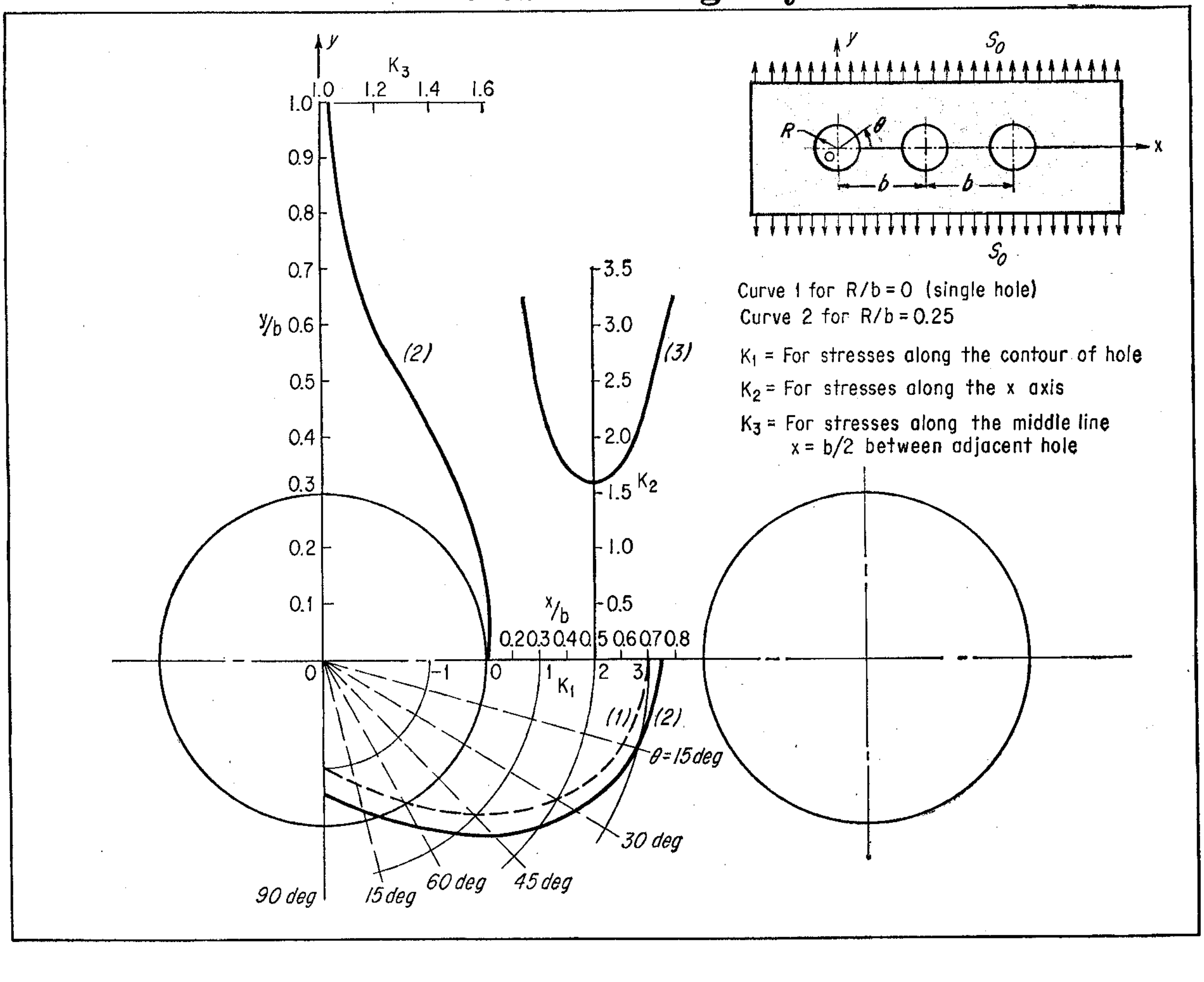

Residual Stress Can Help Design Tool for Springs

Put residual stresses to work when designing springs. You can double load-carrying capacity and quadruple life.

George Kurasz & W. R. Johnson

EFFECTS OF RESIDUAL AND SERVICE STRESSES in a flat spring. Spring is formed for a preset. Stress-relieving takes out unfavorable residual stresses; presetting puts favorable residual stresses back in. Service stress in 6 is algebraic sum of 3 and 5.

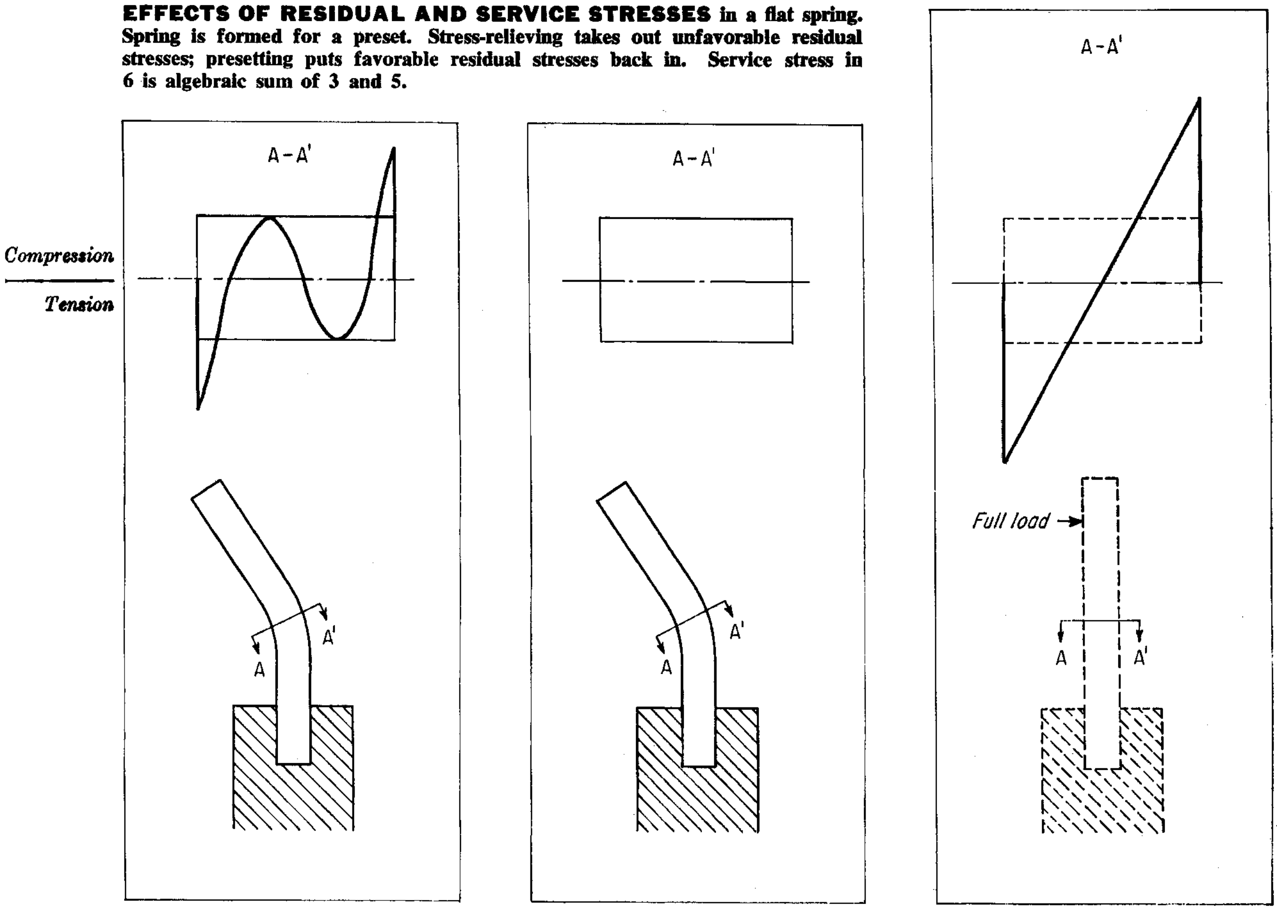

No stress relief (unfavorable residual stress)

1

Stress-relieved (no residual stress)

2

Stress-relieved (service stress only)

3

If properly controlled, residual stresses in a finished spring can be a valuable design tool, measurably improving spring performance. When the spring is stressed in only one direction (not subjected to reverse bending or torsion) residual stresses can more than double static-load capacity and can increase dynamic-load life by 400%. Although residual stresses do not alter the elastic modulus of the material (spring rate), they do change apparent yield strength and fatigue limit.

Residual stresses are introduced in two ways: in processing the spring material itself and in the manufacture of the spring. The stresses produced when the material is being processed are introduced by the cold-working operations and reduce load-carrying capacity of a spring. Severely cold-worked or hard-drawn materials show an extremely low yield point with almost no elastic limit because the *micro-strains originating from* the plastic deformation are unfavorably oriented and cause small amounts of slip at low applied stresses. These undesirable residual stresses can be mostly eliminated by a stress-relief heat treatment. Stress-relieving raises yield point as much as 50%.

Residual stresses introduced in the manufacture of the spring are the ones that can be controlled. They are introduced by overstressing the spring. Here's how it is done:

Residual stresses introduced during forming are unavoidable and may be unfavorable. For this reason the spring is first stress-relieved by heat treatment. Afterward controlled, favorable residual stresses of the desired magnitude and direction are introduced by setting or truing or setting and shot-peening the spring. To be favorable, residual stresses introduced by setting must oppose service stresses.

There are actually three levels of performance possible from springs, depending on treatment after forming: no stress relief, stress relief only, and stress relief plus prestressed with favorable residual stresses. For example, tests indicate that U-shaped springs loaded in a direction to open the U and stress-relieved after forming performed 300% better than conventionally formed springs with no stress relief. Performance was another 200%, or a total of 500% better when the springs were prestressed by truing for favorable residual stresses. The same proportions hold true for cold-formed pretempered spring-steel strip.

Setting or truing, of course, means bending the spring beyond its elastic limit, then permitting it to spring back to its new position. This introduces residual stresses opposing the direction of the overload. So the overload must

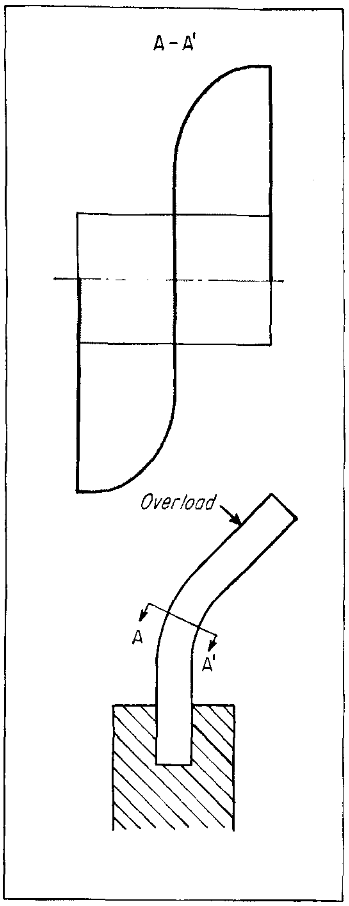

Presetting the spring (to induce residual stresses)

4

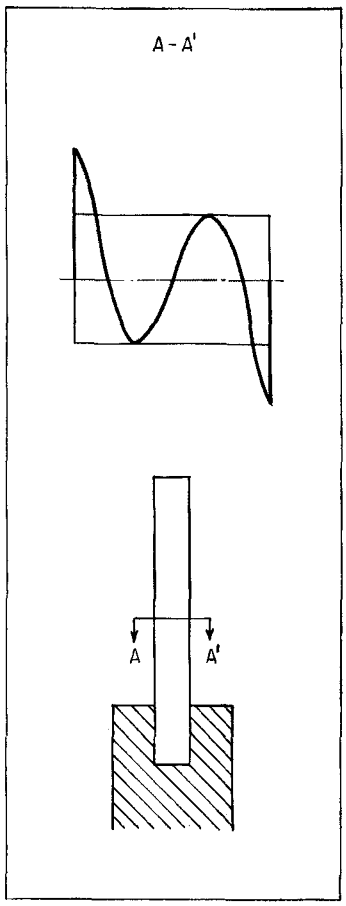

Preset spring ready for service (favorable residual stresses)

5

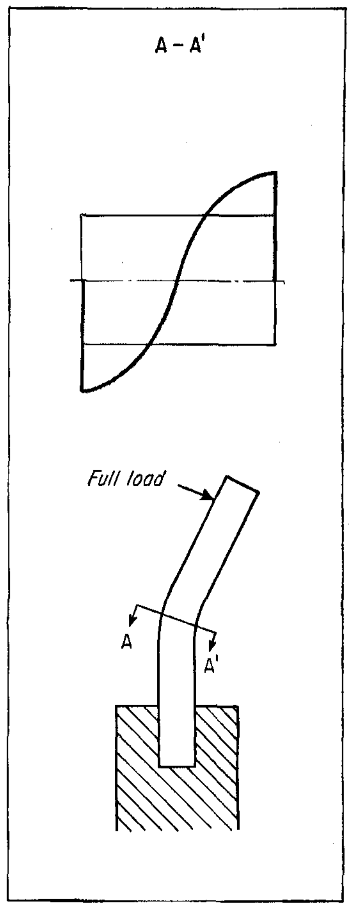

Compression

Tension

Preset spring under full service load (3 + 5)

6

PREDICTING FATIGUE FAILURE IN BELLEVILLE SPRINGS

Fatigue tests on Belleville springs show that they ultimately fail in tension. In two series of tests, springs were preset for favorable residual stresses, then cycled with the inside diameter loaded in compression. On the first spring, initial fatigue cracks started in the compression-loaded ID area after 1½ million cycles, but since they did not interfere with load-carrying ability, the test was continued. The spring finally failed after 6 million cycles. The critical crack originated in the concave side with the 120,000-psi tensile stress near the OD rather than the area of 270,000-psi compression stress (convex side) near the ID where the initial cracks were located.

In the second test, springs also failed in tension after only 48,000 cycles under 170,000-psi tensile stress and 370,000-psi compressive stress.

Both types of springs had an OD of 0.750 in. and were 0.028 in. thick. The standard spring had an ID of 0.380 in. and a total height of 0.023 in. compared to the 0.300 ID and 0.026-in. total height of the special spring. Two different ID's were chosen so that the ratio of OD to ID would vary in order to get two levels of stress.

Maximum compressive stress at the ID on the convex side was calculated by the well-known Almen and Laszlo formula from "The Uniform Section Disk Spring," Almen and Laszlo, ASME, *Trans,* Vol 58, No. 4, May 1936, pp 305-314.

$$S_D = \frac{4Ef}{(1-\mu^2)\,(g-1)^2 d^2}\left[\left(\frac{g-1-\ln g}{\ln g}\right)\left(h-\frac{f}{2}\right)+\left(\frac{g-1}{2}\right)t\right]$$

Maximum tensile stress at the OD on the concave side was calculated by the Ashworth formula from "The Disk Spring or Belleville Washer," Ashworth Institution of Mechanical Engineers, *Proc,* Vol 155, 1946, pp 93-100 (When $2h - f/t \ln g$ is greater than 1):

$$S_T = \frac{4Ef}{g\,(1-\mu^2)\,(g-1)^2 d^2}\left[\left(\frac{g\ln g - g+1}{\ln g}\right)\left(h-\frac{f}{2}\right)+\left(\frac{g-1}{2}\right)t\right]$$

In both formulas, g = OD/ID ratio, d = ID, h = force height, t = thickness, f = deflection, E = elastic modulus, and μ = Poisson's ratio. All dimensions are in inches.

be in the same direction in which the service stresses will be applied. The magnitude of the residual stresses is determined by the amount of overload. When the spring is formed, its shape after the heat treatment must allow for a final set of the proper degree and in the proper direction.

When a spring is bent beyond its elastic limit, its outer, convex surface is stressed in tension; the inner, concave surface is stressed in compression. The outer surface fibers become permanently stretched, preventing return of the spring to its original position when the overload is removed. The inner surface fibers are shortened. When the spring returns to its new relaxed position, the outer surface fibers are now in compression and the inner surface fibers in tension. This is residual stress. When the service load is applied, the residual (compressive) stress on the outer surface fibers cancels out an equal amount of the tensile stress introduced by the service load. Therefore, at full service load, total tensile stress on the outer surface equals tensile stress due to load minus residual compressive stress. The spring can operate above original yield point.

Calculating stress

Although residual-stress systems are very complex, formulas for spring de-

DESIGN STRESSES FOR HELICAL OR COILED SPRINGS

Wire material	Static		Dynamic	
	Normal maximum stress (Wahl corrected), % of tensile strength	Maximum stress using favorable residual stress (Wahl corrected) % of tensile strength	Normal maximum stress, psi	Maximum stress after shot peening, psi
Music wire, SAE 1085....	40	60	75,000	95,000
Oil-tempered, SAE 1066...	45	67½	......	......
Stainless steel, SAE 302...	35	52½	60,000	75,000
Alloy spring, SAE 6150....	45	67½	75,000	95,000
Phosphor bronze........	35	52½	20,000	25,000
Beryllium copper, alloy 25.	45	67½	50,000	60,000

sign have been purposely simplified for easy manipulation, often to the point where many stress factors are ignored, and must be compensated for by other design data.

Furthermore, whereas formulas for calculating load-deflection curves in spring designs are generally accurate, stress formulas are not. Stress cannot be measured directly—only by its effect on strain as it alters the spacing in the atomic structure. All spring formulas postulate stress-free, homogeneous, elastic materials for an oversimplified shape. For example, on compression and extension coil springs, designs have been computed with the same formula used for stress in torsion of straight round bars:

$$S = \frac{MC}{J}$$

which converts to $S = \dfrac{8PD}{\pi d^3}$

where S = torsional stress, psi; M = moment, lb-in.; C = distance from neutral axis to surface, in.; J = polar moment of inertia, in.^{4}; P = load, lb; D = pitch diameter of spring, in; and d = wire diameter, in.

A correction factor, K, devised by Dr A. M. Wahl of Westinghouse Electric Corp, improves the formula. The factor recognizes that a helical spring is not a straight torsion bar but a highly curved beam and compensates for the beam curvature.

In theory, the modified stress formula

$$S = \frac{K8PD}{\pi d^3}$$

should predict the stress of an ideal spring, whereas spring behavior should be predictable from the torsional properties of the material. Although disagreements exist about design formulas because of the complexity of residual stress, tests show that the Wahl formula, devised for elastic behavior only, predicts spring stress in wire elements up to the torsional yield point and beyond, owing to the favorable residual stress included.

The table shows allowable design stresses and stresses for fatigue loading based on the Wahl formula. To induce favorable stresses for static applications, the spring must be preset, which may add 50% to maximum stress; for dynamic applications, the spring must be shot-peened, which adds 25% to stress range. Shot-peening static springs or presetting dynamic springs does not increase design level.

For flat springs, a very slight amount of set will permit operation up to the tensile strength. Most successful flat spring design is by trial and error, not by formula.

Favorable stresses in flat springs

Stress levels were improved in the suspension springs of the 1962 Chevrolet II by making the most of favorable residual stresses. The springs are tapered, single-leaf blades instead of conventional multi-leaf design. They eliminate liner and friction problems and proportionally raise stress levels at reduced unit weight. Stress levels of the single-leaf springs are from 180,000 to 220,000 psi compared to 140,000 psi for multi-leaf springs, which they supersede.

The spring stock is rolled so that stresses are induced uniformly from end to end when the spring is shaped to specifications. The effectiveness of the design depends largely on the shot-peening process employed. The process is unusual because the spring is peened while under exceptionally high stress to induce a favorable residual stress. Using 10-12 Almen C-2 shot, peening reduces the spring's cambered height when the spring is subsequently preset at its final operating stress range.

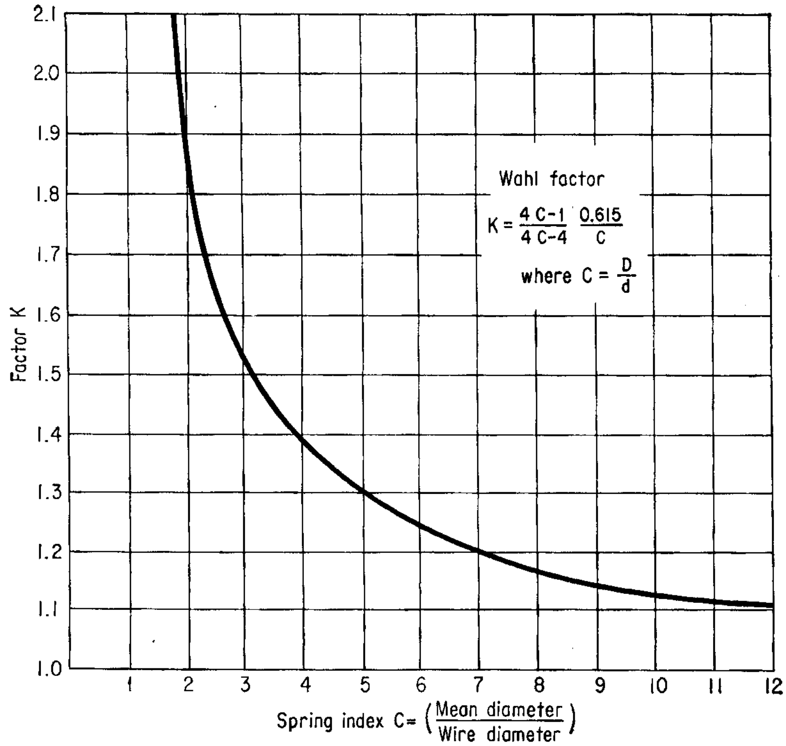

CLASSIC WAHL factor curve

Quick Calculations for Corrugation Stiffness

Equations and graph find moment of inertia and location of neutral axis for a wide range of cross-sections.

Earl A. Phillips

Corrugations add stiffness to sheets and plates—but how much? One of the equations given here quickly and accurately estimates the additional stiffness by solving for moment of inertia of the cross-section. And to help in calculating stresses, a second equation finds the neutral axis in the corrugated sheet.

The equations were derived for pressed corrugations (top sketch). Sheets corrugated in this manner do not undergo any reduction in width. Horizontal parts remain as thick as they were in the original sheet; but when the convolutions are formed—by stretching—the webs become thinner.

Another method of corrugation reduces the width of the finished sheet, but retains a constant thickness throughout (bottom sketch). The equations hold for these constant-thickness corrugations as well—except when the corrugations are nearly rectangular: then the equations are accurate for the pressed corrugations only.

As a guide to using the graph, representative cross-sections have been sketched in to show where they fall.

EQUATIONS

Height of neutral axis above reference line ($y = 0$):

$$\bar{y} = K_1 t(2 - K_2 - K_2 K_3)/2$$

Moment of inertia:

$$I = Lt^3(K_1^2 A + 1)/12$$
$$= Lt^3 B/12$$

A is found from the graph on page 77. B is a magnification factor that tells how many times stronger the corrugation has made the sheet. If comparisons, and not absolute values are needed, simply compute B for each corrugation cross-section.

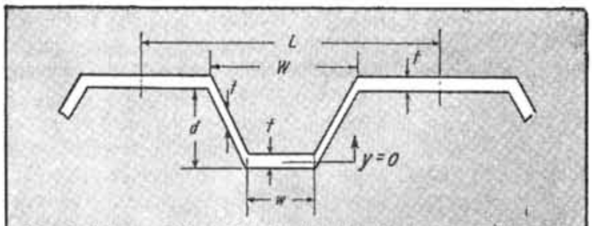

Pressed Corrugation (Model Used to Derive Equations)

SYMBOLS

A = Parameter depending on K_2 and K_3
B = Ratio, stiffness of corrugation to stiffness of flat sheet ($K_1^2 A + 1$)
d = Depth of corrugation, in.
I = Moment of inertia, in.^{4}
K_1 = Ratio, d/t
K_2 = Ratio, w/W
K_3 = Ratio, W/L
L = Corrugation pitch length, in.
t = Thickness of sheet, in.
w = Width of bottom of corrugation, in.
W = Width of top of corrugation, in.
y = Height of neutral axis, in.

EXAMPLE I —Constant Thickness (curved webs)

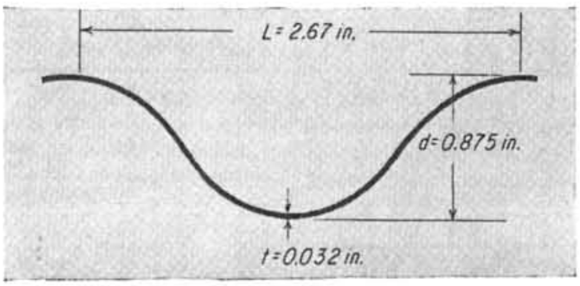

When webs are curved, as they are in this case, draw analogous straight-web cross-section and find W and w by measurement or, if possible, simple geometry. In this example, assume web slope is 45° and horizontal parts at top and bottom of corrugations are equal.

$$W = L/2 + d = 2.67/2 + 0.875 = 2.21 \text{ in.}$$
$$w = L/2 - d = 2.67/2 - 0.875 = 0.56 \text{ in.}$$

Ratios are:

$$K_1 = d/t \quad = 0.875/0.032 = 27.4$$
$$K_2 = w/W = 0.56/2.21 = 0.25$$
$$K_3 = W/L = 2.21/2.67 = 0.83$$

From chart, A = 1.75. Thus

$B = K_1^2 A + 1 = (27.4)^2\, 1.75 + 1 = 1310$

$I = Lt^3B/12 = 2.67(0.032)^3\, 1310/12 = 0.0095$ in.^{4} per corrugation.

$I = 0.0095 \times 12/2.67 = 0.043$ in.^{4} per foot of width.

Actual value of I is 0.041 in.^{4} per foot of width.

EXAMPLE II—Constant Thickness (straight webs)

Find W and w by measurement.

$K_1 = d/t \quad = 4.0/0.3125 = 12.8$

$K_2 = w/W = 3.4/8.8 = 0.386$

$K_3 = W/L = 8.8/12 = 0.73$

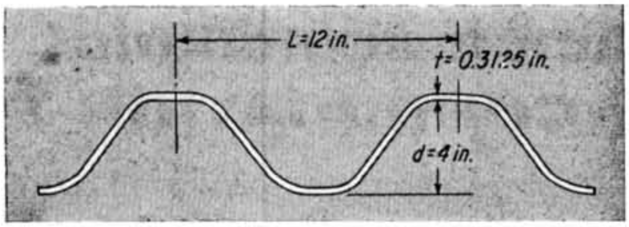

From chart, A = 2.1. Thus

$B = K_1^2 A + 1 = (12.8)^2\, 2.1 + 1 = 345$

$I = Lt^3B/12 = 12(0.3125)^3\, 345/12 = 10.5$ in.^{4} per corrugation.

Actual value of I is 9.84 in.^{4}. The 6% error results mainly because this method neglects rounded corners.

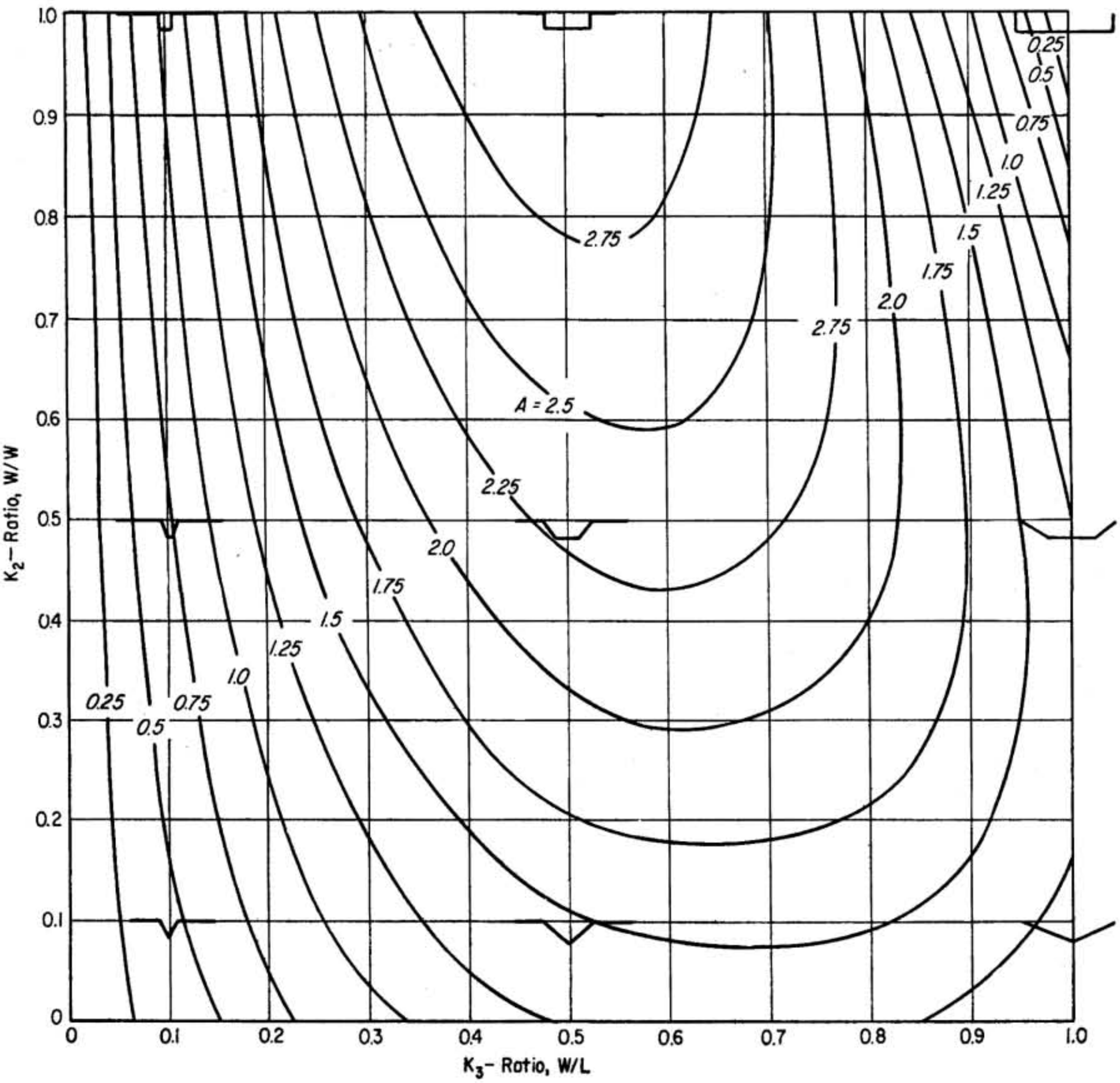

When Thin-Wall Cylinders Carry the Load

These new equations give quick answers for stress and deflection caused by skirts or reinforcing rings.

Robert I. Isakower

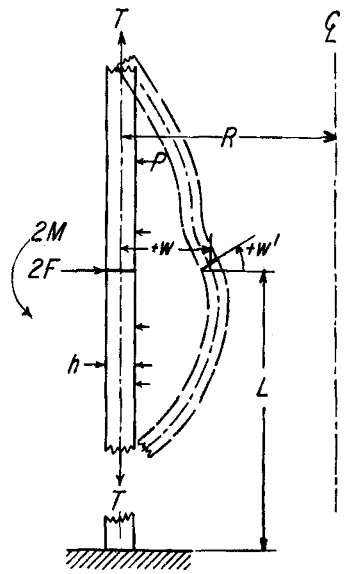

SYMBOLS

E = Young's modulus, psi
e = external-load moment arm, in.
$2F$ = radial load, lb per in. of circumference
h = cylinder-wall thickness, in.
K = ratio, R/h
L = distance to point of restraint, in.
$2M$ = moment, in.-lb per in. of circumference
P = internal pressure, psi
R = mean cylinder radius, in.
T = axial membrane load, lb per in. of circumference
w = radial displacement, in.
w^1 = rotational displacement, radians
μ = Poisson's ratio
σ_θ = hoop stress, psi
σ_x = axial stress, psi
$\phi_{1,2,3}$ = equation factors

For accurate results: $K \geq 10$, $L \geq \frac{5}{\beta}$,

where $\beta = \frac{3(1-\mu^2)}{\sqrt{Rh}}$

Thin-wall cylinders often act as structural members or as supports for external loads. These loads are transmitted to the cylinder through rings, skirts, clips or guy-wire supports. Stresses and deflections in the cylinder depend on internal pressure as well as external moments and radial loads.

Calculating these values usually involves time-consuming simultaneous equations. But the new equations presented below give answers faster, and with less chance for error. The key: three factors that eliminate many of the calculations ordinarily needed. These factors, ϕ_1, ϕ_2, and ϕ_3 are charted for various values of Poisson's ratio on the continuing page.

1. **Stresses** (add for inner fiber; subtract for outer)

Axial:

$$\sigma_x = \frac{T}{h} \pm \frac{6}{h^2}[\sqrt{Rh}\,\phi_1 F + M]$$

Hoop:

$$\sigma_\theta = PK \pm \frac{\mu 6}{h^2}[\sqrt{Rh}\,\phi_1 F + M] - \frac{\phi_2 K^{1/2} F}{h}$$

2. **Displacements**

Radial:

$$w = (K^{3/2}\phi_2 F - PRK + \mu TK)/E$$

Rotational:

$$w^1 = \frac{K^{1/2}\phi_3 M}{h^2 E}$$

$$T = \frac{PR}{2} + T_{external}$$

EXAMPLE: A steel cylinder with a support skirt has $T_{external} = 0$, $P = 0$, $R = 10$ in., $h = 0.20$ in., $\mu = 0.30$, $E = 30 \times 10^6$ psi, $e = 1.0$ in., $2F = 60$ lb/in.

SOLUTION: $2M = (2F)e = 60$ in.-lb/in.
From chart, $\phi_1 = 0.3891$, $\phi_2 = 1.2865$, $\phi_3 = 4.2488$

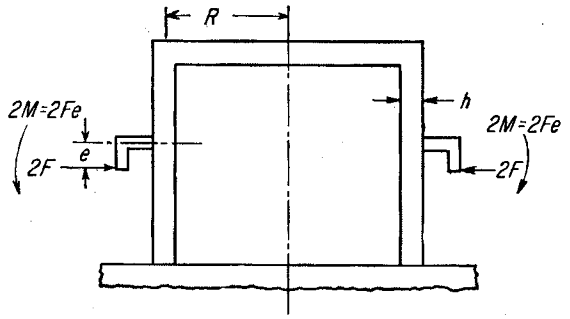

Stresses

Axial:

$$\sigma_x = \frac{0}{0.20} \pm \frac{6}{(0.20)^2}\left[\sqrt{10(0.20)}\,(0.3891)30 + 30\right]$$
$$= \pm 6975 \text{ psi}$$

Hoop:

$$\sigma_\theta = 0 \times 50 \pm 0.30\,(6975) - \frac{1.2865\ \sqrt{50}\,(30)}{0.20}$$
$$= -3456 \text{ psi inner fiber}$$
$$= +750 \text{ psi outer fiber}$$

Displacements

Radial:

$$w = \frac{(50)^{3/2}(1.2865)30}{30 \times 10^6} - \frac{0 \times 10 \times 50}{30 \times 10^6}$$
$$+ \frac{0.30 \times 0 \times 50}{30 \times 10^6} = 4.50 \times 10^{-4} \text{ in.}$$

Rotational:

$$w^1 = \frac{\sqrt{50}\,(4.2488)\,30}{(0.20)^2\,30 \times 10^6}$$
$$= 7.49 \times 10^{-4} \text{ radians}$$

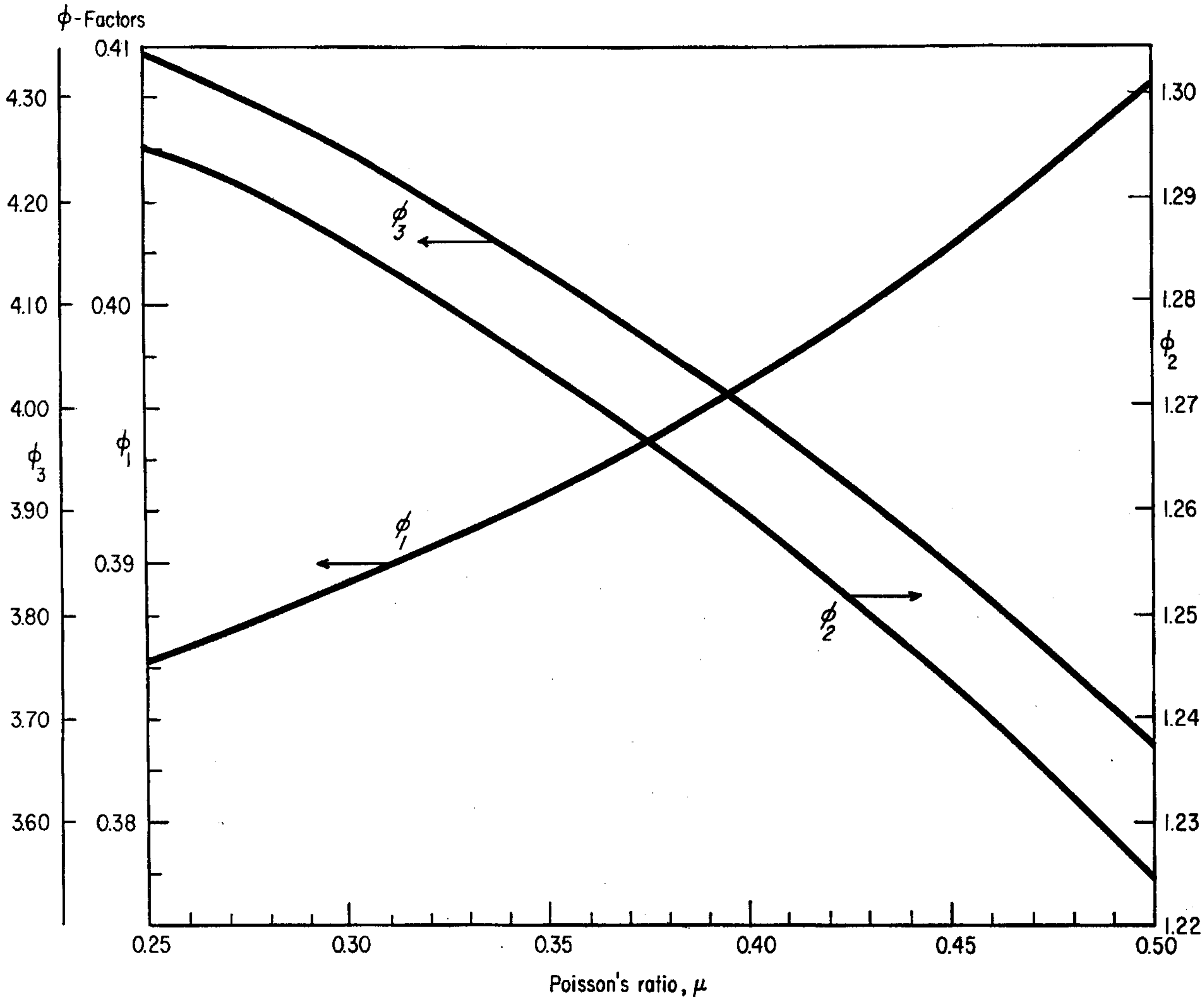

Thick-end Cylinders: Stress-correction Factors

Formulas and examples show how correct maximum stresses can quickly be found.

Robert I. Isakower

What effect does a thick end have on stresses in a thin circular cylinder? It's important to know because the stresses may be more than quadrupled in some cases. For example, proceed with caution whenever a thick flange supports a tensile-loaded cylinder—stresses at the flanged end will usually be increased. Moreover, the restraint imposed by the fixed end invites bending as well as direct membrane stresses. This changes the stress pattern. A thick end-closure for a pressure vessel has the same effect.

Formulas:

1. Cylinders with internal pressure (Add δ for inner fiber; subtract for outer)

$$S_A = (PR/2h)\,(1 \pm \delta_1)$$

$$S_H = (PR/h)\,(1 - \delta_4 \pm \delta_3)$$

2. Cylinders with tensile load only (Subtract δ for inner fiber; add for outer)

$$S_A = (T/h)\,(1 \mp \delta_2)$$

$$S_H = (\mu T/h)\,(1 + \delta_5 \mp \delta_2)$$

Correction factors (δ) for various values of Poisson's ratio are charted on the continuing page (excepting δ_5, which equals 1 for all values of μ).

SYMBOLS

h = cylinder-wall thickness, in.
P = internal pressure, psi
R = mean cylinder-radius, in.
S_A = max axial stress, psi
S_H = max hoop stress, psi
T = tensile load, lb/in. (=PR/2 when cylinder is loaded with internal pressure.)
δ = correction factor
μ = Poisson's ratio

For accurate results R/h should be not less than 10.0 approx.

SAMPLE PROBLEMS

1. A tensile-loaded cylinder has R = 12 in., h = 0.4 in., T = 1000 lb/in., Poisson's ratio = 0.30. Find max stresses at flange end. (See sketch below.)

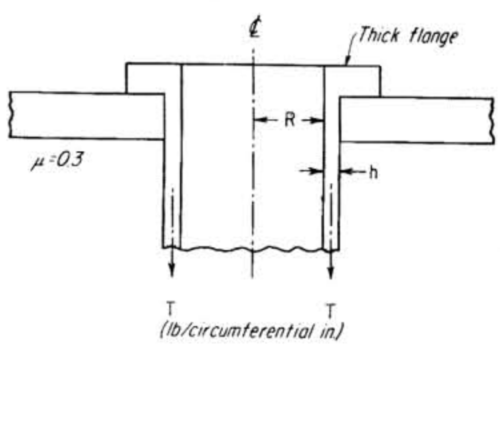

The Solution:

From chart, $\delta_2 = 0.545$; formula for case 2 gives

$$S_A = \frac{1000}{0.4}\,(1 + 0.545)$$
$$= 2500 \times 1.545$$
$$= 3860 \text{ psi}$$

$$S_H = 0.3\left(\frac{1000}{0.4}\right)(2 + 0.545)$$
$$= 750 \times 2.545$$
$$= 1905 \text{ psi (outer fiber)}$$

Both stresses have been increased; without correction factors, axial and hoop stresses are respectively 2500 and 750 psi. (These are the stresses that exist in the tube where the bending effect is damped out.)

2. A pressure vessel has R = 10 in., h = 0.3 in., H = 2.0 in., P = 500 psi, μ = 0.3. Find max stresses at closed end.

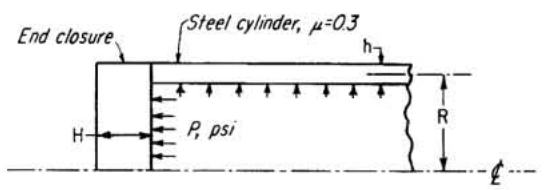

The Solution:

Since H is large compared to h, the flat plate may be considered infinitely rigid compared to the thin cylinder. It is therefore valid to assume the condition

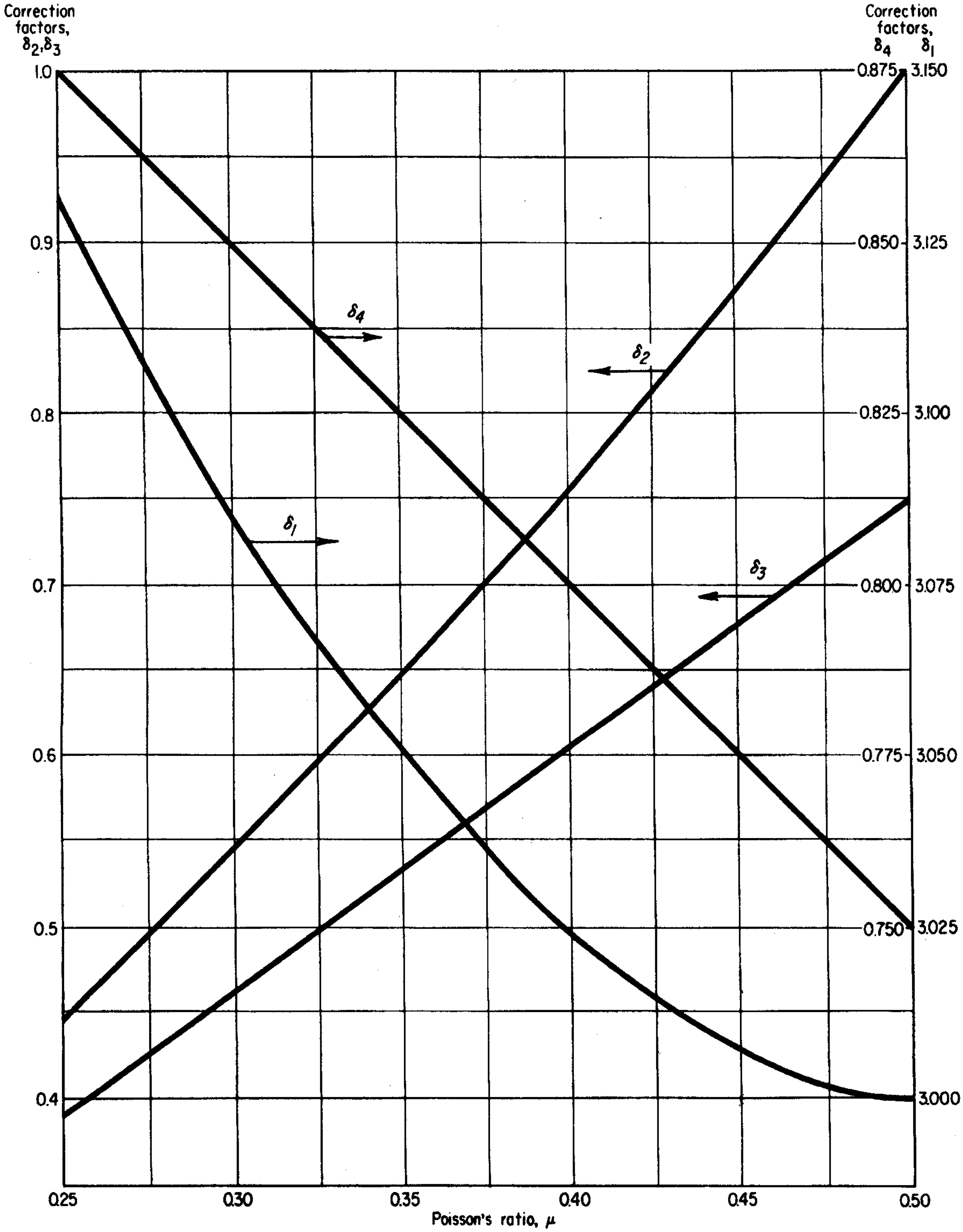

here is that of a fixed-end cylinder.

From the chart, $\delta_1 = 3.086$, $\delta_4 = 0.850$, $\delta_3 = 0.4625$

Formula for case 1 gives

$$S_A = \frac{500 \times 10}{2 \times 0.3}(1 + 3.086)$$

$$= 8330 \times 4.086$$

$$= 34{,}100 \text{ psi (inner fiber)}$$

$$S_H = 16{,}660 \times 0.6125$$

$$= 10{,}200 \text{ psi (inner fiber)}$$

In this case, axial stress is increased while hoop stress is decreased owing to the local bending.

Three Nomographs Aid in Designing Pressure Vessels

Use these charts to find wall thickness, hoop stress or pressure limit.

F. Kaplan

SYMBOLS

D = Cylinder diameter, in.

P = Internal pressure, psi

S = Hoop stress (circumferential tensile stress), psi

t = Wall thickness, in.

Barlow Thin-wall Equation

Wall thickness $t = PD/2S$

Hoop stress is assumed to be uniformly distributed through the thickness of the shell wall.

EXAMPLE: An 8-in.-dia. cylinder must hold 2000-psi internal pressure. What wall thickness will limit hoop stress to 20,000 psi?

SOLUTION: Diameter of 8 in. is off the scale, so solve using 0.8 in., then multiply t by 10.

Draw a line between 0.80-in. diameter at left to 2000-psi pressure, and extend to pivot line at right. From intersection at pivot line draw a line through 20,000-psi hoop stress to wall thickness at left, 0.040. Required wall thickness is $0.040 \times 10 = 0.40$ in.

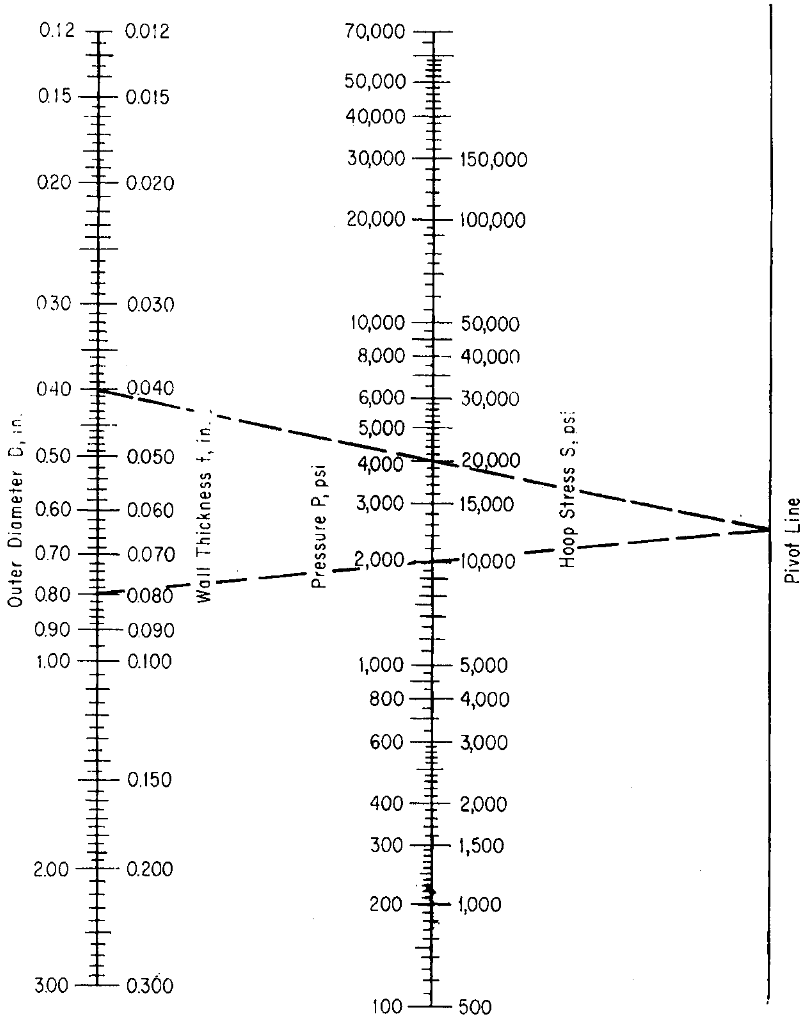

Pressure Vessel Design

Follow this simple procedure for determining how tight a gasket should be, and then relate it to required bolt preload via the charts on page 29-6.

via the charts on page 29-6.

Gasket Materials and Contact Facings

Gasket material		Gasket factor m	Shape	Use Facing sketch	Use column at right
Rubber without fabric or a high percentage of asbestos fiber: Below 75 Shore Durometer		0.50			
75 or higher Shore Durometer		1.00			
Asbestos with a suitable binder for the operating conditions	1/8 thick	2.00		1(a,b,c,d) 4,5	2
	1/16 thick	2.75			
	1/32 thick	3.50			
Rubber with cotton fabric insertion		1.25			
Rubber with asbestos fabric insertion, with or without wire reinforcement	3-ply	2.25	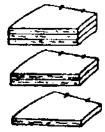		
	2-ply	2.50			
	1-ply	2.75			
Vegetable fiber		1			
Spiral-wound metal, asbestos filled	Carbon	2.50		1(a,b)	2
	Stainless or Monel	3.00			
Corrugated metal, asbestos inserted or Corrugated metal, jacketed asbestos filled	Soft aluminum	2.50			
	Soft copper or brass	2.75			
	Iron or soft steel	3.00			
	Monel or 4-6% chrome	3.25			
	Stainless steels	3.50			
Corrugated metal	Soft aluminum	2.75		1(a,b,c,d)	2
	Soft copper or brass	3.00			
	Iron or soft steel	3.25			
	Monel or 4-6% chrome	3.50			
	Stainless steels	3.75			
Flat metal jacketed asbestos filled	Soft aluminum	3.25	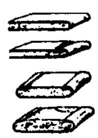	1a,1b,1c*, 1d*,2*	2
	Soft copper or brass	3.50			
	Iron or soft steel	3.75			
	Monel	3.50			
	4-6% chrome	3.75			
	Stainless steels	3.75			
Grooved metal	Soft aluminum	3.25		1(a,b,c,d) 2,3	2
	Soft copper or brass	3.50			
	Iron or soft steel	3.75			
	Monel or 4-6% chrome	3.75			
	Stainless steels	4.25			
Solid flat metal	Soft aluminum	4.00		1(a,b,c,d) 2,3,4,5	1
	Soft copper or brass	4.75			
	Iron or soft steel	5.50			
	Monel or 4-6% chrome	6.00			
	Stainless steels	6.50			
Ring joint	Iron or soft steel	5.50	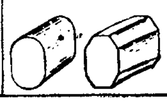	6	1
	Monel or 4-6% chrome	6.00			
	Stainless steels	6.50			

Facing sketch
Exaggerated

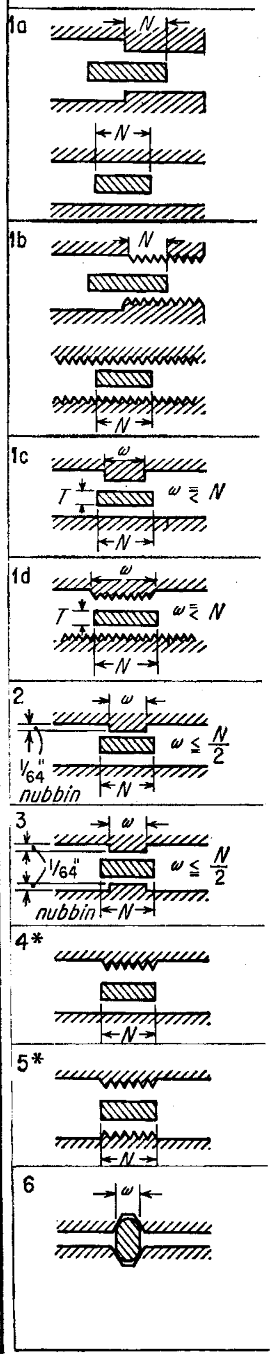

* The surface of a gasket having a lap should not be against the nubbin.

	Basic gasket seating width, b_0		Effective gasket seating width, b
	Column 1	Column 2	
	$\frac{N}{2}$	$\frac{N}{2}$	$b = b_0$, when $b_0 \leq 1/4''$ $b = \frac{\sqrt{b_0}}{2}$, when $b_0 > 1/4''$ Location of gasket load reaction 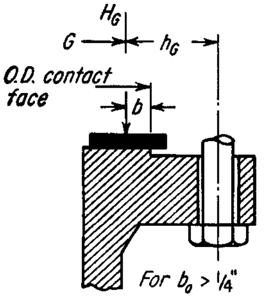
	$\frac{N}{2}$	$\frac{N}{2}$	
	$\frac{\omega+T}{2}$ $\left(\frac{\omega+N}{4} max\right)$	$\frac{\omega+T}{2}$ $\left(\frac{\omega+N}{4} max\right)$	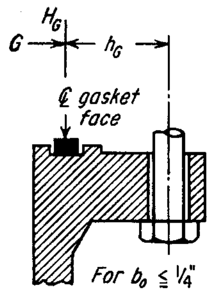
	$\frac{\omega+N}{4}$	$\frac{\omega+3N}{8}$	
	$\frac{\omega}{2}$; $\left(\frac{N}{4} min\right)$	$\frac{\omega+N}{4}$; $\left(\frac{3N}{8} min\right)$	
	$\frac{3N}{8}$	$\frac{7N}{16}$	NOTE: The gasket factors listed only apply to flanged joints in which the gasket is contained entirely within the inner edges of the bolt holes
	$\frac{N}{4}$	$\frac{3N}{8}$	
	$\frac{\omega}{8}$		*Where serrations do not exceed 1/64" depth and 1/32" width spacing, sketches 1b and 1d shall be used

The American Society of Mechanical Engineers has recently compiled very useful data on the amount of bolt pressure necessary to prevent a gasket from blowing out in a cylinder or pressure vessel. The tables below are from the new ASME Boiler and Pressure Vessel Code (Section III Nuclear Vessels).

The proper amount of tightening torque can be obtained from the charts on the previous page—or you can use your own method for determining this value.

Assume that you have a pressure vessel similar to that shown at right.

The required bolt preload in gasketed joints of pressure vessels to maintain the joint tightness can be computed from the following ASME formula:

$$P_t = 0.785\, G^2p + (2\pi bGmp)$$

where

P_t = total minimum required bolt load; divide by the number of bolts for the required preload per bolt

p = internal pressure, psi

b = effective gasket or joint-contact-surface seating width, in. (see table at left)

G = diameter at location of gasket load reaction. G is defined as follows: When $b_o \leq 1/4$ in., G = mean diameter of gasket contact face, in. When $b > 1/4$ in., G = outside diameter of gasket contact face less $2b$, in.

m = gasket factor (from Table II)

Given: A pressure vessel with a 1/16 in. thick asbestos gasket. The internal pressure at 100F is 350 psi. Also, the gasket geometry is:

$b = .306$ in.; $G = 19.388$ in.; $m = 2.75$.

Thus from the ASME formula: $P_t = 139{,}200$ lb.

Pressure vessel, gasket and bolted head

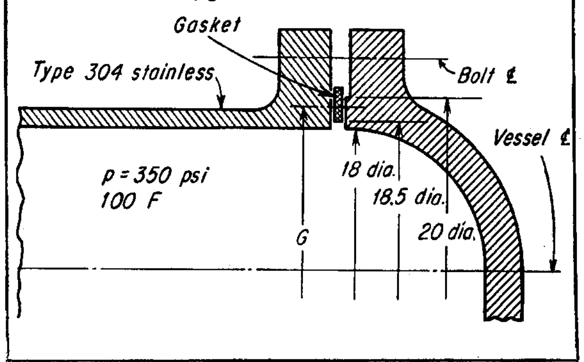

As first choice, try 1-in. bolts of 5A 193 Gr B8. For this material, design to two-thirds yield value (see the table on p 83), or 20,000 psi.

From Fig 4, p 85 the required preload bolt must be kept to less than 10,000 lb. With 16 bolts in the bolt circle, the predicted load per bolt is 139,200/16 = 8700 lb, and the average stress intensity in the bolts will be 18,000 psi—well within the allowable value.

Fig 4 further shows that the bolts (at 8700 lb load and 18,000 psi) should be installed with 145 ft-lb torque.

A Graphical Aid for Combined Stress Problems

John P. Hatch

Two dimensional combined stress problems involve the following formula:

$$T = \sqrt{S_s^2 + (S_t/2)^2} \quad (1)$$

where

S_t = simple direct tensile stress, psi
S_s = simple direct shear stress, psi
T = max. resultant shear stress, psi

When the problem is such that the ratio, $S_s/\frac{1}{2}S_t$ can be computed and the allowable value of T is known, the graphical construction shown in Fig. 1 can be used.

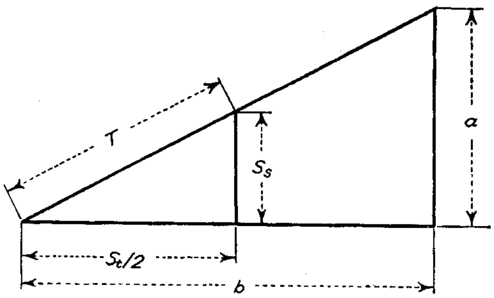

Fig. 1—Construction: Lay off a right triangle with legs a and b such that $a/b = s_s/\frac{1}{2}s_t$. On the hypotenuse lay off T to a convenient psi scale. Drop perpendicular s_s. Using the same psi scale, measure the two stresses, s_s and $s_t/2$.

EXAMPLE: Tension and Shear Loading of Bolt.
Given:
T is not to exceed 7,000 psi
Bolts are loaded as shown in Fig. 2.
PROBLEM: Find bolt diameter required.
SOLUTION:

$$L_s = \text{shear load per bolt} = \frac{3{,}000}{2} = 1{,}500 \text{ lb}$$

$$L_t = \text{tensile load per bolt} = \frac{6 \times 3{,}000}{2 \times 3.5} = 2{,}570 \text{ lb}$$

a = area of bolt, sq. in.

Then
$$\frac{L_s}{L_t} = \frac{1{,}500}{2{,}570} = \frac{a\,S_s}{a\,S_t}$$

Thus,
$$\frac{S_s}{S_t/2} = \frac{1{,}500}{1{,}285}$$

See Fig. 3 for the graphical solution.

The following calculations are not necessary if the foregoing construction is made. In lieu of the construction, the solution is:

$$\tan\alpha = \frac{1{,}500}{1{,}285} = 1.168$$
$$= 49.4 \text{ deg (approx)}$$
$$S_s = T\sin\alpha = 7{,}000 \times 0.759 = 5{,}313 \text{ psi}$$

This value is satisfactory since it is less than the allowable stress. Based on the maximum shear stress theory of failure, the bolt dia, d, is:

$$d = \sqrt{4L_s/\pi S_s} = \sqrt{\frac{4 \times 1{,}500}{3.1416 \times 5{,}313}} = 0.60 \text{ in.}$$

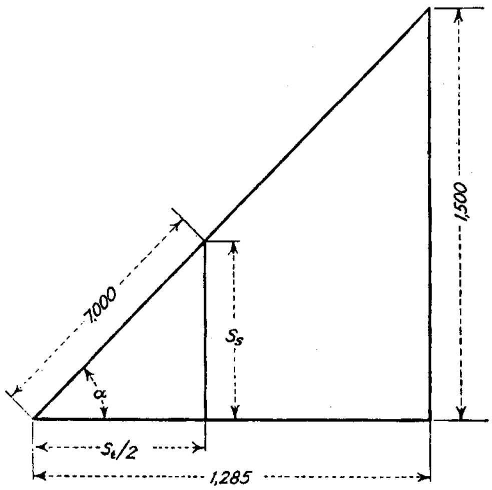

Fig. 3—Legs L_s and $L_t/2$ correspond to a and b in the sample construction. After dropping the perpendicular, s_s and $s_t/2$ are measured with the psi scale used to layout T=7,000 units on the diagonal.

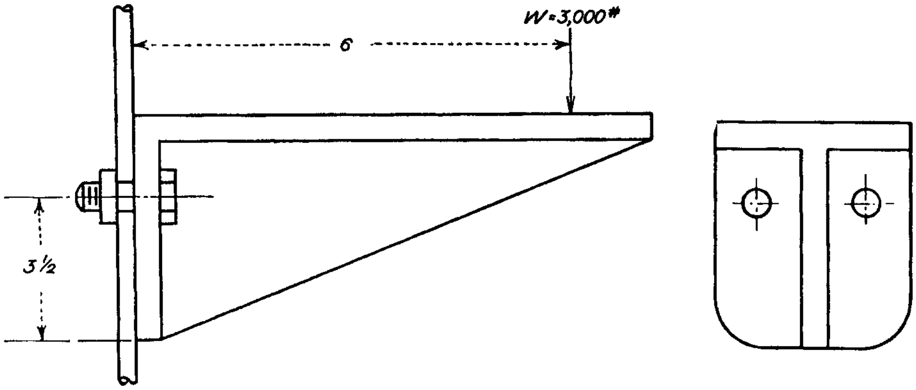

Fig. 2—Bolts in sample problem are loaded as shown. Graphical construction is shown in Fig. 3.

Pin and Shaft of Equal Strength

Herman J. Scholtze

THE ACCOMPANYING TABLE gives the sizes of round driving pins and round shafts drilled to receive the pin in which both parts are equally strong in shear, for the condition that the shaft and pin are made of the same material.

The author has discovered that when the pin diameter equals 40 percent of the shaft diameter, the shearing stress in the pin equals the shearing stress in the shaft, also that the polar moment of inertia of the drilled shaft equals the shaft radius to the fourth power.

Values given in the table in columns headed "Torque," and "Load on One End of Pin" have been computed for a shear stress of 12,000 lb. per sq. in. For other values of shear stress, the load on one end of pin equals the cross-section area of the pin multiplied by the allowable shear stress, and the torque equals the load on the pin multiplied by the shaft diameter.

R = radius of shaft, in.
r = radius of pin, in.
S_s = shearing stress in shaft, lb. per sq. in.
S_p = shearing stress in pin, lb. per sq. in.
J = polar moment of shaft cross-section through the axis of pin bore
T_s = torque on shaft, in. lb.
T_p = torque delivered by pin, in. lb.
θ = central angle subtended by one half the chord of circular segment section or drilled shaft, radians

$$T_p = 2\pi r^2 R S_p$$

$$T_s = J S_s / R$$

$$r = \sqrt{J}/(R\sqrt{2\pi})$$

$$J = R^4\theta - r^4\left(\frac{\sin\theta}{3\cos^3\theta} + \frac{2\tan\theta}{3}\right)$$

$$r = \frac{1}{R\sqrt{2\pi}}\left[R^4\theta - r^4\left(\frac{\sin\theta}{3\cos^3\theta} + \frac{2\tan\theta}{3}\right)\right]^{1/2}$$

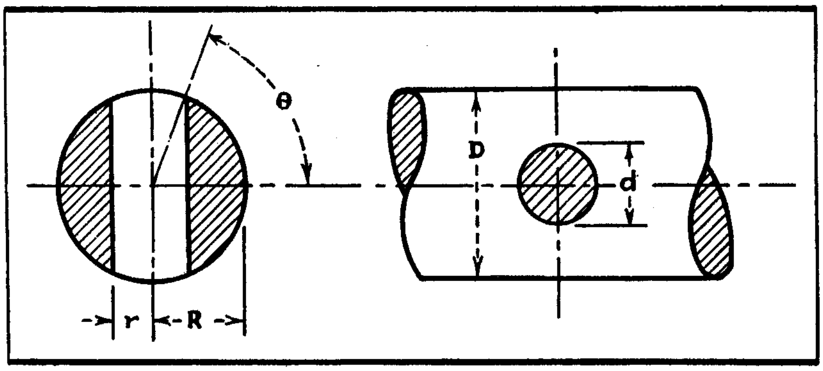

Equal Strength Shafts and Pins of Similar Material

Dia. of Shaft, in. D	Dia. of Pin, in. d	Polar Moment of Inertia, J	Polar Section Modulus, J/R	Torque, in. lb. at 12,000 lb. per sq. in. Shear Stress T	Load on One End of Pin, lb. $P = T/D$	Cross-Section Area of One End of Pin, sq. in.
1/4	0.100	0.000244	0.001952	23.5	94	0.00785
5/16	0.125	0.000597	0.003820	45.8	146	0.01277
3/8	0.150	0.001236	0.006579	79	210	0.01767
7/16	0.175	0.002290	0.01047	125	286	0.02405
1/2	0.200	0.003906	0.01562	187	374	0.03142
5/8	0.250	0.009537	0.03051	366	590	0.04909
3/4	0.300	0.01977	0.05273	635	845	0.07069
7/8	0.350	0.03663	0.08374	1,010	1,160	0.09621
1	0.400	0.06250	0.1250	1,500	1,500	0.1257
1-1/4	0.500	0.1526	0.2442	2,940	2,350	0.1963
1-1/2	0.600	0.3164	0.4218	5,100	3,400	0.2827
1-3/4	0.700	0.5862	0.6700	8,000	4,570	0.3848
2	0.800	1.0000	1.0000	12,000	6,000	0.5027
2-1/4	0.900	1.6018	1.4238	17,000	7,550	0.6362
2-1/2	1.00	2.4414	1.9531	23,400	9,350	0.7854
2-3/4	1.10	3.5745	2.6000	31,200	11,350	0.9500
3	1.20	5.0625	3.3750	40,500	13,500	1.131
3-1/2	1.40	9.3789	5.3593	64,000	18,200	1.539
4	1.60	16.000	8.0000	96,000	24,000	2.011
4-1/2	1.80	25.629	11.390	125,000	27,700	2.545
5	2.00	39.062	15.625	187,000	37,500	3.142
5-1/2	2.20	57.191	20.797	240,000	43,750	3.801
6	2.40	81.000	27.000	324,000	54,000	4.524
7	2.80	150.062	42.875	515,000	73,500	6.158
8	3.20	256.000	64.000	770,000	96,000	8.042
9	3.60	410.062	91.125	1,090,000	121,000	10.18
10	4.00	625.000	125.000	1,500,000	150,000	12.57
11	4.40	915.062	166.375	2,000,000	182,000	15.21
12	4.80	1,296.000	216.000	2,600,000	216,000	18.10

Design for Shock Resistance

Alignment charts based on the shock-rise time concept have established the performance requirements and deflections for shock mounts.

Raymond T. Magner

IF you know the form and intensity of shock a product sustain during assembly, trans n and use, you can determine ptibility to damage Test results will establish whether the product must be redesigned, partially protected, or isolated from certain kinds of shock altogether. Sometimes all three steps are necessary.

Shock damage is caused by acceleration forces developed during impact. These forces can be measured by accelerometers placed on critical parts of the product, although the instrumentation required for precise measurements under heavy impact loads is complex. Useful values for maximum acceleration can be computed from the shock-rise time and drop height by the formula

$$G = \frac{72}{t} \sqrt{h}$$

where G = acceleration, g
t = shock-rise time, millisec
h = drop height, in.

Drop height can usually be determined with fair accuracy. The shock-rise time is dependent on the elasticity of the striking mass, resilience of impact surface, and extent of contact area, which may be a flat or a curved surface, an edge, or a point. Shock-rise time has been determined for a variety of conditions by careful instrumentation. For point contact between a rigid steel frame and a concrete surface, assuming that the mass of the struck surface is at least 10 times the mass of the striking body, the rise time is 1 to 2 millisec; for a flat face contacting soft earth or sand, the rise time is about 6 millisec.

The most severe shock, such as

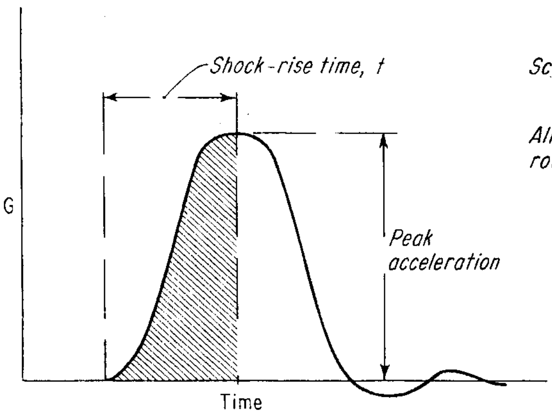

PEAK ACCELERATION felt by a dropped mass is inversely proportional to shock-rise time, which is dependent on rigidity of materials and area of contact.

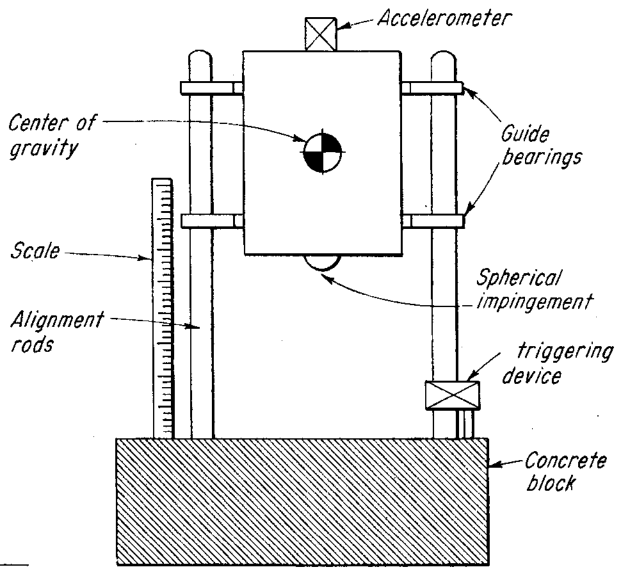

FREE-FALL IMPACT on concrete, measured using a hardwood surface of 1-in. radius, provided a point contact; shock-rise time under these conditions was 2 millisec.

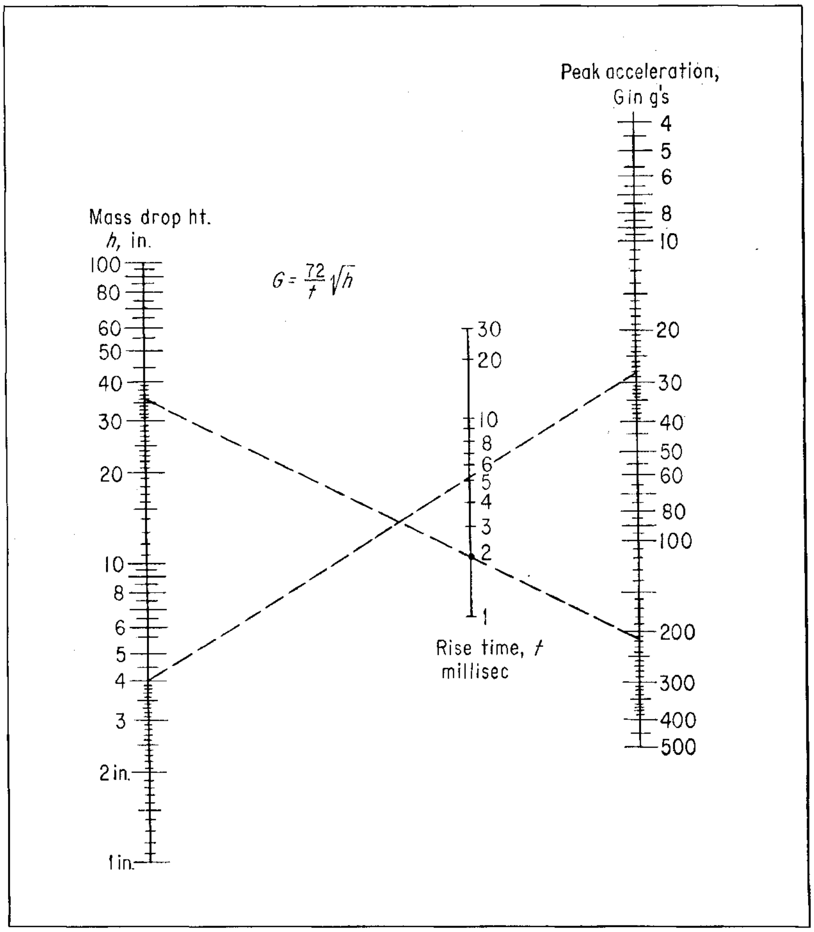

DROP HEIGHT alone will establish the peak acceleration when rise time is known for the impacting conditions. For a 3-ft fall from a truck tailgate to a concrete road, peak acceleration will be over 200 g; a 4-in. flat drop to sand will develop about 30 g.

TYPICAL VALUES FOR SHOCK-RISE TIME

CONDITION	FLAT FACE	POINT
RIGID STEEL AGAINST CONCRETE	1	2
RIGID STEEL AGAINST WOOD OR MASTIC	2-3	5-6
STEEL OR ALUMINUM AGAINST COMPACT EARTH	2-4	6-8
STEEL OR ALUMINUM AGAINST SAND	5-6	15
PRODUCT CASE AGAINST MUD	15	20
PRODUCT CASE AGAINST 1-IN. FELT	20	30

Note. Mass of struck surface is assumed to be at least 10 times the striking mass. Point contact with spherical radius of 1 in.

dropping from a truck tailgate to a concrete road surface, involves rise times so short that they are difficult to measure. Extensive tests for this type of impact were made using a spherical steel impingement surface with a radius of 1 in. striking smooth concrete. The striking mass was rigid enough to have a resonance frequency above 400 cycles. Under these test conditions a repeatable value of rise time was 2 millisec.

For free-fall shock conditions where the drop height is known and the rise time can be determined, the alignment chart, left, solves the equation for peak acceleration. For example, a rigid product falling off a truck tailgate 36 in. high and making point contact on a solid concrete surface (rise time 2 millisec) will experience an acceleration force greater than 200 g.

Impact on less rigid surfaces such as wood, mastic, compact earth, or sand produces rise times of 5 to 15 millisec, see table. A 3-ft drop to mastic or wood with a rise time of 5 millisec will produce 85 g; against a sand or mud surface with a rise time of 10 to 15 millisec, 25 to 40 g. A unit slipping from the hands of an operator and dropping 4 in. onto a felt pad 1 in. thick will have a shock-rise time of about 30 millisec and receive a shock of 2 to 4 g.

Transportation shocks

Vertical accelerations on the body of a 2-ton truck traveling at 30 mph on good pavement range from 1 to 2 g, with a rise time of 10 to 15 millisec. Higher speeds, rougher roads, stiffer truck springs, and careless driving all decrease the rise time and thus double or triple the acceleration loads.

Highest acceleration forces in railroad freight cars are encountered in humping, where impact loads on the product container may be from 4.5 to 28 g. Loading on car, speed at impact, and type of draft gear are important variables, as shown in the curves on page 86 for horizontal shock during humping.

Military service calls for two series of shock tests. The first imposes 18 shocks of 15 g and 5.5 millisec rise time, three on each axis and in each direction; performance of the equipment must be unaffected. The second or "crash" series calls for 2 shocks on each axis with a peak acceleration of 30 g and 5.5 millisec rise time; the equipment must remain captive but is not required to operate after this test. Most commercial airborne specifications are similar to military requirements except that acceleration levels are somewhat lower.

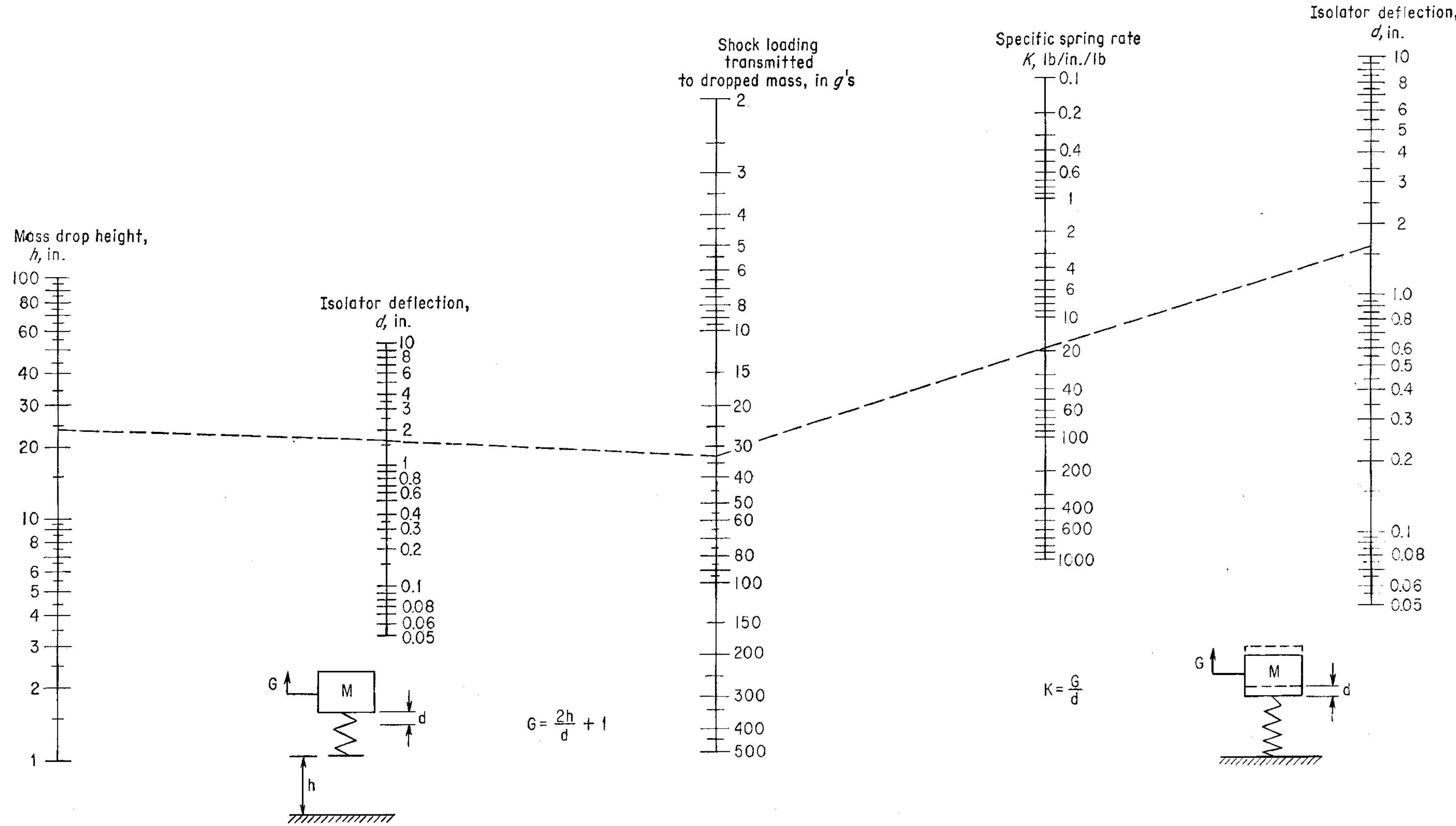

DEFLECTION AND STIFFNESS of an isolator are obtained in two steps: 1) drop height and maximum acceleration of product determine isolator deflection. 2) maximum acceleration and isolator deflection establish spring-rate factor which, multiplied by the dead weight load on the isolator, gives the deflection rate in pounds per inch.

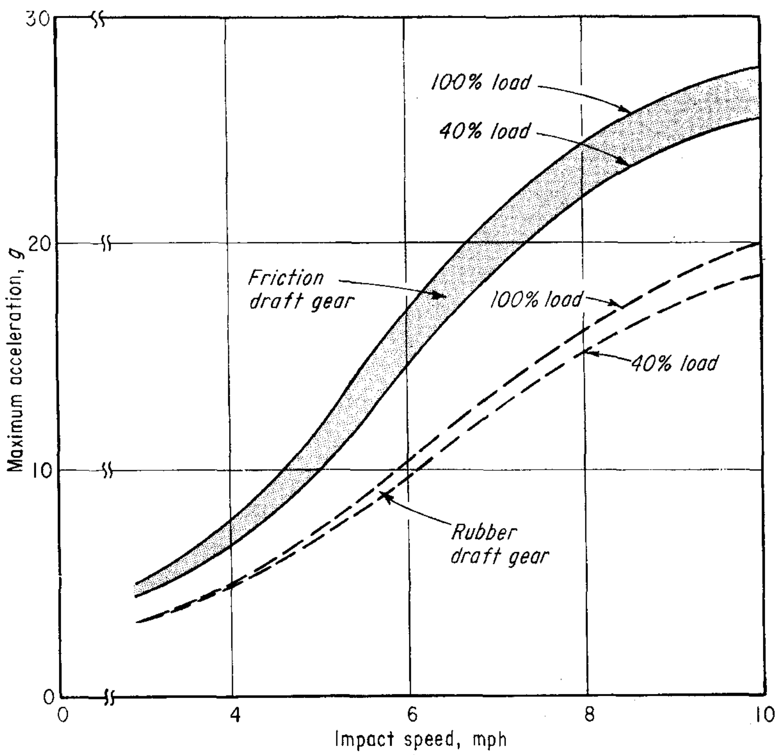

HORIZONTAL SHOCK forces imposed on product container in freight cars during humping. Rubber draft gear reduces shock at all speeds.

Maximum shock the product can withstand is determined by the rigidity and resonance frequencies of the structure and the shock sensitivity of its components. Two levels of failure are significant: momentary malfunction at instant of shock, and catastrophic or permanent damage.

As a first step in evaluating the shock sensitivity of a product the structure should be subjected to static loads equal to the peak shock loads anticipated, and the deflections should be measured. The location of sensitive components and the rigidity of their supporting structures determine how much of the imposed shock will reach them. Ample space must be provided for deflection of components under shock.

For most components that are sensitive to shock, suppliers include maximum safe acceleration loads in catalog data. Maximum loads on vacuum tubes are 2 to 5 g; relays may withstand higher accelerations, depending on the type and direction of acceleration. Transistors are of low mass and good rigidity, and when properly supported are highly resistant to shock. Ball bearings races may be indented by the balls; sleeve bearings are usually much more resistant to shock.

When expected shocks exceed the maximum safe value, a shock isolator must be incorporated in the product between the shock-sensitive elements and the point of impact. The major practical problem is trade-off between isolator deflection and the maximum shock load that can be accepted. Increased margin of safety requires increased allowance for movement.

To help you reach a compromise, the left half of the large alignment chart gives the isolator deflection for a selected acceleration when the drop height is known. The chart assumes a drop on concrete, and a 2-millisec shock-rise time. For a drop of 24 in. with a maximum transmitted shock of 33 g, the isolator deflection will be 1.65 in.

The right half of the chart shows the specific spring rate for the selected isolator deflection. Multiplying the specific spring rate by the weight carried by each isolator gives the deflection rate, in pounds per inch, that should be specified for the isolator.

Continuing the example, the specific spring rate is 19 for 33 g and 1.65 in. deflection. If the equipment weighs 25 lb and the load is divided equally between four isolators, the spring rate for each isolator will be $19 \times 25/4 = 118$ lb/in.

This chart gives a quick and ready answer for preliminary design, particularly in developing clearance requirements and isolator capacity. To simplify the various charts a linear, undamped system with one degree of fredom is assumed; results given are conservative, particularly if such design refinements as nonlinear deflection rate and some damping are added.

An isolator with a nonlinear deflection rate (stiffness increasing with deflection) will reduce the isolator deflection for a given transmitted acceleration and will also give added protection against bottoming under a shock of higher intensity than anticipated. Addition of damping for control of excursion at resonance frequency will also reduce isolator deflection by a small amount.

Most mounting systems provide six degrees of freedom; they are free to move in vertical, lateral, and longitudinal axes and to rotate about these axes. The deflection rate of an isolator may be substantially different in vertical and horizontal directions if this is required by expected service conditions.

The function of a shock mount is to provide enough protection to avoid damage under expected conditions, but overdesign can be costly, both in the design of the product and in the shock-mount components. To avoid underdesign and service failures on one hand, and overdesign and added cost on the other, shock-mount specialists should be asked for their assistance and recommendations before the design is frozen.

K Factor for Impact Loading

This allowance for loss of energy on impact gives more accurate values for stress and deformation.

S. Warran Kaye

Usual formulas for impact loading assume complete recovery of the kinetic energy of the moving body. This isn't so. Some kinetic energy is dissipated. The K factor in following equations is a measure of this energy loss.

The corrected formula for deformation and stress with vertical impact is:

$$d_i/d = S_i/S = 1 + \sqrt{1 + 2Kh/d}.$$

The corrected formula for deformation and stress with horizontal impact is:

$$d_i/d = S_i/S = \sqrt{Kv^2/(384.6)d}.$$

SYMBOLS

d = Deformation for static loading, in.
d_i = Deformation for impact loading, in.
h = Initial height of striking body above struck body, in.
K = Impact-loading factor
M = Mass of striking body, lb-sec²/in.
M_1 = Mass of struck body, lb-sec²/in.
S = Stress in struck body for static loading, psi
S_i = Stress in struck body for impact loading, psi
v = Velocity of striking body, in./sec

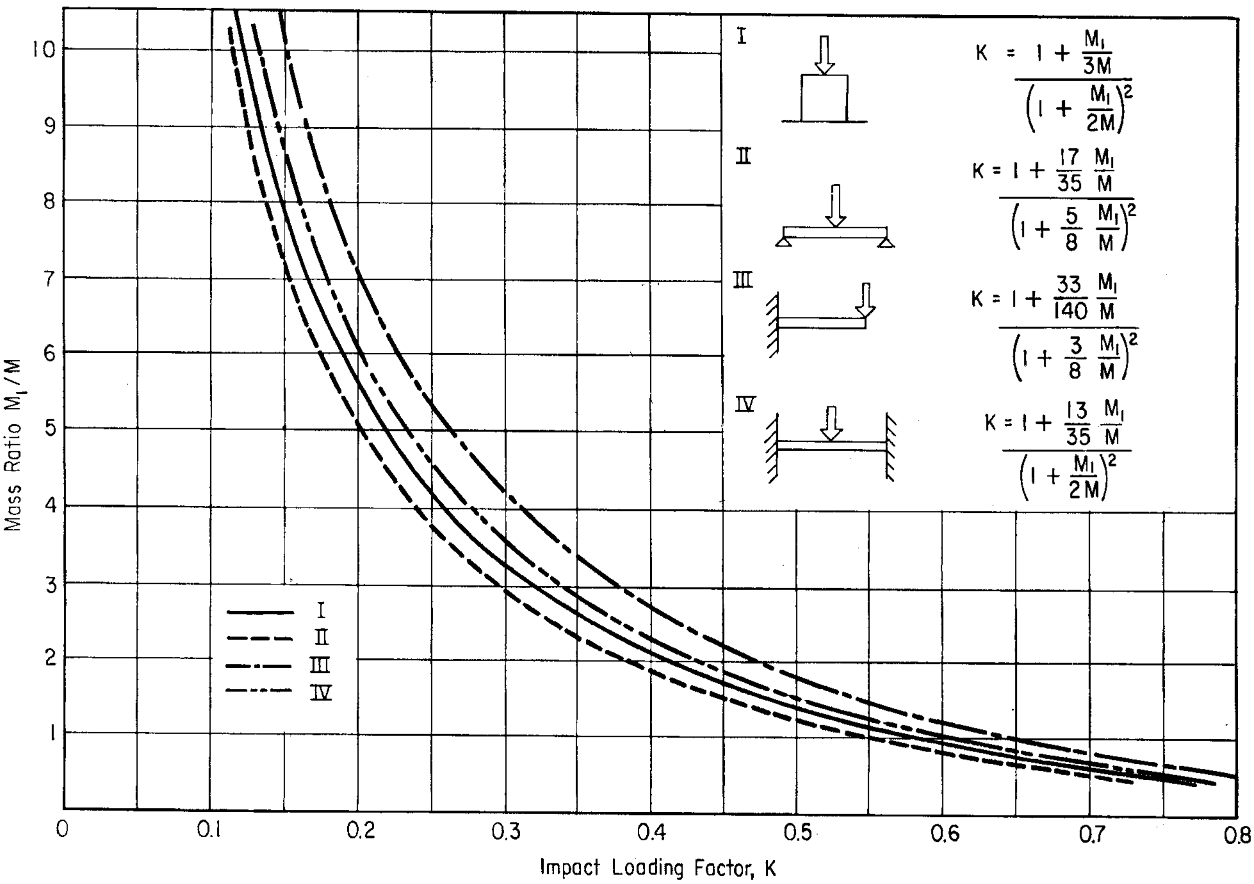

SECTION 30

NOMOGRAMS

Nomogram for Angles in Constructed Shares

H. F. Bariffi

FROM THE ALTITUDE, h, and the differences $(a—d)$ and $(b—c)$ in lengths of corresponding sides of upper and lower bases, the dihedral angle A can be calculated.

To calculate S_b connect the given value of $(a—d)$ on the right hand outer scale with the value of h on the h-scale and read the value of S_b. In like manner, the value of S_a can be calculated from $(b—c)$ and h. Connect the value of S_a to the value of S_b on the diagonal scale and project to the Q-ine. Connect the intersection of this line and the Q-line with the given value of $(a—d)$ on the inner left hand scale. Connect the intersection of this line and the diagonal T-line with the $(b—c)$-scale. Project this line to the left hand scale and read the angle A.

EXAMPLE: When $h = 17$ in., $(b—c) = 25$ in. and $(a—d) = 28$ in., find S_a, S_b and A. Connecting 28 in. on the outer right hand $(a—d)$-scale and 17 in. on the h-scale gives a line crossing the S_b-scale at 22 in. Also, connecting 25 in. on the outer right hand $(b—c)$-scale and 17 in. on the h-scale gives a line crossing the S_a-scale at 21.1 in. A line connecting 21.1 in. on the inner right hand S_a scale with 22 in. on the diagonal S_b scale intersects the Q-line at the indicated point. A line connecting this point with 28 in. on the inner left hand $(a—d)$-scale crosses the diagonal T-line at the indicated point. A line connecting this point with 25 in. on the $(b—c)$-scale passes through the point 112.1 deg on the A scale.

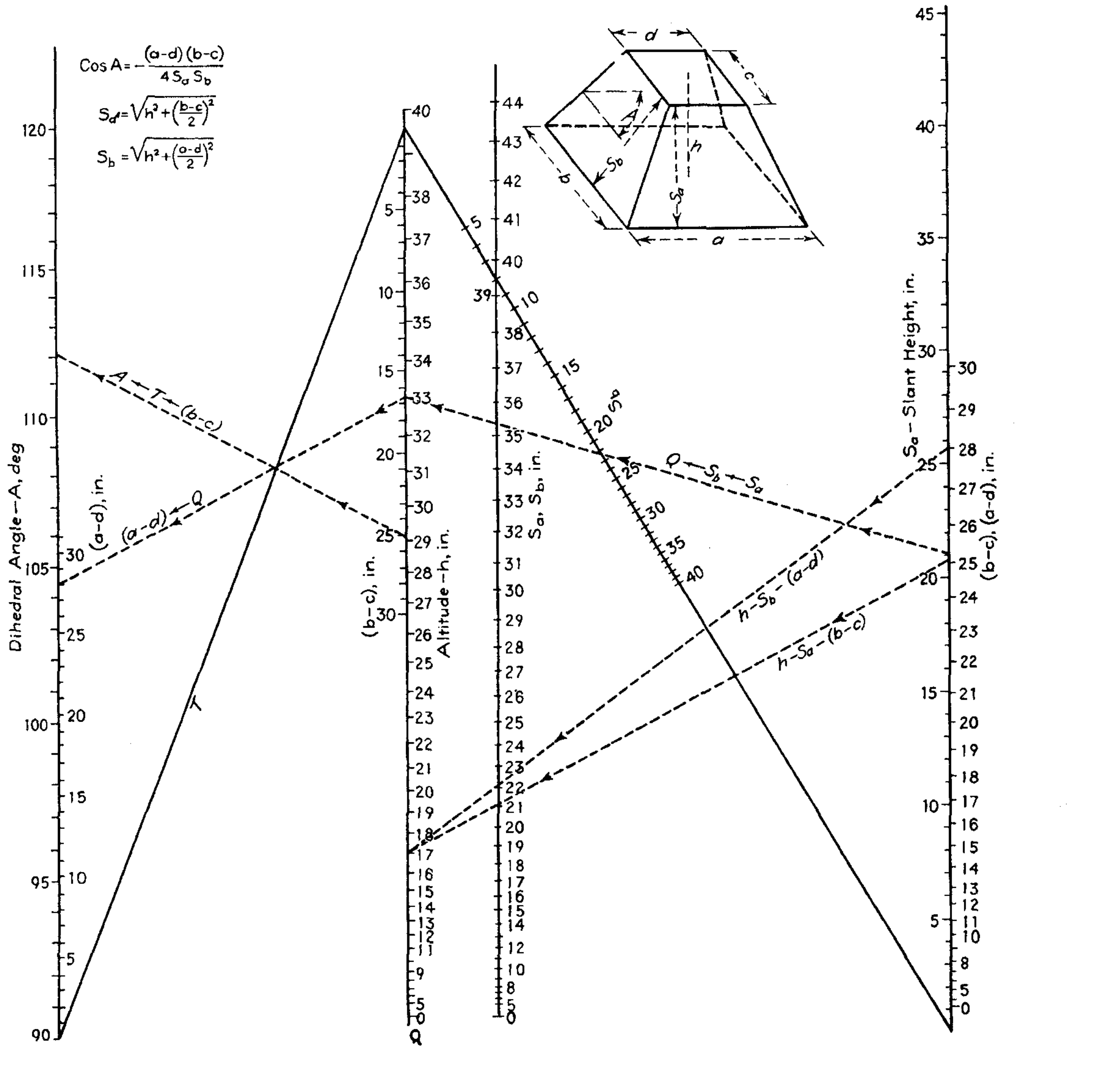

Arc Length Versus Central Angle

(Angle of Bend, Length, and Radius)

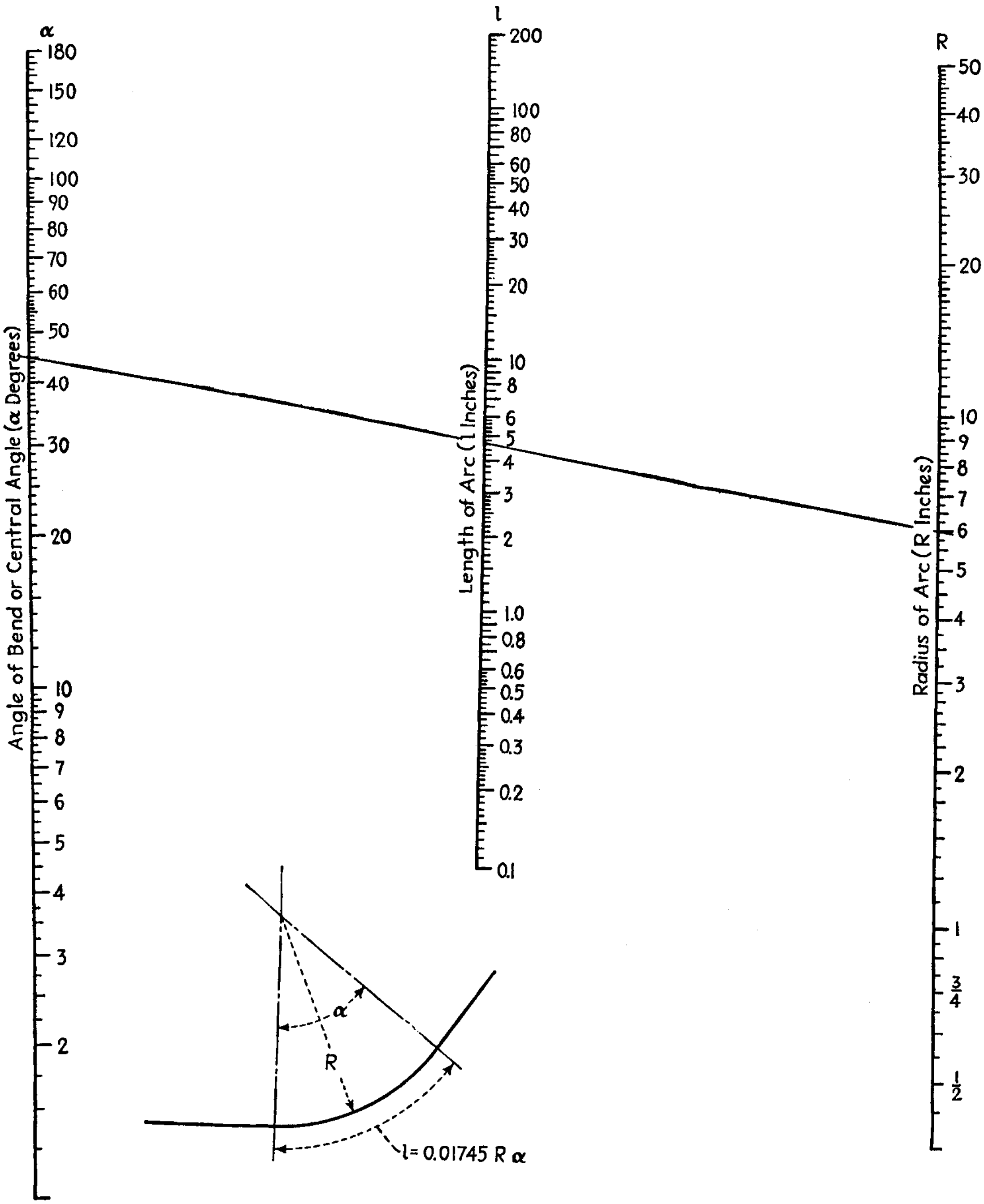

Draw a straight line through the two known points. The answer will be found at the intersection of this line with the third scale.

Example: For a 6-in. radius and 45-deg. bend, length of arc is 4.7 in.

Chordal Height and Length of chord

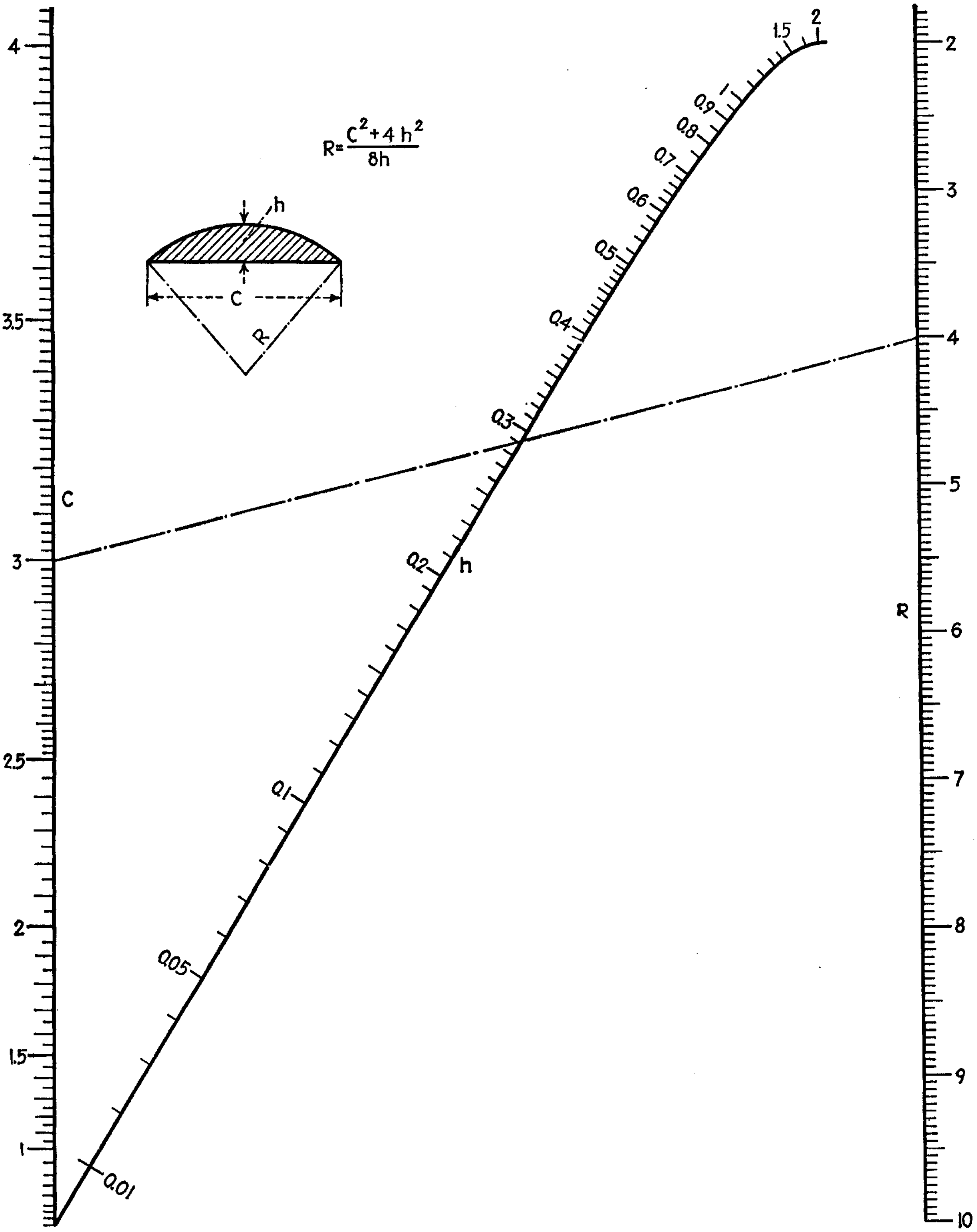

Draw a straight line through the two known points. The answer will be found at the intersection of this line with the third scale.

Example: Length of chord is 3 in., and radius of circle is 4 in. The height *h* of the chord is 0.29 in.

Forces in Toggle Joint with Equal Arms

$$\frac{P}{F} = \frac{S}{4h}$$

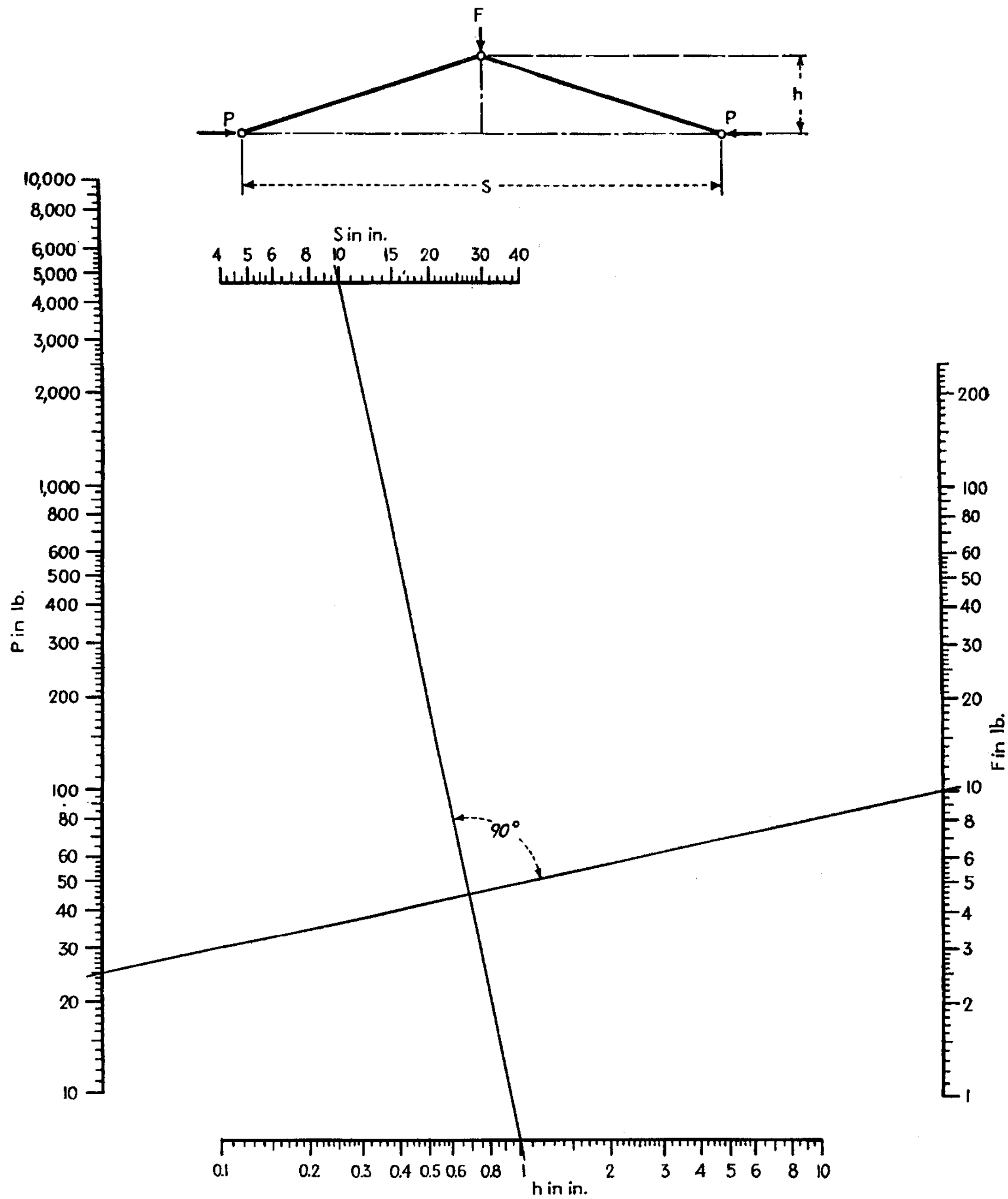

Example: Use mutually perpendicular lines drawn on tracing cloth or celluloid. In the example given for $S = 10$ in. and $h = 1$ in., a force F of 10 lb. exerts pressures P of 25 lb. each.

Radial Deflections of Rotating Disks: With Constant Thickness and Central Hole

L. M. Porter

THE NOMOGRAM SOLVES the equations for the total radial deflection at the inner and outer radius of rotative disks with constant thickness. The equations[1] are based on steel disks with $E = 29 \times 10^6$ psi and Poisson's ratio of 1/3. Since the ratio of density to Young's modulus is almost the same for steel, magnesium, and aluminum, the nomogram can be used for all three materials with an error of about 0.5 per cent for aluminum and 2.5 per cent for magnesium. While the nomogram will solve the equations for any values of the independent variables within the limits of the chart, the resulting values of the deflection are of no practical value if the elastic limit of the material has been exceeded.

The tangential stresses can be found by dividing the total radial deflection by the original radius and multiplying the quotient by the modulus of elasticity, E of the metal.

EXAMPLE:

A steel disk with inner radius 2.0 in., outer radius 10.0 in. rotates 10,000 rpm. Find deflection and stress at inner radius.

SOLUTION:

Ratio K of outer to inner radius is 5.0. K scale is graduated on both sides: the left for finding the deflection at the outer radius and the right side for determining the deflection at the inner radius. Line I connects a value of 2.0 on the r scale with 5.0 on the right side of the K scale, establishing a point on the turning line. Line II drawn through this turning point to 10,000 rpm gives δ_1 of 0.0046 in. for the radial deflection. The tangential tensile stress is then found to be:

$$\sigma_t = \frac{0.0046}{2} \times 29 \times 10^6 = 66{,}700 \text{ psi.}$$

1. Reference: Derived from equations of A. Stadola in *Turbo-Blowers and Compressors* by W. J. Kearton.

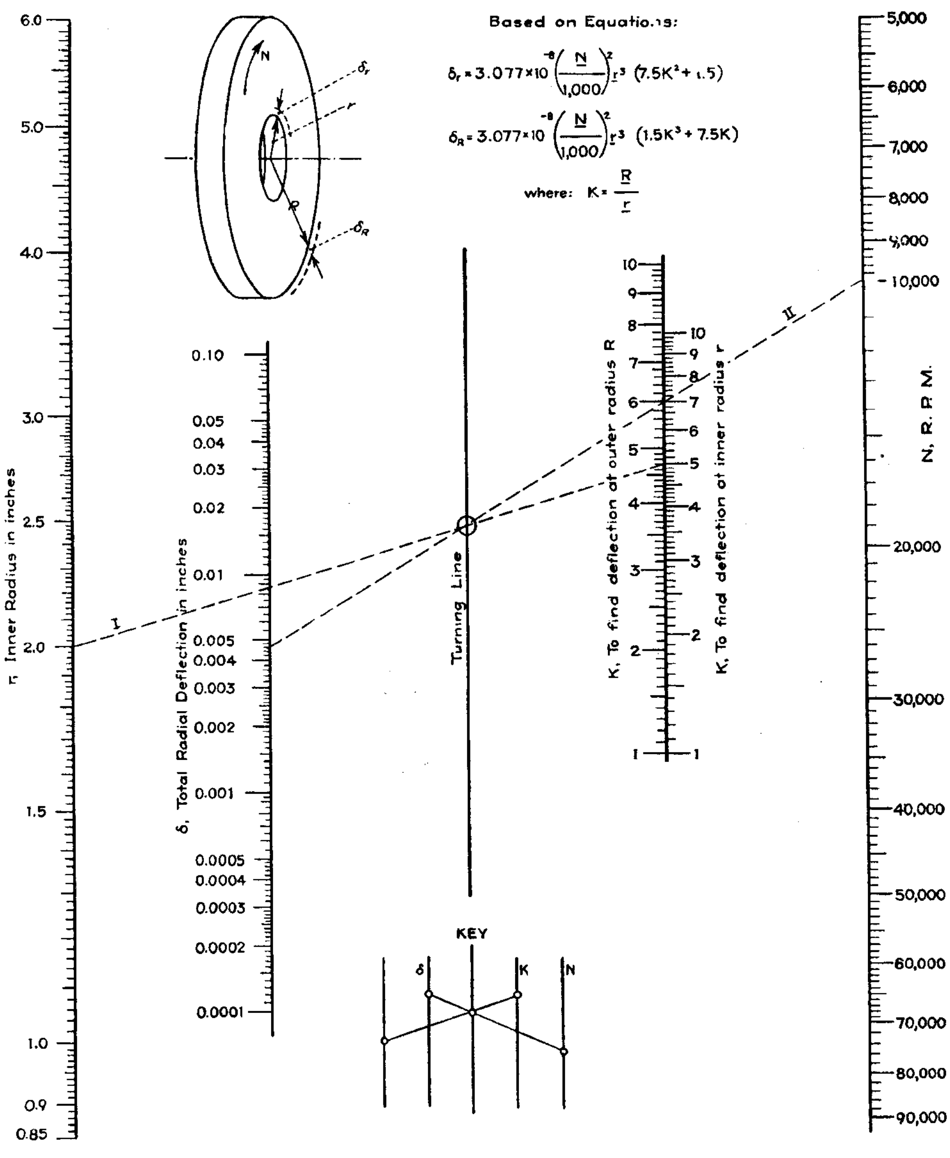

Power Capacity of Spur Gears

Charles Tiplitz

MAXIMUM RATED HORSEPOWER that can safely be transmitted by a gear depends upon whether it runs for short periods or continuously. Capacity may be based on tooth strength if the gear is run only periodically; durability or wear governs rated horsepower for continuous running.

Checking strength and surface durability of gears can be a lengthy procedure. The following charts simplify the work and give values accurate to 5 to 10%. They are based on AGMA standards for strength and durability of spur gears.

Strength Nomograph is used first. Apart from the

Strength of Spur Gears.
Based on AGMA 220.01

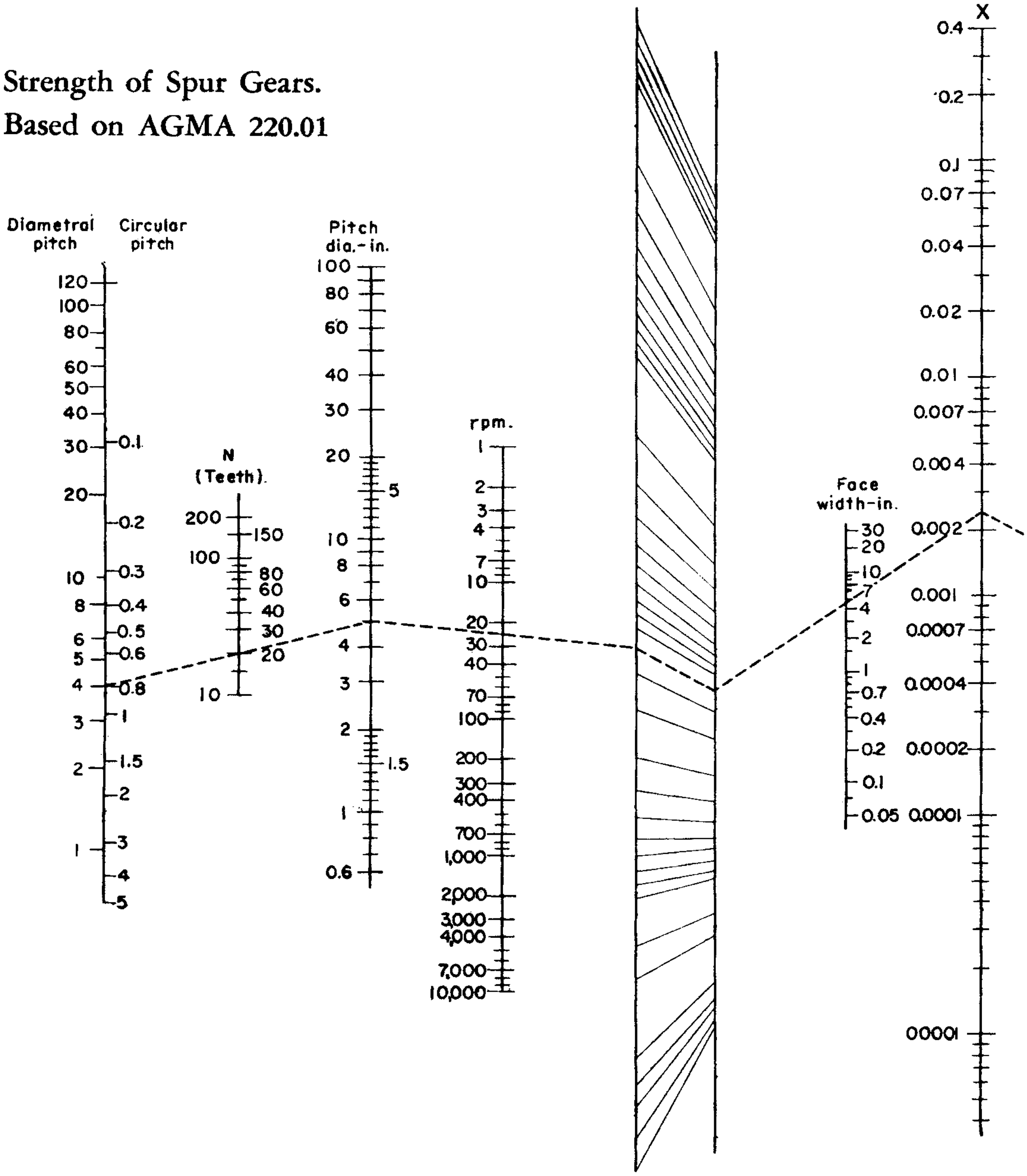

usual design constants only two of the following three need be known: pitch, number of teeth and pitch diameter. To use the charts connect the two known factors by a straight line, cutting the third scale. From this point on the scale continue drawing straight lines through known factors, cutting the pivot scales. Between the double pivot scales the line should be drawn parallel to the adjacent lines.

Durability nomograph must be entered on scale X at the same value that was cut on the X scale on the strength chart. Both pinion and gear should be checked if made of different materials and the smaller of the values obtained should be used.

Strength of Spur Gears (cont.)

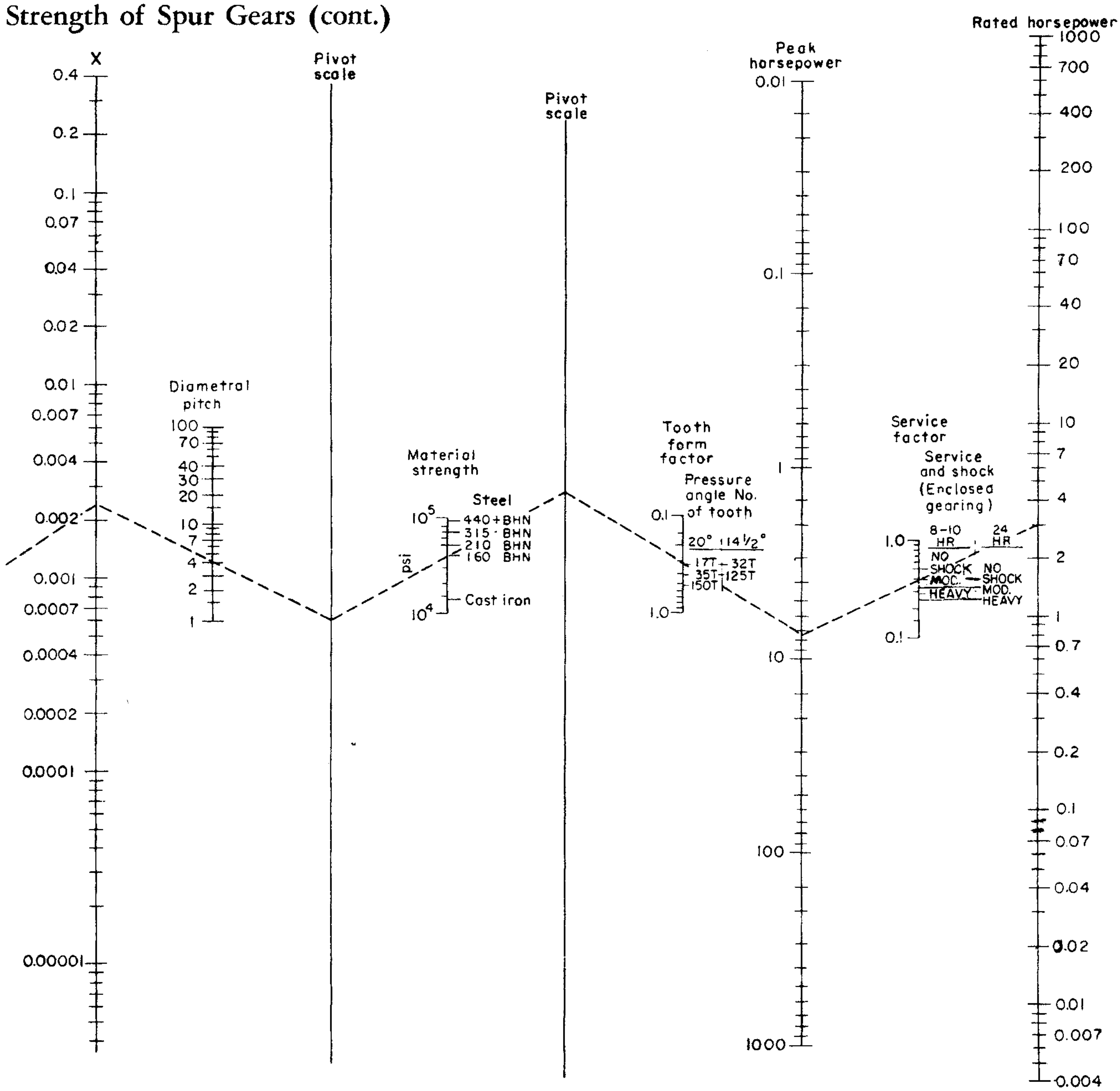

Surface Durability of Spur Gears. Based on AGMA 210.01

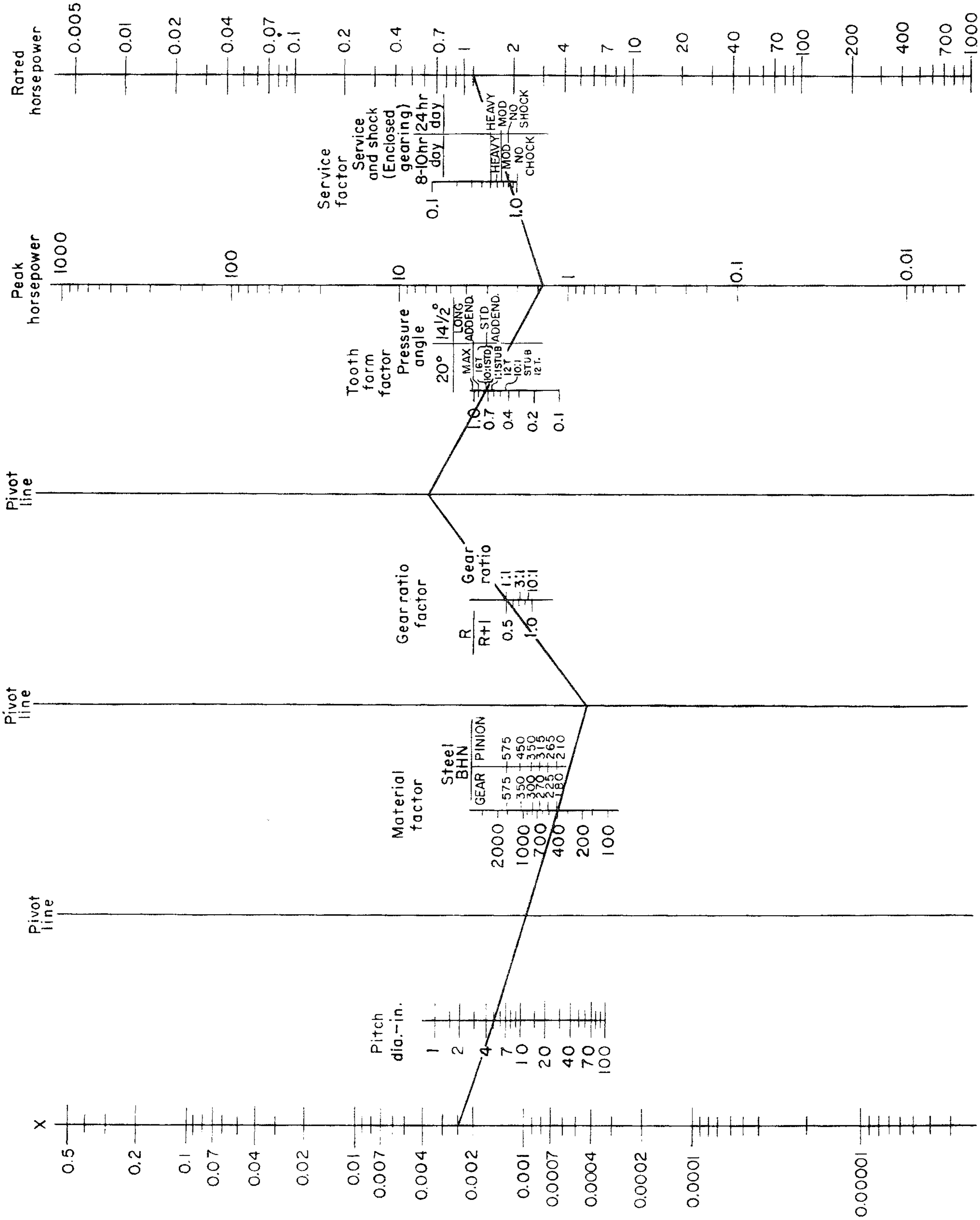

Alignment Chart for Face Gears

B. Bloomfield

THE MAXIMUM PRACTICAL DIAMETER for face gears is that diameter at which the teeth become pointed. The limiting inside diameter is the value at which tooth trimming occurs. This is always larger than the diameter for which the operating pressure angle is zero. The two alignment charts that follow can be used to find the maximum OD and the minimum ID if the numbers of teeth in the face gear and pinion are known. They eliminate lengthy calculations.

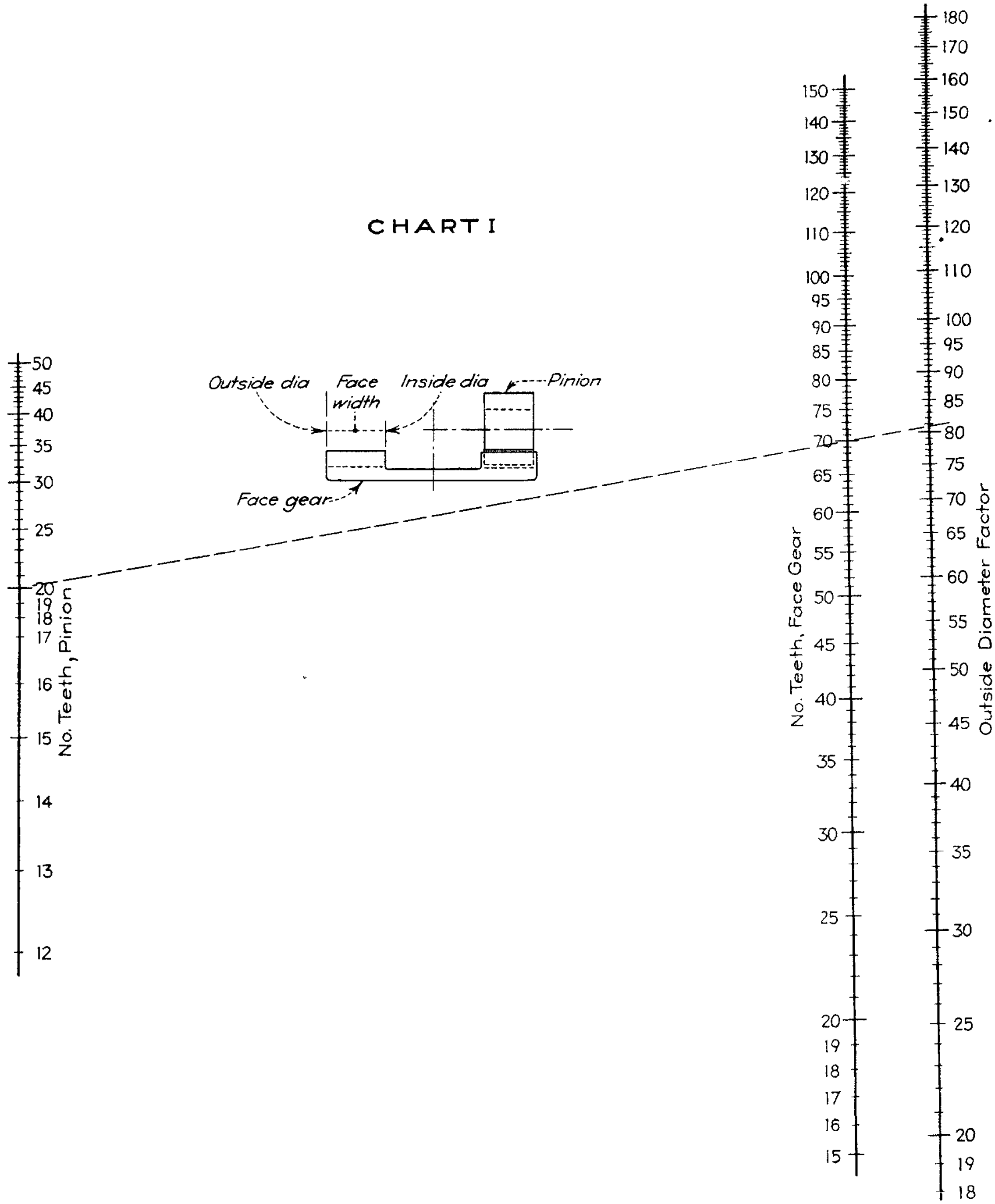

FOR BOTH CHARTS the pinions are assumed to be spur gears of standard AGMA proportions, and the axes of the face gear and pinion are assumed to intersect at right angles. Both should be used only for tooth ratios of 1.5 to 1 or larger. Smaller ratios require pinion modifications not allowed for in these data. For both charts, the appropriate face gear diameter is found by dividing the factor from the chart by the diametral pitch of the pinion.

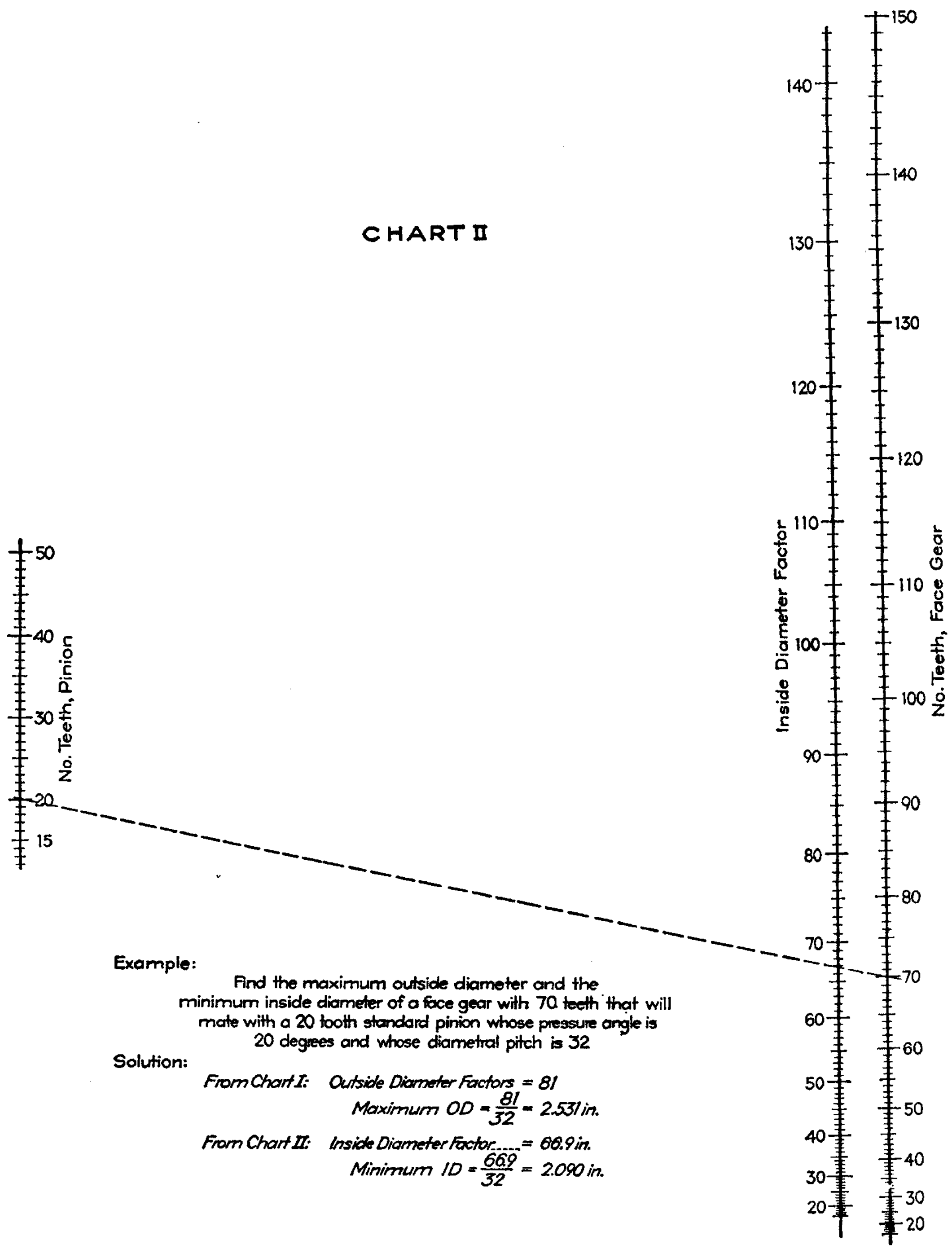

Linear to Angular Conversion of Gear-Tooth Index Error

For pitch diameters up to 200 inch, chart quickly converts index error from ten-thousandths of an inch to seconds or arc.

Harold R. Ronan JR.

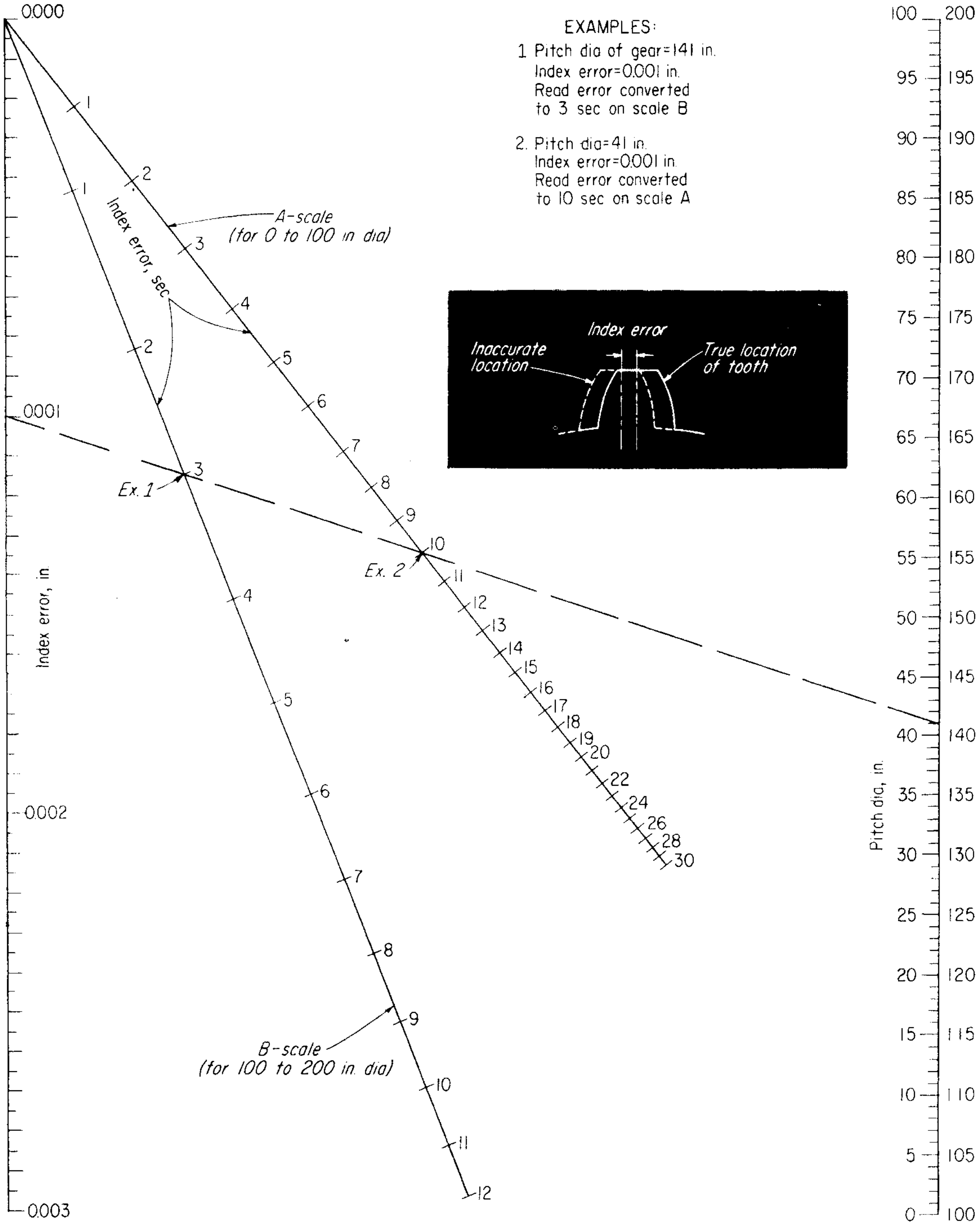

Determine Parallel Axis Moment of Inertia

Herbert F. Bariffi

ONE METHOD of determining the moment of inertia of a mass through its center of gravity is to suspend the mass from a knife-edge. Such an arrangement, using a piece of keystock for a knife-edge, is shown in Fig. 1. If this compound gravity pendulum, which is in effect what the setup amounts to, is set swinging and the arc of swing is limited to about 6 deg double amplitude, the moment of inertia about the support axis is equal to

$$I_o = \frac{W}{4\pi^2} t^2 L \tag{1}$$

where

I_o = moment of inertia about support axis
W = weight of mass, lb
t = oscillation period, sec
L = distance between center of gravity and support axis, in.

To find the moment of inertia about center of gravity the following equation can be used.

$$I_{cg} = I_o - L^2 \frac{W}{g} \tag{2}$$

where

g = acceleration of gravity, ft per sec²

Substituting I_o value from Eq (1) into Eq (2)

$$I_{cg} = \frac{W}{4\pi^2} t^2 L - L^2 \frac{W}{32.2 \times 12}$$

Simplifying

$$I_{cg} = WL\,[0.02533\, t^2 - 0.002588 L] \tag{3}$$

This Eq (3) will give values of I_{cg} in in. lb sec².

The nomogram illustrated can be used to solve for I_{cg} with values of t, L and W known. To use this nomogram start with a value t on the inner left-hand A scale, pass through a value of L on the A curve to the right-hand, or turning axis. Then, follow a straight line from the turning point through a value of W on the A diagonal, and return to the left-hand axis, reading I_{cg} on the outer scale. By using the right-hand I and t scales, and working to the left over the B curve for L, the same problem can be solved with larger values of t.

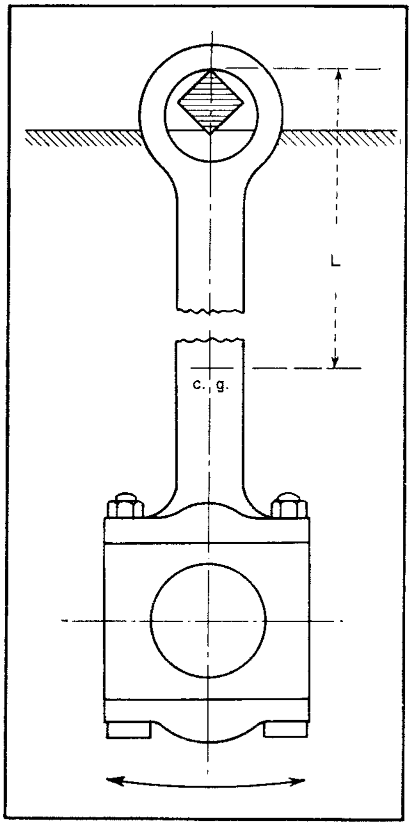

Fig. 1—Connecting rod suspended from keystock.

EXAMPLE: Given a pulley of 8 lb weight, L equals 10 in., t equals 1.5 sec. Find I_{cg}.

SOLUTION: Starting at t equals $1\frac{1}{2}$ on inner A scale of left-hand axis, follow the dotted line through curve A at L equals 10 to the turning line; go back through W equals 8 on diagonal A to I_{cg} equals 2.5 in. lb sec ².

It should be noted that the effects of L and t are screened in the equation. However, I_{cg} is directly proportional to W, and this fact permits the unlimited extension of the nomogram's use.

Suppose, in the above example, W had been 880 lb. It would appear that this value is too large for the W scale, but Eq (3) can be written:

$$\frac{I_{cg}}{k} = \frac{WL}{k}\,[0.02533 t^2 - 0.02588\, L]$$

So, in this case, assume k equals 110, and use the nomogram as above with W equaling 8, and read I_{cg}/k equals 2.5. Now merely multiply this value by 110 to find 275 in. lb sec². This is the true value of I_{cg}.

An unusual feature of this nomogram is the relation between the values of t and L; these quantities cannot be assumed at random for trial of nomogram accuracy. For example, a scant passing through $t = 1.81$ and $L = 30$ also passes through $L = 2$, thus suggesting that two different suspension lengths will satisfy the same result. One of these lengths is an extraneous value as the previously outlined experiment will indicate. Furthermore, t is always larger than $0.31936\sqrt{L}$ when inch and second units are used.

Nomogram to Determine Parallel Axis Moment of Inertia

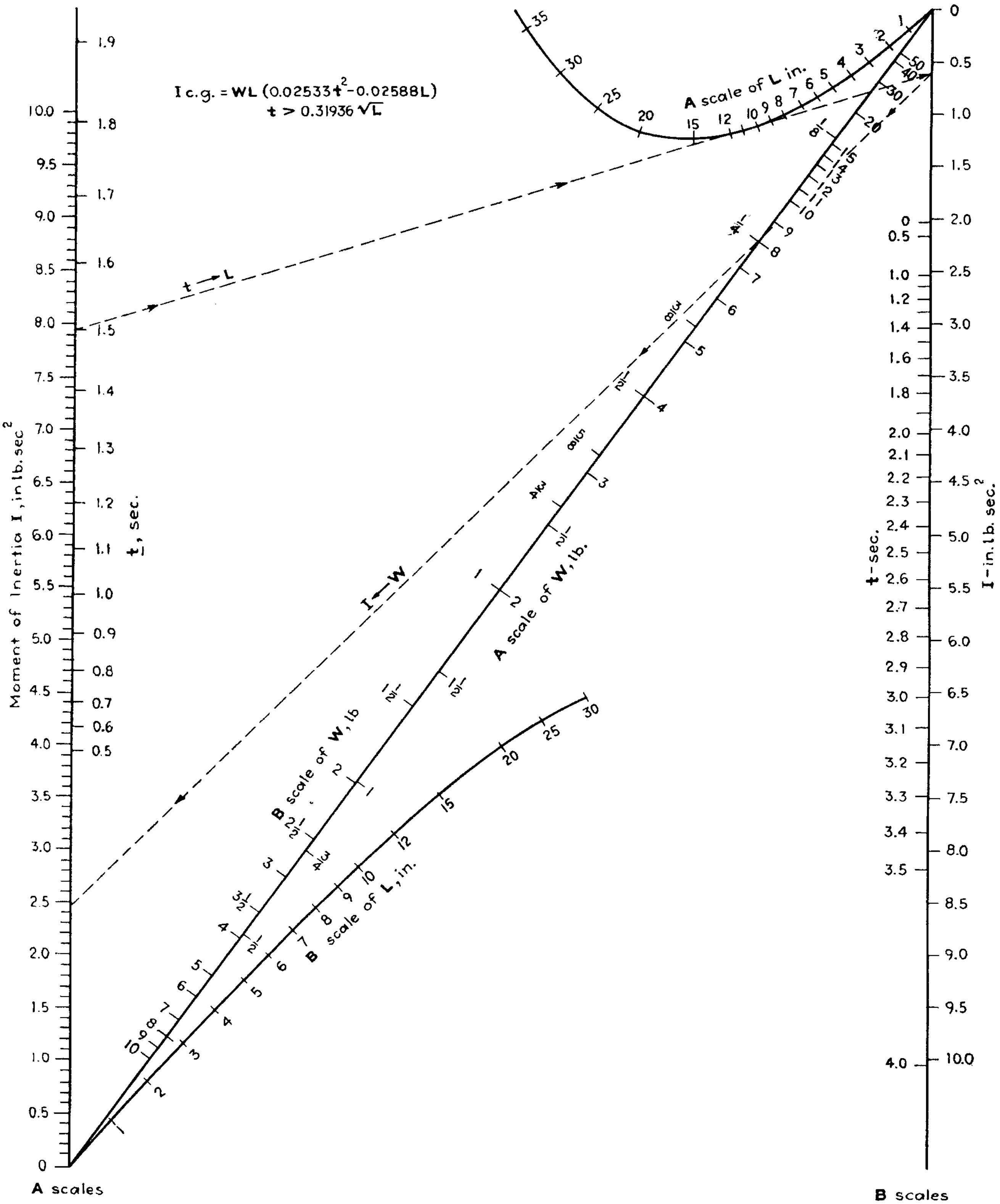

Moment of Inertia of a Prism about the Axis aa

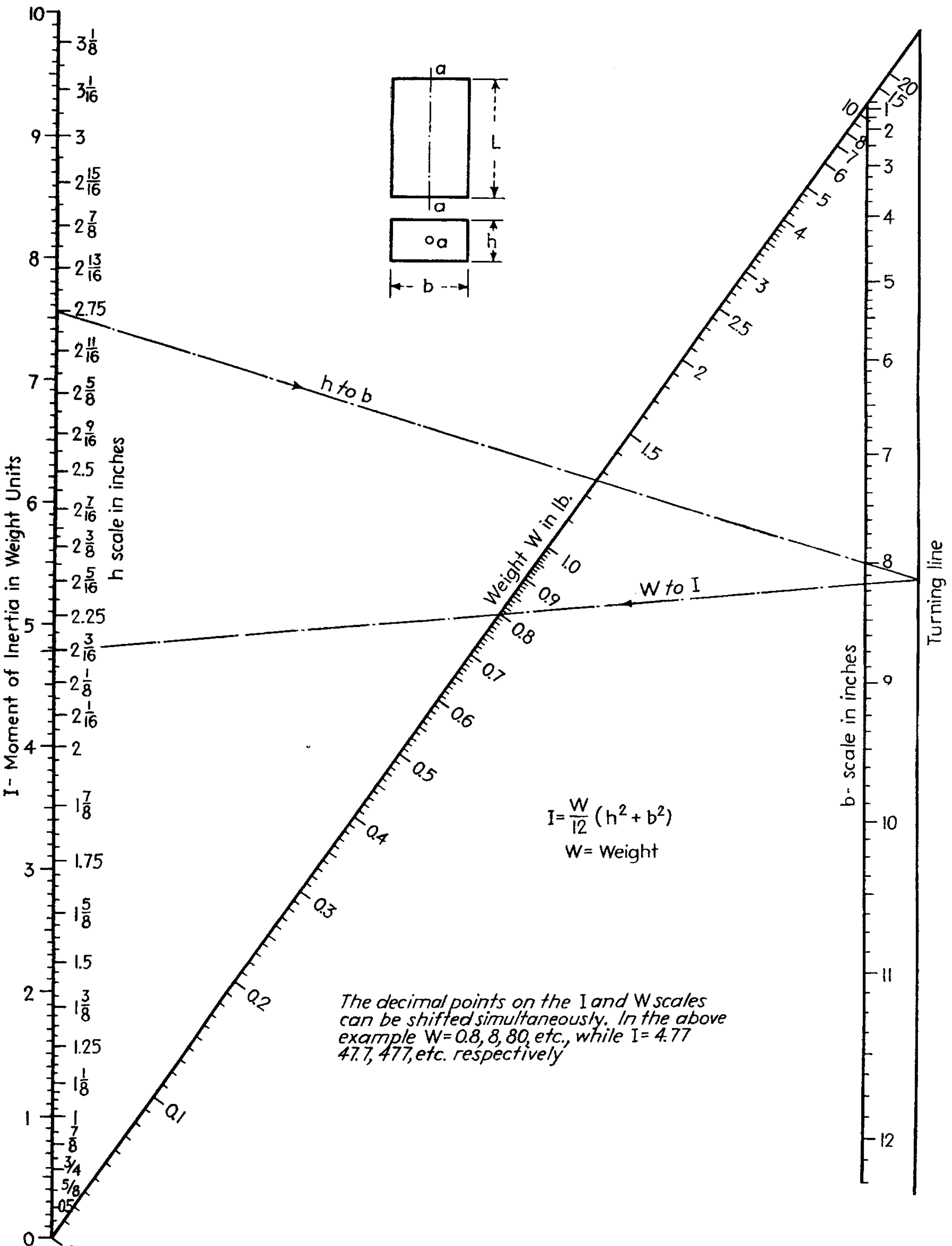

Chart for Transferring Moment of Inertia

$$I = I_0 + WX^2$$

To use chart, draw two mutually perpendicular lines on a sheet of transparent material. For example, the cross-lines show that, when the weight of the mass is 12 lb., its moment of inertia I_0 about a given axis is 30 lb.-in. squared and the distance to another parallel axis is 2.5 in.; then the moment of inertia I about the second axis is 105 lb.-in. squared.

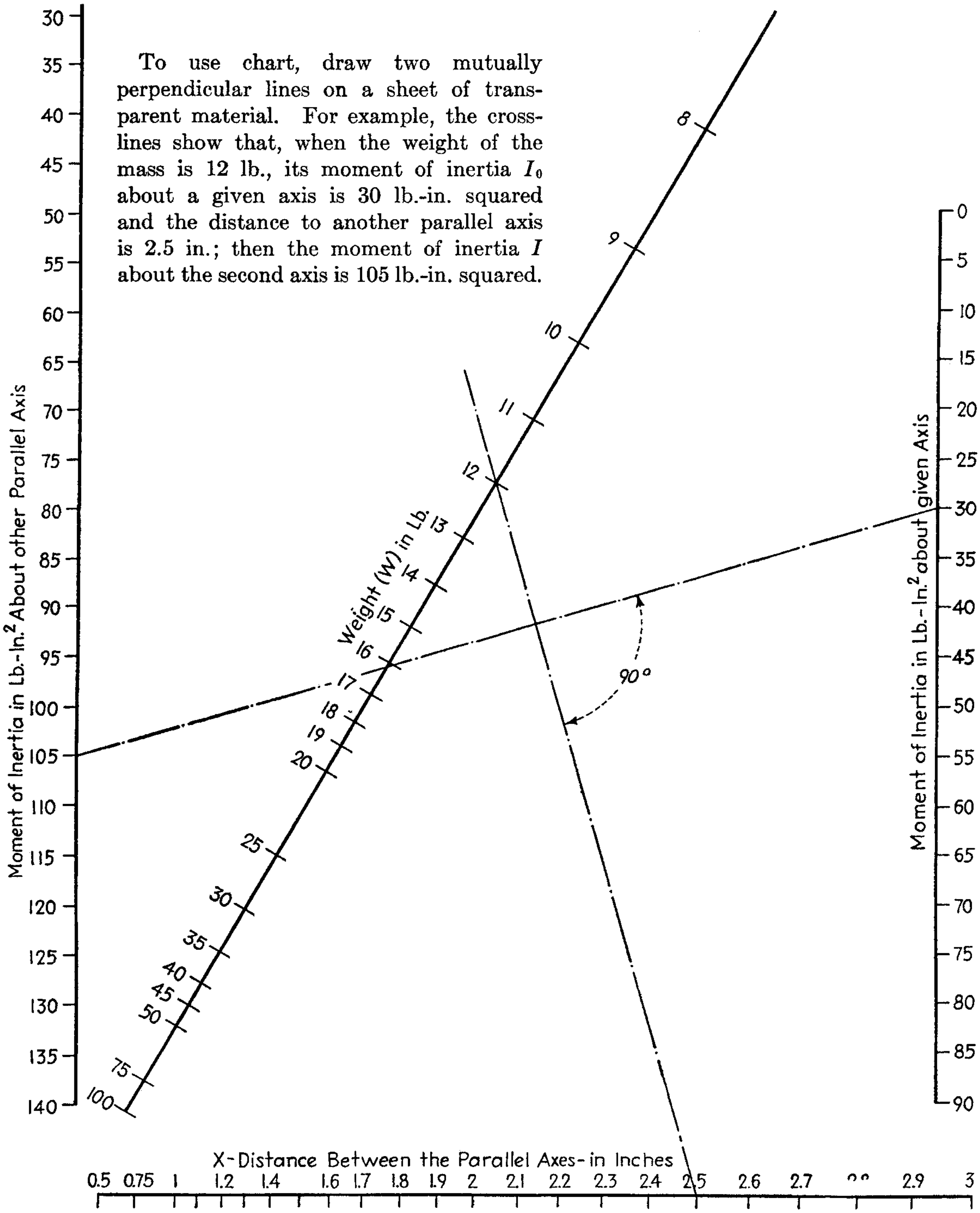

Rotary Motion

$$V = \frac{P}{F} = \frac{S}{T} = \frac{2\pi R n}{12 \times 60}$$

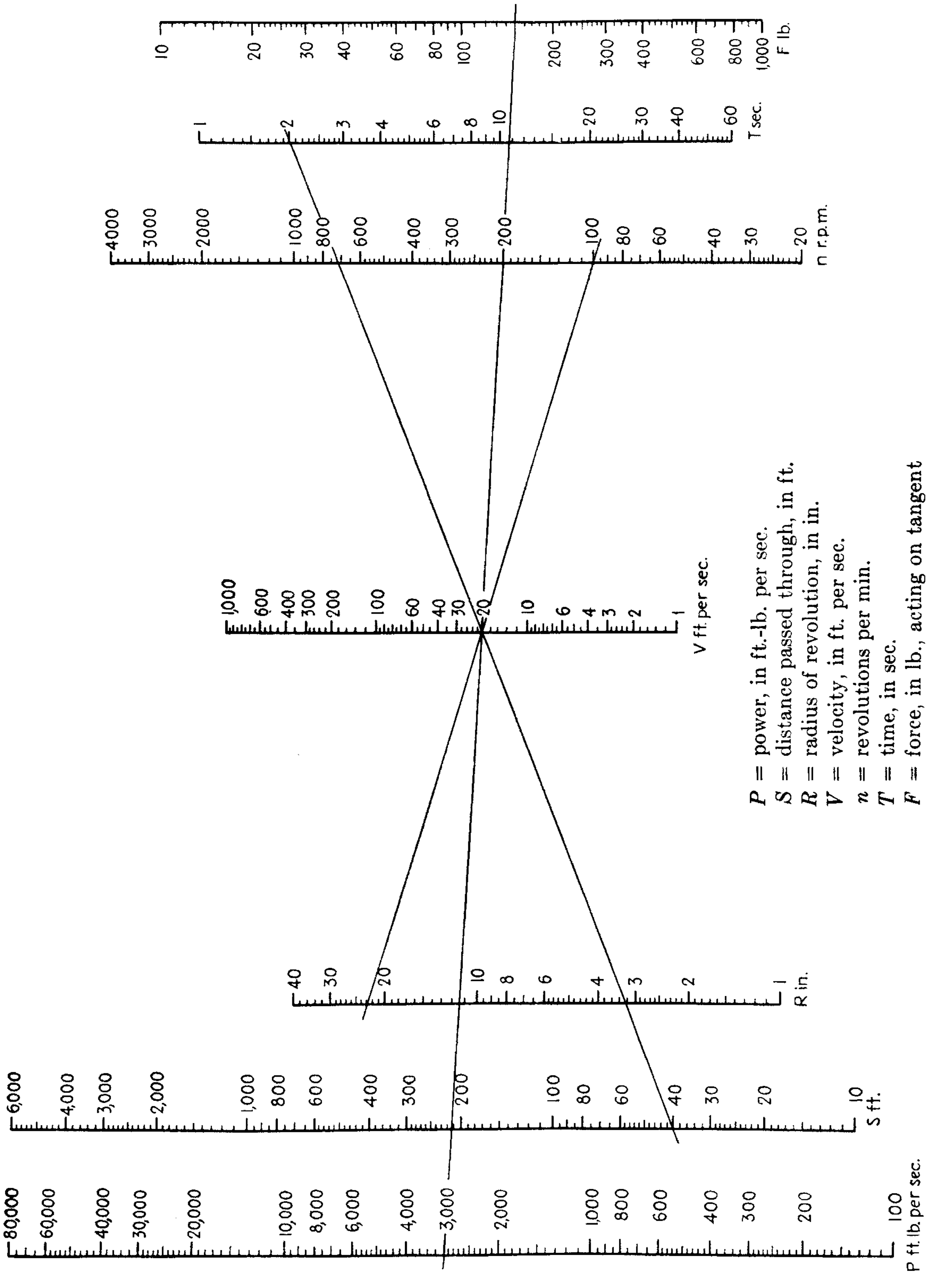

Accelerated Linear Motion

$$\frac{2S}{T^2} = \frac{V}{2S} = \frac{V}{T} = \frac{32.16F}{W} = G$$

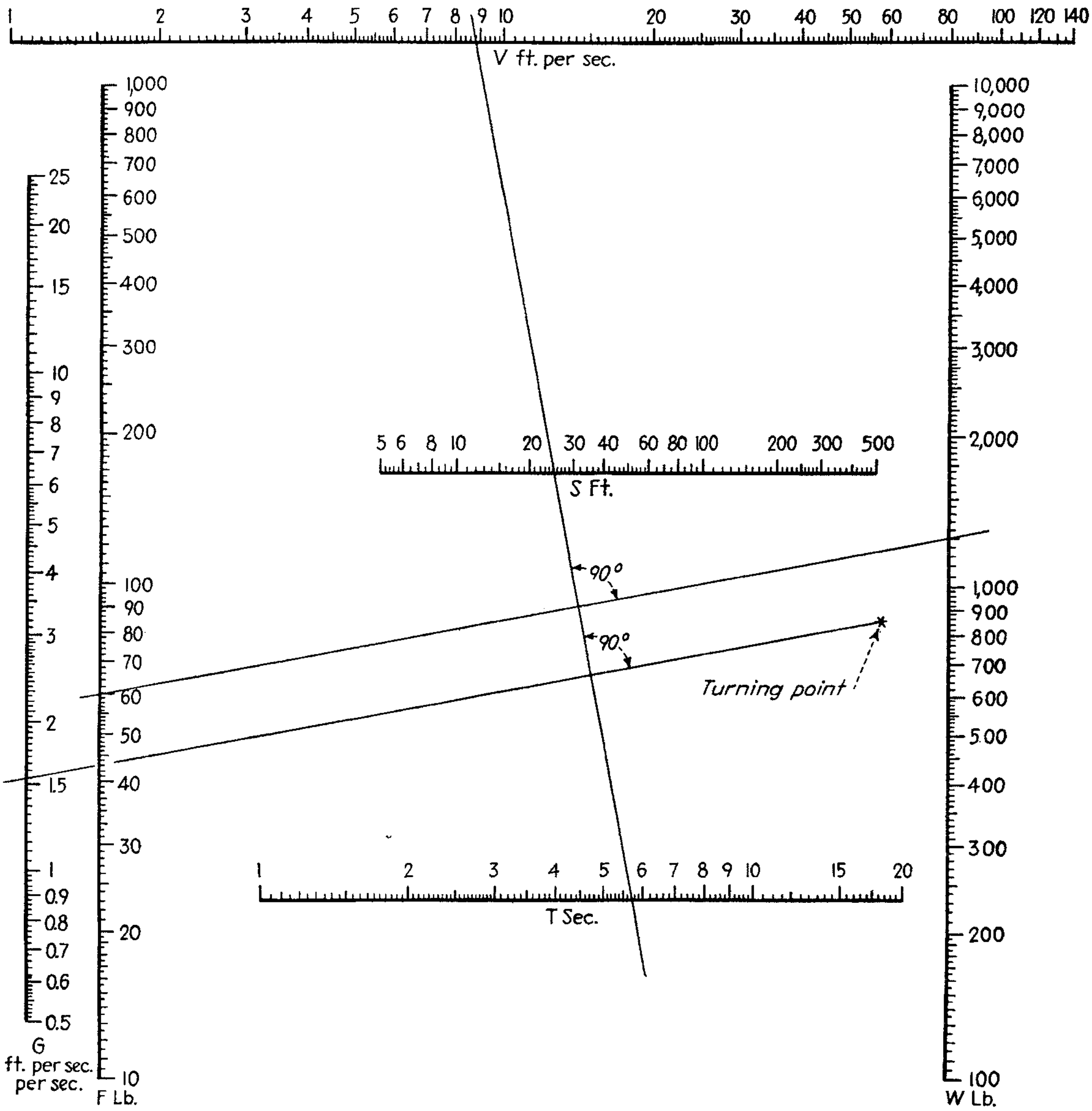

* = turning point
V = velocity at time T, in ft. per sec.
S = distance passed through, in ft.
T = time during which force acts, in sec.
F = accelerating force, in lb.
W = weight of moving body, in lb.
G = constant acceleration, in ft. per sec.

Theoretical Capacity of Gear Pumps and Motors

A. E. Maine

This nomogram is based on the equation

$$F = 0.0036\, D^2Sw/P$$

where F = flow, gpm
D = pitch dia of gear, in.
S = speed, rpm
w = width of gear teeth, in.
P = gear tooth factor

EXAMPLE—At what speed must a gear pump operate to deliver 50 gal/min assuming 2 in. pitch dia gears, 1¼ in. tooth width, and each gear has 10 teeth.

Line I connects the pitch dia and number of teeth. From the point representing 50 gal/min, Line II is drawn through the intersection of Line I and the reference line. Since Range 1 was used to establish the left end of Line II, the required speed is read at 4350 rpm.

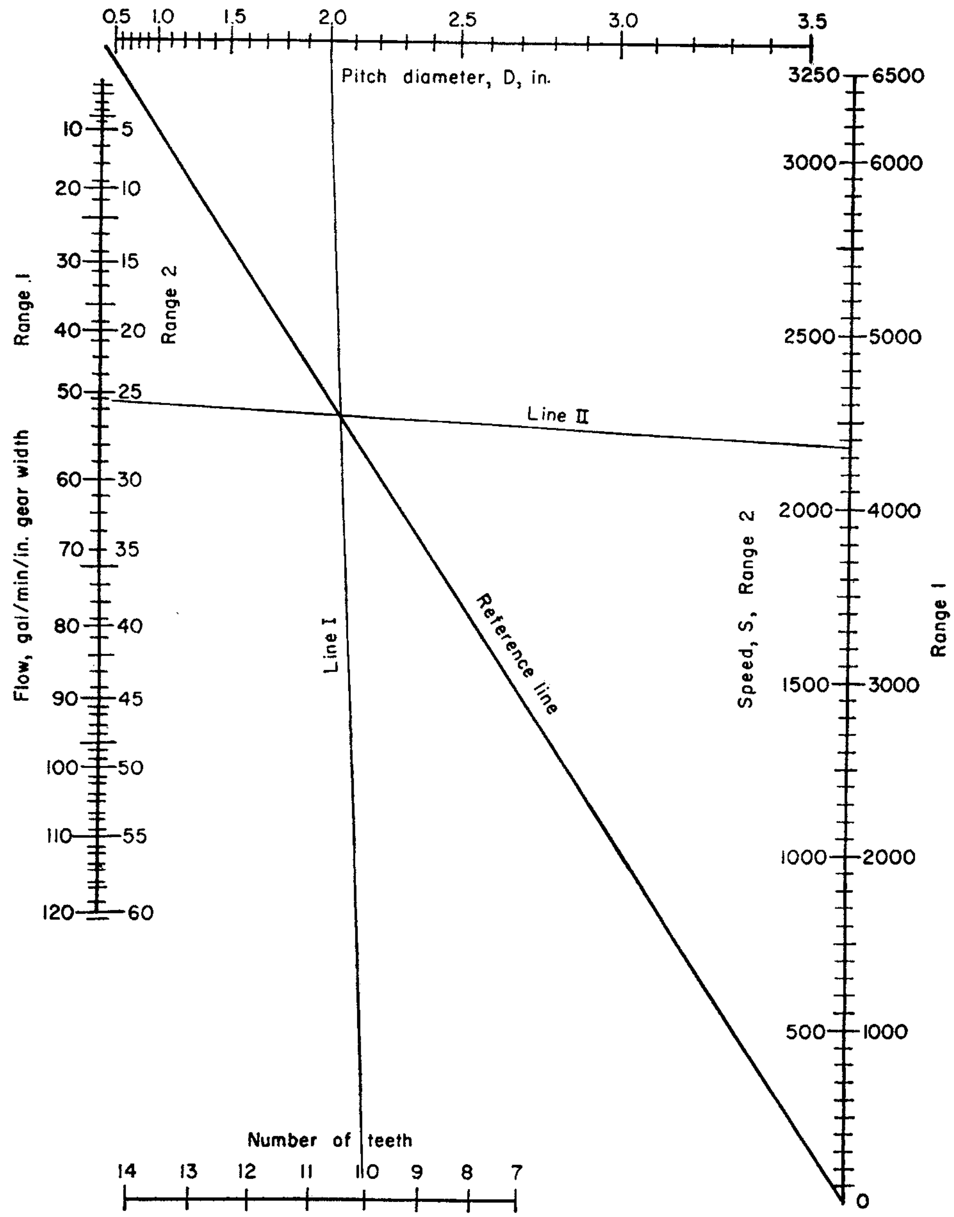

Nomogram for Piston Pumps

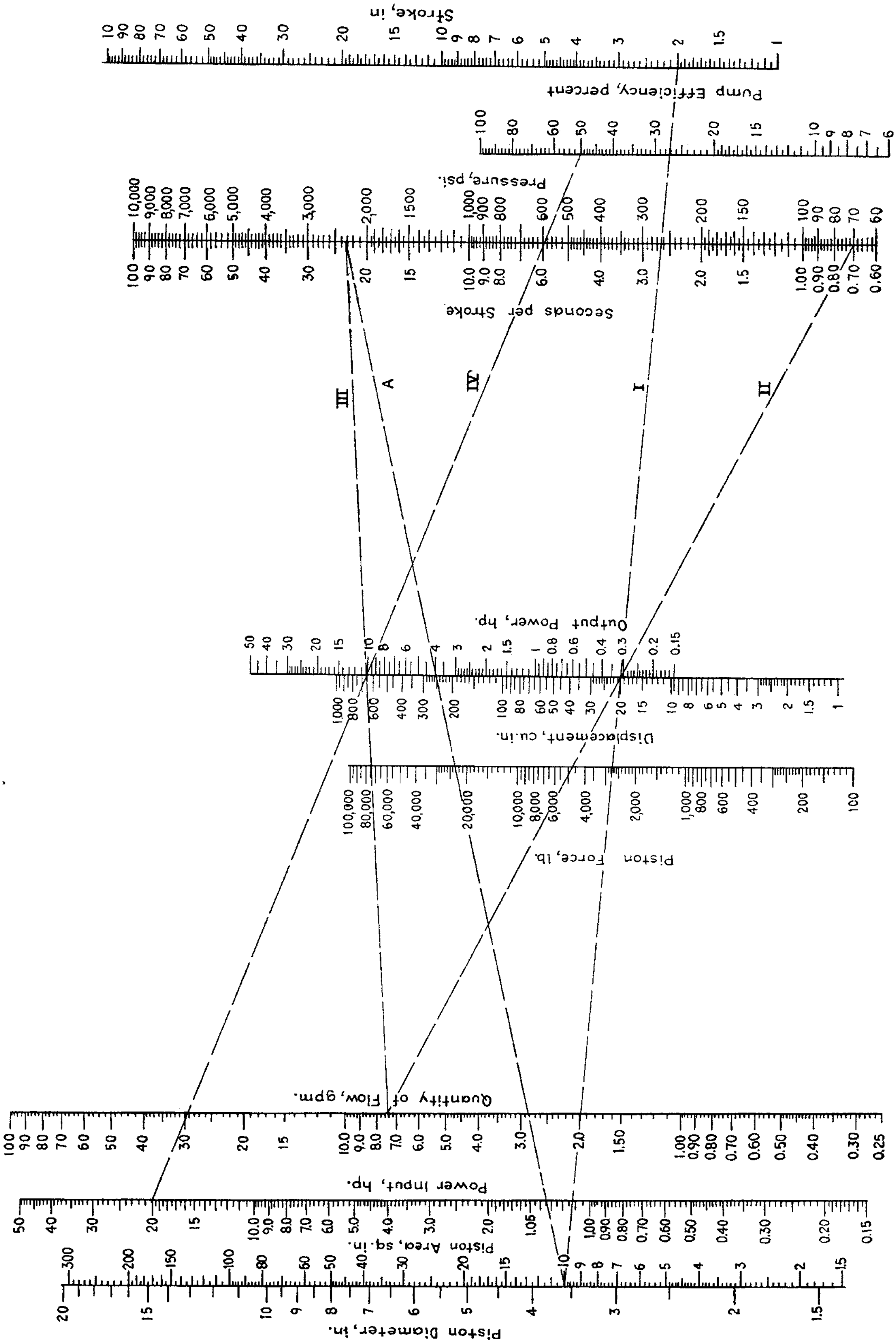

Weight and Volume

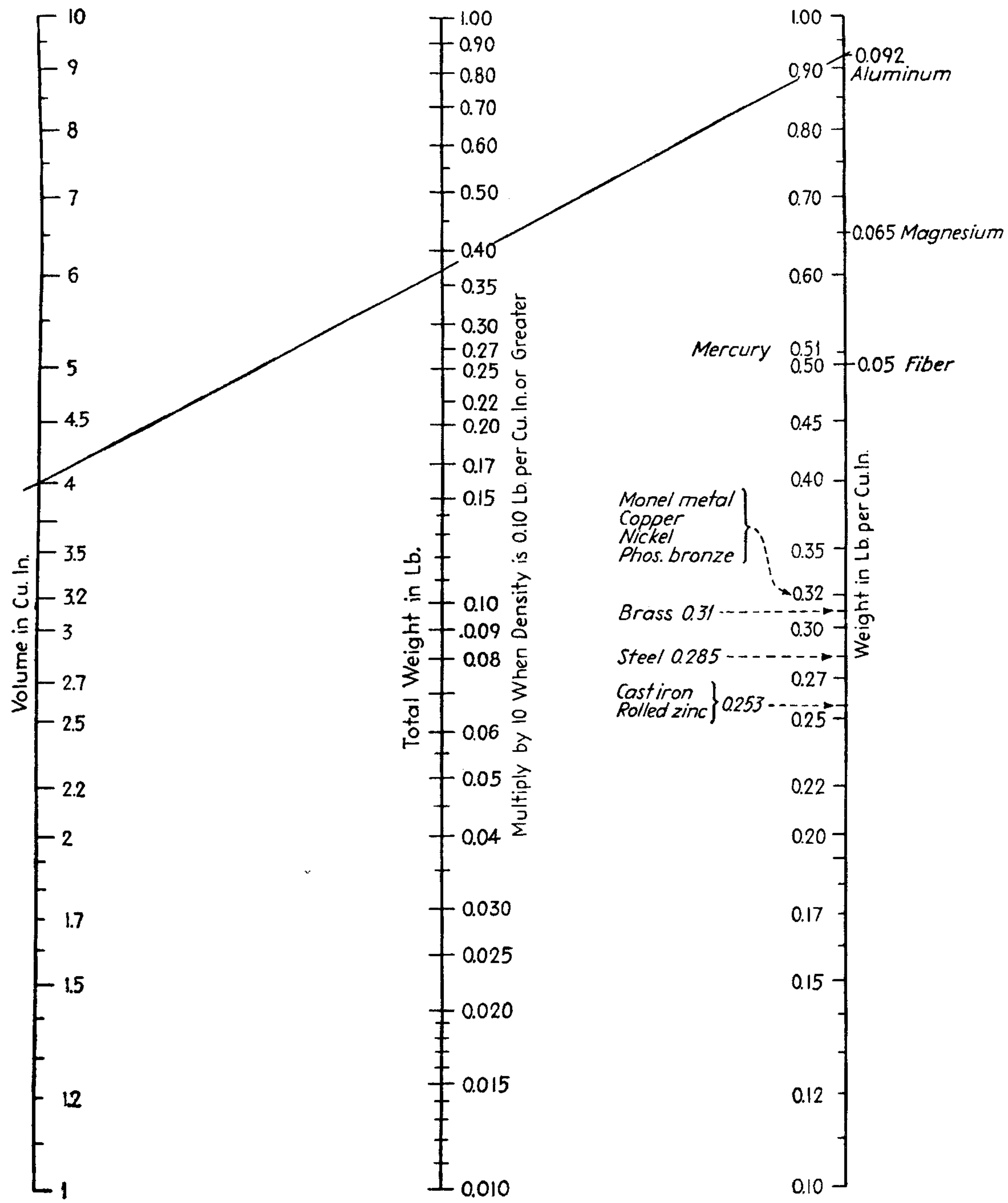

Draw a straight line through the two known points. The answer will be found at the intersection of this line with the third scale.

Example: 4 cu. in. of aluminum weighs 0.37 lb.

Volumes of Spherical Segments

C. P. Nachod

THIS nomogram is designed for calculating graphically the volume of a spherical segment such as would be used for the rounded ends of tanks.

The chart is based on the equation

$$V = \pi h^2\left(r - \frac{h}{3}\right) = \pi h^2\left(\frac{d}{2} - \frac{h}{3}\right)$$

in which

V = volume of the segment
h = height of segment
r = radius of sphere
d = diameter of sphere

The nomogram gives h up to a hemisphere for d up to 10. For a greater range of values, the volume of the spherical segment can be found by proportion since the volumes of similar segments are proportional to the cubes of their diameters. For example, let the diameter d of the sphere equal 15 in. and h equal 6 in., V' can be found as follows:

$$\frac{h}{d} = \frac{6}{15} = \frac{4}{10}$$

Chart shows for d equal to 10, and h equal to 4, that V equals 184 cu. in.

Then for d equal to 15, and h equal to 6

$$V' = \left(\frac{15}{10}\right)^3 \times 184 = 1.5^3 \times 184 = 621 \text{ cu. in.}$$

Scales are shown for drawing more h lines so that the precise one needed for any calculation can be drawn.

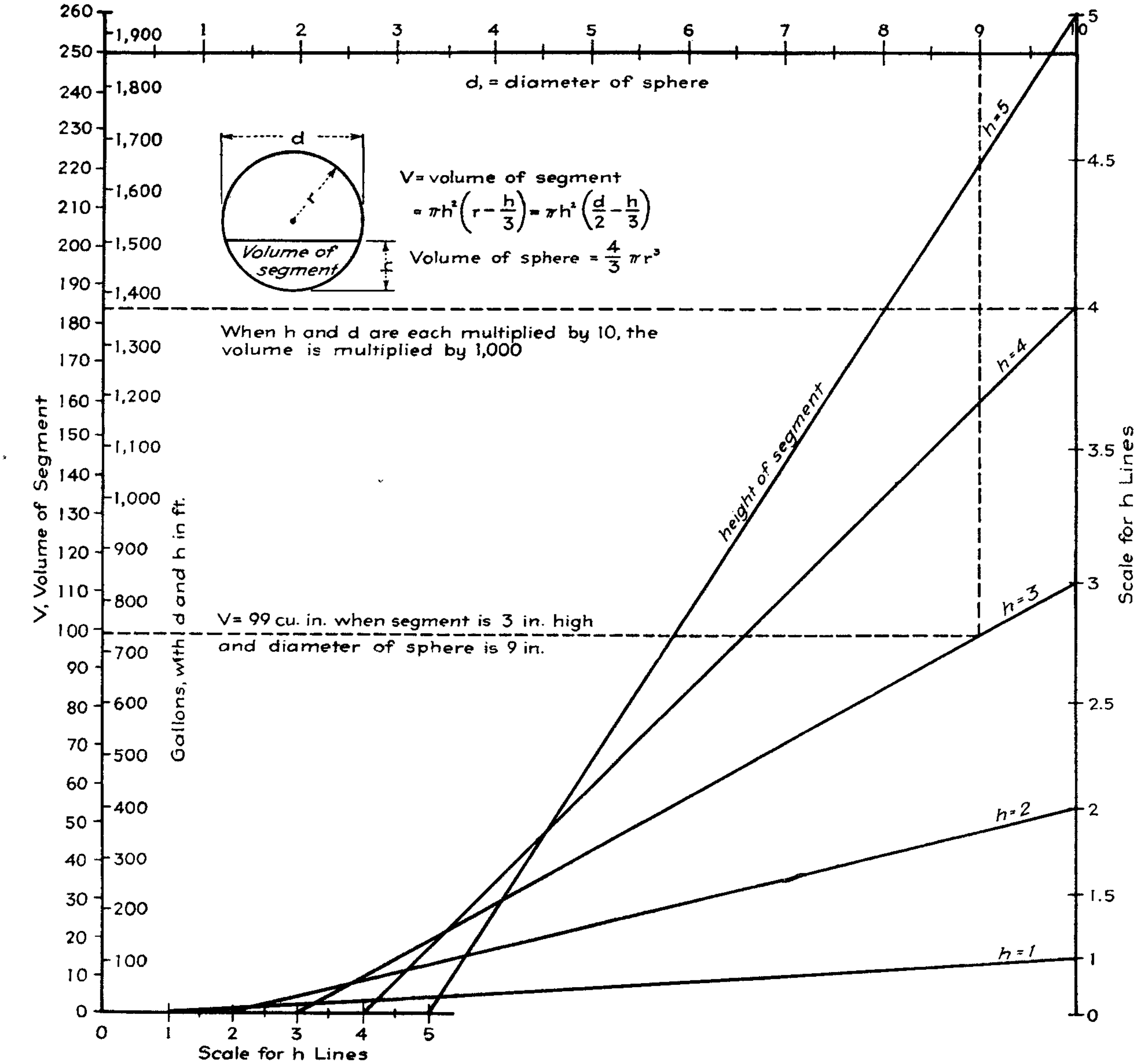

Volumes in Horizontal Round Tanks with Flat Ends

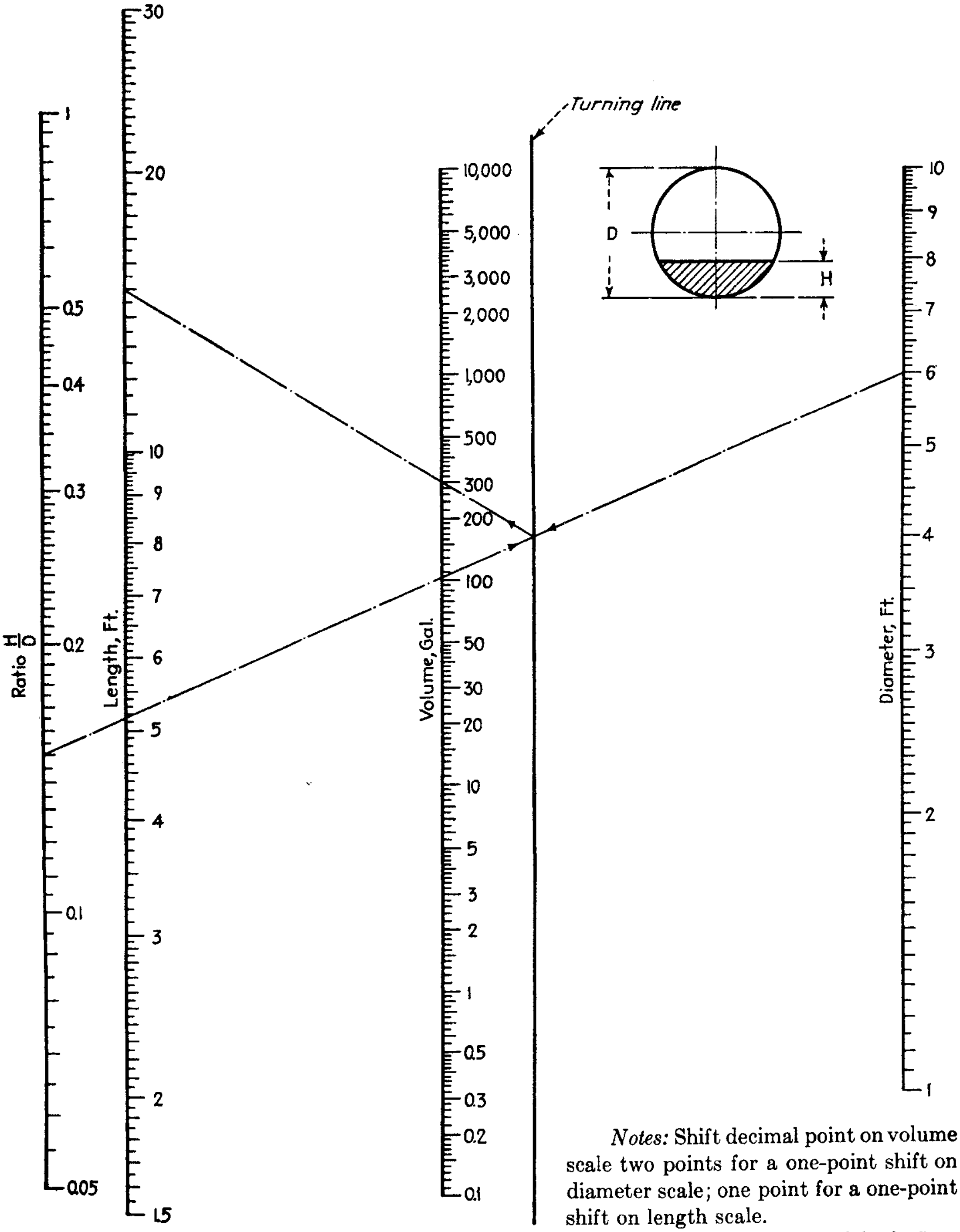

Notes: Shift decimal point on volume scale two points for a one-point shift on diameter scale; one point for a one-point shift on length scale.

Example: Tank is 6 ft. in diameter and 15 ft. long. $H = 0.9$ ft. $H/D = 0.15$. Join 0.15 on H/D scale with 6 on diameter scale. From point of intersection with turning line, draw line to 15 ft. on the length scale. The volume scale shows 300 gal. If D had been 0.6 ft., H 0.09 ft., and length the same, the answer would be 3.00 gal.

Another Shortcut to Torsion-Bar Design

This nomograph supplies values for a mass moment of inertia of torsion bars–or any round or rectangular bar.

D. A. Derse

Answers read directly off the nomograph are for torsion bars, fixed at one end, made of material with a density of 0.280 lb/in.^{3} For other materials, multiply moment of inertia I by density/0.280. If the bar isn't fixed at either end, double the value of I.

Example

Find moment of inertia of a circular torsion bar with diameter $d = 0.50$ in., length $L = 26$ in. Draw two lines intersecting at right angles on a piece of transparent paper or plastic. Line up the cross on the three knowns on the nomograph and read off $I = 5.8 \times 10^5$ lb-in.-sec^2.

SYMBOLS

a = Half width of rectangular bar, in.

b = Half height of rectangular bar, in.

d = Diameter of round bar, in.

I = Effective mass moment of inertia, lb-in.-sec^2

L = Length of bar between restraint and plane where torque is applied, in.

M = Mass of bar, lb-sec^2/in.

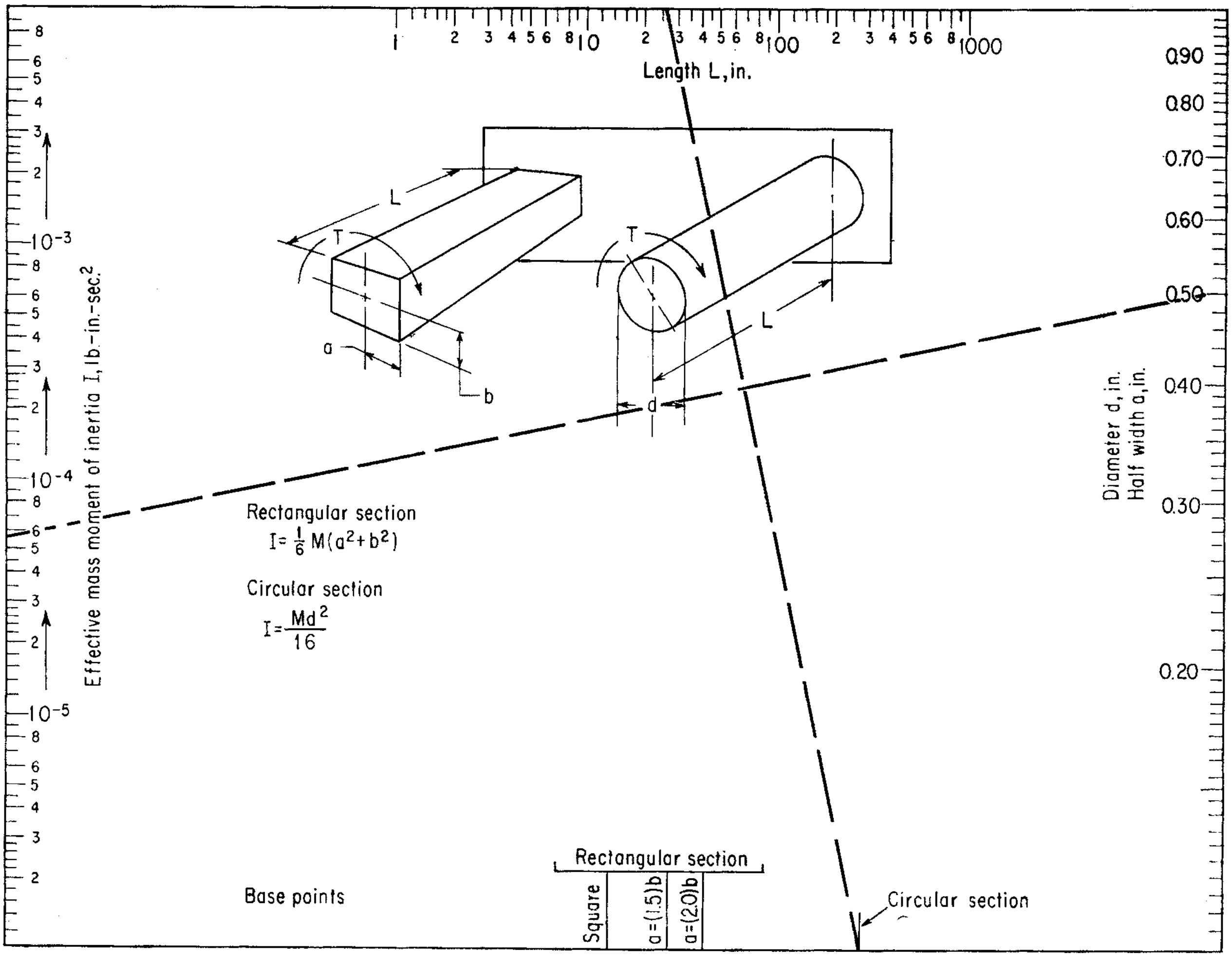

INDEX

NOTE: Subjects are followed by double numbers to indicate each page reference. The (first) bold-face number indicates the section; the (second) light-face number is the page number of that section.

A

B

C